Copyright © 2003, 2014 Vytenis Babrauskas

Ignition Handbook

Copyright © 2003, 2014 Vytenis Babrauskas

By the same author:

Babrauskas and Grayson, eds., HEAT RELEASE IN FIRES, 1992

Krasny, Parker, and Babrauskas, FIRE BEHAVIOR OF UPHOLSTERED FURNITURE AND MATTRESSES, 2001

Copyright © 2003, 2014 Vytenis Babrauskas

Ignition Handbook

Principles and applications to fire safety engineering, fire investigation, risk management and forensic science

Vytenis Babrauskas, Ph.D.

Fire Science Publishers

◆

Society of Fire Protection Engineers

Disclaimer
The information presented has been carefully evaluated and is believed to be reliable. Nonetheless, no warranty, expressed or implied, is offered as to the accuracy of the information. Neither the author nor the publishers assume any responsibility for the use of the information contained herein. Any individual using this information is obligated to obtain professional guidance and must not make decisions based solely on the information provided herein if such use of information has a potential to affect safety of people or property.

Copyright © 2003, 2014 by Vytenis Babrauskas

No part of this publication may be reproduced, stored in a retrieval system, or transmitted in any form or by any means, electronic, mechanical, photocopying, recording, scanning or otherwise, except as permitted under Section 107 or 108 of the 1976 United States Copyright Act, without the prior written permission of the Publisher.

ISBN 0-9728111-3-3

Library of Congress Control Number: 2003090333

Published by Fire Science Publishers
A division of Fire Science and Technology Inc.
Issaquah, WA 98027
USA

Distributed in Europe by:
Interscience Communications Ltd.
London SE10 8JT
United Kingdom

Printed and bound in the USA.

10 9 8 7 6 5 4 3 2 1

Foreword

While there has been significant scientific study into the ignition of fires and explosions, the results of this research have not been utilized to their maximum potential. This book is a significant step towards correcting the under-utilization of this body of knowledge.

Vytenis Babrauskas has a reputation for the thoroughness of his literature searches, and this book demonstrates that that reputation is well deserved. Dr. Babrauskas left no stone unturned, and the result is arguably the most comprehensive work on a single subject in the area of fire science or fire protection engineering.

This book is written for a broad audience, ranging from beginners who are new to the scientific study of ignitions to experts who have a well developed scientific background. The author presents fundamental science relating to combustion, which is presented in a manner suitable for beginners with only a rudimentary understanding of chemistry, then expands upon this treatment at a level that would be suitable for most advanced experts in areas relating to ignitions of fires and explosions. For each topic covered, this book thoroughly presents the relevant underlying science, then uses this science to explore the strengths and weaknesses of typical applications such as regulatory requirements and test methods.

While the author states that the primary use of this book will be in the investigation and understanding of past fires, there is another important application of this information: the design of buildings and facilities. In any design where the prevention of ignition is an objective, the concepts presented in this book provide an invaluable resource for the design engineer.

Morgan J. Hurley
Technical Director
Society of Fire Protection Engineers

Preface

The present work is the first book attempting to cover the entire subject of ignition of unwanted fires. The only areas where coverage has been intentionally limited are:

(1) Fundamental theory of reacting flows. A number of modern ignition theories are simply specialized applications of general computational fluid dynamics (CFD) models. The CFD field has become highly developed in recent years and an assortment of good textbooks already exists.

(2) Preventive measures. Chapter 12 presents material in several, selected areas where systematic, research-based studies exist. But the field is vast and hundreds of codes, standards, and handbooks dealing with preventive issues involved in design, installation, and maintenance of facilities have been published by NFPA and other organizations. The reader should consult these for their detailed recommendations.

(3) Flash point compilations. Chapter 15 contains information on a wide variety of pure and 'practical' fuels where, apart from flash points, additional data, e.g., flammability limits or minimum ignition energies, exist. For an authoritative compilation of flash point data on roughly 2000 substances, NFPA 325 is recommended.

(4) Brand-name listings of defective or recalled products. This is ephemeral information and should be obtained from CPSC or from specialty periodicals.

Even with the limitation #1 stated above, some readers may find that much less space is devoted to coverage of theory than to coverage of practical applications. This, however, is due to availability of material. The author believes that a theory is valuable only if:

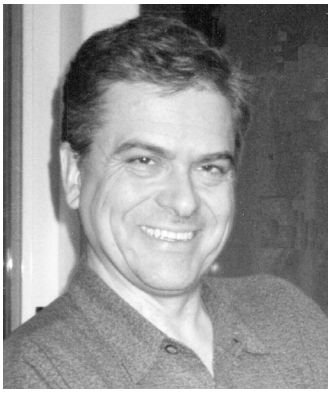
(a) it leads to a conceptual understanding of the problem; or

(b) it provides a framework for making useful practical calculations.

The author reviewed a very large number of theory papers which did not meet either of these objectives and, consequently, are not covered in this Handbook. Typically, such theoretical studies did not lead to physical insights and either (a) produced only wholly-numeric solutions, which were illustrated with a few example problems but with no means for users to apply to their own cases, or (b) were so ambitious that a huge number of input constants is required, but there exists no practical means by which users can obtain such constants for their problems. If such theories had been included, the size of the Handbook would likely have doubled, but it is hard to see that its value would have increased.

Several of the author's friends have suggested that coverage should also be limited in the areas where information might prove of value to lawless individuals. Apart from the fact that he doubts a book can be made useful for technical specialists, yet devoid of value to the criminal, the author believes in the wisdom of Isaac Bonewits: *"Evil acts cannot be prevented by keeping the public ignorant."*

About the author



Vyto Babrauskas was the first person to ever earn a doctoral degree in Fire Protection Engineering (University of California, Berkeley), where he studied fire endurance of buildings and created the first computer room fire model to be released in the US. Subsequently, he conducted fire research at the National Institute of Standards and Technology for 16 years, where he developed the Cone Calorimeter, the large-scale open calorimeter, and other test methods. He also developed various fire safety engineering design methods and models and has written extensively on fire safety topics, which includes more than 200 articles and reports. Since 1993 he has headed Fire Science and Technology Inc., a firm providing consulting, contract R&D services to manufacturers and laboratories, and fire science support to fire investigations and litigations.

.

Acknowledgements

Writing this book proved to be a bigger undertaking than I envisioned at the start. Thus, the decision by the Society of Fire Protection Engineers' Education and Scientific Foundation to provide some support for the effort has been much appreciated.

Many individuals graciously provided various materials helpful towards preparing this book, with special thanks due to: Marty Ahrens, Kathleen Almand, John Amerongen, Ralph Anthenien, Jesse Aronstein, Kiyomi Ashizawa, Arlene Barnhart, Chris Bloom, Joe Bloom, Regina Burgess, Mary Cahill, Monica Carnesi, Kenneth Cashdollar, Judd Clayton, Hugh Council, Michel Curtat, John D. DeHaan, Fred Dryer, Dougal Drysdale, David Edenburn, Ulf Erlandsson, Charley Fleischmann, Ross F. Firestone, Michael Fitz, Mario Fontana, Mark E. Goodson, Cecile Grant, Yasuaki Hagimoto, John R. Hall jr., Yuji Hasemi, David Higday, Irma M. Hill, David B. Hirsch, Marcelo Hirschler, Donald Hoffmann, Blake Holt, Ron Hrynchuk, Morgan Hurley, David Icove, Nora Jason, Mohammed Khan, Richard Kithil, jr., Ingolf Kotthoff, Ulrich Krause, Christian Kubainsky, Peter Lambrineas, John Lentini, Neville McArthur, Roy Merrifield, Keith Moodie, Steven Nowlen, Jack Olsen, Birgit Östman, Roger Parker, David Peace, Ulrich von Pidoll, Chris M. Pietersen, Albert Reed, David Reiter, Terry A. Roberts, Kuma Sumathipala, Takeshi Suzuki, Ken Swan, Russell Thomas, Robert J. Tuchman, Kathy Whisner, Robert H. White, Ulf Wickström, Fred Williams, and R. Brady Williamson.

Sincere thanks is due the reviewers whose comments were greatly valued and helped to make this a better book: Norman Alvares, Andrew Armstrong, Larry Arnold, Robert Barker, Bruce Ettling, Irvin Glassman, Mark Goodson, Brian Gray, Yasuaki Hagimoto, Martin Hertzberg, Robin Holleyhead, Gordon Jones, Takashi Kashiwagi, Ronald Kilgore, Ulrich Krause, Graeme Leiper, Bob Levine, Keith Moodie, Howard Needles, Thomas Ohlemiller, Thomas Peacock, Albert Reed, John Rockett, Jack Sanderson, Eckart Schmidt, Thomas Shefchick, Joel Stoltzfus, Hugh Talley, Craig Tarver, Elizabeth Weckman, and Robert Witter. I am especially grateful to those reviewers—Michael Fitz (who read the book's manuscript as a graduate-student assignment for a course I was teaching at Worcester Polytechnic Institute) and John Staggs (and anonymous reviewers recruited by him)—who undertook to review the entire manuscript.

Ross F. Firestone wrote the section on Arc-discharge lamps; Michael M. Fitz wrote the section on Welding and portions of the sections on Chimneys and flues and on Coffeemakers and teapots.

Thanks to Carol Heywood-Babrauskas and Doris Heywood for proofreading the book, and to Viki Mason and David Heywood for designing the cover and the titlepage. Chau Nguyen and Noel Putaansuu helped prepare some of the figures for this book.

Acknowledgements and sources of copyrighted materials

Permissions to reproduce copyrighted material from a number of sources are gratefully acknowledged.
Chapter 1. Figure 4: Reprinted with permission from NFPA 921 Guide for Fire and Explosion Investigations, Copyright © 2001, National Fire Protection Association, Quincy, MA 02269. This reprinted material is not the complete and official position of the National Fire Protection Association on the referenced subject which is represented only by the standard in its entirety.
Chapter 4. Figure 2: Reprinted by permission from The Combustion Institute. Figure 13: Reprinted by permission from The Combustion Institute. Figure 55: Copyright American Institute of Physics, used by permission. Figure 57: Reprinted by permission from The Combustion Institute. Figure 58: Copyright Royal Society, used by permission. Figure 67: Reprinted by permission from The Combustion Institute. Figure 72: Reprinted by permission from Fig. 3 of Khalturinsky, N. A., and Berlin, Al. Al., Polymer Combustion, pp. 145-294 in *Degradation and Stabilization of Polymers*, H. H. G. Jellinek, ed., Elsevier, Amsterdam (1989). Figure 79: Reprinted by permission from The Combustion Institute.
Chapter 5. Figure 2: Reprinted by permission from The Combustion Institute. Figure 4: Reprinted by permission from The Combustion Institute. Figure 5: Reprinted by permission from The Combustion Institute. Figure 17: Reproduced with permission of the AIChE. Copyright © 1995 AIChE. All rights reserved. Siwek, R., and Cesana, C., Ignition Behavior of Dusts: Meaning and Interpretation, *Process Safety Progress* vol. 14, 107-119 (1995). Figure 24: Reprinted by permission from The Combustion Institute. Figure 27: Reprinted by permission from The Combustion Institute. Figure 28: Reprinted by permission from The Combustion Institute. Figure 39: Reprinted by permission from Springer-Verlag. Figure 50: Reproduced with permission of the AIChE. Copyright © 1999 AIChE. All rights reserved. Siwek, R., and Cesana, C., Ignition Behavior of Dusts: Meaning and Interpretation, *Process Safety Progress* vol. 14, 107-119 (1995). Figure 58: Reproduced by permission from ASTM International.
Chapter 6. Figure 4: Reprinted by permission from The Combustion Institute. Figure 6: Reproduced with the permission of The Institute of Energy, London. Figure 7: Reproduced with the permission of The Institute of Energy, London. Figure 9: Reprinted by permission from The Combustion Institute. Figure 17: Reproduced with permission of Elsevier Science. Figure 32: Reprinted by permission from The Combustion Institute. Figure 57: Reprinted with permission from NFPA, Electrical Installations in Hazardous Locations, Copyright © 1988, National Fire Protection Association, Quincy, MA 02269. Figure 58: Reprinted with

permission from NFPA, Electrical Installations in Hazardous Locations, Copyright © 1988, National Fire Protection Association, Quincy, MA 02269. Figure 59: Reprinted with permission from NFPA, Electrical Installations in Hazardous Locations, Copyright © 1988, National Fire Protection Association, Quincy, MA 02269. Figure 60: Reproduced by permission from ASTM International.
Chapter 7. Figure 11: Reprinted by permission from The Combustion Institute. Figure 12: Copyright Royal Society, reprinted by permission. Figure 13: Reprinted by permission from The Combustion Institute. Figure 14: Reprinted by permission from The Combustion Institute. Figure 15: Reprinted by permission from The Combustion Institute. Figure 16: Reprinted by permission from The Combustion Institute. Figure 17: Reprinted by permission from The Combustion Institute. Figure 39: Reprinted by permission from The Combustion Institute. Figure 43: Reprinted with permission from *Aspects of Degradation and Stabilization of Polymers*, H. H. G. Jellinek, ed., Elsevier, Amsterdam (1978). Figure 45: Copyright John Wiley & Sons; reprinted by permission. Figure 74: Reproduced with permission of Elsevier Science. Figure 84: Reproduced by permission from ASTM International.
Chapter 9. Figure 8: Copyright Royal Society of Chemistry; used by permission. Figure 9: Reprinted by permission from The Combustion Institute. Figure 10: Reprinted by permission from The Combustion Institute. Figure 12: Copyright Associacio D'Enginyers Industrials de Catalunya, used by permission. Figure 13: Reprinted by permission from The Combustion Institute. Figure 15: Reproduced with permission of the American Institute of Chemical Engineers. Copyright © 1995 AIChE. All rights reserved. Chong, L. V., Shaw, I. R., and Chen, X. D., Thermal Ignition Kinetics of Wood Sawdust Measured by a Newly Devised Experimental Technique, *Process Safety Progress* vol. 14, 266-270 (1995). Figure 16: Copyright The Institute of Physics, used by permission. Figure 17: Copyright Royal Society of New Zealand, used by permission. Figure 19: Copyright Elsevier Science, used by permission. Figure 30: Reprinted by permission from The Combustion Institute. Figure 31: Reprinted with permission from Elsevier Science. Figure 35: Reprinted with permission from Elsevier Science. Figure 37: Reprinted with permission from Elsevier Science. Figure 43: Reprinted with permission from Elsevier Science. Figure 44: Reprinted with permission from Elsevier Science. Figure 47: Reproduced by permission from ASTM International. Figure 48: Reprinted with permission from Elsevier Science.
Chapter 10. Figure 22: Copyright © 1999 AIChE. All rights reserved. Figure 24: : Reprinted by permission from Springer-Verlag.
Chapter 11. Figure 16: Reprinted with permission from NFPA, Fire Protection Handbook, 16th ed., Copyright © 1986, National Fire Protection Association, Quincy, MA 02269. Figure 29: Copyright BRE Ltd.; reproduced by permission. Figure 31: Reprinted by permission from The Combustion Institute. Figure 33: Reprinted by permission from The Combustion Institute. Figure 34: Copyright Elsevier Science, used by permission. Figure 39: Copyright Institute of Physics; used by permission. Figure 54: Reprinted courtesy of Exxon Mobil Corporation. Figure 56: Copyright Institute of Physics; used by permission. Figure 59: Copyright Dover Publications; used by permission.
Chapter 12. Figure 2: Copyright © 1975 AIChE. All rights reserved. Howard, W. B., Rodehorst, C. W., and Small, G. E., Flame Arresters for High-Hydrogen Fuel-Air Mixtures, pp. 46-55 in *Loss Prevention*, vol. 9, AIChE, New York (1975).
Chapter 13. Figure 3: Copyright Elsevier Science, used by permission.
Chapter 14. Figure 27: Copyright NEMA; used by permission. Figure 39: Copyright © IEEE 1975. Figure 45: Reprinted with permission from the July 13, 1987 issue of *Air Conditioning, Heating & Refrigeration News*. Figure 52: Reprinted with permission from NFPA, Béland, B., Considerations on Arcing as a Fire Cause, *Fire Technology* vol. 18, 188-202 (1982), Copyright © 1982, National Fire Protection Association, Quincy, MA 02269. Figure 60: Copyright Fire Findings, LLC; reprinted by permission. Figure 94: Copyright ASAE, reprinted by permission. Figure 99: Copyright Fire Findings, LLC; reprinted by permission. Figure 116: Copyright HMSO; used by permission. Figure 127: Copyright BRE Ltd.; reproduced by permission.
Color Plates. Plate 15: British Crown copyright © 1995, courtesy HSL. Plate 16: British Crown copyright © 2001, courtesy HSL. Plate 17: British Crown copyright © 2001, courtesy HSL. Plate 43: British Crown copyright © 1995, courtesy HSL. Plate 111: Copyright Fire Findings, LLC; reprinted with permission.

Crown copyright material is reproduced with the permission of the Controller of HMSO and the Queen's Printer for Scotland. Additional photographs are British Crown copyright © and have been provided courtesy of the Health and Safety Laboratory, HSL.

Photographs provided by Chris Korinek, P.E. of Synergy Technologies, www.synergytech.net are © Chris Korinek.

Table of contents

Detailed Contents are given at the start of the individual chapters.

Foreword, by Morgan J. Hurley iii

Preface iv

Acknowledgements v

Chapter 1. Introduction 1

Chapter 2. Terminology 13

Chapter 3. Fundamentals of combustion 24

Chapter 4. Ignition of gases and vapors 41

Chapter 5. Ignition of dust clouds 141

Chapter 6. Ignition of liquids 182

Chapter 7. Ignition of common solids 234

Chapter 8. Ignition of elements 352

Chapter 9. Self-heating 367

Chapter 10. Explosives, pyrotechnics and reactive substances 444

Chapter 11. Characteristics of external ignition sources 497

Chapter 12. Preventive measures 591

Chapter 13. Special topics 609

Color Plates. 637

Chapter 14. Information on specific materials and devices 675

Chapter 15. Tables 1022

Index. 1081

Copyright © 2003, 2014 Vytenis Babrauskas

Chapter 1. Introduction

Background **1**
Fire ignition statistics **2**
The fire triangle and taxonomy of ignitions **6**
Some complications of definition *8*
Types of combustion and combustion-like reactions *8*
Apparatus-dependent nature of ignition **9**
The probabilistic nature of ignition and negative proof **9**
Comments to the fire investigator **10**
Computer methods **11**
References **12**

Background

All fires start with ignition. In olden times, by the way, ignition used to be called *inflammation*, and that term is still occasionally found in some literature. When a fire is investigated, many things may be checked, but one of the essential ones is an attempt (it is not always successful!) to determine the cause of the fire. To determine the cause, it is important to know the ignition characteristics of combustibles. Can a material have undergone self-heating and spontaneous combustion? Is the radiant heat output of a certain malfunctioning device sufficient to ignite a hypothesized first-ignited material? Often, when one of these questions arises, the issue of testing and analysis must then be handled. How shall the material be tested? and how shall the results be presented so that a hypothesis could properly be accepted or disproved? Conversely, the fire protection engineer and the chemical engineer must have knowledge about ignition characteristics so that environments could be designed which minimize the possibility of unwanted ignition.

The present book is the first ever to attempt to encompass the total field of ignition of unwanted fires. (We will generally not deal with *desired* ignitions, such as the ignition of gasoline vapors in an engine cylinder, although in some cases wanted ignitions have to be studied due to their potential for leading to further ignitions that are unwanted.) Because ignition is of concern both to fire investigators and to engineers, the needs of two different groups must be addressed and the intended readership of this tome encompasses both these groups. This is an experiment, since very few publications have been written which attempt to be useful to both. However, the author feels that this is possible. The more theoretical or mathematical sections can be skipped by those without a science background and continuity will not be lost. Most of the chapters which contain heavy doses of theory also contain a section entitled *Highlights and summary of practical guidance*; this can be the first recourse to the fire investigator, who can then use it as a basis to explore other sections of particular relevance in that chapter. Additionally, Chapters 14 and 15 function as a mini-encyclopedia of practical information on substances and devices commonly encountered in fires.

While it is true that ignition begins a fire, this book is not an introduction to fire science, nor to the investigation of fires. While the reader is not expected to have a background both in fire science/engineering and in fire investigation, he or she is expected to have a background in *one* of these. Individuals from scientific fields would be expected to have first studied Dougal Drysdale's **An Introduction to Fire Dynamics**[1]; this is a unique introduction to fire science and there is currently no 'or-equal.' In the fire investigation area, the two most essential prerequisites are John DeHaan's **Kirk's Fire Investigation**[2] and NFPA 921—Guide for Fire and Explosion Investigations[3]. Also valuable is a British fire investigation textbook issued by The Institution of Fire Engineers[4].

While much here may be useful to the researcher, nonetheless the book is primarily addressed to the practitioner. Thus, even in the theory sections, lengthy or highly complex mathematical solutions have not been presented in detail. Instead, ample references are given to those researchers who will want to look up (and maybe improve upon!) various lengthy mathematical procedures reported in the literature. The summaries of theoretical proofs and conclusions given in this book, however, should suffice in most cases even for the advanced practitioner.

Much of the literature of this field was developed quite a few years ago. Thus, the best way of presenting numeric guidance was generally by means of graphs. Today, however, it is reasonable to assume that any engineer or investigator will have access to spreadsheet programs on the computer. Thus, the author has taken many such older results which were given only in graphical form and, by digitizing and curve-fitting them, converted them into simple equations which can readily be set up in a spreadsheet. It is also worthwhile to point out that some old solutions are only available as trial-and-error equations, commonly ones where the unknown quantity appears on both sides of the equation. Such equations were laborious to evaluate in slide-rule days, but by setting up an expression for each side of the equation into two cells of a spreadsheet, iterations can be made almost as fast as evaluating a simple algebraic expression.

Fire ignition statistics

In many countries, death rates due to fire improved remarkably over the course of the 20th century, as illustrated by US data[5, 6] in Figure 1. Reliable national statistics are not available prior to 1913, but fire losses in the 19th century were evidently very large. For example, in 1875 it was estimated

Table 1 Causes of US structure fires (average per annum over the years 1994-1998)

Cause	Fires	Civilian deaths	Civilian injuries	Direct property damage (in Millions)
Cooking equipment	107,500 (19.0%)	339 (9.0%)	4,928 (23.1%)	$514.7 (7.1%)
Stove	71,000 (12.5%)	248 (6.6%)	3,645 (17.1%)	$282.9 (3.9%)
Oven	15,800 (2.8%)	25 (0.7%)	488 (2.3%)	$71.4 (1.0%)
Incendiary or suspicious	90,300 (15.9%)	628 (16.8%)	2,468 (11.6%)	$1,598.1 (22.1%)
Match	16,000 (2.8%)	70 (1.9%)	362 (1.7%)	$168.5 (2.3%)
Unknown-type open flame	8,600 (1.5%)	46 (1.2%)	263 (1.2%)	$162.2 (2.2%)
Heating equipment	70,100 (12.4%)	486 (13.0%)	1,828 (8.6%)	$778.5 (10.8%)
Fixed space heater	18,300 (3.2%)	145 (3.9%)	402 (1.9%)	$192.1 (2.7%)
Central heating unit	11,500 (2.0%)	50 (1.3%)	259 (1.2%)	$111.1 (1.5%)
Chimney or flue	10,500 (1.8%)	13 (0.3%)	46 (0.2%)	$65.3 (0.9%)
Water heater	8,400 (1.5%)	37 (1.0%)	379 (1.8%)	$92.1 (1.3%)
Fireplace	7,800 (1.4%)	28 (0.7%)	114 (0.5%)	$85.3 (1.2%)
Portable space heater	6,100 (1.1%)	178 (4.7%)	492 (2.3%)	$135.6 (1.9%)
Other equipment	64,000 (11.3%)	298 (8.0%)	2,164 (10.2%)	$1,045.8 (14.4%)
Electrical distribution	54,700 (9.6%)	372 (9.9%)	1,664 (7.8%)	$971.4 (13.4%)
Fixed wiring	17,400 (3.1%)	138 (3.7%)	400 (1.9%)	$359.0 (5.0%)
Light fixture or sign	8,700 (1.5%)	33 (0.9%)	162 (0.8%)	$101.4 (1.4%)
Cord or plug	8,100 (1.4%)	99 (2.6%)	450 (2.1%)	$149.2 (2.1%)
Appliances, tools, or air conditioning	39,200 (6.9%)	136 (3.6%)	1,223 (5.7%)	$352.7 (4.9%)
Clothes dryer	18,100 (3.2%)	17 (0.5%)	418 (2.0%)	$92.5 (1.3%)
Open flame, ember or torch	34,300 (6.0%)	138 (3.7%)	1,014 (4.8%)	$456.0 (6.3%)
Torch	8,300 (1.5%)	15 (0.4%)	283 (1.3%)	$190.6 (2.6%)
Open fire	6,200 (1.1%)	18 (0.5%)	93 (0.4%)	$45.2 (0.6%)
Rekindle or reignition	5,800 (1.0%)	1 (0.0%)	5 (0.0%)	$47.8 (0.7%)
Hot ember or ash	5,400 (1.0%)	16 (0.4%)	108 (0.5%)	$66.2 (0.9%)
Smoking material	29,000 (5.1%)	850 (22.7%)	2,256 (10.6%)	$341.0 (4.7%)
Cigarette	25,700 (4.5%)	735 (19.6%)	2,025 (9.5%)	$292.6 (4.0%)
Exposure (to other hostile fire)	25,200 (4.4%)	35 (0.9%)	190 (0.9%)	$358.1 (4.9%)
Convection or direct flame	9,400 (1.7%)	17 (0.5%)	77 (0.4%)	$148.3 (2.0%)
Radiated heat	7,100 (1.3%)	10 (0.3%)	47 (0.2%)	$57.5 (0.8%)
Child playing with fire	22,600 (4.0%)	296 (7.9%)	2,119 (10.0%)	$271.2 (3.7%)
Match	8,700 (1.5%)	84 (2.2%)	634 (3.0%)	$96.0 (1.3%)
Lighter	7,700 (1.4%)	140 (3.7%)	1,039 (4.9%)	$110.2 (1.5%)
Other heat, flame, or spark	16,800 (3.0%)	152 (4.1%)	1,196 (5.6%)	$263.1 (3.6%)
Candle	8,000 (1.4%)	95 (2.5%)	838 (3.9%)	$112.7 (1.6%)
Natural causes	13,400 (2.4%)	16 (0.4%)	243 (1.1%)	$291.4 (4.0%)
Lightning	7,700 (1.4%)	10 (0.3%)	63 (0.3%)	$179.0 (2.5%)
Total	**567,100**	**3,744**	**21,293**	**$7,241.9**

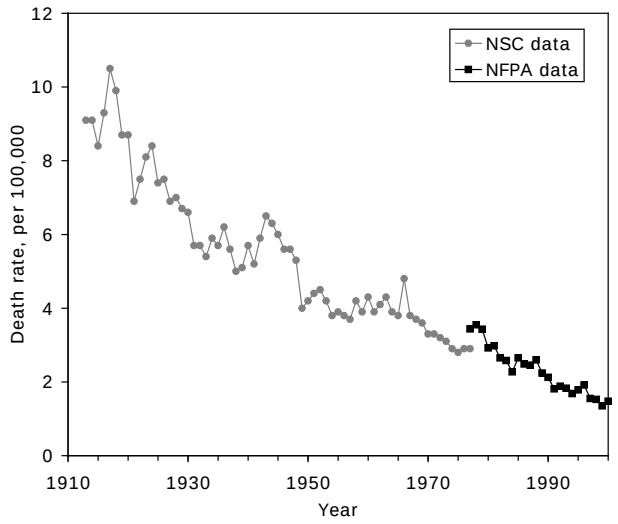


Figure 1 Death rate due to fire in the United States

(but possibly overestimated) that 5,000 to 6,000 deaths[7] were occurring annually in the US due to kerosene ignition accidents alone. Today, there are around 4,000 deaths annually from *all* fire causes. No single factor accounts for this impressive record of improvement. Smoke detectors are perhaps the modern invention that has had the most significant impact on fire deaths. The fraction of households equipped with smoke detectors in the US[8] jumped from 10% in 1974 to 67% in 1982 and is currently over 90%; yet the statistics show a relatively smooth decline, without a sharp downward jump during that period. A number of ignition sources which were notorious in earlier years became insignificant a century later. As an example, gas and kerosene lighting were very prominent fire sources in the 19th century but are rare today. But it is not entirely clear that sufficient categories of this type exist to account for the steady improvement. Two factors which may account for a steady improvement are (1) increased education among the population, and (2) more strict codes, standards, and regulations, although their effects are hard to quantify.

Detailed causes of US structure fires are given in Table 1, as provided by NFPA[9]. These are fires reported to U.S. municipal fire departments and so exclude fires reported only to Federal or state agencies or industrial fire brigades. The table presents fires in *all* buildings and is not restricted to homes. First-level cause categories are based on a hierarchical sorting developed by the US Fire Administration. Hierarchical sorting means the numbers tend to be lower than those calculated if a cause is considered in isolation. Second-level causes are calculated within the first-level categories and are shown only if they accounted for at least 1.0% of fires. Also, second-level causes that are totally lacking in detail (e.g., unknown form of heat) are omitted. Most fires classified as "Other equipment" lack all detail on the equipment involved. Fires are shown to the nearest hundred, civilian deaths and injuries to the nearest one, and direct property damage to the nearest hundred thousand dollars. Sums may not equal totals because of rounding errors. Fires with first-level cause category of "unknown" have been proportionally allocated.

Table 2 Fraction of US fires that are incendiary or suspicious

Location of fire	1980	1998
structure fires	23.4	19.2
vehicle fires	8.7	14.9
outdoor and other	67.9	65.9

Two things must be kept in mind in connection with the US national statistics, such as given in Table 1:

(1) The only fires counted are those reported to the local fire departments, but *most* fires are unreported. The majority of these are small nuisance fires which are successfully extinguished by individuals who do not subsequently feel a need to contact the fire department. A 1974 study in one city found that only about 11% of the total residential fires were reported[10]. A much larger, more recent study of US households[11] found that only 4% of the total residential fires were reported. The study also identified that many householders tend to forget events that occurred as recently as a year ago, and it was necessary to restrict surveying to just the most recent 3-month period. On the basis of all, rather than just reported, fires, the conclusion was that nearly 30% of US households experience a fire in any one year. Of *all* residential fires, 69.1% were due to human carelessness, 21.3% due to failure of products or equipment, 0.1% due to children playing with fire, and the remainder due to miscellaneous or unknown causes. The majority (76.4%) of *unreported* fires took place in the kitchen.

(2) The determination of cause is made by the local fire department. Their primary obligation with regards to

Table 3 Deaths due to fire for 1993, per year, per 100,000 population

Country	Rate
Argentina	1.0
Australia	0.6
Canada	1.2
Chile	2.0
Cuba	1.9
Finland	2.0
Germany	0.9
Greece	1.3
Hungary	2.8
Italy	0.7
Japan	1.0
Poland	1.4
Russia	5.9
Spain	0.6
Sweden	0.9
UK	1.0
USA	1.5
Venezuela	0.5

investigation of fires is to determine if a crime has been committed. If no crime is found, then the resources in many communities do not permit a detailed investigation. Private investigators working for insurance companies may have greater resources to investigate fires, but there is no mechanism whereby their findings would enter into the national statistics.

In the US, incendiary and suspicious fires declined in structures over the last two decades[12], but rose for vehicles (Table 2).

The statistics of other countries are significantly different. Annual death rates due to fire in selected countries[13] is shown in Table 3. Such wide discrepancies have been studied, but a clear rationale does not always emerge; the topmost reasons are, perhaps: cultural differences, building construction differences, quantities and types of occupant goods, widely disparate rates of utilizing energy, effectiveness of firefighting forces and occupant devices (smoke detectors), and—perhaps most important of all—incompatible schemes for collecting statistical data. Table 5 shows the breakdown of fire causes in Sweden[14]; clearly lightning is a large problem in that country.

Table 4 Fire causes in São Paolo residential buildings during 1995-97

Cause	Percent
carelessness at cooking	14.4
inadequate electrical wiring	11.7
arson or incendiarism	9.6
negligence with candles	5.4
LPG leakage	3.9
children playing	2.7
overheating of appliances	1.9
carelessness at smoking	1.6
balloons	1.2
carelessness at handling flammable liquids	0.3
accumulation of grease on appliances	0.3
negligence at welding works	0.3
other known causes	1.6
unknown	45.0

Table 5 The causes of fires reported in Sweden, 1982-1991

Cause	Percent
lightning	22
electrical	16
deliberately set	10
fireplace	6
chimney	3
welding	1
explosions	1
spontaneous combustion	1
other known causes	15
unknown	25

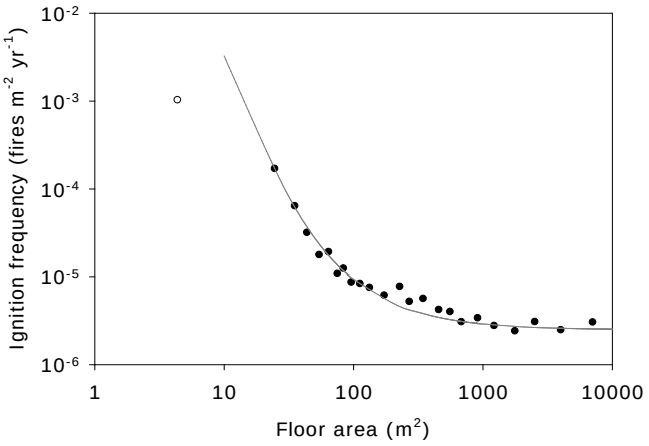


Figure 2 Ignition frequency in Finnish buildings, normalized per unit floor area

Fire statistics in developing countries tend to be quite different from those in industrialized countries. For example, some recent statistics from Brazil[15] are shown in Table 4. It is also interesting to note the focus on blame, which is generally absent in Western statistics.

To a first approximation, one might expect that the frequency of ignition per unit floor area is constant. Few countries publish fire statistics on that basis, but data from Finland[16] indicate something else. Figure 3 shows that for buildings larger than about 100 m^2, the frequency of ignition does increase with increasing floor area. But the increase is not linear, as made clear in Figure 2, except for buildings of floor area greater than 10,000 m^2. It is also not immediately evident why very small structures (< 100 m^2) have a disproportionately high incidence of ignitions, but some of these would evidently be outbuildings, not occupied structures.

Not all ignitions have the same probability of leading to a large fire, as shown in Table 7, compiled by NFPA[6]. Apart from the obvious case of exposure fires, it is clear that in-

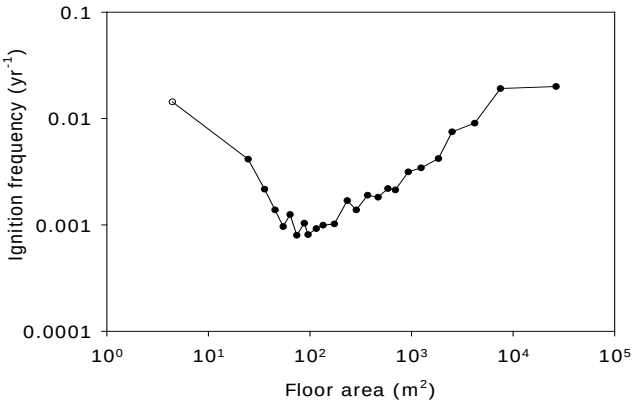


Figure 3 Ignition frequency in Finnish buildings, as a function of floor area of building

Table 6 UK statistics for 1993 – 1996 on the probability of *dwelling* fires spreading beyond room of origin

Source of ignition	Prob. (%)	Source of ignition (cont'd)	Prob. (%)
Total	7.9	smokers materials	10.4
chimney etc	37.1	electric central heating	10.2
electric weld & cut	27.6	candle	10.0
motor vehicle related	24.3	other and unspecified fuel space heater	10.0
hot metal, molten glass	17.9	other non-electric cooking appliance	9.4
other blowlamps	17.8	lighting	9.2
malicious	17.7	electric space heater	9.2
other and unspecified fuel central heating	17.3	liquefied petroleum gas other appli-ance/installation	9.2
liquid petroleum gas cooker	17.0	oil and petroleum space heater	8.1
LPG blowlamp	16.4	other electrical appliance/equipment	8.0
rubbish	16.3	blanket, bedwarmer	8.0
LPG space heater	16.2	sockets and switches	8.0
slow combustion stove etc	15.8	lightning	7.5
oil and petroleum central heating	15.3	television	7.5
fireworks	15.1	other and unspecified other appli-ance/installation	7.1
non-motor vehicle related	14.9	gas central heating	6.4
matches	14.0	plugs	5.9
computer/VDU	13.9	gas space heater	5.3
cigarette lighters	13.8	spontaneous combustion	5.3
electric water heating	13.5	iron	4.7
solid fuel: fire in grate	13.3	gas blowlamp	3.7
ashes, soot	13.3	tumble and spin driers	3.6
spread from fire	13.2	dishwasher	3.6
oil and petroleum other appli-ance/installation	13.1	other and unspecified fuel water heating	3.3
wire and cable	13.1	other cooker	3.2
acetylene weld & cut	12.7	gas water heating	3.2
gas (mains) other appliance/installation	11.6	gas cookers	2.2
taper, lighted paper, other naked light	11.4	other electric cooking appliance	1.7
audio visual	11.3	kettle, urn, etc	1.6
other welding and cutting appliances	11.0	electric cookers	1.5
electric blowlamp	10.8	microwave cooker	0.8
leads to appliances	10.5	washing machine	0.7
refrigerator	10.5	other	11.7
		unspecified	29.7

tentional ignitions are disproportionately likely to lead to large fires; conversely cooking-equipment fires are likely to be confined to the kitchen. Generally, the results suggest that open-flame ignitions cause the probability of fire extension to be high. It should also be noted that the top six include three causes – exposure, natural causes, electrical distribution equipment – where fire origin often is not inside a room and so flame spread beyond the room of origin may be hard to define. The effect of children playing with matches on causing large fires is especially extreme judging from another set of statistics. In the nationwide US study on unreported fires referred to above[11], it was found that while only 4% of the total fires were reported, 47% of the fires started by children playing with fire were reported. This is evidently because these fires are much more likely to overwhelm the householders' personal ability to extinguish.

Similar UK statistics[17], but more detailed and restricted to dwelling fires are shown in Table 6. Cox et al.[18] reported the results of a 1977 survey of fires and explosions in the chemical industry; these are given in Table 8; the study is also of significant interest in that it is one of the few ambitious efforts to analyze ignitions as part of an overall effort to quantify risk in a particular industry. The authors also reported the results of a British survey covering 1987/88, these results are given in Table 9.

More recent, but less specific data have been published in a world-wide survey[19] encompassing hydrocarbon/chemical industry losses during 1970 – 1999 that exceeded a $10,000,00 loss. These are given in Table 10 through Table 12.

Table 7 US statistics for 1994 – 1998 on the probability of fire spreading beyond room of origin

Major cause of fire	Percent
exposure (to other hostile fire)	54.7
incendiary or suspicious causes	47.9
open flame, ember or torch	34.7
child playing with fire	32.0
natural causes	31.7
electrical distribution equipment	27.9
other heat source (e.g., candle)	23.6
other equipment	23.1
smoking	22.8
heating equipment	21.5
appliances or tools	13.3
cooking equipment	6.9

Table 8 Breakdown of the nature of fires and explosions in the chemical industry

Event	Percent
fires	32
explosions outside equipment, but inside buildings	24
explosions inside equipment, because of runaway reactions or explosive decomposition	23
explosions inside equipment because air got in	11
vessels bursting due to corrosion, overheating, or overpressure	7
explosions in the open	3

Table 9 Causes of 668 known chemical industry fires/explosions studied by HSE in 1987/88

Cause	Percent
open flames (except LPG-fired equipment)	35.5
hot work	18.0
electrical current	10.5
hot surfaces	7.2
smoking	5.7
friction	5.4
spontaneous combustion	3.9
autoignition (gases)	3.7
open flames, LPG-fired equipment	3.6
hot particles	3.0
static electricity	2.8
other	0.7

Table 10 World-wide major losses in the hydrocarbon/chemical industry during 1970-1999

Event	Percent
fire	47
explosion	30
vapor cloud fire/explosion	15
mechanical breakdown	3
other	5

Table 11 Equipment associated with the major losses in the hydrocarbon/chemical industry during 1970-1999

Equipment	Percent
piping	20
vessels	20
tankage	12
pumps	6
heaters	4
heat exchangers	4
compressors	2
other	32

Table 12 Operating units associated with the major losses in the hydrocarbon/chemical industry during 1970-1999

Event	Percent
catalytic cracking	12
hydrotreating	12
storage	12
crude distillation	11
coking	6
alkylation	4
reforming	3
jetties	2
other	27

In a survey[20] covering only 1999 within the US petroleum refining industry, 25 incidents were described as given in Table 13.

Table 13 Survey results from US refineries experiencing fires or explosions during 1999

Event	Percent
Fire	72
Explosion	20
Fire+explosion	8

The fire triangle and taxonomy of ignitions

The fire triangle should already be well-known to any reader coming to this book. It says that fuel, an oxidant, and heat are necessary for combustion. Ignition is, of course, *the initiation of combustion*, but it may be surprising that, among the many available combustion textbooks, most do not provide any definition of combustion! There are a few that do. Demidov[21] defines it as: "Any chemical reaction accompanied by liberation of heat and emission of light." Lewis and von Elbe, in their classical textbook[22] define it as: "A spontaneously accelerating chemical reaction with large energy release." Fristrom[23] considers it to be: "Any relatively fast exothermic gas-phase chemical reaction." Griffiths and Barnard[24] define it as: "A self-supporting exothermic reaction."

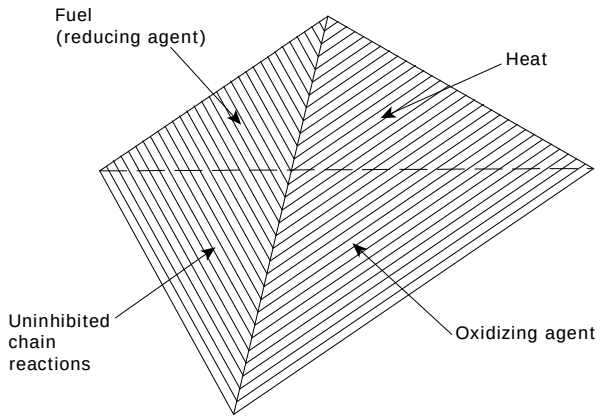


Figure 4 The tetrahedron of fire
(Copyright NFPA, used by permission)

For our purposes, it is best to define combustion as "**A self-sustained, high-temperature oxidation reaction**," a definition very close to that adopted by Turns[25]. Now, we can consider what the implications of this definition are. First, "reaction" identifies that the process is one where a chemical reaction occurs. Next, "high-temperature" excludes phenomena such as rusting, which is self-sustained oxidation, but one occurring at low temperatures. "Self-sustained" means that the process can occur without the continued presence of external energy. The opposite phenomenon is called "oxidative pyrolysis." If a material requires continued external heating for it to sustain an oxidation reaction, then it is being pyrolyzed rather than combusted. Finally, "oxidation" means that there are two participants to the reaction, with one substance being oxidized (losing electrons, or increasing in oxidation number), the other being reduced (acquiring electrons, or decreasing in oxidation number). It may be noted that while a combustion reaction is indeed exothermic, this does not need to be separately included in the definition since it is encompassed within "self-sustained."

Thus, for the fire triangle, we have explained the need for fuel and oxidant. The need for heat must be understood in a broad sense. Something must bring the system to a self-sustained, high-temperature condition. Commonly, it will be an external source of energy, with the system being able to continue reacting once a small area has been raised in temperature. But in other circumstances (spontaneous combustion), the material itself generates enough heat due to a chemical reaction occurring in it, that no external energy source is needed. Thus, a source of heat *is* present, but it is internal.

Based on this, it would be possible to divide ignitions into the form of fuel (gas, liquid, or solid), then into the form of heat used (internal or external). This type of taxonomy would be simple, but not comprehensive. A number of real-world complications exist. Some substances are mixed-phase, e.g., oil-soaked rags. Dust clouds are composed of solid particles, but their ignition behavior is specialized, and much more resembles that of gases. The oxidizer is usually gaseous air. But it may be a liquid or, in certain cases, a solid substance.

The definition of combustion we have adopted is appropriate, since it is consistent with other NFPA definitions. What it does, however, is exclude rapid, high-temperature events which are not an oxidation reaction. These include primarily decomposition reactions. A decomposition reaction is where a single molecule splits up into two pieces. These are common in pyrotechnics and explosives, also in chemical manufacturing accidents. Such will fall outside of our narrow definition of combustion. Nonetheless, initiation of these types of non-oxidative reactions will be considered in this work. The reason is that a very similar theory is used for their analysis, and many practical strategies for measuring, quantifying, or preventing them are also similar to those pertinent to oxidation reaction.

Finally, as explained in NFPA 921, modern textbooks usually invoke the fire tetrahedron (Figure 4), where uninhibited chain reactions are also considered[*]. The reason that the tetrahedron concept is introduced has to do with halogenated fire extinguishing agents. These work largely by terminating chain reactions, not by cooling or removing fuel or oxygen. Thus, if the nature of chain reactions were not considered (see Chapter 3 for a further discussion of combustion chemistry), then it would not be possible to explain the high effectiveness of halogenated fire extinguishing agents. In terms of our definition of combustion, this leg of the tetrahedron assures that the reaction *is* self-sustaining.

The reader will note that, in due accordance with their practical importance, the four sides of the tetrahedron are not equally represented in this handbook. In the vast majority of fires, it is evident that fuel, oxygen, and chain reactions are available. Thus, the largest emphasis is placed on ignition sources—examination of all aspects that make or do not make a potential ignition source a *competent ignition source* in a given situation. Conversely, chain reactions only become crucial to consider when chemical extinguishing media are involved or flame-retardant materials are being developed. Extinguishment is outside the scope of this Handbook. FR materials are considered only in the context that a certain amount of experimental ignition data on FR materials is presented, otherwise, as indicated in the Preface, the Handbook also does not delve into the topic of designing FR formulations.

[*] The present author does not think that it is a useful idea to teach the fire tetrahedron. For students at an elementary level, the additional concepts introduced can be needlessly confusing, while for more advanced students the tetrahedron concept does not provide any needed chemistry tools.

Table 14 Primary types of combustion and combustion-like reactions (and corresponding ignition types)

Combustion type	Reaction zone temp.	Fuel	Oxidizer	Where reactions occur	External ignition energy needed	Notes
normal flame	H	G	G	G	Y/N	
cool flame	M	G	G	G	Y/N	
catalytic	M	G	G	surface	Y	a
glowing	M/H	S	G	surface	Y	
smoldering	M	S	G	surface	N	b
condensed-phase				S/L	Y/N	c

G – gas
H – high
L – liquid
M – medium
N – no
S – solid
Y – yes

a – catalytic surface is needed
b – porous, char-forming fuel is needed
c – reactions are not limited to oxidation and may be decomposition, polymerization, isomerization, etc.

SOME COMPLICATIONS OF DEFINITION

In the majority of cases, the ignition event is clear when it occurs. If a piece of newspaper is lit, or a match is thrown into a gasoline pool, there is no doubt when ignition has occurred. In some cases, however, things are not so clear. The three main cases of difficulties concern:

(1) Flashing, or transient ignition, even with sustained source of heat. If visible flaming occurs, but very quickly dies out, leaving most of the fuel unburnt, the event is clearly different from one where ignition leads to nearly-complete consumption of combustibles.
(2) Cessation of burning upon removal of heat source. A number of substances can exhibit a behavior whereby combustion stops as soon as the external source of heat is removed. Is this "self-extinguishment" indicative of the fact that the product will be nearly non-participating in a fire?
(3) Cool flames. We have agreed above to only consider high-temperature reactions. Cool flames can be considered intermediate-temperature (a few hundred ºC). They are not common to most fire scenarios, but in certain situations need to be recognized. Cool flames are considered in Chapter 4. The initiation of cool flames is termed *sub-ignition*.

Issues #1 and #2 have troubled standards-makers for years, with no clear solution being at hand. Arbitrary divisions of ignition into "sustained flaming," "transient ignition," and "flashing" have sometimes been made, as seen in the next Chapter. In many cases, a substance which only exhibits transient ignition or flashing *in the full-scale fire* would qualify as relatively safe. Yet, the difficulties arise because such properties are normally measured in bench-scale tests, and the extrapolation to much larger scales is uncertain, especially for borderline phenomena. In some cases, even flashing can be problematic, for instance in burns to exposed skin. The vivid term "self-extinguishment" has a history of mis-use, and this is explored further in Chapter 7.

From the definition of combustion, it immediately follows why fuel and oxidizer need to be present to have an ignition. It is not an entirely trivial question to ask why heat or other form of energy must be added. The explanation for this requires that the concept of activation energy be considered. Chapter 3 presents some rudiments of combustion theory and provides a brief introduction to chemical kinetics.

TYPES OF COMBUSTION AND COMBUSTION-LIKE REACTIONS

Since ignition is the initiation of combustion, it is important to be aware that several types of combustion (or combustion-like) reactions exist. For our purposes, the primary combustion types can be divided into 6 main types, as shown in Table 14. Normal flames are, of course, the most commonly known form of combustion. A flame is a gas-phase manifestation and the proximate fuel and oxidizer are both gaseous. The ultimate source of the fuel, however, may be a vaporizing liquid or a solid which is degrading (pyrolyzing) and releasing combustible gases. Cool flames are rarely observed outside a laboratory environment, but for many substances the manifestation of a normal (hot) flame is preceded by a cool flame. Catalytic combustion can occur on the surface of certain substances, especially platinum, which are only mildly heated. It is not a common cause of accidental ignitions, apart from certain industrial accidents. Glowing ignition is seen when a surface which is receiving some heat suddenly exhibits a jump in temperature and begins to glow. When exposed to modest heating conditions, wood and cotton fabric sometimes ignite initially in a glowing mode, possibly changing to flaming combustion later. Glowing combustion differs from catalytic combustion in that the surface itself acts as fuel and is consumed; in catalytic combustion, the surface is not consumed and fuel and oxidizer molecules merely combine while on the surface. Smoldering also involves a glowing, but by definition, it is a self-sustained process—external heating is not needed to sustain it, although it may be needed to start the process. Combustion-like exothermic reactions in con-

densed-phase (i.e., solid or liquid) substances can show a wide variety of behaviors. These are most common in explosives, pyrotechnics, and as runaway reactions in chemical processing plants.

Normal-flame ignitions are considered throughout the book. Cool flame ignitions are covered in Chapter 4. Catalytic combustion is treated in Chapters 3 and 4. Apart from ignitions which are due to self-heating, glowing and smoldering combustion modes have not been extensively studied; the basic principles are treated in Chapter 7, while specific substances are discussed in Chapter 14. Self-heating and spontaneous combustion are covered in Chapter 9. Some metals and certain other non-metallic elements ignite and burn in a glowing mode. The ignition of these substances is covered in Chapter 8, with additional details given in Chapter 14. Condensed-phase ignitions are covered in Chapter 10.

Explosions can be physical or chemical. Chemical explosions are due to combustion or combustion-like reactions considered above. Physical explosions are forceful pressure disturbances not caused by a chemical reaction, for example, caused by dropping a large hot piece of metal into water. Physical explosions are outside the scope of this book, for an introduction, see Leiber and Doherty[26].

The definition of ignition is often a source of rich controversy to theoreticians, and some of this is alluded to in Chapters 7 and 9. Experimentalists generally do not face this difficulty, it being usually visually clear whether a substance is ignited or not. Thus, we shall be content to use the simple definitions of ignition and related concepts as given in Chapter 2.

Apparatus-dependent nature of ignition

Many physical or chemical properties can be measured in a way which is independent, or at least almost independent, of the measuring apparatus. In many practical cases, the complications introduced by the measuring apparatus are but a minor nuisance. This may lead the casual observer to feel that ignition must also be an intrinsic property. Since heat losses in a particular system are clearly an apparatus-dependent feature, maybe these losses should be eliminated? But some thought will serve to reveal that if two substances which can interact exothermically—a fuel and an oxidizer—are put together in an adiabatic system, they will always ignite and will reach the adiabatic flame temperature. In real life, of course, we know that ignitions occur in some circumstances and not in others. What prevents the potential occurrence of ignition is the presence of heat losses. In any experiment, these heat losses, which are wholly an artifice of the experimental rig are, in fact, the crucial variable which determines ignition. Thus, it becomes important to design measuring rigs which reflect some real-life characteristic which we wish to embody, since striving for the 'ideal' would lead trivial results. This will become

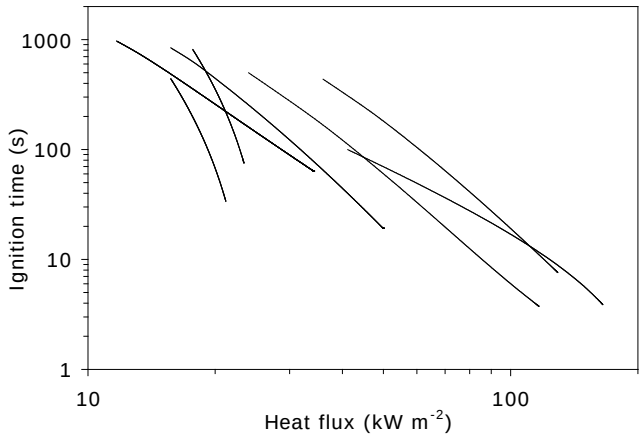


Figure 5 Piloted ignition of wood, as measured by various investigators prior to 1970

clear throughout this book, in that most of the chapters include a lengthy section on test methods. Without the availability of test methods—credible and applicable test methods—it would not be possible to say anything useful on the ignition topic.

In many important cases for ignition, for example, the ignition of solids from an applied heat flux, progress has been rather slow. As late as 1970, Ulrich and Sasine[27] examined the available data for the piloted ignition of wood. Figure 5 shows the results they found by reviewing the literature. A small part of the scatter is accounted for by genuine differences—wood species, thickness, moisture content, etc. The major differences, though, stem from the fact that the investigators all used different apparatuses and different calibration techniques, without the benefit of standardization. For this specific problem, it turned out that accurate calibration of heat flux meters is a crucial requirement, but concerted efforts to establish a minimum quality for heat flux meter calibrations did not take place until the 1980s.

The probabilistic nature of ignition and negative proof

The fire safety engineer and the risk manager involved in designing or assessing facilities can generally work with existing data and common scenarios. However, when investigations are made to find why a particular fire occurred, questions often arise as to whether *X* could have ignited *Y*, under certain circumstances. The question can be tackled by basic science principles, by data correlations, or by wholly-specific testing. In any of these approaches, the individual must exercise great care if an attempt is made at negative proof, that is, proving that something cannot happen. In the world of science, many things can happen which are unexpected or not intuitive. If one performs only a few experiments and obtains a negative result, this can mean that (1) the event is indeed impossible; or (2) the investigator was either not smart enough or not patient enough in order to discover the rare circumstances under which the event actu-

ally occurs. Many ignition phenomena have a strong probabilistic aspect to them—if the event is rare and only a few experiments were done, a wrong conclusions can be arrived at.

Can a cigarette dropped into a wastepaper basket start a flaming fire? In a study on this question[28], the experimenter had to conduct 132 trials before obtaining the first positive result. At the end of the study, 5 positive results from 300 trials were found. Had he stopped at 100 trials—a large number, already—the conclusion would have been reported that "dropped cigarettes cannot start flaming wastepaper baskets."

The issue is especially germane for electrical fires. The failure rate of electrical outlets has been estimated as 2×10^{-6}/year, as based on an estimated 1.62 billion outlets that are in use and are carrying current[29]. This is a very low failure rate, lower than that for most products whose failure rates are known. But this low failure actually corresponds to 3290 fires/year from this cause. This is a significant number and worthy of attention, yet to re-create the fires may be very difficult. The only way that this might feasibly be done is by over-stressing the device, in comparison to its typical use condition. Such studies are discussed in Chapter 14, but are always open to challenge that the over-stressing protocol may not fully simulate reality.

Patience may simply be required in waiting during a single test, apart from the issue of needing to run many trials. Most published values show that somewhere over 20 kW m^{-2} radiant heat flux must be applied to a wood surface to cause autoignition. These experiments are typically concluded in 10 – 30 minutes. But in one case[30], the experimentalists waited for over 3 hours and discovered that wood can autoignite at a heat flux of 5 kW m^{-2}. An even more extreme example has been presented by Cawley[31]. He conducted tests to determine the probability of igniting a methane/air mixture from an electric 'break-spark.' His results (Figure 6) show that, at low enough currents, probabilities on the order of 10^{-6} are found. It requires some highly automated experimental equipment to be able to generate enough trials to determine such low probabilities. Even if 1000 trials were made—which is an enormous number for most conventional experiments—a notably higher minimum igniting current would have been reported than was actually found at the $P = 10^{-6}$ level.

For risk managers, it is especially important to appreciate the probabilistic nature of the entire fire triangle. The probability P of a fire or an explosion occurring can be expressed as:

$$P = P_f P_o P_s$$

where P_f = probability of ignitable fuel being present; P_o = probability of necessary oxidizer being present; and P_s = probability of an ignition source being present. P_o will commonly be ≈ 1, but an inerting atmosphere may turn out to be practical. But the other two terms can vary widely. The role of the risk manager has to be to minimize P, and all too often this is misunderstood and focus is placed only on reducing P_s. Hertzberg has given some good examples of improving the overall level of safety by carefully evaluating the possibility of reducing each of the three factors[32].

Redundancy is an important concept in safety systems. In many areas of product design, it is accepted practice (or a legal requirement) that any single failure should not result in a grievous consequence. For example, design of electrical appliances against electric shock hazard is often done on that basis. If a metal enclosure is used, two failures must occur before a user will be subject to active endangerment: (1) a short from the phase conductor to the cabinet must occur; (2) a failure must take place in the grounding arrangement for the enclosure. But in the majority of situations, redundancy is not provided against the hazard of ignition—it generally takes only one failure or one thoughtless action for fire to be started. There are, however, a few areas of fire safety where redundancy is provided, for example, in the design of electric equipment to be used in potentially flammable atmospheres; this topic is covered in Chapter 12.

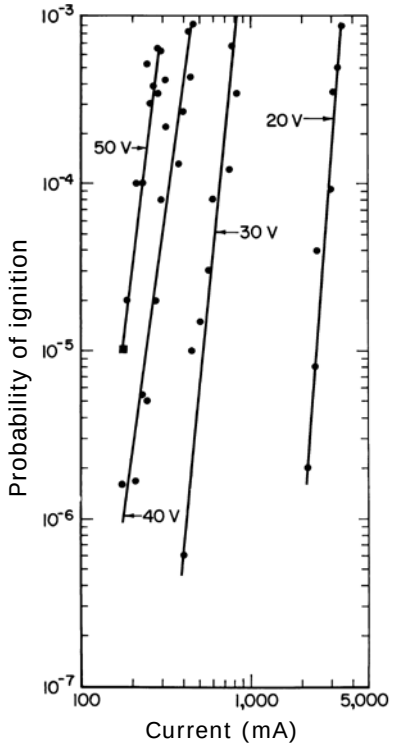


Figure 6 Probability of igniting methane/air mixtures with a break-spark from a resistive circuit

Comments to the fire investigator

A fire is investigated by first determining the area of origin, and then establishing the cause. To establish the cause, it is necessary to consider all combustibles that could have been located in the area of the origin, and then determined that

there was an ignition source capable of igniting one of the combustibles. It is also necessary to rule out other causes by determining that available ignition sources were not capable of igniting other combustibles. Thus, once the origin area has been found, much of the work of the investigator consists of trying to match various possible ignition sources against various fuels, and determining which pairs can and which cannot lead to ignition. This book has been organized to facilitate being used for this purpose.

This Handbook contains much material dealing with theory or mathematical aspects of fire. These will be of importance to fire science and fire engineering specialists, but will not be of main interest to fire investigators. Consequently, even though a great deal of mathematical material is presented, the book has been organized so that schooling in mathematics or science is not necessary in order to obtain practical guidance. The information of greatest importance to the investigator will be found in Chapters 14 and 15, which contain alphabetically organized material on various combustibles and on ignition sources. This information is given largely in non-mathematical terms and emphasizes the qualitative aspects of ignition. In some cases, quantitative data are also given, for example, E and P values for describing the temperature-versus-size relation of self-heating solids. The reader wishing to make computations by using these variables will have to consult Chapter 9, where the theory of self-heating is developed. To understand the theory requires a fair bit of mathematical background. Lacking this, the reader can simply be aware that the substance discussed has been known to self-heat, and that calculational formulas are available for estimating the minimum size of material needed for spontaneous combustion.

The fire investigator may want to know why science is useful at all to his or her task. This is an important question and deserves a serious answer. The reasons are the following:

- by studying the science, an improved qualitative understanding can be achieved of the phenomena involved, even if no quantitative calculations are undertaken;
- if testing is required, guiding principles will be known which will allow selection of the most appropriate tests and minimize unfruitful explorations;
- when data are collected, knowledge of the scientific principles will enable sensible plots to be made and errors to be avoided in making extrapolation or interpolations.

It must also be mentioned that the status of the science underlying ignition phenomena is such that it will rarely be possible to compute desired answers from first principles alone, unless the individual is willing to expend a dissertation's worth of effort. Instead, recourse to tests will almost always be needed.

Chapter 11 presents extensive general information on ignition sources. It should be used in conjunction with material in Chapter 14 on specific ignition sources. Chapters 4 through 10 contain a systematic presentation of ignition principles, theory, and test methods, as pertains to each of the various classes of combustibles. Each of these chapters begins with a section on *Highlights and summary of practical guidance*. This gives a brief overview of the substance of the chapter and sets out the basic principles in non-mathematical terms. These chapters do contain extensive mathematical developments, but the investigator can skip over those sections, while still getting benefits from the rest of the material. Sections of special interest to investigators will include those dealing with effects of various variables on the ignition process and on test methods used.

Computer methods

The reader may note that no review is made in this book of computer programs for ignition problems. This is not due to an oversight but, rather, due to an absence of material to review. Problem-solving in engineering and applied sciences can be viewed as falling into three procedural categories:

(1) looking up data in tables and using simple formulas;
(2) using computer programs which have been set up to solve well-known categories of problems for which systematic procedures had been developed;
(3) conducting research by setting up conservation equations, expressing them in the form of differential equations (commonly partial differential equations, with possibly three spatial dimensions) and solving them by advanced mathematical techniques.

Category #3 describes how Ph.D. dissertation research is commonly pursued in science and engineering, but the present work is not intended as a primer towards that purpose. Category #1 generally only requires that equations be typed into a spreadsheet, and there is a great deal of material in the present handbook compiled for this purpose. A few computer programs are also available for solving simple formulas in the ignition field (e.g., ignition of building façades from radiant heat of a neighboring building). Category #2 can best be illustrated in fire science by room fire models. These have been developed since the 1970s and have become a highly valuable engineering tool. A survey identified several dozen of those[33], and a number of them are available at low cost or gratis from the developers. These tools require some science background to use intelligently, but are a far cry from the 'Ph.D. candidate with a white sheet of paper' of Category #3. To this author's knowledge, no Category #2 tools have become available in the ignition area. But there are a number of aspects of ignition (self-heating of geometrically non-simple shapes is one that immediately comes to mind) that could benefit from the availability of competent, affordable computer programs.

Concerning Category #3, the utility is often less than meets the eye. The literature contains a wide proliferation of theoretical studies (all categories of engineering, not just fire-safety-related) that are accompanied by numerical solutions to example problems but, regrettably, only occasionally

accompanied by validation. This scheme is of little value to a potential user, unless his company can sponsor a Ph.D. candidate. The reason is because the solutions are typically published only for example problems which will generally be unrelated to the user's need.

References

1. Drysdale, D. D., **An Introduction to Fire Dynamics**, 2nd ed., John Wiley, Chichester, England (1999).
2. DeHaan, J. D., **Kirk's Fire Investigation**, 5th ed., Brady/Prentice-Hall, Englewood Cliffs, NJ (2002).
3. Guide for Fire and Explosion Investigations (NFPA 921). National Fire Protection Assn., Quincy, MA (1998).
4. Cooke, R. A., and Ide, R. H., **Principles of Fire Investigation**, The Institution of Fire Engineers, Leicester, England (1985).
5. **Injury Facts**, 2000 ed., National Safety Council, Itasca IL (2000).
6. Statistics provided by J. Hall, NFPA (2001).
7. Moore, F. C., **Fires: Their Causes, Prevention and Extinction**. Combining also A Guide to Agents respecting Insurance against Loss by Fire. The Continental Insurance Company of New York, New York (1877).
8. Ahrens, M., U.S. Experience with Smoke Alarms and Other Fire Alarms: Who Has Them? How Well Do They Work? When Don't They Work? Fire Analysis & Research Div., NFPA (1998).
9. Statistics provided by J. Hall, NFPA (2001).
10. Crossman, E. R. F. W., Zachary, W. B., and Pigman, W., FIRRST: A Fire Risk and Readiness Study of Berkeley Households, 1974, *Fire J.* **71**:1, 67-73 (Jan.1977).
11. 1984 National Sample Survey of Unreported, Residential Fires (Contract No. C-83-1239), prepared for CPSC, Audits & Surveys, Princeton NJ (1985).
12. Hall, J. R. jr., U.S. Arson Trends and Patterns, Fire Analysis & Research Div., NFPA (2001).
13. International Accident Facts, 2nd ed., National Safety Council, Itasca IL (1999).
14. Rosenberg, T., Statistics for Fire Prevention in Sweden, *Fire Safety J.* **33**, 283-294 (1999).
15. Ono, R., and Da Silva, S. B., An Analysis of Fire Safety in Residential Buildings through Fire Statistics, pp. 219-230 in *Fire Safety Science—Proc. 6th Intl. Symp.*, Intl. Assn. for Fire Safety Science (2000).
16. Rahikainen, J., and Keski-Rahkonen, O., Determination of Ignition Frequency of Fire in Different Premises in Finland, *Eurofire '98, Third European Symp.*, Brussels (1998).
17. Tzortzis, S., and Sugg, D., private communication, UK Home Office, London (2001).
18. Cox, A. W., Lees, F. P., and Ang, M. L., **Classification of Hazardous Locations**, Institution of Chemical Engineers, Rugby (1990).
19. Large Property Damage Losses in the Hydrocarbon-Chemical Industries—A Thirty-year Review, 19th ed., J. C. Coco, ed., Marsh Risk Consulting, [n.p.] (2001).
20. Flowers, M., 1999 Process Safety Performance Measurement Report, American Petroleum Institute, Washington (2000).
21. Demidov, P. G., **Combustion and Properties of Combustible Substance**, NTIS No. AD 621 738, National Technical Information Service, Springfield, VA (1965).
22. Lewis, B., and von Elbe, G., **Combustion, Flames and Explosions in Gases**, 3rd ed., Academic Press, Orlando, FL (1987).
23. Fristrom, R. M., **Flame Structure and Process**, Oxford University Press, New York (1995).
24. Griffiths, J. F., and Barnard, J. A., **Flame and Combustion**, Blackie Academic and Professional/Chapman and Hall, London (1995).
25. Turns, S. R., **An Introduction to Combustion**, McGraw-Hill, New York (1996).
26. Leiber, C. O., and Doherty, R. M., Review of Explosion Events—A Comparison of Military and Civilian Experiences, pp. 1-15 in **Prevention of Hazardous Fires and Explosions: The Transfer to Civil Applications of Military Experiences**, V. E. Zarko et al., eds., Kluwer Academic Publishers, Dordrecht (1999).
27. Ulrich, R. D., and Sasine, K. P., A Survey of Literature on the Pyrolysis of Wood and Other Cellulosic Solids (NWC TP 5045), Naval Weapons Center, China Lake CA (1970).
28. Cigarette Fires in Paper Trash, *Fire Findings* **6**:1, 1-3 (Winter 1998).
29. Babrauskas, V., How Do Electrical Wiring Faults Lead to Structure Ignitions? pp. 39-51 in *Proc. Fire and Materials 2001 Conf.*, Interscience Communications Ltd., London (2001).
30. Shoub, H., and Bender, E. W., Radiant Ignition of Wall Finish Materials in a Small Home (NBS 8172), [U.S.] Natl. Bur. Stand, Washington (1964).
31. Cawley, J. C., Probability of Resistive Spark Ignition Caused by Very Low Currents (RI 9114), Bureau of Mines, Pittsburgh (1987).
32. Hertzberg, M., Explosion Hazards of Combustible Gases, Vapors, and Dusts, pp. 2687-2733 in **Patty's Industrial Hygiene**, Vol. 4, 5th ed., R. L. Harris, ed., Wiley, New York (2000).
33. Friedman, R., International Survey of Computer Models for Fire and Smoke, *J. Fire Protection Engineering*, **4**, 81-92, (1992).

Copyright © 2003, 2014 Vytenis Babrauskas

Chapter 2. Terminology

Terms used in this book **13**
Definitions **13**
Abbreviations and acronyms **20**
References **22**

Terms used in this book

Many of the terms discussed in this book do not have an absolute meaning. Instead, they refer to the findings from certain tests or procedures. Thus, when using ignition-related terms it becomes very important to know the specifically-applicable definitions. In some cases, there are conflicting definitions issued by standards-making bodies; the reader must be aware of such discrepancies. Thus, in this Chapter, a collection of definitions is presented that are useful to the study of ignition. A number of them may not be intuitively obvious to the reader and they all deserve careful study if misconceptions are to be avoided.

Abbreviations of names for various explosive compounds are given in Chapter 14 under *Explosives*.

Following modern practice, units are written without the use of the solidus ("/") symbol. Thus, for example, instead of writing kg/m^3, the notation kg m^{-3} is used.

Definitions

Adiabatic flame temperature. The temperature of a flame in the absence of any heat losses.

Aerosol. A colloidal suspension of liquids or solids in a gaseous medium.

Afterflame. ISO 13493[1] defines it as: "Flame which persists after the ignition source has been removed."

Afterglow. ASTM E 176[2] defines it as: "Emission of light, usually subsiding, from a material undergoing combustion, but occurring after flaming has ceased."

Air terminal. A lightning rod.

Arc. See: *electric arc.*

Arc tracking. A phenomenon whereby an arc between two or more wires, on initiation, will sustain itself through a conductive path provided by degradation of the insulation for a measurable length[3]. See also: *Tracking*.

Autocatalytic reaction. A reaction which is accelerated by an accumulation of the reaction products.

Autogenous ignition temperature. Archaic variant of *autoignition temperature*.

Autoignition. The sudden inflammation of a gaseous charge when it is exposed to a particular temperature and pressure[4]. NFPA 921[5] defines it as: "Initiation of combustion by heat but without a spark or flame." It is also normally understood that the heat is to be applied uniformly; thus, ignition facilitated by localized hot surfaces is a form of piloted ignition, not autoignition.

Autoignition temperature. NFPA 325[6] defines it as: "The ignition temperature of a substance, whether solid, liquid, or gas, is the minimum temperature required to cause self-sustained combustion, independently of the heating or heated element."

Backdraft. NFPA 921[5] defines it as "An explosion occurring from the sudden introduction of air into a confined space containing oxygen-deficient superheated products of incomplete combustion."

Basis weight. The mass of a thin material expressed per unit area; customary units are g m^{-2}. This quantity is used since thickness of fabric, paper, etc. is not a quantity that can be reliably determined, thus density (kg m^{-3}) is not appropriate as a quantitative descriptor for these materials.

Bead. NFPA 921[5] defines it as "A rounded globule of resolidified metal at the end of the remains of an electrical conductor that was caused by arcing and is characterized by a sharp line of demarcation between the melted and unmelted conductor surfaces."

BLEVE. Boiling liquid, expanding vapor explosion. It is the explosive release of expanding vapor and boiling liquid when a container holding a pressure-liquefied gas fails catastrophically[7].

Bolted short. An electrical short circuit where good metal-to-metal contact is made and arcing does not occur at the location of the short.

Catalyst. A substance which promotes chemical reaction without itself being significantly consumed.

Combustible liquid. According to NFPA 30[8], a combustible liquid is any liquid that has a closed-cup flash point at or above 100ºF (37.8ºC). Combustible liquids are further subdivided as:

- Class II liquids have a flash point at or above 100°F (37.8ºC) and below 140ºF (60ºC).
- Class IIIA liquids have a flash point at or above 140ºF (60ºC), but below 200ºF (93ºC).
- Class IIIB liquids have a flash point at or above 200ºF (93ºC).

Liquids having lower flash points are identified as *flammable liquids*. The NFPA system is being made obsolete by UN/DOT regulations, which define 60.5°C as the limit, not 37.8ºC See also: *flammable liquid*; *ignitable liquid*.

Combustion. A self-sustained, high-temperature oxidation reaction.

Condensed phase. The term refers to substances which are liquids or solids, but not gases.

Cookoff. Explosion of weapons due to external flames or fire.

Cool flames. Slow combustion reactions which occur only under limited conditions and produce temperatures of only 200 – 300ºC.

Critical diameter. Minimum diameter of an explosive charge capable of maintaining detonation.

Deflagration. A subsonic wave supported by combustion[18]. Also defined as the propagation of a combustion zone at velocity that is less than the speed of sound in the unreacted medium[9]. The flame front and the reaction products travel in opposite directions. If within a gaseous medium, a deflagration is the same as a *flame*.

Detonation. A reaction propagating at a velocity greater than the local speed of sound in the unreacted material. In a detonation, the shock front and the reaction products travel in the same direction.

Detonator. The US government[10] defines it as: "Blasting caps, electric blasting caps, delay electric blasting caps, and nonelectric delay blasting caps."

Diathermancy. Partial transparency. Diathermanous solids absorb radiant energy in-depth, while opaque substances absorb it only at the surface.

Ease of ignition. ISO 13943[1] declares this to be: "Deprecated term, see *ignitability*." However, on a practical basis, since *ignitability* is just as imprecise a term as *ease of ignition*, declaring a preference for one term over the other would seem unnecessary.

Electric arc. A continuous, luminous discharge of electric current crossing a gap or an insulating surface between two conductors. It has been more precisely defined as[11]: "A stable discharge between two electrodes in which thermionic emission is the feedback mechanism for sustaining the discharge." An arc is distinguished from an electric spark by being a continuous discharge, whereas a spark is a transient discharge.

Electric contact. Holm[12] defines it as: "A releasable junction between two conductors which is apt to carry current."

Electric spark. See: *spark (electric)*.

Emissive power. The radiant flux received from a source object if the view factor is unity. The units are kW m^{-2}.

Endothermic reaction. A chemical reaction which requires that energy be supplied to the system from an external source for the reaction to occur.

Energy fluence. Flow of energy per unit area. Typically reported in units of kJ m^{-2}, the term is most commonly used in the munitions field.

Enthalpy. The thermodynamic quantity that is the sum of the internal energy of the system and the product of its volume multiplied by its pressure.

Equicylinder. A cylinder having a height equal to its diameter.

Equivalence ratio. The fuel/air ratio, divided by the fuel/air ratio for a stoichiometric mixture.

Exothermic reaction. A chemical reaction which releases energy. The opposite is *endothermic reaction*, which denotes that the reaction requires an external heat source in order to take place. It must be borne in mind that, if the temperature of a substance is progressively raised, many substances will show both endothermic and exothermic reactions. Exothermic reactions encountered in self-heating problems may be oxidative, that is, needing oxygen. But they may also be decomposition reactions that do not require oxygen.

Explosion. As Stecher[13] points out, "The term 'explosion' has no fixed and definite meaning either in ordinary speech or in law." Cook[14] defines explosion as "A release of energy creating a sudden outburst of gas." This broad definition includes chemical, atomic, and physical explosions. Physical explosions can occur due to overpressures of boilers or pressure vessels. They also include steam explosions, which occur when a large, hot body is quickly inserted into water*. In combustion science, an explosion is any rapid, high-temperature combustion. It excludes such low-temperature phenomena such as *cool flames*. Thus, in the broadest sense, a sound is not necessary as part of an explosion, and explosions are considered to encompass normal *flames*[15]. Confusingly, some detonation experts consider 'explosion' and 'detonation' to be mutually-exclusive terms, with 'ex-

* The largest known steam explosion was the underwater volcano eruption which demolished the island Krakatoa in 1883. Its shock waves in air and water circled the entire planet several times.

plosion' referring only to deflagrations. The term 'thermal explosion' denotes the self ignition of self-heating materials[16]. The latter phenomenon is normally not accompanied by any sudden outburst of gas, nor by any sound or appreciable pressure rise. Definitions of 'explosion' have been reviewed by Martin et al.[17]

Explosion limits. In colloquial speech, *explosion limit* is taken to be a synonym for *flammability limit*. In combustion science, however, the meanings are different. The flammability limits for a given temperature and pressure are the lean and rich fuel concentration values beyond which no flame will propagate. Explosion limits, by contrast, are[18]: "the pressure-temperature boundaries for a specific fuel-oxidizer ratio that separate regions of slow and fast reaction." Thus, explosion limits are presented as a line on a graph where temperature is plotted on the x-axis, pressure is plotted on the y-axis, and the fuel/air ratio is specified (typically, the stoichiometric value).

Explosive substance. The UN definition is[19]: "Explosive substance is a solid or liquid substance (or a mixture of substances) which is in itself capable by chemical reaction of producing gas at such a temperature and pressure and at such a speed as to cause damage to surroundings. Pyrotechnic substances are included even when they do not evolve gases."

Fire. ASTM E 176[2] defines it as: "Destructive burning as manifested by any of all of the following: light, flame, heat, smoke." Another definition is[20]: "Any incident that results in flames or smoke and can cause damage to life or property if left unchecked."

Fire point. NFPA 850[21] defines it as: "The lowest temperature at which a liquid in an open container will give off sufficient vapors to burn once ignited. It generally is slightly above the flash point." Taking a more narrow approach, NFPA 30[22] defines it as: "The lowest temperature at which a liquid will ignite and achieve sustained burning when exposed to a test flame in accordance with ASTM D 92, Standard Test Method for Flash and Fire Points by Cleveland Open Cup." ISO[1] defines it much more generally as: "The minimum temperature at which material ignites and continues to burn for a specified time after a standardized small flame has been applied to its surface under specified conditions." Perhaps the best definition is from BSI[23]: "The lowest temperature at which a liquid gives off sufficient flammable vapours in air to produce sustained combustion after removal of the ignition source." In addition to ISO, some authorities consider fire point to be a general term, also applicable to solids, not just liquids.

Firedamp. Natural gas. The term refers to gas found in mines. It consists mostly of methane, with small amounts of ethane and other hydrocarbons and possibly of carbon monoxide or carbon dioxide.

Flame. A rapid, self-sustaining propagation of a localized combustion zone at subsonic velocities through a gaseous medium. Since they are rapid, flames also represent high-temperature combustion. In a gaseous medium a flame is identical to a *deflagration*. A slow form of combustion which can exist under certain conditions is differentiated as a *cool flame*.

Flame kernel. The initial gaseous breakdown zone during spark ignition of a fuel/oxidizer mixture.

Flammable. NFPA 921[5] defines it as: "Capable of burning with a flame."

Flammable liquid. According to NFPA 30[8], a flammable liquid is any liquid that has a closed-cup flash point below 100ºF (37.8ºC) and a *Reid vapor pressure* not exceeding 276 kPa at 100ºF (37.8ºC) Flammable liquids are further subdivided as:

- Class IA liquids have flash points below 73ºF (22.8ºC) and boiling points below 100ºF (37.8ºC).
- Class IB liquids have flash points below 73ºF (22.8ºC) and boiling points at or above 100ºF (37.8ºC).
- Class IC liquids have flash points at or above 73ºF (22.8ºC), but below 100ºF (37.8ºC).

Liquids having higher flash points are identified as *combustible liquids*. See also: *ignitable liquid*.

The UN defines[19] liquids as 'flammable' if their closed-cup flash point is less than or equal to 60.5ºC (141ºF) or their open-cup flash point at or below 65.6ºC (150ºF). The UN system has been adopted by the US Dept. of Transportation[24] and is expected to eventually make the NFPA definitions obsolete.

Flammable solid. This definition is problematic because standards bodies have adopted definitions which conflict with both combustion science and everyday understanding of fire. In combustion science, a flammable solid is merely any solid substance which can burn; this includes newspapers, wood, fabrics, etc. The standards bodies, however, effectively consider "highly hazardous flammable solids," but omit the "highly hazardous" phrase. The UN definition is[19]: "Solids which, under conditions encountered in transport, are readily combustible or may cause or contribute to fire through friction; self-reactive and related substances which are liable to undergo a strongly exothermic reaction; desensitized explosives which may explode if not diluted sufficiently." Substances having a heat of decomposition $\geq$ 300 kJ kg^{-1} or an SADT $\leq$ 75ºC for a 50 kg specimen are construed to be self-reactive. UN excludes from the definition substances which fall into other, more specific classifications: Class 1 explosives, oxidizing substances, and organic peroxides.

Flash ignition temperature. Piloted ignition temperature. There is only one common test which uses this definition, ASTM D 1929. This test method does not distinguish between flashing and sustained-flaming ignition, and many substances do not show flashing prior to initiation of sustained flaming, but the nomenclature unfortunately implies that flashing and not sustained-flaming is being recorded.

Flash fire. Rapid combustion of a flammable gas cloud which does not result in a significant overpressure.

Flash point. The NFPA 325[6] definition is: "The flash point of a liquid is the minimum temperature at which the liquid gives off sufficient vapor to form an ignitable mixture with air near the surface of the liquid or within the test vessel used. By 'ignitable mixture' it is meant a mixture that is within the flammable range (between the upper and lower limits) and, thus, is capable of propagation of flame away from the source of ignition. Some evaporation takes place below the flash point, but not in quantities sufficient to form an ignitable mixture." ISO[1] defines it as: "The minimum temperature to which a material or product must be heated for the vapours emitted to ignite momentarily in the presence of flame under specified test conditions." For completeness, the definitions must be understood to include the requirement that the test conditions involve air at a pressure of 1 atm. The actual value of the flash point is dependent on the type of test equipment that is used for its determination. Flash point differs from *fire point* in that at the flash point temperature the vapors are only required to flash and not to continue burning.

Flashover. This term is used in two different, unrelated contexts. In fire safety science, it means the full involvement in flames of a room or other enclosed volume. In electrical engineering, it means the electrical breakdown of insulation along a surface.

Forced ignition. See *piloted ignition*.

Gas discharge. Gas discharges refers to a group of phenomena which accompany the flow of current through a gas under the influence of an applied electric field. Such discharges may be classified as self-sustaining (e.g. arc) or non-self-sustaining (e.g., photoionization discharge), a transition from the latter to the former occurring via an electrical breakdown (e.g., spark). In the case of a non self-sustaining discharge, the current flow ceases as soon as the external ionizing source is removed even though the electric field remains. Conversely a self-sustaining discharge persists as long as the driving electric field persists.

Glow. ASTM E 176[2] defines it as: "(1) the visible light emitted by a substance because of its high temperature; (2) visible light, other than flaming, emitted by a solid undergoing combustion."

Glowing combustion. NFPA 921[5] defines it as: "Luminous burning of solid material without a visible flame."

Ground fault. NFPA 921[5] defines it as: "A current that flows outside the normal circuit path, such as (a) through the equipment grounding conductor, (b) through conductive material other than the electrical system ground…, (c) through a person, or (d) through a combination of these ground return paths.

Halogenated. Containing atoms from one of the halogen-series elements (fluorine, chlorine, bromine, etc.).

Heat flux. The rate at which energy flows across an imaginary plane of 1 m^2. The units are power/area, or kW m^{-2}. This is the definition normally used in engineering; in physics, the quantity is termed *heat flux density*.

Heat flux density. See *heat flux*.

Heterogeneous reaction. A reaction in which the reactants are not all in one phase, for instance, a gas and a solid. In combustion systems, this is often illustrated by a reaction at a surface, e.g., air + charcoal. This type of combustion exhibits a glow or a bright light, but not flames.

Homogeneous reaction. A reaction in which the reactants are all in the same phase. An example is homogeneous combustion in the gas-phase, where flaming combustion occurs throughout a volume of space.

Hypergolic. A reaction is hypergolic if two substances ignite directly upon contact.

Ignitability. ISO[1] defines it as a: "measure of the ease with which an item can be ignited, under specified conditions." This is clearly a very loose term, and it can be used in various different ways. In recent years, it is most typically used in describing the response of a solid material to a flame or a radiant heat source.

Ignitable. ISO[1] defines it as: "capable of being ignited."

Ignitable liquid. An ignitable liquid is a liquid which is either a *flammable liquid* or a *combustible liquid*.

Ignite. ISO[1] defines it two ways: "(Intransitive verb). To catch fire with or without the application of an external heat source. (Transitive verb). To initiate combustion."

Ignited. ISO[1] defines it as: "The state of a body undergoing combustion."

Ignition. ISO[1] defines ignition as: "Initiation of combustion."

Ignition source. ISO[1] defines it as "Source of energy that initiates combustion."

Ignition temperature. ISO[1] defines "ignition temperature (minimum): (Minimum) temperature at which combustion can be initiated under specified test conditions."

NFPA 921[5] defines it as: "Minimum temperature a substance must attain in order to ignite under specific test conditions. Reported values are obtained under specific test conditions and may not reflect a measurement at the substance's surface. Ignition by application of a pilot flame above the heated surface is referred to as piloted ignition temperature. Ignition without a pilot energy source has been referred to as autoignition temperature, self-ignition temperature, or spontaneous ignition temperature."

Note that NFPA limits the definition to the material surface temperature, while the ISO definition is broad and can encompass criteria based on either surface temperature or test-furnace temperature.

Ignition time. The time from beginning of exposure to heat, until ignition occurs. The ignition time is highly dependent on the conditions of the test or the experiment.

ISO[1] declares it to be: "Deprecated term; see *minimum ignition time*." This is an unfortunate stance, since *ignition time* (**not** minimum) is an essential term in describing the results of radiant-heating tests for ignition of solid materials. In such tests specimens of the material are presented with various radiant heat flux values, and the ignition times corresponding to each are tabulated. Furthermore, at any particular heat flux value, if multiple test runs are made, the report should sensibly document the average time for ignition and not just the minimum from the runs.

Incendive. Able to cause ignition. The NFPA 77[25] definition is: "A spark that has enough energy to ignite an ignitable mixture is said to be incendive. Thus an incendive spark can ignite an ignitable mixture and cause a fire or explosion. A nonincendive spark does not possess the energy required to cause ignition even if it occurs within an ignitable mixture."

Incendivity. The ability to cause ignition. The NFPA 77[25] definition is: "The ability of a spark to ignite an ignitable mixture." Morgan[26], who coined the term, felt that the term was needed to clearly differentiate the concept from 'inflammability.' Morgan, however did not restrict it to sparks and defined it as: "That property of an igniting agent (such as a spark, flame, or hot solid) whereby it is able to cause ignition." It is sometimes viewed that incendivity is a property of a heat source, while ignitability is a property of a fuel but, in fact, the two are not independent.

Induction period. This term is mainly used in combustion chemistry studies, and generally means *ignition time*.

Initiation. The start of detonation, as applied to explosives.

Intrinsically safe circuit. NFPA 70, the National Electrical Code[27] defines this as: "A circuit in which any spark or thermal effect is incapable of causing ignition of a mixture of flammable or combustible material in air under prescribed test conditions." It then refers to UL 913[28] for test requirements.

Intrinsically safe system. NFPA 70 defines this as: "An assembly of interconnected intrinsically safe apparatus, associated apparatus, and interconnecting cables in that those parts of the system that may be used in hazardous (classified) locations are intrinsically safe circuits."

Laminar flame speed. Glassman[18] defines it as: "The velocity at which unburned gases move through the combustion wave in the direction normal to the wave surface." Also called burning velocity, flame velocity, normal combustion velocity, and fundamental flame speed.

Layer ignition temperature. For a layer of dust upon a hot surface, this is the lowest temperature of the hot surface that can cause ignition.

Lightning. A transient, high-current electric discharge whose path length is measured in kilometers[29].

Liquid. In chemistry, a liquid is defined as[30]: "An amorphous form of matter intermediate between gases and solids in which the molecules are much more highly concentrated than in gases, but much less concentrated than in solids." In practice, it is often necessary to distinguish between gases and low-boiling point liquids. For this purpose, a substance is a liquid and not a gas if its boiling point at 1 atm is 25ºC or higher; other slightly different reference temperatures are also sometimes used. The NFPA 30[22] definition of a flammable liquid requires that it have a Reid vapor pressure not over 276 kPa at 37.8ºC; substances with a higher vapor pressure are flammable gases. This definition is not identical to the preceding. In some cases, liquids must be distinguished from highly viscous substances; see NFPA 30 for details of a definition of liquids that is used to exclude highly viscous substances. Note that a particular substance may be in a gaseous, liquid, or solid state, depending on its pressure and temperature.

Limit flame temperature. The flame temperature at the lower flammability limit.

Lower explosive limit; **lower explosion limit**. See *explosion limits*.

Lower flammability limit. The lowest concentration of a gas or vapor that will just support the propagation of flame away from a pilot ignition source. The LEL is commonly measured in volume percent, which is the same as mole percent, but *not* the same as mass percent. Occasionally it is reported in mass concentration units (g m^{-3}). The value of the LFL also depends on the atmosphere: its composition, temperature, and pressure. By convention, the LFL values are reported for a normal atmosphere of 21% (by volume) oxygen, at 25ºC (77ºF) and a pressure of 1 atmosphere (760 mm Hg) unless specified otherwise. Sometimes called *lean limit of flammability*.

Lower temperature limit. It is the minimum temperature to which a saturated fuel vapor-air mixture must be heated for flame propagation to be possible. It differs from the flash point only in that different test equipment is used for its measurement and a different criterion is prescribed for interpreting the results.

Maximum experimental safe gap. The maximum permissible gap, between flanges of defined geometry, separating the internal volume of a vessel from an external explosive atmosphere. A gap larger than this figure may allow an internal ignition in the vessel to propagate to the external atmosphere[31].

Minimum explosible concentration. ASTM E 1515[32] defines it as: "The minimum concentration of a combustible dust cloud that is capable of propagating a deflagration through a uniform mixture of the dust and air under specified conditions of test." The units are g m^{-3}, and the term is identical to LFL, if the latter is expressed in mass concen-

tration units. For consistency, in this book 'LFL' is generally used, irrespective of whether the substance is a gas or a dust cloud.

Nonincendive circuit. NFPA 70 defines this as: "A circuit in which any arc or thermal effect produced, under intended operating conditions of the equipment or due to opening, shorting, or grounding of field wiring, is not capable, under specified test conditions, of igniting the flammable gas, vapor, or dust-air mixture." It then refers to ISA-S12.12[33] for test requirements.

Ohmic heating. Heating created by an electrical current, as determined by Ohm's Law. The power dissipated is expressed as $P = I^2R$, where P = power, I = current, and R = resistance.

Overcurrent. NFPA 921[5] defines it as: "Any current in excess of the rated current of equipment or the ampacity of a conductor. It may result from an overload (see definition), short circuit, or ground fault."

Overload. NFPA 921[5] defines it as: "Operation of equipment in excess of normal, full-load rating, or of a conductor in excess of rated ampacity, which, when it persists for a sufficient length of time, would cause damage or dangerous overheating. A fault, such as a short circuit or ground fault, is not an overload."

Oxidation. A chemical reaction in which a compound or a radical loses electrons. The opposite reaction, in which electrons are gained, is called "reduction."

Oxygen index. The ratio of moles of oxygen to moles of oxygen + diluent; it is usually expressed as a percentage.

Pilot source of ignition. ASTM E 176[2] defines it as: "A discrete source of energy, such as, for example, a flame, spark, electrical arc, or glowing wire."

Piloted ignition. ISO[1] defines it as: "Ignition of combustible gases or vapours by a secondary source of energy, as by, for example, a flame, spark, electrical arc or glowing wire." Sometimes referred to as 'forced ignition' or 'induced ignition.' Piloted ignition occurs when a localized heat source is present; if a substance ignites due to being raised uniformly in temperature, then *autoignition* occurs.

Piloted ignition temperature. The surface temperature of a substance that occurs at the moment that ignition is observed, under conditions that a pilot is used for ignition. The term is applied primarily to solids; see also *fire point*.

Plosophoric materials. NFPA 495[34] defines them as: Two or more unmixed, commercially manufactured prepackaged chemical ingredients (including oxidizers, flammable liquids or solids, or similar ingredients) that are *not* classified as explosives but that, where mixed or combined, form a blasting explosive.

Porosity. The volume of void spaces, divided by the gross volume. The definition is used in connection with substances having internal voids.

Pressure limit. The pressure below which a combustion or decomposition reaction cannot take place.

Pressure piling. MSHA[35] defines it as: The development of abnormal pressure as a result of accelerated rate of burning of a gas-air mixture (frequently caused by restricted configurations within enclosures).

Primer. The US government[10] defines it as: A cartridge or container of explosives into which a detonator or detonating cord is inserted or attached.

Propellant. An explosive material that normally burns but not detonates and is used for propulsion purposes.

Pyrolysis. The chemical degradation of a substance by the action of heat. In fire science, sometimes *pyrolysis* is used to refer to a stage of fire before flaming combustion has occurred. In gas chromatography, *pyrolysis* is sometimes restricted to the heating of a substance without oxygen, but in fire science no implications of presence or absence of oxygen are made.

Pyrophoric. Following the recommendations of UN[19], the US Dept. of Transportation[36] classifies pyrophoric substances into its Division 4.2 and defines them as: "A pyrophoric material is a liquid or solid that, even in small quantities and without an external ignition source, can ignite within 5 minutes after coming in contact with air when tested according to UN Manual of Tests and Criteria." NFPA 471[37] uses the identical definition, but omits mention of the UN tests. NFPA 49[38] defines pyrophoric material as "A substance capable of self-ignition upon short exposure to air under ordinary atmospheric conditions," thereby omitting both a quantitative time element and a test method. Another meaning of the word *pyrophoric*, now obsolete, used to be "producing sparks when ground or abraded."

The temperature comprising "ordinary atmospheric conditions" is made more precise in certain other definitions. According to the Chemical Manufacturers Association, a pyrophoric substance is one which will ignite spontaneously in dry or moist air at or below 130ºF (54ºC). NFPA 318[39] uses essentially the same definition: "A chemical with an autoignition temperature in air at or below 130°F (54.4°C)."

Pyrotechnic substance. The UN definition[19] is: "Pyrotechnic substance is a substance or mixture of substances designed to produce an effect by heat, light, sound, gas or smoke or a combination of these as a result of non-detonative self-sustaining exothermic chemical reactions."

Quenching distance. Minimum dimension that a flame kernel must acquire in order to establish a freely propagating flame. Below this minimum size, heat losses exceed heat gain from the chemical reaction and the kernel will self-extinguish[31].

Reid vapor pressure. The vapor pressure as determined by the ASTM D 323 test method[40]. Note that real vapor pressures are generally not identical to the Reid vapor pressure, because the measurement is affected by the vapor/liquid

volume ratio, and generally the real situation will not entail a ratio of 4:1.

Rekindle. NFPA 921[5] defines it as: "A return to flaming combustion after apparent but incomplete extinguishment."

Self-accelerating decomposition temperature. This term does not have a specific scientific meaning, but is used in UN Regulations[19] is different contexts, depending on which test method is being described. It generally connotes a temperature at which a self-heating reaction either surpasses a criterion value or becomes critical.

Self-heating. ISO[1] defines it as: "A rise in temperature in a material resulting from an exothermic reaction within the material." The US Dept. of Transportation[36] classifies self-heating materials into the same division as pyrophoric ones, Division 4.2, and defines them as: "A self-heating material is a material that, when in contact with air and without an energy supply, is liable to self-heat. A material of this type which exhibits spontaneous ignition or if the temperature of the sample exceeds 200ºC (392ºF) during the 24-hour test period when tested in accordance with the UN Manual of Tests and Criteria, is classed as a Division 4.2 material."

NFPA provides several definitions. NFPA 471[41]: "Self-heating material — a material that, when in contact with air and without an energy supply, is liable to self-heat." NFPA 921[5]: "Self-Heating. The result of exothermic reactions, occurring spontaneously in some materials under certain conditions, whereby heat is liberated at a rate sufficient to raise the temperature of the material."

An entirely different meaning of the term exists in electrical engineering[1]: "Heat generated by a powered electrotechnical product resulting in a rise in temperature of the product."

Self-ignition. This term is ambiguous and can be understood two different ways: as *autoignition* or as *spontaneous combustion*. NFPA 921[5] defines it as: "Ignition resulting from self-heating. Synonymous with spontaneous ignition." ISO[1] defines it as: "Spontaneous ignition resulting from self-heating."

Self-ignition temperature. This term is usually understood to mean *autoignition* temperature. Because it is prone to being interpreted in various ways, ISO[1] declares it as: "Deprecated term (see *spontaneous ignition temperature*)." NFPA 921[5] defines it as: "The minimum temperature at which the *self-heating* properties of a material lead to ignition." This is needlessly narrowing the scope of the term, since it is often taken to mean an unpiloted ignition due to any cause, which could include radiant heating just as well as self-heating. NFPA 53[42] more appropriately treats self-ignition temperature as a synonym for *autoignition temperature*.

Sensitivity. The sensitivity of an explosive is the minimum stimulus that must be imparted to the explosive, within limited time and space, to detonate it. The term can only be used in a qualitative way, since the results are highly dependent both on the mode in which the energy is supplied, and on the details of the test apparatus.

Short circuit. IEEE[43] defines it as: "An abnormal connection (including an arc) of relatively low impedance, whether made accidentally or intentionally, between two points of different potential." NFPA 921[5] defines it as: "An abnormal connection of low resistance between normal circuit conductors where the resistance is normally much greater. This is an overcurrent situation but it is not an overload."

Smoldering. A propagating, self-sustained exothermic reaction wave deriving its principal heat from heterogeneous oxidation of a solid fuel. The term does not apply to situations where an external source of heat drives the exothermic reaction. See: *pyrolysis*.

ISO[1] defines "smouldering: The combustion of a material without flame and without light being visible. NOTE: smouldering is generally evidenced by an increase in temperature and/or by effluent." ASTM E 176[2] defines it as: "Combustion of a solid without flame, often evidenced by visible smoke."

Spark. The term is used in connection with two different phenomena. **Electric spark**: Dielectric breakdown of a gas between two electrodes in which the liberation of secondary electrons from one of the electrodes is the major feedback mechanism necessary to sustain the discharge[11]. NFPA 77[25] defines it as: "A short-duration electric discharge due to a sudden breakdown of air or some other insulating material separating two conductors at different electric potentials, accompanied by a momentary flash of light." A *spark* is a transient event, while an *electric arc* is a sustained event. **Mechanical spark**: A small, incandescent particle.

Inconsistent with NFPA 77 and general scientific usage, NFPA 921[5] uses the term *arc* to encompass both arcs and electrical sparks, and defines *spark* solely as "a small incandescent particle," excluding electric breakdown phenomena.

Spontaneous combustion. Visible smoldering or flaming caused by thermal runaway. ISO[1] declares it to be: "Deprecated term; see *self-ignition*." Despite ISO's stance, the term is useful and properly descriptive.

Spontaneous ignition. This term is commonly used interchangeably with *spontaneous combustion.* The latter term is preferred, however. *Spontaneous ignition* has another meaning: the ignition of an object due to external heating, without the use of a pilot flame. To avoid confusion, *autoignition* is the preferred term for the latter.

ISO[1] defines it as: "Ignition resulting from a rise of temperature without a separate ignition source." This definition is notably ambiguous, and it is not clear whether *autoignition* of all sorts is contemplated, or solely that due to self-heating.

Spontaneous ignition temperature. ISO[1] defines it as: The minimum temperature at which ignition is obtained under specified test conditions without any source of pilot ignition. NOTE: This temperature may be caused either by self-heating or by induced heating." Thus, unlike its definition of *spontaneous ignition* itself, here ISO is including all forms of *unpiloted ignition*.

Stoichiometric mixture. A stoichiometric mixture of chemical reactants (more correctly referred to as a stoichiometrically balanced mixture) is one in which the proportion of reactants is such that there is no surplus of any reactant after the reaction is completed. The reaction products must be known (or defined) for the concept to be applicable. In systems which are capable of partial reaction, the ultimate reaction products are normally used (example: carbon is taken as oxidizing to CO_2, not to CO).

Stray current. Current flowing through paths other than the intended circuit.

Subcritical. In self-heating theory, denotes conditions that will not lead to thermal runaway.

Supercritical. In self-heating theory, denotes conditions that will lead to thermal runaway.

Surface flash. ISO[1] defines it as: "Movement of transient flame over the surface of a material without ignition of its basic structure." It also states in a note that "This period of time is usually shorter than 1 s.

Surface ignition. Ignition caused by an imposed heat flux accompanied by a pilot flame placed directly onto the surface of a specimen. The term is rarely used.

Sustained flaming. ISO[1] defines it as: "Persistence of flame on or over a surface for a minimum period of time. NOTE: the period of time required will vary across different standards, but it is usually of the order of 10 s." In the military research community, this term is sometimes understood to mean that flaming persists after the source of heating is removed, which is a fundamentally different definition from the one given by ISO.

Thermal explosion. Runaway self-heating of a substance, the exothermicity of which can be represented as a single chemical reaction of the Arrhenius form. Runaway self-heating may not cause any detectable pressure rise nor make a noise that is commonly considered a trait of explosions. If the reaction is a chain reaction, rather than a single-step reaction, then ignition is referred to as a "chain-reaction explosion."

Thermal runaway. Self-heating which rapidly accelerates to high temperatures. Under many practical conditions of organic substances stored in air, thermal run-away will lead to ignition. Under some conditions, a stable elevated temperature is reached rather than a runaway condition. Note that self-heating does *not* need to result in a thermal runaway and may simply result in a moderate temperature rise.

Thermally-thick solid. A solid which, while heated from one face, shows a negligible temperature rise at its opposite face. This characteristic is not simply a property of a material, but also depends on the time of exposure and the heat flux.

Thermally-thin solid. A solid which, while heated from one face, shows a back-face temperature which is nearly identical to the temperature of the heated face. This characteristic is not simply a property of a material, but also depends on the time of exposure and the heat flux.

Tracking. IEC[44] defines it as: "Progressive formation of conducting paths, which are produced on the surface and/or within a solid material, due to the combined effects of electric stress and electrolytic contamination." The phenomenon is also referred to as *arc tracking*.

Tracking resistance. ISO[1] defines it as: "The ability of a material to withstand a test voltage, under specified conditions, without creating conducting paths on the surface of the specimen and without the occurrence of flame."

Tramp metal. Loose metal objects present in places where they should not be, for example, among pulverized agricultural products.

Transient flaming. Flaming ignition which does not exhibit *sustained flaming*. ISO uses the variant term *transitory flaming*.

Transitory flaming. ISO[1] defines it as: "Existence of flame on or over the surface of the specimen for a period of time longer than that of *surface flash*, but shorter than that of *sustained flaming*."

Triboelectrification. The generation of static electricity by friction between two dissimilar materials.

Unpiloted ignition. ASTM E 176[2] defines it as: Ignition caused by one or more sources of energy without the presence of a pilot source of ignition." *Autoignition* is the preferred synonym.

Upper explosive limit; **upper explosion limit**. See *explosion limits*.

Upper flammability limit. The highest concentration of a vapor or gas that will ignite and burn with a flame in a given atmosphere (air, pure oxygen, etc.).

Upper temperature limit. The maximum temperature for which a saturated fuel vapor-air mixture can show flame propagation.

Abbreviations and acronyms

A. amperes.
abs. absolute.
ABS. acrylonitrile-butadiene-styrene.
AES. Auger electron spectroscopy.
AIChE. American Institute of Chemical Engineers.
ARC. Accelerating Rate Calorimeter.

ASTM. American Society for Testing and Materials, now called ASTM International.
ATF. automatic transmission fluid.
atm. atmospheres (unit of pressure).
AWG. American Wire Gauge.
AWS. American Welding Society.
BAM. Bundesanstalt für Materialprüfung (a German research institute)
BATF. Bureau of Alcohol, Tobacco, and Firearms.
BM. the former Bureau of Mines; remaining functions are now part of the Center for Disease Control.
BSI. British Standards Institution.
ca. approximately [Latin: *circa*].
cc. closed cup.
CDC. Center for Disease Control.
CEN. Comité Européen de Normalisation.
CFD. computational fluid dynamics.
CFR. Code of Federal Regulations.
CMHR. combustion-modified, high-resilience (foams).
CSA. Canadian Standards Association.
CSIRO. Commonwealth Scientific and Industrial Research Organization, Australia.
CTI. Comparative tracking index.
DSC. differential scanning calorimetry.
DTA. differential thermal analysis.
EBW. exploding bridgewire.
EDS. energy-dispersive X-ray spectrometry.
e.m.f. electromotive force.
ESCA. electron spectroscopy for chemical analysis.
EU. European Union.
EPS. expanded polystyrene foam.
ETFE. ethylene-tetrafluoroethylene.
EVA. ethylene-vinyl acetate.
FAA. Federal Aviation Administration.
FAE. fuel-air explosive.
FEP. fluorinated ethylene propylene.
F-K. Frank-Kamenetskii (developer of a self-heating theory).
FM. Factory Mutual, now called FM Global.
FMRC. Factory Mutual Research Corp.
FP. flash point.
FR. flame retardant; fire-retarded.
FRP. fiber-reinforced plastic.
FRS. Fire Research Station (UK).
g. grams.
GFCI. ground-fault circuit interrupter.
GRP. glass-reinforced plastic.
GWIT. Glow-Wire Ignition Temperature (test).
h. hours.
ha. hectares.
HAI. High-current Arc Ignition (test).
HRR. heat release rate.
HSE. Health and Safety Executive (UK).
HVAR. High-Voltage Arc Resistance (test).
HVTR. High-Voltage Arc-Tracking-Rate (test).
HWI. Hot-Wire Ignition (test).
IAAI. International Association of Arson Investigators.
ICBO. International Conference of Building Officials.
IEC. International Electrotechnical Commission.
IED. improvised explosive device (i.e., home-brew bomb).
IEEE. Institute of Electrical and Electronics Engineers.
IMDG Code. International Maritime Dangerous Goods Code.
ISO. International Organization for Standardization.
J. joules.
K. kelvins.
kg. kilograms.
LEL. lower explosive limit.
LFL. lower flammability limit.
LIT. layer ignition temperature.
LTL. lower temperature limit.
m. meters.
MC. moisture content.
MEC. minimum explosible concentration.
MESG. maximum experimental safe gap.
min. minutes.
MLR. mass loss rate.
MOC. minimum oxygen concentration needed for combustion.
N. newtons.
NA. not available
NACA. National Advisory Committee for Aeronautics (became NASA).
NASA. National Aeronautics and Space Administration.
NBS. National Bureau of Standards; now, National Institute of Standards and Technology.
n.d. no date of publication given.
NEC. National Electrical Code.
NEMA. National Electrical Manufacturers Association.
NFPA. National Fire Protection Association.
NI. no ignition.
NIOSH. National Institute for Occupational Safety and Health.
NIST. National Institute of Standards and Technology; formerly: National Bureau of Standards.
n.p. no place of publication given.
NSC. National Safety Council.
NTIS. National Technical Information Service.
NTSB. National Transportation Safety Board
OC. open cup
OSB. oriented-strand board.
OSHA. Occupational Safety and Health Administration.
Pa. pascals.
PBI. polybenzimidazole.
PCTFE. polychlorotrifluoroethylene.
PE. polyethylene
PEEK. polyetheretherketone.
PES. polyester.
PET. polyethylene terephthalate; often known by the trade name Dacron when used in fiber form.
PIR. polyisocyanurate.
PLC. Performance level category.
PMMA. polymethylmethacrylate.
PP. polypropylene.

pph. parts per hundred
PRV. pressure relief valve.
PTB. Physikalisch-Technischen Bundesanstalt (German research institute)
PTFE. polytetrafluoroethylene.
PUR. polyurethane.
PVC. polyvinyl chloride.
RF. radio frequency.
RH. relative humidity.
rms. root-mean-square.
RVP. Reid vapor pressure.
s. seconds.
S. siemens.
SADT. self-accelerating decomposition temperature.
SIMS. secondary ion mass spectrometry.
SLT. superheat limit temperature.
SP. Swedish National Testing and Research Institute.
St. stokes.
TAM. Thermal Activity Monitor.
TCO. thermal cutout.
temp. temperature.
TRP. thermal response parameter.
typ. typically
XPS. extruded polystyrene foam.
UEL. upper explosion limit.
UFL. upper flammability limit.
UK. United Kingdom.
UL. Underwriters Laboratories, Inc.
UMTA. Urban Mass Transportation Administration.
UN. United Nations.
US. United States.
UTL. upper temperature limit.
UVCE. unconfined vapor cloud explosion.
V. volts.
VAC. volts AC.
VDC. volts DC.
vol%. percent by volume.
W. watts.
XLPE. crosslinked polyethylene.
XLPO. crosslinked polyolefin.

References

1. Fire Safety – Vocabulary (ISO 13943), International Organization for Standardization, Geneva.
2. Standard Terminology of Fire Standards (ASTM E 176), ASTM.
3. Dricot, F., and Reher, H. J., Survey of Arc Tracking on Aerospace Cables and Wires, *IEEE Trans. Dielectrics and Electrical Insulation* **1,** 896-903 (1994).
4. Griffiths, J. F., and Gray, B. F., Fundamentals of Autoignition of Hydrocarbons and Other Organic Substrates in the Gas Phase, *24th Loss Prevention Symp.*, AIChE, New York (1990).
5. Guide for Fire and Explosion Investigations (NFPA 921), 2001 ed., NFPA (2001).
6. Guide to Fire Hazard Properties of Flammable Liquids, Gases, and Volatile Solids (NFPA 325), NFPA.
7. Birk, A. M., and Cunningham, M. H., The Boiling Liquid Expanding Vapour Explosion, *J. Loss Prev. Process Industries* **7**, 474-480 (1994).
8. Flammable and Combustible Liquids Code (NFPA 30), NFPA.
9. Standard on Explosion Prevention Systems (NFPA 69), NFPA.
10. Code of Federal Regulations, 29 CFR 1926.914.
11. **Encyclopedia of Explosives and Related Items**, B. T. Fedoroff, et al., eds., Picatinny Arsenal, Dover NJ (1960-1983).
12. Holm, R., **Electric Contacts: Theory and Applications**, 4th ed., Springer-Verlag, Berlin (1967).
13. Stecher, G. E., and Lendall, H. N., **Fire Prevention and Protection Fundamentals (Comburology)**, The Spectator, Philadelphia (1953).
14. Cook, M. A., **The Science of High Explosives** (ACS Monograph 139), Reinhold Publishing, New York (1958).
15. Médard, L. A., **Accidental Explosions**, 2 vols., Ellis Horwood, Chichester, England (1989).
16. Thomas, P. H., The Effect of Reactant Consumption on the Induction Period and Critical Condition for a Thermal Explosion (FR Note 409), Fire Research Station, Borehamwood, England (1959).
17. Martin, R. J., Reza, A., and Anderson, L. W., What Is an Explosion? A Case History of an Investigation for the Insurance Industry, *J. Loss Prevention in the Process Industries* **13**, 491-497 (2000).
18. Glassman, I., *Combustion*. 3rd ed., Academic Press, San Diego (1996).
19. **Recommendations on the Transport of Dangerous Goods**. Vol. 1: Model Regulations, 10th ed., 1997. Vol. 2: Manual of Tests and Criteria, 2nd ed., 1995. United Nations, New York.
20. 1984 National Sample Survey of Unreported, Residential Fires (Contract No. C-83-1239), prepared for CPSC, Audits & Surveys, Princeton NJ (1985).
21. Recommended Practice for Fire Protection for Electric Generating Plants and High Voltage Direct Current Converter Stations (NFPA 850), NFPA.
22. Flammable and Combustible Liquids Code (NFPA 30), NFPA.
23. Glossary of Terms Associated with Fire. Part 1: General Terms and Phenomena of Fire (BS 4422 Part 1), British Standards Institution, London (1987).
24. Code of Federal Regulations, 49CFR173, Shippers—General Requirements for Shipments and Packagings, Dept. of Transportation, Washington.
25. Recommended Practice on Static Electricity (NFPA 77), NFPA.

26. Morgan, J. D., **Principles of Ignition**, Pitman, London (1942).
27. National Electrical Code (NFPA 70), NFPA.
28. Standard for Safety—Intrinsically Safe Apparatus and Associated Apparatus for Use in Class I, II, and III, Division 1, Hazardous (Classified) Locations (ANSI/UL 913), UL.
29. Uman, M.A., **The Lightning Discharge**, Academic Press, Orlando FL (1987).
30. Lewis, R J. sr., **Hawley's Condensed Chemical Dictionary**, 14th ed., Wiley, New York (2001).
31. Carleton, F. B., Bothe, H., Proust, Ch., and Hawksworth, S., Prenormative Research on the Use of Optics in Potentially Explosive Atmospheres—PROPEX (EUR 19617 EN), European Commission, Luxembourg (2000).
32. Standard Test Method for Minimum Explosible Concentration of Combustible Dusts (ASTM E 1515), ASTM.
33. Electrical Equipment for Use in Class I, Division 2, Hazardous (Classified) Locations (ANSI/ISA-S12.12), American National Standards Institute, New York.
34. Explosive Materials Code (NFPA 495), NFPA.
35. Code of Federal Regulations, 30 CFR 18.2.
36. Class 4, Divisions 4.1, 4.2, and 4.3—Definitions, 49 CFR 173.124 (1998).
37. Recommended Practice for Responding to Hazardous Materials Incidents (NFPA 471), NFPA.
38. Hazardous Chemicals Data (NFPA 49), NFPA.
39. Standard for the Protection of Cleanrooms (NFPA 318), NFPA.
40. Standard Method of Test for Vapor Pressure of Petroleum Products (Reid Method), ASTM D 323, ASTM.
41. Recommended Practice for Responding to Hazardous Materials Incidents (NFPA 471), NFPA.
42. Guide on Fire Hazards in Oxygen-Enriched Atmospheres (NFPA 53), NFPA.
43. Standard **Dictionary of Electrical and Electronics Terms**, IEEE, New York (1998).
44. Method for the Determination of the Proof Tracking and Comparative Tracking Indices of Solid Insulating Materials (IEC 60112), 4th ed., International Electrotechnical Commission, Geneva.

Copyright © 2003, 2014 Vytenis Babrauskas

Chapter 3. Fundamentals of combustion

Introduction **24**
Thermochemistry **24**
Heat of combustion *25*
Constant-volume heat of combustion *27*
Effective heat of combustion; heats of explosion and detonation *28*
Relations between fuel and air *28*
Adiabatic flame temperature *30*
Reaction kinetics **32**
Branching chain reactions *33*
Autocatalytic reactions *34*
Flame speed **35**
Types of explosions **36**
Pressure piling *37*
Deflagration to detonation transition *38*
Catalytic combustion **38**
Tests for fundamental combustion properties **39**
Further readings **39**
References **39**

Introduction

In this Chapter, a brief review is made of some simple fundamentals of combustion theory. Here, we present some of the basic ideas of the chemical reactions involved in oxidation of materials. A *chemical reaction*, by the way, is simply a rearrangement of atoms into a different configuration. In other words, it occurs when molecules split up, and new molecules are formed out of the original collection of atoms. A *change of state*, however, is a physical change, not a chemical reaction. Thus, ice melting and becoming water, then being boiled off and becoming steam does not comprise any chemical reaction, only a change of state of matter. The molecules at all times continue to remain H_2O.

The branch of science which is concerned only with the state of the initial reactants and the final products is termed *thermochemistry*. The study of how fast the reactions take place is termed *reaction kinetics*.

Rapid, high-temperature oxidation is referred to as *combustion*. There is sometimes a distinction made between fire and explosion. According to one author[1], an *explosion* is a gas-dynamic process by which a marked increase in system pressure generates destructive forces. By contrast, he considers *fire* to be slower combustion process in which the overall rate of fuel oxidation is limited by its rate of mixing with the surrounding air. Definitions something of this nature are commonly used both by scientists and by laymen. However, these terms are not intended to be highly precise, and all manner of subtle difficulties can arise. For example, the process leading to spontaneous combustion is often termed a *thermal explosion*, yet gas-dynamics plays a negligible role in it. *Detonation* is a unique, narrowly defined form of explosion (a reaction propagating at a velocity greater than the local speed of sound in the unreacted material), but apart from that, explosion and fire should be viewed simply as points of emphasis on a continuum.

Thermochemistry

Fuels and oxidizers, when combined, cause heat to be liberated. If the heat is sufficient, visible flames can be seen. Why are, then, all fuels not spontaneously igniting? In other words, why is the "heat" side of the fire triangle needed? To understand the answer to this simple-seeming question, we must examine some chemistry of combustion. In such study, we will learn that the fuel + oxidizer reaction usually* has an energy hump: external energy must be put into

* Some pairs of substances do not need energy input in order to ignite. Such pairs of substances which ignite directly upon being mixed are termed *hypergolic*. In many hypergolic reactions, the oxidizer needed for such ignition is not oxygen, thus the more general concept of "pairs of substances" is used for clarity.

the system, before fuel and oxidizer molecules can actually combine and form products. To understand this process, some concepts of combustion thermochemistry and kinetics must be understood. This will be the theme of the present chapter.

HEAT OF COMBUSTION

The heat of combustion is actually more precisely defined as the *enthalpy of combustion* and sometimes casually denoted as *calorific value*. Thus, it is essential that the concept of *enthalpy* be briefly reviewed from thermodynamics. The First Law of Thermodynamics states that:

$$\Delta E = Q - W$$

where ΔE = change in the internal energy of a system; Q = heat added to the system; and W = work done by the system. The units for all of these quantities are joules, although in fire studies it is more convenient to use kJ (1000 J) or MJ (10^6 J). The internal energy can be understood as the energy stored in the molecules themselves. As it turns out, in thermodynamics we do not try to determine the absolute value of this energy, but are only interested in changes which occur when the system interacts with the outside world. This is why the First Law is couched in terms of the change, ΔE. The reason for the minus sign is that due to the definition of W, whereby a positive W means work is done by the system. Since work done *by* the system lowers its energy, whereas heat added to the system raises the energy, there is a minus sign in front of W, but not in front of Q.

We must now consider some details of the work term. We will mainly be concerned with work due to expansion of gases. Suppose a reaction occurs which causes the volume of the system to expand from V_1 to V_2. Then the work that is done *by* the system *on* the atmosphere surrounding it is

$$W = P(V_2 - V_1) = P\Delta V$$

In SI units, pressure is measured in Pascals (Pa), where 1 Pa = 1 N m^{-2}. The Newton (N) is basic SI unit of force. It can be expressed as 1 N = 1 kg m s^{-2}. The work term is *absent* if the reaction occurs in a constant-volume vessel, since then $\Delta V \equiv 0$; otherwise, an expansion that occurs corresponds to a positive ΔV and therefore to a positive W term. Chemical reactions taking place under constant-pressure conditions are very common. If the only work involved is that due to the expansion of the gases and the pressure P is constant throughout the process, then the First Law becomes:

$$\Delta E = Q - P\Delta V$$

We now define enthalpy H as:

$$H = E + PV$$

The heat added to the constant-pressure system in going from state 1 to state 2 is:

$$Q = (E_2 - E_1) + P(V_2 - V_1) = (E_2 + PV_2) - (E_1 + PV_1)$$

But by the definition of H, this becomes:

$$Q = H_2 - H_1 = \Delta H$$

In other words, in a constant-pressure process, the heat added to the system is equal to the change in its enthalpy. Since in thermochemistry the main task is to account for the heat absorbed or eliminated from a system, the use of the enthalpy concept simplifies things by developing expressions for heat that do not require accounting for volume changes. The units of enthalpy are the same as energy, e.g., J, kJ or MJ.

Now, consider a general reaction where:

$$(\text{reactants}) \rightarrow (\text{products})$$

Using the concept of enthalpy, the *heat of reaction*, h_r, is the heat which must be *added* to the system to produce the products from the reactants:

$$\Delta H_r = \sum n\Delta H_f^o\Big|_{\text{products}} - \sum n\Delta H_f^o\Big|_{\text{reactants}}$$

where the n is the number of moles of a particular reactant or product species, ΔH_f^o is the *standard heat of formation* for the species, and the summation is taken over all products and all reactants. The heat of formation of any chemical species, in turn, is defined as the heat which is required to be added in order to form that species out of its constituent elements, with the elements being in their standard state. By convention, the standard state is defined to be at a temperature of 298 K and a pressure of 1 atm, and the "o" superscript reminds us of that. To fully specify the standard state, the state of aggregation must also be specified. This is taken to the be normal or common state at 298 K. For example, the normal state for oxygen at 298 K is as the molecule O_2, not as the atom O; thus, the standard state for oxygen is defined as $O_2(g)$, where the "g" denotes the gas state. The standard heat of formation is sometimes written as ΔH_{f298}^o, where the "298" denotes the standard temperature of 298 K. There are several other slight permutations of this symbol that will be found in the literature. The reason for establishing such conventions is to facilitate making published tables of values; if the conditions were not standardized, it would be very difficult to collect the needed data for solving problems.

A simple example of the arithmetic of heats of formation will make this clear. Suppose we combine hydrogen and carbon to form methane:

$$C(s) + 2H_2(g) \rightarrow CH_4(g)$$

If the process takes place at room temperature, the hydrogen will be gaseous, but the carbon will be solid (graphite); this is reflected in the equation written above. Since the (s) state for carbon and the (g) state for H_2 are the standard states for both of these substances, the heats of formation are $\equiv 0$ for both. Gaseous methane is not an element, so we expect it to have a non-zero ΔH_f^o. From thermochemical reference tables[2,3], the value of ΔH_f^o for CH_4(g) is found to be -74.81 kJ mol^{-1}. Thus, H_r = -74.81 – 0 = -74.81 kJ mol^{-1}. The negative sign indicates that heat must be *removed* from the system for the products to stay at 298 K and not to rise in temperature. In other words, the negative sign indicates an *exothermic* (heat producing) reaction. This

example might suggest that one could take a slab of graphite, discharge some hydrogen gas on it, and convert the graphite into methane. If one were to do this at room temperature, one would find that nothing would happen and no CH_4 could be detected. The reason is because the reaction rate is exceedingly slow for this reaction, in other words, chemical kinetics, which we have not considered yet, prohibits the easy occurrence of this reaction. However, if we were to wait a very long time, we might find that eventually it would be possible to detect some reaction products.

This same problem can be turned around in a useful way. Suppose we have a cylinder of methane gas. Is it likely to spontaneously decompose and revert into C and H_2? To consider this, all that is needed is to reverse the reaction, that is, switch the products and the reactants. Now, the heat of reaction of the reverse reaction becomes +74.81 kJ mol^{-1}. This means that a large amount of heat would have to be added to the system in order to decompose methane, in other words the reverse reaction is *endothermic*. Here, since thermodynamics alone suggests to us that the process will not happen spontaneously and there is no need to consider whether slow reactions would further prohibit the occurrence.

Now consider another simple gas, acetylene, C_2H_2. This time, instead of writing the equation for formation, let us ask whether the decomposition reaction is likely to spontaneously occur:

$$C_2H_2(g) \rightarrow 2C(s) + H_2(g)$$

The heat of formation of $C_2H_2(g)$ is +226.7 kJ mol^{-1}, and two substances on the right side of the equation are both in their reference state, so their heats are $\equiv$ 0. Thus, the heat of reaction is:

$$2(0) + 0 - 226.7 = -226.7 \text{ kJ mol}^{-1}$$

The decomposition reaction of acetylene, having a minus sign for its heat of reaction, is exothermic. Furthermore, the value of –226.7 kJ mol^{-1} is a very high negative number, so the reaction is highly favored by thermodynamics to occur. There is a slight energy barrier to this occurring, however, so acetylene can be handled relatively safely under certain conditions. The role of the heat of formation in evaluating unstable substances is discussed further in Chapter 10 and specific compounds are discussed in Chapter 14.

Next consider a combustion reaction:

$$CH_4(g) + 2O_2(g) \rightarrow CO_2(g) + 2H_2O(l)$$

whereby gaseous methane burns and produces gaseous CO_2 and liquid water. In thermochemistry, the standard reaction which is considered occurs at 298 K: the reactants enter the system at 298 K, the reaction occurs, and then either enough heat is added or removed from the system, so that the products also return to the same 298 K temperature. Real combustion systems, of course, rarely have the products returning to 298 K. For example the exhaust from a car engine is much cooler than the combustion taking place within the cylinder, but it is still above room temperature. Such computations will be considered below.

To find the heat of reaction for the above combustion reaction, it is necessary to look up the heats of formation of the four substances involved. The ΔH_r can then be evaluated as:

$$\Delta H_r = \big(-393.51 + 2(-285.83)\big) - (-74.81 + 0)$$
$$= -890.36 \text{ kJ mol}^{-1}$$

Since we all know that methane, when burned, releases heat, it is not surprising to find a minus sign for the heat of reaction. The *heat of combustion*, ΔH_c is defined as the negative of ΔH_r, in order to conveniently have a positive number for combustible substances. Therefore, the heat of combustion, also called *calorific value*, of methane is +890.36 kJ mol^{-1}. In many cases, the unit of measurement which is convenient is mass, not moles. The molar mass* of methane is 16.04 g mol^{-1}, thus the heat of combustion is more commonly expressed as Δh_c = 55.50 MJ kg^{-1}. When mass-based, instead of mole-based, quantities are used, it is common to adopt the lower-case letters *h*, *q*, and *e* for enthalpy, heat, and internal energy.

There are actually two different heats of combustion which need to be kept straight. In the reaction above for the burning of methane, the water was written as $H_2O(l)$, specifying the liquid state. If the reaction products are actually cooled down to 298 K, then water will condense and be in liquid form. In most combustion systems, however, water remains as vapor and does not condense. The arithmetic needed to correct for the fact that condensation did not occur is then just a burden. Thus, the heat of combustion with water going to $H_2O(l)$ is defined as the *gross (or upper) heat of combustion*. The same reaction, but with water going to $H_2O(g)$, is defined as the *net (or lower) heat of combustion*. Consequently, one must always specify which heat of combustion is being referred to. To keep this straight, the nomenclature ΔH_c^u and ΔH_c^l is often used. The heat of formation of $H_2O(g)$ is –241.82 kJ mol^{-1}. Thus, the heat of reaction when $H_2O(g)$ is the product becomes:

$$\Delta H_r = \big(-393.51 + 2(-241.82)\big) - (-74.81 + 0)$$
$$= -802.34 \text{ kJ mol}^{-1}$$

and ΔH_c^l = +802.34 kJ mol^{-1}, or Δh_c^l = 50.01 MJ kg^{-1}. For any substance, if Δh_c^u is the only published value that is available, the net heat of combustion can be calculated as:

$$\Delta h_c^l = \Delta h_c^u - 0.2183[\%H] \quad \text{MJ kg}^{-1}$$

where [%H] is the percent of hydrogen, by mass, in the fuel, and both heats of combustion are to be expressed in units of (MJ kg^{-1}). Thus, for the methane example, one mole of CH_4 weighs 16.04 g, in which there are 4 atoms of H, the latter having an atomic weight of 1.008 g. Then, to obtain Δh_c^l from Δh_c^u, it is necessary to subtract

* Molar mass used to be known as *molecular weight* to those who studied chemistry not so recently.

0.2183×100×4×1.008/16.04, or 5.49 MJ kg^{-1}, which gives Δh_c^l = 50.01 MJ kg^{-1}, exactly as above.

In most handbook compilations, listings are given for the heats of formation, rather than the heats of combustion. Thus, the user must be able to perform the arithmetic of starting with heats of formation and computing the heat of combustion. For the heat of combustion,

$$\Delta H_c = -\sum n\Delta H_f^o\Big|_{\text{products}} + \sum n\Delta H_f^o\Big|_{\text{reactants}}$$

Now writing a fairly general expression for combustion of a fuel in oxygen:

$$\begin{aligned} &C_cH_hO_oN_nS_sX_xB_bSi_i \\ &\quad + \frac{1}{2}\left[2c + \frac{h}{2} - o - \frac{x}{2} + 3s + 3b + 2i\right]O_2 \\ &\rightarrow cCO_2 + \frac{1}{2}(h - x - 2s - 3b)H_2O + \frac{n}{2}N_2 \\ &\quad + xHX + sH_2SO_4 + bH_3BO_3 + iSiO_2 \end{aligned} \qquad (1)$$

The above expression is unchanged for combustion in air, except that an identical number of nitrogen molecules become added to both sides. The letter *X* is used to indicate any of the halogen atoms (F, Cl, Br, etc.) that may be present. Noting that there will always be only 1 fuel mole on the left side of the equation, and that $\Delta H_f^o\Big|_{O_2} \equiv 0$,

$$\begin{aligned} \Delta H_c = &-c\Delta H_f^o\Big|_{CO_2} - \frac{1}{2}(h - x - 2s - 3b)\Delta H_f^o\Big|_{H_2O} \\ &- x\Delta H_f^o\Big|_{HX} - s\Delta H_f^o\Big|_{H_2SO_4} - b\Delta H_f^o\Big|_{H_3BO_3} \\ &- i\Delta H_f^o\Big|_{SiO_2} + \Delta H_f^o\Big|_{fuel} \end{aligned}$$

In handbook tabulations it will be found that, in general, values of ΔH_f^o are given separately for the crystalline-solid, amorphous-solid, liquid, and gas phases, generally abbreviated as (c), (a), (l), and (g). By convention, the products are generally taken to be CO_2 (g), HX (l), $H_2SO_4 \cdot 115H_2O$ (l), H_3BO_3 (c), and SiO_2 (a), although there is not universal agreement. For water, if the lower heat of combustion ΔH_c^l is computed, then the H_2O (g) state is used, while for ΔH_c^u the H_2O (l) state applies. The state of the reactants is *not* standardized. It is possible for fuel to be in solid, liquid, or gas phases, so the value of ΔH_f^o to be used for the fuel must correspond to the actual state of the substance. If we want to compute the standard (net) heat of combustion, then it is defined to be at a temperature of 298 K. For this purpose, the (g) state should be picked for substances with a boiling point ≥ 25ºC, and the (l) state for liquids having T_b < 25ºC. For substances which are solids at 25ºC, the (c) or (a) state should be used. Inserting the appropriate values for the heats of formation of standard products,

$$\begin{aligned} \Delta H_c^u = &393.51c + 142.92(h - x - 2s - 3b) - x\Delta H_f^o\Big|_{HX} \\ &+ 887.81s + 1094.33b + 903.49i + \Delta H_f^o\Big|_{fuel} \end{aligned}$$

$$\begin{aligned} \Delta H_c^l = &393.51c + 120.91(h - x - 2s - 3b) - x\Delta H_f^o\Big|_{HX} \\ &+ 887.81s + 1094.33b + 903.49i + \Delta H_f^o\Big|_{fuel} \end{aligned}$$

where for $\Delta H_f^o\Big|_{HX}$ the values used are –318.97 kJ mol^{-1} for HF, –166.62 kJ mol^{-1} for HCl, and –121.16 kJ mol^{-1} for HBr, and all of these values refer to these acids in dilute aqueous solutions.

Example Compute the net heat of combustion of methyl chloride, CH_3Cl. Its T_b = –24ºC, so we will take the state to be (g). The heat of formation of CH_3Cl (g) = –80.83 kJ mol^{-1}. Then,

$$\begin{aligned} \Delta H_c^l &= 393.51\times 1 + 120.91(3-1) - 1\times(-166.62) - 80.83 \\ &= 721.12 \text{ kJ mol}^{-1} \end{aligned}$$

or, since the molar mass is 50.49, Δh_c^l = 721.12/50.49 = 14.28 kJ g^{-1}, or 14.28 MJ kg^{-1}. Because of the low heat of combustion, we would not expect methyl chloride to burn easily.

If we wanted to compute the gross heats of combustion, it would be necessary to consider some more details of the products of reaction. Because definitions need to be standardized, products of reaction are standardized. This does *not* means that these particular products will occur in actual combustion, but rather that chemists have agreed to use certain reaction products for developing tables and handbook data. CO_2 and N_2 remain gaseous products even for the gross heat of combustion.

CONSTANT-VOLUME HEAT OF COMBUSTION

The standard definition of heat of combustion entails a process occurring at constant pressure, this being the reason why the heat of reaction is expressed as an enthalpy. It is possible for combustion processes to occur at constant volume. In fact, the standard oxygen bomb calorimeter for measuring heats of combustion is a constant volume device. The constant-volume heat of combustion, i.e., the energy of combustion, ΔE_c, is experimentally obtained, then from it ΔH_c can be calculated as:

$$\Delta E_c = \Delta H_c - RT\Delta n$$

where R = universal gas constant (= 8.314 J mol^{-1} K^{-1}), T = 298 K, and Δn = (gaseous moles of products – gaseous moles of reactants). Note that any reactants or products which are in condensed phase are ignored in the above arithmetic. Fuels are often in condensed phase, but for explosive or pyrotechnic substances, combustion products (e.g., metal oxides) can also be in condensed phase.

EFFECTIVE HEAT OF COMBUSTION; HEATS OF EXPLOSION AND DETONATION

In actual combustion, not all products are simply the standard products discussed above. For instance, in every fire a fraction of carbon becomes CO—all of the carbon does not go just into CO_2. Similarly, other minor species may be produced. The heat of combustion for actual, as opposed to standard, conditions are termed *effective heat of combustion*. This is not a unique value for a substance, since different fire conditions will produce different reaction products. In a large fraction of practical fire situations, the effective heat of combustion is 90% or more of the net heat of combustion. Thus, in many cases it is not necessary to consider actual reaction products and their effects on the heat release.

One situation where (minus) the heat of reaction is greatly different from the heat of combustion is for solid explosives. If the substance were reacted with a sufficient amount of gaseous oxygen, then bomb calorimeter determinations would produce the standard heat of combustion. However, in a real explosion of a solid explosive, the time scales are such that there is not an opportunity for the explosive substance to react with atmospheric oxygen. Thus, the *energy of explosion*, ΔE_{exp}, is measured by using the same bomb calorimeter as for the determination of the heat of combustion, but filling the bomb with nitrogen instead of oxygen. The igniter wire ignites the substance and heat evolved is measured calorimetrically. For this measurement, the pressure of nitrogen in the bomb at the start of the test is set at a recommended value of either[4] 2.53 MPa or[5] 3.1 MPa. The energy of explosion is also referred to as the *heat of explosion*. The *energy of detonation*, ΔE_{det} (more commonly called the *heat of detonation*) is the negative of the heat of reaction, but using a special definition for the reaction products. The reaction products are taken to be at ambient pressure and temperature, but having the composition that the products would have if their temperature and pressure values were those which prevail at the Chapman-Jouguet (C-J) point[4]. The latter—a value calculated from hydrodynamics of detonations—is chosen because it approximates the temperature/pressure conditions found in a detonation. At the C-J point, the temperature may reach 5000 K and the pressure 35 GPa. Thus, substantial calculations need to be made to obtain this value. The difference between the heat of explosion and the heat of detonation is small, unless the oxygen balance (see Chapter 10) is quite negative. Fedoroff[4] reports that the distinction is often ignored by experimentalists, that disagreements exist concerning the exact definition of the heat of detonation, and that, in any case, experimental results show a wide scatter. Values of the heat of explosion and heat of detonation, while numerically rather similar, will be much lower than the heat of combustion, if the substance has a *negative oxygen balance*. The latter concept is discussed in detail in Chapter 10, but briefly it means that a substance having a negative oxygen balance can be further oxidized, if it can react with the oxygen in air, once its initial self-reaction is completed. Consequently, for many explosives, the heat of explosion is only ¼ to ½ of the heat of combustion. Some typical values are given in Chapter 14 under *Explosives*.

Table 1 Gas explosions—explosion energies for stoichiometric fuel/air mixtures

Fuel	Net ht. of comb. (MJ kg^{-1})	Ht. of comb. per unit vol. of fuel* (MJ m^{-3})	Stoich. air/fuel ratio (m^3/m^3)	Explosion energy per volume of fuel/air mixture* (MJ m^{-3})
ammonia	18.6	13.0	3.6	2.8
butane	45.7	108.6	31.0	3.4
cyclohexane	43.4	149.4	42.9	3.4
ethylene	47.2	54.1	15.3	3.5
hydrogen	120.0	9.9	3.4	2.9
methane	50.0	32.8	10.5	3.1
propane	46.3	83.5	23.9	3.4
vinyl chloride	18.4	47.0	13.1	3.3

* for volume of gas at 298 K

In addition, in recent years it has been suggested that the energy of explosion be limited further still to the energy that can be realized as thermodynamic work (e.g., pressures of blast waves moving walls). Not 100% of the energy of the reaction can be converted into work, and the rest can only become heat. Since the heat released in explosions is not destructive in the same manner that mechanical work is, the concept of *available energy of explosion* allows the maximum destructive potential of explosions to be quantified and compared[6].

For *gas explosions*, the energy released, per volume of stoichiometric fuel/air mixture, does not depend much on the nature of the fuel. Table 1 shows that most fuels release close to 3.4 MJ for each cubic meter of stoichiometric fuel/air mixture. As a related quantity, the ratio (heat released)/(mass of oxygen consumed) is nearly constant for most organic fuels, and it comprises the *oxygen consumption principle*. The latter has been the basis of current-day measurements of heat released in fires[7].

RELATIONS BETWEEN FUEL AND AIR

As will be seen throughout the Handbook, the air/fuel ratio is a variable of primary importance in determining the conditions of combustion. The proportion between fuel and air can be expressed in various ways. In many cases, volume-percent of a fuel gas is specified, it being tacitly assumed that the remainder is air. For mixtures which contain special diluents, simply identifying the vol% of each component is appropriate. Next, it is necessary to introduce the concepts of *stoichiometric*, *fuel-lean* and *fuel-rich*. A fuel/oxidizer mixture is referred to as being stoichiometric if the amount

of fuel is exactly such that, upon combustion, there is no extra fuel left unburned and no oxygen left unreacted. If more fuel than needed for stoichiometric combustion is present, then the mixture is fuel-rich. Similarly, if less is present, then the mixture is fuel lean.

The general reaction for the stoichiometric combustion of a fuel can be written as:

$$1\,\text{kg fuel} + r\,\text{kg air} \rightarrow (1+r)\ \text{kg products}$$

In other words, for complete combustion, each kg of fuel requires r kg of air. Thus, the air/fuel ratio for complete combustion is r, on a mass basis. In combustion engineering, the air/fuel ratio is often used on a mole (or volume) basis. If γ is the air/fuel mole ratio, then it can be obtained as:

$$\gamma = r\frac{M_f}{M_a}$$

where M_f = molar mass of fuel and M_a = molar mass of air = 28.96 g mol^{-1}. When the ratio of the fuel and air is not the stoichiometric one, then the fuel/air mixture can be represented by the use of the *equivalence ratio*[*], which is a dimensionless number assigned the symbol φ:

$$\varphi = \frac{(fuel/air)}{(fuel/air)_{st}}$$

where *st* denotes stoichiometric conditions. All values of $\varphi > 1$ correspond to fuel-rich conditions; similarly all values of $\varphi < 1$ correspond to fuel-lean conditions. The equivalence ratio can also be expressed as:

$$\varphi = r \times \frac{\text{mass of fuel}}{\text{mass of air}} = \gamma \times \frac{\text{moles of fuel}}{\text{moles of air}}$$

And it can be shown that the value of φ is the same, regardless if the amounts are all evaluated as moles or as masses.

For example, methane burning fully in air is:

$$CH_4 + 2(O_2 + 3.76N_2) \rightarrow CO_2 + 2H_2O + 7.52N_2 \qquad (2)$$

In the above equation, the amount of oxygen is such that there is no oxygen left among the products; neither is there any fuel left, thus the reaction, as written, is stoichiometric. Suppose now that there are two moles of methane going into the reaction, with the amount of air unchanged:

$$2CH_4 + 2(O_2 + 3.77N_2) \rightarrow CO_2 + 2H_2O + 7.52N_2 + CH_4 \qquad (3)$$

We first compute γ using the stoichiometric reaction, Eq. (2). For each mole of fuel burned, the number of moles of air is 2 × (1+3.77) = 9.54. Thus, γ = 9.54/1 = 9.54. Now compute the fuel/air mole ratio for our desired reaction, Eq. (3). This fuel/air mole ratio is = 2/9.54 = 0.210. Thus, φ = 9.54×0.210 = 2.0.

Consider now what would happen if the ratios were computed as masses. The mass of two moles of air is = 2 × (32.00 + 3.77 × 28.01) = 275.2 and the molar mass of CH_4 is 16.04. Thus, the value of r is 275.2/16.04 = 17.16. Considering now our desired reaction, Eq. (2), the mass of two moles of CH_4 is 2 × 16.04 = 32.08 g. Then, the fuel/air mass ratio is 32.08/275.2 = 0.117 (this, of course, is *not* the same as the mole ratio of 0.210). The value of φ = 17.16×0.117 = 2.0, which is the same as when computed by ratioing volume ratios.

In cases where the fuel is a liquid aerosol or a dust cloud, it is common to express the fuel as a fuel mass concentration in air (g m^{-3}). In such cases, it can be shown that the equivalence ratio can also be expressed as:

$$\varphi = \frac{\text{fuel mass concentration}}{(\text{fuel mass concentration})_{st}}$$

For the fairly general fuel discussed above, the value of γ is obtained as:

$$\gamma = 4.77\left[c + \frac{h}{4} - \frac{o}{2} - \frac{x}{4} + \frac{3}{2}s + \frac{3}{2}b + i\right]$$

where the variables are defined as indicated in Eq. (1). In some cases, the ratio γ_o is desired:

$$\gamma_o = \frac{\text{moles of oxygen}}{\text{moles of fuel}}$$

This, of course, is evaluated simply as:

$$\gamma_o = \left[c + \frac{h}{4} - \frac{o}{2} - \frac{x}{4} + \frac{3}{2}s + \frac{3}{2}b + i\right]$$

For methane γ = 4.77×(1 + 4/4) = 9.54. Similarly, the value of r is obtained as:

$$r = 4.77\frac{28.85}{M_f}\left[c + \frac{h}{4} - \frac{o}{2} - \frac{x}{4} + \frac{3}{2}s + \frac{3}{2}b + i\right]$$

Thus, since the molar mass of methane is 16.04, its value of r is obtained as 9.54×28.85/16.04 = 17.16. Occasionally, the stoichiometric oxygen/fuel mass ratio, r_o is needed. This can be evaluated as:

$$r_o = \frac{32.00}{M_f}\left[c + \frac{h}{4} - \frac{o}{2} - \frac{x}{4} + \frac{3}{2}s + \frac{3}{2}b + i\right]$$

For methane, r_o = 32.00×2/16.04 = 4.0.

The stoichiometric concentration of fuel in a fuel/air mixture, C_{st}, is an often-used quantity. It is defined on a vol% basis and thus it is:

$$C_{st} = \frac{100}{1+\gamma}$$

For the general fuel C_{st} can be evaluated as:

$$C_{st} = \frac{100}{1 + 4.77\left(c + \frac{h}{4} - \frac{o}{2} - \frac{x}{4} + \frac{3}{2}s + \frac{3}{2}b + i\right)}$$

It is often necessary to convert between values of φ and the vol% of fuel, C_f, in a non-stoichiometric fuel/air mixture. This can done according to:

[*] The definition given here is the customary one, but the reader must be warned that some researchers use a definition which is exactly the inverse of the one used here.

$$C_f = \frac{100}{1+\frac{\gamma}{\varphi}} = \frac{100}{1+\frac{\left(\frac{100}{C_{st}}-1\right)}{\varphi}}$$

and

$$\varphi = \frac{\frac{100}{C_{st}}-1}{\frac{100}{C_f}-1}$$

For methane, C_{st} = 100/(1+9.54) = 9.49%. Thus, if a methane concentration of 15 vol% is measured in air, the equivalence ratio φ = (100/9.49–1)/(100/15–1) = 1.68. Thus, this concentration represents a mixture which is 68% fuel-rich.

ADIABATIC FLAME TEMPERATURE

The adiabatic flame temperature, T_{ad}, is the temperature which a fuel-air mixture would reach if it could react without losing any heat in the process to the environment. This, of course, is impossible, but it is a very useful concept since it establishes the upper limit for combustion temperatures. In a real system with heat losses, the actual temperature achieved must be less than T_{ad}. Consider a stoichiometric methane/air mixture:

$$CH_4 + 2(O_2 + 3.76N_2) \rightarrow CO_2 + 2H_2O + 7.52N_2$$

As discussed in the previous section, the heat of this reaction is –890.36 kJ mol^{-1}. This amount of heat would need to be removed from the system (by using cooling coils, for example) in order to bring the combustion products back to room temperature. But here, we will assume that the system is perfectly insulated and will rise to a high temperature. To start with the general case, for a constant-pressure system where the reactants and the products are at two different temperatures T_1 and T_2, with neither one being the standard 298 K reference temperature, and no heat is added or removed from the system, conservation of energy gives:

$$Q = \Delta H = \sum_{i \text{ products}} n_i \left[\left(H^o_{T_2} - H^o_{298}\right) + \Delta Hf^o_{298}\right]_i - \sum_{j \text{ reactants}} n_j \left[\left(H^o_{T_1} - H^o_{298}\right) + \Delta Hf^o_{298}\right]_j$$

Same as with internal energy, the absolute value of enthalpy is undefined. Only the difference in enthalpy between that at one temperature and that at a second temperature can be quantified. The reference temperature can, in principle, be anything, but the reference handbooks compile all use 298 K. Thus, the notation $\left(H^o_{T_2} - H^o_{298}\right)_i$ does not mean that two different numbers are to be looked up and then subtracted—this is a *single* quantity which is looked up in the tables. This term, not to be confused with the enthalpy of formation, discussed above, is the increase in enthalpy sustained when a mole of substance i which is at 1 atm pressure goes from a temperature of 298 K to a temperature T_2. Continuing the example of methane burning adiabatically, the heat entering the system ≡ 0. Simplifying the problem now by assuming that the reactants entered at a temperature of 298 K and not at some different value of T_1,

$$0 = \sum_{i \text{ products}} n_i \left[\left(H^o_{T_2} - H^o_{298}\right) + \Delta H^o_{f298}\right]_i - \sum_{j \text{ reactants}} n_j \left[\Delta H^o_{f298}\right]_j$$

To solve this equation, it is convenient to remember from chemistry the definition of the constant-pressure heat capacity C_p:

$$C_p(T) = \left(\frac{\partial H}{\partial T}\right)_P$$

C_p is a function of the temperature, and at any given temperature it represents the slope of the enthalpy curve with respect to temperature. Enthalpy rises notably with temperature, but its slope, C_p, is rather less affected by temperature. If C_p were a constant, independent of T, then we could write

$$\left(H^o_{T_2} - H^o_{298}\right) = C_p\left(T_2 - 298\right)$$

Since we have assumed the system is adiabatic, $Q \equiv 0$, and

$$0 = C_p(CO_2)\cdot(T_{ad} - 298) + \Delta H^o_{f298}(CO_2) + 2C_p(H_2O)\cdot(T_{ad} - 298) + 2\Delta H^o_{f298}(H_2O(g)) + 7.52C_p(N_2)\cdot(T_{ad} - 298) + 7.52\Delta H^o_{f298}(N_2) - \Delta H^o_{f298}(CH_4) - 2\Delta H^o_{f298}(O_2) - 7.52\Delta H^o_{f298}(N_2)$$

where we have explicitly stated that the T_2 which must be solved for is, in fact, T_{ad}. To simplify this fairly lengthy expression, we can realize that

$$\Delta H^u_c(CH_4) = -\Delta H^o_{f298}(CO_2) - 2\Delta H^o_{f298}(H_2O(g)) + \Delta H^o_{f298}(CH_4)$$

while the heats of formation of O_2 and N_2 are ≡ 0. Thus,

$$0 = \left[C_p(CO_2) + 2C_p(H_2O) + 7.52C_p(N_2)\right](T_{ad} - 298) - \Delta H^u_c(CH_4)$$

If we make the approximation that C_p = constant, then a suitable temperature needs to be selected at which to pick these values. This temperature should roughly be halfway between 298 K and T_{ad}. For the sake of simplicity, we will pick T = 1300 K. At this temperature, C_p (CO_2) = 57.1 J K^{-1} mol^{-1}; C_p (H_2O) = 44.9 J K^{-1} mol^{-1}; and C_p (N_2) = 34.1 J K^{-1} mol^{-1}. Thus,

$$T_{ad} \approx 298 + \frac{890.36\times10^3}{57.1 + 2\times44.9 + 7.52\times34.1} = 2506 \text{ K}$$

which is somewhat higher than the actual value of 2225 K. In the above equation, it was necessary to multiply the heat of combustion results by 1000, since their original units were in kJ, while the units used for C_p in the denominator are in J.

If adiabatic flame temperatures were manually computed in a way as described, even if an approximation for C_p were not needed, the results would still be higher than the true value. The reason is that the actual combustion products are not simply CO_2 and H_2O. For any organic fuel, some products of incomplete combustion (CO, soot, unburned hydrocarbons) will exist, although these are likely to be negligible if the combustion is fuel-lean, instead of stoichiometric or fuel-rich. In addition, however, the actual combustion products will contain *dissociated* species, such as H, OH, O, and will also tend to contain some molecular hydrogen (H_2) and some NO. Since dissociation is endothermic, this means that enthalpy contribution is reduced from the expected value.

Since most unwanted combustion occurs under constant, or nearly-constant, pressure conditions, the above derivation focused on the *constant-pressure* T_{ad}. There is a second type of adiabatic flame temperature which can be derived, a constant-volume T_{ad}. The difference between the two computed T_{ad} values is not trivial. For methane burning stoichiometrically in air, the constant-pressure T_{ad} is 2225 K, while the constant-volume T_{ad} is 2889 K. The reason the constant-volume process gives a much higher temperature is because all of the energy of the reaction goes solely to heating the combustion products. In a constant-pressure system, a portion of the energy is dissipated as a work term, $p\Delta V$. Henceforth in this book we will only concern ourselves with constant-pressure T_{ad}.

The adiabatic flame temperature of most fuels is in the range of 2000 to 2500 K when burned in normal air. For combustion in pure oxygen, T_{ad} is typically 3000 to 3500 K, but in the extreme case of carbon subnitride (C_4N_2), which is a highly endothermic compound, a value of 5300 K is found. One might think that any value of T_{ad} > room temperature would mean a substance can burn. This is not true; to learn why, we must consider combustion reaction kinetics. Empirically, gases and vapors which have an adiabatic flame temperature below about 1600 K will normally not undergo self-sustained combustion in a 21% oxygen environment. The LFL and UFL values for any gas ought to correspond to the same value of T_{ad}, and one would expect the same value to be shared by gases which have the same chemical oxidation mechanism. Actual LFL and UFL values are somewhat apparatus-dependent, but Hertzberg et al.[8] demonstrated for methane that using experimental values of LFL = 4.9% and UFL = 18.5%, T_{ad} is computed to be 1450 K at both the LFL and the UFL.

Since the availability of computers, adiabatic flame temperatures are computed by using standard computer programs for complex equilibrium calculation. A collection of computed results by Egerton[9], BM[10], Melhem[11] and the author are shown in Table 2. It can be seen that for most gases, T_{LFL} values are in the range 1300 – 1600 K. Acetylene, carbon disulfide, hydrogen, and hydrogen sulfide are exceptions having much lower values. But, apart from acetylene—which has the rare triple carbon bond—the others are inorganics, so should not properly be compared to organic gases. Shebeko et al.[12] recently reported T_{LFL} summary results for various families of organic compounds (but not for individual compounds): most results clustered around 1600 K. The T_{UFL} values are much more scattered and are generally lower than T_{LFL}. Hertzberg et al.[8] provided additional data showing that (a) for hydrocarbons, the limit flame temperature increases with increasing number of carbon atoms; and (b) most organic compounds, including substituted hydrocarbons, show an asymptote of $T_{LFL} \rightarrow 1600$ K, as the number of carbon atoms becomes large. The above values assumed that the oxidant is air. For fuel mixtures in oxygen, the values are typically 200 – 300 K lower. A very similar notion of a limiting flame temperature is often used in studying the effectiveness of inert diluents in quenching combustion.

Table 2 Limit flame temperatures and stoichiometric adiabatic flame temperatures in air

Gas	T_{LFL} (K)				T_{UFL} (K)	T_{ad} at stoich. (K)
	Melhem	Egerton	BM	Author	Melhem	
acetaldehyde	1552				977	2300
acetone	1541				1229	2210
acetylene	1268	1280		1250		2541
ammonia	1632	1773			1825	
n-butane		1718	1613			2280
1-butene	1479				1254	
carbon disulfide		720				2250
carbon monoxide	1394	1386			1268	
dimethyl ether	1565				980	
ethane	1534	1564	1483		1399	2259
ethanol	1492				1041	
ethyl acetate	1571				1047	2125
ethylene	1370	1485		1347	1216	2369
n-heptane		1842	1643			2275
hexane		1841	1653	1609		2273
1-hexene	1583				1091	
hydrogen		981				2345
hydrogen sulfide	1045				1383	
iso-octane			1703			2210
methane	1481	1527	1483	1483	1774	2225
methyldichlorosilane	1543				847	
methyltricholorsilane	1602					
n-octane		1848	1683			2275
n-pentane		1758				2275
propane		1656	1553			2267
propylene	1431	1756			1444	2320
trichlorosilane	1260				915	

In a related study, Ogawa and coworkers[13] reported that limiting values of the flame temperature (experimentally measured, not a computed value for adiabatic conditions). are independent of fuel type, but dependent of (a) mixture fraction, and (b) flame stretch. High flame stretch rates (> 10 s^{-1}) led to a measured flame temperature of around 1470 K for mixtures near the LFL; this value dropped to around 1320 K for a stretch rate of 2.5 s^{-1}. For mixtures near the UFL, values were generally about 200 K higher for a given stretch rate. The topic of flame stretch will not be covered in this book and interested readers should consult text-books suggested in *Further Readings*, below.

Real flame temperatures in accidental fires are normally much smaller than the adiabatic flame temperature. Flashed-over room fires commonly show 900 – 1000ºC. Jet fires and pool fires typically show 1000 – 1300ºC. Perhaps surprisingly, dust cloud explosions[14] also typically show 1000 – 1300ºC, despite the presence of solid particles. In general, temperatures close to the adiabatic flame temperature are not achieved except in specialized burners where heat losses have been carefully minimized. The practical examples cited above are all turbulent diffusion flames and the values cited represent those measured by normal sensing instruments. Since turbulent combustion comprises packets of air and fuel mixing and reacting, at any one place there will be a range of temperatures that vary rapidly and average out to the measured value. These turbulent combustion peaks are higher, but they are difficult to measure and have rarely been studied.

In the case of solid and liquid explosives, the detonation temperatures[15-17] are typically 3000 – 4500 K. These values are higher than for ordinary combustibles burning in air and roughly similar to ordinary combustibles burning in oxygen. The higher temperatures can be understood as being due to the efficient reaction, in that it is not necessary to heat an inert diluent such as the nitrogen in air.

Reaction kinetics

For a chemical reaction to occur, molecules must collide. But at ordinary temperatures, it is possible to create a gaseous mixture containing large amounts of both fuel and oxidizer molecules, yet no reaction will be observed, despite the fact that numerous collisions are occurring. In the 19th century, the Swedish chemist Svante Arrhenius first suggested that this was because these collisions did not have sufficient energy. He considered that there was an energy 'hump' which must be overcome by the reactants, even if the reaction itself is exothermic (Figure 1).

The reactants must be raised to an energy E_a above the ambient in order for the reaction to take place. This *activation energy* may be supplied by raising the temperature of the system, which will raise the kinetic energy of all of the molecules. The energy hump exists because—generally—bonds must be broken before new ones can be formed.

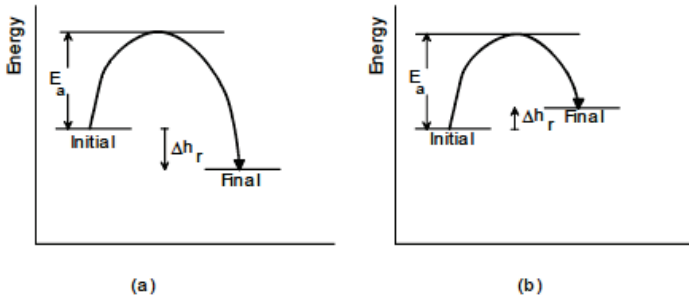


Figure 1 The activation energy needed to complete a reaction. (a) Exothermic reaction. (b) Endothermic reaction.

There are some particles, however, which can enter into reactions directly, without first needing to have external energy supplied to break bonds. These are free atoms or molecules which either have excess electrons or are missing electrons, in other words, species that possess free chemical bonding sites. Such particles are called *free radicals*. Since they are extremely highly reactive, this means they are also very short-lived. As a result, free radicals must normally be created by starting a reaction by raising the thermal energy of the system. The first bond breaks, and one or more free radicals are created. Energy to get over the 'hump' can also be supplied by other means; for example, there are light-sensitive reactions, where light energy is sufficient to cause the reaction to occur.

We may represent a simple reaction as two reactants, A and B, going into products C and D.

$$A + B \rightarrow C + D$$

Arrhenius[18] also discovered that the rate at which the reaction occurs can be represented as:

$$-\frac{dc_A}{dt} = -\frac{dc_B}{dt} = \frac{dc_C}{dt} = \frac{dc_D}{dt} = c_A^n c_B^m A e^{-E/RT}$$

where the concentrations of the various species are c (kg m^{-3}), A is the pre-exponential factor, R = the universal gas constant (8.314 J mol^{-1} K^{-1}), the activation energy E_a (kJ mol^{-1}) has been simply denoted as E, and T = temperature (K). Here, the c and A variables should not be confused with the schematic representation of the molecules in the reaction as A, B, C, and D. The exponents n and m are experimentally determined constants. Most commonly, both n and m will have values ≈ 1. If the amounts of the two reactants are present in the exactly-needed ratios (i.e., the reactant mixture is stoichiometric), then for the above reaction, c_A will always remain identical to c_B as both reactants are progressively consumed. In such a simple case, we can write:

$$-\frac{dc_A}{dt} = c_A^n A e^{-E/RT}$$

where now $n \approx 2$. Such a reaction is termed a 2nd order reaction. This is often a reasonable representation for a mixture of gases. In a different example (considered in detail in Chapter 9) of a pile of porous solids in air, it is often assumed that the oxygen in the air in infinite and inexhaustible. Then the concentration of "B" cannot go down, and it is found that the above equation also applies, but with $n = 1$. This type of reaction is termed a 1st order reaction.

The units of the pre-exponential factor A will depend on the order of the reaction and are: $(\text{kg/m}^3)^{1-n}\ \text{s}^{-1}$. Thus, for a first order reaction, the units are s^{-1}, while for a second order reaction they are $\text{m}^3\ \text{kg}^{-1}\ \text{s}^{-1}$.

It is often stated in elementary presentations that the rate of a chemical reaction is increased by 2× to 3× for each 10ºC rise in temperature. This, however, is only a very crude expression and, in addition, it implies that temperatures only close to room temperature are considered. Figure 3 shows that a 2× increase in reaction rate, going from 25ºC to 35ºC implies that E = 54 kJ mol^{-1} while a 3× increase implies E = 84 kJ mol^{-1}. But if E = 54 kJ mol^{-1} and the temperature is raised from 300ºC to 310ºC, the reaction increases by a factor of 1.2×, not 2.0×. To obtain a 2× increase starting from 300ºC requires that E be 199 kJ mol^{-1}.

A number of researchers[19-21] noted that the two main kinetic parameters—the activation energy E and the pre-exponential factor A—are not independent. Instead, a relation can be found of the form:

$$\ln(QA) = f(E)$$

where E = activation energy (kJ mol^{-1}), A = pre-exponential factor (s^{-1}), and Q = heat of reaction (kJ kg^{-1}). The following relation (Figure 2) has been found to hold for coal[21]:

$$\ln(QA) = 0.95 + 0.314\,E$$

Studies, however, have been performed only on a few families of rather similar substances, so it is not clear to what extent general relationships could be evolved.

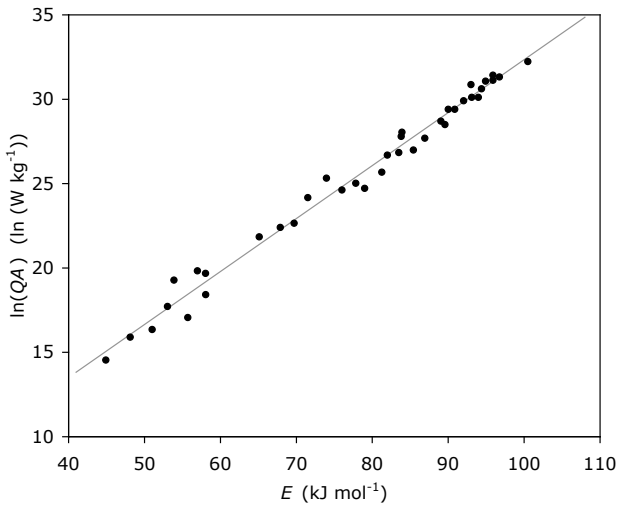


Figure 2 Relation between E and $\ln(QA)$ for coal

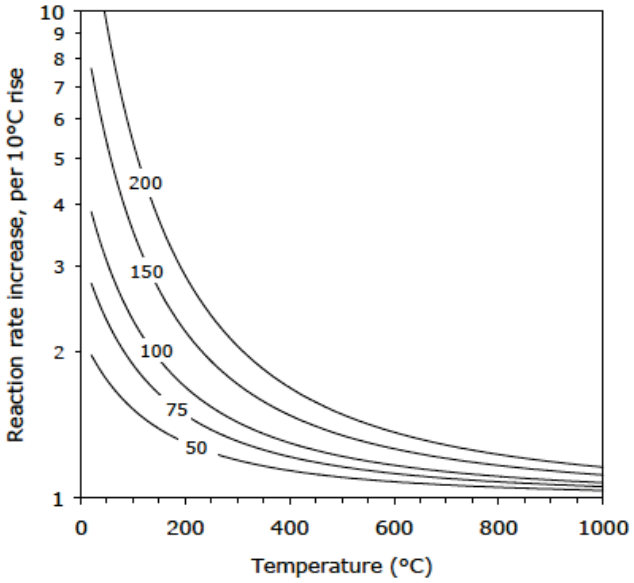


Figure 3 Effect of activation energy E on the reaction rate increase that occurs for each 10ºC rise in temperature (curves given for E = 50, 75, 100, 150, and 200 kJ mol^{-1})

BRANCHING CHAIN REACTIONS

There is no common organic substance which would actually burn by means of a single, simple reaction as depicted above. We can consider why this is so. The formal reaction of methane burning in oxygen is:

$$CH_4 + 2O_2 \rightarrow CO_2 + 2H_2O$$

This would require that three molecules meet and collide: one methane molecule and two O_2 molecules. Statistically, for three molecules to collide is a rare event. What is not rare is for two molecules to collide and thereby to form products which include one of more highly reactive, unstable species, called *free radicals*. We will consider the low temperature oxidation of methane to CO and water as an example. This reaction,

$$2CH_4 + 3O_2 \rightarrow 2CO + 4H_2O$$

clearly cannot occur directly, by waiting for the rare event of 5 molecules to collide! Instead, *initiation* can occur by the reaction[22]

$$CH_4 + O_2 \rightarrow \dot{C}H_3 + H\dot{O}_2$$

where the dots denote a reactive species. In this particular reaction, two free radicals were created in the initiation, but in general, initiation of a chain reaction will occur if at least one radical is created. The next steps can involve chain propagation. For methane, these can include:

$$\dot{C}H_3 + O_2 \rightarrow CH_2O + \dot{O}H$$

$$\dot{O}H + CH_4 \rightarrow H_2O + \dot{C}H_3$$

$$\dot{O}H + CH_2O \rightarrow H_2O + H\dot{C}O$$

The above three reactions are termed *chain propagation* because the same number of free radicals are produced in each as are consumed. With just these two types of reactions, no significant amount of substance could react. Acceleration is introduced by a *chain branching* reaction:

$$CH_2O + O_2 \rightarrow H\dot{O}_2 + H\dot{C}O$$

In a chain branching reaction, intermediates react and produce more free radicals than are consumed; in the above case, two radicals are produced and none are consumed. Further chain propagating steps include:

$$H\dot{C}O + O_2 \rightarrow CO + H\dot{O}_2$$

$$H\dot{O}_2 + CH_4 \rightarrow H_2O_2 + \dot{C}H_3$$

$$H\dot{O}_2 + CH_2O \rightarrow H_2O_2 + H\dot{C}O$$

The above set of all the equations can be seen to produce the desired products, CO and H_2O. It would also leave some unreacted free radicals, thus, it is found that the following *chain termination* reactions also need to occur:

$$\dot{O}H \rightarrow \text{wall}$$

$$\dot{C}H_3 \rightarrow \text{wall}$$

$$H\dot{O}_2 \rightarrow \text{wall}$$

The latter occur simply by collisions of active species with the walls or other molecules not showing reactivity.

The above scheme is one of the simplest realistic oxidation reactions. Most reaction schemes are more complex and can entail hundreds of separate reactions.

Chain reactions differ from simple reactions (sometimes termed *thermal reactions*) in one crucial way: if the reaction is kept isothermal, the reaction rate does not always monotonically decrease. In a simple reaction conducted at a clamped temperature, since the abundance of the reactants decreases with time, so must the reaction rate. In this manner, chain reactions resemble autocatalytic reactions, which we consider next.

AUTOCATALYTIC REACTIONS

Many explosions or fires occurring in chemical plants which produce liquid substances occur when the process undergoes an unwanted autocatalytic reaction. If a *constant-temperature* environment is considered, and the reaction is of the zeroth order, then reactants are never depleted and the reaction rate never changes with time. For 1st, 2nd, etc., order of reaction, the reaction rate continuously drops with time, since it is proportional to some (positive) power of the reactant concentration, and the concentration monotonically drops with time. There is another class of behaviors, however, that can occur—in these reactions, the reaction rate first increases, then reaches a maximum, and finally begins to decrease. These are called *autocatalytic reactions*. To understand this, first consider the normal effect of a catalyst. A *catalyst* is a substance which is not consumed during reaction, but which enhances the rate of a chemical reaction. Thus, an autocatalytic reaction can be viewed as if the reaction product which is being created is a catalyst for the reaction itself. If it were not (and remembering that the temperature is held constant in this simplest illustrative case), then there would be no mechanism for the reaction rate to increase over time.

The autocatalytic reaction of substance *A* going into *B* proceeds as:

$$A + B \xrightarrow{k} 2B$$

Note that it is necessary to postulate that there is at least a tiny amount of *B*, greater than 0, at the start, or the reaction would never start. It is convenient to define a 'conversion fraction' x as the fraction of substance *A* which has been converted into *B*. With this definition, the reaction rate can be expressed as:

$$\frac{dx}{dt} = k\left(x+\beta\right)\left(1-x\right)$$

with the original, tiny fraction of *A* already converted into *B* at the start being β, which is called the autocatalysis parameter. The above is a differential equation in x, and a solution for x, the fraction of substance reacted is:

$$x = \frac{\beta\left(e^{(1+\beta)kt} - 1\right)}{1 + \beta\, e^{(1+\beta)kt}}$$

and the rate at any given time is:

$$\frac{dx}{dt} = \frac{\beta\left(1+\beta\right)^2 k e^{(1+\beta)kt}}{\left(1 + \beta\, e^{(1+\beta)kt}\right)^2}$$

which for $\beta \ll 1$ can be approximated as:

$$\frac{dx}{dt} \approx \frac{\beta\, k e^{kt}}{\left(1 + e^{kt}\right)^2}$$

Since β is assumed to be tiny, at $t = 0^+$ the reaction rate is a small value, $\beta k/4$. For $t \rightarrow \infty$, not surprisingly $dx/dt \rightarrow 0$. But shortly after time zero, a sharp peak is reached. Differentiating the reaction rate equation with respect to x shows that when $\frac{d^2x}{dt^2} = 0$,

$$\beta\, e^{\lambda t}\left(\beta + 1\right) = \left(\beta + 1\right)$$

where we have set $\lambda = \left(1+\beta\right)k$. But this equation can only be true if

$$e^{\lambda t} = \frac{1}{\beta}$$

Thus, at the peak:

$$x = \frac{1-\beta}{2}$$

$$\frac{dx}{dt} = \frac{\left(1+\beta\right)^2 k}{4}$$

But if the starting amount of substance converted was small ($\beta \ll 1$), then the peak occurs at $x \approx$ ½ and peak reaction

rate is $\frac{dx}{dt} \approx \frac{k}{4}$. The time at which the reaction reaches its peak rate is: $t_{pk} \approx -\frac{\ln(\beta)}{k}$.

Many reactions involving autocatalysis are not 'pure' autocatalytic reactions, but also have a non-autocatalytic component. For these, it is not necessary to assume an arbitrary 'seed' fraction of the product, since products are already being produced by the non-autocatalytic portion of the reaction rate. A reaction of this kind can be represented as:

$$-\frac{d(1-x)}{dt} = k_1(1-x)^m + k_2(1-x)^n \cdot x^p$$

since the remaining mass fraction at any time is $(1–x)$. Here, there are two different rate constants k_1 and k_2, and in the general case, the reaction orders m, n, and p may assume various values. The rate constants are assumed to depend on temperature according to the relations $k_1 = A_1 e^{-E/RT}$ and $k_2 = A_2 e^{-E/RT}$.

Flame speed

If one increases the gas flow to a Bunsen burner, it is noticed that the flame, which is roughly conical-shaped, becomes taller. One might suppose that there is a constant speed at which a premixed gas/air volume element tends to burn at. Thus, increasing the mixture flow speed up the tube increases the flame size, so that the burning rate normal to the plane of the flame remains constant. There are a number of nuances about the Bunsen burner flame, and these have been studied. The earliest study, however, that unraveled the flame speed story was a series of experiments by Coward and Hartwell[23] in 1932. They considered the simpler case of a horizontal tube filled with a stagnant fuel/air mixture. The tube is closed at the far end and ignited at the open end. Experimentally, it was found that the flame progresses at a steady speed along the tube. For 10% methane/air mixtures in tubes of 50 – 100 mm diameter, Coward and Hartwell found that the axial motion (with respect to a stationary observer) was ≈ 1.0 m s^{-1}. The flame front, however, was not straight, instead, it was seen to bulge at the top and slump at the bottom. Consequently, the effective area of the flame front was much larger than the cross-section of the tube. By measuring the flame front area and the volume flow rate, however, they were able to determine that $S_L = \frac{\text{volume flow rate}}{\text{area of flame front}}$ was a constant, and that it was a constant irrespective of the propagation direction: horizontally, upward, or downward. Coward and Hartwell called S_L the *fundamental flame speed*. Today, it is commonly referred to as the *laminar flame speed* or *laminar burning velocity*, but numerous other terms are found in the literature. The laminar flame speed is the velocity component that is normal to the flame surface and is measured with respect to the unburned gas; thus, it is commonly also designated S_u, with *u* denoting unburned. Unlike other velocities in the system, e.g., the velocity with respect to the fixed observer, the fundamental flame speed is a characteristic of the chemical reaction and is independent of the geometrical arrangements. The velocity of the flame with respect to the burned gas, S_b, is related to S_L according to:

$$S_b = S_L \frac{\rho_u}{\rho_b}$$

Where ρ = density (kg m^{-3}), *u* denotes unburned, and b burned. Commonly, the density ratio can be ≈ 6; thus if S_L = 0.45 m s^{-1}, S_b = 2.7 m s^{-1}. Thus, the velocity with respect to the burned gases will be much greater than with respect to the unburned*. The velocity that a stationary observer will see depends on the geometrical arrangement. The simplest case is a flat-flame burner. Here, the gas velocity flowing up the tube is exactly = S_L.

The value of S_L depends on the stoichiometry, and is generally maximum close to, but not exactly at, $\varphi = 1$. The tabulated values of S_L normally refer to the composition at which it is the maximum; for methane/air mixtures it has been determined to be 0.45 m s^{-1}. For most hydrocarbon fuels, $S_L \approx 0.3$ to 0.8 m s^{-1}. Hydrogen shows a very large flame speed, with a maximum of about 3 m s^{-1}. Acetylene is also unusual, in having a peak $S_L \approx 1.5$ m s^{-1}. For tubes of widely differing sizes, Coward and Hartwell also found that the axial motion speed increased with increasing diameter, but that S_L remained a constant.

A theoretical explanation of the fundamental flame speed can be developed in the following way. In the flame zone, the temperature will rise from T_o to T_f, where the latter is the flame temperature. If, for the sake of simplicity, it is assumed that no heat is lost to the external environment, then all the combustion products flow away at T_f. Now, the heat release rate of the flame is:

$$QA\dot{m}'''\delta_f$$

where Q = heat of reaction (kJ kg^{-1}), A = flame area (m^2), $\dot{m}''$ = mass consumption rate (kg s^{-1} m^{-2}), and δ_f = flame zone thickness (m). But the HRR is used to raise the gases from T_o to T_f, thus:

$$QA\dot{m}'''\delta_f = \rho_o S_L AC(T_f - T_o)$$

where ρ_o (kg m^{-3}) = density of unburned gas mixture. Solving for the flame zone thickness,

$$\delta_f = \frac{\rho_o S_L C(T_f - T_o)}{Q\dot{m}'''}$$

The heat conducted across the flame zone is

$$\frac{\lambda}{\delta_f} A(T_f - T_o)$$

* The nomenclature in the literature is highly inconsistent and some authors use *laminar flame speed* to refer to S_b and *burning velocity* to refer to S_L; the magnitude of the numbers is usually sufficient to decide which is meant.

where λ (kW m^{-1} K^{-1}) = thermal conductivity of the gas. Now the heat being released is removed from the reaction zone by conduction, thus the equality holds:

$$Q A \dot{m}''' \delta_f = \frac{\lambda}{\delta_f} A \left(T_f - T_o \right)$$

From the above equation, a second expression for δ_f can be obtained:

$$\delta_f = \sqrt{\frac{\lambda \left(T_f - T_o \right)}{Q \dot{m}'''}}$$

The unknown flame thickness δ_f can then be eliminated by equating the two expressions for δ_f to each other:

$$\frac{\rho_o S_L C \left(T_f - T_o \right)}{Q \dot{m}'''} = \sqrt{\frac{\lambda \left(T_f - T_o \right)}{Q \dot{m}'''}}$$

Giving

$$S_L = \frac{Q \dot{m}'''}{\rho_o C \left(T_f - T_o \right)} \sqrt{\frac{\lambda \left(T_f - T_o \right)}{Q \dot{m}'''}}$$

Equating the HRR to the heat required to heat the product gases,

$$Q \rho_o = \rho_o C \left(T_f - T_o \right)$$

$$S_L = \sqrt{\frac{\lambda \ \dot{m}'''^2}{\rho_o^2 C \dot{m}'''}}$$

But the definition of thermal diffusivity, α (m^2 s^{-1}) is:

$$\alpha = \frac{\lambda}{\rho C}$$

Thus

$$S_L = \sqrt{\frac{\alpha \ \dot{m}'''}{\rho_o}}$$

The above computation of the flame speed was developed in 1883 by Mallard and Le Chatelier, and it is a *thermal theory*, since diffusion of gas species is not explicitly treated. Theories which take much more of the actual chemistry into account do exist, and can be found in Glassman's book[22]. An extensive review of experimental studies has been compiled by Andrews and Bradley[24].

Real combustion systems are commonly turbulent rather than laminar. Since turbulence increases the transport of heat and species, it is not surprising that turbulent flame speeds are higher. Turbulent flame speeds, S_T, can sometimes be approximated as:

$$S_T = S_L \sqrt{\mathrm{Re}}$$

where the Reynolds number Re = uD/v is a dimensionless velocity, with u = flow velocity (m s^{-1}), D = characteristic dimension of the system (m), and v = kinematic viscosity (m^2 s^{-1}). Thus, for turbulent systems, S_T is *not* a constant of the fuel/oxidizer mixture, but is also proportional to local turbulent flow velocity.

As considered above, if the fuel/air mixture is in a pipe with two open ends, or if the pipe has one closed end and the mixture is ignited at the open end, then reasonably steady flame propagation will be seen, well below the speed of sound. A steady state is possible since thermal expansion of the combustion products pushes the burnt mixture out the open end. However, if the mixture is ignited at the *closed end*, then a very different situation takes place. The heated combustion cannot escape, except by compressing the unburnt gases. Thus, the combustion wave will accelerate, and the process may lead to a detonation, as shown[25] in Figure 4. The resulting shock wave has been studied extensively in classical combustion literature.

Types of explosions

An ignition may lead to a form of combustion that is considered an explosion. 'Explosions' encompass a very wide range of meanings; some, such as steam explosions or pressure-vessel explosions are not related to combustion phenomena, and we shall not consider them here. In common English usage, 'explosion' connotes a loud sound, but some combustion explosions do not produce a sound. Concerning explosions related to combustion phenomena, it is considered that there are three types[26] (Table 3).

Thermal explosions occur due to bulk self-heating of a substance. The autoignition of a flammable gas mixture is an example, as is the spontaneous combustion of a haystack. Note that there is no sound associated with the latter exam-

Table 3 Types of chemical explosions

Explosion type	Characteristics
Thermal explosion	No defined reaction zone. Self-heating throughout the substance.
Deflagration	Traveling reaction wave. Velocities of 10^{-5} – 300 m s^{-1} (subsonic speeds). Energy transfer ahead of the reaction zone by conduction, convection and radiation Reaction products are usually gases but may be liquids or solids.
Detonation	Traveling reaction wave. Velocities of 1000 – 9000 m s^{-1} (supersonic speeds). Energy transfer by shock compression. Pressure rise of 20 – 80 atm in gases, 25,000 – 350,000 atm in solids. Reaction products are usually gases.

ple. Thus, spontaneous combustion of a haystack would only be considered an explosion by chemists, but not in everyday English usage. To produce a loud sound requires that an abrupt pressure rise propagate through the air, but combustion reactions which are unconfined may not necessarily produce a significant pressure rise.

A deflagration is a combustion wave that is sustained by heat transfer from the combustion zone to unreacted material. A deflagration is not limited to gas phase. Liquid and solid substances can also undergo deflagration. Deflagrations in liquids have been studied by Grewer[27] and Verhoeff[28]. A detonation is a reaction propagated at a velocity greater than the local speed of sound in the unreacted material.

The question may well be asked, What types of combustion are *not* explosions? Apart from the issue of thermal explosions, combustion is not an explosion if the process is not accelerative[29]. Thus, for example, a flame on a Bunsen burner or on a candle is not an explosion because the rate of reaction is fixed by the mechanism that regulates fuel supply and combustion proceeds at a constant (more or less) rate.

If a fuel-oxidizer mixture is contained within a vessel of fixed volume that does not break during the explosion, then the maximum pressure can be computed that can occur within the vessel. In analogy to the adiabatic flame temperature, the maximum vessel pressure will occur if no heat is lost to the outside in the process. If a detonation is not involved, then the pressure can be obtained from the Ideal Gas Law. If '1' denotes the ambient condition and '2' denotes the combusted mixture, then

$$\frac{P_1 V_1}{n_1 T_1} = \frac{P_2 V_2}{n_2 T_2}$$

At ambient conditions, P_1 = 1 atm and T_1 = 298 K. If the vessel does not break, then $V_2 \circlearrowleft V_1$. The n_2/n_1 denotes the moles of product, divided by the moles of reactant*. In the simplest case, a fuel such as CH_4 produces the same amount of product moles as there were reactant moles. Thus, we will take $n_2/n_1 = 1$ here, although the exact value can easily be computed for any substance with a known chemical formula. The peak adiabatic flame temperature occurs for mixtures which are very close to being stoichiometric, and for many organic fuels, $T_{ad} \approx 2200 - 2300$ K. This is our T_2. Thus,

$$P_2 = \frac{1.0 \times 2250}{298} = 7.55 \text{ atm or, say, 8 atm}$$

For substances with $n_2/n_1 > 1$, this value will be slightly higher. In the case of an air atmosphere, however, the preponderance of nitrogen makes it hard for the mole ratio to deviate greatly from unity. If the mixture is within its flammable limits, but far from stoichiometric, then a lower T_{ad} will be found and, consequently, a lower P_2 will be found.

If the initial temperature is colder than 298 K, then higher explosion pressures will be achieved since the adiabatic flame temperature does not change anywhere nearly as much as does the ambient temperature. If the change in T_{ad} is ignored, from an initial temperature of –40ºC, a peak pressure would be expected of:

$$P_2 = \frac{1.0 \times 2250}{233} = 9.65 \text{ atm}$$

or 28% higher than from 298 K; actual experimental results[30] show about a 30% increase.

PRESSURE PILING

There are deflagrations where substantially higher pressures are recorded than 7 or 8 atm, and values of 20 – 30 atm have been experimentally measured. The effect is termed *pressure piling* and arises due to geometrical complexities. In 1906, Beyling[31] first observed that if two interconnected chambers are filled with a flammable gas mixture and ignited in one chamber, the explosion pressure in the second chamber is often much higher than in the chamber where the explosion originated (Figure 5). The Bureau of Mines[32] later conducted more systematic tests with natural gas/air mixtures in a small-scale steel box and found a maximum pressure of 5.4 atm when the box had no subdivisions. Upon dividing the box into two chambers, separated by a plate having a 100 × 100 mm opening, the maximum recorded pressure was 15.6 atm, under the conditions that the larger chamber had a volume 7× times that of the smaller one. They also found that the location of the ignition source within the initially-ignited chamber affected the results.

Conn[33] reviewed various studies of pressure piling and suggests the following explanation. Within a single chamber,

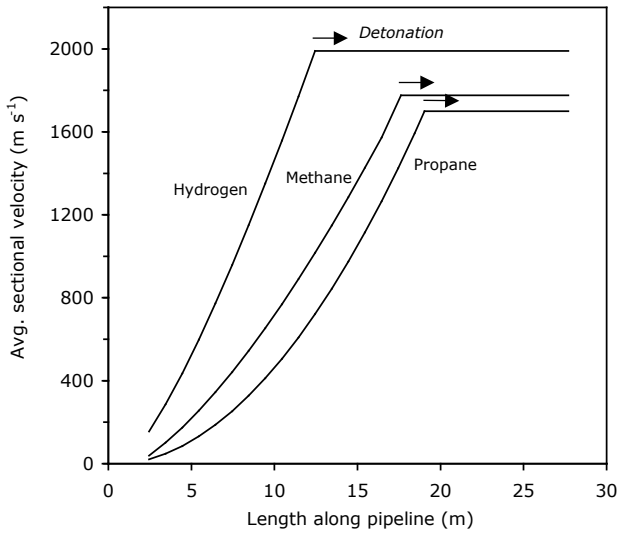


Figure 4 Acceleration of flame along a 200 mm diameter pipeline; ignition by flame jet at closed end.

* Only moles of gaseous substances are considered.

the 7 or 8 atm explosion pressure that is recorded should be viewed as a 7- or 8-fold *rise* in original pressure. Thus, if the starting pressure becomes much higher than 1 atm, the ultimate explosion pressure will also be increased. Pressure piling, then occurs because: (1) the pressure wave in the primary chamber leads to an elevated pressure in the secondary chamber; and (2) the starting temperature in the secondary chamber is elevated since compression happens rapidly and nearly adiabatically. Conn also developed a simple hydrodynamic model of the pressure piling process which predicts that pressures of over 30 atm are possible as the volume of the secondary chamber becomes small compared to the primary chamber. Nonetheless, he points out that even worst-case accident scenario planning will hardly ever entail the specific combination of conditions needed to

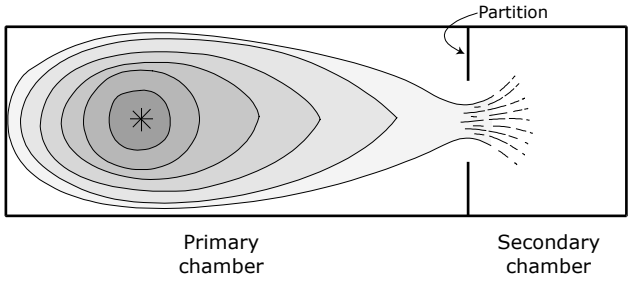


Figure 5 A simple geometry leading to pressure piling

attain such high pressures. Extreme cases of pressure piling may lead to detonation (see below), and this is a problem of some concern in certain industrial facilities.

DEFLAGRATION TO DETONATION TRANSITION

Combustion can start as a deflagration then transition to a detonation. This process of acceleration can occur since the propagation velocity of a shock wave increases with density and a compression wave is being generated in a deflagration ahead of the flame. If such a transition occurs, it is sudden. Transition is promoted by any phenomenon that increases flame speed, the most common being the presence of obstructions. Obstructions create turbulence and a local acceleration of the gas, creating regions of increased velocity.

In pipes, transition to detonation is possible if both the diameter and the pipe length are large enough. For methane and propane, a minimum diameter of 25 – 100 mm is needed, although other gases may be detonated in pipes as small as 12 mm. For detonations, the peak pressure is **not** limited to ca. 8 atm, and may be about 20 atm for gaseous fuels. In some circumstances, however, gas mixtures in larger-diameter pipes can lead to a 'double-discontinuity shock piling,' with pressures in the range of 400 atm being attained[34]. Deflagration-to-detonation transition is considered in more detail in Chapter 4.

Catalytic combustion

Normal combustion occurring in the gas phase is the dominant form of combustion which is of interest for both wanted and unwanted fires. There is a very different category of combustion possible: combustion by means of chemical reactions on an 'active' surface. This is called catalytic combustion. The reactants are a gaseous fuel and a gaseous oxygen, but a third participant—the surface—is needed. The catalyst is normally a noble metal, e.g., platinum. By definition of the term *catalyst*, it is meant that the substance is not consumed. Thus, for example, powdered iron can be ignited in air and it will burn up once ignited. This is not catalytic combustion. But in certain situations iron can act as a catalyst so that it promotes the ignition or combustion of some other substance, without being consumed itself. Such behavior is illustrated at a number of places throughout this Handbook. In any catalytic reaction, one or more reactants are temporarily adsorbed onto the catalyst surface, while reaction products are eventually desorbed from the surface, returning the catalyst to its original chemical form. Apart from the fact that a flame does not accompany catalytic combustion*, two other special traits are found: the reaction temperatures are generally lower than in flaming combustion; and catalytic combustion is not limited to taking place within the flammable limits that are defined for flaming combustion.

In the process of inventing his miner's safety lamp in 1816, Sir Humphry Davy discovered that methane can be burned in a flameless manner on platinum. He did not make use of this discovery, but the German chemist Johann Döbereiner, who had been studying reactions with platinum, learned about it and discovered that when using finely-divided platinum ('platinum black'), ignition is possible, not just sustained combustion. He realized that its ability to produce fire without use of flint or tinder could lead to practical devices. The simultaneous discovery of catalysis and catalytic ignition became a sensation in scientific circles and resulted in more than a dozen publications within 3 months of the invention. This became the basis of Döbereiner's lamp (*Döbereinersches Feuerzeug*, Color plate 3), and during the 19th century it became the first widely used device based on catalytic combustion[35]. The device is ingenious. There is an open-bottom glass vessel held inside a larger glass container. The lamp is part-filled with dilute sulfuric acid. A piece of zinc, suspended on a wire, reacts with the sulfuric acid to produce hydrogen gas. The gas leaves the inner bottle and goes through a stopcock and then through a mass of sponge platinum, where it ignites and burns. When the stopcock is turned off, the H_2 no longer leaves the inner bottle, the pressure consequently rises inside it, and the acid level drops (while rising in the outer container). The reaction then stops once the liquid level drops below the zinc[36].

* In some systems, it is possible to have catalytic combustion on the surface, while flaming combustion also takes place in the gas phase.

Today, catalytic combustion is primarily being exploited in applications where it is desired to reduce pollution-causing nitrogen oxides. The latter are formed only at high temperatures, thus, combustion systems which can run efficiently at lowered temperatures can be made cleaner. An example is the catalytic converter, fitted to modern cars to re-burn some pollutants which are generated in main engine combustion.

Catalytic combustion is also found in various space heater designs. Available since the 1960s, such heaters normally use a porous panel, the front surface of which is impregnated with a platinum catalyst[37]. Fuel gas is supplied to the back of the panel, as is an air stream, for which a fan is used. The catalyst cannot burn the fuel until it has come up to its operating temperature. To preheat the panel, an electrical heating element is included. The operation is safety-interlocked so that fuel gas flow does not start until the needed operating temperature has been reached. The preheating takes 10 – 15 minutes; normal operation involves a 400 – 500ºC temperature of the catalyst.

Some other combustion systems use a combination of catalytic action (heterogeneous combustion) and homogeneous combustion (normal flaming combustion). The analysis of such systems is difficult and can only be done with complex mathematical modeling. For further details, the paper by Park et al.[38] presents a current, state-of-the-art perspective.

Tests for fundamental combustion properties

ASTM provides several test methods which describe the calibration and operation of oxygen bomb calorimeters and the reporting of heat of combustion data. ASTM D 240[39] and the higher precision ASTM D 4809[40] are used for liquids while ASTM D 2015[41] applies to solids. General safety precautions for running oxygen bomb tests are given in ASTM E 144[42].

Further readings

Stephen R. Turns, **An Introduction to Combustion**, 2nd ed., McGraw-Hill, New York (1999). Jürgen Warnatz, **Combustion**, Springer-Verlag, New York (1999). Both of these are excellent, all-around combustion textbooks which are up to date and are aimed at undergraduate, not graduate, engineering students.

Irvin Glassman, **Combustion**, 3rd ed., Academic Press, San Diego (1996). Glassman's book is the most widely used graduate-level engineering textbook on combustion. He steers a careful course in providing adequate mathematical development of theory, but not presenting the subject matter as simply a branch of applied mathematics.

Roger A. Strehlow, **Combustion Fundamentals**, McGraw-Hill, New York (1984). The late Prof. Strehlow was an expert in detonations and this graduate-level book is strong on that topic; also, it contains a more comprehensive section than usual on setting up conservation equations for combustion modeling.

J. Clifford Jones, **Combustion Science: Principles and Practice**, Millenium Books, Newtown NSW, Australia (1993). This textbook is aimed at the undergraduate engineering student, but emphasizes qualitative presentation and industrial applications over the development of mathematical theory.

M. J. Pilling, ed., **Comprehensive Chemical Kinetics**, vol. 35 (Low-temperature Combustion and Autoignition), Elsevier, Amsterdam (1997). R. G. Compton and G. Hancock, eds., **Comprehensive Chemical Kinetics**, vol. 37 (Applications of Kinetic Modelling), Elsevier, Amsterdam (1998). This set of companion volumes is the most recent of treatises which cover research in combustion kinetics.

References

1. Hertzberg, M., Explosion Hazards of Combustible Gases, Vapors, and Dusts, pp. 2687-2733 in **Patty's Industrial Hygiene**, Vol. 4, 5th ed., R. L. Harris, ed., John Wiley, New York (2000).
2. Wagman, D. D., et al., The NBS Tables of Chemical Thermodynamic Properties. Selected Values for Inorganic and C1 and C2 Organic Substances in SI Units, *J. Phys. and Chem. Ref. Data* **11**, Supplement 2 (1982).
3. Stull, D. R., Westrum E. F., jr., and Sinke, G. C., **The Chemical Thermodynamics of Organic Compounds**, John Wiley, New York (1969).
4. **Encyclopedia of Explosives and Related Items**, B. T. Fedoroff, et al., eds., Picatinny Arsenal, Dover NJ (1960-1983).
5. Baroody, E. E., and Peters, S. T., Heat of Explosion, Heat of Detonation, and Reaction Products: Their Estimation and Relation to the First Law of Thermodynamics (IHTR 1340), Naval Ordnance Station, Indian Head MD (1990).
6. Crowl, D. A., Calculating the Energy of Explosion Using Thermodynamic Availability, *J. Loss Prev. Process Industries* **5**, 109-118 (1992).
7. Babrauskas, V., and Grayson, S. J., eds., **Heat Release in Fires**, E&FN Spon, London (1992).
8. Hertzberg, M., Zlochower, I. A., and Cashdollar, K. L., Volatility Model for Coal Dust Flame Propagation and Extinguishment, pp. 325-333 in *21st Symp. (Intl.) on Combustion*, The Combustion Institute, Pittsburgh (1986).
9. Egerton, A. C., Limits of Inflammability, pp. 4-13 in *4th Symp. (Intl.) on Combustion*, Williams & Wilkins, Baltimore (1953).
10. Zabetakis, M. G., Lambiris, S., and Scott, G. S., Flame Temperatures of Limit Mixtures, pp. 484-487 in *7th Symp. (Intl.) on Combustion*, Butterworths, London (1958).
11. Melhem, G. A., A Detailed Method for Estimating Mixture Flammability Limits Using Chemical Equilibrium, *Process Safety Progress* **16**, 203-218 (1997).

12. Shebeko, Yu. N., Fan, W., Bolodian, I. A., and Navzenya, V. Yu., An Analytical Evaluation of Flammability Limits of Gaseous Mixtures of Combustible-Oxidizer-Diluent, *Fire Safety J.* **37**, 549-568 (2002).
13. Ogawa, Y., Saito, N., and Liao, C., Burner Diameter and Flammability Limit Measured by Tubular Flame Burner, pp. 3221-3227 in *27th Symp. (Intl.) on Combustion*, The Combustion Institute, Pittsburgh (1998).
14. Andrews, S. P., Jet Ignition of Dust Clouds (IR/L/EC/98/01/IS), HSE, Buxton, UK (1998).
15. Kato, Y., et al., Detonation Temperature of Nitromethane and Some Solid High Explosives, pp. 558-566 in *Proc. 8th Symp. (Intl.) on Detonation*, Office of Naval Research, Dept. of the Navy, Arlington VA (1985).
16. He, X.-C., Han, C.-B., and Kang, S.-F., The Measurement of Detonation Temperature of Condensed Explosives with Two Colour-Optical Fiber Pyrometer, pp. 567-574 in *Proc. 8th Symp. (Intl.) on Detonation*, Office of Naval Research, Dept. of the Navy, Arlington VA (1985).
17. Burton, J. T. A., Hawkins, S. J., and Hooper, G., Detonation Temperature of Some Liquid Explosives, pp. 759-767 in *Proc. 7th Symp. (Intl.) on Detonation*, Naval Surface Weapons Center, China Lake CA (1981).
18. Arrhenius, S., Über die Reaktionsgeschwindigkeit bei der Inversion von Rohrzucker durch Säuren, *Zeitschrift für physikalische Chemie* **4**, 226-248 (1889).
19. Tanaka, T., Predicting Ignition Temperature, Minimum Explosive Limit, and Flame Propagation Velocity, pp. 79-99 in *Proc. Intl. Symp. on Grain Dust Explosions*, Grain Elevator and Processing Society, Minneapolis (1977).
20. Cuesta, A., Martínez-Alonso, A., and Tascón, J. M. D., Correlation between Arrhenius Kinetic Parameters in the Reaction of Different Carbon Materials with Oxygen, *Energy and Fuels* **7**, 1141-5 (1993).
21. Nugroho, Y. S., McIntosh, A. C., and Gibbs, B. M., On the Prediction of Thermal Runaway of Coal Piles of Differing Dimension by Using a Correlation Between Heat Release and Activation Energy, *Proc. Combustion Inst.* **28**, 2321-2327 (2000).
22. Glassman, I., **Combustion**, 3rd ed., Academic Press, San Diego (1996).
23. Coward, H. F., and Hartwell, F. J., Studies in the Mechanism of Flame Movement. Part II. The Fundamental Speed of Flame in Mixtures of Methane and Air, *J. Chem. Soc.* 2676-2684 (1932).
24. Andrews, G. E., and Bradley, D., Determination of Burning Velocities—A Critical Review, *Combustion and Flame* **18**, 133-153 (1972).
25. Bartknecht, W., **Explosions: Course, Prevention, Protection**, Springer-Verlag, Berlin (1981).
26. Groothuizen, T. M., Hartgerink, J. W., and Pasman, H. J., Phenomenology, Test Methods and Case Histories of Explosions in Liquids and Solids, pp. 239-251 in *Loss Prevention and Safety Promotion in the Process Industries—Proc. 1st Intl. Loss Prevention Symp.*, Elsevier, Amsterdam (1974).
27. Grewer, T., **Thermal Hazards of Chemical Reactions**, Elsevier, Amsterdam (1994).
28. Verhoeff, J., Experimental Study of the Thermal Explosion of Liquids (Ph.D. dissertation), Prins Maurits Laboratorium TNO, Rijswijk, Netherlands (1983).
29. Liñán, A., and Williams, F. A., **Fundamental Aspects of Combustion**, Oxford University Press, Oxford (1993).
30. Bossert, J., and Hurst, R., **Hazardous Locations**, Canadian Standards Assn., Rexdale, Ont. (1986).
31. Beyling, C., Versuche zwecks Erprobung der Schlagwettersicherheit besonders geschützter elektrischer Motoren und Apparate sowie zur Ermittlung geeigneter Schutzvorrichtungen für solche Betriebsmittel, ausgeführt auf der berggewerkscahftlichen Versuchstrecke in Gelsenkirchen-Bismarck [Experiments for the Purpose of Testing the Safety in Firedamp of Certain Protected Motors and Equipment, as Well as the Determination of Suitable Protective Arrangements for such Equipment, Carried out at the Experimental Gallery in Gelsenkirchen-Bismarck], *Glückauf (Essen)* **42**, 129-138 (1906).
32. Gleim, E. J., and Marcy, J. F., A Study to Determine Factors Causing Pressure Piling in Testing Explosion-proof Enclosures, Paper 5 in *7th Intl. Conf. of Directors of Safety in Mines Research*, Safety in Mines Research Establishment, Buxton, England (1952).
33. Conn, J. W., Pressure Piling (Engineering Report 8706201), Mine Safety and Health Admin., Triadelphia WV (1987).
34. Craven, A. D., and Greig, T. R., The Development of Detonation Over-pressures in Pipelines, pp. 41-50 in *Proc. 3rd Symp. on Chemical Process Hazards with Special Reference to Plant Design* (Symp. Series No. 25), The Institution of Chemical Engineers, London (1968).
35. Kauffman, G. B., The Origin of Heterogeneous Catalysis by Platinum: Johan Wolfgang Döbereiner's Contributions, *Enantiomer* **4**, 609-619 (1999).
36. Williams, W. D., Döbereiner's Hydrogen Lighter, *Bull. Hist. Chem.* **24**, 66-68 (1999).
37. Lardeux, P., Catalytic Combustion Heaters, *Fire Prevention Science and Technology*, No. 6, 4-12 (Aug. 1973).
38. Park, Y. K., Bui, P.-A., and Vlachos, D. G., Operation Regimes in Catalytic Combustion: H_2/Air Mixtures near Pt, *AIChE J.* **44**, 2035-2043 (1998).
39. Standard Test Method for Heat of Combustion of Liquid Hydrocarbon Fuels by Bomb Calorimeter (ASTM D 240), ASTM.
40. Standard Test Method for Heat of Combustion of Liquid Hydrocarbon Fuels by Bomb Calorimeter (ASTM D 4908), ASTM.
41. Standard Test Method for Gross Calorific Value of Coal and Coke by the Adiabatic Bomb Calorimeter (ASTM D 2015), ASTM.
42. Standard Practice for Safe of Oxygen Combustion Bombs (ASTM E 144), ASTM.

Copyright © 2003, 2014 Vytenis Babrauskas

Chapter 4. Ignition of gases and vapors

Highlights and summary of practical guidance **43**
Exothermic reactions in gases **44**
Slow oxidation *44*
Cool flames *45*
Multiple ignition temperatures *45*
Autoignition of premixed gases **46**
Theory *46*
Ignition of specific fuels 53
Experimental determination of the AIT *54*
Variables affecting the AIT *55*
Molecular structure 55
Fuel concentration 56
Pressure 57
Oxygen concentration 57
Vessel size and operating conditions 58
Wall material 59
Flow velocity and turbulence 59
Other relations *60*
AIT of mixtures *60*
Ignition time *60*
Effect of fuel type and mixture composition 61
Effect of pressure 63
Effect of flow rate 63
Sub-ignition, two-stage, and multi-stage ignitions *63*
Ignition due to compression or shock *64*
Piloted ignition of premixed gases **65**
Ignition with the presence of excited species *65*
Spark ignition phenomema 65
Theories for spark ignition, MIE, and quenching distance 66
Ignition from breaking wires or moving contacts 70
Pilot flame ignition 73
Ignition by burning particles 74
Variables affecting ignition of gases when piloted with the presence of excited species *74*
Chemical nature of the fuel 74
Oxygen concentration 75
Diluents 75
Fuel concentration 76
Temperature 77
Pressure 78
Gravity 78
Test geometry 79
Mixture velocity and turbulence 79

Wall materials ... 79
Circuit topology ... 79
Spark duration ... 80
Electrode arrangement ... 81
Electrode materials ... 83
Ignition in the absence of excited species and hot-wire ignitions of all types ... 83
Hot surface ignition and catalytic effects ... 83
Fused wire ignition ... 94
Ignition by hot, non-flaming gases and MESG ... 96
Ignition by laser energy ... 101
Direct thermal heating of gas ... 101
Photochemical excitation of gas ... 101
Laser-induced breakdown of gas ... 101
Radiative heating of small particles in the atmosphere ... 102
Laser-induced breakdown of gas aided by presence of small particles ... 104
Flammability limits ... 104
Theory ... 107
Flammability limits in mass units ... 108
Estimation of flammability limits ... 109
Flammability limits for mixtures ... 111
Variables affecting flammability limits ... 112
Oxygen concentration ... 112
Pressure ... 112
Temperature ... 113
Velocity ... 115
Gravity ... 116
Turbulence and sloshing ... 116
Measuring apparatus ... 116
Ignition source ... 118
Additives ... 118
Minimum oxygen concentration for flammability ... 118
Unified theories of gas ignition ... 120
Ignition of non-premixed gases ... 120
Initiation of gaseous detonations ... 121
Minimum energy for detonation ... 123
Detonation limits ... 123
Tests for ignition properties of gases ... 123
Autoignition temperature ... 123
Early methods ... 123
Heated tube tests ... 124
Tests primarily for liquids ... 124
Other test methods ... 124
Heated-surface ignition ... 124
Flammability limits ... 124
Bureau of Mines flammability tube ... 124
ASTM E 681 ... 125
Proposed EN method ... 126
ASTM E 918 ... 126
ASTM E 2079 ... 126

UL tests 126
Research tests 126
Minimum ignition energy *126*
ASTM E 582 test 127
Quenching distance *127*
MESG *128*
IEC/PTB and HSE 20 mL spheres 128
Westerberg apparatus (UL) 128
Further readings **128**
References **128**

Highlights and summary of practical guidance

The ignitability of flammable or combustible gases depends on how air (or another oxidizer) is mixed with the fuel gas. If the fuel gas and air are mixed together first, then ignited, *premixed* combustion occurs. If the premixed mixture is supplied in modest amounts at a controlled rate, then the situation basically describes a burner. But if a large volume is filled up with a fuel gas/air mixture and then ignited, a *gas explosion* results. The ignition and combustion of premixed mixtures have been studied extensively. Another possibility is that the fuel gas and the air are not well mixed before being ignited. This situation has been studied less, and is more complicated since there can only be one fully-mixed condition, but an infinity of possibilities of poor or limited mixing. The gases would not ignite at all, of course, if no mixing occurred, but a limited amount of mixing will always occur due to molecular diffusion. Flames that are observed when a fuel gas enters the atmosphere (for example, by evaporating from an open tank of solvent) not having been otherwise mixed with the air are generally known as *diffusion* flames, since mixing can take place through diffusion (molecular-scale motions of gas). The distinction between diffusion and premixed combustion is not absolute, thus, for example, if natural gas escapes from a broken pipe and burns as a jet in the air, this is considered a diffusion flame, even though the strong outflow velocity creates some local mixing and that mixing is much more rapid than would be possible through molecular diffusion alone.

Gas mixtures can be ignited in two basic ways: (1) *autoignition*: by raising the temperature of the whole volume of gas; or (2) *piloted ignition*: by introducing a local source of heat or energy. The minimum temperature which a gas mixture must reach by heating the whole volume is called the autoignition temperature (AIT), sometimes also called spontaneous ignition temperature (SIT). Autoignition suggests that the temperature of the environment is uniform, in both space and time. This is an idealization and practical tests fall short of this ideal. The AIT of a gas mixture is *not* the lowest temperature *of the flame*; rather, it is the lowest temperature to which the mixture must be heated before it 'takes off.' The time between when the mixture was first subject to AIT conditions and the time that a visible flame is seen is termed the *induction period*, or *ignition time*. The word 'piloted' is not limited to a gas pilot, it also includes other localized energy sources, such as a spark, a hot wire, etc. Sometimes the terms 'forced' or 'induced' ignition is used in place of 'piloted ignition' to indicate the broad nature possible for the localized source of energy.

AIT values are extensively tabulated in the literature, but only rarely does the AIT have relevance to actual accidental ignitions of gases. By far the most dominant way in which gases are ignited accidentally is by sparks, flames, or hot surfaces. Hot surfaces have to reach a temperature substantially higher than the AIT of a gas or vapor for ignition to occur. For example, the AIT of methane is 640ºC, but a hot metal bar may have to be raised to over 1000ºC before a methane/air mixture will be ignited. The reason is because the heat losses are different in the two cases. For the AIT determination, a flask is used which is heated throughout, while in hot-surface tests only a small fraction of the surfaces contacted by the gas is at the high temperature, the rest are at the cooler ambient temperature. Because of simplification and conservativeness, regulatory bodies often do not differentiate between AIT and hot-surface ignition and prescribe limits based on AIT when guarding against hot-surface ignition hazards. A rule of thumb is sometimes used that hot surfaces have to be 200ºC higher than the AIT for a hot-surface ignition to occur, but rules of thumb should not be relied upon in critical situations. Even relative rankings of AIT values do not correspond to ease of ignition by hot surfaces. For example, hydrogen (AIT = 520ºC) is easier to ignite by a hot body than is hexane (AIT = 223ºC).

In Chapter 9 it is explained in detail that the concept of a fixed-value ignition temperature is meaningless for the self-heating of solids and that their tendency to thermal runaway must be presented as a temperature/size graph or equation, instead. But the chemical process whereby a gas self-heats to ignition is essentially the same. Thus, the question arises, Why is a fixed-value ignition temperature meaningful for gases? This simple question does not have a simple answer, but the following factors should be considered. (a) As stated above, fuel gas/air mixtures are rarely ignited by bodily

raising their temperature to a high value, thus the situation is only sporadically encountered in practice. (b) As explained in detail in this Chapter, there *does* exist a size dependence for the AIT of gases. (c) Self-heating solids are commonly stored at or near room temperature, where accurate values must be known, i.e., it is not useful to know that the critical temperature is 40ºC±30ºC. But for a gas mixture, a knowledge that a 400ºC AIT has an uncertainty of ±30ºC may be perfectly acceptable.

It is found experimentally that when a fuel gas is mixed with air, flame propagation cannot occur if the fuel gas concentration is too small or too great. The limiting concentration values are known as the *lower flammability limit* (LFL) and the *upper flammability limit* (UFL). They are normally expressed as percent of fuel, by volume, in air, but occasionally are provided in other units, for instance, grams of fuel per m^3 of mixture. In older literature, they are often identified as the LEL (lower explosion limit) and UEL (upper explosion limit). In a rough way, flammability limits can be understood to arise because flames need a minimum temperature to exist. Too much air or too much fuel dilutes the mixture enough that a sufficient temperature rise cannot be achieved. This explanation is extremely simplified and actual prediction of flammability limits from basic science concepts is very difficult. A few gases (e.g., acetylene) have reported values of UFL = 100%. In those cases, the gas does not require oxygen to react, since the fuel molecule itself can explosively decompose. Normal combustion where the fuel combines with oxygen is also possible with acetylene, and this is the reaction that occurs in useful activities such as welding.

Flames cannot propagate through small openings. This is the concept of *quenching distance* and it forms the basis for most designs of flame arresters. These distances are quite small, on the order of 1 – 3 mm for most gases under optimal conditions. In accidental fires, however, gas/air mixtures will rarely be at their optimal ratio, thus, significantly larger distances may suffice to suppress propagation of many mixtures.

Very little energy input is required to ignite any fuel gas/air mixture within its flammability limits, although the energy must be in the 'right' form. A spark having an energy of 1 millijoule will easily ignite many gas mixtures. Yet, the mixture may not ignite if a 100 W bulb is placed in it and electric power is supplied to it for a whole day. In the latter case, the power delivered into the bulb is 100 W = 100 J s^{-1}, while the time is 8.64×10^4 s; thus the energy is 8.64×10^6 J. A wide variety of studies show that, for gases, ignition occurs most easily when energy is delivered fast (microseconds) and into a small volume. This same reasoning must not be applied to solids, where a fast, high intensity application of energy to a small area may vaporize the material, but not leave it burning.

What fraction of a spark discharge goes into heating the gas, versus that which is wasted in the circuit? This question is of significant importance in being able to accurately quantify ignitability, yet the current status of research is unsettled. As indicated both in this Chapter for gases and in Chapter 5 for dust clouds, estimates range from 'nearly all' to '1 to 10%'. Part of the variability comes from well-known circuit parameter effects, but further research is still needed in this area.

Under worst-case conditions, sparks created with electric circuits of very low voltage can ignite flammable gas atmospheres. Limited data show that 4 – 5 V can be sufficient if a high current can be delivered in a resistive circuit during the opening of a contact or the breaking or melting of a wire; voltages as low as 0.5 V, or lower, can suffice in inductive circuits.

Explosions of fuel gas/air mixtures in enclosures tend to be deflagrations if the enclosure has dimensions not too different in the three directions and is not filled with obstructions. Otherwise, for long, narrow enclosures or ones which effectively have baffles within the space, a detonation may be possible.

The Model Regulations promulgated by the United Nations and adopted by various countries (the Dept. of Transportation in the US) define a *flammable gas* as a substance which is in the gas state at a temperature of 20ºC and 101.3 kPa pressure; and has an LFL of 13% or less, or has a flammable range of at least 12 percentage points, irrespective of the value of the LFL. As discussed in Chapter 14, ammonia is a gas which has been involved in numerous explosions and fires but, according to this legal definition, it is not flammable. Thus, one needs to be aware that legal definitions may not be of much use in understanding actual fire hazards.

Exothermic reactions in gases

Exothermic reactions in gases are of three types:

(1) slow oxidation;
(2) cool flames
(3) combustion, or rapid oxidation, or normal flames.

In this section some general features of these reactions are considered. Details of ignitions involving normal flames are then pursued throughout the rest of this Chapter.

SLOW OXIDATION

If a fuel is in contact with an oxidant, then oxidation is expected to occur, even if it is so slow as to give no visible signs. At room temperature, this is the kind of reaction that may be expected between a fuel gas and the oxygen in the air. Even without combustion ('rapid oxidation') occurring, over time a measurable amount of fuel may be consumed during slow oxidation. Figure 1 shows the results of placing a methane/air mixture into an 0.44 L vessel held at 8ºC below the ignition temperature[1]. By the end of the 20 minute

experiment, a sizable fraction of the methane was consumed in slow oxidation. Such results are to be expected only at high temperatures; at room temperature the mixture could have been stored for a very long time without there being a detectable drop in methane concentration.

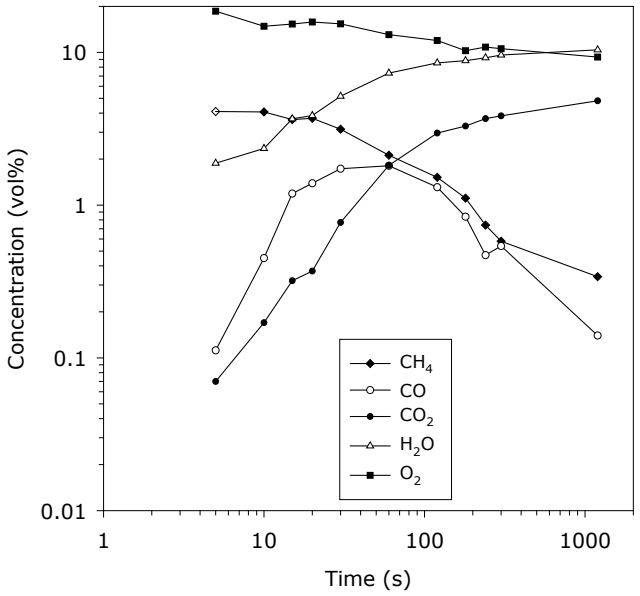


Figure 1 Reactions taking place in a vessel containing a methane/air mixture at 624ºC, which was 8ºC below the ignition temperature of the mixture under the given experimental conditions.

COOL FLAMES

At higher temperatures, some fuel gases start to exhibit cool flames. These flames are pale blue and a darkened room is commonly required in order to observe them. This type of oxidation is possible if the fuel molecule has a primary carbon bond ($–CH_3$) or a secondary carbon bond ($–CH_2–$) available for attack by oxygen and can form hydroperoxides and aldehydes (other than formaldehyde) as reaction products. Such products are partially-oxidized, which accounts for the low heat release in cool flames. The pale blue-white light associated with cool flames is emitted by formaldehyde (CH_2O) in an excited state. Temperature increases of only 10 – 150ºC accompany a cool flame. Cool flames may occur with many common hydrocarbon gases, but most commonly are found at pressures below 1 atm and in highly fuel-rich regimes. Cool flames have been studied extensively in the combustion literature, but since this research has largely been at pressures much below 1 atm, the findings have tended to have only limited application to safety problems. Cool flames have been observed at ambient pressure conditions for acetaldehyde, diethyl ether[2], divinyl ether, glycols[3], MIL-H-83282 hydraulic fluid (but not MIL-H-5606), MIL-L-7808 lubricating oil[4], and a variety of other substances. A safety concern exists, because if enclosed, or if present in large quantities, cool flames can transition to normal flames. Cool flames are also observed for CO burning in air; the pale blue glow is attributed to a combined effect of numerous radicals in the flame[5].

The minimum temperature at which cool flames may be initiated is called the *sub-ignition temperature*. Commonly, the sub-ignition temperature may be 50 – 100ºC lower than the AIT, but bis(2-methoxyethyl)phthalate has an AIT of 393ºC, while the sub-ignition temperature is 204ºC[3]. Cool flames cannot be predicted from thermal ignition theory; if cool flames are found, this implies that branching-chain theory must be used to explain autoignition. Cool flames consume only a small amount of reactants, otherwise the multiple flames seen in many cases would be impossible. Unlike normal-flame ignitions of gases, which are normally very quick, the induction period for cool flames may be on the order of 0.5 h. Cool flames are also associated with *negative temperature coefficient* regions. Most reactions show an increasing reaction rate with a rise in temperature, thus it is unusual when the contrary occurs. It arises because more than a single reaction is involved and the negative temperature coefficient is the net outcome of several competing reactions[6]. Fish[7] and Lignola and Reverchon[8] reviewed chemical kinetics studies on cool flames. It is normally understood that (at 1 atm) gases which show AIT values less than about 300ºC ignite initially with a cool flame, then subsequently transition to a normal flame. Conversely, gases which show AIT values greater than about 400ºC ignite only with a normal-flame. However, there are other views on the subject[9]. Unlike normal flames, the conditions for the ignition of cool flames are highly dependent on the condition of the surface of the test vessel. Some limited data discussed later in this Chapter imply that cool flames are likely to be seen only in vessels having a surface area greater than 80 cm^2; for a sphere this would be equivalent to 67 mL.

Regimes in which cool flames occur are prone to show oscillatory combustion phenomena. Yang and Gray[10] first proposed a theory which can explain the origin and nature of these oscillations. Griffiths and Scott[11] reviewed the oscillatory flames theory from the point of view of the continuous-flow, stirred-tank reactor (CSTR).

MULTIPLE IGNITION TEMPERATURES

In some cases, a substance can have more than one ignition temperature. For low pressures (≈ 0.1 atm), a number of organic compounds show multiple ignition temperatures, that is, a situation where there is a band of temperatures at which ignition does not occur, but ignition occurring at values both higher and lower. On occasion, this behavior is also found at 1 atm. For example, Dykstra and Edgar[12], studying gasoline vapors at 1 atm, found that using a mixture of 4.6% gasoline vapors, 37.7% O_2 and 57.7 N_2, no ignition would occur below 280ºC. Mixtures between 280ºC and 314ºC were ignitable. Mixtures between 314ºC and 444ºC, however, were non-ignitable, but mixtures of all

higher temperatures were. The phenomenon was not seen in 21% oxygen atmospheres, but only in enriched ones. Furthermore, extrapolation of data suggested that the multiple ignition phenomenon also disappears at very high O_2 concentrations, but this was not tested experimentally.

The same phenomenon was found by Frank and Blackham[13] in studying the autoignition of *n*-decane and *n*-dodecane in a normal 21% oxygen atmosphere (Figure 2). Decane showed ignition at 235 – 330ºC and again at over 365ºC, but not for intermediate values. Similarly, dodecane showed ignition at 232 – 325ºC and at over 350ºC. The authors consider this to occur because the lower regime exhibits a cool-flame ignition, while the upper regime is a normal hot flame ignition. For the intermediate region, neither mechanism is sufficient. Other hydrocarbons, e.g., *n*-hexadecane, were ignitable over a continuous range, but for a certain intermediate-temperature range ignitions were possible only for a narrow range of fuel/air ratios. Sortman et al.[14] documented dual ignition temperatures at room pressure and oxygen concentration for cetane, *n*-decane, heptane, decahydronaphthalene, and propylcyclopentane. It must be noted that both Sortman and Frank and Blackham conducted their experiments by dropping liquid droplets into heated crucibles. These types of test methods create a complex combustion environment where some phenomena might be attributable solely to spatial or temporal non-uniformities, as discussed in detail in Chapter 6. Dykstra and Edgar, however, used a concentric-tube method that is not confounded by problems of non-uniform heating and evaporation. An additional example is shown in Figure 20, where multiple ignition regimes can be seen on a P-T diagram, as it would be intersected by a line at 1.0 atm. As explained above, intermediate regimes of non-ignition are due to negative-temperature-coefficient behavior. This phenomenon, however, requires detailed chemical reaction modeling and cannot be represented by a simplified theory.

Autoignition of premixed gases

THEORY

Suppose that a fuel gas and an oxidizer gas (say, air) are quickly introduced and perfectly mixed in a vessel. If the vessel is at room temperature and pressure, in most cases no fire will take place. Only with the most exceptionally reactive gases would a fire result. Suppose now, however, that this vessel is heated. Even with 'ordinary' gases, at a certain temperature *autoignition* may take place. In this Section, we attempt to quantify the conditions under which such ignitions can be expected.

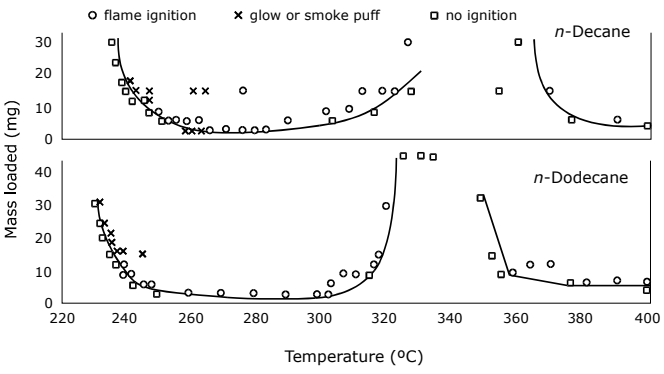


Figure 2 Regimes of ignition and non-ignition for two gases

The simplest concept of autoignition envisions that fuel and oxidizer, which are at a low temperature and non-reacting initially, at some point become immediately raised to a high temperature; most theoretical treatments are based on this assumption. In practice, however, it is difficult to achieve a starting point like that. An experimental rig may comprise a heated, evacuated flask into which gas is suddenly introduced. Figure 3 shows two example time-temperature curves for a centrally-placed thermocouple in the flask[15]. Observe that the y-axis shows not the actual temperature, but the temperature difference between the gas and the original flask wall temperature. The negative excursion is due to cold gas flowing into the hot flask. In analyzing results of this kind according to a theoretical model, the time origin is normally taken from the zero-crossing, not from the actual time when the gas was first admitted to the flask. This appears to be a straightforward treatment, but note that only the readings of the central thermocouple are shown. Thermocouples placed closer to the walls would show a zero crossing at a slightly different time; thus, determining the proper starting time does involve some uncertainty. It can also be seen in Figure 3 that even the non-ignition (slow oxidation) case shows a perceptible temperature rise, but the maximum temperature rise associated with a non-ignition case is modest. Finally, note that both curves eventually go back to zero because reactants become depleted.

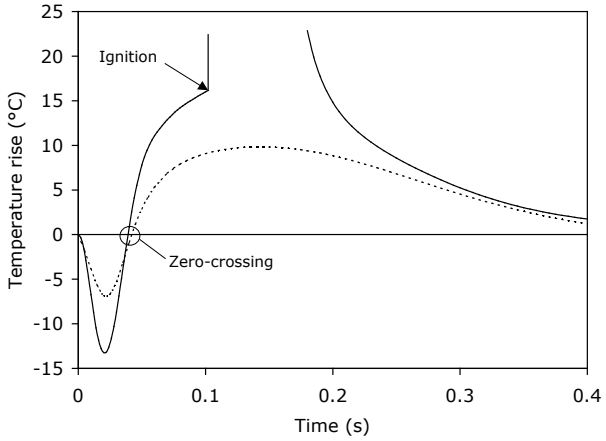


Figure 3 Temperature at the center of an evacuated, heated vessel into which a gas mixture was rapidly introduced. Solid line shows a mixture which ignited, dotted line shows a mixture which did not.
(Copyright The Combustion Institute, used by permission)

If a gas mixture capable of undergoing fast, exothermic reactions is introduced into a vessel, given a high enough starting temperature and a long enough waiting time (generally called *induction period* by chemists and *ignition time* by engineers), the mixture may combust spontaneously, without use of any spark or other ignition device. The Russian scientists Nikolai Semenov and David Frank-Kamenetskii are considered the originators of a theory which can quantify such ignitions. Semenov worked in this area from the late 1920s, and Frank-Kamenetskii since the late 1930s. English-language textbooks by both have been published[16,17,18], but these are quite advanced, and the reader wanting to go beyond our presentation here would best next turn to a modern-day combustion textbook[19,20].

In the simplest analysis, we do not consider the actual details of the chain reactions that carry combustion forth. Instead, the fuel/oxidizer mixture can be considered as having a single exothermic overall reaction, described by Arrhenius kinetics. If such a system were perfectly insulated ('adiabatic'), then it would invariably self heat, go into thermal run-away, and ignite. Thus, in even the most idealized conception, it is necessary to describe in some way the real-world heat losses which the vessel sustains at its boundaries.

If we have, for example, a spherical vessel, then there will be a temperature distribution inside, with the gases being hottest at the center and coolest at the edges. This is because the edges are cooled while the center is far away from this cooled boundary. This difference may be ignored, which was Semenov's initial approach, or it may be expressed according to laws of heat conduction, as done by Frank-Kamenetskii. The thermal conditions at the edges may also be represented in several ways. The simplest is an assumption that the external atmosphere is at one temperature T_o, while the walls of the vessel are at a higher temperature, T_w, and that heat is being exchanged according to simple convective cooling:

$$\dot{q}_c'' = h\,(T_w - T_o)$$

where h is a heat transfer coefficient (kW m^{-2} K^{-1}).

Before undertaking quantitative solutions, it is highly instructive to consider what happens qualitatively. This is best done on a diagram where the heat losses and the heat gains are considered separately, and both are plotted as a function of temperature (Figure 4). Even though time is clearly of great import to the problem, it turns out that one can learn much of the rudiments by considering only steady-state solutions. The solutions, even with numerous simplifications, are mathematically difficult, and our development will show that much can be learnt from considering the steady-state problem.

Figure 4 shows that three different relations are possible between heat losses and heat generation in a volume of gas. The lowest heat loss curve never intersects the heat generation curve. Thus, if the wall temperature and the convective heat loss coefficient are such that the lowest curve holds, then the system will immediately self-ignite. Now consider the situation with the uppermost heat loss curve. Here, there are two points, denoted X and Z, where a solution is possible. Suppose the system is initially at some temperature below that corresponding to point Z. Then, the system will heat or cool until it reaches point X. Point X is a stable solution, since if any random temperature variation moves temperatures to the right, heat losses will rise faster than heat gains, and the system will return to point X, and conversely for cooling excursions. Point Z is also a solution which could be obtained, but any slight increase of temperature will result in heat gains exceeding heat losses. Thus, if it originally started at Z, a small random fluctuation in temperature could take it to a very high temperature, i.e., ignition. Point Y is a unique value, since it corresponds to the highest value of initial environment temperature (T_o) for which a stable solution can be obtained. The gas temperature at point Y can be denoted T_c and is referred to as the *critical temperature*[*]. The rise in gas temperature from T_o to T_c is actually quite small, and is the maximum temperature increase that can occur without thermal runaway. The chemical reactions taking place are more than zero, but slow enough not to give visible signs of combustion.

Defining the heat gain term as Q_G and the heat loss term as Q_L, we may note that the critical point is characterized by two conditions:

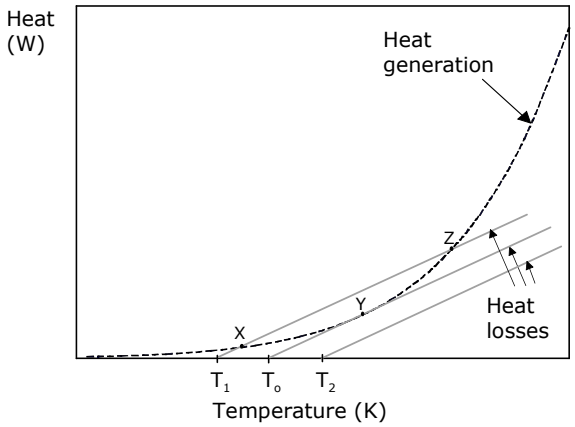


Figure 4 The heat generation and heat loss in a volume of gas; heat losses corresponding to 3 different heat transfer coefficients are shown. The heat loss curve passing through point Y represents the critical condition for 'thermal explosion'

[*] The nomenclature in the literature is not always clear or consistent—sometimes T_o is referred to as the critical temperature, other times it is the temperature at point Y. The physical meaning, however, is different: T_o is the maximum permissible temperature of the environment, while the temperature at point Y is the maximum temperature of the reacting substance that is possible without runaway.

(1) $Q_G = Q_L$

(2) $\dfrac{dQ_G}{dT} = \dfrac{dQ_L}{dT}$

in other words, (1) the values of the two terms are equal; and (2) the slopes are equal. Historically[21], the first condition was discovered by van't Hoff in 1883, while second one by Taffanel and le Floch[22] in 1913, consequently these two conditions sometimes bear their names.

As described in Chapter 3, if the reactant's temperature is T, then the rate at which reactant mass is consumed is:

$$\dot{m}''' = c^n A e^{-E/RT}$$

If the volume is V and the heat of the reaction is Q, then the heat generated* by the reaction is:

$$\dot{q} = QAVc^n e^{-E/RT}$$

The heat loss is

$$\dot{q} = hS(T - T_o),$$

where h = convective heat transfer coefficient and S = surface area. Expressing the equality of values gives:

$$QAVc^n e^{-E/RT} = hS(T - T_o)$$

Now, if we define θ as:

$$\theta = \frac{E}{RT_o^2}(T - T_o)$$

The heat balance equation can be expressed in terms of θ:

$$\frac{E}{RT_o^2}\frac{QAVc^n}{hS}e^{-E/RT} = \theta$$

To arrive at an analytical solution, at this point an approximation is necessary for $e^{-E/RT}$. If $(T - T_o)/T_o << 1$, then we make use of the approximation that for any $x << 1$,

$$\frac{1}{1+x} \approx 1 - x$$

This allows the exponential to be approximated as:

$$e^{-E/RT} = \exp\left(-\frac{E}{R(T_o + [T - T_o])}\right)$$

$$= \exp\left(-\frac{E}{RT_o}\left[\frac{1}{1 + \dfrac{T - T_o}{T_o}}\right]\right) \approx \exp\left(-\frac{E}{RT_o}\left[1 - \frac{T - T_o}{T_o}\right]\right)$$

$$= \exp\left(\frac{E}{RT_o}\frac{(T - T_o)}{T_o} - \frac{E}{RT_o}\right) = \exp(\theta)\cdot e^{-E/RT_o}$$

With this approximation, the heat balance equation can be rewritten as:

$$\frac{E}{RT_o^2}\frac{QAVc^n}{hS}e^{-E/RT_o}\cdot\exp(\theta) = \theta$$

The entire group of quantities preceding the second exponential is a constant and is defined as the Semenov number, ψ:

$$\psi = \frac{E}{RT_o^2}\frac{QAVc^n}{hS}e^{-E/RT_o}$$

Thus, the heat balance equation can be written as:

$$\psi\cdot\exp(\theta) = \theta \qquad (1)$$

To express the equality of slopes, we take the derivative with respect to T of each side of the above equation:

$$\psi\frac{d\theta}{dT}e^{\theta} = \frac{d\theta}{dT}$$

or,

$$\psi e^{\theta} = 1 \qquad (2)$$

The only way that Eq. (1) and Eq. (2) can be true is if $\theta \rightarrow 1$. But substituting that back into the heat balance equation gives:

$$\psi = 1/e$$

We can denote the critical condition by the subscript c, thus

$$\psi_c = 1/e$$

And $\theta_c = 1$

The meaning can be made a bit more clear by writing out the relations in dimensional terms. Thus

$$\frac{E}{RT_o^2}\frac{QAVc^n}{hS}e^{-E/RT_o} = \frac{1}{e}$$

And rewriting it as:

$$\frac{V}{S} = \frac{1}{e}\frac{RT_o^2 h}{EQAc^n}e^{+E/RT_o}$$

This means that for a given ambient temperature T_o, the maximum size of the object is limited to the value of V/S given above. Any larger size will result in thermal runaway and, therefore, ignition.

We must now consider briefly whether the assumption we made, that $(T - T_o)/T_o << 1$, is reasonable. Since we found that the critical condition corresponded to $\theta = 1$, we may express that as

$$\theta = \frac{E}{RT_o^2}(T - T_o)$$

and divide both sides of the inequality by $RT_o^2/(E[T - T_o])$. Thus, the approximation is also equivalent to $RT_o/E << 1$. Now, typical values might be $T_o \approx 600$ K, $E \approx 100{,}000$ J mol^{-1}, and $R = 8.314$ J mol^{-1} K^{-1}. Thus, $RT_o/E \approx 0.05$, which is <<1. For order-of-magnitude estimates, it is also useful to note that ratio E/R will often be in the range of 10,000 – 20,000 K.

* It can be seen that the exponential factor in the equation below does not monotonically keep rising with temperature. Instead, at very high temperatures a plateau is reached, since exp(–E/RT) → 1 as $T \rightarrow \infty$. Thus, in addition to the two intersections of the heat generation curve with the heat loss curve shown in Figure 4, a third intersection occurs at very high temperatures. This is not of concern in our solution, however, since the process already either stabilizes or runs away in the lower-temperature portion shown.

It is also instructive to see in dimensional units the maximum temperature rise that can occur without thermal runaway. Since $\theta_c = 1$, then

$$\frac{RT^2}{E} = T_c - T_o$$

where the gas temperature at criticality is denoted as T_c. This gives a quadratic equation in T_c, whose solution is:

$$T_c = \frac{E}{2R} \pm \sqrt{\left(\frac{E}{2R}\right)^2 - \frac{T_o E}{R}}$$

and it can be shown that physical results correspond only if the minus sign is taken for the second term. This gives

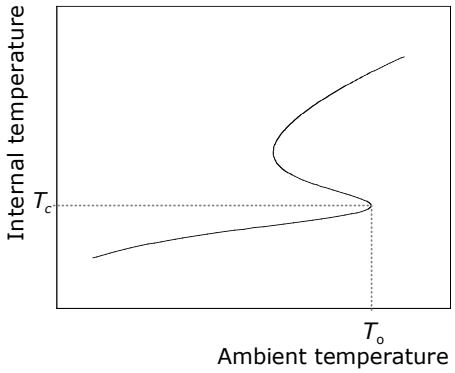


Figure 5 Full solution for T, as function of T_o (schematic)

$$T_c = \frac{E}{2R} - \frac{E}{R}\sqrt{1 - 4R\frac{T_o}{E}}$$

Now, since $RT_o/E << 1$, we can expand the square root expression as a power series in T_o/E, giving

$$T_c \approx \frac{E}{2R} - \frac{E}{2R}\left[1 - \frac{2RT_o}{E} - \frac{2RT_o^2}{E^2} + \ldots\right]$$

or

$$T_c - T_o \approx \frac{RT_o^2}{E}$$

Using the above example values, the difference $(T_c - T_o) \approx$ 30 K. The above treatment was simplified, since only the physically stable part of the solution was developed. In fact, the curve of the steady-state Semenov solution has two additional branches[23], as shown in Figure 5. For certain ambient temperatures below T_o, three solutions for T are possible, but only the lowest value corresponds to a stable, unignited state—the middle branch is unstable, while the top branch would represent an ignited state if the Semenov model were suitable for describing for actual combustion, not just conditions leading up it (which it is not).

A number of authors[24,25] give a further-approximated version of the above development by explicitly assuming that $T_c \approx T_o$. In that case, the equation giving the AIT, i.e., the value of T_o which corresponds to critical conditions, which in our development is:

$$eQAVc^n e^{-E/RT_o} = hS\frac{RT_o^2}{E}$$

becomes, instead:

$$QAVc^n e^{-E/RT_o} \approx hS\frac{RT_o^2}{E}$$

For common hydrocarbon combustion reactions, $n = 2$, and therefore, $c^n \sim \left(\frac{P}{RT}\right)^2$, where P = pressure. Substituting this, and taking logarithms of both sides gives:

$$\ln\frac{P}{T_o^2} = \frac{E}{2RT_o} + \text{const}$$

This relation indicates that raising the system pressure causes ignition to take place at a lower temperature, and vice versa. The relation between the pressure and the temperature can best be represented by plotting $1/T_o$ on the x-axis and $\ln\frac{P}{T_o^2}$ on the y-axis (Figure 6).

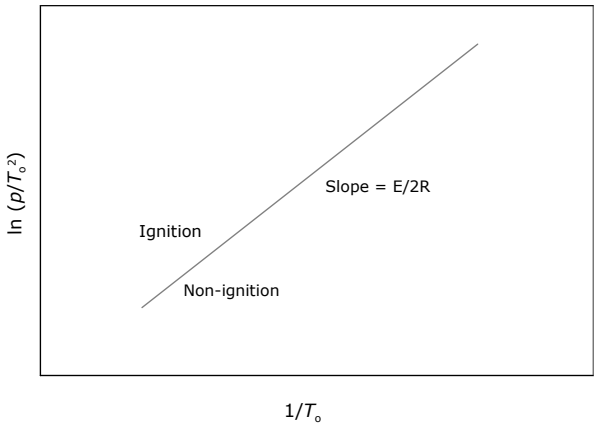


Figure 6 The relation according to Semenov theory between the pressure and the temperature needed for ignition

The above development comprised a *stationary state theory*, that is, we were only seeking to find the conditions necessary for criticality, not the time involved in heating up the system. For actual ignition problems, if the ambient temperature is larger than the T_o corresponding to critical conditions, thermal runaway will occur, that is, the gas will ignite. It then becomes of interest to assess the time required for ignition, t_{ig}. To evaluate this time, the heat released per unit volume during the period from $t = 0$ to $t = t_{ig}$ is:

$$QAc^n e^{-E/RT_o} \cdot t_{ig}$$

Assuming that there are no losses to the outside (that is, the system is adiabatic), this same heat goes to raise the temperature from T_o to T_c:

$$\rho C(T_c - T_o)$$

where ρ = density and C = heat capacity. Thus,

$$\rho C(T_c - T_o) = QAc^n e^{-E/RT_o} \cdot t_{ig}$$

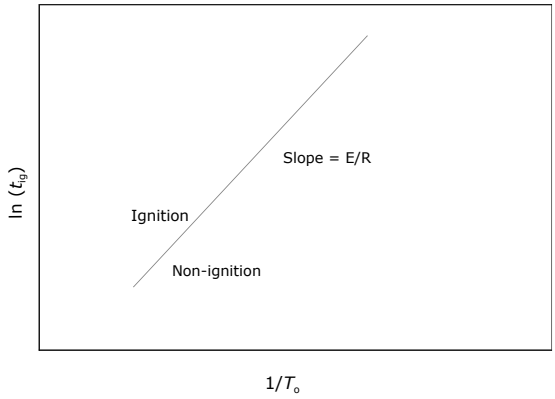


Figure 7 The dependence of the induction period on the gas temperature

But

$$\left(T_c - T_o\right) \approx \frac{RT_o^2}{E}$$

Thus

$$\frac{\rho CRT_o^2}{E} = QAc^n e^{-E/RT_o} \cdot t_{ig}$$

For a second-order reaction, $n = 2$, and $\rho \equiv c$, thus

$$t_{ad} = \frac{CRT_o^2}{cQAE} e^{+E/RT_o}$$

where the subscript *ad* denotes that external heat losses have not been taken into account. Despite the fact that this result was obtained by some highly simplified reasoning, a full solution to the time-dependent problem[26] gives the identical expression for t_{ad}. Now, if we roughly assume in the above equation that the dependence on T_o in the first factor is small compared to the exponential dependence on T_o of the second factor, we can take logarithms of both sides and write:

$$\ln(t_{ad} \cdot c) = \frac{E}{R}\frac{1}{T_o} + \text{const}$$

Since pressure is proportional to concentration, this also implies:

$$\ln(t_{ad} \cdot P) = \frac{E}{R}\frac{1}{T_o} + \text{const}$$

If the above equation holds, then plotting $1/T_o$ on the x-axis and $t_{ad} \cdot P$ on the y-axis should give straight lines if the x-axis is linear and the y-axis is logarithmic (Figure 7); the values of T_o must be in Kelvins for this plot. Spadaccini and TeVelde[27], however, attempted to validate this for cetane and found that the experimental data did not fall into straight lines. Instead, a straight line was obtained if the following equation was plotted:

$$\ln(t_{ad} \cdot P^2) = \frac{E}{R}\frac{1}{T_o} + \text{const}$$

which requires that $t_{ad} \cdot P^2$ be plotted on the y-axis. Figure 8 shows that, with the exception of the leanest mixture (φ = 0.3), the points do fall along a single straight line. Since $1/T_o$ gives very small numbers, Figure 8 was plotted with $1000/T_o$, instead of $1/T_o$, on the x-axis. The slope of the line is 24.54. From this, the value of E can be found, since

$$24.54 = \frac{E}{R}\frac{1}{1000}$$

giving E/R = 24,540 K, and, since 8.314 J mol^{-1} K^{-1}, this gives E = 204 kJ mol^{-1}.

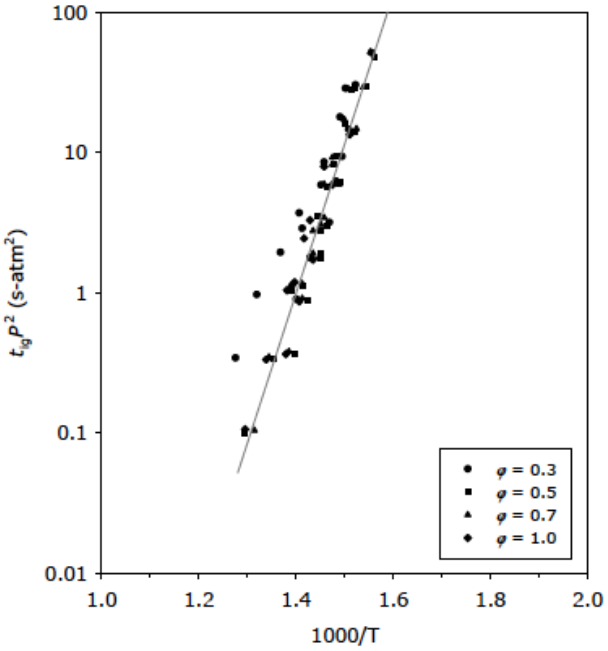


Figure 8 Autoignition data for cetane at several equivalence ratios, plotted as suggested by Spadaccini and TeVelde

For some purposes, it may be useful to make corrections for the non-adiabatic nature of real systems. A suitable correction is[28]:

$$t_{ig} = (n\gamma)^{-1/3} t_{ad}$$

where n = order of reaction ($n \geq 1$), and γ is given by:

$$\gamma = \frac{C}{Q} \cdot \frac{RT_o^2}{E}$$

giving the heat-loss corrected ignition time as:

$$t_{ig} = n^{-1/3} \frac{1}{A}\left[\frac{CRT_o^2}{QE}\right]^{2/3} e^{+E/RT_o}$$

Semenov assumed that there are only two distinct temperatures in the system, the outside environment being at one temperature and the gas inside at another. The assumption that the volume of gas is at a single temperature is a strong simplification. In fact, a gas has a finite thermal conductivity, and this will cause the center to be hotter than the periphery. Frank-Kamenetskii recognized this and created a theory which takes finite gas conductivity into account. His theory, however, discards a p iece of physics which Semenov treated realistically—he assumes the vessel wall is

'clamped' at the environment temperature T_o. The differences are summarize in the table below. A 'blend' of these two theories is possible and this is discussed in Chapter 9.

Table 1 Main differences between Semenov and Frank-Kamenetskii theories

Theory	Temperatures inside the vessel	Temperatures outside the vessel
Semenov	uniform	decrease over a certain boundary-layer thickness from a high value at the wall, to a lower value in ambient air
Frank-Kamenetskii	non-uniform; highest at the center, lower towards the walls	uniform: both the vessel wall and the ambient air are at the same temperature

Frank-Kamenetskii starts by applying the fundamental heat conduction equation to a fixed volume of gas:

$$\rho C \frac{\partial T}{\partial t} = \frac{\partial}{\partial x}\left(\lambda \frac{\partial T}{\partial x}\right) + \frac{\partial}{\partial y}\left(\lambda \frac{\partial T}{\partial y}\right) + \frac{\partial}{\partial z}\left(\lambda \frac{\partial T}{\partial z}\right) + \dot{q}'''$$

where

ρ = gas density (kg m^{-3})
C = heat capacity (kJ kg^{-1} K^{-1})
T = temperature (K)
t = time (s)
λ = thermal conductivity of the gas (kW m^{-1} K^{-1})
$\dot{q}'''$ = heat generation rate (kW m^{-3}).

The heat generation term is a simplified representation of the overall combustion reaction which can take place. Note that here it must be expressed in per-volume units. To make the equation simpler, the 'del operator' can be introduced,

$$\rho C \frac{\partial T}{\partial t} = \nabla \cdot (\lambda \nabla T) + \dot{q}'''$$

We then assume that the thermal conductivity is a constant, allowing it to be taken outside the differential:

$$\rho C \frac{\partial T}{\partial t} = \lambda \nabla^2 T + \dot{q}'''$$

In developing his simplest 'stationary' solution, Frank-Kamenetskii considers only the steady-state solution, by dropping the time-dependent term and only considering the spatial variations. Thus,

$$\lambda \nabla^2 T = -\dot{q}'''.$$

If the heating is symmetrical, for various geometries the 'Laplacian operator' ∇^2 can be evaluated as:

$$\nabla^2 = \frac{d^2}{dx^2} + \frac{j}{x}\frac{d}{dx}$$

where $j = 0$ for a slab, $j = 1$ for radial heat flow in a cylinder, and $j = 2$ for in a sphere.

Now, the heat generation term can be expressed as a product of the heat of reaction, Q (kJ kg^{-1}) and the reaction rate $\dot{m}'''$ (kg s^{-1} m^{-3}). If the reaction rate is assumed to be represented by a first-order Arrhenius expression (which is the simplest assumption, but not generally a realistic one for most gases), then

$$\dot{m}''' = \rho A e^{-E/RT}$$

Here, the pre-exponential factor A has the units of (s^{-1}) since the exponential has to be dimensionless. Thus, the governing equation becomes:

$$\nabla^2 T = -\frac{Q\dot{m}'''}{\lambda} = -\frac{QA}{\lambda}\rho e^{-E/RT}$$

The entire chemistry of the combustion process is then embedded into two constants: A and E. All other variables are either thermochemical constants of the system (conductivity, density), universal constants (R), or distance variables. The boundary conditions for the above differential equation must express the wall temperature, which is taken as a constant,

$$T = T_o \quad \text{for} \quad x = r$$

where x is the radial distance from the center, and r is the radius of the vessel. Furthermore, due to symmetry, $\frac{\partial T}{\partial x} = 0$ at $x = 0$.

Frank-Kamenetskii then made the approximation that the temperature rise at which the system starts to 'run away towards ignition' is small compared with the ambient temperature of the system. To express this, it is instructive to define a temperature rise term T*, where $T^* = T - T_o$. Then, the approximation becomes $T^* << T_o$. The exponential term can then be written as

$$\exp\left(\frac{-E}{RT}\right) = \exp\left(\frac{-E}{R(T_o + T^*)}\right) = \exp\left(\frac{-E}{RT_o}\left[\frac{1}{1 + T^*/T_o}\right]\right)$$

and using the fact that $T^* << T_o$:

$$\exp\left(\frac{-E}{RT}\right) \approx \exp\left(\frac{-E}{RT_o}\left[1 - \frac{T^*}{T_o}\right]\right) = \exp\left(\frac{-E}{RT_o}\right)\exp\left(\frac{ET^*}{RT_o^2}\right)$$

Using this expression, the heat conduction equation becomes:

$$\nabla^2 T^* = -\frac{QA\rho}{\lambda}\exp\left(\frac{-E}{RT_o}\right)\exp\left(\frac{ET^*}{RT_o^2}\right)$$

The equation is then put into nondimensional form by defining two nondimensional variables:

$$\theta \equiv \left(\frac{E}{RT_o^2}\right)T^*$$

and

$$\eta \equiv \frac{x}{r}$$

This gives

$$\nabla_\eta^2 \theta = -\frac{QA\rho}{\lambda}\left(\frac{E}{RT_o^2}\right)r^2 \exp\left(\frac{-E}{RT_o}\right)e^\theta$$

where the subscript η denotes that the Laplacian operator is with respect to η. The boundary conditions become:

$$\theta = 0 \qquad \text{at} \quad \eta = 1$$
$$d\theta/d\eta = 0 \qquad \text{at} \quad \eta = 0.$$

The solution for the temperature distribution can be obtained from the above differential equation and its boundary conditions. For determining ignition, however, the question becomes: Under what conditions is *any* steady-state solution impossible? This condition is, perforce, the ignition point, since the process is encountering thermal runaway.

The analysis is simplified by noting that all the physical constants remaining in the equation show up in a single group, which is defined as δ, sometimes referred to as Frank-Kamenetskii's δ:

$$\delta = \frac{QA\rho}{\lambda}\left(\frac{E}{RT_o^2}\right) r^2 \exp\left(\frac{-E}{RT_o}\right)$$

and the differential equation then is:

$$\nabla_\eta^2 \theta = -\delta\, e^\theta$$

This equation does not have any solution if the value of the constant δ becomes too large. Frank-Kamenetskii showed that the largest value of δ for which a physical solution exists for a sphere is 3.32. Similarly, for an infinite cylinder of radius r, the critical value is 2.0, while for a slab of thickness $2r$ it is 0.88. This solution clearly demonstrates that 'ignition temperature' is not a property of a particular gas mixture; instead, it is related to the size of the vessel in which gas is contained.

In the development above, we assumed a first-order reaction, i.e., that the reaction rate is proportional to ρ. For a second-order reaction, the concentration of reactants to the second power, c^2, would be substituted for ρ.

The above expression for δ can be usefully employed to find the effect of pressure on the autoignition temperature. Noting that the Ideal Gas Law can be expressed as $\rho = MP/RT$, where M = molar mass (kg mol^{-1}), P = pressure (Pa), and T = temperature (K), the expression for δ becomes:

$$\delta = \frac{QA}{\lambda}\frac{MP}{RT_o}\left(\frac{E}{RT_o^2}\right) r^2 \exp\left(\frac{-E}{RT_o}\right)$$

Temperature cannot be explicitly solved from this equation, but a P versus T (or r^2 versus T) relation could be plotted and would show the form of a modified hyperbola. Egeiban et al.[29] explored the ignition behavior at low pressures of di-tertiary-butyl peroxide. The latter was selected as a substance which shows simple ignition kinetics (due to exothermic decomposition). The *P-T* diagram (Figure 9) shows the hyperbola shape which is characteristic for a substance whose oxidation can be modeled by the thermal theory.

When the thermal theory is valid, for spherical vessels of various sizes, plotting $\ln(P\, r^2/T_o^3)$ against $1/T_o$ should give a

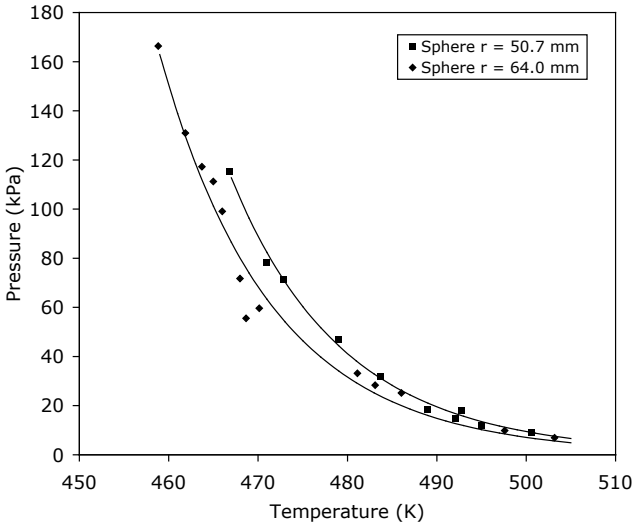


Figure 9 The *P-T* diagram for the ignition of di-*tert*-butyl peroxide

straight line with a slope of $-E/R$. The slope in Figure 10 is –18989, which gives E = 158 kJ mol^{-1}, a value identical to that determined for di-*tert*-butyl peroxide from other means. The authors, however, also determined that the experimental value of δ corresponding to ignition was 6.0 – 6.7, which is quite far from the theoretical 3.32. Thus, the theory, while giving the exact E value and also being able to predict very well the functional dependences of pressure, temperature, and size, does not correctly predict the absolute location of the ignition curve on the $P - T$ plane. For many purposes, however, a simple theory which succeeds to this extent will be more than adequate.

The theoretically-motivated plotting, as shown in Figure 10, is not convenient for illustrating the dependence of T_{ig} on

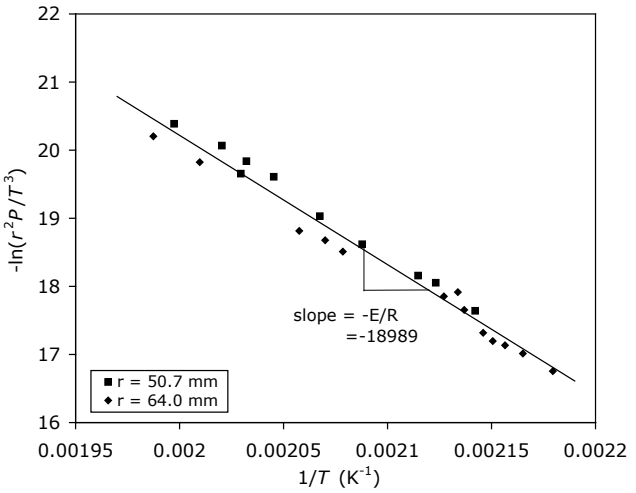


Figure 10 Application of thermal autoignition theory to di-*t*-butyl peroxide (Egeiban et al.)

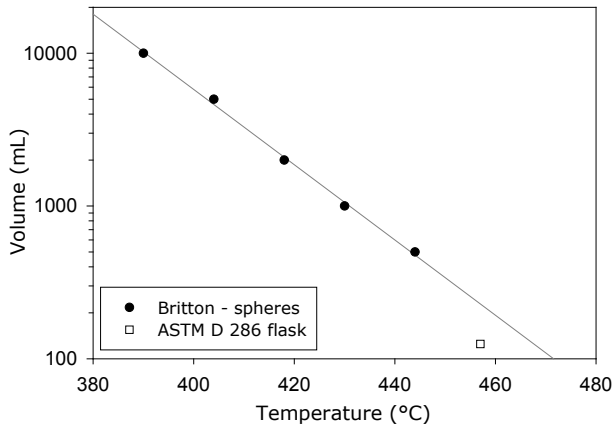


Figure 11 Effect of vessel size on autoignition of ethylene oxide in air

volume, since T_{ig} shows up on both axes. Britton[30] pointed out that, for practical purposes, straight lines will be found if T_{ig} is plotted on a linear x-axis and V on a logarithmic y-axis. This is illustrated in Figure 11 for ethylene oxide in air. Note that since the temperature plot is linear, degrees Celsius can be used just as well as Kelvins. Much early data on autoignition has been reported using the ASTM D 286 flask, and this is also shown for comparison.

Figure 12 shows the ignition regions for a stoichiometric mixture of H_2S in oxygen[31]. At a temperature of 330ºC, for instance, it indicates there are three ignition/non-ignition limits. At very low pressures, no ignition occurs, then at 0.4 kPa ignition can occur up to 1.5 kPa, after which ignition does not occur until 8.2 kPa is surpassed. A diagram of this kind does not arise if purely thermal theory is considered. Instead, the 1st and 2nd limits come about due to the role of chain branching. Note that these pressures are all well below 1 atm (101.3 kPa).

Similarly, most real fuels show ignition time vs. temperature relationships that do not conform to the thermal theory. For example, Figure 13 shows experimental and calculational results[32] for *n*-heptane. Observe that over a certain range of temperatures increasing the temperature makes it harder to ignite the mixture. The calculational results were from a chemical kinetics model which tracked 556 different chemical species.

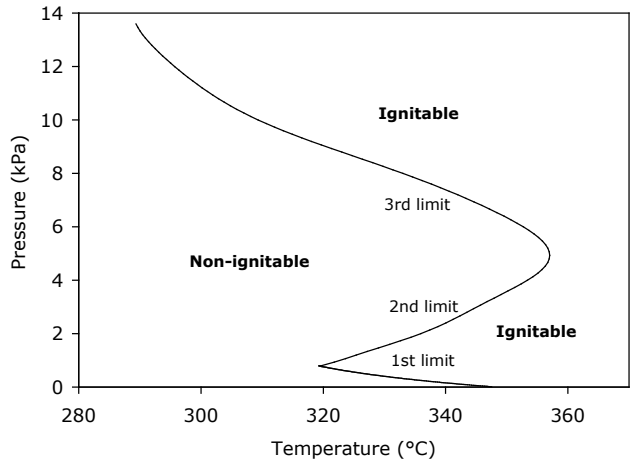


Figure 12 The P-T diagram for the ignition of a stoichiometric mixture of H_2S in oxygen

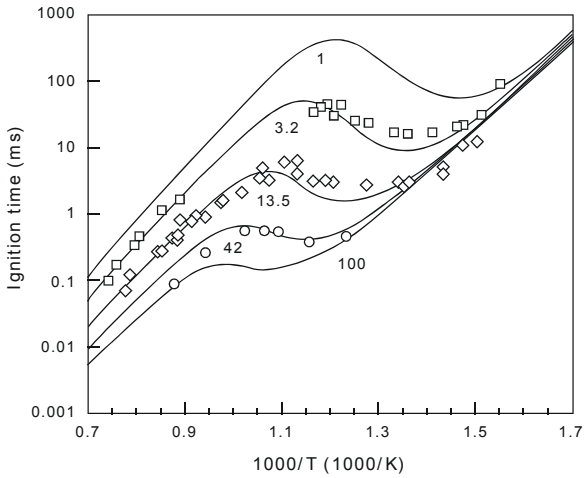


Figure 13 Ignition time vs. temperature for stoichiometric *n*-heptane/air mixtures at pressures of 1 to 100 atm. Solid lines represent calculational results.
(Copyright The Combustion Institute, used by permission)

Both the Semenov and the Frank-Kamenetskii theories were based on the assumption of a simple, single-step chemical reaction. An ignition under such circumstances is termed *thermal explosion* in the combustion literature. As we have seen in Chapter 3, however, combustion reactions normally fail to satisfy this requirement and are, instead, chain reactions. Such ignitions constitute *chain-reaction explosions*, also referred to as *branching-chain explosions*. Setting up and solving equations describing branching-chain reactions is very complex and does not lead to any approximate, closed-form solutions. Instead, solutions must be obtained by elaborate mathematical computer modeling.

IGNITION OF SPECIFIC FUELS

The three simplest fuel molecules of general interest are hydrogen (H_2), carbon monoxide (CO), and methane (CH_4). Since it has only two atoms and both are identical, hydrogen is the simplest fuel that can be studied. CO is important since many organic fuels burn by first oxidizing to CO and then later to CO_2. Methane is, of course, the primary component in natural gas. Theories have been created for the oxidation—including ignition phenomena—of all three. The reaction chemistry of even these simplest molecules is extraordinarily complex. Even though the 'global' reaction mechanism of hydrogen,

$$2H_2 + O_2 \rightarrow 2H_2O$$

represents the simplest possible combustion reaction, in actuality the mechanism is complicated, and Foo and

Yang[33] identified the need for 12 reactions to study the H_2 + O_2 system.

The kinetics of CO combustion is unusual, since a pivotal role is played by moisture in the atmosphere: wet CO is easy to ignite, whereas dry CO is highly resistant to ignition. Even minuscule amounts of H_2O (or H_2, or any other hydrogen-containing species) tend to promote certain reactions that are not possible in truly dry systems. But since very little of hydrogen needs to be present for a mixture to be moist, experimental studies of truly dry CO combustion are difficult. These were not being attained until the painstaking studies of Gray et al.[34,35], who elucidated the following types of exothermic responses.

Wet mixtures (> 2000 ppm H_2)

- Ignition. A visible flash occurs suddenly; fuel is completely consumed.
- Slow reaction. No light is emitted. Temperature increases due to self-heating are immeasurably small. pressure and concentration changes are small, even over long time periods.

Intermediate mixtures (200 ppm < H_2 < 2000 ppm)

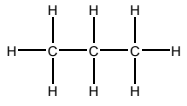
- *Ignition*.
- *Glow*. This is chemiluminescense. It is observable in a dark room as a blue emission. Reaction is relatively slow; temperature increases are limited; not all fuel is consumed. This response is only found for pressures of less than 0.1 atm.
- *Oscillatory glow*. This is seen as pulses of light. Analogous to cool flames seen with hydrocarbons. Reaction consumption occurs mainly during spikes of light emission.
- *Slow reaction*.

Dry mixtures (H_2 < 50 ppm)

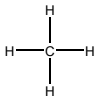
- *Glow*. This is the only reaction that occurs. Ignition is not achieved. The fuel is not 100% consumed. The glow is steady, except for a small range of pressure/temperature conditions (500 < T < 565ºC; 0.011 < P < 0.063 atm) where oscillatory glow is observed[36].

In flow-through systems where sufficient hydrogen is present, if ignition occurs, it is oscillatory in nature[36]. Gray et al. also developed a kinetic model that is able to reproduce most of the experimental features of ignition in a flow-through system[37].

Hydrocarbon molecules of higher molar mass have carbon-carbon and carbon-hydrogen bonds. For example, propane



is . But methane is



and it has no C–C bonds. Normally, the C–C bond is the weakest and the combustion chain reaction can begin with its attack. But in methane, the more difficult-to-break C–H bond must first be broken. Quantitatively, 439 kJ mol^{-1} must be supplied to break a C–H bond in methane, but only 356 kJ mol^{-1} to break the C–C bond in propane, and 305 to 320 kJ mol^{-1} in larger hydrocarbon molecules[38]. Thus, methane oxidation is

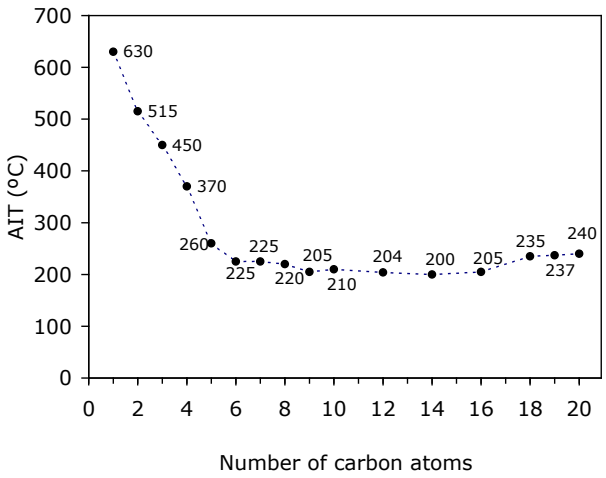


Figure 14 The AIT of *n*-alkane hydrocarbons in air, as a function of the number of carbon atoms

anomalous among hydrocarbons and methane shows an exceptionally high AIT. A recent study[39] has identified some 150 elementary reactions which needed to be computed in order to accurately predict methane oxidation reactions; in another recent study[40], some 177 reactions were used. However, reasonable prediction was obtained using only (!) 55 reactions[41].

If methane's AIT is unusually high, how come that, in the case of spark ignition, the ignition energy required is not higher than for other hydrocarbons? The reason is because the bond strength issues only come into play for starting a chain reaction by providing radicals or other excited species. When a spark is discharged, highly excited species are already introduced in large quantities.

Ignition of other organic fuels. The chemistry of the combustion and, hence, of the ignition, of most organic substances is enormously complex. In the words of chemical mathematician Peter Gray[42]: "In general, hydrocarbon oxidations are chemically the most complex systems studied outside the biological sphere." That the calculational effort needed for modeling is huge can be seen from another example: a recent study on the oxidation of propylene[43] involved solving 377 equations. Fortunately, for many practical applications, details of chemical kinetic steps taking place do not need to be mastered. Readers wishing to delve into these "complex systems" can start with the major monographs that have been published in the field, those by Minkoff and Tipper[44], Bamford and Tipper[45], Hucknall[46], Pilling[47], and Compton and Hancock[48].

EXPERIMENTAL DETERMINATION OF THE AIT

Conceptually, the AIT of a gas mixture is a simple idea. To construct an apparatus which measures it, however, is not simple at all. If substances showed no reaction at a certain temperature, and reacted fully at a slightly higher one,

things would be simpler, but this is not the case. One can imagine, for example, a vessel in which a mixture is placed at room temperature, then heated very slowly. At a certain temperature, flaming ignition will be observed. Things become less simple when it is realized that if the vessel were heated at a different rate, a different temperature of ignition would be recorded. The first experiments on this topic were done by Mallard and Le Chatelier[49] in 1880, who used an evacuated, heated porcelain vessel to which gas mixtures were quickly admitted. The mixture was injected cold, and it, of course, heated non-uniformly. The time required for heating could be eliminated by feeding the fuel and the oxidizer in separate heated tubes to a region where they would mix and potentially ignite. Dixon and Coward designed such an apparatus in 1909, but this was not a perfect answer, either, since an uncontrolled time of mixing was substituted for an uncontrolled time of heating. A detailed review of the various test methods that have been used to measure the AIT is given in the last section of this Chapter.

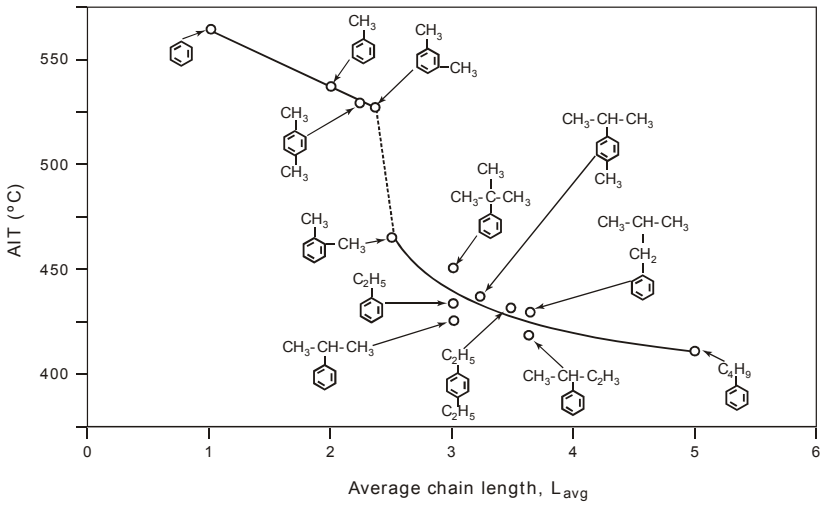


Figure 15 The AIT of aromatic hydrocarbons in air, as a function of average chain length (note the two ignition regimes—high temperature and low temperature)

VARIABLES AFFECTING THE AIT

MOLECULAR STRUCTURE

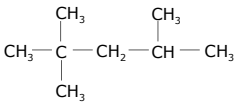
Molecular structure, not surprisingly, influences AIT results and the AIT depends on the bond strength of the weakest bond in the fuel molecule (or the O–O bond in oxygen, in case that is weaker than any fuel bonds). For *n*-alkane* series hydrocarbons, the AIT decreases with increasing number of carbon atoms, going from CH_4 to C_5H_{12}, as shown in Figure 14[50]. For higher alkanes, the AIT becomes nearly constant at 200 – 220ºC. The hydrocarbons starting with pentane (C_5) show a uniformly low AIT values because cool-flame ignitions are possible for them at atmospheric pressure. The much-higher values for C_1 through C_4 molecules reflect the fact that cool-flame ignitions are possible only at sub-atmospheric pressures. For very large molecules C_{16} and higher, the AIT starts to rise because the high molar mass brings about low volatility.

More complex molecules, i.e., branched-chain alkanes can be handled by the more generalized concept of carbon-chain length. Zabetakis[51] describes that the AIT is determined by the average carbon-chain length, L_{avg}, defined as:

$$L_{avg} = \frac{2\sum_{i=1}^{n} g_i N_i}{M(M-1)}$$

where N_i is the number of carbon atoms in any particular chain i, g_i is the total number of chains which have their number of carbon atoms equal to N_i, and M is the number of methyl ($–CH_3$) groups. This is illustrated for a series of aromatic hydrocarbons in Figure 15. None of these compounds show cool-flame ignition at ambient pressure.

Branched molecules typically have higher AIT values than straight-chain molecules. An important example can be cited in connection with *knock* in engines. Knock, which can be damaging to gasoline engines, occurs when the fuel ignites prematurely due to autoignition, instead of igniting from a spark at the correct time in the engine cycle. As is well known, knock propensity is measured as *octane numbers*. This is confusing, however, since the term is a misnomer—the correct term would be 'iso-octane numbers.' The straight-chain molecule, *n*-octane, in fact, has an AIT of 220ºC and an octane number of –18. It is not a suitable motor fuel. Iso-octane, which has the structure



has an AIT of 415ºC and an octane number of 100, by definition. Egolf and Jurs[52] developed a proprietary model for predicting the AIT on the basis of various molecular-structure descriptors. They claim their model shows standard deviations approaching the experimental uncertainty of AIT measurements.

* The series of hydrocarbons methane (CH_4), ethane (C_2H_6), propane (C_3H_8), butane (C_4H_{10}), etc. is alternately referred to as *n*-alkanes or as *n*-paraffins. The prefix '*n*' denotes 'normal,' that is, a molecule with carbons in a straight chain and not branched.

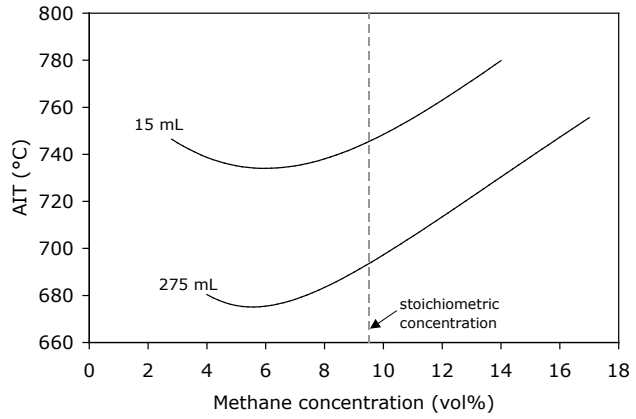


Figure 16 Effect of fuel concentration on AIT for methane, tested in vessels of two different sizes

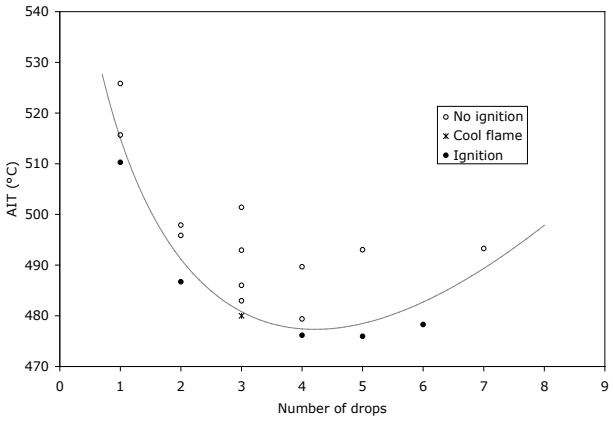


Figure 17 Ignition of 1,1-dineopentylethane in a heated crucible test

FUEL CONCENTRATION

There is an optimum fuel concentration in terms of obtaining the lowest AIT value, as shown in Figure 16 for methane[22]. Note that the optimum is around 5.5 – 6%, which is much lower than the stoichiometric concentration of 9.5%.

The bulk of the AIT data available in the literature were obtained in various heated flask or crucible test apparatus by dropping cold droplets of fuel into a heated volume. Typical results[53] are shown in Figure 17 and these indicate a minimum, which is reported as the tabulated AIT value. However, the results, when obtained in this manner, cannot be related to actual fuel/air ratios. Numerically, a fuel/air ratio could be computed, but it would not have significance because: (1) the fuel concentration is non-uniform in apparatuses of this kind, and (2) the apparatuses are leaky and even the total amount of air cannot be accurately determined.

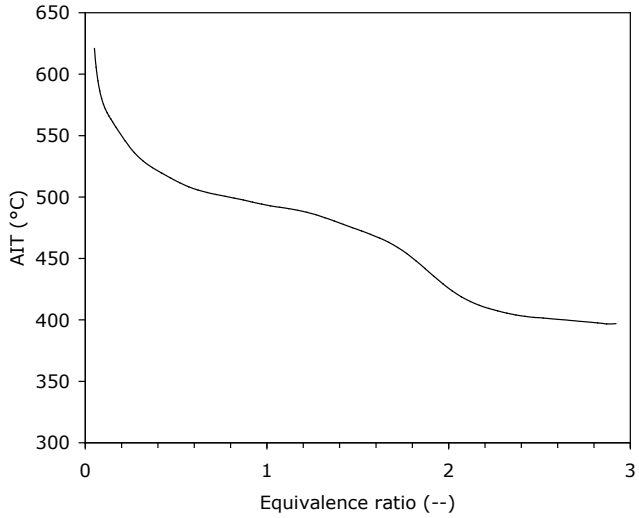


Figure 18 Effect on AIT of the fuel concentration for butane/air mixtures
(Copyright AIChE, used by permission)

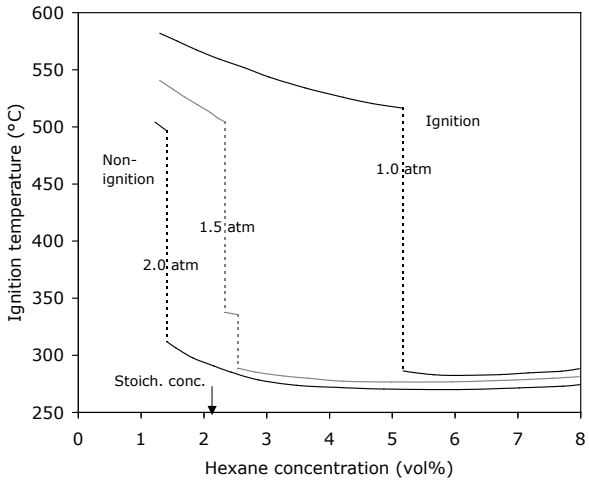


Figure 19 The effect of fuel concentration on the ignition temperature of hexane

A more careful study was done by Griffiths and Gray[54], who determined the AIT as a function of the equivalence ratio for butane/air mixtures in a heated 0.6 L spherical vessel (Figure 18). Their results does not show a minimum at intermediate fuel concentration values, but rather a value which decreases with increasing fuel concentration. The Bureau of Mines AIT value for butane is 370ºC, which is somewhat lower than the lowest value (397ºC) shown by Griffiths and Gray. The authors also studied other gases and showed some exceedingly irregular functions describing the AIT dependence on equivalence ratio.

The above results were obtained, as are most AIT data, at 1 atm pressure. But pressure can have a pronounced effect on

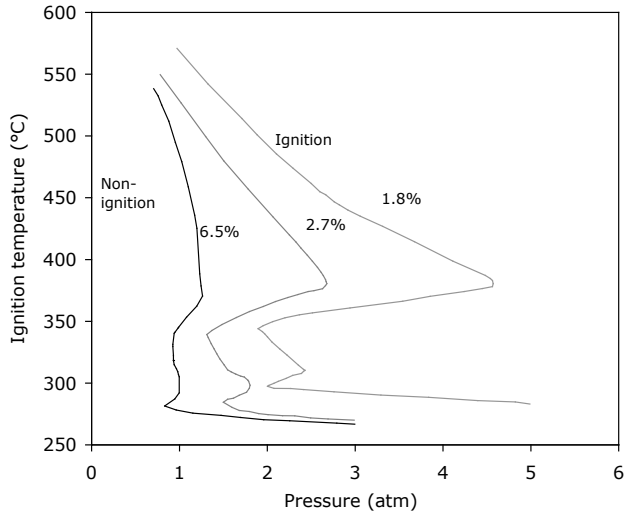


Figure 20 The dependence of ignition regimes on fuel concentration for hexane/air mixtures

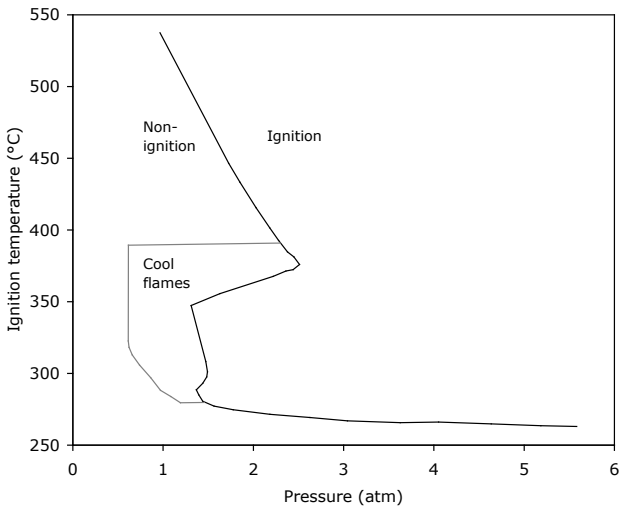


Figure 21 The ignition regimes for a mixture of 3.1% hexane in air

AIT, as shown in Figure 19 for hexane/air mixtures, determined by Townsend et al.[55]. The reaction kinetics for mixtures in the 'upper branch' of the curves is different from that in the 'lower branch.' As with all AIT measurements, there is a significant apparatus-dependence; thus, the minimum value of AIT obtained by Townsend et al. for 1 atm conditions (282 C) is higher than the value adopted by the Bureau of Mines (225 C). The existence of two ignition regimes is common for more complex organic fuel molecules and corresponds to the possibility of cool flames and two-stage ignitions.

PRESSURE

Raising the pressure generally lowers the AIT. The theory discussed above indicates that:

$$\ln\frac{P}{T^2} = \frac{A}{T} + B$$

and over a small enough range this may also be true in experiments. But Figure 22 shows results from Demidov[56], Furno et al.[63], Gödde et al.[57], and Kuchta[50,150] and they indicate that the exact relation will depend on the substance involved. Furthermore, the effect tends to be more pronounced when smaller experimental vessels are used[50,63].

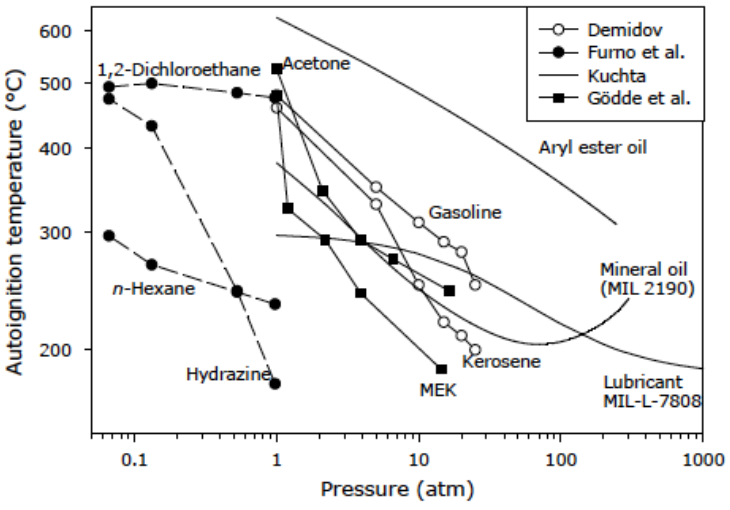


Figure 22 The effect of pressure on the AIT of various vapors

The effect is even more pronounced when there are several combustion modes in which the fuel can burn. Figure 21 illustrates this for a 3.1% hexane mixture in air[55]. The effect of fuel concentration on these ignition/non-ignition boundaries is illustrated in Figure 20. Each of the mixtures also has associated with it a separate cool-flame region, but, for legibility, these are not illustrated in Figure 20. Many practical devices, e.g., air compressors, are operated at high pressures. Thus, the large drop in AIT when going to high pressures must be considered both for lubricants and for any adventitious contaminants.

OXYGEN CONCENTRATION

The effect of oxygen concentration on the AIT is hard to discern from tabulations (e.g., Table 1 in Chapter 15) which combine the results from numerous investigators, but it becomes more evident when data from a single apparatus are assessed, e.g., the results of Ono[58]. Zabetakis[51] considers that there are two distinct possibilities. The compounds that show 'low-temperature' ignitions (< 300ºC) are ones that also show cool flames and a two-stage ignition process.

For these substances, the AIT values in oxygen are nearly identical to those in air. Compounds that show 'high-temperature' ignitions (> 400ºC) undergo direct, normal-flame ignitions. The AIT in oxygen for such substances can be greatly below its air value. This happens because, in oxygen, the ignition regime changes to the two-stage ignition process.

Increasing the oxygen concentration generally decreases the ignition time. Experiments show that the oxygen concentration effect is:

$$t_{ig} = \frac{\text{constant}}{[O_2]^n} e^{E/RT}$$

where $[O_2]$ = oxygen concentration (vol%) and n = constant, but there seems to be little agreement as to what the value of n is, or what influences it. Jackson and Brokaw[86] got 0.25, Freeman and Lefebvre[59] 0.6, Chang et al.[60] 0.74, Miller[61] 1.0, while Mullins[62] obtained 2.0. There is a huge difference in these results, and it would appear that some intervening variable has been neglected. The data of Miller suggest that for AIT values greater than about 1000ºC, the above equation is no longer obeyed at all.

VESSEL SIZE AND OPERATING CONDITIONS

Increasing the vessel size lowers the AIT[63.] Figure 23 shows this relation for a range of common gases and vapors[56,64,65]. The pertinent quantity is the surface/volume ratio, but for vessels of similar shapes, volume or surface alone can be used to plot data. The effects of surface losses were already recognized in 1922 by Mason and Wheeler[66], who suggested plotting AIT values against the surface/volume ratio of the vessel, with the implication being that a 'true' value could be obtained by extrapolating the data down to a ratio of 0.

Kuchta et al.[67] noted that a change in regime is possible with certain substances, leading to large changes in AIT with modest changes in critical dimension of the system. As an example, the AIT of *n*-decane was found to be 224ºC for a radius of 11 mm, 214ºC for 18 mm, but a huge 602ºC for 4 m m. In addition, ranking of fuels was drastically changed when vessel sizes < 11 mm were explored. This is indicative of a change in ignition chemistry, with cool flames and two-stage ignitions not being possible for the smaller vessel sizes. Figure 24 shows AIT values given by White[68] for aviation kerosene, with sizes expressed as the area/volume ratio. Gray analyzed these results and note that a discontinuity of slope for the ignition/no-ignition boundary can indicate that there is a negative-temperature coefficient region in the heat generation vs. temperature relation for the substance, that is, over a certain region, raising the temperature decreases the reaction rate. In that case, there can be two-stage ignitions, with these occurring as sketched out between the gray curves.

Table 2 Effect of using a sealed vessel for conducting AIT tests

Substance	AIT (ºC)		
	Open vessel, DIN 51794 test	Open 0.5 L vessel	Sealed 0.5 L vessel
acetone	535	525	NA
methyl ethyl ketone	475	480	325
2-pentanone	445	470	285
methyl butyl ketone	420	NA	210

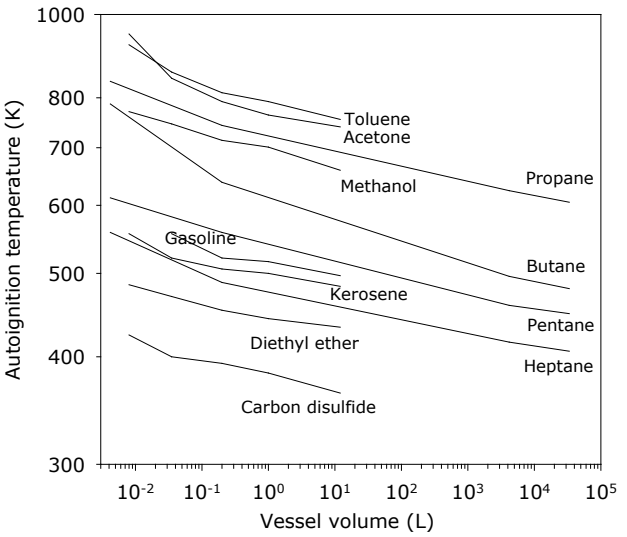


Figure 23 Effect of vessel volume on the AIT of various gases and vapors

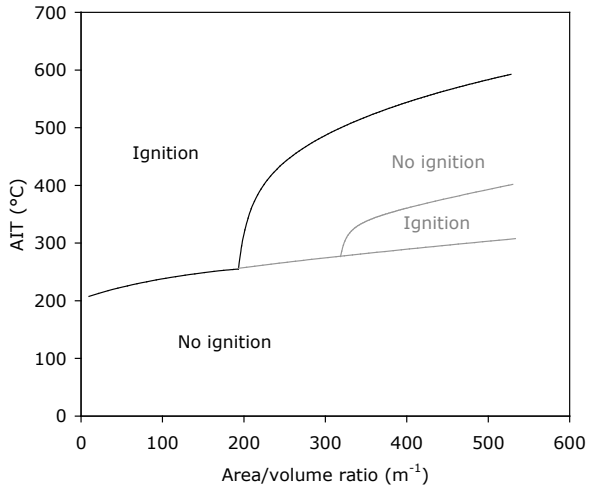


Figure 24 Effect of vessel area/volume ratio on the AIT of aviation kerosene. Experimental results are shown in black; potential second ignition region shown in gray (qualitative only).

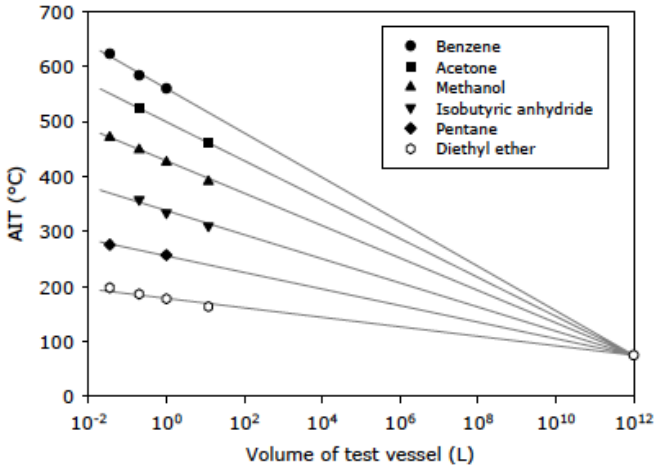


Figure 26 Universal asymptote proposed by Beerbower for scaling AIT results

It is evident that if AIT data are obtained from laboratory equipment of 1 L or so in size, and applied to chemical factory reactors where sizes are several orders of magnitude greater, accidental autoignitions may be observed 'below the AIT.' HSE have warned against this type of misapplication of data[90]. But since it is very difficult to run tests in production-scale vessels, an estimating technique is needed for AIT values applicable to large-size vessels. A. Beerbower (quoted by Coffee[69]) suggested that for common C,H,O compounds (i.e., ones without halogen, sulfur, or other heteroatoms) a universal asymptote exists, so that knowing the AIT for one vessel size, it is possible to estimate the AIT for another size. He proposed that, if extrapolated to a vessel volume of 10^{12} L, all gases and vapors will show AIT = 75ºC. Thus, if the measured AIT = T_1 at volume = V_1 (L), then the AIT (= T_2) for any other volume V_2 is computed as:

$$T_2 = 75 + (T_1 - 75)\left[\frac{12 - \log_{10} V_2}{12 - \log_{10} V_1}\right]$$

Figure 25 illustrates the data obtained by Beerbower demonstrating that the agreement is rather good.

Standard tests are run in vessels which are open or otherwise in pressure equilibrium with ambient atmosphere. But since increased pressure lowers the AIT, if tests are run in sealed vessels, much lower AIT values are found. This was demonstrated by Gödde et al.[57], as shown in Table 2.

WALL MATERIAL

As discussed above, wall surfaces have a chain-termination effect in chain reactions. Not surprisingly, different materials can show different efficiency for chain-termination reactions. For some common materials, the order is[70]:

lowest AIT	clean dry Pyrex, quartz
medium	porcelain; surfaces coated with KCl, $BaCl_2$
highest AIT	silver

Demidov[56] shows data that for some vapors, changing the wall material of the test vessel changes the AIT results by hundreds of degrees. For example, in one set of experiments the AIT of diethyl ether was found to be 188 C in a glass retort, 193 C in a steel block, 533 C in an iron tube, and 549 C in a quartz tube. For many substances, a platinum crucible gave the lowest AIT values, but in the case of ethanol, the platinum crucible value was more than 100 C higher than the value in a steel block. Frank and Blackham[13,71], however, found that the AIT of diethyl ether was 207 1 C, when tested in aluminum alloy, black iron, brass, copper, Inconel, or stainless steel vessels. Based on a large number of compounds studied, they concluded that the material of the walls does not affect substances with AIT < 290 C (i.e., those that show cool flames and multistage ignitions), but can have an effect on substances with high ignition temperatures. The results of Ono[58], however, show that numerous exceptions exist to such a simple rule. In a series of comparison tests using stainless steel vessels with oxidized and bright-metal surfaces, in the worst case, a 48 C difference was found, but in most cases the agreement was within 10-30 C. In an interesting series of explorations, Setchkin[72] used a 1 L glass flask, where the material on the *outside* of the flask (i.e., in between the glass flask and the surrounding heating elements) was varied. Results for a copper layer showed AIT values about 10ºC higher than those for a refractory material. However, a mirrored surface gave values another 5ºC or so lower than for the refractory. These results are hard to interpret and Setchkin merely noted that a mirrored surface was not practical for routine work.

FLOW VELOCITY AND TURBULENCE

The tabulated values of AIT refer to stagnant gas conditions. For ignition to take place at a given temperature, a time period equal to the induction period is needed. If a gas moves very fast through and past a heated tube or vessel,

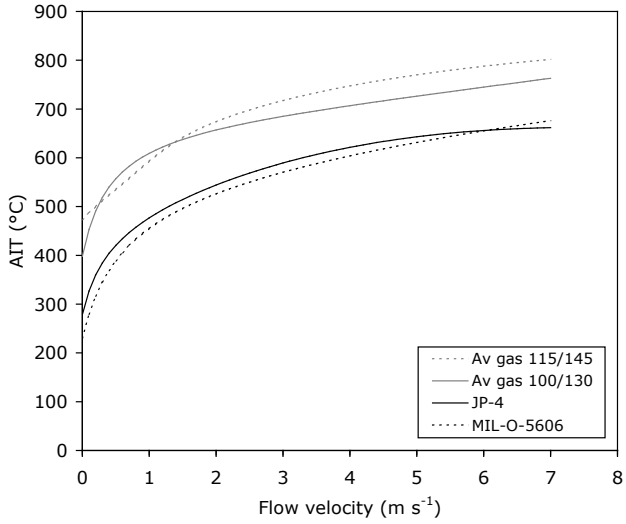


Figure 25 Effect of flow velocity on the AIT of several aviation fluids

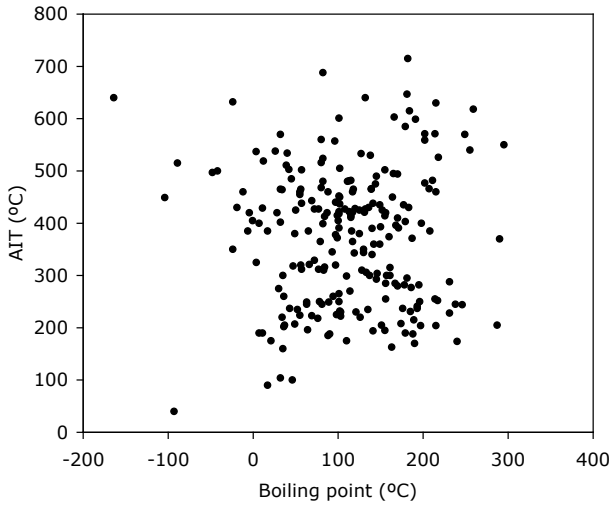


Figure 27 The absence of relation between boiling point and AIT

ignition will not occur if the residence time spent by the gas there is less than the induction period pertinent to the temperature in question. In practice, things get more complicated, since gases rapidly flowing through areas of changing temperature cannot be approximated as all being at a single temperature. Consequently, the residence time vs. induction period relationship may be more helpful for qualitative studies than for actual numerical determination. A limited amount of available data[73] indicates that the AIT rises steeply as flow velocity goes from zero to about 2 m s^{-1}, then rises at a slower rate for higher velocities (Figure 26). The authors suggest that these data can be approximately represented by:

$$\frac{1}{T_u} = \frac{1}{T_o} - a\,u^{1/4}$$

where T_o = AIT (K) at zero velocity, T_u = AIT (K) at a given velocity, u = velocity (m s^{-1}), and a = fuel-dependent constant. Observe that the temperatures have to be expressed in Kelvins in this equation. The effects of turbulence have been found to be inconsistent[74]

OTHER RELATIONS

Wiezevich et al.[75] proposed that there is a relation between the AIT and the boiling point, but Figure 27, which presents data for some 228 pu re compounds, shows that there is none. Indeed, none should be expected, since the AIT is primarily determined by the compound's reactivity (i.e., kinetics) while the boiling point is simply an expression of the volatility of the compound.

AIT OF MIXTURES

The AIT of mixtures has rarely been studied. Figure 28 shows the relation for acetaldehyde/ethylene oxide mixtures[30]. It is clear that the relation is not linear and that it is dominated by the lower-AIT component over most of the range. Similar, non-linear relations have been found for methane/ethane and methane/butane mixtures. The non-linearities arise due to chemical kinetics effects and complex kinetic models are able to reproduce most of the features of these curves[76]. See also *Ethylene oxide* in Chapter 14.

IGNITION TIME

The time needed for a gas mixture to ignite, when exposed to an elevated temperature environment, can range from about 0.01 ms to hundreds of seconds. Decreasing the temperature increases the ignition time[66] (Figure 29), but for any substance, there is a maximum time for ignition. In the case of gases, this time is fairly short, e.g., in one study on methane in a 1.2 L apparatus, it was found that, at any temperature, if ignition did not occur in 30 s, it will never occur[77]. Same as with ignition temperature, the ignition time is not independent on the size of the system, as shown in Figure 35.

As indicated in the Theory section above, if simple Arrhenius kinetics is used and Semenov's theory is adopted, then a relation of form:

$$\ln t_{ig} = \left(\frac{E}{R}\right)\frac{1}{T} + a$$

is expected, where a is an experimental constant. Thus, if $1/T$ is plotted on the x-axis, and $\ln(t_{ig})$ on the y-axis, the results should be straight lines with a slope of E/R and a y-axis intercept of a. Note that T must be in absolute units, that is Kelvins and not degrees Celsius. For convenience, actual plots are generally presented whereby a $\log_{10}$ scale is used for plotting t_{ig} on the y-axis, as illustrated in Figure 30 using the data of Anagnostou et al.[84]. A number of other experimental results collected by the Bureau of Mines[78] are shown in Figure 32. If a single Arrhenius expression for

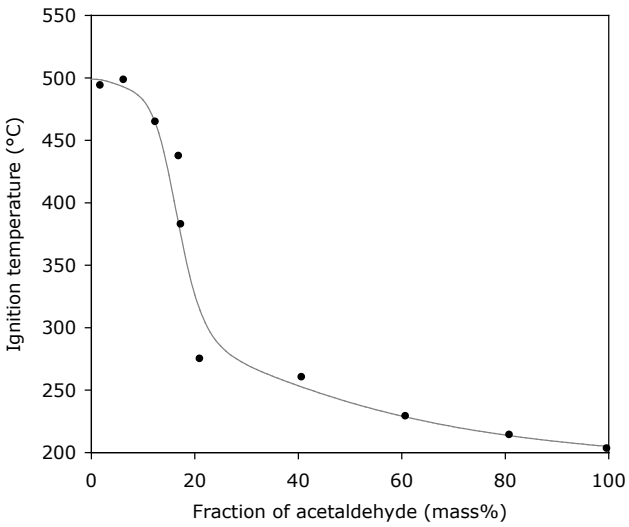


Figure 28 AIT of acetaldehyde/ethylene oxide mixtures in air

global kinetics would be sufficient for any gas, then results for any particular gas would fall along a single, straight line. Instead, most gases show lines with two slopes: a higher temperature and a lower temperature regime. In the high-temperature regime, the effective activation energy E is 50 to 90 kJ mol^{-1}, while in the low-temperature region values are E 140 to 190 kJ mol^{-1}. Not surprisingly, hydrogen, which is the simplest molecule, shows only a single regime. Perhaps surprisingly, given the large number of reactions that take place in real gases, the curves are all composed of two straight lines, rather than being complex shapes. As shown by Sano and Yamashika[79], this straight line relationship emerges even from complex computer modeling of detailed chemical reactions.

Experimental results for much shorter ignition times were reviewed by Goodger[80] and his collation of data for *n*-heptane is shown in Figure 31. In addition to the two regimes identified by the BM work (2 – 100 s), two more regimes can be seen. From the shortest times experimentally examined, around 0.01 ms, to about 0.5 s, a single slope of $E \approx 170$ kJ mol^{-1} can be seen; in the range of 0.5 s to 2 s, a shallow slope of $E \approx 30$ kJ mol^{-1} is found. Chemically, it is more appropriate to attribute the regimes to changes in temperature than changes in time, and thus the results are summarized in Table 4 as temperature regimes. For most other hydrocarbons, the data were not as extensive as for heptane, but Goodger generally found similar trends, with there being four different regimes. For the short ignition times, since the data primarily come from tests where liquid drops were used to produce the vapor, it may be appropriate to take the advice of Zabetakis et al.[81], who suggest that the results can be strongly affected by the evaporation time and not be any direct reflection of actual chemistry.

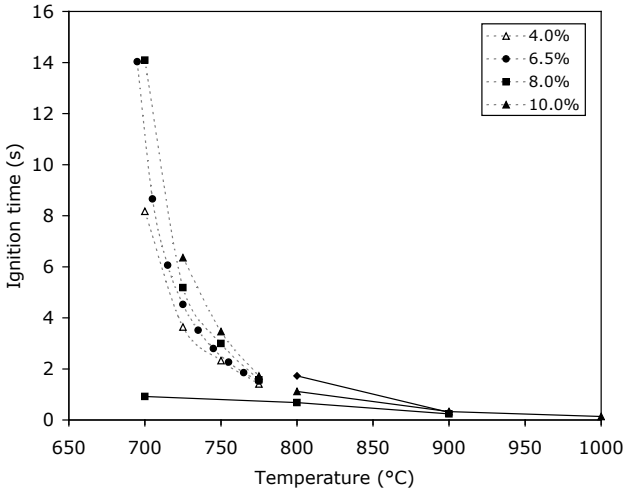


Figure 29 Ignition times for several concentrations of methane in air, as measured in two different apparatuses (dotted lines: Mason & Wheeler, solid lines: Taffanel & Le Floch)

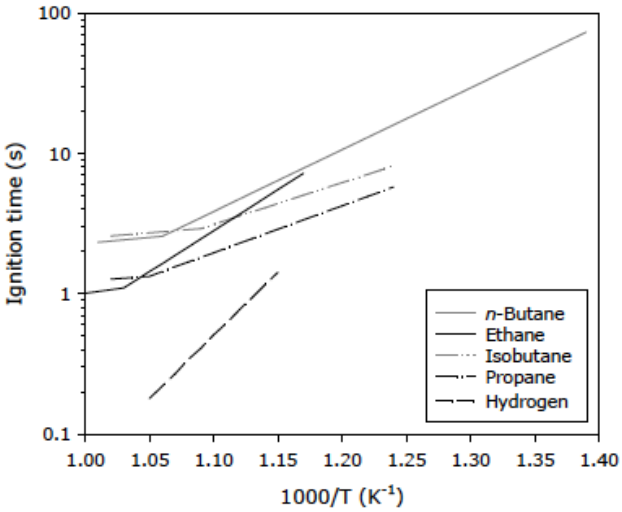


Figure 30 Ignition times for several fuel gases (stoichiometric concentration of the fuel gas in air), as measured by Anagnostou et al.

EFFECT OF FUEL TYPE AND MIXTURE COMPOSITION

For hydrocarbons, the Bureau of Mines developed some general guidance, shown in Table 3. This may be useful when data are available for certain compounds that are similar to the desired one.

The effect of the mixture composition on ignition time was studied in the 1920s by Mason and Wheeler. For methane[66], they found that the shortest times were recorded for the leanest fuel mixtures, and that increasing the fuel concentration increased the time to ignition. No special feature was observed near the stoichiometric value—the induction period just kept increasing with increasing equivalence ratio, φ.

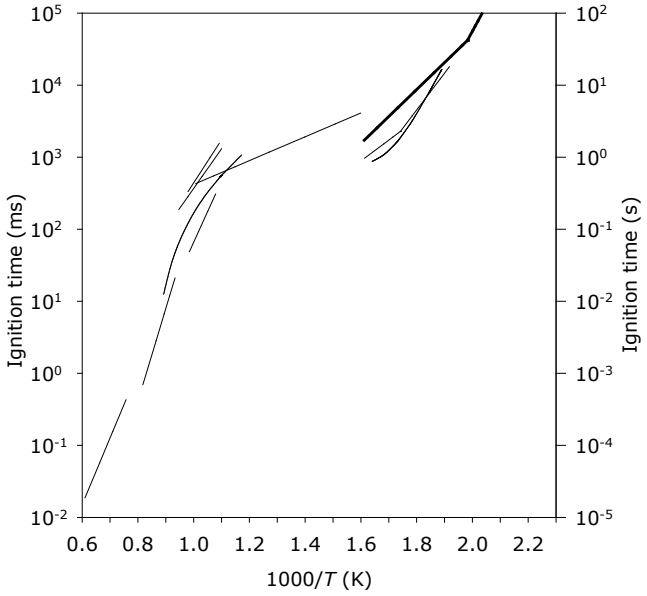


Figure 31 Experimental data for ignition times of *n*-heptane (BM data shown in bold)

Table 3 Effect on ignition time of changing chemical structure of hydrocarbons

Change in chemical structure	Example		Effect on ignition time
	Change from	To	
lengthening chain	*n*-heptane	*n*-octane	decreases
adding side chain	cyclohexane	methyl-cyclohexane	decreases
lengthening side chain	methyl-cyclohexane	ethyl-cyclohexane	decreases
cyclization	1-octene	ethylcyclohexane	increases
saturation	1-octene	*n*-octane	decreases
shifting double bond	1-octene	2-octene	nil

The exact opposite was found for other alkanes: ethane, propane, butane, and pentane[82]. For these gases, the ignition time, at any particular temperature, decreased monotonically with φ. Salooja[83] confirmed the latter finding for a number of other gases. For temperatures in the range of 550 – 750ºC, over concentrations spanning $0.5 < \varphi < 2.0$, the fuels showed a monotonically decreasing ignition time as φ increased. At 800ºC, however, all of the fuels he examined showed very short ignition times which did not detectably vary with φ. Anagnostou et al.[84] used a heated-tube apparatus and found that the results were quite dependent on apparatus minutiae. Nonetheless, they were able to observe that (a) ignition time drops monotonically with fuel concentration, extending even to very rich mixtures; and (b) the ignition time drops monotonically with oxygen concentration, at least over the range 5 – 40% for several hydrocarbon gases that they tested. For kerosene/air mixtures[85], some experimental data show that fuel concentration does not influence the ignition time, if only very lean mixtures are considered. Figure 33 illustrates that a roughly power-law relation is obeyed for ethane/air mixtures even up to extremely rich mixtures. For ethane, the 50% fuel concentration is way above its UFL (12.4%), but combustion is possible since the temperatures involved are very high.

For propane/oxygen/nitrogen mixtures, Jackson and Brokaw[86] found that:

$$t_{ig} \propto X_F^{-1} X_O^{-0.25}$$

where X_F = fuel concentration (mole fraction), and X_O = oxygen concentration. For kerosene/air mixtures, Mullins[87]

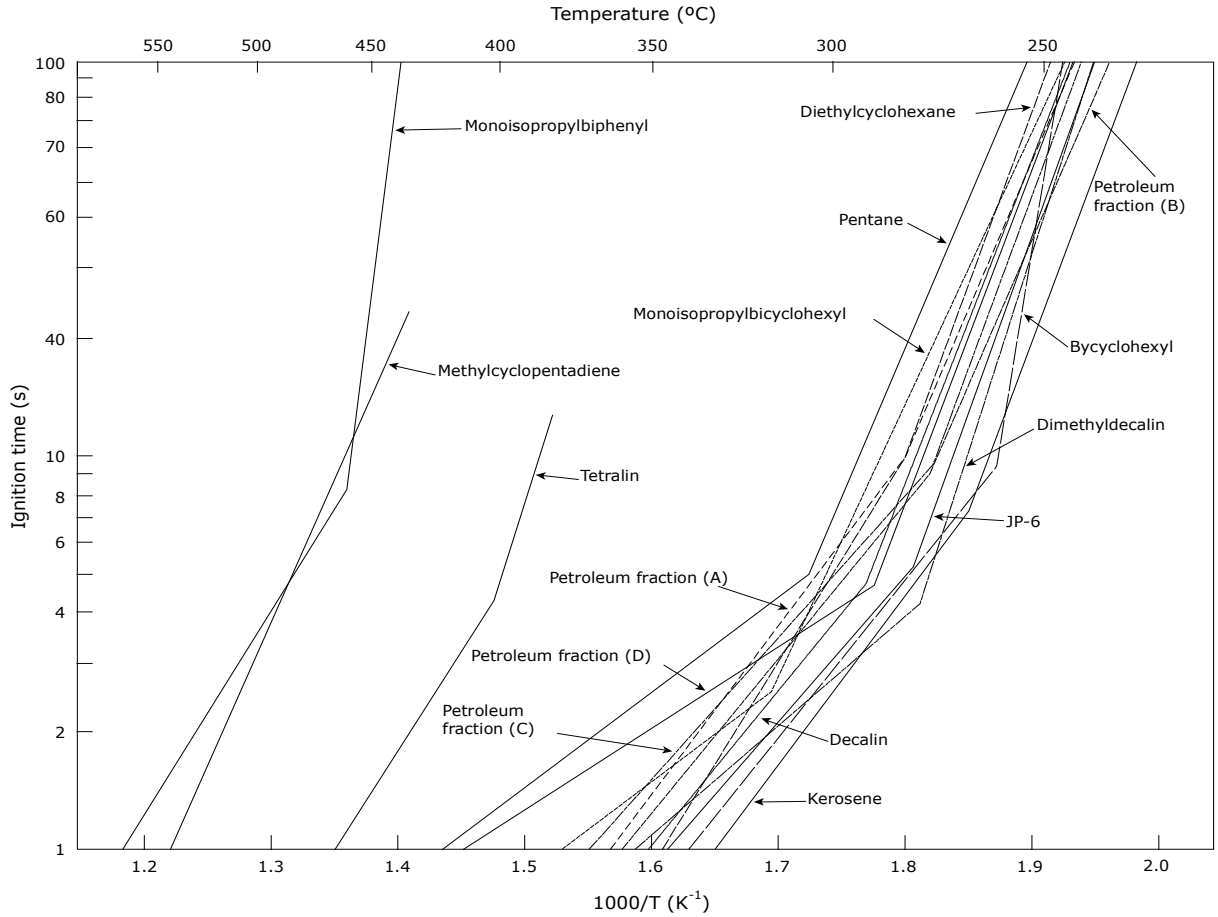


Figure 32 Ignition times for a number of gases measured by the Bureau of Mines

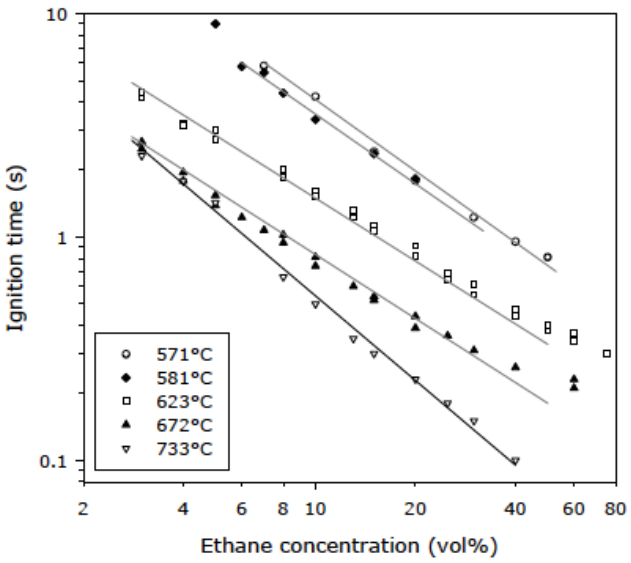


Figure 33 Effect of fuel concentration on the ignition time for ethane

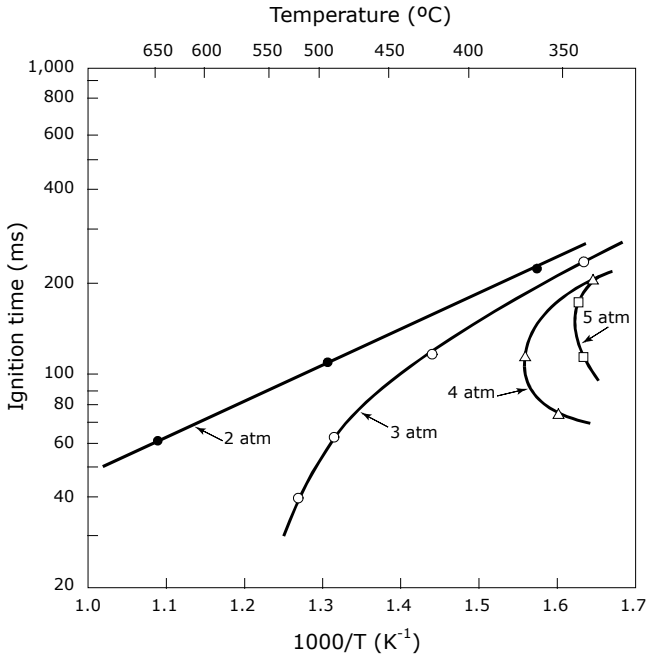


Figure 34 Effect of pressure on the ignition time of pentane

stated the results that

$$t_{ig} \propto (OI)^{-2}$$

where OI = oxygen index (--), but he did not provide experimental details. The most extensive studies, although only on a single fuel, LPG, were done by Miller[61]. Over a very wide range of fuel concentrations, he found no fuel concentration effect and found that the only mixture property that governed ignition times was the oxygen index, OI. His results were given by:

$$t_{ig} = \left(\frac{1}{OI}\right) 4.88 \times 10^{-13} \exp(32{,}400 / T)$$

where T = temperature (K). The conclusion from the above research studies, unfortunately, must be that the experimental results and their derived correlations are in very wide disagreement and that useful recommendations of some generality do not emerge.

EFFECT OF PRESSURE

Increasing the mixture pressure generally shortens the ignition time, as measured by the Bureau of Mines[78] (Figure 34). It has typically been proposed that the pressure-dependence has the form:

$$t_{ig} \propto P^{-n} e^{E/RT}$$

or, alternatively, as:

$$\ln t_{ig} = \left(\frac{E}{R}\right)\frac{1}{T} - n \ln P + a'$$

where the constant a' is different from the a used before. As shown above, Spadaccini and TeVelde concluded that n = 2, but not all experimental results obey this power law. Schihl et al.[88] surveyed the literature and found proposed values to span $0.4 \le n \le 2.5$, although most of the values were between 1.0 and 1.25. Unfortunately, Figure 34 shows that, apart from the pressure dependence, even the temperature dependence no longer follows the expected exponential form at higher pressures.

EFFECT OF FLOW RATE

Jackson et al.[89] studied the ignition of propane/air mixtures using a test apparatus where the fuel and oxygen were separately preheated to the same temperature, then introduced as a flow stream into a mixing chamber. They found that (a) there was an optimum flow rate at which the minimum ignition time was recorded; and (b) this flow rate increased with increasing fuel concentration.

SUB-IGNITION, TWO-STAGE, AND MULTI-STAGE IGNITIONS

Many organic substances, when tested in flask-type AIT tests, show a surprisingly long time to reach flaming ignition—minutes, rather than seconds[90]. This is taken as indirect evidence that much of the induction period is taken up by slow oxidation reactions, and that fast oxidation takes place only at the very end of that period. For some hydrocarbon fuels, over a certain range of pressures and temperatures, ignition occurs as a two-step process. First, a 'sub-ignition,' that is, a cool-flame (weak blue) ignition occurs,

Table 4 Effective activation energy for *n*-heptane ignition

Temperature range (C)	E (kJ mol^{-1})
220 – 300	130
300 – 350	75
350 – 650	30
650 – 1300	170

then some time later this is followed by a hot-flame (orange) ignition. The process is important to designers of internal combustion engines, since it manifests itself as 'knock.' Kane's study[91] provides an example of experimental research on the topic. Photos obtained by Pearlman[92] (Figure 36) illustrate the two-stage ignition process and also show the effect of buoyancy due to normal gravity. In the presence of buoyancy, a heated zone first develops at the top of the test vessel, consequently, reactions are also earliest completed at the top. For unwanted fires, it may be important because a cool ignition could lead to a hot-flame ignition. In systems not involving cool flames, raising the temperature shortens the time needed for reactions to take place. But because of the competing-reactions nature of cool flames, fuel/air systems involving cool flames sometimes show a minimum when ignition time is plotted against temperature. In other cases, a single straight line plot is obtained for both regimes. Figure 35 shows experimental results obtained by D'Onofrio[3]. Since both regimes are correlated by a single line, it can be concluded that, for ethylene glycol, the limiting step of reaction kinetics is identical, irrespective of whether the mixture ignites in a cool flame or in a hot one. Under some pressure/temperature/concentration conditions, multi-state ignitions may occur[11,93]. The whole field of multi-stage and oscillatory ignitions has produced rich possibilities for research in mathematical chemistry, but it has not been readily possible to reduce the findings to tabular or simplified data that might be then applied to safety issues.

IGNITION DUE TO COMPRESSION OR SHOCK

A gas volume can be ignited without the use of a localized external source of energy by raising the pressure of the system. This particular mode is occasionally the cause of unwanted fires or explosions. The primary examples are air compressors (see Chapter 14) and high-pressure oxygen systems (Chapter 13). As far as wanted fires go, in a Diesel engine the fuel/air mixture is ignited by compressing the volume by about 15-fold. The Diesel engine, however, uses

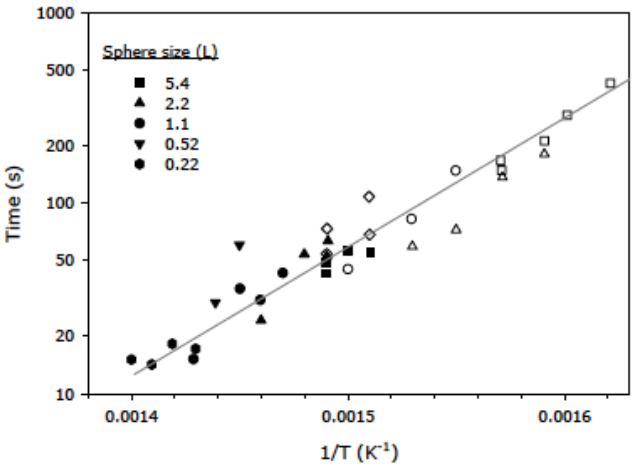


Figure 36 Ignition (solid symbols) and sub-ignition (open symbols) times for ethylene glycol

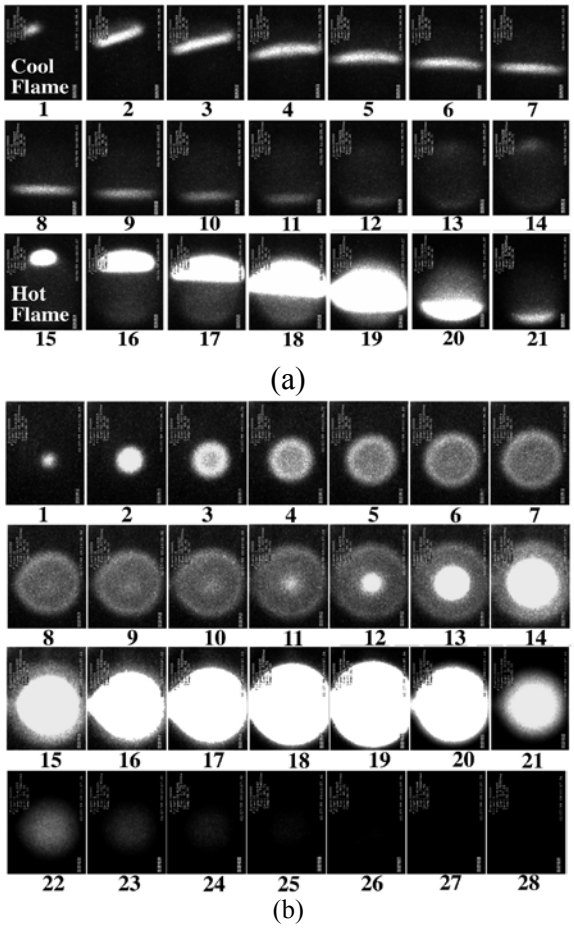


Figure 35 Two-stage ignition in butane/oxygen (50/5) mixture, P = 0.33 atm, T =310°C. (**a) Normal gravity**; time between sequential frames = 1/10 s. (**b) Microgravity**; time between sequential frames = 1/30 s. *(Courtesy Howard Pearlman)*

a mixture which is a liquid aerosol, not a premixed gas mixture. The mathematical basis for predicting compression ignition is treated in Chapter 11.

If compression is rapid, the process can be treated as being adiabatic, since the time available for heat losses to occur is small. Ignition temperatures have been reported from such 'rapid compression machines,' but these have little applicability to non-engine applications, since the ignition temperature is evaluated at some high pressure (typically 10 – 20 atm), and ignition temperature is pressure-dependent (as shown above). In addition, the limits of flammability reported from compression ignition experiments are much wider than for ignition of stagnant mixtures. For example, Shepherd[94] found a flammability range of 2 – 75% for methane/air mixtures undergoing compression ignition. He also found that there is a *maximum* pressure for ignition to occur, and at very high compressions it was not possible to obtain ignition. An additional complication is the need to keep the gas mixture at an elevated temperature for some

time (induction period) before ignition will take place. The fluid dynamics and heat transfer in a rapid-compression environment are highly non-steady, and it becomes hard to interpret the time variable.

Shock waves also form a potential ignition source which acts by compression. However, the same quantitative relations cannot be applied since, unlike piston compression, (a) the compression is not isentropic and (b) multiple wave reflections can be involved, which serve to increase local pressures. Wolański and Wójcicki[95] conducted experiments showing that an abrupt discharge of a fuel gas into the atmosphere can cause a shock ignition if a certain Mach number is exceeded; they also described a numerically-solved model for predicting the necessary ignition conditions. The situation can arise in practice if a pipe containing a fuel gas under high pressure breaks.

Piloted ignition of premixed gases

A mixture of fuel and oxidizer gases does not need to be heated to an elevated temperature for ignition to occur. A mixture of methane and air that is at room temperature and pressure will readily ignite if (a) the mixture proportions are within certain bounds; and (b) a small source of energy (typically, a spark or a pilot flame) is introduced into the mixture. In this Section, we examine the conditions under which piloted ignition will occur. When the ignition energy source is something other than a pilot flame, the term *forced ignition* is sometimes used to emphasize the more general nature of this ignition energy. We shall use *piloted ignition*, however, to include all forms of introduced energy, and not limiting it to pilot flames. Laser ignition is a mode that has some very specific peculiarities and it will be treated by itself.

In this Section, we shall first consider the basic phenomena involved in piloted ignition. Then, we shall examine applied engineering concepts of flammability limits, and the requirements for the ignition energy source. The two main requirements for the latter are the energy amount and a size limit (quenching distance). Concepts behind these energy source requirements are also presented in this Section.

For piloted ignition, it is important to appreciate the distinction between localized combustion and flame propagation. Sources of adequate energy or temperature will cause a *localized* combustion to take place, sometimes referred to as a "flame cap." If the mixture is not within the *flammability limits*, however, combustion will not propagate to other parts of the gas volume. The localized combustion then is basically of no hazard. Flammability limits are addressed later in this Chapter. It will generally be seen that there is no direct connection between the AIT of a particular gas mixture and the temperature which a local-heating agent, such as a hot surface or a hot gas jet, must attain in order to propagate flame throughout the gas mixture.

There have been a variety of dissimilar theories proposed to quantify piloted ignition. In this Chapter, we will discuss only a few selected simpler or newer theories. We refer the reader to Jones[96] for a review of some other theories.

IGNITION WITH THE PRESENCE OF EXCITED SPECIES

The simplest mode of 'forced' ignition involves just a heated surface. In that case only heat energy is added to the system. An electric spark or arc, apart from high temperatures, also contributes excited species and those can help get the combustion chain reaction started. Quite obviously, an existing zone of combustion, i.e., a pilot flame, will also contribute excited species. Ignition of gases by ignition sources involving excited species are thus considered as a group in this section. Ignition by mechanical breaking of current-carrying wires clearly involves ignition by an electric spark. When wires break due to melting out (fusing), the ignition mechanism also involves excited species, as produced by the electric spark the occurs when the wire ends separate. However, to consolidate the presentation of all of the material concerning hot wires, fused-wire ignitions are discussed together with hot-surface ignition in the section dealing with ignition in the absence of excited species.

SPARK IGNITION PHENOMEMA

The theory and fundamental physics of electric spark and arc discharges are presented in Chapter 11. The theory of gas ignition from a spark is given in the next section. Following that, experimental results, apparatus-dependent factors, and data for common gases will be considered. The most important variable relevant to the spark ignition of gases is the *minimum ignition energy* (MIE). A related variable of great importance is the quenching distance. It is found experimentally that flames cannot propagate through very small spaces, and the minimum distance between solid surfaces (which act as heat sinks) is called the *quenching distance*. Quenching distance is of great importance in various flames, not just those ignited by sparks, but it has traditionally been studied—both theoretically and experimentally—in conjunction with spark ignition work. A quantity related to the quenching distance is the *maximum experimental safe gap* (MESG). For reasons to be made clear later, MESG concepts are discussed under piloted ignition in the absence of excited species.

In general, ignition from a spark or an arc between two metallic electrodes can be caused in two ways: (1) by applying a sufficiently large voltage across electrodes held a fixed distance apart, or else, (2) by opening or closing and electric contact. As will be seen in detail below, for fundamental research studies only the first method is suitable. The second possibility, however, can represent actual industrial ignition scenarios, if for instance, a wire breaks and a flammable gas mixture is ignited. Thus, significant research has also been done in geometries where contacts are

rapidly opened and closed in order to test for ignitability. These studies are taken up in a later section.

Even if the fuel/oxidizer ratio is within the flammability limits, ignition will not occur if the gas mixture is confined in a very narrow tube or other enclosure. The walls of such a tube serve to break the chain reaction necessary for combustion to continue. The active radicals which propagate the chain reaction are able, instead, to react with the walls. Such radicals cannot then continue on to reactions which would increase the 'radical pool.'

The first experimental work on quenching distances was published in 1782 in Vienna by Jan Ingen-Housz[97]. This received little notice until the phenomenon was rediscovered in 1815 by Sir Humphry Davy[98]. Davy determined that flames of a methane/air mixture would not travel along a metal tube with a diameter less than 3.6 mm. He also considered that metal tubes were more effective to suppress flame propagation than glass, since the conductivity of metal was much higher. The idea of a minimum diameter was correct, but the notion of ranking the effectiveness according to conductivity was soon disproved. The subject was approached systematically by Holm in 1932 who conducted extensive experiments using a variety of gas mixtures[99]. A minimum diameter of about 3.4 mm was needed for the worst-case CH_4/air mixture, 9.9% methane in air. For 6.5% or 13% mixtures, a diameter of 8 mm was sufficient to prevent propagation, with a parabolic-shaped curve for intermediate mixtures. For coal gas*, the smallest needed diameter was 1.8 mm, for a 21% mixture. For hydrogen, 0.8 mm diameter was found, under the worst-case of 35% mixture. The needed diameters were roughly the same for both tubes and orifices, but Holm learned that an orifice which was adequately sized to prevent initial flame passage must not be heated for a protracted period. If it is , then flame-arresting action no longer holds, and flame is able to break through.

The minimum opening size through which a flame can pass differs, depending on whether the opening is circular, or slot-like (e.g., between parallel plates). Unfortunately, the term 'quenching distance' is often used for both conditions, so the context must make clear which geometry is being considered. The term 'quenching diameter' is applied only to circular openings.

THEORIES FOR SPARK IGNITION, MIE, AND QUENCHING DISTANCE

In this section we consider theories that attempt to predict the conditions necessary for a spark to ignite a gas mixture and the related topic of the minimum size of a flow channel below which a mixture, even if ignited, will not propagate flame. We will generally see that simple theories for spark ignition give results which are only semi-quantitative. Conversely, sophisticated theories have been developed in recent years which appear to be able to predict experimental results to a reasonable accuracy, but these involve a large computational effort and fall into the realm of fundamental research, rather than fire safety applications. The simplest theories are those which endeavor just to relate the MIE to the quenching distance, with one of these two quantities being required to be experimentally determined. Theories for predicting quenching distance without the aid of experimental MIE data have thus far failed to become useful or, as Jarosiński[100] described the situation: "Numerous existing theories connected but loosely with the facts create considerable bewilderment."

The nature of the spark discharge itself is considered in Chapter 11. Here, the question to be addressed is the following. A spark has been discharged into a combustible mixture: Under what conditions will the spark result in an ignition? To answer this question, the microscopic behavior of the *flame kernel* must be considered. A spark raises a small volume of gas to a very high temperature so that any fuel within the volume can be burned. This kernel flame will proceed to grow if the heat that is released in the process of fuel combustion exceeds the heat losses from this volume. The heat release is proportional to the volume of the kernel, but the heat losses are proportional to its surface area. For a sphere, the volume is $^4/_3\pi r^3$ while the surface area is $4\pi r^2$. Thus, the heat release/heat loss ratio is proportional to volume/surface, which in turn is proportional to r. Given this fact, it is not surprising that there exists a minimum size of kernel flame that is necessary for ignition. It is also evident that ignition is simply to be viewed in this case as a growth of the initial flame volume. Conversely, if no ignition occurs, then the volume of flame will not grow. Only a fraction of the energy delivered by the spark is actually available for heating and sustaining the temperature of the flame kernel. The remainder is dissipated as shock wave energy and as heat conduction and radiation. It is empirically found that if the amount of energy delivered by the spark is insufficient, then the flame kernel rapidly decays and extinguishes after consuming only a small amount of fuel. If, on the other hand, the amount of energy is greater than a certain value, a steadily propagating flame occurs, which consumes all of the fuel available. A successful spark ignition theory, then, should be able to predict this minimum energy.

The simplest theory is Litchfield's[181]. He suggested that the MIE and the quenching diameter can be related by means of a simple conceptual model. The flame kernel is viewed as an expanding gas bubble, and the mechanical work needed to expand the bubble to the quenching diameter d_T is taken as being equal to the MIE. In ambient atmosphere tests, the bubble will be at nearly atmospheric pressure, thus $W = PV$, where $P = 1$ atm and $V = \frac{1}{6}\pi d_T^3$. Therefore,

* Coal gas is a mixture of about 50% H_2, 18% each CH_4 and CO, and rest CO_2, O_2, N_2, and miscellaneous hydrocarbons.

$$MIE = 0.053 d_T^3$$

where MIE (mJ) is given solely as a function of d_T (mm). Litchfield noted that experimental data showed this relation to be true, to within about a factor of 2.

Litchfield's theory considers no chemical or thermal properties of the gas mixture. A number of authors suggested taking the basic thermochemical properties into account by considering the energy that must be put into a sphere of diameter d_T in order to raise its temperature to the adiabatic flame temperature T_f:

$$MIE = mC\left(T_f - T_o\right) = \frac{\pi}{6}\rho C\left(T_f - T_o\right) d_T^3$$

In this formulation, the MIE also varies as d_T^3, but with different numeric constants. If a stoichiometric fuel/air mixture in air is considered, then $\rho \approx 1.18$ kg m^{-3}, $C \approx 1.0$ kJ kg^{-1} K^{-1}, and $(T_{ad} - T_o) \approx 1900$ K. Inserting these constants gives:

$$MIE = 1.17 d_T^3$$

This formulation turns out to be of limited use, since the predicted MIE values are about 20× higher than experimentally measured ones.

Pursuing a slightly more sophisticated thermal theory, Lewis and von Elbe[70] proposed the relation:

$$MIE = K\frac{\pi}{4} d_T^3 \rho C T_o \left(1 - \frac{T_o}{T_f}\right)$$

where K (--) is a 'flame stretch factor.' The flame stretch factor is not easily obtained, but if one sets $K = 1$, and inserts the same ambient-air properties as above, then their equation becomes:

$$MIE = 0.24 d_T^3$$

This is more reasonable than the previous result, but is still not as satisfactory as Litchfield's result.

Various simplified conceptual models have also been proposed to predict the needed value of d_T. Lewis and von Elbe[70] consider that the spark rapidly raises the kernel to a very high temperature, many times greater than the adiabatic flame temperature of any fuel/oxidizer mixture. This kernel then grows in size, but decreases in temperature. If flame propagation (i.e., ignition) is to occur away from this kernel, then by the time that the temperature of the kernel has dropped to T_f, the diameter of the kernel needs to have grown to such a size that the temperature gradient between the burned gas in the core and the unburned gas at the edge has approximately the same slope as the temperature gradient in a steady-state laminar flame through this particular fuel/oxidizer mixture. This theory is a *thermal model*, which considers the heat and mass balance within a spherical or cylindrical body. We will assume that the kernel is spherical, which is a fairly reasonable assumption for a spark created by capacitive discharge between two closely-spaced electrodes. Following Turns[101] we express the heat balance of the flame kernel as

$$\dot{Q}''' V = \dot{Q}_{cond}$$

where $\dot{Q}'''$ = heat generated (W m^{-3}), V = volume (m^3), and $\dot{Q}_{cond}$ = conduction heat loss to the cold gas at the edge of the sphere (W). The volume of a sphere is $\frac{1}{6}\pi d^3$, while its surface area is πd^2. The heat generation term can simply be expressed as fuel mass production × heat of combustion. Since fuel is being lost, the latter is a negative quantity $-\dot{m}_F'''$, while the heat of combustion is simply Δh_c. The gas volume inside the kernel is viewed as all being at one temperature; therefore, this is equivalent to a sphere which has infinite thermal conductivity. Outside the sphere, the temperature goes down from T_f at the edge to T_o as $r \to \infty$. To evaluate the conduction losses at the sphere edge, then, the standard expression[102] for a sphere is:

$$\dot{Q}_{cond} = 2\pi d\lambda\left(T_f - T_o\right)$$

Substituting this into the heat balance equation gives the critical kernel diameter d_T as:

$$d_T^2 = \frac{12\lambda\left(T_f - T_o\right)}{-\dot{m}'''\Delta h_c}$$

To obtain a useful expression for the mass loss occurring per unit of flame kernel volume requires a development of laminar flame theory. This is not trivial, since coupled equations are to be solved for chemical reaction, heat transfer, and diffusion. Instead, we shall simply quote the results from Turns:

$$\dot{m}_F''' = \frac{-\rho S_L^2}{2\alpha\left(r_o + 1\right)}$$

where α = thermal diffusivity (m^2 s^{-1}), S_L = laminar flame speed (m s^{-1}), and r_o denotes the stoichiometry of the combustion reaction according to the definition:

$$1\,\text{kg fuel} + r_o\ \text{kg oxidizer} \rightarrow \left(r_o + 1\right)\text{kg products}$$

In laminar flame theory, a chemical kinetics calculation can be made in order to estimate the laminar flame speed S_L. For our purposes, it will be sufficient to treat S_L as an experimentally determined quantity (see Chapter 3). Thus, d_T can be evaluated as:

$$d_T^2 = \frac{12\lambda\left(T_f - T_o\right)2\alpha\left(r_o + 1\right)}{\rho S_L^2 \Delta h_c}$$

But the heat of combustion Δh_c of 1 kg of fuel goes into raising the temperature of $(r_o + 1)$ kg of products from T_o to T_f. Thus

$$\Delta h_c = \left(r_o + 1\right) C\left(T_f - To\right)$$

This gives an expression for the critical flame kernel diameter as:

$$d_T = \sqrt{24}\frac{\alpha}{S_L} = 4.9\frac{\alpha}{S_L}$$

As Turns points out, the multiplying constant of 4.9 should not be viewed as anything more than qualitative, due to

some extreme simplifications which were made in solving the problem. Not only was the whole system assumed to be isothermal, but even for temperature-dependent variables such as α it is not at all clear what reference temperature needs to be selected. Having said that, however, the dependence of d_T on α/S_L is a useful result, and one which recurs in some much more ambitious theories.

Another approach was taken by Ballal and Lefebvre[103], who undertook to predict both the MIE and the d_T for: (a) quiescent, slightly turbulent, and very turbulent flow conditions; (b) gases, monodisperse aerosols and polydisperse aerosols; and (c) various stoichiometry conditions. Their theory was primarily based on dimensional reasoning and was not a detailed solution of conservation equations. Nonetheless, they found agreement with experimental data. The equations, although closed-form, were lengthy and cumbersome, so we give here solely their results for gases under quiescent conditions. For these,

$$d_T = \frac{10\alpha}{S_L}$$

This is the same as our previous result, but with a different multiplying constant.

A slightly different thermal theory was proposed by Friedman[104] who suggested the relation:

$$\frac{d_T S_L}{\alpha} = k\left(\frac{T_f - T_{ig}}{T_{ig} - T_o}\right)^{1/2} = Pe$$

where d_T = quenching diameter (m), S_L = laminar flame speed (m s^{-1}), α = thermal diffusivity (m^2 s^{-1}), k = a constant, and the subscripts denote f = flame, ig = ignition, and o = ambient. The non-dimensional grouping of constants Pe is identified as the *Peclet number*. The temperature at which quenching occurs is not known *a priori*. But, if it can be approximated that T_{ig} is roughly proportional to T_f, then the whole right hand side of the equation becomes approximately constant, and for most fuels Pe ≈ 46. Expressed[105] on the basis of the parallel-late quenching distance d_{II} instead of d_T, Pe ≈ 40. Subsequently, Mayer[106] showed that Pe increases slightly with increasing T_{ad}, and increases significantly with increasing activation energy of the combustion reaction. However, since lumping all of flame chemistry into a single activation energy is a gross empiricism and its value cannot be foretold from more fundamental considerations, it did not appear that such relations were going to be helpful. Furthermore, even if this were successful, it would be much easier to actually measure d_T than to accurately determine both S_L and α. A large number of later, more sophisticated theories have been reviewed by Potter[107]. None of them offer any greater help in interpreting, collapsing, or extending empirical results than the simple relationships given above.

Experimentally[100], it has been found that:

$$\frac{d_{II}}{\delta_L} = 2.0 \text{ to } 2.2$$

where δ_L = laminar flame thickness. That is unsurprising, although the relation is not all that useful, since δ_L is not a quantity that is simple to measure, nor is it widely tabulated.

The relation between the parallel-plate quenching distance d_{II} and the quenching diameter in a tube, d_T, has been found to be[107]:

$$d_{II} = 0.65\, d_T$$

Note that there is no difference between the parallel plate geometry and the geometry where flanged electrodes are used (described later in this Chapter).

For turbulent, flowing gas mixtures, Ballal and Lefebvre[161] proposed the relations:

$$d_{II} = \frac{10\alpha}{S_L - 0.16u'} \qquad \text{if } u' < 2S_L$$

$$d_{II} = \frac{10\alpha}{S_T - 0.63u'} \qquad \text{if } u' > 2S_L$$

where S_T = turbulent flame speed (m s^{-1}), and u' = turbulence intensity (m s^{-1}).

More accurate results might be expected if additional phenomena involved in the flame initiation are included. The phenomena are very complex, since the spark discharge causes a tiny, localized shock wave to be propagated and the energy going into this shock wave is a crucial factor determining ignition or non-ignition. Thus, it was not until 1980 that a model was developed which includes some of these advanced features[108]. According to Adelman, the critical kernel diameter is the same as the critical quenching diameter d_T which is experimentally found to be $b\alpha/S_L$, where b = 10 to 16. For ignition to occur, when kernel reaches the critical diameter, the kernel must be expanding at a speed at least equal to the laminar flame speed. From his theory, a relation for MIE was developed:

$$MIE = \frac{\pi}{4}\left(\frac{\gamma}{\gamma - 1}\right) d_g P d_T^2$$

where d_g = spark gap (m), P = pressure (Pa), d_T = critical kernel diameter (m), and = 1.4 for air. To compare with the simpler theories, if $d_T = d_g$ = 2 mm and P = 1 atm, then Adelman's theory predicts MIE = 2.3 10^{-3} J = 2.3 mJ. Experimental values of MIE for gases having d_T ≈ 2 mm are typically found to be 0.3 – 0.5 mJ, so the prediction is not very accurate. By contrast, Litchfield's simplistic theory predicts MIE = 0.4 mJ, so unfortunately the more sophisticated theory does not give better results. Adelman also predicted that the time period for the energy pulse must be greater than about 1 μs for ignition to occur.

A new theory was offered by Frendi and Sibulkin in 1990[109], which required knowing the diameter over which

the spark energy will be deposited. At the smallest diameters, it led to a predicted MIE for methane about 70× lower than the measured value. Sloane and Ronney[110] concluded that the huge discrepancy was because Frendi and Sibulkin simplified the chemistry by using only a 1-step global Arrhenius reaction rate. Their own model, using detailed chemical kinetics, indicated an MIE, valid over a b road range of small deposition diameters, which quite closely matched the experimental value; as might be expected, their model is highly complex and requires detailed computer simulations to be run for each case. Sloane and Ronney's detailed calculations also showed that the energy required for ignition rises if the spark energy is deposited over too-broad a region. For a minimum value of ignition energy to be reached for methane/air mixtures, the region over which the energy is deposited had to be no greater than ca. 0.6 mm diameter. Even though a reasonable result is computed by the Sloane/Ronney theory, it requires as input the diameter over which the spark energy is deposited. Clearly, the theory is incomplete, because this diameter is not under the control of the experimenter. Other purely-computational theories have also been presented[111].

The usefulness of a particular theory depends on the time scale of the spark discharge. For very rapid spark discharges (1 μs), high pressures (> 200 atm) are created in the spark region, and complex hydrodynamic phenomena, including shock waves, become important[112]. For the more typical slower discharges (50 – 100 μs), these phenomena play a smaller role and thermal theories can have a reasonable utility, at least qualitatively.

It has been proposed[56] that there is a relationship between the induction period measured under autoignition conditions, and the minimum spark energy needed for ignition for spark-induced ignition. If the time required for the spark to cool down to the AIT is shorter than the induction period, then ignition will not occur.

All of the theories give the basic result that $MIE \propto d_{II}^3$. A large amount of Bureau of Mines data that Lewis and von Elbe collected are shown in Figure 37 along with the correlation:

$$MIE = 0.07\, d_{II}^2$$

where MIE = min. ignition energy (mJ) and d_{II} = quenching distance (mm). It can be seen that the experimental data follow a proportionality to the power 2, and not to the power 3. The reason why the data do n ot fall along a line of slope 3 is because of the flanged electrodes that were used in the Bureau of Mines studies. Ballal and Lefebvre[161] conducted experiments where the electrodes were 2 mm rods, and found that a power-of-3 relation *was* obtained.

Pitt et al.[113] argued that the poor agreement of even the complex theories was because of an incorrect assumption as to the basic fluid dynamics. As shown in Chapter 11, the spark kernel has a *toroidal* shape over most of the critical

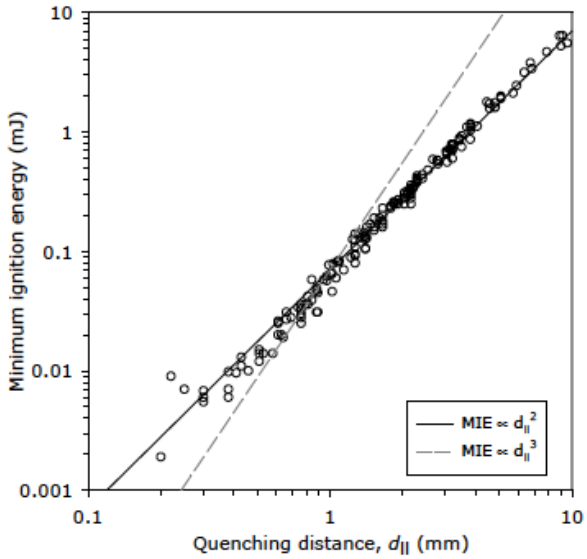


Figure 37 The relation between d and MIE, based on data with flanged electrodes (data for hydrogen, methane, ethane, and propane are included, but there is no effect of fuel type on the relation)

time period, but modeling of this shape is very complicated, partly because the structures become turbulent after an initial laminar growth period. Pitt et al. themselves made substantial progress in fluid-dynamical modeling of the problem, but did not evolve a theory to the point of providing a predictive equation. Most other modelers simplify matters by presuming the shape to be *spherical*. Anderson and Lim[114] concluded that sphericity is a very reasonable assumption despite the toroidal appearance. They measured separately the volume and the surface area for a large number of spark kernels and found the relation is $V \propto A^{1.51}$. This is very close to the relation for a sphere, which is $V \propto A^{1.5}$.

The minimum energy MIE decreases with increasing pressure or increasing initial temperature. Fenn[115] proposed that the relation is:

$$MIE \propto \frac{(T_f - T_o)T_o}{X_o^{3/2} P^2} \exp(3E / 2RT_f)$$

where T_o = initial mixture temperature (K), T_f = adiabatic flame temperature (K), X_o = mole fraction of oxygen in mixture, P = ambient pressure (Pa), and E = activation energy (kJ mol^{-1}). Since the activation energy will differ for each gas and is not necessarily easily obtainable, Fenn further proposed it can be estimated as:

$$E = 67\, T_{LFL}$$

and T_{LFL} = flame temperature at the LFL (K). If the LFL is known from experiment, then the flame temperature at the LFL can be calculated from theory. Fenn provided extensive validation data showing that the agreement with his equation, while not highly precise, is accurate enough for many practical purposes.

IGNITION FROM BREAKING WIRES OR MOVING CONTACTS

UK coal mines in the early years of the 20th century used to have bell signaling circuits powered by 24 VDC. Originally it was thought that arcing from such power supplies would be non-incendive, but accidents soon proved this wrong[116]. These circuits contained inductive elements, such as iron-core bell coils, relays, and other devices. Thus, for many years the Safety in Mines Research Establishment (SMRE) conducted studies on ignition of gases from low-voltage, inductive circuits. Contact arcs or sparks are not limited by Paschen's Law (see Chapter 11), thus discharges can occur at low voltages.

In laboratory breaking-wire experiments, a wire is notched, then pulled apart by two opposing rollers. Once the wire breaks, the two ends comprise electrodes of finite size and their mass can act as a quenching mechanism. Thus, Lord et al.[117] showed that broken-wire ignitions take place at lower currents if the wires are broken very fast or if the wire gauge is very fine. They used the same 24 VDC power supply and an inductance coil of 95 mH, similar to what was used for standard testing by SMRE. For an 8.3% methane/air mixture, the SMRE 'Break-flash No.3' apparatus* which uses a pair of electrodes moving at slow speed to create the arc, gave a minimum current of 185 mA. In Lord's tests, thin copper wires notched and then broken by rapidly pulling apart required currents of 100 – 115 mA. Thick copper wires broken apart needed 160 mA. Very thin tungsten wires (0.025 mm) needed a current of 82 mA. The differences were attributed to quenching. When a flame kernel is forming, the metal parts act to quench it. This quenching will be minimized if the metal parts are either removed very fast from the kernel, or else if they are very small to begin with. The theoretical value of energy that can be stored in an inductor, and therefore delivered from it into a contact spark is $\frac{1}{2} LI^2$, where L = inductance (H) and I = current (A). Based on this theoretical value, in early SMRE experiments[118], about 1.0 to 2.5 mJ was needed to ignite methane/air mixtures. But building on the ideas of Lord and using an optimum circuit inductance and 0.025 mm wire, Berz[119] found a minimum ignition energy of 0.3 mJ which is very close to the 0.2 mJ value commonly cited for capacitive discharge. In actual testing of the potential for breaking parts to ignite gas mixtures, ultimate limits such as the one shown by Berz will not be reached. Thus, practical testing devices (see Chapter 12) simulate realistic heat sink effects, not minimal ones.

Circuits with capacitive elements are also likely to be found in modern electronics. Zborovszky[120] studied in detail the current needed to cause a break-spark discharge in a capacitive circuit. There can, in the general case, be three resistances in such a circuit, one is series each with the power supply, the capacitor, and the break-spark contacts. She considered the simplest case where a resistor exists in series only with the power supply (Figure 38). There are four basic regimes of ignition from such a circuit. To the left of point A, the circuit acts as a purely-resistive circuit. Between point A and point B, the charge on the capacitor contributes some energy, but the major part of the energy comes directly from the power supply. Between point B and point C, the bulk of the energy comes from the charge on the capacitor, while beyond point C, ignition energy is drawn only from the charge stored on the capacitor, and the energy flowing from the power supply is negligible. Observations also indicated that to the left of point B, ignition occurs at a break-spark, while to the right of point at a make-spark.

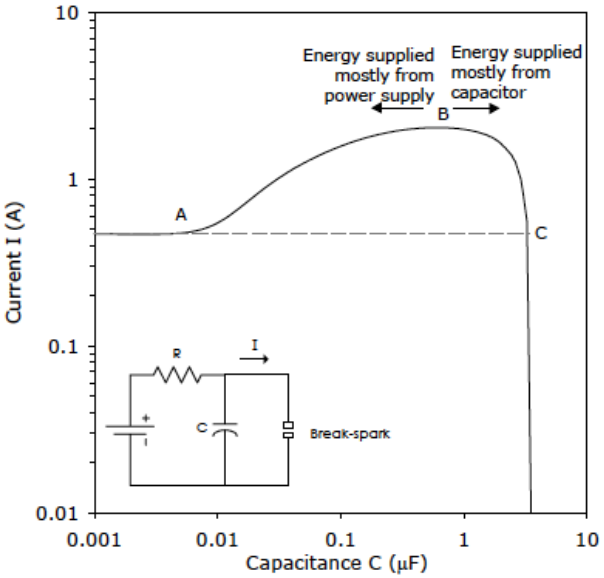


Figure 38 Current needed for ignition of an 8.3% CH_4/air atmosphere using the IEC/PTB break-flash apparatus (IEC 60079-11) fed from a 30 V power supply. At lower supply voltages, the curve would move up and to the right.

In a circuit where resistance plays a minimal role, the loss of energy into the electrodes of a break-spark arrangement can be demonstrated in a plot of capacitance versus voltage required for ignition. If there were no losses, then the voltage required would be:

$$V = \sqrt{\frac{2 \times MIE}{C}}$$

in other words, the results should fall on a line of slope = – ½, when plotted on a log-log scale. The data collected by Magison[149] on methane/air mixtures are shown in Figure 39; the slope is ≈ – ½ for higher voltages, but deviates significantly at lower voltages and a plateau is reached at around 10 – 20 V. This is consistent with a minimum voltage of 10 – 15 V needed to sustain an arc discharge (see Chapter 11).

Some similar data were obtained by Thomas[129], even though he used a capacitive discharge circuit having a non-

* A break-flash or break-spark apparatus involves a cam-operated set of contacts which keep being opened and closed as the cam rotates. This type of test equipment is further discussed in Chapter 12.

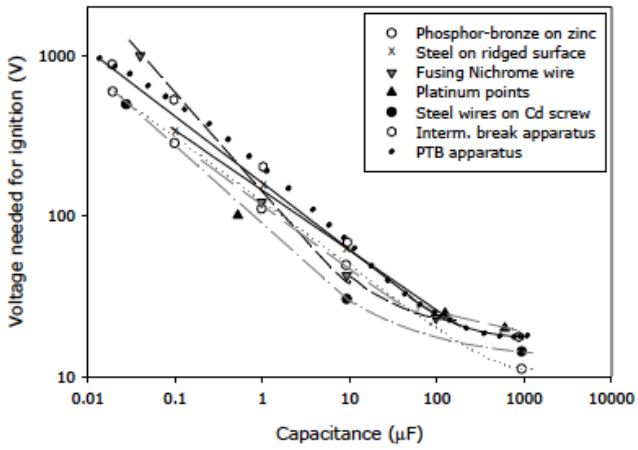


Figure 39 Ignition of methane/air mixtures from break-spark capacitive discharge

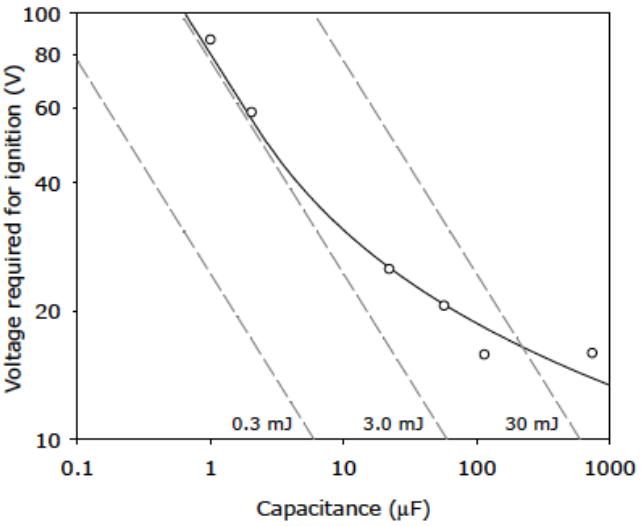


Figure 40 Ignition of 8.5% methane/air mixtures by low-voltage capacitive-discharge sparks (shown in gray are constant-energy contours)

standard arrangement where two pointed electrodes were brought slowly together. Figure 40 shows that, due to quenching effects at small electrode spacings, substantially more energy is needed than the 0.3 mJ that would be required in a circuit where a capacitor charged to a high voltage is discharged across stationary electrodes. The data points are for a circuit where there was essentially zero resistance in series with the capacitor. Thomas also noted that for capacitances greater than about 100 µF and a non-zero resistance (not shown), the ignition curves are nearly horizontal, indicating that a minimum voltage—rather than minimum energy—criterion is governing.

The most common arrangement for break-spark testing is an inductive circuit, with the reported result being the minimum igniting current (MIC). The MIC is dependent both on the circuit voltage and on its inductance[121], as shown in Figure 41. The circuit inductance of 0.095 mH is commonly selected for use in standardized testing, since it corresponds, in most cases, to the end of the plateau portion of the curve. The numerical values refer only to the SMRE Intermittent Break-flash apparatus; Zborovszky[237] has shown that somewhat different results are obtained in the IEC/PTB break-flash apparatus. Methane concentration of 8.3% is used, since this was found to be the most easily ignitable concentration. For a circuit containing a resistance R and an inductance L in series with a power supply of voltage V_o, the energy delivered into the discharge is[122]:

$$E_d = V_m\left[(V_o - V_m)\frac{t_d}{R} + \left(\frac{V_o}{R} - I_m\right)\frac{L}{R}\right]$$

where V_m and I_m are the minimum voltage and current pertinent to the contact materials in question (see Chapter 11) and t_d = discharge duration:

$$t_d = \frac{L}{R}\ln\left(\frac{V_m}{V_m - V_o + I_m R}\right)$$

The value of E_d is greater than the stored energy in an inductor, $\frac{1}{2}LI_o^2$, since part of the energy comes directly from the power supply and not from the inductor; here $I_o = V_o/R$. Note that the equation for t_d indicates that the discharge stops once the current decreases to I_m. The derivation of the above equations presumes that the voltage across the gap is V_m; this is not true if the separation speed is very high, and no simple equations exist in that case.

Figure 42 shows data collected by Magison[149] on the effect of experimental conditions and of inductance for high-inductance circuits. A slope very close to –½ is seen in the high-inductance regime. Also shown are Gehm's data[123] on the minimum current necessary to create a spark that is visible in a dark room.

In a circuit where resistance is the only impedance element present, there is a definite—although not simple—relation between circuit voltage and the MIC and Figure 43 shows results obtained in the SMRE Intermittent Break-flash Apparatus. The results should be viewed as indicative and not absolute, since different values are found using different test rigs[124,129]. UK authorities have used relations of this kind to approve dry cells for use in intrinsically-safe mine equipment that are intended for use in non-inductive circuits. The effect of adding inductance to a resistive circuit is to lower the two leftmost branches of the curve shown in Figure 43; the rightmost branch is unaffected by inductance. Sufficient data points are not available in Figure 41 to derive smooth curves, but it can be seen that they would fall as indicated if plotted on Figure 43. Note also that the minimum voltage of 4 V found needed to ignite a flammable mixture with the SMRE Intermittent Break-Flash apparatus is close to the limit of 5 V that Vogt found needed in fused-wire experiments, as discussed below. These are extreme

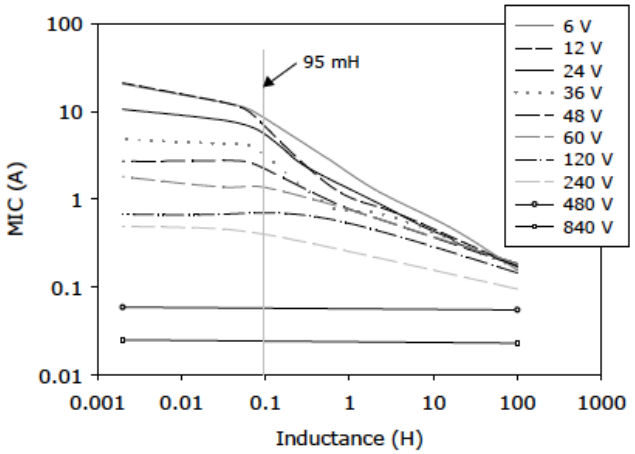


Figure 41 Effect of voltage and inductance on MIC for methane/air mixtures using the SMRE Intermittent Break-flash Apparatus

cases and typically a lower limit of 8 – 15 V is reported in purely resistive circuits. In inductive circuits, however, ignitions have been reported at the 0.5 V level[125], and lower-yet values are not precluded.

The speed at which a contact is opened or pulled apart influences the results. Apart from the quenching effect already discussed above, the voltage/current/time/gap-distance relationship for the spark channel and the associated circuit must be considered. For inductive circuits, at high levels of inductance, a fast break is the most incendive, while for low inductance values a slow break or repeated (intermittent) breaks are most incendive[149].

The role of the discharge time in break-spark experiments with inductive circuits is not fully clear. In one series of tests[126], it was found that conditions were most incendive if spark duration was around 3 ms; discharges that only lasted

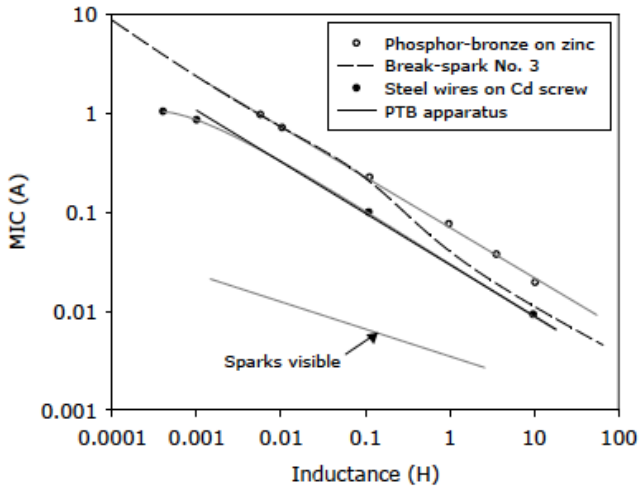


Figure 42 Effect of circuit inductance on the ignition of 8.3% methane/air mixtures in high-inductance circuits

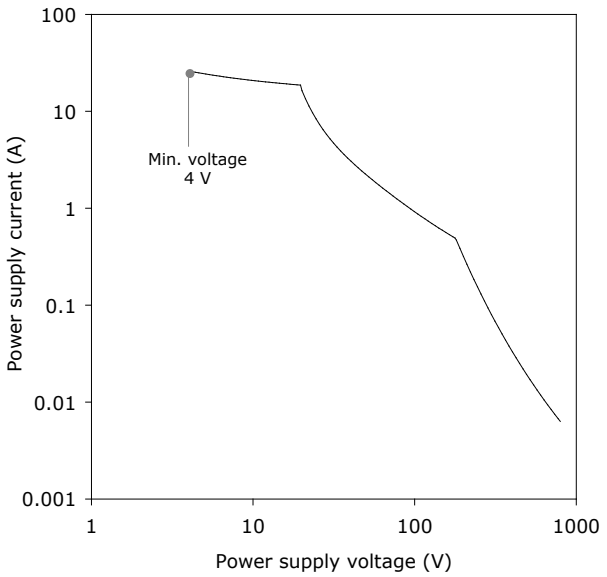


Figure 43 Ignition of 8.3% methane/air mixtures with a resistive circuit: relation between voltage and MIC (SMRE Intermittent Break-flash test apparatus)

microseconds were typically non-incendive (Figure 44). But in another study, varying the spark duration over the range 10 – 30 µs showed no systematic effects on the minimum energy required for ignition[127]. Most of the studies with capacitive discharges have been under conditions of a high voltage causing a breakdown between stationary electrodes, not the creation of an arc or spark by opening a contact in a low-voltage circuit. The issue of spark duration for those conditions is considered later in this Chapter.

The metal used for the electrodes affects the results. The relation is not simple, since different rankings are obtained when testing under conditions of (a) rapid separation, low voltage, and high inductance; or (b) slow separation, high voltage, low inductance. In the former case, it is necessary that the metal be both hard and of a high boiling point for

Table 5 Effect of contact metal on incendivity for slow-separation, high-voltage, low-inductance break-sparks

Metal	Melting point (°C)	Resistivity (nΩ-m)	Incendivity of sparks
tin	232	115	most incendive
cadmium	321	68	
zinc	420	59	
beryllium	1287	35.6	
chromium	1907	125	
aluminum	660	26.5	
nickel	1455	69.3	
iron	1538	96.1	
copper	1085	16.8	
silver	962	15.8	least incendive

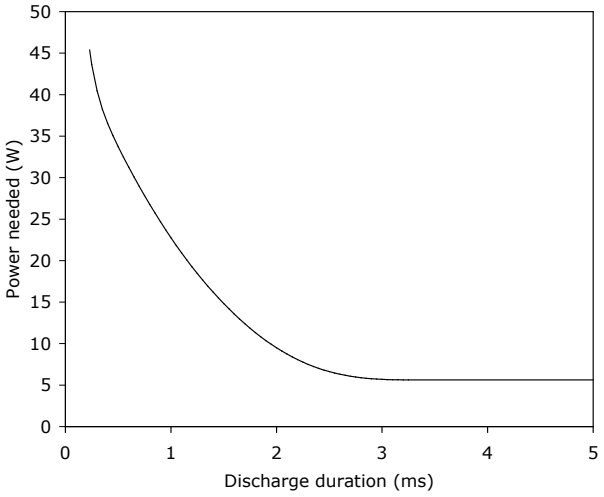


Figure 44 Circuit power necessary for ignition of an 8.3% methane/air mixture using the IEC/PTB break-flash apparatus (27 VDC power supply, resistive circuit, spark at a tungsten wire separating from a cadmium plate)

the most incendive results to be obtained. Tungsten is the most incendive under those conditions. In the latter case, the opposite prevails—soft, low melting-point metals are found the most incendive. These include cadmium, zinc, and magnesium. According to German studies[128], the rank ordering of contact metals under those conditions is as shown in Table 5. Thomas[129] summarized some of the early research on this topic, but simple guidance was not possible under all conditions.

Fuel concentration strongly affects the MIE value in the case of high-voltage capacitive discharge sparks. But for break-sparks, experiments showed that it affects the results only to a small extent, provided the mixture is well within the flammability limits[237].

From the above discussion, it can be seen that, apart from details of test electrodes, the main parameters determining whether or not a given flammable gas atmosphere can be ignited are:

- the voltage available from the power supply
- the current available from the power supply
- the nature of the circuit elements.

To determine if an actual electric device can ignite the given atmosphere, testing is normally required, since the effective values of circuit capacitance or inductance may not be easy to calculate. Procedures for used for this type of testing are described in Chapter 12.

PILOT FLAME IGNITION

The introduction of a pilot flame into a fuel/oxidizer mixture well within its flammable limits will not necessarily result in ignition of the mixture. As early as 1906, Beyling[130] pointed out that a flame may be ejected from

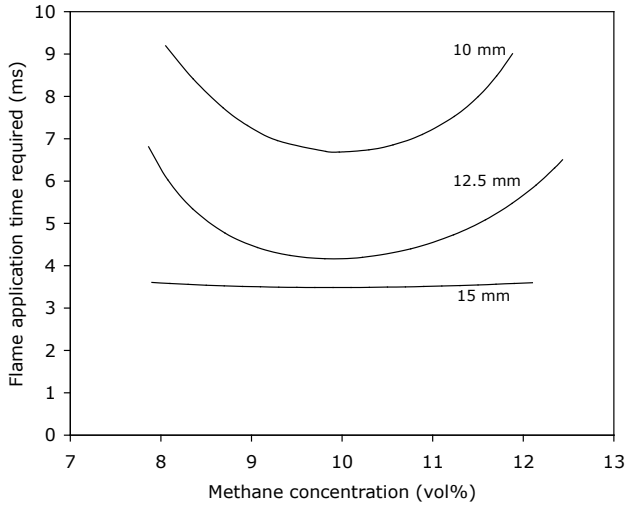


Figure 45 Ignition of methane/air mixtures by a pilot flames of various lengths

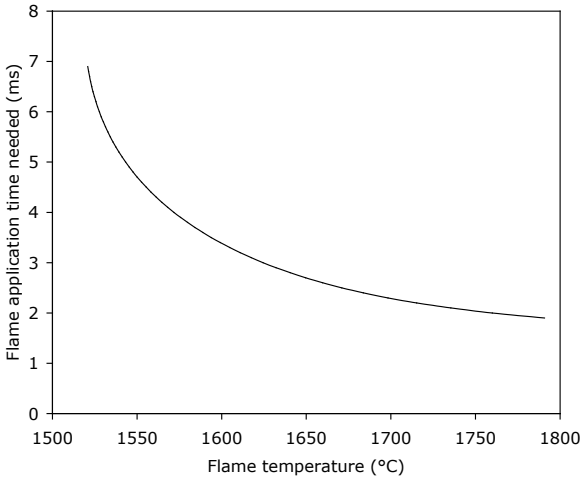


Figure 46 Flame application time needed to ignite methane/air mixtures of optimum ignitability with a small flame

small openings of a vessel wherein an explosion was taking place, yet fail to ignite a flammable mixture located outside the vessel. The concept is also well-known in the testing of 'permissible explosives,' which may emit a flame yet fail to ignite a flammable atmosphere. In general, studies have shown that for ignition to occur, the flame has to:

- have a sufficient temperature
- be of sufficient size (i.e., high enough HRR)
- be applied for a sufficient time

In 1926 Walls et al.[131] measured the time that it takes for a small, downward-pointing pilot flame to ignite methane/air mixtures. The results (Figure 45), not surprisingly, show that the minimum time required is near the stoichiometric concentration (9.5%), although slightly above it. Perhaps less expected is the substantial effect of the igniting flame

size on the time required. In additional tests using a different apparatus, where flame shape and dimensions were not specified, the authors varied the flame temperature and measured the application time needed for ignition (Figure 46).

Wolfhard and Burgess[132] later demonstrated that the temperature of a pilot flame capable of igniting the mixture is unrelated to the AIT of the mixture. In studying methane/nitric oxide (NO) mixtures, they determined an AIT value of 1110ºC, but the temperature of pilot flames had to reach 2100 – 2300ºC (varying slightly with the fuel type used for the pilot) for pilot-flame ignition to occur. Somewhat higher pilot flame temperatures were required at very low pilot-flame flow rates. Observations indicated that ignition of the mixture occurs not near the main reaction zone of the pilot flame, but above the visible tip of the pilot flame. It was also found that fuel-lean pilot flames ignited mixtures more readily than pilot flames operating at stoichiometry. Wang et al.[133] proposed a s teady-state theory relating the length and velocity of the pilot flame to the burning velocity of the gas mixture, but its experimental validity is not clear.

A number of anomalies have been discovered with pilot flame ignition of fuel/air mixtures. Sawerysyn[134] et al. found that, under some circumstances, introducing a pilot flame into a stagnant methane/air mixture somewhat above its LFL did not result in flame propagation. They attributed this to the dilution effect of the pilot flame's combustion products. For ignition to occur, a location has to exist where the fuel/air mixture ratio is favorable and the temperature is sufficient. The experiments of Sawerysyn indicated that there can be an absence of a location of this kind. Not surprisingly, then, their work also showed that, under some circumstances, a smaller pilot flame was more effective in causing rapid, complete combustion of the gas/air mixture than was a larger flame. Conversely, Karim et al.[135] studied the ignition of flowing fuel/air mixtures with pilot flames and found that these were flammable in some cases at lower fuel concentrations than published in standard tabulations. This was attributed to the heating effect of the pilot flame on the flowing gas mixture.

Gases which contain halogen atoms can be difficult to ignite with a flame, since halogens interfere with chain propagation needed for combustion. According to Jones[136], such substances are more easily ignited by a spark but his study did not establish quantitative trends.

IGNITION BY BURNING PARTICLES

It is not difficult to ignite gas mixtures with burning particles, which may be friction sparks, flying brands, etc. Sparks caused by metal tools impacting upon solid objects are a well-known cause for coal mine explosions. In warfare, burning particles are exploited in incendiary weapons. Homan and Sirignano[137] examined the propensity of burning aluminum particles to ignite methane and propane mixtures. For methane/air mixtures near $\varphi = 1$, the minimum particle diameter was found to be 20 μm. For $\varphi = 0.6$, about 80 μm particles were needed, while for $\varphi = 1.4$ about 40 μm. For propane, the minimum size was found to occur not at $\varphi = 1$, but rather at φ of 1.3 to 1.8; a diameter of 20 μm being needed in that range. For $\varphi = 1$, a diameter of 40 m was needed, for $\varphi = 0.6$ around 100 μm, and for $\varphi = 2.1$ around 40 μm. The energy delivered by the burning metal particle is the product of the particle's mass times Δh_f, the heat of formation of the metal oxide (minus sign disregarded). Thus, a 20 μm diameter aluminum particles delivers

$$E = \frac{1}{6}\pi d^3 \rho \cdot \Delta h_f = \frac{1}{6}\pi \left(20\times10^{-6}\right)^3 2700\times31\times10^6$$
$$= 0.35 \text{ mJ}$$

where the heat of formation of Al_2O_3 is -31×10^6 J kg^{-1}. A comparison of the aluminum particle results with those for spark ignition showed that, to within the expected accuracy of the determination, there was no difference in the MIE obtained by the two methods. By comparison, an aluminum particle which was at the same 2300 K temperature as a burning one, but without combustion taking place, would have to be of 140 μm size under conditions where a 20 μm burning particle sufficed for ignition. Additional information on this topic is given in Chapter 11.

VARIABLES AFFECTING IGNITION OF GASES WHEN PILOTED WITH THE PRESENCE OF EXCITED SPECIES

In this section we consider the effects that various variables have on the piloted ignition of gases that involves the presence of excited species. The information is generally restricted to ignition from a high-voltage capacitive discharge circuit. There is almost no information of this type for ignition from pilot flames, burning particles, or other forms of ignition that entails the presence of excited species. As discussed above, the behavior of fuel-air mixtures when ignited from low-voltage sparks generated by making or breaking electric contacts can be quite different from that when ignited by a high-voltage spark passed between stationary electrodes. However, again there is not much systematic information on the effects of chemical or physical variables.

CHEMICAL NATURE OF THE FUEL

The theories considered above indicate that the quenching distance depends on the laminar flame speed (S_L) of the gas and that, in turn, MIE depends on the quenching distance. Thus, MIE should be a function of S_L. This was explored to a very limited extent by researchers in the 1950s. Metzler[138] proposed a correlation that $S_L \propto \text{MIE}^{-0.8}$. Potter and Berlad[139] suggested that the laminar flame speed and the quenching distance are related as:

$$S_L d_{ll} = 1.2\times10^{-4} T_o T_f$$

where S_L = laminar flame speed (m s^{-1}), d_{ll} = quenching distance (m), T_o = ambient temperature (K), and T_f = flame temperature (K). Further research appears not to have been

pursued in this vein. The reason is a practical one—it is much easier to obtain a reliable value for MIE or d_{II} than it is to measure S_L to a reasonable accuracy.

Within a given chemical family, for fuel-rich mixtures, the quenching distance decreases with increasing molar mass of the fuel[107]. A dependence has not been documented for lean mixtures.

OXYGEN CONCENTRATION

Increasing oxygen concentration lowers the MIE as does increasing the total pressure of the mixture. This is illustrated in Figure 47 and Table 6. Chin[140] proposed that MIE is proportional to oxygen concentration to the –4 power. This appears to be a rather high exponent, and Ural et al.[141] noted that the data of Lewis and Von Elbe[70] are better represented by $MIE \propto (OI)^{-2.5}$, where OI = oxygen index, $O_2/(O_2+N_2)$, with the propane data following the power law:

$$MIE_{propane} = 0.0034 P^{-2.1} (OI)^{-2.5}$$

where at any OI value, the propane concentration used was the one giving the lowest ignition energy. Whether this has applicability to other gases can be tested, to a limited extent, by plotting Litchfield's data from Table 6 according to a –2.5 power law. Figure 48 shows that the results for acetylene are well predicted; however, for the remaining three gases the expected slope is not followed.

The effect of oxygen concentration on the quenching distance of methane is illustrated in Figure 49[142]. For tests run in O_2 instead of air, quenching distances about a factor of 5 smaller are found experimentally[50]. As an example, ethylene shows 1.25 mm in air, but 0.19 mm in O_2. The number of substances where quenching distances in O_2 have been reported is small, however. Most of these reported values are in the 0.15 to 0.30 mm range. Table 6 shows additional data.

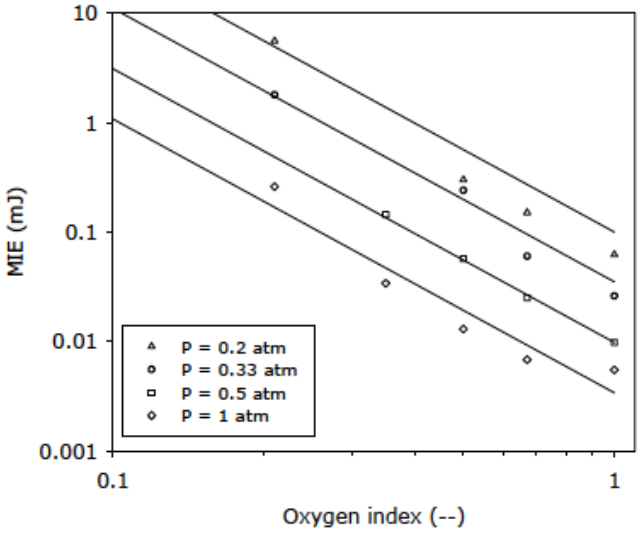


Figure 47 The MIE of mixtures of propane/oxygen/nitrogen as a function of oxygen index and total pressure

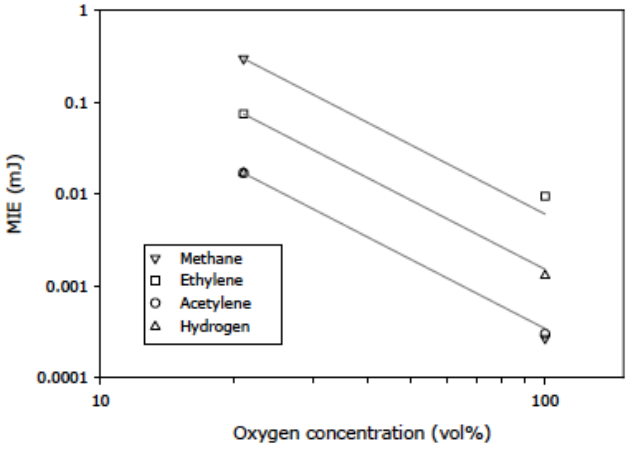


Figure 48 Correlation of MIE according to a -2.5 power law dependence on oxygen concentration

DILUENTS

If the fuel is mixed into an atmosphere which comprises oxygen and a diluent gas other than nitrogen, then MIE values and quenching distances can be expected to change. Lewis and von Elbe[70] present a illustrative data for a few gases. Not enough experimental data are available to draw quantitative conclusions, but basically the dominant effect is the heat capacity of the diluent gas—gases with higher heat capacity values show higher MIE values and greater quenching distances. Anomalous results, as often in combustion, are found when very small molecules, such as He, are involved.

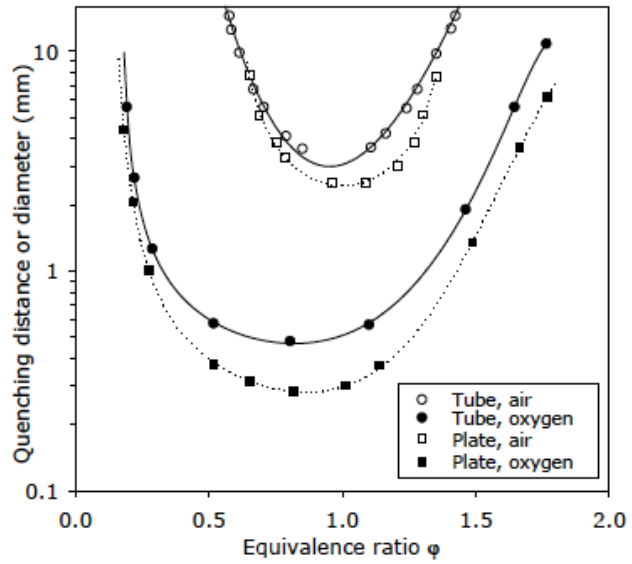


Figure 49 The effect of equivalence ratio and oxidizer type on methane quenching distance (between flat plates) and quenching diameter (in tube)

Table 6 Effect of oxygen concentration on MIE[181] and on quenching distance[107]

Fuel	MIE (mJ)		Quenching distance *d* (mm)	
	Air	O_2	Air	O_2
acetylene	0.017	0.0003	0.52 – 0.65	0.08 – 0.10
ethylene	0.075	0.00095	1.25	0.19
hydrogen	0.017	0.0013	0.5 – 0.64	0.2 – 0.34
methane	0.3	0.00027	2.2 – 2.5	0.3
propane	NA	NA	1.75 – 2.28	0.21 – 0.27

FUEL CONCENTRATION

The effect of the fuel/air ratio on the MIE, as measured at the Bureau of Mines[143] for various alkane-series hydrocarbons is shown in Figure 50. If the fuel and the oxidizer had identical diffusivities, the minimum energy would fall at the stoichiometric mixture condition ($\varphi = 1$). Molecules lighter than air (hydrogen, methane) have higher diffusivities and the MIE for those occurs at $\varphi < 1$. This is because it is more difficult for oxygen molecules to diffuse into the reaction zone than for fuel molecules, consequently, a super-proportional amount of oxygen molecules is needed. Conversely, most other fuel molecules are heavier than air, and for them the MIE occurs at $\varphi > 1$.

Ural et al.[141] noted that the value of φ at which the minimum ignition energy occurs depends on the molar mass in a predictable way. For alkane-series hydrocarbons, a correlation can be found (Figure 51) which is:

$$\varphi\big|_{\text{MIE miminum}} = 0.29 + 0.155\sqrt{W}$$

where W = molar mass (g mol^{-1}) and it is assumed that the atmosphere contains 21% oxygen.

In the experiments represented in Figure 50, varying amounts of fuel gas were introduced into an atmosphere which was at 21 vol% oxygen, prior to the introduction of the fuel. If the oxygen/nitrogen proportions are different, then the MIE will be strongly affected. Figure 52 shows this for methane[70]. The concentration of oxygen is expressed as the oxygen index, OI = $O_2/(O_2 + N_2)$. For alkane-series hydrocarbons (e.g., ethane, propane, etc.), *except* methane, Chin[140] noted that the value of for which the minimum MIE is obtained decreases with OI at the same rate. This enables the following equation that includes the effect of both molar mass and oxygen index to be derived:

$$\varphi\big|_{\text{MIE miminum}} = 0.41 + 0.155\sqrt{W} - 0.57(OI)$$

Thus, for example, for propane W = 44.1 and at room conditions (OI = 0.2095) the value φ to obtain the lowest MIE is = 0.41 + 0.155×6.64 – 0.57 (0.2095) = 1.32, while in pure oxygen (OI = 1.0) it falls to 0.87. A limited amount of validation data indicates that the equation is valid at ambient and sub-atmospheric pressures and for both still and flowing mixtures.

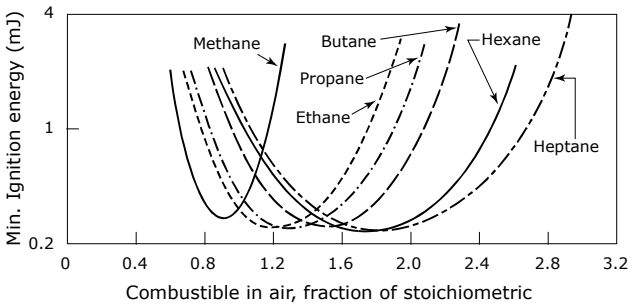


Figure 50 The effect of fuel/air mixture on the MIE for alkane-series hydrocarbons

The means used to cause ignition has some effect on the most-easily-ignitable gas concentration. Singer et al.[144] collected data on this issue for methane/air mixture, shown in Table 7. Stoichiometric concentration of methane in air is 9.5%. This limited study emphasizes that extrapolation of capacitive-spark results to other applications may not necessarily be valid.

The MIE values for hydrocarbons in air are seen to be generally in the range 0.2 – 0.4 mJ. It is important to appreciate that these energies are extremely small quantities. The potential energy equivalent of 0.2 mJ consists of raising a 2 g weight by about 1 cm. For ignition of hydrocarbons in O_2, the values drop further by about a factor of 10. In considering the above information, it must be remembered kept in mind the role of the MIE, versus the ignition energy needed at other fuel/air ratios. For safety purposes, it is imperative that the lowest value be used, since the most-unfavorable mixture can occur. But in explaining events and non-events in real life, it must be remembered that mixtures will very rarely be close to the worst-case proportion. Thus, it may be that an ignition source was available which was above the MIE for a particular fuel in air, but ignition did not occur. Apart from probabilistic aspects of ignition, this may simp-

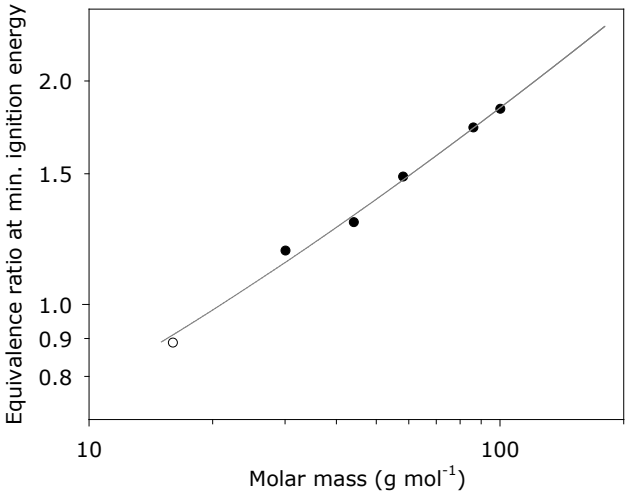


Figure 51 Effect of molar mass on the equivalence ratio at which the minimum ignition energy is found

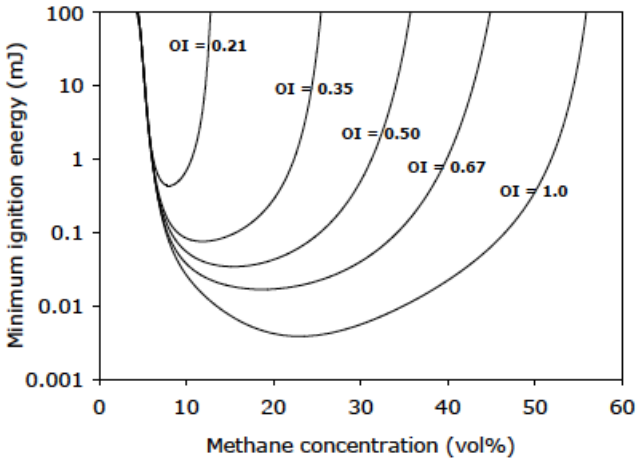


Figure 52 The effect of oxygen index and fuel concentration on the MIE of methane

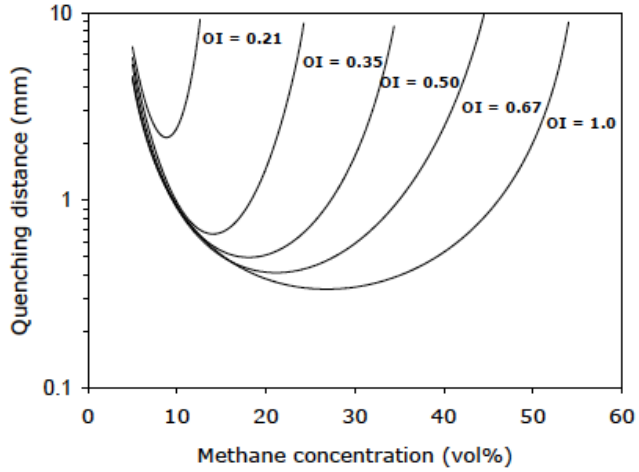


Figure 53 The quenching distance for methane, as a function of oxygen index and fuel concentration[70]

ly be because the mixture had an equivalence ratio far from 1.0. At the lower and upper flammability limits, maybe 100× more energy can be needed for ignition to occur than is needed for the worst-case mixture. It must also be remembered that 'flammability limits' can become an indistinct concept if very large ignition sources are contemplated; this is discussed in more detail later in this Chapter.

The quenching distance is normally reported at the fuel concentration where the smallest distance is found. As shown for methane in Figure 53, the minimum value is close to the stoichiometric. Similar curves are available for a few other gases[145,154]. For many hydrocarbons, the lowest quenching distance is found at φ = 1.1 to 1.3. As a mixture approaches the flammability limits, the value of the quenching distance increases greatly. A recent study[146] confirmed that for methane in air, at the lean limit $d_{\|} \approx 9$ mm. This distance is the same irrespective of whether the propagation is upward or downward, however the lean limit for upward

Table 7 Effect of means of ignition on the most-easily-ignitable concentration for methane

Means of ignition	Methane conc. (vol%)
electrically heated surfaces, large	4.0 – 5.0
heated bomb	5.0
hot gas stream, laminar	5.0
heated plane surfaces, small	5.0 – 6.0
hot quartz tube surface	6.0
sparks from impacts of iron alloys against steel	6.4
wires, electrically heated	6.7
hot jets, pulsed	6.5 – 7.5
sparks from impact of rocks against steel	7.0
hot metal surface, electrically heated	7.0
cannon shots of permissible explosives	8.1
spark, inductive	8.3
spark, capacitive	9.5
flames	9.9

propagation is lower than for downward propagation (5.3% versus 6.0% in one study[100], but varies slightly with experimental conditions). A study of the fuel concentration effect for propane was reported by Jarosiński et al.[147]

TEMPERATURE

Increasing temperature lowers the MIE, as illustrated by the data of Fenn[115] and King and Calcote[148] in Figure 54, with additional data of King and Calcote showing the equivalence ratio effect in Figure 55. In rough terms[50], a 100ºC increase in temperature decreases the MIE by a factor of 2. The straight-line relationship indicates that $\ln(MIE) \propto 1/T$. Furthermore, since the slopes for the various gases are essentially identical, a universal relation can be used for estimating the MIE at one temperature, if it is known at another:

$$E_2 = E_1 \exp[0.008(T_1 - T_2)]$$

where E_2 is the MIE (mJ) at T_2 (K) and E_1 is the MIE (mJ) at T_1 (K). This temperature effect will only be found if the test is run so that the spark electrodes are far enough apart to be out of the quenching distance; otherwise little temperature effect is seen[149]. This point is especially pertinent to breaking wire and break-spark test arrangements, where the gap perforce starts at zero and thermal losses can be high. The temperature effect on MIE becomes more complicated when the fuel/air mixture is not a predefined mixture, but rather is the fuel vapor in equilibrium with the liquid fuel. This situation is considered in Chapter 6.

The quenching distance decreases with increasing temperature according to:

$$d \propto \frac{1}{T^n}$$

where $n \approx 0.5$ to 0.85[104]; a more precise relation has not been evolved. If more specific data are not available, Potter[107] recommends using n = 0.5. The temperature dependence has practical implications, since it means that in heated

environments strategies for flame arresting may not work, if they were tailored for cooled conditions.

PRESSURE

Increasing pressure lowers the MIE[150]. The relationship is generally considered to go as $MIE \propto P^{-n}$, where n is in the range 1.72 to 2.1[151]. Example data for ethane[151] and methane[155] are shown in Figure 56.

The quenching diameter decreases with increasing pressure as:

$$d_T \propto \frac{1}{P^n}$$

where $n \approx 0.8$ to 1.0. Potter[107] shows that there is a complex relation between n and the effective reaction order of the combustion reaction, n', but that the relation can be approximated as $n \approx 0.55\ n'$. Note that in this type of relation the value of n' is not constrained to be a whole fraction, but assumes various values in the range of about 1.3 to 2.2. Where specific details are lacking, Barnett and Hibbard[152] suggest using $n = 0.9$, Friedman and Johnston[153] $n = 0.91$, and Glassman[19] $n = 1$. Even with all else held constant, the air/fuel ratio of the mixture affects the n value to a limited extent[154]. The pressure effect on quenching diameter is important in situations where a gas mixture is in a closed space and flame will or will not propagate out small openings.

A high pressure *gradient* along the length of a tube through which a flame may pass can significantly lower the value of the quenching distance. High pressure gradients will occur if along the vent path from a nearly-sealed vessel undergoing an explosion, to the outside. This is closely related to the MESG problem, but with the difference that the issue here is the physical propagation of a flame through the passage, not necessarily the ignition of an atmosphere on the far side of the vessel. Potter[107] reports some very old data which indicate that an explosion pressure of 8 atm will lower the quenching distance by about a factor of 2 for most fuels. For hydrogen, the reduction was 3×, while for acetylene a higher-yet value was reported. However, the sole available study is sufficiently old that questions may be raised about the general validity of its results.

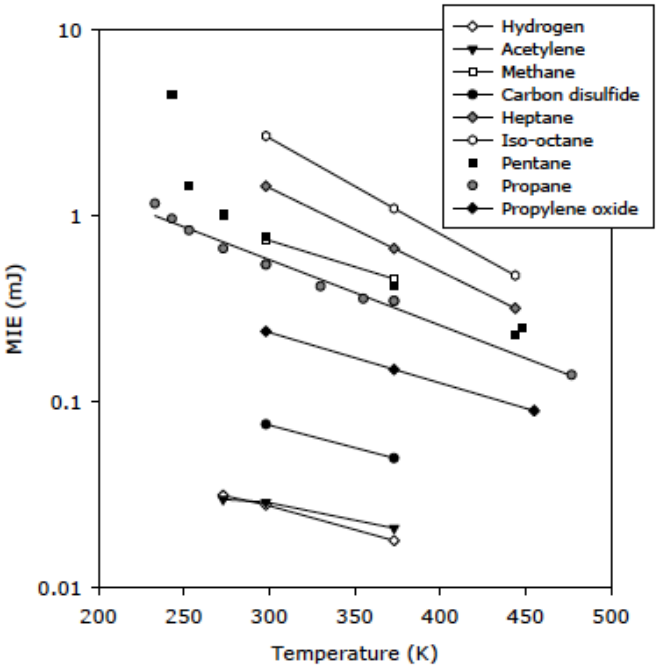


Figure 55 Temperature effect on MIE

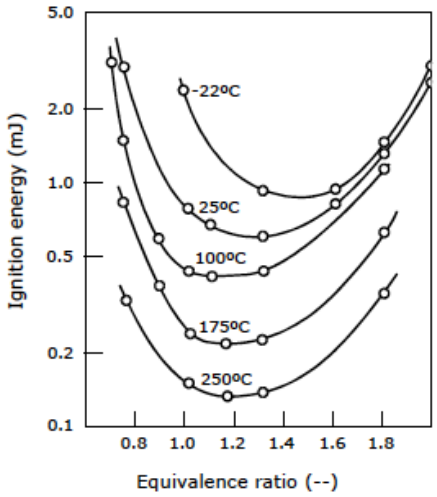


Figure 54 Temperature effect on the MIE of pentane/air mixtures

(Copyright American Institute of Physics, used by permission)

GRAVITY

Ronney[155] examined the effect of zero-g conditions on the spark ignition of methane/air mixtures. Under test conditions where the LFL was 4.68% at 1-g, the LFL rose slightly to 5.08% at 0-g.

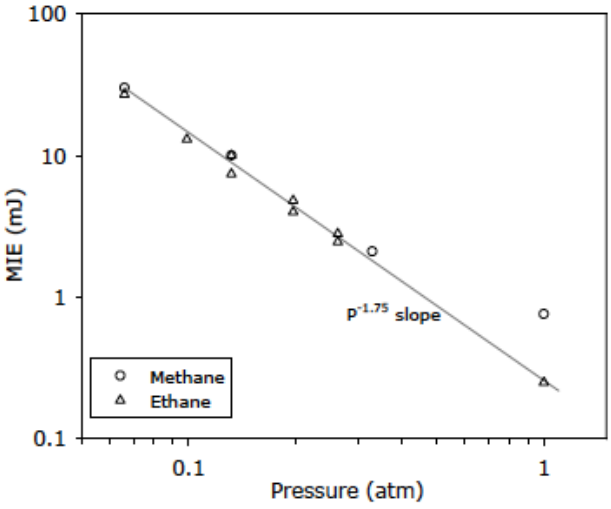


Figure 56 Pressure effect on MIE

TEST GEOMETRY

When the quenching distance is measured in tubes, the direction of propagation has an effect, but quantitative relations are not available[107].

MIXTURE VELOCITY AND TURBULENCE

Theoretical predictions are that flow velocity has an influence on the MIE, but only if it is appreciably higher than the burning velocity of the mixture[156]. The available experimental data indicate that if a mixture has a non-zero velocity, the quenching distance will become larger than the standard value measured in stagnant conditions. But if the mixture has a sufficient outflow velocity, flashback may be avoided as the mixture will be moving faster forward than flame can propagate backwards in it. In an early study, Swett[169] examined the effect for several gases and concluded that, for $u >> 0$, there is linear dependence on velocity in the form:

$$MIE(u) = a + c\,u$$

where u = velocity (m s^{-1}) and a and c are fuel-specific constants. Russian data on propane/air mixtures[157], obtained over the range 1.3 – 17 m s^{-1}, showed that MIE increases monotonically with velocity according:

$$MIE(u) = MIE(0) + c_1 u^{3/2}$$

where MIE (0) refers to a stationary mixture and c_1 is a duel-specific constant. Kono and Hatori[179] studied the effect of velocity for propane/air mixtures using very small-diameter electrodes (< 0.8 mm). For an electrode gap of 3 mm, velocity had no effect until it exceeded ca. 8 m s^{-1}; for larger velocities, the MIE increased steeply, so that at 20 m s^{-1} it was about 10× that for stagnant conditions. For spark gaps smaller than the quenching distance, however, the relationship was complicated. A minimum MIE was found at a velocity of 3 – 5 m s^{-1} and, again, a steep increase at high velocities. But for smaller velocities there was also a sharp increase and also a local minimum at around 1 m s^{-1}. The authors consider that the local hump is caused by details of heat loss to the electrodes.

The effect of turbulence has been investigated in several studies. Swett[158] found that high turbulent velocities raise the MIE. For low-pressure propane-air mixtures, the MIE rose by about 2× as turbulent intensity went from nil to 2.3 m s^{-1}. Akindele et al.[159] investigated smaller turbulent velocities both experimentally and by theoretical modeling and found the turbulence effect to be minimal. Furthermore, they concluded that the initial development of the flame kernel cannot be affected by turbulence when its size is less than the scale of turbulence. For times greater than ca. 0.1 ms, they found that kernel radius growth rates were very slightly increased by turbulence. De Soete[160] presented extensive data on propane/air mixtures, showing that turbulent intensity raises the MIE; he also evolved a calculation formula for predicting the effect. Ballal and Lefebvre[161] concluded that bulk velocity, by itself, has no effect on MIE, but that the turbulent intensity does.

Table 8 Effect of capacitance and electrode diameter on MIE (mJ)

Gas	Capacitance (pF)	Electrodes			
		15 mm	1.6 mm	0.5 mm	points
28% hydrogen/air	6.1	0.022	0.016	0.019	
	30	0.094	0.079		0.034
	50		0.160		
	146	0.390	0.260	0.210	0.073
8.5% methane/air	6.1	0.21			
	13		0.40		
	30	0.94	0.87		
	50		1.06		
	146	4.67	2.21	2.09	0.75

The general conclusion is that both flow velocity and turbulent intensity normally lead to increases in MIE, but that sufficient data are not available on which to base a robust calculational formula. Ballal and Lefebvre[162] showed that in propane/air mixtures, the quenching distance shows a modest increase both with increasing velocity and with increasing turbulent intensity.

WALL MATERIALS

In tests to determine the quenching diameter, the tube material has been found not to materially affect the results. Since heating is not sustained, the wall temperature does not rise significantly above its original ambient value, and, thus, the actual thermal conductivity does not play a role.

CIRCUIT TOPOLOGY

The entire topology of the electric circuit used to create spark ignition must be carefully considered, including values of resistance and capacitance or inductance. In capacitive discharge testing, the capacitance and the charging voltage can be independently controlled. The energy stored in a capacitor, from fundamental physics can be expressed as:

$$E = \frac{1}{2} C V^2$$

But all of this energy is not available for igniting the gas mixture. Some of the energy is lost in the circuit resistance, and, furthermore, a practical circuit cannot discharge a capacitor to zero voltage during the time frame when the energy can contribute to the flame kernel. While circuit topology influences the effectiveness of the energy delivery, other factors must be considered too. The most effective gap size is slightly greater than the quenching distance. If a typical quenching distance may be 2 mm, then the voltage needed to cause a spark discharge across say 2.3 mm is (3×10^6 V m^{-1}) (2.3×10^{-3} m) ≈ 7 kV. If the MIE is 0.25×10^{-3} J, the needed capacitance can be solved from the above equation:

Table 9 Effect of capacitance and electrode diameter on voltage needed for ignition (V)

Gas	Capacitance (pF)	Electrodes			
		15 mm	1.6 mm	0.5 mm	points
28% hydrogen/air	6.1	2700	2300	2500	
	30	2500	2300		1500
	50		2500		
	146	2300	1900	1700	1000
8.5% methane/air	6.1	8300			
	13		7850		
	30	7900	7600		
	50		6500		
	146	8000	5500	5350	3200

$$C = \frac{2 \times MIE}{V^2} = \frac{2 \times 0.25 \times 10^{-3}}{\left(7 \times 10^3\right)^2} = 10 \times 10^{-12} \text{ F} = 10 \text{ pF}$$

Thus, it can be seen that a primary constraint is the breakdown voltage of the gap. If the capacitance is increased beyond the optimum value needed, the voltage cannot be decreased to compensate, because the voltage would drop below the breakdown voltage needed to cause a spark at all. This has been found experimentally—the voltage stays constant, but as the capacitance increases so likewise does the ignition energy needed [163,164,176]. If it is realized that breakdown requires a constant voltage, rather than a constant energy, then the results[176] shown in Table 8 for energy and Table 9 for voltage are seen as consistent. Values of capacitance less than about 5 pF are very difficult to create, since stray capacitance cannot be eliminated. In addition, stray inductance begins to dominate[165], and its value is hard to reduce below 15 μH. Consequently, discharges from low C-L-R circuits tend to be oscillatory in nature.

The role of circuit resistance comes into play in another manner, again not directly related to the energy distribution in the circuit. In 1951 Roth et al.[166] attempted to measure the energy delivered into the gas directly. Their instrumentation was not fast enough to capture the full event, but with extrapolation of the measured values they inferred that close to 95% of the nominal stored energy was being delivered. Later studies[165] indicated that the actual energy dissipated in the spark generally decreases with increasing resistance, although not monotonically. Despite this, lowest MIE values are not found for lowest circuit resistances. Experimentally, it is found that there is an optimum value of resistance, and that too small a value of resistance in series with the capacitor will lead to excessively high values of energy being needed for ignition[167]. This is because it is not just the delivery of energy that matters, but also the time over which it is delivered. In one study[177], optimum discharge times were found to be ca. 1.2 μs, but a broad-based study of this topic does not exist. For an overdamped circuit, if the effective discharge time τ is taken to be the time required for the response to decay down to 1%, then $\tau = 4.6RC$. This simple relation however does not describe the small-capacitance circuits that lead to the most incendive discharges. According to it, a 50 kΩ resistor would be optimal for a 5 pF capacitance, even though only 50% of the stored energy is delivered into the gap under these conditions[165], compared to 90% with R = 100 Ω.

Rose and Priede[165] examined a wide range of discharge times and found that—with practical values of circuit impedances—at short discharge times (microseconds), the waveform was oscillatory and the spark gap resistance was a constant. But at large discharge times (milliseconds), the waveform was overdamped and the resistance was an inverse function of current, much as found for arcs. The experimental measurements indicated that:

$$R_g I^{1.36} = \text{constant}$$

where R_g = spark gap resistance (Ω), and I = current (A). When using large capacitances (> 1 00 pF), a series resistance > 20 Ω was needed for the waveform to be overdamped; for small capacitance circuits, a general guideline was not given.

The *quality* of the capacitor used can affect greatly the energy losses, especially for higher capacitance values. In one series of experiments, Pidoll[168] showed that the largest losses were found with paper capacitors, smaller losses with plastic-film types, and smallest yet with low-loss pulse capacitors.

Workers researching intrinsic safety of industrial instrumentation systems studied at great length the effects of resistance in both capacitive and inductive discharge circuits but much of this work has been aimed at the break-spark arrangement and these results have been considered in the section above dealing with breaking wires and moving contacts.

SPARK DURATION

The duration of the spark also influences the results. Swett[169] originally showed that an optimum duration of spark discharge exists, and that sparks discharged in a longer or shorter time result in the observed value of MIE rising. Results from a later study by Kono et al.[170] are shown in Figure 57. The data were obtained using 0.3 mm diameter wire electrodes and a gap spacing equal to the quenching distance. An optimum duration of 50 – 60 μs is seen. In another study, using 1 mm diameter electrodes and a gap of 1 mm, Kono et al.[171] obtained data showing a flat region for spark durations of 20 – 50 μs, with MIE values rising for spark durations over 50 μs. Kravchenko et al.[172] studied the spark ignition of mixtures of 8.5% methane in air. They found an optimum spark duration of 110 μs under all circumstances. For a resistive circuit, the energy required for ignition was unchanged at over the range from 60 μs (the shortest duration explored) to 110 μs, then increased mono-

tonically with increasing spark duration. For an inductive circuit, however, the 110 µs value was a sharp minimum and both increasing and decreasing spark duration served to raise the energy required for ignition. In experiments with 20% hydrogen in air, they found that the optimum spark duration was only 10 µs. Ziegler and Herweg[173] explored the effect of spark duration on the ignition of methane/air mixtures at an equivalence ratio $\varphi = 0.67$. Using a technique for measuring efficiency of discharge identical to that used by Hertzberg for dust clouds (see Chapter 5), they found that the efficiency increased from 20% for a duration of 20 µs up to 33% for a duration of 200 µs. Beyond 200 µs, a plateau at the same 33% value was seen up to the longest duration explored, 400 µs.

The above results pertain only to tests where stationary electrodes are spaced for optimum ignitability, typically at slightly greater than the quenching distance. In a break-spark, the situation is different, since the gap starts at zero and may still be much smaller than the quenching distance when the bulk of the energy is transferred into the spark. Much longer discharge times are optimal in that arrangement, as discussed above.

Testing is commonly done with DC power, but experiments have also been reported using AC sources. Early work by Wheeler suggested that the minimum igniting current needed for low-frequency AC power sources was the same as the value needed for DC, when the crest value of the AC current was used in the comparison. Subsequent Russian work[129] showed the minimum igniting current rises with frequency until a peak is obtained (ca. 10 kHz for hydrogen/air mixtures), then falls again at higher frequencies. The two factors coming into play are the shorter discharge times being available before a zero-crossing is reached as the frequency is increased, but the ease of re-striking an arc as the de-ionization time is shortened. Later, much more

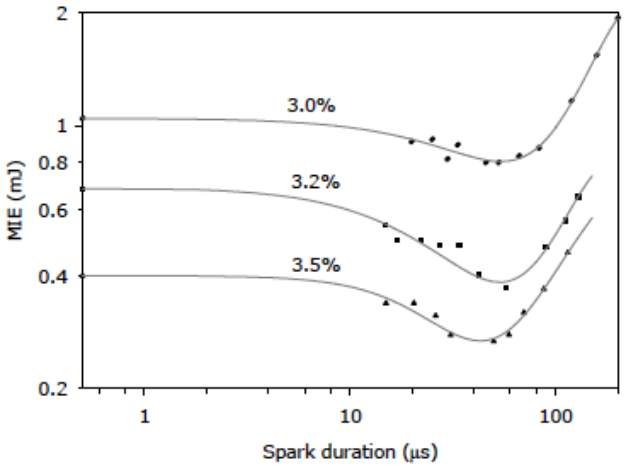


Figure 57 Effect of spark duration on MIE for several concentrations of propane in air
(Copyright The Combustion Institute, used by permission)

detailed studies were undertaken by Kono et al.[174]. They found that there was an optimum frequency which varied on other test conditions, but tended to be around 100 – 200 kHz. At both lower and higher frequencies, the ignition propensity decreased. They then expanded the study to a train of two pulses, representing the igniting effect of a single cycle of sine wave. An optimum pulse duration of around 50 µs was found. Under conditions where the two-pulse method was just sufficient to ignite the mixture, it was found that a single pulse, delivering the same energy as the two separate pulses, did not cause ignition.

Some ignition circuits, both in laboratory experiments and in automotive use, employ an arrangement whereby a capacitor is discharged into the primary side of a step-up transformer. The high voltage from the secondary winding is then directly connected to the spark gap. The combination of the capacitor and the inductance of the primary winding of the transformer forms a *resonant circuit*. Kono et al.[171] determined that an optimum resonant frequency ca. 100 kHz exists for this topology, at least within the context of their experimental arrangement.

When *repetitive sparks* are used, with a cycling rate greater than a certain minimum, the energy discharged by each individual spark can be substantially less than the minimum ignition energy, and yet ignition may still occur. This was demonstrated for methane/air mixtures at a low pressure of 0.2 atm, for which MIE = 6.4 mJ. Repeated sparks with a per-spark energy as low as 0.21 mJ successfully ignited this mixture[175]. Apart from very small volumes where an overall warming effect might be created, the main reason for the enhanced ignitability is because previous sparks have created breakdown products of the fuel gas which are more readily ignitable than the parent gas.

ELECTRODE ARRANGEMENT

If electrodes are placed closer together than the quenching distance, then they will act as a large heat sink in removing heat from the developing flame kernel. Consequently, correct values of the minimum ignition energy can only be determined correctly if the gap width exceeds the quenching distance*. This point was not known in the early days of spark ignition research, and consequently there was no agreement among the MIE values that were published. Figure 58 illustrates the effect of gap size obtained when testing with 2 mm diameter wire electrodes having flat tips[161]. Similar data have been reported by Movilliat and Giltaire[176] for H_2/air and CH_4/air mixtures.

The electrode diameter also influences the minimum energy results. Large electrodes introduce a substantive body into the system to which heat is lost. However, for electrode

* MIE values specific to a breaking-wire or moving-contacts geometry may also be measured, but they should not be expected to be the same as the standard values obtained between fixed electrodes.

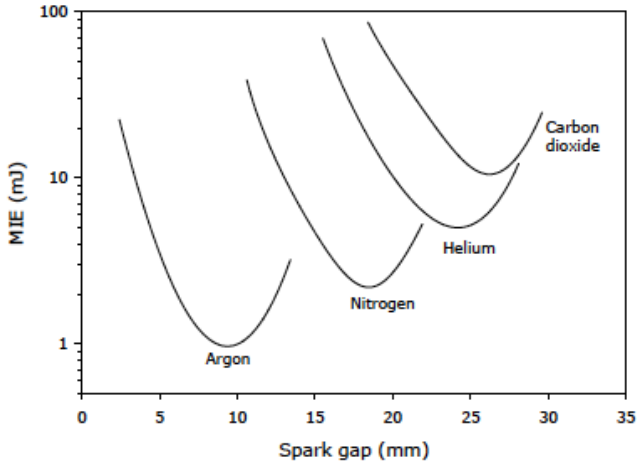


Figure 58 Effect of spark gap size on MIE (stoichiometric propane mixtures with oxygen and various diluents, P = 0.17 atm; 2 mm electrodes with flat tips)
(Copyright Royal Society, used by permission)

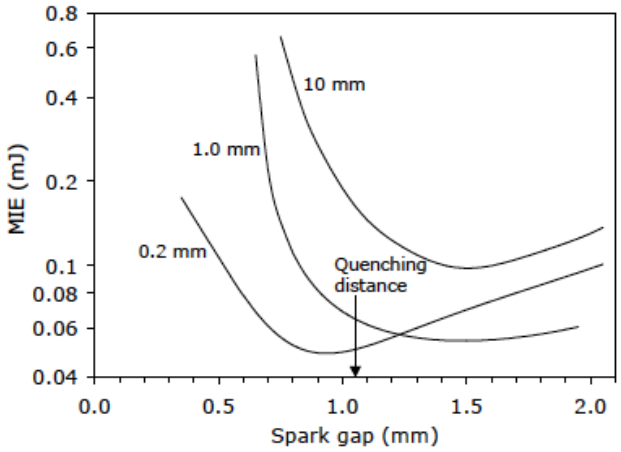


Figure 59 Effect of electrode size (two spherical electrodes) on the ignition of H_2/air

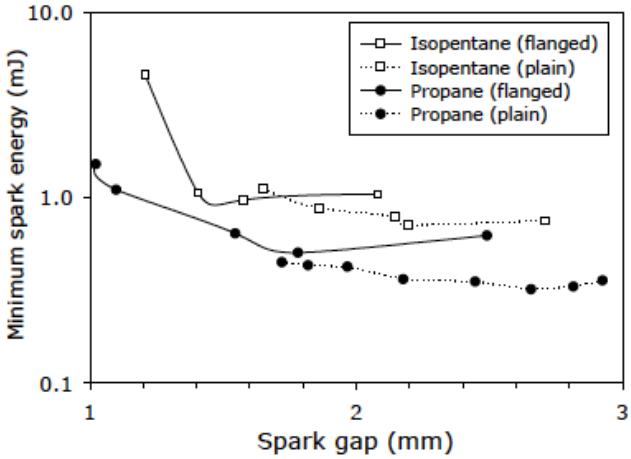


Figure 60 Effect of electrode spacing and construction[180]

diameters below ca. 2 mm, a corona discharge is formed instead of a spark. The diameter which can reliably produce the lowest minimum energy results, thus, tends to be just larger than what is needed for corona discharge to occur. Some results of Rose and Priede[177] on hydrogen are shown in Figure 59. Krämer[178] used spherical electrodes to ignite ammonia/air mixtures and found substantially lower MIE values for 5 mm diameter electrodes than for 15 mm. Kono and Hatori[179] studied the effect of electrode diameter on the ignition of propane/air mixtures in the range 0.05 – 0.8 mm. They found lowest MIE values with the smallest electrode diameter. Table 8 gives further examples of the diameter effect.

Matters are further complicated because the optimum spark gap is a function of *pressure*; limited testing at sub-ambient pressures[157] indicates that for low pressures the optimum gap size is roughly $\propto 1/P$.

The extreme sensitivity of results to gap size can be avoided if flanged* electrodes are used. Flanged electrodes also allow the simultaneous determination of the quenching distance, since if the gap length is smaller than the quenching distance, a developing flame kernel is physically quenched on the flanges. By contrast, even though heat losses occur to the electrodes, if plain-tip electrodes are spaced closer together than the quenching distance, expansion of a flame kernel is still possible, although the value of energy required increases drastically.

Use of flanged electrodes was explored by Calcote et al.[180] In their tests, they had an asymmetrical arrangement where the negative electrode was flanged, while the positive electrode was a plain 3.2 mm diameter wire with a hemispherical tip. The flange was a stainless steel disc, 12.7 mm diameter and 0.25 mm thick, fitted to the electrode at a distance of 0.25 mm down the shaft from the hemispherical electrode tip. Differences in results between tests using two plain electrodes, versus tests using one flanged electrode

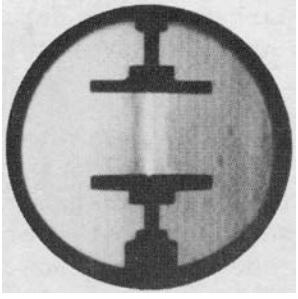


Figure 61 Spark channel developing between two flanged electrodes in a methane/air mixture (time = 50 μs)

* A flanged electrode is one where a glass disc surmounts the end of the wire.

are illustrated for two gases in Figure 60.

Calcote et al. compared the results from tests run under their two conditions. For a large number of gases, a satisfactory correlation was found:

$$MIE_{flanged} = 0.793\, MIE_{plain}^{1.18}$$

where $MIE_{flanged}$ denotes the results for the one flanged/one plain pairing, while MIE_{plain} refers to a pair of plain, hemispherical-tip electrodes; both values are in mJ.

In further studies, the Bureau of Mines found[181] that the most reliable data come from experiments where both electrodes were equipped with 12.7 mm diameter glass flanges (Figure 61). They also found that the best results involved an electrode tip which was flush with the glass disc; Calcote used an electrode which slightly protruded beyond the disc. A non-conductive material such as glass is used, since it can provide thermal quenching without providing a spurious surface for the discharge to wander onto. Under those test conditions, varying the gap width produced results such as illustrated in Figure 62—there is no detectable effect of electrode spacing over a wide range, until a minimum spacing is reached, at which point the ignition energy effectively becomes near-infinite. This critical spacing is identified as the parallel-plate quenching distance, $d_{||}$. If at least one of the electrodes does not have a wide enough flange, then even at small electrodes spacings the developing flame kernel can 'escape sideways' and ignitions, albeit at higher energy remain possible. This is illustrated in Figure 62 for the data points where only one flanged electrode was used, with the second electrode being a fine-point needle. In all of the cases where the electrodes used were not both flanged, a less distinct relation of energy vs. spacing distance has been found and the MIE measurements have been judged to be of poorer repeatability. If very large electrode spacings are used, then the ignition energy needed again starts to rise. Thus, the proper measurements of MIE are made at an electrode spacing just a bit larger than the quenching distance. The electrode arrangement evolved at the Bureau of Mines appears to be unique. Most studies with various other kinds of electrodes show a distinct minimum, not a plateau, in spark gap distance vs. MIE curves.

ELECTRODE MATERIALS

In an early study, Rose and Priede[177] showed that metal used for the spark electrodes has a distinct effect on the MIE. For H_2/air mixture, platinum showed the highest ignition energy, cadmium the lowest, with silver and aluminum giving intermediate results. Later, Ballal and Lefebvre[103] conducted more extensive experiments and proposed the relationship:

$$E_{\min} \propto T_b^{1/4} d^{1/2}$$

where T_b is the boiling point (K) of the electrode and where d is the electrode diameter (m). The boiling-point dependence comes from a known relationship for the ionization of gases. Similar results were obtained by Ziegler et al.[182] The

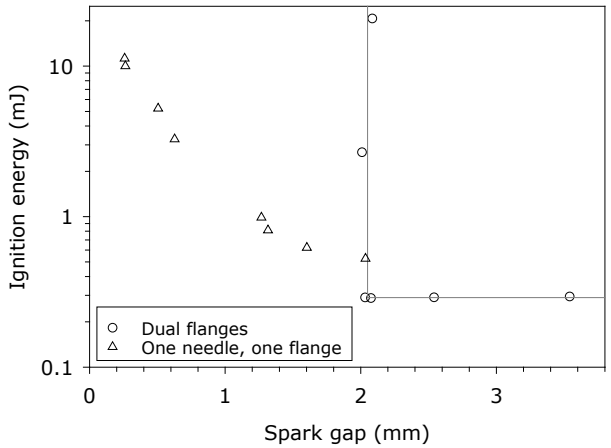


Figure 62 Effect of spark gap on ignition energy for a mixture of 8.3% methane in air (the flanges were 12.7 mm glass discs)

electrodes used by BM for their main studies were made of 1.6 mm diameter stainless steel.

Not surprisingly, if at least one of the electrodes is *heated*, the energy needed for ignition will change. This has been shown in limited testing[183], but not enough studies exist to generalize the trends.

IGNITION IN THE ABSENCE OF EXCITED SPECIES AND HOT-WIRE IGNITIONS OF ALL TYPES

The most common way that a localized source of heating can be created without the presence of excited species is by heating a surface, generally a metal surface. The only other mode that has received some systematic study is one where ignition is caused by a jet of hot, non-flaming gas. Wires that melt (fuse) due to electric heating will generate excited species once an arc is created. Thus, they do not comprise a mode where excited species are absent, however, we treat them directly following the treatment of non-melting wires in order to present all work on hot wires together.

HOT SURFACE IGNITION AND CATALYTIC EFFECTS

In this section we consider hot-surface ignition aspects for pure gases. In many practical cases, hot surface ignitions involve liquid sprays, droplet, or spills. These are considered in Chapter 6. Sir Humphry Davy[98] observed in 1815 that plunging an iron bar "at the highest degree of red heat and at the common degree of white heat" into firedamp (mostly methane)/air mixture did not ignite the mixture. The first scientists to suggest an explanation for this were Mallard and Le Chatelier[49], who in 1880 proposed that while a gas volume directly next to the heated surface does heat up to a high temperature, convective effects quickly sweep it out of that area, where it is cooled down. In other words, they suggested that if the residence time of the heated volume of gas is less than the induction period, ignition is not observed.

By contrast, in an AIT test vessel, all of the surroundings of the gas mixture are at a uniform temperature and any convective motion of the gas mixture does not result in the gas volume 'running away' from the hot surface. Apart from an AIT-testing environment, the 'running away' effect would also be avoided in a stably-stratified environment—for example, a cylinder where only the top surface was heated—but no experiments of this kind have been reported.

Most surfaces are chemically nonreactive, but a few, platinum and palladium for example, provide a catalytic action. Thus, these surfaces behave systematically differently with regards to homogeneous (visible flames) ignitions and also can support heterogeneous (glowing surface) ignitions that are not exhibited by non-catalyst materials. In practical applications, catalysts can be used for either the ignition of a mixture, or for facilitating continuing combustion which would otherwise be impossible. A well-known example of the latter application is the catalytic converter used in current-day automobiles. It provides an extra step of reaction which would not occur if the exhaust gases simply flowed through the same pipe, minus the catalyst.

Experimental studies

In this section, experimental ignition studies will be reviewed where the surfaces studied were primarily non-catalytic. Studies focusing specifically on catalytic effects will be discussed in the following section. The first extensive work on hot-surface ignition was published in 1919 by Prof. Thornton[184], the father of oxygen consumption calorimetry[185]. In his study, he mainly reported the current necessary to cause ignition from an electrically heated wire; temperature was only estimated in a few cases. For many gases, the needed current was roughly independent of the fuel/air ratio over much of the flammable range. For 0.1 mm diameter platinum wires, methane required about 2 A, while gasoline vapors only 0.9 A; all other fuels were intermediate. The metals explored were silver, gold, molybdenum, tungsten, platinum, and iron. For all metal types and for all gases (except H_2 and CO), ignition occurred for the same electric power per unit wire length. In the absence of reliable temperature measurements, however, these results would be difficult to place in context.

In 1927, Coward and Guest[186] studied ignition of natural gas/air mixtures in a large test vessel by heated strips of various metals, with the natural gas being 93.2% methane. They noted that even though the flammability limits (i.e., the range wherein flame propagation fully resulted) were 5.5% to 13.5% for the fuel, mixtures over the range 2.4 – 16% could be "ignited," but such ignitions did not propagate throughout the vessel. One might expect that results would have shown that stoichiometric mixtures are ignitable at the lowest temperatures, with mixtures being progressively fuel-lean or fuel-rich being harder to ignite. Instead, Coward and Guest found a monotonic relation for most metals tried: the lowest temperatures required were at the lowest fuel concentration, with progressively higher temperatures needed for richer mixtures. For copper, gold, Monel, nickel, steels of various sorts, and tungsten, temperatures of 1000–1060ºC were required at the LFL, rising to ca. 1070–1200ºC at the UFL. For molybdenum, an opposite trend was found, since the metal itself ignited. Later investigators[187] found that tungsten wires behave similarly to molybdenum in that tungsten also readily oxidizes in air at high temperatures and hot tungsten wires normally do not ignite flammable gas atmospheres until the metal itself ignites; this phenomenon is further discussed under *Fused wires*, below.

Vogt[188] used 0.2 mm wires, stretched horizontally, and measured the electric current, rather than wire temperature. His results are shown for methane in Figure 63 and hydrogen in Figure 64. For platinum wires igniting methane, over the concentration range of 8 – 12%, the wires fused, but no ignitions were obtained. In most cases, leaner mixtures were more easily ignitable, but there was not a strong effect of fuel concentration. Vogt's results for platinum wires were the opposite from those of Coward and Guest: he also found that it is most difficult to ignite methane near its stoichiometric concentration, but elsewhere in his experiments the mixtures ignited more easily with platinum than with any other metal. The test conditions, however, were not identical, and wires of different materials heated by the same current will not attain identical temperatures. Vogt conducted a more limited test series to measure the temperatures and found these results for 8% methane/air mixtures: tungsten 1530ºC; Nichrome 1430ºC; nickel 1390ºC; and platinum 1290ºC. Thus, the ranking order was only reversed for nickel vs. Nichrome when temperature, rather than current, was taken as the independent variable.

Vogt concluded that the differences among the metals are due to chemical and not due to physical (e.g., thermal or electrical conductivity) factors. He tested tinned 0.2 mm iron wires and found that they readily ignited methane/air mixtures, whereas an untinned 0.2 mm iron wire fused without igniting. There was also a fuel effect, in that the conclusion with respect to tinning was reversed when testing hydrogen mixtures—tinned wires made ignition harder, not easier. Vogt also observed that copper wires could not ignite methane mixtures, even for large wire sizes. In these explorations, the largest conductor he used was a 6 5 mm wide strip, which fused but did not ignite the mixture. Very low circuit voltages (< 5 V) were needed so that an incendive spark would not be emitted upon fusing the wire[*]. Vogt's finding with regards to inability of copper wires to ignite methane/air mixtures was confirmed by Powell[189], although, as stated above, Coward and Guest could obtain

[*] This strategy has normally not been used by other researchers. Consequently, when a hot wire ignites a gas mixture upon fusing, it is commonly ignited from the spark caused by opening the circuit.

ignitions of natural gas even though they used narrower (12.7 mm wide, by 1 mm thick) copper strips. It is unclear if the small amount of non-methane constituents was crucial to the outcome or whether some other experimental factors governed.

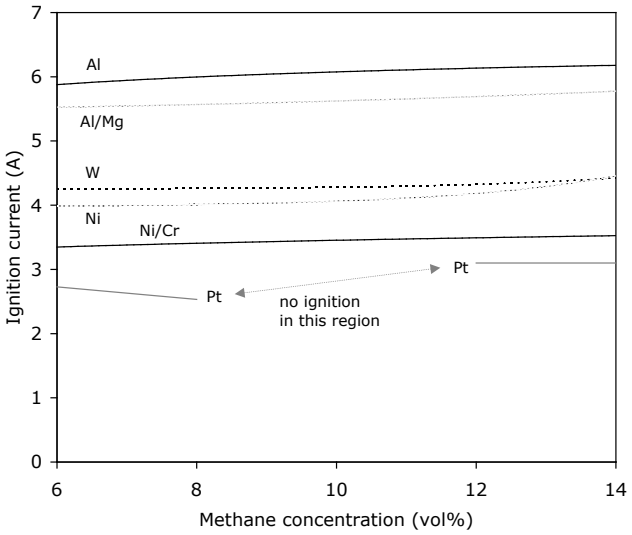


Figure 63 Ignition of methane/air mixtures by 0.2 mm wires of various materials

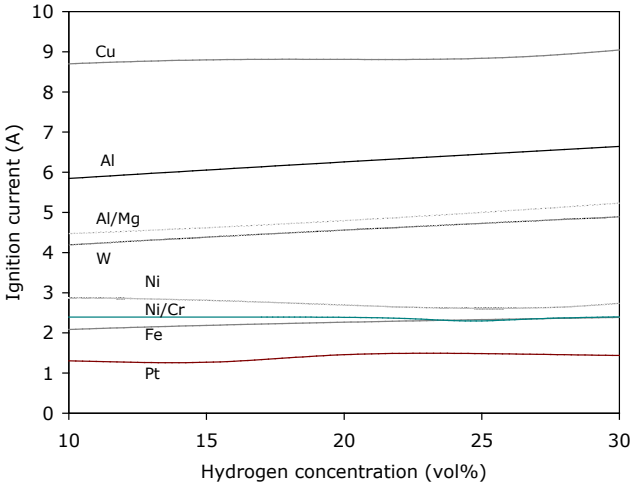


Figure 64 Ignition of hydrogen/air mixtures by 0.2 mm wires of various materials

Kuchta and Cato[248] ignited mixtures using a 10 mm diameter Nichrome rod, with the mixtures being at their most-readily ignitable (but unspecified) concentrations. Their results were: hexane 682ºC, octane 671ºC, and decane 660ºC. Duarte and Drysdale[190] measured the ignitability of a 3% propane mixture in air using a 5 mm Nichrome strip. In their experiments, they located the strip in the bottom of a groove and found a modest geometric effect in the results. The ignition temperature without a groove was 900ºC; in the deepest groove (40 mm) the temperature dropped to 820ºC, with intermediate values for smaller depths. Other experiments with Nichrome wires were conducted by Vanpée and Bruszak[249] who use a 1 mm wire, 90 mm long (Figure 65). Several trends of temperature with equivalence ratio are seen, but the majority of the fuel gases showed only a small dependence on equivalence ratio. Markworth and Schebsdat[191] ignited CS_2/air mixtures with an overheated, wirewound resistor of 6.5 mm diameter and 20 mm length. They found that ignition temperature increased notably with fuel concentration, going from 250ºC at 1% up to 365ºC at 9%. Diethyl ether/air mixtures showed the opposite trend, with temperatures decreasing with increasing concentration over the range 6 – 15%; for concentrations of 15 – 30%, a plateau region was found.

Ignition of gases from heated tungsten surfaces do not require ignition of the metal itself if the hot body is something bigger than a small wire. Cutler[192] used an 11.1 mm wide heated tungsten strip and obtained the results shown in Figure 66. The experiment was unusual in that he provided a brief pulse of heating, instead of keeping a strip at a constant temperature, thus, his results are hard to compare to other workers', although some additional transient heating data were also obtained by Adomeit[193].

In the case of ignition by incandescent particles, the *sphere* is a suitable geometry to study. Also, in such cases the sphere will usually be moving through the flammable atmosphere, so flow velocity must be considered. Experimentally, work on spheres is unique, since in all of the other geometrical arrangements, the surface is electrically heated. For a sphere, on the other hand, experimentalists invariably have taken the approach that in practical cases a sphere will be ejected from some source and then proceed to cool in the atmosphere—it will not be maintained at a fixed temperature electrically. Thus, one will expect that much higher (initial) temperatures will be needed for a sphere to ignite a given atmosphere than would be the case for an electrically

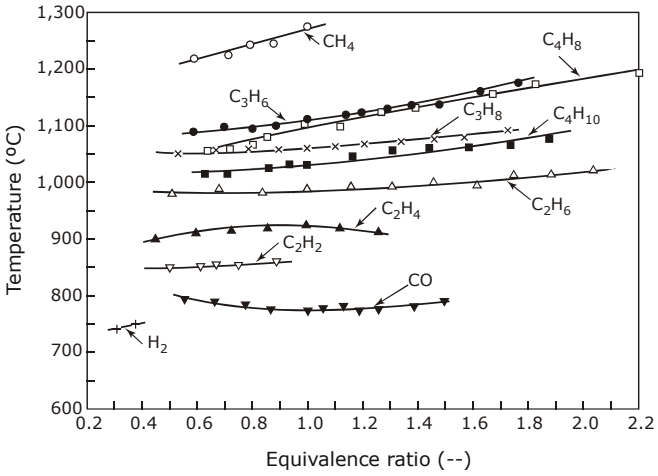


Figure 65 Temperatures needed to ignite various gas/air mixtures using a 1 mm Nichrome wire

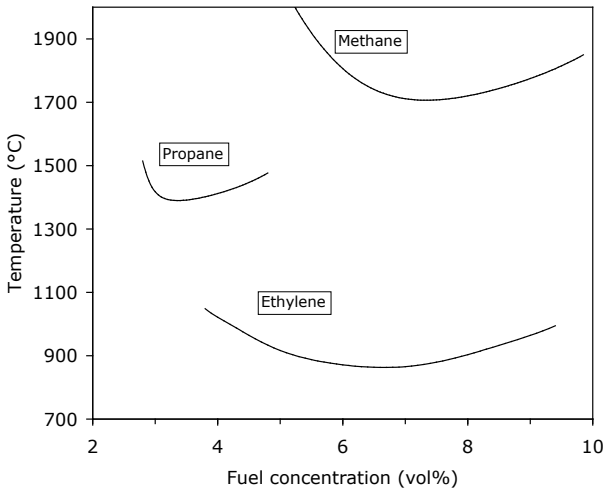


Figure 66 The ignition of gas mixtures in air using a transiently heated tungsten strip

heated body of the same size. Silver[194] and Paterson[195] were the first to study this problem at Glasgow University. For a large variety of materials—aluminum, alundum, nickel, platinum, quartz, slate, titanium dioxide, etc.—the effect of material type was found to be minimal. Newly made platinum spheres were less effective in igniting than other materials; however, the results for aged platinum spheres were essentially identical to all the other materials tried. For a 10% H_2/air mixture, ignition temperature was 900ºC for 0.5 mm diameter spheres and 800ºC for 2.0 mm spheres. Pentane/air mixtures in the range 1.5 to 5% showed 1150ºC for 2 mm diameter and 1030ºC for 4.0 mm. In general, the minimum ignition temperature varied inversely with sphere diameter over the range studied, 0.5 to 5.5 mm. Methane/air mixtures could not be ignited at temperatures up to 1200ºC. For lean mixtures, the necessary temperature for ignition increased very steeply with sphere velocity over the range 10 – 60 m s^{-1}. For a given sphere velocity, higher (but lean) fuel concentrations resulted in lower ignition temperatures being necessary. The temperature of the fuel/air mixture itself did not affect the results, when varied over a range of 200ºC. The researchers did not compare the outcome in the same experimental rig with zero velocity particles. Tolson[196] used an exploding wire technique, which creates an electric arc that disintegrates and scatters tiny metal particles and found that microgram-size particles can ignite methane/air mixtures when they are at temperatures on the order of 3000ºC. Aluminum, iron, copper, and graphite particles ignited the gas mixtures readily, but it was much more difficult to ignite with tin, lead or zinc, and perhaps impossible to get methane/air ignitions with cadmium. Except for aluminum (which most readily caused ignitions, but does not have the highest boiling point), the results otherwise indicate that the incendivity of metal particles is roughly proportional to their boiling points (cadmium's T_b is 767ºC, while zinc's is 907ºC). It was possible, however, to ignite hydrogen/air mixtures by intense laser-energy vaporization of cadmium wires. Tolson did not make particle size measurements, so the results cannot be related to theory.

The effect of *air velocity* was studied by Mullins et al.[197] for pentane/air mixtures ignited with a heated 6.4 mm stainless steel rod. Figure 67 shows that for flow velocities less than about 30 m s^{-1} (which is a substantial value!), the effect is minor. On the other hand, for some hydraulic fluid vapors, it has been found that the surface temperature needed for ignition increases starting at flow velocities barely above zero[198].

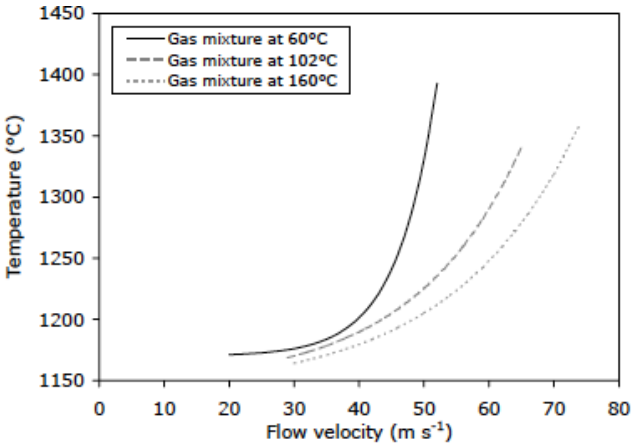


Figure 67 The temperature of a 6.4 mm stainless steel rod needed to ignite stoichiometric pentane-air mixtures of various initial temperatures
(Copyright The Combustion Institute, used by permission)

Geometric variables influencing natural convection were found to have an influence in experimental studies by Bull[210]. In confining a mixture between an upper hot plate and a parallel cold plate below it, he found that when the spacing became less than 50 mm, exceedingly high hot-plate temperatures became necessary to ignite hexane mixtures having less than 4% fuel concentration. For richer mixtures, the plate spacing had no effect. Hamer et al.[199] tested the rotors of industrial electric motors as a potential source of hot-surface ignition for flammable atmospheres. Atmospheres containing heptane, hexane, or tetrafluoroethylene required hot-surface temperatures 72 – 122ºC above the AIT of the particular vapor for ignition to occur with a locked rotor. With rotor rotating, it proved impossible to ignite any of the mixtures, up to the maximum attainable equipment temperature of ca. 350ºC. As in nearly all of its characteristics, diethyl ether was anomalous, in that its hot surface ignition temperature was 180ºC, essentially the same as its AIT value. With a rotating rotor, it ignited at 229ºC. The environment inside an electric motor is a highly enclosed one, with a marked similarity to an AIT tester, thus it is not surprising that locked-rotor temperatures only about 100ºC higher than the AIT were recorded. The authors note that it was very difficult to make accurate temperature measurements and that, consequently, the actual

rotor temperatures were probably higher than the measurements indicated. The authors also concluded that "any air movement inhibits ignition" in such geometries.

There are almost no studies on *ignition times* for hot-surface ignitions. In one small study, Rae et al.[204] examined the effect of stoichiometry on ignition time of methane from heated surfaces. They found minimum times at $\varphi \approx 1$, with concentrations further away from $\varphi = 1$ showing progressively longer ignition times.

Size effect is clearly a major factor in hot-surface ignitions and a number of workers endeavored to capture the essence of this variable. Bartels[200] showed that there is a size effect, but that the effect is not large once the surfaces are centimeter- and not millimeter-sized. But his results (Table 10) also show that hot-surface ignition temperatures for the larger cylinder sizes approach the AIT values.

Table 10 Hot-surface ignition temperatures for cylinders of several diameters and materials

Fuel	AIT (ºC)	Hot-cylinder ignition temp. (ºC)		
		60 mm brass	38 mm glass	51 mm glass
diethyl ether	195	239	235	227
dimethoxymethane	237			327
heptane	223			302

Powell[189] attempted to generalize the size effect on the minimum temperature needed for a hot body to cause ignition. His conclusions (Figure 68) show that for bodies with a size greater than about 10 mm, the effect of size becomes nearly insignificant. For bodies of size < 1 mm, for example, mechanical sparks, there is an extremely steep relation between size and minimum temperature. Most experimental ignition temperature data reported for individual gases tend to imply an accuracy which is not borne out when data from several investigators are compared. Thus, Powell's representation of results simply according to IEC 'Groups' of gases* has a merit of realism. Group I comprises methane alone. Group IIA has gases with MESG > 0.9 mm (e.g., propane, heptane, methanol, etc.). Group IIB has gases for which 0.5 < MESG < 0.9 mm; it includes ethylene, ethylene oxide, pentane, etc.). Group IIC pertains to MESG < 0.5 mm and comprises only acetylene, carbon disulfide, and hydrogen. An examination of the data discussed by Powell does not make clear the basis for the very steep rise in the trendlines of Figure 68 for very small sizes. It appears Powell intermixed results for hot-particle ignitions with those for hot wires and surfaces. That would appear to be hard to justify, because small particles cool very rapidly, and an initial temperature will have decreased greatly by the time the induction period is over. Duarte and Rohatgi[201] undertook a review of original literature addressed at the same question. They only found reliable data for $d \geq 1.6$ mm; at this size and greater the effect of size on the required temperature was moderate, not steep.

The quantitative effect of surface dimension on the required temperature for ignition is not particularly clear from a plot such as Powell's, especially in view of the steepness of the curves. Müller[202] obtained data on the ignition of town gas/air mixtures showing that straight lines can be plotted if a semi-log graph is used and if the hot surface area, not lineal dimension is used. Scaling according to diameter or thickness, in fact, is a rather poor idea, since for many heated bodies used in experiments the biggest dimension, by far, is their length and presumably the whole length presents a surface available for reaction. Müller's data are shown in Figure 69, as are more recent results from HSE for other gases[203]. The results of Rae et al.[204] on methane are shown in a plot of this kind in Figure 70. A reasonably good fit is seen, except for the smallest areas tested. A configuration where the ceiling is heated is the only stably-stratified geometry and would, in principle, be free of convective effects. This should lead to the lowest ignition temperatures. Rae et al. did not find this, and it appears that this is because they did not create a true ceiling geometry, but rather inserted a heated surface, face-down, but below the actual ceiling of the chamber. Such a configuration is not stably stratified and hot gases will still move convectively. Rae et al. also explored higher methane concentrations and results showed increasing ignition temperatures with increasing concentrations, up to the highest value tested (13%). Ignition temperatures were about 100ºC higher at 13% than at 6%.

Kuchta[50] subsequently illustrated the straight-line relationship for a number of other vapors (Figure 71). The functional relationship represented by all of the straight lines is:

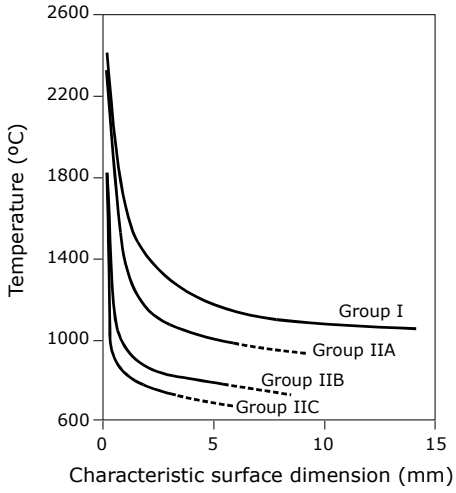


Figure 68 General trends for ignition of gases from hot surfaces

* The IEC Groups of gases are discussed in Chapter 12.

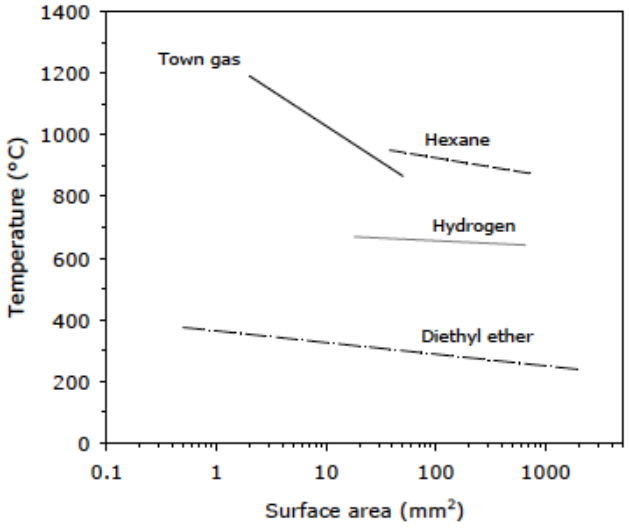


Figure 70 Effect of hot surface area on ignition of several fuel gas/air mixtures

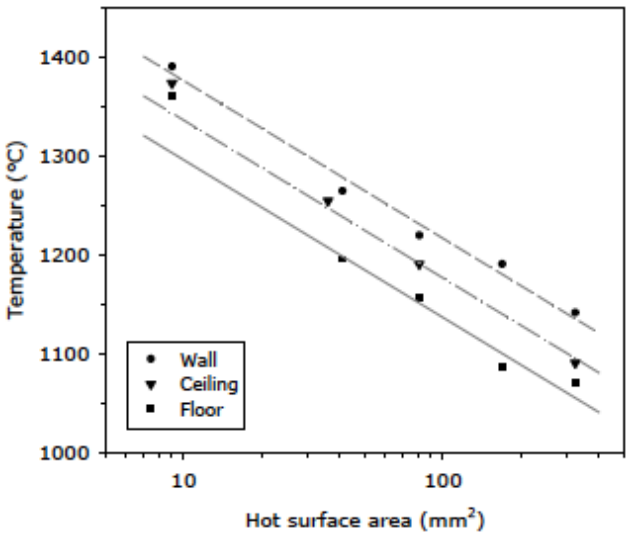


Figure 69 Effect of hot surface area and orientation on ignition of mixtures of 6% methane in air

$$T_{ig} = a - b \ln A$$

where A = surface area (cm^2) and a and b are different constants for each fuel. The data in Figure 71 show two distinct behaviors. JP-6 and *n*-hexane exhibit kinked curves, with a strong discontinuity at ca. 90 c m^2. For these fuels, cool-flame ignition is possible, and this is observed if the vessel size is large enough. Motor oil does not show cool flame ignition, while the other fuels were not tested with large enough heated areas to assess their trends. It is interesting to note that there is no discontinuity at the boundary between heated rods and heated vessels. This finding, in fact, denotes that there is a continuum of 'enclosedness,' with AIT test vessels being at one extreme and heated wires at the other.

The size effect on ignition time was explored for methane/air mixtures by Sano and Yamashita[79] using a computation model. They found a roughly similar relation for time as did Powell for temperature—size mattered little, once it exceeded about 10 mm; for very small sizes, the effect was quite large.

Oxygen concentration may have an effect on h ot-surface ignition, but there is little information on it apart from a study by Khalturinsky and Berlin[205] who used a 2.1 mm diameter heated cylinder, 21 m m long. Their results (Figure 72) indicate a strong effect up to about 40%, with no further effect at greater oxygen concentrations.

The *surface material* used makes a strong effect on catalytic ignitions, but it is also a factor for flaming ignitions from hot surfaces. This has historically been explored mostly in connection with autoignition tests for liquids, and details in Chapter 6 should be consulted. Bannister et al.[206] provide an explanation based on ionic effect. In their theory, the thermoelectric (Seebeck) effect at the hot surface increases the electron density and provides a negatively charged surface which polarizes oxygen molecules in the air, with the resulting induced O_2 dipole serving to promote rupture of

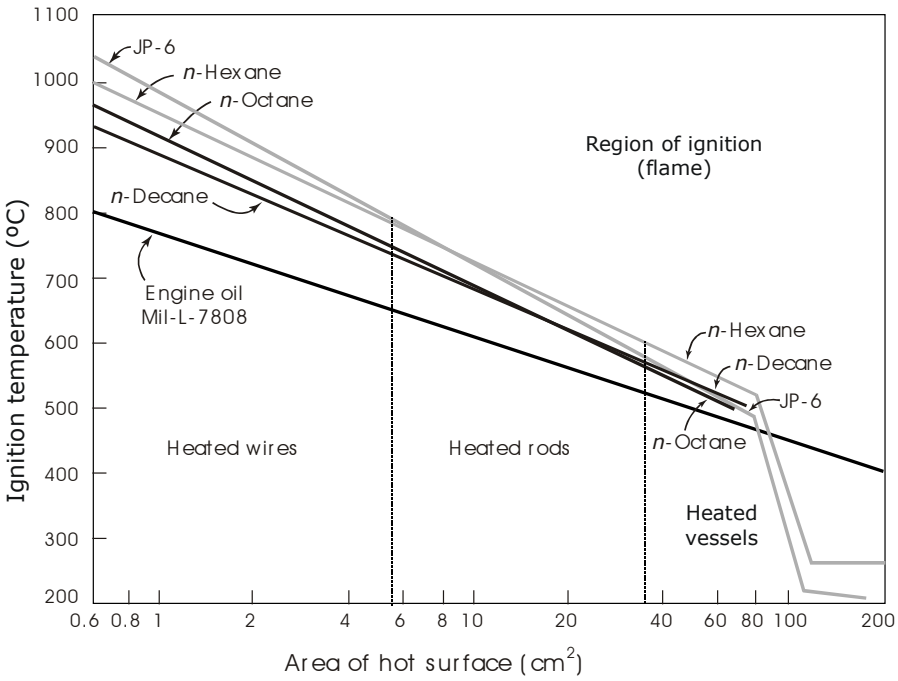


Figure 71 Ignition of vapors from hot surfaces: the effect of surface area

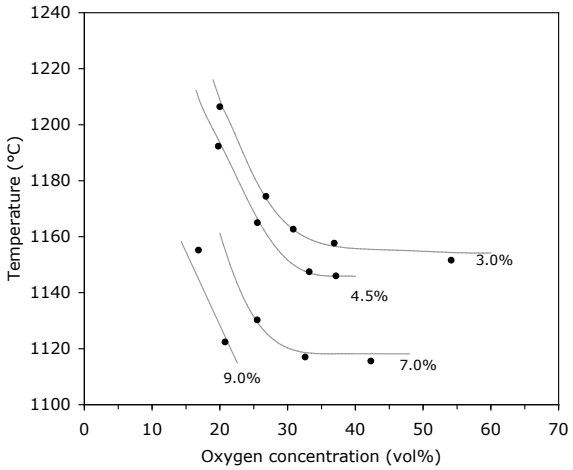


Figure 72 Effect of oxygen concentration on the hot-surface ignition temperature of various concentrations of methyl methacrylate vapor in air
(Copyright Elsevier, used by permission)

Table 11 Effect of surface material according to the theory of Bannister

Surface	Seebeck coefficient (μV K^{-1})		Ignition temp.
	At 25°C	At 300°C	
quartz	NA	NA	lowest
iron	+10	+8	
titanium	+5	+2	
zinc	+2		
aluminum	–1.6	–2.2	
platinum	–5.3	–11.6	highest

C–H bonds. Consequently, the more positive the Seebeck coefficient the more readily will ignition occur. Table 11 indicates that ignition trends are related to the Seebeck coefficient for metals. Non-metals do not have a Seebeck coefficient and Bannister provides another explanation why a quartz surface is expected to be negatively charged.

The effects of *gravity* were studied by Nagata et al.[207] on methane mixtures, who found that the results were identical in microgravity and in normal gravity, if the oxidizer was air. If the oxidizer was O_2, however, then ignition in microgravity was substantially faster than in normal gravity.

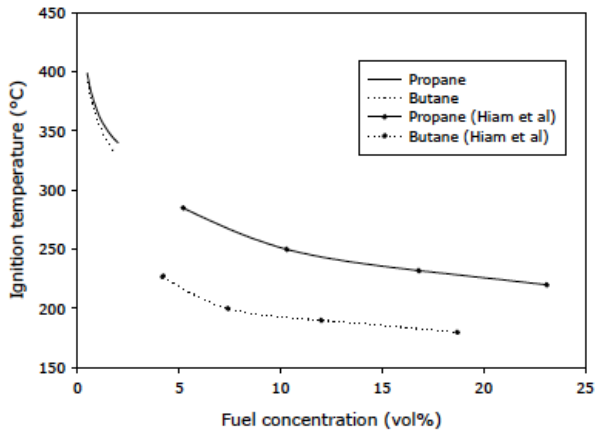


Figure 73 Platinum wire ignition of propane and butane

Catalytic (surface) ignition

Coward and Guest[186] were the first investigators to explore the effects of catalytic materials, but they only examined catalyst effects on gas-phase ignitions, rather than studying the surface-ignition phenomenon. Fundamentally, a catalyst functions by lowering the activation energy required for a reaction to occur. But the sequence of events comprising a surface (also called glowing, or heterogeneous) ignition is rather complex and there are five steps involved in the catalytic reaction process[208]:

(1) diffusion of the reactants to the catalyst surface
(2) adsorption of reactant molecules onto the surface, forming a catalyst-reactant molecule complex
(3) a chemical reaction, which may be between two adsorbed molecules or between an adsorbed molecule and one in the gas phase
(4) desorption of the products from the surface
(5) diffusion of the products back into the gas stream.

Cho and Law[208] examined the catalytic ignition of six fuels over a thin, heated platinum wire at near-zero flow velocity; increasing velocities had the effect of slightly raising the ignition temperature, therefore a very low, 'creeping-flow' velocity was used. Fuel, oxygen, and nitrogen were independently introduced in these experiments and, therefore, the O_2/N_2 ratio was not limited only to its atmospheric value. They found that the fuels fell into two groups: those whose ignition temperature dropped with increasing fuel concentration, and those which rose with increasing fuel concentration. The dropping-temperature fuels were propane (C_3H_8) and butane (C_4H_{10}). The rising-temperature fuels were carbon monoxide (CO), hydrogen (H_2), ethylene (C_2H_4), and propylene (C_3H_6).

The results for propane and butane are shown in Figure 73. The results are presented using fuel concentration as the main variable since it was demonstrated that varying oxygen in the range 4 – 20% had nearly no effect on the results. Since this is true, it can also be realized that plots against the equivalence ratio φ fail to give a single curve expressing the results. It is also interesting to observe that, when plotted against φ, the ignition temperature relationship does not change at $\varphi = 1$. In both the fuel-lean and the fuel-rich regimes, ignition temperature continues to decrease with increasing φ, although oxygen concentration never disappears as the second parameter. Figure 73 also shows some older data obtained by Hiam et al.[209] on propane and butane at higher concentrations. These authors used a 0.1 mm platinum wire coiled into a helix shape. Their propane data appear to be almost an extension of Cho and Law's, but the butane data are clearly lower than found by Cho and Law.

The remaining fuels all show a second type of behavior (Figure 74). With these fuels, the ignition temperature monotonically *increases* with fuel concentration. However, each fuel reaches a near-plateau value, and further fuel concentration increases do little to raise the ignition temperature. Unlike for the first group, where ignition temperature plotted against O_2 showed little variation (except very near to the $\varphi = 1$ value), for the second group of fuels the ignition temperature monotonically decreases with increasing O_2 concentration in the fuel-lean regime. The fuel-rich regime was not sufficiently explored for the second group of fuels.

Cho and Law concluded from the results, first, that catalytic ignition cannot be represented by any generalized Arrhenius form of reaction rate such as $c_f^a c_{ox}^b \exp(-E/RT)$ even for general powers a, b of the concentrations of fuel (c_f) and oxygen (c_{ox}). They also pointed out that the interaction of some very simple molecules with surfaces has been quantitatively studied at sub-ambient pressures, but that there is nearly no systematic information on interactions of common fuels with surfaces at atmospheric pressure. Qualitatively, they observed that data exist showing that the ranking of the adsorption strength of the molecules studied goes as:

$$O_2 > C_3H_6 > C_2H_4 > CO > H_2 >> C_4H_{10} \approx C_3H_8$$

The grouping of the fuels according to surface adsorption strength, then, corresponds to the two groups of ignition results, with propane and butane being difficult to adsorb since a C–H bond must be broken, rather than a C=C bond. Oxygen is more strongly surface-bonded than any of the fuels. In the case of propane fuel, most of the surface sites will be occupied by oxygen molecules and propane molecules will have difficulty getting adsorbed. Thus, reactivity will increase if a greater abundance of fuel is provided. Increasing oxygen however is not expected to change the reactions, since the surface is mainly populated by oxygen molecules. This qualitatively explains why increasing propane concentration lowers the ignition temperature, but increasing oxygen concentration does not change it. Other organic molecules which do not have C=C bonds, e.g., methane[211] and hexane[210], behave similarly to propane. Deutschmann et al.[211] consider that the adsorption strengths of CO and H_2 are greater than of oxygen, thus, at low temperatures the surface is going to be populated largely by fuel molecules, in the case of these fuels. Despite this difference in interpretation, the experimental trends observed by them are identical to those of Cho and Law.

In the case of propylene and other fuels of the second group, the adsorption strengths of the fuel are of the same order of magnitude as that of oxygen. Thus, it means that fuel and oxygen will be competing for surface sites. So, for lean mixtures, the effect on temperature should be similar whether the concentration of fuel is raised or the concentration of oxygen is lowered. The experimental results bear out this hypothesis.

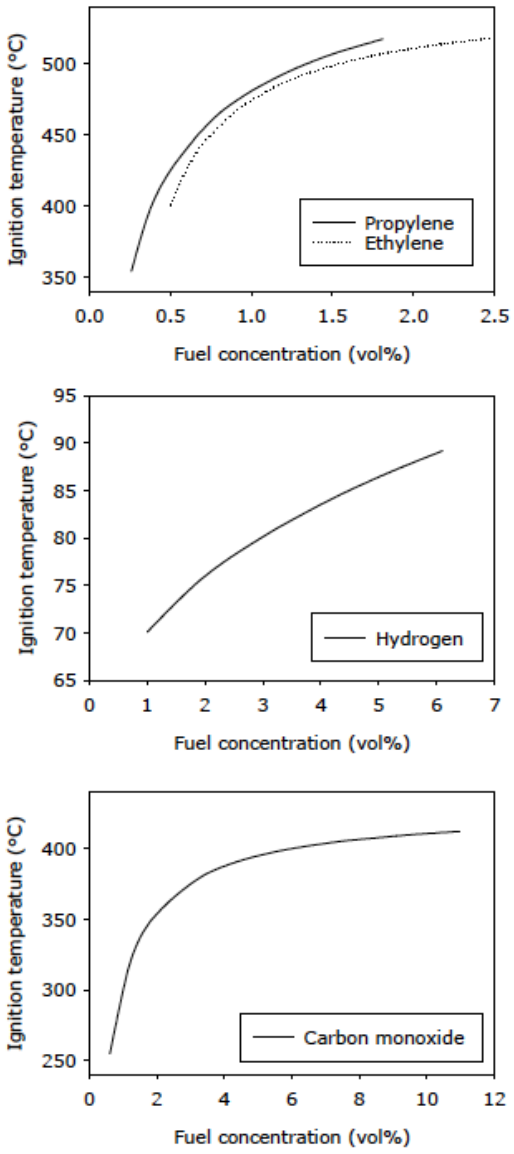


Figure 74 Platinum wire ignition of other fuels

Song and coworkers[212] constructed a test rig where a gas stream impinged upon a heated platinum foil ('stagnation flow' condition). In that arrangement, the size of the foil is immaterial, since it is much larger than the reaction zone of the gas mixture. In their experiments, they were able to separately identify homogeneous and heterogeneous ignition. Homogeneous ignition was evidenced by a visible flame; heterogeneous ignition was noted by a change in the power consumption of the electrically heated foil. Figure 75 shows their results. The 'flammability limits' for heterogeneous ignition were found to be much broader than for normal flaming ignition: for methane, these were 3 – 74%, in comparison to 5 – 15%. Over a substantial middle portion of the heterogeneous ignition range, a behavior was found which the authors dubbed 'autotherm.' In that range of concentrations, removing the electrical power from the platinum foil did not cause the combustion to stop.

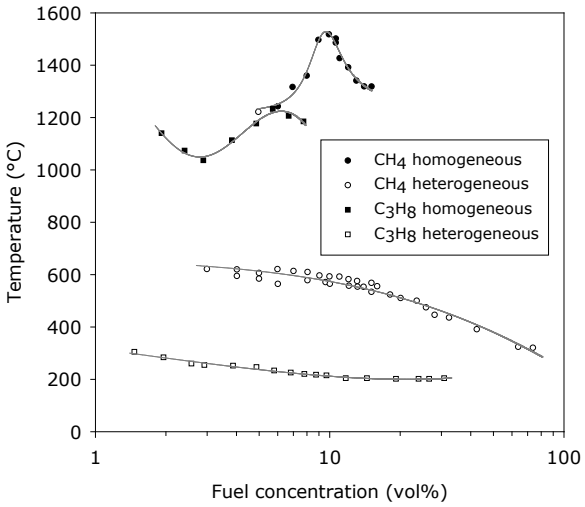


Figure 75 Platinum foil ignition temperatures for stagnation flow geometry of methane and propane

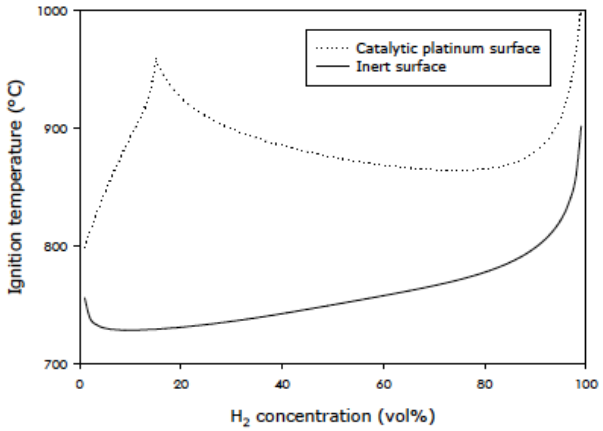


Figure 76 Ignition temperatures necessary for gas-phase ignition of hydrogen/air mixtures

Methane is a difficult to ignite gas, and early experiments[186] suggested a curiosity: for mixtures very close to stoichiometric, substantially higher temperatures of a platinum surface are needed than for mixtures with $\varphi < 0.9$ or $\varphi > 1.1$. For many chemical reactions, the condition of the mixture being near-stoichiometric is one that results the $\varphi = 1$ condition occur the most easily, thus, all sorts of chemical explanations were attempted to elucidate this anomaly. A good explanation did not come until careful experiments were done by Griffin and Pfefferle in 1990[213]. They found that gas-phase and surface ignitions must be considered separately and that, furthermore, these two forms of ignition may interact in order to create anomalous-seeming results. The anomaly stems from transient heat losses, since the heating time for a solid surface is much greater than the time scale according to which chemical reactions take place. Once a suitable experimental arrangement was developed, the authors found that surface ignition (glowing), temperatures ranged from 575ºC at $\varphi = 0.5$ to 545ºC at $\varphi = 1.5$, with no jumps in between. For gas-phase ignitions (flaming), the temperatures ranged from 1120ºC at $\varphi = 0.5$, to 1320ºC at $\varphi = 1.0$, to 1410ºC at $\varphi = 1.5$, with the range again being smooth and continuous. In neither case is there a jump at $\varphi = 1.0$. A surface ignition was possible even for the lowest value of φ explored, 0.025, although the temperature required was not reported. The authors also reported some data for surface ignition temperatures of ethane/air mixture; generally, temperatures about 240ºC lower than corresponding ones for methane were found. Over the range 76 – 250 μm, the wire diameter used did not influence the results.

The effect of using an inert versus a catalytic surface for flaming ignition of hydrogen was explored by Bui et al.[214]. Figure 76 shows how a catalytic surface interferes with a gas-phase ignition; also, compare these values to the vastly lower values shown in Figure 74 for glowing ignition of hydrogen. For inert surfaces, very similar results to those of Bui that are shown in Figure 76 were also obtained by Enomoto et al.[215]. However, they found increased temperatures with a platinum surface only for highly fuel-lean conditions. For mixture ratios with $\varphi > 0.4$, their platinum results were indistinguishable from the their inert surface results; possibly this was due to a lesser catalytic activity of their platinum surface.

The effect of oxygen concentration has been explored only to a very limited extent. Cho[216] obtained the CO data shown in Figure 77; he also reported a small amount of scattered data for propane.

Rogowski and Pitt[217] explored the ignition of various gas jets on the platinum covered surface of a catalytic room heater. The jet was 100% fuel, while the heater was situated in normal room air. For propane, they found that ignition occurred without any heating, the catalytic surface being at 21ºC. The most common application of hot surface ignition is for igniting modern gas furnaces and gas clothes dryers, wherein a silicon carbide *glow bar* is heated electrically. Such an arrangement has been found to be more reliable than the historically-used gas pilot; advice on practical troubleshooting of such ignition systems has been published[218].

Theories

Semenov theory. A simple thermal theory can be used to explain the minimum temperature T_c which a sphere of radius r must have in order to ignite a gas mixture flowing past it. The sphere is taken to have a given initial temperature and it is not supplied with electric heating. Assume that the temperature drops from T_c at the surface of the sphere to the ambient T_o in a small distance L. The area of this heated gas layer is approximately $4\pi r^2$ and the volume of the thin

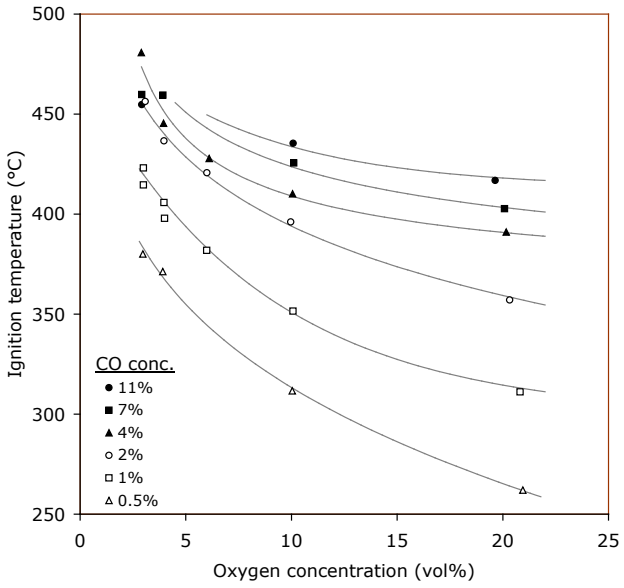


Figure 77 Effect of oxygen concentration on the catalytic ignition of CO

layer is $4\pi r^2 L$. If we assume a first-order reaction, then the HRR of the layer is

$$\rho QA(4\pi r^2 L)\, e^{-E/RT_c}$$

The conductive heat loss is

$$4\pi r^2 \frac{\lambda}{L}(T_c - T_o)$$

Equating the HRR to the heat loss gives:

$$\rho QA\left(4\pi r^2 L\right) e^{-E/RT_c} = 4\pi r^2 \frac{\lambda}{L}(T_c - T_o)$$

The heat transfer can be expressed by means of the nondimensional Nusselt number Nu. The general definition of Nu is:

$$Nu = D\frac{h}{\lambda}$$

where D = critical dimension (m) and h is the heat transfer coefficient (W m^{-2} K^{-1}). For a sphere, $D = 2r$. The heat transfer coefficient is defined as the thermal conductivity, divided by the thermal boundary layer thickness:

$$h = \frac{\lambda}{\delta_t}$$

In the present case, the thermal boundary layer thickness, by assumption, was L. Putting these together, we can replace L by $2r$/Nu, giving

$$\rho QA\; e^{-E/RT_c} = \frac{\lambda}{L^2}(T_c - T_o) = \frac{\lambda\, Nu^2}{4r^2}(T_c - T_o)$$

Or

$$e^{-E/RT_c} = \frac{\lambda\, Nu^2}{4r^2 \rho QA}(T_c - T_o)$$

By taking logs of both sides,

$$\ln\left[e^{-E/RT_c}\right] = \ln\left[\frac{\lambda\, Nu^2}{4\rho QA}\right] + \ln\left(\frac{T_c - T_o}{r^2}\right)$$

$$\ln\left(\frac{T_c - T_o}{r^2}\right) = -\frac{E}{R}\frac{1}{T_c} - \ln\left[\frac{\lambda\, Nu^2}{4\rho QA}\right]$$

Thus, by plotting experimental data with $1/T_c$ on the x-axis and $\ln\left(\frac{T_c - T_o}{r^2}\right)$ on the y-axis, a straight line will be obtained with a slope of $-E/R$ if simple, single-step kinetics, in fact, controls the ignition process. Ashman and Büchler[219] presented a theory which is variant of the above.

Laurendeau theory. Semenov's theory does not address the details of the heat losses from the hot surface, which are important in establishing data trends. Thus, Laurendeau[220] proposed a theory for hot-body ignitions that includes stagnant gas, natural convection, and forced convection possibilities. Laurendeau starts from the postulate of van't Hoff, who considered that ignition at a hot surface can be defined as the moment at which the net heat flow at the surface is zero. To understand the physical basis for this criterion, it is helpful to consider Figure 78. If a volume of gas is not ignited, then heat is being delivered from the hot surface to the gas. Thus, the heat flow is into the gas, and the temperature gradient at the surface is negative. If a gas is already ignited, then heat from combustion is available to be delivered into the boundary surface; thus the temperature gradient at the surface is positive. The condition where the temperature gradient is zero represents no net heat flow (adiabatic condition) and corresponds to the ignition event. Of course, the theory could not be used if the hot surface were so hot that its temperature would exceed the flame temperature of the gas mixture.

Laurendeau assumes that the surface is convectively cooled, i.e.,

$$\dot{q}''_{x=0} = \frac{\lambda\, Nu}{L}(T_w - T_o)$$

where T_w is the temperature at the wall (K) and T_o is the temperature of the surrounding gas (K). By equating this value to the heat transfer due to combustion, an ignition criterion is obtained:

$$\left(\frac{\theta_w - 1}{\theta_w}\right)^2 \theta_w^{n/2} e^{E^*/\theta_w} = \frac{2D_1 D_2}{E^*}$$

where $_w = T_w/T_o$, $E^* = E/RT_o$, and two Damköhler numbers D_1 and D_2 are defined as:

$$D_1 = A\left(\frac{P}{RT_o}\right)^{n-1} \frac{X_o^{m_o} L^2}{\alpha\, Nu}$$

$$D_2 = \frac{X_f^{m_f} Q}{C_p T_o}$$

X_o = mole fraction of oxidizer, X_f = mole fraction of fuel, the reaction rate is defined to be:

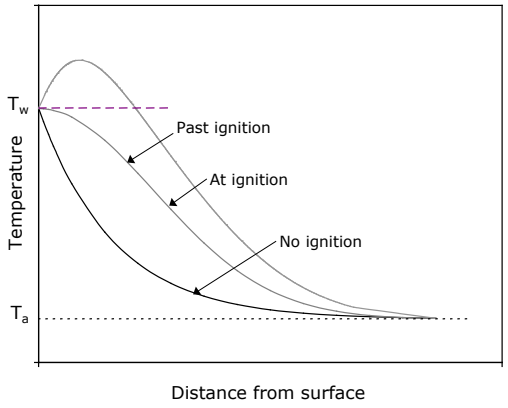


Figure 78 Temperature distribution near the heated wall

$$\dot{w} = -X_f^{m_f} X_o^{m_o} A e^{-E/RT}$$

$$n = m_f + m_o$$

α = thermal diffusivity ($m^2\ s^{-1}$), and L = characteristic dimension (m). The evaluation of Nu depends on the flow conditions. If flow is assumed not to be turbulent, then

Nu = constant	stagnant
$Nu \propto L^{3/4}(T_w - T_o)^{1/4} P^{1/2}$	natural convection
$Nu \propto L^{1/2} u^{1/2} P^{1/2}$	forced convection

where u = flow velocity ($m\ s^{-1}$). For the combustion of hydrocarbons, $n = 2$ is commonly the order of the reaction. Furthermore, the effect of T_w is mostly concentrated in the exponential term; thus, dropping the other factors containing T_w, one obtains:

$\ln(P^2 L^2) \propto E/RT_w$	stagnant
$\ln(PL^{1/2}) \propto E/RT_w$	natural convection
$\ln(PL/u) \propto E/RT_w$	forced convection

The application of the theory to Cutler's data[221] is shown in Figure 79. When plotting 2 ln (L) as a function of $1/T_w$, the results for stagnant conditions should fall along a straight line whose slope is E/R. For methane, an appropriate value of E/R is 25,000. The solid line in Figure 79 shows that the three lowest-temperature points follow this relationship. Why do the others not? The reason is that at high strip temperatures, it is no longer appropriate to assume stagnant conditions—elevated metal temperatures induce natural convection in the gas atmosphere. For pure natural convection, the slope would be 25,000 if 0.5 ln (L), instead of 2 ln (L) were plotted on the y-axis. In other words, if the y-axis remains 2 ln (L), then data points should follow a line of $4E/R$. The dotted line bears this conclusion out, and indicates that points following that line must be considered as being in a natural convection flow, not in a stagnant gas.

Laurendeau's theory does less well when applied to Kuchta's data[67,248]. Figure 80 shows that at higher temperatures, the same slope of 25,000 (note that, for convenience, the x-axis variable is plotted as $1000/T_w$) is found. But at lower temperatures, the slope is roughly 10,000, which is neither 2× nor 4× the high-temperature slope. It is of some interest to observe that the break in slope for Cutler's data is at 1800ºC, while for Kuchta's data it is at 700ºC. Both values are much higher than the regime in which cool flames occur.

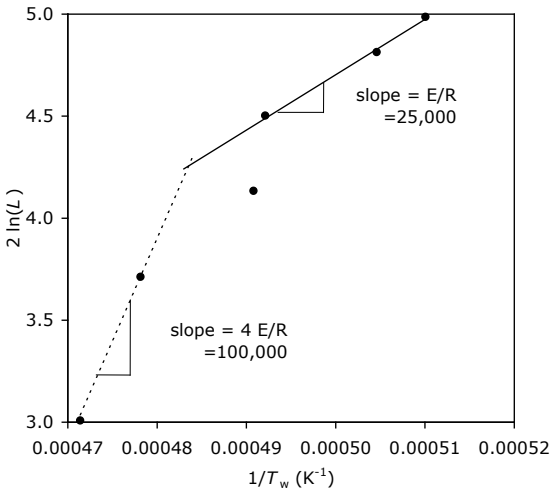


Figure 79 Laurendeau theory applied to Cutler's data: hot-metal-strip ignition of 7% methane/air mixtures; L = width of strip (mm)
(Copyright The Combustion Institute, used by permission)

Kumagai and Kimura[222] obtained a large amount of data for hot-wire ignition of town gas. According to Laurendeau, for forced convection, the correlating function should be $\ln(L/u)$. This did not collapse their data, but the data can be collapsed by a more general treatment of the Reynolds number. In general, the heat transfer coefficient[223] is proportional to:

$$h_c \propto \frac{(Lu)^k}{L}$$

Laurendeau's suggested correlation form implies $k = 0.5$. Collapse of data onto a single line was possible by taking $k = 0.25$, in other words, by plotting $\ln(L^2/(uL)^{1/2})$, as shown in Figure 81.

Ono et al.[224] studied the natural convection case for a number of gases. Applying a modification of Frank-Kamenetskii theory, they were able to correlate their experimental data according to:

$$\ln(P^{n-1} L^{1/2}) = C_1/T_w + C_2$$

This equation differs from Laurendeau's in that (a) a constant term C_2 is added; and (b) a variable order of reaction n is assumed. Their data for propane gave $n = 2$, but methane, ethanol and diethyl ether gave $n = 1.7$. The additive term was seen to become important for temperatures greater than

about 1300 K; for such temperatures, a straight line is no longer found and the additive term accounts for the curvature. The conclusion with regards to Laurendeau's theory and related theories is that while they are tractable, they do not offer any notable improvement in correlating experimental data over the plots based on area as correlating variable, discussed above. Perhaps it is too much to expect significant accuracy from Laurendeau's simple theory when applied to electrically heated bodies—it must be kept in mind that it does not include any heat-balance term for the electrical power supplied.

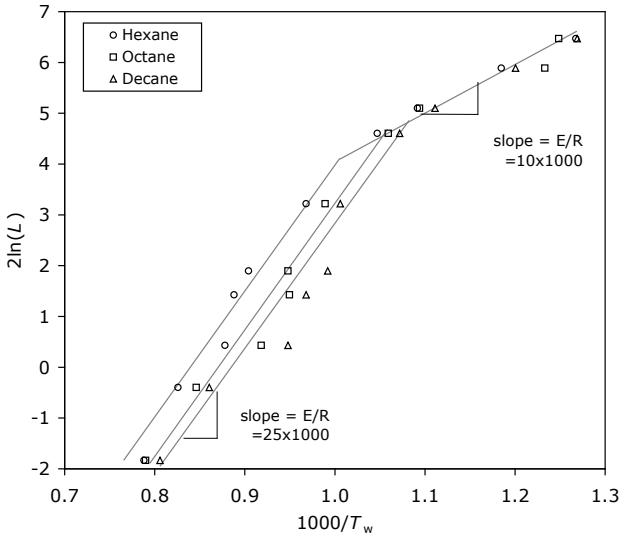


Figure 80 Laurendeau theory applied to Kuchta's data: hot Nichrome or Inconel wires

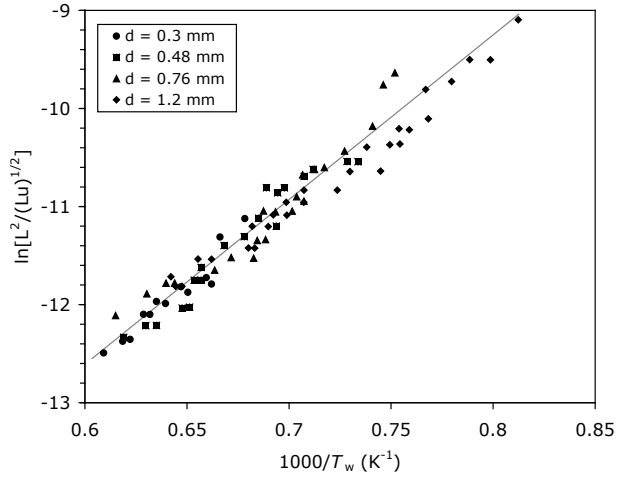


Figure 81 Correlation of forced-convection results of Kumagai and Kimura for hot wires in town gas

Other theories. A model was developed by Goyal et al. that endeavors to predict hot-sphere ignition temperatures from fundamental chemical kinetics data[225]. Sharma and Sirignano[226,227] constructed an elaborate model and obtained some numerical solutions with it. Their calculations showed the expected behavior—smaller size or higher velocity of the hot body require higher temperatures for ignition to be attained, but no closed-form solutions were derived. Cairnie et al.[228] proposed another model requiring significant computational effort. Boczek et al.[229] developed a theory for the ignition of a hydrogen-air mixture by a stationary hot sphere. They considered a single-step Arrhenius reaction in the gas phase and solved the problem numerically. A minimum particle diameter of 8 μm was predicted necessary to ignite an 8% hydrogen/air mixture. Toong[230] developed a theory for the ignition of gases by an infinitely-large plate, i.e., a laminar boundary layer solution for a gas flowing past a hot plate where the sides and the end of the plate are infinitely far away. In principle, solutions of this problem could make a good comparison for the infinite-size asymptote obtained from studies of finite-size objects. In practice, however, closed-form solutions or approximations were not obtained for Toong's theory that would be needed to make a comparison. Chen and Faeth[231] further developed the laminar boundary layer theory. Their theoretical calculations showed a large dependence on the Arrhenius parameters, but actual correlation to experimental data was not attempted. A number of authors have proposed ignition theories for *catalytic surfaces*, which may be heated or not. The one by Fakheri[232] is among the most ambitious; he also provides an extensive review of previous work on the topic. The problem generally modeled is one of forced convection over a long catalytic plate; this is relevant to some cases of purposeful combustion but is not a particularly common geometry for accidental ignitions.

FUSED WIRE IGNITION

In 1922, Ilsley and Hooker[233] studied the ignition of natural gas/air mixtures by heated 22 AWG (0.643 mm) copper and iron wires. They found that ignition took place only if the wires fused. Since two different metals could be brought up to just below their melting temperature without ignition taking place, yet ignition would occur upon fusing, the findings were suggestive that more than simply a hot-surface temperature effect was involved. Later, Shepherd and Wheeler[234] conducted more extensive experiments using platinum and tungsten wires. They found that the platinum wire needed to be heated to 1200 – 1300ºC, which was below the fusing temperature of the metal; ignitions with tungsten wires could be obtained far below the melting point. Subsequently, Davies[235] discovered that very thin (0.127 mm) gold wires only ignited methane/air mixtures upon fusing (T_m = 1064ºC). Repeating his experiments with platinum wires, he found that when the wire was heated to about 600ºC, the temperature took an abrupt jump to 1600ºC. This signified a heterogeneous ignition. The wire was then heated to its melting point (T_m = 1768ºC) by applying further electric power, but a gas-phase ignition never occurred. Davies concluded that when gas-phase ignitions did occur, it was because fusing of the wire caused a spark to appear and to ionize the gas mixture, and that these

should not properly be considered hot-surface ignitions. In further experiments, Davies found that heterogeneous ignition was strongly dependent on the nature and history of the platinum surface—fresh wires did not show a low-temperature heterogeneous ignition, only ones which were 'pre-conditioned' did.

Very thin (0.127 – 0.16 mm) copper wires were used by Silver[236] in 5% diethyl ether/air mixtures. Fusing the wires did not lead to any ignitions. However, when he used a slightly smaller (0.114 mm) wire, but configured as a long (0.3 m) spiral, he obtained an ignition even without fusing the wire. Wires of 0.33 – 0.63 mm diameter did lead to ignition, but only after fusing. Silver also showed that small (5A or less) glass cartridge type fuses (with glass removed) did not lead to ignitions of diethyl ether/air mixtures when fusing. Zborovszky[237,238] conducted constant-current tests using various wires (Table 12). Whether or not ignition took place after fusing was found to be dependent on the duration of the spark discharge caused by fusing. If the duration was 16 μs or less, there was no ignition, while durations of 70 μs or more did lead to ignition; intermediate values were not examined. In testing tungsten wire, Shepherd and found a special phenomenon taking place. Ignition could be achieved with very low currents if they waited for the wire to oxidize. As it oxidized, it lost thickness and eventually the tungsten itself ignited and flamed. At that point, the gas mixture would become ignited. Under these conditions, 0.065 mm wires required only 1.04 A for ignition, while 0.1 mm wires needed 1.56 A. Although copper does not ignite in this type of experiment, Zborovszky[237] found that with copper wires there was also an oxidation effect, which could lead to thermal runaway. If the wire temperature was raised above ca. 950ºC, then the wire started to undergo a runaway condition, leading to fusing. At temperatures below this value, the wire could be maintained at a given temperature without appreciably changing with time, without fusing, and without ignition. In her experiments on copper wires, ignition versus non-ignition cases showed a color difference. After the experiment, the wires which both fused and caused ignition were lavender or dark lavender in color, while ones which fused but with no ignition were grey. In her tungsten wire tests, Zborovszky found that ignition could be achieved without fusing, and with as little as 3.5 A, but this took 1174 s. In all her other experiments, ignition took place in 260 s or less, and was later followed by fusing. Thus, for tungsten wires the ignition mechanism was determined to be hot surface, with the subsequent fusing and arcing playing no role in the ignition process.

Lewis and von Elbe[70] considered that the minimum energy for fused-wire ignition should be the same as for spark ignition, but corrected for the energy needed to heat up the wire. Using the experimental results of Stout and Jones[239], they plotted MIE as a function of the heat sink variable ρVC (density × volume × heat capacity) for the wire and found that the energy extrapolated to $\rho VC = 0$ was very close to MIE as determined from spark ignition experiments; for higher values of ρVC, MIE increased linearly with ρVC.

Table 12 Zborovszky's results on the ignition of 8.3% methane in air by heated wires

Wire	Diameter (mm)	Current needed for ignition (A)	Must fuse for ignition to occur
copper (100 mm long)	0.254	*	
	0.327	*	
	0.381	46	yes
	0.508	32	yes
	0.635	80	yes
beryllium/copper (80 mm long)	0.178	4.25	yes
	0.38	11	no
tungsten (11 mm long)	0.178	4.5	yes
	0.178	3.5	no
tungsten (80 mm long)	0.178	4.25	yes
	0.38	9 – 12	no
* wire fused, but no ignitions obtained			

Craven and Foster[240] claimed that ignitions from fused wires occur because, when a wire fuses, hot metal particles are ejected into the gas volume and these particles present a large surface area in contact with the gas. Furthermore, a larger gas kernel becomes effectively 'seeded' with such particles. But Zborovszky showed that such special assumptions are unnecessary by conducting two parallel experiments—in one case ignition took place upon fusing of the wire. In the second case, wires of the same diameter (0.635 mm) and the same electrical current (79.3 A) were used, but two wires were originally butted together, then quickly separated at a speed matching that at which fused wire ends separate. This experiment likewise led to ignition, leading Zborovszky to conclude that the ignition mode in fused-wire experiments is simply normal spark ignition. She did document that multiple flame kernels could be observed in some wire fusing experiments, but evidently these do not play a crucial role. The spark discharge produced 5 – 20 mJ in her experiments, and this energy sufficed for ignition.

A comprehensive recent study[241] by Takahashi and coworkers explored the effect of a wide variety of fused wires on the ignitability of a methane/air mixture at room pressure and temperature. This type of experiment is carried out by selecting a DC or AC power supply of a given voltage. A wire of a given metal type, diameter and length is then connected to the power supply. A current recording circuit determines the total current which flowed through the wire, up to the point that the wire fails due to fusing. The total power delivered is simply determined as the integral over time of the voltage times the current. By monitoring the current, the authors were able to elucidate the *time* element in such ignitions. For mixtures at the LFL, ignition occurred during the wire's heating-up period, before fusing. But for mixtures at the UFL, ignition corresponded to the

fusing event. This difference implies that less heating energy must be delivered for ignition at the LFL than at the UFL. Within certain broad ranges, the results did not depend significantly on the diameter of the wire nor on the voltage used for fusing. A very high voltage (100 VAC), however, was found to cause such a vigorous scattering of particles that results had poor repeatability. Takahashi also found that a different ignition mode occurred if the voltage was low enough so that a long preheat time occurred before fusing. In such cases, they believe that the fuel gas is able to decompose prior to ignition and that the subsequent ignition, effectively, represents a different fuel. When tungsten wires were fused under long-preheat conditions, an additional phenomenon was observed. The actual ignition was preceded by observable chemiluminescence, which is attributed to a tungsten-carbon reaction. Under such conditions, the UFL was increased from 16.3% to ca. 17.5%. Takahashi's main conclusion was that metals of high melting point, such as molybdenum (T_m = 2892 K), and tungsten (T_m = 3663 K) give higher UFL values than do low melting point metals, such as copper (T_m = 1357 K), Nichrome (T_m = 1673 K), or platinum (T_m = 2043 K). A limited exploration with copper wires indicated that fusing of an 0.3 mm diameter wire was never sufficient to cause ignition; copper wire of 0.5 mm diameter was able to cause ignition, but only by using a very large amount of energy. Thus, for the purposes of conducting standard, conservative tests, only the high melting point metals should be used. When various exceptional ignition modes were excluded, the flammability limits for methane/air under fused-wire ignition conditions were found to be 4.6% to 16.3%, which is slightly broader than the 5.0% to 15.0% spark-ignition range reported by Coward and Jones[242]. The authors consider this to be insignificantly different, since a German test method (DIN 51 649 Part 1) employing an apparatus similar to Coward and Jones, but with somewhat different dimensions, gives a flammable range of 4.4% to 16.5%.

When a current-carrying wire is fused, the diameter of the *droplets* formed normally does not exceed the wire diameter[237].

IGNITION BY HOT, NON-FLAMING GASES AND MESG

There are a number of safety problems where the ignition problem is as shown schematically in Figure 82. Two chambers are connected by a narrow passage. The primary chamber has a flammable atmosphere and an explosion takes place there. It is desired to prevent an explosion in the secondary chamber, which also may contain a flammable atmosphere. With this arrangement, the ignition in the secondary chamber may be due to:

- a jet of hot gases expelled into it
- a flame expelled into it
- hot particles expelled into it.

Ignition by flames was already considered earlier in this Chapter, while ignition from small hot particles moving through a narrow passage has only been studied to a limited extent and it is considered in Chapter 12 under explosionproof enclosures. The phenomenon which generally tends to govern ignition in practical situations of this kind is a jet of hot, non-flaming gases and this mechanism will now be considered. The problem is typically important in chemical manufacturing plants, where electrical equipment, even under failure conditions, must be prevented from igniting flammable atmospheres. In such equipment, it may be impractical to insist on zero gaps at junctures such as mating flanges, and finite-size gaps can be permitted, if it is reasonably certain that an explosion will not be initiated through this path. In safety regulations, this is done by limiting the size of the gap to a prescribed maximum size, called the MESG (maximum experimental safe gap).

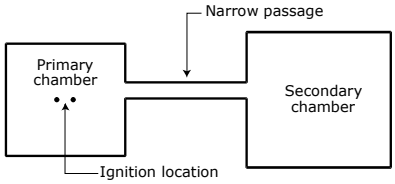


Figure 82 Basic geometry of the secondary chamber ignition

A jet of hot, but non-flaming gases has the ability to act as a pilot for igniting a mixture. The earliest investigations of this phenomenon were by Wolfhard and coworkers. In one study[243], using jets of hot air or nitrogen, they showed that mixtures of hydrocarbon gases in air required very high temperatures for ignition, typically 900 – 1100ºC. The flow rate of the hot gas jet, however, had nearly no effect. The effect of oxygen percent in the atmosphere was negligible, for concentrations > 21%, and modest for concentrations between the MOC and 21%. Using a jet of nitrogen to ignite H_2/air mixtures[244] required a temperature less than 755ºC; a temperature of 870ºC sufficed for a hot air jet to ignite a CO/air mixture. Later, they examined[245] methane/oxygen/nitrogen jets escaping through a narrow channel into an 'outer' methane/air atmosphere. They first determined that gaps smaller than 3 mm in diameter would not pass through a methane/air flame, but ignition of a flammable 'outer' mixture could still occur due to the issuing hot gas jet. When the gap diameter became less than about 2.75 mm, hot-gas-jet ignition became impossible, unless the escaping jet's composition contained more than 21% oxygen. For gaps below about 0.5 mm, even highly oxygen-enriched jets were unable to cause ignition. For methane/21% O_2/nitrogen jets escaping into an outer atmosphere where the fuel was a mixture of CO and H_2, however, a much smaller gap of 1.2 mm was required to prevent ignition. The problem has another size variable, the length of the channel. Functionally, this corresponds to the width of the flanges containing the gap. The longer the gap length, the greater the cooling effect that might be expected on the jet. Thus, for lengths greater than about 5 – 10 mm, it was found that increasing gap length increased the minimum oxygen concentration of jet required for ignition to occur. However, it was found that very short gaps (< 5 mm) made

ignition more, not less, difficult. This is because flows emerging from short channels diverge rapidly, with attendant cooling.

In other experiments, Wolfhard et al.[246] documented that a stoichiometric hydrogen/air 'inner' mixture was more incendive than a stoichiometric methane/air mixture. They also deduced that shock waves do not play a role in igniting the outer mixture. Vanpée and Wolfhard[247] showed that there is quite a good correlation (but not a straight line relation) between the gas-jet ignition temperature and an unusually-defined limit flame temperature of a particular fuel gas. The limit flame temperature (see Chapter 3) is normally defined as the flame temperature at the LFL, but Vanpée and Wolfhard defined it as the flame temperature when a stoichiometric fuel/oxygen mixture is diluted with sufficient nitrogen so as to be at extinction.

In a study encompassing a variety of fuels, Kuchta and Cato[248] found that the lowest temperatures were required when the fuel/air mass ratio exceeded about 0.5. At a fuel/air ratio of 0.25, igniting temperatures were about 50ºC higher. The results are hard to present in some universal way because ignition temperatures decrease with increasing jet diameter[249]. This relation appears to be monotonic and does not show a minimum. The authors also studied several permutations of the basic situation of discharging a hot-air jet into a flammable atmosphere:

- a hot-air jet is discharged into a volume of pure fuel (without an oxidizer).
- a hot-nitrogen jet is discharged into a flammable atmosphere.

These test conditions likewise led to a plethora of disaggregated results. Qualitatively, however, the authors observed some important effects. As an example, injecting a hot nitrogen jet from a 17 mm diameter hole into CO/air mixtures produced no visible phenomena if the jet temperature was below 750ºC. But when the jet temperature was between 750 and 875ºC, a luminous column appeared in the CO/air mixture. The color was generally deep blue at the base of the column, progressing to green further downstream. The length of the column increased with temperature and reached about 250 mm at 875ºC. For temperatures in excess of this value, flame originated at a location roughly corresponding to the tip of the luminous column. This flame then propagated throughout the vessel, denoting a true ignition of the mixture. With the exception of hydrogen mixtures, lowering the *pressure* of the system caused an increase in the ignition temperature, but the effect was not large until pressure dropped to ca. 0.2 atm. Methane[250] generally behaved in a different manner from other fuels. Flaming ignition without a preceding luminous column occurred if the methane concentration in the target atmosphere was ≥6%. But for methane concentrations in the range of 1.5 – 5.5%, a bright luminous column was seen, but no flaming ignition. Some typical laminar-jet ignition data obtained by BM are shown in Figure 83.

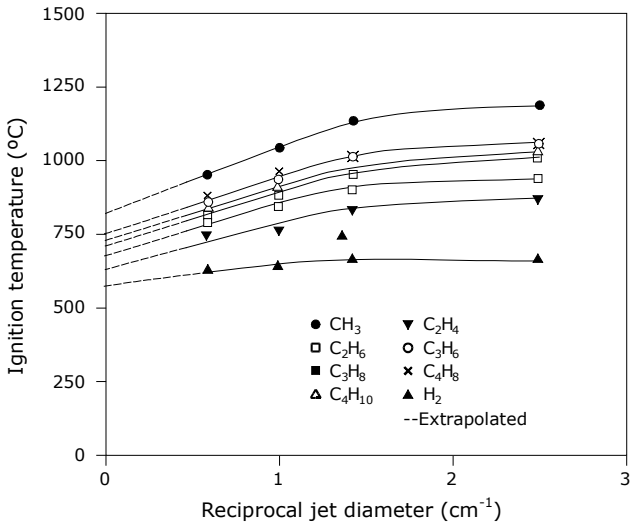


Figure 83 The effect of jet diameter on ignition with a laminar hot-gas jet[250]

For a given diameter of hot source, the temperatures of hot gas jets needed for ignition are always higher than the temperature of a hot, non-catalytic wire[251].

The above discussion was limited to laminar jets. Turbulent-jet ignition temperatures are generally higher than those for laminar jets. For turbulent jets, it has been shown that ignition, if it occurs, tends to occur at about 10 mm away from the exit[252]. A theory has also been proposed for the turbulent jet case[252], but it does not lead to closed-form solutions. The exit velocity of the gases (and whether they are laminar or turbulent) will, of course, be affected by the pressure developed in the primary chamber, thus, the fluid-mechanical regimes within the primary chamber must be considered next.

Upon an explosion in the primary chamber, the pressure in it will rise significantly, and an increase of roughly six-fold is common[253]. The role of pressure in the primary chamber is important, complicated, and not necessarily intuitive. Thibault et al.[254] explained that, as the outflow velocity from the primary chamber is increased, progressively three different regimes are encountered:

(1) A laminar flow regime, where the MESG pertinent to the narrow passage corresponds to the conventionally-measured quenching distance.
(2) A turbulent-mixing controlled regime, where turbulent mixing of the combustion products at the entrance to the secondary chamber causes the temperature of the jet entering the secondary chamber to drop. Consequently, increased pressure in the primary chamber (and flow velocity into the secondary chamber) lead to larger spacings being sufficient for quenching.
(3) A gas-dynamic regime, where flow is sonic at the inlet into the secondary chamber. In this regime, quenching distances are about an order of magnitude greater than

Table 13 Effect of flange breadth on the MESG of methane in air

Flange breadth (mm)	MESG (mm)
3	0.7
5	0.85
8	0.9
10	0.9
12.5	0.975
15	1.0
25	1.15
50	1.3
75	1.35

the MESG values for that particular mixture. An overpressure in the primary chamber of only about 0.8 atm can suffice to cause sonic outflow.

The highest pressure and velocity are developed if the ignition source is located at the center of the primary chamber. As a consequence of this, the safest *location* for the ignition source in the internal chamber is at the center and the least safe is near the flanges. Experiments where the igniter was located in different locations within the primary chamber will generally yield quite different results. For example, in some early tests, Walls et al.[131] found that a circular orifice of 5.1 mm diameter (in a 3 mm thick wall) was required for ignition of a methane/air mixture, whereas its MESG is reported as 1.14 mm when measured in current-day test equipment. Larsen and Eckhoff[255] showed that for gap sizes slightly greater than the MESG, there is only a very small range of igniter-to-gap spacings for which propagation can occur. Maekawa and Takeichi[256] demonstrated that when the igniter was located in the center of the primary chamber and not close to the flange, values of MESG were found which were higher than the quenching distance. Smith[257] studied the igniter location effect for methane/air mixtures in three different vessels and found that the effect ranged from negligible to about 30%; the effect was generally largest for very small flange breadths (< 6 mm). Phillips[258] directly studied the effect of flow velocities when the igniter location was changed.

Most of the MESG studies have used small spark ignition sources, since the application of the results is typically to electric-control equipment that only uses small currents. But if ignition in the first chamber is from a large arc, then smaller gaps are needed in order to avoid transmitting the explosion into the second chamber. Bartels[259] found, for a limited number of tests, that the required gap size dropped with increasing arc current. Additional data have been presented by Birtwhistle and coworkers[260,261].

The annular space between the flanges through which the primary chamber gases escape has three dimensions. The MESG itself corresponds to the smallest dimension, but the other two dimensions can affect the outcome and, thereby, have an effect on the MESG value. Phillips[262] documented that the MESG value increases with increasing flange breadth (i.e., the distance along the flow stream), up to a very wide 50 mm flange (Table 13). Riddlestone and Nethercot[263] also published similar data. Maekawa and Taeichi[256] showed that, under some circumstances the distance along third dimension (perpendicular to the gap and to the flow velocity) can also affect MESG values.

Brown et al.[264] showed that the volume of the space wherein the explosion originates must have a certain minimum size (ca. 900 mL for H_2) so that an incorrectly high value of MESG would not be reported (Figure 84).

Later investigators found that curves typically have a 'knee' at a much smaller volume. For instance, Redeker[265] provided data which provides the basis for the selection of a 20 mL internal test volume by PTB, the German safety testing organization (Figure 85). Redeker also showed that for the values to reach a constant asymptote, the secondary chamber must be configured as a pressure-relieving (constant-pressure) chamber. If the secondary chamber is sealed, then a constant plateau is not obtained, but that latter situation would not likely pertain to actual industrial explosions.

Phillips[266] attempted to create a model to predict MESG values. Basically, the exiting jet is cooled by air being entrained into it, while its temperature is raised by reactions. It is assumed that at the issuing gap there is zero fuel fraction. Now, in the outside atmosphere, combustible gas is present and this is being entrained, along with air. Thus, a competition is set up between cooling and heating. Phillips showed that the maximum entrainment rate is proportional to a group of constants representing the fuel, primarily its reaction rate. A plot of this 'fuel chemistry' variable against the MESG showed a good relationship, but Phillips did not

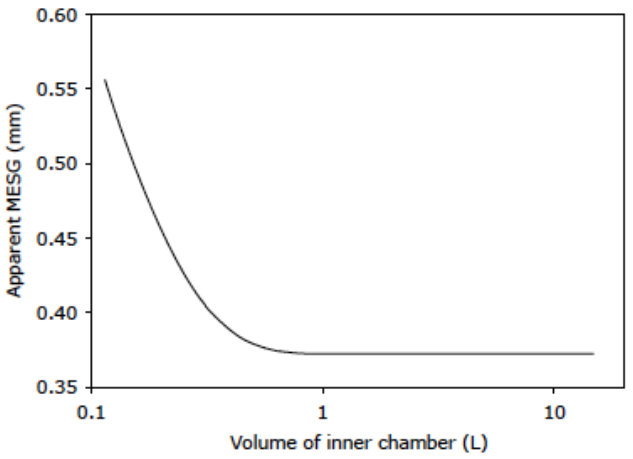


Figure 84 Brown's results on the effect of volume of the space wherein the explosion originates on the apparent MESG of mixtures of 29.6% H_2 in air (determined at the 50% probability level)

present verifiable computational details, and his theory has been criticized by Prof. Roger Strehlow as being unacceptably oversimplified[267]. Lunn[268] also attempted to relate the MESG to chemical structure. Qualitatively, he found it depended on the initial decomposition of the fuel molecule at pre-ignition temperatures, especially the bonds that were susceptible to earliest attack and the products which were being formed. Such considerations, however, did not lead to numeric predictions or correlations. In general, MESG values are lowest for gases which have unsaturated bonds (C=C or C C), since these tend to be least stable. Burgess and Hertzberg[269] proposed that MESG will be governed by the dimensionless ratio LFL/C_{st}, where C_{st} = stoichiometric fuel concentration (vol%). Unfortunately, checking this relation for a number of substances listed in Table 1 of Chapter 15 reveals that a correlation is non-existent.

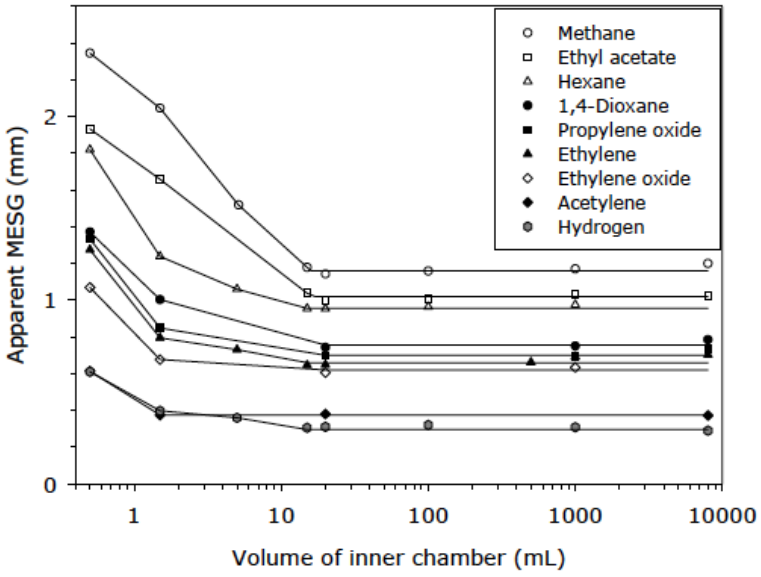


Figure 86 Redeker's results on the effect of volume of inner chamber on the apparent MESG (flange width = 25 mm in all cases)

If the flanges are heated, as by continued flame activity in the inner chamber, the effective MESG value will decrease. This dependence on *temperature* was documented by James[270] for the case of natural gas/air mixtures (Figure 86). In systems at elevated pressure, *pressure*[262] has an effect on the MESG, as illustrated in Figure 87. The curves for the three gases are quite similar and can be well represented by:

$$\frac{MESG}{MESG_{1\,atm}} = 0.13 + \frac{0.86}{P}$$

where P = total pressure (atm). *Humidity* has a negligible effect on results[271].

The MESG is normally quite a bit smaller than the minimum quenching diameter. This is because the quenching diameter is determined for a stagnant mixture, while in MESG testing an explosion is created in the inner chamber, which expels gases at high velocity. Helwig and Nabert[272] showed that for 20 common gases and vapors the relation:

$$MESG = 0.5\,d_{II}$$

is obeyed very closely (Figure 88), with only CS_2 showing a discrepancy. However, there are other exceptions. Wolfhard and Bruszak[245] found for a configuration where the inner volume comprised a nitric oxide/hydrogen mixture while the outer volume contained methane/air that MESG = 0.7 mm while d_{II} = 15 mm, which is a ratio of 0.062. Redeker[265] showed that values of MESG and the quenching distance would become identical, to within experimental error, if the MESG were measured using an inner chamber of very small dimensions instead of the 20 m L or larger volume that is needed for standard testing. This can be seen by noting that the data points in Figure 85 for the smallest test vessel are close to the published values of d_{II}.

The *test apparatus* used makes a difference. The values of MESG as determined by the UL's Westerberg apparatus (details of the test apparatuses are given at the end of this Chapter) are sometimes similar to the UK results and sometimes grossly different. The disparities were originally examined by Strehlow et al.[267], later by Phillips[273], and finally by Bartkus[422]. Strehlow conducted some modeling of explosions in the Westerberg apparatus, in the 20 mL HSE sphere and in the 8 L UK sphere. These results were inconclusive, but did point out a strong role of the flange configuration: in the UL test, the breadth (i.e., the travel distance for the escaping gases) of the flange is 19 mm, while it is 25 mm in both UK tests. Phillips considered it a serious draw-

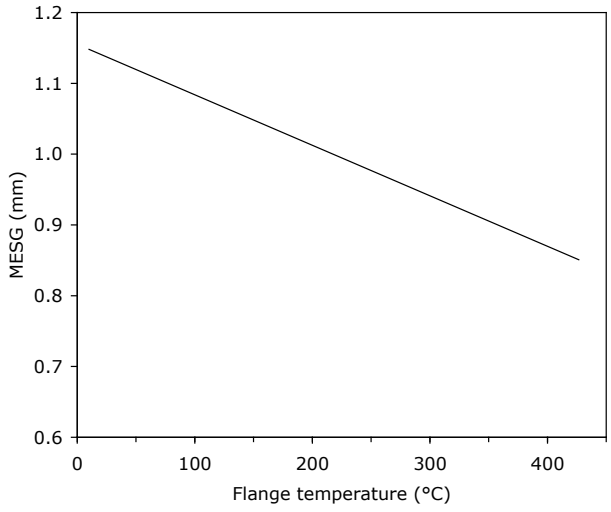


Figure 85 Effect of elevated temperature on effective MESG for the case of natural gas/air mixtures

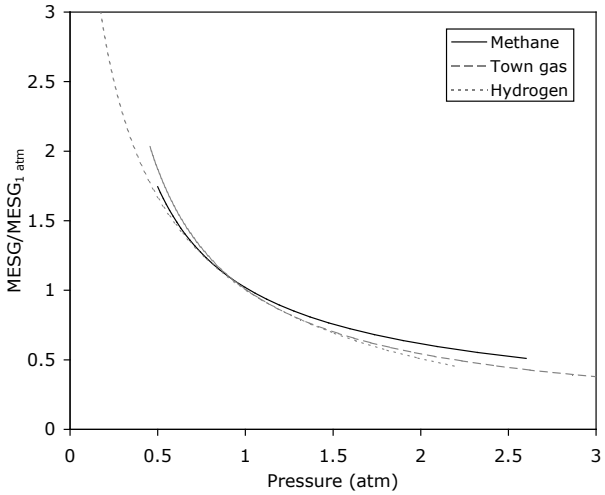


Figure 87 Effect of pressure on MESG

back of the UL rig that the secondary chamber is smaller in volume than the primary and consequently, the environment there becomes strongly vitiated by the entering gas jet. This has a pronounced effect only if the fuel has a low AIT, in which a spurious autoignition can occur in the secondary chamber due to the hot vitiated gases. Bartkus considered Phillips' hypothesis to be validated by further testing at UL, where new tests were run with the volume of the primary chamber reduced by 30%. This resulted in the MESG for hydrogen rising from 0.086 mm to 0.23 mm and for diethyl ether from 0.30 to 0.64 mm. Other values were unaltered by UL, despite their questionable status. Figure 89 shows a comparison of results; the UL values for hydrogen and diethyl ether are the corrected ones. Acetylene, ammonia, and carbon disulfide are clearly strong outliers and have not been corrected. Generally, only a very weak dependence on AIT can be seen, so effects other than a low-temperature

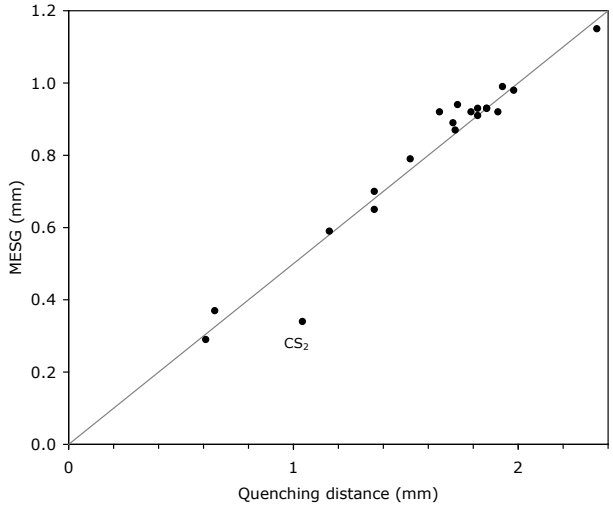


Figure 88 Relation between quenching distance and MESG

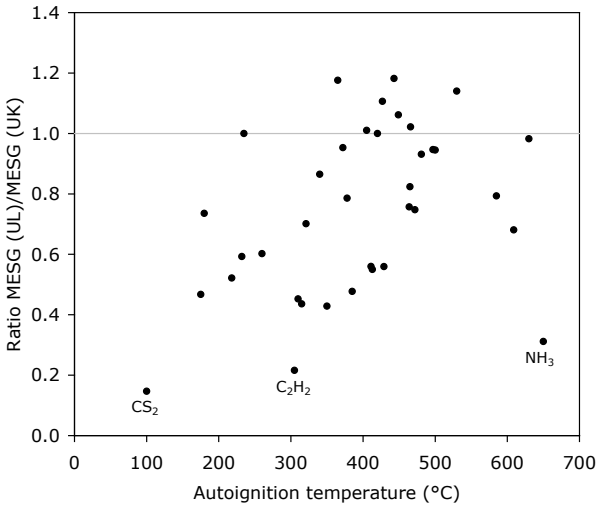


Figure 89 Comparison of MESG values obtained by the UL procedure and by the UK procedure

autoignition in the secondary chamber appear to be dominating. Britton[274] considers that the IEC/PTB apparatus should be used and that the UL apparatus is poorly designed. He pointed out that MESG data are mostly used for designing small electrical instrumentation cabinets and that creating pressure piling and bulk heating in the test system grossly misrepresents the intended use of the data.

As was pointed out by Slack and Woodhead[275], there is a relation between the MESG and the MIE. For industrial safety applications, the results of testing are often reported not in energy units but simply as the minimum value of current—'*minimum igniting current*'—needed for ignition. Figure 90 shows the results from PTB[272]. Their correlation line is:

$$MESG = 0.022 \times MIC^{0.87}$$

The correlation between MESG and MIC is used in the IEC scheme for design of electrical equipment for hazardous locations (Chapter 12). In there, the value of MIC is reported as the 'MIC ratio,' which is the MIC for the desired substance, divided by the MIC for methane. By using only the ratio, it was felt that some interlaboratory discrepancies would be eliminated. The MIC for methane is determined as 85 mA at PTB. Note that MIC values are even more test-apparatus-dependent than MESG values. The German researchers concluded that the UK values reported using the HSE Break-flash Apparatus No. 3 can be related to the PTB values as:

$$MIC_{HSE} = 2.17 \times MIC_{PTB}$$

The PTB values are the ones of more general interest, since their test apparatus was the one adopted as an international standard by IEC. Bartels and Howes[276] showed that values of the MIC, as determined in the IEC/PTB breakflash apparatus, decrease with increasing pressure, oxygen concentration, or temperature. A limited amount of data obtained by

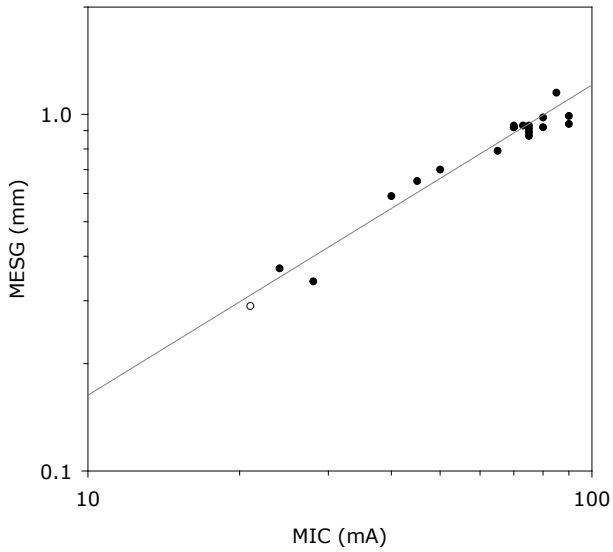


Figure 90 Relation between MESG and MIC using German data from PTB

Zborovszky[237] pertinent to the pressure effect suggests that $MIC \propto \frac{1}{P}$. Raising the oxygen concentration[277] from 21% to 35% causes the MIC to decrease by about 3×.

MESG data are compiled in Chapter 15. Brandes et al.[278] proposed a method for estimating the MESG of *mixtures* of gases.

IGNITION BY LASER ENERGY

The ignition of gases by lasers can be in one of six ways[156,279]:

(1) direct thermal heating of gas
(2) photochemical excitation of gas (photodisssociation)
(3) laser-induced breakdown (spark) of gas; a subcategory of this termed resonant breakdown is possible but has been demonstrated only for some unusual gases.
(4) radiative heating of small particles in the atmosphere
(5) laser-induced breakdown of gas aided by presence of small particles
(6) laser-induced heating of particles of explosives.

The last possible mode is very specialized and will not be considered. The modes that depend on direct use of laser energy to produce a spark kernel (#2 and #3) are inefficient—the bulk of the energy is not absorbed by the gaseous medium. Ignition by simple heating of a solid target (i.e., dust particle) can be much more efficient, and ignition by that mechanism requires much lower heat fluxes. With laser energy it is possible to initiate detonations, not just deflagrations, and Ronney[156] reviewed this topic.

DIRECT THERMAL HEATING OF GAS

Thermal heating is typically feasible if suitable molecules are present that can effectively absorb radiation at the laser wavelength. Trott[280] provided extensive data for ignitions in this mode on low-pressure (11 – 13 kPa) fuel/air mixtures using ethylene, methanol, ethanol, dimethyl ether, *p*-dioxane, *n*-propyl nitrate, and *iso*-propyl nitrate. The laser wavelengths used were 9.2 – 10.8 μm in his experiments. Successful thermal ignitions were also reported for $SF_6/CH_4/O_2$ mixtures from CO_2 laser radiation[281]; even though methane and oxygen are transparent to laser radiation, SF_6 does absorb and this suffices. The temperatures the gas needs to attain for ignition to occur are much higher using laser heating than using conventional heating arrangements. Trott typically found that T_{ig} values were 200 – 500ºC higher than standard AIT values. Apparent activation energies, however, as computed from $\ln(t_{ig})$ versus $1/T$ plots, were nearly the same as reported in conventional experiments.

PHOTOCHEMICAL EXCITATION OF GAS

If sufficient UV radiation is imposed, molecular oxygen can be dissociated into atomic oxygen. This creates the initial radicals needed to start a chain reaction, and combustion can then begin. Photochemical excitation was already studied by Norrish[282] in 1964, who used a photoflash tube for his experiments, before lasers for this purpose were available.

LASER-INDUCED BREAKDOWN OF GAS

Extremely intense laser radiation can cause a gas to break down in the form of a plasma, visible as a spark which, under the right circumstances, can be incendive. The irradiance needed (10^{11} – 10^{12} kW m^{-2}) is several orders of magnitude greater than necessary for ignition by directing laser energy onto a target surface or particle, with actual gas ignition then resulting from the elevated temperature of the target. Several groups[283,284] studied the effect of the wavelength of the laser used on the energy needed for ignition, but clear trends were not found. In laser-spark ignition, a plasma is created that has extremely high temperatures (100,000 to 1,000,000 K), along with high local pressures (ca. 10^3 atm) and a concomitant shock wave[291]. The laser pulse duration needed for ignition is very short. As an example, Phuoc[285] ignited stoichiometric methane/air mixtures at ambient pressure using pulse lengths of 5.5 ns. Because of the short duration, the energy needed was only 7.5 mJ. Detonable mixtures can be detonated by laser-induced breakdown. When atmospheric pressure is varied, Lee and Knystautas[286] showed for equimolar C_2H_2/O_2 mixtures that an inverse energy/pressure relation exists that characterizes the boundary between deflagrations and detonations.

In describing the ignition of methane/air mixtures, Phuoc and White[291] observed that initially a loud 'crack' is heard upon the breakdown of the gas and the formation of a spark channel, the kernel then grows and is followed later by a burst of blue flame enveloping the spark. For producing a spark (as contrasted to an incendive spark), about 2.5 mJ was found to be needed at 1 atm, with greater energies at

lower pressures. For sparks to be incendive at 1 atm, about 4 mJ was needed; this is about an order of magnitude greater than for ignition from a capacitive-discharge spark. Also, unlike for capacitive discharge spark ignitions, the minimum energy was found at rather high methane concentrations of 10 – 14%. In their experiments, where Phuoc and White had incendive results with irradiances of $10^{13} – 10^{14}$ kW m^{-2}, the corresponding beam powers were $10^6 – 10^7$ W and beam diameters were ca. 17 μm. For a spark kernel to continue growing and lead to ignition, a minimum size of ca. 0.4 mm was needed in the short axis; the kernels were cylindrical or ellipsoidal, and lengths were about double the width.

The sparks created by laser breakdown differ from sparks produced by capacitive discharge primarily in two ways: (1) the laser-induced plasma is hotter and of shorter duration than from spark discharge; and (2) heat transfer and flow effects due to metal electrodes are absent. Despite these differences, the energy required for ignition through laser-induced breakdown of gases is roughly similar to the MIE found in capacitive discharge testing. In an early study, working in a low-pressure regime ($0.2 \leq P \leq 0.4$ atm), Weinberg and Wilson[287] found the energy required for methane ignition by the laser mechanism was within about a factor of 3 to the value found at the same pressure in capacitive discharge testing. More recently, Lim et al.[288] conducted tests at 1 atm and found that there is a strong effect of pulse duration. Figure 91 shows that using shorter pulses (picosecond duration) more energy is required than for longer duration (nanosecond) pulses. The same trend was found by Syage et al.[289], who tested hydrogen/air mixtures. By extrapolating from their experiments with theoretical modeling, they showed that, while pulse durations on the order of 10 μs give MIE values about 10× higher than do capacitive sparks, pulses of 1000 μs give laser-ignition values similar to the capacitive ones. The latter is an exceedingly long time, however, and it is not clear if this a realistic extrapolation. Under many test conditions, the energy required for breakdown is inversely proportional to pressure, at least over a range of about 0.1 – 10 atm[290].

There is no detectable delay period between initiation of the beam pulse and spark breakdown if short-wavelength (ca. 1 μm or less) radiation is used. For long-wavelength radiation, e.g., a CO_2 laser at 10.6 μm, delay may be detectable[290].

Since one mode of ignition with laser radiation involves an electron cascade process, environments leading to the presence of initial electrons facilitate ignition; this includes the presence of impurities such as aerosols or low-ionization potential organic vapors[291].

A hybrid technique has also been used[292], whereby laser energy is focused onto a 'beam dump.' The latter is an open conical cavity where multiple reflections of the beam energy occur from the walls, with the energy being mostly deposited into the gas phase near the point of the cavity. The walls aid the focusing of energy in this case, but do not directly act as a hot-surface ignition source.

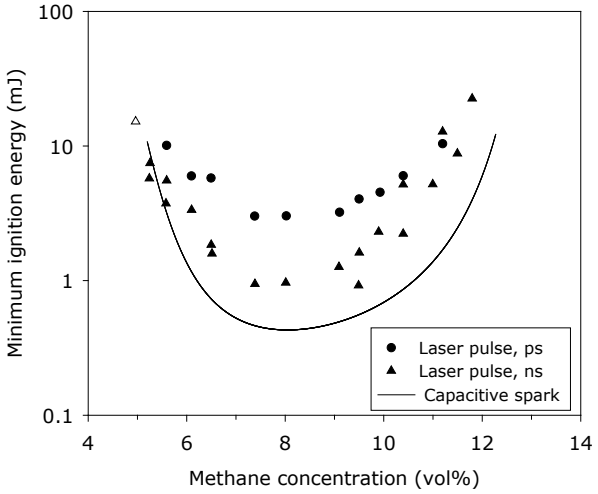


Figure 91 Effect of laser pulse duration on MIE for methane/air mixtures at 1 atm pressure

RADIATIVE HEATING OF SMALL PARTICLES IN THE ATMOSPHERE

If a gas mixture contains some suspended particles and a laser beam is hits a particle, under certain circumstances the heating can ignite the flammable gas mixture. This mode of ignition is considered to have potential for accidental ignitions, since laser measuring and sensing devices are more actively being introduced into manufacturing and extractive industries. Two types of target particles, in general, may be involved—combustible and non-combustible. Dubaniewicz et al.[293] explored this mode of ignition for methane/air mixtures. In their experiments, they used an optic fiber to deliver laser energy to particles which were adhered to the end of the fiber. Smaller fiber diameters were found to require less energy, with an 0.2 mm fiber requiring typically less than 1 W. Calculations showed that the non-combustible iron oxide particles used as targets heat up to roughly 1500 K in the ignition process. Bituminous coal particles (combustible) required more power than black iron oxide (Fe_3O_4) particles (non-combustible); this is attributable to the higher radiant absorptivity of the iron oxide particles. The same authors[294] also explored the ignition of hydrogen/air mixtures by laser beams impinging on coal dust particles. Their data, along with those of Carleton et al.[299], Zhang[295], Bothe[296], and Tortoishell[297] are shown in Figure 92. The role of very small particles is not fully clear. Experimental ignition data from other investigators exist down to very small particle sizes (Figure 92), but Tortoishell[297] reported in his study that he failed to ignite particles smaller than 0.25 mm diameter because the particles tended to vaporize, rather than to cause an ignition. Furthermore, in his

study he observed that combustible particles of any size decomposed without causing ignition.

When the area of the target becomes large compared to the quenching distance of the fuel, an area effect should disappear. Adler et al.[298] measured the minimum heat flux needed using large-size, inert targets and their results are shown in Table 14. If the target itself is combustible, lower heat fluxes are sufficient for ignition. For small charcoal particles in a carbon disulfide mixture, the authors found that 9 kW m^{-2} sufficed; large charcoal particles are themselves ignited by laser heating and do not make a viable target.

Generally, the optimally-ignitable gas concentration is lower with laser heating of target particles, than it is with spark ignition. For example, the optimal concentration for methane was found to be 5 – 6%, versus 8.3% for spark ignition testing.

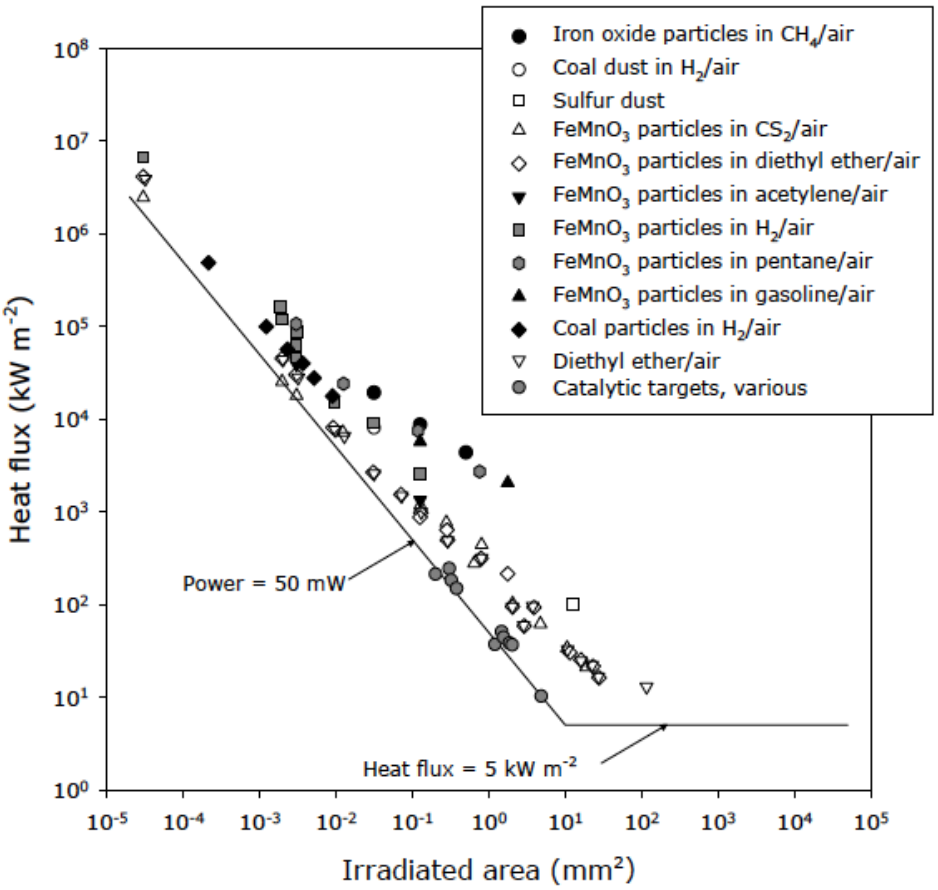


Figure 92 Summary of data on minimum laser heat flux required for ignition of gases by heating of solid target particles

Carleton et al.[299] examined the effect of varying oxygen concentrations over the range 15 – 28% and concluded that the effects were minor. They also explored the effect of the chemical nature of the fuel gas. These results are shown in Table 15. The target powder was chosen because it led to lowest power ignitions; coals, carbon black, and black toner particles generally needed higher power for ignition. Visually, it was found that ignition occurs above the target, not directly adjacent to it. The authors also reported that, with very small beams "the target appears seriously disturbed by the beam and a hole is instantaneously drilled into the target at the hot spot." Quite evidently, a target cannot be raised to a high temperature for a sufficiently long time to ignite a gas atmosphere if it has vaporized; however, general guidelines for conditions under which vaporization occurs were not evolved. The ignition power results shown in Table 15 are roughly correlated to MESG, especially for the 400 μm fiber tests, with the exceptions of hydrogen, propane, and 2-propanol.

Table 14 Minimum heat flux needed for ignition using large, inert targets

Fuel	Min. heat flux (kW m^{-2})
carbon disulfide	22
hydrogen	80
ethylene	87
diethyl ether	90
propane	110
pentane	112
methane	167

In the case of dust clouds, a separate target and combustible gas mixture are not needed, since ignition can be obtained by absorption of radiation by particles of the dust cloud. Carleton et al. also obtained some results in dust clouds; these generally proved to be harder to ignite than targets in gas atmospheres. For example, a minimum ignition power of 1.9 W was found for a starch target in gas atmospheres, but this rose to 4.0 W for a starch target in a starch-dust atmosphere. Additional work is considered in Chapter 5.

The data summary shown in Figure 92 indicates that no ignitions occur at power levels less than about 50 mW. Based on this, the European Commission has selected a 35 mW level as intrinsically safe[299]. The heat flux $\propto$ 1/area relation holds over a very wide range of target areas, but clearly, as the heat flux is decreased and the area is increased, eventually a finite limit for the heat flux must be

Table 15 Effect of chemical nature of fuel for laser ignitions of $FeMnO_3$ targets

Gas	Conc. at min. ignition power (vol%)	Min. ignition power for 62.5 µm fiber (W)	Min. ignition power for 400 µm fiber (W)
carbon disulfide	1.5	0.050	0.149
diethyl ether	12.0	0.089	0.127
acetylene	25.0	0.110	0.167
hydrogen	10.0	0.140	0.331
ethylene	7.0	0.202	0.494
n-heptane*	3.0	NA	0.502
propionaldehyde*	2.0	NA	0.617
propane	5.0	0.250	0.842
tetrahydrofuran	6.0	0.267	NA
2-propanol	4.5	0.273	0.660
methyl ether	8.0	0.280	NA
methane	5.0	0.304	1.125
n-pentane	3.0	0.315	0.847
* tested at 110ºC			

reached. The Commission guidelines set forth 5 kW m^{-2} as the minimum heat flux below which ignitions are not expected. For gases other than diethyl ether and CS_2, the Commission criteria would offer a very large safety factor.

It is not a trivial task to explain why a 'power' limit exists in Figure 92. Carleton and Weinberg[300] proposed that the breakpoint separating the 'power' limit from the 'heat flux' limit should correspond to a size of the quenching distance for the gas. If the area over which the energy is deposited is smaller than the quenching distance, then the actual area has no role in the problem, since the energy from the entire area can be used in heating the flame kernel. For diethyl ether, the quenching distance is about 2 mm, while for CS_2 it is around 0.5 mm. For most other gases, it is generally 1 – 2 mm. Thus, according to this reasoning, the breakpoint should be at about 0.5 – 2 mm, or at an area of roughly 1 mm^2. In Figure 92, the breakpoint is found at ≈ 10 mm^2, but this value very much depends on data points taken to define the 'heat flux' limit, and latter, as mentioned above, is highly uncertain. Thus, given the fact that the experimental data span 8 orders of magnitude, agreement to within a factor of 10 seems entirely reasonable.

Based on data for large-area ignitions, Carleton et al. found an inverse correlation between the temperature of the target and the AIT of the gas. For silicon carbide targets (the only ones for which these data were provided), a relation was derived:

$$\theta_{ig} = 6.876\theta_a - 1.778\times10^{-2}\theta_a^2 + 1.392\times10^{-5}\theta_a^3$$

where $\theta_{ig} = (T_{ig} - T_o)$, T_{ig} = surface temperature at ignition (K), T_o = ambient temperature (K), $\theta_a = (AIT - T_o)$, and AIT = autoignition temperature (K). The relation, along with experimental data, are shown in Figure 93. Apart from ethylene and hydrogen, the relation fits the data rather well. The authors attributed the divergent behavior of the latter two gases to their exceptionally high laminar flame velocities. A number of mathematical theories[279,301,302] have been offered, but the solutions have been solely computational in nature and closed-form approximations were not offered. Note that at much higher laser irradiances than shown in Figure 92 (ca. 10^{11} kW m^{-2}) it is possible to achieve direct ignition of gases without converting the energy into thermal heating of a solid target; this mode was discussed above.

LASER-INDUCED BREAKDOWN OF GAS AIDED BY PRESENCE OF SMALL PARTICLES

This is, effectively, a combined mode of action and it requires much less power than breakdown without the presence of particles. Kingdon and Weinberg[303] explored this mode by focusing the laser beam sufficiently to cause a breakdown of the gas, but at the same time introducing particles into the focal region. In this mode, high heat fluxes are not required to break down the gas, and the authors considered the breakdown threshold to be smaller than they could measure. The actual energy needed for ignition in this mode turned out to be of the same order of magnitude (0.5 mJ) as the MIE for spark ignition (0.2 mJ) when igniting methane/air mixtures The proviso is that the energy which must be considered is the net energy developed in the plasma, not the gross energy supplied from the laser.

Flammability limits

Assuming that a substance shows an exothermic behavior due to oxidation and not due to self-decomposition, polymerization, or another form of a unary reaction, then it is evident that if an atmosphere contains 100% fuel or 100% oxidizer, no ignition and no fire can occur. What may not be necessarily evident is that the fuel/oxidizer ratio has to be within certain bounds, or else ignition is impossible, even if the 'fire triangle' is met, that is, fuel, oxidizer, and source of ignition are all present.

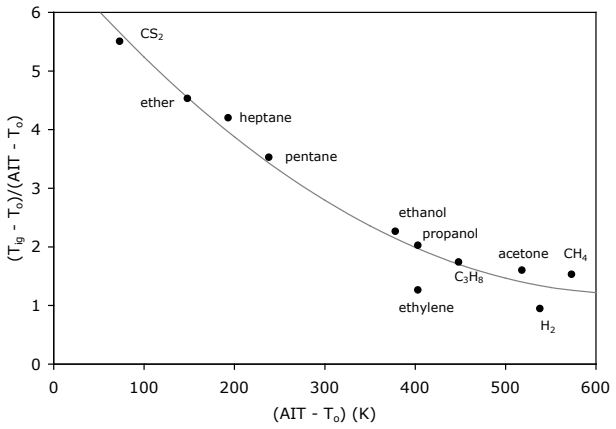


Figure 93 Relation between AIT and target surface temperature for ignition of gases by laser radiation heating of target surfaces

Qualitatively, the reason for the existence of flammability limits is because—apart from 'cool flames'—a flame of very low temperature cannot be sustained. The lowest possible flame temperature describes the minimum temperature below which reaction kinetics become so slow that rapid oxidation, i.e., flames, cannot occur. In the definition, it is important to realize that a continuous combustion is described, not a momentary phenomenon. Thus, a flammability limit can theoretically be considered to be a state at which a 1-dimensional, planar, premixed flame in an infinite medium becomes impossible. In addition to reaction kinetics, heat losses also come into play in any practical combustion situation.

The concept of *flammability*, as applied to gas mixtures, is more specific than is what is used in general in the English language. A mixture is flammable if a flame can *propagate* through it. Thus, if a local heat source, when applied to a mixture, results in combustion which does not propagate through the volume of the gas, the mixture is considered *non-flammable*. But if a heat source is introduced into a fuel/oxidizer mixture through which propagation cannot occur, a local 'cap' of flame may nonetheless be visible. The upper and the lower *flammability limits*[*], then, refer to the lowest and highest fuel concentration, by volume, for which the mixture is flammable. More precisely, the LFL is defined as the value half-way between the lowest concentration at which flame propagation occurred, and the highest concentration at which it did not. The UFL is defined in a similar manner. As with most aspects of ignition, the concept of flammability limits is not absolute, but rather depends on the details of the test apparatus by which the determination is made. Flammability limits are pertinent only to *premixed* fuel/oxidizer atmospheres; the concept is not meaningful if a volume contains significant spatial concentration non-uniformities.

The concept of flammability limits is applied only to normal flames. *Catalytic combustion* can take place outside of the normal flammability limits, since the process does not entail a flame propagation but rather a surface reaction. Thus, for example, the flammability limits of hydrogen in air are 4.0 – 75%, but using a platinum catalyst[304], combustion can be sustained over 1.0 – 80%.

Mixtures can come in a wide range of complexity, but commonly will be a fuel-oxygen-nitrogen mixture. Data presentation becomes somewhat complex, since a *ternary* system must be considered. Figure 94 shows the BM results for methane-oxygen-nitrogen on a triangular plot[51]. The flammable region is the fin-shaped area inside. A few geometric constructions are of interest in this kind of plot. To determine the minimum O_2 concentration which can result in a flammable mixture, given the worst-case fuel and N_2 percentages, a line is drawn that is tangent to the fin and parallel to the 'C-N' axis. This tangent line is seen to correspond to O_2 = 12%. By referring to the other coordinates at the point of tangency, it is found that CH_4 = 8%, and N_2 = 80%. The ratio of O_2 to N_2 in air is fixed at 0.2095/0.7905. Thus, a line labeled "air" is drawn which represents the line upon which any fuel/air mixture must be located, unless O_2 or N_2 are introduced into the system separately, not in their in-air ratio.

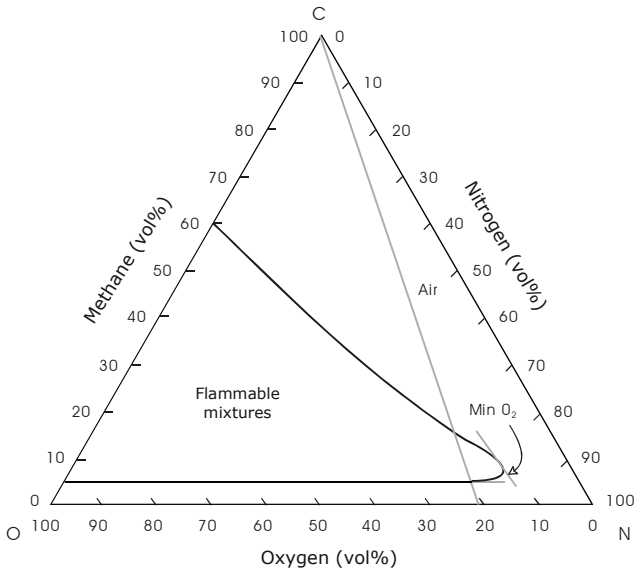


Figure 94 The flammability limits for the methane-oxygen-nitrogen system[51]

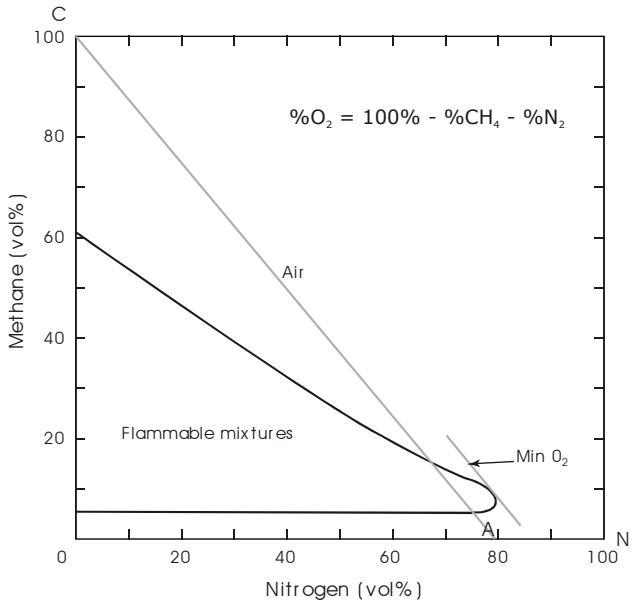


Figure 95 The methane-oxygen-nitrogen system represented on a two-axis plot[51]

[*] Older literature often refers to these as *explosion limits*. This terminology is not preferred today, partly because of the realization that, close to the limits, the gas mixture may be flammable, but it burns slowly and is hardly 'explosive.'

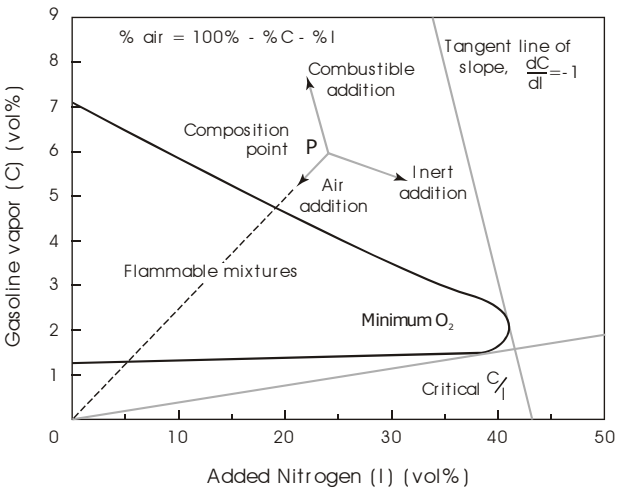


Figure 96 Flammability diagram for 100/130 grade aviation gasoline[50]

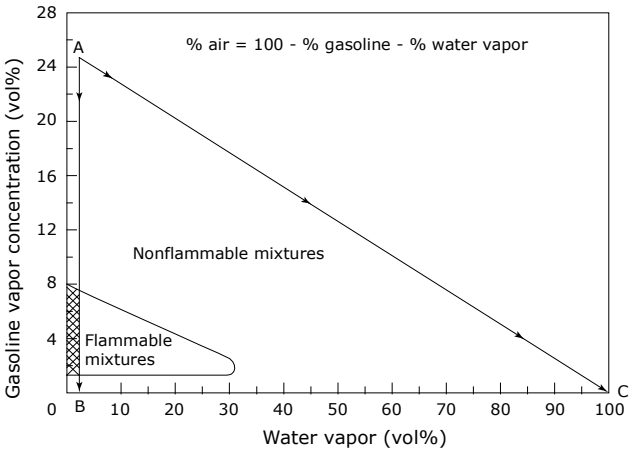


Figure 97 Flammability diagram of the gasoline vapor-air-water vapor system[51]

Since fuel + O_2 + N_2 must equal 100% in the system, this means that if, say the percent of CH_4 and N_2 are known, the oxygen value is pre-determined and cannot vary. Thus, it is possible to make a two-axis plot of the same data, as shown in Figure 95. A similar two-axis plot could be made by using CH_4 and oxygen as the two explicit quantities.

Some practical problems arise where inerting is being considered. It is assumed that fuel concentration will be originally plentiful, but that nitrogen will be added to the system until the mixture is no longer flammable. In a practical case, the atmosphere would be measured with a gas analyzer reading percent O_2. A diagram showing fuel vapor on the y-axis and *added* nitrogen on the x-axis is then convenient (Figure 96). In such a diagram, the minimum O_2 value is found by first drawing a line at the slope of dC/dI = -1, and finding the point at which it is tangent to the 'nose' of the curve. At this point of contact, the fuel vapor (C) and the added nitrogen (I) percents can be found on the graph. The percent of air is then = 100 – percent C – percent I. Having obtained the percent air, multiplying by 0.2095 gives the oxygen percent. Also illustrated in Figure 96 is an arbitrary point P. Suppose a certain amount of nitrogen has already been added, and the composition is now at point P. From this point, three lines are shown. If more fuel vapors are added, the point P will shift along the line marked "Combustible addition." Similarly, if more air or more nitrogen are added, the point will shift along the other two directions. Note that the line for fuel addition has the slope of dC/dI = –1, while the line for air addition goes between P and the origin of the graph.

Table 16 Effect of methane concentration on the pressure rise sustained upon ignition

Methane in air (vol%)	Pressure rise (atm)
5.0	0.06
5.5	0.7
6.0	3.9
8.0	6.5
10.0	7.5

Quaternary mixtures are encountered in some practical circumstances. Zabetakis illustrates the case of a gasoline tank which is to be cleaned by pressure-washing with either water or steam[51]. This involves gasoline–O_2–N_2–H_2O vapor, and such a quaternary system is rather difficult to graph. A simplification can be made if the O_2/N_2 ratio is always invariant, as it is in normal air. Figure 97 shows such a representation. Suppose the original mixture, upon draining the liquid from the tank, contains 24% gasoline vapor at a temperature of 21ºC. If the air has 100% RH at this temperature, its water-vapor content is 2.5 vol%. Point B denotes this water vapor content. Point A then denotes a mixture which is 2.5% water vapor, 24% gasoline vapor, and the rest being air. If pressure-washing with water is done, then the operation will introduce additional air which is at 21ºC and is saturated with water vapor (along with some liquid water). Thus, the mixture will start moving in a straight line from point A and eventually approach point B. But by doing this, it will pass through the flammable region; thus an explosion is possible, if a spark ignition occurs. Now consider what happens if steam is used for cleaning. Pure steam is point C. Steam contains 100% water and thus the mixture composition will move in a straight line from point A to point C, a route which does not pass through the flammable region; thus an explosion is precluded. The above analysis ignores the effect of temperature on the LFL, which is reasonable here since the temperature rise is not high and line A-C does not pass close to the flammable region.

The lower flammability limit (LFL) in air and in pure oxygen are normally found to be identical. This can be understood easily. Under lean conditions, there is a surplus of air. Therefore, air is acting as a diluent. But the heat capacities

of oxygen and nitrogen are very similar. Therefore, the two gases can be viewed as interchangeable, for purposes of absorbing heat through dilution.

The term flammability limits suggests that there is a sharp demarcation between combustion and non-combustion, as the fuel gas concentration is changed. This is partly true, and the exact value is highly dependent on both the test apparatus and the criteria selected. The latter issues are addressed under Test Methods at the end of the Chapter, but the sharpness or lack thereof can be considered in the context of some experimental data[305]. Table 16 shows the pressure rise recorded when methane/air mixtures were ignited in a 120 L sphere. The LFL for methane is normally quoted as 5.5%. It can be seen that some combustion activity (although small) is registered for smaller concentrations and, conversely, at 5.5% there is a 'slight' explosion, rather than the full-force explosion achievable with richer mixtures.

Example We want to find out how much propane can leak out into a 1200 m^3 space before the LFL is reached. In this example, we will assume that the propane is evenly distributed although, as seen later, this would often be a poor assumption in practical cases. The LFL of C_3H_8 is 2.1 vol% and its molar mass is 44.1. We use the ideal gas law:

$$PV = nRT = \left(\frac{m}{M}\right)RT$$

where for this calculation it is convenient to use the following self-consistent set of units: m = mass (g), P = pressure (atm), M = molar mass (g mol^{-1}), R = 82.1 10^{-6} m^3 atm K^{-1} mol^{-1}, and T = temperature (K). The total pressure = 1 atm, but the pressure of C_3H_8 is at the LFL is 2.1% of that, or 0.021 atm. The mass m which corresponds to the LFL is computed as:

$$m = \frac{VPM}{RT} = \frac{1200 \times 0.021 \times 44.1}{82.1 \times 10^{-6} \times 293} = 46.2 \times 10^3 \text{ g} = 46.2 \text{ kg}$$

This is not a small leak, but would more closely correspond to a sizeable broken cylinder.

THEORY

It has proven to be quite difficult to evolve a good theory of flammability limits. The difficulties arise because the problem is intrinsically a dynamic one: not only must flame propagation be quantified, but mechanisms must be described which may only be second-order effects with regard to flame velocities of stoichiometric mixtures, yet assume a dominant role for limit mixtures.

The limits of flammability occur because, as with any ignition phenomenon, there is a balance between heat generation and heat losses. The heat loss mechanisms are:

(a) natural convection
(b) wall losses
(c) radiation
(d) selective, diffusional demixing
(e) flow gradient effects (flame stretch).

The first two attempts to formulate a quantitative theory were in 1957. Spalding[306] focused on radiative losses, while Mayer[106] added convective losses. It, however, turns out that the dominant mechanisms are (a) and (e). Hertzberg presented a unified theory[307] whereby each of the mechanisms is unraveled in turn. For the LFL in horizontal propagation, Hertzberg performs a force balance at the flame, defining a combustion force as the gradient of the kinetic energy (KE) across the flame:

$$\text{combustion force} = \frac{\Delta(KE)}{\Delta x} = \frac{\rho_b S_b^2/2 - \rho_u S_u^2/2}{\alpha / S_u} = \frac{S_u^3}{2\alpha}\left(\frac{\rho_u}{\rho_b}\right)(\rho_u - \rho_b)$$

where u denotes unburned mixture and b denotes burned. The combustion force is then set equal to the buoyancy force, which is:

$$\text{buoyancy force} = (\rho_u - \rho_b)g$$

Setting these expressions equal to each other allows us to solve for S_u, the flame velocity at the LFL:

$$S_u = \left[2\alpha g \frac{\rho_b}{\rho_u}\right]^{1/3}$$

For many gases, $\alpha \approx 0.55 \times 10^{-4}$ m^2 s^{-1}, and at near-limit conditions $\rho_b / \rho_u \approx 1/5$, giving $S_u \approx 0.06$ m s^{-1}. To determine the LFL then requires that a computation be made of the laminar flame velocity S_L as a function of the equivalence ratio φ. The LFL then corresponds to that value of φ at which the limiting-value S_u is identical to S_L (φ). Experimentally, for many gases S_L (φ) $\approx$ 0.06 – 0.08 m s^{-1} at the LFL, confirming that the theory is in the right order of magnitude.

For upward propagation, Hertzberg extends the theory and determines that the value of φ must be sought at which S_L (φ) = $S_{u\uparrow}$, with

$$S_{u\uparrow} = \left[\frac{3}{16}\left(\frac{\rho_u - \rho_b}{\rho_u + \rho_b}\right)\right]^{1/3} \approx \frac{1}{2}\left[2\alpha g \frac{\rho_b}{\rho_u}\right]^{1/3}$$

or, in other words, upward propagation corresponds to a value of S_L (φ) which is ½ that for horizontal propagation. For methane/air mixtures, the theory predicts that the lean limit occurs at S_u = 0.06 m s^{-1} for horizontal propagation and 0.03 m s^{-1} for upward propagation. These correspond to fuel volume fractions of 5.3% and 4.8%, respectively. Since the measured values are 5.4% and 5.0%, the agreement is quite close. Hertzberg also derives a theoretical expression for the downward propagation LFL, but since this is always the highest of the three and therefore of less interest in fire safety concerns, we refer the reader to the original study for its details.

Hertzberg later extended his theory[308] to encompass the effect (b), which is of importance when small-diameter tubes are used. Radiation losses, mechanism (c), were found to be unimportant in terrestrial flames, but possibly

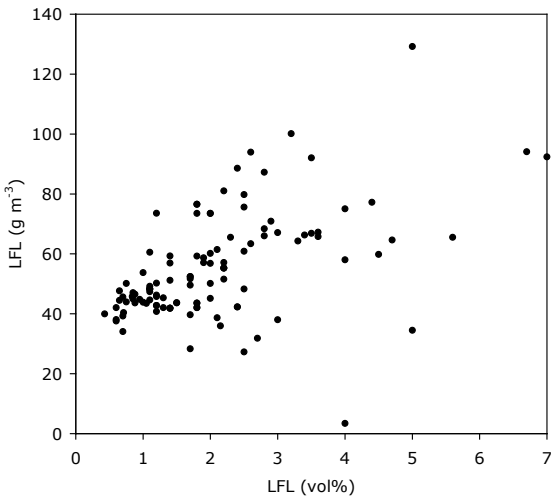


Figure 98 The relation between LFL (volume units) and LFL (mass units) for a number of simple organic molecules

crucial in determining flammability limits at microgravity conditions[309]. Selective diffusional demixing is an effect which comes into play when fuel molecules are much smaller or much larger than molecules of air (or other media present). Hertzberg provides correction factors which cover these cases[309]. In the final part of this theory[310], Hertzberg provides additional considerations of mechanism (e). While Hertzberg's theory is sound, in that it accounts for most of the important flame effects, its engineering applicability is limited, because it is normally much easier to measure the LFL of a mixture directly than to accurately compute a S_L (φ) curve.

Since the same chemistry governs both flammability limits and laminar burning velocity, Westbrook[311] proposed that the flammability limit corresponds to a laminar burning velocity $S_L \approx 0.05$ m s^{-1}. Any mechanisms which would reduce S_L below this value would also quench the flame. Law and Egolfopoulos[312] compiled a large collection of data to this point, but their results disproved the utility of the proposed criterion. The mean value was indeed not far from 0.05 m s^{-1}, but the range of S_L at the LFL was found to be 0.005 – 4.38 m s^{-1}. Instead, they determined that what stays roughly constant at the lean flammability limit is the adiabatic flame temperature, which was between 1450 and 1520 K for all of the mixtures that they examined. This conclusion, they point out, does not apply to the rich limit, nor to systems where halogenated species are present.

In current-day work, a number of authors[313,314] have shown that computational schemes which take into account both reaction kinetics and heat losses are able to correctly predict flammability limits for arbitrary mixtures, but the computations are laborious and the computed results do not lead to phenomenological insights.

FLAMMABILITY LIMITS IN MASS UNITS

To solve practical problems, it is sometimes convenient to express the fuel amount on a mass, rather than the volume, basis. The conversion can be made knowing the general relation for converting from a mole-fraction Y_1 to a mass-fraction X_1. For simplicity, here we illustrate with only 2 components, which we can identify as 1 = fuel, 2 = air:

$$X_1 = \frac{M_1 Y_1}{M_1 Y_1 + M_2 Y_2}$$

Since mol% and vol% are identical, we only need to convert from percent to fractions. Thus, for example, since propane has an LFL of 2.1 vol%, $Y_1 = 0.021$. Everything which is not propane must be air, thus $Y_2 = 0.979$. The molar mass of air = 28.96, thus

$$X_1 = \frac{44.1 \times 0.021}{44.1 \times 0.021 + 28.96 \times 0.979} = 0.032$$

Thus, the LFL of propane can be expressed as 3.2 mass%.

Sometimes the opposite operation needs to be performed, converting mass% to vol%. For such cases, the formula is:

$$Y_1 = \frac{X_1 / M_1}{X_1 / M_1 + X_2 / M_2}$$

where again we have illustrated only two components, but the generalization to more can easily be made.

Fuel mass, expressed as a percent of total mass, is only occasionally used. What is much more common is an expression of fuel mass as a *concentration*, i.e, fuel mass, per total system volume:

$$LFL_{(mass)} = \frac{LFL}{100 - LFL} \times \frac{1000\,M}{24.46}$$

where 24.46 is the molar volume at 25ºC. The factor (100 – LFL) will generally be ≈ 100, at least within the experimental error of LFL measurements. Thus, a suitable expression is:

$$LFL_{(mass)} \approx LFL \times \frac{10\,M}{24.46}$$

Thus, for example, propane has LFL_{25} = 2.1 vol%, and this is converted to a concentration of 38.7 g m^{-3} using the exact equation or 37.9 g m^{-3} using the simplified. Some authors[51] use a factor of 22.41, instead of 24.46, to obtain values at 0ºC, instead of 25ºC; but since combustion processes normally take place in environments closer to 25ºC than to 0ºC, the 24.46 factor is more realistic. Figure 98 shows the relation for a wide variety of organic molecules containing only C, H, O, and N atoms. The bulk of data in volume units span a range from about 0.5 to 4%, a range of 8:1. In mass units, the range collapses to 30 to 90 g m^{-3}, a span of only 3:1. The figure also suggests that, in the absence of any other information, assuming that LFL ≈ 50 g m^{-3}, is not a bad assumption. Halogenated molecules (not shown on the figure) have values much in excess of that, so the estimate is fairly conservative, since the only data points below

50 g m^{-3} are generally ones which are well-studied and not likely to need estimation.

The utility of expressing the LFL on a mass-concentration basis is shown in another way in Figure 99. This illustrates this for *n*-alkanes (straight-chain alkanes, e.g., methane, ethane, propane, etc.) the LFL is nearly.

ESTIMATION OF FLAMMABILITY LIMITS

When measured data are not available, various methods have been proposed for estimating flammability limits. There is no 'best' method; what method, if any, is appropriate, will depend totally on the user's needs and the information that is already available or can be obtainable. Thus, a number of estimation rules published in the literature are summarized below. As with all estimating rules, none are as good as a reliable test result on the substance itself.

Zabetakis[51] suggests that the LFL *for alkane-series hydrocarbons* (that is, fuels with a formula of C_nH_{2n+2}), can be estimated at 25ºC as:

$$LFL \approx 0.55\, C_{st}$$

where C_{st} = stoichiometric concentration (vol%) of the fuel in air, and the equation for computing C_{st} has been given in Chapter 3. That equation assumes that the real products will be the standard products and that no incomplete combustion products (CO, soot, etc.) will be produced. For alkane-series hydrocarbons, the general combustion reaction expression simplifies to:

$$C_cH_{2c+2} + \frac{1}{2}(3c+1)(O_2 + 3.77N_2) \rightarrow$$

$$cCO_2 + (c+1)H_2O + \frac{1}{2}(3c+1)(3.77N_2)$$

Thus the mole (or volume) fraction of fuel in air is

$$= \frac{1}{1+(1.5n+0.5)(4.77)}$$

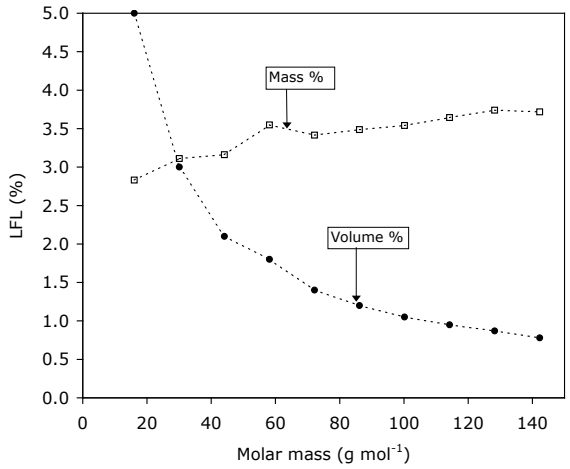


Figure 99 Straight-chain alkanes: the effect of computing LFL on a mass basis

and converted to percent becomes:

$$C_{st} = \frac{100}{1+(1.5n+0.5)(4.77)}$$

As an example, *n*-decane is $C_{10}H_{22}$. Its C_{st} = 1.33% and the estimated LFL would be 0.73%. The actual LFL is 0.75%, so the agreement is very good. While approximately correct results may often be obtained, nonetheless the estimating formula cannot be assumed to apply to hydrocarbons other than the alkane series. For example, if it were applied to acetylene, an LFL of 4.2% would be computed. The actual LFL = 2 .5%, so a l arge, unconservative error would be made.

Using a larger data set than Zabetakis, Pintar[315] proposed a slightly better fit for LFL of hydrocarbons:

$$LFL \approx 0.512\, C_{st}$$

The same expression is also a good approximation for *esters* (substances with the formula $C_nH_{2n-1}OOC_mH_{2m+1}$), but the user must take care to correctly balance the reaction for combustion of the fuels.

For *alcohols* (which have the general formula $C_nH_{2n+1}OH$), *ethers* ($C_nH_{2n+1}OC_mH_{2m+1}$), and *aldehydes* and *ketones* (C_nHC_nO) the LFL_{25} can be estimated as[51]:

$$LFL \approx 0.5\, C_{st}$$

The advantage of such an approximation is that no experimental data are required. It only requires knowing the value of C_{st}, which can always be computed, if the formula of the substance is known.

Hilado[316] proposed that the LFL can in general be approximated as:

$$LFL = A \cdot C_{st}$$

where the constant *A* assumes the following values:

C, H, O compounds	0.537
amines	0.692
chlorides	0.609
dichlorides	0.716
bromides	1.147
sulfur-containing compounds	0.577

He also proposed a rule for the UFL, but it does not exhibit much generality.

Shimy[317] proposed estimating rules for some of the more common families of organic compounds (Table 17).

Some investigators have advocated developing estimating schemes that are universal, i.e., independent of a particular organic family. Kanury[318] attempted to do this on a theoretical basis, but the results were not encouraging. Other investigators have met with more success by taking a purely empirical approach. Firth et al.[319] suggested that the LFL can be estimated as:

$$LFL \approx k / \Delta h_c^l$$

Table 17 Estimating rules proposed by Shimy

Compounds	LFL	UFL
n-alkanes, *n*-alkenes	6/c + 0.2	60/h + c/20 + 2.2
iso-alkanes, *iso*-alkenes	6/c + 0.1	60/h + 2.3
benzene series	8/c	86/(2h_r +h')
alcohols	8/c – 0.7	(80 – 2h)/2c + 3
c – number of carbon atoms h – number of hydrogen atoms h' – number of hydrogen atoms not in radicals h_r – number of hydrogen atoms in radicals		

where k is a constant and Δh_c^l = net heat of combustion (kJ mol^{-1}) and is taken to be a positive number. Figure 100 shows that this relation is acceptable only if significant outliers can be tolerated; it can also be shown that the suggestion[336] to use values of the heat of combustion on a per-mass basis does not give better results. Suzuki[320] proposed another formula based on the heat of combustion but cautioned that its applicability extends to compounds containing only C, H, and O atoms. Hshieh[321] extended the scheme to include compounds containing Si and halogen atoms. His relation is:

$$LFL = 1145\left(\Delta h_c^l\right)^{-0.8} - 0.38$$

Hshieh's method can be considered the best of these, but still only fair accuracy is to be expected. Hshieh found 95% confidence intervals of about 0.5 vol%. Since many substances show an LFL of 1.0 vol% or less, the accuracy is clearly limited; consequently, such methods should only be used for rough estimating purposes.

Pintar[315] suggested that a relation between LFL and flash point be considered as another estimating method:

$$LFL = 100 \times \frac{P(T_{FP} - 3)}{P}$$

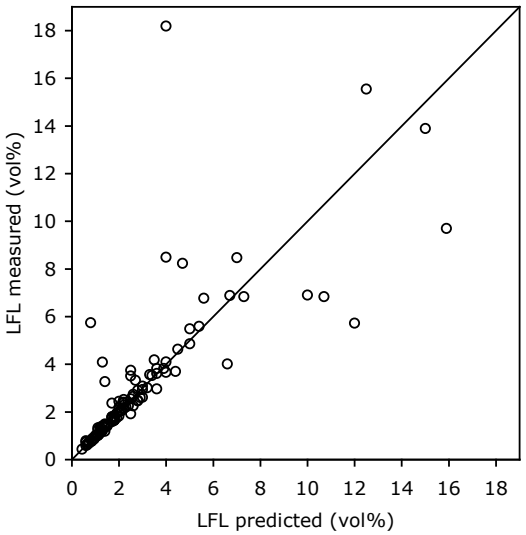


Figure 100 The prediction of the LFL by the method of Firth et al.

where $P(T_{FP} - 3)$ = vapor pressure (Pa) at a temperature 3ºC lower than the flash point, and P = total pressure (Pa). He empirically determined that better results are obtained if the value at $T_{FP} - 3$ is used, instead of at T_{FP}. The converse problem, of predicting the flash point from the LFL is considered in Chapter 6.

The simplest estimating formula[322] for the UFL is:

$$UFL \approx 3.3\, C_{st}$$

although there is a very large amount of scatter. Pintar[315] recommends the similar formula:

$$UFL \approx 3.8\, C_{st}$$

While all estimating methods for UFL give only very rough results, Pintar points out that the results from this simple rule are almost as good as from the DIPPR method. For *alkane-series hydrocarbons*, again, when LFL_{25} is known, the upper flammability limit may be estimated as:

$$UFL \approx 6.5\sqrt{LFL}$$

The UFL often cannot reasonably be predicted on the basis of simple rules because values can vary widely even for isomers. As an example, considering substances with the formula C_3H_6O, the UFL for propionaldehyde is 17%, but for propylene oxide it is 37%.

Monakhov[323] offers approximate methods for computing the LFL and the UFL.

$$LFL \approx \frac{100}{a\beta + b}$$

and

$$UFL \approx \frac{100}{c\beta + d}$$

where

$$\beta = n_C + n_S + \frac{n_H - n_X}{4} - \frac{n_O}{2}$$

with n_C being the number of carbon atoms in the fuel molecule, n_S sulfur, n_H hydrogen, n_O oxygen, and n_X denoting any halogen (F, Cl, Br, I) atoms. The values of the other constants are: a = 8.684; b = 4.679. The upper-limit constants depend on the value of β. For $\beta \le 7.5$, c = 1.55 and d = 0.56. For $\beta > 7.5$, c = 0.768 and d = 6.554. This relation is applicable to a wider range of fuels, including ones with oxygen, sulfur, and halogen atoms. For many compounds, the values predicted are reasonable. As an example, for phthalic anhydride ($C_8H_4O_3$), the predicted LFL is 1.4%, compared to the actual value of 1.2%. But it likewise should not be applied to such 'badly behaved' gases as acetylene, where unreasonable values would be predicted.

For hydrocarbons, in some cases, the UFL of a straight-chain ('normal') compound will be known but not the values for the branched-chain ('iso-') isomer (or vice versa). For such cases, Monakhov[323] offers an approximation:

$$\frac{UFL_{iso}}{UFL_n} = \frac{T_{b,iso}}{T_{b,n}}$$

where T_b is the boiling point (K). Monakhov also offers an approximation for the LFL, but examining experimental data it is clear that for most substances the difference between the *iso-* and the *n-* molecule's LFL would be within the experimental data scatter; thus it would appear to be more appropriate to simply assume that $ULF_{iso} \approx ULF_n$.

FLAMMABILITY LIMITS FOR MIXTURES

For mixtures of fuel gases, the lower flammability limit can be computed by Le Chatelier's Law[324], if the LFLs are known for the constituent components:

$$LFL = \frac{100}{\frac{C_1}{LFL_1} + \frac{C_2}{LFL_2} + ... + \frac{C_n}{LFL_n}}$$

where C_1 ... C_n are the concentrations of the n components and LFL_1 ... LFL_n are their respective flammability limits.

Example The LFL of propane is 2.1 vol% and that of butane is 1.8 vol%. For a gas mixture comprising 70% propane and 30% butane, the LFL is computed as:

$$LFL = \frac{100}{\frac{70}{2.1} + \frac{30}{1.8}} = 2.0$$

Chemically, the Law depends on all substances having the same T_{ad} at the LFL condition. As shown in Chapter 3, this is true for most organic fuels, but exceptions do exist. Thus, Le Chatelier's Law is generally accurate when applied to most mixtures[325], except those containing hydrogen, hydrogen sulfide, carbon disulfide, formaldehyde, or acetylenic compounds[326]. The Law *is* obeyed for CO + H_2 mixtures[327]. The Law will normally not be applicable for substances which burn by decomposition, rather than oxidation[336]. Sizable (and unconservative) errors can also be introduced if the Law is applied to halogenated species[136]. For a number of mixtures, Hustad and Sønju[328] demonstrated that, using Le Chatelier's Law, all results were within 20% of the predicted value and 83% were within 10%. Le Chatelier's Law is not restricted to LFL values at room temperature, and can also be applied to elevated temperature data.

Le Chatelier's Law can also be applied to the UFL[329], but more deviations must be expected, even if the fuel mixture does not contain any halogenated species[330]. This is because chemical kinetics plays a stronger role in the UFL.

The more recent *DIPPR method* [331,332] attempts to predict, within the same framework, both the LFL of a single compound, and the LFL of a mixture. According to the method, the LFL (vol%) is estimated as:

$$LFL = \frac{100}{\sum_i \left[X_i \sum_j n_j GF_j \right]}$$

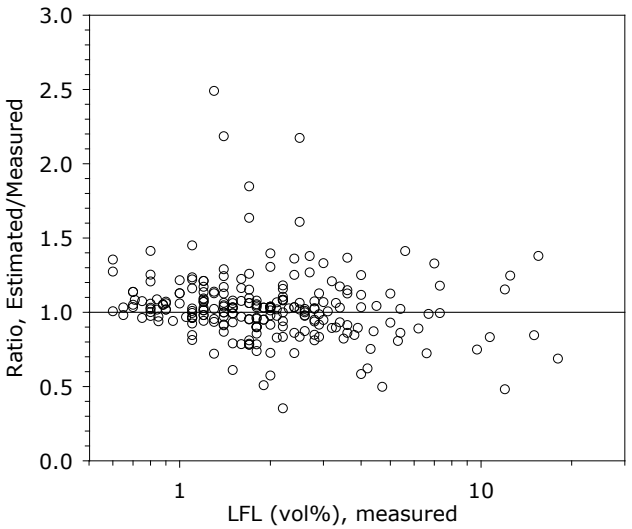


Figure 101 Comparison of LFL predicted according to DIPPR method with experimental results for 241 pure substances

where X_i = mole fraction of gas i in mixture (considering fuels only; air and diluents are ignored); n_j = number of groups of type j in compound i; and GF_j = group factor for group j, to be obtained from Table 18. Negative values denote suppression, rather than combustion, effect. Thus, the computed LFL for pure CCl_4 would be 100/(–8.42), which is a negative number and this denotes a non-flammable compound. For a set of 40 mixtures, Liekhus et al.[332] demonstrated that the DIPPR method showed a mean predicted value that was +0.8%, compared to the experimental results; for the Le Chatelier rule, the mean predicted value was –8.5%. The standard deviation for the DIPPR method was ±12.6%, compared to ±7.6% for the Le Chatelier rule. A comparison of LFL values as estimated by the DIPPR method to measured values is shown in Figure 101. Recently the DIPPR scheme has been extended by Pintar[315], who developed a group-factor method which treats 61 groups, it is known as the *MTU method*, after the Michigan Technological University where the author is based. A separate

Table 18 Group factor values for the DIPPR method

Group	GF
C	9.10
C≡C	14.07
H	2.17
H_2	20.
O	–2.68
N	1.38
F	–4.18[a] –2.55[b]
Cl	–4.38
I	17.5
S	10.9
P	9.6
Si	1.3
a – if $n_H \geq n_F$ b – if $n_H < n_F$	

scheme is used by DIPPR for predicting UFL values. That scheme is significantly more complex and can be found in the DIPPR manual[331]. Pintar has also provided an elaborate MTU method for predicting the UFL.

VARIABLES AFFECTING FLAMMABILITY LIMITS

OXYGEN CONCENTRATION

The LFL does not vary with an increase in oxygen concentration, and its value in pure oxygen is generally identical to the value in atmospheres of 21% oxygen[333]. Since the LFL is a fuel-lean condition, excess oxygen is available at 21% and any further excess oxygen is simply acting as a diluent. The molar heat capacities of O_2 and N_2 are similar and, consequently, the LFL value is not changed by going to a 100% oxygen atmosphere. If O_2 concentration is progressively decreased below 21%, then eventually a minimum oxygen concentration is reached; this is discussed in the following section. The UFL, however, greatly increases with oxygen concentration, as shown in Figure 102. The data illustrated are from Kuchta[50], and curve fit is:

$$UFL(oxygen) = 120 - \frac{216}{\sqrt{UFL(air)}}$$

When measured values of the UFL are available in both O_2 and in air, but an estimate of the UFL is desired at some intermediate oxygen concentration, the following equation[323] can be used:

$$UFL = 0.12\left(UFL(oxygen) - UFL(air)\right)\sqrt{x - 21} + UFL(air)$$

where x denotes the vol% of O_2 at which the UFL is to be computed.

PRESSURE

Increasing the initial pressure of the gas mixture generally increases both the LFL and the UFL, as illustrated in Figure 103 for natural gas. The relations can be represented by the formulas:

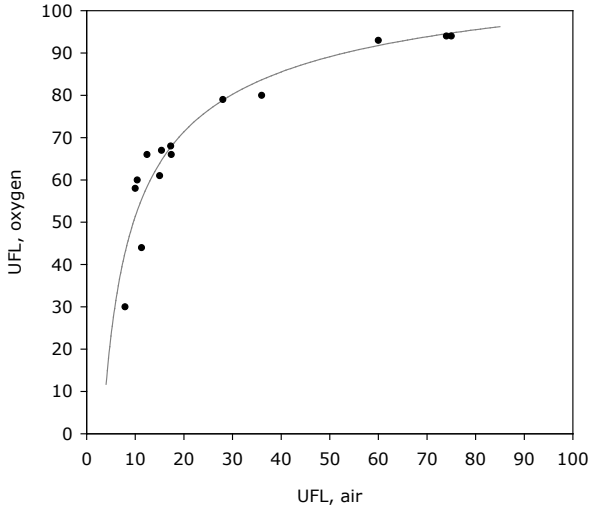


Figure 103 The relation between UFL in air and UFL in oxygen

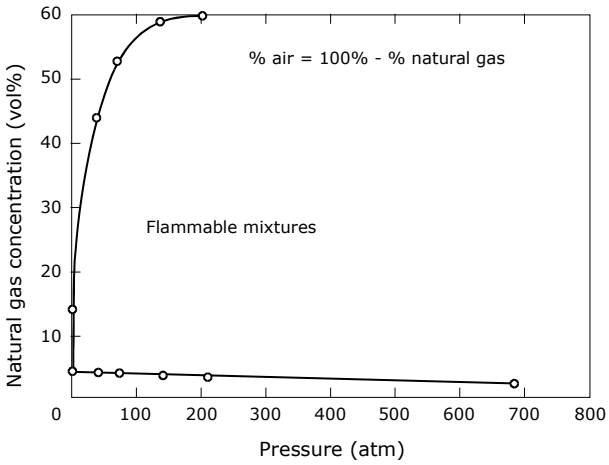


Figure 102 The effect of very high pressures on the flammability limits of natural gas[51]

$$LFL = LFL_a - 0.31\ln P$$
$$UFL = UFL_a + 8.9\ln P$$

where P = pressure (atm) and the subscript a denotes conditions at ambient (1 atm) pressure. Similar expressions are generally not available for different fuels.

A more detailed study on the effects of pressure for methane has been done by Ronney and Wachman[334], who conducted both downward and upward propagation experiments (Figure 104). The downward propagation results show a functional form as indicated in the equation above; the upward propagation results indicate a curvature at very low pressures.

Somewhat different results have been obtained on several other gases by Zabetakis[51] (Figure 105). Here, he found a similar effect as did the other researchers for the LFL, but the UFL results showed a peak at around 0.2 atm pressure. The reason for this is not clear.

Melhem[335] computed flame temperatures for several gases as a function of concentration and pressure and observed that increasing pressure raises the flame temperature for fuel-rich mixtures, but not for lean ones. Thus, if the flame temperature is assumed to be constant at the flammability limits, then the UFL will rise with increasing pressure, but the LFL will not change.

As the pressure is lowered, a *pressure limit* is reached, where the LFL and the UFL become identical, as illustrated in Figure 106[355]. Below this pressure, the propagation of flame becomes impossible. For most combustion reactions, the pressure limit is so low that safety measures cannot be based upon its existence, as shown in Table 19[336]. But for decomposition reactions of unstable substances, not exceeding the pressure limit of the substance sometimes can be a useful safety strategy. Brandes et al.[337] reported data on acetone, ethyl acetate, and hexane vapors at an elevated

Table 19 Pressure limits for several gases and vapors

Substance	Reaction	Pressure limit (atm)
acetylene	combustion in oxygen	< 0.001
methane	combustion in air	0.066
chloroacetylene	decomposition, pure fuel	0.066
ethylene oxide	decomposition, pure fuel	0.7
acetylene	decomposition, pure fuel	1.4
propadiene	decomposition, pure fuel	2.2
methyl acetylene	decomposition, pure fuel	4
ethylene	decomposition, pure fuel	70
propylene	decomposition, pure fuel	1000

temperature of 100ºC. For all these substances, the pressure limit was roughly 3 kPa. For natural gas at room temperature[338], the pressure limit is approximately 6.8 kPa.

The above discussion presumed that certain amounts of fuel gas and air were mixed together, and then the pressure of the system lowered or raised. With vapors of liquids, there is another way that the pressure effect comes in. Suppose a large open container of the liquid is sitting in a closed chamber. Now raise or lower the pressure in this chamber—What will be the effect? Assuming that the temperature remains constant and the total pressure is lowered, the partial pressure of the vapor will remain unchanged, but the partial pressure of air will drop. Thus, mixtures which were too lean at room pressure may become flammable at a lowered pressure; conversely, mixtures within the flammability limits at room pressure may become too rich for combustion. On the assumption that there is not a total-pressure

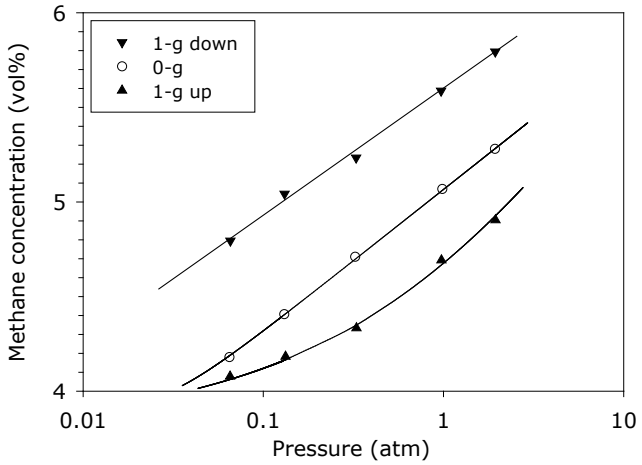


Figure 104 Effect of pressure, gravity, and propagation direction on the LFL of methane

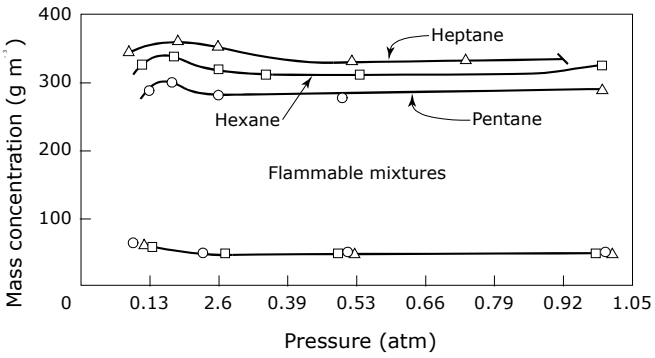


Figure 105 Effect of pressure on the LFL and UFL of several hydrocarbons

effect on the flammability limits (i.e., that the lines in Figure 105 are flat-horizontal), conditions at the new pressure may be computed by simply knowing the vapor pressure of the liquid. Example calculations for a number of common liquids have been published[339].

The *temperature limits of flammability* (explained below), change with total pressure according to the effect considered above. As the system pressure is lowered, both the LTL and the UTL drop downward. This effect is illustrated for aviation fuels in Chapter 14.

TEMPERATURE

The most general formulation of the problem involves a vapor which is in equilibrium with a pool of liquid, so this problem will be analyzed here, even though ignition of liquids is separately considered in Chapter 6. An example is shown for *n*-decane in Figure 107. The fuel vapor concentration is plotted on the right y-axis. Since the vapor con-

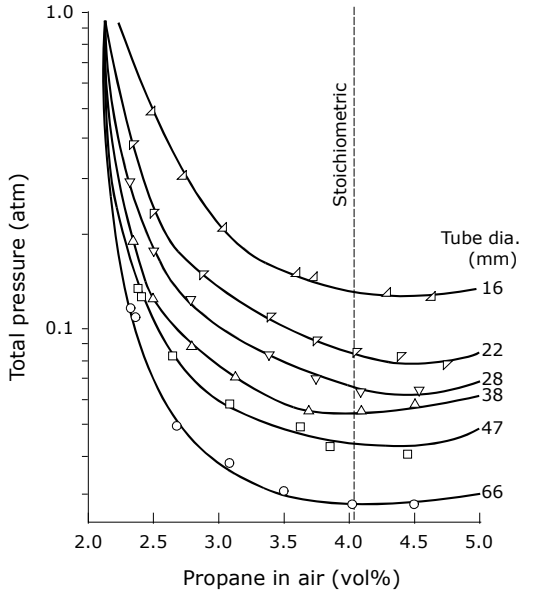


Figure 106 Pressure limits for propane, as a function of tube diameter

centration is related to the vapor pressure through the Ideal Gas Law, the left y-axis is used to denote the fuel vapor pressure. The vapor pressure above a liquid and in equilibrium with it represents the saturated vapor-air mixture and is shown as the steep diagonal line. The region to the left of this line represents an aerosol. It can only be created by mechanically atomizing the fluid into the air, not by simple evaporation from the surface of a liquid. The region to the right of this line represents vapor-air mixtures which are not saturated. Such mixtures can be created if a certain volume of vapor is introduced into a closed space but a liquid pool of the fuel does not exist. For these mixtures, the concentration of fuel vapor is less than what would be reached if a liquid pool were available from which further vaporization could take place.

It will be noted on Figure 107 that the flammable range widens with temperature, i.e., the lower flammability limit decreases and the upper limit increases. The presence of the liquid phase establishes the existence of a special point on each flammability limit vs. temperature line. The point labeled T_L is termed the *lower temperature limit* (LTL), and is the minimum temperature to which the system must be heated for flame propagation to be possible. Similarly, the point labeled T_U is termed the *upper temperature limit* (UTL), and is the maximum temperature to which the system can heated and still show flame propagation. The diagram also points out that cool flames are not encompassed within the standard definition of flammability limits. Note that LTL and UTL are meaningful only under conditions where the fuel vapor is saturated, i.e., it is in equilibrium with a reservoir of liquid. The LTL would be identical to the *flash point* (see Chapter 6), if flash point and flammability limits were measured under identical conditions, which they are not. Figure 108 shows the relation between LTL and the flash point. The LTL values are as reported by Zabetakis[51], while the flash point values (closed-cup) are from various sources. The scatter from a 45º line amounts to no more than the reproducibility of the measurements.

Some examples of LTL and UTL are given in Table 20. It can be seen that for most of the substances either summer or winter ambient temperatures will fall between the LTL and the UTL. Thus, for many common substances, tanks that are not completely full can be anticipated to contain mixtures which can explode, given an ignition source.

As might be expected, there is a probabilistic aspect to temperature limits. Figure 109 shows results from experiments by Vaivads et al.[340] where a 'strong' spark was used. The use of a strong ignition source tends to broaden the probability curves; if a weak spark is used, the LTL and UTL lines are nearly vertical.

For refined petroleum products, the following correlations have been evolved for the LTL and the UTL[341]:

$$\text{LTL} = 0.82\ \ \text{IBP} - 86$$

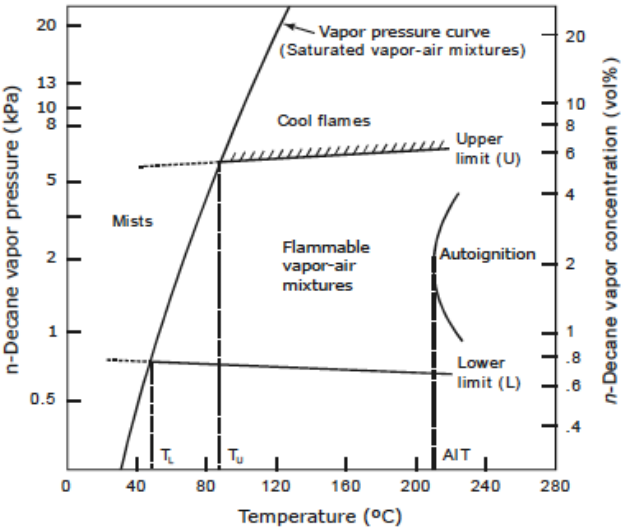


Figure 107 The effect of temperature of the flammability limits of *n*-decane[50]

$$\text{UTL} = 0.70\ \ \text{IBP} - 42$$

where IBP = initial boiling point (ºC), as determined by ASTM D 86[342]. The relations are shown in Figure 110.

In 1925 White[343] observed that, as the mixture temperature is raised, the adiabatic flame temperature at the LFL remains constant. Zabetakis et al.[344] observed that for most hydrocarbons the LFL decreases by about 8% for each 100ºC rise in mixture temperature. By this rule, mixtures containing an infinitesimal concentration of fuel could sustain flame propagation if the temperature were raised to about 25 + 100/0.08 ≈ 1275ºC. This was confirmed by further work at the Bureau of Mines[51], illustrated in Figure 111. The asymptote temperature is seen to be 1300ºC. At a temperature of 1300ºC or higher, even minuscule amounts of fuel gas are thus likely to lead to a propagating fire. A later study by Hustad and Sønju[328] concluded that 1200ºC is a better fit than 1300ºC for the asymptote, however, this

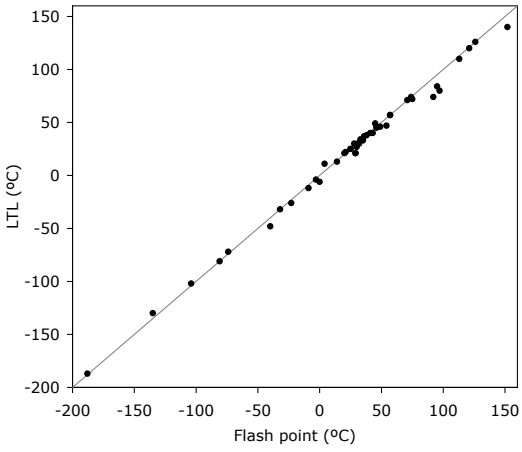


Figure 108 Relation between LTL and flash point

difference is probably within the experimental reproducibility for making flammability limit measurements.

Table 20 The flammable region for some common organic liquids[345]

Substance	Lower limits		Upper limits	
	LFL (vol%)	LTL[a] (C)	UFL (vol%)	UTL (C)
acetone	2.6	-18	12.8	7
benzene	1.4	-12	8.0	16
carbon disulfide	1.0	-30	50	25
cyclohexane	1.3	-17	7.8	15
diethyl ether	1.9	-45	36.5	9
ethanol	3.3	13	19	43
heptane	1.1	-4	6.7	26
methyl ethyl ketone	2	-7	12	22
styrene	1.1	31	6.1	62
toluene	1.3	4	7	37
xylene	1.0	29	7.0	62

[a] – the values are reported by the authors as LTL, but are probably actually flash point measurements.

With this value in hand, if the LFL is known at a temperature T_1 (normally this will be 25ºC), then it can be evaluated at another temperature T_2 according to:

$$LFL_{T_2} = LFL_{T_1}\left(1 - \frac{T_2 - T_1}{1300 - T_1}\right)$$

If T_1 is, in fact, 25ºC, then the expression becomes:

$$\frac{LFL_{T_2}}{LFL_{25}} = 1 - 0.000784\left(T_2 - 25\right)$$

An equation of this form is sometimes known as the *Burgess-Wheeler law*. The asymptote value ought to correspond to the adiabatic flame temperature at the LFL condition. Actual values, shown in Chapter 3, are not far from the value of 1300ºC derived as an asymptote to experimental data.

The general relation above does not hold for hydrogen, and for hydrogen the expression is[328]:

$$\frac{LFL_{T_2}}{LFL_{25}} = 1 - 0.00129\left(T_2 - 25\right)$$

The general relationship above will also not hold if the substance starts to *decompose* at elevated temperatures. Thus, Schrödter[346] showed for ethyl acetate and methanol that the diminution in the LFL with increasing temperature tends to stop or be reversed at a temperature close to the decomposition temperature (325ºC for ethyl acetate, 300ºC for methanol).

For the UFL, BM recommends that the increase with temperature be computed according to:

$$UFL_{T_2} = UFL_{T_1}\left(1 + \frac{T_2 - T_1}{1412 - T_1}\right)$$

If T_1 is 25ºC, then the expression becomes:

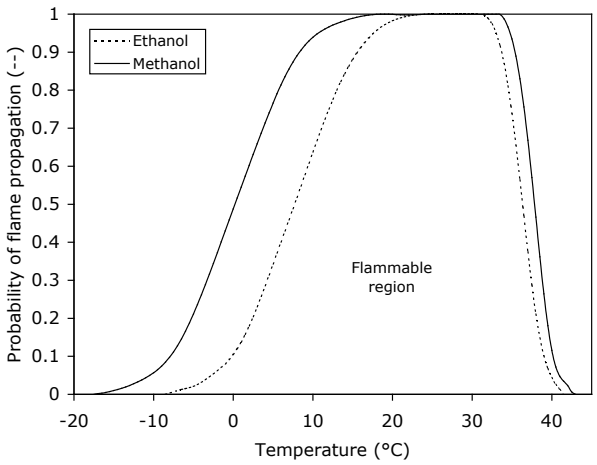


Figure 110 Temperature limits for alcohols expressed on a probabilistic basis, based on experiments using a 'strong' spark source; if a weak spark is used, nearly-vertical lines are found, instead.

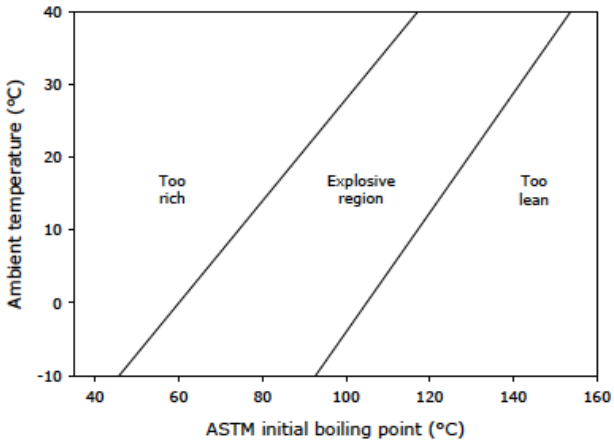


Figure 109 Flammability temperature limits for petroleum products, as a function of ASTM initial boiling point

$$\frac{UFL_{T_2}}{UFL_{25}} = 1 + 0.000721\left(T_2 - 25\right)$$

However, while the predicted temperature effect on the LFL is very similar to the measured data, for the UFL there are substantial discrepancies. Figure 112 shows that even the higher alkanes (hexane, heptane, and octane) do not follow the general relationship. One reason that non-linearities arise is due to cool-flame ignitions with some gases, at some temperatures, and not at others.

VELOCITY

When mixtures are not quiescent, but are flowing at an appreciable velocity, the LFL rises and the UFL falls. Starkman et al.[347] illustrated this with data for propane/air mixtures, but general relations have not been proposed.

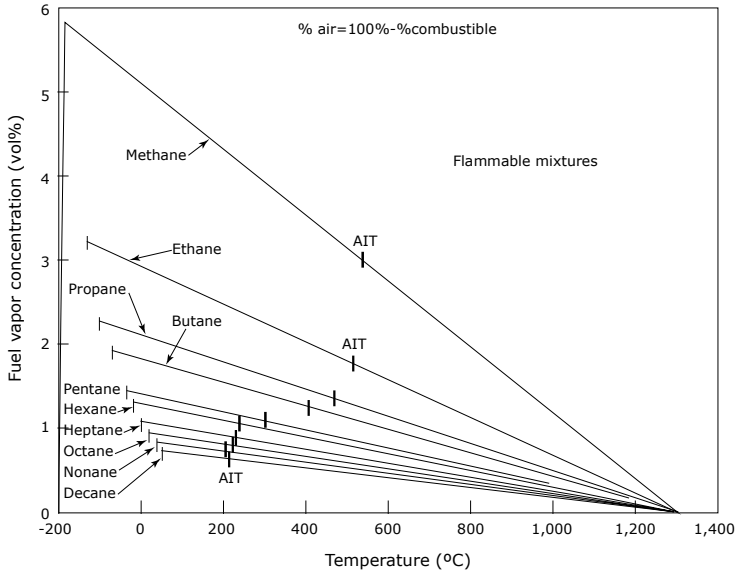


Figure 111 The effect of temperature on the LFL of *n*-alkanes

GRAVITY

Gravity affects the propagation of flame by introducing buoyancy, which distorts the flame shape. Thus, there has been interest in studying flammability limits under zero-gravity conditions. A set of results[334] for methane is shown in Figure 104. The LFL under 0-g conditions lies between the upward and the downward propagation results obtained at 1-g conditions.

For gravity greater than normal, the upward propagation limits, both LFL and UFL, are nearly unchanged. For downward propagation, however, the limits progressively narrow. Downward propagation becomes impossible at any fuel concentration for natural gas/air mixtures at over 100 G[348].

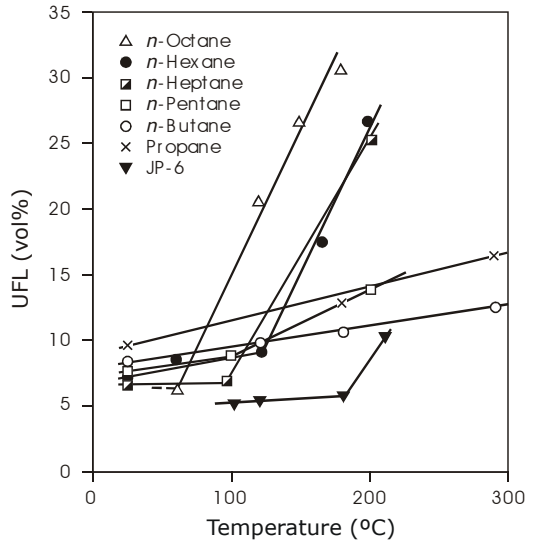


Figure 112 The effect of temperature on the UFL for several hydrocarbons[50]

TURBULENCE AND SLOSHING

For pure gases, a limited amount of data suggests that turbulence narrows the flammability range. When fan-stirring was introduced into a test chamber, it was found that the LFL rose (and the UFL fell) with fan speed and consequently with the turbulence ty[349,350]. The effect requires a sizable stirring speed, however, to become significant. A fan speed of 2000 rpm only increased the LFL by about 0.75 percentage points for methane in air. The narrowing of observed flammability limits has been interpreted as being an MIE effect: if experiments are conducted at the same ignition energy and it requires more energy to ignite mixtures that are either turbulent or have an equivalence ratio far away from stoichiometric, then turbulent mixtures will be observed as having a smaller flammability range. Lovachev[351] reviewed some other, mostly older, studies and concluded that a wide variety of trends have been reported. The effect generally seems small, but it must be remembered that if faith is rigidly (and improperly) placed in tabulated values, then even small effects can lead to flame propagation in 'non-flammable' mixtures.

When a liquid aerosol (mist) is present, increasing turbulence lowers the LFL. Similarly, if the system comprises a part-full reservoir of flammable liquid, sloshing the liquid will lower the LFL of the vapor. This is due to creation of a mist, and the effects are considered in more detail in Chapter 6.

MEASURING APPARATUS

Several factors directly related to the test apparatus design affect the flammability limits. These include the energy of ignition source, the size of the propagation tube, and the direction of flame propagation (upward or downward).

Most of the flammability data reported in the literature has been obtained with the technique developed by the Bureau of Mines (BM). The method is based on a flame tube, and either upward or downward propagation can be measured. It has been determined that the limits for upward propagation are wider, and therefore this is the orientation that BM adopted. This is illustrated in Table 21, where results are given using an early apparatus with a diameter of 75 mm and a length of 1.5 m. Close to the limits, flame cannot travel downward, because buoyancy creates an upward convective current. But upward propagation can remain possible, since buoyancy aids propagation. This is evidenced by the shape of the flame—at the LFL, a downward traveling flame is approximately flat, while an upward traveling flame 'bulges' upward[352]. The effect has also been interpreted in terms of greater flame stretch in downward propagation[70]. Even wider limits would be reported from

flat-flame burners; however, it has been concluded that such results do not correlate to real fire situations and, therefore, flat-flame burners are not used for determining flammability limits. The data of Table 21 show that the UFL values are much more affected by the direction than are the LFL values; indeed for the LFL the differences are mostly within experimental data scatter. For fundamental combustion chemistry studies, downward propagation is preferred precisely because the extra effects of buoyancy do not come into play.

Table 21 Effect of propagation direction on flammability limits[353]

Mixture	Direction	LFL (vol%)	UFL (vol%)
methane/air	upward	5.35	14.85
	horizontal	5.40	13.95
	downward	5.95	13.35
pentane/air	upward	1.42	8.0
	horizontal	1.44	7.45
	downward	1.48	4.64
benzene/air	upward	1.45	7.45
	horizontal	1.46	6.65
	downward	1.48	5.55

Numerical simulations[354] for methane have suggested that, over the pressure range 0.25 – 1.0 atm, tube diameter has a strong influence for diameters < 100 mm, and very little influence for diameters > 200 mm. Since the standard apparatus used by the Bureau of Mines (see below) has a diameter of 50 mm, this suggests that somewhat wider limits might be found in real-scale applications. The reason for the wider limits is because a h igh flame speed is found for higher tube diameters. This flame speed, as measured by Levy[352], is nearly identical to the speed of an air bubble rising in a fluid-filled tube, which increases with tube diameter.

For sub-atmospheric pressures, the tube diameter plays an important role. Simon et al.[355] showed that the lowest mixture pressure at which flame propagation is possible ('pressure limit') depends inversely on the tube diameter (Figure 106). This was determined to be a quenching-diameter effect. The quenching diameter increases with decreasing pressure, and, in fact, the pressure limit corresponds to the reduced-pressure quenching diameter.

The spark energy required to ignite a mixture varies both with the chemical nature of the gases and with the stoichiometry, with mixtures close to $\varphi = 1$ being the easiest to ignite and those farther away requiring progressively greater spark energies. The spark energy specified for the test apparatus may, therefore, influence the exact flammability limits determined.

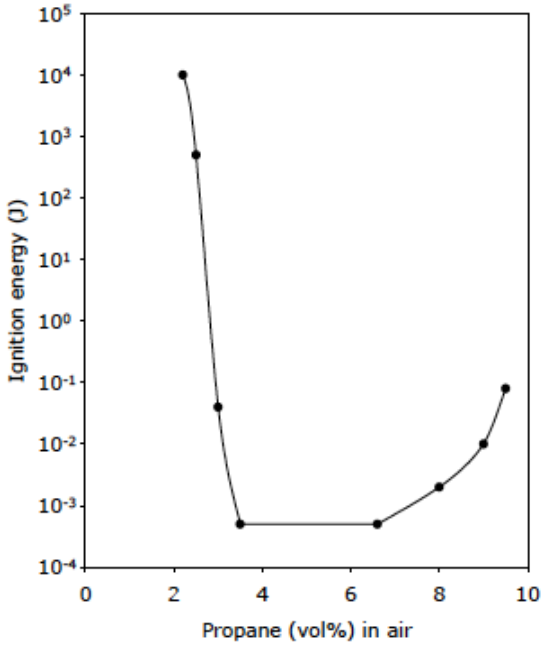


Figure 113 Propane flammability limits as a function of ignition energy, as measured under turbulent conditions in a 1 m^3 sphere

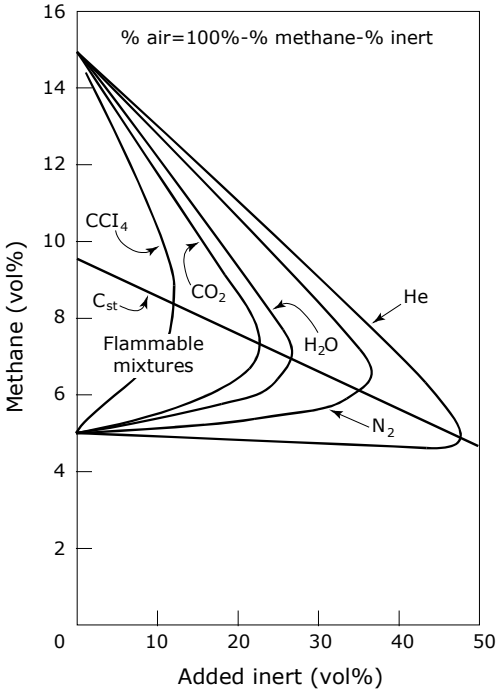


Figure 114 The effect of additives on the flammability limits of methane[344]

IGNITION SOURCE

A small amount of data exists for flammability limits determined by use of igniters other than electric spark discharges. Cashdollar et al.[305] assessed the flammability limits for several gases using pyrotechnic igniters, in addition to electric sparks. For methane, a 1 000 J igniter in a 1 20 L spherical chamber gave LFL results very similar to those obtained with an electric spark. For hydrogen, however, a 5000 J igniter (the smaller igniter was not tested) gave an LFL of 5%, compared to 6.5% found using spark ignition. But hydrogen was considered to be an anomaly, since its results are highly dependent on test apparatus details and on the exact experimental definition of LFL adopted. If very large ignition sources are used, significant turbulence is created, which tends to lower the LFL; in addition, sizable flame volumes are presented within the chamber, making the results perforce dependent on igniter characteristics. Pellmont[356] measured the ignition energy dependence of propane/air mixtures under turbulent conditions in a 1 m^3 sphere. His results (Figure 113) show that a huge increase in igniter energy is needed to sizably lower the LFL, but the moderate increases in igniter energy raise the UFL. Bartknecht[357] showed similar data for methane, indicating that very large ignition sources are needed to sizably widen the flammability limits.

ADDITIVES

Inert additives (that is, substances which are neither fuels nor oxidizers), are sometimes added to mixtures in order to decrease their flammable limits or to make the mixture entirely outside the range of flammability.

For inert additives, the effect is proportional, in the first approximation, to their heat capacities. The heat capacities, at 298 K and 1 atm, of some inert additives are given in Table 22.

Experimental data indeed show that the effectiveness of inert additives is in the order:

$$CO_2 > H_2O > N_2 > He > Ar.$$

Since their C_p values are identical, the effectiveness of Ar and He would have been estimated to be identical, but experimentally it is found that Ar is more effective than He. Molecules with halogen atoms (e.g., F, Cl, Br) are not inert, since their action contributes to chain termination, not simply dilution. Thus, halogenated compounds such as CCl_4 are more effective than their C_p values would suggest.

From Figure 114 it can be seen that, for moderate amounts of inert additives, the effect is mainly on the UFL. All of the additives are able to make a mixture non-flammable if added in sufficient quantities. However, adding lesser amounts of N_2 has negligible effect on the LFL, while adding less than 45% of helium actually decreases the lower limit of methane.

For most hydrocarbon gases, nitrogen in the amount of 40 – 50 vol% must be added to a fuel/air mixture in order to make them 'non-flammable,' that is, to prevent flame propagation. These are very high amounts, whereas much lower concentrations are sufficient when using many halogen-containing ('halon') gases. The most popular and effective of these, however, have been banned due to environmental ozone considerations.

MINIMUM OXYGEN CONCENTRATION FOR FLAMMABILITY

Under the conditions of the flammability test apparatus, when the oxygen level is below a certain value, flame propagation is no longer possible. That is, the mixture is not flammable below such oxygen conditions. The problem was first investigated by Rhead in 1918[358]. Currently used data are primarily from the Bureau of Mines[50,359]; these and values from NFPA 69[360] are shown in Table 23. It can be seen that, with the exception of a few unusual or highly flammable fuels, the rest of the fuels show a remarkably consistent pattern. The minimum oxygen concentration below which flame propagation is impossible (at 1 atm and 298 K) is approximately 12 vol% if air is diluted with nitrogen. Very often, however, dilution occurs because the burning substance vitiates a closed atmosphere in which the burning is occurring. In such cases, it is reasonable to assume that CO_2 is the main diluent. Table 23 then indicates that for vitiated burning, flame propagation is no longer to be expected once the oxygen concentration drops below 14%.

Concentration is normally defined with the denominator comprising the total contents of the volume, so that oxygen concentration, for example, is defined as $= O_2/(N_2 + O_2 + \text{fuel})$. In some cases, however, it is more convenient to work with the oxygen concentration of the atmosphere to which the fuel is being introduced, rather than with the atmosphere that results when the fuel is actually mixed in. Such a definition, for example, was used by Rhead in his original study. If this definition is used, it should actually be called the *minimum oxygen index*, since oxygen index is defined as: $OI = O_2/(N_2 + O_2)$. In practice, the distinction is normally not made, since numerically the effect is smaller than the experimental data scatter.

If the LFL is known and the diluent is N_2, then the MOC can be predicted by the following relation:

Table 22 Heat capacities of some gases

Gas	C_p (J mol^{-1} K^{-1})
Ar	20.79
He	20.79
N_2	29.13
H_2O (g)	33.58
CO_2	37.11

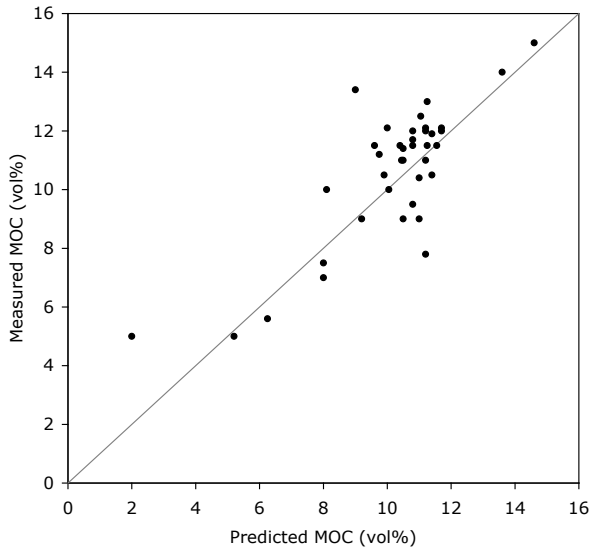


Figure 115 Prediction of MOC on the basis of measured LFL

$$MOC = LFL \times \gamma_o$$

where γ_o = stoichiometric oxygen/fuel mole ratio. The latter quantity is not tabulated in Chapter 15, but it can also be seen that the prediction can be made as:

$$MOC = LFL \times \frac{1}{4.77}\left(\frac{100}{C_{st}} - 1\right)$$

where C_{st} = stoichiometric fuel concentration (vol%). This latter relation is plotted in Figure 115 and it is seen that there is no systematic deviation, although there is a fair bit of scatter. The basis of this prediction can best be seen from an example. For *n*-hexane, LFL = 1.2% and C_{st} = 2.16%. Thus, at the LFL, the mixture composition is 1.2% fuel, (100 – 1.2)×0.21 = 20.7% O_2, and 78.1% N_2. Now, the MOC implicitly assumes that—to be a minimum—the percent of fuel is at optimal value to allow combustion at the minimum O_2 concentration. The optimum amount of fuel will be close to the stoichiometric amount, so it assumed that the oxygen/fuel mole ratio is exactly the stoichiometric one. For hexane, this ratio is 9.50. The minimum amount of fuel is 1.2%, therefore the minimum amount of oxygen is 1.2×9.50 = 11.4%. The experimentally-determined value is 11.9%, which is quite close. An entirely different prediction method—based on functional-group contributions has been proposed[361], but there is not enough validation data to assess its quality of prediction.

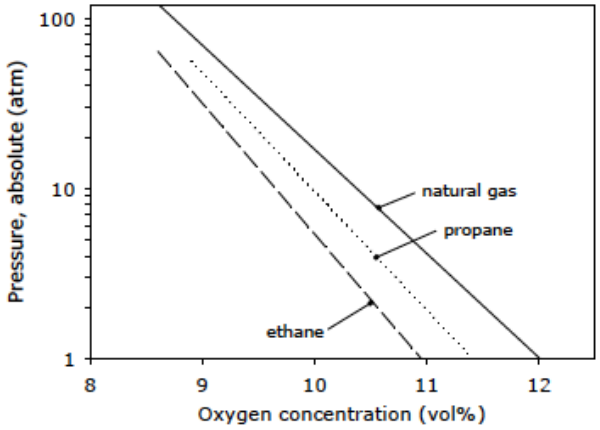


Figure 116 The effect of pressure on the minimum oxygen concentration for combustion[50]

Table 23 Minimum oxygen concentration (MOC) for flame propagation of various combustibles, expressed as vol%, for two diluents—nitrogen and carbon dioxide

Substance	For N_2	For CO_2
acetone	11.5	14
aviation gasoline (70/100)	12	15
aviation gasoline (115/145)	12	14.5
benzene	11.2	13.9
butadiene	10.4	13.1
n-butane	12.1	14.5
1-butene (butylene)	11.5	14
carbon disulfide	5	7.5
carbon monoxide	5.6	5.9
cyclopropane	11.7	13.9
diethyl ether	10.5	13
ethane	11.0	13.4
ethanol	10.5	13
ethylbenzene	9.0	
ethylene	10.0	11.7
ethylene dichloride	13	
gasoline	11.6	14.4
n-heptane	11.5	14.5
n-hexane	11.9	14.5
hydrogen	5.0	5.2
hydrogen sulfide	7.5	11.5
isobutane	12.0	14.8
isobutylene	12	15
isobutyl formate	12.5	15
isopentane	12	14.5
jet fuel JP-3	12	14.5
jet fuel JP-4	11.5	14.5
methane	12.1	14.6
methanol	10	12
methyl acetate	11	13.5
3-methyl-1-butene	11.5	14
methyl ethyl ketone	11	13.5
methyl formate	10	12.5
natural gas, Pittsburgh	12	14.5
n-pentane	12.1	14.4
propane	11.4	14.3
propylene	11.5	14.1
propylene oxide	7.8	
styrene	9.0	
toluene	9.5	
1,1,1,-trichloroethane	14	
UDMH	7	
vinyl chloride	13.4	
vinylidene chloride	15	
vinyl toluene	9.0	

Elevated pressure lowers the minimum oxygen concentration at which burning is sustained. Figure 116 illustrates this for several gases.

While flammability limits are not applicable to *non-premixed* conditions, e.g., diffusion flames, the concept of minimum oxygen concentration does apply. Not only that, but the numerical values are very close (Table 24). Since combustion, perforce, is less efficient for diffusion flames, it is not surprising that the minimum O_2 values are all about 1% higher than for the premixed case.

Unified theories of gas ignition

Yang made the observation that, in the simplest theoretical formulation, there will be no difference between autoignition and piloted ignition. If a volume of gas is below the AIT, a non-zero energy needs to be introduced in order to give ignition. If the volume is above the AIT, the ignition energy needed is zero. Using these concepts, he produced a mathematical ignition formalism[362]. The formalism, however, is too simplified to describe experimental results. Specifically, only single-step Arrhenius kinetics is used, while heat losses are represented as a radiant loss of the entire gas volume. More current theories of spark ignition, described earlier in this Chapter, clearly indicate that complex phenomena take place in the flame kernel, and that performing heat transfer analysis on the lumped gas volume will not suffice to give results of quantitative utility. Yang was able to demonstrate qualitative agreement in modeling the spark gap as a thermal volume. For large gap lengths, the heated volume was considered to be roughly cylindrical, and his theory correctly predicts the experimental fact that MIE increases linearly with increasing gap length[363]. Similarly, for short gap lengths, the MIE is independent of gap length, and Yang's theory, considering the thermal volume as a sphere, correctly predicts that MIE is independent of gap length.

A unified theory in a different context was later set out by Yang and Gray[365,366]. In the early days of combustion modeling, the simplest theory was that of Semenov, discussed earlier in this Chapter; it is called a 'thermal' theory. Later, the concept of chain-branching was introduced, which allowed more complex chemical reactions to be treated. Like Semenov's thermal theory, the unified theory focuses primarily on criteria for instability, rather than detailed tracking of reaction progress. The first achievement of the theory was to predict the P-T relation for ignition of hydrogen.

Ignition of non-premixed gases

By far, the most research on ignition of gases has been done for the premixed case. This is not surprising, since there is only one premixed possibility, but an infinity of non-premixed fuel/air arrangements possible. As the simplest geometry, Maksyutov et al.[367] studied the case where a hemisphere of fuel gas suddenly comes into contact with a hemisphere of oxidizer. This was found to be a relatively tractable problem, but its practical applicability would be rare.

It is sometimes taken that hazard will be small if an amount of fuel gas is introduced into a closed space which yields a computed concentration below the LFL. This is incorrect, if the gas happens to be introduced (as nearly always will happen) in a way that it is not uniformly premixed. Hirano[368] studied situations where (a) a methane layer was evenly created above a layer of air; and (b) a fuel gas was injected, but measures were not taken to premix. In both cases, ignitions were easy to achieve. For the latter case, the pressure rise upon ignition smoothly increased with mean fuel concentration, with no jump occurring as the concentration rose beyond the LFL. The pressure rise was sufficient for collapsing structural elements before the LFL was reached.

If a layer of denser-than-air fuel gas is deposited, unpremixed, at floor level, ignition and a layer-type burning, without explosion, is possible. A more likely outcome is that the initial burning will sufficiently stir up the layer that eventually an explosive behavior will be seen. Recently Tamanini[369] reported brief results of experiments where propane was leaked at floor level and most of the room was initially below the LFL.

Liebman et al.[370] studied the flammable regions of a tank being filled with liquid JP-4. For both top-filling and bottom-filling conditions, they found that initially four distinct layers formed, bottom to top: (1) liquid, (2) vapor above the UFL, (3) vapor within the flammable region, and (4) vapor below the LFL. With time, however, the regions moved up until some vanished at the top of the tank. With modest filling rates, the upward movement of the three gas layers occurred faster than the rise in liquid level. Eventually, except at extremely low temperatures, the entire vapor space came to be above the UFL. Similar results were obtained with gasoline filling, except that the fully fuel-rich layering occurred much earlier. Ignitions of atmospheres were generally violently explosive, unless the over-rich layer occupied the bulk of the vapor space. In those cases, 'mild' ignitions were observed.

Table 24 Minimum oxygen concentration for premixed versus diffusion flames[364]

Fuel	Min. O_2 conc. (vol%)	
	Premixed	Diffusion flames
propane C_3H_8	11.4	12.3
pentane C_5H_{12}	12.0	13.0
hexane C_6H_{14}	11.7	13.1
octane C_8H_{18}	11.9	13.1
decane $C_{10}H_{22}$	11.9	13.2
methanol CH_3OH	9.8	10.0
ethanol C_2H_5OH	10.7	11.9

The explosion of enclosed spaces such as tanks that have a composition nominally above the UFL, but where the atmosphere is not well-mixed, can occur as a two-stage process. An initial hot spot or spark ignites a portion of the volume which is readily flammable. This causes relief devices to operate or other means to vent. The venting then causes temperatures and pressures to drop, with atmospheric air being sucked in through openings. A bulk of the interior volume now becomes lower than the UFL and better mixed, so a much larger second explosion follows the first. This sequence has been observed on a number of ship explosions[371].

The flammability limits within *partly-mixed* mixtures have been reported to be slightly wider, under some conditions, than in well-mixed environments, but the effect numerically was quite small[372].

The topics of fuel gas/vapor distribution in rooms and other near-closed spaces from gaseous discharges and from liquid spills are further treated in Chapter 13.

Initiation of gaseous detonations

Most mixtures of fuel gases in oxygen can be detonated, and many fuel gas/air mixtures can also. Detonation can occur by two means: (1) direct detonation, which occurs when a powerful ignitor is used; (2) deflagration-to-detonation transition (DDT). The latter process is one of 'flame acceleration,' and the ignition source which caused the initial deflagration is not relevant towards determining if a transition to detonation will occur. Two mechanisms are identified[373] as causing a laminar deflagration to transition to a detonation: (a) Interaction of pressure waves with the flame. Pressure waves cause the initially-smooth flame front to become wrinkled, due to an interface instability mechanism. Since the heat release rate per unit flame area remains roughly constant, increasing the flame area causes an increase in HRR, and this interaction sets up a positive-feedback condition. Eventually, detonation occurs at a local hot spot in the highly turbulent flame. The onset of detonation from accelerating laminar flames was initially modeled by Oppenheim and associates[374]. (b) The onset of turbulence in the flow of the unburned ahead of the flame, which occurs when the Reynolds number gets sufficiently high. In the simplest case of a tube open at one end and closed at the other, if the mixture is ignited at the open end, a combustion wave will propagate steadily through the mixture and a transition to detonation will not occur. But in the converse situation of a mixture ignited at the closed end, the combustion wave will progressively accelerate as it moves through the mixture and a DDT may take place. Thus, a prerequisite for a DDT to develop is an attainment of a minimum velocity turbulence component.

A transition to detonation is found not to occur in short pipe, and a minimum pipe length is necessary. The minimum tube length ('run-up distance' or 'detonation induction distance') decreases with increasing pressure or decreasing pipe diameter and is also strongly dependent on the chemical nature of the fuel molecule. Ginsburgh and Bulkley[375] provided some data on needed run-up distances for ammonia, ethylene, hydrogen, methane, and propane and proposed that $\frac{(\text{run-up distance})W^{3/2}}{(\text{pipe diameter})}$ can be correlated as a decreasing function of the burning velocity, where W = molar mass. Their correlation was poor, however, and the effect of pressure was not successfully represented. Also, they did not study enough gases to determine whether correlating molar mass against burning velocity successfully captures the chemistry involved. The chemistry effect is significant, as shown by the data of Westbrook[376] in Table 25. Bartknecht[357] and Steen and Schampel[377] conducted more extensive tests and their results (Figure 117) suggest that, even if the approach of Ginsburgh and Bulkley has merit, it should be modified to include an additive constant in the run-up distance within the correlating variable. They also obtained data as a function of fuel concentration and found that the minimum run-up distance is required at stoichiometric fuel concentration. The results should only be viewed as indicative, since pressure, head-end volume, and other factors affect the actual numerical values. Additional data obtained by Chatrathi et al.[378] are also shown in Figure

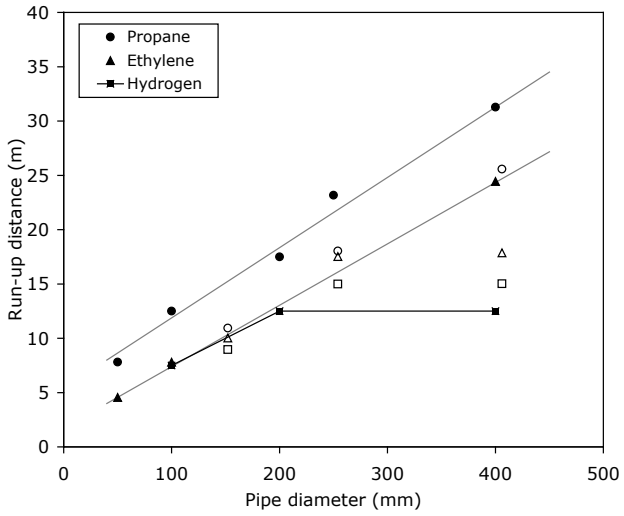


Figure 117 Effect of pipe diameter on run-up distance for detonation (dark symbols: German data; open symbols: Chatrathi)

Table 25 Relative run-up distances required for detonation to occur in circular tubes

Gas	Length (mm)
acetylene	0.1
ethylene	2
methanol	2
ethane	4
methane	20

Table 26 Cell sizes and minimum tube diameters necessary to detonate an unconfined vapor cloud

Fuel gas	Cell size (mm)	Min. tube diam. to detonate cloud (mm)
acetylene	10	150
hydrogen	15	200
ethylene	29	430
ethane	54 – 62	900
propylene	52	
propane	69	900
n-butane	50 – 62	900
methane	250 – 310	

117. Pure methane is extremely difficult to detonate, but small amounts of ethane and other hydrocarbons, as present in natural gas, make detonations in the latter notably easier. In one experimental study, it was found that 0.08 kg of tetryl sufficed to detonate an ethane/air mixture, but 22 kg was required for methane/air[379]. The above results should not be taken to mean that larger diameters are safer—in fact, detonations are precluded if the diameter becomes small enough. This is discussed below and a quantitative example for acetylene is given in Chapter 14.

For a pipeline detonation to be feasible, it is also necessary that the pipe not be too narrow. Fuel/air detonations have a cellular structure and this structure establishes a lower limit to the diameter of the pipe, which is very roughly equal to this cell size. Experimental determinations of cell size differ substantially, but some indicative values are shown in Table 26[380]. These results are all obtained at the most-readily detonable mixture, which is a composition usually close to the stoichiometric one. Methane is anomalous in that a tube diameter ca. 50 mm is sufficient, which is only about 1/6 the cell size[381]. For any gas, a much larger tube diameter is needed if the detonation is to emerge from the end of the tube and be capable of detonating an unconfined vapor cloud at that location. The data indicate that the diameter must be about 15× the cell size for a cloud detonation to be feasible.

Table 27 Minimum energy needed for detonation of various gases in oxygen and in air

Gas	In oxygen		In air	
	Fuel conc. (vol%)	MIE (J)	Fuel conc. (vol%)	MIE (J)
acetylene	40	3.83×10^{-4}	12.5	1.29×10^{2}
ethane	28.6	1.07	7.7	5.09×10^{6}
ethylene	33	7.2×10^{-2}	9.5	1.20×10^{5}
ethylene oxide	40	1.2×10^{-2}	12.3	7.62×10^{3}
hydrogen	60	1.58	29.6	4.16×10^{6}
methane	40	5.07×10	12.3	2.28×10^{8}
propane	22.2	5.77×10^{-1}	5.7	2.52×10^{6}
propylene	25	2.03×10^{-1}	6.6	7.55×10^{5}

Table 28 Constants for computing the relation between tube diameter and the minimum pressure needed for detonation

Fuel	Mixture	K	n
acetylene	8.8% C_2H_2 in air	1.15	0.915
	12.5% C_2H_2 in air	0.83	0.912
	$C_2H_2 + 4O_2$	0.049	0.884
	$2C_2H_2 + 5O_2$	0.022	0.882
	$C_2H_2 + O_2$	0.012	0.924
ethane	$C_2H_6 + 7O_2$	0.15	0.976
ethylene	$C_2H_4 + 3O_2$	0.081	0.918
hydrogen	$2H_2 + O_2$	0.23	0.928
methane	$CH_4 + 2O_2$	0.54	0.955
propane	$C_3H_8 + 5O_2$	0.13	0.933
propylene	$2C_3H_6 + 9O_2$	0.099	0.970

Lee[373] developed a semi-quantitative model for predicting the onset condition to transition to detonation. Based on this, he identifies a minimum turbulent flame speed of around 230 m s^{-1} as needed in air; in oxygen, only ca. 65 m s^{-1} is needed. Since laminar flame speeds in air are typically 0.5 m s^{-1}, this means that mechanisms must exist for increasing the speed about 460-fold for detonation to occur. In oxygen, however, typical laminar flame speeds are 10 m s^{-1}, thus an amplification of only 6-fold is needed. This explains why transitions to detonation are much more likely in oxygen atmospheres. The laminar flame speeds of acetylene and of hydrogen are much greater than those of other fuel gases; thus the hazards of detonation are also proportionately greater for these fuels.

Table 29 Some reported values of detonation limits (to be used as rough guide only, since values are highly dependent on experimental conditions)

Gas	Limits (vol%)	
	In O_2	In air
acetylene	3.5 – 92	4.2 – 50
butane	2.1 – 38	2.0 – 6.2
butanol	2.6 – >40	2.8 – 4.5
ammonia	25 – 76	
carbon monoxide	40 – 82	
cyclohexane	1.4 – 29	
ethane	3.6 – 46	2.87 – 12.2
ethanol		5.1 – 9.8
ethylene	4.1 – 60	3.3 – 14.7
ethylene oxide	2.6 – ?	2.8 – 4.5
hexane	1.6 – 36	1.6 – 5.6
hydrogen	15 – 90	18 – 59
MAPP		3.0 – 10.1
methane	1.9 – 15	6.3 – 13.5
methanol	9.5 – 65	
octane	1.6 – 17	1.5 – 2.9
propane	2.5 – 43	2.6 – 7.4
propylene	2.5 – 50	3.6 – 10.4
propylene oxide	3.3 – 40	
xylene	1.1 – 27	

Since flame speeds are increased by obstructions, passage of flame through a wire mesh or grid which is not fine enough to act as an effective flame arrester can lead to a detonation. The passage of flame through a grid increases its 'wrinkling,' and this acts to increase the flame speed.

Direct detonations of gas mixtures can be achieved by energetic sparks, in addition to condensed-phase explosives. A theory exists for predicting such detonations[373]. Spark energies several orders of magnitude greater than for igniting deflagrations are needed; however, values in the range of 0.1 J, sufficient for acetylene/air mixtures, are large enough that they would be uncommon for static electricity discharges.

MINIMUM ENERGY FOR DETONATION

In some industrial situations, the possibility of a detonation must be considered, thus it is of interest to have some measure of the energy needed to initiate one. Matsui and Lee[382] made a series of determinations using an indirect technique, whereby detonations were caused in a tube and then propagated (or not) into a large spherical vessel. The minimum energies were computed from a theoretical relationship based on the gas pressure and the minimum tube diameter needed for detonation. Table 27 shows the results obtained. The fuel concentrations given have been found to be the concentrations corresponding to the least energy needed. Note that 228 MJ are needed to detonate methane in air; even though the numbers should be understood only as relative indicators, nonetheless this suggests that it is very difficult to detonate methane in air (but not too hard in oxygen).

There is a relation[382] between the initial pressure and size of the tube that forms a minimum requirement for detonation,

$$P_i = Kd^{-n}$$

where P_i = minimum initial pressure needed for detonation (atm), and d = tube diameter (mm). Example values are shown in Table 28.

DETONATION LIMITS

It is sometimes of interest to know the lower and upper limits between which a detonation can occur. These have not been documented as extensively as have normal flammability limits, but several studies[112,336,382- 387] indicate that they are somewhat more narrow than flammability limits (Table 29). The values shown generally pertain to experiments in tubes; for unconfined detonations, the limits, especially the lower limit, become narrower. In addition, there are various other experimental details which can affect the results, and no measurement technique has been standardized. Almost any gas can be detonated, including such low-combustibility ones as carbon tetrachloride and tetrachloroethylene[388]; although detonation limits are not published on those.

Table 30 Effect of ignition energy on detonation limits of acetylene/oxygen mixtures

Ignition energy (J)	Detonation limits (vol%)
4.5	15 – 60
6.5	14 – 60
12	14 – 62
84	10 – 65
320	10 – 67

Detonation limits are affected by the ignition energy, but this makes results often difficult to apply to actual explosion incidents. BM data[389] illustrate this for acetylene (Table 30).

Tests for ignition properties of gases

AUTOIGNITION TEMPERATURE

EARLY METHODS

The most famous method for determining the autoignition temperature of gases was that developed by Mallard and Le Chatelier[49] in 1880. They used an evacuated, heated vessel into which a pre-measured quantity of a gas mixture (at ambient temperature) was suddenly admitted. This seemingly simple technique is actually complicated and non-ideal. There are several problems: (a) the volume is not at a uniform temperature, since a cold gas is admitted into a hot vessel; (b) there is an unaccounted-for 'physical' temperature rise which occurs because the vessel, originally at a low pressure, becomes pressurized; and (c) ignition delay times cannot be correctly determined, since the mixture takes some time to warm up. For a reversible, adiabatic process, thermodynamics would predict that the temperature rise from admitting a gas into an evacuated vessel would be:

$$T_f - T_o = T_o(\gamma - 1)$$

where $\gamma = C_p/C_v$, C_p = constant-pressure heat capacity, and C_v = constant-volume heat capacity. For an ideal gas, $C_p - C_v = R$, where R = universal gas constant. An ideal monatomic gas will have $\gamma = 5/3$, and a diatomic gas $\gamma = 1.4$, but fuel gas molecules normally have a much greater number of atoms and, for them, the effect is smaller. Fine et al.[391] explored the effect experimentally. A temperature rise (above the original vessel temperature) of 139 – 225ºC were found

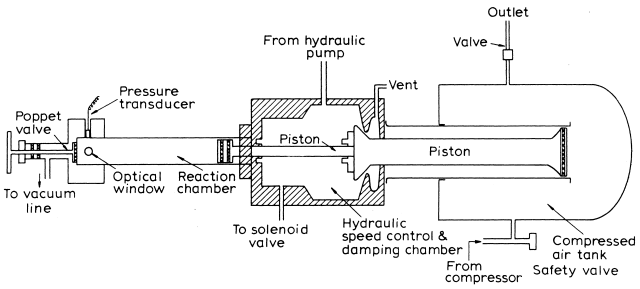


Figure 118 A rapid compression machine[390]

at the center of the test vessel when monatomic inert gases at 0.105 atm were introduced into a preheated, evacuated vessel.

Other early test methods included: (1) A sealed glass bulb containing the gas mixture is plunged into a constant-temperature bath, and ignition or lack thereof is observed. (2) The gas mixture in a tube is led through a rising-temperature bath. (3) Rapid compression machines (Figure 118), using a cylinder generally reminiscent of an automotive engine cylinder. This technique was highly favored in early 20th century testing, due to the similarity of conditions created there, compared to those in the automotive engine. For compression to be adiabatic, it must be very rapid. However, if the cylinder is compressed rapidly, it will overshoot the final temperature. Slowing down the cylinder helps reduce the overshoot, but introduces an unknown heat loss term. If an automotive engine is not the application of concern, then this technique has the additional disadvantage that elevated pressure is used rather than atmospheric. Consequently, AIT values will be inappropriately low (by as much as 300ºC), due to the inverse effect of pressure on AIT. Such data are not readily correctable to reflect 1 atm conditions. Recent studies with rapid compression machines have been reviewed by Griffiths[395].

HEATED TUBE TESTS

One of the few methods which allows a reliable determination of the induction period is a heated tube test. In this test, pure fuel and oxidizer gases are introduced into two separate, heated tubes[392]. The gases emerge into a cavity which is also at the same temperature as the preheat temperature of the supply tubes. Variants of this technique have been used in the UK[393,394] and in Russia[56]. Most of the studies with this arrangement are quite old and the reliability of the test apparatuses may be questionable, but the apparatus built by Jackson et al.[89] in 1954 was sophisticated, and a recent version was developed at the University of Leeds in 1996, which also includes provisions for atomization of liquid fuels[395]. While the scheme seems to be the one with the fewest drawbacks, nonetheless the results can be quite sensitive to apparatus details[84], so it is not necessarily evident that this geometry produces more 'fundamental' data.

TESTS PRIMARILY FOR LIQUIDS

The number of chemical substances which are gases at room temperature is vastly outnumbered by those which are liquids. Consequently, there has not been much interest in developing test methods solely for gases and most of the development efforts historically focused on liquids. These typically take the form of some heated apparatus into which drops of the liquid are dropped in and which rapidly vaporize at the elevated temperature. Such test methods are discussed in Chapter 6.

OTHER TEST METHODS

Griffiths et al.[396] developed a modern variant of the heated flask test used by Mallard and Le Chatelier. One new feature is a magnetic stirrer that is located in the flask. Some experimental results on methane with and without stirrer suggest that, at least for that gas, the effect of the stirrer on the value of AIT is small[41].

Sage and Weinberg[397] developed an innovative test where a flow-through vessel is used with two heaters, a main 'preheat' heater and a secondary 'supplement' heater. The gas mixture is preheated to a temperature below its AIT, then various temperatures of the supplement heater are used and the AIT is determined by extrapolation.

HEATED-SURFACE IGNITION

Smyth and Bryner[398] at NIST developed a hot-surface test method for the US Air Force. It was considered that in jet engine applications the flow velocities would be fast enough that a specially designed test method was needed which provided for short-duration exposures. Their test method comprises an electrically heated foil, which may be nickel, stainless steel, or titanium. The mixture is introduced as a jet impinging at 45º to the heated foil. The boundary-layer contact time is estimated at 90 ms. The results obtained with the test apparatus gave, with a few exceptions, highest T_{ig} values using the nickel foil and lowest values using the stainless steel foil. Similar to other research investigations, the dependence on the equivalence ratio was monotonically downward, with richest mixtures showing lowest T_{ig} values. Using the stainless steel foil and $\varphi = 1$, of the 15 hydrocarbons tested, all showed T_{ig} values within a narrow range of 720 – 840ºC except for acetylene, which gave 662ºC.

FLAMMABILITY LIMITS

BUREAU OF MINES FLAMMABILITY TUBE

The best known apparatus (Figure 119) for measuring the flammability limits of premixed gases is that developed by BM[242]. It consists of a 50 mm I.D. glass tube, 1.5 m long. The glass tube is closed off with a ground glass plate *b* and sealed in a pool of mercury *c*. It is evacuated with a vacuum pump through tube *j*. For testing vapors of combustible substances which are liquids at room temperature, the liquid is held in container *p*. Air (or oxygen, or diluents) is admitted through a drying tube *q*. Mixing is accomplished by repeatedly raising and lowering mercury reservoir *g*. The mixing time is generally 10 – 30 min. A test is then started by removing the mercury seal *c*, removing the plate *b*, and introducing a spark or a small flame at the open bottom of the glass tube. For spark ignition, platinum electrodes with a 6.3 mm spark gap and an AC power source of ca. 7.5 kV are used. For a mixture to be declared flammable, propagation has to occur at least halfway up the tube; if only a shorter propagation distance is found, this is deemed to

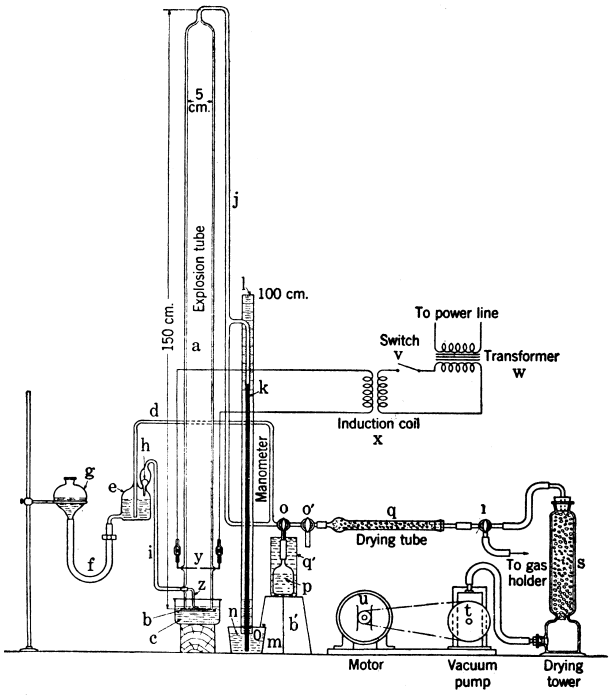


Figure 119 The standard Bureau of Mines apparatus for determining flammability limits of gases and vapors

occur due to localized heating from the igniter, and is not considered representative of the substance. A number of higher-molecular-mass compounds would be 'non-flammable' if tested in the standard apparatus, since at room temperature they do not vaporize sufficiently. The substances may propagate flame, however, if warmed up to a higher temperature. Thus, the Bureau of Mines evaluated the LFL of a number of such compounds at temperatures high enough (up to 203ºC) so that their flammability limits are attained. This was done using a similar apparatus, but with the propagation tube being located in an air oven[344].

There is an effect of the tube diameter on the results from the Bureau of Mines test. When the diameter was doubled, in a very limited series of tests it was found that the LFL limit stayed constant, but the UFL limit decreased[399]. During the 1970s, BM discontinued the use of the traditional apparatus and replaced it with the apparatus of ASTM E 681; however, very few data have been published from the later apparatus.

ASTM E 681

BM research showed that for some halogenated compounds the 50 mm tube apparatus may give 'non-flammable' results, but a special 100 mm version indicates that modest flammability does exist. The latter was

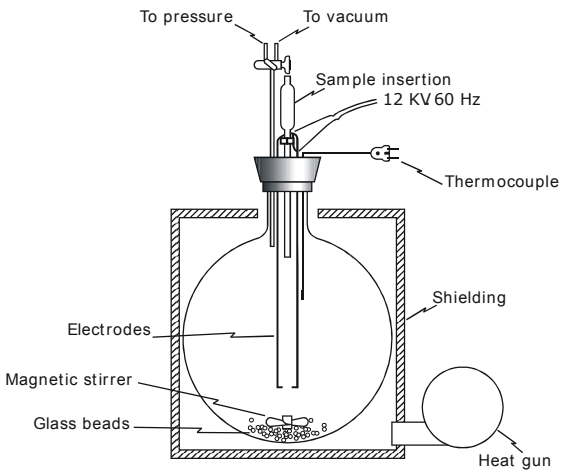


Figure 120 ASTM E 681 apparatus (5 L sphere)

not standardized and eventually, when Eastman Kodak developed the 5 liter sphere[400], BM also installed one in their laboratories. The Kodak apparatus became the ASTM E 681 test[401], which uses a 5 L glass sphere (Figure 120) to determine the flammability limits of substances in air at 1 atm or lower pressures and at temperatures below 150ºC. Pure-oxygen is not permitted to be used as the oxidizer in this test method. Samples may be introduced either as a gas, or a liquid which vaporizes within the test vessel. A magnetic stirrer is provided at the bottom of the vessel to aid mixing. Ignition is by electrodes which are 3.2 to 4.8 mm diameter and have a spark gap of 6.4 mm. The spark gap is located somewhat below the mid-height of the sphere. The test method also provides for a 12 L sphere, to be used for specimens which do not readily ignite in the 5 L apparatus. The test basically measures upward flame propagation, although the flame will also have a spherically-expanding aspect to it. Figure 121 compares results[402] obtained in the BM vertical propagation apparatus to those obtained in the ASTM E 681 sphere. With a few exceptions, the results are generally quite close. The same apparatus is called out in the ASTM E 1232 method[403], which is used to determine

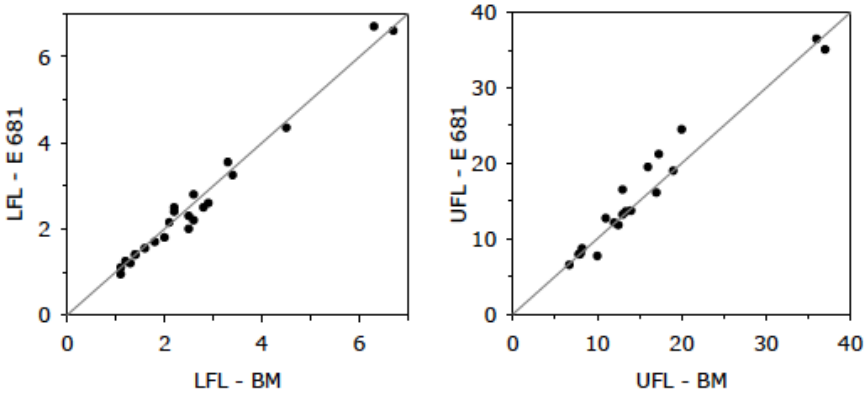


Figure 121 Comparison of LFL and UFL values obtained in BM flammability tube to values in the ASTM E 681 sphere

the lower temperature limit of flammability (LTL), as contrasted to determining the flammability limits at a preselected temperature. Few research studies have been published with the ASTM E 681 apparatus, although researchers at the University of Edinburgh[404] documented rather extensively the performance of a similar apparatus using a 6 L stainless steel sphere.

PROPOSED EN METHOD

In Europe, the original work at the Bureau of Mines was the inspiration for a German test, DIN 51649[405]. The test uses a vertical glass tube 300 mm long and 60 mm ID. Ignition is by means of spark electrodes at 60 mm above the bottom. For elevated temperatures, a hot-air jacket is used or the apparatus is placed in an oven. For gas mixtures, a steady flow rate is established within the tube, then flow is stopped prior to testing. For mixtures where a vapor is involved, a heated-tube vaporizer is used[406]. The method has become the basis for the proposed European standard EN 1839[407]. The latter expands the original concept by allowing the user the choice of either the tube apparatus or a sphere apparatus. The tube apparatus has been expanded somewhat to 80 mm diameter. The sphere apparatus similarly follows the ASTM E 681 scheme, with sizes of 5 L or greater being allowed. Ignition for the sphere apparatus is a fused-wire device, not the electric spark which is used in ASTM E 681. Curiously, there is no US standard test today which retains vertical tube type apparatus. A small amount of data cited in the EN standard indicate that the flammability limits are slightly broader when using the tube apparatus, but the data do not encompass any halogenated compounds.

ASTM E 918

If flammability limits at elevated pressures and temperatures are required, ASTM E 918[408] test allows determinations to be made at pressures up to 1.38 MPa and temperatures up to 200ºC. The vessel is a 1 L, 76 mm diameter, metal cylinder with spherical ends. Ignition is by means of a fuse wire which is located somewhat above the bottom of the vessel. Flame propagation is defined to have occurred when a pressure rise of more than 7% above initial pressure (absolute) occurs.

ASTM E 2079

The ASTM E 2079 method[409] describes a test where a spherical vessel is placed in a heating oven and is initially evacuated. The vessel may be as small as 4 L, with vessels up to 35 L reported to have been used. The test mixture is introduced and ignited by one of 5 optional igniters. The purpose of the test is solely to establish the MOC, so various concentrations of oxygen are supplied by trial-and-error until the minimum value is found. A 7% rise in the initial vessel pressure is used as the criterion of flame propagation, and visual observations are not made. The only paper that describes the test method is a study by CDC[305] describing the use of a 20 L vessel for making flammability limits measurements; no data on MOC measurements using this test method have yet been published in the literature. The physical hardware used by CDC is identical to the 20 L BM vessel described in Chapter 5 for testing dust clouds; the latter is standardized as ASTM E 1515.

UL TESTS

UL has used a 28 L steel cylindrical vessel for making LFL determinations at various temperatures. In this procedure, which apparently was only used for testing vapors and not gases, the vessel was first preheated to a desired temperature. Then the test liquid was injected with a syringe and a stirring fan activated inside the vessel. After a time of stirring, the fan was stopped, an electric spark was discharged through electrodes located near the bottom, and presence or absence of upward flame propagation observed.

RESEARCH TESTS

In the standard ASTM E 681 test method, the convection currents set up by the flame are a factor which influences the numeric value of the flammability limits reported. This reproduces the situation in accidental fires, but leads to complications and difficulties in modeling. More theory-friendly burner arrangements are possible, but Lewis and von Elbe[70] clearly warned: "It has been found possible to obtain limits considerably outside those obtained from practical testing by using flat-flame burners." A number of researchers worked with flat-flame, tubular-flame, and similar burners, although, following the *caveat* of Lewis and von Elbe, their results should not be considered as safety characteristics of the substances tested. Studies in this vein include those of C. K. Law et al.[410], Ishizuka[411], Liao et al.[412,413], and NIST[414].

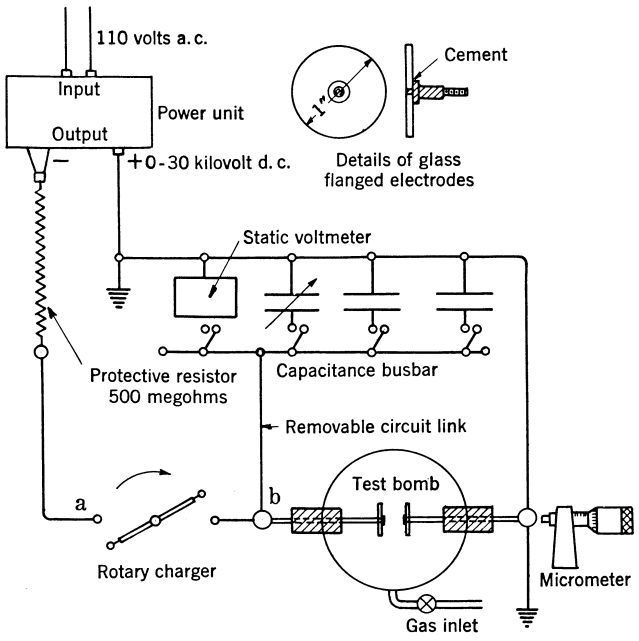


Figure 122 General arrangement of the Bureau of Mines MIE testing rig

MINIMUM IGNITION ENERGY

Apart from the ASTM test described below, several other tests of the 'break-flash' type are described in Chapter 12.

ASTM E 582 TEST

The ASTM version[415] is based on the Bureau of Mines procedures[181,416] (Figure 122) for determining the MIE and quenching distances of gases and vapors. The apparatus uses a 1 L stainless steel sphere, with capacitive discharge between flanged electrodes. The electrodes are 3.2 mm diameter and tipped with glass flanges which have a diameter of 5 – 10 times the spark gap distance. A high voltage power supply is used which can deliver 1 – 30 kV. The minimum voltage that can be used will, of course, depend on the breakdown voltage (Paschen's Law) for the particular gap distance and pressure selected. The capacitance is normally comprised solely of the stray capacitance and is in the range of 8 – 12 pF. To obtain a true MIE value requires that assurance be had that more than one spark does not occur. The Bureau of Mines recommends that the relaxation time of the flame kernel first be estimated as:

$$\tau = \frac{r^2 \rho C_p}{\lambda}$$

where r = half-width of spark gap (m), ρ = density of gas mixture (kg m^{-3}), C_p = heat capacity of gas mixture (J kg^{-1} K^{-1}), and λ = thermal conductivity (W m^{-1} K^{-1}). The RC value of the discharge circuit is then to be chosen so that it is greater than the value of τ computed above. This will normally require a resistor in the range of 10^9 to 10^{11} Ω. The ASTM standard, however, recommends that a fixed value for the series resistor of 10^{12} Ω (10^6 MΩ) be used. The test procedure involves first determining the quenching distance, then setting the spark gap to be slightly greater than the quenching distance and determining MIE. Both procedures have to be done by trial-and-error. The test apparatus may be used for temperatures up to 400ºC and pressures up to 3 atm. The BM report points out that for certain substances, larger spheres or spheres made of glass or metal are needed, but these have not been standardized by ASTM.

QUENCHING DISTANCE

There are no standard tests for measuring quenching distance. Experimentally, four different techniques have been used[107].

(1) Flowing the fuel/oxidizer mixture through a small burner tube, then quickly shutting off the flow. If the flame flashes back down into the tube, this means that the diameter is greater than d_T, the quenching diameter (mm). A smaller diameter tube is then tried and the process continued until the maximum diameter is found for which flashback does not occur. This diameter is d_T.

(2) Putting a stationary fuel/oxidizer mixture into a tube, then determining if propagation down the tube will or will not occur. Experimentally, this is commonly done in an all-glass apparatus. A portion of the apparatus is of a sizeable diameter and it contains a pair of spark electrodes. Attached to the large apparatus is a small-diameter, thin tube which is closed at the far end. The entire volume of the apparatus is filled with a mixture and the spark is ignited. The propagation or not of the mixture down the small tube is recorded. Since pressure has an effect on the results, the large cavity must be adequately vented to the atmosphere or to a plenum of controlled pressure. Practical details are illustrated by Potter et al.[417] A modified method uses a conically-shaped closed-end tube. In that method, propagation stops at a certain distance and knowing the inside diameter at that place the quenching diameter can be directly determined without need of a trial-and-error procedure using tubes of various sizes.

(3) Measuring the distance between flanged electrodes. In this technique, the standard Bureau of Mines flanged-electrode apparatus (e.g., the ASTM E 582 version) is used that is normally used to measure the MIE. As the electrode spacing is reduced, below a certain spacing a near-infinite rise occurs in the energy required for ignition. The spacing between the two electrodes is taken to be the parallel-plate quenching distance d_{II}. The results from this method are considered to be less precise than from the preceding two methods.

(4) Extrapolation from blowoff-flashback stability diagrams. This method[5] is somewhat convoluted and is of limited precision, so it would rarely be the tool of first choice.

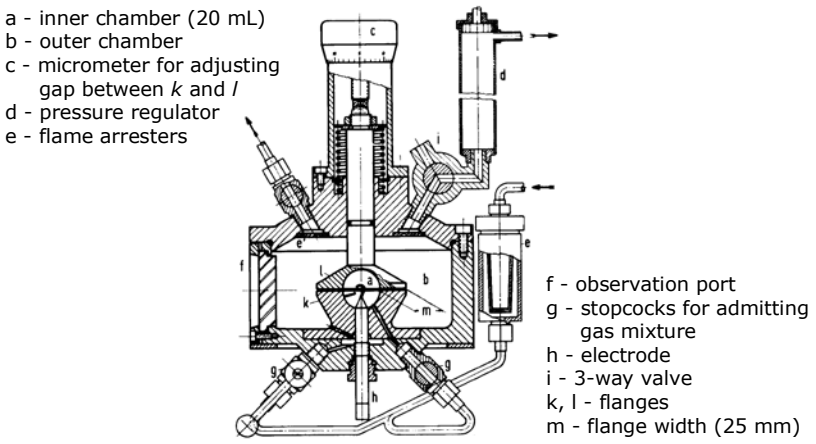


Figure 123 The 20 mL sphere developed by PTB and standardized by IEC

MESG

IEC/PTB AND HSE 20 mL SPHERES

Outside of the US, most MESG data have been obtained using a 20 mL sphere apparatus developed at the Physikalisch-Technische Bundesanstalt (PTB) in Germany[272]. Figure 123 shows the main features of the apparatus. The same gas mixture is admitted into the inner chamber (20 mL sphere) and into the outer explosion chamber (4.5 L). For an explosion to propagate from the inner chamber to the outer chamber, the gases must travel through a flange gap. The gap is adjustable, but the flange width is fixed at 25 mm. The apparatus has been standardized by IEC as IEC 60079-1A[418].

Much experimental MESG data have been published on the basis of testing with the 20 mL apparatus of the Health and Safety Executive laboratories[419]. The operating portions of the HSE apparatus are identical, but the equipment was redesigned so that it can be heated up to 130ºC, so that MESG values could more easily be determined for substances which have too low a vapor pressure at ambient temperature. Such substances are studied in the IEC/PTB apparatus by placing the test apparatus within an oven. Even though 20 mL is a small volume, HSE compared the results from the 20 mL apparatus to a large, 8 L apparatus[420] and found good agreement.

WESTERBERG APPARATUS (UL)

The apparatus in which testing of MESG values has been done in support of the National Electrical Code was developed by W. C. Westerberg at Underwriters Laboratories[421] and is described in UL's Technical Report No. 58[422]. The primary explosion chamber comprises a section of nominal 12-inch (0.3 m) pipe with a volume of 28.3 L. The secondary chamber into which the explosion does or does not propagate is 18 L. UL explored various breadths for the flange gap through which the gases escape, but adopted a 19 mm flange for their standard tests. The procedure involves running five tests and taking the worst results obtained:

(1) quiescent mixture in primary explosion chamber; ignition near flange;
(2) quiescent mixture in primary explosion chamber; ignition at opposite end of chamber from flange;
(3) turbulent mixture in primary explosion chamber, created with a small fan in the chamber; ignition near flange;
(4) turbulent mixture in primary explosion chamber; ignition at opposite end of chamber from flange;
(5) a pressure-piling configuration, wherein a 3.05 m long, closed-ended pipe (nominal 1.5 inch size) is connected onto the primary explosion chamber; no fan is used in this configuration.

Further readings

Bernard Lewis and Günther von Elbe, **Combustion, Flames and Explosions in Gases**, 3rd ed., Academic Press, Orlando FL (1987). This is the most famous, classical textbook on the combustion of gases. It includes a plethora of experimental observations no more recent author has attempted to encompass. The authors were associated for many years with the Bureau of Mines.

Guide to Fire Hazard Properties of Flammable Liquids, Gases, and Volatile Solids (NFPA 325), NFPA. This is the standard guide to autoignition temperatures. Note that the philosophy taken by the compilers has been exceptionally conservative: Instead of evaluating the data for accuracy and discarding dubious values, the authors have chosen to report the most conservative value found in the literature for a particular substance. Consequently, in many cases what is reported is an outlier, rather than a best estimate of the value.

Dag Bjerketvedt, Jan Roar Bakke, and Kees van Wingerden, Gas Explosion Handbook, *J. Hazardous Materials* **52**, 1-150 (1997). This study, prepared Christian Michelsen Research, is a technical, but highly readable, monograph on gas explosions.

References

1. Naylor, C. A., and Wheeler, R. V., The Ignition of Gases. Part VI. Ignition by a Heated Surface. Mixtures of Methane with Oxygen and Nitrogen, Argon or Helium, *J. Chemical Soc.* **130**, 2456-2467 (1931).
2. White, A. G., and Price, T. W., The Ignition of Ether-Alcohol-Air and Acetone-Air Mixtures in Contact with Heated Surfaces, *J. Chem. Soc.* **115**, 1462-1505 (1919).
3. D'Onofrio, E. J., Cool Flame and Autoignition in Glycols, *13th Loss Prevention Symp.*, AIChE (1979).
4. Johnson, A. M., Roth, A. J., and Moussa, N. A., Hot Surface Ignition Tests of Aircraft Fluids (AFWAL-TR-88-2101), Air Force Wright Aeronautical Labs., Wright-Patterson AFB, OH (1988).
5. Gaydon, A. G., and Wolfhard, H. G., **Flames: Their Structure, Radiation and Temperature**, 4th ed., Chapman and Hall, London (1979).
6. Bardwell, J., and Hinshelwood, C. N., The Cool Flame of Methyl Ethyl Ketone, *Proc. Royal Soc. London* **A205**, 375-390 (1951).
7. Fish, A., The Cool Flames of Hydrocarbons, *Angewandte Chemie Intl. Edition* **7**, 45-60 (1968).
8. Lignola, P. G., and Reverchon, E., Cool Flames, *Prog. Energy and Combustion Science* **13**, 75-96 (1987).
9. Affens, W. A., and Sheinson, R. S., Autoignition: The Importance of the Cool Flame in the Two-stage Process, *13th Loss Prevention Symp.*, AIChE (1979).

10. Yang, C. H., and Gray, B. F., On the Slow Oxidation of Hydrocarbons and Cool Flames, *J. Phys. Chem.* **73**, 3395-3406 (1969).
11. Griffiths, J. F., and Scott, S. K., Thermokinetic Interactions: Fundamentals of Spontaneous Ignition and Cool Flames, *Prog. Energy Combustion Science* **13**, 161-197 (1987).
12. Dykstra, F. J., and Edgar, G., Spontaneous Ignition Temperatures of Liquid Hydrocarbons at Atmospheric Pressure, *Ind. and Eng. Chem.* **26**, 509-510 (1934).
13. Frank, C. E., and Blackham, A. U., Investigation of Hydrocarbon Ignition (NACA TN 2549), NACA, Washington (1952).
14. Sortman, C. W., Beatty, H. A., and Heron, S. D., Spontaneous Ignition of Hydrocarbons: Zones of Nonignition, *Ind. and Eng. Chem.* **33**, 357-360 (1941).
15. Gray, P., and Lee, P. R., Studies on Criticality: Temperature Profiles in Explosive Systems and Criteria for Criticality in Thermal Explosions, pp. 1123-1131 in *11th Symp. (Intl.) on Combustion*, The Combustion Institute, Pittsburgh (1966).
16. Semenov, N. N., **Chemical Kinetics and Chain Reactions**, Oxford University Press, London (1935).
17. Semenov, N. N., **Some Problems of Chemical Kinetics and Reactivity**, vol. 2, Pergamon Press, London (1959).
18. Frank-Kamenetskii, D., **Diffusion and Heat Transfer in Chemical Kinetics**, 2nd ed., Plenum Press, New York (1969).
19. Griffiths, J. F., and Barnard, J. A., **Flame and Combustion**, Blackie Academic and Professional/Chapman and Hall, London (1995).
20. Glassman, I., **Combustion**, 3rd ed., Academic Press, San Diego (1996).
21. Gray, P., Auto-Inflammation (Spontaneous Ignition) in Gases, pp. 52-69 in *1st Specialists Meeting (Intl.) of the Combustion Institute*, Bordeaux, France (1981).
22. Taffanel, J., and Le Floch, G., Sur la combustion des mélanges gazeux et les retards à l'inflammation, *Comptes rendus* **156**, 1544-1546; **157**, 469-471, 595-597, 714-717 (1913).
23. Vulis, L. A., **Thermal Regimes of Combustion**, McGraw-Hill, New York (1961).
24. Khitrin, L. N., **Physics of Combustion and Explosion**, Israel Program for Scientific Translations, Jerusalem (1962). Russian original: **Fizika goreniya i vzryva**, Izdatelstvo Moskovskogo Universiteta, Moscow (1957).
25. Kanury, A. M., **Introduction to Combustion Phenomena**, Gordon & Breach, New York (1975).
26. Semenov. N. N., Thermal Theory of Combustion and Explosion, *Prog. of Physical Science (USSR)* **23**:3 (1940), NACA Tech. Memo. No. 1024, National Advisory Committee for Aeronautics, Washington (1942).
27. Spadaccini, L. J., and TeVelde, J. A., Autoignition Characteristics of Aircraft-type Fuels (NASA CR-159886), NASA, Washington (1980).
28. Merzhanov, A. G., and Abramov, V. B., Thermal Explosion of Explosives and Propellants, A Review, *Propellants and Explosives* **6**, 130-148 (1981).
29. Egeiban, O. M., Griffiths, J. F., Mullins, J. R., and Scott, S. K., Explosion Hazards in Exothermic Materials: Critical Conditions and Scaling Rules for Masses of Different Geometry, pp. 825-833 in *19th Symp. (Intl.) on Comb.*, The Combustion Institute, Pittsburgh (1982).
30. Britton, L. B., Thermal Stability and Deflagration of Ethylene Oxide, *Plant/Operations Progress* **9**, 75-86 (April 1990).
31. Gray, P., and Sherrington, M. E., Explosive Oxidation of Hydrogen Sulphide: Self-Heating, Chain-Branching and Chain-Thermal Contributions to Spontaneous Ignition, *J. Chem. Soc. Faraday Trans.* Series 2, **70**, 2338-2350 (1974).
32. Seiser, R., Pitsch, H., Seshadri, K., Pitz, W. J., and Curran, H. J., Extinction and Autoignition of n-Heptane in Counterflow Configuration, *Proc. Combustion Inst.* **28**, 2029-2037 (2000).
33. Foo, K. K., and Yang, C. H., On the Surface and Thermal Effects on Hydrogen Oxidation, *Combustion and Flame* **17**, 223-235 (1971).
34. Gray, P., Griffiths, J. F., and Bond, J. R., Carbon Monoxide Oxidation: Chemiluminescence and Ignition, pp. 811-819 in *17th Symp. (Intl.) on Combustion*, The Combustion Institute, Pittsburgh (1979).
35. Bond, J. R., Gray, P., and Griffiths, J. F., Oscillations, Glow and Ignition in Carbon Monoxide Oxidation. I. Glow and Ignition in a Closed Reaction Vessel and the Effect of Added Hydrogen, *Proc. Royal Soc. London* **A375**, 43-64 (1981).
36. Gray, P., Griffiths, J. F., and Scott, S. K., Oscillations, Glow and Ignition in Carbon Monoxide Oxidation in an Open System. I. Experimental Studies of the Ignition Diagram and the Effects of Added Hydrogen, *Proc. Royal Soc. London* **A397**, 21-44 (1985).
37. Gray, P., Griffiths, J. F., and Scott, S. K., Oscillations, Glow and Ignition in Carbon Monoxide Oxidation in an Open System. II. Theory of the Oscillatory Ignition Limits in the CSTR, *Proc. Royal Soc. London* **A402**, 187-204 (1985).
38. Kerr, J. A., Strengths of Chemical Bonds, pp. 9-51 to 9-73 in **CRC Handbook of Chemistry and Physics**, D. R. Lide, ed., CRC Press, Boca Raton FL (1995).
39. Hidaka, Y., Sato, K., Henmi, Y., Tanaka, H., and Inami, K., Shock-Tube and Modeling Study of Methane Pyrolysis and Oxidation, *Combustion and Flame* **118**, 340-358 (1999).
40. Li, S. C., and Williams, F. A., NOx Formation in Two-Stage Methane-Air Flames, *Combustion and Flame* **118**, 399-414 (1999).
41. Reid, I. A. B., Robinson, C., and Smith, D. B., Spontaneous Ignition of Methane: Measurement and Chemical Model, pp. 1833-1843 in *20th Symp. (Intl.) on Combustion*, The Combustion Institute, Pittsburgh (1984).
42. Gray, P., Thermal Explosion Fundamentals; Unification of Thermal and Chain-branching Theories of Reaction and Ignition; Thermokinetic Interpretation of Hydrocarbon Oxidation, pp. 171-191 in **Fast Reactions in Energetic Systems**, C. Capellos and R. F. Walker, eds., D. Reidel, Dordrecht (1981).
43. Heyberger, B., Battin-Leclerc, F., Warth, V., Fournet, R., Côme, G. M., and Scacchi, G., Comprehensive Mechanism for the Gas-Phase Oxidation of Propene, *Combustion and Flame* **126**, 1780-1802 (2001).
44. Minkoff, G. J., and Tipper, C. F. H., **Chemistry of Combustion Reactions**, Butterworths, London (1962).
45. Bamford, C. H., and Tipper, C. F. H., eds., **Comprehensive Chemical Kinetics**, vol. 17 (Gas Phase Combustion), Elsevier, Amsterdam (1977).
46. Hucknall, D. J., **Chemistry of Hydrocarbon Combustion,** Chapman and Hall, London (1985).

47. Pilling, M. J., ed., **Comprehensive Chemical Kinetics**, vol. 35 (Low-temperature Combustion and Autoignition), Elsevier, Amsterdam (1997).
48. Compton, R. G., and Hancock, G., eds., **Comprehensive Chemical Kinetics**, vol. 37 (Applications of Kinetic Modelling), Elsevier, Amsterdam (1998).
49. Mallard, E., and Le Chatelier, H. L., Sur les températures d'inflammation des mélanges gazeux, *Comptes Rendus Academie Sciences Paris* **91**, 825-828 (1880).
50. Kuchta, J. M., Investigation of Fire and Explosion Accidents in the Chemical, Mining, and Fuel-Related Industries—A Manual (Bulletin 680), Bureau of Mines, Pittsburgh (1985).
51. Zabetakis, M. G., Flammability Characteristics of Combustible Gases and Vapors (Bulletin 627), Bureau of Mines, Pittsburgh (1965).
52. Egolf, L. M., and Jurs, P. C., Estimation of Autoignition Temperatures of Hydrocarbons, Alcohols, and Esters from Molecular Structure, *Ind. and Eng. Chem. Res.* **31**, 1798-1807 (1992).
53. Frank, C. E., Blackham, A. U., and Swarts, D. E., Investigation of Spontaneous Ignition Temperatures of Organic Compounds With Particular Emphasis on L ubricants (NACA TN 2848), NACA, Washington (1952).
54. Griffiths, J. F., and Gray, B. F., Fundamentals of Autoignition of Hydrocarbons and Other Organic Substrates in the Gas Phase, *24th Loss Prevention Symp.*, AIChE (1990).
55. Townsend, D. T. A., Cohen, L. L., and Mandlekar, M. R., The Influence of Pressure on the Spontaneous Ignition of Inflammable Gas-Air Mixtures, III—Hexane and Isobutane-air Mixtures, *Proc. Royal Soc. London* **A146**, 113-129 (1934).
56. Demidov, P. G., **Goreniye i svoystva goryuchikh veshchestv**, Izdatel'stvo Ministerstva Kommunal'nogo Khozyaystva RSFSR, Moskva (1962). English translation: **Combustion and Properties of Combustible Substance**, NTIS No. AD 621 738, NTIS, Springfield, VA (1965).
57. Gödde, M., Brandes, E., Möller, W. O., and Cammenga, H. K., Zündtemperatur bei erhöhtem Ausgangsdruck [Effect of Elevated Pressure on Autoignition Temperature], pp. 71-75 in Tagungsbericht zum 8. Koll. zu Fragen der chemischen und physikalischen Sicherheitstechnik: Recht und Technik zum Schutz von Mensch und Umwelt, BAM und PTB, Berlin (1999).
58. Ono, S., On the Effects of Surfaces upon the Spontaneous Ignition of the Liquid Fuels, *Review of Physical Chemistry of Japan* **20**, 42-49 (1946).
59. Freeman, G., and Lefebvre, A. H., Spontaneous Ignition Characteristics of Gaseous Hydrocarbon-Air Mixtures, *Combustion and Flame* **58**, 153-162 (1984).
60. Chang, C. J., Thompson, A. L., and Winship, R. D., Ignition Delay of Propane in Air between 725 – 880ºC under Isothermal Conditions, pp. 431-435 in *7th Symp. (Intl.) on Combustion*, Butterworths, London (1958).
61. Miller, R. E., Some Factors Governing the Ignition Delay of a Gaseous Fuel, pp. 417-424 in *7th Symp. (Intl.) on Combustion*, Butterworths, London (1958).
62. Mullins, B. P., Combustion in Vitiated Atmospheres. Part III—Effect of Oxygen Concentration on Ignition Induction Period, *Fuel* **32**, 205-207 (1953).
63. Furno, A. L., Imhof, A. C., and Kuchta, J. M., Effect of Pressure and Oxidant Concentration on Autoignition Temperatures of Selected Combustibles in Various Oxygen and Nitrogen Tetroxide Atmospheres, *J. Chem. and Eng. Data* **13**, 243-249 (1968).
64. Snee, T. J., and Griffiths, J. F., Criteria for Spontaneous Ignition in Exothermic, Autocatalytic Reactions: Chain Branching and Self-Heating in the Oxidation of Cyclohexane in Closed Vessels, *Combustion and Flame* **75**, 381-395 (1989).
65. Lewis, D. J., Autoignition Temperature Determinations & Their Relationship to Other Types of Potential Ignition Sources & Their Application to Practical Situations, pp. 257-273 in *7th Intl. Symp. on Chemical Process Hazards with Special Reference to Plant Design* (IChemE Symp. Series No. 58), The Institution of Chemical Engineers, London (1980).
66. Mason, W., and Wheeler, R. V., The Ignition of Gases. II. Ignition by a Heated Surface. Mixtures of Methane and Air. *J. Chem. Soc.* **121**, 2079-2091 (1922).
67. Kuchta, J. M., Bartkowiak, A., and Zabetakis, M. G., Hot Surface Ignition Temperatures of Hydrocarbon Fuel Vapor-Air Mixtures, *J. Chem. and Eng. Data* **10**, 282-288 (1965).
68. White, R. G., Spontaneous Ignition of Kerosene (AVTUR) Vapor: The Effect of the Ratio, Vessel Surface Area to Volume. Technical Report 67107, Royal Aircraft Establishment, Farnborough Hants, England (1967).
69. Coffee, R. D., Cool Flames and Autoignitions: Two Oxidation Processes, *13th Loss Prevention Symp.*, AIChE (1979).
70. Lewis, B., and von Elbe, G., **Combustion, Flames and Explosions in Gases**, 3rd ed., Academic Press, Orlando FL (1987).
71. Frank, C. E., and Blackham, A. U., Spontaneous Ignition of Organic Compounds, *Ind. and Eng. Chem.* **44**, 862-867 (1952).
72. Setchkin, N. P., Self-Ignition Temperatures of Combustible Liquids, *J. Research NBS* **53**, 49-66 (1954).
73. Fire Protection Research Program for Supersonic Transport (APL TDR-64-105), Air Force Aero Propulsion Laboratory, Wright-Patterson AFB, OH (1964).
74. Belles, F. E., and Swett, C. C., Ignition and Flammability of Hydrocarbon Fuels, pp. 277-320 in Basic Considerations in the Combustion of Hydrocarbon Fuels with Air (NACA Report 1300), NACA, Washington (1957).
75. Wiezevich, P. J., Whiteley, J. M., and Turner, L. B., Spontaneous Ignition of Petroleum Fractions, *Ind. and Eng. Chem.* **27**, 152-155 (1935).
76. Griffiths, J. F., Coppersthwaite, D., Phillips, C. H., Westbrook, C. K., and Pitz, W. J., Auto-Ignition Temperatures of Binary Mixtures of Alkanes in a Closed Vessel: Comparisons between Experimental Measurements and Numerical Predictions, pp. 1745-1752 in *23rd Symp. (Intl.) on Combustion*, The Combustion Institute, Pittsburgh (1990).
77. Conti, R. S., and Hertzberg, M., Thermal Autoignition Temperatures from the 1.2-L Furnace and Their Use in Evaluating the Explosion Potential of Dusts, pp. 45-59 in **Industrial Dust Explosions** (ASTM STP 958), ASTM, Philadelphia (1987).
78. Kuchta, J. M., Lambiris, S., and Zabetakis, M. G., Flammability and Autoignition of Hydrocarbon Fuels Under Static and Dynamic Conditions (RI 5992), Bureau of Mines, Pittsburgh (1962).
79. Sano, T., and Yamashita, A., Flame Ignition of Premixed Methane Air Mixtures on a High-Temperature Plate, *JSME Intl. J. Series B: Fluids and Thermal Engrg.* **37**, 180-186 (1994).
80. Goodger, E. M., Spontaneous Ignition Research: Review of Experimental Data, *J. Inst. Energy* **60**, 84-94 (June 1987).

81. Zabetakis, M. G., Furno, A. L., and Jones, G. W., Minimum Spontaneous Ignition Temperatures of Combustibles in Air, *Ind. and Eng. Chem.* **46**, 2173-2178 (1954).
82. Mason, W., and Wheeler, R. V., The Ignition of Gases. IV. Ignition by a Heated Surface. Mixtures of the Paraffins with Air. *J. Chem. Soc.* **125**, 1869 (1924).
83. Salooja, K. C., Effects of Temperature on the Ignition Characteristics of Hydrocarbons, *Combustion and Flame* **5**, 243-247 (1961).
84. Anagnostou, E., Brokaw, R. S., and Butler, J. N., Effect of Concentration on Ignition Delays for Various Fuel-Oxygen-Nitrogen Mixtures at Elevated Temperatures (Tech. Note 3887), NACA, Washington (1956).
85. Mullins, B. P., **Spontaneous Ignition of Liquid Fuels**, AGARDograph no. 4. Butterworths, London (1955).
86. Jackson, J. L., and Brokaw, R. S., Variation of Spontaneous Ignition Delays with Temperature and Composition for Propane-Oxygen-Nitrogen Mixtures at Atmospheric Pressure (NACA RM E54B19), NACA, Cleveland (1954).
87. Mullins, B. P., Studies of the Spontaneous Ignition of Fuels Injected into a Hot Air Stream. III. Effect of Chemical Factors upon the Ignition Delay of Kerosine-Air Mixtures, *Fuel* **32**, 327-341 (1953).
88. Schihl, P., Atreya, A., and Bryzik, W., Development of a Shear Layer Ignition Model for Application to Direct-Injection Diesel Engines, *Combustion and Flame* **121**, 453-470 (2000).
89. Jackson, J. L., Brokaw, R. S., Weast, R. C., and Gerstein, M., A Flow Apparatus for the Determination of Spontaneous Ignition Delays, *Ind. and Eng. Chem.* **46**, 2547-2550 (1954).
90. Snee, T. J., Auto-ignition, Slow Combustion and the Variation of Minimum Ignition Temperature with Vessel Size, *Loss Prevention Bulletin* No. 81, 25-38 (1988).
91. Kane, G. P., The Two-Stage Auto-Ignition of Hydrocarbons and "Knock," *Proc. Royal Soc. London* **A167**, 62-80 (1938).
92. Pearlman, H., Diffusion-controlled Cool Flames and Multistage Ignition at Reduced Gravity, pp. 483-493 in *Fire & Explosion Hazards—Proc. 3rd Intl. Symp.*, Univ. Central Lancashire, Preston, England (2000).
93. Gray, P., Griffiths, J. F., Hasko, S. M., and Lignola, P. G., Novel, Multi-stage Ignitions in the Spontaneous Combustion of Acetaldehyde, *Combustion and Flame* **43**, 175-186 (1981).
94. Shepherd, W. C. F., The Ignition of Gas Mixtures by Impulsive Pressures, pp. 301-316 in *Third Symp. on Combustion and Flame and Explosion Phenomena*, Williams & Wilkins, Baltimore (1949).
95. Wolański, P., and Wójcicki, S., Investigation into the Mechanism of the Diffusion Ignition of a Combustible Gas Flowing into an Oxidizing Atmosphere, pp. 1217-1223 in *14th Symp. (Intl.) on Combustion*, The Combustion Institute, Pittsburgh (1972).
96. Jones, J. C., **Combustion Science: Principles and Practice**, Millennium Books, Newtown NSW, Australia (1993).
97. Ingen-Housz, J., **Vermischte Schriften phisisch-medizinischen Inhalts**, N. K. Molitor, ed., Johann Paul Krauss, Wien (1782).
98. Davy, H., On the Fire-Damp of Coal Mines, and on Methods of Lighting the Mines so as to Prevent Its Explosion, *Phil. Trans. Royal Soc.* 1-24 (1816).
99. Holm, J. M., On the Ignition of Explosive Gaseous Mixtures by Small Flames, *Phil. Mag.* Series 7 **14**, 18-56 (1932) and **15**, 329-359 (1933).
100. Jarosiński, J., Flame Quenching by a Cold Wall, *Combustion and Flame* **50**, 167-175 (1983).
101. Turns, S. R., **An Introduction to Combustion**, McGraw-Hill, New York (1996).
102. Incropera, F. P., and DeWitt, D. P., **Fundamentals of Heat and Mass Transfer**, 4th ed., John Wiley, New York (1996); p. 240.
103. Ballal, D. R., and Lefebvre, A. H., A General Model of Spark Ignition for Gaseous and Liquid Fuel-Air Mixtures, pp. 1737-1746 in *18th Symp. (Intl.) on Combustion*, The Combustion Institute, Pittsburgh (1980).
104. Friedman, R., The Quenching of Laminar Oxyhydrogen Flames by Solid Surfaces, pp. 110-120 in *3rd Symp. on Combustion and Flame and Explosion Phenomena*, Williams & Wilkins, Philadelphia (1949).
105. Jarosiński, J., A Survey of Recent Studies on Flame Extinction, *Prog. Energy and Combustion Science* **12**, 81-116 (1986).
106. Mayer, E., A Theory of Flame Propagation Limits Due to Heat Loss, *Combustion and Flame* **1**, 438-452 (1957).
107. Potter, A. E. jr., Flame Quenching, *Prog. Comb. Science and Technology* **1**, 145-181 (1975).
108. Adelman, H. G., A Time Dependent Theory of Spark Ignition, pp. 1333-1342 in *18th Symp. (Intl.) on Combustion*, The Combustion Institute, Pittsburgh (1980).
109. Frendi, A., and Sibulkin, M., Dependence of Minimum Ignition Energy on I gnition Parameters, *Combustion Science and Technology* **73**, 395-413 (1990).
110. Sloane, T., and Ronney, P. D., A Comparison of Ignition Phenomena Modeled with Detailed and Simplified Kinetics, *Combustion Science and Technology* **88**, 1-13 (1993).
111. Tromans, P. S., and Furzeland, R. M., An Analysis of Lewis Number and Flow Effects on the Ignition of Premixed Gases, pp. 1891-1897 in *21st Symp. (Intl.) on Combustion*, The Combustion Institute, Pittsburgh (1986).
112. Chomiak, J., **Combustion: A Study in Theory, Fact, and Application**, Abacus Press, New York (1990).
113. Pitt, P. L., Clements, R. M., and Topham, D. R., The Early Phase of Spark Ignition, *Combustion Science and Technology* **78**, 289-314 (1991).
114. Anderson, R. W., and Lim, M. T., Experimental Study of a Developing Spark Kernel, pp. 511-514 in *GD85 – 8th Intl. Conf. on Gas Discharges & Their Applications*, Leeds Univ. Press, Leeds, UK (1985).
115. Fenn, J. B., Lean Flammability Limit and Minimum Spark Ignition Energy, *Ind. and Eng. Chem.* **43**, 2865-2869 (1951).
116. Wheeler, R. V., Report on Battery Bell Signalling Systems as regards the Danger of Ignition of Firedamp-Air Mixtures by the Break-Flash at the Signal Wires, Safety in Mines Research Board, HMSO, London (1915).
117. Lord, H., Widginton, D. W., and Gordon, R. L., The Use of Breaking Wires to Produce Incendive Electrical Discharges, pp. 7-14 in *Flameproofing—Intrinsic Safety and Other Safeguards in Electrical Instrument Practice* (IEE Conf. Report Series No. 3), Institution of Electrical Engineers, London (1962).
118. Allsop, G., and Guénault, E. M., The Incendivity of Electric Sparks in Relation to the Characteristics of the Circuit, pp. 341-353 in *3rd Symp. on Combustion and Flame and Explosion Phenomena*, Williams & Wilkins, Philadelphia (1949).
119. Berz, I., On Inductive Break Sparks of High Incendive Power, *Combustion and Flame* **3**, 131-132 (1959).

120. Zborovszky, Z. K., New Concepts and Experimental Results on the Ignition Limits of CR Circuits, pp. 123-128 in *3rd Intl. Conf. on Electrical Safety in Hazardous Environments*, Institution of Electrical Engineers, Power Div., London (1982).
121. Berz, I., and Khan, M. A. A., An Extension of Existing Design Parameters Relevant to Intrinsically Safe Electrical Circuits, *The Mining Electrical & Mechanical Engineer* **46**, 259-263 (1966).
122. Zborovszky, Z., Study of Incendiary Potential of Low Voltage High Current Inductive Discharges (BuMines OFR 46-79), Bureau of Mines, Pittsburgh (1978).
123. Gehm, K.-H., Sonderschutzarten für den Explosionsschutz von elektrischen Betriebsmitteln [Special enclosures for explosion safety of electrical factory equipment], *Elektro Welt B (Industrielle Elektrotechnik)* **4**:10, 187-188 (Oct. 1959).
124. Ikeda, T., Difference in Experimental Data From IEC Data in the Ignition Limit of Propane, *Mining Technology [UK]* **73**:841, 18-20 (Jan 1991).
125. Bartels, A. L., Bradford, M., and Thompson, M. G., Incendivity of Electrical Sparking due to Circulating Currents in the Enclosure of Large Electrical Machines, pp. 141-148 in *4th Intl. Conf. on Electrical Safety in Hazardous Areas* (IEE Conf. Publ. 296), Institution of Electrical Engineers, London (1988).
126. Zborovszky, Z., Study of Intrinsic Safety Basics and Testing Machines: Study of the Effects of Discharge Duration, Electrode Materials and Surface Conditions on the Minimum Ignition Current (BuMines OFR 68-79), Bureau of Mines, Pittsburgh (1977).
127. Gordon, R. L., West, L. C. W., and Widginton, D. W., The Ignition of Methane-Air Mixtures by Arc Discharges of Controlled Duration, pp. 15-20 in *Flameproofing—Intrinsic Safety and Other Safeguards in Electrical Instrument Practice* (IEE Conf. Report Series No. 3), Institution of Electrical Engineers, London (1962).
128. Olenik, H., Rentzsch, H., and Wettstein, W., **Handbuch für Explosionsschutz—Explosion Protection Manual**, 2nd ed., Brown, Boveri & Cie im Verlag W. Girardet, Essen, Germany (1983).
129. Thomas, V. M., Design of Intrinsically Safe Apparatus for Use in Coal Mines: A Review of Data ancd Techniques, *The Mining Electrical & Mechanical Engineer* **44**, 295-308 (May 1964); Part II, 321-329 (June 1964).
130. Beyling, C., Versuche zwecks Erprobung der Schlagwettersicherheit besonders geschützter elektrischer Motoren und Apparate sowie zur Ermittlung geeigneter Schutzvorrichtungen für solche Betriebsmittel, ausgeführt auf der berggewerkscahftlichen Versuchstrecke in Gelsenkirchen-Bismarck [Experiments for the Purpose of Testing the Safety in Firedamp of Certain Protected Motors and Equipment, as Well as the Determination of Suitable Protective Arrangements for such Equipment, Carried out at the Experimental Gallery in Gelsenkirchen-Bismarck], *Glückauf (Essen)* **42**, 1 (1906).
131. Walls, N. S., Wheeler, R. V., Rintoul, W., and White, A. G., The Ignition of Firedamp by Momentary Flames (Paper 24), Safety in Mines Research Board, London (1926).
132. Wolfhard, H. G., and Burgess, D. S., The Ignition of Combustible Gases by Flames, *Combustion and Flame* **2**, 3-12 (1958).
133. Wang, T. S., Zhang, Y. F., Zhao, H. F., Qi, Z. M., and Ren, A. F., A Study of Ignition by Flame Torches, pp. 1729-1736 in *18th Symp. (Intl.) on Combustion*, The Combustion Institute, Pittsburgh (1980).
134. Sawerysyn, J.-P., Meriaux, B., and Lucquin, M., Interaction of a Preexisting Flame with Flowing Flammable Fuel-Air Mixtures, *Combustion and Flame* **41**, 221-233 (1981).
135. Karim, G. A., Wierzba, I., Metwally, M., and Mohan, K., The Combustion of a Fuel Jet in a Stream of Lean Gaseous Fuel-Air Mixtures, pp. 977-991 in *18th Symp. (Intl.) on Combustion*, The Combustion Institute, Pittsburgh (1981).
136. Jones, G. W., The Flammability of Refrigerants: Mixtures of Methyl and Ethyl Chlorides and Bromides, *Ind. and Eng. Chem.* **20**, 367-370 (1928).
137. Homan, H. S., and Sirignano, W. A., Minimum Mass of Burning Aluminum Particles for Ignition of Methane/Air and Propane/Air Mixtures, pp. 1709-1717 in *18th Symp. (Intl.) on Combustion*, The Combustion Institute, Pittsburgh (1980).
138. Metzler, A. J., Minimum Spark-Ignition Energies of 12 Pure Fuels at Atmospheric and Reduced Pressure (NACA RM E53H31), NACA, Cleveland OH (1953).
139. Potter, A. E. jr., and Berlad, A. L., A Relation between Burning Velocity and Quenching Distance (NACA TN 3882), NACA, Washington (1956).
140. Chin, J. S., The Analysis of the Effect of Oxygen Addition on Minimum Energy, *J. Energy* **7**, 710-715 (1983).
141. Ural, E. A., Zalosh, R. G., and Tamanini, F., Ignitability of Jet-A Fuel Vapors in Aircraft Fuel Tanks, pp. 14-1 to 14-13 in *Aircraft Fire Safety* (AGARD Conf. Proc. No. 467), AGARD (1989).
142. Harris, M. E., Grumer, J., von Elbe, G., and Lewis, B., Burning Velocities, Quenching, and Stability Data on Nonturbulent Flames of Methane and Propane with Oxygen and Nitrogen, pp. 80-89 in *3rd Symp. on Combustion and Flame and Explosion Phenomena*, Williams & Wilkins, Baltimore (1949).
143. Blanc, M. V., Guest, P. G., von Elbe, G., and Lewis, B., Ignition of Explosive Gas Mixtures by Electric Sparks. III. Minimum Ignition Energies and Quenching Distances of Mixtures of Hydrocarbons and Ether with Oxygen and Inert Gases, pp. 363-367 in *3rd Symp. on Combustion and Flame and Explosion Phenomena*, Williams & Wilkins, Philadelphia (1949).
144. Singer, J. M., Cook, E. B., and Grumer, J., Equivalences and Lower Ignition Limits of Coal Dust and Methane Mixtures (RI 6931), Bureau of Mines, Pittsburgh (1967).
145. Guest, P. G., Sikora, V. W., and Lewis, B., Static Electricity in Hospital Operating Suites: Direct and Related Hazards and Pertinent Remedies (RI 4833), Bureau of Mines, Pittsburgh (1952).
146. Jarosiński, J., Strehlow, R. A., and Azarbarzin, A., The Mechanisms of Lean Limit Extinguishment of an Upward and Downward Propagating Flame in a Standard Flammability Tube, pp. 1549-1557 in *19th Symp. (Intl.) on Combustion*, The Combustion Institute, Pittsburgh (1982).
147. Jarosiński, J., Lee, J. H., Knystautas, R., and Crowley, J. D., Quenching Distance of Self-Propagating Dust-Air Flames, *Archivum Combustionis* **7**, 267-278 (1987).
148. King, I. R., and Calcote, H. F., Effect of Initial Temperature on Minimum Spark Ignition Energy, *J. Chem. Phys.* **23**, 2444-2445 (1955).
149. Magison, E. C., **Electrical Instruments in Hazardous Locations**, 4th ed., ISA, Research Triangle Park NC (1998).

150. Kuchta, J. M., and Clodfelter, R. G., Aircraft Mishap Fire Pattern Investigations (AFWAL-TR-85-2057), Aero Propulsion Laboratory, Air Force Systems Command, Wright-Patterson AFB, OH (1985).
151. Metzler, A. J., Minimum Ignition Energies of Six Pure Hydrocarbon Fuels of the C_2 and C_6 Series (NACA RM E52F27), NACA, Cleveland OH (1952).
152. Barnett, H. C., and Hibbard, R. R., Properties of Aircraft Fuels (Tech. Note 3276), NACA, Washington (1956).
153. Friedman, R., and Johnston, W. C., Pressure Dependence of Quenching Distance of Normal Heptane, Iso-Octane, Benzene, and Ethyl Ether Flames, *J. Chem. Phys.* **20**, 919-920 (1952).
154. Friedman, R., and Johnston, W. C., The Wall-Quenching of Laminar Propane Flames as a Function of Pressure, Temperature, and Air-Fuel Ratio, *J. Appl. Phys.* **21**, 791-795 (1950).
155. Ronney, P. D., Effect of Gravity on Laminar Premixed Gas Combustion. II. Ignition and Extinction Conditions, *Combustion and Flame* **62**, 121-133 (1985).
156. Ronney, P. D., Laser versus Conventional Ignition of Flames, *Optical Engineering* **33**, 510-521 (1994).
157. Kravchenko, V. S., and Bondar', V. A., **Vzryvobezopasnost´ elektricheskikh razriadov i frik-tsionnykh iskr** [Explosion Safety of Electrical Discharges and Frictional Sparks], Nedra, Moscow (1976). Part 1. Chapter 1 (HSE Translation 8346), Health and Safety Executive, London.
158. Swett, C. C. jr., Spark Ignition of Flowing Gases. IV. Theory of Ignition in Nonturbulent and Turbulent Flow Using Long-Duration Discharges (RM E54F29a), NACA, Washington (1954).
159. Akindele, O. O., Bradley, D., Mak, P. W., and McMahon, M., Spark Ignition of Turbulent Gases, *Combustion and Flame* **47**, 129-155 (1982).
160. De Soete, G. G., The Influence of Isotropic Turbulence on the Critical Ignition Energy, pp. 735-743 in *13th Symp. (Intl.) on Combustion*, The Combustion Institute, Pittsburgh (1970).
161. Ballal, D. R., and Lefebvre, A. H., Ignition and Flame Quenching in Flowing Gas Mixtures, *Proc. Royal Soc. London* **A357**, 163-181 (1977).
162. Ballal, D. R., and Lefebvre, A. H., The Influence of Flow Parameters on Minimum Ignition Energy and Quenching Distance, pp. 1473-1481 in *15th Symp. (Intl.) on Combustion*, The Combustion Institute, Pittsburgh (1974).
163. Morgan, J. D., **Principles of Ignition**, Pitman, London (1942).
164. Li, G., and Wang, C., Comprehensive Study on Electric Spark Sensitivity of Ignitable Gases and Explosive Powders, *J. Electrostatics* **11**, 319-332 (1981).
165. Rose, H. E., and Priede, T., An Investigation of the Characteristics of Spark Discharges as Employed in Ignition Experiments, pp. 454-463 in *7th Symp. (Intl.) on Combustion*, Butterworths, London (1958).
166. Roth, W., Guest, P. G., von Elbe, G., and Lewis, B., Heat Generation by Electric Sparks and Rate of Heat Loss to the Spark Electrodes, *J. Chem. Phys.* **19**, 1530-1535 (1951).
167. Eckhoff, R. K., Towards Absolute Minimum Ignition Energies for Dust Clouds? *Combustion and Flame* **24**, 53-64 (1975).
168. Pidoll, U. von, The Ignition of Clouds of Sprays, Powders and Fibers by Flames and Electric Sparks, *J. Loss Prevention in the Process Industries* **14**, 103-109 (2001).
169. Swett, C. C. jr., Spark Ignition of Flowing Gases (NACA Report 1287), NACA, Washington (1956).
170. Kono, M., Kumagai, S., and Sakai, T., The Optimum Condition for Ignition of Gases by Composite Sparks, pp. 757-766 in *16th Symp. (Intl.) on Combustion*, The Combustion Institute, Pittsburgh (1976).
171. Kono, M., Iinuma, K., Kumagai, S., and Sakai, T., Spark Discharge Characteristics and Igniting Ability of Capacitor Discharge Ignition Systems, *Combustion Science and Technology* **19**, 13-18 (1978).
172. Kravchenko, V. S., Erygin, A. T., and Yakovlev, V. A., Critical Duration of an Electrical Discharge for Ignition of Methane-Air and Hydrogen-Air Mixtures, *Combustion, Explosion and Shock Waves* **9**, 532-524 (1973).
173. Ziegler, G. F. W., and Herweg, R., Low-Current Arc Discharge Characteristics of Cadmium Electrodes for Ignition Studies, pp. 534-537 in *GD85 – 8th Intl. Conf. on Gas Discharges & Their Applications*, Leeds Univ. Press, Leeds, UK (1985).
174. Kono, M., Kumagai, S., and Sakai, T., Ignition of Gases by Two Successive Sparks with Reference to Frequency Effect of Capacitance Sparks, *Combustion and Flame* **27**, 85-98 (1976).
175. Litchfield, E. L., and Monroe, J. S., Ignition of Gaseous Mixtures with Repetitious Sparks, *Combustion and Flame* **7**, 393-394 (1963).
176. Movilliat, P., and Giltaire, M., Mesure de l'énergie d'inflammation de mélanges gazeux par décharge capacitive. Inflammation par décharge d'une personne chargée d'electricité statique, *J. Electrostatics* **6**, 307-331 (1979).
177. Rose, H. E., and Priede, T., Ignition Phenomena in Hydrogen/Air Mixtures, pp. 436-445 in *7th Symp. (Intl.) on Combustion*, Butterworths, London (1958).
178. Krämer, H., Minimum Ignition Energy of Ammonia/Air Atmosphere, pp. 504-506 in *GD85 –8th Intl. Conf. on Gas Discharges & Their Applications*, Leeds Univ. Press, Leeds (1985).
179. Kono, M., and Hatori, K., Ignition of Low Flow Velocity Mixtures by Short Duration Sparks, pp. 500-503 in *GD85 – 8th Intl. Conf. on Gas Discharges & Their Applications*, Leeds Univ. Press, Leeds (1985).
180. Calcote, H. F., Gregory, C. A. jr, Barnett, C. M., and Gilmer, R. B., Spark Ignition: Effect of Molecular Structure, *Ind. and Eng. Chem.* **44**, 2656-2662 (1952).
181. Litchfield, E. L., Minimum Ignition-Energy Concept and Its Application to Safety Engineering (RI 5671), Bureau of Mines, Pittsburgh (1960).
182. Ziegler, G. F. W., Wagner, E. P., and Maly, R. R., Ignition of Lean Methane-Air Mixtures by High Pressure Glow and Arc Discharges, pp. 1817-1824 in *20th Symp. (Intl.) on Combustion*, The Combustion Institute, Pittsburgh (1984).
183. Rogulski, W., Ignition of Gas Mixtures by Electrical Discharges between a Heated and a Cold Electrode, *Nature* **194**, 858-859 (1962).
184. Thornton, W. M., The Ignition of Gases by Hot Wires, *Phil. Mag.* Series 6, **38**, 613-633 (1919).
185. Janssens, M., and Parker, W. J., Oxygen Consumption Calorimetry, pp. 31-59 in **Heat Release in Fires**, V. Babrauskas and S. J. Grayson, eds. E&FN Spon, London (1992).
186. Coward, H. F., and Guest, P. G., Ignition of Natural Gas-Air Mixtures by Heated Metal Bars, *J. Amer. Chem. Soc.* **49**, 2479-2486 (1927).

187. Coward, H. F., and Wheeler, R. V., The Ignition of Firedamp (Paper 53), Safety in Mines Research Board, London (1929).
188. Vogt, G., Die Zündquelle "Heisse Oberflächen" [Hot Surfaces as an Ignition Source], *Glückauf* **113**:20, 1000-1005 (20 Oct. 1977). HSE Translation 7578, HSE, London.
189. Powell, F., Ignition of Gases and Vapours by Hot Surfaces and Particles—A Review, pp. 267-299 in *Report of the 9th Intl. Symp. on Prevention of Occupational Accidents and Diseases in the Chemical Industry,* Intl. Social Security Assn., Lucerne (1984).
190. Duarte, D., and Drysdale, D. D., The Effect of Local Confinement on the Ignition of Flammable Vapour/Air Mixtures at a Hot Surface, pp. 665-673 in *Interflam '93*, Interscience Communications Ltd., London (1993).
191. Markworth, D., and Schebstadt, F., Zündverhalten kleiner Heisser Bauteile in Explosionsfähiger Atmosphäre [Ignition Behavior of Small Heated Components in an Explosive Atmosphere] (PTB-W-25), Physikalisch-Technische Bundesanstalt, Braunschweig, Germany (1985).
192. Cutler, D. P., Further Studies of the Ignition of Gases by Transiently Heated Surfaces, *Combustion and Flame* **33**, 85-91 (1978).
193. Adomeit, G., Ignition of Gases at Hot Surfaces under Nonsteady Conditions, pp. 237-243 in *10th Symp. (Intl.) on Combustion*, The Combustion Institute, Pittsburgh (1964).
194. Silver, R. S., The Ignition of Gaseous Mixtures by Hot Particles, *Phil. Mag.* Series 7, **23**, 633-657 (1937).
195. Paterson, S., The Ignition of Inflammable Gases by Hot Moving Particles, *Phil. Mag.* Series 7, **28**, 1-23 (1939); **30**, 437-457 (1940).
196. Tolson, P., The Ignition of Flammable Atmospheres by Small Amounts of Metal Vapor and Particles, *Combustion and Flame* **18**, 19-26 (1972).
197. Mullins, J. W. II, Fenn, J. B., and Irby, M. R., The Ignition of High Velocity Streams of Combustible Gases by Heated Cylindrical Rods, pp. 317-329 in *3rd Symp. on Combustion and Flame and Explosion Phenomena*, Williams & Wilkins, Philadelphia (1949).
198. Kuchta, J. M., Fire And Explosion Manual for Aircraft Accident Investigators (AFAPL-TR-73-74). Prepared by Bureau of Mines, Pittsburgh, for Air Force Aero Propulsion Laboratory, Wright-Patterson Air Force Base, Ohio (1973).
199. Hamer, P. S., Wood, B. M., Doughty, R. L., Gravell, R. L., Hasty, R. C., Wallace, S. E., and Tsao, J. P., Flammable Vapor Ignition Initiated by Hot Rotor Surfaces within an Induction Motor: Reality or Not? *IEEE Trans. on Industry Applications* **35**, 100-113 (1999).
200. Bartels, A. L., Ignition by Hot Surfaces in Electrical Equipment, pp. 109-114 in *Conf. on Electrical Safety in Hazardous Environments* (Conf. Publ. No. 74), Institution of Electrical Engineers, London (1971).
201. Duarte, D., and Rohagi, J., Mechanics of Ignition by Hot Surfaces, *J. Applied Fire Science* **7**, 165-180 (1997/98).
202. Müller, R., Einfluss der Zündenergie auf die Zündgrenzen von Gas/Luft-Gemischen unter Variation von Druck und Temperatur, Universität Erlangen-Nurnberg, Germany (1977).
203. Cutler, D., and Brearley, D., Frictional Ignition of Dusts and Vapours (IR/L/EC/98/01), HSE, Buxton, UK (1998).
204. Rae, D., Singh, B., and Danson, R., The Size and Temperature of a Hot Square in a Cold Surface Necessary for the Ignition of Methane (Research Report 224), Safety in Mines Research Establishment, Sheffield, England (1964).
205. Khalturinsky, N. A., and Berlin, Al. Al., Polymer Combustion, pp. 145-294 in **Degradation and Stabilization of Polymers**, H. H. G. Jellinek, ed., Elsevier, Amsterdam (1989).
206. Bannister, W. E., Walker, J. L., and Morehouse, E. T., Autoignition. Part 1. Thermoelectric Effects of Hot Surfaces: An Ionic Mechanism for Spontaneous Ignition, The Combustion Institute/Eastern States Section, 1988 Technical Mtg., Clearwater Beach FL (1988).
207. Nagata, H., Kim, H. M., Sato, J., and Kono, M., An Experimental and Numerical Investigation on the Hot Surface Ignition of Premixed Gases under Microgravity Conditions, pp. 1719-1725 in *25th Symp. (Intl.) on Combustion*, The Combustion Institute, Pittsburgh (1994).
208. Cho, P., and Law, C. K., Catalytic Ignition of Fuel/Oxygen/Nitrogen Mixtures over Platinum, *Combustion and Flame* **66**, 159-170 (1986).
209. Hiam, L., Wise, H., and Chaikin, S., Catalytic Oxidation of Hydrocarbons on Platinum *J. Catalysis* **9**, 272-276 (1968).
210. Bull, D. C., Autoignition at Hot Surfaces, pp. 165-172 in *2nd Intl. Symp. on Loss Prevention and Safety Promotion in the Process Industries*, European Federation of Chemical Engineering, Publication Series No. 1; 189th Event. DECHEMA, Frankfurt (1978).
211. Deutschmann, O., Schmidt, R., Behrendt, F., and Warnatz, J., Numerical Modeling of Catalytic Ignition, pp. 1747-1754 in *26th Symp. (Intl.) on Combustion*, The Combustion Institute, Pittsburgh (1996).
212. Song, X., Williams, W. R., Schmidt, L. D., and Aris, R., Ignition and Extinction of Homogeneous-Heterogeneous Combustion: CH_4 and C_3H_8 Oxidation on Pt, pp. 1129-1137 in *23rd Symp. (Intl.) on Combustion*, The Combustion Institute, Pittsburgh (1990).
213. Griffin, T. A., and Pfefferle, L. D., Gas Phase and Catalytic Ignition of Methane and Ethane in Air over Platinum, *AIChE J.* **36**, 861-870 (1990).
214. Bui, P.-A., Wilder, E. A., Vlachos, D. G., and Westmoreland, P. R., Hierarchical Reduced Models for Catalytic Combustion: H_2/Air Mixtures Near Platinum Surfaces, *Combustion Science and Technology* **129**, 243-275 (1997).
215. Enomoto, K., Furuhama, S., and Kobayashi, Y., Ignitability of Hydrogen-Air Mixture by Hot Surfaces and Hot Gases, *Hydrogen Energy Progress* (Proc. 3rd World Hydrogen Energy Conf., 1980), Vol. 2, 1149-1163 (1981).
216. Cho, P., Catalytic Ignition and Heat Release of Fuel/Air Mixtures (Ph.D. dissertation), Northwestern Univ., Evanston IL (1984).
217. Rogowski, Z. W., and Pitt, A., Ignition of Flammable Vapours, Gases and Sheet Materials by Catalytic Heaters (Fire Research Note 1023), Fire Research Station, Borehamwood, England (1975).
218. Spilt Coil Gas Burner Has Few Parts but Is a Complex System, *Fire Findings* **6**, No. 4, 12-13 (1998).
219. Ashman, L. E., and Büchler, A., The Ignition of Gases by Electrically Heated Wires, *Combustion and Flame* **5**, 113-121 (1961).
220. Laurendeau, N. M., Thermal Ignition of Methane-Air Mixtures by Hot Surfaces: A Critical Examination, *Combustion and Flame* **46**, 29-49 (1982).
221. Cutler, D. P., The Ignition of Gases by Rapidly Heated Surfaces, *Combustion and Flame* **22**, 105-109 (1974).

222. Kumagai, S., and Kimura, I., Ignition of Flowing Gases by Heated Wires, pp. 554-558 in *6th Symp. (Intl.) on Combustion*, Reinhold, New York (1956).
223. Gebhart, B., **Heat Transfer**, 2nd ed., McGraw-Hill, New York (1971).
224. Ono, S., Kawano, H., Niho, H., and Fukuyama, G., Ignition in a Free Convection from Vertical Hot Plate, *Bull. JSME* **19**, 676-683 (1976).
225. Goyal, G., Warnatz, J., and Maas, U., Numerical Studies of Hot Spot Ignition in H_2-O_2 and CH_4-Air Mixtures, pp. 1767-1773 in *23rd Symp. (Intl.) on Combustion*, The Combustion Institute, Pittsburgh (1990).
226. Sharma, O. P., and Sirignano, W. A., Ignition of Stagnation Point Flow by a Hot Body, *Combustion Science and Technology* **1**, 95-104 (1969).
227. Sharma, O. P., and Sirignano, W. A., On the Ignition of a Pre-mixed Fuel by a Hot Projectile, *Combustion Science and Technology* **1**, 481-494 (1970).
228. Cairnie, L. R., Harrison, A. J., and Morgan, P. A., Autoignition in a Free Convection Boundary Layer, pp. 1799-1806 in *18th Symp. (Intl.) on Combustion*, The Combustion Institute, Pittsburgh (1980).
229. Boczek, B., Glinka, W., and Wolański, P., Ignition of a Combustible Mixture by a Burning Metal Particle, *Oxidation Communications* **5**, 157-173 (1983).
230. Toong, T. Y., Ignition and Combustion on a Laminar Boundary Layer over a Hot Surface, pp. 532-540 in *6th Symp. (Intl.) on Combustion*, Reinhold, New York (1956).
231. Chen, L.-D., and Faeth, G. M., Ignition of a Combustible Gas near Heated Surfaces, *Combustion and Flame* **42**, 77-92 (1981).
232. Fakheri, A., Analytical and Experimental Investigations of Catalytic Combustion (Ph.D. dissertation), Univ. Illinois, Urbana (1985).
233. Ilsley, L. C., and Hooker, A. B., Ignition of Gases by Electric Detonators (RI 2383), Bureau of Mines, Pittsburgh (1922).
234. Shepherd, W. C. F., and Wheeler, R. V., The Ignition of Gases by Hot Wires (Paper 36), Safety in Mines Research Board, London (1927).
235. Davies, W., The Ignition of Methane by Hot Wires, *Fuel* **22**, 72-76 (1943).
236. Silver S., A Review of the Ignition of Flammable Gases or Vapors by Hot Wires, Internal Report FMP-62/186-EEC (EEC No. 54), Dept. of Mines and Surveys, Mines Branch, Ottawa (1962).
237. Zborovszky, Z., Study of Intrinsic Safety Basics and Testing Machines: A Comparison of Tungsten and Copper Hot Wire Ignition Capability and Discharge Duration in the Ignition Process of Explosive Atmospheres in Testing Apparatus (BuMines OFR 116-77), Bureau of Mines, Pittsburgh (1976).
238. Zborovszky, Z., Intrinsically Safe Supporting Research (Report DRI 5628), Denver Research Institute, University of Denver, Denver (1980).
239. Stout, H. P., and Jones, E., The Ignition of Gaseous Explosives Media by Hot Wires, pp. 329-336 in *3rd Symp. on Combustion and Flame and Explosion Phenomena*, Williams & Wilkins, Baltimore (1949).
240. Craven, A. D., and Foster, M. B., The Limits of Flammability of Ethylene in Oxygen, Air and Air-Nitrogen Mixtures at Elevated Temperatures and Pressures, *Combustion and Flame* **10**, 95-100 (1966).
241. Takahashi, A., Urano, Y., Tokuhashi, K, Nagai, H., Kaise, M., and Kondo, S., Fusing Ignition of Various Metal Wires for Explosion Limits Measurement of Methane/Air Mixture, *J. Loss Prevention in the Process Industries* **11**, 353-360 (1998).
242. Coward, H. F., and Jones, G. W., Limits of Flammability of Gases and Vapors (Bulletin 503), Bureau of Mines, Pittsburgh (1952).
243. Wolfhard, H. G., and Vanpée, M., Ignition of Fuel-Air Mixtures by Hot Gases and Its Relationship to Firedamp Explosions, pp. 446-453 in *7th Symp. (Intl.) on Combustion*, Butterworths, London (1958).
244. Wolfhard, H. G., The Ignition of Combustible Mixtures by Hot Gases, *Jet Propulsion* **28**, 798-804 (1958).
245. Wolfhard, H. G., and Bruszak, A. E., The Passage of Explosions through Narrow Cylindrical Channels, *Combustion and Flame* **4**, 149-159 (1960).
246. Wolfhard, H. G., and Bruszak, A. E., Communication of Flame Through Cylindrical Channels (RI 5457), Bureau of Mines, Pittsburgh (1959).
247. Vanpée, M., and Wolfhard, H. G., Comparison between Hot Gas Ignition and Limit Flame Temperatures, *ARS J.* **29**, 517-519 (1959).
248. Kuchta, J. M., and Cato, R. J., Hot Gas Ignition Temperatures of Hydrocarbon Fuel Vapor-Air Mixtures (RI 6 857), Bureau of Mines, Pittsburgh (1966).
249. Vanpée, M., and Bruszak, A. E., The Ignition of Combustible Mixtures by Laminar Jets of Hot Gases (RI 6293), Bureau of Mines, Pittsburgh (1963).
250. Vanpée, M., and Wolfhard, H. G., Ignition by Hot Gases (RI 5627), Bureau of Mines, Pittsburgh (1960).
251. Kuchta, J. M., Summary of Ignition Properties of Jet Fuels and Other Aircraft Combustible Fluids (AFAPL-TR-75-70), Air Force Aero Propulsion Lab., Wright-Patterson AFB, OH (1975).
252. Phillips, H., Ignition in a Transient Turbulent Jet of Hot Inert Gas, *Combustion and Flame* **19**, 187-195 (1972).
253. Rozlovskii, A. I., and Zakarnov, V. F., Effect of Gas Expansion During Combustion on the Possibility of Using Flame Arresters, *Combustion and Flame* **17**, 215-221 (1971).
254. Thibault, P., et al., Transmission of an Explosion through an Orifice, pp. 599-606 in *19th Symp. (Intl.) on Combustion*, The Combustion Institute, Pittsburgh (1982).
255. Larsen, Ø., and Eckhoff, R. K., Critical Dimensions of Holes and Slots for Transmission of Gas Explosions—Some Preliminary Results for Propane/Air and Cylindrical Holes, *J. Loss Prevention in the Process Industries* **13**, 341-347 (2000).
256. Maekawa, M., and Takeichi, M., Non-Ignition of an Ejected Flame through a Gap Greater than the Quenching Distance, *Fire Research* **1**, 317-322 (1978/79).
257. Smith, P. B., The Role of Flanges in Conferring Protection on Flameproof Electrical Enclosures (Research Report 77), Safety in Mines Research Establishment, Sheffield, England (1953).
258. Phillips, H., The Basic Theory of the Flameproof Enclosure, pp. 99-103 in *Conf. on Electrical Safety in Hazardous Environments* (Conf. Publ. No. 74), Institution of Electrical Engineers, London (1971).
259. Bartels, A. L., Low Power Arcing in Flameproof Enclosures, pp. 104-108 in *Conf. on Electrical Safety in Hazardous Environment* (Conf. Publ. No. 74), Institution of Electrical Engineers, London (1971).

260. Birtwhistle, D., Byers, K., Crisp, J., and Das Gupta, S., Arcing in Flameproof Enclosures, pp. 164-167 in *Proc. 10th Intl. Conf. on Gas Discharges and Their Applications (GD '92)*, Univ. College of Swansea, Swansea, UK (1992).
261. Crisp, J., and Birtwhistle, D., Modelling of Methane Explosions and Fault Arcing in Flameproof Mining Enclosures, pp. II-288 to II-291 in *Proc. 11th Intl. Conf. on Gas Discharges and Their Applications (GD '95)*, The Institute of Electrical Engineers of Japan, Tokyo (1995).
262. Phillips, H., The Mechanism of Flame-proof Protection. (SMRE Research Report 275), Safety in Mines Research Establishment, Sheffield, England (1971).
263. Riddlestone, H. G., and Nethercot, W., Explosionproof Electrical Equipment for Aircraft, pp. 26-28 in *Flameproofing—Intrinsic Safety and Other Safeguards in Electrical Instrument Practice* (IEE Conf. Report Series No. 3), Institution of Electrical Engineers, London (1962).
264. Brown, G. K., Dainty, E. D., and Silver, S., Laboratory Investigations of Hydrogen Explosion Phenomena Relating to Electrical Apparatus (Res. Rep. R182), Dept. of Mines and Technical Surveys, Mines Branch, Ottawa (1966).
265. Redeker, T., Classification of Flammable Gases and Vapours by the Flameproof Safe Gap and Incendivity of Electrical Sparks (PTB-W-18), PTB-Bericht, Physikalisch-Technische Bundesanstalt, Braunschweig, Germany (1981).
266. Phillips, H., A Reaction-rate Theory for Flameproof Enclosures, pp. 22-25 in *Flameproofing—Intrinsic Safety and Other Safeguards in Electrical Instrument Practice* (IEE Conf. Report Series No. 3), Institution of Electrical Engineers, London (1962).
267. Strehlow, R. A., Nicholls, J. A., Magison, E. C., and Schram, P. J., An Investigation of the Maximum Experimental Safe Gap Anomaly, *J. Hazardous Materials* **3**, 1-15 (1979).
268. Lunn, G. A., The Influence of Chemical Structure and Combustion Reactions on the Maximum Experimental Safe Gap of Industrial Gases and Liquids, *J. Hazardous Materials* **6**, 341-359 (1982).
269. Burgess, D., and Hertzberg, M., The Flammability Limits of Lean Fuel-Air Mixtures: Thermochemical and Kinetic Criteria for Explosion Hazards, *ISA Trans.* **14**, 129-136 (1975).
270. James, R. S., Effect of Temperature on Flame-Arresting Properties of Flat Joints in Explosion-proof Mine Equipment (RI 4639), Bureau of Mines, Pittsburgh (1950).
271. Torry, R., Flameproof Enclosures for Mining Electrical Equipment: Influence of Atmospheric Moisture on M aximum Safe Gaps (Research Report 202), Safety in Mines Research Establishment, Sheffield, England (1962).
272. Helwig, N., and Nabert, K., Zusammenhänge zwischen Kenngrössen für explosionsgeschützte Betriebsmittel [Correlation between Characteristic Values for Explosion Safety in Processing], PTB Mitteilungen, *PTB-Mitteilungen* 287-293 (April 1968).
273. Phillips, H., Differences between Determinations of Maximum Experimental Safe Gap in Europe and USA, *J. Hazardous Materials* **4**, 245-256 (1981).
274. Britton, L. G., Using Maximum Experimental Safe Gap to Select Flame Arresters, *Process Safety Progress* **19**, 140-145 (2000).
275. Slack, C., and Woodhead, D. C., Correlation of Ignitabilities of Gases and Vapours by a B reak Spark and at a F lange Gap, *Proc. IEE* **113**, 297-301 (1966).
276. Bartels, A. L., and Howes, J. A., The Variation of Minimum Igniting Currents with Pressure, Temperature, and Oxygen Enrichment, pp. 120-125 in *Conf. on Electrical Safety in Hazardous Environments* (Conf. Publ. No. 74), Institution of Electrical Engineers, London (1971).
277. Tolson, P., The Use of Oxygen-Enriched Mixtures to Provide a Factor of Safety in the Ignition Testing of Intrinsically Safe Circuits, pp. 131-135 in *Conf. on Electrical Safety in Hazardous Environments* (Conf. Publ. No. 74), Institution of Electrical Engineers, London (1971).
278. Brandes, E., März, G., and Redeker, T., Normspaltweiten von Mehr-Brennstoffkomponenten-Gemischen in Abhängigkeit der Brennstoffzusammensetzung [Computational Method for MESG Values of Mixtures of Combustibles] (PTB-W-69), PTB-Bericht, Physikalisch-Technische Bundesanstalt, Braunschweig, Germany (1997).
279. Hills, P. C., Zhang, D. K., Sampson, P. J., and Wall, T. F., Laser Ignition of Combustible Gases by Radiative Heating of Small Particles, *Combustion and Flame* **91**, 399-412 (1992).
280. Trott, W. M., CO_2-Laser-Induced Deflagration of Fuel/Oxygen Mixtures, *J. Appl. Phys.* **54**, 118-130 (1983).
281. Hill, R. A., and Laguna, G. A., Laser Initiated Combustion of $CH_4 + O_2$ Mixtures, *Optics Communications* **32**, 435-439 (1980).
282. Norrish, R. G. W., The Study of Combustion by Photochemical Means, pp. 1-20 in *10th Symp. (Intl.) on Combustion*, The Combustion Institute, Pittsburgh (1964).
283. Raizer, Y. P., **Gas Discharge Physics**, Springer-Verlag, Berlin (1991).
284. Ma, J. X., Alexander, D. R., and Poulain, D. E., Laser Spark Ignition and Combustion Characteristics of Methane-Air Mixtures, *Combustion and Flame* **112**, 492-506 (1998).
285. Phuoc, T. X., Single-Point versus Multi-Point Laser Ignition: Experimental Measurements of Combustion Times and Pressures, *Combustion and Flame* **122**, 508-510 (2000).
286. Lee, J. H., and Knystautas, R., Laser Spark Ignition of Chemically Reactive Gases, *AIAA J.* **7**, 312-317 (1969).
287. Weinberg, F. J., and Wilson, J. R., A Preliminary Investigation of the Use of Focused Laser Beams for Minimum Ignition Energy Studies, *Proc. Royal Soc. London* **A321**, 41-52 (1971).
288. Lim, E. H., McIlroy, A., Ronney, P. D., and Syage, J. A., Detailed Characteristics of Minimum Ignition Energies of Combustible Gases using Laser Ignition Sources, pp. 176-184 in **Transport Phenomena in Combustion**, vol. 1, S. H. Chen, ed., Taylor & Francis, Washington (1996).
289. Syage, J. A., Fournier, E. W., Rianda, R., and Cohen, R. B., Dynamics of Flame Propagation Using Laser-Induced Spark Initiation: Ignition Energy Measurements, *J. Appl. Phys.* **64**, 1499-1507 (1988).
290. Morgan, C. G., Laser-induced Breakdown of Gases, *Reports on Progress in Physics* **38**, 621-665 (1975).
291. Phuoc, T. X., and White, F. P., Laser-Induced Spark Ignition of CH_4/Air Mixtures, *Combustion and Flame* **119**, 203-216 (1999).
292. Morsy, M. H., Ko, Y. S., and Chung, S. H., Laser-Induced Ignition Using a Conical Cavity in CH_4-Air Mixtures, *Combustion and Flame* **119**, 473-482 (1999).
293. Dubaniewicz, T. H. jr., Cashdollar, K. L., Green, G. M., and Chaiken, R. F., Ignition of Methane-Air Mixtures by Laser Heated Small Particles, *J. Loss Prevention in the Process Industries* **13**, 349-359 (2000).

294. Dubaniewicz, T. H. jr., Cashdollar, K. L., Green, G. M., and Cucci, G. R., Ignition Tests with a Fiber-Optic Powered Instrument, *Proc. 41st Annual ISA Analysis Division Symp.,* **29**, 175-184 (1996).
295. Zhang, D.-K., Hills, P. C., Zheng, C., Wall, T. F., and Samson, P., Fibre Optic Ignition of Combustible Gas Mixtures by the Radiative Heating of Small Particles, pp. 1761-1767 in *24th Symp. (Intl.) on Combustion*, The Combustion Institute, Pittsburgh (1992).
296. Bothe, H., Johannsmeyer, U., and Schenk, S., Explosion Protection Concepts for Optical Radiation in Explosion Hazardous (Classified) Locations, *ISA Expo/2000*, Vol. 4 (2000).
297. Tortoishell, G., The Safety of Optical Systems in Hazardous Areas, pp. 115-124 in *In-Process Optical Measurements and Industrial Methods*, Proc. SPIE vol. 1266, SPIE, Bellingham WA (1990).
298. Adler, J., Carleton, F. B., and Weinberg, F. J., Ignition of Flammable Atmospheres by Radiation-Heated Fibrous Agglomerates, *Proc. Royal Soc. London* **A440**, 443-460 (1993).
299. Carleton, F. B., Bothe, H., Proust, Ch., and Hawksworth, S., Prenormative Research on the Use of Optics in Potentially Explosive Atmospheres—PROPEX (EUR 19617 EN), European Commission, Luxembourg (2000).
300. Carleton, F. B., and Weinberg, F. J., Correlating Minimum Ignition Criteria, *Proc. Royal Soc. (London)* **A447**, 513-526 (1994).
301. Scott, S. K., and Smith, J. D. B., Modelling of Ignition of Flammable Atmospheres by Radiation-Heated Fibrous Agglomerates, *Proc. Royal Soc. London* **A450**, 199-217 (1995).
302. Adler, J., Laser Ignition of a Combustible Gas: A Composite Layer Steady-State Model, pp. 1769-1776 in *24th Symp.(Intl.) on Combustion*, The Combustion Institute, Pittsburgh (1992).
303. Kingdon, R. G., and Weinberg, F. J., The Effect of Plasma Constitution on Laser Ignition Energies, pp. 747-756 in *16th Symp. (Intl.) on Combustion*, The Combustion Institute, Pittsburgh (1976).
304. Park, Y. K., Bui, P.-A., and Vlachos, D. G., Operation Regimes in Catalytic Combustion: H_2/Air Mixtures near Pt, *AIChE J.* **44**, 2035-2043 (1998).
305. Cashdollar, K. L, Zlochower, I. A., Green, G. M., Thomas, R. A., and Hertzberg, M., Flammability of Methane, Propane, and Hydrogen Gases, *J. Loss Prevention in the Process Industries* **13**, 327-340 (2000).
306. Spalding, D. B., A Theory of Inflammability Limits and Flame-Quenching, *Proc. Royal Soc. London* **A240**, 83-100 (1957).
307. Hertzberg, M., The Theory of Flammability Limits. Natural Convection (RI 8127), Bureau of Mines, Pittsburgh (1976).
308. Hertzberg, M., The Theory of Flammability Limits. Conductive-Convective Wall Losses and Thermal Quenching (RI 8469), Bureau of Mines, Pittsburgh (1980).
309. Hertzberg, M., The Theory of Flammability Limits. Radiative Losses and Selective Diffusional Demixing (RI 8607), Bureau of Mines, Pittsburgh (1982).
310. Hertzberg, M., The Theory of Flammability Limits. Flow Gradient Effects and Flame Stretch (RI 8865), Bureau of Mines, Pittsburgh (1984).
311. Westbrook, C. K., Inhibition of Hydrocarbon Oxidation in Laminar Flames and Detonations by Halogenated Compounds, pp. 127-141 in *19th Symp. (Intl.) on Combustion*, The Combustion Institute, Pittsburgh (1982).
312. Law, C. K., and Egolfopoulos, F. N., A Kinetic Criterion of Flammability Limits: The C-H-O-inert System, pp. 413-421 in *23rd Symp. (Intl.) on Combustion*, The Combustion Institute, Pittsburgh (1990).
313. Law, C. K., and Egolfopoulos, F. N., A Unified Chain-Thermal Theory of Fundamental Flammability Limits, pp. 137-144 in *24th Symp. (Intl.) on Combustion*, The Combustion Institute, Pittsburgh (1992).
314. Lakshmisha, K. N., Paul, P. J., and Mukunda, H. S., On the Flammability Limit and Heat Loss in Flames with Detailed Chemistry, pp. 433-440 in *23rd Symp. (Intl.) on Combustion*, The Combustion Institute, Pittsburgh (1990).
315. Pintar, A. J., Predicting Lower and Upper Flammability Limits, *Proc. Intl. Conf. on Fire Safety*, Vol. 28, Product Safety Corp., Sissonville WV (1999).
316. Hilado, C. J., A Method for Estimating Limits of Flammability, *J. Fire and Flammability* **6**, 130-139 (1975).
317. Shimy, A. A., Calculating Flammability Characteristics of Hydrocarbons and Alcohols, *Fire Technology* **6**, 135-139 (1970).
318. Kanury, A. M., Flaming Ignition of Solid Fuels, pp. 2-190 to 2-204 in **The SFPE Handbook of Fire Protection Engineering**, 2nd ed., NFPA (1995).
319. Firth, J. G., Jones, A., and Jones, T. A., The Principles of the Detection of Flammable Atmospheres by Catalytic Devices, *Combustion and Flame* **21**, 303-311 (1973).
320. Suzuki, T., Note: Empirical Relationship between Lower Flammability Limits and Standard Enthalpies of Combustion of Organic Compounds, *Fire and Materials* **18**, 333-336 (1994).
321. Hshieh, F.-Y., Predicting Heats of Combustion and Lower Flammability Limits of Organosilicon Compounds, *Fire and Materials* **23**, 79-89 (1999).
322. Mullins, B. P., Bubble-points, Flammability Limits and Flash-points of Petroleum Products, pp. 55-75 in **Combustion Researches and Reviews 1957**, Butterworths, London (1957).
323. Monakhov, V. T., **Metody issledovaniya pozharnoi ospasnosti veshchestv**, Khimya, Moscow (1972). English translation: **Methods for Studying the Flammability of Substances**, published for U.S. National Bureau of Standards by Amerind Publishing Co., New Delhi, India (1985).
324. Le Chatelier, H., Note sur le dosage du grisou par les limites d'inflammabilité [Estimation of Firedamp Concentration according to Flammability Limits], *Annales de Mines* (8th series) **19**:8, 388-395 (1891).
325. Jones, J. W., Inflammability of Mixed Gases (Tech. Paper 450), Bureau of Mines, Pittsburgh (1929).
326. Bunev, V. A., and Babkin, V. S., Deviations from the Le Chatelier Rule for the Limits of the Propagation of a Flame, *Combustion, Explosion and Shock Waves* **9**, 525-527 (1973).
327. Jorissen, W. P., General Discussion, *Trans. Faraday Soc.* **22**, 291-297 (1925).
328. Hustad, J. E., and Sønju, O. K., Experimental Studies of Lower Flammability Limits in Gases and Mixtures of Gases at Elevated Temperature, *Combustion and Flame* **71**, 283-294 (1988).
329. Coward, H. F., Carpenter, C. W., and Payman, W., The Dilution Limits of Inflammation of Gaseous Mixtures, *J. Chem. Soc.* **115**, 27-36 (1919).
330. Wierzba, I., Karim, G. A., and Cheng, H., The Flammability of Rich Gaseous Fuel Mixtures Including Those Containing Propane in Air, *J. Hazardous Materials* **20**, 303-312 (1988).

331. **Manual for Predicting Chemical Process Design Data: Data Prediction Manual**, R. P. Danner, T. E. Daubert, eds., Design Institute for Physical Property Data, AIChE (1983-1987).
332. Liekhus, K. J., Zlochower, I. A., Cashdollar, K. L., Djordjevic, S. M., and Loehr, C. A., Flammability of Gas Mixtures Containing Volatile Organic Compounds and Hydrogen, *J. Loss Prevention in the Process Industries* **13**, 377-384 (2000).
333. Lewis, B., and von Elbe G., Theory of Flame Propagation, pp. 183-188 in *2nd Symp. on Combustion*, 1937, The Combustion Institute, Pittsburgh (1965).
334. Ronney, P. D., and Wachman, H. Y., Effect of Gravity on Laminar Premixed Gas Combustion. I. Flammability Limits and Burning Velocities, *Combustion and Flame* **62**, 107-119 (1985).
335. Melhem, G. A., A Detailed Method for Estimating Mixture Flammability Limits Using Chemical Equilibrium, *Process Safety Progress* **16**, 203-218 (1997).
336. Médard, L. A., **Accidental Explosions**, 2 vols., Ellis Horwood, Chichester, England (1989).
337. Brandes, E., Pawel, D., Alpers, J., and Scheffler, J., Sicherheitstechnische Kenngössen bei reduzierten Ausgangsdrücken, pp. 85-90 in Tagungsbericht zum 8. Koll. zu Fragen der chemischen und physikalischen Sicherheitstechnik: Recht und Technik zum Schutz von Mensch und Umwelt, BAM und PTB, Berlin (1999).
338. Jones, G. W., and Kennedy, R. E., Inflammability of Natural Gas: Effect of Pressure upon the Limits (RI 3798), Bureau of Mines, Pittsburgh (1945).
339. Mitchell, F. C., and Vernon, H. C., Effect of Pressure on Explosion Hazards, *NFPA Q.* **31**, 306-313 (1938).
340. Vaivads, R. H., Bardon, M. F., Rao, V. K., and Battista, V., Flammability Tests of Alcohol/Gasoline Vapours (SAE Paper 950401), Society of Automotive Engineers, Warrendale PA (1995).
341. Klinkenberg, A., and van der Minne, J. L., **Electrostatics in the Petroleum Industry**, Elsevier, Amsterdam (1958).
342. Standard Test Method for Distillation of Petroleum Products (ASTM D 86), ASTM.
343. White, A. G., Limits for the Propagation of Flame in Inflammable Gas-Air Mixtures. Part III. The Effect of Temperature on the Limits, *J. Chem. Soc.* **127**, 672-684 (1925).
344. Zabetakis, M. G., Scott, G. S., and Jones, G. W., Limits of Flammability of Paraffin Hydrocarbons in Air, *Ind. and Eng. Chem.* **43**, 2120-2124 (1951).
345. Britton, L. B., and Smith, J. A., Static Hazards of Drum Filling, Paper 54e, *21st Loss Prevention Symp.*, AIChE (1987).
346. Schrödter, W., Die untere Zündgrenze von Lösemitteln bei höheren Temperaturen, pp. 245-266 in *Report of the 9th Intl. Symp. on Prevention of Occupational Accidents and Diseases in the Chemical Industry*, Intl. Social Security Assn., Lucerne (1984).
347. Starkman, E. S., Haxby, L. P., and Cattaneo, A. G., A Study of Free Flames in Turbulent Streams, pp. 670-673 in *4th Symp. (Intl.) on Combustion*, Williams & Wilkins, Baltimore (1953).
348. Lovachev, L. A., et al., Flammability Limits: An Invited Review, *Combustion and Flame* **20**, 259-289 (1973).
349. Abdel-Gayed, R. G., Bradley, D., and McMahon, M., Turbulent Flame Propagation in Premixed Gases: Theory and Experiment, pp. 245-254 in *17th Symp. (Intl.) on Combustion*, The Combustion Institute, Pittsburgh (1978).
350. Boston, P. M., et al., Flame Initiation in Lean, Quiescent and Turbulent Mixtures with Various Igniters, pp. 141-149 in *20th Symp. (Intl.) on Combustion*, The Combustion Institute, Pittsburgh (1984).
351. Lovachev, L. A., Flammability Limits—A Review, *Combustion Science and Technology* **20**, 209-224 (1979).
352. Levy, A., An Optical Study of Flammability Limits, *Proc. Royal Soc. London* **A283**, 134-145 (1965).
353. White, A. G., Limits for the Propagation of Flame in Inflammable Gas-air Mixtures, *J. Chem. Soc.* **125**, 2387-2396 (1924).
354. Gerstein, M., and Stine, W. B., Analytical Criteria for Flammability Limits, pp. 1109-1118 in *14th Symp. (Intl.) on Combustion*, The Combustion Institute, Pittsburgh (1972).
355. Simon, D. M., Belles, F. E., and Spakowski, A. E., Investigation and Interpretation of the Flammability Region for Some Lean Hydrocarbon-Air Mixtures, pp. 126-138 in *4th Symp. (Intl.) on Combustion*, Williams & Wilkins, Baltimore (1953).
356. Pellmont, G., Explosions- und Zündverhalten von hybriden Gemischen aus brennbaren Stäuben und Brenngasen [Explosion and Ignition Behavior of Hybrid Mixtures of Combustible Dusts and Combustible Gases] (dissertation), Eidgenössischen technischen Hochschule, Zürich, Switzerland (1979).
357. Bartknecht, W., **Explosions: Course, Prevention, Protection**, Springer-Verlag, Berlin (1981).
358. Rhead, T. F. E., Residual and Extinctive Atmospheres of Flames, *J. Soc. Chemical Ind.* **37**, 274-278 (1918).
359. Lewis, B., Report of Research and Technologic Work on Explosives, Explosions, and Flames—Fiscal Years 1947 and 1948 (RI 4502), Bureau of Mines, Pittsburgh (1947).
360. Standard on Explosion Prevention Systems (NFPA 69), NFPA.
361. Subramaniam, T. K., and Cangelosi, J. N., Predict Safe Oxygen in Combustible Gases, *Chem. Engineering* **96**:12, 108-113 (Dec. 1989).
362. Yang, C. H., Theory of Ignition and Auto-Ignition, *Combustion and Flame* **6**, 215-225 (1962).
363. Blanc, M. V., Guest, P. G., Von Elbe, G., and Lewis, B., Ignition of Explosive Gas Mixtures by Electric Sparks. I. Minimum Ignition Energies and Quenching Distances of Mixtures of Methane, Oxygen, and Inert Gases, *J. Chem. Phys.* **15**, 798-802 (1947).
364. Maček, A., Flammability Limits: A Re-Examination, *Combustion Science and Technology* **21**, 43-52 (1979).
365. Yang, C. H., and Gray, B. F., The Determination of Explosion Limits from a Unified Thermal and Chain Theory, pp. 1099-1106 in *11th Symp. (Intl.) on Combustion*, The Combustion Institute, Pittsburgh (1966).
366. Gray, B. F., and Yang, C. H., Unified Theory of Explosions, Cool Flames and Two-Stage Ignitions, *Trans. Faraday Society* **65**, 1603-1622, 2133-2137 (1969).
367. Maksyutov, S. S., Novozhilov, B. V., and Tsyganov, S. A., Thermal Self-Ignition of Previously Unmixed Gases, *Combustion, Explosion, and Shock Waves* **18**, 407-411 (1982).
368. Hirano, T., Methodology for Hazard Assessments, pp. 119-136 in *Proc. Intl. Workshop on Safety in the Transport, Storage and Use of Hazardous Materials*, National Research Institute of Fire and Disaster, Tokyo (1998).

369. Tamanini, F., Partial-Volume Deflagrations—Characteristics of Explosions in Layered Fuel/Air Mixtures, pp. 103-117 in *Fire & Explosion Hazards—Proc. 3rd Intl. Symp.*, Univ. Central Lancashire, Preston, England (2000).
370. Liebman, I., Spolan, I., Kuchta, J. M., and Zabetakis, M. G., Ignition of Tank Atmospheres During Fuel Loading, 30th Midyear Meeting, American Petroleum Institute, Montreal, Canada (11 May 1965).
371. Knowles, R. E., Discussion, *Trans. Inst. Marine Engineers* **77**, 137-138 (1965).
372. Karim, G. A., and Lam, H. T., Ignition and Flame Propagation within Stratified Methane-Air Mixtures Formed by Convective Diffusion, pp. 1909-1915 in *21st Symp. (Intl.) on Combustion*, The Combustion Institute, Pittsburgh (1986).
373. Lee, J. H. S., Initiation of Gaseous Detonations, *Annual Review of Physical Chemistry* **28**, 75-104 (1977).
374. Laderman, A. J., Urtiew, P. A., and Oppenheim, A. K., On the Generation of a Shock Wave by Flame in an Explosive Gas, pp. 265-274 in *9th Symp. (Intl.) on Combustion*, The Combustion Institute, Pittsburgh (1962).
375. Ginsburgh, I., and Bulkley, W., Industrial Aspects of Hydrocarbon-Air Detonations, pp. 198-205; 220 in **Fire Protection Manual for Hydrocarbon Processing Plants**, vol. 1, C. H. Vervalin, ed., 2nd ed., Gulf Publishing, Houston (1973).
376. Westbrook, C. K., Chemical Kinetics of Hydrocarbon Oxidation in Gaseous Detonations, *Combustion and Flame* **46**, 191-210 (1982).
377. Steen, H., and Schampel, K., Experimental Investigation of the Run-up Distance of Gaseous Detonations in Large Pipes, pp. E23-E33 in *4th Intl. Symp. on Loss Prevention and Safety Promotion in the Process Industries*, vol. 3, Pergamon, Oxford (1983).
378. Chatrathi, K., Going, J. E., and Grandestaff, B., Flame Propagation in Industrial Scale Piping, *Process Safety Progress* **20**, 286-294 (2001).
379. Bull, D. C., Elsworth, J. E., and Hooper, G., Susceptibility of Methane-Ethane Mixtures to Gaseous Detonation in Air, *Combustion and Flame* **34**, 327-330 (1979).
380. Moen, I. O., Transition to Detonation in Fuel-Air Explosive Clouds, *J. Hazardous Materials* **33**, 159-192 (1993).
381. Lindstedt, R. P., and Michels, H. J., Deflagration to Detonation Transitions and Strong Deflagrations in Alkane and Alkene Air Mixtures, *Combustion and F lame* **76**, 169-181 (1989).
382. Matsui, H., and Lee, J. H., On the Measure of the Relative Detonation Hazards of Gaseous Fuel-Oxygen and Air Mixtures, pp. 1269-1280 in *17th Symp. (Intl.) on Combustion*, The Combustion Institute, Pittsburgh (1978).
383. Burgess, D. S., Murphy, J. N., Hanna, N. E., and Van Dolah, R. W., Large-Scale Studies of Gas Detonations (RI 7196), Bureau of Mines, Pittsburgh (1968).
384. Nettleton, M. A., Detonation and Flammability Limits of Gases in Confined and Unconfined Situations, *Fire Prev. Science & Tech.* No. 23, 29-30 (Jun. 1980).
385. Furno, A. L., Cook, E. B., Kuchta, J. M., and Burgess, D. S., Some Observations on Near-Limit Flames, pp. 593-599 in *13th Symp. (Intl.) on Combustion*, The Combustion Institute, Pittsburgh (1970).
386. Williams, A., and Smith, D. B., The Combustion and Oxidation of Acetylene, *Chem. Reviews* **70**, 267-293 (1970).
387. Benedick, W. B., Kennedy, J. D., and Morosin, B., Detonation Limits of Unconfined Hydrocarbon-Air Mixtures, *Combustion and Flame* **15**, 83-84 (1970).
388. Munday, G., Detonations in Vessels and Pipelines, *Chemical Engineer (London)* No. 248, 135-144; 152 (Apr. 1971).
389. Litchfield, E. L., Hay, M. H., and Cohen, D. J., Initiation of Spherical Detonation in Acetylene-Oxygen Mixtures (RI 7061), Bureau of Mines, Pittsburgh (1967).
390. Griffiths, J. F., A General Model to Predict the Safe Lifetime of Slowly Reacting Explosives and Propellants, pp. 241-247 in *4th Symp. on Chemical Problems Connected with the Stability of Explosives*, Sektionen för Detonik och Förbränning, Sundbyberg, Sweden (1977).
391. Fine, D. H., Gray, P., and MacKinven, R., Thermal Effects Accompanying Spontaneous Ignitions in Gases. I. An Investigation of the Heating Effects Which Accompany the Rapid Admission of Inert Gas to an Evacuated Vessel, *Proc. Royal Soc. London* **A316**, 223-240 (1970).
392. Dixon, H. B., and Coward, H. F., The Ignition-Temperatures of Gases, *Proc. Chem. Soc. London* **25**, 67-68 (1909).
393. Dixon, H. B., and Coward, H. F., The Ignition Temperatures of Gases, *J. Chem. Soc.* **95**, 514-543 (1909).
394. Coward, H. F., Ignition Temperatures of Gases. "Concentric tube" experiments of (the late) Harold Baily Dixon, *J. Chem. Soc.* **135**, 1382-1406 (1934).
395. Griffiths, J. F., Spontaneous Ignition of Hydrocarbon Fuels at Temperatures in the Range 750 – 1500 K (Contract No. F61775-98-WE103), University of Leeds, Leeds UK (1998).
396. Griffiths, J. F., Gray, B. F., and Gray, P., Multistage Ignition in Hydrocarbon Combustion: Temperature Effects and Theories of Nonisothermal Combustion, pp. 239-248 in *13th Symp. (Intl.) on Comb.*, The Combustion Institute, Pittsburgh (1970).
397. Sage, J. A., and Weinberg, F. J., An Attempt at Measuring Homogeneous Ignition Temperatures, pp. 464-469 in *7th Symp. (Intl.) on Combustion*, Butterworths, London (1958).
398. Smyth, K. C., and Bryner, N. P., Short-Duration Autoignition Temperature Measurements for Hydrocarbon Fuels (NISTIR 4469), NIST (1990).
399. Zabetakis, M.G., Flammability Characteristics of Combustible Gases and Vapors (Bulletin 627), Bureau of Mines (1965).
400. Coffee, R. D., Vogel, P. C., and Wheeler, J. J., Flammability Characteristics of Methylene Chloride (Dichloromethane), *J. Chem. and Eng. Data* **17**, 89-93 (1972).
401. Standard Test Method for Concentration Limits of Flammability of Chemicals (ASTM E 681), ASTM.
402. Kuchta, J. M., and Bajpayee, T. S., Classification Test Methods and Criteria for Flammable Gases (Internal Report No. 4827, prepared for US Dept. of Transportation), Bureau of Mines, Pittsburgh (1990).
403. Standard Test Method for Temperature Limit of Flammability of Chemicals (ASTM E 1232), ASTM.
404. Hirst, R., Savage, N., and Booth, K., Measurement of Inerting Concentrations, *Fire Safety J.* **4**, 147-158 (1981/82).
405. Bestimmung der Explosionsgrenzen von Gasen und Gasgemischen in Luft (DIN 51649), Deutsches Institut für Normung, Berlin (1986).
406. Conrad, D., Grewer, T., Hentschel, B., and Redeker, T., Development of a Standard Method for Flammability Limits of Vapour-Air Mixtures, Vol. 2, pp. 79-1 to 79-12 in *7th Intl. Symp. on Loss Prevention and Safety Promotion in the*

Chemical Industries, European Federation of Chemical Engineering (1992).
407. Determination of Explosion Limits of Gases, Vapours and Their Mixtures (prEN 1839), Comité Européen de Normalisation, Brussels.
408. Standard Practice for Determining Limits of Flammability of Chemicals at Elevated Temperature and Pressure (ASTM E 918), ASTM.
409. Standard Test Methods for Limiting Oxygen (Oxidant) Concentration in Gases and Vapors (ASTM E 2079), ASTM.
410. Law, C. K., Zhu, D. L., and Yu, G., Propagation and Extinction of Stretched Premixed Flames, pp. 1419-1426 in *21st Symp. (Intl.) on Combustion*, The Combustion Institute, Pittsburgh (1986).
411. Ishizuka, S., Determination of Flammability Limits Using a Tubular Flame Geometry, *J. Loss Prevention in the Process Industries* **4**, 185-193 (1991).
412. Liao, C., Saito, N., Saso, Y., and Ogawa, Y., Flammability Limits of Combustible Gases and Vapors Measured by a Tubular Flame Method, *Fire Safety J.* **27**, 49-68 (1996).
413. Ogawa, Y., Saito, N., and Liao, C., Burner Diameter and Flammability Limit Measured by Tubular Flame Burner, pp. 3221-3227 in *27th Symp. (Intl.) on Combustion*, The Combustion Institute, Pittsburgh (1998).
414. Grosshandler, W., Donnelly, M., and Womeldorf, C., Lean Flammability Limit as a Fundamental Refrigerant Property (NISTIR 6229), NIST (1998).
415. Standard Test Method for Minimum Ignition Energy and Quenching Distance in Gaseous Mixtures (ASTM E 582). ASTM.
416. Litchfield, E. L., Hay, M. W., Kubala, T. S., and Monroe, J. S., Minimum Ignition Energy and Quenching Distance in Gaseous Mixtures (RI 7009), Bureau of Mines, Pittsburgh (1967).
417. Potter, A. E., jr. and Anagnostou, E., Reaction Order in the Hydrogen-Bromine Flame from the Pressure Dependence of Quenching Diameter, pp. 347-351 in *7th Symp. (Intl.) on Combustion*, Butterworths, London (1959).
418. Electrical Apparatus for Explosive Gas Atmospheres - Part 1: Construction and Verification Test of Flameproof Enclosures of Electrical Apparatus – First Supplement: Appendix D: Method of Test for Ascertainment of Maximum Experimental Safe Gap (IEC 60079-1A), International Electrotechnical Commission, Geneva (1975).
419. Lunn, G. A., An Apparatus for the Measurement of Maximum Experimental Safe Gaps at Standard and Elevated Temperatures, *J. Hazardous Materials* **6**, 329-340 (1982).
420. Dickie, P., and Lunn, G. A., The Maximum Experimental Safe Gap: Comparison of Results from 8-litre and 20-cm^3 Explosion Vessels, *J. Hazardous Materials* **8**, 271-278 (1984).
421. Westerberg, W. C., Testing Electrical Equipment for Chemical Atmospheres, *Fire Technology* **2**, 226-233 (1966).
422. Bartkus, A. A., et al., An Investigation of Flammable Gases or Vapors with Respect to Explosion-proof Electrical Equipment (Tech. Rept. No. 58), Underwriters Laboratories Inc., [n.p.] (1993).

Copyright © 2003, 2014 Vytenis Babrauskas

Chapter 5. Ignition of dust clouds

Highlights and summary of practical guidance **142**
General principles **143**
Chemistry of combustion **144**
Flammability limits **145**
Lower flammability limits *145*
Upper flammability limit *148*
AIT, quenching distance and MESG **148**
Theory of ignition of dust clouds **149**
Hybrid gas/dust-cloud ignitions **151**
Ignition sources for dust clouds **152**
Mechanical sparks *153*
Electric sparks *153*
Hot surfaces *153*
Glowing nests *153*
Others *154*
Clouds of powdered fibers (flock) **154**
Analysis and application of data **154**
Variables affecting the AIT *154*
Dust concentration 154
Volatile content 154
Particle diameter 155
Moisture 156
Oxygen concentration 156
Residence time 156
Turbulence 156
Test apparatus volume 157
Variables affecting the flammability limits *157*
Probability level used for the definition of the LFL 157
Particle diameter 157
Temperature 158
Pressure 158
Moisture 158
Oxygen concentration 159
Igniter energy supplied 159
Variables affecting the MIE *161*
Dust concentration 161
Particle diameter 161
Temperature 162
Pressure 162
Moisture 162
Oxygen concentration 162
Turbulence 163

Charge on particles 163
Spark electrodes: material and gap size 163
Spark circuit parameters 163
Air velocity and turbulence 166
Test vessel size 166
Risk management based on the MIE *167*
Diluting with inert gases *167*
Diluting with inert dusts *169*
Tests for ignition properties of dust clouds 170
ASTM E 1491 ..... *170*
ASTM E 2019 ..... *170*
Godbert-Greenwald furnace *171*
Bureau of Mines 1.2 L furnace *171*
BAM oven *171*
Hartmann apparatus *172*
Bureau of Mines 6.8 L chamber *173*
Spheres and other 20 L chambers *173*
Nordtest 15 L apparatus *175*
1 m³ spheres *175*
ASTM E 1232 ..... *175*
IEC 61241-2-3/Mike 3 ..... *175*
CMI mechanical impact test *176*
Further readings 176
References 177

Highlights and summary of practical guidance

Dusts can present three types of ignition hazards: (1) layers of dust can ignite if they pile up on hot surfaces; (2) dust clouds in the air can ignite and lead to a flash fire; (3) dust clouds in air can explode (Color Plate 1). The present chapter deals with the explosion hazard; the layer heating hazard is treating under Self-heating in Chapter 9. In some cases, stirring up and igniting dust may lead only to a flash fire, instead of an explosion. But, because an explosion is a more severe consequence than a flash fire, there has not been much research on flash fires.

Dust explosions are generally possible only in unoccupied spaces. This is because the dust concentrations needed for an explosion are high enough that the spaces would not be habitable. But in a habitable space, stirring up dust that has settled on various surfaces may produce an explosive concentration.

Much of the ignition and combustion behavior of dust clouds resembles that of fuel gas/air mixtures. Thus, ignitability of dust clouds is characterized by flammability limits, minimum ignition energy values, and AIT values. As with gases, the AIT value has been much used by regulatory bodies, but is generally not a reasonable descriptor of actual hazards, since ignition almost never occurs by uniformly raising the temperature of the dust cloud to an elevated value.

Because of the added complexity of the solid phase, dust clouds are significantly more difficult to study, and furthermore, have traditionally been less researched than have gas mixtures. Thus, guidance available is often sparse or contradictory. It must be noted, however, that in the last two decades or so there has been a substantial increase in research and currently dust cloud explosions are probably receiving every bit as much study as are gas explosions.

Safety specialists in dust explosions have mostly focused on small-scale test methods, yet the ability of these methods to predict real-scale reality has been at best uncertain, and at worst non-existent. This is hardly reliable, economical, or conservative. Hopefully future work will either lead to

well-validated small-scale methods or to other procedures which reliably—yet not over-conservatively—assess real-scale hazards. The most serious problem with present-day tests is poor uniformity of the dust concentration within the chamber. Since results are reported on the basis of the nominal concentration (mass of dust released, divided by volume of chamber), published LFL* values are often erroneously low, sometimes extremely so.

Dust particle diameter is a critical variable, yet tabulated data will hardly ever pertain to the size that is of specific interest. Thus, tabulated data (such as given in Chapter 15) must only be viewed as a rough guide, not as a quantitative indicator. Tests must be performed on the dust of interest to determine actual values, but even then great faith should not be placed in results from small-scale tests.

In some cases, the system of interest is a hybrid mixture (dust cloud + flammable gas). This is quite common in coal mines, where methane + coal dust is encountered. In hybrid mixtures, the presence of one component reduces the amount of the other component that can be present to maintain the atmosphere below its explosive limit. The LFL can often—but not always—be computed by a simple linear proportioning formula.

For flammable gas atmospheres, one of the main tools available for avoiding ignition is dilution. If sufficiently high ventilation rates can be assured in a system that the fuel concentration is well below the LFL, then ignition is avoided. This is generally not possible to do for dusts. Ventilation flow rates sufficiently high to avoid the LFL are often impractical. In addition, high ventilation velocities can serve to stir up dust layers and introduce new dust into the atmosphere. In some systems and machinery where effective dilution is not possible, inerting, for example, with nitrogen gas, must be utilized.

In 1977 Prof. Essenhigh[1] noted that: "Most research since the explosion hazard was recognized in 1785 by the Turin Academy of Sciences has been experimental." This is still largely the case, and while a number of theories have been put forth, little has emerged in terms of calculational equations suitable for practical assessment of dust cloud ignition hazards. As in many other fields of applied science, some practical problems (when sizable resources can be allocated!) are already being solved by advanced modeling schemes based on computational fluid dynamics. However, review of CFD methodologies is not within the scope of this handbook.

* In the dust explosion literature, it is more common to find the abbreviations LEL or MEC used; however, for consistency and generality, LFL is used here for dust clouds, just as well as for gases.

General principles

Dusts are solids; however, a suspension of dust in air (a *dust cloud*, or a *solid aerosol*) shares many more ignition characteristics with gases than it does with solids, as far as the ignition behavior is concerned. The particles comprising a dust cloud can have a wide variety of shapes. Many are roughly spherical, but platelets, needles, and other shapes are also found. Grain elevators and other agricultural product handling or processing facilities have proven particularly susceptible to dust explosions, since movement of the product tends to create dust and then to transport it. The dusts in grain handling facilities are typically particles of 17 to 120 μm diameter[2]. Also problematic have been the explosions in coal mines of mixtures of methane gas and coal dust. Other explosions tend to occur in chemical industry and in sundry manufacturing processes where dusts are generated. Curiously, the scientific world was not always convinced of the reality of dust explosions, and it was well into the 20th century before certain scientists stopped doubting that the phenomenon can occur. On the other hand, already in 1882, Marreco and Morrison[3] were conducting experiments by firing pistols into a 25 m long dust chamber containing coal dust. One of their findings was that a mixture of coal dust + methane ignites more readily than coal dust alone. Shortly thereafter, in 1885 Engler[4] documented that that a mixture of charcoal dust + methane can be explosible, even if the concentration of neither one alone would be high enough for ignitability. The term *hybrid explosions* is applied to such combinations.

It is a common rule of thumb that a dust cloud of explosive concentration is one in which the hand cannot be seen when the arm is stretched straight out in front of its owner[5]. Under normal conditions, few habitable spaces would have housekeeping so poor that this level of dustiness was present. But dust explosions tend to happen under abnormal circumstances, and high levels of dust can be introduced by a failure of machinery, events which stir up dust previously laying on horizontal surfaces, etc.

An important difference between gas and dust explosions concerns the physical nature of the fuel. For gases, only the chemical nature of the molecule has to be known. For dusts, however, physical properties such as diameter, shape, agglomeration, and sorption of moisture can play an important role. Thus, any theoretical treatment becomes more complicated and difficult. Also, aerodynamics plays a much more crucial role. Gas explosions can occur in quiescent atmospheres, but a dust explosion cannot, since air movement must exist in order to make the dust airborne. If dusts are fully settled in a layer, then ignition may be possible, but the combustion will resemble the combustion of normal solids, and not be an explosion. This problem is identical to the problem of self-heating of porous or granular materials and is treated in Chapter 9. The possibility must also sometimes be considered that quiescent burning of a dust layer

could get stirred up and lead to an explosion, although this chain of events has not been systematically studied.

Because of the possibility of lofting previously settled material, dust explosions often are a 2-stage event: (1) an initial ignition occurs and a certain amount of dust which was present in the air explodes; (2) the explosion makes airborne a large amount of dust which was previously settled out on various surfaces, this new fuel then explodes. The two stages are sometimes identified as *primary* and *secondary* explosions. In coal mining, a variant is encountered, where the primary explosion occurs due to a methane 'pocket.' The methane explosion then stirs up dust and the secondary explosion is a coal dust explosion. Experiments[6] have shown that dust explosions often tend to generate their own secondary explosion, although this question is poorly understood. Recently, Scherpa[7] conducted small-scale experiments on the dispersal of dust from settled layers into a dust cloud, but his technique involved an air blast and not an actual primary explosion. Apparently, the initial explosion acts to drive pyrolyze more fuel vapors from the dust cloud than can be burned locally, and this surplus amount is then available for burning later or at a different place. It is not always necessary to have a primary explosion in order to convert a dust layer into a dust cloud and to explode it. A case is reported where a smoldering layer of wood dust was found and a water stream applied to it for extinguishment[8]. Instead, the hose stream stirred up the dust and an explosion occurred. Dust explosions are normally deflagrations; detonations have been created in experimental studies[9-12] but have not been reported in practice.

Apparatuses developed for testing dusts necessarily differ from those for gas mixtures, because of their different characteristics as regards mixing. Gases are easy to mix uniformly and, once mixed, will not separate out. On the other hand, it is very difficult to create a uniformly mixed dust cloud and, once created, it does not remain in the same condition for long. Solid dispersions in air can be relatively stable if the particles are of very small size (< 0.1 μm), but this is much smaller than the dust clouds generated in typical processing or storage applications. These traits also make measurements on dust clouds less accurate than those on gases, since the basic starting point of an accurately-known concentration comes into question.

A specialized form of combustion is when a primary explosion stirs up a settled dust layer, but the ensuing secondary explosion has the character of propagating in a layer, rather than volumetrically. Explosions of this kind, where fuel is progressively driven into the air by entrainment, rather than being first lofted then burned, were studied by Srinath[13].

Chemistry of combustion

van der Wel[14] classified the chemistry of dust clouds into three types:

Type 1. The combustion reaction occurs on the surface (heterogeneous) and produces gas-phase combustion products. Example: graphite.
Type 2. The combustion reaction occurs on the surface; the products are solid or liquid. Example: most metals.
Type 3. The material pyrolyzes first, and the fuel actually combusting is in the gas phase. Example: most organic substances.
The main steps required to take place for ignition of Type 3 dust clouds are basically the same as for common solids (bulk material):

- the material is heated
- heat causes pyrolysis
- the pyrolysis process produces combustible gases
- the pyrolysis gases are liberated from the solid
- the pyrolysis gases mix in the atmosphere with oxygen
- ignition and explosion occur in the gas phase.

For organic materials, any effects of direct surface oxidation are considered to be small-to-nil, although in earlier years some researchers[15] argued the converse, that dusts ignite primarily by surface oxidation. The process of ignition of metals is discussed in detail in Chapter 8, although example data pertinent to ignition of metals dust clouds are also included throughout this Chapter.

A fourth type of ignition that can take place, not elaborated by van der Wel, involves solid-state decomposition or auto-oxidation, as for explosives and pyrotechnics. A few studies of explosions of dust clouds of propellants exist[19], but the problem is rarely encountered in practice, since most production processes for explosives are not accompanied by the generation of dense dust clouds.

The combustion of a dust cloud differs from combustion of gas mixtures due to the discrete nature of the particles, each one of which forms a local combustion zone. For an explosion to take place, the zones have to be close enough, so that what has been charmingly called[16] "the cooperative mechanism" can sustain flaming. In addition, a dust cloud is rarely created without turbulence, unlike flammable gas atmospheres. The consequence is that the flame thickness in a dust cloud explosion is on the order of centimeters, instead of the 1 mm or so found for flames of gases.

There is not much data on flame temperatures or laminar burning velocities for dust clouds, but limited results for cornstarch and lycopodium[6,17] showed stoichiometric flame temperatures of 1500 – 1600ºC and velocities of 0.13 – 0.59 m s^{-1}. The peak flame temperatures reported in another study[18] for cornstarch, coal, and toner powder were 1100 – 1400ºC. In detonations of various dusts, temperatures up to 2400 – 2600ºC were found. An adiabatic flame temperature of 1720ºC has been calculated for corn dust[13]. Some other researchers found higher laminar burning velocities[13], on the order of 0.5 – 1.5 m s^{-1}; it appears that results are highly dependent on the experimental arrangement used. Turbulent burning velocity, of course, depends on the nature of the

turbulence—experimental values in the range 5 – 1000 m s^{-1} have been reported[13]. The *duration* of flaming in a dust cloud explosion[18] is generally 0.2 – 0.5 s, as measured in test chambers of 2 – 20 m^3 volume.

Flammability limits

LOWER FLAMMABILITY LIMITS

Analogous to the lower flammability limit for gases, a minimum explosible concentration of dusts can be defined. Most explosible dusts have reported lower limits in the range of 20 to 200 g m^{-3}, but the realism of values at the low end of this scale has to be judged in the context of LFL measurements on gases. The lowest reported value is 3.3 g m^{-3}, for hydrogen. The only two organic gas molecules that show LFL values below 30 g m^{-3} are acetylene at 26.6 g m^{-3} and 1,2-propadiene at 27.8 g m^{-3}. These results (see Chapter 15) were obtained by the Bureau of Mines using their flame propagation tube apparatus (see Chapter 4). The ignition source is an electric spark in that apparatus. As Eckhoff pointed out[19], dust combustion can be less efficient than that of gases, but cannot be more efficient—so higher, not lower, LFL values must be expected for dust clouds. The LFL for a dust cloud could, in principle, be identical to that of a gas, if volatilization is rapid enough, such that all of the dust material is pre-volatilized and if the dust suspension were truly uniform.

In 1924 Trostel and Frevert[20] noted that "One of the weak points in any work done with dusts lies in the inability to create and maintain for much more than a second or so a fair homogeneous suspension of definite dust-air proportions." This problem has not been fully solved to date. In 1967, researchers at the Southwest Research Institute[21] reported that LFL values obtained with the Hartmann apparatus, the still-most-common apparatus for this purpose, are roughly a factor of 2× too low, since visible observations indicate that the dust fills only about half the chamber, yet calculations assume that the given mass of dust is dispersed evenly throughout the entire volume. They also noted that the concentration is uneven radially, being higher near the tube walls and lower near the center. Quite recently, Wolański made a study on anomalously-low reported LFL values and similarly concluded that they were due to improperly mixed dust suspensions[22,23]. It remains very difficult to achieve a uniform mixture of dust within a given volume of air. Most typically, there will be pockets of more dense mixtures, interspersed with less dense pockets. If the igniter is so located that pockets of more than average density can flow by it, then it is possible that what was recorded as ignitable was a local concentration that was significantly greater than the average concentration value that was computed. Wolański further pointed out that an LFL of 20 g m^{-3} would mean an adiabatic flame temperature of ca. 500 K at the lean limit; this is grossly unreasonable, since all true limit flame temperatures (see Chapter 3) are generally ca. 1500 K. The same conclusion was reached by Lesikar et al.[24] who reported on tests not of materials showing anomalously low LFL values, but rather, ones in the 'normal' range. Wheat dust shows LFL ≈ 65 g m^{-3} when tested in the standard way in the Hartmann apparatus. But using high-speed photography, they documented that only a portion of the chamber actually contains dust at the moment of explosion, and that the effective LFL value is 110 – 150 g m^{-3}, depending on the particle size distribution. Even more problematic was lignite dust. Standard values, as obtained from Bureau of Mines testing[25] are in the range 25 – 50 g m^{-3}, but a value of 290 g m^{-3} was found by Lesikar et al.

The issue of spatial non-uniformity is also quite real in actual explosions, since mixing will not be perfect in these either. But there does not seem to be any basis for claiming that a small-scale test showing poor uniformity is predictive of a full-scale situation where mixing is imperfect. Eckhoff[19] reviewed various physics details of the mixing process, but it became clear that little progress has been made in dealing with the consequences of poor uniformity on test results or on accidental explosions.

Makris and Lee[26] perhaps best summarized the unsatisfactory state of the art by pointing out that most of the apparatuses used for determining LFL values produce values which have little relation to reality, with the main reasons for this being:

(1) some apparatuses, e.g., the Hartmann apparatus, are so small as to be below the quenching diameter for some dust types;
(2) most apparatuses produce a highly non-uniform dust concentration, and it is not clear that the average concentration has any physical meaningfulness;
(3) since flammability limits innately refer to the potential for flame to propagate through a large, open space, the realism of testing in small, closed volumes (e.g., 20 L spheres) is questionable;
(4) often excessively large ignition sources are used in the laboratory-scale apparatuses, unrealistically enlarging the flammability limits;
(5) the criteria adopted for the test influence the outcome, yet have no fundamental basis that could be related to real-scale performance;
(6) while attempts have been made to provide real-scale validations, the multiple apparatus-dependent features interact in such a way that it is not reasonable to conclude anything positive, in the absence of a large number of validation data points.

As an example of the apparatus-dependent problem, they observed that reported LFL values for cornstarch range from 8 to 380 g m^{-3}. They especially cautioned that a sizable pressure rise recorded in a fixed-volume chamber (the normal criterion applied in determining LFL values in such experiments) does *not* imply that the same mixture would generate an indefinitely propagating flame in a large environment. Instead, it simply means that a fixed quantity of dust ignited and burned enough to raise the pressure to the

criterion value. At the end of their study, the authors concluded that several apparatuses—the Nordtest 15 L apparatus, an experimental 5 m^3 sphere, and their own 180 L cylinder—gave values which were nearly identical (70 – 80 g m^{-3}) and appeared to be the optimum experimental value determined by pressure-rise methods. The extreme outlier (8 g m^{-3}) was obtained in the 20 L Siwek sphere. An entirely different set of results was obtained, however, from experiments done in tubes (similar to the Hartmann apparatus, but larger in scale) where actual flame front propagation was monitored, with the criterion being that the flame propagate at least ¾ of the tube length. Here, the authors found that in large-diameter tubes, LFL = 200 g m^{-3} if the tube is closed (constant volume). For open tubes (constant pressure), LFL = 400 g m^{-3} was measured. Finally, they found that certain coal dusts would not propagate flame at any concentration in their 180 mm diameter tube, which they attributed to the fact that the quenching diameter for this dust was ca. 190 mm. Their conclusions from this experimental work was that "All flammability limits of dust-air mixtures determined in closed-bomb experiments have no fundamental significance at all and are thus meaningless." Instead, they concluded that an open tube apparatus must be used, but that its diameter must exceed the quenching diameter of the dust. Additional data in related studies were reported by Jarosiński et al.[27,28]

A secondary dust explosion will be ignited by an extremely powerful ignition source—an ongoing explosion. Thus, to characterize the intensity of explosions it is prudent to assume that the secondary explosion is the one which does the major damage and therefore, to conduct tests using a very powerful ignition source. In view of this, within the dust explosion testing community over the last several decades, the concept of using pyrotechnic igniters has been developed. These igniters are appropriate for testing the maximum pressures developed in explosions, but when applied to determining of LFL values, three problems can be seen: (1) A highly energetic igniter is logically applicable only to situations where the primary explosion is a gas explosion. Yet, igniters of this kind have been applied to testing of all sorts of dusts even in situations where a primary gas explosion is unlikely or impossible. (2) When highly energetic ignition sources are employed, a non-parallelism is created in regards to the testing of gases, where such schemes are not used: dust clouds are effectively 'proven' to be more readily ignitable than gases. (3) The ignition flame from these devices is highly directional and non-spherical, making analysis or comparison to other igniters difficult.

To examine the effect on gases when highly energetic ignition sources were used, Hertzberg et al.[29] conducted comparative tests on methane using a conventional spark igniter and a series of pyrotechnic igniters. When tested in a 20 L chamber, methane showed LFL = 4.9 vol% (32.1 g m^{-3}) using a spark igniter and using pyrotechnic igniters up to 1000 J nominal rating. For a 2500 J pyrotechnic igniter, however, they found that the recorded LFL dropped to 4.4 vol% (32.4 g m^{-3}). When a larger 120 L chamber was used, then the LFL value associated with the 2500 J igniter rose back to 4.9% and only when going to a 5000 J igniter did it drop to 4.7% (30.8 g m^{-3}). A similar decrease in reported LFL with increasing igniter energy was found for dust clouds (Figure 1). Note, however, that the dust cloud data in Figure 1 are not given for ignition sources smaller than 500 J. Yet, typical ignition sources for dust clouds are mechanical sparks, electrostatic discharges, and other low-energy sources (dust cloud ignition statistics are discussed in Chapter 14).

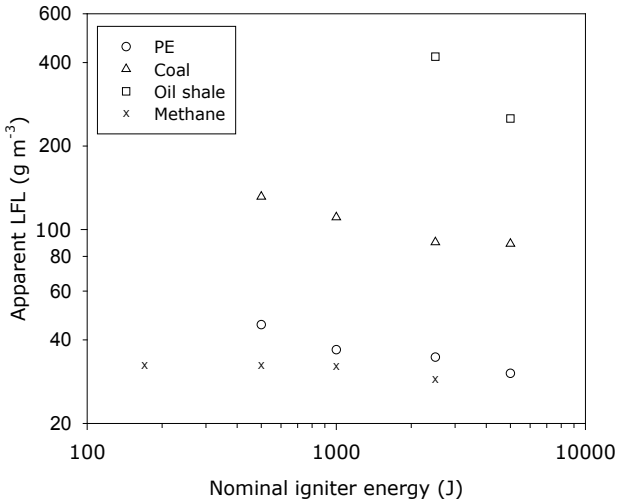


Figure 1 Effect of igniter energy on LFL values, as measured in the 20 L chamber used by the Bureau of Mines

Cashdollar et al.[30] conducted a series of experiments where they characterized coal and other dusts by their volatilizable mass fraction. It is a bit hard to view this mass fraction (termed 'volatility' by the authors) as being independent of the test conditions, but they were able to pin down the ends of the scale by using the definition that volatility of graphite dust ≡ 0, and volatility of polyethylene dust (which melts and gasifies before burning) = 100%. For other substances they used a laser pyrolysis method to determine the fraction that is volatilizable, and produced a relation between volatility (mass fraction volatilizable) and the measured LFL (Figure 2).

Their results show a straight line relation when 1/LFL is plotted against volatilizable fraction. The rightmost point on the graph is polyethylene (PE) with no graphite, and the authors found LFL = 33 g m^{-3} for the PE dust. Cashdollar et al. indicate a line which almost, but not quite, passes through the origin. If this small offset is ignored, then their results can be represented as:

$$LFL = \frac{3300}{VF}$$

where VF = volatilizable fraction (%). Conceptually, this is undoubtedly correct, although the numerical values ob-

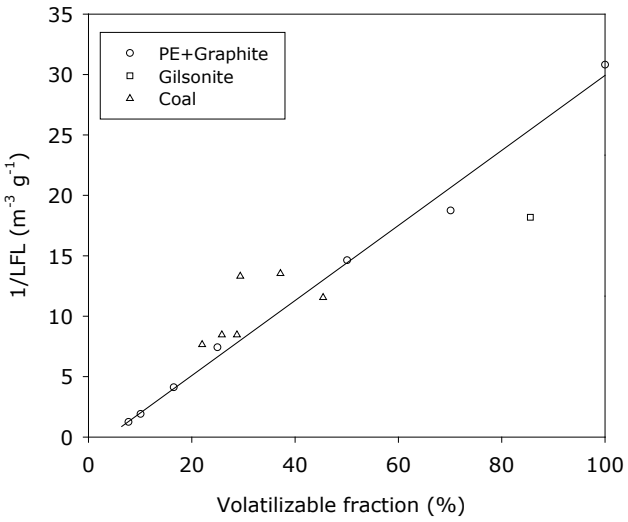


Figure 2 Effect of volatilizable fraction on LFL of dusts
(Copyright The Combustion Institute, used by permission)

tained in their experiments can be considered too low. These results are tantamount to concluding that the PE dust burns as a gas with LFL = 33 g m^{-3}. Table 1 in Chapter 15 shows that only 6 organic substances could be found in the literature with LFL values ≤ 33 g m^{-3}, and it appears questionable that the pyrolysis products for PE comprise only those six. Instead, as discussed later in this Chapter under Test Methods, the questionably-low values can be attributed to the use of a 2500 J pyrotechnic igniter in the 20 L Bureau of Mines test apparatus. The volatilizable fraction concept is fascinating and might possibly correlate the LFL of a wide variety of nonmetallic dusts. But at the moment only results for the three dusts in Figure 2 are available, as measured on a common basis.

The prediction scheme of Cashdollar et al. implies that all plastics which volatilize 100% without leaving a char have an identical LFL value. This, of course, is not true. Dividing the dust matter into volatiles and non-volatiles is the simplest subdivision. But as far as the volatiles are concerned, the heat of combustion might be expected to come into play. On this basis, Wolański[22] proposed that the LFL (g m^{-3}) can be approximated by:

$$LFL = 3634\ \Delta h_c^{-1.21}$$

where Δh_c = gross heat of combustion (MJ kg^{-1}) of the dust. In a practical scheme, the heat of combustion should actually pertain only to the volatile matter, setting as zero the contribution of the portion going into char. This next step of development has not yet been explored. Agricultural dusts normally have Δh_c < 24 MJ kg^{-1}, thus by this approximate formula they should show LFL > 78 g m^{-3}. According to extensive measurements that Wolański made, he finds that the minimum experimental LFL for agricultural dusts, when done with great care to obtain uniform mixtures, is 65 g m^{-3}. As mentioned above, he points out that many LFL values reported in the literature are systematically too low, due to insufficiently adequate uniformity of the tested mixture. The cornstarch studies of Makris, Lee, and Jarosiński, discussed above, must also be considered. They indicate that a realistic LFL for cornstarch is in the range 200 – 400 g m^{-3}, yet since cornstarch is nearly 100% volatilizing, LFL ≈ 33 kg m^{-3} would be obtained according to the scheme of Cashdollar et al. The heat of combustion of cornstarch is around 17.6 MJ kg^{-1}, so use of the Wolański relation would raise this to 113 g m^{-3}, which is much more reasonable, although still low.

Shevchuk et al.[31] proposed a simplified theory whereby:

$$LFL = \frac{C\rho\left(T_{ig} - T_o\right)}{0.5\Delta h_c - C_s\left(T_{ig} - T_o\right)}$$

where T_{ig} = autoignition temperature of dust (K), C_s = heat capacity (J kg^{-1} K^{-1}) of dust, and C and ρ are the room-temperature heat capacity and density, respectively, of air. Reasonable prediction of experimental results was claimed for an assortment of metal dusts; other dust types were not explored. In view of both theoretical and experimental problems in determining T_{ig}, however, it is not clear how robust such a method can be; in any case, no other workers have attempted a validation.

A general flammability diagram can be prepared for dust clouds using concentration vs. temperature axes, which establishes three basic regions of non-flammable atmospheres, atmospheres that ignite with the use of a pilot, and atmospheres which autoignite. Such a diagram is shown for coal dust in Figure 3[32].

Instead of expressing the LFL as a concentration, it is also possible to express it as an equivalence ratio. For example, the LFL for 5 µm PMMA dusts is 100 g m^{-3}. Stoichiometric combustion of PMMA in air is:

$$C_5H_8O_2 + 6\left(O_2 + 3.76N_2\right) \rightarrow 5\,CO_2 + 4H_2O + 22.56N_2$$

The molar mass of PMMA is 100.06. Thus, at φ = 1.0,

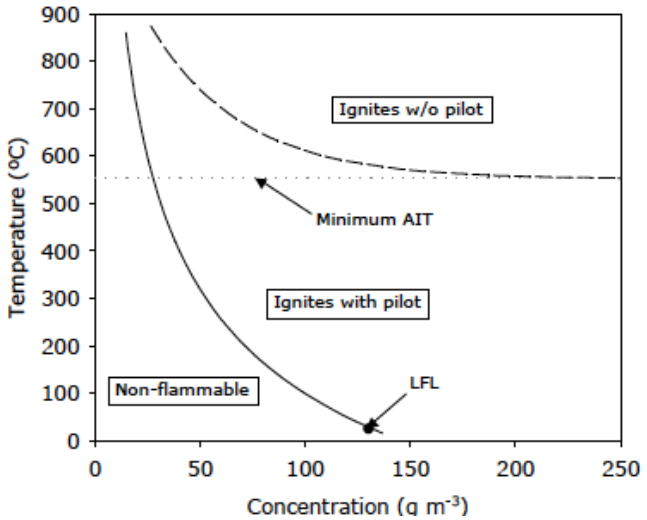


Figure 3 Regions of flammability for coal dust
(Bureau of Mines)

100.06 g of PMMA react with 28.56 mol of air. Assuming that ambient temperature is 20ºC, then 1 mol of an ideal gas = 0.024055 m^3, and 28.56 mol of air takes up 0.687 m^3. Therefore, the stoichiometric PMMA concentration is 100.06/0.687 = 146 g m^{-3}. At the LFL concentration of 100 g m^{-3}, the equivalence ratio = 100/146 = 0.69. This is not surprising. What is interesting is to consider the equivalence ratio for 50 μm particles, which have a reported LFL of 180 g m^{-3}. For such particles, the LFL corresponds to φ = 180/146 = 1.23, in other words, for the *lower* flammability limit to be reached, fuel-rich conditions must be attained! The explanation, of course, has to do with the fact that, for large particles, the fuel is not readily available—it must first be pyrolyzed and, thus, only a small fraction of the fuel can participate in the early stages of combustion.

In summary, if LFL values of dust clouds were to be obtained that have quantitative validity, rather than solely being an apparatus-dependent rank ordering, it would be necessary to follow Wolański's requirements[23]:

- the dust should be uniformly dispersed;
- ignition energy should be sufficient to ignite the mixture, but not so high as to enhance combustion of lean mixtures;
- flame propagation should be observed far enough away from the ignition so that the influence of the ignition source is negligible;
- if an alternate criterion is used to determine the LFL, it should be well correlated to the flame propagation criterion given above.

Unfortunately, none of the major data tabulations that are available conform to these requirements, although a few individual studies exist that do. It is especially noteworthy that there exist no validation experiments which would endeavor to quantify LFL values under conditions approximating those in real-scale explosions. Thus, while numerous combustion science considerations suggest that LFL values for dust clouds have to be appreciably higher than for gas explosions, a quantitative means of 'adjusting' the tabulations derived from conventional small-scale tests is not available. For agricultural dusts, values below 65 g m^{-3} can be considered to be erroneous. For any organic dust, values below 50 g m^{-3} must be considered spurious[22].

UPPER FLAMMABILITY LIMIT

Experimentally, an upper flammability limit (UFL) can be found for dusts, and it is generally around 2 – 3 kg m^{-3}, but as high as 13 kg m^{-3} for some substances. Very few studies exist in the literature where UFL values have been determined; Eckhoff[19] made a survey of a number of these studies. The UFL values are highly dependent on the ignition energy used, so even in a single apparatus, many different UFL values can be assigned[33]. At these enormous concentrations, it becomes very difficult to get any kind of uniformity of dispersion, so experimental uncertainties are large. In practice, huge concentrations can be created in processing and conveying machinery, but will not occur in habitable atmospheres, since there would be zero visibility if one were to enter a space with concentration above the UFL. Even in processing machinery, there is little assurance that a concentration reliably above the UFL could be created. Thus, since opportunities generally do not exist to operate a process above the UFL, there has been little impetus to quantify UFL values.

The chemical process occurring at the UFL is not analogous to gases. Apart from unique issues associated with metal dusts, dusts must first pyrolyze, or gasify, before they can combust. In a gaseous mixture of fuel/oxidizer, all of the material is already in gas phase and can react. The UFL in gases, thus, arises because the heat sink effect of a large excess of fuel molecules prevents high temperatures from being reached at which appropriate reactions could take place. In a dust cloud, however, the combustion takes place in a different phase than the one which comprises the fuel 'reservoir.' A stoichiometric flame sheet can propagate in the gas phase, where it has only a secondary thermal contact with the mass of yet-unpyrolyzed fuel. If expressed as an equivalence ratio, the UFL of dust clouds may be $\varphi \approx 30$, which is, of course, enormously higher than for gases ($\varphi \approx 2$ to 5, except for unstable gases).

With the above considerations in mind, for the general case, one of two mechanisms can limit the flame propagation in dust clouds: (1) diffusion and reaction in the gas phase; or (2) pyrolysis of the solid particle. The latter limit can come about due to either very large concentrations of particles, or else particles of very large diameter.

AIT, quenching distance and MESG

The autoignition temperature of dust clouds is measured in a furnace of one kind or another, and the value reported is the minimum temperature needed for ignition. In terms of fundamental interpretation of the results, difficulties arise because of the ill-defined environment for the test substance. The test dust is injected by means of a cold-air stream into the heated cavity. This makes it impossible to assume a single, fixed temperature for the volume. Since the walls are, perforce, at a higher temperature than the dust volume, hot-surface ignition aspects can come into play. The AIT concept would suggest that ignition is to be expected if the dust cloud experiences any temperature higher than the AIT. But a Bureau of Mines study[34] showed that one type of dust tested, polyethylene, gave an anomalous behavior—not only was there a minimum temperature below which ignition did not occur, but also a maximum temperature above which ignition was impossible. The reason for this is unclear, and six other materials tested did not exhibit such a non-ignition regime.

Same as for gases, dust clouds show a minimum distance below which propagation of flame cannot occur. The quenching distance for dust clouds, however, has not been extensively studied. Jarosiński et al.[27] designed a special

tube apparatus containing a series of quenching plates in the center. A dust cloud is generated in both halves of the tube, ignited in the bottom half, and propagates or not into the top half. Results for cornstarch are shown in Figure 4. The authors also found a minimum quenching distance of 10 mm for aluminum flakes and atomized aluminum, and 25 mm for coal dust of less than 5 µm. A very large value of 190 mm was found for polydisperse coal dust passing through a 200 mesh sieve. The coal tested was one of low volatility, and this accounts for the high values of quenching distance. Cornstarch, on the other hand, was found to be nearly 100% volatilizing, thus quenching distances, much as LFL values, can at least qualitatively be seen to depend on the fuel volatility.

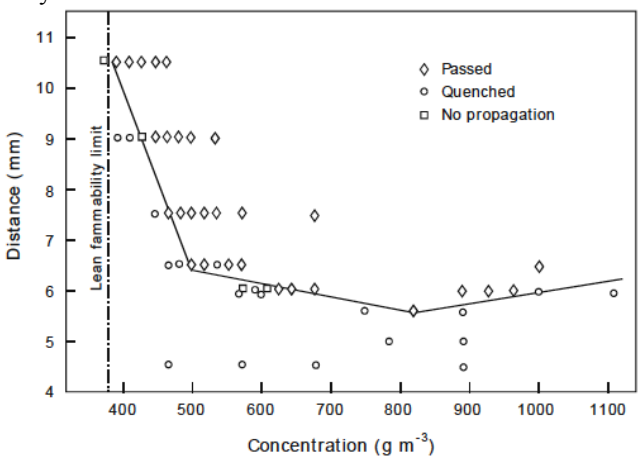


Figure 4 Quenching distance for 15 µm cornstarch dust
(Copyright The Combustion Institute, used by permission)

In design of explosionproof equipment the related concept of MESG (maximum experimental safe gap) is used, and the principles have been described in Chapter 4. MESG values can also be obtained for dust clouds, although the data are sparse. Jarosiński et al.[28] obtained a value of 1.5 mm for cornstarch at 600 g m^{-3}. Figure 4 shows that the quenching distance for the dust was 6 mm. Schuber[35] provided MESG data for a number of dust types. Using a flange breadth of 15 mm, he found typical values of 1 – 3 mm, but for two dusts, however, he found very low values. Lycopodium showed 0.75 mm, while a mixture of 80% sulfur and 20% lignum sulfate showed only 0.20 mm. There was generally a smoothly-increasing dependence of MESG value on the flange breadth, up to breadths of about 35 mm, beyond which point plateau values were reached. The lowest reported MESG value for a gas is 0.29 mm for hydrogen. The tabulated standard MESG values for gases were obtained in the IEC/PTB apparatus using a 25 mm flange breadth, so the 0.20 mm measurement would rise somewhat if referenced to the same flange breadth. Nonetheless, the reason why a dust cloud should show an MESG value essentially identical to the hydrogen mm is unclear. Schuber also provided a correlation for MESG (mm) as:

$$MESG = \left(MIE \times \frac{T_{ig} + 273}{273} \right)^{0.157}$$

where MIE is measured in mJ and T_{ig} is the AIT in ºC. The results pertain to a flange width of 25 mm and AIT values as measured in the BAM oven. The MESG values are typically several-fold smaller than the quenching distances.

Theory of ignition of dust clouds

In Chapter 4 it was pointed out that numerous theories for predicting the LFL of gases have been proposed, but that they are either seriously inaccurate, or unvalidated, or computationally very difficult. Thus, so far it has not been found viable to predict the LFL of gases from theory. For dust clouds, there are many further complications. Primary of these are: (1) the need to account for the volatilization of the solid; (2) a strong coupling of fluid dynamics—unlike for gases, the problem cannot be studied in a quiescent state; and (3) interactions between particles, especially the dominant role of heating by radiation[36]. Despite these daunting complexities, some progress has been made.

Several workers have put forth ambitious mathematical theories which try to cover comprehensively the phenomena involved in dust cloud combustion. Klemens and Wojcicki[37] offered such a comprehensive theory, but even with numerous simplifications, few conclusions could be drawn from the numerically computed results. Smirnov and coworkers[38] developed a numerical model that includes the effects of turbulence. The model was detailed enough so that a number of features, e.g., slow ignition, could be examined.

For predicting experimental trends through graphs or closed-form equations, simpler theories appear to hold more promise. Such theories generally postulate a limiting factor to the HRR, and this factor can be either (a) reaction kinetics or (b) external heat transfer. A theory based on reaction-kinetics limiting factor was proposed by van der Wel[14], who suggested that the autoignition temperature of dust clouds could be modeled in an analogy to the Semenov model for the AIT of gases (Chapter 4). In the Semenov theory, for a volume of gas, the HRR expression is:

$$\dot{q} = QAVc^n e^{-E/RT}$$

For dust clouds, van der Wel suggested that the HRR be considered proportional to the total surface area of particulate, and to be driven by the oxygen concentration. Thus,

$$\dot{q} = QAsVc_{O_2} e^{-E/RT}$$

where c_{O_2} = oxygen concentration (kg m^{-3}), V = volume (m^3), and s = surface area of particulates per volume (m^2/m^3). The latter can be evaluated as:

$$s = \frac{6c_s}{d_p \rho_s}$$

where c_s = dust concentration (kg m^{-3}), d_p = particle diameter (m), and ρ_s = particle density (kg m^{-3}). An expression for the AIT, T_{ig}, is then obtained from the implicit equation:

$$eQAsVc_{O_2}e^{-E/RT_{ig}} = hS_v\frac{RT_{ig}^2}{E}$$

where S_v = surface area of vessel (m^2).

A simple theoretical equation as the above lacks realism in a number of areas, as van der Wel points out:

- The theory assumes that as long a waiting time as needed is available for an explosion to develop. In practice, the explosion has to occur within a very short time, or the dust cloud settles out.
- The heat of pyrolysis is not taken into account.
- It is not possible to create a truly uniform-temperature environment in actual test apparatuses.
- Solid, unvolatilized particulates act as localized heat sinks.

Zielinski[39] was the first to suggest that better predictions of experimental results might be obtained if it were postulated that heat transfer, not chemical reaction, limits the HRR. Part of his reasoning was that chemical-reaction theories are likely to be systematically wrong numerically, since the numerical results from these theories are dominated by the particle temperature, yet this temperature is very hard to measure accurately and is usually overestimated. This line of thinking was subsequently extended by Hertzberg et al.[40] and Litton et al.[41] at BM. Litton proposed that a tractable theory could be formulated by considering the problem to be dominated by radiation. A propagating fire cannot be sustained unless a mass concentration of volatiles greater or equal to that of the LFL is produced. Energy is radiated from the ignition source and can be expressed as a source radiance I_o (W m^{-2}). The Beer-Lambert Law is assumed to be valid for attenuation of radiation by small particles:

$$I_a / I_o = 1 - e^{-\sigma c_s D}$$

where I_a = absorbed heat flux (W m^{-2}), σ = specific absorption area (m^2 kg^{-1}), c_s = mass concentration of dust (kg m^{-3}), and D = path length (m). It is assumed that the absorbed energy, E_a (J), is related to the mass of volatiles released M_v (kg) by an effective heat of vaporization L_v (J kg^{-1}):

$$E_a = M_v L_v$$

Using the Beer-Lambert Law, the absorbed energy can be expressed as the absorbed heat flux, times the area of the absorbing particles, times the time. The area of the absorbing particles is $\sigma c_s V$, where V = volume (m^3), thus:

$$E_a = \left(1 - e^{-\sigma c_s D}\right) I_o t_{ig} \sigma c_s V$$

where t_{ig} is an ignition time (s). Ignition will be propagated only if the available E_a is $\geq$ the required E_a, thus:

$$\left(1 - e^{-\sigma c_s D}\right) I_o t_{ig} \sigma c_s V \geq M_v L_v$$

Dividing by the volume gives:

$$\left(1 - e^{-\sigma c_s D}\right) I_o t_{ig} \sigma c_s \geq \frac{M_v L_v}{V}$$

If the volatilizable fraction of the dust is f_v (--), then $c_s = \frac{M_v}{f_v V}$, and substituting:

$$\left(1 - e^{-\sigma c_s D}\right) I_o t_{ig} \geq f_v L_v$$

Litton also noted that experimentally for coal dust it i s found that $L_v = 8.0 / f_v$, while I_o and t_{ig} are fixed properties of the ignition source. Thus, ignition (propagation) is possible if:

$$\left(1 - e^{-\sigma C D}\right)\sigma \geq \frac{8.0}{I_o t_{ig}}$$

where D = characteristic length (m) of the dust cloud; for example, for the BM 20 L test chamber it is 0.168 m. The specific absorption area σ depend both on the particle diameter and on the volatile fraction. Since the typical wavelength of radiation will be around 1 μm and explosible dusts are normally larger in size, it can be noted that for particle sizes >> the wavelength, $\sigma \propto \frac{1}{d_{32}}$ where d_{32} is the Sauter mean diameter (μm), or the diameter of a particle having the same volume/surface ratio as the entire cloud. The volatilizable fraction comes in because only the non-volatilizable portion of the particle is effective in absorbing radiation, thus σ will be proportional more or less to $(1 - f_v)$. Litton computed[42] that $\sigma = \frac{600}{d_{32}}$ m^2 kg^{-1} for HVB coal dust, and similarly $\sigma = \frac{672}{d_{32}}$ m^2 kg^{-1} for LVB coal dust. Since increasing particle diameters lead to decreasing σ values, the theory predicts that higher concentrations will be needed to achieve flammability as the particle size increases. This is borne out in the rising portion of the curves in Figure 18, although the theory does not describe the plateau region at small diameters.

Hertzberg et al.[43] suggested that examining the detailed behavior of a single particle could form the basis for understanding the greater complexity of dust clouds. Thus, they conducted an extensive series of tests on dusts of metals and some non-metallic elements; their data are summarized in Chapter 14. From these experimental studies, the authors proceeded to evolve some rudiments of a theory. Much as for gases, an adiabatic flame temperature, T_{ad}, corresponding to stoichiometric fuel concentration can be computed. Also in analogy to a gaseous fuel, an adiabatic limit temperature T_{LFL} can be defined as the adiabatic flame temperature corresponding to the fuel/air ratio found at the LFL. Finally, Hertzberg et al. consider that the propensity for the fuel to volatilize can roughly be represented by T_v, which is the temperature at which the amount of fuel vaporized is between 0.01 and 0.1 of the stoichiometric amount. In their model, the 'driving force' for the combustion of the fuel is then expressed as $(T_{ad} - T_{LFL})/T_v$. This group of variables should then be able to predict the LFL. The results of this

computation is shown in Figure 5. The authors point out that this is only a rough correlation, since it assumes that the solid and the surrounding gas are at the same temperature, which is not true. It is also not clear that this relation would be useful for predictive purposes, since T_{LFL} can only be determined once the LFL is known and there does not seem to be a useful recipe for computing T_v.

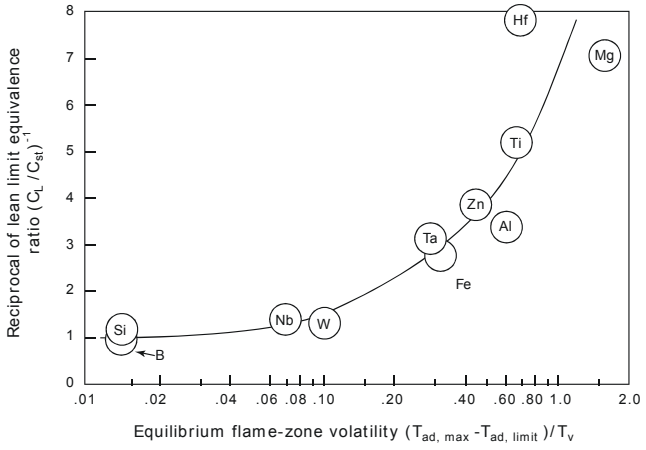


Figure 5 Prediction of the LFL of dusts on the basis of a volatility parameter
(Copyright The Combustion Institute, used by permission)

Yuasa and Takeno[44] conducted detailed studies of the early time history of a dust cloud explosion and concluded that a minimum kernel diameter exists, much as it does for gases. The events forming a kernel in dust cloud are more complicated, and the authors did not derive a quantitative theory. They did observe that the minimum kernel size was highly dependent on the size of the particles. For magnesium/aluminum alloy particles, the kernel was 1 – 3 mm for 18.5 μm particles and 5 – 11 mm for 63.5 μm particles.

Nomura and coworkers[45] proposed a simplified flame-sheet theory intended to predict the LFL, the UFL, and the MOC of a dust cloud. The validity of such a scheme is dubious, since dust clouds have all of the combustion complexities of gas mixtures, plus complications of their own—yet no simple theory has succeeded in accurately predicting the LFL values for gas mixtures.

Ballal[46] developed a theory for the minimum ignition energy (MIE) and quenching distance of dust clouds. Closed-form, but quite complex expressions were provided, based on an extension of Spalding's vaporization model[47]. Thus, the primary variable driving the system is viewed as the 'Spalding B-number,' which is a parameter that combines a number of thermochemical constants. Unfortunately, most of these constants will be unavailable except in the case of simple, pure compounds. An interesting aspect of Ballal's theory is that it unifies the treatment of dust clouds and liquid aerosols. The validation of his theory is uncertain. Ballal did not publish any of his raw data, and no other researchers have undertaken to attempt a validation.

Mittal and Guha[48] constructed a theory for predicting the AIT of polyethylene dust. The dust was assumed to pyrolyze primarily to butylene gas and their mechanism contains a number of empirical relations for this process. It is not readily evident how the theory might be generalized to dusts not already tested. Eckhoff[19] reviewed a variety of other dust cloud ignition theories.

Theoretical expressions for quenching distance are normally not sought with dust clouds, since inter-particle distances are large enough that the concept of a homogeneous mixture cannot be applied[14].

Hybrid gas/dust-cloud ignitions

Atmospheres containing a mixture of ignitable gases and dusts are common in some fields, for example, coal mines commonly contain a mixture of methane and coal dust. In other industries, dust clouds which also contain vapors of organic solvents are found. In Chapter 4, Le Chatelier's Law was presented, and it is a simple linear relation which states that the contribution of a substance to a mixture's property is directly proportional to its abundance. The Law is applicable to predicting the LFL of mixtures whenever the values of T_{ad} at the LFL condition are similar for the substances involved. As it turns out, the limit temperature of ca. 1500 K is found not only for most hydrocarbons, but also for many dusts. Perhaps of most practical import, it does hold for mixtures of coal dust and natural gas or methane. Figure 6 illustrates the linear relationship found in large-scale tests at the Bureau of Mines[49]. Similar relationships are also found in laboratory-scale tests[78,80], as shown in Figure 7. (It must be noted, however, that a German study[50] did not find a linear relation for coal dust/methane mixtures, but rather one with a complex S-shape.)

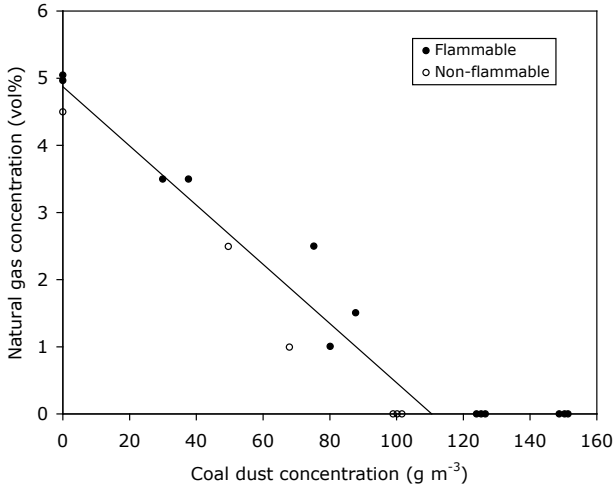


Figure 6 Flammability limits for natural gas/coal dust mixtures tested in a large-scale mine test by the Bureau of Mines

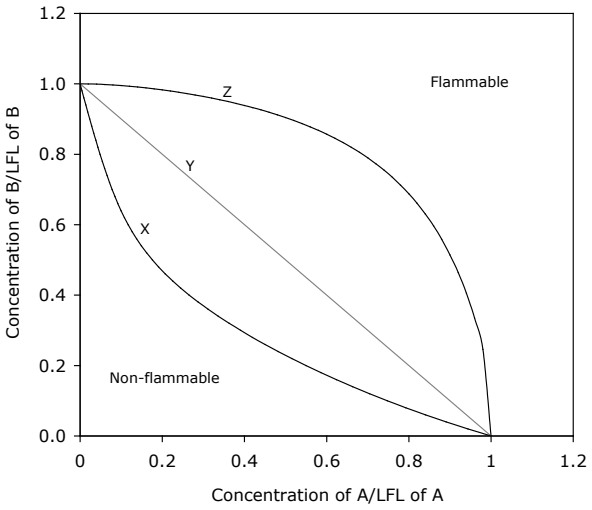


Figure 7 The LFL of mixtures. Line Y (linear) is found to be obeyed by many mixtures. Curve X (synergism) represents the combination A = PVC dust, B = methane. Curve Z (antagonism) represents the combination A = cornstarch dust, B = hydrogen.

Hybrid mixtures can also show much lower MIE values than expected for the dust alone. Pellmont[51] examined a series of dust/propane mixtures (Figure 8). Dusts which already showed low MIE values were little affected, but dusts needing high energy levels for ignition exhibited dramatic drops. Also shown in Figure 8 are the results for propane/air mixtures without dust, using the same turbulent conditions as used in testing for the hybrid mixtures. A number of other studies on this topic were reviewed by Eckhoff[19].

Britton noted that the results such as shown in Figure 8 fall along straight lines on a semi-log plot. This can be expressed in equation form as[52]:

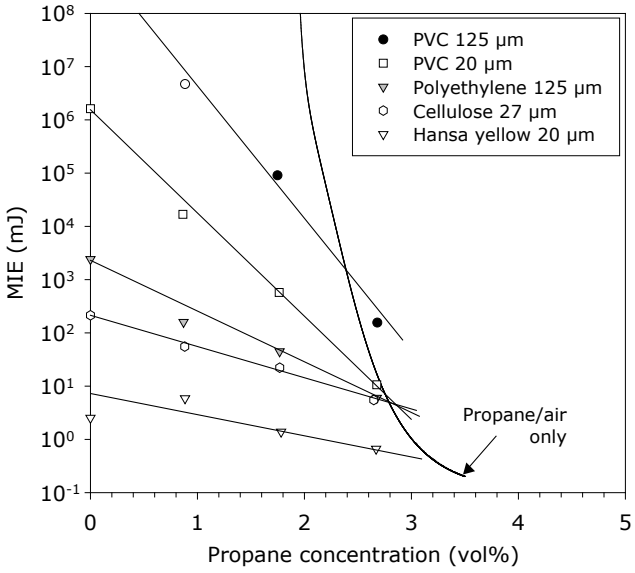


Figure 8 Hybrid dust/propane mixtures studied by Pellmont

$$MIE_h = \exp\left[\ln MIE_d - \frac{c}{c_o}\ln\frac{MIE_d}{MIE_g}\right]$$

where MIE_h = MIE of hybrid mixture; MIE_g = MIE of gas alone, obtained at a gas concentration of c_o; MIE_d = MIE of dust cloud alone; and c = concentration of gas in hybrid mixture (vol%).

Ignition sources for dust clouds

Common ignition sources for dust clouds include:

- *Open flames.* Combustion equipment using flames or pilot lights should not be used where ignition of dust suspensions is possible.
- *Hot surfaces.* These can be of various types and if a minimum ignition temperature is exceeded, an ignition can result.
- *Hot particles.* A dust cloud can be ignited from burning embers, including those generated by welding or cutting operations.
- *Friction, grinding sparks, or impact sparks.* Overheated bearings or jammed machinery can cause friction heating. Grinding sparks can ignite certain dust clouds under certain conditions. Impact sparks can result from tramp metal. The latter consists of inadvertent metal being included in processes where metal is not intended to be processed. A study has shown[53] that brief impacts of steel hand tools against steel or against concrete surfaces are not able to ignite dust clouds, however.
- *Sparks from electric devices, including electrostatic discharge.* The sensitivity of dusts to electrostatic discharges is dependent on the volume resistivity of the dust suspension. For the six electrostatic discharge types (see Chapter 11), the possibility for causing dust cloud ignitions is: (1) Corona discharge—too feeble to ignite. (2) Brush discharge—can ignite dust/flammable gas mixtures, but not pure dust clouds. (3) Powder heap discharge—can ignite most combustible dusts. (4) Spark ignition—can ignite any combustible dust, if appropriate MIE. (5) Propagating brush discharge—can ignite any combustible dust. (6) Lightning-like discharge—hypothetical; could conceivably ignite giant piles.

Statistics on ignition sources for grain dust explosions are given in Chapter 14.

Dust explosions are normally deflagrations. Limited research suggests that to achieve a d ust detonation would require a detonating initiator. With the possible exception of terrorist attack, such an event is unlikely. Unlike for gases, where unconfined vapor cloud explosions are possible, dust cloud explosions are normally considered impossible in open air. But Baker and Tang[54] consider that this possibility does exist if a detonating initiator were used, although there is no specific research on topic. A detonation would

also be possible if the cloud comprised a powdered explosive.

MECHANICAL SPARKS

The possibility of sparks created by tramp metal to act as an ignition source for dust explosions was already being studied as early as 1888[3]. More recently, Morse conducted experiments where she dropped broken files a distance of 26 m into a dust cloud explosion chamber[56]. No explosions were obtained, although in 215 trials there were several instances of "possible flame" reported. Experiments have shown that both sparks generated from grinding and those due to impacts can only ignite dust clouds having MIE values below about 13 mJ[53]. For this to happen, an especially susceptible metal, such as titanium, must be involved. Sparks from steel against steel, or steel against concrete, will not ignite dust clouds. It is also understood that a cluster of sparks is required to ignite a dust cloud, and that ignition could not occur if only a single spark was presented. The latest view[70] is that ignition from mechanical sparks is possible only if:

(1) the dust cloud has an MIE < 10 mJ; *and*
(2) the autoignition temperature of the dust cloud is < 500ºC.

In this context, the values of MIE refer to the use of an inductive circuit, while AIT measurements are taken in the BAM furnace.

ELECTRIC SPARKS

Any dusts that are capable of being charged to a high electric potential by friction or flow effects could possibly be self-ignited by electrostatic discharge. Many years ago, this question was of much interest[55], but little systematic guidance has been produced. The incendivity to grain dust clouds (only described as < 74 μm) of electric sparks from motor commutators was examined by Morse[56]. Using small electric motors rated at 1.7 A or less, she found that light, 'normal' sparking at the commutator was not incendive, but when the condition of the brushes was made poor by artificial roughening, incendive sparks were obtained.

HOT SURFACES

Dust clouds are ignitable by hot surfaces, but either very large areas or very high temperatures are needed. Not much data exists on this subject, with results from Zeeuwen[57] and Eckhoff[19] being shown in Figure 9. Similar trends are seen, but values differ substantially (note that wheat flour was tested by both authors). The differences are presumably due to experimental conditions, but details that might explain this have not been published.

Gibson and Schofield[58] compared data for a large number of dusts tested for the AIT by the Godbert-Greenwald furnace, and for the hot-surface ignition temperature by a British test (the 'No. 1 Wheeler test') which uses a 0.27 mm coiled wire as the hot surface. The largest cluster of AIT results was at 500 – 800ºC, but was at 900 – 1200ºC for the hot-wire test. In addition, around 45% of the total was found non-ignitable (over 1300ºC) by the hot-wire test, while only 8% were non-ignitable (over 1000ºC) in the Godbert-Greenwald furnace. These results imply that, roughly speaking, temperatures of a 0.27 mm hot wire must be about 400ºC greater than the AIT of the dust cloud for an ignition to be expected.

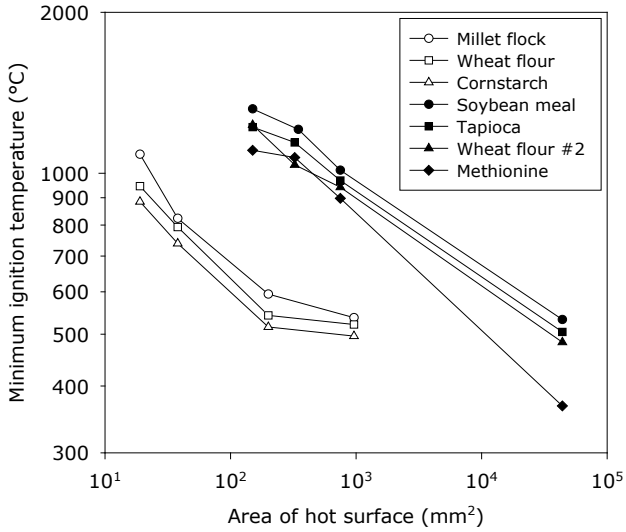


Figure 9 Relation between area of hot surface and minimum temperature needed for ignition (solid symbols: Zeeuwen; hollow symbols: Eckhoff)

Gibson and Rogers[59] found that there is a small effect of the bulk temperature of the dust cloud on the minimum hot surface temperature for ignition. Using a heated coil in a modified Godbert-Greenwald furnace, they found that the coil temperature needed for ignition of lycopodium dust* dropped from 920ºC to 890ºC as the dust cloud was preheated from ambient to 100ºC. Similarly, for hydroxy propyl methyl cellulose, the temperature dropped from 950ºC to 860ºC.

GLOWING NESTS

Most of the ignition mechanisms for dust cloud explosions are the common ones that have been studied extensively in connection with various other forms of substances. A type of ignition which is largely unique to dust clouds is the glowing nest. Various ignition sources may ignite an organic material while it is in the form of a layer or in storage, i.e., not in an air suspension. If the material is then conveyed by conveyors, pneumatic tubes, etc., the glowing nest may come to a region where an explosible dust concentration exists. The question then arises whether the glowing

* Lycopodium spores come from the club moss family and are roughly spherical and about 25 – 35 μm diameter; they are commonly used as a standard substance in dust explosion studies. Originally, they were used as flash powder in early photography.

nest has the capability of igniting the dust cloud. Eckhoff[19] surveyed a number of studies on the topic. While universally applicable guidance did not emerge, some salient conclusions were:

- Nests of 700ºC falling through dust clouds were non-incendive during flight, but caused some ignitions when landing at the bottom. Nest weights of at least 15 g were required for those ignitions to occur.
- Nests having a temperature ≥ 900ºC and a surface area ≥ 75 cm^2 were able to ignite dust clouds that had AIT values of ≤ 600ºC, as tested in the BAM oven.
- If nests disintegrate in free-fall, they may be able to create a fireball which then ignites the dust cloud. But nests of this type cannot be conveyed for any significant distance, because they would already disintegrate in transport.

OTHERS

Singer[60] reported on a study where laminar jets of hot nitrogen gas were used as an ignition source for coal dust + methane mixtures. Temperatures of 1100 – 1220ºC were needed, depending on the relative concentrations of dust and methane. HSE studied the ability of a flame-jet originating in one vessel to ignite a dust cloud present in an interconnected vessel[61]. Larger-diameter pipes were found more likely to lead to ignition, as did the presence of baffles, the latter because they cause flame acceleration. General guidelines, however, were not evolved. Studies have been reported where lasers were used to ignite dust clouds[14]. Taniguchi et al.[62] used a laser to ignite dust clouds of low-volatile bituminous coal in a pure oxygen atmosphere and found that 0.2 J was required to ignite clouds of 63 μm particles, but only 0.1 J for 22 μm particles.

Clouds of powdered fibers (flock)

In textile mills and other industries, airborne small fibers can be generated. These will be the thickness of a single fiber and maybe on the order of 1 mm in length. The ignitability characteristics of flock have some differences from clouds of particles having more compact shapes. Bartknecht[80] studied the problem and evolved a conservative estimate of the LFL (g m^{-3}) for flock. His graph can be simply represented as:

$$LFL \geq \left(3.7 + 16.75\,M^2\right)^2$$

where M is the mass per particle (μg). Similarly, the results for MIE (J) can be approximated as:

$$MIE \approx 0.0082\,e^{20.8\,M}$$

Analysis and application of data

VARIABLES AFFECTING THE AIT

DUST CONCENTRATION

The AIT varies inversely with dust concentrations at lean concentrations (< 100 g m^{-3}) and is nearly independent of the concentration at high concentrations. Figure 10 provides several examples[63].

VOLATILE CONTENT

Substances which liberate significant volatiles ignite at a lower temperature than ones which do not[63], but this tendency is hard to capture in a simple test. Total volatile content, as opposed to details on when and how they are evolved, is relatively easy to measure, so efforts have been made to see if it is useful for prediction purposes. Nagy and Verakis[68] explored whether it could be correlated to the AIT. Some trend for lower AIT values with increasing volatile content was found, but the data scatter was huge. For example, for volatile contents of 30 – 40%, AIT values

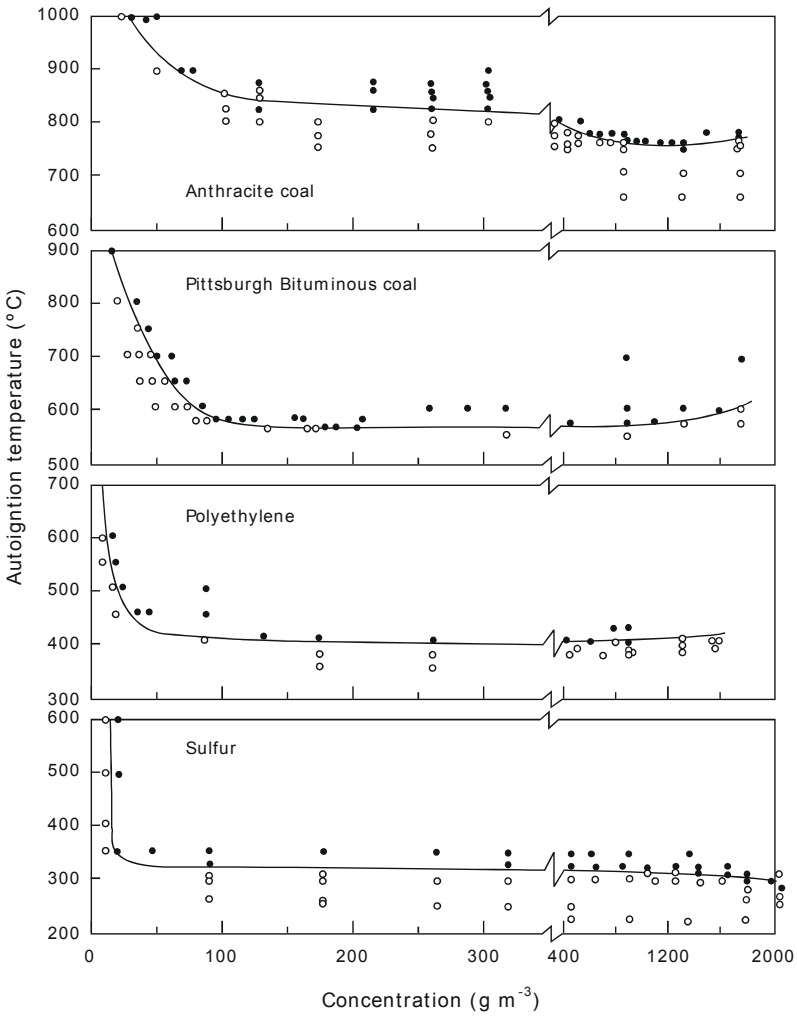


Figure 10 Effect of dust concentration on the AIT

ranged from 350 to 800ºC. Many years earlier, Wheeler[64] conducted a similar study and concluded that no correlation exists.

PARTICLE DIAMETER

Similar to its effect on the LFL, particle diameter does not affect the AIT for small particles, but large particles, beyond a certain size, show an increase of AIT with size (Figure 11)[63,65]. Nomura and Calcott[66] developed a theoretical model which predicts the rise in AIT with increasing particle diameter. Their theory also predicts that there is a minimum AIT value and that the AIT begins to rise again as the diameter becomes small; this is generally not observed in experiments. According to their theory, the rise in AIT for large-diameter particles is due to residence time effects—if residence times could be made very long in the test furnace then large particles would show a decrease, not an increase, in AIT. This is a bit academic, however, since dust clouds, especially of large particles, cannot be kept in suspension for long time periods.

A small amount of available data[16] indicates that the effect is opposite for dusts of metals, at least in dilute atmospheres (Figure 12). Mitsui and Tanaka[67] used a Semenov-type theory to explain this difference in trends, which they consider to be due to radiant emissivity effects, emissivity being low for metals and high for organics. The heat release term is proportional to the number of particles × the surface area of each particle. But for a fixed concentration, the number of particles $\propto 1/d^3$, while the surface area is $\propto d^2$. Thus, the heat release rate is $\propto 1/d$. But the heat losses scale differently. The convective heat losses are assumed to be equal to the number of particles, which for a fixed dust mass is $\propto \frac{1}{d^3}$, times the loss of each one $\propto d^2 \times \frac{1}{d}$, giving an overall dependence as $\propto \frac{1}{d^2}$. Radiation losses, on the other hand, are taken as being due to the entire cloud, not due to individual particles, thus, radiation scales according to the size of the cloud and has a $\propto d^0$ dependence with respect to particle diameter. The net result is that clouds having a high convection/radiation loss ratio show an AIT which decreases with increasing diameter, while the converse holds if the loss ratio is low. The authors obtained good predictive results and were able to correctly account for the difference in diameter-dependence between organics and metals, but caution that many of the needed constants are unavailable and estimates must be made.

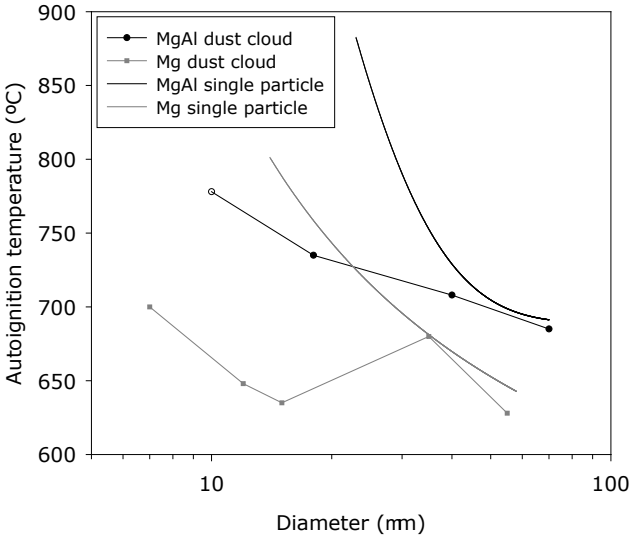


Figure 12 Effect of particle diameter on the AIT for two metal dusts (dust cloud concentration = 80 g m^{-3})

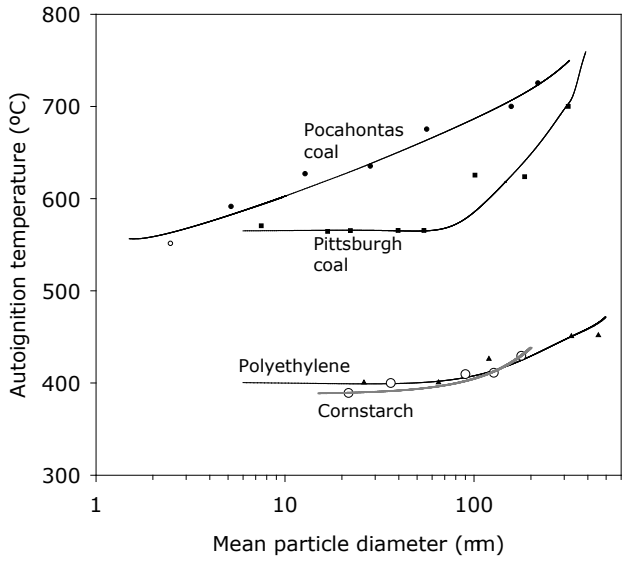


Figure 11 Effect of particle diameter on the AIT for some organic substances

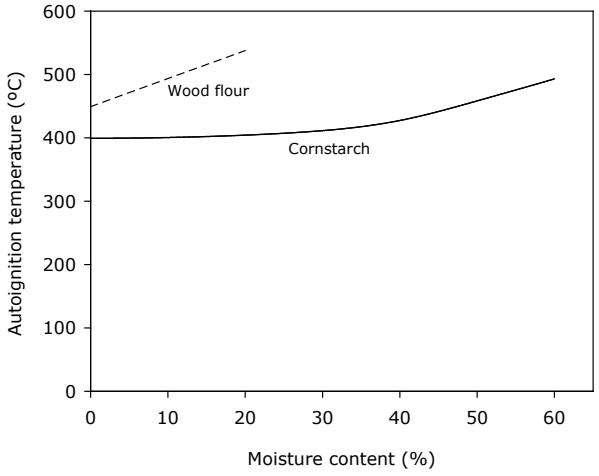


Figure 13 Effect of moisture on AIT

MOISTURE

Not surprisingly, if moisture is added to an organic dust, the AIT is raised. Some Bureau of Mines data[68] on this point are shown in Figure 13. Very little other data is available on the moisture effect, so a quantification of the effect is not possible.

OXYGEN CONCENTRATION

Nagy and Verakis[68] provided a limited amount of Bureau of Mines data on the effect of lowering the oxygen concentration. Figure 14 shows that lowering the oxygen concentration raises the AIT. Ignitions were possible down to as low as 5% oxygen concentration, in the case of cornstarch.

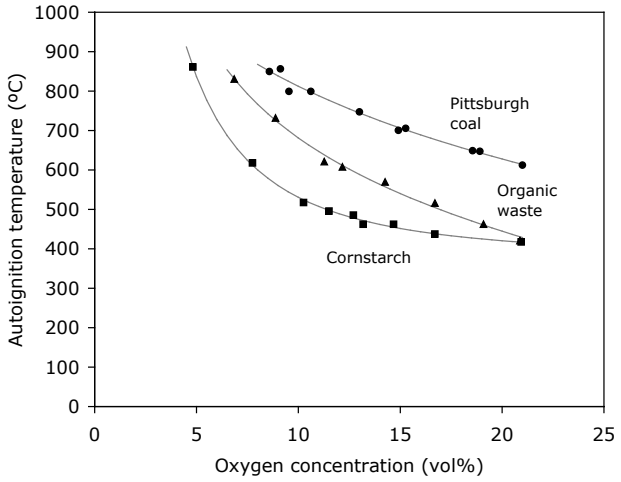


Figure 14 Effect of oxygen concentration on AIT

RESIDENCE TIME

When the AIT of gases is being determined, the test substance is mechanically stable and a long induction time is not problematic. For dusts, however, the suspension is inherently unstable and a long waiting time is not feasible. In an early study made before the design for the Godbert-Greenwald furnace was finalized, Wheeler[64] obtained the data shown in Figure 15. The residence times were extremely long and presumably the uniformity was poor, but the results are indicative nonetheless. More recent results of Griesche and Brandt[69] from the Godbert-Greenwald furnace are shown in Figure 16. When AIT values are determined in the BAM furnace, an anomaly in the test procedure prevents a similar comparison. Since the BAM furnace is horizontal, the dust settles out on the bottom, instead of leaving the apparatus as in the Godbert-Greenwald furnace. The dust can then ignite as a dust layer, rather than a dust cloud, which the BAM test protocol considers as an equally-valid determination of the AIT.

Siwek and Cesana[70] made a comparison of results obtained in the BAM furnace to those in the Godbert-Greenwald furnace. Figure 17 shows that sometimes the results for the

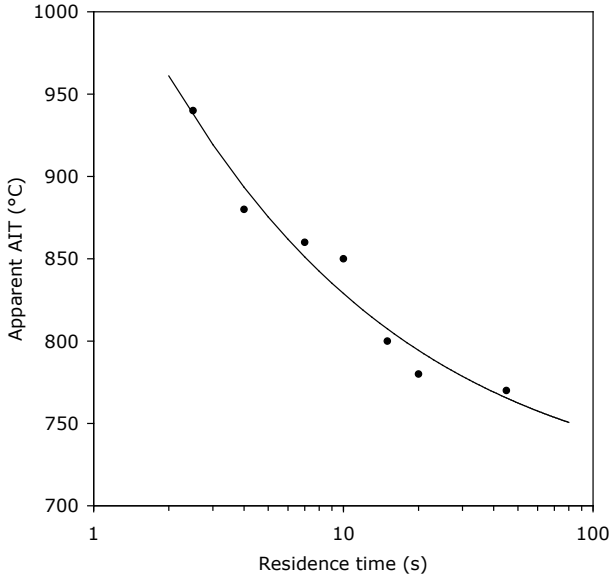


Figure 15 Effect of residence time in an early version of the G-G furnace, as determined for a coal dust by Wheeler

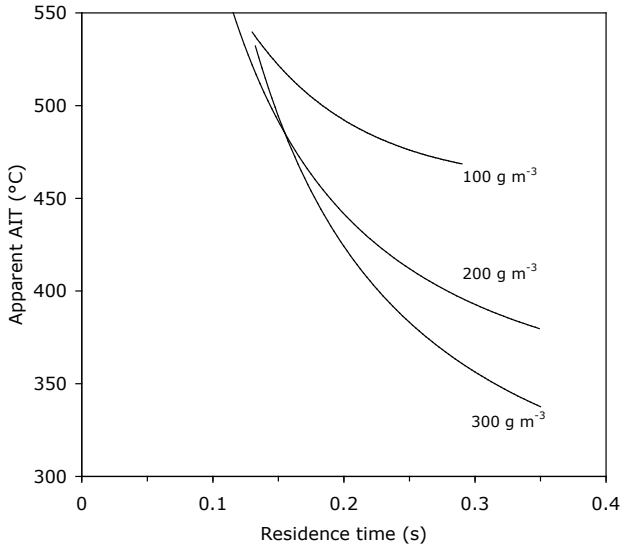


Figure 16 Effect of residence time in the G-G furnace as determined by Griesche and Brandt

two furnaces are close; rarely are the BAM results higher, but commonly they are lower than for the Godbert-Greenwald furnace. Some of the difference may be attributable to local heating effects. Some of the particles going through the BAM furnace are likely to impinge on the reflector and receive hot-surface heating there; a comparable effect does not exist in the G-G furnace.

TURBULENCE

For wheat and oats, experiments[6] showed that at a high dust concentration (800 g m^{-3}) turbulence does not affect the

AIT. But at a lower concentration of 300 g m^{-3}, the AIT was found to rise linearly with the intensity of turbulence, increasing by about 200ºC as the intensity went from 0 to 30%.

TEST APPARATUS VOLUME

Theory and experiments on gases show that if the system volume is increased, the AIT can be expected to decrease. This raises the question if dust clouds tested in small-size experimental rigs can reasonably be used to characterize explosibility in larger spaces. No data are known for dust clouds on this important issue.

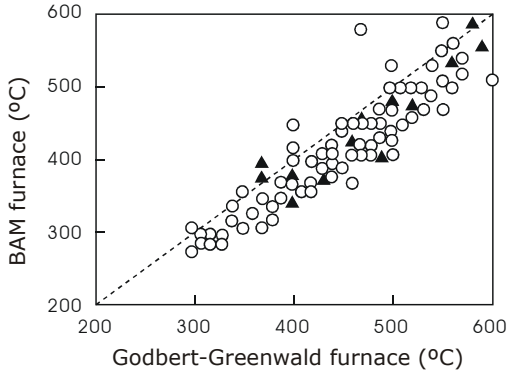


Figure 17 Ignition temperatures compared between two test apparatuses; the two symbols denote two different laboratories conducting tests
(Copyright © 1995 AIChE)

VARIABLES AFFECTING THE FLAMMABILITY LIMITS

PROBABILITY LEVEL USED FOR THE DEFINITION OF THE LFL

To be able to develop reproducible values for the LFL, the probability level at which ignition is deemed to have taken place needs to be defined. This is not a major concern for gases, since the range of energy values spanned by going from slightly above 0 to slightly below 1.0 probability is not large. The same is not true for dusts, however. For polyethylene dust, for example[71], at P = 0.04, the concentration is 50 g m^{-3}, but when the concentration has increased to 300 g m^{-3}, P is still only ca. 0.5. Rare events are unlikely to be encountered, of course, if few trials are made. Thus, in German and Swiss studies[80] it has generally been a convention to run 20 trials.

PARTICLE DIAMETER

For organic dusts, the matter which is ignited and burns are the volatiles, not the original solid. Thus, increasing the diameter while keeping the mass loading fixed decreases the amount of fuel that is potentially available in the gas phase. When the particles are of large enough size, the atmosphere will be non-explosive at any loading that can be actually generated. Figure 18 shows how increasing particle size increases the LFL. The data are from Hanai et al.[72] and the Bureau of Mines[32,65]. The curves are flat for particles below a certain size; for very large particles, the curves become very steep. When very strong ignition sources, e.g., 10 kJ pyrotechnic igniters[78], are used, however, particle diameter does not affect the LFL for particles smaller than about 40 – 120 µm (the value depends on the substance). Note that in the graph the near-vertical portion of the curve scales according to the volatile fraction of the fuel. Low-volatile bituminous coal (LVB) is to the left of high-volatile bituminous coal (HVB). Even though PMMA and polyethylene are both thermoplastics, Hertzberg and Zlochower[73] found that a much higher fraction of PE is volatilized in a dust cloud than of PMMA. Xu et al.[75] consider that the reason most of the curves show a flat portion followed by a rising curve is because the particle size at the 'knee' represents the maximum size that can be fully volatilized within the available thickness of the flame zone.

Explosions do not occur with very large particles. Not a great deal of studies have been done on this point, but it appears that for most substances the largest explosible diameter is found at around 300 – 500 µm, given any practical igniter energy[74,75]. NFPA[76] considers that, by definition, dusts are not explosible if they are of size greater than 420 µm. In the case of halogenated substances, e.g., PVC dust, the combustion process is hindered by the halogen atoms; thus, UFL values of around 150 µm are found for these substances[19].

In research, it is customary to study dusts which have been sieved in order to be relatively monodisperse. In actual processing operations where dusts are involved, this may not be the case; in fact, the dust cloud may have a very wide distribution of particle sizes (polydisperse). Polydisperse systems are greatly more difficult to study since now at least one other parameter apart from diameter must be considered—some measure of spread of diameters. If the distribution does not lend itself to a mathematical function

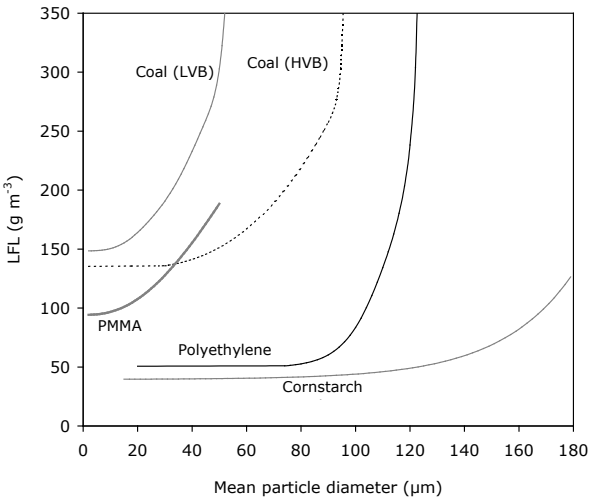


Figure 18 Effect of particle diameter on the LFL

needing only 2 variables, then even more cumbersome numerical treatments would have to be considered.

TEMPERATURE

Similarly as for gases, when the temperature increases,3 the LFL decreases. Data from Glarner[77] and Wiemann[79] illustrate this in Figure 19.

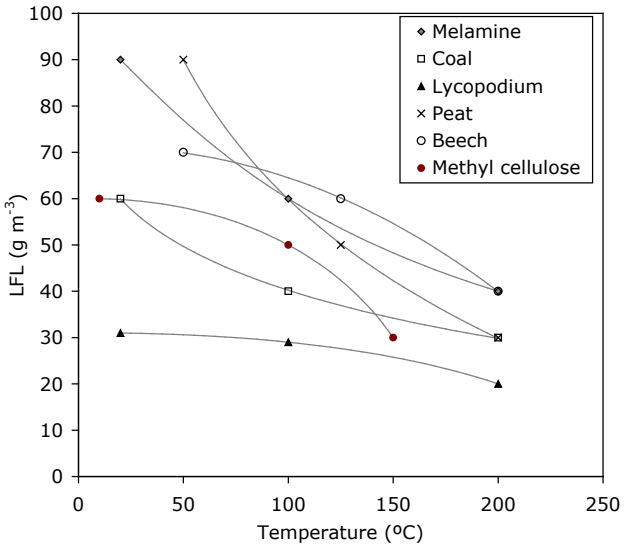


Figure 19 Effect of temperature on the LFL

BM[78] suggests that a prediction can be made by assuming that the temperature dependence is linear:

$$\frac{LFL_{T_2}}{LFL_{T_1}} = \left[1 - \beta\left(T_2 - T_1\right)\right]\frac{T_1}{T_2}$$

where LFL_T denotes the LFL (g m^{-3}) at a temperature T (K), and β = constant ≈ (6 to 7)×10^{-4} K^{-1}. Normally, standard test results will be available at T_1 = 293 or 295 K. The experimental data of Wiemann suggest that the relation holds only in a very rough sense and that, furthermore, the value of β is hardly a constant, with values needed to fit the data ranging from about 1×10^{-4} to 35×10^{-4}. The prediction results for two substances—melamine dust (measured by Glarner) and lycopodium dust (measured by BM[102])—are shown in Figure 20. For lycopodium dust, using the value β = 6.4×10^{-4} K^{-1} recommended by BM gives a rather poor fit, especially in the 100 – 400ºC region. For melamine dust, a value β = 17×10^{-4} was required, which is quite outside the range of β values recommended by BM and would have not been possible to anticipate without running the actual tests.

PRESSURE

Increasing pressure raises the LFL for dusts. For a few example dusts, this effect was shown to be linear. Figure 21 shows coal data from Wiemann[79], with the other data being from the Bureau of Mines[78]. Note that the gas data here are reported in the same mass units as for the dusts. Generally,

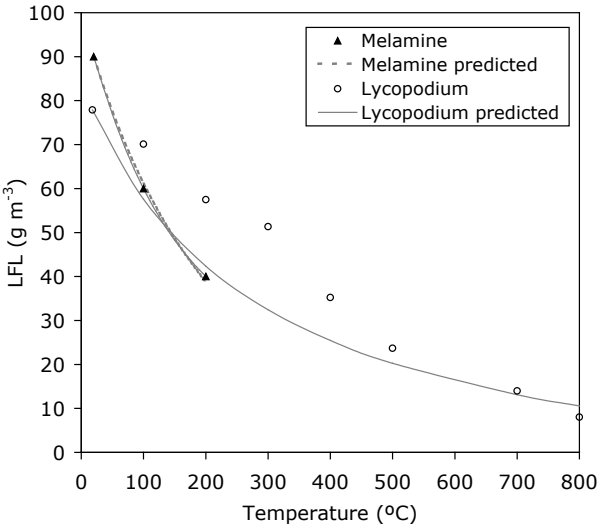


Figure 20 Prediction of the temperature dependence of the LFL of melamine, as compared to measured values

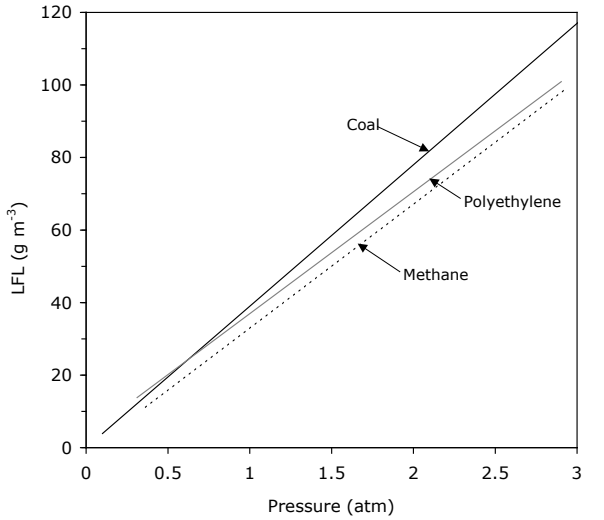


Figure 21 Effect of pressure on the LFL

LFL data for gases are reported in volume units and, in those units, the effect is much smaller.

MOISTURE

Moisture can affect many aspects of dust clouds and their ignitability. For organic, hygroscopic materials, high moisture promotes clumping. If the effective particle size becomes large due to moisture-induced agglomeration, then (a) it might become unlikely that a significant amount of dust will become airborne; and (b) ignition will be more difficult for the product that is airborne. Bartknecht[80] considers that, for many materials, it is unlikely that dusts having more than 10% moisture content will get lofted and dispersed sufficiently in order to become explosible. Simi-

larly, Eckhoff[81] concluded that agricultural dusts having more than 15% moisture, by mass, are unlikely to be ignitable. As a preventive strategy, however, introducing high levels of moisture will rarely be acceptable, since moisture may interfere with the primary function of the product being handled or produced. While increasing the moisture content always increases the minimum ignitable concentration of the dust, the dependence does not follow a universal law. Bureau of Mines results for cornstarch[65] and Pittsburgh coal[68] are shown in Figure 22, as are those of Monakhov[82] for 5-nitrofurfural diacetate. Studies on charcoal dust[83] indicate that moisture has a sizable effect on LFL for dusts with low volatile content, but the effect becomes smaller as the volatile content increases.

Mok et al.[84] studied the effect of RH on the LFL for dusts of a polymer resin, methacrylate-butadiene-styrene. They found no effect below 60% RH, but from 60% to 80% there was a very steep, linear increase, whereby the LFL went from 50 g m^{-3} to 150 g m^{-3}.

OXYGEN CONCENTRATION

Over the range tested by BM[85], increasing oxygen concentrations progressively decreased the LFL (Figure 23). This is in sharp contrast to the behavior for gases (methane is illustrated in Figure 23), where there is no difference between LFL measured at 21% versus at 100% oxygen. The authors hypothesized that the dust behavior is seen because increased oxygen concentrations promote volatilization of the dust. The combined effects[32] of particle diameter and oxygen concentration are illustrated in Figure 24.

IGNITER ENERGY SUPPLIED

Similar to the situation for gases, as greater amounts of spark energy are supplied, the apparent LFL of a dust cloud decreases. This issue was already known in 1924[20], and the problem has been discussed at the start of this Chapter. Additional studies on this topic were conducted by the Bureau of Mines using their smaller 7.8 L dust explosion cylinder. These results[85] are shown in Figure 25. The effect for methane gas is rather small. But for the dusts it is evident that increasing the igniter energy beyond about 10 J causes a sizable drop in the apparent LFL value.

Matsuda and Itagaki[86] explored the effect of igniter energy using a 1 m^3 sphere and a Japanese 30 L sphere on the flammability limits of activated carbon dusts using samples with a broad particle distribution of 1 – 400 μm. Their results (Figure 26) showed that in the 30 L sphere there is a substantial effect, down to the lowest igniter energy exam-

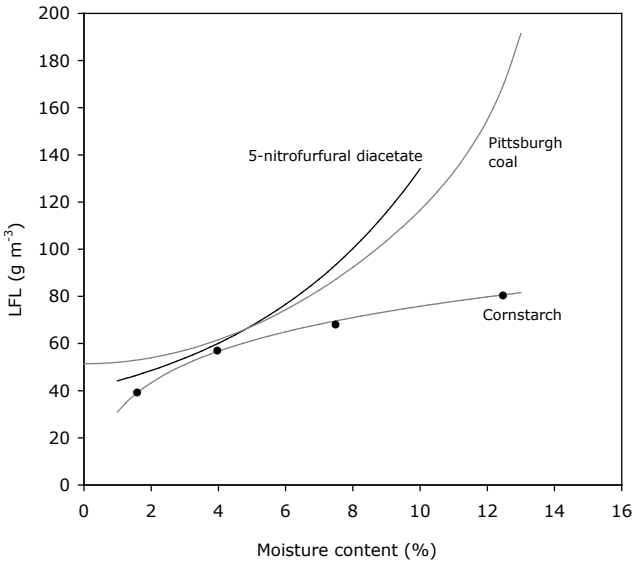


Figure 22 Effect of moisture content on the LFL

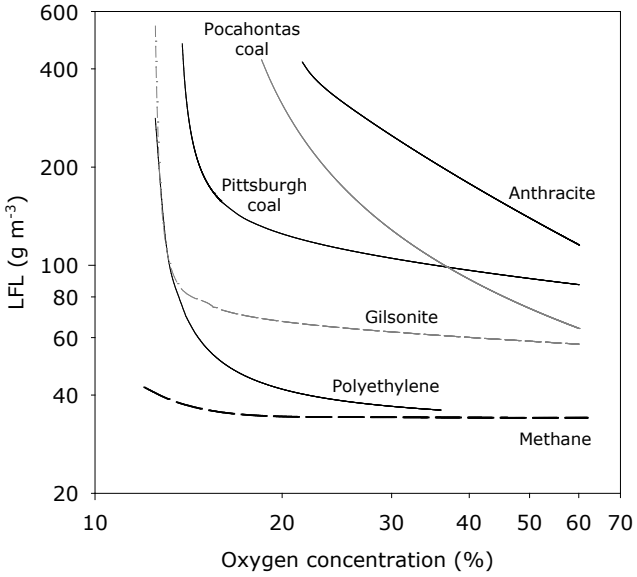


Figure 23 Effect of oxygen concentration on LFL

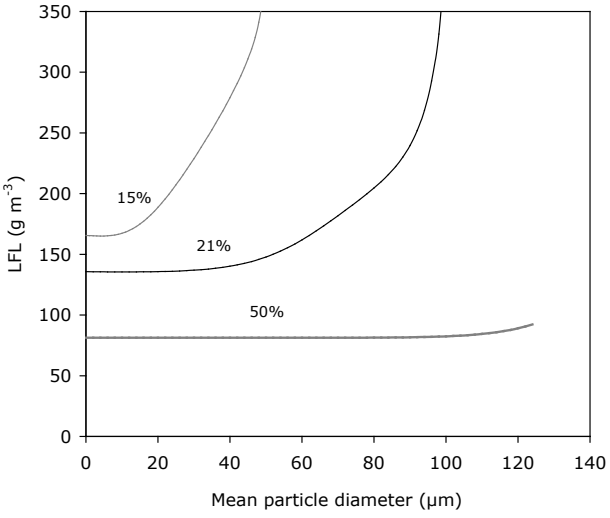


Figure 24 Combined effects of particle diameter and oxygen concentration on the LFL of coal dust
(Copyright The Combustion Institute, used by permission)

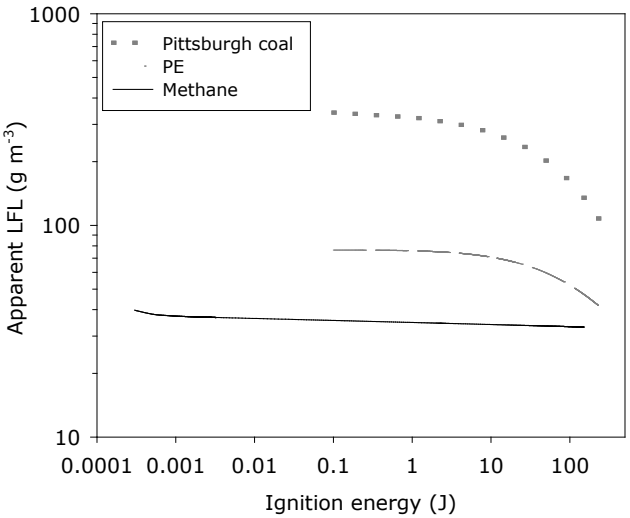


Figure 25 Relation between ignition energy and LFL for several dust types, as measured in the 7.8 L cylinder used by the Bureau of Mines

ined (0.9 kJ). Furthermore, if it is considered that 'overdriving' a test chamber is evidenced by a non-vertical curve on a concentration/energy plot, there was range of igniter energies that could be identified as 'non-overdriving' the chamber. The effect of igniter energy in the 1 m^3 chamber was much less significant. Observe also that the LFL, as determined in the larger chamber, was about 2× that found in the 30 L chamber. This suggests that LFL values measured in chambers of less than 1 m^3 size may quite generally have a large error due to the smallness of the test volume.

Their results obtained in the 1 m^3 chamber also illustrate that if the igniter energy is too small, no ignition at all will be observed. The minimum energy required for the activated carbon dust (ca. 1.8 kJ) is, of course, huge, and such dusts could not be ignited from limited-energy sources such as normal static electricity discharges. There is clearly a volume effect for the minimum igniter energy, with < 0.9 kJ sufficing in the 30 L chamber. But if one assumes that a location with a potentially ignitable dust cloud will generally be greater than 1 m^3 in size, the ignition energy required to cause an explosion in a real-scale application will presumably be > 1.8 kJ. Gibson et al.[87] presented data showing that large chemical igniters, while totally atypical of spark discharges, do rank materials more or less similarly as do open-flame ignition sources.

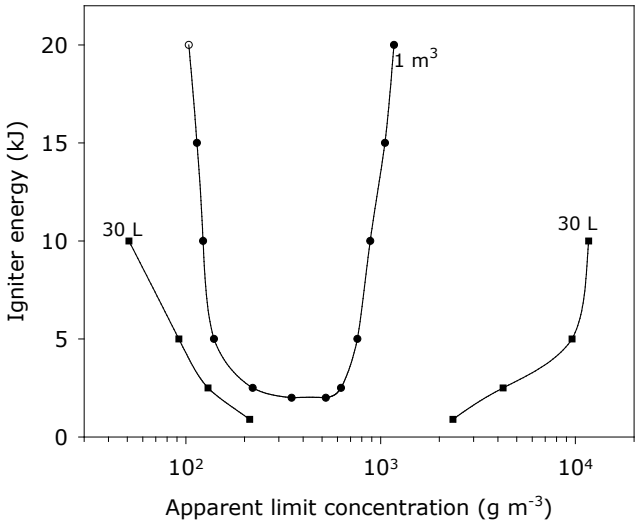


Figure 26 Effect of igniter energy on the apparent flammability limits for polydisperse activated carbon dust in test chambers of two sizes

The combined effects on the flammability limits of temperature and igniter energy are illustrated in Figure 28 and Figure 27[101]. The lines identified as 'lean flammability limit' were determined using a pyrotechnic igniter of 2500 or 5000 J. For coal dust, the LFL determined using the pyrotechnic igniter is about 3 times lower than when determined using a 1.36 J (effective) spark. In the case of polyethylene dust, the highly anomalous curves are a consequence of the melting of polyethylene at around 115 C.

Glowing-wire ignition sources have been used by some European investigators as an alternate ignition source for the Hartmann apparatus, but without published data comparing the results against the standard spark source. The only study on the topic appears to be a 1924 paper[20], which gave data on a handful of dust types showing that LFL values were lower by about a factor of 2 when tested with a 1200ºC platinum glow wire, compared to values obtained by an inductive spark. For gases, glowing-metal ignition sources are much *less* effective than sparks, so it is surprising that the opposite should be true for dusts. There is, however, some limited modern corroboration on this point, as indicated under the presentation of the Hartmann Apparatus test, below.

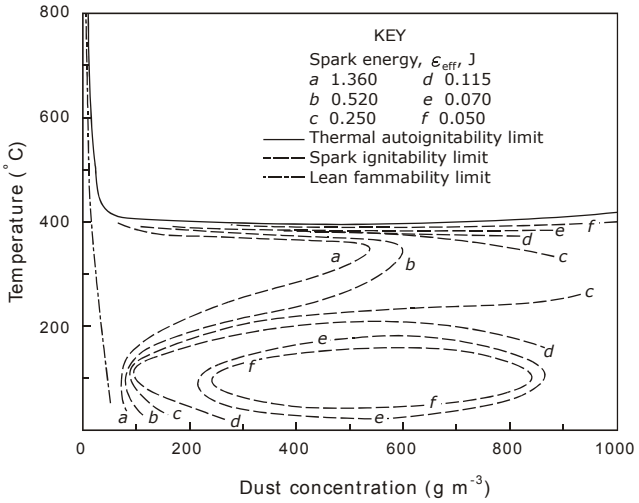


Figure 27 Effects of igniter energy and temperature on the flammability limits of polyethylene dust
(Copyright The Combustion Institute, used by permission)

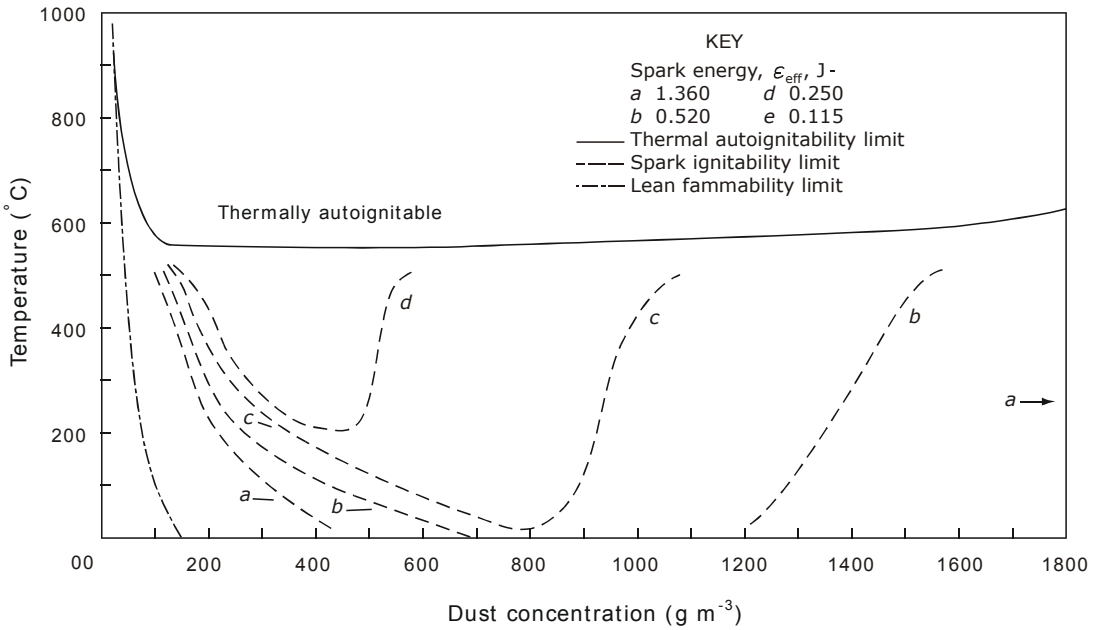


Figure 28 Effects of igniter energy and temperature on the flammability limits of Pittsburgh bituminous coal *(Copyright The Combustion Institute, used by permission)*

VARIABLES AFFECTING THE MIE

DUST CONCENTRATION

Studies with gases (Chapter 4) show a concentration dependence that is roughly parabolic: somewhere in the vicinity of stoichiometric conditions there is a minimum value, with needed ignition energy rising smoothly to either side of that minimum. For dust clouds, the minimum value occurs at a concentration substantially greater than the stoichiometric one. To compute the stoichiometric concentration, all of the fuel present is taken into account. In the case of a dust explosion, the pyrolysis is neither complete nor instantaneous, thus, in effect, a sizeable fuel fraction cannot contribute to the early development of the explosion and only becomes combusted later. Some experimental results of Bartknecht[80] on three plastics, of Matsuda and Naito[97] on cork dust, and of Maranda et al.[88] on aluminum dust are shown in Figure 29. The aluminum dust was in the form of flakes with two different mass-mean diameters, 11 μm and 68 μm. The behavior of the polyester and the cork dust is probably the most representative of a wider variety of substances—same as with gases, increased difficulty of ignition becomes evident as the LFL is approached.

PARTICLE DIAMETER

For particle diameters greater than a certain value, particle diameter influences the MIE. Some examples are given in Figure 30. The data for cornstarch, ethyl cellulose, and sugar were taken in a conventional Hartmann apparatus[65,89,90], while the data for methyl cellulose[19], polyethylene and aluminum[80] used the European spark ignition procedures (see below). Theories have been proposed by Kalkert and Schecker[91] and Ballal[46] to explain the dependence on diameter, and they predict that MIE $\propto d^3$. For the results shown in Figure 30, polyethylene and aluminum show close to a d^3 dependence, while the other products do not. Dust clouds of particles larger than about 300 – 500 μm are non-explosible[80,19], given any practical igniter energy. Eckhoff[19] points out that metal dusts show ignitability increasing with decreasing diameter all the way down to 1 μm. He cautions that testing which is done for poorly-determined sizes, or at sizes larger than may be involved in actual use can lead to unconservative conclusions being drawn.

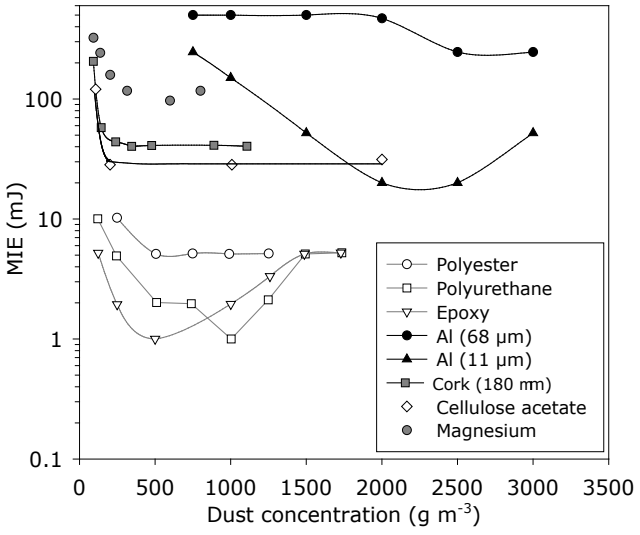


Figure 29 Effect of dust concentration on MIE

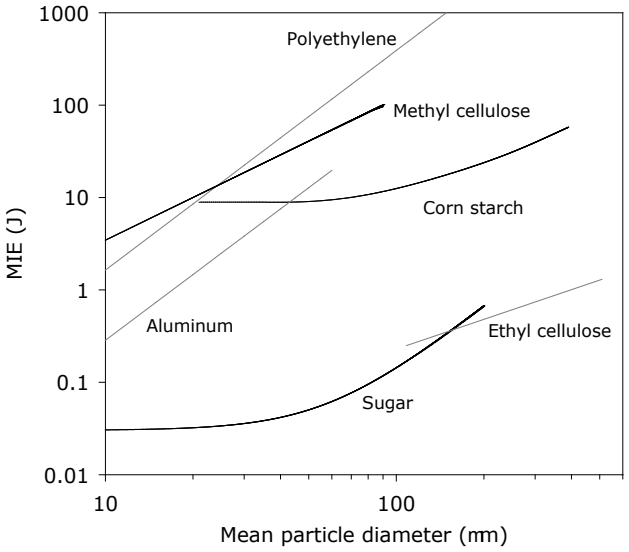


Figure 30 Effect of particle diameter on MIE

TEMPERATURE

Glarner[77] studied the effect of temperature on the MIE of various dusts. His results (Figure 31) show linear behavior on a log-log scale, with lines converging at the value of 0.088 mJ at a temperature of 1000ºC. If the value MIE_{25} is known at 25ºC, then the MIE value at an arbitrary temperature T (ºC) is:

$$MIE_T = 10^{-4.056+(1.873-0.624\log T)(4.056+\log MIE_{25})}$$

Glarner's equation, however, rests on poor theoretical foundation, since it would predict that MIE $\rightarrow \infty$ as $T \rightarrow$ 0ºC. In fact, the behavior of dust clouds at 0ºC is insignificantly different from that at 25ºC. Thus, not surprisingly, some substances do not obey this form at all. BM data[102] indicate that for coal there is a complex temperature/concentration interaction (Figure 28) which would not lead to such simple formulas.

PRESSURE

Over a limited range, Glarner[77] examined the effect of pressure on the MIE. In all cases, he found no difference in MIE at 1.6 atm, versus at 1.0 atm pressure. In tests at 0.65 atm, however, most dusts showed about a factor of 2 increase of MIE, compared to 1.0 atm results. The exceptions were very-hard-to-ignite dusts (e.g., melamine) that require kilojoule levels of energy—these showed no change even at the sub-atmospheric pressures. The conclusion is that values determined at 1 atm can be conservatively used at higher pressures.

MOISTURE

For agricultural dusts, raising the moisture content increases the MIE. This is illustrated in Figure 32; the cornstarch data are from BM[65], the others are from TNO[109]. The minimum MC needed in agricultural dusts to prevent explosion has variously been reported as between 14%[92] and 23%[93]. These values were obtained in small-scale test apparatuses and should not be taken as reflecting real-scale conditions. Grain will rot if stored at excessively high moisture contents (greater than ca. 20%), so a strategy of raising the MC may have limited practicality.

OXYGEN CONCENTRATION

If oxygen concentration is lowered, the MIE values will generally rise. Figure 33 shows some results for various dusts[68,80]. With organic dusts, a steep dependence on oxygen concentration is seen, but with metal dusts, only a very gradual one.

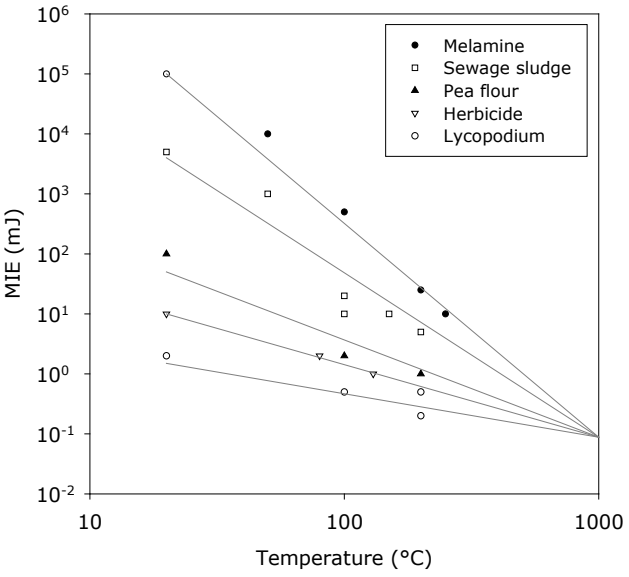


Figure 31 Temperature effect on MIE

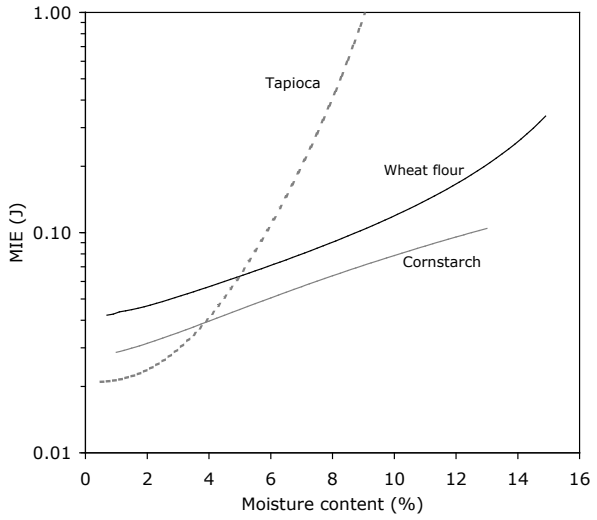


Figure 32 Effect of moisture content on the MIE for several agricultural dusts

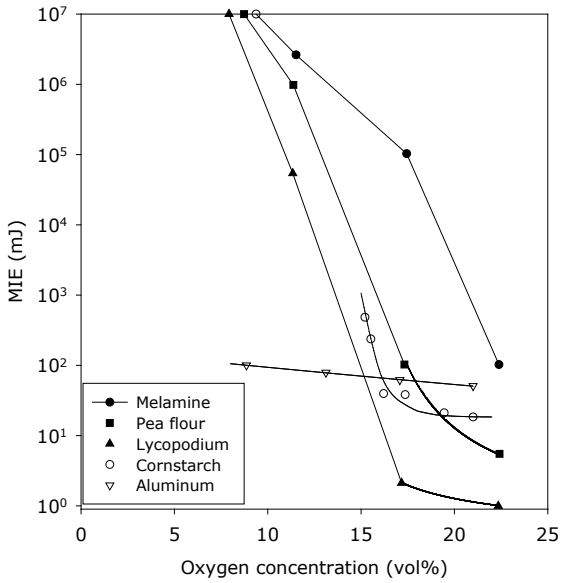


Figure 33 Effect of oxygen concentration on MIE

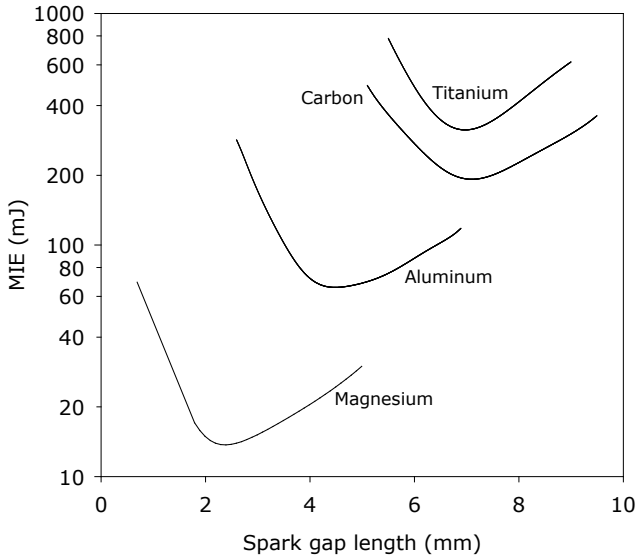


Figure 34 Effect of spark gap length on MIE (equivalence ratio = 0.65; Sauter mean diameter = 40μm)

TURBULENCE

Increased turbulence causes the MIE to rise. This has been documented qualitatively[94], although quantitative relations are lacking. Even if they were available, the turbulence in most real-life scenarios is hardly ever quantified, so the ability to use such relations would be questionable.

CHARGE ON PARTICLES

It has been found that if the particles in a dust cloud are not electrically neutral but are already carrying a charge, the MIE value decreases. Choi et al.[95] tested PAN powder and found that the MIE was about 25% lower for particles carrying a charge of 20 – 30 nC g^{-1} than for neutral particles. The polarity of charge did not make much difference.

SPARK ELECTRODES: MATERIAL AND GAP SIZE

The metal from which the electrodes are made can influence the results, but not drastically. Glarner[77] showed that, of 5 metals tried, tungsten invariably gave the lowest MIE results; other metals typically showed values 1 – 4 times as great. Same as for gases, there exists an optimal spark gap size, with smaller or larger spacings leading to higher reported values of MIE. Some example curves[96] are shown in Figure 34. From relations on this type a gap of 6 mm is commonly chosen as being reasonable for testing a variety of dust types. This gap is several times greater than what is optimally selected for testing gas mixtures. The optimum gap length also decreases when the dust concentration increases; except for very dilute mixtures, however, the latter effect is small[97].

SPARK CIRCUIT PARAMETERS

In 1950 Boyle and Llewellyn[98] found that inserting a series resistor into the firing circuit for capacitive discharge ignition of a dust cloud led to lower MIE values being reported. With zero resistance, it required 490 mJ to ignite an aluminum powder dust cloud, while inserting a 50 kΩ resistor dropped this down to 55 mJ. It is even more remarkable considering that their reported energy values were nominal, taking into account only the energy stored on the capacitor and ignoring the large energy loss within the resistor when a resistor is introduced. The answer was found in the time response of the circuit. When a circuit has only stray resistance, the discharge time will be exceedingly fast (a few microseconds). If the time constant is increased by a series resistor, the energy can be more effectively delivered. This occurs because the role of the discharge time for dust clouds is very different from that for gases. A very fast, vigorous discharge creates a pressure which literally blows the dust out of the spark gap. As the time constant is increased, the force is decreased and more dust remains accessible to ignition. To relate the discharge time to the circuit parameters, the expression for current decay in an RC circuit is:

$$I(t) = \frac{V_o}{R}\exp(-t/RC)$$

where V_o = initial capacitor voltage. If the spark duration time is defined, somewhat arbitrarily, as the time that it takes for the current to drop to 1% of its original value, then the time constant τ is:

$$\tau = 4.6RC$$

Line et al.[99] subsequently found a very similar effect, but the optimum resistance in their case was 100 kΩ.

Hay and Napier[100] conducted tests on polystyrene and cornstarch dusts in a modified Hartmann apparatus where they were able to vary both the capacitance and the series resistance. In addition, they directly measured the voltage and current flowing through the spark gap and computed the

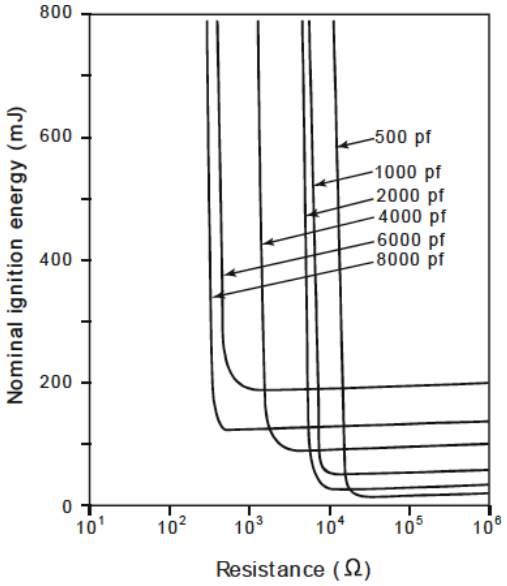


Figure 35 Nominal MIE of stoichiometric mixture (87 g m^{-3}) of polystyrene dust in air

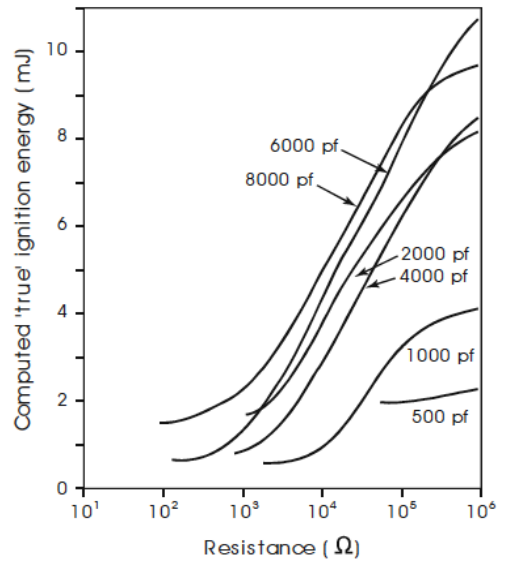


Figure 36 Computed 'true' MIE of stoichiometric mixture of polystyrene dust in air

actual energy delivered. In their rig, they concluded that only 1 – 10% of the nominal energy (expressed as $\frac{1}{2}CV^2$, where C = capacitance and V = voltage) is actually delivered into the spark gap. The rest is presumably dissipated in the circuit, but the authors did not attempt to compute losses in the circuit, which—had it been done—could have been used to double-check the accuracy of their 'true' values. The curves of nominal energy vs. resistance showed an optimal value at ca. 500 – 20,000 Ω (Figure 35), but their computed 'true' energy was found to be monotonically decreasing with resistance (Figure 36). The authors did not try values lower than 500 Ω in their experiment.

At BM, Hertzberg and coworkers conducted studies[101,102] using an arrangement where a charged capacitor is discharged into a spark gap through an intervening step-up transformer. This would be a poor choice of circuit arrangement for understanding the fundamental physics, but it is the one that has traditionally been used in the Hartmann apparatus (see below). For spark energies below 2 J, they determined the spark energy efficiency to be approximately 25%. In other words, if the nominal available energy is defined as $\frac{1}{2}CV^2$, then only 25% of that energy was computed to have entered the kernel. But for larger nominal energies, efficiency dropped drastically, so that at 100 J, the efficiency was only 2%. They found that a significant fraction of the input energy is expended simply in doing work of compressing the gas outside the spark kernel. Typically, 25% was delivered into the spark kernel itself, 7% went into compression work, while the rest represented circuit losses. Concerning effects of the circuit parameters, in their rig, discharge energy was increased mainly by raising the capacitance of the capacitor, rather than raising the voltage. The results indicated efficiency progressively dropped as larger capacitance values were used, but they did not explore the converse possibility of raising voltage rather than capacitance. All of their reported efficiencies were obtained by an indirect technique using a theoretical model which produced the relation:

$$E_{eff} = 2.5 V_o \Delta P$$

where E_{eff} = energy delivered into the spark kernel (J), V_o = volume of test chamber (m^3), and ΔP = pressure rise in chamber (Pa). Values of ΔP were measured and efficiency was then determined by dividing E_{eff} by the nominal spark energy. Most of Hertzberg's results were obtained with a spark gap of 6 mm, but he did find that efficiency generally increased with gap size, up to about 8 mm.

Matsuda and Naito[97] explored empirically the optimal discharge time for lycopodium and cork dust clouds. They found that increased discharge times were needed for greater particle diameters. Their results showed that minimum energies corresponded to spark duration times in the range 0.1 – 1.0 ms. This conclusion, however, depends on the dust type. Eckhoff[19] showed that the optimum time for polyacrylonitrile dust is 0.01 ms, with even lower values for some other dusts. On the other hand, Nifuku and Katoh[103] showed for coal dust that spark durations of 2 – 10 ms give identical (lowest) ignition energy values, whereas if the discharge time drops below 2 ms, the energy needed increases sharply. Without further studies, it is not possible to derive general guidance on a relation between particle diameter and optimum discharge time.

Traditional experience had indicated that to ignite dust clouds requires ignition energies several orders of magnitude higher than for gases. But, starting in the 1970s, several European research groups discovered specialized spark arrangements which lead, in some cases, to values being reported for dust clouds in the same range as for methane

(0.3 mJ). The first research group to develop a super-low-energy method was the one at Christian Michelsen Institute (CMI) in Norway*. Eckhoff observed that sparks of short duration (1 μs) are less incendive than ones of about 0.1 to 10 ms duration[104,105]. Thus, CMI developed a special ignition circuit, described by Alvestad[106]. Basically, capacitors are discharged into the spark electrodes via a transformer, into which is coupled a trigger circuit. Diodes are used to chop the waveform to minimize oscillations. The voltage and current waveforms are highly complex and depend on both the capacitor used and its charging voltage. The discharge time is dependent on the spark energy, being about 0.04 ms for a 1 mJ spark and 2 ms for a 10 J spark. Field[107] compared MIE values obtained using the CMI circuit to those obtained using the circuit of the traditional Hartmann apparatus. This comparison is shown in Table 1 and also plotted in Figure 37. In the figure is also shown the correlation recommended by Eckhoff[19]:

$$MIE(CMI) = \frac{[MIE(Hartmann)]^{4/3}}{21.5}$$

Eckhoff specifically points out that the correlation should only be applied in the range 10 mJ ≤ MIE(Hartmann) ≤ 10,000 mJ, but judging from Field's data the entire correlation must be considered to be only qualitative. Clearly, the MIE values differ greatly between the two circuits. However, it is hard to choose the 'right' one, since the Hartmann circuit has large, unquantified losses, while the CMI circuit represents a 'minimum' that is not likely to ever occur in an accident.

In 1926, Wynne-Williams[108] studied the discharge produced by a three-electrode spark gap. He found that a small spark discharge between an auxiliary electrode (located to one side of a main electrode) and the main electrode would pre-ionize the space between the main electrodes and to allow a later 'main' spark across the primary electrodes to be produced at a lower voltage than otherwise possible. Much later, this principle was put to use by TNO[109] in Holland (Figure 38) and by Glarner[77] and Bartknecht[80] in Switzerland. Glarner's main electrodes have a 6 mm gap. The auxiliary electrode is located 2 mm away (perpendicular) from one of the main electrodes. In operation, a spark is fired across the 2 mm auxiliary gap first, using an energy low enough so that this firing would not ignite the test atmosphere. Since this spark ionizes the gas in main spark gap, a subsequent spark can be fired across the main 6 mm gap using a drastically lower energy than would be necessary for ignition of the atmosphere had the gas not been pre-ionized. Glarner's electrodes are made of 2 mm dia. stainless steel and have pointed tips. The main spark circuit uses an inductance of 1.32 – 46.4 mH but no series resistance. Studies have shown that the MIE values determined with this scheme are about 10 – 100 times lower[80,110] than when using a simple capacitive-discharge circuit. A few dusts however (e.g., melamine and sulfur) are exceptions, and do not show a large decrease in MIE when using this special circuit. The meaningfulness of the data obtained by this pre-ionization scheme is fundamentally questionable, however, since the process does not simulate a sequence of events encountered in accidental explosions. Additional data on the effect of inductance has been presented

Table 1 Effect on MIE of the ignition circuit used

Substance	MIE (mJ)	
	Hartmann	CMI
aluminum flakes	10	0.3
cornstarch	30	0.3
iron, atomized	40	0.12
lycopodium	22	6.0 – 6.5
methyl cellulose	40	4.9
polystyrene	40	0.3
sulfur	15	0.3

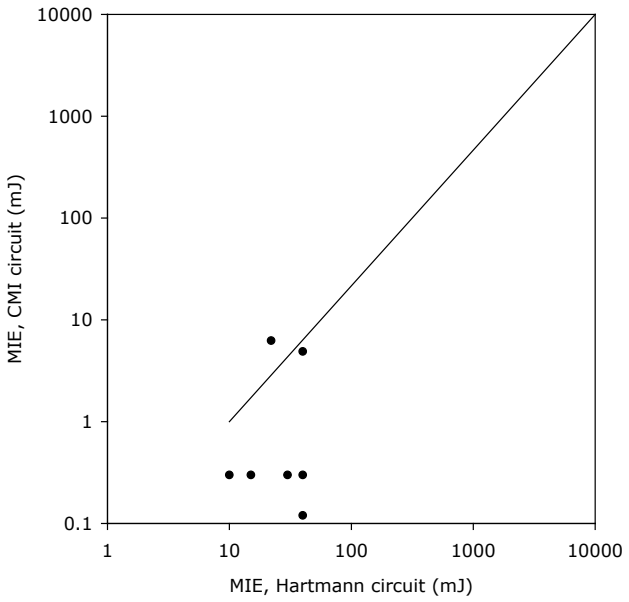


Figure 37 Relation between MIE values obtained using the Hartmann circuit and the CMI circuit; also shown is Eckhoff's proposed correlation

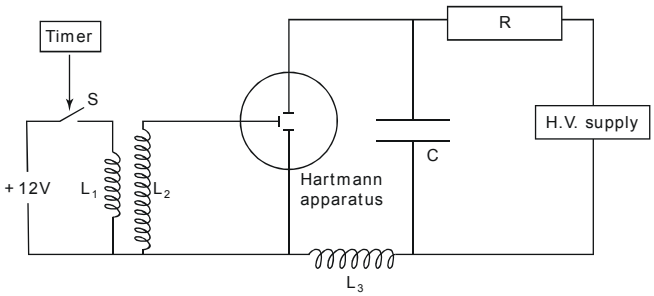


Figure 38 TNO 3-electrode arrangement, as implemented on the Hartmann apparatus

* Now named Christian Michelsen Research.

by Pidoll[111], who showed that MIE values are insensitive to the presence of induction for dusts with very low MIE values. But at higher MIE values, inserting a 1 mH inductance into the circuit often lowered the MIE value by about tenfold. Britton[112] has described several other circuit arrangements, including the trickle charge circuit of BS 5958, a moving electrode method, and a variant of the CMI circuit used at several US chemical manufacturers.

As a conservative measure, one or the other of the above schemes have come into wide use, at least in Europe. However, their use would appear to be unjustified, excessive conservatism, since no studies exist that would relate the values found under these test conditions to explosions that occur in actual accidents. Especially, the 3-electrode device is so peculiar that there does not seem any possibility that it would represent events in an actual accident. Interestingly, Bartknecht recommends that his circuit *not* be used for the testing of flock (Figure 39), for the reason that ignition sources in flock machinery are unlikely to be inductive in nature. Indeed, going further, Eckhoff[19] has advised that the circuit should not be used for electrostatic hazard assessment in industrial plant, since "high inductance values are unlikely to occur in accidental electrostatic discharge circuits in industry." In the same vein Bailey et al.[113] studied a wide variety of equipment used in chemical plants and found that with one exception (a rubber hose with a metal coil, 220 μH) all of the inductances were less than 3 μH. Glor[114] also concluded that equipment with significant inductance is sufficiently rare that general-purpose data should not be based on simulating them. Conversely, Smallwood[115] hypothesized that if discharges are to poorly conducting (e.g. plastics) surfaces, then the discharge time length might be lengthened, making inductive or resistive elements a reasonable surrogate for the lengthened discharge time.

Unlike a gas mixture, a dust cloud does not just stay in place after being created—unless continuously agitated, it settles out quickly. Thus, with any given test apparatus, there will be an optimum time at which the spark should be fired. If it is fired too early, then a uniform mixture will not have had a chance to be created. If it is fired too late, then settling out of the dust will result in non-minimum ignition energy values being reported. Bartknecht[80] documented some of these details. For the Siwek 20 L sphere, a delay time of 0.12 s was found to be optimal; for several other test apparatuses, both larger and smaller, values of around 1.2 – 1.5 s were found best.

AIR VELOCITY AND TURBULENCE

Increasing the air stream velocity raises the MIE value roughly linearly. A modest amount of experimental data exists[19] and can be generalized to the following predictive relation:

$$MIE_2 = MIE_1 + \alpha\left(u_2 - u_1\right)$$

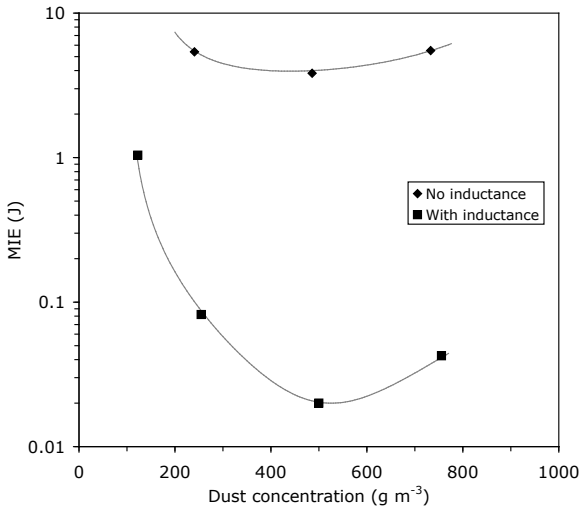


Figure 39 MIE for acrylic flock—effect of spark circuit parameters
(Copyright Springer-Verlag, used by permission)

where MIE_2 denotes the ignition energy (mJ) corresponding to velocity u_2 (m s^{-1}), and similarly for MIE_1. The empirical constant α is in the range 0.3 – 0.5, and a typical value of 0.4 can be used.

Dust clouds are difficult to create in laminar flows. Turbulent conditions are present in all of the test methods and in most practical applications. Since turbulence increases the MIE, the values of MIE associated with dusts will perforce be higher than those for gases, since the latter are measured under quiescent conditions. Bartknecht[80] showed for some materials that going from "low turbulence" to "medium turbulence" conditions increased the MIE values by a factor of about 80. A practical means does not exist to quantify the turbulence in various test apparatuses, nor indeed have even semi-quantitative comparisons been reported. A unique experimental rig[9] has been proposed, however, where dust clouds are in a 'cycling' laminar motion due to an ingenious electrostatic charging arrangement. The apparatus is primarily designed to measure quenching distances, but so far only a single material has been studied.

Line et al.[99] conducted interesting experiments where they ignited dust clouds both in a tube (as in the Hartmann apparatus) and as a free jet in open air. It took significantly more energy to ignite the dust cloud when it was in a tube. The authors explained that this is because the rapid expansion induces significant turbulence in a tube, while expansion in open air is less turbulent.

TEST VESSEL SIZE

The effect of test vessel size on MIE has not been explored in depth. Glarner's study[77] (Table 2) suggests that higher values are reported in a larger test apparatus, which would imply that applying test results to a large-scale end-use environment may be fundamentally conservative.

Table 2 Effect of test vessel size on MIE

Dust	MIE (mJ)	
	20 L sphere	1 m^3 sphere
antioxidant	1	2
lycopodium	2	2
paint A	2	3
paint B	1	5
epoxy polyester	2	5
cellulose	10	50
pea flour	100	1000
melamine polymer	100,000	1,000,000

RISK MANAGEMENT BASED ON THE MIE

A British Standard exists which classifies dust suspensions according to their liability to static electricity ignition. BS 5958[116] classifies dust suspensions according to the minimum ignition energy, as given in Table 3. The precautions listed in this table pertain to dust suspensions having a volume resistivity of less than 10^{12} Ω-m; dusts of higher insulating value require additional precautions.

DILUTING WITH INERT GASES

The effect of inert dilution gases on making a co al dust cloud non-flammable is illustrated in Figure 40 and compared to the effect for methane.

Another way of considering dilution is to examine the *minimum oxygen concentration* (MOC) that is needed for explosion. Krause et al.[117] argued that a similar relation should be found between the LFL and the MOC for dust clouds as for gases (see Chapter 4). The main differences are that the LFL for dust clouds must be measured in units

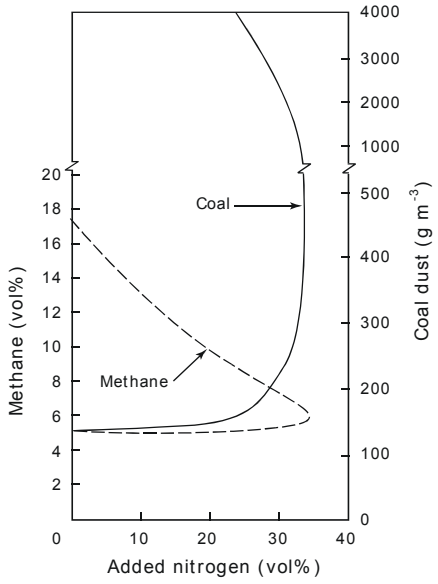


Figure 40 Comparative effect of adding nitrogen to methane and to coal dust atmospheres[78]

Table 3 Recommendations of BS 5958 for dust cloud precautions

Min. ignition energy (mJ)	Recommended precautions
500	Low sensitivity to ignition. Earth plant when ignition energy is at or below this level.
100	Consider earthing personnel when ignition energy is at or below this level.
25	The majority of ignition incidents occur when ignition energy is below this level.
10	High sensitivity to ignition. Consider restrictions on the use of high resistivity non-conductors when ignition is at or below this level.
1	Extremely sensitive to ignition. The presence of explosible dust-air mixture should be avoided wherever possible. Handling operations should be such that they minimize the possibility of suspending the powder in air. All possible steps should be taken to encourage the dissipation of charge and to discourage charge operations.

of g m^{-3} rather than in vol% and that the elemental composition of the fuel is normally reported as mass-fractions. based on requirements of oxygen for combustion. On this basis,

$$MOC = LFL \times \frac{r_o}{\rho_{O_2}}$$

where LFL = (g fuel)/m^3, r_o = stoichiometric oxygen/fuel mass ratio (--), ρ_{O_2} = density of oxygen (g O_2/m^3) and at 298 K it is 1290 g m^{-3}. For a fuel containing only the elements C, H, and O, r_o can be evaluated as:

$$r_o = \frac{32}{12}\mu_c + \frac{32}{4}\mu_h - \mu_o$$

where μ_c, μ_h, and μ_o are the mass fractions (--) in the fuel of C, H, and O, respectively. An analogous expression can be derived for dust that include additional elements. Krause's data are plotted according to this relation in Figure 41 and it is seen that the prediction is generally conservative. However, as Chapter 4 shows, the MOC for most organic gases is in the range of 10 – 12%. By contrast, the dust cloud results show a lot of values in the range 6 – 8% (the two lowest data points represent metal dusts and not organic fuels). Dust cloud MOC values that are below the values for gases are presumably too low due to experimental difficulties.

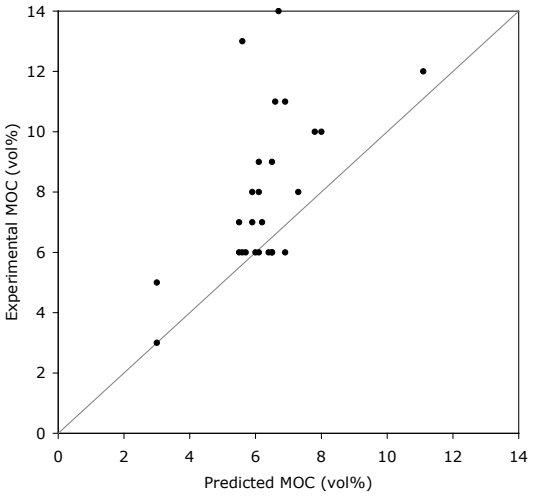


Figure 41 Prediction of MOC for dust clouds based on the LFL

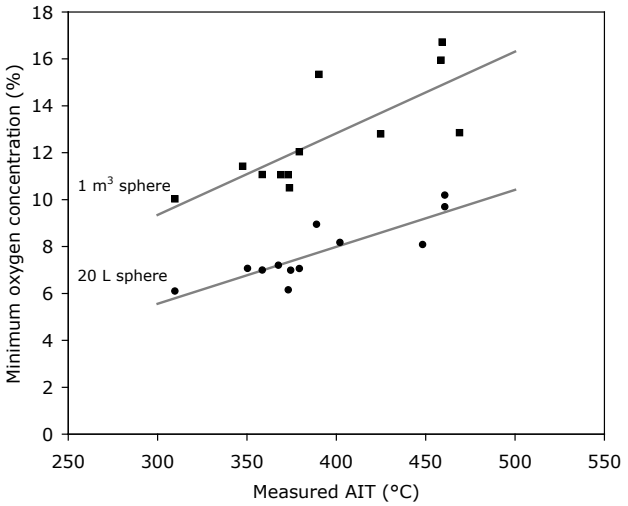


Figure 42 Predicting the minimum oxygen concentration on the basis of the AIT

Bartknecht[80] found that the MOC is roughly dependent on the AIT of the dust, as measured in the BAM oven (Figure 42). The MOC values were measured in the 20 L Siwek sphere and in the Bartknecht 1 m^3 sphere. With only a few exceptions, the values found for gases are 11.5 – 12%, thus the values from the 1 m^3 sphere that are below 12% are presumably attributable to an overdriving of the chamber by the pyrotechnic igniter. Much more striking are the lowest MOC values of 6 – 8% found in the 20 L sphere, which are substantially lower than MOC values for gases. The combustion of a dust cloud cannot be any more efficient than that of a premixed gas atmosphere, although it can definitely be less efficient. Thus, results which suggest contrariwise are evidently due to unrealistic test arrangements. Specifically, the pyrotechnic igniter evidently overdrives the 20 L sphere to a remarkable degree. Siwek and Cesana[70] proposed a correlation for *MOC*:

$$MOC = 12.9 + 1.62 \log\left(MIE\left[1 + \frac{AIT}{273}\right]\right)$$

where *MIE* is in joules and AIT (ºC) is as determined in the BAM oven. Scant details have been made available for the basis of this correlation, so its intended range of validity is not clear.

A correlation between MOC and AIT is also curious on chemical grounds. Gases do not show any such correlation and it would appear that the correlation arises due to some unanalyzed intervening variable. The value of MOC for most organic, non-halogenated gases is nearly constant and bears no relation to AIT values, which span a wide range.

The above results were obtained at 20ºC. If the ambient atmosphere is at an elevated temperature, then lower values of oxygen concentration will suffice for combustion to be possible. This is indicated in Figure 43. The values were obtained by Wiemann in a 1 m^3 sphere[79,118], so the results can realistically be applied to real-scale problems. Most of the data can be represented well by a linear trend, whereby the MOC at any temperature T_2 can be estimated from its value at T_1:

$$MOC_{T_2} = MOC_{T_1} - 0.014\left(T_2 - T_1\right)$$

Essentially identical trends are seen from the 20 L sphere[77], although in the latter case the absolute values do not seem to be applicable.

Wiemann obtained a results for the MOC of a number of dusts at room temperature using the 1 m^3 sphere. These values are given in Table 4. Again, values below 12%, or so, for organic fuels must be viewed as questionable, since they are lower than what is attained by gases.

Table 4 MOC values, as determined by Wiemann

Dust type	Diameter (µm)	MOC (%)
aluminum	22	5
barium stearate	<63	13
bisphenol A	34	9.5
cadmium laurate	< 63	14
cadmium stearate	<63	12
coal, anthracite	17	14
coal, brown	63	13
cornstarch	17	9
dibenzoyl peroxide	59	10
methyl cellulose	70	10
β-naphthol	<30	9.5
pea flour	25	15.5
paraformaldehyde	23	6
polyethylene	26	10
rye flour	29	13
soot	13	12
sulfur	30	7
wheat flour	60	11
wood	27	10

The effect of particle diameter on the MOC was explored by several researchers[68,119]. Figure 44 shows that there is little effect for diameters < 100 µm. For larger diameters, some dusts show strongly rising MOC values, while for others the increase is mild.

Less dilution is needed if the dust concentration is not near its worst-case value, in other words, there is a dust concentration dependence also. The values reported in the literature are generally for dust concentrations giving near-lowest MOC values. Larger or smaller dust concentrations will raise the MOC value. Figure 45 illustrates the effect for phenol formaldehyde dust[120].

The above discussion assumed that the system is composed of only three substances—oxygen, nitrogen, and dust. In some cases, diluting is done not by nitrogen but by water vapor or CO_2. The latter molecules have higher heat capacity and thus, a lesser dilution is required for non-flammable conditions to be reached. Guidance is not as extensive for water vapor, CO_2, or other diluents, but Wiemann has illustrated that coal dust showing at 150ºC an MOC of 10.9% could be inerted with water vapor by dropping oxygen to 12.3% or with CO_2 by dropping oxygen to 13.0%.

DILUTING WITH INERT DUSTS

If it is required to make an atmosphere non-flammable, then inerting with nitrogen is possible, although costly. Diluting with excess air is generally impractical, since additional flow velocities introduced may tend to stir up and create greater dust quantities. In some specific cases, the most practical and economical solution is dilution with inert dusts. This has found application in coal mines for a long time, where limestone dust is used. When the mass fraction

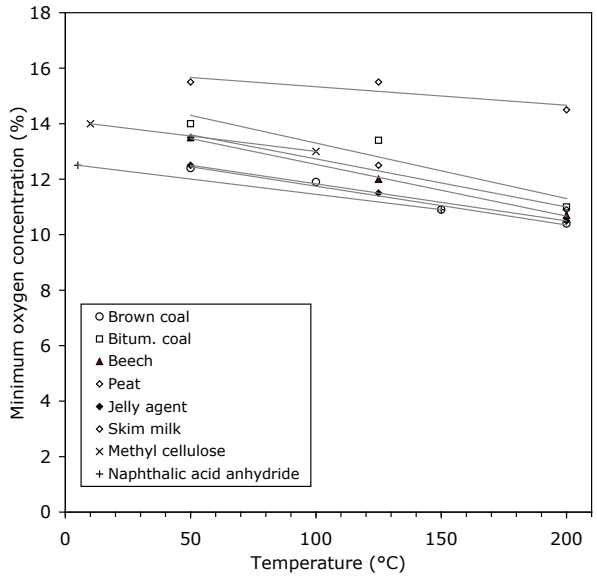


Figure 43 Effect of temperature on MOC using a 1 m^3 sphere

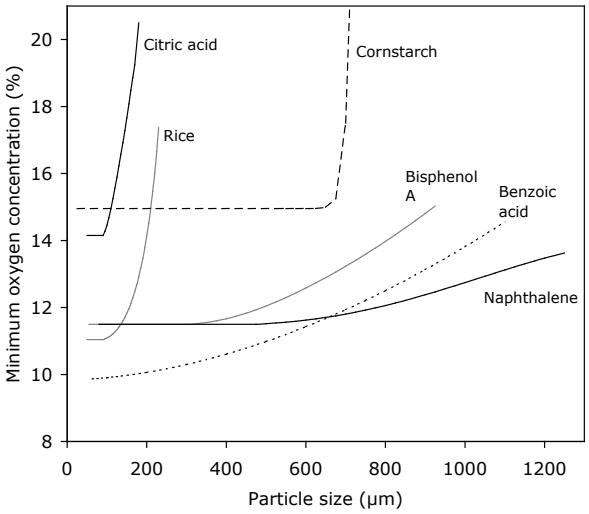


Figure 44 Effect of particle size on MOC

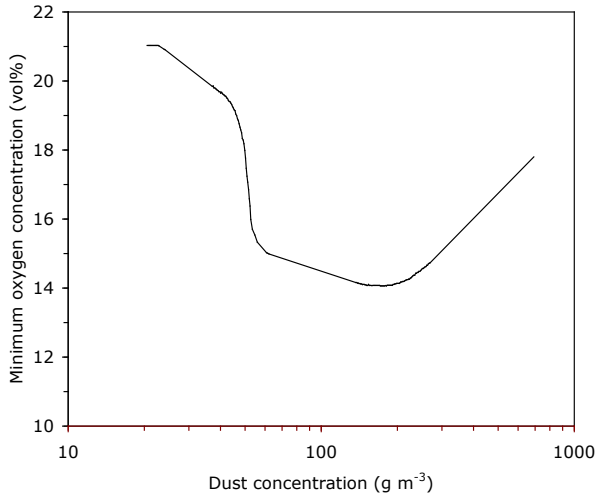


Figure 45 Minimum oxygen concentration for 15 µm phenol formaldehyde dust

of limestone dust reaches about 75-80% of the combined mass of coal+limestone dust, mixtures become non-flammable[78]. Limestone dust, however, is ineffective against methane gas explosions. BM[30] reported on a series of measurements in their 20 L apparatus using a 5000 J pyrotechnic igniter that showed that 92% inert dust was needed for inerting polyethylene dust.

Tests for ignition properties of dust clouds

There is a wide variety of test equipment that has been used to characterize explosible dust clouds. The primary variables which are of interest are:

- minimum ignition energy, MIE
- lower flammability limit, LFL
- autoignition temperature, AIT
- minimum oxygen concentration, MOC
- maximum pressure rise
- maximum rate of pressure rise

The latter two variables are only of post-ignition concern and are not further discussed here. The MIE and the LFL can be measured in any of the devices discussed below. The AIT can be measured in any of the devices which have the capability of being heated.

The methods described below are ones that have received significant use in recent decades. The early history of test methods developed in Germany and elsewhere in Europe has been reviewed by Bartknecht[80]. Brown and Woodhead[121] reviewed the history from an apparatus designer's point of view. Essenhigh et al.[122] reviewed the design principles and details of a majority of the current apparatuses and it is important to note their conclusions. The state of the art of test apparatus design is acceptable, at best, only if comparative values are needed. If data need to be obtained that have fundamental credibility, *all* of the currently-common test methods must be considered as unsatisfactory. This is because:

- cloud uniformity is poor
- motions exist in the system which are uncharacterized and of varying velocity
- particles are rapidly lost from the test section or segregate according to size
- the ignition sources used have an effect on the result, and the effect is neither theoretically characterized nor a realistic representative of the end-use environment
- the residence time of the particles within the apparatus affects the test outcome, but it is neither quantified nor controlled.

Thus, it becomes very difficult to compare test results and theories, if the test apparatuses cannot be relied upon to generate data under known, fixed, simple boundary conditions.

ASTM E 1491

ASTM E 1491[123] is a peculiar standard which does not describe a specific apparatus, but rather lets the user choose from a list of four entirely different test apparatuses: (1) the Godbert-Greenwald furnace; (2) the BAM oven; (3) the heated version of the Bureau of Mines 1.2 L Hartmann apparatus; and (4) the Bureau of Mines 6.8 L furnace. The standard recommends that samples be prepared by sieving to have 95% at the minus 200 mesh size, i.e., smaller than 75 μm. Since it is known that results obtained with these apparatus show systematic differences, and, in some cases, large differences, testing according the standard evidently can yield quite disparate results.

ASTM E 2019

This standard[124] for the MIE of a dust cloud allows for testing in either a Hartmann tube of 0.5 L or 1.2 L capacity, or a 20 L sphere, despite the fact that correlation between those is poor. An electric spark ignition is used, with a spark gap of 6 mm. The value of the capacitance is not specified. The ignition energy is computed as $\frac{1}{2}C\left(V_i^2 - V_f^2\right)$, where V_i is the initial voltage of the charged capacitor and V_f the voltage remaining upon discharge. Energy losses are ignored. Four calibration substances are specified: tetrakis-methylene(3,5-di-(tert)-butyl-4-hydroxyhydrocinnamate)methane: MIE = 1 – 6 mJ; anthraquinone: MIE = 1 – 11 mJ; lycopodium: MIE = 10 – 30 mJ; and Pittsburgh coal: MIE = 30 – 140 mJ. As can be seen from these ranges for standard substances, highly accurate results are not being sought. The minimum ignition energy is computed at the 10% probability level. The results are to be prepared as a plot of concentration vs. MIE. Four entirely different spark circuits are permissible: (1) A 3-electrode system, where a spark breakdown caused by an auxiliary electrode triggers the main discharge. (2) An arrangement where a pneumatic cylinder rapidly moves one electrode into position, causing discharge when a critical distance has been attained. (3) A fixed system where a trickle-charge circuit keeps raising the capacitor's voltage until break-

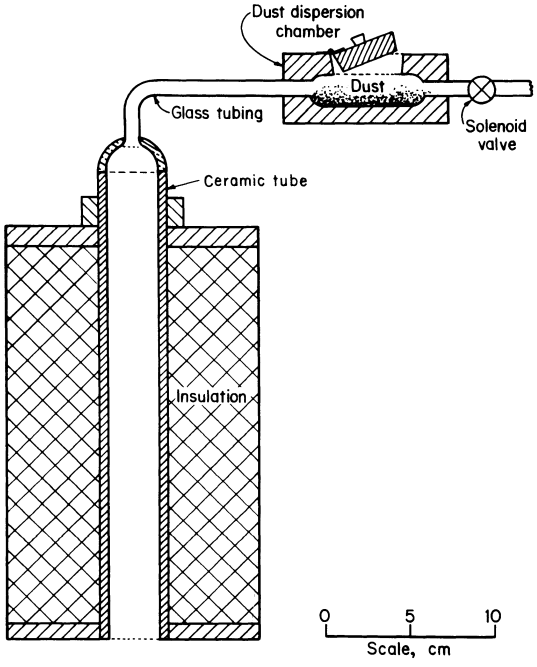


Figure 46 A cross-section view of the Godbert-Greenwald furnace

down occurs. Or, (4) A circuit whereby a secondary charged capacitor is quickly connected to a transformer which received a pulse and couples it into the discharge circuit of the primary capacitor.

GODBERT-GREENWALD FURNACE

The earliest of the apparatuses from which data are still used, this 0.27 L furnace (Color Plate 4) was developed cooperatively by BM and SMRE in 1935[125,126] as an elaboration of a design that was originally described by the French combustion scientist Taffanel in 1911. A dust dispersion tank of 150 mL is connected to the top (Figure 46) and a puff of air through that chamber is used to disperse the dust into the furnace chamber. The furnace itself uses Nichrome wire as the heating element and can be heated up to 1000ºC. The furnace does not have an ignition mechanism and therefore is used only for AIT studies. Milligram-to-gram quantities of dust are injected, using an air pressure which is varied according to the characteristics of the dust. Ignition is taken to occur if flame becomes visible below the mouth of the furnace. The apparatus has been criticized for its poor uniformity of both temperature and dust concentration[63].

BUREAU OF MINES 1.2 L FURNACE

Since uniformity of dust dispersion in the G-G furnace was considered to be poor, in 1981 BM developed a replacement test apparatus, the 1.2 L furnace[34, 63] (Figure 47 and Figure 48). Unlike the G-G furnace, which is only suitable for making AIT measurements, the 1.2 L furnace was developed to allow both AIT and MIE studies to be made, in other words, it was also viewed as a heated replacement for the Hartmann apparatus (see below). The most significant change from the G-G furnace is that dust is blown up, not down, into the apparatus, helping to establish uniformity inside it. The dust is dispersed into the volume by manually loading the disperser with dust, inserting it into the bottom of the chamber, then dispersing it using 60 mL of air, delivered in a 30-ms pulse. Ignition is judged to occur if the fiberglass diaphragm at the top of the furnace ruptures and flame is emitted from the port within 3 s of dispersion.

BAM OVEN

In Europe, and especially in Germany, the BAM oven[127] is commonly used. This apparatus is a horizontal tube oven, at the far end of which is a parabolic metal plate (Figure 49, Figure 50, and Color Plate 2). Testing is started by setting the oven to 600ºC and blowing in 1 to 2 mL of dust using a squeeze-bulb, which is deflected by the parabolic plate. If ignition results, then the heaters are turned off and new samples injected at every 50ºC as the oven is cooling down. If ignition is not obtained at 600ºC, then higher temperatures are used. The temperatures reported from the BAM oven are generally lower than from the Godbert-Greenwald furnace.

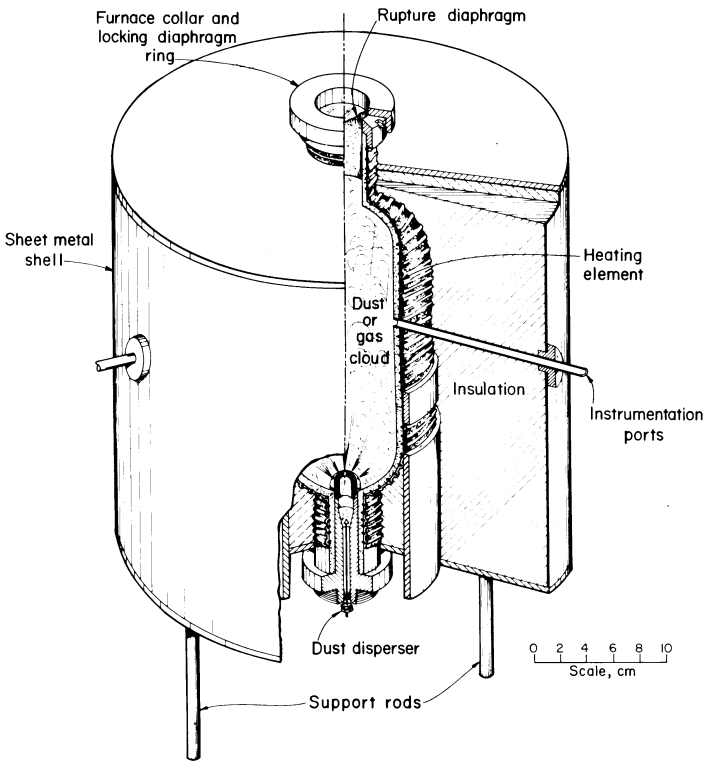


Figure 47 The Bureau of Mines 1.2 L furnace

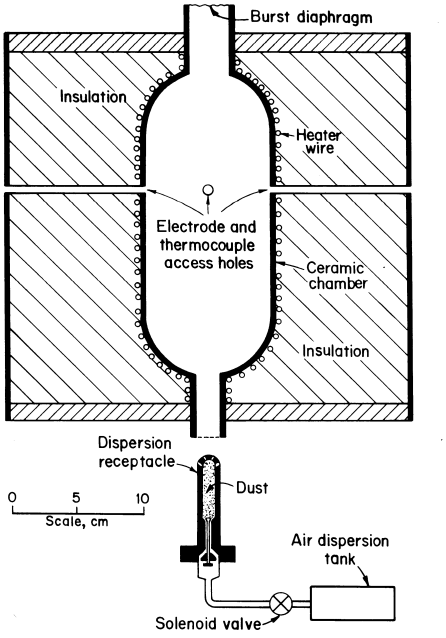


Figure 48 Cross-section view of the Bureau of Mines 1.2 L furnace (the dust receptacle is shown in the loading position; it is pushed up into the chamber just before an air blast is activated to start the test).

HARTMANN APPARATUS

The Hartmann apparatus designation can be confusing, since a number of devices have been described which differ significantly in some of their crucial features. The original device[128], also called the Hartmann tube, is a 1.2 L cylinder, 305 mm tall and 70 mm dia., into which dust is injected from the bottom. The tube is an open-top PMMA cylinder, and the apparatus uses an electric spark ignition source (Figure 51 and Color Plate 5). The bottom contains a cup where a quantity of dust is placed and dispersed with a puff of air from a 1.3 L air reservoir. The pressure to be used for dispersion needs to be determined in preliminary trials. Tungsten spark electrodes are located 100 mm above the base. The spark circuit involves a capacitor which is discharged through a transformer. The discharge time is adjustable, and the operator is required to optimize it by preliminary trials. The criterion of ignition is a flame propagation distance of 100 mm or greater in the tube. The transformer-coupled circuit was adopted for the Hartmann apparatus presumably because it prolongs the discharge time, compared to a simple capacitor discharge.

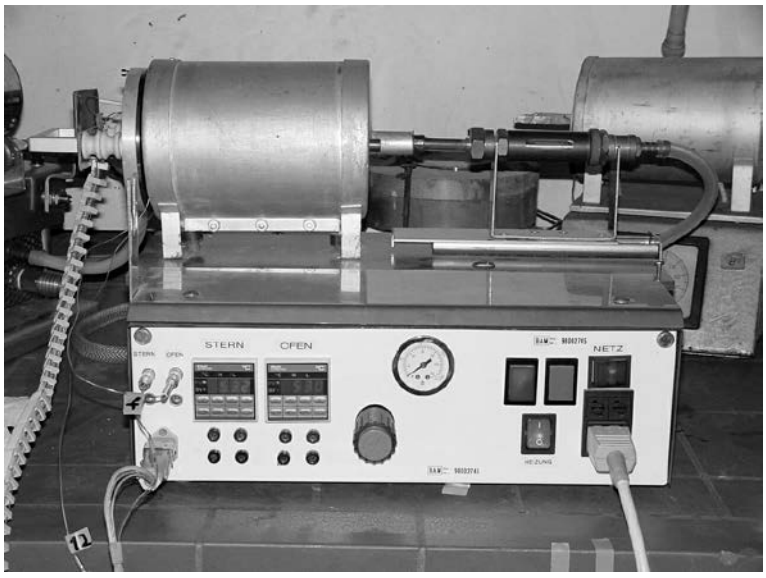


Figure 49 BAM oven, external view
(Courtesy Ulrich Krause, BAM)

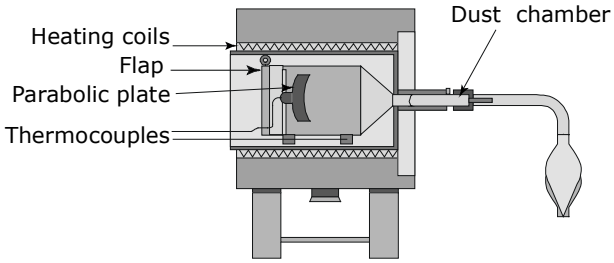


Figure 50 Section view of the BAM oven
(Copyright AIChE, used by permission)

When the LFL (as opposed to the MIE) is to be determined, a filter-paper rupture disk is installed with a locking ring to cover the top of the apparatus. The disk has a 1.6 mm hole in the center to avoid excessive pressure rise due to the introduction of the air puff. The criterion for occurrence of ignition in LFL determinations is the bursting of the disk. Thus, the flame propagation criterion is a pressure rise equal to the bursting pressure of the paper disk, about 0.2 atm. For determining the MOC, the Hartmann apparatus is modified so that a controlled-oxygen atmosphere is presented to the unit.

For determining pressure rise, a steel pressure-vessel version of the Hartmann apparatus is used, often referred to as a *Hartmann bomb*. The latter has been standardized as ASTM E 789[129]. The ASTM version is the unheated steel cylinder. A heated bomb version evolved into the 1.2 L apparatus, discussed above. In 1978 Lütolf[130] described a modified Hartmann apparatus, where (a) the tube of the apparatus is a Pyrex cylinder; (b) an alternative for the electric spark is provided by a Kanthal glow coil, operated at 1200ºC; and (c) a flapper vent is located on the top of the cylinder. The latter is graduated in degrees of opening angle, and is intended to be used for rough preliminary screening. Field[107] recommends that the glow wire be used for dusts that are not readily ignitable by an electric spark. Glarner has concluded the 1200ºC coil can successfully ignite only dusts which have AIT values ≤ 540ºC, as measured in the BAM oven.

The vast majority of the published ignition data using the 'Hartmann apparatus' pertain to the open-top PMMA-cylinder version and not to the later versions. Even though the electric spark ignition used with the Hartmann apparatus is at the extremely weak end of the scale amongst today's test methods, Eckhoff has pointed out that "none of the dusts that were classified as 'non-explosible' in the [spark-ignited Hartmann tube] ever caused any explosions in the chemical industry." This observation certainly implies that tests using more energetic igniters are excessively conservative.

The criteria adopted for the Hartmann apparatus can have a strong effect on the reported values. In studies of the LFL of gases, it is well understood that for the flammability limit to be reached, extensive flame travel has to be observed—flaming in the nearby vicinity of the ignition source is not sufficient. Lunn[131] noted that LFL values reported in the UK at the Fire Research Station using their version of the Hartmann tube are often lower than those from the Bureau of Mines, since, for unexplained reasons, the UK procedures[107] deem the flammability limit to be reached if any flames are observed moving away from the igniter.

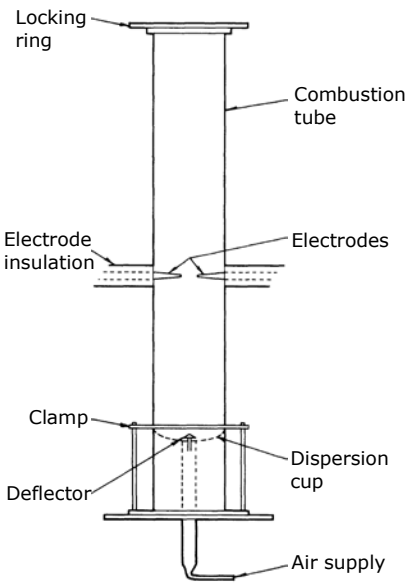


Figure 51 General-use version of Hartmann apparatus

The reproducibility of MIE data obtained in the Hartmann apparatus does not appear to be especially good. In a roundrobin conducted by ASTM in 2000, 9 laboratories agreed reasonably well on the value (ca. 20 mJ) for lycopodium dust. But for Pittsburgh coal, which should also not be a difficult-to-test substance, reported values from 5 laboratories ranged from 50 to 1000 mJ. Part of the problem appears to be attributable to the ignition circuits, which are not all identical at the laboratories using this equipment. Several studies[21,132] document shortcomings of the Hartmann apparatus.

An apparatus conceptually similar to the Hartmann apparatus, although actually not sharing any parts in common has been invented in Norway and described by Eckhoff[133]. The apparatus comprises an open steel tube, 140 mm diameter and 400 mm tall. Dust is introduced by an air blast at the bottom. Also located at the bottom is an igniter, which consists simply of an oxyacetylene welding torch. The apparatus was developed because a number of dust cloud explosions have originated due to careless welding.

BUREAU OF MINES 6.8 L CHAMBER

The BM 6.8 L chamber[63] is very similar to the heated version of the Hartmann apparatus, except for the increased size (Figure 52). The main innovation is an automated device for loading the dust disperser into the chamber. The rupture diaphragm is also replaced with a flapper vent. Ignition is judged to occur if the vent opens and flame is emitted within 6 s after dispersion of the dust. For most dusts, the AIT results are found to be within 30 C of the values obtained with the 1.2 L Hartmann apparatus.

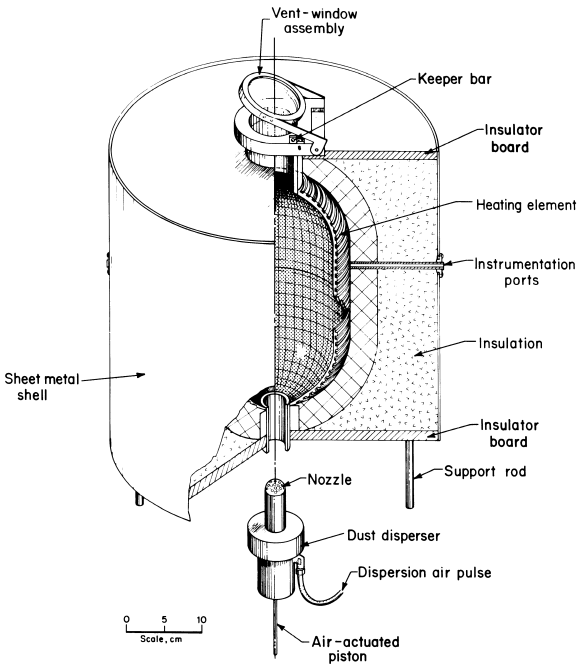


Figure 52 View of the Bureau of Mines 6.8 L apparatus

SPHERES AND OTHER 20 L CHAMBERS

Recent work has shown that values of pressure rate of rise determined in a too-small apparatus cannot be scaled suitably to real-scale applications. Thus, much current research focuses on chambers of 20 L size and greater. Note, however, that this issue does not refer to determinations of ignition parameters, only of explosion pressures. The ASTM E 1515 test method[134] is based on a 20 L chamber developed

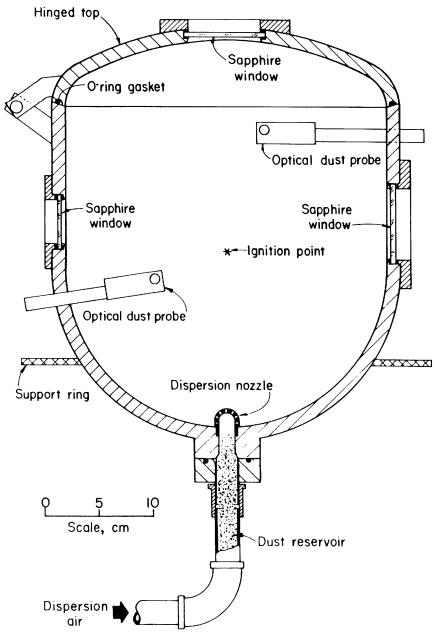


Figure 53 The Bureau of Mines 20 L dust explosion sphere



Figure 54 Siwek 20 L sphere
(Courtesy Sicherheitsinstitut: Swiss Institute of Safety & Security)

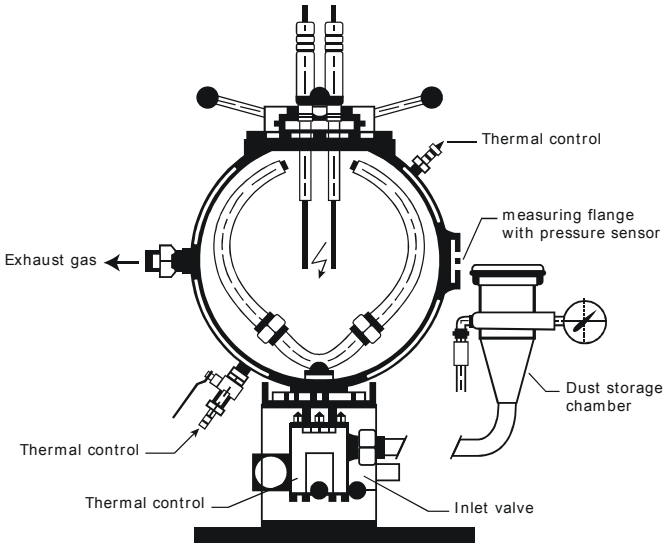


Figure 55 The 20 L Siwek sphere—cutaway view[138]

Table 5 Minimum oxygen concentrations for explosibility of Pittsburgh coal dust

Chamber	Igniter energy (J)	Min. oxygen content (%)
20 liter	1000	13.5
	2500	11.0
	5000	9.5
1 m^3	10,000	13.5

by the Bureau of Mines[135]. The chamber is made of stainless steel and is shaped somewhat between a cylinder and a sphere (Figure 53). Ignition is with a pyrotechnic igniter* of 2500 or 5000 J energy. The ASTM standard recommends that the samples be prepared by sieving to have 95% of the particles at the minus-200-mesh size, i.e., smaller than 75 μm, but that particles much smaller than 75 μm not be included. The moisture is to be below 5%. Concerning ignitability, the test variable reported is the minimum explosible concentration, MEC, which is synonymous with LFL. Other results are also reported from the test that pertain to characteristics of the explosion. The apparatus is not heated, so it cannot be used for AIT determinations.

Table 6 Validation of LFL results in large-scale tests

Test apparatus	Igniter energy (J)	Gilsonite	Pittsburgh coal
20 L	1000	50±5	90±5
	2500	35±5	80±10
	5000	30±5	60±10
	10,000	30±4	50±10
1 m^3	2500	39±3	90±5
	5000	41±3	85±5
	10,000	36±3	80±5
large-scale mine gallery	methane gas explosion	35	60

Going et al.[136] recently reported results from a study using this chamber which indicate that even the 2500 J igniter overdrives the system and that a 1000 J igniter would appear to be more reasonable. This can most clearly be judged from their MOC data for Pittsburgh coal (Table 5). Values ca. 13.5% are typical of many hydrocarbons, while a value of 11.0% would only be characteristic of a few exceptionally flammable ones, amongst which coal dust can hardly be envisioned.

Another way that the realism of ignition energy can be assessed is from large-scale validation. Sapko et al.[137] conducted large-scale mine gallery tests on gilsonite and Pittsburgh coal dust. These results (Table 6) suggest the 2500 J igniter provides the best agreement to large-scale data where the expected real-life ignition source is enormous, i.e., an ongoing gas explosion. For applications where a dust explosion is not foreseeably set off by a gas explosion, these results would not be relevant.

Apart from the very expensive 1 m^3 spheres, the apparatus most widely used in Europe in recent years for testing dusts has been the 20 liter sphere (Figure 54 and Figure 55), developed by Richard Siwek at Ciba-Geigy in Switzerland[138]. The method has a unique way of operation, in that the vessel is first evacuated down to 0.4 atm, then the dust is injected with sufficient air to bring up the starting pressure to

* Pyrotechnic igniters used are a mixture of zirconium (40%), barium nitrate (30%), and barium peroxide (30%). The largest, 10 kJ, contains 1.2 g of mixture, with the other sizes being proportionately smaller.

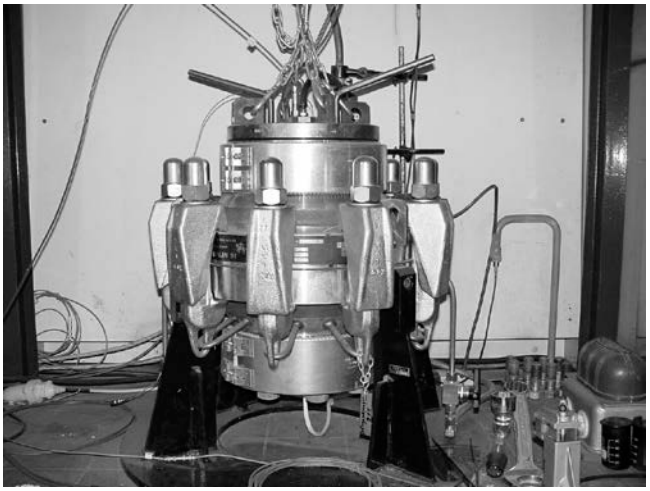


Figure 56 A 20 L bomb, as used at BAM
(Courtesy Ulrich Krause, BAM)

1 atm. The apparatus uses a huge 10,000 J pyrotechnic igniter. Eckhoff[19] points out that "the very strong 10 kJ igniter may cause combustion of dust even if the dust concentration is below that required for self-sustained flame propagation at constant pressure." Dust cloud ignitions occur mainly through cutting, grinding, tramp metal or overheating causes[139], and none of these approach a 10 kJ level. Thus, for situations where a dust cloud explosion is unlikely to be triggered by an ongoing gas explosion, a 10 kJ igniter would be inappropriate. The method is standardized as ASTM E 1226[140]. The method has primarily been used to determine the maximum pressure and the rate of pressure rise that occurs, although LFL determinations can also be made. The apparatus is not designed to be heated to high temperatures for making AIT determinations. However, Bartknecht[80] described a special, heated version which can be operated up to 250ºC for making LFL measurements at moderately elevated temperatures. Another 20 L bomb, as used at BAM, is shown in Figure 56.

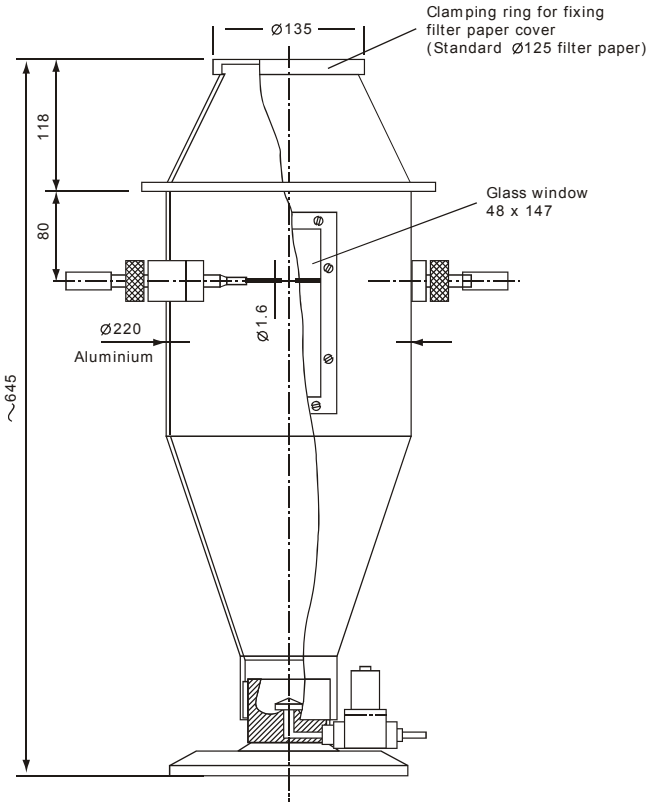


Figure 57 The Nordtest 15 L apparatus

NORDTEST 15 L APPARATUS

A 15 L vessel (Figure 57) was developed by Eckhoff at the Christian Michelsen Institute and adopted by Nordtest as NT Fire 011[141]. An electric arc ignition is used. The criterion for explosion is not clear, but the standard specifies that results are to be reported for the concentration giving ignition at the 50% probability level. The standard uses a clever scheme of a substitute chamber wherein the actual dust concentration is determined in the area near the ignition source by sampling from that area during a dispersion event. Makris and Lee (see above) concluded that this was the most credible of the standard test methods, but it must be noted that they did not consider any of the standard methods to be adequate.

1 M^3 SPHERES

A 1 m^3 sphere (Figure 58) is commonly used in Europe for testing according to the German standard VDI 3673[142]. Some of its development has been described by Bartknecht[80]. A slightly different variant has been described by ISO[143] as ISO 6184-1. Several 1 m^3 spheres of slightly different types have also been used[144]. The 1 m^3 spheres are not heated, so they cannot be used for AIT determinations. Another type of 1 m^3 vessel used at BAM is shown in Color Plate 6.

ASTM E 1232

A specialized question sometimes is asked—Determine whether a smoldering layer of dust in a closed volume can generate enough combustible pyrolysates to create an explosible atmosphere. This is addressed by the ASTM E 1232 test method[145]. The method, whose primary application is to liquids, also contains procedures for granular powdered materials. A 50 cm^3 amount of the test substance is placed in a 5 L heated flask. The flask is heated to a desired test temperature and an electric spark is applied to determine if the atmosphere is flammable. Eckhoff[19] surveyed a number of additional, non-standard tests designed to explore this same question.

IEC 61241-2-3/MIKE 3

An IEC standard[146], IEC 61241-2-3 is based on a highly modified Hartmann tube evolved by Siwek and Cesana[70]. The apparatus is commonly known as 'Mike 3,' after the

model number designation of the commercial version produced by Adolf Kühner AG, in Birsfelden, Switzerland. The test method is developed only for examining the ignitability at certain discrete energy values: 1, 3, 10, 30, 100, 300, and 1000 mJ. For the two lowest energy values, a charging voltage of 15 kV is used and ignition is caused by activating a relay which connects a charged capacitor across a discharge gap. For the higher energy values, a pneumatic activator that quickly moves one electrode from its rest position to the final position, which comprises a 6 mm discharge gap. A voltage of 15 kV is used for 10 mJ energy testing, and 11 kV for higher energies. The apparatus provides for testing either with a 1 mH inductor in series with the charged capacitor, or else with only parasitic inductance (< 0.025 mH). Steel or tungsten electrodes of 2 mm diameter are used. Only a limited amount of data have been published concerning the effect of inductance in this apparatus[113], suggesting that the higher inductance value sometimes—but not always—causes lower MIE values to be reported. The data also suggest that, compared to other test devices, the MIE values from the Mike 3 apparatus are sometimes similar, but sometimes vastly lower. The reasons for this have not been presented.

CMI MECHANICAL IMPACT TEST

No standard test for ignitability of dust clouds from mechanical impact-generated sparks exists. An experimental rig developed at CMI has been described by Pedersen and Eckhoff[53]. A swinging hammer contacts an anvil within a dust-laden environment. The dust dispersion system is a modified version of the dispersion cup used in the Hartmann apparatus.

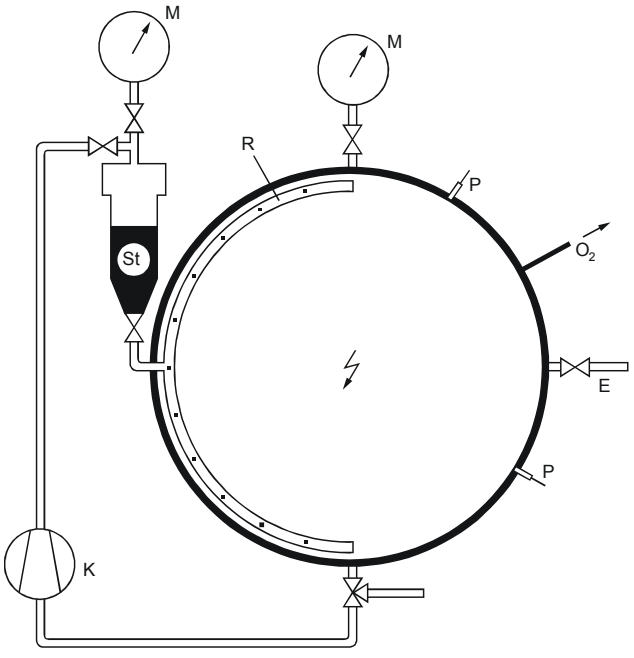


Figure 58 The 1 m^3 sphere, as prescribed by VDE 3673
(Copyright ASTM International, used by permission)

Further readings

Rolf K. Eckhoff, **Dust Explosions in the Process Industries**, 2nd ed., Butterworth-Heinemann, Oxford (1997). The only comprehensive textbook in the field of dust explosions is Eckhoff's. He provides both a plethora of experimental data and theoretical development of numerous aspects of dust explosions.

Wolfgang Bartknecht, **Dust Explosions: Course, Prevention, Protection**, Springer-Verlag, Berlin (1989). Bartknecht is a German researcher who has been highly prolific in the dust explosion research area. His book is valuable for the large amount of photographs and for numerous graphs illustrating data trends. Theory is not covered and there are no data tables.

Peter Field, **Dust Explosions**, Elsevier, Amsterdam (1982). Field was the last in a series of researchers at the Fire Research Station of the UK who studied dust explosions. His book summarizes the experimental results from much of the FRS research, and includes extensive data tables. The book is wholly empirical in scope.

Brenn- und Explosions-Kenngrössen von Stäuben, H. Beck, N. Glienke, C. Möhlmann, eds., (BIA-Report 12/97), Berufsgenossenschaftliches Institut für Arbeitssicherheit, Sankt Augustin, Germany (1997). English edition: **Combustion and Explosion Characteristics of Dusts** (BIA-Report 13/97), Hauptverband der gewerblichen Berufsgenossenschaften, Sankt Augustin, Germany (1997). By far the most ambitious compilation of data in this field, this book comprises a set of tables giving data on 4300 dusts, compiled during a project involving five German safety organizations. The LFL data are from the Lütolf-modified Hartmann tube, or the 1 m^3 sphere, or the 20 L Siwek sphere. Indications are not given as to which of the latter two was used; the Hartmann tube values can be imputed by an absence of K_{st} values. In the case of the Siwek sphere, the 10,000 J igniter was used, with its attendant problem of overdriving the apparatus. MIE and MOC values were apparently also obtained from one of the two spheres. AIT data are from the Godbert-Greenwald furnace or from the BAM furnace, or, in some cases, both; these are clearly identified. Also given are dust layer hotplate test results, using a 50 mm layer depth, and from a German platinum-wire 'combustion test.' The latter (which is similar in spirit, but not in detail, to the UN Test N.1) uses a small pile of material that is briefly ignited by the wire and the results are classified into 6 burning classes.

Schofield, C., and Abbott, J. A., **Guide to Dust Explosion Prevention and Protection. Part 2—Ignition Prevention, Containment, Inerting, Suppression and Isolation**, The Institution of Chemical Engineers, London (1988). This practical guide is addressed to the plant safety engineer and offers extensive suggestions on how to lay out and operate facilities to minimize dust explosion hazards.

References

1. Essenhigh, R. H., Problems of Ignition and Propagation of Dust Clouds, pp. 276-288a in *Proc. Intl. Symp. on Grain Dust Explosions*, Grain Elevator and Processing Society, Minneapolis (1977).
2. Prevention of Grain Elevator and Mill Explosions: Report of the Panel on Causes and Prevention of Grain Elevator Explosions of the Committee on Evaluation of Industrial Hazards (NMAB 367-2), National Academy Press, Washington (1982).
3. Hexamer, C. J., **A Collection of Essays on Spontaneous Combustion**, The Spectator Co., New York (1888).
4. Engler, C., Beitrage zur Kenntniss der Staubexplosionen¸ *Chemische Industrie*, 171-173 (June 1885).
5. Essenhigh, R. H., Dust Explosion Research, *2nd Loss Prevention Symp.*, AIChE (1968).
6. Wolański, P., Grain Dust Explosion and Control, Final Report, Grant No.FG-Po-370, Project No.PL-ARS-135, Warsaw Univ. of Technology, Warsaw (1993).
7. Scherpa, T., Secondary Dust Cloud Formation from an Initiating Blast Wave (M.S. thesis), Worcester Polytechnic Institute, Worcester MA (2002).
8. Fowler, A. H. K., and Baxter, A., Fires, Explosions and Related Incidents at Work in Great Britain in 1996/97 and 1997/98, *J. Loss Prevention in the Process Industries* **13**, 547-554 (2000).
9. Aldis, D. F., and Lai, F. S., Review of Literature Related to Engineering Aspects of Grain Dust Explosions (Misc. Publ. No. 1375), US Dept. of Agriculture, Washington (1979).
10. Lee, J. H. S., Zhang, F., and Knystautas, R., Propagation Mechanisms of Combustion Waves in Dust-Air Mixtures, *Powder Technology* **71**, 153-162 (1992).
11. Wolański, P., Detonation of Organic Dust-Air Mixtures, *Proc. 20th Intl. Pyrotechnics Seminar*, IIT Research Institute, Chicago (1994).
12. Kauffman, C. W., Sichel, M., and Wolański, P., Research on Dust Explosions at the University of Michigan, *Powder Technology* **71**, 119-134 (1992).
13. Srinath, S. R., Flame Propagation due to Layered Combustible Dust (Ph.D. dissertation), Univ. Michigan, Ann Arbor (1985).
14. van der Wel, P. G. J., Ignition and Propagation of Dust Explosions (Ph.D. dissertation), Delft University Press, Delft, Netherlands (1993).
15. Carpenter, D. L., The Explosibility Characteristics of Coal Dust Clouds Using Electric Spark Ignition, *Combustion and Flame* **1**, 63-93 (1957).
16. Cassel, H. M., and Liebman, I., The Cooperative Mechanism in the Ignition of Dust Dispersions, *Combustion and Flame* **3**, 467-475 (1959).
17. Krause, U., and Kasch, T., The Influence of Flow and Turbulence on Flame Propagation through Dust-Air Mixtures, *J. Loss Prevention in the Process Industries* **13**, 291-298 (2000).
18. Andrews, S., and Lunn, G. A., A Report on Some Tests on the Jet Ignition of Dust Clouds, HSE, Buxton, UK (2001).
19. Eckhoff, R. K., **Dust Explosions in the Process Industries**, 2nd ed., Butterworth-Heinemann, Oxford (1997).
20. Trostel, L. J., and Frevert, H. W., The Lower Limits of Concentration for Explosion of Dusts in Air, *Chem. and Met. Eng.* **30**:4, 141-146 (28 Jan. 1924).
21. Eggleston, L. A., and Pryor, A. J., The Limits of Dust Explosibility, *Fire Technology* **3**, 77-89 (1967).
22. Wolański, P., Minimum Explosive Concentration of Dust-Air Mixtures, pp. 206-219 in *Proc. 6th Intl. Colloquium on Dust Explosions*, Shenyang, China (1994).
23. Wolański, P., Dust Explosion Research in Poland, *Powder Technology* **71**, 197-206 (1992).
24. Lesikar, B. J., Parnell, C. B. jr., and Garcia, A., III, Determination of Grain Dust Explosibility Parameters, *Trans. ASAE* **34**, 571-576 (1991).
25. Nagy, J., Dorsett, H. G., jr., and Cooper, A. R., Explosibility of Carbonaceous Dusts (RI 6597), Bureau of Mines, Pittsburgh (1965).
26. Makris, A., and Lee, J. H. S., Lean Flammability Limits of Dust-Air Mixtures, *Archivum Combustionis* **9**, 43-64 (1989).
27. Jarosiński, J., Lee, J. H., Knystautas, R., and Crowley, J. D., Quenching of Dust-Air Flames, *21st Symp (Intl.) on Combustion*, The Combustion Institute, Pittsburgh (1986).
28. Jarosiński, J., Lee, J. H., Knystautas, R., and Crowley, J. D., Quenching Distance of Self-Propagating Dust-Air Flames, *Archivum Combustionis* **7**, 267-278 (1987).
29. Hertzberg, M., Cashdollar, K. L., and Zlochower, I. A., Flammability Limit Measurements for Dusts and Gases: Ignition Energy Requirements and Pressure Dependences, pp. 303-313 in *21st Symp. (Intl.) on Combustion*, The Combustion Institute, Pittsburgh (1986).
30. Cashdollar, K. L., Hertzberg, M., and Zlochower, I. A., Effect of Volatility on Dust Flammability Limits for Coals, Gilsonite, and Polyethylene, pp. 1757-1765 in *22nd Symp. (Intl.) on Combustion*, The Combustion Institute, Pittsburgh (1988).
31. Shevchuk, V. G., Kondratiev, E. N., Zolotko, A. N., and Goroshin, S. V., Effect of the Structure of a Gas Suspension on the Process of Flame Propagation, *Combustion, Explosion, and Shock Waves* **15**, 723-727 (1980).
32. Hertzberg, M., Cashdollar, K. L., Ng, D. L., and Conti, R. S., Domains of Flammability and Thermal Ignitability for Pulverized Coals and Other Dusts: Particle Size Dependences and Microscopic Residue Analysis, pp. 1169-1180 in *19th Symp. (Intl.) on Combustion*, The Combustion Institute, Pittsburgh (1982).
33. Deguingand, B., and Galant, S., Upper Flammability Limits of Coal Dust-Air Mixtures, pp. 705-715 in *18th Symp. (Intl.) on Combustion*, The Combustion Institute, Pittsburgh (1980).
34. Conti, R. S., Cashdollar, K. L., Hertzberg, M., and Liebman, I., Thermal and Electrical Ignitability of Dust Clouds (RI 8798), Bureau of Mines, Pittsburgh (1983).
35. Schuber, G., Ignition Breakthrough Behavior of Dust/air and Hybrid Mixtures through Narrow Gaps, pp. 14-1 to 14-15 in *Proc. 6th Intl. Symp. on Loss Prevention and Safety Promo-*

tion in the Process Industries, Norwegian Society of Chartered Engineers, Oslo (1989).
36. Leuschke, G., The Mechanism of Ignition Propagation in Dust Clouds, *Staub (English ed.)* **25**, 7-16 (1965).
37. Klemens, R., and Wojcicki, S., A Model for Coal Dust-Air Mixture Ignition by Means of An Electric Spark, paper presented at the 1983 Fall Meeting, Western States Section, The Combustion Institute (1983).
38. Smirnov, N. N., Nikitin, V. F., and Legros, J. C., Ignition and Combustion of Turbulized Dust-Air Mixtures, *Combustion and Flame* **123**, 46-67 (2000).
39. Zielinski, E., The Evolution of Volatile Matter from Pulverized Coal Particles, *Fuel* **46**, 329-340 (1967).
40. Hertzberg, M., Zlochower, I. A., and Edwards, J. C., Coal Particle Pyrolysis Mechanisms and Temperatures (RI 9169), Bureau of Mines, Pittsburgh (1988).
41. Litton, C. D., and Chaiken, R. F., The Role of Radiation Absorption in Defining Explosibility of Coal/Rock Dust Mixtures, pp. 1571-1577 in *26th Symp. (Intl.) on Combustion*, The Combustion Institute, Pittsburgh (1996).
42. Litton, C. D., private communication (2001).
43. Hertzberg, M., Zlochower, I. A., and Cashdollar, K. L., Metal Dust Combustion: Explosion Limits, Pressures, and Temperatures, pp. 1827-1835 in *24th Symp. (Intl.) on Combustion*, Combustion Institute, Pittsburgh (1992).
44. Yuasa, S., and Takeno, T., Ignition and Combustion of Magnesium-Aluminum Alloy Particle Clouds in a Hot Gas Stream, pp. 741-748 in *19th Symp. (Intl.) on Combustion*, The Combustion Institute, Pittsburgh (1982).
45. Nomura, S.-I., Torimoto, M., and Tanaka, T., Theoretical Upper Limit of Dust Explosions in Relation to Oxygen Concentration, *Ind. and Eng. Chem.—Process. Des. Dev.* **23**, 420-423 (1984).
46. Ballal, D. R., Further Studies on the Ignition and Flame Quenching of Quiescent Dust Clouds, *Proc. Royal Soc. London* **A385**, 1-19 (1983).
47. Spalding, D. B., **Some Fundamentals of Combustion**, Butterworths, London (1955).
48. Mittal, M., and Guha, B. K., Minimum Ignition Temperature of Polyethylene Dust: A Theoretical Model, *Fire and Materials* **21**, 169-177 (1997).
49. Cashdollar, K. L., Sapko, M. J., Weiss, E. S., and Hertzberg, M., Laboratory and Mine Dust Explosion Research at the Bureau of Mines, pp. 107-123 in **Industrial Dust Explosions** (ASTM STP 958), ASTM (1987).
50. Foniok, R., Hybrid Dispersive Mixtures and Inertized Mixtures of Coal Dust: Explosiveness and Ignitability, *Staub-Reinhaltung der Luft* **45**, 151-154 (1985).
51. Pellmont, G., Explosions- und Zündverhalten von hybriden Gemischen aus brennbaren Stäuben und Brenngasen [Explosion and Ignition Behavior of Hybrid Mixtures of Combustible Dusts and Combustible Gases] (dissertation), Eidgenössischen technischen Hochschule, Zürich, Switzerland (1979).
52. Britton, L. G., Estimating the Minimum Ignition Energy of Hybrid Mixtures, *Process Safety Progress* **17**, 124-126 (1998).
53. Pedersen, G. H., and Eckhoff, R. K., Initiation of Grain Dust Explosions by Heat Generated during Single Impact between Solid Bodies, *Fire Safety J.* **12**, 153-164 (1987).
54. Baker, W. E., and Tang, M. J., **Gas, Dust and Hybrid Explosions**, Elsevier, Amsterdam (1991).
55. Blacktin, S. C., Self-promoted Dust Explosions, *Chemical Age (London)* **47**, 53-57 (1942).
56. Morse, A. R., Ignition of Grain-dust Clouds by Electric Light Bulbs and Motors (NRC No. 4411, ERB-430), National Research Council of Canada, Ottawa (1956).
57. Zeeuwen, J. P., Review of Current Research at TNO into Gas and Dust Explosions, pp. 687-702 in **Fuel-Air Explosions**, J. H. S. Lee and C. M. Guirao, eds., University of Waterloo Press, Waterloo, Canada (1982).
58. Gibson, N., and Schofield, F., Fire and Explosion Hazards in Spray Dryers, pp. 57-66 in *Proc. 6th Intl. Symp. on Chemical Process Hazards with Special Reference to Plant Design* (Symp. Series No. 49), The Institution of Chemical Engineers, Rugby (1977).
59. Gibson, N., and Rogers, R. L., Ignition and Combustion of Dust Clouds in Hot Environments—An Exploratory Study, pp. 209-217 in *7th Intl. Symp. on Chemical Process Hazards with Special Reference to Plant Design* (IChemE Symp. Series No. 58), The Institution of Chemical Engineers, London (1980).
60. Singer, J. M., Ignition of Mixtures of Coal Dust, Methane, and Air by Hot Laminar Nitrogen Jets, pp. 407-414 in *9th Symp. (Intl.) on Combustion*, The Combustion Institute, Pittsburgh (1962).
61. Andrews, S. P., Jet Ignition of Dust Clouds (IR/L/EC/98/01/IS), HSE, Buxton, UK (1998).
62. Taniguchi, M., Kobayashi, H., and Azuhata, S., Laser Ignition and Flame Propagation of Pulverized Coal Dust Clouds, pp. 3189-3195 in *26th Symp. (Intl.) on Combustion*, The Combustion Institute, Pittsburgh (1996).
63. Conti, R. S., and Hertzberg, M., Thermal Autoignition Temperatures from the 1.2-L Furnace and Their Use in Evaluating the Explosion Potential of Dusts, pp. 45-59 in **Industrial Dust Explosions** (ASTM STP 958), ASTM (1987).
64. Wheeler, R. V., The Volatile Constituents of Coal. Part IV. The Relative Inflammabilities of Coal Dusts, *J. Chemical Soc.* **103**, 1715-1722 (1913).
65. Hartmann, I., Cooper, A. R., and Jacobson, M., Recent Studies of the Explosibility of Cornstarch (RI 4725), Bureau of Mines, Pittsburgh (1950).
66. Nomura, S., and Callcott, T. G., Calculations of the Ignition Sensitivity of Dust Clouds of Varying Size Distributions, *Powder Technology* **45**, 145-154 (1986).
67. Mitsui, R., and Tanaka, T., Simple Models of Dust Explosion. Predicting Ignition Temperature and Minimum Explosive Limit in Terms of Particle Size, *Ind. and Eng. Chem.—Process. Des. Dev.* **12**, 384-389 (1973).
68. Nagy, J., and Verakis, H. C., **Development and Control of Dust Explosions**, Marcel Dekker, New York (1983).
69. Griesche, G., and Brandt, D., Einflussfaktoren auf die Zündtemperatur von Staub-Luft-Gemischen [Factors governing the piloted-ignition temperature of dust/air mixtures], *Die Technik* (Berlin) **31**, 504-507 (1976).
70. Siwek, R., and Cesana, C., Ignition Behavior of Dusts: Meaning and Interpretation, *Process Safety Progress* **14**, 107-119 (1995).
71. Napier, D. H., and Roopchand, D. R., Ignition Probability of Hybrid Mixtures, pp. 310-323 in **Industrial Dust Explosions** (ASTM STP 958), ASTM (1987).
72. Hanai, H., Ueki, M., Maruta, K., Kobayashi, H, Hasegawa, S., and Niioka, T., A Lean Flammability Limit of Polymethylmethacrylate Particle-Cloud in Microgravity, *Combustion and Flame* **118**, 359-369 (1999).

73. Hertzberg, M., and Zlochower, I. A., Devolatilization Rates and Interparticle Wave Structures during the Combustion of Pulverized Coals and Polymethylmethacrylate, pp. 1247-1255 in *23rd Symp. (Intl.) on Combustion*, Combustion Institute, Pittsburgh (1990).
74. Parnell, C. B., jr., et al., Grain Dust Explosion Hazard (DEC-84-079), National Grain and Feed Assn., Washington (1979).
75. Xu, B.-W., Zheng, H.-J., and Xu, W.-Q., The Effect of Particle Size of Fibre Dust LEL, pp. 237-246 in *Proc. 5th Intl. Colloquium on Dust Explosions*, Pultusk near Warsaw (1994).
76. Manual for Classification of Gases, Vapors, and Dusts for Electrical Equipment in Hazardous (Classified) Locations (NFPA 497M), NFPA.
77. Glarner, T., Temperatureinfluss auf das Explosions- und Zündverhalten brennbarer Stäuben [Explosion and Ignition Behavior of Combustible Dusts] (dissertation), Eidgenössischen technischen Hochschule, Zürich, Switzerland (1983).
78. Hertzberg, M., and Cashdollar, K. L., Introduction to Dust Explosions, pp. 5-32 in **Industrial Dust Explosions** (ASTM STP 958), ASTM (1987).
79. Wiemann, W., Influence of Temperature and Pressure on the Explosion Characteristics of Dust/Air and Dust/Air/Inert Gas Mixtures, pp. 33-44 in **Industrial Dust Explosions** (ASTM STP 958), ASTM (1987).
80. Bartknecht, W., **Dust Explosions: Course, Prevention, Protection**, Springer-Verlag, Berlin (1989).
81. Eckhoff, R. K., Pressure Development during Explosions in Clouds of Dusts from Grain, Feedstuffs and other Natural Organic Materials, *Fire Research* **1**, 71-85 (1977/78).
82. Monakhov, V. T., **Metody issledovaniya pozharnoi ospasnosti veshchestv**, Khimya, Moscow (1972). English translation: **Methods for Studying the Flammability of Substances**, published for U.S. National Bureau of Standards by Amerind Publishing Co., New Delhi, India (1985).
83. Jones, E., and White, A. G., Gas Explosions and Dust Explosions—A Comparison, pp. 129-139 in *Dust in Industry*, Society of Chemical Industry, Leeds, England (1948).
84. Mok, Y.-S., Lee, D.-H., Choi, J.-W., and Lim, W.-S., The Effect of Humidity in Dust Explosion and the Autoignition Characteristics of MBS Copolymer, pp. 11-14 in *APSS2001—Proc. Asia Pacific Symp. on Safety*, Vol. 1, Japan Soc. for Safety Engineering, Yokohama (2001).
85. Hertzberg, M., Cashdollar, K. L., and Lazzara, C. P., The Limits of Flammability of Pulverized Coals and Other Dusts, pp. 717-729 in *18th Symp. (Intl.) on Combustion*, Combustion Institute, Pittsburgh (1980).
86. Matsuda, T., and Itagaki, H., Effects of Ignition Energy on Dust Explosion Parameters, pp. 245-256 in *Proc. 6th Intl. Colloquium on Dust Explosions*, Northeastern Univ. Press, Shenyang, China (1994).
87. Gibson, N., Maddison, N., Rounsley, J. S., and Stokes, P. S. N., Assessment of Dust Explosion Hazards: Effects of Changes in the Test Methods and Criteria, pp. 63-76 in *Hazards in the Process Industries: Hazards IX* (IChemE Symp. Series No. 97), The Institution of Chemical Engineers, Rugby, England (1986).
88. Maranda, A., et al., Some Aspects of Fire and Explosion Hazards in Comminution of Flaked Aluminum Powders, *Archivum Combustionis* **6**, 39-49 (1986).
89. Hartmann, I., and Nagy, J., Inflammability and Explosibility of Powders used in the Plastics Industry (RI 3751), Bureau of Mines, Pittsburgh (1944).
90. Geysen, W. J., Belmans, R., and Scheys, L., A Sugar Dust Explosion and some Measures to Limit Its Consequences, pp. 234-242 in **Industrial Dust Explosions** (ASTM STP 958), ASTM (1987).
91. Kalkert, N., and Schecker, H.-G., Theoretische Überlegungen zum Einfluss der Teilchengrösse auf die Mindestzündenergie von Stäuben, *Chemie-Ingenieur-Technik* **51**, 1248-1249 (1979)
92. Dirkzwager, L., The Effect of Cornstarch Moisture Content on Explosion Ignition Energy Requirements, pp. 171-181 in *Proc. Intl. Symp. on Grain Dust Explosions*, Grain Elevator and Processing Society, Minneapolis (1977).
93. Chiotti, P., An Overview of Grain Dust Explosion Problems, pp. 13-36 in *Proc. Intl. Symp. on Grain Dust Explosions*, Grain Elevator and Processing Society, Minneapolis (1977).
94. Eckhoff, R. K., Understanding Dust Explosions. The Role of Powder Science and Technology, *Kona Powder and Particle* No. 15, 54-67 (1997).
95. Choi, K. S., et al., Ignitability of Powder Paints in Electrostatic Powder Coating System, pp. 297-300 in *APSS2001—Proc. Asia Pacific Symp. on Safety*, Vol. 1, Japan Soc. for Safety Engineering, Yokohama (2001).
96. Ballal, D. R., Ignition and Flame Quenching of Quiescent Dust Clouds of Solid Fuels, *Proc. Royal Soc. London* **A369**, 479-500 (1980).
97. Matsuda, T., and Naito, M., Effects of Spark Discharge Duration on Ignition Energy for Dust/Air Suspensions, pp. 189-198 in **Particulate Systems—Technology and Fundamentals**, J. K. Beddow, ed., Hemisphere, Washington (1983).
98. Boyle, A. R., and Llewellyn, F. J., The Electrostatic Ignitability of Dust Clouds and Powders, *J. Soc. Chemical Industry* **69**, 173-181 (1950).
99. Line, L. E., Rhodes, H. A., and Gilmer, T. E., The Spark Ignition of Dust Clouds, *J. Phys. Chem.* **63**, 290-294 (1959).
100. Hay, D. M., and Napier, D. H., Minimum Ignition Energy of Dust Suspensions, pp. 73-78 in *Chemical Process Hazards in Plant Design IV (IChemE Symp. Series No. 49)*, Institution of Chemical Engineers, Rugby, England (1977).
101. Hertzberg, M. Conti, R. S., and Cashdollar, K. L., Spark Ignition Energies for Dust-Air Mixtures: Temperature and Concentration Dependences, pp. 1681-1690 in *20th Symp. (Intl.) on Combustion*, Combustion Institute, Pittsburgh (1984).
102. Hertzberg, M., Conti, R. S., and Cashdollar, K. L., Electrical Ignition Energies and Thermal Autoignition Temperatures for Evaluating Explosion Hazards of Dusts (RI 8988), Bureau of Mines, Pittsburgh (1985).
103. Nifuku, M., and Katoh, H., Incendiary Characteristics of Electrostatic Discharge for Dust and Gas Explosion, pp. 240-245 in *Proc. 3rd Intl. Symp. on Hazards, Prevention, and Mitigation of Industrial Explosions*, Tsukuba, Japan (2000).
104. Eckhoff, R. K., Towards Absolute Minimum Ignition Energies for Dust Clouds? *Combustion and Flame* **24**, 53-64 (1975).
105. Eckhoff, R. K., and Enstad, G., Why Are "Long" Electric Sparks More Effective Dust Explosion Initiators Than "Short" Ones? *Combustion and Flame* **27**, 129-131 (1976).

106. Alvestad, B., An Electric Spark Generator for Determination of Minimum Ignition Energies of Dust Clouds (CMI Report No. 803301-3), Christian Michelsen Institute, Fantoft, Norway (1980).
107. Field, P., **Dust Explosions**, Elsevier, Amsterdam (1982).
108. Wynne-Williams, C. E., An Investigation into the Theory of the "Three-Point Gap," *Phil. Mag.* Series 7, **1**, 353-378 (1926).
109. Zeeuwen, J. P., and van Laar, G. F. M., Ignition Sensitivity of Flammable Dust-Air Mixtures, pp. 61-73 in Maitrise des risques la manutention et le stockage des pulvérulents alimentaires/Control and the Risks in Handling and Storage of Granular Foods, Association pour la Promotion Industrie Agriculture, Paris (1985).
110. Lüttgens, G., and Glor, M., **Understanding and Controlling Static Electricity**, Expert Verlag, Ehningen (1989).
111. Pidoll, U. v., The Ignition of Clouds of Sprays, Powders and Fibers by Flames and Electric Sparks, *J. Loss Prevention in the Process Industries* **14**, 103-109 (2001).
112. Britton, L. B., Using Material Data in Static Hazard Assessment, *Plant/Operations Progress* **11**, 56-70 (1992).
113. Bailey, M., Hooker, P., Caine, P., and Gibson, N., Incendivity of Electrostatic Discharges in Dust Clouds: The Minimum Ignition Energy Problem, pp. 233-237 in *Electrostatics 1999* (Conf. Series No. 163), Institute of Physics Publishing, Bristol, England (1999).
114. Glor, M., Hazards Due to Electrostatic Charging of Powders, *J. Electrostatics* **16**, 175-191 (1985).
115. Smallwood, J. M., Dust Cloud Ignition by Electrostatic Discharges and the Mythology of Minimum Ignition Energy—Do We Know Enough? pp. 221-224 in *Electrostatics 1999* (Conf. Series No. 163), Institute of Physics Publishing, Bristol, England (1999).
116. Code of Practice for the Control of Undesirable Static Electricity (BS 5958). Part 1: General Considerations. British Standards Institution, London.
117. Krause, U., Weinert, D., and Wöhrn, P., Diagrams for the Determination of the Limiting Oxygen Concentration of Dust/Air Mixtures, pp. 257-266 in *Proc. 5th Intl. Colloquium on Dust Explosions*, P. Wolański, ed., Oficyna Wydawnicza Politechniki Warszawskiej, Warsaw (1993).
118. Wiemann, W., Einfluss der Temperatur auf die Sauerstoff-Grenzkonzentration bei der Inertisierung [Influence of Temperature on the Minimum Oxygen Concentration for Inerting], pp. 467-488 in *Report of the 9th Intl. Symp. on Prevention of Occupational Accidents and Diseases in the Chemical Industry*, Intl. Social Security Assn., Lucerne (1984).
119. Sweis, F. K., and Sinclair, C. G., The Effect of Particle Size on the Maximum Permissible Oxygen Concentration to Prevent Dust Explosions, *J. Hazardous Materials* **10**, 59-71 (1985).
120. Palmer, K. N., and Tonkin, P. S., Use of Inert Gas to Prevent Dust Explosions, **Combustion Institute European Symposium 1973**, Academic Press, London (1973).
121. Brown, K. C., and Woodhead, D. W., Dust Explosions in Factories: Closed-Circuit Test Apparatus (SMRE Report 86), Safety in Mines Research Establishment, Sheffield, England (1953).
122. Essenhigh, R. H., Mahendra, K. M., and Shaw, D. W., Ignition of Coal Particles: A Review, *Combustion and Flame* **77**, 3-30 (1989).
123. Standard Test Method for Minimum Autoignition Temperature of Dust Clouds (ASTM E 1491), ASTM.
124. Standard Test Method for Minimum Ignition Energy of a Dust Cloud in Air (ASTM E 2019), ASTM.
125. Godbert, A. L., and Greenwald, H. P., Laboratory Studies of the Inflammability of Coal Dusts: Effect of Fineness of Coal and Inert Dusts on the Inflammability of Coal Dusts (Bulletin 389), Bureau of Mines, Washington (1935).
126. Conti, R. S., Cashdollar, K. L., and Thomas, R. A., Improved 6.8 L Furnace for Measuring the Autoignition Temperatures of Dust Clouds (RI 9467), Bureau of Mines, Pittsburgh (1993).
127. Leuschke, G., and Osswald, R., Bedeutung und Ermittlung von sicherheitstechnischen Kengrössen brennbarer Stäube, *VDI-Berichte* **304**, 29-38 (1978).
128. Dorsett, H. G., et al., Laboratory Equipment and Test Procedures for Evaluating Explosibility of Dusts (RI 5624), Bureau of Mines, Pittsburgh (1960).
129. Standard Test Method for Dust Explosions in a 1.2-Litre Closed Cylindrical Vessel (ASTM E 789), ASTM.
130. Lütolf, J., Kurzmethoden zur Prüfung brennbarer Stäube, *VDI-Berichte* **304**, 39-46 (1978).
131. Lunn, G. A., A Note on the Lower Explosibility Limit of Organic Dusts, *J. Hazardous Materials* **17**, 207-213 (1988).
132. Allen, J., and Calcote, H. F., Grain Dust Ignition by Friction Sparks—A Preliminary Investigation, National Grain and Feed Assn., Washington (1981).
133. Eckhoff, R. K., Dust Explosion Hazards in the Ferro-Alloys Industry, *Proc. 52nd Electric Furnace Conf.* (1994).
134. Standard Test Method for Minimum Explosible Concentration of Combustible Dusts (ASTM E 1515), ASTM.
135. Cashdollar, K. L., and Hertzberg, M., 20-L Explosibility Test Chamber for Dusts and Gases, *Rev. Sci. Instruments* **56**, 596-602 (1985).
136. Going, J. E., Chatrathi, K., and Cashdollar, K. L., Flammability Measurements for Dusts in 20-L and 1-m^3 Vessels, *J. Loss Prevention in the Process Industries* **13**, 209-219 (2000).
137. Sapko, M. J., Weiss, E. S., Cashdollar, K. L., and Zlochower, I. A., Experimental Mine and Laboratory Dust Explosion Research at NIOSH, *J. Loss Prevention in the Process Industries* **13**, 229-242 (2000).
138. Siwek, R., Development of a 20 Liter Laboratory Apparatus and Its Application for the Investigation of Combustible Dusts, Ciba-Geigy Ltd., Basle, Switzerland (1985).
139. Billinge, K., Frictional Ignition Hazard in Industry: A Survey of Reported Incidents From 1958 to 1978, *Fire Prevention Science and Technology*, No. 24, 13-19 (1981).
140. Standard Test Method for Pressure and Rate of Pressure Rise for Combustible Dusts (ASTM E 1226), ASTM.
141. Dust Clouds: Minimum Explosible Dust Concentration (Nordtest NT Fire 011), Nordtest, Espoo, Finland (1989).
142. Druckentlastung von Staubexplosionen [Pressure Venting of Dust Explosions], VDI 3673, Verein Deutscher Ingenieure, Düsseldorf, Germany (1995).
143. Explosion Protection Systems. Part 1. Determination of Explosion Indices of Combustible Dusts in Air (ISO 6184-1), International Organization for Standardization, Geneva (1985).
144. Cashdollar, K. L., and Chatrathi, K., Minimum Explosible Dust Concentrations Measured in 20-L and 1-m^3 Chambers, *Combustion Science and Technology* **87**, 157-171 (1993).

145. Standard Test Method for Temperature Limit of Flammability of Chemicals (ASTM E 1232), ASTM.
146. Electrical Apparatus for Use in the Presence of Combustible Dust - Part 2: Test Methods - Section 3: Method for Determining Minimum Ignition Energy of Dust/Air Mixtures (IEC 61241-2-3), International Electrotechnical Commission, Geneva.

Copyright © 2003, 2014 Vytenis Babrauskas

Chapter 6. Ignition of liquids

Highlights and summary of practical guidance **183**
Accidental ignitions of liquids **184**
Properties of liquids **184**
Autoignition of liquids **186**
Ignition of single drops *187*
Liquid aerosols or sprays *190*
Flash point and fire point **192**
Flash point *192*
Upper flash point *193*
The fire point *193*
The pre-flash 'halo' *194*
The distribution of fuel vapors above the surface *194*
Estimations of flash point *196*
Flash points of mixtures *198*
Ideal mixtures 199
Non-ideal mixtures 199
Mixtures with halogenated components 200
Flash points of petroleum distillates 202
Relation between flash point and MIE *202*
Piloted ignition of liquids **202**
Spark ignition of liquid aerosols or sprays *202*
Minimum ignition energy 203
High flash-point liquids 205
Limits of flammability for liquid aerosols 206
MESG of liquid aerosols *207*
Hot surface ignition of droplets, sprays or spills *207*
Single droplets of a pure fuel 207
Hot engine surfaces and related problems 209
Pools *213*
Pools at or above their flash point 213
Pools below their flash point 215
Ignition of fuel in closed vessels **215**
Effect of vapor/liquid volume ratio *216*
Effect of slosh *217*
Radiant ignition of liquids **217**
Thick layers *217*
Thin layers *218*
Ignition of liquids by other means **219**
Tests for ignition properties of liquids **219**
Autoignition temperature *219*
Early test methods 219
ASTM D 286 221

ASTM D 2155 222
ASTM E 659 222
Other Bureau of Mines tests 223
Flash point 223
ASTM D 56 224
ASTM D 92 225
ASTM D 93 225
ASTM D 1310 225
ASTM D 3278 225
ASTM D 3828 226
ASTM D 3934 226
ASTM D 3941 226
Abel flash point test 226
Tests for other properties 226
ASTM D 4206 test for sustained burning 226
Hydraulic fluid sprays 226
Further readings 227
References 227

Highlights and summary of practical guidance

With the exception of certain unstable or reactive substances, liquids do not literally ignite. When ignition of liquids is discussed, this normally refers to vapors which have come from some body of liquid and ignited upon mixing with the atmosphere. If there is a liquid surface exposed to air, at any temperature above absolute zero the liquid exhibits a vapor pressure: it undergoes vaporization. The vaporization is highly temperature-sensitive and also depends on the chemical nature of the liquid. Then, if high temperatures or a localized energy source are present in the air volume into which the vapors have mixed, ignition may occur. Thus, many aspects of ignition of liquids, such as flammability limits or minimum ignition energy are identical to those for gases, and these have been presented in Chapter 4. The reader wishing to study the ignition of liquids is advised to first review Chapter 4. In this chapter, those aspects of the ignition of liquids will be treated that are unique for liquids. The main topics covered in this Chapter are:

- autoignition temperature
- flash point
- fire point
- ignition by hot surfaces
- ignition of droplets, aerosols, and sprays.

In many cases, the temperature limits of flammability are also important. To present together all of the material related to flammability limits, these have been covered in Chapter 4, even though they involve a phenomenon intrinsically dependent on a liquid phase.

Liquids are substances whose vapor pressure at a reference temperature, commonly 25ºC (298 K), is less than 1 atm. However, this does not mean that a substance defined as a liquid cannot be present as a gas, nor that a substance defined as a gas will not be encountered as a liquid. The actual state of a substance—gas or liquid—is dependent on both its pressure and its temperature. Propane is defined as a gas, even though it is commonly sold in liquid form. At 25ºC, its vapor pressure is greater than 1 atm (it is actually 9.5 atm), but if it is compressed it liquefies. NFPA has definitions of flammable and combustible liquids. The 'liquid' portion of these definitions is not identical to the normal chemistry definition (see Chapter 2).

The flash point is the temperature at which a liquid must be raised in order to produce sufficient vapors for flash-ignition and it can be measured by one of many standardized test apparatuses. These devices can either be open-cup or closed-cup arrangements. In North America, ever since 1977 closed-cup testers have been mandated for official purposes. The flash point determined in a closed-cup apparatus is normally somewhat lower than in an open-cup apparatus, but the exact difference varies somewhat with the nature of the substance. Strong regulatory focus is placed on the flash point due to an implicit assumption that ignition of liquids will not readily occur if the flash point of the liquid is above that of its environment. This assumption is only approximate, for three reasons: (1) the flash point as determined by a specific test apparatus is not necessarily

the flash point of the liquid in its end-use environment. (2) Liquids with flash point temperatures greater than the temperature of the liquid or of the environment can sometimes be ignited by wicking, spraying, or other means. (3) Liquids that are mixtures, rather than pure substances, may show a tendency for preferential vaporization and loss of one component, and this process will be different in the real environment compared to the tester.

Flash points can be estimated very roughly by means of a variety of estimating formulas, but such estimates must only be used for preliminary guidance, not for actual quantitative determination.

The vapor above a liquid will establish an equilibrium pressure only in a closed space. For a vessel that is open to the atmosphere, there is a continuous loss of liquid through evaporation. In such a case, also, there is concentration gradient above the liquid—as the height above the surface gets greater, the concentration gets lower. Thus, if an ignition source is brought near an open vessel of a flammable liquid, ignition will not be possible except at certain heights. For large heights, the concentration of the mixture will be below the LFL. Then, approaching the surface there will be a region where ignition is possible (it is assumed here that the vapor pressure of the substance is high enough at the ambient temperature). Finally, as an ignition source is brought yet closer to the surface, ignition will no longer be possible again. The above discussion presumed that the atmosphere is quiescent. If the vessel sits in a place where there is significant motion of air, then concentration gradients may be largely eliminated.

Vehicular gasoline tanks are normally capable of exploding only when welding is attempted on an 'empty' tank. If the tank contains any amount of liquid fuel, the vapor inside the tank is above its UFL, except in extremely cold climates. In a crash, an explosion becomes possible if the tank gets broken apart, and the liquid runs away or enough air mixes in so as to lower the vapor concentration below the UFL.

There is no relation between flash point and AIT. The AIT is primarily determined by a fuel's reactivity (its rate of oxidation) while the flash point is primarily determined by its volatility. Thus, for example, methane shows one of the highest AIT values, 640ºC, and one of the lowest flash point values, –188ºC. Methane is so volatile that, at ambient pressure, it is a gas and not a liquid; but it is of exceptionally low chemical reactivity. Flash point and boiling point, on the other hand, are highly correlated since both are governed largely by the same phenomenon—volatility.

Hot-surface ignition is affected both by the chemical reactivity and the volatility of the fuel. If the hot surfaces create an enclosed volume, then ignition will take place at approximately the AIT. But this condition is relatively rare and assuming that the hot-surface ignition temperature is 200ºC above the AIT generally provides a more realistic estimate.

Finally, it must be kept in mind that there are some liquids used for industrial purposes that can ignite and explode directly as a liquid, without first vaporizing and mixing with air. These are highly specialized and are treated with other unstable substances in Chapter 10.

Accidental ignitions of liquids

A 1975 study[1] examined the fuel involved in ignitable liquid accidents; the results are given in Table 1. It is seen that gasoline outranks all others by a very wide margin. The primary activities associated with the ignitions are listed in Table 2.

Table 1 Consumer injuries from ignitions of liquids

Substance	Percent
gasoline	68.4
lighter fluid	5.3
cooking grease	4.4
alcohol	4.0
adhesives	1.9
paint thinner	1.9
solvents	1.9
kerosene	1.6
fuel	1.2
oils	1.2
charcoal/starter fluid	0.7
cleaning fluid	0.7
cooking oil	0.7
paint	0.7
turpentine	0.7
mix of chemicals	0.6
paraffin and candle wax	0.6
other or unspecified	3.1

Properties of liquids

Liquids are not unique substances, but simply a *state* of matter. In the case of simple, low molecular-weight substances, at low temperatures the substance will be a solid, then a liquid at higher temperatures, and finally a gas at higher temperatures yet. Many practical substances, however, degrade, that is, change chemically, as they are heated, instead of just changing their state. For example, at a pressure of 1 atm, methyl alcohol is a solid below –98°C, then a liquid up to 65°C, and then a vapor only. But wood is a solid at room temperature which, when heated, breaks down into smaller molecules which are liquids or gases. Wood itself does not become a liquid or a gas. A map delineating the states of matter that are possible for a given substance is called a *phase diagram* and these are published in chemical handbooks. In Chapter 4, the principles and applications of gas and vapor ignitions was presented. Thus, in this Chapter only issues directly connected with the liquid state will be discussed.

Table 2 The activities associated with injuries due to accidental ignition of liquids

Activity associated with ignition	Percent
starting/tending open fire	20.1
playing with flammable liquid and an ignition source	10.8
spilling flammable liquid	9.9
using flammable liquid as cleaning agent	6.7
knocking over/dropping flammable liquid	6.6
cleaning/repairing equipment	5.7
priming carburetor	4.8
using matches or lighter	4.4
transporting flammable liquid	3.8
using machinery/equipment	3.2
using work tools	3.1
riding/driving vehicle	2.5
using flammable liquid as adhesive	2.2
other	2.2
refueling equipment	1.8
playing with matches or lighter	1.6
playing with flammable liquid	1.6
standing by an open fire	1.5
standing near flammable liquid	1.5
transferring flammable liquid	1.5
using flammable liquid as exterminating agent	1.5
disturbing open fire	0.9
unknown	0.9
using flammable liquid to ignite heat source	0.7
assault/suicide	0.7

The unique aspect of liquids which affects their ignition is the vapor pressure. At room temperature, solids, except for subliming solids such as naphthalene, have exceedingly low vapor pressures. Thus, solids typically ignite due to pyrolysis, i.e., a reaction which is a chemical degradation and which results in a vapor being generated. Liquids, however, do not need to degrade (although some do) in order to exhibit a substantial vapor pressure. The vapor pressure is a unique function of temperature. The simplest dependence of vapor pressure on temperature is the Clapeyron equation:

$$\ln P_{vp} = A - \frac{B}{T}$$

where P_{vp} = vapor pressure (atm), T = temperature (K), and A and B are constants specific to each particular gas. Most substances are sufficiently non-ideal that the Clapeyron equation is not an accurate representation of vapor pressure. A variant of it, termed the Antoine equation, however, often suffices to represent the data:

$$\ln P_{vp} = A - \frac{B}{T + C}$$

where there are now three constants to be tabulated for each substance: A, B and C. A number of real gases can be satisfactorily represented with the Antoine equation. Not all reference sources are uniform, and data in a number of them use the form $\log_{10}(P_{vp})$, instead of $\ln(P_{vp})$. For many substances, however, more complicated expressions are needed to accurately represent the vapor pressure than is possible using a 3-constant scheme. The book by Reid et al.[2,3] provides a large collection* of these.

Figure 1 shows some typical vapor pressures, as function of temperature. Figure 2 illustrates that by plotting the pressures as a function of 1/T and using a semilogarithmic scale, plots for many liquids will provide very close to straight lines[3,4]. Straight lines in this plot are equations of the form of the Clapeyron equation. Thus, unless results of the highest accuracy are needed, the simple Clapeyron equation will usually suffice.

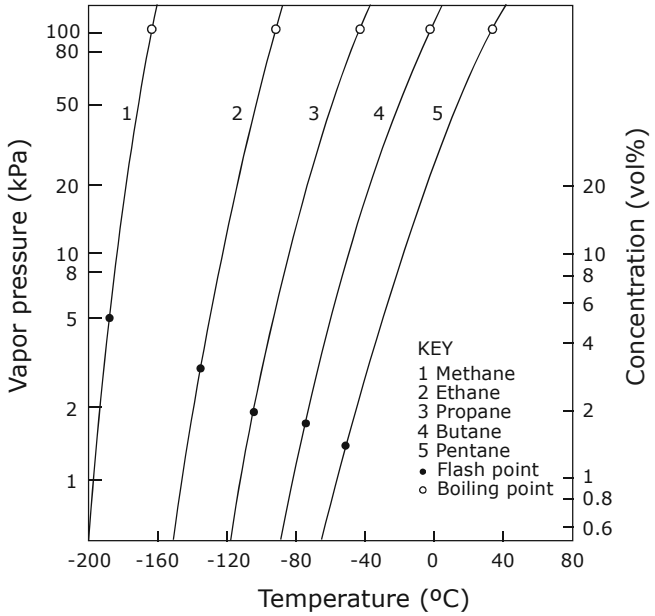


Figure 1 The vapor pressures of some *n*-paraffin series hydrocarbons[5]

For pure hydrocarbons (that is, molecules with only C and H atoms), Butler et al.[6] suggested a universal expression that is suitable for preliminary estimating purposes:

$$\ln P_{vp} = 10.6\left(1 - T_b / T\right)$$

where P_{vp} = vapor pressure (atm), and T_b = boiling point (K).

If a closed volume contains a reservoir of a liquid, the system is not in motion, and the liquid surface is flat, then there can only be a single unique pressure of the vapor above the liquid. This pressure is determined by the temperature of the system. For example, cyclopentene (C_5H_8) obeys the relation:

$$\ln P_{vp} = 9.3154 - \frac{2583.07}{T - 39.70}$$

* The third edition of Reid's book gives simple Antoine-form expressions for many compounds for which the fourth edition only provides more complex expressions. When using the third edition formulas, note that the values of pressure are mm Hg. To convert to atmospheres, subtract 6.6333 from the Antoine constant A.

At a temperature T = 298, ln P_{vp} = –0.687, giving P_{vp} = 0.503 atm. If a tray of this liquid is placed in a closed volume and the amount of liquid is sufficient for there to remain a liquid phase, enough liquid will evaporate so that a vapor pressure of 0.503 atm will be established. Since partial pressures and mole fractions are equal in a gas mixture, this also means that the mole fraction of cyclopentene in the vapor space will be 0.503, and that its concentration will be 50.3 vol%. The equilibrium pressure is referred to as *saturated vapor pressure*. The only way that an equilibrium with smaller concentration of the cyclopentene can be established is by putting in so small an amount of liquid that all of the liquid will evaporate and not enough will be present to establish a liquid/vapor equilibrium. The only way that a larger amount of cyclopentene could be introduced would be by atomizing and spraying the liquid into the air. However, while higher amounts can be introduced in this manner, they are in the form of an aerosol and not a vapor. If time is allowed for equilibration after such a spraying has occurred, the excess amount will rain out into the reservoir of liquid at the bottom of the container.

The *boiling point*, T_b, of a pure liquid, by definition, is the temperature at which its vapor pressure is equal to the ambient pressure. The ambient pressure of interest is generally 1 atm. A liquid which is the mixture of several components does not have a unique boiling point. Instead, as temperature is raised, the lower-boiling-point fractions start boiling off first, with the higher-boiling-point fractions following later. This principle is utilized in the process of fractional distillation, where several relatively-pure substances can be recovered from a mixture.

Normal flammable or combustible liquids are not capable of ignition *as a liquid*. A high-temperature oxidation reaction (combustion) can occur only with the vapors of such liquids, not the liquids themselves. In other words, evaporation must occur first, only then followed by combustion. This process is intrinsically more complicated than the ignition of gases, where no change of state of the substance needs to be considered. While the knowledge that the vapors of flammable liquids burn, rather than the liquids themselves, is now very basic, it was not until 1931 that this fact was conclusively demonstrated.

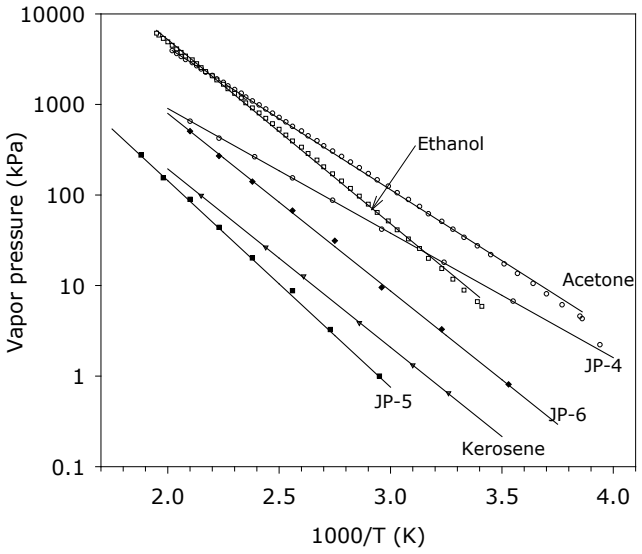


Figure 2 Vapor pressures represented according to the Clapeyron equation

Autoignition of liquids

In the ignition of gases, autoignition is very simple to understand conceptually. A fuel/oxidant mixture is not exposed to any localized energy sources. The temperature of the mixture is raised until ignition occurs. Not only is this notion relatively simple conceptually and experimentally, it also lends itself to a straightforward theoretical treatment. At the start of this Chapter, however, we observed that, apart from certain reactive substances, liquids do not show an ignition event by themselves. As its temperature is raised, a liquid will vaporize more rapidly. If the vapors are removed, however, all of the liquid will boil away and no ignition event will happen. Thus, clearly, just raising the temperature is not a sufficient way to provoke autoignition of liquids.

In fact, autoignition of liquids might best be considered to be a misnomer. To see what actually happens, we need to consider details of how engineering tests for 'autoignition of liquids' are conducted. These are considered in detail at the end of this Chapter. Here, we can succinctly summarize a typical test used for autoignition of liquids. An empty cup, exposed to air or with an air stream directed through it, is heated to a given temperature. One or more drops of the liquid are dropped into the heated cup. An observation is recorded whether ignition occurred. This process is clearly peculiar for several reasons:

(1) While the cup and air may be at a relatively uniform temperature, the rest of the system is clearly not; especially, since the droplet is normally introduced while it is still at room temperature.
(2) Contrary to the notion that autoignition involves the use of no localized sources of high temperature or external energy, the heated cup surface is clearly of a much higher temperature than are the vapors being released from the droplet.
(3) The fuel/air ratio is a fundamental variable affecting the ignition temperature in the gas phase. Yet, the fuel vapor concentration is undefined and uncharacterized.

Thus, perhaps it is best to simply consider 'autoignition' of liquids to correspond to a certain type of empirical testing, but not to be a rigorous, theoretically definable process. A practical question then is: What is the relationship between that AIT of the liquid's vapors and the results of one of the liquid-droplet tests? The answer, unfortunately, is that not enough data is available to make general conclusions.

IGNITION OF SINGLE DROPS

At some temperature above the flash point temperature, an ignitable liquid's vapor that accumulate in a closed space can ignite without the presence of any external pilot. This is known as the autoignition temperature (AIT). To determine the AIT in a practical test, a maximum waiting time (ignition delay, ignition time, or induction period) has to be defined for how long observations are continued in the absence of a flash. For temperatures higher than the AIT, the ignition delay will be shorter than this arbitrarily defined waiting time. An illustration of the relation between temperature, T (K) and the ignition delay t_{ig} (s) is given in Figure 3[7]. If vaporizing liquid drops obeyed the theory presented in Chapter 4 for gases, plotting $\ln(t_{ig})$ against $1/T$ should give straight lines; experimental results show that distinct curvature is found.

Ignition of single drops has been studied for a long time, but without conclusive results of broad generality being achieved. In 1954, Nishiwaki[8] studied the ignition of single drop inserted on a silica filament into a furnace. His data indicted that, at a fixed temperature, the ignition time t_{ig} could be expressed as:

$$t_{ig} = a + bd$$

where d = diameter, and a and b are constants for any particular fuel type. He also found that, in the case of two droplets, there was a proximity effect, and droplets separated by 4 – 5 times their diameter showed a faster ignition time than did droplets spaced closer or farther apart. Similar data were also presented by Masdin and Thring[9], who show that:

$$t_{ig} = a + cd\exp(E/RT)$$

where c is another constant, E = effective activation energy (kJ mol^{-1}), R = universal gas constant (= 8.314 J mol^{-1} K^{-1}), and T = temperature (K). Thus, a single expression is developed which takes into account both diameter and temperature dependence, although they caution that their expression should not be applied to residual oils and other high-molecular-weight petroleum products. By comparing the above equation against the results of Figure 3, it can be seen that straight lines would be achieved if $a \equiv 0$. But the a term will normally be non-zero because it effectively expresses the time needed to vaporize the drop, before reactions in the vapor-phase can commence.

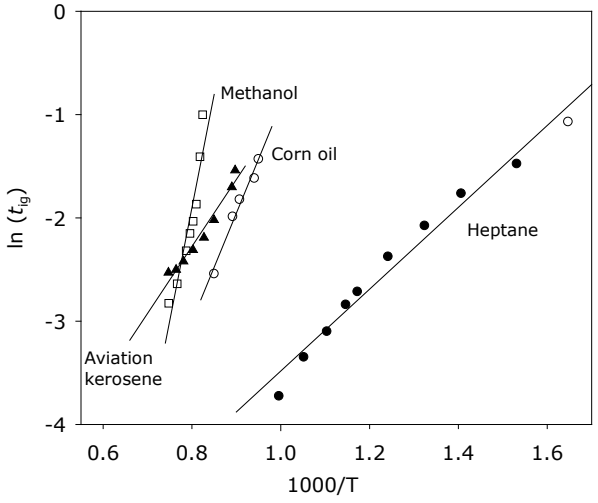


Figure 3 Ignition times for autoignition of single 1.5 mm drops

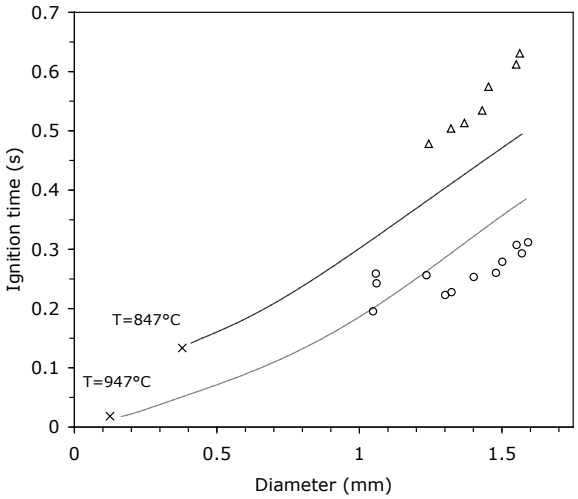


Figure 4 Effect of diameter on ignition for *n*-hexadecane drops in an air stream with 2 m s^{-1} velocity and at two different air-stream temperatures; solid lines indicate predictions from theory; × denotes smallest ignitable diameter *(Copyright The Combustion Institute, used by permission)*

Taylor and Burgess found that the ignition temperature of small drops of residual fuel oil follows the relation[10]:

$$T_{ig} = \frac{76.6}{d} + 218$$

where T_{ig} = temperature of the drop at ignition (ºC) and d = diameter (mm).

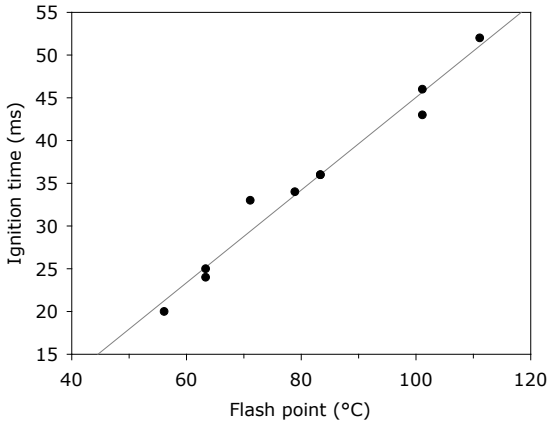


Figure 5 Effect of flash point on ignition time of 1.2 mm drops

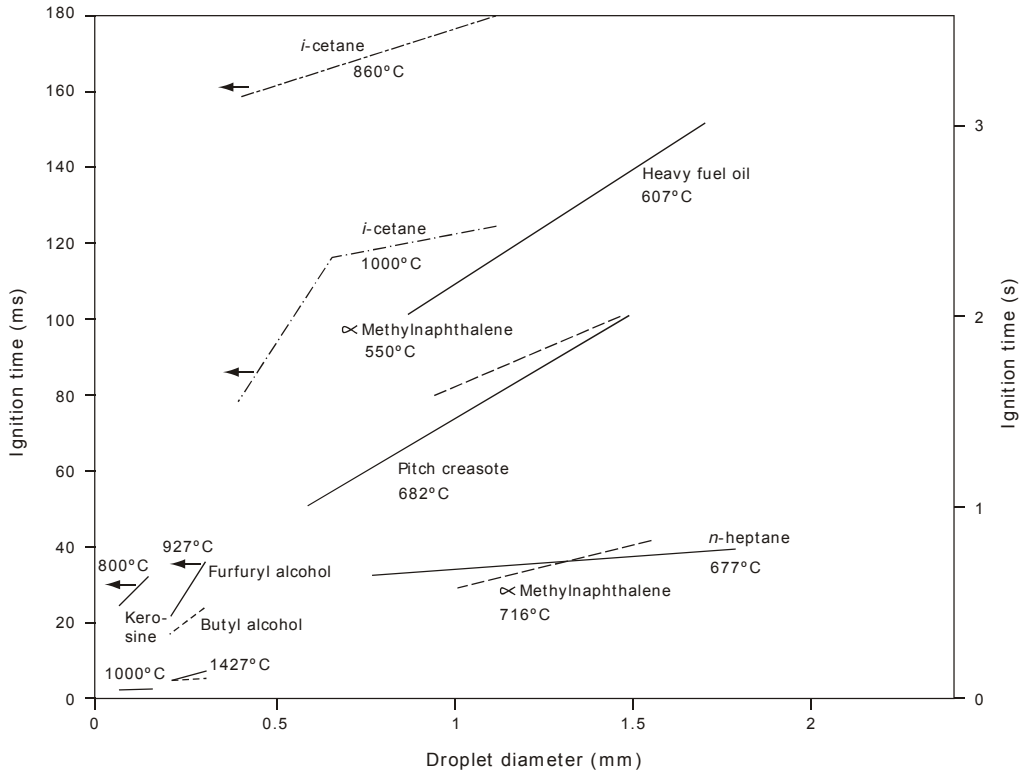


Figure 6 The effect of droplet diameter on ignition time. Note that some fuels are plotted against the left-side time axis *(Reproduced with the permission of The Institute of Energy, London)*

The ignition of single droplets in a forced-convection hot-air stream was studied by Wong et al.[11] They developed a theory (solved numerically only) along with some experimental data (Figure 4). Note that there is a minimum diameter below which the droplet vaporizes without ignition. For the cases where ignition does occur, it generally happens while the droplet diameter is still nearly its original size (>90%). Figure 4 also illustrates that the minimum temperature of an air stream is higher to achieve ignition of a small drop than for a larger drop. The reason is because a small, single drop cannot provide as much flammable vapor as can a larger drop. This relation only holds for single drops in isolation; as will be seen below, for liquid aerosols the opposite trend is found. There is, in general, not much data on critical droplet diameter, but Molero de Blas[12] found a critical diameter of ca. 1.0 mm for a variety of residual oils, when injected into a 600ºC furnace, dropping to 0.5 mm for an 800ºC temperature.

Saitoh et al.[13] conducted experiments with *n*-heptane and *n*-hexadecane. For both fuels, they showed that the minimum furnace temperature needed for ignition decreased, as the droplet diameter increased. For *n*-hexadecane, the ignition time increased with diameter, similar to Nishwaki's findings. But for *n*-heptane, ignition time was roughly constant, except at the smallest diameters, where it increased. Tanabe et al.[14] showed that *n*-heptane droplets undergo a two-stage ignition process, with hot-flame ignition preceded by a cool-flame reaction taking place at ca. 480ºC. Moriue et al.[15] studied the ignition of single droplets of *n*-decane at pressures from ambient to 2 MPa. They found regions of cool-flame, hot-flame and two-stage ignitions, along with interspersed zones of non-ignition. At ambient pressure, they found: below 310ºC, no ignition; 310 – 440ºC, cool-flame ignition; 440 – 650ºC, no ignition; over 650ºC, normal-flame ignition. Two-stage ignitions were found only at pressures over 2 atm.

Bryant[16] studied the ignition of single, 1.2 mm drops suspended on a thin wire and ignited by rapidly presenting the hot exhaust gases of a burner below the specimen. His results (Figure 5) showed an ignition time proportional to the flash point. This was considered reasonable since it requires more time to reach a flammable vapor concentration if the flash point is higher. The actual hot-gas temperature was not characterized, nor were different heating regimes explored. The liquids examined were primarily proprietary. Points for JP-5 (not shown) did not fall on the line and Bryant attributed this to the very wide range on volatilities represented in the fuel mixture.

Goodger[17] reviewed a number of studies on ignition time of liquid droplets. The main trends that he found are shown in Figure 6. Typically, a linear increase in ignition time is found with increasing droplet diameter. This occurs because larger droplets need a longer heating time before their sur-

face reaches a temperature at which an adequate mass flux of vapors is being produced.

The effect of *fuel stoichiometry* on the induction period has also been studied by Goodger, but no general trends emerge. For very short ignition times, however, the mixture ratio appears to be a relatively unimportant variable. For single droplets of iso-octane, Faeth and Olson[18] found a *pressure* effect of the form $t_{ig} \propto P^{-2.6}$. Additional data are shown in Figure 7.

Within a given chemical family, the ignition time tends to increase with the *number of carbon atoms*[19]. This effect is due to physical reasons and not chemical. As shown in Chapter 4, the AIT of vapors generally decreases as the number of carbon atoms increases. But molecules with a larger number of carbon atoms are less volatile and a longer time is needed for a sufficient amount of vapor to be released. *Multi-component fuels* tend to have a complex drop-size/ignition time relationship. Takei et al.[20] explored this for several binary fuel combinations and summarized the general trends in Figure 8.

A number of workers put forth autoignition theories for single-drop ignition[21-24] and Mawid[25] reviewed the efforts up to 1989 in some detail. Thus far, however, none are both validated and reasonably tractable (i.e., not requiring that the user set up and solve differential equations on a computer). The problem is complex due to its highly unsteady nature, so that simple approximations, if made, do not tend to lead to good predictions. The effect of water in a fuel droplet, i.e., an *emulsion*, was studied by means of theoretical model by Jeng[26]. He found that, for water content of less

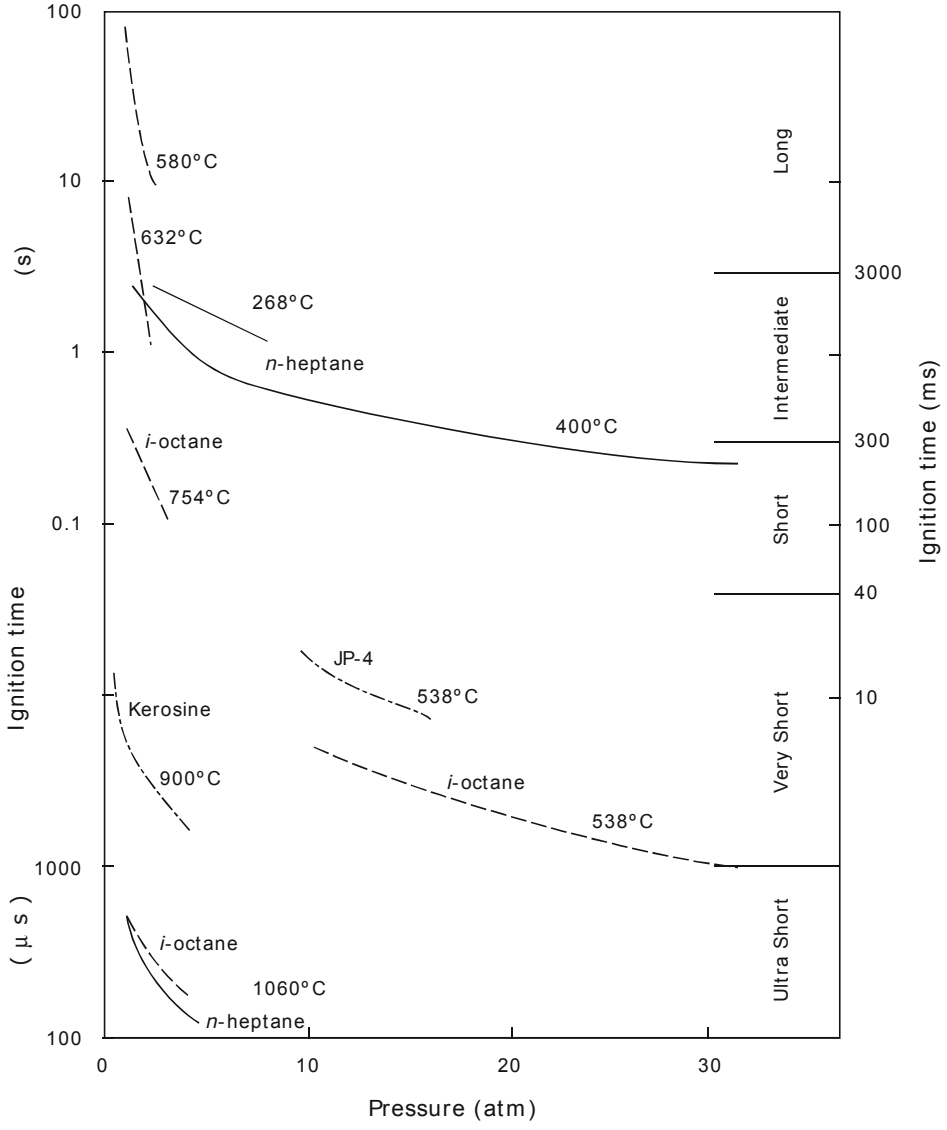


Figure 7 The effect of pressure on ignition time of liquid aerosols
(Reproduced with the permission of The Institute of Energy, London)

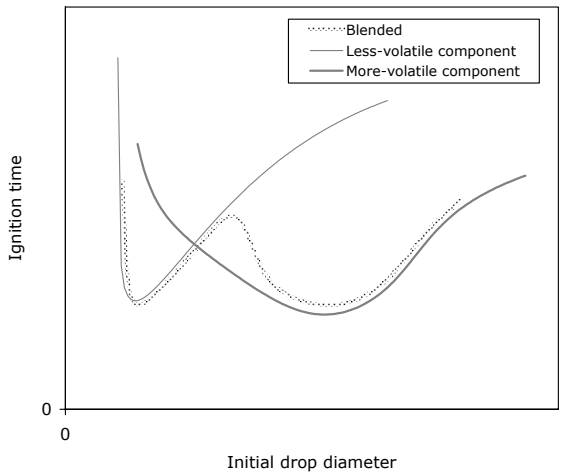


Figure 8 Effect of drop diameter on ignition time of blended fuels

than 20%, the effect on ignition time was negligible; higher water percentages caused an increase in the ignition time.

LIQUID AEROSOLS OR SPRAYS

Boilers, furnaces, and other forms of wanted combustion commonly used liquid fuels in the form of aerosols (also known as *mists* or *clouds*). Unwanted fires involving aerosols often happen subsequent to a piping system springing a leak. Nozzles and other atomizing devices can normally produce droplets in the range 5 – 300 μm although droplets below about 30 μm are more difficult to produce. Smaller diameter particles are often created as *condensation mists*, when an evaporated material begins to cool; for a number of liquids, mists of 0.2 – 2.0 μm can be produced by condensation[27].

Liquid aerosols are sometimes characterized by C, defined as $C = \dfrac{\text{inter - drop distance}}{\text{drop diameter}}$. Thus, a classification has been suggested[28]:

$C >> 10$	Aerosol traits are minimal and droplets behave as individual droplets.
$C \approx 10$	Strong inter-drop interaction, ignites and burns with a flame surrounding entire cloud. Hayashi et al.[29] showed that for *n*-decane the regime corresponds to $C < 30$.
$C < 5$	Very dense sprays; not a common situation.

Wong et al.[30] however showed that C is not the only geometric variable and that the drop diameter continues to play a role. Their experimental investigations led to the conclusion that liquid aerosols can autoignite in one of three modes:

- *Local ignition* – aerosols of large-diameter droplets ignite in a manner similar to single droplets, where there is minimal interaction from adjoining droplets.
- *Global ignition* – for aerosols of smaller-diameter droplets, the reaction zone is distributed between the droplets and droplets no longer behave in an isolated way. When the aerosol ignites, flame surrounds the outside of a region encompassing many drops, while the inside does not exhibit flaming since it is too fuel-rich.
- *Homogeneous ignition* – aerosols of smaller-yet droplets, when exposed to high temperatures, vaporize before igniting; thus, their ignition is indistinguishable from that of a uniform vapor.

These different modes are illustrated in Figure 9. The designations H, G, and L denote the three ignition regimes; the numbers at each curve denote the overall equivalence ratio of the aerosol, with values of C being given in parentheses. The data in the figure pertain solely to an air temperature of 1500 K. At that temperature, the homogeneous ignition regime occurs for droplets smaller than 25 – 45 μm, with the exact value depending on the stoichiometry and the droplet spacing. The air temperature does affect the minimum size; at 1300 K, the regimes goes out to ca. 70 μm, while at 1800 K it exists only below 20 μm.

Rah et al.[31] studied the ignition of aerosols of *n*-dodecane and No. 6 fuel oil as a function of oxygen concentration. Their results (Figure 10) show that the ignition time varies approximately as $t_{ig} \propto C_{O_2}^{-0.5}$.

Wood and Rosser[32] studied the ignition of hexadecane drops in several arrangements—as single drops, as a group of 3 – 5 drops, and as a stream of 60 drops/s. Their results (Figure 11) show that all of the arrangements can be correlated by an equation of the form:

$$d^2 = g \exp(-E/RT)$$

where d = drop diameter (mm), g = a constant which depends on the arrangement, E = effective activation energy

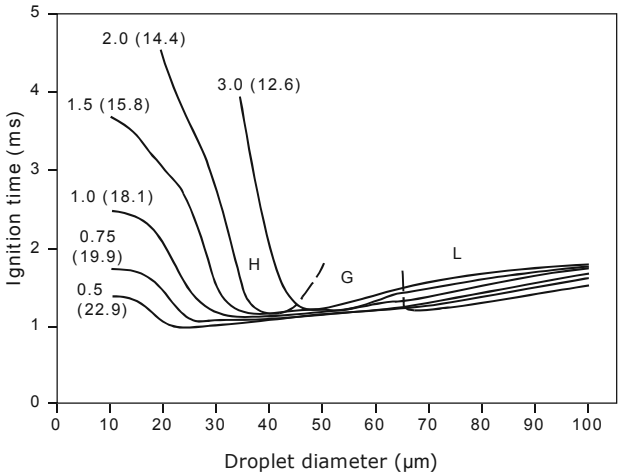


Figure 9 The ignition regimes at 1500 K for heptane aerosol in air

(Copyright The Combustion Institute, used by permission)

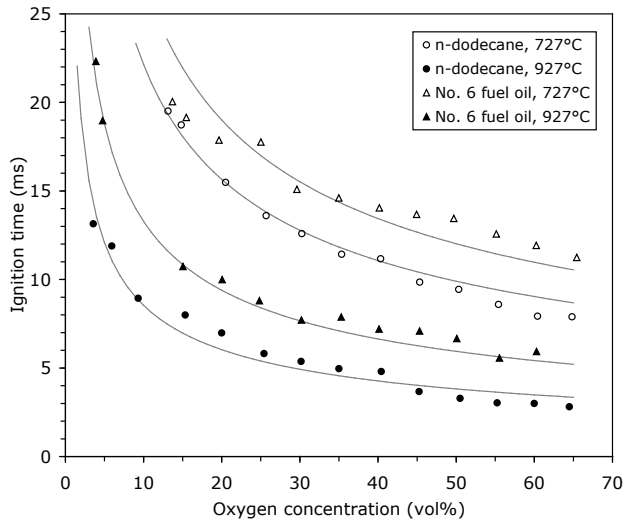


Figure 10 Effect of oxygen concentration on ignition of two fuels in aerosol form (d = 150μm)

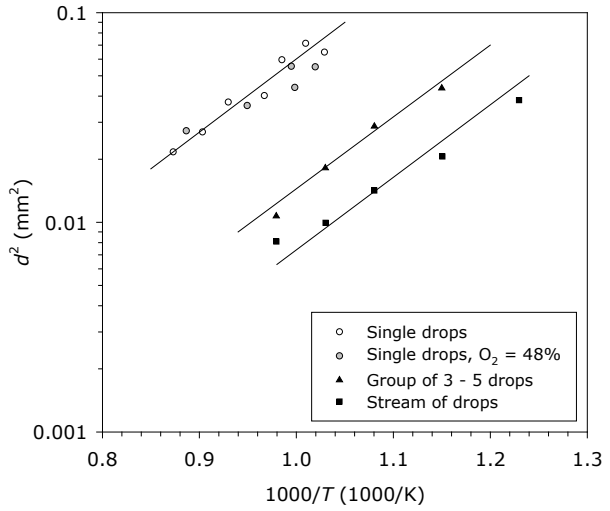


Figure 11 Relation between drop diameter and furnace temperature needed for ignition of hexadecane drops

(kJ mol^{-1}), R = 8.314 J mol^{-1} K^{-1}, and T = furnace temperature (K). For hexadecane, the slope is found to be 8.05, giving E = 1000×8.314×8.05 = 67 kJ mol^{-1}. It is also interesting to note that there was no detectable difference between the results obtained at 21% oxygen concentration and at 48%, although Wood and Rosser point out that theoretically a very small effect should exist.

Hiroyasu[33] measured autoignition times for sprays (of unspecified droplet diameter) in a high-temperature, high-pressure environment and obtained the following equation giving a reasonable correlation of results:

$$t_{ig} = AP^B \varphi^C \exp(D/T)$$

where t_{ig}= ignition time (ms), P = pressure (atm), φ = equivalence ratio (--), and T = temperature (K), with the constants A, B, C, and D being given by:

Fuel	A	B	C	D
light oil	0.276	–1.23	–1.60	7280
heptane	0.748	–1.44	–1.39	5270
dodecane	0.845	–1.31	–2.02	4350
hexadecane	0.872	–1.24	–2.10	4050

Some examples of the effect of droplet concentration are shown in Figure 12, as measured by Laster and Annamalai[34]. Octane becomes progressively easier to ignite as the concentration increases, while dodecane shows a minimum value, and becomes more difficult to ignite at higher concentrations. The authors attribute this difference to the fact that dodecane has a higher boiling point than octane and, thus, is more difficult to vaporize—thus, a large fuel mass effectively acts as a heat sink.

Turbulence decreases the AIT for liquid aerosols[35]. Ignition times for liquid droplets in *microgravity* are shorter than in normal gravity[36]. This is due to the absence of convection.

Because of the large number of variables involved, no simple theories for the ignition of clouds of liquid droplets have emerged. Sichel and Palaniswamy[37] developed an elaborate theory which they solved numerically for the case of an 0.1 m diameter cloud of octane droplets, present at a number density of 10^9 particles/m^3. Their solution gives a cloud ignition temperature of around 190ºC, as compared to 630ºC for a single 100 μm droplet. McIntosh et al.[38] developed a variant of Semenov theory which includes fuel in both droplet and vapor phases. Several reviews[39,40] are available of theoretical models for the autoignition of liquid

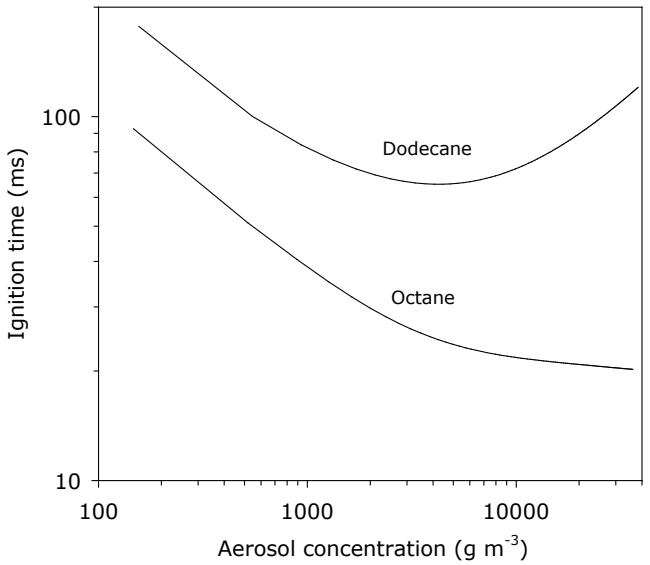


Figure 12 Autoignition time for aerosols of 100 μm dodecane and octane droplets at a furnace temperature of 927ºC

aerosols, but unfortunately it is seen that most of these models are not accompanied by validation against experimental data.

Flash point and fire point

FLASH POINT

The most basic question to be considered in the ignitability of liquids is the following. An open dish of a certain liquid is placed in a certain atmosphere. What are the conditions under which it will ignite from a small flame? To deal with this question, we will first assume that the atmosphere into which the dish is introduced is fully mixed, that is, that there are no concentration gradients anywhere before the dish is introduced. Furthermore, it will be useful to assume that the atmosphere is still. Let the dish contain methanol and the atmosphere be 21% oxygen/79% nitrogen. There are no methanol vapors in the atmosphere before the dish is introduced. In a thought experiment, let us introduce a pilot flame slightly above the methanol dish at time $t = 0$. Ignition will clearly not occur, at any temperature of the atmosphere, because there are yet no methanol vapors in the atmosphere. So, first, evaporation and diffusion must occur. Because the atmosphere is 0% methanol and the dish is 100% methanol, a flow of methanol vapor will start to leave the liquid dish and move into the atmosphere. Piloted ignition will occur—in the gas phase—when at some particular place in the atmosphere,

1. an adequate concentration of the liquid's vapor exists above the liquid,
2. an adequate concentration of an oxidizer is mixed in with the fuel vapors,
3. a localized heat source of sufficient magnitude is present.

If the dish is small and the space into which it is introduced is large, there may be only a very small zone where a flammable mixture will be found. We may also run out of fuel and not reach a significant fuel vapor concentration in the atmosphere. Consider now the more specialized case. Suppose the dish is introduced into a rather small space. Let the space be closed, but with a small hole, so that its pressure will always equilibrate with atmospheric pressure. Under these conditions, it will be easier for the fuel vapors to fill the whole space more quickly and to reach higher ultimate concentrations. The former case may represent a fire accident in a processing facility. The latter case represents a closed-cup flash point test. The conditions have been arranged to represent, more or less, a worst case situation.

If the volume of the space is small, and if we wait for a sufficiently long time, a steady-state concentration of fuel vapor will be found in the atmosphere. The volume percent of fuel vapor y_f is the atmosphere will be:

$$y_f = 100 \times p / P$$

where p is the saturated vapor pressure of the liquid at the temperature T, and P is the atmospheric pressure. Provided that the temperature is not too close to the critical temperature, the vapor pressure of a liquid can be represented as a simple function of T by the Antoine equation, as given above.

If the temperature T is low enough, a steady-state fuel vapor concentration will be achieved, but a small flame introduced into the atmosphere will not cause ignition. This will happen if at T the value of y_f is below the LFL. As the liquid reaches a certain temperature, however, the first possibility of ignition will occur. This temperature is called the *closed-cup flash point*. Thus, theoretically it should be possible to compute the closed-cup flash point by knowing the LFL of the substance, converting it to fuel vapor pressure, and then solving the Antoine equation for T. Such a calculation of the flash point typically gives a value which is close to the measured one, but sometimes significantly farther away than would be due to just the repeatability of the test[41]. This is because both the LFL and the flash point determinations are somewhat dependent on the apparatus details. While these can be standardized, there is no single 'right' way that the test equipment can be constructed.

It is loosely considered that the flash point temperature corresponds to the value LTL (the concept of LTL was explained in Chapter 4). Such a relation is only conceptually true. In practice, the actual value of both the flash point temperature and the LTL are apparatus-dependent and the determinations are made in two entirely different apparatuses: a flash point tester and a flammability limits apparatus. In neither type of apparatus are there absolutely perfect test conditions. The vapor concentrations are not perfectly uniform, there are wall effects, etc. The *ignition source itself* will be a source of turbulent mixing and localized concentration variations. The small flame, spark, etc., causes extremely high temperature gradients and this, in turn, disturbs any pre-existing vapor concentration levels.

In an *open-cup* configuration, a cup holding the liquid is situated in essentially an open atmosphere. The concentration of fuel vapors is highest near the liquid's surface, but progressively diminishes towards zero as the height above the cup increases. Since the igniter cannot be placed directly at the liquid's surface, the location at the igniter has a lower vapor concentration and, consequently the OC flash point is higher than the CC. It is generally found that the CC flash point is several degrees Celsius higher than what would be predicted from the LFL/vapor pressure relationship. In turn, the OC flash point is several degrees higher than the CC value. Factory Mutual[42] tested a number of compounds for which they gave both OC and CC results. Figure 13 shows these data along with the correlation:

$$T_{FP(OC)} = 1.12\, T_{FP(CC)} + 7.1$$

but it has to be remembered (see below) that there are systematic differences between test apparatuses, not just OC vs CC conditions alone.

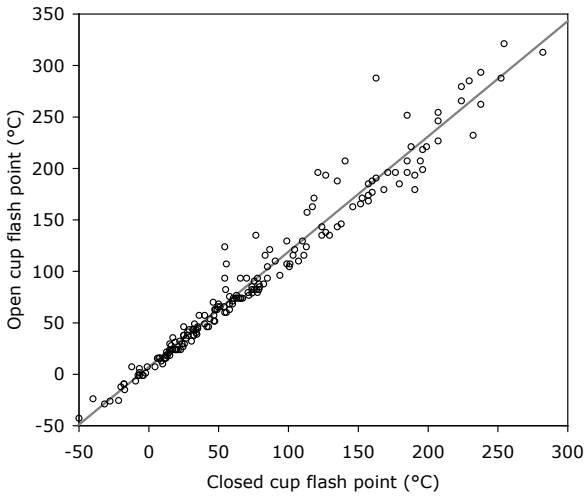


Figure 13 Relation between OC and CC flash point values

A substance does not necessarily have to have its flash point be above its freezing point. While this is true for the vast majority of organic substances, cyclohexane is a notable exception. Its open-cup flash point is –17ºC, while its freezing point is 6.5ºC.

By definition of NFPA 30, a liquid is termed *flammable* if it its flash point is less than 100ºF (37.8ºC), and *combustible* if the flash point is equal or greater than 100ºF. These definitions are somewhat confusing to many people, since it is often desired to refer to liquids that are capable of burning, but whose exact flash point is unknown or unimportant. The term *ignitable liquid* can be used to cover both flammable and combustible liquids, but its use is likely to not be understood by the layman. Flash point values must not be assumed to apply to aerosols, since these can often ignite at lower temperatures than the flash point determined for quiescent liquids.

The flash point is measured in apparatuses using very small quantities of liquids. Since the possibility of explosions will usually concern kilogram, not gram, quantities, the question arises whether the small-scale results adequately represent a large-scale reality. Shepherd et al.[43] concluded that they do not, at least for the Jet A fuel that they examined. In their work, they found that flashing occurred in larger-scale apparatuses at about 10 – 15ºC below the measured flash point. Now, jet fuels are highly complex mixtures, and it is not clear that this conclusion can be generalized to other fuels; nonetheless, the finding is troubling. The authors also pointed out that, with complex mixtures, a stable fuel essentially does not exist, and that they encountered flash point shifts in their work that were not explainable.

UPPER FLASH POINT

For some specialized applications, it is also possible to determine a rich-limit flash point or upper flash point. This corresponds to a temperature so high that the equilibrium vapor mixture of the liquid's vapor and air is at the rich flammability limit. Such a limit can be demonstrated with gasoline by dropping a lighted match into a gasoline can which is equilibrated with air at room temperature. If the mixture is indeed in equilibrium and has not been otherwise stirred or ventilated, it should be possible to watch the match extinguish. An explosion will result, however, if the vapor mixture is not above the rich flammability limit, for instance, by stirring in air into the can.

Measurements of the upper flash point are not commonly made, but Hasegawa and Kashiki[44] reported on a series of results obtained using the closed-cup Setaflash apparatus. Empirically they also derived:

$$T_{ucc} = UTL + 6.4$$

where T_{ucc} = upper closed-cup flash point and UTL = upper temperature limit of flammability (see Chapter 4). The scatter of this relation was reported as ±5.3ºC.

THE FIRE POINT

The fire point of a liquid, in contrast to its flash point, is the minimum temperature at which a *sustained* flame will result upon application of a pilot flame. It must be measured in an open vessel (e.g., an open-cup flash point test apparatus), since oxygen depletion in a closed-cup device would prevent sustained burning from being achieved. The definition is not complete without specifying a time limit for distinguishing between flashing and sustained flaming. ASTM test methods use a 5 s value. Some illustrative values are given in Table 3. The examples given in Table 3 are for simple, non-halogenated liquids. For some other liquids, the fire point can be greatly higher than the flash point; Figure 14 illustrates this for some aviation hydraulic fluids and lubricating oils[45].

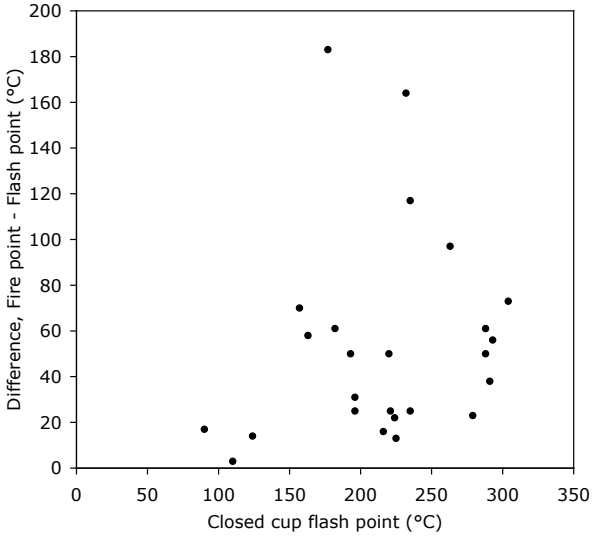


Figure 14 Relation of fire point to flash point—some trends for aviation hydraulic fluids and lubricating oils

Table 3 Example values of closed-cup flash point, open-cup flash point, and fire-point temperatures

Substance	Closed cup FP (°C)	Open cup FP (°C)	Fire point (°C)
n-hexane	–22	–26	
n-heptane	–4	–1	2[47]
methanol	12	1.0[54], 16[42]	1.0[54], 17[47]
n-octane	12	17[51]	18[51]
ethanol	13	22	22[47]
sec-butanol	24		29[51]
m-xylene	25		44[48]
p-xylene	25	31	44[54]
n-butanol	29	36	36[54], 38[51], 50[48]
n-nonane	31	37[51]	42[51]
o-xylene	32	36	42[51]
JP-6		38	43[49]
n-decane	44	52	61.5[54], 66[48]
decalin		57	63[49]
tetralin		71	74[49]
bicyclohexyl		74	79[49]
dodecane	74		103[48]
fuel oil, No. 2	124		129[50]
fuel oil, No. 6	146		177[50]
glycerol	160	176	207[48]
motor oil	216		224[50]

The combustion process associated with the fire point is different from that for a flash point. When a flash point is being determined, a premixed fuel-air mixture has been created and a flame rapidly propagates through the mixture. The fire point, however, is associated with steady burning. For a vaporizing liquid, such steady combustion comprises a diffusion flame. Thus, there is not necessarily a simple, physical relationship between the flash point and the fire point. In general, the relation among the various temperatures pertinent to liquid ignitions is:

$$T_{flash\ point} \quad T_{fire\ point} < T_{s.s.\ surface} < T_b$$

It is clear that there is no more liquid above the boiling point T_b, therefore all of the other characteristic temperatures for a liquid must be lower. Also, from the definition of fire point, it cannot be lower than the flash point. As illustrated in Table 3, for liquids with $T_{flash\ point}$ below about 40°C, the fire point is commonly about 3 – 10ºC above the CC flash point. For liquids with high flash points, however, the difference becomes progressively greater. In the case of certain alcohols, however, the flash point and the fire point have been found to be identical.

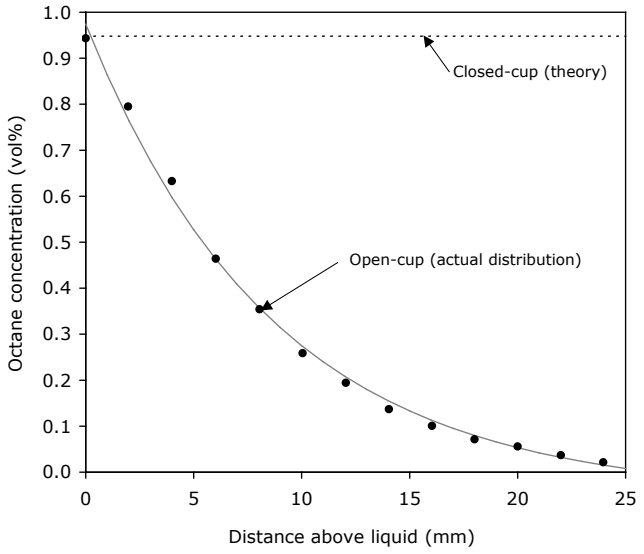


Figure 15 Fuel vapor distribution above an open cup of *n*-octane at 14ºC

Finally, it should not be surprising that if the liquid is ignited and burns in a steady state, $T_{s.s.\ surface}$, the liquid's surface temperature will be higher than $T_{fire\ point}$, but slightly lower than T_b. If a liquid is vaporizing, without burning, then $T_{s.s.\ surface}$ will be slightly lower than the ambient temperature. This occurs because vaporization is an endothermic process, so since heat is removed from the system, its temperature must drop.

THE PRE-FLASH 'HALO'

It is well-known that when some fuels (but not alcohols) are tested in a flash-point apparatus, a blue halo can be seen around the igniter at some temperature slightly below the flash point temperature. This halo does not propagate beyond the immediate vicinity of the igniter and, thus, according to standard testing instructions, does not constitute the flash point. The nature of this halo has been documented[51], but the mechanism is not explained. With other fuels, the ignitor flame gets enlarged and turns from blue to yellowish-green; again, in the absence of overt flame propagation, this is not considered to constitute a flash point. The changed color is attributed to thermal decomposition of the fuel vapors[46].

THE DISTRIBUTION OF FUEL VAPORS ABOVE THE SURFACE

The concentration of fuel vapors above the liquid surface is constant if the vessel is closed, but decreases with height for an open-top vessel. Figure 15 shows a measured concentration distribution obtained for octane filled to the top of a 50 mm diameter open cup[51]; the temperature of the liquid is slightly below its flash point. The vapor pressure of octane is 960 Pa at 14ºC, which is 0.948% of 1 atm. The data shows that a fuel vapor concentration of approximately 0.948% is indeed found next to the surface, with an exponential decrease for other heights. In about 6 mm, the concentration has dropped off to half its value at the surface. Because the concentration changes greatly with small changes in height, it may be surmised that highly precise placement of the ignition flame would be needed in an open-cup flash point tester if reproducible results are to be obtained. Experimental results confirm this (see below).

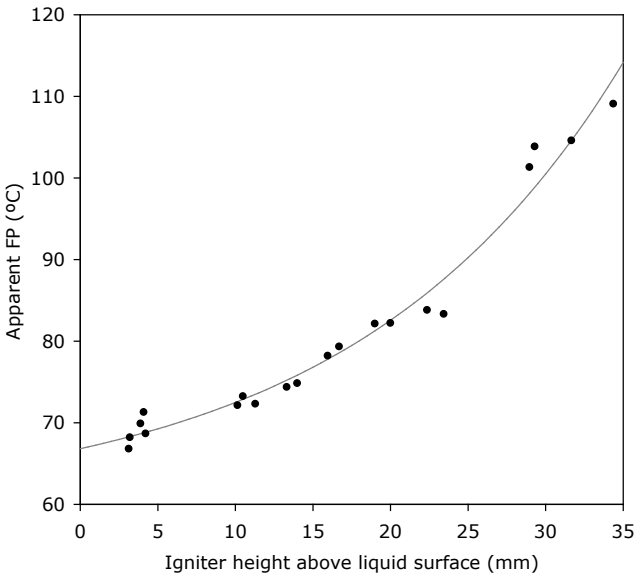


Figure 16 Effect of igniter height on the apparent flash point of hexanol found by using an electric igniter in the Pensky-Martens flash point tester (solid line represents best fit through data points, not a theoretical prediction)

The fuel vapor concentration above an open dish is hard to compute theoretically because 3-dimensional diffusion is involved. But for simpler geometries, the concentration distribution can be computed. The classical problem—called the *Stefan problem*—involves a straight-sided, open-topped tube with a layer of liquid on the bottom. It is assumed that there is a strong cross-wind at the top of the beaker, so that the fuel vapor concentration is zero at the top. With this assumption, the problem can be solved, since the diffusion of vapor is only 1-dimensional. The vapor distribution is exponentially decreasing with height in such a configuration, and details of the solution can be found in textbooks on mass transfer[52]. Additional aspects of the Stefan problem are considered in Chapter 13.

Burgoyne et al.[53] developed a more refined model for predicting the open-cup flash point by (a) examining the effect of tube heights equal to either the actual lip height above the liquid surface, or a height of infinity; and (b) solving a transient problem as occurs in flash-point testers where the liquid is continuously raised in temperature, instead of being preset at a given value. The model was used to predict flash point values as a function of igniter height above the liquid surface. The results from the model only roughly corresponded to the measured values, but the latter are interesting by themselves and are shown in Figure 16. In their tests, the authors used a Pensky-Martens tester modified to use an electric igniter instead of a flame, since a flame was found to have a sizable disturbing effect on the temperatures within the apparatus.

Based on data such as the trend line shown in Figure 16, it might be supposed that the most conservative height for placing a pilot flame would be infinitesimally above the surface. But if the flame is placed very close to the surface, much of its energy is imparted to the liquid phase and becomes unavailable for igniting the vapors. The minimum height for the igniter to be placed is termed the *quench layer height*. Glassman and Dryer[54] measured the effect of igniter location for samples of decane (Figure 17). The flash point determined with the igniter at 6.35 mm above the surface (the standard igniter height in the ASTM D 1310 Tag open-cup flash point test) is 55ºC. However, the lowest flash point found was 52 – 53ºC, which occurred when the igniter was placed closer to the liquid. Placing the igniter closer than about 3 mm produced only a blue 'halo' around the ignition flame, but did not lead to a flash propagating over the surface. Thus, a quench layer height of about 3 mm was found for decane. In principle, a different quench layer height might be obtained in the determination of the fire point. Once above its quench layer height, however, the results suggest there is a plateau over which the fire point value determination would not change. This is different from the flash point, which is seen to increase monotonically with increasing height. At large heights, the flash point

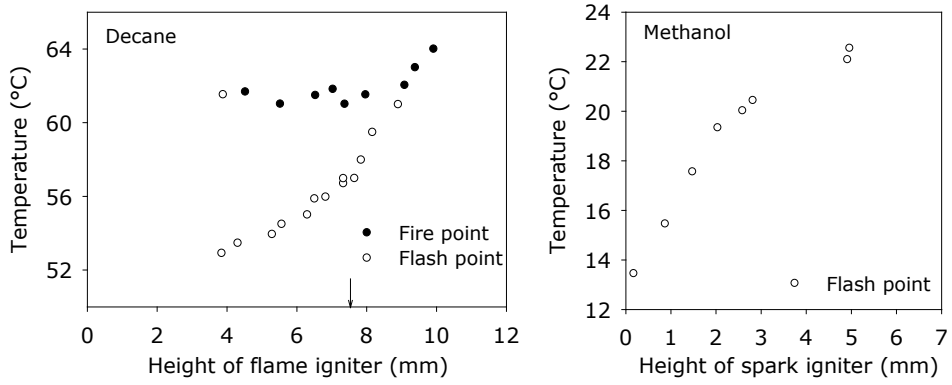


Figure 17 The effect of igniter height for decane and methanol. Arrow indicates height of flame igniter in ASTM D 1310 Tag open-cup test
(Copyright Elsevier Science, used by permission)

keeps increases with height, as shown by Zinn[55] for pools of JP-4 and JP-5. His experiments covered the range of 25 – 125 mm.

Table 4 Flash points and quench layer heights for alcohols determined by Glassman and Dryer

Fuel	T_T (°C)	T_{cc} (°C)	T_{oc} (°C)	$T_{oc\text{-}sp}$ (°C)	δ_q (mm)
methanol	9.5	11.1	1.0	13.5	0.25
ethanol	11.9	13	6.0	18.0	0.25
n-propanol	22.8	26	16.5	26.0	0.30
n-butanol	31.8	35	36	40.5	0.40
45% ethanol/ 55% water	--	27.8	27	29.0	0.30

T_T – theoretical flash point, computed from LFL and vapor pressure curve
T_{cc} – closed cup flash point
T_{oc} – open cup flash point
$T_{oc\text{-}sp}$ – open cup flash point determined by spark
δ_q – quench layer height, determined for spark ignition

Glassman and Dryer also examined in detail the ignition behavior of a series of alcohols. For most fuels, the open-cup flash point is several degrees above the closed-cup value. Thus, their contrary results (Table 4) needed to be explained. The anomaly was found to lie in the fact that, for alcohols, even a minimal igniter flame, placed at the height giving the lowest temperature, causes enough of the heat flux to impinge on the liquid to preheat it locally. Thus, Glassman and Dryer conducted additional open-cup tests using a spark, instead of flame, ignition source. With the exception of *n*-propanol, these results now show the expected relationship that $T_{oc\text{-}sp} > T_{cc}$. The anomalous flash point behavior of alcohols is related to their extremely small quench layer heights, which is a fraction of the value (say, 3.0 mm) seen with other fuels. The study did not elucidate, however, a chemical reason for the anomalous behavior of alcohols. The values of the quenching distance for vapors of alcohols, measured in the normal way, are not particularly different from those for hydrocarbons. Thus, some other relationship governs the quench layer heights measured above liquid pools.

Provided that the igniter is above the quench layer, then flash or sustained ignition will occur if the igniter is placed in a region where the vapors are between the LFL and the UFL. If there is a *cross-draft*, then ignition is possible provided that the draft velocity is less than the laminar flame speed. The flame speed to be evaluated is one which pertains to the local concentration of vapors at the igniter location. Zinn[55] showed that the effect of wind velocities up to 4 m s^{-1} was to cause a moderate increase in the flash point value, provided that the pilot was placed at the leeward edge of the pool.

Bunama and Karim[56] conducted an interesting study where they modeled the transient effect associated with quickly pouring a liquid into the bottom of an open-top tube then following the change of fuel concentration with time at various heights. Initially, all of the volume within the tube will be below the LFL. But then a flammable zone will be established and the heights at which LFL and the UFL are located will rise. Thus, a flammable zone will 'detach' from the bottom and move upwards. Figure 18 shows their calculations for pentane, illustrating that the flammable zone (difference between the LFL height and the UFL height) also expands as it moves upwards. Since the UTL of pentane is below room temperature, eventually the flammable zone moves out of the tube and the entire volume is too rich to ignite. In the calculated results, time was expressed as a dimensionless quantity:

$$\tau = \frac{D_{ab} t}{L}$$

where D_{ab} = diffusion coefficient of the fuel vapors in air (m^2 s^{-1}), t = time (s), and L = tube height (m). Similar calculations for methanol showed an upward movement only of the UFL height—the tube never develops a fuel-rich zone and the final outcome is that the entire volume is within the flammability limits.

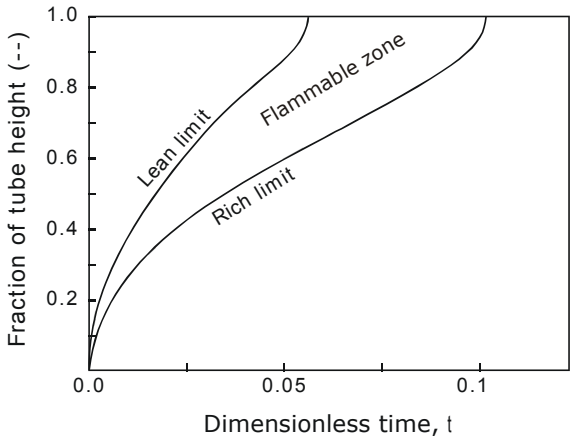


Figure 18 Heights of the LFL and the UFL in a tall tube containing pentane at 22ºC

ESTIMATIONS OF FLASH POINT

For a homologous series of straight-chain organic compounds (e.g., the *n*-paraffins: hexane, heptane, octane, nonane, etc.) flash points form a simple, predictable and extrapolatable series. Thus, if flash points for a number of the members are known, they can be plotted as a function of the number of carbon atoms in the molecule, and unknown members estimated by interpolation or extrapolation. For a group of organic molecules within one chemical family, it is generally found that the flash point:

- increases with increasing number of carbon atoms
- increases with increasing boiling point
- increases with increasing heat of combustion, if the latter is expressed per-mole, rather than per-mass, units.

Relations derived for straight-chain molecules, however, cannot be applied to branched-chain molecules. For instance, when plotted against number of carbon atoms or

boiling point, primary *n*-alcohols (methyl, ethyl, *n*-propyl, etc.) form a smooth curve which, apart from methyl alcohol, is a straight line. But isomers (e.g., isopropyl, isobutyl alcohols) do not necessarily fall on the same line. For impure liquids (e.g., crude oil) the flash point generally increases with increasing specific gravity.

To a rough extent, the flash point varies directly with the boiling point. Figure 19 shows that an approximate, generally conservative estimating rule can simply be given as a linear relationship:

$$T_{FP} = 0.655T_b - 53 \qquad (1)$$

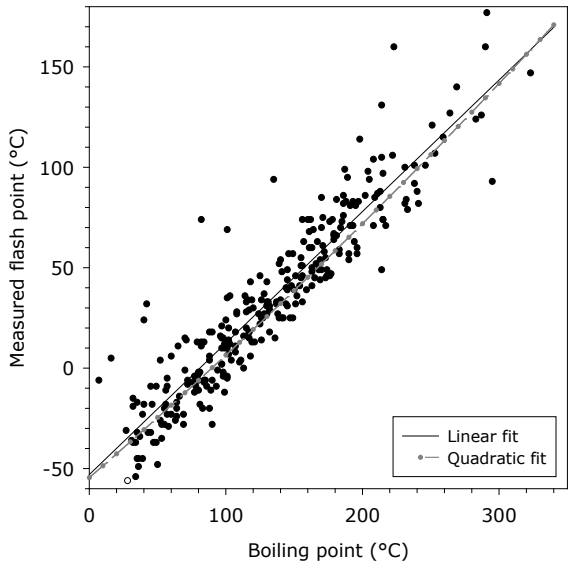


Figure 19 Effect of boiling point on flash point, showing linear fit and Hshieh's equation (quadratic fit)

A number of investigators[57,58] sought more accurate prediction schemes by introducing the possibility of curvature into the prediction line. The latest of these, by Hshieh[59], proposed:

$$T_{FP} = -54.5377 + 0.5883T_b + 0.00022T_b^2$$

His equation is also shown in Figure 19, but, based on 290 organic liquids for which data are plotted, the fit is actually worse. It has sometimes been suggested that a good correlating variable is the *number of carbon atoms* in the molecule, however, these are less successful than simple boiling point correlations, since effects of isomerization, which are ignored when plotting against the number of carbon atoms, can be reasonably taken into account by using the T_b. Another variation on the boiling point theme was suggested by Metcalf and Metcalf[60] who introduced a term for the density of the substance and providing a separate equation for hydroxyl compounds (compounds having an R–OH group):

$$T_{FP} = -87.77 + 0.6223T_b + 0.0383\rho$$

except for hydroxyl compounds

$$T_{FP} = -81.02 + 0.5544T_b + 0.0527\rho$$

for hydroxyl compounds

where ρ = density (kg m^{-3}). Their proposal has not been extensively tested. The *heat of combustion* was proposed as a supplementary variable by Shebeko et al.[61] Their paper gives an erroneous equation, but a correlation based on 290 organic liquids from Table 1 of Chapter 15 gives:

$$T_{FP} = -46.6 + 0.739T_b - 0.00484\Delta h_c$$

where Δh_c = gross heat of combustion (kJ mol^{-1}). The goodness of fit is shown in Figure 20, for which the standard error is 14.52ºC. This compares to a standard error of 16.22ºC for Eq. (1) given above which uses only the boiling point. Hsieh's method gives 17.17ºC, but unlike in his study, no silicone liquids were included in this correlation. The results of Figure 20 show that the larger excursions are almost all on the conservative side, so the corrected Shebeko method appears to be the best of the 'simple' methods.

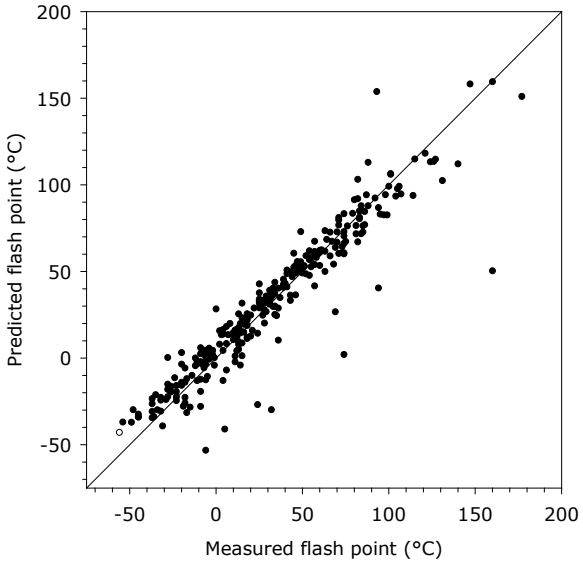


Figure 20 Flash point prediction for 290 organic liquids, based on inclusion of heat of combustion

A large number of researchers have assumed that the flash point ought to correspond to a *fixed value of vapor pressure*, at least within certain chemical families. But for a wide variety of pure chemical substances, Kueffer and Donaldson[62] documented that the vapor pressures at the flash point are mostly in the range from 1.0 to 4.0 kPa, which is a range broad enough to make the concept useless. If attention is focused on a single chemical family, however, more reasonable predictions may be achieved. For example, Fujii and Hermann[63] concluded that average vapor pressure corresponding to the flash point temperature = 1.2 kPa, but the 'family' constant ranges from 0.55 (for alkenes) to 2.3 (for alcohols). Both they and other authors noted that there is no hope of applying a rule of this type to products that are mixtures of substances. This is illustrated

for aviation fuels in Figure 1, which shows that the vapor pressure at the flash point ranges from 0.7 to 2.0 kPa; for low-viscosity petroleum oils, the values range from 0.5 to 2.0 kPa[4].

In 1927, Leslie and Geniesse[64] suggested that an improved predictivity can be obtained by using a value of vapor pressure which contains information on the stoichiometry:

$$p_v = \frac{P_{tot}}{k\gamma_o}$$

where p_v = vapor pressure (atm), P_{tot} = total pressure (typ., 1 atm), k = empirical constant ≈ 8, and γ_o = (moles of oxygen)/(moles of fuel) for stoichiometric combustion (see Chapter 3).

A similar formula was later published by Blinov, the Russian researcher famous for his studies on the burning of liquid pools[65]:

$$T_{FP} = \frac{A_B}{\gamma_o \, p_{FP} D_o} - 273$$

where T_{FP} = flash point (°C); A_B = 4 for calculating the closed-cup flash point, 4.5 for open-cup flash point; and 5.25 for the fire point; p_{FP} = vapor pressure of the substance at the flash point temperature (atm); D_o = diffusion coefficient ($cm^2\ s^{-1}$); and γ_o is the same as before. The equation must be solved iteratively, since the vapor pressure at the flash point will not be known until the flash point temperature is known. The diffusion coefficient D_o will not be found tabulated for uncommon substances, thus, the following equation is used to estimate it:

$$D_o = 1/\sqrt{\sum_i k_i m_i}$$

The constants entering the above equation all come from examining the fuel molecule. The values m_i are the number of atoms of element i present in the molecule, with the summation being over all fuel-molecule elements. The constants k are obtained as follows:

Element	Value of k
hydrogen	1
oxygen	17
nitrogen	16
sulfur	48
chlorine	37
bromine	79

For carbon atoms, however, a more complex strategy is used. For carbon atoms in a benzene ring, k = 25. For carbons in other ring structures, $k = 25 + 2m_C$ if $m_C < 8$, and k = 42 if $m > 8$. For carbon atoms not in ring structures, $k = 25 + 3m_C$ if $m_C \quad 8$, and $k = 50$ if $m_C > 8$.

Two schemes based on vapor pressure data have been offered by DIPPR[66]. One is an iterative scheme similar to Blinov's, but based on more recent Russian research. The second one assumes that the flash point temperature is the temperature at which the vapor pressure reaches its LFL value, that is:

$$P_f(T_{FP}) = LFL \cdot P_{tot} \qquad (2)$$

where LFL is in units of volume-fraction. Since LFL is normally tabulated in units of vol%, using the latter, the relation becomes:

$$P_f(T_{FP}) = \frac{LFL}{100} P_{tot}$$

where $P_f(T_{FP})$ = vapor pressure of fuel at the flash point (Pa) and P_{tot} = total pressure (Pa). To use this scheme, it is necessary to know (1) the LFL, and (2) the vapor pressure for the substance, as a function of temperature. The solution is made by trial-and-error, plugging in various values of temperature and finding the temperature for which the above relation is satisfied. Figure 21 shows that, apart from a small number of outliers (which may well be due to errors of measurement), the method gives reliable results. In practice, however, it is easier to measure the flash point than the LFL, so the method would be more useful for estimating the LFL from a known flash point value.

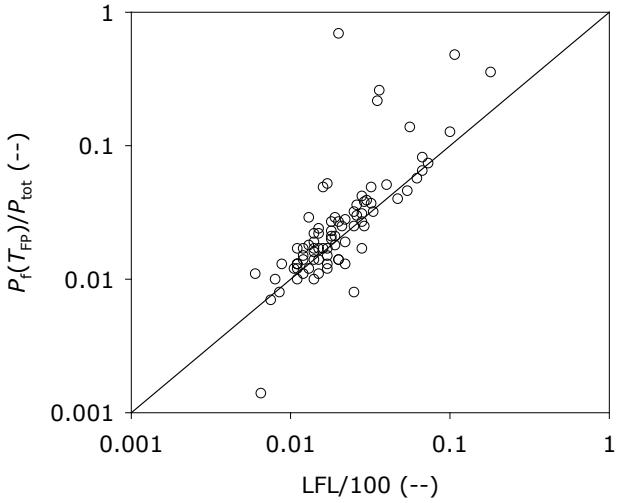


Figure 21 Prediction of T_{FP} according to a DIPPR method (for 81 pure substances[62])

While reasonable predictions may often be achieved, the practicality of schemes based on knowing the vapor pressure of the substance is questionable. Vapor pressure data are available for fewer substances than are flash points; in addition it is much quicker and less expensive to send a sample to a laboratory for flash point testing than it is to experimentally determine a vapor pressure vs. temperature curve.

FLASH POINTS OF MIXTURES

Two liquids may be miscible or not. If they are not, in quiescent conditions one liquid will float on the other. The flash point of two immiscible liquids is determined solely by the flash point of the lower density liquid, that is, the one which floats on top.

For mixtures of miscible fluids, both ideal and non-ideal, Le Chatelier's Law is obeyed. Le Chatelier's Law states that for a multi-component mixture the LFL will be such that:

$$\sum_i \frac{X_i}{LFL_i} = 1 \qquad (3)$$

where X_i is the vapor-phase volume fraction of component i, and LFL_i is its lower flammability limit, expressed as a volume-fraction. Further relations depend on whether the mixture is ideal or not. A rule of thumb is that mixtures are generally ideal if the components are all from the same family of organic compounds (e.g., all alcohols, all ketones) and non-ideal otherwise.

IDEAL MIXTURES

Le Chatelier's Law is not sufficient to compute the flash point of a mixture, since it does not tell us the vapor pressure (and therefore, X_i) of a particular component in the mixture. For an ideal mixture, according to Raoult's Law, the total vapor pressure of the mixture, P_{tot} is:

$$P_{tot} = \sum_i X_{Li} P_i \qquad (4)$$

where X_{Li} = liquid-phase mole fraction of component i in the mixture, and P_i = vapor pressure of the pure component i. From Eq. (2), it is possible to substitute LFL_i by $P_i(T_{FP,i})/P_{tot}$, where $P_i(T_{FP,i})$ = the vapor pressure of component i at the flash point of pure i. On substituting this equality, along with Eq. (4) into Eq. (3), gives:

$$\sum_i \frac{X_{Li} P_i(T_{FP})}{P_i(T_{FP,i})} = 1 \qquad (5)$$

This equation is implicit for T_{FP}, but it can be solved by trial-and-error iteration. As mentioned above, reference sources are available that give Antoine equation expressions for $p(T)$. Thus, since T_{FP} is known for each pure component, $P_i(T_{FP,i})$ can be found for each from its pertinent Antoine equation. A trial value of TP for the mixture is then assumed. T_{FP} values are tried iteratively until the summation in Eq. (5) comes out 1.

Example

An example of an ideal mixture is the ethylene glycol/methanol system. The mixture is ideal, since both components are alcohols. Experimental flash point results are shown in Figure 22[67]. Note that flash points do not follow a linear relation, even for ideal mixtures. The estimated values were obtained by using the following Antoine equations for vapor pressure:

$$p = \exp\left(13.63 - \frac{6022}{T - 28.25}\right) \qquad \textit{ethylene glycol}$$

$$p = \exp\left(11.88 - \frac{3613}{T - 34.85}\right) \qquad \textit{methanol}$$

where p = vapor pressure (atm) and T = temperature (K). The measured flash point for pure ethylene glycol is 114ºC and for methanol 11ºC. The calculated values agree reasonably closely with the measured ones for intermediate compositions.

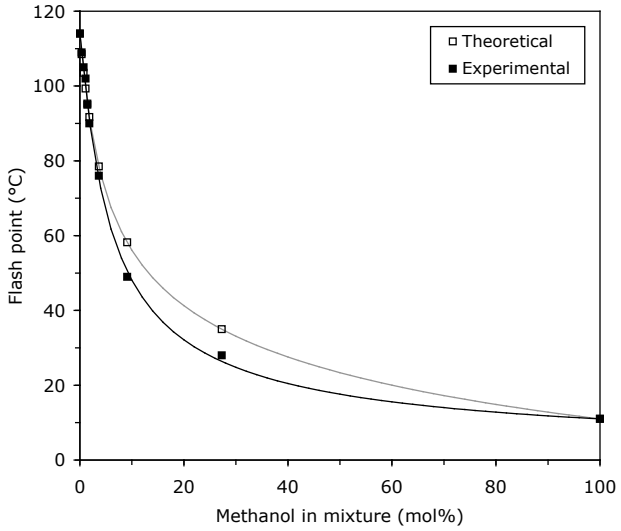


Figure 22 Flash points of ethylene glycol/methanol mixtures

Numerous accidents have occurred when a heater was fueled with kerosene fuel into which gasoline was added. The dominant effect is one of forcing out the fuel from the device due to internal overpressurization, since the vapor pressure of gasoline is higher. Ignition is then promoted due to a lowering of the flash point. Lentini showed[68] that adding 4% gasoline into kerosene drops its flash point from 49°C to ca. 6°C, as measured in the ASTM D 56 flash point apparatus. Data on open-cup flash points and fire points of mixtures of gasoline with automatic transmission fluid, brake fluid, engine oil, and power steering fluid have been reported[69]. The results indicate that (a) about 15 – 20% of gasoline mixed into any of the above fluids brings down their open-cup flash point to room temperature; and (b) while the fire points are significantly higher than the open-cup flash points for the pure fluids, the two values become indistinguishable once 15 – 20% of gasoline is added.

NON-IDEAL MIXTURES

Non-ideal mixtures show behaviors which can be surprising, if the user has not expected it. Adding a higher-flash-point compound may fail to raise the flash point of a particular compound, or even lower it. For example, adding up to 50% of *n*-butanol (FP = 29ºC) to *n*-octane (FP = 14ºC) fails to change the flash point of the mixture.

For non-ideal mixtures, an empirical correction is made to Raoult's Law by introducing an activity coefficient:

$$P_{tot} = \sum_i \gamma_i X_{Li} P_i$$

where γ_i = activity coefficient of component i (--). The activity coefficient varies with the concentration and also depends on the other molecules present in the mixture. Values

greater than 1 denote substances which have a greater vapor pressure in a mixture than proportional to its mole-fraction. The difficulty in using this equation is that activity coefficients may be hard to find for binary systems and impossible for systems of more components. To overcome this problem, Walsham[70] developed an empirical method of prediction based on activity coefficients assigned to different chemical families. He further found that an empirical factor for molar mass improves the correlation. With this additional factor, Eq. (5) becomes:

$$\sum_i \frac{\gamma_i X_{Li} P_i(T_{FP})}{P_i(T_{FP,\,i}) \cdot M_i^{5/4}} M_{mx}^{5/4} = 1.0 \qquad (6)$$

where M_i = molar mass of component i, and M_{mx} = molar mass of the mixture. For a binary mixture, the values of γ_i are found from Table 5. The column headings denote the solute while the row headings denote the solvent. Thus, for example, γ_i for alcohol in water is = 48.0. Apart from tabulated generic values such as Walsham's, group-contribution calculation schemes for activity coefficients exist and more sophisticated predictions can be based on them[71].

Normally, if a non-volatile solid is added to a solvent, the vapor pressure will be reduced and, consequently, the flash point can be expected to be raised. This generalization is implicitly based on Raoult's Law, but Kamarchik[72] has shown it not to be obeyed for xylene/polystyrene mixtures. When polystyrene, which has a negligible vapor pressure, is dissolved into xylene, the flash point of xylene is decreased, and is decreased linearly with the amount of polystyrene dissolved.

If a non-flammable liquid is miscible with a flammable one, there is usually a fraction reached beyond which the mixture becomes non-flammable (i.e., has no flash point), but this limit usually requires a very large amount of the non-flammable liquid. For example[73], pure methanol has a FP of 7ºC; a 40/60 mixture of methanol/water has 30ºC; and it requires reaching a 5/95 mixture before a non-flammable condition is obtained (Figure 23).

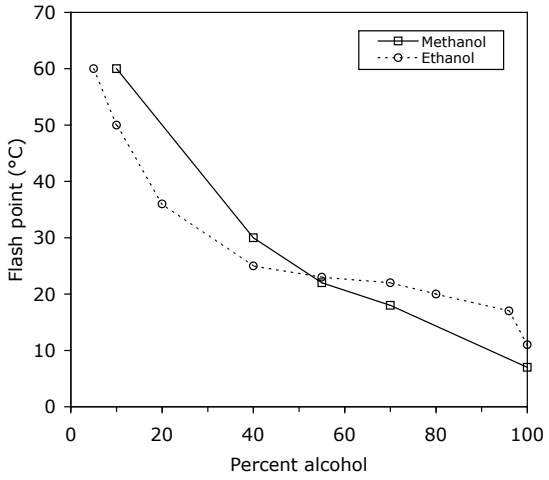


Figure 23 The flash points of alcohol/water mixtures

MIXTURES WITH HALOGENATED COMPONENTS

Great care must be used in interpreting flash point measurements on mixtures containing halogenated substances (substances containing chlorine, bromine, or other atoms from the halogen series of the periodic table). Halogen atoms serve to retard combustion by breaking the chain reactions; thus, mixtures containing halogenated components may show high flash points in a closed-cup flash point tester. However, if the halogenated component is more volatile than the remaining fraction, in case of a spill of the substance in open air, the halogenated component will evaporate first and will subsequently be gone. The non-halogenated portion remaining will then be able to ignite at temperatures significantly below the reported T_{cc} value. A

Table 5 Binary activity coefficients for various chemical families

Type	1	2	3	4	5	6	7	8	9
1	1.0	1.0	12.7	33.9	2.9	2.7	3.7	2.0	48.
2	1.0	1.0	15.0	57.0	2.8	2.2	3.7	2.0	28.
3	5.0	5.2	1.0	1.3	1.0	1.2	2.0	1.3	83000.
4	6.8	25.	1.4	1.0	2.6	2.8	7.4	4.0	300000.
5	3.0	2.1	1.2	2.8	1.0	1.0	1.6	1.1	1200.
6	2.5	2.0	1.5	4.3	1.0	1.0	0.7	1.3	180.
7	13.0	4.4	1.0	3.6	1.0	1.0	1.0	1.5	519.
8	3.1	1.8	1.3	8.8	1.1	0.9	0.7	1.0	350.
9	3.8	2.0	575.	1000.	8.3	12.	16.	2.4	1.0

Key: 1 – alcohols (e.g., *n*-butyl alcohol)
2 – ether alcohols (ethylene glycol monoethyl ether)
3 – aromatic hydrocarbons (cumene)
4 – aliphatic hydrocarbons (nonane)
5 – esters (*n*-butyl acetate)
7 – ketones (methyl isobutyl ketone)
8 – glycol ether esters (ethylene glycol monomethyl ether acetate)
9 – water

number of serious losses have occurred when users were falsely reassured by high T_{cc} values of paint thinners containing methylene chloride. ASTM flash point standards do not give guidance on this issue, but Department of Transportation regulations do address the problem. The DOT regulations (49 CFR 173.120) specify that if the substance is a mixture and if $T_{cc} > -7°C$ is measured, then a second test must be made of a partially-evaporated substance, and the reported T_{cc} must be the lower of the two. The evaporation regimen requires placing the liquid in an open beaker such that the ratio of the volume to the exposed surface area is 6:1. Before sampling, the beaker is to sit at ambient conditions for 4 h, or until 10 vol% has evaporated, whichever comes first.

Apart from validity of measurement, when solvents contain a significant component of methylene chloride, anomalous flash point test results are obtained[74]. In closed-cup testing, a greatly enlarged pilot flame is seen, while in open-cup testing a blue halo results. Either condition prevents a definite flash point from being determined.

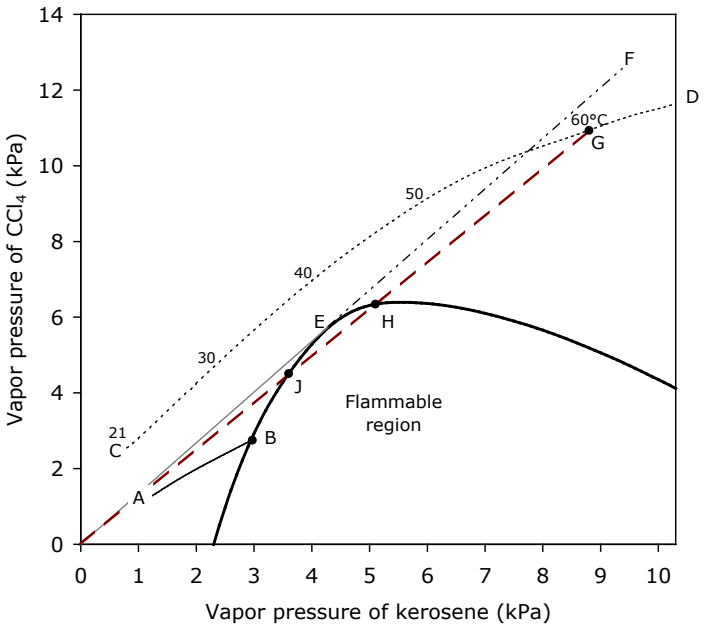


Figure 24 Flash point relations for a mixture of kerosene and CCl_4 (the Gerstein anomaly)

ASTM flash point standards do caution the user about a second mis-application of flash point results for mixtures. For mixtures where the more volatile component is also the more flammable one, vaporization losses from a sample will mean the sample being tested exhibits an incorrectly high flash point result. Thus, sampling procedures must be in place to assure that the more volatile components have not been lost. Unrepresentativeness of tested sample becomes a serious problem when using open-cup flash testers with heavier petroleum products[75].

In addition to the above issues with both the correctness and the meaningfulness of test procedures, a different problem has been found by Gerstein and Stine[76]. When a halogenated component is added to a hydrocarbon, it is possible to observe anomalous results on occasion in using a flash point tester. It will be assumed for illustration that the halogenated component which has no flash point is incapable of burning, although this, of course, is not an iron-clad rule, by any means. Such a mixture may exhibit no flash point, yet, may ignite at locations in the test apparatus where the vapor vents to the outside. This burning does not qualify as a flash point according to the test procedures, yet clearly demands to be understood.

The anomalous behavior can be understood by referring to Figure 24. Suppose the proportions of kerosene and carbon tetrachloride (CCl_4) in the liquid phase are such that the relative vapor pressures at room temperature are at point A on the diagram. This means that the mixture is non-flammable at room temperature. As the temperature of the liquid in the flash-point tester cup is raised, the vapor pressures will move along the line A-B. At point B, the temperature will have just attained its flash point value and a flashing will be observed. Any higher temperatures would move into the flammable region and they would also register flashing, at least until the upper flash point is reached.

Suppose now that there is less kerosene and more CCl_4 in the liquid, so the vapor pressures at room temperature are at point C. As the temperature is progressively increased, the vapor pressures will move along the line C-D. At 60ºC, the vapor pressures will be at point G. The kerosene/CCl_4 vapor at this value of temperature and of relative vapor pressures is non-flammable. Suppose now that some air is mixed in with this vapor. Mixing in air does not change the relative kerosene/CCl_4 proportion, but reduces both by the same measure. Thus, the diluted mixture will now follow the straight line G-0, where 0 is the origin. When the mixture is sufficiently diluted to reach point H, combustion will occur. This is the 'anomalous' behavior identified by Gerstein and Stine. It occurs because the line C-G which was followed by raising the temperature of the liquid and the vapor equilibrated with it is curved, while line G-0 is straight. The behavior will occur any time that a fuel/diluent vapor mixture passes to the right of line E-F. The line E-F is a straight line that starts at the origin and is tangent to the flammability curve (the solid black line).

To discover why line C-G-D is curved, we can consider a mixture where Raoult's Law and Clausius-Clapeyron equations hold. Then the partial pressures of the fuel *f* and the inert *i* in the vapor phase will be:

$$p_f = X_f \, p_f^o$$

$$p_i = X_i\, p_i^o$$

where X_f = mole fraction of fuel in liquid = $(1 - X_i)$, and p^o denotes the vapor pressure of a given temperature of the pure liquid. The pressure-temperature relation can be obtained from the Clausius-Clapeyron equation:

$$p_f^o(T) = \exp\left[\frac{\Delta h_{v,f}}{R}\left(\frac{T - T_{b,f}}{T \cdot T_{b,f}}\right)\right]$$

$$p_i^o(T) = \exp\left[\frac{\Delta h_{v,i}}{R}\left(\frac{T - T_{b,i}}{T \cdot T_{b,i}}\right)\right]$$

where h_v = latent heat of vaporization, and T_b = boiling point. For a given X_f, the above four equations represent a non-linear relation between p_f and p_i, since the temperature effect is non-linear. Thus, the line C-G-D is curved. The Gerstein anomaly is not dependent on the validity of Raoult's Law or the Clausius-Clapeyron equation. Thorne[77] has provided a number of illustrative calculations of the phenomenon for mixtures that do not obey Raoult's Law or the Clausius-Clapeyron equation.

FLASH POINTS OF PETROLEUM DISTILLATES

For paint thinners that are petroleum distillates without significant gaps in their distillation curve, a very good approximation is[78]:

$$T_{cc} = 0.719(T_b - 101)$$

where T_{cc} is the Tag closed-cup flash point (ºC) and T_b is the *initial* boiling point, as determined by ASTM D 86[79]. (For a mixture, the boiling point rises as boiling continues and more volatile fractions are boiled off).

For mixtures of 'middle' distillates (i.e., fractions boiling in the range 90 – 370ºC), a formula was developed by Butler et al.[6] that allows the closed-cup flash point T_f of the mixture to be estimated, if the flash points are known for the constituents:

$$e^{4722/T_{FP}} = \sum_i X_i e^{4722/T_{FP}(i)}$$

where X_i = mole fraction of the i^{th} component, and $T_{FP}(i)$ = flash point (K) of the i^{th} component.

RELATION BETWEEN FLASH POINT AND MIE

For a fuel-gas/air mixture which is at a fixed fuel/air ratio, the MIE decreases with increasing temperature, as shown in Chapter 4. But the situation becomes more complicated when a fuel-vapor/air mixture is established in a closed space, in equilibrium with the liquid. As the temperature changes, the fuel/air ratio also changes under those conditions. This is exactly what happens in a closed-cup flash point tester, but flash-point testers are not equipped with means for changing the energy of the ignition source presented to the sample. In experimental arrangements where a spark of variable energy can be presented to the sample, it is found that there is an optimum sample temperature which gives the lowest value of MIE. Not only does lowering the fuel temperature raise the MIE, but so does raising it. Figure 25 illustrates a correlation developed on the basis of experimental data for Jet A fuel[80]. The high-temperature branch of the curve occurs because the mixture is becoming fuel-rich. For this particular fuel, the optimum temperature is about 11ºC above the flash point, but will vary for other fuels.

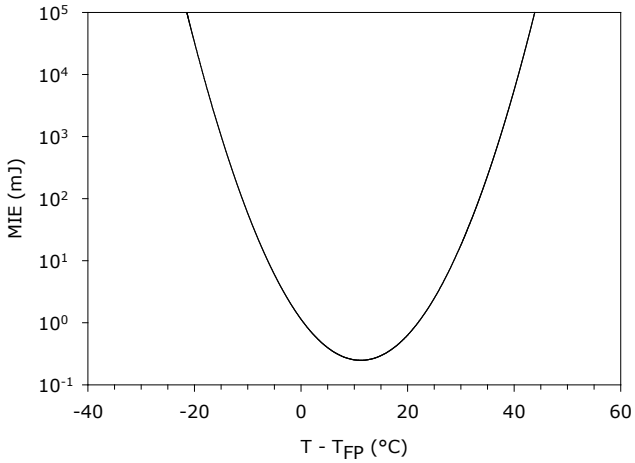


Figure 25 MIE needed for ignition of Jet A fuel in closed tanks, as a function of the difference between the fuel temperature and the flash point temperature

Piloted ignition of liquids

SPARK IGNITION OF LIQUID AEROSOLS OR SPRAYS

A *liquid aerosol* is a suspension of liquid particles in air fine enough (typically < 200 μm) that they are able to stay suspended, at least for a while. A *liquid spray* is generally the term used if the aerosol is being examined at a location close to where it is being generated, so that significant discharge velocities are present. Experimental work[81] has shown that if the droplets have a diameter smaller than 10 μm (0.01 mm), the combustion behavior is identical to the vapor of that substance. Droplets with a diameter > 40 μm burn individually, with a separate flame surrounding each droplet. Once initiated, a flame does not propagate if the nearest droplets are very far away; thus clearly there exists a LFL. The mean distance between droplet centers in the limit mixture is about 22 times the droplet diameter for droplets < 10 μm and about 31 times the droplet diameter for droplets > 40 μm. But larger-diameter aerosols are able to ignite and burn at lower fuel/air ratios, as discussed below. Liquid aerosols can be *detonated*[104], although this is difficult in laboratory experiments and would evidently be rare in real life. Bowen and Cameron[82] have reviewed many aspects, such as flame speeds, of explosions in clouds of liquid aerosols, but not their ignition aspects.

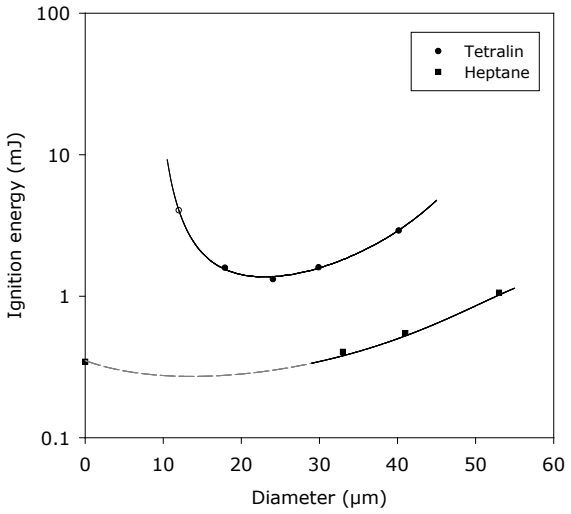


Figure 26 The effect of droplet diameter on the needed ignition energy of two aerosols

A majority of the studies on ignition of liquid aerosols have been done using *monodisperse* (i.e., all droplets are of the same size) particles, since this leads to the easiest interpretation of results. In practice, however, aerosols are commonly *polydisperse* (i.e., all droplets are not of the same size). There are many different ways in which an 'effective' diameter can be defined for an aerosol having a range of particle sizes, but not all will produce quantity which correlates ignition data from polydisperse aerosols with data from monodisperse aerosols. Unfortunately, there is not an agreement on the correct measure. Dietrich et al.[83] concluded that the Sauter mean diameter must be used. The Sauter mean diameter, D_{32}, is defined as:

$$D_{32} = \frac{\int_0^\infty D^3 n(D) dD}{\int_0^\infty D^2 n(D) dD}$$

where D = diameter (m), and $n(D)$ = probability of a particle having a diameter between D and D+dD. By contrast, Aggarwal[84] claims that another variable, D_{20}, is the only one that will give correct results. This is because D_{20} represents the average surface area presented by the particles and Aggarwal suggests that this is the true governing variable.

MINIMUM IGNITION ENERGY

The minimum energy for ignition depends on the *droplet diameter*. For spark ignition of liquid aerosols, droplets of 10 – 30 μm tend to require the least energy. Figure 26 shows this for tetralin[85] and heptane[86]. These results suggest that aerosols with the optimum droplet diameter are more readily ignitable than a pure vapor, but the data for this conclusion are not extensive. In other experiments on the tetralin aerosol, the spark gap width was varied and a shallow optimum of ca. 3.5 mm was found for the spark gap width. An analysis of the flame kernel for a liquid aerosol is very similar to that for gases, since the energy expended in vaporizing the liquid is only a few percent of the total spark energy. The combined effect of stoichiometry and droplet size[87] is illustrated in Figure 27 for tetralin and in Figure 28 for heptane. Over the range that it has been explored, fuel concentration has a monotonic effect on the MIE. In addition to the results shown in Figure 28, a study by Dietrich et al.[83] showed that over the range of equivalence ratios from 0.7 to 2.2 increasing *fuel concentration* invariably decreased the MIE. More limited data show that raising the *oxygen concentration* reduces the MIE[83].

For the regime of particle diameters ≥40 μm, Ballal and Lefebvre[88] obtained data (Figure 29) showing a power law relation:

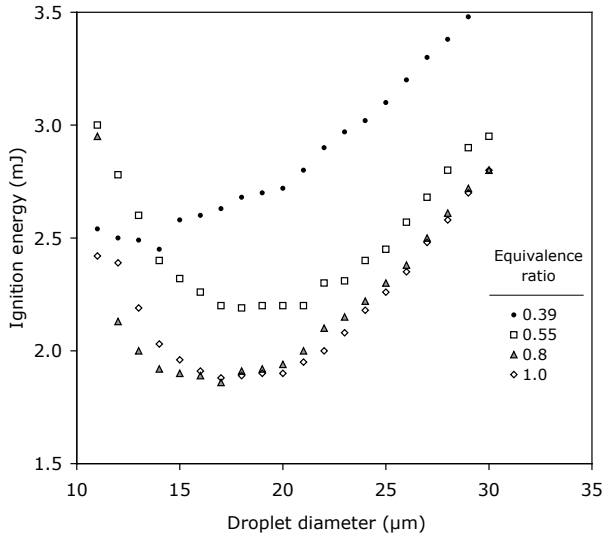


Figure 27 Effect of stoichiometry on ignition energy for tetralin aerosols of various droplet sizes

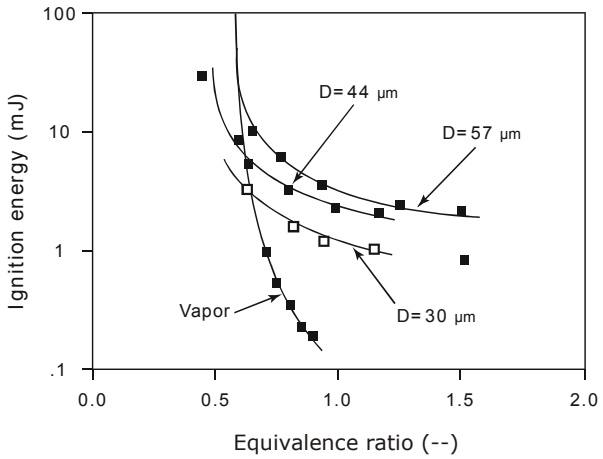


Figure 28 Effect of stoichiometry on ignition energy for *n*-heptane aerosols and vapor

$$MIE \propto D_{32}^{4.5}$$

where D_{32} is the Sauter mean diameter (μm) of the droplets. They, along with other authors[89], consider that $MIE \propto d_{\|}^3$. Ballal and Lefebvre also produced theories for $d_{\|}$ in both stagnant and flowing conditions. Their theory for stagnant conditions or low-velocity conditions[90] gives that:

$$d_{\|} = D_{32}\left[\frac{\rho_f}{\rho_a \varphi \ln(1+B)}\right]^{1/2}$$

where ρ_f = density of liquid (kg m^{-3}), ρ_a = density of air (kg m^{-3}), φ = equivalence ratio (--), and B = Spalding B-number* (--):

$$B = \frac{\Delta h_c / r + C_{pa}(T_f - T_b)}{L + C_{pf}(T_b - T_a)}$$

where Δh_c = heat of combustion (kJ kg^{-1}), r = stoichiometric air/fuel mass ratio (--), C_{pa} = heat capacity of air (kJ kg^{-1} K^{-1}), C_{pf} = heat capacity of liquid fuel (kJ kg^{-1} K^{-1}), L = latent heat of fuel vaporization (kJ kg^{-1}), T_f = flame temperature (K), T_b = boiling temperature of fuel (K), T_a = ambient temperature (K). Their theory for turbulent air stream conditions[88] gives:

$$d_{\|} = \frac{0.32 C_{pa}\rho_f}{\lambda_a \varphi \ln(1+B)}\left[\frac{D_{32}^3 u' \mu_a}{\rho_a}\right]^{1/2}$$

where λ_a = thermal conductivity of air (W m^{-1} K^{-1}), u' = root-mean-square velocity fluctuation component (m s^{-1}), and μ_a = dynamic viscosity of air (18×10^{-6} kg m^{-1} s^{-1} at ambient temperature). In both cases, the authors suggest additional corrections for aerosols which are not monodisperse.

In a related study, Ballal and Lefebvre[91] obtained data which point to the importance of the spark gap distance. Figure 30 shows that the MIE of aviation kerosene is nearly identical for gaseous mixtures and for aerosols of 40 μm diameter. But this presumes that the mixtures were tested at their optimal spark gap distance. If the spark gap is kept constant while droplet diameters are varied, some anomalous results may be found. Note also that the optimum gap distance is smaller for aerosols than for gases. These tests were run with plain-tip spark electrodes, thus they do not show the 'flat-bottom' curves characteristic of data obtained by the Bureau of Mines with flanged electrodes. Chan[87] obtained experimental data on the optimum spark gap distance for monodisperse tetralin aerosols. His results can be approximately represented as:

$$d_g = 0.04 d_p + 0.7$$

where d_g = spark gap distance (mm), and d_p = particle diameter (μm). A comparison to the aviation kerosene results of Figure 30 shows that the same equation would not apply

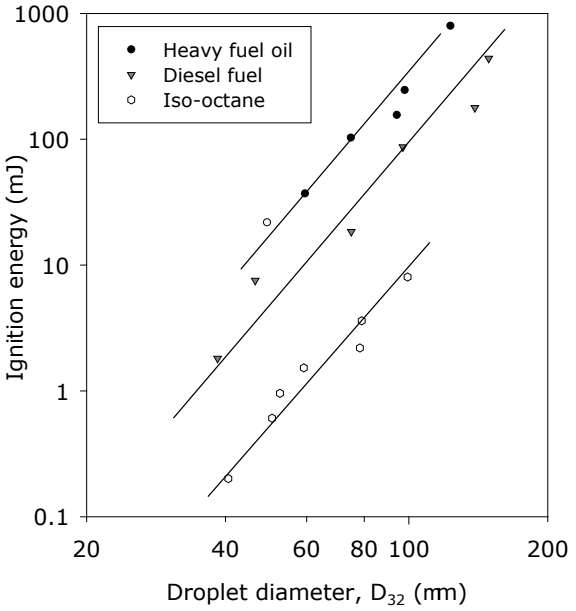


Figure 29 Effect of droplet diameter on MIE of aerosols with larger droplet sizes

to kerosene, but it can at least be concluded that increasing particle diameters will generally require an increased spark gap, if true MIE values are to be obtained.

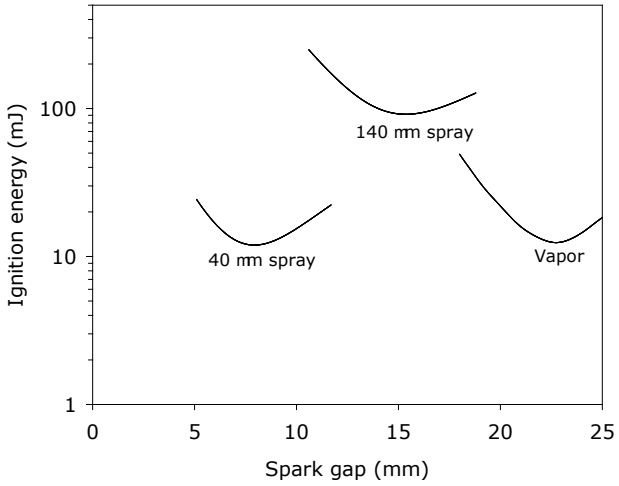


Figure 30 Effect of spark gap width on aviation kerosene vapor and sprays mixtures at 0.2 atm

The minimum ignition energy also depends on the *temperature*. This is illustrated in Figure 31 for various fuel sprays. The data are from Kuchta[92] and from Liebman et al.[93] Kuchta's droplet size was specified as less than 10 μm, while Liebman's drop size distribution was unspecified. Presumably the large differences between results are attributable to different drop size populations. Note that the temperature effect is much greater for liquid sprays than it is for gases (see Chapter 4).

* The Spalding B-number is a flammability parameter commonly used for liquids; a comprehensive presentation of the concept is provided in the textbook by Kanury, cited in *Further Readings*.

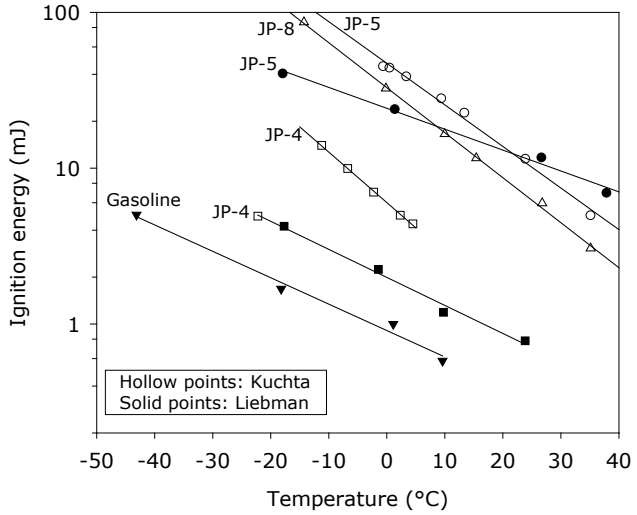


Figure 31 The MIE for various sprays

Reducing the *pressure* tends to raise the MIE, as shown by the data of Ballal and Lefebvre[91] in Figure 32.

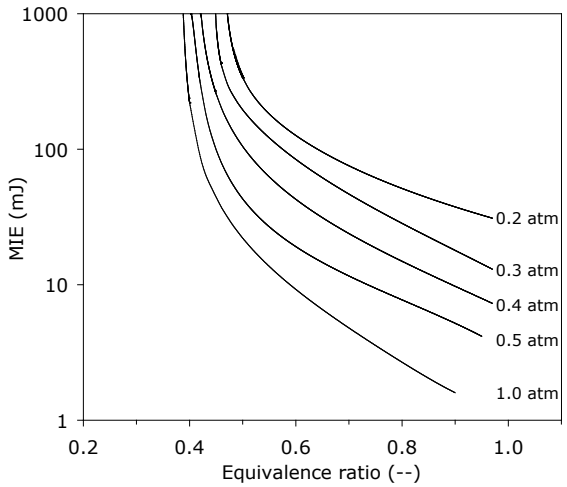


Figure 32 Effect of pressure on the MIE of sprays of aviation kerosene
(Copyright The Combustion Institute, used by permission)

Spark duration has a strong effect on the MIE needed, at least as found in experiments on kerosene sprays[94] in a flow-through environment with velocities of 20 – 50 m s^{-1}. Minimum values were found for spark durations of 35 – 80 μs, depending on various experiment conditions. If spark duration was increased or decreased by a factor of 2 from its optimum value, the needed ignition energy typically rose by roughly 50%.

Flow velocity generally increases the MIE, at least for large velocities. SubbaRao et al.[95] investigated the velocity effect for kerosene and found a steady increase in MIE with velocity for velocities greater than 30 m s^{-1}. Their data were limited in the low-velocity regime, but it seems that perhaps for velocities less than 20 m s^{-1} the effect would not be significant.

HIGH FLASH-POINT LIQUIDS

The flash point temperature of liquids does not apply to situations where the liquid is in the form of a spray, and it has been demonstrated that liquid sprays can be ignited at temperatures well below their flash point[96]. A number of experimental studies illustrate this for a variety of high-flash point liquids. Hydrocarbon mixtures with flash points of up 120ºC have been shown to be ignitable at room temperature by electric sparks when sprayed as large (millimeter-size) droplets[97]; similarly, petroleum products with flash points up to 130ºC have been reported[98] to be readily flammable in air as aerosols. It is also reported[99] that ignition of hydraulic fluid sprays under ambient pressure/temperature conditions is readily achieved with a small natural-gas pilot flame for both MIL-H-5606 (FP = 89 – 102ºC) and MIL-H-83282 (FP = 210 – 221ºC). Cook et al.[100] sprayed OM 13 and OM 33 oils with hypodermic needles into a version of the BM glass-tube flammability tube. These are UK military hydrocarbon oils having flashpoints > 160ºC. Drop sizes were 80 – 300 μm and the authors did not have any difficulty in creating flame propagation. The most important early study was that of Eichhorn[101], who found that mists of peanut oil (FP = 324ºC) could be ignited and burned "as readily" as Stoddard solvent (FP = 43ºC). In his experiments, the aerosol was sprayed into an open glass vessel, so it appears that preheating of the walls was not required for combustion. Eichhorn ignited his sprays with an electric spark, but did not measure the size distribution of the droplets. He also showed that six other liquids, with intermediate flashpoints of 71 to 229ºC, burned readily.

Recently, Hirsch et al.[102] also conducted a study using a wide variety of liquids. They used an open-spraying rig in which a nozzle was simply used to spray the liquid horizontally as a free jet. In addition, they measured explosion pressures by repeating tests inside an explosionproof vessel. Drop sizes were typically 0.35 – 0.9 mm. The test fluids involved a variety of dry-cleaning chemicals and cutting oils which had flash points ranging from 45 to 240ºC and AIT values of 215 – 375ºC; actual identities of the fluids were not given. Their results were:

- No effect of flash point was found on the explosion pressures developed.
- Liquids with FP < 100ºC were all ignited with an electric spark of 1.1 J.
- Liquids with FP > 100ºC were all successfully ignited with a spark of 10 J (intermediate values were not explored).
- Mechanical grinding sparks from a cerium-based (igniter 'flint') rod ignited all sprays; mechanical grinding sparks from 12 different steel alloys ignited no sprays.
- Hot spots created by mechanical rubbing or grinding ignited all liquids if they showed a red glow. Fireballs several meters in diameter were produced in this way.

- Steel rods electrically heated to 800 – 900ºC ignited all sprays (Color Plate 7); the needed ignition temperature bore no relation to the AIT of the liquid.
- When sprayed liquid was deposited as a film upon a surface, low-FP liquids (50°C) resulted in sustained, difficult-to-extinguish fires, but high-FP (> 200ºC) liquids did not sustain this type of surface burning.

In addition, they conducted another series of experiments where ignition sources were introduced into a closed chamber which was filled with mists of very small diameter (< 10 μm) but with actual spraying stopped before introducing an ignition source. No ignitions were obtained in these non-replenished atmospheres and it appeared that it was not possible to reach the LFL under such stagnant conditions. Apart from the study by Hirsch et al., there are additional data which suggest that it is very difficult to create a flammable cloud in air from a high flash point liquid if the spraying is not continuous. Earlier at the same institution, Förster and Steen[103] studied this problem for octanol (FP = 81ºC). Eckhoff[104] summarized their study and noted that coagulation generally prevents such clouds from being flammable a short time after spraying is stopped. He concluded that the inter-drop distance in the explosible range may typically be as small as 10 drop diameters, which leads to rapid coagulation of an initial population of small drops. These now-larger drops will then rain out and the mixture will no longer be in the flammable zone.

A case history of an explosion of a tanker truck being filled with a 65°C flash point gas oil has been described[156]; it occurred due to 'splash filling,' which creates an aerosol in the tank. This appears to be a relatively rare accident, and typically ignitable concentrations of high flash-point fuels such as diesel oil are not reached, except if there is extreme frothing[161]. In the latter case, the froth may become ignitable and, if ignition occurs, flames may then propagate to the previously-too-lean mist above it. *Foams* or *froths* of flammable liquids can be created by mechanical agitation or by depressurizing a vessel which contains dissolved gases. In the latter case, gases which are now no longer able to be dissolved froth up to the surface. Foams share some traits of liquid aerosols, but there are very few ignition studies. BM conducted a few experiments[105] where kerosene, which has a flash point over 38ºC, was foamed up inside a closed container at 20ºC. It could be readily ignited from a spark and led to a full propagating fire of the contents. Britton[161] documented a few case histories involving liquid foams. He also pointed out that if a froth is produced by decomposition of an oxidizing agent (e.g., hydrogen peroxide), the oxygen-enriched froth may be flammable even if within an originally-inerted vessel. Additional laboratory studies with liquids of above-ambient flash points are considered in the next Section. Aerosols of *frozen liquid droplets* can be ignited, if present in sufficient concentration, even though the vapor pressure of a frozen liquid is nearly zero[161].

LIMITS OF FLAMMABILITY FOR LIQUID AEROSOLS

As with other dispersed combustibles, limits of flammability exist for liquid aerosols. Perhaps the earliest study was by Haber and Wolff[106], who reported in 1923 that the LFL for aerosols is the same as for vapors. Later studies showed that for droplets smaller than 10 μm, the LFL is indeed identical to that of the vapor at the same temperature. But for larger diameters, the results apparently vary according to the fuel type. Figure 33 shows that for tetralin[81,107,109] (FP = 71ºC) the LFL decreases with droplet diameter, but for kerosene[105] it rises. The results of Zabetakis that are shown for kerosene may be questionable, however, since Mizutani et al. obtained results for No. 2 fuel oil that were quite similar to their tetralin results (e.g., a straight, downward sloping line) and chemically, fuel oil behaves rather similarly to kerosene. For *n*-decane[29] (FP = 46ºC), the LFL drops from 43.6 g m^{-3} for a gas, to about 10 g m^{-3} for aerosols of droplets having a diameter of 40 – 140 μm. The measurements involved are difficult to make and curves such as shown in Figure 33 should only be viewed as approximate, since using a different experimental method tends to produce significantly different results[100].

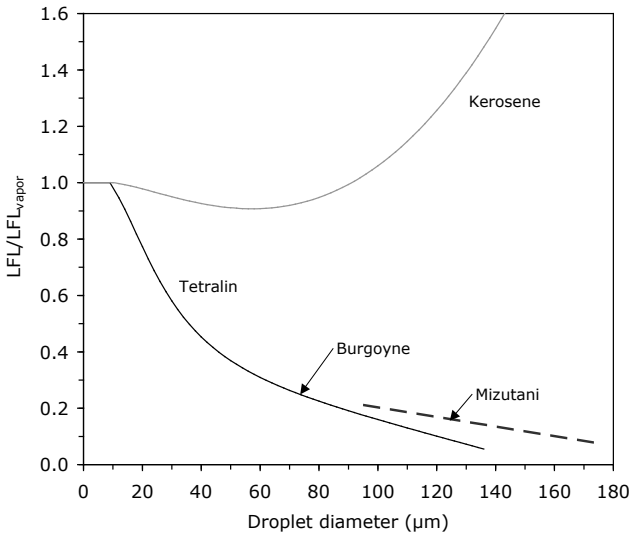


Figure 33 Dependence of LFL on droplet diameter for two liquid aerosols

To consider why larger droplets having a lower LFL than the corresponding vapor, the measuring apparatus must be considered. An apparatus very similar to BM flammability tube (Chapter 4) been used for studying liquid aerosols[108]. A mixture is established in a long cylinder having an open bottom. A small flame is applied at the bottom and it is observed whether a flame can propagate all the way up to the top. If it can, the mixture is considered to be flammable. A diameter of ca. 50 mm is considered to give suitable results. The LFL for an aerosol is expressed in fuel-concentration units (g m^{-3}). This can be presented as a curve of LFL versus mean droplet diameter. In this test environment, Burgoyne[109] explained that the diameter effect is due to sedi-

mentation motion of the larger droplets. The fuel concentration at the flamefront, in fact, remains nearly constant irrespective of diameter. But the flamefront concentration, for such large droplets, is no longer identical to its volume-average concentration. Instead, it is expressed as:

$$c_f = c_m \frac{v_f + v_a + v_s}{v_f + v_a}$$

where c_f = flamefront concentration, c_m = volume-average concentration, v_f = upward flame velocity, v_a = downward air flow velocity, and v_s = sedimentation velocity of the droplet relative to the air. The two concentrations are identical if $v_s \rightarrow 0$, which is true only for very small droplets. For droplets up to ca. 50 μm,

$$v_s = \frac{d^2 \rho g}{18 \mu}$$

where d = droplet diameter (m), ρ = droplet density (kg m^{-3}), and μ is the dynamic viscosity of air (18×10^{-6} kg m^{-1} s^{-1} at ambient temperature). The above results all refer to upward propagation. A limited study was performed by Burgoyne[110] for *downward* propagation of tetralin mists where he found that the LFL did not decrease with diameter and, for large diameter drops (> 0.5 mm), no flame propagation was possible at all, although individual burning droplet could drop down. A theoretical analysis by Mizutani[107] suggests that *horizontal propagation* results may be similar to those for downward propagation, but experimental data are not available.

The LFL of liquid mists is affected by *turbulence*. Förster and Steen[111] conducted tests with 50 μm diameter 1-octanol (FP = 81ºC) droplets. As the turbulent fluctuation velocity was increased from 0.44 m s^{-1} to 1.89 m s^{-1}, the LFL dropped by 60%. Other mists have not been studied in a similarly quantitative manner. A similar effect was found for *flow velocity*—raising the flow velocity of the mixture caused a drop in the LFL[94]. In a high-velocity flow, Anson[112] obtained some anomalous results with kerosene—raising the droplet diameter from 60 to 150 μm caused a monotonic *increase* in the value of the LFL; this issue has not been studied further.

There is one old study on the minimum oxygen concentration needed for combustion of liquid sprays. Sullivan et al.[113] tested a wide variety of liquids in a rig where the spray was spark-ignited at ambient temperature, but with variable oxygen content of the test chamber. For most hydrocarbon liquids, MOC values of 12 – 14% were found. But for chlorinated liquids, silicones, and other FR formulations, some quite-high values (up to 85%) were seen.

MESG OF LIQUID AEROSOLS

On rare occasions, the MESG of liquid aerosols has been studied. Using the procedures of the Health and Safety Executive in the UK, Capp[114] measured the MESG for three sprays of three liquids and found that they were 15 to 23% higher than MESG values on the corresponding vapors. The droplet size of the sprays was around 30 μm. The actual values will depend on the particle diameter, but it was concluded that the increase is generally modest. For design purposes, using the values obtained for the vapor would be conservative, but not excessively so.

HOT SURFACE IGNITION OF DROPLETS, SPRAYS OR SPILLS

SINGLE DROPLETS OF A PURE FUEL

The basic phenomenology has been studied for a single droplet, released at low speed in still air onto a hot surface[115-118]. With many ignition phenomena, ignition time decreases monotonically with increasing temperatures. This—dramatically—is not true with droplet/hot surface ignition. To understand ignition, it is first necessary to study the evaporation of droplets hitting hot surfaces. There are 6 different regimes for the evaporation process, as shown in Figure 34.

(a) When the hot surface temperature is below the fluid's boiling point, the droplet assumes a plano-convex shape and slow evaporation takes place.
(b) At the boiling point, a vapor bubble forms in the center of the drop.
(c) At a certain temperature, the maximum evaporation rate occurs, many small bubbles form within the droplet, and the evaporation process is violent.
(d) At higher temperatures, the drop breaks up into one large drop surrounded by small drops.
(e) At a higher temperature (approximately corresponding to the Leidenfrost temperature*), the droplet lifts entirely off the surface and resembles a squashed sphere.
(f) At the highest temperatures, the drop is spherical and is separated from the surface by a vapor film.

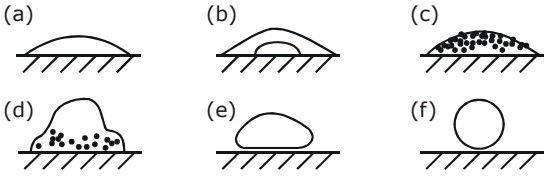


Figure 34 The regimes of drop evaporation on a hot surface

The nature of these six different regimes helps explain the relation between hot-surface temperature and the droplet vaporization time (Figure 35). There is a pronounced minimum in the curve which is, in effect, an optimal temperature for droplet vaporization. The curve of ignition time vs. temperature has a very similar shape, but is offset substantially towards the higher temperatures (Figure 36). The ignition time corresponds to the time that it takes to vaporize a specific drop mass, irrespective of the temperature. Roughly speaking, the ignition time is controlled by chemi-

* The concept of the Leidenfrost temperature is explained in most textbooks on heat transfer.

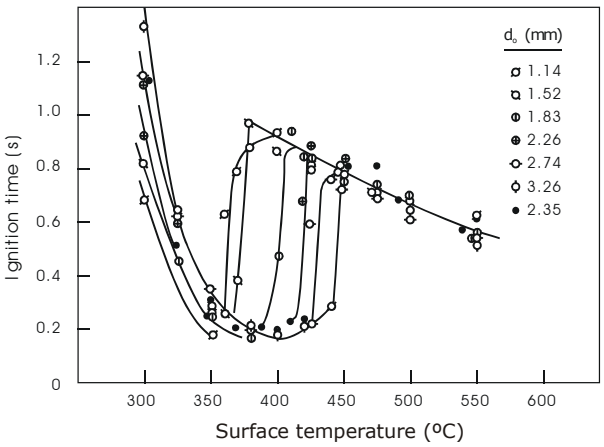


Figure 35 The time for evaporation of a cetane drop of a hot surface

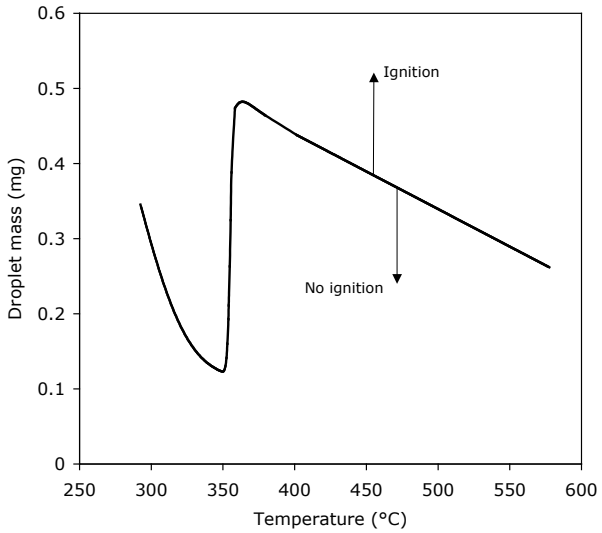


Figure 36 The time for ignition of a cetane drop on a hot surface

cal kinetics for temperatures less than the Leidenfrost temperature, and by physical processes at higher temperatures.

The abrupt increase in ignition time always corresponds to the time at which the drop ceases to have contact with the surface. Finally, there is a cr itical drop size below which ignition cannot occur (Figure 36). This critical size (expressed as either mass or diameter) is dependent on the surface temperature.

When viewed not from the point of view of the physics of evaporation but considering only the temperature needed for ignition, Cho and Law[119] concluded that there are four regimes for most hydrocarbon liquids (Figure 37), with the following temperature limits being roughly characteristic of dodecane:

Temp. (ºC)	Behavior
< 200	no ignition at all
200 – 290	vapor pocket ignition—no ignition is possible while drop is still present; ignition occurs immediately after drop finishes evaporating; flames are conical and sooty
290 – 650	ignition is possible only if atmospheric pressure exceeds a certain minimum value
> 650	no ignition while drop is still vaporizing; some time after completion of vaporization a flash fire is noted

The above results pertain only to 2 mm diameter drops; the authors also stated that for other pressures or diameters, it can be assumed that pd = constant, at least over some range, but the extent of the applicability was not stated.

Karasawa et al.[120] studied the ignition of single droplets in the range of 1.7 – 2.0 mm impinging on a hot surface. They found that heptane and diethyl ether drops could undergo either a n ormal or a co ol-flame ignition; however, most other tested fuels could not, as shown in Table 6, where AIT values are also shown for comparison, taken from Chapter 15.

Sommer[121] propelled single droplets of decane vertically upwards and close to, but not touching, a h eated metal plate. The minimum hot surface temperature needed for ignition was 800ºC for 53 µm particles, and 820ºC for 104 µm particles. Of more interest was the fact that ignition occurred at the lowest plate temperature not when the plate was directly next to the flight path, but rather when it was horizontally a certain distance away. For the smaller droplets, the optimal spacing was 0.2 mm, while for the larger it was 0.4 mm. The interpretation is that at too-close spacings,

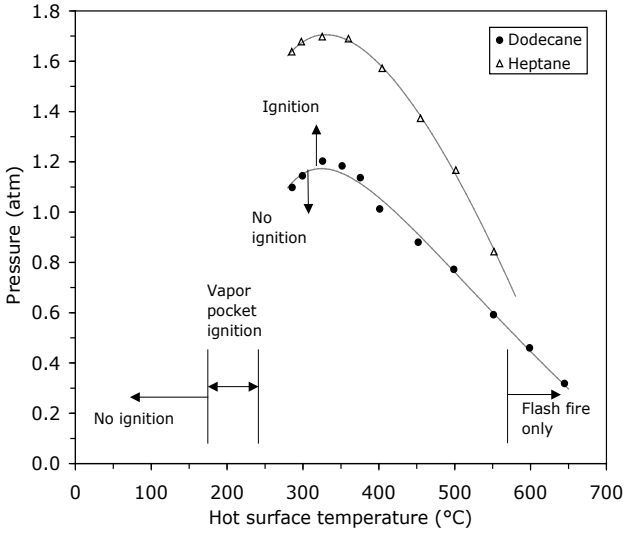


Figure 37 Hot-surface ignition regimes for 2 mm drops, as determined by Cho and Law

Table 6 Single-drop hotplate ignition temperatures found by Karasawa et al.

Fuel	AIT (ºC)	Hot surface ignition temp. (ºC)	
		Cool flames	Hot flames
diethyl ether	195	240	670
n-butanol	345	none	650
heptane	223	360	670
methanol	470	none	690
iso-octane	415	none	704
ethanol	365	none	717
styrene	490	none	738

an overly rich mixture was being created at the locations where temperature would have been optimal for ignition.

Satcunanathan[122] put forth a theory for ignition time of droplets on hot surfaces, but the simple theory, could, at best, only account for the left-hand branch of the curves in Figure 36. Several authors[123-125] developed more advanced theories, but these still ignore the non-spherical shape of actual droplets, their solutions are wholly numerical in nature, and validation data were not presented for the minimum hot-surface temperature needed for ignition of real fuels.

The broad conclusion that can be reached from the above studies is that, except for fuels which show a cool-flame ignition mode, the T_{ig} for a single drop falling onto a hot surface is typically 200 – 300ºC above the AIT.

HOT ENGINE SURFACES AND RELATED PROBLEMS

In this section, we consider the potential ignition of liquid sprays, streams, mists, etc. that come into contact with a heated surface. Here, the fuel originally starts as a liquid. Additional pertinent information in Chapter 4 may be consulted for cases where the fuel is fully pre-vaporized so that only a vapor contacts a hot surface. Ignitions of liquid fuels from hot surfaces most commonly occur in connection with a hot engine exhaust manifold. Exhaust manifold temperatures in passenger cars can vary over a large range[126] of 200 – 600ºC. The dull-red-hot temperature of 600ºC will only be reached if there is a serious engine problem; for a vehicle that is not malfunctioning, the upper limit is considered to be 500ºC[127]. Even 300ºC is above the AIT of many common liquids, thus researchers have needed to explain why such ignition incidents are relatively rare.

In one of the earliest studies on this subject, Wiezevich et al[128] reported in 1935 that individual drops of gasoline and of motor oil, dropped onto a 510ºC hot plate failed to ignite. But it later became clear that the amount of liquid discharged is an important variable, as evident from the experiments of Knowles, who used various quantities of turbine oil falling on a hot surface (Table 7). This is consistent with

Table 7 Ignition of spills of turbine oil on a hot surface[130]

Quantity	Min. ignition temp. (°C)
2 drops	450
5 mL	380
30 – 60 mL	315

a report[129] that lubricating oil ignited when 'poured' over a pipe which was at 293ºC.

In a 1951 report, Scull[131] reviewed the early literature on the subject and concluded that the temperature of a hot surface must greatly exceed the AIT of the fuel in order for ignition to occur. Some of the data he collected on ignition using non-enclosed environments, i.e., heated flat plates, are shown in Table 8. The wide data scatter is noteworthy and is still found among more recent research. The results shown in Table 8 were obtained using iron, steel, or nickel plates. In another study reviewed by Scull, it was reported that ignition temperatures using a copper plate were about 140ºC lower than for an iron plate. Scull hypothesized that this might be a thermal conductivity effect. He also noted that the high temperatures obtained are due to the geometric nature of the problem: only one surface is hot, and the rest of the surrounding environment is essentially at ambient temperature. The standard autoignition tests for liquids, by contrast, release a drop into a geometry where both the surface and the surrounding air are at, roughly, the same elevated temperature.

Table 8 Early research on hot surface ignitions summarized by Scull

Substance	Hot surface temp. (°C)
gasoline	560; 718 – 760
aviation gasoline	454; 585
ethanol	690
kerosene	650
diesel fuel	718 - 760
motor oil	718 - 760
hydraulic fluid	400
lubricating oil	430

Ferguson[132] studied the explosions of crankcases, in which connection he conducted experiments on mists of paraffinic-base and naphthenic-base lubricating oils. The oil was heated, then passed through an atomizing nozzle and into a cylindrical explosion tube which was heated to 65ºC. Air was preheated to the same temperature and supplied at varying velocities. A minimum temperature of 870ºC was needed for a Nichrome strip, 25 × 50 × 0.5 mm, to ignite the mixture. He found negligible effect of the oil type, the air flow rate (over the range 0.13 – 0.6 m s^{-1}) and the fuel/air ratio, provided the mixture was rich enough to ignite. When the system temperature was raised to 121ºC, the ignition temperature dropped to 760ºC. For air velocities higher than about 0.6 m s^{-1}, there was a gradual rise in the

Nichrome strip temperature needed for ignition. Increasing the size of the strip to 25 × 250 × 0.5 mm lowered the ignition temperature by about 110ºC. Adding up to 20% diesel fuel into the lubricating oils did not change the hot-strip ignition temperature. Ferguson's experiments were interesting in that he had an fully-enclosed geometry, and a heated one, at that, yet the T_{ig} values were much greater than the AIT. It emerged that enclosing the volume, by itself, is not a significant contributor towards lowering the ignition temperature. It is necessary that the enclosing surfaces themselves be at a high temperature and not just moderately heated.

The Tokyo Fire Department[133] found that gasoline leakage onto a manifold at 564ºC was not sufficient to cause its ignition, but that electric sparks due to leakage from a high-tension cord did suffice. They also found that engine oil would not ignite when sprayed on an exhaust manifold, but ignited when it collected in a low spot on the surface of the manifold.

Battista et al.[162] used two different test rigs to examine the ignitability of various fuels. For each fuel, 5 mL was applied by a pipette onto the heated surface—a simple heated tube and an actual diesel engine manifold. The results (Table 9) show that the only fuel which ignited at a relatively low temperature was methanol containing 4% of an unspecified 'cetane improver.'

Table 9 Results obtained by Battista et al. using two different hot-surface ignition rigs

Fuel	Hot-surface temp. (ºC) needed for ignition	
	Simple tube	Exhaust manifold
methanol (96%)/ cetane improver (4%)	450	300
methanol	620	> 700
methanol (85%)/ gasoline (15%)	635	> 700
diesel oil	> 650	700
gasoline	> 650	> 700

Goss[134] examined the ignition of several fluids on a hot steel manifold (Table 10), but with test details not specified. Snyder et al.[135] conducted tests on a number of hydraulic fluids tested using Federal Test Method Standard 791 (Method 6053). Their full results are given in Chapter 14; the only two common, commercial fluids were MIL-H-5606 (flash point 102º, manifold ignition 388ºC) and MIL-H-83282 (flash point 230ºC, manifold ignition 322ºC).

Phillips[136] reported results (Table 11) from various hydraulic fluids tested using the European CETOP RP 65H test[137]. In this test, 10 mL of fluid is discharged drop by drop onto a heated manifold.

Table 10 Hot-surface ignition temperatures determined by Goss

Substance	Manifold temp. (°C)
brake fluid (AP brand, DOT 3)	400
brake fluid (Unipart, DOT 3)	400
brake fluid (Castrol Girling Crimson)	650
engine oil	600
silicone oil	600

Table 11 Hot manifold test results for various hydraulic fluids

Fluid	AIT (ºC)	Flash point, open cup (ºC)	Manifold temp. (ºC)
mineral oil	350	200	350
carboxylate ester	415	266	400
phosphate ester	575	245	800
water-glycol fluid	NA	NA	> 800

Severy et al.[138] constructed a manifold simulation rig which was enclosed on 5 sides and open on the front (Figure 38). Using 10 drops of liquid and no forced air flow, they defined two levels of ignition—'consistent' and 'marginal.' Their results are shown in Table 12. A number of their values are identified here as approximate, since the authors only gave those results in a poorly drawn figure.

Table 12 Hot surface ignition temperatures obtained by Severy et al.

Fluid	Marginal ignition (ºC)	Consistent ignition (ºC)
brake fluid	ca. 410	ca. 500
diesel fuel	521	549
gasoline, leaded	ca. 510	610
gasoline, unleaded	ca. 520	627
motor oil	ca. 320	ca. 420
propane (liquid)	ca. 675	ca. 775

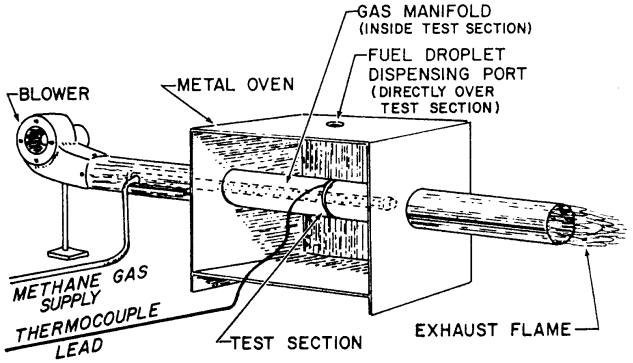


Figure 38 Hot manifold simulation rig used by Severy et al.

Goodall and Ingle[139] examined the hot surface ignition of various fuels in a stainless-steel test rig where the fluid spray was confined between two plates, a bottom plate heated to a higher temperature and a top plate heated to a lower temperature. Thus, it appears that the rig was a half-way mark between a hot plate being hit by fluid in open air, and the all-heated environment of an AIT test apparatus. Under conditions where the upper plate was at room temperature, about 335ºC was required for the ignition of JP-1. Room temperature values for the upper plate were not reached for JP-4 and mineral-base hydraulic fluid, but it appears, by extrapolation, for that case the hot-plate temperatures would have been about 400ºC. As the cold-plate temperature was progressively raised, a lower hot-plate temperature was needed for ignition. For a cold-plate temperature of 270ºC, JP-1, JP-4 and hydraulic fluid all showed hot-plate ignition temperatures of ca. 240ºC. Silicone-based hydraulic fluid and an ester-based turbine oil gave much higher temperatures under similar conditions (270ºC upper-plate temperature), to wit, 440ºC for the turbine oil and 490ºC for the silicone oil. Goodall and Ingle also ran some experiments with various wind velocities and found, as did other researchers, a monotonic increase of minimum ignition temperature with wind velocity. They also examined the effect of substituting aluminum surfaces for stainless steel and found no detectable difference. A comparison of their general results for JP-4 with Clodfelter's data (see below) suggests that their rig provided such a high degree of confinement that their geometry, in fact, approximated that of an AIT test.

A slightly different arrangement was studied by Graves et al.[140], who injected fuel into a forced air stream moving upwards in a circular duct. Downstream of the injection point, the duct walls were heated. The fuel mist was of very small drop size, on the order of 20 to 200 μm (0.02 to 0.2 mm). Under those conditions, they found that the fuel droplets were fully evaporated before they could impact to the walls. For Jet A fuel flowing at a stream velocity of 1 m s^{-1}, the results are illustrated in Figure 39. The wall temperature necessary for ignition was found to depend on the air stream velocity; at a flow velocity of 3 m s^{-1}, needed temperatures were about 70ºC higher.

Several studies focused on the ignition of fluid sprays in *a jet engine nacelle* of an airplane in flight. Since there is a non-zero air velocity in that environment, the studies focused on the effects of velocity. Atkinson and Eklund[141] used a flat plate arrangement, where small streams or sprays of jet fuels were directed onto a horizontal heated plate in various wind conditions. Their ignition results are shown in Figure 40.

A much more realistic geometry, in fact, an actual jet engine located in a wind tunnel, was used by Westfield[142], who was able to simulate flight Mach numbers up to 0.70. Temperatures along the engine were surveyed and a spray

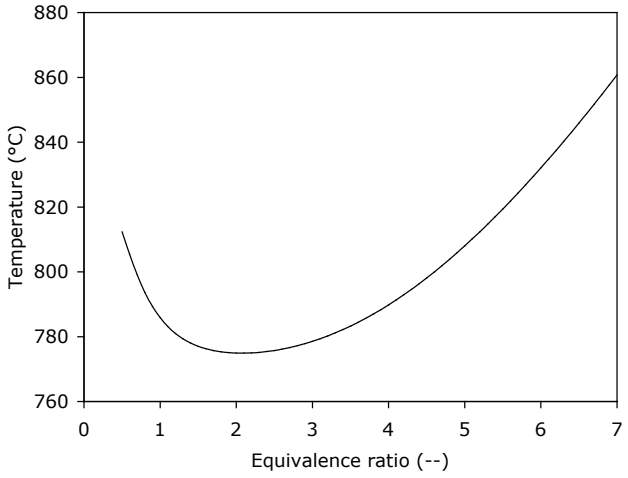


Figure 39 Effect of equivalence ratio on wall temperature needed for ignition of Jet A fuel (flow velocity = 1 m s^{-1})

nozzle was placed at the hottest location. At zero air flow rate, the hot surface temperatures needed for ignition were 450ºC for Jet A, 460ºC for Jet B, and 490ºC for MIL-H-5606 hydraulic fluid. Increasing the air flow rate generally made ignition more difficult, but the relation was not necessarily linear. Based on these results, Westfield concluded that a long-standing aviation industry guideline that hot-surface ignitions are unlikely if the surface temperature does not exceed 260ºC (500ºF) was conservative enough.

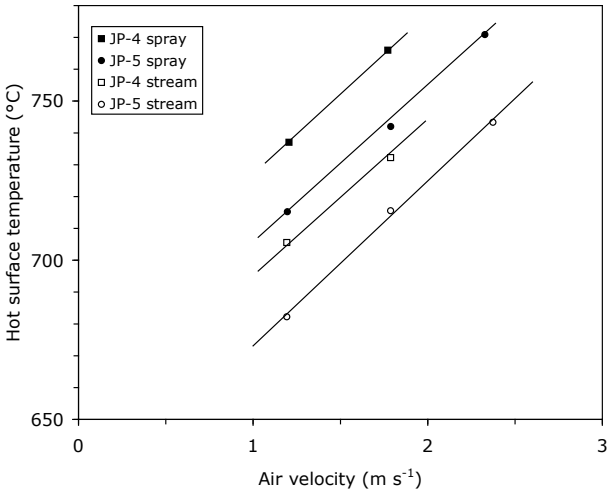


Figure 40 Hot surface (plate) ignition tests of Atkinson and Eklund

Myronuk[143] first conducted flat-plate experiments, but discovered that the residence-time was a critical factor. In his experiments, he was unable to retain the mixture for a sufficient time for ignition to occur. Thus, he then mocked up the fin-like obstructions that can be found on a real engine surface. He considered that the more realistic test geometry both prolonged the residence time and helped to create a

stagnation mixing region. His test results showed that there was no significant difference between the ignition of JP-4 and JP-5 aviation fuels and MIL-H-5606 hydraulic fuels, thus the results are shown in Figure 41 as one band. On the other hand, he found that the type of metal used made some difference. He attributed this to a combination of catalytic effects and of thermal insulation by an oxidation layer. Figure 42 shows ignition time results for JP-4 sprays in the same series of experiments.

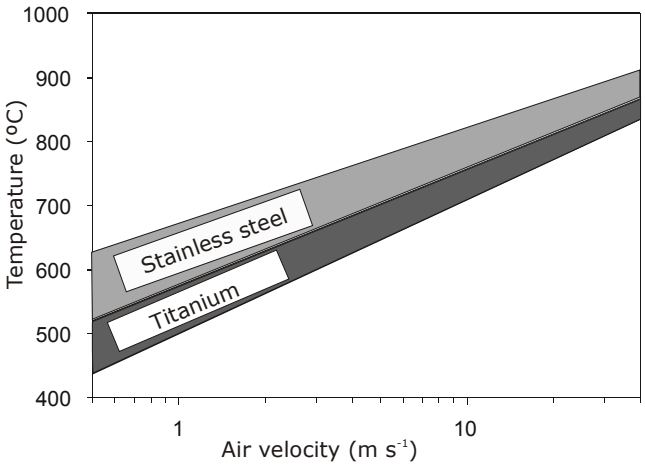


Figure 41 Myronuk's results for ignition of JP-4, JP-5 and MIL-H-5606 hydraulic fluids on hot engine surfaces

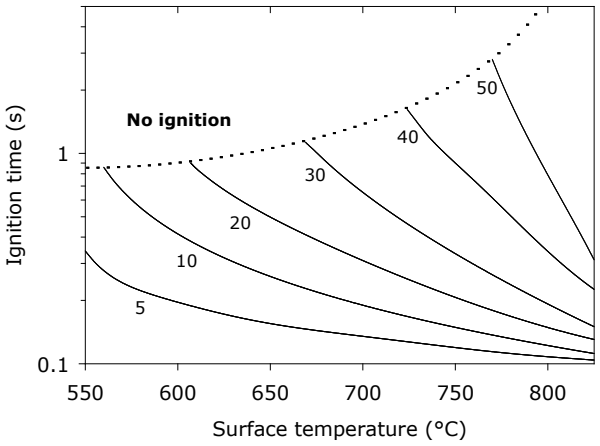


Figure 42 Myronuk's results for ignition of JP-4 sprays onto a hot engine surface, for various air flow rates (m s^{-1})

Similar tests were later performed by Clodfelter[144] using a realistic mockup of a jet engine. His results are shown in Figure 43. Unlike Myronuk, his results showed a clear difference between JP-4 and MIL-H-5606 ignitability. The flash point of JP-4 is –18ºC, versus +89ºC for MIL-H-5606 hydraulic fluid. However, the AIT of JP-4 is 240ºC, versus 227ºC for MIL-H-5606. It may be noted that these AIT values are very close, so if AIT values were controlling, the results should have been very similar. Instead, it is seen that the *lower* flash point liquid is much harder to ignite.

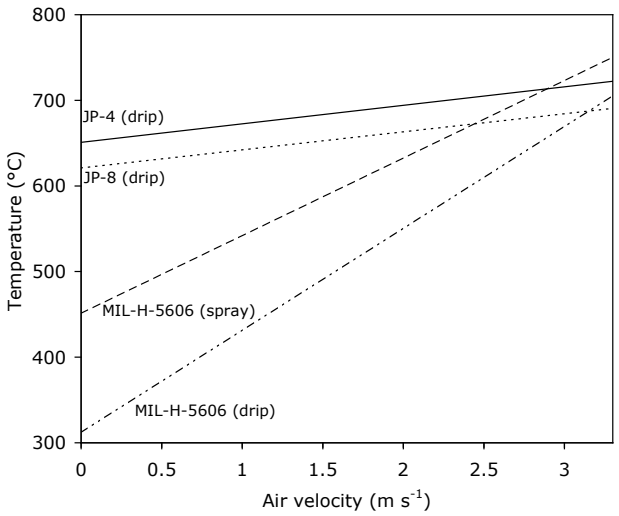


Figure 43 Clodfelter's results for ignition of drips and sprays onto a hot engine surface

Johnson et al.[145] explored the effect of *ambient pressure* on heated surface ignition temperatures. Using aviation fluids sprayed into a heated duct, they found a substantial pressure effect, with lower pressures giving higher ignition temperatures. Lowering the ambient pressure to 0.5 atm corresponded, roughly, to an increase of 250ºC in the hot surface ignition temperature for two hydraulic fluids.

The role of *time* was explored to a limited extent by Geyer and Moussa[146]. They used an engine nacelle simulator where fuel mists were applied for varying durations. Under some conditions, it was evident that fuel application needed to be fairly long (up to 1 min) for ignition to occur, but sufficient results were not obtained in order to derive quantitative relations.

It should not be much surprise to find that if a liquid is introduced into a fully enclosed space, then results similar to those obtained from AIT tests, rather than from hot-surface tests, will be obtained. Glendenning[147] demonstrated this by obtaining a 280ºC ignition temperature for aviation gasoline injected into the inside of a heated exhaust pipe.

While the above comprises a fairly long list of research studies, general guidance emerges only qualitatively. The reason why temperatures significantly higher than the autoignition temperature are necessary has to do with the distribution of fuel vapors in the vicinity of the hot surface. A location *in the gas* has to exist where

(a) the temperature is at or above the autoignition temperature;
(b) the fuel concentration is between the LFL and the UFL, as determined for that particular temperature; and
(c) the fuel/air mixture stays in a high temperature zone for a sufficient time.

Such a location will not exist until the surface is significantly hotter than the autoignition temperature. From these requirements, it can also be seen that if a partly- or fully-enclosed environment is involved, the needed temperature will drop, since there will no longer be a dropping temperature gradient with increasing distance away from the wall.

These considerations also make it clear that the temperature at which a hot-surface ignition can take place is not a constant of a substance, but is equally affected by the chemical nature of the substance and the environmental conditions. The latter include such details such as the amount of material dispersed and any imposed flow velocity. Experimental data indicate that there exists an inverse relation (Figure 44) between the flash point and the hot-surface ignition temperature, although, in view of the many variables governing the hot-surface ignition temperature, this relation is hardly quantitative.

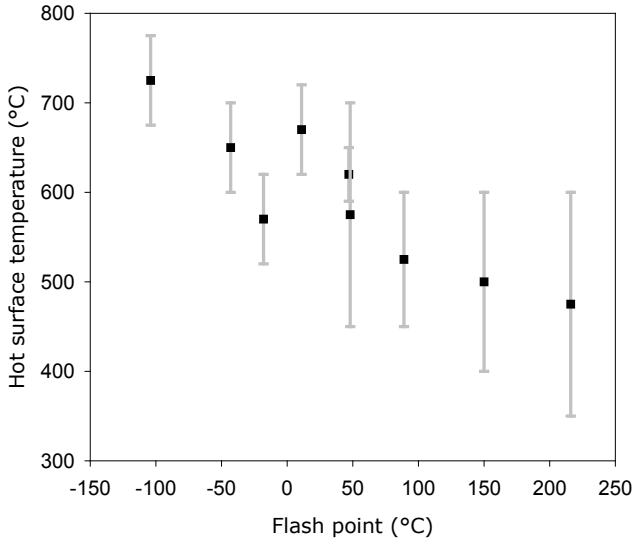


Figure 44 Relation between hot-surface ignition temperature and flash point

Most of the studies where velocity was varied indicate that an imposed velocity above a certain minimum value raises the surface temperature required for ignition. This is consistent with a minimum induction period interpretation, but is hard to evaluate quantitatively without elaborate experiments or complex computer modeling. Even early studies showed that results may be affected by the type of metal used for the heated surface, but no practical guidance has emerged on this point. Surface roughness plays a role in the evaporation process which is complicated and only partly understood. But Bennett[148] has reported on some preliminary research indicating that a surface with micro-cavities may be less prone to igniting some liquids.

The value of AIT is determined solely by the reactivity of the fuel. The value of the flash point is mostly a measure of the volatility of the fuel, although chemical reactivity plays a secondary role. The hot-surface ignition temperature can be viewed as being roughly equally affected by chemical reactivity and volatility. In the limit case, as the heated surface covers an ever-increasing fraction of the periphery of the volume under consideration, the value of the hot-surface ignition temperature must necessarily approach the AIT and volatility no longer plays a role. But this is normally not the type of hot-surface ignition problem that is of interest to the user. Parenthetically, the experimental studies considered in this Section suggest that such highly enclosed, heated geometries are rare, since most investigators (many of which created semi-enclosed environments) reported hot-surface ignition temperatures much higher than the AIT. If the space in question is roughly approximated as a cube and hot surfaces occupy more than one face of the cube, it is prudent to consider that the substance will ignite at the AIT. Otherwise, with the exception of substances whose droplets show a cool-flame ignition, the hot-surface ignition temperature it typically more than 200ºC greater than the AIT. The American Petroleum Institute concluded in its recommendations[149] that hot surfaces are liable to ignite fuel vapors only if the surface temperature exceeds the AIT by at least 200ºC in still air, and by even a larger amount if an appreciable velocity exists. This appears to be as reasonable a statement as can be made on the subject without getting into details on the specific geometry and materials and doing *ad hoc* testing.

There has been almost no theoretical work on the hot-surface problem, with the study by Vaivads et al.[150] being the sole one. Unfortunately, their model gave results which are the opposite of the experimental findings: their computations indicated that the lower-flash-point liquid would be more readily ignitable than one of a higher flash point.

POOLS

POOLS AT OR ABOVE THEIR FLASH POINT

"A pool will ignite if its temperature is above the flash point, and will not if below." This would appear to be a natural conclusion from the principles and results of flash point tests. But complications exist in real-scale pools that are not reflected in flash point testers. Where shall the pool be ignited? This questions was examined by Atkinson and Eklund[141], who studied the ignitability of jet fuels in two pool environments—an open one and a shrouded one. The pools were 250 mm diameter; three ignition sources were used—a small pilot flame, a 10 J spark, and a hot Nichrome wire.

Using the open-pool configuration, visual observations indicated that the vapor behaved differently for the two fuels. In the case of JP-4, a stagnant layer of fuel vapors formed about 25 mm high over the fuel surface, and a convective motion wafting the vapors upward was not seen. For the JP-5, which has a much lower vapor pressure, a stagnant layer did not form and a convective column was seen rising. This behavior in a quiescent environment determined the quanti-

tative results that were obtained. The results (Figure 45) show that for distances of ca. 25 mm above the pool, ignition occurs at about the nominal FP of the fuel. At progressively greater igniter heights, the pool has to be raised to temperatures considerably in excess of the FP. For JP-4, ignition with the spark was problematic, in that results were extremely erratic for heights in the range of 25 – 50 mm, and ignition was impossible at heights over 50 mm. The hot wire, as expected, was found to be a much less effective igniter than the spark. For JP-5, the results indicate that the most effective igniter was the hot wire, the least effective the spark, with the flame being intermediate. This ranking is hard to interpret and probably simply reflects data scatter.

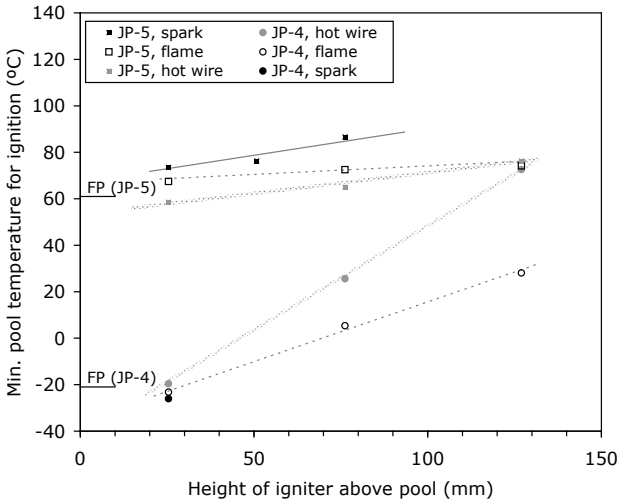


Figure 45 Effect of igniter height and igniter type on ignition of unshrouded pools

The authors then repeated the experiments, but with the pool surrounded by a 300 mm high shroud. Since in a large-size pool the vapors are likely to accumulate to a greater height than possible with a small, open pool, the shroud was considered to represent a sectional slice from a large pool. These results are shown in Figure 46. Similar trends with temperature were seen, but now reliable spark ignitions of JP-4 were possible up to the maximum height tried, 127 mm. In the shrouded pool tests, the effect of the ignition source was no longer anomalous, as it had been with the small, open pool—the flame source was consistently more effective than the spark, for both fuels.

Atkinson and Eklund also examined the effect of wind velocity on the ignitability of pools. The ignition sources were placed at the downstream edge of the pool, slightly above the pool surface. The results (Figure 47) show that modest wind velocities have a small effect, but the effect is to raise the temperature needed for ignition. Again, flame ignition sources provide some local preheating for the pool, so ignition may be possible at temperatures somewhat below the FP; the data on this point should not be considered rigorous, since jet fuels are mixtures, not pure chemicals, and

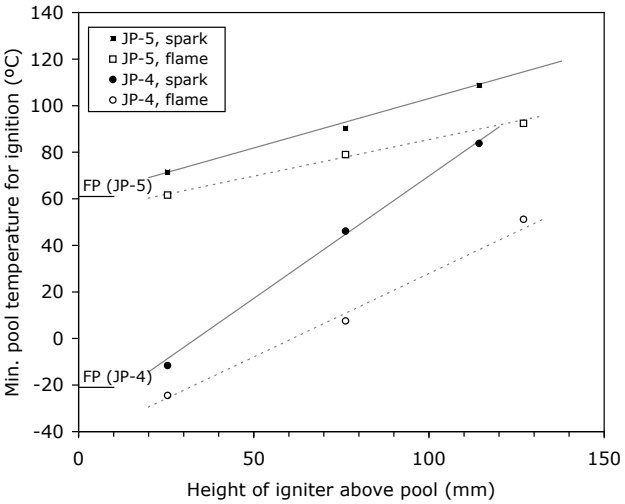


Figure 46 Effect of igniter height and igniter type on ignition of shrouded pools

actual flash points will change with progressive evaporation.

If a liquid pool has a temperature above its flash point, then in still air there is likely to be a large column above the surface where putting in a small spark or pilot will result in ignition. If there is a cross-wind, however, then the vapor rising from the surface forms a thin boundary layer, instead of a tall column. The fuel concentration is highest at the surface and monotonically decreases further out into the boundary layer. Ignition will occur only if the ignition source is placed at a location lower than the place at which the LFL is reached in the boundary layer. Murad et al.[151] applied boundary layer theory to compute the location of the LFL and found that this coincided closely to the maximum experimental height at which ignition could be achieved.

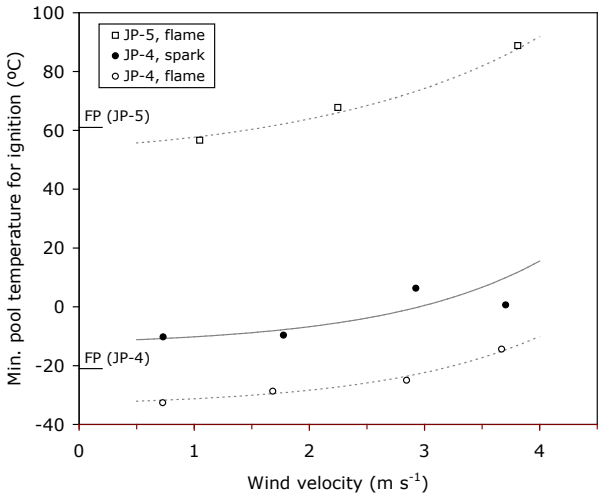


Figure 47 Effect of wind velocity on ignition of pools

POOLS BELOW THEIR FLASH POINT

Ignition of pools having a temperature less than their flash point presents a different situation. Assume for the moment that the flash point is a true material property and is not apparatus-dependent. Then clearly if the temperature of the liquid is below T_{FP} and a small igniter is placed above the surface, neither flashing nor ignition will occur. But what if a larger igniting flame is used and it is played on the surface to cause significant heating of the liquid? For modest heating, there still will be no ignition, but the explanation involves thermally-induced fluid motions. When a strong flame is used, the temperature of the fluid's surface is raised locally. However, the surface temperature remains at its lower original value a short distance away. This difference in temperatures sets up a convective current[152,153], whereby the heat is taken away from the region of the flame and distributed over a wide surface area of the liquid pool. Assuming that the area of the pool is greatly larger than the area being subject to direct flame heating, the rise in the surface temperature is negligible, and a flash does not occur. The flame or hot body, however, does not need to be massive for small pools (say, less than a few centimeters); for these, the effect of heat redistribution becomes limited due to small pool size.

Given the above physics, it is sometimes believed that liquids having a flash point significantly above the ambient temperature cannot be ignited. There are many ways in which this belief can be found to be false. The simplest way is by the use of a wick. An oil lamp would not burn if one attempts to light the vapors with a match. It burns readily when a wick is lighted, however. The physical principle involved is that of *constrained local heating*. The only reason that ignition does not occur in previous example is that the heated fluid elements can escape the heating zone. Thus, any mechanism which restrains fluid elements from escaping may lead to ignition. On a wick, surface tension provides the necessary force to hold in local fluid elements. Alan Roberts studied in detail the process of wick-supported flaming in his dissertation[154]; his results were summarized in a series of papers[155]. In burning pools of isoamyl alcohol, Roberts determined that the temperature of the surface of the wick was slightly above the boiling point of the liquid, indicating that the effective liquid level was slightly underneath the surface of the wick. The effect of the wick is highly localized. By using a tiny test flame, Roberts found that pool vapors were ignitable only for lateral distances no greater than 20 mm from the wick.

Other innovative ways exist whereby constrained local heating can occur. Glassman et al.[152] conducted experiments wherein they added a small amount of a thickening agent into kerosene pools. A polyisobutylene with a molar mass ~20,000 was used. The flash point of such a mixture was found to be no different from pure kerosene. However, they found that whereas a pure kerosene pool cannot be ignited from a small pilot flame, a thickened pool readily ignites. With the thickened fuel, the heated liquid is unable to move away from the source of the heat.

Incidents have been reported[156] where welding operations on 'empty' tanks holding residues of heavy oils caused ignition and explosion, even though these oils had flash points much above the prevailing temperature. There are several possibilities for this. (1) A thin coating of a high viscosity oil is unable to create convective currents when subjected to localized heating; thus such a layer might be viewed as "self-wicking." (2) Tank samples that were taken may not reflect the vapor available for ignition. The lighter fractions which would comprise the ignition problem may all have already been evaporated, so that sampling the liquid simply does not reflect on what is in the vapor phase. (3) Certain areas may release liquid or vapor after initial vapor-freeing of the tank[157]. It would seem simple to just use a combustible gas detector to determine the actual content of the atmosphere, but a study[158] showed that it is very easy to get erroneous readings with these detectors due to sampling problems. Other related issues are discussed under *Asphalt storage tanks* in Chapter 14.

The issue of ignition of *very thin* layers of liquids is not well quantified. Liquid layers thinner than about 0.8 – 2 mm may not ignite due to heat losses occurring to the bottom, possibly augmented by a liquid-film thermocapillary deformation effect which reduces the layer thickness locally[153,155].

Ignition of fuel in closed vessels

A common question concerning flammable liquids is: "For a vessel partially filled with a flammable liquid, what is the temperature range over which the vapors can form an ignitable mixture?" This question may be the most common for motor vehicle gasoline tanks, but can occur in a wide range of circumstances. The vapors in a gasoline tank will not ignite, due to the concentration of the vapors being above the UFL (except under very cold temperatures). An 'empty' gasoline tank will, however, have a lower vapor concentration; this can be within the flammable range. It may be surprising, but this fact was already known in 1877[159], way before the automobile era. For many types of tanks, it may be impractical to get them sufficiently empty. For example, extrapolations based on laboratory tests indicated that a tank of the Boeing 747 airplane would have to be emptied of all but about 4 – 8 L of fuel before assurance could be had that the LFL is not reached within it[160].

In discussions of the flammable range, it is often assumed that the liquid contents of a vessel are all at the same temperature. In tanks which are stirred through the motion of a vehicle, this is likely to be an excellent assumption. But in fixed tanks, especially ones which may be getting substantial heating from sunlight, temperature distributions may be substantially non-uniform. For large industrial tanks that are not fully sealed but are 'air-breathing,' Britton[161] states that

fuel vapor concentrations found escaping the breathing pipe are typically only 30 – 50% of the computed values, if computation is based on the average temperature of the liquid in the tank, but reasons for this deviation have not been studied.

A safety precaution must be emphasized: To fill a tank, at least initially, one has to start with an empty tank! Thus, even for a liquid with a very low UTL, one cannot assume the tank atmosphere will be above the UTL during the initial filling. It may be necessary that the tank first be filled with an inert gas, before introducing the liquid to it, if there is a possibility of ignition from electrostatic or other causes.

Apart from the question of stirring, there are three factors to consider in determining whether or not ignition occurs: (1) the energy of the spark; (2) the amount of fuel in the tank; and (3) the temperature. The amount of fuel is important since it determines the fuel vapor concentration that can be attained. Battista and coworkers[162] set up a device for creating a spark (of unspecified energy) inside a fuel tank which was 1/30 full of fuel. For methanol, they obtained ignition at 19ºC, but this was a very mild event, entirely contained within the tank. For a 85% methanol/13% gasoline/2% butane fuel ignition occurred at –34ºC, with unspecified consequences. For an 85% methanol/15% gasoline fuel, the ignition occurred at –25ºC, and was another mild event contained within the tank. For methanol containing 4% cetane improver, ignition was at 20ºC, but the ignition event resulted in burning fuel discharge and tank bulging. Both of these consequences, however, were also very mild.

The authors then investigated ignition using a small flame at the open neck of the filler. With gasoline in a steel fuel tank, the vapors did ignite and the tank expanded, vented, and the fuel was consumed. Using gasoline in a plastic fuel tank, the results were roughly similar. In neither case, judging by the description of the events, would it appear that the fires would have been threatening to individuals not intimately involved in fueling. For methanol, either with or without cetane improver additive, there was no ignition of fuel from the flame at the open filler neck. Using an 85% methanol/15% gasoline fuel, the results were ignition and burning roughly similar to gasoline, for both the steel and the plastic tanks.

In an interesting companion examination, Battista and coworkers fired explosive projectiles (nails fired from a Ramset explosive-actuated power tool) at steel and plastic fuel tanks. The fuels tested were gasoline, methanol, methanol with cetane improver, and an 85% methanol/15% gasoline fuel. In no case did ignition result due to penetration of the tank.

Battista and coworkers also extended their study in a more fundamental vein by conducting a series of experiments with the 85% methanol/15% gasoline fuel in the IEC spark test apparatus[163]. Figure 48 shows the combined effect of temperature, fuel amount, and ignition current. These results are under idealized laboratory circumstances (such as a stirred vapor space without stratification) and cannot be directly extrapolated to field experience. Nonetheless, they are valuable since the trends are delineated quantitatively.

EFFECT OF VAPOR/LIQUID VOLUME RATIO

When a liquid/vapor equilibrium exists in a part-filled, closed vessel the vapor pressure will be a constant value, irrespective of vapor/liquid volume ratio, if the liquid is a pure compound. If the liquid is a mixture, however, then the vapor/liquid volume ratio will affect the vapor pressure and, consequently, the flammability limits and the flash point. If the volume of the vapor space is very small, even the most volatile component will be able to exist in both liquid and vapor phases. But if the vapor space volume becomes large, then the most-volatile component may entirely evaporate from the liquid and not raise the fuel concentration in the vapor space to the same value which would be possible if there was a larger reservoir of liquid. Then, the temperature of the liquid will have to be raised to vaporize less volatile components, if ignition is to be possible. The standard ASTM Reid vapor pressure test uses a vapor/liquid volume ratio of 4:1. *True vapor pressure* is defined as the vapor pressure as the vapor/liquid volume ratio → 0. An illustration is given in Chapter 14 under *Aviation fuels* which shows how the vapor pressure rises as the vapor/liquid volume ratio drops. For gasoline, the true vapor pressure is about 7% higher than the Reid vapor pressure.

For this reason, closed-cup flash point test methods need to prescribe a fixed vapor/liquid volume ratio to give reproducible results. Actual end-use environments may have a different vapor/liquid volume ratio, however, thus the end-

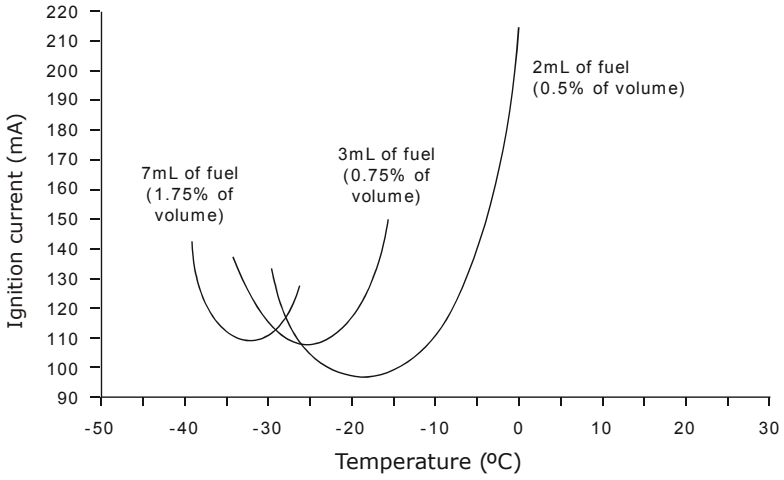


Figure 48 Combined effects of temperature, fuel amount and ignition current on the ignitability of a closed volume containing a motor fuel

use flash point may differ from the one determined in the standard test method. Carhart[172] compiled data for several JP-5 fuels at various ullage percentages and found a clear effect for certain batches and none for others. The variations can occur because specifications for JP-5 fuel control the composition of the fuel only within a broad range.

EFFECT OF SLOSH

The flammability of liquid in a closed container may change if the container is *shaken or sloshed*. Within a closed container that is at rest at a given temperature, a liquid/vapor equilibrium is established and the partial pressure developed by the vapor is simply the equilibrium vapor pressure of that particular substance at the given temperature. This vapor pressure is defined with respect to a flat liquid surface; with a curved liquid surface, as present at a droplet, the vapor pressure becomes higher[164]. Thermodynamically, this is due to a surface contribution to the Gibbs free energy, with convex surfaces raising vapor pressure and concave ones lower it. The vapor pressure at a droplet P_d is related to the vapor pressure at a flat surface P according to the relation:

$$\frac{P_d}{P} = \exp\left(\frac{2k(T_c - T - 6)}{rRT} \left[\frac{M}{\rho} \right]^{1/3} \right)$$

where T_c = critical temperature of the liquid (K), T = temperature (K), r = radius of droplet (m), R = universal gas constant (= 8.314 J mol^{-1} K^{-1}), M = molar mass (kg mol^{-1}), ρ = density of droplet (kg m^{-3}), and the constant k is approximately 2.1×10^{-7} J K^{-1}. The critical temperature of various liquids can be found in standard handbooks[3]. Since all of the remaining variables are fixed at a given temperature, the vapor pressure increases ~ exp (1/r), which means that if the droplets are small, there will be a significant vapor pressure increase. Since the vapor pressure of interest represents a dynamic equilibrium, it can be visualized that the reason why the vapor pressure is higher for small droplets is because it is harder for a vapor molecule to return to a small drop than to a large planar surface.

Ott[165] conducted slosh-tank experiments on various aviation fuels and found that by vigorous sloshing he could lower the LTL by about 33ºC, however the LTL under slosh conditions becomes somewhat poorly defined, that is, as the temperature is lowered, explosion pressures progressively fall, without there being a sharp explosion/no explosion demarcation. He also found experimentally that there was no detectable effect of slosh on the UTL.

Radiant ignition of liquids

Pools which are at a temperature above their flash point can be ignited by a spark, a small flame, and other localized sources of heat which do not provide any substantive heating to the body of liquid itself. But one way in which pools at an initial temperature below their flash point can ignite is if they are subject to radiant heating. Typically, this heat flux may originate from another nearby, but not contiguous burning object. In this section, we consider separately thick and thin layers. For thick layers, both the theory and the engineering treatment are nearly identical to the case of solid combustibles. For this reason, we refer the reader to the pertinent sections in Chapter 7 for a systematic presentation of the principles of radiant ignition. Thin spills of a combustible liquid upon a solid substrate present some unique issues, and its theoretical treatment is given below.

THICK LAYERS

Putorti et al.[166] tested layers of motor oil in the Cone Calorimeter for radiant ignition. Depths of 10, 15, and 42 mm were tested, but no significant effect of layer depth was found. The results are indicated in Figure 49. There was a very modest difference between the two grades tested and it is not clear if this difference would be reproducible. The results can be represented for SAE 30 oil as: $\dot{q}''_{cr}$ = 1.20 kW m^{-2}; B_{ig} = 315. For SAE 50: $\dot{q}''_{cr}$ = 1.21 kW m^{-2}; B_{ig} = 336. Similar tests were also conducted by Wu et al.[167] for pools of 6 – 10 mm depth and, again, no layer depth effect was found.

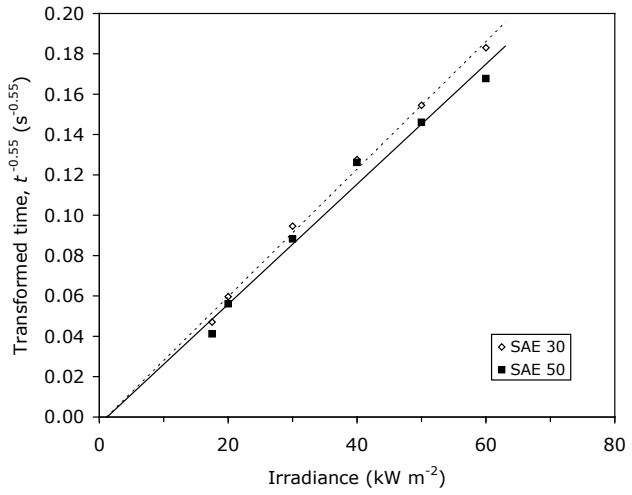


Figure 49 The piloted ignition of thick layers of motor oil

Wu and Torero[168] examined the radiant ignition of crude oil from the Alaska North Slope. Crude oil contains hydrocarbons spanning a wide variety of molar masses and the lighter fractions can be evaporated by prolonged open-air exposure or by heating. Their data are shown in Figure 50. It may be noted that the sample which was 12% evaporated shows a critical ignition flux of about 1 kW m^{-2}, while the 20% evaporated sample shows 4 kW m^{-2}. The non-evaporated and the 8% evaporated samples, however, show a different behavior: their critical flux is less than zero. The authors did not explore the minimum needed flux, but if the minimum flux is not too far from the critical flux, the results would suggest that the 0% and 8% evaporated specimens do not require any radiant heating and a simple spark should suffice to ignite them.

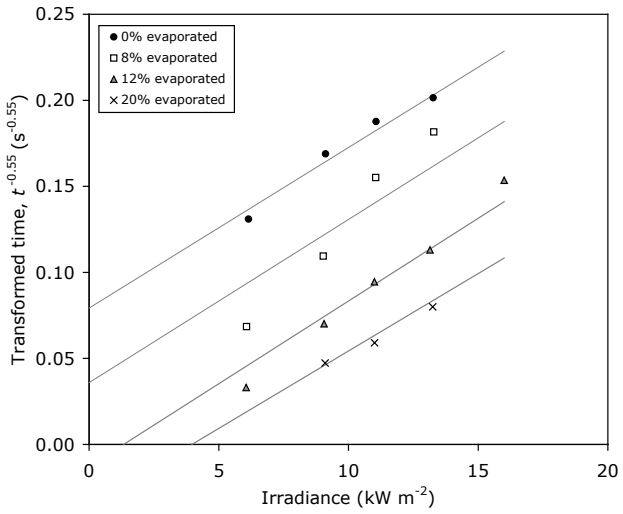


Figure 50 Piloted radiant ignition of Alaska North Slope crude oil

This interpretation is confirmed by the results shown in Figure 51. The ASTM D 56 closed-cup flash point is seen to linearly depend on the percent evaporated of the crude oil. Furthermore, if ambient temperature is around 23°C, then it is seen that samples of less than 9% evaporated fraction show a flash point of less than ambient temperature. Thus, *a negative value of critical flux suggests that the flash point is less than ambient temperature*. This relation should not be taken to be highly precise, however, since results from both radiant ignitability tests and flash point tests are dependent on apparatus details and are not absolute quantities. Wu and Torrero also demonstrated that oil layers as small as 6 mm behave as thermally thick materials, but did not explore ignition of thinner layers.

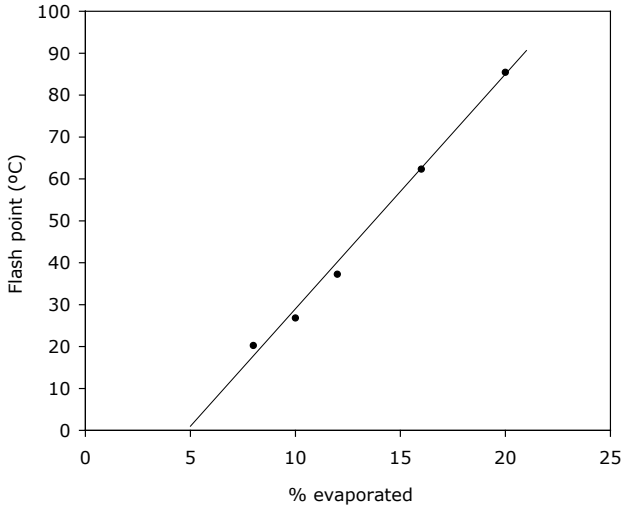


Figure 51 Relation between flash point and % evaporated for Alaska North Slope crude oil

Li et al. measured the ignitability of several liquids using both tungsten-lamp and CO_2 laser sources[169]. Their results are shown in Table 13. The laser results are atypical of other heating mechanisms, since the absorption of radiation occurs solely within a few molecular diameters of the surface. This causes unusual motions both in the vapor plume above the surface and in the liquid itself.

Table 13 Ignitability of liquids determined by Li et al.

Fuel	Flash point (°C)	Min. flux (kW m^{-2})	
		Lamp source	Laser source
kerosene	43	2.9	6700
light diesel	62	3.7	4600
heavy diesel	82	5.2	3200

THIN LAYERS

If a liquid is spilled on a surface, typically, on the floor, two possibilities can occur: (1) Its exposed surface area becomes limited by a 'diked' area, whether it is diked intentionally or not. (2) Either no means of diking exist, or the amount of liquid spilled is small enough that the size of the spill area will be governed by the amount spilled, the surface tension and viscosity properties of the fluid, and the roughness or porosity properties of the surface. In addition, if floors are sloped or warped, a pattern may be established which is centered on the low spots of the surface. Modak conducted an extensive experimental investigation of thin-spill ignitions[50]. He demonstrated that the thermophysical properties of a wide range of common oils (No. 2 fuel oil, SAE 30 motor oil, turbine oil, and fire-retardant hydraulic fuel) are indistinguishable, even though their flash points and fire are, of course different. This means that for a given irradiance and a given depth of spill, the surface temperature versus time relation was found to be identical for these oils. For smooth, non-absorptive surfaces, e.g., steel or epoxy-coated concrete, the depth of spill, computed as the (volume spilled)/(surface area formed) ratio, was found to be a constant value, independent of the amount spilled (Table 14). In the case of normal, uncoated concrete, however, for larger spills resulted in effectively greater depths being computed, due to in-depth absorption by the surface.

Table 14 Effective depth of spill for undiked spills on flat, non-absorptive surfaces

Oil type	Depth of spill (mm)
No. 2 fuel oil	0.22
turbine oil	0.34
SAE 30 motor oil	0.75
fire-retardant hydraulic fluid	0.84

Putorti et al.[170] studied gasoline spills on wood parquet, vinyl floor tiles, and carpeting. The effective depth of spill he found was 0.67 mm for a wood floor and 0.56 mm for vinyl tile. Carpeting did not exhibit a constant depth of spill. His results appear to be at variance to Modak's, since Modak found that depth of spill effectively decreased with viscosity, but gasoline is less viscous than fuel oil.

Modak also provides several different theoretical approximations to predicting the ignition time. Ignition is assumed to be reached at the moment that the fluid's surface temperature first attains the fire point temperature. The agreement between theory and experimental results was limited. However, in view of this, the simplest approximation appears to be a useful starting point. In this approximation, the thermal properties of the liquid are ignored, since a very thin layer does not appreciably change the heat balance of the substrate. Instead, the temperature-time curve of the liquid surface will be governed by the thermal inertia *of the substrate*. Liquids will still differ in their fire point temperatures. But since the thermal inertia of common substrates varies enormously, much more than do the fire points of common liquids, it is clear that ignition time is largely governed by the nature of the substrate, rather than by any property of the liquid itself.

Ignition of liquids by other means

A fundamentally different way of igniting liquid drops or aerosols is by shock waves. Miyasaka and Mizutani[171] conducted experiments igniting liquid droplets and sprays with shock waves. They studied sprays of a high volatility fuel (tetralin) and a low volatility one (cetane). Droplet diameter was ca. 80 μm. For tetralin, there was no effect of droplet injection rate, and the results were in all cases identical to tetralin vapor. Ignition was extremely fast, however, and was orders of magnitude faster than when ignited by other means. The ignition time t_{ig} (ms) was expressed as:

$$t_{ig} = 0.0005 \exp(5680 / T_2)$$

where T_2 (K) is the static temperature of the shock wave, determined from its velocity by use of the Rankine-Hugoniot relationship. For the low volatility fuel, similar exponential relationships could again be obtained, but these differed for each injection rate. The rapidity of ignition was attributed to the fact that the shock wave shatters the initial droplets to a 'micromist' where the diameters are only a few μm.

Tests for ignition properties of liquids

AUTOIGNITION TEMPERATURE

The AIT is a variable which is highly dependent on the test apparatus and the test protocol used. NFPA 32[5] provides the following general guidance in selecting and relying on ignition temperature tests: "Some of the variables known to affect ignition temperature are the percentage of the gas or vapor in the mixture, the shape and size of the test vessel, the rate and duration of heating, the kind and temperature of the ignition source, and catalytic or other effects of materials that may be present. As there are many differences in ignition temperature test methods, such as the size and shape of the test vessel, the material of construction of the test vessel, method and rate of heating, residence time, and method of flame detection, it is not surprising that reported ignition temperatures may differ for the same material."

Carhart[172] noted that AIT values tabulated for common substances in authoritative data compilations sometimes differ by 100ºC or more. One variable that has been studied at some length is the size of the test vessel. Figure 52 shows some data obtained by Setchkin[173] on the size effect using spherical flasks. The size effect should be similar to that found for gases and an orderly decrease of AIT with size is found, except for the largest size (15 L; V/A = 67 mm). This was an artifact of the experiments, since a thicker glass vessel had to be used, giving higher heat losses. Flasks on the order of 12 or 15 L are not practical for laboratory testing, so Setchkin recommended that a 1 L size (V/A = 27 mm) would be sufficient. According to thermal ignition theory (see Chapter 4), plots of $\ln\left(T_{ig}^2 / r\right)$ should give straight lines if plotted as a function of $1/T_{ig}$, where T_{ig} = ignition temperature (K), and r = radius (m). This is shown in Figure 53, where reasonably straight lines are seen, except for the smallest and largest sizes.

EARLY TEST METHODS

The early history of developing test equipment for characterizing the autoignition of liquids took place during the first three decades of the 20th century. It was largely motivated by the desire to develop suitable motor fuels for automobiles, aircraft, and other related applications. Thus, perhaps it is not surprising that the very first test method proposed in 1906[174] involved a compression cylinder. Effectively, this was a h ighly-simplified version of a one-cylinder internal combustion engine. Under assumptions of adiabatic compression, the temperature reached in the en-

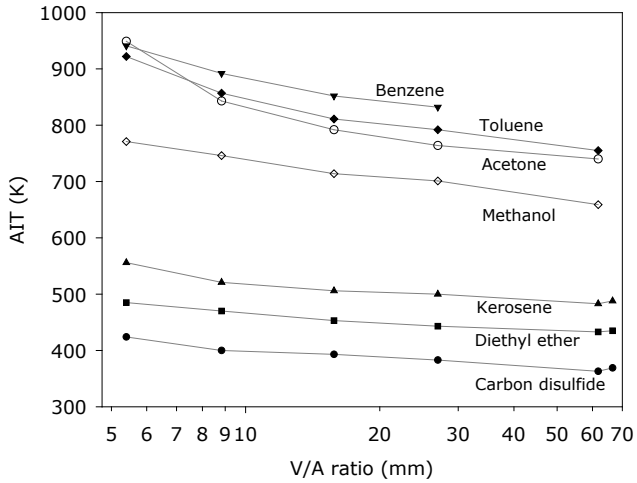


Figure 52 The effect of flask size on the AIT of liquids

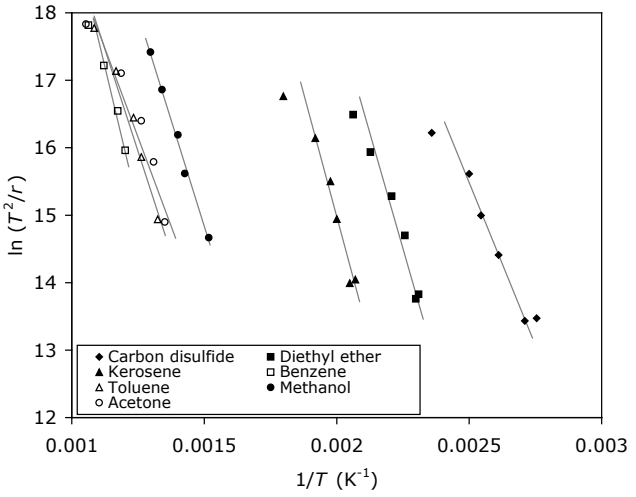


Figure 53 Setchkin's results plotted according to Semenov theory

gine can be computed from the pressure attained. This was certainly an indirect method and one especially problematic because no visual observation was possible.

Since in this Handbook the focus is on unwanted fires, test methods especially tailored for improving the design of internal combustion engines are not within the scope. It is interesting to note, however, that a large number of further adiabatic-compression ignition test methods were described in the literature subsequent to 1906. Mullins[175] reviewed these test methods comprehensively. In more recent decades, there has been a revival of interest in adiabatic compression tests for use within the aerospace industries, because of the possibility of evaluating substances at high pressures. However, values from adiabatic compression tests are systematically high when compared to tests performed in other types of apparatuses[173]. This is due to the basic pressure effect, compounded by non-uniformities in temperature that are a consequence of the rapid compression[176]. The basic compression-ignition principle is presented in Chapter 11, while additional use of test methods based on this principle is discussed in Chapter 4.

The majority of test methods which have been proposed for the purpose of determining an autoignition temperature of liquids are a form of heated-crucible test. The two most-used types of crucible tests have been the Moore test and the Jentzsch test. Moore's apparatus[177] is shown in Figure 54. An electrically heated block forms the crucible onto which a drop of liquid is released. Combustion air is supplied through a separate pipe and is wound for a number of turns through the heated block. This allows the incoming air to assume a temperature close to that of the crucible surface. A thermometer monitors the block temperature, while two cover plates are used to minimize the influence of room air currents. The liquid to be tested is held in a room-temperature dropper. This apparatus shown was Moore's 'improved' tester; his original design dates to 1917[178]. Moore's tester was not the earliest crucible method; two different German crucible test apparatuses were first described in 1913, but these were quickly supplanted by more evolved techniques. Many further elaborations along the same line of design as Moore's apparatus were seen during the subsequent years. The most important one of those was the first standard test method, ASTM D 286, described below. Apart from the general problems with test in this category, the Moore tester has been criticized[179] for giving too-high ignition temperatures on account of having too small a test chamber. The temperatures reported using the Moore tester are often hundreds of degrees higher than those obtained from a better test apparatus. For example, diethyl ether is reported[180] as 487ºC, compared to the 195ºC normally taken as its AIT today; or 520ºC for hexane, compared to 223ºC.

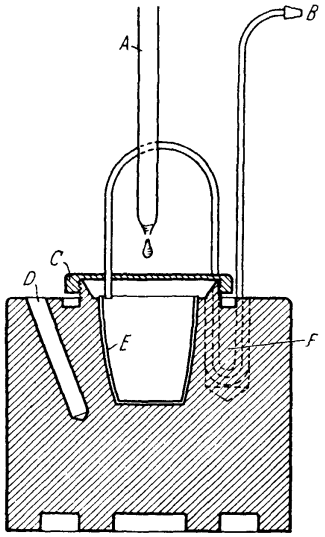


Figure 54 Moore's tester (**A** oil dropper; **B** oxygen feed tube; **C** cap; **D** pyrometer hole; **E** crucible; **F** thermal plug)

The second type of crucible test to achieve an early following was Jentzsch's method. In 1924 Jentzsch[181] designed a four-chamber tester, with one chamber holding a thermometer, while the other three are fed with oxygen and one of those receives a drop of specimen (Figure 55). Oxygen is metered in through a bubble counter. Jentzsch used the latter because he proposed a hazard rating scale which encompassed both the AIT and the amount of oxygen required by the specimen. For reasons not entirely clear, test results from Jentzsch's tester are broadly similar to values obtained in other test methods that use air, not oxygen. There were not many subsequent modifications of this apparatus as there were of the Moore tester, but the Jentzsch method continued to have wide and extensive use, even into the 1950s. At that time, the US Navy conducted some detailed studies of the apparatus and concluded that reproducibility is unacceptable with this test[182].

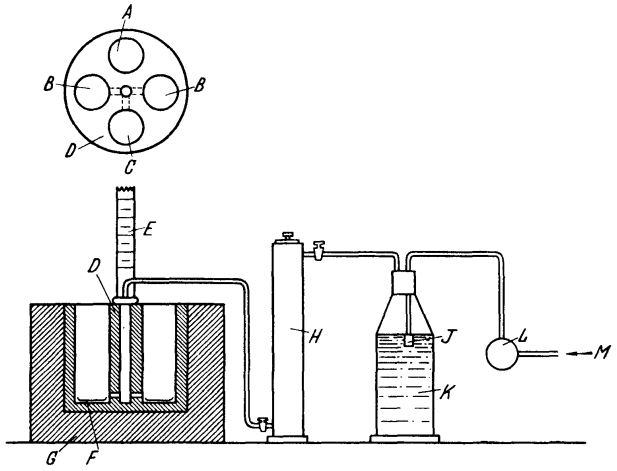


Figure 55 Jentzsch's tester (**A** thermometer well; **B** auxiliary chambers; **C** specimen chamber; **D** crucible; **E** thermometer; **F** vaporization dish; **G** furnace; **H** drier; **J** jet; **K** bubble counter; **L** adjusting valve; **M** oxygen supply)

Another category of autoignition testers differed from Moore's or Jentzsch's methods fundamentally because they did not pump in an oxidant stream into the crucible. The air was stagnant in a flask which was open to the atmosphere. Methods of this type were developed in the 1920s at Factory Mutual[179] and at Underwriters Laboratories[183]. A number of less-frequently used variants have also been reported in the literature. While the air flow was not capable of being varied in such methods, significant emphasis was placed on studying fuel-quantity effects. To that end, flasks of varying sizes and varying *flask materials* were used, and also varying amounts of fuel were introduced in an experiment. In the FM studies, glass and metal (copper, steel, chromium) flasks were compared. In some cases, the differences were small (<10 – 20°C). In other cases, differences on the order of 200°C were seen. This was true especially for alcohols. For example, isopropyl alcohol ignited at 456°C in a 125 cm^3 glass flask, but required 638 C in a 106 cm^3 chromium vessel and failed to ignite at up to the maximum temperature (649°C) that could be attained in a 106 cm^3 copper vessel. Hilado and Clark[184] surveyed available data and recommended that for consistency, tests should only be made in glass vessels. Glass is chosen due to its low reactivity and because, in most cases, it gives the lowest reported AIT values.

All of the above tests share the trait that substances are introduced at ambient pressure. A different scheme is to admit substances into an evacuated vessel. This type of an arrangement was found in some very early research done in 1880 by Mallard and Le Chatelier and later by Mason and Wheeler[185]. Several other researchers also used evacuated vessels, but no schemes of this kind have been proposed for standardized tests.

Certain substances decompose rapidly when exposed to heat. Thus, Frank and Blackham[186] pointed out that when testing ethers, a much larger amount of liquid must be used than for other organic compounds. Otherwise, rapid decomposition of the ether led to insufficient vapor concentration available for ignition. The form in which the liquid is delivered also has an effect. Most substances show similar AIT values when a few drops are dropped in, as compared to spraying the test substance into the chamber, but motor oils were found to exhibit significantly lower AIT values when sprayed in[187].

The range of reported data when experiments from various laboratories using various test apparatuses are considered can be enormous. For example, a comparison of values for benzene ignition in air reported by seven workers showed values of 370, 500, 520, 656, 700, 740, and 1062°C[183]. Larger differences yet may be involved when the substance (e.g., gasoline) is not a pure chemical.

Mullins[175] viewed that 'static' (i.e., no forced air flow) crucible methods, such as those of FM or UL, give poorer results than the Moore, Jentzsch, etc., crucible methods where air is pumped in. This is because he concluded that AIT values from the latter were more reproducible and were generally numerically lower. The exact opposite conclusion was arrived at by NACA[187]. They concluded that tests under zero-flow conditions gave the lowest results and a better correlation with chemical structure. NACA views proved to be more persuasive, since the later test methods (e.g., the ASTM methods) are zero-flow methods.

A number of other designs have been reported through the years. *Heated tube* methods have frequently been used in research studies on the AIT of gases and can be modified for fuels originally in liquid form. This is arguably the most accurate way of determining an AIT value, as discussed in Chapter 4. However, no standardized tests of this type have been put forth. A variety of *bomb methods* has seen significant usage in aviation-fuel research, where they are necessary if conditions other than at atmospheric pressure must be considered.

ASTM D 286

In the 1920s, the Bureau of Mines developed a test method based on a 125 cm^3 flask which is submersed in a bath of liquid solder. A gas burner heats the solder to a desired temperature. This method became standardized as ASTM D 286[188] (Figure 56). Results of a roundrobin using this method were published[189]. Gases can also be tested in the apparatus, by syringe injecting a suitable amount. Lewis[190] has discussed some problems associated with testing of gases, and it is clear that better methods are available for the purpose. The method has been criticized on several grounds[191]:

- the results are markedly affected by the size and shape of the cavity
- a fuel concentration gradient exists vertically in the cavity
- temperatures are non-uniform in the cavity
- because of the non-uniformity of fuel concentration, the minimum ignition temperature corresponds to unreasonably rich fuel vapor concentrations.

On a practical basis, the apparatus was criticized due to the fact that it lacked a way of making visual observations of ignition and also because it was difficult to keep clean[192]. A large compilation of results from a modified version of the test method (using a steel block, instead of liquid bath) has been published by the Bureau of Mines[193]. The test method was subsequently replaced by ASTM D 2155.

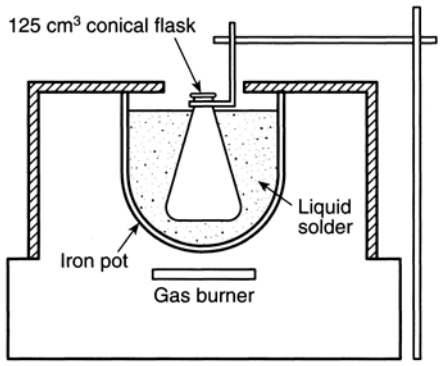


Figure 56 ASTM D 286 autoignition test (withdrawn)
(Copyright NFPA, used by permission)

ASTM D 2155

This test method was developed by the Bureau of Mines as its "I-8" apparatus and involves a heated 200 cm^3 glass Erlenmeyer flask[194]. The apparatus was more modern, with electric heaters being used to heat the flask. In the ASTM D 2155 apparatus (Figure 57), a small amount of the liquid is injected, and the flask is watched for 5 minutes for signs of a flash. If no flash occurs, the flask temperature is reported as being above the AIT. ASTM D 2155 has been withdrawn and superceded by ASTM E 659; however, the method remains an official US government test, used by the Mine Safety and Health Administration[195]. IEC 60079-4[196] is basically similar, except that a new flask must be used for each substance tested.

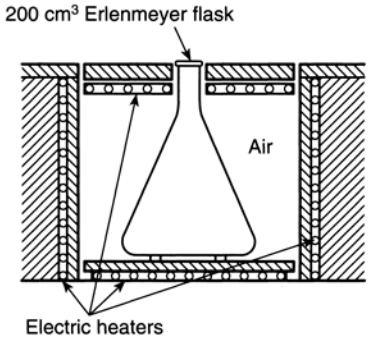


Figure 57 ASTM D 2155 autoignition test (withdrawn)
(Copyright NFPA, used by permission)

ASTM E 659

The ASTM E 659 test[197] (Figure 58) for autoignition of liquids is based on an apparatus developed by Setchkin[173] (Figure 59) at NBS (NIST) in 1954. A glass flask is surrounded by an electrically heated oven and is equipped with measuring thermocouples. To perform a test, an 0.1 mL sample of the liquid is injected with a syringe. The apparatus is observed for 10 min for signs of ignition by viewing in a fully darkened room. If no ignition occurs, another temperature is selected for the oven and the procedure is repeated. When the ignition temperature has been determined to within °3 C using 0.1 mL samples, both larger and smaller amounts are investigated to determine the overall lowest autoignition temperature. If cool flames are observed, these are reported separately as a 'cool-flame autoignition temperature.' Compared to Setchkin's original design, the ASTM version reduced the flask size from 1.0 to 0.5 L, removed the stopper, and provided a mirror for viewing of the inside of the flask. The apparatus itself is the simplest of the various 'autoignition' tests for liquids that have been proposed and contains nothing more than the heated flask and a viewing mirror; no forced air supply is used. It replaced older ASTM tests for autoignition of liquids, ASTM D 286 and ASTM D 2155 which were withdrawn. The method is also described as being suitable for readily-vaporized solids. While detailed studies have not been reported, it does not appear that the ASTM E 659 overcomes any of the fundamental shortcomings of the older tests.

Judging from the limited data of Johnson et al.[145], results obtained from the ASTM E 659 test are lower than from the ASTM D 2155, and the differences are greater for more volatile fuels, as shown in Table 15.

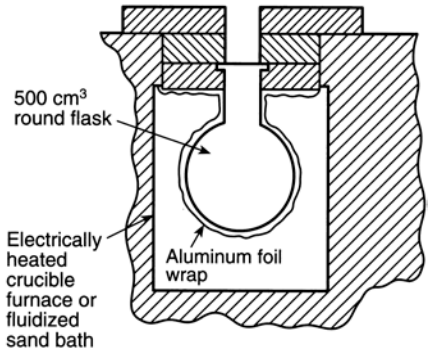


Figure 58 ASTM E 659 autoignition test (Setchkin flask test)
(Copyright NFPA, used by permission)

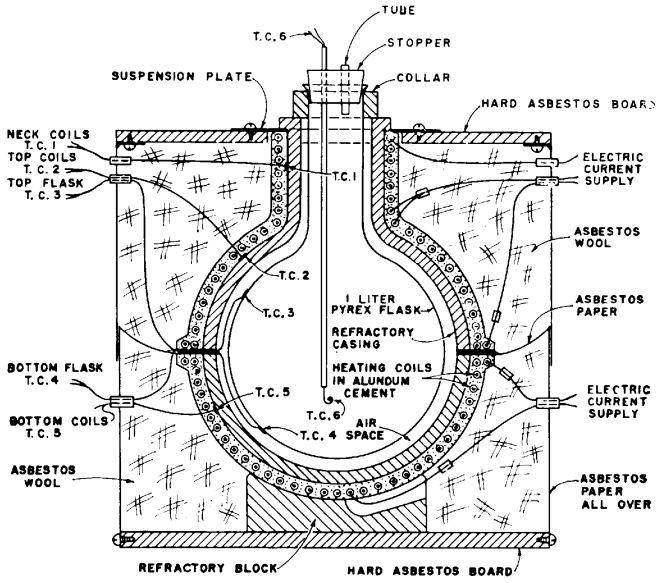


Figure 59 The Setchkin flask apparatus for AIT of liquids

Table 15 Some comparative results from two ASTM tests for AIT

Substance	AIT (ºC)	
	ASTM D 2155	ASTM E 659
MIL-H-5606 hydraulic fluid	227	218
MIL-H-83282 hydraulic fluid	371	366
MIL-L-7808 lubricating oil	382	372
JP-4 jet fuel	254	227
JP-8 jet fuel	246	224

OTHER BUREAU OF MINES TESTS

For tests at low pressures and also for studying vessel size effects, the Bureau of Mines constructed a 4900 cm^3 heated steel vessel[198]. For studying motor engine fuels and related substances, the Bureau developed a bomb able to withstand explosion pressures, and thereby permit characterization of ignition times for a wide range of pressures[199]. The stainless steel bomb had an inside volume of 0.3 L.

FLASH POINT

A flash point tester is a simple device and needs only the following components:

(1) a small cup
(2) a device underneath the cup for heating it
(3) a thermometer
(4) a small flame that can be swung in and out, at a fixed distance above the liquid
(5) a lid (only for closed-cup tests)

The basic test procedure is also very simple. The test liquid is placed in a temperature-controlled cup and is allowed to reach equilibrium at a pressure of 1 atm and a given temperature. When equilibrium is reached, a small premixed flame is introduced into the air/fuel-vapor mixture above the liquid. If this vapor mixture flashes, then the vessel temperature is above the flash point; if not, then it is below. By trial and error, a temperature is determined which is the lowest at which the vapor does flash. This is reported as the flash point of the liquid. Despite this basic simplicity, development of flash point tests has had a very long and rich history. In this section, we review mostly the currently-used devices, with a brief historical look at early developments. A 1913 book[200] discusses some 48 apparatuses that were in use or were described in the literature. Fortunately, most of these are now obsolete but even the number of remaining ones might be considered excessive.

The testing of liquids for flash point properties became necessary in the 1860s, with the introduction of kerosene for kerosene lamps and for house heating. The use of a liquid fuel indoors is much more dangerous if the fuel vapors can ignite at ambient temperatures. These hazards of low flash point fuels became clear early, and during the 1860s the Abel closed-cup apparatus and the Tagliabue open and closed-cup testers came into use. The first UK Petroleum Act of 1862 attempted to restrict fuels having a flash point below 37.7ºC (100ºF), but did not specify a test method. In 1868 this was changed to specify an open-cup apparatus developed by Letheby and Attfield of the UK Home Office. The latter was found out not to be well-reproducible and Keates developed the first closed-cup apparatus, which was suggested for regulatory use in 1871, but never adopted. In 1875 Sir Frederick Abel was asked by the Home Office to help improve Keates' test. Abel's device was a rather strange closed-cup apparatus which used a water bath to maintain a fixed temperature, but interspersed an air space between the bath and the sample cup[201]. The heat to the unit was supplied by an alcohol lamp. A significant advance was the introduction of a controlled flame to replace the lighted string (!) previously used to test for flashing. In 1879 the UK recognized the use of the Abel flash point tester, and since the previous test was an open-cup unit, lowered the value to 22.7ºC (73ºF) on the grounds that this corresponded to a 37.7ºC reading of the open-cup method. Abel's test saw significant use in Germany, where it was early discovered that barometric readings have a substantial influence on the results. In high-altitude cities, values as much as 7°C lower were being determined. Despite this problem, it was noted that the Abel test was considered better than some 20 apparatuses previously invented in Germany. However, since high-altitude cities were not a concern in the UK, the problem was noted but not addressed[201]. In the US, regulation proceeded on a local or State basis, and 19th century fire safety literature contains significant pleas for mandating "100ºF kerosene" in order to reduce fire fatalities.

Barometric pressure has an effect on the flash point since, at any given temperature, it changes the fuel concentration. The fuel vapor pressure is only dependent on temperature (and not on total pressure). But changing the total pressure

changes the ratio (fuel vapor pressure)/(total pressure) and consequently changes the volume fraction of fuel in the atmosphere. To make a fully accurate correction would require knowing the vapor pressure of curve of the fuel in question, which is impractical. Consequently, ASTM E 502[202] recommends a universal correction which is deemed to be sufficiently accurate for physically reasonable variations in barometric pressure:

$$T_{fp}(corr.) = T_{fp}(meas.) + 0.25\,(101.3 - P)$$

where P = barometric pressure during test (kPa).

Prior to 1977, the US Dept. of Transportation regulated chemical hazards by using the Tagliabue (Tag) open-cup flash point tester and defining 'flammable' liquids as those having an open-cup flash point below 80ºF (26.7ºC). Since then, DOT, NFPA, and other US organization have agreed to use the Tag closed-cup test, with 'flammable' liquids being defined as those showing a closed-cup flash point below 100ºF (37.8ºC). This was based largely on demonstrations[74] that the Tag open-cup tester showed poor reproducibility, and the that reproducibility was better in the Tag closed-cup tester, and better yet in the Pensky-Martens tester.

Flash point measurements are occasionally applied to substances not in the liquid phase. NFPA 325 points out that: "Flash point applies mostly to flammable and combustible liquids, although certain solids, such as camphor and naphthalene, that slowly volatilize at ordinary room temperature, or certain liquids, such as benzene, that freeze at relatively high temperatures, will exhibit a flash point in the solid state."

ASTM defines 8 different flash point test methods. Their main traits are categorized in Table 16. Due to the proliferation of test methods, ASTM has a specific standard, ASTM E 502[202], which is devoted solely to giving the user general instructions on how to select and use a flash point test method. Note that the Abel test method, sometimes used in Europe, is not recognized by ASTM.

The Setaflash methods are intended as go/no-go tests at some temperature of interest for regulatory or specifications purposes. In that mode, they are very easy to use. They also avoid some of the inaccuracies associated with the rising-temperature methods. The latter have limitations[203] that can be serious, especially for mixtures (impure substances):

(1) each time the flame is dipped, some volatile components may escape. This can cause an improperly high reading to be registered.
(2) the vapor is not at the same temperature as the liquid, and this difference is exacerbated by the temperature ramping. This is especially a problem for high viscosity or low thermal conductivity liquids. The use of a stirrer is intended to overcome this problem, but it can lead to forming a mist in the chamber, which again will make results erroneous.

It has been stated[105] (but not proven) that for some petrochemical mixtures the flash point is dependent on the rate of heating and that slower heating may lead to a significantly lower T_{fp} being reported.

An extensive interlaboratory study of the reproducibility of closed-cup flash point methods was conducted in Europe[204]. The two primary methods studied were IP 303/74[205] (similar to ASTM D 3278 and D 3828) and IP 304/74[206] (similar to ASTM D 3941). These methods were selected because they are fixed-temperature methods. The investigators initially determined that all rising-temperature methods give apparatus-dependent results (primarily due to temperature non-uniformities in the apparatus and vessel size/shape differences), while results from fixed-temperature methods should be independent of the exact apparatus used. Thus, it was held that only fixed temperature (also called 'equilibrium') methods can be used to assign apparatus-independent values for flash points. Apparatuses normally used in a rising-temperature mode—such as Abel, Abel-Pensky, Pensky-Martens, and Tag—can also be used, provided they are operated with an adequate water bath and that this bath's temperature is only raised slowly. Standard IP 304 provides the instructions for doing exactly that. The results of the study indicated that there was no statistically significant difference between the various apparatuses, when operating in the IP 304-prescribed mode. Furthermore, it was found possible to determine flashpoints for a series of calibrating liquids to a reproducibility of ±0.5ºC (95% confidence interval). Finally, it was found that, when operated in a rising-temperature mode, the Abel apparatus gave results which were indistinguishable from equilibrium determinations; however, the Pensky-Martens test gave rising-temperature results which were significantly higher than when operated in an equilibrium mode.

ASTM D 56

The Tagliabue closed-cup test method, ASTM D 56[207], is the oldest flash point method listed by ASTM, having first been issued in 1918. It is the primary method called out by US Dept. of Transportation regulations. A test cup (Figure 60) holding 50 mL of sample is immersed in a liquid bath,

Table 16 Main features of ASTM flash point tests

Test	Name	Open/ Closed	Rising/fixed temp.	Stirred	Regulatory use
D 56	Tag, closed	C	R	N	DOT
D 92	Cleveland	O	R	N	others
D 93	Pensky-Martens	C	R	Y	DOT
D 1310	Tag, open	O	R	N	others
D 3278	Setaflash	C	F	N	DOT
D 3828	Setaflash	C	F	N	others
D 3934	Flash/no-flash	C	F	Y/N	others
D 3941	Equilibrium	C	slow rising	Y/N	DOT

which is typically a water/ethylene glycol mixture. The liquid bath is heated by a gas burner and is to warm up at a rate of 1°C per minute (for substances with T_{FP} < 60°C) or at 3°C per minute (for substances with $T_{FP} \geq 60$°C). At every 0.5 or 1°C interval, a small flame is briefly lowered down near the surface to test whether a flash occurs. The upper limit for the test method is 93°C. The lower limit is not specified, except for the note that values below 0°C may be unreliable.

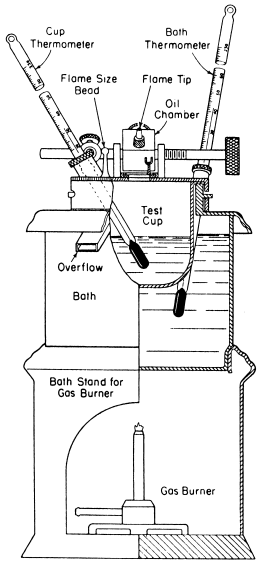


Figure 60 The Tagliabue closed-cup flash point tester
(Copyright ASTM International, used by permission)

ASTM D 92

The Cleveland open-cup test method, ASTM D 92[208], dates to 1921 and finds use in the petroleum industry for products, apart from fuel oils, having a T_{FP} between 79 C and 400 C. It uses a cup in which 70 mL of test liquid is held. There is no liquid bath, but temperature uniformity across the bottom of the cup is provided by a metal plate. Heating can be either by a gas burner or by an electric resistance heater. The heating, once a temperature close to the expected flash point is reached, is done at a rate of 5 – 6ºC per minute. The test method also provides for the reporting of the fire point, in addition to the flash point. The latter is defined as the lowest temperature at which flaming is sustained for at least 5 s. Its reproducibility was found to be the worst of all of the flash point testers[211].

ASTM D 93

The Pensky-Martens closed-cup tester, ASTM D 93[209], was first standardized in 1921 (Color Plates 8 and 9). It is limited to testing substances with a viscosity > 5.5 cSt at 40ºC. It has neither a liquid bath nor a heat sink plate, but relies on a stirrer inserted into the sample cup to ensure temperature uniformity. The Pensky-Martens test basically replaces the water bath of the Abel-Pensky test (not used in the US) with a heavy metal shell. The sample size is 75 mL. Due to absence of a water bath, high temperatures may be attained. The test method is usable for T_{FP} values from 40ºC to 370ºC. The sample is heated at a rate of 5 – 6 ºC per minute. Unlike other tests, there is a freedom to select the ignition source type, and both gas pilots and electric glow wires can be used. Burgoyne et al.[53] showed that a gas pilot used in the apparatus introduces significant aberrations both by localized heating of the liquid and by convection effects throughout the vapor space. Thus, they recommended use of electric spark ignition, but their recommendation was not adopted by ASTM.

The Pensky-Martens test was found to yield flash point values about 7 – 11ºC higher than the Tag Closed-cup tester[51]. Fire points reported in the Pensky-Martens test were found to be 8 – 13ºC higher than corresponding values in the Tag Closed-cup tester. In a research study where electric spark discharge was used at an optimized height[51], it was found that even the Tag Closed-cup fire point values were 1 – 10ºC higher than the 'true' values, while Pensky-Martens values were up to 18ºC higher than the 'true' values.

ASTM D 1310

The Tagliabue open cup test method, ASTM D 1310[210], was first issued in 1952. Flash points from –18ºC to 165ºC can be determined with this method. A water/ethylene glycol water bath is used, and the heat is provided by a gas burner. The sample is heated at a rate of 1°C per minute. Fire points may also be determined with this method, along with flash points. The fire point is defined the same as in ASTM D 92. Its reproducibility was found to be poor[74,211].

ASTM D 3278

While the preceding devices date to the early part of the 20th century, the Setaflash test, ASTM D 3278[212], was standardized in 1973 and reflects newer ideas in instrument design. The scheme was invented by T. Kidd at Esso Petroleum Co. and commercialized by Stanhope-Seat Ltd. Its development has been briefly reviewed by Wray[213]. It is a closed-cup test applicable for T_{FP} between 0°C and 110°C and viscosities less than 150 cSt at 25°C. A very small sample amount of 2 mL is injected with syringe into a preheated sample cup. The sample cup is part of a machined metal block which is directly heated by an electrical resistance heater. To examine higher or lower temperature values, a new specimen must be used. There is no stirring and no liquid bath. For temperatures below ambient, an auxiliary cooling block is used, which is packed with an acetone/dry ice mixture. A special procedure is given for testing organic peroxides. According to ASTM E 502, the Setaflash method is the preferred procedure for testing solid substances. Solids are dropped directly into the sample cup, instead of being injected into the filling orifice. This test method is very similar to ISO 3679[214] and ISO 3680[215] procedures.

ASTM D 3828

The ASTM D 3828 test method[216] is another version of the Setaflash test, developed by a different ASTM committee. It is specified over the temperature range of –20ºC to 300ºC. For temperatures over 100ºC, a 4 mL sample is used. At one time, ASTM also had a rising-temperature ('dynamic') Setaflash standard, ASTM D 3243[217]. Because of the small sample cup size in the apparatus, results from the dynamic procedure proved to be inaccurate, and the standard was withdrawn; it was officially superceded by ASTM D 3828.

ASTM D 3934

ASTM D 3934[218] evolved from studies in Germany that led to the German standard DIN 53213. It is an 'apparatus non-specific' closed-cup, go/no-go testing scheme which, in the ASTM standard, can use the sample cup of either the D 56 (Tag) or the D 93 (Pensky-Martens) test method. The liquid bath to be provided is not specified in detail. The test is intended for compliance verification, where a flash/no-flash result is to be obtained at a single test temperature. Temperatures in the range of 0ºC to 110ºC are encompassed. The method is roughly similar to ISO 1516[219] and is used by the paint and varnish industry. In the Pensky-Martens version, the sample stirrer is retained. A review of the inter-apparatus data correlation using this method has been published[220].

ASTM D 3941

For substances of low thermal conductivity, the rising-temperature Tag or Pensky-Martens tests may not give accurate results. A separate test standard, ASTM D 3941[221], has been developed which—like D 3934—allows the use of either the Tag or the Pensky-Martens sample cups and gives freedom in design of the liquid bath. Unlike D 3034, however, it provides a rising temperature program. The main difference between this standard and D 59 or D 93 is the slow rate of rise, being only 0.5ºC per minute. The method is similar but not identical to ISO 1523[222]; it is specified by the US Dept. of Transportation in regulations, in place of ISO 1523.

ABEL FLASH POINT TEST

The UK and some other countries still use the Abel flash point test. These are standardized by two IP (Institute of Petroleum) standards. IP 33[223] (also issued as BS 3442) is the official UK government test, according to the revised Act of 1928, while IP 170 describes a commercial standard that has been updated through the years. The device comprises a small, covered sample cup heated indirectly by an alcohol lamp. The lamp heats the water bath, but the sample cup is separated from the water bath by an air gap. The water bath is first heated to 54ºC (130ºF) and the source of heat is then removed. A specimen is first inserted at 16ºC (60ºF) and is then to be tested at every 1ºF rise in its temperature. The timing for opening the cover and applying the test flame is to be set by a metronome (possibly the only use ever made of a musician's instrument in fire testing). The peak test temperature is evidently somewhere below 54ºC, since reheating the bath is not allowed. A stirrer is provided for the specimen cup, but this is to be used for "viscous materials" only. A separate procedure is described for testing solid petroleum products.

The commercial IP 170 standard[224] provides a test range of –18ºC to 71ºC (0 to 160ºF). In the commercial procedure, the air space is also filled with water (or an antifreeze). All samples are stirred continuously by hand, not just viscous materials. Heat is continuously applied so as to raise the temperature of the sample at approximately 1ºC per minute.

TESTS FOR OTHER PROPERTIES

ASTM D 4206 TEST FOR SUSTAINED BURNING

The ASTM D 4206[225] apparatus is a small open cup which holds 2 mL of a test liquid and which is maintained at a temperature of 49°C by an electric heater. After the specimen is poured in, a small flame is applied for 15 s above the surface. The specimen fails if it sustains burning for more than 15 s after the removal of the pilot flame, or if it ignites from the pilot flame while it is still in its standby position, prior to having been moved into the test position. The test method is the ASTM equivalent of British standard BS 3900 Part A-11, which is used in the UK to regulate the flammability properties of kerosene.

HYDRAULIC FLUID SPRAYS

In many applications, hydraulic fluids are required to have low combustibility or a measure of resistance to ignition. For this purpose, a large variety of tests have been invented. Totten and Webster[226] reviewed 8 different methods. The methods in most current use are discussed below. The European Commission has issued a handbook—commonly called the 'Luxembourg report'—of test methods for fire-resistant hydraulic fluids[227]. Not all of the methods are for fire, since mechanical properties, toxicity, etc. are also encompassed.

ISO 15029

The method[228] provides three separate tests, a hollow cone nozzle method (ISO 15029-1), a 'small-scale' test (ISO 15029-2) and a large-scale test (ISO 15029-3). The hollow cone nozzle test was developed by the Coal Board of the UK. It is a bench-scale test where the test fluid, heated to various temperatures is sprayed from an 80 hollow-cone nozzle at a pressure of 7 MPa. The spray is ignited with an oxy-acetylene flame which is applied until ignition occurs. Upon ignition, the exposing flame is removed. The test variable reported is the time that it takes for extinction of the flame of the test fluid to occur. This method is little-used, with the Part 2 or Part 3 tests being viewed as more current test strategies.

The ISO 15029-2 test apparatus[229,230] resembles a wind tunnel, about 2 m long and 0.5 m high. It is called the 'Buxton test,' in reference to the town in the UK where the developing HSE laboratories are sited. An atomizer sprays the test fluid horizontally into the flowing air stream. Downstream of the atomizer is a propane burner which does or does not ignite the mixture. Two different propane flow rates are provided (approx. 3 and 10 kW), in order to better discriminate among fluids. The results are reported in terms on an 'ignitability index' RI, which is a complex expression involving various temperature measurements within the test apparatus. Smoke is also measured at the exhaust end and a separate rating is assigned for it. The product is rated into grades A – H, depending on its RI and its smoke measurement.

The large-scale ISO 15029-3 method was derived from an earlier Nordtest test[231]. It uses an arrangement involving a partially-enclosed room, where a nozzle sprays the test fluid into the air at an angle of 60º up from horizontal. Four different nozzle pressures are used: 50, 100, 150, and 250 atm. A propane igniting burner is located nearby, and products of combustion are collected in a large 3 × 3 m hood. The propane burner is used in three sizes, 10, 25 and 100 mm diameters, with the HRR values being 10, 100, and 200 kW, respectively. The results are reported in terms of combustion efficiency, with 0 indicating no ignition, and values greatly less than 1.0 indicating a sporadically igniting fluid. The reference heat of combustion has to first be determined using an oxygen bomb calorimeter. A report has been published giving guidance and example data[232].

Factory Mutual tests

FM uses an Approval Standard[233] that has two tests: (1) a hot surface test; and (2) a spray propagation test. In the hot surface test, a steel channel is place at 30º up from vertical, and its underneath surface is heated by propane burners to give a surface temperature of 704ºC. The heating is then turned off, and the test fluid is sprayed for 60 s onto the channel from a nozzle. If ignition occurs, the nozzle is turned away, and the flame must not follow the movement of the nozzle, for the fluid to pass. In the spray propagation test, a high-pressure spray is directed horizontally into open air. A propane torch is introduced at 0.15 and 0.46 m away from the nozzle. The flame must not persist for more than 6 s after removal of the torch.

MSHA spray test

The official test[234] specified for hydraulic fluids by the US Mine Safety and Health Administration is a spray test where fluid at 10.2 atm and 66ºC is discharged from a 90º cone angle nozzle. Three different ignition devices are used: (1) burning cotton waste in a metal trough; (2) an electric arc; and (c) a hand-held propane plumber's torch. The three hand-held sources are to be moved along the spray pattern in an undefined manner. To pass, the fluid must not burn for more than 6 s after withdrawal of the ignition source, when the ignition source is held for 60 s at any location farther than 0.46 m from the nozzle. Loftus[235,236] has discussed this test in detail, along with some other tests used by MSHA.

Further readings

Brian P. Mullins, **Spontaneous Ignition of Liquid Fuels**, AGARDograph no. 4. Butterworths, London (1955). This work also covers various test methods that can be used to measure the AIT of gases.

A. Murty Kanury, **Introduction to Combustion Phenomena**, Gordon & Breach, New York (1975). This is the best presentation of Spalding's B-number concept which is widely used in combustion modeling of liquids.

References

1. Tyrrell, E. A., Fire Incidents Involving Flammable Liquids, Gas, and Dry Explosives (NBSIR 75-784), NBS (1975).
2. Reid, R. C., Prausnitz, J. M., and Sherwood, T. K., **The Properties of Gases and Liquids**, 3rd ed., McGraw-Hill, New York (1977).
3. Reid, R. C., Prausnitz, J. M., and Poling, B. E., **The Properties of Gases and Liquids**, 4th ed., McGraw-Hill, New York (1987).
4. Sargent, L. B. jr., Volatility Characteristics of Low-Viscosity Petroleum Oils, *Lubrication Engineering* **37**, 513-519 (1981).
5. Kuchta, J. M., Investigation of Fire and Explosion Accidents in the Chemical, Mining, and Fuel-Related Industries—A Manual (Bulletin 680), Bureau of Mines, Pittsburgh (1985).
6. Butler, R. M., Cooke, G. M., Lukk, G. G., and Jameson, B. G., Prediction of Flash Points of Middle Distillates, *Ind. and Eng. Chem.* **48**, 808-812 (1956).
7. Goodger, E. M., Spontaneous Ignition of Falling Droplets in the Cranfield Pressure Rig, *J. Inst. Energy* 199-208 (Dec. 1987).
8. Nishiwaki, N., Kinetics of Liquid Combustion Processes: Evaporation and Ignition Lag of Fuel Droplets, pp. 148-158 in *5th Symp. (Intl.) on Combustion*, Reinhold, New York (1954).
9. Masdin, E. C., and Thring, M. W., Combustion of Single Droplets of Liquid Fuel, *J. Inst. Fuel* **35**, 251-260 (June 1962).
10. Taylor, R. A., and Burgess, A. R., Particulate Formation in Fuel Oil Combustion, *Fuel Science & Technology Intl.* **6**, 41-81 (1988).
11. Wong, S.-C., Liao, X.-X., and Yang, J.-R., A Simplified Theory of the Ignition of Single Droplets under Forced Convection, *Combustion and Flame* **110**, 319-334 (1997).

12. Molero de Blas, L. J., Pollutant Formation and Interaction in the Combustion of Heavy Liquid Fuels (Ph.D. dissertation), University College, London (1998).
13. Saitoh, T., Ishiguro, S., and Niioka, T., An Experimental Study of Droplet Ignition Characteristics Near the Ignitable Limit, *Combustion and Flame* **47**, 27-32 (1982).
14. Tanabe, J., et al., Two Stage Ignition of *n*-Heptane Isolated Droplets, *Combustion Science and Technology* **108**, 103 (1995).
15. Moriue, O., et al., Effects of Dilution by Aromatic Hydrocarbons on Staged Ignition Behavior of *n*-Decane Droplets, *Proc. Combustion Inst.* **28**, 969-975 (2000).
16. Bryant, J. T., Ignition Delay Time of Fuel Droplets, an Empirical Correlation with Flash Point, *Combustion Science and Technology* **10**, 185-187 (1975).
17. Goodger, E. M., Spontaneous Ignition Research: Review of Experimental Data, *J. Inst. Energy* **60**, 84-94 (June 1987).
18. Faeth, G. M., and Olson, D. R., The Ignition of Hydrocarbon Fuel Droplets in Air, *SAE Trans.* **77**, 1793-1802 (1968).
19. Abdou, M. I., The Vaporization and Self-Ignition of Liquid Fuel Drops (Ph.D. dissertation), Univ. Wisconsin, Madison (1962).
20. Takei, M., Tsukamoto, T., and Niioka, T., Ignition of Blended-fuel Droplet in High-Temperature Atmosphere, *Combustion and Flame* **93**, 149-156 (1993); also **96**, 186-189 (1994).
21. Priem, R. J., Borman, G. L., El-Wakil, M. M., Uyehara, O. A., and Myers, P. S., Experimental and Calculated Histories of Vaporizing Fuel Drops (Tech. Note 3988), NACA, Washington (1957).
22. Law, C. K., Asymptotic Theory for Ignition and Extinction in Droplet Burning, *Combustion and Flame* **24**, 89-98 (1975).
23. Law, C. K., Theory of Thermal Ignition in Fuel Droplet Burning, *Combustion and Flame* **31**, 285-296 (1978).
24. Aggarwal, S. K., Effects of Internal Heat Transfer Models on the Ignition of Fuel Droplets, *Combustion Science and Technology* **42**, 325-334 (1985).
25. Mawid, M. A., Analyses of Spray and Droplet Ignition for Pure and Multicomponent Fuels (Ph.D. dissertation), Univ. Illinois, Chicago (1989).
26. Jeng, K.-J., Evaporation and Ignition Delay of Fuel and Emulsion Droplets (Ph.D. dissertation), North Carolina State Univ., Raleigh (1986).
27. Green, H. L., and Lane, W. R., **Particulate Clouds: Dusts, Smokes and Mists**, 2nd ed., E. & F.N. Spon, London (1964).
28. Correa, S. M., and Sichel, M., The Group Combustion of a Spherical Cloud of Monodisperse Fuel Droplets, pp. 981-991 in *19th Symp. (Intl.) on Combustion*, The Combustion Institute, Pittsburgh (1982).
29. Hayashi, S., Ohtani, T., Iinuma, K., and Kumagai, S., Limiting Factor of Flame Propagation in Low-Volatility Fuel Clouds, pp. 361-367 in *18th Symp. (Intl.) on Combustion*, The Combustion Institute, Pittsburgh (1980).
30. Wong, S.-C., Chang, J.-C., and Yang, Y.-C., Autoignition of Droplets in Nondilute Monodisperse Clouds, *Combustion and Flame* **94**, 397-406 (1993).
31. Rah, S.-C., Sarofim, S. F., and Beer, J. M., Ignition and Combustion of Liquid Fuel Droplets, *Combustion Science and Technology* **49**, 169-184 (1986).
32. Wood, B. J., and Rosser, W. A. jr., An Experimental Study of Fuel Droplet Ignition, *AIAA J.* **7**, 2288-2292 (1969).
33. Hiroyasu, H., Fundamental Spray Combustion Mechanism and Structures of Fuel Sprays in Diesel Engines, pp. 237-260 in **Mechanics and Combustion of Droplets and Sprays**, H. H. Chiu and N. Chigier, eds., Begell House, New York (1995).
34. Laster, W. R., and Annamalai, K., Ignition Delay of Droplet Clouds: Results from Group Combustion Theory, *Chemical Engineering Communications* **105**, 201-219 (1991).
35. Mizutani, Y., Nakabe, K., and Chung, J. D., Effects of Turbulent Mixing on Spray Ignition, pp. 1455-1460 in *23rd Symp. (Intl.) on Combustion*, The Combustion Institute, Pittsburgh (1990).
36. Kono, M., Ito, K., Niioka, T., Kadota, T., and Sato, J., Current State of Combustion Research in Microgravity, pp. 1189-1199 in *26th Symp. (Intl.) on Combustion*, The Combustion Institute, Pittsburgh (1996).
37. Sichel, M., and Palaniswamy, S., Sheath Combustion of Sprays, pp. 1789-1798 in *20th Symp.(Intl.) on Combustion*, The Combustion Institute, Pittsburgh (1984).
38. McIntosh, A. C., Gol'dshtein, V., Goldfarb, I., and Zinoviev, A., Thermal Explosion in a Combustible Gas Containing Fuel Droplets, *Combustion Theory and Modelling* **2**, 153-165 (1998).
39. Sirignano, W. A., An Integrated Approach to Spray Combustion Model Development, *Combustion Science and Technology* **58**, 231-251 (1988).
40. Annamalai, K., and Ryan, W., Interactive Processes in Gasification and Combustion. Part I: Liquid Drop Arrays and Clouds, *Prog. Energy and Combustion Science* **18**, 221-295 (1992).
41. Burgoyne, J. H., and Williams-Leir, G., Inflammability of Liquids, *Fuel* **28**, 145-149 (1949).
42. Factory Mutual Engineering Corporation, **Handbook of Industrial Loss Prevention**, 2nd ed., McGraw-Hill, New York (1967).
43. Shepherd, J. E., Krok, J. C., and Lee, J. L., Jet A Explosion Experiments: Laboratory Testing (Explosion Dynamics Lab. Report FM97-5), Graduate Aeronautical Laboratories, California Institute of Technology, Pasadena (1997).
44. Hasegawa, K., and Kashiki, K., A Method for Measuring Upper Flash Point—Practical Method Using Setaflash Closed-Cup Apparatus, *Report of Fire Research Institute*, No. 71, 69-77 (1991).
45. Kuchta, J. M., and Clodfelter, R. G., Aircraft Mishap Fire Pattern Investigations (AFWAL-TR-85-2057), Aero Propulsion Laboratory, Air Force Systems Command, Wright-Patterson AFB OH (1985).
46. Wray, H. A., Flammability of Chlorinated Hydrocarbons and Hydrocarbon Mixtures, *J. Coatings Tech.* **56**, 37-43 (Oct. 1984).
47. Khan, M. M., Spray Flammability of Hydraulic Fluids and Development of a Test Method (FMRC J.I. 0T0W3.RC), Factory Mutual Research Corp., Norwood MA (1991).
48. Roberts, A. F., and Quince, B. W., A Limiting Condition for the Burning of Flammable Liquids, *Combustion and Flame* **20**, 245-251 (1973).
49. Kuchta, J. M., Lambiris, S., and Zabetakis, M. G., Flammability and Autoignition of Hydrocarbon Fuels Under Static and Dynamic Conditions (RI 5992), Bureau of Mines, Pittsburgh (1962).

50. Modak, A. T., Ignitability of High-Fire-Point Liquid Spills (EPRI NP-1731), Electric Power Research Inst., Palo Alto, CA (1981).
51. Ishida, H., and Iwama, A., Some Critical Discussions on Flash and Fire Points of Liquid Fuels, pp. 217-226 in *Fire Safety Science—Proc. 1st Intl. Symp.*, Hemisphere, Washington (1986).
52. Bird, R. E., Stewart, W. E., and Lightfoot, E. N., **Transport Phenomena**, John Wiley, New York (1960). p. 522
53. Burgoyne, J. H., Roberts, A. F., and Alexander, J. L., The Significance of Open Flash Points, *J. Inst. Petroleum* **53**, 338-341 (1967).
54. Glassman, I., and Dryer, F. L., Flame Spreading Across Liquid Fuels, *Fire Safety J.* **3**, 123-138 (1980/81).
55. Zinn, S. V., jr., Crash Fire Hazard Evaluation of Jet Fuels, *Proc. Natl. Business Aircraft Mtg.*, Society of Automotive Engineers, New York (1972).
56. Bunama, R. M., and Karim, G. A., Modeling the Formation of Flammable Atmospheres within Cylindrical Containers Containing Some Liquid Fuel, *Proc. Combustion Inst.* **28**, 2867-2874 (2000).
57. Patil, G. S., Estimation of Flash Point, *Fire and Materials* **12**, 127-131 (1988).
58. Satyanarayana, K., and Kakati, M. C., Note: Correlation of Flash Points, *Fire and Materials* **15**, 97-100 (1991).
59. Hshieh, F.-Y., Note: Correlation of Closed-Cup Flash Points with Normal Boiling Points for Silicone and General Organic Compounds, *Fire and Materials* **21**, 277-282 (1997).
60. Metcalf, E., and Metcalf, A. E. M., Communication: On the Correlation of Flash Points, *Fire and Materials* **16**, 153-154 (1992).
61. Shebeko, Y. N., Korol'chenko, A Y., Ivanov, A V., and Alekhina, E. N., Calculation of Flash Points and Ignition Temperatures of Organic Compounds, *Soviet Chemical Industry*, **16**, 1371-1376 (1984).
62. Kueffer, J., and Donaldson, A. B., Correlation of Flash Point Data with Lower Flammability Limit, pp. 119-124 in *Proc. 1997 Tech. Mtg., Central States Section, The Combustion Institute* (1997).
63. Fujii, A., and Hermann, E. R., Correlation between Flash Point and Vapour Pressures of Organic Compounds, *J. Safety Research* **13**, 163-175 (1982).
64. Leslie, E. H., and Geniesse, J. C., Flash Points of Saturated Vapors of Combustible Liquids, pp. 161-162, **International Critical Tables of Numerical Data, Physics, Chemistry, and Technology**, vol. 2, McGraw-Hill, New York (1927).
65. Monakhov, V. T., **Metody issledovaniya pozharnoi ospasnosti veshchestv**, Khimya, Moscow (1972). English translation: **Methods for Studying the Flammability of Substances**, published for U.S. National Bureau of Standards by Amerind Publishing Co., New Delhi, India (1985).
66. **Manual for Predicting Chemical Process Design Data: Data Prediction Manual**, R. P. Danner, T. E. Daubert, eds., Design Institute for Physical Property Data, AIChE (1983-1987).
67. Finnegan, D. M., Study of Flash Points of Multicomponent Flammable Liquid Solutions (M.S. Thesis). Worcester Polytechnic Institute, Worcester MA (1994).
68. Lentini, J. J., Vapor Pressures, Flash Points and the Case Against Kerosene Heaters, *Fire and Arson Investigator* **40**:3, 16-18 (March 1990).
69. Ohlemiller, T. J., and Cleary, T. G., Aspects of the Motor Vehicle Fire Threat from Flammable Liquid Spills on a Road Surface (NISTIR 6147), NIST (1998).
70. Walsham, J. G., Prediction of Flash Points for Solvent Mixtures, pp. 405-417 in *Papers. ACS Div. of Organic Coatings and Plastics Chemistry, 162nd Natl. Mtg.*, Vol. 31 part 2 (1971).
71. Gmehling, J., and Rasmussen, P., Flash Points of Flammable Liquid Mixtures Using UNIFAC, *Ind. and Eng. Chem—Fundamentals* **21**, 186-8, 321 (1982).
72. Kamarchik, P., Effect of Solution Viscosity on Observed Flash Points by the Pensky-Martens Method, *J. Fire and Flammability* **15**, 33-38 (1982).
73. Demidov, P. G., **Goreniye i svoystva goryuchikh veshchestv**, Izdatel'stvo Ministerstva Kommunal'nogo Khozyaystva RSFSR, Moskva (1962). English translation: **Combustion and Properties of Combustible Substance**, NTIS No. AD 621 738, National Technical Information Service, Springfield VA (1965).
74. Probst, K. G., Flash Point of Mixed Solvents, *J. Paint Technology* **41**, 670-679 (1969).
75. Allen, I. C., and Crossfield, A. S. The Flash Point of Oils (Tech. Paper 49), Bureau of Mines, Government Printing Office, Washington (1913).
76. Gerstein, M., and Stine, W. G., Anomalies in Flash Points of Liquid Mixtures, *Ind. Eng. Chem. Prod. R&D* **12**, 253-255 (1973).
77. Thorne, P. F., Flash Points of Mixtures of Flammable and Non-Flammable Liquids, *Fire and Materials* **1**, 134-139 (1976).
78. Ellis, W. H., Solvent Flash Points—Expected and Unexpected, *J. Coatings Technology* **48**, 44-57 (March 1976).
79. Standard Test Method for Distillation of Petroleum Products (ASTM D 86), ASTM.
80. Hill, R., ed., A Review of the Flammability Hazard of Jet A Fuel Vapor in Civil Transport Aircraft Fuel Tanks (DOT/FAA/AR-98/26), Federal Aviation Admin., Atlantic City NJ (1998).
81. Burgoyne, J. H., and Cohen, L., The Effect of Drop Size on Flame Propagation in Liquid Aerosols, *Proc. Royal Soc. London* **A225**, 375-392 (1954).
82. Bowen, P. J., and Cameron, L. R. J., Hydrocarbon Aerosol Explosion Hazards: A Review, *Trans. IChemE* **77B**, 22-30 (1999).
83. Dietrich, D. L., Cernansky, N. P., Somashekara, M. B., and Namer, I., Spark Ignition of a Bidisperse, *n*-Decane Fuel Spray, pp. 1383-1389 in *23rd Symp. (Intl.) on Combustion*, The Combustion Institute, Pittsburgh (1990).
84. Aggarwal, S. K., and Sirignano, W. A., Ignition of Polydisperse Sprays: Importance of D_{20}, *Combustion Science and Technology* **46**, 289-300 (1986).
85. Singh, A. K., and Polymeropoulos, C. E., Spark Ignition of Aerosols, pp. 513-519 in *21st Symp.(Intl.) on Combustion*, The Combustion Institute, Pittsburgh (1986).
86. Danis, A. M., Namer, I., and Cernansky, N. P., Droplet Size and Equivalence Ratio Effects on Spark Ignition of Monodisperse *n*-Heptane and Methanol Sprays, *Combustion and Flame* **74**, 285-294 (1988).
87. Chan, K.-K., An Experimental Investigation of Minimum Ignition Energy of Monodisperse Fuel Sprays (Ph.D. dissertation), Rutgers Univ., New Brunswick NJ (1982).

88. Ballal, D. R., and Lefebvre, A. H., Ignition and Flame Quenching of Flowing Heterogeneous Fuel-Air Mixtures, *Combustion and Flame* **35**, 155-168 (1979).
89. Peters, J. E., and Mellor, A. M., An Ignition Model for Quiescent Fuel Sprays, *Combustion and Flame* **38**, 65-74 (1980).
90. Ballal, D. R., and Lefevbre, A. H., Ignition and Flame Quenching of Quiescent Fuel Mists, *Proc. Royal Soc. (London)* **A364**, 277-294 (1978).
91. Ballal, D. R., and Lefebvre, A. H., Ignition of Liquid Fuel Sprays at Subatmospheric Pressures, *Combustion and Flame* **31**, 115-126 (1978).
92. Kuchta, J. M., Fire and Explosion Manual for Aircraft Accident Investigators (AFAPL-TR-73-74). Prepared by Bureau of Mines, Pittsburgh, for Air Force Aero Propulsion Laboratory, Wright-Patterson Air Force Base, Ohio (1973).
93. Liebman, I., Spolan, I., Kuchta, J. M., and Zabetakis, M. G., Ignition of Tank Atmospheres During Fuel Loading, *Proc. API* **45 (III)**, 218-230 (1965).
94. Rao, K. V. L., and Lefebvre, A. H., Minimum Ignition Energies in Flowing Kerosine-Air Mixtures, *Combustion and Flame* **27**, 1-20 (1976).
95. SubbaRao, H. N., and Lefebvre, A. H., Ignition of Kerosine Fuel Sprays in a Flowing Air Stream, *Combustion Science and Technology* **8**, 95-100 (1973).
96. Bowen, P. J., and Shirvill, L. C., Combustion Hazards Posed by the Pressurized Atomization of High-Flashpoint Liquids, *J. Loss Prevention in the Process Industries* **7**, 233-241 (1994).
97. Pidoll, U. von, The Ignition of Clouds of Sprays, Powders and Fibers by Flames and Electric Sparks, *J. Loss Prevention in the Process Industries* **14**, 103-109 (2001).
98. Lewis, D. J., Dust Explosions: Their General Relationship to Gas, Vapour and Mist Explosions with Particular Reference to Venting, *19th Loss Prevention Symp.*, AIChE (1985).
99. Benz, F. J., Bishop, C. V., and Pedley, M. D., Ignition and Thermal Hazards of Selected Aerospace Fluids (RD-WSTF-0001), NASA JSC White Sands Test Facility, Las Cruces, NM (1988).
100. Cook, S. J., Cullis, C. F., and Good, A. J., The Measurement of the Flammability Limits of Mists, *Combustion and Flame* **30**, 309-317 (1977).
101. Eichhorn, J., Mists Can Cause Explosions, pp. 190-193; 220 in **Fire Protection Manual for Hydrocarbon Processing Plants**, vol. 1, C. H. Vervalin, ed., 2nd ed., Gulf Publishing, Houston (1973).
102. Hirsch, W., Hempel, D., and Förster, H., Prevention of Fire and Explosion in Industrial Spraying of Hydrocarbons with High Flash Point, pp. 760-769 in *Proc. 9th Intl. Symp. on Loss Prevention and Safety Promotion in the Process Industries*, Associacio D'Enginyers Industrials de Catalunya, Barcelona (1998).
103. Förster, H., and Steen, H., Explosionsfähigkeit von Nebel/Dampf/Luft oder Nebel/Gas/Luft-Gemischen [Explosibility of Mist/Vapor/Air or Mist/Gas/Air Mixtures] (Bericht W-21), Physikalisch-Technische Bundesanstalt, Braunschweig, Germany (1983).
104. Eckhoff, R. K., Generation, Ignition, Combustion and Explosion of Sprays and Mists of Flammable Liquids in Air (CMI-R 91/ A25014), Chr. Michelsen Institute, Bergen, Norway (1991).
105. Zabetakis, M., and Rosen, B. H., Considerations Involved in Handling Kerosine, *Proc. Amer. Petroleum Inst.* **37**(III), 296-306 (1957).
106. Haber, F., and Wolff, H., Über Nebelexplosionen [On Mist Explosions], *Zeitschrift für angewandte Chemie* **36**, 373-377 (1923).
107. Mizutani, Y., and Ogasawara, M., Laminar Flame Propagation in Droplet Suspension of Liquid Fuel, *Intl. J. Heat & Mass Transfer* **8**, 921-935 (1956).
108. Burgoyne, J. H., and Richardson, J. F., The Inflammability of Oil Mists, *Fuel* **28**, 1-6 (1949).
109. Burgoyne, J. H., Mist and Spray Explosions, *Chem. Eng. Progress* **53**, 121M-124M (1957).
110. Burgoyne, J. H., The Flammability of Mists and Sprays, pp. 1-5 in *Proc. 2nd Symp. on Chemical Process Hazards with Special Reference to Plant Design* (Symp. Series No. 15), Institution of Chemical Engineers, London (1963).
111. Förster, H., and Steen, H., Explosionsverhalten von Nebel/Luft- und Nebel/Gas/Luft-Gemischen [Explosive Behavior of Mist/Air and Mist/Gas/Air Mixtures], pp. 439-464 in *Report of the 9th Intl. Symp. on Prevention of Occupational Accidents and Diseases in the Chemical Industry*, Intl. Social Security Assn., Lucerne (1984).
112. Anson, D., Influence of the Quality of Atomization on the Stability of Combustion of Liquid Fuel Sprays, *Fuel* **32**, 39-51 (1953).
113. Sullivan, M. V., Wolfe, J. K, and Zisman, W. A., Flammability of the Higher Boiling Liquids and Their Mists, *Ind. and Eng. Chem.* **39**, 1607-1614 (1947).
114. Capp, B., The Maximum Experimental Safe Gap for a Spray of Higher Flash Point Liquid, *J. Hazardous Materials* **18**, 91-97 (1988).
115. Tamura, Z., and Tanasawa, Y., Evaporation and Combustion of a Drop Contacting with a Hot Surface, pp. 509-522 in *7th Symp. (Intl.) on C ombustion*, The Combustion Institute, Pittsburgh (1959).
116. Mizomoto, M., Hayano, H., and Ikai, S., Evaporation and Ignition of a Fuel Droplet on a Hot Surface. Part 1. Evaporation, *Bull. JSME* **21**, 1765-1771 (1978).
117. Mizomoto, M., and Ikai, S., Evaporation and Ignition of a Fuel Droplet on a Hot Surface. Part 2. Ignition, *Bull. JSME* **21**, 1772-1779 (1978).
118. Mizomoto, M., Morita, A., and Ikai, S., Evaporation and Ignition of a Fuel Droplet on a Hot Surface. Part 3. Effects of Initial Drop Diameter, *Bull. JSME* **22**, 1266-1273 (1979).
119. Cho, P., and Law, C. K., Pressure/Temperature Ignition Limits of Fuel Droplet Vaporizing over a Hot Plate, *Intl. J. Heat & Mass Transfer* **28**, 2174-2176 (1985).
120. Karasawa, T., Shiga, S., and Kurabayashi, T., Ignition Phenomena of a Fuel-Droplet Impinging upon a Hot Surface, *Bull. JSME* **29**, 143-148 (1986).
121. Sommer, H., Ignition Studies of Fuel Droplet Streams, pp. 641-646 in *21st Symp. (Intl.) on Combustion*, The Combustion Institute, Pittsburgh (1986).
122. Satcunanathan, S., Ignition Delay of Individual Liquid Fuel Droplets, *Ind.. and Eng. Chem.—Process Des. Dev.* **10**, 297-304 (1971).
123. Gülder, Ö, and Wong, J. K. S., Spheroidal Evaporation and Ignition of Fuel Droplets on a Hot Surface, pp. 1751-1760 in *20th Symp. (Intl.) on Combustion*, The Combustion Institute, Pittsburgh (1984).

124. Aggarwal, S. K., and Sirignano, W. A., Ignition of Fuel Sprays: Deterministic Calculations for Idealized Droplet Arrays, pp. 1773-1780 in *20th Symp. (Intl.) on Combustion*, The Combustion Institute, Pittsburgh (1984).
125. Aggarwal, S. K., and Cha, S., A Parametric Study on Spray Ignition and Comparison with Experiments, *Combustion Science and Technology* **59**, 213-223 (1988).
126. Cooke, R. A., and Ide, R. H., **Principles of Fire Investigation**, The Institution of Fire Engineers, Leicester, England (1985).
127. Sandel, P., Vehicle Fires: More Accurate Ways of Reporting Causes Are Needed, *Fire* **84**, 22, 28, 30 (Oct. 1991).
128. Wiezevich, P. J., Whiteley, J. M., and Turner, L. B., Spontaneous Ignition of Petroleum Fractions, *Ind. and Eng. Chem.* **27**, 152-155 (1935).
129. Burgoyne, J. H., and Newitt, D. M., Crankcase Explosions in Marine Engines, *Institute of Marine Engineers Trans. (London)* **67**, 255-270 (1955).
130. Knowles, R. E., Discussion, *Institute of Marine Engineers Trans. (London)* **77**, 137-138 (1965).
131. Scull, W. E., Relation Between Inflammables and Ignition Sources in Aircraft Environments (NACA Report No. 1019), Lewis Flight Propulsion Laboratory, Cleveland OH (1951).
132. Ferguson, G. W., Diesel Engine Crankcase-Explosion Investigation, *Trans. ASME* **74**, 7-21 (1952).
133. Takahasi, T., Sugisaki, M., Sada, T., and Tsurumi, T., Ignition Mechanism of Fuel Leaked in Vehicles, *Summary of 1995 Annual Mtg. of Japan Assn. of Fire Science and Engineering* 220-223 (1995).
134. Goss, J. C., Brake Fluid Is a Fire Hazard, *Transport Engineer*, p. 9 (March 1989).
135. Snyder, C. E. jr, Krawetz, A. E., and Tovrog, T., Determination of the Flammability characteristics of Aerospace Hydraulic Fluids, *Lubrication Engineering* **37**, 705-714 (Dec. 1981).
136. Phillips, W. D., Fire Resistance Tests for Fluids and Lubricants—Their Limitations and Misapplication, pp. 78-101 in Fire Resistance of Industrial Fluids (ASTM STP 1284), ASTM (1996).
137. Manifold Ignition Test, CETOP Provisional Recommendation RP-65H, CETOP, Frankfurt (1974).
138. Severy, D. M., Blaisdell, D. M., and Kerkhoff, J. F., Automotive Collision Fires, pp. 113-199 in *Proc. 18th Stapp Car Crash Conf.*, Society of Automotive Engineers, Warrendale PA (1974).
139. Goodall, D. G., and Ingle, R., The Ignition of Inflammable Fluids by Hot Surfaces, *Aircraft Engineering* **38**, 20-24, 29, 35 (Apr. 1966).
140. Graves, C. B., Tang., Y. L., and Skifstad, J. G., Ignition of a Fuel Spray by a Hot Surface, *AIAA J.* **24**, 1994-2001 (1986).
141. Atkinson, A. J., and Eklund, T. I., Crash Fire Hazard Evaluation of Jet Fuels (FAA-RD-70-72), Federal Aviation Admin., Washington (1971).
142. Westfield, W. T., Ignition of Aircraft Fluids on High Temperature Engine Surfaces, *Fire Technology* **7**, 69-81 (1971).
143. Myronuk, D. J., Dynamic, Hot Surface Ignition of Aircraft Fuels and Hydraulic Fuels (AFAPL-TR-79-2095), Air Force Aero Propulsion Laboratory, Wright-Patterson AFB, OH (1980).
144. Clodfelter, R. G., Hot Surface Ignition and Aircraft Safety Criteria (SAE Paper 901950), Society of Automotive Engineers (1990).
145. Johnson, A. M., Roth, A. J., and Moussa, N. A., Hot Surface Ignition Tests of Aircraft Fluids (AFWAL-TR-88-2101), Air Force Wright Aeronautical Labs., Wright-Patterson AFB, OH (1988).
146. Geyer, W. H., and Moussa, N. A., Hot-Surface Ignition and Fire-Suppression Tests in an Aircraft Engine Bay (AIAA PAPER 91-2382), *AIAA/SAE/ASME/ASEE 27th Joint Propulsion Conf.*, AIAA, Washington (1991).
147. Glendenning, W. G., Possible Cause of Aircraft Fires on Crash (R&M No. 1375), Aeronautical Research Committee, HMSO, London (1930).
148. Bennett, J. M., Ignition of Combustible Fluids by Heated Surfaces, *Process Safety Progress* **20**, 29-36 (2001).
149. Ignition Risk of Hydrocarbon Vapors by Hot Surfaces in the Open Air (Publ. 2216), 2nd ed., American Petroleum Institute, Washington (1991).
150. Vaivads, R. H., Bardon, M. F., and Battista, V., A Computational Study of the Flammability of Methanol and Gasoline Fuel Spills on Hot Engine Manifolds, *Fire Safety J.* **28**, 307-322 (1997).
151. Murad, R. J., Lamendola, J., Isoda, H., and Summerfield M., A Study of Some factors Influencing the Ignition of a Liquid Fuel Pool, *Combustion and Flame* **15**, 289-298 (1970).
152. Glassman, I., and Hansel, J. G., Some Thoughts and Experiments on Liquid Fuel Spreading, Steady Burning and Ignitability in Quiescent Atmospheres, *Fire Research Abstracts and Reviews* **10**, 217-234 (1968).
153. Ross, H. D., Ignition and Flame Spread over Laboratory-Scale Pools of Pure Liquid Fuels, *Prog. Energy Combust. Sci.* **20**, 17-63 (1994).
154. Roberts, A. F., Spread of Flame on a Liquid Surface (Ph.D. dissertation), Imperial College, Univ. of London (1959).
155. Burgoyne, J. H., Roberts, A. F., and Quinton, P. G., The Spread of Flame Across a Liquid Surface. I. The Induction Period, *Proc. Royal Soc. (London)* **A308**, 39-53 (1968). Burgoyne, J. H., and Roberts, A. F., The Spread of Flame Across a Liquid Surface. II. Steady-state Conditions, *Proc. Royal Soc. (London)* **A308**, 55-68 (1968). Burgoyne, J. H., and Roberts, A. F., The Spread of Flame Across a Liquid Surface. III. A Theoretical Model, *Proc. Royal Soc. (London)* **A308**, 69-79 (1968).
156. Kletz, T. A., Case History. Some Fires and Explosions in Liquids of High Flash Point, *J. Hazardous Materials* **1**, 165-170 (1975/76).
157. Safe Entry and Cleaning of Petroleum Storage Tanks (API Publ. 2015), 4th ed., American Petroleum Institute, Washington (1991).
158. SubbaRao, L. D., Measurement of Vapor Concentrations in Heated Combustible Liquid Storage Tanks (M.S. thesis), Worcester Polytechnic Institute, Worcester MA (1996).
159. Moore, F. C., **Fires: Their Causes, Prevention and Extinction**, The Continental Insurance Co. of New York, New York (1877).
160. Summer, S. M., Mass Loading Effects on Fuel Vapor Concentrations in an Aircraft Fuel Tank Ullage (DOT/FAA/AR-TN99/65), Federal Aviation Administration, Atlantic City NJ (1999).
161. Britton, L. G., **Avoiding Static Ignition Hazards in Chemical Operations**, AIChE (1999).

162. Battista, V., Campbell, H., and Lobay, G., Further Investigation of the Safety of Methanol Fuels, Presented at the 1989 Summer National Meeting, August 22, 1989, Philadelphia, PA, AIChE, New York.
163. Electrical Apparatus for Explosive Gas Atmospheres. Part 3: Spark Test Apparatus for Intrinsically-Safe Circuits (IEC 60079-3). International Electrotechnical Commission, Geneva.
164. Fried, V., Hameka, H. F., and Blukis, U., **Physical Chemistry**, Macmillan, NY (1977).
165. Ott, E. E., Effects of Fuel Slosh and Vibration on the Flammability Hazards of Hydrocarbon Turbine Fuels within Aircraft Fuel Tanks (AFWAL-TR-70-65), Air Force Aero Propulsion Laboratory, Wright-Patterson AFB, OH (1970).
166. Putorti, A. D. jr., Evans, D. D., and Tennyson, E. J., Ignition of Weathered and Emulsified Oils, pp. 657-667 in *Proc. 17th Arctic and Marine Oil Spill Program Technical Seminar*, vol. 1 (1994).
167. Wu, N., Mosman, T., Olenick, S. M., and Torero, J. L., Effect of Weathering on Piloted Ignition and Flash Point of a Slick of Oil, 633-649 in *Proc. 21st Arctic and Marine Oil Spill Program (AMOP) Technical Seminar*, vol. 2, Environment Canada, Ottawa (1998).
168. Wu, N., and Torero, J. L., Enhanced Burning of Difficult to Ignite/Burn Fuels Including Heavy Oils (NIST-GCR-98-750), NBS (1998).
169. Li, J.-H., and Huang, Z.-H., Study on the Correlation of Ignition Time for Liquid Fuels and Heat Radiation, pp. 108-116 in *Symp. for '97 FORUM—Applications of Fire Safety Engineering*, Tianjin, China (1997).
170. Putorti, A. D. jr., Flammable and Combustible Liquid Spill/Burn Patterns (NIJ 604-00), National Institute of Justice, US Dept. Justice, Washington (2001).
171. Miyasaka, K., and Mizutani, Y., Ignition of Sprays by an Incident Shock Wave, *Combustion and Flame* **25**, 177-186 (1975).
172. Carhart, H. W., Jet Fuel Safety and Flash Point, pp. 35-45 in **Factors in Using Kerosine Jet Fuel of Reduced Flash Point** (ASTM STP 688), ASTM (1979).
173. Setchkin, N. P., Self-Ignition Temperatures of Combustible Liquids, *J. Research NBS* **53**, 49-66 (1954).
174. Falk, K. G., The Ignition Temperature of Hydrogen-Oxygen Mixtures, *J. Amer. Chem. Soc.* **28**, 1517 (1906).
175. Mullins, Brian P., **Spontaneous Ignition of Liquid Fuels**, AGARDograph no. 4. Butterworths, London (1955).
176. Belles, F. E., and Swett, C. C., Ignition and Flammability of Hydrocarbon Fuels, pp. 277-320 in Basic Considerations in the Combustion of Hydrocarbon Fuels with Air (NACA Report 1300), NACA, Washington (1957).
177. Moore, H., Spontaneous Ignition Temperatures of Liquid Fuels, *J. Inst. Petroleum* **6**, 186-223 (1920).
178. Moore, H., Spontaneous Ignition Temperature of Liquid Fuels for Internal Combustion Engines, *J. Soc. Chemical Industry* **36**, 109-112 (1917).
179. Thompson, N. J., Autoignition Temperatures of Flammable Liquids, *Ind. and Eng. Chem.* **21**, 134-139 (1929).
180. Helmore, W., Spontaneous Ignition Temperatures: Determination and Significance, pp. 2970-2975 in **The Science of Petroleum**, vol. 4, A. E. Dunstan et al., eds., Oxford Univ. Press, London (1938).
181. Jentzsch, H., Über Selbstentzündung von Ölen und Brennstoffen [On the Self-ignition of Oils and Fuels], *Zeitschrift des Verein Deutscher Ingenieure* **68**, 1150-1152 (1924).
182. Johnson, J. E., Blizzard, R. H., and Carhart, H. W., An Evaluation of the Jentzsch Fuel Tester (NRL Report 3602), Naval Research Lab., Washington (1950).
183. Bridgeman, O. C., and Marvin, C. F., jr., Autoignition Temperatures of Liquid Fuels, *Ind. and Eng. Chem.* **20**, 1219-1223 (1928).
184. Hilado, C. J., and Clark, S. W., Discrepancies and Correlations of Reported Autoignition Temperatures, *Fire Technology* **8**, 218-227 (1972).
185. Mason, W., and Wheeler, R. V., The Ignition of Gases. II. Ignition by a Heated Surface. Mixtures of Methane and Air. *J. Chem. Soc.* **121**, 2079-2091 (1922).
186. Frank, C. E., and Blackham, A. U., Spontaneous Ignition of Organic Compounds, *Ind. and Eng. Chem.* **44**, 862-867 (1952).
187. Frank, C. E., Blackham, A. U., and Swarts, D. E., Investigation of Spontaneous Ignition Temperatures of Organic Compounds With Particular Emphasis on Lubricants (NACA TN 2848), NACA, Washington (1952).
188. Standard Method of Test for Autogenous Ignition Temperatures of Petroleum Products (ASTM D 286), ASTM (1930).
189. Nuckolls, A. H., Report of Subcommittee XXVIII on Autogenous Ignition of Petroleum Products, *Proc. ASTM* **30**, 788-792 (1930).
190. Lewis, D. J., Autoignition Temperature Determinations & Their Relationship to Other Types of Potential Ignition Sources & Their Application to Practical Situations, pp. 257-273 in *7th Intl. Symp. on Chemical Process Hazards with Special Reference to Plant Design* (IChemE Symp. Series No. 58), The Institution of Chemical Engineers, London (1980).
191. Jackson, J. L., and Brokaw, R. S., Variation of Spontaneous Ignition Delays with Temperature and Composition for Propane-Oxygen-Nitrogen Mixtures at Atmospheric Pressure (NACA RM E54B19), NACA, Cleveland (1954).
192. Boodberg, A., and Cornet, I., Atmospheric-pressure Apparatus for Studying Ignition Delay, *Ind. and Eng. Chem.* **43**, 2814-2818 (1951).
193. Scott, G. S., Jones, G. W., and Scott, F. E., Determination of Ignition Temperatures of Combustible Liquids and Gases. Modification of the Drop Method Apparatus, *Anal. Chem.* **20**, 238-241 (1948).
194. Zabetakis, M. G., Furno, A. L., and Jones, G. W., Minimum Spontaneous Ignition Temperatures of Combustibles in Air, *Ind. and Eng. Chem.* **46**, 2173-2178 (1954).
195. Autogenous-Ignition Temperature Test, 30CFR35.20, Code of Federal Regulations.
196. Electrical Apparatus for Explosive Gas Atmospheres. Part 4: Method of Test for Ignition Temperature (IEC 60079-4), International Electrotechnical Commission, Geneva.
197. Standard Test Method for Autoignition Temperature of Liquid Chemicals (ASTM E 659), ASTM.
198. Furno, A. L., Imhof, A. C., and Kuchta, J. M., Effect of Pressure and Oxidant Concentration on Autoignition Temperatures of Selected Combustibles in Various Oxygen and Nitrogen Tetroxide Atmospheres, *J. Chem. and Eng. Data* **13**, 243-249 (1968).
199. Elliott, M. A., Hurn, R. W., and Trimble, H. M., Autoignition of Fuels in a Constant-Volume Bomb, *Proc. American Petroleum Inst. Sect. III* **35**, 361-373 (1955).

200. Redwood, B., **Petroleum**, 3rd ed., vol. 2, London, Charles Griffin, London (1913).
201. Abel, F., The Flashing Test for Petroleum, *J. Soc. Chemical Industry* **1**, 471-478 (1882).
202. Standard Test Method for Selection and Use of ASTM Standards for the Determination of Flash Point of Chemicals by Closed Cup Methods (E 502), ASTM.
203. Sherratt, M., Recommendations for Change in the Methodology for Flash Point Testing of Residual Fuels, *Petroleum Review* **47**, 429-431 (1993).
204. Lewis, D. J., Gonska, H., and Karchar, W., The Certification of a First Series of Five Hydrocarbon Materials for the Determination of Equilibrium Flashpoint (Temperature Range 15 to 65 C), Report EUR 6102-EN, Commission of the European Communities, Luxembourg (1984).
205. Rapid Tests for Flashpoint (IP 303/74), Institute of Petroleum, London (1974).
206. Flash Testing Using the Cup of Any Standard Closed Cup Apparatus (IP 304/74), Institute of Petroleum, London (1974).
207. Standard Method for Test for Flash Point by Tag Closed Tester (ASTM D 56), ASTM.
208. Standard Test Method for Flash and Fire Points by Cleveland Open Cup (ASTM D 92), ASTM.
209. Standard Test Methods for Flash-Point by the Pensky-Martens Closed Cup Tester (ATM D 93), ASTM.
210. Standard Test Method for Flash Point and Fire Point of Liquids by Tag Open-Cup Apparatus (ASTM D 1310), ASTM.
211. Probst, K. G., Correlation of Apparatus for Measuring Flash Points of Solvents, *J. Paint Technology* **40**, 576-581 (1968).
212. Standard Test Methods for Flash Point of Liquids by Small Scale Closed-Cup Apparatus (ASTM D 3278), ASTM. *Formerly titled*: Standard Test Methods for Flash Point of Liquids by Setaflash Closed Tester.
213. Wray, H. A., New Flash Point Tester for the Paint Industry—Setaflash, *J. Paint Technology* **45**, 44-54 (1973).
214. Paints, Varnishes, Petroleum and Related Products – Determination of Flashpoint – Rapid Equilibrium Method (ISO 3679), International Organization for Standardization, Geneva.
215. Paints, Varnishes, Petroleum and Related Products – Flash/No Flash test – Rapid Equilibrium Method (ISO 3680), International Organization for Standardization, Geneva.
216. Standard Test Methods for Flash Point by Small Scale Closed Tester (ASTM D 3828), ASTM. *Formerly titled*: Standard Test Methods for Flash Point by Setaflash Closed Tester.
217. Flash Point of Aviation Turbine Fuels by Setaflash Closed Tester (ASTM D 3243), ASTM.
218. Standard Test Method for Flash/No Flash Test—Equilibrium Method by a Closed-Cup Apparatus (D 3934), ASTM.
219. Determination of Flash/No Flash – Closed Cup Equilibrium Method (ISO 1516), International Organization for Standardization, Geneva.
220. Bell, L. H., New Flash Test Methods, *J. Inst. Petroleum* **57**, 219-230 (1971).
221. Standard Test Method for Flash Point by the Equilibrium Method with a Closed-Cup Apparatus (D 3941), ASTM.
222. Determination of Flash Point – Closed Cup Equilibrium Method (ISO 1523), International Organization for Standardization, Geneva.
223. Flash Point by the Abel Apparatus—Petroleum (Consolidation) Act 1928 Method (IP 33), Institute of Petroleum, London.
224. Flash Point by the Abel Apparatus (IP 170), Institute of Petroleum, London.
225. Standard Test Method for Sustained Burning of Liquid Mixtures Using the Small Scale Open-Cup Apparatus (ASTM D 4206), ASTM.
226. Totten, G. E., and Webster, G. M., Fire Resistance Testing Procedures: A Review and Analysis, pp. 42-60 in Fire Resistance of Industrial Fluids (ASTM STP 1284), ASTM (1996).
227. Requirements and Tests Applicable to Fire-Resistant Hydraulic Fluids Used for Power Transmission and Control (Hydrostatic and Hydrokinetic), 7th ed., Doc. No. 4746/10/91 EN. Safety and Health Commission for the Mining and Other Extractive Industries, European Commission, Luxembourg (1994).
228. Petroleum and related products – Determination of spray ignition characteristics of fire-resistant fluids (ISO/DIS 15029), International Organization for Standardization, Geneva.
229. Yule, A. J., and Moodie, K., A Method for Testing the Flammability of Sprays of Hydraulic Fluid, *Fire Safety J.* **18**, 273-301 (1992).
230. Holke, K., Testing and Evaluation of Fire-Resistant Hydraulic Fluids Using the Stabilized Heat Release Spray Test, pp. 119-132 in **Fire Resistance of Industrial Fluids** (ASTM STP 1284), ASTM (1996).
231. Fluid Spray: Combustion Efficiency (NT FIRE 031), Nordtest, Espoo, Finland (1987).
232. Simonson, M., Milovancevic, M., and Persson, H., Hydraulic Fluids in Hot Industry: Fire Characteristics and Fluid Choice (SP Report 1998:37), Swedish National Testing and Research Institute, Borås (1998).
233. Approval Standard—Less Hazardous Hydraulic Fluids (Class 6930), FM Global, Norwood MA.
234. Temperature-Pressure Spray-Ignition Tests, 30CFR35.21, Code of Federal Regulations.
235. Loftus, J. J., Juarez, N., Maldonado, A., and Simenauer, J., Flammability Measurements on Fourteen Different Hydraulic Fluids Using a Temperature-Pressure Spray Ignition Test (NBSIR 81-2247), NBS (1981).
236. Loftus, J. J., Assessment of Three Different Fire Resistance Tests for Hydraulic Fluids (NBSIR 81-2395), NBS (1981).

Copyright © 2003, 2014 Vytenis Babrauskas

Chapter 7. Ignition of common solids

Highlights and summary of practical guidance **237**
Types of ignition **238**
General principles of flaming ignition **238**
Qualitative features *238*
The ignition problem for solids *239*
Research into ignition of solids **241**
Ignition temperature as ignition criterion *243*
Mass loss rate as ignition criterion *246*
HRR as an ignition criterion *248*
Other criteria for ignition *249*
Ignition from radiant heating **250**
Gas phase events *250*
Cool flames *250*
Comprehensive theories *251*
Atreya's model 254
Engineering treatments for thermally thick solids *256*
Development of approximate solutions 257
Janssens' procedure 260
Quintiere's procedure 262
Tewarson's procedure 264
Other data treatment procedures 264
Relation between minimum and critical fluxes 265
Engineering treatments for thermally thin solids *265*
Condition 1—back face insulated 266
Condition 2—back face cooled 267
Condition 3—back face also heated 268
Other issues for thin slabs 268
Illustrative data *268*
Composite materials *269*
Criteria for distinguishing thermally thick versus thin materials *271*
General and intermediate-thickness materials *272*
Energy needed for ignition *274*
Laser ignition *275*
Ignition from convective heating or immersion in a hot environment **277**
Ignition theories for convective heating *280*
Lumped-capacitance model 280
Thermally-thick solid—constant heat flux 280
Thermally-thick solid—constant convective transfer coefficient 280
Thermally-thick solid—boundary layer solution 281
Ignition theories for submersion in hot environments *281*
Theoretical solutions for other problem conditions **281**
Thermally-thick inert solid with fixed net heat flux *281*
Thermally-thick inert solid with fixed heat flux and convective cooling *282*
Thermally-thick reactive solid with fixed heat flux *282*

Finite-thickness inert plate with fixed heat flux 283
Finite-thickness reactive plate 283
Finite-thickness polymer undergoing charring 283
Thermally-thick reactive solid held at a fixed face temperature indefinitely 284
Thermally-thick reactive solid held at a fixed face temperature for a finite time 284
Thermally-thick reactive solid receiving fixed radiant heat flux only 284
Solid receiving a brief, high-intensity pulse of radiation 285
Porous solids 285
Diathermanous solids 285
Miscellaneous geometries 285
Depletion of reactants not ignored 285
Ignition from localized sources **286**
Small flames 286
Small-diameter, high-intensity heat sources 287
Hot bodies 287
Ignition from large flames **289**
Duration of ignited burning **290**
Flashing vs. sustained flaming 290
Sustained flaming after initial ignition 290
Variables affecting ignition of solids **292**
Type of pilot (or lack thereof) 292
Orientation 294
Exposed area size 295
Air flow rate 297
Oxygen concentration 299
Piloted ignition 299
Autoignition 299
Chemical composition of diluents 300
Total pressure 300
Moisture and relative humidity 302
Initial temperature of specimen 304
Acceleration of gravity 304
Surface absorptivity, material transparency, surface coatings, and spectral characteristics of the radiant source 304
Polymer structure 308
Porosity 308
Fire retardants 308
Movement of the surface 309
Surface roughness 310
Ignitability of aged, degraded, or charred materials 310
Wetting by water 310
Type of apparatus 311
Mass of sample 311
Long-term radiant exposures 311
Arcing across a carbonized path **312**
Glowing ignition **315**
Smoldering ignition **315**
Theory 318
Effect of layer thickness 318

Effect of packing density or porosity *318*
Smolder promoters and smolder inhibitors *318*
Transition from smoldering to flaming ignition *319*
Indicators of smoldering *320*
Tests for ignition properties of solids **320**
Flame ignition tests *320*
ASTM D 2859 methenamine pill test 321
CS 191-53 (16 CFR 1610) flammable fabrics test 321
FF-3-71 (16 CFR 1615) and FF-5-74 (16 CFR 1616) children's sleepwear tests 322
CPSC 16 CFR 1500.44 flammable solids test 322
NFPA 701 and NFPA 705 methods 322
ASTM D 1692 322
UL 94 test series 323
UL end-product tests 326
Small-flame tests for wire and cable 327
MVSS 302 328
FAR Bunsen burner test 328
ISO 11925-2 small flame test 329
Large-flame tests 329
Radiant ignition tests *330*
The Cone Calorimeter 330
ISO 5657 331
ASTM E 1321 (LIFT) 331
FM Fire Propagation Apparatus—ASTM E 2058 332
ASTM E 1623 (ICAL) 333
Arc tracking and arc ignition tests *333*
ASTM D 495 333
ASTM D 2303 333
ASTM D 3032 334
ASTM D 3638 334
MIL-STD-2223 334
UL tests 334
Electric spark or arc ignition *334*
Bureau of mines electric spark method 334
Nordtest NT Fire 016 method 335
NIST electric arc method 335
Smoldering *335*
Cellulose insulation 335
Mattress tests 335
Burning brand ignition *335*
ASTM E 108 roof test 335
Other types of tests *336*
Convective heating tests 336
Hot wire or bar ignition tests 336
Hot rivet or nut tests 336
Setchkin furnace, ASTM D 1929 336
Limiting oxygen index (LOI), ASTM D 2863 338
Thermal analysis tests 338
Further readings **338**
References **339**

Highlights and summary of practical guidance

Solids can ignite due to external heating, or self-heating (self-heating is discussed in Chapter 9). In some cases, both external heating and self-heating are involved. Despite many limitations, it is often reasonable to use the approximation that a solid ignites due to external heating when its exposed surface reaches a fixed ignition temperature. A quasi-constant ignition temperature is a usable concept only for external heat sources which cause a substance to be ignited in a flaming mode. There is no constant 'handbook' temperature which can characterize the process of smoldering ignition, nor the process of self-heating. The concept of ignition temperature (where applicable) is often valuable because it may allow the deduction that if an external heat source was not as hot as the ignition temperature of the material, the material could not have ignited from that source.

A solid may ignite from self-heating even if it is surrounded by an environment that is at a low ambient temperature, e.g., 20ºC. Almost all organic substances have a potential to self-heat. Self-heating is important, however, only when the mass of the substance is large and the available time is long, e.g., days to years. For ignition times on the order of minutes, only external heating effects will normally need to be considered. Exceptions exist for extremely reactive self-heating materials, such as linseed-oil covered rags, which can ignite in small quantities and in a time frame of only a few hours. For substances subjected to external heating, but at a low heat flux and for a moderately long time (hours), it may also occasionally be necessary to take into account self-heating effects. For most substances, self-heating is caused by oxidation rather than decomposition, thus self-heating is less common among non-porous materials.

Pre-charring most solids at fluxes insufficient to cause ignition, if it has any effect at all, usually makes the substance more difficult to ignite when larger heat fluxes are subsequently applied. This is because readily ignitable volatiles are driven off in the initial heating process.

For most solids, ignition due to external heating occurs in the gas phase, that is, volatiles are driven off which then ignite and burn in the surrounding atmosphere (this is not true for metals and other elements, and these are separately discussed in Chapter 8). Self-heating involves reactions occurring in the solid phase. Thus, a self-heating-caused ignition manifests itself as a smoldering or glowing; this can transition to flaming when the reaction front reaches an open surface. Substances which are self-heating, but have negligible heat flux imposed from the outside show ignition first in the center, because this is where the least heat losses are occurring. If they are cut apart before going to flaming, a charred core is found, surrounded by less-damaged material.

Apart from some specialized mechanisms (ohmic heating, arc tracking, etc.) external heating of solids involves one or a combination of the three classical heat transfer mechanisms:

- conduction
- convection
- radiation.

Heating by radiation is considered to be the most important of these and is the dominant one in flames and in situations where a non-contiguous hot body provides the heating. Heating by conduction is the primary mechanism when a hot body comes into direct contact with an ignitable material. There is a vast body of literature on radiative-mode ignition of solids and the bulk of this Chapter is devoted to this topic. Research on conduction or convection modes of ignition has been extremely limited.

The concept of an ignition temperature is useful in understanding why, using a small flame, it is hardest to ignite a flat surface, easier to ignite an edge, and easiest to ignite a corner. This is because in a corner the heat can flow into the body along three directions, so as to raise its temperature to a given value the quickest.

Reported ignition temperatures (and other ignition properties) of plastics are often vary over a wide range, since common commercially-useful plastics are rarely of high purity. PVC is perhaps the most extreme example, since the pure polymer—which has very good resistance to ignition and burning—is a rigid, brittle material of limited uses. Practical PVC formulations include numerous additives; to make flexible PVC products, large amounts of plasticizers have to be added. Unless halogenated, these additives are more readily ignitable than pure PVC, and flexible PVC formulations reflect this fact.

Hot objects—embers, welding slag, flying brands, etc.—can often be exceptionally effective as ignition sources, even when they are quite small. This is true regardless of whether they are flaming or merely incandescent. But research on ignition from hot objects is scant, although some indicative data is available (see Chapter 14 for specific substances).

Materials which char when subjected to heat are likely to be able to smolder under some circumstances. Smoldering is a complicated phenomenon, yet research in this area has been quite limited. Consequently, very little guidance is available on the quantitative aspects of smoldering. Under the right circumstances, wood products and almost any material of botanical origin can smolder. A few inorganic materials also have the ability to smolder. Smoldering can be started by a variety of ways, including glowing bodies, flames (with flaming then being extinguished but smoldering continuing), or without any external ignition source,

simply by assembling a large enough pile of a self-heating material. Smoldering can also be started by an already-smoldering object, e.g., by inserting a burning cigarette into a pile of smolderable material.

The assumptions are often made that common solids will not be ignited from (1) electric circuits where the current, voltage, or power are below certain values; and (2) by hot objects having less than a certain amount of stored thermal energy. Unfortunately, there is very little research on #1, so that it is not possible to draw useful conclusions. But research on Christmas tree lights (see Chapter 14) indicates that as little as 1.25 W can ignite paper. Assumption #2 is incorrect, both from theoretical principles and according to laboratory measurements: stored energy is not the sole controlling variable of the problem. This is discussed in detail in Chapter 14 under *Forest materials, vegetation, and hay*.

Types of ignition

Ignition of solids can basically be of four types:

- Ignition of the fuel vapors driven off the solid. This is the most common form of ignition and is manifested as flaming. Most of the solids in this category produce flammable vapors by *pyrolyzing*, that is, chemically degrading due to the action of heat[*]. The degraded substance is no longer of the same chemical identity as the virgin substance. A few low molecular-mass solids liquefy and vaporize without pyrolyzing, that is, the substance vaporized is chemically identical to the virgin substance. Naphthalene is an example.
- Smoldering ignition. When a porous or granular substance undergoes self-heating, ignition is commonly manifested first as smoldering. However, smoldering ignition also may be caused by external heating, e.g., a glowing cigarette falling down on a sofa.
- Direct ignition of the surface of a solid. Many metals and a few other substances are examples. A flammable vapor is not released which could then be subject to ignition, instead, the oxidation takes place directly at the solid's surface. Ignition of metals is considered in Chapter 8. Under certain conditions, cellulosic materials (e.g., wood) can ignite in this manner, which is generally called glowing ignition.
- Ignition by a chemical reaction (e.g. thermal decomposition) that occurs directly in the solid phase. Reactive substances, explosives, and pyrotechnics fall into this category. These are considered in Chapter 10. The burning of gases is either not involved at all with these substances, or occurs only to a limited extent after the initial solid-state reaction has started.

[*] Some chemists use a definition whereby pyrolysis is taken to be the degradation due to the action of heat *in the absence of oxygen*. In fire science, however, the term is used to mean degradation due to the action of heat in any atmosphere, including ones that do contain oxygen; this latter definition is used throughout this book.

Pyrolysis can be explained as follows. The molecules comprising most combustible solids are very large, commonly involving thousands of atoms. As such, these molecules are not able to be directly oxidized, at least not in an oxidation rapid enough to be called combustion. So ignition takes place as a 2-step process. Upon initial exposure to heat, the large molecules break apart and release some small fragments. Since the fragments are small and since heating has raised the system temperature, the fragments largely emerge as gas molecules. These now have the potential to ignite in the air above the solid's surface under the right conditions. The nature of the residue remaining when the fragments leave depends on the substance involved. For some substances (e.g., wood) the residue is a solid carbonaceous matrix called a char. But for others (e.g., polypropylene) the residue is essentially a liquid. There are also substances (e.g., PVC) which can leave either a char or a liquid-like material, depending on details of the heat exposure.

In addition to systematic effects due to the of the fuel, there can be three basic physical arrangements:

(1) a single, isolated mass, which may range from a microscopic particle to a huge object
(2) a pile or layer of small particles
(3) a dust cloud.

Dust clouds of solid particles share more characteristics with gases than with solids, and are treated in Chapter 5. Piles or layers of pyrolyzing or otherwise exothermically reacting granular or powdered material are treated in Chapter 9. Thus, in this Chapter only the ignition of a single item of a solid fuel is considered. Furthermore, there is very little information on the ignition of single particles if they are of tiny size; most of the available information concerns metals and other elements and this topic is treated in Chapter 8.

General principles of flaming ignition

QUALITATIVE FEATURES

Before either theory or engineering data are examined, it is worthwhile to consider some general features of the problem of the flaming ignition of solids. First of all, since flames are a gas-phase phenomenon, for a solid to be capable of a flaming ignition it must respond to heat by breaking down and releasing combustible vapors. This is the pyrolysis process discussed in the previous Section. For a pyrolyzing solid to ignite in a flaming mode, the same three conditions must be satisfied as for liquids:

1. the substance must be sufficiently heated so that an adequate concentration of *pyrolysate* (the pyrolyzed vapors) exists at some location away from the surface
2. an adequate concentration of an oxidizer (typically, air) must be mixed in with the fuel vapors so that a flammable fuel/oxidizer gas mixture exists somewhere above the surface
3. either the temperature of the pyrolysate/air mixture must become high enough (for autoignition to occur) or

else a sufficient external energy source such as a pilot flame or a spark must be introduced (for piloted ignition to occur).

There are several fundamental differences between ignition of solids and liquids, apart from their general similarities. If the ignitable liquid is a pure substance (not a mixture, such a gasoline) then in most cases it will produce a vapor which has the identical chemical composition to the liquid. In thermodynamic terms, the vaporization of such a liquid is *reversible*; that is, if the vapors are cooled, they will condense into the original substance. In the case of a solid, the process of heating up the solid is normally destructive, or *irreversible*. If the vapors are cooled down, the original solid is not regained. The term 'pyrolysis' denotes that heating is accompanied by irreversible chemical changes.

The response of a liquid to heat sets up convective currents inside the liquid; these influence the ignition behavior. Such convective currents do not occur in a solid, although pyrolysis manifests itself by the production of vapors from the solid. Some solids form a film of liquid at the surface when exposed to heat. Plastics such as polyethylene are an example. Other solids do not form a layer of liquid, but instead exhibit a flow of gases through a porous matrix which becomes less dense with prolonged exposure of heat. Wood is an example of such a substance.

The ignition may be *autoignition* or *piloted* ignition. The term 'forced ignition' is sometimes used as a synonym for piloted ignition. The use of the term autoignition for solids is rather different than for gases. For a gas, autoignition occurs when the entire substance is raised in temperature to a point that flames appear. For a pyrolyzing solid, however, what becomes raised in temperature sufficiently to ignite is not the solid itself, but the gas that has been pyrolyzed from it. The term 'autoignition temperature' is applied either to the minimum surface temperature of the solid for which the gas-phase flaming event occurs or to the minimum temperature of the furnace needed for ignition to occur. The latter definition is used when testing small samples in a furnace, but the two temperatures are not generally identical.

Ignition of solids may be *transient* or *sustained*. If the ignition is transient, then removing the source of external heating causes combustion to cease. If ignition is sustained, then combustion continues until a substantial fraction of fuel is exhausted, even if the external heat source is removed. Transient ignition (or flashing) can occur in a slightly different context, whereby even if the external heat source is not removed, only a brief period of combustion occurs, and most of the material in unconsumed. While these distinctions would appear to be substantively fundamental, in actual testing of materials they do not play a major role. Surprisingly little is known about the behavior upon removal of the heat source, and even most test methods do not quantify this property. As for brief transient or flashing events, these are observed and recorded, but rarely form any basis for judging of product performance. The length of time that divides flashing or transient flaming from sustained flaming is a matter of definition. In standard test methods for solid substances, a value of 4 to 10 s is typically defined as the minimum time necessary for sustained ignition.

Figure 1 illustrates flashing and sustained flaming ignition during piloted-ignition testing of PMMA. Not all substances show flashing prior to sustained flaming. The terms 'flash point' and 'fire point' can also be applied to solids. In this PMMA example, the flash point is 287ºC while the fire point is 306ºC. Note that, due to flashing, the temperature actually being registered by a thermocouple located at the surface of the sample is 312ºC at the time of ignition. This reading is influenced by the presence of the flashing, and so T_{ig} is assigned the extrapolated smooth-rise value, in other words, the temperature rise solely due to the external heater[1]. The fact that momentary increases in surface temperature due to flashing must not be considered in determining the value of T_{ig} can also be learned from the fact that, at several of the flashes preceding sustained-flaming ignition, the instantaneous surface temperature notably exceeded 306ºC, yet sustained flaming did not occur. A similar graph has been shown by Atreya for red oak[49]. He notes that of over 100 wood samples tested, only one showed flashing prior to sustained flaming. Details of the autoignition phenomenon are generally understood much less well, since testing and research in recent years has focused largely on the piloted ignition problem.

THE IGNITION PROBLEM FOR SOLIDS

For ignition of solids, the practical problem is usually the following: "For a given thermal attack, determine whether ignition will occur. If it does occur, determine how long it will take." This immediately suggests the areas which must

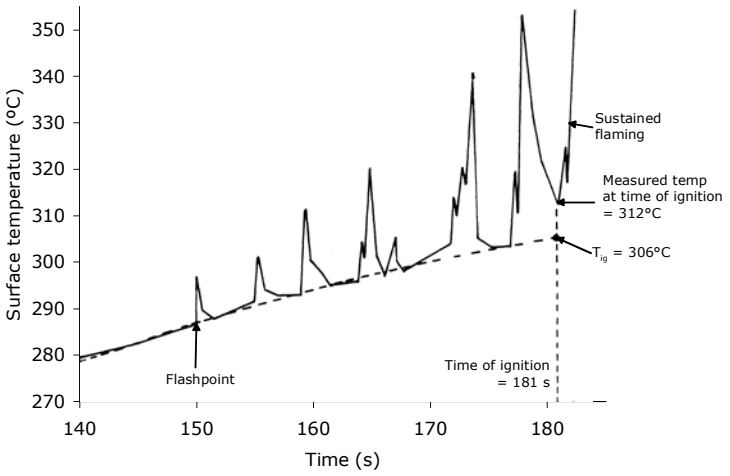


Figure 1 Flashing and sustained flaming ignition of PMMA exposed to radiant heat flux of 20 kW m^{-2} (Thomson[2])

be quantified:

- the thermal attack
- the heating up and pyrolysis of the solid
- the association of the observation of flames with a quantifiable variable.

Ignition of solid substances has been of interest even prior to the 20th century. In most early works, only a very crude notion of the thermal attack existed. It was not until the work of Brown[3] in the 1930s that it became clear to most researchers that, at ignition, the temperature of the substance and the temperature of the test furnace are not necessarily identical. Eventually, as a consequence of defense-related research in the early 1950s, incident heat flux came to be recognized as the primary engineering variable. It was realized that the temperature of the existing fire, test-device heater, etc., was *not* a sufficient description of the thermal attack upon the substance. Two different sources could have identical temperatures, yet cause very different responses of the ignitable substance. The science of heat transfer, of course, had been fairly well developed by the 1950s, but it was not previously used to quantify exposures to ignitable substances. There are known to be three primary mechanisms for transporting heat: conduction, convection, and radiation. Conduction heat transfer is important in certain ignition problems, e.g., firebrands. These problems will be considered later, and in the first part of this Chapter it will be assumed that there is an air space between the heating source and the ignitable substance. Thus, two means of transferring heat from the source to the target will need to be considered—convection and radiation.

The heating up of the solid, once the external thermal attack has been quantitatively and correctly specified, is the heart of ignition theory. Most common combustibles—wood is an excellent example—exhibit a highly complex chemistry of thermal degradation of the solid material. Thus, it is necessary to focus on theories which either lend themselves to a closed-form solution, or which can act as a framework for presenting and analyzing empirical data. More fundamentally ambitious theories have been formulated, but they are currently not able to act as practical tools for solving ignition problems. Consequently, as we shall see below, 'theory' of the ignition of solids normally connotes an engineering data-correlation approach, elevated by the introduction of a limited number of physics principles.

In this Chapter, we will see that—thus far—only theories based on simple heat transfer considerations have led to engineering relationships that can be usefully applied towards practical problem solving. This limitation is not satisfying, since it means that the ignition temperature must be introduced as an *ad hoc* hypothesis. We will also briefly consider theories which do bring in chemistry. The simplest way to do this is to introduce a chemical reaction only into the solid phase. This approach has received a fair amount of usage in the rocket propulsion community. Somewhat surprisingly, it appears that these theories can sometimes predict the correct data trends even for pyrolyzing solids, not just for propellants that ignite directly in the condensed phase. However, even such simplest-possible treatment of chemistry requires more input data than are obtainable in the course of normal testing.

To identify the moment that flames will first occur on the basis of fundamental science requires, in addition to modeling the solid, to model the complex fluid mechanical environment, along with the chemistry, in the gas phase. As was seen in Chapter 4, a comprehensive theory of the ignition of gases must solve hundreds of chemical reactions occurring simultaneously. In principle, this can be accomplished by advanced, 3-dimensional, numerical thermo-fluid-chemical modeling of the gas-phase environment above the ignitable substance. These calculations are currently difficult and lengthy, and it is likely to be a number of years before they might become a routine tool for solving ignition problems.

As we shall see in this Chapter, the research that has been successfully applied to problem-solving has generally had two components: (a) development of mathematical techniques for making the heat transfer problem tractable; (b) development of criteria for ignition, since the simple theories do not 'know' when ignition occurs. To accomplish the latter, it becomes necessary to associate the ignition event with some quantifiable feature of the solid's thermal response. This is not easy to do in a reliable way. Two main stratagems have developed: (1) identification of a certain face temperature of the substance with the ignition event; or (2) identification of the ignition event with a critical rate of mass loss of the substance. Both of these approaches will be considered below. Perhaps the most useful is a third stratagem which has only emerged recently. This stratagem takes a 'black box' approach to the heating of the substance and does not attempt to represent the physics in any direct way. Instead, it calculates the ignition time (or absence of ignition) solely from the input data, i.e., an experimental record of heat fluxes versus ignition times. In addition to these main types of criteria, a number of others have been proposed and have found utility in certain limited applications. We will also consider some of those in brief.

The ignition temperatures of common solids differ less among categories of materials than is sometimes presumed, although sizable differences can be found both due to details of the material's formulation and due to the testing method used. Table 1 shows data compiled from Chapter 15. Only polymers without FR additives have been considered; halogenated plastics, because of their innate FR characteristics, have been grouped separately. Within any of the categories, ignition temperatures typically vary by ±100ºC or less. Not surprisingly, thermosetting plastics typically have higher ignition temperatures. The values for the halogenated plastics group are skewed by the fact that most of the available data are for ordinary PVC, which is less re-

sistant to thermal attack than are some more advanced materials in this family.

Table 1 Ignition temperatures of various plastics grouped by category

Category of solid	Ignition temp. (ºC)	
	Piloted	Auto
thermoplastics	369 ± 73	457 ± 63
thermosetting plastics	441 ± 100	514 ± 92
elastomers	318 ± 42	353 ± 56
halogenated plastics	382 ± 70	469 ± 79

Research into ignition of solids

The current state of the art of ignition of solids from external heating is not necessarily easy to present succinctly or straightforwardly. For the last hundred years, understanding of the phenomenon was gained in spurts and jumps, part of which were empirical and experimental, while the other portion consisted of mathematical theories. To gain a reasonable understanding of the progress of these ideas, it is appropriate to start with a brief historical survey of research into ignition of solids.

One of the earliest systematic studies on the ignition of solids was by Bixel and Moore in 1910[4], who used a small crucible submersed in a constant-temperature bath to examine autoignition of woods and cellulosic materials. Their results are shown in Table 2. The specimens were small and were exposed for up to 6 hours. Bixel and Moore implicitly assumed that the temperature at which ignition occurs is going to be a characteristic value for the tested substance. This assumption had already been made by researchers in the 19th century, but it is by no means a trivial truism (nor is it always true!).

Table 2 Autoignition temperatures determined by Bixel and Moore

Material	Avg. AIT (ºC)
charcoal (moist)	159
charcoal (dry)	216
paper	224
Georgia pine	203
maple	232
cypress	241
chestnut	254
oak	257

The conditions needed for piloted ignition were examined in 1915 by R. E. Prince at the Forest Products Laboratory in Madison, WI, as part of an already ongoing program to develop fire-retardant treatments for wood[5]. For this work, two different test apparatuses were developed. Most of the studies were done in the first apparatus, which was an electrically heated vertical hollow cylinder. Specimens 31.8 × 31.8 × 101.6 mm were suspended in the center of this furnace. The furnace walls were set to various temperatures in the range 175 – 470ºC and the time to ignition recorded. Ignition was with a gas pilot, located at the top of the furnace, a substantial distance above the specimen. Some oven-dried specimens ignited in as short a time as 15 min at 175ºC, but minimum temperatures for ignition were not sought. Neither the heat flux to the specimen, nor the temperature of the specimen itself were studied. The test apparatus itself, with modest modifications, later became the Setchkin furnace, used in ASTM D 1929 and ASTM E 136 tests. Prince also developed a second ignitability test apparatus. The latter was a small electric radiant panel and was used only for testing wood shingles and siding. In the latter studies, Prince was the first experimentalist to focus on the question not only if flaming ignition will occur, but whether flaming will continue if the radiant source is removed. Experimentally, he pulled away the specimen from the radiant panel after 1, 6, or 12 min had elapsed after ignition, and then timed the 'afterflame' duration. Thomas et al.[6] reanalyzed Prince's results and concluded that their data indicated an average ignition temperature of wood of 210ºC. This is somewhat higher than average oven temperature, and the modest increment comes from self-heating of the solid.

The dissertation of Clement Brown[3] was the next significant step in quantifying the ignition of solids. As a starting point, Brown made a very extensive study of 19th and early 20th century literature on ignition problems and his dissertation is a valuable resource for exploring the early scientific history of ignition research. Even though basic fundamentals of heat transfer were already known in 1934, it is clear from Brown's study that researchers of that era were not yet ready to apply them to the study of the ignition problem—the ignition temperature was being treated as a hypothetical 'chemical property,' without any attempts to quantify the transport of heat into the substance, and without an understanding of the mechanisms responsible for raising the temperature of the substance. Even the distinction between external and self-heating was not being appreciated at the time, and test methods for both were being intermingled. Brown's actual test apparatus was roughly similar to Prince's, but he introduced a forced air stream into the furnace cavity and did not use a pilot. Brown used tiny samples (1 to 5 g) and observed mainly the onset of exothermicity. Thus, his study, if anything, more resembled current-day DTA studies rather than ignition tests. Brown's main contribution was the identification of the importance of the specimen-face temperature, as distinguished from the furnace temperature. Generally, he found autoignition temperatures of 220 – 250ºC for woods and other cellulosic materials tested. A few substances were lower, such as tobacco and hay at 172ºC, newsprint at 184ºC and jute at 192ºC.

The earliest ignition studies to adopt some engineering principles were those of British mathematicians Bamford et al.[7] Their first experiments used flames for exposing inter-

mediate-thickness wood panels on both faces, and their results specifically pertinent to intermediate-thickness materials are discussed later in this Chapter. Bamford et al. were the first to propose that the heat conduction equation be used as the primary basis for analyzing ignition. The heat-conduction based theory required knowing the heat flux from the flames, however, they lacked means for measuring it, and were forced to resort to a dubious estimate. Their theory included a heat generation term and they assigned Arrhenius-kinetics constants to it using a rationale which they did not describe, most likely curve-fitting to the experimental results. From this model, they also calculated the mass loss rates as a function of time, and correlated these computed results to the observations of ignition. This led to a postulated criterion that piloted ignition occurs when the mass flux of pyrolysates emerging from the surface (i.e., the mass loss rate of the specimen) first reaches the value $\dot{m}'' = 2.5$ g m^{-2} s^{-1}. Later work by Weatherford and Sheppard[8] indicated that there were errors in the numerical solutions of Bamford et al.; however they were able to demonstrate that, under most conditions, a constant mass-loss-rate criterion for ignition implies a constant face temperature at ignition, and *vice versa*.

Bamford et al. then went on to conduct a second series of experiments, wherein 50 mm thick wood panels were subjected to radiant heating from an electric heater and ignited with an impinging gas pilot. Under such conditions, they reported that wood panels showed a minimum heat flux necessary for ignition of about 2 kW m^{-2} (in light of later work, this value appears to be significantly too low). They also found that with low irradiances, specimens only burned 2 – 6 min, and then flaming stopped, with most of the material remaining unburned. For the specimens to burn up fairly completely, a minimum irradiance of ca. 46 kW m^{-2} was needed.

Heat-conduction theory was next used by Fons[9] in 1950 who studied the ignition of ponderosa pine cylinders. Because accurate surface temperature measurement with thermocouples tends to be very difficult, Fons used interior thermocouples, then computed the surface temperature by using the heat-conduction equation (solving the 'inverse problem'). By this computation, he determined the autoignition temperature of wood to be 343ºC.

Buschman[10] examined the piloted ignition of various wood specimens exposed to a radiant panel. Over the heat flux range of 14 – 37 kW m^{-2}, he found that the computed surface temperature at ignition (Table 3) did not vary with the exposure time or the heat flux. Buschman computed the surface temperature using an inert-solid heat transfer model, but did not actually measure it.

In 1965, Martin[11] attempted to summarize a large volume of ignition studies on sheets of cellulose that were done for the U.S. Department of Defense. He identified three radiant heating regimes: (1) for very low heat fluxes, convective effects are important. In addition, the heat wave is able to reach the back face of the specimen before ignition occurs, thus, the material's thickness is an important variable. (2) For intermediate heat flux levels, sufficiently-thick specimens can ignite before significant back-face heating has taken place. This regime is governed by heat flow expressions pertinent to a thick solid. (3) At very high heat fluxes, ablation (i.e., a mass loss rate so large that the front face recedes rapidly) governs. In this regime, transient ignition is easy to achieve, but sustained flaming may not occur, because a very thin layer of material has been quickly heated to a high temperature. This layer may burn off without transmitting enough heat into the body of the material for combustion to continue. Martin's results for cellulose are shown in Chapter 14, and he effectively considered the ignition problem solved, since he was able to summarize all of his data into a 'universal' graph. It was not possible to use his graph for predictive purposes, however, so more suitably closed-form solutions still needed to be evolved.

Table 3 Surface temperatures for piloted ignition of woods, as computed by Buschman

Wood	Ignition temp. (ºC)
hardboard, tempered	298
maple	343
red oak	348
spruce	376
poplar	389
balsa	391

Shortly after Bamford's study, around 1950 the Fire Research Station in England began an extensive research program on ignition of wood and related materials, which continued into the 1960s. Lawson and Simms[12] were able to measure heat fluxes and produced extensive heat flux vs. ignition time plots for various woods. They also were the first to develop mathematical techniques that would allow predictions of ignition to be made from available test data. Their work in this regards forms the introduction to modern data-correlation methods, discussed below.

The gas-phase problem is moderately decoupled from the response of the solid to radiation. However, several researchers noted that, in certain specialized heating regimes, pyrolysates emitted by the solid cause significant radiative effects. Gardon[13] studied the autoignition of wood under quite high heat fluxes (120 – 200 kW m^{-2}) obtained from concentrating solar radiation using mirrors. He concluded that "the cloud of smoke" that rapidly forms in front of the surface significantly attenuates the radiation. Later, Kashiwagi, in studying the ignition of PMMA and wood using a CO_2 laser (which radiates at a 10.6 μm wavelength) found that extremely high attenuation of the beam could occur due to absorption by the pyrolysates forming in front of the specimen[14], with the radiation fraction reaching the specimen surface being as low as 20% in some cases. The

effect, evidently, can be serious for high-intensity radiation or for laser radiation. There have not been many studies directly examining the effect for non-laser sources in the more important sub-100 kW m^{-2} flux range. Kashiwagi[15] also examined the radiation fraction transmitted through the pyrolysates of PMMA and wood using a 700ºC black body heater and found it dropped below 70%. However, indirect evidence from other sources (for example, the modest effects of orientation, and successful validation studies for models that omit this phenomenon) suggests that the effect is typically not large.

IGNITION TEMPERATURE AS IGNITION CRITERION

The concept that a solid substance should have a unique ignition temperature has been a widespread, tacit assumption ever since scientific study of ignition began. As shall be seen later, this is hardly self-evident and, at best, is an approximation to reality. To make matters more complex, it must be realized that there have been two different meanings assigned to the term *ignition temperature*:

(1) the minimum temperature that the air must be heated to, in order that a specimen placed in the heated air environment would ignite;
(2) the surface temperature of the specimen just prior to the point of ignition.

Definition #1 was the prevalent one until about the last 3 decades. This is also the concept of ignition temperature invoked in the popular ASTM D 1929 ignition test. Definition #2 is generally more useful, both because it is more likely to be relatively constant for a material, and also because definition #1 is not applicable to the common situation, both in real fires and in more modern ignition tests, where the surface of a specimen is heated only by radiation, while convective heat transfer is small and is in the opposite sense (cooling). Use of definition #2 requires an accurate measurement of the surface temperature; this is much harder to do than is measuring the temperature of a test furnace, consequently, only when the importance of this measurement was finally realized, did researchers strive to develop the measurement technology.

To persons not well versed in fire science, it often seems that materials should be simply categorized by their ignition temperature. There are a number of limitations to this approach:

- It does not take into account how fast substances ignite.
- Accurate measurements of ignition temperature #2 (specimen face) are quite difficult to make; values of ignition temperature #1 (furnace) are of uncertain relevance for many applications.
- A great majority of combustible solids have fairly similar ignition temperatures, yet present diverse ignitability hazards; this is largely due to the fact that materials tend to differ widely in their thermal inertia, and the latter variable establishes the time scale of the problem. (Thermal inertia is the product of the solid's thermal conductivity × density × heat capacity and is discussed in detail later in this Chapter).

The concept of a 'handbook' ignition temperature is not without merit, however. In some cases, where time to ignition does not need to be computed, this concept may be sufficient to rule out certain fire causes. If an object ignites from *external* heating, and all temperatures in its environment are lower than a tabulated T_{ig}, then clearly we do not expect the object to be able to ignite. Conversely, if the surrounding temperatures are greatly higher, an ignition might be expected. It is very important not to apply this simple, sometimes-useful idea to *internal* heating. A number of substances are prone to self-heating, or spontaneous combustion. This topic is discussed in Chapter 9. For such substances, if the pile of material is large enough, ignition can occur even with no other source of heat apart from an ambient-temperature atmosphere surrounding the material. *It is in no way logical to assign an 'ignition temperature' to a self-heating substance.* As the size of the pile increases, the environment temperature needed to cause spontaneous combustion decreases. Thus, for a self-heating substance, a graph of size vs. environment temperature required for ignition can be made, but no single value can be assigned. Furthermore, it must be understood that substances prone to self-heating may also be ignited by external ignition. For example, if a pile of linseed-oil soaked rags is placed in front of a radiant heater, it may ignite in a few minutes, due to external heating, rather than in hours, which it would take if the pile were simply left in a 20ºC room. In such a case, the ignition of the pile should be treated by the methods of this Chapter, rather than Chapter 9. Many substances can be driven to ignition by a combination of self-heating, plus some localized heating. Such problems are difficult, but the time scale can be used for reasonable guidance: if ignition occurs in about 1 hour, or less, self-heating can probably be ignored. Conversely, if it takes days, weeks, or years to reach ignition, the problem is dominated by the self-heating aspects. To emphasize: if self-heating is involved, ignition can take place even though the highest temperature of any objects nearby the target substance is much less than the object's 'handbook' T_{ig}.

In the above discussion we have learned that an object may still ignite, even if it is exposed to temperatures well below a 'handbook ignition temperature.' On the other hand, an object may not ignite even if it is exposed to temperatures well above the 'tabulated ignition temperature.' A number of circumstances need to be considered.

- The temperatures usually discussed are the temperatures of hot objects near the material in question. But the surface of the material in question may never come up to a temperature even close to that value. One common situation is for thermoplastic materials, many of which can recede when subjected to heat. If the heat

source is localized, the material may fail to ignite simply by receding.

- A finite time is required for a material's face to rise to a certain temperature when heated. If the hot object is only exposing the target object for a short time, ignition may not occur.
- A tiny amount of material may ignite, but ignition may not be sustained. This occurs when 'flashing' instead of 'sustained flaming' happens. It may also happen that a chunk of the material ignites and falls away burning, while the rest of the material fails to burn because it is now too far away from the heat source.
- Finally, tabulated values may not be representative of the specific material in question. This is especially true for man-made polymers, since, in many of those, the primary ingredient may comprise only half or less of the total mass, the remainder being comprised of various additives.

A practical issue to consider is that ignition temperatures for common combustible solids vary only over a rather limited range of about 300ºC to 500ºC. By contrast, thermal inertia values of common combustibles vary by about a factor of 100 (see Chapter 15). This means that differences in time to ignition of different materials is likely to be determined by their relative values of thermal inertia, not of their ignition temperature. The role of thermal inertia is explored in the succeeding sections of this Chapter. Finally, it has been pointed out that while most researchers assign comfortably small error bars to their own results, comparing ignition temperatures obtained by different researchers often leads to major disagreements[16].

Whether or not T_{ig} is a sensible concept for characterizing materials has to be examined on the basis of experimental evidence. While this is often an oversimplification, for convenience, combustible solids can roughly be considered to be of two types: (1) those that melt when subjected to high temperatures; and (2) those that char. Most of the 'commodity' plastics, that is, excluding expensive 'engineering' plastics, are melting substances. For those, constancy of T_{ig} appears to be well-justified experimentally. One must ask: Constancy with respect to what? The effects of a wide variety of factors on the ignition of solids is considered in detail later in this Chapter, but clearly there should be constancy with respect to heating rate. This is best examined in tests where a specimen is heated by a radiant heater, and typical results obtained by Thomson[2] are shown in Figure 2. Four of the 5 polymers show a T_{ig} which is invariant with heat flux. For PMMA, however, T_{ig} is reasonably fitted by a horizontal line only in the mid-range of the heat fluxes; essentially the same results with PMMA were obtained in a different apparatus by Cordova et al.[17]

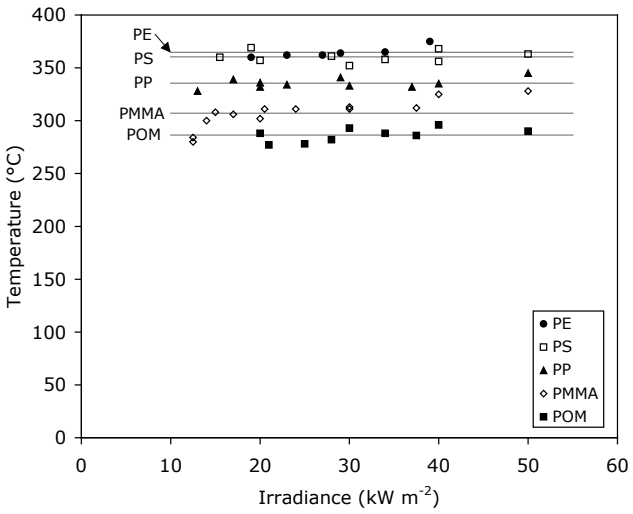


Figure 2 Ignition temperatures of several common plastics, as a function of irradiance

Kokkala[18] attempted to study the ignition of a PMMA ceiling in a somewhat real-life situation by impinging 3 – 10 kW burner flames upon it. He found T_{ig} = 380 – 410ºC, which is significantly higher than reported in most other studies; the higher values are probably attributable to a significant (but not measured) velocity induced by the burner. A minimum heat flux of 20 – 30 kW m^{-2} was needed for the PMMA to ignite; this is, again, much higher than found in radiant heating tests. Not enough results are available from flame-heating tests, however, to generalize these types of observations.

Some rather different results are found for charring materials. Most natural materials, e.g., agricultural products, are charring materials, but only wood has been studied in sufficient detail to draw systematic conclusions. Wood is dis-

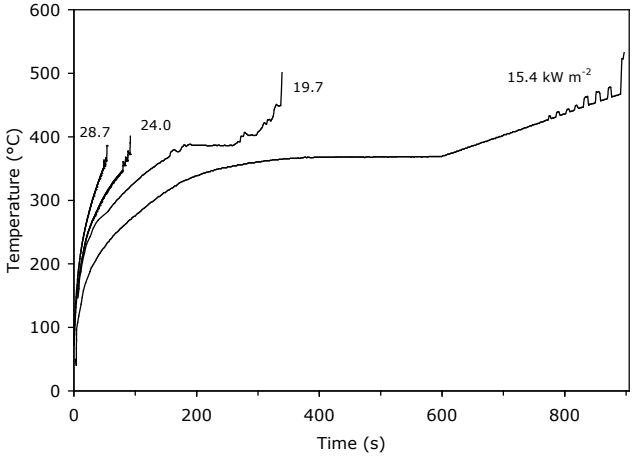


Figure 3 The surface temperature of Mahogany samples exposed to various heat fluxes

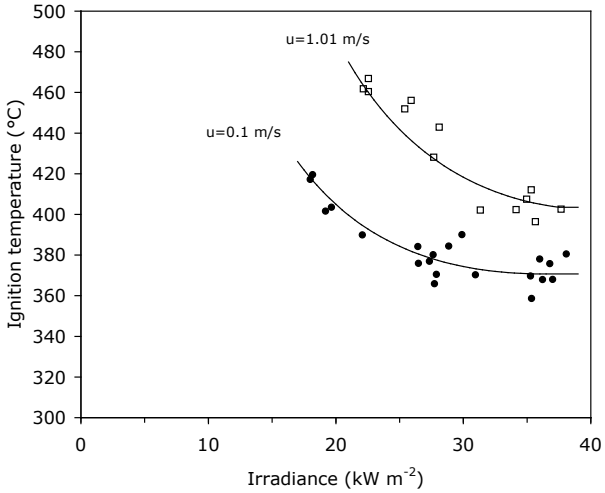


Figure 4 Effect of heat flux and air velocity on T_{ig}: results of Atreya and Abu-Zaid

cussed at length in Chapter 14, but here we present some example experimental data. Li and Drysdale[19] used a careful measurement technique to study the piloted ignition temperature of several wood species. Their results (Figure 3 and Table 4) showed some high T_{ig} values at low fluxes, then a lower, relatively constant, value at larger fluxes. Decreasing T_{ig} values with increasing heat flux were also found by Abu-Zaid[67] for red oak and by Atreya[62] for 8 different species of wood. A joint paper by these two authors[20] gave the results shown in Figure 4. The authors' test environment was a wind tunnel and it is evident that air velocity has quite a sizable effect on the results, with the irradiance effect also being apparently a bit smaller at the lower velocity. Moghtaderi et al.[21] measured the ignition temperature for Monterey pine as a function of both heat flux and moisture. Their results, shown in Figure 5, indicate similar trends. The analysis of a large number of other results for wood, given in Chapter 14, suggests that, as seen in the data of Li and Drysdale, there are two heat-flux regimes and T_{ig} is constant in the higher heat-flux regime, but varies with flux at low heat flux values.

Table 4 Piloted ignition temperatures of various woods

Wood species	Heat flux (kW m^{-2})	T_{ig} (°C)	Plateau temp. (°C)	t_{ig} (s)
Western red cedar (280 kg m^{-3})	15.4	450	366	583
	19.7	431	379	216
	24.0	365	—	57
	28.7	346	—	30
	31.7	354	—	23
obeche (350 kg m^{-3})	15.4	497	359	684
	19.7	442	361	176
	24.0	364	—	60
	28.7	344	—	39
	31.7	340	—	29
white pine (360 kg m^{-3})	15.4	446	354	1094
	19.7	411	380	257
	24.0	397	—	95
	28.7	387	—	48
	31.7	375	—	32
mahogany (540 kg m^{-3})	15.4	465	365	850
	19.7	427	385	324
	24.0	364	—	90
	28.7	360	—	60
	31.7	353	—	38

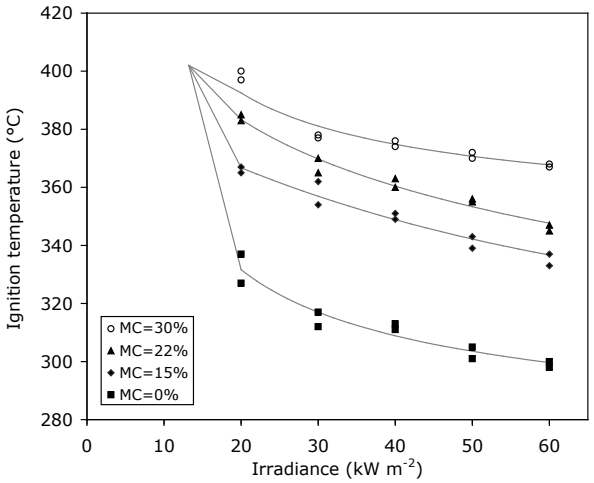


Figure 5 Ignition temperature of Monterey pine, as a function of irradiance and moisture content

These studies on wood materials indicate a number of complications, but foremost is the effect of glowing ignition. For irradiances below a certain value, such charring materials initially ignite in a glowing mode, and they may possibly subsequently transition to flaming. Any substances that ignite in a glowing mode do not show a constant T_{ig}, and details are discussed later in this Chapter. Another factor is self-heating. The effects of self-heating for wood, as for most other materials, are small or negligible if exposed to high external fluxes for a short time. In the opposite situation, heating by a low heat flux for an extended period of time, the surface temperature will rise due to a bulk self-heating effect, apart from what happens at the surface itself. Wood and agricultural materials furthermore are hygroscopic, that is, they have a tendency to take up moisture. Increasing the MC causes a notable increase in T_{ig}, provided the imposed flux exceeds a certain minimum value. For irradiances just barely sufficient to ignite the material, clearly MC cannot have any effect since ignition will not take place until the specimen is thoroughly desiccated.

The above experimental findings suggest that assuming that T_{ig} is a constant which is characteristic of a material is reasonable assumption for melting materials and is also a useful—albeit imperfect—concept for charring materials, so long as glowing-initiated ignitions are not considered.

Nonetheless, there are difficulties with the notion of a constant T_{ig}:

(1) The surface temperature is exceedingly difficult to measure accurately. Very tiny, fragile thermocouples (around 0.05 mm) are needed to avoid gross errors. But even so, errors arise. The foremost is that it is hard to keep a thermocouple fixed to the exact face of a specimen as it is heating up. Most materials tend to shrink, swell, melt, bubble, crack, or otherwise deform prior to ignition; a thermocouple which was accurately located at the start of the exposure may end up elsewhere, or broken, by the time that ignition is reached.
(2) Optical measurements of surface temperature are sometimes made. These avoid certain errors, but are subject to errors of their own—for example, a value of emissivity may need to be specified for the surface, but this can be both temperature-dependent and poorly known.
(3) Some external variables do have an effect on the ignition temperature.
(4) For some materials, if prolonged heating under heat fluxes somewhat lower than those needed to cause ignition is followed by increased heating so that T_{ig} is reached and surpassed, ignition may not occur.

In addition, it must be remembered, as illustrated above for the case of thermoplastics, that T_{ig} values for a large majority of combustible solids are clustered closely together, making this variable not too useful for distinguishing among materials.

For *thin materials*, the concept of a surface temperature is not particularly meaningful, since there is, by definition, negligible difference between the internal temperature and the surface temperature. For most analyses with thin materials, consequently, calculations are based on the specimen's mean temperature. Thus, it has been proposed that for thin materials the mean temperature can serve as the criterion of ignition. In experimental measurements, the surface temperature* at ignition for thin materials is found to be much higher than for the same substance in thick layers; for example, a value of 600ºC has been quoted for cellulose[27].

MASS LOSS RATE AS IGNITION CRITERION

Subsequent to Bamford et al., a number of other investigators explored the values of mass loss rate at the flash point or at sustained flaming under piloted ignition conditions. Melinek[26] developed a simple numerical model of the ignition process, where the mass loss rate of the specimen is treated as a first-order Arrhenius reaction, that is:

$$\dot{m}'''(t) = \left(\rho(t) - \rho_c\right) A \exp\left(\frac{-E}{RT}\right)$$

where $\dot{m}'''$ = volumetric mass loss rate (g m^{-3} s^{-1}), and ρ_c = the density of the char that remains after all volatiles have left. By solving the temperature equation and integrating the mass loss rate term with respect to specimen depth he was able to get an expression for $\dot{m}''(t)$, the mass loss rate per unit surface area (g m^{-2} s^{-1}). Typical results are shown in Figure 6. Because of the exponential dependence on temperature, until quite close to ignition time there are essentially zero pyrolysates generated. The curve reaches a peak and then decays; the decay is due to exhaustion of reactants. The shape of the curve explains why a specimen receiving only marginally sufficient flux for ignition might not sustain burning after a short initial period.

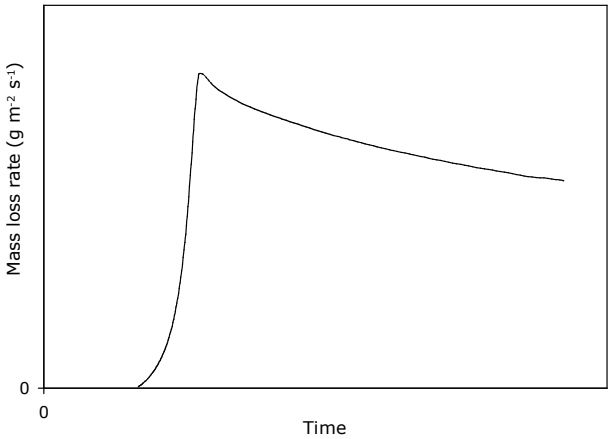


Figure 6 Mass loss rate curve of wood, as computed by Melinek

Kanury[28] attempted to evolve a single, theoretical expression for the needed $\dot{m}''$, but Thomson[2] found that there was an error in his reasoning (he assumed that the gas plume above the specimen reaches the flame temperature prior to ignition).

Table 5 Minimum mass loss rate for piloted ignition, as obtained by various investigators

Material	At flash point (g m^{-2} s^{-1})	At ignition (g m^{-2} s^{-1})
Non-oxygenated materials		
decane (liquid)		0.6[29]
polyethylene		1.3[29], 1.9[22]
polypropylene	0.6[29]	1.2[29], 2.2[22]
polypropylene, FR		3.1[29]
polystyrene	0.55[29]	0.4[23], 1.0[29], 3.0[22]
polystyrene, FR		5.0[29]
Oxygenated materials		
ethylene/vinyl acetate copolymer (EVA)		1.3[24]
PMMA	1.0[29]	0.7[23], 1.9[29], 3.2[22]
PMMA, FR	1.8[29]	4.0[29]
polyoxymethylene	0.85[29]	1.8[29], 3.9[22]
wood		1.5[25],1.8[1], 2.2[29], 2.5[7], 5.1[26]

* It is dubious that, in experimental thermocouple measurements with thin samples, the surface temperature can be differentiated from the mean temperature.

While not much progress has been made towards a workable theoretical basis for the minimum mass flux, a number of experimental results are available. Drysdale and Thomson[29] conducted what is arguably the most carefully prepared set of experiments for the purpose of obtaining minimum values of mass loss rate. Their values, along with those of several other investigators, are shown in Table 5. Tewarson et al.[30] also reported on the mass loss rate needed for piloted ignition for a series of electric cable specimens. The values are not shown in the Table, but ranged from 2.6 to 4.8 g m^{-2} s^{-1}.

It is clear that accurately measuring low values of mass loss rate is difficult and that the data are to some extent apparatus-dependent. Furthermore, it can be concluded that, for any given substance, lower reported values are more likely to be accurate than are higher ones. For example, Deepak and Drysdale[31] obtained a value of 4 – 5 g m^{-2} s^{-1} for PMMA. Upon further development of the experimental rig at the same facility, Drysdale and Thomson[29] found a value of 1.9 g m^{-2} s^{-1}. With this in mind, certain trends emerge:

(1) Non-oxygenated, non-FR solids show flashing when a mass loss rate of around 0.6 g m^{-2} s^{-1} is reached.
(2) Oxygenated, non-FR solids show flashing when a mass loss rate of around 1.0 g m^{-2} s^{-1} is reached.
(3) Non-oxygenated, non-FR solids show piloted ignition when a mass loss rate of around 1.2 g m^{-2} s^{-1} is reached.
(4) Oxygenated, non-FR solids show piloted ignition when a mass loss rate of around 2.0 g m^{-2} s^{-1} is reached.
(5) The ratio of the mass loss rate at ignition (sustained flaming; fire point) to that at flashing (flash point) is about 2:1.
(6) FR materials require about double the mass loss rate than do comparable non-FR materials for flashing or for ignition.

As several theories have suggested, there should be a relation between ignition temperature and $\dot{m}''$ at ignition. Due to the wide scatter of data obtained by different researchers, it is possible to look for trends only by focusing on a single study. Since the best data available are from Drysdale and Thomson, Figure 7 shows the trends from their results. Clearly, oxygenated and non-oxygenated fuels fall along separate trend lines. Polystyrene is seen to be an outlier, but decane follows well the trend of the non-oxygenated polymers. Due to paucity of data, the lines drawn in Figure 7 must be viewed only as indicating qualitative trends.

For a *thermally-thin* solid, some explicit calculations can be made, since, by definition, a thermally-thin solid is all at one temperature. If single-step, zero-order Arrhenius kinetics is assumed, then

$$\dot{m} = -A\,m(0)\exp(-E/RT)$$

where A = pre-exponential constant (s^{-1}), $m(0)$ = initial mass (kg), and E = activation energy (kJ mol^{-1}). But

$$m(0) = \rho(0)LS$$

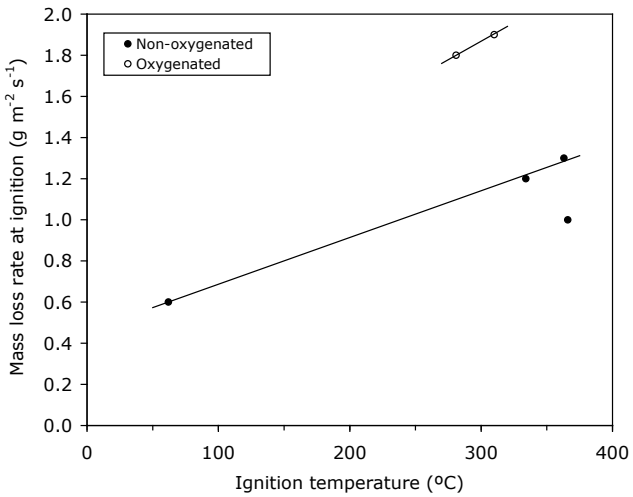


Figure 7 The relation between ignition temperature and mass loss rate criterion

where $\rho(0)$ = initial density (kg m^{-3}), L = thickness (m), and S = surface area (m^2). Then,

$$\dot{m}'' = A\rho(0)L\exp(-E/RT)$$

where any decrease in ρ or L prior to ignition has been ignored. Since A, E, and ρ are fixed, this implies that for the thin material there cannot be a fixed relationship between $\dot{m}''$ and T_{ig} as the thickness L is varied.

The above treatment assumed that $\dot{m}''$ is a constant for a given material and is independent of test conditions. Unfortunately, this is not exactly true. Rasbash et al.[32] examined the effects of certain variables on the $\dot{m}''$ for PMMA tested in the horizontal orientation. The instrumentation used at the University of Edinburgh was of much lower accuracy than subsequently evolved by Thomson, thus the data

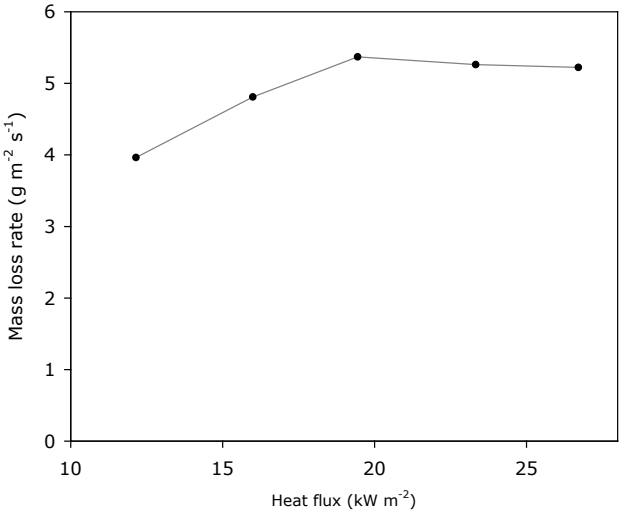


Figure 8 Effect of heat flux on MLR needed for ignition of PMMA

should be viewed as only rough indications. Figure 8 shows a modest drop in $\dot{m}''$ as the flux approaches the minimum value needed for ignition. The air flow rate according to Figure 9 is optimum at intermediate values. The reason for this has not been fully explained, but the same phenomenon is illustrated in Figure 56. Figure 10 indicates that as oxygen concentration is brought down to a critical value, the needed $\dot{m}''$ rises rapidly. The bump at 40% is most likely experimental error.

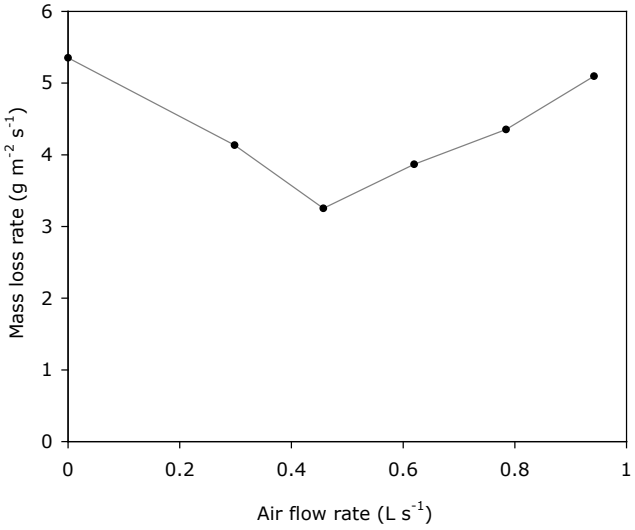


Figure 9 Effect of air flow rate on MLR needed for ignition of PMMA

Little information is available on the mass loss rate needed for autoignition. Melinek[26] observed that for one series of tests on wood, $\dot{m}''$ was 50% higher under autoignition conditions, compared to the piloted ignition value.

HRR AS AN IGNITION CRITERION

As discussed in detail in Chapter 4, flames cannot be sustained for arbitrarily low flame temperatures. Instead, a flame temperature associated with the LFL can be determined, and its value is relatively high. On this basis, a heat release rate (HRR) criterion becomes reasonable to consider. A volume of gases in front of the specimen must be brought up to, and maintained, at this flame temperature for initial combustion (ignition) to occur and then to be sustained. A heat balance on this volume implies that it is the product of the mass loss rate times the heat of combustion (in other words, the HRR) of the evolved pyrolysates that is governing.

Actual values of HRR at ignition can be computed using Thomson's results presented in the preceding Section and values of heat of combustion. Table 6 shows the results obtained; the lowest reported mass loss rate value was used for each material. FR materials could not be evaluated

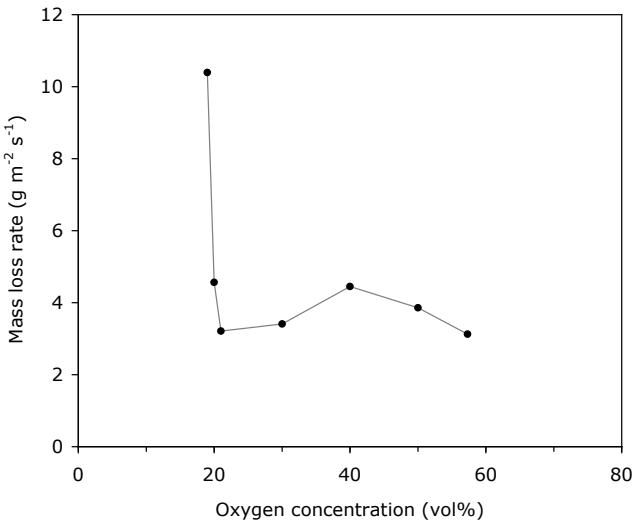


Figure 10 Effect of oxygen concentration of MLR needed for ignition of PMMA

since heats of combustion for the specimens used were unknown. There is quite a lot of data scatter and measurements of low mass loss rates are difficult to make. However, the results of Table 6 generally lie between the two published recommendations: 25 kW m^{-2} (by Hansen[33]) and 50 kW m^{-2} (by Kokkala and Baroudi[34]), irrespective of whether the fuel is oxygenated or not. For a mass loss rate criterion, a substantially higher value was found for oxygenated materials than for non-oxygenated. But the oxygenated materials have correspondingly lower heats of combustion (since they are 'pre-oxidized') and thus it appears that a single value of HRR can serve as an ignition criterion, irrespective of whether the fuel is oxygenated or not. It is unlikely that FR materials will fall in line with this same value, since flame retardants that are chemically reactive in the gas phase are expected to show a higher temperature at the LFL.

A quantitative prediction based on HRR was attempted by Alpert and Khan[35]. They argued that the ignition criterion should be:

Table 6 HRR as a criterion for piloted ignition

Material	MLR at ignition (g m^{-2} s^{-1})	Heat of combustion (MJ kg^{-1})	HRR at ignition (kW m^{-2})
Non-oxygenated materials			
decane (liquid)	0.6	44.2	26.5
polyethylene	1.3	43.2	56.2
polypropylene	1.2	43.2	51.4
polystyrene	1.0	39.7	39.7
Oxygenated materials			
PMMA	1.9	24.9	47.3
polyoxymethylene	1.8	15.7	28.3
wood	1.8	18.5	33.3

$$\dot{q}'' = 54\sqrt{D}$$

where D = fuel base diameter (m). Since the effective diameter of the Cone Calorimeter samples used by Thomson was 0.113 m, this would suggest that the critical HRR = 18.1 kW m^{-2}. However, Alpert and Khan did not provide any data of their own to validate their hypothesis and Thomson's data are not close to 18.1 kW m^{-2}.

OTHER CRITERIA FOR IGNITION

For experimental measurement of ignition, normally observation of flame (or, possibly, glow or explosion) should be sufficient. Yet, much of early experimental work on ignition was done using criteria other than observation of flame. Brown[3] adopted the definition: "The temperature at which the rate of generation of heat becomes greater than its dissipation under certain fixed conditions." This definition—with slight modifications—could form a viable definition of the critical temperature for self-heating; for flaming ignition of externally-heated solids, however, it makes little sense. In practice, Brown used specimens tiny enough that a single thermocouple inserted into the center of the specimens could be taken to represent the entire specimen's temperature. He inserted the specimen into an oven where the temperature rose at a programmed rate. He then plotted the difference between the furnace and the specimen thermocouple readings. The first instance that this signal started to deviate from a straight line was declared to be the ignition temperature. Occurrence of visible flaming was never recorded. Brown did record the crossing-point temperatures, i.e., the temperature at which the thermocouple traces for the furnace and for the sample thermocouples crossed over. This value was generally 30 – 50ºC higher than that which he recorded as T_{ig}, but in some instances the difference reached 100ºC.

Using a philosophy and procedures rather similar to Brown's, Graf[36] used a criterion that "the rate of heating in the substance exceeds the rate of heating induced by the external source of heat and has visible combustion in the form of a glow or flame as an end result." In his experiments, he inserted minuscule specimens into an oven which had a programmed rate of rise of temperature. His actual procedure was a bit unclear, but it appears that he looked, at a location very close to the specimen, for the first time where the slope of the temperature started to rise at a more rapid rate than the oven temperature was rising.

In his study, Brown also surveyed much older literature. His survey indicates that methods similar to his were predominant in that time period. Very few examples were cited of investigators actually using observation of flame as the ignition criterion. In the current era, criteria very similar to Brown's are still being used when thermal analysis instruments are used for determining ignition. No study exists that would document a relation between these 'pseudo-ignition' temperatures recorded for minuscule specimens and real ignition temperatures on materials of end-use size or configuration. The reason why early experimentalists favored these techniques appears to be expediency—tests could be run in an automatic fashion, rapidly and without needing to have an observer present. Despite the inappropriateness of 'non-observational' criteria in experimental work, a large, systematic error cannot be ascribed to such criteria, at least as found in Babrauskas' survey[37] on the ignition of wood.

Simms[38,65] proposed that autoignition occurs only at the time and location where turbulence is first established in the gas stream. It is clear that if turbulence is present, it will enhance the mixing of the fuel vapors into the air and decrease the time at which the LFL first occurs. However, it does not seem to be a primary criterion, and no other researchers have adopted his point of view. For piloted ignition, Alvares et al.[39] suggested that a criterion would be the attainment of a 6% concentration of flammable pyrolysis vapors at the place where the igniter is located. Again, no work using such a criterion has been reported.

Deverall and Lai[40] constructed a model of the solid phase and considered the requirement that ignition will occur when gas temperature first becomes higher than the surface temperature, i.e., the direction of the flow of heat is reversed locally. Their model then predicted that ignition will occur when the irradiance first becomes equal to {conductive heat loss of the solid at the surface + 2× heat of gasification}. Determining either of these quantities accurately enough has been found to be exceedingly difficult, so the criterion lacked practicality. A related criterion sometimes considered[41] is that ignition occurs if the temperature gradient just inside the front face of the solid becomes flat. This instantaneously-flat condition is seen as being followed by a positive slope, i.e., that the solid has now become a net source of heat rather than a net sink. This criterion appears useful for the ignition of solid propellants but has not seen much application to common solids.

Janssens[76] lists 6 other criteria that have been proposed, generally only by a single researcher. Vilyunov[153] lists a total of 10 mathematical criteria that have been proposed for ignition. Kulkarni et al.[42] list 14 mathematical criteria and 6 experimental criteria that have found usage. Most of them have been developed since some purely numerical calculations do not 'know' when ignition has occurred. As such, these will mainly be of interest to researchers planning a particular numerical solution. For example, one of these criteria states that ignition corresponds to the inflection point on the curve of the front-face temperature vs. time. Criteria of this sort are relatively removed from the physics of the problem since it still remains necessary to prove that something of interest actually happens at the time when the particular mathematical condition becomes fulfilled.

Ignition from radiant heating

In this section, we address a major concern of this Chapter: quantifying how materials ignite when exposed to a radiant heat flux from an external heat source. The events taking place in the gas phase are considered first. This is a brief treatment, both because there is very little experimental information and because most current-day theories that lend themselves to practical application ignore the gas-phase events. Next, some comprehensive models that do consider events in both the solid phase and the gas phase are presented. Finally, the remainder of this Section focuses on engineering models which have been specifically developed to treat experimental data.

GAS PHASE EVENTS

For a majority of pyrolyzing solids under most thermal exposure conditions, ignition occurs as a gas-phase event, after the solid has produced a sufficient amount of fuel gases. Yet, surprisingly, the details of the gas-phase ignition have not been probed extensively. Yoshizawa and Kubota[43] studied the ignition of thick (13 mm) cardboard specimens oriented horizontally and exposed to xenon lamp heating at the high heat flux of 300 kW m^{-2}. They found that the first flame kernel (Figure 11) appeared at 7 mm above the surface and proceeded to grow in both directions—towards and away from the surface. About 14 ms later, a second kernel appeared at 10 mm and also proceeded to grow. By about 22 ms, both kernels had expanded to reach the surface, after which a customary diffusion flame continued to propagate. Surprisingly, the point at which the flame originally appeared was found to correspond to an equivalence ratio of about 4.7, which is extremely rich, even given that the temperature at that locale was about 540ºC just prior to ignition. The combustible gases that ignited were found to be mostly CO. To the accuracy that they could determine, the surface temperature at the time of ignition was nearly identical to the 540ºC measured in the gas phase. In a much less detailed study, Mutoh et al.[114] reported temperatures of ca. 500ºC just prior to ignition of PMMA. Again, temperatures on the surface and in the gas phase location where ignition first took place were essentially identical. The only other measurements that could be found in the literature on the topic of gas temperatures at the time of unpiloted ignition of a solid are those of Durbetaki et al.[44] But they reported some exceedingly high temperature and the reasons for this are unclear.

Bukovec and Urbas[45] measured the flame temperatures in the gas phase in front of a vertical Douglas fir specimen. They found peak temperatures of ca. 1300ºC. Much as Yoshizawa and Kubota did in the horizontal orientation, they found that in the vertical orientation the point of the highest flame temperature originally starts out at some distance away from the surface, then draws closer. For specimens exposed to a 65 kW m^{-2} flux, at the moment of ignition the location of peak temperature was 5 – 7 mm in front of the surface. After 400 s of burning, it became about 2 mm and

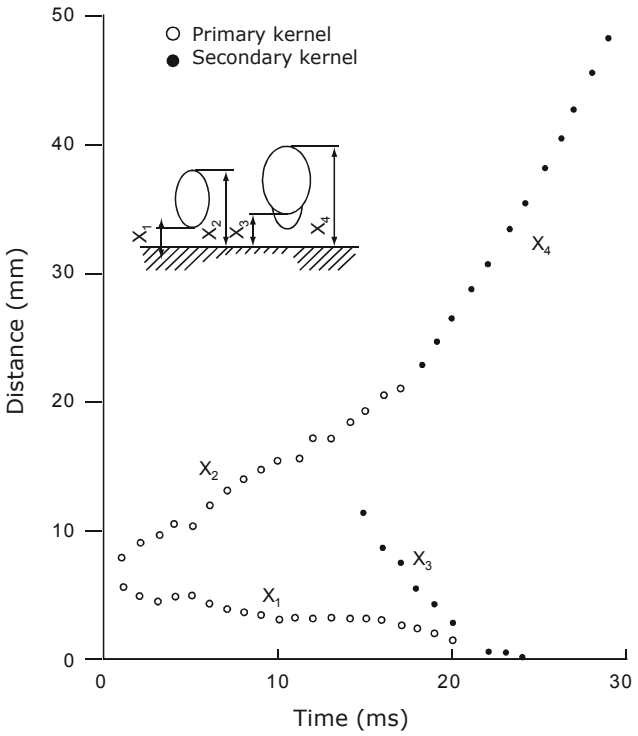


Figure 11 Development of the ignition kernel
(Copyright The Combustion Institute, used by permission)

stayed at that distance subsequently. Flames stayed laminar only for 15 s after ignition, becoming turbulent thereafter.

The gas-phase events during *piloted ignition* are even less well studied than are those during autoignition. Conceptually, one might suppose that a mixed volume of gases exists which, at a certain point, reaches its LFL. The gases, however, are hardly well-mixed unless, possibly, very long ignition times are involved. Furthermore, there does not exist any reasonably simple scheme for computing when this concentration might be attained.

Conceptually, Long et al.[46] pointed out that t_{ig} can be viewed as being a summation of three terms:

$$t_{ig} = t_p + t_m + t_i$$

where t_p is the time needed to raise the surface of the solid to a sufficient temperature so that there would be the minimum needed mass flow rate of pyrolysates; t_m is the time needed for the pyrolysates to mix with air; and t_i corresponds to the induction period of the fuel/air mixture, that is, the time needed for chemical reactions to take place in the gas phase. This type of additive arithmetic has only rarely been explored, unfortunately.

COOL FLAMES

Same as for some gases and liquids (see Chapter 4), solids can also ignite showing 'sub-ignition' in the form of cool flames, or else two-stage ignitions where a cool-flame is followed subsequently by a normal-flame ignition. The

phenomenon was studied by Baillet and coworkers[47,48], who investigated the polyolefin family and found that it occurs in the case of polypropylene, poly-1-butene, and poly-4-methyl-1-pentene, but not in the case of polyethylene. The polyolefins that did show a cool flame ignition only showed it in limited temperature/O_2 concentration regions, with the oxygen limits spanning no more than 20 – 60 vol% for polypropylene and 37 – 60 vol% for poly-4-methyl-1-pentene.

COMPREHENSIVE THEORIES

As a pyrolyzing solid is heated, flammable gases are generated in the chemical breakdown of the solid and these gases leave the heated face of the material. Initially, the concentration of the pyrolysates is low, and ignition is impossible. Since initially there are no pyrolysates in the ambient environment, the difference in concentration acts to diffuse pyrolysates away from the surface. As a result, a fuel/air mixture is created above the surface. When the rate of emission of pyrolysates becomes sufficient to create a zone where the mixture reaches the LFL, ignition can occur if an ignition source is present there. The mixture is premixed, so the initial flame must be premixed. If the production of volatiles from the surface is insufficient, then the event represents a transient flash. If the flow of volatiles is adequate, then a flame gets established some distance above the surface, but this flame now is a diffusion flame, not a premixed one. The entire situation is complex, as illustrated in Figure 12[49]. This figure illustrates the more difficult case of wood or similar materials which possess internal voids, thereby allowing pyrolysates to flow through those spaces. Solid plastics can generally be represented in a slightly simpler manner, since subsurface flows of vapors do not exist. The two cases are sometimes identified[50] as *volumetric decomposition* and *superficial decomposition*.

As will be seen below, 'engineering' theories ignore all features of the gas phase and simply focus on solving a heat transfer problem in the solid phase. A number of studies have been published which attempt to consider both the thermal response of the solid and the gas-phase environment, using at least some chemistry and possibly some fluid mechanics. We shall call these 'comprehensive,' although these vary quite a bit as to the amount of detail incorporated. Both the solid and the gas phase can be formulated as a 1-, 2-, or 3-dimensional problem. Because specimens cannot be infinitely wide nor long, the gas phase concentrations above the fuel surface must necessarily have a 3-dimensional character. But a number of theories which use only a 1- or 2-dimensional treatment of the gas phase have had various degrees of success. However, there is little to be gained by using more than a 1-dimensional treatment of the solid phase, so most theories—even the latest ones—generally treat the solid as a 1-dimensional problem.

Kashiwagi[51] presented an early attempt at calculating the autoignition time for a solid exposed to a radiant heat flux. The formulation was entirely 1-dimensional, so a realistic representation of the plume of combustible gases developing outside the solid could not be made. One of the conclusions from his model was that the surface temperature at ignition should increase with increasing heat flux; this conclusion, however, was not borne out in his later experimental studies[115]. Atreya et al.[52] presented another theory where both the solid and gas phase are treated in a 1-dimensional way. With this theory, Atreya was able to demonstrate that a quenching distance exists for solids, and that locating a pilot closer to the surface will lead to extinction. He also computed that the optimal distance of the pilot above the surface is just slightly greater than the quenching distance, that it increases with increasing fuel mass loss rate, and that ignition times increase as the pilot is moved farther away. Of significant interest is Atreya's conclusion[49] that the presence of a high temperature pilot flame makes details of gas-phase chemical kinetics unimportant. This still leaves the gas phase mixing process as an important aspect that needs to be modeled.

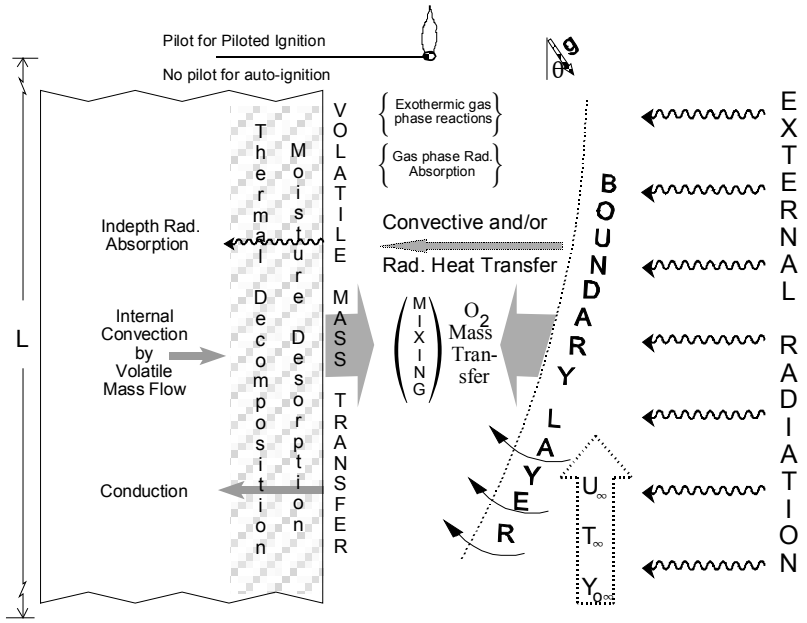


Figure 12 Main physical and chemical processes taking place during the ignition of a solid by radiant heat
(Copyright Royal Society, reprinted by permission)

While studies of simplified geometries, such as Atreya's are highly valuable in understanding the main aspects governing ignition, the fact remains that the gas phase environment may be varied. There can be a strong convective flow, or a minimal one. The surface may be rough, creating local turbulence, or not. Access may be available for oxygen to enter from the sides, close to the surface, or not. Despite some rough assumptions that can be made, the mixture forming above the surface is assuredly *not* uniform. Temperatures are also notably non-uniform in the gas, and their distribution is governed by some of the same factors. Thus, while premixed gas ignition ideas can be applied, they can only be expected to be of qualitative utility.

Gandhi[53] undertook to model a 2-dimensional problem, where a boundary layer over a vertical panel is treated, along with radiant heat flux. The chemistry was represented as separate Arrhenius-form reaction rate equations for the solid and for the gas phase. Gandhi assumed that the criterion of ignition is a change of the gas-phase temperature gradient from negative to positive. The problem formulation was ambitiously encompassing, but the consequence was that there was a very large number of independent variables, and no closed-form or approximate solutions were evolved, nor were comparisons with experiments made.

Amos and Fernandez-Pello[54] presented a 2-dimensional model of ignition in a stagnation-flow geometry where autoignition is assumed to occur due to absorption of radiation by pyrolysate gases. Since the convective flow is an air flow at room temperature, their model predicts that the minimum (radiant) flux for ignition increases linearly with increasing air flow velocity. The model results were presented as numerical calculations, and no comparison to experimental data was made.

The latest research efforts in modeling ignition of solids make use of available computation power to create and solve models which are 1-dimensional in the solid, but 3-dimensional (or axisymmetric, 2-d) in the gas phase. Tsai et al.[55] developed such a model to predict both piloted and autoignition of PMMA in the Cone Calorimeter. The model assumed:

- 3-dimensional conservation equations for continuity, momentum, energy, and species in the gas phase. To represent the Cone Calorimeter geometry, they assumed the flow was laminar and axi-symmetric.
- diffusion represented by Fick's law
- 1-dimensional heat conduction in the solid phase
- radiation from the conical heater represented as 1-dimensional, downward
- absorption of radiation by pyrolysate gases (assumed to be MMA monomer), but neglecting radiative emission from gases.
- single-step Arrhenius kinetics in the gas phase

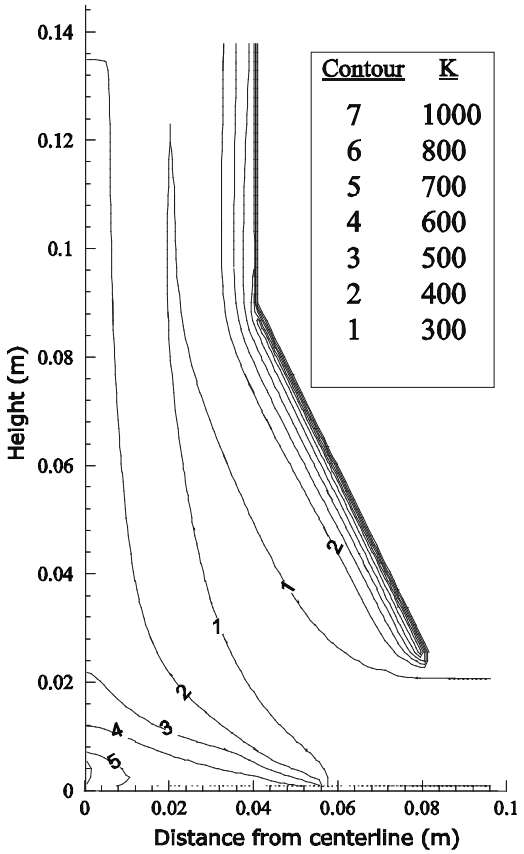


Figure 13 Gas-phase temperatures above specimen at 183.6 s in the model of Tsai et al.
(Copyright The Combustion Institute, used by permission)

- single-step Arrhenius kinetics to represent pyrolysis of the solid
- pyrolysis of fuel occurs only at the surface.
- for piloted ignition, the spark was approximated as a local hot spot of 1000 K.

Autoignition prediction calculations just prior to ignition (Figure 13) show high temperatures mostly localized at the conical heater. However, a small bubble-shaped region of elevated gas temperatures (see contour 5) is forming just above the specimen. Ignition is shown in Figure 14, at which time an 'upside-down tulip' shaped flame surface has formed, and it extends to about 110 mm above the specimen surface. Note that temperature contours now represent much higher temperatures, with small regions indicated as being close to 2400 K. Finally, quasi-steady-state burning is shown in Figure 15. Due to model simplifications, the predicted peak temperatures are higher than measured, nonetheless the calculations capture well the essential features of autoignition.

A somewhat similar model for predicting piloted (only) ignition of wood in the Cone Calorimeter was developed by Yuen[56]. His sub-model for the pyrolysis of the solid is the most ambitious thus far attempted, including, apart

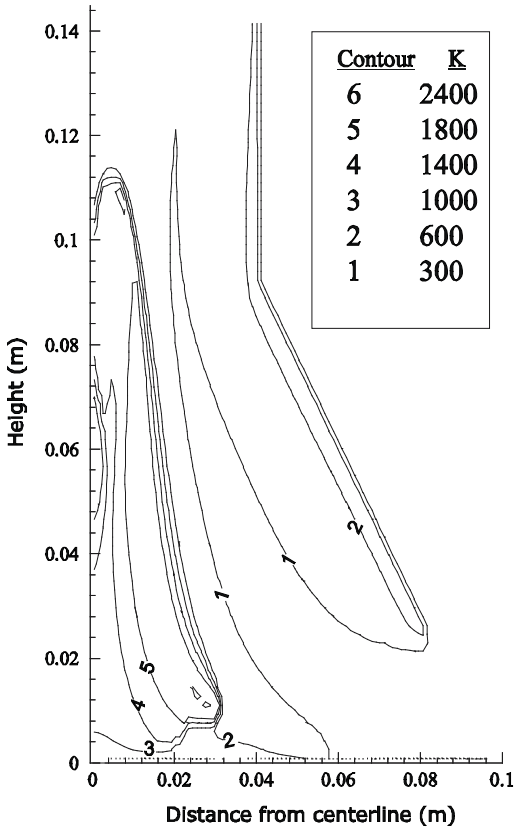


Figure 14 Gas-phase temperatures above specimen at 183.8 s in the model of Tsai et al.
(Copyright The Combustion Institute, used by permission)

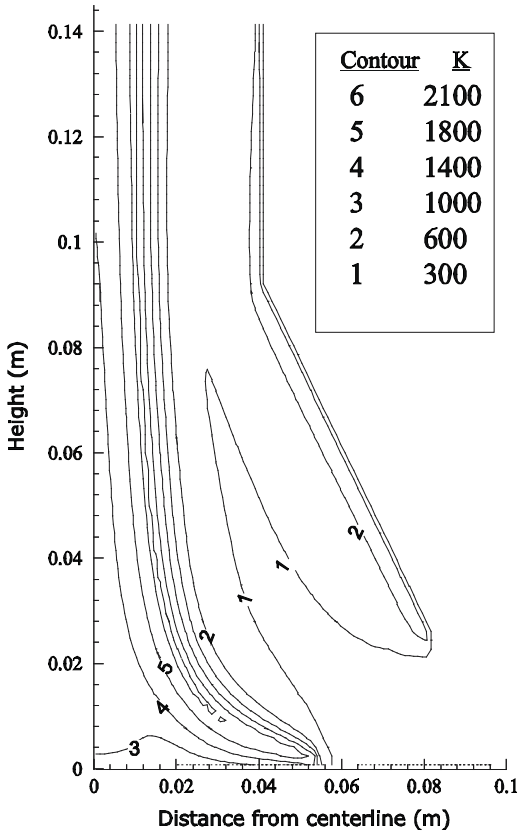


Figure 15 Gas-phase temperatures above specimen at 184.1 s in the model of Tsai et al.
(Copyright The Combustion Institute, used by permission)

from one-step Arrhenius kinetics, movement of moisture and temperature-dependent thermal properties. The model was able to predict adequately the ignition times at heat fluxes of 40 – 70 kW m^{-2}. For a heat flux of 20 kW m^{-2}, predicted ignition times were only about 1/5 of the times actually measured. Yuen's formulation is noteworthy in that he did not use any adjustable factors—all needed constants were obtained from the literature or from experiments different than the environment of the Cone Calorimeter. A total of 18 constants were used to characterize the physics and chemistry of wood pyrolysis; the number of constants needed for solving the gas-phase problem was not specified. The model that Yuen evolved could conceivably be adapted to solving ignition problems other than for wood. However, obtaining the needed material constants would evidently be quite difficult. Results from Yuen's model show[57] the feature that Yoshizawa found experimentally: flames from the initial kernel move outward and downward towards the specimen face.

Most of the more ambitious theories have treated a thick solid, since this more closely corresponds to the majority of real-life problems. The *thermally-thin* case is theoretically easier to analyze, however, since a 0-dimensional treatment of the solid (no gradients of anything in the solid) can be adopted. Nelson et al.[58,59] created a sophisticated model to represent autoignition of a thermally-thin substance in the Cone Calorimeter. Their theory had no spatial variations for any property and assumes that the pyrolysates form a gas 'slab' of uniform thickness above the surface. Nonetheless, five differential equations needed to be solved simultaneously to obtain a solution for the gas temperature, a rapid jump in which indicates ignition. Results computed with their model showed the presence of a minimum flux for ignition and, in certain circumstances, exhibited flashing, in addition to sustained ignition. Despite its mathematical complexities, the model is physically simplified and in its present stage of development is not yet intended for predicting the response of real materials.

Nakamura et al.[60] modeled the autoignition of a thermally-thin solid using a 2-dimensional (axi-symmetric) formulation in the gas phase. Their results for cellulose filter paper indicated that autoignition within the plume above a horizontally-oriented thin slab can occur either near the surface (Type 1) or near the tip of the plume (Type 2). Increasing oxygen concentration of the atmosphere promotes the case where ignition occurs at the tip, while raising the acceleration of gravity promotes occurrence of ignition near the surface. Some of their main results are shown in Figure 16, while vertical plume sections are shown in Figure 17. Their modeling predicts the Type 1/Type 2 breakpoint at a higher

oxygen concentration than is normally observed (see later in this Chapter), but otherwise the model captures the main features of autoignition.

The theoretical problem of the ignition of pyrolyzing solids is identical, apart from minor issues, to that for the ignition of non-hypergolic propellants. Thus, the major review papers in the latter specialty, discussed in Chapter 10, can be viewed as providing additional insights into the problem of ignition of pyrolyzing solids.

ATREYA'S MODEL

As a specific example of one of the simpler comprehensive models, Atreya's 1-dimensional solid+gas phase model[49] sets up the following equations:

Fuel stoichiometry:

1 kg fuel + r_o kg O_2 → (1 + r_o) kg products + Δh_c (heat)

Gas-phase continuity:

$$\frac{\partial \rho}{\partial t} + \frac{\partial (\rho u)}{\partial x} = 0$$

Gas-phase energy conservation:

$$\rho \frac{\partial T}{\partial t} + \rho u \frac{\partial T}{\partial x} = \frac{\partial}{\partial x}\left(\frac{\lambda}{C}\frac{\partial T}{\partial x}\right) + \frac{1}{C}\frac{\partial \dot{q}_r''}{\partial x} + \frac{\Delta h_c}{C}\dot{m}'''$$

Gas-phase fuel conservation:

$$\rho \frac{\partial Y_F}{\partial t} + \rho u \frac{\partial Y_F}{\partial x} = \frac{\partial}{\partial x}\left(\rho D \frac{\partial Y_F}{\partial x}\right) - \dot{m}'''$$

Gas-phase oxygen conservation:

$$\rho \frac{\partial Y_O}{\partial t} + \rho u \frac{\partial Y_O}{\partial x} = \frac{\partial}{\partial x}\left(\rho D \frac{\partial Y_O}{\partial x}\right) - r_o \dot{m}'''$$

Equation of state at constant pressure:

$$\rho T = \rho_\infty T_\infty$$

Gas-phase reaction rate:

$$\dot{m}''' = A \rho^2 Y_F Y_O e^{-E/RT}$$

Solid-phase mass balance:

$$\frac{\partial \rho_S}{\partial t} + \frac{\partial \rho_m}{\partial t} = -\frac{\partial \dot{m}''}{\partial x}$$

Solid-phase energy balance:

$$\rho_S \frac{\partial h_S}{\partial t} + \rho_m \frac{\partial h_m}{\partial t} + \dot{m}'' \frac{\partial h_g}{\partial x} = \frac{\partial}{\partial x}\left(\lambda_S \frac{\partial T_S}{\partial x}\right)$$

$$+ \frac{\partial \dot{q}_r''}{\partial x} + \left(Q_S - h_S + h_g\right)\frac{\partial \rho_S}{\partial t} + \left(Q_m - h_m + h_g\right)\frac{\partial \rho_m}{\partial t}$$

Solid-phase decomposition kinetics:

$$\frac{\partial \rho_S}{\partial t} = -A_S\left(\rho_S - \rho_{Sf}\right)\exp\left(-E_S / RT_S\right)$$

The initial and boundary conditions are:

at $t = 0$, $0 < x < \delta$:

$$Y_F(x,0) = 0, \quad Y_O(x,0) = Y_O \quad , \quad T(x,0) = T$$

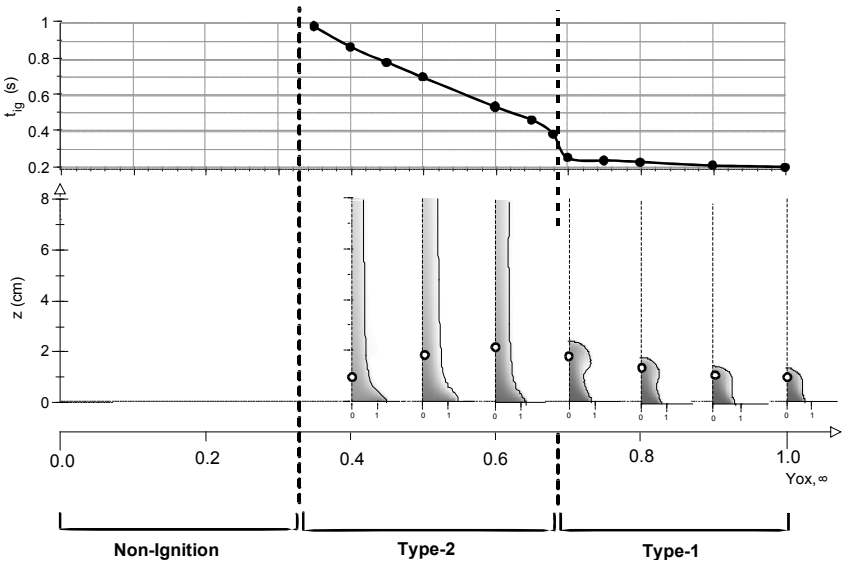


Figure 16 Effect of oxygen concentration on the location of point of autoignition according to the modeling results of Nakamura et al.; hollow black dot indicates location at which flame kernel first appears
(Copyright The Combustion Institute, used by permission)

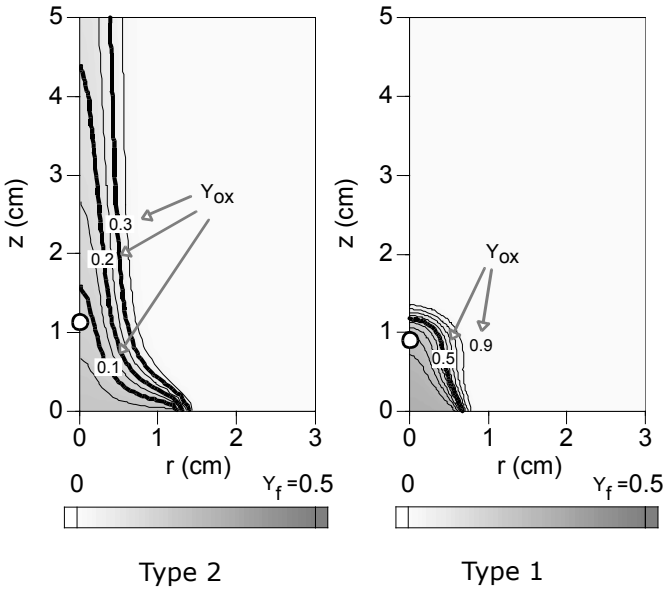


Figure 17 Vertical plume sections for the two ignition modes using the model of Nakamura et al.
(Copyright The Combustion Institute, used by permission)

at the solid/gas interface $t > 0$, $x = 0$:

$$\rho D \left.\frac{\partial Y_F}{\partial x}\right|_{x=0} = \dot{m}_S''\left(Y_F - Y_{FS}\right),$$

$$\rho D \left.\frac{\partial Y_O}{\partial x}\right|_{x=0} = \dot{m}_S''\left(Y_O\right),$$

$$-\lambda_S \left.\frac{\partial T_S}{\partial x}\right|_{x=0} = -\lambda \left.\frac{\partial T}{\partial x}\right|_{x=0} - \varepsilon\sigma\left(T_S^4 - T_\infty^4\right)$$

$$= \alpha_s \dot{q}_e'' - h_c\left(T_S - T_\infty\right) - \varepsilon\sigma\left(T_S^4 - T_\infty^4\right) - \dot{m}_S'' Q$$

at the edge of the boundary layer $x = \delta$, $t > 0$:

$Y_F(\delta,t) = 0$, $Y_O(\delta,t) = Y_{O\infty}$, $T(\delta,t) = T_\infty$, $\dot{q}_r'' = \dot{q}_e''$

at the back face of a thick solid:

$T_S(L,t) = T_\infty$

where:

A = gas-phase pre-exponential factor ($m^3\ s^{-1}\ kg^{-1}$)
A_S = solid-phase pre-exponential factor (s^{-1})
C = gas-phase heat capacity (kJ $kg^{-1}\ K^{-1}$)
E = activation energy of gas phase reaction (kJ mol^{-1})
E_S = activation energy of solid phase reaction (kJ mol^{-1})
h = enthalpy (kJ kg^{-1})
h_c = convective heat transfer coefficient (kW $m^{-2}\ K^{-1}$)
Δh_c = heat of combustion (kJ kg^{-1})
L = fuel thickness (m)
$\dot{m}''$ = fuel mass flux from solid (kg $m^{-2}\ s^{-1}$)
$\dot{m}_S'' = (\rho u)_S$
$\dot{q}_e''$ = specified external heat flux (kW m^{-2})
$\dot{q}_r''$ = radiant flux (kW m^{-2})
Q_m = heat of moisture desorption (kJ kg^{-1})
Q_S = heat of gasification of fuel (kJ kg^{-1})
t = time (s)
T = gas temperature (K)
T_S = surface temperature (K)
u = gas velocity (m s^{-1})
x = distance perpendicular to fuel surface (m)
Y_F = mass fraction of fuel vapors in the gas phase (--)
Y_O = mass fraction of oxygen in the gas phase (--)
α_s = absorptivity of surface (--)
δ = boundary layer thickness (m)
ε = emissivity of surface (--)
λ = thermal conductivity (kW m-1 K^{-1})
ρ = density of gas (kg m^{-3})
ρ_S = density of solid (kg m^{-3})
ρ_{Sf} = density of char (kg m^{-3})
σ = Stefan-Boltzmann constant (5.67×10^{-11} kW $m^{-2}\ K^{-4}$)

and the subscripts F, g, m, O, and S denote fuel, gas, moisture, oxygen, and surface, respectively.

Atreya made certain simplifications in the above equations, based on physical insight. In the gas-phase energy balance, the term $\partial \dot{q}_r'' / \partial x$ was neglected since its effect is small except at very large heat flux values. In the solid-phase equations, the terms with the subscript m denote fuel-moisture and Atreya confined his solutions to situations where moisture effects can be ignored. The term $\partial h_g / \partial x$ represents the heat transfer due to flow of volatiles within the solid; Atreya ignored this contribution since it is small prior to ignition. The term $\partial q_r / \partial x$ represents the diathermancy of the solid and was ignored. A number of other simplifications can be made on the solid-phase energy balance equation, depending on the traits of the material being considered, and Atreya illustrated several of those.

The above model can represent both autoignition and piloted ignition. For piloted ignition, it is necessary to add a pilot energy source. Atreya did this following the scheme of Tzeng[50], whereby a t hin gas layer at some distance above the surface is intermittently brought up to adiabatic flame temperature in order to 'test' for the possibility of establishing a flame.

Atreya's model was able to show very successful predictions for the mass loss rate of wood needed for ignition. Figure 18 shows the graphical solution from his model using parameter values that are representative for wood. The solution is defined by the point where the straight line (representing the gas phase solution) intersects the rising curves. Since the chemical kinetics of the solid phase was not fully known, Atreya used two values for a non-dimensional pre-exponential factor A*, where $A^* = \frac{A_S L^2 \rho_S C_S}{\lambda_S}$. Depending on which one is chosen, $\dot{m}'' \approx 1.5 - 1.6$ g $m^{-2}\ s^{-1}$ was predicted. Since the lowest (and presumably the most accurate) experimental measurement, as shown above, is 1.8 g $m^{-2}\ s^{-1}$, the agreement can be considered excellent. Atreya's theoretical calculations also show that over the heat flux range 20 – 40 kW m^{-2}, both the minimum $\dot{m}''$ and T_{ig} are essentially independent of heat flux.

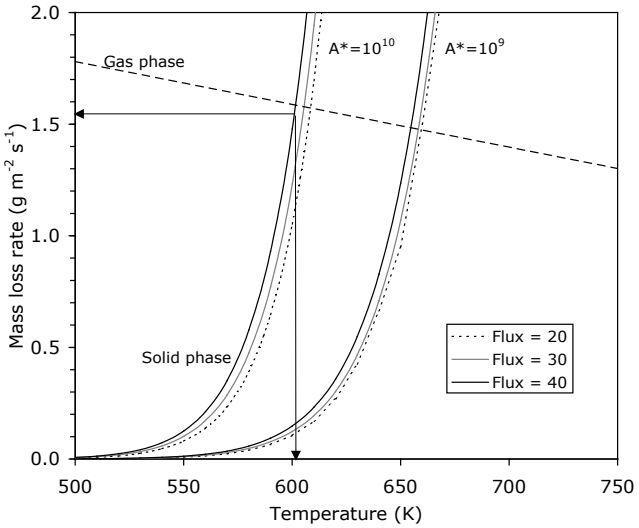


Figure 18 Atreya's theoretical prediction of the MLR of wood needed for piloted ignition. Ignition point occurs at the value where solid phase and gas phase MLR values are identical. The point shown corresponds to heat flux = 40 kW m^{-2}, A* = 10^{10} and gives T_{ig} = 605 K, MLR = 1.59 g m^{-2}.

ENGINEERING TREATMENTS FOR THERMALLY THICK SOLIDS

In the discussion above, it was made clear that, at the present time, computation of the ignition of solids (as with most ignition problems) cannot be done from first principles without a tremendous computational effort. Even if computational effort were not a consideration, all of the advanced theories necessarily require a large collection of input constants which will not be available for most materials, except perhaps if the chosen material has already been the subject of a doctoral dissertation. But this does not mean that only task-specific testing is of value. Theories of modest complexity exist which allow experimental data to be interpolated, extrapolated, and collapsed to just a few constants. The normal radiant ignition experiment consists of exposing a specimen to a known heat flux and recording the ignition time. This can be done at a range of heat fluxes and the result will be a table of data pairs (flux, time). It is the purpose of a simplified theory to enable these data to be analyzed in such a way that all of the information is captured in only a few variables, which can be viewed as 'quasi-properties' of the substance. Thus, as shown below, a data table which may have dozens of entries is collapsed to 3 variables.

Most of the practical work has been done for the 1-dimensional simplification, thus, this will be the focus of the present section. We divide the problem first into thermally-thick and thermally thin materials, then consider the situation when thick/thinness is uncertain. By 1-dimensional, it is meant that width and length of the specimen face are much larger than the depth and that the heated area is either the full size of the face or at least much larger than the specimen thickness. This criterion for 1-dimensional behavior is highly simplified, and we shall also consider experimental data on this point later in this Chapter.

Most of the theoretical analyses intended to be used as aids for data analysis ignore all chemistry, both in the gas phase and in the solid. With models of this type, a mathematical solution cannot be made for the ignition temperature. Instead, the ignition temperature is treated:

- as an experimentally measured value; or
- as a data-fit parameter; or
- by formulating the model to avoid the ignition temperature concept.

Measuring surface temperatures accurately is highly challenging. If thermocouples are used, very fine thermocouples are required and great pains taken to make sure they are truly at the surface, neither standing proud nor being recessed. It has been concluded within the profession that making these measurements accurately is only feasible in the context of research programs, not for ordinary testing purposes. If optical radiation methods are used, different sets of difficulties and errors are encountered, but an accurate measurement is not made easier. This leaves schemes that impute the T_{ig} from quantities that are experimentally measured, versus methods which bypass the need for an ignition temperature. Most of the practical schemes have focused on the former, but it will be shown that, for many purposes, the latter approach has significant merit.

In this section, we will consider the solid as being inert. The assumption that the solid is inert may seem to be an unreasonably drastic one—after all, if the solid were inert, no ignition would ever occur! Nonetheless, several investigators[11,61] found that experimental temperature distributions measured in ignition studies are very similar to those computed for inert bodies, and that effects such as diathermancy (non-opaqueness) and heats of reaction and phase change can often be neglected. Both from experiments and from numerical calculations, it has been found that at modest heat fluxes most of the ignition time is devoted to thermal heating of the solid. Actual chemistry in the solid, at the interface, or in the gas phase plays a significant role only during a short time interval just preceding ignition. For this reason, reasonable agreement between experiment and calculation can be obtained by using solutions which entirely ignore chemistry and simply solve the inert heating of a slab. The above simplification becomes progressively less accurate at high heat fluxes (say, over 200 kW m^{-2}) and short ignition times (milliseconds). The latter conditions will rarely be encountered in accidental fires, but are common in many combustion studies, especially where propellants are being modeled. When using a model that represents the substance as an inert solid, in addition to not being able to obtain a theoretical value of ignition temperature, there is a second limitation—since the substance is assumed inert, the loss of mass during heating is not modeled, thus, a mass loss rate criterion cannot be used to determine when ignition occurs. However, as the review of the topic above showed, it is also difficult to determine accurately the MLR at ignition experimentally. Thus, most engineering treatments ignore MLR.

To formulate the problem, it is first necessary to understand (or to review, as the case may be) concepts of heat conduction. To do this, it is appropriate to begin with the First Law of thermodynamics, which states that—if mechanical work is not involved in the problem—for any control volume:

$$\begin{bmatrix}\text{Amount of energy}\\ \text{added to system}\end{bmatrix} + \begin{bmatrix}\text{Stored energy of mass}\\ \text{entering system}\end{bmatrix} - \begin{bmatrix}\text{Stored energy of mass}\\ \text{leaving system}\end{bmatrix} = \begin{bmatrix}\text{Net increase in stored}\\ \text{energy of system}\end{bmatrix}$$

We will consider the material to be inert, and will consider the simplest case of a slab where changes only in one direction (the x-direction) need to be considered. The second and third terms in the above equation will be zero if no mass is entering or leaving the control volume. The rate at

which heat flows in at any location x is $\dot{q}$ and the rate at which heat flows out at location $x+dx$ is

$$\dot{q} + \frac{\partial \dot{q}}{\partial x} dx$$

Thus, the net heat flow in is

$$\dot{q} - \left(\dot{q} + \frac{\partial \dot{q}}{\partial x} dx \right) = - \frac{\partial \dot{q}}{\partial x} dx$$

For an inert solid, the heat flow at any location is governed by the *Fourier equation*. This empirically-derived equation states that the heat flow per unit area is proportional to the gradient of temperature in the body and to a material property which is termed the *thermal conductivity*. The Fourier equation is:

$$\dot{q} = - \lambda \frac{dT}{dx}$$

where λ = thermal conductivity (W m^{-1} K^{-1}). The minus sign in the above equation comes about because of the axiom of thermodynamics which states that heat flows from the hotter place to the cooler one. Then, the net heat flow (what is coming in one face of the slab, minus what is leaving the other) is:

$$- \frac{\partial}{\partial x} \left(- \lambda \frac{\partial T}{\partial x} \right) = \lambda \frac{\partial^2 T}{\partial x^2}$$

where we were able to take λ outside the outer derivative by assuming that it is a constant, independent of x. If the heat capacity and the density are constant (not necessarily always a realistic assumption) and there are no changes of phase (e.g., melting), then the heat stored in the control volume can be expressed as:

$$\rho C \frac{\partial T}{\partial t} dx$$

Then equating the net heat flow in to the heat stored gives:

$$\rho C \frac{\partial T}{\partial t} = \lambda \frac{\partial^2 T}{\partial x^2}$$

This is a partial differential equation for T, as a function of x and t. By consulting any textbook on heat transfer, the extension of this result to three dimensions can be found. For the three-dimensional case, the heat conservation equation is written as:

$$\rho \, C \frac{\partial T}{\partial t} = \lambda \nabla^2 T$$

where the notation $\nabla^2 T$ denotes $\dfrac{\partial^2 T}{\partial x^2} + \dfrac{\partial^2 T}{\partial y^2} + \dfrac{\partial^2 T}{\partial z^2}$

The initial condition for the problem is:

$$T(x) = T_o \qquad \text{for all } x, \text{ for } t < 0.$$

If the front face is heated by an incident heat flux $\dot{q}''_e$ (kW m^{-2}) and loses heat by convection and re-radiation, then the front-face boundary condition is:

$$- \lambda \frac{\partial T_s}{\partial x} = h_c \left(T_o - T_s \right) + \alpha_s \dot{q}''_e - \varepsilon_s \sigma \left(T_s^4 - T_o^4 \right)$$

where h_c = convective heat transfer coefficient (W m^{-2} K^{-1}), the temperature of the gas near the surface is T_o (K) which is taken to be the same as the solid's initial temperature, σ = Stefan-Boltzmann constant (5.67 $\times 10^{-11}$ kW m^{-2} K^{-4}), ε_s = emissivity of surface (–), and α_s = absorptivity of surface (–). Atreya[62] obtained an approximate analytical solution for this case, however, the solution was cumbersome. Panagiotou and Delichatsios[63] provided another approximate analytical solution, although, again, experimental data could not be evaluated or correlated without the use of a computer program. Consequently, they do not appear to have promise for engineering applications. It is interesting to note that Atreya examined in detail the ignition behavior of wood and concluded that the inert-body assumption is not a serious limitation for that material. The heat of pyrolysis of wood, of course, is not zero, but has both endothermic and exothermic peaks over a range of temperatures. But, unless highly accurate solutions are sought, Atreya concluded that assuming a zero heat of pyrolysis does not lead to appreciable errors.

DEVELOPMENT OF APPROXIMATE SOLUTIONS

Lawson and Simms[12] were the first to consider the inert-heating equation as a starting point for developing a method for treating experimental data. Their solution was based on the solid being very thick. This is called 'semi-infinite' in mathematical terminology and is referred to as a 'thermally-thick' body in heat transfer studies. We will return below to consider what thickness a real solid must have in order to be treatable as a thermally-thick body. Lawson and Simms took the boundary condition at the front face of a semi-infinite solid to be:

$$- \lambda \frac{\partial T}{\partial x} = \dot{q}''_e - h_{eff} \left(T_{ig} - T_o \right)$$

Thus, it is assumed that all of the incident heat flux $\dot{q}''_e$ is absorbed by the body, in other words, that the surface is black ($\alpha_s = 1$). Except possibly for very brief ignition times, realistic solutions will not be obtained if front-face heat losses are ignored. The heat losses are twofold: (1) as the surface temperature starts rising, it begins to exceed the ambient temperature and, therefore, a convective cooling stream starts in motion; and (2) the surface can radiate heat, in addition to absorbing it, and as the surface temperature rises, its re-radiated component will start becoming significant. Since the latter is proportional to T^4, an exact solution would be difficult. Thus, Lawson and Simms lumped the re-radiated term into the convective term by use of a fictitious value of the convective transfer coefficient h_{eff}, where h_{eff} has some value greater than the purely-convective heat transfer coefficient h_c. With this boundary condition, and the initial condition $T(x) = T_o$ for all x, the heat transfer problem has the classical solution[137]:

$$T_{ig} - T_o = \frac{\dot{q}''_e}{h_{eff}} \left[1 - \exp(\tau) \, \text{erfc}\left(\sqrt{\tau} \right) \right]$$

where $\tau = h_{eff}^2 t_{ig} / \lambda\rho C$ is the non-dimensional ignition time. If $\alpha_s \neq 1$, then the results are the same, except that the non-dimensional ignition time becomes defined as: $\tau = h_{eff}^2 \alpha_s t_{ig} / \lambda\rho C$. The above is a mathematically complete solution, but it is not readily usable. A minor obstacle is the fact that the complementary error function *erfc* is a mathematical function which requires use of tables or approximations. If a program is available* which evaluates *erfc*, then the bigger obstacle remains that the solution is not explicit for the dependent variable. Normally, one specifies a value of $\dot{q}_e''$ and wishes to compute the value of t_{ig}. Yet, the above solution is readily workable only if one knows t_{ig} and wishes to solve for $\dot{q}_e''$. Another difficulty is that there are two separate groups of variables which have embedded in them the physical properties: $h_{eff}\left(T_{ig} - T_o\right)$ and $h_{eff}^2 \alpha_s / \lambda\rho C$. If the values of those were known, then $\dot{q}_e''$ could be obtained by specifying t_{ig}. But from the user's point of view, the desired scheme is the following:

(a) measure the ignition time at several values of $\dot{q}_e''$;
(b) obtain some constants from these results;
(c) insert these constants into some simple formula which will give t_{ig} for any value of $\dot{q}_e''$ inputted.

A number of schemes have been proposed to accomplish this, and we now examine some of the better-known ones.

Lawson and Simms proposed that for large τ values an approximation based on a series expansion can be made, giving:

$$T_{ig} - T_o = \frac{\dot{q}_e''}{h_{eff}}\left[1 - \frac{1}{\sqrt{\pi}}\left(\frac{1}{\tau^{1/2}} - \frac{1}{2\tau^{3/2}} + \frac{3}{4\tau^{5/2}} - \ldots\right)\right]$$

$$\approx \frac{\dot{q}_e''}{h_{eff}}\left[1 - \frac{1}{\sqrt{\pi\tau}}\right] = \frac{\dot{q}_e''}{h_{eff}}\left[1 - \frac{1}{h_{eff}}\sqrt{\frac{\lambda\rho C}{\pi\, t_{ig}}}\right]$$

This equation was not highly accurate in correlating their experimental data, which did not extend to very long ignition times. Thus, Simms[64] provided a second approximation, for $\tau \rightarrow 0$:

$$T_{ig} - T_o = \frac{\dot{q}_e''}{h_{eff}}\left[\frac{2}{\sqrt{\pi}}\tau^{1/2} - \tau + \frac{4}{3\sqrt{\pi}}\tau^{3/2} - \frac{1}{2}\tau^2 + \ldots\right]$$

$$\approx 2\dot{q}_e''\sqrt{\frac{t_{ig}}{\pi\lambda\rho C}}$$

It can be noted that the convective heat loss coefficient h_{eff} does not enter the above approximation; thus, it cannot be expected to be realistic for correlating real data, except at very large irradiances, where convective losses are indeed negligible. At high heat fluxes, if a thermally-thick solid ignites very fast, then the effect of convective cooling of the front face can properly be ignored. Simms[65] proposed that convection may be neglected if:

$$h\sqrt{\frac{t_{ig}}{\lambda\rho C}} \leq 0.12$$

The two expressions of Lawson and Simms allowed trends to be identified for very short and very long ignition times, but did not give an equation which would be accurate for correlating a full range of experimental data. It can be shown that range $0.1 < \tau_{ig} < 5$ is not acceptably approximated even by using the 'full' 4-term approximations given above; using only one or two terms leads to a much more serious 'missing middle.'

In a similar vein, Quintiere[66] suggested another two approximations, but he proposed that the whole range of ignition times can be covered by a piecewise-continuous approximation:

$$T_{ig} - T_o \approx \frac{\dot{q}_e''}{h_{eff}}\frac{2}{\pi}\sqrt{\tau} = \frac{\dot{q}_e''}{h_{eff}}\frac{2}{\sqrt{\pi}}\sqrt{\frac{h_{eff}^2 t_{ig}}{\lambda\rho C}} \qquad \text{for } \tau \leq 0.8$$

$$T_{ig} - T_o \approx \frac{\dot{q}_e''}{h_{eff}} \cdot 1 = \frac{\dot{q}_e''}{h_{eff}} \qquad \text{for } \tau > 0.8$$

Or, grouping the constants,

$$T_{ig} - T_o \approx \frac{\dot{q}_e''}{h_{eff}} b\sqrt{t_{ig}} \qquad \text{for } t \leq t_m$$

and

$$T_{ig} - T_o \approx \frac{\dot{q}_e''}{h_{eff}} \qquad \text{for } t > t_m.$$

where t_m is the value of dimensional time that corresponds to the dimensionless $\tau = 0.8$ and b is a constant. Quintiere proposed that, for convenience, the function $[1 - \exp(\tau)\,\mathrm{erfc}(\sqrt{\tau})]$ be designated as $F(\tau)$. Figure 19 shows his approximation, the 4-term versions of Simms' approximations, and the true value of the function.

In order to progress from mathematical approximations to a viable data-handling protocol, Buschman[10] was the first to suggest that what is needed to correlate experimental data is simply a relation between the heat flux and the time. He proposed that:

$$t_{ig}^{-n} = C\left(\dot{q}_e'' - \dot{q}_{cr}''\right)$$

where C, n, and $\dot{q}_{cr}''$ are experimental constants. As discussed above, Atreya had obtained a comprehensive solution to the inert-solid problem, including both convection and re-radiation at the face. Abu-Zaid[67] took Atreya's complex solution and demonstrated that, to a reasonably small error, it could be represented as

* Current-day spreadsheets normally have the function *erfc* built in, however, it must be noted that using directly the *exp* and *erfc* functions of spreadsheet programs leads to gross errors for τ_{ig} greater than about 30; this occurs because a very large number is being multiplied by a very small one. To make a correct evaluation for $\tau_{ig} > 30$, it is necessary to use an approximation that is suitable for large τ_{ig}, instead.

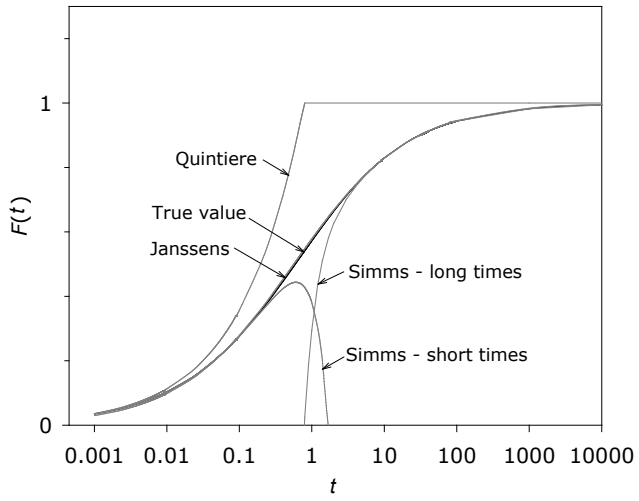


Figure 19 Various approximations to the semi-infinite solid ignition function

$$t_{ig}^{-0.5} = C\left(\dot{q}''_e - \dot{q}''_{cr}\right)$$

and where C and $\dot{q}''_{cr}$ remain experimental constants. Thus, he provided a theoretical justification for Buschman's empirical approach. While the same conclusion can be arrived at by extreme simplifications of the heat transfer problem, Abu-Zaid demonstrated that it is not necessary to ignore re-radiation or convection, nor to limit the validity to very small or very large ignition times. In the same vein, Smith and Satija[68] proposed that the concept be generalized to non-constant heat fluxes by adoption of a *flux-time product*, FTP, where:

$$FTP = \int_0^{t_{ig}} \left(\dot{q}''_e(t) - \dot{q}''_{cr}\right) dt$$

These authors did not provide a mathematical justification for their procedure and replaced n = ½ with n = 1, which would be appropriate only for thermally-thin materials. Later, several authors[69,70] revived the idea, but provided for a variable n, so that thermally-thick and thermally-thin materials could be encompassed:

$$FTP = \int_0^{t_{ig}} \left(\dot{q}''_e(t) - \dot{q}''_{cr}\right)^n dt$$

In what was the most ambitious study of piloted ignition to that time, in 1971 Hallman[71] published a dissertation where he included the first systematic determination of the spectral absorption characteristics for a large variety of plastics and enabled values of α_s to be computed. With these data in hand, Hallman started with the Lawson/Simms approximation for very short ignition times:

$$t_{ig} \approx \frac{\pi}{4} \frac{(\lambda\rho C)\left(T_{ig} - T_o\right)^2}{\left(\alpha_s \dot{q}''_e\right)^2}$$

He then attempted to use the above equation as a basis for a correlation, but with adjustable exponents. Using handbook values of room-temperature $\lambda\rho C$ data, he arrived at the best-fit formula:

$$t_{ig} = \frac{1035\left(\lambda\rho C\right)^{0.75}\left(T_{ig} - T_o\right)^{1.04}}{\left(\alpha_s \dot{q}''_e\right)^2}$$

The results, however, showed a high degree of scatter about the predicted values. The notably low exponent for the ignition temperature term arose because Hallman did not follow the recommendation of Buschman to include the $\dot{q}''_{cr}$ term. In a similar exercise, Tewarson[72] proposed that data be plotted in the form:

$$t_{ig} = \frac{\pi}{4} \frac{(\lambda\rho C)\left(T_{ig} - T_o\right)^2}{\left(\dot{q}''_e - \dot{q}''_{cr}\right)^2}$$

or

$$t_{ig} = \frac{\pi}{4}\left[\frac{TRP}{\dot{q}''_e - CHF}\right]^2$$

where the *thermal response parameter*, TRP (kW s$^{1/2}$ m^{-2}), is defined as: $TRP = (\lambda\rho C)^{1/2}\left(T_{ig} - T_o\right)$ and $CHF \equiv \dot{q}''_{cr}$. In this formula, the value of α_s has effectively been set to 1.0, since in the Factory Mutual Flammability Apparatus, which is the test method used by FM to determine the TRP, the specimen surface is blackened prior to test. Tewarson's procedure uses reasonable exponents for the various factors, since he does not leave out the important $\dot{q}''_{cr}$ term. Koohyar[73] reviewed a variety of additional early approximate treatments.

The *minimum flux for ignition* is also a variable which is amenable to theoretical analysis. By definition, this heat flux is the minimum for which a surface temperature of T_{ig} may be achieved. If it is assumed that the minimum flux for ignition will occur at such a long time that the substance will be in thermal equilibrium, then the temperature gradient at the surface of a semi-infinite solid becomes zero. Consequently, the conduction loss is zero, and the heat balance at the surface is:

$$\alpha_s \dot{q}''_{\min} - h\left(T_{ig} - T_o\right) - \varepsilon_s \sigma T_{ig}^4 - \dot{m}''_{\min} L_v = 0$$

where ε_s = surface emissivity (--), $\dot{m}''_{\min}$ = minimum mass loss rate for ignition (kg m^{-2} s^{-1}), L_v = total heat of gasification (kJ kg^{-1}), and values of temperature are expressed in Kelvins. This equation can be directly solved for $\dot{q}''_{\min}$ if all the other quantities are known. But, in practical applications, the other quantities will rarely be known. The variables α_s, ε_s, and L_v can be obtained only with laborious measurements*, while correct values of $\dot{m}''_{\min}$ are so diffi-

* In many cases, the assumption is made that $\varepsilon = \alpha_s$. This is not necessarily true. According to Kirchoff's Law, ε is equal to α_s at a *given* radiation wavelength. But since the spectral distribution of the source radiation is not the same as that of the target being emitted by the target, the wavelength-averaged ε will generally be somewhat different from the wavelength-averaged α_s. In practice, for most problems there is no alternative but to assume that $\varepsilon = \alpha_s$.

cult to determine that it is still unclear whether the best-available results are sufficiently accurate. By contrast, it is simple and inexpensive to determine $\dot{q}''_{\min}$ experimentally; consequently, this variable is almost always measured, not computed.

JANSSENS' PROCEDURE

In 1966, Keller et al.[74] observed that data from the ignition of propellants at high radiant or convective heat fluxes could be well correlated if heat flux is plotted on the x-axis, square root of ignition time on the y-axis, and a line with a slope of –0.92 is drawn to the points. This, of course, is equivalent to plotting heat flux on the x-axis and $t_{ig}^{-0.543}$ on the y-axis. Some 25 years later, Janssens rediscovered this same fact, and proceeded to place it on a sounder mathematical footing. The procedures he evolved are today the best means of analyzing ignition data for thermally thick solids and for interpolating or extrapolating from those results.

Janssens[75,76] started with the solution for the case of a semi-infinite slab being heated by radiation and cooled by convection (that is, lumping the surface re-radiation term into an effective convection coefficient h_{eff}). The difficulty is that solution for the front-face temperature,

$$T_{ig} = T_o + \frac{\alpha_s \dot{q}''_e}{h_{eff}} \left[1 - \exp(\tau)\operatorname{erfc}\left(\sqrt{\tau}\right)\right]$$

cannot be evaluated by simple means, and most previous efforts at producing an approximation gave expressions which were only accurate at the extremes of $t_{ig} \rightarrow \infty$ or $t_{ig} \rightarrow 0$, but not for a wide range of intermediate values. Janssens attacked the problem by a statistical approach, and found that a good approximation* was:

$$\left[1 - \exp(\tau)\operatorname{erfc}\left(\sqrt{\tau}\right)\right] \approx \frac{1}{1 + 0.73\tau^{-0.55}}$$

Janssens then demonstrated that the approximation also holds for the more realistic case where heat losses include both a convection term, proportional to T^1, and a radiation term, proportional to T^4. At the critical flux, it can be assumed that the ignition time $t_{ig} \rightarrow \infty$ (although we shall later see that this is not exactly true). Thus:

$$T_{ig} \approx T_o + \frac{\alpha_s \dot{q}''_{cr}}{h_{eff}}[1.0]$$

which allows the effective convective coefficient to be expressed as:

$$h_{eff} = \frac{\alpha_s \dot{q}''_{cr}}{\left(T_{ig} - T_o\right)}$$

Combining the above equations and eliminating ($T_{ig} - T_o$) gives:

$$\dot{q}''_e = \dot{q}''_{cr}\left[1 + 0.73\left(\frac{\lambda\rho C}{h_{eff}^2 t_{ig}}\right)^{0.55}\right]$$

This result has great significance for the practical application of radiant ignition data. It implies that if experimental data are plotted such that $\dot{q}''_e$ is put on the x-axis and $t_{ig}^{-0.55}$ on the y-axis, then the data will fall in a straight line, with the x-axis intercept being $\dot{q}''_{cr}$. The plot to be made is illustrated in Figure 20. In some cases, it is found[77] that the minimum flux at which ignition takes place, $\dot{q}''_{\min}$, is substantially greater than $\dot{q}''_{cr}$. The minimum flux is determined experimentally as being halfway between the lowest flux at which ignition was found and the highest flux at which no ignition occurs for long exposure times. The critical flux, on the other hand, is a variable only determined by data plotting, and is simply the x-axis intercept. When $\dot{q}''_{\min}$ is substantially larger than $\dot{q}''_{cr}$, it is empirically found that more realistic predictions of T_{ig} are obtained if $\dot{q}''_{\min}$, and not $\dot{q}''_{cr}$, is used in the above series of equations. This is illustrated in the example problem below. The collection of experimental data points, in any case, is represented by just three variables: $\dot{q}''_{cr}$, $\dot{q}''_{\min}$, and the slope of the straight line.

While the concept has received little study, clearly the existence of a $\dot{q}''_{\min} > \dot{q}''_{cr}$ implies that there is a *maximum time of ignition*. In other words, there are not ignition times that $\rightarrow \infty$, instead, no ignition is feasible beyond some finite time. This is mandated by elementary chemical kinetics, since reactants are progressively exhausted at any finite temperature. In this case, the reaction products, which also diminish if the reactants are consumed, are the combustible pyrolysis gases that will or will not ignite.

Once a plot such as shown in Figure 20 is made, interpolations or extrapolations can be made directly from the straight line plotted. But for some modeling purposes, it is also desired to deduce the effective thermophysical properties of the specimen. Using Janssens' procedure this is done as follows. The assumption is made that values of h_c and α_s are known. The former is a function of the test environment, rather than of the specimen. The actual value of h_c is not a true constant, but has a slight dependence on the temperature difference between the gas stream and the surface. In the case of the Cone Calorimeter apparatus (test method details are presented at the end of this Chapter), a number of slightly different values have been proposed[78-80], but commonly $h_c \approx 0.013$ kW m^{-2} K^{-1} is chosen for both horizontal and vertical specimen orientations. For more precise work, Janssens recently found that that h_c varies somewhat with the irradiance used. This is understood to be due to the fact that the heater acts as a pump of air, thus creating, in effect, some forced convection. For specimens in the hori-

* Janssens also showed that a usable approximation can be made by using $\tau^{-0.5}$, although a less good one.

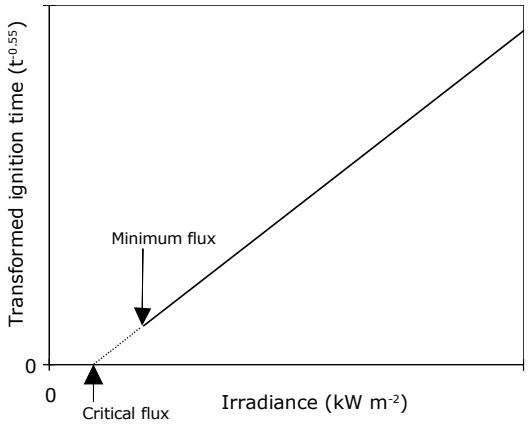


Figure 20 The main variables of the ignitability plot

zontal orientation[81,82] Janssens obtained results that could be well represented by:

$$h_c = 6.56\times10^{-3}\cdot\dot{q}_e''^{0.35}$$

These newly-recommended values are quite a b it higher than found by previous researchers, for unidentified reasons. For example, in his new study, h_c = 0.0202 kW m^{-2} K^{-1} at 25 kW m^{-2} irradiance and h_c = 0.0258 kW m^{-2} K^{-1} at 50 kW m^{-2} irradiance. Janssens further recommended that a linear approximation can be used:

$$h_c = 0.0118 + 3.4\times10^{-4}\,\dot{q}_e'' \qquad \dot{q}_e'' < 50 \text{ kW m}^{-2}$$

$$h_c = 0.0255 + 6.5\times10^{-5}\,\dot{q}_e'' \qquad \dot{q}_e'' \geq 50 \text{ kW m}^{-2}$$

For the vertical orientation, Janssens[83] found values about 10 – 15% than for the horizontal orientation. This is as expected from normal considerations of convective heat transfer. For the LIFT apparatus, which likewise uses vertically-oriented specimens, a value of h_c = 0.015 kW m^{-2} K^{-1} is specified in the ASTM standard[66]. However, Dietenberger showed that this quantity is also flux-dependent[84]. His suggested relation is:

$$h_c = \left(0.0139 - 0.0138x\right)\left(\dot{q}_{50}''\right)^{1/4}$$

where x = lateral distance (m) along specimen, measured from the hot end, and $\dot{q}_{50}''$ denotes the heat flux measured at the 50 mm distance. Using this expression for the location x = 0.05 m, h_c = 0.0295 kW m^{-2} K^{-1} at 25 kW m^{-2} irradiance and h_c = 0.0351 kW m^{-2} K^{-1} at 50 kW m^{-2} irradiance. The LIFT value is higher than for vertical specimens in the Cone Calorimeter because a more powerful heater is present in the LIFT apparatus, and this raises the convective heat flow. Using any of the non-constant expressions makes data analysis difficult. Thus, it may be best to adopt an average, constant value for the flux range of interest. This is especially true in view of the fact that the flux-dependent studies have all thus far been done only in one laboratory each and have not been corroborated by testing in other laboratories.

For the absorptivity α_s, a measured value should be used if available. If it is not, Table 32 indicates that the average value for a wide range of plastics is 0.88, which is also the identically same value as adopted by Janssens for use with wood products; thus α_s = 0.88 should be used for treating Cone Calorimeter data. For LIFT data, the physics is, of course, no different, but the standard data treatment procedure[66] mandates that $\alpha_s \equiv 1.0$ be used. With values of h_c and α_s in hand, the procedure becomes:

1. Obtain a series of ignition times at varying heat fluxes.
2. Plot $t_{ig}^{-0.55}$ on the y-axis, as a function of $\dot{q}_e''$ on the x-axis. Note that the units for the x-axis are to be (kW m^{-2}).
3. Fit a straight line to the data points and determine the critical irradiance $\dot{q}_{cr}''$ as the x-axis intercept.
4. Evaluate the slope of the straight line. The inverse of slope is defined as a constant, B_{ig} :

$$B_{ig} = \frac{1}{\text{slope}}$$

5. Obtain T_{ig} by a trial-and-error solution of the relationship:

$$\frac{\dot{q}''_{\min}}{\left(T_{ig} - T_\infty\right)} = \frac{h_c}{\alpha_s} + \frac{\sigma\left(T_{ig}^4 - T_\infty^4\right)}{\left(T_{ig} - T_\infty\right)}$$

6. Solve for h_{eff} using :

$$h_{eff} = \frac{\alpha_s \dot{q}''_{\min}}{\left(T_{ig} - T_o\right)}$$

7. Compute the apparent $\lambda\rho C$ as:

$$\lambda\rho C = h_{eff}^2\left[\frac{B_{ig}}{0.73\,\dot{q}''_{\min}}\right]^{1.828}$$

In adopting specific procedures for presenting data, such as outline above, it must be kept in mind that the slope of the line (and B_{ig}) is not a general material property, but depends on the exact theory used. For example, if, as in the Tewarson procedure, time to the –0.5, instead of –0.55 power were plotted, the slope will be different. What does *not* change, regardless of theory used, is the value of $\dot{q}''_{\min}$; this is because it is a direct experimental determination and is not subject to interpretation according to a mathematical theory.

Some materials may not show straight lines when plotted in the way suggested. The theory described above only pertains to thermally thick materials, and if the material is too thin, then data points at higher heat fluxes will fall on a straight line, but data points at low heat fluxes will deviate and will lie above that line. Janssens proposes that such cases be treated by only utilizing the data points which do fall on a reasonably straight line in deriving thermal properties. If a material is so thin as to be thermally thin over most of the exposure range, then it should be treated as thermally thin (see below).

Example

The values experimentally determined by Thomson for polyethylene using an apparatus similar to the Cone Calorimeter were:

Flux (kW m^{-2})	15	19	23	27	29	34	39
Ignition time (s)	NI	524	315	223	172	114	85

From these results, the minimum flux is determined as (15+19)/2 = 17 kW m^{-2}. The derived values to be plotted are heat flux on the x-axis and $t_{ig}^{-0.55}$ on the y-axis. These values are:

x-axis: Flux (kW m^{-2})	19	23	27	29	34	39
y-axis: $t_{ig}^{-0.55}$	0.0319	0.0423	0.0511	0.0589	0.0739	0.0869

The results are shown in Figure 21. A least-squares routine was used to pass the line of best fit through the 7 data points, giving an x-intercept of 7.9 kW m^{-2} and a slope of 0.00279. The critical irradiance, $\dot{q}''_{cr}$ thus is 7.9 kW m^{-2}. The value of B_{ig} = 1/0.00279 = 358. The values h_c = 0.013 kW m^{-2} K^{-1} and α_s = 0.88 are also used. If calculations are based on $\dot{q}''_{cr}$, then a trial-and-error solution for T_{ig} is obtained from:

$$\frac{\dot{q}''_{cr}}{(T_{ig} - T_\infty)} = h_c + \frac{\sigma(T_{ig}^4 - T_\infty^4)}{(T_{ig} - T_\infty)}$$

giving T_{ig} = 537 K = 264ºC. Thomson measured T_{ig} = 363ºC experimentally, thus this computed value is much too low. On the other hand, if calculations are based on $\dot{q}''_{\min}$:

$$\frac{\dot{q}''_{\min}}{(T_{ig} - T_\infty)} = h_c + \frac{\sigma(T_{ig}^4 - T_\infty^4)}{(T_{ig} - T_\infty)}$$

this gives T_{ig} = 675 K = 402ºC. The error here is much smaller than with the use of $\dot{q}''_{cr}$. Continuing the problem solution on the basis of using $\dot{q}''_{\min}$, h_{eff} is obtained from:

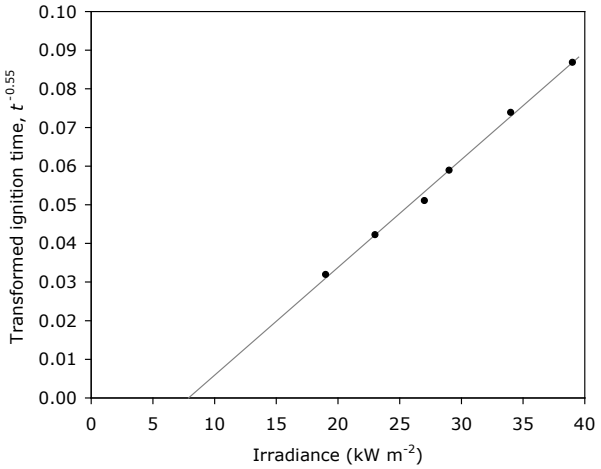


Figure 21 Polyethylene example problem—Janssens procedure

$$h_{eff} = \alpha_s \frac{\dot{q}''_{\min}}{(T_{ig} - T_\infty)}$$

giving $h_{\rm eff}$ = 0.0392 kW m^{-2} K^{-1}. Finally, the apparent thermal inertia $\lambda\rho C$ is obtained as:

$$\lambda\rho C = h_{eff}^2 \left[\frac{B_{ig}}{0.73\,\dot{q}''_{\min}}\right]^{1.828}$$

giving $\lambda\rho C$ = 0.716 kJ^2 m^{-4} s^{-1} K^{-2}.

Non-constant heat flux—generalization of Janssens' procedure

Generally, the external heat flux will not be constant. Then, there are two ways of dealing with this. For very rough approximations, one can simply average the heat flux and insert this value into the pertinent ignitability plot. For a more accurate solution, however, a time-resolved calculation must be made. To do this, we use Duhamel's theorem[85]. In Janssens' methodology, observe that in the ignitability plot, any point above the diagonal line denotes non-ignition, while any point on or below the line denotes ignition. We also note that B_{ig} is 1/slope. To find out if ignition occurs for any given time history of $\dot{q}''(t)$ then, the following integral must be evaluated[86]:

$$B = t^{0.05} \times \frac{1}{2}\int_0^t \frac{\dot{q}''_e(\tau) - \dot{q}''_{cr}}{\sqrt{t - \tau}}\, d\tau$$

The ignition criterion thus becomes: *Ignition occurs if* $B \geq B_{ig}$. The technique can be applied whenever a non-constant irradiance occurs and the $\dot{q}''_e(t)$ history is known. This procedure is only approximate, however, since the loss term is assumed to have a constant value, $\dot{q}''_{cr}$. But this value will only be attained at the moment of ignition—at earlier times, losses will be lower, since the surface temperature will be lower. Consequently, the method leads to lower values of B being computed than is actually the case.

QUINTIERE'S PROCEDURE

Because it has been used to develop a significant amount of published data, it is also important to understand Quintiere's procedure[66]. It is a part of the LIFT test procedure (see the *Test methods* section of this Chapter) but has sometimes also been used in connection with other experimental apparatuses. In this procedure, first a value of $\dot{q}''_{\min}$ is found experimentally. This is assumed to be occurring at steady state, thus

$$\alpha_s \dot{q}''_{\min} = h_c(T_{ig} - T_o) + \alpha_s \sigma(T_{ig}^4 - T_o^4)$$

As explained above, Quintiere assumes $\alpha_s \equiv 1$ and h_c = 0.015 kW m^{-2} K^{-1}. Inserting those values in the above gives:

$$\dot{q}''_{\min} = 0.015(T_{ig} - T_o) + \sigma(T_{ig}^4 - T_o^4)$$

From the above equation, T_{ig} is then calculated. Next, the linearized (effective) heat transfer coefficient h_{eff} is, by definition:

$$\dot{q}''_{\min} = h_{eff}\left(T_{ig} - T_o\right)$$

Thus, it can be solved for as:

$$h_{eff} = \frac{\dot{q}''_{\min}}{\left(T_{ig} - T_o\right)}$$

The expression for the ignition temperature of a thermally-thick slab is approximated as:

$$T_{ig} = T_o + \frac{\dot{q}''_e}{h_{eff}} F\left(\tau_{ig}\right)$$

where

$$F\left(\tau_{ig}\right) = \begin{cases} \dfrac{2h_{eff}\sqrt{t_{ig}}}{\sqrt{\pi\lambda\rho C}} & \text{for small } t_{ig} \\ 1 & \text{for large } t_{ig} \end{cases}$$

According to this, if $\sqrt{t_{ig}}$ is plotted on the x-axis and $\dot{q}''_{\min} / \dot{q}''_e$ on the y-axis, the data will fall along a straight line which passes through the origin and has the slope of $2h_{eff} / \sqrt{\pi\lambda\rho C}$; this slope is identified as b and has units of s^{-1}. In addition to the slope, the user must also determine the x-value at which the line crosses the horizontal line located at y = 1. The time at which this occurs is the break-point between 'small' and 'large' t_{ig} values and is denoted as t_m. Thus, the user procedure is summarized as follows:

1. Determine the value of $\dot{q}''_{\min}$ experimentally (Quintiere refers to this variable as $q_{o,ig}$).
2. Plot the data points by plotting $\sqrt{t_{ig}}$ on the x-axis and $\dot{q}''_{\min} / \dot{q}''_e$ on the y-axis.
3. Pass a straight line going through the origin through the data points. Quintiere's original study implies that data points should be left out of the correlation at the higher x-values if they visually appear to deviate from a reasonable line, but this is not explicitly explained there nor in the ASTM standard. The slope of the line is identified as b.
4. Calculate T_{ig} (K) by trial-and-error using the equation:
$$\dot{q}''_{\min} = 0.015\left(T_{ig} - T_o\right) + \sigma\left(T_{ig}^4 - T_o^4\right)$$
Alternatively, there is a chart provided in the ASTM standard for the LIFT test that presents the relationship between $\dot{q}''_{\min}$ and T_{ig}. Note that this equation, while generally similar to the one used by Janssens, produces significantly higher T_{ig} values, since the minimum, rather than the critical, heat flux is used.
5. Determine h_{eff} from:
$$h_{eff} = \frac{\dot{q}''_{\min}}{\left(T_{ig} - T_o\right)}$$
6. Determine the apparent thermal inertia, $\lambda\rho C$, from
$$\lambda\rho C = \frac{4}{\pi}\left(\frac{h_{eff}}{b}\right)^2$$

The final values that are reported using the Quintiere procedure are: $\dot{q}''_{\min}$, T_{ig}, and $\lambda\rho C$. Note that Quintiere's procedure, unlike Janssens', has no alternative for treating thermally-thin materials—all materials are treated as thermally-thick, irrespective of thickness.

Example

The same example as was used to illustrate Janssens' method will be used to illustrate Quintiere's method. The experimentally determined ignition times for polyethylene were:

Flux (kW m^{-2})	15	19	23	27	29	34	39
Ignition time (s)	NI	524	315	223	172	114	85

From these results, the minimum flux is determined as (15+19)/2 = 17 kW m^{-2}. The derived values to be plotted are obtained as:

x-axis points: $\sqrt{t_{ig}}$	22.89	17.75	14.93	13.11	10.68	9.22
y-axis points: $\dot{q}''_{\min} / \dot{q}''_e$	0.895	0.739	0.630	0.586	0.500	0.436

These values are now plotted as shown in Figure 22. The data point x = 22.89 was omitted from the correlation, since it appeared not to follow a straight line. Passing a straight line through the remaining points gave b = 0.0435. Given $\dot{q}''_{\min}$ = 17, trial-and-error solution gives T_{ig} = 674 K = 401ºC, compared to a value of was 363ºC measured by Thomson. Using T_{ig} = 674 K and solving, gives h_{eff} = 0.0446 kW m^{-2} K^{-1}. Finally, the apparent thermal inertia $\lambda\rho C$ is determined as 1.34 kJ^2 m^{-4} s^{-1} K^{-2}. As Janssens has observed[75], the value of thermal inertia obtained by the Quintiere procedure is higher than obtained by the Janssens procedure, due to the less-accurate approximation used for the analytical solution.

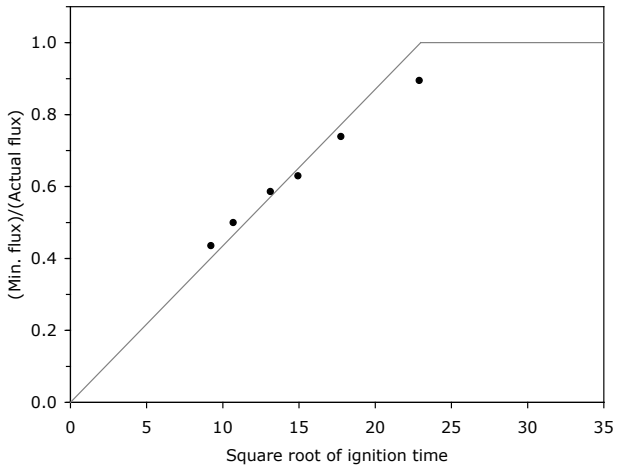


Figure 22 Polyethylene example problem—Quintiere procedure

TEWARSON'S PROCEDURE

Tewarson[72] starts from the equation

$$t_{ig} = \frac{\pi}{4}\frac{TRP^2}{(\dot{q}''_e - \dot{q}''_{cr})^2}$$

which was developed above. The procedure could be applied to any test apparatus, but in practice, most of the data using his analysis procedure has been obtained on the FM Fire Propagation Apparatus (see *Test methods*). In his procedure, ignition tests at even-5 kW m^{-2} irradiance values are run. The lowest value for which ignition is obtained is identified as the CHF, 'critical heat flux.' Note that this definition is not consistent with Janssens'. In fact, the CHF is a rough, biased determination of $\dot{q}''_{\min}$: rough because normally 1 or 2 kW m^{-2}, not 5 kW m^{-2}, steps are recommended; biased because the value of CHF that is reported is the lowest heat flux at which ignition did occur, not the mean between the lowest occurring and the highest non-occurring. The FM Fire Propagation Apparatus exposes specimens to radiation from a source which has a much higher effective radiating temperature than do room fires. Since under these conditions many materials show a much lower absorptivity than they do for radiation from room fires, a systematic error would be introduced into the procedure. An effort is made to reduce the error by blackening the specimens in the Tewarson procedure. For a black surface, $\alpha_s \equiv 1$, and this more closely represents the absorptivity of common materials for room-flame radiation. The ignition data are then plotted with $\dot{q}''_e$ on the x-axis and $t_{ig}^{-1/2}$ on the y-axis. A straight line is passed through the data points, from which TRP, the thermal response parameter, is obtained as:

$$TRP = \sqrt{\frac{4}{\pi}}\frac{1}{slope}$$

The units of TRP are kW s$^{1/2}$ m^{-2}. The only two values reported are TRP and CHF. Since the x-axis intercept will generally not be equal to CHF, the reporting procedure does not allow the user to construct a specific straight line: the slope is known, but the intercept is not. The information is deemed sufficient for FM purposes, since their hazard assessment procedures rank the ignitability of products solely on the TRP values, and actual ability to interpolate or extrapolate ignition times is not sought. Nicolette and Nowlen[87] have criticized Tewarson's procedure on the grounds that straight-line extrapolations can be seriously misleading, if actual data points are not collected to determine $\dot{q}''_{\min}$, since the real curve may be substantially different than an extrapolation from high-flux values.

OTHER DATA TREATMENT PROCEDURES

The procedure described by Janssens is the best available method for deriving thermophysical material properties from ignitability data. It is essential to point out that similar, but slightly different procedures tend to lead to significantly different values of the derived 'constants.' Fangrat has demonstrated[88] this fact quite clearly. This is not unexpected, since the thermal 'constants' are in actual fact temperature-dependent. An example of actual, temperature-dependent values of the thermal inertia is shown in Figure 23. This emphasizes that assigning constants to such non-constant properties over-simplifies the real ignition physics.

Delichatsios et al.[90] offered a procedure for data analysis which is somewhat more complicated than that of Janssens. Unfortunately, when attempting to analyze real experimental data, Dembsey and Jacoby[99] found that, in 7 out of 13 cases, unphysical answers were produced (negative values of minimum fluxes for ignition were computed for ordinary substances that actually require heat fluxes significantly greater than zero to ignite). Similar difficulties were not encountered using the treatments of Janssens or Quintiere. Part of the poor performance of this method may be because, instead of lumping all losses into a single, empirical heat loss term, Delichatsios explicitly treats re-radiation but sets the convective heat loss term to zero. Actual convective heat loss is generally not negligible. Spearpoint[306] offered a method which does take into account both convective and radiative losses, but solves an approximate heat transfer equation by forcing the temperature distribution within the solid to obey a parabolic distribution. Moghtaderi et al.[21] presented a method where the value of T_{ig}, instead of being assumed constant is treated as a variable which is dependent on the irradiance. Experience does not exist with the Spearpoint and Moghtaderi methods apart from the authors' own.

North[89] suggested that if no test data are available, for thick materials the ignition time (s) can be estimated knowing only its room-temperature density ρ (kg m^{-3}):

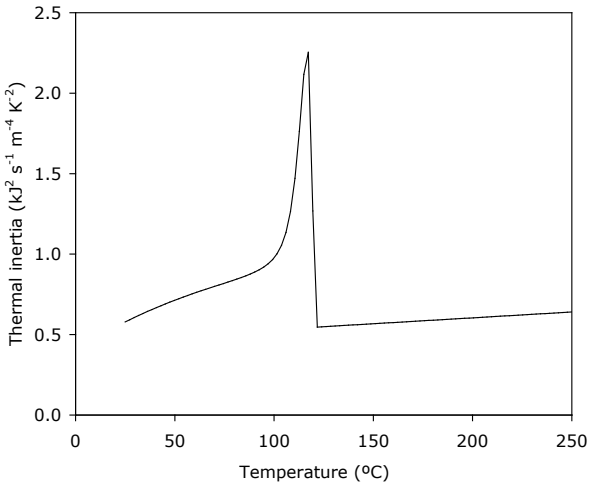


Figure 23 The actual thermal inertia for medium-density polyethylene
(Courtesy J. Staggs and R. Whiteley)

$$t_{ig} = 113 \frac{\rho}{\dot{q}''^{2}_{e}}$$

where t_{ig} = ignition time (s), ρ = density (kg m^{-3}), and $\dot{q}''_e$ = heat flux (kW m^{-2}). For a series of 13 building products tested at heat fluxes in the range of 20 – 75 kW m^{-2}, the formula showed typical errors of 20%, but in extreme cases the errors were up to 200%. The formula, of course, does not take into account variations in T_{ig} among materials, nor factors such as the presence of fire retardants or the effects of the latent heat of phase changes (e.g., melting substances). The formula also cannot predict the minimum flux for ignition, and inserting heat flux values lower than the minimum will give spurious answers. Consequently, heat fluxes lower than ca. 20 kW m^{-2} should not be used in the formula.

Other rough-estimating models have been proposed requiring that the user additionally supply values of thermal conductivity and heat capacity, or that values be provided at some elevated temperature. Since measuring the ignition time in the Cone Calorimeter is simpler than determining these additional properties, methods of that type may not offer much advantage.

RELATION BETWEEN MINIMUM AND CRITICAL FLUXES

Delichatsios et al.[90] proposed that the relation between minimum and critical fluxes should be:

$$\dot{q}_{cr} = 0.7\, \dot{q}''_{\min}$$

To examine whether this relation has enough predictive accuracy to be useful, the results of Babrauskas (Table 8) and Thomson (Table 9) are compiled in Table 7[*]. The average ratio $\dot{q}''_{cr} / \dot{q}''_{\min}$ is 0.4, not 0.7. The range is 0.11 to 0.68, thus even the highest experimental value for the ratio is smaller than Delichatsios' theoretically predicted value. The actual data show that the relation varies substantially and is not a universal constant, nonetheless, for very rough estimating purposes $\dot{q}''_{cr} / \dot{q}''_{\min} \approx 0.4$ might be used. Or, since $\dot{q}''_{cr}$ is more likely to be known than $\dot{q}''_{\min}$, estimation on the basis of $\dot{q}''_{\min} / \dot{q}''_{cr} \approx 2.4$ could be used.

ENGINEERING TREATMENTS FOR THERMALLY THIN SOLIDS

Conceptually, *thermally thin* means responding to heat in such a way that the entire object is being heated to a single temperature. For this to occur, objects need to be physically thin, or have high thermal conductivities (e.g., metals), or both.

Most building products behave as thermally thick materials. Thermally thin materials would include draperies, curtains, decorative bunting and paper decorations, and clothing items. The layman is likely to think that materials such as wallpaper are also 'thin.' This, of course, is true only prior to its being mounted on the substrate. When wallpaper glued on to plaster, for example, responds to heating, it responds as a thick material, since heat flows into the substrate and such a substrate does not rapidly equilibrate to a single temperature.

Table 7 A comparison of the ratio of critical to minimum flux

Code	$\dot{q}''_{\min}$ (kW m^{-2})	$\dot{q}''_{cr}$ (kW m^{-2})	Ratio $\dot{q}''_{cr} / \dot{q}''_{\min}$
PU	13	3.08	0.24
PMMA	8	3.33	0.42
WP	10	3.36	0.34
LD	8	5.44	0.68
CB	12	7.83	0.65
PE	17.5	8.7	0.50
PMMA (PX)	10.6	4.3	0.41
PMMA (FIN)	9.5	4.7	0.50
POM	11.5	2.2	0.19
PP	11.3	1.2	0.11
PS	14	7.1	0.51

The boundary conditions to be considered for thermally-thin objects can be more diverse than those needed to understand thermally-thick ones. For a thermally-thick object, most cases of interest are covered by assuming that the initial object temperature and the initial environment temperature are identical. Furthermore, the object is heated only from one face since the back face is, by assumption, 'infinitely' far away. A thermally-thin object, however, will be exposed on both sides to *something*, and those conditions need not necessarily be identical. In fact, there can be a very diverse collection of front/back boundary condition combinations. For practical work, however, it is sufficient to consider three:

1) the front face is exposed to a radiant heat flux and also undergoes convective cooling and re-radiation; the back face is perfectly insulated (adiabatic).
2) the front face is exposed to a radiant heat flux and also undergoes convective cooling and re-radiation; the back face undergoes convective cooling and re-radiation.
3) the front and the back faces are exposed to identical radiant heat flux and also undergo convective cooling and re-radiation.

In terms of fire incidents, the different boundary conditions can be exemplified in fabric fires. If a person's coat catches fire, and he is wearing several additional layers of clothing underneath, then condition #1 may be approximated. If one side of a room-divider curtain is ignited from a high-power floodlight, while the back side of the fabric is exposed to air, condition #2 will pertain. If a girl tries jumping over a bonfire and misses, the hem of her dress may be exposed to

[*] It must be noted that Delichatsios was working with curve fits of $t^{-0.5}$ power, whereas we adopt Janssens' recommendation of $t^{-0.55}$ power; the above conclusions would change little if replotted to the –0.5 power.

flames fairly evenly from both faces; thus, condition #3 would apply.

CONDITION 1—BACK FACE INSULATED

The theoretical formulation that leads to a simple solution is where the front face boundary condition includes radiation and convection, but the re-radiation term is lumped into an effective convection term, represented by the heat transfer coefficient h_{eff}:

$$2r\rho C\frac{\partial T}{\partial t}=\alpha_s\dot{q}''_e-h_{eff}\left(T_{ig}-T_o\right)$$

where $2r$ is the slab thickness (m). Note that the thermal conductivity λ does not enter this equation. The initial condition is $T = T_o$ at $t = 0$. The solution for the front face temperature is:

$$T_{ig}-T_o=\frac{\alpha_s\dot{q}''_e}{h_{eff}}\left[1-\exp\left(-\frac{h_{eff}t}{2r\rho C}\right)\right]$$

The solution can also be obtained explicitly giving the ignition time:

$$t_{ig}=\frac{2r\rho C}{h_{eff}}\ln\left[\frac{\alpha_s\dot{q}''_e}{\alpha_s\dot{q}''_e-h_{eff}\left(T_{ig}-T_o\right)}\right]$$

For cases where the external radiant flux dominates over convection, the logarithm term can be approximated in a series expansion:

$$t_{ig}\approx 2r\rho C\frac{(T_{ig}-T_o)}{\alpha_s\dot{q}''_e}\left\{1+\frac{(T_{ig}-T_o)}{2\alpha_s\dot{q}''_e}h_{eff}+\ldots\right\}$$

and taking $(T_{ig}-T_o)h_{eff}/2\alpha_s\dot{q}''_e<<1$, this gives:

$$t_{ig}\approx\frac{2r\rho C}{\alpha_s\dot{q}''_e}\left(T_{ig}-T_o\right)$$

This expression suggests the roles of the major variables, but does not give a realistic solution, since it implies that ignition will occur at a heat flux that is only infinitesimally greater than 0. In a similar effort to model the extremely-high radiant flux case, Simms[91] correlated data for radiant autoignition of thin, cellulosic solids subjected to short pulses of extremely high intensities, such as may be expected from nuclear bombs. For $\dot{q}''_e >>$ 100 kW m^{-2}, his data follow the relation:

$$t_{ig}=\frac{2400r\rho}{\dot{q}''_e-110}$$

where r = half-thickness (m).

Janssens[75] obtained numerical solutions and found that, when t_{ig}^{-1} is plotted as a function of $\dot{q}''_e$, most of the data range can be represented by a straight line (Figure 24). The straight line has the following equation:

$$\dot{q}''_e=0.97\dot{q}''_o\left[0.53+\frac{2r\rho C}{h_{eff}t_{ig}}\right]$$

where $t_o=\frac{4r\rho C}{h_{eff}}$, $\dot{q}''_{cr}$ is the x-axis intercept of the straight line, and $\dot{q}''_o$ is the x-value that corresponds to t_o. To obtain the appropriate straight line from the experimental data points, only data points where $t_{ig} \le t_o$ are to be plotted. To illustrate the scope of data that might be included, consider a cellulose paper sheet of 0.5 mm thickness ($2r$ = 0.5 10^{-3} m), density ρ = 600 kg m^{-3}, and heat capacity C = 1200 J kg^{-1} K^{-1}. Then if h_{eff} = 30 W m^{-2} K^{-1}, the criterion is evaluated as t_o = 24 s. Thus, only data points for $t_{ig} \le$ 24 s (or, $1/t_{ig} >$ 0.042 s^{-1}) should be plotted. Now, the effective thermophysical properties contained in the expression for t_o will not be known *a priori*, thus, empirically one would use data points that fall in a straight line, but omit those at the low end that deviate downwards.

The reason for omitting from the data correlation the points at large ignition times is that, theoretically—unlike in the thermally-thick case—data points will not follow a straight line down to the x-axis intercept. Instead, for values of $t_{ig} > t_o$, the curve is approximated as a straight vertical line, as indicated in Figure 24. Janssens showed that the value of $\dot{q}''_o = 1.96\dot{q}''_{cr}$, and it can be taken that $\dot{q}''_{\min} \approx \dot{q}''_o$.

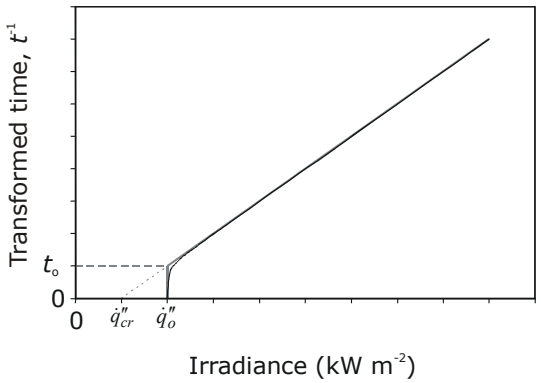


Figure 24 The relation between ignition time and heat flux for thermally thin materials

Thus, having found by data plotting the value of $\dot{q}''_{cr}$, the value of $\dot{q}''_o$ is known. Then, using

$$\dot{q}''_o=\frac{h_c}{\alpha_s}\left(T_{ig}-T_o\right)-\sigma\left(T_{ig}^4-T_o^4\right)$$

the value of T_{ig} can be found. Given that, h_{eff} is solved for as:

$$h_{eff}=h_c+\frac{\alpha_s\sigma\left(T_{ig}^4-T_o^4\right)}{\left(T_{ig}-T_o\right)}$$

There remains the as-yet unknown material property ρC. This is obtained as:

$$\rho C=\frac{1.03h_{eff}B_{ig}}{2r\dot{q}''_o}=\frac{0.53h_{eff}B_{ig}}{2r\dot{q}''_{cr}}$$

where, in parallel with the thermally-thick case, B_{ig} is defined as 1/slope of the straight line.

With the development above, Janssens' thermally-thin procedure becomes:

1. Obtain a series of ignition times at varying heat fluxes.
2. Plot t_{ig}^{-1} on the y-axis, as a function of $\dot{q}_e''$ on the x-axis. Note that the units for the x-axis are to be (kW m^{-2}).
3. Fit a straight line to the data points and determine the critical irradiance $\dot{q}_{cr}''$ as the x-axis intercept. Do not fit the line to any points at the small-flux end of the scale that deviate below a straight line.
4. Evaluate the slope of the straight line. The inverse of slope is defined as a constant, B_{ig} :
$$B_{ig} = \frac{1}{\text{slope}}$$
5. Find $\dot{q}_o''$ from $\dot{q}_o'' = 1.96\dot{q}_{cr}''$.
6. Obtain T_{ig} by a trial-and-error solution of the relationship:
$$\dot{q}_o'' = \frac{h_c}{\alpha_s}\left(T_{ig} - T_o\right) + \sigma\left(T_{ig}^4 - T_o^4\right)$$
7. Solve for h_{eff} using :
$$h_{eff} = \frac{\alpha_s \dot{q}_o''}{(T_{ig} - T_o)}$$
8. Compute the apparent ρC as:
$$\rho C = \frac{1.03 h_{eff} B_{ig}}{2r\dot{q}_o''}$$

There are few experimental studies in the literature where thermally-thin solids were exposed with the use of the adiabatic back-face condition. Thus, data to test the theory directly are lacking.

CONDITION 2—BACK FACE COOLED

Qualitatively, this condition represents a body with the same heat input as for Condition #1, but with 2 the heat losses, since the losses now occur from both faces, instead of just one. In practice, neither the convective loss nor the radiative loss will be the same from the back face as from the front face. There are no known experimental studies where an attempt would have been made to quantify these differences. Thus, a practical treatment is to assume that the back faces losses are identical to those at the front. Then use can be made of Janssens' solution for the adiabatic-back-face case by realizing that the identical heat balance equation will be obtained if, instead of doubling the heat losses, the values of $\dot{q}_e''$ and $2r$ that are used are fictitious values, equal to ½ the real ones.

Example

Pure-cellulose paper is one of the few thermally thin substances that has been explored to any significant extent. Martin and Alvares[92] have provided data on two thicknesses of blackened cellulose paper, exposed to heat from the front only, with the back face free to lose heat by convection and radiation. For the 0.5 mm thick paper, the following ignition data were obtained:

Flux (kW m^{-2})	37.0	38.5	38.3	34.7	41.2	43.3	44.7	
Time (s)	40.6	35.6	33.5	33.4	25.6	25.8	23.8	
Flux (kW m^{-2})	48.2	49.7	46.2	49.9	53.1	68.7	87.7	98.1
Time (s)	22.9	22.3	22.4	19.0	17.7	11.3	7.8	7.0

Find the effective thermal properties of this material.

Solution. The data points to be plotted are the following:

Flux	37.0	38.5	38.3	34.7	41.2	43.3	44.7	
1/*t*	0.025	0.028	0.030	0.030	0.039	0.039	0.042	
Flux	48.2	49.7	46.2	49.9	53.1	68.7	87.7	98.1
1/*t*	0.044	0.045	0.045	0.053	0.057	0.089	0.128	0.143

with the flux plotted on the x-axis and 1/*t* plotted on the y-axis. When the data are plotted (Figure 25), the point at 37 kW m^{-2} appears to be an outlier and is excluded. The remaining points are used in the data fit. The fitted straight line has a slope of 0.00191, giving B_{ig} = 525, and an x-axis intercept of 22.6 kW m^{-2}. To obtain values pertinent to the present case of non-adiabatic back face, the heat flux scale must be divided by ½. Thus, the x-axis intercept becomes 11.3 kW m^{-2}, the slope = 2×0.00191 = 0.00382, and B_{ig} = 525/2 = 263. According to Janssens' scheme, the minimum heat flux is computed as 1.96×11.3 = 22.1 kW m^{-2}. Using h_c = 0.013 kW m^{-2} K^{-1} and α_s = 0.96, T_{ig} is computed by trial-and-error, as 735 K = 462ºC. The value of h_{eff} is computed as 0.0481 kW m^{-2} K^{-1}. Finally, using the value $2r$ = 0.5×10^{-3} m, ρC is computed as 1486 kJ m^{-3} K^{-1}. The room temperature value for cellulose paper is $\rho C \approx 600 \times 1.200$ = 720 kJ m^{-3} K^{-1}.

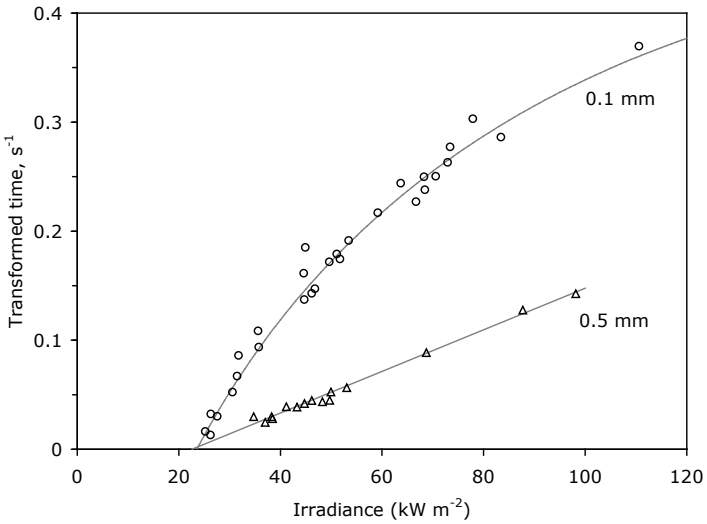


Figure 25 Thermally-thin material—blackened cellulose paper of two thicknesses

As far as $\dot{q}''_{\min}$ is concerned, it will be found that its value is about 2× of that for a thermally thick solid. This is because, roughly speaking, there is twice the amount of cooling available per unit frontal area of solid.

When materials of the same chemical composition, but different thicknesses or densities are encountered, Janssens' governing equation can be re-stated as:

$$\frac{W}{t_{ig}} = A\left(\dot{q}''_e - \dot{q}''_{cr}\right)$$

where $W = 2r\rho$ = the material's mass per unit area or 'basis weight' (g m^{-2}), and A and $\dot{q}''_{cr}$ are constants to be determined empirically. For practical purposes, it is generally much more useful to use W, rather than attempting to separately determine $2r$ and ρ, both of which are difficult to measure for thin materials. The data of Rangaprasad[93] on piloted ignition of off-white cotton fabrics, exposed vertically to flame radiation on one side and to room air on the back face, are plotted according to this procedure in Figure 26. A very good correlation with no systematic deviations is found for fluxes up to 100 kW m^{-2}. At higher fluxes, the ignition times are very short and most likely the deviations are due to difficulties in providing an instantaneous 'turn-on' of the exposure. For these data, the values obtained are $A = 0.744$ g kJ^{-1}, $\dot{q}''_{cr}$ =13.1 kW m^{-2}.

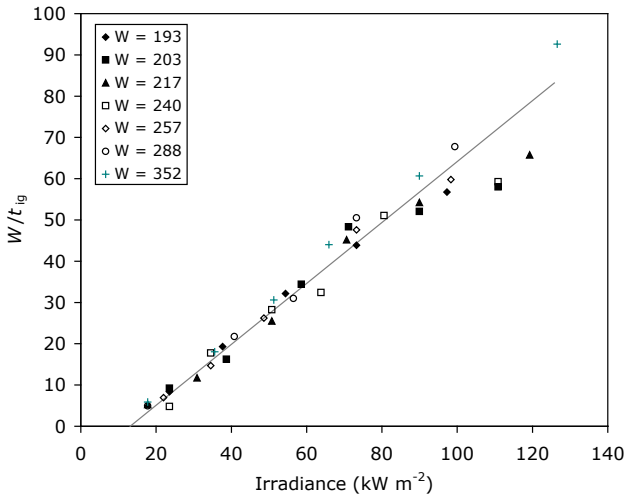


Figure 26 Ignition from flame radiation (single-sided heating, back-face cooled) of cotton fabrics of various weights

CONDITION 3—BACK FACE ALSO HEATED

When the specimen is subjected to heating on both faces (condition #3), by symmetry no heat can flow across the mid-thickness of the specimen. Thus, the mid-thickness is an adiabatic plane. Condition #1 represents a specimen with imposed heat flux on one face and the second face adiabatic. Thus, condition #3 can be represented by the same equations as condition #1, but with the real thickness being $4r$ instead of $2r$.

OTHER ISSUES FOR THIN SLABS

The engineering models for the ignition of thin solids are typically purely-thermal in character, that is, only the time for the temperature to rise to a given T_{ig} is tracked. A thin solid can be readily raised to a high temperature, so this would suggest that thin fuels would always ignite at low $\dot{q}''_{\min}$ values. But experimentally, this does not always occur. For example, Hilado and Brauer[94] reported on a series of fabrics exposed to radiant heating. In many cases, specimens did not ignite at notably high fluxes: 58 – 105 kW m^{-2}. The materials showed smoking and charring early in the exposure period, but ignited late or not at all. Behavior of this kind can be attributed to *fuel exhaustion*. Chemically, the reaching of a specific T_{ig} is merely a correlational indicator of reactions taking place, it does not guarantee that a reaction will actually take place. If there does not exist any location where the fuel-air mixture has reached its LFL and where an ignition source is also present (or, a location with high enough temperatures for autoignition), then ignition will not occur, despite high temperatures elsewhere in the system.

ILLUSTRATIVE DATA

An assortment of data obtained using the Cone Calorimeter are shown in Figure 27 (thermally-thick specimens) and Figure 30 (thermally-thin specimens). The specimens represented are identified in Table 8. The data are from Babrauskas and Wetterlund[95] except CB which is from Grant and Drysdale[79]. The minimum flux for ignition was determined by trial and error, using steps of 2 kW m^{-2}. For example, PMMA ignited at 9 kW m^{-2} but did not ignite at 7 kW m^{-2}; thus its $\dot{q}''_{\min}$ is 8 kW m^{-2}.

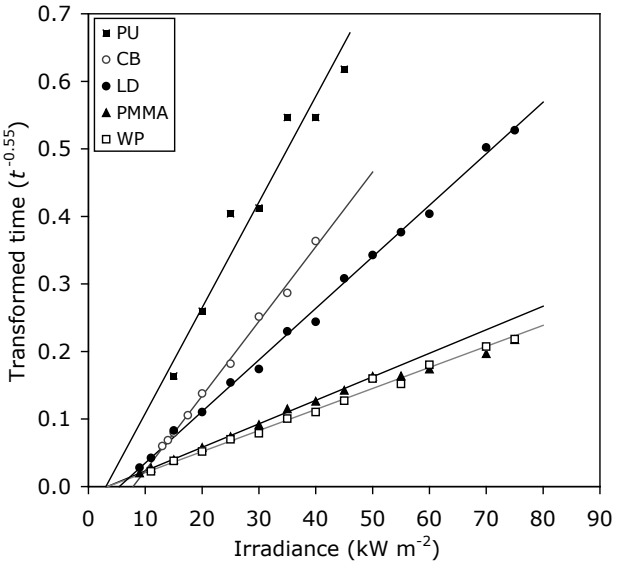


Figure 27 Ignitability plots for a number of different thermally-thick materials

Table 8 Specimen identification and data for the ignition plots

Code	Material	Thick-ness (mm)	$\dot{q}''_{\min}$	$\dot{q}''_{cr}$	B_{ig}	T_{ig} (ºC)	$\lambda\rho C$
PU	polyurethane foam, FR, rigid, 35 kg m^{-3}	40	13	3.08	63.9	350	0.039
PMMA	PMMA, black, 1200 kg m^{-3}	10	8	3.33	287	266	1.01
WP	wood particleboard, 700 kg m^{-3}	19	10	3.36	321	302	0.98
LD	insulating cellulosic fiberboard, 270 kg m^{-3}	13	8	5.44	131	265	0.24
CB	corrugated cardboard, double-wall, FC flute	6	12.5	7.83	90.5	343	0.080
AC	furniture composite: acrylic fabric (546 g m^{-2}) on top of high resilience polyurethane foam (36 kg m^{-3})	50*	7	6.30	510	245	2.05†
CO	furniture composite: cotton fabric (213 g m^{-2}), Kevlar interliner (81 g m^{-2}), HR PU foam (36 kg m^{-3})	50*	7	10.6	305	245	1.23†

- computed.
* - analyzed as thermally-thin
† - value refers to $2r\rho C$ (kJ m^{-2} K^{-1})

Some additional data[96] on solid plastics are given in Figure 28 and Table 9. The materials were all 6 mm thick. It can be noted that the –0.55 power law representation fits most of the data very well, with the exception of the lowest point of PMMA (FIN). The authors repeated their study in the ISO 5657 rig[97] and a comparison of the results is shown in Figure 29. Data obtained in the ISO 5657 test does not show an anomalous data point, but there is a modest systematic difference between the two rigs, with ignition times being slightly lower in the experimental rig. While both apparatuses used a radiant electric heater, numerous other details were different, so a unique reason is hard to assign for the difference.

Table 10 showed that for a number of plastics the effective value of thermal inertia that is pertinent to the whole temperature excursion from T_o to T_{ig} is about 2.7× the value at room temperature. Additional data for wood are shown in Table 11[21]. The effective $\lambda\rho C$ was found to be roughly 1.9× the value at room temperature. Findings of this kind seem to be quite plausible, since thermal conductivity is a strongly-increasing function of temperature. For instance, between room temperature and 300ºC, the thermal conductivity of wood increases[98] by about 3.5×, while that of PMMA increases over 10 .

COMPOSITE MATERIALS

When composites contain a thin combustible face backed by a thick layer of another material, it may not be evident whether ignition data will follow thermally-thin, thermally-thick, or some unique trend. Upholstered furniture often consists of a composite comprising a layer of fabric atop a thick layer of polyurethane foam. Ignitability plots of two different furniture composites are shown in Figure 30. Note that the AC series is almost perfectly fitted to the t^{-1} power. The other series, CO, is also well fitted to t^{-1}, with the exception of the two lowest points, which are slightly above the curve-fit line. It can be readily shown that furniture composites do *not* show a good fit when thermally thick fitting is attempted. The reason is that the ignition behavior is dominated by the fabric alone. The density of the foam layer behind is so much lower than the fabric density, that during the ignition period the foam simply acts as thermal insulation.

If a thin combustible layer is attached to a high-density non-combustible substrate, the opposite result may be found—the data correlate as thermally thick, not thermally thin. Janssens has illustrated this for paper-faced gypsum wallboard (see Chapter 14), which correlates as a thermally-thick material, despite the fact that the only combustible component is the thin paper facing. He also found that the slope of the line reflects the thermal inertia of gypsum, not paper. Composites of this type are likely to show $\dot{q}''_{\min}$ values which are significantly higher than $\dot{q}''_{cr}$. The elevated values of $\dot{q}''_{\min}$ occur since the amount of fuel present in the thin layer is so low that at lower heat fluxes the fuel gets exhausted before the surface temperature can reach to an ignition value.

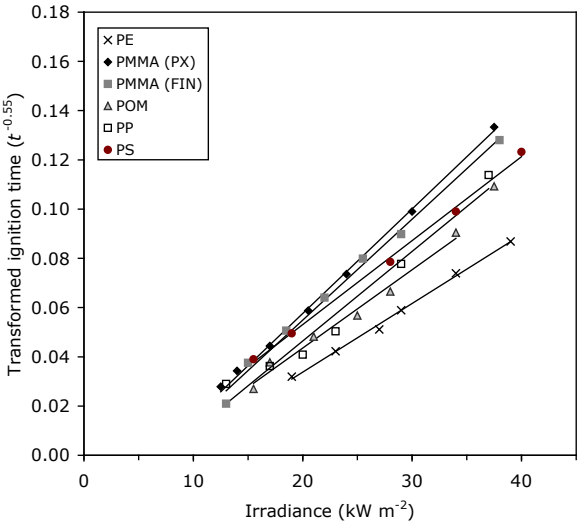


Figure 28 Radiant ignition data on plastics obtained by Thomson and Drysdale in a special rig

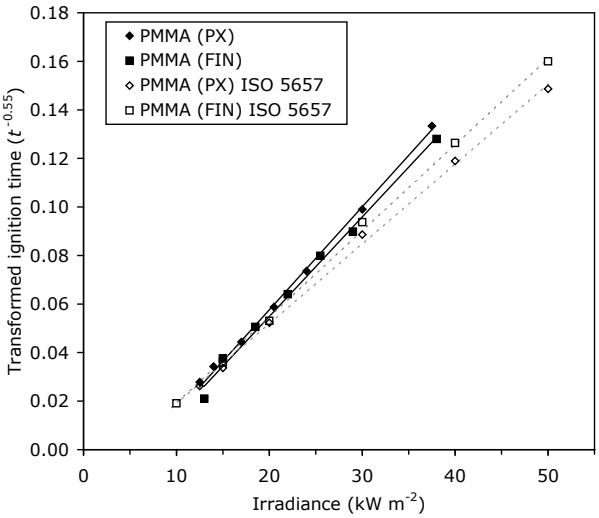


Figure 29 Radiant ignition data obtained by Thomson and Drysdale in two different test apparatuses

Table 9 Properties of polymers tested by Thomson and Drysdale (experimental values derived from tests in the ISO 5657 apparatus)

Code	**Material**	**Density** (kg m^{-3})	**Thermal cond.** (W m^{-1} K^{-1})	**Heat capacity** (kJ kg^{-1} K^{-1})	$\dot{q}''_{\min}$	$\dot{q}''_{cr}$	B_{ig}
PE	polyethylene (Courtalds Polythene)	920	0.33	2.1	17.0	8.7	424
PMMA (PX)	polymethylmethacrylate (ICI Perspex)	1180	0.17	1.5	10.6	4.3	303
PMMA (FIN)	polymethylmethacrylate (Lohja Finnacryl)	1190	0.21	1.46	9.5	4.7	281
POM	polyoxymethylene (DuPont Delrin)	1420	0.37	1.47	11.5	2.2	422
PP	polypropylene (Courtalds)	905	0.21	1.93	11.3	1.2	382
PS	polystyrene (BASF Hyalite)	1040	0.12	1.34	14	7.1	341

Table 10 Further comparisons based on the results of Thomson and Drysdale

Code	**Material**	$\lambda\rho C$ (kJ^2 m^{-4} s^{-1} K^{-2})		T_{ig} (°C)	
		From hand-book	From Janssens proced.	Measured	From Janssens proced.
PE	polyethylene	0.64	0.98	363	402
PMMA (PX)	polymethylmethacrylate	0.30	0.83	311	313
PMMA (FIN)	polymethylmethacrylate	0.37	0.81	311	294
POM	polyoxymethylene	0.77	1.40	281	327
PP	polypropylene	0.37	1.19	334	324
PS	polystyrene	0.17	0.78	366	364

Table 11 Relation between apparent values of thermal inertia of wood measured experimentally and handbook values at room temperature

Species	Moisture content (%)	Thermal inertia ($kJ^2\ m^{-4}\ K^{-2}\ s^{-1}$)	
		Hdbk.	Exp.
Pacific maple	10 – 12	0.087	0.213
Monterey pine	0	0.065	0.111
" "	30	0.230	0.478
sugar pine	10 – 12	0.057	0.071

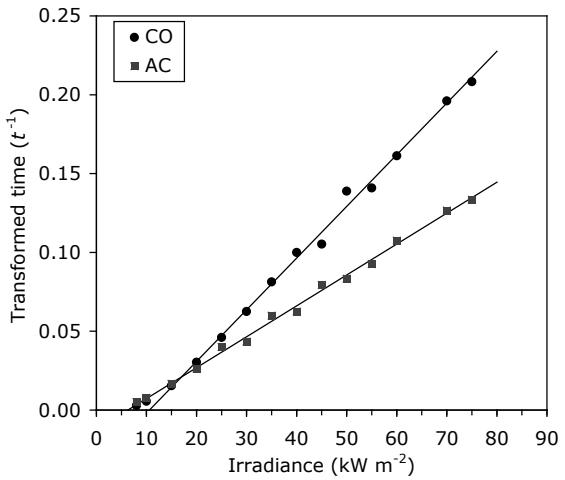


Figure 30 Ignition response of two furniture composites, exemplifying thermally thin behavior

CRITERIA FOR DISTINGUISHING THERMALLY THICK VERSUS THIN MATERIALS

To distinguish thermally thin and thermally thick materials rigorously requires knowing their thermal properties (λ, ρ, C) along with the heating and geometry conditions. For a 1-dimensional slab, a *thermal penetration depth* can be defined as the thickness of the specimen which has been heated to a certain temperature. An expression for thermal penetration depth δ_p that is sometimes used is:

$$\delta_p \approx 4\sqrt{\alpha t}$$

The numerical factor is quite arbitrary. The factor of 4 comes from solving the heat transfer problem for the case of a fixed surface temperature being imposed and defining the penetration depth to occur at the place where the temperature rises to 0.005 of the surface temperature rise[99]. Choosing such a tiny temperature rise creates an exceedingly conservative criterion. A more appropriate factor was suggested by Chomiak:

$$\delta_p \approx \frac{2}{\sqrt{\pi}}\sqrt{\alpha t} = 1.13\sqrt{\alpha t}$$

A similar expression was offered by Dusinberre[100]:

$$\delta_p \approx 1.2\sqrt{\alpha t}$$

Table 12 Minimum estimated fluxes to comprise thermally-thick samples, for the data of Ngu

Type	Minimum flux (kW m^{-2})	
	20 mm	40 mm
beech	17.6	9.9
Macracarpa	15.5	8.3
Monterey pine	13.6	7.9
Rimu	17.0	8.9
MDF	21.8	10.9
plywood	15.2	7.6

Since the elevated temperature zone progressively penetrates the solid after the start of exposure, the thermal penetration depth increases with exposure time t. Thus, all materials start behaving as thermally thick the instant that they are exposed to heat, then behave as thermally thin at infinite time. For the ignition problem, however, the value which is important is the thermal penetration depth at the time of ignition: products can be considered thermally thick if the penetration depth at the time of ignition does not exceed the thickness. Products *exposed to heating from both sides* are thermally thick only if δ_p is less than ½ of the value computed from the above formulas which assume single-sided heating.

A useful rule of thumb is that products of $\leq$ 1 mm thickness will be thermally thin; products thicker than about 20 mm will be thermally thick, unless they are foams. The response of foams varies a great deal according to their melting or charring characteristics and no simple generalization is likely to be adequate. For products falling in between 1 mm and 20 mm, a more detailed examination should be made. A suggested guideline for wood products to be considered thermally thick is[101]:

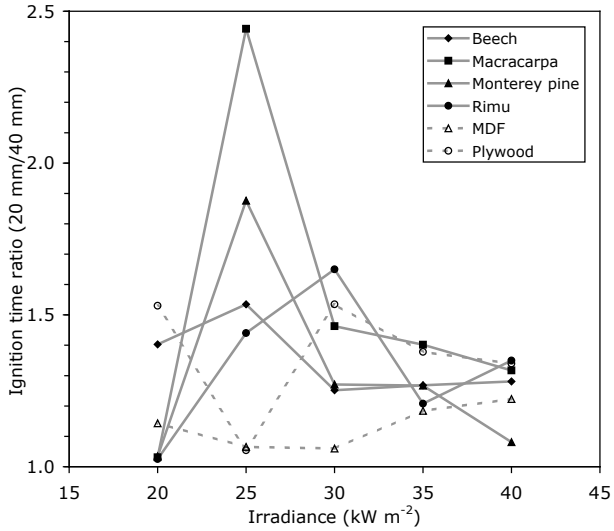


Figure 31 Effect of thickness for various woods tested by Ngu (each test condition represents the average of 5 test results)

$$2r > \frac{0.6\rho}{\dot{q}''_e}$$

where $2r$ = thickness (mm), ρ = density (kg m^{-3}), and $\dot{q}''_e$ = irradiance (kW m^{-2}). As an example, for a density of 310 kg m^{-3}, the prediction is that 6 mm wood samples will behave in a thermally-thick manner at heat fluxes greater than 31 kW m^{-2}. But the formula is not always obeyed, for reasons which are not entirely clear. Akita[271] ran tests on Japanese cedar boards of this density and found that thermally-thick behavior was seen down to 25 kW m^{-2}, the lowest heat flux used. Ngu[102] tested a number of wood types in the ISO 5657 apparatus. These results, shown in Figure 31, imply that even 20 mm samples are not quite thermally thick at 40 kW m^{-2}, yet the estimating formula would predict (Table 12) that thermally-thick behavior should be seen at fluxes less than half of that.

GENERAL AND INTERMEDIATE-THICKNESS MATERIALS

By 'thermally thick,' we mean a substance, in which when exposed to a heat flux on its front face, appreciable temperature rise has not yet occurred on its back face. Conversely, 'thermally-thin' means that, at a given instant, the back face is a temperature which is close to that of the front face. From this elementary consideration, it is clear that the classification is not absolute: at very high heat fluxes, all substances are effectively thermally thick, while at very low heat fluxes, all are thermally thin. A categorical classification becomes sensible only when it is understood that the range of heat fluxes of interest in accidental fires is relatively small, with the bulk of interest being centered on fluxes in the range of 35 – 100 kW m^{-2}. A certain attention also has to be paid to the minimum flux for ignition, which for common building products may be in the range of 10 – 20 kW m^{-2}.

Thus, there will be thicknesses of products where, in the crucial 35 – 100 kW m^{-2} range, at the time of ignition the back face temperature will be roughly halfway between ambient and front face temperature. For engineering purposes, we can identify these as 'intermediate thickness' products. Mikkola and Wichman studied such possibilities[103] and recommended that, for intermediate-thickness products, plots against $t^{-2/3}$ be made; however, they did not give rules for assigning products into the intermediate-thickness category. Much earlier, Lawson and Simms[12] tested various woods of a 19 mm thickness and also concluded that a $t^{-2/3}$ law gave the best representation. But their own data showed substantial deviations from straight lines when thus plotted, so their conclusion was hardly a robust one. Janssens[75] evaluated the possibility of plotting data according a $t^{-2/3}$ law, but found that the results do not yield useful material thermophysical properties. Thus, he recommended that a $t^{-0.55}$ relation still be used, but that only points at the high flux end of the scale be used in fitting a straight line.

Table 13 Cone Calorimeter ignition results obtained at NRCC

Material	Thick. (mm)	Density (kg m^{-3})	Ignition time (s) at flux	
			25 kW m^{-2}	50 kW m^{-2}
wood	3	617	121	43
wood	5	840	277	37
wood	6	780	248	60
plywood	6	528	123	14 - 24
plywood	12.3	583	128	23 - 24

Table 14 Effect of thickness on ignition of spruce panels

Thick. (mm)	Ignition time (s), at a given heat flux (kW m^{-2})					
	15	20	30	40	50	70
2		83±15	32±6	23±4	16±3	
6		285±25	54±7	36±5	14±4	10±3
37	2070±150	470±70	63±10	29±4	16±3	8.5±1.5

Bamford et al.[7] tested panels of an unidentified softwood species, exposed to flames on both sides. On the basis of testing specimens 11 – 51 mm thick, they proposed an empirical formula for ignition time which includes a thickness variable. Their experimental results, however, were anomalous and their proposed scaling relation was mathematically incorrect, since they proposed that the ignition time should be proportional to L^2, where L = specimen thickness. In fact, for thermally thick specimens, the thickness can play no role, while for thermally-thin specimens, the ignition time must be proportional to L, not L^2.

Koohyar[73] tested wood panels of intermediate thicknesses (12 – 19 mm), exposed both from a single side and from both sides. Based on his results, he offered several empirical correlations, which can be expressed as $t_{ig} \propto L^{-n}$. Since in these correlations n ranges from 0.13 to 2.0, they are evidently unphysical, since thicker specimens take a longer time, not shorter, to ignite. At the same laboratory, Wesson[104] later obtained ignition data on oak specimens of various thickness, exposed to tungsten lamp radiation. His results (Figure 32) sensibly show that the thinner specimens do ignite more rapidly, but the data have a large amount of scatter. From these results, along with those for other wood species, Wesson et al.[105] concluded that over the heat flux range 25 – 146 kW m^{-2} wood materials are thermally thick if the thickness is 20 mm or greater. For thinner specimens, they proposed the relation:

$$t_{ig} = \frac{35\rho^{0.9}\left[erf\left(\sqrt{\frac{\rho C_p L^2}{4\lambda t_{ig}}}\right)\right]^{1.2}}{\left(\alpha_s \dot{q}''_e\right)^{2.8}}$$

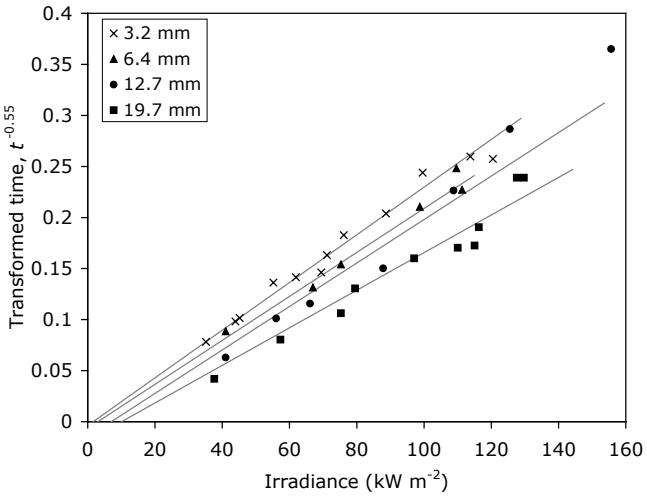


Figure 32 Effect of thickness on the ignition of oak specimens using tungsten-lamp radiant heating

This relation is not particularly satisfying, since t_{ig} shows up on both sides of the equation and, thus, only an iterative solution is possible.

More recent studies[106] were done at NRCC where the Cone Calorimeter was used (Table 13). Standard procedures (electric spark piloting, lightweight fiber blanket substrate) were used. For the irradiances examined, clearly the whole-wood samples show a thickness effect below 5 mm; the results on plywood, however, suggest that for thicknesses greater than 6 mm, any thickness effect is below the repeatability level of the material.

Additional data were obtained by Mikkola[107], who tested spruce specimens of 440 kg m^{-3} and 10% moisture content in the Cone Calorimeter. His results, shown in Table 14, indicate that:

- At heat fluxes of 50 kW m^{-2} or greater, there is no statistical difference even between 2 and 37 mm panels.
- At heat fluxes of 30 – 40 kW m^{-2}, results for 6 – 37 mm panels are indistinguishable, but 2 mm panels ignite quicker.
- At a heat flux of 20 kW m^{-2}, even the 37 mm panel becomes thermally thin.

These are probably the most reliable results so far, and properly verify that the thermally thin/thick breakpoint thickness increases with rising heat flux.

Table 15 Minimum thickness for wood specimens to be thermally thick

Min. thickness to be thermally thick (mm)	Heat flux (kW m^{-2})					
	20	**30**	**40**	**50**	**60**	**70**
Rule-of-thumb	13.2	8.8	6.6	5.3	4.4	3.8
Mikkola results	≈20	≈5	≈5	< 2		< 2

Mikkola's results can be compared to predictions from the rule of thumb mentioned above. Table 15 indicates that the rule provides viable estimates at medium heat fluxes, but that the estimated values become quite conservative at heat fluxes > 50 kW m^{-2}.

Table 16 Results of Cone Calorimeter tests on clear PMMA exposed to a heat flux of 50 kW m^{-2}

Thick. (mm)	Ignition time (s)
1.5	15
3	17
10	24
20	25
25	22

Paul[108] reported data on clear PMMA tested at various thickness; his results are given in Table 16. If 24 s is taken as the ignition time for thermally thick material, then the 1.5 mm material ignites about 38% faster. Some data on polyethylene[109] tested at a heat flux of 50 kW m^{-2} indicate that 1 and 2 mm thick samples ignite faster, but that ignition times for specimens of 3 – 10 mm thickness are essentially independent of thickness.

Jacoby[110] tested several materials where both the thickness and the heat flux were varied. His Cone Calorimeter results for a glass-reinforced vinyl ester composite material are shown in Table 17. The substrate used was not the standard lightweight ceramic fiber blanket, but rather a ceramic board with a density of 258 kg m^{-3}. A distinct difference in ignition time between the 1.5 and the 3.0 mm thick samples is seen up to the highest flux used, 90 kW m^{-2}. But ignition time differences become small between the 3.0 and the 8.0 mm thick samples when a flux around 60 – 75 kW m^{-2} is reached.

Table 17 Ignition times (s) for glass-reinforced vinyl ester composites in three different thicknesses

Thick. (mm)	Heat flux (kW m^{-2})								
	20	**25**	**30**	**35**	**40**	**50**	**60**	**75**	**90**
1.5	291	148	95	64	61	44	26	16	18
3.0	450	239	158	103	99	67	53	34	24
8.0	735	382	284	152	163	91	61	43	

According to Janssens[77], the issue of thermal thickness category should be addressed empirically. If it is not clear *a priori* that the product is thermally-thick or thermally-thin, then a curve-fitting procedure should be used where the exponent n is variable, with the limits of –1.0 and –0.5. Thus, in practice, a general procedure can be suggested as follows:

1. Guess whether the product is thermally thick or thin
2. Plot the data using n = –0.55 (or –1.0)
3. Determine if the line is reasonably straight

4. If neither $n = -0.55$ nor -1.0 give a reasonable straight line, conduct a least-squares curve-fit where the exponent n is allowed to vary.

As mentioned above, intuition does not always provide the correct results. As an example, studies on composite shipbuilding panels having a thickness slightly over 30 mm[111], showed that the optimum n was –0.78 (for one type of core) or –1.0 (for a second core type). The large overall thickness might have induced the user to presume that n = –0.55 was the appropriate value. The explanation lies in the fact that the face coverings on these products had a density of about 20 times that of the core material. Thus, the contribution of the core is effectively unseen in the ignition process. Grenier and Janssens[112] provide further illustrations of curve-fitting for composite products which are possibly of intermediate thermal thickness. Dietenberger[84] has presented a method for intermediate-thickness specimens which is essentially an interpolation scheme.

When data are available only at a single thickness which is judged to be 'intermediate,' it is best to realize that any specimen will show thermally-thick results when irradiated with very high heat fluxes and thermally-thin results when heated at a very low rate. Thus, two different plots can be made from the same data, with a straight line being fitted at the high-flux region to a thermally-thin plot (y-axis = t^{-1}), and a straight line being fitted at the low-flux region using a thermally-thick plot (y-axis = $t^{-0.55}$). Data on 6.4 mm thick plywood provided by de Ris and Khan[25] are plotted this way in Figure 33 and Figure 34. (Note that the data were obtained using the FM procedure with blackened specimen face, so there is a systematic bias with respect to the irradiance scale). The authors consider that the thermal-thickness effect is complicated by moisture movement in the sample, which in a thermally-thin sample will more likely leave through the front face and thereby dilute the gas stream.

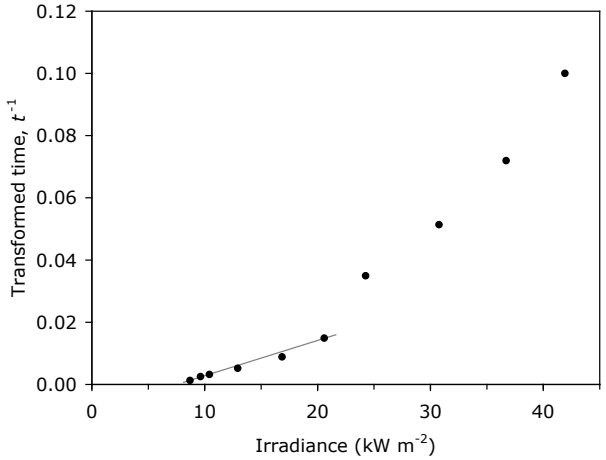


Figure 33 Plywood specimen, 6.4 mm thick: low-flux regime plotted as thermally-thin

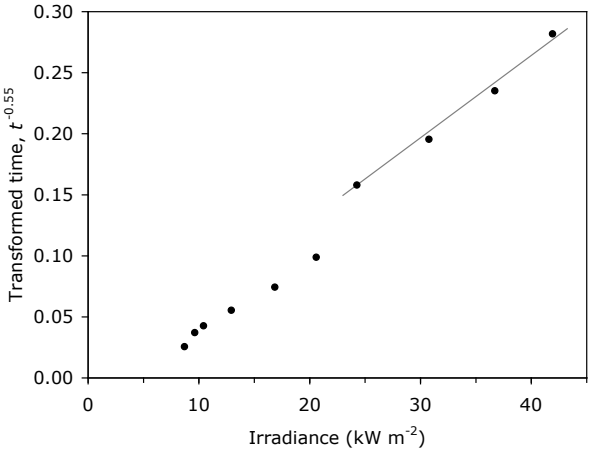


Figure 34 Plywood specimen, 6.4 mm thick: high-flux regime plotted as thermally-thick

ENERGY NEEDED FOR IGNITION

Experimentally, heat flux (kW m^{-2}) is the driving force for ignition. But sometimes it is considered that a substance requires a certain minimum energy fluence (kJ m^{-2}) to ignite (energy fluence is defined as the energy that flowed through a unit surface area). Can the minimum energy fluence be a constant for a substance? If (1) the ignition temperature of the substance were a constant, (2) the substance sustained no heat losses, and (3) it had infinite thermal conductivity, then the answer would be Yes. In such a case, the energy increase occurring during the heating is:

$$Q = \rho L C \Delta T$$

where L is the thickness of the substance and ΔT is the temperature increase from ambient to T_{ig}. But also:

$$Q = \dot{q}'' t_{ig}$$

where $\dot{q}''$ is the heat flux imposed on the specimen. Since none of the three necessary conditions for this simple relation to hold are true for real combustibles, the minimum ignition energy is not a constant and thus is generally not a variable of much utility. To illustrate this, the same materials examined above can be considered for their minimum ignition energy fluence requirements. Figure 35 shows this for thick solids, while Figure 36 illustrates thin solids. For thick solids, the minimum energy decreases with increasing heat flux, although gradually tapering off at higher heat fluxes. It is possible that a plateau might be reached at higher irradiance values than the maximum explored in this work. For thermally-thin specimens, a plateau is reached for irradiances greater than about 35 – 40 kW m^{-2}. The fact that a constant-energy condition roughly holds for thermally-thin bodies at high irradiance could have readily been expected from Janssens' plots. If

$$\left(\dot{q}''_e - \dot{q}''_{cr}\right) \propto t_{ig}^{-1}$$

then clearly $\dot{q}''_e t_{ig} = Q \approx$ constant for $\dot{q}''_e >> \dot{q}''_{cr}$.

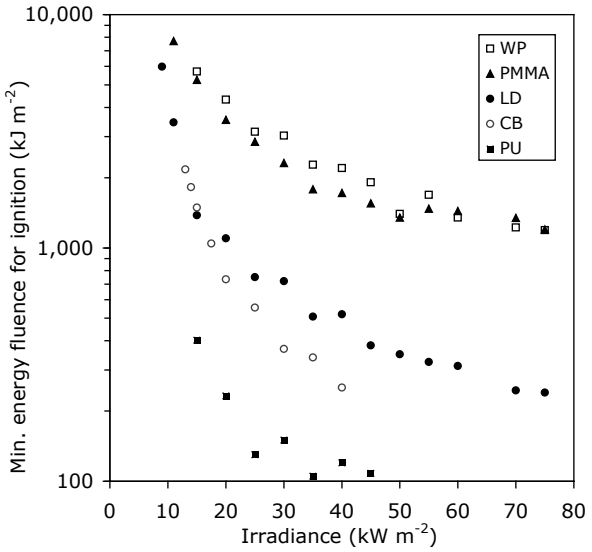


Figure 35 Minimum energy fluence for ignition of some thermally-thick solids

Martin[113] examined this question for thin sheets of cellulose using a carbon arc ignition source. Over a very wide range of high irradiance values (40 – 4000 kW m^{-2}), he found that the minimum ignition energy varied only by a factor of 2.

It must be emphasized that the minimum energy fluence, which is taken as the product of the irradiance × t_{ig}, is only an *apparent* value. The actual energy which enters the body is lower than that which is computed in this simple way, because some of the energy is re-radiation, and also because convective losses occur. There is no simple way to compute the *net* energy that actually entered into the body, thus, calculations requiring this value may not be of practical value. The reason that assuming a constant ignition energy is a fair assumption for thin solids, but a poor one for thick ones is due to the non-uniform temperature distribution which exists within a thick body. For thermally thin bodies, assuming that the entire substance is at a single temperature is a valid assumption, thus at least one of the three requirements outlined above is satisfied.

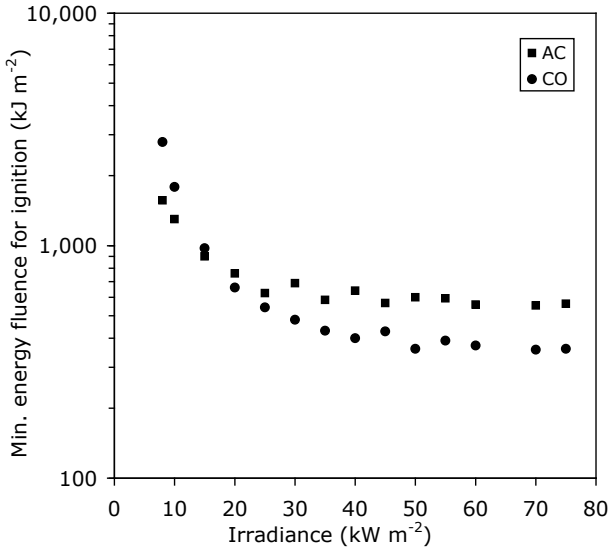


Figure 36 Minimum energy fluence for ignition of some thermally-thin solids

LASER IGNITION

A laser is a high-energy source of electromagnetic radiation in the visible or the infrared portions of the spectrum. Its distinguishing trait, of course, is coherent radiation, which is emitted at one unique wavelength. If the wavelength is one at which a material has substantial absorptivity, then laser energy may cause ignition. Laser ignition has been explored for warfare and is used in industrial processes. Neither of these usages results in significant unwanted fires. However, because lasers are a convenient, precisely controllable source of heating, a large number of ignition experiments have been reported in the literature.

Autoignition. Most laser ignition experiments have been in the autoignition mode. Mutoh et al.[114] exposed 30 mm thick, horizontal PMMA samples to a CO_2 laser beam at the wavelength of 10.6 μm. Lasers cannot heat large-area specimens, and in their experiments the beam diameter was 12 mm. They found that the minimum flux needed for autoignition was 250 kW m^{-2} (Figure 37). Steady-flaming ignition was found for the heat flux range of 250 – 600 kW m^{-2}. For heat fluxes in the range of 600 – 800 kW m^{-2}, only a transient-flaming ignition could be created. The time scale was also notable. Whereas steady ignition took place in ca. 40 s at 600 kW m^{-2}, transient ignition at heat fluxes just slightly greater occurred in only 3 – 4 s. In the same experimental arrangement, the minimum flux for vertical-orientation specimens was 185 kW m^{-2}, with the jump occurring at 340 kW m^{-2}. Also shown in Figure 37 are results from Kashiwagi[15], who exposed 12 mm thick clear PMMA samples and found $\dot{q}''_{min} \approx 160$ kW m^{-2}. In that test series[115], Kashiwagi also reported that $\dot{q}''_{min} \approx 110$ kW m^{-2} for specimens oriented at a 45° angle, and 90 kW m^{-2} for vertical specimens. Mutoh et al. also obtained data in the vertical orientation and found that ignition times were about 5 to 50× shorter than for the horizontal orientation. By contrast, for ignition by typical black-body heat sources, ignition times in the vertical orientation are slightly longer than in the horizontal. This suggests that attenuation of radiation while traversing the pyrolysates plume is a dominant effect with laser radiation, since a much deeper layer must be traversed in the horizontal orientation. However, even with vertical orientation, Mutoh et al. obtained a large value of $\dot{q}''_{min} \approx 180$ kW m^{-2}. For the transient ignition regime, there was essentially no difference between ignition times in the two orientations. This is evidently because transient ignition is primarily a gas-phase phenomenon and differences

in the efficiency of delivering radiation to the surface do not play a major role.

Kashiwagi additionally conducted tests using a gas-fired radiant panel providing 60 kW m^{-2}. Horizontally-oriented samples ignited in about 75 s, while vertically-oriented samples did not ignite at all. Kashiwagi's data indicate that minimum fluxes for autoignition are higher with a laser source than for conventional radiant sources (note that Kashiwagi's determination was not that the minimum flux for ignition with the radiant panel is 60 kW m^{-2}, rather that ignition was possible at that flux; presumably the minimum flux was lower than that). The extraordinarily high minimum heat fluxes found by Mutoh are hard to explain, but suggest that data obtained from laser ignition experiments may not be relevant to building fires. Averson et al.[116] (also shown in Figure 37), did not determine a minimum flux, however their data indicate (a) identical results in horizontal and vertical orientations; (b) no jump. Averson further obtained data for obliquely-upside-down orientations; not surprisingly, longer ignition times were obtained in these orientations.

In later tests[117] Kashiwagi exposed 15 mm thick clear PMMA and found $\dot{q}''_{\min} \approx 90$ kW m^{-2}, in the horizontal orientation, and 100 kW m^{-2} in the vertical. The difference between 160 and 90 kW m^{-2} is substantial, and Kashiwagi considers it may be due to a more drafty environment and a slightly greater beam size (35 mm vs. 30 mm) in the second series.

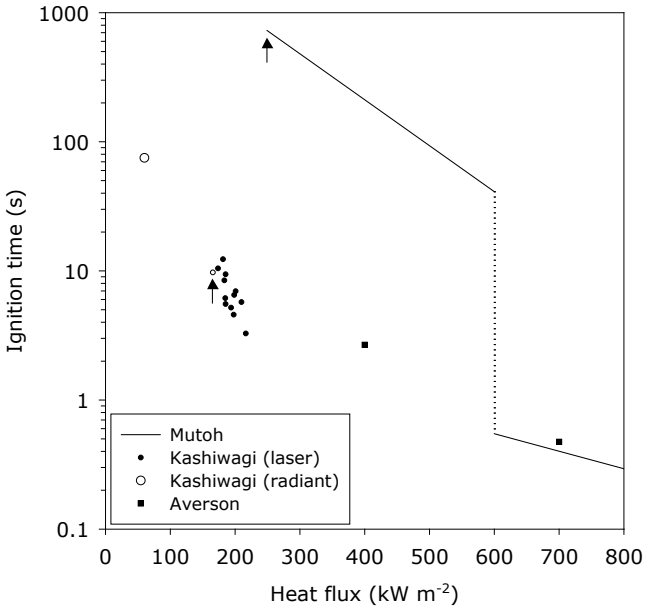


Figure 37 The autoignition of clear, horizontally-oriented PMMA using laser ignition sources (arrows denote minimum flux for ignition)

In his laser exposures, Kashiwagi found that the autoignition temperature for PMMA did not depend on the heat flux, but did depend on orientation, being 400ºC in horizontal and 450ºC in vertical orientation. As can be seen below, these values are at least 100ºC higher than required for piloted ignition. For red oak, he found a very strong dependence on heat flux, with T_{ig} going from 570ºC at 85 kW m^{-2} to 410ºC at 165 kW m^{-2} in the horizontal orientation; in vertical orientation, autoignition temperatures were roughly 80ºC higher.

A study on autoignition of dust layers by focused, high-intensity xenon-lamp radiation has been reported[118]. While not coherent, this radiation source is also very intense and concentrated into a small area. For a variety of dust types, a minimum ignition flux of about 280 kW m^{-2} was found. No comparable data exist for exposures of these substances to conventional radiant heat sources, but the flux value is enormous. Part of the reason for the enormous $\dot{q}''_{\min}$ value might be attributable to the very small heated area used, 3 cm^2. The question why laser ignition is so much different from radiant-panel ignition was indirectly addressed by Hertzberg and Zlochower[119], who studied the mass loss rate of PMMA under radiant-panel and laser heating conditions. They found huge differences between the two sets of results: for example, to obtain an MLR of 10 g m^{-2} s^{-1} required an absorbed radiant flux (incident flux × absorptivity) of about 25 kW m^{-2} with a radiant panel, versus 85 kW m^{-2} using a CO_2 laser. They attributed the differences to (a) the smaller sample dimensions necessary with laser heating, and (b) the indirect effect of higher surface temperatures. Concerning the latter effect, they concluded that the specimen showed T_{ig} values that increase with increasing flux, thus, laser experiments run at high fluxes would intrinsically imply the material is harder to ignite. The authors claimed to have successfully reconciled the two sets of results by calculating the surface heat losses for the two cases, but did not present details to support this.

Piloted ignition. Similarly unusual results are found for pilot-ignition studies with laser sources. Kashiwagi[15] used a CO_2 laser to expose horizontally-oriented samples, with the laser beam providing a heated diameter of 20 – 30 mm on the face of the specimen. He found that 70 kW m^{-2} was the minimum flux for ignition of 12 mm thick samples of clear PMMA (Figure 38). A comparative data point obtained by Thomson[2] using a laser with a 12 mm exposing diameter is also shown. Thomson did not test for the minimum flux, but evidently it was less than 34 kW m^{-2}, which is her data point shown in Figure 38. Also shown are tests done by Thomson using the same specimen material and the same basic experimental rig, but with a radiant heater. It is evident that (1) the slope of the line through Thomson's points is substantially different from that through Kashiwagi's, (2) the *highest* flux used by Thomson was substantially below the *minimum* flux found in the Kashiwagi experiment, and (3) Thomson's ignition time using a laser is about 4 times longer than using a radiant heat source. Thomson speculated that the very long ignition times observed with laser

ignition may be due to certain difficulties that a laser source might create for attaching a weak flame at the surface.

Thomson found little difference in the piloted ignition temperatures for the two types of ignition sources. At a heat flux of 34 kW m^{-2}, the ignition temperature was 320 – 334ºC using the laser source, compared to 305 – 338ºC when igniting specimens of small area with a radiant source (slightly lower values of 306 – 312ºC were obtained when igniting normal-size specimens in radiant-heater ignition tests). Kashiwagi[120], however, obtained different values of T_{ig} for clear PMMA: 360 – 400ºC using a laser source, compared to 280ºC when using a conical radiant very similar to the kind used by Thomson. He attributes this to the fact that his conical heater data were obtained at a low flux of 18 kW m^{-2}, while the laser data were obtained at much higher heat fluxes. But this interpretation must be contrasted to the results of Thomson, who found an extremely small flux dependence for T_{ig}, at least if one leaves aside the question of enormous fluxes, which she did not study. Kashiwagi further considered that the pyrolysis of PMMA has different mechanisms that operate at different temperature regimes, and that this material's chemistry may affect the value of T_{ig} obtained under different heating conditions. Kashiwagi also pointed out that other experiments on the same material indicated that the surface temperature is 390ºC for a sample over which flame is spreading, and is 400ºC for a sample undergoing steady-state burning. Drysdale and Thomson[121] considered that Kashiwagi's high T_{ig} values are unrelated to the nature of the laser radiation, but are simply attributable to the fact that his ignition source was an 0.25 mm platinum wire at 950ºC. As developed in Chapter 4, hot wires are an inefficient form of piloting and some very high temperatures may be needed for ignition to be successful.

It is hard to draw firm and systematic conclusions from studies on laser ignition, apart from the obvious one that the laser ignition mechanism is substantially different from flame or grey-body radiation sources. Consequently, laser-ignition results cannot be intermixed with other types, nor should the results be applied to accidental fires not involving lasers. The following effects may play a role in creating these systematic differences:

(1) Greater attenuation of incident 10.6 μm laser radiation by pyrolysates near the specimen surface than occurs for blackbody radiation which is emitted at shorter wavelengths.
(2) Exposed-area effects, since the exposed area is sometimes very small with laser heating and a smaller exposed area leads to a higher fraction of the heat being lost.
(3) Sample diathermancy effects, since materials may be more diathermanous at 10.6 μm than at the shorter wavelengths characteristic of blackbody sources.

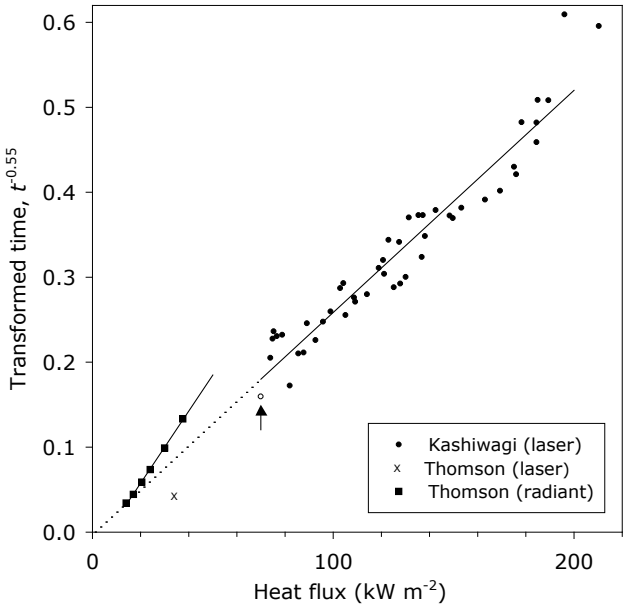


Figure 38 The piloted ignition of clear, horizontally-oriented PMMA (arrow denotes minimum flux for ignition)

(4) Definition of the heat flux used, since the beam from a laser is intrinsically non-uniform (commonly, Gaussian distribution) and it is not clear if the peak, the average, or some other statistic should be considered.
(5) Difficulties in achieving autoignition. The high surface temperatures required for autoignition suggest that there may be gas-phase mixing or autoignition difficulties that are not experienced with other heat sources.
(6) Problems related to rapid turn-off of radiation. Some tests using lasers are run where the beam is turned off after initial ignition, and those results may be influenced by the very rapid rate at which laser radiation can be cut off, which can lead to flame destabilization.
(7) Indirect effects, due to laser experiments commonly being run at much higher heat fluxes than ones using radiant heat sources. The intervening variable here is the surface temperature, which may be higher at very high fluxes, leading to higher surface heat losses and, consequently, a smaller fraction of the incident radiation being available to heat the solid.

Ignition from convective heating or immersion in a hot environment

Until the last few decades, it was most common to study ignition of solid materials by immersing a small specimen into a heated furnaces cavity. The variable being controlled in this type of exposure is the furnace temperature, measured in some arbitrary location. The specimen is heated by a combination of convective and radiative heat flux. Convection—rather than simple conduction—occurs because even if the cavity had no convective currents before the start of test, inserting a cold body into the middle of a hot gas volume will create convective movement. The ASTM

D 1929 test (Setchkin furnace) is the typical example of an environment of this type. The actual convective heat flux is somewhat hard to determine in that environment, and there has not been any research where heat transfer details in the apparatus were probed.

A theoretically more tractable configuration is that of convective heating, where a stream of hot gas with a known velocity and temperature is directed against a specimen. In practice, however, it is hard to arrange this type of heating, since if a high-temperature air stream is being presented to the specimen, there are likely to be equally hot, radiating solid surfaces in the vicinity. Under convective heating, for moderate flow velocities, increasing the velocity simply increases the convective heat flux, and this causes the material to pyrolyze faster and to ignite quicker. Eventually, however, a non-thermal effect comes in: the *residence time* becomes too short for chemical reactions to be completed and this becomes a limit to ignition. The residence time is the time that a molecule has available in an environment where chemical reaction is possible, i.e., where the temperature is high enough. This is sometimes known as a 'Damköhler number effect.' In addition to decreasing the available reaction time, increasing the velocity of the air stream also dilutes the pyrolysates.

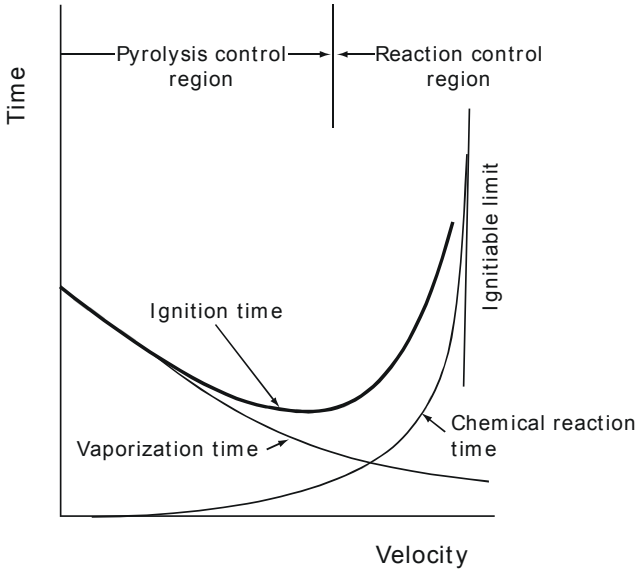


Figure 39 Effect of convective flow velocity on ignition time
(Copyright The Combustion Institute, used by permission)

Niioka et al.[122] illustrated the residence time effect as shown in Figure 39. There is an optimum air flow velocity, and increasing or decreasing it will cause the ignition times to get longer. They also obtained experimental results for several polymers which were configured as hemispherical samples and presented with an impinging-jet flow of heated gas. Figure 40 shows their results for several polymers ignited with an air stream having 60% O_2 and heated to 840ºC (HTPB denotes hydroxyl-terminated polybutadiene). The convective heat flux plotted on the x-axis is the value determined with reference to the specimen's face temperature (20ºC) before its temperature starts rising. For heat fluxes up to 70 kW m^{-2} in the case of PMMA and up to 120 kW m^{-2} for the other two specimens, the ignition time decreases with increasing heat flux. For larger convective heat fluxes, however, the ignition times start rising again. The velocity corresponding to 70 kW m^{-2} was 4 m s^{-1} and for 120 kW m^{-2} it was 10 m s^{-1}. Niioka also showed that for any given gas-stream temperature and oxygen concentration there exists a maximum flow velocity, beyond which ignition is impossible. This maximum velocity increases with increasing gas-stream temperature. Wang and Yang[123] presented some limited data on PMMA spheres, showing that an optimum flow velocity exists and that ignition times get longer for faster or slower flows.

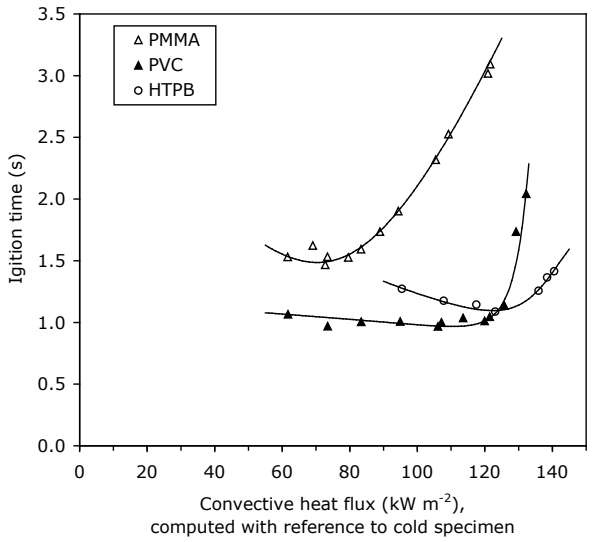


Figure 40 Effective of high flow velocities on convective ignition

Di Blasi et al.[124] studied the autoignition of loosely-packed straw beds (ρ = 50 kg m^{-3}) by subjecting them to a high-temperature air stream. For air stream temperatures below 270ºC, no ignition was obtained. For higher temperatures, increasing the air stream temperature also increased the temperature of ignition, as shown in Figure 41. It may also be that the air stream velocity influences the specimen's T_{ig}, but the effect, if any, was smaller than the data scatter. At a given air stream temperature, ignition times monotonically decreased with increasing velocity. The trends shown in Figure 42 indicate that $t_{ig} \propto u_{\infty}^{-1.2}$. Thus, in the study of Di Blasi et al., an 'optimum' velocity was not found. This is most likely due to two factors: (1) only low ($\leq$ 2 m s^{-1}) velocities were explored, and (2) there may be some peculiarities associated with the material tested, which exhibits a propensity for glowing ignition. Over the range $0.2 < u_{\infty} < 2.0$, their ignition time results can be represented by:

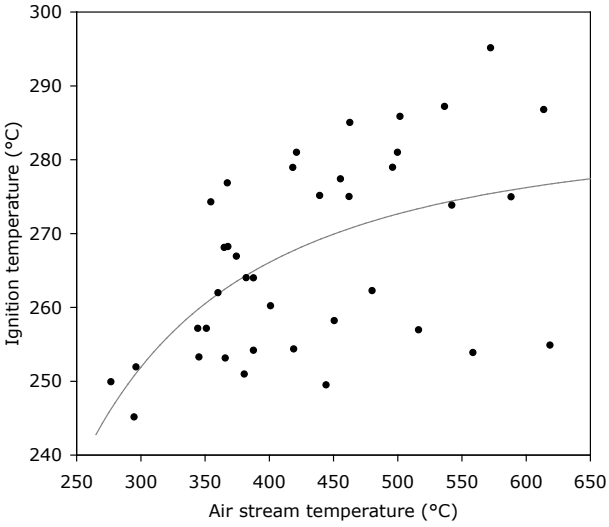


Figure 41 Effect of air stream temperature on the ignition temperature of straw beds

$$t_{ig} = 1.4 \times 10^4 u_\infty^{-1.2} \left(T_g - T_{ig}\right)^{-1.5}$$

however, in view of the limited amount of data collected, this relation should be viewed only as a rough trend.

Akita[125] conducted a convective-ignition study on PMMA samples, independently varying the temperature and the velocity of the hot air stream. Figure 43 shows that the surface temperature at ignition varies with the heating conditions. Using higher velocities requires that higher air-stream temperatures also be used, and this results in a higher surface temperature at ignition. From these results it can be seen that—unlike in radiative ignition—for convective ignition, the heat flux is not a useful data correlating variable, since air stream velocity and temperature affect the results not simply in proportion to the computed heat flux. Akita's results imply that the optimum velocity is very low, below 0.5 m s^{-1}, and this suggests that gas-phase effects militate against a simple inert-solid conceptual model of convective ignition.

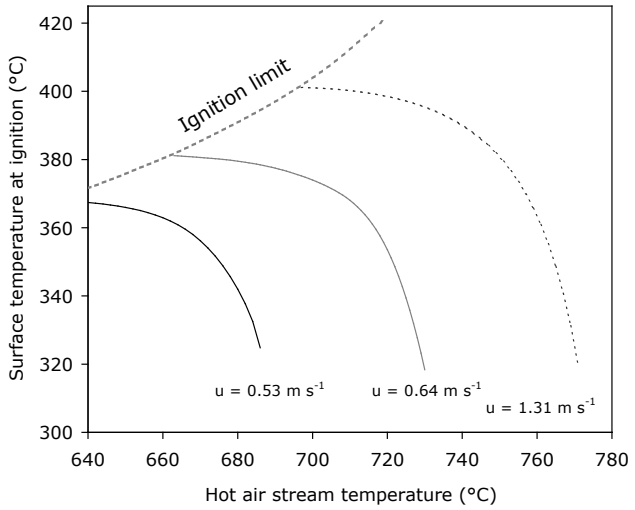


Figure 43 Convective autoignition of PMMA in a hot air stream for three different air-stream velocities
(Copyright Elsevier Science, used by permission)

Convective heating was also used by Clark, who studied the ignition of several polymers[126-128]. In his experiments, he subjected the specimens to the high-temperature products of a very lean H_2/O_2 flame, directed at the specimen in the form of an impinging jet and producing quite low heat fluxes of 11 – 20 kW m^{-2}. Clark found that T_{ig} values for

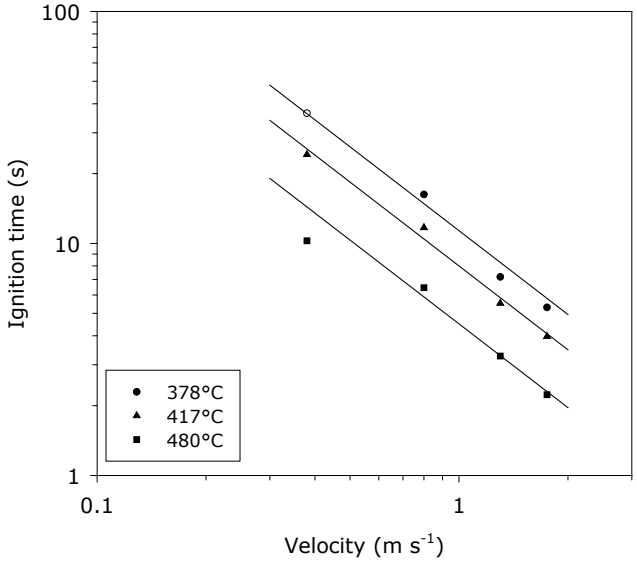


Figure 42 Ignition of straw beds from a hot air stream

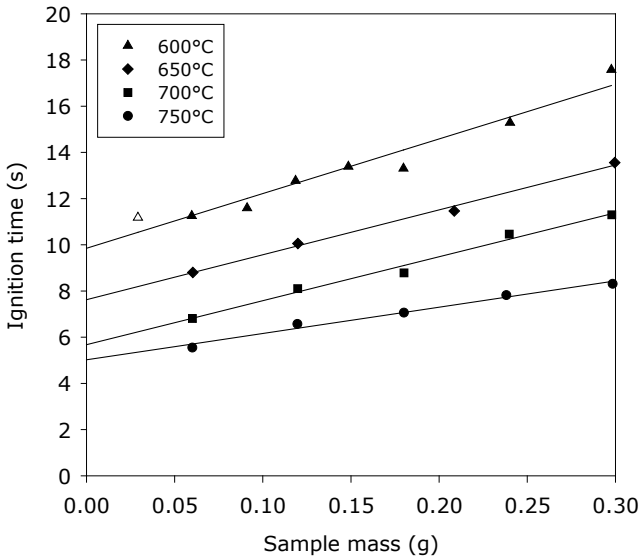


Figure 44 Ignition times for nylon 6,6 specimens

PMMA ranged from 227ºC to 420ºC, depending on temperature/velocity conditions.

Miller and coworkers[16] reported on a study using an apparatus somewhat similar but not identical to the Setchkin furnace to study autoignition of very small specimens. They observed that, for most materials, the ignition time varies linearly with specimen mass (Figure 44). Based on this, they concluded that it is possible to describe a 'characteristic' ignition time which is obtained by extrapolating the mass vs. time data to zero mass. For seven materials tested, this proved to be reasonable for all except polyacrylonitrile (PAN). In the case of PAN, there was no effect of specimen mass on ignition time, except at the lowest temperature examined, 525ºC.

Having obtained 'characteristic' ignition times for each exposure temperature, Miller et al. then correlated the results as shown in Figure 45. As explained by Hertzberg and Zlochower[119], results of this type should not be interpreted to imply that the slope is an activation energy associated with a chemical reaction. The activation energy obtained from the slopes, here typically 35 kJ mol^{-1}, correspond to the energy requirement for a *physical* process* (the gasification of the polymer) and not a chemical one.

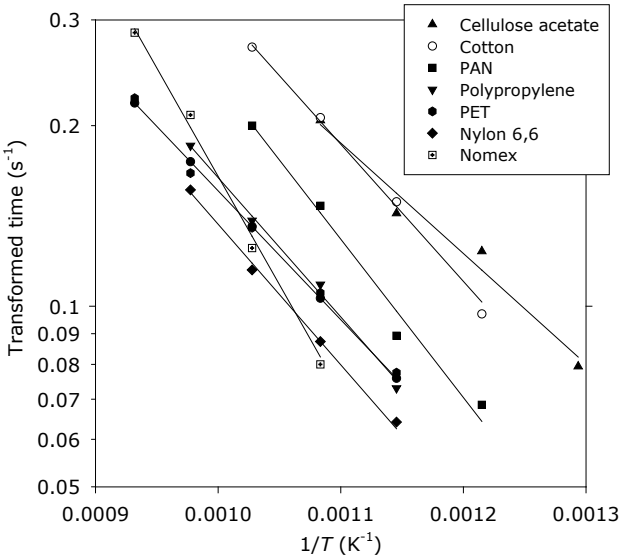


Figure 45 Relation between furnace temperature and ignition time of fabrics, as expressed according to an Arrhenius plot
(Copyright John Wiley & Sons; reprinted by permission)

IGNITION THEORIES FOR CONVECTIVE HEATING

LUMPED-CAPACITANCE MODEL

The simplest analytical treatment of the convective heat transfer environment is by what is called in heat transfer literature a *lumped-capacitance model*. If a solid body is thin enough, then at any instant it can be assumed that it is all at one temperature, $T_s(t)$, which is a function of time, but not a function of location. By heat conservation,

$$\textit{heat in} - \textit{heat out} = \textit{heat stored}$$

or,

$$2h_{eff}\,S\left(T_g - T_s\right) = \rho V C \frac{dT_s}{dt}$$

where we have assumed that heat transfer occurs over two faces, each of area S (m^2). Other terms are: T_g = gas temperature (K), h_{eff} = effective heat transfer coefficient (W m^{-2} K^{-1}), ρ = density (kg m^{-3}), V = volume (m^3), C = heat capacity (J kg^{-1} K^{-1}). If the thickness is $2r$, then $V = 2rS$, giving

$$\frac{dT_s}{dt} = \frac{h_{eff}\left(T_g - T_s\right)}{r\rho C}$$

The initial condition is $T_s = T_o$, at $t = 0$. With this, the solution can be obtained as[129]:

$$T_s(t) = T_g - \left(T_g - T_o\right)\exp\left[-\left(\frac{h_{eff}}{r\rho C}\right)t\right]$$

The heat transfer solution becomes a solution to the ignition problem, once a specific ignition temperature, T_{ig}, is associated with the temperature of the body at ignition.

$$t_{ig} = \frac{r\rho C}{h_{eff}}\ln\left[\frac{T_g - T_o}{T_g - T_{ig}}\right]$$

In some cases, the values of T_{ig} do not vary greatly for a group of materials being considered. The above relation then shows that $t_{ig} \propto r\rho$. In other words, for thin materials the ignition time should be directly proportional to the mass per unit area (kg m^{-2}) of the material. This has been experimentally shown to be true for fabrics (see Chapter 14).

THERMALLY-THICK SOLID—CONSTANT HEAT FLUX

In some cases, materials are ignited by very hot convective heat streams. If $T_g >> T_{ig}$, then the heat flux remains approximately constant during the heating of the specimen. In that case, the same treatment can be used as is described by Janssens for radiant heating; this type of data treatment was originally proposed by Keller et al.[74].

THERMALLY-THICK SOLID—CONSTANT CONVECTIVE TRANSFER COEFFICIENT

In 1954, Hicks[130] published the first study of this problem. He started with the basic equation:

$$\rho C\frac{\partial T}{\partial t} = \lambda\nabla^2 T + \dot{q}'''$$

where $\dot{q}'''$, the energy of pyrolysis per unit volume, is expressed as:

$$\dot{q}''' = \rho Q A e^{-E/RT}$$

* More precisely, a quasi-physical process. Gasification of liquids is a purely physical process but gasification of polymers is accompanied by chemical changes.

and the front face boundary condition is:

$$-\lambda \frac{\partial T}{\partial x} = h_c\left(T_g - T_s\right) \qquad \text{at } x = 0$$

where T_g = temperature of gas (K) and T_s = temperature of front face of slab (K). From this theory, Hicks could construct plots of ignition time versus front-face temperature, given explicit values of the material constants. This unfortunately is the inverse of the problem which is normally encountered—one normally starts with measured data, then a procedure is needed to convert the data into material 'properties,' and only then can the properties be used in calculating what would have happened under different conditions. Later, the Russian researchers Lisitskii and Merzhanov[131] conducted a number of experiments and concluded that $t_{ig} \propto h_c^{-1.64}$. By itself, this is not too useful since one normally wishes to find the dependence on the flow velocity u_∞ and the gas temperature T_g, instead. By using a kinetic model and making a number of approximations, they did produce a closed-form (but not explicit) equation relating t_{ig}, h_c, T_g, T_o, and a number of chemical kinetics constants. In the absence of the latter, the method would not be useful. More problematically, their basic heat-transfer coefficient dependence is questionable. For flow past a flat plate, the dependence of h_c on u_∞ in their theory is such as to give $t_{ig} \propto u_\infty^{-0.82}$, in other words, the ignition time is predicted to monotonically decrease with increasing gas flow velocity. But the available experimental data discussed above indicate that the actual relationship is not monotonic and that different regimes exist where raising the velocity may either help ignition occur quicker or retard it.

THERMALLY-THICK SOLID—BOUNDARY LAYER SOLUTION

Kashiwagi et al.[132] used a shock-tube apparatus to create a heated gas stream, which was directed past a flat plate specimen of polybutadiene-acrylic acid (PBAA). They found that ignition occurred at a varying distance upstream of the leading edge, with this distance decreasing as the oxygen concentration of the air stream was increased. They explained this as a reaction-time effect—since reactions take longer at a lower oxygen concentration, a longer travel time along the flow stream was required for ignition. They also developed a theory based on a self-similar, laminar boundary-layer, treating the gas-phase in a 2-dimensional way, but the solid only as an inert solid subjected to 1-dimensional heating. In a follow-on study[133], they eliminated the similarity assumption. Both models made use of single-step Arrhenius kinetics in the gas phase, but the authors pointed out that the constants needed for a reaction-rate term of this kind were not available. Furthermore, the model solutions required difficult numerical computations and did not lead to any closed-form approximations. A similar theory was presented more recently by Cordova et al.[134]; again, it did not lead to user-accessible solutions. Coffin[135] performed numerical modeling of the autoignition of PMMA in a boundary layer flow with radiative heating. The results showed a decrease in ignition time with increased sample length, the decrease being substantial for laminar flows and small for turbulent.

IGNITION THEORIES FOR SUBMERSION IN HOT ENVIRONMENTS

Unlike in the radiant-heating problem (where the specimen is convectively cooled), in this problem, both the radiant and the convective heat transfer terms are heat gains. The radiant heating term is:

$$\alpha_s \sigma\left(T_f^4 - T_s^4\right)$$

where the view factor, for reasons of thermal submersion, is unity. Unlike in the standard radiant-heating problem, however, *all* of the sides of the specimen are subject to this heating flux. The convective heat transfer term is:

$$h_c\left(T_f - T_s\right)$$

Since typically the tests where this environment is created involve thin specimens, the problem becomes difficult since 3-dimensional heat transfer must be calculated in the solid. No published solutions to this problem have been found.

Hermance et al.[136] treated the case of *conduction* heating, where convective velocity is negligible, as is radiation. They formulated the problem as 1-dimensional and included chemical reactions both in the solid and in the gas phase. Example computed results and extensive sensitivity analyses were presented, but no closed-form approximations were obtained. Furthermore, the simplifying assumptions they needed to make will rarely apply to accidental ignitions of solids. Lack of convective flow can be arranged if the specimen is presented with a hot gas in a face-down orientation, but to ignite solids generally a temperature is needed which is high enough that ignoring radiation is not reasonable.

Theoretical solutions for other problem conditions

For solids being heated in a 1-dimensional way, as we have developed above, the most common practical situation will be radiant heating, with simultaneous convective cooling and re-radiation from the front face. Occasionally, purely convective heating may be a reasonable representation of physical events. A large number of additional theoretical studies have been published that use boundary conditions which are only rarely encountered with practical substances. In this section, we briefly overview studies of this type.

THERMALLY-THICK INERT SOLID WITH FIXED NET HEAT FLUX

For one very simple case, exact solutions can be found in the classical heat conduction literature. If chemical reactions are ignored, the body is assumed to be infinitely thick, and the surface boundary condition is couched in terms of a

net heat flux (convection, plus absorbed radiation, minus surface re-radiation), then the solution is[137]:

$$t_{ig} = \frac{\pi \lambda \rho C_p}{4} \frac{\left(T_{ig} - T_o\right)^2}{\dot{q}''^2_{net}}$$

This solution, while mathematically easy, is unlikely to be useful, since under almost any heating conditions that arise in fires, the net heat flux varies with time even if the externally-imposed radiant flux is fixed.

THERMALLY-THICK INERT SOLID WITH FIXED HEAT FLUX AND CONVECTIVE COOLING

This problem resembles the practical one treated earlier in this chapter, except that re-radiation is omitted. The front face temperature is given by[138]:

$$T = T_o + \frac{\dot{q}''}{h_c}\left[1 - \exp\left(\frac{h_c^2}{\rho C}\right)\operatorname{erfc}\left(\frac{h_c t^{1/2}}{(\lambda \rho C)^{1/2}}\right)\right]$$

THERMALLY-THICK REACTIVE SOLID WITH FIXED HEAT FLUX

For many common solids, exothermic reactions within the solid can be ignored if the solid is heated at a relatively high heat flux. As heat fluxes get progressively lower, however, it becomes less accurate to use an inert-solid model. Already in 1959 Thomas et al.[6] observed that the effect may be significant. Some example data obtained by Urbas are shown in Figure 46. In his experiments, he exposed 16 mm particleboard using the ICAL apparatus and measured the surface temperature without, however, continuing the tests until ignition. The specimens reached a quasi-steady state at about 250 – 260ºC, then self-heating became pronounced and a new quasi-steady-state at 350 – 400ºC was noted.

A large number of studies have been published which consider the fixed-heat-flux case where a single, Arrhenius-form reaction is assumed to occur in the solid. The gas phase is still ignored. Liñán and Williams[139,140] solved the basic heat conservation equation:

$$\rho C \frac{\partial T}{\partial t} = \lambda \frac{\partial^2 T}{\partial x^2} + \rho A Q \exp\left(-E / RT\right)$$

where zero-order Arrhenius kinetics was assumed. They obtained an approximate solution for T_{ig} as:

$$T_{ig} \approx \frac{E}{R}\left[\ln\left(\frac{\lambda \rho C T_o A}{\dot{q}''_e}\right)\right]^{-1}$$

Using the above value, they proposed that the ignition time can be iteratively obtained from:

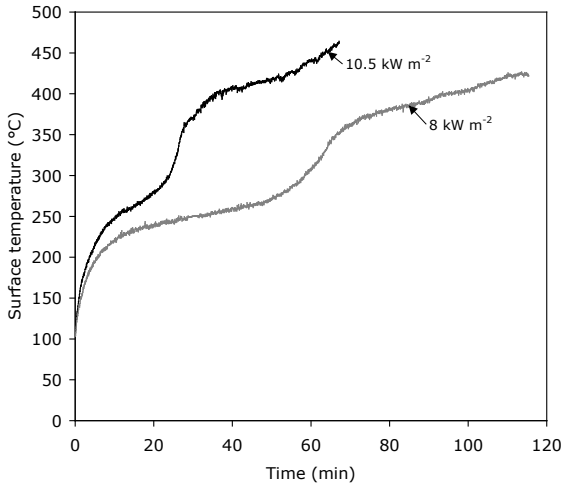


Figure 46 Front surface temperatures on 16 mm thick particleboard (back face open to air) exposed to low heat flux radiant heating
(Courtesy Joe Urbas)

$$t_{ig} = \left(\frac{\pi \lambda \rho C T_o^2}{4 \dot{q}''_e}\right) \times$$

$$\left\{\left[\ln\left(\frac{\lambda \rho C T_{ig} A}{0.65 \dot{q}''^2_e \sqrt{E / RT_o}}\left(\frac{\pi \dot{q}''^2_e t_{ig}}{\lambda \rho C T_o^2}\right)^{1/4}\right)\right]^{-1}\left(\frac{E}{RT_o}\right) - 1\right\}^2$$

Another approximate, closed-form (but not explicit) solution was provided by Harrach[141]:

$$t_{ig}^{1/2} \exp\left[-\frac{E/R}{\dot{q}''_e z t_{ig}^{1/2} + T_o}\right] = \frac{\dot{q}''_e z C}{2QA}$$

where $z = \alpha_s \sqrt{\frac{1.26}{\lambda \rho C}}$

Andersen[142] used a similar starting point, a solid undergoing a single Arrhenius-form reaction. In his case, he assumed a diathermanous solid being heated by a radiant heat flux; convective heat transfer was ignored. He proposed that a quasi-ignition temperature, T_c, can be determined in the following way. The time to ignition is defined as:

$$t_{ig} = t_{inert} + t_{ad}$$

where t_{inert} is the time needed to heat the specimen to the temperature at which reactions start, while t_{ad} is the chemical reaction time needed, considering only events in the solid phase. For t_{ad}, he took the Frank-Kamenetskii expression for the adiabatic induction period of a thermal explosion (this concept is covered in Chapter 9). The value of T_c is then found by making the reasonable, but *ad hoc*, assumption that this temperature corresponds to the time at which the rate of temperature rise due to chemical heating becomes equal to the rate of rise due to external heating. By differentiating the expressions for temperature rise due

to external heating and temperature rise due to chemical reactivity and setting them equal to each other, a value of T_c is found. This value of T_c is then inserted into the inert-substance equation and a time is obtained to reach T_c. The expression for t_{ad} is explicitly available, and the ignition time is then obtained by summing the two times. The procedure, while relatively straightforward, does not yield a single equation for expressing ignition time, thus it has not seen much use.

Another theoretical formulation was developed by Staggs[143,144], who incorporated a more generalized pyrolysis model into the problem. He writes the fundamental energy equation as:

$$\rho C \frac{DT}{Dt} = \lambda \frac{\partial^2 T}{\partial y^2} - \rho L_v A \mu^{n-1} \exp(-E/RT)$$

where y is the distance measured from the initial location of the top surface and D/Dt represents the 'convective derivative,' that is, the derivative with respect to time, following a material element. If the material flows past position y at a speed v, then $D/Dt = \partial/\partial t + v\partial/\partial y$. The chemical reaction term is based on a scalar μ which describes the progress of degradation in the solid phase, evolving according to

$$\frac{D\mu}{Dt} = -A\mu^n \exp(-E/RT)$$

where $v(y,t) = A\int_y^L \mu^{n-1} \exp(-E/RT)dy$. The instantaneous position of the top surface is denoted as $y = s(t)$. Then, the limits of the solid at any time are $s(t) \le y \le L$. The boundary conditions are:

$$-\lambda \frac{\partial T}{\partial y} = \varepsilon \dot{q}'' + h(T_o - T) + \varepsilon\sigma(T_o^4 - T^4) \qquad \text{at } y = s(t)$$

$$\frac{\partial T}{\partial y} = 0 \qquad \text{at } y = L$$

where it is assumed that the specimen is thick enough so that adiabatic rear face conditions will apply. Staggs obtained numerical solutions to the above equations and used them to evaluate the differences between various simplified ignition criteria that have been proposed. If the reaction kinetics is fast, then when the incident heat flux is varied there is little variation in the surface temperature at which a certain critical mass loss rate is reached. For slow reaction kinetics, however, raising the heat flux causes the critical mass loss rate to occur at a notably higher temperature. The model also predicts that, after ignition, the 'quasi-steady' front-face temperature is higher for thin specimens and lower for thick ones. Thus, it becomes clear that, in the general case, the problem does not have a 'characteristic temperature' which would be governed solely by its physicochemical properties: both the ignition temperature and the quasi-steady surface temperature vary with dimensions or heat flux conditions. Kinetics, while not being the only factor controlling the surface temperature, of course does affect it: faster reactions do result in lower quasi-steady surface temperatures.

Other studies of a mathematical nature on the problem have been published by Thomas[145] and by Adler and Thorne[146]. These have not culminated in closed-form expressions for problem solving.

FINITE-THICKNESS INERT PLATE WITH FIXED HEAT FLUX

A solid of finite thickness L is amenable to theoretical solutions if the back face is insulated while the front face receives a fixed heat flux. Carslaw and Jaeger[137] give the front face temperature solution as:

$$\frac{(T_x - T_o)\lambda}{\dot{q}''_{net} L} = Fo + \frac{1}{3} - \frac{2}{\pi^2}\sum_{j=1}^{\infty} \frac{1}{j^2} e^{-j^2\pi^2 Fo}$$

where $Fo = \dfrac{\alpha t}{L^2}$ = Fourier number.

FINITE-THICKNESS REACTIVE PLATE

Annamalai and Durbetaki[147] formulated a solution for a thin, porous plate heated by an impinging hot-gas jet. The plate gasifies according to a single-step Arrhenius kinetics. They were able to obtain an explicit solution (in quite complex form) only under the additional assumption that the rear face of the plate is adiabatic.

FINITE-THICKNESS POLYMER UNDERGOING CHARRING

Staggs and coworkers[148] developed at interesting, first-order theory to represent the ignition of a polymer which undergoes charring when subjected to heat. Ignition was assumed to occur the moment that a specified minimum mass loss rate is first attained. The physics of the model is probably too simple for it to be calculationally useful, but the authors found a number of notable trends:

- materials which produce a low amount of char behave qualitatively similar to non-charring ones;
- materials with an intermediate charring tendency show a time jump below a certain heat flux—ignition times become abruptly much greater at lower fluxes
- materials showing a high char-yield fraction become non-ignitable below a relatively critical heat flux and there is no region of long ignition times below the critical heat flux.

Charring materials tend to produce a two-hump mass-loss-rate curve, and the nature of this behavior becomes more clear when viewed in the context of this curve. If the mass loss rate at, or before, the first peak exceeds the minimum rate needed for ignition, then ignition takes place relatively rapidly. On the other hand, if the mass loss rate at first peak does not reach the minimum MLR value, it may take a long time before sufficient MLR is attained on the second peak. The second peak, by the way, corresponds to a time when the material has become thermally-thin and virgin material

is no longer available deeper into the sample to absorb supplied energy.

THERMALLY-THICK REACTIVE SOLID HELD AT A FIXED FACE TEMPERATURE INDEFINITELY

The front face of a semi-infinite body is held at a temperature T_s indefinitely. The situation physically corresponds to an infinitely thick solid being placed on a hot plate. A flaming ignition is impossible in that case, since there exists no surface open to air, but a smoldering ignition could occur. The problem has no meaningfulness for an inert solid, but can be useful in analyzing test data on explosives or unstable substances. Consequently, it is assumed that there is a temperature-dependent chemical reaction taking place within the solid. The initial and boundary conditions are: $T = T_o$ for all x and for $t < 0$. $T = T_s$ for $x = 0$ and $t > 0$. According to Vilyunov[153], the ignition time is found to be:

$$t_{ig} = \left[1 + \frac{2E}{RT_s^2}(T_s - T_o) + 0.163\left(\frac{E}{RT_s^2}(T_s - T_o) \right)^2 \right] \times \frac{RT_s^2}{E}\frac{C}{QA}\exp(E/RT_s)$$

A solution was also obtained by Cook[149] using a different numerical method and different approximations. His results for the ignition time expressed non-dimensionally[150] are:

$$\tau_{ig} \approx 0.20\theta(\theta + 8)$$

where $\tau_{ig} = \dfrac{t_{ig}}{t_{ad}}$, $t_{ad} = \dfrac{RT_o^2}{E}\dfrac{C}{AQ}\exp(E/RT_o)$, and $\theta = \dfrac{E}{RT_o^2}(T_s - T_o)$.

The results can be represented as:

$$\ln\left[\frac{t_{ig}}{T_s - T_o} \right] = \frac{E}{RT_s} + b_o$$

where the constant b_o is:

$$b_o = \ln\left[\frac{0.2\rho C}{QA}\left(\frac{E}{R}\frac{T_s - T_o}{T_s^2} + 8 \right) \right]$$

Consequently, plotting the left-hand side quantity on the y-axis and $1/T_s$ on the x-axis should give a slope of E/R. The value of b_o, obtained as the x-axis intercept, can then be used to obtain $\rho C/QA$. Experimentally, it was found that data fall on a straight line only in the short ignition time regime[151]. Liñán and Williams[152] provided another solution to this problem.

THERMALLY-THICK REACTIVE SOLID HELD AT A FIXED FACE TEMPERATURE FOR A FINITE TIME

The front face of a semi-infinite body is held at a temperature T_s for a certain length of time, t_*. Then the front face is maintained at adiabatic conditions. What is the shortest time t_* for the front face to be heated so that ignition can occur (ignition occurs at time t_{ig} which is later than t_*)? The substance is assumed to behave according to zeroth order Arrhenius kinetics, with the heat conservation equation being:

$$\rho C\frac{\partial T}{\partial t} = \lambda\frac{\partial^2 T}{\partial x^2} + \rho AQ\exp(-E/RT)$$

and the initial and boundary conditions are: $T = T_o$ for all x and for $t < 0$. $T = T_s$ for $x = 0$ and $0 < t \le t_*$. $dT/dx = 0$ for $x = 0$ and $t > t_*$. Vilyunov[153] solved the problem numerically and determined that

$$t_* = 0.214\left(1 + 1.44\frac{RT_s}{E} \right)\frac{EC(T_s - T_o)^2}{RT_s^2 QA}\exp(E/RT_s)$$

where E = activation energy (kJ mol^{-1}), R = universal gas constant (8.314 J mol^{-1} K^{-1}), T_o = initial temperature (K), C = heat capacity (kJ kg^{-1} K^{-1}), Q = heat of reaction (kJ kg^{-1}), and A = pre-exponential factor (s^{-1}). It is realized, of course, that for most solids the kinetic constants E, Q, and A will not be known and will have to be treated as data fitting parameters.

THERMALLY-THICK REACTIVE SOLID RECEIVING FIXED RADIANT HEAT FLUX ONLY

If the heat reradiated from the front face is ignored, convection is also ignored, and the only external heat entering the body is a net heat flux at the front face, $\dot{q}_r''$, then Vilyunov's approximate solution can be used. His method is indirect since it first requires that an intermediate variable be solved for, a fictitious temperature T_h. This is given by the implicit equation:

$$QA\lambda\rho e^{-E/RT_h}\frac{\pi}{2}(T_h - T_o) = \dot{q}_r''^2$$

If one know all of the thermochemical and kinetic constants of the material, then the only unknown is T_h, since T_o is the given initial condition. The value of T_h is not given explicitly, but can be obtained by a few trial iterations. Having determined T_h, the ignition time is obtained as:

$$t_{ig} = \left[1 + \frac{E(T_h - T_o)}{2RT_h^2} \right]\frac{RT_h^2}{E}\frac{C}{QA}e^{E/RT_h}$$

The surface temperature at ignition, T_{ig}, is determined from:

$$T_{ig} = T_h\left[1 + \frac{RT_h}{E}\left(1 - \frac{RT_h^2}{2E(T_h - T_o)} \right) \right]$$

The condition for thermal-thickness is that the thickness L obey:

$$L > \frac{\pi}{2}\frac{\lambda(T_h - T_o)}{\dot{q}_r''}$$

Vilyunov's solution is interesting in that it captures much, though not all, of the physics of the real problem and allows some illustrative computations to be made. For example, knowing the thermochemical properties, it is not difficult to determine the dependence of the surface temperature at ignition, T_{ig}, on the heat flux, $\dot{q}_r''$. The computations in-

dicate that T_{ig} rises with increasing $\dot{q}''_r$, which is experimentally found to be true, although the simple solution here over-predicts this increase. In contrast with the above set of equations, which slightly underestimated the ignition time, Vilyunov also offers an alternative solution, which slightly underestimates the ignition time:

$$QA\rho e^{-E/RT_q}\frac{2\lambda RT_q^2}{E}=\dot{q}''^2_r$$

$$t_{ig}=\frac{0.7\lambda\rho C}{\dot{q}''^2_r}\left(T_q-T_o\right)^2$$

The variable T_q is, close to, but not exactly, the surface temperature at ignition.

SOLID RECEIVING A BRIEF, HIGH-INTENSITY PULSE OF RADIATION

This problem was important in the 1950s when thermal ignitions due to nuclear weapons attacks were being studied (see Chapter 11). This problem can be complicated because, in many instances, a pulse of this nature will give a flash ignition but not a sustained ignition. Vilyunov[153] discusses some solutions and limitations.

POROUS SOLIDS

Telengator et al.[154] extended the analysis of Liñán and Williams to the case where the solid was porous. The detailed solution, despite numerous simplifications, could only be achieved by numeric computations. However, a first-order approximation was developed:

$$t_{ig(porous)}\approx t_{ig(non-porous)}\times\left(1-\varepsilon\right)\left(1-\varepsilon+\lambda_g\varepsilon/\lambda_s\right)$$

where $\varepsilon=\dfrac{\text{volume of voids}}{\text{total volume}}$, λ_g = gas phase conductivity (W m^{-1} K^{-1}), and λ_s = solid phase conductivity (W m^{-1} K^{-1}). The above relation pertains to the situation where the surface releases the pyrolysis gases readily. If an impervious surface exists, then ignition times are invariably shortened for a porous solid, since expanding gases drive energy further into the body[155].

DIATHERMANOUS SOLIDS

Many materials absorb heat in depth, not being fully opaque. Diathermancy always increases ignition time and thus, as a conservative approximation, might be neglected. When it needs to be treated, the Beer-Lambert Law is invoked, which states that for a parallel beam of monochromatic radiation passing through an infinitesimally thin slice of a homogeneous absorbing medium, the energy absorbed within the slice is proportional to the incident energy times the slice thickness times a material constant. Using this, the energy balance for the 1-dimensional case becomes:

$$\rho\, C_p\frac{\partial T}{\partial t}=\lambda\frac{\partial^2 T}{\partial x^2}+\alpha_s\dot{q}''_e\beta\exp\left(-\beta x\right)+\dot{q}'''$$

where β = in-depth absorption coefficient (m^{-1}). Because a new, entirely independent variable has been introduced into the problem, it becomes much more difficult to seek a closed form solution. Gardon and Michalik presented numeric and graphical solutions to the basic heat transfer problem[156]. The approximation methods of Vilyunov[153], while not giving closed-form solutions, at least provide the possibility of obtaining a solution without computer programming, although some iterative algebraic calculations need to be done. The asymptote at extremely high heat fluxes is[157]:

$$T_s(t)-T_o=\frac{\beta\,\dot{q}''_e t}{\rho\, C_p}$$

thus, the extreme-heat flux t_{ig} can be approximated by setting $T_s = T_{ig}$. If $\dot{q}'''\equiv 0$, then the surface temperature can be obtained from the following equation[158], although further approximations would be needed to solve explicitly for the ignition time:

$$T_s(t)-T_o=\frac{\alpha_s\dot{q}''_e}{\lambda\beta}\times\left[2\beta\sqrt{\frac{\lambda t}{\pi\rho C}}-1+\exp\left(\beta^2\frac{\lambda t}{\rho C}\right)\operatorname{erfc}\left(\beta\sqrt{\frac{\lambda t}{\rho C}}\right)\right]$$

MISCELLANEOUS GEOMETRIES

Vilyunov[153] provides a number of solutions for a semi-infinite cylinder which is heated by conduction or radiation at its end surface and convectively cooled along the sides. Other solutions include pulses of radiation, combustible material behind thin non-combustible slabs, hot wires passing through thick bodies, and imposed heat fluxes which vary with time. In general, solutions are developed in a way where the differential equations are non-dimensionalized with respect to an arbitrary temperature scale, then a separate solution is made for this normalizing temperature, which has only a conceptual, not a physical meaning. All of these procedures require a fair bit of algebraic manipulation and some trial-and-error iterative solutions of auxiliary equations in order to produce results.

DEPLETION OF REACTANTS NOT IGNORED

A zero-order kinetics is generally a poor assumption for charring or pyrolyzing solids, since reaction rates change significantly due to depletion of reactants. For these materials, Martin[11] considers that first-order kinetics should be used. This makes the problem significantly more difficult, since now there are two variables—temperature and density—that need to be solved for, instead of temperature alone. Assume that there is only one reactant that needs to be taken into account and that its initial concentration is c_o. Then

$$\frac{dc}{dt}=-c^n Ae^{-E/RT}$$

where the minus sign reflects that it is the concentration of reactants, not products, that is being evaluated. The initial condition is $c = c_o$ at $t = 0$. For a solid, it is most convenient to consider that the concentration is the density, thus

$$\frac{d\rho}{dt} = -\rho^n A e^{-E/RT}$$

As discussed above, Melinek[26] solved this problem numerically; no closed-form approximations emerged from his study. In general, if a solution for mass loss rate must be made, two different simplifications can be considered:

1. Assume that the front face does not move, but the material progressively loses density, with the density loss being greatest at the front face. This was the assumption taken by Melinek.
2. Assume that the substance simply sloughs material off the front face, without changing the density of the material which remains. This is the ablative limit and might be appropriate for non-porous thermoplastics exposed to very high heat fluxes.

A large number of authors have developed models with explicit first-order kinetics and some other studies of this type are discussed elsewhere in this Chapter.

Ignition from localized sources

SMALL FLAMES

The engineering theory presented above assumes that the response of a small surface area element *dA* is typical of the entire surface being ignited. This will not be true if: (1) the specimen is small, or (2) the ignition source is small. By small, we mean that edge effects will predominate and that no part of the source/specimen is far away from the edge. A Bunsen burner is a small ignition source, since nowhere in its flux field can there be found a region of uniform heating and one situated far from all edges. A room-heating stove igniting a wallboard is probably not a small source, since typically the ignited area will be substantial in size. Here, both the source and target are large. A small target and a large source could be exemplified by an electric cord igniting from the radiant heat of a nearby malfunctioning furnace.

In each of the 'small' ignition cases, the heating conditions and the combustible gas evolution cannot be represented as a portion of a uniform surface. Thus, the heat flow problem becomes 3-dimensional, instead of being 1-dimensional. While mathematical computation of 3-d heat flow is certainly feasible, nonetheless setting up such computational problems is tedious. Worse yet, the results, because of the numerous geometric variables, do not have enough generality to be reduced to simple formulas, nomographs, etc. Thus the problem has rarely been studied; an example is by Thomas[159].

Another issue with small-specimen ignition is the question of dimensional changes. When a small specimen shrinks, flows, thermally deforms, chars, intumesces, etc., it can significantly change the critical distances between the flame combustion zone and its own surfaces. This becomes almost impossible to represent mathematically; we know of no success stories in this area.

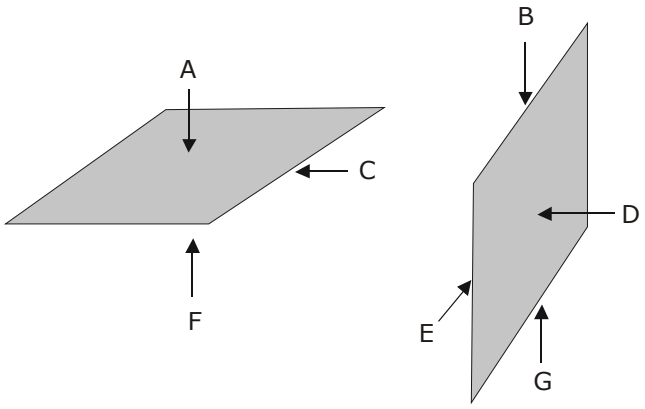


Figure 47 The 7 geometric locations at which it is possible to apply a flame onto a flat solid which has three axes of symmetry

Another problem is the effect of fire retardants. Products treated with FR agents often tend to show very good behavior in the small specimen/small flame situation. Performance may not be as good for the large specimen/large flame geometry. These scale effects are intrinsically 3-dimensional and have not been theoretically studied.

Table 18 Results from ignitability testing on 3.2 mm thick plaques of various materials, using two flame sources

Material	Smaller-flame ignition						Larger-flame ignition					
	A	B	C	D	E	G	A	B	C	D	E	G
Plastics												
ABS	–	+	+	+	+	+	+	+	+	+	+	+
acrylic	+	+	+	+	+	+	+	+	+	+	+	+
GRP type 1	–	–	–	–	–	–	–	–	–	–	–	–
GRP type 2	–	–	–	–	–	–	–	–	–	–	–	–
GRP type 3	–	–	+	–	+	+	–	–	+	–	+	+
nylon 6,6	–	–	–	–	–	–	–	–	–	–	–	–
polycarbonate	–	–	–	–	–	–	–	–	–	–	–	–
polyethylene	–	+	+	+	+	+	–	+	+	+	+	+
polypropylene	–	+	+	+	+	+	–	+	+	+	+	+
polystyrene	+	+	+	+	+	+	+	+	+	+	+	+
PVC	–	–	–	–	–	–	–	–	–	–	–	–
Wood and cellulosics												
ash	–	–	–	–	–	+	–	–	–	–	–	+
beech	–	–	–	–	+	+	–	–	–	–	+	+
birch	–	–	–	+	+	+	–	–	–	+	+	+
cardboard	–	–	–	+	+	+	–	–	+	+	+	+
elm	–	–	–	–	–	+	–	–	–	–	–	+
iroko	–	–	–	–	–	–	–	–	–	–	–	–
hardboard	–	–	–	–	–	+	–	–	+	–	–	+
hornbeam	–	–	–	–	–	+	–	–	–	–	+	+
maple	–	–	–	+	+	+	–	–	–	+	+	+
oak	–	–	–	–	+	+	–	–	–	–	+	+
red softwood	–	–	–	–	+	+	–	–	–	–	+	+
sapele	–	–	–	–	–	+	–	–	–	–	–	+
sycamore	–	–	–	–	–	+	–	–	–	–	+	+

In terms of practical testing, for a planar solid which has three axes of symmetry, there exist 7 distinct locations where a flame may be applied (Figure 47). Taylor[160] conducted tests on a variety of materials using two flames, both applied for a 5 s period. The smaller flame was 12.5 mm long, using a propane burner with a 2.5 mm diameter tube. The larger flame was 50 mm long, using a propane burner with an 8 mm diameter tube. Wilson's results on a variety of 3.2 mm thick samples are shown in Table 18. Preliminary testing showed that results using the **F** position were highly scattered, being greatly affected by the exact specimen to burner tube spacing, consequently, this test position was not used. Otherwise, the results indicate that the propensity to ignition is ranked in the order **A** (least ignitable), **B**, **C**, **D**, **E**, **G** (most ignitable). Additional data on small-flame ignitability are provided in Chapter 14 under *Plastics* and *Wood*.

Taylor did not explore the effect of specimen thickness, but with many materials this variable is important. A limited amount of data exists on wood, as shown in Chapter 14. Some indication can also be had from listing reports of test laboratories using the UL 94 test method, where it is known that it is more difficult for thin specimens to pass and, consequently, the listing is limited to a specified material thickness. Apart from such limited information, data on the thickness effect on small-flame ignitability is basically non-existent.

For experimental testing with small ignition sources, there exists UK standard BS 5852[161] which has a graded series of ignition sources. Table 19 shows the results obtained when 3 mm thick polypropylene sheets were tested with these sources[162]. It must be noted that the wood crib sources are used in the test method by being placed on top of a horizontally-oriented specimen. With wood crib sources, after a certain time of burning, direct conduction from the glowing char is probably more important a heat transfer mode than is radiation from the flames of the crib.

We conclude that, unfortunately, at the present time there are no engineering tools available for treating the general case of ignition with small sources or on small target objects. Some trends can be anticipated using the guidance developed below for large source/target analysis. However, if a specific question must be answered whether a fire could or could not have started on the basis of a small source/target, at the present time one must answer it by experiment. For upholstered furniture and mattresses, small-source ignitability has been studied for a long time. This is partly due to the fact that cigarettes, which may be the smallest commonly occurring ignition source, cause a preponderance of furniture ignitions. Upholstered furniture ignitions are discussed in Chapter 14.

SMALL-DIAMETER, HIGH-INTENSITY HEAT SOURCES

A plumber's or welder's torch can often be applied to a piece of foam plastic with the result that a hole is created in the material, but it is not ignited. Before the US Federal Trade Commission took action against the plastics industry for misrepresentation of flammability[163], this trick was sometimes employed by unscrupulous sales agents to prove that their plastic is 'noncombustible.' No quantitative model of the action of a torch upon a plastic specimen has been produced, but the general principles can be outlined qualitatively. The factors involved are: endothermicity of melting/pyrolysis, shrinkage, and flame blow-off limits. Foam plastics prone to demonstrating this type of phenomenon have some pronounced endotherms in their thermal response curve. Thus, part of the external heat is converted to heat of melting, of vaporization, or of degradative pyrolysis. The flame and hot gas stream issuing from a torch reaches very high temperatures, but is of small diameter. Shrinkage pulls the material out of the direct path of this stream, creating a hole. These plastics do not burn by heterogeneous combustion, thus igniting the surface itself is not the issue; the question is what happens in the boundary layer flowing through the newly-formed hole. It would appear that either violent entrainment disrupts the possibility of a zone where a mixture within its flammable limits can exist, or else that excessive velocities cause blow-off.

HOT BODIES

Hot bodies, in general, include both substances with a finite amount of heat (e.g., a piece of welding slag) and those that are continuously heated, such as an electric heating coil. A hot body placed in contact with combustible material may lead to its ignition. Two possibilities must be considered:

Table 19 The results of small-flame ignition testing of polypropylene sheets

BSI source no.	Type	Avg. HRR of source (kW)	Total heat supplied (kJ)	Duration of exposure (s)	Results for polypropylene
1	gas burner	0.072	1.43	20	no ignition
2	"	0.29	11.4	40	flashing
3	"	0.50	34.9	70	flashing
4	wood crib	0.75	85.9	115	no ignition
5	"	1.54	208	135	sustained ignition
6	"	2.32	777	335	sustained ignition
7	"	4.63	1780	385	sustained ignition

(1) the combustible material is capable of smoldering; or
(2) the combustible material is not smolderable.

If the material does not smolder, then it can only be ignited if the hot body creates sufficient pyrolysis gases, and the gases then ignite either by autoignition or by the surface of the hot body. Most non-porous plastics are not susceptible to smoldering, and it is generally hard to ignite them with hot bodies. When presented with a hot body, thermoplastics melt, gasify, and typically retract from the heated surface. Unless very flammable gases are copiously liberated, the sequence is likely to lead to a non-ignition, with the remaining material separated from the hot body by a gap. Thermosetting plastics, of course, do not melt, but these are typically materials that are much harder to ignite by any means (e.g., radiative heating), since they generally have lower heats of combustion and a lower propensity to gasify. Smolderable materials may first be ignited in a smoldering manner, and this may later transition or not to flaming combustion; or, they may be directly ignited in a flaming mode.

Despite the existence of some standardized tests for hot-surface ignition (described at the end of this Chapter), there has been little experimental work of the ignition of solids by hot surfaces and theoretical studies are equally scarce. Part of the difficulty arises from geometric complications. Several common possibilities must be considered, although the variety is endless:

- a small hot body contacts the much-wider surface of a combustible
- the entire face of the combustible is contacted by a hot body
- a hot body is partly or wholly submersed in the solid.

If the substance is non-smolderable and thermally thick, then ignition can only occur at the edges around the hot surface, since the hot surface is presumed to be impervious to flow of oxygen. The problem, therefore, intrinsically becomes 3-dimensional. If the substance is thermally thin, then flaming can also start on the back face (the assumption is made that the hot body is only pressed against one face), but no studies exist on this arrangement. It must also be noted that, in the case of the small hot body, a convective flow is likely to be created by its presence, and this will influence the thermal response of those parts of the target that are not in direct contact with the hot body.

For a few simple geometries, smolderable bodies can be treated by using self-heating theory (Chapter 9). Reasonably tractable methods are presented there for the cases of a slab with its whole face contacted by a hotplate and for the cylinder geometry that can represent ignition of wire or pipe insulation. Ohlemiller[164] treated these two, along with several more complex geometries, for the case of cellulosic insulation. His study involved mostly numerical solutions and he did not evolve any closed-form approximations. But the most common actual cases of ignition by hot surfaces typically involve a small, flat hot body landing on a large combustible surface. No tractable theory exists for the corresponding cases of a heated disc or a heated small rectangle.

Vilyunov and Sidonsky[165] treated the case on a semi-infinite rod where a hot surface touches its front face for a fixed length of time, then the hot surface is removed and the face becomes adiabatic.

The case of a small hot sphere landing on—and partly embedding itself in—an explosive was treated by Gol'dshleger et al.[166] For the purposes of this discussion, explosives behave similarly to smolderable fuels, in that the exothermic reaction is within the body and there is no need to produce gases and to ignite the gases. In their work, they developed a theory and conducted laboratory tests on nitrocellulose and polyvinylnitrate. For a 2 mm steel ball impacted into nitrocellulose, they found transient flashing for a ball at 430ºC, with sustained ignition occurring for a 450ºC ball. However they defined actual ignition temperature as 410ºC, which was the lowest temperature at which the explosive was largely consumed. For balls of smaller diameter, higher temperatures were required. Over the range of sphere diameters $0.7 \le d \le 2.5$, their results for both explosives (Figure 48) can be fitted by curves of the type:

$$T_s = a + b\exp(-d/c)$$

where T_s = sphere temperature; a, b, and c are constants; and d = ball diameter (mm). This equation, unfortunately, does not have generality, since the constants effectively depend on a combination of the physical and chemical properties of the combustible substance, along with the thermal properties of the hot sphere. With very limited data, Gol'dshleger also showed that a hot sphere of lower thermal conductivity must be raised to a higher temperature. Gol'dshleger's theory itself is discussed in Chapter 9.

A modest collection of purely-experimental data exists, but it is sparse enough that few helpful generalizations can be made. In connection with the development of his furnace, Setchkin[167] reported a small amount of hot-surface ignition data (Table 20). The test details were not stated, but it appears likely that he placed small specimens on a laboratory hotplate which was much larger than the specimens. In his protocol, evidently temperatures were explored only in 50ºC increments.

Kuchta, Furno and Martindill[168] used a 63 × 46 mm heated steel plate which they pressed against various materials in both air and oxygen atmospheres. Some of their results are shown in Table 21. Same as Setchkin, they found that a much higher hot-surface temperature was needed for ignition than the material's T_{ig} obtained under radiant or convective heating conditions. Ignition of solids with a radiant heat flux shows a small-to-nil dependence on oxygen concentration, yet Kuchta's tests revealed a very notable de-

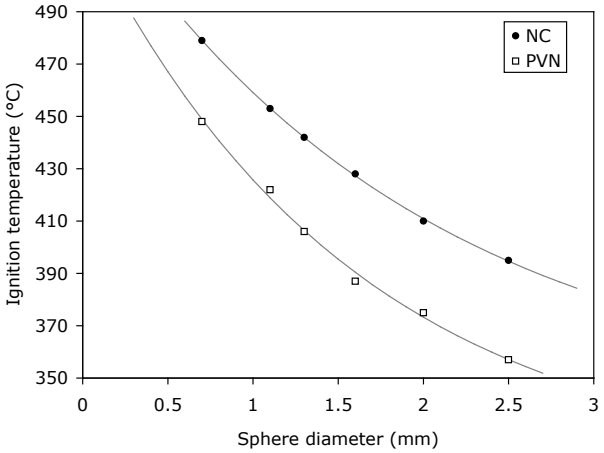


Figure 48 Hot sphere ignition data for two explosives, nitrocellulose and polyvinylnitrate

pendence. In addition, Kuchta et al. found that the minimum hot plate temperature depended on the total pressure, with values at 6 atm being 50 – 100ºC lower than at 1 atm. A direct comparison cannot be made here to radiant ignitability, since pressure dependence is unclear for that mode of ignition. Khalturinskii et al.[169] reported data on the effect of oxygen concentration for hot-surface ignition of PMMA and POM. The needed temperature depended on oxygen concentration at low O_2 values, but beyond a certain minimum concentration (15% for POM, 30% for PMMA) there was no effect at all. Their test conditions are not clear, however, since some exceptionally high temperatures were needed (1000 – 1200ºC).

Table 20 Ignition temperatures determined by Setchkin

Material	Ignition temp. (ºC)		
	Piloted	Auto	Hot-surface ignition
cellulose acetate	305	475	600
cellulose nitrate	141	141	550
melamine formaldehyde, mineral filled	313	455	700
phenol formaldehyde, w. paper reinforcement	306	399	600
PMMA	290	456	600
polyester, w. glass cloth	346	462	600
polystyrene	345	488	600

A small amount of data was presented by Widginton[170] for ignition of coal dust from electrically heated bare wires. Using wires of 0.20 – 0.48 mm diameter, he found that 2.5 to 9.0 A had to be carried by the wire to ignite coal dust, but the spread of the results was not governed by wire diameter. Apparently the thickness of the dust layer was small enough that the problem was not dominated by self-heating effects.

Table 21 Hot surface ignition results by Kuchta et al.

Material	Hotplate temp. needed for ignition (ºC)	
	In air	In oxygen
cellulose acetate	> 600	425
cotton sheets	465	360
cotton sheets, FR	575	310
paper	470	410
PMMA	595	430
PVC	> 600	425
wool	> 600	500

Some further experimental results are compiled in Chapter 11 under *Hot solids or liquids* and in Chapter 14 under *Coal*; *Cotton*; *Fabrics*; *Floor coverings*; *Forest materials, vegetation and hay*; *Plastics*; and *Wood*. These results are typically hot-surface ignition temperatures cited for a particular substance under poorly-defined experimental conditions. Unfortunately, there are no data sets where size, temperature, and thermal conductivity of the hot object were systematically varied. Thus, it is not possible even to provide suitable methods for data plotting and for extrapolation from test data, such as given earlier in this Chapter for the case of radiant heating.

In summary, hot-body temperatures must be substantially greater than normally-reported values of T_{ig} for ignition to occur. It is also evident that increasing the size of the hot body reduces its required temperature, as does increasing the thermal conductivity of the hot body. The sole case for which systematic theoretical treatments and experimental techniques are available is for smolderable (especially granular) materials ignited in hotplate or hot-wire type geometries; these are described in Chapter 9.

Ignition from large flames

Large flames can be characterized in terms of their heat flux (see Chapter 11) and once the pertinent heat flux is known, an ignition analysis as described above for radiant/convective fluxes can be done. A special concern, however, arises in the case of combustible wall/ceiling linings and similar large-surface materials. For those products, the ignition of the material directly adjacent to the flame is often a moot issue; instead, the concern is whether the surface will spread flame or not.

If the flame is in direct contact with the surface, then the convection heat transfer situation is considerably modified from the one customarily adopted for theoretical work, since convection provides heating, not cooling of the surface. Very little data exists for this condition, with the data of Bamford et al. having been discussed earlier in this chapter, while some more current (and more reliable) data on wood are cited in Chapter 14.

Duration of ignited burning

FLASHING VS. SUSTAINED FLAMING

Flashing is often reported in Bunsen burner type tests on solids. In Cone Calorimeter and other radiant-heating tests on solid materials, generally not much use is made of data on the time of occurrence of flashing, since it is not seen as a variable which is useful in predicting hazard in real fires. Consequently, few studies exist where flashing times were reported. Table 22 shows the results from one test series[171] where this point was specifically examined. The data indicate that (a) materials containing FR agents are more likely to exhibit flashing prior to ignition; (b) the difference between the first occurrence of flashing and sustained flaming ignition is usually trivial at heat fluxes of 50 kW m^{-2} or greater. A general comparison concerning effectiveness of FR agents should not be made from these results, since unspecified FR compositions were used, and they differed for the different polymers.

SUSTAINED FLAMING AFTER INITIAL IGNITION

If a solid is exposed to a constant heat flux and the heat flux is discontinued a certain time after ignition, one of two things can happen: (1) the solid will continue flaming; or (2) flaming will cease. The question which will occur is often important for understanding the dynamics of real fires. Conceptually, the reason why extinction takes place is because sustained flaming requires a sustained generation of volatiles to burn, and the latter becomes impossible. A brief, high-intensity heat pulse may be so intense as to vaporize and ignite a certain amount of material, but any given mass of original flammable vapors will stop flaming maybe in 1 s or less. There will subsequently be no fire, unless a mechanism exists that can deliver volatiles at a sufficient rate. A solid which has been heated at a much slower rate but for a long time will have had the opportunity to heat up in depth. Consequently, removing the source of heat may not affect things much for a while, since the solid's temperature will drop only gradually and the mass delivery rate of volatiles is proportional to the temperature of the surface layer. As a result, removing the source of heat a short while after it was first applied is much more likely to cause flaming to stop, than if the heat source is removed after having been applied for a long time.

Actual laboratory research on the topic of sustained flaming is unfortunately very limited. This question was first asked in 1915 by Prince[5], who examined the behavior of Western red cedar shingles. When a 1 min period was allowed between ignition and removal of heat source, he found that unpainted shingles continued burning to completion. Many different paints, though, had the effect that, upon removal of the heat source, burning stopped in a few minutes and most of the specimen was not consumed. When 6 min elapsed before the removal of the heat source, however, all of the tested products continued burning and burned up fully. Much more recently, Tuyen et al.[172] explored the sustained flaming of square wood dowels. The dowels were heated by being inserted horizontally into the cavity of a heated coil. Unfortunately, while the authors describe the coil temperature as being 600ºC, they did not measure the heat flux from the coil. After ignition was achieved, they removed the coil. For specimens of 2 × 2 mm up to 7 × 7 mm, flaming was sustained after heat source removal. For specimens 14 × 14 mm and larger, flaming ceased after heat source removal. Intermediate-size specimens were able to continue flaming only if the heater continued to be applied for 10 – 60 s post-ignition.

Substances which are exposed to extremely high heat fluxes may exhibit only transient flaming, despite the large heat flux. This was shown for thick wood siding which was exposed to nuclear weapons tests[173]. Even though very heavy pyrolysis, massive smoke emission, and some flaming occurred during the nuclear weapon exposure, the wood siding did not continue to burn afterwards. This is strikingly different from other substances, such as cloth, paper, finely-divided combustibles, etc.—all of these ignited in a fully flaming manner and did not self-extinguish. The effect is related to the ability of the heat pulse to establish a sufficiently deep, heated layer within the solid material. As discussed earlier, this effect was studied for cellulose at some length by Martin, but his work did not lead to a general strategy applicable to other materials.

Ohlemiller et al.[174] explored sustained flaming for a double-base propellant. Using very high heat fluxes from a laser source, they found that there was an optimal region in a flux/time plot for maintaining flaming after removal of the radiation source. Excessively high heat fluxes caused extinction due to a 'deradiation' effect, which was under-

Table 22 Cone Calorimeter ignition data for a number of polymers

Polymer	Heat flux (kW m^{-2})	Non-FR grade		FR grade	
		Flash (s)	t_{ig} (s)	Flash (s)	t_{ig} (s)
ABS	25	--	111	98	120
	50	--	38	27	34
	75	14	17	15	17
crosslinked polyethylene	25	--	86	155	162
	50	33	37	61	63
	75			33	37
high impact polystyrene	25	176	206	149	304
	50	--	52	40	106
	75	21	24	20	25
polycarbonate/ABS copolymer	25	--	189	211	267
	50	--	49	51	53
	75	--	21	26	28
unsaturated polyester	25	107	119	--	NI
	50	40	42	150	159
	75			37	79

NI – no ignition

stood to be a rapid change in heat balance at the surface, leading to an abrupt drop in surface temperature. Pantoflíček and Lébr[175] suggested that at high fluxes, there is a limiting temperature gradient within the solid—if the gradient at the surface is steeper than a given value, a sustained ignition is impossible. They also proposed that, apart from a minimum heat flux needed to achieve ignition, there is a minimum energy fluence requirement for combustion to be sustained:

$$q''_e = \frac{\lambda}{u}\left(T_{ig} - T_o\right)$$

where q''_e = energy fluence (kJ m^{-2}), λ = thermal conductivity, and u = regression velocity of surface. The validity of their suggestions would need to be answered experimentally, but suitable data are lacking.

Solids may fail to burn up relatively completely even if the heat source is not removed. This tends to occur if: (a) the material is highly FR-treated or is an 'inherently-FR' substance; or (b) it is exposed at a heat flux which is close to the material's critical flux for ignition. The effect of material type on completeness of combustion when the heat source is not removed is illustrated in Figure 49[176]. At the low flux of 20 kW m^{-2}, there is a very wide range of behaviors among materials. Some, for instance the phenolic/paper, burn up nearly completely. The polyurethane foam example, however, burns only about 35% at this flux, yet burns up fairly completely at 50 kW m^{-2}.

Conceptually, a heat balance for the flame should indicate whether losses are small enough and heat production high enough that flaming can be sustained. In practice, that is hard to do without defining and solving a full 3-dimensional model for the gas phase. Thus, simplified 1-dimensional concepts have been sought. Rasbash[32,177] proposed a concept related to the limit flame temperature idea. The latter states that combustion will not be sustained if the flame temperature drops below a certain value. Rasbash reformulated the concept in terms of heat fluxes, and defined a heat loss factor ϕ which is the maximum fraction of the heat of combustion that can be lost to the solid surface by means of convection. For non-fire-retarded substances, Rasbash suggested that the value of ϕ should range between 0.2 and 0.4. Thomson[2] computed the ϕ values for six plastics and found a range of 0.20 – 0.48 for her materials. This is a very wide spread and does not give a useful numerical criterion. More problematically, the Rasbash formulation is based on assuming that the heat release rate and the heat of vaporization are constants. The reason that some materials show non-sustained burning is precisely because these values are not constant—after an initial peak of HRR, the production of volatiles tails off and flaming is no longer sustained. The HRR curve is easy to measure and could be included into a tractable method. But an accurate determination of the heat of vaporization curve requires a significant research effort, due to noise associated with numerical differentiation of the mass loss curve. Successful research

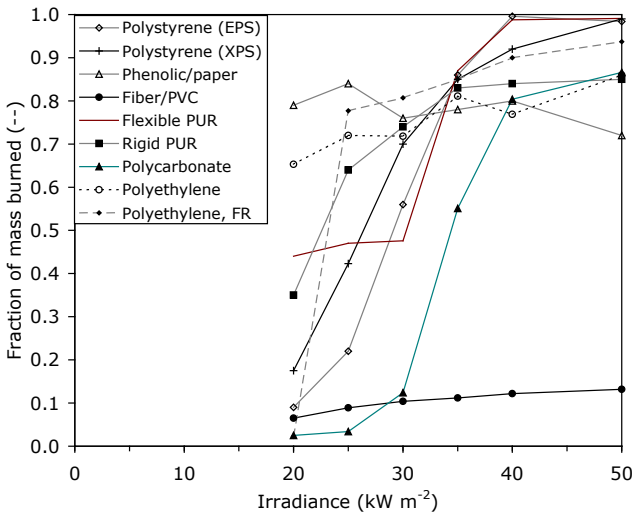


Figure 49 The effect of irradiance on mass fraction burned

studies have been reported[178], but it does not appear that the procedure lends itself to being made routine.

Brindley et al.[179] offered a theoretical solution to the persistence question, solving the case of fixed heat flux at the front face (i.e., no convection or re-radiation). Their solution was wholly numerical and systematic guidance did not evolve from it. In practice, the means of answering the question are currently empirical, e.g., various small-flame ignition tests which limit the 'afterflame' time. In an effort to evolve a closed-form criterion, Lyon[180] suggested that the following expression for heat release be considered:

$$\dot{q}'' = \frac{\Delta h_{c,eff}}{L_g}\left(\dot{q}''_e + \dot{q}''_{fl} - \dot{q}''_{\min}\right)$$

where $\dot{q}''$ = heat release rate (kW m^{-2}), $\Delta h_{c,eff}$ = effective heat of combustion (kJ kg^{-1}), L_g = effective heat of gasification (kJ kg^{-1}), $\dot{q}''_e$ = externally imposed heat flux (kW m^{-2}), $\dot{q}''_{fl}$ = heat flux from specimen's own flame (kW m^{-2}), and $\dot{q}''_{\min}$ = minimum heat flux for ignition (kW m^{-2}). Experimentally, it is found[34,181] that flaming combustion is not sustained unless the heat release rate exceeds a value of about 30 kW m^{-2} to 50 kW m^{-2}. Thus, inserting a value of 40 for HRR and setting the external flux to zero gives the condition for sustained burning as:

$$\frac{\Delta h_{c,eff}}{L_g} \geq \frac{40}{\dot{q}''_{fl} - \dot{q}''_{\min}}$$

The problem with this expression is that it does not readily lend itself to experimental evaluation. Values of effective heat of combustion and minimum heat flux for ignition can easily be found from Cone Calorimeter experiments. Flame flux is difficult to measure accurately, with values determined for specimens in the Cone Calorimeter[182-184] ranging from 5 to 37 kW m^{-2}. More difficult yet is to obtain a realistic value for L_g. In the equations above, L_g is considered a

constant and, in principle, it could simply be obtained experimentally as:

$$L_g = \frac{\dot{q}''_e + \dot{q}''_{fl} - \dot{q}''_c}{\dot{m}''}$$

where $\dot{m}''$ = mass loss rate (kg s^{-1} m^{-2}). However, once actual data are examined, it is found for many materials that (1) rather than being constant, the mass loss rate and the effective heat of combustion vary greatly with time[178,185]; (2) both of these quantities also vary with the externally imposed flux, and it may not be easy to extrapolate to conditions of HRR ≡ 40 kW m^{-2}. Thus, calculationally, this must be considered an unsolved problem. For certain classes of polymers, Lyon[180] suggests an empirical figure of merit be used, based on char fraction and LOI of the material, but the approach is drastically simplified (it assumes that $\Delta h_{c,eff}/L_g$ is a universal constant for all materials) and it lacks corroboration.

In practical applications, ignition and flame propagation are often closely related. Hazard commonly does not exist unless ignition results in propagation, rather than local, non-sustained burning. Propagation can be viewed as a series of ignitions, and it will stop if a necessary ignition along the way cannot happen. This may occur if a zone of low thermal inertia meets up to a zone of high thermal inertia. A practical example is shown in Color Plate 12. The fringe of a rug located close to a fireplace hearth was ignited by a burning ember. A portion of the fringe was consumed, but burning did not propagate into the rug itself. The thermal inertia of the fringe and of the rug were very different, and burning of the fringe could not ignite and cause sustained combustion of the rug, which had a much greater thermal inertia due to its greater density.

Variables affecting ignition of solids

TYPE OF PILOT (OR LACK THEREOF)

For solid materials, a pilot can be viewed as being of one of three types:

(1) no pilot, i.e., autoignition
(2) a pilot located in the gas phase, without direct heating effects to the specimen
(3) a pilot where the flame is directly impinging on the surface of the specimen which is also being radiatively or convectively heated.

For the third case, very little experimental data and no theory exist, thus only a few data will be cited here. Cases #1 and #2 are quite general, but practical application is held back by the unavailability of a tractable theory which would quantify the gas-phase conditions needed to produce autoignition. The simplest conceptual model for autoignition t_{ig} would be that $t_{ig} = t_{ss} + t_{gp}$, where t_{ss} is the identical solid-phase heating time used to predict piloted ignition, and t_{gp} is an induction period needed for autoignition of a gas volume, once it has been brought to a certain temperature. But the temperature history of the pyrolysate+air mixture in front of the solid surface is not well studied, nor is the 3-dimensional distribution of temperatures actually present within this layer. Since the induction period for autoignition is a sensitive function of the gas temperature, t_{gp} appears to not be readily obtainable by any simple approximation. Thus, we resort in this section to simply examining experimental data.

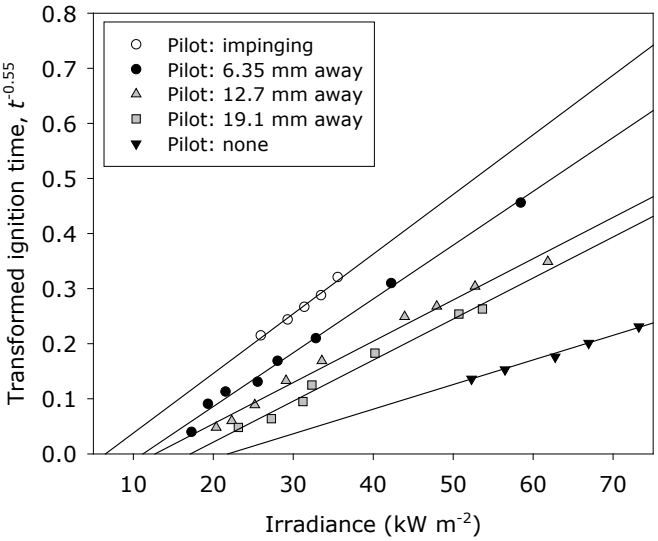


Figure 50 Ignition of vertically-oriented pine samples, for various pilot conditions

For two woods, the Fire Research Station[186] found the following values of the critical flux for ignition (Table 23).

Table 23 Early FRS results on the effect of piloting for ignition of wood

Species	Critical flux (kW m^{-2})		
	Auto	Piloted	Impinging pilot
Western red cedar	27	15	5.0
Douglas fir	28	15	5.0

Later, FRS's Simms and Hird[187] set forth the hypothesis that these three conditions are not separate possibilities, but merely points along a continuum. The variable to be considered is the distance of the pilot from the surface. Zero distance corresponds to impinging pilot; infinite distance corresponds to autoignition; while increasing the distance from the surface (yet still staying within the pyrolysis gas stream) should lead to longer ignition times. To examine their hypothesis, they conducted experiments on vertically-oriented specimens cut to a 51 × 51 mm face size. A gas pilot was located at the top of the specimen, and was positioned at various distances in front of the specimen face. Three oven-dried cellulosic materials were tested: fiber insulating board (250 kg m^{-3}), Colombian pine (500 kg m^{-3}), and oak (700 kg m^{-3}). Their results for Colombian pine are shown in Figure 50. A smooth progression of ignition times is seen, increasing from the impinging condition to the 19.1 mm offset condition. For unpiloted ignition, a

fairly substantial increase in ignition time is seen, even compared to the farthest-away pilot condition. Increasing values of $\dot{q}''_{cr}$ with decreasing pilot effectiveness are clearly to be expected. But the ignition lines also show decreasing slope with decreasing pilot effectiveness. This effectively indicates an increase in $\lambda\rho C$ for far-away pilots or unpiloted ignitions. Under unpiloted conditions, a higher surface temperature will have to be attained before ignition occurs. Presumably, the effective thermal inertia is then higher under such conditions.

The pilot *height* above the top of a vertically-oriented specimen were explored by Muir[207], who found that the effect on ignition time was small until sizable heights (75 – 100 mm) above the top were reached. In a related study, Stockstad[188] used a horizontal tube furnace with very small specimens of unspecified size. For various wood samples, he found that no ignitions occurred up to the maximum furnace temperature of 460ºC if the pilot was located 10 mm or higher above the specimen. Ignition was always possible at a height of 5 – 6 mm, with decreasing probability of ignition for heights of 7 – 9 mm. Other studies comparing piloted ignition to autoignition of wood are reviewed in Chapter 14 under *Wood*. The *length* of a pilot flame does not have an effect on ignition time according to Muir[207], who used pilot flames from 10 to 50 mm long.

Another comparison between piloted and autoignition conditions was made by Starchville[189] who ran Cone Calorimeter tests on flexible PVC electrical tubing and rigid PVC electrical conduit (Table 25). Some estimates on the effect of presence of a pilot on the *minimum flux for ignition* can be made from this study. The steps of 10 kW m^{-2} are very coarse when it comes to minimum-flux studies, but the results are indicative nonetheless. For both the tubing and the conduit, the spark-ignition minimum flux can be taken as 15 kW m^{-2}; the unpiloted flux, however, is 35 kW m^{-2}. Comparing now the ignition times where ignition was achieved in both modes, for the PVC tubing, the spark-ignition times are about 70% of the unpiloted values. For the rigid conduit, the experimental data show a longer ignition time with spark than without. This anomalous result can be explained as being due to data scatter: all of this author's data represent only single trials.

Table 25 Ignition of PVC tubing and PVC conduit

Irradiance (kW m^{-2})	Flexible tubing Ignition time (s)		Rigid conduit Ignition time (s)	
	No pilot	Spark	No pilot	Spark
10	NI	NI	NI	NI
20	NI	375	NI	695
30	NI	210	NI	373
40	195	135	270	293
50	135	90		270
60		75		105
90		45		15
NI – no ignition				

A systematic study of the effect of pilot type was made by Wraight[190], although the study was limited to a single flux of 30 kW m^{-2}. Wraight used the ISO 5657 apparatus for his experiments. His test conditions were the following:

(1) no pilot
(2) a natural gas pilot flame, about 15 mm long and located 15 mm above the specimen
(3) a 0.27 mm diameter Nichrome wire, 40 mm long, located 15 mm above the specimen. The wire was carrying 5 A at 6.4 V.
(4) a 5 mm spark gap, using an 8-15 kV source and located 15 mm above the specimen.

The results are given in Table 24. The values given represent the mean of 3 (in two cases, 2) tests.

Table 24 Results for pilot-type experiments in the ISO 5657 test at a flux of 30 kW m^{-2}

Material	Ignition time (s)			
	No pilot	Flame	Hot wire	Spark
insulating fiberboard, white-finish, type A	31.7	26.7	32.0	30.0
insulating fiberboard, white finish, type B	30.0	21.0	26.0	27.5
insulating fiberboard, unfinished	20.3	9.7	14.3	15.0
hardboard	104.0	57.7	77.0	78.3
hardboard, FR	181.5	6.5	101.5	112.5
polystyrene foam ceiling tile	39.7	18.7	39.0	29.7

The results clearly indicate that, as expected, the autoignition times are always the longest. The hot-wire and spark ignition modes gave statistically indistinguishable results for all products. The flame ignition mode, however, showed a wide variation. For polystyrene foam and unfinished insulating fiberboard, the ignition time for flame mode was about ½ that for hot-wire or spark modes. For plain hardboard and for the two types of finished insulating fiberboard, the flame ignition times were about 20% lower than for hot-wire or spark modes. The FR hardboard clearly showed some special phenomenon, but the author was not able to investigate this. In a more limited comparison, Mikkola[191] compared two products in the ISO 5657 test, using the standard flame and an electric spark igniter. Unlike Wraight, Mikkola observed shorter times with the spark, the two values being 41 vs. 39 s and 5.6 vs. 4.1 s. Cain[192] tested 12 products in the ISO 5657 test and determined $\dot{q}''_{\min}$ for both piloted (flame) and autoignition conditions. His results (Figure 51) show that, on the average $\dot{q}''_{\min}$ for autoignition is 2.37× that for piloted ignition; the range was from 1.6× to 3.7×.

Harkleroad et al.[193] studied the ignition of vertical samples exposed to the radiant panel heat source of the LIFT apparatus, but using various non-standard pilot flame types and

locations. For a flame located 25 mm above the top of a particleboard specimen and 5 mm in front of its surface plane, they found that at low heat fluxes of 17 – 40 kW m^{-2}, ignition took place first in the gas volume above the specimen, and only some 10 – 40 s later flashed down to the face of the specimen. For heat fluxes in the range 13.7 – 15.4 kW m^{-2}, only an ignition of the gas volume above took place, flame never went close to the specimen face. The LIFT apparatus has a strong induced convective flow due to the close-by presence of the gas-fired radiant panel, thus the authors attributed the effect to the relatively high upward flow velocity of the boundary layer at the surface.

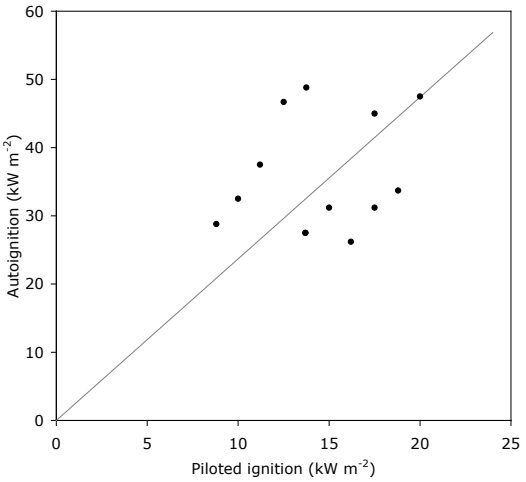


Figure 51 Minimum flux for ignition, as determined in the ISO 5657 apparatus for piloted and autoignition conditions

Shields et al.[195] obtained data for cellulosic products using both a gas flame and spark ignition. Their results can be summarized as:

$$t_{ig}(gas) = \left(1 - 0.00246\dot{q}''_e\right) \times t_{ig}(spark)$$

Thus, for example, at a flux of 50 kW m^{-2}, a gas pilot might be expected to produce 12% shorter ignition times. In a parallel study[80], the same investigators noted that the minimum flux for ignition did *not* decrease when a gas pilot was substituted for the electric spark and that, in the majority of cases it very slightly increased. The reason for this is not clear. The same investigators also compared the ignition times for autoignition and spark ignition, and their results can be expressed as:

$$t_{ig}(autoignition) = \left(2.86 - 0.0172\dot{q}''_e\right) \times t_{ig}(spark)$$

In this case, at a flux of 50 kW m^{-2}, if no pilot is used, ignition times can be expected to be 2.0× those for the spark-ignition case. Additional studies on piloting details and their effects on ignition have been reported by Amos[194].

The results from several of the studies discussed imply that a gas pilot can apply significant local heating to a specimen, even when it is positioned in a 'non-impinging' location. This was early recognized, and was the reason for the arrangement in the ISO 5657 test (see below) whereby a pilot is only periodically swung into position. Such an arrangement minimizes heating, but adds an uncertainty to the ignition time determination. Since part of a pilot flame's heat flux is imposed through radiation, a non-luminous flame, e.g., hydrogen, would be expected to minimize local heating. Thomson[2] explored the effects of a hydrogen pilot. She operated the pilot in two modes—located at a single spot, and hand-circled above the specimen. Her results for PMMA are shown in Table 26. It can be assumed that an electric spark imposes negligibly small heating on the specimen. Thus, even with a non-luminous hydrogen flame located a substantial distance above the face of the specimen, it is evident that when the pilot is fixed at a single location, local heating effects greatly perturb the measured ignition time. By contrast, when the hydrogen pilot is circled around, the ignition times no longer differ statistically from the spark ignition case. Since it is easy to set up spark ignition, but more difficult to carefully circle a hydrogen pilot flame at a fixed height, the recommendation is clear: *standardized piloted-ignition testing should use a spark and not a gas pilot.*

Table 26 Ignition times for 6 mm thick PMMA exposed to a heat flux of 25 kW m^{-2}

Pilot type	Ignition time (s) for height above specimen		
	5 mm	10 mm	20 mm
spark	116 4	112 6	135 5
moving pilot	110 6	105 5	124 8
fixed pilot	68 9	95 4	118 8

ORIENTATION

While materials can be arranged in highly diverse ways, most ignitability testing is done for samples which are either oriented horizontally, face-up, or else vertically. The convective environment for the two conditions is substantively different. For a horizontal specimen, air is entrained from all sides, and a relatively constant surface temperature is found across the face. For a vertical sample, a boundary layer is established, with the bulk of the flow being bottom-up. If the specimen is located in an ambient atmosphere of ambient temperature and is heated with a radiant heater, the air flowing by the face of the specimen will be of ambient temperature at the bottom, and will progressively warm up towards the top. This causes the face temperature of the specimen to be higher at the top than at the bottom; consequently, in some cases of marginal ignition it will be found that a flame will only go down partway on the sample.

During two Cone Calorimeter roundrobins, data on the effect of orientation on ignitability were obtained. Figure 52 shows this relationship, where the results can be correlated as:

$$t_{ig}(V) = 1.20\, t_{ig}(H)$$

There was no irradiance effect, since, if analyzed separately, the 25 kW m^{-2} tests showed a scaling factor of

1.19±0.09, while the ones at 50 kW m^{-2} scaled using 1.26±0.07. Shields et al.[195] also reported results on this point, but based only on tests carried out in a single laboratory and only on cellulosic materials. In their work, the vertical/horizontal ratio comes out to about 1.4. The fact that ignition times should be greater in the vertical orientation is not surprising, if we consider the relevant pyrolysate streams which are igniting. In the case of the horizontal specimen, there exists a roughly-pyramidal volume of pyrolysis gases, and a small electric spark located above the specimen's centerpoint can be situated in a region where a flammable mixture is easily established. In the case of the vertical specimen, a very thin sheet of pyrolysis products flows upwards along the surface. This may require a higher energy concentration due to its thinness, and it may also wander away from the fixed place of the igniter.

If a specimen is exposed in the horizontal, face-down orientation, the environment is somewhat stably stratified. It would be fully stable if the problem were 1-dimensional, but gases heated at the surface will flow across the face, and 'fall off the edge upwards.' A stratified environment does not allow ready mixing of fuel and oxygen, thus ignition should be much delayed. This is exactly what Shields et al. found in using the ISO 5657 apparatus upside-down. The ignition times in the face-down orientation were typically about 3× longer than those found for the face-up orientation. The minimum flux for ignition also rose increased about 3 – 4× compared to that for the face-up orientation. Thus, wood products which can normally be ignited at ca. 12 kW m^{-2}, were requiring around 45 kW m^{-2} for ignition. However, an opposite result was obtained by Moulen and Grubits[196]. They also used the ISO 5657 apparatus, but found ignition times for the face-down orientation to be somewhat *shorter* (Figure 53). Since these are the only two test series reported where these comparisons were made, it is hard to reconcile the opposing conclusions.

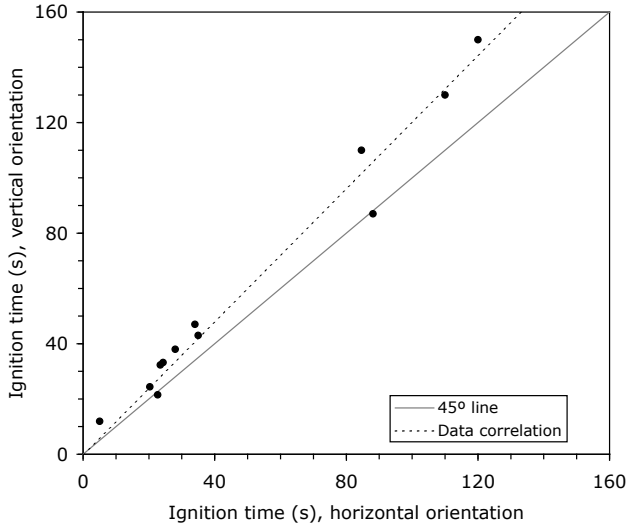


Figure 52 Relation between ignition times in the horizontal and in the vertical orientations, as determined from two Cone Calorimeter round robins

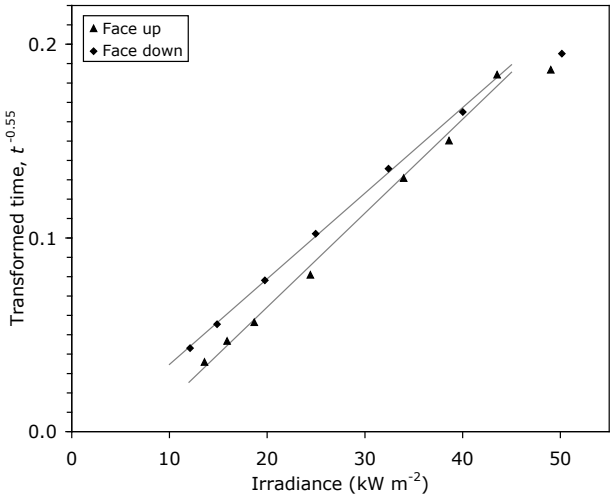


Figure 53 Results of Moulen and Grubits on the effect of orientation for the piloted ignition of hardboard

Materials may, of course, be exposed at angles which are not just multiples of 90º. Results were reported[197] wherein the ignition of PMMA was studied at various angular orientations, not just horizontal and vertical. The minimum ignition time was found to occur at an intermediate orientation (Figure 55). While an effect of irradiance is also seen, nonetheless the average ignition time in the vertical orientation is about 1.2 times that in the horizontal, which is exactly the same conclusion as found in the Cone Calorimeter round robin discussed above. The reason for the 30º position giving the fastest ignition times is presumably related to the details of the boundary layer that is formed above the specimen.

EXPOSED AREA SIZE

For vertical panels exposed in air to radiant heat flux, initially the panel will be at the room temperature and there will be no convective effect. As the face temperature rises, a difference in temperature between the room and specimen will arise, and this will result in a convective flow being induced past the face. The convective heat flux is not uniform along the height. The boundary layer that is formed is progressively thicker towards the top, so the cooling effect is progressively smaller. According to this effect, a tall panel will ignite first at the top, and a taller panel will ignite earlier than a shorter one. A convective effect will be absent entirely if the heat flux is so high that ignition is achieved before the boundary layer attains a steady state. For a specimen of 0.1 m height, it has been estimated that only at irradiance values > 200 kW m^{-2} will the convective effect be totally absent[39].

Apart from the problems of very small specimens or specimens heated only over small portions of their face, the

effects of size ought to be predictable from theory. Long et al.[46] noted that the only scale-dependent term in basic ignition theory is the convective heat transfer coefficient, h_c, which varies with size L according to $h_c \propto \frac{1}{L^{1/4}}$. The effect on ignition time is much smaller than the change in h_c, since heat losses are dominated by radiation. Long et al. estimated that for PMMA reducing the size by a factor of 3 would increase the total heat loss by about 4%. The slight increase in t_{ig} is counteracted by an increase in effectiveness of mixing fuel vapors into the air, since the mass transfer coefficient for this process also varies as $1/L^{1/4}$.

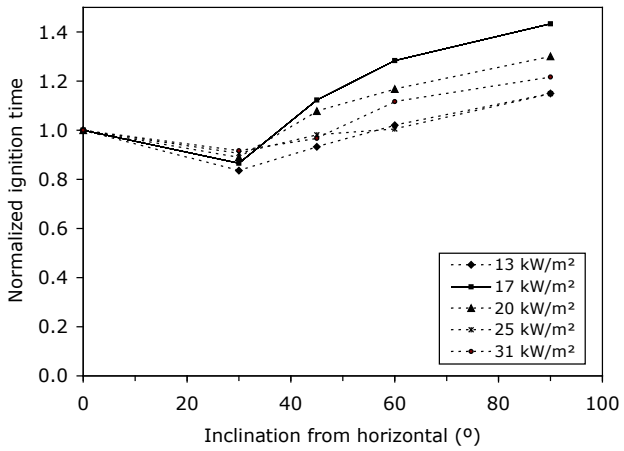


Figure 54 The effect of the angle of inclination on the ignition of 6 mm PMMA slabs

In practice, experimental results indicate that, provided minuscule sample sizes are not being considered, the convective effect is rather small. For example, Kashiwagi[115] examined the effect for PMMA and red oak at an irradiance of 60 kW m^{-2}. A slight decrease in ignition times was found for 150 × 150 mm samples, compared to 75 × 75 mm samples, but the effect was probably within the data scatter. Thomson[2] found that PMMA samples which were heated over a 19 × 19 mm area showed a T_{ig} of 338ºC, compared to 312ºC for samples heated over their entire 65 × 65 mm face area.

Simms et al.[198] showed that for large irradiance values, when the irradiated area was 3 cm^2 on a large-area specimen, the ignition times needed to be increased by 24% over those found when the total specimen face was irradiated. When the absorbed radiation (incident radiation × surface absorptivity) fell below 120 kW m^{-2}, the correction needed increased as shown in Table 27. Data at irradiances lower than 67 kW m^{-2} were not collected. For a 25 cm^2 irradiated area, and an irradiance of 120 kW m^{-2} or higher, the multiplying factor was only 1.03. For an absorbed radiation of 50 kW m^{-2}, the multiplying factor was 1.67. The values quoted are all mean values, and individual materials showed significant deviations from these values, especially for smaller values of absorbed radiation. A general-purpose correction scheme which would take into account the heat flux, the irradiated area, and the material thermophysical properties did not emerge from Simms' study. Also, an explanation did not emerge why the intensity of radiation should be a variable that affects the correction factor.

Hu and Clark[199] tested horizontally-oriented specimens in the ISO 5657 apparatus, using both the standard exposed specimen area of 0.0154 m^2 and a reduced area of 0.0016 m^2, in other words, an area reduced by about a factor of 10. Ignition times for the smaller-specimen size were consistently about 1.14× the values for the standard-size specimens. The 16 cm^2 smaller size is, of course, much larger than the 3 cm^2 areas examined at FRS.

A study with indirect findings was conducted at FRS in connection with ignitability of carpets[200]: actual ignitability was not measured, only onset of specimen melting. Two conditions were examined: a substantial irradiated area of 3000 mm^2, and a tiny area of 10 mm^2. At a given irradiance, it was found that the time to melting was 5 – 6 times longer when the tiny area was exposed, in comparison to the larger one.

Another exploratory study on the same topic was done by Clark[201]. He explored only one value of irradiance, 17 kW m^{-2}. In his arrangement, square specimens, located horizontally, face-up, were embedded in a sand layer. Investigation of heat flows showed that the sand layer adequately simulated samples of larger area, but only pyrolyzing over the actual given face area. In his tests, he first attempted spark ignition. If the spark ignition was unsuccessful after 10 min, a flame was applied at the surface. The results are shown in Table 27. For spark ignition of large irradiated samples, the value of $\dot{q}''_{min}$ for PMMA is about 8 kW m^{-2}; thus, Clark's tests were at about double that. Standard Cone Calorimeter PMMA samples will ignite at about 280 s at an irradiance of 17 kW m^{-2}. Thus, Clark's average value of 311 s is only slightly high. The 10×10 mm sample, however, while showing a modestly raised ignition time, is clearly borderline non-ignition, since 1 out of 3 specimens did not ignite. Thus, for 10×10 mm samples the $\dot{q}''_{min}$ is presumably around 16 kW m^{-2}. While the data are too few to draw general conclusions, the experimental results on wood can be of direct utility in application to fire investigations. If a wood item is thermally-thick, is at least 10 × 10 mm in

Table 27 Effect of absorbed radiation on ignition time correction for 3 cm^2 exposed area

Absorbed radiation (kW m^{-2})	Multiplying factor
120	1.24
100	1.39
84	1.52
76	1.56
67	1.64

Table 28 Effect of specimen area for radiative ignition at 17 kW m^{-2}

Specimen	Size (mm)	Ignition time (s), by spark	Ignition by flame at 10 min.
PMMA	5×5×4	N, N, N	Y, Y, Y
	10×10×4	442, N, 392	NA, Y, NA
	20×20×4	317, 303, 312	NA, NA,NA
polyethylene	5×5×6	N, N, N	Y, Y, Y
	10×10×6	N, N, N	Y, Y, Y
	20×20×6	N, N, N	Y, Y, Y
polycarbonate	5×5×6	N, N, N	Y, Y, Y
	10×10×6	N, N, N	Y, Y, Y
	20×20×6	N, N, N	Y, Y, Y
red oak	5×5×17	N, N, N	N, N, N
	10×10×17	N, N, N	Y, Y, Y
	20×20×17	416, 483, 406	NA, NA,NA

Y – yes
N – no
NA – does not apply

size, and is receiving at least 17 kW m^{-2} irradiance, then in the presence of a flame, ignition will occur.

Mikkola[191] compared ignition times in the Cone Calorimeter (100 100 mm specimens) to the ISO 5657 test (specimen exposed diameter = 150 mm). His results (Figure 55) show a heat-flux dependent relationship. There is a wide scatter of data, but for heat fluxes below 50 – 60 kW m^{-2}, the best-fit line is $\frac{t_{ig(ISO5560)}}{t_{ig(ISO5657)}} = 1.34 - 0.0052\dot{q}''_e$. The data would suggest that at larger heat fluxes the ratio becomes close to unity.

In a similar series of experiments, Nussbaum and Östman[202] tested 13 building products in the Cone Calorimeter and in a specially-constructed version of the Cone Calorimeter which was twice in scale, i.e., specimens of 200 × 200 mm were tested. Their results showed a different trend, as given in Table 29. The values at 75 kW m^{-2} are probably subject to more error than suggested by the standard deviation, since most products ignited in 6 s or less, and a shield was not used.

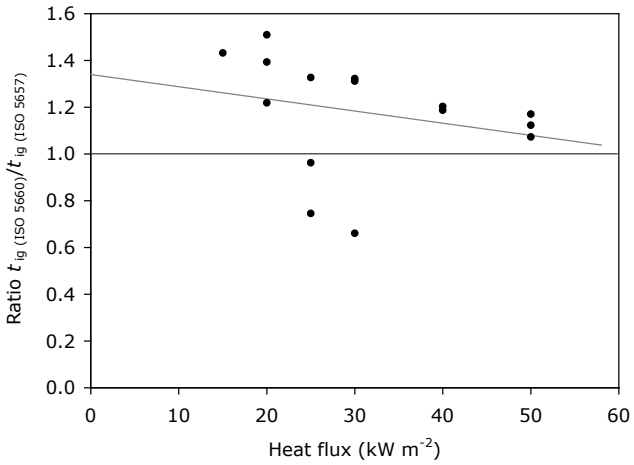


Figure 55 The relation between ignition time in the Cone Calorimeter and in the ISO 5657 apparatus

Table 29 Comparison between ignition times in the Cone Calorimeter and in a similar apparatus using larger, 200×200 mm specimens

Heat flux	Ratio of ignition times, small/large specimens
25	1.32 ± 0.57
50	1.35 ± 0.25
75	1.51 ± 0.34

For *thermally-thin* materials, very little information is available on the area effect. One study[203] concluded that for paper tissues irradiated with a tungsten-lamp source over a 6.5 cm^2 area, the minimum flux for ignition rose 14% from that needed for a large-area exposure.

AIR FLOW RATE

The role of air movement past an ignition specimen is complex. The simplest arrangement to consider is where a specimen is radiatively heated, and convectively cooled. In that case, increased air velocity past the specimen increases convective cooling and shows up directly as a heat loss term. But additional effects are: (1) increased air flow velocity can affect mixing and local concentrations of fuel and oxidizer in the gas stream; (2) for substances which ignite in a glowing mode, air velocity will directly affect the reaction rate in that process. Several studies exist where the effect has been investigated, and these are summarized below. The general guidance is that high velocities inevitably make ignition more difficult. A somewhat different situation pertains to the case of purely-convective heating, where the only source of heat to the specimen is a hot-air stream. This exposure condition was considered above.

In a crude early study, Lullin[204] measured the ignition temperatures of wood samples using a horizontal tube furnace. He found that an optimum flow velocity of 0.4 m s^{-1} existed, with smaller or higher velocities resulting in a higher reported T_{ig}. The specimens were heated at a low enough temperature that ignition of wood was a 2-step process, with an initial glowing ignition followed shortly by flaming. In similar, but better-controlled experiments, Graf[36] later tested a number of materials and found, for some materials, an optimum flow velocity of ca. 0.175 m s^{-1}. There was a great deal of scatter, and some material showed relatively constant T_{ig} values for all velocities below about 0.2 m s^{-1}, down to 0.04 m s^{-1}, which was the lowest velocity used. For velocities significantly greater than 0.2 m s^{-1}, T_{ig} values invariably increased. Bowes[205] used a vertical tube furnace to ignite sawdust and grass meal. Varying velocity over the range 0.003 to 0.03 m s^{-1}, he found no velocity

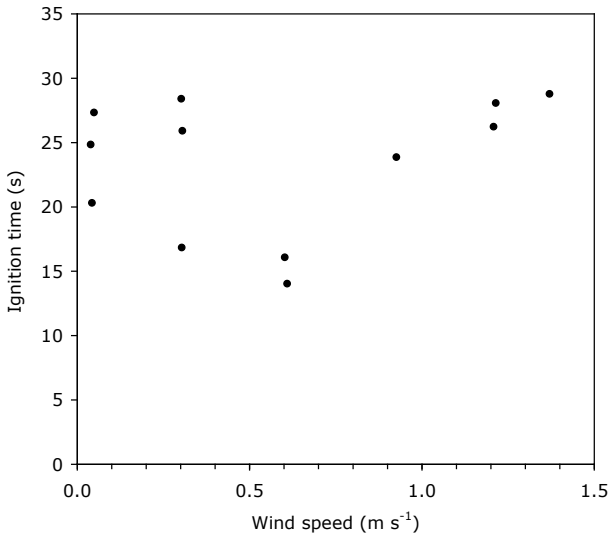


Figure 56 Effect of wind speed on autoignition of horizontally-oriented white pine specimens exposed to radiation from a solar furnace

effect. In a more typical radiant test arrangement, Atreya and Abu-Zaid[20] exposed wood specimens in a horizontal, face-up orientation. Increasing the wind speed from 0.1 m s^{-1} to 1.0 m s^{-1} raised the effective T_{ig} by about 40ºC (Figure 4).

Simms[206] measured the effect of a small draft on the autoignition of wood specimens. The draft did not change the ignition times, but did change the $\dot{q}''_{min}$. For blackened oak and cedar specimens, he found the minimum was 116 kW m^{-2} without a draft, but 100 kW m^{-2} with a draft for oak and 76 kW m^{-2} for cedar. The peculiarities of the experimental rig are unclear, however, since modern researchers have found minimum flux values several-fold smaller than 76 kW m^{-2}. Similarly, Kashiwagi[117] noted that ignition times were longer in still air than in a drafty room. Janssens[75] reported that effects of drafts can alter the results obtained in the ISO 5657 test for horizontally oriented specimens, but quantitative information was not provided.

Weatherford and Sheppard[8] used a test apparatus which subjects specimens to convective heating, efforts having been taken to minimize radiative contribution. In their rig, they found no effect on ignition time when varying air flow velocities over the range of 0.1 to 0.7 m s^{-1}. Muir[207] investigated the effects of air flow on the piloted ignition of vertically oriented samples. Wind speeds greater than 0.75 – 1.0 m s^{-1} led to substantial increases in ignition times. For smaller velocities, the effect was trivial, although at low irradiances (but not at high) he found a statistically-significant but shallow minimum. In one set of results, velocities of 0.2 – 0.3 m s^{-1} gave a slightly lower t_{ig} than did a zero velocity. Ulrich and Butcher[208] reported autoignition measurements on white pine (Figure 56) showing a similar shallow minimum which, in their case, was at around 0.6 m s^{-1}.

Bilbao et al.[209] studied the ignition of 19 mm thick pine specimens in an apparatus somewhat resembling the Cone Calorimeter, but using high velocities of air. The data plotted (Figure 57) all represent flaming, piloted ignition times; the authors also found that at non-zero velocities some flaming ignitions were preceded by a glowing ignition. The effect of an imposed velocity is to increase the convective transfer coefficient, h_c, which in turn raises the value of h_{eff}. The consequence is that increasing the velocity u (m s^{-1}) leads to (a) an increase in $\dot{q}''_{cr}$, and (b) an increase in B_{ig}. Unfortunately, no simplified technique has been developed for directly relating these changes to values of u.

Several studies of air through-flow have been reported for the Cone Calorimeter. In a NIST study[101], three exhaust-system flow rates were used: none, 24 L s^{-1}, and 41 L s^{-1}. Both horizontal and vertical orientations were examined for PMMA and redwood. No systematic effects were found of air flow rate over this range. In the above study, the normal open-air specimen configuration was used. No-exhaust conditions do not indicate zero air flow, since the cone heater alone creates a natural-convection flow, but no attempt was made to quantify this flow. In a similar vein, Thomson[2] examined the effect of whether an extract fan was or was not used with an experimental radiant ignition rig. Using PMMA and polypropylene samples, she also concluded that no effect could be found. Petrella[214] used a special fully-enclosed version of the Cone Calorimeter and again found no effect over the range of 9 – 24 L s^{-1}. Two studies have also been done by VTT on this subject. In the first study[215], no systematic difference was seen for data obtained at 24 L s^{-1} (in open air), as compared to 3 to 6 L s^{-1} (in an enclosed apparatus). In the second study[210], using flow rates of 0.67 – 6 L s^{-1}, longer ignition times were generally found with higher air flow rates, although the data showed a great deal of scatter. Combining results for nylon and polypropylene and excluding some evident outliers, a trend of the following kind can be seen:

$$t_{ig} \approx t_{ig,o}\left(1 + 0.094\dot{V}\right)$$

where $t_{ig,o}$ is a normalizing constant obtained by extrapolation to zero air flow and $\dot{V}$ = air flow rate (L s^{-1}). Thus, for example, a specimen which showed a t_{ig} of 200 s at a flow rate of 6 L s^{-1}, would be likely to show $t_{ig} \approx 140$ s at a flow rate of 1 L s^{-1}.

The OSU Apparatus performs rather differently. In that apparatus[101], PMMA specimens exposed at 35 kW m^{-2} ignited at 209 s with 12 L s^{-1} flow rate and at 403 s with 24 L s^{-1}. Chen[211] reported limited results with a modified ISO 5657 apparatus that used electric spark ignition and found that imposing an air velocity greater than 0.5 m s^{-1} led to longer ignition times than quiescent (< 0.2 m s^{-1}) conditions. Cordova and Fernandez-Pello[212] measured the effect

of an imposed flow velocity on the piloted ignition of PMMA using a wind tunnel apparatus. At zero imposed velocity, ignition took place when a mass loss rate of 1.8 g m^{-2} s^{-1} was reached, while imposing a velocity of 2.5 m s^{-1} doubled the required mass loss rate; at intermediate flow velocities there was a linear relationship between velocity and mass loss rate.

Even though the above list of studies is fairly long, it is difficult to establish firm trends. For velocities greater than about 0.5 m s^{-1}, it is evident that increasing velocity increases cooling and delays ignition. But for small velocities, reported effects are very diverse. The magnitude of the effects in this regime is generally not large, so a practical conclusion might be that velocities < 0.5 m^{-1} do not significantly affect the outcome.

OXYGEN CONCENTRATION

Piloted ignition of a solid might very roughly be considered as occurring when the LFL of a pyrolysate/air mixture is first reached, while autoignition of a solid might be considered to involve the autoignition of pyrolysates. Thus, the effect of oxygen concentration could be anticipated to be different in the two cases.

Both modes of ignition may, in principle, be affected if surface oxidation of the solid is involved. As discussed above, for most materials it is considered appropriate to use an inert-heating model of the solid. The pyrolysates may be generated at a faster rate than expected if oxidation of the solid material is appreciable. The effect is small for most substances, but if the material is capable of glowing combustion (e.g., wood), then the role of oxygen concentration on its pyrolysis rate may have to be considered. For white pine, Kashiwagi et al.[213] showed that, heated at a flux of 40 kW m^{-2}, it showed a peak MLR of 12 g m^{-2} s^{-1} in at O_2 = 21%, 9.5 g m^{-2} s^{-1} at O_2 = 10.5%, and 6.2 g m^{-2} s^{-1} at O_2 = 0.

PILOTED IGNITION

Since the LFL of gases is normally unaffected by varying oxygen concentration over a wide range, it might also be expected that oxygen concentration is not an important variable affecting the piloted ignition of solids. Petrella[214] tested polystyrene and PMMA in the Cone Calorimeter and found that t_{ig} was independent of oxygen concentration. Using an early-identical apparatus, Mikkola[215] tested 6 different materials at 21% and 15% oxygen with a heat flux of 50 kW m^{-2}. Apart from PVC, an average ignition time of 24% higher was found at 15% O_2, compared to values at 21% O_2. PVC was clearly very much affected by O_2 concentration, since the ignition time at 15% O_2 was some 3× as long as at 21% O_2. Interestingly, the results for wood particleboard were essentially identical to those for nylon, polystyrene, and other thermoplastics—a modest rise only. A follow-on study at the same institution[210] examined nylon and polypropylene in more detail and gave the results

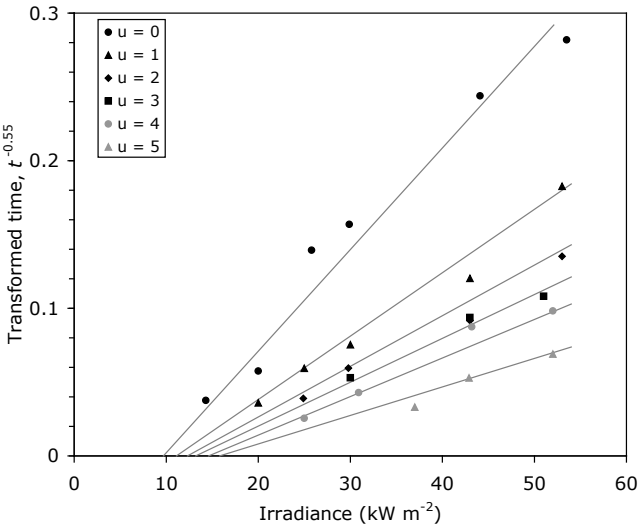


Figure 57 Effect of wind speed on the ignition time of pine

shown in Figure 58. Data obtained by Hirsch et al.[216] on a PVC/acrylic copolymer and on an intumescent FR PUR foam again showed that there is nearly no effect until oxygen concentration approaches its MOC value, at which point ignition times increase precipitously. PMMA shows little variation, down to the lowest flux (15 kW m^{-2}) examined[217]. Results on silicone elastomers[218] showed similar results. Additional data have been collected in a NASA report[219].

AUTOIGNITION

If autoignition of pyrolyzing solids is viewed as occurring when that AIT is first attained for a volume of pyrolysate gas mixed with oxygen, the same relations should hold as

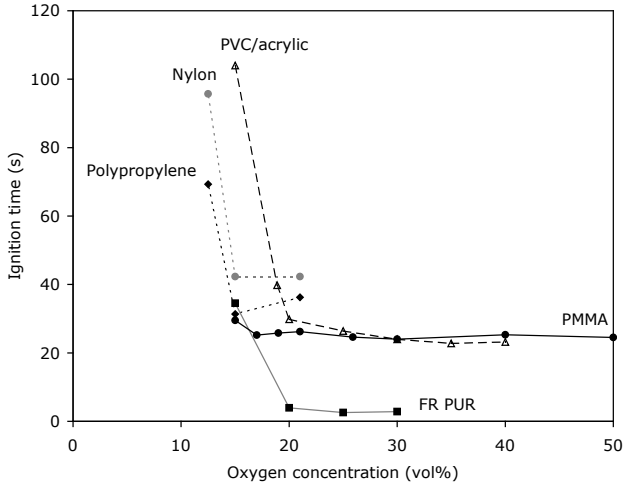


Figure 58 Effect of oxygen concentration on the piloted ignition of several plastics tested at a heat flux of 50 kW m^{-2}

for the AIT of gases. Unfortunately, as seen in Chapter 4, there is a wide spread of results on this point. If it is further assumed that ignition will not involve cool flames or two-stage ignitions, then

$$t_{ig} \propto \frac{\text{constant}}{Y_{O_2}^n}$$

where Y_{O_2} = oxygen mass fraction, and the exponent n is probably somewhat less than 1.0.

Kashiwagi's early model of radiant autoignition[51] predicted a minimum value for the mass fraction of oxygen, Y_{O_2}. This minimum depended on the exact problem being solved, but was often in the vicinity of 0.15. For Y_{O_2} just slightly higher than this minimum value, there was a very narrow range, where ignition time went from infinite to a modest value, as Y_{O_2} was raised slightly. For further increases in Y_{O_2}, the ignition time varied as:

$$t_{ig} \propto Y_{O_2}^{-0.068}$$

Because this dependence on Y_{O_2} is very slight, the result was that the ignition time dropped only about 15% as Y_{O_2} went from 0.23 to 1.00. Alvares[27,220] found a similar behavior in experimental studies on thin cellulose sheets. His results (Figure 59) show that for a partial pressure greater than about 0.18 atm (i.e., from just below ambient) there is a slight effect going as $t_{ig} \propto P_{O_2}^{-1/4}$. However, if the oxygen partial pressure is decreased below about 0.18 atm, ignition times become drastically prolonged and ignition becomes impossible once the partial pressure drops below about 0.16 atm. Nakamura et al.[60] computed the ignition behavior of the same material using a sophisticated axisymmetric, 2-dimensional numerical model, but their results were only qualitatively in line with Alvares' experimental findings.

Ohlemiller and Summerfield[221] examined the ignition of epoxy using enormous (800 – 4000 kW m^{-2}) heat fluxes from a laser. At the low end of this heat flux range (< 1600 kW m^{-2}) ignition time at an oxygen concentration of 43% were slightly longer—but barely more so than the data scatter—as compared to times at 100% oxygen. On the other hand, also using a laser source, Beckel and Matthews[222] found that increasing oxygen fraction over the range of 20 – 100% had a strong effect in reducing the ignition time.

FRS studied the ignition of blocks of wood and sawdust in a tube furnace which incorporated a forced air stream[223]. For 10 mm cubes of wood, they reported that T_{ig} at autoignition dropped from 380ºC to 270ºC when air was replaced with pure oxygen. On the other hand, for sawdust cubes the drop was much smaller, from 310ºC to 280ºC. Moghtaderi[224] showed that for wood, over the range of 14 – 21% O_2, increased oxygen concentration led to shorter ignition times; furthermore, the effect was more pronounced for pre-charred samples. For plastics, the reported effects are inconsistent. Marzani[234] found that changing from an air atmosphere to one of pure O_2 has a negligible effect (5 – 10ºC) on the AIT. On the other hand, Paciorek et al.[225] investigated the difference between AIT values for several materials in air, versus in oxygen, and their results, summarized in Table 30, show large differences. Delfosse[226] examined the autoignition of PVC and found that T_{ig} dropped from 600ºC at 21% to 475ºC at 50% oxygen.

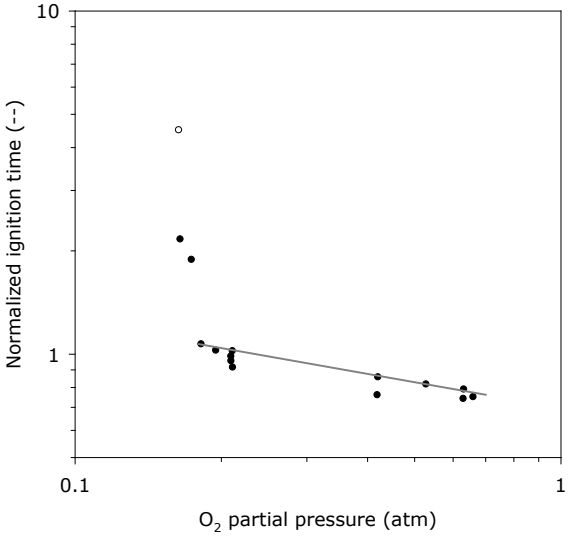


Figure 59 Effect of O_2 partial pressure on the autoignition of cellulose

CHEMICAL COMPOSITION OF DILUENTS

Accidental ignitions in oxygen/nitrogen atmospheres can readily be encountered where the O_2 concentration is not 21%, as discussed above. On rare occasions, accidental ignitions may take place in atmospheres where the diluent is not nitrogen, or is not wholly nitrogen, for example, CO_2 or helium. This has been of some interest to NASA and a review paper is available on this topic[227].

TOTAL PRESSURE

The total pressure affects gas-phase reactions, and it lowers both the AIT and MIE of gases (see Chapter 4). Thus, these same effects may also be expected to manifest themselves in the ignition of fuel vapor/air mixtures pyrolyzed from

Table 30 Effect of oxygen concentration on the AIT of several materials studied by NASA

Material	AIT (ºC)	
	In 21%	In 100%
Fluorel KF 2140	630	400
paint 45B3	495	365
polyisocyanurate foam	> 600	350
PTFE	575	510
Refset	> 610	380

solids. In addition, the total pressure may affect the autoignition of a material indirectly by its effect on the lower flammable limit, but for many materials, over a fairly wide range of pressures, the lower flammable limit is not significantly affected by total pressure[228].

Hermance[229] presented a theoretical model for the autoignition of polymers where the pressure effect is included. His numerically-computed results indicated that $t_{ig} \propto P^{-1/2}$. He did not present any experimental data to validate his theory, but there does exist a limited number of experiments on the effect of pressure for common solids. Kishore and Sankaralingam[230] studied the autoignition of polymers using a DTA apparatus, which is not the best equipment for the task. They found a modest decrease in T_{ig} with pressure, for example, a PVC specimen that ignited at 469ºC at 1 atm, ignited at 394ºC at 21 atm. Wharton et al.[231] also used a DTA technique and obtained similar results for several materials but the opposite result for Neoprene—for this material, raising the pressure increased the T_{ig}.

Attwood and Allen[232] tested 60 mg samples of nylon 6,6 in pure oxygen atmospheres at total pressures of 11 and 131 atm. The ignition temperature at 11 atm was 350ºC, dropping to 300ºC at 131 atm. For several silicone elastomeric materials, however, the order was reversed, with specimens showing a higher T_{ig} at the higher pressure. Wolf et al.[233] studied the ignition of PVC in a pure-oxygen atmosphere and found a marked decrease in T_{ig} with increasing pressure, but they did not quantify their results. Marzani[234] ignited several plastics in a heated bomb at various pressures and using both air and pure O_2. For polyethylene in air, the AIT dropped from 193ºC at 68 atm to 182ºC at 170 atm. But at a pressure of 34 atm or lower, no ignition occurred, up to a maximum bomb temperature of 426ºC. In an O_2 atmosphere, the AIT dropped from 185ºC at 13.6 atm, down to 179ºC at 102 atm, and no ignition was achieved at 6.8 atm or lower. These temperature differences within the 'ignitable range' are trivial, but the existence of a 'non-ignitable range' of pressures is noteworthy. Marzani did not conduct ambient-pressure ignition tests, but the data in Chapter 15 show AIT values in the neighborhood of 400ºC. Thus, it appears that at a certain elevated pressure the AIT drops precipitously by roughly 200ºC. Kuzminskii[235] studied the effect of pressure on the ignition of rubbers in O_2 atmospheres. The AIT for natural rubber dropped from 161ºC at 5 atm to 142ºC at 120 atm. For various synthetic rubber types produced in Russia, the effect was similar or somewhat smaller. Pippen and Stradling[236] tested a number of solid aerospace materials in a flash point tester designed for high pressures and 100% oxygen concentration. The flash point typically dropped 100 – 200ºC as the pressure was raised from 1 atm to 100 atm. Changes in fire point were also quite similar, although a number of the materials did not show sustained burning at all until 1.6 to 3.4 atm was reached.

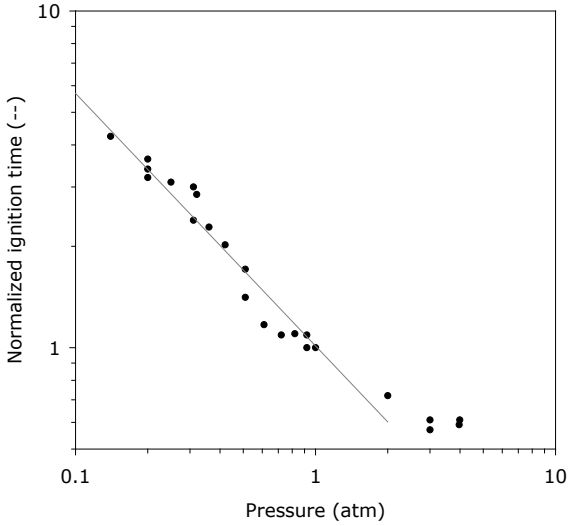


Figure 60 Effect of total pressure on the autoignition of cellulose

Bolod'yan et al.[237] studied the piloted ignition (using a glow coil) and subsequent flame spread of various fabrics in atmospheres of elevated pressure. Plain cotton (and for PMMA) fully burned up at oxygen concentrations below 21% and over the entire pressure range used, 0.1 – 10 MPa. But FR fabrics, including FR cotton and carbon-fiber, and aramid, showed an inverse relationship between pressure and needed oxygen concentration. At ambient pressure, concentrations ca. 40% were needed, but the needed concentration dropped to 15 – 18% as pressure was raised to 10 MPa. In a similar vein, Hirsch and Bunker[238] found that materials such as PTFE and Kel-F which, when ignited with a glow wire but not provided with external heat flux,

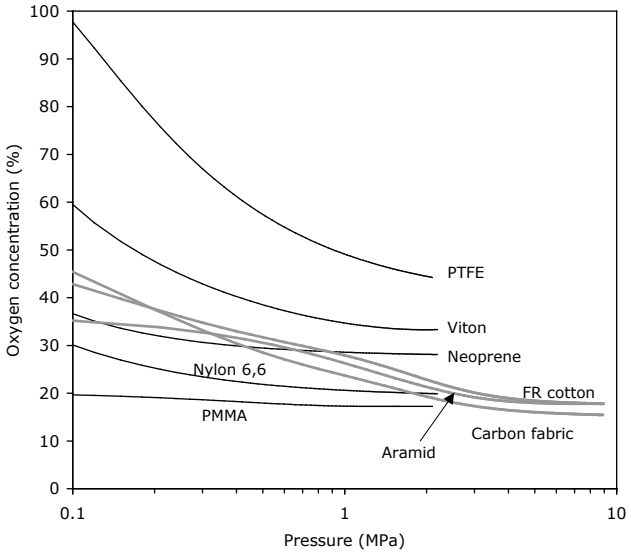


Figure 61 Relation between oxygen concentration and pressure needed for sustained flaming of several materials; data of Benning shown in black, Bolod'yan in gray.

do not burn in 100% O_2 at ambient pressure, do burn in an oxygen atmosphere at 7 MPa. Benning[239] presented similar data for Neoprene, nylon 6,6, PMMA, PTFE, and Viton over the range 0.1 – 2.0 MPa. A summary of trends is shown in Figure 61.

Alvares[220] used an arc furnace to ignite sheets of cellulose at various pressures. His ignition time results, normalized to ignition time at 1 atm, are shown in Figure 60. The fitted line represents $t_{ig} \propto P^{-3/4}$ and is seen to give a good fit for pressures less than 1 atm. At higher pressures, the effect becomes much smaller and it appears that by 3 or 4 atm the effect may be nil.

The topic has been more extensively researched (although not yielding up simple answers) in connection with the ignition of propellants, and this is taken up in Chapter 10. But propellants are not commonly studied in a piloted ignition mode, and there do not appear to be any studies on pressure effects for the piloted ignition of common solids.

MOISTURE AND RELATIVE HUMIDITY

Moisture content could simply be measured as the percent of the total mass of a specimen that is comprised of water. This is done in certain trades and industries, but most commonly, moisture content (MC) is measured on a dry basis. Thus,

$$MC = \frac{\left(W_{wet} - W_{dry}\right) \times 100}{W_{dry}}$$

where W_{wet} = mass wet and W_{dry} = mass dry. This requires using a standard procedure for drying the sample. Typically[240] the specimen is dried in an oven at 103±2ºC until it equilibrates to a constant mass; for specimens of modest size, a 24 h period often suffices. Results are occasionally cited as "xx% ODW," where ODW makes explicit that oven-dry weight was used as the basis. MC values may be greater than 100%, and living vegetation commonly shows values over 100%.

Yuen et al.[241] presented a theory for pressure effects on autoignition of thin materials, but it involves solely a glowing ignition mode.

In 1956, the US Forest Service conducted a study[242] where they examined the relation between the frequency of building fires and moisture, the latter assessed as the equilibrium moisture content of fine fuels. The results (Figure 62) show a very strong effect, with frequency, on the average, being 2 – 6 times greater during the driest periods than the wettest. If the study were repeated today, most likely the effect would be found to be less, since during the study period in the 1940s, a majority of the combustibles were cellulosic; today, a sizable fraction of the fuel load is comprised of man-made polymers, and the majority of these are not hygroscopic. It should also be kept in mind that intervening variables (e.g., use of heating during certain times of year)

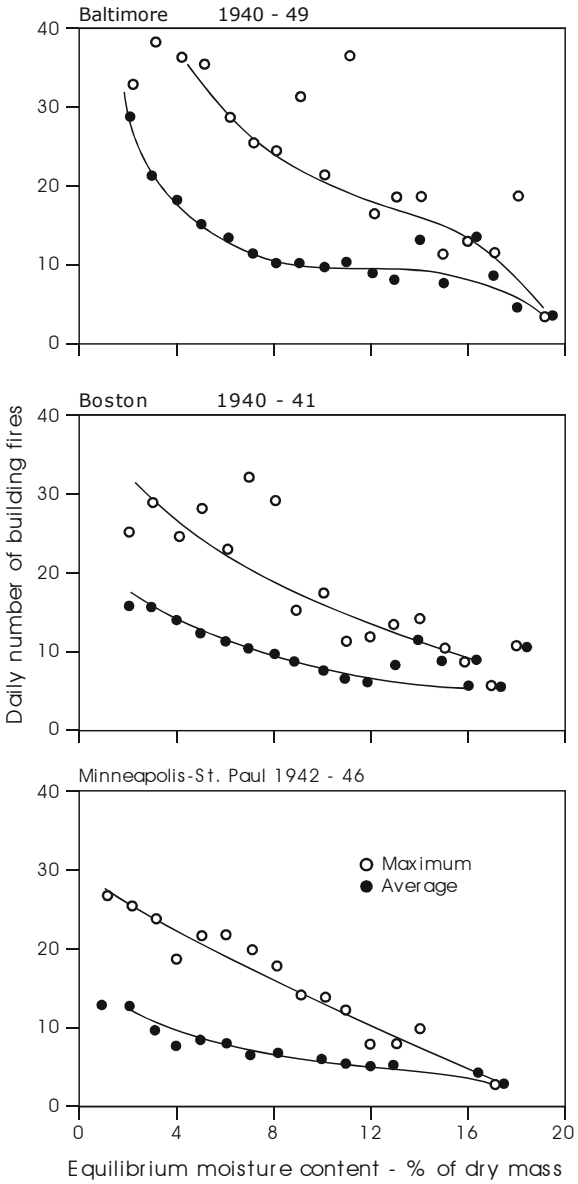


Figure 62 Relation between frequency of building fires and equilibrium moisture content of fine fuels

were not accounted for. Finally, whether a building fire gets reported is influence by flame spread and not by ignition alone. Nonetheless, the trends are striking and suggest that moisture effects should not be overlooked.

The effect of RH on ignition is mostly due to the effect of humidity on the equilibrium moisture content of solid ignitable materials. Few synthetic materials are so affected ('hygroscopic'), but many natural materials of significant interest are hygroscopic: wood and various agricultural products being the most notable examples. The relation between relative humidity and equilibrium moisture content is complex and non-linear; in addition, hysteresis is involved, that is, the adsorption curve is not identical to the desorption curve. These curves are different for various

substances, but for rough purposes, it has been proposed[242] that most cellulosic materials can be roughly represented by a single curve (Figure 64).

The average equilibrium values of moisture in different regions of the US are shown in Figure 63[243]. There is gross variation of about 2:1 between the 'wet' and the 'dry' regions. In addition to the gross climatic differences, there are seasonal differences and smaller-area variations. For example, Peck[244] found moisture contents during the summer of 4% in Salt Lake City and 13.5% in New Orleans. Lumber *outdoors* equilibrates to 12 – 18% MC. *Green wood* is at 50 – 150% MC, depending on the species and on whether heartwood or sapwood is considered. Paints and varnishes applied to wood, even if applied on all sides, delay effects of environmental RH, but do not significantly alter the moisture content to which the piece of wood will equilibrate[244].

The effects of moisture on the ignition of solids can be both in the solid phase and in the gas phase. If a substance is exposed to a high heat flux, so that ignition takes place while moisture still exists in the interior, some of the moisture will be driven out along with the pyrolysates (but some will leave through the back face). This will dilute the fuel vapors and consequently make it more difficult to reach a flammable mixture, but the effect is likely to be small compared to solid-phase effects. Within the material, moisture affects the thermal conductivity and the heat capacity, consequently raising the $\lambda\rho C$. In addition, the endothermic contribution of the heat of vaporization must be considered. This is all possible to track with models that are based on a porous, moist body concept, such as those of Yuen[56] or Moghtaderi[245]. These models require extensive numerical calculations and do not lend themselves to any simplified solutions.

Experimentally, it is found that increasing the moisture content tends to raise the ignition temperature, based on the few available studies. Abu-Zaid[67] found that the autoignition temperature of wood rises was 40ºC higher for MC = 17% specimens, compared to oven-dried ones. Janssens[76] concluded that the piloted ignition T_{ig} of wood rises by 2ºC

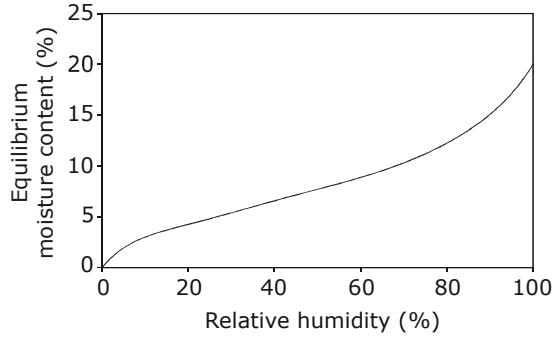


Figure 64 Approximate relation between relative humidity and equilibrium moisture content for fine, cellulosic fuels at room temperature

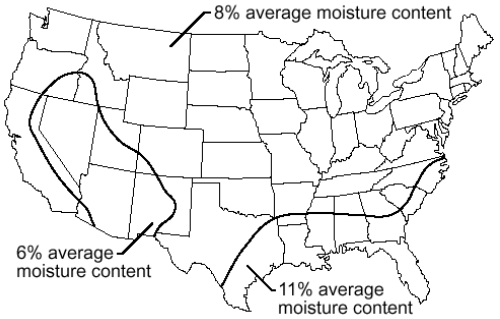


Figure 63 Average equilibrium moisture content of wood indoors, as a function of geographic location in the United States; the southern California coast, up to the San Francisco Bay region, is also at approximately 11% average moisture content.

for each percent of moisture content increase. Both these studies involved fluxes high enough that the specimens were presumably not fully dried out by the time of ignition. At low enough heat fluxes, there should not be a moisture effect since the moisture will be all gone by the time of ignition.

For the ignition of thermally-thin materials, Pickard and Wraight[246] proposed that the MC effect be approximated as an additive term to the ignition time:

$$t_{ig} = t_{ig(dry)} + \frac{\Delta h_{vap} L \rho_o MC}{\alpha_s \dot{q}''_e}$$

where L = thickness (m), ρ_o = dry density (kg m^{-3}), h_{vap} = heat of vaporization of water (kJ kg^{-1}). In tests on cellulose paper, the authors found that the relation was well obeyed for very thin specimens, but less so for specimens greater than about 0.5 mm. Duvvuri[247] showed that for thermally-thick materials, the increase in ignition time also depends on the same variables. But clearly the entire thickness will not be desiccated prior to ignition if a fairly high heat flux is applied. Thus, it may be reasonable to replace h_{vap} with some as-yet unknown parameter a:

$$t_{ig} = t_{ig(dry)} + \frac{aL\rho_o MC}{\alpha_s \dot{q}''_e}$$

Duvvuri's data did not span a wide enough heat flux range to test the above equation, but experimental data from Moghtaderi et al.[21] on intermediate thickness (9 mm) wood specimens show (Table 31) that a is not a constant, but rather decreases strongly with flux. This is not surprising, since at higher fluxes the thermal penetration depth at the time of ignition is smaller, consequently less material needs to be dried out. Agreement with experimental results can be obtained if the following form is taken for a:

Table 31 Piloted ignition times of Monterey pine as a function of moisture content

Heat flux (kW m^{-2})	Ignition time (s)			
	0% MC	15% MC	22% MC	30% MC
20	179	295	420	540
30	19	52	67	93
40	9	18	30	36
50	5	11	11	19
60	3	7	9	11

$$a = 33{,}200\left(\dot{q}''_e\right)^{-2} - 8.7$$

Moghtaderi[248] himself proposed a simpler equation:

$$\frac{t_{ig}}{t_{ig}(dry)} = \left[1 + 0.035MC\right]^2$$

which gives predictions accurate to about a factor of 2. Neither equation has been tested against other materials, so a wider applicability must not be assumed. Simms and Law[249] reported some results on the effect of moisture on the ignition times of wood, both piloted and autoignition. But their heat flux range used was very small, making trends difficult to quantify. Examination of a large set of Cone Calorimeter piloted ignition results showed that differences between ignition times at 0% and at 12% MC are small enough that they are swamped by data scatter[37].

At high heat fluxes, it has been demonstrated for wood[245] that no significant drying occurs at heat fluxes greater than about 35 kW m^{-2}. Conversely, near the minimum flux, the material has very substantially dried out prior to ignition. The latter fact leads to the conclusion that the minimum heat flux should be independent of MC. The sole existing study on topic, by Simms and Law[249], however, produced contrary findings. In their study, $\dot{q}''_{\min}$ for piloted ignition was higher by about 20% for wood with MC = 40%, as compared to oven-dry wood; for autoignition it was higher by about 28%, with the increases being roughly linearly proportional to MC. But these findings would appear to be an experimental artifact due to their short test duration, it being known[287] that some very long test times are needed to reach a true value of $\dot{q}''_{\min}$.

Apart from a few studies on wood, there is very little data on moisture effects. The effect of RH—rather than MC directly—on the ignition of fabrics has been studied[250]. For a 94 g m^{-2} 100% cotton T-shirt fabric, lowering the RH from 90% to 10% dropped the ignition time from 5.4 to 3.1 s under a radiant flux of 23 kW m^{-2}. For an 97 g m^{-2} cotton flannel, however, the change was smaller, going from 5.4 to 4.2 s. For a polyester/cotton blend, there was no significant effect on ignition.

INITIAL TEMPERATURE OF SPECIMEN

Fons[9] examined the effect of varying initial temperature between 10 and 66ºC on the ignition time of ponderosa pine when subjected to thermal immersion testing by insertion into a hot oven. The effect was found not to be significant.

When electric wires and cables are in use, they will generally operate at some temperature above the ambient. Standards bodies such as UL and IEC consider that electrical insulation materials that are used for wires, cables, and other similar applications have an insulation rating temperature, which is the maximum temperature to which the insulation can be exposed for an extended period of time. Since this temperature may be substantially above room temperature, it may be hypothesized that ignitability behavior would be different for specimens at the in-use temperature than at 20º – 25ºC. Lupton et al.[251] conducted a study to determine the effect that running tests at a wire's rating temperature would have on results from testing with a small open flame. They found cases where materials which did not spread flame upwards at ambient temperature did so at the rating temperature; however, the investigation was only exploratory and general guidance could not be evolved. In a similar study, Rodak et al.[252] tested wires used in NASA applications with a small-flame exposure, and found that ignition times decreased when specimens were preheated to elevated temperatures. Again, the study was only exploratory and no systematic guidance resulted.

Baer and Ryan[253] studied the radiant ignition of a propellant comprised primarily of ammonium perchlorate and polysulfide. For heat fluxes in the range 75 – 420 kW m^{-2}, they found that ignition times fell by 50%, as the initial sample temperature rose from –60ºC to +60ºC.

ACCELERATION OF GRAVITY

Older experiments have suggested that the ignitability of a material is not significantly affected by a lowered gravity or by micro-gravity conditions[254]. This is in agreement with the findings of Strehlow and Reuss[255], who concluded that gravity has but a minor effect on the LFL. However, more recently it has been reported[256] that autoignition of paper occurs more readily in micro-gravity. This is understood to be because, in the absence of significant gravity, pyrolysis products are not swept away by convection from the face of the specimen and, thus, a flammable concentration can build up earlier[257]. A recent theoretical study[60] on thin, horizontally-oriented fuels concludes that lowering the acceleration of gravity has a slight effect on promoting autoignition.

SURFACE ABSORPTIVITY, MATERIAL TRANSPARENCY, SURFACE COATINGS, AND SPECTRAL CHARACTERISTICS OF THE RADIANT SOURCE

When a radiant heat flux is incident upon the face of a material, in the general case, the heat flux is apportioned into three ways:

1. absorbed by the material
2. reflected from the face

3. transmitted through the material

Only the portion of the flux which is absorbed by the material can be used to raising its temperature. Thus, most theoretical models are formulated in terms of absorbed, rather than incident heat flux. To know the portion of heat flux which is absorbed requires knowing the material's surface absorptivity. This is not a constant and, rather, depends on the wavelength of the radiation. All radiant sources, apart from lasers, emit radiation at a variety of wavelengths, but the wavelength distribution is controlled both by the temperature of the source and by other factors (e.g., whether the source is a flame or a solid substance heated to a high temperature). Thus, to know the percent of incident flux absorbed requires knowing both the spectral energy distribution of the source and the material's absorptivity, as a function of wavelength.

Thermal radiation in accidental fires comes primarily from two sources: (1) molecular and soot radiation from flames; and (2) radiation from solid surfaces (e.g., walls) that have been heated by fire. The latter radiate similarly to a black body at the given temperature, although they will not be fully black, that is, the emissivity will be less than 1.0. Two black body sources and an exemplar fire source, hexane pool flames, are shown in Figure 66. Room fires with ordinary combustibles will normally not exceed about 1200ºC. Much higher temperatures are found only for fires of metals, in pure-oxygen systems, and other specialized applications.

Considering now the effect of surface absorptivity α_s, a material will have an absorptivity between 0 and 1. For opaque materials other than shiny metals, the value will normally be much closer to 1 than to 0. The absorptivity is a function of the wavelength of the absorbed radiation, and most real substances show a curve which is quite non-uniform. The fact that a substance has a white color only indicates that its absorptivity *in the visible portion of the spectrum* is quite low. For real fires (as contrasted to arc lamps and similar sources), the emitted radiation is primarily in the infrared, not the visible, part of the spectrum. Most 'white' materials are, in fact, of rather high absorptivity in the infrared. Hallman[71] measured the spectral absorptivity of a wide array of plastics and some other commodities. An example is shown for different types of PMMA in Figure 65. For all grades, the absorptivity at wavelengths greater than 2.4 μm is essentially constant at about 0.93. But over the visible spectrum (0.4 to 0.7 μm), the three color types differ greatly. Black PMMA shows an absorptivity of about 0.95, white about 0.3, and clear ≈ 0.

To obtain the integrated value of the absorptivity, Hallman integrated the values of the spectral absorptivity of the materials over the emissive power curves of several sources, as given in Table 32. The results, not surprisingly, show that the absorptivities are nearly identical for the 1000 K black body and the hexane flames, but grossly different for the 3000 K black body. The 3000 K temperature is similar to the temperature of tungsten lamps, so those results could be used to assess experimental studies done with tungsten lamps.

The surface absorptivity of woods was studied by Wesson et al.[105]. For a wide variety of wood species, they found that $\alpha_s = 0.76$ when the source radiation is that of flames. For tungsten lamps operating at 2500 K, Wesson's α_s values ranged from 0.41 to 0.56, with most species being 0.44 to 0.49. Spectrophotometer measurements which are made at room temperature cannot reflect the actual situation of a pyrolyzing solid being degraded in the process of igniting. A number of materials, especially wood, change from a light color to a dark one prior to ignition. This means that the actual absorptivity is dependent on the temperature of the surface which, in turn, depends on the time. For numeric analysis purposes, the effective value will be some value intermediate between the one at room temperature and the one at ignition. Janssens[75] concluded that $\alpha_s = 0.88$ tends to characterize well most woods as they are raised from room temperature to ignition by being heated from a heater having spectral characteristics similar to that of fires.

It is not necessary to know α_s in order to accurately and realistically measure the radiant ignitability of a specimen, provided that the heater in the test apparatus has radiant emission characteristics roughly similar to those of real fires. With this consideration in mind, most fire test equipment designed in the last few decades have used heat sources which are either actual flames, or else are electrical heaters running at 1200ºC or less. During the 1950s and '60s, however, many research studies, especially for the military, were done with apparatuses using tungsten/quartz lamps (effective temperatures ca. 3000 K) or with arc sources, which have an even higher effective temperature. These sources radiate primarily in the visible portion of the spectrum, not in the infrared.

If a test exposure is conducted using an apparatus radiating primarily in the visible portion of the spectrum and it is desired to apply the results to building fires, then one of two things must be done: (1) blacken the surface; or (2) determine the value of α_s pertinent to the spectrum of the heater and correct to a value pertinent to the spectrum of fire. Blackening the surface is not without its drawbacks, since it is not feasible to make a surface black without changing its other characteristics. Typically, blackening is done by applying a coating of some type of soot. Black paint is rarely suitable, since its organic components may contribute to the ignition process. To be effective, the soot layer has to have some minimal thickness, but this then means that there has now been placed an intervening layer in front of the specimen's surface. The intervening layer may change the effective thermal inertia of the substrate.

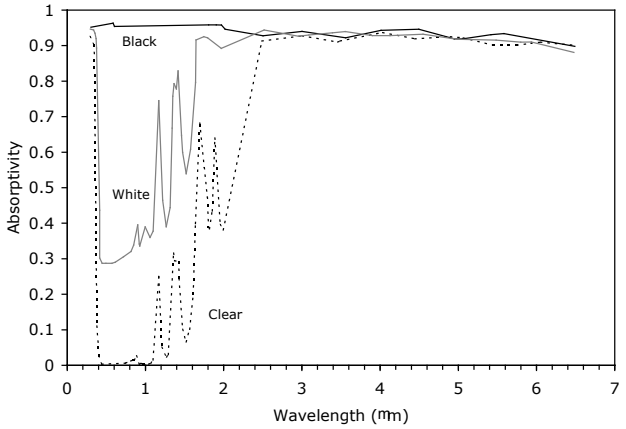


Figure 65 Spectral absorptivity of different types of PMMA

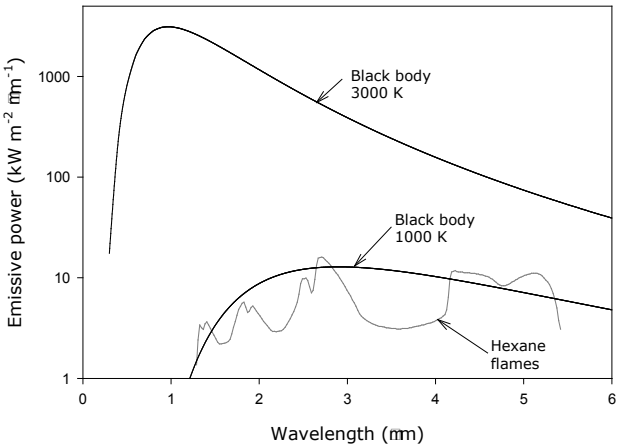


Figure 66 The spectral emissive power of various sources

Issues of surface conditions become important when considering data from the FMRC Flammability Apparatus (see below). In that apparatus, the heat is produced by tungsten/quartz lamps which reach up to ca. 2200ºC. This is much higher than fire temperatures, and in addition, the quartz envelope cuts off all radiation beyond about 4 μm. To address the problem of a spectral distribution strongly biased away from the infrared and towards the visible, FMRC adopted a test protocol of coating the specimen face with a thin layer of graphite powder. The layer of graphite is assumed to have an emissivity very close to 1.0 over the entire radiant spectrum. To examine the effect of a graphite coating, FMRC obtained data[258] comparing the ignition of 25 mm thick black PMMA with identical samples which were coated with graphite (Figure 67). The data show that the uncoated results fall very close to a straight line on a $t^{-0.55}$ plot. The coated results, however, are substantially lower at fluxes over 20 kW m^{-2}, and do not follow one straight line. The FMRC authors' explanation is that the effect is due to the fact that black, but uncoated PMMA specimens are not perfectly opaque, but absorb radiation in depth. However, since all other studies indicate that diathermancy *increases*, not decreases, the time to ignition, this explanation is not plausible. A more credible explanation is that the surface coating of graphite is not of negligible thermal effect, but creates an insulating layer, thereby increasing ignition times at higher irradiances. For comparative purposes, data obtained at NIST on the Cone Calorimeter are also given. These specimens were uncoated and were exposed to a radiant heat source operating at fire temperatures (below 1000ºC). These data points fall along the same line as the FMRC uncoated specimens. In Figure 67, at an irradiance of 60 kW m^{-2}, the ignition times for FMRC's coated specimens are 2.5 times greater than for the coated ones. If the coating associated with FMRC's standard test protocol always leads to such anomalous results, then unconservative errors of up to 250% may be involved in using the coated-specimen protocol.

Most solids are opaque, that is, the fraction of the incident radiant energy which is transmitted through the material is zero. However, some materials show *diathermancy*, that is, they are partially transparent, at least at certain wavelengths. When diathermanous materials are subjected to radiant heating, they absorb radiation in depth, not just at surface. The effect of this partial transparency is to increase the ignition time[221], since the radiant energy is no longer being optimally deposited for raising the surface temperature. Very thin materials, such as paper or facial tissue, are substantially diathermanous, and with these, a portion of the incident energy simply leaves the back face directly, without heating the specimen. When dealing with these materials, Martin et al.[203] pointed out that a factor of $1/(1-\exp(\beta L))$ should theoretically be used to multiply the values of $\dot{q}''_{\min}$ determined on the basis of neglecting diathermancy, where β = extinction coefficient (m^{-1}) and L = specimen thickness (m). However, actual data were not particularly well correlated by this factor, and they concluded that scattering of radiation would also have to be accounted for in order to provide a better fit.

The interaction between the source temperature and the material's diathermancy has been illustrated experimentally by Thomson[2]. She exposed 6 mm thick slabs of PMMA, both black and clear, to an electrical heater which radiates as a gray body. Her results are shown in Table 33. Since the black material has an absorptivity which is essentially independent of wavelength, the operating temperature of the heater does not influence its ignition time. But the absorptivity of clear PMMA progressively drops below about 2.5 μm, thus a smaller fraction of radiation is absorbed as the temperature of the radiant source is increased (and its peak wavelength of radiation correspondingly decreased). Thus, higher heater temperatures produce longer ignition times.

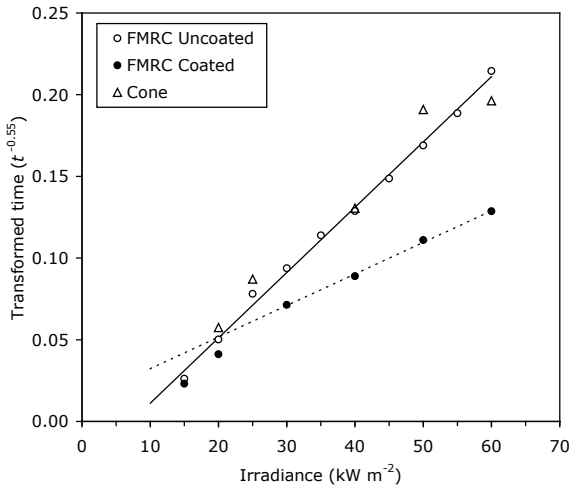


Figure 67 Comparative results on 25 mm thick black PMMA

A question commonly asked is the effect of *paint* on the ignition characteristics of a surface. Paint applied in thick, multiple layers will strongly affect the ignition characteristics of material. The FMRC results discussed above imply that even surface coatings which are applied in quite thin layers may have a measurable effect. In many cases, however, if the thickness is not excessive, a coat of paint may not appreciably affect the ignition results. Moysey and Muir[259] demonstrated this for a number of common paints applied to cedar panels. Vovelle et al.[260] examined three paints on a particleboard surface and found a protective effect with two (ignition times increased by 20 – 65%) and an adverse effect from the third (ignition times decreased by 20 – 26%). In rare cases (e.g., nuclear weapons), ignition from radiation sources having a peak in the visible, rather than infrared, portion of the spectrum must be considered. Then, not surprisingly, painting darker-colored materials with a white paint increases the time to ignition[261]. See also in Chapter 14: *Gypsum wallboard*; *Paints, dyes and related substances*; and *Wood and wood products*.

Table 33 Effect of diathermancy for PMMA specimens exposed to an incident heat flux of 25 kW m^{-2}

Temperature of heater (ºC)	Ignition time (s)	
	Black	Clear
450	124	128
643	120	146
740	134	155
795	128	163

Table 32 Surface absorptivities determined for various radiant sources

Material	Integrated absorptivity for given source			
	1000 K black body	Pool flames	3000 K black body	Solar radiation
ABS	0.91	0.92	0.65	0.55
butyl rubber (isobutylene/ isoprene copolymer)	0.92	0.92	0.95	0.95
cellulose acetate butyrate	0.84	0.88	0.34	0.12
chloroprene rubber	0.72	0.71	0.51	0.62
cork	0.64	0.60	0.44	0.52
melamine formaldehyde	0.91	0.91	0.80	0.80
nitrile rubber (buna-N)	0.92	0.92	0.93	0.94
neoprene rubber	0.91	0.91	0.93	0.94
nylon 6,6	0.93	0.93	0.75	0.62
phenol formaldehyde (phenolic)	0.90	0.91	0.75	0.78
PMMA, black	0.94	0.94	0.95	0.96
PMMA, white	0.91	0.92	0.62	0.42
PMMA, clear	0.85	0.89	0.31	0.10
polycarbonate	0.87	0.88	0.72	0.69
polyethylene	0.92	0.93	0.72	0.57
polyoxymethylene	0.92	0.93	0.64	0.48
polyphenylene oxide	0.86	0.88	0.57	0.48
polypropylene	0.92	0.93	0.72	0.57
polystyrene, white	0.86	0.88	0.45	0.29
polystyrene, clear	0.75	0.78	0.28	0.10
polyurethane elastomer	0.92	0.93	0.72	0.62
PVC, gray	0.90	0.91	0.89	0.89
PVC, clear	0.81	0.85	0.30	0.15
rubber, natural	0.88	0.89	0.69	0.69
silicone rubber	0.79	0.79	0.52	0.62

Some products, notably certain thermal insulations, are manufactured with a shiny aluminum facing. The absorptivity of shiny aluminum is around 0.07 to 0.1 in the near infrared. By contrast, most other common building materials show an infrared absorptivity of around 0.7 – 0.8. If the surface truly maintains an absorptivity below 0.1, then ignition of any combustibles underneath is unlikely, except if flashover conditions develop. However, in fires it is common for copious soot to be produced, and for the soot to deposit on a nearby surface. The absorptivity of a black soot coating is around 0.98. Thus, the same product that might be 'ignition-resistant' originally, may ignite readily once sooted up. This situation has some implications for the ignitability testing of aluminum-faced products. Since one can generally have no assurance that a fire would be soot-free, it is prudent to only do ignitability testing on such products either by blackening their face or by first removing the aluminum facing. If the facing is removed, this will also change the pyrolyzing characteristics of the product. Since aluminum is impervious to vapor flow, if a faced product is heated, the vapors will be retained for a short amount of time; subsequently, the facing will split or delaminate as pressure builds up. This propensity has not been studied in any detail, so it is not

known whether blackening the facing or removing it would result in more realistic testing.

POLYMER STRUCTURE

The main properties of polymer which control the ignition time are the thermal inertia, the surface absorptivity, and the ignition temperature. But chemical details of the polymer, such as its molar mass, can also affect the results. Kashiwagi et al.[262] examined the ignition of two different makes of clear, 12 mm thick PMMA—Plexiglas (Rohm & Haas) and Lucite (DuPont). PMMA is ideal for this type of study, since the material has a simple chemistry and the commercial product is nearly a pure polymer. For piloted ignition of vertical samples at a heat flux of 18 kW m^{-2}, they found nearly identical T_{ig} (275ºC), but the Plexiglas sample's ignition time (255 s) was about 15% shorter than the Lucite's (300 s). The samples had nearly identical values of thermal inertia and are presumed to have had very similar absorptivities. The molar masses were 402,000 for Plexiglas and 179,000 for Lucite. If this were the only difference, however, higher molar mass would lead to longer ignition times. But TGA measurements showed that Plexiglas starts to decompose at lower temperatures. The materials have different activation energies, both in nitrogen and in air, and Plexiglas was also found to be more sensitive to oxygen effects. The measured differences might be due to different ways of manufacturing, impurities, and the very small amount of additives that are contained in the polymers, but a direct explanation is not available.

POROSITY

Piles of forest materials, agricultural products, fibers, dusts, etc., are highly porous assemblies that can be packed to a variety of porosities. Thus, porosity becomes a problem variable. Porosity is a dimensionless quantity defined as:

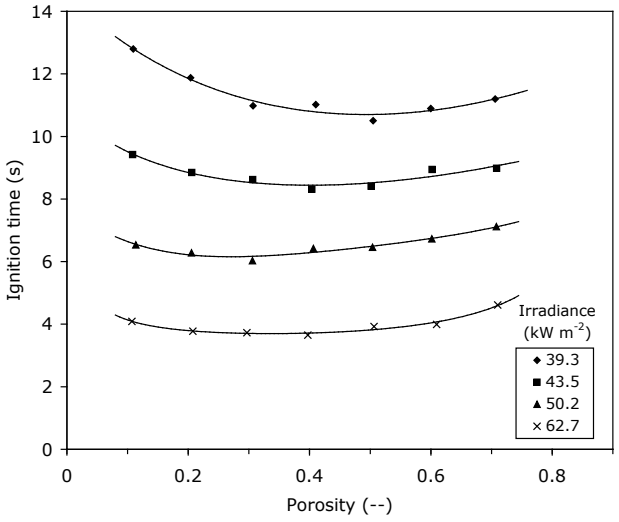


Figure 68 The effect of porosity on piloted ignition of excelsior at MC = 6.7%

$$\varepsilon = \frac{\text{volume of voids}}{\text{gross volume}}$$

Garg and Steward[263] examined the effect of porosity on the ignition of excelsior (Figure 69). Calculations with this model showed that there is negligible effect on ignition time for ε less than about 0.5. The accompanying experiments (piloted ignition conditions) indicated similar trends, but with a pronounced minimum value of t_{ig} at around ε = 0.4 – 0.5. At low irradiance values, assuming the t_{ig} is identical for the porous body as for a solid one could be in substantial error, although at high irradiances this assumption could be reasonable. The authors also tried to model the effect by using an inert-substance model where the thermal properties were modified by substituting $\lambda(1- \varepsilon)$ for λ and $\rho C(1- \varepsilon)$ for ρC, but the predictions of the model did not closely follow the data trends. Similar experiments were also conducted by Varma and Steward[264], but their data showed such high scatter that distinct trends did not emerge

FIRE RETARDANTS

Fire retardants can be of various types. An inert, 'filler' type of retardant, for example, calcium carbonate ($CaCO_3$), functions solely by removing combustible mass fraction and raising the effective thermal inertia. Semi-inert FR agents, for example, alumina trihydrate, $Al(OH)_3$, or magnesium hydroxide, $Mg(OH)_2$, confer the advantages of inert retardants, but also interfere with ignitability and combustion by endothermic decomposition, producing water as the decomposition product. Both of these FR agents tend to be used in high concentrations, possibly as much as 50% of the mass. Such FR agents will change all of the chemical and physical (e.g., thermal inertia) properties of polymer. Other FR agents, however, exist which act to interfere with gas-phase combustion. Most retardants which are halogenated fall into this category. These are normally used in small enough quantities to not change appreciably thermophysical properties such as thermal inertia, but they do raise the ignition temperature of the material. For example, Drysdale and Thomson[265] examined the effect on ignition of a number of polymers, with and without FR agent (Table 34). The FR agents also raised the minimum heat flux for ignition and increased the ignition time at any given heat flux. They also examined inert fillers and found that calcium carbonate did not affect T_{ig}, while alumina trihydrate gave a modest increase in T_{ig}. Large loadings (40 – 50%) of inert fillers raised the minimum flux for ignition. Inert fillers are much denser than the base polymer, so adding the filler causes an increase in the product density. Drysdale and Thomson found that increased times to ignition when adding inert fillers could largely be accounted by the increased specimen density. Hirschler concluded that, since alumina trihydrate is inexpensive and commonly in high loadings, it tends to be the most effective FR agent for improving radiant-flux ignitability performance[266]. The improvement, however, is highly variable and not readily predictable.

Table 34 The effect of halogenated FR agents on the ignition temperature

Material	T_{ig} without FR (°C)	T_{ig}, with FR (°C)
PMMA	306 – 312	370 – 376
polypropylene	320 – 332	392 – 407
polystyrene	360 – 370	430 – 445

The use of FR agents may cause the earliest signs of ignition to occur earlier than for the non-FR material. Grand[267] showed that in most cases the time to sustained flaming either remains the same for the FR material, or else becomes up to several-fold longer. But non-FR polymers which do not exhibit flashing sometimes show a flashing ignition when an FR agent is added, and this flashing ignition comes before the non-FR material would have shown sustained-flaming ignition (Table 35).

Table 35 Effect of FR agents on ignition of some polymers, as tested for piloted ignition in the Cone Calorimeter at a heat flux of 50 kW m^{-2}

Polymer	Flashing time (s)		Sustained flaming (s)	
	Non-FR	FR	Non-FR	FR
ABS	none	27	38	34
HIPS	none	40	52	106
PC/ABS	none	51	49	53
unsaturated polyester	40	150	42	159
XPE	61	33	37	63

Nelson et al.[268] conducted a theoretical study on thermally-thin polymers where they examined the effect of an inert additive. In one example case calculated, when sufficient additive was added so that the mass fraction of resin in the sample dropped to 50%, the critical heat flux for ignition rose from 27.2 to 31.0 kW m^{-2}. This is a modest rise and suggests that very large fractions of inert additive would be needed for the critical heat flux to be raised by a sizeable amount. In general, inert fillers are used for improved arc-tracking performance, to meet the UL 94 HB ratings, and to reduce HRR and smoke, but not normally for improving ignition resistance under radiant heating conditions.

A number of polymer families exist which either intrinsically produce a significant amount of char, or else char-forming can be promoted by additives or chemical modifications. A theoretical paper[269] has recently put forth the thesis that for these polymers there may exist a critical 'jump' at a certain char yield. If the viewpoint is taken that—all else held constant—ignition corresponds to a fixed mass loss rate of combustible volatiles first being attained, then clearly production of char detracts from the ability to produce volatiles. The authors considered the common case where the $\dot{m}''$ versus time curve is double-humped, with the second peak representing the condition that sufficient mass has been lost so that the specimen becomes effectively thermally thin. If with modest char yield the critical value of $\dot{m}''$ is attained prior to reaching the first peak, then when increased charring decreases the volatile production rate, the critical value may only be attained near the second peak—this can correspond to either a large increase in ignition time, or if the second peak is not high enough, no ignition at all.

The compounding of fire-retarded plastics is a highly specialized industrial activity and is generally outside the scope of this Handbook. Current information can be found in the patent literature and in regular conference series of three organizations:

- Fire Retardant Chemicals Association, Lancaster PA. This society of fire-retardant chemical manufacturers holds semiannual technical conferences.
- British Plastics Federation. This society holds biennial conferences. Recent proceedings have been published by Interscience Communications Ltd., London.
- Business Communications Co., Inc., Norwalk CT. This commercial group holds an annual conference on fire retardants.

The above discussion was predicated on the assumption that the substance being treated with FR agents is a synthetic polymer. Entirely different types of FR agents and mechanisms are encountered with wood or other lignocellulosic materials. See *Cellulose insulation* and *Wood and wood products* in Chapter 14.

MOVEMENT OF THE SURFACE

Any material that ignites and burns will eventually show a change of the location of its surface, with respect to its original location. But numerous materials also show movement prior to ignition, and this can affect their ignitability. Plastics can show both swelling and shrinking tendencies. When exposed in the Cone Calorimeter to a uniform radiant flux, many grades of PVC expand considerably. Because the heater is fixed a short distance above the specimen, this would cause them to receive a slightly higher heat flux (the increase is not large, since the movement increases the view factor, but the view factor is already near-maximum). In testing, either wire grids to hold back the surface are used, or else techniques have been adopted where the swelling specimen is tested at a greater than standard distance below the heater. There are no known studies where this phenomenon would have been examined systematically in real fires.

A number of thermoplastic foam materials shrink when exposed to heat. The most notable example is polystyrene foam, although polyethylene foam behaves very similarly. Ignition of polystyrene foams normally does not take place in the solid phase[270]. The material melts at a low enough

temperature so that by the time a sufficient temperature has been reached for ignition, it is in the form of a liquid film.

At present there are no useful quantitative techniques to predict the behavior or the ignitability effects of surface movement. In addition, in certain geometries some materials will undergo a gross movement which is melting and falling out of their original position. This behavior enables them to pass certain unsophisticated fire tests and, on occasion, may represent exactly what happens in real life. In other cases, however, falling down may be precluded and the same material may show rapid ignition.

Intumescent coatings are coatings which are applied over surfaces and whose primary property is rapid, voluminous swelling when exposed to heat. The protective action takes place because the coatings are of limited combustibility, thus, even though they move closer to the source of the heat, the net effect of a successful intumescent coating is to delay ignition and reduce or delay the heat release from the material.

SURFACE ROUGHNESS

If a solid's surface is not smooth, then there can, in principle, be protuberances of lower thermal inertia that are able to ignite more readily than the bulk material. This issue has not been explored, however, in any depth. Akita's study on the radiant ignition of thick wood samples showed that there was no difference in ignition time for smooth-surface, versus rough-sawn, wood boards[271]. On the other hand, Heskestad's[272] work showed that when fabrics are ignited by a small flame and the two sides are dissimilar, there can be a substantial difference in ignition times. But not enough specimens were tested in either study to be able to draw broad-based conclusions.

IGNITABILITY OF AGED, DEGRADED, OR CHARRED MATERIALS

When a solid material is aged, thermally degraded, or charred, a number of physico-chemical changes can occur which may affect its ignitability:

1) lighter fractions (e.g., residual solvents) can vaporize
2) the molar mass can decrease due to scissions, local oxidation, free-radical attack, and other factors
3) water-soluble fire retardant agents may be leached out
4) density may drop, especially if pronounced charring occurs
5) electrical conductivity may decrease due to charring
6) most materials that are not already dark will darken, causing an increase in the radiative absorptivity.

There is a vast body of literature on the degradation of combustible materials, but very few studies have focused on the effects on ignitability.

An aging program was conducted at SP[273] using a variety of products. The test program consisted of exposure in a 70ºC oven for 7 weeks; this was deemed to approximate a 4-year exposure under actual use conditions. Ignition tests were conducted in the Cone Calorimeter at a 50 kW m^{-2} heat flux. Ignition times were unchanged after aging for a wide variety of products (roofing materials, wall coverings, curtains, foam polystyrene, counter-top laminate). Only for an FR paint was there a significant change, but that product improved its performance with aging, going from a t_{ig} of 300 s to 480 s after aging. In another SP program[274], high-impact polystyrene (HIPS) material, of the kind used for making television enclosures, was subject to testing before and after aging. The aging program consisted of 1200 hours at 80ºC, simulating 8 years of normal service life. Two types of samples were tested, non-FR and an FR grade using decabromodiphenylether. The latter showed V0 performance in the UL 94 test both before and after aging. The non-FR material however gave HB results prior to aging, but failed HB classification after aging. Attwood and Allen[232] found an aging effect in ignition of nylon 6,6 in pure-oxygen, hyperbaric atmospheres, with 7-year old material sometimes igniting at greatly lower temperatures than virgin material.

Wood has been the material whose degradation aspects have been studied the most. Details are presented in Chapter 14 under: *Wood and related products*. Briefly, for ignition from external heating, weathering and pre-charring make wood harder to ignite; rotting makes ignition easier. Degradation of electrical wiring insulation is considered in Chapter 14 under *Electric wires and cables.*

WETTING BY WATER

One of the functions of water used in fire extinguishment is to pre-wet surfaces to reduce the potential for further ignitions. A study of this was reported by Josler[275], who tested vertically-orientation wood siding panels in the Cone Calorimeter at an irradiance of 30 kW m^{-2}. Both raw and stained siding boards were examined. In addition to dry control specimens, specimens were wetted with water and with four different fire-fighting 'wetting' additives, i.e., proprietary surfactants. The unstained siding which showed an ignition time of 100 s dry, showed $t_{ig} \approx 140$ s when tested right after wetting with water or with any of the additive systems. The stained siding ignition time rose from 75 s to 90 – 95 s. Tests were also run at 3 h and 6 h after the panels were wetted. The plain-water results showed no improvement over the unwetted controls. However, the best additive system retained nearly full effectiveness after 6 h. The worst one, however, decreased to unwetted-specimen performance. Also explored were the same additives incorporated into a compressed-air foam extinguishing arrangement. A very wide scatter of results was seen for these specimens. Without aging, the best specimen showed $t_{ig} \approx$ 190 s for the unstained siding and $t_{ig} \approx 125$ s for the stained siding. In general, most of the additives did better in the foamed condition than when sprayed from nozzles without foaming. Preliminary testing had indicated that such beneficial results are only obtainable for hydrophilic materials.

Building materials, such as PVC, which are not wetted by water would not show any improvement.

A related issue is *re-ignition*. The question here is: If a fuel was extinguished by applying water, how long will it take before it re-ignites, given a specified irradiance, mass-burned percent, material properties, and amount of water applied? This question has been addressed by some detailed numerical modeling[276], but, due to the large number of variables involved, is difficult to treat in closed form. A limited amount of experimental data has also been published[277,278], but not enough to lead to general guidance. The best illustrations of general trends and magnitude of effects are in papers by Moghtaderi et al.[279,280]. They generally found that, for a given water application rate, re-ignition time decreases linearly with increasing irradiance and with increasing sample porosity. For the samples studied, re-ignition time was also inversely proportional to specimen thickness.

TYPE OF APPARATUS

Even though ignition test apparatuses using a controlled radiant flux should, in principle, give identical results, in practice no two engineering test methods will usually give identical results. Figure 29 shows a comparison of two PMMA materials tested in the Edinburgh University (EU) apparatus and in the ISO 5657 apparatus. At around 20 kW m^{-2}, both apparatuses give identical results. For higher heat fluxes, the EU apparatus gives shorter ignition times, while the converse is true at 10 – 15 kW m^{-2}. Results for two different types of PVC materials tested in the EU apparatus and in the Cone Calorimeter showed shorter times in the Cone Calorimeter at higher fluxes[281]. Of greater interest perhaps is that one grade of PVC showed $\dot{q}''_{\min} \approx 35$ kW m^{-2} in the EU apparatus, but less than 20 kW m^{-2} in the Cone Calorimeter. The samples tested in the EU apparatus were 60 mm diameter, as contrasted to 100 mm squares in the Cone. Also, the EU apparatus used a hydrogen pilot, compared to an electric spark in the Cone.

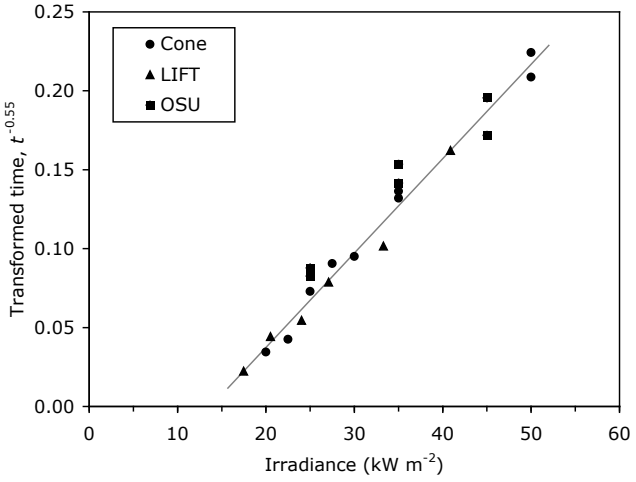


Figure 69 Ignition results for Douglas fir in three different test apparatuses

In other comparisons, however, little systematic difference could be found. Tran et al.[282] tested Douglas fir in three different apparatuses. Figure 69 shows little, if any, systematic difference between the three apparatuses. In Tran's comparison, the minimum flux for ignition was not established, and that might have shown non-trivial differences. Earlier, Quintiere et al.[283] reported on tests of aircraft sandwich panels, tested in the Cone Calorimeter, the LIFT, and the FM Flammability apparatus. There was a great deal of scatter in the results, and any systematic deviations were generally smaller than the data scatter.

MASS OF SAMPLE

The mass of sample does not significantly affect the ignition temperature, except in apparatuses which use minuscule specimen sizes. In a special thermal analysis setup[284] which was equipped with a spark ignition facility (for obtaining real, and not imputed, ignition temperatures), it was found that cotton fabric had an ignition temperature of 270ºC if tested in quantities of at least 350 – 400 mg. For smaller masses, the ignition temperature recorded rose with dropping mass, reaching 300ºC for 50 mg samples. Ignition proved impossible to achieve for samples smaller than 50 mg. Exploring the low end of the mass scale, Davies et al.[285] studied the autoignition of cellulose obtained from cotton using a DTA apparatus. They found an ignition temperature of 349ºC for a 1 mg specimen, and 353ºC for a 15 mg specimen, with intermediate masses also showing essentially identical ignition temperatures. Morimoto et al.[286] reported test results on a wide variety of plastics using a custom-designed test apparatus which was roughly similar to the Setchkin furnace, except that a specimen mass of only 200 mg was used. Their resulting T_{ig} values were much higher than those determined by other workers in the Setchkin furnace. Graf[36] studied the autoignition of wood, paper, and other lignocellulosic materials using a horizontal tube furnace. Over the range explored—0.5 to 10 g—he found that decreasing the specimen mass produced a monotonically increasing T_{ig}. There was a combined effect with air flow rate, and higher air flow rates led to a greater effect of specimen mass. The T_{ig} value for 0.5 g specimens was about 5ºC higher than for 5 g specimens with a reasonably small air flow rate, but at higher air flow rates the difference rose to about 30ºC.

LONG-TERM RADIANT EXPOSURES

Most radiant ignition tests are conducted for periods of 10 – 30 minutes. In one case, Shoub and Bender[287] undertook longer-term exposures using vertical specimens of size 0.92 × 0.92 m. The heat source was an electric radiant panel operating at an effective black-body face temperature of 273ºC and producing a heat flux of 4.3 kW m^{-2} at the center of the specimen, with lower heat fluxes at the edges. Specimens were mounted in two different ways—either onto

Table 36 Ignitions obtained by Shoub and Bender for various materials at a heat flux of 4.3 kW m^{-2}

Specimen	Back	Ignition time (h)	Temperature at ignition (ºC)	
			Face	Back
fiberboard, bagasse (13 mm, 290 kg m^{-3})	a	0.92	260	158
hardboard (6 mm, 960 kg m^{-3})	m	3.93	386	374
paperboard, laminated, primed (10 mm, 560 kg m^{-3})	a	0.58	270	96
paperboard, laminated, painted (10 mm, 560 kg m^{-3})	m	4.75	280	198
plywood (13 mm, 630 kg m^{-3})	a	5.17	254	254
a – air space m – millboard				

furring strips attached to a wall, or directly onto 25 mm thick asbestos millboard. A spark ignition system was installed at ceiling level, far above the specimens. However, all ignitions were observed to take place directly at the specimen and without the help of the igniter; thus, the results represent autoignition and not piloted ignition conditions. Their main results are given in Table 36. No ignitions were obtained for:

- acoustical tile, 12 mm, screwed onto millboard
- polystyrene wall tile, 1.7 mm, cemented onto gypsum wallboard
- wood veneer laminated onto gypsum wallboard
- vinyl-faced gypsum wallboard

The results indicate that self-heating was contributing, at least for some specimens. In the absence of self-heating, the face temperatures of the specimens could not exceed 273ºC, the temperature of the radiant source, and would actually have to be significantly less. A significant amount of convective cooling had to be present since the bottom of the specimens was raised 0.2 m off the floor, and even more cooling in the case of those specimens mounted with an open air space in back. The experimental facility set up by Shoub and Bender was rather crude and it would be important to obtain corroboration by other workers before their results are considered reliable.

Arcing across a carbonized path

Many electrical fire ignitions are due to arcing across a carbonized path. If a carbonized path is created where current may potentially flow, arcing may then occur along this path, possibly leading to ignition either of the combustible insulator itself, or some other nearby fuel. A carbonized path can be created in at least three ways[288]:

(1) arc tracking;
(2) overheating (by electrical overcurrent, external radiant heating, etc.);
(3) impingement of fire upon the insulation.

NFPA 921[289] considers ignitions from arc tracking and from arcing-through-char to be different phenomena, but they are not. A carbonized path need not be created by arc tracking, as discussed in detail below, but by one of the other two mechanisms. The outcome in all cases, however, irrespective of how the carbonized path was created, can be manifested as arcing-through-char.

Systematic research knowledge, what little there is of it, is almost wholly confined to arc tracking. Creation of a carbonized path by overheating is considered in Chapter 14 under *Electric wires and cables*. The existence of arc tracking has been known for a long time, even though details are poorly understood. A German textbook[290] discussed it in 1937, and an ASTM standard was already published in 1948[291]. Arc tracking is a progressive creation by *electrical* means of a carbonized path along the surface of in insulator that separates two current-carrying conductors. Moisture and contaminants are generally responsible for causing arc tracking, although dry tracking also can occur. The electric conductivity of pure water is very low, but when ionic contaminants are dissolved in water, its conductivity increases and it becomes possible to create current flow if the layer of moisture has access to circuit conductors somewhere. The flow of current then has a drying effect on the moisture layer. The drying is non-uniform, and eventually dry patches start to be formed along the current path. The first overt electrical discharges occur as faint, purple-colored *corona discharges* across the dry patches[292]. With buildup of carbonization along the path, small electrical discharges, called *scintillations*, can then occur. These are red or orange-colored. Since part of the current flow is through an electrolyte of significant resistance, these scintillations represent a very small current flow (less than 50 – 100 mA in one series of tests[293]) and would not trip any overcurrent devices. Surprisingly, temperatures up to 1000ºC can be generated by such surface leakage discharges. These elevated temperatures then continue the process of polymer carbonization. Thus, in the tracking process, a carbon track is laid down along the surface, and that track has a low enough resistivity that current can subsequently start to flow along the carbonized track, which, in turn, causes more carbonization and more heating. A runaway situation can then develop. The tracks which occur due to repeated wetting and drying often propagate in a tree-like fashion, thus the condition is sometimes referred to as *treeing*. However, the term 'dielectric treeing' usually refers to microscopic cracks induced by an electric field, not necessarily to the carbonized track of concern here. There has been a large variety of theories[294] attempting to explain the causes and mechanisms of dielectric treeing (sometimes subdivided into electrical trees and water trees).

Eventually, an arc discharge may occur along a carbonized path between the two metal conductors. To create an electric arc in this way requires a vastly lower voltage than does simple breakdown in air between two electrodes. For

example, with many plastics, Yoshimura et al.[292] found that 600 VAC was sufficient to cause an arc discharge across a 4 mm gap. By contrast, breakdown across a 4 mm gap in air requires about 10,000 VAC (see Chapter 11). On cables, arc tracking will normally not be initiated unless a conductive moisture film exists that has electrical contact to two conductors that have a voltage difference between them. This may happen if a cable is mechanically damaged, so that two current-carrying conductors are exposed. Moisture then collects on the damaged area, and pollutants are present which ionize the layer. But on some materials, arc tracking does not require a direct contact between an electrode and the surface of the insulator; tracking over phenolic and melamine surfaces could be initiated even when the electrodes were separated by gaps of about 0.25 mm from the insulator surface.

The process as described above is sometimes referred to as 'wet-tracking' or 'wet fire.' In high-voltage applications it is also common to encounter 'dry-tracking.' This occurs without the presence of moisture or surface contaminants. Instead, it is sufficient that an electric arc occur close to a polymeric surface. If the process continues, the high temperatures create a charred track along the surface of the polymer. In low-voltage circuits, a carbonized path is less likely to be created by an arc near the surface of an insulator. Instead, a carbonized path may be created by a glowing connection or other source of locally-elevated temperatures. These causes are discussed in more detail in Chapters 11 and 14.

In DC circuits, tracking usually starts at the anode, chars a local area right at the anode, then meanders, rather than progressing along the shortest path to the cathode[295]. Similarly, in AC circuits growth of the track occurs mainly from the electrode that is instantaneously acting as the anode. Arcing does not continue unless the conducting path is poor. Thus, in phenolics it was found that arcing very quickly establishes a highly-conductive path, and afterwards arcing is no longer observed. A much lower value of resistance is established along a path which has arc-tracked, in comparison to one which was only thermally charred[295].

Oba[296] conducted experiments where he damaged the insulation on Japanese type VVF power cable (which has two 2-mm solid copper conductors*) to expose the conductors, then sprayed electrolyte onto the area to initiate arc tracking. By varying the AC voltage supplied to the cord, he obtained a char length relation as a function of voltage (Figure 70). Below 50 V, progress of charring was very limited. He repeated the experiments by depositing powdered carbon onto the damaged area and found, in that case, for arc tracking to occur, the applied voltage had to exceed 24 V. Below 50 V, small incandescent spots could

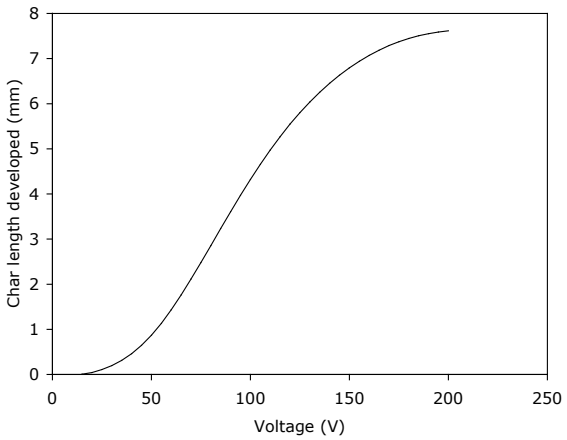


Figure 70 Char length developed after 70 h in the wet arc-tracking experiments of Oba

be produced, but not flaming ignition. Flaming ignition was readily possible for voltages of 100 – 150 V. Above 200 V, flaming ignition readily occurred, but increased char lengths were not obtained since the events were explosively forceful and blew off the carbonized material and the melted conductor portions. Under other conditions, much less than 24 V is sufficient to cause arc tracking. Bernstein[297] reports that arc tracking can occur in 6 V battery circuits, provided the battery has sufficient current capacity to sustain the arc.

In an early theoretical study into the arc tracking problem[298], it was found that the molecular structure of the polymer is the main determinant of arcing propensity. Aliphatic polymers (e.g., polyethylene, PTFE) tend not to undergo arc tracking, while aromatic ones or ones containing alternating double bonds (e.g., phenolic, polyethylene terephthalate, polystyrene) do. This is because the latter, when pyrolyzed, leave residues which are electrically conductive or semi-conductive. Also tending to exhibit arc tracking are polymers which, while lacking aromatic rings or double bonds originally, form rings or double bonds during thermal degradation; PVC and polyacrylonitrile are examples of this. It was also found out that oxygen is not a requisite for the formation of arc tracks, and that materials can be made to arc track in a nitrogen atmosphere. To simplify matters greatly, it can be said that arc tracking can only happen if a polymer can char, since if the degradation product is gaseous rather than a char, a conductive track cannot be established. Practical difficulties arise because charring is not an absolute property of polymers but, rather, is conditional. Despite a black appearance, the track is *not* graphitic carbon, but rather an organic semiconductor[298]. Arc tracking is not necessarily confined to the surface, but may involve subsurface layers, especially if the insulator is heterogeneous, i.e., fiber-reinforced[299].

* The original paper contains a misprint – the conductors were 2 mm diameter, not 2 mm^2 area.

A comparative experimental study[300] using the IEC 60112 test method showed that styrene-butadiene rubber (SBR) readily exhibited arc tracking even in the dry state. This is partly attributed to the use of carbon black in the formulation, but Neoprene samples with a similar loading of carbon black did not exhibit dry arc tracking. Neoprene, however, did show the worst performance in moist tracking. For most polymers, it was shown that the impressed voltage has a significant effect, but that raising the ambient temperature by 100ºC does not. The authors provided data on a large number of other wire insulation polymers.

Wilkins and Billings[301] did some fundamental research on arc tracking propensity and found that each material capable of arc tracking has a minimum current which must be available for arc tracking to occur. Their experimental results were: PVC 0.15 – 0.20 mA, PVA 0.3 mA, Ebonite (butadiene/methylstyrene rubber) 1.1 mA, phenolic/paper 1.15 mA, polycarbonate 1.2 mA, and PTFE 2.3 mA. A thermal model was evolved that could predict this behavior. A minimum current is necessary so that the material could achieve a r equired local breakdown temperature; these values ranged from 186ºC for PVC to 446ºC for PTFE. The breakdown temperature is controlled by the thermal decomposition of the material, and was found to be correlated to TGA results for each material, thus the minimum current could be correlated to the T_{90} in the TGA test, which is the temperature at which 10% of the mass is lost. They also found that materials which show zero residue upon completion of a TGA test are only prone to arc *erosion*, but not arc tracking. Simple thermoplastics are materials which pyrolyze completely in a TGA test. Residual material remains (and therefore arc tracking is possible) either if the polymer innately chars, or else if additives are used which cause residual weight to remain. Materials with a high residual weight fraction are ones which are often thermally resistant and are selected to resist radiant or flame ignition. Thus, the requirements for such resistance versus arc tracking performance can be conflicting. However, alumina trihydrate ($Al_2O_3 \cdot 3H_2O$), a common filler for many polymers, was found to be highly effective in reducing the arc tracking propensity in certain polymers[302,303].

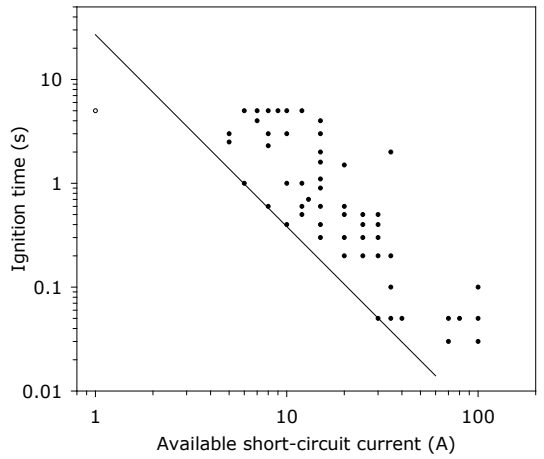


Figure 71 Ignition of electric cords with carbonized section from plugging into branch circuits having various available short-circuit current capacities

In design, the resistance to arc tracking is controlled by two means: (1) selection of well-performing insulation materials; and (2) observing adequate *creepage* distances. The latter concept is illustrated in Figure 72. For arcing from metal to metal, the governing distance is called the clearance distance, d_1. But since arc tracking proceeds only along solid surfaces, the distance across which arc tracking must travel, if failure is to occur, is called the creepage distance, d_2. Creepage distances are set down in numerous military and industrial specifications, but the rationale is usually empirical and not much scientific research is available on the topic. Day and Stonard[304] conducted tests where time to wet arc-tracking failure was measured as a function of creepage distance. With highly aggressive contaminants used, after 20 min most specimens still had not reached ultimate limits, but rank-order differences, not surprisingly, were the same as found in comparative tracking index test results on the materials.

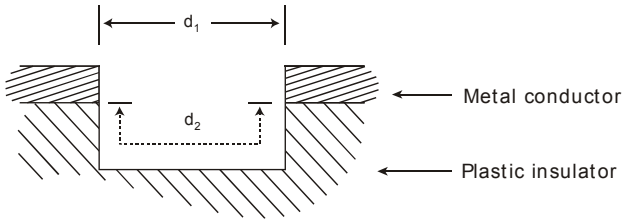


Figure 72 Simplified view illustrating clearance and creepage distances

In an interesting study[305], UL simulated ignitions due to arc tracking in the laboratory. In their tests, they created a carbonized track by faulting a length of 16 AWG cord containing 24 copper strands and insulated with PVC. Insulation was partially scraped off the cord to reveal the two conductors. The path across the now-exposed conductors was wrapped with PVC electrical tape, which presumably is more prone to arc tracking than is bulk PVC cord insulation. The construction was over-wrapped with fiberglass tape and carbonization was initiated by connecting a neon transformer across the cord connections. Ignitions were then examined using the carbonized cord by plugging it into branch circuits having various available short-circuit currents. Surgical cotton was wrapped around the specimen to serve as ignition target. The results are indicated in Figure 71. Apart from one data point, the lower bound to the results can be described by:

$$t_{ig} = 27 A^{-1.83}$$

where t_{ig} = ignition time (s) and A = available short-circuit current (A).

Glowing ignition

When a solid is pyrolyzed by the application of heat, two things happen: (1) gaseous products are liberated; and (2) the solid-phase material is changed. The solid-phase material may respond by either melting or charring, although occasionally both occur. Significantly higher temperatures are normally reached on charring solids than on melting ones. Because of the high surface temperatures, direct surface reactions sometimes become dominant in the case of charring materials. A surface that undergoes rapid oxidation is described as having reached glowing ignition. In an experiment where the surface temperature of the sample is monitored, when glowing ignition occurs, a jump of several hundred degrees Celsius in the surface temperature over the span of a few seconds is registered.

Many charring substances respond when subject to high heat fluxes by igniting with a flame, with the flame first appearing some distance away from the specimen surface in the plume of pyrolysates. The same substances when presented with a low heat flux often ignite by first exhibiting glowing at the surface, and possibly later erupting in flaming. Examples of such substances include wood[19,306], charring fabrics[307], and oats dust[308]. In the case of fabrics, it was observed that minor impurities in the fabric had a strong effect in determining whether, at a given heat flux level, ignition will be glowing or flaming. One type of PVC material was shown to exhibit a glowing ignition when the smoke-suppressant additive ferrocene was added, but not for the virgin material[309].

Glowing ignition has received very little systematic study. Since glowing ignition involves the direct surface oxidation of a material (heterogeneous reaction), Baer and Ryan[253] suggested that the simplest model is:

$$\frac{\partial T}{\partial t} = \frac{\lambda}{\rho C}\frac{\partial^2 T}{\partial x^2}$$

with the boundary condition:

$$-\lambda \left.\frac{\partial T}{\partial x}\right|_{x=0} = \dot{q}_e'' + B_s Q_s \exp(-E_s / RT)$$

where T = temperature, t = time, λ = thermal conductivity, ρ = density, C = heat capacity, $\dot{q}_e''$ = irradiance, B_s = pre-exponential factor, Q_s = heat of reaction, E_s = activation energy for surface reaction, and R = universal gas constant. Based on this, Lengellé et al.[310] proposed an approximate scheme which is essentially a perturbation on the inert solution. They assumed that ignition corresponds to the instant at which the surface temperature rise due to the exothermicity first equals a fraction b of the incident heat flux:

$$B_s Q_s \exp\left(-E_s / RT_{ig}\right) = b\,\dot{q}_e''$$

In a system where E_s, B_sQ_s, and b are known, the above equation can then be solved for $T_{ig}(\dot{q}_e'')$, giving:

$$T_{ig} = \frac{E_s}{R}\left[\ln\left(\frac{B_s Q_s}{b\,\dot{q}_e''}\right)\right]^{-1}$$

where b = non-dimensional temperature rise associated with ignition. The b factor serves as an ignition criterion and they found empirically that $b \approx 0.15$ corresponds to ignition. The equation predicts that T_{ig} decreases with decreasing irradiance. In the Lengellé scheme, plots of t_{ig}^{-n} against $\dot{q}_e''$ give straight lines, just as with the inert solution; the physical meaning of the slope of the line, however, is altered. For ignition of substances other than propellants, where the exothermicity stems from reaction with atmospheric oxygen, the concentration of oxygen can be expected to play a role, that is $B_s \propto C_{ox,\infty}^m$, where $C_{ox,\infty}$ = oxygen concentration far away from the fuel surface, and m = reaction order. Suuberg et al.[311] examined experimental data for a number of chars and concluded that m = 0.68±0.08; a more recent survey[312] suggests that m may range from about 0.6 to 1.0 Thus, glowing ignition sensibly ought to become more difficult as the oxygen concentration drops. All of the experimental data discussed by these authors come from industrial combustion studies with little similarity to accidental ignition scenarios, so the application to fire safety scenarios can only be speculative.

Smoldering ignition

Smoldering can be defined as a propagating, self-sustained exothermic reaction wave deriving its principal heat from heterogeneous oxidation of a solid fuel. As discussed in Chapter 3, heterogeneous oxidation means that the reaction occurs on the surface of the fuel. Since flames are a manifestation of a homogeneous (dispersed within a volume; not at the surface) reaction, flames are not seen in connection with smoldering. This technical meaning is much narrower and more specific than the layman's view of smoldering. The layman often applies 'smoldering' to fires which show small (as opposed to larger) flames, or to situations where an external heat source is charring or pyrolyzing a substance. In this book, we use the term 'smoldering' according to the technical definition given above, unless made clear otherwise. If the smoldering reaction achieves temperatures high enough to exhibit a visible glow, the combustion is often referred to as *glowing* combustion. But glowing combustion can also be caused by applying an external source of heat, rather than as an outcome of smoldering.

Most combustible solids do not smolder. Generally, smoldering is only common with porous or granular materials that can char and that have limited, if any, tendencies to melt. In addition, the char structure must be porous and not clogged by molten material[313]. Common materials which are known, under some circumstances, to smolder include:

- wood and cellulosic products in finely divided form (chips, low-density fiberboard, etc.)
- paper

- leather
- cotton, in the form of batting, fabric, or string
- carbon
- forest duff, peat, and organic soils
- various agricultural products
- latex foam
- some types of polyurethane, polyisocyanurate and phenol formaldehyde foams; open-cell (flexible) foams are more likely to smolder than closed-cell (rigid) foams.
- coal, charcoal, coke, cigarettes, and incense sticks—these are among the few materials which are used to produce *wanted* smoldering.
- dust layers of various sorts.

A very wide variety of organic substances can smolder when arranged into a layer of dust or powder. Examples include coal, cocoa, lycopodium, and sawdust. Powdered iron sulfite can also smolder[314]. Metal powders or dusts (e.g., magnesium [314], brass[315]) can also be made to smolder. For the case of magnesium, however, since the temperatures registered in the process were ca. 1300ºC, it does not entirely appear appropriate to use the term 'smoldering'; for brass, by contrast, 'smolder' temperatures of ca. 400ºC were found.

Under some conditions, certain cellulosic substances—paper, solid wood—can smolder that do not appear to be porous. Cigarette paper, is of course porous, but on a scale too small to be seen with the naked eye. Most other cases of paper smoldering appear to involve layers of paper, where air access is between sheets. Solid wood has limited porosity, and its smolderability is discussed in Chapter 14.

In the end-use environment, porous material is likely to exist in layers or in heaps. The air flow and heat flow which prevail during a smoldering ignition are highly 3-dimensional and analysis is difficult. For this reason, many laboratory studies have been conducted in simplified geometries, where a long, narrow pile is created with impervious barriers on all except the two ends; air is then forced into one open end and exits the other. Under such conditions, a 1-dimensional smolder geometry can be created. If the end facing the wind is ignited, then the mode of smolder is called *forward smolder* since the air flow direction and the direction of smolder-front movement are the same. This mode is also, somewhat confusingly, called counter-current smolder*. If the opposite end is ignited, then the condition is one of *reverse smolder*. In that case, the smolder front moves in the opposite direction from the air movement. The latter mode is also called concurrent smolder, or opposed-flow smolder. Figure 73 is Sato's illustration of the two cases[316]. Laboratory studies done under such conditions have been helpful in understanding the physics of smolder. Nonetheless, it must be remembered that rather different conditions usually prevail in the case of real fires, so numeric data obtained in 1-dimensional laboratory studies cannot be directly applied if the fire conditions involve a 3-dimensional problem.

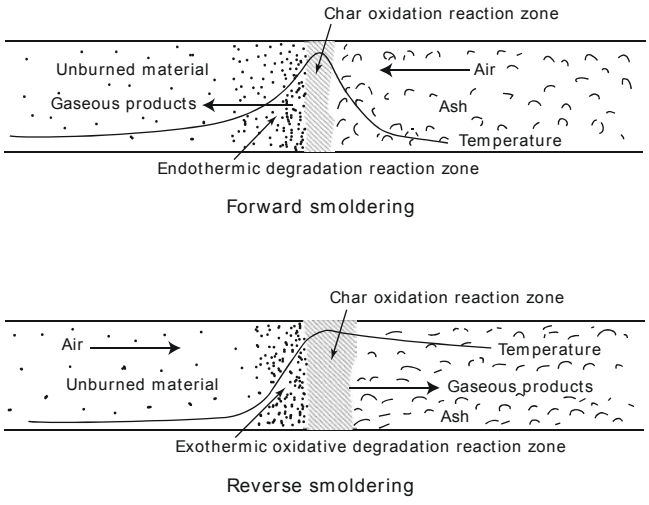


Figure 73 Two types of 1-dimensional smoldering

Forward and reverse smolder geometries differ fundamentally in the nature of the air that is supplied to the smolder front. In the case of forward smolder, the air must travel through the already burned portion. It arrives at the smolder front preheated, but also depleted of oxygen, since some of the oxygen already gets used for reactions in the partly-burned region. In reverse smolder, the air arrives at the smolder front without preheating and without depletion of oxygen. Thus, reverse smolder can establish a steady-state smolder velocity. For forward smolder, the continued transport of heat in a direction to preheat the fuel causes the reaction to continually accelerate. In the smolder wave, the smolder velocity is limited by the influx of oxygen, rather than by the fuel or by the chemical kinetics. The critical role of oxygen supply in opposed-flow smolder can be noted experimentally[317] in the fact that at the end of the smolder zone, oxygen concentration drops to zero; fuel concentration, by contrast, does not. The *rate* of smolder is normally higher for reverse smolder than for forward smolder. Evidently, the oxygen depletion that occurs in forward smoldering is more effective toward decreasing the reaction rate, than is preheating as a means of raising reaction rate.

* 'Forward' denotes that wind and smolder front velocity are both in the same direction; 'counter-current' denotes that the air and the fuel are fed from opposite directions into the smolder front. In the opposite situation, 'reverse' denotes that wind and smolder front velocities are in opposite directions, while 'concurrent' denotes that the air and the fuel are fed from the same direction into the smolder front.

In addition to the fluid mechanics, the chemistry of combustion often differs between forward and opposed-flow smolder. Oxidative pyrolysis of virgin material tends to dominate in reverse smolder, while char oxidation becomes of importance in forward smolder.

Many laboratory studies of smoldering used a flat, thin 'pancake' heater as the external source of heat. The pancake heater can be characterized either by its surface temperature or by the heat flux at its surface. In such studies, it has been found that to create a self-sustained 1-dimensional smolder reaction, the external heat source must be able to raise temperatures to a sufficient value at a distance away from the heater representing a *minimum char thickness*. For forward smolder of flexible polyurethane foam, the minimum char thickness has been experimentally found to be ca. 50 mm; for reverse smolder, the minimum is ca. 100 mm[318]. In terms of 'external' variables, a minimum heat flux exists, below which ignition will not occur, since a steady state temperature will be established in the vicinity of the heater which is below the minimum necessary to create a self-sustained smolder reaction. In the same manner as for radiant ignition of the front face of a solid combustible, the heat flux alone does not characterize the response, but the time of application must also be considered. The heat flux/time relationship necessary for reverse smolder ignition is shown in Figure 74, where comparison to experiment indicates a rough agreement, at least for longer time periods. For forward smolder, the heating times are less.

While a minimum ignition temperature does not exist in general for a substance to sustain smoldering, in 1-dimensional studies it is commonly found that a higher igniter temperature is needed for reverse smolder to occur than for forward smolder. For polyurethane foam in an atmosphere at ambient oxygen concentration, in one experimental rig[318] it was found that T_{min} = 290ºC for forward smolder, but 385ºC for reverse smolder. For forward smolder conditions, changing the oxygen concentration does not change the minimum temperature, but for reverse smolder, decreasing the oxygen concentration raises the minimum needed temperature.

Kellogg et al.[319] ignited heavy cotton fabrics in a smolder mode by pressing an electric cartridge heater onto the fabric surface. They found that a minimum heat flux around 15 kW m^{-2} was needed for ignition and that this did not vary with the basis weight (g m^{-2}) of the fabric. Lowering the oxygen concentration to 14.7% raised the minimum flux to 17.5 kW m^{-2}. The time to ignition, at a given heat flux, however was strongly dependent on the basis weight. Except for heat fluxes barely above the minimum needed for ignition, their data could be represented by a straight line of $1/t_{ig}$ versus (heat flux/basis weight):

$$\frac{1}{t_{ig}} = 0.79\left(\frac{\dot{q}_e''}{W}\right) - 0.0119$$

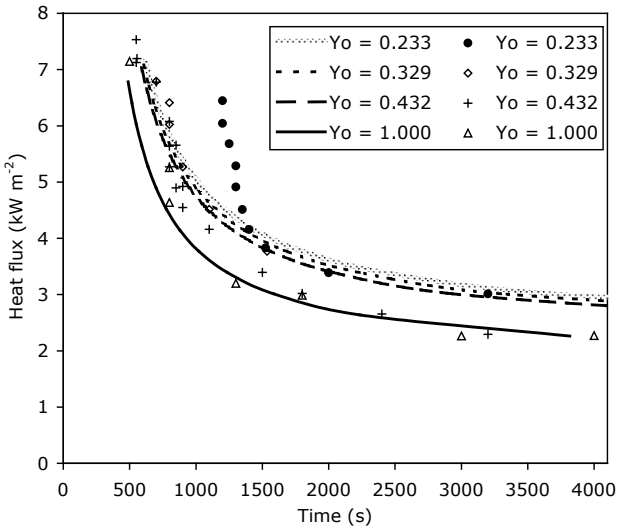


Figure 74 The heat flux needed for reverse smolder ignition of polyurethane foam[318]
(Copyright Elsevier Science, used by permission)

where t_{ig} = ignition time (s), $\dot{q}_e''$ = heat flux (kW m^{-2}), and W = basis weight (g m^{-2}).

Minimum conditions for ignition of smolder-retardant-treated loose-fill cellulose insulation in a smoldering mode were investigated by Ohlemiller[164]. He found, not surprisingly, that larger hot surfaces required a lower temperature. A wire of 4.8 mm diameter required 380 – 385ºC, while an 0.2 0.2 m plate only 255 – 266ºC. The effect of the smolder retardant was judged to be very small, and untreated specimens required only slightly lower temperatures.

There are very few data on smolder started by external radiant heating, as opposed to a heat source which is in contact with the material. In one study[320] on flexible polyurethane foam using a Cone Calorimeter as the heat source, it was found smoldering ignition could only be sustained over the very narrow flux range of 6.1 to 6.8 kW m^{-2}. For heat fluxes less than 6.1 kW m^{-2}, the heat was not sufficient to cause a char zone to propagate. For heat fluxes higher than 6.8 kW m^{-2}, surface melting occurred. This caused the surface to become non-porous, stopping the possibility of smolder. A critical temperature of 300 – 325ºC was found for a self-sustained smolder front. The authors also found that a mass loss rate of 0.8 g s^{-1} m^{-2} was the minimum rate needed for smoldering ignition.

Reproducibility of smoldering-ignition tests is commonly poor, partly because the process is inordinately sensitive to *air flow*. Honeycutt[321] documented in a series of tests on cigarette ignition of upholstered furniture that a velocity of 0.0005 m s^{-1} had no effect, but velocities as small as 0.035 m s^{-1} already detectably affected the results. In most cases, moderate velocities increase the propensity to smoldering ignition. It was also found that the warmth of a person

sitting down on a chair can induce velocities on the order of 0.01 m s^{-1}.

The *velocity* of smolder, once ignition has occurred, is very slow. For a wide variety of smolderable materials[322,323], it was found that smoldering rates encompassed the range between 0.5 mm min^{-1} and 6 mm min^{-1}. For coal dust[324], the range is reported as 0.83 to 8.3 mm min^{-1}. For cellulose insulation, a velocity of 3.1 mm min^{-1} has been reported[164]. For cellulose insulation treated with fire retardant agents, values in the range of 1.3 to 1.75 mm min^{-1} were found. The presence of even high loadings of smolder-retardant agent does not drop the smolder velocity to zero. Denser materials smolder more slowly, and Palmer[325] has suggested that, for a variety of materials, the product (density × smolder velocity) is roughly constant. According to this approximation,

$$v = k / \rho$$

where v = smolder velocity (mm min^{-1}); k = 300 to 670; and ρ = density (kg m^{-3}). Matters become more complex to evaluate when the smolder front has a strongly 3-dimensional aspect. In one interesting experiment[326], a cube of air-dried sawdust, 0.91 × 0.91 × 0.91 m, was assembled with a lit cigarette placed into the center. For 7 days there was no external evidence of combustion, but thereafter the surface slumped slightly and acrid smoke first appeared. By the 12th day, the cube was evidently in active combustion.

Blowing air over a smoldering product increases the smoldering velocity. In a study[327] on grain 'screenings' (small particles) it was found that blowing air at a velocity of 4 m s^{-1} increased the smolder velocity by about a factor of 10. Raising the ambient temperature increases the smolder velocity. For a number of products[323,328], it was found that raising the temperature from 20 to 100ºC roughly doubles the smolder velocity.

The *smoke* emitted from smoldering has not been much studied. For smoldering oil shale dust, it was found[329] that the smoke contained a high enough percentage of flammable gases that a lighted match would ignite the smoke.

THEORY

For cases where a smolderable material is ignited by a large hot surface, the same ignition theory can be used as is used for self-heating of dust layers (see Chapter 9). A successful example of such application to cellulose attic insulation has been published[164]. For small, hot sources, however, it was found that the theory becomes problematic to apply and, of course, it could not be applied at all to smoldering initiated with a flame. A number of theories have been proposed for smolder velocity, but ones based on credible physics[330,331] have so far not led to solutions of practical applicability.

EFFECT OF LAYER THICKNESS

Smoldering cannot be sustained unless the smolderable material has a minimum layer thickness[332]. The amount of practical guidance on this point is limited. Palmer[333] studied layers of several dust types, and his results are shown in Figure 75. For particle sizes below 0.4 mm, the results show a linear dependence on particle diameter. For cork dust, sustained smoldering was possible down to about 1 mm layer thickness, provided very fine dusts were used. Palmer also investigated large diameters of cork dust and found a depth around 50 mm for 2 mm particles; for larger particle sizes, the minimum required layer depth decreased instead of further increasing. In addition, Palmer examined dry grass dust of < 0.065 mm sieve size. This dust was able to smolder in a 2 mm thick layer.

Ohlemiller and Rogers[334] examined the minimum layer depth needed for sustained smoldering of cellulose insulation. For untreated material, a depth of 35 mm was found, while for insulation treated with 20% boric acid, the depth increased to 65 mm. The material is fibrous in nature, so particle diameter is not a meaningful measure. No theoretical treatment of the problem is available, but Ohlemiller considers it likely that physical properties, especially packing density, are the most important in controlling the process[335]. A scale effect was also documented for flexible polyurethane foam[336].

EFFECT OF PACKING DENSITY OR POROSITY

For the smoldering process to be sustained, porosity must neither be so low that access of oxygen is too difficult, nor so high that excessive heat losses, especially from radiation, occur to the external atmosphere. Lawson[337] explored the effect of density on the smoldering ignition of cellulose insulation by a cigarette. He found that material which was resistant to smoldering ignition at a lower density, generally started to smolder if the insulation was packed tighter. In the case of one material, he also found that further increases in density led to non-ignitions, indicating the existence of an optimum density for ignition. Palmer also reported that a maximum density exists beyond which smoldering will not propagate[333]. Pyne et al.[338] suggested that fuel beds will not smolder if porosity is greater than 90%.

SMOLDER PROMOTERS AND SMOLDER INHIBITORS

Experiments, primarily by McCarter[339-341] indicated that certain inorganic impurities often found in wood products, natural-fiber textile, and other substances of lignocellulosic origin are strong promoters of smoldering. These impurities include salts and hydroxides of monovalent metals (e.g., NaCl, NaOH, KCl, etc.), and salts of iron, chromium, and lead (e.g., $FeCl_3 \cdot 4H_2O$, $CrCl_3 \cdot 6H_2O$). The latter group of compounds induced a more complete smolder combustion and McCarter associated this with catalytic activity of these metals. Potassium was the most potent metal found with respect to facilitating smolder. Unfortunately, it is also the

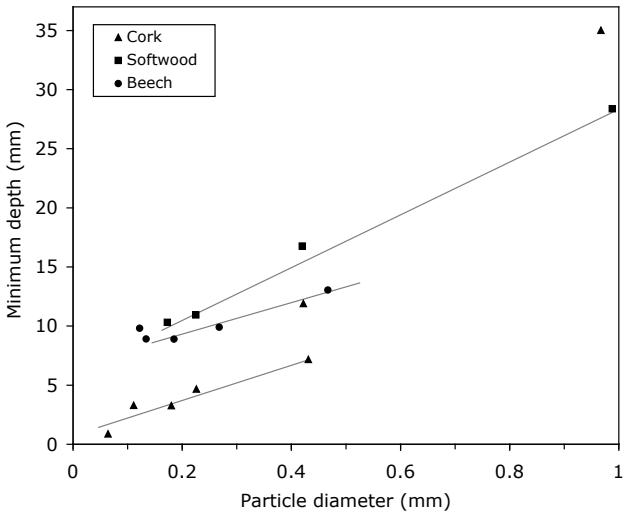


Figure 75 Minimum layer depth for smoldering of several dust types

most dominant inorganic cation found in natural cotton and possibly other lignocellulosics. Smolder was not facilitated by aluminum, antimony, barium, calcium, cobalt, copper, magnesium, molybdenum, nickel, tin, or zinc compounds examined.

With certain materials such as cotton, it is possible to suppress the smolder tendency by thorough washing, since this removes the metal-ion impurities. Kellogg et al.[319] found that untreated cotton fabric had about 6000 ppm potassium ion content. Washing the fabric to the extent of lowering it to 2000 ppm had little effect; reducing to 1000 ppm substantially prolonged the time needed for smoldering ignition, while washing so that only 150 ppm remained made smoldering ignition impossible. Smolder can be inhibited by the application of sulfur (S_8) or compounds containing boron or phosphorus. The most useful of the latter are boric acid (H_3BO_3), and the ammonium phosphates. A number of multivalent metal chloride compounds were also found to be effective, but these have generally not been found commercially viable. The mechanism of action of sulfur is unique[342], in that it entails a reaction of sulfur vapors with carbonaceous radicals, thereby interfering with combustion at the smolder front. The remaining substances commonly used as smolder inhibitors have long been studied as flame-retardants for wood. These work largely by altering the normal pyrolysis chemistry of the material, that is, they act solely in the solid phase; in addition, boron-based compounds may create a glassy film at elevated temperatures which can present a physical barrier to combustion[343]. The early history of smolder-inhibitor compounds and their modes of action was comprehensively reviewed by Browne[344], with a later review by Le Van[345]. Smolder inhibitors are generally developed empirically and theoretical guidance on identifying optimum candidates is non-existent.

Unlike for cotton, washing does not work as a technique for removing smolder-promoters from wood fibers, since these are not water-soluble in wood[340]. Calcium and magnesium were found to be the primary elements serving a smolder-promoter role in wood fibers. These are strictly not inorganic impurities, since they are bound into the carboxyl groups of the cellulose. Removal is possible, however, by the use of an acid wash. Other chemical reactions that replace these metal cations with hydrogen, ammonium, or aluminum cations were also judged likely to reduce the smolderability of wood fibers.

TRANSITION FROM SMOLDERING TO FLAMING IGNITION

The conditions governing when and if a transition to flaming will occur has been the subject of theoretical investigations and of laboratory studies, using simplified geometries. Smoldering to flaming transition can occur in conditions where the material sits in stagnant air[164]. Real-life smoldering in layers of porous material is complex, because heat and mass transfer are not 1-dimensional and because edge conditions may play a crucial role. Smoldering materials are often found to break out into flaming when the smolder front encounters a change of media[346]. For example, smoldering cellulose loose-fill insulation tends to break out in flaming when the smolder front reaches a wood framing member[347]. The mechanism of this has been studied[349], and it was found that the smoldering insulation shrinks and creates a gap between itself and the adjacent wood member. This gap allows a flow of air to develop, which oxidizes the char formed on the cellulose insulation and raises it to a high glowing temperature. The glowing char has a good view factor to the adjoining wood surface and ignites it radiatively.

The time required for a smoldering fire to break out into flaming can be surprisingly long. A case is reported of a smoldering initiation in a Russian grain silo which took 2 years to reach a flaming state, at which point an explosion occurred[348].

Because of the geometric complexities of studying layers of material sitting in stagnant air, many laboratory studies focused on creating flow conditions where air can enter the combustion zone only along one direction, and the conditions are so set up that either reverse or forward smoldering is exhibited. For reverse smolder, a simple theoretical treatment suggests that the smolder velocity will be constant and transition to flaming ignition will not occur. This is based upon a 1-dimensional idealization of material far away from boundaries, and does not necessarily imply that flaming cannot break out when an edge is reached. If the smolder is forward smolder, however, then as smolder velocity increases with time, transition to flaming can be directly anticipated. Laboratory studies, however, prove that transition to flaming is also possible for reverse smolder,

although the minimum air velocity that must flow through the material for this to occur is about doubled[349]. In the laboratory study cited, this meant a doubling from 2 to 4 m s^{-1}, but it is not clear whether in real-life smoldering situations identical velocities (due to wind, or induced by natural convection in some manner) would apply to the transition point. In a study using a more realistic geometry of 2-dimensional, forward smoldering it was learned that transition to flaming is most likely to occur if there is a velocity of 0.25 – 2.0 m s^{-1} across the specimen face[336]. Higher velocities are more likely to lead to extinguishment rather than a transition to flaming. For dusts or powders, the particle size also influences the likelihood of transition to flaming. An old FRS study[326] reported that dust layers with larger particle sizes are more likely to transition but did not provide numerical data.

Even if a sufficient velocity is provided for a transition to flaming to occur, the process takes time. The time to flaming[350] has been found to (a) increase sharply with increasing density of material; and (b) decrease with increasing air velocity. These experimental times ranged from 5 to 75 min, although no general relations were obtained.

The effect of FR or smolder-inhibiting agents has been found to be mixed[349]. Borax or boric acid suppressed smoldering-to-flaming transitions from occurring in the bulk material at air velocities up to 5 m s^{-1}. However, when the smolder front reached a wood framing member, the effect of borax was found to be minimal on the transition to flaming. For boric acid treatment, the air velocity needed for transition to flaming during forward-flaming was raised from 2 m s^{-1} to about 3.7 m s^{-1}.

INDICATORS OF SMOLDERING

In many situations it is useful to establish when signs of a smoldering fire might first have been detectable. The first research paper on this topic appeared recently. Mizuno et al.[351] conducted experiments where smoke was introduced to unexpecting experiment subjects. It took less than 10 mg of combustion products distributed into a medium-sized room to elicit a 100% response, but individual response times were extremely varied (< 1 min to over 30 min). Most subjects (80%) first noted a smell and not visible smoke. Some subjects smelled smoke when the quantity smoldered was less than 0.1 mg.

Tests for ignition properties of solids

There are basically two types of testing strategies that are used for determining the flaming ignition of solids: (1) to create a test exposure which directly mimics an expected fire exposure. This is the strategy used for examining the ignition of substances from small flames. No theory or analysis is used, with credibility resting solely on the fact that the test flame is considered to be very similar to the flame in the actual fire. (2) Testing using highly controlled, simple exposure conditions. These conditions are not necessarily viewed as representing the real environment, except in isolated occasions. Instead, the test results form the input data into some analysis scheme which can predict ignition. For this purpose, radiant heating is inevitably used. Heaters can be designed which impose a uniform radiant heat flux upon a test specimen and which present only a tiny fraction of heat transfer by means of convection. Convective heating is normally not used in tests, since, according to fundamental heat transfer theory, it can be seen that it is very difficult to create conditions on a flat specimen face whereby heat transfer rates do not vary greatly between the leading edge and the trailing edge. Furthermore, it is also not readily feasible to eliminate radiant heating, so there is little hope of creating a tractable convective heating environment. Consequently, test methods can be divided into flame tests, radiant heat tests, and some miscellaneous types.

The listings below summarize the features of the most widely used tests for ignition of solids. An ASTM index[352] is available which lists large numbers of additional fire tests according to end-use application; many of these tests have procedures where ignitability is examined. Some less-commonly used ASTM, ISO, and IEC tests have been examined by Hirschler and Grayson[353]. A wide variety of other test methods are described by Pál[354] and Troitzsch[355]; these references are especially useful for locating foreign and obsolete standards. Because of the enormous variety of publications that IEC has issued on flame ignition tests, it has also published a report[356] providing a history of the development and use of some of the various test flames incorporated in their standards.

FLAME IGNITION TESTS

There is a wide assortment of tests which entail the use of a small flame placed against a test specimen. The most widely used of those are reviewed in this Section. As will be seen below, the objectives for these tests generally go beyond a straightforward issue of ignitability. There are, in fact, very few tests where the test result is simply whether a flame was able to ignite a specimen, and if so, the number of seconds that this took. Most tests in use measure some combination of ignitability and flame spread—specimens pass if flame spread no further than a given criterion. A large fraction of these tests also measure *afterflame* or *afterglow*. As discussed above, whether a substance, once ignited, will or will not continue burning once the ignition source is removed, can be an important question. The afterflame concept is an empirical expression of this performance. Thus, while the information is intended to address a distinct need, the main limitation of such measurements is their lack of generality—it may be that a specimen passes, given a certain exposure flame, but it is impossible to tell what will happen with a different flame or with a different arrangement of the specimen. The concept of afterglow is somewhat more difficult to justify. Apart from issues associated with smoldering or self-heating (which are not ad-

dressed by these tests), it is rarely the case that a hazard will be created if the surface of something continues to glow after having been exposed to flames. After all, flames already existed in the environment and the test article failed to propagate flames.

All of the standard tests for small-flame ignition are conducted at room temperature. But for some products, e.g., electric wire and cable, the normal operating conditions involve a temperature distinctly above ambient. Elevated temperature effects are discussed above under *Variables affecting ignition of solids: Ambient temperature*.

ASTM D 2859 METHENAMINE PILL TEST

The smallest flame used in a standard fire test method is the methenamine pill used in the ASTM D 2859 test[357] for carpets. Methenamine ($C_6H_{12}N_4$) is a subliming, non-melting solid which is commonly used as a urinary antibacterial agent. In the test, an 0.149 g pill is ignited with a match on its top surface and placed upon the carpet. On top of the carpet is placed a steel plate having a 205 mm opening in the middle; the tablet is centered in the middle of this hole. The pill burns about 2 min and produces a heat flux of about 4 – 4.5 kW m^{-2} during the peak burning time[358]. To pass the test, 7 out of 8 specimens must not burn closer than 25 mm to the edge of steel plate's opening. According to CPSC regulations, carpeting sold in the US must pass the methenamine pill test, and an essentially identical description of the test method is contained in the Federal Regulations[359]. In the CPSC scenario, the methenamine pill is intended to simulate a burning particle being ejected from a fireplace and landing on a carpet. It is important to realize that the test simulates a very tiny, flaming object. If ignition from small, incandescent (i.e., non-flaming) objects is to be tested, than there is no assurance that data from the methenamine pill could be used. Apart from strict ignitability issues, when small particles land on lightweight, fluffy, or porous materials, there is a complex reaction of the target which can include melting, shrinking, and charring. Even if a small flaming object and a small incandescent object are the same size, it cannot be concluded, in general, that this type of surface response will be similar and that, therefore, ignitability propensity will be similar.

Methenamine pills have also been used to test other products. In one series of tests on mattresses[360], it was found out that while the methenamine pill may present the smallest flame, it is not always the least-strenuous flame source. When compared to a 20 s application of a butane flame, most test specimens either passed or failed both ignition sources. But 2 out of 20 specimens failed the methenamine test, while passing the butane flame test. Conversely, 2 other specimens passed the methenamine test but failed the butane flame test. The occasional odd results are probably due to the fact that the burning pill can recede into the surface as the flaming progresses.

CS 191-53 (16 CFR 1610) FLAMMABLE FABRICS TEST

The general apparel flammability test was developed in the late 1940s after a series of tragic fires involving highly flammable fuzzy rayon sweaters, evening gowns, and children's cowboy chaps. The development of the test method has been reviewed by Bonnet[361]. The political background for the test, along with its limitations, has been given by Patton[362]. All clothing and clothing fabrics sold in the US must meet this test requirement[363]. The test method clamps a 152 × 51 mm specimen in a metal edge frame and this is placed at a 45º angle inside a test cabinet. A hypodermic needle is used as a butane burner to impose a 16 mm long flame for 1 s to the upper surface of the specimen at 25 mm from the lower end. Burn time is indicated by burn-through of a cotton thread trip cord placed 127 mm upstream of the ignition point, which triggers a timer. There are many other numerous details of preparing and conditioning specimens for test, and these are described in a CPSC manual[364]. ASTM D 1230[365] is somewhat similar, but it is rarely used.

The criteria for the standard are shown in Table 37. They are especially convoluted, since the blatantly political motivations of Congress were apparently not appreciated by the enforcing agency, so they added a footnote without changing the original wording of the standard. Also, the meaningfulness of three classes is obscure, since they are not utilized in regulation.

Table 37 Criteria applicable to the CS 191-53 test standard

Class	Flat-weave fabrics	Raised-fiber fabrics
1	trip time 4 s *	trip time > 7 s; or any trip time is permitted, if specimen only shows a surface flash and base fabric does not ignite or fuse
2	(not used)	4 s trip time 7 s, and base fabric ignites or fuses
3	trip time < 4 s *	trip time < 4 s and base fabric ignites or fuses

* changed to 3.5 s by US Congress.

Because of the extraordinarily brief flame exposure and the lenient criteria, this test method is exceptionally easy to pass. A majority of fabrics weighing more than about 70 g m^{-2} does not even ignite from the flame exposure used in the test. Of fabrics which would functionally be suitable for making apparel, only very lightweight, gauzy fabrics or ones with a highly flammable nap would likely fail. Apart from these types, most other apparel fabrics requires more than 1 s of flame exposure to ignite[366]. Data on ignition times of fabrics are compiled in Chapter 14. CPSC recognized the fact that heavier weight fabrics do not fail the test

by exempting plain-weave fabrics heavier than 2.6 oz/yard (88 g m^{-2}) from testing.

FF-3-71 (16 CFR 1615) AND FF-5-74 (16 CFR 1616) CHILDREN'S SLEEPWEAR TESTS

A standard for the flammability of children's sleepwear was originally issued by the Dept. of Commerce in 1971 as DOC FF-3-71 and was enforced by the Federal Trade Commission. The method comprises a small test cabinet in which fabric specimens 89 mm wide by 254 mm high are clamped in a vertically-suspended metal frame. A special tube burner applies a 38 mm long methane flame at a 25º angle for 3 s to the surface of the specimen, at the bottom edge. The test passes if the average char length for 5 specimens does not exceed 178 mm and if no single specimen burns the full vertical length if 254 mm.

Upon creation of CPSC in 1973, this standard passed into their jurisdiction. Initially, sleepwear manufacturers found that the easiest way to meet the standard was to use polyester fabric and to treat it with the FR agent 'tris,' which is *tris*(2,3-dibromopropyl)phosphate. A major furore arose in the mid-70s when the claim was made that this FR agent was carcinogenic. Despite the fact that (1) no human injuries had been reported from the chemical, and (2) many alternatives were available for producing complying fabrics, CPSC responded by modifying the test method[367] to eliminate the afterflame requirement which was originally a part of the test criteria. Using the modified test method, polyester and nylon fabrics can generally pass without any chemical treatment. The FF-3-71 test method is called out for children's sizes 0 – 6X; the same test, but with different regulatory requirements is called out for children's sizes 7 – 14 as FF-5-74.

CPSC 16 CFR 1500.44 FLAMMABLE SOLIDS TEST

CPSC maintains two definitions for the flammability of solids. (1) *Extremely flammable solid*—Means a solid substance that ignites and burns at an ambient temperature of [26.7ºC] or less when subjected to friction, percussion, or electrical spark. (2) *Flammable solid*—Means a solid substance that, when tested by the method described in § 1500.44, ignites and burns with a self-sustained flame at a rate greater than [2.54 mm s^{-1}] along its major axis. There is no test method associated with "extremely flammable solid." For "flammable solid," the CPSC test method involves holding a burning paraffin candle of at least 25 mm diameter with flame in contact of the specimen surface for 5 s, or less if the specimen ignites in < 5 s. The specimen passes if it does not ignite during the 5 s exposure, or if the fire propagation rate is less than the criterion value. The test requires that the flame be touching the sample "at the end of the major axis." This has been criticized by NIST[368], in that many substances do not have an identifiable major axis and that packing density is not specified for substances which are in loose form. In addition, problems were found in identifying the "substance" when flammable trim of otherwise non-flammable solids was concerned. To solve the difficulties attendant to the testing of several classes of products, NIST developed improved test methods, but these were not adopted by CPSC.

The Bureau of Mines[369] proposed a test method for this topic, but this has not met acceptance. The UN test method on this topic is discussed in Chapter 10.

NFPA 701 AND NFPA 705 METHODS

The NFPA 701 test[370] is a fabric test which is generally used in building codes for curtains, scenery, and decorations in schools and places of public assembly. The standard was originally published in 1938, but has been revised at various later times. The traditional large-scale test in NFPA 701 was developed by UL in the 1930s and comprises a tall metal chimney, inside which was hung a 2.97 m long fabric specimen. This was ignited by applying a Bunsen burner flame for 12 s at the bottom edge. The test method was completely changed in 1996 when the large-chimney test was replaced with two tests. Test 1 is for general use and entails a 400 mm long specimen which is hung vertically in an open-face test cabinet and exposed for 45 s to the flame of a Meeker burner held horizontally against the bottom edge. To pass, the afterflame must not last longer than 2 s nor must more than 40% of the specimen mass be lost. Following a research program[371], Test 2 was developed for fabrics with linings and curtains comprising multiple layers. A 1.2 m high specimen is hung inside a metal chimney and exposed for 120 s to flames of a Bunsen burner held at 25º off vertical at the bottom edge. To pass, the afterflame must not last longer than 2 s, nor must the char length exceed 435 mm (or 1050 mm for folded specimens).

The NFPA 701 also used to contain a 'field test' procedure. This test was sometimes misused and applied to plastics, for which it was never intended. Consequently, in 1992, the 'field test' became a separate standard, NFPA 705[372]. In the field test, a kitchen match is applied for 12 s to the bottom of a vertically suspended specimen; to pass, afterflame must not exceed 2 s, and burn length must not exceed 102 mm. The field test is stated not to be correlated to NFPA 701 results, so its value is only as a rough indicator.

ASTM D 1692

This was a small-flame ignition test[373] which used a wing-tip burner to apply a flame to a test specimen positioned horizontally on a wire mesh. Either sheet or foam specimens were used. The unusual feature of this test method was that specimens which did not burn farther than 127 mm were to be reported as "self-extinguishing by this test." This florid language caused the Federal Trade Commission to view the test method as a tool for deceptive marketing of plastics, and was one of the main reasons that the FTC took action against numerous plastics manufacturers and ASTM in 1973[163]. As part of the settlement, the test method was

withdrawn. The identical hardware still exists in the UL 94HB test, but the deprecated term is not used there.

UL 94 TEST SERIES

Perkins published in 1941 a study which was the forerunner to the UL 94 standard[374]. Plastics at that time were coming into more widespread use, as more polymer types were becoming commercialized. Perkins designed a test method using a gas burner flame to simulate the flame of "a common strike-on-the-box match." In the original study, only a vertical orientation was used, with specimen length being 152 mm. Various widths and thicknesses were explored. Perkins only applied the burner flame a single time, but explored flame application durations from 4 to 60 s. On the basis of the results obtained, Perkins classified plastics into 3 groups: Group 1. Cellulose acetate was taken as the benchmark for this group. Cellulose acetate butyrate, PMMA, polystyrene, and one sample of polyvinyl alcohol were also included. Group 2. This group comprised specimens less combustible—for various reasons—than Group 1. Included were a plasticized PVC/PVA copolymer, casein, phenolic, and urea formaldehyde. Group 3. Specimens in this group did not propagate flame after removal of the test flame. Specimens in this group included plasticized PVC, a number of PVC/PVA copolymers, phenol formaldehyde and another sample of PVA. As described below, the UL 94 test (first published in 1972) is substantially different from Perkins' original scheme.

UL 94[375] is actually a series of different tests; thus, a material cannot be described as "passing UL 94," but may be described, for example, as meeting the requirements for V-0. The individual tests and classifications are summarized in Table 38. These only cover the highlights of the testing procedures; the user should consult the standard for actual procedural details. The specimens tested under UL 94 are plastic materials, cut to standard sizes; other UL tests are provided for examining the ignitability of end-use articles.

A majority of the procedures of UL 94 are based on the use of a Bunsen burner, the construction of which is standardized in ASTM D 5025[376]. The use of the burner for the 20 mm and 125 mm flames is described in ASTM D 5207[377]. Both of these test flames involve operating the burner in a premixed mode. IEC standards 60695-11-3[378] and 60695-11-4[379] are functionally equivalent to ASTM D 5207.

The thickness plays a crucial role in UL 94 ratings. Most materials ignite more readily and burn faster or for greater distances if they are thinner. Thus, an actual rating may be described as "V-1 1/8-inch," which denotes that the material is accepted as V-1, but only provided thicknesses of 1/8" or greater are used. The same material may also be rated "V-0 ¼-inch," indicating that at the greater thickness a better rating is obtained.

The mildest tests in the UL 94 series are the ones where the material is oriented horizontally: 94HB and 94HBF. ASTM D 635 test[380] is functionally identical to the 94HB procedure. The 94HBF, 94HF-2, and 94HF-1 tests are used solely for foam materials; these tests are essentially identical to ASTM D 4986[381], which replaced the withdrawn ASTM D 1692 test. The results from the foam series of tests cannot be directly compared to HB ratings, since different test procedures are involved, but all horizontal-burning tests are milder than is any vertical-test rating (e.g., V-2).

The vertical-burn series tests are more strenuous than the horizontal-burn test. ASTM D 3801[382] is similar to the 94V-x procedures. IEC 60695-11-10[383], ISO 1210[384], ISO 9772[385], and ISO 9773[386] standards comprise test procedures which provide equivalents to both HB and V-x methods. The IEC method, which is becoming the most widely used, has a slightly different procedure for obtaining HB ratings. In the IEC scheme, meeting *either* the maximum flame travel distance or the maximum flame spread rate requirement suffices. In addition, the IEC scheme provides for HB40 and HB75 ratings, depending on which flame spread rate (mm min^{-1}) was obtained; there is no limitation as to specific sample thicknesses to be tested.

The 5V designations (5VA and 5VB) come from the fact that the flame used was originally specified as a 5-inch flame. For a 5VA rating, two entirely different sizes of specimens must be tested and pass in order to receive the appropriate rating. ASTM D 5048[387], ISO 10351[388] and IEC 60695-11-20[389] are essentially identical to the 5V portion of UL 94. The 94VTM (Vertical Test Mandrel) tests are used solely for thin materials which deform or burn up to the holding clamp when subjected to the 94V-x test; ASTM D 4804[390] is similar. The RP test is not an ignition test at all, but rather a radiant panel flame spread test. For the main tests, the order of difficulty of qualifying a specimen is: HB (easiest), V-2, V-1, V-0, 5VB, 5VA (hardest). There is no direct comparability of the results of the HF or VTM series to results from HB or V-x series.

The UL 94 series of tests attempts to screen out rapidly-aging components by requiring that certain replicates be subjected to accelerated-aging conditioning for 7 days at 70ºC. It is not clear there is any relation of this conditioning to actual degradation during the service life of the material.

Generally, there are three ways that a UL 94 V-0 rating can be achieved:

1. use of polymers that contain halogen in their basic structure (e.g., PTFE, polychlorotrifluoroethylene, brominated epoxy);

Table 38 Main features of UL 94 small flame tests

Rating	Specimen size			Burner angle	Time flame applied (s)	No. of times flame applied	Burner flame	Specimens tested	Criteria
	Width (mm)	Thick. (mm)	Length (mm)						
HB	13	(1) actual max., 13 mm (2) 3 mm	125	([a])	30	1	20 mm (50 W)	3	• L_b < 100 mm • ([b]) BR ≤ 40 mm min^{-1} • ([c]) BR ≤ 75 mm min^{-1}
HBF	50	(1) actual max., 13 mm (2) actual min.	150	0°	30	1	wingtip burner	5	• L_b < 125 mm • BR 38 mm min^{-1}
HF-1									• L_d ≤ 60 mm • AF ≤ 2 s for 4/5 specimens • AF ≤ 10 s for all specimens • AG ≤ 30 s for all • no cotton ignited below specimen
HF-2									• L_d ≤ 60 mm • AF ≤ 2 s for 4/5 specimens • AF ≤ 10 s for all specimens • AG ≤ 30 s for all
V-0	13	(1) actual max., 13 mm (2) actual min.	125	0° ([c])	10	2	20 mm (50 W)	5	• AF ≤ 10 s per flame application • AF ≤ 50 s total for 5 specimens • (AF + AG) ≤ 30 s for each specimen after 2nd flame application • no AF or AG reaches clamp (at 119 mm) • no cotton ignited below specimen
V-1									• AF ≤ 30 s per flame application • AF ≤ 250 s total for 5 specimens • (AF + AG) ≤ 60 s for each specimen after 2nd flame application • no AF or AG reaches clamp (at 119 mm) • no cotton ignited below specimen
V-2									• AF ≤ 30 s per flame application • AF ≤ 250 s total for 5 specimens • (AF + AG) ≤ 60 s for each specimen after 2nd flame application • no AF or AG reaches clamp (at 119 mm)

Main features of UL 94 small flame tests…continued

Rating	Specimen size			Burner angle	Time flame applied (s)	No. of times flame applied	Burner flame	Specimens tested	Criteria
	Width (mm)	Thick. (mm)	Length (mm)						
VTM-0	50	(1) actual max. (2) actual min.	200 ([e])	0º ([d])	3	2	20 mm (50 W)	5	• AF ≤ 10 s for any application • AF ≤ 50 s total for 2×5 applications • (AF + AG) ≤ 30 s for each specimen after second application • no AF or AG reaches clamp • no cotton ignited below specimen
VTM-1									• AF ≤ 310 s for any application • AF ≤ 250 s total for 2×5 applications • (AF + AG) v 60 s for each specimen after second application • no AF or AG reaches clamp • no cotton ignited below specimen
VTM-2									• AF ≤ 310 s for any application • AF ≤ 250 s total for 2×5 applications • (AF + AG) ≤ 60 s for each specimen after second application • no AF or AG reaches clamp
5VA	13	(1) actual max., 13 mm (2) actual min.	125	20º	5	5	125 mm (500 W)	5	• (AF + AG) ≤ 60 s after 5th application of flame • no cotton ignited below specimen
	150	(1) actual max., 13 mm (2) actual min.	150					3	• no burn-through holes
5VB	13	(1) actual max., 13 mm (2) actual min.	125	20º	5	5	125 mm (500 W)	5	• (AF + AG) ≤ 60 s after 5th application of flame • no cotton ignited below specimen
RP	(see standard for details)								

L_b – burned length
L_d – damaged length
BR – burn rate
AF – duration of afterflame
AG – duration of afterglow

([a]) flame is held vertically; specimen is oriented so that long axis is horizontal, while short axis is tilted 45º with respect to horizontal
([b]) for actual thickness specimen
([c]) for 3.2 mm thick specimen
([d]) angle may be up to 45º if melting/dripping is encountered
([e]) twisted into a modified cylinder shape

2. use of polymers that, upon thermal decomposition, leave more than about 60% of their mass as char (e.g., polyphenylsulfone, polybenzimidazole, or Kevlar);
3. incorporating suitable flame retardants into the formulation.

Lyon and Walters[391] proposed that a V-0 rating will be obtained by materials which show a HRR less than about 250 kW m^{-2}, on the basis of the average HRR determined at an irradiance of 50 kW m^{-2}. Materials which show a HRR > 400 kW m^{-2} are almost certain to be rated no better than HB, with intermediate values giving scattered results. The rule was based on studying only 15 materials, and a later study by Bergendahl et al.[392] show that there is only a modest relationship between performance in the UL 94 test, versus that in radiant heating tests. The latter investigators studied 6 materials in UL 94 and in the Cone Calorimeter and found that, while long ignition times and low HRR tended to correlate to a good UL 94 rating, there were specimens with essentially identical results in the Cone Calorimeter that were classified as HB for one versus V-0 for the other.

The reason for the existence of UL 94 series of tests, presumably, is because they are felt to reflect the propensity of plastics to ignite when presented with small flames. Surprisingly, validation of the tests has rarely been undertaken. The most comprehensive effort so far is discussed in Chapter 14 under *Television sets and computer monitors*. That study indicates significant problems with the test series. The V-2 rating appears to be especially problematic—the range of performance for specimens qualified as V-2 was found to be huge, overlapping both HB and V-0. UL themselves ran a small series of tests[393] on computer monitors where only HB and V-0 specimens were examined. The salient findings were:

- An HB rated monitor ignited readily with a paper match, when held at a corner or underneath. The sides and top could not be ignited with a wooden match. A candle was able to ignite in all configurations except on burning completely down and challenging the underneath surface.
- Four V-0 rated monitors resisted paper matches, wood matches, and candles placed in variety of locations. In one case, however, when the candle flame was next to a ventilation opening, an ignition occurred (due to thickness variations and edge burning), but the monitor eventually self-extinguished without full consumption of test article.
- A burning HB rated monitor placed close to a V-0 rated monitor was able to ignite the latter, with full consumption occurring. This, of course, emphasizes that the V ratings are not intended to reflect behavior when the ignition source is large.
- A monitor which had a HB-rated base, with the remainder being V-0-rated ignited and burned completely when ignited by a candle flame to the base.

V-1 rated materials were not considered in the test work since V-1 ratings are rare. Most materials, if they burn for 10 s, will burn for 30 s. It would be difficult for polymer chemists to produce a V-1 material by design.

As part of an international harmonization effort, the next edition of UL 94 will no longer contain technical provisions, but rather will refer the user to IEC/ISO standards:

- HB ratings: IEC 60695-11-10
- V ratings: IEC 60695-11-10
- 5V ratings: IEC 60695-11-20
- FH ratings: ISO 9772
- VTM ratings: ISO 9773

UL END-PRODUCT TESTS

For many appliances and devices, UL provides that plastics may be qualified in two different ways: (1) by conducting small-flame, arc-tracking, and other tests on the plastic material used; or (2) by subjecting the actual product to fire testing. Thus, UL 746C[394] and UL 1950[*395] prescribe a series of fire tests to be conducted on actual finished products. The decision *where* to apply the flame can be crucial, but this is left up to the discretion of the laboratory. UL 746C in general considers that passing *either* the 12 mm flame test or the 20 mm flame test is equivalent to using an HB-rated plastic.

The *12 mm flame test* ('Needle-flame test') is published as UL 1694[396] but is also separately described in a number of end-use product standards. The test is mainly used by manufacturers of electronic components. It provides for two, 30 s applications of flame (estimated at 45 W) to be made to the item. For this test, the burner is a hypodermic needle of 0.5 mm I.D., with the end cut flat. No air supply is introduced into the burner. Two flame applications are made, with the length of flame exposure being dependent on the specimen volume. Specimens of less than 250 mm^3 are exposed for 5 s, those between 1750 and 2500 mm^3 for 30 s, with intermediate sizes being exposed for 10 or 20 s. The item passes if the afterflame time following each application does not exceed 30 s, if the afterflame plus afterglow time following the second application does not exceed 60 s, if cotton placed below the specimen is not ignited, and if the specimen is not completely consumed. Parts which are made of plastics rated at least V-2 do not need to be tested. This is the mildest test used by UL for general-purpose testing of plastics and it does not have an equivalent in the UL 94 series. Some of its history has been provided by Moltzan and Hall[397]. The IEC equivalent to this test is IEC 60695-2-2[398].

The *20 mm flame test* (50 W; also described as the *¾ inch flame test*) provides for two, 30 s applications of flame to the item. The burner conditions earlier were different, but

[*] Apart from minor deviations, UL 1950 is identical to IEC 60950 and CSA C22.2 No. 950 tests.

currently are standardized to be identical to UL 94. While the test burner used is essentially identical to that employed in the UL 94 V tests, the criteria are more lenient than for V-2: the item passes if afterflame does not exceed 60 s after the 2nd flame application and if the entire object is not consumed. No flame travel limits are set (and, similar to V-2, no limits on molten flaming material). Under UL 746C, parts which are made of plastics rated at least V-2 are presumed to pass the 20 mm test. However, for the purposes of the UL 1950 test, plastics must be rated at least V-1 in order to be presumed to pass the 20 mm flame test.

The *130 mm flame test* (500 W; also described as the *5 inch flame test* and sometimes identified as 125 mm or 127 mm flame test) uses a Bunsen burner with air supply adjusted so the flame has a 38 mm inner blue cone. The test involves the application of a flame 5 times, each time being applied for 5 s then removed for 5 s. The item passes if afterflame does not exceed 60 s after the final flame application, if cotton placed below the specimen does not ignite, and if the specimen is not sufficiently destroyed to reduce the integrity of the device. Parts which are made of plastics rated 5VA do not need to be tested.

In addition to the above tests, UL 746C also describes a test which is conducted on plaques, rather than on the real-scale object. The *746-5VS enclosure flammability test* uses the 5-inch burner flame, but exposes 152 × 152 mm plaques of the material for 60 s. The item passes if neither afterflame nor afterglow exceed 5s, if cotton placed below the specimen does not ignite, and if the plaques do not burn through.

For large plastic enclosure or exterior parts, defined as those having an area > 10 ft^2 (0.93 m^2) or a dimension > 6 ft (1.83 m), UL 746C also requires that the Steiner Tunnel (ASTM E 84) or the radiant panel (ASTM E 162) tests be run. Both of these tests are flame spread tests and do not examine the ignition behavior of the specimen.

The *hot flaming oil test* is prescribed by UL 1950 for the testing of certain full-scale enclosures of electronic equipment. This specialized test is used to examine whether openings in the bottom of an enclosure can set fire to combustibles underneath. A ladle holding 10 mL of burning oil is used to pour the oil into the bottom of the enclosure, and cheesecloth below the enclosure must not ignite.

In addition to flame tests, UL procedures for end-use product testing also include tests for other ignition modes. These are published in UL 746A and are described below under *Arc tracing and arc ignition tests* (the High-Current Arc Ignition Test) and *Other types of tests* (the Glow-Wire Ignition Test and the Hot Wire Ignition Test).

SMALL-FLAME TESTS FOR WIRE AND CABLE

ASTM D 2633

A small-burner flame test for wire specimens is described in Par. 63 of ASTM D 2633[399]. A 560 mm long specimen is used, stretched taut vertically, with a paper flag attached 254 mm above the location at which the flame is applied. The flame is applied from a gas burner which is inclined 20º from vertical. The flame is applied 5 times for 15 s each, with a 15 s interval between applications. Passing results are reported if the flag is not more than 25% burned during test and if cotton placed underneath the specimen does not ignite.

UL 1581

UL standards for various types of wires and cables (e.g., UL 44, UL 62[400], and UL 83) specify the requirement to test the wire/cable according to one or more of small-scale tests* that are delineated in UL 1581[401]. Apart from several narrowly specialized methods, the general-purpose methods for small-scale ignitability testing are the following:

Horizontal flame/FT2 test, Par. 1100. A 254 mm long specimen is supported horizontally, and surgical cotton is placed 241 mm below the specimen. A Tirrill burner positioned at 20º off vertical is used to apply a flame to the center of the specimen for 30 s. The specimen fails if it ignites the cotton or if the total length of char exceeds 100 mm. The "FT2" designation refers to the designation of the test originally promulgated by the Canadian Standards Association.

Vertical flame/FT-1 test, Par. 1060. The method is similar to ASTM D 2633, except that: (a) the specimen length is 457 mm; (b) an additional failure criterion is applied that the specimen shall not flame longer than 60 s after the end of the 5th application of flame; (c) a 4 m^3 test chamber is used.

VW-1 (vertical-wire) test, Par. 1080. The method, which was originally designated the FR-1 test, is identical to the Vertical Flame test, except that: (a) instead of there being a fixed 15 s waiting interval in between flame applications, if the specimen is still flaming after waiting 15 s, the next application of flame does not occur until the specimen's flaming stops; and (b) the afterflame time length criterion is ≤ 60 s after *each* flame application, instead of only after the 5th one. This procedure is tougher for certain specimens than the Par. 1060 test, since it was found that re-applying the flame while the specimen was still burning caused flaming to be extinguished for certain specimens, due to local velocity effects, and the specimen would not re-ignite[402]. ASTM D 3032 describes a test method (Sec. 18, Test Method A) which is similar; this test method is anticipated to be moved into another ASTM standard in the near future. At that time, the procedures will specifically identify the flame as being 500 W.

* Some standards also require large-scale flammability tests to be performed, but these are not primarily tests for ignition.

IEC tests

IEC provides two different small-flame tests for wires or cables, IEC 60332-1 and IEC 60332-2. The test method IEC 60332-1[403] uses a vertical specimen 600 mm long, clamped between two clamps 550 mm apart. A 1000 W burner flame is applied at 45º to the specimen and is placed so that the inner blue cone of the flame is 10 mm from the surface of the specimen and 475 mm below the top clamp. The period of flame application varies with the specimen diameter, being 60 s for specimens ≤ 25 mm, 120 s for specimens of 25 – 50 mm, 240 s for specimens of 50 – 70 mm, and 480 s for specimens > 75 mm. In all cases, the charred area must extend no closer than 50 mm to the top clamp and 10 mm to the bottom clamp. The test method IEC 60332-2[404] uses an identical specimen and clamp arrangement, but the burner flame is specified by a total flame length of 125 mm, not by HRR. The flame is applied for only 20 s, irrespective of specimen size. To pass, the charred area must not extend closer than 50 to the top clamp. There is a separate IEC test for grouped (bunched) cables, but this large-flame test does not have much relation to ignitability.

MVSS 302

The only requirement of the US Federal government for fire behavior of interior materials of automobiles is the extremely lenient MVSS 302 test[405]. A 102 mm × 356 mm (4" ×14") is tested in a maximum thickness of 12.7 mm (½") by being clamped in a metal U-shaped edge frame and exposed to 38 mm high Bunsen burner flame for 15 s. The material passes if it burns for no longer than 45 s after the removal of the flame, or if the flame does not spread farther than 51 mm (2"), or if the flame spread rate does not exceed 1.69 mm s^{-1} (4" min^{-1}). ASTM D 5132[406] and ISO 3795[407] are functionally equivalent to MVSS 302, except that they do not include criteria for passing. The MVSS 302 represents a minimum performance level, even less strenuous than UL 94HB.

FAR BUNSEN BURNER TEST

The Federal Aviation Administration requires various aircraft materials to pass a vertical Bunsen burner test. This test is described in Appendix F of Federal Aviation Regulations (FAR) Part 25. The apparatus originates with a 1951 Federal test, identified as Method 5902. In a 1968 revision, this was replaced by Method 5903, which adds a requirement that "Matheson B-gas" be used as the fuel gas. The latter is a mixture comprising 55% hydrogen, 24% methane, 3% ethane, and 18% carbon monoxide. Its origins date back to the World War II era, when it was desired to standardize a controlled mixture which would be representative of 'manufactured gas' or 'producer gas' which was a common fuel preceding the widespread use of natural gas (which is predominantly methane). An FAA

Table 39 Results from round-robin testing with the ISO 11925-2 small-flame ignition test

Material	Thick. (mm)	Percent reported ignitions[a]			Notes
		Surface location	Bottom edge location	Side edge location	
extruded PS foam, FR	20	57/55	59/59		melted away from flame, but ignited
expanded PS foam, FR	40	16/12	12/24		melted away from flame; only occasional transient ignition
expanded PS foam	60	74/85	88/96		burned completely
PMMA	3	10/70	100/100		bottom edge ignition and 30 s exposure needed for successful ignition
birch plywood	12	10/10	78/78	71/71	no ignition from surface or bottom exposure; occasional ignition w/o flame spread for side edge ignition
PVC	0.1	74/74	46/47		shrank back, sometimes pulled out of holder; ignited and burned, but only for duration of exposure
paper wall covering on gypsum	13	30/47	33/30		rare ignitions; probably occurred where imperfect adhesion to gypsum
pine	19	40/53	89/100		required 30 s exposure to ignite
medium density fiberboard	9	20/30	96/97		no ignition with surface exposure; ignites with bottom edge exposure
PVC coated polyester fabric	0.5	100/100	100/100		shrank away severely, ignited, but ignition not sustained
PUR foam w. aluminum facing	40	80/87	100/100	100/100	flame pierced aluminum and caused rapid burning of foam
PUR foam w. bitumen paper facing	40	59/78 100/100[b]	100/93 100/100	100/100	bitumen facing ignited, but only burned during exposure; when tested with foam side out, burned rapidly

a – first number refers to 15 s exposure, second to 30 s exposure
b – second set of data refers to foam-side exposure

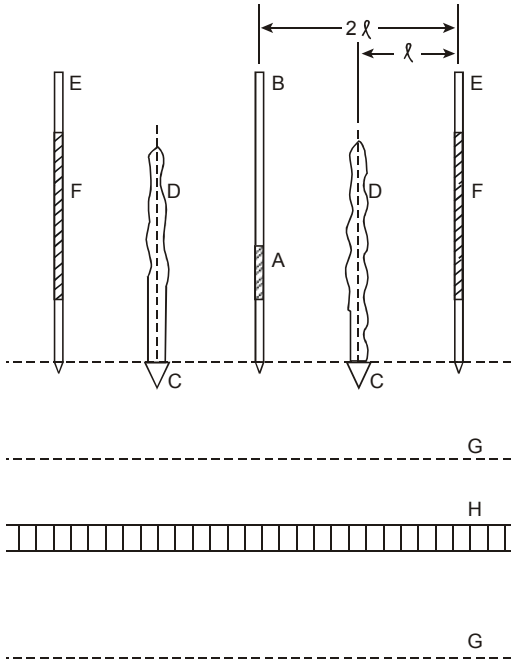


Figure 76 Vertical cross-section through large-flame test used by Koohyar (**A** specimen; **B** specimen holder; **C** liquid pan burners; **D** flame; **E** shroud; **F** viewing ports; **G** screens; **H** honeycomb air diffuser)

study[408], however, found a problem with this gas, in that it tends to give irreproducible flames. This is attributed to iron pentacarbonyl, $Fe(CO)_5$, which is formed when the CO gas component reacts with rust in the gas cylinder. It was determined, by contrast, that 99% purity methane, used as a fuel, did not show any such irreproducibility problems. The same study also examined the influence of thermocouple diameter on measurement of the flame temperature. An inverse relationship between diameter and maximum temperature reading was found.

ISO 11925-2 SMALL FLAME TEST

The ISO small-burner test[409] has mainly derived from the German 'Kleinbrenner' test. An Annex for materials which melt and shrink was developed on the basis of research at the French laboratory LNE. Its basic concept was adopted by the European Commission as one of the test methods for regulating the lower-rated classes of building products. Consequently, the test further evolved under CEN work. A 90 mm wide by 250 mm specimen is mounted vertically in an edge-frame specimen holder. The complicated burner is used to produce a flame of 20 mm height, which is applied at a 45º angle to the specimen. Because of European standardization issues, numerous alternatives and reporting schemes are involved. The burner flame may be applied for 15 or 30 s. Each product is to be tested 6 times by applying the flame to the broad surface and another 6 times by applying the flame to the bottom edge. Multi-layer products over 10 mm are subject to additional testing regimens. Data to be reported include: whether ignition occurs; whether flame spreads as far as 150 mm; if flaming droplets are observed; and if filter paper placed underneath the specimen ignites. If the product shrinks away from the flame without igniting, then an entirely different moving-flame procedure is to be done.

A round-robin with 12 materials was conducted using the 1997 version of this test method[410]. The main results are summarized in Table 39. Despite the seemingly routine nature of the test, it was rare to find 0 or 100% ignitions reported for any material. The Notes in the table refer to typical behavior of specimens.

LARGE-FLAME TESTS

A few flame-ignition test methods have been developed where it is intended to impose a relatively constant heat flux from a flame onto a flat specimen surface. The geometry envisioned is similar to that of the radiant ignition tests, described below. A specimen is used which is much larger in its two face dimensions than it is in the depth. The edges are protected in some manner, so that ignition would not occur at the edges or corner of the specimen. One such test was developed by Koohyar[73]. In his rig, a vertical specimen (100 × 100 mm) was heated by two flames, one on each side, with neither flame touching the specimen (Figure 76). The flames stood upright because combustion air flow to the flames was fed from the bottom and was balanced to be equal from both sides. The heat flux imposed on the specimen was adjusted by varying the spacing distance *l* of the flames. The geometry suggests that the view factor of the flame sheet was quite close to 1.0, so it is not clear how the diminution in heat flux was achieved; perhaps there was a sizable contribution from convection.

Later, Lawson and Parker[411] created a geometry where there was one flame, but two specimens, with the single flame occupying a central position between two specimens spaced 53 mm apart (Figure 77). Unlike in the Khooyar rig,

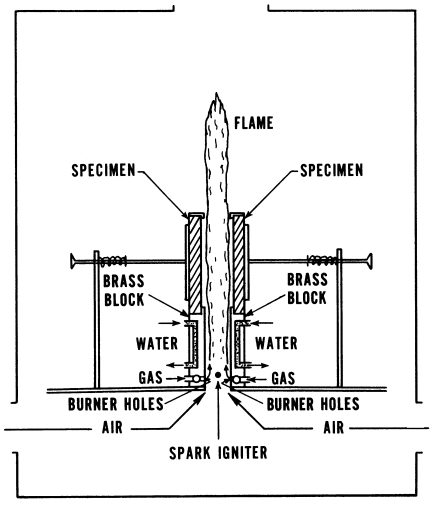


Figure 77 Flame ignition test by Lawson and Parker

a methane burner was used, supplied with fuel at a rate of 8 kW (57 kW m^{-1}, if computed per length of line burner). The flame was positioned relatively close to the specimen face and ignition was declared to occur at the time that the flame 'attached' to the face. The gas flow was set so that the flame would impose an average heat flux of 32 kW m^{-2} to the specimen; unlike in the Khooyar rig, provisions were not made for varying the heat flux.

In both these rigs, it was evident that heat flux uniformity could not have been particularly good, although documentation was not provided on this point. Subsequent test development efforts were generally based on the view that a radiant heat source is much easier to control reproducibly and that it can also simulate an actual large-flame exposure, simply by selecting an appropriate irradiance.

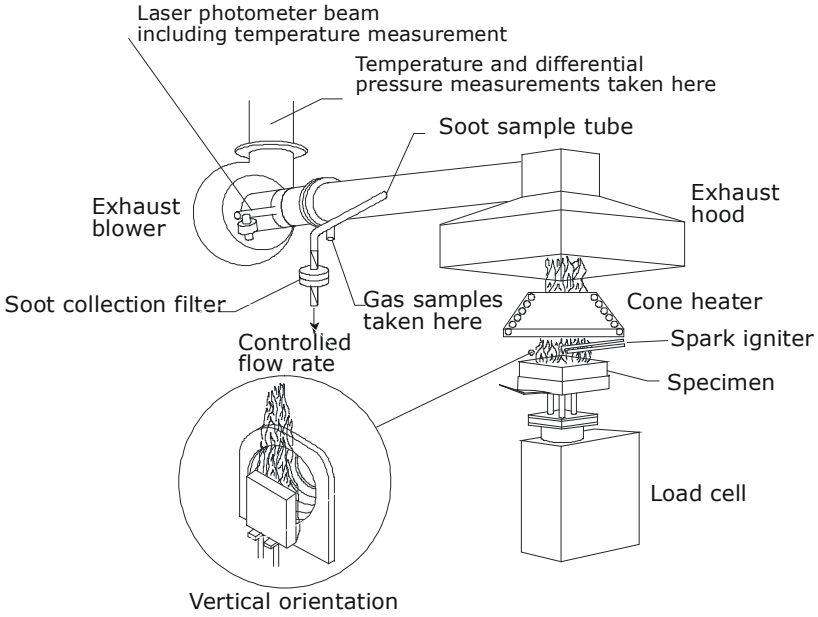


Figure 78 General view of the Cone Calorimeter

RADIANT IGNITION TESTS

THE CONE CALORIMETER

The Cone Calorimeter was developed by Babrauskas[412-414] at NIST during the 1980s as an apparatus primarily for measuring the HRR of small-scale specimens (Figure 78). Until its development, there was not available any standardized test where samples can be heated radiatively with a uniform, feedback-loop stabilized heat flux. The method has been published as ASTM E 1354[415], ISO 5660[416], and in various specialized standards. Because of the uniform exposure provided to specimens, it has become widely used for measuring additional fire properties: mass loss rate, ignitability, smoke production rate, and toxic gas production. Currently it is the most common apparatus used in laboratories worldwide for measuring the radiant ignitability of materials. Babrauskas and Parker[101] described the early ignition testing work with the Cone Calorimeter.

Apart from specialized units that have been constructed to operate in controlled atmospheres[417], specimens are tested in room air. A radiant heater can impose up to 100 kW m^{-2} upon the face of the specimen, which may be horizontally or vertically oriented. Some specimens melt, collapse, or otherwise behave anomalously when in the vertical orientation, thus standard testing is done in the horizontal orientation, with vertical orientation only being used for special research purposes.

The conical heater of the Cone Calorimeter was inspired by the earlier one found in the ISO 5657 test, as described below. The heater in the Cone Calorimeter is not identical, however, since certain improvements were made to enhance reliability and to increase the maximum obtainable heat flux. The emissivity of the heater[418] is approximately 0.99 and the emissivity × view factor product[75] for the cone heater is 0.73, thus the radiant flux going to a cold specimen is:

$$\dot{q}''_e = 0.73\,\sigma\left(T_h^4 - T_o^4\right)$$

where T_h = heater temperature (K) and T_o = room temperature (K). The heater radiates as a grey body operating at a maximum temperature of about 1273 K (1000ºC). Thus, the radiation of the heater falls in the same portion of the spectrum as do most building fires, which are commonly at or below 1000ºC.

Because, in the horizontal orientation, the radiant heater essentially surmounts the pyrolysate plume emerging from the sample, attenuation of radiation by the pyrolysate stream is not as large as it would be in test arrangements where the radiant heat flux arrives straight-down from a remote radiator and has to pass through the thickest part of the plume. In the vertical orientation, the boundary layer of pyrolysates adjacent to the surface is innately thin and the issue does not arise.

In any ignition test where uniform face-heating is provided, effects at the edges must be shown not to be significant. A study was done on samples for the Cone Calorimeter prepared in three different ways: (1) a steel edge frame around the specimen; (2) no edge frame; specimens terminate in a cut edge; (3) an insulated edge frame[419]. For most products, ignition time effects differed only to within the data scatter. For foam plastics, there was a more significant effect, but it is found that many of these cannot be studied in a truly apparatus-independent way.

Figure 78 does not show it, but the current version of the Cone Calorimeter requires the use of a retractable shield between the heater and the specimen. It takes the operator a

finite amount of time to insert the specimen holder into the apparatus and seat it down on the load cell. For products where ignition times are of several minutes duration, small errors in heat flux exposure at the start of the test will not make a d etectable difference. But for specimens which ignite in only a few seconds, uncertainty in starting the test can cause an error. The benefits of using a shield were documented during a research program where extensive testing of upholstered furniture composites was done[420].

ISO 5657

The ISO 5657 test [421] was the first standardized ignition test to be made available which used an electric radiant panel for exposing specimens to a nearly-uniform heat flux. It was originally developed in 1970 by Stephen Grubits[422], at the Experimental Building Station in Australia, now part of CSIRO. Grubits' original version had optional provisions for a spark igniter, or a gas pilot. CSIRO later dropped the gas pilot in favor of a hot wire igniter[196]. Subsequent development of the test in Germany by Peter Topf led to the adoption of the 'dipping duck' pilot. Grubits used the test apparatus in the upright (specimen held face-up), turned sideways (specimen vertical), and upside-down orientations. The ISO version only adopted the face-up orientation.

The most unusual feature of the ISO 5657 test is the 'dipping duck' gas pilot. It was designed to bring a gas pilot close to the specimen surface, yet to avoid imposing a significant amount of added heat flux locally. The pilot is attached to an motorized arm which briefly brings it down once every 4 s, then retracts it to a standby position. It was found that halogenated test specimens tend to extinguish the gas pilot, thus, in the standby position the pilot approaches a r e-igniter flame, which is an auxiliary, non-moving pilot which re-ignites the main pilot if it had been extinguished. The 4-s dipping cycles places a limit on the accuracy, which clearly cannot be better than ±2 s. Another unusual feature is the arrangement whereby a deadweight device presses the specimen up against a masking plate. This device is intended to compensate for specimens which shrink and recede from a heat source, although the squeezing of a test specimen is arguably unreasonable.

The emissivity × view factor product[192] for the apparatus has been determined to be 0.67. The geometry and construction of the conical heater are similar (but not identical) to those on the Cone Calorimeter, thus the value is rather close to the 0.73 obtained for the Cone Calorimeter.

For most testing and research work, ISO 5657 h as been superceded by the Cone Calorimeter, the design of which was inspired by certain features of the ISO 5657 test. Thus, the features of the ISO 5657 test will be described mainly by the differences between it and the Cone Calorimeter, as shown in Table 40. In comparing test results between the two apparatuses, it was found that ignition is typically slightly faster in the ISO 5657 test than in the Cone Calorimeter, although in many cases the differences are no more than the scatter of the data[423]. There may be many reasons for this, but possibly the lack of temperature control on the ISO 5657 equipment is the largest cause.

ASTM E 1321 (LIFT)

This test[424] is primarily designed to obtain material properties pertinent to opposed-flow flame spread. A separate portion of the test is designed for the measurement of ignition times of samples exposed to a nearly-uniform radiant heat flux. Vertically-oriented specimens of 155 × 155 mm are used, with ignition being by an acetylene/air pilot flame. The pilot flame is 180 mm long and horizontally projected about 25 mm above the top edge of the specimen. The gas-fired radiant heat panel is capable of imposing heat fluxes up to 65 kW m^{-2} on the specimen. The ASTM stand-

Table 40 A comparison of features of the ISO 5657 and Cone Calorimeter tests

Feature	ISO 5657 test	Cone Calorimeter
Heating source	electrical element, shaped as truncated cone	electrical element, shaped as truncated cone
Max. power of heater	3000 W	5000 W
Maximum heat flux	50 kW m^{-2}	100 kW m^{-2}
Control of heat flux	set temperature, maintained by servo loop	set temperature, maintained by servo loop
Pilot	propane gas flame, dipping every 4 s	continuous electric spark; optionally, may be tested without pilot
Specimen orientation	horizontal only	horizontal; vertical (optional)
Specimen size	165 165 mm	100 100 mm
Specimen holder	pressure plate forcing specimen against mask plate having a 140 mm circular opening; specimen rests on high density (825 kg m^{-3}) board	horizontal orientation: placed on a pad of low-density (65 kg m^{-3}) ceramic fiber blanket, supported in stainless steel holder vertical orientation: in stainless steel holder, backed by low-density ceramic fiber blanket, supported by calcium silicate board

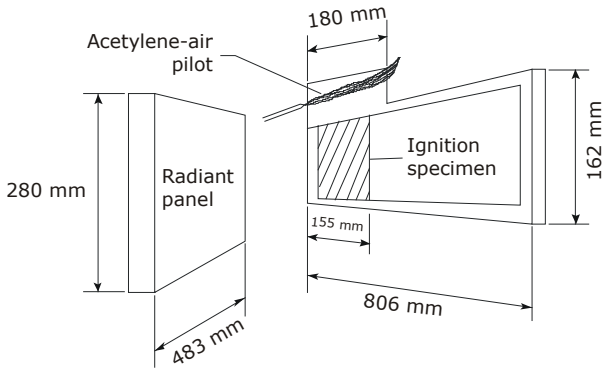


Figure 79 The LIFT test apparatus

ard uses the Quintiere analysis method, which was discussed in detail earlier in this Chapter. The value of $\dot{q}''_{\min}$ is required to be obtained to 2 kW m^{-2} precision in conducting the ignition tests. Due to the nearby presence of the gas-fired heating panel, there is a strong convective flow established across the face of the specimen. Thus, Drysdale[425] has found that values of $\dot{q}''_{\min}$ determined from the LIFT test are consistently higher than those from other apparatuses. In a similar vein, Janssens[75] documented that values of $\dot{q}''_{cr}$ measured in the LIFT test are about 1.0 to 1.5 kW m^{-2} higher than measured in the Cone Calorimeter. He also discovered that systematic errors in measured ignition times occur for heat fluxes > 45 kW m^{-2}; this is because the heater panel is not thermostatically controlled and inserting a cold specimen upsets the panel temperature significantly at higher heat fluxes. Finally, the standard ASTM E 1321 procedure provides for a method for determining an effective value of the thermal inertia, $\lambda\rho C$, but Janssens considers that the values are over-estimated, due to the use of asymptotic approximations.

There have been several variants of this test. The HIFT test[426] involves turning the entire rig around by 90º so that the specimen is in the horizontal plane and melting substances can be tested. The FIST test[427] involves adding a forced air flow of 1 m s^{-1} over the face of the specimen.

FM FIRE PROPAGATION APPARATUS—ASTM E 2058

This apparatus[428] (Figure 80), earlier referred to as the FM Flammability Apparatus, is a specialized test method used by the Factory Mutual system for measuring HRR, ignitability, and flame spread. In many aspects, the apparatus is not too dissimilar to the horizontal orientation of the Cone Calorimeter, but there are two notable peculiarities. (1) The apparatus uses a tungsten/quartz lamp heat source operating at up to a 2200ºC effective radiation temperature, which results in a radiant spectrum much different from the type of heating obtained from flames, room fires, or hot surfaces, which are almost invariably below 1200ºC. The radiation from the FM source is largely in the visible spectrum, where many substances show a much lower absorptivity than in the infrared spectrum. Consequently, the standard procedure with this test involves blackening of the surface to raise what might otherwise be a very low absorptivity. This does not necessarily result in the same amount of radiant flux being absorbed by a specimen as would happen if the surface were not blackened, but radiation from a lower-temperature source were provided. (2) The apparatus can be operated using atmospheres of various oxygen concentrations, but it is normally operated at 40% oxygen instead of at 21%. This is due to a desire to use the HRR data in the context an FM scaling rule which holds that small-scale data collected at 40% oxygen agree better with large-scale data than if this test apparatus were operated at 21% oxygen. Because of the radiant spectrum and the blackening procedure, results from the FM Flammability Apparatus may be systematically different from those obtained in other test methods.

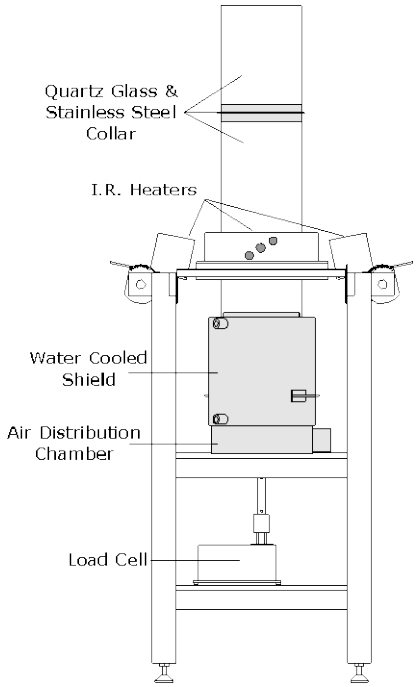


Figure 80 Factory Mutual flammability apparatus

Other differences include a maximum irradiance of 65 kW m^{-2} and an ethylene/air gas pilot. Specimen mounting details in the FM apparatus depend on the particular commodity which is being tested, but wires and cables are commonly tested as single lengths, rather than as a packed array, such as is standard in the Cone Calorimeter. This creates a major difference in response, especially with thinner cables, which are then exposed on all sides and tend to respond in a thermally-thin manner, even if they would respond as thermally-thick in other installations. This was illustrated by Gandhi[429], who tested 9 communications cables in the Cone Calorimeter and in the FM apparatus. Because of these mounting differences, specimens in the FM apparatus ignited much more rapidly (Figure 81) despite

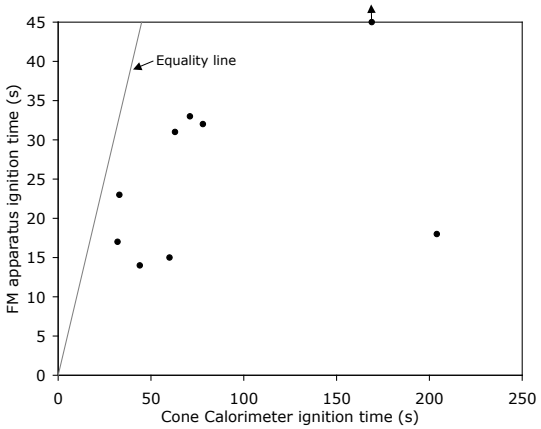


Figure 81 A comparison of piloted ignition times in the FM apparatus and in the Cone Calorimeter for thin communications cables

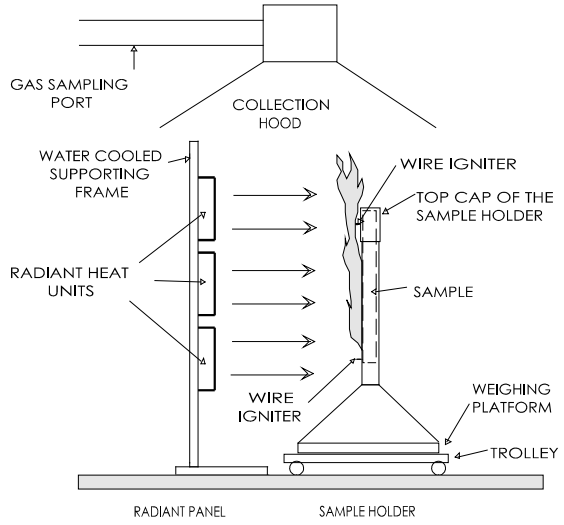


Figure 82 The ICAL apparatus

the fact that both sets of specimens were tested by Gandhi at 21% oxygen. In normal operation, users follow additional testing prescriptions which are given in a large assortment of FM in-house standards; the ASTM standard merely prescribes basic instrument construction and operation principles.

ASTM E 1623 (ICAL)

The ASTM E 1623[430] test is known as the 'ICAL,' which denotes Intermediate-scale CALorimeter. This method (Figure 82) is intended for testing complicated assemblies, where bench-scale testing might not provide sufficiently usable characterization. Vertically-oriented 1.0 × 1.0 m specimens are used, with a thickness of up to 152 mm. Unlike the Cone Calorimeter, heating is by a gas fired panel. Ignitability may be measured at heat fluxes of up to around 60 kW m^{-2}. Piloting is by hot wire igniters, located at both top and bottom of the specimen holder.

Some years after the ICAL was developed, it was noticed that ignition times were consistently longer than in the Cone Calorimeter. This was identified to be due to the greater convective velocity that a large specimen induces[431]. The solution was to mount a ledge below the sample, which has the effect of stopping the boundary layer flow and creating a local eddy, with downward air velocity at the lower portion of the specimen face. The ledge also served a flameholder function once ignition took place and ensured a more steady burning.

ARC TRACKING AND ARC IGNITION TESTS

A 1994 survey[432] identifies 26 different tests which have been published for determining arc tracking resistance, although some of them were drafts rather than formal test methods. A number of the more widely used tests are described below. Others of occasional interest include ASTM D 2132[433], ISO 2678[434], IEC 60587[435], and NASA Handbook NHB 8060 (Test 18)[436].

ASTM D 495

This test[437] creates a high voltage, low current exposure condition and only evaluates arc tracking under dry, clean conditions. Dry tracking can be induced by HV discharges over an insulator's surfaces in real applications, and the test simulates this situation. The method provides a 12,000 V arc across tungsten rod (alternatively, stainless steel strip) electrodes placed on the surface and spaced 6.38 mm apart (Figure 83). The test method is used in UL 746A, and the latter classifies the ASTM D 495 numeric performance into Performance Level Categories (PLC) 0 through 7, with PLC 0 being the best and PLC 7 the worst.

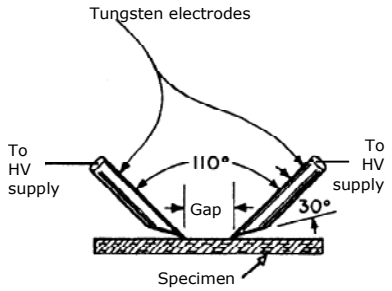


Figure 83 Electrode arrangement of the ASTM D 495 arc tracking test

ASTM D 2303

The method[438], referred to by UL as the Inclined Plane Tracking test, uses a 50 × 130 mm flat specimen where an AC voltage is applied to the surface by two electrodes spaced 50 mm apart, and the surface is continually doused with a stream of liquid contaminant. This rather intricate test can be run in two modes: (1) the initial tracking voltage mode, or (2) the time-to-track mode. For the first case, increasing voltages are applied and the lowest voltage reported which results in progressive tracking during a 1 h exposure. For the time-to-track mode, a desired voltage (up to 6

kV) is applied and the time recorded for progressive tracking to develop.

ASTM D 3032

This ASTM document[439] is a compilation of a large number of different test methods for wire insulation. Three of the methods are directly related to flammability, two being for arc tracking and the third one (see above under UL 1581) being a flame test. Section 26 describes a procedure for damage from dry-arc propagation, wherein a reciprocating guillotine blade slices through a wire bundle to create a short circuit. A specific arrangement of 7 wires is connected to a 3-phase, 400 Hz AC supply circuit, and resistance is inserted in the lines to provide a 1 A current flow. The blade sawing through the assembly initiates an arc, and the test criteria involve the arc-damaged length of wires, both those in contact with the blade and those that are not. The test is considered to be an arc-tracking test, but the connection is tenuous, since no arc-tracking is actually induced. The ASTM D 3032 standard is being reorganized and the VW-1 flame test procedure and some others are being devolved onto a separate test standard.

Section 27 is a wet-arc tracking test. A bundle of seven wires connected in a specified way to a 3-phase, 400 Hz AC supply circuit is used, with resistance being inserted in the lines to provide a 1 A current flow. The insulation is stripped off two of the wires and a 3% NaCl solution is dripped onto the exposed conductors at a rate of 8 – 10 drops per minute. The primary result is the length of wire damaged by arcing.

ASTM D 3638

According to ASTM D 3638[440], the Comparative Tracking Index (CTI) is defined as the voltage which will cause failure by tracking when 50 drops of electrolyte are applied, simulating wet conditions. The maximum test voltage does not exceed 600 VAC. In the procedure, two platinum electrodes are placed on a specimen 4 mm apart; a test voltage is selected and 50 drops of ammonium chloride solution are dispensed into the gap at 30 s intervals. The test method is used in UL 746A, and the latter classifies the ASTM D 3638 numeric performance into Performance Level Categories (PLC) 0 through 5, with PLC 0 being the best and PLC 5 the worst. *IEC 60112*[441] is identical, except that it also describes the Proof Tracking Index, which is a go/no-go test at a single, specified voltage. Research with the IEC 60112 test has been described by Centurioni et al.[442] A roundrobin was conducted in the late 1990s to assess the IEC 60112 test[443]. As a consequence, a number of changes to the procedure are expected to occur. The data collected can also be used to reflect on general categories of materials. For a series of board products (no wire insulation was tested), FR polyamide, non-FR polybutylene terephthalate, and unsaturated polyester gave results of > 600 V. FR polybutylene terephthalate and polycarbonate were ca. 225 V, while phenolic laminate gave ca. 175 V.

MIL-STD-2223

This military standard[444] contains two test methods used by the military for testing of arc-tracking propensity of wires and cables. Test Method 3006 for wet-arc tracking is similar to Section 27 of ASTM D 3032, while Test Method 3007 follows Section 26 of ASTM D 3032 for dry-arc tracking.

UL TESTS

For rating arc-tracking and arc-ignition performance of plastics, the UL 746A standard[445] refers to ASTM D 495 (for D 495 ratings), D 2303 (for inclined-plane tracking) and D 3638 (for CTI ratings) tests. It also establishes three other tests which are not standardized by ASTM. The High-Voltage Arc-Tracking-Rate test applies 5200 V AC across two electrodes onto the specimen surface. The arc is applied multiple times during 2 minutes, and an arc-tracking rate is computed as the length of track established, divided by 2 min. The numeric results (HVTR ratings) are grouped into 5 PLC categories, ranging from PLC 0 to PLC 4.

The High-Voltage Arc Resistance test uses the same power source as the High-Voltage Arc-Tracking-Rate test, but only applies the arc in a single, fixed location for a maximum time of 300 s. The test result is the time that it takes for ignition to occur. The numeric results (HVAR ratings) are grouped into four PLC categories, ranging from PLC 0 to PLC 3.

Finally, in the High-Current Arc Ignition test (HAI), a fixed copper electrode and a movable stainless steel electrode are connected to a 240 VAC power source and an arc is struck between them at the surface of the test specimen, which is a 12.7 × 127 mm bar. Forty arcs per minute are applied, and the primary measurement is the number of arcs it takes to cause ignition. The performance is grouped into 5 PLC categories, ranging from PLC 0 to PLC 4. Middendorf[446,447] describes some of the practical problems with this test method. The UL 1950 standard[395] utilizes HAI ratings for certain equipment. But more commonly, for circuit voltages less than 600 V, UL end-product standards utilize CTI ratings.

Generally, if the manufacturer cannot provide material which qualifies under one or more of the necessary standards, the option is available to perform whole-device tests. The *End-Product Arc Resistance Test* is described in UL 746C[394].

ELECTRIC SPARK OR ARC IGNITION

BUREAU OF MINES ELECTRIC SPARK METHOD

In the 1940s, the Bureau of Mines developed a test method for ignitability of dust layers using an electric spark source[448]. In the method, a 1.6 mm layer of dust is placed on a steel platen, to which one electrode is connected. The

second electrode is a steel needle which is lowered manually onto the dust layer until a spark discharge occurs. The charging voltage for the capacitor is 400 V. Results are reported as MIE values, similar to normal procedures used for gases.

NORDTEST NT FIRE 016 METHOD

The Nordtest method[449] is conceptually very similar to the Bureau of Mines method. A powder or granular sample fills a chrome-steel specimen cup which is 2 mm deep and 12 mm diameter. The second electrode of the spark circuit comprises an 0.5 mm tungsten wire which is brought to within about 1 mm of the specimen's surface. A standard charging circuit is not prescribed, but Eckhoff[450] has described procedures that are implemented at Christian Michelsen Research. Unlike the Bureau of Mines method, the Nordtest method has primarily been used for pyrotechnics and explosives.

NIST ELECTRIC ARC METHOD

Peacock and Vaishnav[368] designed a test method for testing substances that might be highly prone to electric arc ignition on behalf of CPSC, who have a regulation against "extremely flammable" solids. CPSC regulations do not provide a test method and the NIST development work was intended to provide a regulatory test. The apparatus uses a 10 kV (AC) source to create an arc between two copper electrodes placed 5 mm apart and 3 mm above the specimen surface. Black powder and smokeless powder ignited in about 0.1 s, as did human hair. The head of a safety match ignited in 0.2 s, while common consumer goods such as paper, plastic and rubber took about 0.5 to 1.0 s. The authors recommended that an arc application time of 0.3 s would distinguish between the hazardous substances and the normal ones, but noted that common solids, in general, are more readily ignitable by a match than by a small electric arc. Thus, they questioned the need for a regulation specifically based on electric arc ignitability of consumer goods. CPSC did not adopt the proposed method into regulation.

SMOLDERING

Smoldering ignitions can occur due to self-heating or due to external ignition sources. The ignitability of materials from self-heating is considered in Chapter 9. As far as ignition from external sources, there does not exist any test method suitable for all materials. The primary consumer goods for which external-source smoldering ignitions are problematic are cellulose insulation and articles containing resilient padding; tests for these are given below.

Mintz[451] has proposed that the Setchkin furnace be used for examining the smoldering ignition of materials by monitoring the specimen temperature rise and looking for evidence on an exotherm as a point of inflection on the temperature curve. But a s moldering ignition is evidence of self-heating, so it appears to be more desirable to test by one of the methods presented in Chapter 9, which recognize the role of self-heating, rather than adapting a test method designed for another purpose.

CELLULOSE INSULATION

In the US, the smoldering ignitability of loose-fill cellulose insulation is regulated by CPSC[452]. Functionally, ASTM C 739[453] provides the same testing instructions. As part of this test method, a procedure is described whereby the material is used to fill an open-top box, 200 × 200 mm. A lit cigarette is inserted into the center, and flaming or continued smoldering are monitored. The specimen passes if no flaming occurs and if the mass loss does not exceed 15%.

MATTRESS TESTS

The smoldering potential of mattresses is tested according to CPSC regulations[454]. This is a full-scale test, whereby 18 cigarettes are placed on the test mattress and the extent charring is observed. Nine cigarettes are placed on the bare surface and 9 are placed on a b edsheet-covered mattress and then covered by a s econd cotton sheet. To pass, the charring must not extend more than 51 mm from the cigarette in any direction. For initial screening purposes, a bench-scale test is available as ASTM D 5238[455], however, the latter is restricted to cotton batting, whereas the Federal standard applies to all mattress types, including foam types, some of which are susceptible to smoldering.

BURNING BRAND IGNITION

ASTM E 108 ROOF TEST

In the US, roof coverings are normally tested by ASTM E 108[456]. This method originated at UL shortly after 1900 and comprises five different tests, including two which pertain to ignition: the burning brand test and the flying brand test. In each of the tests, a roof deck is constructed at the end of a wind tunnel, with the wind tunnel blowing onto the deck at a speed of 5.36 m s^{-1} (12 mph). In the burning brand test, which simulates the roof-as-victim scenario, wood cribs are used to simulate a brand which has landed upon the test roof. Roof performance is graded into Classes A, B, and C. The test brand for Class A roofs is a 2 kg, 305 × 305 mm crib; for Class B a 500 g, 152 × 152 mm crib (Color Plate 10); and for Class C twenty 9.25 g, 38 × 38 mm cribs (Color Plate 11). The criteria for the test method are given in the parallel UL standard, UL 790[457]. To pass, no flying brands may be generated from the roof assembly during the burning brand exposure, nor may glowing pieces of the deck fall down, nor may there be sustained flaming underneath the deck, nor may the underlying deck (apart from non-combustible decks) become exposed due to failure of the roof covering. In the flying brand test, which simulates the roof-as-source-of-brands scenario, a l arge gas burner and a wind tunnel apply a wind-blown flame to the top side of the roof. To pass, no glowing or burning particles may be produced by the roof. Studies[458] indicated that the 5.36 m s^{-1} wind speed is rough-

ly optimum—doubling or halving its value decreases the likelihood of test failure. The Class A brand is an exceptionally heavy object with respect to the aerodynamic lift that it could create. Thus, it would be unlikely to become airborne for any significant distance—it might more appropriately be viewed as a burning portion falling from a building. In any case, the Class A requirements are remarkably stringent.

OTHER TYPES OF TESTS

CONVECTIVE HEATING TESTS

No standard tests have been developed in this category, although a number of research studies have been reported (described earlier in this Chapter).

HOT WIRE OR BAR IGNITION TESTS

ASTM D 3874 method[459] uses a Nichrome heating wire which is wrapped around a bar-shaped specimen and heated at a rate of 0.26 W mm^{-1}; the actual temperature of the hot wire is not specified. The test result is the length of time that it took for the specimen to ignite. The early development of the method is described by Schwarz[460]. The statement is given in the ASTM Standard that the results from the test are equivalent to those from the IEC 60695-2-20 standard. Hot wire ignition (HWI ratings) from the test are also used in UL 746A[445], which groups performance into six performance categories, PLC 0 (best) through PLC 5 (worst) according to the ignition time. Test on various plastics using the method have been reported by de Aruajo and Wagner[461]. The ignition time was found to generally increase with increasing thickness of the sample. In several cases, the authors found that their measurements disagreed significantly with the manufacturer's reported PLC category.

In the *ASTM D 6194* 'glow-wire' method[462], a 4 mm Nichrome wire is formed into a tongue shape and is held against the specimen at a single point for 30 s. The variable is the temperature of the wire needed to achieve ignition during a 30 s exposure. The reported glow wire ignition temperature is 25ºC higher than the highest temperature which led to no ignitions of three specimens. GWIT ratings (Glow-Wire Ignition Temperature) described in UL 746A[445] are functionally equivalent, as is the IEC 60695-2-13 test[463]. Compared to the ASTM D 3874, the glow-wire test method has more physical significance, since the temperature measured is in some way characteristic of the material, not just an arbitrary performance index. In the IEC test, traditionally, the only test temperatures used were 550, 650, 750, 850, and 960ºC, although recently the test method also permits temperatures in even-100 units. In principle, the GWIT results could be used for any of a wide variety of purposes. In practice, the tests tend to be used for only one purpose: as a part of a test procedure for approval of electric or electronic equipment. In that context, it is expected that electric faults may occur, that the faults may cause gross overheating of wires, and this condition should not lead to a fire hazard from burning plastic parts inside the equipment. Now, most of the wiring will be in copper, which has a melting point of 1085ºC. Electric faults in equipment which does not have special current-limiting features can be expected to melt wiring and to cause even higher temperatures associated with the post-fusion arc. It might possibly be considered that certain types of arcing will be short enough not to be an ignition hazard, but it seems much harder to claim that electric faults cannot cause wires to reach their melting point temperature. Thus, it seems unduly lax that the IEC recipe permits testing at temperatures as low as 550ºC and does not even encompass testing at 1085ºC.

Although the concepts are generally similar, an unpublished UL study[464] indicated that there is no correlation between the PLC ratings obtained in the HWI test and the temperatures reported in the GWIT.

In the 1981 edition of IEC 707[465] test, which has been withdrawn, the *Schramm-Zebrowski incandescent rod test* was described, wherein a 10 × 125 × 4 mm bar-shaped specimen was held horizontally and a glowing silicon carbide rod pressed into its end. The glowing rod was 8 mm dia. and controlled to a temperature of 955ºC. The results were grouped into three classes, depending on whether the specimen did not ignite, ignited but failed to progress a distance of 100 mm, or else spread beyond that. This method was also issued by ASTM as D 757.

The specialized *bad-connection test* of IEC 60695-2-3[466] is specifically intended to simulate the ignition potential of a faulty electrical connection which is glowing due to abnormally high resistance having been formed (see Chapter 11). Only screw connections are tested with this method. A Nichrome heater wire is inserted into the screw connection for 30 min, and it is observed whether or not the test device ignites.

Glow temperature is sometimes tested for. There is a specific Russian test[467] for this property.

HOT RIVET OR NUT TESTS

A hot rivet or nut, if it falls on a combustible material, might start a fire. This thinking led to an old US Navy test where a hot rivet was used to test latex foams. A British test of this nature still exists, BS 4790[468], which is applicable to the testing of carpets. Tests of this type are relatively mild, since the specimen is always oriented horizontally and the heat flux from the hot object drops to zero in a short distance.

SETCHKIN FURNACE, ASTM D 1929

When empirical determinations of 'ignition temperature' are made, the test method used is usually the Setchkin Furnace, ASTM D 1929[167,469,470]. This test method uses a hot-air furnace (Figure 84) wherein a 3 g specimen is placed

into a cup. The furnace is pre-equilibrated to a desired test temperature, and the ignition temperature is determined by a trial-and-error procedure, narrowing the temperature down to within 10ºC. If autoignition ('spontaneous ignition,' or SIT, in the terminology of the method) is to be determined, no pilot is used; if the test is for piloted ignition ('flash ignition' or FIT), then a small propane gas pilot flame located high above the specimen is used. The ignition/no-ignition determination is made at the moment when 10 min have elapsed after insertion of the specimen. An air flow at a velocity of 0.025 m s^{-1} is provided through the specimen cavity. An identical method is published by ISO as ISO 871[471].

The apparatus was developed by Nicholas Setchkin at the National Bureau of Standards and is a further development of the early apparatus of Prince[5]. The same apparatus is also used in the ASTM E 136 t est for 'non-combustibility'[472]. Early versions of ASTM D 1929 included an alternative rising-temperature method and a trial-and-error procedure for determining the optimum air flow velocity. The latter procedure was abandoned since it was discovered that for most materials the 0.025 m s^{-1} velocity provides close to worst-case results[473].

The temperature reported as the 'ignition temperature' is the one registered by thermocouple T_2, which is in the air space, 10 mm below from the specimen pan. The thermocouple actually placed at the specimen surface, T_1, is used only in the context that the standard states: "Flaming or glowing combustion can also be observed by a rapid rise in temperature T_1, as compared to T_2." For materials that shrink or melt, T_1 will probably end up in the gas phase, above the specimen, once heating has progressed.

Just prior to ignition, a specimen usually undergoes some detectable self-heating, thus there is not a fixed relationship between the specimen temperature and the furnace temperature at the instant of ignition. This is true for both the unpiloted and the piloted modes. Yoshida et al.[474] reported a series of results on electric wire/cable materials. Differences of 20 – 40ºC were common, while differences of up to 70ºC were seen occasionally. Even the sign of the difference was seen to be random. The authors also found that, for temperatures above the minimum required for ignition, $1/t_{ig}$ increased linearly with increasing furnace temperature. The reason for this is not entirely clear, since heat flux is not linearly proportional to temperature. In addition to the standard ASTM procedure, the authors also conducted tests where a spark igniter was installed inside the furnace cavity, a short distance above the specimen. For a set of 9 different materials examined, the average specimen temperature at the flash-ignition point using the D 1929 pilot flame was 382ºC, versus 337ºC when using spark ignition. A 45ºC difference is striking. As discussed earlier in this Chapter, ignition by a flame pilot is normally a more strenuous condition than ignition by a spark. The fact that in the

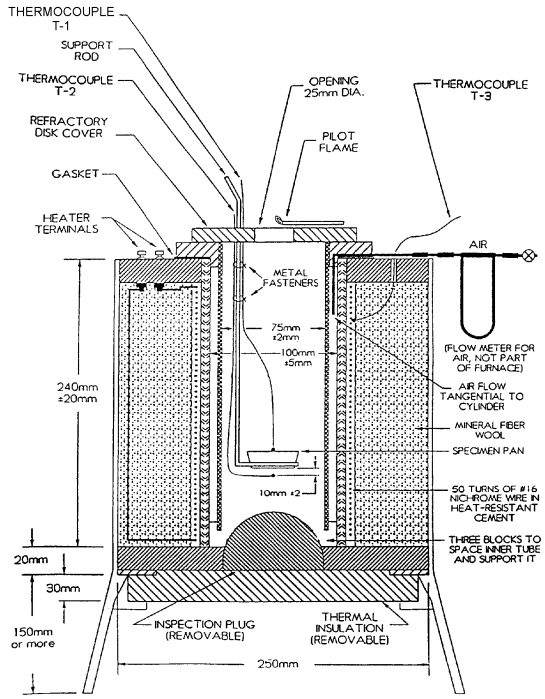


Figure 84 The Setchkin Furnace, ASTM D 1929
(Copyright ASTM International, used by permission)

apparatus a s park igniter is significantly more effective indicates that the pilot flame is very poorly sited. This should not be surprising upon examining the drawing of the test furnace: good practice normally suggests placing a pilot flame close to where combustible gases are being generated, not far downstream. It has been observed[473] that the difference between the autoignition and the piloted ignition temperature, as determined by the standard ASTM D 1929 procedure is generally less than 20ºC. A difference this small again points out the unsatisfactory location for the ignition device in the test apparatus.

Wulff et al.[475] attempted to conduct ignition tests on fabrics in the standard apparatus, but temperature measurements in the vicinity of the specimen indicated unacceptable non-uniformities. They then modified the apparatus by (a) replacing the ceramic cylinder core with one made of steel, which has a much higher thermal conductivity; a nd (b) introducing preheated air into the furnace. It does not appear that any other researchers have considered these particular difficulties of the test method.

Masařík[476] reported on a study using the Czech test method ČSN 64 0149, which is very similar to the Setchkin furnace. He examined three design alternatives for the apparatus:

(1) furnace inner tube: ceramic vs. stainless steel
(2) specimen pan: nickel vs. stainless steel
(3) ignition source: glowing wire vs. pilot flame.

where the underlined alternatives are the ones specified in the Setchkin furnace. Plastics showed little sensitivity to the variables examined. But for wood fiberboard, there were large effects, confounded with reproducibility problems. The piloted ignition temperature obtained ranged from 240 to 380ºC. The combination of nickel specimen pan and glowing wire ignition appeared to cause much higher recorded ignition temperatures in some, but not all laboratories. Since neither of these conditions pertains to the Setchkin furnace, the results suggest that those two variables have been well chosen in the ASTM D 1929 method.

Results of interlaboratory trials ('roundrobins') have been reported on the method. The data (see *Plastics* in Chapter 14) indicate adequate precision, with reproducibility standard deviation of typically 20 – 30ºC. The problem with relying on data from the test method is, thus, not that the reproducibility is poor, but, rather, that the test conditions do not simulate actual fire ignitions very well, and that substantially different results may be obtained in a real end-use environment.

Hilado and Kosola[477] proposed that it makes more sense to measure the air temperature above the specimen, rather than below an impervious specimen pan. They constructed a rig based on a horizontal tube furnace; their results are given in Chapter 15.

LIMITING OXYGEN INDEX (LOI), ASTM D 2863

The oxygen index test, or limiting oxygen index test, ASTM D 2863[478] is commonly used for plastics. The Oxygen Index for a given fuel is defined as:

$$\mathrm{OI} = \frac{X_{O_2}}{X_{O_2} + X_{N_2}}$$

where X denotes the mole (or volume) fraction of a substance. Thus, it is not identical to the oxygen volume fraction X_{O_2}, since the latter is (moles O_2)/(moles total gases), while the OI is (moles O_2)/(moles O_2+N_2). But since the only difference between (moles total gases) and (moles O_2+N_2) is the moles of fuel vapors, and the latter are a small fraction of the total, in fact $\mathrm{OI} \approx X_{O_2}$. The objective of the test is to determine the lowest OI value at which burning (downward flame propagation) can be sustained, thus the test is usually referred to as the limiting oxygen index test.

The concept of LOI testing is based on a plausible, but flawed idea: By testing small cylinders of material in a candle-like configuration, it should be possible to determine whether the material is able or not to sustain burning in an environment of a certain oxygen concentration. The problems with the LOI test are that (1) The results are strongly apparatus-dependent. (2) The apparatus presents a minimally challenging geometry. For example, burning associated with upward flame spread is much more severe than burning in a candle-like geometry. (3) The test is conducted at room temperature. Raising the temperature lowers the oxygen concentration at which burning is sustained, and ignition incidents may occur in connection with overheating of equipment or devices. The test method has also been used for liquids, but it has been shown that the LOI results do not correlate to flash point values[479]. In addition, LOI results for hydrocarbons liquids are typically 15 – 16%, yet limits of flammability testing on these fuels indicate that oxygen must be lowered to around 11 – 14% before upward propagation becomes impossible. Thus, reliance on LOI data would err unconservatively.

Routley[480] and Abbott and Chalabi[481] proposed a heated oxygen index, where the variable reported is a 'temperature index,' defined as the temperature at which the material will burn in air having the ambient oxygen concentration. This is more realistic, since elevated temperatures are common in fire environments, while elevated oxygen levels less so. Nonetheless, the technique fails to overcome the other problems of the LOI test concept.

THERMAL ANALYSIS TESTS

It is occasionally considered that thermal analysis (TGA, DTA, DSC) techniques can be used to determine an ignition temperature of solid materials. Unfortunately, the values of T_{ig} (generally ignition is taken to mean the occurrence of the first significant exotherm) obtained using specimens of a few milligrams exposed to a pre-programmed temperature rise rate in a thermal analysis instrument may not necessarily be related to ignition temperatures of bulk solids igniting under radiant flux or flame-heating exposure. The ignition temperature obtained from such a thermal analysis test will depend on the heating rate of the sample, and there is no particular heating rate that is 'correct.' As an example, for pure cellulose, it was found that the ignition temperature determined in a DTA apparatus[285] increased from 288ºC for a heating rate of 1ºC min^{-1}, to 351ºC when heated at 20ºC min^{-1}. Wharton et al.[231] also documented that the heating rate makes a large difference on the ignition temperatures obtained from DTA tests. For testing in a more realistic scale, as discussed earlier in this chapter, the heat flux does not appreciably affect the T_{ig} for most materials, apart from ones igniting in a glowing mode. On the other hand, Fangrat et al.[88] found a number of instances where the ignition temperature determined in thermal analysis tests was very close to that observed in Cone Calorimeter testing.

Further readings

Vladimir N. Vilyunov and V. E. Zarko, **Ignition of Solids**, Elsevier, Amsterdam (1989). A comprehensive review of the Russian literature on the mathematical theory of ignition of solids.

References

1. Atreya, A., and Wichman, I. S., Heat and Mass Transfer During Piloted Ignition of Cellulosic Solids, *J. Heat Transfer* **111**, 719-725 (1989).
2. Thomson, H. E., Ignition Characteristics of Plastics (Ph.D. dissertation), Univ. Edinburgh, Scotland (1988).
3. Brown, C. R., The Determination of the Ignition Temperatures of Solid Materials (D. Sc. thesis), The Catholic University of America, Washington (1934).
4. Bixel, Edward C., and Moore, Howard J., Are Fires Caused by Steam Pipes? (B. S. thesis), Case School of Applied Science, Pittsburgh (1910).
5. Prince, R. E., Tests on the Inflammability of Untreated Wood and of Wood Treated with Fire-Retarding Compounds, *Proc. NFPA*. **19**, 108-158 (1915).
6. Thomas, P. H., Simms, D. L., and Theobald, C. R., The Interpretation of Some Experimental Data on the Ignition of Wood (FR Note No. 411), Fire Research Station, Borehamwood, UK (1959).
7. Bamford, C. H., Crank, J. and Malan, D. H., The Combustion of Wood. Part I, *Proc. Cambridge Phil. Soc*. **42**, 166-182 (1946).
8. Weatherford, W. D., and Sheppard, D. M., Basic Studies of the Mechanism of Ignition of Cellulosic Materials, pp. 897-910 in *10th Symp. (Intl.) on Combustion*, The Combustion Institute, Pittsburgh (1965).
9. Fons, W. L., Heating and Ignition of Small Wood Cylinders, *Ind. and Eng. Chem.* **42**, 2130-2133 (1950).
10. Buschman, A. J., Ignition of Some Woods Exposed to Low Level Thermal Radiation (NBS Report 7306), NBS (1961).
11. Martin, S. B., Diffusion-Controlled Ignition of Cellulosic Materials by Intense Radiant Energy, pp. 877-896 in *10th Symp. (Intl.) on Combustion*, The Combustion Institute, Pittsburgh (1971).
12. Lawson, D. I., and Simms, D. L., The Ignition of Wood by Radiation, *Brit. J. Appl. Phys.* **3**, 288-292 (1952).
13. Gardon, R., Temperatures Attained in Wood Exposed to High Intensity Thermal Radiation (Ph.D. dissertation), Univ. London, England (1959).
14. Kashiwagi, T., Effects of Attenuation of Radiation on Surface Temperature for Radiative Ignition, *Combustion Science and Technology* **20**, 225-234 (1979).
15. Kashiwagi, T., Experimental Observation of Radiative Ignition Mechanisms, *Combustion and Flame* **34**, 231-244 (1979).
16. Miller, B., Martin, J. R., and Meiser, C. H., jr., The Autoignition of Polymers, *J. Applied Polymer Science* **17**, 629-642 (1973).
17. Cordova, J. L., Walther, D. C., Torero, J. L., and Fernandez-Pello, A. C., Oxidizer Flow Effects on the Flammability of Solid Combustibles, *Combustion Science and Technology* **164**, 253-278 (2001).
18. Kokkala, M., Heat Transfer to and Ignition of Ceiling by an Impinging Diffusion Flame (Research Reports 586), Valtion Teknillinen Tutkimuskeskus, Espoo, Finland (1989).
19. Li, Y., and Drysdale, D., Measurement of the Ignition Temperature of Wood, pp. 380-385 in *Fire Science and Technology—Proc. First Asian Conf.*, Intl. Academic Publishers, Beijing (1992).
20. Atreya, A., and Abu-Zaid, M., Effect of Environmental Variables on Piloted Ignition, pp. 177-186 in *Fire Safety Science—Proc. Third Intl. Symp.*, Elsevier Applied Science, London (1991).
21. Moghtaderi, B., Novozhilov, V., Fletcher, D. F., and Kent, J. H., A New Correlation for Bench-scale Piloted Ignition Data of Wood, *Fire Safety J.* **29**, 41-59 (1997).
22. Tewarson, A., Experimental Evaluation of Flammability Parameters of Polymeric Materials, pp. 97-153 in **Flame Retardant Polymeric Materials**, vol. 3, M. Lewin, et al., eds., Plenum Press, New York (1982).
23. Kashiwagi, T., and Omori, A., Effects of Thermal Stability and Melt Viscosity of Thermoplastics on Piloted Ignition, pp. 1329-1338 in *22nd Symp. (Intl.) on Combustion*, The Combustion Institute, Pittsburgh (1988).
24. Staggs, J. E. J., Ignition of Char-forming Polymers at a Critical Mass Flux, *Polymer Degradation and Stability* **74**, 433-439 (2001).
25. de Ris, J. L., and Khan, M. M., A Sample Holder for Determining Material Properties, *Fire and Materials* **24**, 219-226 (2000).
26. Melinek, S. J., Ignition Behaviour of Heated Wood Surfaces (FR Note 755), Fire Research Station, Borehamwood, England (1969).
27. Alvares, N. J., and Martin, S. B., Mechanisms of Ignition of Thermally Irradiated Cellulose, pp. 905-914 in *13th Symp. (Intl.) on Combustion*, The Combustion Institute, Pittsburgh (1970).
28. Kanury, A. M., Ignition of Cellulosic Solids: Minimum Pyrolysate Mass Flux Criterion, *Combustion Science and Technology* **16**, 89 (1977).
29. Thomson, H. E., and Drysdale, D. D., Flammability of Plastics. II. Critical Mass Flux at the Firepoint. *Fire Safety J.* **14**, 179-188 (1989).
30. Tewarson, A., Lee, J. L., and Pion, R. F., Categorization of Cable Flammability. Part 1: Laboratory Evaluation of Cable Flammability Parameters (EPRI NP-1200 Part 1). Electric Power Research Institute, Palo Alto (1979).
31. Deepak, D., and Drysdale, D. D., Flammability of Solids: An Apparatus to Measure the Critical Mass Flux at the Firepoint, *Fire Safety J.* **5**, 167-169 (1983).
32. Rasbash, D. J., Drysdale, D. D., and Deepak, D., Critical Heat and Mass Transfer at Pilot Ignition and Extinction of Material, *Fire Safety J.* **10**, 1-10 (1986).
33. Hansen, A. S., and Hovde, P. J., Prediction of Time to Flashover in the ISO 9705 Room Corner Test based on Cone Calorimeter Test Results, *Fire and Materials* **26**, 77-86 (2002).
34. Kokkala, M., and Baroudi, D., A Thermal Model for Upward Flame Spread on a Combustible Wall (Raportti A.2), Valtion Teknillinen Tutkimuskeskus, Espoo, Finland (1993).
35. Alpert, R. A., and Khan, M. M., Rating Product Components as Noncombustible, pp. 555-565 in *Interflam 2001—Proc. 9th Intl. Conf.*, Interscience Communications Ltd., London (2001).
36. Graf, S. H., Ignition Temperatures of Various Papers, Woods, and Fabrics (Oregon State College Bull. 26), Oregon State College, Corvallis (March 1949).

37. Babrauskas, V., Ignition of Wood: A Review of the State of the Art, pp. 71-88 in *Interflam 2001—Proc. 9th Intl. Conf.*, Interscience Communications Ltd., London (2001).
38. Simms, D. L., Ignition of Cellulosic Materials by Radiation, *Combustion and Flame* **4**, 293-300 (1960).
39. Alvares, N. J., Blackshear, P. L., and Kanury, A. M., The Influence of Free Convection on the Ignition of Vertical Cellulosic Panels by Thermal Radiation, *Combustion Science and Technology* **1**, 407-413 (1970).
40. Deverall, L. I., and Lai, W., A Criterion for Thermal Ignition of Cellulosic Materials, *Combustion and Flame* **13**, 8-12 (1969).
41. Bradley, H. H., jr., Theory of Ignition of a Reactive Solid by Constant Energy Flux, *Combustion Science and Technology* **2**, 11-20 (1970).
42. Kulkarni, A. K., Kumar, M., and Kuo, K. K., Review of Solid-Propellant Ignition Studies, AIAA Paper 80-1210, AIAA, New York (1980).
43. Yoshizawa, Y., and Kubota, H., Experimental Study on Gas-Phase Ignition of Cellulose under Thermal Radiation, pp. 787-795 in *19th Symp. (Intl.) on Combustion*, The Combustion Institute, Pittsburgh (1982).
44. Durbetaki, P., Tingle, W. J., Ryszytiwskyj, W. P., and Tincher, W. C., Self-Ignition of Pyrolyzate-Air Mixtures, *Fire Research* **1**, 243-254 (1977/78).
45. Bukovec, P., and Urbas, J., Use of Bench Scale Methods to Predict Room Fire Growth (Status report for the period from 9/1/1990 to 8/31/1991). Dept. of Chemistry and Chemical Technology, Univ. Ljubljana, Ljubljana, Yugoslavia (1991).
46. Long, R. T. jr., Torero, J. L., Quintiere, J. G., and Fernandez-Pello, A. C., Scale and Transport Considerations on Piloted Ignition of PMMA, pp. 567-578 in *Fire Safety Science—Proc. 6th Intl. Symp.*, Intl. Assn. for Fire Safety Science (2000).
47. Baillet, C., Delfosse, L., and Lucquin, M., On the Cool Flame Self Ignition of Polyolefins, pp. 148-152 in *Combustion Institute European Symposium 1973*, Academic Press, London (1973).
48. Baillet, C., Delfosse, L., and Lucquin, M., Étude de phénomène pulsatoire periodique observe au cours de la reaction de certains polymères fondus avec l'oxygene. III. Cas des copolymères ethylene-propylene et autres polyolefines, *European Polymer J.* **17**, 791-795 (1981).
49. Atreya, A., Ignition of Fires, *Phil. Trans. Royal Soc. London* **A356**, 2787-2813 (1998).
50. Tzeng, L.-S., Theoretical Investigation of Piloted Ignition of Wood (Ph.D. Dissertation), Michigan State University, East Lansing MI (1990).
51. Kashiwagi, T., A Radiative Ignition Model of a Solid Fuel, *Combustion Science and Technology* **8**, 225-236 (1974); also **14**, 119-122 (1976).
52. Atreya, A., Wichman, I. S., Tzeng, L. S., Abu-Zaid, M., Effect of Water on Piloted Ignition of Cellulosic Materials (NIST-GCR-88-552), NIST (1988).
53. Gandhi, P. D., and Kanury, A. M., Thresholds for Spontaneous Ignition of Solids Exposed to Radiant Heating, *Combustion Science and Technology* **57**, 113-128 (1988).
54. Amos, B., and Fernandez-Pello, A. C., Model of Ignition and Flame Development on a Vaporizing Combustible Surface in a Stagnation Point Flow: Ignition by Vapor Fuel Radiation Absorption, *Combustion Science and T echnology* **62**, 331-343 (1988).
55. Tsai, T.-H., Li, M.-J., Shih, I-Y., Jih, R., and Wong, S.-C., Experimental and Numerical Study of Autoignition and Pilot Ignition of PMMA Plates in a Cone Calorimeter, *Combustion and Flame* **124**, 466-480 (2001).
56. Yuen, R. K.-K., Pyrolysis and Combustion of Wood in a Cone Calorimeter (Ph.D. dissertation), The University of New South Wales, Australia (1998).
57. Yuen, R., Casey, R., de Vahl Davis, G., Leonardi, E., Yeoh, G. H., Chandrasekaran, V., and Grubits, S., Prediction of Piloted Ignition and Combustion of Wood, *Symp. on Thermal Science and Engineering in Honor of Chancellor Chang-Lin Tien*, Univ. California, Berkeley (1995).
58. Nelson, M. I., Brindley, J., and McIntosh, A., A Mathematical Model of Ignition in the Cone Calorimeter, *Combustion Science and Technology* **104**, 33-54 (1995).
59. Nelson, M. I., Ignition Mechanisms of Thermally Thin Thermoplastics in the Cone Calorimeter, *Proc. Royal Soc. (London)* **A454**, 789-814 (1998).
60. Nakamura, Y., Yamashita, H., Takeno, T., and Kushida, G., Effects of Gravity and Ambient Oxygen on a Gas-Phase Ignition over a Heated Solid Fuel, *Combustion and Flame* **120**, 34-48 (2000).
61. Thomas, P. H., and Simms, D. L., Thermal Damage to Solids by Radiation and Chemical Decomposition (FR Note 331), Fire Research Station, Borehamwood, England (1958).
62. Atreya, A., Pyrolysis, Ignition and Fire Spread on Horizontal Surfaces of Wood (Ph.D. dissertation), Harvard Univ., Cambridge MA (1983).
63. Panagiotou, T., and Delichatsios, M. A., A Numerical Solution for the Surface Temperature Rise History of a Material Including Surface Reradiation Losses (FMRC J.I. 0Q0J1.BU), Factory Mutual Research Corp., Norwood MA (1989).
64. Simms, D. L., On the Pilot Ignition of Wood By Radiation, *Combustion and Flame* **7**, 253-261 (1963).
65. Simms, D. L., Comment on "A Radiative Ignition Model of a Solid Fuel," *Combustion Science and Technology* **14**, 119-120 (1976).
66. Quintiere, J. G., and Harkleroad, M. F., New Concepts for Measuring Flame Spread Properties (NBSIR 84-2943), NBS (1984).
67. Abu-Zaid, M., Effect of Water on Ignition of Cellulosic Materials (Ph.D. thesis), Michigan State Univ., East Lansing MI (1988).
68. Smith, E. E., and Satija, S., Release Rate Model for Developing Fires, *ASME J. Heat Transfer* **105**, 282-287 (1983).
69. Mitler, H. E., and Walton, G., A Computer Model of the Smoldering Ignition of Furniture (NISTIR 4973), NIST (1992).
70. Silcock, G. W. H., and Shields, T. J., A Protocol for Analysis of Time-to-Ignition Data from Bench-scale Tests, *Fire Safety J.* **24**, 75-95 (1995).
71. Hallman, J. R., Ignition Characteristics of Plastics and Rubber (Ph.D. dissertation), Univ. Oklahoma, Norman (1971).
72. Tewarson, A., Generation of Heat and Chemical Compounds in Fires, pp. 3-53 to 3-124 in **SFPE Handbook of Fire Protection Engineering**, 2nd ed., NFPA (1995).
73. Koohyar, A. N., Ignition of Wood by Flame Radiation (Ph.D. dissertation), Univ. Oklahoma, Norman (1967).

74. Keller, J. A., Baer, A. D., and Ryan, N. W., Ignition of Ammonium Perchlorate Composite Propellants by Convective Heating, *AIAA J.* **4**, 1358-1365 (1966).
75. Janssens, M. L., Fundamental Thermophysical Characteristics of Wood and Their Role in Enclosure Fire Growth (Ph. D. dissertation), Univ. Gent, Belgium (1991).
76. Janssens, M., Piloted Ignition of Wood: A Review, *Fire and Materials* **15**, 151-167 (1991).
77. Janssens, M. L., Improved Method of Analysis for the LIFT Apparatus. Part 1. Ignition, pp. 37-46 in *Proc. 2nd Fire and Materials Conf.,* Interscience Communications Ltd, London (1993).
78. Green, A. R., Apte, V. B., and Bilger, R. W., Flame Spread along Horizontal Conveyor Systems, pp. 127-137 in *Proc. of the 23rd Intl. Conf. of Safety in Mines Research Institutes*, Bureau of Mines, Washington (1989).
79. Grant, G. B., and Drysdale, D. D., The Use of Ignitability Data from the Cone Calorimeter to predict T_{ig}, the Surface Temperature at Ignition for Cellulosic Packaging Materials, pp. 35-63 in *Industrial Fires: Workshop Proceedings* (EUR 15340 EN). Published for the Commission of the EC, Apeldoorn, Netherlands (1993).
80. Shields, T. J., Silcock, G. W., and Murray, J. J., Evaluating Ignition Data Using the Flux Time Product, *Fire and Materials* **18**, 243-254 (1994).
81. Janssens, M. L., Dillon, S. E., and Allwein, S., Characterizing the Thermal Environment of the Cone Calorimeter for Analyzing Ignition Data of Materials, pp. 125-135 in *Interflam 2001—Proc. 9th Intl. Conf.*, Interscience Communications Ltd., London (2001).
82. Janssens, M. L., and Dillon, S. E., Predictions Based on Quintiere's Model of ISO 9705 Room Fire Test Performance of Marine Composites (SwRI Project No. 01-2854-001), prepared for US Coast Guard, Southwest Research Institute, San Antonio TX (1999).
83. Janssens, M. L., Kimble, J., and Murphy D., Computer Tools to Determine Material Properties for Fire Growth Modeling from Cone Calorimeter Data, *Fire and Materials 2003*, Interscience Communications Ltd., London (2003).
84. Dietenberger, M. A., Protocol for Ignitability, Lateral Flame Spread, and Heat Release Rate Using Lift Apparatus, pp. 435-449 in *Fire and Polymers II: Materials and Tests for Hazard Prevention* (ACS Symp. Series 599), G. L. Nelson, ed., American Chemical Society, Washington (1995).
85. Öziçik, N., **Heat Conduction**, John Wiley & Sons, New York (1980).
86. Baroudi, D., private communication (1994).
87. Nicolette, V. F., and Nowlen, S. P., A Critical Look at Nuclear Qualified Electrical Cable Insulation Ignition and Damage Thresholds (SAND-88-2161C). Sandia National Laboratories, Albuquerque NM (1988).
88. Fangrat, J., Hasemi, Y., Yoshida, M., and Hirata, T., Surface Temperature at Ignition of Wooden Based Slabs, *Fire Safety J.* **27**, 249-259 (1996); **28**, 379-380 (1997).
89. North, G. A., An Analytical Model for Vertical Flame Spread on Solids: An Initial Investigation (Fire Engineering Research Report 99/12), School of Engineering, Univ. Canterbury, Christchurch, New Zealand (1999).
90. Delichatsios, M. A., Panagiotou, Th., and Kiley, F., The Use of Time to Ignition Data for Characterizing the Thermal Inertia and the Minimum (Critical) Heat Flux for Ignition or Pyrolysis, *Combustion and Flame* **84**, 323-332 (1991).
91. Simms, D. L., Damage to Cellulosic Solids by Thermal Radiation, *Combustion and Flame* **6**, 303-318 (1962).
92. Martin, S. B., and Alvares, N. J., Ignition Thresholds for Large-yield Nuclear Weapons (USNRDL/TR-1007), Naval Radiological Defense Laboratory, San Francisco (1966).
93. Rangaprasad, N., The Piloted Ignition of Thin Materials (Ph.D. dissertation), Univ. Oklahoma, Norman (1972).
94. Hilado, C. J., and Brauer, D. P., Effect of Construction, Substrate, and Piloting on Ignitability of Furniture Upholstery Fabrics, *J. Fire and Flammability* **10**, 26-40 (1979).
95. Babrauskas, V., and Wetterlund, I., Comparative Data from LIFT and Cone Calorimeter Tests on 6 Products, Including Flame Flux Measurements (SP Report 1999:14), Swedish National Testing and Research Institute, Borås (1999).
96. Thomson, H. E., and Drysdale, D. D., Flammability of Plastics. I. Ignition Temperature, *Fire and Materials* **11**, 163-172 (1987).
97. Thomson, H. E., and Drysdale, D. D., Piloted Ignition of Plastics, pp. 151-164 in **Fundamental Aspects of Polymer Flammability**, G. Cox and G. Stevens, eds., The Institute of Physics, London (1987).
98. Daikoku, M., and Saito, K., Measurement of Thermophysical Properties of PMMA and Cellulose, pp. 137-146 in *Proc. Fire and Materials '98 Conf.*, Interscience Communications Ltd., London (1998).
99. Dembsey, N. A., and Jacoby, D. J., Evaluation of Common Ignition Models for Use with Marine Cored Composites, *Fire and Materials* **24**, 91-100 (2000).
100. Dusinberre, G. M., **Heat Transfer by Finite Difference Methods**, Wiley, New York (1961).
101. Babrauskas, V., and Parker, W. J., Ignitability Measurements with the Cone Calorimeter, *Fire and Materials* **11**, 31-43 (1987).
102. Ngu, C. K., Ignition Properties of New Zealand Timber (Report 2001/5), Dept. of Civil Engineering, Univ. Canterbury, Christchurch, New Zealand (2001).
103. Mikkola, E., and Wichman, I. S., On the Thermal Ignition of Combustible Materials, *Fire and Materials* **14**, 87-96 (1989).
104. Wesson, H. R., The Piloted Ignition of Wood by Radiant Heat (D. Eng. dissertation), Univ. Oklahoma, Norman (1970).
105. Wesson, H. R., Welker, J. R., and Sliepcevich, C. M., The Piloted Ignition of Wood by Thermal Radiation, *Comb. and Flame* **16**, 303-310 (1971).
106. Kim, A., and Onno, R., Evaluating the Fire Hazard of Lining Materials Using the OSU, Cone Calorimeter and Full-Scale Fire Test Methods (Internal Report No. 625), Natl. Research Council, Ottawa (1992).
107. Mikkola, E., Puupinnan syttyminen [Ignition of Wood Surface] (Research Notes 1057), Valtion Teknillinen Tutkimuskeskus, Espoo, Finland (1989).
108. Paul, K. T., Cone Calorimeter: Initial Experiences of Calibration and Use, *Fire Safety J.* **22**, 67-87 (1994).
109. Whiteley, R. H., Elliot, P. J., and Staggs, J. E., Steady State Analysis of Cone Calorimeter Data, pp. 71-78 in *Flame Retardants '96*, Interscience Communications Ltd., London (1996).
110. Jacoby, D. J., Ignition Characteristics of Marine Cored Composites: Effect of Skin Thickness and Core Composi-

tion (M.S. thesis), Worcester Polytechnic Institute, Worcester MA (1998).
111. Grenier, A. T., Dembsey, N. A., and Barnett, J. R., Fire Characteristics of Cored Composite Materials for Marine Use, *Fire Safety J.* **30**, 137-159 (1998).
112. Grenier, A. T., and Janssens, M. L., An Improved Method for Analyzing Ignition Data of Composites, pp. 253-264 in *Proc. 23rd Intl. Conf. on Fire Safety*, Product Safety Corp., Sissonville WV (1997).
113. Martin, S. B., Ignition-Ablation Responses of Cellulosic Materials to High Radiant Heat Loads, *Pyrodynamics* **2**, 145-150 (1965).
114. Mutoh, N., Hirano, T., and Akita, K., Experimental Study on Radiative Ignition of Polymethylmethacrylate, pp. 1183-1190 in *17th Symp. (Intl.) on Combustion*, The Combustion Institute, Pittsburgh (1978).
115. Kashiwagi, T., Effects of Orientation of Sample on Radiative Ignition of Combustible Solids, pp 6-1 to 6-3 in Eastern States Section, Combustion Institute 1978 Fall Technical Meeting, Miami Beach FL (1978).
116. Averson, A. E., et al., Effect of Orientation on the Inflammation of PMMA by Laser Radiation, *Combustion, Explosions, and Shock Waves* **21**, 57-59 (1985).
117. Kashiwagi, T., Effects of Sample Orientation on Radiative Ignition, *Combustion and Flame* **44**, 223-245 (1982).
118. Glinka, W., Klemens, R., and Wolański, P., Radiative Ignition of Dust Layer, *Archivum Combustionis* **13**, 149-161 (1993).
119. Hertzberg, M., and Zlochower, I. A., Devolatilization Wave Structures and Temperatures for the Pyrolysis of Polymethylmethacrylate, Ammonium Perchlorate, and Coal at Combustion Level Heat Fluxes, *Combustion and Flame* **84**, 15-37 (1991).
120. Kashiwagi, T., Letter to the Editor: Flammability of Plastics I: Ignition Temperatures, *Fire and Materials* **12**, 141-142 (1988).
121. Drysdale, D., and Thomson, H., Letter to the Editor, *Fire and Materials* **12**, 142 (1988).
122. Niioka, T., Takahashi, M., and Izumikawa, M., Gas-phase Ignition of a Solid Fuel in a Hot Stagnation-point Flow, pp. 741-747 in *18th Symp. (Intl.) on Combustion*, The Combustion Institute, Pittsburgh (1980).
123. Wang, G.-G., and Yang, J. T., Convective Thermal Ignition of an Individual Polymethylmethacrylate Particle, *J. Thermophysics and Heat Transfer* **6**, 333-340 (1992).
124. Di Blasi, C., Portoricco, G., Borrelli, M., and Branca, C., Oxidative Degradation and Ignition of Loose-Packed Straw Beds, *Fuel* **78**, 1591-1598 (1999).
125. Akita, K., Ignition of Polymers and Flame Propagation on Polymer Surfaces, pp. 501-525 in H. H. G. Jellinek, **Aspects of Degradation and Stabilization of Polymers**, Elsevier, Amsterdam (1978).
126. Clark, F. R. S., Ignition of Polymethylmethacrylate Slabs by a Small Flame, *J. Polymer Science,* Polymer Chemistry Ed. **21**, 2323-2334 (1983).
127. Clark, F. R. S., Ignition of Low-Density Polyethylene Slabs by a Small Flame, *J. Polymer Science,* Polymer Chemistry Ed. **21**, 3225-3232 (1983).
128. Clark, F. R. S., The Role of Oxygen in the Ignition of Polystyrene by a Small Flame, *J. Polymer Science,* Polymer Chemistry Ed. **22**, 263-268 (1984).
129. Incropera, F. P., and DeWitt, D. P., **Fundamentals of Heat and Mass Transfer**, 4th ed., John Wiley, New York (1996).
130. Hicks, B. L., Theory of Ignition Considered as a Thermal Reaction, *J. Chem. Phys.* **22**, 414-429 (1954).
131. Lisitskii, V. I., and Merzhanov, A. G., Ignition of Condensed Substances by a Stream of Hot Gas, *Combustion, Explosion and Shock Waves* **1**, 45-52 (1965).
132. Kashiwagi, T., MacDonald, B. W., Isoda, H., and Summerfield, M., Ignition of a Solid Polymeric Fuel in a Hot Oxidizing gas Stream, pp. 1073-1086 in *13th Symp. (Intl.) on Combustion*, The Combustion Institute, Pittsburgh (1970).
133. Kashigawi, T., and Summerfield, M., Ignition and Flame Spreading over a Solid Fuel: Non-similar Theory for a Hot Oxidizing Boundary Layer, pp. 1235-1247 in *14th Symp. (Intl.) on Combustion*, The Combustion Institute, Pittsburgh (1972).
134. Cordova, J. L., August, M., and Fernandez-Pello, A. C., Auto-ignition of a Flat Solid Fuel in a High Temperature Oxidizer Boundary Layer Flow, *Combustion Science and Technology* **113/4**, 573-595 (1996).
135. Coffin, D. B., Effects of Turbulence on Radiation Induced Ignition of Solid Fuels (Ph.D. dissertation), Georgia Inst. of Technology, Atlanta (1999).
136. Hermance, C. E., Shinnar, R., and Summerfield, M., Ignition of an Evaporating Fuel in a Hot Oxidizing Gas, Including the Effect of Heat Feedback, *Astronautica Acta* **12**, 95-112 (1966).
137. Carslaw, H. S., and Jaeger, J. C., **Conduction of Heat in Solids**, Clarendon Press, Oxford (1959).
138. Steward, F. R., Ignition Characteristics of Cellulosic Materials, Fall 1971 Meeting, Eastern States Section, The Combustion Institute, Waterloo (1971).
139. Liñán, A., and Williams, F. A., Theory of Ignition of a Reactive Solid by a Constant Energy Flux, *Combustion Science and Technology* **3**, 91-98 (1971).
140. Liñán, A., and Williams, F. A., **Fundamental Aspects of Combustion**, Oxford University Press, Oxford (1993).
141. Harrach, R. J., Estimates on the Ignition of High Explosives by Laser Pulses, *J. Appl. Phys.* **47**, 2473-2483 (1976).
142. Andersen, W. H., Theory of Surface Ignition with Application to Cellulose, Explosives and Propellants, *Combustion Science and Technology* **2**, 213-221 (1970).
143. Staggs, J. E. J., A Theoretical Investigation into Modelling Thermal Degradation of Solids Incorporating Finite-rate Kinetics, *Combustion Science and Technology* **123**, 261-285 (1997).
144. Staggs, J. E. J., A Theory for Quasi-steady Single-step Thermal Degradation of Polymers, *Fire and Materials* **22**, 109-118 (1998).
145. Thomas, P.H., On the Surface Ignition of Self-heating Materials, *Combustion Science and Technology* **36**, 263-283 (1984).
146. Adler, J., and Thorne, P. F., Ignition/Extinction Criteria for Combustible Solid Surfaces, pp. 127-149 in Proc. Joint One Day Meeting, Combustion Physics Group/Polymer Physics Group, The Institute of Physics, London (1987).
147. Annamalai, K., and Durbetaki, P., Ignition of Thermally Thin Porous Pyrolyzing Solids under Normally Impinging Flames, *Combustion and Flame* **27**, 253-266 (1976).
148. Watt, S. D., Staggs, J. E. J., McIntosh, A. C., and Brindley, J., A Theoretical Explanation of the Influence of Char For-

mation on the Ignition of Polymers, *Fire Safety J.* **36**, 421-436 (2001).
149. Cook, G. B., Some Developments in the Theory of Thermal Explosions, pp. 626-631 in *6th Symp. (Intl.) on Combustion*, Reinhold, New York (1956).
150. Merzhanov, A. G., and Averson, A. E, The Present State of the Thermal Ignition Theory: An Invited Review, *Combustion and Flame* **16**, 89-124 (1971).
151. Boddington, T., Cottrell, A., Laye, P. G., and Singh, M., Times-to-Ignition of Pyrotechnics, *Thermochimica Acta* **106**, 253-261(1986).
152. Liñán, A., and Williams, F. A., Ignition of a Reactive Solid Exposed to a Step in Surface Temperature, *SIAM J. Applied Math.* **36**, 587-603 (1979).
153. Vilyunov, V.N., and Zarko, V.E., **Ignition of Solids**, Elsevier, Amsterdam (1989).
154. Telengator, A. M., Margolis, S. B., and Williams, F. A., Analysis of Ignition of a Porous Energetic Material (SAND98-8546), Sandia Natl. Labs., Albuquerque NM (1998).
155. Telengator, A. M., Margolis, S. B., and Williams, F. A., Ignition Analysis of a Porous Energetic Material—II. Ignition at a Closed Heated End (SAND98-8655), Sandia Natl. Labs., Albuquerque NM (1998).
156. Gardon, R., and Michalik, E. R., Radiant Heating of Transparent Materials (ASME Paper 57-A-51), American Society of Mechanical Engineers, New York (1957).
157. Price, E. W., Bradley, H. H. jr., Dehority, G. L., and Ibiricu, M. M., Theory of Ignition of Solid Propellants, *AIAA J.* **4**, 1153-1181 (1966).
158. Zenin, A. A., Zanotti, C., and Giuliani, P., Obtaining Macrokinetic Characteristics of Propellants by Laser Ignition, pp. 1509-1520 in **Transport Phenomena in Combustion**, vol. 2, S. H. Chen, ed., Taylor & Francis, Washington (1996).
159. Thomas, P.H., Some Conduction Problems in the Heating of Small Areas on Large Solids, *Quart. J. Mech. and Applied Math.* **10**, 482-493 (1957).
160. Taylor, W., Proposed Methods of Fire Testing of Materials Used in the Contents of Buildings (Members Report No. 8), RAPRA, Shawbury, England (1977).
161. Methods of Test for Assessment of the Ignitability of Upholstered Seating by Smouldering and Flaming Ignition Sources (BS 5852), British Standards Institution, London (1990).
162. Zhang, J., Shields, T. J., and Silcock, G. W. H., Fire Hazard Assessment of Polypropylene Wall Linings Subjected to Small Ignition Sources, *J. Fire Sciences* **14**, 67-84 (1996).
163. Federal Trade Commission Complaint on the Flammability of Plastic Products, File No. 732-3040, May 31, 1973.
164. Ohlemiller, T. J., Smoldering Combustion Hazards of Thermal Insulation Materials (NBSIR 81-2350), NBS (1981).
165. Vilyunov, V. N., and Sidonsky, O. B., Theory of Ignition of Condensed Systems by a Glowing Surface, *Doklady Akademii Nauk SSSR.***152**, 131-133 (1963).
166. Gol'dshleger, U. I., Barzykin, V. V., and Ivleva, T. P., Ignition of Condensed Explosives by a Hot Spherical Object, *Combustion, Explosion, and Shock Waves* **9**, 642-647 (1973).
167. Setchkin, N. P., A Method and Apparatus for Determining the Ignition Characteristics of Plastics, *J. Research NBS* **43**, 591-608 (1949).
168. Kuchta, J. M., Furno, A. L., and Martindill, G. H., Flammability of Fabrics and Other Materials in Oxygen-Enriched Atmospheres. Part I. Ignition Temperatures and Flame Spread Rates, *Fire Technology* **5**, 203-216 (1969).
169. Khalturinsky, N. A., Popova, T. V., and Berlin, A. A., Polymer Combustion and Inhibition Mechanisms, *Russian Chemical Reviews* **53**, 326-346 (1984).
170. Widginton, D. W., Some Aspects of Design of Intrinsically Safe Circuits (SMRE Research Report 256), Safety in Mines Research Establishment, Sheffield, England (1968).
171. Priest, D. J., Fire Calorimetry of Flame-retarded Polymers, pp. 279-291 in Fire Resistant Materials: Progress Report (DOT/FAA/AR-97/100), R. E. Lyon, ed., Federal Aviation Administration, Atlantic City NJ (1998).
172. Tuyen, B., Loof, R., and Bhattacharya, S. C., Self-sustained Flaming Combustion and Ignition of Single Wood Pieces in Quiescent Air, *Combustion Science and T echnology* **110/111**, 53-65 (1995).
173. Glasstone, S., and Dolan, P. J., **The Effects of Nuclear Weapons**, 3rd ed., US Dept. of Defense and US Dept. of Energy, Washington (1977).
174. Ohlemiller, T. J., Caveny, L. H., DeLuca, L., and Summerfield, M., Dynamic Effects on Ignitability Limits of Solid Propellants Subjected to Radiative Heating, pp. 1297-1307 in *14th Symp. (Intl.) on Combustion*, The Combustion Institute, Pittsburgh (1972).
175. Pantoflíček, J., and Lébr, F., Comments on "Surface Exotherm during Ignition of Ammonium Perchlorate Propellants," *AIAA J.* **6**, 1435-1436 (1968).
176. Babrauskas, V., Specimen Heat Fluxes for Bench-scale Heat Release Rate Testing, *Fire and Materials* **1**9, 243-252 (1995).
177. Rasbash, D. J., Relevance of Fire Point Theory to the Assessment of Fire Behaviour of Combustible Materials, pp. 169-178 in *Intl. Symp.—Fire Safety of Combustible Materials*, Univ. Edinburgh, Edinburgh, Scotland (1975).
178. Janssens, M., Cone Calorimeter Measurements of the Heat of Gasification of Wood, pp. 549-558 in *Interflam '93,* Interscience Communications Ltd., London (1993).
179. Brindley, J., Griffiths, J. F., McIntosh, A. C., and Zhang, J., Initiation of Combustion Waves in Solids and the Effect of Geometry, *J. Australian Math. Soc. Series B* (2000).
180. Lyon, R. E., Solid-State Thermochemistry of Flaming Combustion (DOT/FAA/AR-99/56), Federal Aviation Administration, Atlantic City NJ (1999).
181. Grexa, O., Janssens, M., and White, R., Analysis of Cone Calorimeter Data for Modeling of the Room/Corner Test on Wall Linings, pp. 63-71 in *Proc. 4th Intl. Fire and Materials Conf.*, Interscience Communications Ltd., London (1995).
182. Shorter, J., Burning Rate of Wood Measured in a Cone Calorimeter (B.Eng. thesis). Dept. of Mechanical Engineering, Univ. Sydney, Australia (1993).
183. Hopkins, D. jr., and Quintiere, J. G., Material Fire Properties and Predictions for Thermoplastics, *Fire Safety J.* **26**, 241-268 (1996).
184. Opstad, K., Modelling of Thermal Flame Spread on Solid Surfaces in Large-Scale Fires (Ph.D. dissertation), Norges Tekniske Høgskole, Trondheim, Norway (1995).

185. Jackson, J. L., Direct Measurement of Heat of Gasification for Polymethylmethacrylate (NISTIR 88-3809), NIST (1988).
186. Pickard, R. W., Simms, D. L., and Walters, J. E. L., The Ignition by Radiation of Wood Protected by Some Common Paints (FPE Note No. 61/1951), Fire Research Station, Borehamwood (1951).
187. Simms, D. L., and Hird, D., On the Pilot Ignition of Materials by Radiation (FR Note 365), Fire Research Station, Borehamwood, England (1958).
188. Stockstad, D. S., Modifications and Test Procedures for the Stockstad-Lory Ignition Furnace (Res. Note INT-166), US Forest Service, Intermountain Forest & Range Experiment Station, Ogden UT (1972).
189. Starchville, M., unpublished results, NIST.
190. Wraight, H. G. W., A Note on the Performance of Various Ignition Methods in the ISO Ignitability Test, unpublished note, Fire Research Station.
191. Mikkola, E., Ignitability Comparisons between the ISO Ignitability Test and the Cone Calorimeter, *J. Fire Sciences* **9**, 276-284 (1991).
192. Cain, M. W., An Investigation into the Ignitability Characteristics of Several Common Materials (IR/L/FR/85/10), HSE, Buxton, UK (1985).
193. Harkleroad, M. F., Quintiere, J. G., and Walton, W. D., Radiative Ignition and Opposed Flow Flame Spread Measurements on Materials (DOT/FAA/CT-83/28), Federal Aviation Administration, Atlantic City Airport NJ (1983).
194. Amos, B. T., Ignition and Flame Propagation Studies Over a Flat Fuel Surface (NIST-GCR-92-604), NIST (1992).
195. Shields, T. J., Silcock, G. W., and Murray, J. J., The Effects of Geometry and Ignition Mode on Ignition Times Obtained using a C one Calorimeter, *Fire and Materials* **17**, 25-32 (1993).
196. Moulen, A. W., and Grubits, S., Ignition and Smoke Properties of Building Materials (Technical Record TR 44/153/435), Experimental Building Station, North Ryde, NSW, Australia (1977).
197. Thomson, H. E., and Drysdale, D. D., Effect of Sample Orientation on the Piloted Ignition of PMMA, pp. 35-42 in *Interflam '90*. Interscience Communications Ltd., London (1990).
198. Simms, D. L., Law, M., Hinkley, P. L., and Pickard, R. W., The Effect of Size of Irradiated Area on the Spontaneous Ignition of Materials. Part 1: The Effect on Ignition Time (FR Note 307), Fire Research Station, Borehamwood, England (1957).
199. Hu, X.-F., and Clark, F. R. S., The Use of the ISO/TC92 Test for Ignitability Assessment, *Fire and Materials* **12**, 1-5 (1988).
200. Goldstone, B. M., Hazards from the Concentration of Solar Radiation by Textured Window Glass (BRE Report), Building Research Establishment, Garston, UK (1982).
201. Clark, F. R. S., Radiative Ignition of Thermoplastic and Char-forming Materials, *Fire and Materials* **8**, 196-198 (1984).
202. Nussbaum, R. M., and Östman, B. A.-L., Larger Specimens for Determining Rate of Heat Release in the Cone Calorimeter, *Fire and Materials* **10**, 151-160 (1986).
203. Martin, S. B., and Alvares, N. J., Critical Irradiance for Ignition of Cellulosic Fuels (WSCI-66-23), 1966 Spring Meeting, Western States Section, The Combustion Institute, Pittsburgh (1966).
204. Lullin, A., Recherches sur les températures d'inflammation du bois et sur les enduits ignifuges [Studies on the temperatures of inflammation of wood and on fireproof coatings] (D.Sc. dissertation), Eidgenössischen technischen Hochschule Zürich, Imprimerie Albert Kundig, Genéve (1925).
205. Bowes, P. C., The Determination of the Ignition Temperature of Solids by a Rising Temperature Method (FR Note 10), Fire Research Station, Borehamwood, England (1952).
206. Simms, D. L., Experiments on the Ignition of Cellulosic Materials by Thermal Radiation, *Combustion and Flame* **5**, 369-375 (1961).
207. Muir, W. E., Studies of Fire Spread between Buildings (Ph.D. dissertation), Univ. Saskatchewan, Saskatoon, Canada (1967).
208. Ulrich, R. D., and Butcher, A. G., Post-Ignition Burning of Horizontal Wood Surfaces (NWC TP 5271), Naval Weapons Center, China Lake CA (1971).
209. Bilbao, R., et al., Experimental and Theoretical Study of the Ignition and Smoldering of Wood Including Convective Effects, *Combustion and Flame* **126**, 1363-1372 (2001).
210. Hietaniemi, J., Kallonen, R., and Mikkola, E., Fires at Chemical Warehouses: A Cone Calorimeter Study on t he Burning Characteristics and Fire Effluent Composition of Selected Chemical Compounds (VTT Research Note 1810), Valtion Teknillinen Tutkimuskeskus, Espoo, Finland (1997).
211. Chen, F. F., Radiant Ignition of New Zealand Upholstered Furniture Composites (M.S. thesis), Univ. Canterbury, Christchurch, New Zealand (2001).
212. Cordova, J. L., and Fernandez-Pello, A. C., Convection Effects on t he Endothermic Gasification and Piloted Ignition of a Radiatively Heated Combustible Solid, *Combustion Science and Technology* **156**, 271-289 (2000).
213. Ohlemiller, T. J., Kashiwagi, T., and Werner, K., Wood Gasification at Fire Level Heat Fluxes, *Combustion and Flame* **69**, 155-170 (1987).
214. Petrella, R. V., Assessment of Full-Scale Fire Hazards and Cone Calorimeter Data, *J. Fire Sciences* **12**, 14-43 (1994).
215. Mikkola, E., Effects of Oxygen Concentration on Cone Calorimeter Results, pp. 49-56 in *Interflam '93*, Interscience Communications Ltd., London (1993).
216. Hirsch, D., Haas, J., Hshieh, F.-Y., and Beeson, H., Effect of Oxygen Concentration on Materials' Ignitability and Flammability Using a Controlled-Atmosphere Cone Calorimeter, pp. 227-234 in *Proc. Intl. Conf. on Fire Safety*, Vol. 25, Product Safety Corp., Sissonville WV (1998).
217. Hshieh, F.-Y., Motto, S. E., Hirsch, D. B., and Beeson, H. D., Flammability Testing Using a Controlled-Atmospheres Cone Calorimeter, pp. 299-325 in *18th Intl. Conf. on Fire Safety*, Product Safety Corp., Millbrae, CA (1993).
218. Hshieh, F.-Y., and Buch, R. R., Controlled-Atmosphere Cone Calorimeter, Intermediate-scale Calorimeter, and Cone Corrosimeter Studies of Silicones, pp. 213-239 in *Proc. Intl. Conf. on Fire Safety*, Vol. 23, Product Safety Corp., Sissonville WV (1997).
219. Hshieh, F.-Y., and Beeson, H. D., Evaluation of the Controlled-Atmosphere Cone Calorimeter for Determining Fire Properties of Materials According to NASA Handbook

8060.1C Test 2 (NASA Reference Publication 1345), NASA, Washington (1995).
220. Alvares, N. J., The Effect of Pressure on Ignition by Thermal Radiation (WSCI 66-27), Western States Section, The Combustion Institute, 1966 Spring Mtg. (1966).
221. Ohlemiller, T. J., and Summerfield, M., Radiative Ignition of Polymeric Materials in Oxygen/Nitrogen Mixtures, pp. 1087-1094 in *13th Symp. (Intl.) on Combustion*, The Combustion Institute, Pittsburgh (1970).
222. Beckel, S. A., and Matthews, R. D., Ignition of Polyoxymethylene, *Combustion and Flame* **57**, 71-86 (1984).
223. Prolonged Heating of Wood, pp. 8-11 in *Fire Research 1948*, Dept. of Scientific and Industrial Research and Fire Offices' Committee, London (1949).
224. Moghtaderi, B., Short Communication: Effects of Char Oxidation on Re-ignition Characteristics of Wood-Based Materials, *Fire and Materials* **24**, 303-304 (2000).
225. Paciorek, K. L., Kratzer, R. H., and Kaufman, J., Fundamental Ignition Study for Material Fire Safety Improvement (NASA-CR-114402), NASA, Moffett Field, CA (1971).
226. Delfosse, L., Study of Self-Ignition of PVC, *J. Macromol. Sci.—Chemistry* **A11**, 1491-1501 (1977).
227. Hirsch, D. B., Bunker, R. L., and Janoff, D., Effects of Oxygen Concentration, Diluents, and Pressure on Ignition and Flame-Spread of Nonmetals, pp. 179-190 in *Flammability and Sensitivity of Materials in Oxygen-Enriched Atmospheres: Fifth Volume* (ASTM STP 1111), ASTM (1991).
228. Zabetakis, M.G., Flammability Characteristics of Combustible Gases and Vapors (Bulletin 627), Bureau of Mines, Pittsburgh (1965).
229. Hermance, C. E., Ignition of Polymeric Materials Stimulated by Rapid External Heating, Flammability Characteristics of Polymeric Materials, Polymer Conference Series, College of Engineering, Univ. Utah, Salt Lake City (1971).
230. Kishore, K., and Sankaralingam, S., Effect of Pressure on Polymer Ignition, *J. Fire Sciences* **4**, 94-99 (1986).
231. Wharton, R. K., Nolan, P. F., and Swindells, I., Further Studies of Factors That Affect the Spontaneous Ignition Temperatures of Non-metallic Materials in Gaseous Oxygen, pp. 106-124 in *Flammability and Sensitivity of Materials in Oxygen-Enriched Atmospheres: 4th Volume* (ASTM STP 1040), ASTM (1989).
232. Attwood, H. C., and Allen, G. R., On the Spontaneous Ignition Temperature of Organic Materials in Oxygen (ARC-CP-1172), Royal Aircraft Establishment, Farnborough, UK (1971).
233. Wolf, G. L., McGuire, J. G., Nolan, P. F., and Sidebotham, G. W., Spontaneous Ignition Temperature of Tracheal Tubes, pp. 57-65 in *Flammability and Sensitivity of Materials in Oxygen-Enriched Atmospheres* (ASTM STP 1197), ASTM (1993).
234. Marzani, J. A., Spontaneous Ignition of Solid Materials at Elevated Pressures, presented at Eastern Section (Provisional), The Combustion Institute Symposium on Heterogeneous Combustion (Oct. 1968).
235. Kuzminskii, A. S., Some Urgent Problems in the Ageing and Stabilization of Elastomers. Review. *Polymer Science USSR* **19**, 2509-2523 (1977).
236. Pippen, D. L., and Stradling, J. S., Techniques for Determination of Flash and Fire Points and Impact Sensitivity of Materials in a Gaseous Oxygen Atmosphere, *Materials Research and Standards* **35**, 35-43, 52-53 (June 1971).
237. Bolod'yan, I. A., Denisyuk, A. P., and Zhevlakov, A. F., Critical Conditions of Polymer Combustion at Increased Pressure, *Fizika goreniya i vzryva* **4**, 146-147 (1981).
238. Hirsch, D. B., and Bunker, R. L., Effects of Diluents on Flammability of Nonmetals in High-Pressure Oxygen Mixtures, pp. 74-80 in *Flammability and Sensitivity of Materials in Oxygen-Enriched Atmospheres: 6th Volume* (ASTM STP 1197), ASTM (1993).
239. Benning, M. A., Measurement of Oxygen Index at Elevated Pressures, pp. 68-83 in *Flammability and Sensitivity of Materials in Oxygen-Enriched Atmospheres* (ASTM STP 812), ASTM (1983).
240. Skaar, C., **Water in Wood**, Syracuse Univ. Press, Syracuse NY (1972).
241. Yuen, W. W., Greer, D., Lin, G., and Bryan, C., Modeling of the Transient Ignition of a Nonmetal/Oxygen System by Heterogeneous Reaction: Effects of Oxygen Pressure, pp. 191-205 in *Flammability and Sensitivity of Materials in Oxygen-Enriched Atmospheres: Third Volume* (ASTM STP 986), ASTM (1988).
242. Pirsko, A. R., and Fons, W. L., Frequency of Urban Building Fires as Related to Daily Weather Conditions (Interim Tech. Report 866, Armed Forces Special Weapons Project), California Forest and Range Experiment Station, Berkeley CA (1956).
243. Vick, C. B., Adhesive Bonding of Wood Materials, chapter 9 in **Wood Handbook: Wood as an Engineering Material**, Forest Products Laboratory, Madison WI (1999).
244. Peck, E. C., Moisture Content of Wood in Dwellings (Circular No. 239), Dept. of Agriculture, Washington (1932).
245. Moghtaderi, B., Novozhilov, V., Fletcher, D. F., and Kent, J. H., Mathematical Modelling of the Piloted Ignition of Wet Wood Using the Heat-Balance Integral Method, *J. Applied Fire Science* **6**, 91-107 (1996/97).
246. Pickard, R. W., and Wraight, H., The Effect of Moisture on the Ignition and Flame Propagation of Thin Cellulosic Materials (FR Note 450), Fire Research Station, Borehamwood, England (1961).
247. Duvvuri, M. S., Ignition Characteristics of Wet Wood by Thermal Radiation (M.S. thesis), Univ. Oklahoma, Norman (1970).
248. Moghtaderi, B., Combustion Characteristics of Solid Fuels under Fire Conditions (Ph.D. dissertation), Univ. Sydney, Sydney, Australia (1996).
249. Simms, D.L., and Law, M., The Ignition of Wet and Dry Wood by Radiation, *Combustion and Flame* **11**, 377-388 (1967).
250. Backer, S., Tesoro, G. C., Toong, T. Y., and Moussa, N. A., **Textile Fabric Flammability**, The MIT Press, Cambridge MA (1976).
251. Lupton, E. C., Tahlmore, C. D., and Obsasnik, J., Some Differences Noted in the Flammability of Wire Constructions between Testing at Room Temperature and at Elevated Conductor Temperatures, pp. 1-3 in *Proc. 24th Intl. Wire and Cable Symp.,* US Army Electronic Command, Cherry Hill NJ (1975).
252. Rodak, E. M., Taylor, R. J., Hirsch, D. B., and Linley, L. J., Effects of Sample and Test Variables on Electrical Wire Insulation Flammability, *J. Testing and Evaluation* **22**, 447-450 (1994).
253. Baer, A. D., and Ryan, N. W., Ignition of Composite Propellants by Low Radiant Fluxes, *AIAA J.* **3**, 884-889 (1965).

254. Kimzey, J.H., Flaming during Weightlessness (NASA TM-X-58001), NASA, Washington (1966).
255. Strehlow, R.A., and Reuss, D., Flammability Limits in a Standard Tube, Chapter 3 in **Combustion Experiments in a Zero-gravity Laboratory**, (Vol. 73 in Progress in Astronautics and Aeronautics), T. H. Cochran, ed., AIAA, New York (1981).
256. Kashiwagi, T., and Olson, S. L., Radiative Ignition and Transition to Spread Investigation (RITSI), pp. 97-117 in *Proc. One Year Report, Third U.S. Microgravity Payload*, NASA, Washington (1997).
257. Olson, S. L., and Kashiwagi, T., Three Dimensional Radiative Ignition and Flame Spread over Thin Cellulose Fuels, pp. 67-68 in Annual Conference on Fire Research. Book of Abstracts, K. A. Beall, ed. (NISTIR 6242), NIST (1998).
258. Tewarson, A., and Ogden, S. D., Fire Behavior of Polymethylmethacrylate, *Combustion and Flame* **89**, 237-259 (1992).
259. Moysey, E., and Muir, W., Pilot Ignition of Building Materials by Radiation, *Fire Technology* **4**, 46-50 (1968).
260. Vovelle, C., Akrich, R., and Mellottée, H., Thermal Degradation of Painted Wood: An Experimental Study, *J. Fire Sciences* **1**, 191-199 (1983).
261. Hinkley, P. M., The Effect of Coatings on the Ignition of Fibre Insulating Board by High Temperature Radiation (FR Note 364), Fire Research Station, Borehamwood, UK (1958).
262. Kashiwagi, T., Inaba, A., and Brown, J. E., Differences in PMMA Degradation Characteristics and Their Effects on Its Fire Properties, pp. 483-493 in *Fire Safety Science—Proc. 1st Intl. Symp*., Hemisphere Publishing Corp., Washington (1986).
263. Garg, D. R., and Steward, Pilot Ignition of Cellulosic Materials Containing High Void Spaces, *Combustion and Flame* **17**, 287-294 (1971).
264. Varma, A., and Steward, F. R., Spontaneous Ignition of High Voidage Cellulosic Materials, *J. Fire and Flammability* **1**, 154-165 (1970).
265. Drysdale, D. D., and Thomson, H. E., The Ignitability of Flame Retarded Plastics, pp. 195-204 in *Fire Safety Science—Proc. 4th Intl. Symp.*, Intl. Assn. for Fire Safety Science (1994).
266. Hirschler, M. M., Fire Retardant Activity: Quantitative Comparison of Additives, pp. 195-217 in *Fire Safety and Technology. Turmoil—Progress—Opportunities 1973-2000+. Papers Presented at 1998 Spring Conf.*, Fire Retardant Chemicals Assn., Lancaster PA (1998).
267. Grand, A. F., Interpretation of Results from Cone Calorimeter Testing on Fire Retardant and Fire Resistant Polymers, *11th Annual BCC Conf. on Flame Retardancy: Recent Advances in Flame Retardancy of Polymeric Materials*, Business Communications Co., Norwalk CT (2000).
268. Nelson, M. I., Brindley, J., and McIntosh, A. C., Ignition Properties of Thermally Thin Thermoplastics—The Effectiveness of Inert Additives in Reducing Flammability, *Polymer Degradation and Stability* **54**, 255-267 (1996).
269. Watt, S. D., Staggs, J. E. S., McIntosh, A. C., and Brindley, J., A Theoretical Explanation of the Influence of Char Formation on the Ignition of Polymers, *Fire Safety J.* **36**, 421-436.
270. Cleary, T. G., and Quintiere, J. G., Flammability Characterization of Foam Plastics (NISTIR 4664), NIST (1991).
271. Akita, K., Studies on the Mechanism of Ignition of Wood, *Report of the Fire Research Institute of Japan* **9**, 1-44, 51-54, 77-83, 99-105 (1959).
272. Heskestad, G., Ease of ignition of Fabrics Exposed to Flaming Heat Sources (NTIS No. COM-73-10955), NBS (1973).
273. Thureson, P., and Nilsson, M., Degradation of Fire Properties of Approved Products as a Result of Ageing (SP Report 1994:61), Swedish National Testing and Research Institute, Borås (1994).
274. Simonson, M., Blomqvist, P., Boldizar, A., Möller, K., Rosell, L., Tullin, C., Stripple, H., and Sundqvist, J. O., Fire-LCA Model: TV Case Study, Swedish National Testing and Research Institute, Borås (2000).
275. Josler, W. J., Fire Exposure Protection, Chapter 3 in Demonstration of Biodegradable, Environmentally Safe, Non-Toxic Fire Suppression Liquids (NISTIR 6191), D. Madrzykowski and D. W. Stroup, eds., NIST (1998).
276. Moghtaderi, B., Dlugogorski, B. Z., Kennedy, E. M., and Fletcher, D. F., Effects of the Structural Properties of Solid Fuels on Their Re-ignition Characteristics, *Fire and Materials* **22**, 166-165 (1998).
277. Takahashi, S., Experiments and Theory in the Extinction of a Wood Crib, pp. 1197-1206 in *Fire Safety Science — Proc. 1st Intl. Symp.*, Hemisphere, Washington (1986).
278. Moghtaderi, B., and Poespowati, T., Application of a Surrogate Material in Assessing the Impact of Porosity on Re-ignition of Wood-based Materials, *Fire and Materials*, to be published.
279. Moghtaderi, B., Novozhilov, V., Kent, J. H., Fletcher, D. F., and Apte, V. B., Effect of Water Spray on Re-ignition Characteristics of Solid Fuels, pp. 829-840 in *Fire Safety Science—Proc. 5th Intl. Symp.*, Intl. Assn. for Fire Safety Science (1997).
280. Poespowati, T., Moghtaderi, B., Dlugogorski, B. Z., and Kennedy, E. M., Effects of Porosity on Re-ignition Characteristics of a Surrogate Material, pp. 228-237 in *Fire Science and Technology—Proc. 5th Asia-Oceania Symp.*, Univ. Newcastle, Australia (2001).
281. Wang, Z., Fan, W., Wang, Q., and Yuan, H., Ignitability of Polyvinyl Chloride Materials, pp. 73-79 in *Symp. for '97 FORUM—Applications of Fire Safety Engineering*, Tianjin, China (1997).
282. Tran, H. C., Cohen, J. D., and Chase, R. A., Modeling Ignition of Structures in Wildland/Urban Interface Fires, pp. 253-262 in *Proc. First Intl. Fire and Materials Conf.*, Interscience Communications Ltd, London (1992).
283. Quintiere, J. G., Babrauskas, V., Cooper, L., Harkleroad, M., Steckler, K., and Tewarson, A., The Role of Aircraft Panel Materials in Cabin Fires and Their Properties (DOT/FAA/CT-84/30), Federal Aviation Administration, Atlantic City Airport NJ (1985).
284. Mórotz-Cecei, K., Beda, L., and Simon, J., Flammability Characterized by Flash-Ignition Temperatures, *J. Thermal Analysis* **33**, 343-349 (1988).
285. Davies, D., Horrocks, A. R., and Greenhalgh, M., Ignition Studies on Cotton Cellulose by DTA, *Thermochimica Acta* **63**, 351-362 (1983).
286. Morimoto, T., Mori, T., and Enomoto, S., Ignition Properties of Polymers Evaluated From Ignition Temperature and Ignition Limiting Oxygen Index, *J. Applied Polymer Science* **22**, 1911-1918 (1978).

287. Shoub, H., and Bender, E. W., Radiant Ignition of Wall Finish Materials in a Small Home (NBS 8172), NBS (1964).
288. Bernstein, T., Electrocution and Fires Involving 120/240-V Appliances, *IEEE Trans. Ind. Appl.* **IA-19**, 155-159 (1983).
289. Guide for Fire and Explosion Investigations (NFPA 921), 2001 ed., NFPA (2001).
290. Vieweg, R., ed., **Elektrotechnische Isolierstoffe**, Julius Springer, Berlin (1937).
291. Tentative Method of Test for High-Voltage, Low-Current Arc Resistance of Solid Electrical Insulating Materials (ASTM D 495-48T), ASTM (1948).
292. Yoshimura, N., Nishida, M., and Noto, F., Light Emission from Tracking Discharges on Organic Insulation, *IEEE Trans. on Electrical Insulation* **EI-19**, 149-155 (1984).
293. Choi, C.-S., Kim, H.-R., and Kim, D.-O., A Study on the Electrical Properties of RCD(ELB) Case Deteriorated by Tracking, pp. 275-278 in *APSS2001—Proc. Asia Pacific Symp. on Safety*, Vol. 1, Japan Soc. for Safety Engineering, Yokohama (2001).
294. Dissado, L. A., and Fothergill, J.C., **Electrical Degradation and Breakdown in Polymers**, Peter Peregrinus, London (1992).
295. Olyphant, M. jr., Arc Resistance. I. Tracking Processes in Thermosetting Insulating Materials, *ASTM Bull.* No. 181, 60-67. II. Effect of Testing Conditions on Tracking Properties of Thermosetting Insulating Materials, No. 185, 41-38 (1952).
296. Oba, K., Identification of Melting Marks of Electric Wires (unpublished report), Yamagata Prefecture Police Headquarters, Criminal Scientific Laboratory, Japan (1980).
297. Bernstein, T., Electrical Fires: Causes, Prevention, and Investigation, pp. 116-134 in Greenwald, E.K., ed., **Electrical Hazards and Accidents: Their Cause and Prevention,** Van Nostrand Reinhold, New York (1991).
298. Billings, M. J., Smith, A., and Wilkins, R., Tracking in Polymeric Insulation, *IEEE Trans. on Electrical Insulation* **IE-2**, 131-137 (Dec. 1967).
299. Mandelcorn, L., and Dakin, T. W., Wet Surface Tracking of Insulation: A Differential Test with Controlled Short Discharges to a Water Electrode, *AIEE Trans. Power Apparatus & Systems* **81**:Part 3, 291-298 (1962).
300. Paciorek, K. J. L., Kratzer, R. H., Lee, F. F. C., Nakahara, J. H., Harris, D. H., and Perzak, F. J., Moist Tracking Investigation of Organic Insulating Materials, *IEEE Trans. on Electrical Insulation* **IE-17**, 423-428 (1982).
301. Wilkins, R., and Billings, M. J., Effect of Discharges between Electrodes on the Surface of Organic Insulation, *Proc. IEE* **116**, 1777-1784 (1969).
302. Norman, R. S., and Kessel, A. A., Internal Oxidation Mechanism for Nontracking Organic Insulation, *AIEE Trans.* **77**, 632 (1958).
303. Noto, F., and Kawamura, K., Tracking and Ignition Phenomena of Polyvinyl Chloride Resin under Wet Polluted Conditions, *IEEE Trans. on Electrical Insulation* **EI-13**, 418-425 (1978).
304. Day, A. G., and Stonard, D. J., Creepage and Clearance Distances in Electrical Equipment for Shipboard Use, *IEEE Trans. on Electrical Insulation* **EI-12**, 191-199 (1977).
305. Dini, D. A., Skuggevig, W., Wagner, R., Boden, P. J., and Dubiel, D. G., Report of Research on Arc-Fault Detection Circuit Breakers for National Electrical Manufacturers Association (Project 95NK6832), Underwriters Laboratories Inc., Northbrook IL (1996).
306. Spearpoint, M. J., Predicting the Ignition and Burning Rate of Wood in the Cone Calorimeter Using an Integral Model (NIST GCR 99-775), NIST (1999).
307. Alvares, N. J., and Wiltshire, L. L., Ignition and Fire Spread in a Thermal Radiation Field (USNRDL-TR-68-56), US Naval Radiological Defense Lab., San Francisco (1968).
308. Glinka, W., Klemens, R., and Wolański, P., Experimental and Theoretical Studies on Radiative Ignition of Dust Layer, *14th Intl. Colloquium on Dynamics of Explosions and Reactive Systems*, Univ. Coimbra, Portugal (1993).
309. Descamps, J. M., Delfosse, L., and Lucquin, M., An Application of the Self-Ignition Method of Polymers: Anti-smoke Additive Induced Glowing Effect in the Combustion of Poly(vinylchloride), *Fire and Materials* **4**, 37-41 (1980).
310. Lengellé, G., Bizot, A., Duterque, J., and Amiot, J.-C., Ignition of Solid Propellants, *La Recherche Aérospatiale—English Edition*, No.2, 1-20 (1991).
311. Suuberg, E. M., Wójtowicz, M., and Calo, J. M., Reaction Order for Low Temperature Oxidation of Carbons, pp. 79-87 in *22nd Symp. (Intl.) on Combustion*, The Combustion Institute, Pittsburgh (1988).
312. Hurt, R. H., and Calo, J. M., Semi-Global Intrinsic Kinetics for Char Combustion Modeling, *Combustion and Flame* **125**, 1138-1149 (2001).
313. Ohlemiller, T. J., and Rogers, F. E., A Survey of Several Factors Influencing Smoldering Combustion in Flexible and Rigid Polymer Foams, *J. Fire and Flammability* **9**, 489-509 (1978).
314. Cohen, L., and Luft, N. W., Combustion of Dust Layers in Still Air, *Fuel* **34**, 154-163 (1955).
315. Miron, Y., and Lazzara, Hot-Surface Ignition Temperatures of Dust Layers, *Fire and Materials* **12**, 115-126 (1988).
316. Sato, K., Smoldering Combustion of Cellulosic Materials, *'93 Asian Fire Seminar*, Science University of Tokyo (1993).
317. Ohlemiller, T. J., and Lucca, D. A., An Experimental Comparison of Forward and Reverse Smolder Propagation in Permeable Fuel Beds, *Combustion and Flame* **54**, 131-147 (1983).
318. Walther, D. C., Anthenien, R. A., and Fernandez-Pello, A. C., Smolder Ignition of Polyurethane Foam: Effect of Oxygen Concentration, *Fire Safety J.* **34**, 343-359 (2000).
319. Kellogg, D. S., Waymack, B. E., McRae, D. D., Chen, P., and Dwyer, R. W., Initiation of Smoldering Combustion in Cellulosic Fabrics, *J. Fire Sciences* **16**, 90-104 (1998).
320. Anderson, M. K., Sleight, R. T., and Torero, J. L., Downward Smolder of Polyurethane Foam: Ignition Signatures, *Fire Safety J.* **35**, 131-147 (2000).
321. Honeycutt, R. H., The Effect of Low Level Air Flow on Smoldering Ignition of Soft Furnishings by Cigarette Prototypes, pp. 135-143 in *Proc. 4th Intl. Fire and Materials Conf.*, Interscience Communications Ltd., London (1995).
322. Friedman, R., Ignition and Burning of Solids, pp. 91-111 in *Fire Standards and Safety* (ASTM STP 614), ASTM (1976).
323. Krause, U., and Schmidt, M., The Influence of Initial Conditions on the Propagation of Smouldering Fires in Dust Accumulations, pp. 230-239 in *Proc. 3rd Intl. Symp. on Hazards, Prevention, and Mitigation of Industrial Explosions*, Tsukuba, Japan (2000).

324. Hardy, V. O., The Smouldering of Coal Dust and the Effect of Lubricants (Research Report 136), Safety in Mines Research Establishment, Sheffield, England (1956).
325. Palmer, K. N., Explosions in Flammable Smokes from Smouldering Fires, pp. D11-D21 in *4th Intl. Symp. on Loss Prevention and Safety Promotion in the Process Industries* (Symp. Series No. 82), vol. 3. Institution of Chemical Engineers, London (1983).
326. Fire Research 1954 (Report of the Director of Fire Research for 1954), pp. 12-13, HMSO, London (1955).
327. Leisch, S. O., Kauffman, C. W., and Sichel, M., Smoldering Combustion in Horizontal Dust Layers, pp. 1601-1610 in *20th Symp. (Intl.) on Combustion*, The Combustion Institute, Pittsburgh (1984).
328. Krause, U., and Schmidt, M., Smouldering Fires in Bulk Materials, pp. 389-400 in *Fire & Explosion Hazards—Proc. 3rd Intl. Symp.*, Univ. Central Lancashire, Preston, England (2000).
329. Litchfield, E. L, Kubala, T. A., Schellinger, T., Perzak, F. J., and Burgess, D., Practical Ignition Problems Related to Intrinsic Safety in Mine Equipment: Four Short-Term Studies (RI 8464), Bureau of Mines, Pittsburgh (1980).
330. Ohlemiller, T. J., Modeling of Smoldering Combustion Propagation, *Prog. Energy & Combustion Science* **11**, 277-310 (1985).
331. Schult, D. A., Matkowsky, B. J., Volpert, V. A., and Fernandez-Pello, A. C., Propagation and Extinction of Forced Opposed Flow Smolder Waves, *Combustion and Flame* **101**, 471-490 (1995).
332. Bakhman, N. N., Smoldering Wave Propagation Mechanism. I. Critical Conditions, *Combustion, Explosion, and Shock Waves* **29**, 14-17 (1993).
333. Palmer, K. N., Smouldering Combustion in Dusts and Fibrous Materials, *Combustion and Flame* **1**, 129-154 (1957).
334. Ohlemiller, T. J., and Rogers, F. E., Cellulosic Insulation Material. Part 2. Effect of Additives on Some Smolder Characteristics, *Combustion Science and Technology* **24**, 139-152 (1980).
335. Ohlemiller, T. J., Smoldering Combustion, pp. 2-171 to 2-179 in **SFPE Handbook of Fire Protection Engineering**, 2nd ed., Society of Fire Protection Engineers, Boston; and National Fire Protection Association, Quincy MA (1995).
336. Tse, S. D., and Fernandez-Pello, A. C., Some Observations of Two-dimensional Smoldering and the Transition to Flaming, pp. 689-700 in **Transport Phenomena in Combustion**, vol. 1, S. H. Chen, ed., Taylor & Francis, Washington (1996).
337. Lawson, J. R., Environmental Cycling of Cellulosic Thermal Insulation and Its Influence on Fire Performance (NBSIR 84-2917), NBS (1984).
338. Pyne, S. J., Andrews, P. L., and Laven, R. D., **Introduction to Wildland Fire**, 2nd ed., Wiley, New York (1996); p. 22.
339. McCarter, R. J., Smoldering Combustion of Cotton and Rayon, *J. Consumer Product Flammability* **4**, 346-358 (1977).
340. McCarter, R. J., Smoldering Combustion of Wood Fibers: Cause and Prevention, *J. Fire and Flammability* **9**, 119-126 (1978).
341. Richards, G. N., and Hshieh, F.-Y., Influences of Oxygen Chemisorption and of Metal Ions in Ignition and Combustion of Wood, pp. 361-377 in *Fire and Polymers: Hazards Identification and Prevention* (ACS Symp. Series 425). American Chemical Society, Washington (1990).
342. Gann, R. G., Earl, W. L., Manka, M. J., and Miles, L. B., Mechanism of Cellulose Smoldering Retardance by Sulfur, pp. 571-578 in *18th Symp. (Intl.) on Combustion*, The Combustion Institute, Pittsburgh (1980).
343. Knopfler, N. B., Gentry, W. T., and Madacsi, J. P., Resistance of Mattresses Containing Boric Acid Treated Cotton Batting to Open Flame Ignition, *J. Consumer Product Flammability* **4**, 169-187 (1977).
344. Browne, F. L., Theories of the Combustion of Wood and Its Control (Report No. 2136), Forest Products Lab., Madison WI (1958).
345. Le Van, S. L., Chemistry of Fire Retardancy, pp. 531-574 in **The Chemistry of Solid Wood**, R. M. Rowell, ed., American Chemical Society, Washington (1984).
346. Alexopoulos, S., and Drysdale, D. D., Transition From Smoldering to Flaming Combustion, pp. 37-44 in *Interflam '88*, John Wiley, Chichester (1988).
347. Davie, B. W., jr., A Report on Cellulose Insulation, *The Alberta Fire News*, Alberta Firefighters Assn. (Nov. 1994).
348. Nelson, M., Detection and Extinction of Fire and Smouldering in Bulk Powder, pp. 64-139 in British Materials Handling Board, CREDIT Project Report, EV5V-CT92-0082 (1992).
349. Ohlemiller, T. J., Forced Smolder Propagation and the Transition to Flaming in Cellulosic Insulation, *Combustion and Flame* **81**, 354-365 (1990).
350. Chen, Y., Kauffman, C. W., Sichel, M., Fangrat, J., and Guo, Y., The Transition from Smoldering to Glowing to Flaming Combustion, paper 68 in The Combustion Institute/Eastern States Section Fall Technical Meeting (1990).
351. Mizuno, M., Wakamatsu, T., Ohmiya, Y., Ueno, H., and Nohmi, T., Experimental Study on Human Response in Wood Smoldering, pp. 89-92 in *APSS2001—Proc. Asia Pacific Symp. on Safety*, Vol. 1, Japan Soc. for Safety Engineering, Yokohama (2001).
352. Standard Guide for Locating Combustion Test Methods for Polymeric Materials (ASTM D 3814), ASTM.
353. Hirschler, M. M., and Grayson, S. J., International Fire Tests for Electrical Cables, pp. 138-162 in *Proc. Intl. Conf. on Fire Safety*, Vol. 29, Product Safety Corp., Sissonville WV (2000).
354. Pál, G., and Macskásy, H., **Plastics: Their Behaviour in Fires**, Elsevier Science Publishers, Amsterdam (1991).
355. Troitzsch, J., **International Plastics Flammability Handbook. Principles—Regulations—Testing and Approval**, 2nd ed., Carl Hanser Verlag, Munich (1990).
356. Fire Hazard Testing. Part 11-30: Test Flames—History and Development 1979 – 1999 (Technical Report), Intl. Electrotechnical Commission, Geneva (1999).
357. Standard Test Method for Ignition Characteristics of Finished Textile Floor Covering Materials (ASTM D 2859), ASTM.
358. Tu, K. M., and Davis, S., Flame Spread of Carpet Systems Involved in Room Fires (NBSIR 76-1013), NBS (1976).
359. Standard for the Surface Flammability of Carpets and Rugs (FF 1-70), Code of Federal Regulations, 16 CFR 1630.
360. Pakkala, L., Ignitability of Beds and Bedding (Research Reports 247), Valtion Teknillinen Tutkimuskeskus, Espoo, Finland (1984).

361. Bonnet F., Flammability of Textiles for Garment Purposes, *ASTM Bull.* 29-33 (Jan. 1948).
362. Patton, A. J., **Fire Litigation Sourcebook**, 2 vols., Wiley Law Publications, New York (1994).
363. Standard for the Flammability of Clothing Textiles (CS 191-53), Code of Federal Regulations, 16 CFR 1610.
364. Compliance Testing of General Wearing Apparel (Test Manual), Engineering Laboratory, Consumer Product Safety Commission, Washington (1981).
365. Standard Test Method for Flammability of Apparel Textiles (ASTM D 1230), ASTM.
366. Weaver, J. F., Rate of Burning of Apparel Fabrics, *Textile Chemist and Colorist* **8**, 46-51 (Nov. 1976).
367. Standard for the Flammability of Children's Sleepwear: Sizes 0 through 6X (FF 3-71), Code of Federal Regulations, 16 CFR 1615.
368. Peacock, R. D., and Vaishnav, M. P., Flammability Testing of Solids Under the Federal Hazardous Substances Act (NBSIR 78-1580), NBS (1980).
369. Kuchta, J. M., and Smith, A. F., Classification Test Methods for Flammable Solids (RI 7593), Bureau of Mines, Pittsburgh (1972).
370. Standard Methods of Fire Test for Flame-Resistant Textiles and Films (NFPA 701), NFPA.
371. Davis, S., and Villa, K. M., Development of a Multiple Layer Test Procedure for Inclusion in NFPA 701: Initial Experiments (NISTIR 89-4138), NIST (1989).
372. Recommended Practice for a Field Flame Test for Textiles and Films (NFPA 705), NFPA.
373. Standard Method of Test for Flammability of Plastic Sheeting and Cellular Plastics (ASTM D 1692), ASTM (1968).
374. Perkins, A. J., Comparative Burning Tests of Common Plastics (Bull. of Research No. 22), Underwriters' Laboratories, Inc., Chicago (1941).
375. Tests for Flammability of Plastic Materials for Parts in Devices and Appliances (UL 94), UL.
376. Standard Specification for a Laboratory Burner Used for Small-Scale Burning Tests on Plastic Materials (ASTM D 5025), ASTM.
377. Standard Practice for Confirmation of 20 and 125 mm Test Flames for Small-Scale Burning Tests on Plastic Materials (ASTM D 5207), ASTM.
378. Test Flames—500 W Flames: Apparatus and Confirmational Test Methods (IEC 60695-11-3), International Electrotechnical Commission, Geneva.
379. Test Flames—50 W Flames: Apparatus and Confirmational Test Methods (IEC 60695-11-4), International Electrotechnical Commission, Geneva.
380. Standard Test Method for Rate of Burning and/or Extent and Time of Burning of Plastics in a Horizontal Position (ASTM D 635), ASTM.
381. Standard Test Method for Horizontal Burning Characteristics of Cellular Polymeric Materials (ASTM D 4986), ASTM.
382. Standard Test Method for Measuring the Comparative Burning Characteristics of Solid Plastics in a Vertical Position (ASTM D 3801), ASTM.
383. Determination of the Burning Behaviour of Horizontal and Vertical Specimens in Contact with a 50 W Nominal Ignition Source (IEC 60695-11-10), International Electrotechnical Commission, Geneva.
384. Plastics—Determination of the Burning Behaviour of Horizontal and Vertical Specimens in Contact with a Small-Flame Ignition Source (ISO 1210), International Organization for Standardization, Geneva.
385. Cellular Plastics – Determination of Horizontal Burning Characteristics of Small Specimens Subjected to a Small Flame (ISO 9772), International Organization for Standardization, Geneva.
386. Plastics – Determination of Burning Behaviour of Thin Flexible Vertical Specimens in Contact with a Small-Flame Ignition Source (ISO 9773), International Organization for Standardization, Geneva.
387. Standard Test Method for Measuring the Comparative Burning Characteristics and Resistance to Burn-Through of Solid Plastics Using a 125 mm Flame (ASTM D 5048), ASTM.
388. Plastics—Determination of Combustibility of Specimens Using a 125-mm Flame Source (ISO 10351), International Organization for Standardization, Geneva.
389. Determination of the Burning Behaviour of Specimens Using a 500-W Flame Ignition Source (IEC 60695-11-20), International Electrotechnical Commission, Geneva.
390. Standard Test Method for Determining the Flammability Characteristics of Nonrigid Solid Plastics (ASTM D 4804), ASTM.
391. Lyon, R. E., and Walters, R. N., Heat Release Capacity, pp. 285-300 in *Proc. Fire and Materials 2001 Conf.*, Interscience Communications Ltd., London (2001).
392. Bergendahl, C. G., Andersson, D., Simonson, M., and Axelsson, J., FIRESEL—A New Approach to Fire Safety in Electronics, pp. 11-22 in *Flame Retardants 2002*, Interscience Communications Ltd, London (2002).
393. ITI/UL Flammability Task Force, Initial Findings Report, [Northbrook IL] (3 Sept. 1999).
394. Polymeric Materials—Use in Electrical Equipment Evaluations (UL 746C), UL.
395. Safety of Information Technology Equipment, Including Electrical Business Equipment (UL 1950), UL.
396. Tests for Flammability of Small Polymeric Component Materials (UL 1694), UL.
397. Moltzan, H., and Hall, L., UL 1694 and Plastic Encapsulated Integrated Circuits, *8th Annual BCC Conf. on Flame Retardancy: Recent Advances in Flame Retardancy of Polymeric Materials*, Business Communications Co., Norwalk CT (1997).
398. Fire Hazard Testing - Part 2: Test Methods - Section 2: Needle-flame Test (IEC 60695-2-2), International Electrotechnical Commission, Geneva.
399. Standard Test Methods for Thermoplastic Insulations and Jackets for Wire and Cable (D 2633), ASTM.
400. Flexible Cord and Fixture Wire (UL 62), UL.
401. Reference Standard for Electrical Wires, Cables, and Flexible Cords (UL 1581), UL.
402. Gaffney, J., The Significance of the New FR-1 Flame Test, *Wire J.* **6**, 82-84 (Oct. 1973).
403. Tests on Electric Cables under Fire Conditions – Part 1: Test on a Single Vertical Insulated Wire or Cable (IEC 60332-1), International Electrotechnical Commission, Geneva.
404. Tests on Electric Cables under Fire Conditions – Part 2: Test on a Single Small Vertical Insulated Copper Wire or

Cable (IEC 60332-2), International Electrotechnical Commission, Geneva.
405. Standard No. 302; Flammability of interior materials, US Code of Federal Regulations, 49 CFR 571.302.
406. Test Method for Horizontal Burning Rate of Flexible Cellular and Rubber-like Materials Used in Occupant Compartments of Motor Vehicles (ASTM D 5132), ASTM.
407. Road Vehicles and Tractors and Machinery for Agriculture and Forestry—Determination of Burning Behaviour of Interior Materials (ISO 3795), International Organization for Standardization, Geneva.
408. Cahill, P., An Investigation of the FAA Vertical Bunsen Burner Flammability Test Method (DOT/FAA/CT-86/22). Federal Aviation Administration, Atlantic City Airport NJ (1986).
409. Reaction to Fire Tests for Building Products—Part 2: Ignitability When Subjected to Direct Impingement of Flame (ISO 11925-2), International Organization for Standardization, Geneva.
410. Results of Round Robin on I gnitability Test (CEN/TC127/Ad Hoc 2), unpublished [ca. 1998].
411. Lawson, J. R., and Parker, W. J., Development of an Ease of Ignition Test Using a Flame Exposure (NBSIR 82-2503), NBS (1982).
412. Babrauskas, V., Development of the Cone Calorimeter—A Bench Scale Heat Release Rate Apparatus Based on Oxygen Consumption, *Fire and Materials* **8**, 81-95 (1984).
413. Babrauskas, V., and Grayson, S. J., eds., **Heat Release in Fires**, E&FN Spon, London (1992).
414. Babrauskas, V., The Cone Calorimeter, pp. 3-63 to 3-81 in **SFPE Handbook of Fire Protection Engineering**, 3rd ed., NFPA (2002).
415. Standard Test Method for Heat and Visible Smoke Release Rates for Materials and Products using an Oxygen Consumption Calorimeter (E 1354), ASTM.
416. International Standard — Fire Tests — Reaction to Fire — Part 1: Rate of Heat Release from Building Products (Cone Calorimeter method) (ISO 5660-1), International Organization for Standardization, Geneva (1993).
417. Babrauskas, V., Twilley, W. H., Janssens, M., and Yusa, S., A Cone Calorimeter for Controlled-Atmospheres Studies, *Fire and Materials* **16**, 37-43 (1992).
418. Wilson, M. T., Dlugogorski, B. Z., and Kennedy, E. M., Uniformity of Radiant Heat Fluxes in Cone Calorimeter, presented in *Fire Safety Science—Proc. 7th Intl. Symp.*, Intl. Assn. for Fire Safety Science (2002).
419. Babrauskas, V., Twilley, W. H., and Parker, W. J., The Effects of Specimen Edge Conditions on Heat Release Rate, *Fire and Materials* **17**, 51-63 (1993).
420. Sundström, B., ed., Fire Safety of Upholstered Furniture—The Final Report on the CBUF Research Programme (Report EUR 16477 EN). Directorate-General Science, Research and Development (Measurements and Testing) of the European Commission (1995). Published by Interscience Communications Ltd., London.
421. Fire tests — Reaction to fire — Ignitability of building products (ISO 5657), International Organization for Standardization, Geneva (1986).
422. Grubits, S. J., Ignitability Test for Building Materials and Textiles (Technical Record 44/153/392), Commonwealth Experimental Building Station, North Ryde, NSW, Australia (1970).
423. Östman, B. A.-L., and Tsantaridis, L. D., Ignitability in the Cone Calorimeter and the ISO Ignitability Test, pp. 175-182 in *Interflam '90,* Interscience Communications Ltd., London (1990).
424. Standard Test Method for Determining Material Ignition and Flame Spread Properties (E 1321), ASTM.
425. Drysdale, D. D., **An Introduction to Fire Dynamics**, 2nd ed., Wiley, Chichester, England (1999).
426. Motevalli, V., Chen, Y., Gallagher, G., and Sheppard, D., Measurement of Horizontal Flame Spread on Charring and Non-charring Material Using the LIFT Apparatus, pp. 23-32 in *Proc. First Intl. Fire and Materials Conf.*, Interscience Communications Ltd, London (1992).
427. Beck, J. T., Roslon, M., Stevanovic, A., Walther, D. C., and Fernandez-Pello, A. C., Piloted Ignition of Composite Materials Under External Heat Flux, pp. 163-178 in *Proc. Intl. Conf. on Fire Safety*, Vol. 29, Product Safety Corp., Sissonville WV (2000).
428. Standard Methods of Test for Measurement of Synthetic Polymer Material Flammability Using a Fire Propagation Apparatus (FPA), ASTM E 2058, ASTM.
429. Gandhi, P. D., Comparison of Cone Calorimeter Data with FM 3972 for Communication Cables, pp. 86-94 in *Proc. Fire Risk & Fire Hazard Assessment Research Application Symp.*, National Fire Protection Research Foundation, Quincy MA (1998).
430. Standard Test Method for Determining of Fire and Thermal Parameters of Materials, Products, and Systems using an Intermediate Scale Calorimeter (ICAL), (ASTM E 1623), ASTM (1994).
431. Urbas, J., and Parker, W. J., Impact of Air Velocity on Ignition in the Intermediate Scale Calorimeter (ICAL), *Fire and Materials* **21**, 143-151 (1997).
432. Dricot, F., and Reher, H. J., Survey of Arc Tracking on Aerospace Cables and Wires, *IEEE Trans. Dielectrics and Electrical Insulation* **1**, 896-903 (1994).
433. Standard Test Method for Dust-and-fog Tracking and Erosion Resistance of Electrical Insulating Materials (ASTM D 2132), ASTM.
434. Environmental Tests for Aircraft Equipment—Insulation Resistance and HV Tests for Electrical Equipment (ISO 2678), International Organization for Standardization, Geneva (1985).
435. Test Method for Evaluating Resistance to Tracking and Erosion of Electrical Insulating Materials Used under Severe Ambient Conditions (IEC 60587), International Electrotechnical Commission, Geneva (1984).
436. Flammability, Odor, Offgassing, and Compatibility Requirements and Test Procedures for Materials in Environments That Support Combustion (NHB 8060. 1C), Office of Safety and Mission Quality, NASA, Washington (1991).
437. Test Method for High-Voltage, Low-Current Dry Arc Resistance of Solid Electrical Insulation (ASTM D 495), ASTM.
438. Standard Test Method for Liquid-Contaminant, Inclined-Plane Tracking and Erosion of Insulating Materials (ASTM D 2303), ASTM.
439. Standard Test Methods for Hookup Wire Insulation (ASTM D 3032), ASTM.
440. Standard Test Method for Comparative Tracking Index of Electrical Insulation Materials (ASTM D 3638), ASTM.

441. Method for the Determination of the Proof Tracking and Comparative Tracking Indices of Solid Insulating Materials (IEC 60112), International Electrotechnical Commission, Geneva.
442. Centurioni, L., Coletti, G., and Operto, A., A Contribution to the Study of the Tracking Phenomenon in Solid Dielectric Materials under Moist Conditions, *IEEE Trans. on Electrical Insulation* **EI-12**, 147-152 (1977).
443. Report of the Results of the Round Robin Series of Tests to Evaluate Proposing Amendments to IEC 60112 (TR 62062), International Electrotechnical Commission, Geneva (2000).
444. Test Methods for Insulated Electric Wire (MIL-STD-2223).
445. Polymeric Materials—Short Term Property Evaluations (UL 746A), UL.
446. Middendorf, W. H., Successful Performance of the High Current Arc Test, *IEEE Trans. on Electrical Insulation* **IE-17**, 429-433 (1982).
447. Middendorf, W. H., and Kirshteyn, M., The High Current Arc Ignition Test, *IEEE Electrical Insulation Magazine* **4**:6, 21-25 (Nov./Dec. 1988).
448. Dorsett, H. G., et al., Laboratory Equipment and Test Procedures for Evaluating Explosibility of Dusts (RI 5624), Bureau of Mines, Pittsburgh (1960).
449. Dust and Powder Layers: Electric Spark Sensitivity (Nordtest NT Fire 016), Nordtest, Espoo, Finland (1982).
450. Eckhoff, R. K., **Dust Explosions in the Process Industries**, 2nd ed., Butterworth-Heinemann, Oxford (1997).
451. Mintz, K. J., Ignition Temperatures of Dust Layers: Flaming and Non-flaming, *Fire and Materials* **15**, 93-96 (1991).
452. Interim Safety Standard for Cellulose Insulation, Code of Federal Regulations, 16 CFR 1209.
453. Standard Specification for Cellulosic Fiber (Wood-Base) Loose-Fill Thermal Insulation (ASTM C 739), ASTM.
454. Standard for the Flammability of Mattresses and Mattress Pads (FF 4-72), Code of Federal Regulations, 16 CFR 1632.
455. Standard Test Method for Smoldering Combustion Potential of Cotton-Based Batting (ASTM D 5238), ASTM.
456. Standard Test Methods for Fire Tests of Roof Coverings (ASTM E 108), ASTM.
457. Tests for Fire Resistance of Roof Coverings (UL 790), UL.
458. Williamson, R. B., private communication (2001).
459. Standard Test Method for Ignition of Materials by Hot Wire Sources (ASTM D 3874), ASTM.
460. Schwarz, K. H., Prüfung von Isolierstoffen auf Wärme- und Feuerbeständigkeit [Testing of Insulating Materials for Heat and Fire Resistance], *Elektrotechnische Zeitschrift* **B14**, 273-279 (1962).
461. de Aruajo, L., and Wagner, J. P., Investigation of Ignition of Thermoplastics Through the Hot Wire Ignition Test, pp. 236-253 in *Proc. 27th Intl. Conf on Fire Safety*, Product Safety Corp., Sissonville WV (1999).
462. Standard Test Method for Glow-Wire Ignition of Materials (ASTM D 6194), ASTM.
463. Fire Hazard Testing—Part 2-13: Glowing/hot Wire Based Test Methods—Glow-wire Ignitability Test Method for Materials (IEC 60695-2-13), International Electrotechnical Commission, Geneva.
464. Report of the Meeting of the Industry Advisory Group of UL Plastic Materials, Subject 746(94), December 29, 2000, Underwriters Laboratories Inc., Melville NY (2000).
465. Methods of Test for the Determination of the Flammability of Solid Electrical Insulating Materials When Exposed to an Igniting Source (IEC 707), International Electrotechnical Commission, Geneva (1981).
466. Fire hazard testing. Part 2: Test methods. Bad-connection test with heaters (IEC 60695-2-3), International Electrotechnical Commission, Geneva.
467. Monakhov, V. T., **Metody issledovaniya pozharnoi ospasnosti veshchestv**, Khimya, Moscow (1972). English translation: **Methods for Studying the Flammability of Substances**, published for US National Bureau of Standards by Amerind Publishing Co., New Delhi, India (1985).
468. Method of Determination of the Effects of a Small Source of Ignition on Textile Floor Coverings (BS 4790), British Standards Institution, London.
469. Setchkin, N. P., Discussion of Paper on the Ignition Temperature of Rigid Plastics, *ASTM Bull.* No. 151, 66-69 (1948).
470. Standard Test Method for Determining Ignition Temperature of Plastics (ASTM D1929), ASTM.
471. Plastics—Determination of Ignition Temperature Using a Hot-Air Furnace (ISO 871), International Organization for Standardization, Geneva.
472. Standard Test Method for Behavior of Materials in a Vertical Tube Furnace at 750ºC (E 136), ASTM.
473. Brown, J. R., and Gellert, E. P., The Combustion of Organic Polymeric Materials—Ignition Properties (Tech. Note MRL-TN-414), Materials Research Laboratories, Dept. of Defence, Ascot Vale, Vic., Australia (1978).
474. Yoshida, S., Ito, K., Tamamoto, Y., Aida, F., and Hosokawa, E., Flash and Ignition Characteristics of Flame Retardant Materials, pp. 318-325 in *Proc. 38th Intl. Wire and Cable Symp.*, US Army Communications-Electronics Command, Fort Monmouth NJ (1989).
475. Wulff, W., Zuber, N., Alkidas, A., and Hess, R. W., Ignition of Fabrics under Radiative Heating, *Combustion Science and Technology* **6**, 321-334 (1973).
476. Masařík, I., Ignitability and Burning of Plastic Materials: Testing and Research, pp. 567-577 in *Interflam '93*, Interscience Communications Ltd., London (1993).
477. Hilado, C. J., and Kosola, K. L., A Laboratory Technique for Determining Ignition Temperatures of Materials, *Fire Technology* **14**, 291-296 (1978).
478. Standard Test Method for Measuring the Minimum Oxygen Concentration to Support Candle-like Combustion of Plastics (Oxygen Index), ASTM D 2863. ASTM.
479. Nelson, G. L., and Webb, J. L., Oxygen Index of Liquids—Technique and Applications, *J. Fire and Flammability* **4**, 210-226 (1973).
480. Routley, A. F., Development of the Oxygen Index Concept for the Assessment of the Flammability Characteristics of Materials (CDL Report 5/73), Central Dockyard Laboratory, Portsmouth, UK (1973).
481. Abbott, C., and Chalabi, R., Heated Oxygen Index Test, pp. 296-303 in *Intl. Symp.—Fire Safety of Combustible Materials*, Edinburgh, Scotland (1975).

Copyright © 2003, 2014 Vytenis Babrauskas

Chapter 8. Ignition of elements

Highlights and summary of practical guidance **352**
Ignition of metals **353**
General principles *353*
Theories *356*
Theories for a single, isolated mass 356
Theories for metal dust layers 358
Effect of oxygen concentration *359*
Effect of pressure *359*
Effect of flow velocity *359*
Effect of moisture *359*
Ignition of carbon **359**
Graphite and other relatively pure forms of carbon *359*
Coal, coke, and other relatively impure forms of carbon *360*
Single particles 360
Dust clouds 363
Test methods **364**
References **364**

Highlights and summary of practical guidance

A substance which is a pure chemical element cannot pyrolyze since it cannot degrade into any simpler structure. Thus, it is impossible for a substance of this kind to thermally degrade, release volatile vapors, and then have these vapors ignite. Elements can ignite and burn, but their mechanisms are unique. Most of ignitable elements are metals, for example, aluminum, magnesium, and iron. Some non-metal elements also ignite and do so by mechanisms similar to metals. Examples of non-metal elements that can ignite include carbon (graphite), boron, phosphorus, and sulfur. Metals are subject to low-temperature oxidation, which means that a pure metal placed in the atmosphere soon becomes coated with a metal oxide on its surface. For most metals, the metal oxide is a solid product and—to a lesser or greater extent—it adheres to the surface. The oxidation of carbon is unique in many ways because the oxides of carbon, CO and CO_2, are gases. Except for those metals capable of pyrophoric behavior, at room temperature the oxidation process is self-limiting, since (a) as a thicker oxide layer builds up, the layer progressively interferes with the metal/oxygen reaction; and (b) the layer itself serves as heat sink. At high temperatures, reactions proceed fast enough that ignition becomes possible, but details of the process vary according to chemical and thermodynamic constants of the metal. Thus, there is not a single theory that is universally applicable. Detailed theoretical models exist, but these are generally limited to a single element. Specific information on various metals and other ignitable elements is given in Chapter 14.

Some elements exhibit pyrophoric behavior when they are in the form of extremely-small particles. As the particle diameter decreases, the volume/surface ratio goes down. Since the heat generated is proportional to the surface area and (ignoring losses) it must all go towards raising the temperature of the particle, the smaller the particle the higher is the temperature attained. The critical sizes are so small (about 0.03 μm or less) that pyrophoric problems arise only in specialized industries.

Ignition of metals

GENERAL PRINCIPLES

Metals are used as fuels in certain rocketry and pyrotechnic applications, because their combination of high heat of combustion and high density means that a great deal of energy can be delivered from a given volume of fuel. Unfortunately, unwanted metal fires tend to be especially severe and problematic, thus, their ignition behavior must be studied.

The vast majority of solid substances encountered in fires initially respond to heat by pyrolyzing, that is, by degrading chemically into substances of smaller molar mass, which are then able to gasify. The ignition event then corresponds to the initial flaming combustion of the gasified vapors. But pure elements, being the simplest chemical arrangement, cannot further break down into smaller, more readily vaporizable fragments; they can only change state. Thus, they can only burn either by a direct surface oxidation reaction (*heterogeneous combustion*) or else they must be raised to such a temperature that the rate of vaporization becomes sufficient to sustain *homogeneous combustion*, that is, combustion which takes place throughout a volume. A normal flame is an example of homogeneous combustion. The most common examples of solids capable of undergoing heterogeneous combustion are certain metals. However, wood and some synthetic polymers also undergo heterogeneous combustion late in a fire, after all of the available components that can gasify have finished gasifying and flaming. The term *glowing combustion* is sometimes applied to charcoal, wood (in its non-flaming stage) and other substances which exhibit medium-temperature heterogeneous combustion. This term is usually not applied to heterogeneous combustion of metals, since they burn white-hot.

For any substance susceptible to exothermic reactions, ignition occurs if a heat balance cannot be established at a low, steady temperature. Thus, before considering any details, it is convenient to establish a qualitative picture of the basic heat flow terms involved in ignition. This is difficult to do when heating and reactivity are spatially highly non-uniform, such as in a pyrolyzing solid or in the gas plume above a liquid pool. But for other types of substances a useful comparison can be made (Table 1). It can be seen that metals are a 'parallel universe' to other substances. Ignition is facilitated for metals when the particles are made smaller. But for a haystack or a beaker of unstable liquid undergoing self-heating, ignition probability is increased when the volume of the material is made larger.

Table 1 The role of volume and surface area in the ignition of substances

Substance	Heat generation	Heat losses
Gases Porous self-heating solids Unstable liquids	Proportional to the volume	Proportional to the outside surface area
Metals	Proportional to the surface area	Proportional to the volume (during the initial heating)

Under the right conditions, most metals can burn except for the noble metals (gold, silver, platinum, etc.). When a metal burns, the product of combustion is its metal oxide (or its metal nitride). For example aluminum:

$$4Al + 3O_2 \rightarrow 2Al_2O_3$$

The situation is complicated by the fact that most metals form a film of the oxide on their surface simply from low temperature oxidation in air. For those metals, surfaces which are not covered in oxide can be created by producing metal particles in an inert atmosphere, but these are highly specialized applications. The oxide film cannot burn, since it already is the product of the metal's oxidation. Before the bulk metal can burn, the oxide skin must be removed in some way. The rupture of the oxide layer plays a critical role in the ignition process, and it is considered that the rupturing is highly influenced by boundary conditions.

One of the rare similarities which metal combustion shares with hydrocarbon combustion is that dissociation occurs. Thus, in the high-temperature zone there is to be found both elemental oxygen and gas-phase elemental metal.

Ignition can be influenced by oxygen solubility in the metal, for those metals where the solubility is relatively high, such as titanium or zirconium.

Bahn[1] proposed that there are three mechanisms for the ignition of small metal particles:

(1) oxidation of a pure metal surface in an oxidizing atmosphere;
(2) reaction between an oxidizing atmosphere and a reactive chemical that has formed on the surface of the metal;
(3) reaction between an oxidizing atmosphere and a metal induced by mechanical energy, e.g., friction or rupture energy.

The third mechanism is often of interest in hyperbaric oxygen systems and is further considered in Chapter 13.

The first major experimental study of the ignition temperatures of metals was by Grosse and Conway[14]. They classified metals into three groups in regards to their ignition characteristics:

(1) Metals that ignite at or below their melting points (barium, calcium, iron, magnesium, molybdenum, strontium, thorium). These metals all have melting points above 650 – 660ºC. These metals generally do not form a protective oxide layer.
(2) Metals that ignite after they melt (aluminum, antimony, bismuth, cadmium, lead, lithium, potassium, sodium, tin, zinc). These metals all have melting points below

650 – 660ºC. All of these metals (except for alkali metals) form a protective oxide layer. Markstein noted that this group of metals tends to show ignition temperature results that are much less dependent on the experimental conditions than the metals of the first group[2].

(3) Metals that do not ignite (silver, platinum, mercury).

The simplest theory to explain ignition of metals was propounded by Monroe et al.[3], based on a heat-balance concept. They proposed two criteria, the melting-point burn ratio and the boiling-point burn ratio. Sustained combustion cannot occur if the amount of heat liberated in combustion is not enough to bring the metal to its melting point. Thus, the melting-point burn ratio is defined as:

$$BR_{mp} = \frac{\Delta h_c}{\Delta h_{mp} + L_{mp}}$$

where Δh_c = heat of combustion, Δh_{mp} sensible heat to raise metal to its melting point temperature, and L_{mp} = latent heat of melting. Similarly, the boiling-point burn ratio is defined as:

$$BR_{bp} = \frac{\Delta h_c}{\Delta h_{mp} + L_{mp} + \Delta h_{bp} + L_{bp}}$$

where Δh_{bp} sensible heat to raise metal from its melting point to its boiling point and L_{bp} = latent heat of vaporization. Then, according to their theory:

(1) if $BR_{mp} < 1$, the metal cannot be burned;
(2) if $BR_{mp} \geq 1$, but $BR_{pb} < 1$, the metal can burn, but only heterogeneously;
(3) if $BR_{pb} \geq 1$, the metal can burn homogeneously.

Some data[4] based on their theory are shown in Table 2.

It will be noted that Monroe considered that the metal is initially at room temperature and that no external energy is supplied to the system. Thus, it would seem that his ratios could only be applicable to pyrophoric metals, which ignite starting from room temperature. As shown later, however, to describe ignition of pyrophoric metals requires consideration of the oxide film which develops on the surface of most metals, and Monroe does not treat this film at all. Thus, his concept is inapplicable to pyrophoric metals but can have some value in other cases. As discussed in Chapter 13, accidents in pure-oxygen systems often involve a surface ignition of an otherwise not-preheated metal. Monroe's BR_{mp} should be able to suggest which metals can burn up under these circumstances, versus those not igniting or exhibiting only a surface flash. Nickel-rich alloys tend to be hard to ignite in oxygen systems, as shown in Chapter 13, and this is consistent with nickel having a low BR_{mp} value, even though it does exceed Monroe's suggested 1.0 value.

Table 2 Burn ratios for some metals, computed according to the theory of Monroe et al.

Metal	BR_{mp}	BR_{bp}
Ag	0.4	0.05
Cu	2.0	0.2
Ni	3.7	0.5
Fe	3.8	0.56
Sn	44.8	0.8
Pb	18.6	0.9
Cr	6.4	1.2
Ti	10.9	1.4
Be	12.6	1.6
Li	41.7	1.6
Al	29.0	2.2
Zn	19.3	2.4
Ca	17.4	3.1
Mg	22.9	3.6

A more comprehensive theory was put forth by Glassman, who postulated that the flame temperature of many metals is limited to the boiling point of its oxide[5]. This is due to the very high heat of vaporization* of metal oxides, which is greater than the heat available from the combustion process. The heat available from the combustion is simply minus the heat of formation of the metal oxide (since the heats of formation of metals and O_2 are both ≡ 0). The heat required to raise the metal oxide from a solid at 298 K to a vapor at T_b is the sum of the sensible enthalpy of raising its temperature from 298 K to T_b, plus the heat of vaporization at 298 K. Data for some metals are given Table 5. It is seen that—except for boron†, tungsten, and a few others—enough heat is not available to fully vaporize the oxide at its T_b. Thus, the metal's flame will have liquid particles in it and is not fully gasified.

Upon ignition, Glassman[6] considers that the conditions which determine whether heterogeneous or homogeneous burning will happen are based on the boiling points of the metal and its oxide, as given in Table 3. Glassman's theory has not been fully validated, and has been criticized by Steinberg et al.[7]. Their criticism centers around the fact that 'boiling' is not what metal oxides tend to do; rather, many tend to dissociate. This is not a serious limitation to the theory, since a temperature of rapid dissociation can equally well be used.

Table 3 Glassman's concept of metals combustion

Boiling point relation	Type of combustion	Nature of condition
T_b (metal) > T_b (oxide)	heterogeneous	sufficient, but not necessary
T_b (metal) < T_b (oxide)	homogeneous	necessary but not sufficient

There are a number of additional thermochemical subtleties involved, including the fact that the composition of the atmosphere—air or oxygen—can sometimes govern whether the combustion will be heterogeneous or homogeneous.

* Some metal oxides decompose before vaporizing so, for them, it is more correct to refer to the heat of decomposition.

† Chemically, boron is classed as a non-metal, however, its combustion characteristics are similar to those of metals, thus it is often included in theories for the combustion of metals.

Table 4 Controlling phenomena of metals ignition, as classified by Breiter et al.

Group	General features	Controlling variable	T_{ig}	Examples
1	Non-protective oxide	direct oxidation of metal	variable	Ba, Ca, Mg
2	Protective oxide; oxide soluble in metal	melting of oxide and its dissolving in metal	variable	Ti, Zr
3	Protective oxide; oxide not soluble in metal; metal is volatile, oxide is not	melting and oxidation of metal	$\approx T_{mp(metal)}$	Zn
4	Protective oxide; oxide not soluble in metal; non-volatile metal and oxide; $T_{bp(metal)} > T_{mp(oxide)}$	melting of oxide	$T_{mp(oxide)}$	Al, Fe, Ni, Si
5	Protective oxide; oxide not soluble in metal; non-volatile metal and oxide; $T_{mp(metal)} < T_{mp(oxide)}$	boiling of metal	$T_{mp(metal)}$	Be
6	Protective oxide; oxide is volatile	oxidation of metal; boiling of oxide	$\approx T_{bp(oxide)}$	B

Numerous other material properties of the metal and its oxide come into play in determining the nature of combustion. Price[8] considers that the following factors can affect the ignitability of a metal:

(1) Ratio of the molar volume for the solid oxide to that of the metal. Values less than 1 cause the surface oxide layer to be non-protective.
(2) Ratio of the coefficients of thermal expansion of the solid metal to that of its oxide. Values greater than 1 tend to cause the oxide film to crack during heating.
(3) Melting point of the metal. Flow of metal facilitates ignition.
(4) Melting point of the oxide. If the melting point of the oxide is higher than that of the solid metal, the oxide may dissolve in the molten metal or may retract from the surface.
(5) Solubility of the molten oxide in the molten metal. If the solubility is high, the molten metal may diffuse to the surface through the oxide layer. If the solubility is low and the interface surface tension is high, the oxide layer inhibits further oxidation. If the solubility is low but the oxide surface tension is high and the interface surface tension is low, then the oxide tends to accumulate on the surface, retract, and expose the metal.
(6) Boiling point of the metal. If the boiling point is low (e.g., magnesium), then the oxide skin is easily destroyed and ignition occurs at or near the surface. If the boiling point is high (e.g., titanium, tungsten, zirconium boron), then it may not be reached and burning will be primarily by a surface reaction
(7) Boiling point or dissociation temperature of the oxide. If this temperature can be attained, then the oxide layer can be removed and direct surface oxidation results.

Point #1 was first proposed in 1923 by Pilling and Bedworth[9] and the ratio is sometimes referred to as the P&B ratio; unfortunately, later research[10] showed that knowing the P&B ratio does not suffice to determine whether the oxide coat will be protective or not. Mellor[11] concluded that the oxides of most metals are protective at low temperatures and non-protective at high temperatures, with each metal having a unique 'transition temperature' separating the two regimes. The largest group of metals (e.g., Ca, Mg, Mo, Ta) had transition temperatures at 400 – 600ºC. Additionally, for some metals, thin oxide layers are protective, but after the layer grows to larger thickness, it proceeds to crack and break up.

On considerations similar to Price's, Breiter et al.[12] proposed placing metals into 6 different groups of behavior (Table 4). This scheme can be especially helpful in understanding the ignition of metal alloys, where changes in T_{ig} often are seen to correspond to different regimes in a metallurgical phase diagram for the system. Breiter et al. illustrated their theory with data on Mg-Zn, Mg-Al, Zn-Al, Al-Ni, Ti-Zr, and Ti-Ni alloys. As always with metals, actual details of the combustion are highly dependent on the specifics of the combustion situation, and quite different regimes are commonly observed when some test conditions are changed.

Hardt[13] proposed that pyrophoric metals are generally distinguished chemically by largely-unfilled *d* electron orbitals (d_0 to d_2), but it is evident that a number of other factors, some chemical rather than physical, also are involved.

Unlike for hydrocarbon fuels, a metal's flame temperature is essentially independent of the fuel/air ratio over a wide range. Certain metals burned in oxygen can attain very high flame temperatures. The metals showing the highest flame temperatures form a diagonal band on the left side of the periodic table[14] and include beryllium, magnesium, aluminum, and zirconium.

Many metals which require high temperatures for ignition will ignite at ambient temperature if they lack the normal oxide coating on the surface. This can occur in processes where finely divided metals are produced.

Table 5 Thermophysical properties of some metals and their oxides

Metal	**Metal oxide**	T_m (K)		T_b (K)		Δh_v (kJ mol^{-1})	$\Delta h_v + (h_{Tb}-h_{298})$ (kJ mol^{-1})	Δh_f (kJ mol^{-1})	Δh_c (MJ kg^{-1})
		Metal	Oxide	Metal	Oxide				
Al	Al_2O_3	933	2327	2792	3800	1860	2550	-1676	31.06
B	B_2O_3	2348	723	≈3900	2316	429	709	-1272	58.83
Ba	BaO	1000	2286	2170	3273	436		-554	4.03
Be	BeO	1560	2780	2744	4200	745	1065	-608	67.48
Ca	CaO	1115	3200	1757	3123	679		-635	15.85
Cd	CdO	594	273	1040	1832	340		-258	2.30
Ce	CeO_2	1072	2673	3697	≈2900	423		-1089	7.77
Cr	Cr_2O_3	2180	2603	2944	≈4300	1160	1700	-1121	10.78
Cu	CuO	1358	1719	2835	≈2100	399		-157	2.48
Fe	FeO	1811	1650	3134	3673	610	830	-272	4.87
Hf	HfO_2	2500	3060	4876	≈4800			-1145	6.42
K	*	336		1032					
Li	Li_2O*	454	1843	1615	2836	437		-598	43.08
Mg	MgO	923	3099	1363	3873	670	920	-601	24.73
Na	Na_2O	371	1405	1156	†			-414	9.00
Si	SiO_2	1687	1986	3538	3223	581	737	-911	32.44
Sr	SrO	1050	2938	1655	≈3300	600		-592	6.76
Th	ThO_2	2023	3663	5061	4673	729		-1227	5.29
Ti	TiO_2	1941	2116	3560	3273	634		-939	19.6
U	UO_2	1408	3100	4404	3850	619		-1085	4.56
W	WO_3	3695	1745	5828	1997	550	688	-843	4.59
Zn	ZnO	693	2248	1180	2523			-351	5.37
Zr	ZrO_2	2128	2983	4682	4280	811	1021	-1097	12.03

bold symbols indicate heterogeneous combustion expected, according to Glassman's rule
* forms a mixture of oxides, not a single oxide.
† sublimes.
Δh_v = heat of vaporization of metal oxide at 298 K
$h_{Tb} - h_{298}$ = sensible enthalpy to raise the gaseous oxide from 298 K to its boiling temp.
Δh_f = heat of reaction (= heat of formation of solid metal oxide)

An additional complication of metals is that some can burn in atmospheres of pure N_2 or CO_2. In the former case, metal nitrides are formed instead of metal oxides. In the latter, the CO_2 is reduced to CO or C, and the metal is oxidized to its metal oxide.

Some metal particles explode or fragment shortly after ignition. Those with a propensity for showing this behavior—at least under some heating conditions—include aluminum, plutonium, samarium, tantalum, titanium, zirconium[15].

THEORIES

As some of the discussion above indicated, the ignition of metals is a very complicated phenomenon. Partly, this is because of the uniquely tightly coupled physics and chemistry. Phase changes, surface oxide formation, breakage of oxide films, etc., play little or no role with other fuel types, yet are dominant in the ignition and combustion of metals. Because there is not a great deal of commonality in the combustion of the various metals, most Western researchers have endeavored to develop a theory for a single element. A number of them are briefly cited in Chapter 14. Russian researchers took a more global view where a single theory to fit all metals is strived for. Merzhanov[16] has briefly outlined the numerous Russian studies on this topic. Generally, the Russian theories focused on a thermal self-heating formulation, with only a subsidiary role being allocated to the physical phenomena. The studies are wholly computational in nature, and Merzhanov did not capture any of their trends in closed-form equations or approximations.

Apart from differences among elements in their chemical traits, the physical arrangement is also important. Same as for pyrolyzing solids, there are three basic physical arrangements, each one of which needs to be treated by a separate theory:

(1) a single, isolated mass, which may range from a microscopic particle to a huge object
(2) a pile or layer of small particles
(3) a dust cloud.

Theories for #1 and #2 will be considered below. Theories for dust clouds—including metal dusts—have already been considered in Chapter 5; some additional ones are considered later in this Chapter under *Ignition of carbon*.

THEORIES FOR A SINGLE, ISOLATED MASS

Reynolds[17] developed an ignition theory which is based on a variation of the Taffanel and le Floch postulate (see Chapter 4) that, at the ignition temperature:

$$\frac{d\dot{q}''_G}{dT} = \frac{d\dot{q}''_L}{dT}$$

where $\dot{q}''_G$ = heat generation rate (kW m^{-2}) and $\dot{q}''_L$ = heat loss rate (kW m^{-2}). Assuming heat loss is solely by radiation,

$$\frac{d\dot{q}''_L}{dT} = 4\varepsilon\sigma T_{ig}^3$$

while the heat generation term will depend on the actual chemistry at the surface. Reynolds assumed that metals fall into two categories—those that show a linear oxidation law and those with a parabolic law. The linear law is:

$$\dot{q}''_{G1} = QA\exp\left(-E/RT\right)$$

while the parabolic law (as corrected by Markstein[2]) is:

$$\dot{q}''_{G2} = \frac{\gamma QA}{2\delta\rho_{ox}}\exp\left(-E/RT\right)$$

where Q = heat of reaction (kJ per kg of oxygen), A = pre-exponential factor (kg m^{-2} s^{-1} for linear law, kg^2 m^{-4} s^{-1} for parabolic), E = activation energy (J mol^{-1}), R = universal gas constant (8.314 J mol^{-1} K^{-1}), δ = oxide layer thickness (m), and γ = stoichiometric ratio of mass of oxide/mass of oxygen. The dimensionless solution to the equation is:

$$\exp\left(-1/\theta\right) = \frac{\theta^5}{\eta}$$

where $\theta = RT_{ig}/E$ and $\eta = \frac{QA}{4\varepsilon\sigma}\left(\frac{R}{E}\right)^4$ for the linear law and $\eta = \frac{\gamma QA}{8\varepsilon\sigma\delta\rho_{ox}}\left(\frac{R}{E}\right)^4$ for the parabolic law. The solution would seem to be of limited utility, since obtaining the needed constants, especially A, E, and δ, would be much more of a challenge than measuring ignition temperatures. Reynolds presented some data showing fairly good agreement of experiment with theory for a number of metals but did not describe a procedure for obtaining the constants, nor for deciding whether to apply the linear law or the parabolic. Even worse, Reynolds' data showed that, in most cases, A and E are in fact not constants but depend strongly on the temperature.

Mellor[11] noted that, due to certain simplifications, Reynolds' theory predicts that neither specimen size nor ambient pressure affects the ignition temperature, both of which are at variance with a number of experimental studies. He then formulated an improved theory that generalized Reynolds' theory by assuming that each metal oxidizes according to a parabolic law below its 'transition' temperature and according to a linear law above it*.

Mellor based his generalized theory on Frank-Kamenetskii's scheme[18] where the reaction rate at a surface is limited by a combination of diffusion and chemical kinetics. In addition, he included radiative losses from the heated surface. This led to a complicated formulation, however, and Mellor did not even attempt to solve the model he had set up. Mellor did point out that his theory had the possibility of correctly predicting that for small particles T_{ig} varies inversely with diameter. He noted that, for simplicity, many of the more-tractable theories assume a constant Nusselt number and thereby assume that heat losses vary inversely with diameter. Consequently, such theories are unable to predict the experimental results for small particles. Surprisingly, there is not a great deal of literature on the size effect (see Chapter 14), so Mellor conducted experiments which showed that 0.127 mm thick magnesium foils ignited in oxygen at about 100ºC lower than did ones of 0.254 mm thickness; similar results were also shown for calcium foils of two thicknesses.

Yuen[19] proposed an ignition theory which had many required constants but lacked a systematic means for obtaining them. As a result, even though he also presented some experimental data, he was not able to validate the theory. In addition, a number of the Russian theories (e.g., those by Arutyunyan[20] and Gremyachkin[21]) are available in English, but these require wholly-numerical solutions and have generally not been validated against experimental data. Khaikin's[22] is interesting in that it effectively represents a generalization of Reynolds' theory but, again, obtaining suitable data is also a major limitation with its use.

Most simple theories of the ignition of metals treat heat losses in such a way that their predictions are the opposite of Mellor's experimental findings: small particles are predicted to be harder, not easier to ignite. The theory of Friedman and Maček[23] is perhaps the best known of these. Dealing solely with aluminum combustion, they found that experimental data support the concept that, at ignition, the temperature of the particle is always that of the melting point of aluminum oxide, T_{mo}, which is 2327 K. But, because of the exothermic reactions, the environment temperature T_o needed for ignition is lower than T_{mo} and decreases with decreasing particle size. They assumed that the reaction is first-order with respect to oxygen (which is not true in the general case of metals combustion). Then, they postulated that, at the critical temperature T_c, the heat generated $\dot{q}''_G$ must be identical to the heat loss $\dot{q}''_L$. But, in turn, they assumed that the reaction rate is equal to the amount of oxygen that can be delivered to the surface by diffusion, $\dot{q}''_D$. Thus,

$$\dot{q}''_G = \dot{q}''_L = \dot{q}''_D$$

Now $\dot{q}''_G = QAC\exp\left(-E/RT_{mo}\right)$, where Q = heat of reaction, A = pre-exponential factor, and C = concentration of oxygen in the gas phase at the fuel surface. The heat losses were assumed to be solely due to gas-phase conduction loss, $\dot{q}''_L = \frac{2\lambda}{d}\left(T_{mo} - T_c\right)$, where λ = gas-phase conductivity

* But beryllium was found to be an exception to the rule, in that it oxidizes according to a linear law at low temperatures, and parabolic at high.

and d = particle diameter. The diffusion limit to the reaction rate is taken as $\dot{q}''_D = \frac{2QD}{d}(C_o - C)$, where D = diffusion coefficient and C_o = ambient oxygen concentration. The solution for T_c is obtained as:

$$T_c = T_{mo} - \frac{QC_o}{\lambda[(1/D) + (2/dA\exp(-E/RT_c))]}$$

The authors then note that the $1/D$ term is very small and thus the solution simplifies to:

$$T_c = T_{mo} - \frac{QAC_o \exp(-E/RT_c)}{2\lambda} d$$

Thus, in their theory, the particle surface temperature needed for ignition (T_{mo}) is independent of size, but the furnace temperature needed for ignition (T_c) decreases linearly with increasing particle diameter. Numerically, however, the effect is small. For a 35 μm particle, their theory predicts that $T_c - T_{mo} = 7°\text{C}$. This, of course, is below the experimental uncertainty level. They also obtained a simplified expression for ignition time using their theory:

$$t_{ig} = \frac{\rho d^2}{12\lambda}\left[C_p \ln\left(\frac{T_g - T_\infty}{T_g - T_{mo}}\right) + \frac{L}{T_g - T_m}\right]$$

where ρ = density of metal, C_p = heat capacity of metal, λ = thermal conductivity of air, T_g = the furnace temperature ($\geq T_c$), T_∞ = initial particle temperature, and T_m = melting point of metal. The prediction that ignition time should be proportional to d^2 was validated by experimental data. A number of other theories have been reviewed by Glassman et al.[24], but the less well-known ones were also seen to either not predict experimental trends successfully or else to be based on dubious assumptions.

More recently, Glassman et al.[25] proposed a heat balance model for assessing the propensity of various metal particles to undergo pyrophoric ignition. The basic principle is that, for pyrophoric ignition to take place, a particle, when initially in an unoxidized state, must be small enough so that the initial oxide layer that develops due to heterogeneous reaction with air generates sufficient heat to vaporize the metal and to raise the oxide layer temperature to T_m. Assuming that the metal particles are spheres of diameter r (including the oxide coat) and that δ is the thickness of the oxide layer, Glassman et al. consider the following heat balance.

heat available:

$$\frac{4}{3}\pi\left[r^3 - (r-\delta)^3\right]\rho_{ox}\left(-\Delta H^o_{298}\right)_{ox}$$

heat needed to vaporize the metal:

$$\frac{4}{3}\pi(r-\delta)^3\,\rho_m\left[\left(H^o_{bpt} - H^o_{298}\right) + L_v\right]_m$$

heat needed to bring the oxide layer to T_m:

$$\frac{4}{3}\pi\left[r^3 - (r-\delta)^3\right]\rho_{ox}\left(H^o_{bpt} - H^o_{298}\right)_{ox}$$

where H^o_T = standard-state enthalpy at T; $\left(\Delta H^o_{298}\right)_{ox}$ = standard-state heat of formation of the oxide at 298 K; *bpt* denotes the metal vaporization temperature; *m* denotes metal; and *ox* denotes oxide. Solving the heat balance equation gives the thermal runaway condition as:

$$\frac{\rho_{ox}}{\rho_m} \times \frac{\left(-\Delta H^o_{298}\right)_{ox} - \left(H^o_{bpt} - H^o_{298}\right)_{ox}}{\left[\left(H^o_{bpt} - H^o_{298}\right) + L_v\right]_m} \geq \frac{\left(1 - \delta/r\right)^3}{1 - \left(1 - \delta/r\right)^3}$$

The left hand side of the above equation is a group of constants with known values for any particular metal, thus, the maximum radius r for pyrophoric ignition will occur can be obtained if a value for δ is known. Metals with a greater pyrophoric tendency have a larger critical r, or a smaller value of δ/r. Empirically, the data in Chapter 14 show that pyrophoric properties, if exhibited at all, require a diameter roughly 0.03 μm or smaller. Since the physical thickness of oxide layers is normally in the range of 0.0025 – 0.0050 μm, this led Glassman to the criterion that pyrophoric metals are those corresponding to $\delta/r < 0.2$; in other words, if $\delta \leq 0.03$ μm and

$$\frac{\rho_{ox}}{\rho_m} \times \frac{\left(-\Delta H^o_{298}\right)_{ox} - \left(H^o_{bpt} - H^o_{298}\right)_{ox}}{\left[\left(H^o_{bpt} - H^o_{298}\right) + L_v\right]_m} \geq 1.05$$

Metals that satisfy this requirement include aluminum, calcium, cesium, lithium, magnesium, potassium, rubidium, and sodium. But it turns out that uranium and zirconium, which are exceptionally problematic in terms of pyrophoric behavior, do not qualify as pyrophoric metals under Glassman's definition. The reason they exhibit rapid combustion is because the oxide coat which is formed is non-protective—crevices form and oxidation continues to attack the metal through the crevices, thereby maintaining combustion, even though the heat balance is not sufficient to account for total vaporization.

THEORIES FOR METAL DUST LAYERS

If the metal is in the form of a powder or a dust then, under storage conditions it will be held in a container or settled into a layer. This introduces additional complexity, since there are now two separate sizes involved in the problem—the diameter of each particle and the dimension of the pile. Tetenbaum et al.[26] suggested that Frank-Kamenetskii theory (see Chapters 4 and 9) can be applied, with some modification. The basic theory envisions a reaction which is volumetrically uniform throughout the system. But for oxidizing metal particles, reaction can only occur at the surface of each particle. Thus, they concluded that the concentration of substance should be replaced by the total surface area of the all of the particles, divided by the gross system volume. In other words, the mass loss rate due to chemical reaction is taken to be:

$$\dot{m}''' = sA' e^{-E/RT}$$

where s = total surface area/gross volume (m^{-1}), and A' is now a pre-exponential factor which has the units kg m^{-2} s^{-1}. Then the Frank-Kamenetskii parameter δ becomes:

$$\delta = \frac{QA's}{\lambda}\left(\frac{E}{RT_o^2}\right) r^2 \exp\left(\frac{-E}{RT_o}\right)$$

and r (the half-thickness of the layer, sphere, etc.) can be solved for once the other variables are known; the meaning of the variables is the same as given in Chapters 4 and 9. Tetembaum et al. validated their theory against data for uranium powder. Values of E and A' were obtained from unpublished chemical kinetics studies, while the effective thermal conductivity λ was estimated on the basis of data for other metal powders. This effective conductivity is not constant, but decreases with decreasing particle size. The experimental ignition temperature data were obtained by using a fixed-diameter crucible and varying the particle size. The results showed a straight-line plot when the specific area (m^2 kg^{-1}) is plotted against $1/T_o$. Specific area can be measured by any number of experimental techniques and allows particles to be treated which are not necessarily spheres. Results for several metals are shown in Chapter 14 in this format. Note, however, that no data exist where both the particle size and the size of the pile would have been varied, thus, this crucial aspect of the theory is not validated.

EFFECT OF OXYGEN CONCENTRATION

The effect of oxygen concentration on the ignition of metals is generally small, at least in comparing results at 21% and at 100% oxygen. In a study on pressed metal powder tablets, Rozenband et al.[27] found a small effect, as shown in Table 6. The particular metals tested were not able to ignite in pure nitrogen atmospheres. The specimens incandesced at higher temperatures, but did not show overt ignition, due to the stable nature of the nitride film on the surface.

Table 6 Effect of oxygen concentration on ignition of pressed metal powder tablets

Metal	Ignition temperature (°C) at given oxygen concentration			
	25%	50%	75%	100%
hafnium	410	360	370	370
titanium	572	560	535	520
zirconium	350	322	310	300

Maček studied the ignition of single particles of aluminum as a function of the partial pressure of oxygen, and found the T_{ig} to decrease slowly with increasing oxygen pressure[28]. The amount of data collected was not large, but a relation of the form $T_{ig} \propto P_{O_2}^{1/2}$ was found to be reasonable.

EFFECT OF PRESSURE

The effect of pressure on ignition of metals is generally minimal.

EFFECT OF FLOW VELOCITY

The effect of flow velocity on ignition of metals is generally minimal, even for high-speed convective flows.

EFFECT OF MOISTURE

The effect of moisture on the ignition of metals is complex. Some require a dry atmosphere for this to occur (e.g., cerium amalgams, Raney nickel, thorium-silver alloys). However, while zirconium is easier to ignite in a dry atmosphere, moist powder, if ignited, burns more violently[29]. In some cases, introducing water into a pile of finely-divided metal powder will lead to explosion because of the rapid oxidation that is thereby caused[13]. This can have the additional complication in that hydrogen is liberated from the water and so the potential for a hydrogen explosion is created. Aluminum, magnesium, titanium, zinc, and zirconium powders are especially susceptible to this effect.

Ignition of carbon

Pure carbon in the form of graphite can ignite but cannot pyrolyze. Graphite can vaporize, but in common with metals, the vapor pressure is exceedingly low. Thus, surface phenomena play a strong role in its combustion. Coal, coke, char and other materials composed mostly, but not wholly, of carbon have a wide spectrum of ignition responses since some non-carbon material is present and consequently there is an ability to pyrolyze and to release combustible gases at moderate temperatures.

GRAPHITE AND OTHER RELATIVELY PURE FORMS OF CARBON

Goard and Mulcahy[30] studied the ignition of pure graphite rods in an oxygen stream and found T_{ig} values of 815, 803, and 769ºC for three commercial varieties tested. The first variety was re-tested in air and showed an ignition temperature there of 931ºC. These results pertain to the minimum gas flow rate they used, 0.3 m s^{-1}. At higher flow rates, T_{ig} values progressively rose. The authors also presented a theoretical model, but this was complicated by the fact that diffusion of oxygen into pores of the specimen needs to be considered. Actual ignition was found to invariably originate inside the pores for the specimens tested which ranged in porosity from 20 to 30%.

Makino et al.[31,32] studied the ignition of 10 mm graphite rods in a stagnation flow geometry and found that below ca. 800ºC reaction rates are minimal. Over the range 800 – 1200ºC, non-flaming surface combustion is found to occur. At about 1200ºC, flaming ignition occurs, with a CO flame being observed. When O_2 was used instead of air as the oxidizer, the appearance of a CO flame was found at ca. 900ºC. If the velocity of oxidizer gas was increased to higher values, the ignition temperatures rose. In additional studies in room air, Makino and Law[33] found that the lowest T_{ig} values were around 1100ºC, while at 100% O_2 the lowest value was 1000ºC, but the flow velocities were not identical

for the two cases. Under comparable conditions, the specimens in pure O_2 ignited at about 250ºC lower than ones in ambient air. The authors also offered a rather complicated theory which appeared to predict trends reasonably well, but did not include closed-form explicit solutions.

Visser and Adomeit[34] measured the ignition temperatures (homogeneous ignition only) of highly pure graphite in a stagnation-point geometry by subjecting specimens to a high-temperature convective flow field. They found effects of flow velocity, oxygen concentration, and moisture. The latter effect was quite pronounced, with very dry atmospheres leading to ignition temperatures about 250ºC higher than moist ones (> 0.1% H_2O by mass). The moisture effect arises since graphite contains no hydrogen and, consequently, a 'dry' CO flame occurs unless moisture can be picked up from the atmosphere. For ambient oxygen concentration, slow velocities, and moist conditions, an ignition temperature ca. 1100ºC was found. Makino et al.[35] conducted similar experiments and found a specimen temperature of ca. 1000ºC at ignition for moist conditions; for very dry atmospheres, the value rose by about 80ºC.

The effect of the partial pressure of oxygen was studied in the ignition of carbon powder having a particle diameter of 0.025 μm[36]. Ignition took place at 600ºC for an oxygen pressure of 0.5 atm and at 560ºC for 1.0 atm. It was reported that half the mass was already depleted by the time that ignition took place. At lower oxygen pressures, ignition did not occur.

Graphite can pyrophorically ignite in air, if it is first cooled down in liquid argon[37]. This is because available surface sites are first occupied by argon, when the argon evaporates, oxygen can rapidly get to the surface layer, and a heterogeneous ignition occurs.

The ignition temperature of diamond has been quoted as 700 – 800ºC in pure oxygen[38], although in view of the generally higher values found for graphite it is not clear if this is correct.

COAL, COKE, AND OTHER RELATIVELY IMPURE FORMS OF CARBON

Coal is a complex substance which is mostly carbon (for higher-rank coal), but may contain large amounts of volatile matter (for lower-rank coal). Thus, for a number of years, there has been a controversy in the scientific community as to whether coal particles ignite heterogeneously (at the surface) or homogeneously (that is, pyrolyzing first, with the pyrolysis gases igniting and burning at some distance away from the surface). A good introduction to some of the basic principles—and complexities—of coal combustion is provided by Chomiak[39].

The ignition temperature of coal particles has also been an exceptionally controversial issue. Essenhigh et al.[40] observed that: "Typically, the range of values cited for ignition temperatures of coals is 500º to 1000ºC. This is totally at variance with standard practice in the boiler industry, where decades of experience have established that there is a risk of explosion unless the temperatures leaving air-swept mills grinding bituminous coals are limited to about 70ºC; lignites and brown coals generally require grinding to be in inert gases. The discrepancy between recognized industrial safe practice and the reported laboratory measurements is too great for the latter to be credible to design engineers." Presumably this is because industrial hazards generally involve stockpiles where self-heating governs and not a single-particle ignition mode. Self-heating of carbonaceous materials is examined in Chapter 9 (theory) and Chapter 14 (empirical studies). In this Chapter ignition of single particles and dust clouds is considered, although for dust clouds Chapter 5 should also be consulted.

SINGLE PARTICLES

A simplified theory for the heterogeneous ignition of individual carbonaceous particles can be formulated along similar principles as the Semenov theory of the ignition of gases, discussed in Chapter 4, except that the reaction occurs at the surface and not in the volume. Thus, the heat generation is:

$$Q_G = AQc_O^n S \exp(-E/RT)$$

and the heat loss is:

$$Q_L = \frac{2\lambda}{d}(T_s - T_o)S$$

where A = pre-exponential factor, Q = heat of reaction, c_O = oxygen concentration, n = order of reaction, S = particle surface area, λ = conductivity of air, d = particle diameter. To obtain a closed-form solution requires a number of approximations, but the final result for the *gas* temperature needed to cause ignition is obtained as[40,41]:

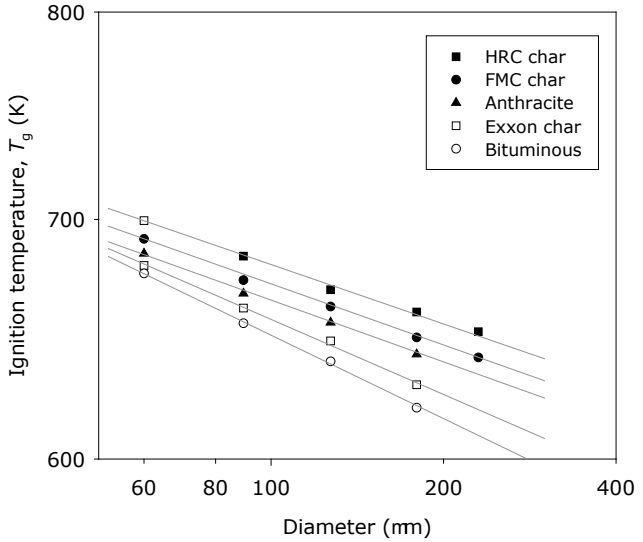


Figure 1 Plots of ignition data of five different coal types according to heterogeneous ignition theory

$$T_g^{\alpha-2} c_O^n d = b$$

The particle *surface* temperature, T_s, at ignition will be higher and can be computed from:

$$T_s = \frac{\alpha}{\alpha - 1} T_g$$

where α is obtained from:

$$E = \frac{\alpha^2}{\alpha - 1} RT_g$$

or

$$\alpha \approx \frac{E}{RT_g} \approx \frac{E}{RT_s}$$

In the above relations, α, b, and n are empirical constants, to be obtained from a fit of the data by log-log plots of T_g as a function of d, and T_g as a function of c_O. Figure 1 shows some results obtained by Chen et al.[42], as plotted according to the heterogeneous ignition theory. From the slopes of the line, values of α are found ranging from 15 (for bituminous coal) to 21 (for HRC char). This means that activation energies of 88 to 125 kJ mol^{-1} are found.

In their study, Chen et al. used specimen with volatile matter ranging from 3 to 45% and tested them by injecting single particles into a tube furnace. The authors estimated that the particle surface temperatures were 20 – 40ºC higher than the furnace temperature. No effect of volatile matter was found on the results.

Results giving the opposite trend are also to be found in the literature. Sinnatt and Moore[43] conducted ignition tests on a variety of coal types. In their experiments, 5 mg samples of powdered material were ignited using a modified Moore tester (see Chapter 6). Using only two particle sizes, they found that lower AIT values were obtained for the smaller particle size for the case of all the 5 coal types studied. Their results, consequently, fall along similar lines as do experimental data for the size effect on very fine metal particles. The coal particles, however, were relatively large, being those that pass through 75 and 150 μm sieve openings. Wall et al.[44] reviewed the literature through 1991 on this topic in some detail. For single-particle experiments, they found:

- T_{ig} decreases with increasing particle size: 9 studies
- T_{ig} increases with increasing particle size: 4 studies

In all of these studies, T_{ig} refers to the furnace temperature and not the particle temperature. Unlike in Chen's study, Wall et al. found that there is a roughly-linear decrease in T_{ig} with increasing volatile content. Generalizing from 6 studies, T_{ig} drops, on the average, from 800ºC for particles of zero volatile content, to 500ºC for particles with 50% volatile content.

Tomeczek[45] proposed a variant on the Semenov solution, whereby the loss term includes a radiant loss term $\varepsilon\sigma\left(T_s^4 - T_g^4\right)$ and conservation of energy gives:

$$AQY_o^n \exp(-E/RT_s)\, S = \left[\frac{2\lambda}{d}\left(T_s - T_g\right) + \varepsilon\sigma\left(T_s^4 - T_g^4\right)\right] S$$

Differentiating with respect to surface temperature gives:

$$\frac{AQEc_o^n}{RT_s^2} \exp(-E/RT_s) = \frac{2\lambda}{d} + 4\varepsilon\sigma T_s^3$$

Tomeczek suggested that in the intermediate temperature regime, n = ½ should be taken and that $E \approx 60 - 120$ kJ mol^{-1}, but he did not provide a full validation.

Brooks and Essenhigh[46] found that the effect of oxygen concentration progressively diminishes with increasing oxygen concentration. For 15 – 25 vol% O_2, raising the concentration significantly reduces T_{ig}, but as 100% is approached, further changes become small. Essentially identical results were obtained by Tognotti et al.[47] This is due to reaction rates being governed by Langmuir-Hinshelwood kinetics at low c_O values (wherein the reaction rate is proportional to c_O^n, with $n \approx$ ½ – 1.0), while at high c_O values T_{ig} becomes independent of c_O since desorption of the adsorbed O_2 film becomes the governing step. Bews et al.[48], analyzing data from a series of experiments on carbon particles where hydrogen impurities were very low, concluded that n = ½ on the basis that the governing step is one of chemisorption of oxygen atoms:

$$C_{(s)} + ½O_2 \rightarrow (C–O)_{(s)}$$

followed by a slow production of gaseous CO according to:

$$(C–O)_{(s)} \rightarrow CO$$

where the subscript (s) denotes solid state. Since intra-particle diffusion can play a role, however, such single-exponent treatments are rather approximate.

The above treatment is very simplified, since radiation, which will dominate at higher temperatures, is ignored. Bar-Ziv et al.[64] considered a theory which includes a radiative loss term, but they did not derive general correlations with it.

Another theory, with a different set of approximations, has been put forth by Annamalai and Durbetaki[49]. It predicts that ignition temperature should vary inversely with the $Y_O d$ product, where Y_O = oxygen mole fraction. Phuoc and Annamalai[50] included radiation losses from the particle and showed that the monotonic decrease of T_{ig} with increasing diameter does not continue for large diameters, if radiation is taken into account. Instead, they predicted that for $d >$ 200 μm, ignition temperatures would start to increase. Unlike most other theories, their theory was able to correctly anticipate a minimum oxygen concentration which is needed for ignition; using typical values for chemical constants, they estimated this at about 11 vol%. Du and Annamalai[51] developed a fairly comprehensive theory which encompassed both surface reactions and gas-phase reactions, thus being able to simulate the entire range of conditions involved in heterogeneous or homogeneous ignition. Homogeneous ignition was shown to occur at low oxygen con-

centrations or for large particle sizes (> 500 μm), with ignition being heterogeneous otherwise. Their calculations, while plausible, were not compared against any experimental data. Jüntgen and van Heek[52] did evaluate experimental data and concluded that the issue of heterogeneous/homogeneous ignition is influenced also by the heating rate to which the specimen is subjected: a medium heating rate (ca. 300 K s^{-1}) facilitates heterogeneous ignition, while particles subjected to much higher or much lower heating rates are more likely to show homogeneous ignition. In their study, all particles larger than about 120 μm also showed homogeneous ignition. The volatile content also affects the outcome, but was not examined by them as a variable.

In general, reported experimental ignition temperatures of coal, coke, char and other forms of impure carbon vary over a tremendous range, and known physical/chemical factors do not account for the spread. Volatile content and size are probably the two most important variables, but the study of Wall et al. found that these cannot adequately explain the data spread. As examples of extreme values, the ignition temperature of carbon soot, in the form of dust of unspecified particle diameter[53], was reported by NIST in 1947 as being 186ºC but details of their procedure are not available. Conversely, Khitrin[54] reported some extraordinarily high ignition temperatures, with the gas temperature needed for ignition of anthracite coal particles in the 75 – 100 μm size being 1027ºC in an environment of 21% oxygen, dropping to 805ºC in 100% oxygen. The surface temperature of the particle was stated to be about 100ºC higher, due to self-heating. Smaller particles required a yet-higher temperature for ignition, with a 20 μm particle igniting at about 1287ºC in 21% oxygen. Tomeczek and Wójcik[55] measured the ignition temperatures of single particles of coal. For 400 μm particles of anthracite coal (volatile matter 5.2%), they found T_{ig} = 970ºC at 21% oxygen. Sub-bituminous coal (volatile matter 32.3%) showed T_{ig} = 640ºC, while coal char gave T_{ig} = 660ºC. Larger particle sizes gave lower ignition temperatures. For example, sub-bituminous coal dropped to 600ºC for a particle size of 1000 μm. Raising oxygen concentrations lowered the ignition temperatures over the whole range of values explored, 10 – 100%. For very large particles, Fu et al.[56] found that varying the particle diameter did not change T_{ig} values. Using 3 – 6 mm coal chars, they found ignition temperatures of 500 – 700ºC, depending on the rank of the coal.

Boukara et al.[57] dropped single particles into a furnace supplied with pure O_2. Two, opposite trends for T_{ig} vs. particle size were found. Char particles showed decreasing T_{ig} values with particle diameter, dropping from 865 – 880ºC for 110 μm diameter, to 740 – 790ºC for 285 μm. Conversely, a high-volatile bituminous coal rose from 800ºC to 875ºC. In all cases, the temperatures refer to the temperature of the furnace.

Essenhigh et al.[40] surveyed a number of other studies and found that reported ignition temperatures spanned the range 300 – 1350ºC, without sufficient reasons being evident for the wide spread. Another recent survey is by Annamalai and Ryan[58]. Most of the studies have focused on a relatively few material types, making it hard to discern systematic trends. A systematic, although old, study by Blayden et al.[59] is thus of high value for illustrating trends. They exposed a small cup containing 0.25 g of powdered sample in a vertical tube furnace, with the samples being various coals that had been carbonized at a variety of temperatures. Their results (Figure 2) show a roughly-linear increase in ignition temperature with carbonization temperature. For a number of the specimens, they also obtained elemental analysis results, and this correlation is shown in Figure 3. For carbon content > 92%, the ignition temperature rises directly with carbon content. Furthermore, other aspects of the coal chemistry appear to be unimportant, in that data for three different coals fall on the same line. Thus, it can be concluded that, while the temperature of carbonization partly controls the carbon content of the char, it is the carbon content which is the controlling physical variable.

Apart from their work with the heterogeneous ignition theory, Essenhigh et al.[40] considered at length the arguments in favor of homogeneous ignition of coal particles, at least for some combinations of particle size and thermal environment conditions. The most persuasive argument was found to be the one concerning the effect of oxygen concentration. If coal particles ignited homogeneously, then the ignition temperature, according to homogeneous ignition theory, would *rise* with increasing oxygen concentration. However, the opposite has been found to be true in experiments. This is consistent with heterogeneous ignition theory which, as outlined above, predicts a fall in ignition temperature. It should be noted that actual coal particle combustion sometimes involves three stages: (1) ignition at the surface; (2) a transition to homogeneous (a flame away from the surface) combustion a while later; (3) followed by exhaustion of volatiles and re-ignition of char (surface burning).

Austin[60] conducted ignition experiments on individual carbonaceous particles in a high-temperature furnace and found that ignition times could be correlated by:

$$t_{ig} = a\frac{\rho d^{3/2}}{T_\infty^7} + b$$

where a and b are constants, ρ = particle density (kg m^{-3}), T_∞ = furnace temperature (K), and d = particle diameter (m). The very strong dependence on furnace temperature implies that radiant heat transfer predominates.

Laser ignition has been studied by several researchers. Phuoc et al.[61] used laser radiation at a wavelength of 1.06 μm to ignite single 3 mm coal particles. Using a pulse duration of 5 ms, they found that a minimum heat flux of 8000 kW m^{-2} was needed for ignition, but that up to 80% of the

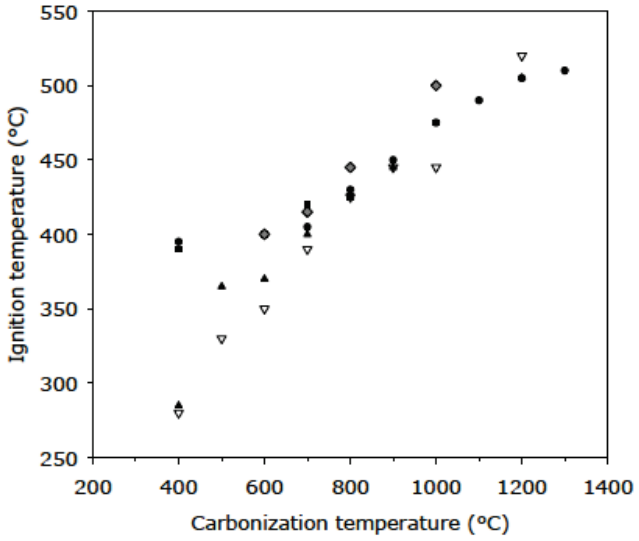


Figure 2 Effect of carbonization temperature on the ignition temperature of 5 different coal chars

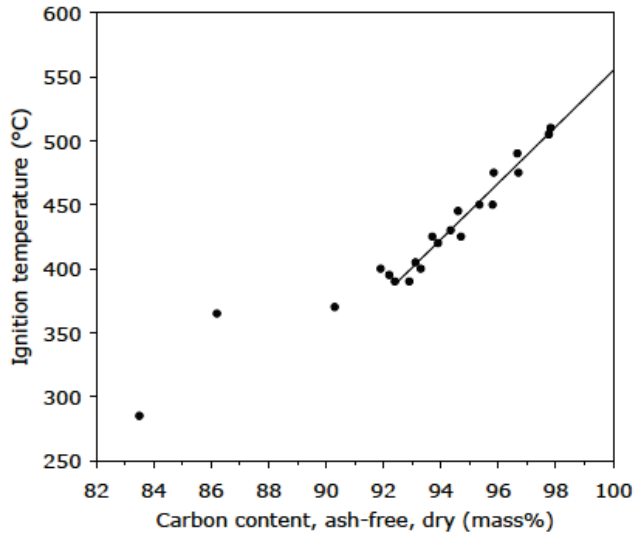


Figure 3 Ignition temperature of coal, expressed as a function of carbon content (data for 3 different coal types)

beam energy was absorbed by the pyrolysis gases emitted from the fuel. In their experiments, bituminous coal samples ignited solely in the gas phase, but subbituminous coal ignited in two stages, first at the surface, followed by a gas phase ignition. Temperature non-uniformities in particles undergoing laser ignition have been studied by Chen et al.[62] Zhang[63] ignited particles of various coals and chars with a laser; the particles were of 50 – 100 μm diameter. He observed that the percent of volatile matter was a crucial factor in determining the mode of ignition. Chars and cokes ignited only heterogeneously, coals of 17 – 30% VM ignited in a two-stage manner, while coal of 30 – 40% VM ignited homogeneously. He pointed out, however, that these conclusions should not be interpreted as general findings, since the thermal exposure conditions are also expected to play a role.

Small particles are difficult to study, since they must somehow be supported, or else studied in free-fall. More recently, it has been found possible to levitate small particles in an electric field by imparting to them an electric charge. Bar-Ziv et al.[64] and Wong et al.[65] ignited coal char particles with laser energy, while suspended in air with this arrangement. They found an ignition temperature of 1227ºC for 150 μm Spherocarb (nearly pure carbon) particles in O_2. In air, apparently a higher temperature would have been required, but the apparatus was not suitable for higher temperatures.

DUST CLOUDS

When a number of particles are suspended in the air in the form of a dust cloud, ignition may be achievable more easily than for single particles, but the phenomenon proved difficult to quantify, and little progress was made until rather recently. As shown above, for single particles, results are inconsistent, but more studies have found that the ignition temperature decreases with increasing particle size than the opposite. But in dust clouds, studies are generally consistent (see Chapter 5) in showing that the ignition temperature increases with particle size, although a lower asymptote is found, so that for smaller particles, there is a negligible effect of diameter. Krishna and Berlad[66] developed a theory based on heterogeneous ignition of the particles themselves and convective (but not radiative) heat transfer in the cloud. For dense clouds, they provided the solution:

$$\frac{1}{T_s}\exp\left(-E/RT_s\right) = d\,\frac{h_c\rho_p}{R_e c}\,\frac{R}{EQA\rho_g Y_o}$$

where d = particle diameter, h_c = convective heat transfer coefficient towards external environment, ρ_p = density of particle, R_e = radius of cloud, c = concentration of particles in dust cloud (g m^{-3}), E = activation energy, Q = heat of reaction, A = pre-exponential factor, ρ_g = density of air, and Y_o = oxygen mole fraction. Essenhigh et al.[40] pointed out that this relation can be approximated as:

$$T_s^{\alpha-1} = const. \times d$$

Since α is around 5 – 20, the relation is consistent with the experimental observation that the dust cloud ignition temperature decreases as particles become smaller. For dilute clouds, theory would predict the opposite effect, that is:

$$d \times T_s^{\alpha-1} = const.$$

however, available data do not suggest that there are ignition regimes for clouds of carbonaceous particles where decreasing the particle diameter would cause an increase in the ignition temperature. Higuera et al.[67] formulated a theory which does include radiation, but with no attempts at validation against experimental data.

Experimentally, Howard and Essenhigh[68] studied the ignition of bituminous coal dust clouds containing 36% volatile matter and found an ignition temperature of 1100ºC. For the samples studied (polydisperse, with particle size mode = 15 μm), they concluded that ignition is heterogeneous, and that volatiles do not play a significant role until after ignition. A much lower value, 550ºC was found by Hertzberg et al.[69], who studied dust clouds of bituminous coal particles; over the smallest particle size range of 17 – 55 μm, no significant size effect was found. For larger particles, increasing ignition temperatures were found, with 400 μm particles requiring 875ºC.

Lucas and Wall[70] conducted experiments where clouds of coal particles were introduced into a vertical furnace, but 'cloud ignition' and 'particle ignition' were separately identified. The latter occurred at low enough temperatures that only a very few particles ignited and there was no 'cooperative mechanism.' Cloud ignition, by contrast, comprised an explosion involving the entire combustible mass. For coals having very high volatile matter (32 – 51%), they found that 70 μm particles showed particle ignition at 420 – 540ºC, decreasing to 380 – 530ºC for 150 μm size. Cloud ignition temperatures were 540 – 670ºC for 70 μm particles and 550 – 670ºC for 150 μm particles. In all cases, the temperature reported were those of the furnace. It is not clear why the cooperative mechanism should result here in higher ignition temperatures being needed.

When dust clouds are dilute enough, experimental trends simply follow those for single-particle. Rybak et al.[71] released 'small clouds' of ca. 10 mg into a furnace. For 90 μm particles of nearly pure carbon (97%), they found T_{ig} = 740ºC at ambient oxygen concentration. Char particles derived from sub-bituminous coal (17% volatile matter) gave T_{ig} = 460ºC. Both materials showed a smooth decrease of ignition temperatures vs. oxygen concentration over the range 8 – 50%. The same group[72] later reported on results where smaller quantities (0.2 – 0.5 mg) of particles were introduced into the furnace. Using 97%-pure carbon, they obtained lower ignition temperatures, indicating the expected lowering of ignition temperature due to the cooperative mechanism. Particles of 60 μm size gave T_{ig} = 560ºC, decreasing to 500ºC for 150 μm. They considered that their results indicated homogeneous, rather than heterogeneous ignition. Flashing was reported to occur at lower temperatures than sustained ignition. In both sets of experiments, the temperatures reported were the furnace temperature needed for ignition.

The state of research must be assessed as being incomplete and contradictory at this point. Not only are widely disparate values reported, but even qualitative trends seem to depend greatly on the details of the experimental procedure adopted. In addition, it is not clear that research findings and actual fire experience have converged sufficiently since Essenhigh's warning in 1989.

Test methods

Unlike for other substances, there are no standard test methods for ignition of metals. Almost every research study on the ignition of metals has been based on a different experimental technique. References are given in Chapter 14 under *Metals*. Schmitt[73] considers that experimental arrangements generally fall into the following categories:

- rising temperature method (similar concept to thermal analysis studies)
- shielded ignition method (specimen is preheated in an inert atmosphere, then oxidizer is introduced)
- flame or torch heating
- crucible tests and pot furnaces
- tube furnaces
- high-pressure reactor
- centrifugal reactor
- electrically heated wire in an air stream
- bell jar combustion
- liquid metal spray
- plus various general techniques for small particles—single particle dropped in furnace, particles introduced into flat-flame burners, and dust cloud/dust layer methods.

ASTM considers[74] that testing of metals for autoignition is not an appropriate endeavor, because ignitions of metals generally occur by means other than a homogenous, bulk raising of the temperature. For use of metals in high-pressure oxygen systems, a number of specialized tests have been developed, and these are covered in Chapter 13.

References

1. Bahn, G. S., On Pyrophoricity of Metals, and on Fine Metal Powders in Particular, *Pyrodynamics* 3, 29-41 (1965).
2. Markstein, G., Combustion of Metals, *AIAA J.* **1**, 550-562 (1963).
3. Monroe, R. W., Bates, C. E., and Pears, C. D., Metal Combustion in High-Pressure Flowing Oxygen, pp. 126-149 in **Flammability and Sensitivity of Materials in Oxygen-Enriched Atmospheres** (ASTM STP 812), ASTM (1983).
4. Werley, B. L., et al., A Critical Review of Flammability Data for Aluminum, pp. 300-345 in **Flammability and Sensitivity of Materials in Oxygen-Enriched Atmospheres** (ASTM STP 1197), ASTM (1993).
5. Glassman, I., Combustion of Metals: Physical Considerations, pp. 253-258 in **Solid Propellant Rocket Research**, Academic Press, New York (1960).
6. Glassman, I., **Combustion**, 3rd ed., Academic Press, San Diego (1996).

7. Steinberg, T. A., Wilson, D. B., and Benz, F., The Combustion Phase of Burning Metals, *Combustion and Flame* **91**, 200-208 (1992). Response by Glassman: **93**, 338-342 (1993); response by authors: **93**, 343-347 (1993).
8. Price, E. W., Combustion of Metallized Propellants, pp. 479-513 in *Prog. in Astronautics and Aeronautics*, vol. 90: Fundamentals of Solid-Propellant Combustion, AIAA, New York (1984).
9. Pilling, N. B., and Bedworth, R. E., The Oxidation of Metals at High Temperatures, *J. Inst. Metals* **29**, 529-591 (1923).
10. Kofstad, P., **High-Temperature Oxidation of Metals**, Wiley, New York (1966).
11. Mellor, A. M., Heterogeneous Ignition of Metals: Model and Experiment (Ph.D. dissertation), Princeton Univ., Princeton NJ (1967).
12. Breiter, A. L., Maltsev, V. M., and Popov, E. I, Models of Metal Ignition, *Combustion, Explosion, and Shock Waves* **13**, 475-484 (1977).
13. Hardt, A. P., **Pyrotechnics**, Pyrotechnica Publications, Post Falls ID (2001).
14. Grosse, A. von, and Conway, J. B., Combustion of Metals in Oxygen, *Ind. and Eng. Chem.* **50**, 663-672 (1958).
15. Nelson, L. S., Combustion of Metal Droplets Ignited by Flash Heating, pp. 409-416 in *11th Symp. (Intl.) on Combustion*, The Combustion Institute, Pittsburgh (1966).
16. Merzhanov, A. G., Thermal Theory of Metal Particle Ignition, *AIAA J.* **13**, 209-214 (1975).
17. Reynolds, W. C., Investigation of Ignition Temperatures of Solid Metals (Tech. Note D-182), NASA, Washington (1966).
18. Frank-Kamenetskii, D. A., **Diffusion and Heat Transfer in Chemical Kinetics**, 2nd ed., Plenum Press, New York (1969).
19. Yuen, W., W., A Model of Metal Ignition Including the Effect of Oxide Generation, pp. 59-78 in *Flammability and Sensitivity of Materials in Oxygen-Enriched Atmospheres: Second Volume* (ASTM STP 910), ASTM (1986).
20. Arutyunan, A. B., Kharatyan, S. L., and Merzhanov, A. G., Theory of the Ignition of Metal Particles. II. Ignition of Metal Particles with the Simultaneous Formation of a Product Film and a Solid Solution, *Combustion, Explosion, and Shock Waves* **16**, 139-147 (1980).
21. Gremyachkin, V. M., Istratov, A. G., and Leipunskii, O. I., Theory of Combustion of a Boron Particle in Oxygen in High-Temperature Environment, *Combustion, Explosion, and Shock Waves* **15**, 691-698 (1979).
22. Khaikin, B. I., Bloshenko, V. N., and Merzhanov, A. B., On the Ignition of Metal Particles, *Combustion, Explosion, and Shock Waves* **6**, 412-422 (1970).
23. Friedman, R., and Maček, A., Ignition and Combustion of Aluminium Particles in Hot Ambient Gas, *Combustion and Flame* **6**, 9-19 (1962).
24. Glassman, I., Mellor, A. M., Sullivan, H. F., and Laurendeau, N. M., A Review of Metal Ignition and Flame Models, Paper 19 in *Reactions between Gases and Solids* (NATO Conf. Proc. No. 52), North Atlantic Treaty Organization, Advisory Group for Aerospace Research and Development, Neuilly-sur-Seine, France (1970).
25. Glassman, I., Papas, P., and Brezinsky, K., A New Definition and Theory of Metal Pyrophoricity, *Combustion Science and Technology* **83**, 161-165 (1992).
26. Tetenbaum, M., Mishler, L., and Schnizlein, G., Uranium Powder Ignition Studies, *Nuclear Science & Engineering* **14**, 230-238 (1962).
27. Rozenband, V. I., Chichev, V. A., and Afanaseva, L. F., Ignition of Certain Transition Metals in a Gaseous Oxidizer, *Combustion, Explosions, and Shock Waves* **12**, 26-30 (1976).
28. Maček, A., Fundamentals of Combustion of Single Aluminum and Beryllium Particles, pp. 203-217 in *11th Symp. (Intl.) on Combustion*, The Combustion Institute, Pittsburgh (1966).
29. Schmitt, C. R., Pyrophoric Materials—A Literature Review, *J. Fire and Flammability* **2**, 157-172 (1971).
30. Goard, P. R. C., and Mulcahy, M. F. R., A Study of the Ignition of Graphite, *Carbon* **5**, 137-153 (1967).
31. Makino, A., Araki, N., and Mihara, Y., Combustion of Artificial Graphite in Stagnation Flow: Estimation of Global Kinetic Parameters from Experimental Results, *Combustion and Flame* **96**, 261-274 (1994).
32. Makino, A., Kato, I., Senba, M., Fujizaki, H., and Araki, N., Flame Structure and Combustion Rate of Burning Graphite in the Stagnation Flow, pp. 3067-3074 in *26th Symp. (Intl.) on Combustion*, The Combustion Institute, Pittsburgh (1996).
33. Makino, A., and Law, C. K., Ignition and Extinction of CO Flame over a Carbon Rod, *Combustion Science and Technology* **73**, 589-615 (1990).
34. Visser, W., and Adomeit, G., Experimental Investigation of the Ignition and Combustion of Graphite Probe in Cross Flow, pp. 1845-1851 in *20th Symp. (Intl.) on Combustion*, The Combustion Institute, Pittsburgh (1984).
35. Makino, A., Araki, N., and Mihara, Y., Combustion of Artificial Graphite in Stagnation Flow: Estimation of Global Kinetic Parameters from Experimental Results, *Combustion and Flame* **96**, 261-274 (1994).
36. L'Homme, G. A. and Boudart, M., The Ignition of Carbon and Its Catalysis by Platinum, pp. 197-202 in *11th Symp. (Intl.) on Combustion*, The Combustion Institute, Pittsburgh (1966).
37. Veselovskii, V. S., Surface Oxidation of Coals, pp. 68-71 in **Surface Chemical Compounds and their Role in Adsorption Phenomena** (AEC TR 3750), Kiselev, A. V., ed., US Atomic Energy Commission, Washington (1957).
38. Ellern, H., **Military and Civilian Pyrotechnics**, Chemical Publishing, New York (1968).
39. Chomiak, J., **Combustion: A Study in Theory, Fact, and Application**, Abacus Press, New York (1990).
40. Essenhigh, R. H., Misra, K. M., and Shaw, D. W., Ignition of Coal Particles: A Review, *Combustion and Flame* **77**, 3-30 (1989).
41. Cassel, H. M., and Liebman, I., The Cooperative Mechanism in the Ignition of Dust Dispersions, *Combustion and Flame* **3**, 467-475 (1959).
42. Chen, M.-R., Fan, L.-S., and Essenhigh, R. H., Prediction and Measurement of Ignition Temperatures of Coal Particles, pp. 1513-1521 in *20th Symp. (Intl.) on Combustion*, The Combustion Institute, Pittsburgh (1984).
43. Sinnatt, F. S., and Moore, B., A Method of Determining the Relative Temperatures of Spontaneous Ignition of Solid Fuels, *J. Soc. Chemical. Ind.* **39**, 72T-78T (1920).
44. Wall, T. F., Gupta, R. P., Gururajan, V. S., and Zhang, D., The Ignition of Coal Particles, *Fuel* **70**, 1011-1016 (1991).

45. Tomeczek, J., **Coal Combustion**, Krieger, Malabar FL (1994).
46. Brooks, P. J., and Essenhigh, R. H., Variation of Ignition Temperatures of Fuel Particles in Vitiated Oxygen Atmospheres: Determination of Reaction Mechanism, pp. 293-302 in *21st Symp. (Intl.) on Combustion*, The Combustion Institute, Pittsburgh (1986).
47. Tognotti, L., Malotti, A., Petarca, L., and Zanelli, S., Measurement of Ignition Temperature of Coal Particles Using a Thermogravimetric Technique, *Combustion Science and Technology* **44**, 15-28 (1985).
48. Bews, I. M., Hayhurst, A. N., Richardson, S. M., and Taylor, S. G., The Order, Arrhenius Parameters, and Mechanism of the Reaction between Gaseous Oxygen and Solid Carbon, *Combustion and Flame* **124**, 231-245 (2001).
49. Annamalai, K., and Durbetaki, P., A Theory on Transition of Ignition Phase of Coal Particles, *Combustion and Flame* **29**, 193-208 (1977).
50. Phuoc, T. X., and Annamalai, K., A Heat and Mass Transfer Analysis of the Ignition and Extinction of Solid Char Particles, *J. Heat Transfer* **121**, 886-893 (1999).
51. Du, X., and Annamalai, K., The Transient Ignition of Isolated Coal Particle, *Combustion and Flame* **97**, 339-354 (1994).
52. Jüntgen, H., and van Heek, K. H., An Update of German Non-Isothermal Coal Pyrolysis Work, *Fuel Processing Technology* **2**, 261-293 (1979).
53. As cited in: Stecher, G. E., and Lendall, H. N., **Fire Prevention and Protection Fundamentals (Comburology)**, The Spectator, Philadelphia (1953).
54. Khitrin, L. N., **Physics of Combustion and Explosion**, Israel Program for Scientific Translations, Jerusalem (1962). Russian original: **Fizika goreniya i vzryva**, Izdatelstvo Moskovskogo Universiteta, Moscow (1957).
55. Tomeczek, J., and Wójcik, J., A Method of Direct Measurement of Solid Fuel Particle Ignition Temperature, pp. 1163-1167 in *23rd Symp. (Intl.) on Combustion*, The Combustion Institute, Pittsburgh (1990).
56. Fu, W. B., Ge, Y., Tang, M. H., and Liu, T. F., A Study on Ignition Criterion of a Large Carbon/Char Particle, *Combustion Science and Technology* **108**, 91-101 (1995).
57. Boukara, R., Gadiou, R., Gilot, P., Delfosse, L., and Prado, G., Study of Ignition of Single Coal and Char Particles in a Drop Tube Experiment by a Probability Method, pp. 1127-1133 in *24th Symp.(Intl.) on Combustion*, The Combustion Institute, Pittsburgh (1992).
58. Annamalai, K., and Ryan, W., Interactive Processes in Gasification and Combustion. Part II: Isolated Carbon, Coal and Porous Char Particles, *Prog. Energy and Combustion Science* **19**, 383-446 (1993).
59. Blayden, H. E., Riley, H. L., and Shaw, F., A Study of Carbon Combustibility by a Semi-micro Method, *Fuel in Science and Practice* **22**, 32-38; 64-71 (1943).
60. Austin, P. J., Ignition and Combustion of Cellulosic Dust Particles (Ph.D. dissertation), Univ. Michigan, Ann Arbor (1994).
61. Phuoc, T. X., Mathur, M. P., and Ekmann, J. M., High-Energy Nd-Yag Laser Ignition of Coals: Experimental Observations, *Combustion and Flame* **93**, 19-30 (1993).
62. Chen, J. C., Taniguchi, M., Narato, K., and Ito, K., Laser Ignition of Pulverized Coals, *Combustion and Flame* **97**, 107-117 (1994).
63. Zhang, D.-K., Laser-induced Ignition of Pulverized Coal Particles, *Combustion and Flame* **90**, 134-142 (1992).
64. Bar-Ziv, E., et al., Measurement of Combustion Kinetics of a Single Char Particle in an Electrodynamic Thermogravimetric Analyzer, *Combustion and Flame* **75**, 81-106 (1989).
65. Wong, B. A., Gavalas, G. R., and Flagan, R. C., Laser Ignition of Levitated Char Particles, *Energy & Fuels* **9**, 484-492 (1995).
66. Krishna, C. R., and Berlad, A. L., A Model for Dust Cloud Autoignition, *Combustion and Flame* **37**, 207-210 (1980).
67. Higuera, F. J., Liñán, A., and Treviño, C., Heterogeneous Ignition of Coal Dust Clouds, *Combustion and Flame* **75**, 325-342 (1989).
68. Howard, J. B., and Essenhigh, R. H., Mechanism of Solid-Particle Combustion with Simultaneous Gas-Phase Volatiles Combustion, pp. 399-408 in *11th Symp. (Intl.) on Combustion*, The Combustion Institute, Pittsburgh (1966).
69. Hertzberg, M., Cashdollar, K. L., Ng, D. L., and Conti, R. S., Domains of Flammability and Thermal Ignitability for Pulverized Coals and Other Dusts: Particle Size Dependences and Microscopic Residue Analysis, pp. 1169-1180 in *19th Symp. (Intl.) on Combustion*, The Combustion Institute, Pittsburgh (1982).
70. Lucas, J. A., and Wall, T. F., Volatile Matter Release, Particle/Cloud Ignition, and Combustion of Near-Stoichiometric Suspensions of Pulverised Coal, pp. 485-491 in *25th Symp. (Intl.) on Combustion*, The Combustion Institute, Pittsburgh (1994).
71. Rybak, W., Zembruski, M., and Smith, I. W., Kinetics of Combustion of Petroleum Coke and Sub-Bituminous Coal Char: Results of Ignition and Steady-State Techniques, pp. 231-237 in *22nd Symp. (Intl.) on Combustion*, The Combustion Institute, Pittsburgh (1988).
72. Wall, T. F., et al., The Ignition, Burning Rate and Reactivity of Petroleum Coke, pp. 1177-1184 in *23rd Symp. (Intl.) on Combustion*, The Combustion Institute, Pittsburgh (1990).
73. Schmitt, C. R., unpublished study (1996).
74. Standard Guide for Evaluating Metals for Oxygen Service (ASTM G 94), ASTM.

Copyright © 2003, 2014 Vytenis Babrauskas

Chapter 9. Self-heating

Highlights and summary of practical guidance **369**
Introduction **371**
Basic phenomena **373**
Theory of self-heating **374**
Steady-state theory for symmetrically cooled bodies *377*
Peak temperatures under subcritical conditions 379
Bodies of other shapes 380
Steady state theory for unsymmetrically cooled bodies *382*
Infinite slab 382
Hollow infinite cylinder 383
Steady-state theory including oxygen diffusion *383*
Steady-state theory including fuel depletion *384*
Correction for low activation energy *385*
More complex reactions *386*
Hot work, cold work, and hot spots *387*
Hot work 387
Cold work 389
Inert hot spots 390
Reactive hot spots 390
Applied heat flux 391
Transient theory *391*
Estimating time to criticality 391
Linearly increasing surface temperature 394
More advanced models 394
Applications **395**
Ignition from self-heating *395*
Effects of different variables on self-heating *395*
Chemical and physical nature of the substance 395
Pile size and shape, and porosity of the substance 395
Particle size 396
Temperature 396
Time of storage 396
Access of air 396
Oxygen concentration 397
Insulation 398
Multiple packing 398
Moisture and rain 398
Density 400
Antioxidants 400
Contaminants 400
Multiple-component substances 401
Ignition of dust layers *401*
Electrical heating problems 402
Hot spots *402*
Self-heating in liquids *403*
Liquid-soaked porous solids *403*

Detonation or deflagration upon self-heating ... *404*
Preventive measures ... *404*
Tests for self-heating or reactivity ... **405**
Real-scale tests ... *406*
UN Test H1—The US SADT test ... 406
Geometric-scaling tests ... *406*
Scaling according to Frank-Kamenetskii theory ... 406
Oven-basket tests: FRS method ... 406
Oven-basket tests: crossing point methods ... 414
Oven-basket tests: Nordtest method ... 417
Oven-basket tests: IMO test ... 417
Oven-basket tests: UN Test N4 ... 418
Hotplate tests ... 418
Scaling according to Semenov theory ... 420
General Dewar flask testing ... 420
UN Test H2—Adiabatic storage test ... 421
UN Test H4—Heat accumulation storage test ... 422
Calorimeter tests ... *422*
Adiabatic calorimeters ... 423
Isothermal calorimeters ... 425
ARC and APTAC tests ... 425
Other industrial reaction calorimeters ... 428
Thermal analysis methods ... *428*
DTA, DSC, and related techniques ... 429
Simple screening test based on DSC ... 430
Quantitative ASTM procedures ... 431
ASTM E 698 ... 431
ASTM E 793 ... 431
ASTM E 1641 ... 431
ASTM E 1231 ... 432
Qualitative ASTM procedures ... 432
UN Test H3—Isothermal storage test ... 432
Empirical or qualitative tests ... *433*
Mackey test and related tests ... 433
Ordway test ... 433
Mackey test ... 433
ASTM E 771 test ... 434
ASTM E 476 ... 434
UN Test O1 for oxidizing solids ... 434
UN Test O2 for oxidizing liquids ... 435
UN Test S1—Trough test for fertilizers containing nitrates ... 435
Bureau of Mines dust layer ignition temperature test ... *435*
Oxygen consumption calorimetry ... *435*
Further readings ... **436**
References ... **436**

Highlights and summary of practical guidance

Spontaneous combustion is the general topic of this Chapter. Specific theories and examples in this Chapter deal with porous or granular solids, although many concepts are also applicable to non-porous solids or to liquids, which are considered in Chapter 10. For open flaming to occur due to self-heating of a porous solid material, it is necessary that:

(1) the material be capable of self-heating;
(2) self-heating of the material must be sufficient to lead to thermal runaway;
(3) thermal runaway must initiate self-sustained smoldering;
(4) the smolder front must reach the outside of the material (or the process must create large enough cavities) where flames can be established.

The basic process of smoldering was already considered in Chapter 7. The new concepts introduced in this Chapter are defined as follows:

Self-heating: an increase in temperature due to exothermicity of internal reactions.

Thermal runaway: self-heating which rapidly accelerates to high temperatures.

Spontaneous combustion: visible smoldering or flaming caused by thermal runaway.

Thus, the *process* is called 'self-heating,' a critical *intermediate outcome* of 'thermal runaway' may or may not occur, while the *final outcome* (if thermal runaway does occur) may be 'spontaneous combustion.' There is no single, universally accepted definition of 'spontaneous combustion,' but the definition above can be considered to be the most reasonable one. Sometimes spontaneous combustion is understood in a more restricted sense, whereby it is said to occur only if open flaming occurs. Much of this Chapter is concerned with theories of self-heating and their application to testing. There exists essentially no systematic knowledge on the question of whether thermal runaway will lead to self-sustained smoldering, but it is often conservatively assumed that if thermal runaway occurs, then the process will continue until spontaneous combustion is seen. The question of whether smoldering will or will not lead to flaming has been discussed in Chapter 7, where it was shown that there is little useful guidance available. Again, it is often conservatively assumed that flaming will automatically occur if thermal runaway occurs.

Since almost all organic substances (and many inorganic ones) can undergo exothermic reactions, it is necessary to understand why everything is not going into thermal runaway and manifesting spontaneous combustion. Self-heating involves an exothermic chemical reaction which serves to raise the temperature of a substance. The most common type of chemical reaction which is encountered in substances showing this problem is oxidation, whereby molecules of the substance react with molecules of oxygen from the air. Almost all organic substances can exhibit exothermic oxidation. For self-heating to be a problem, however, rather than merely a scientific curiosity, normally requires that the substance being oxidized be porous, since oxygen reacts with the solid only at the surface and non-porous materials have a small surface-area/volume ratio. Thus, most solids and liquids do not show the problem, since they are not porous. The problem commonly arises in agricultural products, such as grains or hay, in porous wood products, and in rags oiled with certain vegetable oils. In all of these situations, there is a large surface area over which oxygen may contact the organic substance. In addition, it is necessary that natural cooling, which occurs by convection on any surfaces exposed to air, be insufficient to remove the heat being generated.

If only a small pile of material is present, or if access of oxygen is poor to the interior (for reactions that need oxygen) then self-heating, but not thermal runaway may occur. The material will rise in temperature slightly above ambient, but the rise will not be sustained and eventually the temperature will start going down since reactants will become depleted.

The mechanism involved in spontaneous combustion is fundamentally different from ignition of solids from external heating. When a solid is externally heated, ignition typically occurs due to a gas-phase oxidation reaction. But when a substance goes into spontaneous combustion, the chemical reactions involved are those of the solid phase, which are exothermic pyrolysis or surface oxidation reactions. As a result, there is no correlation between ease of ignition from external heating and propensity to spontaneous combustion.

Industrial accidents involving self-heating often involve non-oxidative reactions, such as polymerization or decomposition. These reactions are a problem with certain liquids, and self-heating reactions in those cases can be exceptionally violent (explosions, not just fires). For oxidizing porous bodies, molecular diffusion is necessary to supply oxygen to the reaction, and it is a relatively slow process. In the case of a liquid which is polymerizing or decomposing, no such slow step exists to limit the reaction rate. The problems of reactive liquids are treated in Chapter 10.

The self-heating reactions in porous solids (or oiled, porous materials) occur at the surfaces of the solid or liquid, not in the gas phase. Thus, if self-heating 'runs away,' it manifests itself initially as a propagating smolder front. The process most commonly starts at the center of the material. Thus, piles may sometimes be cut open to reveal a charred center, but virgin outer areas. Eventually, flaming can occur if the reaction front reaches an open-air surface. Self-heating may be localized to an area that is not at the center if the material is heated from one side, or if it is sufficiently non-homogeneous that hot spots occur. Flaming normally can-

not occur inside porous bodies (unless the process creates large cavities) because (a) pore sizes are typically less than the quenching distance for flames; (b) the oxygen concentration may be too low for flaming; and (c) the internal flow rate of flammable pyrolysis gases within the pores of the material may be too small to sustain a flame.

For some materials, bagging a self-heating commodity into modest size bags is an effective strategy, even if the bags are then stacked in large stacks. This is attributed to the cooling that becomes available through the gaps between the bags. It is helpful if the material from which the bags are made is relatively air-tight, but even materials having a measurable permeability can reduce oxygen availability.

When laboratory data are put into theoretical relationships, predictions can be made of the maximum size of pile that can be stored at a given temperature without undergoing spontaneous combustion. Example results are shown in Figure 1. These were obtained from laboratory data (E and P values) provided for various substances in Chapter 14. It was assumed that the pile is a cube and that cooling is inefficient (Bi = 1.7). The two extreme substances shown are fire-retarded cellulosic attic insulation, which is highly resistant to self-heating, and linseed oil spread on cotton cloth, which is highly prone. The same graph also illustrates that blind faith cannot be placed in theoretical computations. Actual experiments (see Chapter 14) show that as little as 50 g worth of rag, well-covered in linseed oil, can lead to spontaneous combustion. Yet, the theoretical results of Figure 1 suggest that, at a room temperature of 25ºC, a cube of 0.3 m (1 ft) on a side is the minimum. Part of the problem may be that the input data used for the theoretical calculation are of uncertain accuracy. It may be noted that the lines in Figure 1 are all curved. This means that it would not be reasonable to plot a few points and then extrapolate graphically. Instead, methods are developed in this Chapter which transform the size/temperature relationship so that linear plots can be made and extrapolations—if there is confidence in the underlying theory—can be undertaken. It must be emphasized that the temperature of interest is the critical ambient temperature, which is the temperature of the *environment* which must not be exceeded to avoid thermal runaway. The material itself will be at a higher temperature (critical stacking temperature), as shown in Figure 3, where T_o denotes the critical ambient temperature and T_c denotes the critical stacking temperature. T_c may be 20 – 30º higher than T_o.

As with any other type of fire safety problem, the most reliable results are obtained if full-scale tests are done. The present Chapter contains details on conducting a variety of small-scale tests, but it must be appreciated that uncertainty is much higher when only small-scale tests are run. The

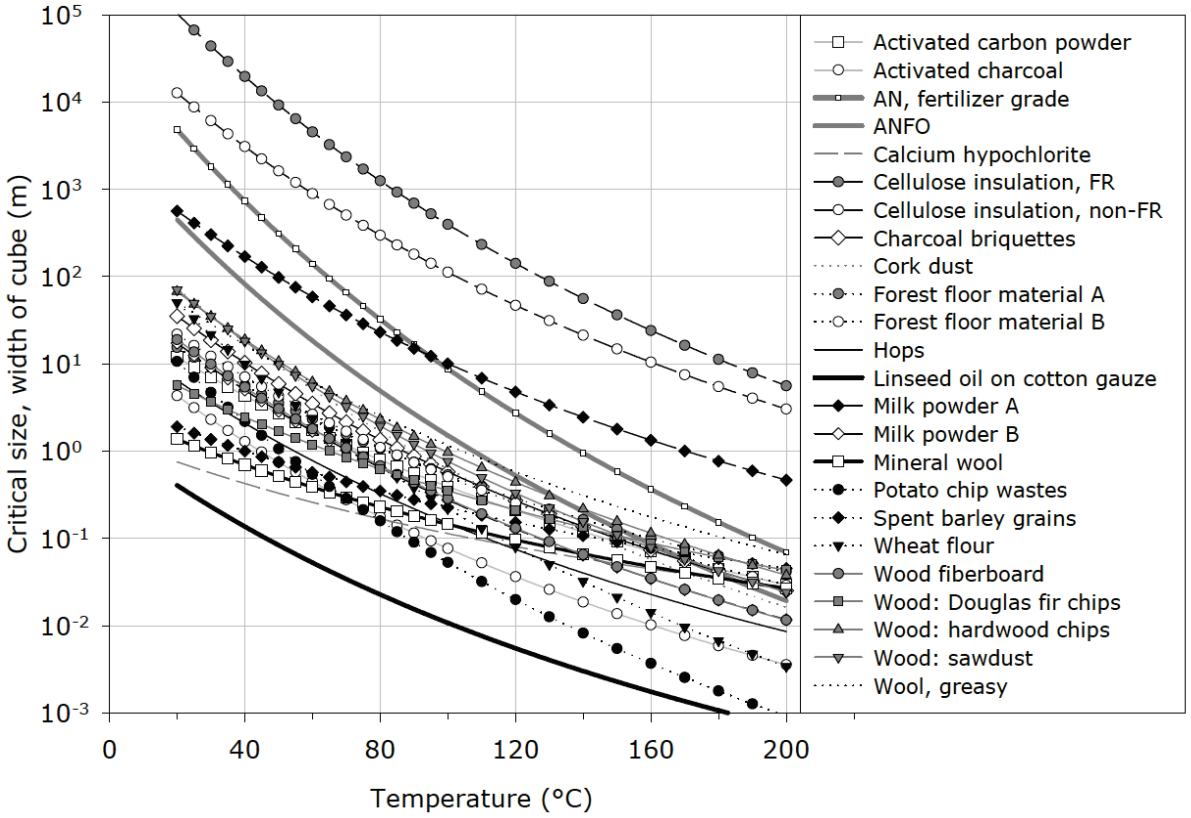


Figure 1 Relationship between size and critical ambient temperature estimated for various substances by applying a theoretical relationship to small-scale test results

basic principle of the small-scale testing is that putting a smaller sample into a higher-temperature environment is equivalent to putting a larger sample into a lower-temperature environment. But unquestioningly using scaling rules can lead to wrong predictions. For example, test results for calcium hypochlorite (see Chapter 14), indicate that two different temperature regimes exist. If extrapolations were made from the high-temperature (small size) data only, an unconservative estimate of the full-scale critical conditions would be produced.

The standard theory presented in this chapter has been shown not to be applicable to (at least some types of):

- bagasse (due to pivotal role of moisture flow)
- benzoyl peroxide (due to multiple reactions and effects of phase change)
- calcium hypochlorite (due to two different reaction regimes)
- coal (due to strong role of oxygen and moisture flow; also since the problem time constants are typically so long that a full time-dependent solution must be sought, rather than being able to rely on steady-state results)
- fertilizers (due to multiple reactions, high variations in thermal conductivity, moisture flow, and melting)
- haystacks (due to biological heating by micro-organisms)
- liquid-soaked pipe insulation (in cases where the fluid is of high volatility and low exothermicity)
- sodium dithionite (due to two exotherms)
- synthetic dyestuffs, certain types (due to complex reactions)
- synthetic rubber, SBR type (due to presence of both endothermic and exothermic reactions).

For such products, either full-scale testing or a comprehensive computer model is required. Each of these products is discussed in Chapter 14.

Theoretical and empirical (e.g., data extrapolations) methods exist for predicting the *time* to runaway, but all of these methods are highly uncertain, due to chemistry complications in the reactions of real materials.

Introduction

Self-heating can occur in any of the states of matter—gas, liquid, or solid. The use of self-heating theory to explain the autoignition of gases was already presented in Chapter 4. Self-heating of liquids is a specialized problem which will be taken up in Chapter 10. In this Chapter, the development will center around self-heating of solids, specifically porous solids. This state of aggregation covers a very wide range of practical problems of spontaneous combustion, ranging from coal mines, to hay stacks, to linseed-oil soaked rags.

Self-heating problems have been known in connection with hay and other agricultural products since time immemorial. However, the science of self-heating is relatively young, largely because it is such a complicated phenomenon. In 1760 the Frenchman Montet wrote a paper about the problem. Active research was triggered when the Russian frigate MARIE caught fire in Cronstadt harbor on 20 April 1781. Count Ivan Tschernichev, the Vice-President of the St. Petersburg Admiralty College, suspected that this may have been due to storage of a hammock which had soaked up a staining preparation—boiled hempseed oil and pine soot. Thus, during the spring of 1781, he conducted a series of experiments to determine the self-heating properties of oil-soaked materials[1]; this is perhaps the first scientific series of experiments on ignitability recorded in the world's literature. Tschernichev's work immediately aroused great interest, and similar experiments were conducted almost imme-

Table 1 US structure fires (average annual data for 1994-1998) involving spontaneous heating or chemical reaction, by type of material first ignited

Type of Material	Fires	Civilian deaths	Civilian injuries	Direct property damage (in millions)
Cotton or rayon fabric or finished goods	905 (16.6%)	1 (9.6%)	27 (19.5%)	$14.1 (12.1%)
Oily rags	710 (13.0%)	0 (0.0%)	11 (8.2%)	$18.8 (16.2%)
Grass, leaves, or brush	568 (10.4%)	0 (0.0%)	6 (4.4%)	$12.7 (10.9%)
Manmade fabric or finished goods	244 (4.5%)	0 (0.0%)	6 (4.0%)	$2.8 (2.4%)
Sawn wood	239 (4.4%)	1 (11.8%)	3 (2.0%)	$5.1 (4.4%)
Grain or natural fiber	190 (3.5%)	0 (0.0%)	1 (0.8%)	$3.3 (2.8%)
Food fat or grease	173 (3.2%)	1 (6.8%)	7 (5.3%)	$1.2 (1.0%)
Unclassified type of material	163 (3.0%)	0 (0.0%)	4 (2.9%)	$3.0 (2.6%)
Adhesive, resin or tar	135 (2.5%)	0 (0.0%)	2 (1.3%)	$1.1 (1.0%)
Untreated, uncoated paper	135 (2.5%)	0 (0.0%)	1 (0.7%)	$3.2 (2.8%)
Other known item	1,803 (33.1%)	7 (73.9%)	65 (47.1%)	$47.5 (40.9%)
Unknown-form item	178 (3.3%)	0 (0.0%)	5 (3.8%)	$3.2 (2.8%)
Total	5,444	9	139	$116.0

Table 2 US structure fires (average annual data for 1994-1998) involving spontaneous heating or chemical reaction, by form of material first ignited

Form of Material	Fires	Civilian deaths	Civilian injuries	Direct property damage (in millions)
Trash	624 (11.5%)	1 (11.8%)	11 (7.9%)	$11.5 (9.9%)
Cleaning supplies	608 (11.2%)	0 (0.0%)	13 (9.2%)	$16.0 (13.8%)
Agricultural product	536 (9.8%)	0 (0.0%)	3 (2.3%)	$13.6 (11.7%)
Linen other than bedding	484 (8.9%)	0 (0.0%)	15 (10.5%)	$7.6 (6.6%)
Unclassified form of material	409 (7.5%)	0 (0.0%)	20 (14.1%)	$6.3 (5.4%)
Clothing not on a person	235 (4.3%)	0 (0.0%)	6 (4.2%)	$2.2 (1.9%)
Structural member or framing	170 (3.1%)	0 (0.0%)	0 (0.0%)	$4.4 (3.8%)
Cooking materials	157 (2.9%)	0 (0.0%)	9 (6.7%)	$0.8 (0.7%)
Dust, fiber or lint	150 (2.8%)	0 (0.0%)	4 (3.0%)	$2.2 (1.9%)
Multiple items first ignited	146 (2.7%)	6 (67.8%)	5 (3.8%)	$4.9 (4.2%)
Other known item	1,715 (31.5%)	2 (21.7%)	46 (33.0%)	$42.3 (36.5%)
Unknown-type item	212 (3.9%)	0 (0.0%)	7 (5.4%)	$4.1 (3.6%)
Total	5,444	9	139	$116.0

diately afterwards by the German pharmacist Johann Georgi and the British scientist Joseph Banks[2]. Despite practical experiments demonstrating the phenomenon, there was not yet any understanding of the basic principles. Indeed, scientific writers of the era were viewing self-heating and 'spontaneous human combustion' (see Chapter 14) as one and the same phenomenon[2].

A century later, while still there was no basic understanding, a proliferation of books dealt with the topic. One of the earlier to focus on spontaneous combustion as a whole was Francis Moore's 1877 work[3], intended as a primer to insurance agents on fire hazards. A British book devoted solely to the topic of self-heating of coal in ships' holds was written by Thomas Rowan in 1882[4]. Shortly thereafter, in New York, John Hexamer was the author of an 1888 book[5] covering diverse aspects of spontaneous combustion. It pulled together in book form a number of articles the author had previously contributed to THE SPECTATOR. In Germany, Hapke[6] wrote a textbook in 1893 devoted wholly to self-heating problems. This was followed by another German textbook on the subject by Medem in 1895[7]. Another German textbook with significant discussions of self-heating was written by Schwartz in 1901, which became popular in its English translation[8]. By 1907 Miehe[9] understood, albeit in qualitative terms, some of the fundamental aspects of self-heating theory, such as the role of heat transfer and of the size of the pile. It is perhaps interesting that publishing of books on this topic tapered off in the 20th century. The first, and only, book on the general subject of self-heating to approach it from a unified, systematic point of view was published in 1984 by the late Philip Bowes[10], a researcher for many years at the Fire Research Station in the UK.

Table 3 Self-heating accidents in American railroads, 1910-1927

Material	Percent
charcoal	62.0
alfalfa and molasses feeds	12.7
rags, oily or wet	3.9
tankage, fertilizer	3.3
coal, pulverized	3.1
oiled or varnished textiles and paper	2.9
fish scrap	2.5
distiller grains, dried	2.5
sponge iron	2.1
rubber scrap, reclaimed rubber	1.6
bran	1.2
wool waste	1.0
baled hay	0.7
cotton waste, oily	0.5

Subsequent to the publication of Bowes' book, there has been quite a large number of research papers published on some of the more theoretical aspects of self-heating. Many of these have originated from a research group at the University of Leeds. Researchers in Australia and New Zealand have also had significant interest in the topic over the last couple of decades. The topic has also been of interest to researchers in Germany and in Russia, and the basic theoretical treatments all start with an adaptation of theories by the Russian researchers Semenov and Frank-Kamenetskii (as originally developed for gases, see Chapter 4). Curiously, scientific interest in the US in self-heating problems has been limited, and there is no American research group that has had long-standing or extensive research programs in this area.

Moore's 1877 book[3] provides some detailed loss experiences with various substances liable to spontaneous combustion. He included the following substances as being considered to be causes of spontaneous combustion fires in that era:

- charcoal, especially if powdered
- coal
- coffee (roasted)
- cotton (wet; or saturated with cotton-seed oil)
- fabrics and yarns dyed black (the author felt that the radiant absorptivity of black surfaces was to blame)
- felt (tarred)
- guano (wet)
- hay
- hemp (moist)
- iron or steel powder
- lampblack, especially when mixed with linseed oil
- rags soaked in linseed, cotton-seed, or rape-seed oil
- oatmeal, bran, and other grains (damp)
- saw dust
- silk, when treated with certain nut oils (this was used in 19th century tassel-making)
- tan bark
- tracing paper, made transparent with linseed oil and not cooled prior to storage
- varnish made from softwood soot and rape oil.

He also listed some pyrophoric substances, which in this Handbook are covered in Chapter 10. Moore already presented as a well-known fact that only vegetable-origin oils are prone to self-heating, and not petroleum-based oils. For an explanation of self-heating fires, he invoked heating due to oxidation, heat of wetting, and presence of pyrites.

Current US statistics, as compiled by NFPA[11], are given in Table 1 and Table 2. It is reasonable to consider that the top two categories both comprise oily rags, even though the coding "cotton or rayon fabric or finished goods" does not make this explicit. Since NFPA obtains its statistics only from municipal fire departments, the statistics will not reflect wildland fires, agricultural operations, or industrial incidents that are dealt with by plant staff without obtaining fire department assistance.

The above current statistics can be compared to a very old study where self-heating accidents in American railroads were tabulated (Table 3)[12]—charcoal is a rare enough cause today so that it is not even on the current list of top materials.

Basic phenomena

"Any material, regardless of its chemical nature, if it can either decompose or be oxidized by air exothermically (giving out heat), is capable of spontaneous combustion." This succinct explanation of the problem is by Prof. Brian Gray[13], who has made a number of mathematical studies of the self-heating problem. Since *runaway self-heating* is one of the ways in which unwanted ignitions occur, it is important to first understand the concept of self-heating, then to be able to quantify runaway conditions. A temperature rise occurs in any body where internal heat is being generated—this is the self-heating process. Whether the temperature rise is immeasurably small, small but measurable, or so large as to lead to thermal runaway depends on the relative rates of heat generation and heat removal.

Heat generation occurs primarily through one (or a combination of several) of the following processes:
(1) exothermic chemical reactions
(2) biological metabolic reactions
(3) heat-producing physical processes.

Heat losses from a body that is self-heating normally occur at the surface. For bodies at a relatively low temperature, convection will tend to be dominant. In places where the body is touching other solid substances, instead of being exposed to air, heat conduction needs to be considered. In principle, thermal radiation also has to be quantified. Radiative effects, however, only become important at high temperatures, and if a body subject to self-heating is at a high temperature, it may already be presumed to have ignited. Thus, thermal radiation heat transfer is typically treated as a correction to the convective heat loss term.

The most common sources of heat generation are exothermic chemical reactions. A wide variety of chemical reactions can occur that are exothermic in nature. In terms of self-heating caused ignitions, the dominant ones are:
(a) oxidation
(b) polymerization
(c) isomerization
(d) decomposition.

Oxidation is the most common of the chemical reactions. The oxidant that is usually involved is oxygen from ambient air, although in pyrotechnic and other less common substances, the oxidant may be a component within a solid body. Some porous and granular materials often suffer from self-heating problems, because air from the atmosphere can flow into the interior of a pile of such material. If oxidation from atmospheric oxygen is the cause of self-heating problems, a sufficient remedy may be to encapsulate the substance in an impermeable barrier material.

Polymerization occurs when molecules combine in order to form a chain. Such a chain can become thousands of units long. Polymerization is a desired process in making plastics, which are man-made polymers. It is undesired when it occurs in other circumstances unexpectedly. Polymerization cannot be stopped by excluding air since no 'external' molecule is required for this type of reaction—the substance is simply agglomerating on a molecular scale.

Isomerization is a somewhat similar process to polymerization. In this process, the atoms in a molecule rearrange themselves in a different way. Oxygen is not a general requirement for isomerization but, in some specific cases, may be involved.

The final type of chemical reaction that is common in self-heating is decomposition. Here, again, no second reactant is needed—the molecule simply flies apart into two or more pieces.

Until the World War II era, it was often believed that self-heating of many substances is caused by chemical impurities (e.g., sulfur in coal), and that pure materials would not self-heat. This has generally been found not to be true, with impurities generally playing a limited, minor role at best.

Biological activity occurs with living matter of all kinds, including plants and microbes. Cell respiration is an exothermic process which is not just confined to living plant matter—it continues for some time after a plant has been harvested. This process stops, however, if the material is dried to below about 30% moisture content. Thus, adequately drying agricultural products can remove one source of self-heating. Even if re-wetted later, metabolic activity is not reestablished. To metabolize their food, plants, fungi, and most bacteria also need oxygen. Thus, metabolic activity also stops at extremely high moisture contents, when water starts to exclude oxygen from the cells. Self-heating also occurs due to microbial action, especially when plant matter is rotting. The self-heating of compost heaps occurs mainly due to microbial action. Biological self-heating activity in plant matter has been reviewed by Kubler[14].

Finally, there are some cases where physical heat-producing processes need to be considered. The only one common in self-heating is the adsorption of water. Many substances prone to self-heating tend to adsorb ("stick onto the surface") large amounts of water. This physical process releases a significant amount of energy and is important with many practical products, e.g., charcoal. Adsorption of water rarely is the sole cause of self-heating; usually it is a contributing factor. When adsorption of water is occurring, other thermophysical effects also need to be considered, apart from the generation of heat. One important one is the effect on the thermal conductivity of the substance. The thermal conductivity of wet, porous substances at temperatures in the range 60 – 100ºC is significantly affected by the moisture content. Friction is another physical phenomenon that has been known in rare instances to contribute to self-heating[15].

In studying problems with electronic equipment, one may find the term 'self-heating' used in a slightly different context. Certain semiconductor devices can have operating regimes where increased temperatures cause increased current flow, which in turn causes higher temperatures and can lead to thermal runaway, if the circuit lacks proper design precautions. For the purpose of understanding fires, however, any ignitions that occur from such devices are simply treated as occurring due to an overheated component; only the manufacturer will generally be interested in detailed theory of why the component overheated.

As the points discussed above indicate, materials subject to self-heating exhibit a wide variety of chemical mechanisms by which heat generation occurs. In the theory portion of this Chapter, a rather simple view of chemistry will be taken, but one which many researchers have verified to yield good results. We leave details of the chemistry of specific materials to Chapter 14.

Theory of self-heating

The theory of self-heating is considered to have been established by three researchers. In 1928, the Russian Nikolai Semenov first described a theory for a substance which rises in temperature, but where the entire substance is at a uniform temperature. Semenov's theory has applications to gases and liquids, but for porous solids the assumption that the substance is at uniform temperature is generally a poor one. In 1939 another Russian, David Frank-Kamenetskii, offered a theory wherein the substance can heat in a realistic manner inside, but it is subjected to a fixed, invariant temperature along all of its edges. This was more realistic, but many porous solids subject to self-heating are simply exposed to air on most of their sides. In that case, convective cooling occurs at the edges (once the substance starts showing a temperature rise) and a more articulated theory is needed. Such a theory was provided by the British researcher Philip Thomas in 1958, who described a substance that is convectively cooled externally and which can assume a natural temperature distribution inside, one set by the interplay between heat generation, thermal conductivity, and convective edge cooling. We will mostly delve into Thomas' theory in this Chapter, along with various later extensions and alternatives. Despite the important role of Thomas in today's understanding of the problem, in the technical literature any theoretical analysis which takes into account internal temperature differences is commonly referred to as an 'F-K theory,' on the basis that Frank-Kamenetskii was the first to develop a way of treating non-uniform temperatures within the material.

The basic ideas on which self-heating theory is founded are simple. The generation of heat occurs throughout the interior of a substance. The total amount of heat generated is proportional to the mass (or volume) of the substance. The amount of heat being generated is also dependent on the temperature, and increases very rapidly with increasing temperature. The mathematical details of this dependence will be considered in the next section. If heat were being generated but not lost, very soon the system would reach an 'infinite' temperature. This, of course, does not occur, since substances normally receive cooling at their edges. This occurs due to convection, as soon as the substance's temperature rises above the ambient temperature.

With increasing temperature, the heat loss due to cooling at the edges increases. This increase is commonly found to be roughly linearly-dependent on the temperature. But the heat generation rises sharply with temperature. We note that

under steady conditions, when a body's temperature is not changing, the heat gained and lost by it must be identical, according to the law of Conservation of Energy. The situation can be illustrated with the aid of Figure 2. This figure is drawn in the context of Semenov theory, since, according to it, the substance is at a single temperature. The heat balance concept equally applies to F-K theory, but a more complicated presentation would be needed since the body is allowed to have internal temperature gradients.

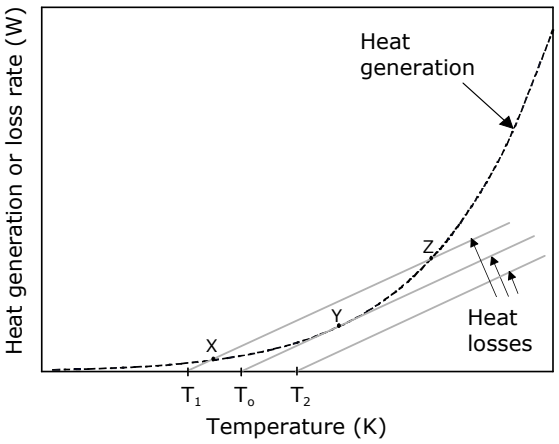


Figure 2 Heat losses and gains, as represented in the Semenov theory

Let us suppose that the substance is initially at temperature T_1. At that temperature, the heat losses and heat gains are not in balance, therefore the substance will heat up until point X is reached. At that point, the heat losses and gains are equal and the substance will be in thermal equilibrium at the temperature of point X. The heat losses and gains would also be at equilibrium at a much higher temperature, marked Z on the graph. Some consideration of the shapes of the curves will indicate that point X is a stable equilibrium, while point Z is not. Suppose, while the system is at point X, that a tiny increase in temperature takes place, meaning the system will move to the right. But as the system moves to the right off point X, the slope of the heat generation line is less than the slope of the heat loss line. Thus, more heat will be lost than generated. The consequence is that the system will return back to point X. In the same manner, if a small excursion to the left of point X would take place, then the heat gains would exceed the losses, the system would heat up and would also return to point X. At point Z, however, the situation is different—a small temperature rise would cause heat generation to exceed heat losses and the system would run away (ignite). A small temperature drop while at point Z would result in the system dropping back down to point X. Thus, we conclude that the equilibrium at point Z is unstable, and a real system would be able to spend more than a moment only at point X.

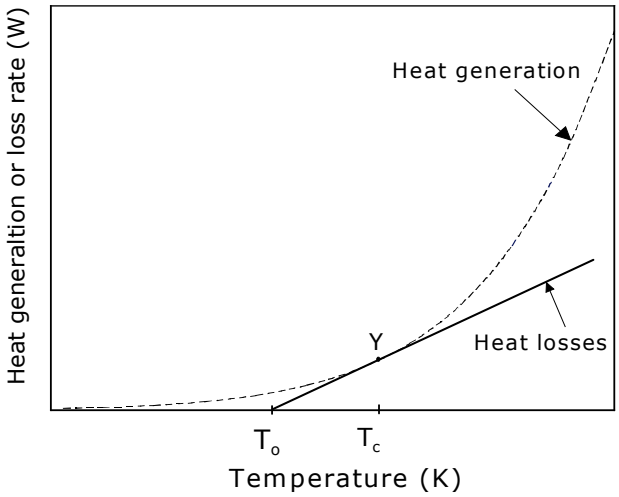


Figure 3 The critical condition

Now, if we consider the system starting at a higher room temperature T_2, it can be seen that there will be no place that the heat gains and the heat losses will be in equilibrium. Thus, the system will just keep rising in temperature until ignition occurs. A system such as this is called *supercritical*; a system which starts at T_1 is *subcritical*.

It can also be seen that the starting room temperature T_o is the highest value at which heat losses and gains could be in equilibrium. Point Y represents an equilibrium condition, but it is an unstable equilibrium. However, any room temperature lower than T_o will lead to a stable solution. Thus, for all room temperatures less than T_o, stable, non-igniting behavior will be found. The substance itself will become warmer than the room temperature and, in principle, will stay indefinitely at some temperature below T_c (Figure 3). In practice, we shall see later, other effects preclude a system from staying at a fixed elevated temperature forever.

It can be confusing to learn that the term 'critical temperature' is often used ambiguously and can refer either to the maximum permissible value of the environment T_o, or else the maximum permissible temperature of the material T_c. In most cases, however, it refers to T_o, since the latter can be externally controlled, while the material's own temperature can only be determined by theory or experimental instrumentation. To make this point more clear, T_o, is sometimes referred to as CAT, critical ambient temperature, while the material's own temperature, T_c, is referred to as CST, critical stacking temperature.

It is interesting to consider what happens when the critical conditions are reached. The above graphs are simplified by only presenting one temperature of the substance. In fact, the temperature of the substance is not uniform: it is the highest at the center and the lowest at the edges. Thus, for a body that is uniformly cooled along all its exterior, the runaway heating must start at the center and progress from there. However, flaming is generally only possible at the

edges. This is because the porous channels of the substance will normally be smaller than the quenching diameter (see Chapter 4). Thus, the typical history of such an incident is that *smoldering* starts at the center, then propagates towards the edges. Commonly, but not always, flaming may break out when the smolder front first reaches an edge exposed to air. In a simplified view, the smolder spread would be uniform, and there could be nothing (or little) left to flame once the smolder front reached the edge. In practice, the material will rarely be uniform, and the smolder spread will rarely also be uniform. Thus, in a typical incident the smolder front can break out to the surface at a single spot, flaming starts there, then the remaining substance starts flaming combustion outside-in, in addition to continuing smoldering inside-out.

In addition to changing the initial temperature of the environment, it may be that the heat transfer coefficient can be changed, for instance by directing air flow from fans onto the substance. The possibilities are shown in Figure 4. Note that there are also two extreme conditions. If infinite heat transfer could be provided, then the *isothermal* line would be followed. Runaway conditions could never be reached, regardless of the temperature at which the isothermal conditions are established. Conversely, if the heat losses are made zero, then the *adiabatic* line would be followed. From any starting point, an adiabatic system will, in time, run away. Adiabatic situations do not occur in normal practice, but a number of test apparatuses have been developed where this condition is approximated.

To be treatable under the F-K theory, the self-heating substance must show rather simple exothermic chemistry. If there is only one pertinent reaction and it can be represented by an Arrhenius-form kinetic expression, then the substance can be analyzed. In general, self-heating solids may show two types of reactions:

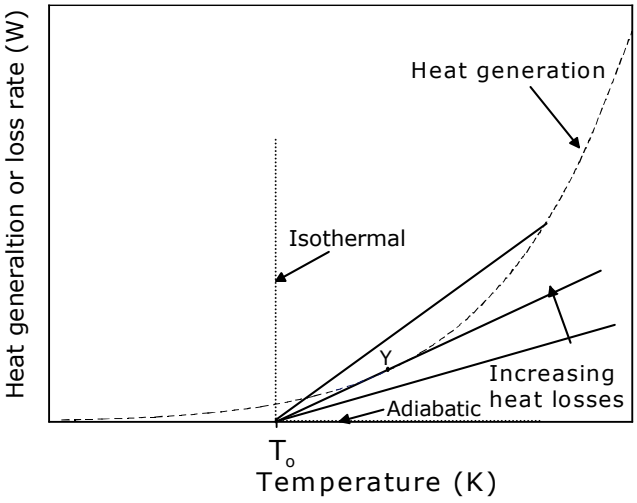


Figure 4 The effect of changing the heat transfer coefficient

- Unimolecular—these include decomposition and isomerization. Such problems would appear to be very simple, since there is not a second reactant to consider. In practice, however, many such reactions have multiple steps, often involving autocatalytic reactions, so real-world complications can arise. Polymerization reactions are not strictly unimolecular, since at least two molecules must be present, but behave the same way as unimolecular reactions, since only one kind of molecule is needed.
- Polymolecular—this is most commonly an oxidation reaction. F-K theory assumes that the necessary oxidant is available in abundance. This is often a good assumption for porous materials since oxygen can simply flow in as needed from the ambient environment. Standard F-K theory cannot treat situations where a reaction may be limited by paucity of oxygen, but some extensions to the theory are considered later in the Chapter.

F-K theory cannot treat situations where more than one reaction takes place, or autocatalytic reactions are involved, or there are non-chemical sources or sinks of energy (e.g., enthalpy of phase change). These complications are briefly considered towards the end of the Chapter.

The above discussion suggests that the most important question in self-heating is *whether* a runaway condition can occur and has ignored the role of *time*. If critical conditions are to be attained, then the time to achieve criticality is an engineering variable of considerable importance. This will be discussed later in this Chapter. If cooling is sufficient that critical conditions are not reached, then the simplest thing that could happen is that the substance just reaches a temperature mildly higher than ambient and stays at that temperature indefinitely. This would be possible if the chemical reaction took place without depletion of reactants[*]. Theoretical treatment is generally much simpler if depletion of reactants is ignored, so this assumption is often made. In the real world, depletion of reactants inevitably occurs, thus, for a subcritical system a modest peak is attained, then temperatures start to drop because of depletion of reactants.

Time is also handled somewhat artificially in defining the problem to begin with. If the chemical reaction is relatively fast, it may be difficult to imagine the 'creation' of the substance at a known temperature. How did it get to be at some one, fixed temperature if the system has a tendency to self-heat (either to runaway, or at least to a stable, higher temperature than the initial one)? It is best to envision that the substance was initially dispersed in very small sizes, so that self-heating would be negligible. At time $t = 0$, it is sudden-

[*] Most authors use the term 'consumption of reactants.' This term seems self-contradictory, since no products could be formed, if no reactants were consumed. The simplification alluded to, on the other hand, does not demand no consumption, merely no depletion of supply.

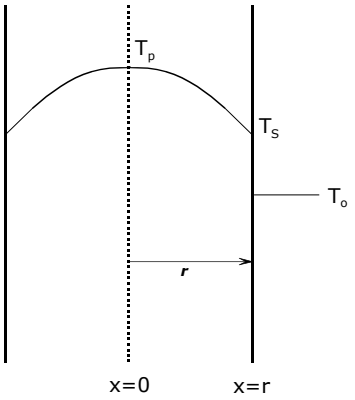


Figure 5 The geometry of a self-heating substance, in the form of a symmetric slab

ly agglomerated into its actual size. This starts the self-heating problem.

STEADY-STATE THEORY FOR SYMMETRICALLY COOLED BODIES

The formulation of the steady-state theory is due to Frank-Kamenetskii[16], with later extensions by Thomas[17]. A number of approximations are made in order to obtain a tractable solution. As we shall see later, some approximations can be relieved with more detailed theoretical solutions, and this can be necessary to get good numerical agreement for various practical problems. Runaway self-heating is sometimes known as a *thermal explosion* and much of Russian literature in this field uses the term. When applied to solid self-heating materials, the term 'explosion' does not denote an audible noise. Instead, it signifies that an extreme change in reaction rate has occurred, from some modest value to near-infinite.

The primary assumptions made are the following:

- The substance is in the form of an infinitely wide/long slab, with thickness 2*r*.
- The surfaces are convectively cooled with a convective coefficient *h*.
- The cooling of both faces is identical (i.e., the problem is symmetrical).
- Natural convection occurring inside the body is ignored.
- The reaction rate proceeds according to zero-order Arrhenius kinetics.
- There is an infinite supply of fuel and oxygen (that is, fuel depletion is ignored, as is any limitation to free diffusion of air into the interior).
- The only temperature gradients are in the thickness direction.

This slab problem is illustrated in Figure 5. T_o is the temperature of the air, T_s is the temperature of the surface of the slab, while T_p is the peak temperature at the center of the slab.

For one-dimensional heat flow with heat generation, the basic energy conservation equation is:

$$\lambda \frac{d^2T}{dx^2} + \dot{q}'''(T) = \rho C \frac{dT}{dt}$$

But in steady state, the right-hand side, by definition, is zero. Thus,

$$-\lambda \frac{d^2T}{dx^2} = \dot{q}'''(T)$$

where λ = thermal conductivity (kW m^{-1} K^{-1})
T = temperature (K)
x = distance (m)
$\dot{q}'''$ = heat generation rate per unit volume (kW m^{-3})

We must now consider the nature of that volume-heating term. It is assumed that the reaction rate has the form of Arrhenius' Law, which was already considered in Chapter 3. For a solid, homogeneous reactant, its concentration is equal to its density. In addition, it is assumed that the heat of reaction is constant, with Q heat being released for each kg of reactant consumed. Thus,

$$\dot{q}'''=\rho Q A e^{-E/RT}$$

where
ρ = density (kg m^{-3}); this is the initial density of the material* and is assumed not to change as the reaction proceeds
Q = heat of reaction (kJ kg^{-1})
A = pre-exponential factor (s^{-1})
E = apparent activation energy (kJ mol^{-1})
R = universal gas constant (= 8.314 J mol^{-1} K^{-1})

To the basic differential equation expressing conservation of energy, we must add boundary conditions to obtain a solution. For moderate temperature increases, it is experimentally found that the heat flow at the boundaries of the slab can be represented by convective cooling:

$$\dot{q}'' = h\,(T_s - T_o)$$

where
$\dot{q}''$ = the heat loss rate per unit area of surface (kW m^{-2})
h = convective heat transfer coefficient (kW m^{-2} K^{-1})
T_s = surface temperature (K)
T_o= ambient air temperature (K)

But performing a heat balance on an infinitesimal layer at the surface, the same amount of heat that is leaving the air side by convection must also be flowing from the substance by conduction:

$$-\lambda \frac{dT}{dx} = h\,(T_s - T_o) \qquad \text{at } x = r$$

Also, the same conditions must hold on the other face of the slab:

* The basic F-K theory presented in this Section assumes a zero-order chemical reaction. Thus, the density of the fuel is a constant and does not change with time. If fuel is significantly depleted before thermal runaway occurs, then a theoretical treatment is needed where the fuel's density (or concentration) is time varying; this is treated in a later Section.

$$\lambda \frac{dT}{dx} = h(T_s - T_o) \qquad \text{at } x = -r$$

Finally, by symmetry it can be seen that:

$$\frac{dT}{dx} = 0 \qquad \text{at } x = 0$$

In the general solution to the energy conservation equation, initial conditions would also be needed, which would describe the 'starting point' of the system. The steady-state theory, by definition, has no time element, so this does not need to be considered here.

To get analytic problem solutions, it is customary to make various approximations. The above system of equations is not solvable in any closed form. Thus, the innovation of Frank-Kamenetskii was to realize that a solution may become possible if the exponential expression is approximated. In many practical cases, the values of E and T_o will be such that

$$\frac{E}{RT_o} >> 1$$

Furthermore, the temperature rise ($T - T_o$) will generally be much less than T, keeping in mind that the temperatures are absolute (K). Starting with the identity:

$$\frac{1}{T} = \frac{1}{T_o}\left[1 - \left(\frac{T - T_o}{T_o}\right) + \left(\frac{T - T_o}{T_o}\right)^2 \frac{T_o}{T}\right]$$

and using the approximations that $E/RT_o >> 1$ and $(T - T_o) << T$, the expression is obtained:

$$\frac{E}{RT} \approx \frac{E}{RT_o}\left[1 - \frac{T - T_o}{T_o}\right]$$

In more recent times, a number of authors have pursued theories where the exponential term is not approximated[18]. It does not appear that any such refined theories have led to improved engineering methodologies, so we will not discuss them here. In some specialized cases, however, the approximation that $E/RT_o >> 1$ is not fulfilled. A practical approach to treating such 'low activation energy' problems is presented later in this Chapter.

Next, a variable θ is defined which is a non-dimensional temperature:

$$\theta = \frac{E}{RT_o^2}(T - T_o)$$

A non-dimensional distance z is defined as:

$$z = \frac{x}{r}$$

Finally, a non-dimensional heat generation rate δ can be defined as:

$$\delta = \frac{E}{RT_o^2}\frac{r^2 \rho Q A}{\lambda} e^{-E/RT_o}$$

Then the energy conservation equation, expressed in the non-dimensional variables becomes:

$$\frac{d^2\theta}{dz^2} = -\delta e^{\theta}$$

The boundary conditions also have to be expressed in the same non-dimensional variables:

$$Bi\,\theta + \frac{d\theta}{dz} = 0 \qquad \text{at } z = 0$$

$$\frac{d\theta}{dz} = 0 \qquad \text{at } z = 1$$

where the convective heat transfer coefficient was expressed as the non-dimensional Biot number* Bi:

$$Bi = \frac{hr}{\lambda}$$

It can then be shown that a suitable solution[17] to the non-dimensionalized conservation equation is:

$$\theta = \ln C_1 - 2\ln\left[\cosh\left(z\sqrt{\delta C_1 / 2} + C_2\right)\right]$$

where C_1 and C_2 are constants of integration. For this solution, $C_2 = 0$, but a numerical evaluation was needed to obtain C_1. However, the primary variable of interest in solving this equation is not the temperature rise itself, but, rather, the critical value of heat generation which corresponds to the runaway condition. This critical value of δ is denoted as δ_c. Physically, any bodies which have a $\delta > \delta_c$ have too little cooling at the boundaries, or they are too large, or their chemical reaction rate is too high for a stable condition. Mathematically, a solution of the conservation equation does not exist for any value $\delta > \delta_c$. Figure 6 shows the results for δ_c as a function of the Biot number. Also shown are the corresponding values for two other common geometries—the cylinder and the sphere. Note that the x-axis represents, in non-dimensional terms, the amount of convective cooling available, while the y-axis is the non-dimensional heat generation rate. Thus, the asymptotes are as expected: for very large cooling, a sizeable heat generation rate can be tolerated without thermal runaway. As the convective cooling is progressively reduced, the system can only tolerate smaller heat generation rates. As the cooling rate goes to zero, the heat generation rate must also go to zero.

An analytical approximation[19] to the results for $\delta_c(Bi)$ shown in Figure 6 is:

$$\delta_c(Bi) = \frac{1}{\dfrac{1}{\delta_c(Bi \to \infty)} + \dfrac{e}{(j+1)Bi}}$$

where $j = 0, 1, 2$ for slab, infinite cylinder, and sphere, respectively, and the values of $\delta_c(Bi \to \infty)$ are given in Table 4.

* There are two similar-seeming nondimensional numbers related to convection which must not be confused: Bi is the ratio (resistance to heat transfer due to conduction inside the solid)/(resistance to heat transfer due to convection in the fluid). The Nusselt number Nu is the ratio (resistance to heat transfer due to conduction in the fluid)/(resistance to heat transfer due to convection in the fluid).

In certain cases, it is useful to consider even simpler approximations valid for very small or very large cooling. For very large cooling ($Bi \rightarrow \infty$), the surface temperature is forced to be identical to that of the surrounding air; this is the original Frank-Kamenetskii problem, before its generalization by Thomas. Conversely, if the edge cooling is very small, then $Bi \rightarrow 0$, and we have what is called the Semenov condition. Thomas' limiting values for those two conditions are given in Table 4. In the Table, e denotes the value 2.718.

Table 4 Thomas' computation of the critical values

Geometry	Surface/ volume ratio	δ_c for Semenov condition (Bi→0)	δ_c for F-K condition ($Bi \rightarrow \infty$)
slab	1/r	Bi/e	0.88
infinite cylinder	2/r	2Bi/e	2.0
sphere	3/r	3Bi/e	3.32

The interpretation of the δ results is as follows. If $\delta < \delta_c$, then after infinite time the substance will reach a finite, subcritical temperature. If $\delta = \delta_c$, then the temperature will reach the critical (runaway) condition, but this will take an infinite time. For $\delta > \delta_c$, the temperature will tend to infinite values after a finite time. For such 'supercritical' systems, the increase of temperature with time does not proceed in a smooth manner. The substance first rapidly heats up to a temperature slightly less than T_c, then it rises in temperature only gradually for a period of time, then finally it again rises rapidly in temperature and shoots up to and past the T_c. Since the runaway condition represents the criticality in the balance between heat generated by a volume and heat lost by the surface, the surface/volume ratio would be expected to be of importance. This is confirmed in Table 4—the Semenov condition is exactly proportional to the surface/volume ratio, and the Frank-Kamenetskii condition is quite close.

The variable δ is sometimes called the *Frank-Kamenetskii number*, but it can also be identified as a type of *Damköhler number*, being a non-dimensional representation of the ratio

$$\delta = \frac{\text{characteristic heating time}}{\text{characteristic reaction time}}$$

PEAK TEMPERATURES UNDER SUBCRITICAL CONDITIONS

The classical theory of thermal ignition also considers in some detail what happens to temperatures in the course of self-heating. The temperature T_p at the center of the body is expressed in terms of a nondimensional temperature θ_p, defined as:

$$\theta_p = \frac{E}{RT_o^2}\left(T_p - T_o\right)$$

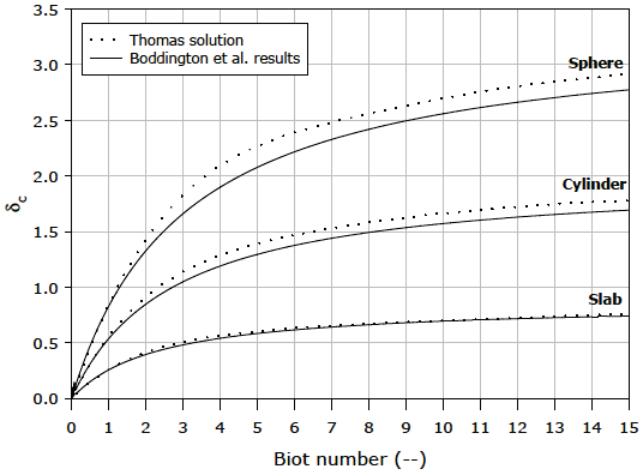


Figure 6 The critical values of the non-dimensional F-K parameter, as a function of the Biot number

Critical values[17,20] of θ_p are given in Table 5—these are the maximum values that can be attained in a stable system. It is interesting to consider an example to gain an appreciation of the magnitude of the values that can be expected. A value of $\theta_p = 1.1$ might be appropriate for moderate cooling. Assume that T_o = 40ºC = 313 K. The value of E will typically be in the range 60 – 140 kJ mol^{-1}. If E = 60 kJ mol^{-1}, then $(T_p - T_o)$ = 14.9ºC degree rise. For E = 140 kJ mol^{-1}, then $(T_p - T_o)$ = 6.4ºC. With small-scale testing, the value of T_o will typically be higher while the Biot number will be higher and the $Bi \rightarrow \infty$ condition might be approximated. Figure 17 shows laboratory data obtained by Read et al. for wool specimens in an equicylinder container. These indicate that if T_o = 155.5ºC = 429 K, then $(T_p - T_o) \approx$ 31ºC was possible prior to reaching criticality. Chapter 14 indicates that E = 91.5 kJ mol^{-1} for wool; and taking θ_p = 1.78, gives a predicted value of $(T_p - T_o)$ = 29.8ºC. The agreement is quite close but, because of various neglected effects, the theory somewhat underestimates the permissible rise. Bowes[10] showed examples of wood sawdust sustaining a subcritical rise of 31ºC and wood sawdust covered with olive oil a rise of 98ºC. The sawdust + olive oil case showed complex reactions not conforming to the assumptions of F-K theory, but the 31ºC rise for sawdust alone is identical to that found by Read for wool. Nugroho et al.[21] presented some more data showing that the actual temperature rise that can be sustained is generally under-predicted by theory.

Table 5 Critical temperature values

Geometry	θ_p		Θ_s
	$Bi \rightarrow 0$	$Bi \rightarrow \infty$	$Bi \rightarrow \infty$
slab	1.0	1.19	0.252
infinite cylinder	1.0	1.39	0.254
equicylinder	1.0	1.78	
sphere	1.0	1.61	0.257
cube	1.0	1.89	

Table 6 Constants for other body geometries

Geometry	j	$F(j)$	$(r/R_o)^2$	(r/R_s)	$\theta_{p,c}$
infinite slab, thickness $2r$	0	0.857	0.3333	0.3333	1.187
thin circular disk, thickness $2r$, radius $10r$	0.4370	0.9243	0.3340	0.4000	1.241
infinite cylinder, radius r	1	1.0000	0.6667	0.6667	1.386
long circular cylinder, radius r, length $10r$	1.418	1.050	0.6671	0.7333	1.489
infinite square rod, side $2r$	1.443	1.051	0.5455	0.6667	1.492
sphere, radius r	2	1.111	1.0	1.0	1.622
equicylinder, radius r, height $2r$	2.728	1.178	0.8047	1.0	1.778
cube, side $2r$	3.280	1.222	0.7009	1.0	1.888
regular tetrahedron, side $2\sqrt{6}\ r$	4.187	1.284	3.4702	2.449	2.058

In some cases, it is useful to estimate the self-heating for much smaller sizes than necessary to reach criticality. Thomas and Bowes[22] showed that for r values small enough so that δ is significantly less than δ_c, T_p for a sphere is given by:

$$T_p - T_o \approx \frac{2+Bi}{Bi}\frac{r^2 Q\rho A}{6\lambda}e^{-E/RT_p}$$

This is not an explicit equation, but knowing all the pertinent constants, the value can be found by a few iterations of trial-and-error. Similar expressions are not available for other shapes, although a reasonable estimate for a cube may be made by replacing the 6λ in the denominator with 4λ.

Of additional interest is the surface temperature. The best solution for that is probably from Gill and coworkers[23]. Their nondimensionalization is different from other authors, however, and uses the absolute temperature value, rather than the temperature rise above ambient. Their relationship for the critical values of the surface temperature, T_s, are also given in Table 5, expressed in terms of the non-dimensional surface temperature Θ_s:

$$\Theta_s = \frac{RT_s}{E}$$

The maximum stable temperature values are of practical import, in that if a temperature at the center of a body (or at the surface) is measured which is greater than the critical value, it indicates that according to the theory, at least, the substance is already in the process of thermal runaway. This is sometimes used in monitoring industrial stockpiles of materials that have a propensity for self-heating. To make this comparison, of course, the relevant nondimensional temperature first should be converted to the dimensional temperature T_p or T_s. The limitation to this strategy is that, at least for small-scale testing, theory may underestimate the permissible temperature rise, however, this at least makes the strategy conservative.

BODIES OF OTHER SHAPES

Closed-form solutions are possible only for some very simple geometric shapes. Even so, there are significant mathematical complexities, regardless of how simple the shape is. Yet, in some applications it is desirable to estimate the self-heating potential of other shapes, for instance, a short cylinder. For this purpose, Boddington and coworkers[24] developed generalized expressions which are able to treat a wide variety of shapes. The method is an approximation, albeit a very good one. For perspective, even 'exact' solutions for this class of problems tend to vary among different researchers, since simplifications must be made in order to obtain any closed-form solutions.

Boddington's general expression for δ_c is in terms of $\delta_c(R_o)$, which is defined in terms of a 'mean radius' R_o, rather than the conventional physical distance r:

$$\frac{1}{\delta_c(R_o)} = \frac{1}{3F(j)} + \frac{e}{j+1}\frac{1}{Bi(R_S)}$$

It is standard in many differential equation solutions to generalize the geometry by the use of the j parameter, where j = 0 is the infinite slab, j = 1 is the infinite cylinder, and j = 2 is the sphere. Boddington's innovation is to extend this 'dimensionality index' concept to other geometries, where it assumes non-integral values. His values are given in Table 6.

Converting then to the physical dimension r, the expression becomes:

$$\delta_c(r) = \frac{(r/R_o)^2}{\frac{1}{3F(j)} + \frac{e}{j+1}\frac{1}{Bi(R_S)}}$$

The final conversion which has to be made is for the Biot number. Boddington gives it as a function of the 'Semenov radius' R_S, but we need to have it in terms of the physical dimension r. This relation is simply:

$$Bi(R_S) = \left(\frac{R_S}{r}\right)Bi(r)$$

Thus,

$$\delta_c(r) = \frac{(r/R_o)^2}{\frac{1}{3F(j)} + \frac{e}{j+1}\left(\frac{r}{R_S}\right)\frac{1}{Bi(r)}}$$

where values of $(r/R_o)^2$ and r/R_S can be found in Table 6. The asymptotic behavior for large and small Bi is:

$$\delta_c = (r/R_o)^2 3F(j) \qquad Bi \to \infty$$

$$\delta_c = \frac{\left(\frac{r}{R_o}\right)^2}{\left(\frac{r}{R_S}\right)} \frac{(j+1)Bi(r)}{e} \qquad Bi \to 0$$

For some common geometries, Boddington's method works out to:

Sphere $$\delta_c(r) = \frac{1}{0.3 + \frac{0.906}{Bi(r)}}$$

Infinite cylinder $$\delta_c(r) = \frac{1}{0.5 + \frac{1.359}{Bi(r)}}$$

Infinite slab $$\delta_c(r) = \frac{1}{1.167 + \frac{2.718}{Bi(r)}}$$

Equicylinder* $$\delta_c(r) = \frac{1}{0.3516 + \frac{0.906}{Bi(r)}}$$

Cube $$\delta_c(r) = \frac{1}{0.3892 + \frac{0.906}{Bi(r)}}$$

A comparison between Boddington's approximations and Thomas' results is shown in Figure 6. For the $Bi \to \infty$ condition, the comparative results are given in Table 7; for the $Bi \to 0$ condition, Boddington's results are essentially identical to Thomas'.

Table 7 Accuracy of Boddington's approximations for δ_c as $Bi \to \infty$

Geometry	Exact	Boddington
slab	0.88	0.857
infinite cylinder	2.0	2.0
sphere	3.32	3.333
equicylinder	2.76	2.84
cube	2.52	2.57

Boddington's simplified method pertains to bodies which can be described by use of only a single dimension, identified here as r. Many practical bodies, however, do not have such a high degree of symmetry. For such more general shapes, Bowes[10] has provided additional results, applicable specifically to the $Bi \to \infty$ condition:

General cylinder with r = radius and d = half-height

$$\delta_c(r) = 2.0 + 0.84\left(\frac{r}{d}\right)^2$$

and $\delta_c(r)$ denotes that the length dimension to be used in evaluating δ is r.

Hollow infinite cylinder with a = inner radius and b = outer radius

Bowes[10] provides a graphical solution for this problem, to which a good analytic approximation is:

$$\delta_c(s) = \frac{1}{6 - 4\exp(-1/z)}$$

where $z = b/a$ is the ratio of the radii, and $s = (b - a)/2$ is the half-thickness of the solid portion. For a solid cylinder, $a = 0$, therefore $z = \infty$, and $\delta_c(s) = 1/2$. To compare to the results for a solid, infinite cylinder, note that its normal δ_c is defined as a function of the full radius r, rather than the half-radius s. Thus, for the solid cylinder we regain the previous result that $\delta_c(r) = 2$. For a hollow cylinder with a very thin wall, as $z \to 1$, $\delta_c \to 0.22$, which is the same result as for an infinite slab of half-thickness s. This particular solution, however, cannot be applied to the most common practical case of self-heating of an annulus: pipe insulation. The boundary conditions for pipe insulation involve a fixed, elevated temperature at the inner radius, rather than convective cooling. For such conditions, the theory of the next Section, below, must be applied instead.

Rectangular brick with sides = $2a$, $2b$, $2c$

$$\delta_c(a) = 0.840\left(1 + \frac{1}{p^2} + \frac{1}{q^2}\right)$$

where $p = b/a$, $q = c/a$, and the notation $\delta_c(a)$ denotes that the length dimension to be used in evaluating δ is a. Beever[54] gives the same formula, but with the constant being 0.873.

Cone with base radius = a, height = d

$$\delta_c(d/2) = 1.2 + \frac{2}{p^2} \qquad \text{for } p \geq 0.5$$

where $p = a/d$. The above approximate relation is derived from a graph of results given by Bowes. For tall, slender cones, where $p < 0.5$, no comparable simplification is offered; however practical piles of materials are less likely to have such a shape. On the other hand, the short-cone configuration is common, since granular material poured on the ground will assume such a shape.

General bodies

No precise expression is available for bodies of general shape. However, Boddington et al.[25] proved that, for the $Bi \to \infty$ condition, a body of any shape (but without internal cavities) will have a higher critical ambient temperature than does a sphere of the same volume. Thus, determining the results for a sphere of the same volume will give a worst-case limit to the desired solution for critical T_o.

* An equicylinder is one of a height identical to its diameter.

STEADY STATE THEORY FOR UNSYMMETRICALLY COOLED BODIES

INFINITE SLAB

The case of uniform cooling on all surfaces of a body is relatively easy to create in oven tests, as discussed later in this Chapter. However, in actual fires such conditions are rarely encountered. One condition which is often encountered is dust layers accumulating on a hot surface. Such a condition can be well approximated by considering a slab which is at a fixed, elevated temperature on one face and convectively cooled on the other face (Figure 7). The conservation equation to be solved is identical to the one already considered in the symmetrical steady-state, but the problem becomes more complicated because now there are two different temperatures associated with the boundary conditions—T_h, the hotplate temperature, and T_o, the ambient air temperatures. Because of this complication, slightly different definitions of the non-dimensional variables θ and δ must be adopted:

$$\theta = \frac{E}{RT_h^2}(T - T_h)$$

$$\delta = \frac{E}{RT_h^2}\frac{r^2 Q \rho A}{\lambda} e^{-E/RT_h}$$

The boundary conditions are:

$$T = T_h \qquad \text{at } x = 0$$

$$-\lambda \frac{dT}{dx} = h\left(T_s - T_o\right) \qquad \text{at } x = 2r$$

where T_s denotes the temperature of the slab at the surface that is exposed to air. After the equation is non-dimensionalized, the boundary conditions become:

$$\theta = 0 \qquad \text{at } z = 0$$

$$-\frac{d\theta}{dz} = Bi\left(\theta_s - \theta_o\right) \qquad \text{at } z = 2$$

For the symmetrically-cooled case, solutions for δ_c were obtained as a function of just a single variable, Bi. In the present case, solutions for δ_c must involve both Bi, defined as before, and a second variable, θ_o, defined as:

$$\theta_o = \frac{E}{RT_h^2}(T_o - T_h)$$

Thomas and Bowes obtained a numerical solution[26] for this problem, shown graphically in Figure 8.

Note that the values of θ_o are all negative. This is because the problem has been defined for a case where the ambient temperature T_o is less than the hot face temperature T_h. Not shown on the figure is the asymptotic behavior for small Bi. As $Bi \rightarrow 0$, $\delta_c \rightarrow 0.22$, which is different from the symmetric case, where $\delta_c \rightarrow 0$. There is a direct comparison to the symmetric case, however. For the symmetric case, as $Bi \rightarrow \infty$, $\delta_c \rightarrow 0.88$. Now, under those conditions, the symmetric case represents a body which has a fixed boundary temperature, since infinite convective heat transfer means the surface temperature of the body is identical to the (fixed) temperature of the fluid. So we establish that the $x = 2r$ boundary is at a fixed temperature. But, by symmetry, under all conditions for a symmetrically-cooled body, the centerline ($x = r$) position is an adiabatic surface. Thus, in the $Bi \rightarrow \infty$ limit, the symmetrically-cooled body has exactly the same boundary conditions as the unsymmetrically cooled case in the $Bi \rightarrow 0$. However, our unsymmetric case was for a width = $2r$, while the analogue of the symmetric case is to be considered for its half-width, which is = $1r$. But note from its definition that $\delta \propto r^2$. Now, since the unsymmetric problem is twice the width, for the same physical conditions to be

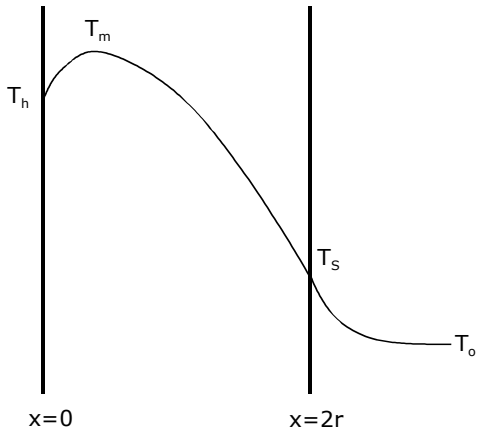


Figure 7 The geometry for the unsymmetric slab with one side (at $x = 0$) at a fixed temperature, the other side (at $x = 2r$) convectively cooled

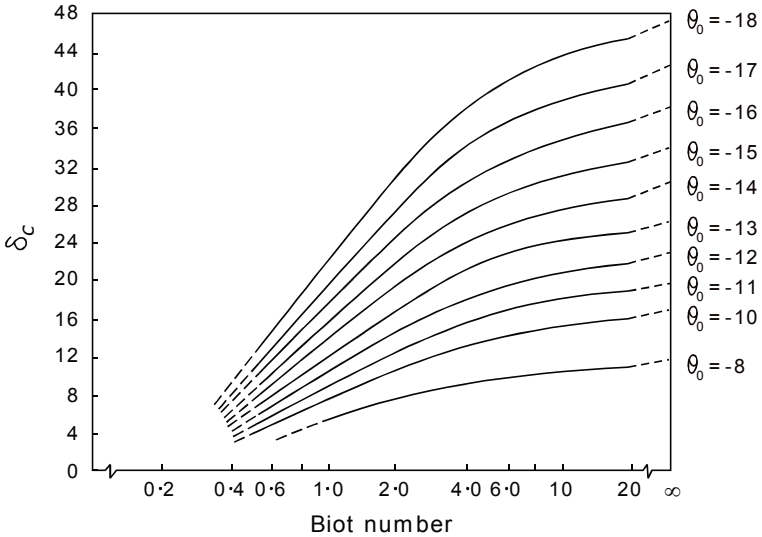


Figure 8 The solution for δ_c in the case of a slab with one face at a constant temperature

(Copyright Royal Society of Chemistry, used by permission)

reached, its δ_c must be = 0.88/4 = 0.22.

There is a closed-form approximation[10] to the results presented graphically in Figure 8 if $\delta_c > 5$:

$$\delta_c \approx \frac{1}{2}\left(\frac{Bi}{1+2Bi}\right)^2 (1.4-\theta_o)^2$$

A somewhat different problem of unsymmetric cooling is when one side is exposed to a constant temperature, but the other side sees a constant heat flux, rather than a heat flux driven by a convective coefficient. This case might occur in practice with a reactive material which is photosensitive, but such problems are not as frequently encountered as convective cooling. A solution was developed by Clemmow and Huffington[27] and is reprised by Bowes[10].

HOLLOW INFINITE CYLINDER

This geometry is most commonly encountered in self-heating of pipe insulation. The pipe insulation is kept at a fixed temperature at its inner radius, while its outer radius is convectively cooled in ambient air. Bowes[29] provides a solution for this geometry. The solution is not exactly parallel to the infinite slab, unfortunately, and is derived in terms of the actual (unknown) outer surface temperature T_s, rather than the known ambient temperature T_a. For pipes of large diameter, the solution perforce must collapse to that of the infinite slab, so the simpler solution given above can conveniently be used. The graphical solution provided by Bowes can be approximated by:

$$\delta_c^* = 0.39|\theta_s|^{1.62} z_s^{0.27+0.49|\theta_s|}$$

where δ_c^* is the critical value of δ^*, and the latter is defined with the space dimension being the wall half-thickness $(b - a)/2$ and the temperature being the inner wall temperature T_h:

$$\delta^* = \frac{E}{RT_h}\left(\frac{b-a}{2}\right)^2 \frac{\rho Q A}{\lambda} e^{-E/RT_h}$$

The nondimensional temperature θ_s is defined as:

$$\theta_s = \frac{E}{RT_h^2}(T_s - T_h)$$

where T_s is the outside surface temperature of the cylinder. The nondimensional distance z_s is defined as:

$$z_s = \frac{b}{a}$$

where b is the outer radius and a is the inner radius. To obtain a solution, T_s is still needed and Bowes points out that, under subcritical conditions, T_s will not be much different from the case where the pipe insulation is chemically inert, thus it can be obtained by solving this equation:

$$h_c(T_s - T_o) = \frac{\lambda(T_h - T_s)}{\ln z_s}$$

where h_c = convective heat transfer coefficient (W m^{-2} K^{-1}). Thus, the practical solution strategy is to first use the above equation to obtain T_s, then use T_s to obtain θ_s, then solve for δ_c^*, and finally solve for δ^*. If $\delta^* < \delta_c^*$, then the system is subcritical, otherwise it is supercritical.

STEADY-STATE THEORY INCLUDING OXYGEN DIFFUSION

The basic steady state theory assumed that there is an infinite supply of both reactants, the fuel and the oxygen. For a porous body, the oxygen must come in from the outside. A certain amount of oxygen is contained within the voids of a porous body, even if its boundaries are sealed and flow cannot take place. Computations typically show, however, that using up all of the local oxygen would allow for a rise of only a few degrees Celsius. Thus, for substances which show exothermicity due to reaction with air, no self-heating hazard will occur unless a continued inflow of oxygen exists.

In a real porous body, however, even if the boundaries are not sealed, there will be limits to how much oxygen can flow into the inside of the body. If this flow is insufficient for the reaction, then the reaction will slow down. To express the oxygen diffusion effect, an equation for the diffusion of oxygen is added[30]:

$$D\left(\frac{d^2c}{dx^2} + \frac{j}{x}\frac{dc}{dx}\right) = \frac{\varepsilon \dot{m}_{ox}'''}{\rho_{ox}}$$

where D = the diffusion coefficient for oxygen in the porous solid (m^2 s^{-1}), c = concentration of oxygen in the gas phase (kg m^{-3}), ε = void fraction (--), ρ_{ox} = density of oxygen (kg m^{-3}), and $\dot{m}_{ox}'''$ = mass consumption rate of oxygen,

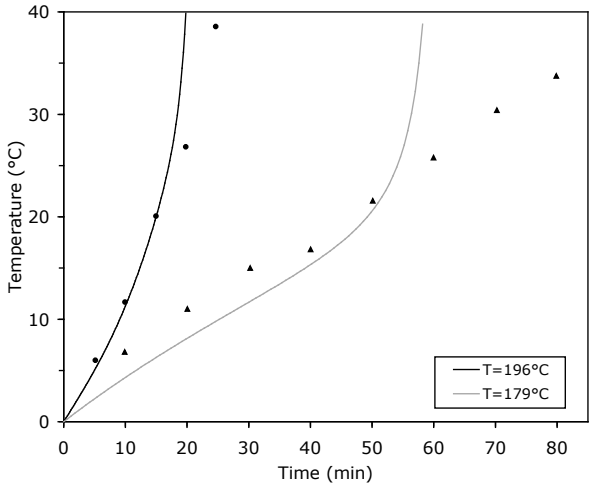


Figure 9 The effect of depletion of reactants on temperature rise[28]. Two different sizes of sawdust spheres were tested—the one exposed to T_o = 196ºC was 37 mm diameter, while the one exposed to T_o = 179ºC was 52.5 mm. The data points are experimental, while the lines are a numerical solution which neglects depletion of fuel.

(Copyright The Combustion Institute, used by permission)

per unit volume (kg m^{-3} s^{-1}). The dimensionality variable j is: 0 for slab, 1 for cylinder, and 2 for sphere; this simplified notation allows all three common geometries to be represented by a single equation. Numerically, D can be evaluated as $D = 1.8 \times 10^{-5} \varepsilon \left(\frac{T}{273} \right)^{7/4}$.

The rate of oxygen consumption can be expressed as:

$$\dot{m}'''_{ox} = \varepsilon A c^n e^{-E/RT}$$

where the Arrhenius rate expression is written to the general power n of the concentration. Since the units for the mass consumption term must be kg s^{-1} m^{-3}, the units of the pre-exponential factor A are seen to depend on the order of the reaction and are: $(kg/m^3)^{1-n}$ s^{-1}. In the same format, the steady-state energy conservation equation is written as:

$$\lambda \left(\frac{d^2T}{dx^2} + \frac{j}{x} \frac{dT}{dx} \right) = -\dot{q}'''$$

Here, the expression for the heat release rate term becomes:

$$\dot{q}''' = \frac{Q_{ox} \varepsilon \dot{m}'''_{ox}}{\rho_{ox}}$$

where Q_{ox} = heat of reaction per mass of *oxygen* consumed (kJ kg^{-1}). The energy conservation equation is then:

$$\lambda \left(\frac{d^2T}{dx^2} + \frac{j}{x} \frac{dT}{dx} \right) = -\frac{Q_{ox} \varepsilon \dot{m}'''_{ox}}{\rho_{ox}}$$

This formulation puts into parallel form the energy conservation equation (diffusion of heat) and the equation for diffusion of oxygen. The simplest boundary conditions are:

$$\frac{dT}{dx} = \frac{dc}{dx} = 0 \qquad \text{at } x = 0$$

$$T = T_o$$

$$c = c_o \qquad \text{at } x = \pm r$$

Note that in this simplified theory, the convective coefficient is *not* taken into account; thus, only a solution for $Bi \rightarrow \infty$ is sought. Thus, this theory relaxes the assumptions of infinite oxygen supply and of zero-order kinetics, but introduces a new limitation of a fixed temperature at the boundaries. To obtain a solution to the above theory, the classical approach has been to make a series expansion of the Arrhenius term around the ambient temperature T_o. Takeno and Sato[31] improved the accuracy by developing a series expansion around the to-be-solved maximum temperature T_m, instead. For their analytical solutions, they also introduced an additional approximation incorporating the diffusivity term. Their analytical solution for the slab case is shown in Figure 10.

The definition of δ_c for the limited-oxygen case is:

$$\delta_c = \frac{E}{RT_o^2} \frac{r^2 c_o^n \varepsilon Q_{ox} A}{\lambda} e^{-E/RT_o}$$

Note that, unlike for the base case, the heat of reaction is here on an oxygen basis and the porosity ε also enters into the equation. Figure 10 indicates that two variables affect

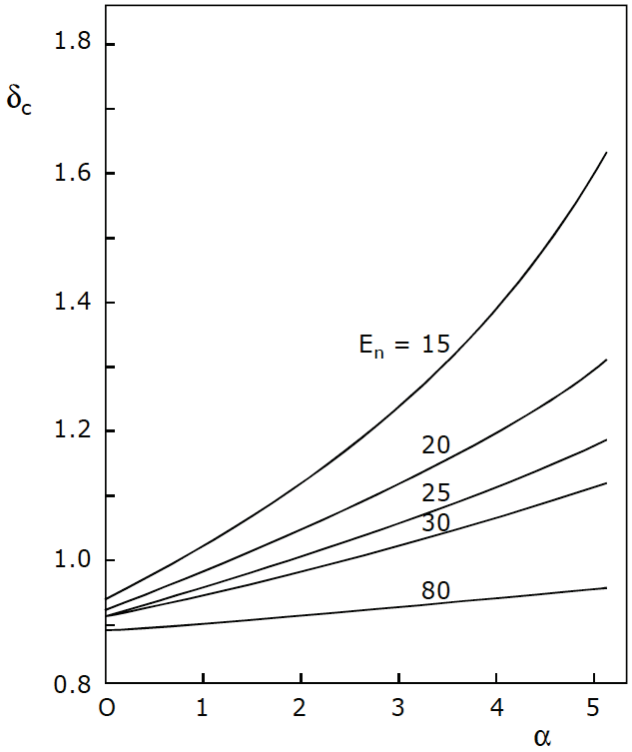


Figure 10 Effect of limited oxygen supply in raising δ_c according to the solution of Takeno and Sato
(Copyright The Combustion Institute, used by permission)

the oxygen-diffusion-limited value of δ_c: α and E_n. These new non-dimensional variables are defined as:

$$\alpha = \frac{n \lambda T_o}{c_o Q_{ox} D}$$

$$E_n = \frac{E}{RT_o}$$

and c_o, as before, is the initial concentration of oxygen. When oxygen supply does not limit the reaction, effectively $D \rightarrow \infty$. This corresponds to the classical solution, thus the $\alpha \rightarrow 0$ limit here should recover the Frank-Kamenetskii limit (i.e., $Bi \rightarrow \infty$). For the slab case, this value was 0.88. Here, one can see a value of $\delta_c \approx 0.9$. The slight difference is due to the different nature of the exponential approximation made by Takeno and Sato. A similar theory was also offered by Nakajima and Takeno[32].

STEADY-STATE THEORY INCLUDING FUEL DEPLETION

Fuel exhaustion occurs in all cases where an ongoing reaction can continue. This causes temperatures to be lower than a numerical solution of the heat flow equation would indicate (Figure 9). The bulk of the fuel depletion occurs after very rapid heating (i.e., runaway) has started. But if reactant depletion is significant, the onset of criticality will be estimated in an over-conservative way, thus a method to take reactant depletion into account is advantageous. The mathematics of the case which includes reactant depletion

changes in a fundamental way[33]. By ignoring reactant depletion, a limiting condition is computed whereby the system temperature →∞. This simplified result is then taken to correspond to thermal runaway, where large but not infinite temperatures will occur. The mathematical solution when reactant depletion is included does not show this same trait. Instead, temperatures run up to a high value, then proceed downward. Physically, this corresponds to the fact that temperatures must start dropping when fuel becomes scant.

Solutions which fully incorporate fuel depletion do not lend themselves to tractable, closed-form approximations. But Thomas presented a theoretical analysis[34] which was obtained by assuming that the fuel depletion case is a perturbation upon the no-depletion case. In his solution, he also generalized the Arrhenius Law reaction rate used to include reactions of arbitrary order. This gives the initial heat release rate as:

$$\dot{q}''' = c_f^n QA e^{-E/RT_a}$$

The fuel concentration c_f can be expressed either in mole units (mol m^{-3}) or density units (kg m^{-3}). The units of A depend on the value of n. For c_f in mole units, they are mol^{1-n} m^{3n-3} s^{-1}, while if c_f is in density units, then A is in units of kg^{1-n} m^{3n-3} s^{-1}. For a first-order reaction, the units of A are s^{-1}. Then δ is expressed as:

$$\delta = \frac{E}{RT_o^2}\frac{r^2 c_f^n QA}{\lambda} e^{-E/RT_o}$$

where c_f is the initial concentration of fuel. In Thomas' solution, an additional nondimensional term B is needed, which represents the temperature rise under adiabatic conditions:

$$B = \frac{E}{RT_o^2}\frac{Q}{C}$$

The results for the critical condition can be expressed as a 'corrected' δ_c:

$$\delta_c(B,n) = \frac{\delta_c(\infty)}{1 - 2.85(n/B)^{2/3}}$$

where $\delta_c(\infty)$ is the value obtained without considering reactant depletion. The value of n will not be known *a priori* without a detailed study of the material's chemistry, but for rough estimating purposes, it may be reasonable to assume $n = 1$. Small values of B promote a high degree of reactant depletion. A correction may be appropriate if B is less than about 100. Boddington[35] worked out a similar solution and obtained 2.703 instead of 2.85 in the above equation. He points out, however, that all such solutions contain steps which are logically somewhat shaky. Thomas and Bowes[36] have discussed the accuracy which is needed for fuel depletion effects calculations in order to preserve the accuracy of predictions, concluding that very simple corrections are sufficient. A number of alternative, possibly more exact solutions to the problem have subsequently been offered. Bowes[10] reviewed several of them in some detail and concluded that the best approximation is:

$$\delta_c(B,n) = \frac{\delta_c(\infty)}{0.97 - 2.35(n/B)^{2/3}}$$

The permissible temperature rise θ_p that can be incurred before criticality is reached also increases if reactant depletion is considered. Tyler and Wesley[37] offered the following correction equation for this:

$$\theta_p(B,n) = \theta_p \times \left[0.326 + 0.553\exp(3.47\varepsilon) + \left[3.69 + 1.91\exp(16.0\varepsilon)\right](n/B)^{2/3}\right]$$

where $\varepsilon = RT_o/E$. The correction equation was derived only for $B \geq 100$, but in view of the absence of other tractable prediction methods, it may be applied, with lower expected accuracy, even to B values outside this range. It is useful to estimate the magnitude of the correction that might be obtained with this equation. Taking values similar to those of some wood products, for example, E = 100 kJ mol^{-1}, Q = 500 kJ kg^{-1}, C = 1.4 kJ kg^{-1} K^{-1}, and taking T_o = 373 K gives B = 31 and ε = 0.031. Assuming that n =1, then $\theta_p(B, n)/\theta_p$ = 1.63; this is a fairly sizable increase in the permissible temperature rise.

The above discussion assumed that the solid in question was a symmetrically heated sphere, cylinder, or slab. For an unsymmetrically heated slab, some numerically-obtained guidance[38] is also available.

CORRECTION FOR LOW ACTIVATION ENERGY

The standard theory assumes that

$$\frac{RT_o}{E} << 1$$

If the activation energy is not large enough to justify that, then the values of δ_c will not be the standard tabulated values. By making full numerical calculations without approximation, Enig et al.[39] obtained tables for δ_c as a function of RT_o/E. For example, if RT_o/E = 0.25, then the slab δ_c = 1.12 instead of 0.88. In practice, no corrections need to be considered if E > 40 kJ mol^{-1}. For smaller values, Boddington et al.[24] provide the following approximation:

$$\delta_c(\varepsilon) = (\delta_c)_{\varepsilon=0}(1 + 1.07\,\varepsilon)$$

where $\varepsilon = RT_o/E$. This equation is valid for $\varepsilon \leq 0.05$. To make the correction, the value of δ_c is found from the basic theory, then the correction is applied according to the equation above.

For extremely small activation energies, the concept of criticality entirely vanishes. Such systems will self-heat continuously and a small-enough 'safe' diameter cannot be sought. This limit occurs at

$$\frac{RT_o}{E} \geq \text{ca. } 0.25$$

The limit value, in principle, varies with *Bi*, but the whole range of *Bi* numbers is encompassed[40] by about 0.24 to 0.25. For T_o = 20ºC, this limit will occur for E < 9.7 kJ mol^{-1}, which would only be seen for certain highly unstable substances.

MORE COMPLEX REACTIONS

Easily-tractable forms of theoretical treatment are all based on there being only a single, Arrhenius-form reaction. But some real materials show chemical reactions that are more complex. The forms of more-complex reactions include the following:

- A single reaction, but with a temperature dependence that is not of the Arrhenius form.
- Two sequential reactions.
- A substance comprised of a mixture of two pure substances, each of which exhibits a separate reaction chemistry.
- A substance that has two parallel reactions taking place, but those reactions cannot be attributed to two separate constituents of the substance.
- Single-step or multi-step autocatalytic reactions.

It is common to find substances where the best-fit kinetic expression shows a temperature dependence of the following form:

$$k \propto T^{1/2} \exp(-E/RT)$$

Boddington et al.[41] studied this case numerically. The results for δ_c are identical to those for the Arrhenius case in the case of no reactant depletion and nearly identical otherwise. Simple solutions have not been offered for more complex temperature-dependent factors.

If a material shows two sequential Arrhenius reactions, matters become very complicated. Forbes et al.[42] described some of the oscillatory behavior that can occur in a system where:

$$A \xrightarrow{k_1} B \xrightarrow{k_2} C$$

with k_1 and k_2 being two different, Arrhenius-form reaction rate terms.

Sawdust contaminated with an oil is the classical example of a two-component system where the self-heating behavior has been studied in detail for each component. Bowes developed a theory[43] for this case and provided experimental results[44] for the sawdust/oil example. Boddington et al.[45] developed another theoretical treatment for the case of two pure substances mixed together, and a calculational example has been published[46]. Wake et al.[47] discussed the case of two parallel reactions and provided numerical solutions for two example cases. Nunziato et al.[48] presented a theoretical solution, but without practical illustration. All of these theories are mathematically complicated and none are straightforward to apply in practice.

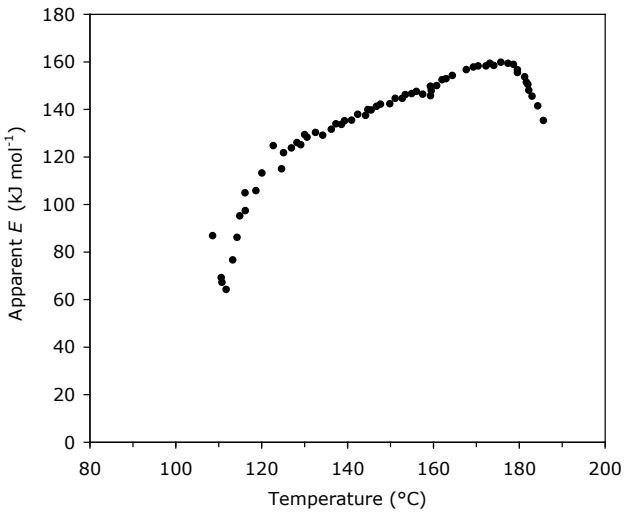


Figure 11 Apparent value of E obtained by analyzing ARC results for di-*tert*-butyl peroxide as having only a single Arrhenius-form reaction

In some cases, several parallel reactions occur in a substance which is a single, complicated substance and the reactions cannot be attributed to components that might be studied in isolation. Analyzing such a substance by assuming a single reaction will produce erroneous results. If a substance has a single, Arrhenius-form reaction, then the value of E must necessarily be a constant. Bowler[49] showed (Figure 11) that presenting data obtained from an accelerating rate calorimeter for di-*tert*-butyl peroxide (which exhibits two parallel reactions) gives an apparent value of E

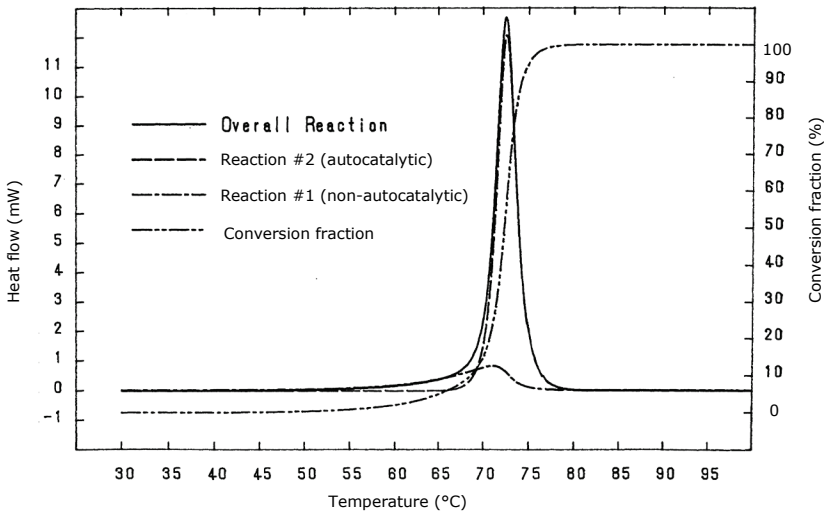


Figure 12 Two reactions during decomposition of bis(2-chlorobenzoyl) peroxide
(Copyright Associacio D'Enginyers Industrials de Catalunya, used by permission)

which is strongly temperature-dependent. A mild case of this has been documented for wood fiberboard[22], although adequate experimental accuracy is obtained by simply treating this material according to a single-reaction Arrhenius expression. Coal exhibits several simultaneous reactions and these cannot be attributed to individual constituents (Chapter 14). In some cases, a practical treatment can ignore the presence of two parallel reactions. A good illustration is provided by some explosives, which often show two temperature regimes (Chapter 10). Within each temperature regime, a single-reaction analysis can be used. This is possible because of the exponential nature of the temperature dependence—for temperatures a little bit away from the breakpoint, one reaction dominates and the second one becomes quantitatively insignificant. For substances of this kind, care must be taken to only use experimental data from the same temperature regime as the proposed environmental temperature into which the substance will be put.

As discussed in Chapter 3, autocatalytic reactions obey somewhat different relationships than do normal bimolecular reactions. In general, if a substance shows a small amount of autocatalytic activity, this may well be ignored. But if the reaction is strongly autocatalytic, extensive research may be needed. Grewer's book[72] examines autocatalytic reactions at great length, but no simple treatment emerges. Li and Hasegawa[50] studied bis(2-chlorobenzoyl) peroxide, whose decomposition has both an autocatalytic and a non-autocatalytic reaction. Allowing for both contributions to be of arbitrary reaction order, they developed an experimental technique for obtaining the kinetic constants from microcalorimeter data. Results can be obtained with a modest amount of trial-and-error because at the very start of the reaction no products yet exist, thus heat production must be solely due to the non-autocatalytic term contribution. Once its kinetic constants are obtained, then the higher temperature regime is used to obtain the constants for the autocatalytic portion of the reaction. The heat release contributions of the two reactions are shown in Figure 12. Another complicated reaction scheme involving autocatalytic reactions was examined by Tyler and Henderson[51], who studied sodium dithionite ($Na_2S_2O_4$), a self-heating powder. The reaction did not conform to a simple autocatalytic reaction, and to obtain agreement with experimental results, they found it necessary to perform numerical calculations using an empirically-derived reaction-rate law.

HOT WORK, COLD WORK, AND HOT SPOTS

Most of the discussion thus far has involved systems with only a single characteristic temperature: a body which is quickly assembled at T_o and placed in an environment which is at T_o. Subsequently, the system can heat up, but only a single temperature is needed to describe the initial system conditions. Apart from the unsymmetrically-heated slab already considered, two other classes of problems occur where there are two different initial temperatures: hot spots and hot/cold work. Theories have been developed to address both these situations. The hot work problem involves a material assembled or stacked which is initially at some elevated temperature T_h, higher than the ambient air temperature T_o. Hot spots may arise as a potential ignition problem in granular material if a hot body (a hot rivet, for example) is dropped into a pile of granular material. The granular material is initially at some lower temperature than the hot body. In such a case, the hot spot itself is inert, but the granular material is reactive. Hot spots may also arise due to non-uniformities of the substance, where localized nuclei of heating develop. The formation of such nuclei appears to still be largely unexplained. However, there has been a fair number of mathematical theories for the self-heating of a system where both the hot body and the surrounding body are reactive. Mathematically, these two problems have only one real difference: The hot work problem comprises a substance which is put into the atmosphere while at an elevated temperature; thus its edges are cooled by *convection*. The hot spot, on the other hand, is immersed in the reactive material; thus its cooling is only by solid-phase *conduction*. Cold work problems are the opposite of hot work, but have received only limited study.

HOT WORK

The problem of the initially-warm material is called the 'hot work' or 'hot stacking' problem. It can arise whenever a heat-treatment of a reactive material is used. For some materials, cooling under conditions of oxygen exclusion may be needed. The hot work problem has some special features, among them is that the upper (unstable) equilibrium point of Figure 2 can serve as a starting point for the process, since heat losses will decrease afterwards. When a system of this kind is placed in the air, there is internal heating but cooling at the boundaries. Thus, inevitably the center of the material rises in temperature. If the system is subcritical, after a modest increase, the temperatures begin to fall. But if the system is supercritical, then temperatures keep growing (Figure 13)[52].

Since there are two different characteristic temperatures, either one can be taken as the reference, but the development of the theory is quite different, depending on the choice. The more intuitively obvious choice is to select the ambient temperature T_o as the reference temperature. This was done by Gray and Scott[52] and the choice leads to δ_c values which sensibly drop as T_h is raised, indicating that if our conventional definition of δ_c is kept, permitted sizes must become smaller as T_h becomes larger. The other choice is to select T_h as the reference temperature. In that case, δ_c rises as T_h increases. The meaning of this is that a certain size would be permitted if both the initial body temperature and the ambient temperature were at the high value of T_h. But since T_o is in fact lower than T_h, a size increase is permitted, with respect to that starting point. This is equally viable as a calculational procedure, albeit less transparent. In the Gray/Scott method, the definition of δ_c is:

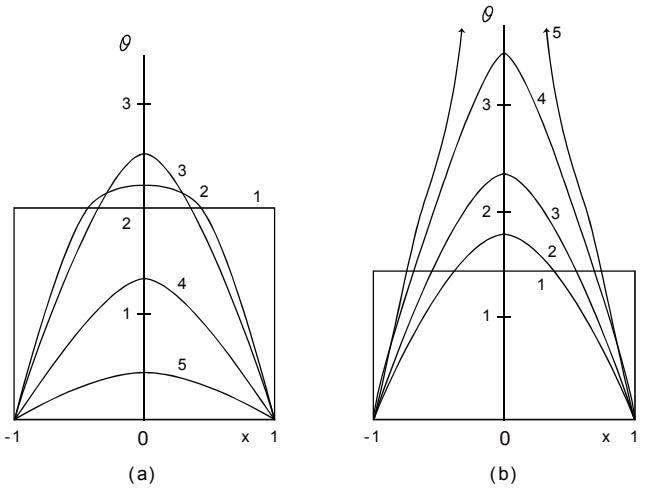


Figure 13 Hot work problem: (a) subcritical and (b) supercritical behavior; shown at time of assembly **1** and at later times **2**…**5**
(Copyright The Combustion Institute, used by permission)

$$\delta = \frac{E}{RT_o^2}\frac{r^2 \rho Q A}{\lambda} e^{-E/RT_o}$$

and the definition of the nondimensional initial temperature is:

$$\theta_i = \frac{E}{RT_o^2}(T_h - T_o)$$

Gray and Scott solved the problem numerically, and obtained results for the slab case as shown in Figure 14. They provided solutions only under the condition of $Bi \rightarrow \infty$, but for several values of ε, where

$$\varepsilon = \frac{RT_o}{E}$$

Note that if $\varepsilon = 0$ and $\delta_c = 0.88$ (that is, the value for the normal, non-hot-work case), then the maximum permitted initial temperature corresponds to $\theta_i = 1.115$, but for smaller δ_c values the permitted θ_i rises rapidly. The authors also provide similar graphs for the infinite cylinder and the sphere. Unfortunately, they did not analyze the case of a cube—which is often the shape of most interest. Griffiths and Kordylewski[53] did treat the case of the cube, but their solution was wholly computational and did not lead to closed-form approximations.

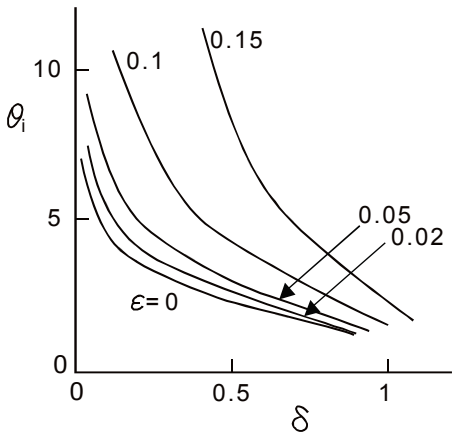


Figure 14 The critical values of initial temperature excess for the infinite-slab case (for values of $\varepsilon = 0$, 0.02, 0.05, 0.1, and 0.15)

An earlier solution to the problem was provided by Thomas[63], who took as a reference temperature the hot work temperature T_h:

$$\delta = \frac{E}{RT_h^2}\frac{r^2 \rho Q A}{\lambda} e^{-E/RT_h}$$

and using the definition of the nondimensional initial temperature as:

$$\theta_h = \frac{E}{RT_h^2}(T_h - T_o)$$

With these definitions, the value of δ_c rises as θ_h rises since, in this case, a rising θ_h must be interpreted as a falling T_o, in other words, T_h is viewed as fixed and that the hot work item is plunged into progressively cooler ambient environments. The Thomas solution was simplified by Bowes[10] and given as:

$$\delta_c = Bi(1+j)\theta_h\, e^{Bi(1+j)/\delta_c}$$

where $j = 0$, 1, and 2 pertain to the cases of the slab, cylinder, and sphere, respectively. This equation allows for finite values of Bi, but the unknown, δ_c, is present on both sides, so the equation can only be solved by trial-and-error. For the case where $\theta_h >> 1$, the very simple approximation can be used:

$$\delta_c \approx Bi(1+j)\theta_h$$

For high rates of convective cooling, where $Bi \rightarrow \infty$, Beever[54] presented graphical solutions. The following equations represent good curve fits to her results in the range $2 < \theta_h < 14$:

Infinite slab $$\delta_c = \frac{1}{0.0544 + 0.3603/\theta_h}$$

Infinite cylinder $$\delta_c = \frac{1}{0.04196 + 0.1382/\theta_h}$$

Equicylinder $$\delta_c = \frac{1}{0.0404 + 0.1180/\theta_h}$$

Sphere $$\delta_c = \frac{1}{0.0366 + 0.0610/\theta_h}$$

Cube $$\delta_c = \frac{1}{0.0458 + 0.1316/\theta_h}$$

All of the solutions above for the hot work problem assume that the substance is not of low activation energy, that is, that $E/RT_o >> 1$. If this condition is not fulfilled, then a simple, closed-form treatment is not available.

Results from a set of validation experiments on the hot work problem have been published[55]. In the experiments, wood sawdust was heated to steady state temperatures of 140 – 160ºC. The material was placed in thin, long cylinders to avoid runaway self-heating while in the oven. After reaching steady state, the sawdust was quickly emptied into cubical wire baskets sitting in open air. A linen lining was used inside the baskets to allow the material to be retained. An agreement within 21% to the theoretical results was obtained. The necessary material properties for the sawdust had been obtained previously from standard oven tests for self-heating of cubes.

COLD WORK

There exists an exact inverse to the hot work problem—a body initially at the temperature T_1 is plunged into an environment at T_o, where $T_1 < T_o$. In practice, this is how oven-basket testing, which is explored later in this Chapter, is done. To conform to simple F-K theory, the material should be dispersed in the oven in the form of an infinitesimally-thin layer, then quickly pulled together at $t = 0$ into a basket. It is rather hard to do this, so normally a basket is prepared at room temperature, then inserted into an oven that is preheated to some elevated temperature. For practical purposes, the time $t = 0$ is then declared to be the time at which the temperature at the center of the specimen first attains the oven temperature. This is entirely acceptable from the point of view of determining the critical size/temperature relationship, but actual temperatures during the initial warm-up period will not correspond to those pertinent to a theoretical treatment where the body is quickly assembled at T_o. The cold work problem has not been studied extensively from a theoretical viewpoint, because assuming that the entire system was equilibrated to T_o at $t = 0$ is a conservative assumption. Chong et al.[56] performed some illustrative numerical calculations for a cube, and these are shown in Figure 15. The substance showed only mild exothermicity, and thermal runaway eventually took place at the center, although early heating showed an initial 'shoulder' rise near the edges. If the substance is strongly exothermic, then runaway will occur close the edge and not at the center. Zinn and Mader[57] made some experiments and provided numerical calculations which illustrates this for the case of a sphere, as shown in Figure 16.

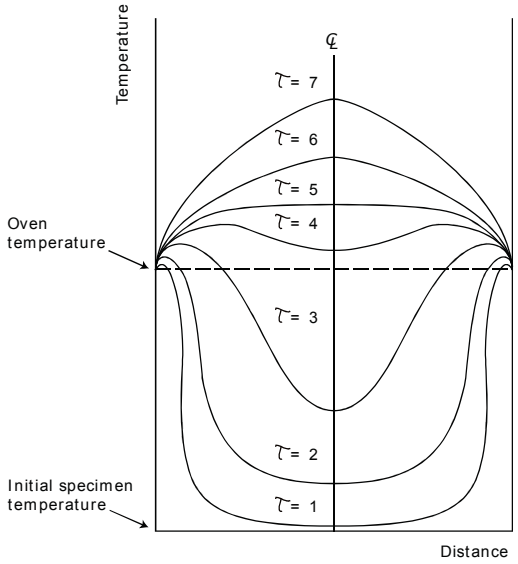


Figure 15 The heating of a cold cube of an exothermic substance after insertion into a test oven held at a hotter temperature; increasing times are denoted by higher τ values
(Copyright © 1995 AIChE)

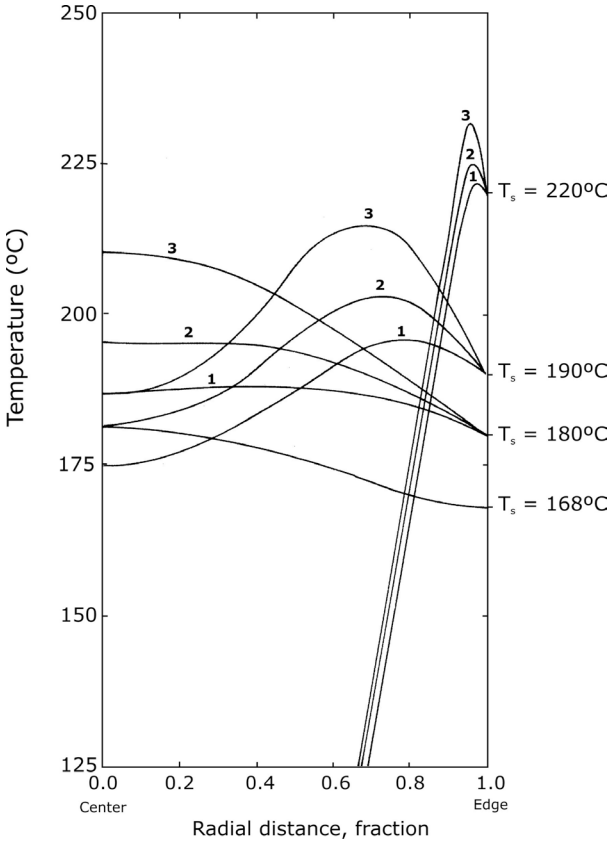


Figure 16 Calculated results for the heating of a 25 mm diameter sphere of RDX, initially at 25ºC, plunged into environments of various elevated temperatures (T_s). Curves shown were obtained for three different times: **1** denotes time which is 90% of critical time, **2** is 95%, **3** is 98%. T_s = 168ºC is the highest subcritical temperature. It is assumed that $Bi \rightarrow \infty$, therefore the surface temperature T_s is identical to the environment temperature T_o.
(Copyright The Institute of Physics, used by permission)

Abramov et al.[58] obtained example solutions in terms of δ_c', which is the critical value of δ beyond which thermal runaway will no longer occur at the center. Their computed values, obtained only for θ_i = 11.7, are shown in Table 8.

For δ slightly in excess of δ_c', thermal runaway will take place only slightly offset from the center and it requires $\delta \approx$ 1000 before the peak temperature approaches close to the edge.

Table 8 Critical values of δ_c' for the condition that θ_i = 11.7

Geometry	δ_c'
infinite plane	9.25
infinite cylinder	12.25
sphere	14.25

INERT HOT SPOTS

An inert hot spot can comprise, for example, a piece of hot metal that falls into a bed of ignitable fuel. Whether a self-sustaining reaction is thereby caused in the fuel bed depends on the size and the temperature of the hot spot, along with the properties of the fuel. The problem becomes intrinsically complicated, since now several new variables—those describing the characteristics of the hot spot—are introduced. Of the various proposed solutions, Bowes[10] recommends the use of Gol'dshleger's method[59] as being reasonably accurate, yet still tractable. In the Gol'dshleger method, the critical value δ_c is approximated as:

$$\delta_c = Z\left[1+\frac{(\theta_h-3)^2 b(j+1)}{30k_\lambda^{2/3}(1+3b^{2/3})}\right]^2$$

where

$$\delta = \frac{E}{RT_h^2}\frac{r^2\rho Q A}{\lambda}e^{-E/RT_h}$$

$$\theta_h = \frac{E}{RT_h^2}(T_h - T_o)$$

$$Z = 0.4\left[\theta_h + 2.25(j-1)\right]^2 \times\left[1+0.5\varepsilon\theta_h\right]\sqrt{b^2+0.25\,j(j+1)(b+0.1b^3)}$$

T_h = initial temperature of hot spot
T_o = initial temperature of surrounding body

$$b = \frac{\rho C}{\rho_h C_h}$$

$$k_\lambda = \frac{\lambda_h}{\lambda}$$

$$\varepsilon = \frac{RT_h}{E}$$

and the suffix *h* denotes properties of the inert hot spot.

Finally, j = 0, 1, and 2 for the infinite slab, infinite cylinder, and sphere geometries, respectively. The approximate solution was derived assuming the following range of variables: 7.5 $\theta_h \le 25$; $0.01 \le \varepsilon \le 0.9/\theta_o$; $1 \le k_\lambda \le \infty$; $0.05 \le b \le 10$. An example of the use of the Gol'dshleger method is given in Chapter 14 under *Forest materials, vegetation, and hay*.

Another solution to the same problem was offered by Liñán and Kindelán[60]. Their solution is based on a different definition of a non-dimensional heat generation parameter, which for distinction is identified as δ^{LK}:

$$\delta^{LK} = \frac{2RT_h^2 QAr^2\rho_o}{E(T_h-T_o)^2\lambda_o}\exp(-E/RT_h)$$

where T_h = temperature (K) of the hot spot, T_o = initial temperature (K) of the self-heating body, ρ_o = density (kg m^{-3}) of the self-heating body, and λ_o = thermal conductivity (W m^{-1} K^{-1}) of the self-heating body. The solution is presented in terms of the variable Λ, defined as:

$$\Lambda = \frac{RT_h^2}{(T_h-T_o)(j+1)E}\frac{\rho_h C_h}{\rho_o C_o}$$

where j = 1 for cylinder or 2 for sphere, ρ_h = density (kg m^{-3}) of the hot spot, C_o = heat capacity (J kg^{-1} K^{-1}) of the self-heating body, and C_h = heat capacity (J kg^{-1} K^{-1}) of the hot spot. Over the range $10^{-2} < \Lambda < 10^3$, the solution for the critical value δ_c^{LK} is shown as a graph, which can be expressed as:

$$\delta_c^{LK} = 1.15 + 1.32\Lambda^{-0.5} + 3.47\Lambda^{-1} + 0.302\Lambda^{-2}$$

The solution is valid provided that $\lambda_h\rho_h C_h >> \lambda_o\rho_o C_o$, which will commonly be the case for granular or porous materials.

A simpler solution, but applicable only to the infinite cylinder geometry was obtained by Friedman[61]. His approximation for δ_c is:

$$\delta_c \approx \ln\left[0.608\frac{E}{RT_h}\left(1-\frac{T_o}{T_h}\right)\right]$$

where the definition of δ is:

$$\delta = \frac{E}{RT_h^2}\frac{r^2\rho Q A}{\lambda}e^{-E/RT_h}$$

REACTIVE HOT SPOTS

Theories for reactive hot spots assume that the hot spot and the fuel bed are comprised of the same substance, with the distinction being that the hot spot is smoldering and the main fuel is not (yet). In principle, theories could also be produced for a situation where the two substances are chemically different, but none of this kind have been published. Thomas reviewed in 1965 the early work[62]. Two concerns emerged: (1) predicted values for δ_c varied by close to a factor of ten among the theories. In fact, under the same circumstances, some theories predicted that immediately after t = 0, the hot spot itself will start rising in temperature, while others predicted that it will start dropping. (2) Adequate experimental data were not available for validation. Several years later, additional new theories were available, leading to a second review of the subject by Thomas[63]. In the latter study, Thomas concluded that Merzhanov's[64] approach is the most suitable. The physical assumptions in that theory are:

(1) the hot substance and the surrounding substance are the same material.
(2) a transient solution is needed, therefore, time terms are not dropped in the conservation equation.
(3) Arrhenius kinetics applies.
(4) reactant depletion can be ignored.
(5) the approximation $RT_h/E \rightarrow 0$ can be made.

The theory then considers a hot zone of radius r which is originally at $T = T_h$ at $t = 0$. The nondimensional temperature rise is defined as:

$$\theta = \frac{E}{RT_o^2}(T - T_h)$$

and the nondimensional difference between the initial hot spot temperature (T_h) and the initial temperature of the surrounding body (T_o) is defined as θ_h:

$$\theta_h = \frac{E}{RT_h^2}(T_h - T_o)$$

A further approximation is then made that $\theta_h >> 1$. The nondimensional heating rate δ is defined as:

$$\delta = \frac{E}{RT_h^2}\frac{r^2 \rho Q A}{\lambda} e^{-E/RT_h}$$

Note that in this formulation the value of temperature used to define δ is T_h (the initial hot spot temperature), not the ambient temperature of the surrounding body. The mathematics of the solution is complex and we will proceed straight to the engineering approximation:

$$\delta_c = M(\ln \theta_h)^N \quad \text{for } 4 < \theta_h < 25$$

where the constants M and N, for various geometries, are given in Table 9.

Table 9 Constants for Merzhanov's theory of reactive hot spots

Geometry	M	N
plane slab	2.66	1.3
infinite cylinder	7.39	0.83
sphere	12.1	0.60

APPLIED HEAT FLUX

A related problem is the ignition of a self-heating material by the application of a specified heat flux at a boundary. Brindley et al.[65] formulated this problem for a slab, a spherical annulus, and a cylindrical annulus; the face not receiving the specified heat flux is, in all cases, subjected to convective cooling. Their method only produced numerical results and did not lend itself to a closed-form solution.

TRANSIENT THEORY

ESTIMATING TIME TO CRITICALITY

The steady state theory tells us only if runaway conditions will result. But it is often of interest to estimate not only *whether* ignition can occur, but *how long* it will take, if the system is one which does lead to ignition. The practical relevance is because many piles of materials prone to self-heating are not being stored indefinitely. If runaway conditions are anticipated to occur in, say 1 month, but the average storage period (before the pile is segregated into small piles and removed) is 3 days, then there is little danger in the process. Since, thus far, time-dependent solutions have not been considered, we first start with an example of some laboratory data showing histories of self-heating. Figure 17 illustrates the temperatures obtained for several equicylinders (height ≡ diameter) of wool, placed in an oven at various temperatures[66].

To estimate the ignition time from theory requires either a numerical computation of the governing equation, or approximations, or both. For the problem of constant surface temperature, Zinn and Mader[57] solved the time-dependent equations for the non-dimensional ignition time τ as a function of the ratio δ/δ_c. under the assumption that $Bi \rightarrow \infty$. Their definition of τ is:

$$\tau = \frac{t_{ig}\lambda}{\rho C r^2} = \frac{t_{ig}}{t_{Fo}}$$

where t_{Fo} denotes the 'Fourier time,' which is the characteristic time for cooling. Thus, the physical ignition time t_{ig} is computed as:

$$t_{ig} = \tau \cdot t_{Fo} = \tau \frac{\rho C r^2}{\lambda}$$

A closed-form approximation to their results is:

$$\tau = \frac{1}{a + b(\delta/\delta_c) - c(\delta/\delta_c)^{-1/2}}$$

where the numerical constants are given in Table 10. A graph of Zinn and Mader's original results (x's) and the curve fits (lines) are shown in Figure 18. Note that only points for $\delta > \delta_c$ are shown, since there is no thermal runaway if $\delta < \delta_c$.

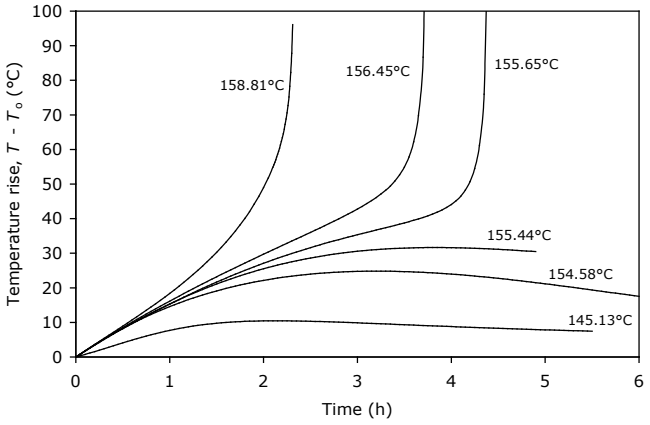


Figure 17 The temperature rise for 6 L equicylinders of wool, when placed into an oven held at various temperatures
(Copyright Royal Society of New Zealand, used by permission)

Table 10 Constants for the Zinn and Mader approximation

Geometry	a	b	c
slab	1.07	0.00380	0.941
cylinder	2.30	0.0187	1.95
sphere	3.90	0.0390	3.46

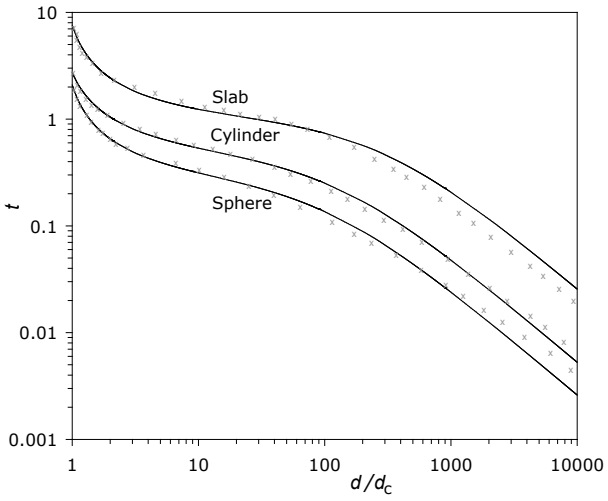


Figure 18 Estimating of the ignition time, Zinn and Mader method

Another method for estimating the ignition time was developed by Boddington et al.[67]. Using the same nomenclature as above, their expression is:

$$\tau = \frac{M(Bi)}{(\delta/\delta_c - 1)^{1/2}}$$

with values of the function M (Bi) given in Table 11. In their paper, Boddington et al. also provide values of M for intermediate values of Bi. However, since the limit values are quite similar, it should suffice to simply select either the $M(0)$ or the $M(\infty)$ value.

The calculations can be alternately presented, as Boddington et al. did in their original work, by using the concept of the *adiabatic induction period*, which pertains to a system with no heat losses. The adiabatic induction period is defined as:

$$t_{ad} = \frac{C}{AQ}\frac{RT_o^2}{E}\exp\left(\frac{E}{RT_o}\right)$$

where C = heat capacity of the reactants (kJ kg^{-1} K^{-1}) and T_o is the initial temperature (K). But, according to definition of δ_c,

$$\delta_c = \frac{t_{Fo}}{t_{ad}}$$

The ignition time t_{ig} can then be expressed as a function of t_{ad}:

$$\frac{t_{ig}}{t_{ad}} = \frac{M(Bi)}{(\delta/\delta_c - 1)^{1/2}}$$

Table 11 Estimating ignition time by Boddington's method: limiting values of $M(Bi)$

Geometry	*M* (*Bi*)	
	Semenov condition (*Bi*→0)	**Frank-Kamenetskii condition (*Bi*→∞)**
slab	1.6344	1.5336
cylinder	1.6344	1.4288
sphere	1.6344	1.3160

This method presumes that the actual conditions are only marginally supercritical, i.e., that δ is not vastly greater than δ_c. For strongly supercritical systems, Boddington et al. provide another expression:

$$\frac{t_{ig}}{t_{ad}} = \frac{M(Bi)}{(\delta/\delta_c - 1)^{1/2}} - 0.8 + 0.8(\delta/\delta_c - 1)^{1/2}$$

Boddington provided an experimental validation of the above equation[68], although the system studied was a highly explosive gas, where criticality times were all less than 5 s. A comparison of the results of Zinn and Mader to those of Boddington et al. indicate that for $1.05 \le \delta/\delta_c \le 5$, where most practical problems are likely to occur, differences of about a factor of 2 are found.

Thomas[34] derived several estimates for the induction period. The most useful is a simple lower limit:

$$\tau \ge \frac{0.89}{\delta}$$

Or,
$$t_{ig} \ge \frac{0.89}{\delta}\frac{\rho C r^2}{\lambda}$$

Another method for estimating the lower bound was developed by Gray et al.[69] They used the assumptions of a slab geometry, no reactant depletion, and $Bi \to \infty$, but performed a full numerical solution, without making approximations for the exponential term. Numerical solutions were obtained, to which they provided an analytical approximation*:

$$\tau_{ig} \ge u^2 \exp(1/u)[1 - \exp(-\Delta/u^2]$$

where $u = RT_o/E$, $\tau_{ig} = \frac{QAR}{CE}t_{ig}$, $\Delta = RT_p/E$, and the units of QA are W kg^{-1}. Here Δ is the nondimensional temperature rise corresponding to runaway, and Gray suggests that for practical purposes it is sufficient to set $\Delta = 0.003$. Since all of the constants can be determined from tests, a conservative estimate can be computed for any desired ambient temperature T_o. Note that the actual size of the pile does not enter into the expression, thus it is indeed a conservative bound. Even though the expression was specifically derived for slabs, Gray suggests that it is equally applicable to other shapes. Gray recommends[70] that for accurate results, an experimental data point for ignition time should be used.

* The equation given here corrects a misprint in the original paper's expression for τ_{ig}.

The procedure, then, is as follows. Conduct standard oven-basket tests (see below), from which a value of E is determined. Select one of the test temperatures, $T_{o,x}$, where the subscript x denotes experimental value. The observed time to runaway at that temperature is found to be $t_{ig,x}$. Then for that condition $u_x = RT_{o,x}/E$. Knowing u_x, the equation can be solved to determine $\tau_{ig,x}$. Finally, the needed group of constants is solved for as:

$$\frac{QAR}{CE} = \frac{\tau_{ig,x}}{t_{ig,x}}$$

Actual computations of t_{ig} for end-use temperature conditions are then made using this value for the group of constants.

A number of other approximate solutions (of much higher complexity) have been reviewed by Bowes[10]. Squire[71] has pointed out that predicted times from all theories will generally be shorter than actual, since fuel depletion is not taken into account in any of the simplified formulas.

For Newtonian cooling of the surfaces with a convective heat transfer coefficient h of finite value, Grewer[72] provided a solution based on knowing the half-time, $t_{1/2}$ (s), of the container, which is defined by the equation:

$$\frac{1}{2} = \exp\left(-\frac{hS}{\rho CV} t_{1/2}\right)$$

where S = surface area, and V = volume. The half-time is then obtained as:

$$t_{1/2} = 0.693 \frac{\rho CV}{hS}$$

Physically, the half-time is determined by taking a block made to the same dimensions as occurs in the problem in question, but of a non-reactive, high thermal conductivity material having a well-known value of C. Suitable materials can be aluminum or copper. The block is heated (or cooled) to equilibrium at some temperature, then quickly removed and plunged into an environment (typically, air) at another temperature. The half-time is simply determined by finding time that it takes for the block to fall (or rise) by ½ of the ultimate value of its temperature change. Grewer then obtained a relation for t_{ig}/t_{ad} as a function of $t_{ad}/t_{1/2}$. This can be numerically represented as:

$$\frac{t_{ig}}{t_{ad}} = \left(\frac{1 + 0.0012\, t_{ad}/t_{1/2}}{1 - 0.255\, t_{ad}/t_{1/2}}\right)^{0.65}$$

The half-time can also be expressed as:

$$t_{1/2} = 0.693\, t_N$$

where $t_N = \dfrac{\rho C}{hS}$ and is identified as the Newtonian cooling time—it is the time scale representing the cooling. We may also note that the Semenov number, ψ_c, is defined as: $\psi_c = t_N / t_{ad}$. Thus, Grewer's relation could have equally well been expressed by replacing $t_{ad}/t_{1/2}$ with 0.693 ψ_c.

Grewer's method is useful in connection with a number of UN tests (see at the end of this Chapter) where $t_{1/2}$ is determined. One would naturally expect that if one "blows harder" on a pile of self-heating material, that the time to criticality would be delayed. Grewer's expression is perhaps the one which most clearly illustrates the effect, since $t_{1/2}$ is decreased with increased cooling, while the expression for t_{ig} increases monotonically (albeit non-linearly), with $1/t_{1/2}$ (Figure 19). Apart from this alternate solution for problems with Arrhenius kinetics, Grewer also developed[72] a numerical solution for the ignition time in the case of autocatalytic reactions.

The above presentation focused solely on the simplest classical case, a body reacting to a uniform ambient temperature. Practical predictions are not available for other situations. For example, a theoretical model[38] was developed to predict the runaway time in systems with one face held at an elevated temperature (e.g., hotplate tests), but comparison with experimental data indicated that success was not achieved.

In practice, it may be best to simply extrapolate from experimental data, and this is what Thomas[73] and Bowes[10] both recommend. Figure 20 illustrates results from Mitchell[161]. In his tests, he used octagonal parallelepipeds with height = face width. The times plotted all pertain to the $\delta \equiv \delta_c$ condition. The lines drawn represent $t_{ig} \propto r^2$. Thomas points out that a dependence on r^2 will be found for any system which is diffusion-limited, and it is not necessary for Arrhenius kinetics to be applicable. Thomas also examined the effect of reactant depletion on the criticality time[74]. He concluded that there is a strong effect, unless the conditions are such that $\delta > 2.5\delta_c$.

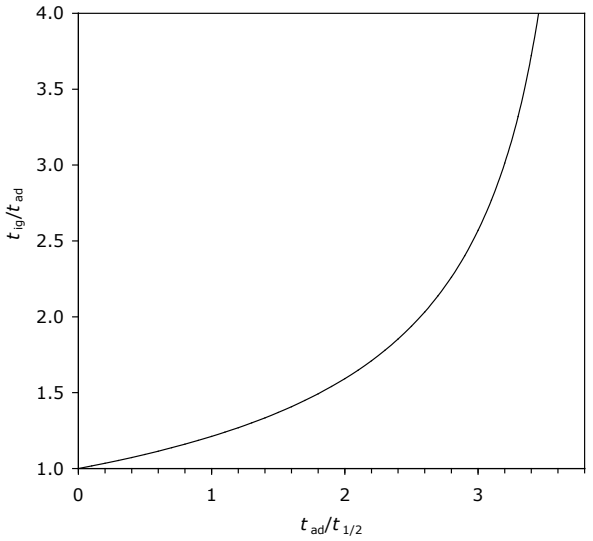


Figure 19 Grewer's method for estimating time to ignition
(Copyright Elsevier Science, used by permission)

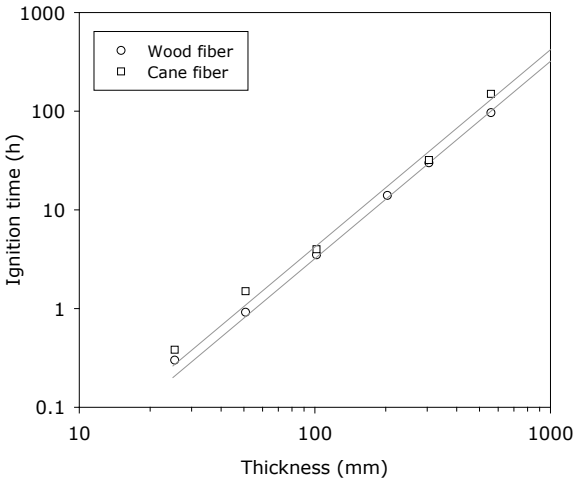


Figure 20 Times to criticality for 'equi-octagons' of two different fiberboards (the oven temperature is different for each data point, in each case corresponding to the critical temperature for the particular thickness)

Gray[75] has pointed out that all methods of computing or estimating time to criticality may be subject to gross errors. The basic reason is that few substances truly possess only a single exothermic reaction. Instead, various chemical reactions (e.g., catalytic reactions) may be important towards establishing the early time scale, but these same reactions are not ones that determine the actual temperature/size criticality relationship. No form of clever mathematical treatment can overcome this potential difficulty.

LINEARLY INCREASING SURFACE TEMPERATURE

In some situations, the boundary conditions for a self-heating substance can be approximated by assuming that the exposed surface temperature is rising at a linearly increasing temperature. Creighton[76] considered a slab with its face subject to the boundary condition

$$T_s = T_o + \beta t$$

and obtained numerical solutions for the cases (a) simple Arrhenius kinetics; and (b) more realistic 3-step reaction kinetics suitable to the explosives HMX and TATB. Unlike bodies with Newtonian cooling conditions at the edges, when peak temperatures are found at the center, the peak temperature rise for this problem is close to the surface. The critical surface temperature T_c at ignition was found in all cases to obey a relation of the form:

$$T_c = \frac{a}{1 - b \ln \beta}$$

where a and b are constants to be fitted.

MORE ADVANCED MODELS

The models discussed so far have largely been simplified sufficiently so that either approximate closed-form solutions could be obtained or, at least, that the number of variables be small enough so that some 'universal' graph could be obtained. This means that important physical/chemical factors had to be ignored. A more comprehensive treatment would include not only transient effects, but also encompass 3-dimensional bodies not having symmetry; more detailed chemistry, variation of thermophysical properties with temperature and degree of charring, flow of moisture, etc.

The disadvantage of comprehensive numerical models is that they lack instructive value. If all the necessary input data can be assembled (and that may be a very large "if"), then a precise, specific result can be computed. However, it is difficult to develop an intuitive understanding how the physics and chemistry really work, when such a model is used. Brute-force, numerical modeling has been used for a very long time in computational fluid dynamics (CFD), in civil engineering thermostructural studies, and in a plethora of other disciplines. Thus, perhaps it is a bit surprising that there have not been a great number developed of multi-component, multidimensional, fully-featured numerical models of self-heating. There has been a handful, however.

Nordon[77] presented a computational model for coal. His initial model was 1-dimensional, but included conservation equations for heat, oxygen, and water vapor. One aspect that Nordon was able to study which is not incorporated into the classical model is forced convection blowing through a porous pile, for example, due to effects of wind. Large amounts of *air flow* reduced self-heating below the no-forced-convection case. On the other hand, a small amount of forced convection, with velocities of the order of 10^{-5} m s^{-1}, served to greatly increase the temperature rise of the pile. More recent work reformulated the model to be 3-dimensional, with the objective of examining the effect of porosity[78]. Under the standard theory, porosity would only be accounted for by the density term of the substance. But increasing porosity decreases the density and, according to Frank-Kamenetskii theory, would decrease the self-heating. Instead, the detailed modeling showed that increasing the porosity from 0.2 to 0.3 caused a significant increase in self-heating. This result indicates that at the lower porosity the coal's heat generation was limited by insufficient oxygen access. A much more comprehensive model for the self-heating of coal was developed by Schmal[79], and it is discussed in Chapter 14.

Another numerical model was illustrated by Takeda and Akita[80], who investigated the case of symmetric bodies having a boundary condition at the edges consisting of a steady rate of temperature rise. The number of variables in such a case exceeds what can be readily represented in closed form, but the authors provided computational results showing that increasing the heating rate raises the computed value of T_c. The effect is not major, however, and in their example increasing the boundary rate of rise by 10× caused only about a 9ºC increase in T_c. A two-dimensional, transient model for self-heating of powders in a silo has been described[81]. Despite the fact that a few models have been

documented in the literature, it does not appear that there are any that are available to the public in the form of a computer program.

Applications

IGNITION FROM SELF-HEATING

When a critical condition occurs in a substance undergoing self-heating, the question becomes: What happens then? In general, one can expect a smoldering type ignition. If the substance is homogeneous and its initial temperature is identical to that of its environment, then the temperature rise will be highest in the center, therefore, this is where the ignition is expected to occur. But if a body is plunged into a very hot temperature environment, then ignition must occur at the edges, since heating only a surface layer of small thickness will suffice to cause thermal runaway. For this to happen requires the system to be greatly supercritical. Bowes[10] provided some practical guidance on this topic. For a sphere, if $\delta > 14.25$, then runaway will occur at the edges first. For an infinite cylinder the transition value of δ is 12.25, and for a plane slab it is 9.25.

In general, flaming ignition is not expected to occur—if it occurs at all—until a substantial amount of fuel is consumed and either a large inside cavity is formed or else the smolder front breaks through to the surface. The reason that flaming conditions are not expected inside a pile of material has to do with the quenching distance, discussed in Chapter 4—the porous material effectively acts as a flame arrester. With sufficient material being consumed, this may no longer be true and flaming ignition can occur inside the cavity. The topic of transition from smoldering to flaming is discussed in Chapter 7.

The aftermath of a spontaneous combustion fire can have some surprising features. One aspect may be the presence of multiple 'chimneys' of burned material; these tend to follow paths of least air resistance[75]. Another is that virgin material may remain unburned at the lowest level of the origin of the fire; this is due to poor access of oxygen downward into the material.

EFFECTS OF DIFFERENT VARIABLES ON SELF-HEATING

In the theory sections, the primary variables influencing self-heating were developed on a quantitative basis. Here we examine the effects from a simple qualitative viewpoint, and also provide experimental data, where available, to guide the individual making an application to fire incidents. Additional variables are considered in the Section *Oven-basket tests: FRS method*.

CHEMICAL AND PHYSICAL NATURE OF THE SUBSTANCE

These factors cannot be controlled by the user, but they may be controllable by the maker of the material. The effects can be determined by referring to the basic equation for the non-dimensional heat release rate:

$$\delta = \frac{E}{RT_o^2}\frac{r^2 \rho Q A}{\lambda} e^{-E/RT_o}$$

Thus, lowering the heat of reaction Q or raising the thermal conductivity λ of the substance will decrease the self-heating tendency. Also, any changes which lower the reactivity of the substance (lowering the pre-exponential factor A, or raising the activation energy E) will reduce the self-heating tendency. The activation energy effect is dominated by the exponential factor.

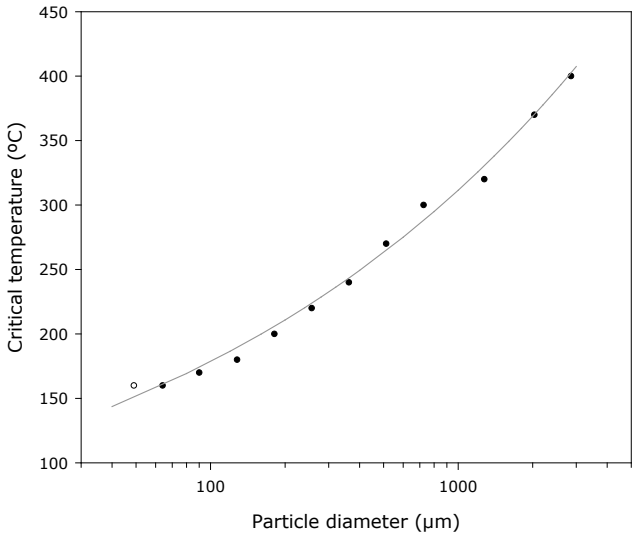


Figure 21 Effect of particle size on hotplate critical temperature for Pittsburgh coal dust

PILE SIZE AND SHAPE, AND POROSITY OF THE SUBSTANCE

The larger the pile of substance, the less efficient is the cooling from the ambient environment, which can only occur at the edges. The heat generation is proportional to the volume of the substance, while the amount of cooling is proportional to the exposed surface area. Thus, the propensity to self-heat is proportional to the volume/surface ratio V/S. This ratio is the highest for the most compact possible body shape, a sphere. It is progressively lower for various elongated shapes, such as a thin, long layer of material.

The most common solids which exhibit self-heating problems are porous materials. Thus, porosity clearly may come into play. In the basic F-K theory, porosity is not a factor, since its primary effect relates to inflow of oxygen and the theory assumes there are no reaction limits due to oxygen insufficiency. Higher-order effects, however, can come into play. Moisture uptake, which can be significant under some circumstances, is affected by porosity, as are surface reactions of various kinds. Materials may change their porosity as chemical reactions take place. Wood is a good example of this. The porosity of virgin whole wood is very small.

This limits the amount of oxygen that can be made available for self-heating, but self-heating nonetheless can proceed, albeit slowly. As oxidation further progresses, the material becomes more porous and oxygen availability becomes greater. No theory is available to treat such a 'self-modifying' substance, but some experimental data are cited under *Wood* in Chapter 14.

PARTICLE SIZE

If the chemical reaction occurred on the surface of the particles (heterogeneous reaction), then particle size would be the most critical variable. F-K theory assumes the opposite extreme, that the reaction occurs evenly dispersed through the volume (homogeneous reaction). The latter assumption appears to be well suited to most substances. But there are exceptions. Coal particles are largely impervious and unreactive except at the surface. Thus, it is not surprising that coal dust tests show a particle size dependence. In testing Pittsburgh coal in a hotplate test, Nagy and Verakis[92] found a strong influence of particle size. Figure 21 shows that the relation was found:

$$T_h = 7.8 + 54\, d^{1/4}$$

where T_h = critical hotplate temperature (ºC) and d = particle diameter (μm). Akgün and Arisoy[82] reviewed a number of other studies on the effect for coal and conducted tests of their own. They concluded that the HRR can be represented as:

$$\dot{Q} \propto Y_{O_2} d^n$$

namely that it depends linearly on the oxygen mole fraction and to a fractional power on the particle diameter d. Their results showed that n itself was temperature-dependent, going from –0.33 at 25ºC up to –0.74 at 75ºC, but this partial expression did not lead to a full calculational method. Their literature review indicated that no diameter effect is present when the particles are very small, but there is wide disagreement as to the limit for this regime (ranging from 0.05 to 5 mm).

Even less data exist for other substances. Demidov[83] reports that in one series of experiments, sulfur pyrite showed a $T_c \approx 400$ºC for various particle sizes > 0.10 mm, but the value dropped to 340ºC for a particle size of 0.086 mm. For wood-bark chips, the size of the particles was found not to affect the self-heating behavior[84].

TEMPERATURE

The cooler the ambient air is, the more effective is the cooling. Thus, a pile of substance which may be stored without reaching critical conditions in the winter may undergo spontaneous combustion in the summer. Similarly, self-heating tendencies are exacerbated if the material is originally stored at an elevated temperature, instead of at ambient temperature.

A factor which should not be overlooked for outdoor storage is *solar heating*. On a clear day, solar heating radiant flux may approach 1 kW m^{-2}, and this is not insignificant. If solar heating is expected to be a factor, numerical evaluation schemes need to be used, since boundary conditions involving natural convection cooling and an external radiant flux are not amenable to closed-form solutions.

TIME OF STORAGE

If conditions for a substance (size, temperature, cooling, etc.) are such that it is sub-critical, then indefinite storage time may be acceptable*. Otherwise, the time to inception of high heating rates—which occurs before the actual point of runaway—must be greater than the storage time. From heat transfer principles, the ignition time may be expected to scale with the size r and the thermal diffusivity α as:

$$t_{ig} \propto \frac{r^2}{\alpha}$$

In practice, the exponent is not necessarily identical to 2, so correlations of the form

$$t_{ig} = b r^n$$

should be sought, where the constants b and n are determined from the data fit. Read et al.[85] recommend a similar form of correlation:

$$t_{ig} \propto \left(\frac{r^2}{\alpha} \right)^{2/3}$$

For practical purposes, Bowes[10] points out that if a series of experimental data is available, extrapolations may be simply made since a plot of r versus t_{ig} will usually produce straight lines on a log-log scale. Or, volume can be used, as shown by the data of Leuschke[86] in Figure 22. A plot of this type is based on test data where each data point was obtained at a different temperature: the minimum temperature needed to exhibit criticality for the particular size being tested. Thus, it can only be used to extrapolate criticality times for just-critical conditions. If the storage temperature is greater than the critical temperature, then the allowable time will be shorter.

In many practical cases, it may be more relevant to plot the time to criticality at a fixed ambient temperature, rather than at the critical one. Such data obtained from a finite-element model of the self-heating of milk powder[87] are shown in Figure 23. The data appear to have a sigmoid shape rather than following a straight line. Thus, extrapolation should not be done and interpolation must be done cautiously.

ACCESS OF AIR

Many—but not all—substances prone to self-heating need oxygen for the chemical reaction to occur. Any conditions which limit oxygen access to the material can, therefore, reduce the self-heating tendency. For example, air infiltra-

* Some substances, e.g., certain agricultural products, may be ruined due to elevated temperatures, even without thermal runaway.

tion into porous substances can be greatly reduced by wrapping them in plastic film (but note that plastic films differ widely in their permeability to air). A more subtle variation of this effect is observed for substances such as linseed-oil soaked rags. It is possible to saturate rags with such a high amount of oil that air is effectively blocked from flowing in. Thus, if one keeps adding linseed oil to a pile of rags, the self-heating propensity will first increase (because the heat of reaction per unit volume is being raised, due to the increased amount of oil), but then with further addition the propensity will start to drop due to difficulties being created for oxygen diffusion.

In most cases of self-heating, air will be pulled through the material by diffusion and natural convection. But air can also be moved through the material by forced ventilation. Apart from allowing oxidation reactions to contribute heat, moving air through the material has an opposite effect also, in that it carries away heat. Thus, especially if a forced ventilation is established, it is not necessarily evident whether air movement will increase or decrease self-heating. A few experiments have been described on this effect. Bowes[88] used a modified Mackey apparatus, where he tested jute fibers soaked in linseed oil. An optimum air flow rate, as defined by the maximum temperature achieved, was found. Gibson et al.[89] reported statistical results from tests on a series of unidentified industrial powders where they conducted self-heating tests with and without forced air movement through the material. Both positive and negative results were obtained, but there were more specimens for which blowing air through the material led to a temperature increase. Neither of these studies led to any systematic guidance and the user will have to tackle the problem experimentally if air movement through the material is considered to be of possible importance.

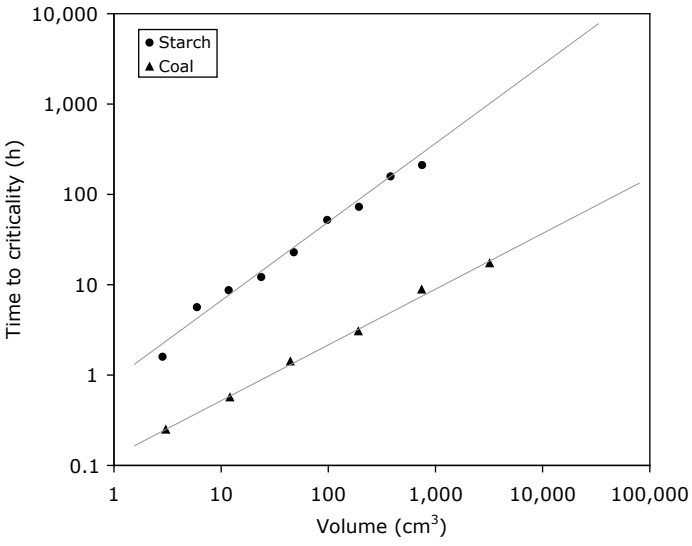


Figure 22 Time to criticality data for two dusts; each data point represents a test run at the lowest temperature leading to criticality

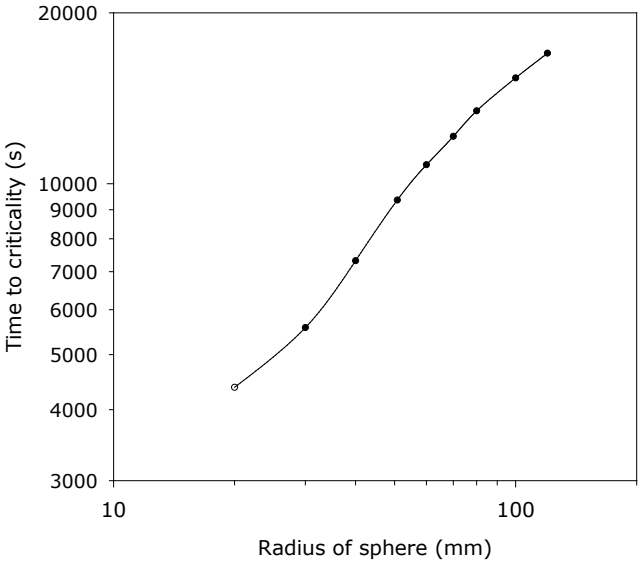


Figure 23 Times to criticality for milk powder spheres of various radii placed in an environment at 195ºC

OXYGEN CONCENTRATION

In addition to the theory refinement which considers limitation of oxygen diffusion, a related effect can be considered: the value of the oxygen concentration for systems not at 21% oxygen. The effects of oxygen concentration are primarily two: (1) lowering the oxygen concentration lowers the HRR of the reaction; and (2) lowered O_2 concentration serves to raise the effective value of δ_c. The value of E is unchanged by changing the oxygen concentration, however.

Bowes and Thomas[30] conducted oven experiments on cubes of wood sawdust at various oxygen concentrations. With the material properties of sawdust having been characterized, they concluded that at an oxygen concentration of 4%, the value of δ_c is raised by 9% over its value in ambient air. In view of general uncertainties of such experiments, this increase can readily be ignored. The effect of oxygen concentration on the heat release rate, however, is noteworthy. In their studies, they observed that the reaction rate should include the factor c_o^n. A value of $n \approx 2/3$ was found for substances as diverse as foodstuffs and coal[90], suggesting that this value has a certain generality. Thus, changing the concentration from 21% to 4% causes a decrease in the reaction rate to $(4/21)^{2/3} = 0.33$ of its ambient-air value. In the standard plot of oven-basket test results (see below), when oxygen concentration is changed only the value of P changes; the slope remains constant since E does not change. Other authors, however, have reported different values for n. Zimbardi[91] examined a variety of powdered agricultural materials and concluded that $n = ½$, irrespective of botanical details. In simple empirical hotplate testing of coal dust, Nagy and Verakis[92] found that over the oxygen concentration range 11.5 –

100%, the critical temperature stayed at 160 – 170ºC, implying that $n \approx 0$ over this range. Below 11.5%, the critical temperature rose sharply, reaching 250ºC for 9.7% oxygen. Conversely, Akgün and Arisoy[82] concluded that, for coal dust, $n = 1.0$.

Bowes[10] concludes that for typical organic substances which show $n \approx 2/3$ and have values of E/RT that are not unusually low, the effect of oxygen concentration on the value of δ_c will be negligibly small and that use of standard values will normally suffice. Thus, for example, in the case of a slab $\delta_c = 0.88$ is taken and use of Figure 10 is not necessary. Under those circumstances, the beneficial effects of partial-inerting can readily be calculated since then $\delta_c \propto c_o^{2/3} r^2$ and consequently the critical value of r varies as $c_o^{-1/3}$. For example if at a given temperature the maximum sub-critical size of a cubical pile of material at 21% O_2 is 1 m, then if inerted down to 5% O_2, and all else remains the same in the expression for δ_c, the critical size will increase to $1.0(0.21/0.05)^{1/3} = 1.63$ m. Care should be taken in extending this arithmetic down to very low values of oxygen concentration, however, since not all organic substances will be devoid of exothermic peaks at zero-oxygen conditions.

INSULATION

A substance prone to self-heating will have this tendency exacerbated if it is wrapped in any form of thermal insulation, since this will diminish the cooling available at the edges. In some cases, the substance may be wrapped in something which both provides thermal insulation and restricts the access of air. In such cases, the analysis is not simple, since the two effects are in opposite directions.

MULTIPLE PACKING

In many cases, self-heating goods are packed into boxes, drums, etc., but the package is not exposed in open air. Instead, multiple units of the package are packed into a larger container, e.g., an intermodal shipping container. Any particular package is obviously receiving poorer cooling at the boundaries because (a) the heat transfer coefficient is likely to be lower when inside an environment where convective flows are interfered with; and (b) the air circulating past one package has already been preheated by another. This problem is only beginning to see some study. Gray[93] proposed that the effective Biot number for such packages be derived as:

$$Bi' = \frac{Bi}{1 + nsh/SH}$$

where Bi' = effective Biot number, Bi = Biot number for a single package in well-stirred air, n = number of packages, s = surface area of each package, h = heat transfer coefficient for a single package, S = surface area of outside container, H = heat transfer of outside container. Gray also developed a more evolved theory[94] which led to the conclusion that thermal runaway will occur if the number of packages n inside the container exceed a certain value:

$$n \geq \frac{SH}{sh}\left\{\frac{shR}{vEQA}u^2 \exp\left[1/u(1+u)\right] - 1\right\}$$

where $u = RT_o/E$, v = volume of each package, T_o = ambient temperature.

MOISTURE AND RAIN

Moisture has an influence on the self-heating of most granular materials. For piles not sealed against air flow, there will be convective and diffusion moisture flows. These can be in or out, depending on the relation of the moisture inside the pile versus that in the environment. In addition, piles of self-heating material such as coal may be stored outdoors. In such case, they may be subject to periodic rains and undergo wetting/drying cycles with large moisture fluctuations. Rain falling on haystacks has been known to cause rapid self-heating; this is discussed in Chapter 14.

The main effects of moisture on self-heating fall into three groups:

(1) the effect of moisture in raising the thermal conductivity λ of the material;
(2) the direct effects of heat loss/gain due to evaporation/condensation of water; and
(3) any chemical or biological reactions which are water-dependent.

Walker[95] examined these effects in some detail and presented extensive historical information. In the theory of self-heating, λ enters into the expressions for both δ and Bi. While expressions exist for the moisture contribution to λ under precisely-specified conditions, a simple correction cannot be included in self-heating computations, because of the gradients of moisture and temperature that exist within the material. For materials such as wet wood chips, the effect of moisture on thermal conductivity is enormous[96]. Moisture effects can be very pronounced in the range 60 – 90ºC, but once the temperatures exceed 100ºC, moisture contribution to self-heating may not be significant. Thus, oven-basket tests, which, due to size limitations, are almost always run at temperatures over 100ºC, can only capture the behavior of a dry specimen in a dry atmosphere. Even apart from this issue, Gray and Wake[97] have demonstrated that scaling does not apply to criticalities induced by wetting. In other words, samples smaller than a certain size will be unconditionally stable against wetting-induced ignition, while larger ones may not.

Heat loss/gain due to evaporation/condensation of water will have the opposite effect depending on whether a hygroscopic material is initially dry or moist. If it is initially at a moisture content which is equilibrated to the RH of the environment, and then is aggregated into large piles which can self-heat, the main effect of the moisture will be an endothermic evaporation term as self-heating proceeds to raise the temperature. This endothermic effect will serve to

delay the self-heating process. Using a computational model, Chong and Chen[98] showed that even a small amount (3% MC) can lead to large delays in time to criticality. McIntosh[99] analyzed some additional features of the problem. He discovered that, depending on the heating regime, conditions can occur whereby vapor is condensing in certain regions of the sample—this would add to the heat evolution.

If the material is originally dry, however, and is then introduced into a moist atmosphere, the chemical self-heating will be augmented by the exothermicity associated with moisture uptake. This heating involves two contributions: (1) the heat of condensation, and (2) the heat of sorption of liquid water. The heat of condensation is sizeable, varying from 2443 kJ kg^{-1} at 20ºC to 2265 kJ kg^{-1} at 100ºC. This is the heat which is released upon converting an amount of water vapor to liquid water at the same temperature. The heat of sorption is the heat which is released when free water at a given temperature becomes sorbed onto the surface of a solid. The heat of sorption is not a constant, but depends both on the substance and on its pre-existing moisture content. For wood materials, it has a value of 1170 kJ kg^{-1} *of water* for completely dry material. But for a material with 8% moisture content, it drops to about 15% of its dry-substance value. If wood is taken from an oven-dry to a fiber-saturated condition, then the amount of heat gained can also be expressed as being 78 kJ *per kg of wood*. Back[100] calculated that if a wood product originally at 5% moisture content were raised to 9.5% moisture under adiabatic conditions, its temperature would rise from 20ºC to 100ºC due solely to the exothermicity of the moisture uptake process. But Hallström and Werling[101] pointed out that Back did not properly account for the sorption isotherm of wood and, if that is done, the temperature will only rise to a maximum of 34ºC under adiabatic conditions, and to a much smaller value if heat losses are included. Real products, of course, are not stored under adiabatic conditions, but Back provides some details of several cases where such self-heating is said to have led to smoldering or charring. This included dry wood fiberboard which ignited a day to a week after being produced and then stored in a high humidity area. This was also observed with rolls of freshly produced cardboard. What Back's analysis apparently overlooks is that the material was not cooled before being stored. If its internal temperature was significantly above ambient, then the self-heating will directly correspond to a 'hot work' problem, and will not necessarily reflect any moisture problems.

Coal is another substance whose self-heating can be affected by moisture. The heat of sorption has also been measured for coal[102] and it is smaller than for wood, being 670 kJ kg^{-1} of water at 0% MC. Introducing completely dry coal dust into an atmosphere at 65% RH will lead to a temperature increase of 2.5ºC. McIntosh[103] considers that moisture is, overall, favorable to avoiding runaway self-heating of coals, and that about 8% water, by weight, would be adequate to prevent it. Complicating testing and analysis somewhat is the observation[104] that, in certain circumstances where significant moisture is present, self-heating to ignition can occur in a substance which has been showing a temperature *decrease* up to a certain point. With exceedingly moist coals, significant problems were noted in analyzing oven-basket test data[105]. These results for coal suggest a relatively modest effect, but one study found a very large effect for coke; this work is discussed in Chapter 14 under *Charcoal, coke and activated carbon*.

Chen and Wake[106] developed a simplified theory for estimating the effect of the RH of the environment on self-heating of a wet, porous material, when hydrolysis or other chemical reactions involving moisture are not present. They suggest that an RH-modified value of δ_c be used, to be computed as:

$$\delta_c^* = \delta_c \exp\left[- RH \frac{E}{RT_o^2} \frac{Q_L \varepsilon D_w C_{w,sa}}{\lambda} \right]$$

where δ_c^* = the RH-modified value of δ_c; RH = relative humidity (on a 0 to 1 scale); Q_L = latent heat of condensation = 2443 kJ kg^{-1}; ε = porosity (--); D_w = diffusion coefficient of water vapor in gas stream = 0.25×10^{-4} m^2 s^{-1}; and $C_{w,sa}$ = density of water vapor in saturated gas ≈ 0.173 kg m^{-3}. Use of this correction factor lowers the value of δ_c, in other words it shows thermal runaway occurring at a lower ambient temperature. The correction is intended to give only a conservative bound, not an exact answer, since the time-varying moisture remaining in the material is not modeled. Physically, Chen and Wake explain the reduction in temperature as occurring since a high ambient RH will reduce the driving force available for drying, and consequently reduce the dissipation into the environment of the heat generated by oxidation. McIntosh et al.[107] gave solutions for the time-dependent heating, but these did not lead to any simple equation. Chong et al.[98] developed another numerical model for self-heating which includes the effects of moisture.

Chemical and biological effects from moisture are only seen with certain classes of products, but these can dominate the self-heating behavior for that type of substance. The most detailed example which has been studied is hay, as presented in Chapter 14. Gray et al.[20] discussed moisture problems in connection with the self-heating of bagasse and pointed out that moisture makes possible hydrolysis reactions, which is precluded if the material is fully desiccated. Their studies are presented in Chapter 14 under *Bagasse*. In general, the effect of moisture on self-heating may be very complicated and simple treatments may be insufficient. Gray[108] has presented a theory which includes a moisture-dependent reaction, in addition to an oxidation reaction. Its results show that regimes with oscillations and other complex behavior will occur under certain combinations of problem conditions.

DENSITY

Increasing the density of a porous, self-heating material will increase the amount of substance available to chemically react, per given volume. Thus, this will increase the reaction. Noting that

$$\delta_c = \frac{E}{RT_o^2}\frac{r_c^2 \rho Q A}{\lambda} e^{-E/RT_o}$$

it is evident that increasing ρ decreases the critical size r_c, and vice versa. Thus, if data were obtained at a density ρ_1 and now it is desired to compute the critical size for material of density ρ_2, the relation is:

$$r_2 = r_1\sqrt{\frac{\rho_1}{\rho_2}}$$

This is illustrated in Figure 24 by some old and only semi-quantitative data on wood fiberboard and jute[109]. Also shown are some experimental data on linseed-oil soaked jute[10], tested in the Mackey test. At high densities, it also follows the same trend; for lower densities, there is an opposite trend, details of which have not been modeled. Data on coal dust were published by Hardy[110]. His data showed a density/thickness interrelation: raising the density always lowered the critical temperature, but the effect was sizeable only for very small layer thicknesses (3 – 6 mm); for 12 mm layers, the density effect became minimal.

With moist substances susceptible to microbial heating, increased density decreases ventilation, diminishes the rate of drying, and thereby can increase the rate of self-heating. This was observed by Frandsen for wood-waste-chip piles[111]. Quantification or modeling is not easy for situations involving both chemical and microbial heating, however.

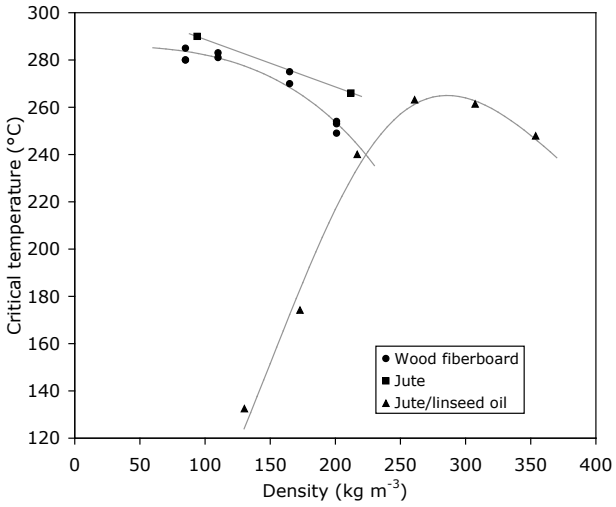


Figure 24 Effect of density of the critical ambient temperature for several materials

ANTIOXIDANTS

Some substances (e.g., foodstuffs, polymers) are formulated with antioxidants. A wide variety of chemicals (e.g., phenols, amines) can serve this role. These will effectively suppress oxidative self-heating, but only until the antioxidant is used up. This effect can be seen in oven heating tests[112]. Figure 25 shows a thermal arrest period t_b during which the antioxidant is being consumed. Oven temperature #1 was slightly below the critical temperature for the given size of sample and criticality did not occur. Oven temperature #2 was slightly above the critical temperature, but an accelerating rise towards criticality did not occur until the time that the antioxidant was used up.

An antioxidant is consumed with the passing of time and eventually offers no protection. Thus, it may be necessary to estimate the duration of time during which protection will remain available. Beever[113] suggests that the following procedure be used. For oven baskets tested at various temperatures, plot $\ln(t_b)$ as a function of $1/T_o$. The data points should fall onto a straight line. Extrapolate to the temperature T_o at which storage is to be done. This will give the approximate length of time for which the antioxidant will remain effective. If additives against deleterious reactions involving more than just oxidation are employed, the broader term *stabilizers* is used. The effect of stabilizers on explosives is discussed in Chapter 10.

CONTAMINANTS

Although the topic has received only minimal study, there are substances which increase the self-heating reactivity of different substrate materials, if introduced as a contaminant. Among compounds which have been identified as playing that role for various substrates (see Chapter 14) are fatty acids and vegetable oils, iron, iron oxides, iron sulfides, cobalt, copper, magnesium, manganese, lead carbonate, potassium carbonate, lead acetate, sodium acetate, and vanadium pentoxide. Consequently, results of testing on specimens, whether small-scale or real-scale, will not be properly indicative of product behavior if criticality in a particular case occurred due to contamination and exemplars are test-

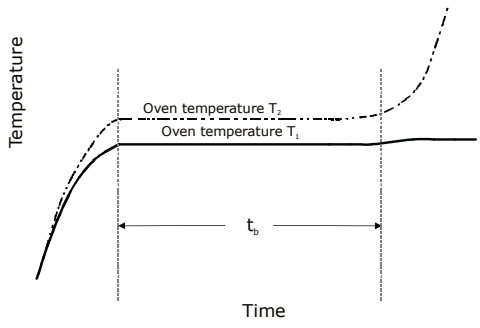


Figure 25 Oven heating results for specimen with antioxidant

ed that are uncontaminated. A case is described in Chapter 14 under *Paper* where a roll of sealed paper towels was found smoldering in the storeroom of a government laboratory. An uncontaminated product would have required an enormously larger volume for critically to occur, and the investigation determined that the product had become contaminated either in manufacture or in packaging.

MULTIPLE-COMPONENT SUBSTANCES

In the common case of the self-heating of linseed-oil soaked cloth, there are two components to consider: the oil and the cloth. Neither a 0% nor a 100% fraction of oil will constitute the worst-case condition. By itself, cotton cloth shows negligible exothermicity compared to linseed oil, so cloth alone would not be the worst case. Oil, however, is not porous if in bulk, so the 100% condition is also reasonably benign. Somewhere in between the worst case condition can be found. A ratio of approximately 1 part oil (by mass) to 1 part cloth is found to be the worst case.

If a large pile is assembled of a material which has two components, each moderately exothermic, then a two-component system has to be considered. An example is sawdust coated with an oil of modest self-heating propensity, which was studied by Bowes[44]. By running oxygen consumption experiments on control samples comprising oil on an inorganic substrate, he was able to demonstrate that the oxidation of the two components is not additive. Both make a positive contribution, but the wood additionally acts as an antioxidant for the oil, with the oil not contributing as much (on top of the wood's contribution) as it would on an inorganic substrate. This he considered to be plausible chemically in terms of what is known of the chemical constituents of wood. No general procedures for such cases are available and, if needed, research would have to be done on the specific system.

IGNITION OF DUST LAYERS

A common problem in many industrial installations is the ignition of dust layers which have accumulated on a hot surface. This usually occurs as a self-heating process. The theory to be used for analysis is the unsymmetric slab problem, presented above. Testing to determine the material properties can be done by any of the tests suitable for engineering determination of self-heating properties. In addition, hotplate tests are sometimes recommended on the grounds that their results can be used without recourse to theory.

Defining the actual ignition event is not necessarily trivial, since the process starts at the hidden surface. Bowes[10] considers the ignition to have occurred when at least one of the following has been observed:

- visible evidence of flaming or glowing in the layer
- melting of the dust layer
- a temperature rise of 50ºC above the hot surface temperature.

A *layer ignition temperature* (LIT) is commonly defined as being the lowest temperature of the hot surface that can cause an ignition according to the above requirements. Some results[10,114] of hotplate tests on several types of dust layers are given in Table 12. Additional data[115] are shown in Table 13 and in Figure 33.

Table 12 Results of some dust layer ignition tests conducted by Bowes

Layer depth (mm)	Ignition temperature (ºC)			
	Beech sawdust	Coal	Cork	Lycopodium
5	350	235	350	283
10	315	205	315	261
20	285	173	280	217

Table 13 Results of some dust layer ignition tests conducted by the Bureau of Mines

Pittsburgh coal		Brass	
Layer depth (mm)	Ignition temp. (ºC)	Layer depth (mm)	Ignition temp. (ºC)
6.5	310	13.3	160
10	265	26.7	140
12.7	240	40	135
25.4	210		

Some additional data on dust layer self-heating ignitions were reported by Reddy et al.[116] They examined Pittsburgh coal, Prince coal and sodium dithionite ($Na_2S_2O_4$). The latter is an interesting material since its exotherm does not require the presence of oxygen. They obtained values of E and QA from hotplate experiments by developing a computer program for the data analysis. From the hotplate tests and additional experiments, the material properties were found to be as shown in Table 15. Note that in the case of sodium dithionite, the Arrhenius-kinetics parameters are, in fact, a poor representation of the actual reaction that takes place, as was shown in detail by Tyler and Henderson[51].

In some cases, the physical condition may be better represented by a surface through which there is a constant power flow into the porous material, rather than there being a hot surface of a fixed temperature. A closed-form solution is not available, but Hensel et al.[117] presented 1-dimensional finite element computations for coal dust and cork dust under such conditions. A heat flux of ca. 0.18 kW m^{-2} was

Table 14 Results for reactive hot spot ignitions

Substance	Bulk density (kg m^{-3})	Min. dia. of hot spot (mm)
cork dust (< 100 μm)	59	19-24
cork dust (500-3000 μm)	171	40
beech wood dust (<400 μm)	382	34
cocoa powder (<40 μm)	369	15

found necessary to cause thermal runaway of a 50 mm thick layer, 0.46 kW m^{-2} for a 25 mm layer, and 1.5 kW m^{-2} for a 10 mm layer. Such values are rather low and might readily be found near motors or heat-producing equipment.

There is no theoretical treatment of induction times for ignition of an unsymmetrically heated slab. Thus, apart from fully-numerical solution strategies[118], it is appropriate to use a data-fit extrapolation as described above.

ELECTRICAL HEATING PROBLEMS

An interesting special case is the deposition of a layer of dust on electric *power cables*. Gray et al.[119] showed that ignition can occur due to two separate phenomena: (1) a non-combustible dust simply acts as insulator and prevents the effective cooling of the wire by convection; this can lead to overheating, melting, or ignition of the wire insulation. (2) If the dust is combustible, the dust layer itself can ignite. Gray showed that formulation of the problem is not particularly difficult, but solutions have to be obtained numerically and these are complicated by the presence of a large number of independent variables. In addition to the variables present in all self-heating problems, this problem adds:

- wire insulation thickness
- electric current
- electric resistance of the copper conductor
- thermal conductivity of copper
- thermal conductivity of the wire insulation.

The authors provided a table giving solutions for selected values of the problem parameters. They also calculated an example case showing that an 0.15 m dust layer thickness can suffice for thermal runaway, given some reasonable problem parameters. They also showed an example of the insulation effect for a wire carrying 14 A. With no dust, the temperature rise was 36ºC; with a dust layer thickness equal to the wire insulation thickness, 77ºC; and with a dust layer thickness of 9× the wire insulation thickness, 300ºC. The latter condition would likely suffice to short out a cable, if not to ignite it. Similar calculations were reported by Dong and Yang[120].

The case of asymmetric accumulation of dust has also been studied[121]. It was shown that, provided the thermal conductivity of the dust is much smaller than that of the cable, the asymmetric case is more conservative than the symmetric, thus, the symmetric results can be used to develop an upper bound.

Another type of electrical heating problem is an electrically heated hot spot (sphere) inserted into a body of smolderable material. Brindley et al.[122] formulated a problem where an electrically heated sphere of radius r_o is embedded at the center of a sphere of granular material having a radius r_1. The problem has no closed-form approximations, so they provided some example calculations using a numerical solution. The problem turned out, at least using a first-order theory, to have an unusual trait. Over a certain range of r_o values, there were multiple zones of stability and runaway, when plotting electric input power as a function of r_o. Validation was not undertaken, so it is not clear if this multiple-zone behavior is real or an artifact of the theory. Nelson[123] considered the same problem and used a purely numerical solution of theory, accompanied by validation experiments. His modeling indicated that:

- r_o – raising it greatly increases the required power, but does not change the surface temperature of the hot spot needed for criticality
- r_1 – changing it has a very small effect on required power
- thermal conductivity – raising it produces a near-linear increase in required power
- heat capacity – no effect
- activation energy – raising it produces a near-linear increase in required power
- heat of reaction – raising it gives a hyperbolic decrease in required power
- ambient temperature – raising it causes a decrease in required power, but the effect is not as large as when raising thermal conductivity or activation energy

Experiments did not support the first of the theoretical predictions and indicated, instead, that the power needed to achieve criticality is roughly independent of r_o. The effects of r_1 and of ambient temperature were found to be broadly consistent with theoretical calculations; other predictions were not investigated experimentally.

HOT SPOTS

Self-heating due to hot spots has only rarely been measured experimentally, thus in this Section we discuss some available results. Krause and Schmidt[124,125] reported data on hot-spot ignitions of cork dust, beech wood powder, and cocoa powder. For an inert hot spot, they used porcelain spheres of various diameter and initial temperatures. The powder was held in a 6 – 12 L cylindrical basket which was always originally at room temperature. For a 25 mm diameter sphere placed in cork dust, a minimum initial temperature of 496ºC was needed to initiate self-sustained smoldering. Larger spheres required lower temperatures: 454ºC for 35 mm, and 427ºC for 40 mm. Sphere size notwithstanding, however, a minimum ignition temperature of 400ºC was observed. Using a 30 mm sphere in beech dust, an initial temperature of 550ºC was needed.

Table 15 Self-heating data for some dust layers

Material	***E*** (kJ mol^{-1})	***Q*** (kJ mol^{-1})	***A*** (s^{-1})	***QA*** (W kg^{-1})
Pittsburgh coal	65.4	N.A.	N.A.	3.04×10^{9}
Prince coal	95.7	N.A.	N.A.	7.0×10^{12}
$Na_2S_2O_4$	177	78.5	2.70×10^{16}	7.7×10^{22}

In a parallel experiment, they buried a 25 W rated electric heating coil in the center of an 0.8 L volume of fine cork dust. The coil produced a surface temperature of ca. 600ºC. They found that a minimum heating time of 5 min, in other words, 7.5 kJ of energy, was needed to cause sustained ignition of the whole volume.

The authors also explored the effect of a reactive hot spot (their term is a 'glowing nest'), wherein a preheated small cubical wire basket of the same substance was inserted into the center of the ambient-temperature specimen. The initial temperature of such a reactive hot spot could not be experimentally varied, they discovered. This is because the smoldering body assumes a characteristic smoldering temperature which is a trait of the material itself. The results for the minimum hot spot diameter needed to cause continuing self-heating of the bulk substance are given in Table 14.

The authors explored the effect of varying the size of the bulk, ambient-temperature specimen into which the hot spot was plunged, but over the range of 6 to 50 L the effects were not pronounced. A very small container of 0.8 L, however, led to substantially greater hot spot diameters being needed for sustained propagation.

Once ignited, the characteristic smolder front temperature varied with both the dust type and the volume of the cylinder. For a 12 L cylinder, fine cork dust showed a temperature of ca. 355ºC, while cocoa powder showed ca. 280ºC, with the other substances giving intermediate values. A 1.5 L cylinder of fine cork dust showed 375ºC, while a 200 L cylinder gave 310ºC. The authors attributed the size effect due to oxygen depletion; this was verified in one experiment.

SELF-HEATING IN LIQUIDS

Self-heating in liquids is treated in detail in Chapter 10, where reliance is placed primarily on Semenov theory. A few studies have been made using an adaptation of Frank-Kamenetskii theory, and we consider one of these here. Liquids differ from the porous solids that have more commonly been the subject of self-heating studies in that the bulk material can be subject to convective currents. In a detailed numerical study of a vertical cylindrical tank, Sheu et al.[126] found that, in addition to δ, the Rayleigh number Ra needs to be taken into account to determine limits of stable regimes. For this problem, they define

$$Ra = \frac{gH^3RT_o}{\alpha\nu E}$$

where g = gravitational acceleration (9.91 m s^{-2}), H = height (m), R = universal gas constant (8.314 J mol^{-1} K^{-1}), T_o = initial temperature (K), α = thermal diffusivity (m^2 s^{-1}), ν = kinematic viscosity (m^2 s^{-1}), and E = activation energy (J mol^{-1}). Solving a cylinder with $H = r$, they found that $\delta \approx 5.4$ for Ra = 0, that is, if the fluid cannot move due to buoyancy. As buoyant effects increase, however, the system is stabilized, and $\delta \approx 17$ for Ra = 150,000. For all greater values of the Rayleigh number, however, three regimes become possible: steady stable, stable oscillatory, and thermal explosion. The limits of the steady stable regime shrink for large Ra numbers, going down to $\delta \approx 10$ at Ra = 500,000. Thus, the conclusion is that by ignoring possible buoyancy effects, a conservative prediction value will be obtained. Shtessel et al.[127] also investigated the problem by numerical computation. Their recommendation was to use an internal-convection-modified value δ_c^* which is obtained as:

$$\delta_c^* = \delta_c\left(1+\frac{0.062Ra^{4/3}}{11{,}000+Ra}\right)$$

LIQUID-SOAKED POROUS SOLIDS

In industrial environments, it is common for a liquid to leak and to soak into pipe insulation, for instance, mineral wool (rock wool). There has been at least one disastrous large fire[128] due to self-heating ignition of ethylene oxide soaked insulation (also known as *thermal lagging*). More common, but less spectacular, fires have occurred on ships when diesel fuel permeated porous insulation. The self-heating problem is similar to that in solids, with the exothermicity being oxidation of the liquid. A number of experimental studies were conducted by Bowes[29]. Two different types of experiments were made: oven-basket tests, and tests in a pipe simulator, where a heated pipe was covered with insulation and raised to various temperatures. To apply the results, Bowes endeavored to use conventional self-heating theory. According to his procedure, one first determines E and P from the oven-basket tests. Next, to apply the theoretical treatment pertinent to the hollow infinite cylinder (p. 383) a value of the outer surface temperature is estimated from:

$$T_s = \frac{hT_o + \dfrac{\lambda}{b\ln(b/a)}T_h}{h+\dfrac{\lambda}{b\ln(b/a)}}$$

This allows θ_s to be determined. Knowing θ_s and z_s (= b/a) the theory gives the value of δ_c^*. Then, using the definition of δ^* one determines whether thermal runaway is expected to occur, depending on whether $\delta^* \geq \delta_c^*$.

Bowes' treatment ignores the evaporation of the liquid. But evaporation is an important process, and it shows up both in the energy balance (as an endothermic contribution) and as a depletion of reactant. Evaporating substances do not behave in a way treatable by F-K theory, since initially there is a time period where no appreciable heating occurs and the main manifestation is evaporation of the liquid. When oven-cube tests are conducted, a long time period is observed during which the sample's temperature shows a steady-state plateau value which is below the oven temperature and does not forebode thermal runaway[129]. Yet thermal runaway can occur later on, and can occur quickly. A theory has been developed by McIntosh et al.[130-133] which takes these additional effects into account. The theory is mathe-

matically complex, even with numerous simplifications of physics. The systems are complex partly because it is not sufficient to consider whether an ultimate steady state is achievable. Conditions exist where calculations would indicate a steady (no thermal runaway) ultimate state, yet the transient temperature behavior earlier is one which is basically an ignition. Matters are also complicated because oxygen availability is poor, especially in the early stages of heating, and diffusion of oxygen needs to be explicitly taken into account[134]. The authors conducted oven-basket experiments with a series of alcohols (C_6 to C_{11}) soaked into cubes of insulation and noted that it was possible to get each one of the alcohols tested to self-heat. They did not report a procedure whereby experimental test results could be used to make calculations based on their theory. The procedure would need to be more complex than Bowes', since additional Arrhenius terms are used in their model to express the evaporation process, and constants for these terms would also need to be obtained. In a later study[135] they considered the limiting case where there is so much liquid that it covers all of the fibers. In that case, the amount of liquid is no longer a problem variable. Even the simpler problem did not have closed-form solutions, but the authors noted that such a system can behave in a deceptive way. Under some conditions, the system may start showing a temperature drop, even though it is super-critical and a while later temperatures will again increase and go towards thermal runaway.

It was also noted that, under some circumstances, ignition within thermal insulation can occur as the autoignition of the liquid's vapor within the void spaces. McIntosh et al.[136] considered here the case where the fibers are fully soaked in liquid (so the amount of liquid does not matter) and determined that a critical size exists for the assembly beyond which vapor ignition is predicted. They express the maximum safe size as a critical volume/surface ratio, so that to avoid criticality the size $\ell \equiv V/S$ must not exceed the following critical value:

$$\ell_c = 1.847\left(\frac{\Delta h_v}{\Delta h_c - \Delta h_v}\right)\frac{hW}{A\rho_L R}$$

where V = volume of insulation (m^3), S = exposed surface area (m^2), Δh_v = latent heat of vaporization (J mol^{-1}), Δh_c = heat of combustion of the vapor (J mol^{-1}), h = convective heat transfer coefficient (W m^{-2} K^{-1}), W = molar mass of the fluid (g mol^{-1}), A = pre-exponential factor for reaction of vapor (s^{-1}), ρ_L = density of the liquid (kg m^{-3}), and R = universal gas constant (= 8.314 J mol^{-1} K^{-1}). The value of A can be estimated from the reaction of the vapor which is usually a hydrocarbon gas. One interesting result of this solution is that the initial temperature does not affect the outcome, and the only variable apart from the chemical constants of the liquid is the size of the system. McIntosh also considered the case where a small leak continually places new liquid into the insulation[137]. For that case, he derived an estimate for the critical feed rate (beyond which dangerous oscillatory temperature behavior develops) as:

$$\dot{m} = \frac{RT_o^2 ShW}{EQ}$$

where T_o = ambient temperature (K), E = activation energy (J mol^{-1}), and Q = heat of reaction (J mol^{-1}), and the Sh product represents the convective heat loss (W K^{-1}) at the surface. This formula is at first sight counter-intuitive since as ambient temperature is increased one needs more supply of fuel to cause critical conditions to occur. This is because at the greater temperature, there is a greater evaporative loss of fuel to be overcome, in order to induce the oscillatory behavior. But of course the equilibrium temperature solution (without oscillations) may in fact already be dangerously high. The formula has greatest practical relevance for low ambient temperatures where the oscillatory behavior is deceptively slow. If the loss of heat at the surface (Sh) is poor, then even a small leak (on the order of grams per hour) is dangerous.

DETONATION OR DEFLAGRATION UPON SELF-HEATING

As mentioned in Chapter 7, certain solid substances, upon self-heating, are capable of undergoing deflagration or detonation, not merely thermal explosion. Ammonium dichromate is a substance which can undergo deflagration; Grewer[72] provides color illustrations of this process as it occurs. Detonation upon self-heating is encountered with explosives and unstable substances and is further considered in Chapter 10.

PREVENTIVE MEASURES

Measures to prevent ignitions due to self-heating can take a wide variety of forms.

1. Chemical modification of the substance. Changes in the chemical makeup of the substance are often limited by the fact that the substance has some practical use and arbitrary changes in formulation may negate its primary function. For oxidative self-heating, one simple strategy often used is to add antioxidant agents, commonly seen in foodstuffs and in synthetic polymers. Such antioxidants have a primary benefit which transcends self-heating issues. For foodstuffs, antioxidants retard spoilage; for polymers, they slow down degradation processes such as yellowing, hardening, or crazing.

2. Inerting. If placed in an inert atmosphere, reactions dependent on atmospheric oxygen will stop. For general storage, this is not practical, but it is employed in specialized applications, including agricultural products where inerting, typically with nitrogen, helps retard spoilage.

3. Reduction in size of piles. This is probably the most common and practical tactic. Since size of pile is a dominant variable in governing the self-heating, a good

preventive measure is to reduce the pile size. This has the advantage that no other modification of the substance nor the environment is necessary.

4. Sealing of the substance. Porous substances only contain a very limited amount of oxygen within the bulk material. For self-heating which depends on atmospheric oxygen, most of the oxygen comes from diffusion or convection through the pile. If packed into airtight containers or otherwise sealed, only the most unstable of substances will be able to self-heat to critical conditions by using the available oxygen sealed in. The most economical form of sealing may be use of impermeable plastic film wraps or bags. In practice, such bags cannot be guaranteed to be 100% intact. Thus, in a fascinating study, Bowes[10] examined activated charcoal packed in plastic bags which were damaged by tears or by cutting away rectangular strips of material. Even with a 613 × 51 mm strip removed from a 25 kg bag, self-heating in the damaged bags did not reach critical conditions at 75ºC, while comparable-size permeable bags were shown to reach thermal runaway if stored at 65ºC. Smaller damaged areas produced undetectable self-heating.
5. Monitoring of temperature rise or products of combustion. A study on grain dust heating showed that an ionization detector can detect conditions quite early, before thermal runaway has commenced[138].

Tests for self-heating or reactivity

In this Section we present an overview of the test methods most commonly used for assessing self-heating or reactivity. Some methods are suited only for solids or only for liquids, etc., while others are of wider applicability. Since there is a some overlap between the theme of this Chapter and the following one, all of the self-heating tests, including those on unstable substances, are discussed as a group here. There has been a huge variety of tests invented for characterizing self-heating materials. The ones discussed in this section are modern tests based on fundamental theory, or are well-known tests used for regulatory purposes, or tests commonly used in industry for exploratory studies. Grewer[139] has reviewed a number of additional tests, which are mainly empirical self-heating tests used in Germany and showed the very wide spread of data obtained in comparative testing.

Hazardous materials basically can be viewed as having two aspects of hazard: (1) the potential for ignition, reaction, explosion, etc.; and (2) the consequences of an ignition, reaction, explosion, spill, etc. When hazardous materials are in transport, governmental regulations commonly apply. The United Nations publish the Recommendations on Transport of Dangerous Goods[140,141] based on recommendations of a Committee of Experts. This work comprises two volumes, first being a model regulation, while the second being a collection of test methods. By itself, the Recommendations do not have a special standing. They acquire the force of law when adopted by treaties or regulations. Treaties have resulted in adoption or partial adoption of the Recommendations for various modes of transport. Transport by ship is governed by the International Maritime Dangerous Goods Code, administered by the International Maritime Organization; air transport by the International Civil Aviation Organization's Technical Instructions for the Safe Transport of Dangerous Goods by Air; and European road transport by UN's European Agreement Concerning the International Carriage of Dangerous Goods by Road. In the US, the Department of Transportation has adopted many of the UN tests for interstate transport requirements. The UN Recommendations are revised rather frequently, and worldwide harmonization efforts are expected to result in substantive technical changes. There is no official commentary to the Recommendations which might provide a rationale for the classification and testing decisions taken; however, a recent symposium[142] was devoted largely to discussions of various aspects of these test methods. Some comments from a test laboratory on certain of the methods are especially valuable[143].

The UN Recommendations propound the concept of a *self-accelerating decomposition temperature*, SADT, defined as "the lowest ambient temperature at which self-accelerating decomposition may occur in the packaging as used in transport." In practice, the Recommendations offer numerous tests for determining the SADT and substantially different definitions are found among the individual test method requirements. As the theory portion of this Chapter makes clear, it is illogical to seek a handbook value of a temperature at which self-heating or decomposition begins. This is because the actual temperature at which runaway occurs depends not just on the chemical nature of the substance, but on the way it is held (e.g., insulated or well-cooled convectively), and most especially, on the amount of substance that is aggregated. The UN regulations try to respect these variables in a rough way by making classifications limits according to sizes of packages and by requiring that a quantity L be measured. L is defined as the heat loss per unit mass (W kg^{-1} K^{-1}) and is to be determined by filling the package with "another substance having similar physical properties" and then observing the half-time of cooling, $t_{1/2}$. The user must also determine the heat capacity of the substance, then compute $L = (C_p \ln 2)/t_{1/2}$. Despite these attempts to provide some realism, Whitmore pertinently concludes[144] that "SADT is not universally the most useful measure." This is because the methods do not produce fundamental data, on the basis of which, the behavior of any desired package might be computed. Part of the problem in providing a solid tie-in to theory is that many of the potentially 'hazardous' substances that need to be considered have complex reaction mechanisms and do not conform to Arrhenius kinetics, specifically, many reactions are autocatalytic.

The UN Recommendations provide four SADT tests, H1, H2, H3, and H4, which are described below. If the SADT is 50ºC or less for self-reactive substances (55ºC for organic peroxides), special temperature control measures are mandated for shipping. Test H1 is a real-size test method, while Tests H2, H3 and H4 are reduced-scale tests, but even these may be unsuitable for initial examination of potentially very unstable substances, thus a number of screening tests have been developed and these are also considered below.

REAL-SCALE TESTS

The size of the substance involved plays a very strong role in determining its self-heating behavior. Thus, the best self-heating test, by far, is a real-scale test. The substance is configured in the shape and with the boundary conditions that it will experience in its end-use application and is placed in an environment at the maximum temperature it is expected to encounter. The results then are directly indicative and require no theory, computations, or extrapolations to produce the final answer. In many cases, due to limitations of cost, time, or supply of material, real-scale testing is impossible and reduced-scale testing must be undertaken. Even the best of these methods leave larger doubts, since the theory according to which extrapolations are undertaken is invariably simplified and certain phenomena are neglected.

UN TEST H1—THE US SADT TEST

UN Test H1 is a real-scale test, where specimens of the actual size are tested in an oven. The oven is intended to be a disposable device, which may be lost in case of explosion. The SADT is defined arbitrarily as the lowest oven temperature for which the specimen shows a 6ºC rise. A substantial safety factor is built into this definition, since, as explained previously in this Chapter, a substance that is approaching thermal runaway will normally show a temperature rise several times greater than 6ºC. The test is run for 7 to 10 days; the exact time is not fixed due to a complicated specification of the start of the data-taking period. The test method is poorly designed, since the air velocity within the oven is not controlled and so results can be irreproducible and susceptible to large unconservative errors[152]. The test method also does not make clear that the "packaging" to be tested should be the full shipping container and not an individual container within it, since grossly unconservative results will be obtained if only the latter is tested. In fact, the test method explicitly limits the test specimen size to no more than 220 L. Finally, if larger packages, such as a rail car, were tested, the time limit of the test would be much too short, since train voyages can be longer and thermal runaway can take place beyond the time limit set in the test.

GEOMETRIC-SCALING TESTS

SCALING ACCORDING TO FRANK-KAMENETSKII THEORY

Most of the test methods based on using the Frank-Kamenetskii theory are oven-basket tests, and these are all presented in this section. A number of regulatory oven-basket tests also exist where the connection to theory is limited, at best. Nonetheless, for convenience these are also described in this section.

Oven-basket tests: FRS method

The most common technique for conducting bench-scale tests with an objective of predicting large-scale behavior is an oven-basket test and, in turn, historically the most common way of doing those has been as developed by the Fire Research Station. The method requires that the sample be held in a wire-mesh basket, thus it is only suitable for solids. Each individual test run is made at a fixed oven temperature, thus the method is classified as an isothermal oven test. This test condition is sometimes described as *isoperibolic*. The technique was refined over several decades of research by Philip Bowes and coworkers[10] and has been described in summary by former FRS researcher Paula Beever[54]. In this technique, a powder, granular, etc. specimen is prepared by packing it into a wire gauze basket; the latter is usually in the form of a cube. Stainless steel wire gauze having openings of ca. 0.25 mm is used. The basket is placed in an oven where the temperature can be controlled accurately to better than ±1ºC. The oven must also be equipped with a fan to keep the temperatures uniform and to provide a reasonably high convective heat transfer coefficient to the specimen. Runaway fires must be expected to occur, so the oven construction should be able to withstand fire temperatures, even though a controlled-heating range of only up to about 400ºC is needed.

The sample is normally prepared at room temperature, then inserted into the oven which is at a desired test temperature substantially above room temperature. As a consequence, the specimen heats up to the oven temperature, but if it is not inert, it also continues to heat to a higher temperature. The initial heating occurs near the edges, but subsequent heating is mainly at the center (see Figure 15). This actual problem is the cold-work problem and is theoretically more difficult to treat than the simple F-K theory, which assumes that initially the substance is already at the oven temperature, but is thinly spread out so it does not self-heat. Within the simple F-K theory, at $t = 0$ the specimen is then assembled instantaneously into the desired oven-basket configuration. In analyzing oven-basket results, it is customary to ignore all times prior to the instant that the central thermocouple reaches the oven temperature, and to declare $t = 0$ to occur at that moment. This is illustrated in Figure 17.

As a minimum, two thermocouples are required—one at the center of the specimen, and the second monitoring the oven

air temperature. In many cases, a third thermocouple is used, located at the surface of the specimen. This third thermocouple is used to monitor whether the $Bi \rightarrow \infty$ condition is reasonably fulfilled, that is, to see if the specimen surface temperature is very close to the oven air temperature. A Type K thermocouple made of 0.19 to 0.27 mm dia. wires and having a bare junction is used. Experiments must be conducted on a number of different-sized cubes. Commonly, cubes of 25, 50, 100, and 200 mm dimensions ($2r$) are used. The density must be controlled so that it is nearly identical for all the specimens tested, and it should approximate the density to which the substance is packed in the real-scale environment. The material must be carefully tamped or shaken in order to ensure that the packing is uniform throughout the sample.

The basic procedure is to determine by trial and error the critical value of T_o for each basket size. For any given size and oven temperature (T_o) setting, there are two possible results: (1) the temperature at the center of the sample rises only a modest amount over the oven temperature (if indeed it reaches it), establishes a plateau, then eventually decreases*; or (2) either initially or after possibly some plateau is reached, a very sharp increase in temperature occurs and the temperature climbs way over the oven temperature. The first event and second event temperatures are denoted as subcritical and supercritical, respectively. By means of bracketing, it is eventually possible to find a subcritical and a supercritical temperature separated by only 1 or 2ºC. The critical value of T_o is then deemed to be halfway in between the two. When a critical T_o has been found for one basket size, experiments are started for the next size. A table is then compiled of r versus critical values of T_o. Since repeated testing (which may take days or weeks) is needed for each specimen size and at least 3—preferably more—sizes must be studied, the procedure is somewhat lengthy.

Simple form of analysis

Once a set of data has been obtained for critical size vs. temperature, the simplest form of analysis is that recommended by Leuschke[146]. The volume/surface ratio (m) is obtained for each specimen and these values are plotted on a log-scale x-axis. The quantity $1000/T_o$ is plotted on the y-axis, where T_o is the oven temperature (K). Leuschke demonstrated (Figure 26) that the results fall into a straight line. In addition, he demonstrated empirically that the shapes of the test containers, provided they are reasonably compact, do not make a significant difference.

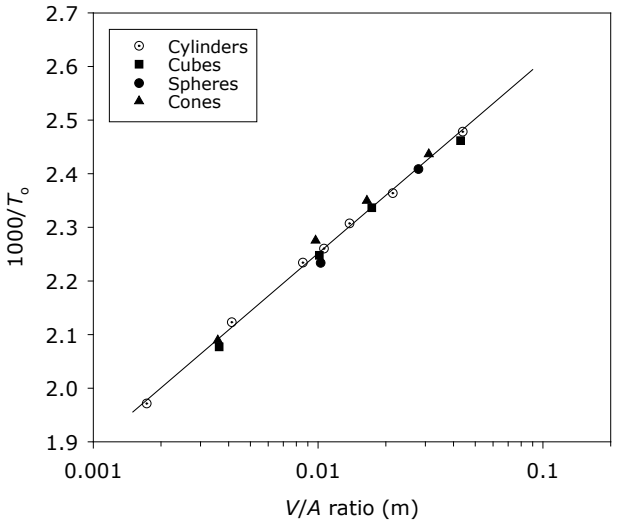


Figure 26 Analysis of cork dust oven-test data using the plot recommended by Leuschke

Example

Using the data of Leuschke in Figure 26, determine what would be the maximum permitted storage temperature for a 2 m conical pile of cork dust.

Solution. The volume of a cone is $\frac{1}{3}\pi r^2 L$, where L = height. We will assume that $L = r$. The area of the base of a cone is πr^2, and the area of the slant surface is $\pi z r$, where z = slant length. For the case $L = r$, $z = \sqrt{2}r$. Then $A = \sqrt{2}\pi r^2$. In the case of an oven-test specimen, the specimen can exchange heat convectively on all sides. For the case of the pile on the ground, there will be no convective cooling of the bottom (of course, conduction heat transfer will exist, but we will ignore this in solving the problem). Thus, the value of A will be taken as only that which comprises the slant-sides. Then, $V/A = \frac{r}{3\sqrt{2}}$. Since in this problem $r = 2.0$ m, $V/A = 0.47$ m. The value of $1000/T_o$ could be determined graphically, by simply extrapolating the data fit line. Instead, we will compute numerically the extrapolated value. The straight line shown in Figure 26 corresponds to the equation:

$$y = 2.97 + 0.156 \ln(x)$$

For $x = 0.47$ m, $y = 1000/T_o = 2.852$, giving $T_o = 351$ K = 78ºC.

FRS method of analysis

The analysis method recommended by FRS and Beever involves using a fair bit of theory to interpret and extend the data, not just making a straight-line plot. As a result, a more refined and accurate estimation can be made, and several corrections incorporated where needed.

After collecting the data, to perform the analysis, one must first determine the value of δ_c that is pertinent to the exper-

* In most oven basket tests, when a specimen is tested at a subcritical oven temperature, the temperature reaches a peak then drops down to about the oven temperature value. Some drop is expected, since a steady-state value would be achieved only if no reactants were consumed. However, questions have been raised[145]—but not answered—as to how it is possible for the excess temperature to drop to near zero, if after removing the specimen from the oven very little is found to have been consumed.

imental situation. To present the data in a form suitable for analysis, we start with the definition of δ

$$\delta = \frac{E}{RT_o^2}\frac{r^2 \rho Q A}{\lambda} e^{-E/RT_o}$$

Taking logarithms of both sides, re-arranging, and noting that the values of δ to be obtained are the critical ones, δ_c, the following relation is obtained:

$$\ln\left(\frac{\delta_c T_o^2}{r^2}\right) = P - \frac{E}{RT_o}$$

where T_o = the critical oven temperature value found for a particular size r, and P is a material constant, since it is a grouping of variables which, under the assumptions of the theory, are neither dependent on T nor r:

$$P = \ln\left(\frac{E}{R}\rho\frac{QA}{\lambda}\right)$$

This suggests that it is appropriate to plot the experimental results by putting $1/T_o$ on the x-axis and $\ln\left(\frac{\delta_c T_o^2}{r^2}\right)$ on the y-axis. This gives a straight line, with a slope of $-E/R$ and a y-axis intercept of P.

To evaluate whether a product stored at a given temperature will exhibit thermal runaway, one first finds the value of δ_c that is given by theory. Note that the end-use geometry need not be the same as the test geometry. For instance, the tested configuration may be a cube, while the end-use product is in the shape of a rectangular box. However, all necessary theoretical corrections to δ_c (for finite Bi number, fuel depletion, etc.) must be made. Then, one can express δ as:

$$\delta = \frac{r^2}{T_o^2}\exp(P)\cdot\exp\left(-\frac{E}{RT_o}\right)$$

where P and E/R were obtained from the plot of experimental data, while the values of r and T_o to be used are those that pertain to the end-use condition. The above equation gives the value of the actual δ. This is to be compared to the value of δ_c obtained from the theory. If the $\delta < \delta_c$, then thermal runaway is not expected; otherwise, it is.

A value of QA is also needed if some of the methods for estimating time to runaway (assuming the system is found to be supercritical). It can be obtained from the values of P and E/R by the relation:

$$QA = \left(\frac{1}{E/R}\right)\frac{\lambda}{\rho}\exp(P)$$

Treatment for initially-hot substances

Using Thomas' hot-work theory, oven tests on cubes or cylinders are conducted in the standard manner and from these results, a value of E/R is found. The value of θ_h can then be solved for:

$$\theta_h = \frac{E}{RT_h^2}(T_h - T_o)$$

where T_h is the initial temperature of the hot material, and T_o is the temperature of the environment. Knowing θ_h, a value of δ_c is then found from the theoretical expression for to the geometrical shape being used. As usual evaluation is made by comparing the δ_c with the value of δ for the actual system.

Treatment for substances varying in density

In some cases, density of a particular substance can vary significantly. Thus, test data may be available from specimens of diverse densities, or else, application of test results needs to be made to substances of various density. In the latter case, it may be simplest to just use the correction:

$$r_2 = r_1\sqrt{\frac{\rho_1}{\rho_2}}$$

If test data of diverse densities are to be used, however, it is possible to modify the standard data correlation procedure and plot $\ln(\delta_c T^2/\rho r^2)$ on the y-axis, instead of $\ln(\delta_c T^2/r^2)$. A consistent treatment may be achieved in this way, but it is important to realize that the y-axis intercept will no longer be the value P, and thus the intercept value cannot be directly compared to P values reported in the literature.

This type of data treatment, while recommended by a number of authors, leaves out the important issue of thermal conductivity. For most organic solids, the thermal conductivity is roughly proportional to the density, although reliable data quantifying this dependence are not necessarily common. If $\lambda \propto \rho$ then *no* correction should be made, since $\delta \propto \rho/\lambda$, and thus the joint density/conductivity dependence would cancel out. In any case, for a given substance, judgment should be used as to whether to correct for ρ alone, to do no corrections, or to correct for both ρ and λ. If for some substance accurate data are available for both the density and the conductivity, then the process is simply generalized and $\ln(\delta_c T^2 \lambda/\rho r^2)$ is plotted on the y-axis when samples of diverse densities are to be correlated.

Variations in loading

In some cases, systems are considered where there is a reactive component which is dispersed on an inert component. Spokoinyi and Eidukyavichus[147] treated a case of mineral wool where the active component is the phenolic binder, while the inert matrix is the mineral wool itself. They concluded that the effects of varying the loading of binder can be represented by taking $Q = \beta Q_p$, where Q_p = heat of reaction of pure reactive component, and β = mass fraction of reactive component in total mass. An estimating rule of this kind can be applied to other substances, keeping in mind that it will only be valid within the context of the F-K theory. Thus, for example, estimates should not be made of a

high enough loading of the reactive component that the reaction becomes oxygen-limited.

Estimating the Biot number

It is generally quite difficult to determine the Biot number, especially for a real-scale commodity. There are no known studies of the transfer coefficient for large stacks of sundry goods and, even if there were, to obtain the Biot number would require knowing the thermal conductivity of the material, which is, again, rarely known or easily determined. Beever[54] suggests that for large piles the assumption that $Bi \rightarrow \infty$ is appropriate. Presumably the justification for this is that, if h_c is size-independent, Bi will increase directly with increasing size and will, in some sense, become 'large.' Thus, the assumption that $Bi \rightarrow \infty$ is commonly applied to the real-scale situation.

For the small-scale oven tests, the choice is to either determine the Bi value quantitatively, or else set the experiment up in such a way the $Bi \rightarrow \infty$ asymptote is valid. Bowes suggests[10] that if the flow velocity is greater than 10 m s^{-1}, then the $Bi \rightarrow \infty$ can be assumed. This advice is important, since oven-basket testing has indicated that, unless high velocities are achieved, significant errors will occur if $Bi \rightarrow \infty$ is assumed[148]. In the procedure described above for evaluating the chemical constants from oven basket testing, if $Bi \rightarrow \infty$ is assumed for a case where a finite Bi value should have been used, the consequences will be: (1) a higher-than-true value of E will be reported; and (2) a higher-than-true value of P will be reported.

The Biot number is expressed as a convective effect, but in actuality there is also radiant heat exchange at the surface. Thus, 'effective' values must be derived for the heat transfer coefficient (which we will denote as h_{tot} here for clarity) that include an extra contribution from radiation. In the general case, for a body of arbitrary shape and arbitrary surface radiant absorptivity, the calculations become unwieldy (and probably unjustified by other approximations already being made in the problem). As a practical approach, when there is natural convection only and no wind, Bowes[10] offers the following equation:

$$h_{tot} = \frac{\lambda_{air}}{D}\left[2.0 + 0.6\left(\frac{gD^3RT_o}{\nu_{air}\alpha_{air}E}\right)^{1/4}\right] + 4\sigma T_o^3$$

where D = diameter or other critical dimension of specimen, λ_{air} = thermal conductivity of air, ν_{air} = dynamic viscosity of air, α_{air} = thermal diffusivity of air, g = 9.8 m s^{-2}, R = 8.314 J mol^{-1} K^{-1} and $\sigma = 5.67\times10^{-8}$ W m^{-2} K^{-4}. The needed values of the thermal properties for air at a particular temperature T_o can be found in Incropera[151]. Bowes also worked an example where h_{tot} was computed for various specimen sizes r. An analysis shows that a good fit through his data can be obtained by a simple expression:

$$h_{tot} = 13 + 1.033\,r^{-0.7}$$

where the units of r are m and the units for h_{tot} are W m^{-2} K^{-1}. This approximation should only be applied to 'compact' shapes, that is, ones where no one dimension is very different from the other two. Gray and Halliburton[149] reviewed available measurements and procedures for determining the Biot number pertinent to testing specimens in wire baskets in ovens having reasonable circulation rates and recommend that the constant value h_{tot} = 14 W m^{-2} K^{-1} can be used as a general expression.

In oven testing, for best accuracy, the value of h_{tot} should be determined in the oven used. To do this, a series of cubes (or whatever shape is used) is made up in copper or aluminum. The internal thermal resistance of these two metals is low enough that it can be ignored. A cube originally at room temperature T_i is plunged into the oven which is at T_∞ and the cube's temperature T is measured as a function of time. A solution for h_{tot} can then be obtained from the lumped-capacitance equation:

$$h_{tot} = \frac{\rho VC}{St}\ln\left(\frac{T_i - T_\infty}{T - T_\infty}\right)$$

where V = volume of cube (m^3), C = heat capacity (J kg^{-1} K^{-1}), S = surface area (m^2), and t = time (s). An example of this kind of experiment has been given by O'Connor[87]. Jones[150] proposed a similar technique, but using an inert substance of arbitrary, but known thermal diffusivity, instead of a metal which has effectively infinite diffusivity. The analysis of results using a low thermal diffusivity block is less straightforward but can be done with the help of Heisler charts, which are given by Incropera[151] and in other heat-transfer textbooks. Having a value for h_{tot}, the value of Bi can then be computed from:

$$Bi = \frac{h_{tot}r}{\lambda}$$

where λ is the thermal conductivity of the substance being investigated and has the units W m^{-1} K^{-1}. The problem is not finished, however, because a value for λ is needed for the substance being evaluated for self-heating.

A simpler but less general technique for finding the Biot number was proposed by Bowes[10]. Oven test specimens (see below) normally require only a central thermocouple (T_m) and a thermocouple recording the oven air (T_a). However, a specimen surface thermocouple, T_s, may also be fitted. In that case, the value of Bi can be estimated directly from steady-state readings (for specimens that did not lead to thermal runaway):

$$Bi = \beta_\infty \frac{T_m - T_s}{T_s - T_o}$$

and the value of β_∞ is 2.36 for a cube and 2.70 for a long cylinder. In the case of hotplate tests for a dust layer,

$$Bi = 0.5\frac{T_p - T_s}{T_s - T_o}$$

where T_p is the hotplate temperature[51]. Determining steady-state temperatures may not be trivial, since some substances

show multiple peaks or significant reactant depletion effects rather than smoothly approaching a steady state.

Halliburton[152] measured the heat transfer coefficients of shipping drums, tested in open air. For an 0.35 m diameter drum, h_{tot} = 10.3 W m^{-1} K^{-1} was found, while for an 0.55 m diameter drum, h_{tot} = 7.9 W m^{-1} K^{-1}. The smaller drum was then measured inside a test oven, where it showed a higher value of h_{tot} = 16.4 W m^{-1} K^{-1} due to the forced-air stirring. Halliburton additionally measured the heat transfer coefficient of a standard shipping container (2.4 m wide × 2.6 m high × 6.0 m long) in open air and found h_{tot} = 3.5 W m^{-1} K^{-1}. If the functional form derived above for forced convection is used, this gives

$$h_{tot} = 1.13 + 2.78\, r^{-0.7}$$

for free convection results in open air. This relation should of course be viewed only as a qualitative trend, since quantitative curve-fitting cannot be done on the basis of only 3 data points.

Estimating the thermal conductivity

For *powders, dusts, and granular materials*, the thermal conductivity is highly dependent on the porosity ε. The extreme cases are trivial, as $\varepsilon \to 0$, $\lambda \to \lambda_s$, where λ_s is the density of the bulk solid. Conversely, as $\varepsilon \to 1$, $\lambda \to \lambda_g$, where λ_g is the conductivity of air. These extremes are not particularly helpful in estimating the actual λ value and unfortunately the relation is not linear. Numerous relations have been proposed for estimating λ, but none is universally valid or applicable. Gorring and Churchill[153] and Dawson and Briggs[154] reviewed a number of studies on the subject. One of the more usable expressions is the Maxwell-Eucken formula[155]:

Table 16 Thermal conductivity of dry air, λ_g

Temperature (ºC)	λ_g (W m^{-1} K^{-1})
0	0.024
20	0.026
40	0.027
60	0.029
80	0.031
100	0.032
120	0.033
140	0.035
160	0.036
180	0.038
200	0.039
220	0.040
240	0.041
260	0.043
280	0.044
300	0.045

$$\lambda = \lambda_s \frac{1 - \varepsilon\left(1 - a\lambda_g / \lambda_s\right)}{1 + \varepsilon\left(a - 1\right)}$$

where

$$a = \frac{3\lambda_s}{2\lambda_s + \lambda_g}$$

Values of λ_g are shown in Table 16. Intermediate values can be computed as:

$$\lambda_g = A + BT + CT^{3/2}$$

where A = 0.0240, $B = 9.24\times10^{-5}$, $C = -1.28\times10^{-6}$, and T = temperature (ºC). The effect of moisture on the conductivity of air is small, raising the value by 1% for a 5% MC.

If a granular material is wetted, thermal conductivity can rise drastically, with a factor of 10 increase not being rare. Palosaari and Cornish[156] discuss thermal conductivity estimating techniques for wet granular materials.

When materials with void spaces are involved, conductive heat transfer can be augmented by radiation and convection. These effects present notable complications for materials of high porosity (e.g., glass fiber thermal insulation), but for relatively compact powders, dusts, grains, etc., usually can be ignored.

For *non-granular cellulosic and lignocellulosic materials* (e.g., cotton, wood products, paper, etc.), the data of Sauer[157] indicate that a good correlation can be produced on the basis of the material's density. Figure 27 gives the experimental data points, along with two fitted lines. On the basis of these results, a practical strategy can be:

If $\rho < 300$ kg m^{-3}, then $\lambda = 0.043$ W m^{-1} K^{-1}.

If $300 < \rho < 1100$ kg m^{-3}, then $\lambda = 1.6\times10^{-4}\,\rho$.

This is indicated as the dashed straight line on the graph.

If $\rho > 1100$ kg m^{-3}, then $\lambda = 0.042 + 1.14\times10^{-7}\,\rho$.

This is indicated as the solid-line curve on the graph. These data only pertain to room-temperature conductivity values, but self-heating theory itself does not provide for changes in λ with temperature, so this should not be a major limitation. A rather similar, but slightly lower curve has been obtained for wool products by Baxter[158]. Most materials of interest in self-heating problems will typically have densities greater than 50 kg m^{-3} or so, but for extremely lightweight materials, effective thermal conductivity rises, since convective and radiative effects begin to dominate[159].

For *granular cellulosic materials*, Bowes et al.[160] concluded that $\lambda \propto \rho$ is a good assumption, at least within the range studied, $250 < \rho < 450$ kg m^{-3}.

Worked examples

Bowes[10] has given a detailed example how data for low-density wood fiberboard are analyzed and presented. Here, we work three versions of this example, following generally

Table 17 Data on low-density wood fiberboard

Shape	Size r (m)	Critical temp. T_o (K)	δ_c for $Bi\to\infty$	$\varepsilon = RT_o/E$	B	h_{tot} (W m^{-2} K^{-1})	Bi	Corr. δ_c
Cube[161]	0.0016	590	2.52	0.049	8.8	107	3.4	4.61
	0.0032	523	2.52	0.044	11.2	71	4.5	3.94
	0.0064	485	2.52	0.041	13.0	48	6.2	3.85
Cube[22]	0.0127	475	2.52	0.040	13.6	35	8.9	4.08
	0.0254	450	2.52	0.038	15.1	27	13.5	4.10
	0.051	425	2.52	0.036	16.9	21	21.7	4.09
Octagon[161]	0.0127	473	2.77	0.040	13.7	35	8.9	4.06
	0.0254	450	2.77	0.038	15.1	27	13.5	4.10
	0.051	420	2.77	0.035	17.3	21	21.7	4.04
	0.102	398	2.77	0.033	19.3	18	36.9	4.00
	0.152	389	2.77	0.033	20.2	17	51.3	3.99
	0.279	382	2.77	0.032	21.0	16	86.6	4.00
Slab[22]	0.0068	475	0.88	0.040	13.6	47	6.4	1.26
	0.0137	445	0.88	0.037	15.5	34	9.3	1.27
	0.021	435	0.88	0.036	16.2	28	11.9	1.29

the method* used by Beever[54]. The example is especially illustrative, since experimental data from three different geometries of oven-test specimens are combined: Mitchell's[161] data on octagonal piles and on cubes, and the data of Thomas and Bowes[22] on cubes and on vertical slabs. The experimental data are given in Table 17. We first solve an example problem where no corrections are made, then solve it again with corrections, and finally compute a hot-work example.

Simple problem

Problem: Using the data obtained, compute the critical height of a layer of wood particleboard placed on the ground, if the stack width and depth are very much greater than the height.

Solution: The first step is to obtain the material properties from the oven test data. This is done as a plot presenting $1/T_o$ on the x-axis and $\ln\left(\delta_c T_o^2 / r^2\right)$ on the y-axis. The values of T_o to plot are simply the critical temperature of the oven environment which was recorded for each different specimen size. The values r are the half-thickness for the slab, the half-edge-length for the cube, etc. The data from experiments on different shapes can be combined in one plot, making sure to use the δ_c pertinent to each geometry. It is assumed that the oven tests were well stirred, so that in the oven the condition $Bi \to \infty$ was fulfilled.

The plot is shown in Figure 29; note that neither of the axes is extended to the zero origin, in order to present the data more legibly. The straight line of best fit was found to be:

$$y = 47.54 - 12053\,x$$

The slope is –12053 and has the units of K. The slope is equal to $-E/R$, thus the activation energy E = 12053 K × 8.314 J mol^{-1} K^{-1}, or 100.2 kJ mol^{-1}. The y-axis intercept is 47.5; the units are ln(K^2 m^{-2}) and it is identified as the variable P in Beever's nomenclature.

The problem to be solved is that of a plane slab. Since the material is placed on the ground and there is no cooling along the bottom surface, it is appropriate to assume that the height of the physical slab is r, and not $2r$. With this assumption, the bottom surface is then equivalent to the midplane of a 'logical' slab which is twice the thickness of the actual slab. The reason is made clear by remembering that zero heat transfer occurs across the midplane of a slab with symmetrical heating and boundary conditions. We will assume that cooling is unrestricted at the top surface and that $Bi \to \infty$ there. If we want to compute the just-critical value of size, then we must evaluate δ under conditions that

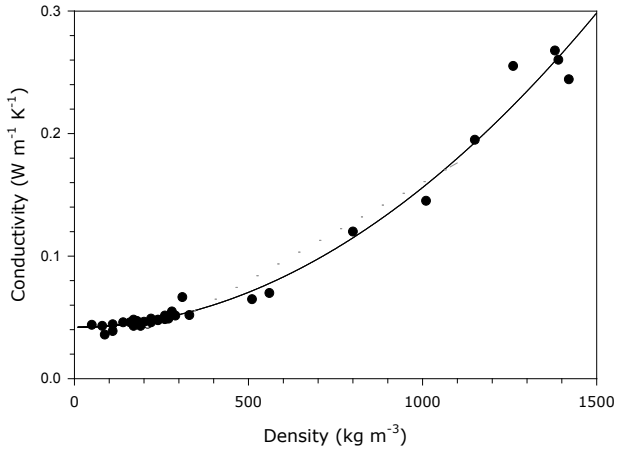


Figure 27 Estimating the thermal conductivity of lignocellulosic solids on the basis of density

* For consistency, we adopt the nomenclature and units used by Beever. Bowes defines $-E/R$ as P, and defines the y-axis intercept (our P) as M. Also note that he uses mm and not m as the unit of measure, with the result that his values of M are lower than our values of P by $\ln(10^6) = 13.82$.

(a) δ is exactly equal to its critical value, δ_c; and (b) T_o is the initial ambient temperature, which we will take as 20ºC = 293 K. For a slab, the critical value $\delta_c = 0.88$. Now

$$\delta_c = 0.88 = \frac{r^2}{T_o^2}\exp\left(P - \frac{E}{R}\frac{1}{T_o}\right)$$

and since all the values are known, we directly get r = 11.4 m. This means that the pile would have to be 11.4 m high for runaway self-heating to occur. This is substantially higher than would normally be stacked in any facility. Thus, if the pile is stacked with its initial temperature being 20ºC, no spontaneous combustion would be expected. Note also that if the pile had been stacked on pallets which permitted good access of cooling air to the bottom, then an even higher critical condition of 2×11.4 m would be computed.

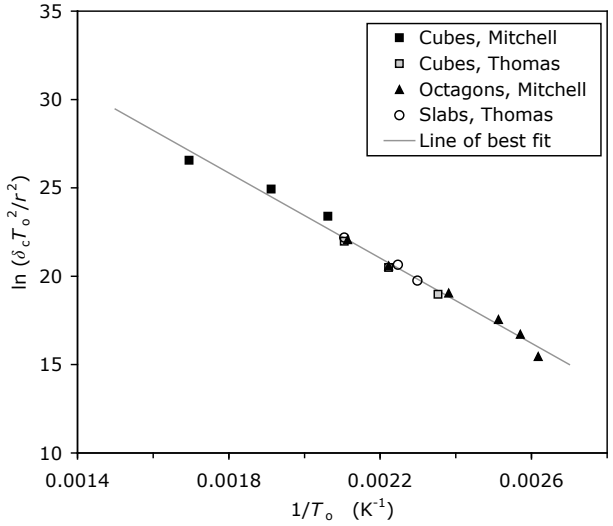


Figure 28 Simple analysis of wood fiberboard data

Problem using corrections

Problem: Using the above experimental data, make corrections for finite Biot number and reactant depletion, check if a correction for low activation energy is needed, then apply the results to determine if a 3 m cube of material, stacked on pallets at 20ºC, is safe.

Solution: Estimates of E and P were already obtained in the previous problem. To correct for a finite Bi, a value of the thermal conductivity λ of fiberboard is needed, which can be taken as 0.050 W m^{-1} K^{-1}. Knowing the size and the thermal conductivity, Bi can be estimated as:

$$Bi = \frac{\left(13 + 1.033 r^{-0.7}\right) r}{\lambda}$$

These values are listed in Table 17. Then values of δ_c corrected for finite Bi values can be obtained from Boddington's relationships. Very little error is introduced if the octagonal parallelepiped is treated as a cube, so two shapes only need to be considered:

$$\delta_c(Bi) = \frac{1}{0.3892 + \dfrac{0.906}{Bi}} \qquad \text{for the cube}$$

$$\delta_c(Bi) = \frac{1}{1.167 + \dfrac{2.718}{Bi}} \qquad \text{for the slab}$$

Reactant depletion correction is computed by first evaluating the nondimensional temperature rise B:

$$B = \frac{E}{RT_o^2}\frac{Q}{C}$$

A good estimate of E was already obtained in the preceding Example problem. A value for the heat of reaction, Q, is difficult to determine without a thermal analysis study of the material. Bowes recommends a value of 350 kJ kg^{-1}, based on a detailed investigation of wood pyrolysis. A knowledge of C for wood fiberboard is also required, this being 1400 J kg^{-1} K^{-1}. A value of B can then be computed as $\left(E/RT_o^2\right)\left(Q/C\right) = 3.0\times10^6/T_o^2$. The reactant-depletion correction factor is:

$$\delta_c(B,n) = \frac{\delta_c(\infty)}{1 - 2.85(n/B)^{2/3}}$$

where n = 1 is appropriate for a first-order reaction.

A low-activation-energy correction is needed if E < 40 kJ mol^{-1}. In the present case, $E \approx$ 100 kJ mol^{-1}, so a correction is not needed.

Thus, the final expression for δ_c, using the two corrections needed, becomes:

$$\delta_c(corrected) = \delta_c(Bi) \times \frac{1}{1 - 2.85\,B^{-2/3}}$$

The final results are shown in Figure 29.

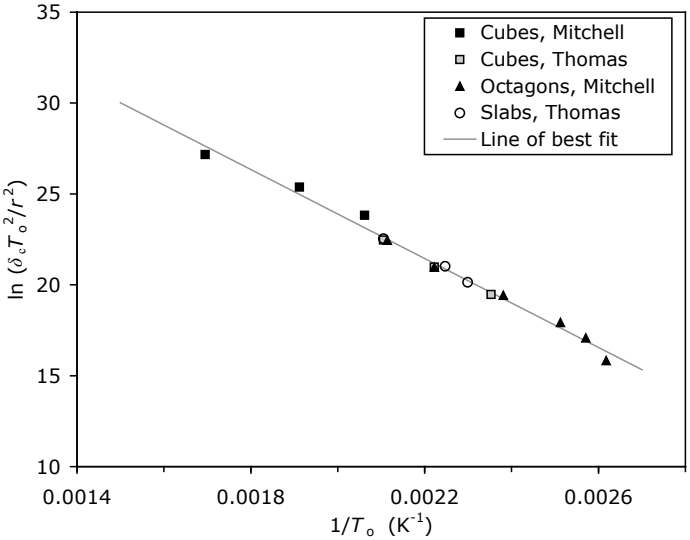


Figure 29 Analysis of wood fiberboard data with corrections included

The line of best fit has a y-intercept (that is, P) of 48.38 and a slope of –12,242 K. Since the latter = $-E/R$, a final value for E of 101.8 kJ mol^{-1} is found. These values are not noticeably different from the ones computed in the preceding problem. To apply the results to a 3×3×3 m cube of wood fiberboard stacked in 20ºC ambient temperature, first we find the value of r is 3/2 = 1.5 m. To estimate Bi:

$$h_{tot} = 13 + 1.033\, r^{-0.7} = 13 + 1.033\,(1.5)^{-0.7}$$
$$= 13.78 \text{ W m}^{-2} \text{ K}^{-1}.$$
$$Bi = \frac{h_{tot} r}{\lambda} = \frac{13.78 \times 1.5}{0.05} = 413$$

This is a very large value, so the $Bi \to \infty$ results (for a rectangular brick with all sides identical) can be used: δ_c = 2.52. As computed above, $B = 3.0\times10^6 / T_o^2$ and n = 1. This gives

$$\delta_c(corrected) = \delta_c \times \frac{1}{1 - 2.85\,(n/B)^{2/3}}$$
$$= 2.52 \times \frac{1}{1 - \dfrac{2.85\,(293)^2}{3\times10^6}} = 2.74$$

Now, the value of δ for the actual conditions is computed as:

$$\delta = \frac{r^2}{T_o^2} \exp\left(P - \frac{E}{R}\frac{1}{T_o} \right)$$
$$= \left(\frac{1.5}{293}\right)^2 \exp\left(48.38 - \frac{12{,}242}{293}\right) = 0.020$$

Since 0.020 << 2.74, the pile is much too small for criticality to occur. The critical condition will occur at:

$$\frac{r^2}{T_o^2}\exp(6.60) = 2.74$$

Which can be solved to give r_c = 18.0 m, in other words, a cube of 36.0 m on a side, which is a large value indeed. Thus, the hazard from storing such piles in 20ºC temperature air should be minimal.

Problem in estimating criticality time

Problem: A very large storage compartment is filled with milk powder to the depth of 2 m. The ambient temperature is 321 K and the self-heating constants have been determined for the product as ρ = 508 kg m^{-3}, λ = 0.127 W m^{-1} K^{-1}, C = 2000 J kg^{-1} K^{-1}, E = 99.6 kJ mol^{-1}, P = 48.1, and $QA = 1.46\times10^{13}$ W kg^{-1}. How long will it take for the bin to reach criticality.

Solution: In order to be able to use any of the time-to-criticality formulas, it is first necessary to determine whether thermal runaway will occur. We will assume that the bottom of the layer represents an adiabatic surface, then r = 2 m. Using the given values, δ = 1.69. Ignoring any corrections for reactant depletion, δ_c = 0.88. Since 1.69 > 0.88, criticality is expected. Using the Zinn & Mader method, $t_{Fo} = \rho C r^2 / \lambda = 3.27\times10^7$ s. Also, δ/δ_c = 1.69/0.88 = 1.92. From Figure 18 or from the equations, $t_{ig} = 8.0310^7$ s = 930 days. Using Boddington's method, take M = 1.53. Then, $t_{ad} = 1.90\times10^7$ s and $t_{ig} = 1.60 t_{ad} = 3.04\times10^7$ s = 352 days. Using Thomas' method for estimating the lower limit, $t_{ig} \geq (0.89\rho C r^2)/(\delta\lambda) = 1.69\times10^7$ = 195 days. Using Gray's method for estimating the lower limit, $u = RT_o / E$ = 0.0268. This gives $\tau_{ig} = 1.14\times10^{13}$. Then, $t_{ig} \geq \tau_{ig} CE / QAR$ = 1.87×10^7 s = 217 days. Note that Gray does *not* recommend that the numerics be worked by substitution in this manner. Instead, his preferred procedure is based on scaling from an experimental datum point for critical time. Unfortunately, this example problem illustrates that theoretical treatments of criticality time are widely divergent.

Hot work problem

Problem: The same wood fiberboard material is now emerging from a manufacturing plant at 80ºC and is then immediately stored at an air temperature of 20ºC. Will a 3×3×3 m pile stacked on pallets reach critical conditions? If so, how long will it take?

Solution: First, a value for θ_o is computed as:

$$\theta_o = \frac{E}{R}\frac{T_i - T_o}{T_i^2} = 12{,}242\frac{353 - 293}{353^2} = 5.90$$

Then, the expression for the δ_c of a hot-work cube is evaluated:

$$\delta_c = \frac{1}{0.0458 + 0.1316/\theta_o} = 14.68$$

Next, the expression of δ is evaluated, with the temperature to be used being the hot-work temperature T_h and not the ambient temperature T_o:

$$\delta = \frac{r^2}{T_h^2} \exp\left(P - \frac{E}{R}\frac{1}{T_h} \right)$$
$$= \left(\frac{1.5}{353}\right)^2 \exp\left(48.38 - \frac{12{,}242}{353}\right) = 16.09$$

Since 16.09 > 14.68, the pile is expected to sustain thermal runaway. Under such circumstances, we wish to estimate the time until critical self-heating will occur. To evaluate this for a slightly-supercritical system, first compute t_{ad}. To evaluate this quantity, we must provide values for QA, but the frequency factor A has not been determined in the solution so far. The product QA can be solved by knowing the value of P and the density ρ, which for wood fiberboard of the present example is 270 kg m^{-3}.

$$QA = \left(\frac{1}{E/R}\right)\frac{\lambda}{\rho}\exp(P)$$
$$= \frac{1}{12{,}242}\,\frac{0.05}{270}\exp(48.38) = 1.55\times10^{13} \text{ W kg}^{-1}$$

$$t_{ad} = \frac{RT_i^2}{E}\frac{C_p}{AQ}\exp\left(\frac{E}{RT_i}\right)$$

$$= \frac{353^2}{12{,}242}\frac{1.4\times10^3}{1.55\times10^{13}}\exp\left(\frac{12{,}242}{353}\right) = 1.06\times10^6\,\text{s} \approx 12.3\ \text{days}$$

The value of $M(Bi)$ for cubes is not given by Boddington, but we can get approximate results by taking the value for a sphere, 1.3. Then, the expected time under real, non-adiabatic conditions can then be computed as:

$$t_{ig} = t_{ad}\frac{M(Bi)}{(\delta/\delta_c - 1)^{1/2}}$$

$$= 1.06\times10^6\,\frac{1.3}{\left(\frac{16.09}{14.68}-1\right)^{1/2}} = 4.4\times10^6\,s$$

= 51 days. This time may be entirely adequate if stock is normally broken up into small shipments within, say, one week.

Limitations and validation of small-scale test procedures

The standard oven-basket test procedure is practical, but it is simplified. For the sake of tractability, the method is based on standard theoretical development which uses a linearized approximation to the Arrhenius rate kinetics, rather than the full expression thereof. Furthermore, the treatment ignores such conditions and factors as:

- irregular product shapes found in practice
- products of more than one material
- materials having more than one exothermic peak; or endothermic and exothermic peaks
- materials having antioxidants
- variation of thermal properties with temperature
- variation of thermal properties with reaction progress (the thermal properties of char are generally different from that of the virgin material)
- mass flow of pyrolysates or water vapor
- natural convection occurring inside the body
- variation of thermal properties with the instantaneous moisture content (this can be an especially strong effect on thermal conductivity when moisture content approaches fiber saturation)
- non-uniform dispersion of the substance if, for instance, finer particles tend to segregate in a pile
- cooling behavior which is not represented by a constant, linear heat transfer coefficient
- forced convection blowing through the porous body
- products that have different exposures on their different sides (e.g., the bottom on a shelf, the sides exposed to air).

Furthermore, to avoid unmanageably large specimen sizes, oven heating typically needs to be conducted at temperatures over 100ºC. Thus, self-heating effects due to biological activity (which ceases at temperatures greater than ca. 80ºC) and due to the presence of moisture cannot be evaluated.

For some of these real-world complications, there has been discussion in the literature, however, none of the above factors lend themselves to any simple correction scheme. Composite products, however, would lend themselves to improved treatment by a modified testing strategy, e.g., by making up cubes of composite rather than cubes of a single material.

A somewhat unanticipated advantage of the oven-basket method is that the results often have a wider range of validity than the F-K theory itself, when it comes to temperature-dependent constants. Material properties, such as thermal conductivity, which vary with temperature cannot be treated by any tractable form of F-K theory. Yet when data are plotted using the FRS procedure for substances having such temperature-dependent properties, it is often seen that straight lines are obtained. This suggests that the effects of various temperature-dependent constants can cancel out sufficiently to produce the linear plots. The FRS procedure, consequently, can be more robust than thermal analysis procedures (see below), which do not provide any satisfactory solutions for situations where the properties are temperature-dependent.

Finally, it is important to point out that oven-basket test procedures, even though they are the most robust form of small-scale testing currently known, have only limited *validation data* and that it may not be prudent to extrapolate to larger sizes. The largest oven-basket sample reported to have been used[44] is 0.9 m, which is much smaller than piles of material are commonly stacked in various industries. Few actual validation studies have been published. A study on activated charcoal[162] concluded that small-scale data followed a linear relationship well up to a size of 0.2 m, but an 0.6 m size oven-basket sample deviated substantially, as did real incidents involving a material size of 2 – 3 m. Both the latter deviations were on the conservative side. For a number of substances, effects such as listed above (e.g., flow of moisture) may dominate in real-scale piles and the effect may be inadequately or incorrectly treated using F-K based extrapolations. In summary, Beever[54] wisely advises of "…risks of extrapolating over orders of magnitude in size" even with this most-refined of the small-scale test procedures.

Oven-basket tests: crossing point methods

This class of tests has often been suggested as quick, small-scale laboratory procedures for self-heating. In a traditional crossing-point scheme, a sample is equipped with at least one thermocouple, located in the middle, and is placed in a temperature controlled oven. The oven temperature is ramped up at a relatively slow rate. If at a certain time the specimen thermocouple reading exceeds the oven temperature, then this is declared to be the 'critical temperature.' The test implicitly relies on the assumption that the small oven sample will undergo thermal runaway at the same temperature as the real-scale pile. As discussed extensively

earlier in this Chapter, both theory and practical experience indicate that the runaway temperature is very strongly affected by the size of the sample, thus simple crossing-point test results are without much value. The results of such testing can, at best, be used to compare the self-heating proclivity of two very similar substances. They are not capable of predicting real-scale thermal runaway conditions[78].

A much improved scheme was proposed by Chen et al.[56] In their scheme, a variant of the crossing-point method leads to quantitative data essentially similar to what is obtained in the standard oven-basket test. In this technique, the oven is held at various constant temperature values and is not ramped. A cubical basket is inserted cold and the temperature is monitored at the center of the specimen and at the edge of the specimen. When the two temperature readings become identical, then, by definition, no heat is being transferred between these two locations within the specimen. Using the equation for conservation of energy and assuming that there are no space-wise gradients gives:

$$\rho C \left.\frac{dT}{dt}\right|_p = \rho\, QA \exp\left(-E / RT_p\right)$$

where the subscript p denotes conditions at the center of the sample. Figure 30 shows results for a coal sample tested at slightly super-critical conditions[21]. The critical value of T_p for 50 mm cubes of this material was 401.5 K (128.4ºC). At 135.6 min, it can be seen that the temperature profile is flat. By repeating the test at various oven temperatures (which do not come explicitly into the above equation), a series of pairs of data points T_p vs. dT/dt is obtained.

Then, by plotting $(1/T_p)$ on the x-axis and ln(dT/dt) on the y-axis, a straight line is obtained according to the relation:

$$\ln\left(\left.\frac{dT}{dt}\right|_p\right) = \ln\left(\frac{QA}{C}\right) - \frac{E}{R}\frac{1}{T_p}$$

The slope is $-E/R$ and the y-axis intercept is ln(QA/C), as illustrated for the same coal material in Figure 32. Often for convenience in dealing with small numbers, $1000/T_p$ is plotted on the x-axis, instead of $1/T_p$. The slope obtained in Figure 32 is –9.378. The actual slope on a graph where $1/T_p$ would have been plotted would be = –1000×9.378 = –9378. Then, E = 9378×8.314 = 77970 J mol^{-1} = 78.0 kJ mol^{-1}. Knowing C, a value for QA may also be obtained. By contrast, in the standard oven-basket procedure, to get QA from the plotted data requires knowing the thermal conductivity λ. Since values of thermal conductivity for porous, possibly moist, substances are generally less certain than their C values, the crossing-point procedure can determine QA more robustly. In the present example, the y-axis intercept of the straight line is found to be 22.32, thus

$$22.32 = \ln\left(\frac{QA}{C}\right).$$

If the value of C = 1000 J kg^{-1} K^{-1} is used, then QA = 1000 exp(22.32) = 4.9×10^{12} W kg^{-1}. Observe that the size of the oven-basket sample does not enter into the calculations. If various sizes are used, the points will all follow the same line. For comparison purposes, the value P, which is the y-axis intercept in conventional plotting of oven-basket data, can be obtained as:

$$P = \ln\left(\frac{E}{R}\right) + \ln\left(\frac{QA}{C}\right) - \ln(\alpha)$$

where we note that the thermal diffusivity α (m^2 s^{-1}) is defined as $\alpha = \lambda / \rho C$. The first two terms in the above equation are directly obtained as results from the plot. The value of thermal diffusivity however, is not determined by the test, and a handbook value needs to be found.

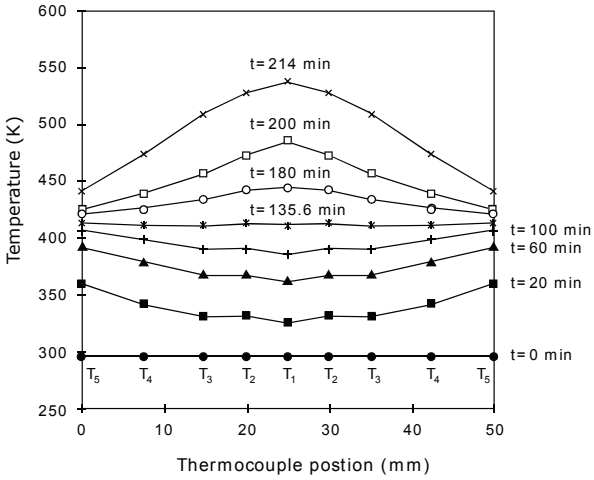


Figure 30 A test of a 50 mm oven-cube sample of coal at slightly supercritical conditions: oven temperature = 402 K (128.9ºC), critical temperature = 401.5 K (128.4ºC)
(Copyright The Combustion Institute, used by permission)

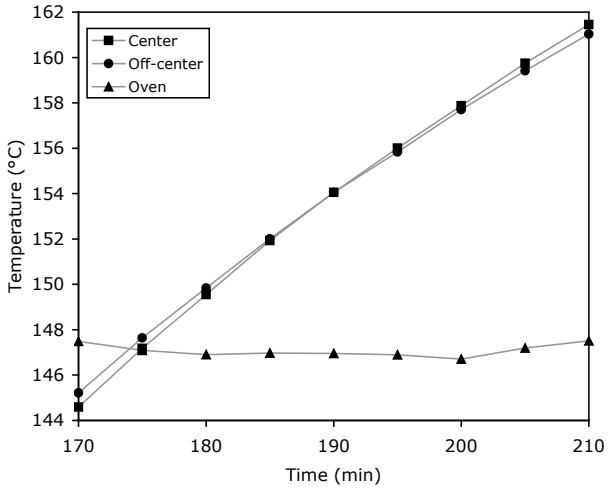


Figure 31 The crossing point illustrated for 60 mm cube of milk powder; off-center thermocouple is 8 mm away from center[164]
(Copyright Elsevier Science, used by permission)

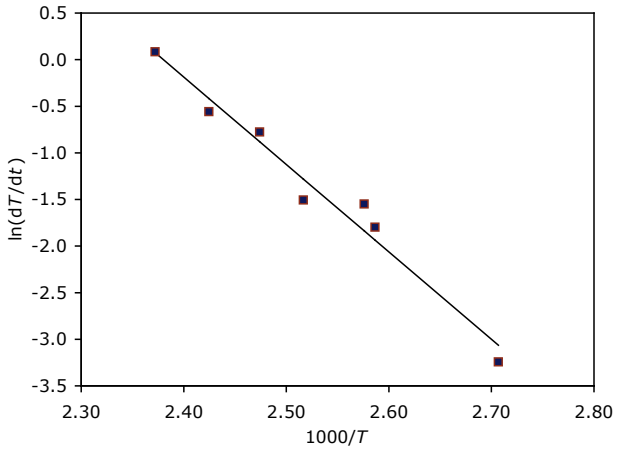


Figure 32 The results for coal self-heating tests plotted according to the crossing-point method of Chen et al.

McIntosh and coworkers[21] also studied coal and found that results using the standard oven-basket method and the crossing-point method were indistinguishable. They further studied the same sample with thermal analysis and obtained a value of E = 109 kJ mol^{-1} from DTA tests. This, they observe, is distinctly erroneous, since the thermal regime in the DTA test did not correspond to the low-temperature chemistry observed in actual self-heating. Sujunti et al.[163] applied the crossing-point method to an Australian coal and demonstrated that (a) the kinetic parameters derived were insignificantly different from the ones obtained from standard oven-basket tests; and (b) the size of the baskets used in the crossing-point tests did not have a noticeable effect on the results.

The best place to put thermocouples using the cross-point method is a crucial issue. Clearly, one thermocouple should always be at or close to the center. Various proposals have been made concerning where the second thermocouple is best located. In the example of Figure 30, it would seem that placing the thermocouple at or near the edge would be best, since greatest sensitivity to a relative difference of temperatures would be had. But in the example shown in Figure 15, placing the thermocouple at the edge does not make much sense, since only the central portion ever gets reasonably flat. In their work, McIntosh et al. recommended that the best place to measure the peripheral temperature is 10 mm away from the center. Chen et al. made many of their measurements using an 8 mm spacing[164].

In doing crossing-point tests, it is important to understand under what conditions and where the temperature profile across the specimen can ever be flat. In general, a theoretical study[165] has indicated that a substance that is originally at a uniform ambient temperature and is then quickly inserted into an elevated temperature environment will never show a flat temperature profile. A specimen quickly assembled of materials that are originally at oven temperature but disaggregated would, of course, show a flat profile, but only for the trivial case at time = 0.

Jones[166] developed an alternative crossing-point method wherein he does not instrument the sample with off-center thermocouples, but rather uses the oven temperature as the second temperature. Figure 31 shows that, at the time that the flat profile occurs in the center of the specimen, the oven temperature is notably lower, being 7ºC less in the example graph. If the Jones method had been used on these data, equality of central thermocouple and oven thermocouple would have occurred at 175 min, which is different from the 190 min at which the temperatures from the two in-sample thermocouples became equal. In making the data plot, both a different temperature and a different dT/dt would have been recorded at that instant. Chen[167] illustrated this in a comparison plot and showed that the kinetic properties that would have been derived would have been different by more than just the amount of data scatter. Chen's examples suggest that the value of the y-axis intercept is more notably altered than the value of E, if the oven temperature is substituted for the specimen peripheral temperature. In addition to Chen's experimental analysis, Gray et al.[165] performed theoretical computations which demonstrated that if the specimen's center has become equal to the oven temperature, the center temperature has to be the *minimum* temperature that is found in the profile of the specimen at that instant. In other words, dT/dx cannot be equal to zero at that time at the central axis of the body.

Comparing among the methods, the Jones method is somewhat easier to use, but the Chen method has better theoretical justification. Comparing either of the crossing-point methods against the FRS oven-basket method, the advantages are:

(a) Only one specimen size is required and no trial-and-error procedure is needed.
(b) Any symmetric shape of specimen (cube, cylinder, sphere, etc.) may be selected without needing to perform computations that are geometry-related.
(c) Because the convective boundary condition drops out[168], it is neither necessary to ensure that $bi \rightarrow \infty$ nor to correct for a non-infinite value.

They also have these drawbacks:

(a) The theoretical foundation for the method is somewhat shaky and Prof. Brian Gray[75], one of the ranking theoreticians on the subject of self-heating, concluded that crossing-point methods "can give dangerously flawed results."
(b) As an entirely separate test procedure, a value of thermal diffusivity must be obtained for the specimen, and this can be difficult, especially for moist materials.
(c) More precise workmanship is required.
(d) The method cannot be used for specimens (e.g., oil-soaked cloth) that show hot spots or other non-uniformities. For this reason, it is desirable with the crossing-point methods to include additional thermo-

couples in the basket so that uniformity can be assessed. Routine testing using only 1 or 2 thermocouples and no visual observation of the outcome should never be done.

(e) A highly accurate specimen center temperature measurement must be made. In the standard oven-basket technique, no quantitative use is made of these data—the reading only has to indicate thermal runaway. In the crossing-point methods, by contrast, errors in measuring that temperature would directly reflect an error in heat balance. This is not a trivial concern, since metallic thermocouple wires may have a thermal conductivity of a thousand times that of the lightweight, porous substances being tested. To avoid significant 'stem loss' errors, a spiral-shape thermocouple has been proposed[169]. In any case, the crossing-point method requires a much higher accuracy of temperature measurement than is demanded in the FRS oven-basket procedure, and this may be quite difficult to achieve[170].

(f) The methods rely on being able to draw a robust straight line through an $\ln(dT/dt)$ versus $1/T$ plot. But Jones[171] found that some materials—sawdust, coconut waste, and bagasse—produce data plots with a high degree of scatter through which a reliable straight line cannot be passed. This is said to be a chemical as opposed to an instrumentation issue, since using the identical equipment and procedures other types of substances do produce good straight lines.

To obtain the needed value of the thermal diffusivity α, several authors[172,173] used the following scheme. Graphical solutions in Carslaw and Jaeger[174] are provided that, with some manipulation, can be used to compute the temperature rise at the center of a cylinder, T, originally equilibrated to a temperature T_i, then plunged at $t = 0$ to an environment at T_f. Defining $\theta = (T–T_i)/(T_f–T_i)$, and knowing the height/diameter ratio of the cylinder, L/D, and its radius r, the value of $\alpha t/r^2$ can be determined for which $\theta = 0.5$, as given in Table 18. Experimentally, the procedure depends on being able to abruptly establish a new temperature on the surface of a cylinder. Consequently, while a cylinder containing the test material may originally be equilibrated to T_i in an air environment, it must be plunged into a water bath and not an air oven at T_f. A thin-walled copper cylinder is typically used which is sealed at one end and contains a removable end-cap made water-tight with an O-ring seal. A thermocouple is passed through the sealed end and fixed at the center of the cylinder. A viable procedure is to equilibrate the specimen in an air oven to a modestly elevated temperature, say 50 – 100ºC, then plunge it into an ice-water bath at 0ºC. The thermocouple output is used to determine the time at which a temperature exactly halfway in between the two endpoint temperatures is attained. Knowing the L/D of the cylinder, a value of $\alpha t/r^2$ is found from Table 18. Since the values of t (s) and r (m) are known, the value of α ($m^2\ s^{-1}$) can be determined. In conducting the experiments, it is important to weigh the cylinder before inserting into the oven and after removal from the ice-water bath. If the weight has increased, it indicates that water has leaked into the cylinder. The specimen should also be examined visually to make sure its condition has not altered, for example, that a lightweight material has not become compacted.

Table 18 Values of $\alpha t/r^2$ which correspond to $\theta = 0.5$

L/D	1	1.1	1.2	1.3	1.4	1.5	1.8	2.5
$\alpha t/r^2$	0.167	0.175	0.182	0.187	0.191	0.195	0.200	0.204

Oven-basket tests: Nordtest method

The Nordic country standards group Nordtest published a novel oven-basket procedure as NT Fire 045[175,176]. Similar to the crossing-point methods, it was developed to eliminate the need for time-consuming, trial-and-error testing. The Nordtest method replaces isothermal heating with a linearly-rising oven temperature regimen. Two specimen thermocouples are used: one at the center, the other halfway between the center and the edge. At least three different specimen sizes are to be used, with the sizes to scale by 2× from each to the next. The test method requires that a suitable heating rate be guessed, or developed by experience, so trial-and-error aspects are not entirely eliminated. There is no published validation of results from this method, nor is there even a comparison to data obtained from FRS-type oven-basket testing. Thus, in view of the fact that at least the latter comparison does exist for Chen's crossing-point method, it would be hard to consider the Nordtest method as the preferred time-saving technique.

Oven-basket tests: IMO test

This method[177] which never became an official IMO test, but has been widely used in its draft form, is based on a highly simplified version of the FRS oven-basket procedure. The simplification is justified since it is intended for pass/fail rating of products and not for product development or risk management purposes. A single oven temperature of 140ºC and a single basket size of 100 mm are used. The oven test is run for 12 h and failure is declared if the temperature at the center exceeds 200ºC (400ºC in the case of activated carbon or activated charcoal). The method is based on the assumption that a value of $E \approx 77$ kJ mol^{-1}, which has been found to be a good value for US bituminous coals[178], will also hold approximately true for any organic substances. With the assumption that the slope (given by $–E/R$) is a fixed, known value, a single point suffices to establish a straight line. The real-life conditions are presumed to correspond to a shipping package of a 3 m cube and a ship's hold temperature of 38ºC. Thus, if the 100 mm cube does not lead to thermal runaway at 140ºC, neither will the 3 m package at 38ºC. But the range of values of E which can be found for common substances is wide. If the true value is 100 kJ mol^{-1}, then critical conditions will occur for 9 m and not 3 m. Even higher values ca. 130 kJ mol^{-1} are common; for such a case the true critical size would rise to

over 37 m. A scheme which inserts unexpected factors of up to 12× is evidently rather crude.

Oven-basket tests: UN Test N4

The UN version of the oven-basket test generally resembles the IMO test, but with some differences. A unique feature is the basket-inside-a-basket arrangement. The inner basket of 25 or 100 mm cube size is put into an outer wire-mesh cubical basket of 150 mm size. This is ostensibly to keep material from being scattered by air flow velocity. This is contrary to what the many decades of research at FRS indicated as being appropriate and has been criticized by Jones[179]. The outer basket creates a poorly defined convective heat transfer situation, making results less amenable to quantitative interpretation.

In the procedure, a test is first conducted using the 100 mm basket at 140ºC for 24 h. Failure occurs if a temperature rise of ¤ 60ºC is recorded by a thermocouple placed in the center of the sample. If the specimen passes, then no further testing is done and the substance does not need to be classified into Division 4.2. If it fails the 100 mm basket test, then another test is run using a 25 mm basket. If the test using the 25 mm basket at 140ºC also fails, then the substance is classified as requiring Division 4.2 Packaging Group II. If the second test is passed, then a third test is run using a 100 mm basket. The third test is run at 100ºC if it is desired to qualify the substance for shipping in sizes no greater than 450 L. Alternatively, it is run at 120ºC if the substance is to be qualified for shipping in sizes of 450 L to 3 m^3. If the substance passes either of these versions of the third test, then it is classified as requiring Division 4.2 Packaging Group III, with appropriate size limits.

Hotplate tests

A testing strategy is possible where the substance is arranged as a uniform layer on a hotplate. The hotplate provides uniform heating, while the upper surface of the specimen is exposed to ambient cooling. The geometry has been used most commonly for examining the self-heating propensity of dust layers, on the grounds that it closely resembles the end-use geometry. In this context, hotplate tests have normally been used just as a rough pass/fail screening procedure, but the experimental arrangement is sometimes also used to derive quantitative data in the context of the F-K theory. Use of theory for this problem, along with example data, have already been presented above under *Ignition of dust layers*. The precision attainable with hotplate testing is lower than with oven-basket testing, but the tests can be conducted quicker[180]. Since the test methods typically use layer thickness of 25 mm or less, higher temperatures must be used in conducting the test in order to reach critical conditions. Consequently, correction for reactant depletion may be needed. The test apparatus must provide for a specimen diameter which is much greater than the depth. Limited testing[181] showed that reported layer ignition temperatures for a 20 mm depth decreased when going from a diameter of 100 mm to 140 mm, but did not further decrease on going to 180 mm. This suggests that, for a 20 mm depth, 140 mm is the minimum diameter for obtaining accurate results. Another study[182] showed that, for layers of 10 – 25 mm depth, in going from 100 mm to 150 mm diameter test specimens the critical hotplate temperature decreased by ca. 10ºC. The accuracy of this work is not clear, however, since the authors reported erroneous critical heat fluxes for ignition.

Analysis of data from hotplate tests according to a theoretical model is more complex than that for oven-basket tests, since there are two temperatures that must be considered—the ambient temperature and the hotplate temperature—whereas with oven-basket testing only a single temperature enters the problem. Thus, theory-based calculations are fairly onerous. For practical purposes, it can be sufficient to plot $\ln\left(T_h^2 / d^2\right)$ as a function of $1/T_h$, where T_h = hotplate temperature (K) and d = layer depth (m). Example plots are shown in Figure 33 using the sawdust data of Bowes[30] and Palmer[183]. Reasonably straight lines are usually produced, and these plots can be used to estimate the value of d for a given T_h. In the example graph, values of d ranged from 5 mm to 100 mm. This includes most of the depth range likely to be encountered in practical testing and a deviation is only seen for the 100 mm data point; the experimental accuracy of the latter is questionable, since the reported value is identical to that given for the 75 mm depth. The value of E might be estimated by assuming that the slope = $-E/R$, but this is a crude estimate. For the given data, a value $E \approx 140$ kJ mol^{-1} would be estimated, but the actual value is around 100 kJ mol^{-1}.

The reason for the poor accuracy is because, same as for oven-basket testing, the value that should be plotted on the

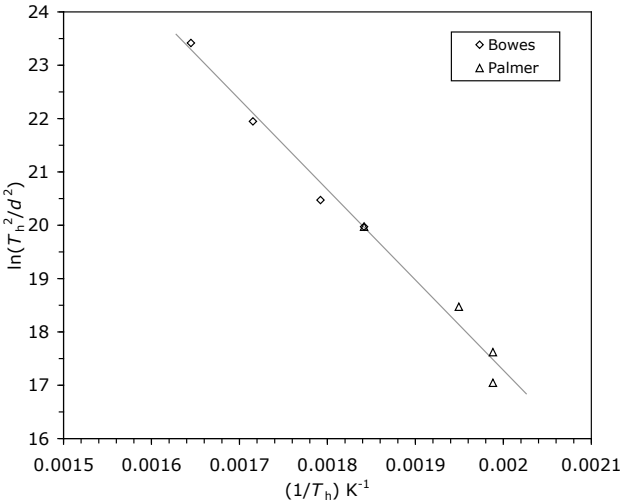


Figure 33 Sawdust hotplate results plotted according to simple correlation

y-axis is $\ln\left(\frac{\delta_c T_h^2}{r^2}\right)$ and not $\ln\left(T_h^2/d^2\right)$ or $\ln\left(T_h^2/r^2\right)$. For oven-basket testing at the $Bi \rightarrow \infty$ limit, the value of δ_c is a simple geometric constant for a given shape. Consequently, whether it is included or omitted simply changes the y-axis intercept of the plot but does not change the slope. For the hot-surface problem, however, the value of δ_c is never a constant, consequently, omitting it causes an incorrect slope to be obtained.

To obtain an accurate solution from theory is cumbersome. As shown above in the theory section, a non-dimensional variable θ_o is needed, which is defined as:

$$\theta_o = \frac{E}{RT_h^2}(T_o - T_h)$$

The value of ambient temperature T_o and hotplate temperature T_h are known. But the value of E is generally not known a priori, and using the slope in a simple data correlation plot will give the wrong result. Thus, the value must be obtained from some other test results, e.g., oven-basket testing. Having a value for θ_o, the value of δ_c is found from Figure 8; note that for each experimental point where a different value of T_h was used, a different value of δ_c will be obtained. Now, the same procedure as involved in plotting oven-basket test results can be used. Using that procedure, $\ln\left(\frac{\delta_c T_h^2}{r^2}\right)$ is plotted on the y-axis, versus $1/T_h$ on the x-axis. But the only useful output of that exercise is that a value for *QA* can be computed; the procedure will also give an improved estimate of *E*. This suggests that hotplate testing has only very limited value as a tool for obtaining material self-heating properties. Because of this, it is not a suitable alternative to oven-basket testing, but does have utility for simple interpolating and extrapolating of data.

With some materials, additional difficulties are encountered if hotplate tests are to be used to impute material properties. Henderson and Tyler found that two criticality temperatures can be reported for sodium dithionite, depending on whether testing proceeds from high temperatures to lower, or vice versa[184]. This is due to two exotherms that the material possesses, one at a higher temperature and one at a lower. When temperatures starting at 400ºC and going down were used, a pseudo-critical temperature at ca. 380ºC was found. But when starting testing at 185ºC, a lower critical temperature at ca. 188ºC was seen. It appears that in the high temperature regime, the low-temperature exotherm is lost in the very rapid temperature rise during the 'assembly' of the dust layer.

Tyler and Henderson[51] further tested sodium dithionite in hotplate tests where they measured the Biot number. Apart from the fact that this substance shows non-Arrhenius kinetics, they discovered a complication in representing the heat transfer at the upper surface. Using the highest ventilation velocity that was possible without scattering the powdery sample, they found that the Biot number varied greatly with layer depth, going from 0.42 for a 5 mm depth to 4.3 for 40 mm. Conversely, if no forced ventilation was used, then the air temperature above the sample rose to very high values (ca. 60ºC), making it impossible to assume a fixed, known ambient temperature value. Thus, they concluded that plots based on the assumption of a constant δ_c value would be in serious error, since δ_c is strongly affected by the value of *Bi*, and *Bi* is notably dependent on layer depth. To obtain data on real material properties, they concluded that it was necessary to measure *Bi* and evaluate δ_c for each data point using the measured *Bi* value for that test run.

Ohlemiller and Rogers[185] presented a detailed analysis of cellulose insulation tested with a hotplate method. They encouraged its use, but with the proviso that predictions from the method to end-use situations be considered, at best, semi-quantitative. Nagy and Verakis[92] claimed that a correlation exists between the critical hotplate temperature when dusts are tested in a 13 mm layer hotplate test and the AIT, as determined in the Godbert-Greenwald furnace (see Chapter 5). This claim was based on only 7 data points and an examination of larger data sets[186] shows that no general correlation exists (nor should one be expected).

ASTM E 2021 test

The rather recent ASTM E 2021 test[187] for self-heating of dusts uses a standard hotplate (Figure 34), on top of which is placed an aluminum plate, 200 mm dia. and 20 mm thick. Due to the plate's high thermal conductivity and high mass, its top surface is much more nearly isothermal than is the surface of the hotplate itself. A steel ring of 100 mm dia. and 12.7 mm depth is placed on top of the aluminum plate and filled with the dust to be tested. The dust tested is to be sub-200 mesh (< 75 μm). The test is discontinued if, after 60 min, self-heating is not apparent. The maximum test temperature is 390ºC. Three standard substances have been characterized with this test. Fine-flake brass dust (sub-325 mesh) coated with stearic acid gives 144 – 160ºC, Pittsburgh coal dust gives 230 – 240ºC, and lycopodium spores give 240 – 250ºC. It is not intended that the data from this test method be used for calculation purposes. Instead, if the assumption is made that dust layers will not exceed 12.7 mm in real life, then the results (adjusted by some prudent safety factor) are simply to be used to limit maximum temperatures of devices upon which dust layers may accumulate. Some of the background of this test has been described by Miron and Lazzara[115] and by the National Academy of Sciences[188]. The test, as specified in the ASTM standard, is very simplistic in that no variations in layer depth are examined. In addition, as mentioned above, several experimental studies exist showing that, to avoid excessive edge effects, a diameter of at least about 140 mm should be used. Thus, for most purposes apart from strict regulatory compliance, it is more appropriate to construct rings of 150 – 200 mm diameter and to vary the layer depth over a significant

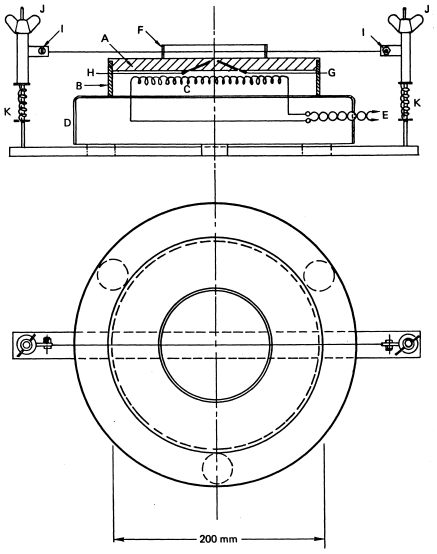


Figure 34 Hotplate test, general arrangement[188]

range. The European standard[189] EN 50281-1-2 is similar but uses a very small layer depth of 5 mm.

SCALING ACCORDING TO SEMENOV THEORY

Tests based on Semenov theory are mostly Dewar-type tests. For convenience, all Dewar tests are grouped into this section, even though the regulatory ones do not have much relation to theory.

General Dewar flask testing

A Dewar flask is a laboratory vessel similar to the well-known Thermos bottles. The sides and bottom of the container (Figure 35) are made of silvered glass in a double-wall construction, with a small vacuum gap in between. Conduction and convection do not exist in a vacuum, but radiation still occurs; thus, the silvered coating is intended to reflect the bulk of the radiation back into the contents. The top cover is typically a lightweight foam plug.

Dewar tests are commonly used for liquids, but one of the earliest devices was developed by the Bureau of Mines in the 1920s for the studying of coal[190]. A 4 L Dewar was filled with oil and in the center was inserted a small glass tube holding 35 g of coal sample. The tube also contained one junction of a thermopile, with the other end being immersed in the oil. The oil bath also contained a heater and a stirrer, with a temperature controller operating the heater so as to maintain very close to zero temperature difference between the coal sample and the enveloping oil bath. The system could maintain an accuracy of 0.15ºC per hour. Thermal explosion theory was not yet developed at that time, so the authors did not analyze their results in the context of a theory.

While the heat losses from a Dewar flask are low, they are high enough that they must be explicitly modeled. It is assumed that the temperature of the liquid within the Dewar flask is uniform. This allows analysis according to Semenov theory. For a small flask, it would seem to be a reasonably accurate assumption, but no error analysis exists. If the substance in the flask is at a uniform temperature, then the cooling of the flask can be represented by a lumped capacitance model. In that case, the only resistance to heat transfer is at the boundary via the convective heat transfer coefficient h_c. If the ambient temperature is T_o and the initial temperature of the Dewar's contents is T_i, then the temperature of the contents at any time t is T, given by:

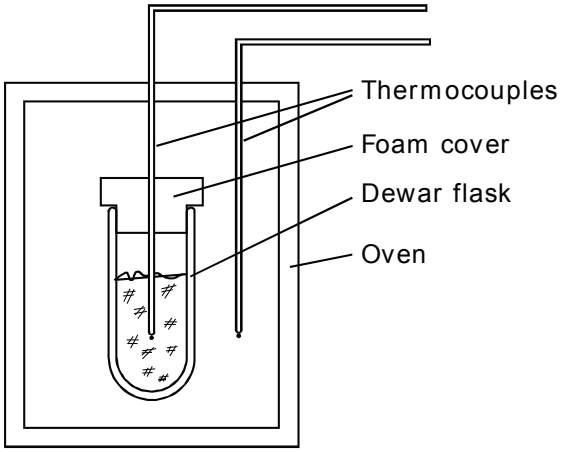


Figure 35 Dewar flask test
(Copyright Elsevier Science, used by permission)

$$T - T_o = (T_i - T_o)\exp\left[-\frac{h_c S}{\rho V C}t\right]$$

where S = surface area, ρ = density, V = volume, and C = heat capacity. It is not necessary to determine all of the factors within the exponential separately, however. Heat losses from Dewars are normally characterized by the half-time $\tau_{1/2}$, that is, the time it takes for a substance to cool to half its original temperature elevation above ambient. Experimentally, a hot liquid (commonly, a low heat capacity substance such as dimethyl phthalate) is poured into the Dewar and its temperature monitored. When $T - T_i$ has dropped to $\frac{1}{2}(T_i - T_o)$, the half-time has been reached. The relation according to the above equation then gives:

$$\frac{h_c S}{\rho V C_p} = \frac{\ln(2)}{\tau_{1/2}}$$

and

$$T - T_o = (T_i - T_o)\frac{1}{2}\exp\left[-\frac{t}{\tau_{1/2}}\right]$$

Thus, $\tau_{1/2}$ is the only property of the Dewar that one needs to know in order to compute how the starting-point temperature decays over time. Values of $\tau_{1/2}$ for an 0.5 L Dewar flask may be on the order of 7 h.

The laboratory-scale results would be directly usable, without additional hypotheses or mathematical manipulation, if

the ratio $h_cS/\rho VC$ in the laboratory test were the same as in the large-scale. The surface/volume ratio S/V will, by definition, be much greater for a small-scale experiment. But since the (heat loss)/(heat generation) ratio actually goes according to $h_cS/\rho VC$, the role of the convective transfer coefficient h_c can be exploited. In a Dewar vessel convective losses are much smaller than the convective losses from a cube, sphere, etc. which is simply exposed to air. Thus, by using the low h_c of the Dewar, the high S/V ratio of the bench-scale experiment can be largely overcome, and the data—approximately at least—taken to be representative of large-scale conditions.

A rigorous analysis of the data according to Semenov theory can be done, as outlined in Chapter 10. But many chemical manufacturing processes involve a relatively short time for which the material exists in a heated state. Thus, time to thermal runaway is often the needed information, not a determination that thermal runaway can/cannot occur. For those cases, Grewer[72] suggests that results of adequate accuracy can be obtained simply by plotting $\log(t_{ig})$ on the y-axis and $1/T$ on the x-axis, where t_{ig} is the thermal runaway time (s) and T = temperature (K). The results should fall along a straight line and the maximum permitted temperature at any desired storage time can be picked off the plot. For comparing substances, the value ADT_{24} is commonly reported. This is the Adiabatic Decomposition Temperature for a 24 h period of exposure. It can be determined by simply reading the temperature at t_{ig} = 24 h from the graph. If the ρVC ('thermal mass') of the Dewar is not small in comparison to thermal mass of the sample, then a correction for the thermal mass of the Dewar may be needed before data are plotted. A more accurate treatment of the data can be made by using the Semenov ψ variable, as explained in Chapter 10.

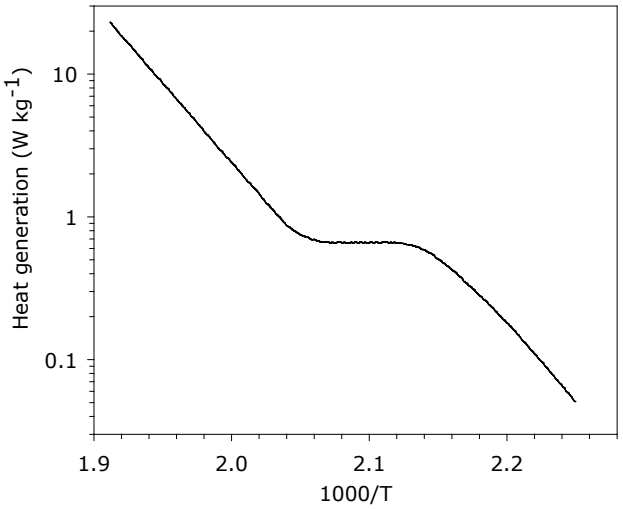


Figure 36 Ammonium nitrate (liquid) tested in the adiabatic storage test (note: this plot is presented using axes best suited for chemical interpretation, not the axes mandated by the test standard)

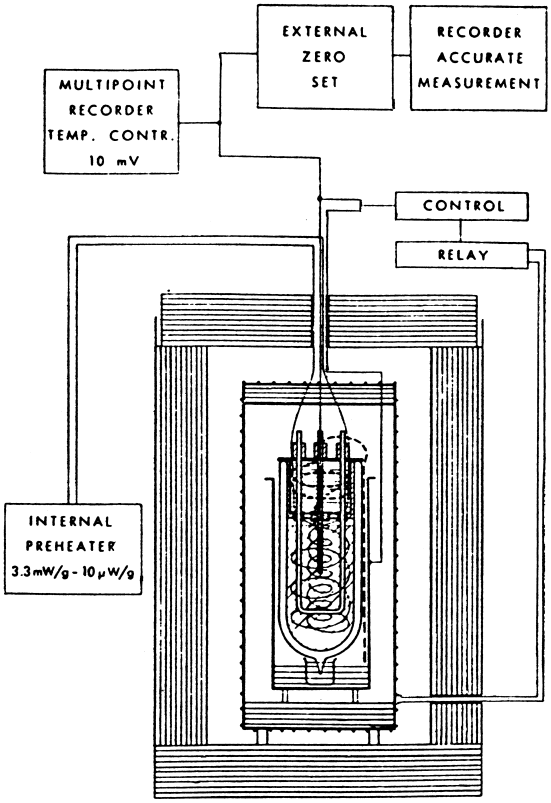


Figure 37 The adiabatic storage test
(Courtesy Elsevier Science, used by permission)

It is important to note that tests are expected to be destructive of the Dewar, so suitable safety precautions are needed in running Dewar tests. The walls of a Dewar flask are, of course, impermeable. Thus, difficulties would exist if a substance were tested where the self-heating reaction depends on atmospheric oxygen being supplied. Flow-through schemes can be arranged, but such gas flow is a non-adiabatic process, so complex corrections and calibrations can be necessary. In general, Dewar tests are only useful when the exothermicity comes from non-oxidative reactions.

A standard Dewar test method does not include any internal heaters. Some schemes have been described[191-193] where an internal heater is associated with the Dewar flask, in addition to the external oven. If properly controlled, a Dewar of this kind is effectively an adiabatic calorimeter.

UN Test H2—Adiabatic storage test

This apparatus comprises a 1.0 – 1.5 L Dewar, located inside a test oven and equipped with a feedback loop control to keep the oven with 0.1ºC of the Dewar contents (Figure 37)[194]. In addition, heating and cooling coils are placed within the specimen area—the former to rapidly bring up the substance to a desired starting point, the latter to help avoid an active explosion, if needed. The apparatus is first calibrated by passing known heating power into the sample

space and using the measured data to determine the heat capacity and the heat loss of the Dewar vessel and the heat capacity of the specimen. The actual testing is done by making numerous 24 h test runs at various temperatures. At each temperature, the heat generation Q_T (W kg^{-1}) is determined as:

$$Q_T = \frac{D(MC + H) - K}{M}$$

where D = rate of rise of temperature (K s^{-1}), M = mass of specimen (kg), C = heat capacity of specimen (J kg^{-1} K^{-1}), H = thermal mass (mass × heat capacity) of the Dewar (J K^{-1}), and K = heat loss (W). The heat loss term K is a temperature-dependent quantity and is obtained in a separate calibration procedure. The presentation of the data is done using the basic Semenov graph (Figure 3). The heat generation curve is simply values of Q_T, plotted as a function of the temperature T. The convective heat loss of the Dewar L (W kg^{-1} K^{-1}) is obtained using a separate test procedure, as described on page 405. Knowing this value of L, the heat loss line on the Semenov graph is plotted as a straight line of slope L and tangent to Q_T curve. The x-axis intercept of the heat loss curve gives T_o, which, upon being rounded to the next higher multiple of 5ºC, is defined in this test as the SADT. The sensitivity of the apparatus is about 10 mW kg^{-1}. An example of results from testing of ammonium nitrate[239] in the adiabatic storage test is shown in Figure 36 (the data in this figure are plotted not on a Semenov graph, but using axes that better illustrate the chemical reactions involved). Three regions are seen in the example graph. For temperatures < 200ºC (the sloping line corresponding to large 1/T values), the water formed from the decomposition reaction remains in the products. Over the range 200 – 220ºC, the water is boiled off; above 220ºC (the sloping line corresponding to small 1/T values), the water content remaining is nearly nil.

UN Test H4—Heat accumulation storage test

The test method is a Dewar test for liquids and wetted solids. An 0.5 L Dewar is used and it is stated that the heat loss characteristics of such a Dewar are similar to a 50 kg package of the intended commodity. The Dewar is inserted into an oven at a given temperature and it is noted whether the sample's temperature rises to 6ºC above the oven temperature during 1 week after the time when the sample's temperature first reached 2ºC below the oven temperature. The SADT is the oven temperature, to the nearest ºC, which turns out to be required to obtain the 6ºC rise within a week.

CALORIMETER TESTS

A calorimeter is any device for measuring energy in the form of heat, commonly heat produced in a chemical reaction. There has been a very wide variety of calorimeters invented, the best known being oxygen-bomb calorimeters used to determine heats of reaction, especially heats of combustion and heats of formation. The four most common calorimeter designs are adiabatic, isothermal, isoperibol, and heat flux meter. Figure 38 shows the basic features of an adiabatic calorimeter. It is based on the principle that, if there is no temperature drop across a body then there can be no heat flow through the body. In the case illustrated, this is the 'bomb,' which is a small vessel holding the sample. Since if $T_2 \equiv T_1$, there is no heat loss from the sample-holding vessel, this adiabatic condition can be created by heating the liquid bath into which the bomb is immersed. The two thermocouples T_2 and T_1 are connected to an electronic controller regulating the power fed to a heater immersed in the oil bath. A stirrer helps keep the oil bath temperature uniform. Practical devices are generally more complex; for instance, the sample bomb is commonly immersed in an inner liquid bath. The temperature measured by thermocouple T_1 is the temperature of the reaction taking place under adiabatic conditions.

Another common arrangement is the isothermal calorimeter (Figure 39). A sample undergoing a reaction can be forcibly maintained at a fixed temperature by cooling or heating it. Commonly, both an electric heater and a cooling device need to be provided. The latter may be a refrigerant loop or electrical cooling (Peltier effect) can be used. A rather sophisticated control circuit is necessary that can control the two devices. The reaction temperature always stays at T_1. The heat released is equal to the electric power consumed by the heater, minus any cooling power used.

For fundamental thermochemistry studies, the isoperibol (constant temperature bath) calorimeter is most commonly used (Figure 40). The bath liquid is generally water, and its temperature can be maintained by circulating it through a water chiller (not shown). Since finite heat transfer takes place between the specimen at T_1 and the water bath at T_2, a substantial calculational effort is needed to derive a corrected value of T_1 which represents adiabatic conditions. This type of arrangement is uncommon for the studying of self-heating materials' hazards.

In a similar vein, external conditions can vary widely if the heat flow from the specimen volume can be quantified and its temperature appropriately corrected. Devices based on this principle are known as heat flux meter calorimeters (Figure 41). The apparatus requires that the sample volume be surrounded by a material of accurately known thermal conductivity. A series of thermocouples are installed on the inner and the outer surfaces of this insulator layer and the heat losses computed using the Fourier Law. Once the heat losses are known, the sample temperature can be corrected to reflect adiabatic conditions.

For self-heating studies, determining the rate of reaction is essential. Thus, standard calorimeter devices which have been developed for measuring heats of reaction (total heat) must be extended to encompass a determination of rates, not just ultimate values. The most common devices which have been used in industrial practice are discussed below. DSC is also a calorimetric technique, but is discussed under

Thermal analysis techniques, below, since historically it evolved from earlier, non-calorimetric thermal analysis techniques and it is used as part of the general thermal-analysis tests toolkit. There are a number of scaled-up off-shoots of DSC developed solely for industrial safety studies and these are covered in the present Section.

The above discussion focused on device types and their differences. But it is also useful to consider the types of calorimetry data from a chemical point of view, irrespective of how they were obtained. These fall into three types:
(1) adiabatic
(2) isothermal
(3) not adiabatic and not isothermal.
The ultimate purpose of the isoperibol and the heat flux meter calorimeters is to produce adiabatic data, thus only adiabatic and isothermal data production has been discussed so far. Another type of data that is possible to collect is constant-rate-of-rise. A small sample may be heated in such a way that its temperature rises at a fixed rate. This principle is widely used in thermal analysis instruments.

ADIABATIC CALORIMETERS

An adiabatic calorimeter, by definition, is one where means have been taken to provide a volume from which no heat losses occur. A truly adiabatic condition, despite the nomenclature, is an impossibility, but relatively-low heat loss devices can be built. The first modern adiabatic calorimeter design to become widely used for self-heating studies was that of Raskin and Robertson[195] (Figure 42). Extensive data using this apparatus were reported by Gross and coworkers[196,197]. A later design by Güney and Hodges[198] involves an inner Dewar which contains the sample and a thermocouple. The inner Dewar is placed in an outer Dewar, with the space between being filled by a highly conductive oil. The space also contains a heater, a stirrer, and the reference junction for the specimen's thermocouple. The thermocouple is used to operate a temperature controller which controls the heater. A more recent form of guard-heater type of adiabatic calorimeter has been described by Kotoyori[199]. More modern devices used by the chemical manufacturing industry are individually discussed below.

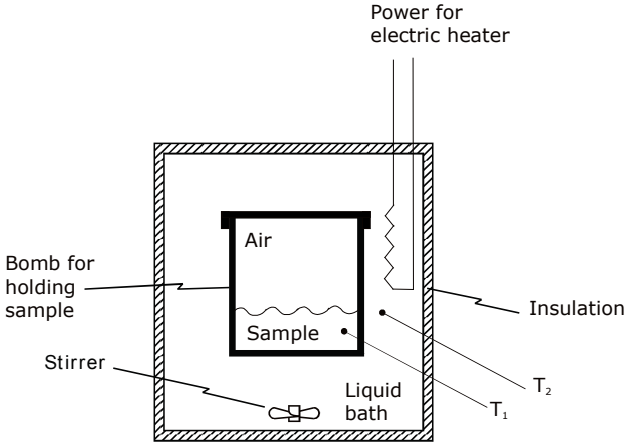


Figure 38 Adiabatic calorimeter (highly simplified)

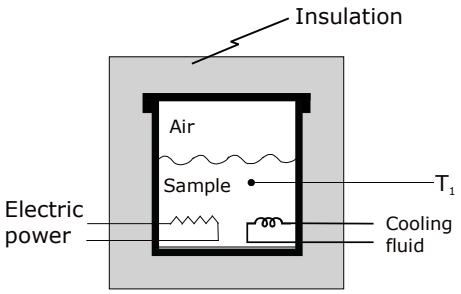


Figure 39 Isothermal calorimeter (highly simplified)

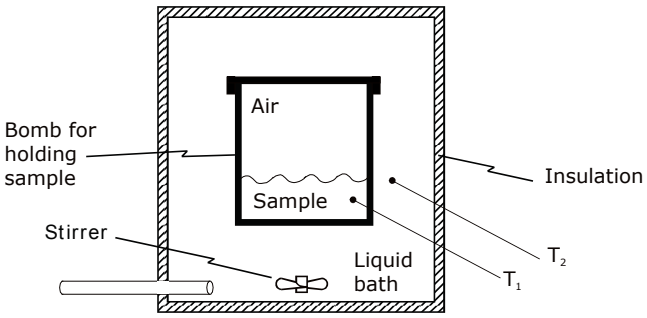


Figure 40 Isoperibol calorimeter (highly simplified)

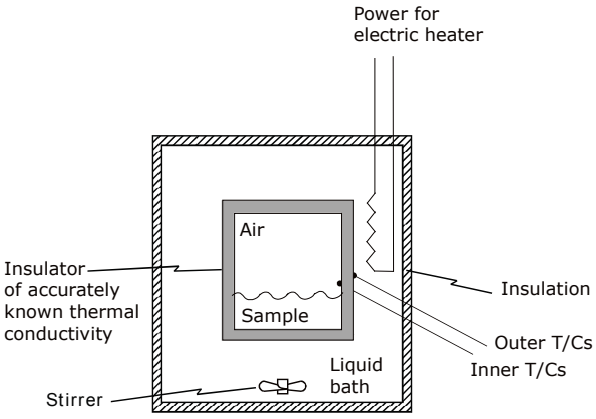


Figure 41 Heat flux meter calorimeter (highly simplified)

A proper analysis of an adiabatic calorimeter is quite complex, if thermodynamic errors are not to be committed. One immediate problem is that many industrial self-heating situations involve constant-pressure systems, and are not operated in closed-volume devices. The concept of an adiabatic system is easily applied only to closed systems. It can also be applied to a system which is leaking mass to the outside (due to thermal expansion), but in practice this is difficult, since accurate measurements of the convective outflow have to be made. Adequately accurate studies can be made in a closed, adiabatic calorimeter, if mass and heat balance terms are not simplified willy-nilly. Yin[200] gave a systematic derivation of the equations for an adiabatic calorimeter.

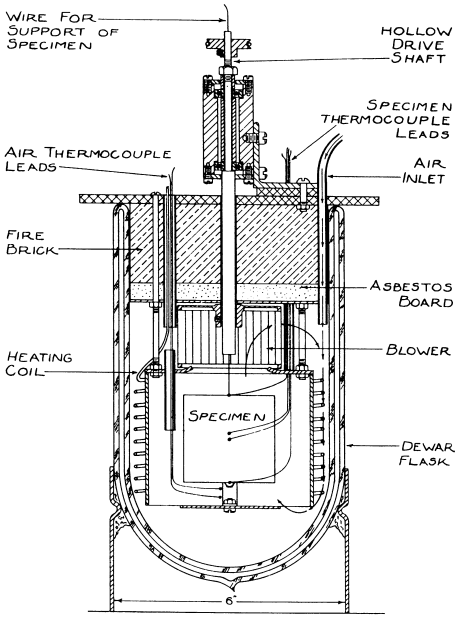


Figure 42 The adiabatic calorimeter of Robertson and Raskin

He also discusses the simplifying assumptions that are usefully made to render the problem tractable. Thus, it is often assumed that the heat capacity C_{vi} for any given chemical species i is independent of temperature and that change of the effective system heat capacity as the reaction takes place is zero:

$$\sum_i \nu_i C_{vi} = 0$$

where the summation is over all the species, both reactant and product. ν_i denotes the number of moles of substance i and is taken positive for products and negative for reactants. Note that if the number of moles in the system does not change as the reaction takes place, then automatically $\sum_i \nu_i \equiv 0$ and the above relation is satisfied. Many reactions are of this type, but others, of course, are not. In addition, it is assumed that only a single reaction takes place, that the reaction goes to completion, and that its reaction rate is:

$$\frac{dC_A}{dt} = k(T)\nu_A C_A^n$$

where concentration of the single reactant is C_A (mol m^{-3}); $k(T)$ = reaction rate constant (mol^{1-n} m$^{3(n-1)}$ s^{n-1}); ν_A = moles of reactant = moles of product; and n = the order of reaction (--). Then, a relatively simple equation is obtained for the rise in temperature of the system:

$$\frac{dT}{dt} = -\nu_A k(T)\left[\frac{T_f - T}{T_f - T_o}\right]^n \left(T_f - T_o\right) C_{Ao}^{n-1}$$

The ultimate temperature rise is:

$$T_f - T_o = \frac{\Delta U(T_o)\, C_{Ao}}{\nu_A \sum_i \left(C_{io} C_{vi}\right)}$$

where the subscript o denotes initial condition, thus, the summation over i includes all the components present at the start of the reaction, that is, both the reactants and the inerts. The inerts include any vessel in which the reactant is situated and, in Yin's formulation, its role is defined systematically, not as an arbitrary correction. The heat of reaction, $\Delta U(T_o)$ is obtained as:

$$-\Delta U(T_o) = \frac{\sum_i N_{if} C_{vi}}{\left(N_{Af} - N_{Ao}\right)/\nu_A}\left(T_f - T_o\right)$$

where N = number of moles; f denotes final (i.e. the state of the products); and i again is to be summed over reactants, products, and inerts. But it was already assumed that no reactants remain at the end of the reaction, the summation is only over the products and the inerts, and likewise $N_{Af} \equiv 0$ in the denominator.

In reality, a large fraction of studies in 'adiabatic' calorimeters are found in the literature where no thermodynamic rigor can be perceived and ill-defined systems are treated in a very casual way. Thus, one commonly finds a development of the following sort. It is assumed that the fraction of mass leaving an open system can simply be ignored and a heat balance performed on the portion that has not departed. In that case, the heat released by chemical reaction goes solely to raising the temperature of the sample and a heat balance gives:

$$C_p \frac{dT}{dt} = QAe^{-E/RT}$$

Since a vessel is present in the system, apart from the chemical reactants, it is then assumed that the mass of the vessel (commonly the inner liner of a Dewar) is also being raised to the same temperature. Thus,

$$\left(W_s C_{ps} + W_d C_{pd}\right)\frac{dT}{dt} = W_s QAe^{-E/RT}$$

where W_s = mass of specimen (kg), W_d = effective mass of Dewar that is being heated (kg), and the subscripts on C_p refer to specimen and Dewar. In reducing the data, $\ln(dT/dt)$ is plotted as a function of $1/T$. The slope of the line is $-E/R$, giving a value for E. The y-axis intercept is $\ln(QA/C_p)$ and from that a value of QA/C_p can be found. The data analysis procedure is only started when the specimen's temperature first equals that of the calorimeter. Substances which show autocatalytic reactions need a different treatment; as discussed by Grewer[72]. Empirically, autocatalytic behavior can be identified if, at the moment the specimen's temperature first reaches the calorimeter temperature, an exponential rise occurs, with no period of linearly-increasing temperature rise. Bowes[201] cautions that results of adiabatic calorimeter testing for specimens showing autocatalytic or parallel reactions can easily be misinterpreted, leading to unconservative predictions. He considers that isothermal methods should be used, instead, if there is any concern about this issue.

Another way that adiabatic calorimeter data are applied to practical problems is to plot the $\ln(t_{ad})$ on the y-axis and $1/T$

on the x-axis. If the reaction is not autocatalytic, the results will form a straight line with the slope $+E/R$. In many cases, the question to be answered is: Can this substance be kept safely for t time at T temperature? Since actual safe storage time will be greater than t_{ad}, simply extrapolating the results to the desired temperature and checking if the t_{ad} at that temperature is greater than the needed t can suffice.

ISOTHERMAL CALORIMETERS

Isothermal calorimeters, especially microcalorimeters, are a well-established tool of thermochemistry for studying Q, the heat of reaction. This does not suffice to pin down all of the needed problem variables, but a direct measurement can often be helpful. The measurement output of a microcalorimeter at any given temperature is a curve of 'specific power,' i.e., power/mass (W kg^{-1}), as a function of time. An instrument of modern design has been described by Nordon[202], who also reviewed some design history of earlier instruments. The method has only occasionally been applied to engineering studies of self-heating, see Tharmalingham[203] and Jones[204,205]. Jones suggested that microcalorimeter data can be used directly, as a routine go/no-go acceptance test, once the kinetic variables have been established for a particular chemical substance by other means. At any given temperature T_o, according to F-K theory, q, the specific power measured by the instrument is:

$$q = QAe^{-E/RT_o}$$

Thus, in his scheme, a value of q_c, the critical HRR per mass (W kg^{-1}) is first determined as:

$$q_c = \frac{\delta_c \lambda R T_o^2}{\rho E r^2}$$

where T_o is the critical ambient temperature for a given value of the radius, r. The evaluation process then simply involves measuring q in the microcalorimeter and determining whether or not $q < q_c$.

ARC AND APTAC TESTS

For the analysis of certain substances, it is important that the combustion products be retained in a constant-volume cavity. Thermal analysis equipment can use closed specimen cells, but these are typically not suited to explosive substances. Another limitation of DSC equipment was that, in the 1970s, the best DSC apparatuses had a resolution limited to about 20 W kg^{-1}; for certain reactions, however, it is necessary to probe lower values. The Accelerating Rate Calorimeter (ARC) was invented in 1978[206] by Townsend and Tou of Dow Chemical Co. to address these limitations. It was specifically developed for industrial screening, rather than fundamental research purposes, so the basic mode of operation was designed to allow rapid, unattended testing.

The ARC (Figure 43) comprises an oven in which is placed a spherical metal bomb. Unlike thermal analysis apparatuses, which are programmed only at one rate of rise, the ARC uses electronics which control the temperature in a 'heat-wait-search' mode (Figure 45). A starting temperature is programmed and the instrument heats up to this temperature, then holds the temperature. The reaction rate is monitored, and, if the rate is too small, the controller heats up to a higher temperature, and again holds that value. The reaction rate is monitored, and the process is repeated for as many steps as required. When the first temperature is found at which a pre-set minimum reaction rate occurs, the instrument then goes into adiabatic mode and tracks the HRR as a function of temperature from that 'final starting point.' Any 'adiabatic' apparatus based on a guard heater principle has a maximum rate at which the reaction can proceed so that control is not lost; for the ARC, it is 15ºC min^{-1}. Under poorly-selected test conditions, the adiabatic limit of the instrument may be exceeded; thus, the raw data must be examined to make sure that that the process has stayed within control. The standard bomb is a 25 mm sphere loaded with 5 – 10 g of sample, although variant bombs are available. A single test takes about 1 day to complete. The ARC test is only suitable for self-reactive substances; the specimen does not have access to air, and therefore it would not be a suitable test for self-heating substances where the exothermicity is caused by oxidation in air. Some of the advantages and limitations of the ARC method have been reviewed by Coates[207].

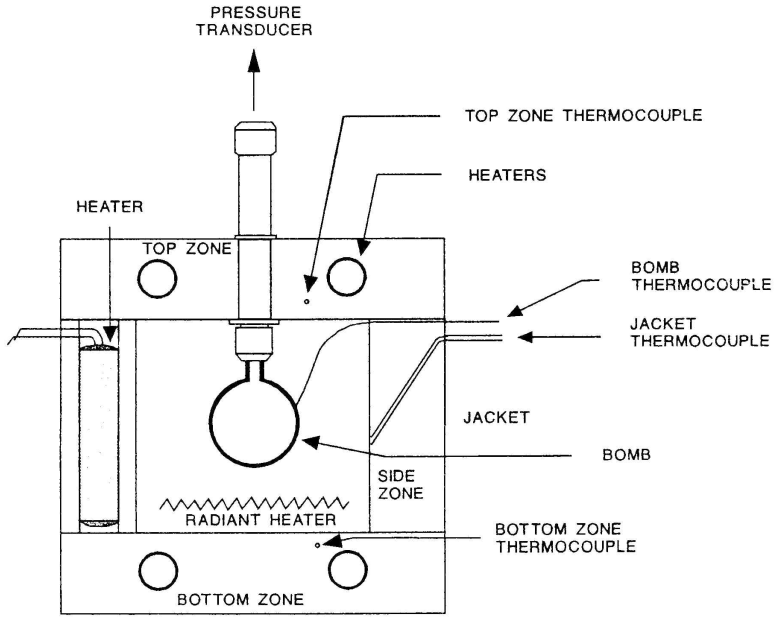


Figure 43 The ARC apparatus
(Copyright Elsevier Science, used by permission)

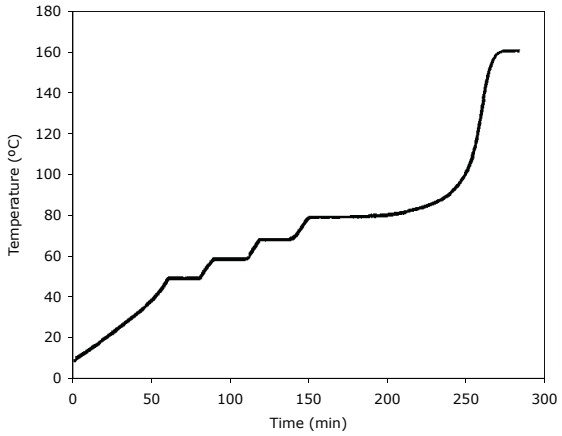


Figure 44 Example of a testing regime used in the ARC
(Copyright Elsevier Science, used by permission)

The success of the ARC test motivated Young and Chippett[208] at Union Carbide Corp. to develop an improved apparatus termed the APTAC, Automatic Pressure Tracking Adiabatic Calorimeter (Figure 45). They saw that the need for a low thermal mass of the vessel and the ability to withstand high reaction pressures were not incompatible requirements, if the outside of the reaction vessel was pressurized. The differential pressure across the reaction vessel walls then becomes small and thick walls were not needed. The basic operating scheme is the same 'heat-wait-search' mode used in the ARC, although more sophisticated monitoring and control instrumentation is fitted. The APTAC is rated to stay in control up to 400ºC min^{-1}, which is a major improvement on the ARC.

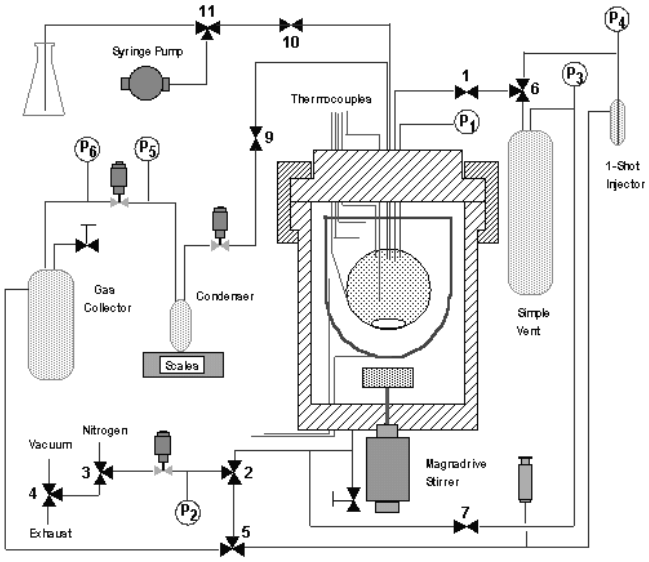


Figure 45 Cross-section view of APTAC
(Courtesy TIAX)

The presentation of the data from the ARC that was developed by Townsend and Tou has been followed by most later users of the equipment, but unfortunately the nomenclature adopted is confusing. In heat transfer theory, the term 'thermal inertia' denotes the product: thermal conductivity × density × heat capacity. Townsend and Tou, however, defined *thermal inertia* as Φ:

$$\Phi = 1 + \frac{M_b C_{vb}}{M C_v}$$

where M = mass, C_v = heat capacity, the subscript b denotes values for the bomb, while the quantities without subscript refer to the sample. The heat capacity used is constant-volume, since the experiments are run in a fixed volume. Unless it is already known, the needed value of the sample heat capacity is obtained by using a DSC instrument. The quantity Φ, in fact, represents the 'inefficiency' of the calorimeter, or the total energy divided by the energy that goes into heating the specimen alone. Wilberforce[209] has more correctly termed it the *thermal dilution factor*. If the bomb had zero mass, then $\Phi \equiv 1$. The values of the measured temperature rate of rise dT/dt, or $\dot{T}$, are multiplied by Φ in order to obtain the true $\dot{T}$. In ARC terminology, the critical ambient temperature T_o is termed the *self-accelerating decomposition temperature*, T_{SADT}, while the critical stacking temperature, T_c, is termed the *temperature of no return*, T_{NR} (see Figure 46).

If Semenov theory is used (see Chapter 4), then the two temperatures are related according to:

$$T_{NR} = T_{SADT} + \frac{RT_{NR}^2}{E}$$

In an adiabatic system, the heat balance equation is:

$$\rho C_v \frac{dT}{dt} = Q\rho A e^{-E/RT}$$

Therefore,

$$\frac{dT}{dt} = \dot{T} = \frac{QAe^{-E/RT}}{C_v}$$

Now, the equation for the adiabatic induction period t_{ad} was earlier shown to be:

$$t_{ad} = \frac{C_v RT^2}{QAE} e^{+E/RT}$$

So substituting the value of $\dot{T}$ into this expression gives

$$t_{ad} = \frac{RT^2}{E}\frac{1}{\dot{T}}$$

In the ARC scheme, the experimentally-found quantity is the peak value of the rate of temperature increase, i.e., the peak $\dot{T}$. Zero-order Arrhenius kinetics would predict an ever-increasing rate of temperature rise until reactants are exhausted; at that point, reaction rate would immediately go to zero. The only reason that a peak is seen, followed by a diminished reaction rate, is that zero-order kinetics is not being obeyed. In ARC measurements, the *time to maximum rate*, TMR, or t_{MR}, is taken to be the same as t_{ad}. Clearly,

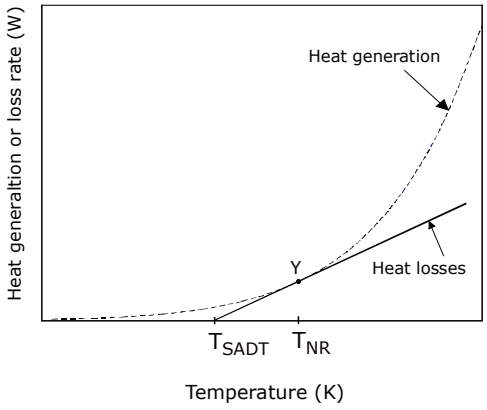


Figure 46 Nomenclature used in ARC testing

this is some form of approximation, since reactant depletion does not enter into the definition of t_{ad}, while t_{MR} could not exist, were it not for reactant exhaustion. Be that as it may, the experimental data are treated by plotting $T^2/\dot{T}$ on the x-axis and t_{MR} on the y-axis; the slope of the line gives R/E.

The energy of the reaction is determined as:

$$\Delta u = \phi \overline{C}_v \Delta T$$

where Δu = energy of reaction, per mass of reactant (J kg^{-1}), $\overline{C}_v$ = constant-volume heat capacity, mass-averaged for the sample and the bomb (J kg^{-1} K^{-1}), and ΔT = ultimate temperature rise (K). The resultant expression can be given in mole, instead of mass, units upon dividing by the molar mass. Reaction enthalpy Δh (J kg^{-1}) can be obtained as:

$$\Delta h = \Delta u + \frac{V \Delta P}{M}$$

where ΔP = pressure change within the bomb (Pa), V = volume of the bomb (m^3), and M = specimen mass (kg).

Since the order of the reaction n is not necessarily $\equiv$ 1, the general relation for reaction rate:

$$\frac{dc}{dt} = -kc^n$$

can be used. The kinetic constants are obtained from the ARC data by noting that the temperature rate of rise is expressible as:

$$\dot{T} \frac{(\Delta T)^{n-1}}{(T_f - T)^n} = A c_o^{n-1} e^{-E/RT}$$

where T_f = the ultimate value of T. By taking logarithms it can be seen that:

$$\ln\left[\dot{T} \frac{(\Delta T)^{n-1}}{(T_f - T)^n}\right] = \ln\left(A c_o^{n-1}\right) - \frac{E}{RT}$$

Thus, by plotting $1/T$ on the x-axis, and the left hand side of the above equation on the y-axis, a line of constant slope $-E/R$ will be found, if the value of n chosen was the correct one. The procedure thus entails trial-and-error plots using various values of n, with n = 1 being a reasonable starting place. When a straight line is found, the value of E is obtained from the slope of the line. The y-axis intercept is $\ln\left(A c_o^{n-1}\right)$ and, from that, the value of A can then be obtained. A substantially different data reduction technique was presented by Huff[210], where kinetic constants are not obtained, but scale-up to the real-scale problem is directly computed.

The ARC technique is not appropriate if a reaction is multistage or autocatalytic, and incorrect conclusions may be drawn from testing such materials[49]. Explosives expert Raymond Rogers[211] strongly cautioned that "the ARC has serious limitations and gives spurious results" when applied to solid explosives or propellants.

Even though it is not one of the UN tests, the ARC has received a lot of industrial use as a simple, quick tool for estimating the SADT that is required under the UN regulations. The original ARC apparatus had a sensitivity of 0.5 – 1.0 W kg^{-1}, and this was not adequate to estimate SADT values without extrapolation. Even with extrapolation, it has been found that SADT values are close to those of the official tests *on the average*, but with substantial plus and minus deviations. Thus, newer apparatuses having a sensitivity of 0.1 – 0.25 W kg^{-1} are considered to be necessary for acceptable predictions[213]. By contrast, it is estimated that the sensitivity of a typical DSC current-day apparatus is around 5 W kg^{-1}. Thus, if for screening purposes, the temperature of 'onset of reaction' is reported, values determined with the ARC are typically 50 – 100ºC lower than a comparable measurement with DSC. However, it must be re-iterated that the thermal stability problem contains three main variables: size, temperature, and time; focusing in on one of them to the exclusion of the other two cannot give a sound procedure. Industrial safety philosophies exist which deem it sufficient to use some convenient apparatus for obtaining an 'onset of reaction temperature,' then apply the results to industrial processes without considering size/time issues, but merely obtaining a 'safe working temperature' by decreasing the 'exothermic onset temperature' by some rule-of-thumb value such as 100ºC. Needless to say, the realism of this kind of approach is not reassuring[212].

A general technique for estimating the SADT from results in two different apparatuses having distinctly different heat loss characteristics has been presented by Whitmore and Wilberforce[213] who proposed a technique which involves using two apparatuses such as DTA, ARC, TAM, etc. Each apparatus is characterized by its own value of Φ, taken as Φ_1 and Φ_2. The heat capacity C of the substance can be computed in either apparatus. Also, in each apparatus the self-heat rate $\dot{T}$ (K s^{-1}) is experimentally determined at the temperature T of the onset of exothermicity. The specific power P (W kg^{-1}) is computed for both apparatuses according to:

$$P = \dot{T}\Phi C$$

An apparent activation energy E is computed as:

$$E = \frac{RT_1T_2}{T_1 - T_2}\ln\left(\frac{P_1}{P_2}\right)$$

The times to maximum rate at each T are computed as:

$$t_{MR} = \frac{RTC}{PE}$$

The values of t_{MR} are then plotted against $1/T$. The time constant of the package $t_{1/2}$ is then located along the t axis and from this a value of T pertinent to the desired package is found. This is the estimated SADT. The authors state that even though the method implicitly conforms to Semenov theory rather than Frank-Kamenetskii theory, it has been found to be accurate for solids, not just liquids.

OTHER INDUSTRIAL REACTION CALORIMETERS

Already in 1949 a reaction calorimeter was developed at VTT[214]. This apparatus was used to determine the heat released when air is bubbled through 20 g of substance held at 100ºC for 1 h. It was, effectively, an improvement over a 1905 test by Proctor and Holmes[215]. Using this device, it was found that the worst product, a linseed-oil based varnish, showed a heat of reaction of 250 kJ kg^{-1}, with various other paints and varnishes showing lower values. The method did not yield usable results for cellulosic products, since exotherms could not be detected at 100ºC.

Despite the long history of reaction calorimeters, the devices in current industrial use are all relatively recent inventions. Devices of some popularity within the chemical manufacturing industry include the Ciba-Geigy/Mettler reaction calorimeter; the PHI-TEC adiabatic calorimeter; isothermal microcalorimeters (heat flux calorimeters) such as the Setaram C80 and MS80, the Hart heat flux calorimeter, or the Thermal Activity Monitor (TAM) by ThermoMetric AB; the reflux heat flow calorimeter[216]; and the Fauske/Fike VSP (Vent Sizing Package). The reflux heat flow calorimeter is designed to study reactions near their boiling point, while the VSP is an adiabatic calorimeter which is intended to study liquids with a high potential of explosion. An advantage of some of these devices is their very high sensitivity. For example, the Hart heat flux calorimeter can detect a temperature rise of about 10^{-6} ºC min^{-1}, while an ARC may detect 0.01ºC min^{-1}, and a standard DSC no better than 0.1ºC min^{-1}. Sun et al.[217] demonstrated that quite misleading data can be reported if the sensitivity of the instrument is not sufficient for the substance being studied. Their study is especially interesting since it was based on a substance which led to an industrial spontaneous combustion accident. A highly sensitive instrument might be thought necessary when huge quantities are assembled of a substance that has only minimal self-heating tendencies. But the amount in the accident was moderate—a 220 L drum—yet the ARC method gave results very much different from the more sensitive C80 apparatus.

Many reaction calorimeters are operated in a similar stepwise manner as is the ARC. A temperature is selected and held for a few hours until a steady heat flow (mW) reading is obtained. A higher temperature is then selected, and the process is repeated. From the stepwise curve, a table of temperature vs. heat flow can then be created. Once this is done, Yu and Hasegawa[218] suggest that reaction calorimeter data be analyzed by allowing the reaction to have a to-be-determined order n:

$$\dot{q} = QAW^n \exp(-E/RT)$$

where $\dot{q}$ = heat flow (W), Q = heat of reaction (J kg^{-1}), A = pre-exponential factor, W = mass (kg), E = activation energy (kJ mol^{-1}), and T = temperature (K). If n =1, then the units of A are s^{-1}. Taking logarithms of both sides and restricting consideration to the initial stage of the reaction, when the mass W is still close to the original mass W_o (i.e., ignoring depletion of reactants):

$$\ln(\dot{q}) \approx \ln(QA) + n\ln(W_o) - E/RT$$

Thus, by plotting $\ln(\dot{q})$ on the y-axis versus $1/T$ on the x-axis, the value of E can be obtained from the slope, which is $-E/R$. Tests are then run at a single temperature, but for different mass loadings W_o. By plotting this second batch of results as $\ln(\dot{q})$ on the y-axis versus $\ln(W_o)$ on the x-axis, the slope obtained is n, the order of the reaction. Furthermore, if the y-axis intercept on this second graph is denoted as Y_i, then QA is obtained as:

$$QA = \exp\left(Y_i + \frac{E}{RT}\right)$$

These results are then applied to determining T_{NR} and T_{SADT} for the package size under consideration. Using Semenov theory, the value of T_{NR} is obtained by a trial-and-error solution of:

$$\frac{E}{RT_{NR}} - 2\ln\left(\frac{1}{T_{NR}}\right) + \ln\left(\frac{h_c SR}{QAW_o^n E}\right) = 0$$

where h_c = convective heat transfer coefficient (W m^{-2} K^{-1}), and S = surface area of package (m^2). The surface area will be known, while the convective heat transfer coefficient has to be measured or estimated. Finally, the value of T_{SADT} is determined from:

$$T_{SADT} = T_{NR} - \frac{RT_{NR}^2}{E}$$

Yu and Hasegawa point out that reactant depletion can indeed be ignored if the instrument is properly operated at sub-critical temperatures low enough that the mass lost during the test is less than 1%.

THERMAL ANALYSIS METHODS

Thermal analysis methods are, by definition, any of a variety of techniques where small amounts of substance are subjected to a specific temperature or temperature regime and their properties measured. The techniques originated in the 19th century, but only became popular after World War II, being used most extensively in the polymer industry. Some

thermal analysis methods are intended to be used only in qualitative, indicative ways. But other thermal analysis methods are intended to determine the relevant reaction chemistry variables E, A, Q, and possibly other variables (depending on what the detail level of the solution being sought is). Because the amount of specimen used and sensitivity of the different instruments are widely disparate, this effectively means that the operating range in which a specimen will be studied will perforce differ for the different instrument types. The unfortunate consequence of this is that, with many substances, the values reported for E, A, and Q depend on the instrument that was used. Jones[219] reported results on peat where it was illustrated how going from an instrument using large samples to a microcalorimeter decreases the apparent value of E. Some thermal analysis methods are calorimetric, but for convenience, discussion of all the methods is grouped together in this section.

For any reduced-scale test method, validation must be available if credence is to be placed in the method's ability to predict the real-scale situation. With thermal analysis methods, a few reports for a few substances exist in the literature comparing the results to other types of tests. But, in general, it must be considered that—for any of the thermal analysis methods—validation is unavailable and may be impossible. The methods are highly sensitive to experimental technique, to data-reduction procedural details, and to the assumptions of reaction chemistry. Larger-scale methods such as oven-basket testing are often somewhat tolerant towards violations of their underlying assumptions, e.g., the unanticipated presence of autocatalytic reactions. But with the micro-scale thermal analysis methods, any experimental work that uncovers something other than a single, simple, Arrhenius-form reaction leads to a situation that not even a framework exists for extrapolating results to the real-scale environment. And unfortunately, few substances of self-heating interest exist where thermal analysis results *do not* show such complications. Thus, the recommendation has to be that these methods are suited only for preliminary screening purposes; to obtain credible quantitative predictions of real-scale behavior, larger-scale tests must be run.

DTA, DSC, AND RELATED TECHNIQUES

It is possible to obtain the necessary variables (E, A, Q, and C, although not λ, if the latter is also needed) from thermal analysis techniques. Thermal analysis apparatuses of interest here are ones designed for monitoring the production of heat, or the loss of mass, of a tiny sample. The techniques include TGA (thermogravimetric analysis), DTA (differential thermal analysis), and DSC (differential scanning calorimetry). All use milligram samples (ca. 5 mg) of substance and expose it to heating conditions where the entire sample is essentially at a single temperature. Because of the small amount of sample tested, the accuracy of measurements are limited. Furthermore, while DSC is a calorimetric technique, it is not a calorimetric technique which has been optimized for producing results of the highest precision. Thus, thermal analysis techniques are more likely to be used for rough estimating purposes, rather than as best-possible sources of data.

TGA is of limited applicability to the self-heating problem; since heat is not being measured, only E and A, but not Q or C can be deduced. Using DTA or DSC, all four variables can be determined. DTA normally requires that a reference material be used which has nearly-identical heat capacity to the test specimen. This is relatively easy to arrange for some liquids, but difficult for most solids. DSC testing is the most versatile and has the fewest limitations, thus this is the preferred thermal analysis technique. The only drawback is that the equipment may be more costly.

Obtaining reasonably reliable self-heating information from thermal analysis techniques usually requires a degree of chemical expertise and a substantial analysis effort. Thus, if other screening techniques are viable (e.g., if sufficient sample exists for Dewar tests), these may be preferred as a more direct source of guidance. Bowes[10] provides a good example of using thermal analysis to obtain self-heating data on the explosive dioxyethylnitramine dinitrate (DINA). When thermal analysis results are obtained on a sample, they may show (1) a single, definite peak; or (2) multiple peaks or other complicated features. In the former case, results may be directly applied as input data to F-K or Semenov theories. In the latter case, the appropriate course of action is either to begin an extensive investigation of the material's chemical nature, or else to turn to techniques which require less interpretation: optimally, full-scale testing, if not, then FRS-style oven-basket testing. Kubler[220] noted that results obtained from any thermal analysis techniques that use only small quantities of sample may be intrinsically misleading for certain categories of substances. With a very small sample, gases released during pyrolysis escape freely from the test cell, but for some substances the initial reaction step of generating the volatiles is endothermic, while subsequent reactions among the gaseous products, or between the gaseous products and the residual solid, are exothermic. This error would not occur with apparatus designs where heating takes place in a closed cell, but the latter arrangement is common only in laboratories studying explosive substances.

When running thermal analysis tests, most users will follow one of the ASTM standards discussed below. Apart from these standards, a few other analysis techniques exist. For TGA data, Flynn and Wall[221] conducted an extensive review of data reduction techniques and one of their methods has been adopted in ISO 11358-2[222]. For DTA data, the data reduction technique of Borchardt and Daniels[223], later elaborated by Reed et al.[224], is normally used.

Various researchers have sought non-isothermal methods for determining the kinetic parameters of a reaction without

any assumptions about the reaction order or the form of the rate law beforehand. These attempts at 'model-free kinetics' usually rely on *differential* methods of analyzing data obtained from constant heating rate experiments, e.g., change in peak reaction rate temperature with heating rate. The drawback to the differential approach is the assumption that the peak reaction rate temperature corresponds to a particular extent of conversion*, typically ½. *Integral* methods obviate this need by allowing the extent of conversion to be determined experimentally from the partial areas of the reaction rate versus time (temperature) curve. Although more general and accurate, integral methods have been less popular because an exact, closed-form (analytic) solution of the Arrhenius integral does not exist, necessitating the use of cumbersome series approximations. Lyon[225] proposed an integral method which gives both E and A using the following procedure. It starts with a simple new approximation for the Arrhenius integral:

$$\int_{T_o}^{T} e^{-E/RT'} dT' \approx \frac{RT^2}{E+2RT} e^{-E/RT}$$

In his approximation, the lower limit is ignored since, in practical cases, at the starting (room) temperature of T_o, $E/RT \ll E/RT_o$. Compared to the numerical solution, he shows that the error is less than 1% when $E/RT > 10$. Practical values of E/RT might span from 5 to 100, and even for $E/RT = 5$, errors are less than 4%. Using this approximation, Lyon obtains

$$E(\alpha) = -R\left[\frac{d\ln\beta}{d1/T(\alpha)} + 2T(\alpha)\right]$$

where β (K s^{-1}) is the heating rate, and α is the conversion fraction. The method then depends on: (1) numerically integrating and normalizing the reaction rate data obtained at different heating rates to obtain α as a function of temperature; (2) determining several 'iso-conversion' (i.e., constant α) temperatures, $T(\alpha)$, at each heating rate β; (3) plotting the $(T(\alpha), \beta)$ data pairs for each α as $1/T(\alpha)$ on the x-axis and ln β on the y-axis. The slope of the curve, $d\ln\beta / d1/T(\alpha)$, at each $T(\alpha)$ is incremented by $2T(\alpha)$ and the total multiplied by the gas constant R to obtain the global activation energy for the reaction at a particular conversion $E(\alpha)$. The incipient temperature at complete conversion $T(\alpha = 1) \equiv T_\infty$, is determined for a series of heating rates β from the numerically integrated and normalized reaction rate data. In practice, T_∞ is the temperature at which the partial area under the reaction rate versus temperature (time) curve just equals the total area. The (β, T_∞) data pairs so obtained are plotted according to:

$$\ln\left(\frac{\beta}{T_\infty}\right) = \ln A - \left\{\ln\left(2 + E/RT_\infty\right) + \left(E/RT_\infty\right)\right\}$$

which is a linear equation of the form $y = a - bx$, with $y = \ln(\beta/T_\infty)$ and $x = \ln(2 + E/RT_\infty) + E/RT_\infty$. The global activation energy E is used as a fitting parameter to obtain unit slope (slope $b = 1$) and the pre-exponential factor is obtained directly as the intercept, $a = \ln A$.

DSC equipment can be operated in a temperature-scanning mode or in isothermal mode. Rogers[211] recommends that only the isothermal mode be used for explosives and similar unstable substances. If a DSC is operated in an isothermal mode, Rogers[226] showed that plotting ln (b) versus time will give a slope which is equal to $-A$, where b = chart deflection (arbitrary) and A = pre-exponential factor (s^{-1}).

Analysis becomes complicated when a liquid reacts to produce a gas and the depletion of the reactant cannot be ignored, since the masses and enthalpies of two different phases must be tracked. A technique has been developed[227] for producing kinetic data for reactions of this kind.

Users without a sufficient background in the subject matter sometimes feel that thermal runaway is precluded if thermal analysis techniques indicate that there is no detectable exotherm in the temperature region in question. Uehara et al.[228] provide a vivid example of the inappropriateness of this conclusion. In examining calcium hypochlorite, they found the first detectable sign of exothermic activity at 180ºC. Yet tests of a rather small (r = 191 mm) cylinder showed that thermal runaway occurred at 75ºC, some 105 degrees lower. The reason is because a DSC, being a device limited to milligram samples of material, cannot be made sensitive enough to detect the needed low values of reaction rate. To overcome the sensitivity limitation, apparatuses such as the ARC (see above) have been developed.

SIMPLE SCREENING TEST BASED ON DSC

In the most crude sense, DSC tests are sometimes used to simply identify whether exothermic peaks are located sufficiently above the working-temperature range of some chemical process or not. If the DSC peaks are located well above the working range, such reactions would be considered non-hazardous. This is not a robust screening strategy, however, since the indicated temperature at which exothermic peaks are found is not an absolute measurement, but is dependent on apparatus conditions, such as specimen size and heating rate. Furthermore, when comparative studies have been done it was commonly found that the exothermicity onset temperatures reported by DSC are not conservative. Thus, for initial screening of reactive liquids the current preference is for the running of ARC tests, instead.

While simple 'peak picking' using DSC is not a recommended screening test, an easy-to-use screening method has been proposed which is more usefully indicative. Hellmiss and Schwanebeck[229] recommend running a single DSC test in an air atmosphere. The heat of reaction Q_r is determined from the DSC curve (Figure 47) as follows:

$$Q_r = \frac{F}{m \cdot dT/dt}$$

* In reaction kinetics, 'conversion' means conversion of reactants into products, thus a conversion fraction of 0.5 means that 50% of the reactants have been consumed.

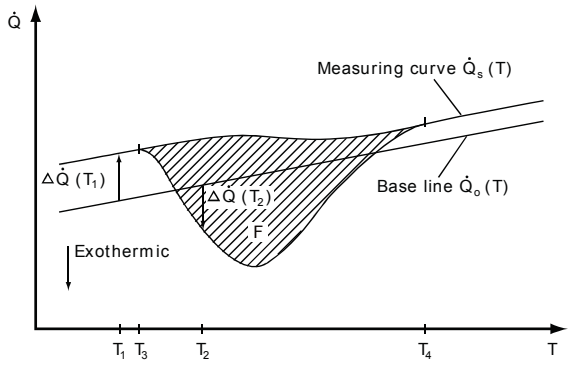


Figure 47 The parameters measured from a DSC curve
(Copyright ASTM International, used by permission)

where F = area under the curve (J K s^{-1}), m = specimen mass (g), and dT/dt = rate of heating (K s^{-1}). Note that for exothermic reactions, Q_r is a negative number. Endothermic reactions, i.e., those which show a positive deflection above the baseline, of course do not exhibit a hazard. If only endothermic peaks are found, no further evaluation of the self-heating safety need be done. The heat capacity C_p is determined as:

$$C_p = \frac{\dot{Q}_s(T_1) - \dot{Q}_o(T_1)}{m \cdot dT/dt}$$

where the quantity in the numerator (J s^{-1}) denotes the offset between the baseline $\dot{Q}_o$ generated with empty specimen and reference holders, and the baseline $\dot{Q}_s$ exhibited by the specimen.

The maximum temperature that could occur for an adiabatic self-heating specimen (that is, with zero heat losses) is:

$$T = T_o - \frac{Q_r}{C_p}$$

where T_o is the ambient temperature at which the substance will be stored. The principle of the screening method is then very simple. If the T computed above is small, say below 200ºC, then the material will not self-heat to ignition in a practical application, since losses will be present in reality and the true temperature will be lower. On the other hand, if the T computed is many hundreds of ºC, then the hazard is real and more detailed tests should be done to determine how large a pile can safely be stored.

QUANTITATIVE ASTM PROCEDURES

ASTM contains two types of recommendations for the use of thermal analysis data in evaluating self-heating substances. The first approach is a quantitative one, leading to simple predictions of the behavior of a real-scale substance. The standards involved for doing this are discussed in the present Section. In addition, ASTM also offers several methods for very rough screening, where no attempt is made to relate the results to the amount of the substance present (reminder: the amount of substance present is the single most important variable governing the self-heating potential). These very rough methods are discussed separately, below.

ASTM E 698

For quantitative estimation, ASTM provides the user with brief and basic experimental procedures for conducting thermal analysis tests using DTA or DSC equipment in ASTM E 698[230]. The standard recommends that hermetically-sealed containers or ampoules be used and that various heating rates β between 1 and 10ºC min^{-1} be used. The data reduction method of Duswalt[231] is recommended to obtain the activation energy and pre-exponential constant. The use of heating-rate corrections and non-linearity corrections is also explained. Doyle's method is described as an alternate. The ASTM standard presumes first-order kinetics and does not delve into a determination of the order of the reaction. The activation energy E is determined by plotting ln(β) on the y-axis and $1/T_p$ on the x-axis, where T_p = peak temperature (K). The slope of the line is $-1.08E/R$ and this gives the initial estimate of E. The approximation involves a numerical error of around 3%, and this can be reduced by performing a series of corrections to this initial value, based on the ratio E/RT. Knowing E/RT, where T is the value midway through the data set, a correction factor D is provided in a table. The next estimate of E is then $E = -\frac{R}{D}\frac{d(\ln\beta)}{d(1/T)}$. The method is predicated on the observation that the conversion fraction is constant at the peak of the reaction. A value for A is obtained from:

$$A = \frac{\beta E}{RT_p^2}^{+E/RT_p}$$

The test method also includes an additional procedure for cross-checking the values obtained.

ASTM E 793

Method E 698 does not include calculation of the heat of reaction, Q. Instead, ASTM provides a separate method for this, ASTM E 793[232]. It is suggested that a heating rate of 10ºC min^{-1} be used. The value is obtained simply by integrating the peak area and comparing the results to a reference substance.

ASTM E 1641

Within ASTM standards, there exists an alternative method for determining the values of E and A. ASTM E 1641[233] is based on the use of a thermogravimetric analyzer. However, since heats of reaction cannot be obtained from a TGA apparatus, most users will presumably find it more convenient to obtain both sets of data from a single apparatus. In the ASTM E 1641 method, E is determined essentially identically as in ASTM E 698. The value of A is found using Doyle's method[234], according to which:

$$A = \beta \frac{R}{E} \ln(1-\alpha) p(E/RT)$$

where $p(E/RT)$ is a tabulated function.

ASTM E 1231

The standard ASTM E 1231[235] is ASTM's procedure for using thermal analysis data as input into the F-K theory. It assumes that the user has obtained values of E and A from ASTM E 698, Q from ASTM E 793, and the thermal conductivity λ from any of a number of possible measurement techniques. Based on these input data, the critical size is computed by the standard F-K equation, without use of any corrections. The time to runaway conditions is estimated as being identically equal to the adiabatic induction period:

$$t_{ad} = \frac{C}{AQ} \frac{RT_o^2}{E} \exp\left(\frac{E}{RT_o}\right)$$

A value of the 'adiabatic decomposition temperature rise' T_{ad} is also computed as:

$$T_{ad} = \frac{Q}{C}$$

This is simply the temperature which a specimen would attain if all of the heat of reaction went into raising the specimen's temperature. This computation, of course, contradicts the assumptions of Frank-Kamenetskii's theory, since it presupposes that the substance is all at a single temperature means assuming that $\lambda \rightarrow \infty$.

QUALITATIVE ASTM PROCEDURES

A number of ASTM tests are intended as screening procedures. While the data are reported in quantitative units, no account is taken of the amount of self-heating substance that is actually present in the real-life application. Thus, the numbers can only, at best, have a qualitative significance.

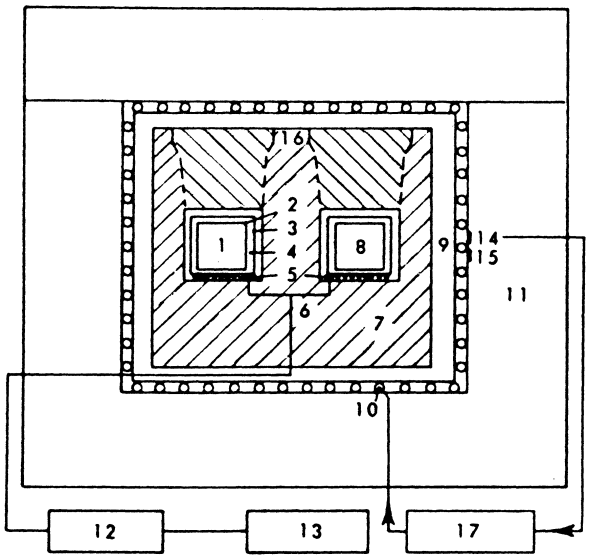
ASTM E 537[236] is a brief standard which instructs the user of DSC equipment how to calibrate the equipment, conduct a test, and to report the values of the 'onset temperature,' the 'extrapolated onset temperature,' and the peak temperature for the substance. These data are not analyzed further to make predictions for real-scale substances.

ASTM E 487[237] is a vague thermal analysis procedure which instructs the user to procure an undefined amount of substance (but preferably less than 50 mg), to place it in an undefined heating apparatus equilibrated to a desired temperature, and to observe it for 2 h. If, for a given temperature, exothermic activity is observed during this period, but is not observed at a temperature of 10ºC less, then the specified temperature is reported as being the 'constant-temperature stability (CTS) value.

ASTM D 2883[238] method is a screening procedure whereby a liquid or solid specimen is placed in glass ampoule which is located in a test oven. Various amounts of substance may be introduced, and the results depend on the amount of substance that was used. Relative temperature rises are measured and a procedure is offered to extrapolate the results to 'incipient' temperature values. While based on a test oven and not a thermal analysis apparatus, the technique is very similar to screening methods based on DTA tests.

UN TEST H3—ISOTHERMAL STORAGE TEST

The apparatus was developed in the Netherlands at TNO and can be viewed as a larger-scale DSC apparatus and comprises an aluminum block surrounded by a heater and thermal insulation (Figure 48)[194]. A sample and reference cup, each of 70 cm^3 capacity and holding up to 20 g of sample, are embedded in the block. Peltier-effect heat flow meters are located between the bases of the cups and the



1 – sample
2 – sample vessel
3 – cylindrical holder
4 – air spaces
5 – Peltier elements
6 – electric circuit
7 – aluminum block
8 – inert material
9 – air space
10 – heating wires
11 – glass wool
12 – amplifier
13 – recorder
14 – platinum resistance sensor for temperature control
15 – platinum resistance sensor for safety control
16 – platinum resistance thermometer
17 – temperature controller

Figure 48 The isothermal storage test
(Copyright Elsevier Science, used by permission)

aluminum block. The device is calibrated and used similarly to a DSC instrument. A test is generally 36 h long. Tests are conducted at multiple temperatures and the result is a plot of Q_T versus T. The calculation of the SADT is done similarly to UN Test H2. The sensitivity of the apparatus is about 1 mW kg^{-1}. Example of results from the testing of TNT[239] is shown in Figure 49.

Apart from the UN instructions, Van Geel[240] developed an analysis method for computing the safe storage radius for materials based on results of the isothermal storage test. The substance is to be tested in the apparatus at a temperature 10ºC higher than is the intended storage temperature. The basic input variable is the peak value of the heat generation rate (W kg^{-1}). Van Geel provides an example case where nitrocellulose powder was studied, but the results were rather anomalous and, in any case, he did not provide any validation data to back up his claim that his method will work in circumstances where the F-K theory fails.

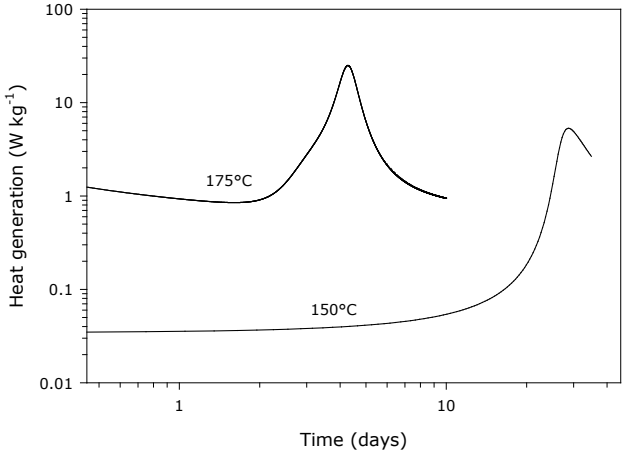


Figure 49 Performance of TNT using the isothermal storage test

EMPIRICAL OR QUALITATIVE TESTS

MACKEY TEST AND RELATED TESTS

Ordway test

In the late 19th century, insurance companies were seeking a reliable method whereby they could categorize oils by their self-heating propensities. Mills using the more hazardous oils would be assigned higher insurance rates. Much of the problem was due to oxidizable double C=C bonds; thus the standard chemistry technique of iodine number (see Chapter 14) was sometimes applied in the hopes that it would correlate to self-heating propensity. Iodine number results, however, were only partially indicative of the problem, thus efforts were made to develop a performance-based test, i.e., one which would actually examine self-heating. The earliest test described in any detail was that of Prof. Ordway of MIT, invented in 1884[241]. He configured a 100 mm diameter horizontally-oriented sheet-steel cylinder in which two balls of cotton were placed 300 mm apart. One 50 g ball was saturated in 50 g of test oil, while the other was an unoiled control. The cylinder was placed inside a larger, 150 mm wrought-iron cylinder (Figure 50), and the latter was heated at the midpoint by a Bunsen burner. Three thermometers were installed in the apparatus, and the procedure called for controlling the flame so that the center thermometer reached 125ºC, while the thermometer at the control sample attained 100ºC. It does not appear that specific failure criteria were laid down for the test.

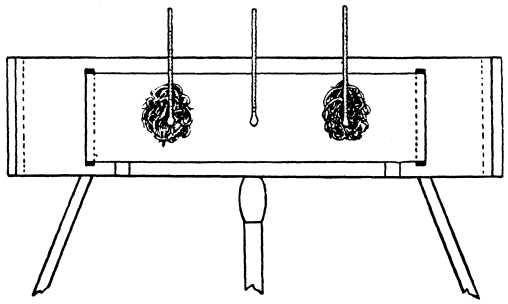


Figure 50 Ordway's test of 1884

Mackey test

Mackey's apparatus of 1895[242] was an improvement, since a definite shape was established for the sample, and a more reproducible heating arrangement evolved. He used 7 g of cotton wool, soaked with 14 g of the oil in question. This was wrapped into a cylinder shape using a piece of wire gauze 125 mm square. The upright cylinder was placed in an oven the temperature of which was held at 100ºC by means of a water jacket. No special provisions for air flow, were made, which entered in through gaps in the oven. A thermometer was used to record the specimen temperature, with an experiment lasting more the 5 h, unless active flaming resulted earlier. From these initial results, Mackey recommended that observing for only 1.5 or 2 h was sufficient to identify problematic oils. In the discussion on the paper, a number of comments were made to the effect that the test apparatus was not well controlled. A year later, Mackey improved his apparatus. The second version[243] of Mackey's 'Cloth-Oil Tester' (Figure 51) is essentially a percolator, holding a 150 mm long gauze cylinder, 37 mm in diameter. The gauze cylinder is filled with 7 g of cotton wool, soaked with 14 g of the test oil. A flow of air by natural convection is created by placing a low inlet and tall outlet into the cavity area. The vessel is placed on a ring stand and heated with a Bunsen burner. If the specimen temperature does not exceed 100ºC during a 1 h exposure period, a passing result is reported. Since the specimen is surrounded by a water jacket held at 100ºC, even with no exothermicity, a specimen will equilibrate to a temperature of only slightly under 100ºC. In Mackey's data, olive oil, which is to be considered a passing substance, attains 97 – 98ºC at 1 h, but it reaches a maximum temperature of 228 – 241ºC in 3.5 – 4.5 h, which is actually higher than some products which fail

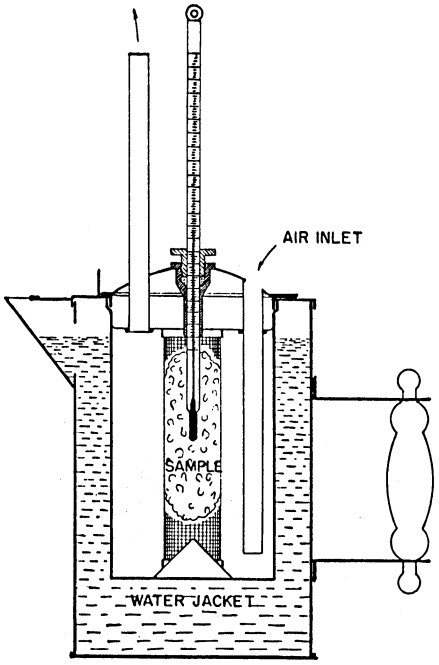


Figure 51 The Mackey apparatus for testing of self-heating propensity of materials

the test. Additional data indicated that the method, using Mackey's criteria, did not have any reasonable margin separating failing from passing specimens. In a much later paper[244], Mackey recommended ranking substances according to the time it takes to reach 200ºC, but it does not appear that this time-to-effect criterion was adopted by users of the test.

Gill compared results from the Ordway apparatus and the two versions of Mackey's[245]. He concluded that Mackey's old version was the most reliable. His data for the second version show that oils with widely varying iodine numbers were exhibiting very similar temperature rises. Bowes[246] has pointed out that, because of the time limit, misleading results can be obtained with oils which have an antioxidant or which are diluted with another liquid. In these cases, there can be a prolonged period during which temperatures do not rise much, but after this period is over, serious self-heating can still be possible.

A radically modified Mackey test was proposed by Factory Mutual in 1927[247], but did not win acceptance. Another modification to the Mackey test was proposed in 1934 by J. B. Firth, who fitted a steam-jacketed chimney and reduced the specimen insertion aperture to 38 mm[248]. In this version the specimen roll occupies the middle 65 mm of a 100 mm long stainless steel gauze cylinder. With oil-covered cotton, visible darkening of the specimen is generally noted at around 150ºC, and charring at around 240 – 260ºC. In 1953 UL described the use of a scaled-up Mackey tester which used a specimen size of 305 mm diameter and 584 mm height[249]. Yet another modification of the Mackey test was standardized as ASTM D 3523[250] in 1976. The reason why such a crude test was put forth so late is unclear. In any case, the ASTM version is a 'Siamese percolator,' with two vessels in one water bath. Thus, it appears conceptually to be a cross between the Ordway and the Mackey schemes. No criteria have been proposed in connection with the test results, which simply comprise the temperature difference of the two containers at the 4 h mark.

ASTM E 771 test

The ASTM E 771 test[251] was specifically intended for examining the self-heating of liquids impregnating inert fibers and can be viewed as an offshoot of the Mackey test. A heated oil bath is used, in which is placed a sample well made of stainless steel pipe. Some 10 mL or more of test liquid is soaked into 5 – 10 g of inert fibers, which is then shaped into a cylindrical shape and placed in a 63 mm diameter, 153 mm tall iron-mesh cylinder. An air flow of 0.8 L min^{-1} is forced through the sample well. The test is conducted for 24 h and the lowest bath temperature at which a 5ºC rise occurs is recorded as the spontaneous heating temperature. The test method was withdrawn in 2001.

ASTM E 476

The thermal stability bomb, ASTM E 476[252] is a small, stainless steel pressure vessel wherein an 0.3 g sample is placed. The bomb is then put into a Wood's metal bath capable of being raised up to 500ºC, and the bath is heated at 8 – 10ºC min^{-1}. The test is stopped when either the pressure-relief diaphragm bursts or a desired temperature is reached. A 'threshold temperature' is reported as the extrapolation to baseline of the runaway exotherm peak.

UN TEST O1 FOR OXIDIZING SOLIDS

This test is a combination ignition and burning rate test. The test is not one that truly examines hypergolic behavior, since an external ignition source is presented. The substance is tested by being mixed with dry cellulose fibers, poured into a conical pile, and presented with an igniter in the form of a 150 W Nichrome wire heater applied for 3 min. Two ratios of oxidizer : cellulose are tested, 4:1 and 1:1, by mass. Reference tests of potassium bromate + cellulose fibers are run in three different oxidizer/fuel ratios. Assignment of the substance into 'Not Division 5.1,' or into Division 5.1 Packing Group I, II, or III is based on comparison of burning time results with those for the reference mixtures. Koseki et al.[253] reported on a number of difficulties in using this test, most important of which is a great sensitivity both to the type of cellulose fibers used and the moisture content.

UN TEST O2 FOR OXIDIZING LIQUIDS

This test method is intended to test for liquids with hypergolic reactivity and also for liquids that promote very rapid burning. The test apparatus comprises a small pressure vessel wherein a mixture of 2.5 g of the test liquid and 2.5 g of cellulose fibers is placed. If the mixture self-ignites during mixing or filling, then it is classified into Division 5.1 Packaging Group I. If it does not, then the test is continued: the mixture is packed into the vessel, a Nichrome heater applies heat for 60 s, and pressure is monitored. Three different reference standards are run and assignment of the substance into 'Not Division 5.1,' or into Division 5.1 Packing Group I, II, or III is based on comparison of the time/pressure results with those for the reference mixtures.

UN TEST S1—TROUGH TEST FOR FERTILIZERS CONTAINING NITRATES

The test method uses a 150 × 500 × 150 mm deep stainless-steel mesh tray which is filled with the fertilizer to be tested. One end of the tray holds a steel plate which is heated either by two Bunsen burners or by an electric plate heater. The test is intended to measure self-sustained exothermic decomposition, but the small amount of unconfined substance never leads to an explosion in the apparatus. The substance is heated for up to 2 h, until a decomposition front is determined to be well established. Heating is then stopped and the specimen is monitored to see if the decomposition front reaches the far end of the device. If it does, then a failing result is recorded. The test does not normally require instrumentation, but Kiiski[254] installed thermocouples at various locations along the trough and obtained typical results shown in Figure 52. Temperature rate-of-rise is shown in Figure 53, with ignition corresponding to the time at which the rate of rise begins to increase again (265ºC). The method is further discussed in Chapter 14 under *Fertilizers*.

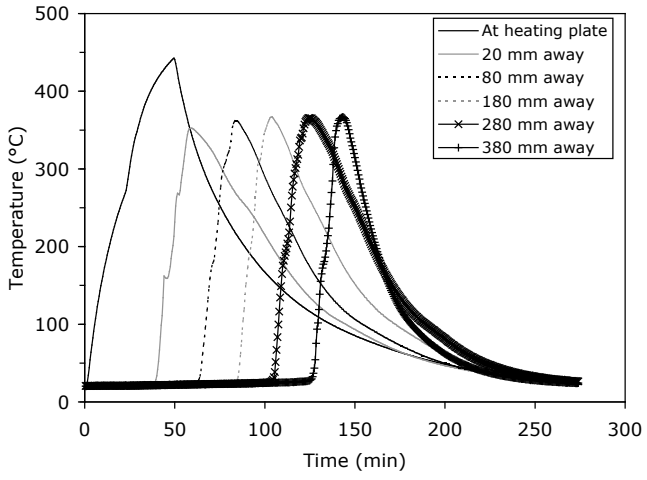


Figure 52 Temperatures measured at various locations while testing an NPK fertilizer in the UN Test S1; a 250 W electric heater was used
(Courtesy Harri Kiiski)

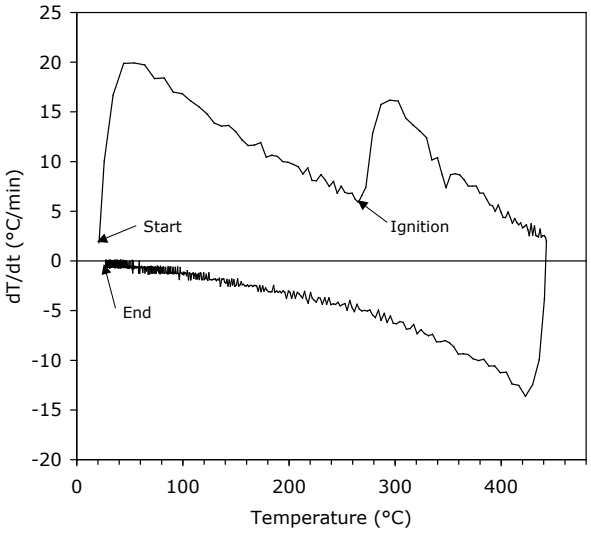


Figure 53 Rate of temperature rise at the heating plate in the UN Test S1
(Courtesy Harri Kiiski)

BUREAU OF MINES DUST LAYER IGNITION TEMPERATURE TEST

The BM test[255] was developed in the early 1940s, predating the concepts of modern self-heating theory. A 12.7 mm layer of dust is placed in a 25 mm dia. wire-mesh basket and suspended in the middle of the Godbert-Greenwald furnace (described in Chapter 5). A thermocouple is placed in the middle of the specimen and ignition is deemed to occur if a point of inflection (in the rising-temperature direction) is found on the temperature trace. The Bureau of Mines collected and reported a very large amount of data using this procedure, especially on agricultural dusts, but its results do not find a role in current evaluation strategies for self-heating hazards. In standard testing, the dust size was specified by passing it through a 200-mesh sieve, i.e., particle size of < 75 μm.

OXYGEN CONSUMPTION CALORIMETRY

A number of studies have been reported where the oxidation of a substance was studied directly by using a means of measuring the oxygen consumed. An early example is the 1949 method developed by the Technical Research Center of Finland (VTT)[214]. In this test, a flask containing the test substance was placed in a heated oil bath and the drop of oxygen pressure over time was monitored. From the results, the oxygen consumption (volume of oxygen consumed, per gram of specimen, per unit time) was computed. The authors showed that mineral oils exhibited no oxygen consumption, but some vegetable-origin liquids showed large consumption. Two measuring temperatures, 50 and 100ºC, were used. A later variant has been described by Carras[78]. Oxygen consumption calorimetry is an easy, standard procedure[256] when it comes to fast oxidation, e.g., substances

actually burning. However, measuring the tiny amounts of oxygen consumed during slow self-heating is a much more difficult task. Because of this, no standardized test method of this type has been developed.

Further readings

Brian F. Gray, Spontaneous Combustion and Self-Heating, pp. 2-211 to 2-228 in **The SFPE Handbook of Fire Protection Engineering**, 3rd ed., NFPA (2002).

Peter Gray and P. R. Lee, Thermal Explosion Theory, *Oxidation and Combustion Reviews* **2**, 1-183 (1967). Peter Gray and M. E. Sherrington, Self-heating, Chemical Kinetics, and Spontaneously Unstable Systems, pp. 331-383 in **Gas Kinetics and Energy Transfer**, vol. 2, The Chemical Society, London (1977). Peter Gray, Chemistry and Combustion, pp. 1-19 in *23rd Symp. (Intl.) on Combustion*, The Combustion Institute, Pittsburgh (1990). For readers wishing a more fundamentally mathematics-based treatment of self-heating, Gray's major review papers are the best starting point.

David A. Frank-Kamenetskii, **Diffusion and Heat Transfer in Chemical Kinetics**, 2nd ed., Plenum Press, New York (1969). The English translation is adequate and this work provides the basic reference to Frank-Kamenetskii's theory.

Philip C. Bowes, **Self-Heating: Evaluating and Controlling the Hazards**, Her Majesty's Stationery Office, London (1984). This large tome collects a wide array of mathematical treatments of the self-heating problem.

A. G. Merzhanov and V. B. Abramov, Thermal Explosion of Explosives and Propellants, A Review, *Propellants and Explosives* **6**, 130-148 (1981). Russian researchers have done some of the most extensive studies on self-heating, but much of it has not been available in English. This review paper presents the highlights of the Russian research.

References

1. Tschernischev, I. G., Physique expérimentale, *Acta Academiae Scientiarum Imperialis Petropolitanae* **1**, 3-18 (1779). Published in 1782. Tschernischev's paper was added as late-breaking news to the journal which otherwise comprised 1779 material.
2. Fullmer, J. Z., On Spontaneous Combustion, *Annals of Science* **17**, 65-80 (1961).
3. Moore, F. C., **Fires: Their Causes, Prevention and Extinction**, The Continental Insurance Co. of New York, New York (1877).
4. Rowan, T., **Coal Spontaneous Combustion and Explosions Occurring in Coal Cargoes—Their Treatment and Prevention**, E&FN Spon, London (1882).
5. Hexamer, C. John, **A Collection of Essays on Spontaneous Combustion**, The Spectator Co., New York (1888).
6. Hapke, L., **Die Selbstentzündung von Schiffsladungen, Baumwolle und anderen Faserstoffen, Steinkohlen, Heuhaufen, Tabak, etc., sowie deren Verhuntung**, 2nd ed., C. E. Muller, Bremen (1893).
7. Medem, R., **Die Selbstentzündung von Heu, Steinkohlen und geolten Stoffen**, J. Abel, Greifswald (1898).
8. Schwartz, E. von, **Fire and Explosion Risks**, Charles Griffin & Co., Ltd., London (1904). Original German edition: **Handbuch zur Erkennung, Beurtheilung und Verhütung der Feuer- und Explosionsgefahr chemisch-technischer Stoffe und Betriebsanlagen**, Ackermann, Konstanz (1902); 2nd ed. 1907; final (6th) ed.: **Handbuch der Feuer- und Explosionsgefahr**, Jung, München (1964).
9. Miehe, H., **Die Selbsterhitzung des Heus: eine biologische Studie**, Fischer, Jena (1907).
10. Bowes, P. C., **Self-Heating: Evaluating and Controlling the Hazards**, Her Majesty's Stationery Office, London (1984). Also published by Elsevier Science.
11. Hall, J. R. jr., NFPA, private communication (2001).
12. Beistle, C. P., Spontaneous Heating and Ignition in Transportation by Railroad, pp. 40-45 in *Report of Conf. on Spontaneous Heating and Ignition of Agricultural and Industrial Products*, NFPA and US Dept. of Agriculture, Washington (1929).
13. Gray, B. F., Arson and Spontaneous Combustion—Can They Be Confused?, lecture notes, n.d.
14. Kubler, H., Heat Generating Processes as Cause of Spontaneous Ignition in Forest Products, *Forest Products Abstracts* **10**, 299-327 (1987).
15. Gray, B. F., and Wake, G. C., Criticality in the Infinite Slab and Cylinder with Surface Heat Sources, *Combustion and Flame* **55**, 23-30 (1984).
16. Frank-Kamenetskii, D. A., **Diffusion and Heat Transfer in Chemical Kinetics**, 2nd ed., Plenum Press, New York (1969).
17. Thomas, P. H., On the Thermal Conduction Equation for Self-heating Materials with Surface Cooling, *Trans. Faraday Society* **54**, 60-65 (1958).
18. Adler, J., and Thorne, P. F., Ignition/Extinction Criteria for Combustible Solid Surfaces, pp. 127-149 in *Proc. Joint One Day Meeting*, Combustion Physics Group/Polymer Physics Group, The Institute of Physics (1987).
19. Asseva, R. M., and Zaikov, G. E., **Combustion of Polymer Materials**, Hanser, Munich (1985).
20. Gray, B. F., Griffiths, J. F., and Hasko, S. M., Spontaneous Ignition Hazards in Stockpiles of Cellulosic Materials: Criteria for Safe Storage, *J. Chem. Technology & Biotechnology* **34A**, 453-463 (1984).
21. Nugroho, Y. S., McIntosh A. C., and Gibbs, B. M., Using the Crossing Point Method to Assess the Self-Heating Behavior of Indonesian Coals, pp. 2981-2989 in *27th Symp. (Intl.) on Combustion*, The Combustion Institute, Pittsburgh (1998).
22. Thomas, P. H., and Bowes, P. C., Some Aspects of the Self-heating and Ignition of Solid Cellulosic Materials, *British J. Applied Physics* **12**, 222-229 (1961).
23. Gill, W., Donaldson, A. B., and Shouman, A. R., Reply to Comments of Zaturska, *Combustion and Flame* **43**, 219-220 (1981).

24. Boddington, T., Gray, P., and Harvey, D. I., Thermal Theory of Spontaneous Ignition: Criticality in Bodies of Arbitrary Shape, *Phil. Trans. Royal Soc.* **270**, 467-506 (1971).
25. Boddington, T., Gray, P., and Scott, S. K., Temperature Distributions, Critical Conditions and Scaling for Exothermic Materials under Different Boundary Conditions. Part 2. Intermediate Boundary Conditions (Arbitrary Biot Number) and Bodies of Low Symmetry, *J. Chem. Soc., Faraday Trans.* Series II **77**, 813-823 (1982).
26. Thomas, P. H., and Bowes, P. C., Thermal Ignition in a Slab with One Face at a Constant High Temperature, *Trans. Faraday Society* **467**, 2007-2017 (1961).
27. Clemmow, D. M., and Huffington, J. D., An Extension of the Theory of Thermal Explosion and Its Application to the Oscillatory Burning of Explosives, *Trans. Faraday Society* **52**, 385-396 (1956).
28. Kinbara, T., and Akita, K., An Approximate Solution of the Equation for Self-Ignition, *Combustion and Flame* **4**, 173-180 (1960).
29. Bowes, P. C., Fires in Oil Soaked Lagging (CP 35/74), Building Research Establishment, Garston (1974).
30. Bowes, P. C., and Thomas, P. H., Ignition and Extinction Phenomena Accompanying Oxygen-dependent Self-heating of Porous Bodies, *Combustion and Flame* **10**, 221-230 (1966).
31. Takeno, T., and Sato, K., Effect of Oxygen Diffusion on Ignition and Extinction of Self-heating Porous Bodies, *Combustion and Flame* **38**, 75-87 (1980).
32. Nakajima, Y., and Tanaka, T., Theoretical Discussion on Two Types of Critical State for Ignition of an Autoxidative Powder Bed, *J. Loss Prevention in the Process Industries* **9**, 59-63 (1996).
33. Boddington, T., Gray, P., Kordylewski, W., and Scott, S. K., Thermal Explosions with Extensive Reactant Consumption: A New Criterion for Criticality, *Proc. Royal Society* **A390**, 13-30 (1983).
34. Thomas, P. H., Effect of Reactant Consumption on the Induction Period and Critical Condition for a Thermal Explosion, *Proc. Royal Society* **A262**, 192-206 (1961).
35. Boddington, T., Gray, P., and Wake, G., C., Criteria for Thermal Explosions with and without Reactant Consumption, *Proc. Royal Society* **A357**, 403-422 (1977).
36. Thomas, P. H., and Bowes, P. C., Reactant Consumption and the Application of Simple Thermal Ignition Models, *New Zealand J. Science* **13**, 509-512 (1970).
37. Tyler, B. J., and Wesley, T. A. B., Numerical Calculations of the Critical Conditions in Thermal Explosion Theory with Reactant Consumption, pp. 1115-1122 in *11th Symp. (Intl.) on Combustion*, The Combustion Institute, Pittsburgh (1966).
38. Tyler, B. J., and Jones, D. R., Thermal Ignition in an Asymmetrically Heated Slab: Effects of Reactant Consumption, *Combustion and Flame* **42**, 147-156 (1981).
39. Enig, J. W., Shanks, D., and Southworth, R. W., The Numerical Solutions of the Heat Conduction Equation Occurring in the Theory of Thermal Explosions (NAVORD Report 4377), US Naval Ordnance Laboratory, White Oak MD (1956).
40. Fenaughty, K. F., Lacey, A. A., and Wake, G. C., The Disappearance of Criticality for Small Activation Energy with Arbitrary Biot Number, *Combustion and Flame* **45**, 287-291 (1982).
41. Boddington, T., Feng, C.-G., and Gray, P., Thermal Explosions, Criticality and the Disappearance of Criticality in Systems with Distributed Temperatures. I. Arbitrary Biot Number and General Reaction-rate Laws, *Proc. Royal Society* **A390**, 247-264 (1983).
42. Forbes, L. K., Myerscough, M. R., and Gray, B. F., On the Presence of Limit-Cycles in a Model Exothermic Chemical Reaction: Sal'nikov's Oscillator with Two Temperature-dependent Reaction Rates, *Proc. Royal Society* **A435**, 591-604 (1991).
43. Bowes, P. C., Thermal Ignition in Two-Component Systems. Theoretical Model, *Combustion and Flame* **13**, 521-530 (1969).
44. Bowes, P. C., Thermal Ignition in Two-Component Systems. Part II—Experimental Study, *Combustion and Flame* **19**, 55-68 (1972).
45. Boddington, T., Gray, P., and Wake, G. C., Theory of Thermal Explosions with Simultaneous Parallel Reactions. I. Foundations and the One-dimensional Case, *Proc. Royal Society* **A393**, 85-100 (1984).
46. Jones, J. C., Rahmati, H., and Wake, G. C., The Unpiloted Ignition of Eucalyptus Leaves Treated as a Parallel Reaction System, *J. Fire Sciences* **9**, 311-329 (1991).
47. Wake, G. C., Sleeman, M., Chen, X. D., and Jones, J. C., Theory and Applications of Ignition with Variable Activation Energy, *J. Thermal Science* **1**, 208-212 (1992).
48. Nunziato, J. W., Kennedy, J. E., and Amos, D. E., The Thermal Ignition Time for Homogeneous Explosives Involving Two Parallel Reactions, *Combustion and Flame* **29**, 265-268 (1977).
49. Bowler, A. N., Critical Appraisal of Thermo-Analytical Test Methods (IR/L/HM/84/33), HSE, Buxton, UK (1984).
50. Li, Y., and Hasegawa, K., On the Thermal Decomposition Mechanism of Self-reactive Materials and the Evaluating Method for their SADTs, pp. 555 in *Proc. 9th Intl. Symp. on Loss Prevention and Safety Promotion in the Process Industries*, vol. 2, Associacio D'Enginyers Industrials de Catalunya, Barcelona (1998).
51. Tyler, B. J., and Henderson, D. K., Spontaneous Ignitions in Dust Layers: Comparison of Experimental and Calculated Values, pp. 45-59 in *Hazards from Pressure: Exothermic Reactions, Unstable Substances, Pressure Relief, and Accidental Discharge* (IChemE Symp. series no. 102), Institution of Chemical Engineers, Rugby, England; and Pergamon Press, Elmsford NY (1987).
52. Gray, B. F., and Scott, S. K., The Influence of Initial Temperature-Excess on Critical Conditions for Thermal Explosion, *Combustion and Flame* **61**, 227-236 (1985).
53. Griffiths, J. F., and Kordylewski, W., Combustion Hazards Associated with the Hot Stacking of Processed Materials, pp. 1777-1784 in *24th Symp.(Intl.) on Combustion*, The Combustion Institute, Pittsburgh (1992).
54. Beever, P. F., Self-heating and Spontaneous Combustion, pp. 2-180 to 2-189 in **SFPE Handbook of Fire Protection Engineering**, 2nd ed., NFPA (1995).
55. Anthony, E. J., and Greaney, D., Short Communication: The Safety of Hot Self-Heating Materials, *Combustion Science and Technology* **21**, 79-85 (1979).
56. Chong, L. V., Shaw, I. R., and Chen, X. D., Thermal Ignition Kinetics of Wood Sawdust Measured by a Newly Devised Experimental Technique, *Process Safety Progress* **14**, 266-270 (1995).

57. Zinn, J., and Mader, C. L., Thermal Initiation of Explosives, *J. Applied Physics* **31**, 323-328 (1960).
58. Abramov, V. G., Gontkovskaya, V. T., and Merzhanov, A. G., Theory of Thermal Ignition. I. Some Conditions Governing the Transition from Self-ignition to Induced Ignition, *Bull. Academy of Sciences of the USSR, Division of Chemical Sciences* No. 3, 404-410 (1966).
59. Gol'dshleger, U. I., Pribytkova, K. V., and Barzykin, V. V., Ignition of a Condensed Explosive by a Hot Object of Finite Dimensions, *Combustion, Explosion, and Shock Waves* **9**, 99-102 (1973).
60. Liñán, A., and Kindelán, M., Ignition of a Reactive Solid by an Inert Hot Spot, pp. 412-426 in *Prog. in Astronautics and Aeronautics*, vol. 76, AIAA, New York (1981).
61. Friedman, M. H., A Generalized Thermal Explosion Criterion—Exposition and Illustrative Applications, *Combustion and Flame* **11**, 239-246 (1967).
62. Thomas, P. H., A Comparison of Some Hot Spot Theories, *Combustion and Flame* **9**, 369-372 (1965).
63. Thomas, P. H., An Approximate Theory of "Hot Spot" Criticality, *Combustion and Flame* **21**, 99-109 (1973).
64. Merzhanov, A. G., On Critical Conditions for Thermal Explosion of a Hot Spot, *Combustion and Flame* **10**, 341-348 (1966).
65. Brindley, J., Griffiths, J. F., McIntosh, A. C., and Zhang, J., Initiation of Combustion Waves in Solids, and the Effects of Geometry, *ANZIAM J.* **43**, 149-163 (2001).
66. Read, A. J., Harrison, W. J., and Walker, I. K., Ignition of Wool in Air. Part 2. Effects of Sample Size, *New Zealand J. Sci.* **10**, 964-978 (1967).
67. Boddington, T., Feng. C.-G., and Gray, P., Thermal Explosion and Times-to-ignition in Systems with Distributed Temperatures. I. Reactant Consumption Ignored, *Proc. Royal Society* **A385**, 289-311 (1983).
68. Boddington, T., Griffiths, J. F., and Hasegawa, K., Induction Times to Thermal Ignition in Systems with Distributed Temperatures: An Experimental Test of Theoretical Interpretations, *Combustion and Flame* **55**, 297-305 (1984).
69. Gray, F. B., Merkin, J. H., and Griffiths, J. F., The Prediction of a Practical Lower Bound for Ignition Delay Times and a Method for Scaling Times-to-ignition in Large Reactant Masses from Laboratory Data, pp. 1775-1782 in *23rd Symp. (Intl.) on Combustion*, The Combustion Institute, Pittsburgh (1990).
70. Gray, B. F., private communication (2000).
71. Squire, W., A Mathematical Analysis of Self-Ignition, *Combustion and Flame* **7**, 1-8 (1963).
72. Grewer, T., **Thermal Hazards of Chemical Reactions**, Elsevier, Amsterdam (1994).
73. Thomas, P. H., Comments on Experiments on the Self-heating of Fibre Insulating Board (FR Note 306), Fire Research Station, Borehamwood, UK (1957).
74. Thomas, P. H., The Effect of Reactant Consumption on the Induction Period and Critical Condition for a Thermal Explosion (FR Note 409), Fire Research Station, Borehamwood, UK (1959).
75. Gray, B. F., Spontaneous Combustion and Self-Heating, in **SFPE Handbook of Fire Protection Engineering**, 3rd ed., NFPA (2002).
76. J. R. Creighton, Ignition Temperatures of Solid Explosives Exposed to a Fire (UCRL-JC-114201), Lawrence Livermore National Laboratory, Livermore CA (1993).
77. Nordon, P., A Model for the Self-Heating Reaction of Coal and Char, *Fuel* **58**, 456-464 (1979).
78. Carras, J. N., and Young, B. C., Self-heating of Coal and Related Materials: Models, Application and Test Methods, *Prog. Energy Combustion Science* **20**, 1-15 (1994).
79. Schmal, D., Spontaneous Heating of Stored Coal, pp. 133-215 in **Chemistry of Coal Weathering**, C. R. Nelson, ed., Elsevier, Amsterdam (1989).
80. Takeda, H., and Akita, K., Thermal Explosion with Linear Time Dependent Boundary Condition, pp. 331-335 in *First Specialists Meeting (Intl.) of the Combustion Institute*, Bordeaux, France (1981).
81. Davis, E. J., Hampson, B. H., and Yates, B., Analysis of the Development of Runaway Reactions in Powders, pp. 1/D:1-1/D:19 in *Runaway Reactions, Unstable Products and Combustible Powders* (Symp. Series No. 68), The Institution of Chemical Engineers, London (1981).
82. Akgün, F., and Arisoy, A., Effect of Particle Size on the Spontaneous Heating of a Coal Stockpile, *Combustion and Flame* **99**, 137-146 (1994).
83. Demidov, P. G., **Goreniye i svoystva goryuchikh veshchestv**, Izdatel'stvo Ministerstva Kommunal'nogo Khozyaystva RSFSR, Moskva (1962). English translation: **Combustion and Properties of Combustible Substance**, NTIS No. AD 621 738, National Technical Information Service, Springfield, VA (1965).
84. Zoch, L. L., jr., Rusch, J. J., and Springer, E. L., Changes in Aspen Bark Stored in Outdoor Piles, *Forest Products J.* **32**, No. 6, 31-34 (1982).
85. Read, A. J., Harrison, W. J., and Walker, I. K., Ignition of Wool in Air. Part 2—Effects of Sample Size, *New Zealand J. Science* **10**, 964-978 (1967).
86. Leuschke, G., Induction Times of Dust Deposits Stored at and Above Self-Ignition Temperatures, pp. 8/647-8/656 in *3rd Intl. Symp. on Loss Prevention and Safety Promotion in the Process Industries*, Swiss Society of Chemical Industries, Zürich (1980).
87. O'Connor, J. F., Self-Heating and Self-Ignition in Dairy Powders (Ph.D. dissertation), Michigan State Univ., East Lansing (1991).
88. Bowes, P.C., Methods for assessing spontaneous heating and ignition hazards. II: The heating of oiled fibre in a modification of the Mackey tester (Fire Research Note No.53), Fire Research Station, Borehamwood (1953).
89. Gibson, N., Harper, H. J., and Rogers, R. L., Evaluation of the Fire and Explosion Risk in Drying Powders, *Plant/Operations Progress* **4**, 181-189 (1985).
90. Elder, J. L., Schmidt, L. D., Steiner, W. A., and Davis, J. D., Relative Spontaneous Heating Tendencies of Coals (Tech. Paper 681), Bureau of Mines, Pittsburgh (1945).
91. Zimbardi, F., Evaluation of Reaction Order and Activation Energy of Char Combustion by Shift Technique, *Combustion Science and Technology* **156**, 251-269 (2000).
92. Nagy, J., and Verakis, H. C., **Development and Control of Dust Explosions**, Dekker, New York (1983).
93. Gray, B. F., Interpretation of Small Scale Test Data for Industrial Spontaneous Ignition Hazards, pp. 719-729 in *Interflam 2001—Proc. 9th Intl. Conf.*, Interscience Communications Ltd., London (2001).
94. Gray, B. F., On the Critical Conditions for an Assembly of Interacting Thermons, *ANZIAM J.* Part 1, **43**, 1-13 (2001).

95. Walker, I. K., The Role of Water in Spontaneous Combustion of Solids, *Fire Research Abstracts and Reviews* **9**, 5-22 (1967).
96. Walker, I. K., and Manssen, N. B., Self-heating of Wet Wood. 2. Ignition by Slow Thermal Explosion, *New Zealand J. Science* **22**, 99-103 (1979).
97. Gray, B. F., and Wake, G. C., The Ignition of Hygroscopic Materials by Water, *Combustion and Flame* **79**, 2-6 (1990).
98. Chong, L. V., and Chen, X. D., A Mathematical Model of the Self-heating of Spray-dried Food Powders Containing Fat, Protein, Sugar and Moisture, *Chemical Engineering Science* **54**, 4165-4178 (1999).
99. McIntosh, A. C., A Semenov Approach to the Modelling of Thermal Runaway of Damp Combustible Material, *IMA J. of Applied Mathematics* **51**, 217-237 (1993).
100. Back, E. L., Autoignition in Hygroscopic, Organic Materials—Especially Forest Products—as Initiated by Moisture Absorption from the Ambient Atmosphere, *Fire Safety J.* **4**, 185-196 (1981/82).
101. Hallström, A., and Werling, K., The Role of Moisture Adsorption in the Auto-Ignition of Hygroscopic Materials, *Fire Safety J.* **6**, 143-145 (1983).
102. Nordon, P., and Bainbridge, N. W., Heat of Wetting of a Bituminous Coal, *Fuel* **62**, 619-621 (1983).
103. McIntosh, A. C., and Tolputt, T. A., Critical Heat Losses to Avoid Self-Heating in Coal Piles, *Combustion Science and Technology* **69**, 133-145 (1990).
104. McIntosh, A. C., and Gray, B. F., The Ignition of Damp Combustible Material where the Fibres Are Entirely Covered with H_2O, *Combustion Science and Technology* **104**, 235-248 (1995).
105. Jones, J. C., and Henderson, K. P., Note on the Effects of Sample Collapse in Self-Heating Tests for Coals and Carbons, *J. Fire Sciences* **15**, 222-226 (1997).
106. Chen, X. D., and Wake, G. C., Thermal Ignition Kinetics of a Moist Combustible Porous Solid in Either Dry or Humid Environment Obtained Using Frank-Kamenetskii Theory, *Trans Instn. Chem. Engrs.* **72B**, 135-141 (1994).
107. McIntosh, A. C., Gray, B. F., and Wake, G. C., The Ignition of Combustible Material in the Presence of a Damp Atmosphere, *Physics Letters A* **191**, 61-70 (1994).
108. Gray, B. F., Analysis of Chemical Kinetic Systems over the Entire Parameter Space. III. A Wet Combustion System, *Proc. Royal Society* **A429**, 449-458 (1990).
109. Bowes, P. C., The Determination of the Ignition Temperature of Solids by a Rising Temperature Method (FR Note 10), Fire Research Station, Borehamwood, UK (1952).
110. Hardy, V. O., The Smouldering of Coal Dust and the Effect of Lubricants (Research Report 136), SMRE, Sheffield, England (1956).
111. Frandsen, W. H., Spontaneous Combustion, It Can Happen in the Forest, *12th Conf. on Fire and Forest Meteorology*, Jekyll Island GA (1993).
112. Beever, P. F., Spontaneous Combustion—Isothermal Test Methods (IP 23/82), Building Research Establishment, Garston, England (1982).
113. Beever, P. F., Isothermal Methods for Assessing Combustible Powders (CP5/82), Fire Research Station, Borehamwood, UK (1982).
114. Bowes, P. C., and Townsend, S. E., Ignition of Combustible Dusts on Hot Surfaces, *British J. Applied Physics* **13**, 105-114 (1962).
115. Miron, Y., and Lazzara, Hot-Surface Ignition Temperatures of Dust Layers, *Fire and Materials* **12**, 115-126 (1988).
116. Reddy, P. D., Amyotte, P. R., and Pegg, M. J., Effects of Inerts on Layer Ignition Temperatures of Coal Dust, *Combustion and Flame* **114**, 41-53 (1998).
117. Hensel, W., Krause, U., John, W., and Machnow, K., Critical Parameters for Ignition of Coal Dust, paper 13f in *28th Loss Prev. Symp.*, AIChE (1994).
118. Hwang, C.C., and Litton, C.D., Ignition of Combustible Dust Layers on a Hot Surface, *J. Applied Fire Science* **2**, 189-204 (1992-93).
119. Gray, B. F., Dewynne, J., Hood, M., Wake, G. C., and Weber, R., Effect of Deposition of Combustible Matter onto Electric Power Cables, *Fire Safety J.* **16**, 459-467 (1990).
120. Dong, X., and Yang, Y., Mathematical Modeling of the Self-Heating Behaviour of Dusts around a Power Cable, pp. 603-610 in *Fire Safety Science—Proc. 6th Intl. Symp.*, Intl. Assn. for Fire Safety Science (2000).
121. Weber, R. O., and Renkema, K. A., Spontaneous Ignition in the Presence of a Power Source, *Combustion Science and Technology* **104**, 169-179 (1995).
122. Brindley, J., Griffiths, J. F., and McIntosh, A. C., Ignition Phenomenology and Criteria Associated with Hotspots Embedded in a Reactive Material, *Chem. Eng. Sci.* **56**, 2037-2046 (2001).
123. Nelson, M., Detection and Extinction of Fire and Smouldering in Bulk Powder, pp. 64-139 in British Materials Handling Board, CREDIT Project Report, EV5V-CT92-0082 (1992).
124. Krause, U., and Schmidt, M., Initiation of Smouldering Fires in Combustible Bulk Materials by Glowing Nests and Embedded Hot Bodies, *J. Loss Prevention in the Process Industries* **10**, 237-242 (1997).
125. Krause, U., and Schmidt, M., Propagation of Smouldering in Dust Deposits Caused by Glowing Nests or Embedded Hot Bodies, pp. 388-403 in *8th Intl. Colloquium on Dust Explosions* (Intl. Symp. on Hazards, Prevention, and Mitigation of Industrial Explosion), Safety Consulting Engineers, Schaumburg, IL (1998).
126. Sheu, L.-J., Lin, J.-D., and Chen, J.-R., Numerical Analysis on the Hot Spot in Reactive Chemical Storage, *J. Loss Prevention in the Process Industries* **12**, 125-136 (1999).
127. Shtessel, E. A., Pribytkova, K. V., and Zhukova, L. A., Characteristics of Thermal Self-ignition under Conditions of Natural Convection, *Combustion, Explosion, and Shock Waves* **15**, 555-562 (1980).
128. Mellin, B. E., Explosion at the BASF Antwerp Ethylene Oxide/Glycol Plant, *IChemE Loss Prevention Bulletin* **1**, 100 (1991).
129. Brindley, J., Griffiths, J.F., McIntosh, A. C., and Zhang, J., Effects of Vaporization, Diffusion and Condensation on the Combustion of Reactive Fluids in Hot Porous Media, *Proc. Royal Society* **A456**, 997-1017 (2000).
130. McIntosh, A. C., Bains, M., Crocombe, W., and Griffiths, J. F., Autoignition of Combustible Fluids in Porous Insulation Materials, *Combustion and Flame* **99**, 541-550 (1994).
131. McIntosh, A. C., and Griffiths, J. F., On the Thermal Runaway of Combustible Fluids in Lagging Material, *IMA J. Applied Math.* **54**, 83-96 (1995).
132. Brindley, J., Griffiths, J. F., Zhang, J., Hafiz, N. A., and McIntosh, A. C., Critical Criteria for Ignition of Combustible Fluids in Insulation Materials, *AIChE J.* **44**, 1027-1037 (1998).

133. Brindley, J., Griffiths, J. F., Hafiz, N., McIntosh, A. C., and Zhang, J., Criteria for Autoignition of Combustible Fluids in Insulation Materials, *Trans. Instn. Chem. Engrs.* **77B**, 61-68 (1999).
134. Truscott, J. E., McIntosh, A. C., Griffiths, J. F., and Brindley, J., The Effect of Oxygen Depletion on the Thermal Runaway of Combustible Fluids in Porous Insulation Materials, pp. 207-217 in **Transport Phenomena in Combustion**, vol. 1, S. H. Chen, ed., Taylor & Francis, Washington (1996).
135. McIntosh, A. C., and Gray, B. F., Self-Heating of Combustible Vapour in Porous Material When the Fibres Are Entirely Covered by Fluid, *Combustion Science and Technology* **113**, 503-515 (1996).
136. McIntosh, A. C., Gray, B. F., and Wake, G. C., Analysis of Bifurcational Behaviour of a Simple Model of Vapour Ignition in Porous Material, *Proc. Royal Society* **A453**, 281-301 (1997).
137. McIntosh, A. C., Lagging Ignition of Combustible Fluids in Porous Media—Effect of Fuel Supply Rate, *Combustion Theory and Modelling* **2**, 179-192 (1998).
138. Gibson, E. D., Morris, V., and Chiotti, P., Thermal Decomposition of Grain Dust: An Early Warning for Incipient Fire or Explosion, *Trans. Amer. Soc. of Agricultural Engineers* **20**, 380-385 (1977).
139. Grewer, T. H., On the Self-Ignition of Dust Deposits, *Staub und Reinhaltung der Luft* **31**, 7-12 (1971).
140. **Recommendations on the Transport of Dangerous Goods: Model Regulations**, 10th ed., United Nations, New York (1997).
141. **Recommendations on the Transport of Dangerous Goods: Manual of Tests and Criteria**, 2nd ed., United Nations, New York (1995).
142. *Proc. Intl. Workshop on Safety in the Transport, Storage and Use of Hazardous Materials*, National Research Institute of Fire and Disaster, Tokyo (1998).
143. Cutler, D. P., Current Techniques for the Assessment of Unstable Substances, pp. 133-141 in *Hazards in the Process Industries: Hazards IX* (IChemE Symp. Series No. 97), The Institution of Chemical Engineers, Rugby, England (1986).
144. Whitmore, M. W., Estimation of Stability Temperatures from Differential Thermal Analysis and Thermal Activity Monitor Data in Combination, pp. 597-607 in *Hazards XII—European Advances in Process Safety* (Symp. Series No. 134), The Institution of Chemical Engineers, London (1994).
145. Jones, J. C., Steady Behaviour of Long Duration in the Spontaneous Heating of Bituminous Coal, *J. Fire Sciences* **14**, 159-166 (1996).
146. Leuschke, G., Experimental Investigations on Self-ignition of Dust Deposits in Hot Environments, pp. 2/G:1-2/G:15 in *Runaway Reactions, Unstable Products and Combustible Powders* (Symp. Series No. 68), The Institution of Chemical Engineers, London (1981).
147. Spokoinyi, F. E., and Eidukyavichus, K. K., Mechanism of Spontaneous Ignition during Storage of Mineral Wool Objects, *Combustion, Explosion, and Shock Waves* **24**, 649-651 (1988).
148. Griffiths, J. F., Hasko, S. M., and Tong, A. W., Thermal Ignition in Packed Particulate Solids: Criticality under Conditions of Variable Biot Number, *Combustion and Flame* **59**, 1-9 (1985).
149. Gray, B. F., and Halliburton, B., The Thermal Decomposition of Hydrated Calcium Hypochlorite (UN 2880), *Fire Safety J.* **35**, 223-239 (2000).
150. Jones, J. C., and Wade, M., Direct Determination of the Biot Number in Oven Heating Tests, *J. Fire Sciences* **17**, 421-429 (1999).
151. Incropera, F. P., and DeWitt, D. P., **Fundamentals of Heat and Mass Transfer**, 4th ed., John Wiley, New York (1996).
152. Halliburton, B. W., Investigation of Spontaneous Combustion Phenomenology of Bagasse and Calcium Hypochlorite (Ph.D. dissertation), Macquarie Univ., Sydney, Australia (2002).
153. Gorring, R. L., and Churchill, S. W., Thermal Conductivity of Heterogeneous Materials, *Chem. Eng. Prog.* **57**:7, 53-59 (1961).
154. Dawson, D. M., and Briggs, A, Prediction of the Thermal Conductivity of Insulation Materials, *J. Materials Science* **16**, 3346-3356 (1981).
155. Lin, F., and Ford, J. D., Thermal Diffusivity of Some Porous Oxides, *Canadian J. Chemical Engineering* **62**, 125-134 (1984).
156. Palosaari, S. M., and Cornish, A. R. H., Approximate Method for Prediction of Effective Thermal Conductivity of Wetted Porous Materials, *Acta Polytechnica Scandinavica-Chemistry including Metallurgy Series* No. 126, 1-24 (1975).
157. Sauer, F. M., Ignition of Black Alpha-Cellulose Papers by Thermal Radiation (AFSW 869), US Forest Service, California Forest and Range Experiment Station, Berkeley (1956).
158. Baxter, S., The Thermal Conductivity of Textiles, *Proc. Phys. Soc. London* **58**, 105-118 (1946).
159. Stephenson, M. E. jr., and Mark, M., Thermal Conductivity of Porous Materials, *ASHRAE J.* **3**, 75-81 (1961).
160. Bowes, P. C., Harris, M. D., and Townshend, S. E., Ignition of Dust Layers on Hot Surfaces (FR Note 374), Fire Research Station, Borehamwood, UK (1959).
161. Mitchell, N. D., New Light on Self-Ignition, *NFPA Q.* **45**, 165 (1951).
162. Bowes, P. C., and Cameron, A., Self-Heating and Ignition of Chemically Activated Carbon, *J. Appl. Chem. Biotechnology* **21**, 244-250 (1971).
163. Sujanti, W., Zhang, D.-K., and Chen, X. D., Low-Temperature Oxidation of Coal Studied Using Wire-mesh Reactors with both Steady-state and Transient Method, *Combustion and Flame* **117**, 646-651 (1999).
164. Chong, L. V., Shaw, I., and Chen, X. D., Exothermic Reactivities of Skim and Whole Milk Powders as Measured using a Novel Procedure, *J. Food Eng.* **30**, 185-196 (1996).
165. Gray, B. F., Little, S. G., and Wake, G. C., The Prediction of a Practical Lower Bound for Ignition Delay Times and a Method of Scaling Times-to-Ignition in Large Reactant Masses from Laboratory Data—II., pp. 1785-1791 in *24th Symp. (Intl.) on Combustion*, The Combustion Institute, Pittsburgh (1992).
166. Jones, J. C., Chiz, P. S., Koh, R., and Matthew, J., Kinetic Parameters of Oxidation of Bituminous Coals from Heat-Release Measurements, *Fuel* **75**, 1755-1757 (1996).
167. Chen, X. D., On Basket Heating Methods for Obtaining Exothermic Reactivity of Solid Materials: The Extent and Impact of the Departure of the Crossing-point Temperature from the Oven Temperature, *Process Safety and Environ-*

mental Protection: Trans. Institution Chem. Engineers **77B**, 187-192 (1999).
168. Chen, X. D., and Chong, L. V., Several Important Issues Related to the Crossing-Point Temperature (CPT) Method for Measuring Self-ignition Kinetics of Combustible Solids, *Process Safety and Environmental Protection: Trans. Institution Chem. Engineers* **76B**, 90-93 (1998).
169. Kubler, H., Wang, Y.-R., and Barkalow, D., Generation of Heat in Wood between 80 and 130°C, *Holzforschung* **39**, 85-89 (1985).
170. Jones, J. C., Correspondence, *Process Safety and Environmental Protection: Trans. Institution Chem. Engineers* **78B**, 68-72 (2000).
171. Jones, J. C., A Means of Obtaining a Full Kinetic Rate Expression for the Oxidation of a Solid Substrate from a Single Criticality Data Point. II. Identification of Suitable Substrates for Application, *Fuel* **78**, 507-508 (1999).
172. Nordon, P., and Bainbridge, N. W., Some Properties of Char Affecting the Self-Heating Reaction in Bulk, *Fuel* **58**, 450-455 (1979).
173. Jones J. C., Bailey R. S., and Bale K., Thermal Diffusivities of Simulated Fuel-Mineral Blends, *J. Fire Sciences* **19**, 69-80 (2001).
174. Carslaw, H. S., and Jaeger, J. C., **Conduction of Heat in Solids**, 2nd ed., Clarendon Press, Oxford (1959).
175. Solid Materials: Spontaneous Ignition Temperature by Continuous Heating (NT Fire 045), Nordtest, Espoo, Finland (1992).
176. Björkman, J., and Keski-Rahkonen, O., Test Method for Self-Ignition of Materials (VTT Publications 96), Valtion teknillinen tutkimuskeskus, Espoo, Finland (1992).
177. Class 4.2 – Spontaneously Combustible. Self-heating Test for Carbon (draft), IMCO, London (1974).
178. Braun, E., Self Heating Properties of Coal (NBSIR 87-3554), NBS (1987).
179. Jones, J. C., Commentary on the UN Test for Spontaneous Heating of Solid Substances, *J. Loss Prevention in the Process Industries* **13**, 177-178 (2000).
180. Beever, P. F., Hazards in Drying Thermally Unstable Powders, pp. 223-231 in *Hazards X: Process Safety in Fine and Specialty Chemical Plants* (Symp. Series No. 115), The Institution of Chemical Engineers, Rugby (1989).
181. Lunn, G. A., et al., Testing Methods for Electrical Apparatus Installed in a Dusty Environment with a Potential Risk of Explosion (Project No. SMT-PL97-1528), HSE, Buxton, UK (2001).
182. El-Sayed, S. A., and Abdel-Latif, A. M., Smoldering Combustion of Dust Layer on Hot Surface, *J. Loss Prevention in the Process Industries* **13**, 509-517 (2000).
183. Palmer, K. N., and Tonkin, P. S., The Ignition of Dust Layers on a Hot Surface, *Combustion and Flame* **1**, 14-18 (1957).
184. Henderson, D. K., and Tyler, B. J., Dual Ignition Temperatures for Dust Layers, *J. Hazardous Materials* **19**, 155-159 (1988).
185. Ohlemiller, T. J., and Rogers, F. E., Cellulosic Insulation Material. II. Effect of Additives on Some Smolder Characteristics, *Combustion Science and Technology* **24**, 139-152 (1980).
186. Nagy, J., Dorsett, H. G. jr., and Cooper, A. R., Explosibility of Carbonaceous Dusts (RI 6597), Bureau of Mines, Pittsburgh (1965).
187. Standard Test Method for Hot-Surface Ignition Temperature of Dust Layers (ASTM E 2021), ASTM.
188. Classifications of Combustible Dusts Relative to Electrical Equipment in Class II Hazardous Locations (NMAB 353-4), National Materials Advisory Board, National Academy of Sciences Press, Washington (1982).
189. Electrical Apparatus for Use in the Presence of Combustible Dust. Part 1-2. Electrical Apparatus Protected by Enclosures—Selection, Installation and Maintenance (EN 50281-1-2), CEN Central Secretariat, Brussels.
190. Davis, J. D., and Byrne, J. F., An Adiabatic Method for Studying Spontaneous Heating of Coal, *J. American Ceramic Soc.* **7**, 809-816 (1924).
191. Cronin, J. L., Nolan, P. F., and Barton, J. A., Strategy for the Thermal Hazard Evaluation of Chemical Reactions, Illustrated by an Analysis of the Nitration of Toluene, pp. 633-659 in *Intl. Symp. on Runaway Reactions*, AIChE (1989).
192. Walker, I. K., and Harrison, W. J., The Self-Heating of Wet Wool, *New Zealand J. Agricultural Research* **3**, 861-895 (1960).
193. Güney, M., and Hodges, D. J., Adiabatic Studies of the Spontaneous Heating of Coal. Part 1, *Colliery Guardian* **217**, 105-109 (1969).
194. Groothuizen, T. M., Hartgerink, J. W., and Pasman, H. J., Phenomenology, Test Methods and Case Histories of Explosions in Liquids and Solids, pp. 239-251 in *Loss Prevention and Safety Promotion in the Process Industries—Proc. 1st Intl. Loss Prevention Symp.*, Elsevier, Amsterdam (1974).
195. Raskin, W. R., and Robertson, A. F., Adiabatic Apparatus for the Study of Self-Heating of Poorly Conducting Materials, *Rev. Sci. Instrum.* **25**, 541-544 (1954).
196. Gross, D., and Robertson, A. F., Self-Ignition Temperatures of Materials from Kinetic-Reaction Data, *J. Research NBS* **61**, 413-417 (1958).
197. Gross, D., and Amster, A. B., Thermal Explosions: Adiabatic Self-Heating of Explosives and Propellants, pp. 728-734 in *8th Symp. (Intl.) on Combustion*, The Combustion Institute, Pittsburgh (1960).
198. Güney, M., and Hodges, D. J., Adiabatic Studies of the Spontaneous Heating of Coal. Part 2, *Colliery Guardian* **217**, 173-177 (1969).
199. Kotoyori, T. J., Critical Ignition Temperatures of Chemical Substances, *J. Loss Prevention in the Process Industries* **2**, 16-21 (1989).
200. Yin, F., Adiabatic Calorimeter: Fundamentals and Application in Thermal Hazard Evaluation, pp. 58-94 in *Proc. Intl. Symp. on Runaway Reactions and Pressure Relief Design*, AIChE (1995).
201. Bowes, P. C., A General Approach to the Prediction and Control of Potential Runaway Reaction, pp. 1/A:1-1/A:35 in *Runaway Reactions, Unstable Products and Combustible Powders* (Symp. Series No. 68), The Institution of Chemical Engineers, London (1981).
202. Nordon, P., Bainbridge, N. W., Szemes, F., and Myers, C., A Low Temperature Reaction Calorimeter of the Calvet Type for the Measurement of the Heat of Oxidation of Coal, *J. Phys. E: Sci. Instrum.* **18**, 338-341 (1985).
203. Tharmalingham, S., The Evaluation of Self-Heating in Bulk Handling of Unstable Solids, pp. 293-312 in *Intl. Symp. on Runaway Reactions*, AIChE (1989).
204. Jones, J. C., On the Extrapolation of Results from Oven Heating Tests for Propensity to Self-Heating, *Combustion and Flame* **124**, 334-336 (2001).

205. Jones, J. C., New Concepts and Test Procedures in the Assessment of Hazards Due to Spontaneous Heating of Transported Combustible Solids, pp. 1313-1320 in *Energy Engineering in the 21st Century Symp.*, The Hong Kong University of Science and Technology (2000).
206. Townsend, D. I., and Tou, J. C., Thermal Hazard Evaluation by an Accelerating Rate Calorimeter, *Thermochimica Acta* **37**, 1-30 (1980).
207. Coates, C. F., The ARC in Chemical Hazard Evaluation, *Thermochimica Acta* **85**, 369-372 (1985).
208. Young, M. A., and Chippett, S., Design and Operation of an Automatic Pressure Tracking Adiabatic Calorimeter (APTAC), pp. 23-57 in *Proc. Intl. Symp. on Runaway Reactions and Pressure Relief Design*, AIChE (1995).
209. Wilberforce, J. K., The Use of the Accelerating Rate Calorimeter to Determine the SADT of Organic Peroxides, CSI Corp., London (1981).
210. Huff, J. E., Emergency Venting Requirements, *Plant/Operations Progress* **1**, 211-229 (1982).
211. Rogers, R. N., and Rogers, J. L., Explosives Science, unpublished paper (1999).
212. Hofelich, T. C., and Thomas, R. C., The Use/Misuse of the 100 Degree Rule in the Interpretation of Thermal Hazard Tests, pp. 74-85 in *Intl. Symp. on Runaway Reactions*, AIChE (1989).
213. Whitmore, M. W., and Wilberforce, J. K., Use of the Accelerating Rate Calorimeter and the Thermal Activity Monitor to Estimate Stability Temperatures, *J. Loss Prevention in the Process Industries* **6**, 95-101 (1993).
214. Virtala, V., Oksanen, S., and Fridlund, F., Om självantändlighet, dess bestämning och förekomst [On spontaneous ignition and its occurrence; methods for the determination of the tendency to spontaneous ignition] (Julkaisu 14), Valtion Teknillinen Tutkimuslaitos, Helsinki (1949).
215. Proctor, H. R., and Holmes, W. E., The Oxidation of Oils, *J. Soc. Chemical Industry* **24**, 1287-1291 (1905).
216. Steele, C. H., and Nolan, P. F., The Design and Operation of a Reflux Heat Flow Calorimeter for Studying Reactions at Boiling, pp. 198-231 in *Intl. Symp. on Runaway Reactions*, AIChE (1989).
217. Sun, Y., Li, Y., and Hasegawa, K., A Study of Self-Accelerating Decomposition Temperature (SADT) using Reaction Calorimetry, *J. Loss Prevention in the Process Industries* **14**, 331-336 (2001).
218. Yu, Y., and Hasegawa, K., Derivation of the Self-accelerating Decomposition Temperature for Self-Reactive Substances Using Isothermal Calorimetry, *J. Hazardous Materials* **45**, 193-205 (1996).
219. Jones, J. C., On the Low-temperature Oxidation of Processed Peat, *J. Fire Sciences* **15**, 162-171 (1997).
220. Kubler, H., Self-Heating of Lignocellulosic Materials, pp. 429-449 in *Fire and Polymers—Hazards Identification and Prevention* (Symp. Series 425), American Chemical Society, Washington (1990).
221. Flynn, J. H., and Wall, L. A., General Treatment of Thermogravimetry of Polymers, *J. Research NBS* **70A**, 487-523 (1966).
222. Plastics—Thermographimetry—Part 2: Determination of Kinetic Parameters (ISO 11358-2), ISO (to be published).
223. Borchardt, H. J., and Daniels, F., The Application of Differential Thermal Analysis to the Study of Reaction Kinetics, *J. Amer. Chem. Soc.* **79**, 41-46 (1957).
224. Reed, R. L., Weber, L., and Gottfried, B. S., Differential Thermal Analysis and Reaction Kinetics, *Ind. and Eng. Chem.—Fundamentals* **4**, 38-46 (1965).
225. Lyon, R. E., An Integral Method of Nonisothermal Kinetic Analysis, *Thermochimica Acta* **297**, 117-124 (1997).
226. Rogers, R. N., Simplified Determination of Rate Constants by Scanning Calorimetry, *Anal. Chem.* **44**, 1336-1337 (1972).
227. Ahmed, M., Fisher, H. G., and Janeshek, A. M., Reaction Kinetics from Self-Heat Data—Correction for the Depletion of Sample, pp. 331-349 in *Intl. Symp. on Runaway Reactions*, AIChE (1989).
228. Uehara, Y., Uematsu, H., and Saito, Y., Thermal Ignition of Calcium Hypochlorite, *Combustion and Flame* **32**, 85-94 (1978).
229. Hellmiss, G., and Schwanebeck, W., Aspects of the Investigation of the Chemical Processes of Self-Heating by Means of Quantitative Thermal Analysis, *J. Forensic Sciences* **30**, 535-540 (1985).
230. Standard Test Method for Arrhenius Kinetic Constants for Thermally Unstable Materials (ASTM E 698), ASTM.
231. Duswalt, A. A., The Practice of Obtaining Kinetic Data by Differential Scanning Calorimetry, *Thermochimica Acta* **8**, 57-68 (1974).
232. Standard Test Method for Enthalpies of Fusion and Crystallization by Differential Scanning Calorimetry (ASTM E 793), ASTM.
233. Standard Test Method for Decomposition Kinetics by Thermogravimetry (ASTM E 1641), ASTM.
234. Doyle, C. D., Kinetic Analysis of Thermogravimetric Data, *J. Applied Polymer Science* **5**, 285-292 (1961).
235. Standard Practice for Calculation of Hazard Potential Figures-of-Merit for Thermally Unstable Materials (ASTM E 1231), ASTM.
236. Standard Test Method for the Thermal Stability of Chemicals by Differential Scanning Calorimetry (ASTM E 537). ASTM.
237. Standard Test Method for Constant-Temperature Stability of Chemical Materials (ASTM E 487), ASTM.
238. Standard Test Method for Reaction Threshold Temperatures of Liquid and Solid Materials (ASTM D 2883), ASTM.
239. van de Putte, T., Determination of the Thermal Stability of Unstable Substances, pp. 179-190 in *Selfheating of Organic Materials*, Intl. Symp. 18th and 19th February 1971, Delft. Delft University (1971).
240. Van Geel, J. L. C., Safe Radius of Heat Generating Substances, *Ind. and Eng. Chem.* **58**, 24-32 (1966).
241. Richards, E. N., An Apparatus for Determining the Liability of Oils to Spontaneous Combustion, *Technology Q. and Proc. of the Society of Arts* **4**, 346-349 (1893).
242. Mackey, W. M., Spontaneous Combustion of Oils Spread on Cotton. II, *J. Soc. Chemical Industry* **14**, 940-941 (1895).
243. Mackey, W. M., Apparatus for the Determination of the Relative Liability to Spontaneous Combustion of Oils Spread on Cotton Wool, *J. Soc. Chemical Industry* **15**, 90-91 (1896).
244. Mackey, W. M., and Ingle, H., Oxidation of Oils in the Presence of Soluble Metallic Catalysts, *J. Soc. Chemical Industry* **36**, 317-319 (1917).
245. Gill, A. H., A Comparison of Apparatus for Testing Liability of Oils to Produce Spontaneous Combustion, *J. Soc. Chemical Industry* **26**, 185-186 (1907).

246. Bowes, P.C., Methods for assessing spontaneous heating and ignition hazards. I: The Mackey test (FR Note 45), Fire Research Station, Borehamwood, UK (1953).
247. Thompson, N. J., Spontaneous Heating of Oils: Methods of Testing, *Ind. and Eng. Chem.* **19**, 394-397 (1927).
248. Bowes, P. C., Factors Limiting General Application of the Mackey Test for Spontaneous Heating and Ignition, *J. Applied Chemistry* **4**, 140-144 (1954).
249. Dufour, R. E., and Clogston, C. C., The Spontaneous Ignition and Dust Explosion Hazards of Certain Soybean Products (Bull. of Research No. 47), Underwriters Laboratories Inc., Chicago (1953).
250. Standard Test Method for Spontaneous Heating Values of Liquids and Solids (Differential Mackey Test), ASTM D 3253, ASTM.
251. Standard Test Method for Spontaneous Heating Tendency of Materials (ASTM E 771), ASTM.
252. Standard Test Method for Thermal Instability of Confined Condensed Phase Systems (Confinement Test), ASTM E 476, ASTM.
253. Koseki, H., Masugi, K., and Mak, W., Some Problems in Test Method for Oxidizing Solids in the UN Recommendations, pp. 45-48 in *APSS2001—Proc. Asia Pacific Symp. on Safety*, Vol. 1, Japan Soc. for Safety Engineering, Yokohama (2001).
254. Kiiski, H., private communication (2001).
255. Dorsett, H. G., et al., Laboratory Equipment and Test Procedures for Evaluating Explosibility of Dusts (RI 5624), Bureau of Mines, Pittsburgh PA (1960).
256. Janssens, M., and Parker, W. J., Oxygen Consumption Calorimetry, pp. 31-59 in **Heat Release in Fires**, V. Babrauskas and S. J. Grayson, eds., E&FN Spon, London (1992).

Copyright © 2003, 2014 Vytenis Babrauskas

Chapter 10. Explosives, pyrotechnics and reactive substances

Highlights and summary of practical guidance **445**
Unstable substances **446**
Heat of formation *447*
Heat of decomposition *447*
Self-heating of liquids *448*
Theory 449
Experimental studies 451
Self-heating of solids *451*
Runaway exothermic reactions **451**
Reactive substances **451**
Explosives **452**
Types of explosives *454*
Chemistry of explosives *455*
Oxygen balance 456
Initiation and ignition *457*
Self-heating, stability in storage, and exposure to heat 457
Impact and shock 459
Flames 464
Radiant heating 465
Hot bodies in contact 465
Friction 466
Compression 466
Electricity 466
Light energy and ionizing radiation 468
Crystal growth 469
RF initiation 469
Modeling detonation *469*
Ignition of air/fuel-gas atmospheres by condensed-phase explosives *470*
Variables affecting the behavior of explosives *470*
Practical applications *472*
Initiating devices 472
Permissible explosives 473
Blasting agents 474
Insensitive munitions 474
Safe distances for storage 474
Propellants **475**
Ignition theory and experimental data *476*
Pyrotechnics **479**
Chemistry of pyrotechnic reactions *480*
Practical applications *481*
Test methods **482**
UN tests *482*
Drop-hammer tests 483
Koenen/BAM friction sensitivity test 483
Card-gap test 484

Readily combustible solids....484
Pyrophoric solids....484
Pyrophoric liquids....484
Water-reactive solids or liquids....485
Oxidizing solids....485
Oxidizing liquids....485
US military standard tests....*485*
Vacuum stability and chemical decomposition tests....485
Laboratory scale impact test....486
Electrostatic sensitivity test....486
Adiabatic sensitivity test....487
Cookoff tests....487
Shock initiation sensitivity test....487
Henkin test for explosion temperature....487
Sensitivity to initiation....488
Permissible explosives....*488*
Other tests....*488*
Pendulum friction test for glancing blows....488
NOL thermal sensitivity test....488
Bureau of Mines test for oxidizing solids....489
LLNL Steven test....489
Further readings....489
References....490

Highlights and summary of practical guidance

In this Chapter we treat a wide variety of solids and a smaller number of liquids which have a propensity for reacting very rapidly. Substances specifically designed to release energy very rapidly are, of course, known as *explosives*. *Pyrotechnics* are substances which are used to create sound, light, smoke or limited force, but do not normally detonate. *Propellants* are used for various propulsion purposes, including armaments and rockets. These three classes of substances are sometimes collectively referred to as *energetic materials*. *Unstable* and *reactive substances* are normally understood to be substances which are not intended to explode, but which can react or decompose in an explosive manner under accidental conditions. There is no fundamental difference in chemistry between the behavior of explosives and of unstable substances; instead, they are differentiated simply according to whether or not there is a purposive use for explosion from the substance.

The unifying theme of these materials is that they do not require oxygen from the air as their primary reaction partner (although they may undergo secondary reactions that involve oxygen from the air). The reaction rates of reactions where gaseous oxygen must arrive at the flame front from the air are limited by the intrinsically slow process of diffusion through a gaseous medium. Since the process is slow, the heat release rate cannot be large. This is why burning of 'common solids' proceeds at a modest rate, compared to explosives or unstable substances. Many explosives or unstable substances, however, do undergo later, secondary reactions with oxygen from the air; the concept of *oxygen balance* is a first-order estimate of this propensity.

Unlike with 'common solids,' the distinction between autoignition and piloted ignition is not meaningful for explosives and unstable substances. The exothermic reaction responsible for explosion or flaming occurs within the solid or liquid, and the presence of a pilot in the gas phase outside it would not affect matters, except as a slight supplemental heating.

To the non-chemist, it may be confusing to find out that some hazardous compounds are referred to as 'endothermic.' The meaning of this designation is that energy would have to be externally supplied in order to assemble them from the constituent elements, as indicated by a positive heat of formation. From the point of view of simple thermodynamics, it might be thought that these compounds should immediately fly apart, i.e., be so unstable as to not exist as a substance that can be produced and warehoused. In practice, not all endothermic compounds are grossly unstable, since the kinetics of the decomposition process must also be taken into account and, if it takes a very long time for the decomposition to take place, the compound may be functionally stable. Nonetheless, relative hazard for unstable compounds is often estimated on the basis of the energy

of decomposition, which quantifies the degree of endothermicity.

Theoretical methods are probably of less use to the hazard specialist in connection with explosives, than with any other class of ignitable substances. A preliminary estimation of reaction hazards is often made with the ASTM CHETAH program[1], which is computer code widely used as first-recourse tool to estimate instability or reactivity of chemical compounds. Highly advanced theoretical computation methods, based on molecular dynamics, have been developed by explosives researchers, but these would be exceptionally difficult to use by the non-specialist. And even with the availability of advanced theories, most hazard assessment of explosives is done on a purely empirical basis. Thus, testing is the cornerstone of hazard assessment and the more widely used test methods are reviewed at the end of this Chapter. Unfortunately, even here things are difficult, since there is little standardization and each research group working in the area generally prefers to invent its own test methods. Furthermore, there is an intrinsic need for a diverse collection of test methods since explosives can be ignited or initiated in various ways, ranging from self-heating to electric spark discharge, and there is generally no correlation between a material's sensitivity to two different types of ignition stimuli.

Commercial uses of explosives are generally driven primarily by economics or availability. This is the reason why, for instance, ANFO has been predominantly used in blasting operations in recent decades as opposed to, say, liquid oxygen explosives, which could also do the job, but not economically. Among the armed forces, over the last two decades, there has been a move to switch over, as much as possible, to 'insensitive munitions.' These utilize energetic compounds that still achieve their intended military purpose, but are not easily exploded by accidental energy sources, such as external shock or heating from a fire.

Unstable substances

Some substances may easily or spontaneously react with certain other substances. Such *reactive* substances are considered in the next Section. Other substances, sometimes called *self-reactive*, are hazardous not necessarily because they can easily react with other substances, but because the molecule itself can 'fly apart.' Common porous solids such as hay or wood fiberboard can be 'unstable' insofar as they are capable of self-heating to ignition. But this form of instability does not lead to an energetic event and substances showing such behavior will not be identified as 'unstable substances.' The self-heating of energetic substances is an important topic, however, and the work in Chapter 9 also lays the basis to understanding some of this behavior. Thus, references will be made in this Chapter to the theory developed in Chapter 9. Also, for convenience all test methods pertinent to self-heating properties have been compiled in Chapter 9, irrespective of whether they are used for energetic materials or materials that self-heat relatively slowly by reacting with the oxygen from the air. Test methods specifically for explosives are presented at the end of this Chapter; these same methods can be applied to the testing of compounds that are not purposive explosives, if their potentially explosive behavior is to be studied. In testing for detonability of unstable substances, it must be kept in mind that there exists a minimum size, below which detonation will not occur. The size is lowered if confinement is provided, but still a minimum exists. Thus, very-small-scale test methods will not be suitable for determining this tendency.

Table 1 Structural features of compounds associated with unstable behavior

Feature	Examples
unsaturated carbon bonds	acetylenes, acetylides, dienes
contiguous nitrogen atoms	hydrazines, azo compounds, diazonium salts, azides
N–O	nitrosos, nitros, nitrates, N-oxides, oximes, 1,2-oxazoles
N–halo	chloramines, fluoramines
O–halo	chlorates, perchlorates, iodosyls
C–metal, N–metal	Grignards, organo-lithium compounds
P–O	phosphates, phosphites
S=O	sulfonyl halides, sulfonyl cyanides
strained rings	epoxides, aziridines
polymerizable groups	compounds with unsaturated groups
mutually reactive groups	amino nitriles, organic salts of oxidizing acids

The UN[2] considers substances containing the following functional groups to be potentially unstable:

(a) aliphatic azo compounds (–C–N=N–C–)
(b) organic azides (–C–N≡N≡N)
(c) diazonium salts ($–CN_2^+Z^-$, where Z^- is a negative-valence group)
(d) N-nitroso compounds (–N–N=O)
(e) aromatic sulfohydrazides ($–SO_2–NH–NH_2$)
(f) organic peroxides (–O–O–); these unstable substances are classified by UN into a category of their own.

Other functional groups identified as potentially unstable include[3,4,5]:

(g) nitro ($–NO_2$). This is generally considered to be the most important group of unstable or explosive compounds[3].
(h) nitrate esters ($–ONO_2$)
(i) nitroso (–NO)
(j) azo and diazo (–N=N–)
(k) azido ($–N_3$)
(l) fulminates (–OCN)
(m) cyano (–C≡N); isocyano
(n) hydrazines (–HN–NH–)
(o) ethynyl (–C≡CH)
(p) alkynes (–C≡C–)
(q) hydroperoxy (–O–OH)

(r) ozonides (–O–O–O–)
(s) chlorates ($–OClO_2$) and perchlorates ($–OClO_3$)
(t) halogenated amines (–NX; $–NX_2$; $–NX_3$)
(u) polymerizable compounds, including certain substituted olefins, epoxides, aziridines, and diketene.
(v) certain organic heavy metal compounds.

A more general list[6] of structural features of compounds potentially unstable has been offered (Table 1).

HEAT OF FORMATION

One way of estimating the stability of compounds is to consider their heats of formation. The heat of formation is the enthalpy which is required to be added in order to form a compound out of its elements. Thus a substance with a high positive value of Δh_f is one which is difficult to 'unite' into a compound and, therefore, one which may have a tendency to spontaneously decompose into its elements or into some larger fragments. Conversely, a substance with a high negative value of Δh_f is one which gives off a lot of heat when formed from its parent elements. Thus, it requires the addition of substantial heat into the system from the outside for such a compound to decompose. Table 2 illustrates this for some common substances. The values shown are all for the vapor state. Compounds showing positive Δh_f values are called *endothermic compounds*.

Molecules of methane, propane, and butane are all known to be stable against disintegrating into pieces. They show heat of formation values well below zero. Acetylene, carbon disulfide, and ethylene are known to be unstable compounds which can decompose under certain conditions. These all have highly positive Δh_f values. Propylene shares some traits with ethylene, but is not as unstable. This is reflected in the fact that its Δh_f value, while positive, is lower than that of ethylene.

Table 2 The heats of formation for some common substances at 298 K

Compound	Prone to decompose spontaneously	Lowest pressure for decomposition (atm)	Δh_f (kJ mol^{-1})
vinylacetylene (C_4H_4)	yes	≈1.0	304.6
acetylene (C_2H_2)	yes	≈1.0	226.7
monochloroacetylene	yes	0.079	214
propadiene (C_3H_4)	yes	2.22	192
methylacetylene (C_3H_4)	yes	3.95	185
propargyl bromide (C_3H_3Br)	yes	0.002	≈170
ozone (O_3)	yes		142.7
carbon disulfide (CS_2)			117.1
hydrazine (N_2H_4)	yes	0.016	95.4
ethylene (C_2H_4)	yes		52.3
propylene (C_3H_6)			20.4
ethylene oxide (C_2H_4O)	yes	0.069	-52.7
methane (CH_4)	no	--	-74.8
propane (C_3H_8)	no	--	-103.9
n-butane (C_4H_{10})	no	--	-126.2
ethyl nitrate ($C_2H_5NO_3$)	yes	< 0.033	-154

For the substances which are prone to decomposition, the lowest pressure under which spontaneous decomposition may occur at 0% oxygen and room temperature conditions is also listed[7]. In all practical cases, details of the test conditions are very important and a tabulation such as this should only be used for preliminary screening. In any case, there is not seen to be a quantitative relation between Δh_f and the pressure sensitivity of the substances.

HEAT OF DECOMPOSITION

Heats of formation are readily found in chemical reference handbooks, since that is one of the most fundamental thermochemical properties of a substance. Minus-one times the heat of formation is the heat which would be evolved, under constant pressure, if the molecule were to fly apart into the constitutive elements. This is exactly what happens with hydrogen peroxide, for example:

$$H_2O_2 \rightarrow H_2 + O_2$$

More complex molecules rarely disintegrate into their elements, and may produce many reaction products. Thus, a more realistic measure is often sought. The heat of decomposition is what describes the heat which is evolved for actual reaction products. Furthermore, unstable chemicals are more likely to be held in a constant-volume environment rather than constant pressure, thus, the 'heat' is preferably an energy rather than an enthalpy. Determining heats of decomposition requires more than simple thermochemistry, since one must know the identity of the pieces into which the molecule will decompose. If this identity is known, then the heat of reaction, for producing the known reaction products, is readily calculable. Otherwise, values must be obtained from testing. For highly energetic materials, the oxygen-bomb apparatus is used, but without adding oxygen. Decomposition is initiated by firing the igniter wire. Compounds that are only moderately unstable will not decompose in this manner, thus data on them must be obtained by less direct means. Often this involves using DSC or other tests discussed in Chapter 9. For explosives, the negative of the heat of decomposition is usually termed the *heat of explosion*.

Table 3 lists some example values for decomposition energy compiled by Grewer[8]. Highly unstable substances show ΔE_d values ranging as high as –6070 kJ kg^{-1}. Roughly, it is suggested that substances having ΔE_d values below –3000 kJ kg^{-1} are very highly hazardous and should be evaluated as to possibly being prone to detonating. Substances with $-3000 < \Delta E_d < -500$ are in a lesser category of hazard, while substances with $\Delta E_d > -500$ kJ kg^{-1} are not likely to undergo violent decomposition (but may be subject to mild

self-heating). Grewer also provides some detailed experimental data which illustrate that changing the test apparatus or conditions under which ΔE_d is determined can lead to variations of more than 2× in the results. Grewer's[8] and Bretherick's[9] monographs should be consulted for detailed discussions of the decomposition chemistry of various unstable substances.

Table 3 Decomposition energy of some substances

Substance	Formula	$-\Delta E_d$	
		(kJ mol^{-1})	(kJ kg^{-1})
diazodinitrophenol	$C_6H_2N_4O_5$	1275	6070
picric acid	$C_6H_3N_3O_7$	1010	4400
2,4,6-trinitrotoluene	$C_7H_5N_3O_6$	998	4395
trinitrobenzoic acid	$C_7H_3N_3O_8$	1073	4170
1,3-dinitrobenzene	$C_6H_4N_2O_4$	590	3510
trinitromethane	CN_4O_8	502	3325
3-nitroaniline	$C_6H_6N_2O_2$	350	2530
lead azide	PbN_6	449	1540
mercury fulminate	$C_2HgN_2O_2$	423	1490
benzoyl peroxide	$C_{14}H_{10}O_4$	340	1400
ammonium perchlorate	NH_4ClO_4	172	1465
tert-butyl peroxybenzoate	$C_{11}H_{14}O_3$	260	1340
propylene oxide	C_3H_6O	65	1120
styrene	C_8H_8	58	560
cornstarch	--	NA	460
1,2-diphenylhydrazine	$C_{12}H_{12}N_2$	81	440
sucrose	$C_{12}H_{22}O_{11}$	140	410
glucose	$C_6H_{12}O_6$	73	405
cellulose	--	NA	330
phosphonic acid	H_3O_3P	8	100

The UN defines[2] unstable substances as substances having a decomposition energy < –300 kJ kg^{-1} and a self-accelerating decomposition temperature (SADT) < 75ºC for a 50 kg package. According to Grewer's results, this is an exceedingly conservative stance; presumably only common sense or SADT testing keeps substances such as cellulose or glucose from being classified as unstable. Substances may also be unstable because of the opposite effect to flying away: *spontaneous polymerization*.

SELF-HEATING OF LIQUIDS

Many liquids are subject to self-heating, although this problem is most commonly encountered only in chemical manufacturing or storage facilities. Self-heating of liquids can occur under two opposite conditions: stirred, or stagnant. Stirred conditions will often be found in chemical plants, where reactor vessels are normally stirred. Stagnant conditions will generally prevail when liquids are warehoused. The possibility of being stirred is unique to liquids and gases—solids, by definition, cannot be stirred. Granular materials could, in principle, be stirred, but environments in which they self-heat in practice are usually at rest. Whether or not a container is stirred has major implications for the analysis of the problem. The purpose of stirring is to make uniform the temperature and concentration within a vessel. Thus, a stirred container problem will be analyzed theoretically as being at a uniform temperature. A stagnant volume of liquid, on the other hand, can show temperature gradients. The case here will be more similar, but not identical, to the case of solid material. Convective flows will occur in a volume of liquid which has significant temperature differences (if the layering is not stable). Such self-stirring does not occur in solids.

Self-heating of liquids is a main cause why chemical plants blow up (with or without an additional flaming fire), thus understanding how such ignitions occur is important. In many cases, only a single reactant is involved, that is, it is a *unary* reaction. The nature of the reaction can be:

- decomposition—a molecule splits up into two or more fragments
- polymerization—molecules join up into longer chains; this is normally an exothermic process
- isomerization—a molecule rearranges its functional groups

More complicated reactions in liquid systems can of course also occur that lead to disastrous self-heating. If a chemical plant reactor failure occurs, it may be followed by additional reactions, e.g., the substance may further burn in air, once ejected from the vessel.

Because the density of a gas is about 1000 times less than that of a liquid, a decomposition reaction causing gasification of a liquid can create pressures on the order of 1000 atm. Some compounds can achieve a flame temperature on the order of 3000 K. From the latter heating effect, another factor of 10 increase in pressure can result, leading to expectations of *ca*. 10,000 atm pressures in the worst case.

The chemistry of many potentially hazardous chemical plant self-heating situations is difficult to unravel because the actual decomposition products are unknown. In many cases, even after extensive investigation post-explosion, only a surmise of the actual chemical mechanism can be made. This means that detailed features such as the heat of reaction cannot be computed quantitatively, since knowledge of reaction products is required for such computations. Also, unless the heat of decomposition is large, the decomposition products are likely *not* to be the equilibrium products. An analogy to this situation can be seen from normal open-air burning: low HRR substances generally burn 'dirty' and do not simply produce CO_2 and H_2O.

Decomposition reactions in liquids can be grouped into three types:

(1) homogeneous reactions which can be considered a thermal explosion
(2) deflagrations (a steadily-moving combustion wave)
(3) detonations (a combustion wave propagated by means of a shock wave).

Fortunately, the fraction of substances prone to showing liquid-state deflagrations is small, and the fraction capable of detonations is smaller yet. Explosions of substances with a high heat of decomposition may start as a thermal explosion then change to a deflagration.

The two main theories of self-heating are those due to Semenov and Frank-Kamenetskii, with the latter having been much expanded by Thomas. Semenov's theory assumes that the substance has no thermal gradients within it. This would generally be a very poor assumption for porous solids, which is the reason that the theoretical development in Chapter 9 did not focus on Semenov's theory. But in the chemical engineering arena, reactions often take place in stirred vessels. The chemical engineering application has the difference that, in many cases, the material is not simply held and stirred, but rather flows in and out of a stirred reactor vessel. These are known as continuously-stirred tank reactor (CSTR) problems and self-heating can be analyzed according to Semenov's basic theory, since neither temperature nor concentration gradients are assumed to exist inside the vessel.

The *time* element is often much different in chemical plant liquid reactions, as compared to storage problems of solids. A reaction is normally completed in a matter of several hours, at which point the substance is cooled and taken out of the reactor. Thus, safety investigations often select a 24 h period as the maximum storage time for which the self-heating potential is to be examined. For solid materials, storage times of weeks or months are common, and the extended-period storage problem (ambient temperature starting conditions) is more commonly encountered than the hot work problem (high initial temperature). In the case of reactive liquids, the starting temperature is commonly in the 100 – 200ºC range.

Many unstable liquids (and explosives) can deflagrate or detonate directly in the liquid phase, without first generating a flammable gas. The combustion which takes place after the ignition is notably different in liquids than in solids, and it is not covered by general combustion textbooks. Probably the best introduction to the science is given by Verhoeff[10]. Unstable liquids may also first vaporize, then decompose. The latter occurs if the decomposition temperature T_d is higher than the boiling point T_b. Verhoeff suggests that a functional definition of T_d is the temperature at which the self-heating liquid first attains a heat release rate of 100 W kg^{-1}.

Less well studied are *heterogeneous explosions* involving liquids that are oxidative, rather than decompositional in nature. When some organic liquids are presented with a gaseous oxidizer, especially at high-pressures, surface explosions, bubble explosions, foam explosions, and aerosol explosions can be possible. These reactions are not constrained by the same flammability limits pertinent to normal gas-phase explosions of the vapors. Hieronymus et al.[11] have presented some illustrative examples, but a systematic overview has not yet been attempted. A similar problem is heterogeneous reaction between two liquids that form different phases. A theory for this problem of *liquid-liquid reaction* has been described by Fujimoto[12].

Our approach in this book concerning condensed-phase substances burning directly in the condensed phase will be slightly different than for substances burning in the gas phase. For the latter, it is appropriate to develop some elementary background of the post-ignition aspects of combustion (Chapter 3). But for liquids and solids we will explore solely the ignition event and leave to specialist texts to develop principles and theories describing post-ignition conditions. Even so, our scope will necessarily be restricted, since theoretical concepts that have wide applicability to a variety of substances are scarce. Typically, research on unstable liquids has been focused solely on a particular substance and the ability to generalize that knowledge may be limited.

THEORY

The earliest theory of self-heating is the one due to Semenov, wherein he assumed that there is resistance to the flow of heat at the edges of the body (i.e., a convective cooling coefficient), but that there are no thermal gradients within the body. A condition of no thermal gradients within the body can come about in two ways: (1) if the substance has a high thermal conductivity, or (2) if the substance is mechanically stirred or agitated. Many unstable substances are liquids which have high thermal conductivities, and reaction vessels for liquids are also often stirred. Thus, the Semenov model can be quite useful for chemical reactor vessels. In the Semenov theory, zeroth-order kinetics is assumed and heat generation within the body is then:

$$\rho VQAe^{-E/RT} + G$$

where we have included an optional heat generation term G (W) due to mechanical agitation or electrical heating. Mechanical agitation is common in reaction vessels for liquids, and the heat contribution from this source has been sufficient to account for some industrial accidents[13]. The convective heat losses are represented as:

$$h_c S\left(T - T_o\right)$$

where S (m^2) is the exposed surface area. Equating the two expressions gives:

$$\rho VQAe^{-E/RT} + G = h_c S\left(T - T_o\right)$$

Also at the critical temperature, which we will define as T_c, the *slopes* are identical (Figure 3 in Chapter 9), thus:

$$\frac{d}{dT}\left(\rho VQAe^{-E/RT} + G\right) = \frac{d}{dT}\left(h_c S\left[T - T_o\right]\right)$$

or

$$\rho VQA\frac{E}{RT_c^2}e^{-E/RT_c} = h_c S$$

and after combining with the previous equality, a solution can be obtained for T_c:

$$T_c = \frac{E}{2R}\left(1 - \sqrt{1 - \frac{4GR}{h_c SE} - \frac{4RT_o}{E}}\right)$$

If there is no internal generation of power, then the classical solution is:

$$T_c = \frac{E}{2R}\left(1 - \sqrt{1 - \frac{4RT_o}{E}}\right)$$

Thus, the power generation term raises the effective ambient temperature from T_o to $T_o + G/h_c S$. An extension of the Semenov theory has been developed[14] for treating industrial dryers and fluidized bed processes, where enthalpy is introduced directly into the system via an air stream.

For many applications, the classical solution to the Semenov theory is further approximated by the use of the power series expansion:

$$\sqrt{1 - \frac{4RT_o}{T}} = 1 - \frac{2RT_o}{E} - \frac{2R^2T_o^2}{E^2} + \ldots$$

and keeping only the two leading terms gives:

$$T_c \approx T_o + \frac{RT_o^2}{E}$$

This approximation is valid if E is sufficiently large, specifically if $2RT_o/E << 1$. Since E may be 100 kJ mol^{-1} and $T_o \approx$ 300 K, then 0.02 is indeed much less than 1.

Bowes[15] suggests that, in parallel to the δ parameter based on Frank-Kamenetskii/Thomas theory that was developed in the previous Chapter, practical analysis of stirred liquids should be based on the Semenov number ψ:

$$\psi = \frac{E}{RT_o^2}\frac{QAV\rho}{hS}e^{-E/RT_o}$$

The critical value of ψ, denoted as ψ_c, is found to be $1/e$. Now, the heat transfer coefficient is found to depend on the radius roughly as:

$$h \approx k_1 r^{-1/2}$$

where k_1 is a constant. For regular geometric shapes such as sphere, cylinder, etc., $V/S = k_2 r$, where k_2 is another constant. Then,

$$\psi = \frac{E}{RT_o^2}\frac{k_2}{k_1}r^{1.5}QA\rho e^{-E/RT_o}$$

and $$\psi_c = \frac{1}{e} = \frac{E}{RT_o^2}\frac{k_2}{k_1}r^{1.5}QA\rho e^{-E/RT_o}$$

In a manner similar as developed in Chapter 9, a data analysis strategy can be developed by multiplying out and taking the natural logarithms of both sides of this equation:

$$\ln\left(\frac{T_o^2}{er^{1.5}}\right) = P - \frac{E}{RT_o}$$

where $$P = \ln\left(\frac{E}{R}\rho QA\frac{k_1}{k_2}\right)$$

Thus, if $1/T_o$ is plotted on the x-axis and $\ln\left(\frac{T_o^2}{er^{1.5}}\right)$ on the y-axis, the slope will be $-E/R$ and the y-axis intercept will be P. Once a sufficient number of data points are obtained to allow a straight line to be fitted, the resultant straight line can be used to estimate the critical size for other values of initial temperature T_o.

While standard theories of self-heating—whether Semenov's or the F-K theory discussed in Chapter 9—can often be applied to analyzing unstable substances, there can arise numerous complications. If the substance undergoes a significant volume change in reacting, for example, when the reaction product is a gas, the formulation has to be modified. A method has been described for treating such substances[16], but it does not appear to be readily usable. Heat transfer conditions can often be adequately estimated for porous-substance self-heating problems. But for unstable substances, changes of phase can introduce mixing which affects heat transfer in a way that is difficult to characterize, since the system is continuously self-modifying.

A unique feature of self-heating in liquids that is not found in solids is *convective flows* of the reactant. If the volume of liquid has only small temperature differences, then convective flows are absent. But if the temperature differences become greater than a certain amount, then convective flows may begin. Conduction plays only a small role in the self-heating of liquids, but convection is effective in diffusing away localized packets of heated material. Thus, Verhoeff[10] found that with some unstable liquids, the system is stabilized by a stirrer's introduction of convective flows, rather than being adversely affected by the added energy.

Verhoeff considers that an explosion of a liquid proceeds in the following stages[10]:

1. *Thermal runaway*. Time scale: 1 – 10^4 s. During this stage the liquid is at a uniform temperature, but the temperature is rising.
2. *Initiation*. Time scale: 0.1 – 10 s. During this state the liquid forms a hot spot. Verhoeff considers that non-uniformities of 2 ⌗C are an empirical sign of the start of initiation.
3. *Explosion*. Time scale: 10^{-3} – 1 s. A propagating reaction zone moves through the mass of the liquid. This is a condensed-phase deflagration, but detonations, while rare, are also possible, especially if the liquid is aerated.

The above presentation focused on a fixed control volume. But liquids in a continuous-flow reactor are also able to reach thermal runaway. These systems exhibit some special peculiarities, one of which is a propensity to undergo temperature/concentration cycling[17]. Merzhanov[18] has developed extensive theories for treating flow-through systems.

EXPERIMENTAL STUDIES

For studying the self-heating of liquids, similar equipment to those used for granular solids cannot be used, since pressure rises can be high and the equipment would be destroyed. Thus, autoclaves are used which can withstand the necessary pressures of up to 150 MPa[10]. Because of the design necessary to withstand high pressures, the thermal conditions within the experimental apparatus end up being less straightforward than in test methods such as oven-basket tests. Consequently, data analysis and interpretation becomes more complex.

A complication of self-heating liquids is that often the chemical reactions cannot be described by a single set of Arrhenius constants, but will change over time. This behavior can be correlated to a conversion fraction variable x which is defined as:

$$x = \frac{\text{reactant mass consumed}}{\text{initial reactant mass}}$$

and is thus 0 at the beginning and 1.0 when the reactant is fully reacted. Verhoeff[10] showed that for the organic peroxide *tert*-butylperoxybenzoate (TBPB), the reaction is autocatalytic up to $x \approx 0.05$, and is approximately first-order for $0.05 < x < 0.98$. He also showed that both the test apparatus used and the numerical technique employed to reduce the kinetics data can have a major effect on the values reported.

For liquids contained in a pressure vessel, *pressure* affects the course of an explosion. Much of the chemistry of the reaction has to take pressure in account, both the initial pressure conditions and the influence of confinement on the pressure rise. If the reaction is autocatalytic and involves generation of gaseous products, then a decrease in pressure leads to a decrease in reaction rate, because the catalytic feedback chain is impaired due to removal of products. In open systems, *evaporation* of reactant may occur. This affects the energy balance of the system and, clearly, criticality, if it occurs, will not occur if it requires a temperature greater than the boiling point of the substance.

Apart from self-heating, unstable liquids can also explode by *forced ignition*, i.e., with the presence of a localized source of heat. While this form of ignition may be less common in industrial accidents it has received some experimental study; for example, Verhoeff[10] examined the effects of a Nichrome heating wire on TBPB.

SELF-HEATING OF SOLIDS

Solids undergoing unary reactions (unstable solids and explosives) are often treated by some version of Arrhenius kinetics that was originally developed for gases, deriving values of E and A as constants supposedly characteristic of the reaction. Gomes[19] has pointed out that values derived in this way may be artifacts of the experiment and little else. A justification for developing rate constants does exist if a reaction mechanism can be elucidated, but this is often not known.

A decomposition reaction in a granular solid may lead to a shock wave being produced if gases that are produced are channeled through small openings among the particles, since acceleration of velocity can occur.

Runaway exothermic reactions

A major fraction of industrial explosions occur not because manufactured products are handled which are unstable. Rather, they occur during production—an exothermic reaction is needed in order to produce a certain substance. An exothermic reaction is perfectly acceptable, if a combination of heat removal (e.g., a water-cooled reaction vessel jacket) and controlled rate of substance introduction keeps the reaction at a stable temperature. In the case of explosions, some procedural error, contamination (e.g., a reaction turns out to be very sensitive to moisture as a contaminant), equipment failure (e.g., cooling water, electricity for stirring), or miscalculation, leads to a condition where heat removal can no longer keep up with heat generation, and a runaway condition ensues. Industrial reactions can be quite difficult to quantitatively model, especially if many steps or manual steps are involved. Many explosions have occurred because a process was stable in bench-scale design, but scale-up to production quantities proved to remove needed safety margins. The thermal aspects of these explosions follow the same principles as do single-substance decomposition reactions. In practice, the application can be very difficult when more than one substance must be considered. There have been a series of proceedings on this topic hosted by AIChE[20]. Also, a European symposium[21] was held on this topic, and a textbook has been published by Grewer[8].

Before detailed thermochemical calculations are undertaken, it is often useful to know whether the reactions have a high potential for exothermicity. A number of estimating rules have been proposed for assessing the risk, with the Dutch scheme[22] being given in Table 4.

Table 4 Dutch scheme for classifying the hazard of exothermic reactions

Hazard rating factor	Type of reaction	Examples
0.30	mild exothermic reactions	hydrogenation, hydrolysis, alkylation, isomerization, sulfonation, neutralization
0.50	moderate exothermic reactions	esterification, oxidation, polymerization, condensation
1.00	critical-to-control exothermic reactions	halogenation
1.25	particularly sensitive exothermic reactions	nitration

Reactive substances

Reactive substances are understood to be ones which react violently or 'immediately' upon mixing. These are sometimes divided into pyrophoric, water-reactive, and hypergolic categories. *Pyrophoric substances* are defined by the Department of Transportation[23] as liquids or solids that, even in small quantities and without an external ignition source, can ignite within 5 minutes after coming in contact with air. If the time for ignition is long, then the substance is *self-heating*, not pyrophoric. Some researchers do not restrict the definition to solids and liquids, but also includes gases, e.g., silane; however, such gases are more correctly referred to as being hypergolic. Also, in scientific usage, pyrophoric substances can include ones which react not with air, but with pure gaseous oxygen, or liquid oxidizers of various sorts. Chemical families where many members are pyrophoric include:

- alkali-metal carbides
- aluminum alkyl compounds
- boranes
- alkyl-metal compounds
- aryl-metals compounds
- acetylenic compounds
- metal and non-metal hydrides
- metal sulfides
- hexamethylnitratodialuminate salts
- metal carbonyls
- organometallic compounds
- phosphines
- silanes

Urben[9] provides extensive listings along with literature references. Carson and Mumford[24] provide additional listings and example case histories. Two papers by Zehr comprise essentially an annotated bibliography of pyrophoric dusts through 1966; the first part is in German[25], while the second part is available in English[26]. While many metals are pyrophoric when in a finely divided, reactive state, the size required is usually very small, generally 0.1 – 1.0 μm. Uranium, uranium hydride, thorium, and plutonium are also pyrophoric when in the form of large pieces[27]. Pyrophoric metals are further considered in Chapter 8 and in Chapter 14.

Calcium permanganate and potassium permanganate are strong oxidizers, and pyrophoric reactions occur between these and glycerin, benzaldehyde, or dimethyl sulfoxide. Ignition can also occur when calcium permanganate contacts paper or cotton. The reactivity of the permanganates is further increased if concentrated sulfuric acid is added. Calcium hypochlorite ignites upon being mixed with a number of organic compounds and it is considered in some detail in Chapter 14.

Chemically different, but with similar hazard considerations are *water-reactive* materials. These include alkali metals and their hydrides, carbides, and amides. Some uranium compounds are both highly pyrophoric in air and water-reactive. Certain *mixtures* also react violently when wetted. These include magnesium powder with silver nitrate, aluminum powder with iodine, aluminum or magnesium with sodium peroxide, sodium hydroxide with ferrosilicon (which glows rather than exploding). The major works on water-reactive substances are the survey by Ripley[28] and the handbook by Gibson and Weber[29]. Water-reactive substances have some use in military and commercial applications, but accidental fires due to water-reactive substances have been very rare, so the cited works should be consulted for details on specific substances.

An exothermic reaction is said to be *hypergolic* if ignition occurs immediately upon contact between two substances. Such pairs of substances are common in the rocketry field, where a hypergolic reaction turns out to be a good way to provide a controllable propulsion source. The hypergolic nature makes it easy to quickly start up the process without a period of preheat. In other circumstances, such a combination of ingredients, if inadvertent, would be highly dangerous. Typical fuel portions of a hypergolic pair include hydrogen, ammonia, hydrazine, and various amines. The oxidizer portion can include hydrogen peroxide, fluorine, white fuming nitric acid, and nitrogen dioxide. Not all pairings have the hypergolic property. For instance, hydrogen will react with fluorine in a hypergolic manner but not with nitric acid. Conversely, ammonia will produce a hypergolic reaction with nitric acid, but not with hydrogen peroxide. Fletcher and Morrell[30] have reviewed research on the ignition of hypergolic rocket propellants. The physical aspects of the explosion that occurs when two hypergolic substances are combined have been studied in high-speed photography by Daimon et al.[31]

Apart from in the rocketry field, some hypergolic reactions find use in mundane applications. One such is a type of self-lighting welding torch which uses chlorine trifluoride and hydrogen. These gases ignite upon mixing, and yield HF and HCl as products. Fire bombs have also been made which depend on the hypergolic reaction between sulfuric acid and a sugar/potassium chlorate mixture.

Explosives

Explosives*, pyrotechnics, and propellants are substances which share some common traits: they are solids or liquids, not gases; and their main utility lies in the fact that they burn very fast. In the latter trait, they differ from liquid or solid combustibles of other types, which are substances that burn slowly, in comparison. The relative HRR differences are enormous. Where a solid combustible might show HRR values of 200 kW m^{-2} and a liquid 2000 kW m^{-2}, a detonating explosive may show 10,000,000 kW m^{-2}. Explosives are typically designed to detonate, while propellants and pyrotechnics must deflagrate rapidly, but not detonate. The pressures attained in a detonation are enormous, commonly

* More precisely, *condensed-phase explosives*.

being around 250,000 atm. Propellants comprise a wide variety of substances which are used for propelling rockets or ammunition. The main distinction between propellants and explosives is the time frame over which the energy is released. Whereas explosives may release their energy in a microsecond, a propellant, in order to deliver useful propulsion, may deliver it in a millisecond up to many seconds. Pyrotechnics are substances which react rapidly but are used for purposes other than shattering objects or propelling rockets or ammunition. The uses of pyrotechnics are for creating light, sound, gasses, motion, or smoke. The distinctions between these classes of substances are not always rigid. The term 'propellant' only came into use in the mid-20th century; earlier these substances were simply categorized as 'low explosives.' There is no substantive difference between propellants and pyrotechnics used for producing gas or motion.

Explosives do not necessarily always react by exploding; they may simply burn in a quiescent manner. This depends on the mode of ignition, as originally discovered by the British chemist Frederick Abel. In 1866 he documented that guncotton will simply burn if ignited by a flame, but will detonate if hit by a hammer with a heavy blow[32].

In this Section, we will first consider explosives and develop general principles for them. Many of these apply directly to pyrotechnics and rocket propellants, thus the following two sections are somewhat more brief in coverage. Some broad differences among combustibles are illustrated in Table 5. Note especially the low energy of explosion for TNT. This is the energy which can be delivered in an explosion, utilizing only the condensed-phase substances. The actual heat of combustion of TNT is 14.5 MJ kg^{-1}. To release this amount of heat requires that some of the carbon of TNT combine with gaseous oxygen from the atmosphere. Such further combustion can occur, but it is not part of the main explosion. Most pyrotechnic substances produce solids, rather than gases, as their primary reaction products. Thus, the volume of products is very small compared to ordinary combustibles or most explosives (some pyrotechnics used as airbag inflators, etc., are designed to produce substantial quantities of gaseous products). The examples in Table 5 make vividly clear that the hazard of explosives is not because there is a large amount of heat produced, but because the heat is produced very rapidly.

Table 5 A comparison of characteristics of some condensed-phase combustibles

Combustible	Formula	Gross Δh_c (MJ kg^{-1})	Volume of products, per mass of combustible (m^3 kg^{-1})
gasoline	$\approx CH_2$	46.9	3.20
wood	$\approx C_{24}H_{60}O_{28}$	19.5	1.52
TNT	$C_7H_5N_3O_6$	2.8[e]	0.740
photoflash mixture	$Ba(NO_3)_2$ + 13Al + $2KClO_4$	8.9	0.025
gunpowder	NA	2.0	NA

[e] energy of explosion

Most common liquids or solids burn by first evaporating or pyrolyzing to produce a flammable gas, then the gas combines with oxygen in a combustion reaction. These types of processes involve two steps, and both can be slow. (1) Evaporation or pyrolysis is limited by the time needed by heat to diffuse into the liquid or solid. (2) When the flammable vapor has been generated, it then still has to go through a slow process where fuel and oxygen molecules diffuse towards each other before the combustion reaction can occur. Explosives also acquire some of their energetic properties from the fact that heat transfer between the burned and the unburned substance is very high, since it occurs in the solid. By contrast, for pyrolyzing solids, the heat feedback from the burning gas back to the solid is inefficient. Thus, many of the unique properties of solid explosives and pyrotechnics come about because the basic reactions follow the form of:

solid A → solid B + gas (reaction #1)

or

solid C + solid D → solid E + gas (reaction #2)

in other words, either a single substance flies apart into fragments, or two types of molecules in intimate physical contact undergo a reaction. Explosives based on reaction #1 are referred to as *single-component explosives*, *molecular explosives*, *intramolecular explosives*, or *monomolecular explosives*. The reaction is one simply of decomposition. RDX (cyclo-1,3,5-trimethylene-2,4,6-trinitramine) is an example of a single-component explosive. Explosives based on reaction #2 are referred to *multi-component explosives*, or *intermolecular explosives*. Physically, the reactants in reaction #2 can be mixed and pressed powder, a particulate phase dispersed in a polymer matrix, a eutectic[33] formed by melting two substances together, etc. ANFO is an example of a multi-component explosive. Even though finely-ground powders and similar mixtures establish close contact between substances, nonetheless the possibility of reacting fast is greatest if a second substance is not needed at all, in other words, if a monomolecular reaction takes place. While there are exceptions and untypical substances, nonetheless many of the common explosives represent reaction #1, while pyrotechnics all correspond to reaction #2. This is because the speed of reaction should be maximized in an explosive, but if a pyrotechnic reacts too fast (i.e., detonates) it becomes a serious hazard rather than a technological tool. In some explosives, features of both reaction #1 and #2 exist—there exists more than one reactant, but at least one of those reactants itself acts as both a fuel and an oxidizer.

The role of the speed of the controlling processes that govern the rate of combustion can also be seen in reactions

between a fuel gas and air. If a fuel gas starts to leak into the air and is immediately ignited, it burns slowly, since diffusion of oxygen molecules to combine with the fuel molecules is necessary. But if a mixture of a fuel gas and oxygen is well stirred, then ignited, a forceful explosion will result.

TYPES OF EXPLOSIVES

Traditionally, explosives were subdivided as low explosives or high explosives according to the scheme below. In modern times, the substances that used to be termed low explosives are classed as propellants, although the traditional classification still sees some use. Flash powder has also been classed as a low explosive, but is currently classified as a pyrotechnic.

- *Low explosives* are fuel/oxidizer mixtures which burn when ignited but do not detonate. Low explosives must be confined for an explosion to be produced and tend to burn without explosion if unconfined.
- *High explosives* are capable of detonation under unconfined conditions.
  - *Primary explosives* are explosives that can detonate by means other than shock waves, for example, mechanical impact, heat or electric discharge. Primary explosives often serve as *initiators*. Examples: mercury fulminate, lead azide, lead styphnate, tetrazene.
  - *Secondary explosives* require a shock wave to detonate; the shock wave is typically supplied by a primary explosive. They tend to deflagrate, not detonate, when initiated by heat or sub-sonic shock. Examples: dynamite, nitroglycerin, PETN, RDX (cyclonite), TNT.

In explosions which do not reach the velocity of sound, i.e., in deflagrations, the damage is mostly from flying pieces of the container which was exploded. By contrast, in detonations the primary damage is from the blast wave itself, except for devices specifically designed to create shrapnel, such as bombs.

Explosives take the form of several *states of aggregation*:

- liquid
- slurry, gel or emulsion
- homogeneous solid
- granular solid

Liquid explosives are relatively rarely used, despite their long history of development. Nitroglycerin is an example of a liquid explosive, but as a pure substance it is not a practical explosive due to its instability. Instead, nitroglycerin is used as an ingredient in the manufacture of other explosives. *Sprengel explosives*, named after the German inventor Hermann Sprengel, are explosives where an oxidizer and a liquid fuel are mixed by the user just before use. At least one of the two components is a liquid. A wide variety of fuels and oxidants was explored by Sprengel. The oxidizer can include potassium chlorate, liquid NO_2, etc. The fuel can be CS_2, picric acid, petroleum, etc. While viable for commercial use, the actual use has been rare. LOX (liquid oxygen) explosives[34] are a still-used example of Sprengel explosives. A wide variety of substances can be used for its fuel component. During World War II, the Russians used the mixture KD in aerial bombs, which comprised 60% nitric acid and 40% dichloroethane[35].

Many explosive mixtures are neither liquid nor solid, but in a state of aggregation which is somewhat intermediate. These are commonly identified as slurries, gels, and emulsions. *Slurries or gels* often consist of ammonium nitrate, a fuel such as aluminum powder, and a thickening agent. The consistency is typically somewhat firmer than that of fresh concrete. The US military has explored a wide variety of liquid explosives, including sensitized nitromethane and hydrazine-based materials, with an eye toward developing gels that use the liquid explosive plus a gelling agent. These have been described[36], but have not come into significant use. *Emulsions* are typically water-in-oil emulsions which comprise a saturated nitrate solution and mineral oil. These are available as packaged cartridges but may also be site-mixed. Slurries, gels and emulsions also require entrained air to be sensitive enough for useful work; this is commonly accomplished by including air-filled microballoons. Additional sensitizing components are often added; these may be aluminum flake, methyl amine nitrate, isopropyl nitrate, hexamethylene triamine trinitrate, ethyl glycol mononitrate, PETN, or TNT.

Many explosives are homogeneous solids, e.g., nitrocellulose. The physical properties are also homogeneous when an explosive is prepared from two or more components as a solid colloidal solution, for example, nitrocellulose and nitroglycerin. *Plastic explosives* contain a polymer such as polybutadiene or polyurethane in which is dispersed a granular explosive (e.g., octogen, RDX). The plastic explosive can be formed into thin sheets or into other desired shapes. Plastic explosives became very successfully commercialized by the Czech firm VCHZ Synthesia (formerly, Semtin) in the form of Semtex. While various grades exist, Semtex generally consists of PETN and RDX in a plastic substrate (styrene-butadiene copolymer), along with dye, antioxidant, and plasticizer. Semtex became a favorite of terrorists due to its ease of concealment and the difficulty of detecting it by chemical sensing outside the package. Thus, a 1991 treaty, the Convention on the Marking of Plastic Explosives for the Purpose of Detection, to which US is a signatory, was enacted which requires that all plastic explosives be 'tagged' by adding an agent to the explosive which has sufficient vapor pressure and a unique signature allowing detection. Synthesia is currently using para-mononitrotoluene or dimethyl-dinitrobutane as taggants for its products. In military applications, C-4 is the most common; it comprises 91% RDX, 5.3% di-(2-ethylhexyl)sebacate, 2.1% polyisobutylene, and 1.6% motor oil. Various types of explosives are also prepared as *putties*, *extrusions*, *castings*, *rubber sheets*, etc.

Granular solids comprise a large category of commercial and military explosives. *Dynamite* was originally a trade name of the Nobel company and referred to powders impregnated with nitroglycerin. Later, gel forms of dynamite came into use. The term has become very broad in meaning, and one definition is[37]: an organic nitrate ester (e.g., NG) along with optional presence of oxidizing salts, carbonaceous filler, sulfur, NC, or microballoons. In US Army usage, a dynamite does not contain any nitroglycerin but, rather, is based on RDX and TNT. For commercial blasting purposes, dynamites have largely been supplanted by ammonium-nitrate based ANFO explosives (see Chapter 14).

Forensics experts often classify explosives according to their origin as:

- commercial explosives
- military explosives
- improvised (i.e., home-brew) explosives.

A bomb concocted from improvised explosives is designated as an IED, an *improvised explosive device*. Improvised explosives are often formulated because raw materials are more readily available for them then for making commercial or military explosives. Unfortunately, many of these are substances which are of poor stability, even in normal handling. In recent years, improvised explosives encountered by authorities included urea nitrate (used in the 1993 bombing of the World Trade Center), TATP (triacetone triperoxide), and HMTD (hexamethylenetriperoxidediamine).

CHEMISTRY OF EXPLOSIVES

The vast majority of explosives are based on molecules which contain nitrogen atoms. The most common functional groups include:

- nitro ($-NO_2$). Example: TNT (2,4,6-trinitrotoluene), $C_7H_5(NO_2)_3$
- nitroso ($-NO$). Example: hexanitrosobenzene, $C_6N_6O_6$
- nitrate ($-ONO_2$). Example: PETN, pentaerythritol-tetranitrate, $C_5H_8(ONO_2)_4$
- nitramine ($>NNO_2$). Example: RDX (cyclotrimethylene trinitramine), $C_3H_6N_3(NO_2)_3$
- azide ($-N_3$). Example: lead azide, $Pb(N_3)_2$

The combustion of pyrotechnics and solid or plastic explosives is sometimes viewed as being based on *solid-state reactions*. In chemistry in general, most reactions occur between liquids or gases, not between solids. The same is true of combustion. A piece of wood is able to ignite and burn because localized high temperatures break down the molecular structure of the solid and release low-molar mass gases. These gases combine with the oxygen in the air to exhibit flaming combustion. A second reaction in the combustion of wood occurs when the heated, charred solid material is directly attacked by oxygen—this exhibits glowing. In no case, however does wood show a reaction involving two solids. Explosives and pyrotechnics, in fact, constitute the only important examples where combustion may involve solid-solid reactions. Whether or not direct solid-solid reactions are important has been debated. McLain[38] considers that they are pivotal, while Hardt[39] feels that they are secondary, at best. In McLain's view, the reactions of solids cannot be viewed in terms of simplified idealizations which are possible with gases. For gases, use of ideal-gas relationships often provides accurate answers, at least if extremes of pressure or temperature are avoided. With solids, however, the defects of their crystal structure tend to govern much of their chemistry. A unique feature of solid-solid reactions is that they must be exothermic. According to the Second Law of Thermodynamics, the Gibbs Free Energy, ΔG, must be negative for a reaction to occur. But $\Delta G = \Delta H - T\Delta S$, where H = enthalpy, T = temperature, and S = entropy. If the reaction products are solids, then $\Delta S \approx 0$. Thus, to have a negative ΔG requires a negative ΔH, in other words, an exothermic reaction.

In Hardt's view, by the time the ignition temperature has been reached, for the majority of explosives or pyrotechnics, at least one component has already melted; thus, the actual reaction is solid-liquid. Furthermore, in his view, many explosive reactions are actually controlled by the diffusion of heat and not by chemical reaction rates. Thus, a number of explosives exist where the reaction rate is independent of temperature but dependent on the thermal conductivity. In actual fact, both types of behaviors must be recognized. In general, solid explosives can be organic, inorganic, or organometallic compounds. These will innately show different thermal and explosive behaviors, since organic materials usually melt before decomposing, while inorganic and organometallic explosives generally decompose before melting. This is why a melting point temperature for many explosives cannot be stated, and chemical handbooks instead state "decomposes." The basic difference stems from the covalent bonds in organic solids, versus ionic bonds in inorganic. The above grouping is very rough however, and some inorganic azides, for example, melt before exploding. There can be difference in the type of chemical bonds even within one chemical family. As an example, inorganic azides range widely in their sensitivity—lead azide is highly sensitive and has covalent bonds, sodium azide is insensitive and has ionic bonds.

Even metal-metal reactions sometimes turn out to be solid-liquid, rather than solid-solid. Hardt cites Pyrofuze as an example. Pyrofuze is made by cladding an aluminum wire with an outer layer of 95% palladium/5% ruthenium. When heated to a critical temperature, a rapid exothermic reaction takes place, but it requires initial melting. The rate of reaction is then limited by diffusion, not by chemical kinetics. *Solid-gas* reactions are also involved in some explosives, and the gas referred to here is not oxygen from the air, but, rather, a gas which is evolved from one of the solid components during early stages of decomposition.

In addition to unwanted detonations, the other hazard which can exist with explosives is *thermal decomposition*. The chemical reactions and reaction products are different for

the two cases. In a detonation, commonly most of the reactants become converted to their maximum oxidized state, such as CO_2 or water vapor. In decomposition, however, it is usual to find that molecule fragments are formed which are far from being fully oxidized. The decomposition reactions of explosives can be complicated, and may often include autocatalytic regimes. The decomposition of cellulose nitrate is discussed in some detail in Chapter 14.

OXYGEN BALANCE

For a condensed-phase explosive to be most effective, the needed oxygen must come from the condensed phase. It should not be necessary to use oxygen diffused from the air, since the diffusion process is much slower than is the process of reaction when molecules of fuel and oxidizer are in close physical contact. However, if an explosive contains too much of oxidizing components, then these cannot be reacted because there is not enough fuel. Thus, the concept of oxygen balance arises. It is defined as the amount of oxygen contained in the explosive, minus the amount needed for complete oxidation, expressed as mass percent of the initial explosive. An effective explosive will have an overall oxygen balance close to zero. Each of the components, however, may have a negative or positive contribution. For an explosive having the general composition $C_cH_hN_nO_o$, the oxidation can be expressed as:

$$C_cH_hN_nO_o \rightarrow n_cCO_2 + \frac{n_h}{2}H_2O + \frac{n_n}{2}N_2 + \left(\frac{n_o}{2} - n_c - \frac{h_c}{4}\right)O_2$$

If the amount of oxygen atoms is large in the explosive, then there is some oxygen left over in the form of O_2, and that amount is $\left(\frac{n_o}{2} - n_c - \frac{n_h}{4}\right)$. Conversely, if the amount in parentheses is negative, then it means that the reaction will seek out the deficit from atmospheric oxygen. Consequently, the oxygen balance OB (percent) is expressed as:

$$OB = 100 \times \frac{32}{M}\left(\frac{n_o}{2} - n_c - \frac{n_h}{4}\right)$$

where 32 is the molar mass of O_2 and M denotes the molar mass of the explosive. Substances which function as oxidizers have a positive OB, substances which are fuels that have a negative OB. As an example, TNT has the formula $C_7H_5N_3O_6$ and a molar mass of 227.1, so

$$C_7H_5N_3O_6 \rightarrow 7CO_2 + \frac{5}{2}H_2O + \frac{3}{2}N_2 + \left(\frac{6}{2} - 7 - \frac{5}{4}\right)O_2$$

then its oxygen balance is:

$$OB = 100 \times \frac{32}{227.1}\left(\frac{6}{2} - 7 - \frac{5}{4}\right) = -74\%$$

This number is highly negative and implies that, for the most efficient explosion, it should be paired with another component which has a positive oxygen balance. Figure 1 shows the relation between OB and the heat of explosion, as evaluated for 13 different propellants. It is evident that OB = 0 correlates to the highest heat of explosion and deviations to either side cause a reduction. The oxygen balance concept should not be used heedlessly as a measure of hazard across widely disparate chemical families[40], but is otherwise a highly useful 'first indicator.' The propellant at the cusp of the graph, by the way, is EGDN. It should be noted that while the definition given above is the most common, some authors have used different definitions. For example, Kamlet and Adolph[41] proposed that (a) carbon atoms should end up in CO, not in CO_2; (b) that the COO group (carboxyl) should be considered non-participating in the combustion reaction; and (c) that the equation be normalized by dividing through by 8. Thus, their definition of oxygen balance becomes:

$$OB_{Kamlet} = 100\left(2n_o - 2n_c - n_h - 2n_{coo}\right)$$

According to Kamlet, then, TNT would have OB_{Kamlet} = –3.08%.

If the oxygen balance is significantly negative, then a *fireball* should be expected to follow after the detonation wave is finished. If large amounts of black smoke are visible, this is likely to be because the oxygen balance was negative and carbon was left over unreacted. A positive oxygen balance does not mean that a fireball is precluded, since fuel can be made available by the blast wave itself if, for instance, a combustible material is pulverized and dispersed into the air.

For the oxygen balance concept to be meaningful, the oxygen contained in the solid-phase material must be readily available for reaction, not just be present. Thus, for multicomponent solid explosives it is important to make sure the powder is finely ground, where the grains of fuel and oxidizer are closely intermixed.

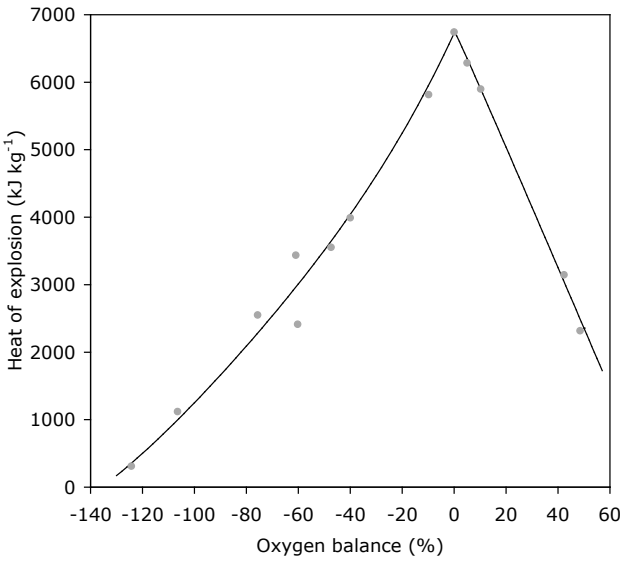


Figure 1 The relation between OB and heat of explosion for a number of propellants

INITIATION AND IGNITION

The beginning of a detonation in explosives is normally termed *initiation*, whereas the term *ignition* implies the start of combustion, but not necessarily of detonation. There can be many modes of initiation for explosives, with some examples being:

- self-heating
- flames or external heat flux
- friction, impact, shock, vibration
- electricity
- light energy, including photochemical excitation
- compression
- sympathetic explosion due to shock waves from an initiating explosion
- crystal growth.

Despite the variety of forms by which energy is delivered, most of these processes ultimately express their effect through thermal means. The actual mode of ignition is often not clear in accidents, and there may be more than one mode involved. For example, nearly a century ago, BM[42] documented three fatal explosions that each took place when wooden tools were driven into the top of a wood keg of black powder in an effort to remove the top. Wood-against-wood will not produce sparks and black powder would not be expected to explode from a small amount of compression, although perhaps a large amount of compression was sustained to particles trapped between two chimes.

In military usage, *sensitivity* is a measure of the amount of energy required for initiation[43]. This general concept has been very difficult to quantify in an acceptable manner, since the energy required for initiation not only depends on the mode by which it is supplied, but also depends on details of the test apparatus. For instance, even results from several types of drop-hammer tests for initiation by impact agree—at best—only qualitatively. It has been proposed that, within a particular chemical family, the sensitivity of an explosive can be related directly to its heat of reaction. Table 6 illustrates this for inorganic azides.

Table 6 Relative sensitivity of inorganic azides[53]

Sensitivity	Substance	$-\Delta h_r$ (kJ mol^{-1})
Most sensitive	$Pb(N_3)_2$	481
↓	TlN_3	234
↓	$Ca(N_3)_2$	46
Least sensitive	LiN_3	13
Non-explosive	KN_3	0
	$Ba(N_3)_2$	-21

SELF-HEATING, STABILITY IN STORAGE, AND EXPOSURE TO HEAT

Until the middle of the 19th century, the only available explosive was black powder, and it is quite stable against self-heating. Subsequently, nitrocellulose, nitroglycerin, and other nitrate ester explosives were invented. The RO–NO_2 bond in these is of limited stability, and numerous accidental explosions began to demonstrate this fact. A stabilizer is added to such explosives in order to increase their useful lifetime; it is a substance that interferes with the decomposition reaction in some manner. The stabilizer is typically sacrificial, and when it is largely used up, the explosive becomes unstable. Thus, the effective lifetime of stabilization is finite. For explosives in the nitrate ester family (nitrocellulose, nitroglycerin, etc.) testing can be done by monitoring for the production of NO_2, which is a decomposition product. This product will not be produced in significant quantity until the stabilizer is used up, after which point rapid production sets in and the explosive becomes unstable. If the explosive has become highly unstable, sufficient NO_2 may be produced so that reddish-brown fumes are actually visible. In laboratory studies, simply monitoring weight change is often sufficient. Figure 2 shows the decomposition of two nitrocellulose-based propellants[44] when tested at an elevated temperature of 90ºC. Propellant B becomes unstable at about 50 days, while Propellant A has a lifetime about half that.

The effective storage lifetime of the explosive can be estimated by determining the decay of the stabilizer's concentration with time. Volk[45] has shown how a plot can be created on the basis of a simple study using thin-layer chromatography (Figure 3). Since the plot is found to be linear using semi-log axes, extrapolation can readily be made to longer periods and lower temperatures.

Assuming that any necessary stabilizer has *not* been depleted, an explosive may still go into thermal runaway if its storage temperature/size relationship is unfavorable. The theory commonly used is the same 'thermal explosion theory' as was already presented in Chapter 9 for self-heating substances. In other words, the explosive is assumed to comprise a volume of substance which is homogeneous. Its chemistry can be represented by a single-step reaction, whose rate follows the Arrhenius form. Many different conditions are possible at the boundaries, same as in the self-heating problem: convective cooling; conduction; a fixed surface temperature; an imposed heat flux, etc. Looking at the details of actual ignition of explosives, it has been demonstrated[46] that initiation occurs at small hot spots rather than homogeneously throughout the body of the substance. However, generally successful correlations based on thermal explosion theory have been achieved ignoring the hot spot complication. A more serious problem is that a computationally useful form of the theory has to assume that the heat of reaction is a constant, whereas for some unstable explosives, this is not true. van Geel and Verhoeff[47] proposed that a test method similar to UN Test H3 (see Chapter 9) be used, along with standard Frank-Kamenetskii theory. Based on the theory as given in Chapter 9, the maximum dimension r that is permissible without thermal runaway is given by, with slight re-arrangement:

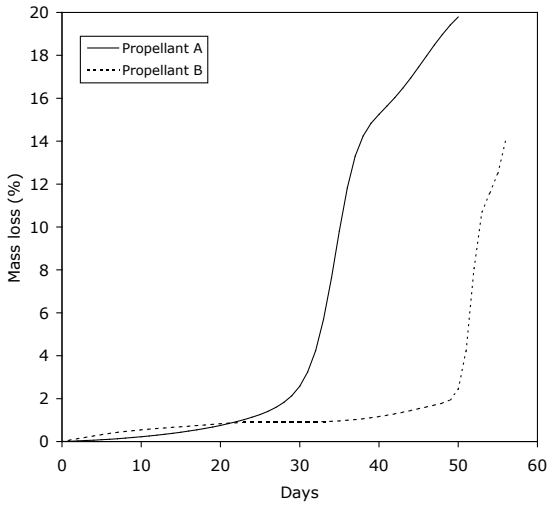


Figure 2 Mass loss of two nitrocellulose propellants, tested at a temperature of 90ºC

$$r = \sqrt{\frac{RT_a^2}{E}}\sqrt{\frac{\delta_c \lambda}{\rho q}}$$

where $q = QA\exp(-E/RT_a)$. The latter heat evolution variable is used since that is what is measured experimentally in the H3 test. van Geel and Verhoeff point out that when the heat release is measured at a standardized, higher temperature T_m, and the end-use ambient temperature is T_a, the relation can be modified to give:

$$r = \sqrt{\frac{RT_a^2}{E}\exp\left[\frac{E}{R}\left(\frac{1}{T_a}-\frac{1}{T_m}\right)\right]}\sqrt{\frac{\delta_c \lambda}{\rho q_{T_m}}}$$

They further assumed that the HRR in the laboratory is measured at T_m = 358 K (85ºC), and that T_a will mostly be 30ºC, but with possible short-term excursions up to 71ºC

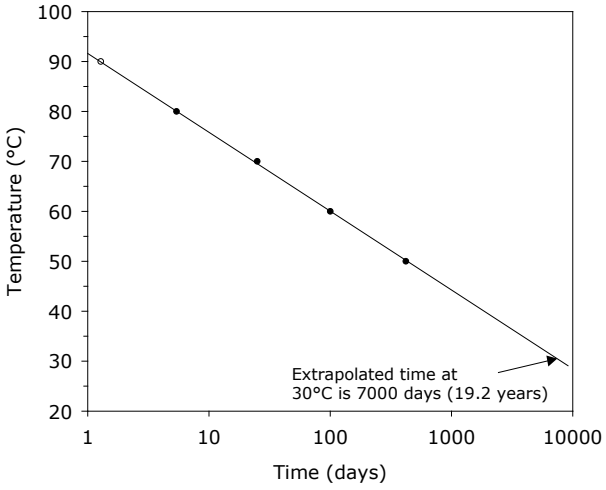


Figure 3 Effect of storage temperature on the lifetime of a commercial propellant (Ball powder K 503) preserved with diphenylamine

(344 K), consequently the latter value is used. Then for values of E in a practical range (between 40 and 200 kJ mol^{-1}), the first factor in the above equation does not vary much, and they suggest that it can conservatively be taken as 6.05. The predictive relation becomes:

$$r = 6.05\sqrt{\frac{\delta_c \lambda}{\rho q_{\max}}}$$

where the value of q_{max} used is the maximum heat release (W kg^{-1}) measured during a 1-week test at 85ºC. For ten different commercial single-, double-, and triple-base propellants they measured q_{max} values between 40 and 200 W kg^{-1}. Safe storage radii were found to range between 0.15 and 0.35 m. If a necessary stabilizer becomes depleted, the HRR measured in the H3 test would shoot up dramatically, however, the method assumes that storage lifetime based on stabilizer depletion will be determined separately and only non-depleted explosives subjected to the HRR testing.

In tests where a small sample is heated isothermally, for very short ignition times, heat losses can be ignored. Then, it can be shown[53] that ignition time data can be represented in the form:

$$\ln(t_{ig}) = \frac{E}{RT} + B$$

where B is a constant for a given substance. For example, Johansson et al.[48] obtained ignition time data for PETN as:

$$\ln(t_{ig}) = \frac{23256}{T} - 44.38$$

valid for $T < 528$ K.

Many explosives fail to conform to Arrhenius kinetics if a substantially wide temperature range needs to be considered. Rogers et al.[49] provided an illuminating example of an explosive comprised of three components which was analyzed extensively both by DSC and in various medium-scale tests. It was found that Arrhenius kinetics could not describe satisfactorily the self-heating behavior, but a reasonable representation was obtained by using an autocatalytic model. A theory has been developed that entails two parallel, Arrhenius-form reactions[50], however, it does not lead to closed-form solutions or approximations. Many explosives become less stable with protracted storage. Chemically, this means that the substance is undergoing an autocatalytic reaction, since the definition of an autocatalytic reaction is one which is accelerated by an accumulation of reaction products. Russian researchers[184] proposed that most thermal decomposition reactions of explosives are autocatalytic. This was demonstrated for several explosives by Tarver et al.[51], who showed that reaction rates increased 3- to 5-fold when gaseous decomposition products were not allowed to escape. They also showed[52] that HMX and RDX decomposition entails three consecutive reactions, NC has a 2-step autocatalytic reaction, while TNT exhibits a 3-step autocatalytic reaction. Some additional practical implications of this are discussed below, under the Henkin Test.

The exceptional sensitivity of explosives can be judged better by considering the quantities needed to cause explosion from runaway self-heating. For example, in Chapter 9 it was seen that generally many kilograms of various common materials were needed for thermal runaway to occur. By contrast, Bowden and Yoffe[53] report that a 1 mg quantity of silver azide will undergo thermal runaway at 375ºC. Similarly, a single crystal of mercury fulminate held at 170ºC will lead to thermal runaway if its thickness is larger than 22 μm.

In terms of chemical families, those containing the nitrate functional group (cellulose nitrate, nitroglycerin, etc.) are of low stability, while those containing the nitro functional group (TNT, tetryl, RDX, etc.) are of high stability. Some data from Rogers[54] illustrate this trend (Figure 4).

Many organic explosives have limited stability, even if stored at room temperature. Some details are given in connection with cellulose nitrate (Chapter 14). But even lead azide, which is a simple, inorganic molecule, shows problematic stability[55]. To prolong its storage life, it is typically stored in an alcohol-water solution. But even stored this way, it gradually decomposes by liberating hydrazoic acid, HN_3.

Sometimes explosives are subjected to a certain amount of heating during packaging. Thus, Persson and Jerberyd[56] presented a model for the detonation of a thin layer of dynamite as it is being heated during ultrasonic welding of the surrounding plastic packaging material. Explosives may also be exposed to heat in various other circumstances and the question then arises if, once cooled back to ambient, they have been substantively altered. Freeder et al.[57] exposed a series of explosives to 75ºC temperature for 1 or 10 days, then cooled them and retested their performance in a drop-hammer test and in the Koenen/BAM friction test. For black powder, black-powder-based explosives, ANFO, and an emulsion explosive, there was no effect. A flash composition, blasting gelatin, and two slurries (RDX and HMX based) showed significant increase in sensitivity. A final group, comprising a single-base propellant, a double-base propellant, a slurry, and an emulsion explosive, showed anomalous behavior: heating for 1 day made performance worse, but heating for 10 days proved less deleterious. The reason for the anomalous behavior was not elucidated.

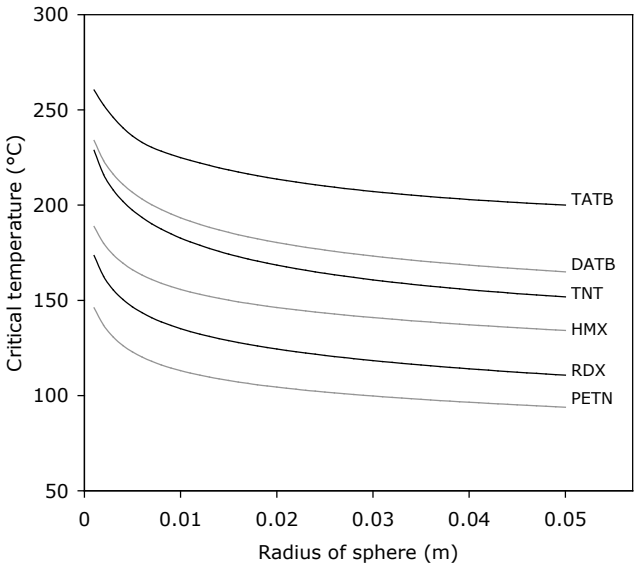


Figure 4 Relative self-heating tendencies of several common explosives

IMPACT AND SHOCK

Impact is usually understood to be created by impulsive mechanical loading, i.e., not created by an existing shock wave. *Shock* initiation of explosives, on the other hand, refers to initiation from an already-detonating substance. *Sympathetic detonation* refers to shock initiation by a detonating substance that is not in intimate contact with the target explosive. The initiation occurs within the body of the receptor, and not at the surface, and it occurs at a point, rather than spread out along a plane[58]. Sympathetic detonation is the principle utilized in card-gap tests, discussed at the end of this Chapter.

Wanted initiation of primary explosives can be by fire, such as from a fuse, mechanical energy such as by a firing pin, or electrical energy as in a blasting cap. But secondary explosives are ones which, by definition, need to be initiated by a shock wave, normally created by the use of a primary explosive. With many secondary explosives, using a form of energy other than shock waves may result in deflagration rather than detonation. Conversely, since primary explosives are highly sensitive to various forms of energy input, it is not necessary to use an initiation source as powerful as a shock wave for them.

Bowden considers that impact can act to initiate an explosive in any of the following ways[59]:
(1) by adiabatic heating of compressed gas spaces
(2) a frictional hot spot on the confining surface or on a grit particle
(3) intercrystalline friction of the explosive itself
(4) viscous heating of the explosive at high rates of shear
(5) heating of a sharp point when it is deformed plastically
(6) mutual reinforcement of gentle shock waves

The impact needed can come from a wide variety of sources. For example, flying fragments of a crystal of an explosive can initiate a detonation. Lead azide can be initiated this way, but not TNT or tetryl[53].

The action of an external impact or an impinging shock wave is highly complex, since mechanical deformations (occurring in both the casing and the explosive) are coupled to shear, viscous flow, and wave propagation phenomena in the explosive. The mechanical work, if converted uniformly to heating the whole mass of explosive, would generally not

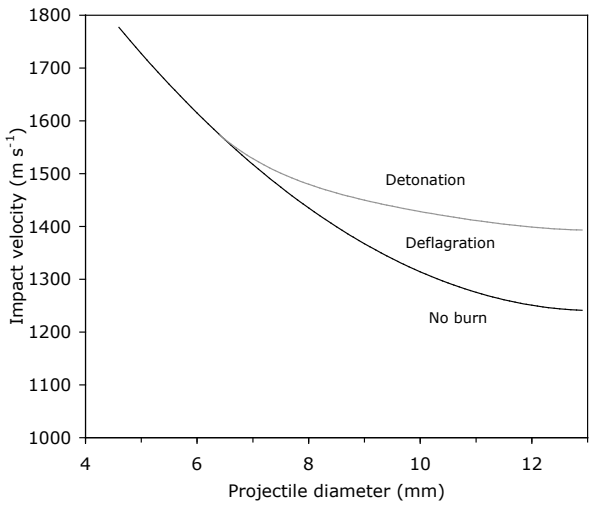


Figure 5 Impact regimes for HMX/polyurethane propellant

be sufficient for ignition. Ignition can occur because the distribution of energy is concentrated and non-uniform[60]; the high pressures and high temperatures thus created then can act as a hot spot to ignite the rest of the material. In liquid explosives, non-uniform distribution of energy commonly occurs due to the presence of gas bubbles[61]. The bubbles may be either in the volume or at the boundary. This bubble can be created as the solid surface is impacting the liquid, possibly aided by asperities in the surface. The bubble is effective in initiating explosion due to the heating effect of adiabatic compression. Some very high pressures can be created in a bubble by applying only modest overall pressure to the volume of substance, since a liquid is nearly incompressible, compared to an air bubble. This rapidly created high pressure causes high temperatures within the bubble. The explosion actually begins in the gas phase, even though the fuel vapor concentration within the bubble may be very low. This initial combustion is analogous to cool flames, with temperatures being in the range of 300 – 500ºC. For liquids, if no bubbles are trapped anywhere, then it is found that impact energies some 3 – 4 orders of magnitude higher are needed for the initiation. In these cases, it is considered that most of the energy is transferred by viscous heating of the plastically-flowing explosive. Médard[3] described an injury that occurred when 20 g of nitroglycerin was dropped 1 – 1.5 m onto a floor. Laboratory experiments were then conducted where glass flasks with 100 g of nitroglycerin were dropped 80 m from a cliff onto a steel armor plate. These resulted in zero explosions in 20 tries and Médard concluded that air bubbles were trapped in the case of the accident, but not in the experiments.

According to Bowden, small voids play a similar role in a solid when gas is trapped in the spaces between crystals. Upon impact, initial plastic flow seals off individual gas packets, then compression can raise the temperature of the gas volume in the same way that it does for bubbles in liquid explosives. The impact energy required to detonate solid explosives, however, is much greater than for liquids. In addition to requiring a high energy, the face of the colliding object ('striker') must be hard enough to plastically deform the explosive, rather than being itself deformed. The hot spot temperature needed to initiate an explosion from impact is similar to that needed to cause initiation from friction. Same as with friction ignitions, grit serves to facilitate ignition from impact, provided the melting point of the grit is higher than the temperature needed for initiating the particular explosive. Frey[62] attempted to create a fairly comprehensive model of initiation through collapse of voids. His solutions were wholly numeric in nature, but he did demonstrate that there is a critical size for a void, beyond which peak temperatures that are reached increase greatly.

The effects of impact are especially complicated for multicomponent explosives. Bowden[63] studied the ignition of black powder (potassium nitrate, sulfur, charcoal) and found that ignition generally occurs at 300 – 350ºC. But the formation of a liquid phase appears to be a necessary precursor, and this occurs at 120ºC, which is the melting point of sulfur.

Bowden's theory, as applied to solids, was contested by Russian researchers[184], who proposed the alternative theory that sizable regions of inelastic deformation (plastic flow) are needed for initiation to occur, and that included voids do not act as a facilitating mechanism for solids. A version of this theory was also adopted by Heavens and Field[64], who conducted extensive experiments on a wide variety of explosives and concluded that, with certain materials, rapid plastic flow leads to the formation of hot spots, which become the locations of ignition. From their drop-hammer experiments, they concluded that plastic flow was the impact ignition mechanism for AP, HMX, PETN, and RDX. US military researchers have had mixed opinions on the matter, with some holding that inelastic deformation of crystals is the main cause of impact initiation in solids[65]. Others[66] however have concluded that gas compression is important, but so is the explosive's tendency to break up into small particles during cavity collapse. A number of theories (e.g., Frey[67]) have been put forth that detonation during impact can originate at a shear band, which is a localized zone of thermal softening that can develop. Experiments have also been devised where direct failure in a shear mode causes initiation[68]. Dienes[69] demonstrated that shear bands can be modeled by an application of F-K theory.

Kondrikov and Tchubarov[70] tested a number of secondary explosives in a drop-hammer test and concluded that there are three stages leading to ignition:

(1) Slow deformation of the pellet under continually increasing pressure, accompanied by a temperature rise of only about $0.8(T_m - T_o)$, where T_m = melting point temperature and T_o = ambient temperature.

(2) Destruction of the pellet, with the energy accumulated during the first stage being released as kinetic energy of the fragments, which fly off as jets of powdered substance; this is accompanied by partial melting of the material.
(3) Pressure begins to rise again in the material that remains; if the velocity of the escaping material in this stage attains a critical value, ignition occurs. The measured critical velocities ranged from 250 m s^{-1} for PETN to 550 m s^{-1} for DINA.

Chaudri[71] showed that causing a rapid fracture of single crystals of sensitive primary explosives by using a high-speed chisel does *not* lead to initiation. He concludes that initiation would only be possible if very high strains could be induced in the crystals, but that this does not appear to be the case. He also presented theoretical calculations showing that the maximum temperature rise that could be caused by inducing plastic flow in explosives crystals is of the order of 20ºC, which he considered as disproving that mechanism. But the temperature rise predicted from friction between grains was on the order of 200ºC, which makes inter-grain friction a much more plausible mechanism. Chaudri's interpretation is that the main mechanisms are:
(1) adiabatic heating within bubbles;
(2) inter-grain friction;
(3) fast gas jets formed at bubbles, when presented with a strong shock.

The initiation by impact is, unfortunately, as much dependent on physical properties of the explosive as it is on its chemistry. For crystalline materials, even size of crystals is an important variable. Figure 6 illustrates the effect for drop-hammer testing of lead azide crystals[72]. When granular material is prepared by pressing, the effect of the pressed density can overwhelm other effects in the system. Seay[73] reports that PETN requires 45 times greater impact pressure to initiate it in single-crystal form (1786 kg m^{-3}) than in pressed form at 1000 kg m^{-3}.

Somewhat surprisingly, it was demonstrated[74] that certain polymer/explosive formulations are more sensitive in drop-hammer tests than is the pure explosive. This tendency was especially strong in polymers having a high glass transition temperature, e.g., polycarbonate or polystyrene. In addition, a low heat capacity, low heat of fusion, and high strength of polymer promoted sensitization. The mechanism was considered to be one of localized, brittle cracking.

As might be expected, sensitivity to shock initiation[107] is decreased by decreasing the temperature or the duration of exposure. The effect of packing density is complex and is considered later in this Chapter. Particle size is also important, there being an optimum size for ease of initiation, with larger or smaller particles being less sensitive. Very small particles give a low sensitivity since hot spots become small. Homogeneous explosives are less sensitive to shock

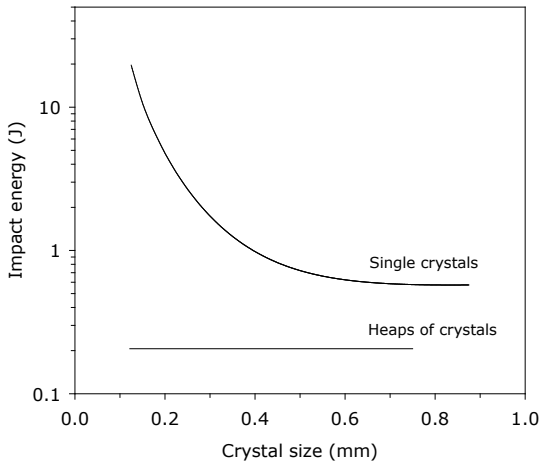


Figure 6 Effect of crystal size on drop-hammer test results for lead azide

initiation than are heterogeneous ones. In tests where the explosive is highly confined, as the packing density approaches the theoretical maximum density, sensitivity to shock greatly decreases. This is because initiation at voids becomes increasingly unlikely[75].

When a projectile hits an unconfined explosive or propellant substance, there can, in general, be three results: (1) no burn; (2) deflagration; or (3) detonation. Anderson et. al.[76] conducted tests on a propellant made of HMX and polyurethane by subjecting specimens to impact from cylindrical gun-fired projectiles of various diameters and velocities. Their results, shown in Figure 5, indicate that for small diameter projectiles, only two outcomes are possible: no-burn, or detonation. For larger diameters, however, a third regime of deflagration becomes possible. The authors computed the critical energy fluence for the results and concluded that it was roughly constant for the deflagration threshold, but not constant for the detonation threshold. The velocities required for initiation were very high in Anderson's study; it is not clear if similar relations are obeyed for more sensitive explosives.

Explosives are commonly tested for impact initiation by use of one of the many drop hammer tests (see below). If the specimen is unconfined, then the failure mode has been found to be radial cracks[77] that are generated at the periphery of the specimen. For shock initiation, the most common test arrangement is a card-gap test.

Theories of impact and shock initiation

Uniform heating of an explosive by a shock wave plays no role in initiation. In general, a uniform temperature rise of only 100 – 200ºC would occur under shocks sufficient to initiate detonation[107]. The essential trait of shock wave heating, instead, is that the heating is not spatially uniform. The increase in internal energy from a shock occurs as visco-

plastic heating and is concentrated in small hot spots of the shocked material. The microscopic mechanism is the collapse of individual pores under shock pressure. The sensitivity to shock has been shown to be not correlated to thermal (self-heating decomposition) sensitivity of explosives[84]. This is not surprising, since it has been learned that the actual reaction mechanisms are different for moderate temperature/pressure decomposition and for shock wave initiation. For some explosives, e.g., liquids, the reaction rates within the heated volume can be modeled by thermal explosion theory[78], but in granular explosives grain burning needs to be modeled.

Friedman[79] provided a one-dimensional treatment where the impact-caused hot spot is approximated as a plate of finite thickness in a substance which is infinite in extent along both directions of the face. The critical half-thickness d_c is found as:

$$d_c = \left(\frac{\lambda (T_h - T_o)}{\rho Q A} \right)^{1/2} \exp\left(\frac{E}{2RT_o} \right)$$

where T_h is the hot spot temperature and T_o is the ambient temperature. A correlation to impact sensitivity as measured by the Explosives Research Laboratory Machine was given as:

$$0.287 \ln h + \ln F + \frac{0.0602E}{300 + 22.9h^{0.574}} + 0.684 = 0$$

where h = drop height (cm), E = activation energy (kJ mol^{-1}) and $F = \sqrt{\lambda / \rho Q A}$. Thus a relation is obtained between drop height and the thermochemical quantities E, Q (heat of reaction), A (pre-exponential factor), λ (thermal conductivity), and ρ (density). Coffey[75] suggested that drop hammer test results can be roughly correlated by noting that G^2h is approximately a constant, where G = shear modulus (N m^{-2}) and h = drop height (m).

Kamlet[41,80] conducted a large number of drop-hammer tests (see Test Methods) on a wide variety of explosives. His tests showed that substances with a higher OB need a smaller amount of energy for initiation, and on that basis they found a relation between oxygen balance and drop-hammer results. For aliphatic compounds, the results were found to depend on whether NO_2 is attached to a nitrogen or to a carbon atom, with the latter requiring higher drop heights for initiation. He also observed that if an aromatic ring has a hydrogen atom bonded directly to a carbon atom of the ring, this constitutes a weak spot for initial decomposition of the molecule. As an example, Kamlet compared TNT and TNB (1,3,5-trinitrobenzene). TNT has an alpha C–H bond, and decomposes at about 200ºC, while TNB does not, and decomposes at about 300ºC. This weakness is reflected in the correlations—for a given *OB* value, explosives with an alpha C–H bond need a smaller drop height for initiation. Note that Kamlet's definition of oxygen balance, OB_{Kamlet}, is not the standard one, however, as discussed above. The correlations of Kamlet's results are:

aliphatic compounds with N-NO_2 group:

$$PE = 5.78 \exp(-0.39 \times OB_{Kamlet})$$

aliphatic compounds with $C(NO_2)_3$ group:

$$PE = 13.88 \exp(-0.54 \times OB_{Kamlet})$$

aromatic compounds, alpha C-H bond present:

$$PE = 5.25 \exp(-0.60 \times OB_{Kamlet})$$

aromatic compounds, alpha C-H bond absent:

$$PE = 13.18 \exp(-0.65 \times OB_{Kamlet})$$

where PE = potential energy for initiation at the 50% probability level (J). In drop-hammer testing, the design of the apparatus has a sizeable effect on the results, thus correlations of this nature should be taken as expressions of trends, not as absolute values of required energy. The drop-hammer apparatus used by Kamlet was the version developed at the Naval Surface Weapons Center.

The theory propounded by the Russians Afanasev and Bobolev in their textbook[184] is substantially different from US methodologies. It is quite convoluted, but basically describes a substance which is compressed to a degree enough to greatly raise its temperature and which then fails in a brittle way. Two separate versions of the theory are formulated, one for thin bodies and one for thick, with separate initiation criteria being given. Applied force is the variable that governs whether initiation will occur, not energy. Roth analyzed the theory in detail in an extensive review article[107] and found it to be less than convincing, nor did he find it to be in tolerable agreement with experimental trends.

Baker and Mellor[81], however, considered that the Russian theories were based on some important experimental work, and the further development must consider these results. The basic finding is that details of the drop-weight testing machine greatly affect the test results. Specifically, if the geometric design is such that the explosive is prevented from flowing out laterally when impacted, initiation fails to occur. This suggests that plastic flow and shear or fracture play a dominant role, and that simply high pressures achieved due to compression alone do not suffice. They also suggested that impact initiation should be viewed as a two-step process: (1) the impact energy, by means of localized material failures, creates hot spots; (2) chemically-reacting hot spots become sufficient to cause a thermal explosion. In line with the first step of this scheme, Baker and Mellor reviewed much of the recent literature where fracture mechanics modeling was used to predict explosives initiation. Their review suggests that a viable theory of some generality might eventually be achieved, but that current efforts to construct a general explanation of explosives initiation on this basis are not yet proving to be successful.

The initiation of an explosive due to the impact of a projectile is experimentally found to depend upon the diameter d of the projectile, with a critical velocity for initiation v_i having the form:

$$v_i = A/d^{1/2} + B$$

where A and B are constants for a given explosive. Andersen[82] has demonstrated that the above relation implies a constant energy fluence for ignition.

Walker and Wasley[83,84] proposed a *critical energy fluence* for initiation concept as defining the ignitability requirements of explosives exposed to shock waves. The concept has meaningfulness only in cases where the impact is delivered uniformly over the front face of the explosive. Thus, flying plate experiments are commonly used, where a projectile impacts upon a flat plate and the flat plate, in turn, applies impact onto the face of the explosive. Walker and Wasley first determined that no correlation existed in a given series of experiments to velocity of flying plate alone; in one case the highest velocity tested showed no explosion, while the lowest did. But correlations based on energy fluence proved successful. The kinetic energy of the plate is simple $\frac{1}{2}mv^2$, where m = mass (kg) and v = velocity (m s^{-1}). Per unit area, the energy of the flying plate becomes:

$$E_P = \frac{mv^2}{2A}$$

Not all of this energy can be transferred into the target to become shock energy. If the plate and the target are made of the same material, then ½ the flying plate energy can be transferred to the target. Otherwise, numerical hydrodynamic calculations are needed. The data developed for the LX-04 explosive show that

$$\frac{E_T}{E_P} = 0.31 - 0.015x + \frac{0.203}{x}$$

where $x = \rho_P/\rho_T$, ρ = density (kg m^{-3}), P denotes plate, and T denotes target. Values lower than 0.5 can be viewed as occurring due an impedance mismatch in coupling the energy. In terms of energy actually received by the target,

$$E_T = \frac{P^2 t}{\rho_o U_s}$$

where E_T = energy fluence (J m^{-2}), P (Pa) = shock pressure, t = duration of shock pressure (s), ρ_o = initial density of explosive (kg m^{-3}) and U_s = shock velocity (m s^{-1}) in the explosive. The quantity $\rho_o U_s$ is known as the *shock impedance*. Note that none of the variables on the right hand side are independent variables—they cannot be specified aforehand, only measured or simulated. Walker and Wasley obtained the following values of critical energy fluence:

PBX 9404	500 kJ m^{-2}
LX-04	1100 kJ m^{-2}
TNT	1400 kJ m^{-2}.

A more extensive tabulation is given in Chapter 14. The concept has also been applied to wedge and card gap tests.

Experimental studies with explosives to test the minimum energy fluence theory were conducted by Howe et al.[85] They conducted tests on PBX 9404 and compared the results to a detailed numerical model, and also to the simplified expression P^2t (Figure 7). The trends were clearly reasonably accounted for. Next, they examined whether an Arrhenius-type self-heating expression could account for the trends; the results (Figure 8) were obviously at complete variance with the expected trends. Small pressure changes imply small temperature changes, yet according to an Arrhenius dependence, these create a very large reaction rate change. Their conclusion was that a hot-spot mechanism is only part of the answer. In addition to the chemical kinetics expressed by applying an Arrhenius form of reaction rate to a hot spot, heat transfer limitations must be taken into account, and these correspond to grain boundaries. Their experimental results also indicated that density and grain size play a strong role, and that values of critical energy fluence are not independent of these parameters. Stresau and Kennedy[86] examined a variety of alternatives to the critical energy fluence criteria, but available data were not extensive enough to suggest an optimal alternative. It has been suggested[87] that the Walker/Wasley criterion is applicable

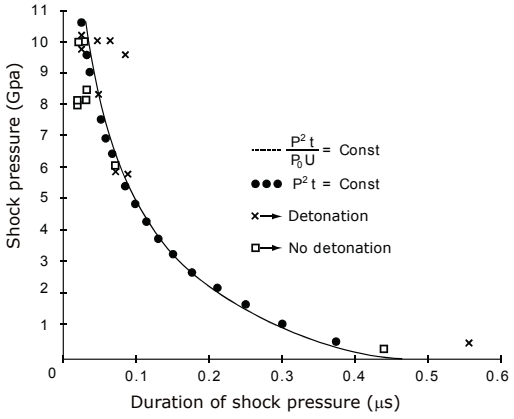


Figure 7 Experimental data for PBX 9404 compared to energy fluence criterion

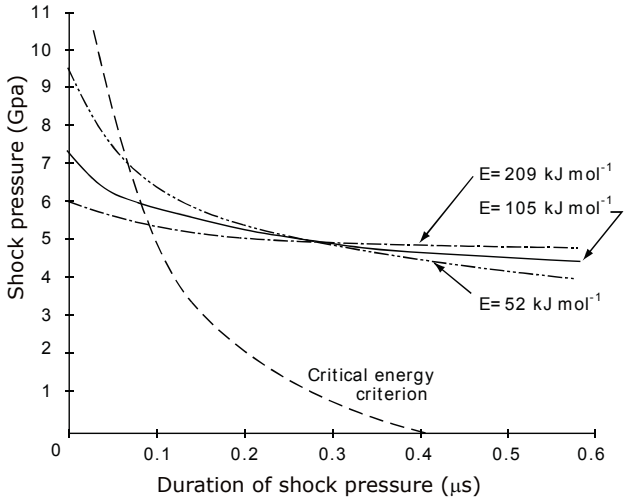


Figure 8 Comparison of experimental results to thermal explosion theory

when the explosive is uniformly exposed over its face, but breaks down when exposed over a partial face area, so that 3-dimensional effects predominate (Figure 9).

Some inconsistencies in the fluence concept were understood once it was learned that the critical fluence is not independent of the area of projectile. Experimental data[88] suggest that if critical energy fluence is plotted as a function of reciprocal area, then a linear plot is obtained (Figure 10), with finite projectile areas requiring more energy fluence than the asymptote for infinite area (zero reciprocal area). The Walker/Wasley theory does not provide for the effect of confinement. Frey et al.[89] demonstrated that for some explosives the degree of confinement will affect the energy fluence needed for initiation.

A modification of the hot spot theory used in self-heating was used by Maiden and Nutt[90] to compute a critical hot spot radius and a time to ignition for shock wave initiation. According to this theory, shock initiation of a given material requires a critical value of the product P^2t, where P = pressure and t = time of pulse. A more detailed approximation for ignition time was also derived:

$$t_{ig} = 4\rho C\mu \frac{T_{ig} - T_o}{\left(P_s - P_y\right)^2} + \frac{2\rho CRT_{ig}^2}{AQE} \exp\left(E / RT_{ig}\right)$$

where ρ = density (kg m^{-3}), C = heat capacity (J kg^{-1} K^{-1}), μ = viscosity (kg m^{-1} s^{-1}), A = pre-exponential factor (s^{-1}), Q = heat of reaction (J kg^{-1}), E = activation energy (J mol^{-1}), R = the universal gas constant (8.314 J mol^{-1} K^{-1}), T_{ig} = ignition temperature (K), T_o = ambient temperature (K), P_s = applied pressure (Pa), and P_y is given by the expression:

$$P_y = -2Y_o \ln \phi_o$$

FLAMES

The earliest weapons contained only black powder and this was ignited with a hot wire or a small flame. Flames can be

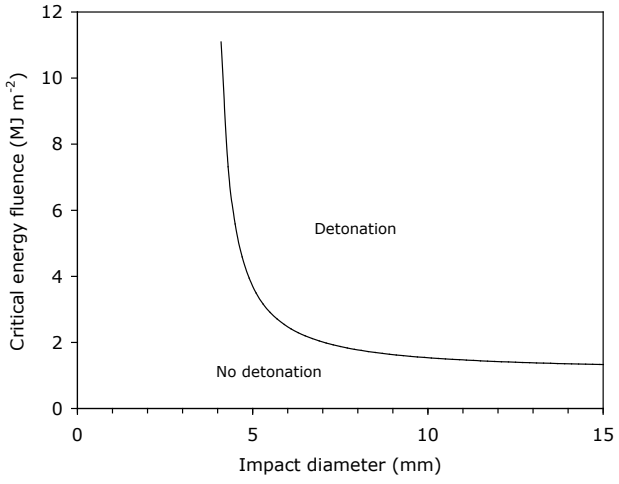


Figure 9 Effect of impact area on critical energy fluence (Composition B tested in flyer-plate experiments)

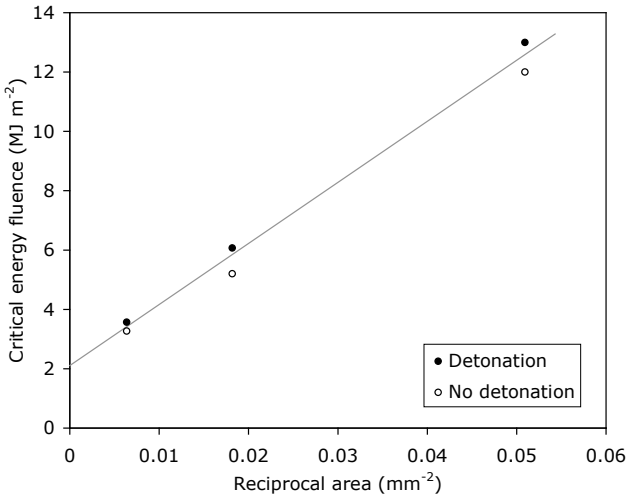


Figure 10 Dependence of critical energy fluence on projectile area for Composition B

used to ignite secondary explosives also, but their trait is that, if so ignited, they will typically burn but not detonate. However, fires of secondary explosives can turn into detonations under some circumstances. There are few systematic studies on the ignition of explosives by flames. Kondrikov[91] reviewed the details of a number of Russian accidents where RDX, PETN, HMX, TNT, or AN detonated after attack by fire. He concluded that one of the following mechanisms is responsible:

(1) confinement or partial confinement;
(2) flame penetration into cracks, slits, or pores;
(3) melting sufficiently large amounts of the explosive;
(4) formation of a vapor or aerosol cloud; or
(5) chemical transformation during initial heating which results in a more sensitive compound being created.

The last mechanism was concluded to have been operative for TNT explosions, where a diazo derivative was postulated.

Initiation or ignition of explosives from flames has most commonly been researched in the context of the military *cookoff* problem, but it is often simulated via radiant heating. In military applications, it can be expected that any place that munitions are located some event can occur, in accident or wartime, that causes flames or hot gases to expose the munitions. In US military work, the cookoff problem is divided into two types:

- *Fast cookoff*. This is simulated by submersion in a large pool fire.
- *Slow cookoff*. This is simulated by testing the explosive in an environment where the temperature rises at 3.3ºC per hour.

Fast cookoff usually produces a less violent reaction than slow cookoff. In slow cookoff, a nearly-constant temperature is established throughout the item; when explosion does occur, the entire device is usually exploded at once. By contrast, in fast cookoff, the temperatures are highly

non-uniform, and reaction first starts in the highest-temperature locations. Involvement of the rest of the item can then take place over a longer time scale than in slow cookoff, leading to lower destructiveness. In basic terms, slow cookoff is very similar to self-heating, except that self-heating studies are often done on bulk (unconfined) material, while slow cookoff testing involves cased explosives.

Traditionally, assessment of cookoff has been by testing. More recently, calculational methods have also been used. The explosive will normally be encased in a metal casing which has thermal conductivity several orders of magnitude higher than for the explosive. Thus, in the calculational methods, the problem is commonly assumed to be of cylindrical geometry, with uniform temperature around the periphery. A first-order solution is not particularly difficult, and methods have been put forth to provide a 1-d solution by spreadsheet calculations[92].

RADIANT HEATING

The use of lasers to ignite explosives has been investigated as a military munitions design option. de Yong et al. have reviewed the literature of this field[93]. Most of the experimental studies involved pulsed lasers producing enormous heat fluxes (on the order of 10^{10} kW m^{-2}) but for very brief time periods (on the order of 10^{-8} s). The ignition is dominated by beam absorption effects, due to the generation of highly absorptive plasmas with these heat fluxes. A minimum beam spot size (typ. 1 mm or less) has been found to exist in laser ignitions and beams focused to smaller diameters do not cause ignition. Despite beam absorption issues, the actual mode of ignition from laser energy has been determined to be thermal, and not involving photochemical or light-pressure effects. In some studies, longer exposure times were also used. In those, it was commonly found that there is both a minimum heat flux for ignition and a minimum fluence. For example, in a study on a pyrotechnic composed of Mg and $NaNO_3$, for exposure times < 2×10^{-3} s, ignition requirement was defined by $E'' \geq 21$ kJ m^{-2}, while for exposure times > 0.1 s, by the requirement that $\dot{q}''_{\min} \geq 1000$ kW m^{-2}. The interpretation of heat flux values from laser experiments is not straightforward, however, due to the typically small beam sizes used, which make assumption of 1-dimensional heat transfer inappropriate. Because of the small beam sizes, actual power levels required to achieve ignition can be tiny—in one series of experiments, ignitions were successfully achieved using a 1 W laser diode and beam diameters of 0.05 – 0.20 mm. For a variety of pyrotechnic compositions[39], laser ignition typically requires an energy fluence of 10 – 100 kJ m^{-2}.

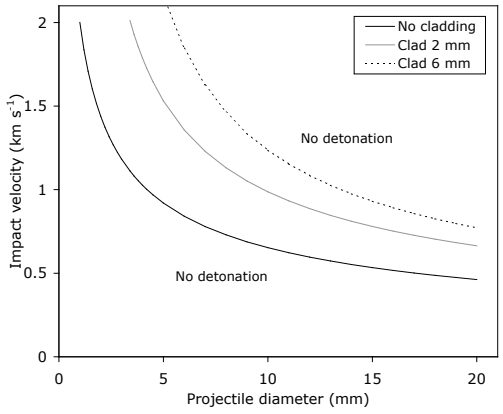


Figure 11 Effect of tantalum cladding thickness on the impact velocity needed for detonation of PBX 9404

Liau et al.[94] reviewed a variety of experimental results on laser ignition of RDX and found close agreement, but only up to 1800 kW m^{-2}; from that point on, up to 6000 kW m^{-2} there were two different trend lines—theory predicted a continuation of the same slope, as did some of the experimental data. But other experimental data reached a plateau at about 1800 kW m^{-2}, and ignition times were roughly constant at 0.03 s for all greater fluxes. Many more studies have been reported on radiant-heating ignition of propellants than of explosives; this is discussed in a later Section, but many of the findings can also have application to explosives.

An issue which is of some interest is whether there is an oxygen concentration effect on the ignition time of explosives or propellants. Explosives with OB ≥ 0 carry their own oxidizer and do not depend on oxygen from the air. Thus, it would be expected that there would be no effect of ambient oxygen concentration. Not much data is available one way or the other to answer this question.

In many practical cases, the explosive is not exposed directly to thermal radiation but, rather, there is an inert layer of some kind in front of the explosive. A theoretical ignition model has been developed[95] for this case when the initiation of the explosive is by purely thermal means.

HOT BODIES IN CONTACT

Explosives and propellants can be ignited by conduction heat flux from a hot body in contact with the surface of the substance. Energetic materials can also be ignited by internal heaters, and this principle is utilized in electrical detonators. In a pioneering study, Jones[96] embedded electrically heated wires in solid explosives and determined the minimum energy needed for ignition. He found that the energy required was directly proportional to the length of the wire. This would imply that the governing variable was the temperature of the hot wire, rather than the energy supplied to it. To a certain extent, this is true, but the thermal capacity (heat capacity × density × wire area) of the wire forms an integral part of the experiment and Jones did not find a constant-temperature criterion when comparing wires of various diameters. Instead, he noted that the energy per unit length of wire is a function of the thermal capacity, and that a minimum value can be obtained by extrapolating the results to zero thermal capacity.

Inami et al.[97] studied the ignition of several propellants from an electrically-heated niobium ribbon which was inserted into the middle of a propellant 'sandwich.' There was a large amount of data scatter, but trends could be correlated by solutions to the heat conduction equation with an Arrhenius heat release term for the solid and a constant-temperature boundary condition. Baer and Ryan[98] studied a similar 'sandwich,' but with a wire running down the length of a cylindrical specimen. They developed a combined heterogeneous/homogeneous model, with one Arrhenius reaction term describing a reaction within the volume of the solid, and a second one pertaining to a surface reaction. Excellent agreement was found with experimental data, but the model is rather unwieldy. Furthermore, it is not evident that the two assumed reactions correspond to actual chemical reactions that occur. More likely, the approach should be viewed as simply empirical fitting of a fairly large number of adjustable constants. A fairly reasonable agreement (errors of up to 2.5×) was obtained with a simpler scheme where no surface reaction was used, but, rather, ignition was taken to occur when a fixed temperature of the wire/explosive interface is reached.

FRICTION

In a classic study, Bowden et al.[99] examined the conditions needed to explode nitroglycerin by rubbing against various surfaces. The experiment involved placing the test material in between a rotating disk and slider. He first determined that the size and shape of the slider did not influence the results. Then, if frictional energy rate (power) is taken as being proportional to (frictional force × rubbing speed), then it turned out that the power was constant for these explosions, with a critical value of (frictional force × rubbing speed) being 20 W. This value was reasonably independent of the actual speed, load, or coefficient of friction used. His next series of tests showed, however, that thermal conductivity of the surface materials was another relevant variable—if conductivity was varied, the value of (frictional force × rubbing speed) needed for explosion did change. Surfaces of lower thermal conductivity required less frictional energy to be expended. Bowden concluded that the governing variable was actually the temperature attained in hot spots on the surface, and that lower thermal conductivity made it possible to more readily reach a high temperature.

For explosives which are in crystalline form, intercrystalline friction can cause initiation if the melting point of the substance is above the temperature at which rapid reactions begin. This condition is usually fulfilled for primary explosives, but not for secondary explosives. It has been found that for secondary explosives, a foreign particle 'grit' is usually necessary, but simple rubbing of clean surfaces suffices to initiate primary explosives. Furthermore, grit particles have the ability to enable explosion only if the grit has a high enough melting point; low-melting point grits do not increase the explosibility. If the melting point of a grit particle exceeds the minimum pertinent to the particular explosive, then increasing the hardness of grit particles serves to increase the ease of explosion.

Most tests that examine the sensitivity of military explosives combine frictional loading with impact, e.g., drop-hammer tests that include sandpaper. Results from 'pure' frictional testing are less often reported, the most common nearly-pure-friction test being the Koenen/BAM friction sensitivity test.

Stab initiation of explosives occurs in some detonators and in tests. Chaudri[100] has demonstrated that the mechanism is frictional in nature.

COMPRESSION

Solid explosives may be initiated by rapidly compressing a gas volume adjacent to the explosive's surface. The principle of adiabatic compression of gases has already been discussed in connection with the ignition of gases. Here, the gas itself (which will usually be air) is not being ignited, but acts upon the solid explosive. Evans and Yuill[101] found that initiation in this manner can readily be achieved for primary explosives, but only partially or not at all for secondary explosives. The compression ignition temperatures that need to be reached for initiation are about 2 to 3 times higher than the temperature values found in direct thermal initiation.

ELECTRICITY

The electrical ignition mechanisms of explosives are of four types[102]:

(1) short-arc discharge
(2) high-voltage arc discharge
(3) resistive heating and semiconductor action
(4) radiation from electric arcs or other high-energy radiant fields

A short-arc discharge occurs when contacts having a potential difference of around 50 V approach within ca. 0.2 μm. The actual resulting arc voltage is 11 to 16 V and the energy is primarily dissipated in heating the anode surface to its boiling point. This creates a vapor cloud which migrates to the cathode. Showers of molten metal usually accompany this discharge. A high-voltage arc discharge occurs at potential differences of more than about 300 V and spacings greater than 5 μm.

In recent years, concern about electrostatic discharge (ESD) initiation of explosive materials was raised due to a 1985 accident where a Pershing II rocket motor was accidentally initiated due to electric spark discharge[103]. Its propellant composition had been considered safe, since prior tests had indicated that Joule-level energies would be required for initiation. Explosives and propellants vary widely in their minimum energy requirements for spark ignition. Commonly, testing is done by simply placing a needle electrode

close to the surface, while holding the substance in a metallic cup to which the other electrode is connected. A spark discharge using a conventional capacitive-discharge apparatus is used. Results from several testing programs using this scheme are given in Chapter 14. These results, unfortunately, are exceedingly dependent on the details of the test. Kirshenbaum[104] examined the performance of various grades of lead azide in a number of these tests; Table 7 indicates that little consistency can be found. Observe, however, that the lowest values reported are much smaller than the lowest MIE values found for spark ignition of gases in air (ca. 2×10^{-2} mJ).

As with the testing of gases, using a low capacitance and a high voltage generally leads to lower MIE values being reported, as contrasted to high-capacitance, low-voltage test conditions. In addition, Kirshenbaum found a strong role of series resistance in the circuit, much as seen in spark ignition studies of gases or dust clouds. The fraction of the nominal energy $\frac{1}{2}CV^2$ that was actually delivered to the spark gap dropped from 80 – 90% for a resistance of 0.15 Ω, down to 10 – 14%, for resistances of 1 kΩ to 1.2 MΩ. Spark gap distance, polarity of the upper-surface electrode, electrode shape, and the metal used for making the electrodes are other factors which have also been found to influence the results. Some factors depend on a highly-specific interaction with the explosive. For instance, for granular materials, a needle electrode has been found to be less effective than a plane electrode, because the spark can 'blow away' the material in the case of the needle[104].

Some testing has been done on electric ignition where both electrodes actually touch the specimen, instead of a spark gap being created between an electrode and the test substance. Ignition can be achieved at much lower energies in this situation (Figure 12), which is termed a *contact discharge*[105]. The mechanism in a contact discharge is ohmic heating, due to high temperatures caused by very small areas of actual contact. A contact discharge is sometimes accompanied by ejection of hot metal particles.

Experimentally it has been found that capacitive discharge of 10 mJ through an electric blasting cap is enough to detonate it if discharged directly across the two legwires[106]. For discharge between a legwire and the metal shell, 30 mJ was found necessary. The charge has to come from some external source, since the small capacitance represented by a blasting cap precludes electrostatic charging from accumulating sufficient charge on the blasting cap itself. The ignition mechanism from an arc is not the same as from a spark. For lead azide, it was found that for spark discharge, the peak probability of ignition occurs at 300 V, and that the probability is nearly independent of the capacitance[107]. For voltages below the Paschen minimum (see Chapter 14), ignitions are also possible, but the probability for any voltage does not exceed 35%.

A viable theory for describing the ignitability of solid explosives from electric spark discharges does not yet exist. Skinner et al.[108] examined single-component explosives and proposed that the mechanism should be largely thermal, and that it should be possible to base analysis on a hot-spot ignition theory. Based on their empirical testing results (tabulated in Chapter 14), they made several correlations to self-heating theory. The best correlation was based on evaluating δ_c for a 20 μm sphere, which was assumed to be the diameter of the hot spot. They solved the expression for critical T_o, then plotted the MIE against $1/T_o$. This was seen to give largely a straight line. Values of the pre-exponential were taken from the literature.

For multi-component propellants, recent studies indicated that compression can have a very large effect and that substances which would have required > 1 J for initiation in a conventional test may only require ca. 10 mJ under certain confinement situations. Specifically, it was found[109] that much lower MIE values will be found if the confinement is sufficiently effective that the hot gases which are formed are prevented from expanding freely. The development of an arc channel in a propellant is complicated, because of its inhomogeneity—there are discrete particles of oxidizer and metal in the polymeric binder, and the three components have widely disparate thermochemical properties. Lee[109] determined experimentally that the arc channel is serpentine (Figure 13), going through the polymeric binder and avoiding the larger particles of oxidizer. The arc channel does not

Table 7 ESD sensitivity of several grades of lead azide, as determined by a variety of test methods

Grade of lead azide	Reported MIE (mJ)
RD1333	4×10^{-7} to $2\times10^{+1}$
service	1.6×10^{-3} to 1×10^{0}
dextrinated	1×10^{-2} to $1\times10^{+2}$
PVA	2×10^{-4} to $2\times10^{+1}$

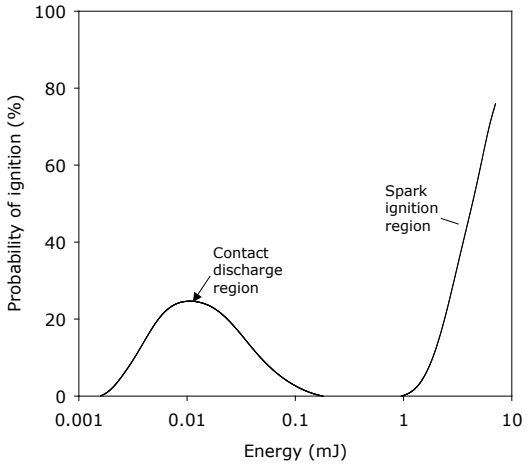


Figure 12 Two ignition modes exhibited by lead azide

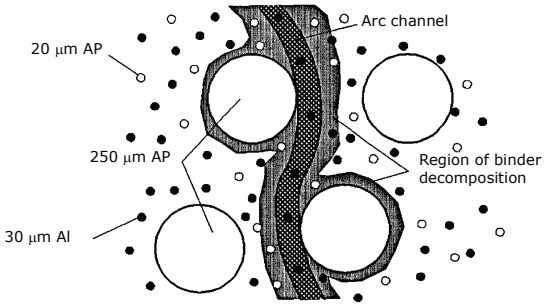


Figure 13 Serpentine arc channel formed in a heterogeneous propellant (typ. width: 140 μm)

avoid the small metal particles, and the conductivity of the metal strongly influences the discharge. During a short-duration discharge, the arc channel expands to its ultimate width largely by compressing the bulk solid, not by ablation of the solid into the channel. Physically, ignition of the propellant takes place adjacent to the arc channel and is governed primarily by three reaction mechanisms: (1) decomposition of oxidizer particles; (2) pyrolysis of the polymeric binder and exothermic reaction between the pyrolysate gases and close-by particles of oxidizer; and (3) reaction of the high-temperature plasma gases with the oxidizer. The latter is especially complicated since, due to the high temperatures involved (ca. 13,000 K), radiation plays a dominant role. Lee suggested some features which a detailed model should incorporate, but actual development of a model along these lines was not undertaken. Lee's work does emphasize that conventional spark discharge studies which expose the surface of a specimen to a spark using small-to-nil confinement cannot be relied upon as giving conservative data for cases where confinement effects are important.

Silver azide has been found to explode at room temperature when a voltage greater than 67 V is impressed across a crystal[110]. The mechanism is understood to involve semiconductor action, not simple ohmic resistivity. Gora et al.[111] conducted extensive studies into semiconductor action for azides. The nature of the metallic contact to the azide surface was found to play a crucial role, whether the contacts are ohmic (allowing free carrier injection) or Schottky-barrier contacts.

A US Navy study on a series of lightning-initiated deflagrations of magazines storing smokeless powder determined that the proximate cause of the explosions was a design of the fiberboard drums that was conducive to internal arcing[112].

LIGHT ENERGY AND IONIZING RADIATION

A number of primary explosive are sensitive to initiation by a sufficient amount of light energy. Results from flash-tube experiments are shown in Table 8[53,113]. The energy density values are obtained by dividing the energy delivered to the crystal by the total surface area of the crystal. Certain nitrides and perchlorates are also susceptible to light energy initiation[107].

Experiments indicate that silver azide is a compound where photochemical excitation can be assigned as the mechanism of initiation. For many other primary explosives, it is not clear whether the light energy is simply being converted to heat, or if a photoexcitation process is involved. Most secondary explosives are organic compounds with covalent bonds. These tend to melt first and then the explosion occurs in the liquid or gas phase. As a result, their sensitivity to initiation from light energy is minimal. For some crystals, e.g., PETN, it has been found that certain intensities of UV light can fracture the crystal without causing initiation[59]. Avrami and Haberman[115] reviewed a number of other studies of light-energy initiation of explosives.

Boddington and coworkers analyzed the problem theoretically by assuming it to be a variation on the self-heating problem[114]. In their theory, thickness plays a critical role, in the same way as in the self-heating problem. This treatment is appropriate for thin materials subjected to very high rates of light heating. For very high heating rates, and with the material in the form of a slab of modest thickness whose front face is irradiated and the back face is kept at ambient temperature, they provided the solution:

$$\delta_c \approx \frac{\beta e^{-\beta}}{e}$$

where the dimensionless heating rate, β is:

$$\beta = \frac{\alpha_s \dot{q}''_e E}{\lambda R T_o^2}$$

The authors did not treat a case analogous to thermally-thick solids being ignited by radiant heating, nor did they

Table 8 Minimum energies for flash-tube ignition

Compound	Formula	Energy for ignition (kJ m^{-2})
nitrogen iodide	$NI_3 \cdot NH_3$	1.6
silver nitride	Ag_3N	2.0
cuprous acetylide	Cu_2C_2	6.3
benzene diammonium nitrate	$C_6H_5N_3O_3$	9.2
diazobenzene perchlorate	$C_6H_5N_2ClO_4$	9.2
ammonium perchromate	$(NH_4)_3CrO_8$	11.0
mercuric fulminate	$Hg(ONC)_2$	16.5
lead azide	$Pb(N_3)_2$	20.
silver fulminate	AgONC	21.
silver azide	AgN_3	26.
mercuric azide	$Hg(ONC)_2$	26.

attempt to use theory to explain the large differences found experimentally in the light energy needed for initiation of various explosives.

Since the 1920s there has been interest in studying the initiation of explosives by radiating them with electrons, neutrons, α-particles, γ-radiation, X-rays, and other high-energy forms of radiation. Gamma radiation has generally been found to have no effect, while modest effects have been found with various other forms of radiation. Avrami and Haberman[115] reviewed a large amount of experimental data on this topic.

SASIN was an explosive developed in a joint effort between Southwest Research Institute and Sandia Laboratories. The explosive comprises silver acetylide and silver nitrate in a solvent which can be alcohol or acetone. The substance can be sprayed onto a surface without detonation, but once it dries it can be detonated by light energy from a powerful source.

CRYSTAL GROWTH

Some of the most sensitive explosives undergo initiation spontaneously, simply due to crystal growth, when crystals are being grown out of a liquid solution. This has primarily been observed with various azides. Chaudri and Field[72] have reviewed a number of research studies in this area. Various theories have been proposed as to why this happens, but it does not appear that a unique explanation is yet in hand.

RF INITIATION

An indirect ignition mechanism is often of concern in blasting operations—the possibility that RF transmissions might induce a voltage into an electric firing mechanism, leading to inadvertent initiation of an explosive charge. Anke et al.[116] studied the problem for several detonator types and produced guidance charts. In general, they found that the portion of the spectrum where the least power is sufficient for detonation is 0.5 – 10 MHz. A transmitter in this frequency range with an effective radiated power of 100 W would need to be about 50 m away to ensure that inadvertent detonation will not occur; a large broadcasting station of 50 kW would need to be about 500 m distant. A British standard[117] exists on this topic. Some additional results were reported by Collett[118].

MODELING DETONATION

As already discussed in Chapter 3, detonation is fundamentally different from normal burning (which is called deflagration). In a deflagration, a combustion wave moves smoothly through the substance leaving reaction products at its conclusion. A detonation is a special hydrodynamic phenomenon which involves shock waves. A chemical reaction is caused by the high speed, high pressure compression of the shock wave, and not by the much slower diffusion of heat or molecules associated with a deflagration wave. A detonation wave may progress in the explosive substance at around 5000 m s^{-1}, and can be compared with the speed of sound in air, which is around 340 m s^{-1} at room temperature.

For about 100 years, the theory to analyze the behavior of explosives has been based on the theory of Chapman and Jouguet (C-J), which strictly applies only to gaseous systems. The C-J theory can answer many practical questions about the behavior of explosives. But it also has failures. For example, it cannot explain why some pairs of isomers show a ranking one way for thermal sensitivity, and an opposite ranking for shock sensitivity. The basic limitations of the theory were eventually found to be (a) the assumption of thermal equilibrium in a shock wave; and (b) the absence of realistic chemistry. The molecules in a shock wave are not in thermal equilibrium, so treating them by classical equilibrium thermodynamics is an oversimplification. Likewise, if many common substances reacting at ambient pressure are known to be poorly represented by global, single-step Arrhenius kinetics, it is not surprising that systems involving highly excited molecules and very high pressures should fail to conform. The width of shock wave progressing through an explosive is typically only ca. 5 nm, which is the span of 15 water molecules. Actual rise times are in the range of picoseconds, although physical instrumentation does not capture such short rise times.

Modern approaches to studying detonations are commonly based on molecular dynamics calculations, in other words, on quantum mechanical calculations for the molecule in question. Needless to say, studies of this type are mathematically and computationally difficult and do not lend themselves to any simple presentation. Bardo[119,120] was the early pioneer of quantum-mechanical theories. These are very computationally intensive and require a much larger number of fitting parameters than classical theories. There is also continuing research on advanced classical-mechanics theories. For example, Ruderman et al.[121] have been studying the ignition of HMX, representing it as a nonlinear viscoelastic solid which is reactive and can also undergo phase transitions to a viscous liquid and to a gas. Politzer and Alper[122] have reviewed the state of the art in molecular dynamics modeling of explosives and placed recent efforts in the context of other modeling strategies. Tarver and Urtiew[123] described a reactive-flow model, where the reaction proceeds in three steps: (1) initial ignition at hot spots, which involves only the amount of explosive represented by its void fraction; (2) reaction of most of the rest of the explosive, involving exothermic chain reactions that form highly-excited gaseous reaction products, which then expand and thermally equilibrate; and (3) slower, diffusion-controlled forms of energy release, such as solid-carbon coagulation or aluminum particle oxidation.

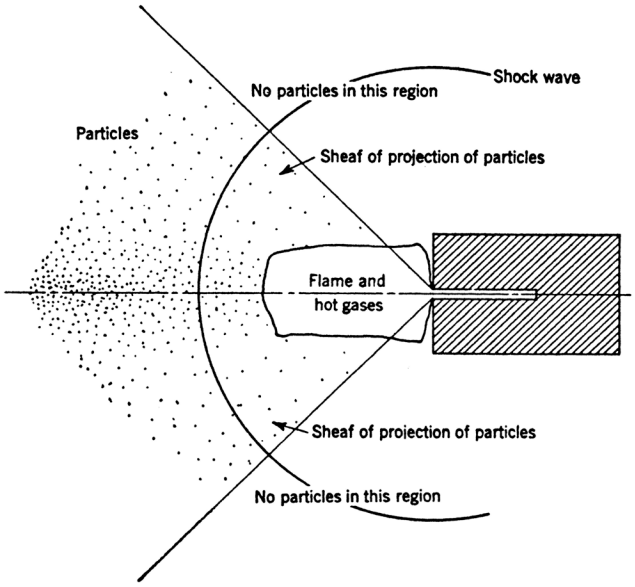


Figure 14 Emissions from a borehole with potential for igniting an air/fuel-gas atmosphere

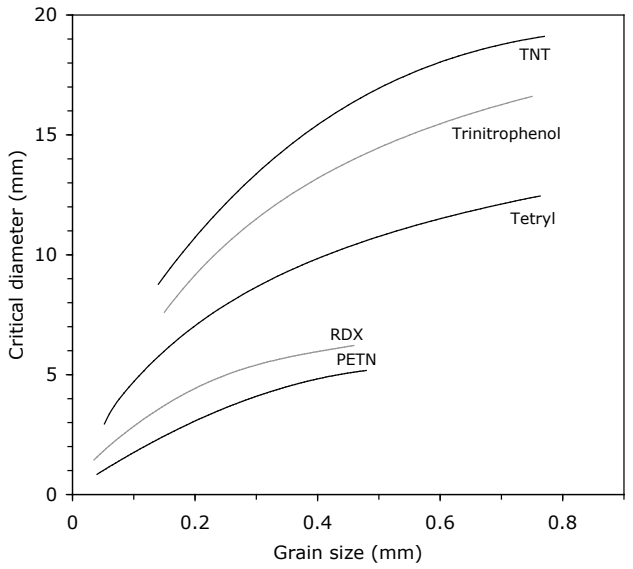


Figure 15 Effect of grain size on critical diameter (density = 1000 kg m^{-3})[184]

IGNITION OF AIR/FUEL-GAS ATMOSPHERES BY CONDENSED-PHASE EXPLOSIVES

In the coal mining industry, it is often necessary to employ explosives for blasting. But coal mines may be 'gassy,' that is, containing a significant amount of methane; thus, a methane explosion may be created by blasting. Consequently, the ignition of air/fuel-gas atmospheres by condensed-phase explosives has been studied. Since even 'permissible explosives' (see below) can produce temperatures of 1500 – 2000ºC, the question of interest is not why the firing of explosives sometimes ignites flammable atmospheres but, rather, why it does not do so every time! Ignition can, in general, be caused by several mechanisms (Figure 14):

- flames
- hot gases
- shock waves, or
- hot particles.

These have been studied by many investigators[124], without simple insights emerging. Coward[126] reviewed in depth the early work in the field, but studies have largely tapered off along with the general reduction in coal-mining safety research. Of the mechanisms, shock waves are probably the most important, especially when in geometries where they can be reflected from a surface, with consequent additive effects. Grant et al.[125] conducted reduced-scale tests in a simulated mine gallery and documented that the oxygen concentration in a methane/oxygen/nitrogen atmosphere is a crucial factor in determining whether a given shot will or will not ignite the atmosphere. They concluded that there are two dominant mechanisms: the shock wave heats the atmosphere to an elevated temperature, but turbulent mixing of the products of detonation has a cooling effect. Ignition by means of incandescent particles ejected from the shothole[126] has been studied by only a few researchers, some of whom doubt the mechanism and consider that ignition will only happen due to impact of particles on solid surfaces and the consequent conversion of kinetic energy into heat. When high explosives are used, the methane/air atmosphere can potentially undergo detonation, not just deflagration. The amount of high explosive needed for this is not large; Benedick[127] demonstrated that it is possible with ca. 2 kg of a plastic explosive (not a permissible explosive).

VARIABLES AFFECTING THE BEHAVIOR OF EXPLOSIVES

The role of *pressure* on explosions is complicated. Since the reactants are at lower pressure than the products, all else being equal, increasing the pressure should decrease the reaction rate (Le Chatelier's Principle). This indeed is what is found for lead azide[53]. But for PETN there are two possible reaction pathways, and high pressure causes explosion, rather than non-explosive decomposition, to be preferred. It turns out that there is a countervailing mechanism due to heat transfer. When an explosive is confined in a rigid casing, the reaction causes the pressure to rise, which would lower the reaction rate. But at the same time, the hot products are retained in intimate contact with the reactants, which they would not be if containment were not provided. In the case of detonations, the main effect of confinement is not thermal, but, rather, directly related to reinforcement of the shock waves. In practice, black powder and smokeless powder will burn, rather than explode, if not confined. Many secondary explosives, however, do not need confinement in order to explode. Even without confinement, if a sizeable pile of explosive material is exposed to slow, gradual heating, then self-heating effects will predominate

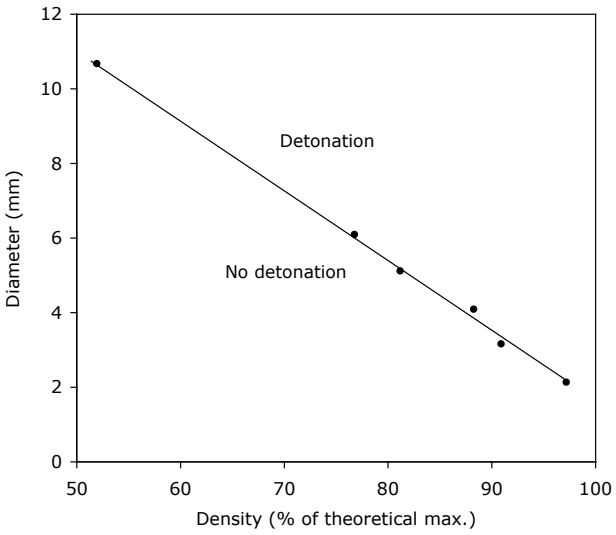


Figure 16 Effect of density on critical diameter ('Group I' - TNT)

and a violent explosion can be expected. On the other hand, some explosives which undergo deflagration within a confinement, may stop reacting entirely once the confinement is breached.

The *physical form* of the explosive affects the minimum energy needed for ignition. Explosives in powder form are much more readily ignitable than are ones which are cast or pressed. *Grain size* has an effect under certain circumstances. For TNT, it has been shown that the energy fluence required for ignition from impact is about 5% lower for fine-grain than for coarse-grain size[128].

For detonation to occur, a minimum *amount* of material must be present. The exact amount depends on numerous factors, but for primary explosives it may be on the order of milligrams, for secondary explosives on the order of grams-to-tons, while for 'non-detonating' substances such as gunpowder and ammonium nitrate it may be hundreds of tons. If a lesser amount is present, a deflagration but not a detonation is possible. There also exists a *critical diameter* of an explosive, and if the explosive is produced in a smaller diameter, detonation does not propagate throughout the substance. This has a practical implication, in that charges intended to be detonated must exceed this diameter. Unfortunately, the critical diameter is highly dependent on grain size and density. Smaller grain sizes give lower critical diameters (Figure 15), but the effect of density is complicated. Price[129] determined that two different behaviors can be found. Figure 16 shows an example of a 'Group 1' material, TNT. Its critical diameter decreases with density (in the explosives field, density is commonly reported as a percent of maximum theoretical density, the latter representing a porosity of zero). By contrast, Figure 17 shows AP, a 'Group 2' material, which exhibits an increasing diameter with density. Price's results only cover a practical range of densities; when extremes of density are investigated, non-monotonic behavior is sometimes seen, as shown in Figure 18 for TNT. Price reports that other Group 1 explosives include PETN, RDX, and tetryl. Other Group 2 explosives are ammonium nitrate and dinitrotoluene. The groups do not exhibit disparate behavior with regards to effect of grain size and temperature on the critical diameter—for both groups, increasing grain size raises the critical diameter, while increasing the temperature lowers it. The critical diameter concept means that certain materials may be 'non-detonable' in laboratory-scale tests, yet detonate in real-scale sizes. Strehlow[130] points out that, in the early part of

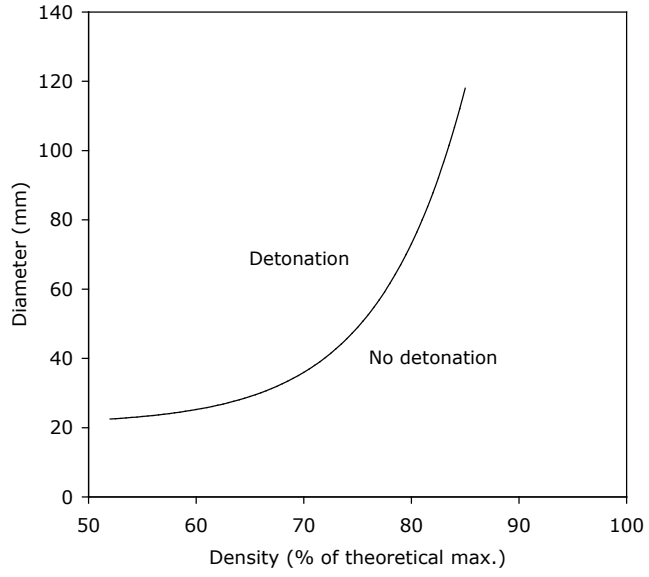


Figure 17 Effect of density on critical diameter ('Group 2' – AP)

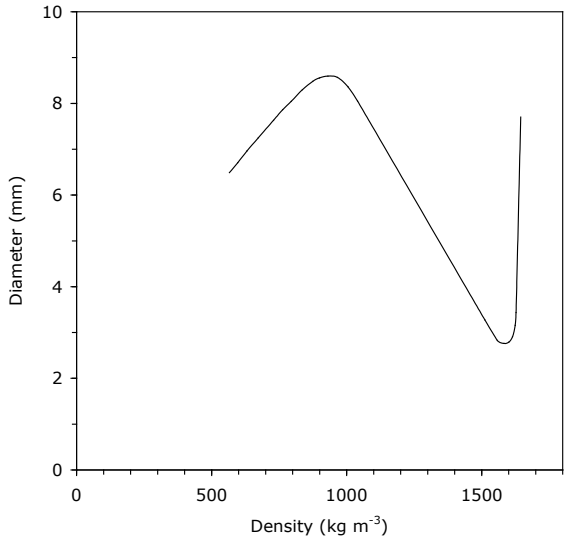


Figure 18 Effect of density on critical diameter (TNT, mean grain size 0.06 mm)[184]

the 20th century, ammonium nitrate (whose history of disasters is reviewed in Chapter 14) was considered 'non-detonable' for this reason.

Increasing the degree of confinement serves to reduce the critical diameter, thus testing to determine the critical diameter is done under conditions of minimal confinement. In some cases, the effect of confinement can be drastic. For example, when ammonium nitrate[131] at a density of 1060 kg m^{-3} is minimally confined (wrapped in plastic tape), the critical diameter is 100 mm; confined in glass, it is 80 mm, while confined in steel, it is below 30 mm. Apart from the density, the mode of preparation of the explosive—cast or pressed—also affects the critical diameter. For thin sheets, a comparable quantity, the critical thickness, can be determined. In early Russian literature, there was a claim that the critical diameter and the critical thickness were related by a simple formula; more extensive test work in the US, however, disproved that[131]. Apart from critical diameter results, the degree of confinement also affects results from gap tests. Most gap tests use a confined acceptor geometry, in which case the sensitivity decreases as the density increases. In one series of experiments[132] where a gap test design was used where the acceptor charge was unconfined, the opposite trend was found—the sensitivity increased as the density increased.

Raising the *temperature* decreases the critical diameter and increases the sensitivity[133]. In a study on AP[134], it was found that raising the temperature from 25ºC to 240ºC decreased the critical diameter from 23 mm to 11 mm.

For some explosives that are hard to initiate, microballoons or small, hard particles with sharp edges and a high melting point are added as *sensitizers*. In addition, impurities can act as sensitizing agents for certain explosives. Substances such as lubricants, waxes, hydrocarbon liquids, camphor, or even water act as *desensitizers* or *phlegmatizers*. The effect of a desensitizer is to quench the explosion after initiation; it does not prevent initiation[53,59]. In many cases, for the effect to be sufficiently beneficial, sizable amounts of a desensitizer have to be added and the desired properties are degraded.

PRACTICAL APPLICATIONS

INITIATING DEVICES

In purposeful firing, a secondary explosive is initiated by an initiating device which typically contains a primary explosive and a base or booster charge. The primary explosive is chosen so that it is easily initiated by a modest amount of externally-supplied energy. It then shock initiates the base charge and the latter provides the shock wave needed to initiate the secondary explosive. But explosives may be initiated by a variety of methods. Initiating devices that produce a flame or flash, but not a detonation are generically termed *igniters*, while those that do produce a shock wave are termed *primers*. The most common means of initiation are the following, which include a few that do not use a primary explosive:

- Friction. This is the simplest initiation device and is used on flares and on some military devices. A matchhead does not detonate nor does it initiate a second explosive, but it comprises a pyrotechnic mixture which is also ignited by friction. The military makes use of stab igniters where the stabbing motion of a conical-shaped pin into a mixture causes sufficient friction for initiation.
- Mechanical impact. The trigger on a hand weapon applies mechanical impact onto the primer composition of the bullet. In the explosives field, any initiating device based on simple mechanical impact is a *percussion primer*. Early compositions of percussion primers were often a mixture of mercury fulminate, antimony sulfide, and potassium chlorate. Primer mixtures today may have lead styphnate, barium nitrate, tetracene, aluminum powder, lead azide, etc.; small amounts of secondary explosives such as TNT and PETN also sometimes show up in a primer mixture.
- Flame. A *safety fuse* is a common examples of initiation by flame. A safety fuse contains a black powder mixture which cannot detonate itself; thus, it is used to initiate a primary explosive, which then applies shock waves to a secondary explosive. In practice, the safety fuse usually leads to a *non-electric blasting cap*, which then initiates the bulk explosive.
- Electric heating. An electric igniter uses a thin Ni-chrome wire (bridgewire) which is rapidly heated by applying an electric current. They can be of two types. An *electric squib* contains only a low explosive and is used for initiating pyrotechnics or propellants. An *electric blasting cap* (commonly called a *detonator* in military applications) contains charges of primary and secondary explosives and is intended to initiate a cap-sensitive secondary explosive which needs a substantial detonating charge to detonate itself. It consists of a copper or aluminum cylinder containing both a primary (e.g., DDNP; formerly, lead azide and mercury fulminate/potassium chlorate mixtures were also common) and a secondary explosive (e.g., tetryl, PETN, RDX). The commonly used No. 8 blasting cap (Figure 19) is 7 mm in diameter and contains 0.3 g of primary charge and 0.8 g of secondary. A firing current of somewhere in excess of 300 mA is normally used. A blasting cap may be used as a means of initiating a detonating cord (also called *detonating fuse* or *Primacord*), where the cord itself contains a high-order explosive, commonly PETN. The detonating cord acts as an intermediate device which propagates detonation into the bulk explosive.
- Exploding wire (in military terminology, exploding bridgewire or EBW). This specialized detonator was developed to impart an immunity to electric detonators against stray voltage or electromagnetic radiation. An EBW detonator does not use a primary explosive

but only a charge of secondary explosive, hence its lower sensitivity to unwanted initiations. An EBW is a particularly energetic form of initiation and can detonate a secondary explosive whereas a normally melting wire would not. The principle is discussed in Chapter 11.

A number of illustrations and practical details of a variety of initiating devices are given by Voreck et al.[135] Commercial detonators are intended to be set off only by application of flame or electricity, but BM[136] documented a number of mishaps where modest mechanical mishandling sufficed.

PERMISSIBLE EXPLOSIVES

In coal mines, flammable methane/air atmospheres will commonly occur, as will flammable coal dust/air atmospheres. Explosives are a convenient way to remove coal, but use of explosives should not result in unwanted explosion of flammable atmospheres which may be spread throughout the mine. Dust clouds will arise from blasting activity, so even if originally there was little dust, after the first blast there is likely to be dust loading that must be allowed for. Early blasting in coal mines involved the use of black powder, and this sometimes had disastrous consequences if a 'gassy' condition was encountered or if a dust cloud arose. It was then noticed that black powder burned relatively slowly and, consequently, produced a fair amount of flaming outside the shothole. High explosives, however, burned more rapidly and were less prone to cause a mine explosion. It was also noticed that the size of the gallery had an important effect on the outcome: gases or dust clouds were much more likely to be ignited if the gallery was narrow. The extreme case is when the explosion vents into a fissure, which is viewed as highly dangerous. Later, it was concluded that ignition of a gas/air or dust/air atmosphere requires a minimum induction period if it is to occur. If the detonation produced by the mining explosive is shorter than this induction period, then ignition will not occur. Explosives having this characteristic were initially developed in 1914 and are termed 'permissible explosives,' also known as 'short-flame' explosives. In 1989, the official term in the US was changed to 'MSHA permitted explosives,' in parallel to the 'permitted explosives' term used in the UK. Methane/air atmospheres are generally more easily ignitable than are dust clouds, but there are enough exceptions to the rule so that candidate permissible explosives must also be demonstrated not to ignite the latter[126]. Permissible explosives may be required not just in coal mines, but in other underground mines where gas or dust hazards exist. Hopler[137] has reviewed the history of permissible explosives in the US.

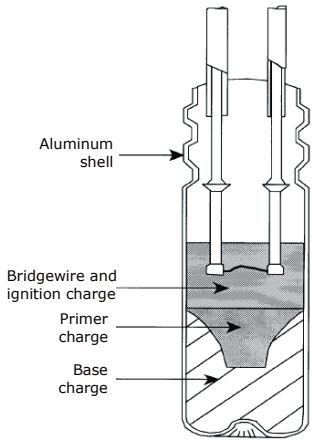


Figure 19 The No. 8 blasting cap

An explosion of methane or dust in a coal mine caused by firing an explosive is an extremely rare event. UK statistics[138] indicate that there are about 6 unwanted explosions per 10^8 shots fired, which is an exceptionally low failure rate. This also implies that tests for permissible explosives must create conditions substantially more favorable towards causing a gas or dust explosion if their safety is to be assessed with a feasible number of experiments.

The allowable duration of the detonation depends on the maximum temperature it develops. All high explosives can be made permissible by adding to it components which reduce the flame temperature. Black powder, however, cannot be made permissible, since it does not detonate and burns slowly. But in the US, since the federal government did not regulate mining safety until 1952, it was still possible to use black powder in underground mining until that date. In general, the principle involved in the design of a permissible explosive is simple. A relation between time to ignition and the needed temperature for the ignition of a methane/air mixture is used. If the time/temperature curve of the explosive is always below the methane/air curve, then the methane/air mixture cannot be ignited. Such a curve is readily obtained for methane, however, obtaining a time/temperature curve for an explosive is more difficult. In practice, the design proceeds in a simpler way. The adiabatic flame temperature for an explosive is not difficult to compute, and this value should no more than 2200ºC, decreased by some suitable safety factor[139]. To ensure that burning time will not be excessive, it is normally sufficient to ensure that the oxygen balance is zero or positive; if OB were negative, this would entail prolonged flaming, since there would be an insufficiency of oxidant within the solid material and oxygen from the air would be used later in the burning process. In general, a flame duration of < 1 ms is required; by contrast, black powder shows 1539 ms, when tested according to BM procedures[34]. In addition to their flame possessing a short time duration, permissible explosives should produce flames of short spatial length, since this minimizes flame extension beyond the borehole, but here the difference between permissible explosives and others is much smaller.

The flame temperature may be lowered by effectively raising the creating ρC of the combustion products. This includes using an excess of fuel in the mixture, incorporating

water molecules into it, or adding substance which decompose endothermically. Physically, permissible explosives are available as granular materials, gels, emulsions, or sheathed explosives. Incorporating a large fraction of ammonium nitrate into an explosive is a common way of making it permissible[140]; this is because of the low detonation temperature of AN. *Cooling salts* (e.g., sodium chloride) are sometimes included in the formulation to reduce the flame temperature and cause an earlier extinction of flaming. Nitroglycerine or nitroglycol are commonly added in small amounts to ensure that a No. 6 detonator will detonate the explosive completely and not just partially[141]. Since permissible status may be achieved by lowering the combustion temperature, sheathing is a way to help an explosive be permissible. This involves a sheath which is either non-explosive (e.g., potassium fluoride, sodium bicarbonate) or of low explosibility and acts mainly as a heat sink. In using permissible explosives, the miner is still responsible for correctly drilling a borehole and placing and stemming the charge therein. Thus, permissible explosives are only 'permissible' if properly fired in boreholes (sufficiently depth, adequate stemming, etc.); if they are fired into open air, methane or dust clouds may be ignited[140]. Finally, the mass of explosive used also affects the probability of unwanted ignition.

There are fewer permissible explosives in the marketplace today than earlier. In the US, the number dropped from 174 in 1952 to 94 in recent years. In general, use of explosives in mining is diminishing, as blasting techniques are being replaced by mechanical ones[137].

BLASTING AGENTS

The US Geological Survey defines blasting agents as "any material or mixture consisting of fuel and oxidizer intended for blasting, not otherwise defined as explosive, provided the finished product, as mixed for use or shipment, cannot be detonated by means of a No. 8 test blasting cap when unconfined." The practical meaning of this is that an explosive designated as a blasting agent will typically require a booster charge for successful detonation, in addition to a detonator. One common form of blasting agent is ANFO (see Chapter 14). Blasting agents do not contain nitroglycerin. Explosives for blasting use which do not fall under the definition of blasting agents are termed *blasting explosives*.

The sensitivity of explosives to detonation from a high-power hunting rifle is essentially identical to that from a No. 8 blasting cap. This was demonstrated by Watson et al.[142] in a study using aluminum-cased No. 8 blasting caps, copper-cased No. 8 blasting caps, and three different hunting rifles. The kinetic energy available from the rifle bullets in these tests ranged from 2400 to 4500 J. They also showed that the results from the two different types of blasting caps were nearly identical.

Table 9 Relative separation distances (m) required for various combinations of donor and acceptor explosives, as determined in Bureau of Mines tests

Donor → **Acceptor ↓**	**AN 1.0 m PE**	**AN 1.0 m steel**	**AN 1.5 m PE**	**AN 1.5 m steel**	**AN 1.0 m steel**	**AN 1.5 m steel**
	Unbarricaded				**Barricaded**	
AN	3.8	5.8	7.0	12.2	1.8	2.3
ANFO	5.8	17.7		46.6	2.4	
ANFO, bagged	8.2	32.9				
dynamite	20.4	50.9				

INSENSITIVE MUNITIONS

If a ship, tank etc. is attacked which contains stored munitions, then the major destruction may occur from the detonation of the stored munitions, rather from direct damage from the attack. Thus, in the US during the mid-1980s, military policies were established to use insensitive munitions wherever possible; other Western countries have also had similar programs[43]. Consequently, much research work was carried out to develop insensitive munitions. These are munitions that can still function properly when fired, but which are unlikely to be detonated by shrapnel, blast, or a fire impinging externally. In the military studies, the objectives have been expressed functionally, rather than in terms of basic energy transfer modes. According to the US Navy[81], the following tests must be successfully passed for munitions to be labeled as 'insensitive':

- fast cookoff—no reaction more severe than burning
- slow cookoff—no reaction more severe than burning
- bullet impact—no reaction more severe than burning
- sympathetic detonation—no propagation
- fragment impact—no reaction more severe than burning
- spall—no sustained burning
- shaped-charge jet impact—no detonation

The above are all large-scale tests, since adequate predictability from small-scale tests has not been considered to be established. A slightly different series of tests has been described by the US Air Force[143]. A recent review of the design issues associated with insensitive munitions has been published by Victor[144]. Insensitive munitions can be created by selecting substances of suitable chemistry or by the addition of desensitizers, or both.

SAFE DISTANCES FOR STORAGE

Given fixed details of the originating detonation and the target explosive, sympathetic detonations are to be expected only up to a certain distance of separation between the pile of explosives originally detonating and the target pile. This concept is embodied in tables of separation distances. Various countries have established such tables, usually based on a small amount of incident data, augmented by expert opin-

ion. In the US, the Institute of Makers of Explosives first promulgated such a table in 1910, with the current version being one published in 1971. This has been adopted by OSHA and BATF as Federal regulations. A modest amount of research has been done on the topic, but not enough to upgrade the tables to the point that they would no longer be primarily expert-opinion-based. A Bureau of Mines study[145,146] produced the results given in Table 9 using several types of originating ('donor') and target ('acceptor') explosives. Both the donors and the targets were equicylinders, with the dimensions specified. The 1.0 m donors weighed 726 kg, while the 1.5 m donors weighed 2452 kg. The end caps on the donors were either a reinforced polyethylene (PE) or a 1.5 mm thick steel sheet. The sand-filled barricades were 0.25 m thick for the 1.0 m donor charges and 0.38 m thick for the 1.5 m charges.

Propellants

The useful function of propellants is that they produce large volumes of gas at a controlled rate. Thus, they differ from explosives, where it is not necessary to limit the rate of reaction. Propellants are used in guns and rockets, but also in various industrial applications (propellant actuated devices) where a high force of short duration is wanted. The peak pressures developed by propellants are considerably lower than by explosives. For rockets, pressures of up to 20 MPa are found, whereas for gun propellants pressures up to 700 MPa. The physical state of propellants may be solid or liquid, although liquid propellants currently have applications only in rocket propulsion.

Propellants for small-arms applications are classed as:

- black powder (potassium nitrate, charcoal, sulfur)
- 'improved,' proprietary derivatives of black powder, with some common examples being:
  - Pyrodex (primarily potassium nitrate, charcoal, sulfur, potassium perchlorate, dicyandiamide, and sodium benzoate, along with wax and wetting agents)
  - Golden Powder, Black Canyon powder (potassium nitrate, ascorbic acid).
- smokeless powder, as three distinct types:
  - single-base powder (NC)
  - double-base powder (NC, NG)
  - triple-base powder (NC, NG, NQ); used only in limited military applications.

In the rocket propulsion field, solid propellants are functionally divided into four classes:

(1) *Single-base propellants*. These comprise only plasticized nitrocellulose as the main ingredient. However, a small amount of stabilizer is added, and other minor ingredients may also be present.
(2) *Composite propellants*. These contain an oxidizer in granular form dispersed throughout an organic binder that acts as fuel. The most common oxidizer is ammonium perchlorate, with potassium perchlorate and ammonium nitrate sometimes also being used. The most common fuel is hydroxyl-terminated polybutadiene (HTPB), but polystyrene, polysulfide, polyurethane, PVC, epoxy, or even asphalt have also been used. A typical formulation can comprise ammonium perchlorate, polybutadiene, aluminum, and a burning-rate modifier such as copper chromite or ferrocene. Another common formulation is based on ammonium perchlorate oxidizer and a Thiokol fuel, the latter being a family of polysulfide rubbers.
(3) *Double-base propellants*. They were discovered by Alfred Nobel, who found that a mixture of nitrocellulose and nitroglycerin produced a reasonably safe, practical propellant of broad applicability.
(4) *Triple-base propellants*. They are similar to double-base propellants, but nitroguanidine is also added into the mixture.

Aluminum is useful due to its high heat of combustion and is often added as a fuel component to single-base and composite propellants. Most practical formulations also include minor ingredients for stabilizing, cross-linking, catalysis of burning, anti-flash, and as aids in processing. Tricalcium phosphate is commonly added to ammonium chlorate-based compositions as an anticaking agent.

A solid propellant composition will contain three 'logical' components: an oxidizer, a fuel, and a binder. However, the number of physical components can be smaller, since the binder is often the same substance as the fuel. Nitrocellulose can be used as a propellant by itself since it effectively comprises all three 'logical' components. The fuel and the oxidizer in solid propellants are in intimate contact: in the case of nitrocellulose, these are simply parts of the same molecule. Where a separate fuel is used, the physical mixture, nonetheless, places fuel and oxidizer molecules into close contact.

The oldest gun propellant, *black powder*, is a multicomponent substance. It is made by grinding potassium nitrate, sulfur, and charcoal individually into fine, uniform powders. The powders are then mixed and milled together, pressed in a hydraulic press, granulated, and finally tumble-polished. The ratio, by mass, of the three components is generally 75:15:10. The combustion products are highly complex and include both gaseous and solid aerosol components. The main product gases are CO_2, CO, and N_2. The white smoke is formed by the solid products, the main ones being K_2CO_3, K_2SO_4, and K_2S.

Black powder has been obsolete for decades in military uses and has been replaced by propellants based on *nitrate esters*, such as nitrocellulose or nitroglycerin. Nitrocellulose is the primary ingredient in *smokeless powder*, so called because it was developed to minimize the large quantities of black smoke emitted by black powder. The term encompasses a wide variety of powders based on nitrocellulose. Usually other ingredients include potassium nitrate or bari-

um nitrate. Recently, attention has been focused on the *nitramine* based propellants (e.g., RDX plus polymeric binder) as insensitive replacements[147].

Liquid rocket propellants may comprise separate fuel and oxidizer sources, or may be a *monopropellant* (a propellant which does not need a reaction partner) such as hydrazine (N_2H_4). In a 'catalytic decomposition engine,' hydrazine decomposes into H_2, N_2, and NH_3 without the need for another reactant in the system. Since hydrogen and ammonia are flammable themselves, further heat release occurs from subsequent combustion reactions. Where separate fuel and oxidizer substances are used, the most common combinations are:

(1) liquid hydrogen (LH_2) with liquid oxygen (LOX or LO_2)
(2) kerosene with liquid oxygen. The grade of kerosene used is designated by NASA as RP-1.
(3) a fuel consisting of either monomethyl hydrazine or a 50/50 mix of unsymmetrical dimethylhydrazine ($C_2H_8N_2$; UDMH; 1,1-dimethylhydrazine) and nitrogen tetroxide (N_2O_4) as oxidizer. Some use is also made of nitric acid (HNO_3) as oxidizer.

Only the third of these combinations is hypergolic, but in practice the hazards may be greater with non-hypergolic pairings. Maximum explosive effect can only occur if a mixed, but unignited fuel/air mixture subsequently is ignited. Thus, if combustion starts immediately upon mixing, the effects may not be as major. In disastrous events, however, the mixing is occurring because of failures of tanks or fuel systems, thus the entire fuel and oxidizer stock is effectively at risk.

Ignition of rocket propellants using LO_2 occurs due to electrostatic discharge as a natural consequence of very vigorous mixing[148]. The mixing is peculiar, since when LH_2 and LO_2 are thrown together, the LH_2 boils while the LO_2 freezes. Conversely, in mixing kerosene and LO_2, the kerosene freezes while the LO_2 boils. No external ignition sources are needed for these combinations when vigorous mixing is provided.

Confinement increases the reaction rate of propellants, more so for gun propellants than for rocket propellants. The sensitivity of unmixed propellants to shock, impact, or friction is generally low.

IGNITION THEORY AND EXPERIMENTAL DATA

For intentional ignitions of solid-propellant rocket motors, three types of igniters are used: (1) pyrotechnic, (2) pyrogen, or (3) hypergolic. A pyrotechnic igniter is a small basket of pyrotechnic material which is ignited itself with an electric squib; once ignited, hot gases and hot particles from it impinge upon the main rocket fuel. A pyrogen igniter is essentially a miniature rocket motor; only hot gases emanate from it onto the rocket propellant. A hypergolic igniter is typically liquid chlorine trifluoride, which is injected onto the propellant; ignition is solely by heterogeneous reaction at the surface. Since the ignition mechanisms vary, it is appropriate that theories of ignition have been developed which emphasize different aspects of the ignition process. The number of theoretical ignition models that have been developed within the propellants community is large, to say the least. For readers interested in the specific details, there have been three reviews that have attempted to list and briefly discuss each of the published theories: Price et al.[149], Kulkarni et al.[150], and Hermance[151]. Hermance's review of 1984 is the most current one, but the publication of new propellant ignition models in the subsequent years diminished considerably. Hermance[151] has grouped theories of propellant ignition into three families:

1. reactive-solid models
2. heterogeneous reaction models
3. gas-phase ignition models.

The reactive solid models share much in common with self-heating theory, as developed in Chapter 9. Heterogeneous reactions do not play a role in the ignition of most other types of combustibles, apart from metals. Thus, the propellant theories of this ilk are basically specialized. Gas-phase ignition is, of course, the type of ignition that is studied for common solids, as presented in Chapter 7. A basic difference is that for common solids the effects of ambient pressure are usually not of interest; the contrary is true for propellant ignition. In addition to elevated pressure, there are further effects related to the rate of rise of pressure; these are also treated in detail by some of the propellant ignition theories.

Some of the reactive-solid models have been of great mathematical elegance (e.g., Liñán and Williams[152]), but Hermance concluded that important trends predicted by them—for example, the pressure-dependence—are at variance with experimental data. Hermance concludes that the best representation is to treat the problem as a gas-phase ignition for all types of propellants (homogeneous, double-base, composite, etc.) that are not ignited hypergolically. For accidental ignitions due to self-heating in storage conditions, the reactive-solid theory would be appropriate. But the needed theory will be of the same type as the ones developed in Chapter 9. The theories developed within the rocket research community have generally been more ambitious but less tractable than the development given in Chapter 9, thus, they will not be reviewed here.

Composite propellants (or pyrotechnics) are unique in their fuel/oxidizer geometric arrangement. Thus, some theories have been developed specifically to model the composite aspects in the ignition process. Summerfield et al.[153] provided the first viable theory of composite propellant combustion. The oxidant and fuel components are both gasified at the surface but do not interact chemically in the condensed phase. A very thin flame forms above the surface, and this flame is laminar, even in generally turbulent flow. The peak flame temperature is reached within 0.1 mm of

the surface. While not conventionally turbulent, the flame is 'granular,' which corresponds to the granular nature of the fuel being burned. Later, Kumar developed a general theory taking into account the physical nature of a composite propellant where grains of oxidizer are embedded in a matrix of fuel[154]. Subsequently Kumar et al.[155] specifically tailored the theory to a propellant where ammonium perchlorate is the oxidizer and polybutadiene-acrylic acid (PBAA) is the polymeric fuel. Solutions were obtained numerically, but Kumar's theory did lead to the explicit conclusion that $t_{ig}^{-2/3} \propto \dot{q}_e''$, unfortunately, as discussed below, experimental data usually do not show a –2/3 power dependence.

Most theories have been based on radiant heating. But Kumar and Hermance[156] formulated a theory for *convective heating* by a stream of hot oxidizing gas. The theory was specifically developed for a composite propellant. The equations were highly complex and the illustrative numerical solutions did not yield simple generalizations. Grain size affects the ignition results and the authors were able to illustrate this in their numerical solutions.

Very few theories provide explicit, closed-form solutions. Bradley[157] considered the ignition of a propellant from an external heat flux (which may be either radiative or convective) and produced numerical solutions and an approximate expression:

$$\frac{QA\lambda T_o}{\dot{q}_e''} = \frac{\sqrt{E'}\exp\left[E'/\left(1+2\sqrt{\tau_c/\pi}\right)\right]}{(\pi\tau_c)^{1/4}\left(1+2\sqrt{\tau_c/\pi}\right)}$$

where $\dot{q}_e''$ is the external heat flux, A = pre-exponential factor, Q = heat of reaction, T_o = initial temperature, λ = thermal conductivity, $E' = E/RT_o$ is a dimensionless parameter, C = heat capacity, and $\tau_c = \dot{q}_e'' t_{ig}/\lambda\rho C T_o^2$ is a dimensionless time. This equation does not give an explicit solution for the ignition time t_{ig}, but it can be solved with simple trial-and-error calculations. One interesting conclusion of Bradley's numerical study was that the order of the reaction does not play a significant role. The computed ignition time varied less than 3% as the reaction order was varied between 0, $^1/_2$, 1, and $^3/_2$.

The heterogeneous ignition condition was modeled by Bradley and Williams[158], who also included an external heat flux in their formulation. In their model, the hypergolic reaction involves a solid and gas that come together suddenly. On the basis of numerical solutions, they proposed that the ignition time should vary as:

$$t_{ig} \propto \dot{q}_e''^{-b}$$

where $b = 2 - \dfrac{8.4RT_o}{E}$

and T_o is the initial temperature of the interface. It is simply the initial temperature if both the solid and gas are initially at the same temperature; otherwise, T_o is to be solved for, knowing the initial temperatures and thermal inertias of the two media. The activation energy E refers to the heterogeneous surface reaction, and it is not exactly clear how it would be obtained experimentally.

Many studies have been published where experimental data trends were established or controlling variables studied, but generally the studies only offer trends, not precise quantitative predictions. Williams et al.[159] reviewed much of the early experimental data on radiant-heating ignition of propellants. The results were seen to follow the trends established in Chapter 7 for thermally-thick solids. In addition, they demonstrated the same finding as obtained in Chapter 7: ignition results from a radiant-heating test cannot be expressed as a constant energy fluence. If energy fluence is plotted against irradiance, the result is not a straight horizontal line but a V-shaped curve showing a distinct minimum at one particular irradiance value.

Propellants carry their own oxygen, but the dominant reaction generally occurs either in the gas phase or at the boundary, not within the bulk of the solid. Thus, propellants might be expected to exhibit an oxygen-dependence more akin to pyrolyzing solids, rather than to explosives. In some cases, however, the solid-state reaction dominates. Keller et al.[160] showed that results of igniting AP/PBAA (copolymer of polybutadiene and acrylic acid) with radiative and convective heat fluxes in pure oxygen and in pure nitrogen atmospheres were indistinguishable, although their data scatter was quite large and a small effect would not have been evident. On the other hand, Price et al.[149] showed a variety of results where there is a large effect of ambient oxygen concentration. A theory by McAlevy et al.[161] for convective ignition of propellants suggests that the ignition time should depend on the oxygen mass fraction as:

$$t_{ig} \propto m_{O_2}^{-2/3}$$

however their experimental results show:

$$t_{ig} \propto m_{O_2}^{-n}$$

where n = 1.2 to 1.5. Kumar and Hermance[162] also conducted a theoretical study of propellant ignition. Evaluated for various material properties, their results typically showed

$$t_{ig} \propto m_{O_2}^{-n}, \text{ where } 1 < n < 2, \text{ for } m_{O_2} > 0.2$$

and

$$n \to 0 \qquad \text{for } m_{O_2} \le 0.2$$

Thus, their theory was much more in line with the experimental data of McAlevy than was McAlevy's own theory. In a similar vein, Kashiwagi et al.[163] obtained experimental results which show a high-oxygen-concentration and a low-oxygen-concentration regime. They conducted an inspired series of convective heating tests in a shock tube, where pure polymers (PBAA and polyurethane) were tested, as were propellants using these polymers + AP as oxidizer. For $m_{O_2} > 0.6$, all four test specimens showed essentially identical ignition time results, with the dependence being:

$$t_{ig} \propto m_{O_2}^{-1.4}$$

But for $m_{O_2} < 0.5$, each system gave a different slope. The two pure fuels showed $n \approx 2.0$ to 4.7, while the two propellants showed $n \approx 0.33$ to 1.0. The authors concluded that at high m_{O_2} values, there are abundant possibilities of oxidation with the gaseous oxygen, but at low values, ignition is longer, and opportunity arises for the solid-state oxygen (when present) to be liberated and to react. Williams et al.[159] gave data similar for polystyrene and a polystyrene-based propellant; both sets of results showed $n \approx 2.0$. An inverse dependence on m_{O_2}, but with a non-constant value of n, was found for a thermal-immersion condition[164], that is, ignition by a stagnant hot gas.

Increasing the total pressure of the atmosphere above the propellant generally decreases the ignition time, but in many cases the relation does not follow a power law[151]. In some experiments[165], no effect of pressure has been found. The early studies of McAlevy[161] showed a theoretical dependence of

$$t_{ig} \propto P_{tot}^{-1.44}$$

while corresponding experimental measurements gave

$$t_{ig} \propto P_{tot}^{-1.77}$$

Very similar results were also reported by Kumar and Hermance[162]. The work of Beyer and Fishman[166] suggests that the pressure dependence becomes small at low heat fluxes (such as might be expected from an accidental fire), provided the value of P_{tot} is not also low. The results of Niioka and Williams[167] on ignition of double-base propellants were similar. They studied two double-base propellants and found negligible effect of going from 1 to 6.8 atm when heat fluxes were below 200 kW m^{-2}. At 2000 kW m^{-2}, however, the higher pressure led to ignition times about 1/10 of time at 1 atm. In a more comprehensive study, Shannon[168] obtained detailed ignition times plots for a number of propellants, covering a wide range of pressures and heat fluxes. The effects of pressure were not well-represented as a power law. Instead, for P_{tot} greater than about 2 atm, there was negligible effect on t_{ig}. For $P_{tot} < 2$ atm, however, the negative exponent was increasingly greater for lower values of P_{tot}. The experiments of Kashiwagi et al. on both pure fuels[169] and on propellants[163] indicate a behavior at very large values of P_{tot} (> 20 atm) where instead of becoming independent of P_{tot}, the ignition times vary according to

$$t_{ig} \propto P_{tot}^{-1}$$

Ohlemiller and Summerfield[170] in a similar study, also show a continued dependence of t_{ign} on P_{tot}, even at high P_{tot} values. Östmark and Gräns[171] found that for TNT, Composition B-3, and Torpex there was a smooth power-law type pressure effect on the energy fluence needed for ignition. But for PETN and RDX there were two regimes: below 2 – 4 MPa, they were very hard to ignite, while at higher pressures ignition became much easier and then the required fluence dropped smoothly with further increases in pressure. The authors noted that all the explosives they tested have a negative OB, and thus they partly react in the gas phase.

The work of both Kashiwagi[163] and Ohlemiller[170] suggests that a combined correlation of the effects of oxygen fraction and the total pressure should not be sought in the use of partial O_2 pressure as a correlating variable, unless only the regime of large m_{O_2} and P_{tot} values is considered, and only approximate results are sought.

For high incident heat fluxes (e.g. heating by lasers), many propellants are sufficiently diathermanous that ignoring in-depth absorption would lead to seriously erroneous results. Figure 20 illustrates this for RDX[172]. The calculations were based on ignoring gas-phase effects. This is seen to be a reasonable assumption at the lower heat fluxes; at higher heat fluxes, modeling of the gas phase would have to be done to produce reasonable predictions. Physically, at high fluxes significant blowing occurs at the surface and, at ignition, the flame is no longer close to the surface but far downstream. This occurs when the ignition temperature reaches the boiling point. Furthermore, at very high heating rates, the surface temperature can surpass the boiling point, since phase equilibrium no longer exists at the surface and the vapor pressure can surpass the atmospheric pressure. Another effect that comes in at high fluxes is a thickening of the vapor zone and, consequently, increased absorption of radiation by the vapors. At the extreme condition for radiation at wavelengths where the explosive is nearly transparent, some highly anomalous effects occur. The surface temperature at ignition does not appreciably rise above ambient, with ignition developing solely at hot spots. A further complication is that propellants often show in-depth absorption which varies greatly with wavelength. For example, for RDX, it was found[173] that the in-depth absorption coefficient β (see Chapter 7) went from 18,000 m^{-1} to 146,000 m^{-1}, as the wavelength went from 9.29 to 10.76 One simplification that is not available for treating the ignition of common solids is usefully applied to propellant ignition: at the high incident heat fluxes of concern in research on propellants, convection and re-radiation terms are normally completely negligible.

Despite these complications, for fluxes that are not too enormous, straight lines can be obtained when ignition time is plotted against the incident heat flux on a log-log plot. Strakovskiy et al.[172] examined 14 different compositions and found that the slope ranged from –0.54 to –0.58; this is very close to the –0.55 power dependence found for common solids, as discussed in Chapter 7. The main difference in the treatment of propellants is that, because of the high heat fluxes involved, $\dot{q}''_{cr}$ can be effectively set to zero. But because of the diathermancy of propellants, Strakovskiy et al. proposed a two-step procedure, whereby the ignition time is initially predicted on the basis of an opaque solid.

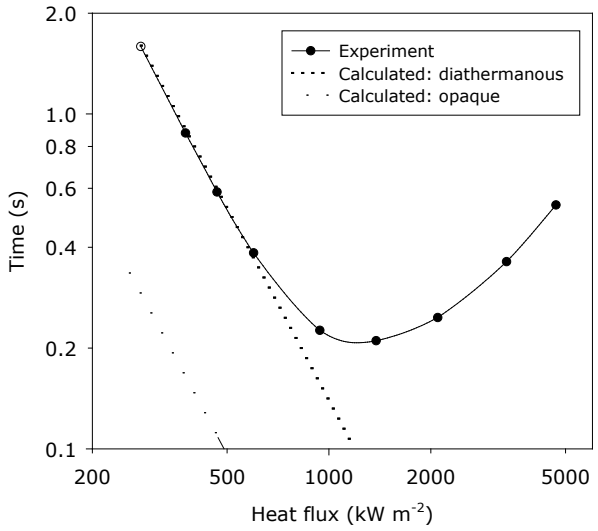


Figure 20 Ignition of RDX propellant with laser radiation at 10.6 μm (1 atm pressure)

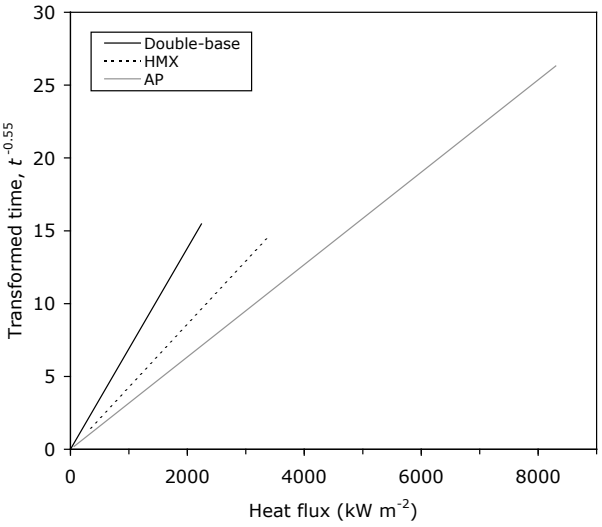


Figure 21 Response of various propellants to high convective heat fluxes and laser radiation

Then, a correction for ignition time is made, taking into account the diathermancy of the propellant.

For many common propellants, however, diathermancy issues can be ignored and straight lines nonetheless obtained. Lengellé et al.[174] studied a number of families of propellants ignited by lasers, hot-gas jets, and other forms of external heat flux. Despite the peculiarities of the laser-ignition problem, by combining results from diverse researchers, they found general correlations showing that ignition could be treated in the same manner as for thermally-thick common solids. The main difference is that, instead of being a constant, the surface temperature at ignition varies somewhat with the applied heat flux, but notwithstanding this, straight lines could be produced as for common solids. Figure 21 shows the results plotted using time to –0.55 power; the authors' plots using –0.5 power also gave results indistinguishable from straight lines. From lowest to highest heat fluxes used, the measured surface temperatures at ignition increased by about 140ºC for each of the propellant families. The differences in slope are accounted for mainly by the different values of thermal inertia, with ammonium perchlorate having the highest thermal inertia and double-base propellants the lowest. The authors concluded that there was no difference in results on the mode of thermal exposure used—radiant or convective—nor whether the radiant source is a laser or an arc-image furnace.

The thermal decomposition of propellants is normally treated by the same theory as developed in Chapter 9. However, it is often found that propellants do not show a constant heat of reaction, that is, at any given temperature, Q is not independent of time. van Geel[175] treats this situation empirically by determining the maximum value of Q that is obtained in testing. This maximum value is used in an equation for determining the critical radius r_c. The value thus determined then comprises an upper limit and is termed the *safe diameter*.

Shannon[168] examined the effect of grain size on the ignition of some composite propellants. Ignition time was about 2× for grains of 150 – 300 μm size, as compared to grains of ≤ 100 μm. He also found that for propellants containing ammonium perchlorate and various polymers, T_{ig} was in the range of 330 – 395ºC at an irradiance of 630 kW m^{-2}.

Pyrotechnics

Pyrotechnics are devices which use a chemical reaction in order to create light, sound, motion, gasses, or smoke. Fireworks are the prime example of pyrotechnics, although the category also includes matches, highway flares, automotive airbag inflators, actuators for airplane slides, and others. Pyrotechnics have military applications, primarily for signaling, but our main concern will be civilian uses, most of which are for the purpose of entertainment.

Most pyrotechnics rely on a physical mixture wherein both the fuel and oxidizer are solid, powdered materials. In a few cases, however, the oxidizer provided in the solid phase is not sufficient for full combustion and additional oxidation takes place using atmospheric oxygen. Liquid-phase materials are not used as commercially sold pyrotechnics, but are sometimes employed in creating special effects for movies. For explosives, there is often an advantage if an oxygen balance close to zero is achieved. For pyrotechnics, however, safety is enhanced if each constituent substance (*not* the whole mixture) has a notably positive or negative oxygen balance. This then assures that the rate of reaction is determined by the slower intermolecular reactivity rather than by the faster intramolecular combustion.

The US government classifies fireworks into *consumer fireworks* and *display fireworks*. Fireworks for use by consumers were designated as Class C explosives until the US adopted the UN classification scheme, under which they are Group 1.4G explosives. Display fireworks are permitted only for licensed individuals and were designated as Class B explosives and are now identified as UN Group 1.3G explosives. The US Consumer Product Safety Commission imposes a number of further regulations concerning the manufacture of fireworks to be sold to consumers. Those are issued in Title 16, Part 1507 of the Code of Federal Regulations.

CHEMISTRY OF PYROTECHNIC REACTIONS

The science of pyrotechnics is rather different from most other aspects of combustion in that it is very poorly developed. Because the commercial marketplace for pyrotechnics is so specialized and limited, there has been little incentive for scientific research. Furthermore, the chemistry is made more difficult because many reactions depend crucially on physical details (e.g., grain size) of the reacting substances. Because of this, the technology has been more of an art than a science, and industry involved is generally secretive of its techniques and knowledge.

A pyrotechnic device normally contains a powder which is a physical mixture of at least two components: a fuel and an oxidizer. Both of these are solids, including the oxidizer. The powder is normally very finely and uniformly ground in order to create optimal propinquity of the ingredients, then packed into some form of casing. While pyrotechnic compositions are required to burn fast, they must not detonate. Such behavior would not be productive towards creating the desired effects and instead would be highly dangerous.

The oxidizer can supply oxygen, chlorine, or some other atom which can oxidize fuels. Common pyrotechnic oxidizers include potassium chlorate ($KClO_3$), potassium perchlorate ($KClO_4$), potassium nitrate (KNO_3), and ammonium perchlorate (NH_4ClO_4). Fuels can include metals, organic compounds, sulfur, etc. Common metals are magnesium, aluminum, or an alloy of magnesium and aluminum. Organic fuels used include anthracene ($C_{14}H_{10}$), charcoal, naphthalene ($C_{10}H_8$), nitrocellulose, red gum, various resins (plastics), shellac, and an almost endless array of other substances.

The adiabatic flame temperatures of many pyrotechnic mixtures are higher than for organic fuels burning in air, but rather similar to organics burning in pure oxygen, namely 3000 – 3500ºC. Mixtures whose function is producing colored effects normally have a much lower flame temperature since many of the latter reactions cannot occur at high temperatures, or they would be overwhelmed by the black-body (i.e., white) radiation of other components.

Despite the paucity of research, some of the basics of pyrotechnics chemistry have come to be well enough understood. Pyrotechnics are generally viewed* as composites where the primary reactions occur in the solid state and are diffusion-controlled. Pyrotechnic reactions fall into three main types:

1) fuel-oxidizer reactions
2) thermite reactions
3) intermetallic reactions

The most common reaction is of the fuel-oxidizer type. However, the oxidizer comes from a solid substance, not from the air. To be useful, the preparation must be reasonably stable. Thus, the oxidizer is usually generated by endothermic decomposition of one of the granular components of the mixture. For example, potassium perchlorate generates oxygen according to the reaction

$$KClO_4 \rightarrow KCl + 2O_2$$

Suppose the composition contains shellac (approx. $C_{16}H_{32}O_5$) as a fuel. Then, a fuel-oxidizer reaction occurs between the O_2 and the shellac.

The most common thermite formulation involves powdered Fe(III) oxide and aluminum:

$$Fe_2O_3 + 2Al \rightarrow Al_2O_3 + 2Fe$$

Another formulation uses Fe_3O_4, which reacts as:

$$3Fe_3O_4 + 8Al \rightarrow 4Al_2O_3 + 9Fe$$

In the thermite reactions, iron oxide acts as the oxidizer and oxidizes the aluminum, which is the fuel. The reaction achieves temperatures of ca. 2200ºC. The reaction is easily sustained since the iron which is produced is a high-temperature liquid which stays in the vicinity of the reactants instead of removing energy from the system as would a gaseous combustion product. Rae[176] studied the minimum temperature needed to ignite various thermite mixtures in a tube furnace and obtained the results given in Table 10. He systematically varied the metal/metal oxide ratios, but only results for the proportion giving the lowest ignition temperature are shown. The ignition temperatures found are all below the melting point of the pertinent metal.

Intermetallic reactions involve an exothermic reaction between two metals. For pyrotechnic applications, these would normally be in the form of a powdered, compressed mixture. Systems exhibiting high heats of reaction include Ce/Zn, Ni/Al, Ni/Al/B, Pd/Al, Ta/B, Ti/B, Ti/B/Al, Ti/C, Zr/B, Zr/C, and others. An example of a device using an intermetallic reaction is the Pyrofuze-type igniter system which uses a platinum or palladium coating on an aluminum wire. When the flow of electric current raises the temperature of the wire, a highly exothermic alloying reaction occurs between the aluminum and the noble metal. Intermetallic reactions are somewhat rare in civilian pyrotechnics, however, they have military applications and have been studied extensively by Hardt[177].

* But see the discussion under 'Chemistry of explosives' above.

Because of the nature of the solid state, the reactivity of pyrotechnic/explosive reactants is often determined by physical factors, and cannot be assessed just be examining the chemical purity of the substance. The physical nature of the substance, in turn, depends strongly on how it was prepared, i.e., its chemical history. McLain[38] points out that in thermite reactions the reaction rate depends on how the Fe_2O_3 was prepared (apart from mode of preparation, it also ages and is quite sensitive to moisture).

Over the centuries, it has been found by experience that many pyrotechnic substances require milling in order to make them effective reactants. Apart from the obvious reduction in size, the milling process also imparts strains into the crystal lattice structure ('lattice looseness'). Actual heats of reaction have been measured and it has been found that the milling increases the heat of reaction[38]. The reaction rates of pyrotechnic compositions are determined much more by the oxidizer than by the fuel. Oxidizers with the lower melting points (or transition temperature, in case of substances showing solid-phase transitions) are more effective than those with higher temperatures.

Certain impurities increase the rate of solid-solid reactions by acting to reduce the eutectic temperature of the mixture. With many compositions, water is such a catalyst and small variations in moisture content affect the reaction rate. The highest reaction rate occurs at a given moisture content and increasing or decreasing it lowers the rate. Thus, the ignition temperature can be affected by both the RH and the storage time of a mixture[38].

The propagation of a gas-phase flame is due to the diffusion of chemical species and heat along the combustion wave. In solid explosives and pyrotechnics, a means also must exist for propagating the reaction. This occurs by heat conduction through the packed, porous mixture. Experimentally, it is found that the mass burning rate is relatively independent of packing density once a certain minimum density is exceeded; mixtures of lower density do not show good thermal contact between grains[38].

The activation energies for pyrotechnic compositions are generally very low, compared to gas-phase combustion reactions. These are often in the range of 13 to 30 kJ mol^{-1}, which is about an order of magnitude lower than for gas-phase combustion reactions. An important issue, however, is that global, single-step Arrhenius expressions tend to have a narrow range of applicability.

Table 10 Temperature needed for a 50% probability of ignition at the most sensitive proportion of reactants

Combination	Ignition temp. (ºC)
aluminum/Fe_2O_3	590
aluminum/Fe_2O_3	525
magnesium/Fe_2O_3	490
magnesium/Fe_2O_3	445
titanium/Fe_2O_3	710

All else being equal, pyrotechnic materials with lower melting points are more easily ignitable[178]. They are also more liable to sustaining unwanted ignitions. Some pyrotechnic powder mixtures are inordinately sensitive to spark ignition, with a little as 0.01 mJ being sufficient[179]. The ignition temperature of the fuel component of a pyrotechnic mixture does not have a significance, since all components of the mixture influence the ignition temperature. There is no standardized test method for ignition temperature measurement of pyrotechnic mixtures and numerical values will depend on the testing technique used, same as with other types of ignition tests.

Much as for explosives, a critical diameter exists, below which steady burning of a pyrotechnic mixture will not occur[178].

McLain[38] has proposed that a theoretical treatment of the ignition of pyrotechnics be patterned after the thermally-thick theory for ignition of solids. In this scheme, the TRP becomes the primary variable to determine. Little, if any, data however appear to be available on the TRP of practical pyrotechnic compositions.

In *theatrical applications*, one sometimes finds formulas which are an exception to the general rule that pyrotechnic substances are mixtures of solids. For example, an exploding volcano can be simulated by dropping glycerin onto potassium permanganate, or by putting a drop of concentrated sulfuric acid onto a mixture of potassium chlorate and powdered sugar[180].

Some *chemical lighting devices* are based on pyrotechnic principles. For example, Coolite light sticks[180] comprise trichlorocarbobutoxyphenyl oxalate, hydrogen peroxide, and bisphenylethynylanthracene, the latter being a fluorescing compound.

PRACTICAL APPLICATIONS

The most common fuels used in pyrotechnic mixtures are magnesium, aluminum, and magnesium-aluminum alloys. Charcoal and sulfur are also commonly used. Common oxidizers are: potassium chlorate ($KClO_3$), potassium perchlorate ($KClO_4$), potassium nitrate (KNO_3), and ammonium perchlorate (NH_4ClO_4). A wide variety of other oxidizers are used, including the chlorates, perchlorates, chromates, bichromates, and nitrates of barium, calcium, sodium, strontium, and ammonium. Metal oxides (Fe_3O_4, Fe_2O_3, MnO_2, Pb_3O_4, PbO_2) are often used, as are some sulfates and iodates. Sulfur is also able to act in certain mixtures as an oxidizer instead of a fuel.

It is rare, however, that a pyrotechnic mixture would only comprise two components, a fuel and an oxidizer. Typical-

ly, 4 to 6 ingredients may be present, determined generally according to empirical experimentation, not fundamental chemistry. One of the additional components which is usually necessary is a binder. Common binders include red gum, dextrin, and various man-made polymers. Other components are often added to produce specific colors.

A firecracker is a particularly simple form of fireworks and may contain only $KClO_3$, S, and Al. The aluminum powder used is firecrackers is a specialized grade known as pyro aluminum which has an especially high surface/mass ratio.

The wanted ignition of fireworks can be accomplished by many means. These include electric matches, electric squibs, or simply a fuse cord made of black powder and paper or twine. In some cases, a *first fire* composition is ignited initially, and this is then used to propagate the reaction to the main charge. A special composition for igniting purposes can also be called *starter mix*, *priming mix*, *primer*, or *torch*.

Highway flares often use a mixture of strontium nitrate with potassium perchlorate, sulfur, wax, and sawdust. A friction igniter is used which may use red phosphorus and a binder such as lacquer or phenol-formaldehyde resin for one surface, and potassium chlorate or potassium perchlorate for the other.

Photoflash flares have a military application for nighttime photography. World War II compositions comprised a mixture[38] of $Ba(NO_3)_2$, Al or Al-Mg, and $KClO_4$. These have a propensity for detonating under impact. More current compositions use $NaNO_3$, Mg, and a small amount of fuel such as varnish.

Where sulfur is used, substitution of the 'flowers of sulfur' form for 'flour of sulfur' can lead to unstable mixtures, since the former contain high amounts of acidic impurities.

Humidity control must often be provided for fireworks manufacture. If the atmosphere is excessively dry, black powder, for example, can be ignited from a static buildup on a person[180].

Test methods

Over the years, an extremely wide variety of tests for explosives has been evolved. The tests described below are ones of more current interest. Médard[3] has described various other European tests of limited usage. Sućeska[181] likewise describes some less-common tests. Fedoroff et al.[107] provide a history of much of the early test method development. Generally, tests for explosives are highly empirical and there tends not to be much correlation between the results from any two test methods. Indeed, traditionally little correlation has been found even between the rank-order results from various sensitivity tests[184]. However, Weston et al.[182] tested 12 different explosives and concluded that if only tests for impact sensitivity are considered, then some rough correlations can be obtained between data from:

- energy fluence in flying-plate test
- small-scale gap test
- large-scale gap test
- run distance to detonation experiments
- minimum priming charge radius required
- critical detonation diameter.

They also showed that correlations of this kind do not extend to ammonium perchlorate-based propellants, which behave substantially differently. Gross and Amster[183] have suggested that there is a rough correlation between the impact sensitivity of explosives and their self-heating behavior (critical temperature for a given size), but according to Russian researchers, such a correlation does not exist[184].

UN TESTS

The UN scheme classifies explosive substances into Class 1, organized into six Divisions:

Division 1.1. Substances and articles having a mass explosion hazard.

Division 1.2 Substances and articles having a projection hazard, but not a mass explosion hazard.

Division 1.3 Substances and articles which have a fire hazard and either a minor blast hazard or a minor projection hazard, or both.

Division 1.4 Substances and articles which present no significant hazard.

Division 1.5 Very insensitive substances which have a mass explosion hazard.

Division 1.6 Extremely insensitive articles which do not have a mass explosion hazard.

To implement this classification, the UN Manual[185] contains a whole battery of tests intended to classify explosive substances. They are organized into 7 series:

Test series 1. To determine if a substance has explosive properties.

Test series 2. To determine if a substance is too insensitive for inclusion in Class 1.

Test series 3. To determine if a substance is thermally stable and not too dangerous to transport in the form in which it was tested.

Test series 4. To determine if an article, packaged article or packaged substance it too dangerous to transport.

Test series 5. To determine if a substance may be assigned to Division 1.5.

Test series 6. To assign a substance or article to Division 1.1, 1.2, 1.3, or 1.4 or exclude it from Class 1. Some of the background of this series of tests is given by Rees[186].

Test series 7. To determine if an article may be assigned to Division 1.6.

Each test series consists of at least two, but as many as 10 tests which might need to be performed to determine a classification question. This is all placed in context via elaborate flow charts which delineate the required testing and

decision-making sequence. Below, we review some of the main ones pertinent to initiation. The entire testing scheme has been developed through a process which is political in nature, and the non-equivalence of tests which are supposedly equivalent has been criticized[187].

DROP-HAMMER TESTS

For practical use of explosives, it becomes important to rate their sensitivity. The sensitivity of an explosive can be defined as the minimum energy that must be imparted to the explosive, within limited time and space, to initiate an explosion of the substance. This energy cannot be measured in a way which does not depend on apparatus details[188]. The impact test is the oldest way of testing for sensitivity, with the first test being one promulgated in 1902 in German railroad shipping regulations; the early-development history has been reviewed by Boyars and Levine[188]. The drop-hammer test is a simple mechanical arrangement (Figure 22, Color Plate 13) whereby a small amount of explosive, usually less than 1 g, is held in a steel anvil and covered by a cylindrical steel striker[215]. A hammer falls upon the striker from various heights. The sensitivity rating is the potential energy which gives a 50% probability of explosion. A stochastic approach is necessary, since it is found that test results have a wide scatter. The potential energy is expressed as:

$$PE = Wgh$$

where PE = potential energy (J), W = mass (kg), g = acceleration of gravity (9.81 m s^{-2}), and h = drop height (m). The units are made clear if it is realized that 1 J = 1 kg m^2 s^{-2}. If in the particular test procedure the mass of the hammer is kept constant, then the sensitivity rating can be expressed simply as the drop height. It has been suggested[189] that the drop-hammer results be interpreted in the following way:

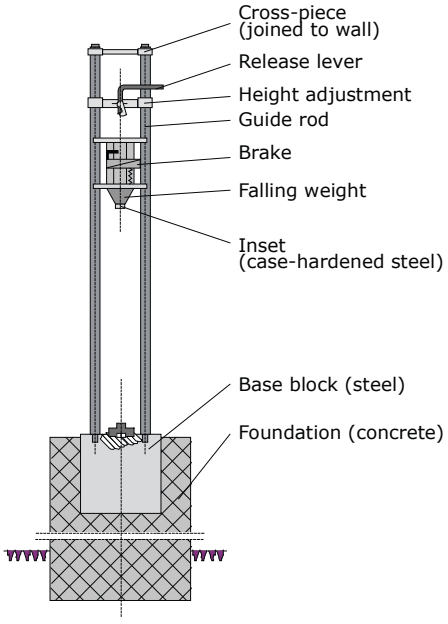


Figure 22 A typical drop-hammer test
(Copyright © 1999 AIChE used by permission)

insensitive:	PE > 30 J
moderately sensitive:	20 ≤ PE ≤ 30 J
sensitive:	5 ≤ PE < 20 J
very sensitive:	PE < 5 J.

In many cases, however, the results of drop-hammer tests are reported not as potential energy, but simply as kg-m or even simply as meters (for a fixed hammer mass).

The drop-hammer test simulates a direct hit onto the explosive and does not address the issue of initiation by a glancing blow. While impact is the way that energy is transferred into the specimen, drop-hammer tests provide substantial sample confinement and may cause initiation through other modes, such as adiabatic compression or hot spots. If one should conclude that dropping hammers is a very crude way of quantifying explosives, the opinion would be one that was already expressed by explosives expert Prof. Frank Bowden[59]: "Hitting a solid with a hammer…is perhaps an experiment more proper to a carpenter than to a physicist."

The reason that results from different drop-hammer tests commonly disagree is largely because not all of the potential energy is first converted into kinetic energy and then into energy of deformation of the explosive. A fraction of the energy is also converted into elastic strain energy of the drop hammer itself and of the anvil. These two pathways do not contribute to initiating the explosive. Coffey et al.[65] in fact consider that in common drop-hammer tests the bulk of the potential energy is realized as elastic deformation energy in the machine and does not go towards plastic deformation of the explosive. They point out[190], however, that at high velocities the fraction of energy going into elastic deformation of the machine itself becomes small, so test types should be preferred that are of the high-velocity type (greater than 8 m s^{-1}).

The drop-hammer test has been published for solids by ASTM as E 680[191] and for liquids as ASTM D 2540, but the UN has standardized on the German BAM version as its Test 3(a)(ii). Ranking of results from drop-hammer tests differs from another widely used explosives sensitivity test, the gap test, since the initiating event—being mechanical rather than a detonation—provides much lower pressures, but over a longer time scale.

KOENEN/BAM FRICTION SENSITIVITY TEST

Developed by Koenen[192] at Germany's Bundesanstalt für Materialforschung und Prüfung (BAM), in this bench-top test, designated by UN as Test 3(b)(i), a 10 mm^3 sample is placed on a rough porcelain plate (Figure 23). On top of the sample is placed a porcelain-tipped arm which can be weighed down with various weights. A reciprocating mechanism drives the plate back and forth for a distance of 10 mm. The load arm does not move in the horizontal direction. The test result is the lowest force at which there is one explosion in 6 trials. An explosion is defined as "report, crackling, sparking, or flame." Typical results are: lead az-

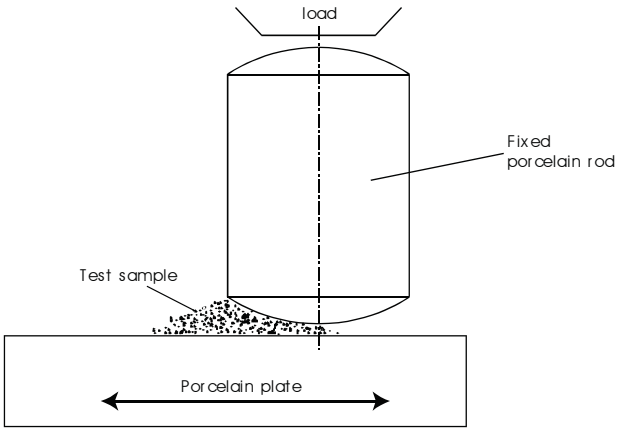


Figure 23 BAM friction sensitivity test
(Copyright Springer-Verlag, used by permission)

ide, 10 N; PETN 80 N; RDX, 120 N; TNT, 360 N. Some additional values have been reported by Moody[193]. The maximum load is 360 N, so specimens which do not initiate with this load are reported as "greater than 360 N." Bazaki and Kubota[194] studied ammonium perchlorate and related compounds in this test and examined correlations between its results and those from other explosives tests. Generally, positive correlations were found to most tests, but no highly predictive relation emerged. Négyesi[189] published a small database of UN impact and friction test results for 36 compounds that are not intentional explosives but may be susceptible to explosion under impact or friction conditions. Most impact test results resulted in non-explosion, with only 5 compounds showing measurable values. Friction test results ranged from 20 to 346 N. The test is sometimes known as the Julius Peters friction test, since the Peters company was its first commercial maker. The Koenen/BAM friction sensitivity test should not be confused with several other tests also invented by Koenen.

CARD-GAP TEST

The card-gap test evolved from simultaneous studies done at US and UK explosives research laboratories in 1953[46]. The test was further developed by the Bureau of Mines in 1968[195] by providing it with instrumentation, and naming it the 'instrumented card-gap test.' Subsequently, numerous researchers have proposed modest variants to the test method. Its purpose is to rank explosives according to their sensitivity to shock initiation. It is a simple mechanical arrangement where a gap, comprised of a variable thickness stack of metal or plastic cards, separates a standardized 'donor' charge from the target 'acceptor' charge. The acceptor charge is butted up to a witness plate, and the damage to the latter is judged by the test procedure. Explosives which are sensitive require a high gap value, while insensitive ones, a low one. The UN Manual[185], provides for three versions of the test. Test 1(a) places the test substance into a steel cylinder of 48 mm OD and 400 mm long. The donor charge, 'booster' in UN's terminology, can be a 50 mm cylinder of either RDX/wax or PETN/TNT. The donor is

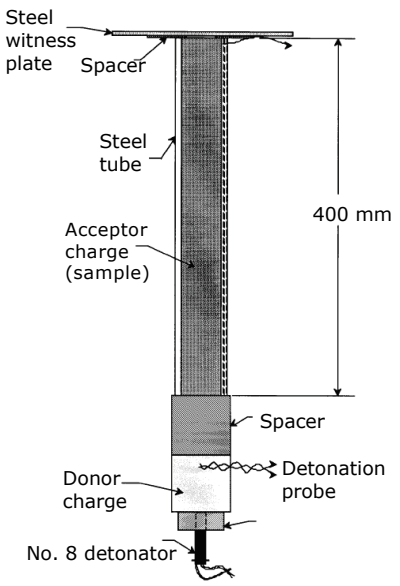


Figure 24 The UN gap test, Test 2(a)

initiated by a No. 8 detonator. This version uses no gap spacer. Test 2(a) is basically identical, but includes a 50 mm thick PMMA spacer (Figure 24); thus the conditions are less severe than for Test 1(a). Test No. 7(b), is dimensionally quite different and is used for qualifying extremely insensitive detonating substances (EIDS).

Apart from the UN versions, there are dozens of variants of the gap test in use. The US Armed Forces use the card gap test described in TB 700-2[196]. ASTM D 2539[197] is a card gap test for liquid monopropellants. Price[198] has compared results from several of the more common gap tests.

READILY COMBUSTIBLE SOLIDS

UN Test N1 for readily combustible solids uses a nonmetallic, non-combustible triangular trough, wherein the substance, which must be in powdered form, is placed (Color Plate 14). The trough width is 20 mm, height 10 mm, and length 250 mm. A flame is applied for 2 min to one end of the powder train. The substance fails, i.e., is classified as a combustible solid, if it ignites and propagates combustion for 200 mm during a 20 min period. The combustion may be either flaming or smoldering.

PYROPHORIC SOLIDS

UN Test N2 is a very simple test not requiring any apparatus. Some 1 – 2 mL of the test substance (which must be in powder form) is dropped from a height of 1 m onto a noncombustible surface. The substance is classified as pyrophoric, if it ignites during the drop or within 5 min of settling.

PYROPHORIC LIQUIDS

UN Test N3 for pyrophoric liquids uses only a 100 mm diameter porcelain cup as the test apparatus. A 5 mm layer

of diatomaceous earth or silica gel is first placed in the cup. Then, 5 mL of the test liquid is poured in. The substance is classified as pyrophoric if ignition occurs within 5 min. If ignition does not occur, then the second part of the test is executed. Here, 0.5 mL of the substance is placed on an indented filter paper. If ignition or charring of the filter paper occurs within 5 min, then the substance is also classified as pyrophoric.

WATER-REACTIVE SOLIDS OR LIQUIDS

The UN criteria for classifying a substance as a water-reactive substance is that either spontaneous ignition occurs upon combining with water, or that flammable gases are evolved at a rate greater than 1 L per kg of substance, per hour. The accompanying Test N.5 describes four simple procedures for combining a substance with water. No description is given of how the rate of flammable gas evolution might be measured, nor how the gases should be analyzed for flammability.

OXIDIZING SOLIDS

UN Test O1 for oxidizing solids involves pouring a pile of the substance, which must be in powdered form, onto a low-conductivity non-combustible board. The substance is first mixed with dry, fibrous cellulose in a ratio of 1:1 or 1:4 of sample to cellulose, by mass. The pile is ignited with a Nichrome wire applied for 3 min. Three reference substance must also be tested, which comprise potassium bromate, mixed 3:2, 2:3, and 3:7 with cellulose. The substance is classified into one of the Packing Groups of Division 5.1 if any of its burning times are shorter than those of any of the reference substances.

OXIDIZING LIQUIDS

UN Test O2 for oxidizing liquids uses a small pressure vessel equipped with a Nichrome wire igniter. The substance is combined 1:1, by mass, with dry, fibrous cellulose. Three reference substances are used, 50% perchloric acid, 40% sodium chlorate solution, and 60% nitric acid, in each case combined 1:1 with cellulose. The main test result is the time it takes for the pressure to rise from 690 to 2070 kPa (gauge). If the test substance shows a pressure-rise time less than any of the three reference substances, then it is classified into one of the three Packing Groups of Division 5.1

US MILITARY STANDARD TESTS

In the US, explosives tests were initially developed at the Bureau of Mines during about 1910 – 1940. After World War II, much of the development activity became localized at the US Army's Picatinny Arsenal in New Jersey. Many of these tests are for categorizing various capabilities of explosives which are outside the interest from the point of view of ignition. The ones related to ignition include: stability, friction sensitivity, heat sensitivity, and impact sensitivity.

The standard tests of the US military currently are grouped into three main documents, each of which contains numerous different test methods: (1) Department of Defense Ammunition and Explosives Hazard Classification Procedures[196]. This document does not describe any unique military tests; instead it authorizes the military to use the tests of the UN Manual[185] and provides administrative details implementing these. (2) Military Standard MIL-STD-1751 (USAF)[199] describes numerous physical performance tests that explosives for US military use must meet. (3) Military Standard MIL-STD-650[200] is a collection of basic chemistry laboratory tests for explosives, a few of which are pertinent to initiation.

The primary test methods of ignition interest are described below. These are not the entire repertoire, and the standards describe a number of more specialized methods. Additional methods described in MIL-STD-1751 pertinent to initiation include: Gas chromatographic reactivity test; Friction sensitivity test; Hot wire initiability test; Impact vulnerability (flying plate) test; Thermal detonability (bonfire) test; Card gap sensitivity test; Small-scale gap test (SSGT); and Stab initiability test. The Friction sensitivity test is similar in general principles, but not in operating details, to the Koenen/BAM friction tests. The gap tests are similar in principle to the UN tests described above. Additional methods described in MIL-STD-650 pertinent to initiation include 75ºC and 100ºC oven stability tests and a reactivity test.

VACUUM STABILITY AND CHEMICAL DECOMPOSITION TESTS

Testing for the storage stability of explosives can be done by any of the tests for self-heating or unstable materials discussed in Chapter 9. But there are also some methods specifically developed for the testing of explosives. Since the production of any gaseous species in significant amount is an indicator of instability, laboratory testing can simply consist of monitoring the increase in pressure of a sample placed in a closed vessel which is heated to a desired temperature. The earliest was Farmer's test of 1920. It comprised a glass beaker in which 5 g of substance is placed. The beaker was evacuated and placed in a constant temperature bath at the desired temperature. After 40 h, the test is stopped and the volume of gas produced is determined by a change in manometer reading. This was followed in 1921 by the Italian Taliani test which was rather similar in principle and became widely used. This has evolved into the Vacuum Thermal Stability test (Test 1 of MIL-STD-1751; also Method 503 of MIL-STD-650) which is regularly used by the US military. The early history has been given by Boyars and Gough[201], while later development has been described by Simmons[202]. The apparatus is a test tube which immersed in a heated liquid bath. A long capillary connects the test tube to a mercury cup. The test tube is charged with 0.2 g of a primary explosive (1.0 g, if per Method 503) or 5 g of secondary. The capillary is then

evacuated and the mercury height recorded. A calibration procedure relates the mercury height to the pressure within the test tube and, therefore, to the volume of gas that is liberated by the specimen after evacuation. The test is run at 100ºC for 48 h (for 40 h if per Method 503). The Method 503 procedure also allows a variant of running at 120ºC. To pass the MIL-STD-1751 criteria, the specimen must evolve no more than 2 mL gas, per gram of test substance. The Chemical Reactivity Test developed by the Lawrence Livermore National Laboratory can be viewed as a modern offshoot of this test. Gas chromatographic analysis is made in the LLNL test in order to quantify the major decomposition products.

LABORATORY SCALE IMPACT TEST

The version of the drop-hammer test described as Test 2 in MIL-STD-1751 (Figure 25) was developed by the Bureau

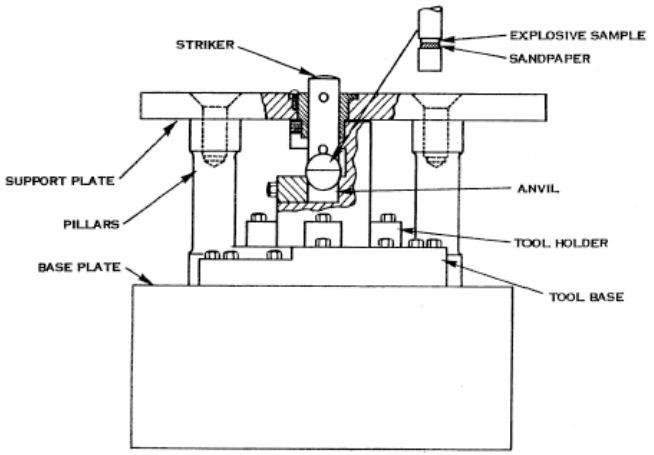


Figure 25 MIL-STD-1751 Test 2 for impact

of Mines during World War II. Hammer weights of 2, 2.5 or 5 kg are available, with a maximum drop height of 3.2 m. The sample consists of 35 mg of material resting unconfined on a piece of sandpaper and is weighted down by a cylindrical steel striker. A total of 25 drops are made with each new drop height to be used being selected according to an 'up-and-down' procedure developed for this test. The final reported value is the drop height which causes explosion at the 50% probability level. There is no specific pass/fail criterion for the test. Method 505 of MIL-STD-650 describes a similar, but not identical, test.

ELECTROSTATIC SENSITIVITY TEST

Test 4 within the MIL-STD-1751 series was developed by the Bureau of Mines in the early 1950s[203]. It uses a phonograph needle as an 'approaching electrode' that, when activated, springs down and punctures and penetrates the sample. The second electrode is a steel support cup for the specimen. There are several procedures within this test method. One procedure uses a 20 mJ discharge (a 0.002 mF capacitor charged to 4.5 kV). There must be no firing in 25 tests,

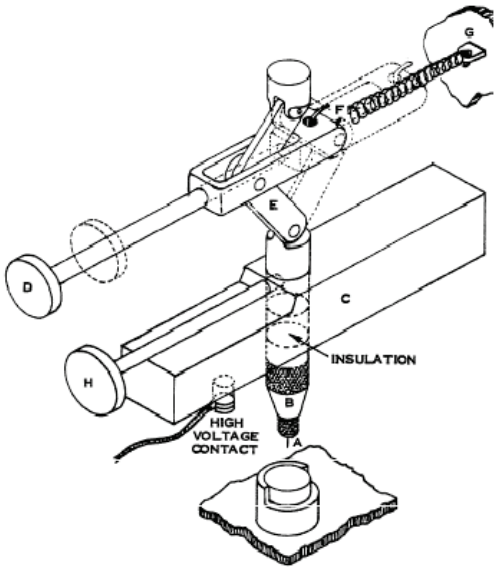


Figure 26 MIL-STD-1751 Test 4 for electrostatic sensitivity (A–needle electrode; B–actuating rod; C–guide housing; D–handle; E–toggle assembly; F–spring; G–wall hook; H–release rod)

with failure determined by the severing of the electrical tape which is used to tape down the top of the specimen. Other procedures are of a screening nature and do not have associated pass/fail criteria.

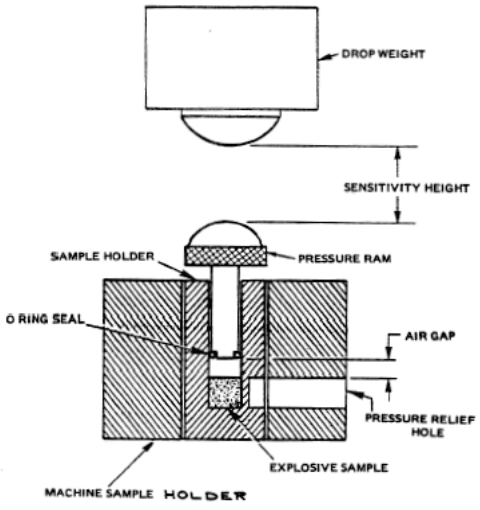


Figure 27 MIL-STD-1751 Test 12 for adiabatic sensitivity

ADIABATIC SENSITIVITY TEST

Test 12 in MIL-STD-1751 (Figure 27) is a modified drop-hammer test whereby the hammer compresses a volume of air, which, in turn, provides pressure to the sample. A 1 g sample is press-loaded into the sample cup, which is compressed by the force of the drop-weight dropping onto the pressure ram. The sample is packed to the same density as intended for the as-used explosive. The operating procedures and the treatment of data and results are similar to Test 2 of the Standard.

COOKOFF TESTS

The initiation of explosives when engulfed in an ongoing fire, or when sustaining another form of unplanned temperature rise, is termed 'cookoff.' There has been a wide variety of variant methods described, but most use a physical arrangement that resembles a pipe bomb with heaters attached to the perimeter (Figure 28). Test 13 in MIL-STD-1751 is a small-scale cookoff test intended as a screening test to find out the sensitivity of munitions to being detonated by unintended heating. It consists of a small steel bomb, 62.5 mm dia. and 127 mm tall, half-filled with the test explosive. When filled, a lid is tightly screwed on and the bomb is placed in a steel heating well. Three thermocouples are located inside the sample space and a pressure gauge is fitted to the bomb.

In general, explosives behave differently when presented with an environment where the temperatures rise fast or slow, thus two types of tests are found to be needed. The US Navy Variable Confinement Cookoff Test was developed at the Naval Surface Warfare Center, in Indian Head MD to simulate a slow cookoff of explosives[205]. The fixture comprises a steel tube clamped between two steel endplates. The steel tube is lined inside with an aluminum tube in order to improve heat transfer uniformity; the inner tube is filled with the explosive to be tested. External heaters heat the assembly at a rate of 3.3°C per hour. The test is concluded when the confinement bursts. A number of other small-scale tests, most of which resemble a pipe bomb in arrangement, have been described by de Yong and Redman[206] and by Kondrikov[207].

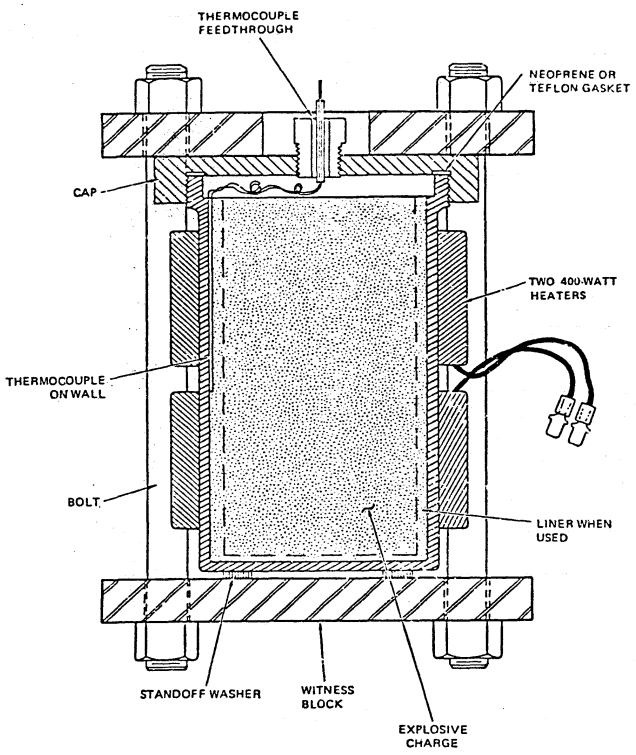


Figure 28 The small-bomb cookoff test developed at the Naval Weapons Center[204]

SHOCK INITIATION SENSITIVITY TEST

Test 14 in MIL-STD-1751 (commonly known as a Wedge test) is intended to determine the sensitivity of a high explosive to shock initiation. The principle is that it takes a certain run distance within the explosive for a shock wave to create a detonation. The testing is highly specialized and the monograph of Gibbs and Popolato should be consulted for details.[208]

HENKIN TEST FOR EXPLOSION TEMPERATURE

In this test[209] a milligram sample of the explosive substance is placed in a hollow copper cylinder (i.e., the tube of a No. 8 blasting cap), loosely capped, and lowered into a Wood's metal bath which is at some pre-selected temperature. An ingenious electric circuit is used to time the explosion. One lead of a circuit connects to the sample case, while the other lead to the cap; when the explosion blows the cap off, the timer is stopped. Times as short as 50 ms can be determined; at the other end of the scale, a maximum time of 1200 s is used. The small quantity of explosive used gives

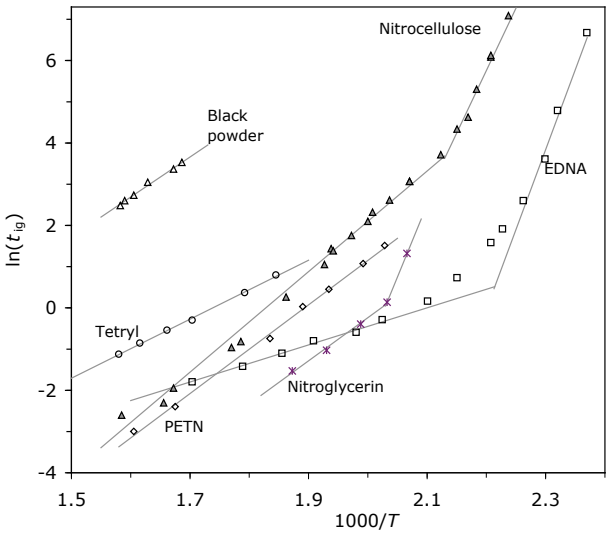


Figure 29 The relation between temperature and ignition time in the Henkin test (25 mg specimens, except nitroglycerin, which was 3 mg)

rather high minimum temperatures for explosion. For example, cellulose nitrate is reported as 175ºC, in contrast with 141ºC being determined for larger samples in the Setchkin furnace[210]. Henkin et al. mainly used the data not for absolute values but to obtain effective values of the activation energy according to the Semenov relation:

$$\ln\left(t_{ig}\right) = \frac{E}{RT} + C$$

where C is a constant. For most explosives, they found a straight-line relation when plotting ln (t_{ig}) as a function of $1000/T$, where T = temperature (K), as shown in Figure 29. Many explosives (EDNA, nitrocellulose, and nitroglycerin in Figure 29) show a low-temperature slope and a different high-temperature slope, indicating that there are two different values of E pertinent to two different temperature regimes. The numerical value of E (kJ mol^{-1}) is obtained by multiplying the slope by R (8.314 J mol^{-1} K^{-1}). The factor of 1000 in the x-axis variable means that the units of E come out directly as kJ mol^{-1}, instead of J mol^{-1}. The test conditions in the Henkin test are such that the values of E are determined for a rather high temperature regime, typically 200 – 300ºC. Many explosives show initial exothermic activity at temperatures lower than the range which is encompassed in the Henkin test; the Henkin data would not be appropriate for those situations. In the cases where the Henkin test shows a high- and a low-temperature regime, the low-temperature values are the ones that will probably be more pertinent to actual explosive performance. Brill and Brush[211] conducted a modern series of experiments in a similar vein and concluded that the 'high-temperature' values of E are effectively spurious, since heat transfer, not chemical kinetics, is the rate limiting mechanism in that regime.

Method 506 of MIL-STD-650 describes the US Army version of the Henkin test. This differs in that the quantity of explosive used is 20 mg and an 'explosion temperature' is defined as the temperature at which t_{ig} = 5 s.

The Henkin test is done under unconfined conditions. Catalano et al.[212] studied explosives confined to a rigid anvil so that products of combustion were not able to escape until the ultimate explosive release. They got entirely linear plots of $1/T$ vs. ln(t_{ig}) over the full range of temperatures studied. The slopes, however, were at strong variance to results computed by using published, single-step Arrhenius kinetics values. Thus, their conclusion was that multiple reaction steps must be considered. The Los Alamos National Laboratory[213] uses a variant of the test where a 40 mg specimen is lightly confined in an aluminum shell.

SENSITIVITY TO INITIATION

The original sand bomb test was developed by the Bureau of Mines[215] in 1916. Method 507 of MIL-STD-650 (Sand test bomb) uses the same concept, but with a complex procedural scheme. It is a test for primary explosives used to determine the minimum amount of detonating materials that will initiate an 0.4 g sample. The test explosive is put into a No. 6 or No. 8 blasting cap and compressed with a plunger by applying a pressure of 20.7 MPa. A safety fuse is crimped onto the end of the blasting cap, the cap is placed into a steel bomb, and the bomb cavity filled with 200 g of sand which has been sieved to have a narrow size range. The fuse is lit and after the explosion the size is sieved and the mass of sand that has been pulverized is determined. There are a number of sequences to this test where the test explosive is fired alone and in conjunction with lead azide and tetryl. The results are reported either as "sensitive to flame initiation alone" or as the mass of tetryl needed for initiation.

PERMISSIBLE EXPLOSIVES

The testing of permissible explosives was originally done by the US Bureau of Mines but is currently under the jurisdiction of the Mine Safety and Health Administration (MSHA). The test series was reorganized in 1989 and the tests that currently must be passed[214] include an air-gap sensitivity test (to ascertain that the explosive can be successfully detonated), a rate-of-detonation test (to determine if an undesired tendency exists for partial detonation), a pendulum-friction test (to determine if the explosive is excessively sensitive), a toxicity test (for personnel safety), and most importantly, two gallery tests. These involve firing a special steel cannon into a test gallery. In 'Test 7,' the gallery is filled with an 8% methane mixture while in 'Test 8' the gallery contains 4% methane plus a dispersion of coal dust. A different series of tests is prescribed for sheathed explosives. The early history of testing permissible explosives was described by Munroe and Tiffany[215].

OTHER TESTS

Apart from the more common tests discussed below, Avrami and Hutchinson[216] have discussed some less commonly used friction tests. Tests that were used by the Bureau of Mines are described by Mason and Aiken[217].

PENDULUM FRICTION TEST FOR GLANCING BLOWS

The Bureau of Mines developed a test[215] where an anvil holds 7 g of explosive, while a swinging pendulum is released and pushes a friction shoe past the explosive 18 times. The glancing blow represents a weight of 20 kg released from a height of 1.5 m. A smaller-scale version of this test was also developed.

NOL THERMAL SENSITIVITY TEST

This test method was developed for the US Department of Transportation as a possible means of identifying hazardous materials. A 2.1 µL sample is enclosed in a 63.5 mm length of stainless steel tubing which is then pulse-heated by a capacitive discharge. The apparatus is capable of heating up to 1000 °C. The induction period for the explosion to occur is determined by using the tubing itself as a resistance thermometer. The primary variables reported are the threshold initiation temperature and the temperature

achieved at 250 μs. Some typical results are given in Chapter 14.

BUREAU OF MINES TEST FOR OXIDIZING SOLIDS

In 1972, the Bureau of Mines described a method[218] for examining the ignition and burning propensity of solid, inorganic oxidizers when mixed with sawdust. The test uses a metal channel, 50 mm wide, 25 mm high, and of an unspecified length (apparently, 178 mm). The test substance, which must be in powdered form, is mixed with red oak sawdust in varying proportions, ignited with a propane torch at one end, and a burning rate is determined. Apart from this terse description, the BM publication provided very few other experimental details. Consequently, test development was continued at General Electric Co.[219]. The GE report contains detailed performance data on 16 oxidizers.

LLNL STEVEN TEST

One of the latest impact tests that has become popular in the US research community is the Lawrence Livermore National Laboratory's Steven Test, developed by Steven Chidester[220]. The test explosive is confined between a 3.175 mm steel front plate and a 19.05 mm steel back plate. A 60.1 mm diameter steel projectile is fired from a gas gun onto the target and pressures developed are monitored with two embedded gauges and four external gauges. The results are presented as a plot of impact velocity vs. average overpressure, as measured at the external gauges, located 3.05 m away. Unlike some other impact tests, the Steven test has a definite threshold velocity, below which zero overpressure is recorded. This allows ranking the results on the basis of the threshold velocity, with less sensitive explosives showing a higher threshold.

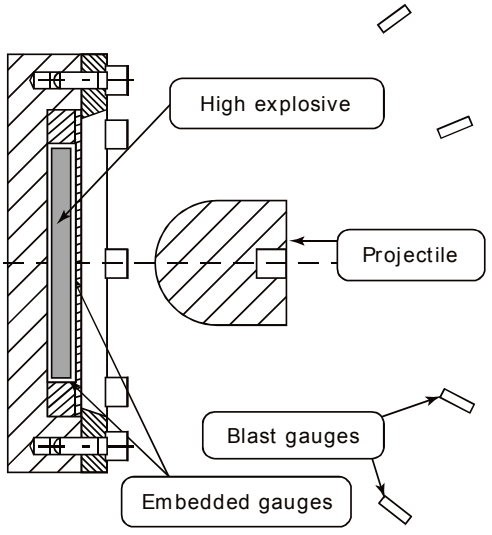


Figure 30 The LLNL Steven Test for impact

Further readings

Frank P. Bowden and A. D. Yoffe, **Initiation and Growth of Explosion in Liquids and Solids**, Cambridge University Press, Cambridge (1952). This was the first book to examine explosives from a fundamental science point of view. In addition, it is an outstanding example of brilliant, yet clear and engaging technical writing. Prof. Bowden was also thesis advisor to Philip Thomas, who went on to become the foremost fire science researcher in the 1950s and '60s.

Tadeusz Urbański, **Chemistry and Technology of Explosives**, 4 vols., Methuen/Pergamon, New York (1964-84). **Encyclopedia of Explosives and Related Items**, B. T. Fedoroff, et al., eds., Picatinny Arsenal, Dover NJ (1960-1983). The two most comprehensive works on explosives are now a bit old, but no more recent works have been anywhere near as comprehensive. Urbański's covers the subject from a chemist's perspective, while Fedoroff's from a weapons designer's. Both contain a huge amount of information but are short on organization.

Josef Köhler and Rudolf Meyer, **Explosives**, 4th ed., VCH, Weinheim, Germany (1993). This standard reference is a 'pocket encyclopedia' of explosives and is a good first reference for finding brief information about explosives, including trade names from various countries. It has been kept up-to-date by frequent revisions.

Brigitta M. Dobratz, and Patricia C. Crawford, LLNL **Explosives Handbook: Properties of Chemical Explosives and Explosive Simulants** (UCRL 52997), Lawrence Livermore National Laboratory, Livermore CA (1985). F. L. McIntyre and R. M. Rindner, **A Compilation of Hazard and Test Data for Pyrotechnic Compositions** (ARLCD-CR-80047), US Army Armament R&D Command, Dover NJ (1980). These are the two most comprehensive data compilations for explosives/pyrotechnics. The Dobratz tome focuses on thermochemical data and properties of explosives, while the McIntyre book contains mostly ignition/sensitivity data for pyrotechnics, but with some basic thermochemical properties.

The following three monographs are wholly (Sućeska's) or primarily (Yoshida's) devoted to descriptions of test methods for explosives, oxidizers, reactive and hypergolic substances. Muhamed Sućeska, **Test Methods for Explosives**, Springer-Verlag, New York (1995). Tadao Yoshida, **Safety of Reactive Chemicals**, Elsevier Science, London (1987). Tadao Yoshida, Yuji Wada, and Natalie Foster, **Safety of Reactive Chemicals and Pyrotechnics**, Elsevier, Amsterdam (1995). The second Yoshida book supplements, not replaces, the earlier work.

Alexander Beveridge, ed., **Forensic Investigation of Explosions**, Taylor & Francis, London (1998). This is a modern guide to investigating criminal explosions (accidental explosions receive only limited attention), with emphasis on

chemical analysis techniques and on organization aspects of large investigations.

The following two books on pyrotechnics are similar, both being rather brief and focusing mainly on the basic science aspects. Joseph H. McLain, **Pyrotechnics: From the Viewpoint of Solid State Chemistry**, The Franklin Institute Press, Philadelphia (1980). John A. Conkling, **Chemistry of Pyrotechnics: Basic Principles and Theory**, Marcel Dekker, New York (1985). A brief but useful introduction to the chemistry of pyrotechnics is: N. Kubota, Propellant Chemistry, *J. Pyrotechnics* No. 11, 25-45 (Summer 2000).

The following two books cover both the science and the technology aspects of pyrotechnics. Alexander P. Hardt, **Pyrotechnics**, Pyrotechnica Publications, Post Falls ID (2001). This is the most current textbook on fireworks that is of significant size and scope, but it is not quite as current as the imprint date would imply, since the author died in 1989. A. A. Shidlovskii, **Principles of Pyrotechnics**, English translation, American Fireworks News, Dingmans Ferry PA (1997). A good English translation of a classic Russian textbook first published in 1964.

Karl O. Brauer, **Handbook of Pyrotechnics**, Chemical Publishing Co., New York (1974). Offers information primarily on hardware, rather than chemistry. John Donner, **A Professional's Guide to Pyrotechnics: Understanding and Making Exploding Fireworks**, Paladin Press, Boulder CO (1997). Well illustrated, this may be the best reference on the construction of some popular fireworks. Donner has written several earlier editions of this book, under slightly different titles.

D. Harrington, and J. H. East, jr., Accidents due to Misuse of Explosives (IC 7259), Bureau of Mines, Pittsburgh (1943). A useful review of blasting accidents and their causes.

Jack R. Gibson and Jeanne D. Weber, **Handbook of Selected Properties of Air- and Water-reactive Materials** (RDTR-144), US Naval Ammunition Depot, Crane IN (1969). While now quite old, this is the only compilation of properties of pyrophoric and water-reactive substances.

The following textbooks are good general references on rocket propellants: George P. Sutton and Oscar Biblarz, **Rocket Propulsion Elements**, 7th ed., Wiley Interscience, New York (2001). Stanley F. Sarner, **Propellant Chemistry**, Reinhold Publ. Co., New York (1966). Bernard Siegel and Leroy Schieler, **Energetics of Propellant Chemistry**, Wiley, New York (1964).

NFPA has issued a number of publications giving safety advice on explosives, propellants, and pyrotechnics. NFPA 495[221] covers safety precautions in the civilian sector concerning handling and storage of explosives. One of the data items provided in NFPA 495 is the American Table of Distances for Storage of Explosives, as originally compiled by the Institute of Makers of Explosives. A separate table of distances is provided for ANFO. NFPA 1124[222], originally NFPA 44A, describes safe manufacturing, handling and transportation practices of consumer fireworks. NFPA 1123[223] covers the safety practices to be used by licensed technicians in staging outdoor public fireworks displays. NFPA 1126[224] describes safety requirements for staging of fireworks displays in connection with theatrical performances. Three standards pertain to model rocketry operations: NFPA 1125[225] deals with manufacturing of rocket motors, NFPA 1122[226] provides general safety precautions for model rocketry, while NFPA 1127[227] gives guidance on high-power rocketry operations.

References

1. ASTM Computer Program for Chemical Thermodynamic and Energy Release Evaluation—CHETAH, Version 7.3, ASTM (2002).
2. Recommendations on the Transport of Dangerous Goods: Model Regulations, 10th ed., United Nations, New York (1997).
3. Médard, L. A., **Accidental Explosions**, 2 vols., Ellis Horwood, Chichester, England (1989).
4. Gustin, J. L., Thermal Stability Screening and Reaction Calorimetry. Application to Runaway Reaction Hazard Assessment and Process Safety Management, *J. Loss Prevention in the Process Industries* **6**, 275-291 (1993).
5. Guideline TAA-GS-05: Identification and Control of Exothermic Chemical Reactions, pp. 167-191 in Safety and Runaway Reactions, N. Mitchison and B. Smeder, eds. (EUR 17723 EN), Institute for Systems, Informatics and Safety, Community Documentation Centre on Industrial Risk, Ispra, Italy (1997).
6. Baker, G. P., and Whitmore, M. W., Investigation of the Use of a Closed Pressure Vessel Test for Estimating Condensed Phase Explosive Properties of Organic Compounds, pp. 85-104 in *Proc. Intl. Workshop on Safety in the Transport, Storage and Use of Hazardous Materials*, National Research Institute of Fire and Disaster, Tokyo (1998).
7. Kuchta, J. M., Investigation of Fire and Explosion Accidents in the Chemical, Mining, and Fuel-Related Industries—A Manual (Bulletin 680), Bureau of Mines, Pittsburgh (1985).
8. Grewer, T., **Thermal Hazards of Chemical Reactions**, Elsevier, Amsterdam (1994).
9. Urben, P. G., ed., **Bretherick's Handbook of Reactive Chemical Hazards: An Indexed Guide to Published Data**, 2 vols., 5th ed., Butterworth-Heinemann, Oxford (1995).
10. Verhoeff, J., Experimental Study of the Thermal Explosion of Liquids (Ph.D. dissertation), Prins Maurits Laboratorium TNO, Rijswijk, Netherlands (1983).

11. Hieronymus, H., et al., Characterisation of Surface Explosions, pp. 217-223 in *Proc. 3rd Intl. Symp. on Hazards, Prevention, and Mitigation of Industrial Explosions*, Tsukuba, Japan (2000).
12. Fujimoto, Y., Prediction of Heat Release Rate in Heterogeneous Liquid-Liquid Reaction, pp. 167-170 in *APSS2001—Proc. Asia Pacific Symp. on Safety*, Vol. 2, Japan Soc. for Safety Engineering, Yokohama (2001).
13. Snee, T. J., The Influence of a Constant Power Heat Source on the Critical Conditions for Thermal Explosion, pp. 112-131 in *Intl. Symp. on Runaway Reactions*, AIChE (1989).
14. De Faveri, D. M., Zonato, C., Pagella, C., Vidili, A., and Ferraiolo, G., Runaway Reaction and Safety Measures in Organic Processes, pp. 155-175 in *Intl. Symp. on Runaway Reactions*, AIChE (1989).
15. Bowes, P. C., A General Approach to the Prediction and Control of Potential Runaway Reaction, pp. 1/A:1-1/A:35 in Runaway Reactions, Unstable Products and Combustible Powders (Symp. Series No. 68), The Institution of Chemical Engineers, London (1981).
16. Bowes, P. C., **Self-Heating: Evaluating and Controlling the Hazards**, Her Majesty's Stationery Office, London (1984). Also published by Elsevier Science.
17. Caprio, V., Insola, A., and Lignola, P. G., Isobutane Cool Flames in a CSTR: The Behavior Dependence on Temperature and Residence Time, *Combustion and Flame* **43**, 23-33 (1981).
18. Merzhanov, A. G., and Abramov, V. B., Thermal Explosion of Explosives and Propellants, A Review, *Propellants and Explosives* **6**, 130-148 (1981).
19. Gomes, W., Definition of Rate Constant and Activation Energy in Solid State Reactions, *Nature* **192**, 856-866 (1961).
20. *Intl. Symp. on Runaway Reactions*, AIChE (1989 and subsequent).
21. Safety and Runaway Reactions, N. Mitchison and B. Smeder, eds. (EUR 17723 EN), Institute for Systems, Informatics and Safety, Community Documentation Centre on Industrial Risk, Ispra, Italy (1997).
22. van Gils, E., Evaluation and Assessment of Runaway Reaction Hazards—An Inspector's Point of View, pp. 137-152 in Safety and Runaway Reactions, N. Mitchison and B. Smeder, eds. (EUR 17723 EN), Institute for Systems, Informatics and Safety, Community Documentation Centre on Industrial Risk, Ispra, Italy (1997).
23. Class 4, Divisions 4.1, 4.2, and 4.3—Definitions, 49 CFR 173.124 (1998).
24. Carson, P. A., and Mumford, C. J., Fires without External Ignition Sources. Part 2. The Hazards of Pyrophoric Substances, *Loss Prevention Bulletin* No. 109, 11-24 (Feb. 1993).
25. Zehr, J., Pyrophore Stäube in Technik und Industrie, *Staub* **22**, 494-505 (1962).
26. Zehr, J., Pyrophoric Dusts in Technology and Industry (II), *Staub* (English ed.) **26**, 1-6 (1966).
27. Schmitt, C. R., Pyrophoric Materials—A Literature Review, *J. Fire and Flammability* **2**, 157-172 (1971).
28. Ripley, W. L., Air- and Water-Reactive Materials (RDTR 124), US Naval Ammunition Depot, Crane IN (1968).
29. Gibson, J. R., and Weber, J. D., Handbook of Selected Properties of Air- and Water-reactive Materials (RDTR 144), US Naval Ammunition Depot, Crane IN (1969).
30. Fletcher, E. A., and Morrell, G., Ignition in Liquid Propellant Rocket Engines, *Prog. Comb. Science and Technology* **1**, 183-215 (1975).
31. Daimon, W., Tanaka, M., and Kimura, I., The Mechanisms of Explosions Induced by Contact of Hypergolic Liquid Propellants, Hydrazine and Nitrogen Tetroxide, pp. 2065-2071 in *20th Symp. (Intl.) on Combustion*, The Combustion Institute, Pittsburgh (1984).
32. Abel, F. A., Researches on Gun-Cotton, *Philosophical Trans. Royal Society* **156**, 268-308 (1866); **157**, 181-253 (1867).
33. Akst, I. B., Detonation in Intermolecular Explosives: Characteristics of Some Eutectic Formulations, pp. 548-559 in *Proc. 7th Symp. (Intl.) on Detonation*, Naval Surface Weapons Center, China Lake CA (1981).
34. Howell, S. P., Paul, J. W., and Sherrick, J. L., Progress of Investigations on Liquid-Oxygen Explosives (Tech. Paper 294), Bureau of Mines, Washington (1923).
35. Dorofeyev, A. N., Kuznetsov, V. A., and Sarkisyan, R. S., Aviation Ammunition, FTD-ID(RS)T-0459-85, Foreign Technology Div., Air Force Systems Command, Wright-Patterson AFB (1986). Russian original: **Aviatsionnyye Boyepripasy** (1960).
36. Scribner, K., Elson, R., Fyfe, R., and Cramer, J. P., Physical, Stability, and Sensitivity Properties of Liquid Explosives, pp. 466-474 in *Proc. 6th Symp. (Intl.) on Detonation*, Office of Naval Research, Dept. of the Navy, Arlington VA (1976).
37. Beveridge, A., ed., **Forensic Investigation of Explosions**, Taylor & Francis, London (1998).
38. McLain, J. H., **Pyrotechnics: From the Viewpoint of Solid State Chemistry**, The Franklin Institute Press, Philadelphia (1980).
39. Hardt, A. P., **Pyrotechnics**, Pyrotechnica Publications, Post Falls ID (2001).
40. Shanley, E. S., and Melhem, G. A., The Oxygen Balance Criterion for Thermal Hazards Assessment, *Process Safety Progress* **14**, 29-31 (1995).
41. Kamlet, M. J., and Adolph, H. G., The Relationship of Impact Sensitivity with Structure of Organic High Explosives. II. Polynitroaromatic Explosives, *Propellants and Explosives* **4**, 30-34 (1979).
42. Howell, S. P., The Menace of Opening Kegs of Black Blasting Powder with Wooden Tools (RI 2161), Bureau of Mines, Pittsburgh (1920).
43. McQuaide, P. B., Test and Evaluation of Insensitive Munitions, pp. 203-232 in **Test and Evaluation of the Tactical Missile**, (*Prog. in Astronautics and Aeronautics*, vol. 119), E. J. Eichblatt jr., ed., AIAA, New York (1989).
44. Ammann, R., Is There a Critical Composition of Reaction Products of Diphenylamine Stabilized Nitrocellulose Propellants During Aging? pp. 9-27 in *4th Symp. on Chemical Problems Connected with the Stability of Explosives*, Sektionen för Detonik och Förbränning, Sundbyberg, Sweden (1977).
45. Volk, F., Dünnschicht-Chromatographische Ermittlung der Lebensdauer von Treibladungspulvern [Thin-layer chromatographic determination of the lifetime of propellant powders], pp. 29-53 in *4th Symp. on Chemical Problems Connected with the Stability of Explosives*, Sektionen för Detonik och Förbränning, Sundbyberg, Sweden (1977).
46. Maček, A., Sensitivity of Explosives, *Chemical Reviews* **62**, 41-63 (1962).

47. van Geel, J. L. C., and Verhoeff, J., Heat Generation Measurements for the Stability Control of Nitrate Ester Propellants, pp. 299-314 in *4th Symp. on Chemical Problems Connected with the Stability of Explosives*, Sektionen för Detonik och Förbränning, Sundbyberg, Sweden (1977).
48. Johansson, C. H, Persson, A., and Selberg, H. L., Ignition of Explosives, pp. 606-608 in *Sixth Symp. (Intl.) on Combustion*, Reinhold, New York (1956).
49. Rogers, R. N., Janney, J. L., and Loverro, N. P. jr., Thermal Stability and Compatibility Predictions for the Explosive EAK, *J. Energetic Materials* **2**, 293-330 (1984).
50. Nunziato, J. W., Kennedy, J. E., and Amos, D. E., The Thermal Ignition Time for Homogeneous Explosives Involving Two Parallel Reactions, *Combustion and Flame* **29**, 265-268 (1977).
51. Tarver, C. M., McGuire, R. R., Lee, E. L., Wrenn, E W., and Brein, K. R., The Thermal Decomposition of Explosives with Full Containment in One-Dimensional Geometries, pp. 1407-1413 in *17th Symp. (Intl.) on Combustion*, The Combustion Institute, Pittsburgh (1978).
52. McGuire, R. R., and Tarver, C. M., Chemical Decomposition Models for the Thermal Explosion of Confined HMX, TATB, RDX, and TNT Explosives, pp. 56-64 in *Proc. 7th Symp. (Intl.) on Detonation*, Naval Surface Weapons Center, China Lake CA (1981).
53. Bowden, F. P., and Yoffe, A. D., **Fast Reactions in Solids**, Butterworths, London (1958).
54. Rogers, R. N., Thermal Hazards of Explosives (LAL-81-9), Los Alamos National Laboratory, Los Alamos NM (1981).
55. Pollock, B. D., Fisco, W. J., Kramer, H., and Forsyth, A. C., Handling, Storability, and Destruction of Azides, pp. 73-109 in **Energetic Materials**, vol. 2, H. D. Fair and R. F. Walker, eds., Plenum Press, New York (1977).
56. Persson, A., and Jerberyd, L., Thermal Explosion Hazard of Thin Layers of Gelatine Dynamite, pp. 43-49 in *Proc. 7th Symp. (Intl.) on Detonation*, Naval Surface Weapons Center, China Lake CA (1981).
57. Freeder, B. G. P., Wharton, R., and Train, A. W., Changes in the Mechanical Sensitiveness of Explosives as a Result of Previous Exposure to Elevated Temperatures, *Propellants, Explosives and Pyrotechnics* **24**, 232-236 (1999).
58. Eichelberger, R. J., and Sultanoff, M., Sympathetic Detonation and Initiation by Impact, *Proc. Royal Society* **A246**, 274-281 (1958).
59. Bowden, F. P., Introduction, *Proc. Royal Society* **A246**, 146-154 (1958).
60. Dorough, G. D., Green, L. G., James, E. jr., and Gray, D. T., Ignition of Explosives by Low Velocity Impact (UCRL-7360-T), Lawrence Radiation Laboratory, Livermore CA (1963).
61. Bowden, F. P., and Yoffe, A. D., **Initiation and Growth of Explosion in Liquids and Solids**, Cambridge University Press, Cambridge (1952).
62. Frey, R. B., Cavity Collapse in Energetic Materials, pp. 68-80 in *Proc. 8th Symp. (Intl.) on Detonation*, Office of Naval Research, Dept. of the Navy, Arlington VA (1985).
63. Bowden, F. P., The Development of Combustion and Explosion in Liquids and Solids, pp. 161-172 in *Fourth Symp. (Intl.) on Combustion*, Williams & Wilkins, Baltimore (1953).
64. Heavens, S. N., and Field, J. E., The Ignition of a Thin Layer of Explosive by Impact, *Proc. Royal Society* **A338**, 77-93 (1974).
65. Coffey, C. S., DeVost, V. F., and Woody, D. L., Towards Developing the Capability to Predict the Hazard Response of Energetic Materials Subjected to Impact, pp. 1243-1252 in *Proc. 9th (Intl.) Symp. on Detonation*, Naval Surface Warfare Center, White Oak MD (1989).
66. Starkenberg, J., McFadden, D. L., Pilarski, D. L., Benjamin, K. J., Boyle, V. M., and Lyman, O. R., Sensitivity of Several Explosives to Ignition in the Launch Environment, pp. 1460-1479 in *Proc. 9th (Intl.) Symp. on Detonation*, Naval Surface Warfare Center, White Oak MD (1989).
67. Frey, R. B., The Initiation of Explosive Charges by Rapid Shear, pp. 36-42 in *Proc. 7th Symp. (Intl.) on Detonation*, Naval Surface Weapons Center, China Lake CA (1981).
68. Boyle, V., Frey, R., and Blake, O., Combined Pressure Shear Ignition of Explosives, pp. 3-17 in *Proc. 9th (Intl.) Symp. on Detonation*, Naval Surface Warfare Center, White Oak MD (1989).
69. Dienes, J. K., On Reactive Shear Bands, *Physics Letters A* **118**, 433-438 (1986).
70. Kondrikov, B. N., and Tchubarov, V. D., Deformation, Destruction and Ignition of the Layer of a Solid under Impact, *Combustion and Flame* **24**, 143-149 (1975).
71. Chaudri, M. M., The Initiation of Fast Decomposition in Solid Explosives by Fracture, Plastic Flow, Friction, and Collapsing Voids, pp. 857-867 in *Proc. 9th (Intl.) Symp. on Detonation*, Naval Surface Warfare Center, White Oak MD (1989).
72. Chaudri, M. M., and Field, J. E., Fast Decomposition in the Inorganic Azides, pp. 383-447 in H. D. Fair, and R. F. Walker, eds., **Energetic Materials**, vol. 1, Plenum Press, New York (1977).
73. Seay, G. M., Shock Initiation of Granular Explosives Pressed to Low Density, pp. 530-535 in *9th Symp. (Intl.) on Combustion*, The Combustion Institute, Pittsburgh (1962).
74. Swallowe, G. M., and Field, J. E., Effect of Polymers on the Drop-Weight Sensitiveness of Explosives, pp. 24-35 in *Proc. 7th Symp. (Intl.) on Detonation*, Naval Surface Weapons Center, China Lake CA (1981).
75. Coffey, C. S., The Initiation of Explosive Crystals by Shock or Impact, pp. 824-830 in *Proc. 10th Intl. Symp. on Detonation*, Office of Naval Research, Arlington VA (1993).
76. Andersen, W. H., and Louie, N. A., Projectile Impact Ignition Characteristics of Propellants. I. Deflagrating Composite Explosive, *Combustion Science and Technology* **20**, 153-160 (1979).
77. Metzner, A. P., and Coffey, C. S., Hot Spot Initiation of Plastic-Bonded Explosives during the Rapid Flow Phase of the Drop Weight Impact Test, pp. 219-223 in *Proc. 10th Intl. Symp. on Detonation*, Office of Naval Research, Arlington VA (1993).
78. Campbell, A. W., Davis, W. C., and Travis, J. R., Shock Initiation of Liquid Explosives, *Phys. Fluids* **4**, 498-510 (1961).
79. Friedman, M. H., A Correlation of Impact Sensitivities by Means of the Hot Spot Model, pp. 294-320 in *9th Symp. (Intl.) on Combustion*, The Combustion Institute, Pittsburgh (1963).
80. Kamlet, M. J., The Relationship of Impact Sensitivity with Structure of Organic High Explosives. I. Polynitroaliphatic Explosives, pp. 312-322 in *Proc. 6th Symp. (Intl.) on Detonation*, Office of Naval Research, Dept. of the Navy, Arlington VA (1976).

81. Baker, P. J., and Mellor, A. M., Energetic Materials Impact Initiation Mechanisms, pp. 289-316 in **Physical and Chemical Aspects of Combustion: A Tribute to Irvin Glassman**, F. L. Dryer, and R. F. Sawyer, eds., Gordon & Breach, Amsterdam (1997).
82. Andersen, W. H., Critical Energy Relation for Projectile Impact Ignition, *Combustion Science and Technology* **20**, 259-261 (1979).
83. Walker, F. E., and Wasley, R. J., Critical Energy for Shock Initiation of Heterogeneous Explosives, *Explosivstoffe* **17**, 9-13 (1969).
84. Walker, F. E., The Initiation and Detonation of Explosives—An Alternative Concept (UCRL-53860), Lawrence Livermore National Laboratory, Livermore CA (1988).
85. Howe, P., Frey, R., Taylor, R., and Boyle, V., Shock Initiation and the Critical Energy Concept, pp. 11-19 in *Proc. 6th Symp. (Intl.) on Detonation*, Office of Naval Research, Dept. of the Navy, Arlington VA (1976).
86. Stresau, R. H., and Kennedy, J. E., Critical Conditions for Shock Initiation of Detonation in Real Systems, pp. 68-75 in *Proc. 6th Symp. (Intl.) on Detonation*, Office of Naval Research, Dept. of the Navy, Arlington VA (1976).
87. Kleinhanss, H. R., Lugenstrass, F., and Zöllner, H., Initiation Threshold of High Explosives in Small Flyer Plate Experiments, pp. 66-76 in *Proc. 9th (Intl.) Symp. on Detonation*, Naval Surface Warfare Center, White Oak MD (1989).
88. Moulard, H., Critical Conditions for Shock Initiation of Detonation by Small Projectile Impact, pp. 316-324 in *Proc. 7th Symp. (Intl.) on Detonation*, Naval Surface Weapons Center, China Lake CA (1981).
89. Frey, R., Melani, G., Chawla, M., and Trimble, J., Initiation of Violent Reaction by Projectile Impact, pp. 325-335 in *Proc. 6th Symp. (Intl.) on Detonation*, Office of Naval Research, Dept. of the Navy, Arlington VA (1976).
90. Maiden, D. E., A Model for Calculating the Threshold for Shock Initiation of Pyrotechnics and Explosives (UCRL-96360), Lawrence Livermore National Lab., Livermore CA (1987).
91. Kondrikov, B. N., Explosions Caused by Fires at High Explosives Production, pp. 17-28 in **Prevention of Hazardous Fires and Explosions: The Transfer to Civil Applications of Military Experiences**, V. E. Zarko et al., eds., Kluwer Academic Publishers, Dordrecht (1999).
92. Victor, A. C., Simple Calculation Methods for Munitions Cookoff Times and Temperatures, *Propellants, Explosives, Pyrotechnics* **20**, 252-259 (1995).
93. de Yong, L., Nguyen, T., and Waschl, J., Laser Ignition of Explosives, Pyrotechnics and Propellants: A Review (DSTO-TR-0068), Defence Science and Technology Organisation, Melbourne, Australia (1995).
94. Liau, Y.-C., Kim, E. S., and Yang, V., A Comprehensive Analysis of Laser-Induced Ignition of RDX Monopropellant, *Combustion and Flame* **126**, 1680-1698 (2001).
95. Knyazeva, A. G., and Zarko, V. E., An Assessment of Ignition Hazard for Shielded Energetic Materials and Its Relation to Flammable Chemicals, pp. 251-264 in **Prevention of Hazardous Fires and Explosions: The Transfer to Civil Applications of Military Experiences**, V. E. Zarko et al., eds., Kluwer Academic Publishers, Dordrecht (1999).
96. Jones, E., The Ignition of Solid Explosive Media by Hot Wires, *Proc. Royal Society* **A198**, 523-539 (1949).
97. Inami, S. H., McCulley, L., and Wise, H., Ignition Response of Solid Propellants to Radiation and Conduction, *Combustion and Flame* **13**, 531-536 (1969).
98. Baer, A. D., and Ryan, N. W. Evaluation of Thermal-Ignition Models from Hot-Wire Ignition Tests, *Combustion and Flame* **15**, 9-22 (1970).
99. Bowden, F. P., Stone, M. A., and Tudor, G. K., Hot Spots on Rubbing Surfaces and the Detonation of Explosives by Friction, *Proc. Royal Society* **A188**, 329-349 (1947).
100. Chaudri, M. M., Stab Initiation of Explosives, *Nature* **263**, 121-122 (1976).
101. Evans, J. I., and Yuill, A. M., Initiation of Condensed Explosives by Compression of the Surrounding Gas, *Proc. Royal Society* **A246**, 176-180 (1958).
102. Wyatt, R. H. M., The Susceptibility of Primary Explosives to Ignition by Electrical Energy, p. 33 in *Flameproofing—Intrinsic Safety and Other Safeguards in Electrical Instrument Practice* (IEE Conf. Report Series No. 3), Institution of Electrical Engineers, London (1962).
103. Knaur, J. A., Technical Investigation of 11 January 1985 Pershing II Motor Fire, pp. 1005-1013 in Minutes of the Twenty-Second Explosives Safety Seminar, vol. 1, Dept. of Defense Explosives Safety Board, Alexandria VA (1986).
104. Kirshenbaum, M. S., Electrostatic Sensitivity, pp. 163-198 in **Energetic Materials**, Vol. 2: Technology of the Inorganic Azides, H. D. Fair and R. F. Walker, eds., Plenum Press, New York (1977).
105. Wyatt, R. M. H., Moore, P. W. J., Adams, G. K., and Sumner, J. F., The Ignition of Primary Explosives by Electric Discharges, *Proc. Royal Society* **A246**, 189-194 (1958).
106. Litchfield, E. I., Hay, M. H., and Monroe, J. S., Electrification of Ammonium Nitrate in Pneumatic Loading (RI 7139), Bureau of Mines, Pittsburgh (1968).
107. **Encyclopedia of Explosives and Related Items**, B. T. Fedoroff, et al., eds., Picatinny Arsenal, Dover NJ (1960-1983).
108. Skinner, D., Olson, D., and Block-Bolten, A., Electrostatic Discharge Ignition of Energetic Materials, *Propellants, Explosives, Pyrotechnics* **23**, 34-42 (1998).
109. Lee, R. J., Ignition in Solid Energetic Materials due to Electrical Discharge (Ph.D. dissertation), American University, Washington (1996).
110. Bowden, F. P., The Explosion of Silver Azide in an Electric Field, *Proc. Royal Society* **A246**, 197-199 (1958).
111. Gora, T., Downs, D. S., Fair, H. D., jr., and Mark, P., Electric Field Initiation of Explosive Azides, pp. 390-395 in *Proc. 6th Symp. (Intl.) on Detonation*, Office of Naval Research, Dept. of the Navy, Arlington VA (1976).
112. Guthrie, M. A., A Review of Recent Lightning-Related Magazine Deflagrations, pp. 1047-1083 in Minutes of the Twenty-Second Explosives Safety Seminar, vol. I, Dept. of Defense Explosives Safety Board, Alexandria VA (1986).
113. Eggert, J., The Ignition of Explosives by Radiation, *J. Phys. Chem.* **63**, 11-15 (1959).
114. Boddington, T., Feng, C., and Gray, P., Thermal Explosion and the Theory of Its Initiation by Steady Intense Light, *Proc. Royal Society* **A390**, 265-281 (1983).
115. Avrami, L., and Haberman, J., Sensitivity to Heat and Nuclear Radiation, pp. 199-247 in **Energetic Materials**, Vol. 2: Technology of the Inorganic Azides, H. D. Fair and R. F. Walker, eds., Plenum Press, New York (1977).
116. Anke, D., Dahme, M., and Ruffing, K., Influence of Electromagnetic Fields on Electro-Explosive Devices (EED), pp.

571-576 in *8th Intl. Zurich Symp. and Technical Exhibition on Electromagnetic Compatibility*, ETH Zentrum–IKT, Zurich (1989).
117. Guide to Prevention of Inadvertent Initiation of Electro-Explosive Devices by Radio-Frequency Radiation (BS 6657), British Standards Institution, London (1991).
118. Collett, P. C. E., RF Induced Currents in Firing Circuits within Buildings (Contract Research Report 200/1998), HSE, Sheffield, UK (1998).
119. Bardo, R. D., The Role of Excited Electronic States in the Bond Scission Process in Detonation Reactions, pp. 93-103 in *Proc. 7th Symp. (Intl.) on Detonation*, Naval Surface Weapons Center, China Lake CA (1981).
120. Bardo, R. D., The Lattice Density of States Concept and Its Role in Determining the Shock Sensitivity of PETN and Nitromethane, pp. 235-245 in *Proc. 9th (Intl.) Symp. on Detonation*, Naval Surface Warfare Center, White Oak MD (1989).
121. Ruderman, G. A., Stewart, D. S., and Fried, E., Modeling the Mechanical Ignition of Energetic Materials, pp. 573-580 in *11th Symp. (Intl.) on Detonation*, Office of Naval Research, Arlington VA (1998).
122. Politzer, P., and Alper, H. E., Detonation Initiation and Sensitivity in Energetic Compounds: Some Computational Trends, in **Computational Chemistry: Reviews of Current Trends**, vol. 4, World Scientific Publishing Co., Singapore (1999).
123. Tarver, C. M., and Urtiew, P. A., Theoretical and Computer Models of Detonation in Solid Explosives*, Intl. Workshop on New Models and Numerical Codes for Shock Wave Processes in Condensed Media*, St. Catherines College, Oxford, England (1997).
124. Gerhard, S. L., and Huff, W. J., Phenomena in the Ignition of Firedamp by Explosives. Part I. Particles from the Detonation (Tech. Paper 603), Bureau of Mines, Pittsburgh (1940).
125. Grant, R. L., Mason, C. M., von Elbe, G., and Lewis, B., Experimental Investigation of the Mechanism of Ignition of Firedamp by Explosives: Studies with Suspended Shots, paper 31 in *7th Intl. Conf. of Directors of Safety in Mines Research*, Safety in Mines Research Establishment, Buxton, England (1952).
126. Coward, H. F., Research on the Incendivity of Coal-Mine Explosives: A Review (SMRE Research Report 210), Safety in Mines Research Establishment, Sheffield, England (1962).
127. Benedick, W. B., High-Explosive Initiation of Methane-Air Detonations, *Combustion and Flame* **35**, 87-91 (1979).
128. Taylor, B. C., and Ervin, L. W., Separation of Ignition and Buildup to Detonation in Pressed TNT, pp. 3-10 in *Proc. 6th Symp. (Intl.) on Detonation*, Office of Naval Research, Dept. of the Navy, Arlington VA (1976).
129. Price, D., Contrasting Patterns on the Behavior of High Explosives, pp. 693-702 in *11th Symp. (Intl.) on Combustion*, The Combustion Institute, Pittsburgh (1966).
130. Strehlow, R., Accidental Explosions, *American Scientist* **68**, 420-428 (1980).
131. Notes from Lectures on Detonation Physics, Transcribed by Frank J. Zerilli (NSWC MP 81-399), Naval Surface Weapons Center, Silver Spring MD (1981).
132. Spear, R. J., and Nanut, V., Anomalous Shock Sensitivity/Density Relationship for Pressed Booster Explosives from a Small-Scale Gap Test, pp. 98-111 in *Proc. 9th (Intl.) Symp. on Detonation*, Naval Surface Warfare Center, White Oak MD (1989).
133. Urtiew, P. A., Erickson, L. M., Aldis, D. F., and Tarver, C. M., Shock Initiation of LX-17 as a Function of Its Initial Temperature, pp. 112-122 in *Proc. 9th (Intl.) Symp. on Detonation*, Naval Surface Warfare Center, White Oak MD (1989).
134. Bogg, T. L., ed., Response of Ammonium Perchlorate to Thermal and Mechanical Shock Stimuli (NWC TP 7053), Naval Weapons Center, China Lake CA (1990).
135. Voreck, W., Slagg, N., and Avrami, L., The Role of Azides in Explosive Trains, pp. 249-291 in **Energetic Materials**, Vol. 2: Technology of the Inorganic Azides, H. D. Fair and R. F. Walker, eds., Plenum Press, New York (1977).
136. Harrington, D., and East, J. H. jr., Accidents due to Misuse of Explosives (IC 7259), Bureau of Mines, Pittsburgh (1943).
137. Hopler, R. B., The History and Development of Permissible Explosives for Underground Coal Mining, pp. 44-63 in *Proc. 22nd Annual Conf. on Explosives and Blasting Technique*, Vol. 2, Intl. Soc. of Explosives Engineers, Cleveland (1996).
138. Ramsay, H. T., and Seager, J. S., On the Influence of the Permitted Ignition Rate in the Assessment of Explosives (Research Report 209), Safety in Mines Research Establishment, Sheffield, England (1961).
139. Naoúm, P., **Nitroglycerine and Nitroglycerine Explosives**, Williams & Wilkins, Baltimore (1928).
140. Hartmann, I., Nagy, J., McGibbeny, E. B., and Christofel, F. P., Ignition of Coal Dust by Permissible Explosives, Paper 2 in *7th Intl. Conf. of Directors of Safety in Mines Research*, Safety in Mines Research Establishment, Buxton, England (1952).
141. Hanna, N. E., Tiffany, J. E., and Damon, G. H., Factors Affecting the Incendivity of Permissible Explosives (RI 5051), Bureau of Mines, Pittsburgh (1954).
142. Watson, R. W., Brewer, R. L., and McNall, R. L., On the Bullet Sensitivity of Commercial Explosives and Blasting Agents, *J. Hazardous Materials* **1**, 129-136 (1975/76).
143. Corley, J. D., Insensitive High Explosives Evaluation Techniques, pp. 41-85 in Minutes of the Twenty-Second Explosives Safety Seminar, vol. I, Dept. of Defense Explosives Safety Board, Alexandria VA (1986).
144. Victor, A. C., Insensitive Munitions Technology for Tactical Rocket Motors, in **Tactical Missile Propulsion** (Progress in Astronautics and Aeronautics, Vol. 170), G. E. Jensen and D. W. Netzer, eds., American Institute of Aeronautics and Astronautics Washington (1996).
145. Van Dolah, R. W., Gibson, F. C., and Murphy, J. N., Sympathetic Detonation of Ammonium Nitrate and Ammonium Nitrate-Fuel Oil (RI 6746), Bureau of Mines, Pittsburgh (1966).
146. Van Dolah, R. W., Gibson, F. C., and Murphy, J. N., Further Studies on Sympathetic Detonation (RI 6903), Bureau of Mines, Pittsburgh (1966).
147. Lefumeux, A., and Degano, D., Thermal Stability, Safety and Vulnerability of a Composite Gun Propellant, pp. 29-34 in *Symp. on Compatibility of Plastics and Other Materials with Explosives, Propellants, Pyrotechnics & Processing of Explosives, Propellants and Ingredients*, American Defense Preparedness Assn. (1986).
148. Baker, W. E., and Tang, M. J., **Gas, Dust and Hybrid Explosions**, Elsevier, Amsterdam (1991).

149. Price, E. W., Bradley, H. H. jr., Dehority, G. L., and Ibiricu, M. M., Theory of Ignition of Solid Propellants *AIAA J.* **4**, 1153-1181 (1966).
150. Kulkarni, A. K., Kumar, M., and Kuo, K. K., Review of Solid-Propellant Ignition Studies, AIAA Paper 80-1210, AIAA, New York (1980).
151. Hermance, C. E., Solid-Propellant Ignition Theories and Experiments, pp. 239-304 in *Prog. in Astronautics and Aeronautics*, vol. 90: Fundamentals of Solid-Propellant Combustion, AIAA, New York (1984).
152. Liñán, A., and Williams, F. A., Theory of Ignition of a Reactive Solid by a Constant Energy Flux, *Combustion Science and Technology* **3**, 91-98 (1971).
153. Summerfeld, M., Sutherland, G. S., Webb, M. J., Taback, H. J., and Hall, K. P., Burning Mechanism of Ammonium Perchlorate Propellants, pp. 141-182 in **Solid Propellant Rocket Research**, Academic Press, New York (1960).
154. Kumar, R. K., Gas Phase Ignition of a Composite Solid Propellant Subjected to Radiant Heating, *Combustion Science and Technology* **30**, 273-288 (1983).
155. Kumar, M., Wills, J., Kulkarni, A. K., and Kuo, K. K., A Comprehensive Model for AP-Based Composite Propellant Ignition, *AIAA J.* **22**, 526-534 (1984).
156. Kumar, R. K., and Hermance, C. E., Gas Phase Ignition Theory of a Heterogeneous Solid Propellant Exposed to a Hot Oxidizing Gas, *Combustion Science and Technology* **4**, 191-196 (1972).
157. Bradley, H. H., jr., Theory of Ignition of a Reactive Solid by Constant Energy Flux, *Combustion Science and Technology* **2**, 11-20 (1970).
158. Bradley, H. H., jr., and Williams, F. A., Theory of Radiant and Hypergolic Ignition of Solid Propellants, *Combustion Science and Technology* **2**, 41-52 (1970).
159. Williams, F. A., Barrère, M., and Hung, N. C., **Fundamental Aspects of Solid Propellant Rockets** (AGARDograph No. 116), Technivision Services, Slough, UK (1969).
160. Keller, J. A., Baer, A. D., and Ryan, N. W., Ignition of Ammonium Perchlorate Composite Propellants by Convective Heating, *AIAA J.* **4**, 1358-1365 (1966).
161. McAlevy, III, R.F., Cowan, P. L., and Summerfield, M., The Mechanism of Ignition of Composite Solid Propellants by Hot Gases, p. 623 in **Solid Propellant Rocket Research**, M. Summerfield, ed., (Vol. 1, Progress in Astronautics and Rocketry), Academic Press, New York (1960).
162. Kumar, R.K., and Hermance, C. E., Gas Phase Ignition Theory of a Heterogeneous Solid Propellant Exposed to a Hot Oxidizing Gas, *Combustion Science and Technology* **4**, 191-6 (1972).
163. Kashiwagi, T., Waldman, C. H., Rothman, R. B., and Summerfield, M., Ignition of Polymers in a Hot Oxidizing Gas, *Combustion Science and Technology* **8**, 121-131 (1973).
164. Hermance, C. E., Shinnar, R., and Summerfield, M., Ignition of an Evaporating Fuel in a Hot, Stagnant Gas Containing an Oxidizer, *AIAA J.* **3**, 1584-1592 (1965).
165. Rosser, W. A., Fishman, N., and Wise, H., Ignition of Simulated Propellants Based on Ammonium Perchlorate, *AIAA J.* **4**, 1615-1622 (1966).
166. Beyer, R. B., and Fishman, N., Solid Propellant Ignition Studies with High Heat Flux Radiant Energy as a Thermal Source, p. 673 in **Solid Propellant Rocket Research**, M. Summerfield, ed., (Vol. 1, Progress in Astronautics and Rocketry). Academic Press, New York (1960).
167. Niioka, T., and Williams, F., Relationship between Theory and Experiment for Radiant Ignition of Solids, pp. 1163-1171 in *17th Symp. (Intl.) on Combustion*, The Combustion Institute, Pittsburgh (1979).
168. Shannon, L. J., Composite Solid-Propellant Ignition by Radiant Energy, *AIAA J.* **8**, 346-353 (1970).
169. Kashiwagi, T., A Radiative Ignition Model of a Solid Fuel, *Combustion Science and Technology* **8**, 225-236 (1974); also **14**, 119-122 (1976).
170. Ohlemiller, T.J., and Summerfield, M., Radiative Ignition of Polymeric Materials in Oxygen/Nitrogen Mixtures, pp. 1087-1094 in *13th Symp. (Intl.) on Combustion*, The Combustion Institute, Pittsburgh (1970).
171. Östmark, H., and Gräns, R., Laser Ignition of Explosives: Effects of Gas Pressure on the Threshold Ignition Energy, *J. Energetic Materials* **8**, 308-322 (1990).
172. Strakovskiy, L., et al., Laser Ignition of Propellants and Explosives (ARL-TR-1699), Army Research Laboratory, Aberdeen Proving Ground MD (1998).
173. Östmark, H., Carlson, M., and Ekvall, K., Laser Ignition of Explosives: Effects of Laser Wavelength on the Threshold Ignition Energy, *J. Energetic Materials* **12**, 63-83 (1994).
174. Lengellé, G., Bizot, A., Duterque, J., and Amiot, J.-C., Ignition of Solid Propellants, *La Recherche Aérospatiale—English Edition*, No. 2, 1-20 (1991).
175. van Geel, J. L. C., The Rate of Heat Generation as a Function of Temperature and Degree of Conversion, pp. 191-197 in *Selfheating of Organic Materials*, Intl. Symp. 18th and 19th February 1971, Delft. Delft University (1971).
176. Rae, D., The Ignition of Gas by the Impact of Light Alloys on Oxide-Coated Surfaces (Research Report 177), Safety in Mines Research Establishment, Sheffield, England (1959).
177. Hardt, A. P., Incendiary Potential of Exothermic Intermetallic Reactions (AFATL-TR-71-87), Air Force Armament Laboratory, Eglin AFB, Florida (1971).
178. Conkling, J. A., **Chemistry of Pyrotechnics: Basic Principles and Theory**, Marcel Dekker, New York (1985).
179. Lindner, V., Explosives, pp. 561-620 in **Kirk-Othmer Encyclopedia of Chemical Technology**, 3rd ed., Vol. 9, Wiley, New York (1980).
180. Hardt, A. P., Pyrotechnics, pp. 484-499 in **Kirk-Othmer Encyclopedia of Chemical Technology**, 3rd ed., Vol. 19, Wiley, New York (1982).
181. Sućeska, M., **Test Methods for Explosives**, Springer-Verlag, New York (1995).
182. Weston, A. M., et al., Correlation of the Results of Shock Initiation Tests, pp. 887-897 in *Proc. 7th Symp. (Intl.) on Detonation*, Naval Surface Weapons Center, China Lake CA (1981).
183. Gross, D., and Amster, A. B., Thermal Explosions: Adiabatic Self-Heating of Explosives and Propellants, pp. 728-734 in *8th Symp. (Intl.) on Combustion*, The Combustion Institute, Pittsburgh (1960).
184. Afanasev, G. T., and Bobolev, V. K., **Initiation of Solid Explosives by Impact**, Israeli Program for Scientific Translation, Jerusalem (1971).
185. Recommendations on the Transport of Dangerous Goods: Manual of Tests and Criteria, 2nd ed., United Nations, New York (1995).
186. Rees, N. J. M., UK MOD Explosive Storage Principles, pp. 1437-1454 in Minutes of the Twenty-Second Explosives Safety Seminar, vol. II, Dept. of Defense Explosives Safety Board, Alexandria VA (1986).

187. Brown, A. K., Mak, W. A., and Whitmore, M. W., A Review of United Nations Tests for Explosivity, *J. Loss Prevention in the Process Industries* **13**, 33-39 (2000).
188. Boyars, C., and Levine, D., Drop-Weight Impact Sensitivity Testing of Explosives, *Pyrodynamics* **6**, 53-77 (1968).
189. Négyesi, G., The Sensitivity of Non-explosive Compounds to Friction Testing, *Process Safety Progress* **15**, 42-47 (1996).
190. Baker, P. J., Mellor, A. M., and Coffey, C. S., Critical Impact Initiation Energies for Three HTPB Propellants, *J. Propulsion & Power* **8**, 578-585 (1992).
191. Standard Test Method for Drop Weight Impact Sensitivity of Solid-Phase Hazardous Materials (ASTM E 680), ASTM.
192. Koenen, H., Ide, K. H., and Swart, K.-H., Sicherheitstechnische Kenndaten explosionsfähiger Stoffe, *Explosivstoffe* **9**, 4-13; 30-42 (1961).
193. Moody, G. G., Hazard Characterization of Explosives by Use of the Friction Sensitivity Test (UCID-21052), Lawrence Livermore Natl. Lab., Livermore CA (1987).
194. Bazaki, H., and Kubota, N., Friction Sensitivity Mechanism of Ammonium Perchlorate Composite Propellants, *Propellants, Explosives, Pyrotechnics* **16**, 41-47 (1991).
195. Ribovich, J., Watson, R. W., and Gibson, F. C., Instrumented Card-Gap Test, *AIAA J.* **6**, 1260-1263 (1968).
196. Department of Defense Ammunition and Explosives Hazard Classification Procedures (TB 700-2); (also NAVSEAINST 8020.8B; also TO 11A-1-47; also DLAR 8220.1), Headquarters, Departments of the Army, the Navy, the Air Force, and the Defense Logistics Agency, Washington (1998).
197. Standard Test Method for Shock Sensitivity of Liquid Monopropellants by the Card-Gap Test (ASTM D2539), ASTM.
198. Price, D., Gap Tests and How They Grow, pp. 365-380 in Minutes of the Twenty-Second Explosives Safety Seminar, vol. I, Dept. of Defense Explosives Safety Board, Alexandria VA (1986).
199. Military Standard—Safety and Performance Tests for Qualification of Explosives, MIL-STD-1751 (USAF), Dept. of Defense, Washington (1982).
200. Military Standard—Explosive: Sampling, Inspection and Testing, MIL-STD-650, Dept. of Defense, Washington (1962; rev. 1973).
201. Boyars, C., and Gough, W. G., Test for Establishing Residual Safe Life of Stabilized Solid Propellants, *Anal. Chem.* **27**, 957-961 (1955).
202. Simmons, H. T., jr., The Vacuum Thermal Stability Test for Explosives (NOLTR 70-142), Naval Ordnance Laboratory, White Oak MD (1970).
203. Brown, F. W., Kusler, D. J., and Gibson, F. C., Sensitivity of Explosives to Initiation by Electrostatic Discharge (RI 5002), Bureau of Mines, Pittsburgh PA (1953).
204. Pakulak, J. M. jr., USA Small-scale Cookoff Bomb (SCB) Test, pp. 539-548 in Minutes of the Explosives Safety Seminar (21st) Held at Houston, Texas on 28-30 August 1984, Vol. 1 (1984). NTIS AD-A152 062.
205. Maienschein, J. L., and Nichols, A. L. III, Ignition and Initiation Phenomena: Cookoff Violence Prediction (UCRL-ID-125795), Lawrence Livermore National Laboratory, Livermore CA (1997).
206. de Yong, L., and Redman, L. D., Cookoff Behaviour of Pyrotechnics (MRL-TR-91-44), Materials Research Lab., Defence Science and Technology Organisation, Maribyrnong, Vic., Australia (1992).
207. Kondrikov, B. N., Investigation of Cook-off-type Test Methods, pp. 135-142 in *11th Symp. (Intl.) on Detonation*, Office of Naval Research, Arlington VA (1998).
208. Gibbs, T. R., and Popolato, A., eds., **LASL Explosive Property Data**, Univ. of California Press, Berkeley (1980).
209. Henkin, H., and McGill, R., Rates of Explosive Decomposition, *Ind. and Eng. Chem.* **44**, 1391-1395 (1952).
210. Setchkin, N. P., A Method and Apparatus for Determining the Ignition Characteristics of Plastics, *J. Research NBS* **43**, 591-608 (1949).
211. Brill, T. B., and Brush, P. J., Chemical Phenomena Associated with the Initiation of Thermal Explosions, pp. 228-234 in *Proc. 9th (Intl.) Symp. on Detonation*, Naval Surface Warfare Center, White Oak MD (1989).
212. Catalano, E., et al., The Thermal Decomposition and Reaction of Confined Explosives, pp. 214-222 in *Proc. 6th Symp. (Intl.) on Detonation*, Office of Naval Research, Dept. of the Navy, Arlington VA (1976).
213. Rogers, R. N., and Rogers, J. L., Explosives Science, unpublished paper (1999).
214. Requirements for Approval of Explosives and Sheathed Explosive Units, Code of Federal Regulations, 30CFR15.
215. Munroe, C. E., and Tiffany, J. E., Physical Testing of Explosives at the Bureau of Mines Explosives Experiment Station, Bruceton, Pa. (Bulletin 346), Bureau of Mines, Pittsburgh (1931).
216. Avrami, L., and Hutchinson, R., The Sensitivity to Impact and Friction, pp. 111-162 in **Energetic Materials**, Vol. 2: Technology of the Inorganic Azides, H. D. Fair and R. F. Walker, eds., Plenum Press, New York (1977).
217. Mason, C. M., and Aiken, E. G., Methods for Evaluating Explosives and Hazardous Materials (IC 8541), Bureau of Mines, Pittsburgh (1972).
218. Kuchta, J. M., Furno, A. L., and Imhof, A. C., Classification Test Methods for Oxidizing Materials (RI 7594), Bureau of Mines, Pittsburgh (1974).
219. King, P. V., Sr., and Lasseigne, A. H., Hazard Classification of Oxidizing Materials and Flammable Solids for Transportation: Evaluation of Test Methods (TES-20-72-6). Dept. of Transportation, Washington (1972).
220. Chidester, S. K., Tarver, C. M., and Garza, R. G., Low Amplitude Impact Testing and Analysis of Pristine and Aged Solid High Explosives, pp. 93-100 in *11th Symp. (Intl.) on Detonation*, Office of Naval Research, Arlington VA (1998).
221. Explosive Materials Code (NFPA 495), NFPA.
222. Code for the Manufacture, Transportation, and Storage of Fireworks (NFPA 1124), NFPA.
223. Code for Fireworks Display (NFPA 1123), NFPA.
224. Standard for the Use of Pyrotechnics before a Proximate Audience (NFPA 1126), NFPA.
225. Code for the Manufacture of Model Rocket and High Power Rocket Motors (NFPA 1125), NFPA.
226. Code for Model Rocketry (NFPA 1122), NFPA.
227. Code for High Power Rocketry (NFPA 1127), NFPA.

Copyright © 2003, 2014 Vytenis Babrauskas

Chapter 11. Characteristics of external ignition sources

Highlights and summary of practical guidance **498**
Introduction **499**
High ambient temperatures **499**
Hot solids or liquids **499**
Large hot surfaces in contact—Theory *500*
Small hot objects—Theory *500*
Airborne burning objects (flying brands) *500*
Ignition of buildings 501
Ignition of wildland fires 503
Prediction of spotting distances 503
Exhaust particles *505*
Welding spatter *506*
Brands ejected from fireplace *507*
Friction and mechanical sparks *507*
General principles 507
Ignition of flammable gas atmospheres 509
Ignition of dust clouds and layers of porous materials 515
Shock, impact, pressure, vibration **517**
Shock and impact *517*
Dropped objects 517
High-velocity impacting particles (unheated) 517
Pressure (compression ignition) *517*
Vibration *518*
Flames or remote objects **518**
Small burner flames and small burning objects *518*
Larger flaming sources and burners *519*
Kitchen sources 519
Large laboratory burners 519
Jets and high velocity burners *519*
Solid-fuel ignition sources *520*
Burning fabrics *520*
Burning furniture *520*
Large burning objects *521*
Liquid pools , wood cribs 521
Fireballs and jet flames 524
Burning buildings 527
Burning forests and vegetation 531
Burning vehicles *532*
Heat fluxes in pre-flashover room fires *532*
Heat fluxes on burning walls *532*
Heat fluxes in post-flashover room fires *532*
Attenuation of radiation by window glass and window screens *533*

Electric phenomena **534**
Electric discharges *534*
The electric spark 537
The electric arc 540
Electric current *548*
Overheating wires 549
Overheating electrical connections 549
Ejection of hot particles 553
Dendrites 553
Adventitious batteries 553
Static electricity *553*
General principles 553
Discharge types 554
Measuring of discharges 557
Electrostatic charging and discharging of solids 557
Electrostatic charging and discharging of persons and apparel 559
Electrostatic charging and discharging of granular materials 561
Electrostatic charging and discharging of liquids 562
Safety measures 567
Lightning *567*
Ordinary lightning 567
St. Elmo's fire 569
Ball lightning 570
Exploding wires *571*
Electromagnetic waves and particulate radiation *571*
Eddy currents 571
Radio transmitters 572
Nuclear weapons 574
Light energy, lenses and mirrors **575**
Aerodynamic heating **576**
Further readings **576**
References **577**

Highlights and summary of practical guidance

An ignition source can constitute any form of heat or a form of energy (for example, kinetic energy) which can become converted into heat. Energy sources can be characterized by at least four main characteristics:

1. the temperature
2. the total energy supplied
3. the rate at which it is supplied, or the time period over which it is delivered
4. the area over which it is delivered.

Dealing with a phenomenon where there are at least four controlling variables can be complex. In many cases, even more than four variables come into play. For example, in radiative heating, the wavelength distribution of the radiation is important. In convective heating, air velocity affects the outcome, not just temperature. Solid objects (i.e., fire brands) often have an extremely irregular heat flux distribution, so the whole concept of energy supplied over a fixed area loses meaning. Because of complications of this type, it is rarely possible to treat ignition sources as simple black boxes supplying energy. Instead, it is necessary to study details of various ignition sources that have been found to be important in actual fires, and to examine how they interact with different types of combustibles.

Ignition sources consisting of radiant heat flux or a hot air stream (convective heating) are relatively simple. The main issues with sources of this kind involve aspects of proper design of test apparatuses. Otherwise, the heat fluxes can be

treated in a simple way according to elementary heat transfer theory. Thus, simple radiant or convective heating has already been treated in the preceding Chapters under the different material types and is not further studied in this Chapter. Flames, burning buildings, and other similar heat sources require some study before they can be described by their heat fluxes. Thus, these ignition source types are included in the present Chapter. Even though principles governing ignition sources are often poorly known, this Chapter is devoted to examination of ignition source principles, to the extent that they can be established. Specific information dealing with practical ignition sources (for example, candles, cigarettes, matches) is presented in Chapter 14.

The ignition potential of hot, incandescent or burning particles is very poorly known. In certain cases, particles of less than 0.5 mg can ignite some dry forest fuels. Fuel gas/air mixtures, under extreme circumstances, can be ignited by a 1 μg burning magnesium particle. But the probability of ignition decreases as the particle size decreases. There have been a number of studies on this topic, but taken together, they do not allow one to evaluate the probability of ignition, as a function of characteristics of the igniting particle and the target material. General research on fire brand ignitions is presented in this Chapter, while more specific details focusing on various target materials are given in Chapter 14.

Electrostatic charge build-up is likely to occur when motion is involved. The motion can involve rubbing of solids or flow of insulating liquids or powders. The flow of pure gases does not lead to static charge buildup. Systematic understanding of electrostatic ignitions is also often limited, although there has been much empirical research.

Perhaps the most difficult to understand ignition source has been electric current. The basic principles governing ignition from electric current are treated in this Chapter; details of ignitions associated with wiring, connectors, appliances, etc. are taken up in Chapter 14. Despite its importance for understanding real fires, research in this area was nearly non-existent until the 1970s and is still scattered and incomplete.

Introduction

Ignition sources can be of two types: (1) self-caused; or (2) external. Examples of self-caused ignitions include hypergolic, pyrophoric, and unstable substances; self-heating; and some others. For these ignition types, there is no difference between the igniter and the ignited. Thus, these have all been considered under appropriate chapters above. In this Chapter we give detailed consideration to external heat sources, that is, sources which are not one-and-the-same as the item being ignited. In electric arc tracking, the identity of the heat source and the item being heated is perhaps less clear, but nonetheless this form of ignition is treated in Chapter 7.

An external ignition source can basically be anything which can generate or deliver an adequate amount of heat. In practice, this includes a wide variety of devices, situations, and substances. In this Chapter we consider those ignition sources that have been studied sufficiently so that some systematic trends are known or some practical guidance is available.

High ambient temperatures

In desert climates, surprisingly high temperatures can be achieved in interior spaces which are neither insulated nor ventilated. A temperature of 101ºC has been measured[1] under such conditions in Tucson, Arizona, when the outdoor air temperature was 49ºC. A similarly extreme temperature of 93ºC was measured on the exterior surface of a roof in Saudi Arabia[2].

In less extreme climates, a study of attic temperatures[3] in Mississippi showed an outdoor air temperature of 40ºC, with corresponding interior temperature of 58ºC. At the same time, the exterior surface temperature of the black-asphalt shingle roof was 78ºC. In Wisconsin, with an outdoor air temperature of 35ºC, peak interior temperature of 54ºC was recorded, with the corresponding exterior surface temperature being 76ºC. Even these extreme temperatures are normally not a problem for stable, solid materials. Self-heating materials, on the other hand, are very sensitive to ambient temperatures and that topic is dealt with in Chapter 9.

According to a study by Bowes[4], the temperature in ships' holds were found to attain 39 – 48ºC for prolonged periods of time when a ship is traveling through tropical areas, although sustained air temperatures are only 29 – 38ºC. Above-deck temperatures[5] almost never exceed 40ºC.

Hot solids or liquids

This category of ignition sources encompasses a broad array of heating configurations, with the two most common examples being:

a) a large hot surface coming into contact with the large surface of the ignitable solid; or
b) a small, hot object falling onto a large ignitable surface.

Common examples of small, hot objects which can act as an ignition source include aerodynamically buoyant burning objects (generally called firebrands or flying brands), engine exhaust particles, and hot, molten, burning, or incandescent metals. Hot metals typically can be generated from friction or impact, from steelworking activities (e.g., hot rivets), from arc welding, or from other sources of electric arcing. Smoldering objects may also be placed in the category of small hot objects. However, there is not much general, systematic knowledge concerning their ability to act as ignition sources. The most common example is a cigarette and its characteristics are treated in Chapter 14. A flying brand may also extinguish during its flight and land on a target as a smoldering object. Some general aspects of smoldering behavior are treated in Chapter 7.

LARGE HOT SURFACES IN CONTACT—THEORY

For a hot surface to be considered 'large,' the minimum width or length dimension should be much greater than the thermal penetration depth (see Chapter 7) of the ignitable solid. A classic example of a large hot surface coming into contact with an ignitable solid is a clothes iron. The analysis of this category of problem is actually not simple. The interface between the hot object and the ignitable object will assume a temperature that is relatively constant for locations far away from the edges of the hot object. This interface temperature (i.e., the surface temperature of the ignitable object) can be approximately computed using standard heat conduction theory. At the moment of contact, the surface temperature of the ignitable object becomes identical to the surface temperature of the hot object. This temperature T_i will be lower than the original surface temperature of the hot object, but higher than the original surface temperature of the ignitable solid. It can be solved as[6]:

$$T_i = \frac{T_h\sqrt{(\lambda\rho C)_h} + T_c\sqrt{(\lambda\rho C)_c}}{\sqrt{(\lambda\rho C)_h} + \sqrt{(\lambda\rho C)_c}}$$

where T_h = temperature of the hot object (ºC), T_c = temperature of the ignitable object (ºC), and the thermal inertia term $\sqrt{(\lambda\rho C)_h}$ refers to the hot object, while $\sqrt{(\lambda\rho C)_c}$ refers to the ignitable object. The solution for the interface temperature, however, is not exactly the answer that is wanted. Far away from the edges, the surface of the ignitable object will be getting heated to the maximum temperature. However, since a hot surface is in direct contact there, no oxygen can get to this place. Where ignition can take place is at the edges of the hot body, since oxygen is available there. That temperature, however, is lower than the interface temperature computed by the above equation.

In practice, the situation may be more complex yet. We have tacitly assumed that both the hot object and the ignitable object have hard, impermeable surfaces. However, by significant heating the ignitable object may melt or pyrolyze and, thereby, open up cavities or voids. Oxygen may then get into these voids. A plastic foam can be an example of an ignitable object which deforms during heating. Also, given enough time, the pyrolysis may proceed through the thickness of the material and break out the other side where oxygen may be present. This is common when heating appliances are improperly placed on combustible floors and the appliance chars a hole through the floor. Flaming combustion often occurs from below the floor.

SMALL HOT OBJECTS—THEORY

Studies on specific categories of hot objects are presented in several sections below. These are mostly either purely empirical or employ a theory for aspects other than ignitability (e.g., aerodynamics of burning brand flight). There have been only limited theoretical attempts to predict ignition of various substrates upon which a small hot object may fall. Examples include forest floor litter (Jones[7]) and surfaces upon which welding spatter falls (Hölemann[8]). These efforts have been based upon the application of either the inert or the reactive hot spot theory, presented in Chapter 9. It is relatively easy to make the required calculations, however, the realism is uncertain since:

(1) There has been no experimental validation of the theories.
(2) Most practical problems violate the basic assumptions incorporated in the theories. The theories all assume that the hot particle is in full, intimate contact with the substrate, and that the latter is infinite in extent. In the case of fibrous materials such a vegetation, the contact between a small particle and the substrate is likely to be at only a few, tiny spots, not along the whole periphery of the particle. In the case of particles landing on a solid surface, again contact will be limited, unless the material melts or burns enough to envelop the particle. Even then, the front-face conditions of the substrate do not approximate an infinite solid.
(3) The experimental data discussed below indicate that the problem is largely probabilistic, but there exists no theory that incorporates probabilistic aspects.
(4) Necessary thermophysical data for the target material, especially the thermal conductivity, may be lacking.

An example on the use of the self-heating theory to predict the ignition potential of molten aluminum particles falling onto barley grass is given in Chapter 14.

AIRBORNE BURNING OBJECTS (FLYING BRANDS)

Many types of fires generate small burning particles which flow along with the gaseous combustion products. When such particles have the capability of setting additional fires, they become firebrands. The basic aerodynamics is that the brand first gets lofted by the plume of fire gases to a high elevation. The available lift decreases as the plume gets progressively cooler at higher altitudes. Eventually, a terminal height is reached. If there were no wind, the brand would simply burn up vertically above its generation point and no spot fire could result. However, wind acts to carry the brand horizontally away from its origin point. Whether or not a combustible particle has the potential of setting a fire depends on the interplay of several factors:

- a particle must be generated (burned off, broken off by air velocity)
- it must get heated to ignition
- it must not burn up completely before it lands on the potential target, and it must carry enough remaining heat of combustion in order to be able to actually ignite the target.

Under a given set of conditions, there will be an optimum mass of particle that can set the most remote spot fires. This will depend not only on the aerothermodynamic aspects of the fire environment, but also on the shape of the object. A firebrand with a shape that creates a significant amount of aerodynamic lift is the most hazardous firebrand.

Table 1 Terminal velocity of potential firebrand materials (tested unignited)

Material	Terminal velocity ($m\ s^{-1}$)
bark of paper birch	5.6
frond of palmetto palm	4.6
leaves	1.3 – 2.24
moss	3.5 – 4.5
pine cones	8.6 – 16.5
pine needles	2.9 – 4.1

Some basic characteristics of forest materials acting as firebrands were studied by Clements[9]. Terminal velocities, as determined in laboratory drop-tower experiments (on unignited materials) are listed in Table 1. Clements also examined the burning times of cones from various pine species by keeping the specimens suspended in a vertical wind tunnel. The flaming times were relatively short, but some very long glowing times were recorded (Table 2).

Table 2 Flaming and glowing times for pine cones in flight (averages for 25 trials)

Pine species	Flaming time (min)		Glowing time (min)	
	Avg.	Max.	Avg.	Max.
loblolly	0.36	0.83	4.09	6.83
longleaf	0.44	1.20	7.50	13.49
shortleaf	0.15	0.53	2.95	4.60
slash	0.32	0.56	6.13	10.42

The length of time during which a firebrand will flame increases with increasing size of brand. Muraszew[35] conducted experiments on natural vegetation items, wood cylinders, and cedar shingles. For all three categories, he found that the flaming time could be represented as:

$$t_{fl} = 25\left(\frac{V}{S}\right)^{5/4}$$

where t_{fl} = flaming time (s), and V/S = volume/surface ratio (mm). The latter was used instead of a diameter so that irregular-shaped brands could be correlated. After a wood brand has ceased flaming, there still remains a glowing phase and brands can ignite target fuels in the glowing phase, although they become progressively less effective.

IGNITION OF BUILDINGS

A 1960 Japanese study found that, within cities, most spot fires are located within 700 m of the originating fire from which brands were launched[10]; a number of these fires were caused by very small brands which were blown in by the wind through small gaps between roof shingles. In the Sakata City Fire[11] of 1976, brands of 50 mm size were found to have traveled up to 1800 m in a prevailing wind of 12 m s^{-1}. More recently, the investigation of a major hotel fire in Japan revealed that fire spread to surrounding areas was mostly by means of fire brands. Brands of 50 mm size were found[12] to have traveled up to 450 m; brands up to 300 mm size were found at shorter distances[13]. Japanese researchers also determined that mass fires which show extremely high rates of spread are mainly dependent on fire brands for these fast spread rates In the Great Hakodate Fire of 1934, fire spread rates of 1000 – 1400 m h^{-1} were attributed to transport of fire brands. An empirical relation was evolved between wind velocity and the rate of spread of an urban mass fire propagating by means of fire brand transport (Figure 1)[14].

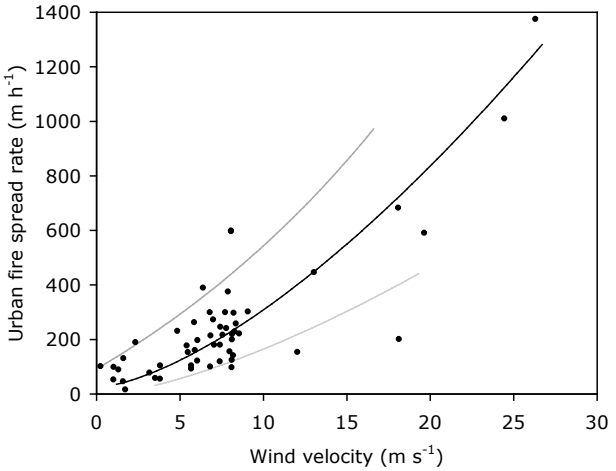


Figure 1 The spread rate of Japanese urban mass fires driven by fire brand propagation

A laboratory study to characterize brands generated by burning roofs was reported by Waterman[15]. Wood shingle roofs were found to be much more effective in producing brands than were roofs covered with asphalt shingles, built-up roofing, or cement-asbestos shingles. Brands comprising asphalt shingles themselves were found to be rarely produced and of little ignition potential; the hazard from asphalt-shingle covered roofs was mainly from brands generated by the supporting wood decking. When an existing wood shingle roof was over-covered by another material, the production of brands was also reduced. When a non-zero wind velocity was present, the generation rate of brands was dramatically increased, by up to an order of magnitude (travel distances of brands were not examined in this study).

Full-scale house burns to quantify the generation of fire brands from burning single-family houses were conducted by Vodvarka[16]. The houses were all of ordinary wood-frame construction. He observed that generation of large amounts of brands was roughly related to the time for fire to vent through the roof—earlier venting caused greater generation. The amount of sizeable brands found was small, but brands of 37 mm width were found up to 75 m away. The limited generation is surprising, since one house had a wood shingle roof, while two more of the five test buildings had wood shingle roofs that had been over-covered by a asphaltic

roofing. In these experimental studies, Vodvarka found that fire brands were mostly generated by roof components: shingles, tar paper, or portions of burnt wood decking.

Vodvarka also discussed some accidental fires. In one bowling alley fire, brands as large as 0.3 m^2 were being lofted even though the structure did not have a wood shingle or shake roof and brands of 100 mm diameter were being carried out as far as 275 m. Fire brands from the burning building started a grass fire 240 m away and structures 120 m away appeared to be in imminent danger of fire brand ignition and had to be wetted down by the fire service. In an accidental fire of a factory building having a slate tile roof, significant brands were found to have been generated and grass ignition occurred up to about 200 m away. This fire, however, had a strong wind of 9 m s^{-1}. In a warehouse fire, tar paper brands traveled over 600 m, crossed the Ohio River, and ignited a roof fire and two awnings. In a factory fire, brands from asphaltic built-up roofing ignited roof fires 800 m away, while additional brands were found 1600 m distant. In an accompanying survey, Vodvarka obtained 250 responses from a questionnaire to fire chiefs asking to list the experiences in their jurisdictions. The most interesting results are given in Table 3.

Table 3 Material first ignited by fire brands from burning buildings, from survey by Vodvarka[16]

Material first ignited	Percent
roof covering	54
vegetation	22
interior of structure	10
trash	8
other	7

Wood roof shakes and shingles have been highly problematic for three reasons: (1) their propensity to generate fire brands is greater than that of any other common building component; (2) they are more readily ignitable than most other roofing materials; and (3) they are exceptionally well aerodynamically shaped. Because of these traits, a wildfire which starts with vegetation and then ignites houses which are roofed with non-fire-retarded wood shakes can generate a conflagration of spot fires well ahead of direct spread of the vegetation fire. Statistics from the 1961 Los Angeles conflagration showed that at a distance of 25 m away from the flame front of a vegetation fire, a roof with some FR properties was 8 times less likely to be lost than one having untreated wood shakes[17]. When compared to the preceding conflagrations in 20th century North America, it was found that the number of buildings lost in the *largest* conflagration not involving wood shakes was less than the number lost in the *average* conflagration which had involved wood shakes. It was also determined that the maximum *spotting distance* (distance at which a secondary fire is ignited by firebrands) recorded from wood shakes was 13 km (8 miles). After the 1991 Oakland Hills fire, it was estimated that each burning house having a non-FR wood shake roof ignited 10 other houses[18].

No fundamental differences exist between the firebrand capabilities of wood shakes versus shingles, nor do differences exist according to whether the cut is edge grain or cross grain, nor if redwood or cedar, nor if heartwood or not. It is difficult to treat a wood shake successfully with fire retardants so that the treatment withstands the adverse effects of water and sunlight for the life of the roof. Nonetheless, some shakes are commercially available these days which have obtained a Class B rating according to ASTM E 108[19]. Roof sprinklers are sometimes proposed for protecting readily ignitable roofs, but these may not be a reliable tool against conflagrations, since the water supply may run dry at a crucial time.

Several laboratory studies exist where the ignition potential of firebrands was examined. Waterman[20] used the Class C brand specified in the ASTM E 108 roof test (see Chapter 7). This brand is a 3 g wood piece, sized 38 ◈ 38 ◈ 20 mm, with one saw-kerf cut across each of the two large faces. The cuts were found to be an important factor in promoting the occurrence of ignition. They simulate large fissures which naturally develop in burning wood pieces. In addition, he studied 0.6 g brands measuring 19 ◈ 19 ◈ 20 mm and several other small brands. Because wind aids the ignition process, several wind conditions were explored: steady at 0.9 – 1.4 m s^{-1}; steady at 2.3 – 2.7 m s^{-1}; alternating calm/bursts at 0.9 – 1.4 m s^{-1}; and alternating calm/bursts at 2.3 – 2.7 m s^{-1}. In addition, tests were run with superimposed radiant heat fluxes of 0 to 8.4 kW m^{-2}. The study was done probabilistically, with probabilities being tabulated for each experimental condition. The results were voluminous, but the main findings were:

- With moderate wind and no imposed external irradiance, 38 mm brands were able to ignite all building materials except Class C-rated roofing and unpainted solid-wood sheathing. They were also able to ignite paper, cardboard, and heavy cloth such as canvas and burlap. Some thinner fabrics resisted ignition. Carpets (both wool and thermoplastic) and fabric/foam upholstered furniture composites typically did not ignite.
- The 19 mm brands ignited canvas, and denim, but did not ignite any construction materials. Paper and cardboard were marginally ignited, requiring a specific wind condition for ignition. Imposed radiation caused ignitions to occur that were not possible without imposed radiation.
- Splintered wood ignited more readily than solid wood.

The RH was not controlled in Waterman's study, nor were elevated ambient temperatures considered. Thus, his findings do not represent the lower limit possible for brand ignitions. Laboratory studies to adequately establish lower-limit conditions as a function of temperature and RH do not exist, but in an old Japanese study, researchers found that glowing wood brands of about 10 mm diameter sufficed to

effectively ignite flat surfaces of building materials such as solid cedar or wood shingles[21]. FRS studied the ignitability of red cedar wood shingle roofs by firebrands[22] and identified the crucial role of a small amount of radiant heat flux on the firebrand ignitability. When 4 kW m^{-2} heat flux was applied, an 0.5 g wood brand sufficed to ignite the roof and maintain flame spread. Without the radiant heat flux, a 100 g wood brand was required. The studies cited above, however, suggest that a 100 g brand would be far greater than the minimum needed, but the relative effect of radiation that was found is nonetheless instructive. Much smaller brands can suffice for ignition in *cracks and corners*, than is required for a flat surface, as discussed in Chapter 14 under *Wood*. The studies discussed in Chapter 14 did simulate high ambient temperature, low RH conditions typical during wildland fires.

IGNITION OF WILDLAND FIRES

In a 1941 study[23], a list of firebrands was put forth, ranking them in order of importance as ignitions of forest fires. Most to least important, the list was given as:
(1) broadcast slash pile burning
(2) large bonfires or burning slash piles
(3) small campfires
(4) burning matches (kitchen matches)
(5) lighted safety and book matches
(6) pipe heels
(7) locomotive sparks and glowing embers
(8) cigarettes
(9) cigars
The list was based on a qualitative review of mostly unpublished studies.

Eucalyptus trees shed strips of bark which are highly efficient as firebrands. It has been documented in Australian wildland fires[24] that spotting distances of 8 – 10 km (5 – 6 miles) are common for high-intensity eucalyptus fires and that spotting distances of 19 – 24 km (12 – 15 miles) were found. An extreme spotting distance of 30 km (18 miles) has been cited[25] in connection with eucalyptus forest fires; this required very strong winds estimated at 90 – 100 km h^{-1}. By contrast, 2 km is the largest spotting distance recorded in Australia for Monterey pine forests, since Monterey pines do not produce aerodynamically well-shaped brands. Size of brand is important in producing long-distance spotting; a brand must remain burning for upwards of 30 minutes in order to produce a spot fire 16 – 24 km (10 – 15 miles) away[26]. In a US study[27], burning California chaparral has been noted to cause ignitions up to 6.5 km (4 miles) away, while mixed-conifers forest fires up to 21 km (13 miles).

PREDICTION OF SPOTTING DISTANCES

The distance away from a main fire that a secondary fire is ignited by brands is termed the spotting distance. To predict spotting distances accurately would require detailed knowledge of:

- The physical characteristics of brands;
- Their burning behavior (including interactions between wind and pyrolysis/combustion of the brand);
- An aerodynamic theory that can predict travel trajectories of particles that change size, shape, and temperature during travel. This travel has three distinct phases which would need to be predicted: (1) lofting, (2) downwind propagation, and (3) deposition or, alternatively, burnout while still airborne.
- A theory that can predict the ignitability of various targets from brands.

Every one of these components is exceptionally difficult, but a small number of studies do exist on the general topic. The last component, a theory of ignition from firebrands, is basically non-existent, apart from the very simple theories discussed at the start of this section. Even empirical research studies are few; the available ones were summarized above or in Chapter 14 under the relevant target fuels: *Dung*, *Fabrics*, *Forest materials and vegetation*, *Paper products*, *Upholstered furniture*, and *Wood*.

An Australian equation[28] has been offered as a simple predictive model for maximum spotting distance:

$$L = r\left(4.17 - 0.033W\right) - 0.36$$

where L = average maximum spotting distance ahead of source fire (km), r = rate of forward fire spread (km h^{-1}), and W = fuel load (tons/hectare). The equation is easy to apply, but it is not clear what are the limits to its validity.

The effect of wind on combustion of airborne objects—which would be pivotal for any comprehensive fire spotting theory—has only been studied to a very limited extent. Refined fluid-mechanical theories of spotting distance begin with the work of Tarifa[29,30] in the 1960s. In a series of wind-tunnel experiments, he characterized the burning of wood particles as a function of wind velocity. As a wood particle burns in air, the consumption of the fuel is such that both the effective density and the effective diameter progressively decrease. Thus, various ways can be used to represent this particle change, but the simplest is just the ratio $m(t)/m_o$, which will be a decreasing function of time, and where m_o = initial mass. A good representation of Tarifa's data is:

$$m(t) = m_o\left[1 - \left(0.0024 + 0.00038\,u\right)t\right]$$

where u = wind speed (m s^{-1}) and t = time (s). The decrease of mass with time stops being linear when the particle stops glowing combustion. This event is velocity-dependent and, at high velocities, the brand burns up completely. But for lower velocities it can be approximated that glowing combustion stops when $m = 0.2m_o$ and after that point, the decrease in mass of the burned-out char particle proceeds more slowly. Other researchers identified that low-density brands are more likely to burn to completion than high density ones[18], but an expression is not available that usefully incorporates the original density. Tarifa collected a great deal of other information in various laboratory tests with firebrands and, on that basis, proposed a theory for spotting

distance. No scheme was provided for users to perform their own predictions, but he did perform calculations which indicated that 22 mm pine spheres have a maximum travel distance of 4.4 km before final break up. Actual spotting distances would be less than that.

Most of the time that a brand made of woody material is in the air, its burning is in a glowing, rather than flaming, mode. In still air, a brand would be able to burn in flaming mode for a substantial length of time, but experiments[24] indicate that firebrands do not flame very long when being subjected even to modest winds. At a wind speed of 4.4 m s^{-1} (10 mph), the flaming time may be 20 – 50% of its value in still air. In some tests, brands which went from flaming to glowing in a wind then re-erupted in flaming when taken out of the wind. This is due to excessive dilution of the pyrolysates being evolved from the brand by high air velocities. Ellis[31] found that eucalyptus bark, even in constant wind, sometimes tends to repeatedly switch between flaming and glowing combustion.

The brands presenting the most problems (i.e., largest spotting distances) are the ones which can generate substantial aerodynamic lift, such as shakes and eucalyptus bark strips. But these are hard to study, both experimentally and theoretically, and only a few workers have even attempted this. More common have been studies of blunt shapes, typically spheres and cylinders. Lee and Hellman[32] analyzed data on burning wood spheres and found that the sphere's radius, at any instant in time, is mainly governed by speed of the air flowing by it. They gave an expression for the radius r (m) as a function of time:

$$\left(\frac{r(t)}{r(0)}\right)^2 = 1 - 1.15\times10^{-14}\left(\frac{u\,t}{r(0)}\right)^{2.5}$$

where u = wind speed (m s^{-1}).

Working in the 1970s, Muraszew and coworkers were the most active US group endeavoring to produce a spotting distance model. Despite studying a number of aspects of the problem in great detail, their efforts did not lead to a usable model. In one study[24] they performed experiments on cylinders and flat plates and provided some expressions for their shrinkage with time under several wind conditions, but were not able to derive a general expression based on a wind speed. The examined how the density decreases with burning time and concluded that (provided wind speed is greater than 2.3 m s^{-1}) a speed-independent density decrease law holds[33]:

$$\rho(t) = \rho_o \exp\left(-t/7600D_o\right)$$

where ρ = density (kg m^{-3}), t = time (s), and D_o = initial volume/maximum cross-section area ratio (m). For brands to be carried a long distance, it is necessary that they be lofted to a significant height. They noted[33] that it is difficult to attain the needed heights from a pure convective plume and that swirl appears to be an essential component. They also developed a strategy for a comprehensive mathematical model[34,35], but the effort was not continued beyond its early stages.

Other investigators have produced models or sub-models with more extensive numerical solutions, but without any closed-form approximations or real-scale validation[36-38]. One nearly-closed-form model was developed at the US Forest Service by Albini[39] and consolidated by Chase[40]. Three options were provided: (1) 'torching tree', (2) pile burning, or (3) wind-driven fire types, and a series of equations is given for each which can solved in a spreadsheet. Equations for the third option were subsequently simplified by Morris[41]. The third option of a 'wind-driven' fire involves firebrands lofted by a *line thermal*[*]. Albini assumed that the brands are non-aerodynamic, and that the thermal is strong, that is, a temperature rise is considered which is not small compared to the ambient temperature (in degrees K). Making a number of other reasonable, but unproven, assumptions, he demonstrated[42] that the maximum lofting height h_{max} (m) is:

$$h_{\max} = 1.73\sqrt{E/P_a}$$

where E = the thermal's energy per unit length (J m^{-1}) and P_a is the ambient pressure (Pa). The horizontal distance that the brand travels until it leaves the thermal is determined by H_e, the vegetation cover height, and the wind velocity. In addition, the wind speed profile—logarithmic, power law, etc.—has a major influence. This model was not developed, nor should it be used, for highly aerodynamic brands such as wood shakes or eucalyptus bark, nor for long-distance spotting. A model which described long-distance spotting would need to include fire whirl phenomena and the representation of large-area crown fires. Albini later developed a theory and a computer program[43] for predicting the maximum distance of spot fires from brands generated by a crown fire.

While a circular plume rarely represents forest fire burning, Woycheese[18] presented a simple model for the lofting and burning of *spherical* wood brands in a circular fire plume. It predicts that the maximum particle diameter d_{max} (m) which can be lofted is:

$$d_{\max} = \frac{143\dot{Q}^{0.4}}{\rho_s}$$

where ρ_s = density of wood (kg m^{-3}) and $\dot{Q}$ = heat release rate of fire (kW). Thus, for example, if ρ_s = 500 kg m^{-3}, then the maximum diameter of a brand that can be lofted by a 50 MW fire is 22 mm, while a 3000 MW fire can loft 111

[*] A 'thermal' in meteorology is a suddenly released buoyant element. The buoyancy remains confined to a limited volume of fluid, which, as it rises, becomes detached from the source that produced it. A plume, by contrast, is generated by a sustained source of buoyancy. In a plume, the buoyant region never separates from the source. A line thermal is one which is 2-dimensional and infinitely long.

mm. Also, for particles of diameters $d > 44\dot{Q}^{0.269}\rho_s^{-0.782}$ the maximum lofting height h_{max} (m) is:

$$h_{\max} = 2.70\dot{Q}^{0.616}\rho_s^{-0.36}$$

Another, more complicated expression pertains to the lofting of small particles, but these are less likely to be the safety concern. The maximum spotting distance x_{max} (m) is:

$$x_{\max} = 2.42GU\dot{Q}^{0.452}\rho_s^{-0.42}$$

where

$$G = \frac{0.090\dot{Q}^{0.368}\rho_s^{-0.28} - 0.108\dot{Q}^{0.2}}{U} + \frac{0.987Q^{0.01}}{U^{0.05}}$$

$$\text{for } 0.23 \le U\dot{Q}^{-0.2} \le 2.32$$

and

$$G = 1$$

$$\text{for } 2.32 \le U\dot{Q}^{-0.2} \le 4.64$$

U = wind velocity (m s^{-1}). As an example, if the wind speed is 15 m s^{-1} and the fire is 1 GW (10^6 kW), then $U\dot{Q}^{-0.2} = 0.95$. Assuming ρ_s = 500 kg m^{-3}, G = 1.05 and x_{max} = 1440 m. It should be noted that, while the theory is relatively sophisticated, Woycheese did not undertake comparison with experiments. Many firebrands are flat objects, for example wood roof shakes, and cannot be approximated as spheres. Woycheese et al.[44] subsequently extended the theory to *disc-shaped* brands, although this work did not produce a closed-form expression for spotting distance.

EXHAUST PARTICLES

The exhaust from the engines of automobiles, trucks, locomotives, farm equipment, etc. can discharge burning carbonaceous particles. These have been known to cause ignitions of vegetation and other combustibles. Trains are a particular likely source of ignitions since not only can firebrands be ejected, but the motion of a train creates a local wind that can help a smoldering fire transition to flaming[48]. In an early study, Fairbank and Bainer[45] found that, in extreme cases, particles as large as 14 mm by 33 mm have been ejected from engines. They first performed laboratory tests on the particles themselves, and found AIT values of 540 – 550ºC for 1 g samples containing particles larger than 0.6 mm and 475ºC for smaller particles. Then, in field tests, they designed an ingenious transportable furnace able to expel hot particles onto test vegetation. The particles flamed for only a short time, then were ejected while glowing. A collection comprising 2 g of particles was ejected in each ejection, irrespective of size. A summary of the results is given in Table 4 and Table 5. For the larger particle sizes, the probability values given in Table 4 may be slightly too low, since the authors only tallied whether or not a test caused a fire and did not further itemize if more than one target location was ignited in any particular test; for the smaller sizes where ignition was a rare event, this factor would not come into play. The actual furnace temperatures used for the tests reported in Table 4 were varied to suit the ignitability characteristics of the type of vegetation being ignited. The largest fraction of the runs were conducted at

Table 4 The effect of particle size on the probability of ignition

Size (mm)	Avg. mass (mg)	Probability of ignition (%)
5.6 – 9.4	50	0.75
4.3 – 4.7	20	0.3
2.3 – 2.4	2.0	0.03
0.6 – 1.2	0.5	0.003
< 0.6	0.01	7×10^{-5}

Table 5 Effect of RH on the furnace temperature to which 4.3 – 4.7 mm particles needed to be heated in order to ignite vegetation

RH (%)	Minimum temp. (ºC)
10 – 29	700
30 – 39	925
40 – 50	1040

750 – 1000ºC, but for some trials temperatures as low as 650 or as high as 1250ºC were used.

Fires were started at up to 9 m away from the test furnace discharge, although glowing particles were visible as far as 18 m away. The authors also conducted experiments where burning carbon particles were deposited on cotton flannel cloth. In the worst cases, holes were burned through the cloth, but actual ignition of the cloth did not occur. In these experiments, the authors learned that the amount of scorching was dependent not only on the temperature and the size of the particles, but also on the type of carbonaceous material. Cotton batting, however, was readily ignited when held 0.5 m behind an exhaust pipe.

Maxwell et al.[46,47] examined exhaust particles from diesel engines as a potential ignition source for wildland. They experimentally generated exhaust particles showing, in some cases, flaming combustion for over 40 s and glowing combustion for over a minute. Temperatures of 400 – 450ºC had to be attained for particles to ignite in a glowing mode. In tests using 1.5 – 2.0 mm particles, 12 out of 186 trials produced glowing or smoldering ignitions of cheat grass (*Bromus tectorum*), while 3 trials resulted in flaming ignitions. The particles averaged about 2 mg in mass, but neither the temperature to which the particles were heated nor the RH of the target fuel were specified. The particles used showed a flaming period of up to 40 s and a glowing time of up to 60 s. In scanning electron microscope studies, they found that the particles were extremely irregular and 'spiky,' thus they doubted that a hot-sphere theory would be adequate. The particles contained a variety of elements and compounds, but CaO tended to be most prevalent mineral constituent. They also found a substantial organic liquid component (up to 2/3 of the total mass) which was determined to be motor oil. The authors concluded that to avoid wildland ignitions, a distance of at least 6 m was needed

from the exhaust to the vegetation. They also observed a notebook was accidentally ignited by 3 mm particles at more than 5 m from the exhaust of a test engine; the ignition, however, was not sustained. Notwithstanding the laboratory tests, Ford[48] deprecated the possibility of extremely small particles being able to start forest fires and pointed out that, in his experience at the California Dept. of Forestry, the minimum particle size found to be an actual cause of forest fires was 3 mm.

The US Forest Service operates a test station in San Dimas, California for testing of spark arresters on engines. They conduct the tests according to SAE test procedures[49-52] and make the results available in a two-volume book of approved-equipment listings[53,54].

WELDING SPATTER

Welding spatter is a well-known source of ignition. The Welding Handbook[55] advises that: "Many fires are started by sparks, which can travel horizontally up to 35 feet from their source and fall much greater distances. Sparks can pass through or lodge in cracks, holes, or other small openings in floors and walls. Materials most commonly ignited are combustible floors, roofs, partitions, and building contents including trash, wood, paper, textiles, plastics, chemicals and flammable liquids and gases. Outside, the most common combustibles are dry grass and brush."

The most famous fire loss caused by welding spatter was the General Motors factory in Livonia, Michigan which burned down in 1952[56]. In that loss, small hot particles from a cutting torch ignited a tray holding a rust-inhibiting liquid of rather low flash point (36.5ºC open cup).

The size of particles ejected from arc welding operations varies widely. In one Japanese study[57], most of the particles were under 0.1 mm, and very few over 0.5 mm. But in another study[58], where a thermographic camera was used to examine the size/temperature/distance relationship for welding spatter, the bulk of the particles were found to be in the range of 1 – 3 mm, although a number of sub-0.5 mm particles were found and two particles (out of hundreds) were found in the range of 6 –7 mm. These differences reflect differences in the collection/identification techniques used and the true particle size distribution presumably includes both the tiny particles and the large ones. Particle temperatures of about 1850ºC were found very near the welding rod. At 1.0 m below, particles were at approximately 1592ºC. From the 1-m location to the lowest drop investigated, 2.8 m, the temperatures decreased very slowly, being an average of 1572ºC at the 2.8-m location. A simple model of convective cooling would indicate that smaller particles cool faster than large ones, but in their experiments the authors did not find any significant effect of particle size on the temperature. Tanaka[59] showed that particle sizes are much greater for oxy-acetylene cutting operations than for arc welding. His experimental data for flame-cutting slag showed no effect of drop distance on measured temperature, with a constant temperature of 2100ºC being obtained. For slag produced by arc welding, he found a slowly decreasing temperature with fall distance. A temperature of 3500ºC was found at the welding location, dropping to 2700ºC in 0.5 m and to 2200ºC in 5 m.

The size of welding spatter particles does not depend on the size of welding rod used[57]. Hagiwara et al.[60] found that the number of particles produced increases when welding current is increased, but the size distribution does not vary appreciably. Most particles in their study were below 1.0 mm, but a small fraction of 3.0 mm particles was found. The amount of spatter produced does vary with the type of coating used. Deep penetrating rods such as the AWS XX11 series spatter more that the filled rods like a XX24 due to the arc action and the thickness of the slag.

The propensity of welding spatter to ignite various materials was tested by Hagimoto et al.[57], as shown in Table 6. They also determined that many particles fractured into pieces if they landed on a concrete or wood floor.

Table 6 Ignitability of various fuels from welding spatter

Target fuel	Particle dia. (mm)	Ignition time (s)
acrylic batting	1.1	< 1
cardboard, corrugated	2.5	7 – 8
cotton cloth	3.1	5 – 6
cotton wool	0.9	< 1
ethanol	1.1	< 1
gasoline	1.4	< 1
kerosene	1.5	NI
kerosene-soaked cloth	1.3	< 1
newspaper	2.5	4 – 5
oil, light	2.0	NI
oil, light, soaked in cloth	1.9	< 1
polyurethane foam	0.9	< 1
polystyrene foam	1.3	3 – 4
sawdust	1.5	< 1*
wood shavings	1.9	4 – 5

* smoldered after 4 – 5 s
NI – no ignition

Tanaka[59] measured the propensity of welding slag to ignite sawdust, simulated by using steel balls of different diameters. He found that 550ºC was the minimum temperature of a steel ball needed for ignition, but that moisture played a major role when specimens had non-zero moisture content. From the experiments (which spanned a particle size range of 3 – 11 mm), a general relation was found:

$$MC = aD + b$$
$$a = 16.46 \log T - 45.06$$
$$b = 5.02 \log T - 13.71$$

where MC = maximum moisture content (%) for ignition, D = particle diameter (mm), and T = particle temperature (ºC). This relation is shown in Figure 2; it should not be used

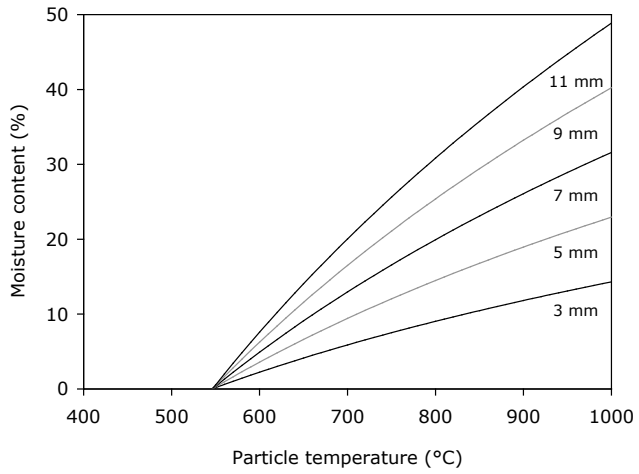


Figure 2 Relation between moisture of sawdust and size and temperature of spherical steel particle needed for ignition

below MC = 9%, which was Tanaka's lowest experimental value.

Okegawa et al.[61] examined the distances to which spatter from oxy-acetylene cutting and electric arc welding operations can travel laterally. When cutting operations were conducted at heights up to about 12 m, the lateral travel distance (including the bounce distance after the first collision with floor) was roughly similar to the welding height, but for larger heights, the travel distances were less than the welding height. In the presence of wind up to 5 m s^{-1}, peak travel distances increased by about 1/3. Cutting greater thicknesses of metal tended to propel particles to somewhat greater distances. The authors then created flammable gas atmospheres and found that arc welding and gas cutting operations readily ignited gasoline, methanol, benzene, and propylene oxide atmospheres, although particle sizes were not measured in the experiment. Particle sizes were measured by Kinoshita et al.[62], who found that a minimum diameter of 0.8 mm was needed for arc welding slag particles to ignite toluene/air mixtures, while 2.0 mm was needed for acetone/air mixtures. In another study[60], it was found that 0.9 – 1.4 mm particles could readily ignite a number of organic vapor atmospheres, but the minimum size needed was not explored.

BRANDS EJECTED FROM FIREPLACE

A British study[63] examined the potential for burning particles from a fireplace to set alight combustible materials. The investigators used particles of coal, which they ignited with a Bunsen burner and then dropped onto various materials in a simulated crevice geometry. A small, unspecified, air flow was used. When testing cotton wool, they found that even the smallest brand they could generate, 0.005 g (about 2 mm diameter) inevitably caused ignition. This is not surprising, since when the material is of low density, fluffy, or finely divided, ignition becomes very easy. This was the historical principle of the tinder box for starting fires using sparks from striking steel against flint. The tinder itself could be any fluffy, low-density combustible material. They also found that a tight-woven cotton rug (1200 g m^{-2}) could not be ignited with the largest brand used, 12 mm diameter. For other brands, the results are given in Table 7. The scrim was more easily ignitable than its surface weight would suggest because it had a brushed-nap finish.

Table 7 Probabilities of ignition of materials from fireplace brands

Material	Brand mass (g) needed for a given ignition probability	
	P = 50%	P = 10%
viscose rayon net (18 g m^{-2})	0.045	0.028
newsprint, layers (55 g m^{-2})	0.065	0.04
cotton (120 g m^{-2})	0.15	0.08
hessian scrim (220 g m^{-2})	0.11	0.04

In practical cases, the question will generally be not whether the brand can ignite a lightweight or fluffy material, but whether the ignition will be carried on to a further substance of heavier density. For example, fireplace brands may ignite and burn up a rug fringe, without the fire propagating to the rug itself.

FRICTION AND MECHANICAL SPARKS

GENERAL PRINCIPLES

Heat generated from friction can serve as an ignition source. Friction is also the cause of small luminous objects being emitted (mechanical sparks). There is a significant overlap between friction and impact, and impact involving friction is covered in the present Section. 'Pure' impact, without friction, is considered in a later Section. The ignition of explosives from friction is treated in Chapter 10.

Most studies on frictional ignition have dealt with ignition of combustibles in the form of flammable gas atmospheres or dust clouds. Because of the high temperatures that can be created, bulk solids can also be ignited, but few studies of those exist. In the 19th century, a common frictional ignition source used to be overheated bearings on rail cars. During the 20th century, frictional ignition of cotton within cotton gins was studied to a limited extent[64].

When two solids are placed together, they do not make uniform contact, since surfaces are always uneven on a microscale. The points of contact are limited and occur where the highest protuberances are found. If the solids are now rubbed against each other, heating occurs primarily at the high spots. The temperature rise is surprisingly high and is, in general, only limited by the melting point temperature of the lower-melting solid. This limit does not apply if one of the materials (e.g., many metals) can be easily oxidized and the oxidation reaction is highly exothermic[65]. Perhaps unexpectedly, a liquid applied between the surfaces does not

prevent the high temperatures. If sufficient properties of the system (surface condition, thermal conductivity, velocity, etc.) are known, then theories exist[66] which allow the interfacial temperature to be calculated. These data will rarely be available, and even if the temperature of the asperities could be calculated, this does not suffice to determine the ignition potential. Thus, the problem is usually approached empirically rather than theoretically. The lifetime of the hot spots is only a few milliseconds or less, thus ignitions directly from the surface hot spot are not able to ignite most gas mixtures. Ignitions become more likely when heated spots break off the surface and become 'mechanical sparks.'

Powell[70] suggests that for many substances it is a good assumption to take the friction coefficient μ as ≈ 0.5. The friction energy developed can then be evaluated as 0.5 × force × rubbing speed. Benz and Stoltzfus[67] considered that an ignition criterion can be expressed as pressure × velocity, or power per unit area (W m^{-2}). Their results obtained in high-pressure, gaseous O_2 environments are discussed in Chapter 13. To be an accurate expression of power delivered in frictional heating, the expression should also contain the friction coefficient. However, Benz and Stoltzfus conducted limited studies to determine friction coefficients and found that the value varied greatly with temperature and, consequently, with interface heating conditions. An ASTM publication[68] has compiled relative data on the pressure × velocity product needed for ignition of a number metal/metal combinations in a high-pressure, pure-oxygen atmosphere.

Billinge[69] studied 106 UK accidents involving ignitions of gases, vapors, or dust clouds due to friction and impact and, on that basis, divided the accidents into three categories:

(1) low energy; can be caused by hand tools. Typical energy: 10 J.
(2) medium energy; can be caused by powered hand tools. Typical energy: 1 kJ.
(3) high energy; can be caused by major collisions on land or sea. Typical energy: over 1 MJ.

Gasoline vapors were reported to have ignited from hammers, boot nails against a concrete floor, metal tools dropped to the floor, and various more energetic sources; Billinge, however, expresses some doubts as to the accuracy of investigation for the lowest-energy of these causes. A screwdriver punching through a metal lid of a can of floor polish was able to cause a flammable vapor ignition. Propane was ignited by a metal wrench against a pipe joint. Ethylene was ignited by unscrewing a valve from a pipe. Hydrogen and carbon disulfide have been readily ignited from low energy actions. Methanol has been ignited from a rubber belt rubbing against a copper tube. Solvents have been ignited by friction between cellulose film and a roller. Grain dust proved readily ignitable from low-energy contact of tramp metal against pipes and hoppers. Flour dust has also ignited from causes where no impact component was involved—overheated motors and overheated pulleys. Corn and sugar dusts have ignited from similar rubbing incidents. Ammonium perchlorate and aluminum powder both have ignited from scraping hand tools. Substances involved in UK case histories studied by Powell[70] and Billinge are summarized in Table 8. From this orientational listing it should not be inferred that every substance can be ignited by a low-energy impact of every moving object listed against every target; detailed case histories should be consulted for specifics.

Table 8 UK case histories on ignitions caused by low-energy friction/impact activities

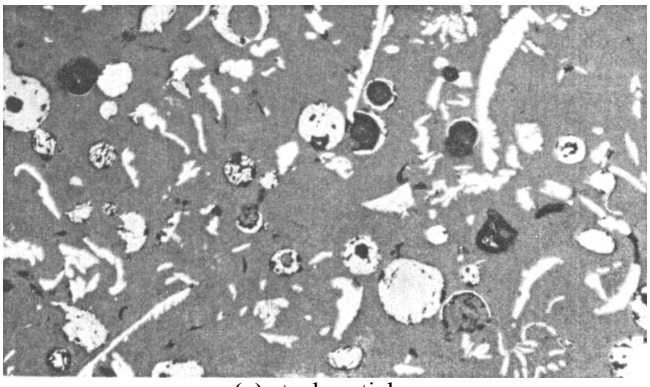
Object moved	Object struck	Substance ignited
aluminum hand tool boot or shoe nails brass rod metal pipe connector steel hand tool various heavy metal objects moved	brickwork caked material concrete steel	ammonium perchlorate carbon disulfide cellulose lacquer denatured alcohol diazonium salt ethylene gasoline grain dust hydrogen LPG paint thinner propane thermite town gas

Mechanical sparks are small incandescent particles (typically, 0.1 mm) created by impact forces or friction or grinding. Some grinding sparks photographed by Blickensderfer et al.[71] are shown in Figure 3. Friction between two objects raises the temperature at the point of contact. Since contact is not smooth, high forces produce high temperatures and can lead to hot fragments of material breaking off. In the case of impact, the kinetic energy is converted to heat energy and the process is otherwise identical. If the material is oxidizable, once a surface is opened up by breaking off material, heating can also occur due to oxidation at the virgin surface, but this relative contribution to heating has not been separately quantified.

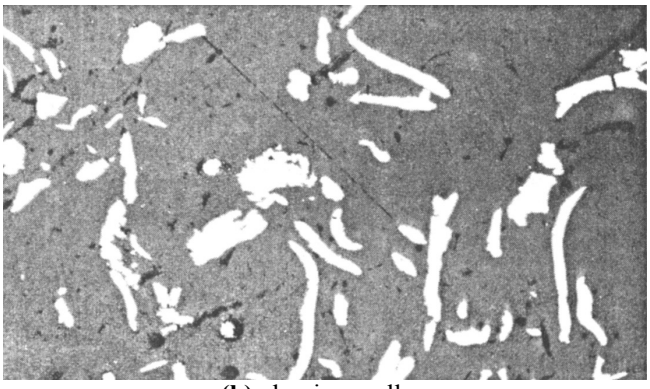
When sparks are generated by impact, it is not generally possible to relate the ignition probability to the potential energy imparted into the colliding solids. The vast bulk of the energy goes into causing elastic and plastic deformations in the solids, which do not contribute to the possibility of igniting a gas or dust cloud. Only a tiny fraction of the energy is released in the form of incandescent particles that may be incendive.

The propensity of materials to cause incendive sparks is related to the *melting point* of the material which has the lowest melting point of the rubbing materials. Since the contact area temperature cannot exceed this value, lower melting point materials tend to be safer.

The metals most likely to cause sizeable sparks upon impact or friction are cerium, zirconium, titanium, and uranium; similar tendencies are predicted in some other elements—samarium, thorium, yttrium, etc.—but these are only rarely used[72]. Depleted uranium has been added to military projectiles specifically to produce sparking[73]. The rare-earth elements cerium, lanthanum, neodymium, and praseodymium are used in making *misch metal*, which is used for cigarette lighter flints, where their sparking propensity is deliberately utilized.



(a) steel particles



(b) aluminum alloy

Figure 3 Grinding particles (100× magnification) from two metal types; particles were mounted in epoxy, then ground and polished to show their cross-sections

Temperatures of certain sparks have been measured optically (Table 9). These values can be misleading in actual applications, since the environment of interest is a fuel/air mixture, not air alone. Studies have indicated that the temperature of mechanical sparks is lower in fuel/air mixtures than in pure air. For example, steel sparks produced by a grinding wheel that were measured at 1850ºC in air, had a temperature of 1750ºC in a methane/air mixture, and less than 1500ºC in mixtures of air with town gas, hydrogen or acetylene[70]. In a nitrogen atmosphere, under the most extreme conditions, a temperature of about 1400ºC can be attained by the friction mechanism, but generally particles may not be visible at all[74] or will only reach a dull-red temperature[71].

Increasing contact pressure, up to a certain point, increases the temperature of the spark. Sparks produced with low contact pressures normally neither reach their melting point nor burn. In most cases, it would appear that actual combustion of the flying particle is taking place and not merely incandescence due to high temperatures. For the same pair of materials, the temperature of grinding-wheel sparks is lower than of mechanical-impact sparks, but the incendivity of grinding-wheel sparks is generally higher than that of impact sparks; presumably this is due to the higher abundance of sparks in a grinding operation.

Table 9 Temperatures of mechanical sparks created in air

Striking object	Target material	Temp. (ºC)	Ref.
mild steel	rusty steel	1730 – 2380	75
mild steel	concrete	2530 – 2730	75
mild steel	rotating grinding wheel	1600 – 1730	75
mild steel	rotating grinding wheel	1730 – 2130	78
alloy steel	rusty steel	1530 – 1980	75
titanium	rusty steel	2030 – 2900	75
titanium	NA	2100 – 2400	76
pyrophor bar	NA	2400 – 2700	76
magnesium	NA	3700	76

Apart from direct heating due to friction, an additional effect can occur with certain materials. Substances which can undergo a local oxidation sustain additional heating and can build up to much higher temperatures. The most common form of this is a *thermite* reaction, occurring between rust (iron oxide) and aluminum. The thermite reaction is discussed in Chapter 10. A thermite-type spark is visually distinguished by a white flash, rather than a small, darker-colored spark. It has been shown that thermite caused sparks can ignite many flammable dust mixtures, not only gases[77].

The *size distribution* of particles generated by rubbing steel against a ceramic grinding wheel[78] has been found to be 40 – 140 μm, with most particles being in the 60 – 100 μm range.

IGNITION OF FLAMMABLE GAS ATMOSPHERES

As a potential ignition problem, mechanical sparks have been recognized for a long time in coal mines. The mines commonly have pockets of methane and other flammable gases which can be ignited if a suitable ignition source arises. Hand picks, coal mining machinery, and rock-against-rock are all causes that have led to mine explosions. The possibility of such ignitions was already known in connection with some early coal mine machines in 1786, although the first mine explosion definitely attributed to spark ignition did not occur until 1896[79]. In the 18th century, it was common in some mines to use a 'Spedding steel mill' for lighting purposes[80]. This was a rotating steel wheel against which a piece of flintstone rubbed, creating a shower of



Figure 4 A Spedding steel mill of the 18th century

bright, long sparks (Figure 4). Accusations were made that such sparks can ignite methane/air mixtures in mines, but tests much later[81] showed that this was not possible.

Coal mine explosions from sparks have been relatively rare, since steel-against-rock sparks are only marginally incendive for methane/air mixtures. During the 1920s it was already identified that friction of quartzitic or micaceous sandstone against other rocks or against metal was typically needed for ignition. Since quartz is known for its piezoelectric characteristics, theories have been proposed relating the ignition from quartz surfaces to electrical effects, but these have not won much acceptance. Later studies[82,83] identified at least a dozen factors which must be considered in determining whether a mechanical spark will be incendive towards a flammable gas or dust cloud atmosphere:

(1) type of fuel
(2) composition of the gas or dust mixture
(3) anvil material
(4) striker material
(5) geometry and roughness of the impacting surfaces.
(6) angle of contact between striker and anvil
(7) frequency of striking
(8) length of striking contact
(9) pressure applied at the interface
(10) energy expended at the point of striking
(11) direction of travel of sparks
(12) nature of the spark: size, temperature, and possibility of strong exothermicity.

Tools cutting into harder rock are more likely to produce incendive sparks than when cutting into softer rock. Striking rock bearing iron pyrites produces dull red particles that start to rapidly oxidize in air and become a brilliant shower of yellow sparks. Despite the copious amount of sparks produced, it was found impossible to ignite methane/air mixtures with such sparks, apparently because they were too short-lived[84]. Negative results were also obtained for ironstone. Furthermore, it was found that when ignition of methane/air atmospheres occurs, upon rare types of vigorous, concerted blows given to sandstone rock, a shower of sparks is not emitted, rather, there is seen only a localized yellow flash at area of impact.

The susceptibility of gases to mechanical-spark ignitions varies greatly with the gas. Mixtures containing a significant component of hydrogen are relatively easily ignitable, whereas methane/air mixtures less easily. A methane concentration of 6.4 – 7% leads to the most incendive conditions[83]; this is leaner than the stoichiometric value of 9.5%. For pentane, the most ignitable concentration is 3.2%, which is richer than the stoichiometric value of 2.6%. For hydrogen, the most easily ignitable concentrations are 10 – 20%, with there being no real peak; the stoichiometric concentration is 30%.

On the order of 50 J impact energy is required to ignite optimum-concentration methane mixtures from a magnesium alloy weight falling onto rusty steel at the optimum angle[83]. By contrast, steel-upon-rusty-steel caused no methane ignitions even at 1000 J energy; about 400 J was found sufficient to ignite hydrogen atmospheres.

Even 'non-sparking' tools made from materials such as copper-beryllium can ignite various flammable atmospheres, if struck against a surface where aluminum particles are lodged on rusty steel. It is has been shown, however, that for ignition to occur, particles of aluminum must first be lodged onto a rusty steel substrate, then struck with another object; striking rusty steel with an aluminum tool is *not* sufficient[75]. This is because a hard collision is required and aluminum, being a soft metal, easily deforms. Striking aluminum-containing paints may be lead to ignition, but only if the surface is preheated and only then under certain circumstances. In one series of tests, such paints were used to coat rusty iron surfaces, then struck with a steel rod[85]. It was found that, with certain paints, bright sparks could be produced, but none were incendive in a town gas mixture. When the painted surface was heated, the brightness of sparks generally increased, but still only non-incendive results were obtained. But other studies showed that most tools, even rubber hammers, struck against a preheated (ca. 175ºC) steel plate painted with aluminum paint were able to ignite various gas mixtures[105].

The current understanding is that the ignition of methane/air mixtures by a frictional contact of two surfaces requires a surprisingly high temperature of 1200 – 1250ºC to be attained[79]. This explains the propensity of quartzitic rocks for mechanical-spark ignitions, since they are one of the few rock types which do not disintegrate at this temperature[86]. Also, it explains why ignitions are not seen against brass (T_{mp} 900ºC) and not readily with copper (T_{mp} 1085ºC), but

more readily with steel (T_{mp} 1450ºC). Such high temperatures needed for ignition also indicate that friction-generated sparking is not very incendive. On the basis of high-speed photography studies, Blickensderfer[87] documented that the ignition normally arises from the hot streak caused on the rock, rather than from the more visible shower of sparks emanating. He was able to model the ignition process by representing the details of the surface heating process, then evaluating the consequences according to the gas ignition requirements of heated area vs. temperature. In some carefully arranged experiments[88], the shower of sparks was also shown independently to be incendive, but this is a moot point, since incendive sparks were only produced from rocks where the hot surface was already capable of causing ignition

Rae[86] conducted experiments where he rubbed a quartz slider against a quartz wheel at various speeds and pressures to determine the potential to ignite a methane/air atmosphere. His results showed that ignition corresponded to $\mu \times$ mass $\times$ rubbing speed = 0.67 $\times$ 114 kg m^{-1} s^{-1}, where 0.67 is the coefficient of friction. This can be converted to power by noting that 1 N = 9.8 kg m s^{-2}, so that $\mu \times$ force $\times$ rubbing speed = 76.4 kg m^{-1} s^{-1} $\times$ (9.8 kg m s^{-2}) = 749 kg m^2 s^{-3}. But 1 kg m^2 s^{-3} = 1 W, therefore the power needed for ignition was 749 W. He also noted that the melting point of pure quartz is 1700ºC, but that quartzitic rock has a melting point around 1250ºC. Some synthetic materials commonly used as grindstones include silicon carbide (carborundum) and aluminum oxide (corundum). These can withstand higher temperatures than can quartzitic rocks, and Rae also obtained ignition data for them. The results were similar for carborundum as for quartzitic rocks, but corundum required about 2200 W for ignition. In earlier tests at the same laboratory[88], it was found that 269 W sufficed for ignition in one case when using 'Derbyshire grit' sandstone, although 400 W or higher was a more typical outcome. These results are all rather approximate, since the coefficient of friction is not a material constant but depends on the actual conditions at the interface[89].

Later in the same laboratories, Cutler and Brearley[90] used a steel cube held against a rotating steel disc as the ignition machine. They considered that the coefficient of friction varied over time, so they presented their results simply as the minimum load, in newtons, needed for ignition at two different rubbing speeds (Table 10). In all cases, stoichiometric fuel/air mixtures were used and test duration was 4 min. The authors point out that they consider their results for diethyl ether to be anomalous, since, under most conditions, this is a very easily ignitable vapor. According to constant-power scaling, the required load at 20 m s^{-1} should be ¼ of that at 5 m s^{-1}. The results, however, do not follow the this dependence. It has also been suggested[71] that ignition propensity should be proportional to (pressure)^2×(speed)^4, but again this apparently holds only in very limited experiments. Thus, in general, it can be concluded that increasing the pressure or the rubbing speed is likely to result in more incendive conditions, but quantitative predictions are likely to be possible only within narrowly-defined experiments.

Table 10 Load required for ignition of fuel/air mixtures by using a rotary rubbing machine

Fuel gas	Min. load for ignition (N)	
	At 5 m s^{-1}	At 20 m s^{-1}
hydrogen	120	<120
propylene oxide	250	500
ethylene	250	600
methanol	850	625
diethyl ether	900	600
propane	1100	800
acetone	1200	500

Many experiments on grinding operations have been reported[91], where it was found that a minimum velocity is needed for the sparks generated to be incendive to gas/air mixtures. Incendive sparks from steel at less than 1 m s^{-1} are considered not possible[92]. But it does not appear that the minimum velocities as measured have much absolute significance—the details of the experimental rig are of paramount importance. A study by the Bureau of Mines[93] indicates that, using conventional US mining machines, it is not feasible to reduce velocities sufficiently to appreciably decrease the probability of ignition simply by this strategy.

The effect of angle on the incendivity of an impact was studied by Titman[83,94] who found that the worst case is around 50° (Figure 5). For worst-case conditions involving an aluminum smear on a steel plate, impact/sliding velocities of about 2 – 3 m s^{-1} are necessary to ignite a methane/air atmosphere[95].

For a specified particle temperature, a minimum mass of particle is required to ignite a given fuel/air mixture. Bowd-

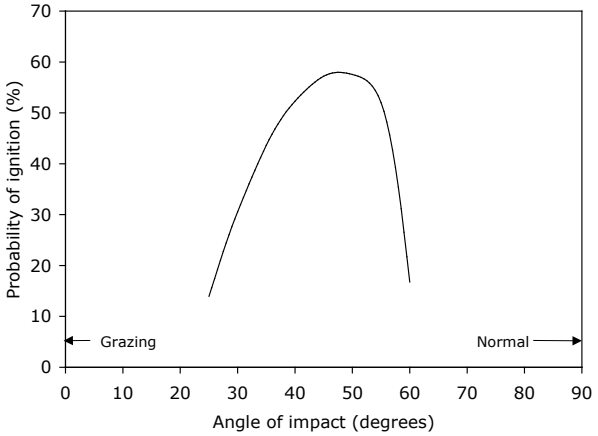


Figure 5 Effect of impact angle on the probability of igniting methane/mixtures by an aluminum-alloy weight falling upon a steel plate

en and Lewis[65] provided illustrative data on some readily oxidizable metals (Table 11). The results were obtained by heating the particles on a surface maintained at 1100ºC, and then permitting them to ignite and reach their combustion temperature. They point out that the mass required is inversely related to the heat of combustion, although the relation is not particularly linear. Under the same conditions, beryllium, carbon, iron, spongy platinum and black platinum were not able to cause ignitions at all. The data are presented at 6.8%, because they found that, in their experiments, this was the most-readily ignitable concentration. In a related study[96] where methane concentration was varied, Bowden found that most of the metals showed a marked increase in mass needed as methane concentrations moved farther away from 6.8%. But for aluminum, magnesium, and pyrophor bar, no change in the mass needed was found over the entire range explored, 5 to 9%.

Table 11 Minimum mass of a burning metal particle needed for the ignition of 6.8% methane in air

Metal	Min. mass (µg)	Heat of comb. (MJ kg^{-1})
aluminum	< 1	31.06
magnesium	< 1*	24.73
titanium	4	19.6
zirconium	6	12.03
pyrophor bar	18	--
cerium	85	7.77
thorium	108	5.29

* In SMRE tests[97], a 0.5 µg magnesium particle of 80 µm diameter was sufficient for ignition.

Bowden also noted that the order of incendivity shown above was *not* duplicated in experiments where metals were pressed against a rotating wheel. In fact, he was unable to cause ignition with aluminum and magnesium at all under these conditions. This was attributed to the fact that these soft metals smeared, rather than launching broken off particles. Titanium did launch small particles, but the particles themselves failed to ignite. Roughly, he concluded that the incendivity of metals in a grinding situation is proportional to their brittleness, not their heat of combustion.

It has been found that, when struck by steel tools, pyrite-bearing rocks readily produce a brilliant shower of sparks, but that the sparks are much less incendive than ones from sandstone rocks. While in experiments, pyrites have required heating to only 200 – 300ºC for oxidation of powdered material to proceed rapidly enough so that flaming of the sulfur component occurs, ignitions in practice have been very rare. The actual ignition mechanism, in contrast to other steel/rock impacts, was found to be the generation of a significant cloud of pyrite dust in the air, a small amount of particles not being able to ignite a methane/air mixture[98]. An experimental study where 30,000 strikes of steel against pyrite were made produced copious sparks but no ignition of 7% methane/air atmospheres[79]. Despite the lesser likelihood, disastrous explosions nonetheless have occurred due to mining tools striking pyrite deposits.

If rock particles are sucked into a ventilating fan (e.g., in a coal mine) in the presence of a flammable atmosphere, an incendive spark may be emitted. The effect of particle size on spark-producing tendencies was studied[99]. It was found that the most powerful sparks were emitted from particles of 3 – 6 mm size. Smaller sparks were emitted from particles of 1 – 3 mm and 6 – 10 mm, with no sparks for particles smaller than 1 mm or larger than 10 mm. The size dependence will vary somewhat with test conditions, nonetheless, the results can be viewed as at least rough guidance.

A coal mine explosion took place when a magnesium alloy drill fell onto a steel surface. Subsequent laboratory testing[100] showed that an explosion in a methane/air atmosphere requires as short a drop as 0.5 m of a 16 kg machine. The sparks seen comprised flaming magnesium particles, not just glowing. A repeat of the tests by dropping a steel machine onto steel plates caused sparks, but no ignitions for drop heights up to 2.3 m. Further testing[101] showed that the steel plate must be rusty, with no ignitions found otherwise. The tests also showed that rust acts due to a thermite mechanism and not due to its rough or abrasive qualities. Other studies[102] showed that ignition can be obtained with clean steel at very high impact velocities (greater than 250 m s^{-1}). Explosions were also found possible by dropping magnesium weights onto brass, but this was fairly difficult and generally required either two successive impacts or dirty surfaces. The reactions involved in dirty surfaces were not explored in detail, but might have been of the thermite type. The Bureau of Mines investigated in some detail a mine explosion triggered by breaking roof bolts and collapse of roof[103]. Laboratory studies, however, were unable to reproduce the conditions needed for ignition by impact involving the particular type of rock and grade of steel.

An old study[104] groups elements into two groups with regards to their potential for incendive sparks:

High sparking potential

calcium, carbon, cerium, copper, iron, nickel, potassium

Low sparking potential

aluminum, beryllium, cadmium, gold, lead, magnesium, palladium, platinum, silver, tin, zinc.

Aluminum, copper, and magnesium do not produce sparks from grinding operations. However, aluminum produces sparks in impacts and magnesium is especially problematic in this regard[105]. Carbon steel against a carborundum grinding wheel produces sparks which ignite carbon disulfide; however, most other substances, including diethyl ether, methane, acetone, ethanol, and benzene are not ignited. The sparking propensity of mild steel and high-carbon steel is the same. If aluminum foil is placed on rusty steel and struck with a hard object, flammable gas mixtures can be ignited much as from aluminum smears[106].

Table 12 Probabilities of ignition for impacts of various materials against quartzitic sandstone

Moving material	Impact energy (J)	Percent ignitions			
		15% hydrogen /air	4% ethylene /air	3% propane /air	7% methane /air
tungsten carbide stud	117		26	1.8	0
	225				0.2
hobnail	117		43	25	0.2
	225				0
tool steel	117		73	24	1
silver steel	117		72	4	1
	255				0
	289				14
mild steel	255				0
	289				0
aluminum bronze	117		82	24	1
copper-beryllium	117		83	20	2
fused quartz	117	100	10		
lamp glass	117	47	5.5	2.8	0
bottle glass	117	39	0.72		

Desy et al.[107] constructed an impact testing machine whereby a head of a chosen material hit a blow onto a target plate made of rusted steel. The angle of contact was at 5º off-normal and the contact velocity was 48 m s^{-1}. The frictional energy dissipated in the contact tended to vary from run to run, due to wear on the head, but was roughly 20 – 35 J. All aluminum alloy heads showed a finite probability of ignition of a 6.4% methane/air mixture, although harder alloys generally exhibited a higher probability than softer ones. No ignitions occurred using structural steel, stainless steel, brass, or fiberglass heads. Aluminum heads were also unable to cause ignition when an aluminum target was substituted for the rusted steel.

Higher machine speed and blunter tool surface lead to a higher probability of ignition. This is due to larger heated areas that are created at higher velocities, not due to raising of peak temperatures. Various other practical matters pertaining to the ignition of methane atmospheres by coal-mining tools have been reviewed by Trueman[108]. Much empirical research has gone on in the coal mining field to develop tools and techniques which reduce the ignition probability. The design of the tool surfaces and the optimized incorporation of water sprays are two salient prevention strategies.

Ignition of flammable gas atmospheres by mechanical impact sparks was studied by Powell[109]. He constructed a rig for simulating the impact of boot nails and other impacting objects onto quartzitic sandstone (Table 12) and steel targets (Table 13). The mixture fractions were selected to correspond to near-worst ignitability conditions. No ignitions were observed against steel targets with methane and propane mixtures. In some cases up to 500 trials were conducted, but there is a lot of randomness evident in the results. In all cases, however, it was seen that the incendivity of the mixtures ranked as:

hydrogen > *ethylene* > *propane* > *methane.*

Magnesium/aluminum alloys become significant more hazardous as a means of producing incendive sparks when the fraction of magnesium rises in the alloy[83], as shown in Figure 6. The hazard stays roughly constant once the composition exceeds about 11% Mg.

Cerium is particularly prone to producing incendive sparks, and this is the reason that cerium alloys are used as cigarette-lighter 'flints' or 'pyrophor bars.' These typically contain 38% cerium and the remainder being rare earth elements. Very small pyrophor sparks are able to ignite methane/air mixtures, with data from Rae[110] being shown in Figure 7. Note that microgram weights suffice and that the leanest mixtures are the easiest to ignite. The temperature of a burning particle was estimated as about 2500ºC. Burning duration of particles in the range 30 – 80 μg was found to be ca. 20 ms, but surprisingly no systematic effect of mass

Table 13 Probabilities of ignition for impacts of various materials against mild, rusty steel

Moving material	Impact energy (J)	Percent ignitions	
		15% hydrogen/air	4% ethylene/air
tool steel	117		90
silver steel	117		0
mild steel	117	42	13
spring steel	117		25
aluminum bronze	117		0
copper-beryllium	117		0

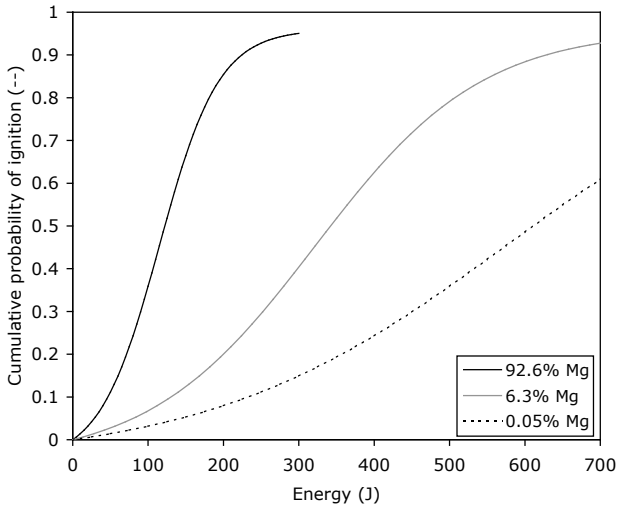


Figure 6 Probability of ignition of a 6.4% methane/air atmosphere by a glancing blow of light alloys on rusty steel

was seen. For other materials tested, ignition of a 5.6% methane mixture with magnesium particles required about 1 μg, while iron pyrite required about 1000 μg (1 mg).

The potential of sparks to ignite flammable gas mixtures has generally been found to increase with increasing *diameter* of the particles. The study of Homan and Sirignano[111] was discussed in Chapter 4. They found that for aluminum particles, a minimum diameter of 0.02 mm was needed for methane/air mixtures. For steel sparks it was found that particles as large as 0.2 mm could be generated and that these were the most incendive[79]. The most incendive of particles tend to ignite mixtures which require about 0.15 mJ for an electric spark to ignite.

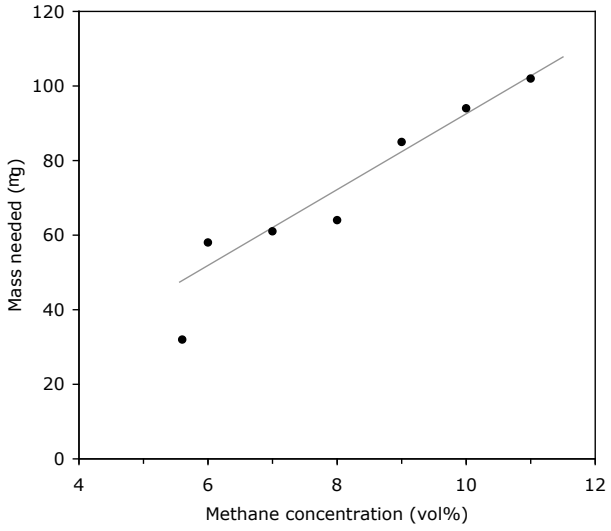


Figure 7 Mass of pyrophor particle needed for ignition of methane/air mixtures

The Bureau of Mines concluded that incendivity of grinding sparks is proportional to the radiance of the spark 'shower' and conducted extensive tests to measure this radiance[112]; the results are given in Table 14.

In actual fire incidents, grinding sparks have ignited ethylene, methanol, and oil vapor[69]. Lean mixtures are more easily ignited by grinding sparks than are rich ones[88]. *Sand blasting*[113] creates numerous, but 'dull,' sparks and tests have shown that these are unable to ignite a propane/air atmosphere.

Campbell[114] conducted large-scale tests to investigate the possibility that dragging metal in an airplane crash might ignite vapors and aerosols of flammable liquids on asphalt or concrete runways. Combustible mixtures were created using spray nozzles attached to the drag sled, and proof-

Table 14 Radiance of spark showers of various metals, as determined by Bureau of Mines

Metal	Radiance ($W\ m^{-2}\ sr^{-1}$)
aluminum	0
beryllium bronze	0
brass	0
copper	0
magnesium	0
zinc	0
chromium	< 0.1
Inconel	< 0.1
molybdenum	< 0.1
Monel	< 0.1
nickel	< 0.1
stainless steel 304	0.30
tungsten carbide	0.30
stainless steel 316	0.55
tungsten	0.60
Fe/20V[a]	1.00
Fe/20Cr	1.62
Fe/20Ni	3.77
Fe/2Si	5.63
Fe/10Al	5.93
Fe/6Si	7.01
titanium	7.43
iron	7.87
Fe/0.3Cu	9.13
Fe/20Co	9.70
Fe/5W	11.00
columbium	13.33
manganese	13.67
Fe/5Mo	17.03
vanadium	17.58
zirconium	21.33
Fe/3Ti	29.11
Fe/20Mn	31.80
steels, carbon[b]	7.5 - 18.0

a – iron compounds designated by percent of second element, with remaining being Fe
b – depends on carbon content

tested using electric spark plug ignition. The test conditions varied were slide speed, slide time, bearing pressure, fuel type and metal type. Despite a large amount of data collected, the main conclusions were straightforward:

- Aluminum (2024-T3 alloy) did not cause any ignitions at speeds up to the maximum explored, 18 m s^{-1}.
- A minimum pressure of about 125 kPa was needed to generate incendive sparks.
- Speed did not greatly affect the results, down to the lowest speed used, 2.2 m s^{-1}.
- Significant differences were not found for ignitability of gasoline, kerosene, JP-4 fuel, or SAE No. 5 lubricating oil.
- Alloys readily causing ignitions at pressures above 125 kPa were titanium (Ti-100A), magnesium (FS1), chrome-molybdenum steel (SAE 4130), and stainless steel (AISI 347). When using one of the steels, generally higher speed, pressure, or time were required for ignition to occur, in comparison to titanium or magnesium. Titanium was somewhat more incendive than magnesium.
- An asphalt surface was marginally safer than concrete. The aggregates in both were slag or limestone, and a higher propensity to ignition would have been anticipated had quartzitic aggregate been used.

Campbell attributed the lack of ignitions from aluminum to the fact that luminous particles were not observed in the drag sled experiments. To further explore the incendive traits of aluminum, he used a grinding wheel to grind the same aluminum alloy in a darkened room. Only rare, tiny, and barely luminous sparks were observed.

'*Non-sparking*' tools for coal mining are made out of brass, bronze, aluminum, wood, etc., which are materials that do not readily produce a burning spark. Powell[115] concludes that no 'non-sparking' metal is safe if it is struck against sandstone or quartz-bearing rock or concrete. Also, small particles can become imbedded in the surface of any tool and then the active surface will be of the inclusion, not of the base material. In the petrochemical industry, studies and experience[116] indicated that (1) it is possible for sparks from hand tools to ignite vapors of petrochemicals; but that (2) it is extraordinarily rare that this will happen, i.e., that the probability of hand-tool sparks being incendive to petrochemical vapors is extremely small. Thus, it was concluded that the only value of non-sparking hand tools may be psychological, but that they are not necessary for actual risk reduction. This recommendation was motivated by the fact actual fire ignitions have been caused in the petrochemical industry by 'non-sparking' tools[118]. Powell points out that steel-against-steel impacts are a hazard in methane/air atmospheres only if the steels are very hard and if a considerable amount of energy (> 250 J) is available[70]. Methane, however, is among the less-readily ignitable gases, so different conclusions may apply to more readily ignitable gases. Power tools can readily ignite some gas mixtures, so their use must be carefully controlled. The US Navy[105] concluded that there would be no reduction of risk from use of non-sparking hand tools in the explosives industry. Overall, however, Powell considers that non-sparking tools have merit, even if they will not prevent all ignitions[70].

IGNITION OF DUST CLOUDS AND LAYERS OF POROUS MATERIALS

The effect of the melting point of the metal on incendivity towards dust clouds was studied by Dahn and Reyes[117]. They found that several types of steel rods contacting a stainless steel surface at high speeds could ignite dust clouds, but that, at the same test conditions, aluminum rods could not. The melting points of carbon steel and stainless steel are not too different, yet stainless steel has less of a propensity to produce incendive sparks. This is held to be due to lower rates of oxidation possible with stainless steel[118]. Brass is also a substance which does not oxidize rapidly; thus, the lack of incendive behavior here is due a combination of low T_{mp} and low oxidation propensity.

Using the same apparatus as described above for gases, Cutler and Brearley[90] conducted rubbing experiments to determine the load necessary to apply to a rubbing block for ignition of several dust clouds (Table 15). St1 and St2 refer to the German classification system for explosion pressures of dust explosions, with St2 being more energetic than St1. The rubbing speed was 20 m s^{-1} for all tests, with a test duration of 90 s. The test specimens differed widely in their particle-size distributions, so it is not clear if chemical or physical factors were dominant.

Table 15 Minimum load needed to ignite dust clouds with a frictional rubbing machine

Dust	Particle size range (μm)	Min. load (N)
sulfur	38 – 180	500
non-dairy creamer powder	38 – 250	700
corn flour (St2)	<38 – 75	750
corn flour (St1)	38 – 75	900
powdered coffee	75 – 500	> 1000
calcium stearate	<38 – 75	< 1125

Most studies have only examined the effect of controlling the velocity. In one study[75], both the velocity and the impact energy were characterized separately. It was found that the incendivity towards corn dust clouds was greater when, for a fixed impact energy, the velocity was *lower*. This was attributed to the fact that higher tool velocities cause greater turbulence, and higher turbulence increases the MIE of dust clouds.

In a study[75] on the incendivity of impact sparks towards corn dust clouds (corn was chosen as having among the lowest MIE values for common dusts), the results shown in Table 16 were found.

Table 16 Incendivity of impact sparks to corn dust clouds

Tool	Ignitions occurred for these targets	Ignitions did not occur for these targets
mild steel	--	mild steel, rusty steel, concrete, all types of rocks
titanium	rusty mild steel, concrete, sandstone	granite, gneiss, quartz, grinding wheel
aluminum	--	rusty steel

Morse[82] found that sparks created by rubbing steel files against an emery grinding wheel would not ignite a wheat dust cloud. Ignitions were also not obtained by striking quartzitic rocks against a steel file, however striking a cerium/iron-alloy flint against a steel file did cause ignitions. In another series of tests, quartzitic rocks of up to 0.91 kg were dropped from various distance up to 26 m onto steel files. During 1824 drops, intense sparks and sometimes local burning was observed, but no propagating explosions occurred. The tests were repeated with magnesium and aluminum alloy items of up to 2.3 kg dropped onto rusted, roughened steel boiler plate. Again, some localized burning was observed, but no propagating explosions.

Ritter[119] conducted extensive tests where grinding sparks of various materials were presented to dust clouds. From these studies, he evolved the generalized boundaries shown in Figure 8—any dust with values of MIE and AIT that fall below the specified line will be ignited by grinding sparks from the given tool-material held against a grindstone. It is seen that flintstone sparks are most incendive, while steel sparks are least, of the materials examined. Similar trends were also obtained for flammable gas atmospheres, but for those, unlike for the dust clouds, an effect of fuel/air ratio was also present. The boundary lines refer only to momentary-contact (0.1 s) events. If a piece of material is forcibly held down to a grindstone, then bulk heating occurs and more incendive sparks are produced. Ritter also examined some of those 'friction' sparks and produced the results of Figure 9. Not shown are Ritter's results on aluminum/rusted steel impact sparks. These were less incendive than any of the combinations portrayed in Figure 8 or Figure 9. Unlike steel, flintstone and titanium showed little difference between the incendivity of grinding and friction sparks.

Allen and Calcote[120] found out that the type of steel used greatly affects the ignitability of dust clouds of corn starch, when pressing steel against a grinding wheel. Iron nails showed a 10% probability of ignition, medium tool steel 30%, and high-carbon steel 70%. They also collected dust from a grain elevator and found that this 'natural' dust had a 15% probability of ignition from the high-carbon steel. The authors also found that the velocity of the sparks produced was 10 m s^{-1} when the peripheral speed of the grinding wheel was 30 m s^{-1}.

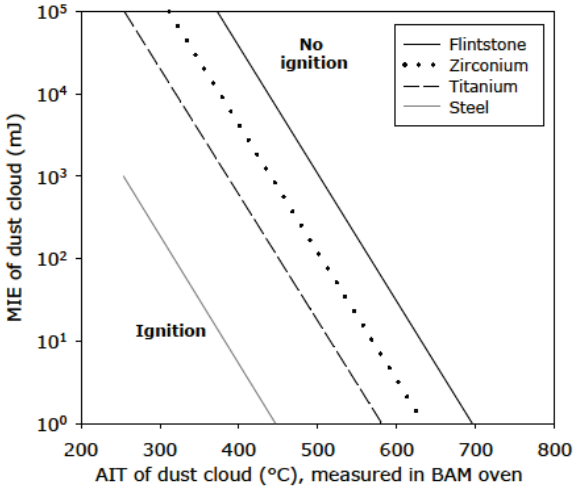


Figure 8 Ignitability of dust clouds by grinding sparks: regions of ignition and non-ignition for brief contact of material (no heating)

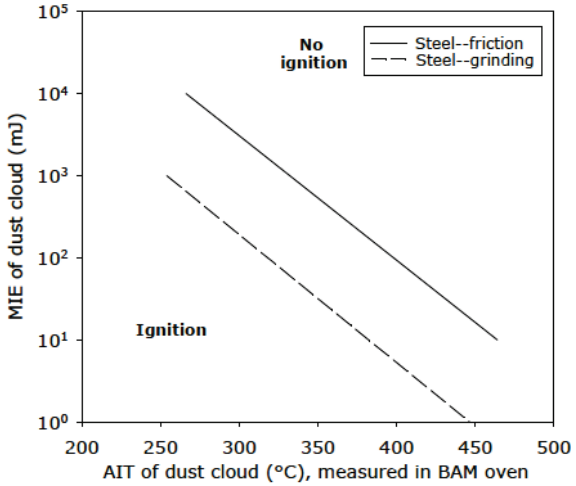


Figure 9 Ignitability of dust clouds by steel sparks: comparison of grinding (momentary) and friction (sustained heating) sparks

In addition to igniting gases and susceptible dust clouds, mechanical sparks can also ignite *dust layers* or other porous materials. Such ignitions are often smoldering rather than flaming, due to the limited amount of energy being delivered to the combustible. A case where grinding sparks flew up through a ceiling vent, and caused a fire by igniting an accumulation of dust in the void space has been reported[121]. In another case, a grinding wheel spark ignited hardwood dust, causing a flaming ignition due to the presence of an air blower[122].

Coal dust can be ignited by friction alone, if speed and force are sufficient, although the phenomenon has received only limited study[123].

Shock, impact, pressure, vibration

Kinetic energy or mechanical work (e.g., rapid compression) are ways in which external energy can be delivered to a substance and which, under some circumstances, may result in ignition.

SHOCK AND IMPACT

Shock waves can ignite gas mixtures and certain solids and liquids. Most solids and liquids are not reactive if shocked. The exceptions include explosives, pyrotechnics and other substances which are liable to decomposition. A number of theories have been developed for the shock and impact sensitivity of explosives, and these are considered in Chapter 10.

The ability of flammable gas mixture to be ignited by compression from a shock wave was first documented by Bradshaw[124] in 1907. Earlier yet work had shown that a rarefaction associated with a shock can also be the cause of ignition.

DROPPED OBJECTS

Broadly speaking, flammable atmospheres may be ignited by dropping forcibly enough one object onto another, if that same pair is also prone to frictional ignitions, but the probability of ignition is generally much lower than for frictional ignition. Bowden and Tabor[125] showed that when two bodies collide in 'normal' impact (no frictional sliding at contact) a temperature rise of only ca. 10ºC occurs for a closing velocity of 1 m s^{-1}. Yet, if the same bodies collide so that frictional sliding does take place upon contact, the temperature at the highest points along the interface will typically reach the melting point of the lower-melting solid.

Many explosives are sensitive to being initiated if dropped. In such an event, the potential energy is converted to kinetic energy and the kinetic energy, in turn, is converted into heat at the interface between the colliding objects. The drop height clearly is an important variable, as is the impact geometry, which governs deformation and, consequently, the effective surface along which the object and the target are tangent. What may not be obvious is that thermal diffusivity of the target is a dominant factor. In a study with an HMX-based explosive[126], three targets were used: quartz, aluminum oxide, and gold. The drop height necessary to initiate the explosive onto a gold surface was found to be about 400× that for the quartz surface, despite the fact that both these materials were prepared with nearly identical coefficients of frictions. The crucial factor was that the thermal diffusivity of gold is about 150× that of quartz.

HIGH-VELOCITY IMPACTING PARTICLES (UNHEATED)

A small particle can have significant kinetic energy if it is flying at high velocities, especially at or above the speed of sound. In an inelastic collision with a fixed object, significant energy can be imparted for the particle to ignite and, in some cases, to also ignite the target. NASA has studied the ignition potential of supersonic 2 mm aluminum spheres colliding into aluminum thimble-shaped targets in a pure-oxygen atmosphere at 28 MPa pressure[127]. The targets were all of the alloy 6061-T6, with a Type III, Class I hard anodization. The test variables were anodized layer thickness and the temperature of the target. A 50% ignition probability for a 3 μm anodized layer occurred for a 200°C target temperature. Specimens with a 20 μm anodized layer did not ignite until 360°C, while a 50 μm layer offered protection which was not exceeded by the maximum test temperature of 400°C. A target with no anodized layer was ignitable at room temperature. In another study[128] using large, 800 μm particles, it was found that stainless steel particles needed about 1/3 lower velocities to achieve the same probability of ignition as aluminum particles. However, steel targets were less ignitable than aluminum and Monel targets less yet.

PRESSURE (COMPRESSION IGNITION)

High temperatures can be created by the compression of gases, and, consequently, ignition can be achieved. This was first described[129] in 1802 by Prof. Joseph Mollet, in Lyon, France. Mollet had learned that a workman in a small-arms factory had accidentally discovered that tinder could be ignited by the hot-air discharge of an air-compression pump. A device to do this became commercially produced in 1806, and it was a hand pump, roughly similar to a bicycle pump. At a compression ratio of 18:1, a temperature of around 674ºC could be achieved, and this was enough to ignite tinder. The principle of compression ignition was put to more important use in 1893, when Rudolf Diesel invented the compression-ignition internal combustion engine. By 1922, Tizard and Pye[130] were presenting a theoretical study of the phenomenon.

During rapid compression, it can be assumed that no heat is lost from a system, that is, the process is adiabatic. If also no work is lost in the process, then the process is reversible and it is termed *isentropic*. For an ideal gas undergoing an isentropic compression, it is demonstrated in elementary thermodynamics that:

$$\frac{T_f}{T_o} = \left(\frac{P_f}{P_o}\right)^{(\gamma-1)/\gamma} = \left(\frac{v_o}{v_f}\right)^{\gamma-1}$$

where the subscripts on the temperature T, pressure P, and volume v are denoted as f for final state and o for initial. The dimensionless constant γ is defined as the ratio of the heat capacities, $\gamma = C_p/C_v$. For air $\gamma = 1.4$. The above equation will not always be quantitatively applicable, since at high temperatures and pressures, the gas may show non-ideal behavior. Bowden and Yoffe[131] treated the case of the non-ideal gas. Using the above equation, the highest final temperature will always be obtained using the lowest initial pressure. But for some forms of ignition, it is important to consider the total energy available in the compressed gas mass, not just its temperature. When starting from a low pressure, the mass is also low, thus it turns out that the peak

nominal energy available to be delivered to heating a specimen[132] does not correspond to $P_o \rightarrow 0$, but rather to $P_o = 0.308\ P_f$.

Ignition can also be obtained if gas compression energy is converted to a sizable pressure by means acoustic resonance. In such a scheme, a gas is introduced at high pressure into a resonant cavity, but is not compressed by piston motion. Some details have been published[73,133] on this ignition mode (sometimes termed *fluidic*, or *flueric*), but it is very rare, although a rifle based on this principle was once briefly marketed.

In addition to gaseous systems, compression ignition can occur if a liquid is compressed which has gas bubbles. Because the volume of the bubbles is more readily reduced than that of the liquid, hot spots develop at the bubbles, and these can serve as a local ignition source, if the substance is susceptible. This topic is discussed further in Chapter 10.

VIBRATION

Sensitive substances may be ignited by vibration. This may be direct mechanical vibration or shaking. But it can also take the form of acoustic energy or ultrasonic energy, both of which are pressure waves created in the air. Normally, objects in the air are highly inefficient in receiving acoustic energy. However, if *resonance* occurs, the efficiency increases many-fold. Resonance can occur when one or more dimensions of the physical object are equal to an integral multiple of the wavelength of the wave.

Vibration of rubber items in a compressed air system has led to cases where the rubber ignited from the heat induced by vibration; the sequence of events was also reproducible in the laboratory[134]. An additional example is given in Chapter 14 under *Fire hoses*. Evidently, the heating is such cases is highly localized, otherwise a gross mechanical failure would occur prior to the ignition temperature being reached.

Flames or remote objects

In some cases, the heat fluxes incident on the target are already known. For instance, they may come from the computations of a room fire model. If the heat source is an overheating object, the heat flux may often be computable by knowing the temperature, size, and emissivity of the object, along with the aid of view factors; these are discussed and tabulated in any textbook on radiant heat transfer.

A somewhat different effort is needed when the heat flux originates from a flame. The heat transfer from a flaming source will depend on numerous parameters. The most important ones include:

- fuel type (gas, liquid, solid; of various chemical compositions)
- heat output of the source
- the direction of the flow of flames (parallel to the target surface, or perpendicular [this is termed 'impinging'] or at various angles)
- distance from source to target
- type of oxidant (typically air, occasionally pure oxygen, as in an oxy-acetylene torch).

While these variables have all been studied in fundamental fluid mechanics or combustion science investigations, practical advice is somewhat scant.

SMALL BURNER FLAMES AND SMALL BURNING OBJECTS

A series of measurements on two Bunsen burner flames have been reported[135]. Natural gas was the fuel, and the burner was operated in two ways—with an inner blue cone, and without. The heights of the inner blue cones were: 25 mm (for the 100 mm flame), and 55 mm (for the 150 mm flame). Flame temperature measurements on these flames are shown in Figure 10.

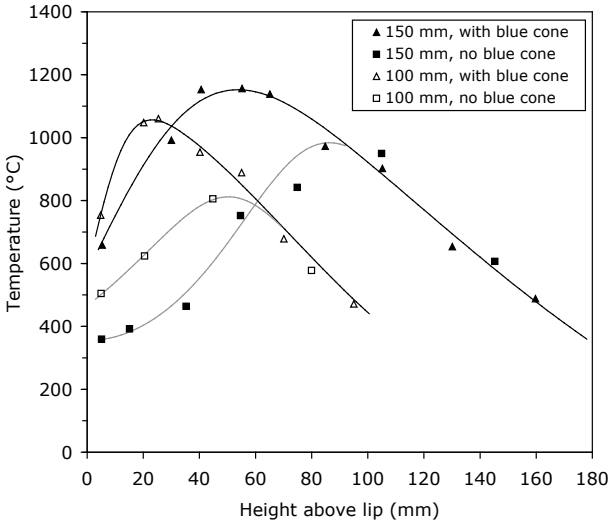


Figure 10 Temperatures in natural gas Bunsen burner flames

For most purposes, however, the heat flux, rather than the temperature, is a more useful measure of an ignition source. A NIST study examined various ignition sources, ranging from 5 W to over 300 kW[136]. The sources included both realistic igniting objects (cigarettes, matches, burning paper lunch bags, etc.) and laboratory sources (small gas burners and wood cribs). It was found that as the HRR of the ignition source increased, the peak heat flux generally did not increase. Instead, only the area covered by the peak heat flux progressively increased. For flames ranging from a 0.3 kW Bunsen-type burner to a 50 kW wastebasket, the peak fluxes were remarkably constant at 30 – 40 kW m^{-2}. Only a methenamine pill was significantly outside this range, a peak heat flux of 4 kW m^{-2} being seen for it. Quintiere[137] examined another set of experimental data and found a range of 20 – 50 kW m^{-2}. Similar conclusions can be seen from the compilation of Paul and Christian[138]. To illustrate

this constancy, Table 17 compiles data from several sources[139-141] on small burner ignition sources. Despite a wide variation in burner power levels, peak irradiance values are all clustered around 35 kW m^{-2}.

Table 17 Relation between HRR and heat flux for small burners

Burner type	Fuel	HRR[b] (kW)	Location	Peak heat flux (kW m^{-2})
needle flame	propane	0.035	45° upward	34 – 38
Kleinbrenner	propane	0.035	impinging	35
gas flame 1[a]	butane	0.081	[c]	35 – 40
gas flame 2[a]	butane	0.289	[c]	31 – 39
gas flame 3[a]	butane	0.633	[c]	20 – 40
tube burner	propane	2.8	45° upward	34
tube burner	propane	14.	45° upward	36
tube burner	propane	21.	45° upward	38
tube burner	butane	3.6	45° upward	36
tube burner	butane	18	45° upward	36
tube burner	butane	27	45° upward	36
tube burner	butane	18	70° downward	40 – 44
tube burner	butane	27	70° downward	50 – 52

[a] As defined according to BS 5852.
[b] Based on the net heat of combustion.
[c] Similar results seen for horizontal and 45° upward orientations.

LARGER FLAMING SOURCES AND BURNERS

KITCHEN SOURCES

Heat fluxes to potentially ignitable objects such as wooden cabinets located above a cooking pan holding burning vegetable oil have been mapped[142]. A 229 mm diameter cast iron pan was used to contain 0.5 L of burning oil. The heat fluxes are shown in Figure 11. Note that even at the highest distance measured, 0.76 m, the heat was 17 kW m^{-2}. The authors found that, at that height, 4 mm thick lauan plywood ignited in 2-3 min. A heat flux of 17 kW m^{-2} is enough to ignite even much thicker wood. For instance, at that heat flux, a 19 mm thick particleboard could be ignited in about 5 min. In the same investigation, it was determined that two gas burners set on maximum output would provide only 9.7 kW m^{-2} heat flux at a 0.23 m height and 1.1 kW m^{-2} at 0.76 m height. Thus, wood construction materials are unlikely to be ignited from gas burners alone, even if located at an unreasonably low height of 0.23 m above the burner.

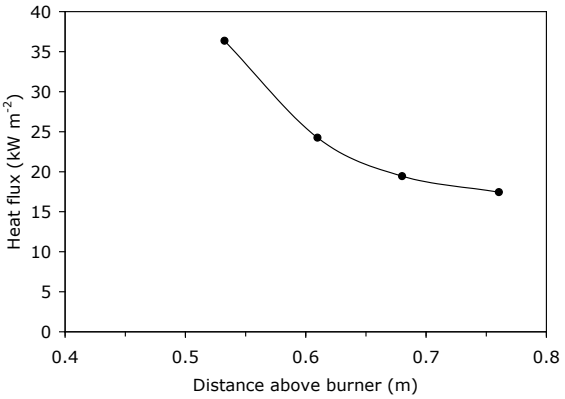


Figure 11 The heat fluxes measured from a pan of burning vegetable oil

LARGE LABORATORY BURNERS

A study done at VTT[143] examined gas burners with HRR values of 40, 100, 160, 230, and 300 kW placed against a wall. The burners released a stream of propane gas upward from a square face, which was filled with sand to diffuse the velocity of the entering fuel gas. Three different face sizes, ranging from 0.17 × 0.17 m to 0.50 × 0.50 m were explored. The peak heat flux to the wall adjacent to the burner was found to be much more dependent on the face size than on the burner HRR. A peak value of around 40 kW m^{-2} was seen with the 0.17 × 0.17 m size and 65 – 80 kW m^{-2} with the 0.30 × 0.30 m size. For the very large face size of 0.50 × 0.50 m, the peak heat fluxes were related to the burner HRR, and the original report should be consulted for those results. Published details are also available for a 50 kW porous-face burner[144] used at NIST for furniture testing.

An examination of the results for small and large burners (except for burners with unusually large face dimensions) shows that the peak flux is almost independent of burner power output, but the wall area adjacent to the burner subjected to a given flux level is nearly linearly proportional to the burner HRR. The latter point is illustrated in Figure 12. For the large-burner data, flame area contours were taken as corresponding to a 20 kW m^{-2} flux level; as a result there is a slight systematic mismatch between the large and small burner data sets. The correlation shown indicates a HRR/area ratio of 100 kW m^{-2}.

JETS AND HIGH VELOCITY BURNERS

A flame which impinges at 90º against a solid object can generate much higher heat fluxes than flames where streamlines flow generally parallel to the surface. The heat fluxes from burners in such orientation can vary from modest to exceptionally severe. On the mild end, a 'T-head' burner is used in some fire tests for upholstered furniture. It consists of a tube with numerous small holes, thus discharging at a higher velocity than is the case of Bunsen-type burners. Ohlemiller and Villa[145] measured heat fluxes as high as 70 kW m^{-2} in the impinging region of this burner's flame. In a parallel study using several different configurations of impinging flames from multi-hole propane and butane burners[140] more typical fluxes of 50 kW m^{-2} were seen. In another study on various commercial burners and plumbers'

blow torches, a maximum impinging-zone heat flux of 140 – 150 kW m^{-2} was seen[146].

For flames from large, premixed, turbulent methane/air burners, impingement region heat fluxes in the vicinity of 200 to 400 kW m^{-2} can be found[147,148]. Heat fluxes from high velocity, non-premixed jet flames[149] of fuel in air can reach around 300 kW m^{-2}. These are extreme cases corresponding to the hottest zone and for gas mixtures which are fairly close to stoichiometric. Moving the target away from the hot zone, or increasing dilution of the combustion stream will, of course, show progressively lower heat fluxes. More typical cases[149] may show values of only 100 kW m^{-2}. Flames with premixed oxygen show very high heat fluxes—for methane/oxygen or propane/oxygen flames, fluxes around 2500 kW m^{-2} have been measured[150]. Away from the center of the impingement, the heat fluxes will fall off. You[151] attempted to provide some scaling relationships for describing the fall-off in flux as radial or axial distances increase between the burner exit and the measuring point. These can give some guidance, but must be used with care, since they were developed using only very small fire sources and not verified against larger ones.

SOLID-FUEL IGNITION SOURCES

The heat flux to adjacent objects from a small wood crib or other solid-fuel ignition source is in the same 30 – 40 kW m^{-2} range as for gas burners. The picture is more complicated, however, for the heat flux from these sources to the object underneath. Data from wood crib sources[152] show small regions where heat fluxes in the vicinity of 90 kW m^{-2} can be found underneath the burning crib. Unlike other sources, where only radiative and convective heating from flames need to be considered, in this case the high heat fluxes originate due to direct conductive heating from a hot, glowing body. Such high values are, in fact, consistent with the temperature of the glowing char. The actual ignition process from such a source has not been characterized, however, since the heat transfer is definitely not 1-dimensional.

For most other solid-fuel ignition sources, localized very high heat fluxes are not found. For instance, Paul and Christian[138] examined the peak heat fluxes found underneath burning balls of crumpled newspaper and underneath wire baskets holding various amounts of shredded paper. The peak heat flux seen in this series of tests was 24 kW m^{-2}, with most experiments indicating substantially lower peaks, down to 7 kW m^{-2}. Another type of solid-fuel source is the 100 g paper cushion stuffed with newspaper used by the German railroads[153]. Döring and co-workers[154] found a maximum of 35 kW m^{-2} underneath the standard paper cushion. Variants of differing types showed flux peaks of 28 to 47 kW m^{-2}. There are some findings contrary to the above, however. Ohlemiller and Villa[145] found substantially higher heat fluxes associated with the newspaper-filled wire basket formerly used as a furniture ignition source by the State of California.

BURNING FABRICS

Miles et al.[155] measured the heat flux from burning clothing textiles. Values of only 5 – 17 kW m^{-2} were reported. These are not likely to be reliable measurements, since flame contact to the heat flux meter appears to have been erratic.

BURNING FURNITURE

One of the few larger-size commodities that have been studied as ignition sources is furniture. The earliest study[156] of burning furniture was relatively non-quantitative—heat fluxes were not measured, but ignitable targets were placed at varied distances. The results are given in Table 18.

To make quantitative heat flux measurements is not simple, since the heat flux varies with time and with the distance away from the object. In addition, the measured heat flux will also vary with the angle of the heat flux meter, but the data which are of primary interest are for vertically-oriented targets. Such measurements were made by Babrauskas[157]. A plot of irradiance values obtained at peak burning time for a 19.9 kg upholstered wicker couch is shown in Figure 13.

If the furniture item presented very small flames, or if the measurement was taken very far away, then radiation scaling would indicate that the heat flux would vary as r^{-2}. However, if either of those two conditions, held, then heat fluxes would be small and there would not be an interest in ignition aspects. Mizuno and Kawagoe[158], correlating measurements at distances of 1.35 – 3.0 m, concluded that scaling according to $r^{-1.8}$ gave better results. The scaling law of $r^{-1.8}$ applied to NIST data[144] gives an approximate predictive formula for the maximum distance at which target ignitions can be expected to occur. Figure 14 shows plots of the relation:

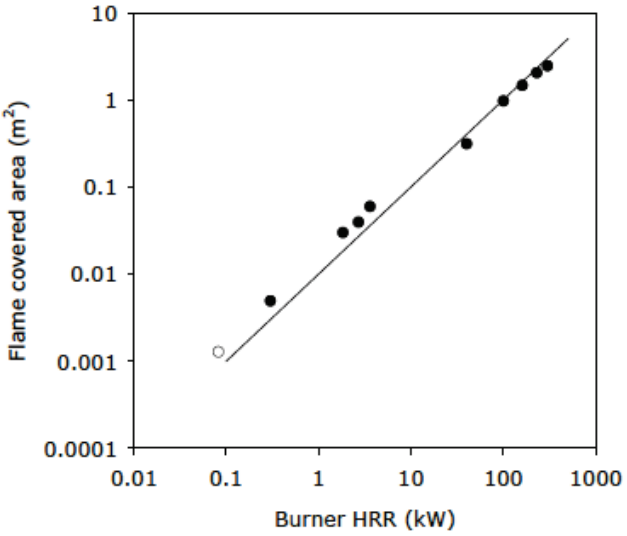


Figure 12 The relation between burner HRR and flame-covered area

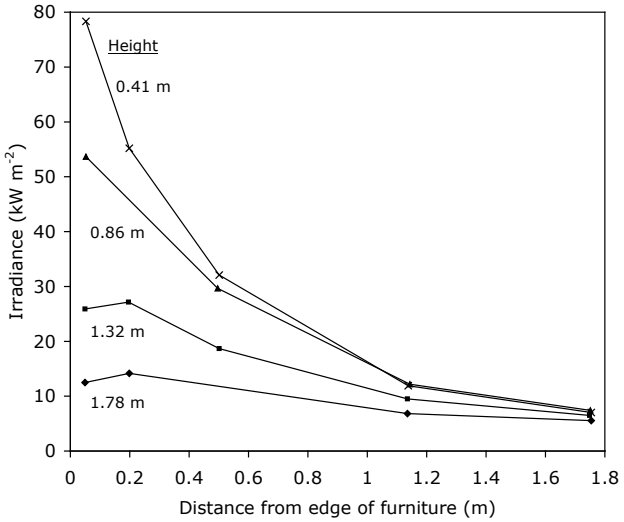


Figure 13 The irradiance to a vertically oriented target measured at the peak burning time of a 19.9 kg couch

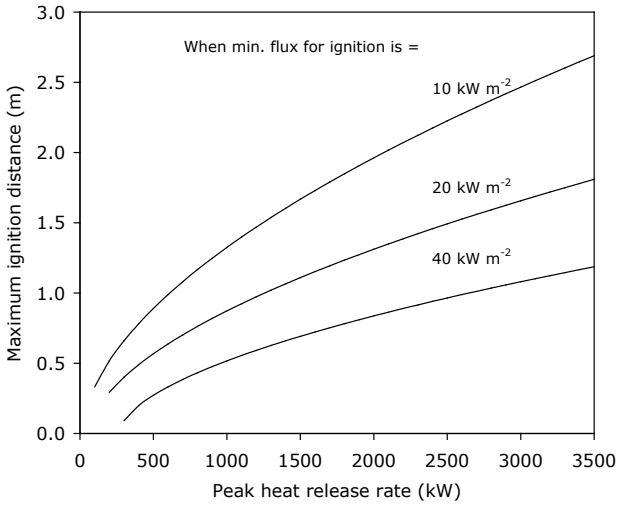


Figure 14 An approximation for the maximum distance at which target ignition is possible, as a function of the HRR of the burning furniture item

$$r = \left(0.0168 \frac{\dot{Q}}{\dot{q}''_{\min}} - 0.0028\, \dot{q}''_{\min} \right)^{0.56}$$

where r = maximum distance from edge of furniture item to target at which ignition is possible (m), $\dot{Q}$ = heat release rate (kW), and $\dot{q}''_{\min}$ = minimum flux for ignition (kW m^{-2}). A heat flux of 10 kW m^{-2} represents an approximate minimum flux for the piloted ignition of easily ignitable targets, such as other items of upholstered furniture. The heat flux of 40 kW m^{-2} represents an upper limit for the autoignition of most building materials and occupant goods. Thus, in most building fires these two values are expected to encompass the range of practical interest.

It is important to realize that burning furniture items, if placed very close to other combustibles, can readily cause ignition by direct flame contact. For instance, if a combustible wall surface is located a short distance behind a burning sofa, flames can directly ignite the wall and radiant flux calculations are not appropriate.

LARGE BURNING OBJECTS

LIQUID POOLS , WOOD CRIBS

The heat fluxes from burning pools or tanks of petrochemicals can be a severe ignition hazard. There are two basic cases to consider: (1) the object is engulfed in the flames; or (2) the object is remote from the flames. Peak temperatures[159] inside large pool fires of hydrocarbon liquids are typically on the order of 1000ºC. Thus, unless the material in question is combustible, yet very highly resistant to ignition, the ignition problem is trivial—ignition can be assumed to occur in a few seconds. Neill et al.[160] examined the heat fluxes to objects submersed in flames from small pool fires. Their measurements did not lead to predictive equations, but it is worth noting their observation that soot deposition occurred in hydrocarbon pool fires, although not in methanol fires. For fires where soot was being deposited, the heat transfer to the target diminished progressively, but slowly, so that at the end of 1 h, the heat flux was typically reduced by 50%. The most useful data on large pool fires come from several studies at Sandia National Laboratories. Net heat flux peaks[161,162] of 120 – 140 kW m^{-2} were found inside the flame volume (i.e., fluxes to objects submersed in

Table 18 Ignition of targets by burning furniture

Burning item	Maximum distance for ignition (m)		
	Cotton cloth	Plywood	Wood blocks
upholstered side chairs	3 specimens caused ignition at 0.15; 5 specimens required < 0.15	1 specimen caused ignition at 0.15; 7 specimens required < 0.15	1 specimen caused ignition at 0.15; 7 specimens required < 0.15
armchairs	2 specimens caused ignition at 0.15; 5 specimens required < 0.15	1 specimen caused ignition at 0.15; 5 specimens required < 0.15	< 0.15 for all
book case	0.45	0.45	0.30
wooden wardrobe	> 1.20	> 1.20	> 1.20

the flames) in a series of tests using 9 × 18 m pools of JP-4. Unlike most other heat flux measurements, the values reported were net fluxes, that is the heat flux actually entering the specimen. The net heat flux is lower than the incident heat flux due to non-unity radiant absorptivity, re-radiation, and the progressive diminution in convection as the specimen warms up. The net heat fluxes decreased during the tests to around 50 kW m^{-2} after a ½ hour. Similar studies in large (20 m diameter) JP-8 pool fires[163] using heat flux meters positioned slightly above the pool and oriented so as to view upwards, showed that the highest heat fluxes (ca. 100 kW m^{-2}) were at the edge; heat fluxes at the center were quite small (15 – 20 kW m^{-2}) due to oxygen starvation.

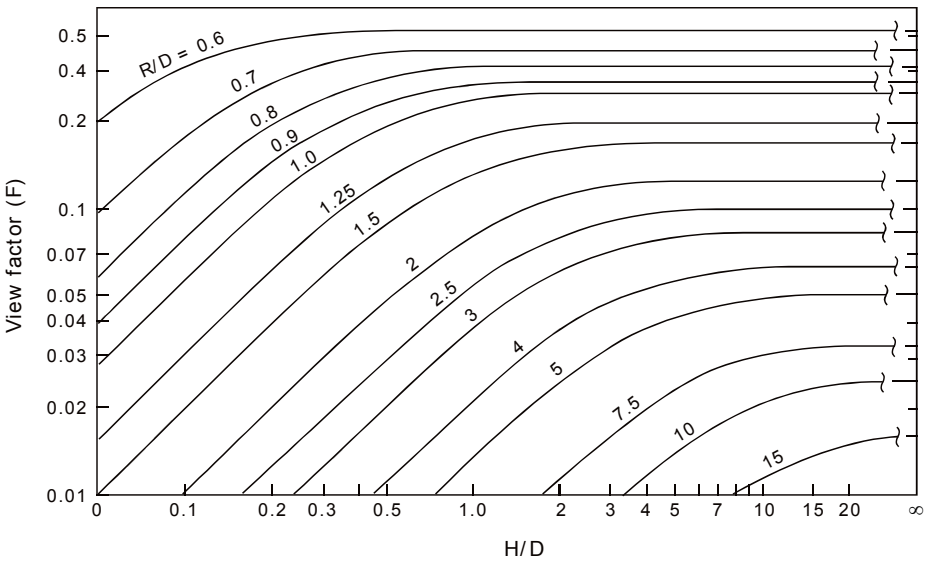


Figure 16 View factor F for a vertical target at ground level
(Copyright NFPA, used by permission)

For the case of objects remote from the flames, the simplest method for estimating the radiant heat flux to a target is that of Shokri and Beyler[164], which was derived from a data correlation and is applicable only to the configuration of a vertical target at ground level (Figure 15):

$$\dot{q}''_{rad} = 15.4 \times \left(\frac{R}{D} \right)^{-1.59}$$

where R = distance from center of pool to target (m), and D = pool diameter (m). This model is very simple indeed, since no chemical characteristics of the pool fire are considered, merely its size.

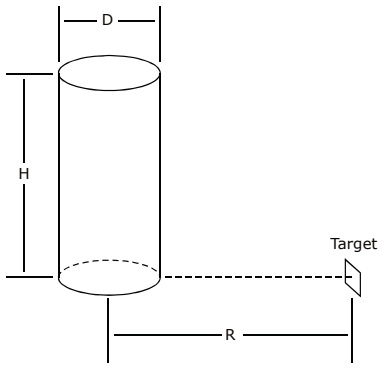


Figure 15 Geometry for vertical target at ground level, exposed to radiant heating from cylindrical-shaped flame body above a liquid pool of diameter D

As the next step in complexity, it can be recognized that the chemical nature of the fuel does play a role in determining the heat flux to a target. The simplest model which takes this into account is the *point source radiation model*. If the size of the burning object is very much smaller than the distance from the fire to the target, and if the fire is radiating equally in all directions, then[165]:

$$\dot{q}''_{rad} = \frac{\chi_r \dot{Q}}{4\pi R^2}$$

where $\dot{q}''_{rad}$ = radiant heat flux (kW m^{-2}), χ_r = fraction of the HRR which shows up as radiant energy (--), $\dot{Q}$ = HRR of the pool (kW), and R = distance from center of pool to target (m). The radiant fraction depends both on the chemistry of the fuel, especially its propensity to produce soot, and on the scale of the problem. Values of χ_r between 0.1 and 0.4 are common, but in the absence of more specific information, χ_r = 0.25 to 0.30 is often taken. A study has been reported on burning pallet loads of organic peroxides[166]. Liquids were packaged in plastic containers within cardboard boxes, while solids were packaged in cardboard drums. Radiation measurements indicated that values of χ_r spanned the small range of 0.20 to 0.28. An SFPE Guide[167] points out that the radiant fraction decreases with pool diameter and suggests a general relation:

$$\chi_r = 0.21 - 0.0034D$$

where D = pool diameter (m). Since the value of χ_r depends on the chemical nature of the fuel and this equation ignores it, obviously it is a simplification.

To improve the accuracy of the estimate, the flame can be treated as a finite geometric area, instead of a point source. The simplest such representation is as a grey-body cylinder, however, this requires additional input data, since the diameter and the height must both be known. The diameter is commonly assumed to be equal to that of the pool, but the flame height must be estimated by some supplemental formula. A number of formulas are available for this purpose, but the simplest is Blinov and Khudiakov's experimental finding[168,169] that, for pools of diameter greater than about 2

m, $H \approx 1.5\ D$. With cylinder diameter and height known, it is possible to perform a radiant-exchange calculation. The radiation from a grey body is:

$$\dot{q}_2 = F_{12} A_1 \varepsilon \sigma T_f^4$$

where $\dot{q}_2$ = radiation leaving source 1 that is intercepted by target 2 (kW), A_1 = area of the source (m^2), ε = flame emissivity (--) and T_f = source temperature (K). The *view factor* F_{12} is a dimensionless number which can range from 0 to 1 and which denotes the fraction of radiation leaving object 1 that is intercepted by object 2. View factors are simply geometric constants which can be calculated (albeit often with difficulty) from the sizes, shapes, and orientations of the objects involved. Next, the identity is used:

$$F_{12} A_1 = F_{21} A_2$$

where F_{21} refers to radiation leaving object 2 that arrives at object 1 and A_2 is the area of the target 2 (m^2). Combining the above two equations gives the desired result for the radiant flux $\dot{q}''_{rad}$ being received by the target:

$$\dot{q}''_{rad} = \frac{\dot{q}_2}{A_2} = F_{21} \varepsilon \sigma T_f^4$$

For practical problem solving, it turns out that there is no need to separately evaluate ε and T_f, but the quantity $\varepsilon \sigma T_f^4$ can be used. It has the units of kW m^{-2} and is termed the *emissive power*. Expressed this way, the basic relation is simply:

$$\dot{q}''_{rad} = FE$$

where we have simplified the F_{21} notation to F. To compute F requires knowing the flame height H and the distance R from the center of the fire to the target. Values of F for a cylindrical flame geometry to vertical target at sitting at the same height as the base of the pool[168] are shown in Figure 16. The width of the cylinder is taken as the pool diameter D and the height of the cylinder H is the flame height, as determined by one of various flame height correlation formulas. The latter assumption has some systematic bias, since the top portion of a flame has very little radiating power, and the effective radiating height is less, but in view of experimental uncertainties in determining flame heights, high precision would scarcely be warranted. The most common flame height equation is Heskestad's[170]:

$$H = 0.224 \dot{Q}^{2/5} - 1.02 D$$

If the approximation that $H \approx 1.5\ D$ is used, then the view factor can be suitably estimated as:

$$F \approx 0.272 \frac{D}{R} - 0.0347$$

The SFPE Handbook[165] and Lees[181] provide equations for computing more view factors from complex flame shapes, while Rew and Hulbert[171] describe a much more elaborate model for all aspects of pool fire radiation, but in view of the various problem uncertainties, it can be questioned whether more elaborate calculations lead to appreciable improvements in accuracy of prediction.

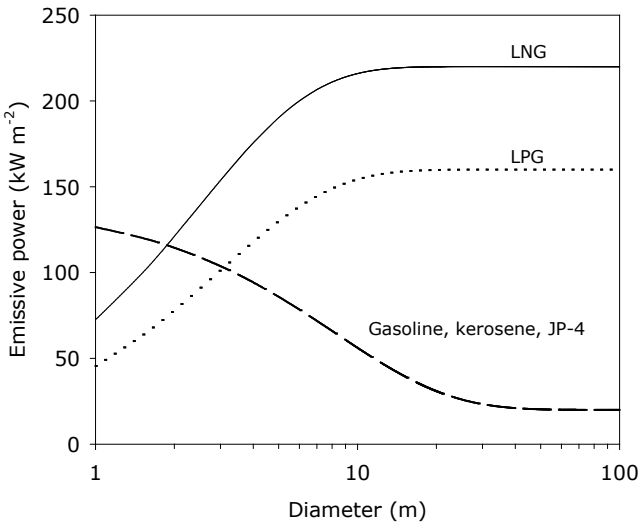


Figure 17 The effect of diameter on emissive power of liquid pool fires

The emissive power E depends on the substance that is burning and on the scale of the fire. Experimental data for the emissive power of several liquid fuels are provided in the SFPE Handbook[165]. Curves expressing these results (Figure 17) are:

LNG: $E = 220 \left(1 - e^{-0.4D}\right)$

LPG: $E = 160 \left(1 - e^{-0.335D}\right)$

gasoline, kerosene, JP-4: $E = 20 + 120\, e^{-0.12D}$

The curves for LNG and LPG are very similar and show that the emissivity increases with increasing size, as is usually found for flames of various types. The results for gasoline/kerosene/JP-4, however, seem anomalous—increasing the size of the fire causes the emissive power to drop. The reason is that these fuels generate a very large amount of black smoke, a certain fraction of which forms a 'cold smoke mantle' around the exterior of the fire. Flames periodically break through this mantle and higher radiation then falls on the surrounding objects. The experimentally reported emissive power for these fuels is a value that averages out these fluctuations. Shokri and Beyler[164] have pointed out that, at least for gasoline/kerosene/JP-4, the SFPE Handbook relations overestimate the peak emissive power that is attainable in practice.

The emissive power of large-size flames has also been studied for square-array cross-piles of wood sticks, which are termed *cribs*. The data of Hägglund and Persson[172] are shown in Figure 18. The equation that represents the data is:

$$E = 190 \left(1 - e^{-0.8D}\right)$$

The curve fit would suggest that $E \rightarrow 190$ kW m^{-2} as $D \rightarrow \infty$, but this is hard to confirm since the emissive power has not reached a plateau for the largest experimental flame depth, which was 2.0 m. Buildings or portions thereof will,

of course, show much greater flame depths. The predictive equation (and those given above for liquid pools) should not be used for $D < 0.3$ m, since convective effects are strong in fires of smaller diameter[173].

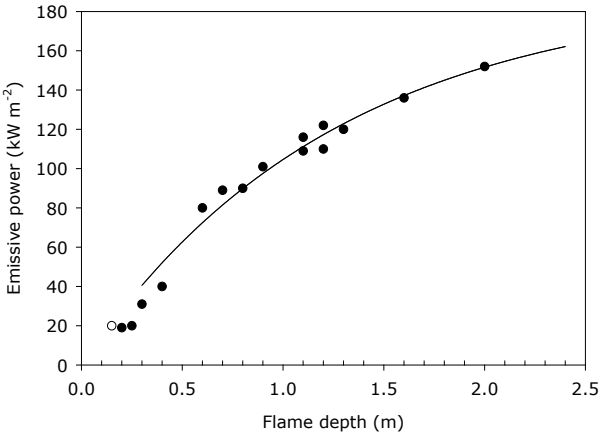


Figure 18 The effect of diameter on emissive power of wood crib flames

FIREBALLS AND JET FLAMES

In a fire safety context, the term *fireball* is generally understood to be the combustion in air of a fixed amount of fuel that is burned up quickly (typically[174] in less than 20 s). A typical fireball is illustrated in Color Plate 15. By contrast, a pool fire is one which is supported by evaporation of a body of liquid and continues to burn for a substantial length of time. If the amount of gas discharged is large, then ignition from a fireball can occur at large distances from the fuel source. A fireball can originate from a BLEVE or some other event that delivers rapidly a large amount of fuel into the air. A large fireball will typically go through three stages[179]:

1. Growth. The diameter of the fireball steadily increases during this stage, but the fireball remains located at ground level.
2. Steady burning. The diameter no longer increases, and at some time during this stage the fireball begins to lift off the ground.
3. Decay. The fireball remains roughly at its maximum size, but radiation from it progressively diminishes.

Methane fireballs were studied by Hardee et al.[174] and their results are summarized in Table 19. On the basis of their own measurements and a review of the literature, including larger-scale data, they offered two estimating equations:

$$d_b = 6.36 W^{0.325}$$

$$t_b = 2.57 W^{1/6}$$

where d_b = maximum fireball diameter (m), t_b = burning time (s), and W = mass of methane (kg).

Johnson and Pritchard[175] conducted large-scale BLEVE tests on railcar-size vessels containing 1000 – 2000 kg butane or propane. They obtained emissive power readings of 250 – 350 kW m^{-2} from the lower part of the fireballs of either fuel. The top of the fireballs registered 500 kW m^{-2} peak values, but combustible targets are unlikely to be situated above one of these fireballs. The duration of a fireball was ca. 4 s. The high heat flux values reported in these tests appear questionable. All available evidence[179] is that flame temperatures in fireballs do not exceed 1200 – 1300ºC. If so, then the emissive power evidently cannot be greater than 347 kW m^{-2} at any time, not just for the average value. Deriving design values from experiments on fireballs is difficult, since actual fireballs vary in effective radiating area with time and their emissive power varies with direction of wind. It is also clear that peak values are not themselves related to hazard and that some credible averaging technique must be used. The peak radiant power of a fireball (E times effective radiating area) is typically reached at the time of lift-off.

Table 19 Small-scale experimental measurements on methane fireballs by Hardee et al.

Mass of methane (kg)	Burning time (s)	Max. dia. (m)	Heat flux at edge (kW m^{-2})	Total energy fluence (kJ m^{-2})
0.15	1.8	3.0		
1.5	2.4	4.4	123	102 – 193
10				251 – 325

Prugh[176] suggested that the following relations can be used to calculate the characteristics of fireballs of any fuel gas:

$$d_b = 6.48 W^{0.325}$$

$$t_b = 0.825 W^{0.26}$$

$$H = 0.75 d_b$$

$$E = 0.0092 \chi_R \Delta h_c W^{0.09}$$

where W = fuel mass (kg), H = center height (m) of fire ball, E = emissive power (kW m^{-2}), χ_R = radiant fraction of heat release rate (--), and Δh_c = heat of combustion (kJ kg^{-1}). The expression for height is a design value that takes into account that fireballs become buoyant early in their combustion stage, and that the peak heat fluxes are seen when they are substantially higher than ground elevation. Suggested values[177,181] of χ_R for a number of common fuels are shown in Table 20, but it must be understood that the values are not completely independent of scale. Scale data are not available in general, but for crude oils, some scale-dependent values for pools[178] are shown in Table 21; comparable values for jets, etc., are not available. If the target is not directly adjacent to the fireball, then the incident heat flux is not E, but is diminished by a view factor. Prugh suggests that the simplest equation for estimating the view factor for radiation from a fireball is:

$$F = \left[\frac{d_b}{2R_f} \right]^2$$

where R_f (m), the distance from the center of the fireball to the target, is given by the hypotenuse:

$$R_f = \sqrt{X^2 + H^2}$$

where X (m) is the lateral distance between the target and the center of the fireball.

Table 20 Radiant fraction of HRR for several gases

Fuel	Radiant fraction χ_R (--)
methane	0.16 – 0.23
hydrogen	0.17 – 0.25
methanol	0.20
natural gas	0.23
butane	0.30
propane	0.33
benzene	0.38
ethylene	0.38
hexane	0.40

Table 21 Effect of pool diameter on radiant fraction of crude-oil fires

Pool diameter (m)	Radiant fraction χ_R (--)
5	0.26
10	0.22
20	0.16

Crawley[179] examined a film from an 80,000 kg actual BLEVE incident which indicated that the duration of burning was 17 s, of which 10 s had a steady state character. Based on this and two other very large-scale incidents, plus various small-scale tests he noted that equations not having an explicit molar mass term gave poor agreement for hydrogen fireballs. Including this molar mass effect, his proposed correlation is:

$$d_b = 10.5\left(\frac{W}{M}\right)^{1/3}$$

where M = molar mass of fuel (g mol^{-1}).

The most authoritative and extensive study has been that of Roberts[180], who correlated data on a number of different combustibles from several studies and concluded that a reasonable representation of fireball diameter is:

$$d_b = 5.8 W^{1/3}$$

The experimental data covered fuel quantities of approximately 10 – 1000 kg. Lees[181] recommended that the above correlation be considered the one of most general applicability. Roberts concluded that the burning time cannot be estimated by a single equation, rather that there is a dependence on the amount of fuel:

$$t_b = 1.1 W^{0.097} \qquad \text{W} < 5 \text{ kg}$$

$$t_b = 0.45 W^{1/3} \qquad \text{W} > 5 \text{ kg}$$

Further, Roberts concluded that for actual estimating of radiant fluxes, an effective radiation duration time, t_r, should be used:

$$t_r = 1.07 W^{0.181}$$

The heat flux found at a distance R_f from the center of the fireball could be estimated as:

$$\dot{q}'' = \frac{8.28 \times 10^5 W^{0.771}}{R_f^2}$$

The relation breaks down for large fireballs, since it would indicate an indefinitely-increasing heat flux, whereas actual experimental data[174] indicate that emissive power does not keep increasing once the fuel mass surpasses about 30 kg.

For very large fireballs, buoyancy effects become stronger, and a British expert panel[181] recommended the following relation:

$$t_b = 2.6 W^{1/6} \qquad \text{W} > 30{,}000 \text{ kg}$$

The same panel recommended that the vapor pressure of the fuel at the moment of release, P (MPa), can be taken into account by the following equation:

$$E = 235 P^{0.39} \qquad P \le 2.$$

More recent data were presented by a Russian group[182], who exploded large steel cylinders filled with gasoline, diesel fuel and kerosene. These conditions create fireballs of maximum compactness, since ignition occurs before diffusion or mixing have taken place. They obtained:

$$d_b = 5.3 W^{1/3} \qquad \text{diesel fuel, kerosene}$$

$$d_b = 4.3 W^{1/3} \qquad \text{gasoline}$$

These diameters are slightly lower than in previous studies, due to the compactness of their fireballs. The authors also reported measurements of E for small diesel-fuel fireballs of 3 – 110 kg and correlated these results as:

$$E = 110\left[1 - \exp\left(-2.6 d_b\right)\right]$$

If $d_b > 1.0$ m, then this equation gives $E \approx 110$ kW m^{-2}. Use of this equation should be limited to fuel amounts no greater than 110 kg, since higher values of E have been measured by researchers who studied larger fireballs. For fireballs within the range of validity, the authors also suggested that, if a time-dependent expression for fireball diameter is available, the above equation can be evaluated for E on a time-dependent basis. Several theories for fireball characteristics have also been developed by Russian researchers[183].

A time-dependent model for fireballs was presented by Martinsen and Marx[184]. Their maximum diameter is the same as given by Roberts,

$$d_{b(Max)} = 5.8 W^{1/3},$$

but during the initial time period, the fireball sits tangent to the grade, and expands in diameter according to:

$$d_b = 8.67 W^{1/4} t^{1/3}$$

Table 22 Emissive power measured from dust explosion fireballs

Dust	Fireball diameter (m)	Max. emissive power[a] (kW m^{-2})	Avg. max. emissive power (kW m^{-2})
aluminum powder	2.5 – 9.2	145 – 2417	858
anthraquinone	7.2 – 11.2	222 – 297	262
coal dust	7.4 – 11.4	107 – 227	162
corn flour	5.4 – 7.9	25 – 57	33
polyethylene	1.8 – 8.4	25 – 87	63
toner dust	9.7 – 15.4	125 – 294	209

[a] – peak with respect to time, average with respect to fireball perimeter

When d_b reaches $d_{b(Max)}$ the fireball stops growing and begins to rise in the air. In their scheme, the fireball duration is:

$$t_b = 0.9 W^{1/4}$$

Williamson and Mann[185] studied propane fireballs and concluded that the lift-off time t_o (s) is:

$$t_o = 1.09 W^{1/6}$$

For other fuels, they suggest the more general expression:

$$t_o = 0.68 r^{1/6} W^{1/6}$$

where r = stoichiometric air/fuel mass ratio for the fuel.

A limited amount of data suggests that the center of the fireball rises to a maximum height of 1.5× $d_{b(Max)}$. Martinsen and Marx approximate the velocity of its rise by assuming that it goes from lift-off to maximum height at a constant velocity, and that this process starts at t = t_b/3 and ends at $t = t_b$.

A plot of the heat flux versus time is quite similar to a triangle[184], thus Jones[186] proposed that it be simplified as an isosceles triangle. In this method, time is scaled according to a dimensionless time t', which is defined as $t' = \frac{\sqrt{g}}{V^{1/3}} t$, where g = acceleration of gravity (9.81 m s^{-2}) and V = volume of vapor leaked, evaluated at ambient temperature and pressure. The triangular plot then has its zero at the time of ignition (t' = 0), peaks at t' = 6, and drops down to zero again at t' = 12.

For fireballs from *dust explosions*, the emissive power has only recently been studied. Holbrow and Hawskworth[187] conducted explosions in 18.3 and 20 m^3 large-scale vessels. Dust concentrations were varied, but generally were at levels designed to elicit peak explosion pressures. Their results are shown in Table 22. A wide range of emissive powers was found, with some organic fuels, e.g., corn flour, showing very low values. The emissive power from aluminum powder was much higher since the adiabatic flame temperature of aluminum burning is air is substantially higher than for organic fuels.

Since *explosives and propellants* have adiabatic flame temperatures which are much higher than normal liquid or solid combustibles, while their heats of combustion are typically low, the fireballs produced by propellants would also be expected to show correlations different than for normal fuels. Figure 19 shows the emissive power measured from a fireball from 1 kg of gunpowder[188]. Unfortunately, 'pyrotechnics,' have diverse characteristics and can only loosely be considered a single family. Data for a number of compositions[189] are shown in Table 23, where the constants a and b pertain to the equation for estimating fireball diameter:

$$d_b = a W^b$$

Peak emissive power was generally 230 – 1000 kW m^{-2}, but no predictive relation was found. The emissive power was mostly dependent on the chemical constitution of the substance, but in most cases there was a small increase with mass of charge. Fireballs from explosives and pyrotechnics are shown in Color Plate 16 and Color Plate 17.

Merrifield and Wharton[190] studied the fireball characteristics for a series of propellants and found that the exponent was generally close to 1/3, but that the scaling factor varied:

$$d_b = (1.5 \text{ to } 3.8) W^{1/3}$$

Matters were also complicated by the fact that the fireballs produced from propellants were often more cylindrical than spherical in shape. Fireball duration was difficult to correlate on a substance-independent basis. A power-law expression for t_b:

$$t_b \propto W^n$$

Table 23 Fireballs from various pyrotechnic compositions: diameter from 1 kg charge and predictive constants for other charge masses

Pyrotechnic composition*	Fireball dia. (m)	a	b
flash (magnesium, potassium perchlorate, graphite)	5.0		
star (magnesium, potassium perchlorate, barium nitrate, PVC)	3.4	3.3	0.40
gunpowder (potassium nitrate, carbon sulfur)	3.2	3.1	0.28
priming (gunpowder, potassium nitrate, silicon)	2.4	2.5	0.29
flare (magnesium, sodium nitrate, calcium oxalate)	2.0	1.9	0.32
star (gunpowder, potassium nitrate, aluminum)	1.6	1.5	0.33
flare (sodium nitrate, magnesium, calcium oxalate, PVC)	1.2	1.1	0.21
priming (potassium nitrate, silicon, sulfurless gunpowder)	0.8	0.74	0.17

* minor ingredients not shown

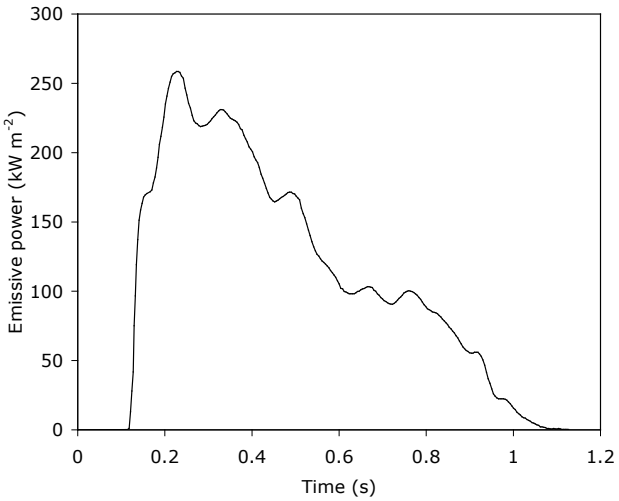


Figure 19 Emissive power from a fireball of 1 kg of gunpowder

required values for n of 0.1 to 0.33, depending on the substance. The emissive power of most of the fireballs measured was roughly 1000 kW m^{-2}, which is consistent with their high flame temperatures.

Jet flames occur when a combustible gas is discharged from a pipe or other opening and burns in the air. These can be intentional (flares at refineries) or accidental. The modeling of their heat flux can be non-trivial since (1) the flame shape is long and narrow and does not lend itself to being approximated as a spherical shape, except for the crudest of estimations; and (2) wind effects may change the lateral location of the higher portions of the flame to a sizable extent. Despite the crudeness of the assumption, the point source radiation model, discussed above, is commonly used in the petrochemical industry[181]. Some experimental data, along with suggestions for extrapolation, have been provided by Brzustowski et al.[191] A large variety of elaborate computational models have been put forth, and these were compiled (but not assessed as to validity) by Lees[181].

See also Chapter 13 for information on heat fluxes and ignition associated with gas explosions in rooms.

BURNING BUILDINGS

When a serious room fire occurs and there are windows in the façade, high heat fluxes can exist. Ignition may possibly occur of: (1) the façade itself, if it is combustible; (2) combustibles such as curtains in rooms on higher stories, if there are windows directly above the fire; or (3) combustibles on or in a building which faces the burning building, thereby creating an *exposure fire*. The ignition of items #1 and #2 will tend to occur only if the room fire is sufficiently advanced so that the window glass breaks and a fire plume is projected above the opening. Distant targets (#3) will be affected by radiation both from the window opening itself and from the fire plume above it. Thus, it is convenient to consider #1 and #2 together, and to relate these potential target locations to the fire plume that emerges from the window opening. The methodology for #3 can then be considered separately.

Heat fluxes to the façade of the burning building

A large fire usually breaks out windows of the building and there comes to be a fire plume (a nearly-vertical column of flame) that rises from the opening. If the façade is combustible, flames lapping directly at it are likely to cause ignition. But additionally, if the plume is tall enough so that the region of high heat fluxes extends to the next storey, its windows may break and fire may directly enter the storey above. Both of these possibilities are sometimes referred to as *autoexposure*. Wade and Clampett[192] have reviewed some case incidents.

The oldest studies on characterizing the fire plume above a window opening mostly only measured temperature distributions, from which some workers tried to compute heat fluxes[214]. An early series of heat flux measurements was conducted by the Fire Research Station in England[193], where for a variety of wood crib fires, the heat flux to the façade above the opening of the burn room window was found to range from about 12 to 40 kW m^{-2}. These values were very low, presumably because the window opening was sufficient to burn most of the pyrolyzed fuel inside the room. Similar experiments using wood cribs were recently reported by Hakkarainen[194]. In her tests, the heat flux was measured at 2.2 m above the top of the window and showed values around 80 – 120 kW m^{-2} after the fire had fully built up, which required around 20 min. With the popularization of the use of plastics in furniture and building materials during the 1970s, it became less likely that burning of the fuel pyrolysates would be confined to the room itself. Two studies using modern furniture fires were performed at Lund University. In the first study[195] values measured for the total heat flux were ca. 145 kW m^{-2} at 0.8 m above the top of the window, dropping to 40 kW m^{-2} at a height of 3.3 m. In a follow-on study[196], primarily the radiant heat flux component was examined, but comparison was made between wood and plastic-fueled fires. Figure 20 indicates the very large increase that plastic fuels give over wood fuels. The authors estimated that this was because the fraction of the fuel mass loss rate showing up as excess pyrolysates was 25% for wood fuel and 65% for plastic fuel. For the plastic fuels, instrumentation for measuring the total heat flux was also used, but only close to the top of the window opening. Values of total heat flux in excess of 200 kW m^{-2} were found at that location. Data obtained by Kotthoff[197] from realistically furnished rooms, mostly with wood materials, are also shown in Figure 20.

Similar magnitudes of results were also found in studies conducted at NRC in Canada[198]. When wood cribs were used, peak heat fluxes of 80 kW m^{-2} at 0.25 m above the top of a square-shaped window were measured, while 115 kW

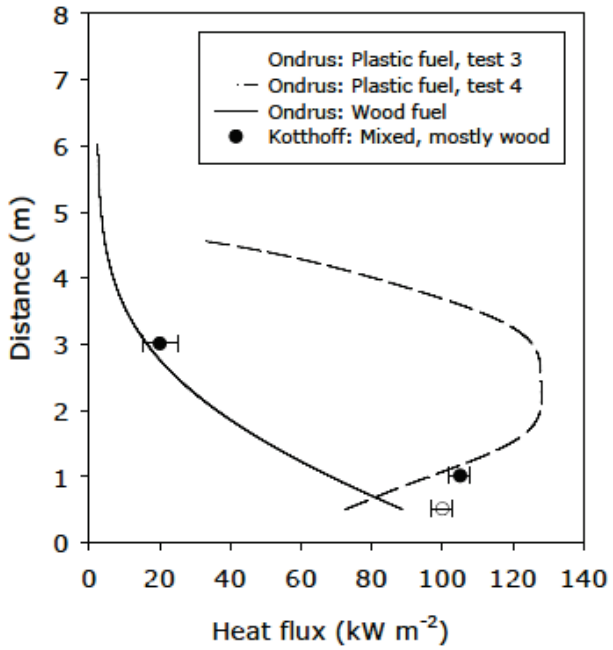


Figure 20 The heat flux to the façade, measured as a function of distance above the top of the window of the fire test room. Ondrus' values are for radiant heat flux, while Kotthoff's are for total heat flux.

m^{-2} was recorded with a tall, narrow window. In the same NRC study, propane burner fires were able to cause heat fluxes of over 200 kW m^{-2}; such extreme heat fluxes, however, require both very large fires (over 10 MW) and very large window openings. Fires under 6 MW did not create façade heat fluxes over 50 kW m^{-2} at a height of 0.5 m above window top.

The effect of combustible façade materials was studied by VTT researchers[199], who used wood boards to cover some, but not all, portions of a test building façade. Heat fluxes were measured at the center of second-storey and third-storey windows, the windows being directly in line above the window of the test room. For a non-combustible façade, a peak heat flux of 70 kW m^{-2} was found at the second-storey window; a peak heat flux of only 14 kW m^{-2} was found at the third storey. For wood board-lined façades, the second-storey heat fluxes were 100 – 112 kW m^{-2}, while 13 – 37 kW m^{-2} was found at the third storey.

The information about heat fluxes to facades presently available does not seem entirely adequate for design purposes. Nonetheless, for design purposes it would be appropriate to assume that heat fluxes of around 100 kW m^{-2} are likely to exist for the first 1 m height above the opening. This means that most combustible materials, if placed on the façade, would quickly ignite. Furthermore, much more than a single-story height (ca. 2.5 – 3 m) would be required for heat fluxes to drop below, say 12 kW m^{-2}. Even if the façade material themselves are non-combustible, the bottom of the window glass of the next higher storey may be only 0.5 – 1.5 m above the window top in the storey below. Some building codes require a non-combustible spandrel panel to separate vertically the windows of one storey from the next. But the typical requirement for a spandrel panel height is 0.6 – 0.9 m, and a 1966 FRS study[200], using a modest cellulosic-materials fuel load, showed that an 0.9 m spandrel is insufficient. Instead, the authors concluded that either fire-resistive glazing or an entire storey's-height of blank wall would be needed. The hazard with fuels having a substantial plastics content, as pointed out above, is higher.

The heat fluxes window glazing that may be permissible for design purposes can be considered in the context of the breakage of window glass. The flux of interest is not the one which will lead to initial cracking but, rather, one that will result in gross fall-out of portions of the glass. If glass both cracks and falls out, then evidently a nontrivial potential exists for ingress of either flames or firebrands from the fire taking place just outside the window. Research on this point is scattered, but it has been documented that 9 kW m^{-2} sufficed for gross fall-out of a single-glazed window[201], while 29.2 kW m^{-2} has led to failure of double-glazed plate glass windows, with gross fall-out of both panes[202]. However, both the details of the window installation and the probabilistic nature of the problem need to be considered, and research is not existent on either point.

Heat fluxes to other buildings

Massive exposure fires have been recorded, especially in earlier years when congested city centers were mainly of wood construction. Even in the 20th century, serious exposure fires have been recorded, and a survey[203] shows that ignitions across 24 m street-widths do take place. Some statistical data were collected in Japan[204] for wood-framed buildings (Figure 21). While their construction practices have not been similar to those in Western countries, nonetheless the general trend of the statistics is revealing. Even at 13 m separation, there is about a 20% probability of ignition of a neighboring façade.

The ignitable materials on the neighboring building may be its façade, such wood siding; but it may also be interior combustibles, which may become ignited once glass breaks out, or may ignite even prior to that, for high heat flux conditions.

The radiation source will vary depending upon the actual conditions. In general, the following may need to be considered:

- radiation from window openings (glazing assumed to be broken early during a serious fire);
- radiation from a fire plume of gases burning outside/above the window opening;
- radiation from a burning combustible façade;
- radiation from the entire structure, if the façade falls off but the remaining structure does not collapse.

In addition, it must be kept in mind that fires are not limited to still conditions, and strong winds may substantially affect most of the governing variables.

The radiant flux incident on a target can be computed as:

$$\dot{q}_r'' = F\varepsilon\sigma T^4$$

where ε = emissivity (--), σ = Stefan-Boltzmann constant (5.67×10^{-11} kW m^{-2} K^{-4}), T = temperature (K), and F = view factor (--). The latter variable depends solely on the geometry of the problem; if a target receives 100% of the radiation of the source, then $F = 1$. The remaining factors in the problem depend only on the combustion characteristics of the source and do not depend on the geometry. The group of factors $\varepsilon\sigma T^4$ is defined as the *emissive power* (kW m^{-2}) and represents the radiant heat flux falling on a target when the view factor $F = 1.0$. Thus, the incident radiant flux is conveniently taken as the product of the view factor and the emissive power of the source.

A fully-involved room fire may register temperatures in the vicinity of 900ºC. Viewed from the outside, if it represents 'cavity radiation' and thus the emissivity is taken as ≈ 1, an emissive power of 107 kW m^{-2} is obtained. The earliest study[205] on the subject, conducted at FRS in 1950, concluded that an effective temperature of 1000ºC should be used for determining the radiation from the window opening. This is somewhat high, and a more recent Swedish study documented values in the range of 800 – 1000ºC for a series of experimental, post-flashover fires[206]. Thus, a range of 75 – 150 kW m^{-2} for the emissive power was found. Window radiation values up to 222 kW m^{-2} were reported in tests by Law[207], but it appears that these were erroneous since the corresponding gas temperatures were measured as only 1060ºC.

There will also be a fire plume extending above the window if the fire is of any appreciable magnitude. The temperatures drop rapidly in the plume and the emissivity is much less than 1. The high radiation temperature value adopted in the FRS study stems partly from the fact that plume radiation was ignored and all of the experimentally-measured radiation was assigned to the window opening, thus creating an 'effective' value higher than the actual value from window radiation alone. In extreme cases, if an adjoining building is placed very close, not only could the external flame impinge on the adjoining structure, but even the convective gas stream emerging from a window opening could suffice for ignition. However, the radiation would be enormous at such a close spacing, so it can be assumed that the adjoining structure is far enough away that there is no direct gas/flame contact. Under those conditions, in one study[208] it was estimated that 12 – 18% of the total radiation received at the façade of a nearby building will come from the radiation of the external flames. Since the problem uncertainty is undoubtedly greater than 20%, this gives some justification to ignoring the contribution of the external flames.

Some experimental data on heat fluxes to adjoining buildings was obtained in Sweden[209]. A small, non-combustible test house having two windows and wood-crib fuel was used. Exposure heat fluxes were measured to an adjoining building located a variable distance away. Except for fires that produced only small heat fluxes, it was found that radiation was invariably higher at the eaves level than at the window level. Peak values found were 40 kW m^{-2} at a 4 m distance and 11 kW m^{-2} at 6 m away. A number of other experimental studies have been made where radiation was measured to remote targets[210,211], but none of them developed data in such a way as to enable radiation calculations to be made for arbitrary target distances. If the fire compartment has a high fuel load of plastics, rather than cellulosic fuels, higher plume emissivities and taller plume heights are expected, but full-scale research on this problem has been nil. When building façades are made of wood or other combustible material, the entire façade may become involved in fire on a burning building. Again, there is not much reliable data for design in this situation. *Wind* is a significant factor many actual exposure fires, but experimental data on its effects are scant. In general, safety factors built into design methods are expected to take into account its effects.

A different façade exposure—heat flux on a façade located adjacent to a simulated urban conflagration was measured in a Japanese full-scale test[212]. Values around 130 kW m^{-2} were recorded on a balcony against which flames were directly being blown from the flame front of the conflagration. However, because the balcony acts to shield the façade itself and to deflect flames, the heat fluxes to flat portions of the façade only registered around 50 kW m^{-2}.

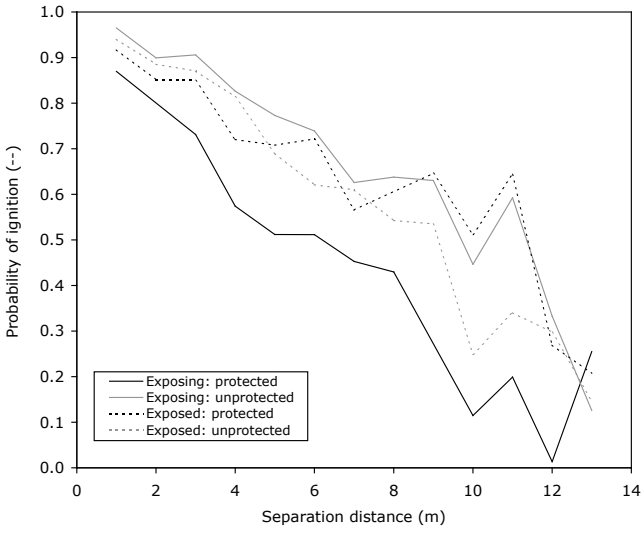


Figure 21 Probability of ignition of buildings from a nearby burning building (results from a Japanese study on wood-framed buildings with combustible and non-combustible claddings)

In an unusual study, Lynam[213] burned a small (2.4 × 5.5 m) plywood sales shack, of the type used in some locales for seasonal retail sales of fireworks. The stand was filled with 418 kg of fireworks of a wide variety, packaged in retail packages. Paper targets placed 4.6 m in front of the shack's open front windows ignited. Heat fluxes of 15 – 18 kW m^{-2} were measured at a location 4.3 m in front of the shack.; the author extrapolated that a heat flux of ca. 40 kW m^{-2} would have been found directly at the window openings. The measured flux values appear to be somewhat low, however, since a heat flux of less than 15 kW m^{-2} (taking into account 4.3 vs. 4.6 m distance) for about 160 s (duration of active burning) would not likely have sufficed to ignite paper targets. Fireworks were scattered to fairly large distances (over 35 m), but it was not determined if any of these projectiles would have been able to ignite combustible targets.

Design methods

Protection against heat fluxes from burning buildings is not normally provided by quantitative design calculations, but, rather, through code prescriptions, as discussed below. The only well-known engineering design method pertinent to the autoexposure problem comes from Law and O'Brien, who developed a method[211,214] for designing heavy-weight steel columns and beams to be used on façades exposed, without fire-protection coatings or coverings. Their method was based on experimental data where (a) the fuel was only cellulosic-based, without plastics; and (b) the ceilings were non-combustible. The second assumption is often enforced by building codes for high-rise structures, but the first assumption seems shaky, at least in today's perspective. Detailed engineering calculations for protection of nearby buildings could be done, but the rudiments thereof are incorporated into building code requirements and these are usually seen to be sufficient.

In view of the serious consequences of exposure fires, most building codes around the world have established some provisions dealing with radiant ignition of neighboring buildings. The provisions commonly require:

- that buildings not be built closer than a certain distance to the property line; or,
- that buildings, if they are built closer than a certain distance to the property line have features to avoid being (a) ignition sources (such as having no windows on that side, using only wired glass, providing steel shutters for all windows, or providing drencher sprinklers at windows); and (b) ignition targets (such as using only non-combustible or difficult to ignite façade materials); and,
- that buildings using combustible façades be separated by larger distances than ones where the façade materials themselves will not burn.

The practice for each building code or country is different, but generally fire temperatures are roughly related to some fuel load concept. Then, some radiation calculations are used to prepare tables or charts of allowable distances. These make additional assumptions about the size of the fire-source façade and the proportion of windows therein. Finally, a criterion is picked for the maximum allowable incident heat flux. Commonly, this is taken as 12.5 kW m^{-2}, which is considered as the nominal value of the minimum flux for ignition of wood products in the presence of a pilot*. Since most products have a higher minimum flux, and since an adequate pilot (e.g., a suitably large flying brand coming to the right place) is by no means assured, this value tends to be conservative, in view of the fact that autoignition fluxes are higher than those for piloted ignition. To complicate matters, the design guides often include concepts of risk management, along with fire physics. Because of this, a deterministic connection to real fire measurements cannot be established.

The earliest system presented for design purposes was developed at FRS[205]. The authors recommended that radiation view-factor arithmetic be done on the basis of radiation emerging solely from windows (and not from flames above windows). On that basis, they recommended that if a view factor is found to be less than 0.056, target ignition will not occur. For a source temperature of 1000ºC and emissivity of 1.0, this corresponds to a limit temperature of 150ºC being reached on the target. A more elaborate design system in the UK was presented in 1963 and the current UK guide[215] on the subject explains their approach. A French scheme was developed by Fackler[216,217] during 1954 – 56, whose studies were remarkably comprehensive. His second paper included a case history where fire propagated by radiation from a burning second story of one building to a parallel building 40 m away. In the US, the design methodology set out in NFPA 80A[218] is taken from McGuire's study[219]. On the basis of analyzing 3 fires (!), McGuire concluded that façades will ignite when the view factor reaches 0.07, for fires of 'normal hazard.' For 'hazardous' fires, a view factor of 0.035 was to be used, while in 'relaxed' conditions, a factor of 0.14 would be used. McGuire also proposed that 1.52 m be added to the required distance to account for the external flame, even though, based on his empirical factors, this was double-counting the flame effect. Flame temperatures did not enter into his scheme, since it was solely based on limiting the view factor. McGuire did not describe how hazard levels might be assigned, which NFPA 80A defines in a notably crude way. The emissive power for McGuire's three cases can be computed as 89, 179, and 357 kW m^{-2}. A value of 179 kW m^{-2} is somewhat higher than would be measured from a room fire, but may be reasonable if external flame contribution is ignored and the emissive power increased proportionally. The 357 kW m^{-2} value is patently unphysical, in the absence of exotic fuels.

* This value is appropriate if moderate exposure times are considered, e.g., 1 h or less. But experimental data are presented in Chapter 14 which indicate that much lower heat fluxes may suffice for ignition if the exposure lasts several hours.

Other design methodologies have tended to preserve more of the physics. Buchanan's guide[220] provides a simple computational approach. Barnett has written several papers[221,222] which form a good introduction to the designer. Collier[223] presented a design method implemented as a simple computer program. Complications arise when structures are involved where the façade is irregular or set back and some calculation schemes can become lengthy. Carlsson[208] reviewed in detail a number of the design methods and computed example cases. His results showed that: (a) the McGuire method gave the longest separation required distances; (b) the FRS method gave the shortest distances; (c) three other methods—those of Collier, Barnett, and NFPA 80A—gave results which were intermediate and were close to each other. In the absence of adequate real-scale validation, this exercise suggests the latter three methods should be preferred. The NFPA 80A method is based on McGuire's scheme and the reason that it was not found to be an outlier, but McGuire's was, is because NFPA 80A is relatively generous with use of the 'light' severity group, while McGuire discouraged its use.

Providing adequate vertical height between the top of one window and the bottom of the window above it is difficult, in view of the fact that approximately a 1-storey blank spandrel panel would need to be created to have a reasonable assurance that fire will not propagate via entry through windows[224]. Thus, in many building codes, the problem of storey-to-storey fire propagation through façade radiation is ignored. The use of checkerboard window arrangements can be made, but this does not necessarily assure safe heat flux levels in the case of wind parallel to the façade. The problem can be solved by use of fire-resistive 'eyebrows' (horizontally cantilevered panels above the windows) or balconies. Experimental evidence is available that balconies[225] or eyebrows[226] are effective as flame deflectors. Limited studies suggest that an 0.6 m projection is insufficient[200], but that a 1 m projection is adequate[224]. Harmathy[227] urged the use of drop-down eyebrows, which would be activated by a fire alarm signal. But the scheme is unlikely to be robust, since failure modes include freezing, rusting, and lack of maintenance.

BURNING FORESTS AND VEGETATION

Heat fluxes from a forest fire burning with flame-front heat release rate of 346 kW m^{-1} have been measured by Packham and Pompe[228]. They concluded that the radiant heat flux (convective heat flux was not measured) was typically 100 kW m^{-2} at the flame edge. At a distance of 7.6 m from the flame front, a radiant heat flux of 57 kW m^{-2} was estimated. The variation of heat flux over time was not studied. Telisin[229] used medium-scale test results to derive an emissivity for the flame front in burning grasslands as:

$$\varepsilon = 1 - e^{-0.16(L+0.375)}$$

where L = flame thickness (m). Measured flame temperatures were approximately 1000ºC.

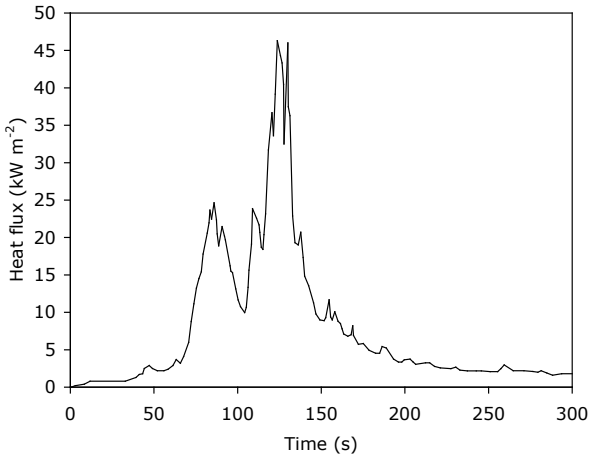


Figure 22 Heat flux measured at 10 m from the flame front of a crown fire

Grishin[230] summarized Russian research on the topic. Grishin distinguishes between a 'general crown fire' and a 'top crown fire.' The latter involves propagation of isolated fire over the crowns, without constituting a steady flame front and without an accompanying surface fire. Based on a series of experimental fires, he determined that temperatures in a 'general crown fire' were typically around 800ºC at the hottest part, although instantaneous fluctuations were some 200ºC higher. Typical heat flux distribution measured at the center of the fire was only 15 kW m^{-2} total. At some 2 m away from centerline (about midway between the center and the edge of the burning), the peak heat flux readings of 120 kW m^{-2} were found, of which about 95% was due to radiation. Peak heat fluxes of 125 kW m^{-2} were recorded in an experimental 'top crown fire,' but most (74%) of the heat was being released as convective flow, so the drop-off of heat flux with distance was apparently precipitous, although unspecified. A fire of this type is very brief: after 15 s, heat flux was no more than 60 kW m^{-2}, while after 40 s, it was no more than 30 kW m^{-2}. By 60 s, combustion had ceased. None of the test fires, of either type, lasted more than 80 s in duration. Grishin's experimental fires did not quite have the fuel load of a mature forest, so his measurements presumably somewhat underestimate severe fires in natural forests.

More recently, Cohen[231] measured the total heat flux at a distance of 10 m from an experimental crown fire that had flame heights of ca. 20 m (Figure 22). A peak of 46 kW m^{-2} was recorded, but this lasted only a few seconds. The tests also included mockup wood building facades placed at several distances away from the flame front. Walls 10 m away scorched, but did not ignite; ignition, however, did occur on a wall that had direct contact with the flame front.

BURNING VEHICLES

The Fire Research Station[232] characterized the radiant heat flux from a burning camper and a burning mobile home. Their results are shown in Figure 23 and Figure 24. The results were obtained at 10 min after ignition, which was close to the peak burning time.

HEAT FLUXES IN PRE-FLASHOVER ROOM FIRES

Heat fluxes occurring in pre-flashover room fires will vary widely. Away from the initial source of fire there will be essentially no heating at all. Near a small initial fire source, heat fluxes of the sort associated with small flames will be seen. With increasing fire spread and involvement, a hot gas layer will build up below the ceiling. The heat fluxes will be significantly hotter within this layer than in lower spaces. Söderbom[233] found values typically < 45 kW m^{-2} at the center of the ceiling during pre-flashover fires. The value at the floor level is, of course, always < 20 kW m^{-2} prior to flashover, since attaining 20 kW m^{-2} at floor level is one definition of flashover[234]. Combustion at floor level, however, is not generally where the attention is focused.

HEAT FLUXES ON BURNING WALLS

For burning walls, a number of studies have explored the heat fluxes from the flame to the yet-unignited portion of the surface. Hasemi studied this problem in detail[235] and provided correlations. For his experiments, peak values of ca. 25 kW m^{-2} were seen for the region downstream of the ignited area, but before the tip of the flames; beyond the flame tip, fluxes were no longer constant, but dropped off further downstream. Additional similar data have also been presented in a summary form[137]. More recent work by Kulkarni et al. has enlarged the diversity of material types examined[236]. The value of 25 kW m^{-2} is seen from these more extensive studies to be the lower bound of where data are clustered—most of the data are in the interval from 25 to 45 kW m^{-2}. Thus, a value of 35 kW m^{-2} might better capture the mean behavior. A 35 kW m^{-2} (or, alternatively, a range of 25 – 45 kW m^{-2}) heat flux, then, can be used to characterize the peak level of heating to a vertical surface element from its own upstream flame, just prior to its ignition. This value needs to be increased if the material is so situated as to be in a hot gas layer that is accumulating in the upper reaches of the room. Apart from the data of Söderbom, discussed above, this additional heating has not been studied.

HEAT FLUXES IN POST-FLASHOVER ROOM FIRES

The maximum temperatures actually seen in post-flashover room fires are ca. 1100ºC. A perfect black-body radiator at that temperature would produce heat fluxes of approximately 200 kW m^{-2}. Peak heat fluxes measured in post-flashover room fires can come close to this value, but are usually somewhat lower. Fang's results from an extensive series of room burns[237] are shown in Table 24.

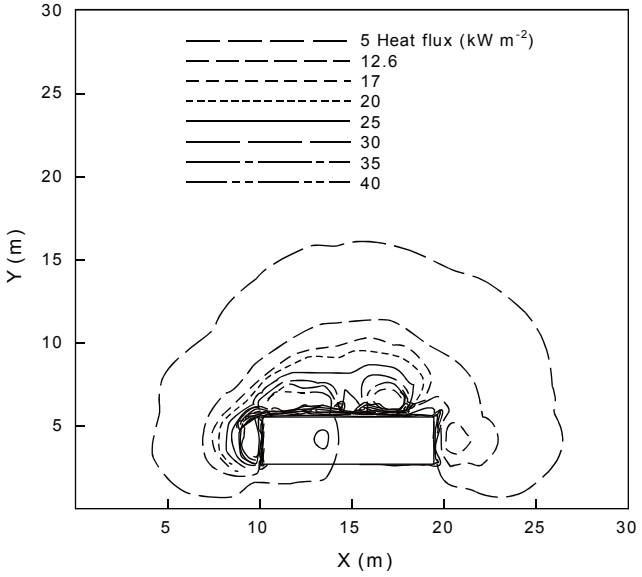


Figure 23 Radiant flux from a burning camper, measured near peak burning time, at a height of 1.8 m

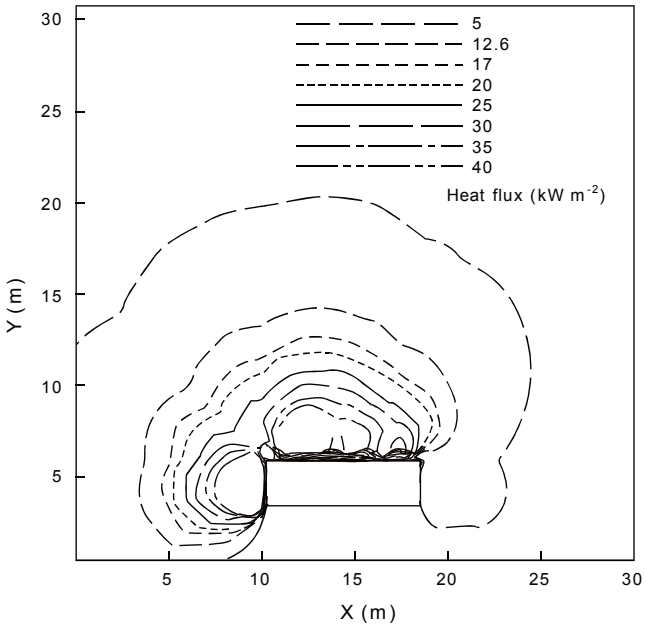


Figure 24 Radiant heat flux from a burning mobile home, measured near peak burning time, at a height of 1.8 m

Table 24 Heat fluxes in post-flashover room fires

	Heat flux (kW m^{-2})		
	Ceiling	Walls	Floor
Average	68 – 147	91 – 194	--
Maximum	106 – 176	116 – 229	119 – 143

ATTENUATION OF RADIATION BY WINDOW GLASS AND WINDOW SCREENS

Window glazing will attenuate radiation but only, of course, if it has not cracked and fallen out. Ordinary window glass can be expected to start falling out (not just to crack) when heat fluxes around 20 kW m^{-2} are reached[202]. The actual value depends on many factors, including the size of the pane. There is some probability of fall-out at a heat flux as low as 9 kW m^{-2}, but the probability of fallout does not become high until about 35 kW m^{-2} is reached. Double-glazed windows can resist approximately 25 kW m^{-2} without fall-out. Tempered glass is able to resist fluxes of 43 kW m^{-2}, at least under some conditions.

Thus, for ordinary window glass, ignition of objects inside a room by flames outside a window is most likely to occur only after the glass has fallen out. In some cases, however, ordinary window glass withstands high temperatures and heat fluxes and responds by slumping rather than cracking, as documented during some Australian wildfires[356]. The latter behavior is evidently somewhat rare and detailed factors have not been studied. There also exist various types of heat-resistant glass which can withstand high heat fluxes, thus the problem of attenuation of thermal radiation through glass needs to be considered.

Ordinary window glass transmits radiation at wavelengths between 0.35 and 2.7 μm very well, moderately between 2.7 and 4.25 μm, and essentially not at all for other wavelengths (Figure 25)[240]. The attenuation is very largely due to the stop-bands of the glass. Within the region of 0.35 to 2.7 μm, Bracciaventi's experimental measurements[238] showed that transmission is between 80 and 90%. Knowing the spectral transmission of the glass and the radiation temperature of the source body, the fraction of fire radiation which is transmitted through an intervening pane of glass can be estimated, as shown in Table 25[239]. Peak temperatures from a fire outside a window are unlikely to be much over 1000ºC. Under those conditions, even a single pane of the thinnest window glass in common use attenuates more than half of the incident radiation. The radiation is attenuated more if the angle of incidence is not perpendicular, but for conservativeness the perpendicular condition may be assumed.

Table 25 Transmission of thermal radiation through 3.2 mm thick window glass

Source temperature (ºC)	Transmission (%)	
	Perpendicular incidence	Diffuse radiation
900	35	31
1000	40	36
1200	49	44
2315	55	--
2727	83	--
4727	84	--
5727	85	--

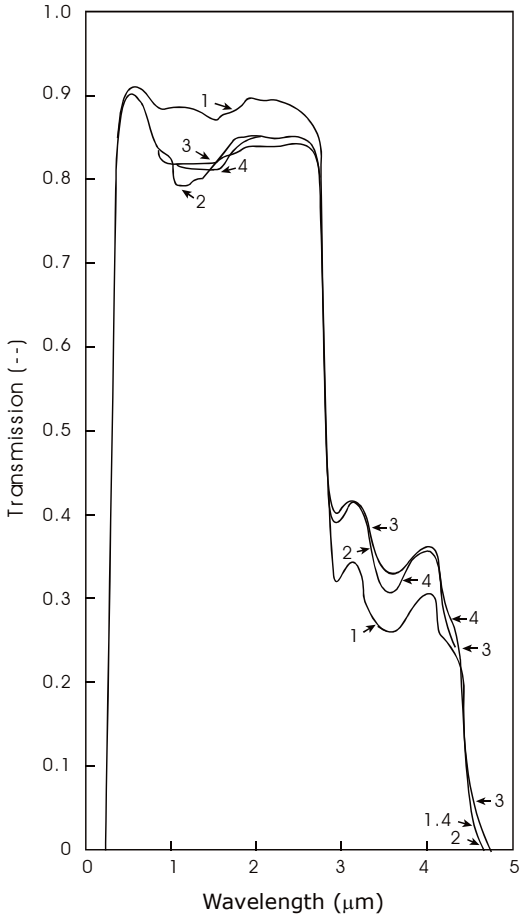


Figure 25 Spectral transmission of window glass (numbers denote four different samples)

Attenuation of radiation from a 2315ºC black-body source, taken as being representative of nuclear blast fireball radiation, was calculated by Downs and Bruce[240] while Bracciaventi[238] made calculations for higher-temperature sources; these additional results are also shown in Table 25. The angle of incidence, if not perpendicular, makes little difference until about 45º, after which point transmission falls drastically[238].

In Bracciaventi's study, the effect of soiling of the glass was also explored. After 44 days of soiling (and a visibly filthy appearance), the transmission decreased only by about 1%.

Since wired, toughened, and other forms of fire-resistive glass are able sustain high temperatures, if the thermal exposure is not of very short duration, then the glass itself will equilibrate to an elevated temperature and will provide a glass-radiated heat flux contribution to the total heat flux found on the far side, not just a transmitted portion. An experimental study where the transmitted and re-radiated heat fluxes were measured through 6 mm plate glass was performed by Moulen and Grubits[241]. Over the heat flux range

of 11.3 – 40.1 kW m^{-2}, about 40 – 45% of the incident heat flux was received on the far side, divided roughly into 60% transmitted and 40% reradiated. Wired plate glass showed slightly lower far-side heat fluxes. In these experiments, the transmitted flux percentage showed a decrease with increasing values of incident heat flux, the reason for this is unclear. Similar studies were conducted by Cowles[242], who conducted a series of 1.5 h fire-endurance furnace tests on several fire-resistive glass types, following the standard time-temperature curve[243] in the furnace. His results are shown in Table 26; the lower values were usually seen late in the test, and the higher ones earlier. The higher transmission measured at BRANZ can be attributed to the higher fluxes used in their tests.

Table 26 Effective transmission of heat flux transmitted through glass (sum of directly transmitted fraction and heat flux radiated from its surface), as determined in fire endurance furnace testing at BRANZ

Glass type	Total heat flux received (% of incident heat flux)
borosilicate glass, heat-strengthened, 6.5 mm	67 – 70
ceramic glass, 5 mm	75 – 89
wired float glass, 6 mm	55 – 62

The spectral transmittance of window screens was measured by Bracciaventi[238]. Within the region of 0.35 and 2.7 μm, transmission was about 66 – 72% for new aluminum screens, 62 – 66% for aged aluminum, 60% for plastic, and 55% for new copper screens. Transmittance was not measured outside this spectral region, so total transmission could not be characterized, but was probably no higher than the above values. In modern energy-efficient housing, it is becoming somewhat common to use double-glazed 'low-e' windows. These have coatings which transmit radiation in the visible spectrum but are reflective for the longer infrared wavelengths. Modeling has suggested that windows of this type may prove substantially more difficult to break out from fire radiation[244], and in addition there will be a much smaller transmittance of infrared energy. Actual test results on fire performance is not yet available. For specialized applications, it is possible to procure fire-resistive glass which is tested and shown to be able to resist post-flashover fire temperatures (and accompanying radiation) for substantial periods of time. At the present, however, this type of glass is costly enough that it is not in general use.

Electric phenomena

In this Section, the basic principles are examined which govern the ability of electric current or static electricity to deliver potentially incendive amounts of energy into a system. Practical aspects of failures associated with electrical wiring and devices are presented discussed in Chapter 14. Ignitions of gases, dust clouds, and solids from electrical energy sources are studied in Chapters 4, 5, and 7, respectively.

ELECTRIC DISCHARGES

Due to cosmic radiation and other factors, a small number of free electrons is always present in air. If an electric field is applied, the electrons move in the direction opposite to the electric field, i.e., to the positive electrode. If the electric field strength is increased (i.e., a sufficient voltage is applied), the electrons move faster, but still collide elastically with molecules in the air. As the field strength increases further, the collisions become inelastic and a collision of a molecule with an electron results in the fragmenting of the molecule, so that an electron is emitted and the remaining molecule becomes positively charged. This is termed *ionization*, since the molecule has become ionized (that is, it has acquired a net electrical charge). Once both positive and negative charges are present in the space, an electric current flow can occur, with electrons moving towards the positive electrode (anode) and positive ions towards the negative (cathode). The current flow that occurs when a sufficiently high voltage is applied is termed a *gas discharge*. If a sufficiently high, uniform electric field is applied, then an electric arc (sustained) or spark (not sustained) can occur. An electric arc requires that a sufficiently high current (more than ca. 0.1 A) be available. If sufficient current is not available, but the voltage is adequate (300 – 400 V), then a *glow discharge* may be sustained. A glow discharge can often be seen in the vicinity of a single pointed electrode. In a glow discharge, electrons are liberated from a cold cathode by collisions of positive ions—heating of the cathode is not involved.

For electrical breakdown of air to occur, the kinetic energy picked up by an electron due to the acceleration by the electric field must exceed the energy needed for ionization of a molecule of air. When ionized, the air molecule emits an electron, and the process accelerates. Soon there is an avalanche of electrons proceeding towards the anode. Additional electrons are emitted, as positive ions collide with the cathode. Ionizing radiation occurs when ion-electron pairs recombine, and this radiation falling on the cathode stimulates more electrons to be liberated at the cathode by photoemission. The whole process is sometimes termed the *Townsend discharge*.

The kinetic energy W gained by an electron when accelerated by an electric field E over a distance L is:

$$W = EeL$$

where e is the charge of the electron (1.6×10^{-19} C). The mean free path (average distance between two collisions) for an electron in air is 4 μm. The energy required to ionize a nitrogen molecule is 15.8 eV and for oxygen is 13.5 eV. An electron volt (eV) is a unit of energy equal to 1.6×10^{-19} J. The above relation can be solved for the minimum electric field E_{min} (V m^{-1}) which will lead to breakdown:

$$E_{\min} = \frac{13.5}{4\times10^{-6}} \approx 3\times10^{6}$$

Thus, when the electric field exceeds about 3 MV m^{-1} breakdown is estimated to occur. This is a very rough estimate, and Paschen in 1889[245] established a relation between breakdown voltage, spacing of electrodes, and gas pressure which has become known as Paschen's Law. According to Paschen's Law, the pressure × gap distance product is the controlling variable and the breakdown voltage V is given by:

$$V = \frac{c_1 pd}{c_2 + \ln(pd)}$$

where p = pressure, d = gap distance, and c_1 and c_2 are constants. Modern measurements[246] of Paschen's Law curves for air and for nitrogen are shown in Figure 26. For discharges from gaps greater than about 0.1 mm, it can be seen that the curve is essentially a straight line. For smaller gaps, however, the breakdown voltage does not go to zero and, instead, a minimum breakdown voltage is found. The Paschen curve goes up at both ends, i.e., for both small and large spacings, because of two different factors affecting the ionizing discharge process. For large gaps, the electric field is small enough that there is not a sufficient number of free electrons to initiate an arc. With a very small gap, the electric field is high and there is a high emission of electrons, but the inter-electrode spacing is very small. Consequently, the probability is low that an electron will strike and ionize a sufficient number of air molecules to start an avalanche breakdown. This minimum of the Paschen curve is approximately 340 V, and it occurs at a *Pd* product of 0.007 atm-mm. In other words, in ambient air, the minimum breakdown voltage occurs for a gap of 0.007 mm (7 μm). This is an exceedingly small distance, and two conductors this far apart would appear to be touching to the naked eye. Experimentally studying the left-hand portion of the Paschen curve requires some specialized techniques, since otherwise discharge may occur over a longer path (but lower voltage) than via the desired minimum-length path. The optimum gap size is on the order of the mean free path length of an electron; if the gap is reduced further, collisions become unlikely and emission from the cathode must primarily be relied upon to supply electrons.

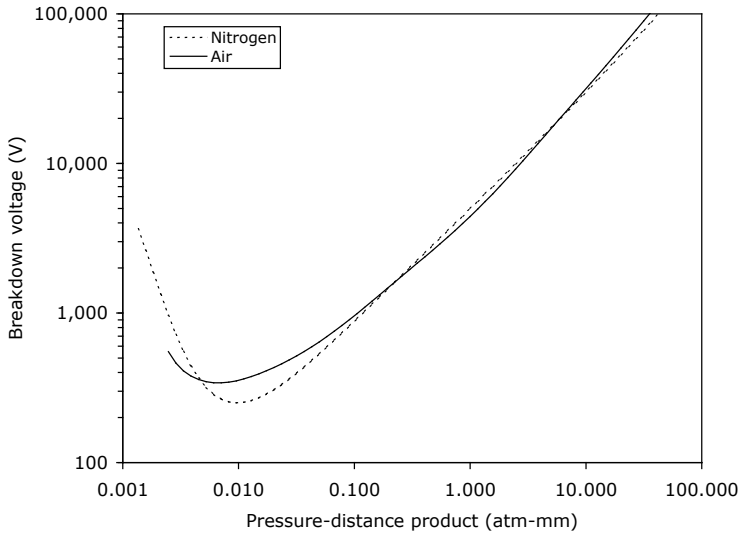


Figure 26 The breakdown voltage (Paschen's Law) between spherical electrodes in air and nitrogen

For practical applications, it can be more convenient to present results in the form of the *dielectric strength* (MV m^{-1}) which is the breakdown voltage, divided by the thickness of the insulator. This is shown in Figure 27 and indicates that for larger distances, the dielectric strength of air is approximately 3.0 MV m^{-1}; the value for nitrogen is quite similar.

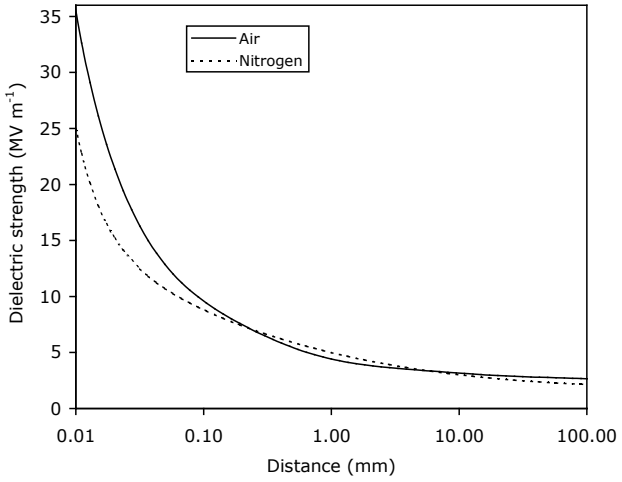


Figure 27 The dielectric strength at 1 atm, as a function of distance

The effect of *humidity* is not large, but humidity can either raise or lower the effective dielectric strength of air. This effect is governed by the voltage/time characteristic of the applied voltage, the polarity, and the details of the electrodes[247]. A fog lowers the breakdown strength to a modest extent[248], but the effect becomes large with a salt fog. At moderate *temperatures*, the dielectric strength of air is directly proportional to density[249], thus it varies also directly with pressure and inversely with temperature. But if the temperature is raised beyond about 450 K, the dielectric strength drops by more than a $1/T$ factor; beyond 2000 K the proportional reduction becomes even greater and at 3500 K the strength has dropped to about ½ that which is accounted for by the $1/T$ factor[250]. At high *elevations*, the decrease in atmospheric pressure becomes significant and the breakdown strength is lower; this affects electric installations in high-elevation locales. *Dust* will lower the breakdown voltage, but quantitatively the effect is small[251]. For atmospheres involving *gases other than air*, the

nature of the molecule involved affects the breakdown characteristics. Molecules differ in their ionization potential (energy needed to lose an electron) and their electron affinity (tendency to capture an electron). Molecules having a higher ionization potential and a higher electron affinity require a higher electric field in order to cause a discharge. When a *fire* is present, the dielectric strength is greatly reduced, as discussed in Chapter 14. Introducing *unignited fuel* into an atmosphere was studied by PTB[252]. Using an 0.6 mm gap where the breakdown voltage in air was 3.3 kV, in pure methane it was 2.0 kV, in pure hydrogen 2.9 kV, and in pure propane 3.7 kV. The effect was not linear with respect to fuel gas concentration, and small amounts of hydrogen actually raised the breakdown strength, with a value of 3.6 kV found for a 10% H_2/air mixture. Breakdown can also occur in a *vacuum*, since field emission of electrons from the cathode is possible. The breakdown strength of vacuum[253] is on the order of 500 MV m^{-1} for short gaps, but the actual value depends quite a bit both on the metal of the electrodes and on whether they are clean or contaminated. Breakdown of air and even traveling fireballs can be created by radiation from extremely powerful *lasers*, but enormous energy fluxes of $10^{11} – 10^{15}$ kW m^{-2} or greater are required[253].

Other variables that can affect the breakdown strength include electrode shape, electrode surface contamination, and the polarity (if electrodes are not identical). The standard Paschen's Law curves assume that the impressed electric field is uniform, which it rarely will be, except in controlled laboratory experiments. Deviations occur if the field has non-uniformities. Field non-uniformities act to raise the breakdown voltage, so they can conservatively be ignored[254]. A higher breakdown voltage is required for steel electrodes than for copper. For nitrogen, the minimum breakdown voltage is ca. 255 V with copper electrodes and 350 V with steel. Even at 1 atm in air, there are deviations from Paschen's Law. For instance, breakdown between two highly polished silver spheres at a gap of 0.25×10^{-3} mm (0.25 μm) was observed at only 50 V by Germer[255]. However, this was the lowest voltage found in a long series of tests—the outcome was highly variable and the average breakdown under these conditions required 200 V. Germer also produced a gap vs. voltage curve showing that the Paschen curve was violated everywhere to the left of its minimum. In the region between 0.001 and 0.008 mm, the breakdown voltage was a constant 340 V, instead of rising with decreasing gap size. Below 0.001 mm, the results showed a constantly falling breakdown voltage, going from 340 V at 0.001 mm to very low values as the zero limit was approached. Unfortunately, it is not clear from these studies under what conditions it can be expected that the Paschen curve will be obeyed—or not. Despite the fact that anomalous characteristics of such very short arcs have been documented, their electrical-safety implications have not been explored, primarily because the design of electrical equipment is based on minimum spacings being much greater.

Paschen's Law curves are identical for both AC and DC voltages. But since AC voltages are normally described by their root-mean-square (rms) values and not the peak values, this means that if results are to be applied to AC voltages, then the values indicated in Figure 26 need to be divided by $\sqrt{2}$. Thus, on an rms basis, the minimum AC breakdown voltage is = 340/1.414 = 240 V(rms). The dielectric strength of liquids and solids can also be characterized by similar graphs, but there are more extensive complications with condensed-phase insulators and specialized references should be consulted[256].

It must be emphasized that Paschen's Law is *not* used in the design of low-voltage equipment. Figure 28 compares the breakdown gap according to Paschen Law to values mandated by IEC 60079[257] for the design of electrical equipment. There are many standards worldwide that govern gap sizes (clearances) required for low or medium-voltage equipment, but they all mandate values much larger than the minimum that would suffice to prevent breakdown. Using the IEC 60079 example, at 10,000 V the safety factor is 41×, increasing to 78× at 1000 V and 700× at 240 V. At 120 VAC, of course, Paschen's Law would predict that breakdown is impossible, but the clearance mandated is 2.5 mm. According to Paschen's Law, to obtain breakdown for a 2.5 mm gap requires 6500 V.

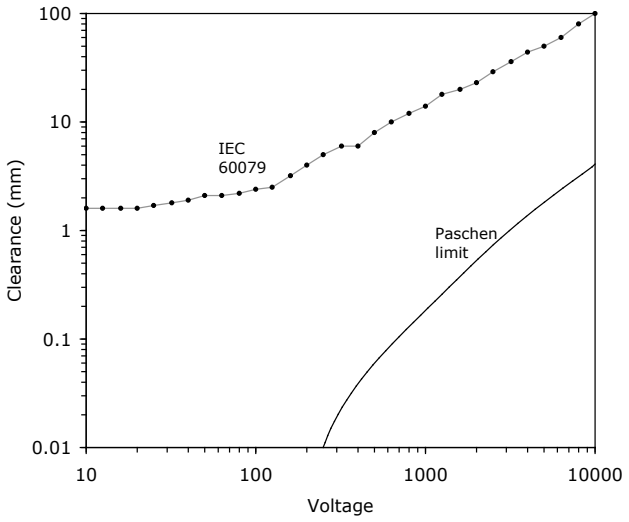


Figure 28 Comparison of Paschen values for an air gap at a given voltage (rms) to clearances required by IEC 60079

Electric 'sparks' and 'arcs' are terms that are basically similar and are sometimes used interchangeably. Thus, the loosest definition is "Electrical arc or spark: The transfer of electrons across a gap." In most cases, however, it is useful to observe differences between the two terms. Both refers to a discharge which occurs in a medium—commonly air—when the impressed voltage exceeds the dielectric strength of the medium. In one set of definitions, the differences are expressed thus:

- An electric *spark* is a dielectric breakdown of a gas between two electrodes in which the liberation of secondary electrons from one of the electrodes is the major feedback mechanism to sustain the discharge.
- An *arc* is a stable discharge between two electrodes in which thermionic emission is the feedback mechanism responsible for sustaining the discharge.

The primary difference is that *spark* denotes a transient phenomenon, while *arc* denotes a sustained event. If a discharge is sustained for prolonged time, eventually the cathode heats up sufficiently so that thermionic emission from the cathode becomes an important mechanism of liberating electrons.

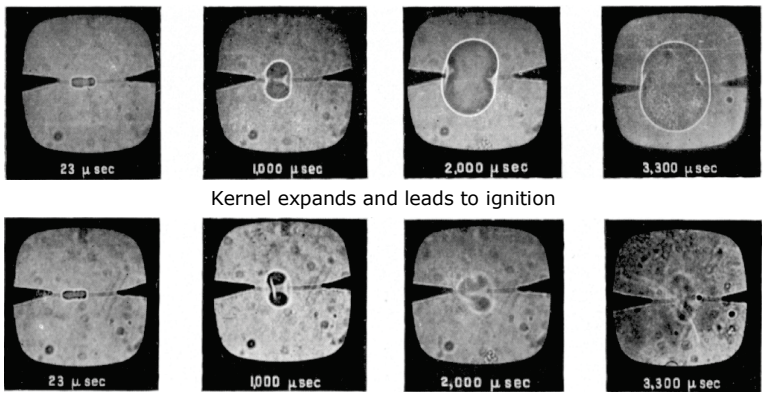


Figure 29 Kernel propagation versus non-propagation[258]
(Copyright HMSO, used by permission)

THE ELECTRIC SPARK

The details of spark ignition are complex and involve an interaction of physics and chemistry effects. Much of the process is now understood, because of its importance to wanted ignitions, specifically, towards improvements in internal combustion engines. However, mathematical theories of all forms of electric discharges are highly complex and specialized, and only the simplest results will be reviewed here.

Maly and Vogel[259] have provided a detailed explanation of the process as it occurs in lean mixtures. The ignition process occurs in three basic phases. When a high voltage (typ. 15 kV) is presented across a small gap, for about 10^{-9} s there is no current flow. After that time, the *breakdown* phase begins. An extremely large current of about 200 A flows for 1–10 ns (1 ns = 10^{-9} s). A cylindrical plasma channel of about 40 μm diameter develops. The plasma rises to a temperature of ca. 60,000 K. Such enormously high temperatures which are localized to a small area are difficult to measure experimentally, and earlier literature had generally given lower values.

The electrical energy supplied is converted into the energy of dissociating and ionizing the molecules in the plasma channel. The dissociated species are typically radicals such as the atoms C, H, O, and N. The pressure in the channel jumps to about 200 atm and is accompanied by the formation of a shock wave. The shock wave causes expansion of the plasma channel, which then causes the temperature to drop. This leads into the *stationary arc* phase. This phase is much longer and lasts for about 1 μs (10^{-6} s). During this phase, the voltage across the gap drops to about 50 V. The current is highly dependent on the impedances of the external circuit, but is several orders of magnitude lower than the current during the breakdown phase. Only about 1% of the molecules remain ionized during the stationary arc phase, but the degree of dissociation remains high. The arc expands to a width of a couple mm, due to a combination of heat conduction and mass diffusion. The temperature during this phase is on the order of 6,000 K, but heat release is negligible. The current continues to fall during this phase. When it drops below about 200 mA, the final phase occurs. This is the *glow discharge*, and it lasts for more than 1 ms (10^{-3} s). During this final phase, the gap voltage rises to 200–500 V, while the current continues falling below the 200 mA level. The temperature is now ca. 3000 K, with less dissociation and only about 0.01% ionized molecules.

For some purposes, it can be useful to characterize the resistance of the spark channel. Eckhoff [260] analyzed a number of studies and concluded that all of the results can be collapsed into a single relation for R (Ω):

$$R = 40 L_s I^{-1.46}$$

where L_s = spark gap (mm), and I = current (A). The studies were all based on capacitive discharge, so the equation should not be applied to other conditions. The relation is

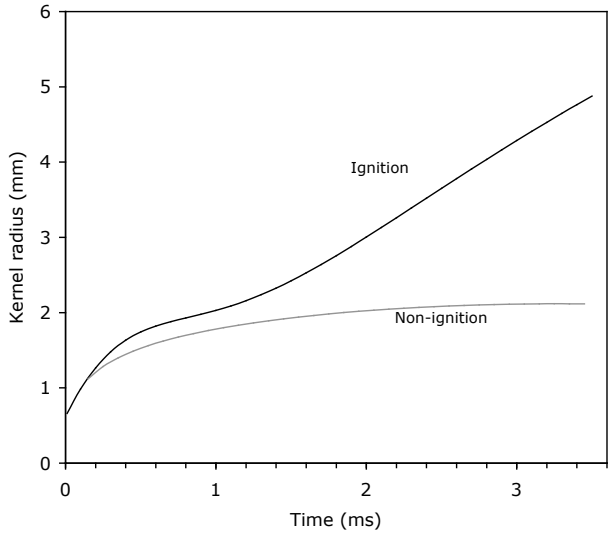


Figure 30 Growth of spark kernel in methane/air mixtures ($\varphi = 0.9$)

valid for discharge currents of 1 mA to 10 A. Chapter 4 contains further information on electric circuit parameters and their effects on spark discharge characteristics.

The spark kernel always dies out if spark discharge is in a non-flammable atmosphere. But if the atmosphere is flammable, the spark kernel, once created, may propagate or die out and not propagate (Figure 29). Conceptually, the problem is that of self-heating, as discussed in Chapter 4. The generation of heat from chemical reactions is proportional to the volume of the kernel, while the heat losses are proportional to its surface area. Thus, if the kernel becomes sufficiently large, it has a chance of surviving, i.e., propagating. Up until it reaches that size, however, it is dependent on there being sufficient electrical energy put into it to sustain its growth.

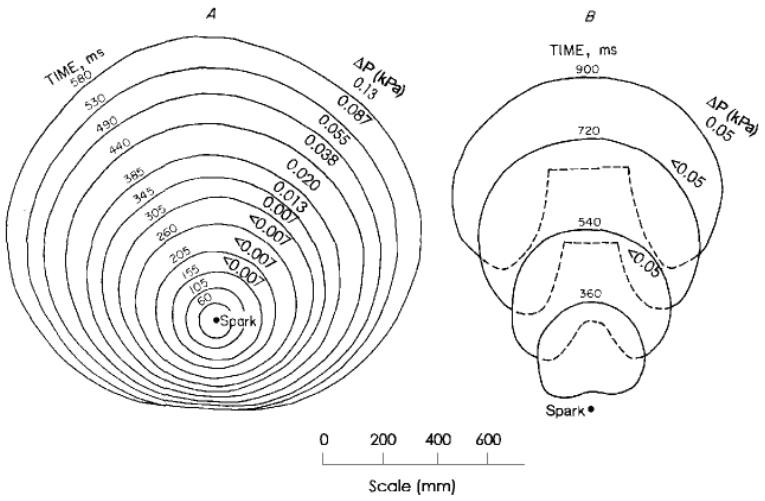


Figure 32 Flame development after spark ignition in methane/oxygen/nitrogen mixtures[270]

If the spark is of short duration, then the flame kernel initially starts out ellipsoidal shaped, then changes into a toroid (doughnut shape), centered on the spark gap. Some illustrative examples photographed by Kono and coworkers are shown in Figure 31, while Figure 33 shows the computed temperature field in the early stages of spark kernel development[261]. At about 200 μs, the kernel either starts decaying or expanding, leading to sustained ignition in the latter case[262,263]. This is taken to suggest that a value of around 200 μs is the minimum time required for ignition. At about 1 ms, the toroid shape becomes spherical.

Lintin and Wooding[264] reported on results of spark kernel growth in methane/air mixtures. Figure 30 shows that up to about 200 μs (0.2 ms) the growth curves of sparks leading to ignition and to non-ignition are identical. After that point, they diverge and after this time, in the non-ignition case, the kernel slows its growth and shortly thereafter stops growing. As a rough criterion, it has been suggested that the spark kernel must grow to a certain size radius by 200 μs if ignition is to occur. The value depends both on the nature of the gas and on its equivalence ratio; for hydrocarbon gases at $\varphi \approx 1$, radii of 2 – 3 mm are needed[262]. The initial volume of the kernel is proportional to the spark energy. Once formed, the size of the flame kernel in the early stages grows with its diameter increasing proportionately to ln (t), as demonstrated experimentally by Chomiak[265]. This growth rate is generally independent of any local flow velocity and is also independent of the exact fuel fraction in an ignitable mixture. These results pertain to still-air conditions; a similar study on turbulent methane/air mixtures was reported by Akindele et al.[266] The time scale discussed above is the one pertinent to normal capacitive discharge sparks. In the case of inductive sparks which are intentionally of long duration (e.g., for internal combustion engines), the time scale is different and the critical radius is much larger[267]. Similarly, the time and distance scales become large for flames at sub-atmospheric pressures[268]. Once kernel growth is established, Xiong et al.[269] documented that the radius continues to grow at a rate which is very close to linear: in methane/air and propane/air mixtures, they saw a linear growth up to the maximum size studied, 35 – 40 mm.

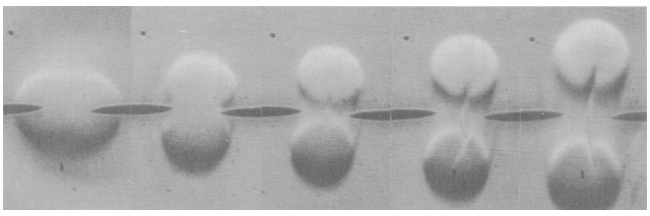


Figure 31 Development of a toroidal kernel (times: 4, 14, 24, 40, and 70 μs)
(Copyright The Combustion Institute, used by permission)

The further development of the flame front from a spark ignition has been studied by the Bureau of Mines[270]. Figure 32 shows flame development for two methane flames, developing in a 3.65 m diameter sphere. The first flame (A) is in a mixture which is well within the flammability limits, with the second one (B) being a near-limit mixture. The near-limit flame shows only vertical flame propagation, while flame A shows also substantial downward propagation, although, because of buoyancy, upward propagation is always greater.

In many practical cases, the flame development is much less uniform and symmetrical than in this example. Figure 34 shows flame kernel development photographed by Dobashi[271] under several conditions. Only when the mixture is uniform and quiescent is there a spherical pattern. Otherwise, even at the early stages the flame shape is already highly irregular.

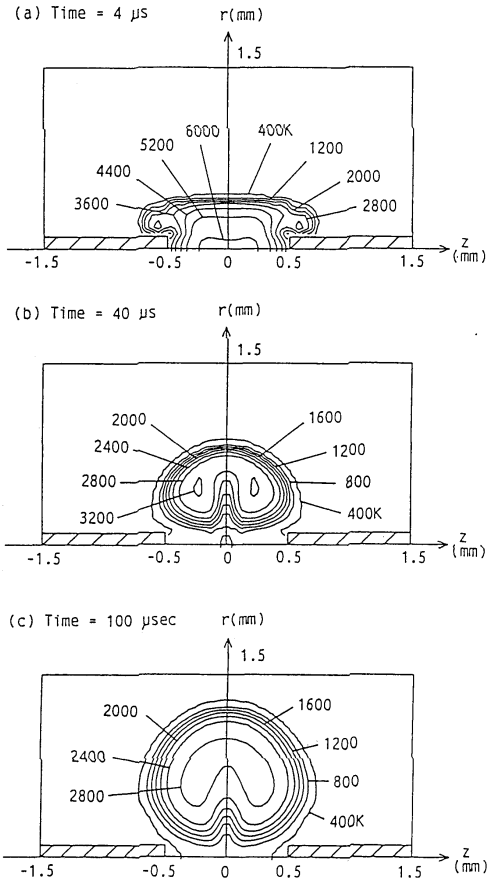


Figure 33 Computed temperature field in the early development of a spark kernel
(Copyright The Combustion Institute, used by permission)

Using their 3.65 m sphere, the Bureau of Mines ignited a mixture of 13% CO in air[272]. The flame development (Color Plate 18) shows strong irregularities, despite the ideal test conditions.

Thiele et al.[273] reported the results of an ambitious numerical modeling effort in representing the growth of a spark, even though their study was restricted to a 2-dimensional, cylindrical representation. This captures most of the important features, but not buoyancy effects. The model includes detailed chemical kinetics, radiative transport, and an electrodynamic model, but not the very earliest stage of breakdown channel development. Using the model, they made detailed calculations of spark development in air, hydrogen/air, and methane/air mixtures, although details of the latter were not given. The model gives realistic predictions of the development of the toroidal shape of the flame kernel. An interesting result from the simulation is that the growth of the flame kernel (radius vs. time) is affected by the shape and size of the electrodes. In a hydrogen/air mixture, flame kernel growth is much faster than in methane/air. By 0.2 ms, the kernel reaches about 4 – 5 mm, whereas in methane/air, the radius is only about 1.3 mm, as shown in Figure 30. In methane/air mixtures at normal gravity[274], a spark kernel initially rises at a speed of about 0.3 – 0.6 m s^{-1}.

In a computational study, Sloane and Schoene[275] examined the optimum fraction of total ignition source energy in the form of energy of dissociation. For stoichiometric methane-air mixtures, about 10% of total energy in the form of dissociation was found to be 'optimum,' i.e., leading to the lowest total ignition energy requirement. The effect was very mild, however. The optimum dissociation fraction lowered the minimum ignition energy only by about 6%. The effect was much greater on the ignition delay time. Under one set of conditions, providing 10% of the energy in the form of dissociation lowered the time from 250 μs to 100 μs.

Spark development has also been studied within the automobile industry using extremely rapid discharge circuits of ca. 50 ns during which time a peak power of 1 MW is reached; however, the characteristics of such ultra-rapid discharge sparks are not identical to those created in normal test circuits, nor to those of accidental electrostatic discharges[276].

The *net energy* available from the spark for ignition purposes excludes those portions developed in the cathode-fall and anode-fall portions of the spark channel[277] (see Figure 36). This concept would have a practical utility if an equation were available relating the fraction of energy that is available to physical details of the electrode arrangement, but such a partitioning rule has not yet been offered.

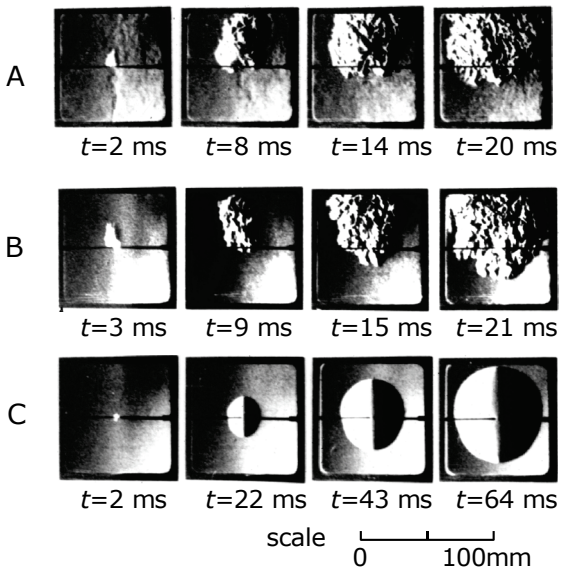


Figure 34 Flame kernels studied by Dobashi. **A**. non-uniform mixture, turbulent; **B**. uniform mixture, turbulent; **C**. uniform mixture, quiescent
(Copyright Elsevier Science, used by permission)

For extremely small gaps on the order of 0.2 μm, a category of spark known as *contact discharge* can occur. In a contact discharge, the bulk of the energy is dissipated at the anode surface, raising it to its boiling point and vaporizing it. A shower of molten metal is sometimes visible in the discharge. Eventually, the vapor condenses on the cathode. The process can ignite certain very sensitive solid explosives[278] and has mostly been studied in the context of susceptibility to electrostatic discharge.

Ignition of various substances by electric sparks is considered in Chapters 4, 5, 6, 7, and 14.

THE ELECTRIC ARC

As discussed above, a spark is, by definition, a non-steady phenomenon. In addition, there are several types of steady-state gas discharges, as shown in Figure 35. Only the arc is important of those from a safety viewpoint, and it corresponds to discharges of the highest current and the lowest voltage.

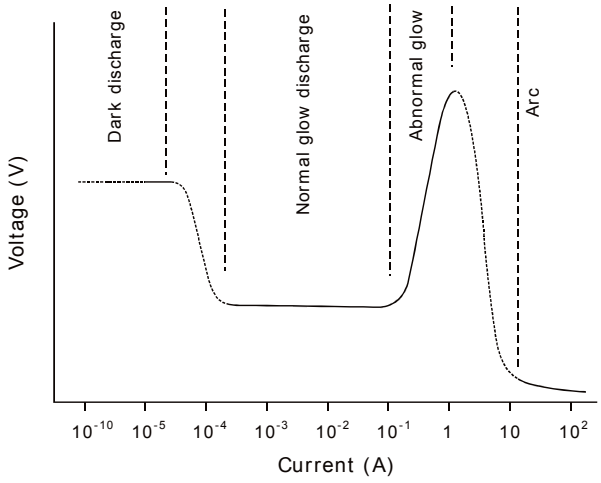


Figure 35 Schematic representation of steady-state voltage and current for several discharge types

Electric arcs have certain general characteristics, but they may be created in some dissimilar ways:

(1) By imposing across an electrode gap a high enough voltage to cause breakdown of the medium, i.e., an electric spark, and arranging that sufficient voltage and current are available from the power source to sustain a steady arc. In other words, the discharge starts as a spark and becomes an arc. The medium of most interest is air, although breakdown of other gases, and also of liquids or solids can be of interest. This form of discharge is normally important only in high-voltage (> 600 V) circuits.

(2) By moving a pair of electrodes (electric contacts) towards each other until they touch, then pulling them away. 'Striking' an arc is a procedure well-known to welders, but it also occurs at the contacts of electric switches. High voltages are not required.

(3) Arcing across a carbonized path.

(4) Glow to arc transition.

An electric arc may often be accompanied by ejection of small incandescent airborne particles. These have been treated earlier in this Chapter under *Hot solids or liquids*; additional information is presented in Chapter 14 under *Forest materials, vegetation and hay*.

Arcs are commonly subdivided into long arcs and short arcs. In a short arc, electrons emitted from the cathode move nearly directly to the anode. In a long arc, however, a region develops in between the electrodes where electrons sustain multiple collisions. Considering first the *long arc*, in steady state, the distance between the two electrodes can be divided into three regions: a *cathode fall* region, a linear region called the *long column*, and an *anode fall* region (Figure 36). In the long column region, the voltage/distance relation is a straight line. But in the spaces close to the two electrodes, voltage changes rapidly and non-linearly with distance. The cathode fall distance is typically 10^{-3} to 10^{-2} mm, over which a drop on the order of 8 – 20 V (typically, 8 – 9 V when using a copper electrode[279]) occurs. Electrodes of other materials give a slightly different voltage drop. The anode fall region is typically 10^{-3} mm and has a voltage drop of 2 – 6 V with a copper electrode. Both the cathode and the anode fall regions are separated from the long column by transition zones (boundary layers) which are significantly longer than the fall regions themselves. Since the temperatures in the long column are at least an order of magnitude greater than the anode and cathode surfaces, the boundary layers serve to change the temperature from that of the metal to that of the plasma. For distances shorter than the combined sum of the cathode fall and the anode fall regions, no linear region exists; these are *short arcs*. The total voltage drop across a short arc is typically 20 – 30 V, but may be as low as a few volts in some cases[253].

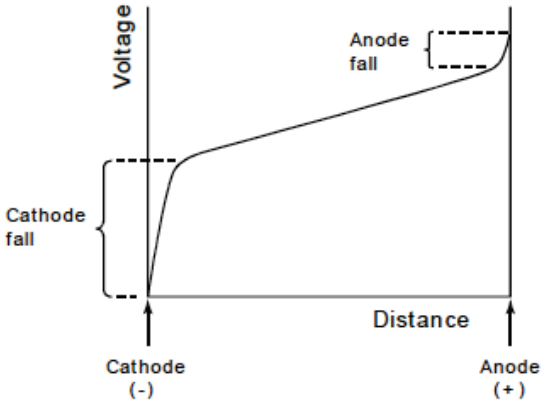


Figure 36 Regions of the long arc (not to scale)

The plasma is chemically reacting and a number of mathematical models have been proposed for its characterization. Due to its extremely high temperature, the plasma radiates very strongly, primarily in the ultra-violet (UV). However, most of the radiation is re-absorbed in the colder regions at the periphery of the plasma channel. The boiling point of the material forming the cathode of an arc has an important effect on the details of the arc. The temperature of the cathode cannot exceed its boiling point. For metals common in accidental arcs, even copper has a low enough boiling point (2562ºC) that it functions as a *cold-cathode arc*. High-temperature arcs include ones where the cathode is made of tungsten, molybdenum, zirconium, or other high T_b metals.

The temperature of an arc can vary widely. Under ambient pressure conditions, it is commonly 6000 – 12,000 K, but can reach 50,000 K. The primary factor governing arc temperature is the arc current. In a theoretical study, Lowke[280] concluded that there are two different regimes of arc operation—below about 30 A, the arc is stabilized primarily by natural convection. Above about 100 A, self-induced magnetic forces predominate. The predictions of his theory, along with data from Pflanz[281], Matsumoto[282], and Lowke, are shown in Figure 37. Also shown is the empirical data fit:

$$T = 6500 \qquad I_a \le 4.5 \text{ A}$$
$$T = 4010 + 1658 \ln I_a \qquad I_a > 4.5 \text{ A}$$

The theoretical predictions are only loosely obeyed, so the empirical data fit should be sufficient for calculational purposes. A temperature is meaningful only for a system whose constituents are in thermal equilibrium and an arc is not necessarily in thermal equilibrium—free electrons, ions, and neutral atoms can be at different temperatures. Arcs at atmospheric pressure, however, tend to be fairly close to thermal equilibrium. Lowke also provided a theory for arc radius. For low-current arcs (< 200 A), there is a complex relationship, but radii are typically between 2.5 to 10 mm. For high-current arcs (> 200 A), the radius can be obtained from the relation that arc current density[280,283] (current per cross-section area) is roughly a constant at 90 – 150 A mm^{-2}.

Once established, an arc does not necessarily last forever. In AC circuits, current goes to zero twice each cycle, and the arc may fail to get re-established once current flow restarts. An arc will also stop if the power source is disconnected so that no more voltage is supplied to the arc. In the design of circuit breakers, it is important to make provisions that the arc which results upon opening the contacts becomes quickly extinguished. Various stratagems are employed, the most universal of which is a scheme whereby the arc progressively lengthens until it can no longer be sustained. Other techniques include using an air blast to blow the arc away and directing the arc into chutes where its path is broken up and heat losses are introduced through baffles.

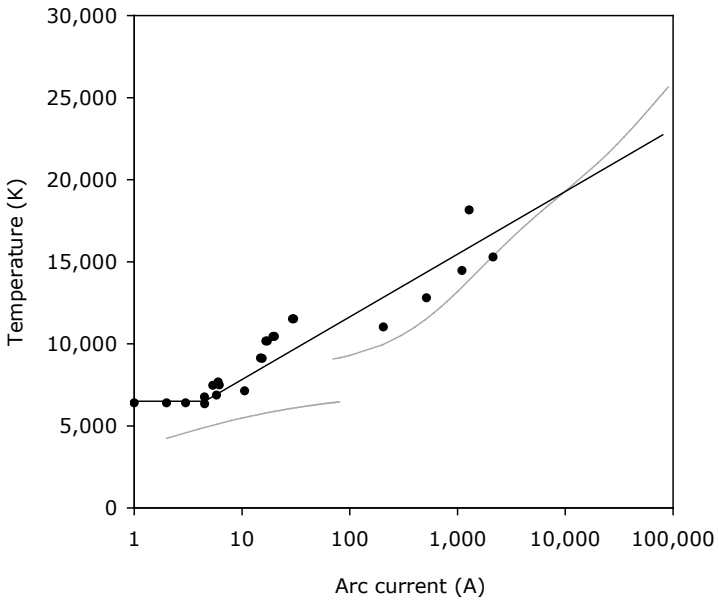


Figure 37 Temperature of arcs in ambient-pressure air, along with predictions from the theory of Lowke (gray lines) and an experimental data fit (black line).

Once a gas breakdown has occurred, the current flow is determined largely by the available voltage and the circuit resistance of the external circuit. In low-voltage circuits, the minimum length of an arc is about 0.1 mm. If electrodes are brought together to a closer distance, the arc jumps out of the gap, so as to maintain a minimum length. As an arc continues to operate, the electrode materials are eroded. Eventually, the arc will be extinguished if the electrodes are not moved closer together. The distances attained before extinction can be surprisingly large. In one series of tests using a 300 VDC supply providing up to 2400 A[284], when two copper electrodes were used, the gap length at extinguishment was 38 mm; with one copper and one steel electrode, it was 51 mm; while with two steel electrodes it was 76 mm. For applications where it is *desired* to create a stable arc (e.g., arc lights) carbon electrodes are commonly used; since carbon does not melt and only oxidizes or gasifies slowly, carbon electrodes provide an arc gap which only slowly changes its dimension.

The effect of buoyancy can act to substantially affect the shape of an arc. Color Plate 19 shows a horizontal arc[285] across a 500 mm gap of a 160,000 VAC power supply and with a measured arc current of 400 A. The arc starts to meander during the 10 ms time frame, but does not yet distend upwards. The latter behavior was examined by Drouet and Nadeau[286], who conducted experiments using currents up to 80 kA and observed that for free-burning arcs in air that lasted up to 0.5 s, the length grew in time according to:

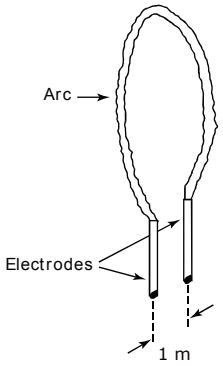


Figure 38 Geometry of electrodes and shape of arc

$$L = 30t$$

where L = length of arc (m) and t = time (s). The minimum length was 1 m, the distance between the electrodes, and the arcs grew up to 15 m long in the space of 0.5 s. As the arc grew, the shape bulged upwards, shown in Figure 38.

In another study, using a 6000 VAC circuit, actual arc lengths up to 2000 mm were observed between electrodes spaced 100 mm apart[287].

It is often of interest to know the voltage/current characteristics of an electric arc. Representing an arc as a circuit element is complicated, since its effective impedance changes dynamically with time. In addition, an arc shows two different current regimes—a low-current, convectively-dominated regime and a high-current regime dominated by self-magnetic effects. Actual voltage/current characteristics are governed by a number of factors, including:

- the gas in which breakdown is occurring (e.g., hydrogen requires a higher voltage than air);
- the pressure of the gas (higher pressure requires a higher voltage);
- gas flow velocity and turbulence (a higher flow velocity requires a higher arc voltage due to convective losses);
- magnetic fields (generally increase the arc voltage due do increased power dissipation);
- electrode material entrainment into the arc (normally reduces the arc voltage);
- ablation of insulating materials (this causes power absorption).

In this Section, characteristics will be considered only for the simplest case of an arc between copper electrodes, in air at 1 atm and without imposed convective flow, magnetic fields, etc. Stokes and Oppenlander[287] found that, for electrode gap in the range $5 \le L \le 500$ mm, the current defining the transition between the low-current and the high-current regimes is:

$$I_t = 10 + 0.2L$$

where I_t = current (A) and L = gap length (mm).

For $I > I_t$, the minimum power dissipated is:

$$P = (20 + 0.534L)I^{1.12} \qquad \text{horizontal or vertical arcs}$$

For $I < I_t$, they found the relations:

$$P = P(I_t) \qquad \text{horizontal arcs}$$

$$P = P(I_t)\left(\frac{I}{I_t}\right)^{0.4} \qquad \text{vertical arcs}$$

In the latter two equations, $P(I_t)$ is to be evaluated by inserting I_t into the large-current P expression. These equations give a good estimate of the *minimum* power dissipated, and the authors validated them over the range 50 W – 30 MW. But the *actual* power dissipated is highly variable and does not lend itself to a systematic representation. Some experimental results are shown in Figure 39. These results indicate that the arc represents a circuit element with a positive conductance for $I > I_t$, but acts as a negative-conductance device at low currents. The arc voltage in their model is obtained by using the relation $V = P/I$. For $I > I_t$, it becomes:

$$V = (20 + 0.534L)I^{0.12}$$

Similarly, since $R = P/I^2$, the arc resistance in the large-current regime is obtained as:

$$R = (20 + 0.534L)I^{-0.88}$$

In the low-current regime, the expressions become:

$$V = (20 + 0.534L)(10 + 0.2L)^{1.12} / I \qquad \text{horizontal arcs}$$

$$V = (20 + 0.534L)(10 + 0.2L)^{0.72} / I^{0.6} \qquad \text{vertical arcs}$$

Quite similar trends were observed by Conrad and Dalasta[288]. They used a 470 VAC power supply and very small electrode gap distances—6.35 to 25.4 mm. Over the current range 270 – 23,000 A, they also got a straight line when plotting the results on a log-log scale, and their lines show the same 0.12 slope as do Stokes'. There is a systematic difference in the constants describing their line, however,

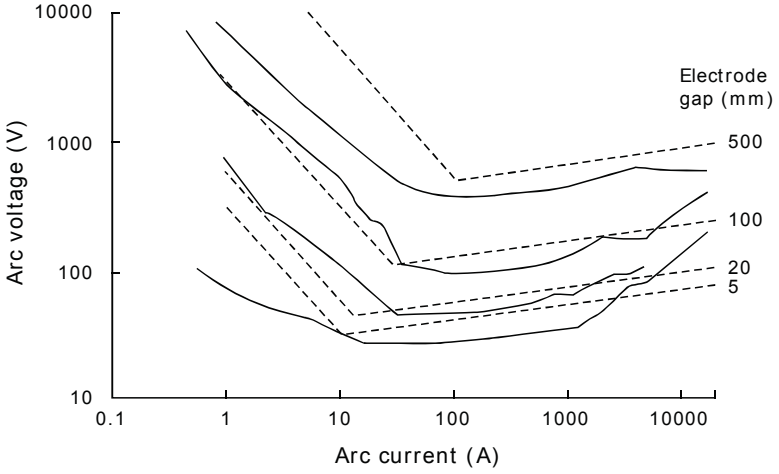


Figure 39 Minimum current/voltage characteristics measured for horizontal arcs between copper electrodes; dotted lines indicate predictions from equations developed by Stokes and Oppenlander
(Copyright Institute of Physics, used by permission)

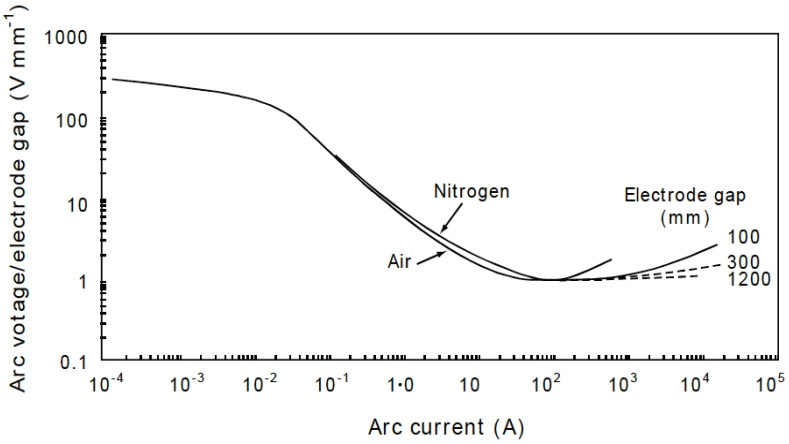


Figure 41 Simplified representation of V-I relation for AC arcs in air and nitrogen as developed by King

with the equation that can be fitted to their results being:

$$V = (16 + 1.0L)I^{0.12}$$

For most purposes, a somewhat simpler representation is adequate, and King[289] showed that in the convectively dominated regime (I < 100 A), it is adequate to assume that the overall voltage gradient (that is, the arc voltage divided by the electrode gap distance) is independent of the gap distance (Figure 40). The following equation represents well enough his results for air in this regime:

$$\frac{V}{L} = 0.961 + \frac{4.04}{0.0156 + I}$$

King's results did extend far enough into the high-current regime to establish firm trends there, however, the fact that the voltage gradient is near-horizontal for large gap distances in that regimes suggests that a limiting value is $V/L \approx 1.0$ V mm^{-1}. Strom[290] conducted experiments with arc currents ranging from 70 A to 22,000 A and electrode gaps of 300 – 1200 mm. In this range, he found a nearly-constant V/L ratio of 1.2 – 1.5 V mm^{-1}, with the lower value being typical for I < 7000 A and the higher for I > 7000 A. Since his range corresponds to the right-hand portion of King's graph, where the V/L values rise above the 1.0 V mm^{-1} minimum, Strom's results can be considered to be quite similar to King's. Strom did not find an electrode-gap effect *per se*.

A number of other workers developed other expressions for arc voltage, current, or resistance. Browne[291] considered the current regime $1.5 \le I \le 15{,}000$ A and gave the expression:

$$V = 30 + 1.18L + \frac{11.8L}{I}$$

The form of this equation is sometimes identified as Ayrton's equation, since Hertha Ayrton[292] first proposed it in 1903. In that same low-current regime, old studies indicate that the dependence on current is not necessarily of the –1 power, but that the power depends on the material from which the anode is made[293]:

$$V \propto A + \frac{BL}{I^n}$$

where $n = 2.62 \times 10^{-4} T_b$, where T_b = boiling point of the anode material (K). Since T_b for copper = 2835 K, according to this relation n = 0.74. Modern data do not exist to determine whether such a power law is useful.

For high-current (7,000 – 80,000 A) long arcs, Goda et al.[294] proposed the following expression:

$$V = 0.95L + \frac{5.0L}{I}$$

This equation shows an extremely tiny drop in voltage with increasing current but it is actually not a good fit to Goda's data, which indicate that a better fit is given by:

$$V = 0.98L + \frac{400L}{I}$$

In the high-current regime, Browne's relation and Goda's (both original and corrected) show a voltage that falls very slightly with current, while King's and Stokes' data give a voltage that increases with current. The four expressions are compared in Figure 41. Sizable differences have always been seen in comparing studies on arc voltages—in the words of Browne[291]: "Actual arc voltages are so sensitive to particular conditions that departures from the equation by 100% or more are to be expected." However, since two equations show an upward trend with increasing current, and two downward, the conclusion that emerges is that current dependence is evidently very small. On that basis,

$$V = 1.2L$$

may best capture the available results. The lack of a universal dependence of voltage on current was confirmed in

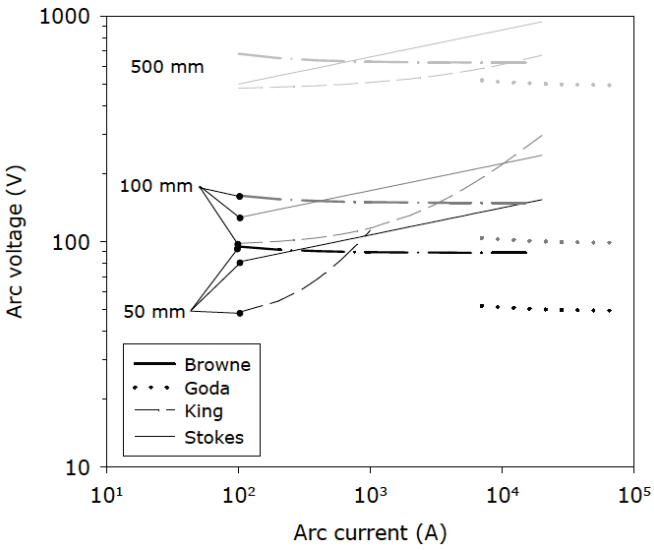


Figure 40 Comparison of three different expressions for arc voltage, applicable to the high-current regime (Goda's expression shown is the corrected equation). Expressions are shown for three different electrode spacings.

studies of Koch and Christophe[296], who created arc faults at splices of underground power cables and found *V–I* characteristics that ranged from (a) voltage decreasing with current, to (b) voltage independent of current, to (c) voltage increasing with current.

When a value of arc resistance are needed, knowing arc voltage and current, it can be computed simply as $R = V/I$. In addition, Fisher[295] recommends the following expression for arc resistance, applicable only to circuits carrying 600 VAC or less:

$$R = 4.96 \frac{\sqrt{L}}{I^{0.85}}$$

In line with the V – *I* relationships studied above, this indicates a dependence on current that is slightly less than unity power. However, while the other researchers typically obtained a linear dependence on *L*, Fisher's expression has a square-root dependence.

To use any of the above relations, it is necessary to estimate the arc current. This topic involves consideration of the details of the circuit and is treated in Chapter 14.

In practical AC circuits, the arc voltage waveforms are strongly non-sinusoidal and generally are non-repetitive as well[296]; that is to say, the waveform looks substantially different in each new current cycle. The latter effect arises because the arc creates a self-modifying environment, since arcing affects both the condition of the electrodes and of the atmosphere in which the discharge is taking place. Thus, a dynamic expression would be needed to model the circuit's time response. Dynamic models for predicting arc voltages and currents have been described by various researchers for low-voltage[291,297] (≤ 600 VAC) circuits, and high age[298-300] systems. In any case, steady-state arc circuit representations cannot be used to estimate whether an arc will burn stably or will self-extinguish, not only because physical meandering of the arc is important, but also because extinguishing criteria are intrinsically based on waveform details.

The voltage across an arc occurring in transformer oil has been represented as[301]:

$$V_a = 8.8 L_a$$

The *enthalpy density*[281,285] of an arc in air at 1 atm is approximately 0.8 – 0.9 MJ m^{-3}.

According to Lee[302], the *power* of an arc, *P*, can be conservatively estimated* as being:

$$P = 0.5 VA_{sc}$$

where VA_{sc} = bolted-short volt-amperes. This relation comes from assuming that the load (arc) impedance is equal to the source impedance, which is the condition at which the maximum power can be transferred to a load. For distribution transformers rated 750 kVA or higher, Lee also recommends that the fault current be estimated as:

$$VA_{sc} = 10 VA_{\text{tranformer nameplate rating}}$$

while for smaller transformers the multiplying factor is 12.5, instead of 10. Using the same assumptions, it can also be shown[308] that for a 3-phase arc,

$$P = 0.5\sqrt{3}\, V I_{3PH}$$

where *V* = rms voltage, and I_{3PH} = phase current during a 3-phase bolted short, while for a phase-to-phase arc the corresponding power is:

$$P = 0.5 V I_{P-P}$$

where $I_{P-P} = I_{3PH} \times \sqrt{3}/2$ or 86.6% of the corresponding 3-phase bolted short current. Thus, the arc power for a phase-to-phase arc becomes:

$$P = 0.25\sqrt{3}\, V I_{3PH}$$

Lee assumed that the entire arc power is dissipated by thermal radiation, which conservatively ignores the portion of the energy dissipated as conduction and as a pressure or shock wave. Convective losses do not enter into the problem since for short time periods buoyancy flows do not get started. However, the entire arc power is not delivered in the form of thermal radiation, and the fraction which is delivered is governed by a number of variables, including:

- the gas in which the discharge is taking place
- the pressure
- entrained contact material.

Latham[303] developed an arc model which also ignores the energy delivered as a pressure wave or a shock wave but does include heat conduction losses. Using this model, he computed the thermal radiation fraction for various arcs currents. Figure 42 shows that, in Latham's model, the radiant fraction becomes high for currents over about 1000 A, but is in the vicinity of only 20% for low arc currents.

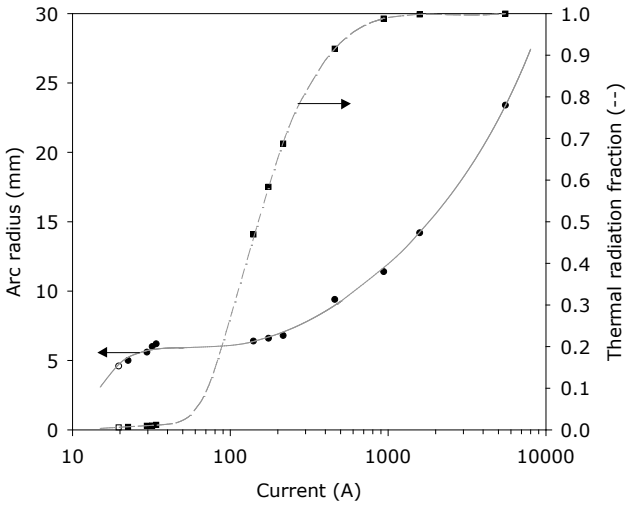


Figure 42 Radius and thermal radiation fraction for long arcs, calculated from Latham's model

* His equations are based on a very simplified view of short-circuit currents. Chapter 14 discusses the topic in more detail.

Lee's assumption of 100% radiant efficiency has been criticized by Stokes[287] as being so overconservative as to be impractical. Stokes points to the studies by Ernst and Strachan as being more realistic. Ernst et al.[304] concluded that assuming 10% of the arc power to be delivered in the form of radiation is more consistent with experimental measurements. Strachan[305] showed data for arcs in an orifice flow geometry, indicating that less than 25% of the arc power is radiated if copper electrodes are used. For other electrode materials, the radiated fraction will differ; for carbon electrodes he found only around 11%. He also studied arcs between fixed, copper electrodes[306] and found that 40 – 50% of the arc power was radiated. Fievet and Maftoul[307] studied high-current moving and motionless arcs. For motionless arcs between copper electrodes, they found that about 25% of the arc power was delivered in the form of radiation. For moving arcs, the value was much lower, ranging from 20% at 1000 A to 7% at 7000 A. In an experimental study[308] on 3-phase arcs in a 600 VAC system, Doughty et al. found that actual arc power was 77% of Lee's assumed value. The value is lower than 100% since Lee's theory assumes that the impedance of the load (i.e., the arc) is identical to the impedance of the source, whereas real arcs establish an impedance governed by actual circuit characteristics. The authors also measured heat fluxes and found a value of 450 kW m^{-2} at a distance of 0.61 m from the center of a 13.5 MW arc, using a 3-phase arc in open air. When the arc was enclosed by a 5-sided metal box, the heat flux at the front face increased by about 3×. For the open-air case, if the arc is assumed to be roughly spherical (which is a reasonable assumption in this case due to the small electrode gaps used), then a radiant power of 2.1 MW is found, which means that 16% of the arc power showed up in the form of thermal radiation. The arc current in these tests averaged around 22,000 A per phase, which according to Latham's theory would have entailed a radiant fraction of 100%. Taken together, the available experimental results are not particularly consistent, but the general conclusion might be that about 20 – 25% of the arc power from a high-current arc between copper electrodes will show up as thermal radiation.

The thermal radiation is commonly referred to as *arc flash*. The consequences of not wearing protective clothing in an arc flash are illustrated[309] in Color Plate 20.

A DC arc will extinguish only if the power supply is removed or if enough material erodes to make the gap too large. In an AC circuit an arc will self-extinguish 2×60 times (2×50 times with 50 Hz power) per second, each time the current goes to zero. But it may re-ignite thereafter, if conditions are right. Whether or not the arc re-ignites afterwards depends whether the arc channel can recover so that it will not break down again with the new imposed voltage. For a recovery to be possible, temperature has to drop and ionized species have to have time to diffuse, encounter reaction partners, and recombine. If that occurs, then the breakdown strength can rise to a sufficient value to avoid a subsequent breakdown. The temperature can drop because heat losses are occurring through conduction, convection and radiation. If wire insulation was incinerated in the process of arcing, an additional factor comes in: the pyrolyzed polymer material may help to promote recombination but it may also lead to arcing across a carbonized path.

Arcs in circuits of less than 150 V tend to extinguish and not re-ignite when the waveform goes through the zero crossing. Arcs in circuits of over 600 V tend to draw very high currents and consequently may be relatively safer since a circuit protection device is likely to open. Voltages between 150 and 600 V are considered the most hazardous in regards to fires being ignited from arcing[310]. This is because the arcs tend to not be extinguished, yet the current flows are small enough that circuit protection devices operate slowly. Typical waveforms[311] for arcing in 120 VAC circuits are shown in Figure 43. Note the intermittent nature of the arc as it extinguishes and reignites. *Restrike voltage* in distribution busbars is considered in Chapter 14.

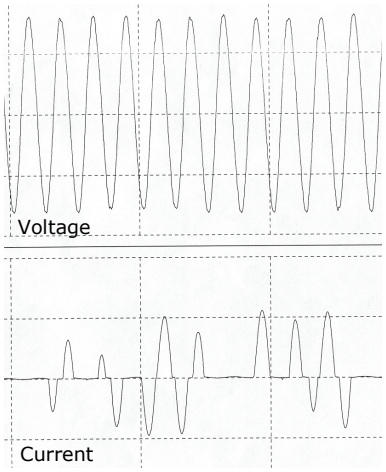


Figure 43 Typical waveforms during a branch-circuit arcing event

Arcing in a 120 VAC branch circuit was experimentally studied by Blades[312]. He found that a stable arc was difficult to create without the presence of polymeric insulation materials that might lead to arcing-through-char. The reason was because metal erosion would quickly increase the arc gap to the point where arcing could no longer be sustained. Sustained arcing was successfully demonstrated by using carbon electrodes, which do not undergo significant erosion. Even with those, for sustained arcing to occur required that the electrodes be preheated to ca. 80ºC. The preheating could be achieved by actually using a heater, or by repetitively undergoing a number of unsustained arcs, which would pre-warm the electrodes. To make the demonstration feasible, he had to construct an electrode spacing drive mechanism of high precision that permitted a very fine adjustment of the gap; without this precision control of the gap, the effect could not be demonstrated. The power dissi-

Table 27 Minimum voltage and current needed in resistive circuits to sustain an arc in air

Electrode material	Min. voltage V_m (V)	Min. current I_m (A)
aluminum	12	0.4
brass	11	NA
cadmium	8.5	0.03
carbon	20	0.01
copper	13	0.45
gold	9.5 – 15	0.38
iron	12 – 14	0.72
iron oxide	14	0.70
lead	9 – 11	0.21
nickel	8 – 14	0.5
palladium	15	0.5
platinum	13.5 – 17.5	0.9
silver	8 – 15	0.4
steel, carbon	14	NA
steel, stainless	15	0.5
tin	11.2	0.4
tungsten	10 – 16.1	1.0
zinc	9	0.03

pated in the arc was about 12.5 W. It is important to realize that arcing will often be *in series* with the load (e.g., at contacts), not in parallel with the line. There is no increased draw of current when a series arc occurs, instead, current flow will decrease, due to the series-flow of current. No overcurrent protective measures can have any effect against a series arc, but sophisticated methods have been developed that detect an arc 'signature'; these are described in Chapter 13.

An arc cannot be sustained unless there is both a minimum voltage and a minimum current available from the circuit[274,313-317], as shown in Table 27. Where available, the values of Zborovszky were preferentially cited, as hers were deemed to be measured most accurately; where not, the entire range found in the literature was cited. Surface contamination may change the V_m value slightly, but only limited results are available[274]. Values in other atmospheres are generally not too different. It must be understood that the voltage/current requirement is roughly hyperbolic, thus an arc will not be sustained if both voltage and current are at their minimum values. An arc running at near-minimum current will require a voltage much greater than the minimum voltage, and vice versa. The current needed for carbon is lower than for any other material. This has the practical implication in that a carbon coating may well be acquired on metallic contacts, and this could lead to very low currents being sufficient to sustain arcing. There are also some indirect data suggesting that hydrocarbon pollution of metallic contacts—without a visible layer of soot—may suffice to cause metallic electrodes to behave similarly to carbon electrodes[318]. Cadmium shows the distinction of having very low values both for minimum voltage and minimum current. Not surprisingly, this has led to the use of cadmium in the IEC/PTB break-flash test apparatus (Chapter 12). The values in Table 27 apply only to resistive circuits; minimum currents in inductive circuits may be substantially smaller[319], as discussed in more detail later. The minimum voltage/current values pertain to an arc of infinitesimal length. If the arc is made longer, the minimum voltage rises sharply, while the current less so. Yokomizu et al.[320] provide some illustrative data showing how the minimum arc voltage rises with increasing arc length or arc current. In a resistive circuit, an arc may be observed upon opening a contact, even if the supply voltage is less than V_m, but the discharge is so short-lived that it is usually not possible to ignite gas mixtures with them[274]. The important question, however, of the minimum voltage sufficient for a spark or arc to be incendive in a flammable atmosphere is poorly researched. Data discussed in Chapter 4 indicate that 4 – 5 V may suffice in resistive circuits and 0.5 V in inductive ones, but conditions under which such low voltages can suffice are not necessarily clear.

For situations where the two electrodes are not made of the same material, the minimum voltage can be viewed as being the sum of the cathode fall and the anode fall voltages, with voltages appropriate to the two materials being summed.

Apart from larger particles being ejected due to gross failure of the electrodes, both the anode and the cathode can generate a stream of tiny particles coming from it, with the particle formation being governed by forces of magnetic compression. The tiny particles have a velocity directed perpendicular to the surface.

Most cases of arcing require that a material such as plastic, wood, etc. be present nearby if the arcing is to lead to fire. But arcing to *aluminum electrodes* can directly lead to ignition of the aluminum metal[321].

Contact arcs regularly occur in electric switches, relays, and similar devices. They also occur inadvertently, when, for example, two bare current-carrying conductors are accidentally shorted. When considering electric switch contacts, the arc caused by closing the switch, is called a *make-arc* (or *closing arc*), while the arc caused in opening the switch is a *break-arc* (or *opening arc*, or *parting arc*). The process of creating an arc (at voltages which may be much less than the Paschen Law minimum of 340 V) is quite similar for both types of contact arcs. In the case of a break-arc the steps involved are:

(1) The electrodes that were originally touching at numerous spots start to touch at only a few very small spots.
(2) A high current density passes through the small metal diameter of contact area that is available.
(3) The 'metal bridge' joining the two contacts starts to melt.
(4) The bridge elongates and rises in temperature.

(5) The bridge reaches the metal's boiling point, becomes unstable and ruptures.
(6) Voltage rises rapidly across the gap, thermionic emission from the hot cathode starts, and eventually the gap becomes ionized and an arc forms.
(7) The diameter of the arc expands from that of the bridge to its eventual free-burning diameter.

The voltage across the gap at the moment of rupture is only ca. 1 V. The reason Paschen's Law does not apply is that is describes the characteristics of room-temperature, non-ionized gases, and the space between the contacts is ionized and at high temperature. Even though 10 – 15 V is needed for the steady-state operation of an arc, the arc is able to initiate with only a 1 V drop due to inductive effects of the two leads. If a current of at least ca. 1 A before the break has been carried and the polarity of the current remains unchanged for at least the time needed for positive ions to traverse the gap, then a stable short arc may be initiated. The circuit must also be such that before the ionization due to the initial spark has dissipated, the voltage between the electrodes rises to a value which is above the minimum. This may be prevented if a capacitor is connected directly across the electrodes, the capacitance of which is sufficient to delay the voltage buildup across the gap. Some devices with mechanical switch contacts incorporate a capacitor across the switch for exactly this purpose of preventing a continuing arc.

The voltage/current relationship for a break-arc at contacts in a low-voltage circuit depends on many physical details of the contacts, including the type of material, the separation speed, and the gap created. Figure 44 illustrates some data reported by Widginton[317]; additional examples have been given by Holm[313]. The asymptotic values (minimum voltage at high currents and the minimum current at high voltages) are higher than those given in Table 27 since the experimental conditions were not optimized so as to give minimum values.

In *closing* switch contacts (make-arc), the sequence of events is very similar. Contact is initially made at only a few high spots. These have limited current-carrying capacity and proceed to melt and rupture, at which point an arc develops. That arc in normally extinguished by heat losses when the contacts close together more tightly.

In circuits where either the minimum voltage or the minimum current requirement is not met for an arc, it might seem that arcing is simply precluded. But this is not necessarily true in real devices where 'parasitic' inductances or capacitances will invariably be present. Parasitic reactance elements are ones that are not purposely installed, but rather created by wiring, terminals, and other necessary physical arrangements. In the simplest example, even in a DC circuit, a parting arc can be created which has an repetitive waveform and higher voltage peaks than the power supply voltage. It may happen that initial vaporization of the metal

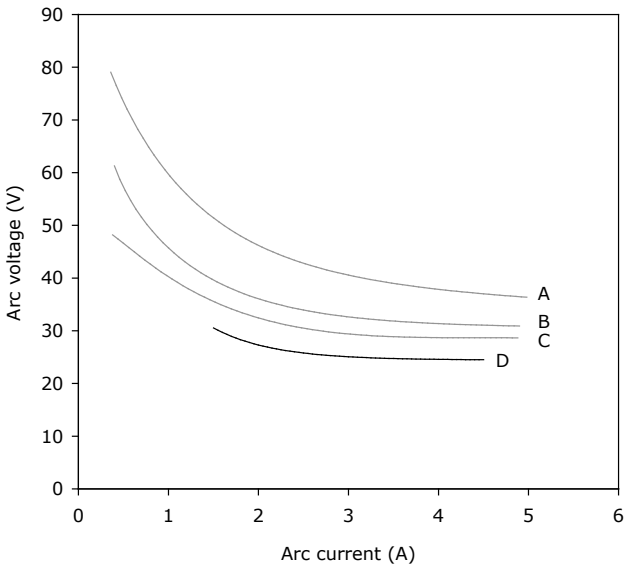


Figure 44 V-I characteristics of break-arcs caused by pulling apart 0.3 mm copper electrodes. **A** and **D** = 1.0 mm gap; **B** = 0.4 mm gap; **C** = 0.2 mm gap. Separation speed of **A**, **B**, **C**: 20 m s^{-1}; **D**: 0.01 m s^{-1}.

bridge allows for an arc to form, but as the contacts pull apart, the arc is not sustained. Current flow now abruptly drops to zero. This creates a back emf, $V = -L\frac{dI}{dt}$, where L = inductance (H) and I = current (A). Because of the abrupt drop in current, high voltages—in the kilovolt range—can be generated even with modest parasitic inductance. Thus, a circuit where power supply voltages and steady state voltages may have only been in the tens of volts can provide enough potential difference to cause a second breakdown in the gap. The process occasionally can go on for a number of cycles before final arc extinction. The discharge involved is not necessarily an arc, but may be a glow discharge or multiple spark breakdown. For example, with a very simple circuit where a copper wire was used to short-circuit a 6.3 V lead-acid battery, peak voltages of 17 – 22 V were measured across the spark gap that opened up due to melting of the wire[322]. Voltages in the vicinity of 300 V can be generated in this manner from a 24 V power supply[323]. In experiments on motor-contactor coils in a 220 VDC circuit, voltage peaks of 11,000 V (55× the supply voltage) were measured in extreme cases upon opening the circuit, although peaks of 10 to 20× were more common[324]. The authors also document an observation of a spark across fixed conductors 12.5 mm apart in a 550 V circuit; according to Paschen's Law, this would imply a discharge voltage of 37,500 V or a voltage ratio of 68×. Statistically, problems will be fewer in AC than in DC circuits, since in an AC circuit many contact openings will take place during a part of the cycle where worst-case behavior is not elicited, while opening a DC circuit is always effectively a 'worst-case' situation. In general, the duration of the spark discharge increases with in-

creasing power supply voltages, and at voltages less than V_m the duration is often only so short (a few microseconds) that the discharge is non-incendive.

A more complicated effect is *tank resonance*, which requires an inductive and a capacitive element. It is due to the formation of an RF resonant circuit between the main energy storage device (capacitor or coil) and parasitic circuit elements. Thus, for example, even if the circuit only has a single inductor as its reactive element, there will be a stray capacitance formed between the wiring. The small value of such a parasitic reactive element means that resonant frequencies are high. The resonant circuit can thus be charged to a much higher voltage than is the steady-state voltage of the connected power supply. Arcing recurs each time that the voltage reaches its breakdown value in the gap. A glow discharge can be especially effective for ignition, since the amount of energy going into a discharge in an inductive circuit is nearly the theoretical $\frac{1}{2}LI^2$ for a glow discharge, but about half that, $\frac{1}{4}LI^2$, for an arc discharge. It is hard to provide simple, general rules for circuits where both L and effects are important, since the problem then has several independent variables. In some situations capacitance in the circuit can be beneficial, since with an optimally chosen value, it can actually suppress arc formation[324].

The condition of the contacts in a break-arc geometry affect the discharge duration and, in turn, the likelihood of ignition. Inorganic surface contaminants (oxides, sulfates) generally increase the duration[274]. Very small amounts of organic contaminants can also prolong the duration of the discharge and thus increase the probability of ignition.

The characteristics of a break-arc are affected by the gases present in the atmosphere. In one study[322], it was found that the presence of methane in air shortens the discharge period and thus, makes the arc less incendive than measured in pure-air conditions.

Glow-to-arc transition has been illustrated by Attwood et al.[325], who studied arcing on 60 Hz AC powerlines. Figure 45 shows typical waveforms for current and voltage across the electrodes. Until a breakdown voltage (typ. 300 – 800 V) is reached, there is no current flow, or only a 'leakage current.' At breakdown, however, a small amount of current begins to flow. The voltage drops to a steady-state glow voltage of around 300 V, while the current continues to rise. At a certain point, depending on circuit characteristics, the voltage abruptly drops, while the current abruptly rises. After a short transient, a nearly-steady (slightly decreasing) arc voltage stabilizes, while the current continues to rise. The jump between glow and arc discharges requires a large current to be available, typically 100 A; conversely, once created, the arc is able to continue until current drops to a very small value (0.1 – 0.5 A). For recurring arcs, the breakdown voltage is called *restrike voltage* and is further discussed in Chapter 14.

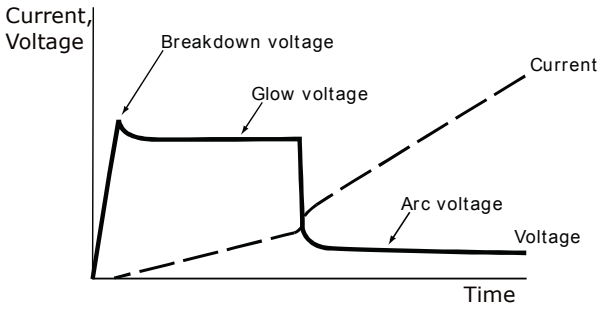


Figure 45 Glow-to-arc transition on an AC powerline (only the initial portion of a half-cycle is shown)

Arcing and vibration

In laboratory experiments, sustained arcing at contacts can be demonstrated by mildly vibrating clean, crossed copper conductors while passing a current[312]. This can create oxide bridges that lead to a glowing connection (see below). Once a glowing connection is established, it persists without needed for further vibration.

Pressures developed by an electric arc

When arcing occurs in sizable power transmission or distribution components, the arc can develop some very substantial pressures. It has been measured[326] that pressures from a 100 kA, 10 kV arc at a distance of 1 m away are about 20 kPa. This pressure is about 10× the capacity of many walls to withstand side-pressure, thus wall collapses can and have occurred. If the arc is not burning in open air, but is confined to a box, some enormous pressures can occur, documented in one case as being 7000 kPa. The pressure is developed due to expansion of metal as it is vaporized and by the heating of air to the high arc temperatures.

ELECTRIC CURRENT

Properly determining electrical causes of fires tends not to be too difficult when high-current or high-voltage circuits are concerned. But in the common scenarios of appliances of modest power or of branch circuits carrying loads of 20 A or less, investigation can be much more difficult. In either high-current or high-voltage situations, electrical failure patterns are typically associated with relatively large metallic parts and the subsequent fire will usually not alter this evidence grossly. Fire originating in small-gauge wiring or at small connection parts, on the other hand, quite often will damage the evidence more seriously, leaving much to speculation. There is a modest body of laboratory research where low-current failures have been simulated, but much is still unknown about details of scenarios leading to actual electrical fires in low-current circuits. In this Section, the basic principles are developed concerning ignitions from current-carrying devices. More detailed discussions on failure modes of wiring, lighting, appliances, etc. are taken up in Chapter 14.

Faults associated with the flow of electric current primarily involve the following phenomena, which are not mutually exclusive:

- sparking or arcing in the gas phase
- arcing across a carbonized path
- glowing, and other forms of overheating
- ejection of hot particles.

The scientific principles of electric discharges (e.g., sparks and arcs) have been covered in the preceding Sections. Arcing across a carbonized path is a phenomenon which is associated with the surface degradation of electric insulators. The ignition source and the substance being ignited, effectively, are identical in this phenomenon. As such, it is covered in Chapter 7. Thus, the rest of the present section focuses on overheating, ejection of hot particles, and some miscellaneous phenomena.

UL considers[327] that a potential risk of fire exists in appliances and devices which (a) use voltages over 30 VAC (rms) and can provide currents over 8 A; or (b) can dissipate more than 15 W. Most consumer appliances fall into one or both of these categories. These limits appear to be based solely on judgment and are unlikely to be actual true limits to ignitability, nonetheless, it is evident that if the power available is lowered, the risk is to some extent reduced.

OVERHEATING WIRES

It is rather hard to ignite the thermal insulation of wires by exceeding the current rating for the conductor, since a large excess is required. Experimental data on this point are examined in Chapter 14. Calculating accurately the temperature rise of a cable is not easy, due to dielectric losses, skin effect, and magnetic and thermal interactions of conductors (and possibly adjoining cables). In addition, many properties needed are temperature-dependent. The IEEE textbook on this topic[328] should be consulted for these details. To make an rough calculation, however, is less complex. VTT researchers[329] offer the following as a simple approximation for a single, insulated conductor:

$$T_{in} = \frac{I^2}{2\pi^2 \sigma \lambda a^2}\left[\frac{1}{Bi} + \ln\left(\frac{b}{a}\right)\right]$$

where T_{in} = temperature of insulator (K), I = current (A), σ = electric conductivity (= 5.8×10^7 S m^{-1} for copper), λ = thermal conductivity of insulation (W m^{-1} K^{-1}), b = outer radius of insulation (m), a = radius of conductor (m), and Bi is the Biot number:

$$Bi = \frac{bh}{\lambda}$$

where h = convective heat transfer coefficient (W m^{-2} K^{-1}). As an example, suppose a 14 AWG wire is considered having a wire insulation thickness = 0.4 mm. For this wire, the diameter = 1.63 mm, so a = 1.63/2 = 0.815 mm = 0.815×10^{-3} m and b = 1.015×10^{-3} m. Assume that the insulation ignites at 400ºC = 673 K , λ = 0.15 W m^{-1} K^{-1}, and h = 50 W m^{-2} K^{-1}. This gives Bi = 0.338. Now, solving for I:

$$I = \pi a \sqrt{\frac{2T_{in}\sigma\lambda}{\left(\frac{1}{Bi} + \ln\left(\frac{b}{a}\right)\right)}} = 135 \text{ A}$$

Since 14 AWG wire has a rated ampacity of 15 A, this is an overcurrent of 9×. This estimate is high, and Chapter 14 indicates that an overcurrents in the range of 3× to 7× suffice to ignite wire insulation.

OVERHEATING ELECTRICAL CONNECTIONS

Overheating at electrical connections is a common cause of fires. The physics and chemistry of electrical connections are very complex, as illustrated by the phenomenological flow chart put forth by Kuroyanagi and coworkers[330]. From Figure 46 it can be seen that numerous phenomena are involved, but not all have been studied systematically and in detail.

Aronstein[331] investigated heating at aluminum–aluminum contacts is some detail. He found that:

- Incipient failing of a connection can be defined as occurring when the contact resistance reaches a value of about 10 mΩ.
- The contact resistance is not a smooth function of contact force. Instead, there is an abrupt drop in contact resistance at a certain contact force.
- A poor connection acts as a current limiter and the current/voltage relation is nonlinear and with hysteresis. If

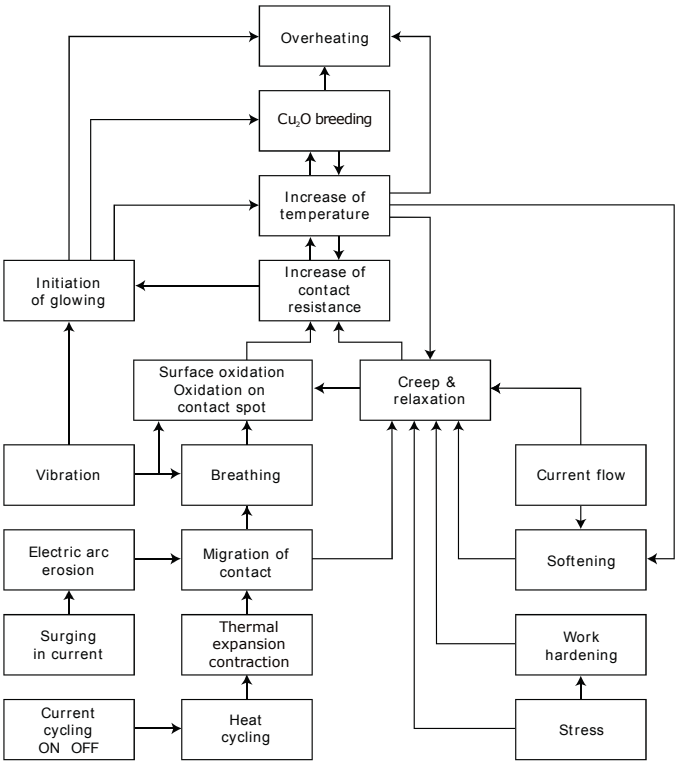


Figure 46 Mechanisms for overheating at electrical connections

current is increased beyond the limit value, unstable operation results and the connection cycles between carrying current and being an open circuit.
- Conduction through a poor connection commonly occurs at only a single spot and involves a process of periodic electric breakdown of the oxide film.

Evidence of overheating is clear when mechanical connections between two current-carrying conductors start to show glowing. Normal, good electric connections should not be subject to a temperature rise much in excess of that for the conductors themselves. This depends on the connection having a very low resistance. Most metals which are used for carrying electrical current are subject to oxidation when exposed to atmosphere. The metal oxide film formed on the surface has a very high resistivity. Thus, a connection where the mating parts are oxidized will be a high resistance connection and will overheat if significant current is passed through it. Temperatures of a glowing connection vary widely, but peak values at the hottest point have been measured from 1100ºC[346] to 1500ºC[332]. Temperatures up to ca. 300ºC have been measured on metal parts some distance away from the hot point[346].

Some metals, such as cadmium, beryllium, and nickel, do not readily form a thick oxide coating, and thus they are often used for contacts of relays and switches. Copper oxidizes slowly, and its oxide is semiconductive. Aluminum oxidizes very rapidly and its oxide has negligible electric conductivity, except for a tiny amount of current that can flow through an aluminum oxide layer due to electron tunneling. For practical purposes, the current that can be carried through an aluminum oxide in nil, and glowing would be unlikely due to insufficient current. Thus, Newbury and Greenwald suggested that the formation of intermetallic compounds (which have intermediate conductivity) is the actual mechanism occurring at the glow site[332].

One of the earliest efforts to study glowing connections was organized by the CEE[333] (now IECEE, and a part of IEC) in 1961. Tests were run in the laboratories of the Verband Deutscher Elektrotechniker in Germany and the Imperial Chemical Industries in the UK. The primary results are shown in Figure 47. The connection acts as a non-linear circuit element. For currents over 10 A, drops of around 2 V are found. But for small currents, voltage drops in the tens of volts can be found. At a maximum current of 20 A, ca. 50 W is dissipated in a copper/brass connection and around 35 W for copper/iron. The study also noted that the power dissipation depends only on the materials involved and not on the nominal size of the contacts. It was also found that to start the glowing process, a current of 4 – 6 A had to be supplied; glowing of freshly-made connections could not be started with smaller currents.

Glowing connections were later studied by Hotta, who identified a number of fire cases attributable to this

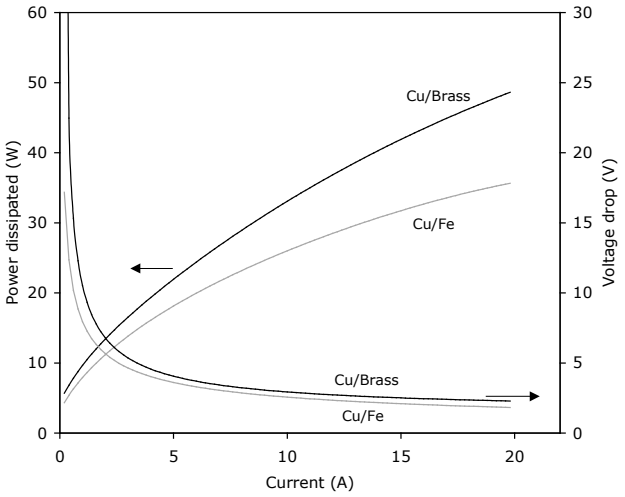
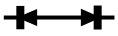


Figure 47 Power dissipation and voltage drop across glowing connections of two types

cause[334]. In laboratory studies on AC circuits, he found that approximately 15 W was dissipated in a glowing copper-copper connection drawing 1 A, and about 25 W at 2.5 A. By means of X-ray analysis, Hotta identified that the high resistance in a copper-copper connection is due to progressive formation of Cu_2O at the junction. He then conducted resistivity studies on pure Cu_2O, which material, he concluded, shows a sharp drop in resistance as temperatures exceed about 900ºC; his quantitative findings, however, have been questioned by Hagimoto[335], who was not able to reproduce the measurements. In a follow-on study, Isa[336] further examined the process and concluded that the glowing connection can be represented in terms of circuit elements as two back-to-back series-connected diodes:



The general sequence of events when the '*Cu_2O breeding process'* occurs at glowing connections has been delineated by Kuroyanagi et al.[330] (Figure 48). Kawase[337] studied the details of the Cu_2O breeding process at copper-to-copper connections. Using an AC source of less than 100 V and of 0.5 to 1.0 A, he noted the following sequence of events when an intermittent connection is made. Initially, when the contact is made and broken, blue sparks are generated. After a number of make/break cycles, the sparks become red, instead of blue. If after this time, contact is made continuously, the Cu_2O breeding process begins to take place. Layers of Cu_2O begin to grow on both contacts (Figure 49). Along the layer of Cu_2O, a single bright filament emerges. Molten metal is located along this thin filament, which meanders "like a worm." Kawase measured the voltage-current relationship of the glowing connection and found that it cycles between high- and low-conductivity states. He interpreted the cycling as a recurring breakdown of the interface between Cu and Cu_2O and confirmed the back-to-back diode circuit model. The CEE work earlier had already noted

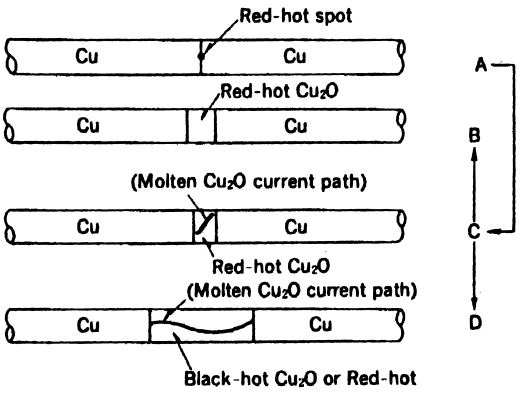


Figure 48 Sequence of events in the Cu_2O breeding process

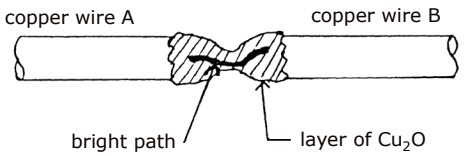


Figure 49 Detailed view of ongoing Cu_2O breeding process

that once a glowing connection is established, if it is interrupted it can resume without first needing to go through a blue spark phase.

Similar experiments were also done by Hagimoto et al.[338], who measured the breeding speed at which Cu_2O is formed in both AC and DC circuits. In AC connections, they found incandescent points occurred at both ends of a meandering, glowing path. The rest of the path was at a lower temperature. In the case of DC connections, they found that an incandescent point was formed only at the (+) electrode. They also found that:

1) The average DC power dissipated at the contacts of 1 mm wires was almost a constant 16 W for currents over 2 A.
2) The average AC power dissipated at the contacts of wires 2 mm in diameter was almost a constant 28 W for currents over 5 A.
3) For 1 mm wires, the maximum breeding speed of Cu_2O was 17 mm h^{-1} in circuits carrying 2 A AC, and 18 mm h^{-1} with 2 A DC. For 2 mm wires, the speed was 6 mm h^{-1} with 2.5 A AC, and 12 mm h^{-1} with 5 A DC.
4) For 1 mm wires, the current necessary for the glow to be sustained was 0.3 – 2 A AC and from 0.3 A to greater than 8 A DC. For 2 mm wires, they were 1 – 2.5 A AC and from 0.5 A to over 8 A DC.
5) The upper limits of these ranges of current were affected by the sputtering caused at the glowing contacts.

Photographs showing glowing connections from the experiments of Hagimoto et al. are shown in Color Plates 21 through 24. They also conducted experiments with stranded cords and found that currents "over a few amperes" were hard to sustain at a glowing connection of a stranded wire—the wire tended to break at the point of heating.

Sletbak et al.[339] studied additional details of the Cu_2O breeding process and found that the filament glows at 1200 – 1300ºC. The process is able to sustain itself, since copper continues to be oxidized underneath. The high temperatures attained can readily lead to ignition. With a current of 1 A, values of 200 – 350ºC were recorded at a 10 mm distance from the glowing point.

If a temperature of ca. 1250ºC is taken to be as typical for the hot part of a glowing Cu-Cu connection, it can be noted that it is very close to 1230ºC, the melting point of Cu_2O. Hagimoto et al.[338] explain that the pulsing waveform found for glowing connections is accounted for by spatter (mechanical sparks) that is sometimes seen to be emitted from the connection. The spatter ejects material and this causes a momentary fluctuation in current. In DC circuits this only takes place from the positive-voltage side of the glowing connection.

Kinoshita et al.[340] examined a variety of metallic contacts using both AC and DC circuits and identified the main reaction products formed at the connections. Their results are summarized in Table 28. The connections differed in their time response. In the DC studies, some connection types showed a basically steady response after a few minutes; others showed a rising drop throughout the test. These results are summarized in Table 29. Interestingly, in the DC studies, the rate of oxidation was non-linearly dependent on the current (Figure 50).

Table 28 Results of Kinoshita et al. on a variety of metals

Metals	Power supply	Outcome	Main products
Cu, Cu	AC	breeding	Cu_2O, CuO
Cu (+), brass (-)	DC	breeding	Cu_2O, CuO
Cu (+), Fe (-)	DC	breeding	Cu_2O, CuO
brass, brass	AC	slow growth	ZnO, Cu_2O, Cu
brass (+), Cu (-)	DC	slow growth	ZnO, Cu_2O, Cu
Fe, Fe	AC	slow growth	Fe_3O_4, Fe_2O_3
Fe (+), Cu (-)	DC	slow growth	Fe_3O_4, Fe_2O_3

Table 29 Voltage drops in DC circuits at a glowing connection carrying 2 A

Metals	Voltage drop
Fe(+) to brass(-) Fe(+) to Fe(-) Fe(+) to Cu(-)	steady ≈ 2 V
brass(+) to brass(-) brass(+) to Fe(-) brass(+) to Cu(-)	steady ≈ 5 V
Cu(+) to Cu(-) Cu(+) to brass (-) Cu(+) to Fe(-)	rising from 5 V at start to 9 V at 90 min

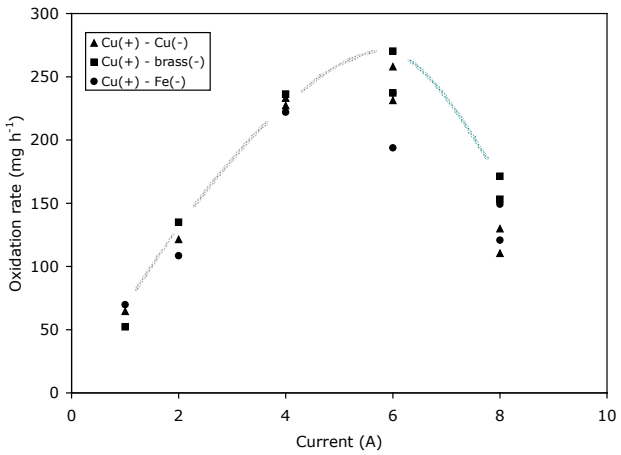


Figure 50 Oxidation rate of several connection types for DC current

In other tests using a variety of metals, Suzuki et al.[341] found that stable glowing connections could be achieved with steel against steel, aluminum, copper, and brass. In their experiments, aluminum against aluminum, copper, or brass gave unsustained glows, while copper against copper or brass could produce no glow. The voltage measured across the connection (for AC currents in the range of 1 – 10 A) was found to be the predictor of glowing performance. If a pair of metals was able to produce more than about a 2 V drop, then stable glowing was possible. Since, for some reason, Suzuki et al. were unable to produce the breeding process often seen in other investigations, their negative results point out that the phenomena are not easy to reproduce.

It has been proposed that a phenomenon identified as 'micro arcing' is involved in a glowing connection. When two metals are separated by a metal-oxide layer, conduction is essentially nil across the layer, which is a dielectric. But the applied voltage can cause a breakdown of the oxide layer. This discharge can cause a fine metal bridge to be created across the dielectric. Substantive current will flow through the metal bridge, but because of its limited current carrying capacity, it shortly overheats, melts, and breaks apart. The process then continues, but because of the high temperatures being created locally, oxide layers are further built up. This theory is not universally espoused, but UL states that their experiments have provided some substantiation[342].

The simplest theoretical model of an overheating connection is obtained by assuming that heat is produced at a constant rate in an infinitesimally-thin plane section across the wire. The wire is represented as a cylinder, without any change of geometry at the point of connection[343]. The solution for the temperature of that cross-section is:

$$\Delta T(t) = q'' \sqrt{\frac{r}{2\pi\lambda h}}\, \gamma(\tfrac{1}{2}, t/\tau)$$

where q'' = power density at the plane section (W m^{-2}), r = radius of the wire (m), λ = thermal conductivity of copper (W m^{-1} K^{-1}), h = effective heat transfer coefficient from the surface of the wire (W m^{-2} K^{-1}), γ = incomplete gamma function[344], and time constant τ(s) is given by:

$$\tau = \frac{r}{2}\frac{\rho C}{h}$$

where ρ = density (kg m^{-3}) and C = heat capacity of copper (J kg^{-1} K^{-1}). The equilibrium value of the temperature rise is:

$$\lim_{t\to\infty} \Delta T(t) = q'' \sqrt{\frac{r}{2\lambda h}}$$

As an example, for a copper wire of 14 AWG, r = 1.63/2 = 0.815 mm, ρ = 8890 kg m^{-3}, C = 385 J kg^{-1} K^{-1}, and λ = 400 W m^{-1} K^{-1}. Assuming that h = 50 W m^{-2} K^{-1}, and that 10 W is dissipated in the connection, giving $q'' = \dfrac{10}{\pi r^2} = 4.8\times10^6$ W m^{-2}. Then

$\Delta T(\infty) = 4.8\times10^6 \sqrt{\dfrac{0.815\times10^{-3}}{2\times400\times50}} = 685$. If the ambient temperature = 20ºC, then the temperature at the overheating connection will be 20 + 685 = 705ºC, which is way over the ignition temperature of most combustibles. This theoretical treatment is highly simplified, nonetheless it indicates that very high temperatures can be anticipated.

The ignition of structural components of a building can be caused by a glowing connection, but there is little data to assess this potential. Aronstein[350] demonstrated in laboratory studies that a connection producing 50 W can ignite wood studs. A minimum time of 25 min was needed for ignition to occur from a 50 W fault. He also found that a connection glowing at a 45 – 50 W level was able to melt aluminum. Electric outlet cover plates made of thermosetting plastic were able to be ignited at the 30 W level; thermoplastic ones, however, were prone to melt away rather than to ignite.

Ettling[345] examined the situation where a nail pierces a conductor in a cable buried in the wall and a resultant glowing connection occurs between the nail and the two pieces of severed conductor. He found glows similar to those studied by Meese and Beausoleil[346]. A fire has been documented[347] which was caused by a glowing connection at a computer unit where the 120 VAC supply was protected by a 1 A fuse, which did not blow. Details of research on glowing connections within electrical receptacles are considered in Chapter 14.

IEC[348] and Sandia National Laboratories[349] both developed different test methods intended to simulate a glowing connection as a means of testing the ignitability of electric wires and cables from this source, but neither method has been validated for ignition of building components. The Sandia apparatus comprises a screw-terminal strip, with a small heater inserted under one screw. The heater provides up to 200 W, although this is time-dependent, due to the negative-temperature coefficient of the heater material. The peak heater power is about 5× greater than the values measured in actual glowing connections, which would imply that the test method is highly conservative. But test results using the method indicated that at a 50 W level, ignition is not observed. Since actual fires evidently involve connection dissipation of less than 50 W, the findings imply that actual fire conditions differ in some ways from the test mockup.

EJECTION OF HOT PARTICLES

Electrical short circuits and arcs sometimes eject incandescent metal particles ('mechanical sparks'). Color Plate 25 shows that even a metal box and cover are not sufficient to retain such material. These can be propelled a modest distance in a residential wiring situation. In the case of short-circuiting in a baseboard heater (Color Plate 26), Aronstein[350] found particles propelled up to 1.5 m (5 ft).

Aronstein also considers that, in low-voltage circuits, the risk of ignition is higher from non-incandescent molten aluminum particles, which can be produced if aluminum wire or connectors are used, than from incandescent particles. While the temperature of molten aluminum is lower than the temperature during its combustion, much larger drop sizes can be attained by molten drops than is normally attained by ejected incandescent particles.

DENDRITES

It has long been known that when a film of water comes onto the surface of an insulator that separates two closely-spaced, bare electric conductors carrying current, electric failures—and possibly ignition—can occur. The details were first studied in 1965 by Elliot[351] who discovered the process of formation of dendrites*. The growth of dendrites is possible with most metals used in electric devices, except aluminum, gold, and platinum. Very little ion content is required in the water; Elliot found that less than 10 ppm NaCl was sufficient. The process does require DC current, so it does not pertain to normal power distribution systems nor AC appliances. The growth is highly voltage-sensitive, but at higher voltages can be surprisingly fast and extensive. For example, Elliot found that at 50 VDC, a gap of 12 mm could be bridged in about 8 minutes. The dendrites are not pure metal, but rather, comprise both metal and metal oxides. Conduction of current across the gap increases with increased formation of dendrites; under heavy formation, a 'sludge' results.

ADVENTITIOUS BATTERIES

A potential difference can be created by electrochemical means any time that an electrolyte is present in conjunction with two dissimilar metals. In one accident, an explosion happened when a worker lowered an aluminum dipstick into a cast-iron tank which contained an acid mixture, along with some produced hydrogen[134]. Subsequent measurements indicated that a potential difference of 1.5 V existed between the two metals.

STATIC ELECTRICITY

GENERAL PRINCIPLES

Static electricity represents electric charges which are 'static,' that is, they are collected upon a surface and are not continuously flowing in an electrical current. The steps involved in a static electricity discharge are schematically illustrated in Figure 51. For significant charge separation (sometimes loosely called *charge generation*) to occur, at least one material must be involved which is an electrical insulator. An electrical insulator is considered to be a substance that has a resistivity above about 10^8 Ω-m, which unfortunately includes most organic substances.

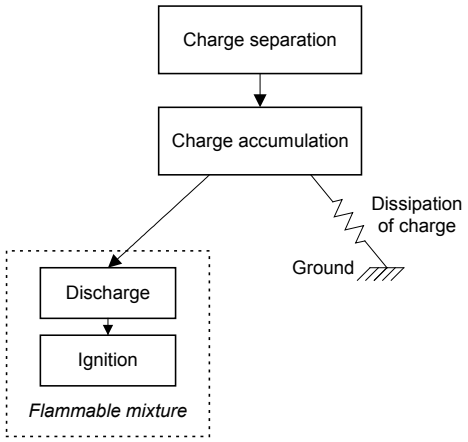


Figure 51 Static electricity fundamentals

Electric charge may be separated by the following means:

1. contact and separation or friction between solids
2. relative motion at a phase interface (liquid-solid; liquid-gas; or between two liquid phases)
3. induction (whereby charge is moved due to the presence of an electric field), also sometimes termed polarization
4. ion collection from a discharge process (e.g., from corona discharge)
5. double-layer charging
6. fragmentation of solids having non-uniform surface charge densities

* These dendrites are not to be confused with dendritic crystals sometimes formed within a molten metal that has cooled. The latter are structures *within* the bulk metal, while the dendrites considered here are growths that protrude from the metal.

7. mechanical fracture (electron emission due to strained or ruptured bonds within solids), also termed piezoelectrification[352]
8. thermal cycling (e.g., charging by freezing[353]), also sometimes termed pyroelectrification.

Contact or friction between two dissimilar substances can produce a charge separation if either of the two substances is an insulator. The contact may be solid/solid, solid/liquid, or liquid/liquid. The most common modes pertinent to fire ignitions are:

a) contact and separation between dissimilar solids
b) flowing powders
c) flowing liquids.

A mild amount of charging can be created simply when two surfaces come into firm contact and are then separated. Friction merely enhances the charging by increasing the effective area of contact. Traditional wisdom is that not only must the materials be dissimilar, but that sizable charging will take place only if they are far apart on the *triboelectric series*, which is a rank-order listing of materials according to how much of a negative or positive charge they tend to pick up[374]. Later studies indicated that, for dielectric materials, the location on the triboelectric series is determined by the material's dielectric constant[361]. Current understanding, however, is that electrification is not precluded in contact between objects made of the same material. Thus, plastic chips falling down a chute made of the same plastic are known to be able to undergo electrostatic charging[354]. It is believed that this may involve both physical factors (e.g., stresses at the surface) and chemical factors (contamination). Temperature differences between the two nominally-identical surfaces increase the likelihood of charging. Electrification is possible due to friction within powders of a single substance. In that case, smaller particles may pick up one polarity of charge while larger ones the other. Gross separation of charge can subsequently occur if the powder is moved or poured in such a way that size segregation occurs[354]. Electrification due to ionized gases flowing past surfaces can arise, but if the gas is at normal temperatures (i.e., not a hot plasma), then the charging that can be achieved is trivial, amounting to less than a volt[436]. Lüttgens[361] points out that this applies only if the gases are not contaminated with solid or liquid particles. Charging to significant voltages that has been attributed to flowing gases turns out to involve small amounts of aerosols. Rapidly expanding gases released from a high-pressure reservoir will cool and this can result in charged droplets being formed. Airplanes pick up a charge by moving past charged particles. Gases which contain solid/liquid aerosols or gas streams which generate liquid or solid particulates (e.g., the discharge of a CO_2 extinguisher; the rapid evaporation of liquid propane) can pick up a charge.

A specific example of relative motion at an interface is the breaking of bubbles. One explosion has been attributed to bubbling of oxygen produced from the dissociation of hydrogen peroxide through a tank that contained an organic liquid at the surface[355]. The discharge was speculated to be a corona discharge, but it was pointed out that some surface inhomogeneities were also needed for it to occur—perhaps a floating metallic object.

Induction charging only pertains to conducting bodies. If a neutral conducting body is brought close to a positively-charged substance, a charge separation will occur in the conducting body, with negative charges flowing towards the positively-charged substance. Positive charges will then accumulate at the opposite end of the conducting body. If contact is now made with the positively-charged substance, local charges will be neutralized, but a net positive charge will remain at the far end.

For certain materials, *moisture* in the air promotes the dissipation of charge since it decreases the electrical resistivity of some materials; it never affects the separation of charge. For many other materials, however, the resistivity is not lowered due to atmospheric moisture. Adding vapor-phase moisture does not actually change the electrical conductivity of the air; adding a mist or spray raises the conductivity, since it traps ions which would otherwise be available to conduct charge[356].

DISCHARGE TYPES

Discharges of static electricity can involve the following geometries:

- discharge between two conductive electrodes
- discharge involving one conductive electrode and an diffuse insulating medium
- discharge from one mist or cloud to another.

Apart from events taking place solely in the atmosphere (which are considered under *Lightning*, below), discharges involved in accidental ignitions are classified as:

(1) spark
(2) corona discharge
(3) brush discharge
(4) powder heap discharge
(5) propagating brush discharge (Lichtenberg discharge)
(6) lightning-like discharge.

Spark

A normal electric spark discharge (Color Plate 27) occurs through the air separating two electrodes when the electric field reaches a value of approximately 3 MV m^{-1}. Thus, for a gap distance d, the voltage V required is $3d$, where V is in megavolts and d is in meters. For a spark to be incendive, the gap distance normally must be equal to or greater than the quenching distance. Considering 2 mm as a typical quenching distance, the voltage required is on the order of 6 kV. Up to about 1000 mJ can be delivered in a spark. This is a sizeable amount of energy, well beyond the MIE of most substances. The charge transferred in an incendive spark is always greater than 10^{-7} coulombs[357]. Spark discharges are distinguished from other electrostatic discharg-

es in that breakdown occurs across the *whole* gap separating two electrodes. MIE values derived from tests using uniform fields between metallic electrodes should not be assumed to apply when one or both of the electrode surfaces is non-metallic, nor when the field is non-uniform. In general, it requires much more energy to ignite a gas mixture when a non-metallic electrode is involved[358].

Corona discharge

A corona discharge (sometimes called *point discharge*) is a slow, diffuse discharge that originates at a metallic electrode and branches out in a diffuse manner into space or towards poorly conducting surfaces. Unlike a spark or an arc, a corona discharge does not create a hot, conducting plasma channel. A corona discharge requires an electrode that has a needle-like point, typically less than 5 mm diameter (Color Plate 28). Charging such an electrode results in an electric field which is distorted, being generally low, but much greater near the point. Corona discharge has the lowest energy of the electrostatic discharge types. It is visible as a violet glow in a darkened room. A corona discharge can also occur in the presence of second electrode, but is still considered a 'one-electrode' discharge since the discharge does actually reach the second electrode. A minimum voltage of about 2 – 6 kV is necessary for a corona discharge to occur, with smaller potentials needed for finer-pointed needles. Characteristics of corona discharges are different, depending on whether the point electrode is positively or negatively charged.

The maximum energy normally realizable from a corona discharge—not much over 0.01 mJ—would even theoretically suffice to ignite only the most ignitable of gases, such as CS_2 or H_2. However, actual ignition requires that the energy be delivered into a small kernel, and the diffuse nature of a corona discharge precludes that. This implies that much more than the tabulated MIE value would be needed and, consequently, that it is unlikely that a corona discharge will ignite flammable atmospheres. Under some conditions, laboratory experiments have demonstrated that combustible mixtures can be ignited, however, the conditions required have been extreme, e.g., charging up to 72 kV[429], or use of circuits that supply a continuous flow of current, rather than being a one-time static discharge[359]. It is evident that a corona discharge cannot ignite dust clouds. Corona discharges are often used in processes and machinery as a safety measure for lowering charge accumulation.

Brush discharge

When a grounded conductor is brought into an electric field that is near its dielectric breakdown strength, a gas discharge can occur in the form of a brush discharge. The discharge is able to occur because of electric field distortion introduced by the electrode, which locally raises the field above its breakdown value. The name comes from the brush-like shape of the discharge, Color Plate 29. It differs from a corona discharge, in that the latter is visually observed to be diffuse. A brush discharge is similar to corona discharge in being a low-energy, one-electrode discharge, but whereas a corona discharge requires a needlelike electrode, a brush discharge occurs when electrodes have a radius of 5 – 50 mm. A minimum potential difference of about 20 – 25 kV is needed for a brush discharge to occur; however, it is considered that discharges at less than about 60 kV are limited to certain laboratory experiments and are unlikely to occur in industrial accidents[360]. Circumstances leading to a brush discharge can include[361]:

- approaching a highly-charged insulator such as plastic films or plastic pipes with a finger or a metal tool;
- discharging of solids from plastic bags in the vicinity of metal parts;
- filling a tank at a high velocity with an insulating liquid, with the charged liquid surface approaching an internal fitting that can act as an electrode;
- lowering a conductive cup, etc., into a highly charged liquid;
- projection of metal parts into a cloud of highly charged dust or aerosol;
- pouring of insulating powders into silos when the fill surface approaches a conductive fitting;
- projection of ships' masts, flagpoles, or antennas into a powerful atmospheric electric field—this is known as St. Elmo's fire.

The incendivity of brush discharges is proportional to the radius—larger-radius conductors are more likely to lead to ignition than ones of smaller radius[361]. Commonly, the high electric field will occur due to the presence of a charged insulator. Only a limited amount of the charge built up on the insulator can be discharged through a brush discharge, due to the limited mobility of charges on the insulator. It is estimated[360] that the energy from a brush discharge will not exceed about 4 mJ. In addition, most of the energy released during a brush discharge does not contribute to incendivity, since the energy is not just localized at the place where a flame kernel is formed. Thus, only 10% of the energy released is actually effective towards ignition[413]. The necessary high electric field strengths are readily found in many powder operations, in mists, and also with movement of plastic films.

While it is most common for brush discharges to occur from a grounded conductor, this is not a fundamental prerequisite, and brush discharges can originate from electrodes at various potentials[361]. This type of brush discharge is called 'spraying' and can occur whenever the potential V (MV) of the electrode and its radius r (m) are such that:

$$\frac{V}{r} > 30 \text{ MV m}^{-1}$$

Brush discharges from a negatively charged insulator (and, therefore, positive charge on the grounded conductor) are much more incendive than from a positively charged one; indeed, there are some doubts that the latter is possible.

This phenomenon appears to be related to the fact that a bright 'root' is formed at the electrode only in the case of a positively-charged grounded conductor[413]. For a brush discharge to ignite a flammable gas mixture, it is necessary that the insulator/conductor gap over which the discharge occurs be greater than 20 – 30 mm. In addition, a minimum surface potential needs to be reached. In most cases, this is about 45 – 60 kV, but under certain extreme cases ignition took place with a potential as low as 20 kV[413]. For a brush discharge to ignite a liquid in a tank, it is necessary that[429]: (1) the liquid be charged negatively, with a surface potential of 30 kV or higher; and (2) a rounded metallic electrode be available, ideally between 10 and 50 mm diameter.

Even though about 3.6 mJ can be delivered in a brush discharge[362] and there are dust clouds that have an MIE ≥ 1 mJ, most studies have concluded that brush discharges will not ignite dust clouds[363], provided that the cloud is not a hybrid dust/gas mixture. A brush discharge has been shown to be capable of igniting dust clouds in certain highly unusual experiments[364]. Larsen et al.[365] painstakingly attempted to ignite clouds of sulfur dust and found that an oxygen concentration of 55% or greater was needed. This is understood to be because a dust cloud fundamentally alters the electric field that leads to a brush discharge.

Powder heap discharge

In some cases, when rapidly filling large containers such as silos or flexible intermediate bulk containers (FIBC) with powders, a much higher charge can build up in the settled powder than was present in the air through which the material moved and a discharge can then take place. This occurs because a growing volume of powder is aggregated, plus when the powder is compacted, its charge likewise gets compacted if the powder is insulating and charge cannot get dissipated. The powder heap discharge is also called a *cone discharge* or a *bulking discharge*. It occurs along the exposed surface of the powder (Color Plate 30). Glor[366] computed certain theoretical limits to this form of discharge. It turns out that a minimum particle size of ca. 0.1 mm is needed for powder heap discharge to occur, but the majority of the actual incidents have involved polymeric resin particles in the 1 – 10 mm range. Early recommendations used to state that up to 10 mJ can be delivered in a single discharge step. But Glor[367] found, on the basis of correlating full-scale test results, that the maximum energy W (mJ) which can be delivered is:

$$W = 5.22\, D^{3.36} d^{1.462}$$

where D = silo or diameter (m) and d = median particle diameter (mm). Thus, Glor concluded that discharges as large as 1000 mJ may be anticipated for large particles flowing into a large silo, although Britton[379] argued that Glor's test methodology may not be realistic.

A minimum product feed rate is needed for a powder heap discharge to occur. This has been estimated at 3000 – 5000 kg h^{-1} for 3 mm particles, rising to 25,000 – 30,000 kg h^{-1} for 0.8 mm particles[361]. The effect of accumulated volume has not yet been quantified. It appears that only a small fraction of the charge accumulated can be dissipated in a powder heap discharge, but this has likewise not been quantified. Powders having a resistivity of less than 10^{10} Ω-m are conservatively judged to not be susceptible to explosions from powder heap discharges[367]; powders which have caused explosions have had resistivities > 10^{12} Ω-m.

In the rapid filling of silos, a propagating brush discharge along the container walls can accompany a powder heap discharge over the surface of the product.

Propagating brush discharge

A very vigorous discharge can occur when certain conditions are met for the charging of a surface. There is a limit to the amount of surface charging that can be sustained on a surface without discharging by ionizing the air (2.65×10^{-5} C m^{-2}). This limit can be increased if a double layer of charges of opposite polarity is accumulated. A way for this to occur is when an insulating layer is directly on top of a grounded metallic layer. This allows opposite polarity charges to build on the second side of the insulating layer (Figure 52). Under those conditions, the maximum surface charge is governed by the breakdown strength of the insulator, which may be on the order of 20 – 40 MV m^{-1}, instead of the 3 MV m^{-1} for air. In addition, the dielectric constant of many common insulators is 2 – 4 times that of air. These two factors combine to give maximum surface charges of around 5×10^{-4} C m^{-2}, and it is considered that 2.5×10^{-4} C m^{-2} is the minimum surface charge needed for a propagating brush discharge. With very thin films of certain plastics, surface charge densities up to 8×10^{-3} C m^{-2} have been measured[368]. A propagating brush discharge (Color Plate 31) can ignite most flammable mixtures, including dust clouds. A discharge occurs in one of two ways: (1) a grounded electrode is brought near the charged insulator surface; or (2) a dielectric breakdown of the insulating layer, resulting in a local puncture. A propagating brush discharge is capable of discharging nearly all of the charge stored in the double layer.

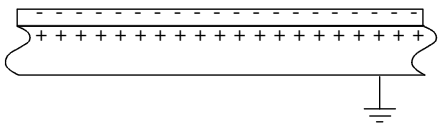


Figure 52 Double-layer charging (charge pairing) occurring when a charged insulator is adjacent to a grounded conductor

A propagating brush discharge (also called *Lichtenberg discharge*) does not occur if the thickness of the insulating layer is greater than 8 – 10 mm, but it also is less likely to occur with very thin insulating layers. For the charge buildup to be successful, the insulating layer has to have a high dielectric strength. A minimum voltage of ca. 4 kV is needed for a propagating brush discharge to occur with very thin films (10 – 20 μm) rising to 8 kV for 0.2 mm thick ones. A

propagating brush discharge will not occur if an insulator has such low dielectric strength that it breaks down prior to charging up to the necessary voltage. Up to ca. 1000 mJ can be delivered in a propagating brush discharge.

A related double-layer charging phenomenon can occur if a plastic sheet is charged with opposing polarity charges on its two surfaces. A significant discharge can then occur if two such sheets are stacked.

Circumstances leading to a propagating brush discharge can include[361,369]:

- conveying an insulating powder at high velocity through plastic pipes or bins that are grounded on their exterior;
- conveying an insulating liquid at high velocity through plastic pipes that are grounded on the outside, or metallic pipes that have an insulating interior coating;
- loading of insulating powders into large, non-conductive silos;
- operating at high velocities conveyor belts that have metallized outer surfaces and an insulating core;
- repeated collisions of dust particles on an insulating surface atop a grounded layer.

In some cases, a propagating brush discharge can occur without an overt grounded layer, for instance when rain is falling on a plastic pipe conveying an insulating powder[370].

A propagating brush discharge does *not* form simply due to the deposition of a thin layer of powder on a metal surface. This is because the breakdown strength of the porous structure is not higher than that of air. Similarly, normal solvent-based paints lead to a porous structure which likewise does not exceed the breakdown strength of air. However, certain insulating coatings on containers and storage vessels are not porous and could sustain a propagating brush discharge.

Lightning-like discharge

Lightning in the atmosphere can occur when water droplets and ice particles are charged to very high potentials. Since particles in dust clouds will also pick up an electric charge, lightning-like discharges have been observed to occur in the dust clouds formed during volcanic eruptions. What is unanswered is whether such discharges can occur on a smaller scale, to wit, in connection with storage silos. A number of accidents have been blamed on such discharges, but the details of the circumstances have never been clear. Lightning-like discharges would presumably be able to ignite almost any combustible matter, so the conditions—if any—that might lead to such lightning would be important to quantify. Boschung et al.[371] conducted experiments whereby a 60 m^3 bunker was rapidly filled with various dusts. They measured peak field strengths of 1000 to 2000 kV m^{-1} during this filling. The peaks were of short duration, but for about 15 – 20 s, the values exceeded the 300 – 500 kV m^{-1} that is needed for lightning discharge. However, no lightning discharges actually occurred. The authors believe that a scale effect was being seen, and that much larger volumes could lead to a lightning-like discharge. The events would be expected to be rare, since normal transport of dusts does not lead to high electrical charging: the experiments reported were set up to be worst-case conditions.

MEASURING OF DISCHARGES

The ignition of a flammable gas mixture or a dust cloud is measured in terms of minimum spark energy that is needed for a capacitive discharge. This is not an absolute measurement, but strongly dependent on the details of the electrical circuit, the electrodes, etc., much as has been discussed in connected with ignition of gases. In a spark discharge, as discussed in Chapter 4, the nominal energy can be determined by measuring the capacitance and the charging voltage. Other forms of discharge, such as corona or brush discharge, do not lend themselves to such measurement. For such discharges, an equivalent energy concept is used. A certain discharge is said to possess a given energy W if it is just able to ignite a mixture which has the minimum ignition energy W, as determined by capacitive discharge testing.

ELECTROSTATIC CHARGING AND DISCHARGING OF SOLIDS

In a common science-class demonstration, cat fur is used to create electrostatic sparks. A live cat, however, can also undergo charging and a subsequent spark discharge. A case is documented where an electrostatically charged cat demolished an execution tank at a pound where town gas was being used and got ignited[372]. Hailstones can occasionally be charged to very high levels, and a case is reported[373] where the discharge occurring upon such hailstones hitting a storage tank sufficed to burn paint on it.

For surfaces in contact to pick up a significant charge, at least one of the surfaces has to be of high surface resistivity. The electrostatic effects of changing the *relative humidity* do not relate to any changes in the conductivity or other properties of air. Instead, increased RH lowers the surface resistivity of some materials and thus decreases the likelihood that surfaces in contact will pick up a high charge. Other materials, however, are but little affected by increases in relative humidity. A sufficient number of materials are affected by RH so that the effect shows up in statistics. A recent study on the topic is not available, but in 1933 Guest[374] compiled data showing that fires and explosions caused by static electricity predominated in winter months, when RH is low indoors, and became several-fold less frequent during summertime. Many insulating materials show a strong drop in surface resistivity at high RH values, for example, fabrics[394] and paper[356]. Waxes are an exception since they have a hydrophobic surface[375]. Plastics show diverse behaviors.

Ranking of solids according to their propensity for picking up an electric charge is inherently misleading, since actual

charge accumulation depends on characteristics of both the surfaces in contact. Henry[376] demonstrated that nylon rubbed with brass picks up more charge than PET, but the PET picks up more charge than nylon when rubbed with wool.

The capacitance with respect to ground that objects represent increases with their size according to the equation:

$$C = 4\pi\varepsilon\varepsilon_o r$$

where C = capacitance (Farads; F), r = radius (m), ε = dielectric constant (--), ε_o = permittivity of vacuum (8.854×10^{-12} S s m^{-1}), where the abbreviation capital S denotes Siemens, the basic unit of electrical conductivity. The dielectric constant for air = 1.0. While this equation is exact only for spheres, objects which are roughly of similar sizes in the three dimensions can be estimated with it. The maximum charge which can be built up on an isolated object in air is governed by the breakdown strength of air E_{max}, which is approximately 3 MV m^{-1}.

The maximum charge density which can be built up on the isolated object is given by:

$$\sigma_{\max} = \varepsilon\varepsilon_o E_{\max}$$

or σ_{max} = 26.5 μC m^{-2}. Since the area of a sphere is = $4\pi r^2$, then the maximum charge which can accumulate on the spherical body is:

$$Q_{\max} = 4\pi r^2 \times 27 = 339\, r^2\ \mu\text{C}$$

The capacitance C is defined as = Q/V. Thus,

$$V = \frac{Q}{C} = \frac{Q}{4\pi\varepsilon\varepsilon_o r} = E_{\max} r = 3.0\times10^6 r$$

As discussed in Chapter 4, assuming that no losses occur, the energy which can be delivered from a capacitive spark is:

$$W = \frac{1}{2} CV^2$$

where we have used W for energy here, in order to avoid confusing with the electric field, designated here as E. Substituting the above, gives:

$$W = 501 r^3$$

where W = energy (J). For many hydrocarbon vapors, a value of MIE ≈ 0.25 mJ is applicable. Then, to cause an incendive discharge from a charged, isolated body, its radius must be at least:

$$r = \left(\frac{0.25\times10^{-3}}{501} \right)^{1/3} = 0.008\ \text{m}$$

Since this limit is only 8 mm, it would be very difficult to develop a safety measure on limiting the physical size of bodies that pick up a charge. In practice, somewhat higher minimum sizes will suffice, since ideally efficient conditions will not be present for discharge. For a propane/air mixture (MIE = 0.26 mJ), a minimum radius of ca. 12 mm was found necessary in order to have an incendive discharge[377]. The capacitance some common objects is given in Table 30.

Table 30 The estimated capacitance of some objects

Object	Capacitance (pF)
buckets, small drums	5
55-gallon drum	100
automobile	500
tank truck	1000
large tractor-trailer	3000

The electrostatic charging of *plastic sheets* can occur by rubbing, by passing over rollers, by rapidly separating sheets, and by various other means. Gibson and Lloyd[378] found that, at RH values less than 40%, many plastics are able to pick up a surface charge of 10 to 23 μC m^{-2}. For higher RH values, the charge densities decreased, the values dropping to about half at 75% RH. In experiments with polyethylene sheets, they found that the surface could be charged to about 75 kV. Sparks occurred when grounded objects were brought close to the charged surface. Incendive sparks could be created in atmospheres containing methane, acetone, toluene, and other vapors. In some cases, the conductivity of plastics is extremely low, and this may help prevent an incendive discharge. Magison[318] documents a case where a hydrogen/air mixture could not be ignited from a plastic case charged to 25 kV. For an incendive discharge to occur, charge must flow at a sufficient rate through the charged material. In testing, it was found that the flow of charge was so small that discharges occurred only as a series of small pulses, with none being able to ignite the gas mixture.

Industrial operations can charge substances to some high potentials[388], as shown in Table 31.

Table 31 Peak charging voltages measured in some industrial operations

Operation	Potential found (kV)
flange on steam ejector	15
conveyor belt moving at 3 – 15 m s^{-1}	80
roll of paper unwound at 10 m s^{-1}	150

A charge accumulated on a solid does not remain there permanently and eventually dissipates (undergoes 'charge relaxation'). This is defined in terms of the relaxation time, which is the time it takes for charge to decay to (1–1/e) = 63% of its initial value. It can be estimated from:

$$\tau = \varepsilon\varepsilon_o \rho$$

where τ = relaxation time (s), and ρ = volume resistivity of the material (Ω-m). Some values[379-381] for ε and ρ are given in Table 32. As an example, for dry wood the relaxation time is computed to be $3.0 \times 8.854\times10^{-12} \times 10^{10} = 0.27$ s. In view of this fast decay of charge, significant electrostatic problems would not be expected. On the other, for PTFE the relaxation time is computed to be 177,000 s, or 49 h, showing that charge decays extremely slowly on PTFE. As

a rough guideline, substances having resistivities below about 10^{10} Ω-m show little propensity for electrostatic discharge hazards. When the initial charge is known, and the constants are available for a material, the charge remaining at any time t is computed as:

$$Q = Q_o \exp(-t/\tau)$$

where Q_o = initial charge (C), and t = time (s).

Table 32 Dielectric constants and volume resistivities for some solid materials

Substance	ε (--)	ρ (Ω-m)
cellulose acetate	3.5 – 7.0	$10^8 – 10^{11}$
cellulose acetate butyrate	3.5 – 6.4	$10^8 – 10^{10}$
cellulose nitrate	6.4 – 8.4	10^9
glass, plate	7.5	2×10^{11}
glass, Pyrex (borosilicate)	5.0	10^{13}
HDPE	2.3	$10^{14} – 10^{15}$
melamine formaldehyde	6 – 9	$10^{10} – 10^{12}$
Neoprene	9.0	10^{11}
nylon	3.5	4×10^{12}
paper, dry	1.7	10^{10}
PCTFE	2.8	10^{16}
PET	3.1	10^{11}
PMMA	3.4	$> 10^{13}$
polycarbonate	3.2	10^{14}
polyester, glass reinforced	4.0 – 5.5	10^9
polypropylene	2.2	$10^{13} – 10^{15}$
polystyrene	2.5	$10^{15} – 10^{17}$
polyurethane	5 – 8	$10^9 – 10^{12}$
PTFE	2.0	10^{16}
PVC	6 – 7	$10^9 – 10^{14}$
rubber, chlorinated	3.0	1.5×10^{11}
rubber, hard	3.0	3×10^{11}
sulfur	3.8 – 4.4	$10^{14} – 10^{15}$
TNT	5.2	9×10^8
wood, dry	3.0	$10^8 – 10^{11}$

Pyrotechnic compositions typically show $\rho = 10^{11} – 10^{12}$ Ω-m when measured at 20% RH, but these mixtures are hygroscopic and values drop greatly at higher humidity[388].

High values of humidity (60 – 70%RH) lead to a microscopic layer of moisture to be accumulated on surfaces. The conductivity of the moisture layer can be higher than for the substrate, allowing a more rapid leaking down of built up charge. In industries where electrostatic discharges can have serious consequences (e.g., explosives manufacturing), it is sometimes recommended[382] that RH be set at ≥ 65%, for an ambient temperature of 20ºC. For other ambient temperatures, a study on the electrostatic charging of 6 fabrics and 3 primary explosives as a function of temperature and RH showed[383] that the same charging voltage would be produced if the RH versus temperature relation is:

$$RH = 80.7 - 0.79\,T$$

where T = temperature (ºC).

Conveyor belts made of high-resistivity materials can build up very high surface potentials due to passing over rollers. Up to 120 kV was measured in one study during periods of extremely low humidity[357]. It was found that charging depended on low values of *absolute* moisture in air, and that RH was not the proper variable for describing the charging tendency. Static eliminators were found to be impractical, since electrostatic charge is re-applied by each roller, so an eliminator would be needed in conjunction with every roller.

ELECTROSTATIC CHARGING AND DISCHARGING OF PERSONS AND APPAREL

A mild shock due to electrostatic discharge is common for human beings. Such discharges can also be incendive. In the early part of the 20th century when gas lighting was used, a parlor trick was common[373] whereby a person would shuffle his feet across a carpeted floor, then light a gas jet by causing an electrostatic spark discharge between his fingers and the metal fixture. Shoes charge the wearer because each time the foot is raised, the capacitance to ground is decreased and charge accumulates on the person.

Charging readily occurs when apparel is worn which is highly insulating and the apparel contacts and separates from external objects. The charge picked up on the apparel then induces a similar charge in the body. A strong spark discharge can be created when one layer of clothing is removed from atop a second one. Or, a discharge may occur from the body to an external object.

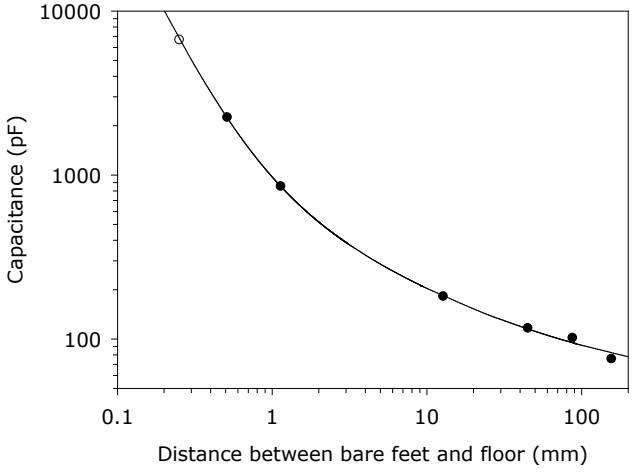


Figure 53 Effect of footwear thickness on the capacitance of a person (assumed standing on a floor of moderate conductivity)

It is generally considered that a human being[384] represents a capacitance to earth of about 120 – 300 pF, with typical values being 150 – 250 pF, and 220 pF sometimes proposed as a 'standard' value[393]. Actual capacitance[385] varies with the thickness of the footwear, as shown in Figure 53. The 'standard' capacitance of 220 pF can be seen to correspond to a footwear thickness of 8.3 mm. An extreme value of 1100 pF has been reported for a male subject wearing leather-sole shoes[386], but its meaningfulness is unclear—the latest experimental study[387] on this subject showed values only within the range 60 – 165 pF. The position of the person affects the capacitance. If the capacitance of a standing person is 250 pF, a sitting individuals may show 280 – 300 pF. An individual infinitely far away from the ground plane[388] would register a capacitance of 30 – 40 pF.

In dry air, the body can charge up to 5 – 25 kV, although voltages towards the high end of this range are uncommon and are limited by corona discharge. Thus, under the worst circumstances, the energy that is stored and is available for release in a spark is:

$$W = \frac{1}{2}CV^2 = \frac{1}{2}\cdot 300\times 10^{-12}\cdot\left(25\times 10^3\right)^2 = 94 \text{ mJ}$$

If this much energy could be effectively applied, it would be enough to ignite all common ignitable vapors and also many dusts. However, more typical values of stored energy due to friction of apparel would be 5 – 20 mJ. A value of 25 mJ has been adopted by a British standard[389] as the maximum practical value needing to be considered. Fisher developed an electrical circuit which creates a rather complex discharge waveform, intended to simulate human discharge under worst-case conditions[384]. At an RH of 50%, a person walking on a carpet will generate no more than about 3 kV, and for RH of 60% or higher it appears to be impossible to create any significant voltage[386]. Thus, the problem is limited to dry atmospheric conditions.

In tests at 20% RH where an individual was doffing laboratory coats of cotton or polyester/cotton blend and the undergarments were of various fibers, charging voltages of 1.8 – 3.6 kV were measured[390]. The charge accumulated by a person repeatedly sliding around on a painted-plywood chair has been measured[391] to be 1.8 μC. At 30 – 35% RH, a person getting up from sitting on a doctor's stool[385] can be charged to 1.0 – 3.0 kV. A person sitting down, then rising from a plastic-covered chair can get charged to about 4 kV under the worst-case conditions (nylon clothing, low RH); but if the RH is raised to 80%, then charging only up to a few hundred volts is possible[392].

The electrostatic charge associated with the changing of linens on hospital beds was studied by Holdstock and Wilson[393]. The metal bedframe (with a measured capacitance of 185 pF), was found to be charged up to 32 kV. The person doing the task was reported as being charged up to 60 kV, although it is not clear why corona discharge did not occur to limit this. When laundry antistatic agents were used, reductions of ¼ to ½ were found. The highest charging voltages all involved modacrylic blankets. In bedding sets that used polyester instead of modacrylic blankets, both the person and the bedframe were charged only to peaks of 17 kV. If a flammable gas atmosphere were present, these values would be much more than sufficient for ignition of even high-MIE gases. If the bed linens are removed by progressively folding them (a common hospital procedure) instead of pulling off, peaks are much reduced. For the best case—cotton bed linens—incendive sparks might be avoided, since peak charging voltages were only ca. 1.5 kV. In extreme circumstances, values up to 2 – 5 kV were found with cotton bed linens by Guest et al. [385]. The reductions achieved by use of laundry antistatic agents would not be sufficient to avoid incendive sparks for the worst case of modacrylic blankets and removal by pulling method.

In an early study, Wilson found that an energy of 18.6 mJ was needed to ignite a CH_4/air mixture from a person forming a capacitance of 220 pF[394]. This is vastly greater than the 0.2 mJ normally considered to be the MIE of methane and gave cause to various speculations concerning resistive losses through the body time effects because not all the energy is released in a single spark. However, a study by Tolson identified the pivotal role of capacitance[395]. For 86 pF, 1.1 mJ was needed; for 150 pF, 4.4 mJ was needed; while for 500 pF, the minimum was 20.2 mJ. A more extensive study by Movilliat and Giltaire[396] gave the results shown in Table 33. Discharges through points give anomalous results (see Chapter 4), but the remaining data show that human capacitor is nearly as effective as the electrical one, provided other circuit parameters are not changed at the same time. Thus, 9 kV is necessary to cause ignition of a CH_4/air mixture from a human being, even though 1 kV has been found sufficient (the lower limit was not explored) to cause non-incendive discharges from a human[397].

Table 33 Incendivity of human body and capacitor discharges

Gas	Electrodes	Human body		Capacitor
		Volts	Energy (mJ)	Energy (mJ)
28% hydrogen /air	15 mm Ø	2800	0.60	0.53
	1.6 mm Ø	2350	0.40	0.35
	points	4900	1.75	0.26
8.5% methane /air	15 mm Ø	9000	5.9	4.7
	points	9600	6.7	0.8

Wilson[398] conducted experiments similar to the above using natural gas/air mixtures. In these experiments, the exact capacitance that the body formed appeared unimportant, but the shape of the electrode did influence the results. A minimum voltage of ca. 6 kV was found to be needed, and a minimum energy of 1.7 mJ. As the size of the electrode was increased from 1 to 12 mm, both the voltage and the energy needed increased. In a continuation of the work[399], 5.5 kV was found needed for mixtures of 8.5% methane in air, while 1.3 kV sufficed for 29% hydrogen in air.

Johnson experimented with stoichiometric acetone/air mixtures and found that the energy required for ignition from a human spark discharge was 3.0 mJ, compared to 1.3 mJ needed for capacitive discharge from a 55 pF capacitor[400]. In Johnson's first experiment, the capacitance of the human was 136 pF. In a second test where the human created 171 pF capacitance, the energy required rose to 3.4 mJ. What proved constant for the three conditions (one capacitor, two humans) was the discharge voltage, which was always 6.7 kV.

A discharge from a person can ignite acetylene/air mixtures at a level of 1.1 mJ[401]. For a human to ignite the explosive PETN, the person would need to be charged to over 70 kV, which is impossible in most practical circumstances[401].

Guidelines are also available (Table 34) which relate the energy discharge from a person to the sensation[418, 379]. A perceptible sensation corresponds requires that the person be charged to about 2 kV[361]. In view of the above results, discharges that are perceptible but not severe are likely to lead to ignition if the person is in a space containing a gas in its flammable range. However, since people do not generally walk around in flammable atmospheres, it is found that electrostatic discharge from humans is actually a rare cause of unwanted ignition of gases[402].

Table 34 Human responses corresponding to various levels of discharge energy

Energy	Response
1 mJ	perceptible
10 mJ	prick
30 mJ	sharp prick
100 mJ	slight jerk
250 mJ	severe shock
> 1 J	possible unconsciousness
> 10 J	possible cardiac arrest

The resistance of the human body[384], measured to a fingertip is about 1300 – 2000 Ω, but if the person undergoes a discharge via a grasped metallic object, the body's effective resistance may be only 360 – 700 Ω.

ELECTROSTATIC CHARGING AND DISCHARGING OF GRANULAR MATERIALS

When granular materials—powders, dusts, grains, etc.—are in motion, they can pick up a charge. Insulating powders—those with a resistivity greater than about 10^{12} Ω-m—do not easily dissipate a surface charge they may acquire and, thus, can be prone to spark discharges. This is especially a problem if they are conveyed or stored in insulating pipes or silos. Perhaps surprisingly, even powdered metals—aluminum and magnesium—become poor enough conductors due to surface oxidation so that explosions of dust clouds of these metals have been caused by electrostatic discharges[403]. The tendency for powders to pick up a charge is roughly proportional to their surface/mass ratio (or inversely proportional to particle diameter)[404,405]. This effect appears to be related to the number of interparticle contact points that are available. There is also a material-specific factor—not all powders of the same surface/mass ratio pick up the same amount of charge under a given set of conditions. One condition which can sometimes be controlled is the nature of the processing operation—these differ substantially in their ability to charge powders. Table 35 shows the specific charge (coulombs per kilogram; note that 1 C = 1 ampere-second) which can be associated with different operations. Clearly, pneumatic transfer is the processing step where the highest ignition hazards may be expected to occur. Recommendations of this kind imply that maximum charge that can be picked up is linearly proportional to the mass of granular of material. Unfortunately, this is often not the case. In studies on granular explosives[405], it was shown that increasing the mass from 50 g to 500 g increases the charge by 1.4× to 3.0×, instead of 10×.

Table 35 Effect of processing type on electrostatic charging of powders[404]

Operation	Specific charge (C kg^{-1})
sieving	10^{-11} – 10^{-9}
pouring	10^{-9} – 10^{-7}
scroll feed transfer	10^{-8} – 10^{-6}
grinding	10^{-7} – 10^{-6}
micronizing	10^{-7} – 10^{-4}
pneumatic transfer	10^{-6} – 10^{-4}

The electrostatic charging is normally much higher if the particles flow along a plastic surface than a metal one. Dahn[406] measured agricultural grains flowing along polyethylene liners and found charging, expressed as an energy/mass ratio, on the order of 2 – 6 mJ kg^{-1}; flowing along metal chutes, the comparable values were 10^{-2} – 10^{-1} mJ kg^{-1}.

As with solids discussed in an earlier Section, charge accumulated on powders decays with time and the relaxation time can be estimated from the equation there. Streaming currents (see below) are possible with flowing powders, just as with flowing liquids. Unlike for liquids, however, little quantitative guidance is available.

Powders where the individual particles are charged and then agglomerated show a *bulking* effect. The maximum surface charge density of a small particle is 26.5 μC m^{-2}. The total charge when N of them agglomerate will be N times the surface charge on each. But the effective radius of the 'macrosphere' becomes small enough that 26 N exceeds the breakdown strength of air, i.e., becomes greater than 26 μC per m^2 of macrosphere surface. A discharge has to occur and this is known as a *bulking discharge.* These sparks that occur across the surface of the heap are known to be able to ignite sensitive gas/air mixtures[407], but have not been extensively characterized.

The resistivity of powders changes drastically with moisture. At conditions of RH > 60 – 65%, any charge formed is rapidly leaked away and hazardous conditions would not be expected[408].

Discharging of dry chemical (sodium bicarbonate or ammonium phosphate/ammonium sulfate) fire extinguishers can cause static electricity buildup. It was found experimentally that this can result in charging voltages which would correspond to discharge energies of up to 54 mJ[409]. Energies of this magnitude would be enough to ignite many dusts, not just gases; however, no actual testing of ignition potential was reported.

During loading or conveying of powders, local non-incendive discharges (corona and possibly brush discharges) may occur which are helpful, rather, than deleterious, since they serve to reduce the charge buildup. Based on this observation, to reduce the incendivity of bulking discharges, it is commonly recommended that a grounded wire be strung through the center of a container receiving insulating powders. This causes small corona-like discharges to occur to the grounding wire, instead of large sparks to the container itself. A ground wire is equally effective if the container is insulating, instead of conductive[407]. The ground wire must be thin (around 1 mm) in order to ensure a corona-like discharge.

While pure gases cannot pick up a charge due to motion, cases of mine explosions have been documented[410] where compressed air nozzles were discharged into atmospheres containing dust and methane.

Pneumatic transport systems cause a build up of charge largely due to bends in the pipeline, but within a few meters of travel distance a steady-state value of charge is reached[411]. For a given air velocity, increasing the product mass flow rate decreases the charging tendency. Charging tendency is also reduced by reducing air velocity and by increasing particle size of the granular material. Electrostatic discharges commonly occur whenever granular materials are pneumatically conveyed. These are typically non-incendive corona discharges. It is the possibility of spark discharges or other more energetic forms that forms the crux of the fire safety problem in these applications.

Silos can build up very high potentials when granular materials are conveyed into them. In one study[411], up to 150 kV was measured, with the highest readings being at the top, close to the product entry location.

Table 36 Electrical conductivity of common liquids

Hazard	Example substances	Typical electrical conductivity (S m^{-1})
Low: conductivity less than 10^{-13}	hexane	10^{-17}
	carbon disulfide	8×10^{-16}
	benzene	5×10^{-15}
	heptane	3×10^{-14}
High: conductivity of 10^{-13} to 5×10^{-11}	xylene	10^{-13}
	dioxane	10^{-13}
	toluene	10^{-12}
	cyclohexane	2×10^{-12}
	styrene	10^{-11}
	kerosene	1.5×10^{-11}
	hexamethyldisilazane	2.9×10^{-11}
	Jet-A fuel	$2 - 3\times10^{-11}$
Low: conductivity greater than 5×10^{-11}	gasoline	10^{-10}
	turpentine	4×10^{-10}
	crude oils	10^{-9} to 10^{-7}
	halogenated hydrocarbons	10^{-8}
	methyl alcohol	10^{-7}
	ethyl alcohol	1.4×10^{-7}
	cetones	10^{-5}
	water: deionized	10^{-5}
	iso-propanol	10^{-4}
	water: acid rain	10^{-2}

Note: resistivity (Ω-m) = 1/conductivity
Above data from[412-414] and other sources; for other substances, Britton's extensive compilation[379] can be consulted. Conductivities of liquids are highly variable and values given are only suggestive. In addition, increasing the purity or decreasing the temperature serves to make the liquid less conductive.

ELECTROSTATIC CHARGING AND DISCHARGING OF LIQUIDS

Many liquids are prone to undergo charge separation when they move past either a solid surface or the interface with another liquid. The charging process arises from minute concentrations of ions present in the liquid. But there is a competition between motion causing charging and innate conductivity causing a relaxation of charge. If a sufficiently high charge is accumulated, an electric discharge may occur. This discharge may cause an ignition under appropriate fuel/air ratio conditions. A negative electric charge is more incendive than the corresponding positive charge on the liquid. Charge relaxation readily occurs if the liquid has a high electric conductivity and for such liquids a high charge does not build up. Unfortunately, many organic liquids (i.e., aliphatic, aromatic, and cyclic hydrocarbons; ethers; some silicones) are good insulators (Table 36). Crude oil, alcohols, aldehydes, cetones, esters, ketones acids, epoxides, and nitriles on the other hand, are typically sufficiently

conductive. As a rough rule, most water-soluble liquids are conductive enough to not raise problems of electrostatic discharge in the course of bulk flow[415]. Liquids with conductivities < 5×10^{-11} S m^{-1} are considered to be of low enough conductivity that electrostatic hazards must be carefully guarded against. However, if the conductivity is extremely low, then ionized species that could cause charge buildup are also largely absent. Liquids with a conductivity of less than 10^{-13} S m^{-1} are considered to be in the latter category[429]. Thus, the peak hazard involves liquids with conductivities from 10^{-13} to 5×10^{-11} S m^{-1}. Low conductivity liquids do not support spark discharges to their surface, but can be subject to incendive brush discharges[379].

Liquids of high conductivity can be involved in static electrification accidents if they are within insulating vessels, or in the form of an aerosol, or in some other environment where a conductive path to ground is absent. A common form of electrification of high-conductivity liquids is spray atomization. As discussed below, water is a substance which can be electrified by atomization.

Since charging of low-conductivity liquids readily occurs, a question that has often been asked is: Why do explosions not occur more frequently in vessels holding ignitable liquids? The reason is generally understood to be because in many cases the vapor space above the liquid where discharges occur is fuel-rich[416].

A study on electrostatically-caused explosions of drums[417] identified the liquids most commonly involved:

- benzene
- toluene
- styrene
- dioxane
- hexamethyldisilazane
- toluene/heptane mix.

These chemicals all shared the traits of: (1) conductivity below $5\diamond10^{-11}$ S m^{-1}; (2) MIE < 1 mJ; and (3) wide temperature limits of flammability.

Pure hydrocarbons do not exhibit electrostatic charging; however, even impurities at the 0.001 ppm level change this situation[418]. The presence of a small amount of *water* in the product can increase the electrostatic charging effect up to 50-fold. Oxygen and sulfur compounds also promote charging in hydrocarbons[429]. Raising the *temperature* increases both the conductivity and the charging tendency, but the increase in charging tendency is usually greater[429]. For some substances, extreme changes have been noted with temperature, for example, with one test substance[419] the charging current increased by 1000× as the temperature was raised from 0ºC to 20ºC.

For insulating liquids flowing in *conducting pipes*, the charge density (C m^{-3}) picked up is linearly proportional to the liquid's flow velocity and the charge density reaches a steady-state value after a certain distance down the pipe. As early as 1913, Dolezalek[420] found that benzene and diethyl ether flowing through metal pipes can charge up to 2000 – 3000 V, with the voltage being roughly proportional to the flow velocity. The charge pickup up is less if the pipe is non-metallic. Flows which consist of two-phase liquids, liquids with suspended solids, or mixtures of immiscible liquids tend to build up higher charges than single-phase liquids. Charge buildup can especially increase if the liquid flows through a fine-pore filter. By passing through such filters, kerosene could be charged up to a voltage of –250 kV; further attempts at charging resulted in a spark breakdown within the liquid[421]. In experiments examining the effect of fill fraction on the charged potential in 100 m^3 kerosene tank[422], it was found that highest voltages were produced for a fill fraction around 50%. In experiments set up to reconstruct an industrial accident[423], it was found that pumping toluene into a metal 55-gallon (208 L) drum required that a voltage of –8500 V and a stored energy of 3.6 mJ be built up before ignition occurred via discharge to a grounded rod.

When a liquid which has picked up a charge enters a tank, at first the charge density Q''' (C m^{-3}) in the tank is identical to the charge density of the entering fluid. Gradually, however, relaxation occurs, that is, the small but finite conductivity of the liquid allows a recombination of charges. The relaxation of charge can be characterized by the fundamental time constant τ which is computed the same way for liquids as for solids (see above), although commonly expressed using the bulk conductivity:

$$\tau = \varepsilon\varepsilon_o / \kappa$$

where κ = bulk conductivity of the liquid (S m^{-1}). For most hydrocarbon liquids*, $\varepsilon \approx 2$. For kerosene, as an example, $\kappa = 15\times10^{-12}$ S m^{-1}, giving $\tau \approx 1$ s.

Bustin and coworkers[424] discovered that liquids of very low conductivity (< 1×10^{-12} S m^{-1}) behave anomalously ('non-ohmically') in that charge relaxation is faster than exponential, decaying approximately hyperbolically. For these very low conductivity liquids, Bustin discovered that the basic governing variable determining the relaxation time constant is no longer the conductivity but, rather, the charge level and the charge mobility. The ohmic theory of charge relaxation is based on the assumption that the total number of charge carriers is constant. But for low conductivity liquids, in the uncharged state the number of charge carriers is small; when a liquid of this kind is charged, charges of one sign are removed and charges of the opposite side added, but the sum greatly exceeds the number of carriers in uncharged liquid. Bustin further assumed that the low initial quantity of charge carriers in the uncharged liquid can be set to zero, and that the charged liquid will then have charg-

* Note that this is not true for oxygenated organic liquids; as an example, for alcohols $\varepsilon \approx 20$.

es of only one sign, assumed as positive. The charge decay with time then goes as:

$$q^+ = \frac{q_o^+}{1 + \mu q_o^+ t / \varepsilon\varepsilon_o}$$

where q_o^+ = initial charge density, and μ = charge mobility ($m^2\ V^{-1}\ s^{-1}$). In practice, the group of variables $\mu q_o / \varepsilon\varepsilon_o$ is taken to be an experimental constant. As an alternative to determining the value experimentally, it has been shown[413] that if the decay is assumed to be exponential, but using a fictional conductivity of 0.5×10^{-12} S m^{-1}, then reasonable relaxation time estimates can be made.

For actual vessels, the relaxation time found experimentally is not the fundamental time constant, but it is related to it. In a theoretical study[425] to characterize this actual relaxation time, it was found that the vessel geometry only matters for fill fractions greater than 90%, and that the relaxation time depends on τ and on $D_t\kappa/\lambda$, where D_t = tank diameter (m), and λ = surface conductivity (S). Thus, both the surface conductivity and the bulk conductivity affect the relaxation time. The actual relaxation times were generally found to be 2 –3 times τ, provided that $D_t\kappa/\lambda$ is greater than about 5. In a similar vein, Strawson and Lewis[426] reported on measurements with an aviation fuel where the at-rest conductivity was compared to the relaxation times for flow past filters. They found that the actual conductivity for the liquid in motion is not identical to the value measured in tests where the fluid is at rest. The values of effective conductivity were found to be between 0.04 and 7 times the at-rest values; most of the values were lower than the corresponding at-rest values, except when at-rest values were already below 1×10^{-12} S m^{-1}. They concluded that the charging process itself causes some ionization, which raises the effective conductivity, but did not delve into reasons why certain conditions lead to effective conductivities lower than the at-rest value.

In many practical arrangements, a metallic fill pipe will exist in the middle of the tank. Its presence has been shown[427] to greatly reduce the maximum potential to which the surface of the liquid charges up to, with the voltages being in some cases reduced to 1/3 those which would occur in the absence of the pipe. It is recommended that the fill pipe extend close to the bottom of the tank[379].

The small size of a flammable liquid container does not preclude ignition due to electrostatic discharge, as documented in a case involving a 2.5 gallon (9.5 L) plastic container containing an alcohol-based solvent[428]. A small explosion took place when a person used a steel knife to puncture the hermetic seal of the container. Laboratory testing suggested that the event was due a charge created by shaking the liquid, and not due to a charge on the person.

For hydrocarbon liquids that pick up some water impurity, relaxation times in tanks can be much lower than predicted, due to sedimentation (settling). The effect arises because of charges associated with the water component and its gradual movement in the tank[429]; the theory has been presented by Klinkenberg and van der Minne[418].

If a liquid is at rest, ion impurities will cause a certain amount of separation of charge, but the net charge in the pipe will be zero. But when a low-conductivity liquid is in motion in a pipe, not just separation, but an actual flow of charge occurs. This flow is called a *streaming current* and it arises because ions in the liquid tend to move with the flow, while the opposite charge on wall dissipates to earth. For it to occur, the liquid must have a conductivity in the range of about 10^{-13} to 10^{-7} S m^{-1}. Higher conductivities lead to rapid neutralization of charge, while smaller ones do not permit a double layer to be formed. It was proposed by Schön[430] for such liquids, that the streaming current is roughly independent of the liquid's exact conductivity and can be approximated as:

$$I = \frac{dQ}{dt} = 3.75\times10^{-6}(uD)^2$$

where Q = charge (Coulombs). Since the cross-sectional area of a pipe is $\pi D^2/4$, the charge density Q''' (C m^{-3}) in a liquid leaving a long pipe depends on the flow velocity u according to:

$$Q''' = \frac{4}{\pi}\frac{I}{uD^2} = 4.78\times10^{-6}u$$

Schön's equations have been used widely. However, more recent experiments[413] revealed that even for smooth-bore pipes (rough-bore pipes are much more hazardous towards accumulating charge and general results cannot be given for them) experimental data are not conservatively represented by Schön's equations. This led to the recommendations of:

$$I = 9.42\times10^{-6}(uD)^2$$

$$Q''' = 1.2\times10^{-5}u$$

But if liquids contain substances which act, effectively, as pro-static agents, then the worst-case condition must be considered:

$$I = 2.5\times10^{-5}(uD)^2$$

$$Q''' = 3.18\times10^{-5}u$$

An even more basic problem is that Schön's assumption that Q''' is independent of pipe diameter was found to be untrue[431]. Instead, the expression should be:

$$Q''' = 5\times10^{-7}u/D$$

where D = pipe diameter (m). A corresponding flow velocity can then be obtained from one of the above equations. Similar values also apply to loading of tanker trucks. It has been found[432] that incendive discharges may be expected if the charge density exceeds 20×10^{-6} C m^{-3} for top loading and 30×10^{-6} C m^{-3} for bottom loading, thus values smaller than these are usually taken as safe.

Moisture and impurities can greatly increase the charge density, but experiments have to be set up carefully to illustrate this. The effect is not found unless the liquid is pumped through filters[433]; charge generation associated with tank-loading in the absence of filtering does not show deleterious effects of impurities. Metallic trash in tanks can act as 'charge collectors' and greatly reduce the charge density necessary to cause an electrostatic discharge[433]. The effect takes place since small metallic objects can be buoyed up by turbulence or by foaming of the product. The combination of filtering + splash loading was found to be highly conducive to discharges; removing either of the two factors greatly diminished the potential for a discharge. In low-viscosity liquids, splash loading by itself produces a charged foam in the tank which can lead to discharges even when the inflowing liquid has little charge on it.

When liquids flow in *insulating pipes*, little streaming current occurs because the charge induced in the pipe walls does not get dissipated to ground. Instead, the primary hazard is of direct breakdown of the pipe material due to an electric discharge. When this occurs, cracks or pinholes may be created; if the liquid is combustible, an external fire hazard can then happen. This is illustrated in one study where kerosene which had picked up a high negative charge from being put through a filter caused an electrostatic discharge that punctured a polyethylene pipe and created a visible leak[434]. Glass pipes are not subject to pinholes, but a discharge may originate in the liquid which extends to the exterior of the pipe (Figure 54)[435]; discharges larger than the one illustrated also were documented and these typically broke the pipe.

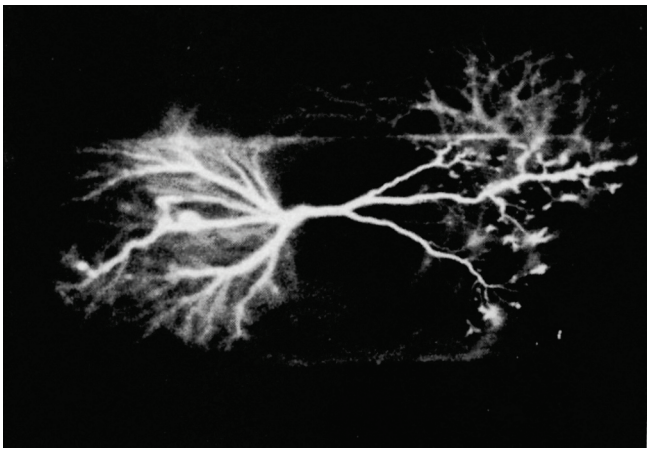


Figure 54 Discharge occurring inside and outside of a 25 mm glass pipe carrying No. 2 fuel oil
(Reprinted courtesy of Exxon Mobil Corporation)

Filters, especially micropore filters (mesh size < 150 μm), are the most significant way that very high charges can be imparted to moving liquids. In fact, in most experiments where it is desired to place a charge on a liquid, vigorous pumping through fine filters is used as the technique. *Rough-bore hoses*, such as ones containing an internal grounding helix, can be almost as effective as microfilters in charging liquids. A *grounded grid* through which a liquid passes can act similarly to a filter in causing charging. Any other arrangement where a two-phase flow is introduced (e.g., bubbles) can also have a similar charging effect.

Liquid sprays can cause intense static electrification; this was first observed near waterfalls in the 19th century and is called *spray electrification*[436]. The process occurs due to the presence of a double layer of charge at the liquid surface. Small pieces of material in the form of droplets removed from the surface can then possess an unbalanced charge. By this process, a water stream may ignite a flammable atmosphere, and this concern arises in operations, for example, where a water spray is used to clean equipment which was used to store flammable liquids. Oil tanker explosions have occurred when water streams have been used to clean 'empty' tankers which contained a flammable atmosphere; this problem came to a head in 1969, when explosions occurred in three very large crude carriers during washing[429,437]. A water mist used in such cleaning[438] may pick up a charge of ca. 30 nC m^{-3}. The solution found was to provide inerting for the tanks, typically using scrubbed flue gas. Potentially incendive charges may also be picked up simply by sloshing of liquids. A similar, but generally larger static charging effect can be produced by jets of *steam*[439]. Predicting charging details is very difficult, but incendive sparks may occur if insulated metallic objects are present in the vicinity or if grounded objects pick up an induced charge and the ground connection is subsequently removed. A small amount of an immiscible component can make a very large change in charging of sprays; in one set of experiments[440], adding 5% water to kerosene increased the charge density by about 1000×.

A laboratory study on the tanker washing problem[441] eventually identified a mechanism for incendive discharges. When a water jet impinges upon a solid surface, upon impact, the jet breaks up into fine and coarse water particles. The coarse drops acquire an electric charge of one polarity, while the fine ones a charge of the other sign. The system is unstable and coarse drops separate and fall out early. The separation of droplets then causes a separation of charge. The result is an atmosphere filled with a charged aerosol. If a tank has been charged this way and contains grounded metal protrusions, then incendive discharges were found to occur when a 'slug' of water falls through the charged aerosol. This slug acquires a charge by moving through the charged aerosol, and incendive discharges were observed in propane/air atmospheres when water slugs fell and passed at 1 – 4 mm from a grounded protrusion within the tank. The study also found that corona discharges occur when droplets fall off grounded protrusions, but no such corona discharges were incendive.

Napier and Rossell[442] studied the charging of sprays of organic liquids, as may occur during a leak or break in piping in a chemical plant. They found that in the aerosol cloud created by the spray the maximum field strength only reaches 0.2 MV m^{-1}, which is greatly below the dielectric breakdown strength of air (3 MV m^{-1}). Thus, direct ignition cannot occur by means of a discharge from the aerosol cloud. However, many joules of energy can be stored in a cloud formed in this manner. Thus, a hazard may still occur if this charge can be transferred to an isolated object, which might then sustain a discharge to ground. Opening the valve of a liquefied gas tank (e.g., butane) will cause a jet of 'gas' to be discharged, but minute droplets of liquid are also carried along. An accident is reported where a jet issued from a butane tank leak and ignited upon impacting a nearby wall[134]. Similar accidents have been reported upon opening the tank valve of a cylinder of dissolved acetylene. In the latter case, droplets of acetone are carried along with the acetylene gas.

Experimental study of discharges

While numerous studies have quantified the separation and movement of charge in liquid systems, studies where details of electric discharges was explored have been few. Wright and Ginsburgh[443] conducted experiments where ball electrodes of various diameters were charged to either a positive or a negative potential and discharges allowed to occur to a liquid surface. The authors concluded that it was very difficult to obtain constant-concentration fuel/air mixtures above liquids that are actually vaporizing, so they simulated the problem by use of a transformer oil (essentially non-vaporizing), above which was a well-mixed atmosphere of 6% propane in air. Their results (Figure 55) indicate that ignition is much harder to achieve when the electrode is negatively charged with respect to the liquid. These discharges were corona discharges, rather than the spark discharges seen when the electrode was positive with respect to the liquid surface. The authors also reported on a number of other experiments where grounded objects, partially or fully submersed in the liquid, led to incendive discharges. These showed the role of 'field concentrators,' whereby discharges occurred due to local distortions of the electric field, despite electric fields being modest when measured over larger distances. Lyle and Strawson[444] conducted similar experiments and found that 4.7 mJ spark energy was needed to ignite a propane/air mixture when the spark went between a metal electrode and the liquid surface (Figure 56). By contrast, the MIE of propane/air mixtures, when ignited by a spark discharged between two optimally-designed metal electrodes is 0.26 mJ; thus using the standard tabulated MIE value would give an unanticipated safety factor of 18. Several additional studies are described in Chapter 14 under *Aviation fuels*.

Gasoline vapors can be ignited from corona discharge if fuel is dripped onto a high-voltage transmission line[249]. For a 55 m diameter conductor, a minimum electric field of 1530 kV m^{-1} was needed; for a smaller 33 mm conductor the value rose to 1740 kV m^{-1}.

Krämer and Asano explored experimentally the minimum conditions necessary inside tanks for spark incendivity[445]. They found that a minimum charge transfer of ca. 0.1 μC (microcoulombs) was necessary. A minimum potential of 58 kV was also found to be needed. The tests were done using electrodes of various diameters, with the electrode simulating a protuberance in a tank to which a discharge would be occurring. A optimum diameter of 20 to 40 mm was found for spherical electrodes. Larger diameters led to a slight increase in the minimum needed discharge potential. A 10 mm diameter led to a significant increase in the needed potential. The minimum charge transfer needed to cause an ignition of a flammable tank atmosphere also depends on the fraction of fuel which was in vapor, versus aerosol, phase. While 0.1 μC could ignite a 100% vapor atmosphere, 1.0 μC was needed when 65% of kerosene fuel was in aerosol phase, and 2 μC when 95% of the fuel was in aerosol phase[421].

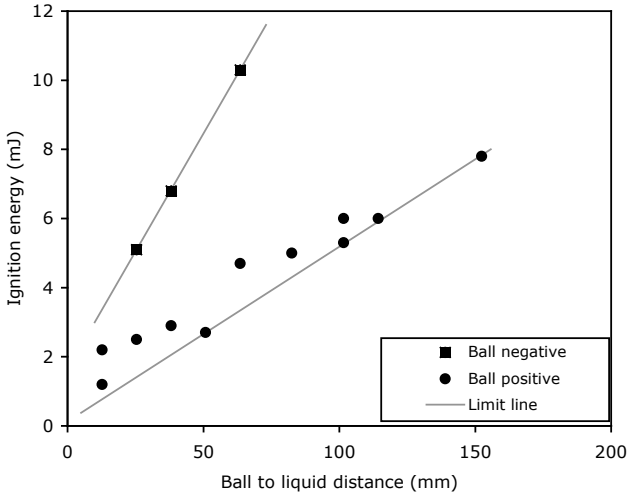


Figure 55 Energy required to ignite flammable atmospheres by electrostatic discharge between ball electrode and liquid surface

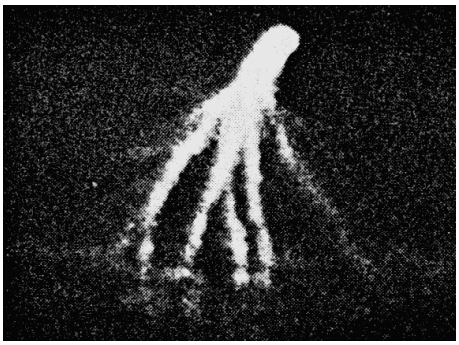


Figure 56 Spark from metal electrode to a liquid surface
(Copyright Institute of Physics, used by permission)

Discharges can also occur within the bulk liquid, although these are common only to a few fuel types[419]. But there is no danger of ignition, if the liquid is without air bubbles.

Additional experimental findings are given in Chapter 14 under *Aviation fuels*.

SAFETY MEASURES

Bonding and grounding of all metallic objects that might become electrostatically charged is the highest priority safety measure. Furthermore, safety is promoted by maximizing the use of metal, as opposed to non-conductive, tanks, pipes, etc. But even if a container is metallic and is suitably grounded, all hazards are not necessarily eliminated, as shown in Figure 57. Inerting eliminates the potential of explosions in flammable atmospheres, but is restricted to situations where it can be affordably provided.

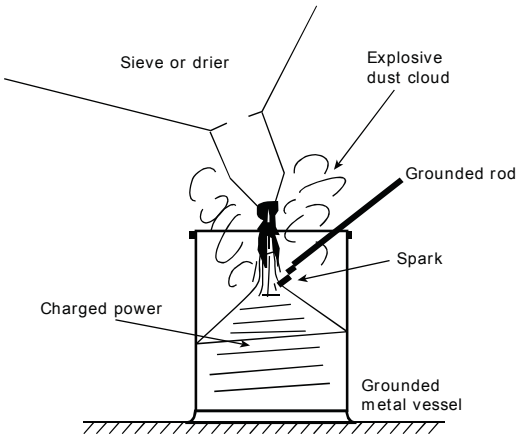


Figure 57 Example of arrangement where an incendive discharge can take place inside a grounded metal vessel

Traditionally, it used to be claimed that *splash loading* promotes electrification. Thus, a generally recommended practice is that liquids should be introduced into the bottom of a tank, not poured openly from the top. However, experimental studies suggest that this is only true in certain circumstances. Bachman's[433] study indicated that filtering is also needed for a hazard to be created, while Lyle and Strawson[444] could not find any measurable effect in their study. Britton[379] agrees that splash loading does not cause significant electrification but considers that, indirectly, splash loading may promote hazardous conditions due to:

(a) an absence of the electric field reduction that is provided when a metal dip pipe is used;
(b) accumulation of excessive charge densities at the liquid surface by stratification;
(c) turbulent mixing causing a dilution of the vapor layer near the liquid surface (which is the most likely place for an incendive brush discharge to occur, but which would normally be above the UFL) by sufficient air to bring it into the flammable region; and
(d) the creation of froth above the liquid surface, which may be more easily ignitable than the vapor from a quiescent liquid.

It has been recommended[446] that for filling tank trucks with petroleum products having a conductivity $< 5\times10^{-12}$ S m^{-1}, the filling velocities be restricted so that the velocity × pipe diameter product $uD \le 0.38$ s^{-1}, while for conductivities in the range of $5 - 10\times10^{-12}$ S m^{-1}, $uD \le 0.5$ s^{-1}. The American Petroleum Institute recommends[429] that flow velocity should:

- be below 1 m s^{-1} until the outlet of the fill pipe is submerged;
- afterwards, be the lesser of (a) 7 m s^{-1}, or (b) $0.5/D$, where D = diameter of pipe (m)

Anti-static agents should be used where needed to increase the conductivity of the liquid. A residence time of 30 s should be allowed for charge relaxation after a petroleum product passes through a filter and before it is exposed to conditions that could lead to an electrostatic ignition[429]. Introducing water into a gaseous atmospheres does *not* help to avoid static discharges. Britton's book[379] provides an extensive, detailed list of additional safety recommendations.

LIGHTNING

ORDINARY LIGHTNING

Lightning becomes possible because electric charge can become separated and accumulated in clouds. Clouds are highly complex entities. There are large temperature gradients, liquid and solid particles, convective flows, and effects due to phase changes. Even today, the physicochemical environment of clouds is by no means comprehensively understood. One recent theory by Ermakov and Stozhkov[447] is illustrated in Figure 58. Thundercloud formation begins when a cold air mass meets a warm one. Ionized, warm, moist air rises, but is then progressively cooled at higher elevations and condensation of water vapor on nucleation centers begins. In the initial phase, condensation proceeds faster on negatively charged nuclei than on positive ones, and the upward air flux produces large-scale separation of charge and a resultant electric field. The latent heat released in condensation assists the buoyancy of the upward air current. Cosmic rays produce ionized showers of particles. When the electric field exceeds 0.2 – 0.3 MV m^{-1}, electron avalanches occur, ionized tracks link with each other and form a conducting tree structure. This allows cloud-to-cloud discharges to occur. In the mature phase, droplets grow and coagulate. There are ascending and descending air flows and the cloud becomes asymmetric, with an excess of negative charge at its base. The electric field between the cloud and earth's surface increases, leading to cloud-to-ground discharges. The maturity phase may last 20 to 30 minutes and produce 50 to 100 cloud-to-ground discharges. This is accompanied by a larger number of cloud-to-cloud dis-

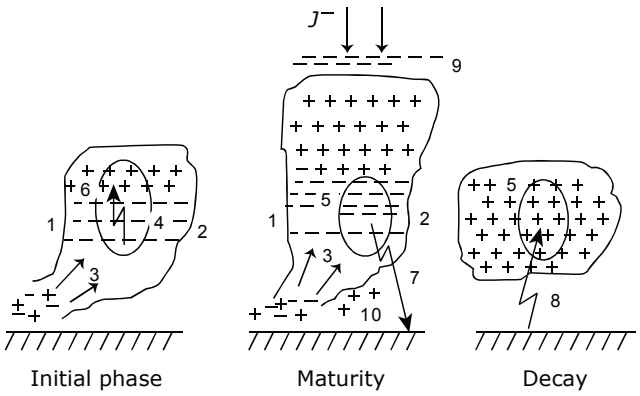


Figure 58 Formation of thunderclouds as described by Ermakov and Stozhkov. **1** warm air front; **2** cold air front; **3** ascending flux of wet ionized air; **4** and **5** extensive air showers produced by primaries with energies over 10^{14} eV or 10^{15} eV, respectively; **6** cloud-to-cloud lightning; **7** cloud-to-ground lightning; **8** ground-to-cloud lightning; **9** negative screen layer; **10** positive charge at cloud base; $\mathbf{J}^-$ current of negative ions from the ionosphere to the top of the cloud.

charges. In the decay phase, vertical air motion is damped out, precipitation occurs, and ground-to-cloud discharges may be observed.

The origins of a lightning strike are due to a separation of charges in clouds. There is most commonly a three-layer 'sandwich': positive charges on top, negative charges in the middle, and positive charges at the bottom[448]. Lightning becomes possible when a potential of 10 – 100 MV with respect to the ground has been reached. A *lightning flash* is composed of several events. The actual discharge begins with the formation of the first *stepped leader*, which is a localized gas breakdown of about 50 m length. The process continues in a stair-step fashion until a leader gets to within about 50 m of the ground (or an object on the ground). The negative charge of the stepped leader induces a positive charge in the earth below. Protruding grounded objects start to conduct heavier point-discharge currents. A streamer then arises from one of these objects or from the earth itself, connects to the leader and starts a *return stroke*. The return stroke is the brightly visible 'lightning stroke.' After the first return stroke, a *dart leader* may descend directly to the ground, without stair-stepping. This dart leader is ball-shaped. It will be followed by a second return stroke. There may be 3 or 4, but occasionally many more, strokes per the total event, which comprises the lightning flash. The total lightning flash may last from 0.01 to 2 s, with 0.2 – 0.4 s being typical, but each individual stroke only lasts about 30 μs. The interval between strokes may be around 40 ms. The current carried by the stepped leader is small, only on the order of 100 A. But each return stroke will typically carry 10 – 20 kA of current and peak currents in excess of 100 kA are occasionally recorded[449]. Somewhat different mechanics govern strokes that do not reach the earth, the cloud-to-cloud discharges. *Thunder* is an acoustic shock wave that originates in the gas breakdown region and then propagates out through the air.

In thunderstorms, a lightning flash may recur twice a minute, but in severe thunderstorms, as many as 25 per minute can be expected. A cloud-to-ground stroke may discharge about 25 coulombs per each stroke. The average length of a stroke is 3 km, and the average energy released is 10^5 J m^{-1}, making an average energy release of 3×10^8 J per stroke[450]. The pressure within a lightning column can reach about 8 atm. A cloud-to-ground flash may be as much as 14 km long; cloud-to-cloud flashed can be much longer.

In calm, sunny weather, the earth is at a slightly negative potential (0.3 to 0.45 MV) with respect to the ionosphere—the earth is continually losing electrons except during lightning events, during which the flow is rapidly reversed. The electric field is approximately 100 to 600 V m^{-1}. When turbulence arises and thundercells start to form, the polarity reverses, and the clouds assume a negative polarity with respect to the earth. The electric field builds up to 10 – 20 kV m^{-1} between the clouds and the earth. Just prior to a lightning strike, the cloud may be charged to a potential of some 30 MV with respect to earth. While the dielectric breakdown strength of normal dry air is 3 MV m^{-1}, within thunderclouds, much smaller electric fields—0.3 to 0.5 MV m^{-1} are sufficient to trigger a lightning flash. Occasionally, especially in connection with tornadoes, lightning discharges take place with the bottom of the cloud being at a positive polarity with respect to earth.

When a lightning strike occurs, nearby metallic objects can have a current induced in them. This includes not only electrical wiring, but other metallic objects such as building beams.

In electrical circuit terms, a lightning stroke can be considered a constant-current source. Therefore, the energy dissipated in object along its path is:

$$\int I^2 R\, dt$$

where I = current (A), R = resistance (Ω), and t = time (s). This accounts for the much higher damage found for objects of poor conductivity, than for metals[451]. Design values for the current of 100 – 200 kA are commonly used[452] since only about 1% of lightning strokes give currents in excess of 200 kA[450]. The current from a second or subsequent stroke is typically less than ½ that from the first one.

Ignitions from lightning

The primary damages[453] to residences from lightning are considered to be:

- brick, concrete and other solid surfaces moved or cracked

- plumbing pipes punctures
- holes burned or punctures in roofs
- arc damage to metal structures such as window frames
- arcs across wiring.

The last three of these, of course, may also be accompanied by ignition of combustible materials. Frydenlund[452] reported on a survey of lightning strikes to private residences (Table 37). Similar statistics are not available for other building types.

Because the temperature rise in an object is proportional to its resistance, a metallic object (e.g., a lightning rod) may sustain limited temperature rise, while a poor conductor such as wood may become ignited. Ignition of an apartment house roof is shown in Color Plate 32. Ignition of structural members inside walls and ceiling is shown in Color Plate 33. Lightning ignitions can assume a wide variety of geometric patterns, as illustrated in Color Plate 34. Multiple ignitions from a single strike are not rare (Color Plate 35).

Table 37 Locations of lightning strikes to private residences

Place struck	Percent
roof or projections	32
TV antenna	29
overhead power line	29
adjacent tree	10

Whether combustibles will be ignited from a lightning flash or not depends critically on whether there is a flow of *continuing current* in the channel after the stroke[463]. About 25 – 50% of lightning strikes exhibit this characteristic—these are sometimes called *hot bolts* (Figure 59). Lightning strikes which are positive (i.e., the cloud being positive with respect to the ground) are much rarer than the converse, but these are precisely the ones that are most likely to cause

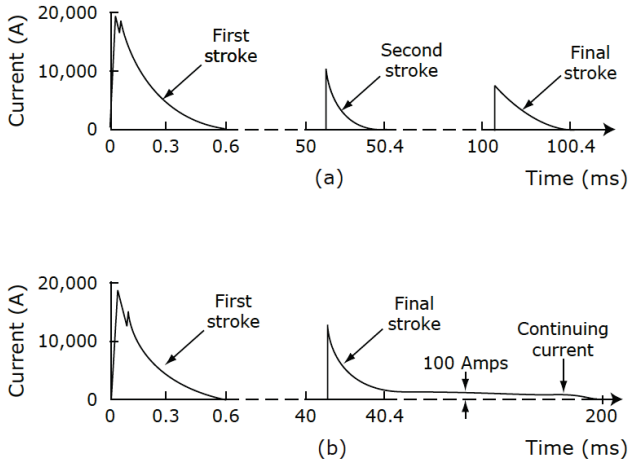


Figure 59 **(a)** Cold bolt, no continuing current; **(b)** hot bolt with a continuing current of ca. 100 A
(Copyright Dover Publications, used by permission)

ignitions, since their peak currents and total charge transfer are much larger. Positive flashes do not have the stepped-leader characteristic of the common, negative strikes, and consist of a single stroke, followed by a period of continuing current flow.

The importance of lightning as an ignition agent for forest fires varies among countries. Lightning strikes account for some 40% of forest fires in British Columbia and 60% of in the western US[454]. However, most lightning strikes only char the tree struck and do not result in a wildland fire. Ignitions in forests usually involve fine fuels (forest floor duff) or punky (rotted) wood; the latter, of course, also exist on living trees[455]. Healthy trees may be damaged by strikes, but are only occasionally ignited when struck, primarily if they are quite dry. The more common effect on living trees is an explosive shattering which occurs due to moisture being rapidly brought to a boil. In milder cases, only a strip of bark gets peeled off (Color Plate 36); in severe cases, the tree is shattered. Occasionally, even very large trees get ignited and some are able to burn comprehensively, not just thinner material burning off[456]. In rare cases, a lightning strike can ignite a living tree in a smoldering mode, and many months can elapse before the smoldering transitions to flaming. In two known cases, redwood trees were involved in such long-term smoldering[457]. It is suspected that the places on the crown of the tree where the lightning struck contained decayed material that facilitated the smoldering process.

Frydenlund[452] considers that the probability of igniting a house fire from a lightning strike is much higher if the house has plastic plumbing pipes, as opposed to metallic ones. This is because the lightning current may flow to ground through a metallic pipe network, but if electric wiring is the only substantive metallic path, the current is likely to go through electric wiring, where heating will be much greater, due to the smaller area of the conductors.

Stevens has reported a case after lightning struck a house where most of the wiring in the house was devoid of copper, all that was left was floppy plastic insulation[458]. He also reports another case of this phenomenon occurring when power was applied to a shorted wire in a house; in the latter case, breakers were not tripped, despite a 4600 kVA short circuit capacity of the electrical feed.

ST. ELMO'S FIRE

Point discharges occur from nearly any sharp, pointed object that is grounded and protrudes above the earth. It requires an electric field of only about 2 kV m^{-1} for a point discharge to begin. Ions are emitted from the sharp object in a point discharge, but there is no visible luminosity. At ca. 100 kV m^{-1}, corona discharge can occur from sharp points. This is a luminous discharge which is also commonly audible. A prominent form of corona discharge in the open air is called St. Elmo's fire; in meteorological literature, it is also

referred to as a brush discharge or a glow discharge, although in electrostatics brush discharge is not synonymous with corona discharge. This non-violent discharge can occur when a sufficient negative charge builds up in the lower layers of a cloud. The discharge occurs because the pointed object creates a distortion in the electric field, with potential lines being concentrated near its tip. A light can be seen when ions and electrons recombine and emit energy in the visible spectrum.

BALL LIGHTNING

Although a meteorological phenomenon termed ball lightning sometimes occurs during stormy weather, it has also been observed during clear weather and in the interior of buildings and aircraft. It is considered to be the least well understood meteorological phenomenon. Despite countless theories and research (a recent monograph[459] contains more than 2400 bibliographic entries), as of this date it remains an unsolved physics problem. There is no doubt among meteorologists and physicists that the phenomenon is real and countless credible case histories exist. But, surprisingly, while a number of photographs have been published, not a single photograph exists which is considered incontrovertibly genuine—apart from a few hoaxes, most have been challenged as mis-identifications (e.g., weather balloons) or as optical illusions[*]. Since the phenomenon is short-lived and its presence cannot be anticipated, evidently few observers have prepared themselves with cameras.

Ball lightning typically has a diameter of 0.1 – 0.5 m, although sizes from 10 mm up to 1 m or more (in rare circumstances) have been reported[460]. It is a vortex of plasma typically of pale red or orange color, but sometimes white or blue-white. The shape is usually spherical, but may be doughnut- or ovoid-shaped. There may be a corona or sparks or rays seen around it. An event lasts from a few seconds to many minutes, with most reports being in the range of 2 – 60 s. Ball lightning has been reported to decay either silently or explosively. A peculiar slow motion is typically associated with the phenomenon—ball lightning does not 'strike' the way that normal lightning does. In several cases, balls of lightning have wafted through in-flight airliners, gliding at about "walking pace"[461]. The ball itself is sometimes seen to roll, spin or tumble. It almost never reported that the balls rise through the air in a convective fashion, which would be typical of an entity at an elevated temperature. Sometimes there are sounds or a sulfurous smell observed. In one case, a ball came down a chimney, approached a person (who avoided it), went up an old papered-over flue, broke through the paper, and finally burst on reaching the flue top, doing considerable damage there[467].

There are unexplained regional variations in ball lightning. European studies report that 95% of ball lightning occurs in connection with thunderstorms, while statistics collected in Japan indicate nearly 90% of events occurring in cloudy weather, but in the absence of rain or thunder[462].

Switching of electrical equipment drawing very large currents is known to occasionally create fireballs that appear to be similar or identical to ball lightning[463]. Laboratory experiments have been reported which produced ball lightning[464-466], but these have tended to produce smaller and shorter-lived luminous entities than ball lightning observed in the field. In addition, the appearance of these structures were rather different from the spherical objects reported in field sightings. Prof. William Thornton, who was the first to investigate a number of topics in fire science, published probably the earliest research paper in English on ball lightning in 1911[467], although earlier scientists were already pondering the phenomenon even in the 18th century. The first full-length book[468] on the phenomenon appeared in 1923; it was mostly a compilation of reported case histories. Very little progress was subsequently made until 1955, when the topic became of interest to plasma physicists, especially in Russia. One Russian theory[133] holds that ball lightning is a consequence of ordinary lightning and occurs when a flux of positively charged particles hits an object. The speed decelerates and the particles start to form a ring vortex, which becomes ball lightning. The ball is said to consist of positively charged particles inside and negatively charged particles outside, kept apart by centrifugal forces. When the rotation decelerates enough due to friction with air so that centrifugal forces become no longer adequate to keep apart the oppositely-charged particles, a discharge occurs. Another theory holds that ball lightning occurs due to bunching of the electric field when encountering a dielectric inhomogeneity. A focusing effect is created and this leads to a localized discharge of plasma. The plasma itself comprises an inhomogeneity and this further concentrates the electric field lines. This theory in effect considers ball lightning to be a corona discharge in mid-air. Another theory has been proposed by Witalis[469], who considers that a branch of plasma theory called Hall-effect magnetohydrodynamics (HMHD) can explain it. Arnhoff[470] considers that ball lightning can occur when the energy of normal lightning rolls up into a ball; solutions of the Helmholtz equation were shown to exist that correspond to a non-expanding sphere. Stenhoff[459] has summarized and categorized dozens of other theories, none of which could be viewed as definitive.

Fatalities are rarely reported from ball lightning. There are reported incidents, but these are few and of unclear veracity; most have been from the 18th and 19th centuries. The most famous report of a fatality is that of Georg Richmann, a physician who was killed by ball lightning in St. Petersburg in 1753, but it is not clear that the cause of death was not ordinary lightning[459].

[*] However, it must be kept in mind that debunkers do not necessarily have preemptive claim on the truth.

Because of the controversial nature of ball lightning, all reports must be viewed in a questioning manner, nonetheless damages reported from ball lightning include splitting of wood, breaking of glass, shattering of TV sets, and fusing of metallic electrical components. Vegetation, clothing, and curtains have been ignited, but generally the event leads to non-sustained ignition, so that propagating fires do not result. Ball lightning ignited and burned off hair on an airline pilot in flight[456]. There have been reports where a house or a ship was burned down, but these date back to the 19th century[459].

EXPLODING WIRES

Passing a large amount of current through a tiny wire, say around 35 μm diameter, results in a vaporization of the metal and very high temperatures being created. Exploding wires were first used to detonate explosives in 1938, but the phenomenon of exploding wires is very complex and poorly understood. Consequently, a detailed explanation of how initiation of high explosives occurs had also been lacking. The situation is further complicated in that the governing phenomena themselves depend on the magnitude of current density that is passed through the wire. At the typically high current densities that are used, a plasma results, but at more modest densities (10^8 – 10^9 A m^{-2}) the wire shatters and disintegrates in the solid phase[471]. The energy required to heat, melt, and vaporize the wire is normally only a small fraction of the energy that is supplied (usually from a capacitor discharge), thus the bulk of the energy is delivered to the plasma[472].

It is normally considered that exploding wires ignite explosives because of the very rapidly rising current that must be provided from a suitable low-inductance discharge capacitor. The melting temperature of the metal is reached, but for a short period of time its inertia keeps it from flowing out. The molten metal is further raised in temperature until its vaporization point is reached. At that time, current starts to flow in the form of an electric arc through the cloud of the metal vapor, heating and expanding it violently. This expansion manifests itself as a shock wave propagated away from the wire. As the arc is stabilized, its resistance drops and the current flow further increases. Recently, it has been suggested that the electric field surrounding the wire ionizes the surface of a high explosive, and thereby pre-sensitizes it so that a weak shock can then initiate a detonation wave[473]. A number of explosives detonators are built around the use of an exploding bridgewire (the term preferred in the munitions field). Because of the creation of a shock wave, an EBW detonator can ignite explosives which would otherwise not be ignited by the melting of the metal that occurs in an ordinary hot wire igniter, e.g., a blasting cap.

ELECTROMAGNETIC WAVES AND PARTICULATE RADIATION

The main regions of the electromagnetic spectrum are shown in Table 38. For electromagnetic radiation to lead to ignition, not only does energy have to be transmitted, but it must be received. In most cases, the received energy of relevance to ignition problems is directly converted into heat at the target. Targets vary widely in their ability to receive electromagnetic radiation, and the ability invariably depends on the frequency of the radiation. The fraction of incident radiation absorbed by a target is termed the *absorptivity*, and it can vary from 0 to 1. Most gases have small-to-nil absorptivity throughout the spectrum and even those gases that show significant absorption only do so within limited wavelength bands. If a radiant heater ignites a flammable gas mixture, it is because a hot radiating surface was present, not because the gas directly absorbed sufficient radiation. Power-frequency and radio waves are significantly absorbed only in metals. Electromagnetic energy emitted from bodies due to their high temperature falls into the infrared region of the spectrum. Hot bodies emit an insignificant fraction of their radiation at lower-frequency portions of the electromagnetic spectrum. Many solids absorb infrared and visible radiation very well. Apart from radiant heaters, there are many devices which intended to generate electromagnetic radiation; typical examples are radio transmitters, lasers, X-ray machines, and ultrasonic generators. Power generators also create electromagnetic fields, but only a small fraction of the generated power is emitted as radiation, the useful portion being transmitted in wires as electric current to the user. Another class of radiation is particulate radiation. Radiation where small, elementary particles are emitted occurs in cosmic rays, in various laboratory high-energy particle sources, and in nuclear reactions and weapons.

Table 38 Primary regions of the electromagnetic spectrum

Region	Frequency (Hz)	Wavelength (m)
power	50 – 60; 400	7.5×10^5 – 6×10^6
radio	10^3 – 3×10^9	0.1 – 3×10^5
microwave	3×10^9 – 3×10^{12}	10^{-4} – 0.1
infrared	3×10^{12} – 4.3×10^{14}	7×10^{-7} – 10^{-4}
visible	4.310^{14} – 7.5×10^{14}	4×10^{-7} – 7×10^{-7}
X-ray	3×10^{17} – 3×10^{19}	10^{-11} – 10^{-9}
cosmic ray	$>3\times10^{22}$	$< 10^{-14}$

Laser ignition of solid objects has been considered briefly in Chapter 7. Ignition by infrared heating has been considered in Chapters 6 and 7. Light energy as an ignition source is considered in a separate Section below. Here, we will only consider three sources: eddy currents, radio and microwave transmitters, and nuclear weapons. Ignition from radiation by energetic particles would be likely to occur only in highly specialized laboratories.

EDDY CURRENTS

If a metallic object is placed in a strong electromagnetic field, an electric current (eddy current) is induced in the object. This principle is exploited industrially for inductive

heating of metals. If the metal is heated sufficiently, and a combustible substance is next to it, an ignition is possible. Such incidents are rare, partly because large electromagnetic fields tend not to be found except in facilities designed for their use. The electromagnetic field from normal power lines is small, because in the balanced geometry of a power line, the fields from the conductors largely cancel.

While ignitions from inadvertent direct-heating effects are probably rare, it is more likely that eddy currents would lead to arcing which, in turn, can cause an unwanted ignition. This is also rare, but has been documented in connection with explosions of motors on offshore oil drilling platforms[474,475]. During the investigations, it was noted that sparking was actually observed at the joints of the enclosures of other similar motors. Measurements showed that currents in excess of 200 A can be induced by a 2-pole induction motor in a steel motor enclosure as the motor is being started. Sizable currents were documented only in large (over 2000 kW, 3000 HP) motors. The induced voltages are minuscule (1 – 2 V), but, because of the inductive nature of the circuit, testing showed that flammable atmospheres may get ignited.

Dielectric heating is a similar form of heating applicable to insulators. Insulators are not perfect, and the dielectric in a capacitor absorbs a certain amount of energy (dielectric loss). Dielectric heating is used in medical and industrial processes, but likewise appears to have minimal potential for causing ignition. Microwave heating is a related process and discussed below.

RADIO TRANSMITTERS

Ignition in the vicinity of radio transmitters can occur in two ways:

(1) by direct heating of substances from the electromagnetic field (see *Induction heating*, above)
(2) by means of RF (radio frequency) sparks.

To ignite flammable gases by means of RF sparks requires not only a huge electric field but also a flammable gas volume and one that is not be electrically shielded (i.e., within a metal tank). This will normally involve an extraordinarily rare combination of circumstances, and there do not appear to be any verified reports of such explosions. Nonetheless, there has been a great deal of design and regulatory interest in the topic in the UK, which includes an HSE guide[476] and British standards[477,478].

Under normal circumstances, devices intended to collect RF energy are called 'antennas' and are designed according basic electrical principles in order to collect the energy efficiently. But metallic buildings or equipment can serve as adventitious antennas, collecting and possibly delivering RF energy to a locale where a spark discharge might occur within a flammable mixture. Research indicated[479] that vertical structures at ground level do not pose a hazard, since they are effectively RF-coupled to the ground. But loop-type structures, for instance, mobile cranes, are more effective antennas. The frequencies at which there is the greatest danger of collecting unwanted RF energy is considered to be 0.5 to 4.5 MHz[480]. The incendivity of RF sparks is, in general, much less well understood than that of DC sparks. Early laboratory tests showed that in spark discharge circuits where the main impedance was a 50 Ω resistance, RF induced power from a few watts (for frequencies below 1 kHz) to a couple of hundred watts (for frequencies over 100 kHz) was needed to cause ignition of methane/air mixtures. In addition to the RF frequency, the metal forming the discharge electrodes had a very large effect on the power needed. Rusty steel or oxidized aluminum required much less power than clean cadmium electrodes. The effect of raising the circuit impedance was to lower the needed RF power for ignition. Later studies[480] quantified the effect of circuit resistance. For a 1000 Ω resistance, 10 W of transmitter power were needed for ignition of methane in air, 7 W for ethylene, and 3 W for hydrogen. The dependence on the circuit impedance was empirically found to be $P \propto Z^{-0.184}$ where P = transmitter power (W) and Z = circuit impedance (Ω). Similar studies have been performed by Widginton[481] for pulsed microwave transmitters. He found that for ignition of methane/air mixtures to occur, the coupling of unwanted microwave RF into a discharge gap must be sufficient so that around 2.5 mJ energy is discharged in the spark. Knight[482] described de-rating factors to be applied to adventitious antennas when the transmission frequency and the self-resonant frequency are not identical (as they rarely will be).

In terms of minimum induced RF voltage needed for an incendive breakflash discharge, measurements by Rosenfeld et al.[483] on methane/air and ethylene/air atmospheres indicated that 300 V peak-to-peak was needed, provided the source impedance was in range 50 – 3000 Ω (and it was considered unlikely that the impedance of an adventitious antenna system should fail to be within this range). In terms of power capable of being induced in the adventitious circuit, a minimum of 12 W was needed for methane and 9 W for ethylene. The authors did some experiments to show that hydrogen mixtures were more readily ignitable, but were not able to get definitive data. Experiments were then done using 'scrape-flash' electrodes, that is, an arrangement where one electrode was scraped past another, prior to separation occurring. The minimum required voltage fell to 75 V under those conditions, but power required remained unchanged. It was considered that the low work function of the metal oxide aided in the production of electrons, thereby lowering the voltage required. A companion study[484] found that, at the P = 0.1% probability level, 290 V peak-to-peak was necessary for igniting hydrogen/air mixtures, and a corresponding power of 5 W. Somewhat different experimental arrangements were employed by Burstow et al.[485], but with results broadly similar.

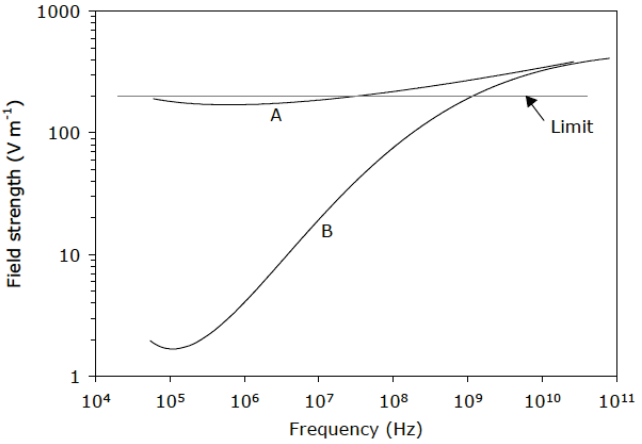


Figure 60 RF transmitter field strength needed for ignition of H_2/air mixtures (**A** antenna of 1 m effective length; **B** longest antenna appropriate to frequency; **Limit** human exposure limit)

Maddocks and Jackson[486] conducted a series of field measurements of voltages induced from transmitters into various antenna-like metal structures. All else being held constant, the induced voltage was found to depend as the square root of the transmitter power. Accompanying the voltage measurements, field measurements were made by connecting up an IEC breakflash apparatus and supplying a hydrogen/air test atmosphere. No ignitions were found for the case of 9 close-by transmitters each putting out 20 kW.

German studies[487] on the same topic concluded that adventitious antennas of about 1 m length would require a field strength of around 200 V m^{-1} to ignite a hydrogen mixture; the 200 V m^{-1} value also happens to be the limit for transmitter field strength that German health regulations consider acceptable for human exposure, so the ignitability potential from short antennas was considered to be inconsequential (Figure 60). A slightly different conclusion was found for extremely long adventitious antennas at low frequencies. The worst-case was found at a frequency around 100 kHz, where a field strength of 2 V m^{-1} would suffice for igniting the most-ignitable concentration of H_2/air.

Burstow et al.[485] also measured the ignition potential in the vicinity of microwave transmitters. The power that can be captured from a given antenna is proportional to the wavelength squared, thus it was found that there was a dominant effect of the frequency of the transmission on the results. In terms of power induced in the adventitious antenna system, very large values were needed for ignition, being 50 – 70 W for hydrogen and 360 W for methane atmospheres.

The ignitions considered above are possible only in the immediate vicinity of a powerful transmitter. Another concern is unwanted RF triggering of blasting circuits. Radio frequency waves can, in principle, spuriously set off an explosion, and this is the reason for signposting against use of transmitters at sites where such work is done. The one extensive study on this subject[488], however, suggests that enormous field strengths would be needed to trigger a blasting cap of reasonable design, e.g., one requiring more than 300 mA to initiate the explosion. In worst-case conditions, 9 V m^{-1} would have been required to reach the 300 mA level. Furthermore, the highest hazard was found to be for frequencies less than 1 MHz, which does not correspond to any legal portable transmission apparatuses usable by civilians. British guidelines (BS 6657[489]) based on this work incorporate a further safety factor of roughly 10×.

Schwab[490] studied gas discharges caused by RF fields and determined that their basic character is essentially identical to DC discharges. Arc discharge, glow discharge, and abnormal glow discharge regimes were found, same as for DC discharges.

The *skin effect* associated with high frequencies confines the flow of current to thin layers at the surface. This has caused some unusual ignitions. A case is reported[410] where a person working on a radio transmitter made contact with an RF-carrying conductor. He felt no sensation until his sock ignited and burned. This was determined to have occurred because a nail through his shoe contacted ground.

It is not difficult to ignite combustible materials inside a microwave oven, but that is a device especially designed to concentrate a large amount of energy within a small space. If a unit produces 700 W and the radiation were uniform across the cross-section, the heat flux would be about 7 kW m^{-2}. If the absorptivity were close to unity, the value would be not much below the minimum heat flux for ignition of some solid combustibles. In addition, hot spots exist and, in those, higher heat fluxes will exist. But the radio frequency used is 2.45 GHz, and most substances are not absorptive at this frequency. The main exceptions are polar molecules (e.g., water) and electrically conductive objects. If metals are introduced into the cavity, an indirect ignition can occur due to high current flow induced in the metallic object and its consequent heating.

Ignition of materials from absorption of microwaves can be treated by theory, since the radiation of electromagnetic energy is described by the well-known Maxwell's equations. The problem of radiation within lossy bodies is far from simple, due to strongly non-linear coupling effects and because the relevant thermal, electrical, and magnetic properties of materials depend on temperature. Many practical substances are non-homogeneous and anisotropic; for those theory can only suggest qualitative outcomes. Microwave heating is used in a number of industrial processes where ignition is possible, but undesired, so a fair amount of effort has gone into trying to understand microwave ignition quantitatively. The studies[491] revealed that hot spots are a phenomenon that is due to the nature of equations themselves, and does not require physical inhomogeneities. Fur-

thermore, the dependence of the material's temperature on applied power commonly takes the form of an S-curve, with a distinct jump. Data properties for a wide range of materials of interest have been compiled by Meredith[492].

NUCLEAR WEAPONS

During the 1950s and '60s, much research was carried on to understand the ignition of combustibles from nuclear weapons. The basic goal was usually to compute the maximum radius of destruction by fire for a given size of weapon. The research studies elucidated the dominant role of atmospheric conditions in the process and even such secondary factors as the reflectivity of nearby large areas. Thus, the results did not lend themselves to being presented as an ignited-radius vs. weapon yield plot, but required numerous other assumptions and calculations. Examples of some of these calculations have been given in a major compendium by Rogers[493].

A nuclear fireball can contain reactions at temperatures of 70,000 K or higher, although an effective radiating temperature of 6500 K is often assumed[497]. About 35 – 45% of the energy is released as thermal radiation, but the fireball thermal radiation characteristics details depend on whether the detonation is at surface level, moderately high, or at a great height. Brode[494] has presented some graphs and calculations for determining fireball radiation. The intensity of radiation varies with time and Thomas et al.[495] found that ignition data can be well correlated by assuming an 'impulse' type of radiation waveform:

$$I(t) = e^2 I_p \left(\frac{t}{t_p} \right)^2 e^{-2t/t_p}$$

where I_p = peak value (same units as I), and t_p = time of peak (s).

Field tests (and experience in Japan) indicated that thick materials, such as wood structural members, are generally not ignited directly from nuclear weapons, but thin materials can be. When structures burn down, it is usually due to initial ignition of lightweight materials. For extremely high heat fluxes, the ignition problem becomes secondary, since blast damage tends to flatten the landscape. In addition, the blast wave sometimes extinguishes the fires that were previously ignited by thermal radiation. Because of its high moisture content, it is difficult to ignite living vegetation[496]. This is partly because initial heating produces a steam cloud and the latter acts to some extent as a radiation shield.

In both field and laboratory studies, the ignitability of relatively thin items from nuclear weapons radiation has conventionally been characterized by use of energy fluence, i.e., kJ m^{-2}. In Chapter 7 it was shown that ignition of a thermally-thick solid does not correspond to a constant value of energy fluence; for thermally-thin solids, use of energy fluence as an ignition criterion seems to be more reasonable. In the case of nuclear weapons, not just the energy fluence, but also the duration of the pulse and its wavelength distribution must be considered as factors determining the ignition of materials. Some example values[497] are listed in Table 39 for low-air bursts of three different weapon yields. In view of the environmental/geometric complications mentioned above, these must be understood to be suggestive values only. Additional data for 15 and 32 kiloton weapons were obtained by Bruce[498].

Table 39 Energy fluence needed for ignition from nuclear weapons

Material	Energy fluence for ignition (kJ m^{-2})		
	35 kilotons	1.4 megatons	20 megatons
Bristol board, 340 g m^{-2}	670	840	1700
cotton, dark blue 270 g m^{-2}	590	790	880
cotton, white 270 g m^{-2}	1300	2000	3600
cotton denim, blue 240 g m^{-2}	500	1100	1800
grass, cheat	210	330	420
needles, pine	420	670	880
newspaper, picture area	210	290	500
newspaper, text area	250	330	630
plywood, Douglas fir	380[a]	670[a]	840[a]
rayon, beige 100 g m^{-2}	540	840	1200
rayon, black 100 g m^{-2}	290	710	1000
rubber, black	420	840	1000
tent canvas, olive cotton 400 g m^{-2}	500	750	1200
window shade, green oiled cotton muslin 270 g m^{-2}	290	540	790

[a] – flames only during exposure.

Rough formulas for explosions in air at intermediate heights are[497]:

$$\dot{q}'' = 1.06 \times 10^9 \frac{\tau W^{0.56}}{r^2}$$

$$q'' = 3.33 \times 10^8 \frac{f \tau W}{r^2}$$

where $\dot{q}''$ = incident heat flux (kW m^{-2}), q'' = energy fluence (kJ m^{-2}), f = thermal radiation fraction (0.35 to 0.45), τ = atmospheric transmissivity (--), W = weapon yield (kilotons TNT[*]), and r = distance from explosion to target (m).

Some primary explosives have been studied for sensitivity to initiation from nuclear particles and ionizing radiation. A compilation of laboratory research has been reported[499]. Modest intensity particle beams, X-rays, gamma rays, etc. have not been found to be effective as initiators.

[*] Nuclear weapons yields are expressed as tons (2000 lb) of TNT equivalent. 1 ton = 4.18×10^{12} J.

Light energy, lenses and mirrors

Light from the sun or from other sources can act as an ignition source. The radiant energy available from the sun in a cloudless sky depends on the latitude, time of year, and hour of day. At peak in temperate climates it is on the order of 1 kW m^{-2}, which is insufficient to ignite any normal building materials or furnishings. The heating can be more severe in high-flying aircraft. It is reported that interior temperatures can reach 95ºC in military airplanes[500]. Even this temperature would suffice to ignite only highly sensitive substances.

But it is possible to magnify solar radiation by optical means. It has been known since antiquity that a convex-shaped mirror can be used for this purpose. Already in the 7th century BC, the Romans were using this method of lighting sacred fires[501]. In a more famous episode, in 212 BC, the Greek scientist Archimedes used a mirror to set fire to a Roman ship in battle. Simms[502] reviewed much of the subsequent research on this topic, which continued through the millennia into modern times. Focusing of sunlight to a point may also be done by a concave-shaped converging-focus lens. Moore's 1877 book mentions that accidental ignitions were not uncommon due to this cause, especially in laboratories where glass vessels may serve as the lens[503]. Other incidents occurred in ships where 'bull's eye' glass with a focusing ability used to sometimes be used before fire incidents led to their replacement. In more recent times, accidental fires caused by magnifying glasses[504] and shaving mirrors[505] have been reported. The former case is especially interesting since the investigator was able to duplicate the ignition in reconstruction testing. It is also not beyond the resources of arsonists to exploit this focusing feature, although its drawbacks would be uncertain timing, possible discovery of the device, and no associated accelerant. The Fire Research Station has estimated that 150 to 200 fires occur annually in the UK due to focused sunlight[506]. Some example fires[506] have occurred due to focusing of sunlight by a chrome-plated reflector of an electrical heater (which ignited cardboard in a shop window), a metal bowl in which clothes were placed (which ignited the clothes), and translucent plastic door handle that ignited a bathrobe hanging on the door. In the latter case, testing was done and it was found that paper readily ignited from the door handle's focusing power[507]. Perhaps the most fascinating case is one where the ignition mechanism was water. Investigation revealed that raindrops on a piece of plastic used as a roof acted as a lens and ignited a silkworm hut.

Glass jugs and similar articles have been found at the origin of forest fires, leading to research on ignitability of forest fuels[508]. The results are summarized in Table 40. Multiplication factor denotes the ratio of the heat flux produced with the aid of the focusing power of the substance being tested, versus the heat flux of the unfocused incident radiation. Normally, glass containers have to be filled with a liquid to act as focusing lenses, since actual wall thickness is fairly uniform. Aerosol cans are able to concentrate sunlight when they have hemispherical, reflective bottom surfaces. The results indicate that objects showing multiplication factors down to the 14 – 12 range are able to cause ignitions, while ones with smaller multiplication factors do not.

Table 40 Ignitability of forest fuels from containers concentrating sunlight radiation

Container	Heat flux multiplication factor	Caused ignition in sunlight
glass jug	28	yes
aerosol can, bright	22	yes
" " (another specimen)	20	yes
spherical rose bowl	14	yes
fish bowl	12	not tested
aerosol can, dull	11	no
syrup bottle	7	no
" " (another specimen)	7	not tested
salad dressing bottle	6	not tested

Bull's eye (sometimes termed bullion) and Flemish glass types are occasionally used as decorative window glass in houses (Figure 61), and the Fire Research Station has investigated fires caused by their focusing ability[509]. FRS tested both glass which had been identified as causing a fire, and also additional commercial examples. Heat flux multiplication factors of 10 – 45 were measured, but this varied widely both with the type of glass and with the particular location within the glass. Solar radiation in the UK does not exceed about 0.85 kW m^{-2}, and testing of the glass recovered from the fire showed that it could produce a peak of 34 kW m^{-2}. A special rig was then constructed which simulated solar radiation upon fabrics, including the effect of a motion of 75 – 80 mm h^{-1} of the focused radiation. A fixed exposure time of 10 min was used. At the peak irradiance used of 35 kW m^{-2}, only one out of 6 upholstery fabrics ignited (a cotton-backed PVC imitation leather) and that one only showed flashing ignition. Six carpet samples were tested at 50 kW m^{-2}, but none ignited. The same findings were obtained for six curtain fabrics. Among the curtain samples tested was a fabric similar to the one in the fire being investigated, but that also showed no ignition. Only when the test procedure was modified by preconditioning the samples to 36°C to simulate a hot summer day, and providing a cotton lining, did the curtain involved in the fire ignite during test. But even this ignition was a 'rapidly spreading glowing,' rather than a flaming. A similar glowing ignition was also observed when tests were repeated at 22ºC, but with pleating of the curtain specimen. Because of the marginal ignitability that was found, the conclusion was that, despite concerted efforts to reproduce a realistic solar-ignition environment, some experimental factors still remained biased against ignition. The above non-ignition results should also not be generalized to other forms of radiant heating, since

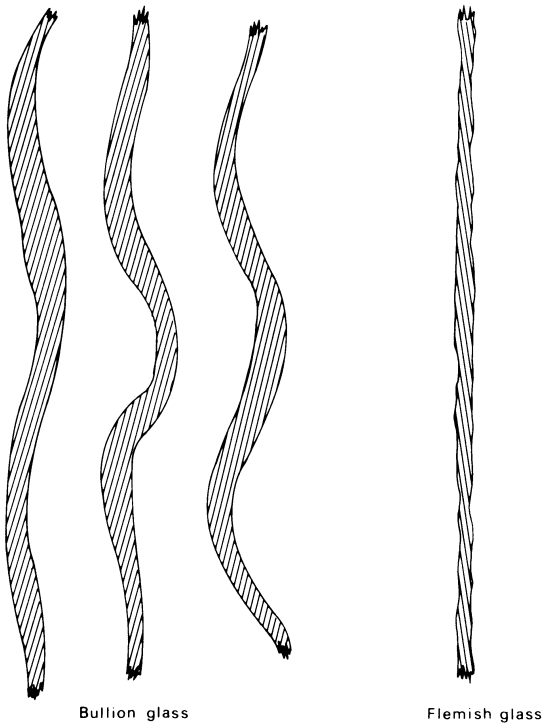


Figure 61 Cross-sections through several types of glass that can intensify radiation
(Copyright BRE Ltd., used by permission)

in the tests here a very small sample area of 30 mm^2 was exposed to radiation. The area selected in the FRS tests was designed to simulate the size of radiation focused from window glass; but as indicated in Chapter 7, materials are substantially more difficult to ignite if very small exposure areas are used.

The above discussion is based on considering light as being converted to thermal energy within the target substance. But there are some highly sensitive explosives which can be initiated by *photochemical excitation*. This occurs if a molecule can absorb a photon of light that has an energy equal to or greater than the energy difference between the ground state and an electronically excited state, the electron can go into the excited state, and this can start a chemical reaction.

It is common for fire investigators who photograph sooty fire scenes to find that the camera flash creates a loud report[510]. This apparently is some form of localized ignition of soot from the light energy, but details have not been studied. No self-sustaining fires from this mechanism have been reported.

Aerodynamic heating

High temperatures can be attained due to supersonic aerodynamic heating. As a potential for ignition, this mode of heating is mainly relevant to aerospace applications, since supersonic movement through air is rare in other circumstances. The stagnation point temperature is given by[511]:

$$T_{stag} = T_o\left[1+\eta_r\left(\frac{\gamma-1}{2}\right)M^2\right]$$

where T_{stag} = stagnation point temperature (K); T_o = ambient temperature (K); η_r = recovery factor (--), often taken as 0.9; γ = ratio of specific heats, $C_p/C_v \approx 1.4$; and M = Mach number (--). Generally, $M \geq 3$ would have to be reached for aerodynamic heating to be of concern.

Further readings

The following recent monographs on electrostatic ignitions cover both principles and practical guidance. The last three also contain copious compilations of case histories; Britton's book, however, offers the most systematic treatment and is the best source of guidance for implementing preventive measures. The topics coverage is sufficiently non-overlapped that the interested reader should refer to all four. All of them assume the reader has at least a moderate familiarity with the principles of electricity.

Laurence G. Britton, **Avoiding Static Ignition Hazards in Chemical Operations**, AIChE (1999).

Thomas H. Pratt, **Electrostatic Ignitions of Fires and Explosions**, Burgoyne Inc., Marietta GA (1997).

Günter Lüttgens and Norman Wilson, **Electrostatic Hazards**, Butterworth-Heinemann, Oxford (1997).

Günter Lüttgens and Martin Glor, **Understanding and Controlling Static Electricity**, Expert Verlag, Ehningen (1989).

H. L. Walmsley, The Avoidance of Electrostatic Hazards in the Petroleum Industry, *J. Electrostatics* **27**, Special issue No. 1&2 (1992). A reprint of a monograph originally issued by Shell Research Ltd. which comprises a code of practice for protecting petrochemical facilities against electrostatic hazards.

Expert Commission for Safety in the Swiss Chemical Industry, Static Electricity: Rules for Plant Safety, *Plant/Operations Progress* **7**, 1-22 (Jan. 1988). A wide-ranging, although terse, guide to good industrial practice for chemical and manufacturing industries.

Recommended Practice on Static Electricity (NFPA 77); Standard for the Installation of Lightning Protection Systems (NFPA 780), National Fire Protection Association, Quincy MA.

F. A. Fisher, J. A. Plumer, and R. A. Perala, Aircraft Lightning Protection Handbook (DOT/FAA/CT-89/22), Federal Aviation Administration, Atlantic City NJ (1989). While only aircraft lightning protection is nominally within its scope, this handbook is exceedingly thorough and may well be the best first-recourse reference on lightning protection in general.

William C. Hart and Edgar W. Malone, **Lightning and Lightning Protection**, Don White Consultants, Gainesville VA (1979).

Len A. Dissado, and John C. Fothergill, **Electrical Degradation and Breakdown in Polymers**, Peter Peregrinus, London (1992). The most current, full-length book on breakdown of electric insulation, it includes extensive theory sections, but limited practical information.

Electrical Contacts, Paul G. Slade, ed., Marcel Dekker, New York (1999). This large tome is the most authoritative reference on arcing associated with electrical contacts.

References

1. Gross, D., Ignition Temperature Tests of Combustible Material—Asphalt Treated Weatherproof Paper (NBS 1498), NBS (1952).
2. Winandy, J. E., and Beaumont, R., Roof Temperatures in Simulated Attics (Res. Pap. FPL-RP-543), Forest Products Lab., Madison WI (1995).
3. Winandy, J. E., private communication (2000).
4. Bowes, P. C., High Mean Temperatures in Ships Holds, *The Marine Observer* **68**, 17 (1968).
5. Sub-Committee Doc. DSC 5/3/30, Sub-Committee on Dangerous Goods, Solid Cargoes and Containers, Intl. Maritime Organization, London (1999).
6. Incropera, F. P., and DeWitt, D. P., **Fundamentals of Heat and Mass Transfer**, 4th ed., John Wiley, New York (1996).
7. Jones, J. C., Improved Calculations Concerning the Ignition of Forest Litter by Hot Particle Ingress, *J. Fire Sciences* **13**, 350-356 (1995).
8. Hölemann, H., and Worpenberg, R., Brandursache Schweissen, Brennschneiden und Löten—Zündmechanismen glühender Partikel [Cause of Fire Welding, Flame Cutting and Soldering—Ignition Mechanism of Glowing Particles], *VFDB Z.*, **41**, 79-89 (1992).
9. Clements, H. B., Lift-off of Forest Firebrands (Res. Pap. SE-159), US Forest Service, Southeastern Forest Experiment Sta., Asheville NC (1977).
10. Kamei, K., Study on the Mechanism of Fire Spread due to Fire Brands, Building Research Institute, Tokyo (1960).
11. Hasemi, Y., private communication (1999).
12. Harada, K., and Ohmiya, Y., Report of the Hotel Fire in Shirahama. Part 1. Damage by Fire Spread, *J. Japan Assn. for Fire Science and Engineering* **49**: 5, 9-15 (1999).
13. Ohmiya, O., and Iwami, T., An Investigation of the Distribution of Fire Brands and Spot Fires due to a Hotel Fire, *Fire Science & Technology* **20**, 27-35 (2000).
14. Fire Spread Velocity in Fires, Fire Fighting Research Note No. 1, Tokyo Metropolitan Fire Fighting Research Committee, Tokyo (1941).
15. Waterman, T. E., Experimental Study of Firebrand Generation (NRDL-TRC-69-15, Project J6130), IIT Research Institute, Chicago (1969).
16. Vodvarka, F. J., Firebrand Field Studies. Final Report. May 24, 1968-August 23, 1969 (IITRI-J6148-FR), IIT Research Institute, Chicago (1969).
17. Wilson, R., The Los Angeles Conflagration of 1961: The Devil Wind and Wood Shingles, *NFPA Q.* **55**, 241-288 (1962).
18. Woycheese, J. P., Brand Lofting and Propagation from Large-Scale Fires (Ph.D. dissertation), Univ. California, Berkeley (2000).
19. Standard Test Methods for Fire Tests of Roof Coverings (ASTM E 108), ASTM.
20. Waterman, T. E., and Takata, A. N., Laboratory Study of Ignition of Host Materials by Firebrands (Project J6142, OCD Work Unit 2539A), IIT Research Institute, Chicago (1969).
21. Hamada, M., et al., Experiments on the Ignition due to Fire Brands, Fire Research—Reports from the Fire Science Research Committee, Property and Casualty Insurance Rating Organization of Japan, Tokyo (1951).
22. Fire Research 1949, Dept. of Scientific and Industrial Research & Fire Offices' Committee, London (1950).
23. Keetch, J. J., Smoker Fires and Firebrands (Tech. Note No. 49), Appalachian Forest Experiment Station, Asheville NC (1941).
24. Muraszew, A., Fedele, J. B., and Kuby, W. C., Investigation of Fire Whirls and Firebrands, Aerospace Rep. ATR-76(7509)-1 prepared for Intermountain Forest and Range Experiment Station, US Forest Service. The Aerospace Corp. El Segundo, CA (1976).
25. Luke, R. H., and McArthur, A. G., **Bushfires in Australia**, Australian Government Publishing Office, Canberra (1978).
26. McArthur, A. G., Fire Behaviour in Eucalypt Forests (Leaflet No. 107), Forestry & Timber Bureau, Dept. of Natural Development, Canberra, Australia (1967).
27. Bunting, S. C., and Wright, H. A., Ignition Capabilities of Non-Flaming Firebrands, *J. Forestry* **72**, 646-649 (1983).
28. Noble, I. R., Bary, G. A. V., and Gill, A. M., McArthur's Fire-Danger Meters Expressed as Equations, *Australian J. Ecology* **5**, 201-203 (1980).
29. Sánchez Tarifa, C., Pérez del Notario P., and García Moreno, F., On the Flight Paths and Lifetimes of Burning Particles of Wood, pp. 1021-1037 in *10th Symp. (Intl.) on Combustion*, The Combustion Institute, Pittsburgh (1964).
30. Sánchez Tarifa, C., et al., Transport and Combustion of Firebrands, Final Report of US Forest Service Grants FG-SP-114 and FG-SP-146, Instituto Nacional de Tecnica Aeroespacial "Esteban Terradas," Madrid (1967).
31. Ellis, P. F., The Aerodynamic and Combustion Characteristics of Eucalypt Bark—A Firebrand Study (Ph.D. dissertation), Australian National Univ., Canberra (2000).
32. Lee, S. L., and Hellman, J. M., Firebrand Trajectory Study Using an Empirical Velocity-dependent Burning Law, *Combustion and Flame* **15**, 265-274 (1970).

33. Muraszew, A., Fedele, J. B., and Kuby, W. C., Firebrand Investigation, Report ATR-75(7470)-1, The Aerospace Corp., El Segundo CA (1975).
34. Muraszew, A., and Fedele, J. B., Statistical Model for Spot Fire Hazard, Report No. ATR-77(7588)-1, The Aerospace Corp., El Segundo CA (1976).
35. Muraszew, A., Firebrand Phenomena, Aerospace Rep. ATR-74(8165-01)-1 prepared for Riverside Forest Fire Laboratory, Pacific Southwest Forest and Range Experiment Station, US Forest Service. The Aerospace Corp. El Segundo, CA (1974).
36. Lee, S.-L., and Hellman, J. M., Study of Firebrand Trajectories in a Turbulent Swirling Natural Convection Plume, *Combustion and Flame* **13**, 645-655 (1969).
37. Garzon, V. E., McDonough, J. M., and Saito, K., Simulation of Forest Fire Spread Due to Firebrand Transport, pp. 151-161 in *ICFRE2: 2nd Intl. Conf. on Fire Research and Engineering*, NIST/SFPE, Gaithersburg, MD (1998).
38. Tse, S. D., and Fernandez-Pello, A. C., On the Flight Paths of Metal Particles and Embers Generated by Power Lines in High Winds—Potential Source of Wildland Fires, *Fire Safety J.* **30**, 333-356 (1998).
39. Albini, F. A., Potential Spotting Distance from Wind-Driven Surface Fires (Research Paper INT-309), Intermountain Forest and Range Experiment Station, US Forest Service, Ogden UT (1983).
40. Chase, C. H., Spotting Distance from Wind-Driven Surface Fires—Extensions of Equations for Pocket Calculators (Research Note INT-346), Intermountain Forest and Range Experiment Station, US Forest Service, Ogden UT (1984).
41. Morris, G. A., A Simple Method of Computing Spotting Distances from Wind-Driven Surface Fires (Research Note INT-374), Intermountain Forest and Range Experiment Station, US Forest Service, Ogden UT (1987).
42. Albini, F. A., Transport of Firebrands by Line Thermals, *Combustion Science and Technology* **32**, 277-288 (1983).
43. Albini, F. A., Maximum Spotting Distance from an Active Crown Fire, to be published.
44. Woycheese, J. P., and Pagni, P. J., Combustion Models for Wooden Brands, pp. 53-71 in *ICFRE3 – Proc. 3rd Intl. Conf. on Fire Research and Engineering*, Society of Fire Protection Engineers, Bethesda MD (1999).
45. Fairbank, J. P., and Bainer, R., Spark Arresters for Motorized Equipment, Bulletin 577, pp. 3-42, University of California Experiment Station (1934).
46. Maxwell, F. D., Fetter, N. R., and Mohler, C. L., Engine Exhaust Particles as Potential Ignition Sources of Wildland Fuels (Paper WSCI-72-19), Western States Section, The Combustion Institute (1972).
47. Maxwell, F. D., and Mohler, C. L., Exhaust Particle Ignition Characteristics (Tech. Report 12). Dept. of Statistics, University of California, Riverside (1973).
48. Ford, R. T. sr., **Investigation of Wildfires**, privately published, Sunriver OR (1995).
49. Multiposition Small Engine Exhaust System Fire Ignition Suppression (SAE Recommended Practice J335), **S.A.E. Handbook**, Society of Automotive Engineers, New York (2000).
50. Spark Arrester Test Procedure for Medium Size Engines (SAE Recommended Practice J350), **S.A.E. Handbook**, Society of Automotive Engineers, New York (2000).
51. Spark Arrester Test Procedure for Large Size Engines (SAE Recommended Practice J342), **S.A.E. Handbook**, Society of Automotive Engineers, New York (2000).
52. Spark Arrester Test Carbon (SAE Recommended Practice J997), **S.A.E. Handbook**, Society of Automotive Engineers, New York (2000).
53. NWCG Fire Equipment Working Team, Spark Arrester Guide. Vol. 1. General Purpose and Locomotive (LP/Loco), National Wildfire Coordinating Group, US Forest Service Technology & Development Center, San Dimas CA. Distributed through National Interagency Fire Center, Boise ID.
54. NWCG Fire Equipment Working Team, Spark Arrester Guide. Vol. 2. Multiposition Small Engine, National Wildfire Coordinating Group, US Forest Service Technology & Development Center, San Dimas CA. Distributed through National Interagency Fire Center, Boise ID.
55. **Welding Handbook**, Vol. 1, L. P. Connor, ed., American Welding Society, Miami (1987).
56. The General Motors Fire, *NFPA Q.* **46**, 105-120 (October 1953).
57. Hagimoto, Y., Kinoshita, K., Watanabe, N., and Okamoto, K., Scattering and Igniting Properties of Sparks Generated in an Arc Welding, pp. 863-866 in *6th Indo Pacific Congress on Legal Medicine and Forensic Sciences (INPALMS)*, Yoyodo, Osaka (1998).
58. Kinoshita, K., and Hagimoto, Y., Temperature Measurement of Falling Spatters of Arc Welding, pp. 145-148 in *Proc. 22nd Annual Mtg. Japan Soc. for Safety Engrg.* (1989).
59. Tanaka, T., On the Inflammability of Combustible Materials by Welding Spatter, *Reports of the National Research Institute of Police Science* **30**:1, 51-58 (1977).
60. Hagiwara, T., Yamano, K., and Nishida, Y., Ignition Risk to Combustibles by Welding Spatter, *J. Japan Assn. for Fire Science and Engineering* **32**:5, 8-12 (1982).
61. Okegawa, S., Watanabe, H., Ikeda, T., and Hoshino, T., Measurement of Distance and Ignition Tests of Gases by Welding Spatter, *J. Japan Society for Safety Engineering* **5**:2, 112-119 (1996).
62. Kinoshita, K., Watanabe, N., and Hagimoto, Y., Discriminating Method of Arc Welding Particles Igniting Combustibles and Ignition Properties of the Particles, pp. 232-235 in *Summary of the 1995 Annual Meeting of the JAFSE* (1995).
63. McGuire, J. H., Law, M., and Miller, J. E., Domestic Fire Hazard Created by Flying Coals and Sparks (FR Note 252), Fire Research Station, Borehamwood, England (1956).
64. Braidech, M. M., and Dean, R. C., Causes and Prevention of Cotton Fires, *NFPA Q.* **43**:4, 240-251 (1950).
65. Bowden, F. P., and Lewis, R. D., Ignition of Firedamp by Stationary Metal Particles and Frictional Sparks, *Engineering* **186**, 241-242 (22 Aug. 1958).
66. Archard, J. F., The Temperature of Rubbing Surfaces, *Wear* **2**, 438-455 (1958/59).
67. Benz, F. J., and Stoltzfus, J. M., Ignition of Metals and Alloys in Gaseous Oxygen by Frictional Heating, pp. 38-58 in **Flammability and Sensitivity of Materials in Oxygen-Enriched Atmospheres**, Second Volume (ASTM STP 910), ASTM (1986).
68. Standard Guide for Evaluating Metals for Oxygen Service (ASTM G 94), ASTM.
69. Billinge, K., Frictional Ignition Hazard in Industry: A Survey of Reported Incidents From 1958 to 1978, *Fire Prevention Science and Technology*, No. 24, 13-19 (1981).

70. Powell, F., Can Non-sparking Tools and Materials Prevent Gas Explosions? *Gas, Wasser, Abwasser = Gaz, eaux, eaux usées* **66**, 419-428 (1986).
71. Blickensderfer, R., Testing of Coal Cutter Materials for Incendivity and Radiance of Sparks (RI 7713), Bureau of Mines, Pittsburgh (1972).
72. Hillstrom, W. W., Thresholds for the Initiation of Pyrophoric Sparking, *4th Intl. Pyrotechnics Seminar*, Steamboat Village CO (1974).
73. Hardt, A. P., **Pyrotechnics**, Pyrotechnica Publications, Post Falls ID (2001).
74. Powell, F., Ignition of Gases and Vapours by Hot Surfaces and Particles—A Review, pp. 267-299 in *Report of the 9th Intl. Symp. on Prevention of Occupational Accidents and Diseases in the Chemical Industry*, Intl. Social Security Assn., Lucerne (1984).
75. Pedersen, G. H., and Eckhoff, R. K., Initiation of Grain Dust Explosions by Heat Generated During Single Impact Between Solid Bodies, *Fire Safety J.* **12**, 153-164 (1987).
76. Rae, D., A Measurement of the Temperature of Some Frictional Sparks, *Combustion and Flame* **5**, 341-347 (1961).
77. Gibson, N., Lloyd, F. C., and Perry, G. R., Fire Hazards in Chemical Plant from Friction Sparks Involving the Thermite Reaction, pp. 26-35 in *Proc. 3rd Symp. on Chemical Process Hazards with Special Reference to Plant Design* (Symp. Series No. 25), The Institution of Chemical Engineers, London (1968).
78. Boczek, B., Glinka, W., and Wolański, P., Ignition of a Combustible Mixture by a Burning Metal Particle, *Oxidation Communications* **5**, 157-173 (1983).
79. Powell, F., Ignition by Machine Picks: A Review, *Colliery Guardian* **239**, 241-253 (1991); and **240**, 21-30 (1992).
80. Wynn, A. H. A., The Ignition of Firedamp by Friction (Research Report 42), Safety in Mines Research Establishment, Sheffield, England (1952).
81. Burgess, M. J., and Wheeler, R. V., The Ignition of Firedamp by the Heat of Impact of Metal against Rock (Paper 54), Safety in Mines Research Board, London (1929).
82. Morse, A. R., Investigation of the Ignition of Grain Dust Clouds by Mechanical Sparks (NRC No. 4968, ERB-494), National Research Council of Canada, Ottawa (1958).
83. Titman, H., and Wynn, A. H. A., The Ignition of Explosive Gas Mixtures by Friction (Research Report 95), Safety in Mines Research Establishment, Sheffield (1954).
84. Burgess, M. J., and Wheeler, R. V., The Ignition of Firedamp by the Heat of Impact of Hand Picks against Rocks (Paper 62), Safety in Mines Research Board, London (1930).
85. Coleman, E. H., and Tonkin, P. S., The Hazard of Sparks from Aluminium Paint. Part 3. The Effect of Ageing of the Paint Film (Fire Research Note 397), Fire Research Station, Borehamwood, England (1959).
86. Rae, D., The Role of Quartz in the Ignition of Methane by the Friction of Sparks (SMRE Research Report 223), Safety in Mines Research Establishment, Sheffield, England (1964).
87. Blickensderfer, R., Methane Ignition by Frictional Impact Heating, *Combustion and Flame* **25**, 143-152 (1975).
88. Burgess, M. J., and Wheeler, R. V., The Ignition of Firedamp by the Heat of Impact of Rocks (Paper 46), Safety in Mines Research Board, London (1928).
89. Rae, D., Danson, R., and Heathcote, N. L., The Coefficient of Friction of Some Rocks and Other High-Melting-Point Materials During Continuous Rubbing (Research Report 237), Safety in Mines Research Establishment, Sheffield, England (1966).
90. Cutler, D., and Brearley, D., Frictional Ignition of Dusts and Vapours (IR/L/EC/98/01), HSE, Buxton, UK (1998).
91. Titman, H., A Review of Experiments on the Ignition of Inflammable Gases by Frictional Sparking, *Trans. Institution Mining Eng.* **115**, 535-557 (1955/56).
92. Bartknecht, W., Ignition Capabilities of Hot Surfaces and Mechanically Generated Sparks in Flammable Gas and Dust/Air Mixtures, *Plant/Operations Progress* **7**, 114-121 (1988).
93. Courtney, W. G., Frictional Ignitions with Coal Mining Bits (IC 9251), Bureau of Mines, Pittsburgh (1990).
94. Titman, H., The Ignition Hazard from Sparks from Cast Alloys of Magnesium and Aluminium (Research Report 90), Safety in Mines Research Establishment, Sheffield, England (1954).
95. Rae, D., The Ignition of Methane-Air by the Glancing Impact of Metals on Smears of Light Alloys formed on Rusty Surfaces (Research Report 190), Safety in Mines Research Establishment, Sheffield, England (1960).
96. Bowden, F. P., Recent Studies of Metallic Friction, *Chartered Mechanical Engineer* **2**, 86-101 (1955).
97. Safety in Mines Research 1953, Thirty-second Annual Report, Safety in Mines Research Establishment, HMSO, London (1954).
98. Allsop, G., and Wheeler, R. V., The Ignition of Firedamp by Pyrites during Coal-Cutting, *Trans. Institution Mining Eng.* **96**, 310-316; 367-368 (1938/39).
99. Yan, P., Lin, Y., Yang, G., Wang, W., Lu, Y., and Zhu, M., Significance of Local-Exhaust Ventilation System in Mines and a Study of the Water Turbine Powered Non-Pyrophoric Light-Alloy Exhaust Fan, pp. 291-308 in *Proc. 23rd Intl. Conf. Safety in Mines Research Institutes*, US Bureau of Mines, Washington (1989).
100. Margerson, S. N. A., Robinson, H., and Wilkins, H. A., The Ignition Hazard from Sparks from Magnesium-base Alloys (Research Report 75), Safety in Mines Research Establishment, Sheffield, England (1953).
101. Rae, D., The Ignition of Gas by the Impact of Light Alloys on Oxide-Coated Surfaces (Research Report 177), Safety in Mines Research Establishment, Sheffield, England (1959).
102. Rae, D., The Ignition of Gas by the Impact of Brass Against Magnesium Anodes and Other Parts of a Ship's Tank (Research Report 229), Safety in Mines Research Establishment, Sheffield, England (1965).
103. Nagy, J., and Kawenski, E. M., Frictional Ignition of Gas during a Roof Fall (RI 5548), Bureau of Mines, Pittsburgh (1960).
104. Weingärtner, J., Die Problematik der nichtfunkenschlagenden Werkzeuge [The Problem of Non-sparking Tools], *Sichere Arbeit* **21**:2, 22-25 (1968).
105. Bernstein, H., and Young, G. C., Sparking Characteristics and Safety Hazards of Metallic Materials (NGF-T-1-57, NAVORD Report 5205), US Naval Gun Factory, Washington (1957).
106. Eisner, H. S., Aluminum and the Gas Ignition Risk, *The Engineer*, 259-260 (17 Feb. 1967).
107. Desy, D. H., Neumeier, L. A., and Risbeck, J. S., Methane Ignition by Frictional Impact between Aluminum Alloys and Rusted Steel (RI 8005), Bureau of Mines, Pittsburgh (1975).

108. Trueman, R., A Literature Review of the Ignition of Methane-Air Mixtures by Coal-Cutting Picks, *J. South African Inst. Mining and Metallurgy* **85**, 209-215 (1985).
109. Powell, F., Ignition of Flammable Gases and Vapours by Friction between Footwear and Flooring Materials, *J. Hazardous Materials* **2**, 309-319 (1977/78).
110. Rae, D., The Ignition of Explosive Gas Mixtures by Small Combustible Particles. Part 1. Ignition by Particles of Pyrophor Bar (Research Report 129), Safety in Mines Research Establishment, Sheffield, England (1956).
111. Homan, H. S., and Sirignano, W. A., Minimum Mass of Burning Aluminum Particles for Ignition of Methane/Air and Propane/Air Mixtures, pp. 1709-1717 in *18th Symp. (Intl.) on Combustion*, The Combustion Institute, Pittsburgh (1980).
112. Kelley, J., and Blickensderfer, R., Spark Shower Radiance of Metal Grinding Sparks (RI 7902), Bureau of Mines, Pittsburgh (1974).
113. Singleton, D. W., Blast Cleaning in Inflammable Atmospheres, *J. Oil & Colour Chemists' Assn.* **59**, 363-368 (1976).
114. Campbell, J. A., Appraisal of the Hazards of Friction-Spark Ignition of Aircraft Crash Fires (NACA Tech. Note 4024), NACA Lewis, Cleveland OH (1957).
115. Powell, F., Ignition of Gas and Vapors*, Ind. and Eng. Chem*. **61**, 29-37 (Dec. 1969).
116. Sparks from Hand Tools, American Petroleum Inst., New York (1956).
117. Dahn, C. J., and Reyes, B. N., Determination of Metal Sparking Characteristics and the Effects on Explosive Dust Clouds, pp. 324-332 in **Industrial Dust Explosions** (ASTM STP 958), ASTM, Philadelphia (1987).
118. Anfenger, M. B., and Johnson, O. W., Friction Sparks, *Proc. American Petroleum Inst. Sect. I* **22**, 54-56 (1941).
119. Ritter, K., Mechanisch erzeugte Funken als Zündquellen von Gas- bzw. Staub/Luft-Gemischen, pp. 185-244 in *Report of the 9th Intl. Symp. on Prevention of Occupational Accidents and Diseases in the Chemical Industry*, Intl. Social Security Assn., Lucerne (1984).
120. Allen, J., and Calcote, H. F., Grain Dust Ignition by Friction Sparks—A Preliminary Investigation, National Grain and Feed Assn., Washington (1981).
121. Shirer, R. J., private communication (1999).
122. Hexamer, C. John, **A Collection of Essays on Spontaneous Combustion**, The Spectator Co., New York (1888).
123. Chaineaux, L., Risque d'inflammation du grisou et des poussières par le choc et la friction [Risk of Ignition Mine Gas and Dusts by Impact and Friction], *Charbonnage de France: Documents techniques*, No. 12, 733-747 (1966), CERCHAR Publication technique No. 1660. SMRE Translation 5473, Safety in Mines Research Establishment, Sheffield, England.
124. Bradshaw, L., The Firing of Gaseous Mixtures by Compression, *Proc. Royal Soc. London* **A79**, 236-241 (1907).
125. Bowden, F. P., and Tabor, D., **The Friction and Lubrication of Solids**, 2nd ed., Oxford Univ. Press, Oxford, England (1954).
126. Randolph, A. D., Hatler, L. E., and Popolato, A., Rapid Heating-to-Ignition of High Explosives. I. Friction Heating, *Ind. and Eng. Chem—Fundamentals* **15**, 1-6(1976).
127. Forsyth, E. T., and Stoltzfus, J. M., Ignition Resistance of Hard (Type III) Anodized Aluminum to Particle Impact, pp. 137-146 in **Flammability and Sensitivity of Materials in Oxygen-Enriched Atmospheres: Eighth Volume** (ASTM STP 1319), ASTM (1997).
128. Benz, F. J., Williams, R. E., and Armstrong, D., Ignition of Metals and Alloys by High-Velocity Particles, pp. 16-37 in **Flammability and Sensitivity of Materials in Oxygen-Enriched Atmospheres**, Second Volume (ASTM STP 910), ASTM (1986).
129. Johansson, S. R., On the History of Fire Tools and Matches, pp. 1-104 in *Pyroteknikdagen 1983*, Sektionen för Detonik och Förbränning, Royal Academy of Sciences, Sundbyberg, Sweden (1985).
130. Tizard, H. T., and Pye, D. R., Experiments on the Ignition of Gases by Sudden Compression, *Phil. Mag.* Series 6, **44**, 79-121 (1922).
131. Bowden, F. P., and Yoffe, A. D., **Initiation and Growth of Explosion in Liquids and Solids**, Cambridge University Press, Cambridge (1952).
132. Werley, B. L., A Perspective on Gaseous Impact Tests: Oxygen Compatibility Testing on a Budget, pp. 27-42 in **Flammability and Sensitivity of Materials in Oxygen-Enriched Atmospheres** (ASTM STP 1197), ASTM (1993).
133. **Encyclopedia of Explosives and Related Items**, B. T. Fedoroff, et al., eds., Picatinny Arsenal, Dover NJ (1960-1983).
134. Médard, L. A., **Accidental Explosions**, 2 vols., Ellis Horwood, Chichester, England (1989).
135. Michel, A., Propane Burner as an External Ignition Source for Fire Testing of Plastic Conduits, IEC ACOS Workshop II—Fire Hazard Assessment of Electrical Equipment, Session III, UL (1988).
136. Babrauskas, V., Specimen Heat Fluxes for Bench-scale Heat Release Rate Testing, *Fire and Materials* **19**, 243-252 (1995).
137. Quintiere, J.G., The Application of Flame Spread Theory to Predict Material Performance, *J. Res. Natl. Bur. Stand.* **93**, 61-70 (1988).
138. Paul, K.T., and Christian, S.D., Standard Flaming Ignition Sources for Upholstered Composites, Furniture and Bed Assembly Tests, *J. Fire Sciences* **5**, 178-211 (1987).
139. Paul, K.T., British Tests and Controls to Limit the Fire Risks of the Contents of Buildings, *Cellular Polymers* **3**, 105-132 (1984).
140. Paul, K.T., and Pugh, A. R., unpublished study on ignition sources for fire tests, conducted by RAPRA Technology Ltd for Fire Research Station (1988).
141. Murrell, J.M., Ignition Sources by Direct Impingement of Flame - A Preliminary Report, unpublished study, Fire Research Station, Borehamwood (1986).
142. Budnick, E. K., and Klein, D. P., Evaluation of the Fire Hazard in a Mobile Home Resulting from an Ignition on the Kitchen Range (NBSIR 75-788), NBS (1976).
143. Kokkala, M., and Heinilä, M., Flame Height, Temperature, and Heat Flux Measurements on a Flame in an Open Corner of Walls, Project 5 of the EUREFIC fire research programme. Valtion Teknillinen Tutkimuskeskus, Espoo, Finland (1991).
144. Babrauskas, V., and Krasny, J. F., Fire Behavior of Upholstered Furniture (NBS Monograph 173), NBS (1985).
145. Ohlemiller, T. J. and Villa, K., Furniture Flammability: An Investigation of the California Bulletin 133 Test - Part II: Characterization of the Ignition Source and a Comparable Gas Burner (NISTIR 4348), NIST (1990).

146. Murrell, J., unpublished study results (Warrington Research Centre) reported to ISO TC 92 SC1 WG2.
147. Fairweather, M., Kilham, J. K., and Mohebi-Ashtiani, Stagnation Point Heat Transfer from Turbulent Methane-Air Flames, *Combustion Science and Technology* **35**, 225-238 (1984).
148. Hargrave, G. K., Fairweather, M., and Kilham, J. K., Forced Convective Heat Transfer from Premixed Flames, Part 2: Impingement heat transfer, *Intl. J. Heat and Fluid Flow* **8**, 132-138 (1987).
149. Duijm, N. J., Jet Flame Attack on Vessels, *J. Loss Prevention in the Process Industries* **7**, 160-166 (1994).
150. Kilham, J. K., and Purvis, M. R. I., Heat Transfer from Hydrocarbon-Oxygen Flames, *Combustion and Flame* **16**, 47-54 (1971).
151. You, H.-Z., An Investigation of Fire-plume Impingement on a Horizontal Ceiling, *Fire and Materials* **9**, 46-56 (1985).
152. Holmlund, C., Burning of small crib ignition sources (Research Report 569), Valtion Teknillinen Tutkimuskeskus, Espoo, Finland (1988).
153. Prüfung von Sitzen für Schienenfahrzeuge des öffentlichen Personenverkehrs (DIN 54 341), Deutsches Institut für Normung e.V., Berlin (1983).
154. Döring, G., Müller, B., Prager, F.H., and Sand, H., Definition of Primary and Secondary Ignition Sources in Conjunction with Fires of Accidental and Malicious Origin, unpublished paper (1986).
155. Miles, L., Bhat, G. R., Sun, R. L., Yeh, K.-N., and Spivak, S., Extinguishability of Flammable Textiles: Part II. Effects of Ambient Oxygen Concentration, *J. Consumer Prod. Flammability* **3**, 166-192 (1976).
156. Theobald, C. R., The Critical Distance for Ignition from Some Items of Furniture (Fire Research Note 736), Fire Research Station, Borehamwood, UK (1968).
157. Babrauskas, V., Will the Second Item Ignite? *Fire Safety J.* **4**, 281-292 (1981/82).
158. Mizuno, T., and Kawagoe, K., Burning Behaviour of Upholstered Chairs: Part 2, Burning Rate of Chairs in Fire Tests, *Fire Science and Technology* **5**, 69-78 (1985).
159. Nakos, J. T., Gill, W., and Keltner, N. R., An Analysis of Flame Temperature Measurements using Sheathed Thermocouples in JP-4 Pool Fires, pp. 283-289 in *Proc. ASME/JSME Thermal Engineering Joint Conf.*, American Society of Mechanical Engineers, New York (1991).
160. Neill, D. T., Welker, J. R., and Sliepcevich, C. M., Direct Contact Heat Transfer from Buoyant Diffusion Flames, *J. Fire & Flammability* **1**, 289-301 (1970).
161. Bainbridge, B. L., and Keltner, N. R., Heat Transfer to Large Objects in Large Pool Fires, *J. Hazardous Materials* **20**, 21-40 (1988).
162. Nakos, J. T., and Keltner, N. R., The Radiative-Convective Partitioning of Heat Transfer to Structures in Large Pool Fires, pp. 381-387 in HTD-106, Heat Transfer Phenomena in Radiation, Combustion, and Fires, American Society of Mechanical Engineers (1993).
163. Gritzo, L. A., et al., Heat Transfer to the Fuel Surface in Large Pool Fires, pp. 701-712 in **Transport Phenomena in Combustion**, vol. 1, S. H. Chen, ed., Taylor & Francis, Washington (1996).
164. Shokri, M., and Beyler, C. L., Radiation From Large Pool Fires, *J. Fire Protection Engineering* **1**, 141-150 (1989).
165. Mudan, K. S., and Croce, P. A., Fire Hazard Calculations for Large Open Hydrocarbon Fires, pp. 3-197 to 3-240 in **SFPE Handbook of Fire Protection Engineering**, 2nd ed., NFPA (1995).
166. Roberts, T. A., Merrifield, R., and Tharmalingam, S., Thermal Radiation Hazards from Organic Peroxides, *J. Loss Prevention in the Process Industries* **3**, 244-252 (1990).
167. Assessing Flame Radiation to External Targets From Pool Fires. Engineering Guide, Society of Fire Protection Engineers, Bethesda MD (1999).
168. Blinov, V. I., and Khudiakov, G. N., Diffusion Burning of Liquids (U.S. Army translation), NTIS No. AD296762 (1961).
169. Babrauskas, V., Fire Modeling and Analysis—Pool Fires: Burning Rates and Heat Fluxes, pp. 21-36 to 21-42 in **Fire Protection Handbook**, 16th ed., A. E. Cote and J. L. Linville, eds., NFPA (1986).
170. Heskestad, G., Luminous Heights of Turbulent Diffusion Flames, *Fire Safety J.* **5**, 103-108 (1983).
171. Rew, P. J., and Hulbert, W. G., Development of Pool Fire Thermal Radiation Model (Contract Research Report 96/199), Health & Safety Executive, Sheffield, UK (1996).
172. Hägglund, B., and Persson, L-E., An Experimental Study of the Radiation from Wood Flames, FOA Rapport C 4589-D6(A3), Försvarets Forskningsanstalt, Stockholm (1974).
173. Babrauskas, V., Estimating Large Pool Fire Burning Rates, *Fire Technology* **19**, 251-261 (1983).
174. Hardee, H. C., Lee, D. O., and Benedick, B., Thermal Hazard from LNG fireballs, *Combustion Science and Technology* **17**, 189-197 (1978); **22**, 185-188 (1980).
175. Johnson, D. M., and Pritchard, M. J., Large Scale Experimental Study of Boiling Liquid Expanding Vapour Explosions (BLEVE), *Gastech '90—14th Intl. LNG/LPG Conf. and Exhibition*, Gastech Ltd., Rickmansworth, UK (1990).
176. Prugh, R. W., Quantitative Evaluation of Fireball Hazards, *Process Safety Progress* **13**, 83-91 (1994).
177. Burgess, D. S., and Zabetakis, M. G., Fire and Explosion Hazards Associated with Liquefied Natural Gas (RI 6099), Bureau of Mines, Pittsburgh (1962).
178. Koseki, H., and Iwata, Y., Effects of Pan Size on Radiation Characteristics of Large Scale Crude Oil Fires, pp. 647-658 in *Interflam 2001—Proc. 9th Intl. Conf.*, Interscience Communications Ltd., London (2001).
179. Crawley, F. K., The Effects of the Ignition of a Major Fuel Spillage, pp. 125-145 in **The Assessment of Major Hazards**, The Institution of Chemical Engineers, Rugby, England (1982).
180. Roberts, A. F., Thermal Radiation Hazards from Releases of LPG from Pressurised Storage, *Fire Safety J.* **4**, 197-212 (1981/82).
181. Lees, F. P., **Loss Prevention in the Process Industries**, 2nd ed., 3 vols., Butterworth-Heinemann, Jordan Hill, England (1996).
182. Dorofeev, S. B., et al., Fireballs from Deflagration and Detonation of Heterogeneous Fuel-rich Clouds, *Fire Safety J.* **25**, 323-336 (1995).
183. Novozhilov, V., Review of Investigations on Rising Fireballs and New Implications for Mitigation of Hazardous Fuel Releases, pp. 144-155 in *Fire Science and Technology—Proc. 5th Asia-Oceania Symp.*, Univ. Newcastle, Australia (2001).
184. Martinson, W. E., and Marx, J. D., An Improved Model for the Prediction of Radiant Heat From Fireballs, *Intl. Conf. and Workshop for Modeling and Mitigating the Conse-*

quences of Accidental Releases of Hazardous Materials, Center for Chemical Process Safety, AIChE (1999).
185. Williamson, B. R., and Mann, L. R. B., Thermal Hazards From Propane (LPG) Fireballs, *Combustion Science and Technology* **25**, 141-145 (1981).
186. Jones, J. C., A Simplified Thermal Treatment of Fireballs, *J. Fire Sciences* **19**, 100-105 (2001).
187. Holbrow, P., and Hawksworth, S. J., Thermal Radiation from Vented Dust Explosions (EC/98/30), Health & Safety Laboratory, Health and Safety Executive, Buxton, England (1998).
188. Harding, J. A., Quantification of the Size, Duration, and Thermal Output of the Fireballs Produced by a Range of Pyrotechnic Compositions (IR/L/EX/94/12), Health & Safety Lab., Health and Safety Executive, Harpur Hill, Buxton, England (1994).
189. Merrifield, R., Wharton, R., and Formby, S., Potential Fire and Explosion Hazards of a Range of Loose Pyrotechnic Compositions, Dept. of Defense Explosives Safety Seminar, Las Vegas NV (1996).
190. Merrifield, R., and Wharton, R., Measurement of the Size, Duration and Thermal Output of Fireballs Produced by a Range of Propellants, *Propellants, Explosives and Pyrotechnics* **25**, 179-185 (2000).
191. Brzustowski, T. A., Gollahalli, S. R., Gupta, M. P., Kapstein, M., and Sullivan, H. F., Radiant Heating from Flares (Paper 75-HT-4), American Society of Mechanical Engineers, New York (1974).
192. Wade, C. A., and Clampett, J. C., Fire Performance of Exterior Claddings (FCR 1), BRANZ, Judgeford, New Zealand (2000).
193. Heselden, A.J.M., Smith, P.G., Theobald, C.R., Fires in Large Compartment Containing Structural Steelwork. Detailed Measurements of Fire Behaviour (FR Note 646), Fire Research Station, Borehamwood (1966).
194. Hakkarainen, T., Post-Flashover Fires in Light and Heavy Timber Construction Compartments, *J. Fire Sciences* **20**, 133-175 (2002).
195. Ondrus, J., Fire Hazards of Facades with Externally Applied Additional Thermal Insulation: Full Scale Experiments (LUTVDG TVBB-3021), Lund Univ., Lund, Sweden (1985).
196. Ondrus, J., and Pettersson, O, Fire Hazards of Window-Frames of Plastics, Aluminium and Wood. Full-scale Experiments–A Comparison (Report LUTVDG/TVBB-3037), Dept. Fire Safety Engrg., Lund Univ., Lund, Sweden (1987).
197. Kotthoff, I., Investigation Report on Fire Tests on Original Scale and in the SBI for Façade Claddings, Materialforschungs- und Prüfungsanstalt für das Bauwesen Leipzig e.V., Leipzig, Germany (1999).
198. Oleszkiewicz, I., Fire Exposure to Exterior Walls and Flame Spread on Combustible Cladding, *Fire Technology* **26**, 357-375 (1990).
199. Hakkarainen, T., and Mikkola, E., Fire Safety of Façades—Recent Large Scale Tests, pp. 139-150 in COST Action E5 Workshop on Fire Safety of Medium-Rise Timber Frame Residential Buildings (Report EUR 17831), Valtion teknillinen tutkimuskeskus (VTT), Espoo, Finland (1998).
200. Langdon-Thomas, G. J. and Law, M., Fire and the External Wall (Fire Note No. 8), Joint Fire Research Organization, HMSO, London (1966).
201. Harada, K., Enomoto, A., Uede, K., and Wakamatsu, T., An Experimental Study on Glass Cracking and Fallout by Radiant Heat Exposure, pp. 1063-1074 in *Fire Safety Science--Proc. 6th Intl. Symp.*, Intl. Assn. for Fire Safety Science (2000).
202. Cohen, J. D., and Wilson, P., Current Results from Structure Ignition Assessment Model (SIAM) Research, presented in *Fire Management in the Wildland/Urban Interface: Sharing Solutions*, Kananaskis, Alberta, Canada (2-5 Oct. 1994).
203. Pingree, D., Some Significant Exposure Fires, *Fire J.* **60**, 17-24 (Jan. 1965).
204. Tsukagoshi, I., Fire Spread Between Wooden Buildings: External Radiation from Wooden House in Fire, pp. 99-106 in *Proc. Wood Frame Housing Conf.*, Oslo, Norway (1986).
205. Bevan, R. C., and Webster, C. T., Investigations on Building Fires, Part III. Radiation from Building Fires (Natl. Bldg. Studies Tech. Paper 5), HMSO, London (1950).
206. Strömdahl, I., The Tranås Fire Tests (Report D3:1972), Swedish National Building Research, Stockholm (1972).
207. Law, M., Radiation from Fires in a Compartment (Fire Research Tech. Paper No. 20), HMSO, London (1968).
208. Carlsson, E., External Fire Spread to Adjoining Buildings—A Review of Fire Safety Design Guidance and Related Research (Report 5051), Dept. of Fire Safety Engineering, Lund Univ., Lund, Sweden (1999).
209. Fredlund, B., et al., Fire Spread in Low Rise, High Density Areas of Small Houses, *FoU-Brand*, No. 1, 7-12 (1974). Published by Svenska Brandförsvarföreningen, Stockholm.
210. Tsukagoshi, I., and Itoigawa, E., External Radiation at a Full Scale Fire Experiment, pp. 901-909 in *Fire Safety Science — Proc.1st Intl. Symp.,* Hemisphere, Washington (1986).
211. Design Guide for Fire Safety of Bare Exterior Structural Steel. Technical Reports. 1. Theory & Validation. 2. State of the Art. Prepared for American Iron & Steel Institute. Ove Arup & Partners, London (1977).
212. Hayashi, Y., et al., Full-Scale Burn Tests of Wooden Three-Story Apartment Building, pp. 100-126 in COST Action E5 Workshop on Fire Safety of Medium-Rise Timber Frame Residential Buildings (VTT Symposium 179), Valtion Teknillinen Tutkimuskeskus, Espoo, Finland (1998).
213. Lynam, D., Fireworks Stand Test Burn, *Fire Technology* **37**, 153-166 (2001).
214. Law, M., and O'Brien, T., Fire-Safe Structural Steel: A Design Guide, American Iron and Steel Institute, Washington (1979).
215. Read, R. E. H., External Fire Spread: Building Separation and Boundary Distances (BRE Report BR 187), Fire Research Station, Borehamwood, England (1991). Contains also: Law, M., Heat Radiation from Fires and Building Separation (Fire Research Tech. Paper 5), Fire Research Station, Borehamwood, England (1963).
216. Fackler, J. P., Securité contre l'incendie dans le bâtiment. Largeurs minima des espaces coupe-feu dans les grandes agglomérations du point de vue des risques de propagation par radiation, *Cahiers du Centre Scientifique et Technique du Bâtiment* No. 24-25. Cahier 217 (1954).
217. Besson, J., and Fackler, J. P., Espaces coupe-feu dans les grandes agglomérations, *Cahiers du Centre Scientifique et Technique du Bâtiment* No. 26. Cahier 224 (1956).
218. Recommended Practice for Protection of Buildings from Exterior Fire Exposures (NFPA 80A), NFPA.
219. McGuire, J. H., Fire and the Spatial Separation of Buildings, *Fire Technology* **1**, 278-287 (1965).

220. Buchanan, A. H., ed., **Fire Engineering Design Guide**, Centre for Advanced Engineering, University of Canterbury, Christchurch, New Zealand (1994).
221. Barnett, C. R., Fire Separation between External Walls of Buildings, pp. 841-850 in *Fire Safety Science—Proc. 2nd Intl. Symp. International Association for Fire Safety Science*, Hemisphere Publishing Corp., New York (1989).
222. Barnett, C. R., Fire-Separation Method, pp. 166-181 in **Fire Safety of Tall Buildings**, Council on Tall Buildings and Urban Habitat, McGraw-Hill, New York (1992).
223. Collier, P., Method for Determining Safe Separation Distances between Buildings in the Event of Fire (Tech. Recommendation No. 13), BRANZ, Porirua, New Zealand (1996).
224. Oleszkiewicz, I., Vertical Separation of Windows Using Spandrel Walls and Horizontal Projections, *Fire Technology* **27**, 334-340 (1991).
225. Babrauskas, V., Full-scale Three-storey House Burned in Japanese Test, *Fire and Flammability Bulletin*, 7-8 (Feb. 1992).
226. Hakkarainen, T., Oksanen, T., and Mikkola, E., Fire Behaviour of Facades in Multi-Storey Wood-Framed Houses (VTT Research Note 1823), Valtion Teknillinen Tutkimuskeskus, Espoo, Finland (1997).
227. Harmathy, T. Z., Flame Deflectors (Building Research Note 96), National Research Council of Canada, Ottawa (1974).
228. Packham, D., and Pompe, A., Radiation Temperatures of Forest Fires, *Australian Forest Research* **5**:3, 1-8 (1971).
229. Telisin, H. P., Flame Radiation as a Mechanism of Fire Spread in Forests, pp. 441-449 in **Heat Transfer in Flames**, N. H. Afgan, and J. M. Beér, eds., Scripta Book Co., Washington (1974).
230. Grishin, A. M., **Mathematical Modeling of Forest Fires and New Methods of Fighting Them**, Publishing House of the Tomsk State University, Tomsk, Russia (1997).
231. Cohen, J. D., Preventing Disaster: Home Ignitability in the Wildland-Urban Interface, *J. Forestry* **98**:3, 15-21 (Mar. 2000).
232. Shipp, M. P., Fire Research Station, private communication (2000).
233. Söderbom, J., EUREFIC—Large Scale Tests according to ISO DIS 9705. Project 4 of the EUREFIC fire research programme (SP Report 1991:27), Statens Provningsanstalt, Borås, Sweden (1991).
234. Lee, B.T., Standard Room Fire Test Development at the National Bureau of Standards, pp. 29-44 in *Fire Safety: Science and Engineering* (ASTM STP 882), T.Z. Harmathy, ed., ASTM (1985).
235. Hasemi, Y., Experimental Wall Flame Heat Transfer Correlations for the Analysis of Upward Wall Flame Spread, *Fire Science and Technology* **4**, 75-90 (1984).
236. Kulkarni, A. K., Kim, C.I., and Kuo, C.H., Turbulent Upward Flame Spread for Burning Vertical Walls Made of Finite Thickness (NIST-GCR-91-597), NIST (1991).
237. Fang, J.B., and Breese, J.N., Fire Development in Residential Basement Room (NBSIR 80-2120), NBS (1980).
238. Bracciaventi, J., Window[s] and Window Screens as Modifiers of Thermal Radiation Released in Nuclear Detonations (Project 9400-90; OCD Work Unit 2534B), Naval Applied Science Lab., Brooklyn NY (1966).
239. McGuire, J. H., Ignition of Materials behind Common 1/8-inch Window Glass (Tech. Note 456), Natl. Research Council, Ottawa, Canada (1965).
240. Downs, L. E., and Bruce, H. D., Effect of Window Glass in Protecting Materials from Ignition by Thermal Radiation (Air Force Special Weapons Project Report AFSWP 792), Forest Products Laboratory, Madison WI (1955).
241. Moulen, A. W., and Grubits, W. J., Water-Curtains to Shield Glass from Radiant Heat from Building Fires (Technical Record TR 44/153/422), Experimental Building Station, Dept. of Housing and Construction, North Ryde, Australia (1975).
242. Cowles, G., Reducing Radiation from Building Fires with Fire Resistant Glazing, BRANZ, Porirua, New Zealand (1999).
243. Fire Resistance Tests — Elements of Building Construction (ISO 834), International Organization for Standardization (1975).
244. Cuzzillo, B., Windows in Wildfires, presented at Wind and Fire II, The Oakland/Berkeley Hills "Tunnel" Fire workshop, Univ. California, Berkeley (1992).
245. Paschen, F., Über die zum Funkenübergang in Luft, Wasserstoff und Kohlensäure bei verschiedenen Drucken erforderliche Potentialdifferenz [On the Required Potential Difference for Spark Discharges in Air, Hydrogen, and Carbon Dioxide at Various Pressures], *Annalen der Physik* **37**, 69-96 (1889).
246. Dakin, T. W., et al., Breakdown of Gases in Uniform Fields—Paschen Curves for Nitrogen, Air, and Sulfur Hexafluoride, *Electra* (CIGRE, Paris) No. 32, 61-82 (Jan. 1974).
247. Gourgoulis, D. E., Mikropoulos, P. N., and Stassinopoulos, C. A., Analysis of Sphere-Rod Gaps under Standard Lightning and Switching Impulse Voltages*, IEE Proc. Science, Measurement and Techn.*, **144**, 11-16 (1997).
248. Kalużny, A., Investigations of the Electric Strength of Air Polluted under A.C. Voltage Stress, pp. 604-607 in *Proc. 10th Intl. Conf. on Gas Discharges and Their Applications (GD '92)*, Univ. College of Swansea, Swansea, UK (1992).
249. Deno, D. W., and Zaffanella, L. E., Field Effects of Overhead Transmission Lines and Stations, Chapter 8 in **Transmission Line Reference Book, 345 kV and Above**, 2nd rev. ed., Prepared by Project UHV, General Electric Co. Electric Power Research Institute, Palo Alto CA (1987).
250. Lee, T. H., Plasma Physics and the Interruption of an Electric Circuit, *Proc. IEEE* **57**, 307-323 (1969).
251. Bruce, F. M., Calibration of Uniform-Field Spark-Gaps for High-Voltage Measurement at Power Frequencies, *J. IEE* **94** Part II, 138-154 (1947).
252. Engel, U., and Lienesch, F., Breakdown Voltage of Combustible Gas/Air Mixture in Relation to the Mixing Ratio, *Ex Magazine* No. 23, 41 (1997).
253. Raizer, Y. P., **Gas Discharge Physics**, Springer-Verlag, Berlin (1991).
254. Held, B., Soulem, N., Peyrous, R., and Spyrou, N., Conditions for a Self-sustained DC Corona Discharge, pp. I-128 to I-131 in *Proc. 11th Intl. Conf. on Gas Discharges and Their Applications (GD '95)*, The Institute of Electrical Engineers of Japan, Tokyo (1995).
255. Germer, L. H., Electrical Breakdown between Close Electrodes in Air, *J. Appl. Phys.* **30**, 46 (1959).
256. Dakin, T. W., Insulating Materials—General Properties, pp. 4-117 to 4-160 in **Standard Handbook for Electrical Engineers**, 13th ed., D. G. Fink and H. W. Beaty, eds., McGraw-Hill, New York (1993).

257. Electrical Apparatus for Explosive Gas Atmospheres. Part 7: Increased Safety "e" (IEC 60079-7), International Electrotechnical Commission, Geneva.
258. Safety in Mines Research 1956, Thirty-fifth Annual Report, Safety in Mines Research Establishment, HMSO, London (1957).
259. Maly, R., and Vogel, M., Initiation and Propagation of Flame Fronts in Lean CH_4-Air Mixtures by the Three Modes of the Ignition Spark, pp. 821-831 in *17th Symp. (Intl.) on Combustion*, The Combustion Institute, Pittsburgh (1979).
260. Eckhoff, R. K., **Dust Explosions in the Process Industries**, 2nd ed., Butterworth-Heinemann, Oxford (1997).
261. Ishii, K., Tsukamoto, T., Ujiie, Y., and Kono, M., Analysis of Ignition Mechanisms of Combustible Mixtures by Composite Sparks, *Combustion and Flame* **91**, 153-164 (1992).
262. Arnold, J. S., and Sherburne, R. K., Observations of the Ignition and Incipient Flame Growth in Hydrocarbon-Air Mixtures, pp. 139-143 in *4th Symp. (Intl.) on Combustion*, Williams & Wilkins, Baltimore (1953).
263. Kono, M., Kumagai, S., and Sakai, T., Ignition of Gases by Two Successive Sparks with Reference to Frequency Effect of Capacitance Sparks, *Combustion and Flame* **27**, 85-98 (1976).
264. Lintin, D. R., and Wooding, E. R., Investigation of the Ignition of a Gas by an Electric Spark, *British J. Applied Physics* **10**, 159-166 (1959).
265. Chomiak, J., Flame Development from an Ignition Kernel in Laminar and Turbulent Homogeneous Mixtures, pp. 255-263 in *17th Symp. (Intl.) on Combustion*, The Combustion Institute, Pittsburgh (1979).
266. Akindele, O. O., Bradley, D., Mak, P. W., and McMahon, M., Spark Ignition of Turbulent Gases, *Combustion and Flame* **47**, 129-155 (1982).
267. Kono, M., Kumagai, S., and Sakai, T., The Optimum Condition for Ignition of Gases by Composite Sparks, pp. 757-766 in *16th Symp. (Intl.) on Combustion*, The Combustion Institute, Pittsburgh (1976).
268. Litchfield, E. L., Chronology and Topology of Sparks at Minimum Energy for Ignition, *Combustion and Flame* **5**, 235-241 (1961).
269. Xiong, Y., Roberts, W. L., Drake, M. C., and Fansler, T. D., Investigation of Pre-mixed Flame-kernel/Vortex Interactions via High-Speed Imaging, *Combustion and Flame* **126**, 1827-1844 (2001).
270. Kuchta, J. M., Investigation of Fire and Explosion Accidents in the Chemical, Mining, and Fuel-Related Industries—A Manual (Bulletin 680), Bureau of Mines, Pittsburgh (1985).
271. Dobashi, R., Experimental Study on Gas Explosion Behavior in Enclosure, *J. Loss Prevention in the Process Industries* **10**, 83-89 (1997).
272. Burgess, D. S., Furno, A. L., Kuchta, J. M., and Mura, K. E., Flammability of Mixed Gases (RI 8709), Bureau of Mines, Pittsburgh (1982).
273. Thiele, M., Warnatz, J., and Maas, U., Geometrical Study of Spark Ignition in Two Dimensions, *Combustion Theory & Modelling* **4**, 413-434 (2000).
274. Zborovszky, Z., Study of Intrinsic Safety Basics and Testing Machines: Study of the Effects of Discharge Duration, Electrode Materials and Surface Conditions on the Minimum Ignition Current (BuMines OFR 68-79), Bureau of Mines, Pittsburgh (1977).
275. Sloane, T. M., and Schoene, A. Y., Energy Requirements for Spherical Ignitions in Atmospheric-Pressure Methane-Air Mixtures: A Computational Study, pp. 1669-1676 in *22nd Symp. (Intl.) on Combustion*, The Combustion Institute, Pittsburgh (1988).
276. Borghese, A., Diana, M., Moccia, V., and Tamai, R., Early Growth of Flames, Ignited by Fast Sparks, *Combustion Science and Technology* **76**, 219-231 (1991).
277. Lim, M. T., Anderson, R. W., and Arpaci, V. S., Prediction of Spark Kernel Development in Constant Volume Combustion, *Combustion and Flame* **69**, 303-316 (1987).
278. Wyatt, R. H. M., The Susceptibility of Primary Explosives to Ignition by Electrical Energy, p. 33 in *Flameproofing—Intrinsic Safety and Other Safeguards in Electrical Instrument Practice* (IEE Conf. Report Series No. 3), Institution of Electrical Engineers, London (1962).
279. Engel, A. von, **Ionized Gases**, Oxford University Press, Oxford (1965).
280. Lowke, J. J., Simple Theory of Free-burning Arcs, *J. Physics D: Applied Physics* **12**, 1873-1886 (1979).
281. Pflanz, H. M., Steady State and Transient Properties of Electric Arcs (Ph.D. dissertation), Technische Hogeschool Eindhoven, Netherlands (1967).
282. Matsumoto, T., Matsuura, H., Shibata, Y., and Fujii, K., Investigation of an Atmospheric Free Arc Discharge, pp. 5-7 in *GD85 –8th Intl. Conf. on Gas Discharges & Their Applications*, Leeds Univ. Press, Leeds (1985).
283. Jones, G. R., **High Pressure Arcs in Industrial Devices**, Cambridge Univ. Press, Cambridge (1988).
284. Hall, P. M., Myers, K., and Vilcheck, W. S., Arcing Faults on Direct Current Trolley Systems, *Rock Mechanics—Proc. 4th WVa University (WVU) Conf. on Coal Mine Electrotechnology*, Morgantown, WV (1978).
285. Stokes, A. D., and Sweeting, D. K., Arc Hazard Issues for Electrical Workers (Dept. report), Dept. of Electrical Engineering, Univ. Sydney, Australia (2001).
286. Drouet, M. G., and Nadeau, F., Pressure Waves due to Arcing Faults in a Substation, *IEEE Trans. on Power Apparatus and. Systems* **PAS-98**, 1632-1635 (1979).
287. Stokes, A. D., and Oppenlander, W. T., Electric Arcs in Open Air, *J. Physics D: Applied Physics* **24**, 26-35 (1991).
288. Conrad, R. R., and Dalasta, D., A New Ground Fault Protective System for Electrical Distribution Circuits, *IEEE Trans. on Ind. and Gen. Appl.* **IGA-3**, 217-227 (1967).
289. King, L. A., The Voltage Gradient of the Free Burning Arc in Air or Nitrogen, pp. 871-877 in *Proc. 5th Conf. on Ionization Phenomena in Gases*, North-Holland, Amsterdam (1962).
290. Strom, A. P., Long 60-cycle Arcs in Air, *AIEE Trans.* **65**, 113-117 (1946).
291. Browne, T. E., jr., The Electric Arc as a Circuit Element, *Electrochemical Society J.* **102**, 27-37 (1955).
292. Ayrton, H., **The Electric Arc**, "The Electrician" Printing and Publishing Co., London [1903].
293. Compton, K. T., The Electric Arc, *Trans. AIEE* **46**, 868-883 (1927).
294. Goda, Y., Iwata, M., Ikeda, K., and Tanaka, S., Arc Voltage Characteristics of High Current Fault Arcs in Long Gaps, *IEEE Trans. on Power Delivery* **15**, 791-795 (2000).
295. Fisher, L. E., Resistance of Low-Voltage AC Arcs, *IEEE Trans. Ind. Appl.* **IA-6**, 607-616 (1970).
296. Koch, B., and Christophe, P., Arc Voltage for Arcing Faults on 25(28)-kV Cables and Splices, *IEEE Trans. on Power Delivery* **8**, 779-788 (1993).

297. Gammon, T., and Matthews, J., Instantaneous Arcing-fault Models Developed for Building System Analysis, *IEEE Trans. on Industry Applications* **37**, 197-203 (2001).
298. Hickery, D. L., Bartlett E. J., and Moore, P. J., Investigation into Physical and Electrical Processes of Power System Fault Arcs, pp, 575-578 in *Proc. 34th Universities Power Engineering Conf*., Iraklio, Greece (1999).
299. Nakamichi, Y., and Tuma, D. T., Analysis of Electric Arcs in AC Circuits, *IEEE Trans. on Power Apparatus and Systems* **PAS-102**, 586-595 (1983).
300. Johns, A. T., Aggarwal, R. K., and Song, Y. H., Improved Techniques for Modeling Fault Arcs on Faulted EHV Transmission Systems, *IEE Proc. Generation, Transmission, and Distribution* **141**, 148-154 (1994).
301. Rønningen, T., Internal Faults in Oil-Filled Distribution Transformers: Fault Mechanisms and Choice of Protection (Ph.D. dissertation), Norges Tekniske Høgskole, Trondheim, Norway (1993).
302. Lee, R. H., The Other Electrical Hazard: Electrical Arc Blast Burns, *IEEE Trans. on Ind. Appl.* **IA-18**, 246-251 (1982).
303. Latham, D. J., A Channel Model for Long Arcs in Air, *Physics of Fluids* **23**, 1710-1715 (1980).
304. Ernst, K. A., Kopiansky, J. G., and Maecker, H. H., The Energy Transport Including Emission and Absorption in N_2 Arcs of Different Radii, *IEEE Trans. on Plasma Science* **1**, 3-16 (1974).
305. Strachan, D. C., High Current Arcs in an Orifice Flow. 4. Radiation Measurements (Arc Discharge Research Project Report ULAP-T35), Dept. of Electrical Engineering & Electronics, Univ. Liverpool (1975).
306. Strachan, D. C., Radiation Losses form High-Current Free-Burning Arcs between Copper Electrodes, *J. Physics D: Applied Physics* **6**, 1712-1723 (1973).
307. Fievet, C., and Maftoul, J., Radiative Power Losses from Moving Laminated Arcs, pp. 46-49 in *Proc. 10th Intl. Conf. on Gas Discharges and Their Applications (GD '92)*, Univ. College of Swansea, Swansea, UK (1992).
308. Doughty, R. L., Neal, T. E., Dear, T. A., and Bingham, A. H., Testing Update on Protective Clothing & Equipment for Electric Arc Exposure (IEEE Paper PCIC-97-35), Institute of Electrical and Electronics Engineers, New York (1997).
309. Third Annual Report to the President and the Congress on the Studies of Deaths, Injuries and Economic Loses Resulting from Accidental Burning of Products, Fabrics, or Related Materials—Fiscal Year 1971, Publication DHEW (FDA) 72-7013, Dept. of Health, Education, and Welfare, Washington (1972).
310. Bernstein, T., Electrical Fires: Causes, Prevention, and Investigation, pp. 116-134 in Greenwald, E.K., ed., **Electrical Hazards and Accidents: Their Cause and Prevention,** Van Nostrand Reinhold, New York (1991).
311. Engel, J. Walz, M., and McCormick, J., Arc Fault Circuit Interrupters, *Third Joint FAA/DoD/NASA Conf. on Aging Aircraft* (1999).
312. Blades, R., The Real Cause of Electrical Fires, RB Laboratories, Boulder CO (1993).
313. Holm, R., **Electric Contacts: Theory and Applications**, 4th ed., Springer-Verlag, Berlin (1967).
314. Holmes, R., Electrode Phenomena, pp, 839-867 in **Electrical Breakdown of Gases**, J. M. Meek and J. D. Craggs, eds., Wiley, Chichester (1978).
315. Zborovszky, Z., and Cotugno, L. A., Evaluation of the Cadmium Disc Breakflash in Testing Electrical Circuits—Safety in Explosive Atmospheres—A Comprehensive Study of Intrinsic Safety Criteria (BuMines OFR 68-76), Bureau of Mines, Pittsburgh (1974).
316. **Electrical Contacts**, P. G. Slade, ed., Marcel Dekker, New York (1999).
317. Widginton, D. W., Ignition of Methane by Electrical Discharges (Research Report 240), Safety in Mines Research Establishment, Sheffield, England (1966).
318. Magison, E. C., **Electrical Instruments in Hazardous Locations**, 4th ed., ISA, Research Triangle Park NC (1998).
319. Suhara, K., Break Arcs in Inductive Circuits and the Minimum Arc Current, *IEEE Transactions on Components, Hybrids and Manufacturing Technology* **14**, 118-123 (1991).
320. Yokomizu, Y., Matsumura, T., Henmi, R., and Kito, Y., Total Voltage Drops in Electrode Fall Regions in SF6, Argon and Air Arcs in Current Range of 10 to 20,000 A, pp. I-86 to I-89 in *Proc. 11th Intl. Conf. on Gas Discharges and Their Applications (GD '95)*, The Institute of Electrical Engineers of Japan, Tokyo (1995).
321. Ryan, H. M., and Jones, G. R., **SF_6 Switchgear**, Peter Peregrinus, London (1989).
322. Zborovszky, Z., Study of Intrinsic Safety Basics and Testing Machines: A Comparison of Tungsten and Copper Hot Wire Ignition Capability and Discharge Duration in the Ignition Process of Explosive Atmospheres in Testing Apparatus (BuMines OFR 116-77), Bureau of Mines, Pittsburgh (1976).
323. Gordon, R. L., West, L. C. W., and Widginton, D. W., The Ignition of Methane-Air Mixtures by Arc Discharges of Controlled Duration, pp. 15-20 in *Flameproofing—Intrinsic Safety and Other Safeguards in Electrical Instrument Practice (IEE Conf. Report Series No. 3), Institution of Electrical Engineers*, London (1962).
324. Taylor, J. R., and Randall, C. E., Voltage Surge Caused by Contactor Coils, *J. IEE* **90** Part II (1943).
325. Attwood, S. S., Dow, W. C., and Krausnick, W., Reignition of Metallic A-C Arcs in Air, *Trans. AIEE* **50**, 854-870 (1931).
326. Lee, R., Pressures Developed by Arcs, *IEEE Trans. Ind. Appl.* **IA-23**, 760-764 (1987).
327. Polymeric Materials—Use in Electrical Equipment Evaluations (UL 746C), UL.
328. Anders, G. J., **Rating of Electric Power Cables**, IEEE Press, New York (1997).
329. Keski-Rahkonen, O., Mangs, J., and Turtola, A., Ignition of and Fire Spread on Cables and Electronic Components (VTT Publications 387), Valtion Teknillinen Tutkimuskeskus, Espoo, Finland (1999).
330. Kuroyanagi, T., Inoue, S., and Suzuki, H., Glowing Phenomena of Copper and Copper Materials and Their Electrical Characteristics, *Copper Promotion Technical Research Group J.* **20**, 198-204 (1981).
331. Aronstein, J., Conduction in Failing Aluminum Connections, *IEEE Trans. Components, Hybrids and Manufacturing Technology* **14**, 170-175 (1991).
332. Newbury, D., and Greenwald, S., Observations on the Mechanisms of High Resistance Junction Formation in Aluminum Wire Connections, *J. Research NBS* **85**, 429-440 (1980).
333. Tests of Insulating Materials for Resistance to Heat and Fire, Report of CEE Working Group "Hot Mandrel Test," CEE (031) D126/61, Deutsches Komitee der CEE beim Verband Deutscher Elektrotechniker, Frankfurt am Main (1961).

334. Hotta, E., On the Phenomenon of Glowing Connections, *J. Japan Assn. for Fire Science* **24**:1, 52-58 (1974).
335. Hagimoto, Y., National Research Institute of Police Science, private communication (2000).
336. Isa, N., On the Phenomenon of Glowing Connections, *J. Japan Assn. for Fire Science* **24**:4, 43-48 (1974).
337. Kawase, T., The Breeding Process of Cu_2O, *IAEI News* **47**, 24-25 (July/Aug. 1975); Second Report, **49**, 45-46 (Nov./Dec. 1977).
338. Hagimoto, Y., Kinoshita, K., and Hagiwara, T., Phenomenon of Glow at the Electrical Contacts of Copper Wires, *Natl. Res. Inst. of Police Science Reports—Research on Forensic Science* **41**, 30-37 (Aug. 1988).
339. Sletbak, J., Kristensen, R., Sundklakk, H., Nåvik, G., and Munde, R., Glowing Contact Areas in Loose Copper Wire Connections, pp. 244-248 in *Proc. 37th IEEE Holm Conf. on Electrical Contacts*, IEEE (1991).
340. Kinoshita, K., Hagimoto, Y., and Watanabe, N., Oxide Production and Phenomenon of Luminous Heat at Electrical Connections, *Reports of the National Research Institute of Police Science* **49**:1/2, 32-37 (1996).
341. Suzuki, H., Tago, M., Inoue, S., and Umemura, T., Glow Phenomena in Electrical Connections, The Furukawa Electric Co. Ltd., Japan (1978).
342. Wagner, R. V., Boden, P. J., Skuggevig, W., and Davidson, R. J., Technology for Detecting and Monitoring Conditions That Could Cause Electrical Wiring System Fires (UL Project NC233, 94ME78760), UL (1995).
343. Keski-Rahkonen, O, and Mangs, J., Electrical Ignition Sources in NPPs: Statistical, Modelling, and Experimental studies, International Atomic Energy Agency, Technical Committee Meeting on "Fire Experience in NPPs and Lessons Learned" (J7-TC-2001.7), Vienna (9-13 July 2001).
344. Abramovitz, M., and Stegun, I. A., **Handbook of Mathematical Functions** (AMS55), NBS (1964).
345. Ettling, B. V., Glowing Connections, *Fire & Arson Investigator* **33**, 3-5 (March 1983).
346. Meese, W. J., and Beausoliel, R. W., Exploratory study of Glowing Electrical Connections (NBS BSS 103), NBS (1977).
347. Shefchick, T. P., Letter to the Editor, *NFPA J.* **85**:2, 117 (Mar. 1991).
348. Fire Hazard Testing. Part 2: Test methods. Bad-connection Test with Heaters (IEC 60695-2-3), International Electrotechnical Commission, Geneva (1984).
349. Spletzer, B. L., and Horine, F., Description and Testing of an Apparatus for Electrically Initiating Fires Through Simulation of a Faulty Connection (NUREG/CR-4570; SAND86-0299), Sandia Natl. Labs., Albuquerque NM (1986).
350. Aronstein, J., Fire Due to Overheating Aluminum-Wired Branch Circuit Connections, Wright Malta Corp., Ballston Spa NY (1983).
351. Elliot, D. K., Wet Electric Faults, Part I. Dendrites, *Suppl. to IEEE Trans. on Aerospace* **AS-3**, 247-251 (1965).
352. Ny, T.-Z., Étude expérimentale des déformations et des changements de propriétés optiques du quartz sous l'influence du champ électrique [Experimental study on deformations and changes in the optical properties of quartz under the influence of an electric field], *Le Journal de physique et le radium* (Series 6) **9**, 13-37 (1928).
353. Gill, E. W. B., Electrification by Freezing, *British J. Applied Physics* **4** (Supl. 2), S16-S19 (1953).
354. Pratt, T. M., Electrostatic Initiation of Explosions in Dusts, *Cereal Foods World* **23**, 601-605 (1978).
355. Pratt, T. H., Electrostatic Ignitions in Enriched Oxygen Atmospheres: A Case History, *Process Safety Progress* **12**, 203-205 (Oct. 1993).
356. Cohn, E. M., and Guest, P. G., Influence of Humidity upon the Resistivity of Solid Dielectrics and upon the Dissipation of Static Electricity (IC 7286), Bureau of Mines, Pittsburgh (1944).
357. Cross, J. A., Study of Static Electricity on Grain Conveying Belts (SMS-80-047), National Grain and Feed Assn., Washington (1980).
358. Barreto, E., Reynolds, S. I., and Jurenka, H., Ignition of Hydrocarbons and the Thermalization of Electrical Discharges, *J. Appl. Phys.* **45**, 3317-3327 (1974).
359. Sloane, R. W., Ignition of Gaseous Mixtures by the Corona Discharge, *Phil. Mag.* 7th Series **19**, 998-1011 (1935).
360. Walmsley, H. L., The Avoidance of Electrostatic Hazards in the Petroleum Industry, *J. Electrostatics* **27**, Special issue No. 1&2 (1992).
361. Lüttgens, G., and Glor, M., **Understanding and Controlling Static Electricity**, Expert Verlag, Ehningen (1989).
362. Glor, M., Ignition of Gas/Air Mixtures by Discharges between Electrostatically Charged Plastic Surfaces and Metallic Electrodes, *J. Electrostatics* **10**, 327-333 (1981).
363. Bartknecht, W., **Dust Explosions: Course, Prevention, Protection**, Springer-Verlag, Berlin (1989).
364. Schwenzfeuer, K., and Glor, M., Ignition Tests with Brush Discharges, *J. Electrostatics* **51/52**, 402-408 (2001).
365. Larsen, Ø, Hagen, J. H., and van Wingerden, K., Ignition of Dust Clouds by Brush Discharges in Oxygen Enriched Atmospheres, *J. Loss Prevention in the Process Industries* **14**, 111-122 (2001).
366. Glor, M., Conditions for the Appearance of Discharges during the Gravitational Compaction of Powders, *J. Electrostatics* **15**, 223-235 (1984).
367. Glor, M., Overview of the Occurrence and Incendivity of Cone Discharges with Case Studies from Industrial Practice, *J. Loss Prevention in the Process Industries* **14**, 123-128 (2001).
368. Maurer, B., Glor, M., Lüttgens, G., and Post, L., Hazards Associated with Propagating Brush Discharges on Flexible Intermediate Bulk Containers, Compounds and Coated Materials, pp. 217-222 in *Electrostatics '87—7th Intl. Conf. on Electrostatic Phenomena (Conf. Series No. 85),* Institute of Physics, London (1987).
369. Edwards, H. R., and Underwood, M. C., The Ignition of Powder/Air Mixtures by Discharges of Static Electricity, *J. Electrostatics* **15**, 123-125 (1984).
370. Cross, J. A., **Electrostatics: Principles, Problems and Applications**, Adam Hilger, Bristol, England (1987).
371. Boschung, P., Hilgner, W., Lüttgens, G., Maurer, B., and Widmer, A., An Experimental Contribution to the Question of the Existence of Lightning-like Discharges in Dust Clouds, *J. Electrostatics* **3**, 303-310 (1977).
372. Gill, A. H., Curious Causes of Gasoline Fires and Gas Explosions, *Ind. and Eng. Chem.* **15**, 140 (1923).
373. Yallop, H. J., **Explosion Investigation**, The Forensic Science Society, Harrogate/ Scottish Academic Press, Edinburgh (1980).
374. Guest, P. G., Static Electricity in Nature and Industry (Bulletin 368), Bureau of Mines, US Government Printing Office, Washington (1933).

375. Cohn, E. M., and Guest, P. G., Influence of Humidity upon the Resistivity of Solid Dielectrics and upon the Dissipation of Static Electricity (IC 7286), Bureau of Mines, Pittsburgh (1944).
376. Henry, P. S. H., Static in Industry, pp. 195-199 in *Proc. 3rd Conf. on Static Electrification* (Conf. Series No. 11), The Institute of Physics, London (1971).
377. Tabata, Y., and Masuda, S., Minimum Potential of Charged Insulator to Cause Incendiary Discharges, *IEEE Trans. Ind. Appl.* **IA-20**, 1206-1211 (1984).
378. Gibson, N., and Lloyd, F. C., Incendivity of Discharges from Electrostatically Charged Plastics, *British J. Applied Physics* **16**, 1619-1631 (1965).
379. Britton, L. G., **Avoiding Static Ignition Hazards in Chemical Operations**, AIChE (1999).
380. Schneider, R. L., Fundamentals of Fire and Explosion Hazards Recognition and Control in Fireworks Manufacturing, pp. 346-377 in *Proc. 1st Intl. Symp. on Fireworks*, Minister of Supply and Services Canada, [n.p.] (1992).
381. Pratt, T. H., **Electrostatic Ignitions of Fires and Explosions**, Burgoyne Inc., Marietta GA (1997).
382. Wheeler, R. V., Dust Explosions, *J. Soc. Chemical Industry* **50**, 650-653 (1931).
383. Cleves, A. C., Sumner, J. F., and Wyatt, R. M. H., The Effect of Temperature and Relative Humidity on the Accumulation of Electrostatic Charges on Fabrics and Primary Explosives, pp. 226-233 in *Proc. 3rd Conf. on Static Electrification* (Conf. Series No. 11), The Institute of Physics, London (1971).
384. Fisher, R. J., A Severe Human ESD Model for Safety and High Reliability System Qualification Testing (SAND89-0194C), Sandia Natl. Labs., Albuquerque NM (1989).
385. Guest, P. G., Sikora, V. W., and Lewis, B., Static Electricity in Hospital Operating Suites: Direct and Related Hazards and Pertinent Remedies (RI 4833), Bureau of Mines, Pittsburgh (1952).
386. Brundrett, G. W., A Review of Factors Influencing Electrostatic Shocks in Offices, *J. Electrostatics* **2**, 295-315 (1976/77).
387. Strojny, J. A., Some Factors Influencing Electrostatic Discharge from a Human Body, *J. Electrostatics* **40/41**, 547-552 (1997).
388. Laib, J., Assessment and Minimization of Electrostatic Discharge Hazards in Pyrotechnic Manipulations, pp. 281-303 in *Proc. 2nd Intl. Symp. on Fireworks*, Minister of Supply and Services Canada, [n.p.] (1994).
389. Code of Practice for Control of Undesirable Static Electricity (BS 5958 Part 1), British Standards Institution, London (1980).
390. Thompson, R. E., Electrostatic Safety in Clothing, *Fire J.* **63**, 15-16 (Nov. 1969).
391. Smith, P. G., The Fire Hazard Due to Static Electricity Produced in a Chair (Fire Research Note 367), Fire Research Station, Borehamwood, England (1958).
392. Henry, P. S. H., Risk of Ignition due to Static on Outer Clothing, pp. 212-225 in *Proc. 3rd Conf. on Static Electrification* (Conf. Series No. 11), The Institute of Physics, London (1971).
393. Holdstock, P., and Wilson, N., The Effect of Static Charge Generated on Hospital Bedding, pp. 7.6.1 to 7.6.9 in *Proc. 18th Electrical Overstress/Electrostatic Discharge Symp.*, ESD Assn., Rome NY (1996).
394. Wilson, N., The Risk of Fire or Explosion due to Static Charges on Textile Clothing, *J. Electrostatics* **4**, 67-84 (1977/78).
395. Tolson, P., The Stored Energy Needed to Ignite Methane by Discharges from a Charged Person, *J. Electrostatics* **8**, 289-293 (1980).
396. Movilliat, P., and Giltaire, M., Mesure de l'énergie d'inflammation de mélanges gazeux par décharge capacitive. Inflammation par décharge d'une personne chargée d'electricité statique, *J. Electrostatics* **6**, 307-331 (1979).
397. Wilson, N., The Nature and Incendiary Behaviour of Spark Discharges from the Body, pp. 73-83 in *Electrostatics 1979* (Conf. Series No. 48), The Institute of Physics, London (1979).
398. Wilson, N., The Ignition of Natural Gas by Spark Discharges from the Body, pp. 21-27 in *Electrostatics 1983* (Conf. Series No. 66), The Institute of Physics, London (1983).
399. Wilson, N., Incendiary Behavior of Electrostatic Spark Discharges from Human Beings, pp. 593-603 in **Performance of Protective Clothing** (ASTM STP 900), ASTM (1986).
400. Johnson, R. W., Ignition of Flammable Vapors by Human Electrostatic Discharge, paper 10d in *14th Loss Prevention Symp.*, AIChE (1980).
401. Berkey, B. D., Pratt, T. H., and Williams, G. M., Review of Literature Related to Human Spark Scenarios, *Plant/Operations Progress* **7**, 32-36 (Jan. 1988).
402. Lüttgens, G., and Wilson, N., **Electrostatic Hazards**, Butterworth-Heinemann, Oxford (1997).
403. Swann, H. W., Survey of Harmful Static Electrification, *British J. Applied Physics* **4** (Supl. 2), S68-S71 (1953).
404. Glor, M., Hazards Due to Electrostatic Charging of Powders, *J. Electrostatics* **16**, 175-191 (1985).
405. Pollock, B. D., Fisco, W. J., Kramer, H., and Forsyth, A. C., Handling, Storability, and Destruction of Azides, pp. 73-109 in **Energetic Materials**, Vol. 2: Technology of the Inorganic Azides, H. D. Fair and R. F. Walker, eds., Plenum Press, New York (1977).
406. Dahn, C. J., Electrostatic Characterization of Grain Products (SMS-80-046), National Grain and Feed Assn., Washington (1980).
407. Blythe, A. R., and Reddish, W., Charges on Powders and Bulking Effects, pp. 107-114 in *Electrostatics 1979* (Conf. Series No. 48), The Institute of Physics, London (1979).
408. Boschung, P., and Glor, M., Methods for Investigating the Electrostatic Behaviour of Powders, *J. Electrostatics* **8**, 205-219 (1980).
409. Collocott, S. J., Morgan, V. T., and Morrow, R., The Electrification of Operating Powder Chemical Fire Extinguishers, *J. Electrostatics* **9**, 191-196 (1980).
410. Smart, R. C., **The Technology of Industrial Fire and Explosion Hazards**, 2 vols., Chapman & Hall, London (1947).
411. Singh, S., Cartwright, P., and Thorpe, D., Silo Electrostatic Hazards (SMS-84-052), National Grain and Feed Assn., Washington (1984).
412. Eynard, P., Contribution à la prevention des inflammations ou explosions provoquées par l'electricité statique dans l'industrie chimique, pp. 623-661 in *Report of the 9th Intl. Symp. on Prevention of Occupational Accidents and Diseases in the Chemical Industry*, Intl. Social Security Assn., Lucerne (1984).
413. Britton, L. B., and Smith, J. A., Static Hazards of Drum Filling, Paper 54e, *21st Loss Prevention Symp.*, AIChE (1987).

414. Harper, W. R., Liquids Giving no Electrification by Bubbling, *British J. Applied Physics* **4** (Supl. 2), S19-S22 (1953).
415. Recommended Practice on Static Electricity (NFPA 77), NFPA.
416. Howard, J. C., The Hazards of Static Electricity, pp. 228-233 in **Fire Protection Manual for Hydrocarbon Processing Plants**, vol. 1, C. H. Vervalin, ed., 2nd ed., Gulf Publishing, Houston (1973).
417. Britton, L. B., and Smith, J. A., Static Hazards of Drum Filling, *Plant/Operations Progress* **7**, 53-78 (1988).
418. Klinkenberg, A., and van der Minne, J. L., **Electrostatics in the Petroleum Industry**, Elsevier, Amsterdam (1958).
419. Rogers, D. T., and Schleckser, C. E., Engineering and Theoretical Studies of Static Electricity, Section VIII, pp. 103-121 in *Proc. 5th World Petroleum Congress*, New York (1959).
420. Dolezalek, F., Electrification of Liquids on Flowing through Pipes, *J. Soc. of Chemical Industry* **32**, 128-129 (1913).
421. Johnson, J. K., The Ignition of Vapour and Droplets by Liquid-to-Metal Sparks, *J. Electrostatics* **4**, 53-65 (1977/78).
422. Matsubara, Y., Matsushima, S., and Jones, T. B., Charge Accumulation in an Oil Tank during Loading Operations, *J. Electrostatics* **40/41**, 191-197 (1997).
423. Pesetsky, B., and Fisher, J. A., Static Problems in Handling Charged Liquids, *9th Loss Prevention Symp.*, AIChE (1975).
424. Bustin, W. M., Koszman, I., and Tobye, I. T., A New Theory for Static Relaxation, *Hydrocarbon Processing* **43**:11, 209-216 (1964).
425. Matsubara, Y., and Jones, T. B., Numerical Modeling for Potential Relaxation of Charged Oil in Containers, *IEEE Trans. on Ind. Appl.* **29**, 117-121 (1993).
426. Strawson, H., and Lewis, A., Electrostatic Charging in the Handling of Aviation Fuels, Aircraft Fuels, Lubricants, and Fire Safety (AGARD Conf. Proc. 84), NATO AGARD (1971).
427. Matsubara, Y., Pazda, R. J., and Jones, T. B., Effect of Fill Pipe on Transient Decay of Surface Potential in a Cylindrical Vessel Containing Charged Liquid, *IEEE Trans. on Ind. Appl.* **30**, 122-126 (1994).
428. Ebadat, V., and Cartwright, P., Electrostatic Hazards from Small Non-Conducting Containers for Flammable Liquids, *27th Loss Prevention Symp.*, AIChE (1993).
429. Bustin, W. M., and Dukek, W. G., **Electrostatic Hazards in the Petroleum Industry**, Research Studies Press, Letchworth, Herts., England (1983).
430. Schön, G., Elektrostatische Aufladungsvorgänge und ihre Zündgefahren, in **Handbuch der Raumexplosionen**, H. H. Freytag, ed., Verlag Chemie, Weinheim, Germany (1965).
431. Walmsley, H. L., and Mills, J. S., Electrostatic Ignition Hazards in Road Tanker Loading: Part 1. Review and Experimental Measurements, *J. Electrostatics* **28**, 61-87 (1992).
432. Lewis, A., and Strawson, H., Static Electrification with Liquid Aviation Fuels: Its Occurrence and Suppression, *Lightning and Static Electricity Conf.*, Royal Aeronautical Society, London (1975).
433. Bachman, K. C., Variables Which Influence Spark Production Due to Static Electricity in Tank Truck Loading, *Lightning and Static Electricity Conf.*, Royal Aeronautical Society, London (1975).
434. Mason, P. I., and Rees, W. D., Hazards from Plastic Pipes Carrying Insulating Liquids, *J. Electrostatics* **10**, 137-145 (1981).
435. Zabetakis, M., and Rosen, B. H., Considerations Involved in Handling Kerosine, *Proc. Amer. Petroleum Inst.* **37**(III), 296-306 (1957).
436. Loeb, L. B., Static Electrification-I, pp. 249-309 in **Progress in Dielectrics**, vol. 4, Academic, New York (1962).
437. Bright, A. W., Hughes, J. F., and Makin, B., Research on Electrostatic Hazards Associated with Tank Washing in Very Large Crude Carriers (Supertankers). I. Introduction and Experiment Modelling, *J. Electrostatics* **1**, 37-47 (1975).
438. Chubb, J. N., Practical and Computer Assessments of Ignition Hazards during Tank Washing and during Wave Action in Part-Ballasted OBO Cargo Tanks, *J. Electrostatics* **1**, 61-70 (1975).
439. Napier, D. H., Generation of Static Electricity in Steam Screens and Water Curtains, pp. 244-264 in *Proc. Symp. on Chemical Process Hazards with Special Reference to Plant Design—V* (Symp. Series 39a), The Institution of Chemical Engineers, London (1974).
440. Gibson, N., Static in Fluids, pp. 71-83 in *Proc. 3rd Conf. on Static Electrification* (Conf. Series No. 11), The Institute of Physics, London (1971).
441. Hughes, J. F., Bright, A. W., Makin, B., and Parker, I. F., A Study of Electrical Discharges in a Charged Water Aerosol, *J. Phys. D: Appl. Phys.* **6**, 966-975 (1973).
442. Napier, D. H., and Rossell, D. A., Hazard Aspects of Static Electrification in Dispersion of Organic Liquids, pp. III-157 to III-164 in *2nd Intl. Symp. on Loss Prevention and Safety Promotion in the Process Industries*, European Federation of Chemical Engineering, Publication Series No. 1; 189th Event. DECHEMA, Frankfurt (1978).
443. Wright, L., and Ginsburgh, I., What Experimentation Shows about Static Electricity, pp. 233-240; 289 in **Fire Protection Manual for Hydrocarbon Processing Plants**, vol. 1, C. H. Vervalin, ed., 2nd ed., Gulf Publishing, Houston (1973).
444. Lyle, A. R., and Strawson, H., Estimation of Electrostatic Hazards in Tank Filling Operations, pp. 234-247 in *Proc. 3rd Conf. on Static Electrification* (Conf. Series No. 11), The Institute of Physics, London (1971).
445. Krämer, H., and Asano, K., Incendivity of Sparks from Surfaces of Electrostatically Charged Liquids, *J. Electrostatics* **6**, 361-371 (1979).
446. Rees, W. D., Static Hazards during the Top Loading of Road Trailers with Highly Insulating Liquids: Flow Rate Limitation Proposals to Minimize Risk, *J. Electrostatics* **11**, 13-25 (1981).
447. Ermakov, V. I., and Stozhkov, Y. I., New Mechanism of Thundercloud Electricity and Lightning Production, pp. 242-245 in *11th Intl. Conf. on Atmospheric Electricity* (NASA/CP-1999-209261), H. J. Christian, ed., NASA, Marshall Space Flight Center AL (1999).
448. Williams, E. R., The Electrification of Thunderstorms, *Scientific American* **259**:5, 88-99 (Nov. 1988).
449. Uman, M. A., **Lightning**, Dover Publications, New York (1984).
450. Hart, W. C., and Malone, E. W., **Lightning and Lightning Protection**, Don White Consultants, Gainesville VA (1979).
451. Robb, J. D., Hill, E. L., Newman, M. M., and Stahmann, J. R., Lightning Hazards to Aircraft Fuel Tanks (NACA TN 4326), NACA, Washington (1958).
452. Frydenlund, M. M., **Lightning Protection for People and Property**, Van Nostrand Reinhold, New York (1993).

453. Recommended Practice for Protecting Residential Structures and Appliances against Surges (Document # PEAC.0545.R), EPRI PEAC Corp., [Knoxville TN] (1999).
454. Taylor, A. R., Lightning and Trees, pp. 831-849 in **Lightning**, vol. 2, R. H. Golde, ed., Academic Press, New York (1977).
455. Fuquay, D. M., Baughman, R. G., and Latham, D. J., A Model for Predicting Lightning-Fire Ignition in Wildland Fuels (Res. Paper INT-217), US Forest Service, Intermountain Forest & Range Expt. Sta., Ogden UT (1979).
456. Viemeister, Peter E., **The Lightning Book**, 2nd ed., MIT Press, Cambridge (1972).
457. Ford, R. T. sr., private communication (2002).
458. Stevens, E., unpublished investigation results (1997).
459. Stenhoff, M., **Ball Lightning**, Kluwer Academic/Plenum, New York (1999).
460. Ritchie, D. J., **Ball Lightning—A Collection of Soviet Research in English Translation**, Consultants Bureau, New York (1961).
461. Davies, P., Great Balls of Fire, *New Scientist*, 64-67 (24/31 Dec 1987).
462. Ohtsuki, Y. H., and Ofuruton, H., Nature of Ball Lightning in Japan, *Il Nuovo Cimento* **10C**, 577-580 (1987).
463. Uman, M. A., **All about Lightning**, Dover Publications, New York (1986).
464. Kondo, N., Ofuruton, H., and Ohtsuki, Y. H., Plasma Luminescence with Water Droplets and Vapor, *J. Atmospheric Electricity* **17**, 47-51 (1997).
465. Golka, R., How to Create Ball Lightning, Vol. 2, pp. 110-1 to 110-2 in *Proc. 1991 Intl. Aerospace and Ground Conf. on Lightning and Static Electricity*, NASA, Washington (1991).
466. Golka, Robert K., In Search of Fireball Lightning, *Radio Electronics* **56**, 46-47 (Mar. 1985).
467. Thornton, W. M., On Thunderbolts, *Phil. Magazine and J. of Science*, Series 6, **21**, 630-634 (1911).
468. **Der Kugelblitz**, Walther Brand, Christian Jensen, and Arnold Schwaßmann, eds. Henri Grand, Hamburg (1923).
469. Witalis, E. A., Ball Lightning as a Magnetized Air Plasma Whirl Structure, *J. Meteorology (UK)* **15**, 121-128 (1990).
470. Arnhoff, G., Is There yet an Explanation of Ball Lightning? *European Trans. Electrical Power Engineering* **2**, 137-142 (May-Jun 1992).
471. Molokov, S., and Allen, J. E., The Fragmentation of Wires Carrying Electric Current, *J. Phys. D: Appl. Phys.* **30**, 3131-3141 (1997).
472. Kumagai, S., and Sakai, T., Ignition of Gases by High-Energy Sparks, pp. 995-1001 in *11th Symp. (Intl.) on Combustion*, The Combustion Institute, Pittsburgh (1966).
473. Frank, A. M., Mechanisms of EBW HE Initiation (UCRL-JC-105647), Lawrence Livermore National Laboratory, Livermore CA (1991).
474. Bartels, A. L., Bradford, M., and Thompson, M. G., Incendivity of Electrical Sparking due to Circulating Currents in the Enclosure of Large Electrical Machines, pp. 141-148 in *4th Intl. Conf. on Electrical Safety in Hazardous Areas* (IEE Conf. Publ. 296), Institution of Electrical Engineers, London (1988).
475. Bredthauer, J., McClung, L. B., Mohla, D. C., and Tretzack, H., Risk of Ignition Due to Transition Currents in Medium Voltage Motors for Hazardous Locations, *IEEE Trans. on Industry Applications* **27**, 1290-1299 (1991).
476. Assessment of the Radio Frequency Ignition Hazard to Process Plants where Flammable Atmospheres May Occur (Guidance Note GS21), Health and Safety Executive, London (1983).
477. Guide to Prevention of Inadvertent Ignition of Flammable Atmospheres by Radio-Frequency Radiation (BS 6656), British Standards Institution, London (1991).
478. Prevention of Inadvertent Ignition of Flammable Atmospheres by Radio-Frequency Radiation (draft document 97/261808 DC), British Standards Institution, London (1997).
479. Robertson, S. S. J., and Loveland, R. J., Radio Frequency Ignition Hazards: A Review, *IEE Proc.* **128-A**, 607-614 (1981).
480. Maddocks, A. J., and Bartels, A. L., Ignition at Radio Frequencies using Simple Tuned and Equivalent Circuits, pp. 144-149 in *3rd Intl. Conf. on Electrical Safety in Hazardous Environments*, Institution of Electrical Engineers, Power Div., London (1982).
481. Widginton, D. W., Ignition Threshold Parameters for Pulsed Microwave Sources, pp. 139-143 in *3rd Intl. Conf. on Electrical Safety in Hazardous Environments*, Institution of Electrical Engineers, Power Div., London (1982).
482. Knight, P., Radio-Frequency Ignition Hazards: The Power Available from Non-Resonant Structures (BBC RD 1982/3), British Broadcasting Corp., Kingswood Warren, UK (1982).
483. Rosenfeld, J. L. J., et al., Experiments on the Incendivity of Radio-Frequency Breakflash Discharges (1.8-21 MHz c.w.), *Radio and Electronic Engineer* **51**, 175-186 (1981).
484. Howson, D. P., Excell, P. S., and Butcher, G. H., Ignition of Flammable Gas/Air Mixtures by Sparks from 2 MHz and 9 MHz Sources, *Radio and Electronic Engineer* **51**, 170-174 (1981).
485. Burstow, D. J., et al., Radio Frequency Ignition Hazards, *Radio and Electronic Engineer* **51**, 151-169 (1981).
486. Maddocks, A. J., and Jackson, G. A., Measurements of Radio Frequency Voltage and Power Induced in Structures on the St. Fergus Gas Terminals, *Radio and Electronic Engineer* **51**, 197-194 (1981).
487. Olenik, H., Rentzsch, H., and Wettstein, W., **Handbuch für Explosionsschutz—Explosion Protection Manual**, 2nd ed., Brown, Boveri & Cie im Verlag W. Girardet, Essen (1983).
488. Bishop, A. E., and Knight, P., The Safe Use of Electroexplosive Devices in Electromagnetic Fields, *Radio and Electronic Engineer* **54**:7/8, 321-335 (Jul./Aug. 1984).
489. Guide for Prevention of Inadvertent Initiation of Electro-Explosive Devices by Radio Frequency Radiation (BS 6657), British Standards Institution, London.
490. Schwab, H. A., Some Properties of Radio-Frequency Gas Discharges in Air at Atmospheric Pressure, *Proc. IEEE* **59**, 613-616 (1971).
491. Hill, J. M., and Marchant, T., R., Modelling Microwave Heating, *Applied Math. Modelling* **20**, 3-15 (1996).
492. Meredith, R. J., **Engineers' Handbook of Industrial Microwave Heating**, Institution of Electrical Engineers, London (1998).
493. Rogers, J. C., Survey of the Thermal Threat of Nuclear Weapons [redacted, unclassified version], SRI Project IMU-4021; contract no. OCD-OS-62-135(III), Stanford Research Institute, Menlo Park CA (1963).
494. Brode, H. L., Fireball Phenomenology, pp. 2-1 to 2-50 in A Collection of Papers on Thermal Effects, Presented at the Symposium at the Fire Service College, Dorking, England. USA/UK/Canada Tripartite Technical Cooperation Program, Sub-Group N, Panel N-3 (Thermal), DASA (1965).

495. Thomas, P. H., Simms, D. L., and Law, M., On the Correlation of the Threshold for Ignition by Radiation With the Physical Properties of Materials (FR Note 381), Fire Research Station, Borehamwood, England (1959).
496. Bush, B. W., and Small, R. D., Note on the Ignition of Vegetation by Nuclear Weapons, *Combustion Science and Technology* **51**, 25-38 (1987).
497. Glasstone, S., and Dolan, P. J., **The Effects of Nuclear Weapons**, 3rd ed., US Dept. of Defense and US Dept. of Energy, Washington (1977).
498. Bruce, H. D., Incendiary Effects on Building and Interior Kindling Fuels (WT-774), Operation Upshot-Knothole, Project 811a, Forest Products Lab., Madison WI (1953).
499. Bowden, F. P., and Yoffe, A. D., **Fast Reactions in Solids**, Butterworths, London (1958).
500. **Kirk-Othmer Encyclopedia of Chemical Technology**, 3rd ed., vol. 19, p. 494, John Wiley, New York (1982).
501. Rossotti, H., **Fire**, Oxford University Press, Oxford (1993).
502. Simms, D. L., Some Early Experiments on Ignition by Radiation (F.R. Note 577), Fire Research Station, Borehamwood, England (1964).
503. Moore, F. C., **Fires: Their Causes, Prevention and Extinction**, The Continental Insurance Co. of New York, New York (1877).
504. Petrovich, W. P., Unusual Origin and Cause of Fires, *Fire & Arson Investigator* **39**:3, 19-20 (Mar. 1989).
505. McGuire, J. H., Mirror-Caused Fire, *Fire J.* **64**, 12-13 (July 1970).
506. Fires Caused by Sun's Rays, *FPA J.* No. 46, 109-110 (July 1959).
507. Uncommon Causes: Number One, *FPA J.* No. 6, 157 (July 1949).
508. Fuquay, D. M., and Baughman, R. G., Can Glass and Metal Containers Start Forest Fires? *Fire Control Notes* **26**, 3-5 (Apr. 1965).
509. Goldstone, B. M., Hazards from the Concentration of Solar Radiation by Textured Window Glass (BRE Report), Building Research Establishment, Garston, UK (1982).
510. Fitz, M., MDE Engineers, private communication (2002).
511. Barnett, H. C., and Hibbard, R. R., Properties of Aircraft Fuels (Tech. Note 3276), NACA, Washington (1956).

Copyright © 2003, 2014 Vytenis Babrauskas

Chapter 12. Preventive measures

General precautions **591**
Measures against static electricity **591**
Lightning protection **592**
Arresters—flame and spark **594**
Flame arresters *594*
Spark arresters *596*
Design of electrical equipment for flammable atmospheres **596**
NEC requirements *596*
Article 500 (traditional classification) 597
Article 505 (IEC classification) 599
Design of equipment for hazardous locations *599*
Explosionproof equipment 600
Dust-ignition-proof equipment 601
Intrinsically safe equipment 601
Increased safety protection 603
Pressurized enclosures 603
Sealed, encapsulated, oil-immersed, and powder-filled devices 603
Miscellaneous protection strategies 604
Design of equipment for mining *604*
Arc fault and cord fault interrupters **604**
Further readings **604**
References **605**

General precautions

Minimizing the occurrence of ignition is one of the essential aspects of the practice of the fire safety engineering profession. The literature of the field is vast, and it is not appropriate to attempt to summarize it here. Thus, in this Chapter we will only (1) cite some salient reference works on the topic; and (2) discuss in some detail a few selected hardware-based ignition prevention concepts.

The National Electrical Code[1] (NEC) is perhaps the most notable work in the reference category. It can be viewed as a codification of good practices to guard against electrocution and against electrically caused ignitions. For designing and operating industrial plant where ignitable dusts are generated, a British guide to recommendations exists[2]; it gives some specific precautions and some checklists for surveying the adequacy of an installation. NFPA has published standards, codes, or guides covering a vast array of industries where specialized means for reducing ignition risk are presented.

Measures against static electricity

The first measure against static electricity is proper grounding and bonding. This is almost always necessary, but may not be sufficient. If liquids, powders, fabrics, etc. are handled which are highly insulating, grounding and bonding may not suffice. If flammable atmospheres are present and conductivities of the substances involved cannot be increased, then—in the worst case—inerting with nitrogen or other inert substances may be needed. For the cases where grounding is effective, it may be surprising that a fairly high resistance, generally quoted as 1 megohm (MΩ), suffices. Some standards specify values as low as 10 Ω, but this is not because a value that low is needed to dissipate charge; rather, it is assumed that the grounding system will corrode and progressively fail, and a still-adequate resistance is expected after serious degradation has taken place. Sometimes, just increasing the humidity in the area can reduce static electricity hazards sufficiently.

Another tactic is the use of *electrostatic eliminators*, which are devices that ionize the air, thereby increasing its conductivity and helping to neutralize charges. It can take the form simply of a grounded array of sharp points. A corona discharge forms at the sharp points, creating ions of the opposite polarity to the original charge, thereby serving to neutralize it. The charge can be reduced down to the point where the surfaces are at a potential that is below the threshold voltage for corona discharge to take place. The device can function safely in fuel/air mixtures having a minimum ignition energy greater than about 0.2 mJ, since a corona discharge itself would only be able to ignite mixtures having minimum ignition energies on the order of 0.01 mJ.

A more effective electrostatic eliminator produces ions of both polarities. One way of creating this is with the use of a small radioactive source, typically polonium 210. The alpha particles emitter by the source collide with air molecules and produce a plasma of ionized air. It has the drawback of a short half-life (138 days), requiring continued replacement. Another technique involves subjecting a grid of needle points or wires to an AC source, with a voltage high enough to cause corona discharge. Its main drawbacks are that (a) ozone is produced; and (b) the needle points must be placed within 10 mm of the surface to be neutralized. Additional advice on static eliminators has been published[3].

Anti-static agents are chemicals which typically increase the conductivity of a substance, so charges could leak away more quickly. This can be done by introducing directly a substance which is more highly conductive, e.g., carbon particles. More fascinating is a technique that increases surface adsorption of water at low humidities, that is, a hydrophilic additive. By use of such techniques, conductive *plastics* can be formulated.

In industrial situations which demand it, it is possible to minimize the risk of electrostatic discharge from persons by having operators wear conductive *shoes* and *wrist straps* and providing conductive *floors*. While most materials not specifically designed to be conductive are, in fact, highly insulating, concrete and terrazzo floors have sufficient natural conductivity that static discharges from persons wearing conductive shoes are unlikely. Conductive *gloves* are also available for operations that need them.

Lightning protection

The lightning rod was invented by Benjamin Franklin in 1752. This is a metallic rod which is grounded at one end and raised in the air at the other. When the initial streamers from the cloud start to form, there is not a highly specific place along the ground level where the initial return stroke is preferentially located. By providing a ground-potential conductor in the air, a preference is established, and the lightning current flows down the rod (which must be of adequate dimension in order not to overheat). Franklin recommended that the tip of the rod (*air terminal*, in the jargon of the lightning protection industry) be pointed, because this leads to a point discharge. In earlier times, this point discharge (corona discharge) was considered necessary to 'attract' the lightning stroke. More recently, experiments showed that a smoothly rounded tip is more successful in attracting lightning to itself and avoid strikes to nearby objects[4]. The first comprehensive engineering guide to proper installation of lightning protection systems was published by Anderson[5] in 1879 and, perhaps surprisingly, few of his recommendations have been overturned by more modern research. Müller-Hillebrand[6] reviewed some of the early concepts of lightning protection.

A lightning protection system basically comprises three main components:

- air terminals
- downconductors
- ground terminals.

Franklin recommended that each air terminal provides a downward 'cone of protection,' with the cone's angle from vertical being 58°. The origin of this recommendation is unclear and it was evidently not evolved from experiments. Subsequent experience suggested that this angle is much too large, and during the 19th century the recommendations slowly went downward to about 30°. However, even using a 30° angle of protection, failures were documented[7]. In more recent times, Lee[7] synthesized a design method for protecting buildings, evolved from advanced calculations used by electric utilities for protection of power lines. The method is applicable only to structures of 45 m height or less and is described in the following way: Imagine a rolling sphere of 45 m radius (Figure 1). The sphere starts rolling along the ground from a distance far away from the structure in question, then roll up to and over the structure and its protective air terminal(s). If the sphere only ends up touching the air terminal(s) and the ground and cannot come into contact with the structure to be protected, then air terminals of sufficient height and quantity have been erected, otherwise additional protection is needed. This more realistic protection concept is more liberal than the 30° fixed-angle scheme for low structures and more conservative for high structures. The 45 m dimension is used because it corresponds to the typical length of the stepped leader, which is about 50 m.

In view of the enormous currents of around 20,000 A that are involved in a lightning strike (see Chapter 11), it is perhaps surprising that gigantic-size downconductors are not required to safely conduct the electricity. The minimum size of conductor does not need to be huge since the flow of current is so brief—much less than 1 s—and heating is proportional to the time of current flow. The simplest model that can predict this is the adiabatic lumped-capacitance model:

$$W = I^2 Rt = \rho CV(T_f - T_o)$$

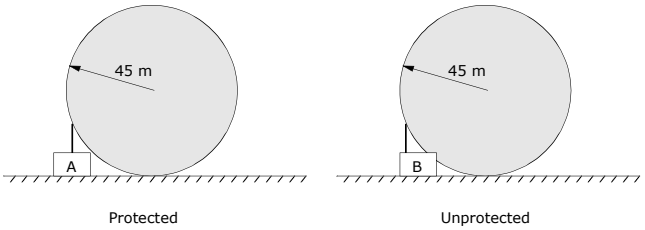


Figure 1 Sphere of protection from an air terminal: structure A is protected, structure B is not

where W = energy (J) flowing into a piece of metal, I = current (A), R = resistance (Ω), t = time (s), ρ = density (kg m^{-3}), C = heat capacity (J kg^{-1} K^{-1}), V = volume (m^3), T_f = final temperature (ºC), and T_o = initial temperature (ºC). This assumes that the current flow is constant over the time t; if the current flow is varying, then the expression becomes:

$$W = R\int I^2\, dt = \rho CV(T_f - T_o)$$

where R is assumed to be time-invariant and has been taken outside the integral. Applying the above relation to copper wire, ρ = 8890 kg m^{-3}, C = 385 J kg^{-1} K^{-1}, $V = A{\cdot}L$, where A = cross-sectional area (mm) and L = length (m). The resistance of a copper wire can be expressed as:

$$R = \rho_e \frac{L}{A}$$

where ρ_e = electrical resistivity of copper = 1.7241×10^{-8} Ω·m. The initial temperature T_o can be taken as 20ºC, while the final (allowable) temperature T_f must be set to some reasonable value below the melting point. Since the downconductor may come into contact with combustibles such as dry leaves, it seems appropriate to limit T_f to 200ºC. Based on studies of lightning discharges, $\int I^2\, dt = 5\times10^6$ $A^2{\cdot}s$ is commonly used. The equation can then be evaluated as:

$$1.7241\times10^{-8}\left(\frac{L}{A}\right)\cdot 5\times10^6 = 8890\times385\,(A\cdot L)180$$

and it can be noted that the actual length of the wire sensibly cancels out of the equation. This gives $A^2 = 1.4\times10^{-10}$ m^4, or $A = 1.18\times10^{-5}$ m^2 = 11.8 mm^2. If the temperature criterion were the melting point of copper (1083ºC), then A = 4.9 mm^2, using the same 'action integral' of 5×10^6 $A^2{\cdot}s$. The lumped-capacitance model is highly simplified since it ignores the variation of resistivity with temperature and ignores reactance in the circuit. Nonetheless, a simple model appears adequate and it formed the effective basis for sizing conductors in Poland; installations sized in this manner were found to be 95% effective[6].

In the US, however, a more conservative approach is taken, with conductor areas being greater than 11.8 mm^2, in order to allow for mechanical damage, some unusually potent lightning strikes, etc. The most commonly followed guidance is that published by NFPA[8]. NFPA 780 divides structures into two Classes, Class I being those up to 75 ft (22.9 m), with Class II being those higher. For Class I structures, the required downconductor area is 29 mm^2 for copper and 50 mm^2 for aluminum. The cross-sectional area required for copper conductors in Class II service is 2× that for Class I. Generally, stranded or braided conductors are used, to minimize loss of current-carrying capacity due to skin effect (this electromagnetic effect pertains to transient current flows and leads to current flowing disproportionately near the surface). A lead coating is often used to minimize loss of metal due to corrosion from flue gases. Properly-installed and maintained lightning protection systems are highly effective, with one report[9] quoting old US studies giving 99.3 and 99.9% effectiveness values.

For configuration of the air terminal, modern studies by Moore et al.[10] concluded that the optimum tip-height to tip-radius ratio is about 680. Thus, a rod erected at 10 m height ought to have a tip of 14.7 mm radius.

For protection of electric installations or electronic equipment, additional protection is often appropriate to provide in the form of *lightning arresters*. These provide a bypass path for current to ground so that it would flow in a path that does not lead to destruction or ignition. A variety of devices are available for this purpose, the most common ones being:

- spark gaps
- gas discharge tubes
- varistors.

High voltage transmission lines are so arranged that a ground conductor is at the topmost position; this plays a similar role to the lightning rod on a building. But a lightning strike can induce excessive current surges in power lines, even if the actual strike current goes into the ground conductor. Thus additional surge protection is usually installed, which often takes the form a spark gap. This is merely a fixed gap between a grounded conductor and one at an elevated voltage. The gap size is chosen so that the air will not break down under normal voltage conditions, but will break down under a lightning-caused surge. The bulk of the current then flows to ground instead of propagating along the network. For low-power equipment, the most common lightning arresters are metal-oxide varistors (see Chapter 14). Telephone companies traditionally used carbon block protectors, which, similar to a varistor, function as a voltage-dependent resistance. Gas discharge tubes, which are basically spark gaps in an enclosed, controlled atmosphere, are used in medium voltage applications where a permanent device is needed (varistors are sacrificial).

Another form of lightning protection is the *Faraday cage*—a cavity within a grounded metallic enclosure. Electric fields may exist outside the cavity, but the cavity remains field-free. The Faraday cage principle is serendipitously

exploited in the motor vehicle, where the occupants inside can expect to be safe from lightning.

Worldwide, the IEC standards[11,12,13] on lightning protection are the most widely followed. The IEC scheme is more calculationally oriented than the primarily-empirical NFPA standard. A good summary guide for the designer on the use of the IEC standards has been published by Wiesinger and Zischank[14]. Other guides to lightning protection include IEEE Std. 142[15], IEEE Std. 1100[16], UL 96A[17], and a variety of military and NASA standards.

Arresters—flame and spark

FLAME ARRESTERS

Flame arresters (sometimes called "flame traps") are devices that typically make use of the quenching distance principle. As was presented in Chapter 4, a flame cannot propagate through a small enough tube or cavity. This principle was recognized in 1815 by Sir Humphry Davy[18] who designed the first practical miner's safety lamp; a comprehensive review of the history of miner's safety lamps has been published[19]. The simplest flame arrester would be just a metal tube with a diameter less than d_T. But unless only a tiny flow is needed, a tube of diameter ca. 1 mm would not be practical. One solution is to make a sufficiently large bundle of tubes. Practical devices using this method have been made, as have ones where the cluster of tubes is replaced by a honeycomb structure. Other configurations include: crimped metal ribbons, sintered metal, metal foam, etc. A crimped metal arrester consists of layers of crimped metal, separated by layers of flat metal. This arrangement creates a series of cells, roughly triangular in shape.

Surprisingly, flame arresters that are effective for certain applications can be made from combustible materials. The US Air Force uses polyurethane foam as a bulk filling material for aircraft fuel tanks, to resist explosions caused by incendiary bullets fired into the tank[20]. The material was found to be about as functional as crimped or honeycomb aluminum arresters, but carrying a smaller weight penalty. The drawbacks are that, when a fuel/air aerosol passes through the foam, electrostatic charging can occur[21] and this has led to some accidents[22]. Thus, in certain applications, metallic flame arresters are required due to electrostatic aspects.

If a bundle of tubes is a viable flame arrester, can it be made short? A very short bundle of tubes or honeycomb, of course, becomes just a perforated metal sheet. Wire gauze is functionally nearly identical. There is disagreement about the efficacy of wire gauze and perforated metal flame arresters. Palmer[23] considers them suitable only for undemanding applications, and not viable elsewhere. The Health and Safety Executive[24] considers that a single-layer gauze arrester is viable if the maximum flame approach speed does not exceed 10 m s^{-1}; higher speeds can be tolerated by multilayer arrangements, but advice is not given. However, an extensive US Coast Guard testing program[25] concluded that wire mesh flame arresters are effective in a rather demanding application of 152 mm pipelines. In their test program, they found satisfactory performance with acetaldehyde, butane, diethyl ether, gasoline, methanol, propane, and toluene; only for ethylene were failures encountered. An arrester can also be made by passing the gas stream through a body of water or other liquid, since flame will not propagate through the bubbles[26,27]; these find use in specialized applications (Figure 2). For gases not compatible with water, fluids such as ethylene glycol or mineral oil are used. An incident is reported where hydraulic flame arresters successfully stopped the propagation of a detonation in a large acetylene pipeline[28].

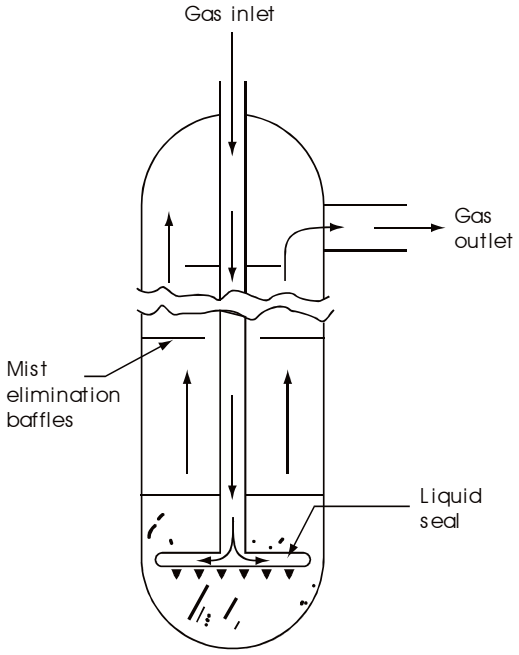


Figure 2 A hydraulic flame arrester
(Copyright © 1975 AIChE)

Certain types of flame arresters use neither quenching distance nor a liquid seal. Instead, they are based on the inability of a flame to propagate backwards into a mixture when the flow velocity through the orifices exceeds the velocity at which flame could propagate backwards[29]. Before this principle is adopted, it is prudent to consider whether there are operating conditions (e.g., startup or shutdown) when unexpected low velocities may occur, yet a flashback hazard still exists. The stoppage of pipeline deflagrations or detonations can also be accomplished by active systems, i.e., a quick-acting gate valve activated by a suitable pressure sensor[28].

The substances with the smallest quenching distances are carbon disulfide, acetylene, and hydrogen. Because acetylene is used in industry more widely than carbon disulfide, performance testing of flame arresters is often focused on

acetylene or acetylene mixtures with air or oxygen. In addition, the AIT of acetylene (ca. 300ºC), is lower than average for industrial gases, although in this respect acetylene is outranked by a number of other gases.

The design or testing of a flame arrester starts with the knowledge of the flame speed of the mixture. The actual flame speed, however, is not a handbook value but depends on turbulence. If long pipe lengths, obstructions, etc., cause a transition from deflagration to detonation to occur, the flame speeds become exceedingly large. This does not preclude design of flame arresters to cope with detonations, but the flame arrester must be robust enough, both mechanically and thermally, to survive an explosion. In some cases, mixtures can be expected to possibly detonate. When flame arresters are designed for such applications, mechanical strength becomes a top issue, since the pressures to be resisted for a detonation may be around 50 atmospheres, contrasted with 8 atm for deflagrations. Metal foam arresters have been shown to be able to resist acetylene detonations, if certain design guidelines are followed[30]. Sintered metal flame arresters have also been studied in connection with detonations of various gases[31].

Based on simple heat loss considerations, Palmer et al.[32] proposed that, provided each hole is smaller than the d_T for the fuel in question, a heat balance for the holes can be developed as follows. The Nusselt number is assumed to be a constant = 2.4. Then, the heat transferred convectively per unit wall area of tube is $2.4\bullet(T_f\text{-}T_w)/d$, where d = diameter of opening. The heat transferred per unit face area of the arrester is then $\dot{q}'' = \frac{2.4\lambda(T_f - T_w)}{d}\cdot\left(\frac{\pi y}{d}\right)\cdot\left(\frac{4F_a}{\pi}\right)$, where y = depth of each opening and F_a = fraction of face area occupied by openings (--). The flame front has a thickness x and travels past the arrester at a velocity v. Then the time that the arrester is exposed to flame heating is x/v. The heat that can be removed from the flame per unit face area of the arrester then is:

$$q'' = \frac{9.6\lambda(T_f - T_w)yF_a}{d^2}\frac{x}{v}$$

Now, if it is assumed that quenching occurs when q''' heat is removed per flame volume, then the maximum flame speed for which a perforated metal, gauze, or crimped metal flame arrester can be successfully used is:

$$v \le \frac{9.6\,\lambda\left(T_f - T_w\right)}{q'''}\frac{yF_a}{d^2}$$

where v = flame speed relative to arrester (m s^{-1}); λ = conductivity of flames (W m^{-1} K^{-1}); T_f = mean temperature of flame gases (K); T_w = temperature of flame arrester (K); and q''' = heat removal for quenching (J m^{-3}). For most hydrocarbons[33], at stoichiometric conditions the group of variables $\frac{\lambda(T_f - T_w)}{q''}$ is approximately 1.34×10^{-3} m^2 s^{-1}. This gives:

$$v \le 0.013\frac{yF_a}{d^2}$$

The relative velocity of flame is given by:

$v = S + |u|$ for flame propagation in the direction of gas flow

$v = S - |u|$ for flame propagation opposing the direction of gas flow

where S = laminar (or turbulent, as appropriate) flame speed (m s^{-1}), and u = bulk flow velocity of gas in pipe or vessel (m s^{-1}). Two cases arise (Figure 3) because the flame propagation may need to be stopped either in the direction of the gas supply or in the direction of products venting. Palmer showed reasonable agreement with experiment, but it must be remembered that theoretical computations can only be viewed as an aid in design of flame arresters, not as a proof of their performance—actual performance can only be evaluated by test.

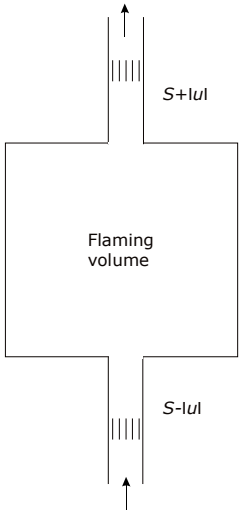


Figure 3 Two cases of flame velocity versus flow velocity

It is essential to appreciate the role of T_w in Palmer's equation. If T_w rises, then the velocity that the arrester is effective against will drop. Thus, if a flame is allowed to play upon an arrester for some time, it will likely break through.

While F_a may, in principle, vary from 0 to 1, in practical devices the range of variations will not be large. Thus, Wilson and Atallah[34] suggested that a useful correlation can be had without including that factor:

$$v \le \frac{0.005y}{d^2}$$

In all of the above equations, if the apertures are not circular, then the diameter should be replaced by the hydraulic diameter $d_H = 4A/P$, where A = area (m) and P = perimeter (m).

Unless the system can tolerate a large pressure drop, it is necessary that the flame arrester be fitted into a pipe section which is of much larger diameter than the normal pipe diameter. Cubbage[35] offers guidance on this point; commonly a diameter 3.5× the pipe diameter is suitable.

The development above assumed that there is negligible pressure rise for the flame. In systems where a substantial explosion pressure may be developed[24], the permissible velocity must be reduced by the ratio P_o/P, where P_o = atmospheric pressure (absolute), and P = explosion pressure (absolute). The performance of many flame arresters is very sensitive to pressure and an unanticipated overpressure can readily cause failure[36]. The condition of flame arresters must be carefully monitored if satisfactory performance is expected. Some large explosions have been attributed to damaged flame arresters, where a previous flame challenge had created void spaces[36].

The Bureau of Mines[37] developed a series of heat transfer models for predicting flame arrester performance; all of these, however, require use of computer programs and do not lead to closed-form equations or graphs.

Some practical advice on selecting flame arresters is given in a UK Guide[38] and by others[24,39]. The testing of flame arresters in the US is according to UL 525[40]. The standard is highly prescriptive and can be viewed as a specification, accompanied by a laboratory testing component. The UL 525 standard has a Continuous Flame test, which is used to examine the flashback potential from the flaming region into the premixed, unignited gas supply. There is also a non-preheated test that devices must pass and an optional test where the flame arrester is subjected to a series of explosions (deflagrations) and has to perform its function under those conditions. Separate test procedures govern devices intended to withstand pipeline detonations. IMO has a standard which governs the testing of flame arresters in tanker vessels[41]. Some practical experience with this test method has been reported by Dyer et al.[42]. In 2002 AIChE published a book[43] dealing with applications for and installation of flame arresters, including detonation arresters. A British method for testing flame arresters has also been published[44]. Howard offers a brief, but instructive guide from the US industry viewpoint[29]. Case histories of failures and design guidance is given by Lapp[45]. Babkin[46] has summarized recent Russian research on flame arresters.

SPARK ARRESTERS

Combustion engines can emit carbonaceous particles in the exhaust stream which may set vegetation and other combustibles on fire. For this reason tractors, locomotives, and other engines are often fitted with spark arresters. Spark arresters fall into two broad categories: screens and cyclones, although designs exist which combine both features. Screens are normally usable only if very few particles are being produced, since they could readily clog otherwise. Cyclones function by creating a swirl flow and using centrifugal force to deposit particles out of the gas flow stream and into a receptacle. Automotive mufflers do not function as effective spark arresters[47], fortunately there are not normally many sparks produced by gasoline-powered automobile engines.

The US Forest Service maintains a facility for testing spark arresters. Detailed descriptions of devices that pass the test are published in separate books for locomotive and general-purpose arresters[48] and for multi-position small engine arresters[49] used on chain saws and hand-held, gasoline-powered gardening equipment. The hazard is considered to be largely due to particles over 0.6 mm diameter, thus, the standards used for testing, SAE J335 and J350, are designed to trap or pulverize particles that are larger than 0.58 mm.

Pellet stoves often produce large quantities of burning particles, yet their exhaust systems rarely contain spark arrester devices. By contrast, fireplaces are often equipped with screens (sometimes called 'spark guards' or 'fire guards'). As discussed in Chapter 11, low density materials can be readily ignited by very small particles, and particle mass must be lower than about 30 mg before the ignition probability drops below 10%. For coal particles, 30 mg corresponds to a diameter of about 3.4 mm. Consequently, commercial screens having a grid size on the order of 12 mm would be of minimal effectiveness. The density of other fuels likely to be used in a fireplace is lower, but the theory discussed in Chapter 9 indicates that particle diameter is of greater importance than the mass in determining the smoldering ignition of a fuel bed, thus brands from other fuels may not require a much greater diameter to achieve ignition.

Design of electrical equipment for flammable atmospheres

In manufacturing, extraction, and related industries, there can be locations where atmospheres may contain flammable amounts of gas or dusts. If electrical equipment needs to be used in such a location, means have to be taken to ensure that the electrical equipment does not cause an explosion. The technology for achieving this has been in existence for a long time, starting in Germany with the massive studies of Beyling[50] in 1906. In the US, the primary guidance on the subject comes from the NEC. In most other countries, the requirements of the International Electrotechnical Commission (IEC) are used. In EU, the regional standards body CENELEC is further interspersed between international and national standards. A number of the concepts used by IEC have recently been introduced into the NEC and are here discussed under NEC Art. 505.

NEC REQUIREMENTS

The Code views that protection measures need to take the following into account:

- the likelihood of the atmosphere being flammable

- the ease of ignition of the atmosphere from an explosion occurring within a nearly-closed apparatus
- the ease of ignition from high temperatures.

To address these concerns, different provisions are made. The likelihood of the atmosphere being flammable is treated by the Classification of locations. The ease of ignition from internal explosions is dealt with by placing fuels into Groups. The ease of ignition from high temperatures is treated by use of 'T ratings.' The NEC then makes provisions for safe installation practices within the various locations. The actual details of design for electrical equipment intended to be suitable for hazardous locations (e.g., intrinsically safe or explosionproof) are left to UL standards to regulate. There is a large number of those, with the primary ones being UL 913[51], UL 1604[52], and UL 2279[53].

Originally, there was only one way according to which Classes, Groups and T-ratings were established. Starting with the 1996 edition, however, there are two parallel schemes—the traditional North American scheme (Art. 500), and the IEC scheme (Art. 505). Since most of the world followed the standards of IEC, it was considered helpful to multinational companies to permit, as an option, the international scheme.

ARTICLE 500 (TRADITIONAL CLASSIFICATION)

According to the traditional scheme, areas in which electrical equipment might need protective features against explosion hazards are divided in the following way:

- Class I, Division 1: flammable gas mixtures exist under normal operating conditions.
- Class I, Division 2: flammable gas mixtures exist only in closed containers or closed systems.
- Class II, Division 1: flammable dust mixtures exist under normal operating conditions; or presence of conductive dusts in hazardous quantities.
- Class II, Division 2: flammable dust mixtures may exist in case of equipment malfunction.
- Class III, Division 1: easily ignitable fibers exist under normal operating conditions.
- Class III, Division 2: easily ignitable fibers are stored or handled.

The Code is deliberately vague in its definitions of the Divisions to allow needed flexibility. Some experts consider[54] that if an explosive concentration is present > 100 h per year, the location should be Division 1, if between 10 and 100 h per year, Division 2, and if < 10 h per year, not Classified. A guide[55] has been developed in the UK which attempts to quantify the classifications by use of hazardous-substance release calculations and risk assessment, but it is not clear that real advantages accrue over 'intuitive' classification.

The actual atmospheres themselves differ in their hazards and their protection requirements. Thus, atmospheres are divided into Groups:

- Group A: acetylene. No other substances are placed into this Group.
- Group B: hydrogen. Also, butadiene, ethylene oxide, propylene oxide, acrolein.
- Group C: diethyl ether. Also, ethylene, cyclopropane, etc.
- Group D: gasoline. Also, numerous other gases and vapors.
- Group E: combustible metal dusts; other dusts having a resistivity less than 1.0 Ω·m.
- Group F: carbon black, charcoal, coal and coke dusts. Resistivity between 1.0 and 10^6 Ω·m.
- Group G: combustible dusts with a resistivity of 10^6 Ω·m or greater.

The Groups for gases/vapors were set out in terms of a 'reference material,' rather than by chemical properties. This establishment of the Groups was a committee action, not derived from a scientific study of the problem, although accompanied by *post hoc* testing at UL. The primary criterion for placing a substance into one of the Groups was the MESG value, as determined from UL's Westerberg apparatus. Only a small number of substances were actually tested and, for most, values were simply derived on the basis of committee opinion. Woinsky[56] attempted to deduce formulas that could assign substances into the NEC Groups, but this was not a fully successful venture, since the Groups were not evolved on the basis of quantitative computations.

In the original testing*, acetylene and hydrogen showed identical MESG values, but were placed in different groups, since acetylene is an unstable substance, while hydrogen is stable. Carbon disulfide was considered to be too hazardous to be included in any Group, even Group A. Unfortunately, the MESG is not the only criterion that has been used in the traditional classification of Groups for NEC. The Committee also factored in the maximum explosion pressure observed during test in the Westerberg apparatus. This is the reason for the dual classification of some substances. If the conduits connected to the electrical equipment placed in the hazardous location are sealed according to certain prescriptions, then the pressure-rise restrictions are considered not to apply, and the milder Grouping is used. For example, ethylene oxide is in Group B, but if the conduits are sealed it becomes Group C. The Groups for various gases and vapors are shown in Chapter 15.

Magison[54] has written at length about the problematic logic of the pressure-rise based Group treatment. There are basically two problems: (1) tests are done in the Westerberg apparatus under conditions that are dissimilar—and much harsher—than would be any explosion propagation that might reasonably be expected to occur in an electrical conduit installed in accordance with NEC provisions; and (2)

* UL later corrected the value for hydrogen, and it rose three-fold; see the discussion of MESG in Chapter 4.

when two rating factors are conflated to produce a single Group, the Group ratings can no longer be used for correlation to any physicochemical variables.

For the classifications of dusts, the NEC does not make this clear, but the National Academy of Sciences (NAS) study (see below) points out that not all combustible dusts fall within the NEC groups. Dusts of low ignition sensitivity and low explosion severity are not classified into the Groups needing special measures. The NAS study also recommended that Group F be abolished and that a breakpoint of 10^3 Ω·m be used to divide Groups E and G. Consequently, in the 1984 edition of the NEC, Group F was abolished. Group F was reinstated in the 1987 edition, because explosionproof motors intended to operate in metal-dust atmospheres need very close tolerances, and those are not required for conductive carbonaceous dusts. The classification of dusts continued to be contentious and substantive changes have been made in this section with nearly every new edition. In general, it has been observed[54] that there is no relation between the conductivity of a dust cloud and either its ignitability or the severity of a consequent explosion. Thus, any classification based on conductivity and, specifically, providing more stringent treatment for conductive dusts does not have a sound basis. The origin of the provision was the perception that conductive dusts might lead electrical parts to short out, and that this creates greater risk than non-conductive dusts. However, the whole purpose of dust-tight, pressurized, intrinsically-safe, etc., apparatus design is to arrange matters so that this does not happen; Magison[54] discusses in some detail the improbability of accidents occurring in the fashion envisioned by this provision.

The classification of gases, vapors, and dusts into the seven Groups has had a complicated history. Expert panels of the National Academy of Sciences were formed on behalf of the US Coast Guard and the Occupational Safety and Health Administration (OSHA). The panels had overlapping membership, but were not identical. Both panels were chaired by Homer Carhart, long-time head of fire research at the Naval Research Laboratory. The work for the Coast Guard resulted in a series of reports[57-61] during 1970 – 1976. These addressed only the classification of gases and vapors. The work on behalf of OSHA spanned 1979 – 1982 and comprised the NMAB 353 series of reports. Reports NMAB 353-1[62] and NMAB 353-5[63] classified gases and vapors, continuing the earlier Coast Guard work. Reports NMAB 353-2[64] and NMAB 353-3[65] were interim studies on the classification of dusts; these were superceded by NMAB 353-4[66]. The summary report was NMAB 353-6[67].

For dusts, arbitrary indices have been developed to determine whether a dust needs to be included in one of the Groups or not. Ignition sensitivity is defined as:

$$\text{Ignition sensitivity} = \frac{T_c \times E \times C}{(T_c \times E \times C)_{\text{Pittsburgh coal}}}$$

where T_c = dust cloud ignition temperature (ºC), as determined in the Godbert-Greenwald furnace; E = MIE of dust (J), as determined in the Hartmann apparatus; and C = minimum explosible concentration (g m^{-3}). The reference values for Pittsburgh coal are: T_c = 610ºC, E = 0.06 J, C = 55 g m^{-3}. Explosion severity is defined as:

$$\text{Explosion severity} = \frac{P \times \frac{dP}{dt}}{\left(P \times \frac{dP}{dt}\right)_{\text{Pittsburgh coal}}}$$

where P = maximum explosion pressure (atm), and dP/dt = maximum rate of pressure rise (atm s^{-1}), with both values being determined in the closed steel Hartmann apparatus. The reference values for Pittsburgh coal are: P = 5.56 atm, dP/dt = 156 atm s^{-1}. The criteria are that if Ignition sensitivity ¤ 0.2, or if Explosion severity ¤ 0.5, then the dust is included in one of the NEC Groups, otherwise it is not.

The actual classifications to be used in connection with NEC requirements are not published within the NEC itself but, rather, are given in NFPA 497[68] for gases and in NFPA 499[69] for dusts. In general, a user would only need to perform tests and use the above criteria if a substance is encountered that is considered to potentially be one that falls into one of the Groups. A number of special hazards, e.g., pyrophoric materials, are not placed under the general Class/Division/Group scheme, but require specific protection measures. In addition, a large number of NFPA standards deal with protection methods for specific industries or installations.

In order to avoid ignitions from hot surfaces, equipment for use in hazardous locations is to be marked with a temperature rating (T-rating). The equipment can then only be used in locations where the AIT of the gas or the layer ignition temperature of the dust is greater than the marked rating. For simplicity (although it hardly seems simpler), the ratings are not actual temperatures, but codes denoting temperature ranges, the code always beginning with the prefix 'T.' For example, T2B denotes a maximum temperature of 260ºC. The user must then find the AIT for the desired gas in NFPA 497 (or NFPA 325[70]) or the layer ignition for the dust in NFPA 499. As discussed in Chapter 4, the use of the AIT as a limit value for hot-surface ignitions is a very conservative approach, since the hot-surface ignition temperature will normally be hundreds of degrees Celsius higher than the AIT.

In the 1997 edition of NFPA 497 and the 1999 edition of NEC, the 'expert judgment' scheme for placing substances into various Groups was fundamentally reoriented and an IEC-based scheme adopted, as shown in Table 2. Curiously, this was not accompanied by a reclassification of actual substances, which remained listed in the groups as previously established.

Table 1 Revised criteria for Article 500 (traditional) classification 'Division system' of gases and vapors

Group	MESG (mm)	MIC ratio (--)
A	Acetylene only	
B	≤ 0.45	≤ 0.40
C	0.45 to 0.75	0.40 to 0.80
D	> 0.75	> 0.80

ARTICLE 505 (IEC CLASSIFICATION)

In this scheme, as originally developed in IEC 60079-10[71] and in use throughout most of the world, the classified areas are termed Zones:

- Zone 0: ignitable concentrations are present continuously, or for long periods of time
- Zone 1: ignitable concentrations are present in normal plant operation
- Zone 2: ignitable concentrations are present only in case of equipment failure.

Roughly, Zone 0 and Zone 1 correspond to Division 1, Zone 2 to Division 2. Within IEC, the classification into zones also extends to dusts, and is done according to IEC 61241-3[72]:

- Zone 20: hazardous atmosphere with regards to dust clouds continuously present
- Zone 21: hazardous atmosphere with regards to dust clouds present in normal operation
- Zone 22: hazardous atmosphere with regards to dust clouds present only for short periods of time

The NEC, however, had not adopted the IEC dust zones as of 2002.

Groups are defined in IEC as an extension of earlier work in the UK by the Safety in Mines Research Establishment:

- Group I: methane only.
- Group IIA: propane, etc.
- Group IIB: ethylene, etc.
- Group IIC: acetylene, carbon disulfide, hydrogen, etc.

Apart from the unique Group I, the others are determined solely by their MESG or MIC data, without need of expert judgment by committee. In the IEC scheme, the MIC (minimum igniting current; see *Ignition from breaking wire or moving contacts* in Chapter 4) is used as a ratio, obtained by dividing the substance's MIC by the MIC of methane. By doing this, it was felt that certain interlaboratory variations would be minimized. The selection rules are shown in Table 2. Note that either MESG or MIC ratio alone is sufficient to classify in most cases, but not all. If the MESG is between 0.5 and 0.55 mm then classification must proceed on the MIC. Conversely, if the MIC ratio is between 0.8 and 0.9, or between 0.45 and 0.5, then classification must be based on the MESG.

As discussed in Chapter 4, the agreement of UL and IEC values for MESG is poor. The reasons for the discordance

Table 2 Criteria for Article 505 (IEC) classification 'Zone system' of gases and vapors

Group	MESG (mm)	MIC ratio (--)
IIC	≤ 0.50	≤ 0.45
IIB	0.50 to 0.90	0.45 to 0.88
IIA	> 0.90	> 0.80

are mostly attributable to design flaws of the UL apparatus[†], thus, there is some expectation that classification will gradually move over to the IEC system. The current edition of NFPA 497 also contains an Appendix suggesting the use of a rule based on Le Chatelier's rule to compute MESG values for gas mixtures. Based on a limited validation, the agreement appears acceptable[73].

The limiting of surface temperatures according to T-ratings is also used in the IEC scheme, however, the groups are fewer in number.

DESIGN OF EQUIPMENT FOR HAZARDOUS LOCATIONS

With low-current electronic and electric equipment, there are two primary ways that they could be the cause of ignition of gases, vapors, or dust clouds: (a) by producing an electric arc; or (b) by becoming so hot that hot-surface ignition occurs. To guard against these eventualities, historically there have been two primary design methodologies: intrinsically safe design, and explosionproof design. For either methodology, one practical tenet is simply to put the minimum necessary electrical equipment into ignitable atmospheres. Thus, it is often possible to only put in simple transducers (thermocouples, float switches, etc.). All of the remaining instrumentation and the control devices (motors, solenoids, etc.) are then ideally located in a non-ignitable atmosphere. In practice, there are instances where such a strategy becomes impossible and, thus, devices such as explosionproof motors can be necessary.

The NEC has traditionally provided for design alternatives as summarized in Table 3. It might be observed that layer ignition temperatures for dusts are hardly similar within each of the NEC dust Groups, thus the logic of across-the-board requirements is unfortunate. With the introduction of Art. 505 in the 1996 edition, the European IEC designs became acceptable, as discussed below.

Letter designations for categories of protection were originally developed in Germany. IEC has taken over the use of these designations and now they are international:

Type 'd' – flameproof. This corresponds to the US terminology 'explosionproof.' Details are given in IEC 60079-1[74].

[†] Some of the problems were corrected when UL redesigned the chamber and provided a corrected (and reasonable) value for hydrogen. No other gases were rerun in the redesigned chamber, however, and there remain flagrant discrepancies (e.g., carbon disulfide, acetylene, pentane) in the official UL data.

Table 3 Summary of design options permitted by the NEC in the traditional scheme

Area	Equipment designs permitted
Class I, Division 1	Explosionproof Pressurized per Division 1 requirements Intrinsically safe *Also*: T-rating for equipment to be ❍ AIT of gas/vapor
Class I, Division 2	Explosionproof (or general-purpose, if only non-incendive or sealed components) Pressurized per Div. 1 or 2 requirements Intrinsically safe *Also*: T-rating for equipment to be ❍ AIT of gas/vapor
Class II, Division 1	Dust-ignition-proof Pressurized Intrinsically safe *Also*: max. temperature according to Group
Class II, Division 2	Dust-tight enclosure General-purpose enclosures permitted in some cases *Also:* surface temperature to be limited to 120ºC
Class III, Division 1	Tight covers, no holes Totally enclosed (in case of rotating machinery) Intrinsically safe
Class III, Division 2	Similar to Division 1

Type 'e' – increased safety. This involves design of equipment so that the probability of failure is made very low. It is described in IEC 60079-7[75].

Type 'i' – intrinsic safety. This is sub-categorized into '*ia*' and '*ib*.' Type '*ib*' is less strenuous than type "ia" and involves only one fault being simulated, instead of two. It is described in IEC 60079-11[76]

Type 'm' – encapsulation. It is described by IEC 60079-18[77]

Type 'n' – this is a catchall category that includes non-sparking apparatus, enclosed-break devices, restricted breathing, and other strategies; formerly called '*s*'. It is described in IEC/TR 60079-15[78]

Type 'o' – oil-immersed. It is described in IEC 60079-6[79].

Type 'p' – pressurization. It is described in IEC/TR 60079-2[80].

Type 'q' – powder filled. It is described in IEC 60079-5[81].

The apparatus itself is marked as "*Ex z*," where z denotes one of the above letters. In addition, the designation *Ex s* is used to denote a mixture of protection methods.

Eckhoff has pointed out that the philosophy of treating, on a more or less similar basis, the possibility of gas and dust explosions inside electrical equipment enclosures is flawed[82]. Enclosures can be easily designed to keep out sufficient dust that an explosible concentration inside cannot build up. Furthermore, it would be extraordinarily unlikely that an internal explosion would then occur at the same time that an explosible concentration continues to exist outside.

EXPLOSIONPROOF EQUIPMENT

Explosion proof equipment typically uses heavy casings to limit energy leakage. Under the explosionproof (also called 'flameproof') philosophy, it is not necessary to limit the generation of arcs or hot spots inside the equipment. Instead, it is presumed that an explosion may occur inside the device, but that the design of the device will prevent it from being communicated to the external atmosphere and causing an explosion in it. Heavy power devices, which could not be engineered to be intrinsically safe, can be qualified as explosionproof. The two main design criteria for explosionproof equipment are:

1. the enclosure must withstand the pressure of an internal explosion
2. all joints of the enclosure must be such that explosion products, as they leave the enclosure, are incapable of igniting gas which may be present in the surrounding atmosphere.

A safety factor is normally applied to the enclosure so that it should withstand 1.5 to 4 times the possible internal explosion pressure. The joints and connections must be tight enough not only to exclude flame from passing through, but also that non-flaming hot gas stream emerging from the enclosure would not be hot enough to ignite the external atmosphere. These requirements mean that physically the device will be enclosed in a heavy casing. In contrast, intrinsically safe devices do not require any special casing.

From an ignitability point of view, the main variable in explosionproof design is the Maximum Experimental Safe Gap (MESG). This is the maximum size opening between two flanges which, for certain specified conditions, will not permit flame propagation from the inside to the outside of the enclosure. There are conflicting constraints on the design process, since smaller gaps lead to higher internal pressures, making it more difficult to design an enclosure that will not shatter during the explosion. For making the experimental determination, IEC has standardized a 20 mL test bomb. Since leakage at flanges in industrial equipment is a common situation that could lead to explosion, the test apparatus creates the gap between two simulated flanges. The test method has already been described in Chapter 4.

For consistency, standard testing and reporting of MESG data on gases and vapors must use a standard flange dimension. The MESG values determined by the IEC or equivalent UK test apparatuses (see Chapter 14) were measured using a 25 mm flange length (length being considered the distance along which escaping gases must travel). The UL

values were obtained with a 19 mm flange. Shorter flange lengths provide less opportunity to cool down the escaping gases, thus effectively requiring smaller gaps in order to avoid flame breakthrough. In actual instruments, flanges greater than 25 mm would be uncommon, but lesser dimensions are common. Magison[54] reviewed literature on the influence of flange length and concluded that each decrease of length by 2× decreases the actual MESG by about 1.3×.

An especially strenuous condition inside explosionproof equipment is a high-power electric arc. Steel enclosures of insufficient strength can be burst, aluminum enclosures burned through by arcing to case, and polymeric enclosures ignited, as shown by a series of German tests[83]. If a high-current arc takes place, it has been shown that transmission of explosion can take place with a flange gap possibly much smaller than the MESG. In one series of tests[83], it was shown that if an arc is so situated that it can directly expel particles through the gap, a gap as small as 0.28 mm may transmit an explosion in methane/air mixtures. But in another study[84] even a 0.2 mm gap transmitted particles that ignited a methane/air mixture. For these incidents, while a flammable mixture explosion inside the case helps to keep the escaping particles hot, it is thought that the phenomenon may also occur without a flammable mixture inside the enclosure at all, merely upon the creation of an energetic arc. The latter would not be likely inside instrument cabinets, but may be very likely within enclosures containing power-switching devices. A practical solution was found to be the introduction of a right-angle bend into the flanges, which effectively decelerates and cools any particles[84]. It was also shown that coal particles exploding inside a case have much too low an energy to cause a particle-ignited explosion outside the case[84].

In some cases, it can take very little leakage to convey a gas to a location where it creates a hazard. Individual wire strands in a stranded-conductor wire have been known to allow a detectable leakage of gas to pass[85].

DUST-IGNITION-PROOF EQUIPMENT

For use in Class II, Division 1 areas, NEC specifies that the design of explosionproof equipment shall be according to UL 1203[86]. The requirements basically involve tight-fitting joints and thick walls. The requirements can be substantially costly, so there is incentive to arrange processes so that areas are in Division 2 rather than Division 1. For Division 2, only normal dust-tightness is required.

INTRINSICALLY SAFE EQUIPMENT

Intrinsically safe equipment is one in which the possible energy/heat sources are such that—under both normal and failure mode operation—an ignition will not occur to an atmosphere where a specific vapor, dust, etc. is present in its most easily ignitable concentration. Such designs normally exhibit the following characteristics:

(1) Very low power consumption.
(2) No electrical components which could store (and later discharge) a significant amount of energy. In practice, this means that values of capacitance and inductance must be kept very low. If higher values are needed, sometimes it is possible to arrange diode shunts which do not interfere with normal function, but which limit the amount of energy that could be made available in case of fault.
(3) Protection circuits to limit the current that can flow into the device. Zener diodes placed across power supplies are a common way of meeting this requirement.

Devices with minimal capability of storing or generating energy can automatically qualify as intrinsically safe equipment. A device which cannot generate or store more than 1.2 V, 0.1 A, 20 mJ, or 25 mW under normal or failure conditions qualifies without further testing. Such a device is exemplified by a thermocouple, which generally produces less than 0.1 V. The limits are very tough to meet and devices other than transducers will rarely qualify. A device within these limits is sometimes referred to as a *simple apparatus*.

In the English-speaking world, the concept of intrinsic safety was first studied by Wheeler[87] in 1915, although only limited research was done until the 1940s. At that time the Safety in Mines Research Board (now the UK Health and Safety Executive) began concerted research which has been the basis of intrinsic safety designs worldwide, not just in the UK.

In US practice, intrinsically safe systems are designed to be safe against two simultaneous failures of components or wiring. This ensures that the probability of actual system failure is very low. When the application is to areas where the presence of a flammable gas atmosphere is itself a rare event, the consideration of only one component failure should be sufficient. This is the tactic taken by IEC 60079-11[76], which provides for two levels of protection. Type '*ia*' is suitable for Zone 0 and involves simulating two faults; Type '*ib*' is suitable for Zone 1 and involves simulating only one fault. Even the '*ib*' philosophy has been criticized as resulting in a grossly over-conservative equipment design[88] if mechanical failure alone is considered; accidental explosions usually involve human errors and not just equipment failures of approved, intrinsically-safe equipment.

A number of subtle points exist in actual equipment design. For instance, no wire strand should be too *small* in diameter. This is because it takes less current to heat up a thin strand to high temperatures than a thick one. The assumption is made that a wire strand can get detached from the wire of which it is part, short out against some other component, then proceed to heat up.

Non-incendive equipment is a less robust category of intrinsically safe equipment, with less stringent requirements. In the NEC, it is permitted in Division 2 areas where there is only a low probability of flammable gas mixture presence. Within Europe, the various forms of protection encompassed within IEC 60079-15[78] are effectively non-incendive designs.

Test methods: UL 913 and IEC 60079-11

The UL 913 standard[89] is primarily a prescriptive document on how intrinsically safe equipment must be designed. Additional parts of the document comprise an extensive series of instructions on how multiple faults are to be created in the test equipment, and a demonstration that must be made that the faults do not lead to potential ignition conditions. Apart from physical testing, the primary test which is called out in UL 913 is the break-flash apparatus developed at the Physikalische-Technische Bundesanstalt (PTB) in Germany and adopted in IEC 60079-11[76]. The apparatus consists of an explosion-proof chamber which is charged with a particular flammable gas mixture pertinent to the certification sought. Components in the equipment under test are identified where a spark discharge might occur under some failure condition. In place of that component, the electrodes of the break-flash apparatus are substituted and electrical conditions imposed which represent a circuit fault condition which it is desired to simulate. The history leading to adoption by the IEC of the PTB apparatus, in preference to devices developed in several other countries, has been reviewed by Bossert[90].

The electrode arrangement consists of two counter-rotating discs. One disc is a metal contact plate, while the other disc holds out 4 tungsten wires. The contact plate has two grooves and the tungsten wires rotating past alternatingly make and break contact. To pass, 400 revolutions without ignition are required for DC circuits and 1000 revolutions for AC circuits. The test apparatus can only be inserted into a low-current device[91], since the 0.2 mm diameter tungsten electrodes are not capable of carrying currents over 3 A.

A break-flash arrangement is used, since at the low voltages present in most intrinsically safe equipment, contact separation is the main means by which an incendive spark might be produced. In the break-flash test, the conditions needed to cause ignition are conventionally described in terms of a current for a given circuit inductance; calculation in terms of actual energy is not undertaken. A cadmium plate is used because it results in the lowest ignition currents being recorded. The test has been criticized[92] for this reason, since cadmium would not reasonably be specified in intrinsically safe equipment (although cadmium is commonly used in general-purpose electrical equipment and a possibility can may exist that cadmium-containing devices might be improperly introduced during repairs or maintenance). A BM study[93] indicated that brass and lead are the next most sensitive materials, with steel being the least sensitive. A UK study showed that the MIC reported in the IEC/PTB apparatus is directly proportional to the minimum arc voltage for the particular metal used for making the disc (see Chapter 11), and cadmium shows one of the lowest values. The sensitivity results are roughly proportional to the boiling point of the metal, cadmium being the lowest boiling point metal used in the testing. As a consequence, UL 913 permits the substitution of a brass plate, if cadmium, zinc, or magnesium are not used in the circuit. It is not clear why the characteristics of the wire electrode do not need come into the relation, especially since tungsten has one of the highest values for minimum arc voltage and for boiling point. Even without the use of a cadmium plate, the UL 913 standard represents an extraordinarily conservative strategy. While, by itself, this cannot be a criticism, the fact that neither a risk analysis nor a cost-benefit analysis ever appear to have been undertaken as tools for identifying desirable safety factors can be viewed as a limitation.

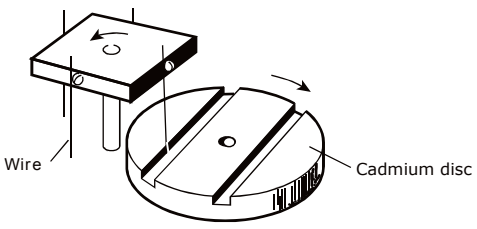


Figure 4 Detail of the counter-rotating mechanism in the IEC/PTB break-flash apparatus

A detailed explanation of the arc behavior in the IEC/PTB apparatus has been provided by Zborovszky[94]. The stochastic nature of ignition in the test apparatus has been studied by Cawley[95], who demonstrated that the probability of ignition has a power-law dependence on the circuit current, $P \propto I^n$. Over the experimental range of $10^{-6} < P < 10^{-3}$, he suggested $n \approx 10$ but Thomas[96] recommends $n \approx 16$. Zborovszky provided experimental details indicating that the large amount of statistical variability is due to the fact that only rare discharges are of a long enough duration (> 1 ms) so that a significant amount of power can get transferred into the arc; for unexplained reasons, in other trials arcing terminates quickly and ignition cannot then take place. Zborovszky[97] criticized the use of tungsten (rather than copper) wire in the IEC/PTB apparatus, since it creates an unrealistic worst-case scenario.

Test methods: HSE high-current apparatus

The IEC/PTB is not designed to cope with conditions that represent battery-operated apparatuses, i.e., a low-voltage, high-current, limited-duration (under short-circuit conditions) power supply. Consequently, HSE recently developed an apparatus for this purpose[98]. The apparatus is called STA, spark test apparatus, and basically involves a further development of the IEC/PTB apparatus to address the needs of the new test conditions.

Test methods: SMRE tests

The Safety in Mines Research Establishment in England conducted extensive research on intrinsically safe equipment for coal mines and developed two test apparatuses: (1) Break-flash Apparatus No.3; and (b) the Intermittent Break-flash Apparatus. The Break-flash No.3 apparatus[99] (Figure 5) simulates a fast snapping break of a wire. The physical device resembles an automotive distributor and provides a current break every 2 s. In a typical circuit, the slow cycling will provide for a potentially incendive spark only at the 'make' position of the contacts. The test method is intended to be used to simulate high-inductance circuits. The Intermittent Break-flash Apparatus simulates a failure where individual strands of wire may brush against another contacting surface in a random manner. This device cycles rapidly and provides a spark at both the 'make' and 'break' positions in most circuits. The test voltage is 24 V, because this corresponds to a voltage commonly found in coal mine equipment. The test method is intended to be used to simulate low-inductance circuits (typ. 1 mH). The history of these test equipment has been reviewed by Haig et al.[100] Thomas has reviewed some more rarely used equipment[101]. It is considered that the SMRE break-flash apparatus No. 3 is not as sensitive as the IEC/PTB apparatus, that is, the values of MIC reported from it are higher than those from the IEC apparatus[54]. The SMRE tests are now only of historical interest.

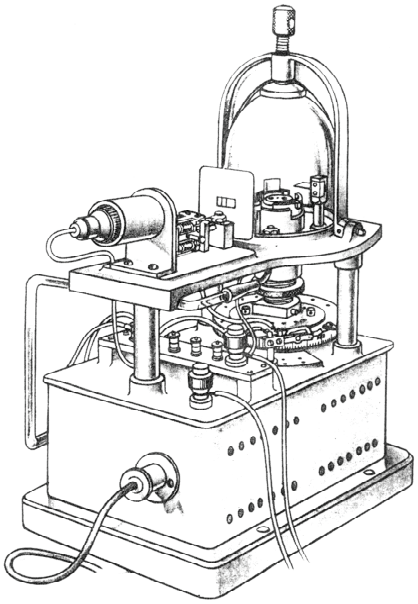


Figure 5 The SMRE Break-flash No. 3 apparatus (the contacts can be seen inside the bell jar)

INCREASED SAFETY PROTECTION

This is an old German protection system which has become part of the IEC system as Type 'e' protection, and in English is known by the very vague '*increased safety*' name. Its application is mainly to devices that use or produce significant amounts of power, e.g., motors, generators, transformers, and power distribution equipment, rather than to instruments and control systems. Conceptually, the scheme is similar, but less robust than intrinsic safety, Type 'i' protection. Consequently, unlike intrinsic safety, which can be used in all Zones, Type 'e' protection can be used in all Zones except Zone 0. Rules for constructing Type 'e' equipment are given in IEC 60079-7[75]. In the US, this document has been the basis of ISA S12.16[102], but usage of this means of protection in North America has been limited.

PRESSURIZED ENCLOSURES

In some cases, it is possible to avoid the cost and complexity of intrinsically safe or explosionproof equipment by providing a clean source of purging air for electrical equipment. These are termed pressurized enclosures (or *purged enclosures*) and design details are specified in NFPA 496[103]. Additional guidance is given in ISA RP12.4[104]. The international equivalent is IEC 60079-2[80]. For Group A or Group B gases, the MESG values are so small that it can be difficult to build large explosionproof equipment to the needed tolerances. Consequently, the pressurized option can allow a more economical design.

SEALED, ENCAPSULATED, OIL-IMMERSED, AND POWDER-FILLED DEVICES

Safety of electrical equipment can be ensured by surrounding the electrical parts with a medium through which flame will not propagate. This is more commonly done for small parts than for entire instruments, and is more common in Europe than in North America. In the case of sealed (sometimes called *hermetic sealed*) equipment, a gas-tight physical barrier creates the separation. The nomenclature implies that no gas can pass the barrier, but this, of course, is not true, since even good seals can be slowly permeated by gas. Thus, in principle, such a scheme should not be used in locations where the external gas concentration is always above the LFL, since eventually a flammable concentration could build up inside the encapsulated equipment. Within the US, ISA S12.12[105] describes testing and qualification of sealed equipment; internationally, IEC 60079-15[78] governs sealed equipment.

Encapsulation is very similar to sealing, but denotes that the device is completely potted in compound of very low gas permeability. Internationally, IEC 60079-18[77] governs encapsulated equipment; no comparable standard exists in the US.

Immersing the contacts in oil can also separate an arc from a flammable atmosphere, but this is not true for all oil-filled equipment, some of which are not intended for use in hazardous atmospheres. In the US, UL 698[106] prescribes requirements for oil-immersed equipment. Internationally, IEC 60079-6[79] governs.

Powder-filling with sand, for example, effectively acts as a flame arrester. Internationally, IEC 60079-5[81] governs; its use in the US is not common.

MISCELLANEOUS PROTECTION STRATEGIES

Several additional design strategies are used in Europe and are outlined in IEC 60079-15[78] but are not common in North America. *Enclosed-break* protection is similar to explosionproof design, but with less stringent requirements. *Restricted breathing* protection is of Swiss origin[107] and involves design of equipment to be used in locations where only temporary excursions above the LFL will occur. The principle ensures that gas concentration within the equipment will stay below the LFL during these events.

DESIGN OF EQUIPMENT FOR MINING

Because of historical reasons, most countries have had (and continue to have) different requirements for explosion safety in mining applications than in manufacturing industries. The requirements in the US for 'permissible electrical equipment' are set out by the Mining Safety and Health Administration (MSHA) under Title 30 of the Code of Federal Regulations (CFR). MSHA carries on the system of approving equipment that was previously administered by the Bureau of Mines.

Arc fault and cord fault interrupters

As discussed in Chapter 14, in branch circuit wiring the current flow through an arc fault is unlikely to trip a circuit breaker. Thus, the patent literature contains a wide variety of devices invented to react to an arc fault. By definition, these devices analyze and act upon a signature of the arcing condition that is not simply an over-current. A survey conducted as part of a 1995 UL study[108] identified that at least 16 US patents had been issued for arc fault protection devices up to that time. According to the National Electrical Code, certain circuits will have to be protected by AFCI (arc fault circuit interrupter) devices starting in 2002[109].

Based on the 1995 study, and a 1996 study[110] which examined various non-sinusoidal waveforms associated with normal-use equipment (e.g., welders, motors, lamp dimmers, etc.), UL issued standard UL 1699 on arc fault interrupters in 1999.

The two best-known solutions to the AFCI problem are those by Blades and by Engel. The Blades invention[111] consists of monitoring for radio-frequency noise induced by arcs. A microprocessor-based signal radio-frequency monitoring device receives signals in the range of 1 – 10 MHz. The signal caused by arcing is unique in that it drops to zero 120 times per second, i.e., at every zero crossing of current. The circuit then identifies an arc as present if (a) a strong enough RF signal is present on the power line; and (b) the signal goes to zero 120 times a second. It was found that it is possible to distinguish the arcing signal from solid-state control devices that might also introduce RF into the lines since the latter introduce spikes of much shorter duration than does arcing. The detector can be incorporated into a conventional circuit breaker. But it is also possible to construct a stand-alone, plug-in detector which sounds an alarm upon decoding the arc fault signal.

The Engel et al. invention[112,113], commercialized by Cutler-Hammer/Eaton Corp., was designed to avoid the cost of a microprocessor. It creates a signal which is proportional to a step-increase in current. An analog integrator is used to cumulate this signal so that either one very large step-increase or a rapid succession of smaller ones suffice to trigger the interrupter. The time constants of a circuit of this kind have to be such as not to lead to nuisance tripping when sizable loads go on-line, nor when dimmers or other devices that create abrupt steps in current go into service. Physically, the device is incorporated into a regular molded-case circuit breaker.

In selecting an arcing signature to detect, an arc fault interrupter must avoid false shutdown due to normal-use devices that exhibit unusual voltage or current waveforms. Such devices include switching-mode power supplies and light dimmers[114]. There will be an arc when some devices are turned on or off and a viable AFCI must not be triggered by such benign arcing[115].

An interesting ignition-preventing concept for electric cords has recently been described[116]. In this cord, termed CFCI—Cord Fault Circuit Interrupter—each conductor is separately shielded with a braid over the individual wire insulation. In normal operation, the braid does not carry any current. Current which does start flowing in the braid indicates a fault has developed and an integrated current-sensing device is triggered which interrupts current to the primary conductors. This scheme is similar to the ground fault circuit interrupter which measures the current flowing in the circuit (hot and neutral) and opens the protection device in the event of an imbalance.

Further readings

NFPA publishes a huge variety of Standards, Guides, and Codes offering guidance on preventive measures. AIChE and its subsidiary, Center for Chemical Process Safety, publish a wide variety of material on preventive topics in connection with the design of chemical manufacturing plants.

Wolfgang Bartknecht, **Explosions: Course, Prevention, Protection**, Springer-Verlag, Berlin (1981). Contains a good, wide-ranging presentation of flame arresters.

Ernest C. Magison, **Electrical Instruments in Hazardous Locations**, 4th ed., ISA, Research Triangle Park NC (1998). This is the most comprehensive US monograph on the topic; it is not an introductory tutorial and presumes that the reader is already familiar with most of the concepts.

Peter E. Schram and Mark W. Earley, **Electrical Installations in Hazardous Locations**, 2nd ed., NFPA, Quincy MA (1997). This book is focused primarily on detailed interpretations of NEC requirements for chemical plant engineers.

Alan McMillan, **Electrical Installations in Hazardous Areas**, Butterworth-Heinemann, Oxford, UK (1998). This is similar to Schram's book, but written for the designer needing to understand how to comply with European CEN requirements for hazardous areas.

Wiring Practices for Hazardous (Classified) Locations Instrumentation. Part I: Intrinsic Safety (ANSI/ISA PR12.6), ISA, Research Triangle Park NC (1995).

References

1. National Electrical Code (NFPA 70), NFPA.
2. Schofield, C., and Abbott, J. A., **Guide to Dust Explosion Prevention and Protection. Part 2—Ignition Prevention, Containment, Inerting, Suppression and Isolation**. The Institution of Chemical Engineers, London (1988).
3. Cross, J. A., **Electrostatics: Principles, Problems and Applications**, Adam Hilger, Bristol, England (1987).
4. Frydenlund, M. M., **Lightning Protection for People and Property**, Van Nostrand Reinhold, New York (1993).
5. Anderson, R., **Lightning Conductors: Their History, Nature and Mode of Application**, E&FN Spon, London (1879).
6. Müller-Hillebrand, D., The Protection of Houses by Lightning Conductors—An Historical Review, *J. Franklin Institute* **274**, 34-54 (1962).
7. Lee, R. H., Protection Zone for Buildings against Lightning Strikes using Transmission Line Protection Practice, *IEEE Trans. Industry Applications* **IA-14**, 465-470 (1978).
8. Standard for the Installation of Lightning Protection Systems (NFPA 780), NFPA.
9. The Basis of Conventional Lightning Protection Technology: A Review of the Scientific Development of Conventional Lightning Protection Technologies and Standards, Federal Interagency Lightning Protection User Group, [n.p] (2001).
10. Moore, C. B., Rison, W., Mathis, J., and Aulich, G., Lightning Rod Improvement Studies, *J. Applied Meteorology* **39**, 593-609 (2000).
11. Protection of Structures against Lightning - Part 1: General Principles (IEC 61024-1), International Electrotechnical Commission, Geneva.
12. Protection of Structures against Lightning - Part 1-1: General Principles - Guide A: Selection of Protection Levels for Lightning Protection Systems (IEC 61024-1-1), International Electrotechnical Commission, Geneva.
13. Protection of Structures against Lightning - Part 1-2: General Principles - Guide B: Design, Installation, Maintenance and Inspection of Lightning Protection Systems (IEC 61024-1-2), International Electrotechnical Commission, Geneva.
14. Wiesinger, J., and Zischank, W., Lightning Protection, pp. 33-64 in **Handbook of Atmospheric Electrodynamics**, vol. 2, H. Volland, ed., CRC Press, Baton Rouge FL (1995).
15. Recommended Practice for Grounding of Industrial and Commercial Power Systems (IEEE Std. 142), "IEEE Green Book," IEEE Standards Dept., Piscataway, NY.
16. Recommended Practice for Powering and Grounding for Sensitive Electronic Equipment (IEEE Std. 1100), "IEEE Emerald Book," IEEE Standards Dept., Piscataway, NY.
17. Installation Requirements for Lightning Protection Systems (UL 96A), UL.
18. Davy, H., On the Fire-Damp of Coal Mines, and on Methods of Lighting the Mines so as to Prevent Its Explosion, *Phil. Trans. Royal Soc.* 1-24 (1816).
19. Hardwick, F. W., and O'Shea, L. T., Notes on the History of the Safety-Lamp, *Trans. Institution Mining Eng.* **51**, 553-724 (1915/16).
20. Kuchta, J. M., Cato, R. J., and Gilbert, W. H., Flame Arrestor Materials for Fuel Tank Explosion Protection (Tech. Report AFAPL-TR-70-40) Wright-Patterson Air Force Base, Ohio (1970).
21. Leonard, J. T., and Affens, W. A., Electrostatic Charging of JP-4 Fuel on Polyurethane Foams (NRL Report 8204), Naval Research Lab., Washington (1978).
22. Bustin, W. M., and Dukek, W. G., **Electrostatic Hazards in the Petroleum Industry**, Research Studies Press, Letchworth, Herts., England (1983).
23. Palmer, K. N., and Rogowski, Z., W., The Use of Flame Arresters for Protection of Enclosed Equipment in Propane-Air Atmospheres, pp. 76-85 in *Proc. 3rd Symp. on Chemical Process Hazards with Special Reference to Plant Design* (Symp. Series No. 25), The Institution of Chemical Engineers, London (1968).
24. Phillips, H., and Pritchard, D. K., Performance Requirements of Flame Arresters in Practical Applications, pp. 47-61 in *Hazards in the Process Industries: Hazards IX* (IChemE Symp. Series No. 97), The Institution of Chemical Engineers, Rugby, England (1986).
25. Bjorklund, R. A., Kushida, R. O., and Flessner, M. F., Experimental Evaluation of Flashback Flame Arrestors, *Plant/Operations Progress* **1**, 254-262 (Oct. 1982).
26. Ministry of Labour, Guide to the Use of Flame Arresters and Explosion Reliefs (Safety, Health and Welfare; New Series No. 34), HMSO, London (1965).
27. Rubach, T., Schecker, H.-G., Jäger, W. R., and Onken, U., Investigations on Increasing Safe Gas Volumetric Flow Rate Through a Water Trap Flame Arrester, *Chemical Engineering & Technology* **15**, 15-20 (1992).
28. Sutherland, M. E., and Wegert, H. W., An Acetylene Decomposition Incident, *Chem. Eng. Prog.* **69**:4, 48-51 (1973).
29. Howard, W. B., Flame Arresters and Flashback Preventers, *Plant/Operations Progress* **1**, 203-208 (Oct. 1982).
30. Barton, R. R., Carver, F. W. S., and Roberts, T. A., The Use of Reticulated Metal Foam as Flash-back Arrester Elements, pp. 223-233 in *Proc. Symp. on Chemical Process Hazards with Special Reference to Plant Design—V* (Symp. Series 39a), The Institution of Chemical Engineers, London (1974).
31. Lietze, D., Limit of Safety against Flame Transmission for Sintered Metal Flame Arrester Elements in the Case of Flashback in Fuel Gas/Oxygen Mixtures, *J. Loss Prev. Process Industries* **8**, 325-329 (1995).

32. Palmer, K. N., and Tonkin, P. S., The Quenching of Flames by Crimped Ribbon Flame Arresters (FR Note 438), Fire Research Station, Borehamwood (1960).
33. Palmer, K. N., and Tonkin, P. S., The Quenching of Flames of Various Fuels in Narrow Apertures, *Combustion and Flame* **7**, 121-127 (1963).
34. Wilson, R. P., and Atallah, S., Design Criteria for Flame Control Devices for Cargo Venting Systems (CG-D-157-75), Office of Research & Development, US Coast Guard, Washington (1975).
35. Cubbage, P. A., The Protection by Flame Traps of Pipes Conveying Combustible Mixtures, pp. 29-34 in *Proc. 2nd Symp. on Chemical Process Hazards with Special Reference to Plant Design* (Symp. Series No. 15), Institution of Chemical Engineers, London (1963).
36. Roussakis, N., and Lapp, K., Comprehensive Test Method for Inline Flame Arresters, *24th Loss Prevention Symp.*, AIChE (1990).
37. Edwards, J. C., Thermal Models of a Flame Arrester (RI 9378), Bureau of Mines, Pittsburgh (1991).
38. Flame Arresters and Explosion Reliefs, Health & Safety Series Booklet HS(G)11, Health and Safety Executive, London (1980).
39. Bishop, K., and Knittle, T., Do you have the 'right' flame arrester in service? *Hydrocarbon Processing* **72**, 99-101 (February 1993).
40. Standard for Flame Arresters (UL 525), UL.
41. Revised Standards for the Design, Testing and Locating of Devices to Prevent the Passage of Flame into Cargo Tanks in Tankers (MSC/Circ. 677), International Maritime Organization, London (1994).
42. Dyer, J. H., Richards, R. C., and Wolverton, C. D. jr., Testing of Flame Screens and Flame Arresters as Devices Designed to Prevent the Passage of Flame (DPPF) into Tanks Containing Flammable Atmospheres According to an IMO Standard (CG-M-3-90), US Coast Guard, Marine Safety Laboratories, Groton CT (1989).
43. **Deflagration and Detonation Arresters**, AIChE (2002).
44. Explosion Protection of Equipment with Flame Arresters—Specification of Methods of Test and Construction (FR Note 974), Fire Research Station, Borehamwood, England (1974).
45. Lapp, K. O., Flame-arrester Failures Illustrate Needed Design Changes, *Oil & Gas J.* **91**, 70, 75-76 (29 Mar. 1993).
46. Babkin, V. S., The Problems of Porous Flame-Arresters, pp. 199-213 in **Prevention of Hazardous Fires and Explosions: The Transfer to Civil Applications of Military Experiences**, V. E. Zarko et al., eds., Kluwer Academic Publishers, Dordrecht (1999).
47. Fairbank, J. P., and Bainer, R., Spark Arresters for Motorized Equipment, Bulletin 577, pp. 3-42, University of California Experiment Station (1934).
48. NWCG Fire Equipment Working Team, Spark Arrester Guide. Vol. 1. General Purpose and Locomotive (LP/Loco), National Wildfire Coordinating Group, US Forest Service Technology & Development Center, San Dimas CA. Distributed through National Interagency Fire Center, Boise ID.
49. NWCG Fire Equipment Working Team, Spark Arrester Guide. Vol. 2 Multiposition Small Engine, National Wildfire Coordinating Group, US Forest Service Technology & Development Center, San Dimas CA. Distributed through National Interagency Fire Center, Boise ID.
50. Beyling, C., Versuche zwecks Erprobung der Schlagwettersicherheit besonders geschützter elektrischer Motoren und Apparate sowie zur Ermittlung geeigneter Schutzvorrichtungen für solche Betriebsmittel, ausgeführt auf der berggewerkscahftlichen Versuchstrecke in Gelsenkirchen-Bismarck [Experiments for the Purpose of Testing the Safety in Firedamp of Certain Protected Motors and Equipment, as Well as the Determination of Suitable Protective Arrangements for such Equipment, Carried out at the Experimental Gallery in Gelsenkirchen-Bismarck], *Glückauf (Essen)* **42**, 1-9, 34-42, 70-74, 93-99, 165-171, 201-206, 237-244, 273-278, 301-306, 338-346, 373-383, 409-418 (1906).
51. Intrinsically Safe Apparatus and Associated Apparatus for Use in Class I, II, and III, Division 1, Hazardous (Classified) Locations (ANSI/UL 913), UL.
52. Electrical Equipment for Use in Class I, and II, Division 2, and Class III Hazardous (Classified) Locations (UL 1604), UL.
53. Electrical Equipment for Use in Class I, Zone 0, 1, and 2 Hazardous (Classified) Locations (UL 2279), UL.
54. Magison, E. C., **Electrical Instruments in Hazardous Locations**, 4th ed., ISA, Research Triangle Park NC (1998).
55. Cox, A. W., Lees, F. P., and Ang, M. L., **Classification of Hazardous Locations**, Institution of Chemical Engineers, Rugby (1990).
56. Woinsky, S. G., Predicting Flammable-Material Classifications, *Chemical Engineering* **79,** 81-86 (Nov. 27, 1972).
57. Fire Hazard Classification of Chemical Vapors Relative to Explosion-proof Electrical Equipment (10 Feb. 1970).
58. Fire Hazard Classification of Chemical Vapors Relative to Explosion-proof Electrical Equipment, Report III (USCGD-92-74), US Coast Guard, Washington (1974).
59. Fire Hazard Classification of Chemical Vapors Relative to Explosion-proof Electrical Equipment (USCGD-109-74), US Coast Guard, Washington (1974).
60. Fire Hazard Classification of Chemical Vapors Relative to Explosionproof Electrical Equipment, Report IV, National Research Council, National Academy of Sciences, Washington (1975).
61. Fire Hazard Classification of Chemical Vapors Relative to Explosion-proof Electrical Equipment (USCGD-71-76), US Coast Guard, Washington (1976).
62. Matrix of Combustion-Relevant Properties and Classifications of Gases, Vapors, and Selected Solids (NMAB 353-1), National Materials Advisory Board, National Academy of Sciences Press, Washington (1979).
63. Classification of Gases, Liquids, and Volatile Solids Relative to Explosion-Proof Electrical Equipment (NMAB 353-5), National Materials Advisory Board, National Academy of Sciences Press, Washington (1982).
64. Test Equipment for Use in Determining Classifications of Combustible Dusts (NMAB 353-2), National Academy of Sciences Press, Washington (1979).
65. Classification of Combustible Dust in Accordance with the National Electrical Code (NMAB 353-3), National Academy of Sciences Press, Washington (1980).
66. Classifications of Combustible Dusts Relative to Electrical Equipment in Class II Hazardous Locations (NMAB 353-4), National Materials Advisory Board, National Academy of Sciences Press, Washington (1982).
67. Rationale for Classification of Combustible Gases, Vapors, and Dusts with Reference to the National Electrical Code (NMAB 353-6), National Materials Advisory Board, National Academy of Sciences Press, Washington (1982).

68. Recommended Practice for the Classification of Liquids, Gases, Vapors, or Vapors and of Hazardous (Classified) Locations for Electrical Installations in Chemical Process Areas (NFPA 497), NFPA.
69. Recommended Practice for the Classification of Combustible Dusts and of Hazardous (Classified) Locations for Electrical Installations in Chemical Process Areas (NFPA 499), NFPA.
70. Guide to Fire Hazard Properties of Flammable Liquids, Gases, and Volatile Solids (NFPA 325), NFPA.
71. Electrical Apparatus for Explosive Gas Atmospheres. Part 10: Classification of Hazardous Areas (IEC 60079-10), International Electrotechnical Commission, Geneva.
72. Electrical Apparatus for Use in the Presence of Combustible Dust. Part 3: Classification of Areas Where Combustible Dust Are or May Be Present (IEC 61241-3), International Electrotechnical Commission, Geneva.
73. Briesch, E. M., NEC Group Classification of Mixtures, *34th Loss Prevention Symp.*, AIChE (2000).
74. Electrical Apparatus for Explosive Gas Atmospheres. Part 1: Construction and Verification Test of Flameproof Enclosures of Electrical Apparatus (IEC 60079-1) International Electrotechnical Commission, Geneva.
75. Electrical Apparatus for Explosive Gas Atmospheres. Part 7: Increased Safety "e" (IEC 60079-7), International Electrotechnical Commission, Geneva.
76. Electrical Apparatus for Explosive Gas Atmospheres. Part 11: Intrinsic Safety "i" (IEC 60079-11), International Electrotechnical Commission, Geneva.
77. Electrical Apparatus for Explosive Gas Atmospheres. Part 18: Encapsulation "m" (IEC 60079-18), International Electrotechnical Commission, Geneva.
78. Electrical Apparatus for Explosive Gas Atmospheres. Part 15: Electrical Apparatus with Type of Protection "n" (IEC/TR 60079-15), International Electrotechnical Commission, Geneva.
79. Electrical Apparatus for Explosive Gas Atmospheres. Part 6: Oil-immersion "o" (IEC 60079-6), International Electrotechnical Commission, Geneva.
80. Electrical Apparatus for Explosive Gas Atmospheres. Part 2: Electrical Apparatus - Type of Protection "p" (IEC/TR 60079-2), International Electrotechnical Commission, Geneva.
81. Electrical Apparatus for Explosive Gas Atmospheres. Part 5: Powder Filling "q" (IEC 60079-5), International Electrotechnical Commission, Geneva.
82. Eckhoff, R. K., Design of Electrical Equipment for Areas Containing Combustible Dust—Why Dust Standards Cannot be Extensively Harmonised with Gas Standards, *J. Loss Prevention in the Process Industries* **13**, 201-208 (2000).
83. Killing, F., and Tielke, M., The Interference Short-Circuit with Arcing Phenomena in Electrical Equipment in Flameproof Enclosures with Special Reference to the So-called Transmission of Ignition by Particles, paper I-3 in *16th Intl. Conf. on Coal Mine Safety Research*, Bureau of Mines, Washington (1975).
84. Hülsberg, F., A New Problem Affecting the Flameproof Enclosure of Electrical Apparatus, Paper 28 in *7th Intl. Conf. of Directors of Safety in Mines Research*, Safety in Mines Research Establishment, Buxton, England (1952).
85. Limiting Electrical Losses—Discussion, *2nd Loss Prevention Symp.*, AIChE (1968).
86. Explosionproof and Dust-Ignitionproof Electrical Equipment for Use in Hazardous (Classified) Locations (UL 1203), Underwriters Laboratories, Inc., Northbrook IL.
87. Wheeler, R. V., Report on Battery Bell Signalling Systems as regards the Danger of Ignition of Firedamp-Air Mixtures by the Break-Flash at the Signal Wires, Safety in Mines Research Board, HMSO, London (1915).
88. Hickes, W. F., and Brown, K. J., Assessment of Explosion Probability for Intrinsically Safe Apparatus, pp. 54-58 in *Conf. on Electrical Safety in Hazardous Environments* (Conf. Publ. No. 74), Institution of Electrical Engineers, London (1971).
89. Standard for Safety—Intrinsically Safe Apparatus and Associated Apparatus for Use in Class I, II, and III, Division 1, Hazardous (Classified) Locations, ANSI/UL 913, Underwriters Laboratories, Inc., Northbrook IL.
90. Bossert, J., and Hurst, R., **Hazardous Locations**, Canadian Standards Assn., Rexdale, Ont. (1986).
91. Bartels, A. L., Bradford, M., and Thompson, M. G., Incendivity of Electrical Sparking due to Circulating Currents in the Enclosure of Large Electrical Machines, pp. 141-148 in *4th Intl. Conf. on Electrical Safety in Hazardous Areas* (IEE Conf. Publ. 296), Institution of Electrical Engineers, London (1988).
92. Morgan, M. J., Electrodes, Wiring, and Barriers, pp. 29-41 in **Electrical Safety Practices** (Monograph 113), Instrument Society of America, Pittsburgh (1972).
93. Peterson, J. S., Influence of Electrode Material on Spark Ignition Probability (RI 9416), Bureau of Mines, Pittsburgh (1992).
94. Zborovszky, Z., and Cotugno, L. A., Evaluation of the Cadmium Disc Breakflash in Testing Electrical Circuits—Safety in Explosive Atmospheres—A Comprehensive Study of Intrinsic Safety Criteria (BuMines OFR 68-76), Bureau of Mines, Pittsburgh (1974).
95. Cawley, J. C., Spark Ignition Probability Estimates for Resistor and Inductor Circuits in Methane-Air Atmospheres, *IEEE Trans. on Industry Applications* **24**, 878-883 (1988).
96. Thomas, V. M., The Design of Intrinsically Safe Apparatus for Use in Coal Mines: A Review of Data and Techniques, pp. 55-56 in *Flameproofing—Intrinsic Safety and Other Safeguards in Electrical Instrument Practice* (IEE Conf. Report Series No. 3), Institution of Electrical Engineers, London (1962).
97. Zborovszky, Z., Study of Intrinsic Safety Basics and Testing Machines: A Comparison of Tungsten and Copper Hot Wire Ignition Capability and Discharge Duration in the Ignition Process of Explosive Atmospheres in Testing Apparatus (BuMines OFR 116-77), Bureau of Mines, Pittsburgh (1976).
98. Cutler, D. P., and Tolson, P., Gas Ignition Test for Heavy Current Low Voltage Circuits (EC/99/59), Health and Safety Executive, Buxton, UK (1999).
99. Lloyd, H., and Guénault, E. M., The Use of Break-Flash Apparatus No. 3 for Intrinsic Safety Testing (Research Report 33), Safety in Mines Research Establishment, Sheffield, England (1951).
100. Haig, J., Lister, H. C., and Gordon, R. L., The Testing of Flameproof and Intrinsically Safe Electrical Apparatus, pp. 39-49 in *Flameproofing—Intrinsic Safety and Other Safeguards in Electrical Instrument Practice* (IEE Conf. Report Series No. 3), Institution of Electrical Engineers, London (1962).

101. Thomas, V. M., Design of Intrinsically Safe Apparatus for Use in Coal Mines: A Review of Data and Techniques, *The Mining Electrical & Mechanical Engineer* **44**, 295-308 (May 1964); Part II, 321-329 (June 1964).
102. Electrical Apparatus for Use in Class I, Zone 1 Hazardous (Classified) Locations: Type of Protection - Increased Safety 'e,' ANSI/ISA-12.16 (IEC 79-7 Mod), ISA, Research Triangle Park NC.
103. Standard for Purged and Pressurized Enclosures for Electrical Equipment (NFPA 496), NFPA.
104. Pressurized Enclosures (ISA-RP12.4), ISA, Research Triangle Park NC.
105. Nonincendive Electrical Equipment for Use in Class I and II, Division 2 and Class III, Divisions 1 and 2 Hazardous (Classified) Locations (ANSI/ISA-12.12), ISA, Research Triangle Park NC.
106. Industrial Control Equipment for Use in Hazardous (Classified) Locations (UL 698), UL.
107. von Angern, K., Theoretical Principles of the Restricted Breathing Properties or Materials in Potentially Explosive Environments and Their Utilization, *IEEE Trans. Ind. and General Appl.* **IGA-14**, 247-254 (1978).
108. Wagner, R. V., Boden, P. J., Stuggevig, W., and Davidson, R. J., Technology for Detecting and Monitoring Conditions That Could Cause Electrical Wiring System Fires (Contract CPSC-C-94-111), conducted by Underwriters Laboratories Inc. for Consumer Product Safety Commission (1995).
109. Gregory, G., AFCIs Target Residential Electrical Fires, *NFPA J.* **94**, 69-71 (Mar./Apr. 2000).
110. Dini, D. A., Skuggevig, W., Wagner, R., Boden, P. J., and Dubiel, D. G., Report of Research on Arc-Fault Detection Circuit Breakers for National Electrical Manufacturers Association (Project 95NK6832), UL (1996).
111. Blades, F. K., Method and Apparatus for Detecting Arcing in Alternating Current Power Systems by Monitoring High-Frequency Noise, US Patent 5,432,455 (1995).
112. Engel, J. C., and MacKenzie, R. W., Low Cost Apparatus for Detecting Arcing Faults and Circuit Breaker Incorporating Same, US Patent 5,691,869 (1997).
113. Engel, J. C., Clarey, R. J., and Doring, T. M., Arc-Fault Circuit Interrupters: New Technology for Increased Safety, *IAEI News*, 24-27 (Nov./Dec. 1997).
114. Gregory, G. D., and Scott, G. W., The Arc-Fault Circuit Interrupter: An Emerging Product, *IEEE Trans. Ind. Appl.* **IA-34**, 928-933 (1998).
115. Lee, D. A., Trotta, A. M., and King, W. H. jr., New Technology for Preventing Residential Electrical Fires: Arc-fault Circuit Interrupters (AFCIs), *Fire Technology* **36**, 145-162 (2000).
116. Brugner, F., and Schiff, N., New Cord Technology Designed to Detect Fire-Causing Conditions, *Fire Findings* **7**, No. 1, 1-3 (1999).

Copyright © 2003, 2014 Vytenis Babrauskas

Chapter 13. Special topics

Explosions in buildings **609**
Diffusion of flammable vapors from spills **612**
Ignition of gas jets from broken pipes **614**
Damages and ignitions from gas explosions **614**
Ignition in room fires **615**
Upper layer ignition in room fires *616*
Backdrafts and smoke explosions **617**
Rekindle ignitions **618**
Unconfined vapor cloud explosions (UVCEs) **619**
BLEVEs (boiling liquid, expanding vapor explosions) **619**
Oxygen-enriched atmospheres **625**
Test methods *628*
ASTM G 72 autoignition test 628
ASTM G 124 piloted ignition test for metals 628
ASTM G 74 gas stream impact test 628
ASTM D 2512 and ASTM G 86 mechanical impact tests 628
ASTM G 125 oxygen-index test for oxygen-enriched atmospheres 629
Wildland-urban interface **629**
Determining ignition properties in fire investigations **631**
Further readings **631**
References **632**

Explosions in buildings

Building explosions generally occur because an enclosed space was accidentally filled with natural gas (which is primarily methane), LP gas (largely propane), gasoline vapors, or some other flammable gas or vapor. Apart from failures of gas piping (Figure 1) and equipment inside buildings, another way that gas enters buildings is through basements or crawl spaces. It is not even necessary that gas piping be provided into a building for entrance of gas to take place. A number of incidents have been recorded where a gas main in the street develops a leak (due to corrosion, shrinkage during cold weather, construction activities, etc.), it finds its way into buildings then through drainage pipes, cracks in walls, and other existing flow paths[1]. The installation practice whereby the gas supply pipe entered a basement underground was a common source for gas inflow, since an annular void is often present around pipes due to settlement. Thus, once an external leak occurred, a preferred path into the building existed. For this reason, the current practice in the US for gas utility companies is not to pipe directly into buildings underground, but rather to bring out the pipe aboveground and make an aboveground entry into buildings. In climates subject to freezing, gas mains should be laid below the frost line[1].

In order to determine the potential for explosion, the question of whether a flammable gas that has entered a building will form a certain layer, or whether it will be mixed relatively uniformly into the existing atmosphere is of utmost importance. It is an intuitive expectation that if a space is unventilated, has minimal thermal gradients, and a light gas is slowly introduced at the top, it will stay as a layer at the top. Similarly, if a heavy gas is introduced at the bottom, layering might also be expected. Since the molar mass of air is 28.96, methane (W = 16) is lighter than air and propane (W = 44) is heavier. Gasoline has a wide variety of constituents, but a value of W ≈ 100 to 105 is normally taken, thus its vapors are much heavier than air. Unfortunately, things quickly become non-simple (and possibly unintuitive) since it takes very little—under some circumstances—



Figure 1 Effects of a massive explosion in a New York high-rise building due to a break in a gas pipe which filled elevator shafts with natural gas[4]
(Photo: NTSB)

to stir and mix the volume. If the fuel gas is introduced with a finite flow velocity, this velocity alone may act to stir the volume of the space. The stirring may be mechanical, for instance, with an HVAC system. Persons walking around also stir air mechanically. But stirring can be done by thermal means, too. Heaters of all sorts will create a rising gas plume above it. The plume entrains air and thereby creates a convective current helping to stir up the environment. Even a very small object such as a gas pilot light will create a plume above and stir the air. The sun shining through a window will create large temperature differences as can cold walls or infiltration from wind blowing on the structure. The heat of a body and breathing can be adequate to mix a small volume, such as within a camper vehicle. Also, buoyancy can be created by density differences alone, temperature gradients are not necessarily required. Releasing a lighter-than-air gas at some non-zero height below the top of the room, or a heavier-than-air gas at some non-zero height above the floor intrinsically sets up convective flows within the room, which help to mix the space[2]. A very important rule is that: *Once mixed, gases do not separate out, even if they are of widely different densities*[3].

A number of experimental studies exist on the topic, but they may not necessarily cover the circumstances of interest to the user. The experimental studies can be grouped into ones using carefully constructed test enclosures that were maintained at uniform temperature, versus real-house experiments. In experiments of the former type, when a lighter-than-air gas is released with negligible velocity at ceiling level, it is normally found experimentally to stay in a layer predominantly at the ceiling level. Conversely, a heavier-than-air gas, if released at floor level, will stay predominantly at floor level. In one study[5], gases were introduced into a 5 × 5 × 6 m high room at very low velocities. For methane introduced at ceiling level at a rate of 0.5 m^3 h^{-1}, even 1.5 h later there was negligible concentration at 1 m below the ceiling. A rather similar result was found for propane introduced slowly at floor level.

Harris[3] conducted experiments where natural gas was introduced into a room which was sealed except for a tiny pressure-relief opening. Figure 2 shows typical results for a leak near the ceiling, which suggest that the concentrations are grouped into 3 zones: Above the position of the leak, there is a zone of nearly-uniform concentration, but below the leak there are two zones: a transition zone and a near-ambient-concentration zone. Harris also showed that better mixing and a deeper ceiling layer occur if the leak's velocity is directed downwards, rather than horizontally or upwards.

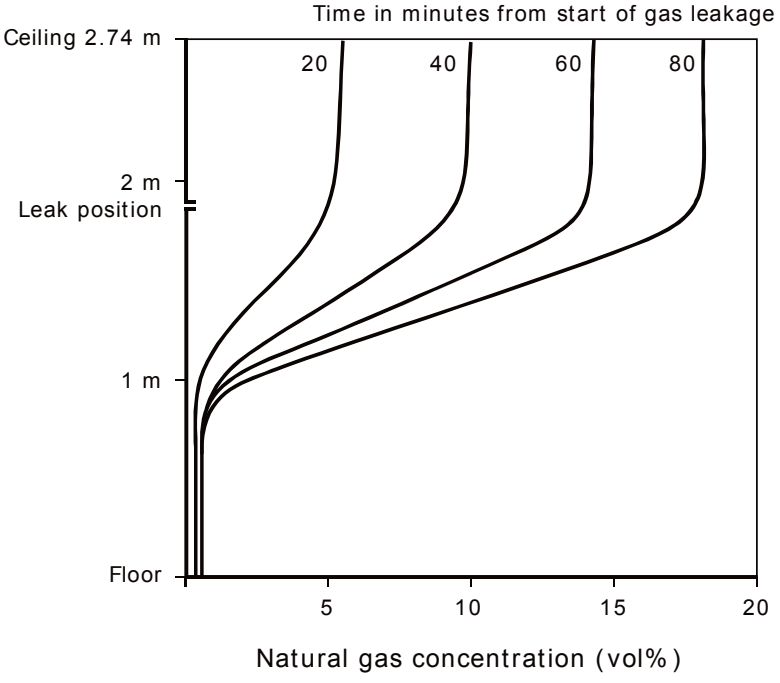


Figure 2 Layering of natural gas in a room with no ventilation (leak near ceiling)

Ventilation, if present, will change the layering of gases. In further tests, Harris explored various ventilation patterns and found that, for natural gas leaks, conditions where air inflow was at the bottom and outflow at the top led to thinnest ceiling layers and the lowest gas concentrations therein. The converse (in at the top, out at the bottom) led to the worst conditions, while various other patterns (e.g., in one side, out the other) led to intermediate results. In practice, of course, unless powerful ventilating systems exist, flows will be created by an interplay between leakage areas and temperatures.

Clodic[6] created leaks of propane and isobutane in a 16 m^3 room and found generally the inverse of the natural-gas results. Leaks created near floor level led to strong concentrations of gas near floor level, while leaks higher in the room resulted in much less steep concentration gradients. Fletcher and Johnson[2] released CO_2 gas into a 3.45 × 3.56 × 2.95 m high unventilated enclosure. This gas is heavier than air and will behave similarly, at least in a qualitative sense, as a release of propane. Figure 3 shows that a two-zone representation is approximately correct—most of the CO_2 remains below the point of discharge and is relatively uniformly mixed in that zone. Above the point of discharge there is only a small concentration found. The authors also conducted several experiments with mechanical ventilation present in the enclosure, but it is harder to capture general trends from these experiments.

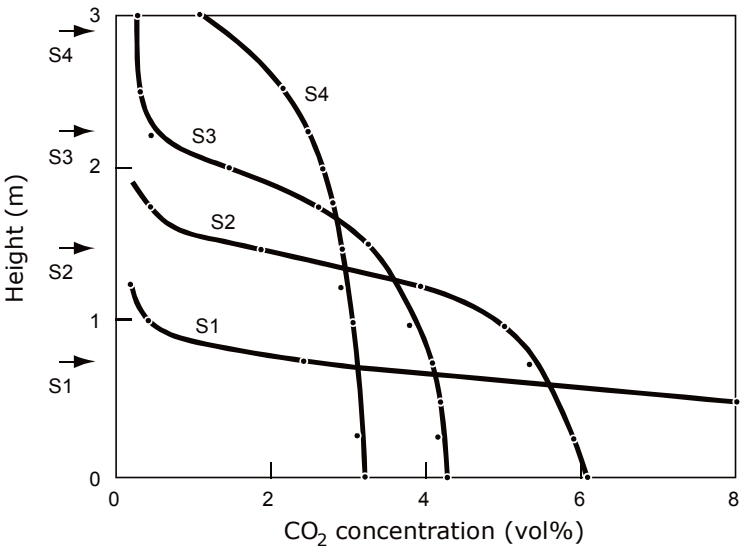


Figure 3 Room concentrations found 1 h after start of CO_2 release at a rate of 15 L min^{-1}. Four different source locations, marked as S1 – S4, were used.
(Copyright Elsevier Science, used by permission)

Very different results from the preceding have been obtained by researchers conducting *whole-house tests*. Weckman[7] created several basement leak scenarios and measured methane concentrations throughout the house. Mixing was nearly complete and only very modest evidence of layering was found, with concentrations at basement floor level being just slightly lower than at ceiling height. Experiments of using natural window ventilation to clear the gas were also performed. The results varied according to wind conditions, but it was found to be quite difficult to clear dead spaces and volumes near ceiling level. Weckman's results, even though limited, are of significant importance, since they point out that houses are generally leaky and are unlikely to be environments of uniform temperature. Essentially the same results were obtained by UL[8] who released propane into a small, unventilated building and found that uniform mixing rather than layering occurred. Existing temperature gradients were apparently sufficient to result in thorough mixing of the volume.

The only type of gas-filling problem that can readily be solved in closed form is one where the volume is assumed to be perfectly stirred and the ventilation (air flow rate), if any, is known. This problem is the standard 'single-compartment model,' as it is known in toxicology. If F_g = inflow rate of fuel gas (m^3 s^{-1}), F_a = ventilation rate (m^3 s^{-1}), V = volume of space (m^3), and t = time (s), then the concentration of fuel gas C (vol%) at any time t after filling has started is:

$$C(t) = \frac{F_g}{F_a + F_g}\left[1 - e^{-\left(F_a+F_g\right)t/V}\right] \times 100$$

Since laboratory experiments described above show a 2- or 3-zone behavior, with significant concentrations present only below the point of discharge for propane (and above the point of discharge for methane), Lapina and Sokalski[9] suggested that the filling with propane be modeled by perfect mixing, but only in the partial volume from the height of the floor up to the leak (or up to the ignition source, if the latter is higher). This is a reasonable strategy for representing the laboratory experiments, however, the few available whole-house experiments suggest that such layering will not happen. Instead, the whole space may have to be treated as a single mixed zone. Cleaver et al.[10] described a more sophisticated 3-zone model, however, no closed-form solutions were provided.

In some cases, a *pocket* of flammable fuel/air mixture may be formed within a larger space. This could be in the early stages of a leak or even much later, if a semi-enclosed volume exists where ventilation by diffusion and convection is poor. Bodurtha[11] suggests that these cases be treated conservatively by assuming that the flammable gas is in a pocket which is uniformly at its stoichiometric fuel/air ratio. Upon ignition, pressure in the pocket will rise to 7 – 8 atm*, and this will then be equilibrated with the rest of the volume. The Bodurtha concept can be visualized as the

* Although if there are numerous partial separations and encumbrances in the volume, *pressure piling* may greatly raise the actual pressures, and the possibility of this must be considered.

explosion of a balloon filled with the specified uniform mixture. But in any actual release of flammable gas, a fraction of gas will be unable to participate in the initial explosion, since not only will it not be at the stoichiometric concentration, but it will be at a location where the concentration is well outside the flammability limits. Thus, the scheme is quite conservative. Nonetheless, a more-conservative-yet scheme was put forth by Ogle[12], but experimental data are lacking that might validate any of these schemes.

Apart from real-house tests and tests within highly-controlled room enclosures, the cylinder geometry has been studied. Valentine and Moore[13] conducted a theoretical study, augmented by experiments where propane was admitted at the bottom of a 2.5 m high cylinder. In one experiment, where they discharged propane at a rate of 0.135 g s^{-1} m^{-2}, at the end of two hours the concentration at floor level was 92%, at 1 m height it was 10%, and at 1.3 m it was at approximately the LFL of 2.2%. Beyond 1.3 m, there was zero detectable concentration of propane. For a smaller filling rate of 0.02 g s^{-1} m^{-2} and a longer filling time of 4 hours, the concentration was 35% at the floor, 2.4% at 1 m, 2.2% at 1.1 m, and zero concentration above 1.3 m. Apart from providing computed and experimental results, the authors did not offer a general prediction scheme.

Diffusion of flammable vapors from spills

The evaporation of liquid fuel spills is a question of great practical importance, both in arson investigations and for certain accidental fires. Under quiescent conditions, with no convective currents, the diffusion of liquid-fuel vapors through air is extremely slow. Liebman et al.[14] demonstrated this in a 200 mm diameter open-top beaker holding gasoline—it took 25 min for the LFL to be reached at 130 mm above the liquid surface. Perhaps surprisingly, they also found that if large petroleum tanks are loaded slowly, then the height of the flammable region does not rise rapidly above the surface of the liquid; this appears to be in contrast to experiments in small tanks, where the contents get stirred relatively quickly. Similarly, Steen[15] reports that, in the absence of wind, butane and propane spills lead to laminar spreading velocities of less than 0.1 m s^{-1}. Another illustration of the extremely slow pace of processes governed by diffusion, without air movement induced by wind or convection, comes from Médard[16] who reports an incident where a hydrogen cylinder was emptied (down to 1 atm), the valve was unscrewed, and the tank left standing, with the top open, for one week. Since hydrogen is some 14 times lighter than air, the expectation was that all of the gas would diffuse out. At the end of that time period, a worker lowered a miniature light bulb into the tank for inspection. The light bulb broke while swinging against the metal and a small explosion ensued, indicating that the tank was not free of hydrogen. Had there been another opening in the bottom, so that a convective through-flow were possible, the hydrogen would undoubtedly not have remained.

When wind, convective currents, movement of persons, or other factors exist that can stir the air space, mixing may be pronounced and vapors may travel large distances. A strikingly long travel distance of gasoline vapors has been reported[17] when a woman cooking at her stove suddenly became enveloped in flames. It turns out that an individual was washing gasoline cans some 90 m away, and sufficient vapors were able to drift to the location where they could be ignited from the flames on the stove. Cooper[18] reports an incident where "Methylated-spirit vapour from a vessel of moderate capacity is believed to have been ignited at a cottage fireplace several hundred yards away." The pilot lights on water heaters sometimes ignite vapors when gasoline has been spilled in the vicinity. This topic is discussed in Chapter 14 under *Water heaters*. Experience indicates that raising the height of this potential ignition source is a useful, but not foolproof, safety strategy. Vigorous stirring can produce a flammable concentration with certain spills even if the water heater has been raised the recommended distance (0.457 m) off the floor.

Because of the complexity of the problem, modeling cannot yet provide practical guidance, even though several models have been presented. The British Government[19] proposed a simple method whereby the liquid vaporizes at a finite rate, but the entire volume is assumed to be fully-mixed. It is assumed that a fraction n of the floor area is covered by the spilled liquid and that the liquid evaporates at a rate $\dot{m}''$ (g m^{-2} s^{-1}). If the LFL of the liquid, expressed on a mass basis, is c (g m^{-3}), then the time for the room volume to reach the LFL is:

$$t = \frac{Vc}{\dot{m}''nA}$$

where V = volume (m^3) and A = area (m^2). But the latter two variables can be eliminated and replaced by the room height h (m):

$$t = \frac{hc}{\dot{m}''n}$$

The evaporation rate, in turn, depends on the local wind speed and on the turbulence; in addition, the evaporation rate is not independent of the spill area but, rather, decreases somewhat for larger areas. The authors suggested that c = 47 g m^{-3} be used as the LFL for gasoline and that very limited, unpublished data for evaporation of gasoline show $\dot{m}''$ = 0.14 to 0.25 g m^{-2} s^{-1}. Unfortunately, the fully-mixed assumption is unconservative, unless the ignition source is located at the ceiling. A flammable region will form at the lower portion of the room much earlier than the average concentration of a full-stirred volume would reach the LFL. The authors also proposed another simple, fully-mixed model for a room that has forced ventilation. In that case, the LFL will never be reached if at least the following ventilation rate is provided:

$$\dot{V} = \frac{\dot{m}''}{c}$$

where $\dot{V}$ = ventilation rate (m^3 air, per second, per m^2 of spill area).

The next more complex treatment considers that the problem resembles that of an open-top beaker which contains an amount of liquid on the bottom. The beaker sits in an environment where the atmosphere to which the top is open is continuously swept away, so the concentration of the liquid's vapor at the top of the beaker is always forced to be zero. This is sometimes known as the Stefan problem and Munoz-Candelario and Alvares[20] applied it to the case of the liquid spill. By simplification of the basic diffusion equation, they evolved the expression:

$$\left(\frac{1-X_A}{1-X_{A0}}\right) = \left(\frac{1}{1-X_{A0}}\right)^{z/h}$$

where X_{A0} = mole concentration of vapors at the surface of the pool, X_A = mole concentration of vapors at height z, and h = height of room (m). Commonly, the question to be answered is whether the vapors have or have not attained the LFL at a certain height where an ignition source is present. Thus, the value of X_A which is of main interest is the value that corresponds to the LFL; to obtain X_A (mole fraction) from a published value of LFL (vol%), simply divide by 100. Despite the fact that a simple solution can be obtained, it is not evident that conditions in real rooms will resemble the assumptions that are needed to be made to produce a tractable solution. In addition, the necessary input data may not be readily obtainable. For a pure substance, e.g., acetone, the value of X_{A0} can easily be obtained from the Clapeyron equation for vapor pressure, as discussed in Chapter 6. Gasoline, kerosene, and other substances which are mixtures, however, do not have a time-independent vapor-pressure/temperature relation, since lighter fractions evaporate first. This means that the flammable region from a spill of these liquids first expands, then contracts, as the lighter fractions are lost. An equation of the kind used by Munoz-Candelario could still be applied if experimental data for the initial (non-aged) vapor pressure of the fuel were available, but this may require special testing. Same as with the British model, no experimental evaporation data for real rooms were offered by the authors to validate their model. Tamanini[21,22] provided a model of greater complexity, where evaporation from a spill in a room under still-air conditions was computed. Despite drastic simplifications, the model is complicated to use and its validity has been examined only to a very limited extent.

Real spills will typically present an intractable problem, since they are unlikely to be symmetric, be exposed to a constant wind speed, be located in a room of a simple, symmetrical geometry, etc. Thus, it must be concluded that at the present time there do not exist methods which allow a reliable estimation to be made of the fuel vapor concentration that develops above a spill. In addition, all models such as discussed above need data (or a sub-model) to quantify the liquid's evaporation rate. Numerous theories[23-28] for this have been proposed, but none have been adequately validated against data of practical interest, e.g., gasoline spills of a practical sizes. Even if a validated theory were available, application would not be easy, due to reasons such as effects of substrate and lack of detailed knowledge of wind velocities. Neither can needed evaporation data be expected to be available from empirical studies, because the latter have been extremely limited for substances of practical concern. Apart from the British study mentioned above, more recently DeHaan[29] studied the gasoline evaporation rate for a single 0.15 m diameter pool and found an initial rate of 2.4 g m^{-2} s^{-1}, decreasing to half that value in about 6 minutes. His finding does not necessarily conflict with the British results, since the per-unit-area evaporation rate decreases with increasing pool diameter and the British results were evidently for much large spills, although the diameter was not specified. In addition, heat losses to a concrete floor would be greater than to DeHaan's insulated glass dish. For camping fuel tested under the same conditions, DeHaan found a rate of about 0.5 g m^{-2} s^{-1}. DeHaan also studied pure pentane pools and found a large decrease in evaporation rate with increasing diameter, but not enough data points were available to justify a quantitative fit. Mackay and Matsugu[30] reported some limited data on evaporation of gasoline from a deep, square pool of 1.22 m dimension. Over the first 10 minutes, evaporation rate was about 3.7 g m^{-2} s^{-1} under unspecified wind conditions. Some indirect conclusions may also be drawn from test data[31] on square, insulated pools of 1.22 m dimension where butane was evaporated. For nearly-still conditions, a rate of 2.0 g m^{-2} s^{-1} was found; this increased to 7 – 8 g m^{-2} s^{-1} in a wind of 5.5 m s^{-1}. Under nearly-still conditions, Lennert[32] found an evaporation rate of 0.4 g m^{-2} s^{-1} from an 0.2 m diameter pool of methyl ethyl ketone. The vapor pressures at 20ºC of these pure liquids are: butane 207 kPa, pentane 59 kPa, MEK 9.7 kPa. As discussed in Chapter 14, the vapor pressure of gasoline is in the range 62 – 108 kPa.

Wren and Martin[33] used a complex calculational model to predict gasoline evaporation rates (but not the concentration of vapors above the pool) for pools for several sizes. For a circular pool of 2 m diameter, they predicted an evaporation rate of 7 g m^{-2} s^{-1}, while for pools of 40 – 80 m diameter, a rate of 9 g m^{-2} s^{-1} was predicted. But since this effort was not accompanied by large-scale validation experiments with gasoline pools, reliance cannot be placed on such computational results.

The above studies show values for the evaporation rate of gasoline that span a range of more than 60 : 1. Some of the differences (e.g., due to pool size or wind conditions) are clearly due to physical environment differences, but nonetheless it must be concluded that credible guidance is currently unavailable. In turn, if the basic evaporation rate is

unknown, then calculational schemes for obtaining vapor concentrations cannot be successful.

Ignition of gas jets from broken pipes

If a pipe carrying a fuel gas at a reasonably high pressure suffers a break, a high velocity jet will be discharged into the atmosphere. Near the mouth, the fuel concentration will be nearly 100% while far downstream it will reach negligible values. In between lies a flammable region. Smith et al.[34] studied the ignitable regions for jets of several fuel gases discharged vertically up into the atmosphere. They concluded that, at the jet centerline, the probability of ignition falls to zero at the height where the mean concentration has fallen to about ½ of the LFL. Ignitions of a free jet are not necessarily sustained, in that the flame may extinguish by blowing off. The height beyond which a flame will blow off was found to correspond to the height of the LFL.

Damages and ignitions from gas explosions

It has sometimes been hypothesized that lighter-than-air gases, layering near the ceiling, will cause more damage at ceiling height and that, similarly, heavier-than-air gases will cause more damage at floor level. In a series of large-scale tests, DeHaan et al.[35] demonstrated that this is not true. The pressures were nearly equal throughout the compartment and greater structural damage would occur in places where the construction was weaker, not in places where the fuel gas was originally localized. Color Plate 38 illustrates this phenomenon from another experimental program on this topic that was conducted in Canada.

When a gas explosion occurs, it is usually accompanied by a fireball. Whether the event leads to a sustained fire depends on the nature of the combustibles present. Because high temperatures occur only briefly during a gas explosion, direct ignition of thermally thick materials is not to be expected. But ignition of lightweight 'kindling,' such as lint, clothing, hair and paper is possible. Ignition of heavy materials and structural components can then occur if there is a chain of kindling fuels (Color Plate 37).

The problem was studied in small-scale by Hagimoto et al.[36], who used a cubical chamber of 0.3 × 0.3 × 0.3 m size. In the first series of experiments, they closed the top and bottom of the chamber with brass plates, but the remaining four sides comprised a thin film held on with grease. Test specimens were sited parallel to the floor and ceiling and at various distances away from the metal surface of the chamber. The following specimens were used: polyethylene film (10 mm × 50 mm × 20 μm); paper (10 mm × 50 mm × 90 μm); cotton fabric (10 mm × 50 mm); and PVC insulation from an electric 'zip cord' (50 mm long). Ignition was with a 1 J spark at the center of the chamber. Table 1 shows the results. They indicate that it is easier to ignite specimens from explosions of mixtures that are near-limit, rather than close to stoichiometric. This is not surprising, in view of slower flame speeds and therefore longer flame contact times. It was also clear that locations near the center of the chamber are more susceptible to ignition than those close to the boundaries, and that it is easier to ignite materials near the ceiling than near the floor.

The authors then did experiments in a similar chamber, but with all 6 sides comprised only of thin film. Tubular rings of paper (130 mm diameter, 10 mm length, 90 and 250 μm thick) placed at the center of the chamber were the ignition targets. In those experiments, it was found that ignition of the paper targets took place at about the time that the flame died out, with shortest ignition times found for mixtures near stoichiometric. For a stoichiometric mixture, flame velocities around 3 m s^{-1} were observed and flame duration

Table 1 Ignitions resulting from explosions in a box with rigid floor and ceiling

CH_4 %	Loc.	PE film				Paper				Cotton fabric				PVC insulation			
		0	1	6	50	0	1	6	50	0	1	6	50	0	1	6	50
6	T	②	③	③	●	–	②	②	●	①	①	①	●	–	–	–	–
	B	–	–	–	–	–	–	–	–	–	–	–	–	–	–	–	–
7	T	②	●	③	●	–	③	③	●	①	①	②	●	–	–	–	–
	B	–	②	③	●	–	–	②	②	①	①	①	①	–	–	–	–
9	T	–	③	③	●	–	②	③	●	①	①	②	②	–	–	–	–
	B	②	③	③	●	–	②	③	③	①	①	②	②	–	–	–	–
13	T	②	●	●	●	–	②	③	●	①	①	②	②	–	–	–	–
	B	②	●	●	●	–	②	③	●	①	①	①	②	–	–	–	–
13.5	T	②	●	●	●	–	②	③	●	①	①	②	●	–	–	–	①
	B	②	③	③	●	–	–	③	●	①	①	①	②	–	–	–	–

Symbols
0, 1, 6, 50: distance of sample from ceiling/floor (mm)
T, B : position: top (ceiling), bottom (floor)
– : no detectable change
①: microscopic change
②: light browning
③: browning
●: burned up

times ca. 0.3 s. Mixtures close to the flammability limits showed velocities ca. 1 m s^{-1} and flame duration times of up to 2.5 s. The thicker paper samples only ignited at gas concentrations near the flammability limits; specimens exposed to near-stoichiometric explosions charred but did not flame.

It is often proposed that an explosion of a fuel-rich mixture is more likely to lead to a serious fire than is a fuel-lean explosion. Hagimoto's data provides only limited support to this notion—the results for PE film do show distinctly more combustion under fuel-rich conditions, but for the other targets it appears that while ignitions are more common in near-limit mixtures, there is not much difference between lean-limit and rich-limit conditions.

A limited amount of data is available from a series of Canadian house explosion tests[37,38]. The experiments showed that the flash fire generates peak heat flux values of up to 230 kW m^{-2}, but in about 2 s the value declines to half that and the fireball is gone in about 6 s (Figure 4). Since the duration is so short and since many locations will receive much less than the maximum flux, it was found experimentally that substantial amounts of fuel can remain unignited. Generally, it was found that only 'spot fires' were present after a test explosion. Upholstered furniture was commonly the item ignited, and this may be due to gas mixtures being trapped within the foam. The organizers concluded, however, that the limited ignitions were not particularly representative of the post-explosion fires that are typically encountered by firefighters.

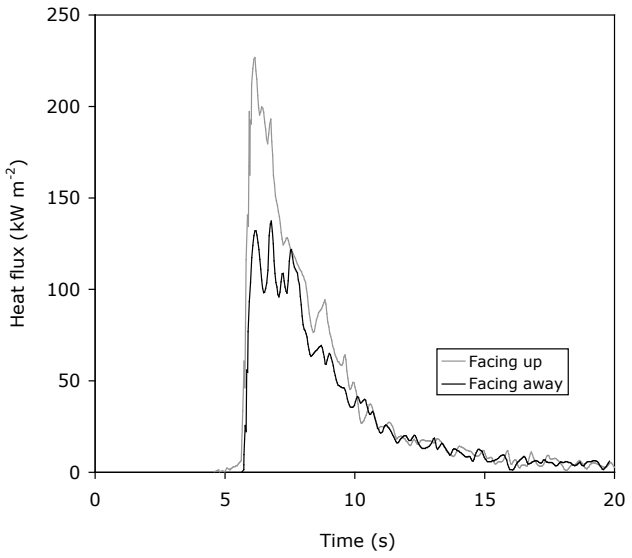


Figure 4 Heat fluxes measured at two sensors in a full-scale experimental natural gas explosion

Ignition in room fires

The question often arises in fire investigations as to what the maximum temperature is that can be expected in room fires. The temperature of a post-flashover room fire is over 600ºC, thus, the ignition temperature of most organic materials will be exceeded in a post-flashover fire. But the question is germane for some hard-to-ignite materials, e.g., metals, which may require a higher temperature for ignition. The adiabatic flame temperature of most common organic materials burning in air is roughly 1900 – 2000ºC. Such high temperatures are approached only in special research burners. In a room fire, much lower temperatures are registered, primarily for three reasons:

(1) The flames are turbulent; consequently the temperature recorded by a thermocouple is an average of reacting flame zones and unreacting 'packets' of air or combustion products.
(2) The combustion is incomplete, with CO, unburned hydrocarbons, and soot being some of the combustion products, not just CO_2 and H_2O; this lowers the temperature.
(3) Radiative losses may be sizable.

Full-scale room fire tests[39] indicate that the peak temperatures in a post-flashover room fire are typically 900 – 1100ºC. Copper electrical wires (T_{mp} 1085ºC) are rarely found bulk-melted (i.e., in areas unassociated with electrical arcing activities) in room fires. It has been reported that some very limited melting of steel (T_{mp} 1350 – 1450ºC) has occasionally been observed in room fires[40], but the caution is also given that reliable determination of whether or not melting or eutectic damage exists needs to be established by metallographic examination with microscopy. Much higher flame temperatures can be attained in the presence of pure oxygen as the oxidizer, or in fires involving exotic fuels (e.g., metals), certain oxidizers, or explosives, although fires with these substances are relatively rare.

The ignition of a second (or subsequent) item from a burning object in a room can occur from direct flame contact or by radiant energy. In the former case, the objects need to be spaced close enough together for such flame contact to occur (maybe < 0.3 m apart). In the latter case, the radiation comes from the flame above the burning object, the hot upper layer in the room, and from the bounding surfaces of the room (ceiling and walls). In hazard analysis calculations, it is most common to only use piloted ignition data, as one cannot be sure that flying brands or other sources of piloting will be absent. For analyzing specific fires which have taken place, judgment should be used as to whether localized sources of ignition could or could not have been present.

For the case of direct flame contact, the ignition time of the second item can be assumed to be the time at which contact occurs. (This assumption is conservative since time is required to pyrolyze fuel and heat the gases produced to their ignition temperature.) For radiant ignition, a simple assumption is that prior to flashover, the radiation from the upper layer and the room surfaces are negligible. Thus, the radiant energy transfer to the surface of the second item all comes from the flame above the first item. Based on this

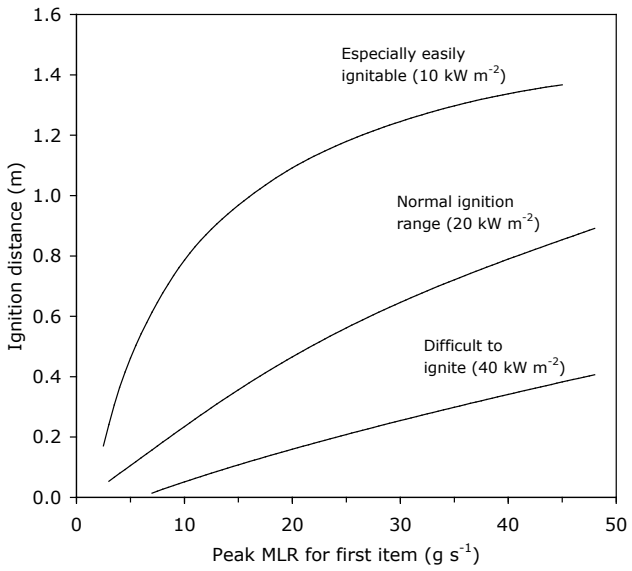


Figure 5 Maximum expected ignition distance for combustibles having various values of minimum flux for ignition, as a function of the mass loss rate of the first burning item

assumption, some years ago Babrauskas[41] developed a procedure for estimating the ignition of the second item. Radiant heat flux values at various distances were obtained as a function of the mass loss rate (MLR) of the first-ignited object. Figure 5 shows results plotted for three values of $\dot{q}''_{\min}$ for the target object (#2 object): 10, 20, and 40 kW m^{-2}. For this purpose, $\dot{q}''_{\min}$ values should be used for a relatively short exposure time, typically 5 minutes or less, since most furniture items do not burn near their peak intensity for longer than that. Curiously, a better fit was found using MLR rather than the HRR of the #1 item; the reason for this is not clear. This estimating procedure is quite conservative, since peak intensity will normally be exhibited only for a short time, and the rest of the time the burning of item #1 will proceed at a slower rate.

A refined strategy is to consider the summation of radiation coming from item #1 and from the room radiation. This is practical to do only in the context of a computer program for computing the time history of a room fire. An example of one way to do the summation has been given by Peacock et al[42]. Once flashover occurs, all remaining combustible items in the room are considered to ignite simultaneously.

UPPER LAYER IGNITION IN ROOM FIRES

In some cases of fire development in rooms, 'flame rollover' is observed. This is a process that can happen (but does not necessarily happen in every fire) if the fuels that burn are located low in the room and their flames are of insufficient height to directly extend to the vicinity of the ceiling. Most fuels in a room fire will burn incompletely, causing a certain amount of heated, unburned, combustible gases to accumulate in a layer below the ceiling. Eventually, the gases in this layer may ignite—this process is termed 'rollover.' If rollover occurs, it is necessarily before flashover, since flashover means not only that the upper layer is ignited and burning, but that it has descended a substantial fraction of the room height below the ceiling. Some room burn tests conducted by DeHaan[43] showed that ignition of the hot gas layer occurred at roughly 500 – 700ºC. Since 600ºC is often taken as the nominal temperature at flashover, it is not surprising that rollover generally preceded flashover by only a brief instant.

Because of the scarcity of controlled experimental studies, details of the rollover process are not well understood. Even the basic question as to whether the process is one of autoignition, or piloted ignition, or either, remains to be answered. Piloted ignition, by the way, might be envisioned as occurring through a flame packet which travels into the upper gas layer. Beyler[44] attempted to quantify the conditions for ignition of the upper gas layer on the assumption that the ignition is piloted. He conducted some small-scale experiments using gaseous and liquid (but not solid) fuels and, based on their results, concluded that Le Chatelier's Rule for flammability of mixtures, along with a temperature dependence of the LFL, as expressed by the Burgess-Wheeler law were sufficient to characterize the ignitability. The actual combustible gas concentrations would rarely be known in practice. What may be possible to compute is the equivalence ratio φ pertinent to the lower-layer burning. If φ is high enough and the upper-layer temperature is also high enough, then ignition may occur. His relation for the minimum value of $\varphi_{\min}$ at which ignition can occur is:

$$\varphi_{\min} = \frac{K}{K - \frac{1}{r} - 1}$$

where

$$K = \frac{2800}{(T_L - T)}$$

r = stoichiometric air/fuel mass ratio (--) for the lower-layer combustion, T_L = adiabatic flame temperature at the LFL (ºC), and T = actual temperature of the upper gas layer (ºC). For this purpose, Beyler suggests using T_L = 1427ºC. Also, usually $r >> 1$, so its contribution may then be ignored in the expression for $\varphi_{\min}$.

Sherman[45] attempted to construct a mathematical model for rollover by incorporating Beyler's results into a two-zone room fire model. A two-zone model, by definition, assumes that the temperature of the hot gases in the upper layer is identical throughout and that there are no variations in concentration of anything. Based on experimental observations of the process in actual rooms[43], it does not appear that uniformity of the upper layer is a good assumption. The effect is rapid, transient, and non-equilibrated; most commonly it appears in the form of an expanding fireball. Thus, while the rollover process should certainly be amenable to mathematical modeling, a more sophisticated model will be

needed if experimentally-observed phenomena are to be reproduced.

Backdrafts and smoke explosions

NFPA 921[46] defines backdraft as "An explosion occurring from the sudden introduction of air into a confined space containing oxygen-deficient superheated products of incomplete combustion." According to NFPA 921, the term 'smoke explosion' is synonymous to 'backdraft,' however, some authors[47] recognize it as a more general term. One way that a smoke explosion can occur is if a smoldering fire releases significant amounts of unburned pyrolysates, which accumulate in the upper portions of the room, but cannot burn there due to low temperatures and an absence of overt ignition source. If the gas layer is within the flammability limits and it descends low enough to encounter a local ignition source, an explosion may result. The term 'gas explosion' is normally reserved for situations where the combustible gas involved is not the unburned pyrolysate of an ongoing combustion. Furthermore, while NFPA 921 limits the backdraft definition to explosions, sudden-combustion events which do not produce a loud report can occur with products of incomplete combustion. The latter have not been studied extensively, however simple room geometries leading to explosive backdrafts have been studied experimentally in some detail[48,49]. Croft[47] has reviewed case histories of backdrafts and smoke explosions; Dunn[50] discusses several cases from a firefighter's viewpoint. Weng and Fan[51] proposed a theoretical model for backdrafts, but have not attempted to validate it with experimental data.

Experimentally, it is very easy to create a backdraft[52,53] by constructing a well-insulated compartment where sizable surfaces of cellulosic materials are burned. There is a door opening, but once the compartment has gotten quite hot, the door is shut. The oxygen level drops and combustion largely ceases, although active pyrolysis (and generation of unburned flammable vapors) continues due to the high temperatures. The door is then quickly opened and a short while later an explosion is heard and a fireball is seen rolling out. Once the door is opened, mixing occurs due to the 'gravity current' which develops as a consequence of the difference in density between the heated gases and the cold incoming air. No ignition source is normally necessary, since it is common for the hot gas layer to be above the AIT of the pyrolysis gases. Backdrafts are facilitated if a combustible ceiling is present, since uncombusted fuel can more readily be accumulated at ceiling level in such cases; saunas are particularly susceptible to this[54]. Color Plate 42 illustrates the fireball from a backdraft created in large-scale experimental studies.

When a backdraft does occur, part of the danger is because there is a substantial delay (typically about 15 s) between opening the door and the time when an explosion propels a large fireball out the opening. This can create a false sense of security to individuals approaching the doorway. It appears that the main variable governing whether or not a backdraft will occur under the conditions described is a presence of a specific amount of fuel vapors in the room. In small-scale tests with methane, Fleischmann et al.[48] experimentally determined that a minimum of 0.10 mass fraction (20 vol%), unburned methane needed to be present in a compartment for backdraft to occur. In a larger-scale follow-on study, Bolliger[55] determined that a mass fraction of methane over 0.15 was needed for a backdraft to be possible. Methane has a combustion chemistry dissimilar to other gases, however, so these results would not necessarily apply to pyrolysis gases of solid or liquid fuels, which rarely contain a significant methane component. Thus, possibly more direct guidance can be taken from the work of Gottuk et al.[49], who determined that for diesel fuel, a mass fraction of 0.16 or more was needed for a backdraft to occur.

While most backdrafts involve a fire where the ventilation conditions were changed at a certain time, studies indicate that opening or closing of doors is *not* necessary, but that simply burning under very poor ventilation conditions can suffice. Sutherland[56] studied smoke explosions in a model scale room where wood cribs were burned under very highly vitiated conditions but the room ventilation was not changed during test. Smoke explosions occurred unpredictably 0, 1, or 2 times during a room fire. By making gas chromatographic measurements of gas samples, Sutherland concluded that the primary fuel for the smoke explosions was unburned hydrocarbons and not CO. He also observed that the process was a direct consequence of *puffing combustion*. Puffing combustion describes burning which periodically oscillates between active combustion inside the room and rapid, vigorous ejection of flames or combustion products; it is a symptom of highly oxygen-starved conditions. Fires exhibiting reasonably steady burning did not involve smoke explosions. The puffing was understood to first extinguish local flaming, leaving a hot fuel surface, and then to bring in fresh oxygen into the volume. A peak pressure of 2.5 kPa occurred in his experiments; this is large compared to pressures in normal fires (around 10 Pa), but much smaller than pressures associated with gas explosions (around 1 MPa). Rather similar experiments were made by Hayasaka et al.[57] They used wood cribs and a wood wall in a model-scale room having a small ventilation opening of 0.20 × 0.24 m at the center of a 0.82 × 0.85 m wall. In a typical experiment, the fire burned in a flaming manner for about 10 min until oxygen concentration near the ceiling (Figure 6) dropped to a very low value. At that point, the fire became a *ghosting* fire for a short while. A ghosting fire is a thin fire of low luminosity that wanders around the room and is not anchored to the fuel bed. At 13 min, the ghosting fire extinguished and the wood only smoldered. Oxygen levels somewhat recovered during this phase. At somewhat over 23 min, the first backdraft occurred, followed by a second and a third. During a backdraft, the fireball originated near the ceiling (Color Plate

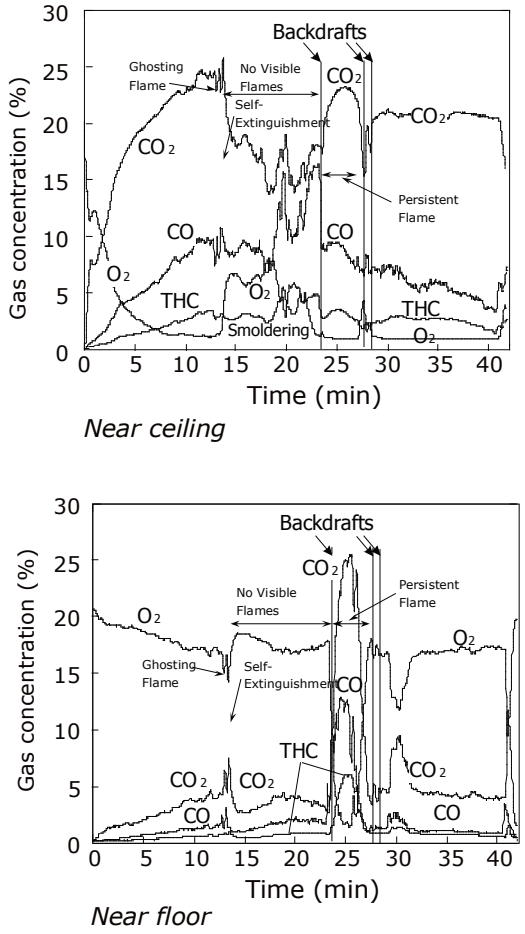


Figure 6 Gas concentrations in the backdraft experiment of Hayasaka et al.

39) and roughly at the center of the compartment, rapidly spreading to the floor and to the ventilation opening.

Chitty[58] studied numerous backdraft incidents and concluded that the following are warning signs of backdraft:

- a fire in a compartment having few openings
- pulsating smoke from openings
- blue flame in the hot gas layer
- roaring or whistling noises
- sudden reversal of smoke flow
- oily deposits on windows (although this is quite common in fires in general).

Backdrafts can occur due to improper firefighting operations. These include use positive-pressure ventilation under inappropriate circumstances[59] and improper roof ventilation. If holes are cut in a roof to ventilate a fire taking place underneath the roof, with sloped roofs care should be taken to cut the openings at the top of the roof. In one case, two backdrafts occurred when the ventilation opening was improperly cut on a lower part of the roof[60].

Color Plate 40 shows a smoke explosion that occurred in a pellet stove. The explosion blew out the glass front which was propelled over 10 m. through a house, and a portion of it penetrated the victim's stomach. The stove was a sealed-combustion system, which employed an air-intake tube that was routed up through the chimney and terminated in open air at the chimney-top level. This is design feature which allows for a counterflow heat-exchanger action between the combustion products and the incoming air. It also creates a system which does not have a pressure differential with regards to atmospheric conditions. The explosion occurred because the air intake tube within the chimney broke and separated, leading to recirculation of combustion products back into the stove.

A smoke explosion that took place in a fireplace is shown in Color Plate 41. It was caused by improperly installing a wood stove by venting it into a large, blocked-off fireplace rather than directly into the chimney.

Rekindle ignitions

A rekindle occurs when a fire has been suppressed to the point of no visible flames, yet later re-erupts in flaming. Why do rekindles occur? To investigate this, it is important to understand what happens when water is applied to a fire. Water may be applied in two ways: (1) as a solid stream, hitting a burning surface, cooling it, and possibly leaving a film of water on it; or (2) as a fog stream, introducing small droplets into the air, which then evaporate and consequently extract heat from the hot gases. Flaming stops when the gas temperature drops below the minimum at which combustion can be sustained. If only the gas-phase cooling were done, then flaming would likely re-erupt very quickly upon stopping the fog stream. This will occur if the burning material is still above its fire point. If the water-vapor laden gases serving as a heat sink are convected out faster than the surface can cool below the fire point, re-ignition will take place. Liquid pools, because of their high thermal inertia, do not cool quickly, thus they may often re-erupt if extinguished only in the gas phase (in practice, restricting oxygen availability to the pool through use of long-lasting foam is a more effective tactic than attempting to cool down the bulk of the liquid).

But if the burning object was extinguished by literally dousing its surface in water, and assuming the fire point is above 100ºC, how can it rekindle? There are several mechanisms. If the mass and heat capacity of an inert object are high, and the surface is abruptly cooled off, the interior portions do not drop in temperature to nearly that level. Thus, once the agent cooling the surface is gone, heat moves back from the center to the periphery, and the surface temperature starts to climb. If the object (as it perforce must be) is not inert, then a self-heating mechanism may need to also be considered. In addition to the heat retained in the central portions, heat is being generated, and that generation can be rapid if the center is sufficiently hot. Finally, the presence of porosity promotes both smoldering and self-heating. If the fire largely involved wood materials, the members were probably originally thick and well-separated from the neighbors. Af-

ter sufficient combustion has taken place, the remainder may now form a heap where each fragment is close to, but not flush against its neighbor. The pieces have gotten smaller and thus there may now be a porous, self-heating body to consider.

Practical aspects of firefighting operations necessary to minimize the possibility of rekindles have been discussed by Dunn[61]. A thorough 'overhaul' procedure is necessary to avoid rekindles. It often requires considerable skill to overhaul sufficiently, yet to leave as much of the scene as possible to fire investigators. The use of a thermal imaging camera can be helpful, since it can pinpoint hot spots that would otherwise not be detected visually. Gustin has suggested that the two most common features associated with rekindles are cellulose insulation and low-density fiberboard[62]; not surprisingly, these are the two most common construction materials that can easily be made to smolder. Rekindles are also common with upholstered furniture, especially those containing latex foam or cotton. Some types of polyurethane foam smolder under certain circumstances and thus can also lead to rekindles. A detailed story on the repeated extinguishments and rekindles of a haystack that had ignited due to self-heating has been published[63]. The use of a surfactant in the overhaul process can help reduce the incidence of rekindles by allowing the water to penetrate the cracks and fibers associated with above mentioned materials.

Unconfined vapor cloud explosions (UVCEs)

An unconfined vapor cloud explosion (UVCE) is an explosion of a flammable gas cloud which is in the open air and not enclosed in a vessel or a room. The explosion must generate a significant overpressure for the term UVCE to be applied; otherwise the event is a *flash fire*. UVCEs are among the most deadly of industrial accidents. Catastrophic events occurred in England at the Flixborough plant of Nypro (UK) Ltd. on 1 June 1974 where a leak of cyclohexane in a nylon-producing plant killed 28 persons[64]. More recently, a UCVE at a Texas plant of Phillips Petroleum Co. on 23 October 1989 killed 24 persons. A UVCE occurs when an ignitable gas or vapor is released into the atmosphere and the cloud subsequently ignites. This type of explosion is 'inefficient,' since much of the fuel is not well enough mixed in order to participate in the combustion. Thus, a maximum yield of only 10% of the theoretical heat of combustion has been reported to be found for UVCEs[65]. A UVCE would not exist at all, of course, if there did not occur a region in which the fuel concentration is within the flammable limits. A UVCE produces a fireball and various blast effects, but these do not include the kind of pulverization which can be seen with high explosives. The definition of UVCE requires that ignition occur subsequent to atmospheric dispersion; explosions where the ignition is concomitant with the release are not classed as UVCEs.

A UVCE can be either a deflagration or a detonation. Only a minority of UVCEs are detonations, but these can show overpressures in excess of 15 atm[66]. One propane cloud detonation incident has been investigated in detail by the Bureau of Mines[67]. If a detonation occurs, it can be the result of either a detonating initiator (e.g., TNT) or by a deflagration-to-detonation transition. The former would be uncommon in peacetime, but the latter can very easily occur. The propensity for deflagration-to-detonation transition can be explained on the basis of the obstacle-laden immediate environment that can be common in a chemical plant near the source of the leak. A release away from any structures would avoid the turbulence creation which leads to flame acceleration and transition to detonation. However, chemical plants are normally laden with assorted piping, stacks, support structures, etc., all of which can serve to promote flame acceleration.

Of all the common gases, acetylene, ethylene oxide, and hydrogen are the easiest to detonate in a UVCE and methane the most resistant. It requires about 1000 times the initiator energy to detonate methane, in comparison to acetylene[65]. Other common gases, such as propane or butane, require 50 – 80 times the energy as for acetylene. When a UVCE does occur, greater damage is also expected with acetylene, due to its greater potential for flame acceleration and higher flame speeds that can be expected. A model has been published for allowing rough damageability estimates to be made[68].

An extensive database of some 165 UVCE incidents has been published[69], primarily covering the period 1945-1977. An important finding is that in 60% of the cases the ignition source (e.g., refinery flare) pre-existed and the explosion occurred when the cloud reached the ignition source. Design guidance for situations involving potential UVCEs is given by the Dutch government[70] and AIChE[71]. The US military has developed weapons which generate a UVCE by releasing and vaporizing a liquid fuel into the air; in their terminology such purposive UVCEs are called *fuel-air explosives* (FAE).

Flash fires have been studied only to a limited extent. AIChE summarized most of the scant data available[71]. Peak heat fluxes in the vicinity of 180 kW m^{-2} are associated with large spills. The effect of size is probably small, since heat fluxes of almost identical magnitude have been measured in much smaller scale house explosions, as shown earlier in this Chapter 13.

BLEVEs (boiling liquid, expanding vapor explosions)

A BLEVE occurs when a tank holding a compressed (pressure-liquefied) gas—commonly propane—undergoes rapid venting. The venting is often caused by overheating, followed by failure of the tank, but this is not a necessary sequence of events. In one case, a BLEVE with a 100 m fire-

ball was produced when pressure was inappropriately released in an industrial autoclave reactor[72]. The majority of cases, however, involve overheating. The overheating can occur due to various sources. It can simply be due to an ongoing fire engulfing a tank. In other cases, overfilling or another cause of overpressure will produce a discharge of the gas through a pressure-relief valve (PRV). If this discharging gas ignites, then an external source of heating exists close to the tank. Further discharge will result in continued flames, which, if impinging on the tank, will progressively raise its temperature and weaken steel that is present above the liquid line. The process leads to runaway, since normally a PRV cannot be practically provided which will keep up with the increasing pressures and flows[*]. The tank then ruptures, resulting in a massive fireball (Color Plate 43) and flying metallic fragments.

While most BLEVE incidents have involved flammable gases, it is not necessary that the gas be flammable for a BLEVE to occur. A BLEVE is basically a physical explosion, and heating from the combustion of the substance itself is only one of the ways that excessive over-pressure can occur. Prugh examined case histories for major BLEVE accidents during the period 1926 – 1986 and identified that, apart from propane/butane/LPG, accidents have volved[73,85]:

acrolein	ethylene oxide
ammonia	gasoline
butadiene	hydrogen
carbon dioxide	methyl bromide
chlorine	phosgene
2-chloro-1,3-butadiene	propylene
diethyl ether	vinyl chloride
ethylene	water

A number of the older accidents happened because of absence of proper valves and safety precautions against overfilling. Shown in Color Plate 44 are views of the fireball from the BLEVE that took place on 21 June 1970 in Crescent City, Illinois upon derailment of a train hauling propane tank cars. After the 1970s, this source of accidents in the US significantly decreased due to tighter regulations and greater safety awareness. But the most disastrous BLEVE took place in relatively recent times—1984—in Mexico[74], killing approximately 500 persons and injuring another 7000. 'Tub rockets' were propelled as far as 1.2 km in the incident, which entailed nine separate explosions, some of which were severe enough to register seismically. BLEVE fireballs from this disaster are shown in Color Plates 45 and 46, while the aftermath is illustrated in Color Plate 47.

[*] This is true for the case of normal *vapor*-discharge PRVs. It would appear to be readily possible to equip many types of tanks with a secondary, *liquid*-discharge PRV. Since the mass of material which can be discharged from a given opening is vastly greater for liquids than for vapors, anti-BLEVE safety could be provided. The secondary PRV would be set to discharge at some suitably higher pressure than the primary PRV.

A BLEVE is defined as an explosive release of expanding vapor and boiling liquid when a container holding a pressure-liquefied gas fails catastrophically[75]. But a failure of a tank holding a pressure-liquefied gas does not necessarily lead to a BLEVE. In general, if, for whatever reason, a fissure arises in a vessel holding a pressure-liquefied gas, there are three outcomes[76]:

(1) The fissure stops growing; there is no BLEVE, only a partial failure with jet release.
(2) Rocketing (partial failure with a liquid and vapor jet propelling the fragments).
(3) Total loss of containment and boiling liquid, expanding vapor explosion (BLEVE). This can occur either all at once or in two stages, as explained below.

For a BLEVE, as opposed to the other two failure modes, to occur, the liquid fill must be *below* a certain level. This is because a minimum energy must be available in the vapor volume to cause the crack in the metal to fully propagate[77]. This finding, of course, should not be taken to imply that tanks should be overfilled. Propane tanks are normally filled to 80% capacity. If a tank is overfilled, when it is subjected to heating (by a rise in ambient temperature, for example) the pressure inside the tank may rise sufficiently to cause discharge from the PRV. Many accidents have been reported where a discharge of this kind ignited, then caused flames to be applied to the tank, heating it further. This chain of events has ended in a BLEVE in many such incidents. Additional studies of non-BLEVE tank failures have been published[78].

Research by Birk and colleagues[76] at Queen's University in Canada and by Venart[79] at the University of New Brunswick identified the following sequence of steps as being characteristic of a BLEVE caused by flame impingement, and these are considered in some detail below.

- When flames impinge upon a tank, the liquid-filled portion stays cool due to heat-sink effects, but the steel around the vapor space rapidly heats up. Stresses increase, while strength has decreased due to the elevated temperature.
- Stresses in the tank wall are especially concentrated at the liquid/vapor interface.
- A crack develops in the tank wall, commonly located in the vapor-space portion, but near the liquid/vapor interface.
- Venting of the vapor results in a pressure drop within the tank and the liquid contents become superheated.
- The superheated liquid flashes, rapidly converting a sizable fraction of the liquid into vapor.
- If the vessel is fairly full, then vapor bubbles in the liquid cause the liquid volume to swell, resulting in a choked, two-phase liquid/vapor flow through the wall break. But if the vessel's fill level is low at the time of the BLEVE, then the two-phase outflow will comprise a mist/vapor discharge, rather than a highly turbulent liquid/vapor discharge.

- The pressure in the tank may drop, rise, or stay steady, depending on a complex interplay of a number of factors. Re-pressurization is discussed further below.
- At some point in the process, the fissure grows along the length of the tank and the tank catastrophically unzips with nearly instantaneous release of its contents. The crack propagation can be as slow as 1 m s^{-1} or as fast as 200 m s^{-1}.

Within this general BLEVE sequence, Birk[80] identifies two sub-categories of BLEVEs:

(1) A very rapid event transpiring once the original hole is formed, with the vessel opening up in 0.1 s or less. The energy in the vapor phase is the driving force in this type of BLEVE, since release of energy by flashing liquid would be too slow to contribute significantly. Vessels of low wall strength typically show this type of BLEVE.

(2) A slower event requiring 1 – 3 s for completion. In this type, crack growth slows down sufficiently after initial formation to let the liquid respond to the pressure drop created by venting. The boiling of the liquid then re-pressurizes the vessel and re-energizes the crack propagation process. This type of BLEVE is typical for vessels of higher wall strength.

Fire impingement upon the portion of the tank comprising the vapor space is much more dangerous than impingement to the liquid portion. When heating is applied to the vapor space, it is not necessary for the liquid phase to sustain an appreciable temperature rise before tank rupture occurs. Birk[81] has documented BLEVEs where the liquid temperature was close to 20ºC. Birk et al. also provided an argument (and limited data) to suggest that, in some cases, a partially-engulfed tank is more likely to BLEVE than a fully-engulfed one. This is related to stratification in the liquid and time required to de-stratify upon initial operation of the PRV.

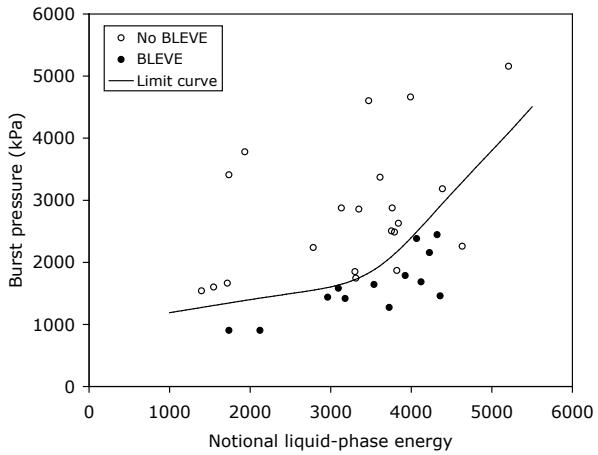


Figure 7 'BLEVE map' proposed by Birk et al. for estimating the likelihood of a tank to undergo a BLEVE

On the basis of a series of medium-scale experimental tests, Birk evolved a 'BLEVE map' (Figure 7) which is intended as a simple estimating tool to characterize the potential for a BLEVE. The x-axis is a simplified representation of the liquid-phase energy, defined as the average liquid-phase temperature (ºC) × fill percentage (%). The y-axis is a measure of the tank's strength, expressed as the burst pressure (kPa):

$$P_{burst} = \frac{2\sigma t_w}{D}$$

where σ = ultimate strength of wall material, taken at the average temperature of the wall surrounding the vapor-phase contents (kPa), t_w = wall thickness (m), and D = tank diameter (m). At failure, for steel tanks the average wall temperatures were measured to range from 580 to 780ºC. A peak value of ca. 800ºC is found; when steel reaches this temperature, very little strength remains (ca. 12%). A suitable expression for the ultimate strength of the grade of steel commonly used to make propane tanks gives:

$$\sigma = 2.85\times10^5 - 1.75\times10^5 \arctan\left(\frac{T-530}{75}\right)$$

where T = temperature (ºC). NFPA's tests[88] showed that, at failure, the wall stresses were 140 to 180% of the *room-temperature* yield stress.

The explosion usually involves a shock wave and must be attributed to more than just fracture of metal. It is found that a pressure *rise* can occur due to rapid depressurization of a tank which is otherwise at a stable pressure and temperature condition. Details of the repressurization process have been studied in small scale by Barbone et al.[82]. They found in their experiments repressurization levels up to 90% of the original pressure drop, but many tests showed a much smaller repressurization. McDevitt et al. conducted tests on small tanks holding R22, a non-flammable refrigerant gas[83]. The tank was heated to 65ºC, then an armor-piercing bullet was fired to open the tank. Pressure measurements showed drop from 2.7 MPa to 2.3 MPa after the bullet was fired in, then rising to 3.4 MPa, before ultimately dropping. Thus, the highest pressure was recorded *after* the hole was made, and the rise occurred due to initiation of boiling of a superheated fluid. The events were rapid, with the ultimate pressure drop only about 1 ms after bullet entry. These results, however, may be influenced by unique aspects of the bullet-firing scenario, i.e., the cavitation that is formed in the liquid behind the bullet, leading to a shock wave formation upon collapse of the bubble.

Reid[72] considers that the explanation involves the boiling process of liquids. Just before tank wall failure, the liquid/vapor system is saturated, that is, there is equilibrium of the vapor with the liquid. After the wall fails, pressure drops rapidly and the liquid should boil and drop its temperature to the value that it would have at 1 atm. But boiling does not start quickly, since initially there are no nucleating sites. Thus, for a while the liquid stays at a temperature above the equilibrium temperature. The explosion

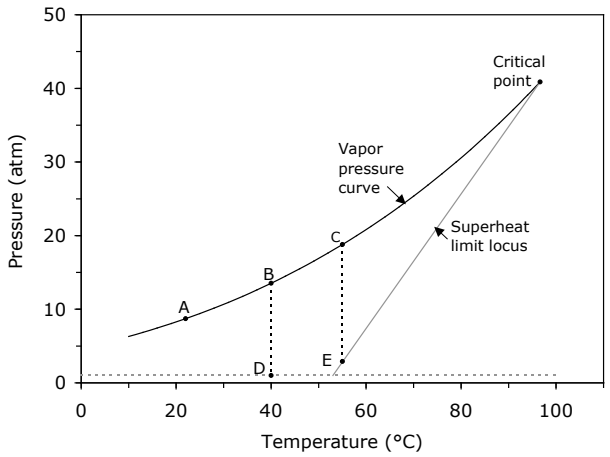


Figure 8 Propane tank depressurization, with and without superheated liquid-vapor explosion

which then occurs follows the theory of superheated liquid/vapor explosions. The conditions for propane are illustrated in Figure 8. In normal storage (point A), propane at room temperature is at a pressure of 8 – 9 atm. If a tank is heated up to point B and rapidly depressurized (to point D), the depressurization will not involve a superheated liquid-vapor explosion. But if the tank is heated up to point C (any temperature above ca. 53ºC) and then depressurized, point E intersects the superheat limit locus, thus the depressurization will generate a superheated liquid-vapor explosion. The temperature at point C is called the *superheat limit temperature* (SLT) and represents the maximum temperature to which a liquid can be superheated without cavitation (boiling).

The pressure in the vessel is the pressure of saturated vapor in equilibrium with the liquid at the vapor/liquid interface. This makes numerical treatment complex, since when heated, the liquid stratifies and the temperature at the vapor/liquid interface becomes higher than the average temperature of the liquid. After the PRV opens, however, the internal boiling tends to mix the liquid and reduce stratification. The flow through the PRV will generally be liquid with bubbles mixed in, as illustrated in the experiments of Sumathipala et al.[84] Data from Birk's tests[76] are shown in Figure 9. They indicate that the *average* liquid temperature is invariably lower than the saturation curve (BLEVE points are all to the left of the curve). If interface temperature and average temperature were identical, then the points would lie along the curve. It is also clear that all points are to the left of the superheat limit line. It is sometimes erroneously thought that BLEVEs can only occur if the average liquid temperature reaches the superheat limit temperature. The results indicate that BLEVEs occur substantially before this limit is reached, as also noted by Prugh[85]. Birk considers that appreciable superheat is uncommon in propane tanks, since nucleation sites are generally abundant[72].

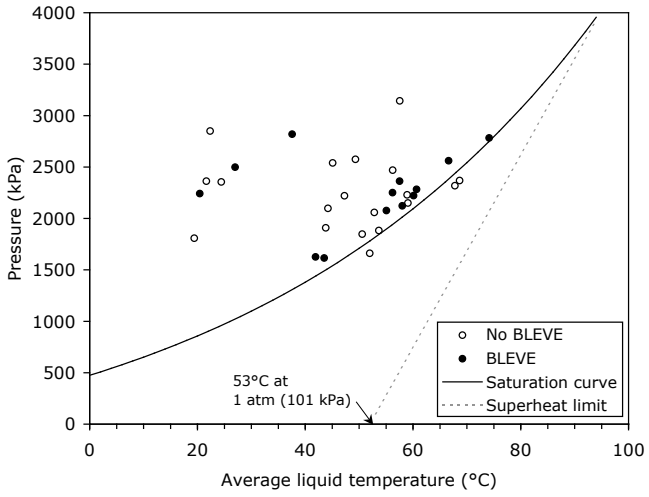


Figure 9 Average liquid temperature and pressure in 400 L propane tanks as a determinant of BLEVE potential

In the US, propane tanks are commonly equipped with a PRV set at 1800 kPa (for small tanks) or 2600 kPa (for large tanks). These correspond to propane saturation temperatures of 52ºC and 70ºC, respectively. Lower pressure settings lessen the likelihood of a BLEVE; to have a reasonable chance of being effective against a BLEVE scenario, Birk et al. urge that the setting be below 1700 kPa, which corresponds to a saturation temperature of 50ºC. It must be kept in mind, however, that PRVs are not designed nor intended to actually prevent BLEVEs, but rather to cope with milder incidents. Birk et al. also found that tank wall thickness has a much greater effect on failure than does the PRV setting, although it must be noted that the tanks in the Mexico City disaster had very thick walls.

Despite the ferocity of the fireball and possible shrapnel, the blast (overpressure) wave in air is moderate, at least as compared to high explosives. In one series of tests on BLEVEs from 400 L propane tanks, peak overpressures of only about 8 kPa (0.08 atm) were measured. The low overpressures are due to the low explosion energy of propane. Birk et al. point out that the explosion energy of TNT is 4680 kJ kg^{-1}, while the explosion energy of propane, evaluated as the isentropic expansion of liquid propane to atmospheric-pressure vapor is only 63 kJ kg^{-1}, or 1.3% of TNT. This figure does not include the energy released due to combustion, but experiments indicate that a BLEVE blast is produced by vapor expansion and not by the subsequent fireball combustion. The character of the blast is different from that of high explosives, since the blast is preferentially concentrated along the cylinder axis, rather than being axisymmetric.

Tank fragments can be propelled to fairly large distances. In one case, metallic fragments from the tank were recovered 229 m away[86]. In another case[87], a rail car fragment weighing more than 18,000 kg was propelled 366 m. In Birk's

tests on 400 L propane cylinders, shrapnel was propelled up to 200 m from the tank (Figure 10). In NFPA's tests on 1893 L propane cylinders[88], shrapnel was propelled also up to about 200 m. Larger distances are possible if the tank becomes propelled as a rocket. This form of propulsion is rare, but in the Mexico City disaster[74], 36 m^3 LPG tanks rocketed up to 1100 m, while projectiles from larger tanks only reached much shorter distances. This accident was extreme and it is rare for projectiles to be propelled farther than about 500 m.

The combustion of flammable material released in a BLEVE can have the character of a jet, a fireball, or a combination of the two. In some cases, a portion of the material remains as a pool, and this can burn as a pool fire on the ground. The effects of a fireball can be estimated with the equations given in Chapter 11 if the mass released is known. The mass that is flash-vaporized corresponds to the heat available to cool the liquid down to its boiling point[25]. While the specific heat and the latent heat are both temperature-dependent, an approximation can be made that they are constants, in which case a heat balance on the vaporization process gives:

$$\Delta h_v \, dm = C \, m \, dT$$

where Δh_v = latent heat of vaporization, m = liquid mass, C = liquid heat capacity, and T = temperature. By integration, the fractional amount of liquid remaining is:

$$\frac{m}{m_o} = \exp\left(-\frac{C}{\Delta h_v}\left(T_o - T_b\right)\right)$$

where m_o = initial mass, T_o is the initial temperature, and T_b the boiling point. The flash-vaporized fraction is then = $(1 - m/m_o)$. But the error from assuming constant Δh_v and C values becomes large unless the critical temperature, T_c, is much higher than the temperatures of interest. This, unfortunately, is not necessarily the case, and Prugh[85] computed more accurate values for the flash-vaporization fraction of a number of liquids (Table 2). Experimentally, it is found for propane that a BLEVE flash-vaporizes 40 – 50% of the contents, with the remainder being either large droplets or left as a liquid pool[77]. Thus, it should be reasonable to estimate fireball effects from LPG BLEVEs by assuming that 50% of the initial mass goes into the fireball. The fireball from a BLEVE can be somewhat different than one from a gas release, since bubbles rapidly develop in the superheated liquid and break, with the expelled fuel being partly an aerosol, not just a vapor. This has not been studied in detail.

Table 2 Flash-vaporization fractions computed from theory by Prugh

Substance	Temperature (°C)			Flash-fraction at SLT (%)
	T_b	SLT at 1 atm	T_c	
ammonia	-33	83	132	40
butadiene	-4	104	152	54
butane	-1	105	152	58
carbon dioxide	-79	-6	31	34
chlorine	-35	93	144	45
cyclohexane	81	220	280	61
ethylene	-104	-24	10	51
hydrogen chloride	-85	11	51	41
octane	126	240	296	67
phosgene	8	126	182	81
propane	-42	53	97	52
propylene	-48	52	92	51
sulfur dioxide	-10	50	158	21
water	100	280	374	36

Estimating the jet fire effects can be done if the mass release rate of the BLEVE is known. This requires modeling the development of the fissure in the tank and is not readily estimated by simple means, although Birk et al. reported

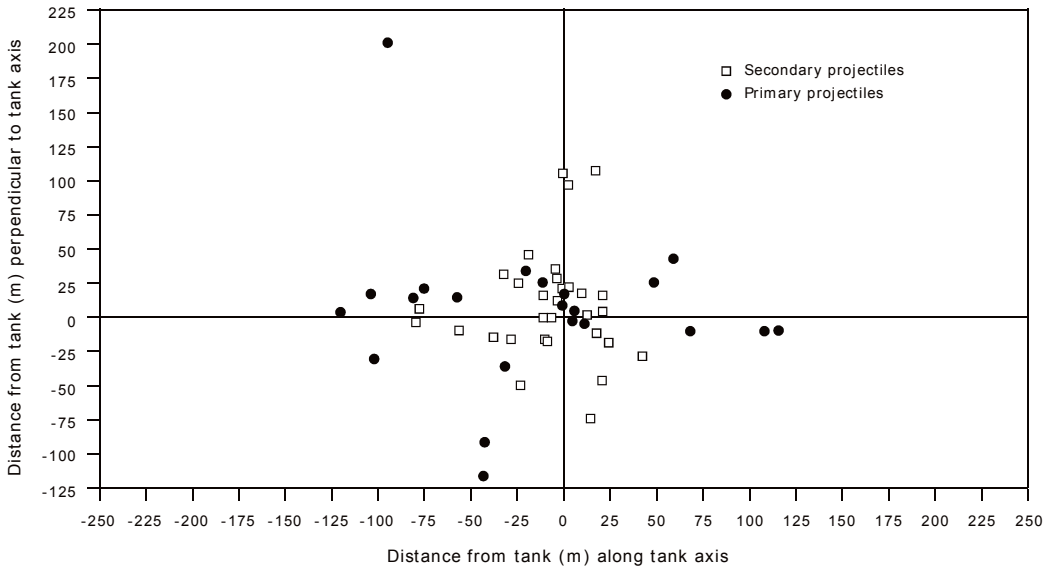


Figure 10 Distances to which shrapnel was propelled in BLEVE tests on 400 L tanks conducted by Birk et al.

reasonable success using a computational model.

According to Leiber[89], some BLEVEs of rail cars do not have external explanation, i.e., they are apparently 'spontaneous.' He studied a series of accidents and concluded that the mechanism is the same phenomenon as Venart's BLCBE: a resonance instability in the liquid, induced by a sudden, coherent collapse of bubbles within it. It is not clear, however, that a 'spontaneous' initiation is possible, i.e., one not precipitated by a mechanical failure causing an initial depressurization.

Some residential (home heating type) propane storage tanks were found to have a design defect that has led to BLEVE incidents[90]. These accidents took place due to corrosion of the tank causing the tank wall to lose sufficient thickness so that it could no longer withstand the pressure. It was found that (a) corrosion preferentially occurs at the tank weld rather than at bulk material; and (b) it is facilitated by accumulation of debris adjacent to it. The design defect consists in locating the weld along the bottom of the tank, where debris is likely to accumulate, rather than at the side, where it would not.

There are some LPG tanks that are made of *aluminum*, not steel. Birk and VanderSteen[91] conducted fire tests to determine the relative performance of small (36 L) LPG tanks of both materials. The test fire exposures were designed to be moderate, rather than severe, and comprised heating the test unit with one, two, or three torch flames, using low-velocity diffusion flames. Of three aluminum tanks tested, all ruptured, with one exhibiting a BLEVE; by contrast, of three steel tanks tested, none failed. These results are not surprising, given the fact that the temperature at which ultimate strength drops to 50% is about 600ºC for steel, but only 260ºC for aluminum. The authors noted that both types of cylinders, steel and aluminum, are claimed to conform to the industry standard, CGA C-14[92], which requires that either a bonfire or a chimney test be passed. The published description of these tests represents them as severe tests and the authors expressed concern that apparently the test methods are either mis-designed or mis-applied, since their own much less intense tests produced gross failures of the aluminum cylinders. Not surprisingly, the authors concluded that "The use of aluminum cylinders for LPG in all applications should be reviewed, along with the appropriate standards that apply to them."

For fire-caused BLEVEs, there are generally three preventive strategies[93]:
(1) prevent the initial fire
(2) prevent the fire from heating and, especially, weakening the tank
(3) prevent the buildup of pressure in the tank.

One of the main preventive measures against BLEVEs is tank insulation. After a slew of LPG rail ranker disasters in the 1970s[87,94-96], the rail industry retrofitted its flammable gas tank cars with external thermal insulation[*]. The thermal insulation serves to break the feedback loop by reducing or eliminating the warming up of the tank when external flames impinge upon it. More recently, thermal insulation jackets have been developed and tested[97] for small (7 to 47 kg) propane tanks. While it will not be typically applicable to tanks except on-site at a chemical plant, an interesting protection strategy is to ensure that a tank is always full, since steel will not be readily weakened if a liquid is available at the back face of the shell to act as a heat sink[93]. An industrial tactic using this approach is to have an auto-fill arrangement that adds water to a tank as the consumable liquid is withdrawn; the liquid, of course, must be compatible with water. Another way to use water in protecting fixed-installation tanks is to install a deluge water spray system. It is generally considered that a safety valve alone cannot be expected to protect against BLEVEs caused by exposure to a fire[93], however Moodie et al.[98] reported on a series of tests where a 5-T uninsulated road tanker was tested. The tanker was filled with LPG from 22 to 75% capacity in a series of 5 tests and subjected to external heating from a kerosene fire producing heat fluxes up to 100 kW m^{-2}. Despite heating for 10 – 30 minutes, no BLEVEs occurred. In each test, however, the PRV valves (two were fitted) operated and resulted in a tall flare burning. Thus, while the possibility of a BLEVE must be seriously considered when uninsulated tanks are engulfed, it is not a foregone conclusion that one will take place. Sometimes pressure regulators and fittings are made of a low-melting-point metal, e.g., a zinc alloy. The melting of this type of component is judged to have contributed to the severity of at least on BLEVE accident[99].

With propane tanks, a BLEVE will generally involve a fire. But there are exceptions. Color Plate 48 shows a tank which was overfilled and on which the PRV was defective and unable to operate. The ambient temperature rise from the time the tank was filled to the warm part of the day suffice to BLEVE the tank, but did not cause a fire.

Many jurisdictions permit 1000 gallon (3785 L) propane tanks to be located within 3 m of buildings. Birk[100] conducted a worst-case theoretical analysis of a tank placed near a re-entrant corner of a combustible building, so that it is 3 m from either of the two walls. The calculations indicated that a BLEVE is highly likely if the tank gets exposed to a fire occurs which involves burning of both walls in the corner, but it must be noted that only the worst-case scenario was treated, and that no validation data were available.

A major Canadian research project[75,81,101] has provided engineering guidelines on calculating the effects of BLEVEs and on appropriate response tactics. Experience has indicated that applying a water stream onto a tank engulfed in flames can itself trigger a catastrophic failure[99]. The TNO

[*] The industry prefers the term *thermal protection*, which includes alternative measures, such as intumescent coatings.

Yellow Book[70] and the AIChE manual[71] contain much useful design guidance for minimizing BLEVE potential at chemical plant installations. A collection of simple design formulas has been compiled by Prugh[73].

Oxygen-enriched atmospheres

In many of the preceding Chapters, oxygen concentration was considered as a variable which can encompass values both higher and lower than 20.95%. Because there are important safety issues associated with elevated-oxygen systems, in this Section we consider these issues specifically. Many metals are relatively safe in atmospheres at normal pressure and oxygen concentration, but turn out to be ignition-prone under elevated oxygen and pressure conditions. Many elevated-oxygen systems and processes are also ones that operate at high pressures, thus the role of high pressure must commonly also be taken into account. Ignitions in high-pressure oxygen systems can be difficult to eliminate since if the materials are functionally usable (e.g., strong enough, not too brittle) then they are also likely to be ignitable—the designer's role then being restricted to choosing less-ignition-prone ones rather than unignitable ones. Apart from industrial and NASA systems, enriched oxygen atmospheres are also common in hospitals; de Richemond and Bruley[102] reviewed a number of case histories. The entire available history of reported accidents within enriched-oxygen or hyperbaric chambers was reviewed by Sheffield and Desautels[103], who provided details on 39 accidents from 1923 through 1996 entailing 82 fatalities. The ignition sources identified by the authors are given in Table 3. In recent decades, most of the accidents have tended to be in countries which do not have strict regulations for enriched-oxygen activities. In pure-O_2 hyperbaric chambers, the consequences of fire are severe—the authors note that "No one has survived such a fire."

Table 3 Ignition sources leading to fires/explosions in enriched-oxygen or hyperbaric chambers

Ignition source	Number of accidents
electric spark/arc	15
electrostatic	8
hand warmer	4
smoking	4
external source	2
child's toy	2
welding	2
unknown	2

Basic guidance is available in a series of ASTM Guides[104-106] which provide useful procedures for identifying and mitigating hazards that might exist in oxygen-enriched environments. NFPA 53[107] provides additional guidance on ignition potential in oxygen atmospheres. The NASA standard on oxygen systems, NSS 1740[109], is comprehensive and offers excellent, practical advice which is useful in all oxygen-enriched applications, not just those of NASA; it has formed the basis of ASTM's newly-issued Manual 36[108]. These guides and standards all stress selecting materials that are more ignition resistant and less flammable as well as the importance of identifying and eliminating ignition sources. In oxygen service, autoignitions are considered rare, compared to situations where a localized form of igniting energy is present. Ignition due to adiabatic compression, however, can occur, and this is one form of non-localized energy that has sometimes been problematic in oxygen systems. Oil contamination can also lead to ignition without a localized source of energy present.

In oxygen-enriched systems, ignition mechanisms have to be considered which may be rare otherwise. NASA[109] considers the following to be important:

- Particle impact. The impact in an oxygen-enriched atmosphere of a small particle upon a surface may cause the mechanical strain energy to be converted to heat and to ignite the particle itself, and to then ignite the impacted surface.
- Mechanical impact. An example is a solenoid-actuated valve striking the valve seat. Aluminum, titanium, lead, and tin alloys are susceptible to this mechanism, but iron, nickel, copper, and cobalt alloys are not.
- Adiabatic compression. High-pressure oxygen released into a dead-end tube can ignite most polymers, although extra high pressures can also ignite metals. Pneumatic impact is considered to be the most common cause of ignition of polymers in oxygen systems. Slow-opening valves are often mandatory in oxygen systems.
- Promoted ignition. Ignition of contaminants, e.g., oils, can ignite adjacent components.
- Galling and friction. Heat from rubbing parts together, especially with the removal of protective oxide film is involved.
- Resonance. Acoustic oscillations in cavities can be sufficient for ignition. This was demonstrated at least for 400-series stainless steels.
- Electric arcing. Even corona discharges (which lack sufficient energy to ignite flammable atmospheres under normal conditions) may be incendive in high-pressure, enriched-oxygen systems since MIE values are much lower under those conditions.
- Flow friction. The interaction of leaking oxygen with a polymer seal or seat has been thought to cause ignition. This has been observe to occur in systems where a pressure differential greater than 6.8 MPa exists across the seal. The specific heat generating mechanism is not understood, but several such ignitions have been observed.
- Metal fracture.

A basic recommendation[106] on suitability of metals for high-oxygen atmospheres is:

Most suitable: Ag, Au, Cu, Ni, Pd, Pt

Least suitable: Ca, Be, Hf, Mg, Ti, Zr

The most-suitable metals are usually characterized by having low heats of formation, while the least-suitable ones have high heats of formation. Alkali metals do not follow this relation, but all of those are wholly unsuitable for oxygen service. Nickel-copper alloys (Monel) are the most ignition- and burn-resistant alloys for use in oxygen systems, followed by copper-based alloys. Nickel-iron alloys (Inconel) are also commonly suitable for use in oxygen systems. Stainless steels are less desirable than nickel-copper alloys because of their poor thermal conductivity, which makes them more reactive in oxygen service[110]. Aluminum alloys, iron alloys (apart from stainless steels), titanium, and magnesium are all readily ignitable in oxygen systems and should be avoided[109]. If these alloys are used, great care must be taken to ensure that the ignition mechanisms are identified and minimized or controlled. In 1997, a large air separation unit exploded in Malaysia, and the cause was determined to be ignition of aluminum used as vaporizer fins in a cryogenic distillation column through which LOX was circulated[111].

It is not necessary that a metal be finely divided for it to ignite and burn, if it is exposed to oxygen-enriched, high-pressure atmospheres. For example, a 6 mm layer of molten stainless steel can ignite and fully burn up if exposed to an atmosphere having over 3.7 atm of O_2 partial pressure[112]. The ignition temperatures of metals in oxygen atmospheres generally decrease with pressure, as shown in Figure 11[110,113], and this effect alone can explain a number of accidents. The results shown in Figure 11 must be viewed as only general guidance—actual ignition temperatures depend a lot on the details of the experiment. For example,

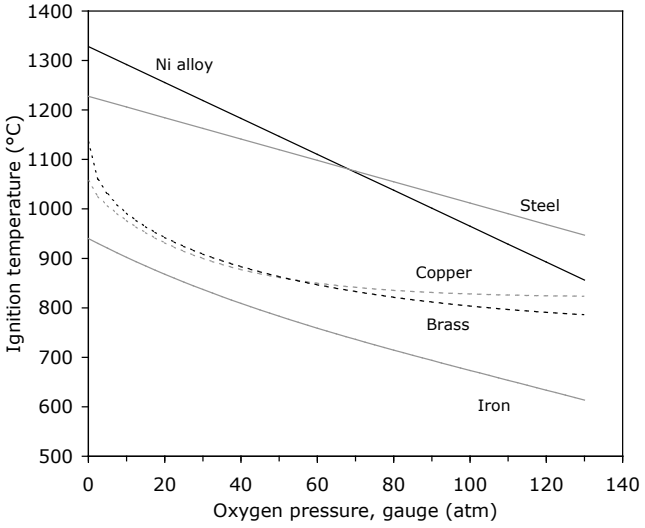


Figure 11 Effect of pressure on ignition temperatures of several solid metals in pure oxygen atmospheres

Bates et al.[114] found ignition temperatures of only 350ºC for ductile iron and for type 304 stainless steel at 50 atm. In addition, it appears that some metals show a reverse trend; data for zinc indicate that ignition temperature rises as the pressure is increased[115].

Enriched-oxygen accidents are mostly confined to industrial and manufacturing uses, however some consumer accidents also occur. Yallop[17] reports that cases have occurred where individuals mistakenly used an oxygen bottle to fill a vehicle tire. The compression was sufficient to ignite lubricants in the tire, with the resultant combustion bursting the tire and causing injury.

Frictional ignitions of metals in high pressure (6.9 MPa) gaseous oxygen environments were studied by Benz and Stoltzfus[116]. They constructed an apparatus where two identical metals were rubbed one against each other at high speeds. The results are given in Table 4. The sensitivities found vary by about 3 orders of magnitude. To be a correct expression of power delivered from frictional heating, the results should also be multiplied by the friction coefficient. Since this was not done in their experiments, the results should only be viewed as relative; in addition, the authors demonstrated that changing various test conditions will also affect the values obtained. The authors measured the bulk temperatures at ignition for a few metals and found that the values were, in certain cases, greatly lower than literature values. For aluminum, a value of 375 – 425ºC was found, compared to a literature value of ca. 2000ºC. This is understood to happen because the rubbing process removes the protective oxide film, which otherwise dominates the ignition mechanism of aluminum. A large set of pressure × velocity data has been compiled by Gunaji and Stoltzfus[117].

Table 4 Relative sensitivity of various metals to frictional ignition in high-pressure gaseous oxygen

Metal alloy	**Pressure ⋄ velocity product (MW m^{-2}) needed for ignition**
nickel 200	228 – 238
Inconel 600	199 – 289
Monel 400	142 – 155
Monel K-500	137 – 163
Hastelloy X	93 – 126
brass 360	69 – 117
Invar 36	60 – 94
stainless steel 316	54 – 72
aluminum 6061-T6	6.3
titanium 6A1-4V	0.39

Metallic components of systems that contain hyperbaric oxygen at elevated temperatures may be ignited by *impact of particles* against the metal. A review of the literature on this topic was presented by Benz et al.[118] Systems not intentionally operated at elevated temperatures are not necessari-

ly safe from ignitions of this type. A case incident was reported[119] where an Australian air force airplane was destroyed during the routine servicing of the crew's oxygen-breathing system. It was hypothesized that a thermite reaction involving aluminum and iron was the cause of the heating, with particle impact being the direct mechanism of ignition. The likelihood of ignition from impact of a polymer particle is minimal according to the experimental findings of Dees et al.[120]

Glassman and Law[121] have offered a relatively simple theory to explain the greatly increased hazards for reactivity of metals as the oxygen fraction in the atmosphere approaches 100%. It helps to explain why, for small-diameter, highly-reactive metals, the reaction rate increases drastically and non-linearly as the oxygen concentration approaches 100%. The increase often is sizeable only for oxygen mass fractions > 99%, and consequently the behavior can be governed by the exact amount of gaseous impurities present in the atmosphere. If oxygen concentration is ≈100%, then no limitation of surface reaction can exist due to a diffusional resistance; but if the value drops below 100%, then oxygen concentration can drop at the surface and this causes a reduction in reaction rate.

A very small amount of *contaminants* can suffice to ignite metals which are otherwise suitable for oxygen service. In one study[122], it was found that 1.5 mg of Buna-N rubber sufficed as an ignition source for Inconel 718 alloy. The ignition and explosion hazards associated with oil films in oxygen-handling equipment have been reviewed by Werley[123]. Shelley et al.[124] studied the ignition properties of PTFE tape contaminated with hydrocarbon oil and concluded that ignition properties can be affected, but unreasonably high levels of contaminant were required for this. Barthélémy and Vagnard[125] extracted contaminants (oil and exuded plasticizers) from used PTFE-lined hoses and found AIT values of only 160 – 220ºC using the ASTM G 72 test. They then tested hoses for adiabatic-compression ignition and were able to reproduce failures of the kind associated with actual incidents. But the results were similar, irrespective of whether the hoses were cleaned or not, so they concluded that basic ignition of PTFE is being involved in this type of accident, with little if any contribution from contaminants. Janoff et al.[126] reproduced these findings and concluded that stainless steel, rather than PTFE, hoses should be used in applications where this form of ignition may be a problem. However, Newton et al.[127] tested oxygen regulators with practically-occurring amounts of contaminants and found that the likelihood of an oxygen regulator fire or explosion is significantly increased by the presence of contaminants.

Under medium pressures, nonmetallic substances such as polymers can be ignited simply by impact of a high-pressure gaseous O_2 stream. This phenomenon was of sufficient concern to NASA that it led to the development of the ASTM G 74 test (see below). NASA researchers[128] tried to elucidate the mechanism of ignition and examined the following possible effects:

(1) adiabatic compression of the initial gas volume by the entering air stream (both real-life accidents and the ASTM test fixture involve an arrangement whereby the polymeric specimen is held in a closed test chamber which is rapidly pressurized);
(2) adiabatic compression of gas bubbles within the specimen;
(3) heating of the material by mechanical compression;
(4) interaction of shock waves with the specimen.

A definitive answer could not be reached, but they did rule out #3 since calculations indicated that, within the ASTM G 74 test chamber, a specimen would sustain less than a 100ºC rise from this mechanism. An effort to measure mechanism #1 experimentally was not successful, but a theoretical calculation suggested that, if mixing between the incoming gas and the gas already present within the volume is small, very high temperatures can be attained, more than sufficient for ignition. Hirsch et al.[129] proposed that the mechanism is primarily one of enhanced polymer gasification. At high pressures (e.g., 700 atm), there are essentially no practical materials which are able to resist ignition from the high temperatures which will be created if such pressures are rapidly imposed upon a system[110]. Ignition of metals by *laser* radiation was studied by Bransford[130].

Ikeda[131] measured the AIT for a number of polymers in pure gaseous O_2 at 1 atm; his results are given in Table 5. Hsieh et al.[132] measured the autoignition temperatures for a number of polymers under 100% oxygen, hyperbaric conditions. Their results are shown in Table 6. Certain polymers which have superior ignition properties at ambient oxygen conditions may not be acceptable in oxygen systems; silicone rubbers are an example[109]. Addition of glass-reinforcing material to polymers may similarly cause an unexpected worsening of ignition performance.

Table 5 Autoignition temperatures for polymers tested in 100% oxygen at a pressure of 1 atm.

Polymer	AIT (ºC)
Buna-N	489
Kalrez	429
Kel F-81, unplasticized	384
Neoprene	306-317
polyethylene	226
polyphenylene sulfide	533
polypropylene	231-262
polytetrafluoroethylene (Teflon)	512-527
PVC	402
silicone rubber	460-473
Vespel SP21	562
Viton	461-484

Table 6 Autoignition temperatures for polymers tested in 100% oxygen at a pressure of 100 atm.

Polymer	AIT (ºC)
ABS	243
butyl rubber	208
EPDM rubber	159
Fluorel	302
Halar	171
Kalrez	355
Neoprene	258
nitrile rubber	173
Noryl (polyphenylene oxide/polystyrene)	348
nylon 6,6	259
polycarbonate	286
polychlorotrifluoroethylene (ECTFE, Kel-F)	388
polyetheretherketone (PEEK)	305
polyetherimide	385
polyethersulfone	373
polyethylene	176
polyethylene terephthalate	181
polymethylene oxide	178
polyphenylene sulfide	285
polypropylene	174
polytetrafluoroethylene (Teflon)	434
polyurethane, flexible	181
polyvinylidene fluoride (Kynar)	268
PVC	239
silicone rubber	262
Teflon FEP	378
Teflon PFA	424
Tefzel	243
Viton A	268-322

Same as with fuel gases, oxygen may linger for surprising lengths of time in spaces supposedly opened up to the atmosphere. An accident is reported where elevated oxygen concentrations remained in an oxygen tanker that had been emptied of its contents and its manhole and all other openings left open for three weeks[16]. Testing of the oxygen level in one part of the tanker did not reveal an elevated concentration in another portion.

Radiation from oxygen-enriched fires is greater than from fires in 21% oxygen atmospheres. In an oxygen atmosphere, flame temperatures can be higher by 1000 K or more than they would be in air. This has strong implications for the ignition of *targets*, since radiant heat flux depends on temperature to the 4th power.

A related hazard of oxygen-enriched atmospheres is that some combustibles which, when ignited in normal air, do not show sustained combustion, may burn well in an oxygen atmosphere.

TEST METHODS

ASTM G 72 AUTOIGNITION TEST

A special test method has been developed for the autoignition of liquids or solids in hyperbaric 100% oxygen atmospheres. The test[133] is normally run at a pressure of 10.3 MPa and can be used for determining autoignition temperatures in the range of 60 – 425ºC. A stainless steel bomb of 0.11 L is surrounded by a heating jacket. A 200 mg sample is placed in a glass sampleholder, which is placed into a glass test tube, and the latter is put into the stainless steel bomb. After being filled with oxygen, the bomb is then heated at a rate of 5ºC per minute. Ignition is recorded as a rapid temperature rise of over 20ºC.

ASTM G 124 PILOTED IGNITION TEST FOR METALS

In this method[134], a stainless steel test chamber is used wherein a cylindrical shaped specimen, 3.2 mm diameter and 150 mm long, is placed. The bottom of the specimen is coated with magnesium or aluminum to act as combustion promoter and is ignited with a Nichrome or Pyrofuze (aluminum/palladium) igniter wire. The test chamber is filled with oxygen to the desired pressure and the igniter wire is powered. If sustained burning of the sample does not occur, a higher pressure is investigated. The basic reported result is the minimum oxygen pressure at which sustained burning occurs. The results are meaningful only in the context of the environment of the test apparatus.

ASTM G 74 GAS STREAM IMPACT TEST

In aerospace, chemical manufacturing, and other applications, situations exist where metals or other solids may be ignited by the high-velocity impact of pure oxygen or other oxidizer streams. ASTM G 74[135] subjects a 1.52 mm thick test specimen at room temperature to an oxidizing gas stream impacting at 69 MPa. Five cycles are performed and ignition or non-ignition is reported. Werley[136] has analyzed some of the test's features. Hirsch et al.[129] demonstrated that there is a strong correlation between the results of this test and the material's AIT, provided the test is run in a way as to determine a quantitative value for the impact reactivity level, not just a go/no-go result. For AIT values in the range 170 – 450ºC, the relation is:

$$I_{50} = 0.423\,T_{ig} - 0.192$$

where I_{50} = impact reactivity level (MPa), calculated at the 50% probability, and T_{ig} = AIT (ºC), as determined in the ASTM G 72 test.

ASTM D 2512 AND ASTM G 86 MECHANICAL IMPACT TESTS

The ASTM D 2512 method[137] is an impact tester developed by the Army Ballistic Missile Agency. Liquids or solids are tested. Liquids are poured as a 1.27 mm layer in a 16.7 mm diameter sample cup. Solids are prepared as a disk of 17.5 mm diameter and 1.52 mm thickness, although other thicknesses may be used. The test cavity is pressured with gase-

ous oxygen, or liquid oxygen may be poured into the test assembly when testing for LOX service. A mechanical drop hammer is released to provide the impact to the specimen. NASA and other agencies have collected extensive data with this test method. ASTM G 86[138] uses the same test apparatus as ASTM D 2512, but adapted for testing at elevated pressures of up to 68.9 MPa.

ASTM G 125 OXYGEN-INDEX TEST FOR OXYGEN-ENRICHED ATMOSPHERES

The ASTM G 125 test[139] is a slight variant of the standard ASTM D 2863 oxygen index test for use by individuals interested in evaluating materials for elevated oxygen service. The same principle of examining the candle-like burning of materials in atmospheres of various oxygen contents is used. Same as with the ASTM D 2863 test, a strong caution must be applied that there is little generality in the results thus obtained.

Wildland-urban interface

A cluster of ignition-related problems tend to occur at the wildland-urban interface, that is, in locations where houses abut wildlands, which can be forests or grasslands. Losses of houses due to ignition from wildland fires has been a serious problem in Australia, California and elsewhere. Ignition of houses from wildland fires involves one or more of these mechanisms:

- radiation
- direct flame contact
- firebrands (embers).

Thus, over the years a number of studies have been conducted to elucidate both the relative contribution of various construction features towards the vulnerability of houses, and to evolve recommendations for improved construction practices.

An early Australian study in 1945 identified the pivotal role of flying brands[140]. The study concluded that:

- the materials of the external walls were of minor importance
- the preponderance of the highly destructive fires started *inside* the house, most commonly due to ingress of flying brands.

Consequently, the recommendations were:

(1) to provide mesh on all openings into attics and subfloor spaces. Eaves should preferably be covered by a board along the bottom and not by mesh.
(2) concerning clay roof tile, to use only types that do not have opening allowing ingress of brands.
(3) both clay-tile and corrugated-iron roofs should use a fascia board which closes off openings at the edge of the roof.

The study also documented brick-veneer houses where window glass sagged, but wood window frames did not ignite. Current Australian recommendations[141] are that, in general, firebrands should be expected to be severe for houses located up to ½ km away from the perimeter of a forest.

In later decades, statistics were collected in Australia about certain characteristics of houses that lead to their ignition and destruction, or not, when confronted with a wildland fire. After a series of 1994 fires, a statistical study[142] focused on the effect of cladding material (Table 7). Clearly, the ignitability of the material plays a strong role, but the authors pointed out that there are intervening 'style' variables. For instance, more wood-clad houses had unenclosed subfloor spaces, which served to promote destruction of houses. Thus, these findings do not necessarily contradict the earlier ones.

Table 7 Effect of exterior cladding materials on house survival

Cladding material	Percent		
	Not ignited	Damaged	Destroyed
masonry	68	15	17
cement boards	48	13	39
wood	33	7	59

In that study, statistics obtained on houses where firebrands were either the sole ignition mechanism, or where ignition was due to a combination of firebrands and heat radiation are shown in Table 8.

Table 8 Materials first ignited by firebrands in Sydney, Australia houses surveyed after the January 1994 wildland fires

Material first ignited	Houses ignited	
	By brands	By brands and radiation
fascia board	9	6
wood deck	13	–
wood window frame	6	6
wood door frame	4	2
wood cladding	5	–
interior contents via broken window	–	4
exposed wood structural member	4	–
wood shingles	2	–
wood stairs	2	–
door mat	2	–
plastic roof panel	2	–
asphalt roofing	1	–
canvas awning	1	–
other	1	–

Another Australian study[143] identified that radiation, by itself, is only rarely the cause of a house to be lost. In a further Australian study[144], it was found that the color of wall cladding did not have a significant effect, but several other factors were quantified with respect to risk of house destruction. Table 9 shows that clay tiles were found the most resistant, presumably due to their low transmission of heat.

It was also found that pitched roofs showed a lower relative risk (0.8, versus 1.0) than flat roofs. A profound difference was found concerning the surrounding vegetation (Table 10); the statistics do not take into account aspects of owner maintenance because evidence was typically destroyed.

Table 9 Effect of roof material on risk of house destruction from a wildland fire

Roof material	Relative risk of house destruction
clay tiles	0.6
steel deck	1.0
corrugated iron	1.4
asbestos-cement	1.5

Table 10 Effect of vegetation type on risk of house destruction from a wildland fire

Vegetation type	Relative risk of house destruction
grass	1.0
shrubs	3.5
trees	8.6

In 1984 Wilson presented a calculational scheme for predicting the probability of house survival in a bushfire[145], based on the study of 450 houses affected by the 1983 Mt. Macedon fire. Six different factors are to be evaluated, as shown in Table 11. If the score is 6.3, then there is a 50% probability of survival; for a score of 4.0 the probability is 90%, while for 8.5 it drops to 10%. Fire intensity is to be estimated on the basis of fuel load (Table 12); a correction factor is applied to the fuel load if the ground slope is not zero. Wilson's scheme indicates that if the fire intensity is very high, the probability of house survival is low, irrespective of how it is constructed or protected. But for lower fire intensities prudent construction practices will affect the outcome, of which the most important is roof material. Nearly as important is the presence of a responsible adult, who may be able to extinguish embers, etc.

Table 11 Factors in the Wilson scheme for estimating the probability of house survival in bushfires

Factor	Points
Fire intensity (kW m^{-1})	
> 10,000	5.2
1,500 – 10,000	3.6
500 – 1,500	2.3
< 500	0.0
Attendance by residents	
unattended	2.2
attended	0.0
Roof	
wood shingles	2.4
metal, fiber, or slate, w. pitch > 10°	1.4
tiled, incl. steel pressed tiles	0.0
any material w. pitch < 10°	0.0
Wall material	
combustible	1.1
non-combustible	0.0
Presence of flammable objects	
present	0.8
absent	0.0
Presence of plants > 5 m high and within 40 m of house	
present	0.6
absent	0.0

Table 12 Fuel loads corresponding to various fire intensities in the Wilson scheme

Fire intensity (kW m^{-1})	Fuel load (tonnes/hectare)	
	Grass fuel	Forest fuel
> 10,000	> 1.7	> 14
1,500 – 10,000	0.3 – 1.7	5.3 – 14
500 – 1500	0.1 – 0.3	3 – 5.3
< 500	< 0.1	< 3

Some examples of ignitions from brands are shown in Color Plate 49 through Color Plate 52. The smoldering combustion of a wood fence post ignited during a wildland fire is shown in Color Plate 53.

Other factors were studied in California[146], where prevalent construction types are different. Roof factors (untreated wood shake roofs have been very popular in California) and vegetation clearance factors are given in Table 13 and Table 14. The combined effect is shown in Table 15. There is an overwhelming probability of house destruction in California wildland fires if the roof is flammable and brush clearance is not maintained. No systematic study exists, but experience in southern California also indicates that houses located in *canyon areas* are more vulnerable than ones in flat terrain.

In general, aspects of house construction or maintenance that can minimize the risk of ignitions include:

1. Removing vegetation from close proximity to buildings; replacing vegetation with types considered to be relatively fire resistant.
2. Providing of roofs that are not easily ignitable by fire brands. Testing is done according to ASTM E 108, and acceptable products are classified at least in Class C, although Class B or Class A provide higher protection.
3. Screening of vents in attics and under-eaves with metal screens that can keep out fire brands.
4. Minimizing eaves projections or cantilevers; avoiding construction on stilts. These forms of construction lend themselves to 'trapping fire.' Eaves should be covered on the bottom with non-combustible material.
5. Using double-glazed window, which better resist breakage due to external radiation. A second pane of glass also attenuates further radiation that might ignite curtains prior to glass breakage. Thicker panes of glass or tempered glass can also better resist breakage. In structures where their use will be acceptable, wired

glass or steel shutters over windows should be considered.
6. Non-combustible cladding (e.g., brick) should be considered in vulnerable locations.
7. Roof sprinklers have been found useful in certain instances.
8. Roofs, gutter, and areas around the structure should be kept free of vegetation litter and other combustibles. In many areas, accumulations of vegetative matter in gutters are easily ignitable and can then serve to ignite the eaves, thus, house designs that do not use gutters are safer[147]. Clearing away debris fully, however, may be a hopeless task. In many cases, even if gutters and decks have been cleared of dry leaves a few days before a wildland fire, they will fill again on the morning of the fire[148].

More detailed recommendations on constructing and maintaining homes to minimize the risk of destruction by wildland fire have been published in several guides on the topic. The US Forest Service has developed a guide[149], as have Australian authorities[150]. Documents intended for possible regulatory adoption include NFPA 1144[151] and the ICBO Urban-Wildland Interface Code[152].

Radiant heat ignition or direct flame contact, while not the dominant ignition causes, are more amenable to systematic analysis, thus, a research program has been conducted at the US Forest Service to model the ignition of structures from radiant heat and from direct flame contact. The initial study[153] suggested that a 15 m tall flame would possibly cause an ignition at a distance of 14 m from a normal wood surface if piloted ignition conditions prevailed and the flame front lasted at least 60 s. The study also entailed experiments where wood siding materials were exposed to burner flames of up to 2 m high. Ignition took place in about 1 min from the burner flames, but flaming was not sustained upon removal of the flame source. Smoldering, however, continued and in some cases active flaming could be brought about by wind.

Table 13 Effect of flammability of roofing on house destruction by wildland fire

Roof	Percent of houses destroyed
flammable	81
non-flammable	30

Table 14 Effect of brush clearance on house destruction by wildland fire

Brush clearance of 9.1 m (30 ft)	Percent of houses destroyed
not maintained	62
maintained	22

Table 15 Effect of combined factors on house destruction by wildland fire

Factors	Percent of houses destroyed
roof flammable, brush clearance not maintained	96
roof non-flammable, brush clearance maintained	14

Crown fires in a forest typically show flame heights of twice the canopy height and heat release rates of 35 – 70 MW per meter of flame front[154], but the duration[155] of a crown fire is only about 60 s. A limited amount of full-scale ignitability data have been collected from large-scale experimental forest fires where a wood façade was exposed[155]. These indicated that scorching, but not sustained ignition occurred from a flame front 10 m away (Color Plate 54). When actual flame contact was made with the wall, however, ignition occurred.

Determining ignition properties in fire investigations

In general, any fire properties can be determined in one of two ways: (1) by looking up values in a handbook, or (2) by conducting tests. The investigator may have identified that a "standard" material or product was involved, one which shows up in handbook tabulations. Thus, there is a temptation to simply analyze the fire by assuming the flash point temperature, minimum flux for ignition, etc., on the basis of handbook data. However, if there is any remaining material to be tested it is generally wiser to actually test the material. For some fire properties, tests can be very expensive, thus they are commissioned only as a last resort. Ignition tests, however, are invariably modestly-priced. One major benefit of having tests conducted on the exemplar substance is that impure or contaminated substances are identified. The tank *may* have held kerosene, but the kerosene was contaminated with gasoline and had a much lower flash point. The flash point test will establish this, and it is simpler to run and less costly than a comprehensive chemical analysis of the specimen, for instance, using GC-MS. However, a flash point test requires a substantial amount of specimen, compared to quantities of less-than-one-drop needed for a GC/MS analysis; thus, specimen availability may be a determining factor.

Further readings

R. J. Harris, **The Investigation and Control of Gas Explosions in Buildings and Heating Plant**, E&FN Spon, London (1983). The only full-length monograph on this topic.

Buildings and the Hazard of Explosion—Proceeding of a Symposium at BRE, Garston, 18 October 1972 (BRE Report), Building Research Establishment, Garston UK (1974).

A Michael Birk et al., Fire Tests of Propane Tanks to Study BLEVEs and Other Thermal Ruptures: Detailed Analysis of Medium Scale Results (TP12498E), Transportation Devel-

opment Centre, Montreal (1997). The most extensive study available on BLEVEs.

Irma M. Hill, **Crescent City Remembers: Father's Day, June 21, 1970**, Scheiwe's Print Shop, Crescent City IL (1995). A book describing in detail one of the most serious rail-car BLEVEs.

References

1. Parker, D. J., and Owings, C. W., Gas Explosions in Buildings: Their Cause and Prevention (IC 7142), Bureau of Mines, Pittsburgh (1941).
2. Fletcher, B., and Johnson, A. E., The Accumulation of Gases in Ventilated and Unventilated Enclosures, pp. 333-353 in *Ventilation '85*, Elsevier, Amsterdam (1986).
3. Harris, R. J., **The Investigation and Control of Gas Explosions in Buildings and Heating Plant**, E&FN Spon, London (1983).
4. Pipeline Accident Report: Consolidated Edison Company Explosion at 305 East 45th Street, New York, NY, April 22, 1974 (NTSB-PAR-76-2), Natl. Transportation Safety Board, Washington (1976).
5. Rabinkov, V. A., The Distribution of Flammable Gas Concentrations in Rooms, *Fire Safety J.* **13**, 211-217 (1988).
6. Clodic, D., Leak Flow Rates and Measurement of Concentration Gradients of Flammable Refrigerants, Centre d'Energétique, Ecole des Mines de Paris, France (1997).
7. Weckman, E. J., HFOG (House Full of Gas) III. Part A: Filling and Venting Experiments, paper presented at Spring Technical Meeting, Canadian Section, The Combustion Institute, Victoria BC (May 1995).
8. Matson, A. F., and Dufour, R. E., Persistency of Odor of Accidentally Released "Pyrofax" Liquified Petroleum Gas (Bull. of Research No. 37), Underwriters Laboratories, Chicago (1946).
9. Lapina, R. P., and Sokalski, M. A., Time to Reach Lower Explosion Limit for Propane, *Fire & Arson Investigator* **51**:2, 42-44 (Jan. 2001).
10. Cleaver, R. P., Marshall, M. R., and Linden, P. F., The Build-up of Concentration within a Single Enclosed Volume Following a Release of Natural Gas, *J. Hazardous Materials* **36**, 209-226 (1994).
11. Bodurtha, F. T., **Industrial Explosion Prevention and Protection**, McGraw-Hill, New York (1980).
12. Ogle, R. A., Explosion Hazard Analysis for an Enclosure Partially Filled with a Flammable Gas, *Process Safety Progress* **18**, 170-177 (1999).
13. Valentine, R. L., and Moore, R. D., The Transient Mixing of Propane in a Column of Stable Air to Produce a Flammable but Undetected Mixture, (ASME Paper 74-WA/HT-39), American Society of Mechanical Engineers, New York (1974).
14. Liebman, I., Spolan, I., Kuchta, J. M., and Zabetakis, M. G., Ignition of Tank Atmospheres During Fuel Loading, 30th Midyear Meeting, American Petroleum Institute, Montreal, Canada (11 May 1965).
15. Steen, H., On the Measurement of the Propagation of Explosive Mixtures in Free Atmosphere, pp. 64-67 in *Conf. on Electrical Safety in Hazardous Environments* (Conf. Publ. No. 74), Institution of Electrical Engineers, London (1971).
16. Médard, L. A., **Accidental Explosions**, 2 vols., Ellis Horwood, Chichester, England (1989).
17. Yallop, H. J., **Explosion Investigation**, The Forensic Science Society, Harrogate and Scottish Academic Press, Edinburgh (1980).
18. Cooper, W. F., Electrical Hazards in Danger Areas, pp. 177-185 in *Conf. on Electrical Safety in Hazardous Environments* (Conf. Publ. No. 74), Institution of Electrical Engineers, London (1971).
19. Precautions Against Fire and Explosion in Underground Car Parks (Post-War Building Studies No. 28), HMSO, London (1950).
20. Munoz-Candelario, R., and Alvares, N. J., Definition of the Concentration Gradient above Flammable Liquids, pp. 377-385 in **Fire Safety Science and Engineering** (ASTM STP 882), ASTM (1985).
21. Tamanini, F., Explosive Volume Formation from the Release of Vapors or Liquids in Enclosures, *Fire Safety Science—Proc. 7th Intl. Symp.*, Intl. Assn. for Fire Safety Science (2002).
22. Tamanini, F., Engineering Predictions of Explosive Layer Formation in Flammable-Liquid Spills, *Combustion Science and Technology* **174**:11/12, 223-239 (2002).
23. Sutton, O. G., **Micrometeorology**, McGraw-Hill, New York (1953).
24. Wade, S. H., Evaporation of Liquids in Currents of Air, *Industrial Chemist* **18**, 55-58 (1942).
25. Clancey, V. J., The Evaporation and Dispersal of Flammable Liquid Spillages, pp. 80-98 in *Proc. 5th Symp. on Chemical Process Hazards with Special Reference to Plant Design* (Symp. Series 39a), The Institution of Chemical Engineers, London (1974).
26. Kawamura, P. I., and Mackay, D., The Evaporation of Volatile Liquids, *J. Hazardous Materials* **15**, 343-364 (1987).
27. Wang, W., Mathematical Model of Vaporization During Gasoline Spills (M.S. thesis), Worcester Polytechnic Institute, Worcester MA (1997).
28. Gauss, A., Fuel and Hydrocarbon Vaporization (Report No. 1661), US Army Ballistic Research Labs., Aberdeen MD (1982).
29. DeHaan, J. D., The Reconstruction of Fires Involving Highly Flammable Hydrocarbon Liquids (Ph.D. dissertation), Univ. Strathclyde, Glasgow, UK (1995).
30. Mackay, D., and Matsugu, R. S., Evaporation Rates of Liquid Hydrocarbon Spills on Land and Water, *Can. J. Chem. Engrg.* **51**, 434-439 (1973).
31. Brighton, P. W. M., Further Verification of a Theory for Mass and Heat Transfer from Evaporating Pools, *J. Hazardous Materials* **23**, 215-234 (1990).
32. Lennert, A. S., Experimental and Theoretical/Numerical Study of Evaporation from Shallow Pools of Organic Liquids, at Simulated Work Place Conditions (Ph.D. dissertation), Danmarks Tekniske Universitet, Lyngby, Denmark (1998).
33. Wren, T., and Martin, D., Evaporation Rates of Motor Spirit Pools in Tunnels (AEAT-0344), AEA Technology, [n.p.] (1995).

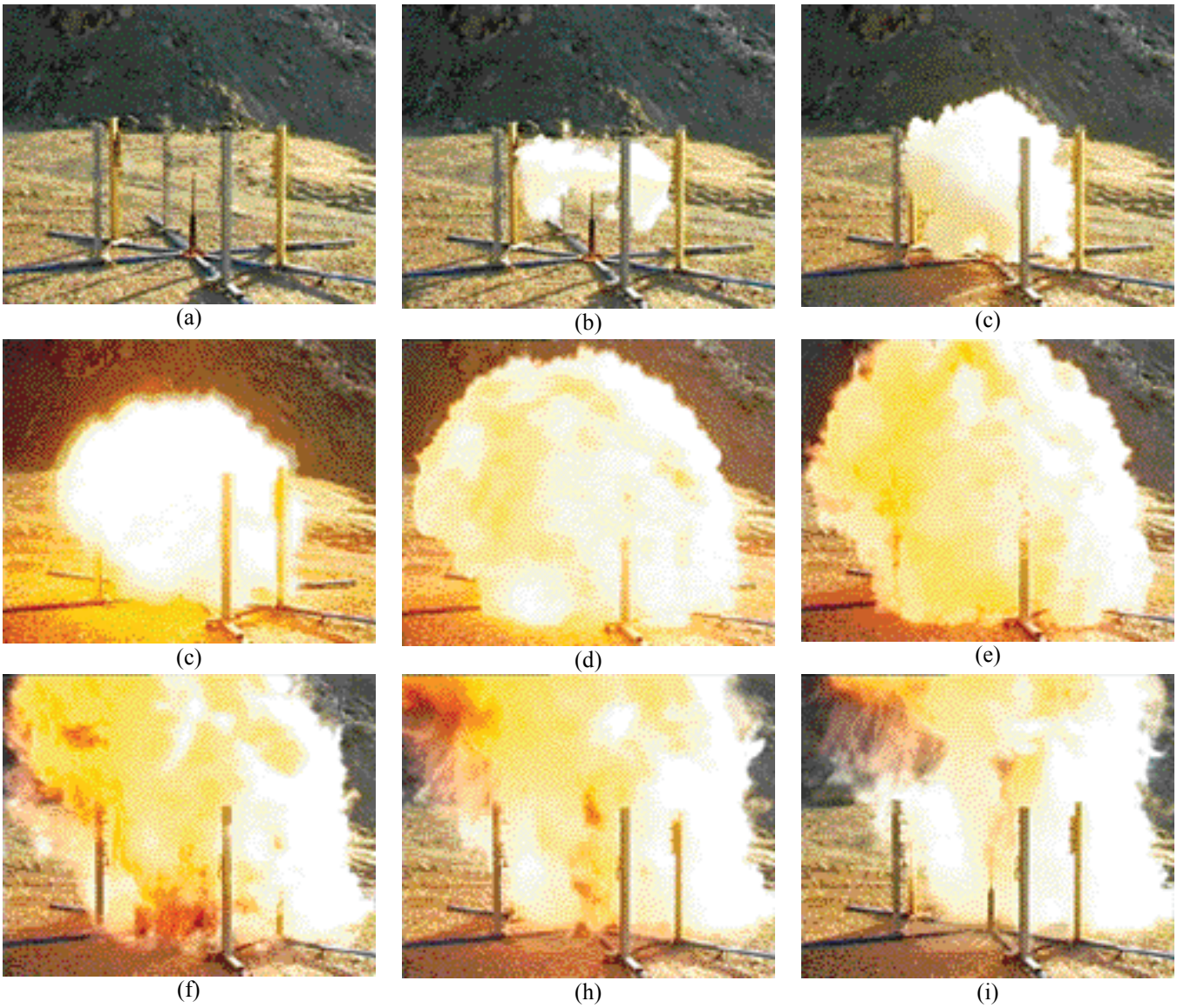
34. Smith, M. T. E., Birch, A. D., Brown, D. R., and Fairweather, M., Studies of Ignition and Flame Propagation in Turbulent Jets of Natural Gas, Propane, and a Gas with a High Hydrogen Content, pp. 1403-1408 in *21st Symp. (Intl.) on Combustion*, The Combustion Institute, Pittsburgh (1986).
35. DeHaan, J. D., Crowhurst, D., Hoare, D., Bensilum, M., and Shipp, M. P., Deflagrations Involving Stratified Heavier-than-Air Vapor/Air Mixtures, *Fire Safety J.* **36**, 693-710 (2001).
36. Hagimoto, Y., Kinoshita, T., and Hagiwara, T., Ignitability of Various Solid Combustibles by Gas Explosion, *Summary of the 14th Annual Mtg. of Japan Soc. for Safety Engineering* 55-56 (1981).
37. HFOG II/III Seminar—House Full of Gas, Fire Investigation Assn. of Alberta and Edmonton Emergency Response Dept., Edmonton (1995).
38. Dale, J. D., Weckman, E. J., and Ackerman, M., HFOG (House Full of Gas) III. Part B: The Explosion and Aftermath, paper presented at Spring Technical Meeting, Canadian Section, The Combustion Institute, Victoria BC (May 1995).
39. Fang, J. B., and Breese, J. N., Fire Development in Residential Basement Rooms (NBSIR 80-2120), NBS (1980).
40. Lentini, J. J., and McCarver, J. F., Melted Steel: How Important? *The National Fire and Arson Report* **10**:4 (1992).
41. Babrauskas, V., Will the Second Item Ignite? *Fire Safety J.* **4**, 281-292 (1981/82).
42. Peacock, R. D., Jones, W. W., Bukowski, R. W., and Forney, C. L., Technical Reference Guide for the HAZARD I Fire Hazard Assessment Method, Version 1.1 (NBS Hdbk. 146), vol. II, NIST (1991).
43. DeHaan, J. D., Full-Scale Compartment Fire Tests, *The CAC News (California Assn. of Criminalists)*, cover, 14-21 (2nd Quarter 2001).
44. Beyler, C. L., Ignition and Burning of a Layer of Incomplete Combustion Products, *Combustion Science and Technology* **39**, 287-303 (1984).
45. Sherman, P. R., Computer Model for the Prediction of Ignition and Burning of an Upper Layer of Products of Combustion (M.S. thesis), Worcester Polytechnic Institute, Worcester MA (1988).
46. Guide for Fire and Explosion Investigations (NFPA 921), NFPA.
47. Croft, W. M., Fires Involving Explosions—A Literature Review, *Fire Safety J.* **3**, 3-24 (1980/81).
48. Fleischmann, C. M., Pagni, P. J., and Williamson, R. B., Quantitative Backdraft Experiments, pp. 337-348 in *Fire Safety Science—Proc. 4th Intl. Symp.*, Intl. Assn. for Fire Safety Science, Boston (1994).
49. Gottuk, D. T., Peatross, M. J., Farley, J. P., and Williams, F. W., The Development and Mitigation of Backdraft: A Real-Scale Shipboard Study, *Fire Safety J.* **33**, 261-282 (1999).
50. Dunn, V., Smoke (Backdraft) Explosions, *Firehouse* 18-24 (Sep. 2000).
51. Weng, W. G., and Fan, W. C., Catastrophic Behaviour of Backdraft in Compartment Fires, pp. 121-130 in *Fire Science and Technology—Proc. 5th Asia-Oceania Symp.*, Univ. Newcastle, Australia (2001).
52. Courtnell, P. M., A Study into the Phenomenon of Backdraught (B.Eng. thesis), Dept. of Built Environment, Univ. Central Lancashire, Preston, UK (1998).
53. Karlsson, B., and Bengtsson, L., Flashover, Backdraft and Smoke Gas Explosion—The Fire Service Perspective, pp. 567-578 in *Interflam '99*, Interscience Communications Ltd., London (1999).
54. Bengtsson, L., and Karlsson, B., An Experimental and Statistical Study of Flashover, Backdraught and Smoke Gas Explosion, pp. 143-154 in *Fire & Explosion Hazards—Proc. 3rd Intl. Symp.*, Univ. Central Lancashire, Preston, England (2000).
55. Bolliger, I. B., Full Residential-Scale Backdraft (Fire Engineering Research Report 95/4), School of Engineering, Univ. Canterbury, New Zealand (1995).
56. Sutherland, B. J., Smoke Explosions (Report 99/15), School of Engineering, Univ. Canterbury, New Zealand (1999).
57. Hayasaka, H., Kudou, Y., Kojima, H., and Ueda, T., Backdraft and Various Backdraft Related Phenomena Observed in Small Compartment Fires, pp. 232-239 in *Proc. 14th Joint Panel Meeting of the UJNR Panel on Fire Research and Safety*, Building Research Institute & National Research Institute of Fire and Disaster, Tsukuba, Japan (1998).
58. Chitty, R., A Survey on Backdraught, Fire Research & Development Group, UK Home Office, London (1994).
59. Gojkovic, D., and Bengtsson, L., Some Theoretical and Practical Aspects on Fire-Fighting Tactics in a Backdraft Situation, pp. 1093-1104 in *Interflam 2001—Proc. 9th Intl. Conf.*, Interscience Communications Ltd., London (2001).
60. Smith, J. P., Roof Truck Work, *Firehouse* 20, 22-23 (Dec. 2002).
61. Dunn, V., Rekindle Fires, *Firehouse* 16-22 (Mar. 2000).
62. Gustin, B., How to Avoid Rekindle Fires, *Fire Engineering* **153**, 69-73 (Nov. 2000).
63. Musselman, H. H., A Case of Spontaneous Combustion of Hay, *Michigan Agricultural Experiment Station Q. Bull.* **17** 175-182 (1935).
64. Tucker, D. M., The Explosion and Fire at NYPRO (UK) Ltd, Flixborough on 1 June 1974 (BRE Note N60/76), Building Research Establishment, Garston, England (1976).
65. Baker, W. E., and Tang, M. J., **Gas, Dust and Hybrid Explosions**, Elsevier, Amsterdam (1991).
66. Moen, I. O., Bjerketvedt, D., Jenssen, A., and Thibault, P. A., Transition to Detonation in a Large Fuel-Air Cloud, *Combustion and Flame* **61**, 285-291 (1985).
67. Burgess, D. S., and Zabetakis, M. G., Detonation of a Flammable Cloud Following a Propane Pipe Leak (RI 7752), Bureau of Mines, Pittsburgh (1973).
68. Wiekema, S. J., Vapor Cloud Explosion Model, *J. Hazardous Materials* **3**, 221-232 (1980).
69. Wiekema, B. J., Vapor Cloud Explosions—An Analysis Based on Accidents, *J. Hazardous Materials* **8**, 295-329 (1984).
70. Committee for the Prevention of Disasters [of The Netherlands], Methods for the Calculation of Physical Effects due to Releases of Hazardous Materials (Liquids and Gases)—'Yellow Book' (CPR 14E), 2 vols., 3rd ed., C. J. H. van den Bosch and R. A. P. M. Weterings, eds. SDU Uitgevers, The Netherlands (1997).
71. **Guidelines for Evaluating the Characteristics of Vapor Cloud Explosions, Flash Fires, and BLEVEs**, Center for Chemical Process Safety of the AIChE, New York (1994).
72. Reid, R. C., Possible Mechanism for Pressurized-Liquid Tank Explosions or BLEVE's, *Science* **203**, 1263-1265 (1979).

73. Prugh, R. W., Quantify BLEVE Hazards, *Chem. Eng. Prog.* **87**, 66-71 (Feb. 1991).
74. Pietersen, C. M., Analysis of the LPG-Disaster in Mexico City, *J. Hazardous Materials* **20**, 85-107 (1988).
75. Birk, A. M., and Cunningham, M. H., The Boiling Liquid Expanding Vapour Explosion, *J. Loss Prevention in the Process Industries* **7**, 474-480 (1994).
76. Birk, A. M., et al., Fire Tests of Propane Tanks to Study BLEVEs and Other Thermal Ruptures: Detailed Analysis of Medium Scale Results (TP12498E), Transportation Development Centre, Montreal (1997).
77. Venart, J. E. S., Rutledge, G. A., Sumathipala, K., and Sollows, K., To BLEVE or Not to BLEVE: Anatomy of a Boiling Liquid Expanding Vapor Explosion, *Process Safety Progress* **12**, 67-70 (1993).
78. Ettling, B. V., Venting of Propane from Overfilled Portable Containers, *Fire & Arson Investigator* **49**, 54-56 (April 1999).
79. Venart, J. E. S., Boiling Liquid Expanding Vapor Explosions (BLEVE): Possible Failure Mechanisms, pp. 112-132 in **Very Large-Scale Fires** (ASTM STP 1336), ASTM (1998).
80. Birk, A. M., Observations from Medium Scale BLEVE Experiments, pp. 23-42 in *Fire & Explosion Hazards—Proc. 3rd Intl. Symp.*, Univ. Central Lancashire, Preston, England (2000).
81. Birk, A. M., Scale Effects with Fire Exposure of Pressure-Liquefied Gas Tanks, *J. Loss Prevention in the Process Industries* **8**, 275-290 (1995).
82. Barbone, R., Frost, D. L., Makris, A., and Nerenberg, J., Explosive Boiling of a Depressurized Volatile Liquid, pp. 315-324 in *ITUAM Symp. on Waves in Liquid/Gas and Liquid/Vapour Two-Phase Systems*, Kluwer Academic Publishers, Dordrecht, The Netherlands (1995).
83. McDevitt, C. A., Chan, C. K., Steward, F. R., and Tennankore, K. N., Initiation Step of Boiling Liquid Expanding Vapour Explosions, *J. Hazardous Materials* **25**, 169-180 (1990).
84. Sumathipala, K., Venart, J. E. S., and Steward, F. R., Two-phase Swelling and Entrainment during Pressure Relief Discharge, *J. Hazardous Materials* **25**, 219-236 (1990).
85. Prugh, R. W., Quantitative Evaluation of BLEVE Hazards, *J. Fire Protection Engineering* **3**, 9-24 (1991).
86. Wolf, A., BLEVE Kills Two, *NFPA J.* **92**, 43-47 (Nov./Dec. 1998).
87. Ryczkowski, J. J., Kingman Revisited, *American Fire J.*, **45**:7, 28-36 (July 1993).
88. Melhem, G. A., Croce, P. A., and Abraham, H., Data Summary & Analysis of National Fire Protection Association's BLEVE Tests, *Process Safety Progress* **12**, 76-82 (Apr. 93)
89. Leiber, C.-O., Approximative Quantitative Aspects of a Hot Spot, *J. Hazardous Materials* **12**, 43-64 (1985).
90. Carley, C. T., and Koelling, H. A., Residential Propane Tank BLEVE, *Fire & Arson Investigator* **52**:3, 24-25 (Apr. 2002).
91. Birk, A. M., and VanderSteen, J. D. J., The Survivability of Steel and Aluminum 33.5 lb Propane Cylinders in Fire, *36th Loss Prevention Symp.*, AIChE, New York (2002).
92. Procedures for Fire Testing of DOT Cylinder Pressure Relief Device Systems (CGA C-14), Compressed Gas Association, Chantilly VA (1999).
93. Martinsen, W. E., Johnson, D. E., and Terrell, W. F., BLEVEs: Their Causes, Effects and Prevention, *Hydrocarbon Processing* **65**, 141-148 (Nov. 1986).
94. Watrous, L. D., Freight Train Derailment and Fire, Crescent City, Illinois, *Fire J.* **64**, 10-13, 30 (Nov. 1970).
95. Hill, I., Crescent City, 25 Years Later, *Firehouse* 34-36 (Dec. 1995).
96. Peige, John D., 25 Killed by LPG Tank Car Blast, Fireball Two Days after Derailment, *Fire Engineering*, **131**:5, 39-44 (May 1978).
97. Jones, S., Reaction of Propane Cylinders to Fire (Report 251), Carboline Europe Ltd., Coventry, UK (1998).
98. Moodie, K., Cowley, L. T., Denny, R. B., Small, L. M., and Williams, I., Fire Engulfment Tests on a 5-tonne LPG Tank, *J. Hazardous Materials* **20**, 55-71 (1985).
99. Tan, D. M., Xu, J., and Venart, J. E. S., LPG Tank Failure: Ste. Élisabeth de Warwick, Quebec, June 27, 1993: The Lessons to Be Learnt, *J. Process Mechanical Engineering*, to be published (2003).
100. Birk, A. M., A Study of Fire Heating of a Propane Tank Located Near a Burning Building, *J. Applied Fire Science* **9**, 173-199 (1999/2000).
101. Birk, A. M., Hazards from Propane BLEVES: An Update and Proposal for Emergency Responses, *J. Loss Prevention in the Process Industries* **9**, 173-181 (1996).
102. de Richemond, A. L., and Bruley, M. E., Insidious Iatrogenic Oxygen-Enriched Atmospheres as a Cause of Surgical Fires, pp. 66-73 in **Flammability and Sensitivity of Materials in Oxygen-Enriched Atmospheres** (ASTM STP 1197), ASTM (1993).
103. Sheffield, P. J., and Desautels, D. A., Hyperbaric and Hypobaric Chamber Fires: A 73-year Analysis, *Undersea & Hyperbaric Medicine* **24**, 153-164 (1997).
104. Standard Guide for Control of Hazards and Risks in Oxygen Enriched Systems (ASTM G 128), ASTM.
105. Standard Guide for Evaluating Nonmetallic Materials for Oxygen Service (ASTM G 63), ASTM.
106. Standard Guide for Evaluating Metals for Oxygen Service (ASTM G 94), ASTM.
107. Guide on Fire Hazards in Oxygen-Enriched Atmospheres (NFPA 53), NFPA.
108. Safe Use of Oxygen and Oxygen Systems; Guidelines for Oxygen System Design, Materials Selection, Operations, Storage, and Transportation (ASTM Manual 36), ASTM (2000).
109. Safety Standard for Oxygen and Oxygen Systems (NSS 1740.15), Office of Safety and Mission Assurance, NASA, Washington (1996).
110. Hust, J. G., and Clark, A. F., A Survey of Compatibility of Materials with High Pressure Oxygen Service, *Cryogenics* **13**, 325-336 (1973).
111. van Hardeveld, R. M., Groeneveld, M. J., Lehman, J.-Y., and Bull, D. C., Investigation of an Air Separation Unit Explosion, *J. Loss Prevention in the Process Industries* **14**, 167-180 (2001).
112. Tench, A. H., Roder, H. M., and Clark, A. F., Combustion of Metals in Oxygen. Phase II. Bulk Burning Experiments (NBSIR 73-345), NBS, Boulder CO (1973).
113. Jakowsky, J. J., and Butzler, E. W., Oxygen-Oil Explosions. Preliminary Report II. Spontaneous Ignition of Metals in Oxygen under Pressure (Serial 2521), Bureau of Mines, Pittsburgh (1923).

114. Bates, C. E., Wren, J. E., Munroe, R., and Pears, C. D., Ignition and Combustion of Ferrous Metals in High Pressure, High Velocity, Gaseous Oxygen, *J. Materials for Energy Systems* **1**, 61-76 (1979).
115. Glassman, I., Mellor, A. M., Sullivan, H. F., and Laurendeau, N. M., A Review of Metal Ignition and Flame Models, Paper 19 in ***Reactions between Gases and Solids*** (NATO Conf. Proc. No. 52), North Atlantic Treaty Organization, Advisory Group for Aerospace Research and Development, Neuilly-sur-Seine, France (1970).
116. Benz, F. J., and Stoltzfus, J. M., Ignition of Metals and Alloys in Gaseous Oxygen by Frictional Heating, pp. 38-58 in **Flammability and Sensitivity of Materials in Oxygen-Enriched Atmospheres, Second Volume** (ASTM STP 910), ASTM (1986).
117. Gunaji, M. V., and Stoltzfus, J. M., Review of Frictional Heating Test Results in Oxygen-Enriched Environments, pp. 146-155 in **Flammability and Sensitivity of Materials in Oxygen-Enriched Atmospheres** (ASTM STP 1197), ASTM (1993).
118. Benz, F. J., Williams, R. E., and Armstrong, D., Ignition of Metals and Alloys by High-velocity Particles, pp. 16-37 in **Flammability and Sensitivity of Materials in Oxygen-Enriched Atmospheres: Second Volume** (ASTM STP 910), ASTM (1986).
119. Grubb, J. W., Case Study of Royal Australian Air Force P3B Orion Aircraft Ground Oxygen Fire Incident, pp. 171-179 in **Flammability and Sensitivity of Materials in Oxygen-Enriched Atmospheres: Second Volume** (ASTM STP 910), ASTM (1986).
120. Dees, J., Forsyth, E., Gunaji, M. V., and Stoltzfus, J. M., An Evaluation of Polymers as Ignition Sources during Particle Impact in Oxygen, pp. 143-151 in **Flammability and Sensitivity of Materials in Oxygen-Enriched Atmospheres: 7th Volume** (ASTM STP 1267), ASTM (1995).
121. Glassman, I., and Law, C. K., Sensitivity of Metal Reactivity to Gaseous Impurities in Oxygen Environments, *Combustion Science and Technology* **80**, 51-57 (1991).
122. Shelley, R. M., Christianson, R., and Stoltzfus, J. M., Evaluation of Buna-N Ignition Hazard in Gaseous Oxygen, pp. 239-251 in **Flammability and Sensitivity of Materials in Oxygen-Enriched Atmospheres** (ASTM STP 1197), ASTM (1993).
123. Werley, B. L., Oil Film Hazards in Oxygen Systems (ASTM STP 812), **Flammability and Sensitivity of Materials in Oxygen-Enriched Atmospheres**, ASTM (1983).
124. Shelley, R. M., Janoff, D. D., and Pedley, M. D., Effect of Hydrocarbon Oil Contamination on the Ignition and Combustion Properties of PTFE Tape in Oxygen, pp. 81-94 in **Flammability and Sensitivity of Materials in Oxygen-Enriched Atmospheres** (ASTM STP 1197), ASTM (1993).
125. Barthélémy, and Vagnard, G., Ignition of PTFE-Lined Hoses in High-Pressure Oxygen Systems: Test Results and Considerations for Safe Design and Use, pp. 289-304 in **Flammability and Sensitivity of Materials in Oxygen-Enriched Atmospheres: Third Volume** (ASTM STP 986), ASTM (1988).
126. Janoff, D., Bamford, L. J., Newton, B. E., and Bryan, C. J., Ignition of PTFE-Lined Flexible Hoses by Rapid Pressurization with Oxygen, pp. 288-308 in **Flammability and Sensitivity of Materials in Oxygen-Enriched Atmospheres: Fourth Volume** (ASTM STP 1040), ASTM (1989).
127. Newton, B. E., Langford, R, K., and Meyer, G. R., Promoted Ignition of Oxygen Regulators, pp. 241-266 in **Flammability and Sensitivity of Materials in Oxygen-Enriched Atmospheres: Fourth Volume** (ASTM STP 1040), ASTM (1989).
128. Moffett, G. E., et al., Ignition of Nonmetallic Materials by Impact of High-pressure Gaseous Oxygen, pp. 218-232 in **Flammability and Sensitivity of Materials in Oxygen-Enriched Atmospheres** (ASTM STP 986), ASTM (1988).
129. Hirsch, D., Skarsgard, E., Beeson, H., and Bryan, C., Predictability of Gaseous Impact Ignition Sensitivity from Autoignition Temperature Data, pp. 521-528 in **Flammability and Sensitivity of Materials in Oxygen-Enriched Atmospheres: 9th Volume** (ASTM STP 1395), ASTM (2000).
130. Bransford, J. W., Ignition and Combustion Temperatures Determined by Laser Heating, pp. 78-97 in **Flammability and Sensitivity of Materials in Oxygen-Enriched Atmospheres: Second Volume** (ASTM STP 910), ASTM (1986).
131. Ikeda, G. K., Oxygen Index Tests to Evaluate the Suitability of a Given Material for Oxygen Service, pp. 56-67 in **Flammability and Sensitivity of Materials in Oxygen-Enriched Atmospheres** (ASTM STP 812), ASTM (1983).
132. Hshieh, F.-Y., Stolzfus, J. M., and Beeson, H. D., Note: Autoignition Temperature of Selected Polymers at Elevated Oxygen Pressure and Their Heat of Combustion, *Fire and Materials* **20**, 301-303 (1996).
133. Standard Test Method for Autogenous Ignition Temperature of Liquids and Solids in a High-Pressure Oxygen-Enriched Environment (ASTM G 72), ASTM.
134. Standard Test Method for Determining the Combustion Behavior of Metallic Materials in Oxygen-Enriched Atmospheres (ASTM G 124), ASTM.
135. Standard Test Method for Ignition Sensitivity of Materials to Gaseous Fluid Impact (ASTM G 74), ASTM.
136. Werley, B. L., A Perspective on Gaseous Impact Tests: Oxygen Compatibility Testing on a Budget, pp. 27-42 in **Flammability and Sensitivity of Materials in Oxygen-Enriched Atmospheres** (ASTM STP 1197), ASTM (1993).
137. Standard Test Method for Compatibility of Materials with Liquid Oxygen (ASTM D 2512), ASTM.
138. Standard Test Method for Determining Ignition Sensitivity of Materials to Mechanical Impact in Pressurized Oxygen Environments (ASTM G 86), ASTM.
139. Standard Test Method for Measuring Liquid and Solid Material Fire Limits in Gaseous Oxidants (ASTM G 125), ASTM.
140. Barrow, G. J., A Survey of Houses Affected in the Beaumaris Fire, January 14, 1944, *J. Council for Scientific & Industrial Research* **18**, 27 (Feb. 1945).
141. Morris, W., and Barber, J. R., Design and Siting Guidelines: Bush Fire Protection for Rural Houses, Country Fire Authority, Victoria, Australia.
142. Ramsey, G. C., and McArthur, N. A., Building in the Urban Interface: Lessons from the January 1994 Sydney Bushfires, presented at *Bushfire '95*, Hobart, Tasmania, Australia (1995).
143. Bell, A., How Bushfires Set Houses Alight—Lessons from Ash Wednesday, *Ecos* No. 43, 3-7 (Autumn 1985).
144. Ramsay, G. C., McArthur, N. A., and Dowling, V. P., Building Survival in Bushfires, *Fire Science '86*, Institution of Fire Engineers, Western Australian Branch (1986).

145. Wilson, A. A. G., Assessing the Bushfire Hazard of Houses: A Quantitative Approach (Tech. Paper No. 6), Rural Fire Research Centre, Vic., Australia (1984).
146. Foote, E. I. D., and Gilless, J. K., Structural Survival, pp. 112-121 in **California's I-Zone**, R. Slaughter, ed., California State Fire Marshal, Sacramento (1996).
147. Cohen, J. D., Examination of the Home Destruction in Los Alamos Associated with the Cerro Grande Fire, July 10, 2000, US Forest Service Rocky Mountain Research Station, Missoula MT (2000).
148. McArthur, N., CSIRO, private communication (2001).
149. Moore, H. E., Protecting Residences from Wildfires: A Guide for Homeowners, Lawmakers, and Planners (Gen. Tech. Report PSW-50), Pacific Southwest Forest and Range Experiment Station, US Forest Service, Berkeley CA (1981).
150. Ramsey, G. C., and Dawkins, D., Building in Bushfire-prone Areas (SAA HB 36-1993), Standards Australia, [n.p.] (1993).
151. Standard for Protection of Life and Property from Wildfire (NFPA 1144), NFPA.
152. Urban-Wildland Interface Code, International Conference of Building Officials, Whittier CA (2000).
153. Tran, H. C., Cohen, J. D., and Chase, R. A., Modeling Ignition of Structures in Wildland/Urban Interface Fires, pp. 253-262 in *Proc. First Intl. Fire and Materials Conf.*, Interscience Communications Ltd, London (1992).
154. Alexander, M. E., Stocks, B. J., Wotton, B. M., and Lanoville, R. A., An Example of Multi-Faceted Wildland Fire Research: The International Crown Fire Modelling Experiment, Canadian Forest Service, Northern Forestry Centre, Edmonton, Alberta (1999).
155. Cohen, J. D., What is the Wildland Fire Threat to Homes? US Forest Service Rocky Mountain Research Station, Missoula MT (2000).

Copyright © 2003, 2014 Vytenis Babrauskas



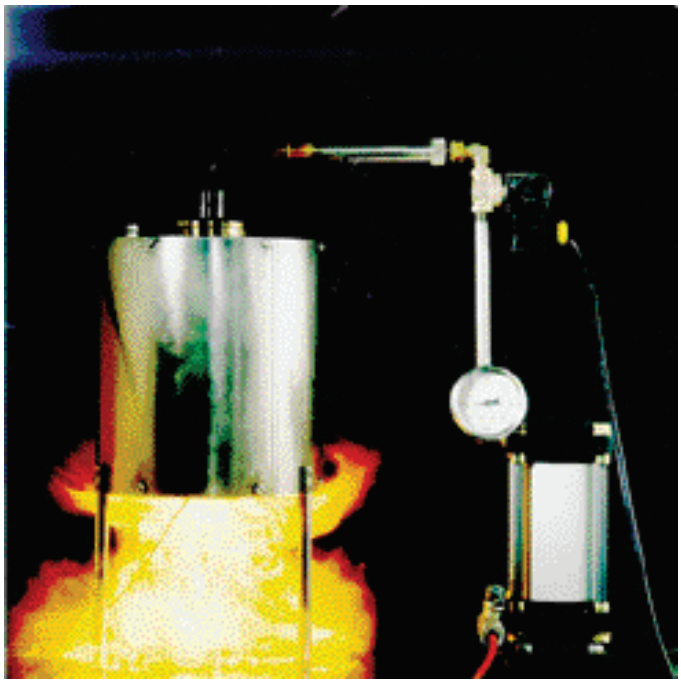
Color Plate 1 An open-air dust explosion. The containers holding dust at the two yellow pillars are pressurized to 20 atm and a quick-open valve ejects the material into the air. The ignitor is located at the center pillar.
(Courtesy Sicherheitsinstitut: Swiss Institute of Safety & Security)



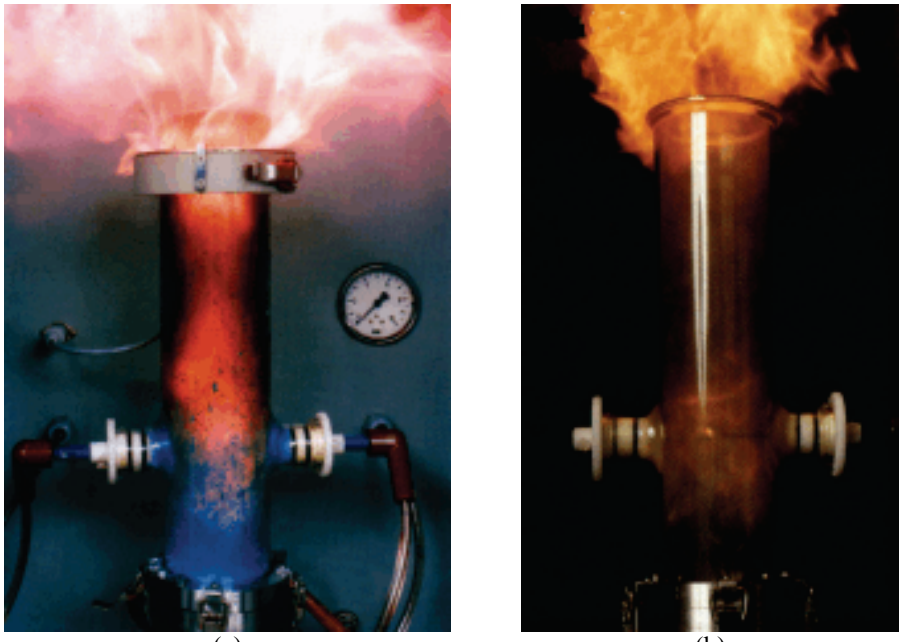
Color Plate 2 BAM oven, view during test
(Courtesy Sicherheitsinstitut: Swiss Institute of Safety & Security)



Color Plate 3 Döbereiner's lamp
(Copyright Platinum Metals Review, used by permission)

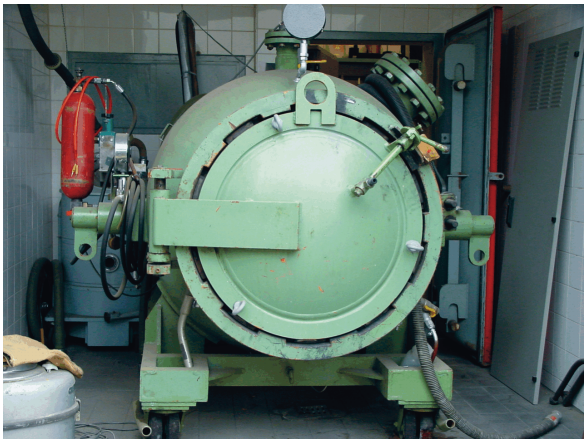


Color Plate 4 An explosion taking place in the Godbert-Greenwald furnace
(Courtesy Chilworth Technologies, Inc.)



(a) (b)

Color Plate 5 Test explosions in the Hartmann apparatus
(Courtesy Sicherheitsinstitut: Swiss Institute of Safety & Security)

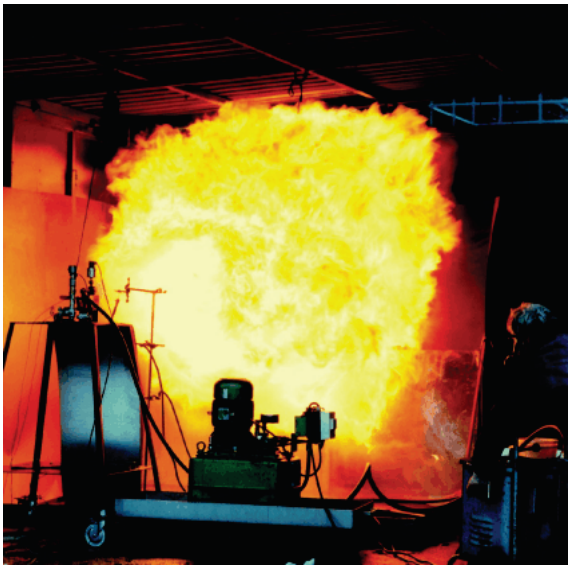


View closed

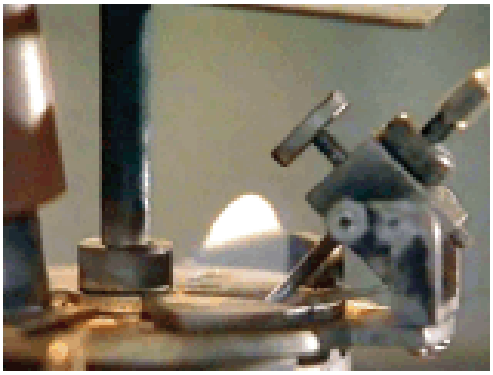


View open

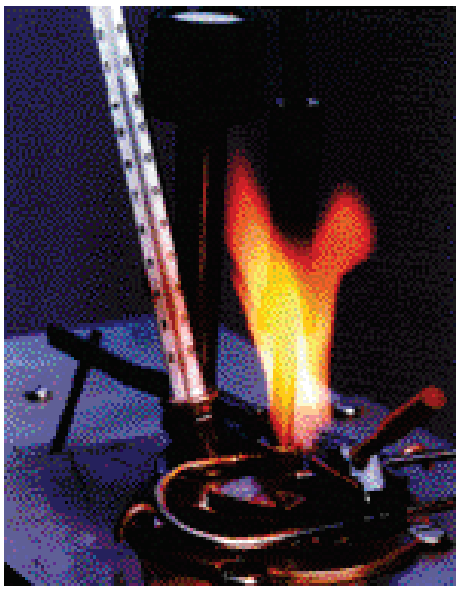
Color Plate 6 A test vessel of 1 m^3 size used at BAM
(Courtesy Ulrich Krause, BAM)



Color Plate 7 Spray of a high-flash point liquid that created a fireball of about 2 m diameter upon ignition. The liquid was an aliphatic ester, FP 235ºC, viscosity 34.2 mm^2 s^{-1}. A 90º full-cone, 4.2 mm diameter nozzle was used, spraying liquid at a pressure of 12 atm. Ignition by a steel rod, 2 mm diameter, 20 mm long, heated to 900ºC. Igniter position from nozzle was 0.2 m away axially, 0.1 m radially.
(Courtesy Hans Förster, PTB)



Color Plate 8 Closeup of the Pensky-Martens flash point tester
(Courtesy Sicherheitsinstitut: Swiss Institute of Safety & Security)



Color Plate 9 The Pensky-Martens flash point tester
(Courtesy Sicherheitsinstitut: Swiss Institute of Safety & Security)



Color Plate 10 Burning Class B brand on a roof
(Courtesy R. Brady Williamson)



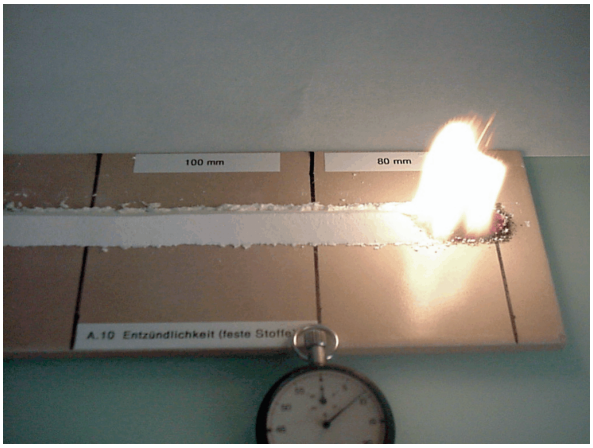
Color Plate 11 Burning and burned-out Class C brands on a roof
(Courtesy R. Brady Williamson)



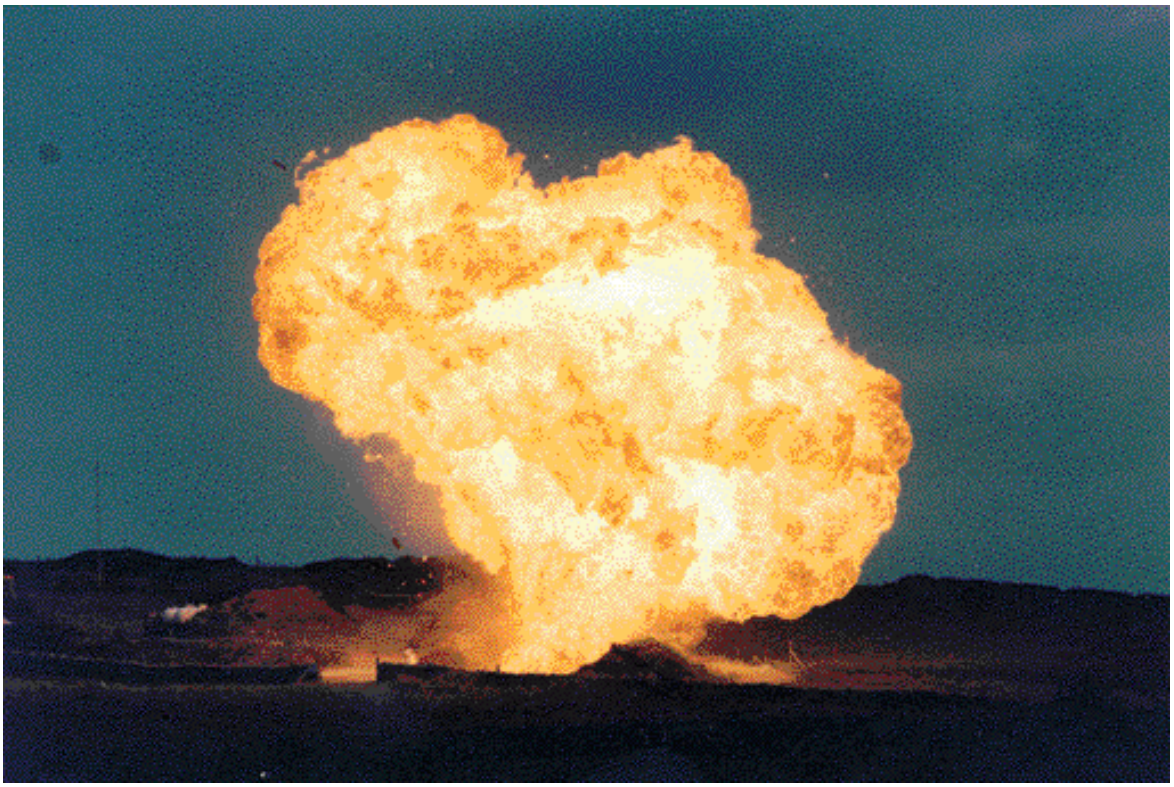
Color Plate 12 Fire non-propagation from a rug's fringe to the rug itself



Color Plate 13 The BAM drop-hammer test, known as UN Test 3(a)(ii)
(Courtesy Sicherheitsinstitut—Swiss Institute of Safety & Security)



Color Plate 14 UN Test N.1 for readily combustible solids
(Courtesy Sicherheitsinstitut: Swiss Institute of Safety & Security)



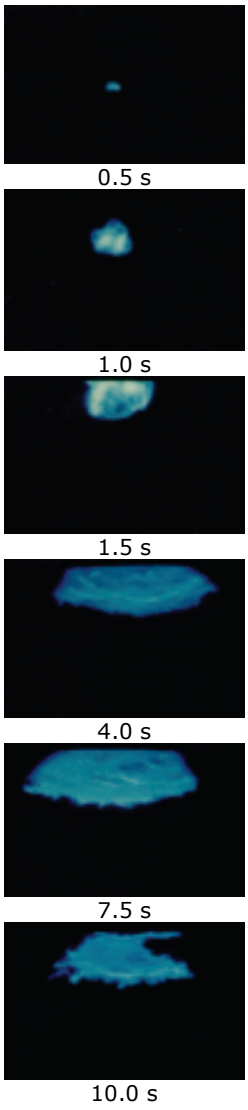
Color Plate 15 Fireball from the BLEVE of a tank with 100% capacity of 2200 kg that held 455 kg and released 280 kg propane
(British Crown copyright © 1995, courtesy HSL)



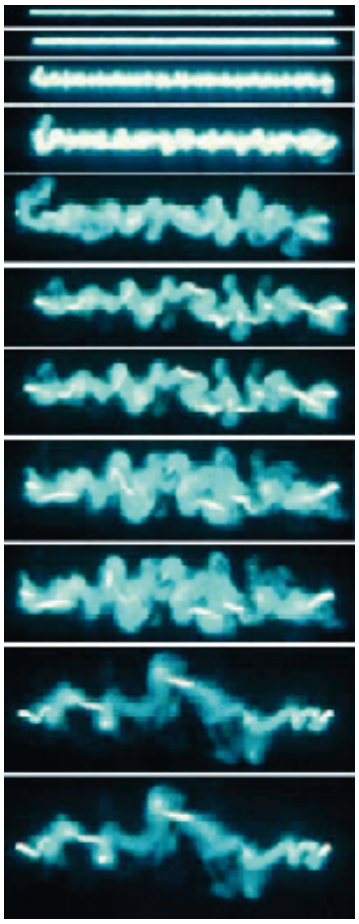
Color Plate 16 Fireball from the ignition of a 23 kg charge of gunpowder; gauge poles are 3 m high at center and 4 m high at periphery
(British Crown copyright © 2001, courtesy HSL)



Color Plate 17 Fireball from the ignition of a 25 kg charge of star composition; gauge pole is 3 m high
(British Crown copyright © 2001, courtesy HSL)



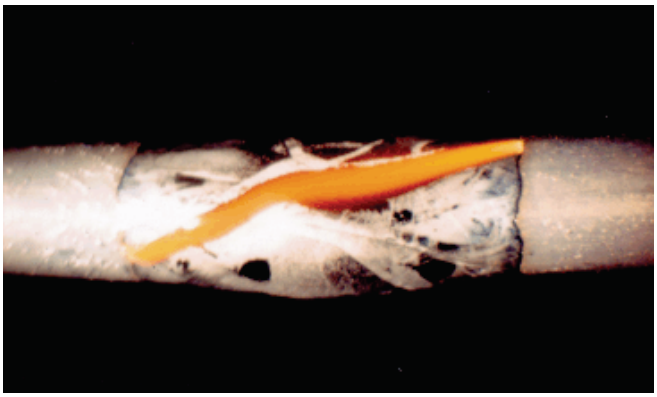
Color Plate 18 Flame development after spark ignition of a CO/air mixture



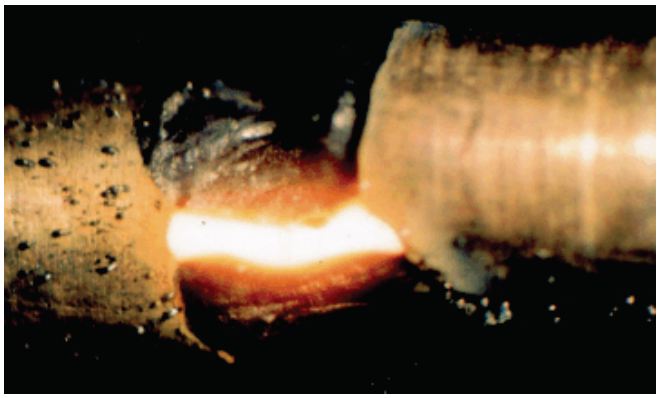
Color Plate 19 A sequence of pictures illustrating the development of a meandering characteristic by a horizontal arc across a 500 mm electrode gap. The time sequence is during the first 10 ms and buoyant flows have not yet had a chance to develop.
(Courtesy Anthony D. Stokes)



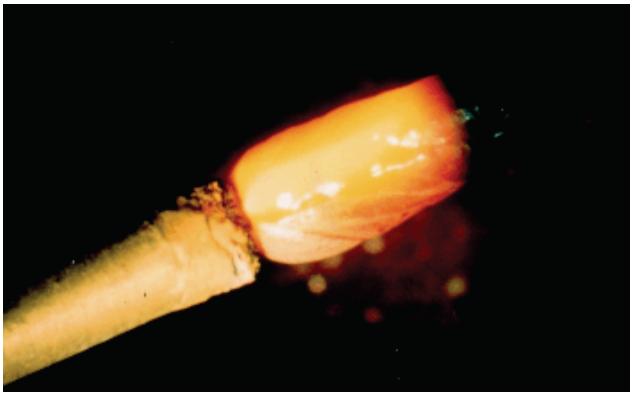
Color Plate 20 An electrician who received burns on 50% of his body due to arc flash
(Photo: Dept. of Health, Education and Welfare)



Color Plate 21 Cu_2O breeding at a Cu-Cu connection drawing 1 A AC
(Courtesy Yasuaki Hagimoto, NRIPS)



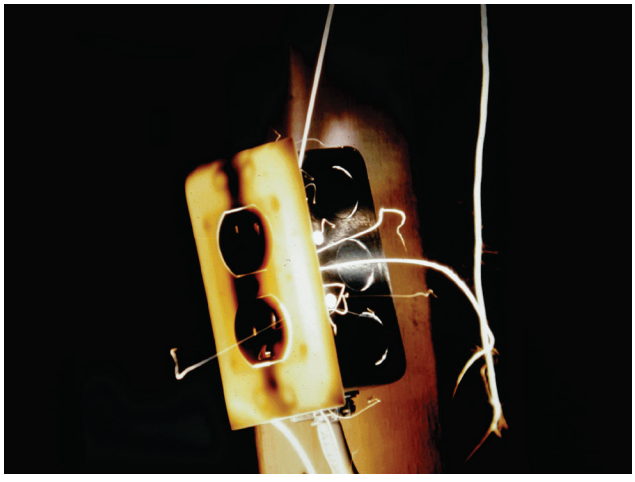
Color Plate 22 Cu_2O breeding at a brass-brass connection drawing 1 A AC; wire size 2 mm
(Courtesy Yasuaki Hagimoto, NRIPS)



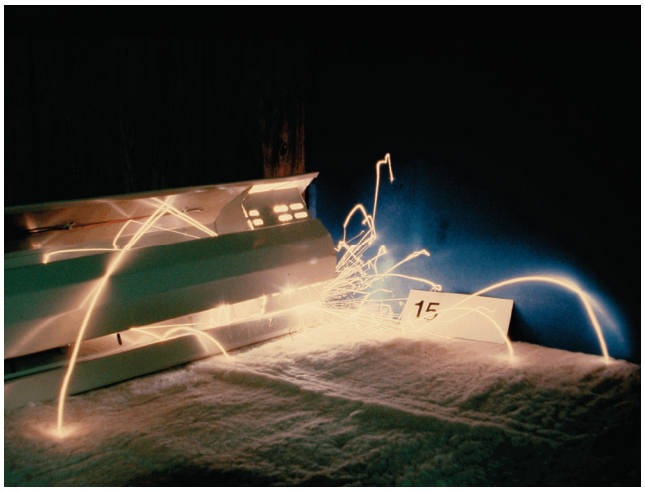
Color Plate 23 Glowing brass (left, +)-Cu (right, –) connection drawing 4 A DC
(Courtesy Yasuaki Hagimoto, NRIPS)



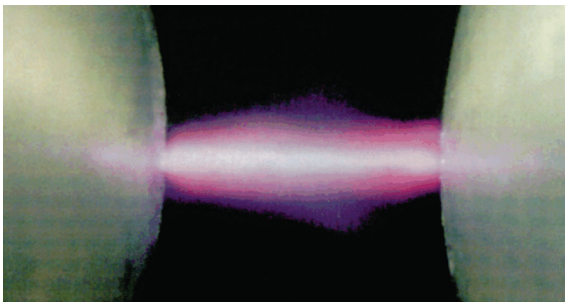
Color Plate 24 Cu_2O breeding at Fe (left, +)-Cu (right, –) connection drawing 1A DC
(Courtesy Yasuaki Hagimoto, NRIPS)



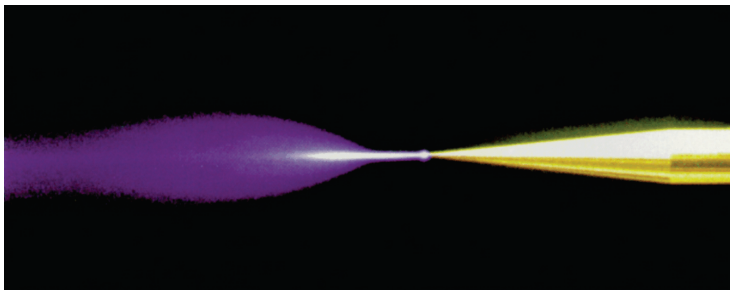
Color Plate 25 Incandescent particles being ejected from a short-circuited duplex receptacle
(Courtesy Jesse Aronstein)



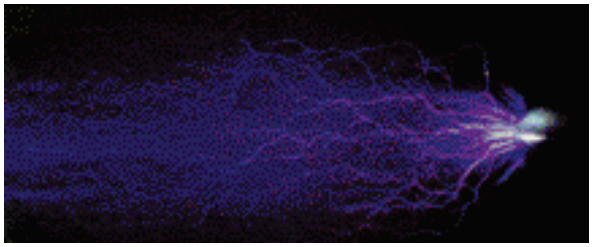
Color Plate 26 Incandescent particles being ejected from a short-circuited baseboard heater
(Courtesy Jesse Aronstein)



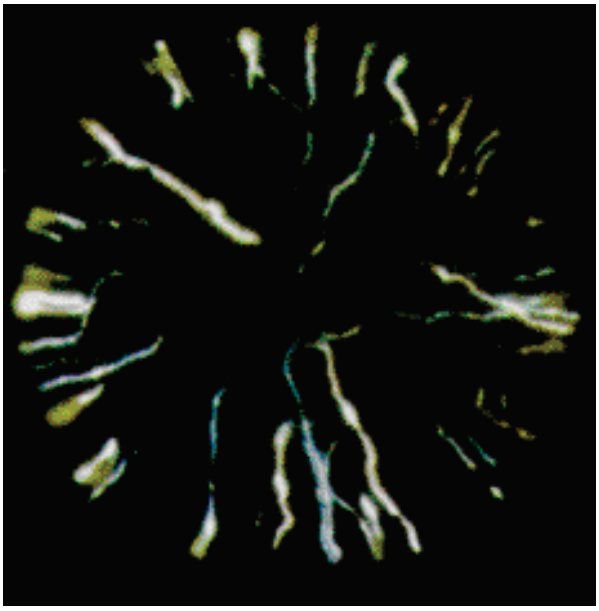
Color Plate 27 Electrostatic spark discharge
(Courtesy Sicherheitsinstitut—Swiss Institute of Safety & Security)



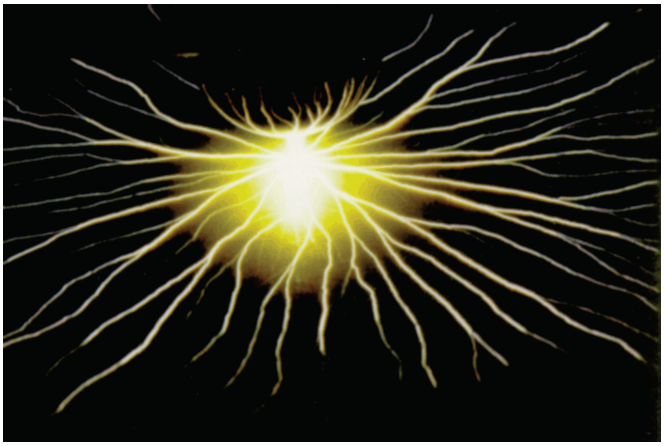
Color Plate 28 A corona discharge form a sharp electrode tip
(Courtesy Sicherheitsinstitut—Swiss Institute of Safety & Security)



Color Plate 29 A brush discharge from a spherical electrode
(Courtesy Sicherheitsinstitut—Swiss Institute of Safety & Security)



Color Plate 30 A powder heap discharge
(Courtesy Sicherheitsinstitut—Swiss Institute of Safety & Security)



Color Plate 31 A propagating brush discharge
(Courtesy Sicherheitsinstitut— Swiss Institute of Safety & Security)



Color Plate 32 Lightning strike to an apartment house roof
(Courtesy Ronnal D. Bewyer)



Color Plate 33 Lightning strike to a corner of a house at a roof, showing ignition and burning of structural members
(Courtesy Roger Parker, South Metro Fire Rescue, Greenwood Village, Colorado)



Color Plate 34 Lightning strike into a bedroom—without a careful investigation the patterns could be mistaken for local burns caused by a use of accelerants
(Courtesy Bruce Brazzle, Fort Riley, Kansas Fire Department)



(a)



(b)

Color Plate 35 Consequences of a lightning strike to an electric service entrance of a restaurant. Two separate fires were ignited, at (**a**) an electric panelboard and (**b**) at combustibles located near gas piping supplying a water heater
(Courtesy Blake Holt, Springdale, Arkansas Fire Department)



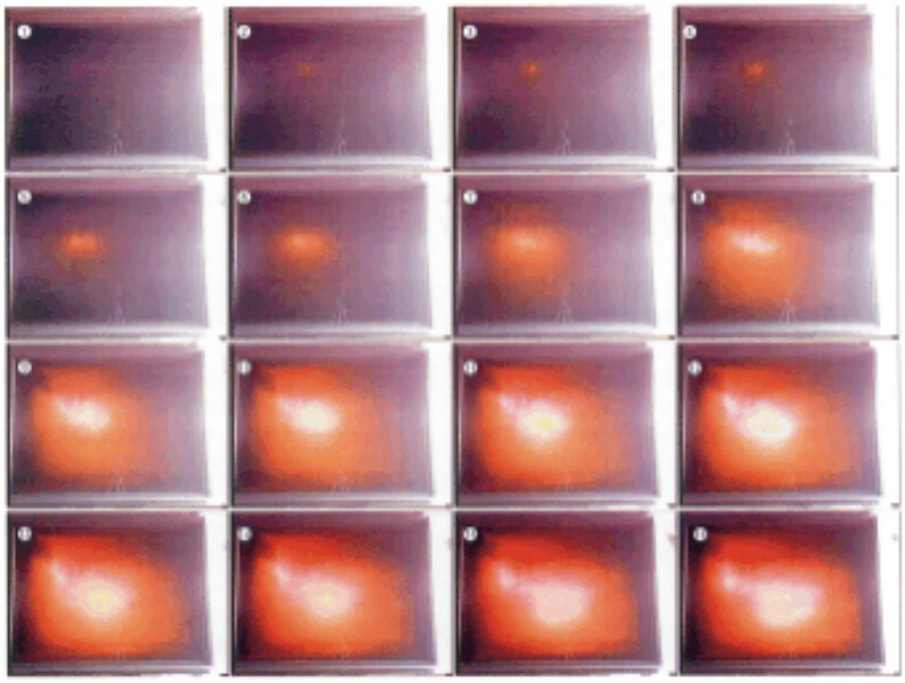
Color Plate 36 Bark stripped from tree by lightning
(Courtesy Richard Kithil, National Lightning Safety Institute)



Color Plate 37 Ignition of the structure of a house as an outcome of a gas explosion
(Courtesy John Amerongen)



Color Plate 38 Fracturing of the pieces of a house during an experimental explosion with natural gas; note destruction occurred preferentially at floor level
(Courtesy John Amerongen)



Color Plate 39 Development of backdraft within the test room; side view—ventilation opening is on the left
(Courtesy Hiroshi Hayasaka)



Color Plate 40 Smoke explosion that took place in a pellet stove
(Courtesy Michael M. Fitz, MDE Engineers)



Color Plate 41 This heating installation sustained a smoke explosion because a stove was improperly installed by venting it into a large, blocked-off fireplace
(Courtesy Michael M. Fitz, MDE Engineers)



Color Plate 42 Backdraft in an experimental compartment: the fireball is over 8 m in diameter and resulted in an internal pressure greater than 300 Pa within the compartment
(Courtesy Charles Fleischmann)



Color Plate 43 Fireball from the BLEVE of a tank with 100% capacity of 2200 kg that held 1930 kg and released 1710 kg propane
(British Crown copyright © 1995, courtesy HSL)

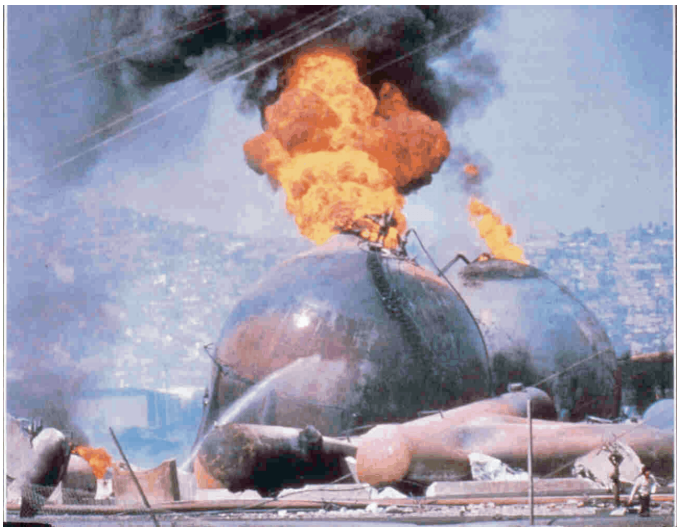


(a) Ground view; note size of water tower for scale



(b) Aerial view

Color Plate 44 Fireball from derailment of train hauling propane tank cars in Crescent City, Illinois
(Courtesy Irma M. Hill)



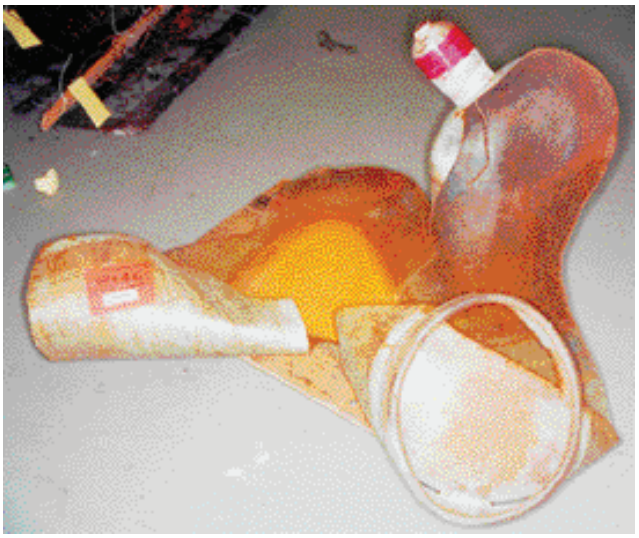
Color Plate 45 Fireball from Mexico City BLEVE disaster
(Courtesy Chris M. Pietersen, Safety Solutions Consultants BV)



Color Plate 46 Fireball from Mexico City BLEVE disaster
(Courtesy Chris M. Pietersen, Safety Solutions Consultants BV)



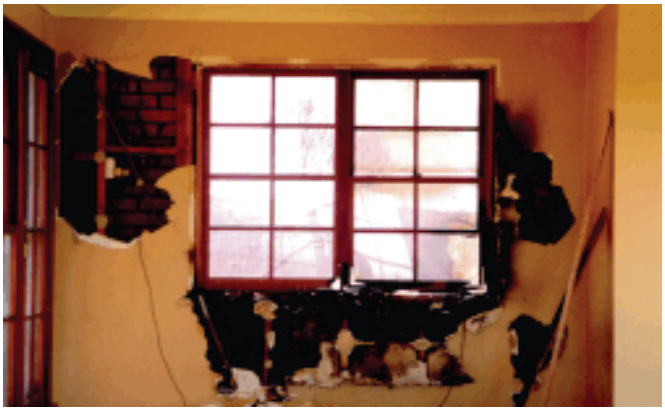
Color Plate 47 Aftermath of Mexico City BLEVE disaster
(Courtesy Chris M. Pietersen, Safety Solutions Consultants BV)



Color Plate 48 A propane tank which underwent a BLEVE (due to overfilling and defective PRV) but without the involvement of fire
(Courtesy Michael M. Fitz, MDE Engineers)



Color Plate 49 Ignition of wood window sill from firebrand
(Courtesy CSIRO Australia)



Color Plate 50 Fire entered the house from another ignited window sill in the same house
(Courtesy CSIRO Australia)



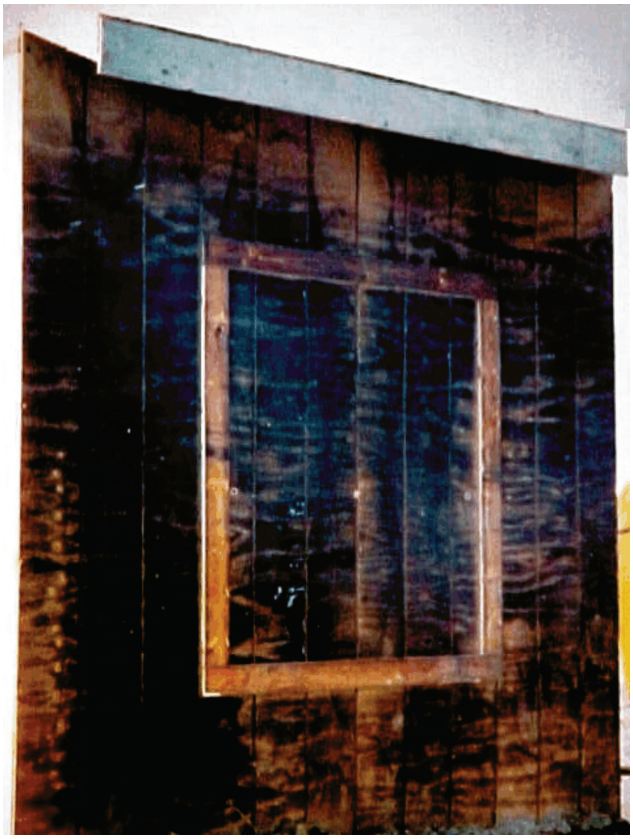
Color Plate 51 Firebrand ignition of wood deck planks
(Courtesy CSIRO Australia)



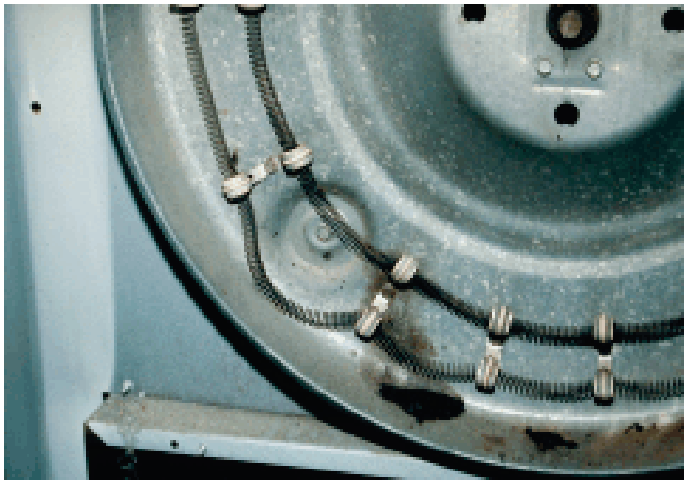
Color Plate 52 Road bridge ignited from brands during 1985 bushfires in Australia. Note lack of combustibles below and the generally low threat of this fire, as evidenced by vegetation still present on the trees.
(Courtesy CSIRO Australia)



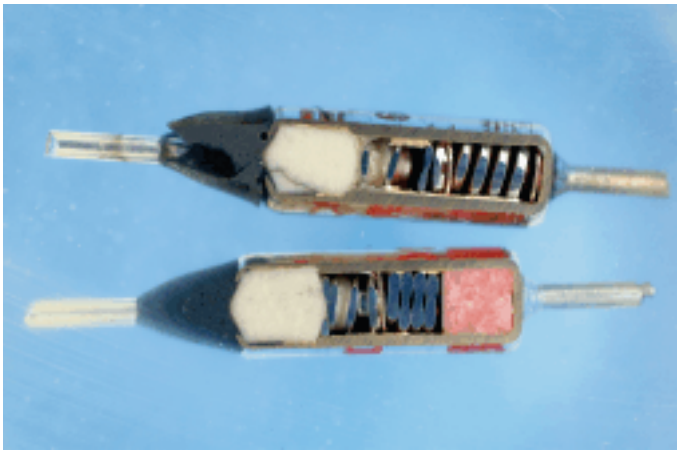
Color Plate 53 Smoldering combustion of chromated-copper arsenate treated pine fence post
(Courtesy CSIRO Australia)



Color Plate 54 Scorched wall without sustained flaming, after exposure to the radiant heat of a crown fire 10 m away *(Courtesy Jack Cohen, USFS)*



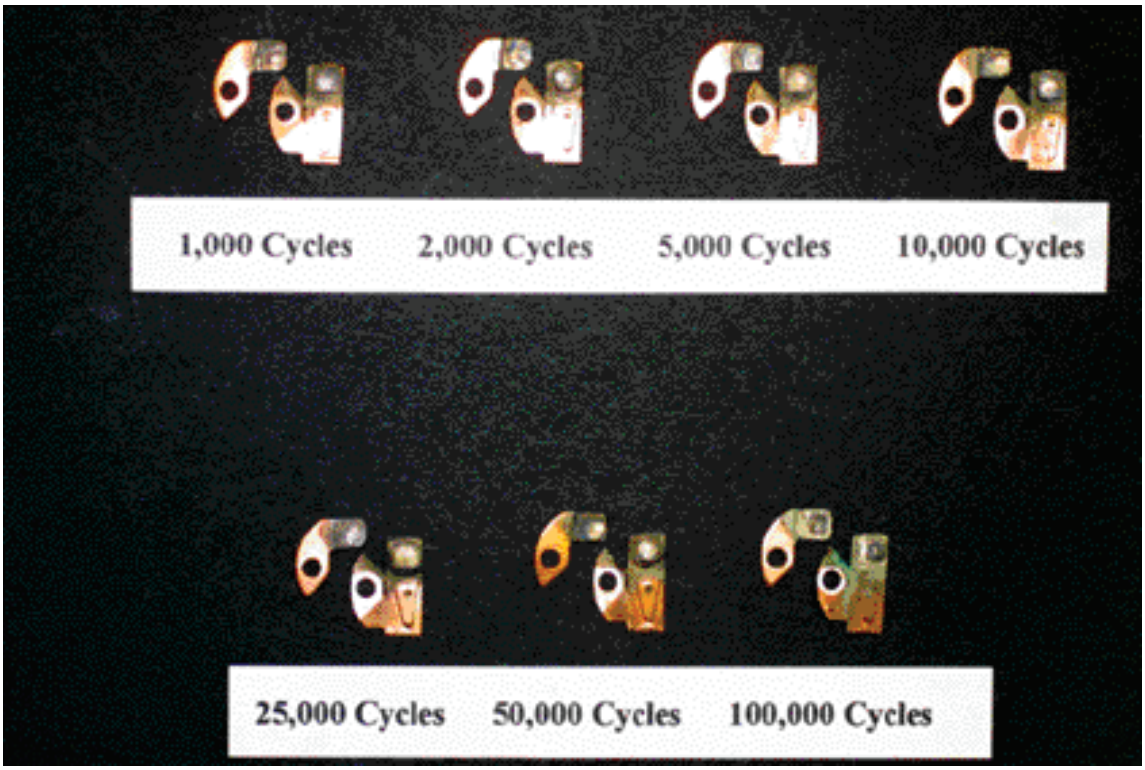
Color Plate 55 Sagging of wire heater element has resulted in a contact with the drum
(Courtesy Jesse Aronstein)



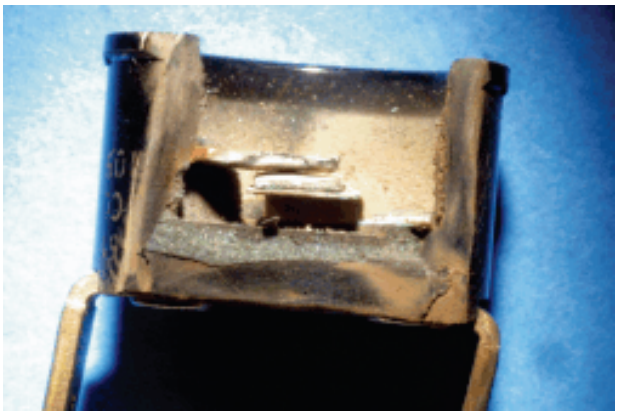
Color Plate 57 Cut-away view of sacrificial TCOs—upper TCO open, lower TCO closed
(Courtesy Kevin Lewis, Schaefer Engineering Corp.)



Color Plate 56 Door is open to the dryer, drum rotation is stopped, but heating of element shorted to drum continues—note red glow of heating element
(Courtesy Jesse Aronstein)



Color Plate 58 Progressive deterioration of contacts with cycling
(Courtesy Kevin Lewis, Schaefer Engineering Corp.)



Color Plate 59 Cut-away of a phenolic body high-limit switch that was subjected to 100,000 cycles (5 cycles a minute) carrying a 10 A load
(Courtesy Kevin Lewis, Schaefer Engineering Corp.)



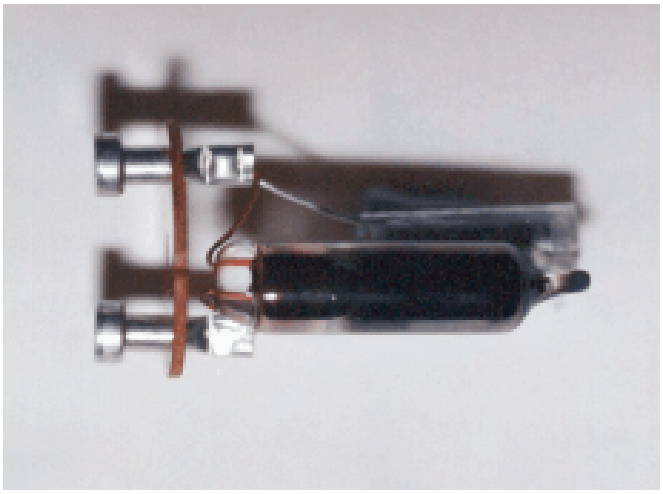
Color Plate 60 Closeup of contacts removed from the above high-limit switch and photographed
(Courtesy Kevin Lewis, Schaefer Engineering Corp.)



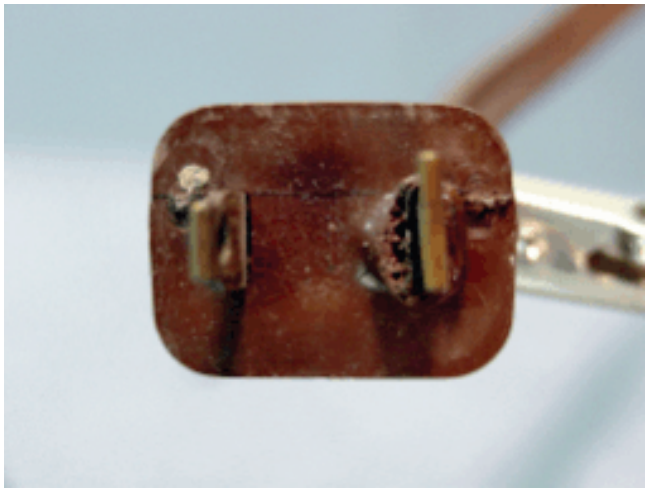
Color Plate 61 Remains of a fire department defibrillator in which its lithium battery exploded



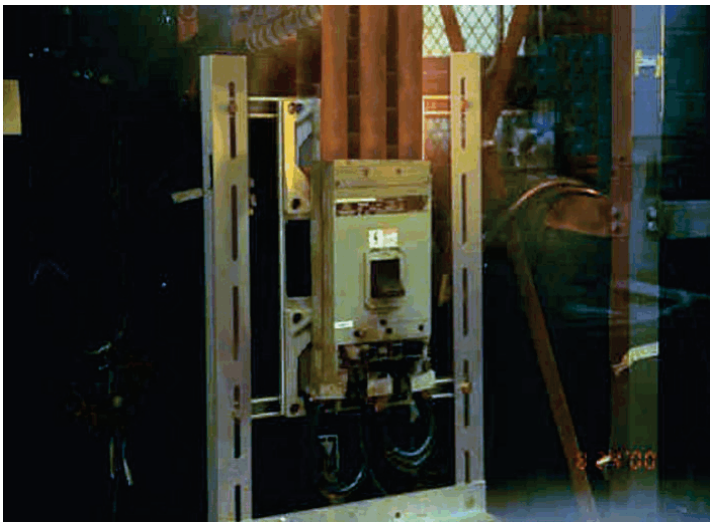
Color Plate 62 Shower of incandescent particles emitted from the operation of an 11 kV expulsion fuse under a short-circuit load of 140 A
(Courtesy Anthony D. Stokes)



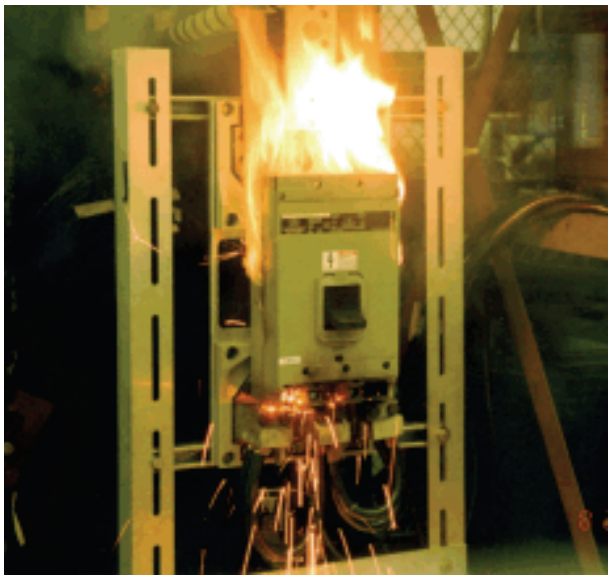
Color Plate 63 Starter with improperly bent wires
(Courtesy Scientific Services Laboratory)



Color Plate 64 Degradation of the plastic found on a hair dryer plug during normal use
(Courtesy Chris Korinek)



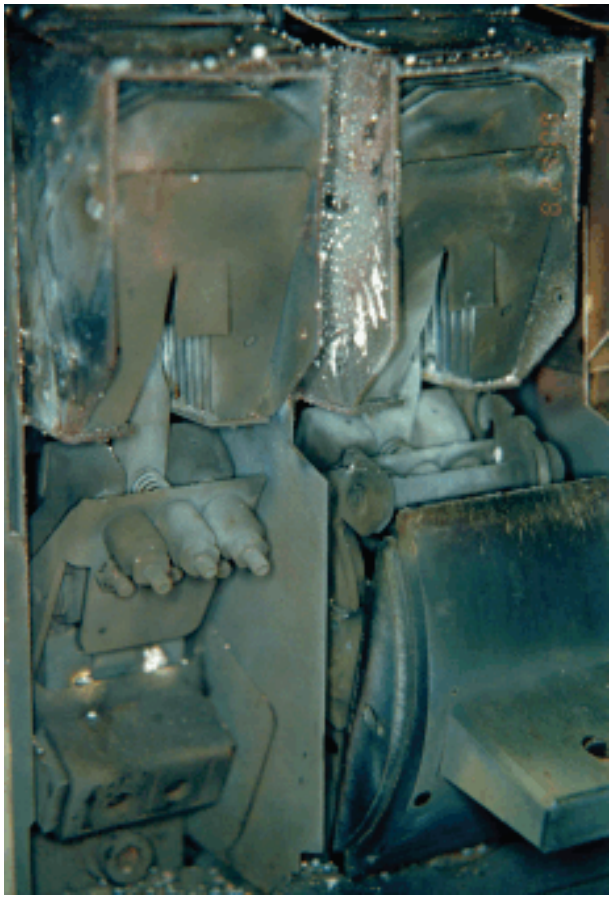
(a)



(c)



(b)

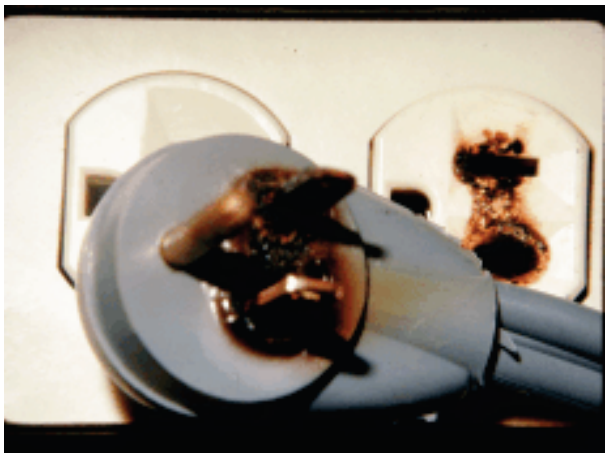


(d)

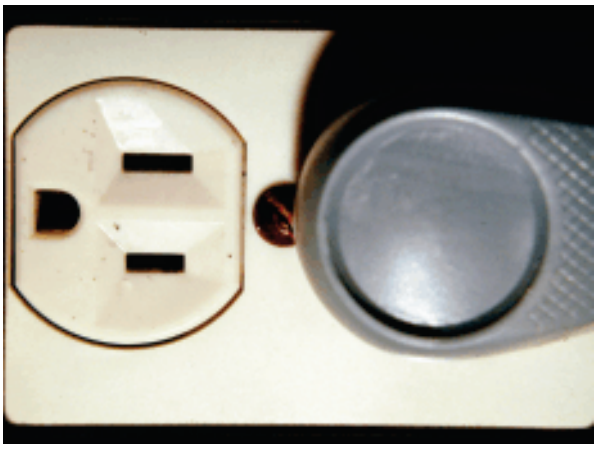
Color Plate 65 Failure and ignition caused by passing excessive current through a circuit breaker **(a)** before test; **(b)** during arcing; **(c)** flaming afterwards; **(d)** damage to circuit breakers.
(Courtesy David Reiter, Verité Forensic Engineering)



Color Plate 66 Fire initiated by arcing at the place where wire strands from a cord were separated from the prong of the plug (note bottom right prong)
(Courtesy M. Uchida)



(a)



(b)

Color Plate 67 (a) Charring occurring at an outlet due to poor grasp of male plug by female receptacle parts. This condition occurred after less than 100 insertion/removal operations and while carrying a load within the ratings (15 A). **(b)** External evidence of overheating is not seen, despite extensive damage.
(Courtesy Jesse Aronstein)

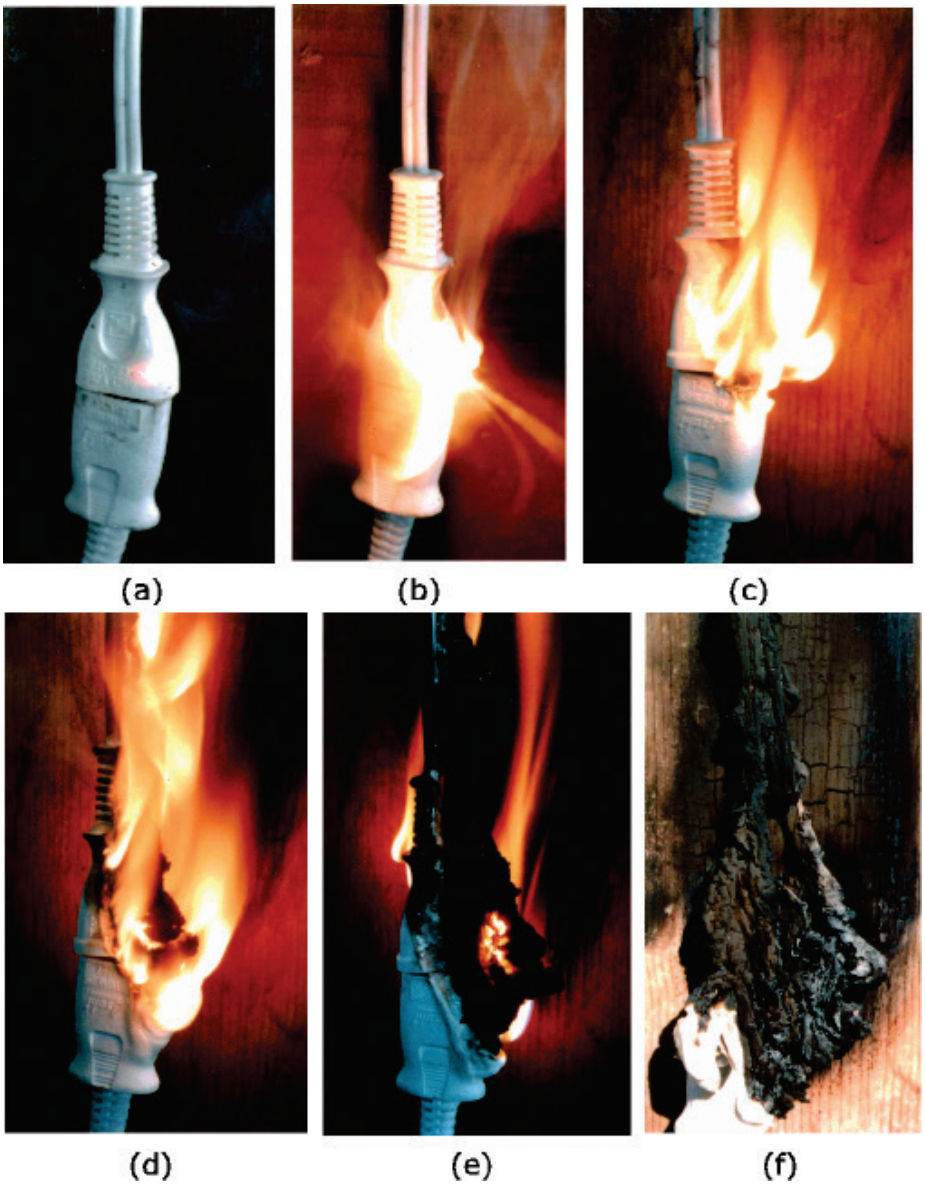


(a)



(b)

Color Plate 68 Ignition of rubber/cotton insulated cord with PVC plug after mechanical failure occurred
(Courtesy Yukio Shimizu)



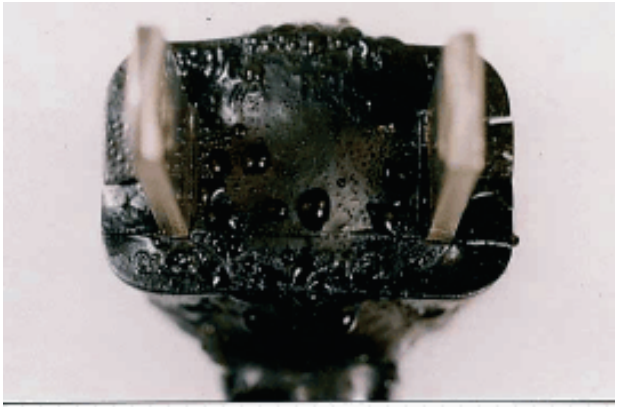
Color Plate 69 Ignition of electric cord with broken wire to male plug; note that the wood board ignited from the burning cord
(Courtesy Yukio Shimizu)



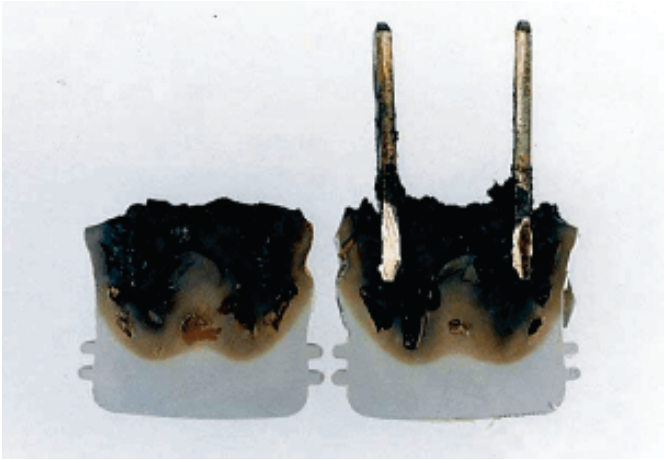
Color Plate 70 Degradation of a molded PVC plug resulting from an experiment where the plug was loosely inserted into an outlet (force = 0.1 N), with a current of 20 A and an exposure period of 25 hours.
(Courtesy Yasuaki Hagimoto, NRIPS)



Color Plate 71 Degradation of a molded PVC plug during laboratory exposure where 200ºC heating was applied to one prong for 100 h
(Courtesy Yasuaki Hagimoto, NRIPS)



Color Plate 72 Degradation of plug after oven aging at 165ºC for 250 hours
(Courtesy Kiyomi Ashizawa)



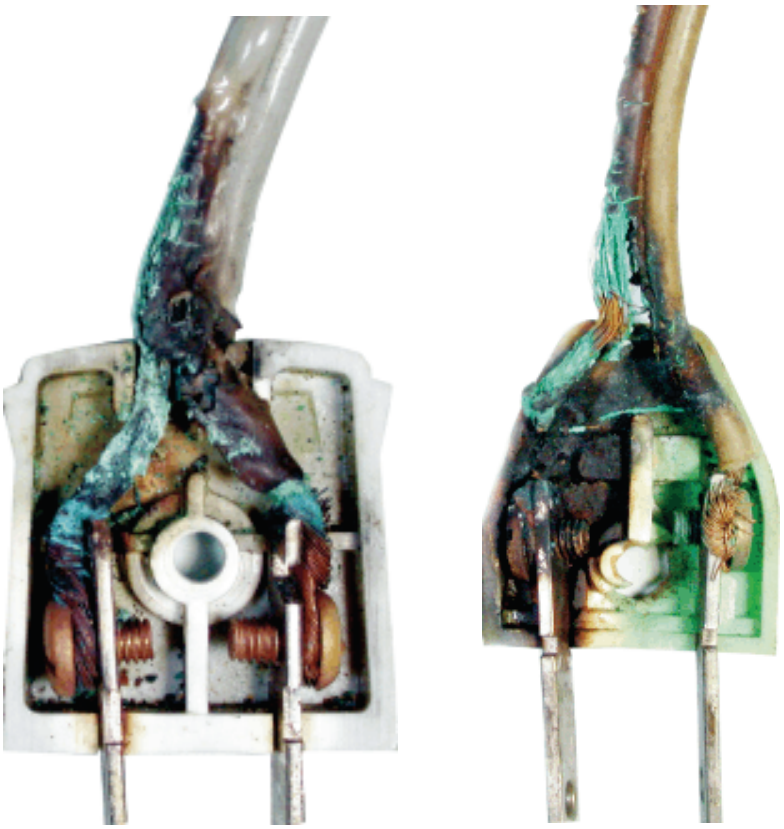
Color Plate 73 Inside view of plug which was thermally degraded and carrying a 12 A load for 1 week; the insulation resistance had dropped to 100 kΩ
(Courtesy Kiyomi Ashizawa)



Color Plate 74 The resistance of this plug had dropped to 1 kΩ due to thermal degradation and absorption of moisture; ignition occurred upon plugging it in with a 10 A load.
(Courtesy Kiyomi Ashizawa)

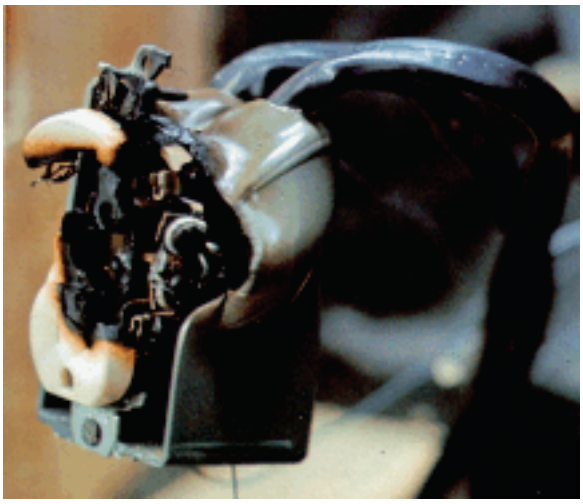


Color Plate 75 Glowing screw connection
(Courtesy David Reiter, Verité Forensic Engineering)

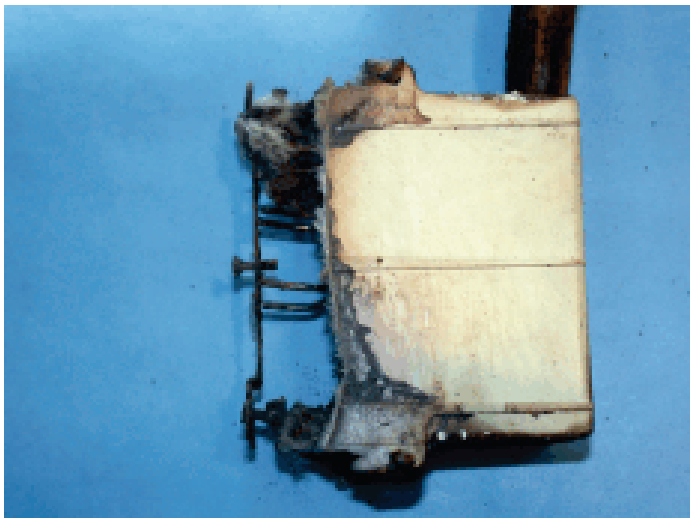


(a) **(b)**

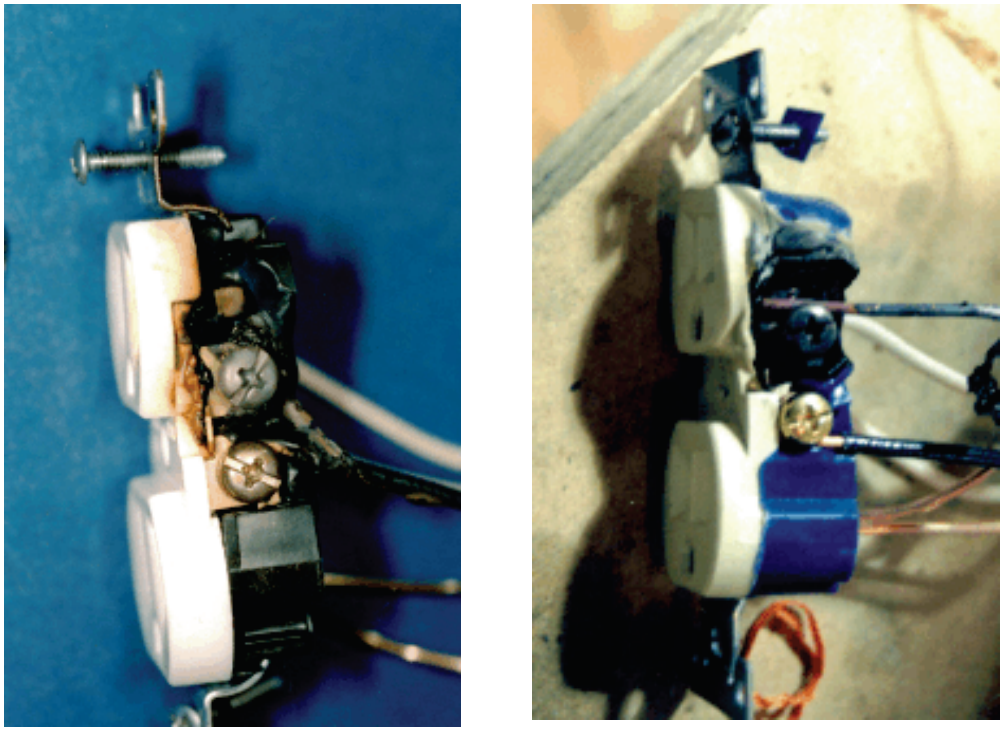
Color Plate 76 Degradation of urea formaldehyde plugs. **(a)** Plug was connected to the end of an extension cord which was used for a coffee maker of 550 W and an electric pot of 840 W for about half a year. **(b)** Plug was at the end of an extension cord which was used for a 1200 W electric heater used during daytime in winter for 4 to 5 years. Note that portions of copper wire have melted out, while other portions have turned to green copper oxide.
(Courtesy Yasuaki Hagimoto, NRIPS)



Color Plate 77 Damage to a duplex outlet from a glowing connection. Observe that damage shows a radial pattern of destruction, emanating from the screw connection. Plastic (PVC, in this case) near the screw connection is gone; further away, plastic is charred; further yet, original undamaged material can be seen.
(Courtesy NIST)



Color Plate 78 Damage to a duplex outlet from external fire. Observe that damage decreases progressively front to back and is not concentrated near terminal screw connections.
(Courtesy Kevin Lewis, Schaefer Engineering Corp.)

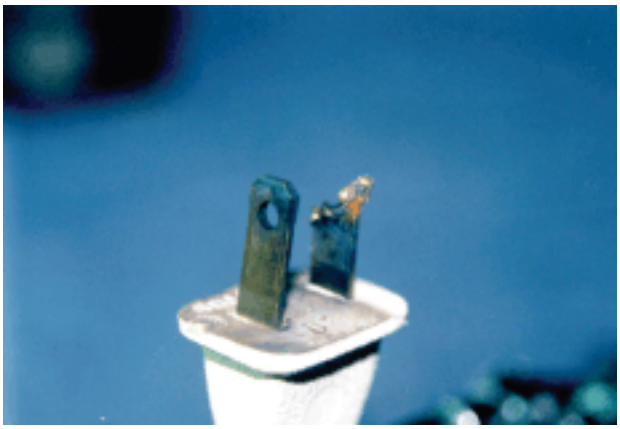


(a) **(b)**

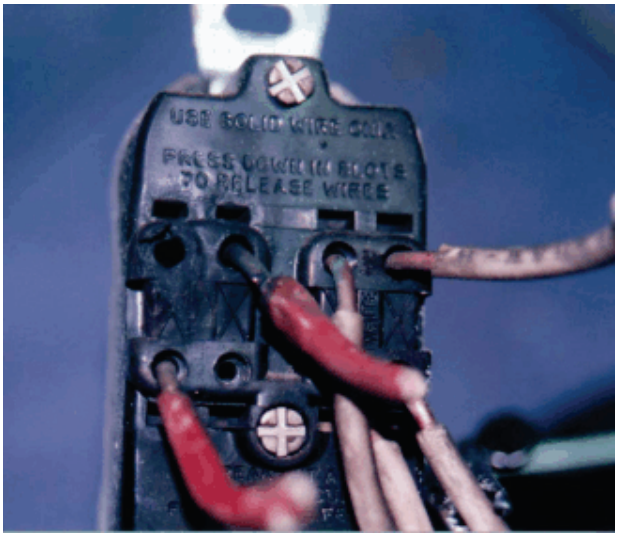
Color Plate 79 Results of laboratory glowing connection tests on **(a)** thermosetting outlet; **(b)** thermoplastic outlet
(Courtesy Kevin Brown, Fire Cause Analysis)



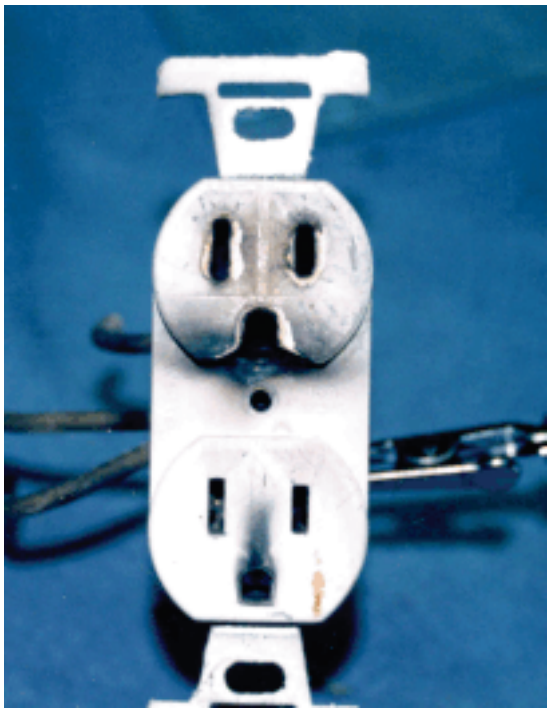
Color Plate 80 A fire originated at a poor aluminum-wire screw connection on this outlet; note the damage to the wire insulation
(Courtesy Kevin Brown, Fire Cause Analysis)



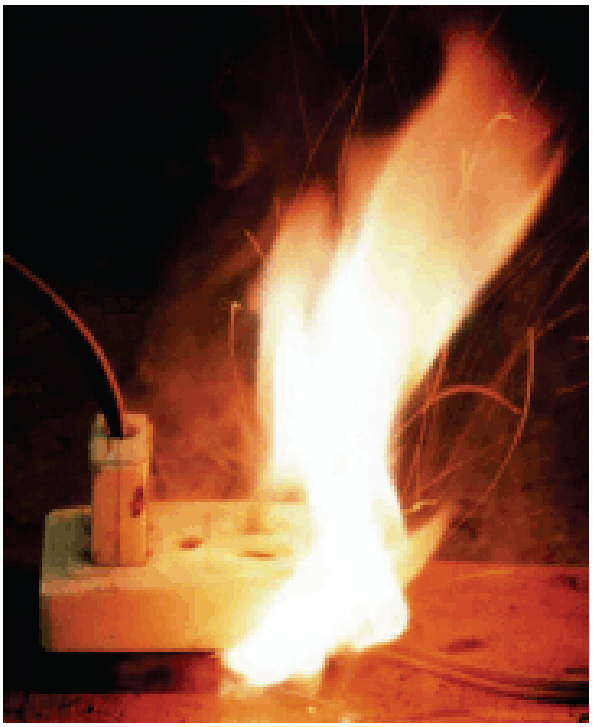
Color Plate 81 Male plug partly burned due to failure of back-wired outlet. Observe that this is an unpolarized plug and it does not cover the ground pin opening.
(Courtesy Al Graps, Electric Forensics, Inc.)



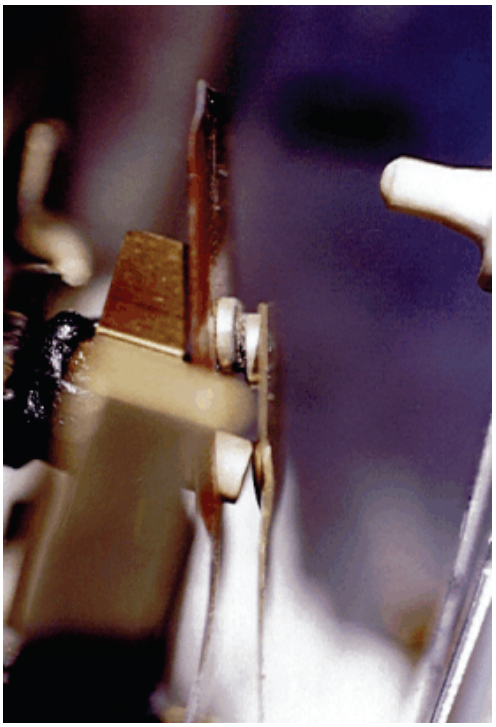
Color Plate 82 Rear view of failed back-wired outlet. A sofa was ignited from incandescent material ejected from this outlet.
(Courtesy Al Graps, Electric Forensics, Inc.)



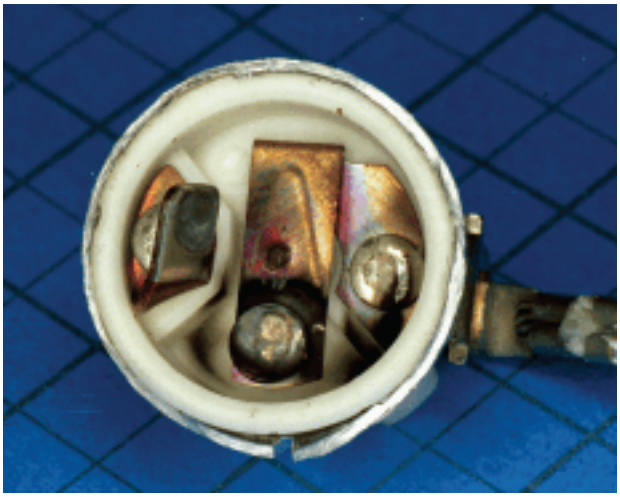
Color Plate 83 Front view of failed back-wired outlet
(Courtesy Al Graps, Electric Forensics, Inc.)



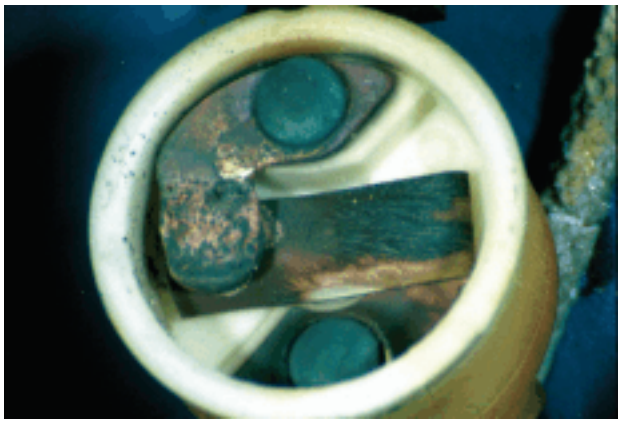
Color Plate 84 Flame projected from duplex outlet box due to arc within it
(Courtesy Yasuaki Hagimoto, NRIPS)



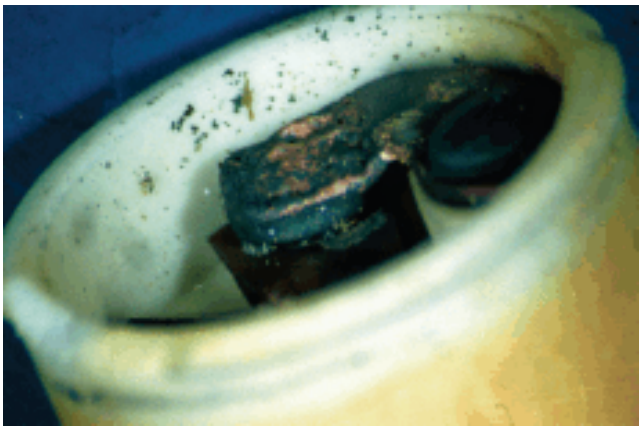
Color Plate 85 A pair of contacts that failed by becoming welded
(Courtesy Thomas Shefchick)



Color Plate 86 Thermostat contacts showing normal wear after 100,000 cycles of operation
(Courtesy Jack Olsen)



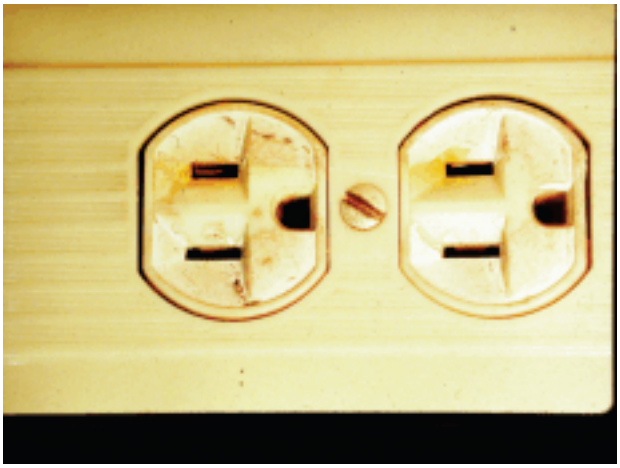
Color Plate 87 Thermostat contacts welded together after a properly-functioning thermostat was subjected to a furnace exposure of 925ºC for 20 minutes
(Courtesy Jack Olsen)



Color Plate 88 Close-up view of thermally-welded contacts shown in Color Plate 87
(Courtesy Jack Olsen)



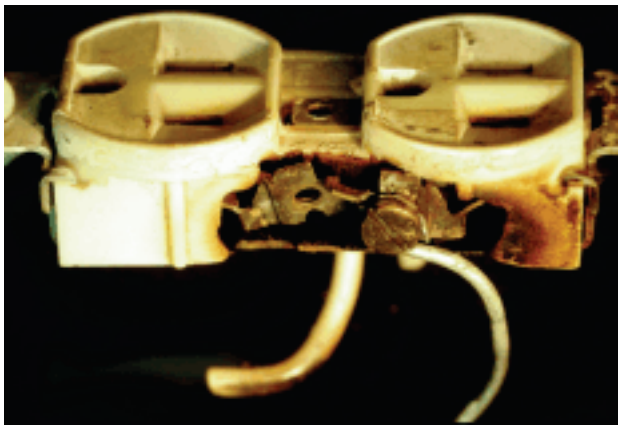
Color Plate 90 Incipient failure of an aluminum wire connection to a duplex outlet; note that insulation has melted and pulled back from both wires
(Courtesy Jesse Aronstein)



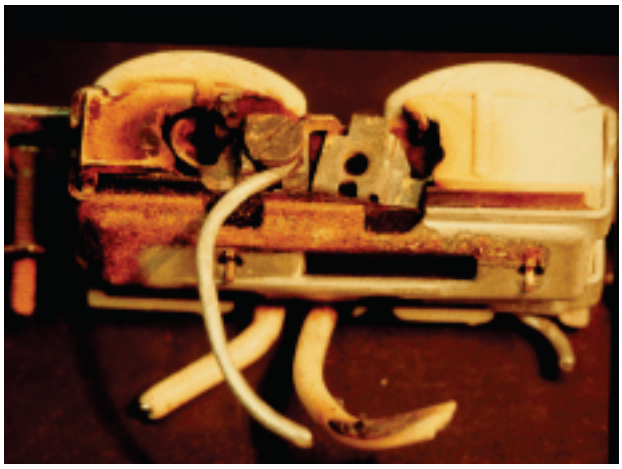
Color Plate 92 Outside view of cover plate of the receptacle shown in Color Plate 91
(Courtesy Jesse Aronstein)



Color Plate 89 Failure of a push-on connector at a dryer safety switch; note molten brass deposited onto the lower portion of the connector
(Courtesy Jesse Aronstein)



Color Plate 91 Gross failure of an aluminum wire connection to a duplex outlet
(Courtesy Jesse Aronstein)



Color Plate 93 Charring of insulation of where two initially-insulated conductors were in contact; note charring on white wire at bottom of photo
(Courtesy Jesse Aronstein)



Color Plate 94 Failure of wire nut used to pigtail one copper wire (12 AWG) from two aluminum wires (10 AWG). Even though carrying only 80% of rated load, a severe failure is seen, with the current being transferred through the steel helix and not by wire-to-wire contact.
(Courtesy Jesse Aronstein)



Color Plate 95 Consequence of arcing across carbonized insulation on a 120 VAC NM cable
(Courtesy David Reiter, Verité Forensic Engineering)



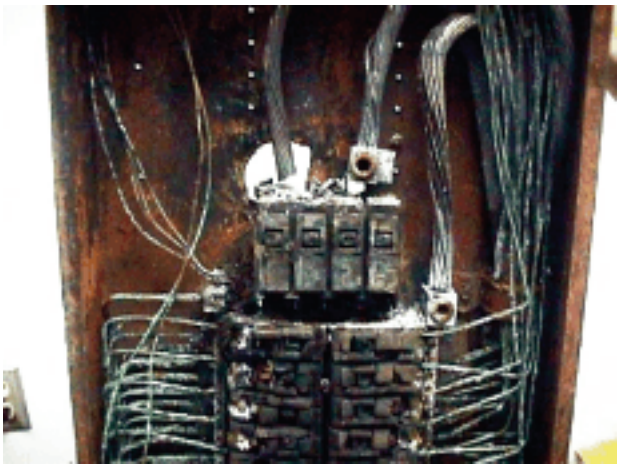
Color Plate 96 Fire due to carbonized insulation of a multi-outlet strip used with a salt-water aquarium
(Courtesy Kevin Lewis, Schaefer Engineering Corp.)



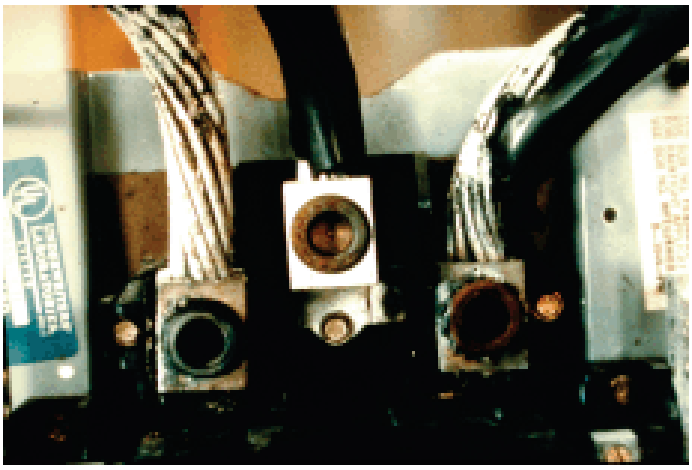
Color Plate 97 PVC cable (12/2, NM) ignited by torch. Note that PVC chars and does not melt
(Courtesy Michael Fitz, MDE Engineers)



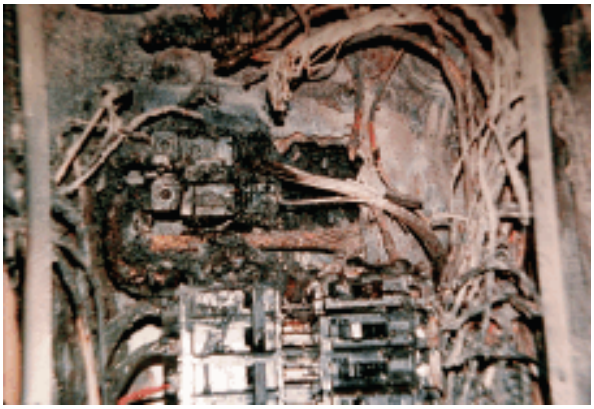
Color Plate 98 PVC cable arcing after being ignited by torch
(Courtesy Michael Fitz, MDE Engineers)



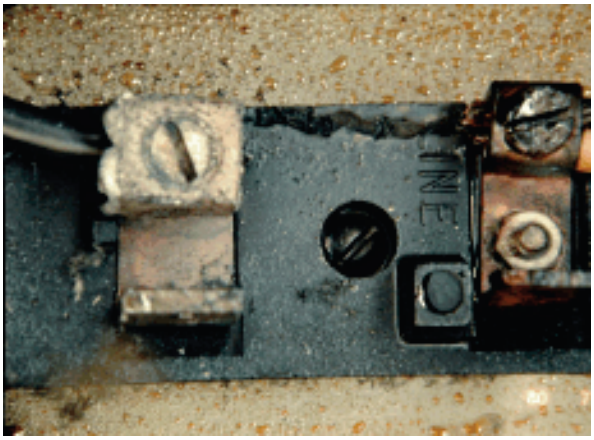
Color Plate 99 Fire starting when a thermoplastic channel used as the support for the main lugs of a panelboard softened and allowed contact with grounded enclosure
(Courtesy John Lentini)



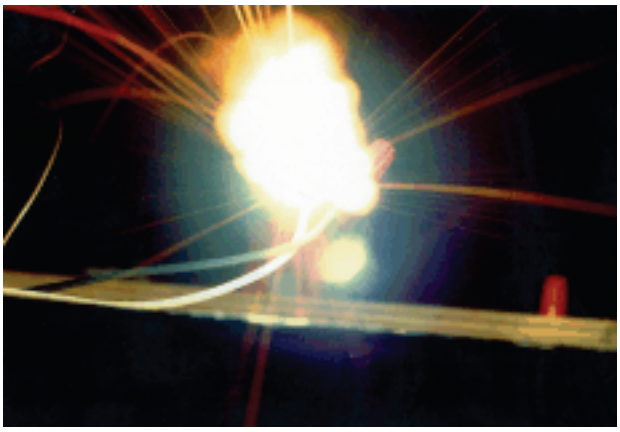
Color Plate 100 Incipient failure at a panelboard due to excessive heating at a connection lug
(Courtesy Jesse Aronstein)



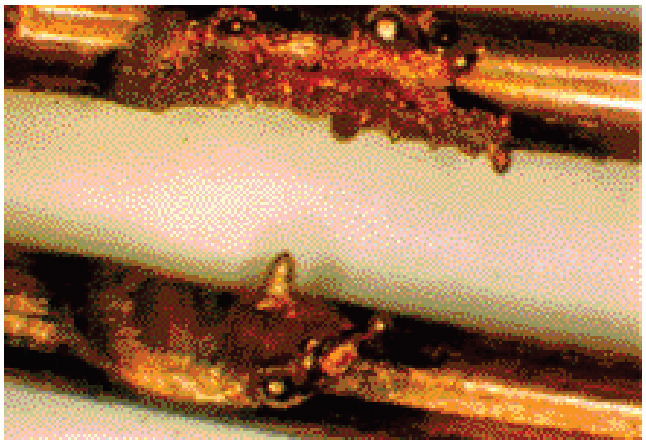
Color Plate 101 Fire originating at a panelboard; note extensive melting of metal enclosure.
(Courtesy Jesse Aronstein)



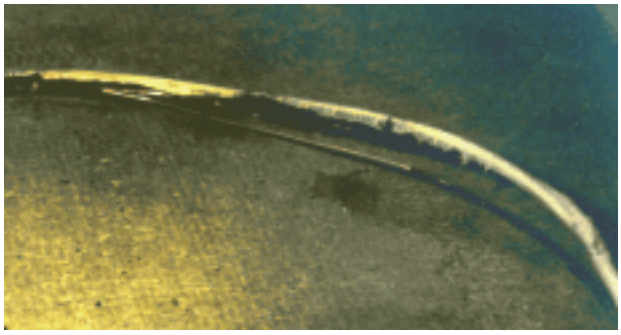
Color Plate 102 Arc tracking in a switch panel. Panel itself was not heated, but heat was applied to a conduit containing a cable feeding the panel. Arc tracking was caused by deposition of pyrolysates upon the insulator; note also the droplets on the back wall of the enclosure, these are condensed pyrolysates that came from the heated section of the cable and traveled through the conduit.
(Courtesy Jesse Aronstein)



Color Plate 103 Arc flash from a short-circuit in a 240 VAC branch circuit
(Courtesy David Reiter, Verité Forensic Engineering)



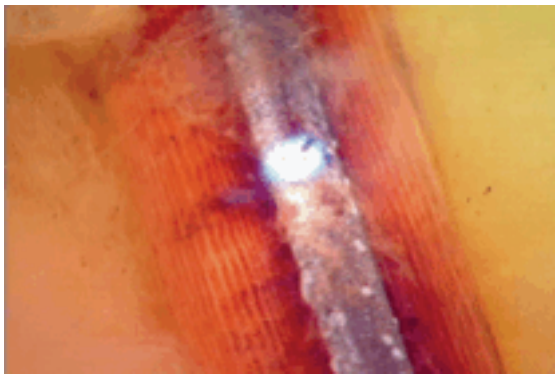
Color Plate 104 Arc beads with an irregular shape (obtained in laboratory testing by making direct contact between uninsulated conductors carrying 240 VAC)
(Courtesy David Reiter, Verité Forensic Engineering)



Color Plate 105 PVC-insulated cable (12/2, NM) melting while carrying a current of 57 A
(Courtesy Michael Fitz, MDE Engineers)



Color Plate 106 PVC-insulated cable (12/2, NM) moments after having ignited when subjected to a current of 150 A
(Courtesy Michael Fitz, MDE Engineers)



Color Plate 107 Arcing taking place on a 14 AWG NM cable degraded due to 1.9× overcurrent and thermal insulation; the thermal insulation was removed prior to photographing
(Courtesy Chris Korinek)



Color Plate 108 Failure of a flexible gas connector due to electric current inadvertently flowing through it
(Courtesy Mark E. Goodson)



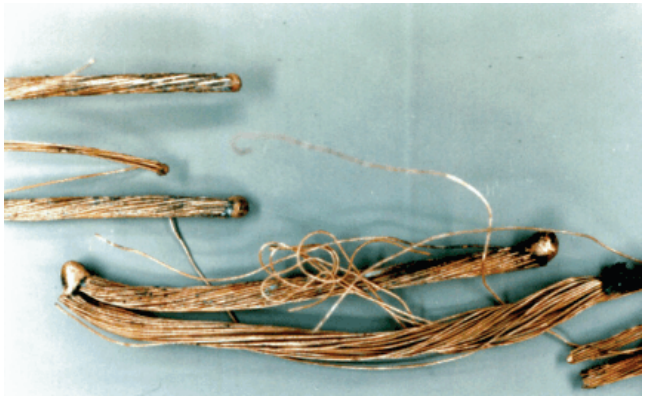
Color Plate 109 Fire originating at a dielectric union ahead of a gas meter
(Courtesy Robert G. Kleinheinz, Libertyville, IL Fire Dept.)



Color Plate 110 Electrified house: ignition of building paper and wood members from electrified plaster mesh
(Courtesy Al Graps, Electric Forensics, Inc.)



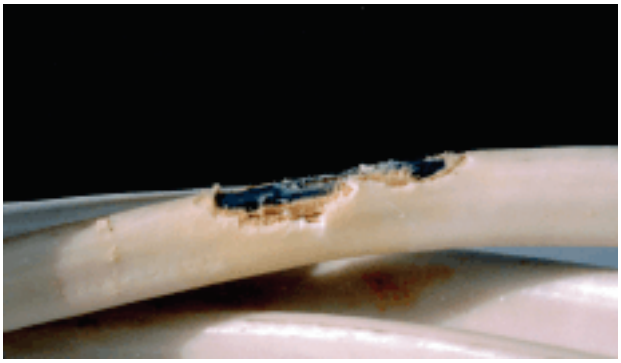
Color Plate 111 Ignitions due to current flow through aluminum siding at an electrified house
(Copyright Fire Findings, LLC; reprinted with permission)



Color Plate 112 Severed ends of SPT-1 power cord showing beads; damage occurred due to flame exposure
(Courtesy Safety Engineering Laboratories Inc. and Kluwer Academic Publishers)



Color Plate 113 Severed ends of SPT-1 power cord showing beads; damage occurred due to radiant heat
(Courtesy Safety Engineering Laboratories Inc. and Kluwer Academic Publishers)



Color Plate 114 Damage from rodents chewing modern electric cable
(Courtesy Chris and Joe Bloom)



Color Plate 115 Electric cable destroyed by ants in a cabin at Riding Mountain National Park (Manitoba, Canada)
(Courtesy Ken Swan)



Color Plate 117 Remains of nail and power cord after fire occurred due to damage of insulation at nail. Note damage due to arcing.
(Courtesy Kevin Lewis, Schaefer Engineering Corp.)



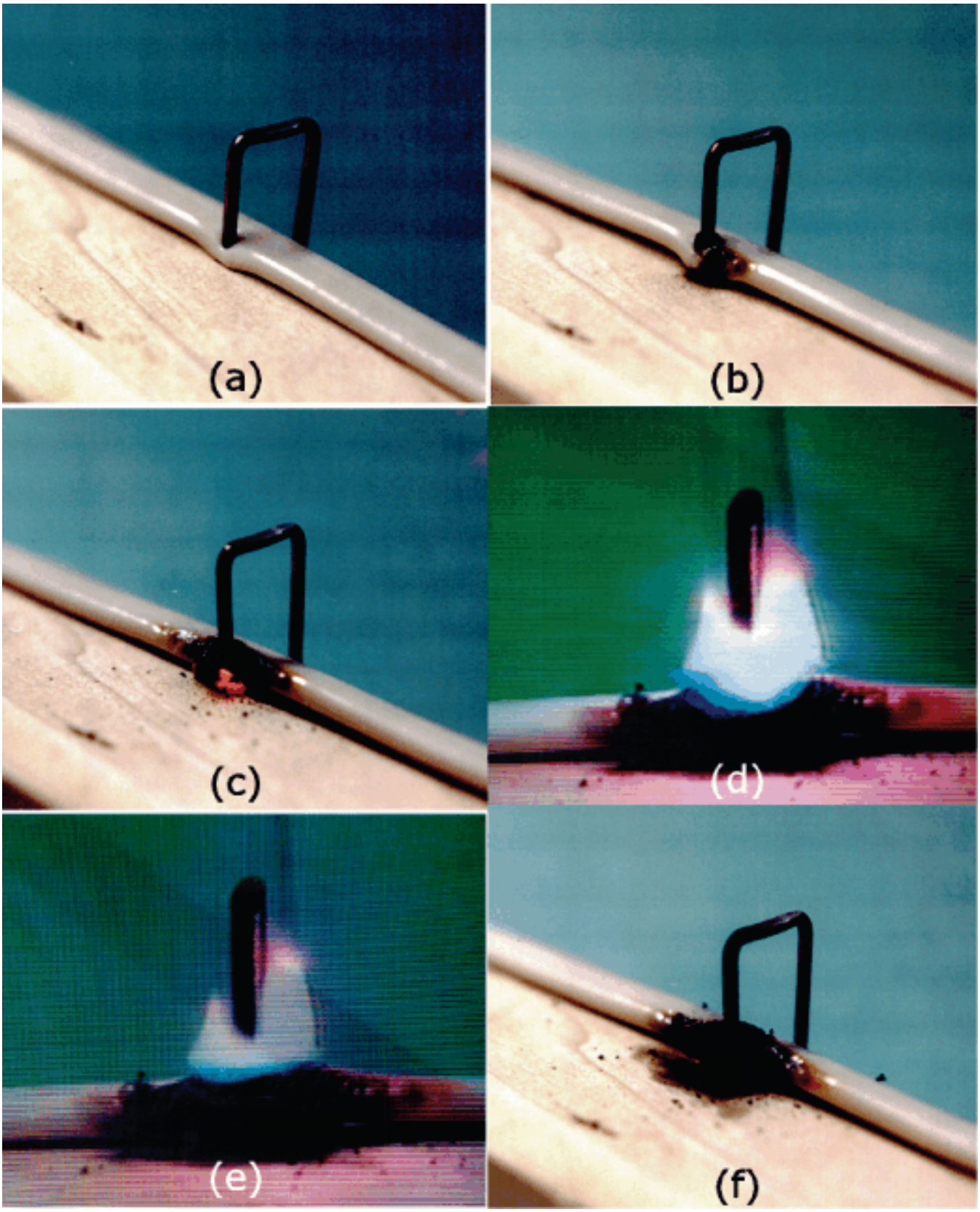
Color Plate 119 Alloying damage of aluminum upon copper
(Courtesy David Reiter, Verité Forensic Engineering)



Color Plate 116 A last-strand failure of a foot warmer cord that led to ignition
(Courtesy Yasuaki Hagimoto, NRIPS)



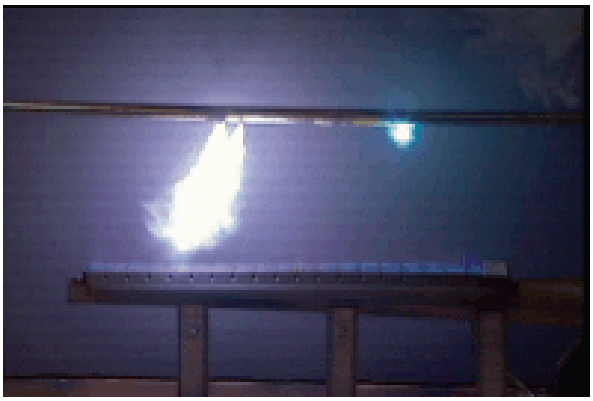
Color Plate 118 A copper wire that simply melted to a nail, but no arcing between the nail and conductor occurred.
(Courtesy Kevin Lewis, Schaefer Engineering Corp.)



Color Plate 120 Laboratory test showing ignition from a staple piercing one of the two conductors of a cable
(Courtesy Richard D. Brugger, PE, Erie PA)



Color Plate 121 Mobile home fire caused by overdriven staple
(Courtesy F. M. Brooks, PE, Baton Rouge LA)



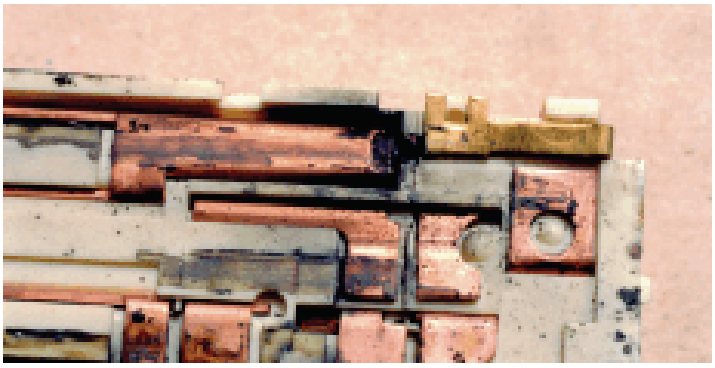
Color Plate 122 Flames from a propane burner (the burner is located below the conduit and the flames are nearly invisible blue color) caused arcing of conductors inside this conduit, having melted holes through the steel
(Courtesy Chris Korinek)



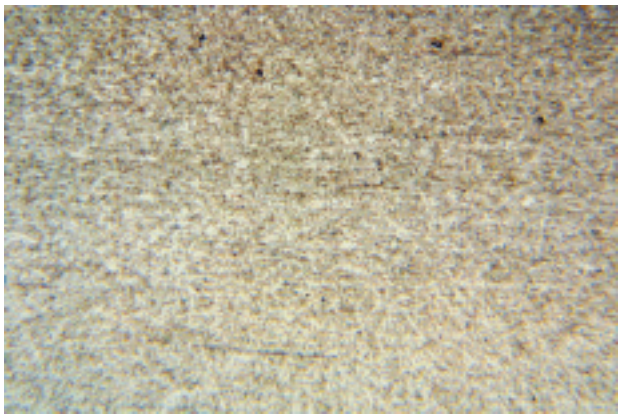
Color Plate 123 Bead created by experimental arcing—cross-section view
(Courtesy Yasuaki Hagimoto)



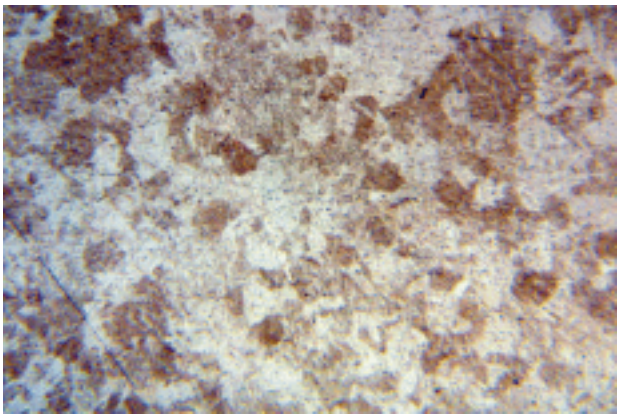
Color Plate 124 'Victim' bead from a real fire
(Courtesy Yasuaki Hagimoto)



Color Plate 125 Arc tracking damage leading to eventual ignition of an ignition switch
(Courtesy Chris and Joe Bloom)

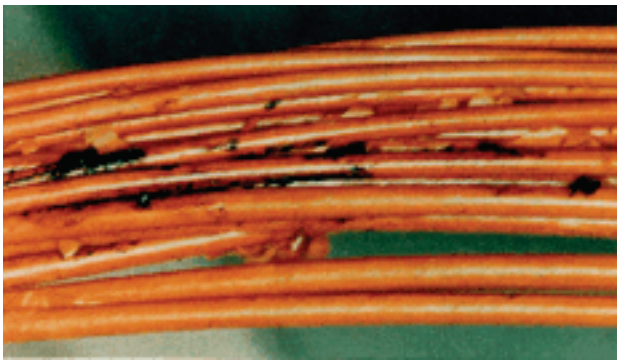


Pre-fire

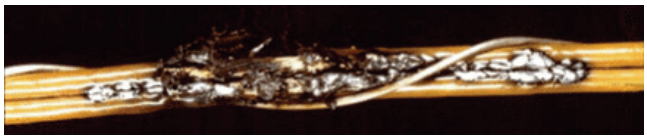


Post-fire

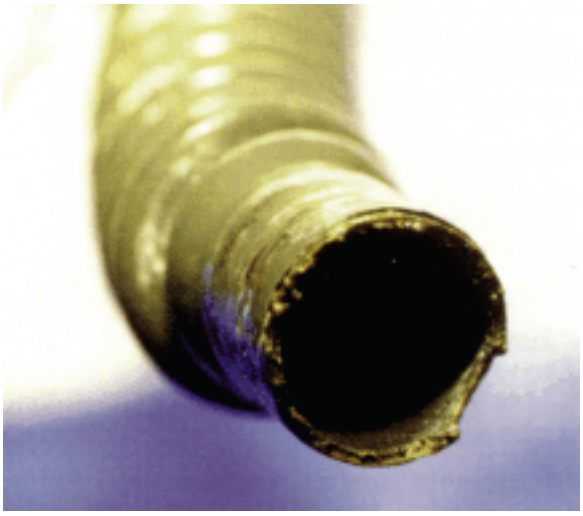
Color Plate 126 Grain structure of thin copper wire; both samples were etched in ammonium hydroxide and photographed through a microscope at 200× magnification. Left: virgin copper—the grains are flat and elongated. Right: after fire—recrystallization and grain growth has occurred creating grains of near-equal dimensions.
(Courtesy Kevin Lewis, Schaefer Engineering Corp.)



Color Plate 127 Arc tracking on MIL-W-81381 wiring



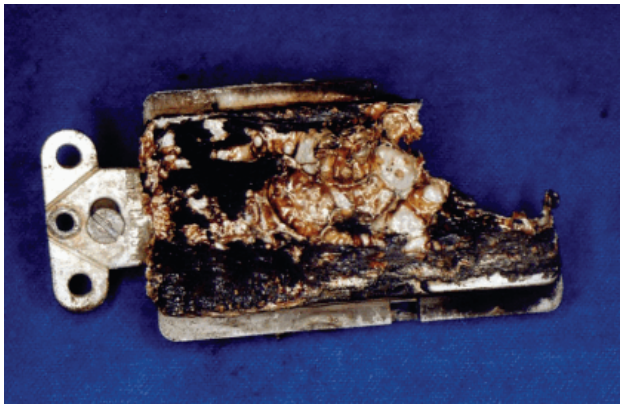
Color Plate 128 Failure of MIL-W-81381 Kapton-insulated wiring during testing for arc tracking by NASA



Color Plate 129 End connection of flexible gas line that failed due to excess electrical current flow
(Courtesy Fire & Arson Investigator)



Color Plate 130 Spark during refueling, going between the metal ring of the filler spout and the conductive rubber membrane connected to the car body (white circle shows location of faint spark).
(Courtesy Ulrich von Pidoll, PTB)



Color Plate 131 GFCI which did not function as a safety device, but rather ignited itself due to corrosion from water splashing upon it
(Courtesy Kevin Lewis, Schaefer Engineering Corp.)



(a)



(b)



(c)

Color Plate 132 Test burn showing use of a rocket-propellant type high-temperature accelerant in an empty building where the only fuel load was a wood ceiling and partial carpeting on the floor. **(a)** View of building before test. **(b)** Shortly after ignition, plumes of white combustion products are rising from buckets holding the accelerant. **(c)** About 4 minutes after the start of the fire the structure was fully engulfed.
(Courtesy Michael Fitz, MDE Engineers)



Color Plate 133 Effects of welding-grade thermite on a kitchen range. **(a)** Ignition of thermite is difficult and a welding torch was used. **(b)** and **(c)** Progression of burning; note how readily thermite burned through the top portion of the range and moved downwards. **(d)** The test range was placed on a 6 mm board of cement-asbestos board; this board was penetrated by the thermite combustion and spalling was caused to the concrete underneath.
(Courtesy Michael Fitz, MDE Engineers)



Color Plate 134 Circular smolder pattern in a self-heating bale of hops
(Courtesy James White, Western Fire Center, Inc.)



Color Plate 135 Spontaneous combustion of hops bales pulled from a warehouse
(Courtesy Yakima, WA Fire Dept.)



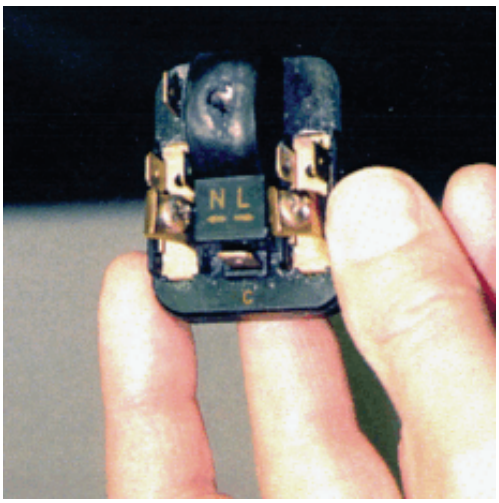
Color Plate 136 Murdered woman, burning with short flames
(Courtesy Oregon State Police and John D. DeHaan)



Color Plate 137 Arc tracking across wet wood from a 9 kV neon transformer circuit
(Courtesy David Reiter, Verité Forensic Engineering)



Color Plate 138 A package of towels found spontaneously smoldering; a comparison package is shown at right
(Courtesy Norman Alvares and LLNL)



Color Plate 139 A failed PTC starting device
(Courtesy Ulf Erlandsson, Rädningsverket, Sweden)



Color Plate 140 Refrigerator fire due to a failed PTC starting device
(Courtesy Ulf Erlandsson, Rädningsverket, Sweden)



Color Plate 141 Glowing ignition of maple at a heat flux of 12 kW m^{-2}, side grain ignition; glow shown in white circle.
(Courtesy Michael J. Spearpoint)



Color Plate 142 Wood siding mockup fully ignited by wood crib weighing 0.8 g. Mockup height 500 mm; crib sticks 2 × 2 mm; crib base 22 × 22 mm.
(Courtesy CSIRO Australia)



Color Plate 143 Ignition of wood floor/ceiling assembly from a hot-water pipe (the left pipe in the photo)
(Courtesy Ken Swan)



Color Plate 144 Close-up of above
(Courtesy Ken Swan)

Copyright © 2003, 2014 Vytenis Babrauskas

Chapter 14. Information on specific materials and devices

Introduction **682**
Accelerants in incendiary fires **683**
Acetylene and related compounds **683**
Aerosol cans **686**
Agricultural products **687**
Self-heating *687*
Electrostatic properties *688*
Air compressors and compressed air systems **688**
Aircraft cabin wall panels **690**
Airplanes **690**
Alcoholic beverages **691**
Aldehydes **691**
Ammonia **691**
Ammonium nitrate and ANFO **691**
Ammonium perchlorate **694**
Antifreeze **695**
Arsenic compounds **695**
Ashes **695**
Asphalt **696**
Automatic transmission fluid **696**
Aviation fuels **696**
Azides **700**
Bagasse and bagasse products **700**
Boranes **701**
Boron **701**
Brake fluid **702**
Calcium resinate **702**
Camping fuel **702**
Candles **702**
Tea candles *704*
Gel candles *704*
Carbon disulfide **704**
Carbon monoxide **704**
Cellulose **704**
Cellulose insulation **706**
Cellulose nitrate, Celluloid, pyroxylin **707**
Charcoal, coke, and related products **710**
Charcoal *710*
Charcoal briquettes *712*
Coke *712*
Activated charcoal *713*
Activated carbon *714*

Chimneys and flues **715**
5-Chloro-1,2,3-thiadiazole **715**
Christmas trees, artificial **716**
Cigarettes and cigars **716**
Clothes irons **719**
CO_2 extinguishers **719**
Coal **719**
Properties of coal *719*
External ignition *720*
Self-heating *720*
Coal dust *724*
Coal pulverizers *724*
Coffeemakers and teapots **725**
Composite materials **725**
Fiber-reinforced plastic *725*
High-pressure laminates, low-pressure laminates, and related products *726*
Compost, manure, garbage, sewage, and landfills **726**
Computer and information technology equipment **726**
Conveyor belts **727**
Cooking appliances **727**
Grills *729*
Cork **729**
Cotton **729**
Crankcase explosions **730**
Crude oil **731**
Curling irons and hair dryers **731**
Curtains **731**
Diapers, disposable **732**
Diesel fuel **732**
Dinitrosopentamethylenetetramine **732**
Dishwashers **732**
Dryers and washers (for clothes) **732**
Dryers (process dryers) **734**
Dung, fecal matter **735**
Dusts **735**
Ignition of layers *735*
Explosions *736*
Earthquakes **737**
Electric (general statistics) **737**
Electric appliances and electronic equipment **740**
High-limit switches *741*
Electric batteries **742**
Electric blankets and mattress pads **743**
Electric circuit interruption devices **744**
Electric fences **746**
Electric lamps and lighting fixtures **746**
Ordinary incandescent lamps *747*
Halogen lamps *749*
Arc discharge lamps *750*

Fluorescent lamps 752
Lighting fixtures: Incandescent 752
Lighting fixtures: Fluorescent 753
Electric motors 755
Electric outlets, plugs and connections 755
Failures at plugs 756
Failures at outlets 759
Miscellaneous connection failures 762
The aluminum wiring problem 762
Incendiarism 765
Electric switches 766
Electric transmission and distribution systems 766
Transformers 766
Busbars, switchboards, and panelboards 769
Insulated distribution cables 772
Service drops and high current capacity conduits 772
High voltage insulators 773
Electric wires and cables 773
Modes of ignition of wiring 773
Contributory factors 787
Appliance cords and extension cords 793
Impaired cooling 794
Wires in steel conduits 794
Electric wiring: Cause or victim? 795
Electric wiring and equipment in motor vehicles 804
Electric wiring in aircraft 804
Electronic components 806
Engines, diesel 806
Ethers 806
Ethylene 807
Ethylene glycol 807
Ethylene oxide 807
Explosives 810
Fabrics 815
Ignition temperature 817
Flame ignition 818
Radiant ignition 821
Convective heating 823
Other forms of heating 824
Elevated oxygen conditions 825
Effects of treatments 825
Farm machinery 826
Feedstuffs 826
Felt 826
Fertilizers 826
Fibers 827
Fibers covered with oil 827
Fire hoses 829
Fishmeal 829

Floor buffers **829**
Floor coverings **829**
Foodstuffs **833**
Forest materials, vegetation, and hay **833**
Ignition by hot gases and hot surfaces *835*
Ignition by matches and small flames *837*
Ignition by cigarettes *839*
Ignition by lightning *840*
Ignition from contact with power lines *840*
Radiant ignition *841*
Ignition by brands or small hot particles *842*
Self-heating *845*
Fuel oil **847**
Furnaces and boilers **847**
Gas-fired *848*
Oil-fired *848*
Furniture **849**
Gas meters, regulators, and piping **849**
Gasoline **849**
Gasoline substitutes *851*
Filling of portable gasoline containers *851*
Fueling vehicles at filling stations *852*
Filling station tanks *853*
Ground fault circuit interrupters **853**
Gypsum wallboard **853**
Hair **854**
Hairdresser chemicals **854**
Heat guns **854**
Heat tapes and heat cables **854**
Heat transfer liquids **856**
Heaters, catalytic **856**
Heaters, electric **856**
Built-in heaters *856*
Portable heaters *858*
House furnaces *858*
Heating equipment (general statistics) **858**
High-temperature accelerants **858**
Hops **859**
Humans **859**
Human skin *861*
HVAC equipment **862**
Hydraulic fluids **862**
Hydrazine **862**
Hydrocarbon gases **863**
Hydrogen **863**
Explosions due to adventitious hydrogen presence *864*
Hydroxylamine **864**
Incendiary timing, delay, and actuation devices **864**
Insecticides, pesticides, fungicides **864**

Iron sulfides **864**
Jute **865**
Kerosene **865**
Kerosene heaters **865**
Lambswool pads, imitation **866**
Lawn mowers **866**
Lime **866**
LNG and LPG **866**
Marijuana and hemp **867**
Matches and lighters **867**
Properties of matches *867*
Ignition potential of blown-out matches *869*
Lighters *869*
Metal alkyls **869**
Metal alloys **870**
Metal carbonyls **870**
Metal hydrides **870**
Metal oxides **870**
Metals **870**
Aluminum *870*
Antimony *872*
Barium *872*
Beryllium *872*
Bismuth *872*
Brass *872*
Cadmium *872*
Calcium *872*
Cerium, pyrophor, and cigarette-lighter 'flints' *872*
Cesium *873*
Chromium *873*
Cobalt *873*
Copper *873*
Hafnium *873*
Iron and steel *873*
Lead *874*
Lithium *874*
Magnesium *874*
Manganese *875*
Molybdenum *875*
Nickel *875*
Plutonium *876*
Potassium *876*
Rare earth elements *876*
Rubidium *876*
Sodium *876*
Strontium *876*
Tantalum *876*
Thorium *877*
Tin *877*

Titanium *877*
Tungsten *878*
Uranium *878*
Zinc *878*
Zirconium *878*
Methane and natural gas **879**
Methyl bromide **880**
Methylene chloride **880**
Microwave ovens **880**
Mineral wool **880**
Motor vehicles **881**
Flammability of interior combustibles *883*
Automobile exhaust systems *883*
Automotive air bags *884*
Flammable refrigerants *885*
Neon lighting **885**
Nitrates **885**
Nitric acid and nitrogen oxides **885**
Nitrides **886**
Nitrogen, liquid **886**
Oils **886**
Vegetable and animal oils *886*
The iodine number test *888*
Mineral and synthetic oils *890*
Oil-water emulsions **890**
Organometallic compounds **890**
Otto fuel II **890**
Oxidizing chemicals **890**
Halogen fluorides *891*
Gaseous fluorine *891*
Liquid chlorine *891*
Water purifying and bleaching chemicals *891*
Carbon tetrachloride *894*
Aircraft oxygen generation canisters *894*
Compressed gaseous oxygen *895*
Liquid oxygen *895*
Oxygen pumps **896**
Oxygen regulators **896**
Paints, dyes, and related substances **896**
Paper products **898**
Paper *898*
Cardboard *899*
Paper vapor barrier *900*
Peat and organic soils **900**
Perchloric acid **901**
Perfluorocarbons **902**
Peroxides **902**
Inorganic peroxides *902*
Organic peroxides *902*

Pharmaceuticals **903**
Phosphines **903**
Phosphorus **903**
Pillows **903**
Pipe insulation **904**
Plastics **905**
Self-heating of solid plastics *909*
Elastomers and foams *909*
Potassium chlorate **912**
Powdered milk **913**
Power steering fluid **913**
Propane **913**
Propylene oxide **913**
Pyrotechnics **913**
Radio and audio equipment **918**
Railroads **918**
Rayon **918**
Refrigerators **918**
Rice husks **919**
Roofing materials **919**
Sanding machines **919**
Saunas **919**
Shredded materials **920**
Siding, plastic **920**
Silane and chlorosilanes **920**
Silicon **921**
Silicone fluids and polymers **921**
Skins and leathers **921**
Soaps **921**
Sodium chlorate and sodium chlorite **921**
Sodium dithionite **922**
Solder and soldering irons **922**
Soots, lampblack, other 'blacks' **922**
Soybeans **922**
Spas **922**
Stearic acid **922**
Steel turnings **922**
Styrene **922**
Sugar **923**
Sulfur **923**
Surge suppressor MOV devices **923**
Surgical tubing **923**
Tanks **923**
Asphalt storage tanks *924*
Tar (wood) **924**
Telephones, cellular **924**
Television sets and computer monitors **924**
Tents **926**
Textile wall coverings **926**

Thatch **926**
Thermostats **926**
Tinder **926**
Tires and wheels **926**
Toasters **928**
Town gas **928**
Turpentine **928**
Unsymmetrical dimethylhydrazine **928**
Upholstered furniture and mattresses **928**
Smoldering and ignition from cigarettes *928*
Ignition from small flames *931*
Ignitability from radiant heat *932*
Ignition from burning brands *934*
Ignitability mode comparisons *934*
Effect of wear and soiling *935*
UFAC and BIFMA requirements for ignitability *935*
California TB 117 standard for ignitability *936*
Flaming-source ignition experiments and proposed test by CPSC *936*
UK furniture regulations *937*
Mattresses *937*
Vacuum cleaners **938**
Wastes **939**
Water heaters **939**
Electric water heaters *939*
Gas-fired water heaters *939*
Welding **941**
Wood and related products **942**
Whole wood *942*
Wood components *961*
Painted wood *962*
Hardboard *962*
Fiberboard *962*
Plywood *964*
Particleboard and oriented strand board *965*
Wood sawdust, chips, and wastes *965*
Oiled sawdust *966*
Wood pulp *967*
Shingles and shakes *967*
Wood-burning appliances **967**
Wool **967**
Further readings **968**
References **969**

Introduction

In this Chapter, detailed information is presented for a variety of substances which are of special interest in regards to their ignition characteristics. Also collected in the same alphabetic arrangement is information on some ignition sources which have been studied in detail. The meaning of various physicochemical constants cited is explained in the pertinent theory chapters, for example, to understand the meaning of E and P, the reader should refer to Chapter 9.

Accelerants in incendiary fires

The breakdown of types of ignitable liquids found by a large commercial testing laboratory[1] during a 5-year period is shown in Table 1. Some older data[2] from a State laboratory are given in Table 2.

Acetylene and related compounds

Acetylene, C_2H_2, is highly combustible, subject to exothermic decomposition, and has a particularly wide flammable range. Much of its special nature is due to the presence of the triple bond (C≡C). Most of the use of acetylene is in gas form, or in its storage form as dissolved in acetone. The rarely-used liquid acetylene has been subjected to various explosion tests and performs roughly similarly to picric acid, a sensitive explosive[26]. Solid acetylene, which has essentially no commercial uses, is fairly insensitive. Additional information on handling liquid or solid acetylene is given by Urben[3]. The standard reported LFL for acetylene is 2.5%, but its UFL can be 100% if it decomposes and is around 80% for normal oxidation. Tested in a 5 L volume, an LFL value of 2.2% was found[26]. The AIT, measured in small vessels or in 12.5 mm tubes[4], is 290 – 300ºC and is surprisingly independent of concentration, over the range of 20 – 80%. For concentrations below 20% or above 80%, the AIT rises to higher values in the 400 – 600ºC range. The AIT is the same regardless of whether the atmosphere is air or pure O_2. The AIT shows a moderate decrease for moderately elevated pressures, but relations have not been reported at higher pressures[9]. For spark ignition, the 0.02 mJ energy required[5] (at the optimal fuel concentration of 9%) is about a factor of ten lower than for most other common hydrocarbons. MIE values in the decomposition regime[9] (fuel concentrations greater than about 80%) are very large, ca. 250 J. At elevated pressures, MIE $\propto P^{-n}$, where n = 2 to 3. The quenching distance in air is 0.65 mm. In oxygen, an accurate value has not been determined, but it has been estimated as about 1/6 that in air[9]. To detonate[6], not just ignite, acetylene/air mixtures at ambient pressure requires, in the worst case, a spark energy of 3.7 mJ; this corresponds to a mixture of 40% acetylene/60% oxygen. The needed detonation energy is very sensitive to pressure, but the effect has only been studied for sub-atmospheric pressures. For pure acetylene (without air or oxygen), explosive decomposition is expected at 800ºC at 1 atm and at 540ºC at 2 atm pressure (absolute), the latter being the highest pressure at which pure acetylene is normally handled[7].

Acetylene is an unstable molecule which can undergo several exothermic reactions—polymerization, 'condensation' reactions, and decomposition. Benzene is the most common polymerization product, but an extensive list of other products has been found when acetylene spontaneously regroups into larger molecules[8]. If the resulting product is not composed of identical repeating units, then the reaction is known as condensation instead of polymerization. The activation energy for some condensation reactions is close to zero, indicating they will not need much heating in order to occur. Heterogeneous condensation reactions also occur—many metals act as catalysts upon which condensation reactions can occur. Surface condensations on finely divided platinum, iron, nickel or cobalt occur at room temperature and incandescent temperatures are found. Rapid heterogeneous reactions on many other surfaces can occur at elevated temperatures.

Table 1 Results of analysis of fire debris samples for accelerants at a large commercial forensic testing laboratory during 1997 – 2001

Ignitable liquid found	Percent
gasoline	20.8
mineral spirits	6.7
naphtha	4.5
kerosene	2.8
diesel fuel	1.1
mixtures	0.6
isoparaffinic solvent	0.5
medium petroleum distillate	0.2
aromatic solvent	0.2
deparaffinated solvent	0.2
normal paraffins	0.2
straight run petroleum	0.1
turpentine	0.1
toluene	0.1
heavy petroleum distillate	0.1
alcohols	<0.1
fuel oil	<0.1
light petroleum distillate	<0.1
other ignitable liquids	2.0
negative findings	59.7

Table 2 Frequency distribution for accelerants (positive findings only) identified by the Ohio Arson Crime Laboratory in 1982

Ignitable liquid found	Percent
gasoline	53
kerosene	11
diesel fuel	7.9
mixtures	7.2
turpentine	5.1
paint thinner	4.9
cigarette lighter fluid	1.9
charcoal lighter	1.5
alcohol	1.3
other	5.5

The decomposition of acetylene occurs as:

$$C_2H_2 \rightarrow 2C + H_2$$

the reaction being exothermic, with a very high heat of reaction of 226.7 kJ mol^{-1}. Decomposition does not occur at room temperature without an ignition mechanism, but if an external energy input is provided, explosive decomposition of pure acetylene (i.e., with no oxygen in the system) can occur at ambient temperature (25ºC) under certain conditions. Apart from flames, the ignition mechanism can com-

prise an electrostatic spark, a hot body, or compression heating due to shock. The probability of any particular energy source sufficing to cause a decomposition explosion increases with increasing pressure of the acetylene[16]. Research into the combustion chemistry of acetylene through 1969 has been reviewed by Williams and Smith[9].

Typical safety recommendation is that end users of acetylene should not use gaseous acetylene at pressures over 2 atm (absolute) or 1 atm (gage). This is probably justified by generally good experience when abiding by this recommendation, but research[10] has indicated that it is possible to explode acetylene in small vessels at pressures as low as 1.4 atm (absolute). The vessels in question were 200 mm by 270 mm and 51 mm by 305 mm. The explosion hazard is related to the size of the pipe or vessel, and Zabetakis[4] has reviewed the literature on decomposition explosions of acetylene in pipelines. His summary (Figure 1) indicates that under initial conditions of atmospheric pressure (1 atm abs), deflagration can occur for tube diameters greater than ca. 130 mm. But with increased pressures, even very small tube sizes can sustain an explosion. Detonation at atmospheric pressure has not been observed, but will generally (in the linear portion of the curves) require a diameter about 2× of what is the minimum for deflagration. While these conclusions of Zabetakis are the best available, nonetheless the experimental data on this must be considered scanty. The data of Nelson[11], not specifically included in Zabetakis' analysis, suggest that beyond about 100 mm diameter, the deflagration limit also reaches a plateau and that further increases in pipe size do not lead to lower minimum pressures required for explosion. In some cases, deflagration flames propagating in pipes can turn into detonations if the pipe is long enough. The length required for this to occur is usually from a few to many meters, but decreases for smaller diameters and for higher initial gas pressures[12]. Thus, a small pipe diameter is helpful towards avoiding an explosion, but is a drawback towards avoiding a transition to detonation if an explosion does occur. The compression heating of a Bourdon gage tube due to rapid opening of a cylinder valve has been evaluated and found not to be sufficient to cause compression ignition[8].

Similar guidance is not available at elevated temperatures. Clearly experimental details (sizes, wall materials, exact pressure used) do make some difference since the data spread is so large, but a systematic accounting for these effects is not available.

The decomposition-explosion of pure acetylene using a heated platinum wire as the ignition source was studied by Detz[13]. He found that the wire temperature needed to be raised to quite high temperatures, as indicated in Figure 2.

The temperature required for acetylene to undergo explosive decomposition can be highly influenced by contaminants. Miller and Penny[14] report that, under certain experimental conditions, a small amount of powdered substances such as rust or pipe scale lowered the temperature from 450ºC to 280–300ºC. The explosive decomposition of acetylene can be readily initiated when copper acetylide is present. This substance, itself highly susceptible to explosive decomposition, can serve as initiator for acetylene explosion. A film of copper acetylide can be formed on the inside of copper tubes exposed to acetylene. Such copper acetylide films, however, are much less prone to spontaneous decomposition than copper acetylide produced by wet-chemistry reactions. But wet-chemistry reactions do happen. In gen-

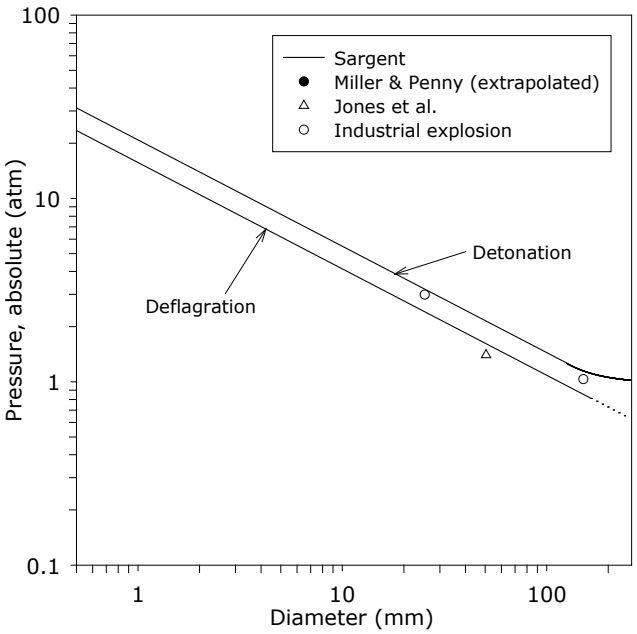


Figure 1 The explosive decomposition limits for acetylene at 25ºC[4]

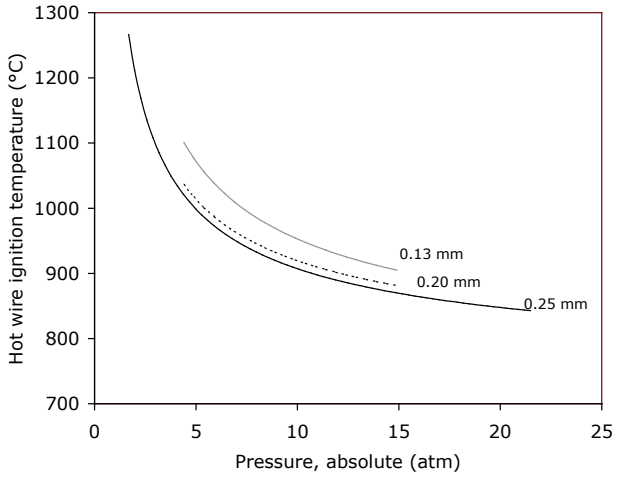


Figure 2 Hot wire temperature needed for decompositional ignition of pure acetylene

eral, the problems found with brass materials are fewer and brass is considered relatively safe[8]. But a series of explosions originating in brass valves of cylinders being filled at a manufacturing plant identified a way that copper acetylide explosions occur[16]. Calcium chloride solution was improperly used for leak testing and this etched some of the brass surface by removing the zinc component and leaving a highly porous, reactive copper surface. The remaining, undried solution reacted with acetylene to form copper acetylide which subsequently detonated. Unfortunately, despite the easy explosibility of copper acetylide under the worst circumstances[15], there does not appear to be any literature quantitatively defining the limits of explosion for copper materials used in conveying acetylene of reasonable purity. Thus, precautions against use of copper fittings are perforce of a vague nature.

It has been found in operating acetylene plants that the most common reason for ignitions is when foreign matter gets on to a valve seat and then gets crushed in operating the valve[16]. Despite this operating experience, the event is difficult to reproduce in laboratory. Miller and Penny[14] conducted numerous laboratory tests under a pressure of 20 atm, but could not produce a single explosion. Their study involved 10,000 tests with a clean valve, 10,000 tests with a valve gritted up with rust and concrete dust, and 10,000 tests where the valve seat was contaminated with a mixture of charcoal and copper acetylide. A standard safety recommendation to minimize the chances of rust or scale sloughing off and getting into valves is to coat the insides of pipes lightly with oil[16]. It has also been found that oil inside valves helps to stop propagation of detonations; the phenomenon is not fully understood, but it is felt to relate to the heat of vaporization needed to gasify the oil.

Admixing other hydrocarbons reduces the explosion potential of acetylene, effectively stabilizing it, although this technique may not always be practicable[10].

Acetylene-air or acetylene-oxygen mixtures in pipes very easily transition from deflagration to detonation, and millimeter lengths (unlike the meters normally required for pure acetylene) may be sufficient for this transition to occur[12].

Detonations in acetylene pipelines can pass through closed valves[16]. Experience indicated that they can pass through any bronze valves, even high-pressure rated ones. Detonations are likely to be stopped by a forged steel valve if the detonation comes from the bonnet side, but not from the under-seat side. Properly installed acetylene plant piping can withstand detonation pressures, but extremely high specification piping is needed.

For a *hot surface* to ignite acetylene, a rather low temperature suffices. Using a brass plate of 1770 mm^2 area, it was found that ignition occurs at 383ºC[17]. Only mixtures within the range of 3 – 40% can be ignited by mechanical sparks[8]. For electric spark ignition, mixtures over 70% acetylene require very large energies—joules, rather than millijoules. At the 100% acetylene limit, about 100 J is needed for ignition.

During the 19th century, acetylene was shipped as a gas, at pressures of 30 – 50 atm. The consequent losses due to explosions proved heavy, and it was soon learnt that acetylene dissolved in acetone is not as sensitive. Thus, it became mandatory that acetylene be shipped in cylinders which are unique in two respects: (1) the volume inside is filled with a porous flame-arrester mass; and (2) the acetylene is dissolved in acetone and not just compressed by itself. In the industry, acetylene shipped this way is known as *dissolved acetylene* (DA). The porous mass traditionally was charcoal and diatomaceous earth. Later, the porous mass used to be a cementitious substance which was reinforced with asbestos and baked in place to provide 90% porosity. This was supplanted by a charcoal-cement matrix, and then by calcium silicate fibers in the cement. Acetone is used because it has the desired properties—acetylene is highly soluble in it at high pressures, but poorly so at ≈ 3 atm (the normal 'empty' pressure of a cylinder). This means that the acetylene can be put solution at the manufacturer, and then obtained in gas form by user. The pressure gage reading of an acetylene tank indicates the actual solution pressure and will change drastically with temperature; the partial pressure of acetylene in a fully-charged tank is around 15 atm.

When an acetylene cylinder is heated externally by a fire or a flame, an explosion may occur. Fatalities have been recorded[18] from explosions that have occurred from modest external flaming impinging upon a cylinder. Heating can also occur due to flashback into the cylinder due to a faulty welding rig or due to improper operation. A standard recommendation[3] states that heating as little as 1 in^2 (6 cm^2) to 185ºC can suffice to start decomposition reactions, which may result in an explosion some hours later; however, it is not clear what quantitative data there may exist to support these values. If the heating is limited, then the hydrogen gas that is evolved from decomposition serves to act as a low thermal conductivity barrier to fresh reactants entering the areas. Thus, curiously, if a partial-pressure relief occurs during an incident like this, a much more disastrous outcome can follow than if the cylinder retains pressure[16]. Bursting discs and fusible plugs are commonly fitted to acetylene cylinders for the purpose of mitigating hazards in such occurrences. But recent HSE experimental studies[19] showed that they may not accomplish their intended purpose and may even make matters worse. Unless a full, early release is obtained, then the partial-release scenario mentioned above comes into play. An undesirable consequence of the operation of a fusible plug may be the overheating of an adjacent acetylene cylinder. Fusible plugs are sometimes mounted in a way as to make them susceptible to mechanical damage in handling the cylinder. In those cases, a leak may occur at the plug and this may be hard to notice.

Fire service operations when acetylene cylinders have been exposed to fire (or localized heating) can become dangerous. The common advice given to alleviate this potential of explosion when heating has taken place is to apply copious cooling water. However, tests have indicated that even cylinders which have been visibly and palpably cooled down can subsequently self-heat and explode up to 24 h later[19-21]. The best advice for situations where an ongoing fire is threatening acetylene cylinders appears to be one offered by the Swedish fire services: When circumstances permit, a sharpshooter is to shoot holes in the cylinder with tracer bullets at top, middle, and bottom. This causes an immediate discharge and ignition of the outflowing gas, eliminating the danger of an unexpected explosion.

Welding torches are designed so that acetylene and oxygen only come together at the torch. Flashback of a flame into an acetylene cylinder is not rare, but generally without serious consequences, due to the design of dissolved acetylene cylinders. But accidents have been reported where flashback followed the hoses into the cylinder and the cylinder exploded[22]. Some accidents have been caused by welders carelessly leaving a torch burning and hanging it over a cylinder; a hole is then burned in the cylinder by the flame[26]. The acetylene in cylinders occasionally undergoes spontaneous decomposition, but the overpressure created normally does not lead to an explosion[26].

Current US practice involves using color-coded and sized check valves in the system to prevent oxygen from being pushed back into the acetylene hose and torch. These check valves can be placed on the inlet to the torch, at every hose connection and at the regulator. Normal acetylene pressures for welding and cutting range from 35 to 50 kPa, but oxygen pressures are generally set relative to the thickness of metal being cut. For torch welding, pressures range from 25 to 175 kPa, but pressures over 700 kPa are not uncommon when cutting steel over 50 mm thick. Even higher pressures may be required if the cutting is conducted underwater. Because of the difference in pressure between the two gasses, it is readily apparent that the high pressure oxygen can easily flow back into the hose and cylinder in the event of a plugged tip and a damaged or missing check valve. Another problem that can occur is when a plugged tip forces the combustion inside the tip which can result in rapid damage to the torch components.

In general, acetylene cylinders can sustain a huge amount of mechanical abuse without exploding. Cylinders have been documented to be crushed into an hourglass shape or have wrinkles in the steel and yet survive[16]. Nonetheless, explosions have occurred in the course of what would appear to be modest mistreatment[23]. It is generally unwise to attempt to cut up acetylene cylinders for scrap, and fatalities have been recorded among individuals doing this[16]. A case has been reported[24] where two individuals filled a plastic bag with a mixture of acetylene and oxygen; the bag exploded while they were transporting it in their car. When the valve of an acetylene tank is opened and a jet of gas is discharged into the air, ignitions have occurred upon the jet impacting a person's hand[26]. The mechanism is electrostatic charging and is made possible by the entrainment of minute acetone droplets into the acetylene stream.

Vinylacetylene (C_4H_4) is the dimer of acetylene:

$$2\ HC{\equiv}CH \rightarrow HC{\equiv}CCH{=}CH_2$$

It has a wide variety of industrial uses and has similar stability problems to those of acetylene[11]. Explosive decomposition can occur in both liquid and vapor phases. This problem has also been studied in certain mixtures which include vinylacetylene[25]. For a given diameter, the pressure required to explode vinylacetylene is somewhat lower than for acetylene[11].

A variety of other *acetylenic compounds* (having the bond C≡C) exist and many are prone to explosive decomposition[3]. Methyl acetylene (propyne, $H_3C–C{\equiv}CH$) is commonly used in welding applications in the mixture MAPP, which is named after its two primary constituents, methyl acetylene and propadiene (allene, $H_2C{=}C{=}CH_2$), but also contains a variety of other hydrocarbons[*]. Diacetylene (1,3-butadiyne, $H–C{\equiv}C–C{\equiv}C–H$) and 1,3,5-hexatriyne ($H–C{\equiv}C–C{\equiv}C–C{\equiv}C–H$) are exceptionally unstable compounds, but without commercial applications. Also unstable are the haloacetylenic compounds, which have the structure $–C{\equiv}CX$, for instance, chloroacetylene ($H–C{\equiv}C–Cl$) and dibromoacetylene ($Br–C{\equiv}C–Br$). Chloroacetylene is a notably unstable compound, with a pressure limit[26] of 0.0065 atm.

Aerosol cans

The compressed gas propellant for aerosol cans used to be Freon or other halogenated gases which were, roughly speaking, fire extinguishants. With the environmental issue of eliminating use of ozone-destroying halogenated chemicals, the Freon propellants have been replaced with highly flammable gases, typically, propane, *iso*-butane, or dimethyl ether. The consequence has been a number of unanticipated accidents; DeHaan and Howard[27] have reviewed some of those. In several cases, houses have been destroyed when excessive numbers of aerosol flea foggers were discharged and the vapors explosively ignited. In another case, a room freshener can fell into a washing machine, the contents discharged and an explosion resulted when the vapors were ignited by a spark. An explosion demolished a 27,000 m^2 warehouse when the operator of a forklift truck ran over an aerosol can[22]. As is general practice in the industry, the truck was not designed for use in flammable atmospheres and could readily present ignition sources once a flammable atmosphere was created. A factory explosion took place when equipment filling spray cans with powdered shampoo and a butane propellant failed and two cans were acci-

[*] One typical analysis gave 37.8% methyl acetylene, 26.1% propadiene, 18% propane, 10% *n*-butane, 7.4% propylene, with minor amounts of other hydrocarbons.

dentally discharged[28]. The investigation revealed that the two-phase flow (solid particles + propellant) is particularly susceptible to electrostatic charging, but that the accident only occurred because the cans were very well electrically insulated and could be charged up to 35 kV. If a can were held by a person, a charging voltage of only about 2.7 kV could be achieved and this would not be incendive. A study concluded that serious accidents involving aerosol cans in Europe have been exceedingly rare[29].

A number of burn injuries have occurred due to aerosol cans failing. In some instances, the discharge occurs due to a valve failure, but a case is also reported[30] where a metallurgical failure caused a can's bottom to separate simply upon manually shaking an aerosol paint can. Aerosol cans should never be heated, but a case is reported where a woman was badly burned in attempting to heat an aerosol can in a microwave oven[31]. An aerosol can which is apparently 'empty' may contain sufficient flammable gas to explode, if it is heated or thrown into a fire[32]. Many explosions have occurred when cans of lubricant spray were used around electrical equipment, dropped and ignited by the arcing. This can occur with a car battery or around energized equipment in buildings.

Aerosol can fires and explosions can have significant consequences in aircraft. To minimize the consequences, improved can designs have been explored[33]. These showed delays in the time needed for a fireball to develop, but the safety implications of this delay is not necessarily clear.

Agricultural products

SELF-HEATING

A wide variety of agricultural products are susceptible to self-heating. These include clover, fishmeal, hay, malt, peat, starch, straw, tobacco, and various types of seed, grain, fodder, fertilizers, yeasts, soybeans and soybean products[34]. The exothermicity can involve any or all of:

- oxidation;
- oxidative polymerization of unsaturated oils;
- fungal (microflora) or bacterial action;
- fermentation (of sugars); and
- moisture (this is not sufficient as a sole cause, but can interact with the other sources of exothermicity).

Specific sections in this Chapter are devoted to *Bagasse; Cotton*; *Feedstuffs*; *Forest materials, vegetation, and hay*; *Hops*; *Jute*; *Marijuana and hemp*; *Peat*; *Rice husks*; *Soybeans*; *Sugar*; and *Wool*.

Some of the very earliest experiments in self-heating and spontaneous combustion are those that were done on grains. Medem[35] reports on studies in this area that an apothecary named Rüde was doing in 1782. Quantitative modeling has occasionally been attempted on agricultural products of various sorts, but the potential of deriving meaningful data is generally limited. Studies have typically been undertaken only on dry, clean, pure substances, but spontaneous combustion problems are the most likely to occur when none of these three conditions hold.

Rail-car loads of wheat being shipped will sometimes self-heat and smolder. In an early study, Bailey[36,37] investigated such occurrences and concluded that moisture was an important factor. He concluded that only wheat with a moisture content over 14.5% will show self-heating.

In general, self-heating in agricultural products has three main causes: (1) cell respiration; (2) thermogenic microflora; and (3) oxidation. Of these, cell respiration is considered to be only a minor contributor[38]. Microflora need a moist environment to flourish; for RH below 74% in the interstitial air space, self-heating due to microflora is unlikely[39].

Self-heating stemming from bacterial and mold growth can be reduced by the use of agents which inhibit such growth. These include acetic, ascorbic, and propionic acids. The latter also arrests biological functions of grain cells, reducing another source of heat generation.

Nut shells, copra, and olive oil presscake residues self-heat readily[40]. Seeds self-heat more slowly than other types of agricultural products, because nature has designed them to oxidize very slowly in order to survive prolonged periods prior to germination[41]. Case histories involving self-heating of corn, fishmeal, fodder, palm products, rapeseed flour, starch, sunflower seeds, wheat bran, and yeast have been reviewed[42]. A fire due to self-heating of bagged rapeseed has been reported[445], but the quantity involved was immense, around 400×10^3 kg, so this is not surprising. An extensive study of palm kernels was one of the earliest investigations in which scientific theory was applied to making practical predictions of self-heating[43]. Spent brewing grains, that is, barley from which malt has been extracted are known to have caused spontaneous combustion fires; their common use is as an animal feedstuff. Walker[44] has studied the self-heating behavior in laboratory tests. His data indicate E = 54 kJ mol^{-1}, P = 33.7. Extrapolation from these values indicate that at room temperature a pile of a couple meters in size would undergo thermal runaway. Bowes[445] reported data on a similar substance, distillers' dark grains, which gave E = 66.9 kJ mol^{-1}, P = 39.1. Self-heating tendency in seeds and seed meals is usually proportional to their fat content[34], but for a given fraction of fats, self-heating must also be considered as proportional to the degree of unsaturation (see *Oils*).

Yeast dusts accumulating in a spray-drying facility have led to self-heating and fire. In one case[45], a layer 40 mm thick at a temperature of 120ºC was the cause. Laboratory tests on 100 mm cubes showed thermal runaway at 165ºC.

A highly detailed manual by Mills[46] gives operators of agricultural facilities guidance for avoiding spontaneous combustion and for firefighting in case of fire.

ELECTROSTATIC PROPERTIES

Solids moved through pipes or tubes can pick up an electric charge. As early as 1919, the US Dept. of Agriculture issued an advisory[47] explaining that the then-rampant fires in cotton gins could be largely prevented by proper grounding of metal machine parts. Electrostatic charging of grains conveyed along metal or polyethylene surfaces was studied by Dahn[48]. Charge accumulation, expressed in units of energy/mass was 0.4 mJ kg^{-1} or less when using a steel surface, but up to 2 – 6 mJ kg^{-1} along the plastic surface. The dielectric constant was typically 4 – 12, but varied greatly with moisture, as lower moisture levels gave lower dielectric constants. The resistivity, measured at 6 kV, was commonly 10^7 – 10^9 Ω-m. In some cases, moisture had a profound effect, with wheat at 11.6% moisture being 4×10^8 Ω-m, while at 13.8% the resistivity dropped to 2×10^7 Ω-m. A typical charge[49] obtained from pouring corn down metal tubes is 2.5×10^{-9} C kg^{-1}.

Air compressors and compressed air systems

Fires and explosions of air compressors occasionally occur, with the combustible being the oil used for lubrication or cooling. Details on a number of incidents have been published[50]. Oil-flooded rotary screw compressors, such as are used in heavy industry, are particularly prone to accidental fire/explosion events[51]. Fowle[52] reported one explosion with 19 fatalities and another with seven. Three main causes have been found to be:

(1) shocks;
(2) excessive temperatures; Fowle suggested that temperatures over 250ºC are excessive, but extensive research studies and accident analyses[59] indicate that temperature over 135ºC are notably hazardous;
(3) sudden pressurization of piping.

Explosions of reciprocating type compressors having oil-lubricated cylinders commonly show the following traits[53]:

(a) the compressor itself is undamaged;
(b) carbonaceous residues are found in the vicinity and immediately downstream of the final stage outlet valves;
(c) faulty operation of the compressor was noted for some time, with high final-stage outlet temperatures (over 135ºC) observed;
(d) the pipe system is blown open at discrete points, separated by unshattered portions.

Empirically, multi-stage reciprocating compressors are safer than single stage. Explosions in turbine compressors are rare, since these do not introduce oil into the working volume. Compressing air to very high pressures in the presence of lubricating oil appears to be an intrinsically unsafe operation, even at low temperatures, as shown by one six-fatality accident[54] in which the explosion occurred on the return side piping of an air compressor where the temperature was only 29ºC. 'Shock' sometimes involves a small explosion which then sets off a more serious one. The Bureau of Mines reviewed several studies on this ignition mechanism[55].

Films of lubricating oils have been shown to ignite at a temperature of 120ºC under a compression of 31:1 and at 160ºC under a compression of 18:1. In rotary compressors, self-heating due to oxidation of oil-soaked reclaimer pads is another cause. Oxidation of mineral oils is generally moderate, but ignitions have been observed when the oil cooling system fails and temperatures rise over 300ºC. Some explosions in various types of compressors are attributed to buildups of oil films that progressively oxidize to a carbonaceous semi-solid mass. Buildup is especially a problem if SAE 10 weight or more viscous oils are used. The buildup level in cases where fires have occurred has typically been extreme—10 mm or more. The area most prone to buildup is the piping between the compressor outlet and the receiver. Rust is considered to catalytically promote the oxidation of lubricating oils. In general, some malfunctions of valves or cooling system, or blocked air filters, or other faults that serve to raise temperature in certain areas of the system are common causes of compressor explosions or fires. In one specific case, operation of a portable compressor in extremely cold weather caused the cooling oil (ATF) to jell and an explosion occurred in the receiver. Loss of cooling oil leads to two forms of overheating: (a) it is not longer possible to remove the heat of compression being produced by the unit; and (b) oil is used to create a seal at the rotor interface; if this seal is lost, then air is internally recirculated and this process can lead to a buildup of high temperatures. This scenario was recreated in a laboratory experiment[56].

Chase[57] studied some of the details of the process and concluded that compression serves to create high gas velocities across the face of the oil film. This causes much more rapid evaporation than would be possible otherwise. The oil film also receives heating from the hot compressed air adjacent to it. With the temperature raised and vaporization mechanism greatly enhanced, sufficient oil can be vaporized to create a flammable mixture. Chase also conducted experimental studies and found that the initial equivalence ratio (representing the vapor in the air prior to compression) along with the compression ratio served to characterize the ignitability of the oil (Figure 3). For an explosion to occur, sufficient oil vapor has to be present to reach the LFL. If the system (and the oil) are initially at a low enough temperature, the LFL will not be attained. But Chase found experimentally[58] that rather modest initial temperatures, on the order of 150ºC for common lubricating oils, suffice to cause the LFL to be exceeded. Even under conditions where sufficient oil cannot be vaporized, it may be put into a mist by the effect of vibrations[59]. Explosions originating in an oil film are likely to be detonations[53].

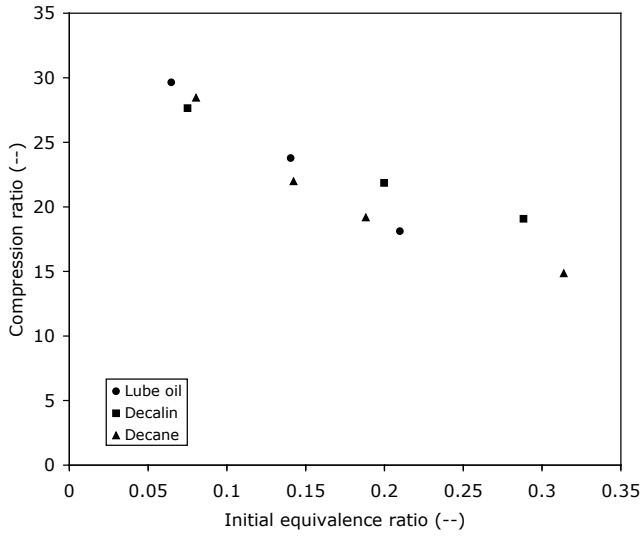


Figure 3 Relation between minimum compression ratio and minimum initial equivalence ratio necessary for compression ignition of several substances

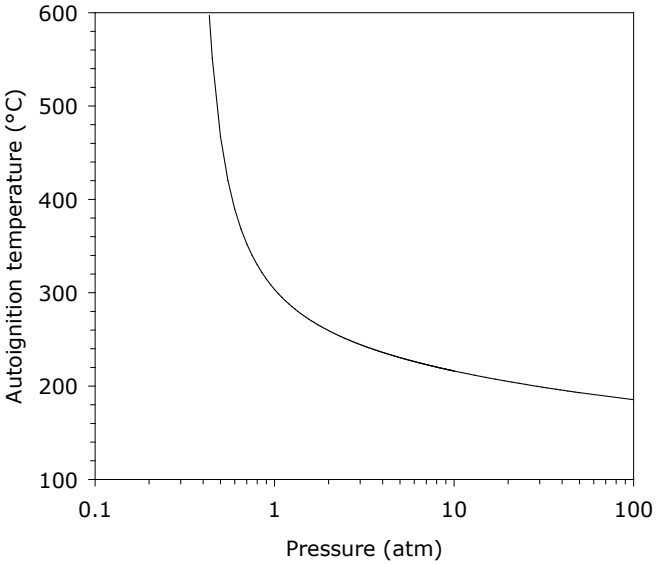


Figure 4 Effect of pressure on the AIT of compressor oil

The major mechanism for explosions however is considered to be not oil film detonations but ignition of carbonaceous residues built up on internal surfaces of a compressor. The Bureau of Mines[60] investigated these carbon formations and found that they are susceptible to exothermic reactions if heated over about 150ºC. Chemical analysis of soots removed from air compressors showed high percentages (15 – 34%, by mass) of oxygen in the soot and this was taken to suggest that an oxygen chemisorption mechanism may be involved. The authors also noted that some incidents of carbon monoxide poisoning have been occurred when breathing air was supplied from an air compressor. This, they concluded, was most likely due to partial combustion within the air compressor, so that an explosion did not result, but CO was generated. High flash-point oils are no longer felt desirable, since these do not reduce the detonation potential, yet lead to greater carbon buildup[53]. Naphthenic mineral oils are safer than paraffinic, since they produce softer residues that are less likely to interfere with outlet valve operation[53]. Narrow-cut fractions are preferred, since these leave fewer residues. Phosphate ester oils can provide enhanced safety, but should only be used on compressors designed for their use.

Laing and Russell[61] conducted experiments which led them to conclude that with oil-flooded rotary-screw compressors, the dominant cause of explosion is failure of oil supply, with an explosion typically occurring when the oil has reached its AIT (Figure 4), which for a compressor delivering air at 8 atm (absolute) is about 220ºC. In their experiments, they noted that the explosion typically originated in the separator and that 15 – 16 atm was commonly the peak pressure attained. For an unexplained reason, it was found that fresh oil was somewhat more prone to explosion than well-used oil.

Another explanation was provided by Loison[62], who considers that the catalytic effect of iron rust is highly dangerous. In the course of investigating some explosions in large-diameter (250 mm) compressed-air piping, he conducted a series of laboratory experiments. In an initial trial, oxygen was flowed through a pipe which was coated with a film of lubricating oil. Ignition occurred when the system reached 300ºC. But when a layer of rust was introduced into the pipe, the ignition temperature dropped to 160ºC, and dropped further to 150ºC when ferric hydrate, $Fe(OH)_3$ was used instead of actual rust. Further experiments were conducted with air. The most dangerous condition found was one where air flow was stopped and then re-started. Under that condition, an ignition temperature of 207ºC was found with iron rust and 151 – 157ºC with ferric hydrate. Loison points out that his experimental arrangement in the second series was a bit unrealistic in that the oil was applied as plug within the pipe and not as a film, nonetheless, he felt that prudent operation should consider ignition likely if temperatures in the vicinity of 150ºC are reached. These temperatures, unfortunately, are readily reached in high-capacity air compressors if they are not clean and scrupulously maintained. In some further experiments, he prepared pipes with various amounts of oil film and initiated an explosion via a frangible membrane connecting to an explosion initiation chamber where a flammable mixture was ignited. The violence of the destruction of the oil-coated pipe proved to be proportional to the amount of oil contained, with about 0.3 mm film thickness being the minimum. It was also observed that after the explosion the oil film was gone and was replaced by a coating of soot. The violent explosions had a detonation character, with velocities up to 1200 m s^{-1} being recorded. In the original accident

investigation, it had been speculated that the pipe explosion possibly was because an explosive was inadvertently set off in the vicinity of the pipe. To test this theory, Loison filled pipes with hydrogen/air mixtures and detonated explosives close by. Small explosions could be produced, but these only yielded one crack per pipe, not the extensive fracturing found in the real accident and in the oil-film experiments. Japanese investigators[63] found that a soot film itself can be detonated and concluded that this can explain certain explosions in compressed-air pipelines.

Apart from autoignition, piloted ignition can occur due to frictional sparks. But unexpected temperature increases, sufficient for autoignition, have been found in connection with malfunctioning valves[59].

Fires involving air compressor lubrication oil may also be externally ignited, for example, a detailed case history is presented of a fire which followed mechanical failure that led to rupture of an oil line and spraying of oil from it[64]. Vibration of fabric or rubber materials in a compressed air system can lead to sufficient heating so as to ignite the material. This was found in accidents and reproduced in the laboratory[26,65]. The materials can be located in flexible couplings, patches, etc. Luzik[66] has provided a check list of maintenance items to check to prevent explosions of oil-flooded rotary screw compressors.

When a valve is rapidly opened from a compressor to an air line, it is common to see a shower of sparks, created by frictional heating of rust and other debris in the air line. But, if upon opening an air valve, an explosion of a dust cloud takes place, the incandescent particles have been found not to be the cause. Instead, it is due to static charging of the dust[67]; experiments[68] indicated that incandescent particles ejected from compressors are of too low temperature/too small size to ignite methane/air atmospheres. Flammable gas atmospheres have also been ignited in the absence of dust clouds, simple by static charging of small debris moving in the air line. If high-pressure air is quickly admitted into a pipeline containing lubricating oil, an explosion is quite possible, due to adiabatic compression. One experimental study[69] showed that temperatures up to 650ºC were easily created by rapid valve operation. Because of the decrease in AIT of lubricating oils with increasing pressure, this mode of ignition presents a severe hazard.

Some large internal combustion engines are started by supplying air pressure to the cylinders from an air compressor. A check valve is used at the cylinder to prevent reverse flow of combustion products into the compressed air line. A number of explosions have occurred upon starting such engines, and Ridgway[70] hypothesized that these normally originate at the engine, not at the air compressor. If the check valve fails to operate properly, then a combustible mixture can be injected backwards into the compressed air line, thereby causing an explosion within the piping.

Aircraft cabin wall panels

Commercial aircraft have cabin walls constructed of a honeycomb composite which comprises fiber/resin face panels and a Nomex honeycomb structure. Harkleroad[71] tested the ignition performance of some commercial and developmental panels. Conventional epoxy/fiberglass/Nomex composites required 20 kW m^{-2} for radiant piloted ignition. Substituting Kevlar for fiberglass raised this value to 23 kW m^{-2}. Panels where phenolic was used instead of graphite required 34 – 36 kW m^{-2}.

Airplanes

Airplanes in flight can become charged to an extremely high potential of ca. 500 kV due to frictional contact with atmospheric particles[72]. Frictional charging is speed dependent, and varies roughly as the third power of velocity. Frictional charging is the strongest from dry particulate matter (e.g., ice crystals or dust); charging due to wet snowflakes is small[73]. The majority of discharges involving airplanes are corona or brush discharges (commonly referred to as St. Elmo's fire) and do not lead to significant damage.

But fires and explosions can occur due to lightning strikes of airplanes. Pilots may not be able to avoid lightning activity, since, according to one study[73], in over 50% of the cases where a strike was reported, there was no lightning activity visible to pilot, and in 11% of the cases there was no precipitation at all. Furthermore, theoretical considerations indicate that the mere entry of the aircraft into a zone of high electric field will increase the potential gradient and this may be sufficient to lead to breakdown and discharge.

Lightning strikes to aircraft are normally innocuous, but on some occasions can puncture fuel tanks and lead to tank explosions. Robb et al.[74] conducted laboratory simulations of lightning strikes to fuel tanks holding aviation gasoline and JP-5 fuel. For strikes that punctured the tank wall, they found that explosions did not occur when the mixture was above the UFL. Explosions did occur in mixtures significantly below the LFL, and this was seen to start with a local ignition by a spark shower from the puncture, escalating to a full explosion of the ullage space. A puncture can also lead to an external fire, but these generally have much less severe consequences and sometimes are even self-extinguished by wind velocity. The authors also noted that lightning-caused explosions of tanks holding aviation gasoline would be extremely uncommon, since the mixture will generally be highly over-rich in flight. By contrast, the temperature range at which most lightning strikes have been recorded, –10 to +10ºC, is within the flammability temperature limits of JP-4, which is thus seen as the most susceptible aviation fuel. Oh and Schneider[75] conducted another series of experiments simulating lightning strikes to airplane skin. The discharge conditions needed to puncture aluminum skin and titanium skin of various thicknesses were characterized. A lightning discharge that transferred about 10 coulombs of charge was found sufficient—in

worst-case circumstances—to cause a puncture (and a likely ignition of fuel) of a 2 mm thick aluminum skin. This is an extreme case and general guidance[76] is that it would take 200 C to puncture 2 mm skin.

See also: *Aviation fuels*.

Alcoholic beverages

Tests have indicated that alcoholic beverages of over 100 proof (US)* can be ignited directly by a match[77]. For such high-proof beverages, one specific hazard can be propagating of fire back into a bottle, whereby the bottle then becomes an effective flame thrower. Plastic inserts are now provided on some bottles that deflect the jet of liquid. Beverages below 100 proof require a wick to be ignited. Flash points[78] for beverages of various concentrations are shown in Figure 5.

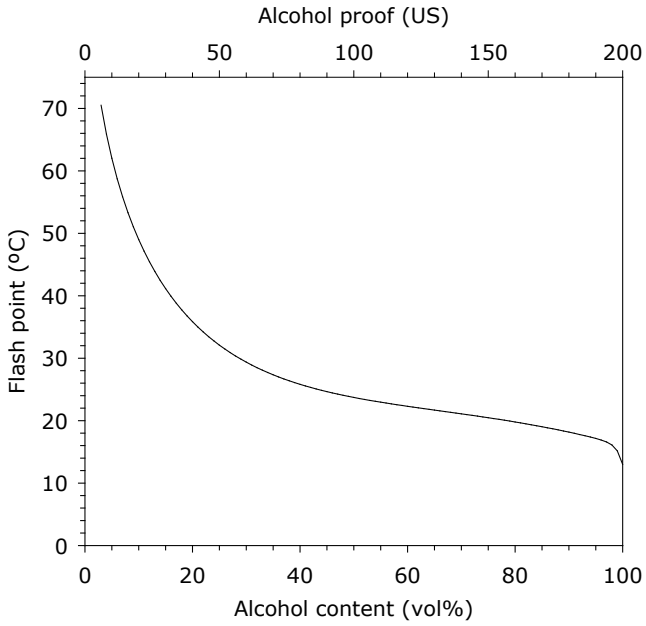


Figure 5 Flash point of alcoholic beverages

Aldehydes

Aldehydes are organic substances having a –CHO group and a number of them are highly reactive and, under certain circumstances, prone to explosion. Britton[79] examined a number of ignition-related features for several aldehydes. The minimum oxygen concentration for combustion of propionaldehyde was found to be 7%, which is unusually low. The AIT for propionaldehyde and butyraldehyde was found to be strongly influenced by pressure, dropping from 185ºC at 1 atm to 90ºC at 9.5 atm. Iron rust was also found to act catalytically towards promoting ignition of aldehydes.

* Proof of alcoholic beverages is defined as proof = 2× alcohol content in the US and as proof = 1.75× alcohol content in the UK.

Ammonia

Anhydrous ammonia (NH_3) is one of the oldest refrigerants and is commonly used in industrial refrigeration facilities. It does not show a flash point in standard flash point testing, consequently, it is sometimes erroneously described as "non-flammable." In fact, ammonia has flammability limits[80] of approximately 15 – 28%, and a high, but a readily measurable AIT of 651ºC. The pressure limit is 9.6 kPa; in other words, ammonia/air mixtures will not sustain flame propagation (at any ammonia concentration) if the total system pressure is lowered below this value. Decomposition begins at 450 – 500ºC. The MOC is around 17% at room temperature decreasing to ca. 11% at 400ºC. The MIE value is usually taken as 680 mJ, although there is a very wide spread of data in the literature[80], all the way down to 8 mJ. At elevated temperatures, ammonia decomposes into nitrogen and hydrogen; the hydrogen then becomes available for burning with oxygen. Not only can ammonia burn, but also detonate[81]. As Urben[3] puts it, "There is a long history of violent [ammonia] gas-air explosions in refrigeration practice." These have continued into modern times[82-86]. In one of the cases[84], the explosion was initiated from the hot filament of an incandescent lamp when cold ammonia gas reached a 300 W lamp and broke the glass envelope. Explosions have also occurred associated with deliveries of the bulk material. If liquid ammonia is accidentally mixed with refrigerant R-22, the tank will overpressurize and a solid residue will be formed in the reaction. Médard[26] claims that explosions inevitably require a confined atmosphere and that ignition is not possible in open air, but it is not clear whether this can always be relied upon. AIChE holds an annual symposium, *Ammonia Plant Safety*, the proceedings of which are published.

Ammonium nitrate and ANFO

Ammonium nitrate, NH_4NO_3, is a white crystalline solid which is widely used as an ingredient of fertilizer mixes. It can also act as an explosive. Its behavior is complicated by the fact that 5 different crystalline forms are found within different temperature ranges at ambient pressure, with a sixth found at high pressures. An additional complication is that it is a strongly hygroscopic material. Pure ammonium nitrate (AN) is stable at room temperature. In his review, Médard[26] concluded that not a single case could be found of an accidental explosion of pure, unheated AN. At elevated temperatures AN can thermally decompose in a variety of different ways, with the two most common ones being:

$$NH_4NO_3 \rightarrow N_2O + 2H_2O$$
$$2NH_4NO_3 \rightarrow 2N_2 + 4H_2O + O_2$$

The first reaction occurs during slow heating, while second reaction is the one which predominates in an explosion. AN has a melting point of 170ºC. In tests on small quantities, it is unstable above 200ºC and shows explosive decomposition[97] at 260 – 300ºC. But since—in at least some of its decomposition pathways—it is an exothermically decomposing material, critical temperatures can progressively drop with increasing sample mass. At about 100ºC, AN

starts reacting directly with organic materials[26] and the process may lead to ignition.

Since the elevated-temperature decomposition reaction produces oxygen, reaction is more potent if a fuel molecule is present. Thus, ammonium nitrate is normally combined with a fuel in order to give a commercially useful explosive. The explosive mixture ANFO is made combining prilled ammonium nitrate (AN), and fuel oil (FO). The amount of fuel oil added is about 6% of the mass of the ammonium nitrate, the amount necessary to make the mixture oxygen-balanced. Such an ANFO mixture is classified as a 'blasting agent,' since it cannot be detonated with a blasting cap. Not all grades of AN can make suitable ANFO. Three grades are commercially available:

(1) Explosive grade. This has a bulk density around 1050 kg m^{-3} and a particle size of 0.15 mm or less. The material is nearly pure, with few if any additives.
(2) Fertilizer grade. This has a bulk density around 1050 kg m^{-3}, a particle size around 2 mm, and includes anti-caking agents such as kaolin or diatomaceous earth. The type of anti-caking agent used has a definite effect on the suitability of the material for use as ANFO.
(3) Porous grade. This has a bulk density of 650 – 800 kg m^{-3} and particle size around 2 mm, with <1% anticaking agents included.

The porosity of the porous prills allows intimate absorption of fuel oil and is needed to produce a good quality explosive. The confusing nomenclature predates the commercialization of ANFO, which occurred during the mid-1950s; explosives based on non-porous AN were used in the 1930s but are not in use today.

For pure ammonium nitrate to explode requires confinement and extreme heating or else the use of a priming charge much more powerful than a blasting cap. It was known in 1835 that AN[87] can detonate, but subsequently many individuals dismissed the possibility. It was very graphically confirmed during an explosion at the BASF factory in Oppau, Germany in 1921 that when blasted with another explosive, ammonium nitrate indeed detonates. The Oppau factory manufactured an ammonium nitrate/ammonium sulfate fertilizer and workers regularly dislodged caked fertilizer with explosives, until the accident that claimed 509 lives. The explosion was 'imperfect,' in that only about 10% of a 4500 tonne cache actually exploded. An essentially identical procedure being performed on 99.5% pure AN in another German town, Kriewald, two months earlier led to only 19 fatalities; consequently its lessons were not learnt. Even after the Oppau disaster, an almost repeat incident cost several hundred lives at Tessenderloo, Belgium in 1942.

The 1947 Texas City disaster proved that large amounts and high heat can detonate ammonium nitrate and initiation with a priming charge is not required. The incident started when S.S. GRANDCAMP, a ship carrying ammonium nitrate fertilizer caught fire[88]. As a consequence, multiple fires were ignited, S.S. HIGH FLYER, a nearby ship with the same cargo also detonated, and 552 lives were lost. The original fire occurred during loading of the ship, so it was not attributable to self-heating; most probable cause was judged to be discarded smoker's materials. A nearby warehouse containing the same fertilizer as loaded on board the ships ignited during the incident, but only burned and did not explode. In 1948, the tragedy was repeated in another AN fertilizer explosion, destroying the ship OCEAN LIBERTY in the harbor of Brest, France, where 21 lives were lost. In 1952, AN exploded in a factory in Nagoya, Japan, killing 22. As recently as September 2001, an AN explosion in Toulouse, France, caused 29 fatalities.

In 1988 an incendiary fire involving a trailer where ANFO was stored led to a massive explosion and firefighter fatalities. The explosive potential of ammonium nitrate was again illustrated on 19 April 1995, when terrorists partly demolished the Alfred P. Murrah Federal Building in Oklahoma City by filling a truck with about 2 tons of ammonium nitrate and nitromethane. The priming charge used was probably a detonating cord. The explosion when using nitromethane is more potent than with fuel oil, since nitromethane is an explosive substance in its own right. Numerous other case histories of accidental AN explosions have been published[87,89]. While accidental detonations certainly have occurred, the record indicates that fires have been more common than detonations. A number of these have been caused by self-heating of impure AN. Scott and Grant[87] published an extensive review of the chemical and explosive properties of AN (but not ANFO) and also provided a number of case histories. Other collections of case histories have been compiled by Médard[26] and by Fedoroff et al.[90]

Van Dolah et al.[91] showed that the sensitivity of AN increases with temperature; results from testing in a card gap test indicated that above 130ºC, AN becomes much more sensitive. There is a strong diameter effect in this relation, with large diameters (greater than about 0.15 – 0.30 m) were found to be detonable at room temperature using a pipe-bomb geometry. When heated to elevated temperatures (as could happen in ship's fire), an 0.075 m diameter pipe bomb detonated in another Bureau of Mines test[97]. In attempting to recreate an AN detonation which occurred in a train wreck, Van Dolah found that a detonation created when fuming nitric acid was poured onto a pool of burning gasoline could sympathetically detonate adjacent AN, provided the latter was present in sizes greater than the critical diameter. AN was found to be detonable by high-velocity rifle bullets, but, unlike the real-life Kriewald incident, preheating was required in the experiments. Shock waves from detonations of gas/air mixtures were found not to detonate AN. A number of unconfined burning experiments, including ones of almost real-scale, were conducted with AN, but none of these resulted in detonations. Another part of the research of Van Dolah was addressed towards attempting to

explain a detonation which leveled a factory where ANFO was being prepared. On the basis of the fire tests conducted, he was not able elucidate the mechanism. In a British study cited by Médard[26], piles of 45 – 70 tonnes of AN were burned but did not explode. The AN was in paper sacks or paper-lined drums, but unconfined in those tests. Médard also collected a number of other research studies which gave negative findings on the explosibility of AN. There is some evidence in small-scale tests that confinement has to permit pressures over 100 atm to be developed for detonation to occur with pure AN, but this is scarcely pertinent to accidental explosions, most of which involved ANFO or AN with another contaminant. In general, it should be noted that very few tests exist where the properties of ANFO would have been explored in realistic scenarios.

A study of AN and ANFO in 1 × 1 m cylinders showed that sympathetic detonations[92] can be occur as far away as 16 m, although most trials gave detonations out to only about 4 m.

At a density of 650 kg m^{-3}, the critical diameter for detonation of pure AN without confinement was found to be 100 mm[26]. At a density of 520 kg m^{-3}, the critical diameter is less than 40 mm. At a density of 1000 kg m^{-3}, the critical diameter surpasses 320 mm. In general, as the density decreases, detonation becomes easier. ANFO is easier to detonate, and the critical diameter even at a high density of 1000 kg m^{-3} was found to be less than 30 mm when tested in a thin metal tube. In tests by Arai et al.[93], steel tubes of 36 mm diameter were found to be sufficient for the detonation of ANFO at a density of 860 kg m^{-3}. When confined in plastic tubes of 40 – 41 mm diameter, the results depended on the type of plastic and the wall thickness. PMMA tubes 2 mm thick sufficed, but PE tubes even of 3.5 mm thickness did not. No detonation was obtained in Pyrex glass tubes of 2.4 mm thickness and 40 mm diameter. The failure of detonation for PE was due to a large deformation that the material could successfully sustain. For Pyrex, the reason was the opposite—the tube fractured so quickly that effective containment was lost. About 0.2% fuel oil is the minimum organic content which causes a detectable increase in the explosibility of AN. Another study[94] found for pure AN a critical diameter of 125 mm at 1020 kg m^{-3} and 200 mm at 880 kg m^{-3}, while ANFO showed 100 mm at 820 – 880 kg m^{-3}. The Bureau of Mines[95] was readily able to detonate most fertilizer-grade AN samples by electrically heating a cylindrical steel bomb having a 75 mm I.D; the temperature of the AN at the time of explosion was typically 300ºC but the density of the tested specimens was not reported.

It is interesting to note that while the ship detonation disasters did not explicitly involve a fuel component, a fuel was in fact present in the form of an anticaking wax applied to the AN in the amount of 0.75% – 1% . Without this adventitious fuel, the explosions might have been much less severe, since even this small amount of wax substantially sensitizes the AN. The sensitization of AN by organic coatings was known as early as 1921, but evidently failed to be appreciated until after the Texas City disaster. Subsequently, in commercial fertilizer production, the wax was replaced by a diatomaceous earth coating, which does not act as fuel. Another factor helping create the large explosions was the reactivity between the paper bags and the AN[96].

Zinc has been found to be a synergist for ANFO[97]. Apart from deliberate introduction in powdered form, zinc could also be available from the coating on galvanized pipes, in the case of pipe bombs. The explosion of the S.S. HIGH FLYER was likely exacerbated by the presence of sulfur. The ship was also hauling a cargo of sulfur and cross-contamination was found. Testing[88] indicated that sulfur-contaminated AN can explode under conditions in which uncontaminated AN will not. An investigation after the Oppau explosion[26] examined the effect of mixture fraction on explosibility of AN/ammonium sulfate mixtures. It was found that results were very sensitive to the ratio and that mixtures with AN at less than 40% were vastly safer than ones with AN > 60%.

For commercial blasting applications in the US, ANFO is currently by far the most common explosive, and its production volume is about 50 times greater than all other explosives combined. Curiously, it does not head the list of favorites for criminal bombers, who vastly prefer black powder, fireworks powders, or dynamite[98].

Watson et al.[99] published data on 16 different ANFO-based explosives tested according to four sensitivity tests: the Koenen/BAM friction test, the Bureau of Mines friction test, a drop-hammer test, and a No. 8 blasting cap. The results showed that generally the mixtures were insensitive, with the exception of ammonium nitrate/nitromethane compositions, which were detonable from a No. 8 blasting cap and showed elevated sensitivity in some of the other tests.

Nabiullah et al.[100] determined the ignition temperature for ANFO as being 260ºC by use of an electric furnace with ramped heating. On the basis of DTA tests, they obtained the kinetic parameters E = 120 kJ mol^{-1} and $A = 8.3\times10^{8}$ s^{-1}. Rogers et al.[101] measured the critical temperature for thermal runaway in 1 mm thick slabs of AN and found T_c = 324ºC for reagent-grade AN and 230ºC for a prilled sample.

Hainer[102] evaluated a number of studies on the self-heating due to decomposition of ammonium nitrate. From his graph, the following values can be obtained. Chemically pure AN: E = 224 kJ mol^{-1}, P = 74. Fertilizer grade AN: E = 149 kJ mol^{-1}, P = 57. Fertilizer grade AN with 7% additional fuel added: E = 135 kJ mol^{-1}, P = 56. The heat of reaction for chemically pure AN is about 60 kJ mol^{-1} at 170ºC, increasing to 68 kJ mol^{-1} at 300ºC. Hainer also determined that pressure plays an important role in self-heating caused explosions of AN. He considers that decomposition in-

volves the simultaneous occurrence of the exothermic reaction:

$$NH_4NO_3 \rightarrow N_2O + 2H_2O$$

(which is then followed by exothermic decomposition of N_2O) and the endothermic reaction:

$$NH_4NO_3 \rightarrow NH_3 + HNO_3$$

A thermal balance between the endothermicity of one and the exothermicity of the other is possible only if significant pressure rise does not occur. If the pressure rises, however, the endothermic reaction is suppressed, temperature begins to rise, and an explosion can follow. This explains why most AN disasters have occurred on board ships and not in warehouses. In ships, the steel hull can allow pressure to build up, but for storage in warehouses, pressure buildup is unlikely. In a contrasting opinion, Scott and Grant[87] consider that self-heating hazards of pure AN are very limited, and that accidents have inevitably involved the presence of impurities. The effect of impurities is attributed to the fact AN is an oxidizing agent and exothermic reactions can occur with oxidizable substances, especially organic ones. Under rapid initiation conditions, it is considered[103] that the reaction of AN goes as:

$$NH_4NO_3 \rightarrow N_2 + 2H_2O + O$$

The oxygen is then available as oxidizer for the fuel oil portion.

ANFO as such cannot be used in wet environments. But it was discovered already in the 1950s that, contrary to the old adage "Keep your powder dry," AN-based explosives can be made that incorporate water into the formulation itself[104]. Initially, this took the form of *slurries*, more currently as *emulsions*, whereby ANFO is dissolved in water, then the liquid is dispersed into the oil and the emulsion is made stable by including an emulsifier (e.g., sorbitan mono-oleate, stearic acid, etc.). A commercial emulsion may contain around 10 – 15% water and can be successfully used in wet applications, but since it is intrinsically insensitive, a sensitizer must be added. For this purpose, air-containing microballoons may be used, or air bubbles introduced by another means. Aluminum may also be added to this emulsion to increase the energy content. Nitro explosives and organic amine nitrates also find some use as sensitizers.

Ammonium nitrate in paper bags should be kept at storage temperatures below 70ºC, since at this temperature acid vapors begin to be released which cause a partial nitration of cellulosic substances and nitrated paper is more flammable[26]. NFPA has a standard (NFPA 490[105]) on the storage of ammonium nitrate; ANFO is also covered in NFPA 495[106].

Ammonium perchlorate

Ammonium perchlorate, NH_4ClO_4, is an inorganic oxidizer used as a component of rocket propellants (but can also be used as a monopropellant) and in pyrotechnic mixtures. The commercial product is a granular solid (commonly 100 – 200 μm), generally coated with an anticaking agent such as tricalcium phosphate. As part of preparation of a rocket propellant, the material is ground to 2 – 5 μm. Unlike the coarse product, the finely-ground material becomes quite sensitive. AP is considered stable at room temperature, but decomposition begins to be detectable at about 150ºC. Early studies of AP decomposition and combustion were reviewed by Jacobs and Whitehead[107]. When heated, ammonium perchlorate does not melt but sublimes and dissociates; the latter takes place by two different reaction pathways, depending on the temperature of exposure:

at ca. 325ºC :

$$2NH_4ClO_4 \rightarrow Cl_2 + 4H_2O + N_2O + 1.5O_2$$

at 380 – 400ºC :

$$2NH_4ClO_4 \rightarrow Cl_2 + 4H_2O + (O_2, N_2, NO, NO_2)$$

where the latter reaction does not include N_2O production[26]. In addition, there are various further reactions among the reaction products. When detonated, the composition of the reaction products is approximately:

$$4NH_4ClO_4 \rightarrow 6H_2O + O_2 + 4HCl + 2N_2$$

The ignition temperature[108] of small, pressed pellets of ammonium perchlorate, NH_4ClO_4, has been reported as 440ºC. DTA measurements[116] gave ignition temperatures of 540ºC for a 15 mg sample, 500ºC for 30 mg, and < 400ºC for 125 mg. Elevated pressures reduce the ignition temperature; in a closed-vessel ignition study, raising the pressure from 1 atm to 50 atm lowered the ignition temperature from 460ºC to 310ºC. In the presence of catalytic compounds[26], ignition can occur at temperatures as low as 225ºC. For pure AP at room temperature to undergo self-sustained burning in a nitrogen atmosphere[116], it must be subjected to a large pressure of over 20 atm; however, in a methane atmosphere burning can take place at ambient pressure. Aging at temperatures substantially below the ignition temperature does not appreciably change the properties of AP[116]. The vapors emitting from the decomposition of AP can be ignited. In a glass cylinder test using 200 g of AP heated to 254ºC it was possible to ignite the vapors by use of either a hot wire or a gas pilot; however the reaction was only "mild burning." A large number of compounds, many of them metallic, act as catalysts for the decomposition or ignition of ammonium perchlorate. In one review[107], ignition temperatures around 400ºC were typically found for pure AP, but dropping to ca. 250 – 300ºC in the presence of C, CdO, Cr_2O_2,CuO, CuCl, ZnO, etc.

Self-heating data based on a small-specimen study in an adiabatic furnace were obtained by Gross and Robertson[109], giving E = 172 kJ mol^{-1}; $QA = 5.6\times10^{19}$ W kg^{-1}; ρ = 910 kg m^{-3}; C = 1500 J kg^{-1} K^{-1}. Later studies indicated that the actual value of E is much lower and the decomposition of AP is possibly autocatalytic. Jacobs and Russell-Jones[110] reported that E = 130 kJ mol^{-1}, and that the reaction is autocatalytic. Bogg[116] found E = 95.8 kJ mol^{-1} and $A = 3.7\times10^4$ for the low temperature regime and E = 117.6 kJ mol^{-1} and $A = 6.0\times10^7$ for the high temperature. Powling[111] correlated a large amount of literature data and concluded that E = 126

kJ mol^{-1}, but without much evidence of autocatalytic behavior.

Pure AP can be detonated at modest heights in a drop-hammer test, but the explosion is notably mild and the explosive has a large critical diameter. The crystal density of AP is 1950 kg m^{-3}. The critical diameter for detonation has been reported as 150 mm for 1050 kg m^{-3} density and 220 mm for 1200 kg m^{-3}. When confined within a strong steel tube, a critical diameter of 35 mm was found for 1200 kg m^{-3} material[26]. For densities greater than 1365 kg m^{-3} of a 95% AP/5% aluminum powder composition, a critical diameter of 70 mm was found. In another study using 200 µm AP particles packed to a density of 1200 kg m^{-3}, a critical diameter of 93 – 100 mm was found[116]. AP becomes much more sensitive when combined with a hydrocarbon; when 1 – 8% oil or grease is added the lowest impact energy for ignition is required[116]. Combining AP with magnesium can lead to spontaneous combustion[1436]. If chlorates (e.g., $KClO_3$) are added to AP propellants, formation of ammonium chlorate will greatly increase the sensitivity of the propellant.

When subjected to radiant heating at 1 atm, pure ammonium perchlorate[112] shows a minimum flux for ignition of ≈ 400 kW m^{-2}. Small amounts of catalyst, however, lower the minimum drastically. For example, with 0.5% copper chromite, the minimum flux drops to ≈ 80 kW m^{-2}. Radiant ignition tests on AP-based rocket propellants typically[107] show ignition temperatures of 350 – 400ºC, but since each investigator generally used both a different experimental technique and a different formulation, wide variations in reported results are seen. The US Army[113] conducted on single steel drums filled with 113 kg of ammonium perchlorate. In one test series, various igniters were placed in the center of the drum; in another test, the drum was placed on, and surrounded by, a burning wood pyre (UN 6c Bonfire Test[550]). In no case did the material explode or detonate. In some cases, AP can sustain a large fire without detonating. Médard[26] reports a case where 5500 kg of AP in a rail shipment burned fiercely, but without explosion. The cause was surmised to be due to friction.

Despite benign results of drum-scale testing, a major US facility producing AP was destroyed by a series of explosions[114,115]. The accident at the production facility of Pacific Engineering Production Co. (PEPCON) in Henderson, Nevada on 4 May 1988 started as a small fire in a dryer building and spread to a large area of 55 gallon (208 L) plastic drums holding AP. The plastic drums tended to burn incompletely, without detonation, and it appeared that the polyethylene played a larger role in the combustion than did the AP. There was also a number of aluminum shipping containers holding AP. Detonations originated at these containers, even though many of them were not pressure-sealed. The particle diameter of the product was > 90 µm, which, according to then-current US Dept. of Transportation advice, was considered to be less hazardous than < 45 µm material. The event was slow-developing, with some 10 – 20 minutes between the start of the fire and the first of 7 explosions. The accident caused a US military committee to be formed to investigate the hazards of AP which prepared an encyclopedic report on AP hazards[116]. A natural gas pipeline traversed the property and was involved in the fires, thus the investigation included the possibility that natural gas played a role. But by conducting tests in a detonation tube, the committee rejected the proposed hypothesis that the event was particularly violent because it entailed the formation and subsequent detonation of an AP/natural gas/air cloud acting as a 'fuel-air explosive.' The factors that led to the PEPCON detonations have not been fully understood. But since the facility and its contents were demolished, the benign results of single-drum testing were demonstrated to be misleading. A paper has been published giving the views on the incident of an engineer retained during the course of litigation by the utility company whose pipeline traversed the site[117].

On 15 October 2001, a much smaller explosion leveled an AP facility, AeroTech Inc., located in Las Vegas, Nevada.

Antifreeze

Automotive antifreeze normally consists of a 50:50 mixture of ethylene glycol and water. Numerous fires have occurred when antifreeze boils over. The typical fire situation involves a discharge of antifreeze onto hot engine surfaces, where the water component, which has a lower boiling point, preferentially boils away. Ethylene glycol is then readily ignitable by a sufficiently hot surface. Cole[118] reports that the flashpoint of the 50:50 mixture is 132ºC, but the conditions of the test, of course, do not simulate these actual occurrences.

Arsenic compounds

A number of fully-alkylated arsenic compounds are pyrophoric, for example, cacodyl (tetramethyldiarsane, $C_4H_{12}As_2$). Urben[3] provides listings along with literature references.

Ashes

Ashes have a low thermal conductivity, consequently it is not rare for an individual to believe that ashes are 'dead,' while in reality hot or smoldering embers are still contained therein. No study has established the maximum limits, but one case history has been published[119] where an individual collected and placed ashes in a plastic bucket upon a wood floor. Seven hours afterwards, flaming erupted. Another

Table 3 Flash points of high-flash point jet fuels

Flash point (ºC)	JP-8 Jet A	Jet A-1
mean	48.1	48.7
range	41 – 58*	41 – 58
* one outlier was at 63ºC		

investigator[120] reported examining with an infrared camera a container of ashes four days after the ashes were deposited in the container and still finding high temperatures.

Asphalt

The minimum flux for ignition of asphalt* has been measured[121] to be in the range of 15 – 20 kW m^{-2}. It was also found that exothermic reactions occur between asphalt and various sodium salts, indicating a potential for runaway self-heating. Franke et al.[45] reported on a fire where cardboard drums filled with 90 kg of an asphaltic adhesive at an initial temperature of 160 – 200ºC self-heated to ignition. See also: *Tanks*

Automatic transmission fluid

An extensive discussion of physical and chemical properties of automatic transmission fluids has been presented by Kemp and Linden[122]. Ohlemiller and Cleary[123] investigated the effect on the flash point and fire point of ATF when contaminated with gasoline. Using a non-standard open-cup test apparatus, they found that the flash point dropped from 185ºC for pure ATF to room temperature (22ºC) when 15 – 20 vol% of the mixture was gasoline. The fire point dropped from 200ºC for pure ATF to 22ºC for a mixture with 25 vol% gasoline. Fitz[124] measured the AIT of ATF using a heated, 0.5 L pressure vessel. At 1 atm, he obtained 255ºC, which dropped slightly to 244ºC at 9.5 atm pressure (absolute). ATF fires are likely to occur when a transmission has been overfilled, if the vehicle is operating under overload conditions, or both[125]. In those cases, fluid can be ejected from filler or vent openings and ignite upon hitting hot exhaust components. While rare, fires that occur in this way have been documented as being potentially very violent[126].

Aviation fuels

Aviation fuels contain an enormous variety of hydrocarbons. Av gas may contain 300 compounds, while JP-4 some 5000 – 10,000. The composition of Jet A is typically[128]: 29% isoparaffins, 28% *n*-paraffins, 20% cycloparaffins, 18% alkylbenzenes, 2% naphthenes, and 3% other. The molar mass[129,130,140] of various aviation fuels is shown in Table 5; other tabulated properties are given in Chapter 15. In the US, aviation fuels for civilian uses are governed by ASTM D 910[131] and ASTM D 1655[132]. Jet fuels are divided into low volatility and high volatility grades.

- High volatility (flash point < –18ºC): JP-4, Jet B
- Low volatility; sometimes referred to as aviation kerosenes (flash point > 38ºC): JP-5, JP-7, JP-8, Jet A.

JP-1 and JP-3 are obsolete, while JP-2 was never designated. The primary fuel used in civil jet aircraft is Jet A, while the military uses mainly JP-8, along with some JP-5. JP-8 differs from Jet A mainly in that it contains anti-icing, anti-corrosion, and antistatic agents. The predominant compounds in the aviation-kerosene type fuels are C_8 to C_{15} hydrocarbons. Vapor pressure curves for a variety of aviation fuels are shown in Figure 6. Jet B, which is uncommon, is the civilian equivalent to JP-4. Occasionally, aviation fuels are referred to by their NATO designations, e.g. F34 (JP-8), F40 (JP-4), F44 (JP-5).

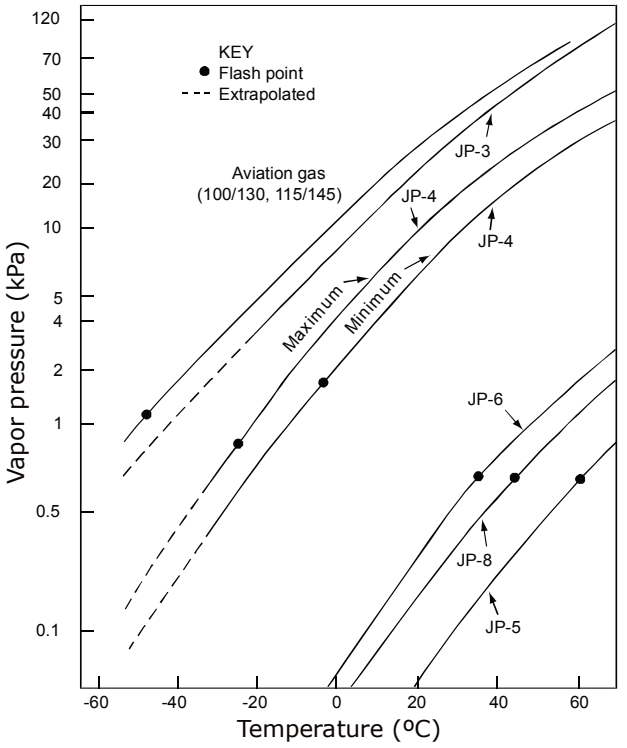


Figure 6 Reid vapor pressure curves for aviation fuels[127] (values are indicative only; actual commercial product can show wide variations)

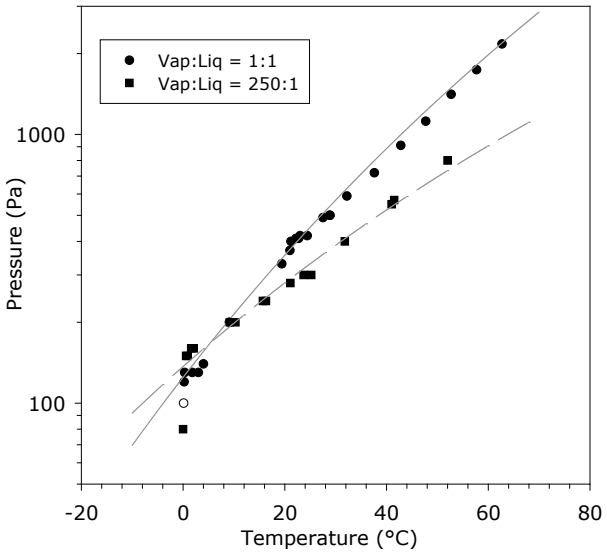


Figure 7 Vapor pressure for Jet A fuel under two different vapor/liquid test ratios

* In the US, asphalt, bitumen, pitch, and tar are considered synonymous terms. However, in some industries and in some countries, distinctions are made.

Table 4 Fractional distillation features of aviation fuels

Fuel	Temperature (°C) at which given % has evaporated		
	0%	50%	100%
Avgas	33	98	210
JP-4	65	160	250
JP-5	180	220	265

For the 'high flash point' fuels, Sochet and Gillard[133] conducted a literature survey and found the results shown in Table 3.

Being blends, aviation fuels do not have a boiling point, but rather show a temperature range over which distillation occurs. Table 4 shows typical properties for avgas and for two jet fuels[134]. Anti-static agents were introduced into military jet fuels and non-US civil aviation fuels around 1970. Subsequently, fires due to static electricity, which were common previously, dropped to low levels[135]. The agents were not seen as necessary for US civil aviation fuels, since electrostatic problems have not been serious in that sector. The agents mainly serve to raise the conductivity of the fuel, shifting the fuel's conductivity out of the region where static discharge susceptibility is the highest. Thus, they can be counter-productive if added to a fuel which has a very low conductivity.

The vapor pressure curve for Jet A was recently measured by Shepherd et al.[136] While Reid vapor pressure is reported using a standard vapor : liquid volume ratio of 4:1, the results are sensitive to this ratio, thus Figure 7 shows it for two different ratios. The authors provided the following data fits:

$$P = 5.75 \times 10^8 \exp(-4191/T) \qquad \text{ratio } 1:1$$

$$P = 4.971 \times 10^6 \exp(-2868/T) \qquad \text{ratio } 250:1$$

with P = pressure (Pa), and T = temperature (K). These results will be reflected in the flash point, which will be lower for the 1 : 1 ratio than for the 250 : 1. This is an example of the effect of liquid/vapor volume ratio for certain complex mixtures, as discussed in Chapter 6.

The flammability of fuel inside airplane tanks is difficult to assess accurately. Four factors are involved:

Table 6 Effect of pressure on aviation fuels

Fuel	Press. (atm)	Flamm. limits (vol%)		MOC (vol%) with diluent:	
		LFL	UFL	N_2	CO_2
Avgas 100/130	1.0	1.3	7.15	11.9	14.8
	0.53	1.25	6.75	11.2	14.1
	0.27	1.3	6.85	11.6	14.1
	0.13	1.4	7.6	11.9	14.8
Avgas 115/145	1.0	1.2	7.1	11.9	14.6
	0.53	1.25	6.9	11.6	14.6
	0.27	1.25	7.0	11.6	14.8
	0.13	1.5	7.85	12.0	14.9
JP-4	1.0	1.3	8.2	11.5	14.3
	0.5	1.3	7.85	11.4	14.5
	0.27	1.35	8.05	11.7	14.6
	0.13	1.35	8.1	12.4	14.9

- pressure
- temperature
- slosh
- oxygen enrichment.

The pressure and temperature effects exist in general for any flammable liquids, as discussed in Chapter 6, but for aviation fuels the pressure effect on LFL and UFL (but not on LTL and UTL) can be ignored, as shown in Table 6[142]. The LTL and UTL are strongly affected by altitude, since they directly decrease with decreasing total pressure.

But temperature limits only pertain to vapors that are vaporized from a liquid under still-air, equilibrium conditions. If significant generation of an aerosol occurs, for instance, due to motion, filling, or agitation, then a flammable aerosol may be created, and this will effectively bring down the lower temperature limit. In flight, if significant non-vertical accelerations are present, then fuel will slosh around and create an aerosol in the tank. As discussed in Chapter 6, the vapor pressure is higher at a curved surface than at a plane surface, thus the fuel's vapor pressure rises due to slosh.

An oxygen enrichment effect occurs since oxygen is more soluble than nitrogen in jet fuel[137]. When an aircraft climbs, oxygen and nitrogen both are de-gassed from the liquid and enter the vapor space, but since a disproportionately higher amount of oxygen was present in the fuel, the vapor space becomes oxygen enriched. In addition, this outgassing cre-

Table 5 Current types of aviation fuels

Fuel	Type	Molar mass (g mol^{-1})	Use
Avgas	gasoline	102	civilian small planes
Jet A	kerosene	140 – 210	civilian jets
Jet A-1	kerosene; lower freeze point that Jet A		civilian jets
Jet B	gasoline/kerosene blend; sim. to JP-4		civilian jets
JP-4	gasoline/kerosene blend; has antistatic additive	122 – 126	military
JP-5	kerosene	169 – 172	military
JP-6	kerosene; lower freeze point than JP-5	147	military
JP-8	kerosene; sim. to Jet A-1, but has anti-static and other additives	162 – 167	military

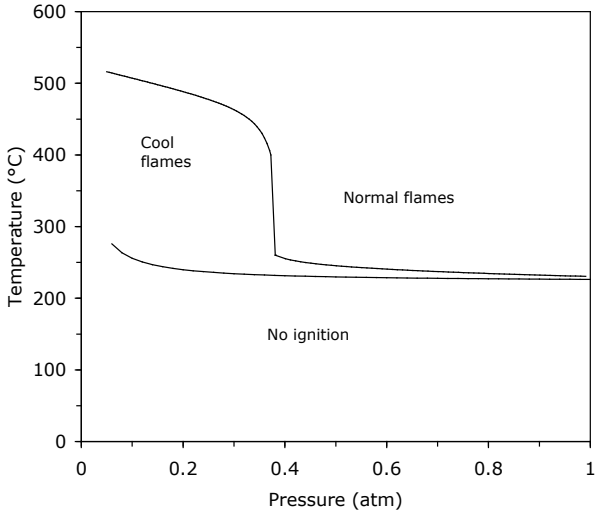


Figure 8 Autoignition regimes for JP-5 fuel

ates a foam at the surface of the liquid[138] and the foam may have different ignition properties than the vapor.

JP-5 fuel has an AIT of approximately 250ºC. But at sub-ambient pressures a substantial cool-flame regime is found[139], as shown in Figure 8. By contrast, JP-4 and JP-8 do not exhibit cool-flame ignition[140]. Figure 8 also shows that at elevated pressures, the AIT of JP-5 falls slightly with pressure, decreasing to 210ºC at 9 atm; similar results have been obtained[141] for JP-1 and JP-4.

For some aspects of jet fuel flammability, it is necessary to know the atmospheric pressure at above-ground elevations. An approximate expression is[142]:

$$P = \exp\left(-1.2\times10^{-4} H - 1.3\times10^{-9} H^2\right)$$

where P = pressure (atm) and H = altitude (m). The MIE increases at higher altitudes, due to decreasing atmospheric pressure. The FAA has suggested[143], based on very limited experimental data, that the effect for Jet A can be approximated as:

$$MIE = \exp\left[\frac{0.207H - 1.395}{\sqrt{1 - 0.049H}}\right]$$

where MIE = minimum ignition energy (mJ), and H = height above mean sea level (km). The dependence of the actual ignition energy E (mJ) on the fuel temperature T (ºC) and the fuel flash point T_{FP} (ºC) was then given as:

$$E = MIE \cdot \exp\left\{\left[9.22\times10^{-4} H + 0.0218\right]\left[T - T_{FP} - 12.2 + 2.73H\right]^2\right\}$$

Contour plots of the above equation are shown in Figure 9. Ignition due to static electricity in a fuel tank, for example, will be limited to certain maximum discharge energy, thus constant-energy contours can be used to distinguish flammable from non-flammable regions. It is reported that many incidents of ignition within airplane fuel tanks have occurred and that most of them involved fueling on the ground[144]. Figure 9 shows that, at ground level, the fuel

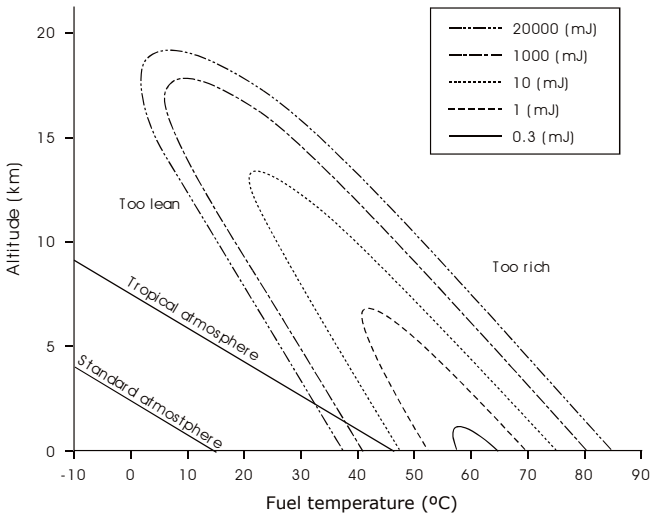


Figure 9 Estimated ignition energy needed for Jet A fuel at various altitudes and fuel temperatures. The large change with altitude is due to effect of total pressure on the LTL and UTL.

tank would be expected to be below the LFL. But this is based on average conditions within a quiescent volume and does not take into account splashing or spraying. Laboratory experiments to reproduce the fuel-tank ignitions have been attempted but have thus far been unsuccessful[144]. Extensive discussions of fuel-tank ignition scenarios are given in an FAA study[143].

Atkinson and Eklund[145] endeavored to find out if a lower temperature limit could be reached with regard to ignitability of jet fuels in mist form from a heated wire. At the lowest fuel temperature they were able to achieve, –40ºC, both JP-4 and JP-5 ignited readily.

Jet A aviation fuel can regularly pick up a charge of up to 4000 μC m^{-3} in handling operations at commercial airports[146] and values up to 5800 μC m^{-3} have been measured on JP-4 fuel[147]. Average charge densities of 30 – 50 μC m^{-3} have been found in airport tests[148]. To place these values in context, general guidance on petroleum-based liquids, given in Chapter 11, indicates that charge concentrations as small as 20 μC m^{-3} can lead to incendive discharges during tank-loading operations. Thus, it is perhaps surprising that so few aircraft fueling explosions have been recorded, even in the absence of antistatic agents.

A number of corrosion inhibitor agents can cause even greater charges to be picked up, but these have a benign effect, since the same agents have been found invariably to raise the conductivity of the fuel to a safe value (> 50 pS m^{-1}). Jet A with no additives of any kind has a conductivity of about 0.1 – 0.3 pS m^{-1}; commercial fuels show about 0.5 – 5.0 pS m^{-1}. JP-4 fuels show typically 1 – 10 pS m^{-1}, but values of 0.7 – 34 pS m^{-1} have been measured. Water was found to be a particularly undesirable component in jet fuel,

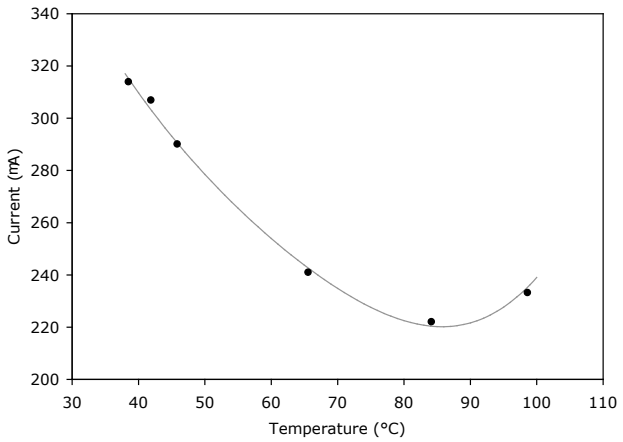


Figure 10 Minimum current needed for ignition of JP-5 in a fuel tank by means of corona discharge

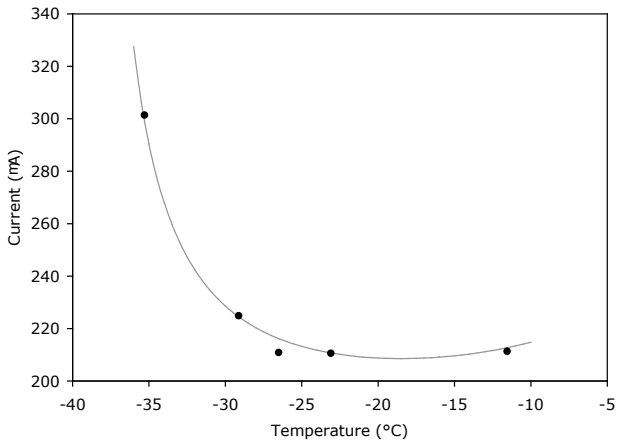


Figure 11 Minimum current needed for ignition of aviation gasoline in a fuel tank by means of corona discharge

since it drastically increased the maximum electrostatic charge, which was not compensated by any increase in the conductivity. The role of water is complex, since its effect of increasing the charge is not intrinsic, and only occurs when the fuel is pumped through filters[149].

Leonard and Carhart[150] noted that ignitions of jet fuel due to electrostatic charging from fuel flow are rare, and determined to find out the detailed reasons. They set up a polyethylene tank with JP-5 jet fuel where the fuel was continuously recirculated and charged by passing through a fiberglass filter. Various grounded electrodes were studied, placed at varying heights above the fuel surface. A parallel series of experiments was conducted where the second electrode was a metal plate, instead of the surface of the fuel. The results are summarized in Table 7 and Table 8. For the two-metal-electrode experiments, the most common result was a spark, especially with larger diameter of grounded electrodes. For discharge to the liquid surface, only a single spark discharge was obtained, the remaining 23 experiments showed either corona or brush discharge. The latter was a form described by the authors as a "pre-breakdown streamer." The brush discharges started out as a single-electrode discharge, but eventually a main stroke spanning to the other electrode was generally attained. The amount of energy available for this main stroke was small, however. Both the corona and the brush discharges were repetitive, with as many as 100 events per minute. For the discharges to the liquid surface, only gaps of 25 mm and greater were used, since it was found that for smaller spacings electrostatic attraction of the charged liquid to the grounded electrode would cause the liquid to rise and come into contact with the electrode, precluding the possibility of a discharge. For a 25 mm sphere, the energy of discharge available at a comparable gap size was about 30× greater for the discharge to the metal plate than to the fuel surface. The authors went on to attempt to ignite mixtures to actually test the incendivity of the discharges. In these tests, they switched to JP-4 fuel, for which a flammable mixture could be created. No successful ignitions could be obtained, but details of the trials were not documented.

Table 7 Summary of experimental results when discharge was to a metal plate

Grounded electrode	Gap (mm)	Discharge obtained	Charge transf. (nC)	Energy of discharge (mJ)
needle	10 – 30	corona	< 1	< 0.001
60º point	2.5	spark	90	0.17
	10 – 80	corona	0.9 – 1.3	0.004 – 0.011
6 mm sphere	2.4 – 8.7	spark	165 – 330	0.68 – 2.64
	9.5 – 12.7	brush discharge	33 – 49	0.27 – 0.49
13 mm sphere	0.24 – 9.5	spark	154 – 443	0.77 – 4.70
25 mm sphere	2.0 – 16.0	spark	128 – 575	0.44 – 12.0

Successful ignitions from a corona discharge were obtained by Newman and Robb[72]. In connection with studies to examine the potential for ignition of fuel tanks by discharges entering the fuel tank through the vent, they conducted experiments on the minimum current needed for ignition of aviation fuel tanks from a corona discharge. The results are shown in Figure 10 for JP-5 and Figure 11 for aviation gasoline; they also obtained data for JP-4, a ramjet fuel, and 'RVP special fuel.' The findings were seen as providing some cause for concern, since corona currents of several hundred microamps were plausible for aircraft in flight.

In the aircraft industry, it is common to use 200ºC as a notional hot-surface ignition temperature for all aviation fuels. This is highly conservative and one maker of aircraft engines, Rolls-Royce[141], found that no ignitions could be obtained below 400ºC.

Table 8 Summary of experimental results when discharge was to a liquid surface

Grounded electrode	Gap (mm)	Discharge obtained	Charge transf. (nC)	Energy of discharge (mJ)
needle	10 – 50	corona	< 1	< 0.001
60º point	25	spark	28	0.27
	10 – 150	corona	0.5 – 0.9	0.003 – 0.012
6 mm sphere	25 – 125	corona	2.0 – 4.0	0.2 – 0.4
13 mm sphere	25 – 125	brush discharge	24 – 97	0.34 – 0.91
25 mm sphere	25 – 125	brush discharge	49 – 84	0.43 – 2.33

Azides

A number of azides, especially silver azide, AgN_3, and lead azide, $Pb(N_3)_2$, are primary explosives which are very sensitive to friction or impact ignition. As little as 4 mg of lead azide has been known to detonate[151]. Hydrazoic acid, HN_3, can explode in either the gas or the liquid phase[151]. Inadvertent reactions producing azide-caused explosions also have been known to occur. In two cases[323], explosions occurred in hospital drain systems, where a saline solution containing 0.1% sodium azide was flushed down. The sodium azide reacted with the copper pipe, producing explosible copper azide. Older automotive air bag inflators used to contain sodium azide (see *Motor vehicles*). See also: *Explosives*.

Bagasse and bagasse products

Bagasse, which is the crushed, juiceless remains after sugar cane is milled, comprises largely cellulosic matter. It typically emerges from the mill[152] having around 50% water by mass and is then stored into piles while still at around 48 – 60ºC. Bagasse is subject to self-heating and, if stored improperly, can lead to spontaneous combustion. A certain amount of self-heating, however, is beneficial, since it allows moisture to be driven off, without needing an external energy source. The moisture is so dominant in determining the self-heating of bagasse, that this is a product where use of the standard oven-basket testing procedure would not only give substantially erroneous large-scale extrapolations, but would produce errors on the unconservative side. Gray and coworkers found that use of self-heating theory based on a dry material undergoing a single chemical reaction grossly overestimates the safe size of stored piles of bagasse[153]. To approximate a correct prediction, they determined that the theoretical formulation must explicitly include water vaporization/condensation and also moisture-dependent chemical reactions[154,155]. In highly wet systems, the major constituent of bagasse, cellulose, has been found to undergo two different reactions, a 'dry' oxidation and a 'wet' reaction which is probably a form of hydrolysis and whose rate is proportional to the liquid-phase water concentration in the material. Their theory involves solving a system of three partial differential equations, representing conservation of energy, liquid water, and water vapor.

In contrast to the simple theory delineated in Chapter 9, numerical solutions of the theoretical model showed three different cases are possible: (1) a rapid decrease in temperature from the original hot-work temperature to a slightly above-ambient equilibrium value; (2) a small initial rise in temperature, followed by a long near-steady plateau at around 60ºC, then a sudden drop of temperature down to a plateau value slightly above ambient (Figure 12); and (3) a runaway behavior with rapid heating at first, then a time when temperature growth tapers off, and finally a steep rise leading to runaway temperatures. This series of behaviors, especially the intermediate-cooling one (#2), is distinctly more complex than that shown by dry materials that are governed by simple kinetics. In practical storage of bagasse, case #2 is preferred, since it allows moisture to be driven

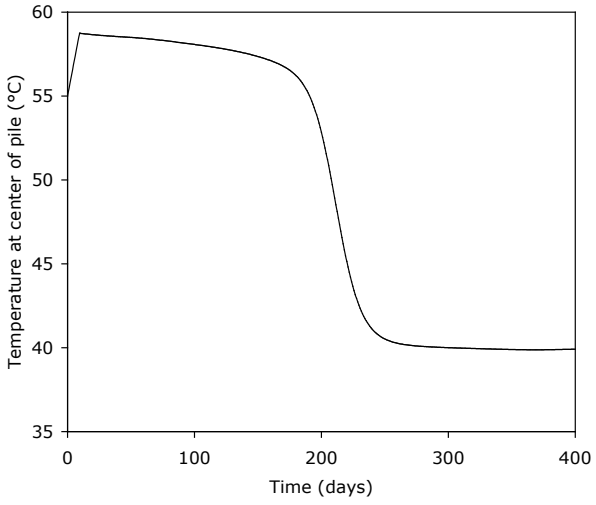


Figure 12 Example temperature history of pile for case #2

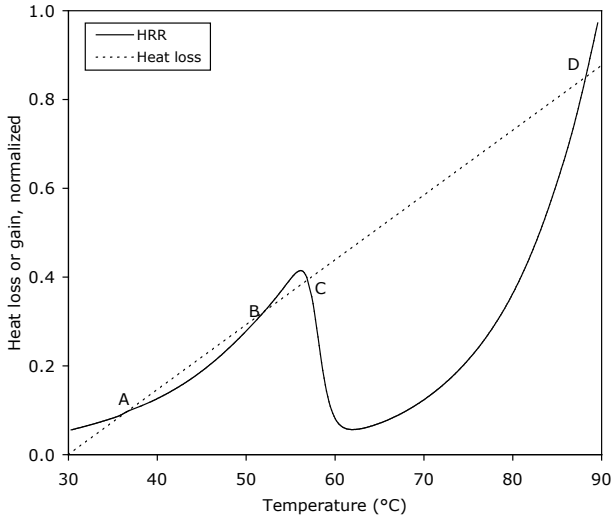


Figure 13 Self-heating curves for bagasse

off. Case #1, by contrast, cools so rapidly that water is not driven off.

Not unexpectedly the energy gain/loss diagram for bagasse looks more complex than for the simple Semenov case. Figure 13 shows an example[154], computed for an ambient temperature of 30ºC. Compared to Figure 2 in Chapter 9, it can be seen that the HRR curve is more complex and that it shows a local maximum and a local minimum. Point C is a quasi-steady equilibrium state which comes about due to the wet reaction term. This point corresponds to the long period of elevated, nearly-steady temperatures observed in a bagasse pile. After sufficient moisture is exhausted, the system drops down to point A. If the original temperature at which the pile was stored were more than 88ºC, then immediate runaway (Case #3) would ensue. The analysis of this problem requires a substantial mathematical effort and does not readily lead to engineering simplifications such as developed in Chapter 9. For a sense of magnitude, given reasonable physical property assumptions, quasi-steady Case #2 solutions were found in the range of 2 – 4.5 m pile size. The plateau in the vicinity of 60ºC can last for a half year, before the rapid drop begins. Piles smaller than 2 m did not show a significant rise in temperature, while piles greater than 4.5 m led to runaway conditions. As for any agricultural product, contribution to self-heating from microbial activity must be considered. But tests[152] where bagasse piles were treated with a biocidal agent showed essentially no difference in self-heating from untreated piles, indicating that for practical purposes this factor might be ignored.

In addition to serving as fuel, bagasse fibers are often used in the manufacture of lightweight fiberboard. The manufactured product is very similar to that which is produced from wood fibers. The AIT of fiber boards derived from bagasse[443] was reported by NIST in 1947 as being 240ºC, but the test method used was only described very sketchily; see *Wood* for details. Mitchell[156] conducted self-heating tests on bagasse fiberboards and found trends similar to wood fiberboard, although the bagasse material was slightly worse. See also: *Wood and related products: Wood fiberboard*.

Boranes

The borane family includes $(BH)_n$, BH_3, B_2H_6 (diborane), B_4H_{10} (tetraborane), B_5H_9 and B_5H_{11} (pentaboranes), B_6H_{10} (hexaborane), and others. Diborane is one of the most hazardous known substances, igniting in ambient air, unless dry and free from impurities[157]. The ignition may take 3 – 5 days, instead of being instant[3]. Diborane also reacts hypergolically with alcohol. Its flammability limits are 0.84 – 93.3%, with combustion possible down to an oxygen content of 1.3%. Polyborane, $(BH)_n$, is similarly reactive. Borane, BH_3, does not exist as a pure substance, since, on formation, it immediately polymerizes into one of the higher boranes. Tetraborane and the higher boranes are reactive similarly to diborane. Additional guidance is given by DOE[158].

Boron

Boron has been proposed as a rocket and ramjet fuel due to its high volumetric heat of combustion, 135,000 MJ m^{-3} (liquid fuels are generally < 35,000 MJ m^{-3}). A common pyrotechnic mixture for igniters (electric matches, squibs) contains potassium nitrate and boron. Boron particles normally contain an oxidized outer layer, and when the particles are heated, their oxide coats tend to stick together, resulting in clustering or agglomeration. In an early study, Talley[159] determined boron to ignite in O_2 at around 1960ºC. Maček and Semple[160] compared several later studies and concluded that, for small particles of about 50 μm, a temperature of around 1630ºC is the ignition temperature in air at room temperature, with the value dropping to ca. 1230ºC when under 15 atm of pressure. In a later paper, Maček concluded[161] that the ignition temperature can be anywhere between 1230ºC and the boiling point of B_2O_3, which is 2043ºC at 1 atm. Moisture affects the ignition process, and ignition temperatures are about 50ºC lower in moist atmospheres than in dry. Unlike some other elements, boron does not burn in low-O_2 environments, with ca. 10% being required for combustion[161]. Yeh and Kuo have reviewed other experimental ignition studies[162].

Boron is understood to ignite by a two-stage process[163]. In the first stage, the oxide layer is removed from the metal, followed by a second stage where oxidation can occur on the metallic surface. Further details of the reactions involved in ignition have been outlined by Li and Williams[164]. Most researchers consider that, due to its low volatility, boron burns heterogeneously, without gas-phase reactions. On the other hand, Yuasa et al.[165] heated small (10 – 13 mg) lumps of boron and concluded that ignition could be either homogeneous or heterogeneous, with homogeneous combustion showing a green-white flame. Glassman[166] challenged this conclusion and suggested that the observed luminosity is from B_2O_3 decomposition products. At the minimum heat flux, Yuasa found that the specimen temperature at ignition was 1400ºC, irrespective of supposed mode of ignition. Commercial boron tends to contain impurities of oxygen and magnesium and this makes the material substantially easier to ignite than the high-purity form.

Mohan and Williams[167] provided an early theoretical model of boron ignition. This indicates that for $1 < d < 50$ μm, diameter makes little difference. But for larger diameters, increasingly higher ignition temperatures are expected. They also pointed out that many of the unique features of boron ignition can be attributed to its highly unusual thermal conductivity properties. Glassman et al.[168] developed a later theory, where they proposed that elemental boron becomes available for combustion by diffusing outward across the oxide coating; most previous theories assumed that oxygen diffuses inward, instead. A recent theory was

published by Zhou et al.[169] They note that the measured ignition time corresponds roughly to the time required to remove the oxide layer, since active combustion is seen very soon thereafter. While the study did not produce closed-form expressions for prediction, the effect of oxide layer thickness was characterized. When all other conditions are held constant, the ignition time equals a constant, plus a term proportional to the oxide layer thickness. The constant represents the heat-up time, while the second term represents the time needed to remove the oxide film, once thermal equilibrium has been reached. The theory also indicates that there is a maximum oxide layer thickness, beyond which ignition will not occur. Their theory states that a layer which is 6.8% of the radius represents this limiting condition.

Clouds of boron particles ignite at lower temperatures than what is needed for single-particle ignition. The minimum ignition temperature decreases with (a) increasing cloud radius, (b) decreasing particle radius, (c) increasing particle concentration, (d) decreasing particle velocity, and (e) decreasing atmospheric pressure. Particles with a radius of 3 μm forming a cloud with a radius of 0.6 m at a mass fraction loading of 5% ignite at an atmospheric temperature of about 1030ºC under zero-velocity conditions[163]. If the mass loading is increased to 25%, ignition becomes possible at 630ºC. A minimum temperature for ignition of boron dusts in air[170] is reported to be 730ºC. Dust clouds with about 12% of magnesium added to the boron show ignition temperatures about 150ºC lower than for boron particles alone[171]. In a CO_2 atmosphere, boron powder (ultra fine, 0.05 μm size) was found not to be ignitable up to the maximum temperature tested, 960ºC[1396].

Brake fluid

Ohlemiller and Cleary[123] investigated the effect on the flash point and fire point of brake fluid when contaminated with gasoline. Using a non-standard open-cup test apparatus, they found that the flash point dropped from 100ºC for pure brake fluid to room temperature (22ºC) when 10 vol% of the mixture was gasoline. The fire point dropped from 130ºC for pure brake fluid to 22ºC for a mixture with 15 vol% gasoline.

Calcium resinate

Used in various paints, leather processing, and cosmetics, calcium resinate ($C_{40}H_{58}CaO_4$) is reported to be a self-heating substance[1542].

Camping fuel

According to DeHaan[172], a typical camping fuel has a Reid vapor pressure of 43.3 kPa at 38ºC. Camping fuel is a complex mixture of hydrocarbons, but dominated by hexane and related compounds. Its flash point is not fixed, but may be around –33ºC. See also: *Gasoline* (white gasoline).

Candles

Candles are one of the oldest forms of open-flame devices in a home, but in a modern residence candles involve some unique ignition hazards. Factors to consider are:

- the combustion is not confined to an engineered combustion device; some candleholders are grossly inappropriate for the application (e.g., they are combustible or are unstable and can be tipped over);
- the open flame has no protection or shielding and candles are often burning while unattended;
- unlike matches and lighters, a candle flame can burn for hours, thus items that take fairly long to ignite can be threatened.
- attempting to extinguish a candle fire with small amounts of water available to a householder is likely to exacerbate the fire in a manner similar to pouring water of burning liquid fires.

Sanderson has documented additional aspects of candle fires[173]. Candle flames were studied very early by Michael Faraday, and his classic 1861 textbook still makes worthwhile reading[174].

Candle fires in the US, while still a small fraction of all residential fires[175], have experienced a significant upsurge in recent years (Figure 14). In response to this, in 2002 ASTM issued a specification, ASTM PS 59[176], establishing safety requirements for candles.

CPSC[177] has compiled US statistics on the general nature of candle fires, see Table 9. NFPA published detailed statistics[175] on US fires for the years 1994-1998, as shown in Table 9 through Table 11. Over the years, CPSC has issued a number of recalls for products that are a combined candle/candleholder due to improper designs where either the candleholder was made from a combustible material and tended to catch fire, or else there was a propensity (typical-

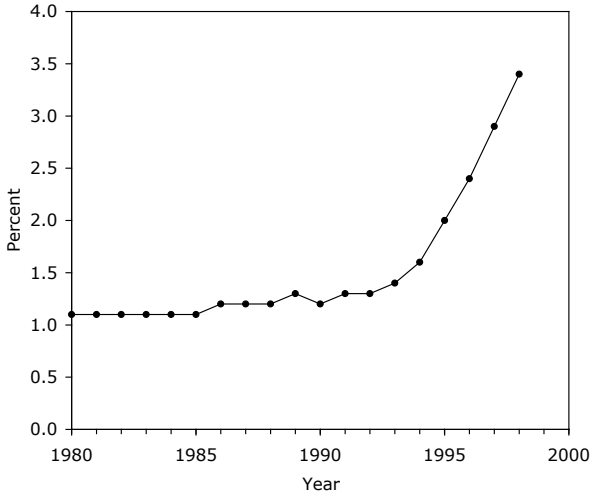


Figure 14 Candle fires in the US, as a percent of total residential fires

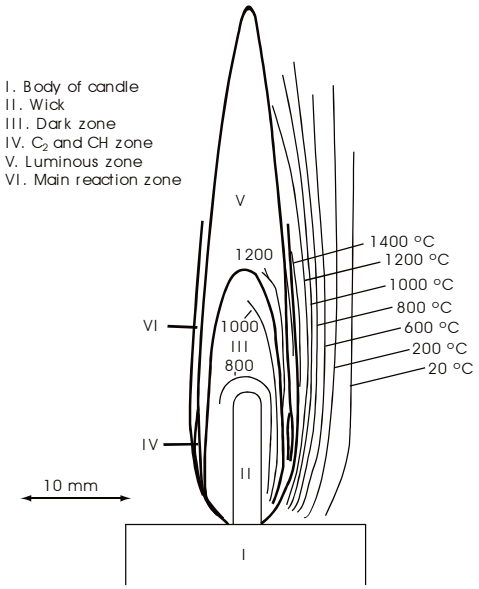


Figure 15 Temperatures in a candle flame, as determined by Gaydon and Wolfhard

ly with a glass or ceramic construction) for the candleholder to shatter and spill out burning material.

Some very high temperatures are found in a candle flame. Gaydon and Wolfhard[170] measured a peak temperature of 1400ºC (Figure 15). Note however that the size of the flame zone is relatively small. Peak temperatures measured in flashed-over room fires are typically around 1000ºC and only rarely reach 1200ºC. Thus, the peak measured temperature in a candle is higher than in a room fire (the candle is not unique in this; other small laminar flames show very similar temperature distributions). The high temperatures in a room fire, of course, encompass a vastly greater area, thus, ignitability comparisons cannot be made solely on values of the temperature peak. A German study[178] reported temperature measurements *above* the tip of visible candle flames (Table 12). The flash points of waxes from various candles were measured by the Cleveland open cup method[179]; three different products showed values of 196, 216, and 236ºC.

Yallop[180] reports that the minimum oxygen concentration needed to sustain a candle flame is typically 10%. Dillon[181] measured heat fluxes above the flame of a 21 mm diameter paraffin-wax candle. He found 50 – 70 kW m^{-2} at the flame tip, dropping to about 20 kW m^{-2} at 200 mm above the flame tip. Less than 10% of the heat was due to radiation. Flame height was 40 – 45 mm.

It is reported[182] that even an overt failure within the candle may not be necessary, if the candle is separated from an ignitable surface only by a relatively modest thickness of metal (e.g., copper, brass). Since metals are substances of high thermal conductivity, in such cases, sufficient heat can pass through the metal to ignite the substrate.

Table 9 Types of candle fire accidents, US statistics (1985-1997)

Type of fire	Percent
ignition, other combustible	49
tipover	19
ignition, clothing	13
candle holder broke, shattered, exploded	12
candle holder fire	6

Table 10 Material first ignited in candle fires

Material	Percent
mattress or bedding	12.8
cabinetry	10.1
curtain, blind, drapery	8.4
interior wall covering	6.2
unclassified form of material	5.8
furniture: unclassified or unknown	5.7
upholstered furniture	5.5
decoration for special event	4.9
wearing apparel not worn	4.6
magazine, newspaper, writing paper	4.4
linen other than bedding	4.0
floor covering or surface	4.0
adornment or recreational material, unclass.	3.5
multiple forms of material ignited together	2.9
appliance housing or casing	2.5
trash or waste	1.7
structural member or framing	1.6
box, carton, or bag	1.5
other material	9.9

Table 11 Leading factors associated with candle fires

Factor	Percent
unattended	19
combustible too close	19
inadequate control of fire	10
children playing	9
abandoned	7
falling asleep	5
incendiary or suspicious	3

Table 12 Temperatures measured at various heights above the tip of visible candle flames

Ht. (mm)	ºC	Ht. (mm)	ºC
20	488	100	280
40	453	120	213
50	400	140	163
80	372	160	89

Candles are sometimes used as incendiary timing devices. A common rate of burning of candles is 25 mm per hour, although larger candles will burn more slowly; candles less than about 20 mm diameter, on the other hand, burn up rapidly. In any case, this is easy to determine experimentally

for a candle of a known type. For common candle types, the heat output is 50 – 100 W.

TEA CANDLES

Tea candles (also called tealights) are small candles self-contained in an aluminum dish and often used without an additional candleholder. A number of fires have been reported where tea candles have ignited combustible surfaces that they were sitting on. These have included European-style, non-FR television cabinets, polystyrene compact disc cases and plastic toilet tank lids[183]. An investigation[184] has revealed that the mode is normally one whereby flaming takes place over the whole top surface since it has reached its fire point temperature. The fire point of wax is fairly high (although it does not appear to have been studied), so the question becomes what raises the wax to its fire point. The investigation determined that several different mechanisms can occur:

- Placing of a spent match in the candle. This is commonly done by users, but it was found that the match sometimes ignites much later and serves as a 'second wick.' The combined effect of two wicks in a small area suffices to heat up the entire wax surface to its fire point.
- Contamination in the wax, leading to 'flaring.'
- Other contaminants (e.g., decorations) that cause multiple-wicking when the candle is nearly regressed to the base.
- Improper wick size; or formation of a lump in the wick, effectively creating an extra-large wick.
- A detached wick that floats up to the surface and causes flaring.

Daéid and Thain[185] measured the temperatures of tea candles at the base of the aluminum dish. Under still-air conditions, they found a peak temperature of 52 – 67ºC, but providing a modest air flow of 0.4 m s^{-1} gave a peak of 89ºC. For such 'normal usage' conditions, the wax did not reach its fire point. Dropping a spent wooden or paper match into the candle led to a gross change in burning—at a certain point the wax ignited and burned as a pool fire. The base temperature at the moment of this ignition was 126 – 182ºC, depending on whether the match was wooden or paper, and whether or not there was an air flow; the actual fire point temperature of the wax itself was not recorded. The peak temperatures at the base under such conditions were 287 – 324ºC. When these candles were placed atop TV cabinets (of unidentified plastic), the cabinet locally melted and the candles fell in once a base temperature of 155 – 226ºC was reached.

GEL CANDLES

Gel candles are made from mineral oil which has been gelled by incorporation of a small amount of a polymer; fragrances, colorings, and other additives are also often added. The resulting substance behaves differently from wax in that it can melt and flow more readily. In case of breakage of container, the burning material may be easier to spread around and harder to extinguish. A comprehensive study of the product category is not available, however. The basic fire performance, in brief, is intermediate between a wax candle and an oil lamp. According to a manufacturer of the raw materials, the open-cup flash point of gel candles is approximately 226ºC, while the fire point is 260ºC.

Carbon disulfide

A versatile solvent, but one of the most hazardous of common industrial chemicals, carbon disulfide, CS_2, has a flash point of –30º, a boiling point of 46ºC, and burns with a nearly colorless flame. It also has an exceptionally low AIT (100ºC) and very wide flammability limits (1.3 – 50%). Carbon disulfide spilled on steam pipes has caused ignitions, especially if the pipes are rusted, and various fires with carbon disulfide have occurred in laboratories. Carbon disulfide was involved in one of the most famous tunnel fires, the Holland Tunnel fire of 13 May 1949[186]. The fire was severe enough to demolish some 180 m of concrete tunnel lining. For a hot surface to ignite carbon disulfide, a rather low temperature suffices. Using a brass plate of 1770 mm^2 area, it was found that ignition occurs at 150ºC[17].

Carbon monoxide

As explained in Chapter 4, the combustion of CO is strongly affected by the presence of moisture, with truly-dry CO being harder to ignite. This also affects the flammability limits, as shown in Table 13. In these tests, 'dry atmosphere' had 15 ppm moisture, while 'normal air' had 0.1 – 0.5%. The tests[187] were run in a rig similar, but not identical, to the one with which standard tabulated values for CO have been reported (the BM values are 12.5 and 74%, respectively).

Table 13 Effect of moisture on flammability limits of CO

Atmosphere conditions	LFL (vol%)	UFL (vol%)
dry atmosphere	18	54
normal air	14	67

Cellulose

Cellulose is one of the three main ingredients of wood, the other two being hemicellulose and lignin. It is found in nearly pure form in laboratory filter paper, and in various purities in commercial papers. The thermal conductivity (W m^{-1} K^{-1}) of cellulose at room temperature can be expressed as[188]:

$$\lambda = \exp\left(1.45 \times 10^{-3}\, \rho - 3.39\right)$$

where ρ = density (kg m^{-3}). In an early study, Brown[189] found an autoignition temperature of 239 – 254ºC. Holm[190] reported in 1913 that cellulose shows a glowing ignition at ca. 360ºC. NBS conducted autoignition tests on 3.3 g of filter paper using a small tube furnace where the air flow rate was said to have been optimized[191] (Table 14). The specimens ignited by a glowing ignition and it was not re-

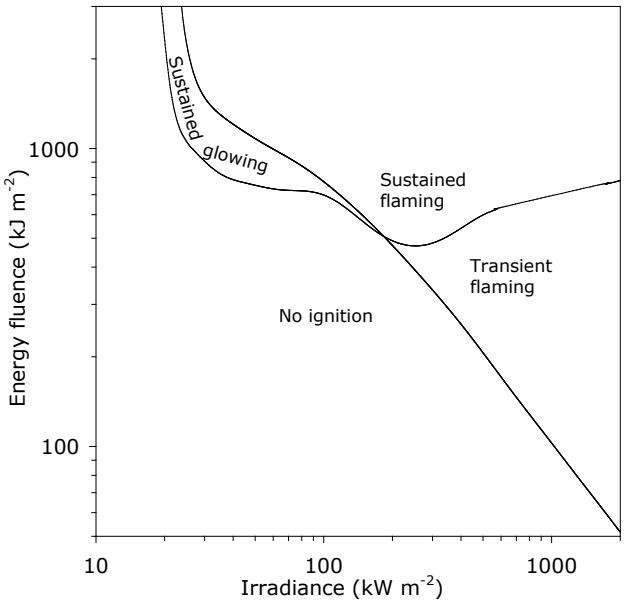


Figure 16 Regimes of ignition for 0.05 mm thick blackened cellulose paper exposed to tungsten lamp radiation

ported whether flaming subsequently ensued. Note that the minimum ignition temperature found for wood is 250ºC (see: *Wood*) and cellulose is one of the main components of wood, so the ignition temperature would be expected to be roughly similar.

Shivadev and Emmons[192] used a radiant heater to ignite Whatman No. 2 white filter paper of 0.18 mm thickness and 85 g m^{-2} basis weight. They found that $\dot{q}''_{min}$ = 42 kW m^{-2} was needed for autoignition. At lower irradiances, the material charred and fell apart, but did not begin flaming. At ignition, they found an average specimen temperature of 350ºC. They concluded that, as far as Arrhenius kinetics was concerned, there were two temperature regimes. For temperatures in the range 260 – 382ºC, E = 109 kJ mol^{-1}, A = 5.9×10^6 s^{-1}, and Q = –368 kJ kg^{-1} (endothermic). For temperatures above 382ºC, E = 226 kJ mol^{-1}, A = 1.9×10^{16} s^{-1}, and Q = +1860 kJ kg^{-1} They also suggested that, throughout the temperature range, the two Arrhenius expressions should be viewed as additive, rather than exclusionary. Martin et al.[1615] conducted experiments where blackened filter paper was exposed to a tungsten lamp source. For

Table 14 Tube furnace tests for the AIT of cellulose filter paper

Furnace temp. (ºC)	Heating time (h)	Ignition
228	70	no
230	45	no
232	7 – 9	yes
246	3	yes
253	2	yes
280	0.5	yes

various types and thicknesses, $\dot{q}''_{min}$ values in the range 20 to 29 kW m^{-2} were found. For these samples, surface absorptivity with respect to the tungsten lamp radiation source was determined to be 0.92. They also assessed ignition by two different means—first observation of surface glow, and first observation of flaming. The values of $\dot{q}''_{min}$ determined at the glowing threshold were about 10% lower than the values cited above for flaming. Martin and Alvares[193] summarized their results in the form of a graph of irradiance versus energy fluence (irradiance × exposure time), and this is shown in Figure 16.

In comparing the results of Martin and Alvares to those of Shivadev, it is not clear why Shivadev's minimum heat flux was so high. A value of around twice the black-material value would be expected for white specimens if a tungsten lamp source were used by Shivadev, but he used a low-temperature coiled-wire heater. For specimens exposed to enormous heat fluxes (180 – 1900 kW m^{-2}), Martin[194] found that the surface temperature at ignition was 600 – 650ºC. This is in line with studies on other substances which show that T_{ig} rises significantly if huge heat fluxes are involved, but a factor also to be considered is that Martin irradiated fairly small areas. Weatherford and Valtierra[195] claimed to have achieved piloted ignition of cellulose sheets using a convective heat flux of only 2.5 kW m^{-2}, but their numbers are inconsistent and it appears that their calibrations were erroneous.

Hinkley et al.[196] conducted experiments on vertically-oriented filter paper (87 g m^{-2}) by impinging an air stream from a hot-air blower onto the paper. Their results are given in Table 15. Air flow velocities were not measured.

Table 15 Autoignition of filter paper from hot-air blower

Distance from outlet (mm)	Hot air temp. (ºC)	Ignition time (s)
25	876	3.8
51	849	3.7
76	705	5.3
102	545	10.5
127	413	N.I.

Walker et al.[197] studied self-heating of cellulose and concluded that the exothermic reaction is of the autocatalytic type. However, Vovelle et al.[198] determined that cellulose oxidation can be represented as a first-order reaction, with E = 250 kJ mol^{-1} and $A \approx 10^{19}$ s^{-1}. Davies et al.[199] examined cellulose in a thermal analysis apparatus at a heating rate of 20ºC min^{-1} and found that autoignition occurs at 350ºC if flowing air conditions are maintained. If the specimen is exposed in stagnant air, an exotherm was found at 341ºC, but no overt ignition. As the heating rate was lowered, the ignition temperature dropped, going down to 283ºC at 1ºC min^{-1}. For oxidation in atmospheres of 21% oxygen, the

same workers[200] concluded that E = 155 kJ mol^{-1}, but noted that the value rises with increasing oxygen concentration.

Cellulose insulation

'Cellulose' insulation is made from ground-up newspaper, which of course, is a wood-pulp product and not wholly just cellulose (it can also occasionally be made from cardboard or wood stock material). Loose-fill cellulose insulation is blown into place using a mechanical blower, and is blown in to a density of 28 – 35 kg m^{-3}. With time, the insulation settles, and a settled density of 50 kg m^{-3} is typical. In making the insulation, FR agents must be added if the product is to pass fire tests required by US Federal regulations mandated by CPSC since 1978: the critical radiant panel test ASTM E 970[201], and a separate smoldering test described in ASTM C 739[202]. Kokkala has provided details for a variety of other test methods designed for cellulose insulation that are occasionally used[203].

Commonly borax (sodium tetraborate, $Na_2B_4O_7 \cdot 5H_2O$) is used to retard flaming ignition and flame spread, while boric acid (H_3BO_3) is added to limit the smoldering potential. These FR agents are added as dry powders. The total amount of retardants added on is about 15 – 25 pph (parts per hundred parts of cellulose insulation, by mass), since attempting higher loadings yields segregation. Siddiqui et al.[204] recommended that about 2 pph borax is needed to pass the critical radiant panel test, and about 18 pph boric acid to pass the smoldering test. In another paper, the same author[205] suggested that the loading be no less than 2 pph borax and 12 pph boric acid. Commercial formulations vary widely, but 4 pph borax and 14 pph boric acid would be fairly typical. In some formulations, another powder, ammonium sulfate is used, but this can show corrosion problems. A liquid FR agent, ammoniated polyphosphoric acid, has occasionally been used.

To pass the required tests, the material must not show a critical flux for 'creeping' flame spread of less than 1.2 kW m^{-2} nor a mass loss over 15% in the smoldering test, which uses a cigarette for the ignition. A cigarette is a very small hot body and, for a successful smolder-retardant formulation, self-sustained smoldering does not occur. However, if a larger-area hot body does cause smoldering to be initiated and the insulation layer depth is greater than about 60 – 100 mm, even large loading (25%) of boric acid will only reduce the velocity of smolder, but not stop smoldering[206]. Gustin reported that a 75 W light lamp placed on a variety of commercial FR-treated cellulose insulation resulted in smolder being initiated in 100% of the trials[207]. Boric acid acts to extinguish the high-temperature afterglow that follows the smolder front; thus, it can help reduce the tendency for a smolder-to-flaming transition to occur. Under conditions of no external wind, the peak temperatures in a smolder front are about 500ºC.

For a given level of FR treatment, the ignition resistance of cellulose insulation increases with fiber diameter. Additionally, larger particle sizes require less FR treatment to achieve the same resistance to smoldering. Some experimental work[208] with an FR system comprising boric acid, borax, and aluminum sulfate in the ratio 2:1:2 showed that increasing the particle diameter from 0.2 to 2.0 mm was equivalent to increasing FR agent loading by about 5 percentage points. The mixture used by the researchers, however, does not represent a common commercial formulation.

Grand[209] conducted a survey where he examined 73 fire incidents involving cellulose insulation. He observed that ignitions of this material are hard to isolate in US statistical fire data bases, due to coding problems. From the actual cases examined, he concluded that the major factors leading to the ignition of cellulose insulation were overheating at an electrical fixture; electric wiring problems; and heating from furnace or flue installations. In addition, he noted that some incidents were due to unobserved ignition of cellulose attic insulation when a fire in another space had occurred and been extinguished. Later, smoldering transitions into flaming. Gustin[207] reported that in one case cellulose insulation ignited simply from heat created by a ceiling-mounted room fan. A large fire occurred when cellulose insulation ignited from mechanical sparks that were emitted by a circular saw used to cut through metal roofing[210].

Belles[211] studied the performance of cellulose insulation and reported a number of problems. He concluded that even properly treated insulation can smolder. As with any porous, smoldering material, extinguishment is very difficult and rekindling can be expected. Belles also reported that the fraction of products in the marketplace not complying with the mandatory regulations was found by CPSC in one study to be 65%. Furthermore, several studies have found that aged, in-place material, when tested, failed the flammability tests, although it is not clear that the material would have passed when new. In one field study[212], only 8 out of 133 samples passed both the ASTM E 970 and the smoldering tests. According to Davie[213], fires occur most commonly when ceiling light fixtures are improperly installed, and adequate clearances do not exist. In a large-scale mockup experiment, he found that, after smoldering for 10.5 h, cellulose insulation then ignited wood joists. He also reports that after extinguishment with water, smoldering was not completely stopped, and resulted in a rekindle 2 days later. Thus, evidence exists that smoldering of cellulose insulation can persist for at least 2 days.

Laboratory studies have confirmed the progressive worsening of performance with age. A NIST study[214] noted that fire retardants may be lost by mechanical settling out, by subliming, or due to moisture effects. After conducting environmental cycling tests, the author concluded that "the long term fire protection provided by fire retardant com-

Table 16 Critical hotplate temperature needed for ignition of 300 m thick layer of cellulose insulation

Condition	Critical hotplate temp. (ºC)
non-FR, ambient = 22ºC	212
treated with 20% boric acid, ambient = 22ºC	232
treated with 20% boric acid, ambient = 80ºC	222

pounds may be limited." Without effective fire retardants, of course, cellulose insulation is just shredded paper, with ignition properties identical to shredded paper. One laboratory study[215] documented that thermal aging of the material may make it more prone to fail the radiant panel test. In an extensive California study[216] using three different manufacturers' products, it was found that after a 3-year exposure all specimens no longer passed the ASTM E 970 test. In the California study, the material was simply stored in a warehouse and was not subjected to either mechanical forces that could cause FR agents to settle out, nor to any accidental wetting which could leach them. Thus, the authors of the study concluded that the diminishing performance is probably due to acidic components being produced by the cellulose itself, which react with, and neutralize the borax. They also pointed that boric acid may slowly be sublimed out of the material. Another possible reason may be that when crude (rather than pure) boric acid is used, the residual sulfuric acid which is contained in crude boric acid reacts to convert borax into boric acid, diminishing the flaming-ignition performance[217].

As discussed in Chapters 7 and 9, smoldering ignition cannot be characterized by a fixed ignition temperature. In testing with hot bodies, the area of the hot body is an essential variable. Issen measured the self-heating parameters of unretarded cellulose[218] and applied standard self-heating theory. Using several different methods, he got substantially scattered data, but his results using an adiabatic furnace are probably most relevant: E = 110 kJ mol^{-1}, QA = 1.7×10^{13} W kg^{-1}, and P = 46.6. In a more extensive study, Ohlemiller[206] found that hot body temperatures of 380 – 385ºC were needed when using a wire of 4.8 mm diameter, but only 255 to 266ºC for an 0.2 × 0.2 m hot plate. For modeling purposes, he concluded that the oxidation chemistry could be represented by a reaction with E = 174 kJ mol^{-1}, λ = 0.053 W m^{-1} K^{-1}, A = 1.17×10^{13} s^{-1}, and Q = 4.2 kJ kg^{-1}, with P = 41.0 being derivable from his given data. These values were obtained from thermal analysis studies[219]. In studies with a hotplate method[220], however, he obtained E = 113 kJ mol^{-1}, QA = 3.7×10^{13} W kg^{-1} and giving P = 40.3 for unretarded insulation of 34 kg m^{-3} density. For insulation retarded with 20% boric acid, the hotplate results were E = 132 kJ mol^{-1}, QA = 9.0×10^{14} W kg^{-1}, and P = 43.9 at a density of 41 kg m^{-3}. These results are perhaps most clear if illustrated for the case of a 300 mm layer, a common insulation depth in attics (Table 16). Over a moderate range of practical densities, Ohlemiller also showed that variations in *density* do not affect the critical conditions[221]. While he discusses the application of the first-order theory to predictions of self-heating, Ohlemiller cautions that no study exists where behavior of cellulose insulation exposed to moderately elevated temperatures over the course of months or years was examined. Cellulose insulation fires are known to have occurred months-to-years after original installation. For example, a CPSC study[222] documented a number of cases where the time between the installation of insulation and a fire originating at a light fixture (not overlamped) was recorded. These times were: 1 day; 4 and 9 months; and 1, 8, and 10 years.

Yereance[223] claims that attic fires have been identified where cellulose insulation self-heated without the presence of any external sources of heat. Using an ambient temperature of 330 K and values of E = 110 kJ mol^{-1} and P = 46.6 gives a critical layer height of 24 m. This is vastly in excess of the 0.3 m or so of attic floor insulation that is typically provided, and—if theoretical extrapolations are justified—indicates that ignition will not occur due to self-heating. However, as further considered in connection with self-heating of wood (see: *Wood*), there must be a general *caveat* applied to using chemical reaction data obtained from short-term experiments to thermal degradation occurring over long time periods.

UK tests[224] on cellulose insulation showed that products treated to pass the cigarette test will not ignite from a lighted match nor from a small wood crib, but can go into smolder from (1) an electric wire drawing excessive current; or (2) from contact with an already smoldering object larger than a cigarette. If smoldering is initiated, it typically proceeds at about 180 mm h^{-1} in unretarded material and 115 – 130 mm h^{-1} in material with insufficient FR agent[203].

Cellulose nitrate, Celluloid, pyroxylin

Cellulose nitrate (also called *nitrocellulose*) is made by the nitration of cellulose. Cellulose belongs to the general chemical family of polysaccharides. It is a major constituent of living plants and is a natural polymer comprising repeating units of a hexagonal structure. Its ultimate formula is $(C_6H_{10}O_5)_n$. Cellulose nitrate is produced by reaction with a mixture of nitric and sulfuric acids. This esterification process, whereby hydroxyl (OH) groups are replaced by ONO_2 groups, is called nitration. The end product consists of high-molecular-mass polymer chains composed of anhydroglucose units, with each unit containing up to 3

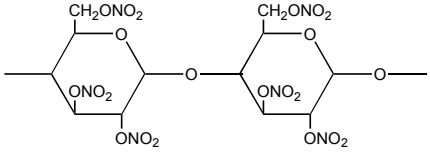


Figure 17 Structure of fully-nitrated cellulose nitrate (OH, instead of ONO_2, groups are present to the extent that the substance is not fully nitrated)

nitrate groups (Figure 17). The general formula is $C_6H_7O_2(OH)_x(ONO_2)_y$, where x+y = 3. Thus, if y = 1, then the formula is $C_6H_9O_7N$ and N content is 6.75 mass%; if y = 2, then the composition is $C_6H_8O_8N_2$ and the N content = 11.11 mass%; while if y = 3, then the formula is $C_6H_7O_{11}N_3$ and the N content is 14.14%. Although maximum nitration corresponding to y = 3 is not practically achievable, nitrocelluloses with the highest practical amounts of nitrogen (13 – 13.5%) are called *guncotton*. The commercial form of the product can be fibers, films, or powders. The end use applications include explosives, Celluloid, lacquers, inks, adhesives, and nail polish. A variety of 'double-base' explosives are prepared by combining nitrocellulose with nitroglycerin. Single-base explosives which do not use nitroglycerin are also made. Celluloid contains 10.5 to 12.2% nitrogen (typ., 11%), material going into lacquers and other coating products 11 – 12%, while material for explosives manufacture ranges from 11.8% to 13.5%. The term *nitrocellulose* is chemically misleading, since the nitrogen-containing groups are nitrate (ONO_2), not nitro (NO_2).

Celluloid, a thermoplastic material, was invented in 1862 and comprises cellulose nitrate, camphor and castor oil, prepared with alcohol solvent. The camphor (typ. 25 – 30%) acts as a gelatinizer and larger amounts increase the flexibility of the product. Castor oil also increases the flexibility of the product, but its softener action is because it is miscible with nitrocellulose, rather than being due to a direct chemical reaction. Celluloid film was the first flexible, transparent material successfully commercialized for use as photographic and movie film. A nitrocellulose 'leathercloth' was another early consumer product used as automobile seat upholstery and in other applications. It is a cotton cloth treated with nitrocellulose, which imparts it an impervious film coating. *Pyroxylin* is a term sometimes used for commercial nitrocellulose-based products.

When cellulose nitrate is detonated, the products are primarily CO_2, CO, H_2O, N_2, and solid C. Nitrocellulose is subject to a slow, spontaneous decomposition, and the products of decomposition are quite different from those of detonation. The decomposition process, sometimes referred to as *denitration*, involves the oxidization of unreacted cellulose by the nitrate group, producing nitrogen oxides which have an autocatalytic effect[225]. It is thought that decomposition begins by cleavage of the O–NO_2 bond, with subsequent interaction occurring between the liberated NO_2 and the bulk material. The decomposition products include nitrogen dioxide (NO_2), nitric acid (HNO_3), and nitrous acid (HNO_2). The nitrogen dioxide which is initially formed then continues to react, undergoing secondary reactions with both the solid material and its decomposition products. The exact mechanism of autocatalysis is not clear. Since the nitrate groups have a destabilizing effect on each other, nitrocellulose compositions with a higher percent of nitrogen are less stable than ones which have a lower nitration level. Some of the decomposition is attributed to hydrolysis, caused by residual sulfuric acid which cannot be fully removed by boiling the nitrocellulose during its manufacture. The gaseous products of thermal decomposition primarily comprise NO, NO_2, and N_2O_4. A reddish-brown color seen in decomposition gases is due to NO_2; NO, N_2O_4 (and N_2O) are colorless. In studying milligram-size samples of nitrocellulose exposed to slow heating[226], it was found that rapid burning or detonation was preceded by liquefaction, which begins slightly above 180ºC. Thus, any visible liquefaction should be taken as a sign of onset of instability. The addition of camphor (as in Celluloid) increases the thermal stability of the product. Decomposition of cellulose nitrate does not require oxygen, thus excluding oxygen is not a viable safety measure. The presence of moisture accelerates the decomposition[227].

Cellulose nitrate is subject to photochemical decomposition by ultraviolet radiation. Stabilizers, e.g., sodium carbonate, can be added to nitrocellulose products to reduce the tendency to decomposition. Cellulose nitrate films have ignited when exposed to direct sunlight, and a Celluloid comb was reported to ignite in a lady's hair[242]. A shoemaker's material called "toe puffs," comprised of cotton or wool cloth impregnated with cellulose nitrate, solvent, rosin, and dye, is associated with a significant danger of spontaneous combustion. Several disastrous fires on ships carrying this material have been described[228]. Gamble[229] provided an extensive listing of fires attributed to ignition of Celluloid.

The cellulose nitrate contained in smokeless powder explosives was traditionally treated with about 1% diphenylamine as a stabilizer[230], later, diethyldiphenylurea also came into use. Stabilizers work in a sacrificial manner, by reacting with the NO_2 that is liberated and forming various nitro- and nitroso derivatives. The stability of cellulose nitrate was in recent years found to depend on the position in the carbon ring which is esterified, with the C_6 position being fully stable, the C_3 intermediate, and the C_2 highly unstable[231]. Since moisture promotes decomposition of smokeless powder, careful drying of the product is necessary.

It is considered[943] that decomposition and instability of cellulose nitrate can first be detected at around 100ºC. A number of empirical tests have been developed specifically for testing the stability of cellulose nitrate materials[225]. At 50ºC, the rate of decomposition is about 4.5×10^{-6} % h^{-1}, and this increases by about 3.5 times for each 10ºC rise in temperature[232]. Gross and Robertson[109] made some of the earliest studies to determine the self-heating data for nitrocellulose. Their results are shown in Table 17, along with later, mostly Russian, determinations. The Gross study has been criticized for being performed in an open-vessel arrangement, so that reaction products could escape. Since it is known that autocatalytic effects exist, this arrangement under-represents the heating that may actually occur if the products are not freely vented[233]. Russian research[234] has indicated that the actual decomposition proceeds as two

parallel reactions, a first-order reaction and an autocatalytic reaction. They concluded, however, that for practical purposes, a zeroth order representation does not lead to large numerical errors, provided that the fraction of substance reacted is not large. Fifer[235] and Brill[236] provided more extensive reviews of the literature and discuss the proposed kinetic mechanisms in some detail. Brill pointed out that data in the range 100 – 200ºC show two parallel reactions, and that widely scattered E and A measurements can be reconciled by plotting ln(A) as a function of E. Two different, straight lines emerge, depending on whether autocatalysis or first-order reaction dominated in the particular experiment.

The sensitivity of various cellulose nitrate products depends highly on chemical and physical details and general guidelines are not possible. Nitrocellulose propellant powder, even if stabilized and in good condition, can be highly sensitive to detonation from electrostatic sparks, as was determined after an explosion in the Netherlands[237]. The ignition of cellulose nitrate from impact by heated small particles was studied by Grossmann and Rele[238]. They concluded that, for particles of 5 mm diameter, ignition will occur even at negligible kinetic energy, if the particle temperature exceeds 300ºC. Conversely, even unheated particles will cause ignition at velocities over 150 m s^{-1}. The radiant ignition of thin (10 μm) films of cellulose nitrate (12.5% N content) was studied by Lenchitz et al.[239] They found that an energy fluence of 14.6 kJ m^{-2} was needed for ignition of film that had its surface blackened. Clear films required about 5× greater energy fluence than did blackened ones. The computed T_{ig} was 270±10ºC. For other thicknesses, the energy fluence required for ignition was related to film thickness as:

$$E'' \propto d^n$$

where d = thickness and $n \approx 0.72$. In addition, they concluded that films thicker than about 20 μm could not be analyzed as thermally thin, since a substantial temperature gradient started to be present. Their study also demonstrated that radiant ignition of cellulose nitrate is a pure-decomposition event which does not require oxygen from the atmosphere—comparative tests run in an N_2 atmosphere yielded essentially identical results.

Numerous fires with X-ray film occurred in the early decades of the 20th century. These have typically involved ignitions from incandescent lamps or from steam pipes. If not extinguished very early, the fires typically lead to forceful explosions. The most systematic investigation of the ignitability of cellulose nitrate film occurred in the aftermath of a fire at the Cleveland Hospital Clinic in 1929[242] which claimed 125 lives. The base stock for the X-ray films of the era comprised cellulose nitrate with 12% nitrogen content, 9% camphor, and a small amount of solvents. The coating on the base stock was gelatin, amounting to 12% of the total weight. The stability of cellulose nitrate film stock is considered intermediate between Celluloid grades and explosives grades. This is attributed to the intermediate level of camphor, typically 9% and much lower than found in Celluloid materials. The camphor component has a tendency to vaporize away in prolonged storage; this, along with the autocatalytic nature of the decomposition, makes aged film more hazardous.

Experimental work in connection with the above investigation involved examining small, 1 g amounts of films in a constant-temperature oven. During a 24 h exposure, no decomposition was seen at 100ºC. For exposure at 120ºC, rapid decomposition occurred at about 12 h. For exposure at 140ºC, rapid decomposition occurred at 5 min and flaming at 15 min. Using 500 g samples at 100ºC, decomposition started at 40 min; at 120ºC, it started at 7 min. However, at 80ºC, a 500 g sample remained undecomposed for 24 h. All experiments, even ones where decomposition was not seen, indicated that the material readily lost 2 – 3% of the mass; this is probably largely solvents, but also some camphor.

Another series of experiments was done exposing film to direct contact with frosted 100 W lamps. Naked film ignited in 310 s. When the film was enclosed in paper envelopes a longer ignition time of 420 s was seen. A wire lamp guard holding the lamp about 8 mm away from the films proved to be of no value in forestalling ignition. Further studies examined the milder exposure of film placed in paper envelopes and exposed only edge-on to the lamps. In these tests, 100 W lamps also caused ignition, and even 60 W lamps were able to start significant decomposition. Companion tests with cellulose acetate safety films showed no ignitions.

The value of 149ºC has been cited as the ignition temperature for nitrate film[250]; the same reference cites data that fresh nitrate film exposed in air at 163ºC ignite in 80 s; at 204ºC in 10 s; and at 260ºC in 3 s. But other studies showed lower values. In experiments on steam pipe contact with cellulose nitrate films in connection with the Cleveland

Table 17 The self-heating chemical kinetic properties of cellulose nitrate

Test method	Temp. range (ºC)	E (kJ mol^{-1})	QA (W kg^{-1})
oven heating in glass tube (Taliani test)[240]	90 – 140	128	NA
radiative ignition[234]	233 – 286	174	2.0×10^{23}
radiative ignition[234]	227 – 268	211	3.2×10^{27}
convective ignition[234]	210 – 250	187	2.1×10^{25}
convective ignition[234]	210 – 220	201	1.5×10^{25}
conduction ignition[234]	211 – 241	185	2.5×10^{24}
conduction ignition[234]	185 – 225	200	9.6×10^{25}
self heating[234]	225 – 255	209	2.1×10^{26}
self heating[241]	--	204	2.0×10^{25}
heat pulse calorimeter[234]	205 – 295	176	6.7×10^{22}
isothermal calorimeter[234]	140 – 165	197	3.1×10^{25}
adiabatic calorimeter[234]	135 – 170	176	1.2×10^{23}

disaster, when temperatures on the outside of the pipe were ca. 145ºC, ignition generally took place in 15 – 30 min, depending on details of the arrangement. For temperatures of ca. 155ºC, ignition took place in 2 min. NBS[243] ran tests on tiny (2 – 5 g) samples and found that, if stored at 135ºC, ignition typically took place in around 2 h. Slightly larger (5 – 10 g) specimens stored at 110ºC typically lost about 25% of their mass in 8 days, but did not ignite. Using large 300 g samples subjected to 100ºC, explosions occurred in about 8.5 h. A Japanese study[244] found an AIT of 167ºC when testing 1 g quantities in a test tube.

The high hazard of cellulose nitrate products, however, comes not from rapid ignition when exposed to high sources of external heat. Rather, the problem is due to the unstable nature of the material and its innate self-heating propensity. Even storage in film vaults under common summertime conditions of 38ºC is believed to have been the cause of nitrate film fires[250]. A study by NBS[245] identified the crucial role of deterioration in determining the self-heating propensity of nitrate films. In their tests, film cans were wrapped with thermal insulation and stored at elevated ambient temperatures of 41 – 49ºC. Films which were visibly deteriorated prior to testing went to thermal runaway, but non-deteriorated films did not.

Some large-scale burning experiments have been reported on cellulose nitrate packed in steel or in cardboard drums[246]. The measurements include emissive power and radiant fraction, and are intended to enable estimations of ignitions of targets from a burning stack of packaged nitrocellulose. Ryan et al.[247] reported results of large-scale fire tests on nitrocellulose storage vaults, but this study did not examine ignition aspects.

In addition to the Cleveland disaster, photographic, radiographic (X-ray), and movie 'nitrate' film has been responsible for other catastrophic fires, but in this use it has been replaced by 'safety film' (generally based on cellulose acetate) for the last half-century. However, stocks of old nitrocellulose films may still exist in archives. Because of the inevitable degradation, cold storage warehouses are used for safety and for preservation. A violent explosion occurred when a pipe containing cellulose nitrate residues was being cut by a hacksaw[248].

Water is often ineffective in extinguishing burning cellulose nitrate, since the material is self-oxidizing and does need access to air; large amounts of water, however, can cool the reaction down. NFPA 40E[249] is a standard describing requirements for warehouses and facilities storing nitrocellulose materials, except those used as motion picture film or in lacquer manufacturing. NFPA 40[250] treats nitrocellulose motion picture film. It is especially intended that film be regularly examined for signs of decomposition (discoloration, blistering, tackiness) and destroyed or segregated if such are found. This is an essential precaution due to the catalytic effect of the decomposition products upon further degradation. NFPA 35[251] describes the safety precautions to be used in the lacquer industry.

Charcoal, coke, and related products

CHARCOAL

Charcoal is produced by the destructive distillation of carbonaceous material. The most common source of carbonaceous material is hardwood. The composition of charcoal depends strongly on the temperature of carbonization (the temperature at which it was produced)[252], as shown in Figure 18. For temperatures exceeding 900ºC, the carbon content exceeds 95%, but commercial charcoal is normally not carbonized at such high temperatures. In general, charcoal made by the traditional process of pit-burning is carbonized at a higher temperature than is charcoal produced in a wood distillation plant, using retorts or ovens. In the absence of measured data, it is often estimated that the mass percent carbon is about 67 – 80%; hydrogen 2 – 3.5%; oxygen 13 – 17%, nitrogen 0.2 – 0.6%, sulfur 0 – 0.04%; and ash 3 – 13%. For many purposes, it is adequate to express it as having a simplified formula of $C_{16}H_{10}O_2$. The gross heat of combustion is 25 – 31 MJ kg^{-1}. Charcoal is largely amorphous, but contains a small amount of ordered, graphitic crystallinity.

In 1816 Sir Davy[253] reported that charcoal heated to the "strongest red heat" would not ignite a methane/air mixture. This is not surprising, since his "strongest red heat" was surely less than the minimum 1000 – 1200ºC which later investigators found a hot object must be heated to in order to ignite methane/air mixtures.

Using a convective heating apparatus, Hill[254] measured the ignition temperature of charcoal to be 403 – 408ºC. Fons[255]

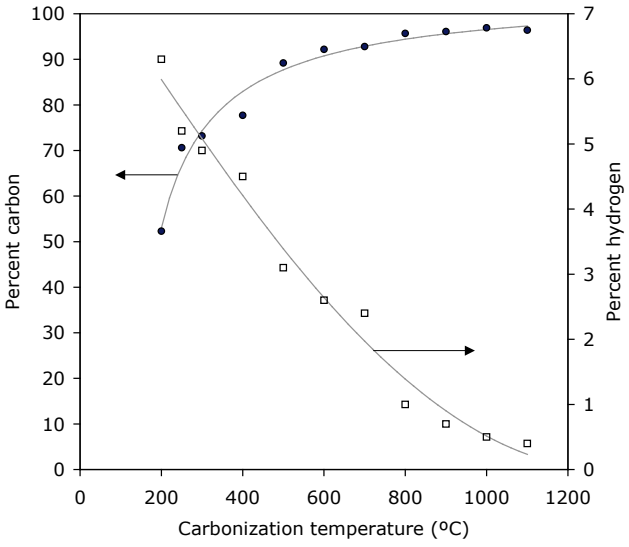


Figure 18 Effect of carbonization temperature on composition of charcoal

reported that 232ºC is the minimum temperature to which charcoal must be raised for glowing ignition to occur, but the experimental basis for his conclusion is unclear. Furthermore, such data would not be of much value, since studies have shown that the ignition temperature of charcoal is strongly dependent on its carbonization temperature. Violette's test results of 1848, as given by Urbański[256], are shown in Table 18. Burgoyne and Richardson[257] performed ignition tests on charcoal in oxygen, not air, and obtained the results in Table 19. Bergström[258,259] also found a dependence on the carbonization temperature, but in his case, lowest ignition temperatures were found for charcoal carbonized at 425ºC, with higher or lower carbonization temperatures both serving to raise the ignition temperature. His lowest reported autoignition temperature was 100ºC, with charcoals carbonized at other temperatures igniting at 110 – 140ºC. These are very low values and are presumably because the material was tested in a finely-ground state. His apparatus was a vertical test tube inserted in a constant-temperature bath, with air being pumped through the test tube. Bergström's data are rather hard to interpret, but Violette's and Burgoyne's results both imply a clear increase of AIT with increasing carbon content of the material. A similar dependence of AIT on carbon content was also found for another carbonaceous material, coal, and those results are given in Chapter 8.

Table 18 Ignition temperatures of charcoal, as reported by Violette

Temp. of carbonization (ºC)	Color of charcoal	Ignition temp. (ºC)
260 – 280	brown	340 – 360
290 – 350	brown	360 – 370
432	black	400
1000 – 1500	black	600 – 800

Table 19 Ignition temperatures of charcoal when ignited in oxygen, as determined by Burgoyne and Richardson

Temp. of carbonization (ºC)	Ignition temp. (ºC)
350	236
450	248
550	268

It has been claimed that the reason why charcoal carbonized at a higher temperature has a higher AIT value is because such charcoal has a lesser ability to adsorb oxygen[260]. However, no reliable experimental studies exist on this point. The heat of adsorption of oxygen onto charcoal was studied to a limited extent by Blench and Garner[261], who showed that it varied with temperature and with the fraction of surface sites already occupied by oxygen. One set of results showed the value rising from 218 J mol^{-1} at 18ºC to 937 J mol^{-1} at 450ºC.

Lumps of charcoal can be highly susceptible to spontaneous combustion, as indicated by this incident[262] described by 19th century Harvard University professor Charles T. Jackson: "While at work in my laboratory, I had occasion to use a piece of charcoal for blow-pipe experiments. I went down to my cellar and brought up a piece of light, fine, round charcoal, suited for that purpose. It was damp. I laid it on the top of a column stove to dry, directly beside a tin pan containing water which was not boiling, and never did boil there. I took the charcoal off the stove and laid it on my table. A short time afterward, I discovered that it was on fire through the piece. I laid it aside, and it burned entirely to ashes. The theory of the ignition of the charcoal under these circumstances struck me at once. Charcoal has wonderful porosity: it has the power of analyzing air, and adsorbing oxygen with comparatively little of its nitrogen. The pores of the charcoal were previously filled with moisture. Drying expelled this moisture. The oxygen of the air was condensed in the charcoal, taking the place of the moisture. The condensation of the oxygen produced enough heat to ignite the charcoal. I repeated this experiment again intentionally, watching it carefully, and with the same result." This incident is especially interesting, since Jackson demonstrated the repeatability of spontaneous combustion at a sub-100ºC external temperature. A moisture effect was again found by Bixel and Moore[263], who reported that in their tests dry charcoal ignited at 216ºC, but moist charcoal at 159ºC. Lucas[449] mentioned an incident of spontaneous combustion of small pieces of freshly-made charcoal, but gave no details.

In 1913, Rosenhain and Gemmell[264] conducted an experiment where they filled a cubical basket (0.35 m on a side, made of perforated brass) with flake charcoal and placed it in an oven. If air supply was restricted to the oven, only modest self-heating was found, but for a larger air supply (but still limited) they found that if the oven temperature was set at 96ºC or higher, spontaneous combustion took place. They then repeated the experiments using air containing 5% SO_2 (used as a fumigating agent on ships). In that case, they found that spontaneous combustion would take place without heating the oven, starting from a room temperature of 16ºC.

Laupper[265] reported in 1926 on sketchily-described experiments where he showed that small amounts of iron strongly catalyze the self-heating of charcoal. He also documented[266] that explosions occur when liquid oxygen is introduced into iron-contaminated charcoal, but do not occur if the charcoal is iron-free. In 1943, Blayden et al.[267] provided quantitative data to demonstrate that quite a few, primarily inorganic compounds (e.g., sodium, potassium or lead carbonate; lead or sodium acetate; vanadium pentoxide, etc.) act as catalysts and reduce the ignition temperature of charcoal by 100 to 230ºC.

Ground charcoal can act similarly to textile fibers in providing a large surface area for oxidation to take place on. Thus,

self-heating fires have been found due to cod-liver oil applied to granulated charcoal[268].

CHARCOAL BRIQUETTES

Commercial charcoal briquettes are comprised of ground charcoal which is combined with a starch paste. The commercial product may also contain additives such as sawdust, coal, limestone, sodium nitrate, and borax[269] to improve the physical characteristics and to achieve a more uniform combustion. Although this has not been studied formally, it is reasonable to assume that these commercial products ignite and burn rather similarly to pure charcoal. Some thermocouple data on commercial briquettes burning meat in a barbecue show peak temperatures of 410 to 470ºC, but with an average temperature around 380ºC during the first 2 to 3 hours of active combustion[269]. Results from seven tests indicated that temperatures dropped to 100ºC in 8 – 13 h after ignition and ashes had returned to room temperature in all cases by 15 h. In another series of tests[270], charcoal briquettes were tested two ways—(1) piled as a pyramid of 2.3 kg (5 lb) on the grill and not disturbed; and (2) spread around the grill after the initial combustion period. When burned untouched, a peak temperature of 1075ºC was recorded and combustion lasted over 26 h, although it is not clear what criterion was used to declare end of test. When spread around, a peak temperature of 600ºC was found with the lid open and 425ºC with the lid and ventilation holes shut. In that case, combustion lasted only 12 – 15 h. The author conducted additional tests demonstrating that slightly burned and extinguished briquettes could cool down to ambient temperature on the exterior, but retain enough heat inside to erupt in fire when placed in a bed of cold ashes at a windy outdoors location. The outcome of this experiment was consistent with situations where a fire is caused by a person attempting to re-use partly burned briquettes by dousing them with water and packing them back in the original bags when they appeared to be cold[271]. See also: *Ashes*.

Wolters et al.[275] conducted oven-basket tests and analyzed the results according self-heating theory to quantify the self-heating behavior of briquettes. Extrapolating from the laboratory results, they concluded that the largest common bag size, 9 kg (20 lb), would require a minimum ambient temperature of 121ºC for critical conditions to occur. At normal room temperature, the amount of briquettes required to reach thermal runaway was computed to be 800,000 kg. For their tested specimens, if the first-order theory encompassed by the testing and analysis is appropriate, then spontaneous combustion cannot occur from one or even a modest collection of 9 kg bags. The authors also examined the effect of high moisture by conditioning some specimens at 32ºC and 85% RH. The critical temperature for those specimens increased about 3ºC over the controls. Advice has occasionally been published that wetting and drying charcoal will lead to spontaneous combustion. To examine this point, the same authors, in another series of experiments[272], took briquettes originally at 4.5% moisture, watered them to reach 30% moisture, then dried them for 4 days until the moisture dropped again to 4.5%. The moisture-cycled specimens showed a critical temperature about 5ºC lower than the controls. This value was just barely statistically significant in the experiments conducted. Aging the briquettes[275] for one year (under unspecified conditions) raised the critical temperature by about 10ºC. Compared to normal production, lignite-based charcoal showed higher critical temperatures.

Despite oven-basket test results which suggest that enormous piles would be needed for spontaneous combustion to occur, fire incidents[273,274] continue to be attributed the self-heating of consumer-size bags of charcoal briquettes. In some cases, it could be that investigations were sloppy and other ignition sources (e.g., discarded cigarettes or ashes) were involved. But if the investigation was done properly, the cause can be attributed to contamination. The section on *Paper* in this Chapter describes a well-documented case where a roll of sealed paper towels was found smoldering on a storeroom shelf. In this Federal laboratory incident, the investigating scientists concluded that the product became contaminated either during manufacture or during packaging. A similar effect may be involved with charcoal briquettes.

Methods to prevent easy access of oxygen to the substance, such as polyethylene bags, were found to be useful to eliminate self-heating ignitions of charcoal[280]. This was confirmed by Wolters et al.[275] for charcoal briquettes. Interestingly, Wolters found that Kraft paper bags lowered the critical temperature. They explained that a Kraft paper bag allows oxygen transfer but inhibits convective cooling of the charcoal.

A very different commodity are 'self-lighting' briquettes which contain a solvent (around 10%) for easy ignition by the user. Tests indicated[275] that not only did the solvent not lower the critical temperature, but slightly raised it. Easier-to-ignite charcoal briquettes may also include paraffin wax, but its role has not been explored.

COKE

Coke is produced by carbonizing coal much in the same manner that charcoal is produced by carbonizing wood. Its self-heating properties can be expected to be broadly similar to those of charcoal, but few self-heating studies are available on coke. Shea and Hsu[276] conducted an interesting study using a 'semi-adiabatic' furnace where they examined the effect of atmosphere composition by passing various gases through the Dewar in which the sample was located. From an initial oven temperature of 66ºC, samples subjected to dry oxygen only showed a rise of 1.5ºC; samples subjected to oxygen which was saturated with water vapor showed a 25ºC rise; while samples subjected to water-vapor-saturated nitrogen or CO_2 showed a rise of 17ºC.

This indicates an extremely large effect of moisture on the self-heating process. In comparing various coke types, they found the highest self-heating propensity with semi-calcined coke; green coke showed a much smaller effect, while calcined* coke nearly nil. Coal itself showed a tendency somewhere between the green and the semi-calcined coke. Activated carbon was roughly similar to semi-calcined coke, while lignite showed the highest self-heating tendency of any substance tested.

ACTIVATED CHARCOAL

Activated charcoal denotes charcoal which has a highly porous structure, and is typically used as filtering and adsorption media. Once produced, charcoal can be activated by use of steam, in a reaction ('water-gas shift') where steam at 900 –1000ºC converts some of the carbon to CO according to:

$$C + H_2O \rightarrow CO + H_2$$

and thereby opens up the pore structure. Or, it can be activated by chemical activation, using phosphoric acid or zinc chloride to swell the wood and open the capillary structure. The substances created are not identical. The oxygen content of steam activated charcoal is less than 2%, while the oxygen content of chemically activated charcoal can exceed 10%. Typical activated charcoal[277] may have a bulk density of 370 kg m^{-3} and an internal surface area of 10^6 m^2 kg^{-1}.

'Weathering' is known to affect the thermal stability of all types of charcoal. It is simply storage of the material in small piles in a place where it can acclimate to the ambient moisture. Typically, about 8 days are allowed for this process. During this time, moisture is adsorbed onto the freshly made charcoal†. For a very long time it has been known that this procedure reduces the later risk of self-heating in shipping or in storage of large quantities. Since adsorption is exothermic, a limited amount of self-heating takes place during the weathering procedure. But since weathered charcoal has already undergone the low-temperature self-heating due to sorption of moisture, if it has been cooled down to ambient temperature after this weathering, the remaining hazard is only from oxidative reactions, and not compounded by water sorption exothermicity. Bags holding 25 kg of activated charcoal sustain a temperature rise of about 37ºC during the peak of this process[277].

Bowes and Cameron studied the problem of self-heating in activated charcoal from the point of view of hazards in ship transportation[277]. They conducted standard oven-test experiments on cubical specimens ranging from 25 to 610 mm and found an activation energy E of 97.4 kJ mol^{-1}. They also obtained some self-heating data on specimens which had first been weathered. Weathering for 7 days at 40ºC was found not to affect the critical temperature. Of course, it would not be expected to, since the oven tests are run at typically > 100ºC and the environmental process of moisture flow into a dry specimen is not replicated in such tests‡. They also conducted accelerated weathering experiments at a temperature of 100ºC. These thermally-treated specimens were found to be more resistant to self-heating than the fresh ones, but it would appear that such high-temperature treatment would also alter the chemical nature of the substance. The authors also undertook to compare the laboratory self-heating results to ship-fire incidents involving several tons of material. Based on approximate values of storage sizes and temperatures, they concluded that reasonable agreement exists.

Modern tests based on self-heating theory provide some additional support for the type of data presented by Violette, discussed above. Over the range 410 – 520ºC, the critical temperature in oven-basket tests using 25 mm cubes rose linearly with the carbonization temperature[277].

At one time, it was hypothesized that activated charcoal can act as a catalyst for the heterogeneous oxidation of some organic compounds. Boden et al.[278] conducted experiments using ethanol and benzene on activated charcoal and demonstrated that such catalysis does not occur and, therefore, that it could not be a contributing factor to the self-heating of activated charcoal. Even in the presence of organic solvents, the self-heating was found to occur due to direct oxidation of carbon. Once this self-heating was occurring, however, the elevated temperatures were able to cause some homogeneous oxidation of the solvents' vapor. Another heating mechanism that can also take place in solvent-soaked beds. The heat of adsorption of ethanol onto carbon is much smaller than that of oxygen. Thus, if oxygen is passed over an ethanol-soaked carbon bed, the displacement of ethanol from the carbon surface will be an exothermic process and contribute to the heating. It was also found that when air is passed over an activated charcoal bed which is at 250ºC, there is no measurable amount of CO being produced, only CO_2. Fires in activated charcoal scrubbers are not uncommon[279] and are ascribed to the exothermic heat of adsorption.

Cameron and MacDowall[280] studied 10 charcoals produced by widely differing processes and conditions. For all except the three minimally-hazardous products, the slopes of the lines in the oven-cube test plots were identical, giving $E \approx$ 97.0 kJ mol^{-1}. The values of P ranged from 49.5 for the most self-heating-prone, to 42.0 for the least. These results implied that a single-size oven cube test (but hopefully with at least some replicates!) would be sufficient to classify the self-heating behavior of charcoal. Another important find-

* Calcined coke is produced by heating green coke to about 1300ºC until the remaining material is over 99% pure carbon.

† It is likely that certain chemical reactions (e.g., oxidation at some surface sites) also occur during the weathering process, but this has not been explored in detail.

‡ The weathered material entered the oven bearing moisture which the originally-dry samples did not. But this moisture was largely (endothermically) eliminated prior to the start of the main self-heating process, which does not begin for a 25 mm cube until ca. 143 C.

ing of this study was the performance of the two charcoal specimens which were unfinished products, not yet activated. Neither specimen was outside of the range of the results of the activated products: one of the specimens was about mid-scale in the test results, while the other one was the second-worst performer. This would imply that the massive increase in internal surface area occurring when the material is activated is not the dominant factor which governs the self-heating performance.

For ship transportation, the maximum expected temperature may be ca. 40ºC with a size of 3 m cube. Thus, Cameron and MacDowall suggested that a critical temperature ≈50ºC for a 3 m cube would be an adequate criterion of safety. A laboratory oven-cube test may conveniently be carried out in a size of 0.1 m. Since

$$\delta \propto \frac{r^2}{T_a^2} \exp\left(-\frac{E}{RT_a}\right)$$

with E = 99.0 kJ mol^{-1}, T_a = 323 K, and r = 1.5 m, the value of δ will the same if r = 0.05 m and T_a = 413 K (140ºC); it is not clear why the authors took E = 99.0 instead of 97.0, which represents their published data plot better. Thus, Cameron and MacDowall concluded that a satisfactory test would comprise a 100 mm cube tested at 140ºC. In their tests with 100 mm oven-cube samples they noted that the time to either a peak temperature or thermal runaway was always less than 7 h; on this basis they concluded that a prudent test time would be 12 h.

Cameron and McDowall concluded that the oxygen content of the original material is the dominant factor. The specimens which were chemically activated and had a high oxygen content were the worst performers, while the low-oxygen content steam-activated ones were the best.

The finding that all charcoals have the same E value was rather unexpected and proved not to be reproducible. Jones[281] studied 11 different activated charcoals and found that the values of E ranged from 88 to 110 kJ mol^{-1}, while the zeroth-order pre-exponential constant A varied between 2×10^5 and 2×10^9 s^{-1}. Jones recommends using a value of Q = 25 MJ kg^{-1} for all charcoal types. He also determined that critical temperatures for 100 mm cubes were 110 – 115ºC for the chemically-activated specimens and 250 – 260ºC for the steam-activated ones. Bowes[445] proposed that λ = 0.055 W m^{-1} K^{-1} is a suitable value for thermal conductivity to be used for activated charcoal, but Jones[282] argued, through some indirect findings, that the actual values are typically 0.15 – 0.27 W m^{-1} K^{-1}.

ACTIVATED CARBON

Activated carbon is a substance which is basically similar to activated charcoal, but is generally considered of higher purity, i.e., the components other than carbon are minor. Its uses are also primarily as filtering and adsorption media. Activated carbon (or finely divided forms of carbon) is an unusually active fuel which possesses adsorptive and catalytic properties to accelerate combustion reactions with virtually any oxidant. Ignition may occur upon intimate contact with oxygen, oxides, peroxides, oxosalts, halogens, interhalogens and other oxidizing species[3].

The autoignition temperature for the ignition of packed beds of activated carbon was studied by Bigg and Street[283] in an environment where hot gas at a specified temperature flowed upwards through the bed. Using 2 mm diameter particles with a large surface area of 8.8×10^8 m^2 kg^{-1}, they found a mild dependence of T_{ig} on the velocity. The lowest temperature, 295ºC, was found for a velocity of 0.1 m s^{-1}. For high velocities, the AIT reached an asymptote of 320ºC. For velocities lower than 0.1 m s^{-1}, there was an inversely relation of AIT on velocity, with a temperature of 370ºC found for near-zero velocity. The authors also developed a complex predictive model, based on Elovich kinetics, that showed good agreement, but required a fully numerical solution. Hardman et al.[284] also found an ignition temperature of 370ºC at zero velocity, but in their experiments the AIT rose monotonically with increase in air flow.

ASTM provides a test method, ASTM D 3466[285], for testing the ignition temperature of activated carbon under conditions where a steady stream of heated air is pumped through a bed of the activated carbon. This is intended to simulate adventitious ignitions in nuclear power plant filtration operations, not to identify storage hazards. The interest in use of the test method is because the activated carbon beds will contain high concentrations of impurities, and it is desired to characterize the ignition hazard of an actual bed containing impurities—the performance of pure activated carbon is not relevant to these applications. Use of the method has been described by Freeman et al.[286] Suzin et al.[287] studied three types of activated carbon and 3 additional types that were impregnated with metals. For the 'pure' carbons, they found AIT values of 365ºC for one type and "over 370ºC" for the other two. The impregnated types ignited at 365 – 300ºC. Using thermal analysis, they also determined temperatures where exothermicity was first detectable to be about 100 – 150ºC lower than the corresponding AIT values. The specific surface area, which spanned 10^3 – 10^6 m^2 kg^{-1}, did not affect the AIT, although the smaller granule size led to lower AIT values; the sizes ranged from 1.5 to 12 mm. Apart from the uses in the nuclear industry, activated carbon beds are also used in semiconductor manufacturing facilities as scrubbing media for oxidizing gases. In self-heating tests using the Accelerating Rate Calorimeter[288], it was found that activated carbon that had adsorbed NO_2 showed rapid exothermic activity at ca. 30ºC; by contrast, pure activated carbon showed exothermic activity starting at 105ºC.

Nelson[1597] conducted oven-cube tests on powdered activated carbon and obtained the following results over the range

50 – 190ºC: E = 83.2 kJ mol^{-1}, P = 42, λ = 0.16 W m^{-1} K^{-1}, C_p = 1.07 – 1.27 kJ kg^{-1} K^{-1}.

Chimneys and flues*

A large number of fires originate in chimneys, or are initiated by the heat of a chimney or flue pipe[289]. Two main modes of ignition are found:

- A chimney fire occurs because unburned and partially burned material builds up to sufficient depth on the walls that it can eventually be ignited. A chimney fire may (a) directly ignite nearby external combustibles; (b) release flaming material from the top of the chimney, which then falls upon and ignites a combustible roof; or (c) the chimney material may crack or warp due to the fire, so that subsequently a hole opens up and enclosing materials may become endangered.
- A single-layer metal flue pipe radiates at a high temperature if a hot fire is created in the heating appliance. If combustibles are inadequately separated or protected, they may become ignited. The NFPA Handbook[290] and NFPA 211[291] provide guidance on necessary clearances. To allow closer spacing of combustibles, flue pipes can be used that have 2 or 3 concentric metal layers, or else have two metal layers with thermal insulation filling the annulus. Fires involving multi-wall flue pipes typically occur when an improper installation creates a gap between two successive pipe sections.

There have been several experimental and theoretical studies[292- 296] on heat transfer from flue pipes, and advice on clearances to be used is derived from these studies. A 1963 report by Shoub surveyed much of the early literature[297]. In 1985, NIST conducted unpublished tests on factory-built insulated chimneys used with wood stoves and coal stoves[298]. Tests were run for roughly 1 – 2 months, with firing being done to simulate a normal winter-time cycle of usage. No chimney fires occurred with coal stoves, but creosote buildup in the wood stove led to a chimney fire which buckled the metal and caused gaps to open up. The study disproved the sometimes-given advice that creosote can be adequately removed "by having a little fire in the chimney once in a while." With a wood stove, flue gas temperatures were typically in the range of 170 – 250ºC, but under some conditions (excluding an active chimney fire) reached as high as 860ºC. By contrast, the highest flue gas temperature obtained in coal-burning tests was only around 380ºC.

Some triple-wall flue pipes are designed on a *thermal siphon* principle. In that type of design, the innermost space is used for the flow of combustion gases. The space between the inner and the middle tube may be filled with a non-combustible insulation, while the space between the middle and the outer tube acts as the thermal siphon. The principle involved is that if this flow path is open at the bottom and properly discharged at the top, room air gets entrained into it and the flow of this air helps keep both the fuel pipe and the heating appliance cooled. With this type of flue pipe, there is lessened danger of ignition from combustibles contacting the outer surface. However, a failure mode exists that is unique to this system. If the installation is improper, and the flow path in the outer annulus is blocked, then overheating of both the appliance and the flue pipe may be encountered. To mitigate these hazards, every installation must be in accordance with the manufacturer's listing and installation instructions. Some appliances are acceptable only when installed with a thermal siphon flue pipe, and any substitution may result in a fire. In a more general context, this *caveat* is very important with any fuel-burning appliances. Many appliances cannot pass safe-temperature requirements contained in UL and similar standards unless a very specific flue pipe installation is made exactly according to instructions.

Fires are sometimes encountered due to a non-obvious hazard created in a situation where a flue pipe was installed in a space that did not contain attic-floor or similar thermal insulation. If previously-empty space between the flue pipe and a nearby combustible member (floor joist, plywood, etc.) is subsequently filled with thermal insulation, the combustible member will become exposed to much higher temperatures than it would otherwise see. This situation is made clear by considering the geometry in Figure 19.

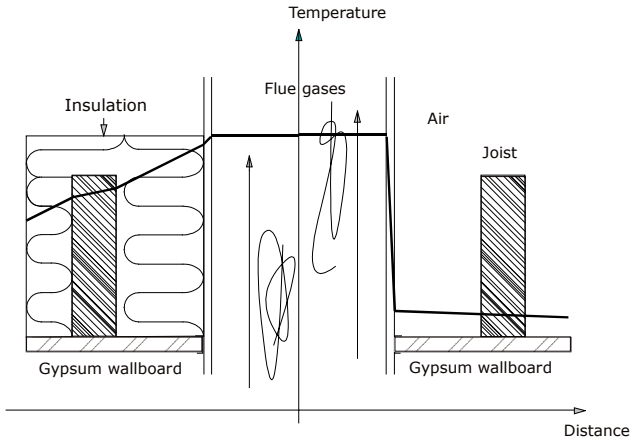


Figure 19 Effect of adding attic insulation on raising the temperature of joists near a flue pipe

Fires in older fireplaces that were site-built using firebricks often occur because there was not a sufficient thickness of brick separating the inside of the fireplace from wood framing members outside[299]. A course of bricks having a thickness around 100 mm is distinctly insufficient and NFPA 211 recommends 150 to 200 mm, depending on whether the fireplace is lined or unlined.

5-Chloro-1,2,3-thiadiazole

Yoshida[300] has reported that this chemical (C_2HClN_2S), an industrial intermediate, has caused two fatal explosions. Its special problem has been that thermal analysis and drop-

* Portions of this section were prepared by Michael M. Fitz.

weight testing failed to reveal the explosive tendencies. In fact, it readily ignites and explodes from friction or impact.

Christmas trees, artificial

The only US standard for testing artificial Christmas trees is UL 411[301]. This includes several tests intended for determining if branches can be directly ignited by faulty electrical lights or wiring, plus a full-scale fire test. It would take an exceptionally flammable plastic material to fail the test portions that simulate electric faults, but the full-scale fire test, on the other hand, is a reasonably tough test. In this test, 0.454 kg shredded newspaper is dispersed at the base of the tree in an 0.61 m circle and is ignited at 4 locations. Failure is declared if the specimen shows flames more than 0.91 m above the top of the tree, if later flame spread takes place in the tree, so that portions not directly over the ignition source catch fire, or if flaming molten drops continue flaming upon hitting the floor. This test simulates ignition from burning gift packages, decorations, or wrappings at the base of the tree. The test was withdrawn in 2002 due to non-use. Currently, artificial Christmas trees sold in the US are largely foreign-made, and these manufacturers have not been submitting products for UL listing, although some of them, in fact, can meet the UL 411 requirements.

Most artificial Christmas trees and properly moist natural ones will resist direct ignition from an electrical source. But ignitions from defective electrical lights or wiring do occur and these are understood to generally take place as a two-stage event. The initial electrical fault produces burning or hot material that drops onto combustibles under the tree. These combustibles, once ignited, then function much like the shredded newspaper source in the UL 411 test to ignite the tree itself. In general, a tree which would not ignite from flames applied onto branches can often ignite and burn vigorously when a burning object is placed underneath it.

Natural Christmas trees are covered under *Forest materials, vegetation, and hay*.

Cigarettes and cigars

Cigarettes are the most common form of ignition which occurs with upholstered furniture and beds; it is also a common source of ignition for a wide variety of other fires. A CPSC study[302] on residential fires initiated from cigarettes gave the results shown in Table 20. The products first ignited in cigarette fires were studied by NFPA[303], as shown in Table 21. The role of cigarettes as an ignition source has been reviewed by Holleyhead[304].

A commercial cigarette[305] typically weighs 0.6 – 1.1 g, is 7.8 to 8.1 mm in diameter, and has a length of 60 to 100 mm. In one series of tests[306] the burn times for 22 different cigarette packings were measured in the range of 11 – 18 min and, surprisingly, there was no relation to length of cigarette—the shortest cigarette (70 mm) burned longer than did any 100 mm cigarettes. In another study, however

Table 20 Materials first ignited in residential fires caused by cigarettes

Material first ignited	Percent
cotton, rayon, or cotton fabric or finished goods	54.3
man-made fabric or finished goods	13.7
untreated, uncoated paper	9.6
fabric, textile or fur, details unknown	3.7
sawn wood	3.2
polyurethane	1.6
tobacco	1.4
multiple items	1.4
PVC	1.2
plastic, unknown type	0.9
other (each less than 0.7%)	6.7
unknown material	2.3

Table 21 Product first ignited by cigarettes (data from 542 fires in 8 US cities during 1991-1992)

Product first ignited	Percent
mattress or bedding	45.4
upholstered furniture	25.4
trash	8.3
clothing	3.5
floor covering	2.5
papers	1.4
curtain or drapery	1.2
multiple items	1.2
structural element or framing	1.1
box or bag	1.1
other known products	7.8
unknown	1.1

burning times of 23 – 29 min were found for 100 mm cigarettes[307]; an extreme duration of 34 min has been reported[308]. The heat output of a cigarette that is not being actively puffed is 4 to 6 W. The autoignition temperature[1418] of tobacco subject to modest air flow velocities below 1 m s^{-1} has been found to be 210ºC. The peak gas temperature inside the cigarette is 800 – 850ºC, however values of 700 – 750ºC are more representative of larger portions of the combustion zone. When a cigarette is smoldering and is not being puffed, temperatures drop by about 100ºC[309]. The temperatures measured on the solids are higher than what is measured in the gas phase. For a puffed cigarette, temperatures of up to 850 – 950ºC are found on the solid 'coal'[309,310]. A temperature of 1110ºC has been reported at an unidentified measuring location[311]. By use of optical measurement techniques, extremely small zones of 1200ºC temperature have been found during puffing[312], the small size, however, makes it unlikely to be of importance in ignition problems. For a cigarette placed on a horizontal surface, the temperature recorded at the cigarette/substrate juncture is about 630 – 690ºC in the case of an insulating material such as upholstered furniture. In the case of a dense, hard surface, e.g., calcium silicate board, values of 370 – 470ºC are found. The peak heat flux[313] from a cigarette to that surface is about 50 – 60 kW m^{-2}. Users tend to

discard non-filter-tip cigarettes[314] when about 32 mm remain, with 95% of the discards ranging from 9 to 43 mm. Krasny has reviewed in more detail the combustion characteristics of cigarettes[1859].

Unlike cigarettes, cigars show much more brand variability. In general, it is considered that cigars do not continue burning to completion unless air is drawn through them, although this may not necessarily be true for all brands in the marketplace. The rate of burning[314] of cigars ranges between 1.8 and 3.8 mm min^{-1}. Left alone, a cigar will burn for 138 – 310 s before self-extinguishing. During that time, 5 – 11 mm will be burned. Some very old data on the temperatures measured in cigars[315] indicate values of 815 – 925ºC when not being puffed; these are indistinguishable from cigarettes.

It may be surprising to realize that cigarettes, puffed or smoldering, are unable to ignite most mixtures of flammable gases in air, at least in laboratory tests. Strese[316] measured a wide variety of gas/air mixtures to determine which ones could and which ones could not be ignited by cigarettes. Ignition was obtained for:

acetylene	hydrogen
carbon disulfide	hydrogen sulfide
ethylene oxide	phosphine
diethyl ether	

Ignition was not obtained for:

acetone	ethylene
acrolein	*n*-heptane
ammonia	*n*-hexane
benzene	methane
butadiene	methanol
butane	methyl amine
butyl acetate	methyl chloride
butylene	methylene chloride
chlorotrifluoroethylene	*n*-octane
cyclohexane	*n*-pentane
cyclopropane	propane
dimethyl ether	iso-propanol
dimethyl amine	propylene
dioxane	propylene oxide
ethyl acetate	town gas
ethanol	trimethyl amine
ethyl amine	vinyl chloride

Strese observed that the fuels which do ignite from cigarettes all have MIE values less than about 0.08 mJ, while most of the gases which do not ignite have values which are higher. Ethylene (which does not ignite) and vinyl acetylene (not tested), however have values which are barely higher than those of ethylene oxide and hydrogen sulfide, which do ignite. Toluene appears to be borderline ignitable. In one set of tests[317], a single ignition of toluene was obtained with a puffed cigarette, but further trials gave negative results. Hards[318] conducted tests where he was able to ignite diethyl ether from cigarettes, but not butane, pentane or propane. Nii[319] showed that diethyl ether and carbon disulfide vapors are readily ignited by cigarettes, especially if the burning end separates and falls into the flammable volume. For diethyl ether, the highest fraction of ignitions was achieved at a vapor concentration of ca. 12% and it proved impossible to ignite mixtures of 7% concentration or less.

Several papers report that gasoline vapors are not ignited in cigarette tests[310,317,320]. A number of theories have been proposed why ignitions do not take place when a cigarette is introduced into a flammable gasoline/air mixture. These include the highly oxygen-depleted conditions in the hot zone, and the 'flame arrester' action of the ash layer[310]. Perhaps most germane is the relation shown in Figure 71 in Chapter 4. In the cigarette, the zone where temperatures over, say 800ºC, exist is only about 2 mm in size. For such tiny heated areas, very high temperatures are required, more than 1000ºC, and these temperatures are more than can be achieved by glowing in the cigarette. For a puffed cigarette, the high temperatures are further counteracted by the very short time that the gases are in contact with the combustion area. If the residence times of the gases is estimated[310] as 1 ms, then only gas mixtures with an induction period (for the appropriate temperature) of less than 1 ms would be prone to ignition. A limited amount of testing indicates that cigars behave the same way as cigarettes with respect to ignition of gases. Neither cigarettes nor cigars are able to ignite dust cloud explosions[506].

Concerning 'non-ignition' results, it must be kept in mind that all of the laboratory tests have entailed only modest numbers of trials and were not set up to explore a wide range of conditions. The test results clearly indicate that ignition of gasoline vapors by a cigarette would be a rare event, but it would be imprudent to assume that the possibility is categorically disproved. As Hards[318] noted: "With negative evidence of this kind one cannot be sure without performing an infinite number of experiments!" Even though often-cited results are that natural gas (largely methane) does not ignite from cigarettes[321], Bureau of Mines tests[315] showed that a cigarette *can* ignite a methane/air mixture, if a velocity of 5 m s^{-1} is present. Combustion in a cigarette is a smoldering process and, presumably, ignition occurs because the imposed air velocity raises the temperature of the smolder front. As shown in Figure 68 in Chapter 4, methane is more difficult to ignite than gasoline, so if methane/air mixtures can be ignited, it would be unreasonable to consider vapors of gasoline and other more-readily ignitable gases to be non-ignitable.

It appears that when a cigarette is *thrown* onto a concrete surface the likelihood of ignition gasoline vapors may be higher. DeHaan[322] reports conducting some trials where such throwing did not result in ignition of gasoline vapors.

However, fire cases have been litigated where this precise scenario has been identified as the cause of the fire. A specific case has also been described by Yallop[323], where a fire was ignited when a man dropped a cigarette near a bowl in which he was using gasoline as a solvent. As with all ignition, a probabilistic aspect must be considered, and it does not appear that DeHaan was able to conduct a large number of trials. Clearly, several aspects of combustion favor ignition in such cases: (1) a large supply of fresh oxygen quickly enters the oxygen-depleted smoldering zone of a cigarette, thereby raising the temperature of the combustion area; (2) the protective ash layer is knocked off and the hot central core is directly exposed to the atmosphere; and (3) a shower of multiple burning fragments often results. What is not in doubt is that matches or cigarette lighters used to light a cigarette can ignite gasoline, methane, and a whole host of other gas mixtures. Thus, in practical cases where a cigarette is considered as a likely ignition cause, the means used to ignite the cigarette itself must be given consideration.

DeHaan[324] suggests that ignitions of gases/vapors from cigarettes that are otherwise identified as 'non-ignitable' may be due to flareups in burning, occasioned by foreign matter in the cigarette. There has not been any study attempting to examine this possibility. A study of smoking-caused methane explosions in coal mines[315] suggests that such incidents are generally due to striking a match in a methane/air atmosphere, not simply due to bringing in an already-lit cigarette. Yallop reports[323] the fascinating information that stubbing cigarettes out on a block of TNT does not cause ignition of the TNT.

With all other factors held constant, a filter-tip cigarette is less likely to ignite a substrate than is a plain-tip cigarette. This was determined in a study[325] which examined the propensity for cigarettes to ignite wood shavings with a cross-wind of 0.75 – 1.0 m s^{-1}. This was attributed to a pulse of high temperature which results when the smolder front in cigarette reaches the butt; the pulse does not occur when a filter is present. The probability of ignition was also found to be dependent on the wind velocity, but this was not studied in detail.

The effectiveness of cigarettes as ignition sources for wastepaper baskets has been examined[326]. For wastebaskets filled with papers, snack wrappers, fast-food bags and polystyrene foam coffee cups, ignitions were not observed. Oily paper towels turned out to be ignitable, but out of a total of 300 tests of dropping cigarettes into wastebaskets, flaming occurred in only 5 instances; the times to flaming ranged from 14 to 18 minutes. A German study[327] provided more comprehensive results (Table 22), but the results were based on only 12 – 15 trials[328]. In fact, much longer ignition times have been observed in real fires. Figure 20 shows documentation of a fire that occurred due to cigarette disposal in a rubbish container. The time between the last human activity at the place of origin and the eruption of flam-

Table 22 Experimental times for flaming ignition to take place after placing a cigarette on a given substrate

Substrate	Time for ignition (min)		
	Min.	Avg.	Max.
corrugated cardboard	12	20	50
cotton	9	16	19
hay, straw	8	15	30
leaves, forest litter	12	46	68
paper	8	17	40



(a)



(b)

Figure 20 Ignition of a wastebasket due to cigarette disposal. **(a)** last human activity at the location of fire origin (lower-left frame: cleaner emptying ashtray contents into rubbish container). **(b)** eruption of flaming 3 h 12 min later.
(Courtesy John D. DeHaan and Washington State Police)

ing was 192 minutes. Some additional research is discussed under *Paper products*.
In a study of comforters filled with feathers, down or polyester fibers, it was found that no ignitions from cigarettes occurred; in each case only local, non-progressive charring was found under the cigarette[329]. The covers tested included cellulosic, thermoplastic, and mixed-fiber fabrics. A computer model has been developed to simulate the ignition of soft furnishings by cigarettes[330]; however, it is a research tool and is not set up for the predictions of real-fire ignitions.

US Congress twice passed legislation to investigate the possibility of reducing cigarette ignitions of upholstered furniture and mattresses. Pursuant to this, NIST completed two major studies of test methods intended to qualify safer cigarettes; these are discussed under *Upholstered furniture*, as are other aspects of cigarette ignition of upholstered furniture and mattresses.

Burning of cigarettes is substantially more hazardous in oxygen-enriched atmospheres. Wharton[331] found that in atmospheres of 30% O_2 or higher, cigarettes flamed, not just smoldered, and burned up rapidly. At 40% O_2, it took only 8 to 9 s for a 50 mm length of cigarette to be consumed. When dipped in liquid oxygen, a cigarette burns like a flare.

Clothes irons

A clothes iron normally shows temperatures of 215ºC or lower on its baseplate if no faults are involved and it is not put down upon an insulating surface[332]. The heating element is typically rated at 1100 W and clothes irons are so designed—unlike many other heat producing devices—that a 100% duty cycle will rapidly destroy it. If for some reason the thermostat fails, then a molten base plate (melting temperature ca. 550ºC) can result[333]. The results of some simple testing on the propensity of clothes irons to set fire to clothing have been published[334]. The study examined the potential for ignition when an electric clothes iron (without an automatic shutoff feature) is placed face down on combustible clothing. A lightweight cotton fabric was used, placed over a cotton ironing-board cover, atop a foam pad. With an iron that had a properly functioning thermostat and thermal fuse protection, no fire resulted during a 168 h test, although substantial scorching resulted. When the thermostat and thermal fuse protection was bypassed, ignition occurred in about 16 min, with visible flaming first occurring on the bottom surface of the particle-board ironing board, then progressing upwards. Another study[335] found that, with a defective thermostat, a 1000 W iron reached a peak temperature of 740ºC in 20 minutes; this is above the melting point of aluminum and the aluminum soleplate did melt out. A different ignition mode is involved when the power cord is damaged by contact with a hot iron surface.

CO_2 extinguishers

When a carbon dioxide extinguisher is discharged, whether fixed or a portable unit, the discharge comprises gaseous CO_2, particles of frozen CO_2, and both condensed and frozen water droplets (from atmospheric moisture). Due to collisions, the stream easily picks up an electrostatic charge. Thus, in a flammable atmosphere, a hazard can be created if an electrostatic discharge occurs. In 1966, such an ignition was the cause of an explosion on the tanker ALVA CAPE which was on fire after a collision took place and CO_2 was discharged for extinguishment. CO_2 discharge was also the cause of several disastrous tank explosions in Germany[336], with one of the cases involving 29 deaths[26].

Leonard and Clark[337] discharged hand-held 6.8 kg (15 lb) CO_2 extinguishers into a flammable, heptane/air atmosphere and obtained explosions in 2 out of 6 trials; tests also showed that charging voltages of 10 – 40 kV were being obtained. Haessler[338] measured up to 50 kV and a typical capacitance of 600 pF; the latter value appears to be very high, but details of experimental arrangements were not given. Up to 20 kV was found near the nozzle of a fixed CO_2 extinguishment system[339]. Butterworth[340] examined the electrostatic charging occurring with fixed, total-flooding CO_2 installations. He concluded that charging rates could be reduced by a factor of 20 – 50 by the implementation of a special discharge nozzle. The two essential traits of the nozzle were (1) non-metallic material, and (2) a sharp-edged orifice at the discharge tip, with no further downstream surfaces available to the flow. Another study explored the electrostatic fields associated with portable CO_2 extinguishers[341]. Maximum field strengths of about 0.6 MV m^{-1} were found, substantially lower than the breakdown value of 3 MV m^{-1}. The authors believe that a shock hazard exists, however, and that electrostatic ignitions are not precluded. In opposite conclusion as for the fixed-installation nozzles, for portable units, the authors found that a metallic discharge horn was helpful, and that a grounding wire included with plastic horns had no beneficial effect.

Coal

PROPERTIES OF COAL

The chemical composition of coal varies widely. Very roughly, coal comprises, by mass, about 80 – 90% carbon, 4 – 5% hydrogen, 3 – 11% oxygen, 1 – 3% nitrogen, 0.5 – 1% sulfur, and much smaller quantities of other elements. For bituminous coals, the percent of hydrogen and oxygen are at the high end, while for anthracite coals they are at the low end of the range. For many purposes, it is adequate to represent the effective formula of coal as $CH_{1.4}O_{0.6}$. A typical value of heat of combustion is 22 MJ kg^{-1} (upper) and 21 MJ kg^{-1} (lower). Coal may appear to be a solid substance, but in fact it is referred to as a "solid colloid"[342]. Its density is typically in the range of 1300 – 1500 kg m^{-3}, although it can range from below 1000 kg m^{-3} to over 2000 kg

m^{-3}. The heat capacity of coal increases with temperature and moisture content and decreases with increasing carbon fraction. The typical range is 0.8 – 1.6 kJ kg^{-1} K^{-1}. A thermal conductivity of about 0.13 W m^{-1} K^{-1} is found. An extensive study on the thermal properties of coal has been published by the Bureau of Mines[343].

POROSITY AND SORPTION OF WATER

A number of studies have been done to elucidate the microstructure of coal, specifically the porosity, and to quantify its relation to the sorption of water. The heat of wetting is approximately 0.4 J per m^2 of internal surface area. To reduce this to a more convenient measure of heat per mass of substance, the internal surface area must be known. The pore structure of coal is complex and has two hierarchies of fine and ultra-fine pores; only small molecules can penetrate the latter. The internal surface area of the ultra-fine pores is in the range of 10 – 200 m^2 g^{-1} of coal. The porosity allows gas diffusion through coal, which, at room temperature, is slow but measurable. The surface area[344] of pores large enough to allow sorption of water is around 10 – 100 m^2 g^{-1}. Using a value of 100 m^2 g^{-1}, the per-mass heat of wetting becomes 40 J g^{-1}. Since the surface of coal is hydrophobic, water is initially adsorbed onto oxygen sites and then additional water molecules cluster due to intermolecular forces of water.

EXTERNAL IGNITION

The temperature needed for the autoignition of pulverized coal varies greatly according to rank, going from 200 – 300ºC for lignite to 450 – 600ºC for anthracite[345], but values in the range 350 – 450ºC are most frequently encountered. A Bureau of Mines study[346] using a vertical tube furnace gave AIT values for a number of coals, along with their chemical composition. For anthracite coals, increasing fraction of carbon gave an increasing AIT. But across the different families of coals, few general trends could be seen. The lowest temperatures (ca. 200ºC) were found for sub-bituminous coals, which had high ash contents (ca. 12%) and high oxygen contents (ca. 13%). It has also been reported that even small amounts of iron oxides lower the ignition temperature as does weathering of the coal, that is, simply letting it sit in air after being mined[355]. The latter effect is typically not large (a drop of 10 – 30ºC), but exact reasons for it have apparently not been elucidated. A number of detailed studies on individual small-particle ignition and on the ignition of coal dust clouds are reviewed in Chapter 8.

SELF-HEATING

When mined out of their original deposits, coals show a tendency for self-heating. In extreme cases, there are deposits of coal that cannot be safely mined, due to their excessive self-heating. Coal was the first self-heating substance of industrialized concern to have been extensively studied. It is reported[347] that in 1646 a scientist was already offering the theory that oxidation of iron pyrites was the cause. The earliest book on the topic of self-heating of coal was a British study by Thomas Rowan[348] on the spontaneous combustion of coal in ship holds, published in 1882. Rowan considered that there were two causes of self-heating: (1) the oxidation of some of the sulfur compounds (primarily iron pyrites) present in coal; and (2) oxidation of the coal itself from atmospheric oxygen. Rowan was also aware, but only in rough terms, that moisture increases the self-heating tendency. He was also aware that increasing the size of the pile will increase the tendency, as will decreasing the size of individual coal lumps.

A few years earlier, in 1876, a Royal Commission[349] appointed by the British Parliament to investigate spontaneous combustion of coal in ships made a number of recommendations, based largely on testimony, not on scientific research. Its primary findings were:

(1) That certain descriptions of coal are intrinsically dangerous for shipment on long voyages.
(2) That the breakage of coal in its transport from the pit to the ship's hold, the shipment of pyritic coal in a wet condition, and, especially, ventilation through the body of coal cargoes, conduce to spontaneous combustion, even though the coal may not be unfit for conveyance on long voyages.
(3) That spontaneous combustion in coal cargoes would be less frequent, if regard were had by shipowners and underwriters to these facts.
(4) That when coal is being carried on long voyages, the temperature in the various portions of the cargo should be tested periodically by thermometer, and registered in the log.
(5) That, with a view to guard against explosion, free and continuous egress to the open air, independently of the hatchways, should be provided for the explosive gases, by means of a system of surface ventilation, which would be effective in all circumstances of weather.

Other recommendations dealt with inspections and similar matters. In related technical findings, the Commission discovered a very strong correlation between the probability of a coal ship's loss due to spontaneous combustion versus the weight of the cargo. The Commission also rightly identified the quantitative importance of time. They studied the time after leaving port before fires broke out, and found that the median value was 60 days. The range for all the ship fires they studied was 37 to 190 days for fire to break out. In addition, testimony indicated that the time from mining to ship-loading ranged from a few hours to 10 days. The Commission also opined that "patent fuel" (fuel briquettes made from powdered, pressed coal) was never a self-heating problem, despite the fact these products were reported in the US to have regularly suffered spontaneous combustion[353].

In his study, Rowan tried to re-examine the Commission's conclusion that iron pyrites are the main cause of coal self-heating in light of more current research. Such newer re-

search, however, was not conclusive. He heartily approved of the Commission's emphasis on increasing the size of individual coal lumps as a preventive strategy. The effects of moisture were also not understood, since explanations were attempted which relate moisture directly to oxidation, instead of considering (as we know now) that the main effect is the heat of sorption. Rowan understood that self-heating is not a process whereby the bulk temperature of the substance rises uniformly, but he was not able to distinguish between hot-spot heating and the temperature distribution which occurs in a porous solid where the local heat generation is uniform, but the heat losses are not.

Self-heating ignitions in ships' holds were often energetic phenomena, and resulted in forcible explosions, some of which continued even after the first event blew hatches off. This, of course, is due to the confined nature of a hold. Rowan accurately noted the early period of slow self-heating, and he described a ship's hold fire as having four stages:

(1) Heat was observed, and this might cover a period of from 10 to 15 days or more. When the temperature increased beyond a certain point the next indication was,
(2) A slight smell of "gas" increasing in intensity, and accompanied by whitish smoke. This rapidly increased, and
(3) Smoke appeared in dense and increasing volume, with a pungent and suffocating small of "gas," which with great rapidity resulted in
(4) General conflagration, with more or less explosion. The occurrence and frequency of explosions being determined by the locality where ignition commenced. The nearer the surface the less likelihood of explosion.

Rowan was impressively perceptive about self-heating, given the limited chemistry knowledge of the era, and the nearly non-existent theory of heat transfer. Thus, he was able to debunk J. W. Thomas, an earlier author, who devoted a chapter in his textbook on coal to spontaneous combustion issues[350]. The latter, writing in 1878, considered that self-heating in charcoal was due to heat of friction caused by air passing through the pores of the substance! Thomas, however, considered that a good remedy would be a means of increasing ventilation to the coal. Rowan dismisses Thomas' suggestion on the basis that it is impractical, but offered a proprietary ventilation system of his own. Clearly, the time was not yet ripe for the realization that increasing the heat losses by "ventilation" can be accomplished by dividing the bulk store into smaller piles, not just by forced-air cooling.

Thomas also considered that "the moistening of coal by rain is very probable the prime mover or cause of the generation of heat." On this point, he was again contradicted by Rowan, who advocated a scheme whereby newly mined coal would be dried in a 150ºF atmosphere. He believed that such heated drying would exhaust the exothermicity of "carbonaceous oxidation of the coal," rather than simply drying the coal.

The first correct interpretation of the self-heating of coal is probably due to the Frenchman Henri Fayol[351,352] (he became famous for his theories of business management), who wrote a 260-page paper on the subject in 1879. He conducted experiments not too different from the sort of oven-basket tests used today and elucidated the effects of oxygen supply, coal rank, particle size, and pile size. During this era, the problem of self-heating was apparently much less for US coals. Hexamer reports[353]: "Fortunately for our country, our soft or bituminous coals are not as prone to ignite spontaneously as the English." Hexamer also reports that in the scientific circles of the time, there was much debate on whether oxidation of organic components of the coal, or oxidation of iron pyrites was the main culprit.

Despite the concerted study of the self-heating of coal, simple answers have not necessarily been produced, although today there is a reasonably good ability to model the self-heating of coal. Many of the practical and theoretical difficulties arise due to the wide-ranging chemical differences among coals of various types. A still-useful monograph on self-heating of coals was published by the Bureau of Mines in 1944[354]. A similar study[355] was produced in the UK in 1957 and serves as a comprehensive review of self-heating studies from the earliest times through the first half of the 20th century. In the modern era, Banerjee[356] reviewed self-heating studies up to 1980.

Coal does not self-heat unless it is exposed to oxygen. Such oxidation of coal is termed 'weathering.' According to Van Krevelen, self-heating proceeds in several sequential stages[342]:

(1) chemisorption of oxygen, with increase in weight (up to 70ºC)
(2) initial release of oxygenated reaction products, and of intrinsic water (70 –150ºC)
(3) production of more fully oxygenated reaction products (150 – 230ºC)
(4) rapid combustion, including the generation of soot (over 230º).

The chemical kinetics of these stages are difficult to unravel, since they overlap as the temperature is raised. The apparent activation energy, to the extent that it can be assigned in such a sequence, steadily increases from around 12 – 16 kJ mol^{-1} in the first stage, up to 100 – 150 kJ mol^{-1} in the fourth. In the first stage, the heat of chemisorption for oxygen has been estimated to be on the order of 400 kJ per mole O_2. If self-heating data are analyzed assuming only a single-step, first-order reaction, then an activation energy of around 120 kJ mol^{-1} is assigned. Braun[357] studied eight different US coals in an adiabatic calorimeter over the range 50 – 130ºC and for five of these coals found that there were two distinct activation energies in this interval. From 50 to

about 80ºC, $E \approx 50$ kJ mol^{-1} was found; from 80 to 130ºC, $E \approx 75$ kJ mol^{-1} was found. In a higher temperature regime of 130 – 170ºC, Jones and Vais[358] found $E \approx 90$ kJ mol^{-1} for several low-rank coals, although individual samples showed the broad range of 75 to 111 kJ mol^{-1}. For a pulverized specimen of low-rank (lignite) coal, Jones[359] obtained the values: $E = 94$ kJ mol^{-1}, $Q = 20$ MJ kg^{-1}, $A = 7\times10^5$ s^{-1}, $\rho = 556$ kg m^{-3}, $C = 1170$ J kg^{-1} K^{-1}, and $\lambda = 0.07$ W m^{-1} K^{-1}. For bituminous South African with a volatile content of 26%, Tognotti et al.[360] found that over the experimental range of 120 – 220ºC, $E = 70$ kJ mol^{-1}, $P = 38.8$. The authors sensibly pointed out that below ca. 125ºC, straight-line relationships no longer hold, and that extrapolations to real storage piles (where ambient temperatures << 100ºC are of concern) should be considered as only rough indications.

Despite the fact that a major contribution to self-heating of coal comes from the sorption of oxygen onto the surface, it turns out that self-heating tendency is increased when the fraction of oxygen that is already chemically incorporated into the coal's structure increases[361]. Highest fractions of oxygen are found in low-rank coals, e.g., lignite. There is a complex interaction between oxygen fraction and particle size, as factors that influence the self-heating propensity of coal. Nugroho et al.[362] showed that for low-rank coals the particle size effect is small, but for high-rank coals decreasing the particle size greatly lowers the temperature of thermal runaway. In addition, in running oven-basket tests they obtained typical self-heating parameter values for Indonesian coals. A high-rank coal with particle size of 0.18 mm and $\rho = 725$ kg m^{-3} gave $E = 90$ kJ mol^{-1}, $QA = 4.48\times10^{12}$ W kg^{-1}, $C = 1240$ J kg^{-1} K^{-1}, and $\lambda = 0.11$ W m^{-1} K^{-1} and the E and QA values are only valid for this specific particle size. At a particle size of 2.3 mm, the corresponding values were $E = 45$ kJ mol^{-1} and $QA = 3.11\times10^6$ W kg^{-1}. A low-rank coal with an 0.18 mm particle size and $\rho = 635$ kg m^{-3} gave $E = 96$ kJ mol^{-1}, $QA = 3.73\times10^{13}$ W kg^{-1}, $C = 1480$ J kg^{-1} K^{-1}, and $\lambda = 0.13$ W m^{-1} K^{-1}. Its variations of E and QA with particle size were much smaller.

As with any self-heating substance, times to criticality are hard to estimate accurately and are rarely examined in connection with case histories. Nonetheless, it has been reported that coal piles most commonly go into thermal runaway within three months of piling, but times as long as 2 years have been noted[354].

The critical temperature for self-heating of coal can be roughly correlated to percent volatile matter. Under one set of test conditions[342], coal with 15% volatile matter showed a critical temperature around 190ºC; for volatile matter of 40%, the temperature dropped to 150ºC.

Moisture is a factor which contributes to the self-heating of coal[363]. For initially-dry coal, Bhattacharyya[364] noted that, while adsorption of both oxygen and moisture are exothermic processes, heat generation due to moisture adsorption is the dominant effect. Matters are complicated because oxidation and moisture are coupled: initial oxidation tends to be inhibited unless there are at least traces of moisture present. There is an optimum level of moisture for maximum self-heating—for coal already holding a lot of water in the pore structure, increasing moisture correlates to a decreased oxidation rate due to flooding of the pore structure: pores which are water-filled cannot be oxidized[372]. In one study[365], the optimum level was identified as 7%. It has been demonstrated that if coal is pulverized and vacuum-dried, and then moisture-saturated oxygen passed through it, even very small amounts of susceptible coal types will reach thermal runaway starting from room temperature[366]. In air, the time scale is longer, but the effect is the same—a 3 kg sample will self-heat to ignition from room temperature[367]. While dramatic, these demonstrations do not seem to reflect on the actual hazard conditions. The oxygen/moisture relationship is complex, because it has been determined that the major portion of the oxygen reacts with coal after first going into solution in the moisture present[368]. The effect is further complicated since it appears to greatly depend on the coal type.

It is now understood that pyrites contribute to self-heating primarily by causing swelling and disintegration of the coal[369]. This disintegration opens up new surface area to oxidation, and the added oxidizable area becomes the ultimate contributing factor. The rate of self-heating is roughly proportional to the third root of the available surface area. The direct effect of heat from the oxidation of pyrites is negligible[376].

Pulverized coal shows the same response as charcoal to 'weathering.' That is, if freshly ground product is exposed to air in small batches before being aggregated into larger volumes, self-heating problems can be minimized, since

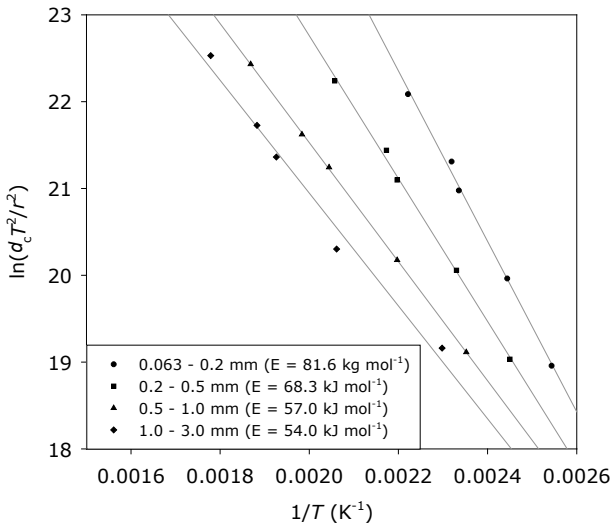


Figure 21 Effect of particle size on self-heating of Derne coal

exothermic sorption of oxygen onto the surface has already taken place[260].

Individual lumps of coal in coal pile can vary from large pieces to ones which are in the 75 µm range. Even though standard self-heating theory considers that there is no effect of *particle size*, researchers studying coal experimentally have generally come to the opposite conclusion. Hardy[370] found that for coal dust layers deposited on hot surfaces, an increase in particle size corresponded to an increased value of temperature needed for ignition. Hensel[371] studied the effect of particle size on self-heating of coal from Derne, Germany using the standard oven-basket method. His results are given in Figure 21 and show a sizeable effect, with larger particle sizes leading to lower values of activation energy and higher values of critical temperature. Hensel considered that this is because simple Arrhenius kinetics is not descriptive of the oxidation chemistry. In his view, latent heats of sorption of molecules at the surface account for the size effect and this effect cannot be represented in the Frank-Kamenetskii theory formulation, although its effect causes the apparent E to change in value. Changing the particle size does change both the density and the thermal conductivity of the substance, but Hensel's data plotted with corrections for both of these effects do not collapse the data towards a single trend line. In a recent survey, Carras and Young[372] examined additional studies on this issue, but Hensel's work can probably be considered the most exhaustive.

Hardy[370] also tested coal contaminated with hydrocarbon oils and greases. Adding these contaminants to coal dust had no effect, or else raised the critical temperature, but some of the greases had a tendency to increase the smolder rate, if ignition did occur. In addition, Hardy conducted a few tests where hot brass balls were dropped into beds of very fine (< 20 µm) coal dust. A 10 mm diameter ball needed to be heated to 400 – 420ºC to ignite the coal, but for a 25 mm ball 315 – 325ºC sufficed. Feng et al.[369] have surveyed various coal characteristics and mining practices with regard to their effect on self-heating. Handa et al.[373] developed a computer program for the numerical calculation of the self-heating of a pile of coal in the shape of a truncated cone. Unlike most other researchers, they included a 2-step reaction mechanism and also modeled the flow of oxygen through the pile. Full-scale results however were not available for validation of the computer code.

Mine *ventilation* can exacerbate self-heating tendencies. This happens when increased air flow rates supply oxygen to locations where previously sufficient oxygen was not available for thermal runaway. In general, the mining environment is considered to be more important in governing whether spontaneous combustion will occur than are details of the coal itself[369].

In view of the inapplicability of the standard F-K theory, as mentioned above, it is not surprising that anomalous results may be found when conducting oven-basket tests. Jones[374] discovered that some coal samples show two peaks, with a trough in between. According to F-K theory, there should never be a drop in temperature except after the (sole) peak is passed. The ultimate drop is due to fuel depletion. Prior to that, the theory recognizes only a rising curve, possibly with horizontal plateaus, the latter due to any antioxidants that may be playing a role. The reason for a trough with some coal samples was not fully elucidated, but tentatively it was suggested that it was due to a liquefaction in the center of the specimen. When a portion of the material is liquefied, access to oxygen would drop precipitously and so would the reaction rate for that portion. In general, researchers in the coal safety field have rarely used standard test methods for self-heating and have generally developed purpose-built test equipment. As an example, the Bureau of Mines considered that relative self-heating tendencies of coal may simply be ranked by determining the propensity of finely-ground specimens to remove oxygen from the atmosphere[375]. For this purpose, they used a sealed Erlenmeyer flask from which air samples are periodically extracted for analysis.

Schmal produced a theoretical model which is probably the simplest that can predict the self-heating of coal over a broad range of conditions[376]. The model is 1-dimensional, but five simultaneous differential equations are solved:

- conservation of oxygen mass
- conservation of heat
- conservation of moisture
- reaction of coal with oxygen
- evaporation and condensation of water.

Of special note is that, unlike most earlier efforts, the model was validated against large-scale data. The modeling was also supported by a large amount of laboratory-scale research at TNO. One of the interesting variables that was documented was a progressive dropping of the heat of combustion with time and temperature of exposure. By contrast, a simple material obeying one-step Arrhenius kinetics would show a mass loss with time, but the heat of combustion of the remaining substance would be unaltered. One of the conclusions from running the model with test cases was that there is a very large exothermic effect from wetting, if dry coal adsorbs moisture from water vapor in the air. One unexpected finding is that within a certain range, if the coal has a higher reactivity, then, in the long run, a lower temperature rise occurs. This was understood to be because higher reactivity coal adsorbs oxygen preferentially closer to the surface, where good heat transfer exists, and this keeps the interior temperature from running away. In line with other studies on moist material, Schmal found that for moist material, until all moisture is used up, the temperature tends to stay 'clamped' at a value way below 100ºC, normally 77 – 87ºC.

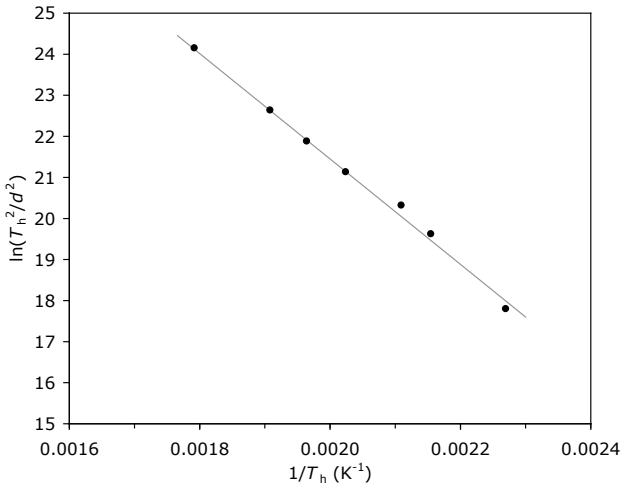


Figure 22 Layer ignition temperatures for Silkstone coal dust as a function of layer thickness

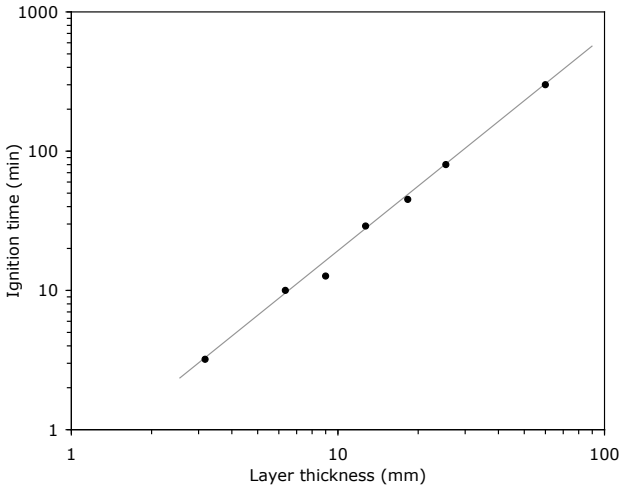


Figure 23 Ignition times for hotplate tests of Silkstone coal dust

The validation exercise confirmed that coal pile porosity has a huge effect on the outcome. Three outcomes were found in modeling and confirmed in validation:

(1) if porosity is very low, diffusion and conduction are mainly responsible for transport of heat and mass. Critical conditions will probably take longer to develop than the pile will be kept in storage.
(2) at intermediate porosities, mass transfer is mainly by convection, while heat transfer is by conduction. Critical temperatures can develop in a relatively short time.
(3) for very high porosities, convection dominates the transport of both heat and mass. Critical conditions will not occur, since the heat generated is being efficiently removed.

It was also found that the initial temperature has a profound impact on the results. Thus, the recommendation follows that any coal arriving at higher than prevailing temperatures be cooled in small piles before being aggregated into large ones. Schmal made the recommendation that a temperature of 77ºC, as measured in the center of the pile, be considered the upper limit for safe storage. Paradoxically, higher peak temperatures were found to be attained in winter than in summer. This is due to the way that convection depends on the ambient temperature. He found it impossible to give simple guidelines with respect to size, since the experimental work showed that coal piles do not behave in an isotropic way. The horizontal dimension is generally less important than the vertical one; but the role of the height of a pile is strongly dependent on the porosity. Finally, he concluded that any relations based on steady-state results would be of little relevance, since the time constants of the system are so long (typ. years) that a coal pile will generally be used up before a steady state would be achieved. Other recent numerical modeling studies have been by Salinger et al.[377] (2-d) and Monazam et al.[378] (1-d).

COAL DUST

Theories and data on the ignition of coal dust are presented in Chapter 8. Extensive data on coal dust in the form of clouds (as contrasted to single particles) are provided in Chapter 5. The percent of volatiles in coal plays a dominant role in determining whether coal dust clouds are ignitable. If the volatile fraction is less than 7 – 8%, than clouds are unlikely to be ignitable. However, if the coal particles are highly porous (specific surface area greater than ca. 100 m^2 g^{-1} as measured by nitrogen adsorption), then dusts of even lower volatility have been shown to be ignitable[512].

In some cases, smoldering ignition of coal is a concern when coal dust accumulates on hot surfaces. For such problems, it is simplest to run hotplate tests. The data from the test can be used with little need for extrapolation, since layer thicknesses to be expected in practice are not very large. Figure 22 illustrates data on Silkstone coal dust[379]; T_h is the hotplate temperature (K) and d is the layer thickness (mm). The times needed to reach ignition are shown in Figure 23.

Bureau of Mine testing[581] showed that, when tested in their test standard depth of 12.7 mm, Pittsburgh coal shows a critical temperature of 233ºC. When tested in a 50 mm depth, a critical temperature of 205ºC was found. Thermal runaway required over 9 h. Smoldering ignitions generally exhibited red glowing and occasional pale blue flames. With one type of British coal, hot glowing sparks were also emitted during smoldering.

COAL PULVERIZERS

Explosions in coal pulverizers have been found to be mainly due to self-heating of layers of coal dust, accumulated upon various machine surfaces which may sustain elevated temperatures[380]. Explosions tend to occur in startup or shutdown, whenever conditions promote an increase in surface temperatures over the normal condition. Within the operating portion of a coal pulverizer, it is possible to arrange things so that explosion potential is minimized by operating

above the UFL of the dust cloud[381]. This is one of the few process types where operation above the UFL of a dust cloud is a viable strategy.

Coffeemakers and teapots*

Modern, electrically-operated coffeemakers are made largely of plastics, generally polypropylene, and prior to the mid-1990s there were large numbers of fire cases involving models that had faulty designs or faulty components, leading to ignition of the plastic case and, subsequently, a possible room fire. The problem is that most consumer models have a sizable electric heater and have casings made of an ignitable plastic. If the heater operates indefinitely, without being turned off, a fire will be likely. Thus, for its basic fire safety, the appliance depends on the proper operation of devices which will shut off the heater at an appropriate temperature level. Up until 1994, coffeemakers typically had one thermostat and one thermal cutout (TCO) device. But a thermostat can fail through fusing of the contacts, due to long use, corrosion, or exposure to moisture[382] and several failure modes are possible for TCOs. In those cases where both the thermostat and the TCO failed, thermal runaway ensued, commonly followed by ignition. In coffeemakers, the TCO is normally a non-resettable component, and service is required after it opens up.

There are several different types of coffeemaker designs in regards to the way in which the water is heated and then the coffee is kept warm. The most common in the past was a high-powered hot-water generator that heated cold (room temperature) water to boiling which allowed the water to percolate up into a filter basket containing the ground coffee. This requires a large heater, up to 1625 W in order to make a pot of coffee in a reasonable length of time. If this same heater is used to keep a pot of coffee warm, then it must be cycled on and off to keep the proper liquid temperature. A cycle time might be 15 seconds on and 2 minutes off. It can be readily calculated that a large number of cycles on the control thermostat will occur. Since thermostats are rated only for a finite number of cycles, eventually a failure in the 'on' position may occur.

Tests on 6 units indicated that when the control devices were bypassed, simulating a failure, autoignition of 4 units occurred within 12 min; the other two units did not go into flaming ignition[382]. Since some of the fires caused by coffeemakers were due to failures of thermal cutout devices, UL tightened up its standard UL 1082[383] in 1994 to require two thermal cutout devices. In that same revision, they also mandated that the thermostat have a ceramic, not a phenolic, body and that it be rated for 300,000 (instead of 100,000) cycles. Under the new UL requirements, coffeemaker fires have become rare and some manufacturers claim that they have never seen a thermal runaway from a dual-TCO design. Apart from fires, coffeemakers are normally very reliable devices, thus, some have been kept in service for many more years than was the manufacturer's life projection. Under these conditions, failures are not unexpected.

Other aspects of coffeemaker design and failures have been discussed by Finneran[384]. During the 1990s, coffeemaker fires became well enough known that arsonists have been found to tamper with coffeemakers in a way as to simulate a well-publicized mode of fire ignition[385]. Owners have also been known to bypass safety devices instead of repairing a faulty device.

Historically, in a now long-discontinued model of coffeemaker, fires were occurring because electrical circuit components were located in places where steam was condensing upon them. This led to arc tracking and sometimes an eventual ignition.

Some electrically-operated teapots are designed for 'attended' use and may not have the same level of thermal protection as a coffeemaker. Some may have thermostats only rated for 100,000 cycles and no thermal protection. If the thermostat fails, there may be melting and a fire. In addition, very inexpensive devices are available for heating tea water which have not thermal protection whatsoever. These comprise a heating coil which is inserted into water and should not overheat, so long as it remains submerged. If the water boils away, or the device is energized while not submerged, a hazardous situation can exist, however.

Composite materials

FIBER-REINFORCED PLASTIC

The term 'composite' can include almost any product which contains two or more distinct components. Perhaps the most widely encountered in fire safety studies, however, are composites which are a fiber-reinforced plastic (FRP). The fiber is often glass, in which case the abbreviation is GRP. GRP panels are in wide use for homeowner construction purposes. Ignitability data for such composites are given under: *Siding, plastic*. Extensive studies have been published on GRP, FRP, and other composite panels used in the shipbuilding and aircraft industries, especially radiant ignitability studies using the Cone Calorimeter[386- 397]. Some example data from a recent test series[398] are given in Table

Table 23 Ignition properties of some glass-reinforced composites for marine applications

Material	Thick. (mm)	Density (kg m^{-3})	Glass content (%)	T_{ig} (°C)	$\lambda\rho C$ (kJ^2 s^{-1} m^{-4} K^{-2})
epoxy, FR	3.9	1910	71	393	1.12
epoxy, coated, FR	3.9	1910	71	483	0.16
modacrylic, FR	5.2	1880	66	349	1.44
phenolic, FR	3.8	1750	58	450	1.52
polyester	4.1	1390	34	323	0.61
polyester, FR	5.2	1650	55	337	1.15
vinyl ester, FR	4.8	1630	58	337	1.33

* Most of this section was prepared by Michael M. Fitz.

Table 24 Ignition temperatures measured in the Setchkin furnace for some high-pressure laminates

Material	Ignition temp. (ºC)	
	Auto-ignition	Piloted
melamine formaldehyde, w. glass reinforcement[399]	475-500	623-645
melamine formaldehyde, w. mineral filler[400]	481	610
melamine formaldehyde, w. mineral filler[399]	313	455
melamine formaldehyde, w. paper reinforcement[401]	398	433
melamine formaldehyde, w. paper reinforcement, FR[401]	554	559
phenol formaldehyde, w. glass reinforcement[399]	520-540	571-580
phenol formaldehyde, w. paper reinforcement[399]	300-311	367-430

23.
A variant of the Cone Calorimeter test method has been promulgated by the US Navy[402] specifically for testing FRP composites. A large number of studies have been conducted by Sorathia and coworkers[403-416] and other investigators[417] using this method. Stevanovic et al.[418] investigated glass-reinforced polypropylene composites using a non-standard test apparatus. They found that the critical flux for ignition varied directly with the volume fraction of the glass reinforcement—for no reinforcement, a critical flux of 8 kW m^{-2} was recorded, rising to 12 kW m^{-2} for 40%.

HIGH-PRESSURE LAMINATES, LOW-PRESSURE LAMINATES, AND RELATED PRODUCTS

High-pressure laminates consist of multiple layers of substrate material interspersed with a thermosetting polymer and heat-cured at high (over 7 atm) pressures. The polymers are typically phenol formaldehyde (phenolic), melamine formaldehyde, epoxy, or silicone. The substrate is paper or cloth. The resulting product can be made in large thicknesses and machined, or it can form as a thin facing to yet-another substrate. As a thin facing, it finds wide usage in kitchen-countertops. Laminates can also be prepared in a low-pressure process. In addition, there are surfacings used for furniture and cabinetry where PVC comprises the face layer. Setchkin furnace ignition data for several laminate types are given in Table 24. Data on radiant, piloted ignition of horizontally oriented specimens tested in the Cone Calorimeter are given in Table 25. Some laminates cannot be successfully studied in bench-scale tests, since they delaminate explosively.

Compost, manure, garbage, sewage, and landfills

Compost self-heats during the decomposition process. This can result in fires if packaged and shipped without being fully 'mature.' To test whether compost is finished and ready for shipment, a Dewar test for self-heating has been proposed[419]. The authors also reviewed the general field of study of compost self-heating. Apart from self-heating, fires in compost facilities are reported to often occur due to welding spatter[420]. Manure also self-heats as it ages. A fire incident and some field measurements on spontaneously combusting manure have been reported[421]. A typical history of spontaneous combustion in a landfill used for demolition wastes has been described[41] where discarded timber constituted the fuel. Compost can also be externally ignited. One fire occurred when a compost turning machine wrapped barbed wire fencing around a wheel during operation which then ignited the compost material when the machine was stopped[422].

Decomposition of vegetable or animal matter, as found in garbage or sewage, or in nature, produces a variety of gases, including methane and hydrogen. In some cases, sufficient amounts of these two gases have accumulated to either reach the LFL within a basement, or to actually result in an explosion. Zabetakis reviewed a number of case incidents[423]. The generation rate of flammable gases is great enough that co-generation plants or flares that capture the gas from sewage treatment plants and capped landfills are common in many locales.

Computer and information technology equipment

For computer equipment, telecommunications equipment,

Table 25 Piloted ignition times (s) for high-pressure laminate products, tested horizontally in the Cone Calorimeter

Material	Thick. (mm)	Irradiance (kW m^{-2})							
		20	25	30	35	40	50	60	75
Formica laminate[424]	3							62	
	6	596		160	138	110	60	35	
	10							40	
melamine-faced particleboard[425]	12		265				34		
melamine-faced particleboard[426]	13		NI	498			42		12
melamine-faced particleboard[424]	15	837		234	161	116	63	40	

and electrical business machines (commonly referred to as *information technology*, IT, equipment), most countries have adopted either verbatim or with modification IEC 60950[427]. In the US, the nationally-modified version of IEC 60950 is UL 1950[428]. From a fire safety viewpoint, this is a weak standard. Low-power devices are permitted to be entirely based on HB plastics, including the outer enclosure. Devices using more than 15 VA are expected to mainly use materials rated V-2 or better in the UL 94 test (see Chapter 7), but there are numerous exceptions. 'Fire enclosures' are required in devices using more than 100 VA. For equipment of less than 18 kg, fire enclosures must meet V-1 while for heavier equipment, the 5V requirement is imposed. However, the permissible size of openings in the sides and top of fire enclosures is effectively unlimited, unless the opening is either directly over a bare-metal part carrying line voltage, or the opening is so situated that objects falling through the opening at 5º from vertical would hit the line-voltage part. The exterior cabinets are declared to be 'decorative parts' and may be made of HB-rated plastics. Some small decorative parts are allowed to be unrated. A tougher standard for exterior cabinetry plastics is only imposed for products intended to be used in computer rooms and having an area over 0.9 m^2 or a single dimension over 1.8 m. For such cases, a flame spread rating of 50 in the Steiner Tunnel is required. The net implication of UL 1950 is that HB-rated plastics are used even for large, vertically oriented surfaces unless the manufacturer voluntarily adopts a higher specification. When HB-rated large, vertically oriented plastics are subjected to a small flame ignition, the expected result is rapid, total consumption of the material.

In actual fact, many IT-equipment manufacturers produce CRT monitors out of V-0 plastics. But computer front panels are commonly made of HB plastics and these can contribute substantial HRR to a fire. A possible ignition scenario is one where a power switch fails (power switches are usually mounted through a hole in the plastic front panel) and the burning switch then ignites the front panel, which serves to propagate the fire outside the device. This type of fire has, in fact, been observed. IBM is on record[429] opposing the use of HB-rated plastics, except for non-power-carrying small parts such as mice and keyboards. Their in-house guidelines require the use of fire enclosures for equipment using more than 15 W, and the fire enclosures (for under-18 kg equipment) must meet V-0, not V-1 requirements.

Computer printers are generally made of HB-rated plastics worldwide. Computer printers from two different, multinational manufacturers were tested by SP[430], who found that both easily ignited from a methenamine pill, burned vigorously, and burned up essentially completely. The plastics for both successfully passed the UL 94 HB requirements.

See also: *Television sets and computer monitors*.

Conveyor belts

Wilcox et al.[431] provided some early UK statistics on ignitions of conveyor belts used in mines (Table 26). Laboratory tests on friction-caused ignitions showed that ignition may generally occur at the time that the belt breaks due to excess temperature and failing mechanical strength. Temperatures up to 500ºC were recorded in such cases.

Elastomeric conveyor belts can pick up an electrostatic charge and this can lead to a spark discharge under some circumstances. If the conveyor is operating in a dust-laden atmosphere, a potential can exist for a dust explosion. It had been proposed that 'conductive' belts would eliminate this potential. But a research study[432] examining belts having surface resistances from 5.3 kΩ/sq to 6.7 GΩ/sq did not bear this out, and showed that the conductive belts did not lead to spark discharges of lower energy than did standard PVC conveyor belts. This was interpreted to occur because the more conductive belts were able to drain charge from a larger area of the belt than did the low-conductivity specimens.

Table 26 UK statistics on ignitions of conveyor belts used in mines

Cause	Percent
faulty bearings in rollers	30.0
overheating of drive head due to load or worn out belt	18.6
improper belt alignment	14.3
obstruction in belt or torn belt	7.1
electrical faults	5.7
faults in compressed air turbines	5.7
other	8.6
undetermined	10.0

Cooking appliances

The majority of cooking appliance fires involves rangetops (Table 27), according to NFPA statistics[433]. A 1963 British study[434] gave the breakdown of causes in 1444 fires originating in electric cooking appliances; Table 28 shows that the vast preponderance involved misuse, not technical faults. A comparison was also made between electric and gas appliance fires (Table 29).

Table 27 US statistics for 1998 on home cooking fires

Appliance	Percent
rangetop	72.1
oven or rotisserie	17.3
portable cooking or warming unit	3.7
open-fired grill	1.8
grease hood or duct	1.1
fixed food warmer	1.0
deep fat fryer	0.5
unclassified	2.5

Table 28 Causes of UK electric cooking appliance fires

Fault	Percent
misuse	97.0
faulty thermostat	1.11
faulty switch	0.35
ground fault	0.55
defective insulation	0.42
faulty installation	0.28
short circuit	0.14
collapse of insulating material	0.14

A much more recent CPSC survey[435] examined the losses during 1994 – 1996. The basic findings are shown in Table 30; breakdowns were not prepared according to fuel type. The action or event leading to ignition are given in Table 31. The detail provided in these two tables is limited, since they were compiled only from national US statistics. A field study with a much smaller sample size (289) gave the results shown in Table 32.

The CPSC study also identified that the risk of ignition (fires per installed appliance, per year) from gas and from electric appliances was nearly equal, but the risk for a fire fatality was about 4× greater with gas appliances. Perhaps surprisingly, this difference appears not to be due to the potential of explosions with gas appliances—in the CPSC field survey, there were no explosions among the 289 cases studied. The CPSC study also identified that the single most common scenario for cooking appliance fires involved frying in fat, with the cook absent from the kitchen. The NFPA study indicated that the risk for a fire fatality was only about 2× greater with gas appliances; furthermore, it indicated greater likelihood of ignition and higher expected dollar losses associated with electric cooking appliances, but did not offer any explanation.

A test where a skillet with corn oil was placed on a gas range and left at the 'high' position showed ignition of the oil at 22 min and flames at the ceiling at 24 min[436]. When repeated with an electric range[437], the ignition took place at 28 min. Self-cleaning ovens can show very high temperatures at certain outside-surface locations when in a self-cleaning cycle. Peak temperatures of 380ºC were recorded and cardboard was ignited on a metal surface near the top of the unit in one test[438]. Switch failures have occurred on electric ranges such that the elements are thought to be off and yet are still heated.

Some gas appliances have had problems with control valves, burners and mountings such that temperatures at the exterior of the housing exceeded acceptable values and adjacent combustible surfaces ignited.

Table 29 A comparison of causes of UK fires with electric and gas cooking appliances

Cause	Percent	
	Electric	Gas
ignition of material being heated or cooked	84.9	69.9
appliance accidentally turned on	2.95	0.85
furniture or fittings too close	2.86	3.37
fabric goods falling onto appliance or being aired too close	2.46	6.74
fat spilt	1.56	1.12
appliance in need of cleaning	1.15	0.56
electric wiring placed too close	1.15	--
curtain blown into appliance	0.98	5.06
flammable liquids, waxes or polishes placed too close	0.66	0.28
portable hot plate used for space heating purposes ignites furniture	0.49	--
paper blown onto appliance of placed too close	0.33	0.84
clothing in contact	0.16	2.53
clothing in contact with hot plate used for space heating	0.16	--
appliance turned off, but still sufficiently hot to ignite fat placed too close	0.16	--
leakage of gas	--	8.7

Table 30 Material first ignited in cooking appliance fires—US national statistics

Material	Percent
material being heated or cooked	71
cabinet, wall covering	5.2
fuel	2.8
textiles	2.4
wire insulation	2.3
other	16

Table 31 Action or event leading to cooking appliance fires—US national statistics

Action or event	Percent [a]	
	Rangetops	Ovens
unattended	57.7	32.3
other misuse	10.8	17.1
mechanical/electrical failure	10.0	21.7
combustible material too close	9.3	12.1
accidentally turned on	5.0	3.6
other (not misuse)	7.2	13.3

[a] – total number of ignitions: 71,600 rangetops, 14,400 ovens

Table 32 Ignitions from cooking appliances—US field survey

Category of failure	Percent
ignition of food	75
product malfunction	9
operational error	5
combustibles too close	1
other	9

GRILLS

The US Fire Administration has compiled some statistics on cooking grill fires[439]. These occur primarily in residential occupancies (71%), with less than 1% being in campsites or recreational areas. The breakdown of causes is shown in Table 33.

Table 33 Causes of fires due to grilles

Ignition cause	Percent
mechanical failure, malfunction	43
operational deficiency	16
misuse of material handled	16
misuse of heat of ignition	15
natural or other factors	4
incendiary or suspicious	3
design, construction, installation deficiency	3

Cork

Cork is obtained as the bark of the cork oak tree, which grows in Mediterranean countries. The chemical composition of cork is approximately 35 – 70% fatty acids and wax alcohols; 15 – 25% lignin; 15 – 25% tannins and catechins; and 3 – 9% cellulose and carbohydrates. In the first half of the 20th century, cork was commonly used as thermal insulation for refrigeration and freezing facilities. Because of its porous nature, it can be ignited in a smoldering mode, although systematic testing has not been reported on this aspect. At least one food-processing facility fire occurred when hot particles from an arc-cutting operation ignited cork insulation. NIST conducted unpublished tests on 9 mm cork board in the Cone Calorimeter and obtained radiant, piloted ignition data shown in Table 34. Hallman[440] examined the piloted, radiant ignition of cork samples of 253 kg m^{-3} density and 12.7 mm thickness. His data show $\dot{q}''_{cr}$ = 22.4 kW m^{-2}, B_{ig} = 124. Cain[441] tested 3 mm tiles in the ISO 5657 apparatus and obtained a minimum flux for ignition of 10 kW m^{-2} for piloted conditions and 32.5 kW m^{-2} for autoignition.

Table 34 Piloted ignition times for 9 mm thick cork board

Heat flux (kW m^{-2})	35	50	75
Ignition time (s)	8.8	3.5	1.1

Self-heating data based on a small-specimen study in an adiabatic furnace were obtained by Gross and Robertson[109]. Their values are: E = 80 kJ mol^{-1}; $QA = 8.0\times10^9$ W kg^{-1}; ρ = 130 kg m^{-3}; λ = 0.42 W m^{-1} K^{-1}; C = 2000 J kg^{-1} K^{-1}. Cork dust samples were also studied by Hensel[442] using the oven basket method. His data indicate E = 114 kJ mol^{-1} and P = 51.0. The above two values of activation energy are exceedingly different, but reasons for this are unclear.

Cotton

Cotton is primarily composed of cellulose, and it is often the commercial source of cellulose for producing filter paper. Tests for the AIT of various forms of cotton were conducted by NIST in 1947, with results reported only in summary form. The data[443] were: absorbent cotton 266ºC, cotton batting 230ºC, and cotton sheeting 240ºC. The test method has only been described very sketchily, see *Wood* for details. The specimens ignited by glowing ignition, with the absorbent cotton test requiring 2.5 h for the ignition of a 1.3 g specimen[191].

Cotton shipped as bales is commonly packed to a density of 360 to 450 kg m^{-3} and a mass of 85 to 227 kg, although in recent years[444] they have been typically at around 218 kg. Bales of cotton are susceptible to self-heating if moist and unclean; dry, clean conditions make self-heating much less likely[445]. A study by the Fire Research Station[446] claimed that most incidents of fire attributed to spontaneous combustion have not been correct. It was considered more likely that either long-term smoldering occurred due to accidental introduction of some hot material, or that contamination with 'drying' oils occurred. It was also concluded that friction of steel bands could cause ignition, but details of this proposed mechanism are not clear. A study by the Southwest Research Institute also deprecated self-heating and concluded that the most common cause of cotton bale fires when shipped in railroad cars is friction of steel bands along with sparking when impact occurs. This study was only published as a news item[447] and experimental results were not cited; the Institute did recommend that strapping be sprayed with a coating that reduces the sparking tendency. Instead, industry found it simpler to over-wrap the strapped bales with a fabric or film covering and this practice is now widespread. Other reports, however, suggest clean material may also, on rare occasions, self-heat, and that wetting appears to promote self-heating[448]. Actual case histories were mentioned by Back where bales of cotton coming from a dry climate ignited when transported to a humid harbor area[2115]. For external ignition, the ease of igniting a bale of cotton depends on its packing density[449], being relatively easily ignitable if 200 – 300 kg m^{-3}, and hard to ignite if around 600 kg m^{-3}. Internal ignition normally takes place due to some smoldering material having been introduced accidentally. This may occur due to sparks or heat of friction association with the ginning process and bales which are in that condition are referred to as 'fire-packed' bales. Once a bale of cotton starts smoldering, the process may be exceptionally long-lived. Several cases are noted of bales that have floated in a river or a canal for 2 – 4 weeks, yet were still smoldering inside at the end of that period[450].

Wakelyn and Hughs[444] conducted a laboratory experiment where they used an electric heater to ignite the center of a high-density (ca. 450 kg m^{-3}) bale. Smoldering ignition could not be sustained from this source, which the authors attributed to the poor access of oxygen into a tightly-packed bale. The authors also stated that bales of less than 225 kg m^{-3} density were able to sustain smoldering, but details were not provided. They also were unable to get cigarettes

and matches to ignite the bales; for this testing, only bales covered with polypropylene film or with burlap fabric were used. The authors also noted that, in recent years, fire incidents generally involved bales of 225 kg m^{-3} or lower density, but not high-density bales. Additionally, tests on clean cotton fibers loosely packed into an cubical oven basket passed the requirements of UN Test N4.

The layer ignition temperature for cotton fibers was studied by Chan and Napier[451] using a hotplate test. Unlike most results for hotplate testing (and unlike predictions from self-heating theory), little effect of layer depth was found. For 23 mm long fibers and a density of 12 kg m^{-3}, a critical hotplate temperature of 265ºC was recorded for a 10 mm layer, decreasing to 255ºC for a 60 mm layer. This may be due to the low packing density of the samples. But the authors found that the density when cotton fiber 'fly' is deposited on surfaces tends to be about 3 kg m^{-3}. At higher densities, the critical temperature does go down, as shown in Table 35. The authors also determined the AIT of the fibers by testing them for ignition in air, using an unspecified method. An ignition temperature of 260ºC was found.

Table 35 Results from hotplate tests on cotton fibers

Layer depth (mm)	Density (kg m^{-3})	Fiber length (mm)	Critical temp. (ºC)	Time to runaway (min)
10	12.2	23	265	2
20	12.2	23	260	17
40	12.2	23	258	13
60	12.2	23	255	14
40	36.7	23	220	11
40	24.4	23	250	12
40	6.1	23	350	13.5
10	12.2	17.5	260	6
20	12.2	17.5	255	7
40	12.2	17.5	254	13
60	12.2	17.5	250	14

Gray et al.[452] conducted oven-basket self-heating tests on cotton fibers, packed to a density of 50 kg m^{-3}. For equicylinders of 75, 115 and 175 mm diameter, they obtained critical temperatures of 230, 212, and 198ºC, respectively, giving E = 93.8 kJ mol^{-1} and P = 42.42. Oven self-heating results were also reported by Mitchell[156]. Self-heating data based on a small-specimen study in an adiabatic furnace were obtained by Gross and Robertson[109]. Their values are: E = 144 kJ mol^{-1}; $QA = 6.93 \times 10^{15}$ W kg^{-1}; ρ = 320 kg m^{-3}; λ = 0.042 W m^{-1} K^{-1}; C = 1300 J kg^{-1} K^{-1}. The activation energy in their results appears to be too high; a more plausible set of results was reported by Jones[453]. He gives: E = 102 kJ mol^{-1}, $Q = 17.3 \times 10^3$ kJ kg^{-1}, $A = 1 \times 10^5$ s^{-1}, λ = 0.04 W m^{-1} K^{-1}. On the basis of these data, Jones also calculated the minimum size/temperature relationship needed for a hot steel particle to ignite a cotton bale. He concluded that a 2 mm diameter particle heated to 700ºC, or an 0.5 mm particle heated to 977ºC would suffice to cause thermal runaway and ignition.

Cotton batting has traditionally been used in providing resilient padding for mattresses and upholstered furniture, although nowadays polyurethane foam in much more common in these applications. Mattresses are required to be resistant to cigarette ignitions (but not open flames) according to Federal regulations (16 CFR 1632). Untreated cotton batting cannot meet this requirement, so typically boric acid is added at about a 10 – 12% level to impart smolder resistance. The boric acid powder is adhered onto the cotton batting by use of a small amount of oil. Mattresses so treated may also resist ignition from matches (although not from burning bedclothes). When using an entire book of 20 paper matches to ignite small mattress mockups, it was found that treated mattresses only charred locally, but did not continue burning[454]. The same results were found by piling up 34 wooden matches in a small bonfire on top. In the same study, all mattresses using ordinary polyurethane foam that were tested ignited fully from both the paper matches and the wooden matches and continued burning the full extent of the specimen. Holleyhead reports tests where in 60 trials lighted cigarettes were placed on untreated cotton waste—charring was observed, but no flaming ignitions could be achieved[304]. For unclear reasons, his results are different from results typically obtained for mattress and upholstered furniture, where both smoldering and flaming are readily found when using non-FR cotton batting.

See also: *Cellulose*; *Fabric*; *Fibers*; *Upholstered furniture and mattresses*.

Crankcase explosions

Since crankcases of internal combustion engines contain both air and a combustible liquid, it is not surprising that there can be a possibility of explosion. Typical causes for explosions in ship engine crankcases include seizure of bearings and restarting the engine while parts are still hot[455]. Four-stroke engines with cylinder bores over 300 mm are most prone to these explosions; the relative risk for two-stroke or smaller four-stroke engines is at least a factor of 3 lower[461]. In addition, V-type engines are much more prone to explosions than are in-line types. Some explosions take place after the engine is stopped and a crankcase door opened for inspection[456]; this suggests that availability of sufficient oxygen may sometimes be the critical factor. In that vein, two-stage explosions have proven to be especially hazardous—the first explosion blows off the crankcase doors, while the second spreads burning oil throughout the engine room[457]. The second explosion takes place when new oxygen is introduced into the crankcase upon blowing off the doors. Serious explosions also have occurred in locomotive engines and in stationary engines, and in external combustion (i.e., steam) engines; similar types of explosions also take place in gear cases and other enclosed, lubricated mechanisms.

Concerted scientific study of the problem dates back to a 1947 crankcase explosion on the REINA DEL PACIFICO which resulted in 28 fatalities. At normal operating temperatures, oil vapor concentrations within a crankcase are negligible, and the oil that is present in the air space is in the form of a mist[458]. The mist in a crankcase is normally not due to mechanical agitation but, rather, due to condensation[457]. Oil is vaporized at hot surfaces, then condenses into a fine mist as it leaves the heated area and cools. The mist particles are very small[459], typically only 1 – 2 μm. Burgoyne and Newitt[460] found that the LFL of engine oil mist was 41 g m^{-3}, which is essentially identical to the LEL of common hydrocarbons in vapor form. They also pointed out that mists at a high enough concentration to reach the LFL have a notably high optical density, that is, even over short distances they will appear to be opaque. In normal marine engine operation, fuel concentrations of the crankcase mist were found not to exceed 1/100 of the LFL. The authors also showed that flame burning velocity and explosion pressures of crankcase oil mist explosions were very similar to those of pentane, allowing pentane to be used as a surrogate test fuel.

If the engine is overheating, then concentrations of oil mist can become significant. Except in the case of hot-spot faults, normal crankcase temperatures[461] are about 65 – 90ºC, which is significantly below the AIT of a lubricating oil mist (about 265ºC). In small-scale tests, Hoare et al.[458] set the crankcase temperature at 85ºC and sprayed mineral oil (flash point 227ºC) to produce a mist. Any practical concentration of mist could be ignited by a small flame when an agitator or an air injector was used. But explosions were hard to create in the absence of agitation and air injection. For atmospheres ignitable with a flame to be ignitable by a hot surface required using a 25 mm tube heated to 600ºC. But explosions did not take place if oil was actually sprayed on the hot tube, rather, the tube quickly dropped in temperature to ca. 200ºC. In some tests, upon attaining an ignitable atmosphere, a door was opened to the chamber. The opening sometimes caused a burst of flame, but never an explosion. In large-scale tests, Hoare used a standard 12-cylinder, 2-stroke marine engine and created a hot spot of unspecified size (possibly around 25 mm) on a metal pipe cap introduced into the crankcase. "Substantial" explosions required a hot spot temperature above 820ºC. None of Hoare's test explosions were detonations and, in fact, the most violent explosions only registered an over-pressure ca. 1 atm. Even this low explosion pressure does not make for an easy design problem, since crankcases of large-size marine engines can typically withstand only about 0.3 atm overpressure. Hoare also observed that none of the explosions were 'instantaneous,' and that they were sometimes preceded by a flaming oil fire. Inerting the crankcase by putting exhaust gas through it was shown to be a satisfactory means of preventing explosions. The oxygen concentration was 9% under these conditions.

Safety features[461] to reduce the potential of a crankcase explosion which are sometimes implemented include: (a) pressure-relief vents; (b) oil mist detectors; (c) emergency inert gas system for the crankcase; (d) ducting of the crankcase breathers to a safe area; (e) exhaust fans on the breathers, to reduce flammable gas concentrations; and (f) gas detectors at the outlets of the crankcase breathers. The latter two features are specific to dual-fuel, i.e., methane and diesel, engines. Flame arresters fitted to pressure relief vents are also beneficial[456]. Lamb provides a number of safety suggestions to minimize the possibility of overheated bearings, pistons, and other engine parts[456].

Crude oil

The properties of crude oil vary enormously, depending on the exact source of the oil. An early study[462] using the Abel apparatus showed flash point values ranging from –18ºC all the way to +170ºC. The distribution was somewhat bimodal, with most results being in the range 10 – 30ºC or 90 to 120ºC. Iwata et al.[463] tested various Iranian crude oils for ignitability by presenting a small flame to open pools of oil held in a 90 mm dish. All samples ignited immediately upon application of flame, suggesting the open-cup flash point was below room temperature for all. Elam et al.[464] conducted ignition tests on various crude oil types using the Cone Calorimeter and piloted ignition conditions. They found that at the lowest heat flux used, 5 kW m^{-2}, not all 2-mm thick layers ignited. But for 4-mm and greater thicknesses, all samples ignited at 5 kW m^{-2}. For thick layers (13 mm), ignition times at 5 kW m^{-2} were 54 – 248 s. Shorter times were recorded when a pilot flame was used, instead of the standard spark device.

Curling irons and hair dryers

Tests have reported on five different makes of domestic electric curling irons to determine if they can set fire to combustibles[465]. As is typical, the irons did not have any thermal cutout devices. When completely wrapped with towels, the irons caused charring of the towels and some melting of plastic parts, but did not start any flaming or smoldering fires. Curling irons have, however, on occasion been found to be manufactured defectively (commonly, a faulty line-cord connection) and caused ignition of fires, although published material does not appear to exist. In use, a curling iron often is repetitively rotated, often in a single direction. Thus, failures have been noted at the connection between the cord and the iron caused by the repeated flexing and twisting of the cord during the normal use of the device. Most modern curling irons, however, have a rotating connection designed to prevent this type of failure. The same failure at the cord connection sometimes occurs with hair dryers and these are normally not equipped with rotating connections.

Curtains

The potential of cotton curtains to ignite room furniture when their burning fragments were blown into a room by a bomb explosion has been studied[466]. The results generally

indicated that probability of ignition increased with increasing basis weight (g m^{-2}) of the fabric. The Fire Research Station[467] tested polyester/cotton curtains using the ISO 5657 test method and found that disintegration occurred at heat fluxes of 20 – 30 kW m^{-2}. Ignition required a heat flux of 40 kW m^{-2}. See also: *Fabrics*.

Diapers, disposable

Holleyhead reports that efforts to ignite the cellulosic-fiber padding of disposable diapers with a dropped cigarette yielded only local scorching, but not sustained smoldering or flaming[304].

Diesel fuel

Diesel fuel is a petroleum distillate which is in the 'gas oil' family of petroleum products; it falls between kerosene and light lubricating oil in the distillation process. The fraction of carbon is 85 – 88%, and hydrogen 11 – 14%; other elements are present only in minor amounts[468]. The flash point is typically controlled to be above 65.6ºC (150ºF), although this is for safety and performance reasons. The specifications of diesel fuel in the US are governed by ASTM D 975[469]. A Chinese study determined the minimum heat flux for piloted ignition to be 3.7 kW m^{-2} for light diesel and 5.2 kW m^{-2} for heavy diesel fuel[470].

Dinitrosopentamethylenetetramine

Yoshida[300] has reported that self-heating of stored dinitrosopentamethylenetetramine (3,7-dinitroso-1,3,5,7-tetraazabicyclo[3.3.1]nonane; DPT; $C_5H_{10}N_6O_2$) caused a harbor explosion. The chemical is used for foaming rubber or for gas generation in propellants.

Dishwashers

A UK study[471] found that the plastic parts of dishwashers were generally ignitable by a tiny 'needle flame' and in some cases even by an electric arc. Cheaper models do not contain a steel shell and a sizable fire was possible with those units. Throughout Europe[472], it was found that the main causes of dishwasher fires were:

- ingress of water, detergent, or rinse-aid onto wiring
- damaged door wiring
- overheating of elements
- faulty internal electrical connections.

Less than 5% of ignitions were attributed to consumer misuse. In the UK[473], two additional causes were identified:

- faults within the programmer/timer
- overheating of the main motor.

While no statistics are noted for the US, similar failure modes have been seen in the US and these types of problems have resulted in several recalls.

Because detergents create a very conductive mixture with water, any leakage onto an electrical component can result in arc tracking. This can be easily seen by making a mixture of detergent and water and inserting a conductor and applying a voltage. For explosions in dishwashers, see: *Hydrogen*.

Dryers and washers (for clothes)

Clothes dryer fires in the US represent about 3 – 4% of the reported residential fires. CPSC[474,475] performed in-depth investigations on 70 clothes dryer fires. The failure modes for fires of known cause are given in Table 36; in 33% of the incidents the cause could not be determined. In 14% of the cases, the timer switch was in the 'off' position when the fire occurred (the timer switch does not fully de-power the unit, however; see below). The proportion of fires with gas dryers (27%) is nearly identical to the fraction of gas dryers sold (24%), the remainder being electric. A breakdown of the point of origin of the fires is shown in Table 37; for 19% of the incidents, the exact origin could not be identified.

In addition to obtaining the statistical data, CPSC also conducted laboratory studies. In one test—a simulation of a bearing failure in the motor—the thermal protective device is supposed to cut out. But the exemplar tested, which was designed for cycling (auto-reset) operation, failed after 50 cycles and lint on the motor ignited. The study also pointed out that, surprisingly, venting to the exterior of the building is only required for gas dryers and not for electric ones. The CPSC study concluded that certain improvements were desirable in standards for both gas[476] and electric[477] dryers.

The Ontario Fire Marshal[478] found that the major causes of fires originating in clothes dryers are:

- lack of maintenance
- improper venting
- drying of 'flammable materials'
- accumulation of lint
- use of plastic ducts

Table 36 Failure modes for dryer fires of known cause

Failure mode	Percent
Electrical ▪ drive motor ▪ thermostat ▪ control malfunction ▪ power cord ▪ timer motor ▪ relay ▪ arcing	36
Restricted airflow ▪ improper venting or installation of vent	19
Heat source ▪ gas control valve ▪ lint ingestion ▪ gas supply line ▪ heat exchanger, gas	13
Mechanical ▪ drum seal bearing ▪ broken drum belt	11
Misuse, abuse	7.5

Table 37 Point of ignition in clothes dryer fires of known origin

Location	Percent
duct, vent	22
lint trap	16
motor	14
drum	9.4
control panel	7.8
electrical system	7.8
timer	6.3
thermostat	4.7
heater coil	1.6
plug, cord	1.6
other known	9.4

Plastic exhaust ducts can play two roles in initiation of fires: (1) they can collapse, bent or be pinched and cause a lint buildup or blockage, that may result in high temperatures within the dryers; (2) they are often the direct mechanism whereby a fire internal to the dryer ignites external combustibles. UL have warned that plastic or aluminum-foil types of vent ducts should not be used[479]. They have had requirements since 1987 for using only metal ducts; however, dryers are commonly self-installed by the user, who may not be aware of safety precautions. Not listed by the OFM, but also known to occur, are fires due to inept repairs or maintenance. Fitz[480] considers the following to be the primary causes of dryer fires (not ranked):

- self-heating materials being dried;
- drying of materials soaked in gasoline or other sources of flammable vapors;
- overfilling the drum with clothing, leading to disruption of design air flow patterns;
- improperly designed dryers where lint tends to accumulate near the heating elements;
- improperly designed dryers that have high discharge temperatures (e.g., one dryer model was found, under normal conditions, to produce a temperature close to 400ºC at the heater discharge into the drum);
- faulty venting of dryer (this may also cause buildup of lint in unexpected locations);
- failure of motor;
- arcing from a wiring failure;
- failure of a gas burner or gas control valve;
- failure of the operating thermostat;
- a cord or receptacle failure.

In rare cases, instances have been reported where friction of clothing alone has been responsible, with the clothes getting trapped between the drum and the housing. Even more rarely, incidents have been found with washers, where excessive friction of clothing against the lid develops.

Statistics on the point are not available, but a certain fraction of dryer fires occur when the drying cycle is unexpectedly stopped, for example, due to a power outage. Case reports exist where self-heating-prone items (e.g., padded brassieres) thereupon ignited; it is not clear if ignitions have been found when drying loads did not contain any items with a known self-heating propensity. Ignitions sometimes happen when metallic objects such as paper clips or coins fall out of clothing and short out some electrical component in the dryer[481].

Dryers usually do not control the heating device (gas or electric) by means of the user-operated timer switch. Instead, the heating device is turned on by a centrifugal switch attached to the motor. If the centrifugal switch fails and remains in the 'on' position, the heating device will operate without the operation of the motor and without there being an airflow through the dryer. A high-limit switch (TCO) is supposed prevent actual overheating, but high-limit switches can be subject to two shortcomings: (1) Same as with high-limit switches on other appliances, these devices are not designed for indefinite life; if the normal control means fails and the appliance operates on the high-limit switch, a fail-unsafe failure might be expected. The use of a manual reset high-limit switch would draw attention to the user that a problem has occurred. (2) In some designs, the location of the high-limit switch is such that excessive temperatures may occur in some location where combustibles could get caught, yet overheating will not be sensed by the high-limit switch.

Some dryer fires occur when the electric heating element sags due to aging and contacts the grounded metal portion of the drum. Current flow becomes possible since dryer manufacturers normally use only single-pole switching to disconnect current flow from the heater element, with one pole remaining live at the 240 VAC connection. Opening the door stops current flow to the motor and to one side of the power line, but not to the other (Color Plate 55, Color Plate 56). Additional information on fires originating from the heating elements is given under *Heaters, electric*.

Sanderson[482,483] has discussed the safety features of clothes dryers and common failures modes of them. The most common cause of fires in commercial-laundry gas-fired dryers is considered to be failure to properly clean the lint trap[484]. Another is improper maintenance or repair by staff.

A number of fire incidents have been reported where terry-cloth towels were laundered and ignited a while after removal from the clothes dryer due to self-heating[485,486]; similar incidents have been reported with mopheads that had been washed, dried, and put in a hamper[487]. Jones[488] convincingly demonstrated that uncontaminated fabrics have such a low HRR due to self-heating, even at dryer temperatures, that thermal runaway is precluded, but that if an oil-contaminated sphere of 100 mm diameter were present[489], then the sphere itself would only need to have self-heated to 170 – 180ºC to successfully drive the entire dryer load to thermal runaway. This is within the range of plausibility. For example, in one case[485] it was found that up to 30% of vegetable oil remained on oily towels after laundering. A

cotton terry-cloth towel can absorb up to 3 times its weight in cooking oil. Since the oils are only partly soluble in water, oil remains after washing. If significant amount of oil having a self-heating potential remains on towels after washing, then a fire can occur during drying. Fires typically occur in commercial laundries, not in residences, since large loads of oil-soaked materials are uncommon in the home environment. Dixon[490] reports of a fire in a prison laundry, which originated in a hamper used to store washed and dried clothing which had been heavily soiled with rapeseed cooking oil. Another fire was reported in a commercial laundry where towels soaked in unidentified oils and greases spontaneously combusted in plastic and canvas containers, where they were placed after drying[491]. In laboratory testing, as a control, Dixon[490] determined that a clean 2 kg cotton-fabric dryer load would not spontaneously combust at a 100ºC drying temperature. The procedure involved placing the clothing into an open-top 25 L plastic tub immediately after drying was completed and monitoring the interior temperatures. For clothes where detergent was entirely omitted from the wash, a minimum of ca. 187 mL of rapeseed oil was found needed to cause spontaneous combustion in a 1 kg load of cotton fabrics dried at 100ºC. A small amount (e.g., half a scoop) of detergent used in the wash did not have a significant effect in counteracting self-heating. Despite claims of the detergent industry that only cotton, and not synthetic-fiber towels have the potential to self-heat[492], polyester and polyester/cotton fabrics were found to also be liable to self-heating. Open flaming did not occur typically until 3 h had elapsed, but in some cases it took more than 4 h. It must be emphasized that these tests all involved spontaneous combustion *after* the clothing was finished drying and removed from the dryer.

Mackey tests on cotton and cotton/polyester towels soaked with 20% oil by weight showed temperature increases of 34 – 60ºC for corn oil and 31 – 76ºC for sunflower oil[485]. This was accompanied by dryer testing, where it was found that dryer fires readily occurred with heavily-oiled towels, especially if a cool-down cycle was not used. Additional tests, conducted by the detergent industry[492], showed that after a single washing, roughly 4 – 15% of soybean oil remained, depending on details of the wash load and the washing procedures. In independent testing, Sanderson[493] examined the fraction of corn oil that gets removed from towels with each washing. Hot water and detergent was used in these tests, but the effects of varying either washing temperature or detergent amount were not examined. The results indicated that each wash/dry operation tended to remove only roughly 1/3 to 2/3 of the oil that was present. The effect of fiber type was also examined, but the results were inconclusive on that point.

After a dryer fire which may have been caused by self-heating of oiled cloths, it is sometimes possible to analyze fatty-acid residues and determine if vegetable or animal fats were involved; a chemical analysis procedure based on ether extraction, saponification, and derivatization was given by Coulombe[494]. Another alternative is to collect samples of wash water from the clothes *washer* and subject these to analysis. The water pump is a place where often some residual water can be found[495].

It has been claimed[496] that use of bleach contributes to the self-heating. This has some credibility in that bleaches are oxidizers; however, apart from anecdotal reports, no studies appear to have been conducted. Furthermore, it would be likely that most highly oil-contaminated cloth would be bleached as part of the washing procedure and it is not clear that self-heating would be less if the circumstances were identical but the bleach was omitted.

It has also been alleged[497] that lint in a clothes dryer's lint trap can self-heat and lead to a dryer fire. This issue was experimentally addressed by Sanderson and Schudel[498]. They conducted tests with dryer lint placed in a temperature-controlled oven at various temperatures in the range of 66 to 121ºC. Even though the upper range was significantly above temperatures found in actual dryers, no self-heating was found. Packing density of the lint, its origin, and its moisture content were varied, but these did not affect the outcome. The authors concluded that cases attributed to such cause were more likely attributable to other malfunctions which resulted in the ignition of plastic dryer parts, a number of which are often associated with the lint trap.

Domestic gas-fired clothes dryers can be a source of ignition if they are located in a garage or other area where an accidental spill of flammable-liquid vapors may occur. In testing[499], it has been found that whether or not a dryer will ignite vapors along the floor depends crucially on the exact setting of the appliance-leveling legs. The gap available at the bottom governs the distribution of entrained air flow through the dryer. The situation is complicated, since safe conditions were found with no gap and with a gap of 37 mm (1.5"), but unsafe conditions at a gap of 13 mm (0.5").

A European study determined that the main causes of clothes *washer* fires were[472]:

- faulty internal wiring or connections
- ingress of water or detergent onto wiring
- overheating of resistors or timers
- vibration and rubbing of cables or other parts
- overheating of motors.

Less than 5% of ignitions were attributed to consumer misuse.

Dryers (process dryers)

Causes of fires in grain dryers have been investigated by Lasseran[500]. Incandescent particles ejected from gas or oil-fire burners were found to be the largest cause of ignitions. Some of these originate as combustible matter inducted through the combustion air supply openings. Cases have been found of this sequence of events even in dryers that

are of the heat-exchanger type, i.e., with sheet metal separating the combustion chamber from the drying chamber. Other ignition causes included blockages and excessive temperature settings. In the case of drying sunflower seeds, these have a fuzz attached to them that can be liberated in the drying process and drawn into the combustion chamber and ignited[46]. Corn kernel debris and rapeseeds are also susceptible to the same behavior.

The potential of dust explosions in spray dryers has been studied by Gibson and Schofield[501]. They pointed out that dusts considered as 'non-ignitable' at room temperature may, in fact, ignite at the 140 – 500ºC found in the dryers. Thus, they recommend that the AIT of the dust be considered as the governing variable, instead. The authors also concluded that ignitable dusts will not be ignited by incandescent particles at 600 – 800ºC, if particle diameter is smaller than 3 – 5 mm. This is best accomplished by having fine-mesh screening at the air intake.

Self-heating of material can occur if deposits of granular or powdery material are allowed to build up in an industrial dryer, leading to dryer fires. Beever[502] points out that this is sometimes due to faulty design where 'dead' corners allow material to accumulate. The remedy is to provide fairings which eliminate dead corners. A book has been published giving extensive loss prevention advice on industrial dryers[503].

Dung, fecal matter

Dried cow dung ('cow chips') has been found to be particularly susceptible to ignition by firebrands. Once ignited, the dung can then cause a propagating fire by igniting adjacent grass. If the dung has been pulverized by cow hooves, Ford[1153] reports that cigarette butts will 'invariably' ignite it. Bunting and Wright[504] conducted field experiments where bulldozed piles of vegetation were set alight and used as a source of generating brands. The target vegetation was generally grass, but the cow chips were found to be the first-ignited target items. Analysis indicated that air temperature was the dominant factor in determining the distance to which spotting would occur, and Figure 24 shows these results. Wind velocities were in the range 5 to 11 m s^{-1}, and relative humidity 11 to 45%. The latter two factors were found to be less important than air temperature. In accompanying laboratory studies, the authors used glowing, non-flaming, cylindrical-shaped juniper brands. For the largest size brand used, 5 × 20 mm, they found that ignition required a minimum air temperature of 4ºC and (with a few exceptions) RH < 50%. Until temperatures exceeded 16ºC, however, for ignition to occur a wind speed > 4.5 m^{-1} was also needed. Also, fuel moisture content of < 13% was found to be a prerequisite for ignition. When brand size was varied, brands of 3 × 15 mm were found able to cause some ignitions, but no ignitions were possible with 2 × 10 mm brands.

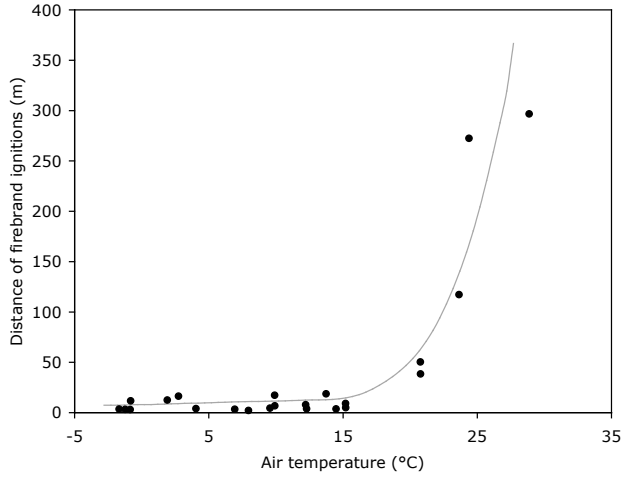


Figure 24 Effect of air temperature on the ignitability of dried cow dung from controlled-burn firebrands

A report exists in the literature[505] where it is claimed that a fire was ignited by the self-heating of a single soiled diaper enclosed in a plastic bag and left in direct sunlight for three days at a location where temperatures were over 38ºC. The mass of potentially reacting material represented by the contents of a diaper is very small and it would be hard to give credence to this report in the absence of confirmatory studies.

Dusts

IGNITION OF LAYERS

Dust layers are generally ignitable in a smoldering mode from glowing cigarettes. van Laar[506] demonstrated this for dusts of tapioca and soybean meal. Radiant ignition of dust layers has occasionally been studied (e.g., Glinka et al.[507]), but not enough studies have been made to draw general conclusions. Leisch et al.[508] studied the smoldering of corn-soy mixed grain dust. Using relatively coarse (2/3 by mass between 106 to 425 μm, 1/3 between 38 to 74 μm) dust at a packing density of 410 kg m^{-3}, they found that smolder velocities were slow, 15 – 60 mm h^{-1}. Using an 0.33 mm platinum wire, a minimum heat flux of ca. 48 kW m^{-2} was needed to cause a smoldering ignition. The ignition source had to be sustained for a very long time in order to effect an ignition: 40 min at 48 kW m^{-2}, 23 min at 200 kW m^{-2}. Using slag from an arc welder, only a transient ignition was obtained for the corn-soy dust, but sustained smoldering was achieved for grain screenings. Identical results were obtained for slag from an oxy-acetylene torch. The slag particle size in both cases was only described as less than 24 g. The authors believe the screenings ignited because of a lower packing density, but a value for the density was not given. In limited testing with cigarettes, it was found that screenings ignited when a minimum wind velocity of 1.5 m s^{-1} was imposed, with no ignition for smaller velocities.

Xu et al.[509] conducted spark ignition tests on several types of dust layers and found the following MIE values: flax 0.365 mJ; cotton 0.456 mJ; and wool 0.41 mJ. The ignitions resulted in smoldering, not flaming.

Palmer[510] examined the hotplate ignitability of tea fluff (i.e., tea dust) and found a temperature of 260ºC for a 25 mm layer and 230ºC for 50 mm. He also noted that the fluff was readily smolder-ignitable by sparks from a cigarette lighter flint.

EXPLOSIONS

Dust explosions have been most prolific and serious in the agricultural products industries, especially in grain elevators. Kauffman[511] presented a detailed survey of grain dust incidents. A German study[512] of the causes of industrial dust explosions gave the results shown in Table 38. The materials involved are listed in Table 39. In view of the major role of pharmaceutical manufacturing companies in dust explosion research, it is perhaps surprising that explosions in their industry are not more frequent. The type of devices associated with dust explosions[513] are listed in Table 40. Despite the relatively high frequency of dust explosions caused by electrostatic discharge, this scenario is very difficult to re-create experimentally. Thorpe et al.[514] noted that sugar dust is one of the substances more frequently involved in actual silo explosions, but could not produce a single explosion in an experimental silo.

A survey[515] of US grain dust explosions for the years 1958 –1975 gave the results shown in Table 41. Extensive tables of BM experimental results on dust explosibility are given in Chapter 15. Since a dust explosion is typically an oxidation (occasionally, a reaction with nitrogen or carbon dioxide), substances which are already stable oxides cannot be involved. Thus carbonates, nitrates, phosphates, silicates, sulfates, etc., will not be involved in dust explosions. The primary members of these families are minerals; in fact, rock dust is used to prevent coal dust explosions. However, some ceramic dusts are explosible. Matsuda reported LFL values for a series of ceramic dusts (metal carbides, metal nitrides, metal borides, and metal silicides)[516,517]. The values ranged from 130 g m^{-3} to 2310 g m^{-3}, apart from a few substances which were non-ignitable.

Table 38 Causes of industrial dust explosions in Germany, 1965-1985

Cause	Percent
mechanical sparks	26.2
smoldering nests	11.3
friction	9.0
electrostatic discharges	8.7
open fires	7.8
hot surfaces	4.9
self-heating	4.9
welding/cutting	4.9
electrical machinery	2.8
other or unknown	19.5

Table 39 Materials involved in dust explosions in Germany

Material	Percent
wood	31.6
agricultural products	24.7
metals	13.2
plastics	12.9
coal and peat	9.2
paper	2.0
others	6.4

Table 40 Equipment associated with dust explosions in Germany

Equipment causing explosion	Percent
silos, bunkers	34.7
dust collectors, filters	20.3
direct heating equipment	9.0
dryers	9.6
crushers	9.0
conveyors	4.2
sieves	5.4
pulp mills	3.6
other	4.2

Table 41 Ignition sources for grain dust explosions in the US

Ignition source	Percent
welding, cutting torch	10.6
open flame other than welding	9.0
foreign material in mill	9.0
friction	7.4
electrical	4.2
lightning	2.1
motors	1.6
spontaneous combustion	1.6
static electricity	0.5
unknown	54.0

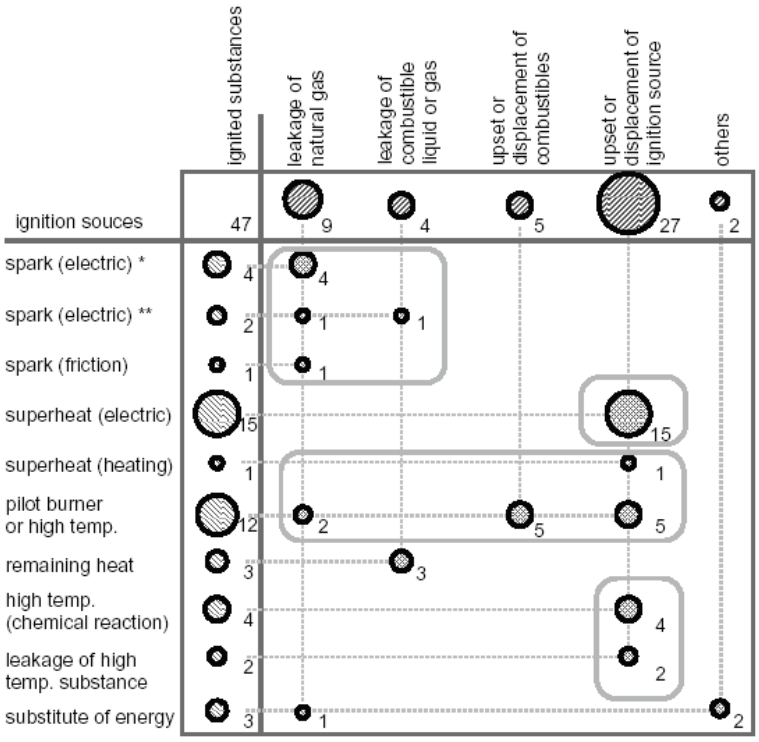


Figure 25 Statistical distribution of fire causes due to the Great Hanshin earthquake of 1995

Earthquakes

Fires after earthquakes have often been of great concern, both because of their prevalence and because firefighting resources may be much reduced, e.g., water mains broken, streets made inaccessible. In one recent fire, the 1995 Great Hanshin fire in Japan, a study was conducted to determine the causes of earthquake-caused fires[518]. The results are shown in Figure 25, with the following being the definitions of the ignition sources:

- spark (electric)*: spark from damaged electric appliances
- spark (electric)**: spark from electric appliances that can occur under normal conditions, e.g., from light switch
- spark (friction): spark from mechanical friction
- superheat (electric): overheating of damaged electric appliances except electric heat source appliances
- superheat (heating): overheating of heat source appliances
- pilot burner or high temp.: pilot burner or high temperature of heat source appliances
- remaining heat: residual heat of heat source appliances
- high temp. (chemical reaction): high temperature caused by chemical reaction of chemicals in vessels which were broken by the quake
- leakage of high temp. substance: leakage of high temperature substance, e.g., leakage of molten metal in a dental laboratory
- substitute of energy: unaccustomed use of energy, e.g., candle for lighting under power failure.

Electric (general statistics)

The US Fire Administration[519] estimates that about 7.7% of all fires are due to 'electrical distribution.' This is the fifth-ranking cause of fires, the fourth-ranking cause of fire fatalities, and the second-ranking cause in terms of dollar losses. Their definition of 'electrical distribution' is: Wiring, transformers, meter boxes, power switching gear, outlets, cords, plugs, and lighting fixtures. Separate categories exist for

Table 42 Average annual losses during 1994-1998 in the US for structure fires involving electrical distribution equipment, arranged by type of equipment involved in ignition

Equipment	Fires	Civilian deaths	Civilian injuries	Direct property damage (in millions)
Fixed wiring	19,100 (32.7%)	131 (37.5%)	415 (24.8%)	$384.4 (37.6%)
Light fixture, lampholder or sign	9,600 (16.4%)	31 (9.0%)	168 (10.0%)	$108.1 (10.6%)
Cord or plug	8,600 (14.7%)	93 (26.7%)	455 (27.2%)	$154.8 (15.2%)
Switch, receptacle, or outlet	5,700 (9.8%)	34 (9.8%)	163 (9.7%)	$82.8 (8.1%)
Lamp or light bulb	4,600 (7.8%)	23 (6.5%)	209 (12.5%)	$64.7 (6.3%)
Fuse, circuit breaker, or other overcurrent protection device	3,400 (5.8%)	8 (2.3%)	93 (5.6%)	$59.3 (5.8%)
Meter or meter box	1,200 (2.1%)	1 (0.2%)	10 (0.6%)	$11.8 (1.2%)
Transformer	1,200 (2.1%)	3 (1.0%)	29 (1.7%)	$23.0 (2.3%)
Unclassified electrical distribution equipment	2,200 (3.8%)	6 (1.6%)	63 (3.8%)	$55.4 (5.4%)
Unknown-type electrical distribution equipment	2,800 (4.7%)	19 (5.4%)	70 (4.2%)	$77.2 (7.6%)
Total	58,300	350	1,674	$1,021.6

Table 43 Factors leading to fires in electrical distribution systems in residences, based on 149 incidents studied by CPSC

Factor leading to failure	Percent
improper alterations	30.4
improper initial installation	16.6
deterioration due to aging	13.8
improper use	12.7
inadequate capacity	12.2
faulty product	9.4
unknown	5.0

Table 44 Equipment associated with low-voltage industrial fires/explosions in the UK

Equipment	Percent
cables and wiring	18.2
cable boxes	1.2
capacitors	0
electric heaters	2.0
instrumentation and miscellaneous	4.5
luminaires and lamps	3.6
motor starters and control gear	25.9
motors, generators, alternators	14.6
plugs and sockets	2.4
switchgear	37.7
transformers	1.6
welding transformers	0

Table 45 Equipment associated with high-voltage industrial fires/explosions in the UK

Equipment	Percent	
Cables		1.5
Capacitor banks		0
Motor starters and control gear		3.4
Switchgear		72.9
circuit breakers	34.0	
switches and switch/fuses	19.5	
current transformers	7.6	
voltage transformers	4.6	
busbar casings and chambers	7.3	
Terminals and connections		4.6
cable boxes, trifurcating boxes	4.6	
bushings	0	
Transformers and appurtenances		17.6
transformer tanks	10.7	
cable boxes	3.1	
tap-changing compartments	2.7	
bushings	1.1	

'cooking,' 'appliances,' and 'other equipment.' The above statistic is based on all fires, which includes vegetation fires, vehicle fires, and others, not just building fires. For residential structure fires, electrical distribution accounts for 9.9% of the total. Fires originating in cords or plugs of appliances are likely to be reported as appliance fires, thus the losses due to cord/plug ignitions will be spread over several categories. More detailed data from NFPA[520] are shown in Table 42. As with all of the statistics available through NFPA, only fires reported to municipal fire departments are tabulated. The data given in Table 42 include all reported structure fires and are not restricted to residential fires.

Table 46 Causes of fires in residential occupancies due to electrical wiring and devices

Cause of fire	Percent (individual cause)	Percent (for categories)
Branch circuit wiring		**29**
mechanical damage or improper installation	8	
poor or loose splice	8	
ground fault	3	
use of improper wiring	3	
knob-and-tube encapsulated	3	
miscellaneous overload	2	
unknown	3	
Cords and plugs		**26**
mechanical damage or poor splice	10	
overloaded extension cord	6	
overloaded plug	2	
damaged plug	2	
miscellaneous (short, water, deteriorated insulation, electric blanket cord)	6	
unknown	1	
Service components		**13**
deteriorated insulation	5	
improper installation (ground fault or overload)	4	
fire due to alterations in progress (e.g., contact with HV wire)	2	
unknown	4	
Lamp and lighting fixtures		**13**
loose or poor connection or splice, mis-wiring	5	
combustibles too close	5	
overlamped	3	
deteriorated insulation	1	
Receptacles and outlets		**11**
loose or poor connection	8	
mechanical damage	3	
overloaded	2	
deteriorated, miswired, plug inserted improperly	2	
unknown	3	
Low voltage transformer	**1**	**1**

These general statistics do not give indications as to the actual reasons for ignition. The only highly-detailed study where an attempt was made to identify reason for ignition of electrical distribution components has been that of Hall et al.[521], who studied 105 residential-occupancy fires (Table 46). CPSC staff[522] continued this work and provided a

Table 47 Causes of electrical fires in Japan during the year 2000

Category			Percent
Power transmission, distribution lines			**37.1**
	wiring in vehicles	15.5	
	distribution lines (interior wiring)	6.2	
	cords	5.2	
	power cords of appliances	4.0	
	transmission lines	2.7	
	other wiring: connections in wiring, outside wiring, etc.	2.7	
	service entrance lines	0.9	
Portable heating equipment			**17.0**
	space heaters, Kotatsu (foot-warming tables)	7.3	
	other portable heating equipment: blankets, carpets, hair dryers, irons, aquarium heaters, etc.	4.6	
	heaters for cooking: cooking stoves, roasters, toasters, ranges, grills, hot plates, rice cookers, etc.	2.4	
	welding machines	2.8	
Appliances			**17.9**
	other appliances: TV sets, refrigerators, washing machines, microwave ovens, air-conditioners, fans, ventilators, grinding machines, etc.	10.5	
	lamps: desk lamps, fluorescent lamps, neon lamps, alley lights, etc.	4.2	
	batteries	3.2	
Wiring devices			**13.2**
	plugs	3.6	
	power strips or extension cords	2.1	
	other wiring devices	7.6	
Heavy electric machines			**8.1**
	other machines: control panels, transformers, etc.	3.6	
	power capacitors	1.7	
	motors	2.1	
	generators	0.7	
Fixed heating equipment			**3.8**
	cooking stoves, ranges or fryers	2.3	
	other fixed heating equipment: furnaces, dryers, sauna heaters, water heaters, etc.	1.5	
Ground leakage/fault			**1.2**
Static electricity			**1.5**
Other electrical origins			**0.2**

breakdown of factors leading to these (Table 43). Many of the faults found were attributable to abusive usage or faulty installation, often by amateurs. These studies reflect similar percentages as found in overall fire department reports[523].

Additional areas where fire department reports showed problems, but which did not occur among the fires studied in detail included overcurrent protection (6%) and meter boxes (1%). Fires initiating from electrical distribution system faults were disproportionately concentrated among older housing and increased substantially with dwelling age, once the age was beyond 20 years.

CPSC also conducted specific studies on problems with several of the electrical distribution system device types, and these are discussed in detail below. For example, the 9.4% attributable to 'faulty product' do not make clear the nature of the problem, but a CPSC study on electrical outlets (see below) found that fires or electrical failures may well arise due to flimsy designs of many devices.

Statistics for fires/explosions in UK factories from low-voltage equipment are shown in Table 44 and are based on 247 incidents. Peck[524] analyzed 262 UK industrial fires or explosions involving high-voltage equipment and provided a summary given in Table 45. Of these incidents, 36.6% involved only an explosion, while the remainder were fires or an explosion with fire. The most common fire/explosion cause was from circuit breakers, of which 93% were oil-filled and 7% dry.

The electrical fire statistics for Japan during 2000[525] are shown in Table 47. Electrical fires comprised 11.8% of the total fires reported. Statistics have been reported from Rus-

Table 48 Causes of 1996 electrical fires in Russia

Cause	Percent
cable, wire	58.6
electric heater	11.3
TV	6.7
switchboard	5.0
switch	3.6
hotplate	3.4
lamp	2.2
refrigerator	2.0
transformer	1.6
bell	1.3
radio, hi-fi	0.9
clothes iron	0.8
automatic switch	0.7
washing machine	0.5
other products	1.4

sia, giving the breakdown of causes for electrical fires[526]. During 1996, electrical fires accounted for 20.5% of the total. For these, the breakdown is shown in Table 48. A Norwegian study identified that, in that country, 1/3 to ½ of the electrical fires in buildings are due to poor contacts or heating/glowing at contacts[527].

Cooper[622] has pointed out that a fire originating in electrical equipment is not necessarily a fire of electrical origin, even though some statistics inappropriately classify them as such. An example is a fire in an electric deep-fat fryer that occurs when the person using it allows the oil to overheat.

Electric appliances and electronic equipment

The statistics in Chapter 1 include information on fires originating in certain primary types of appliances—heating equipment, cooking equipment, and cooling equipment. The major causes of ignition of electrical appliances or equipment, as determined by NFPA[528] are given in Table 49. CPSC estimates[529] for fires originating in miscellaneous appliances are given in Table 50.

For devices which use electricity, such as consumer appliances, computer equipment, telecommunications equipment, etc., there are basically two ignitability issues:

(1) Will an electric fault within the appliance be contained by the housing, so that a fire does not erupt at the outside of the appliance?
(2) Will the exterior surfaces of the appliance resist ignition from a small external ignition source, or, if they do ignite, will they readily self-extinguish or otherwise be limited to only producing a low heat release rate?

Detailed statistics on this point are not available, since in Table 49 ignitions from external sources are lumped into "other known."

There is a widespread opinion that devices which can only consume a very small amount of power cannot cause ignitions. Some authors[530] consider this limit to be 20 W. The UL standard for information technology equipment[428] considers the limit to be 15 W. A more conservative view[527] is "several watts." The realism of such claims is unclear, and there does not appear to be much research on the topic. As shown below under *Electric lamps and lighting fixtures*, even a 1 W incandescent light, upon being broken, can ignite a methane/air mixture, while a 1.25 W source can ignite notebook paper.

In the US, the fire performance of enclosures of electric appliances is effectively governed by the standard UL 746C (see Chapter 7). Safety of electric appliances is covered by a very large number of UL product-specific standards. But, with some exceptions, these standards either refer to the requirements of UL 746C or paraphrase them. In the UL 746C standard, the required performance of enclosures is governed by three variables:

- whether the appliance is portable or not
- whether a portable appliance is intended for 'attended' household use
- whether current-carrying parts inside have a minimum insulation thickness of 0.71 mm.

Stationary appliances must have a 5V rating, while portable appliances need only an HB rating (and no hot-wire ignition requirement), unless they contain electrical parts with less than 0.71 mm insulation thickness. For housings which do have to fulfill an electrical safety function, if intended for 'attended' use, then an HB rating still suffices, but hot-wire

Table 49 US fire statistics on causes of ignition for appliances and equipment (1992-1996)

Cause	Percent
short circuit or ground fault	47.8
other electrical failure	24.0
unclassified or unknown mechanical failure	4.9
lightning	4.9
part failure, leak, or break	4.7
other known	14.0

Table 50 Estimated residential structure fires in 1990 due to miscellaneous appliances (excluding heating, cooking, and cooling appliances)

Appliance type	Fires
clothes dryers	7500
fans	2800
heat tapes	2000
washing machines	1900
television sets	1400
electric blankets	900
audio equipment	700
hair dryers, curling irons	700
clothes irons	500
dishwashers	400
other or unknown	1500

ignitability must be no more than PLC 4. Unattended appliances need a V-2 rating and PLC 4. Decorative parts must be rated at least HB, unless they have a volume smaller than 2 cm^3 and all dimensions smaller than 3 cm. The consequence is that small appliances are normally only HB-rated. Television receivers are a special case and are discussed separately in this Chapter.

In 1998, CPSC reported on the results of a study to determine if the UL 746C provides an adequate level of safety for plastic enclosures[531]. The UL 746C standard provides that either flames be applied to end-use items, or, alternatively, the results obtained from UL 94 tests on plaques of the plastic can be used. Obtaining a V-2 rating is considered equivalent to passing the 12 mm and the 20 mm flame tests of UL 746C. But when subjecting actual enclosures to test flames, only a vague instruction is provided as to where flames should be placed. To examine the adequacy of these provisions, CPSC obtained a number of small consumer appliances and subjected them to tests, using both the UL 94 and the UL 746C procedures. The laboratory findings were:

- Some appliance enclosures failed the HB test, the least stringent test in the UL 94 series.
- Some materials that were Listed by UL as V-2 failed the V-2 test, when CPSC tested samples actually cut out from appliances.
- When tested with the 12 mm or 20 mm flames of UL 746C, a number of appliances made from HB and V-2 materials failed. All appliances made from V-0 materials passed. No V-1 materials were included in the study.

As a result, CPSC made the recommendations that:

- The concept of 'attended' use is vague and is not defined by UL. Consequently, appliances such as toasters and clothes irons can become classified as 'attended.' In the opinion of CPSC, appliances should be classified as 'attended' only if they cannot remain energized when unattended.
- The UL 746C provisions for placing flames on end-use articles are vague and unconservative. An enclosure rating of V-0 should be mandated, unless a more realistic end-use article testing regimen can be evolved within UL 746C that demonstrates adequate resistance to small flames.
- The UL 746C provisions that allow least-stringent performance (HB rating, no hot-wire ignition testing) for housings where current-carrying parts have ¤ 0.71 mm insulation thickness should be abrogated.

UL revised UL 746C during 2000 (effective 2004) to tighten up certain provisions, but for portable attended equipment, HB-rated enclosures continue to be acceptable. UL also clarified that blenders, vacuum cleaners, and hand-held drills are 'attended,' while clothes irons, toasters, electric fry pans, and coffeemakers are 'unattended.' While the new edition of UL 746C is generally intended to require use of V-2 rated materials for unattended equipment, these will still be able to use an HB-rated enclosure as an exception, if certain requirements for the current-carrying components thereof are met. Non-portable equipment continues to require a 5V rating. However, UL are gradually switching over to UL 60335-1[532], which is their version of the international standard IEC standard IEC 60335-1[533] and it will eventually replace UL 746C. Especially noteworthy is that the IEC standard has more strenuous provisions for glow-wire testing, applicable to plastics used within 3 mm of current-carrying conductors. Actual test requirements that must be met are laid down in IEC 60695-13 (glow-wire ignition temperature), and either IEC 60695-2-11[534] (glow-wire flammability index for end products) or IEC 60695-2-12[535] (glow-wire flammability index for plaques). In either case, minimum ratings of 850ºC for glow-wire flammability index and 775ºC for glow-wire ignition temperature must be obtained. The toughened requirements mostly affect parts made from polyester and nylon, which previously tended to be of lesser FR grades[536].

The general philosophy of UL requirements for the flammability performance of appliance housings is that ignition sources are likely to be found only *inside* the equipment, therefore, if certain design features are implemented to keep ignition sources away from the housings, the housings need only a minimal performance level (typically, HB). This means that the housings are unlikely to resist *external* ignition sources. The National Association of State Fire Marshals concertedly, but so far unsuccessfully, endeavored to have this philosophy changed. Some test information on this topic is discussed under *Television sets and computer monitors*. The standards of IEC generally adopt an even more lax philosophy, in that a 13 mm air gap between a possible ignition source and a potential ignition target is deemed to be a fireproof barrier.

CPSC has also expressed concerns that 'push-on' terminals used inside appliances have a disproportionate propensity to cause ignitions. Push-on terminals are mechanical, non-soldered connections where a male spade lug mates with a C-profile female terminal. Faulty connections can result when the fit becomes loosened.

Information on specific appliance categories is located alphabetically in this Chapter.

HIGH-LIMIT SWITCHES

Heat producing appliances are generally required to have a *high-limit switch* (also known as a *thermal cutout* or *thermal cutoff*) apart from the normal thermostat. In some cases, two high-limit switches are used. High-limit switches come in three basic configurations:

(1) Automatically-resetting. This type is functionally identical to a normal-use thermostat—it opens a circuit when a setpoint temperature is exceeded, then re-closes the circuit when cooled down to a lower temperature. Most commonly this is based on the principle of a bi-

metallic element—when two elements of dissimilar thermal expansion characteristics are joined together, a large movement can be generated by a small temperature change. The movement is then used to open a pair of electric contacts. If an overtemperature condition persists, the device will cycle indefinitely.

(2) Manually-resetting. This is most commonly an electromechanical device that opens a circuit and then latches in the open position. Pushing a reset button is required to reset the device.

(3) Sacrificial, one-shot operation. This is most commonly based on a scheme whereby electric contacts are held closed by the mechanical force of a fusible pellet. The pellet has a specific melting point and when it melts out, the contacts open. The device is destroyed by the melting and must be replaced to repair the equipment (Color Plate 57). The fusible pellet principle was first patented[537] in 1960.

In many cases, the pertinent standards allow an automatic-resetting type of high-limit switch to be used. A pervasive ignitability issue exists since in most such appliances there is no audible warning if either the thermostat fails or some other failure mode occurs so that the device 'runs on the high limit,' with the high-limit switch effectively now acting as the thermostat. This situation is hazardous because: (1) high-limit switches are usually rated for only 100,000 cycles and may fail closed, instead of failing open, at the end of their lifetime; (2) since the high-limit temperature is necessarily higher than the range of normal operating temperatures settable by the thermostat, this means that the appliance may equilibrate to a higher temperature and stay at that higher temperature for a long time. Color Plate 58 through Color Plate 60 illustrate the effect of cycling on contacts. An audible buzzer connected to the high limit switch (or use of manual-reset, not automatic reset devices) would solve most of these problems. Some UL standards require a signal, but the signal is permitted to be visual, i.e., a pilot light. It is not at all evident that users understand that a glowing pilot light means "fault," instead of simply "heating."

Electric batteries

Ignition hazards associated with electric batteries can be of three types:

(1) liberation of flammable gases;
(2) providing electrical energy for initiating a fire;
(3) ignition and burning of the battery itself.

The most significant hazard is the generation of flammable gases and their ignition, leading to a battery explosion. Lead-acid batteries, most commonly used in automobiles, are designed to be recharged. The charging process liberates hydrogen and oxygen and this can create a potential fire hazard. Extensive statistics on motor vehicle battery accidents and explosions have been compiled by NHTSA[538]. During a 1-year period, 2280 injuries were reported in the US due to motor vehicle battery explosions. The activities leading up to the explosions are given in Table 51. A common scenario for explosion is if connections are reversed in jump-starting, so that one battery effectively is shorting out the other. However, an error of this type is not required for an explosion to happen. Some accidents are reported when the vehicle is not in use, and there has been a suggestion that in some cases long-term storage of a battery may make a battery explosion more likely[539]. A general study[542] on reported injuries attributed to electrical battery accidents produced the results shown in Table 52. A large fraction of the accidents is due to either inadvertent (e.g., hooking up batteries with inverted polarity) or deliberate abuse (e.g., incineration).

Table 51 Activities leading to reported injuries from motor vehicle battery explosions

Activity	Percent
charging battery	31
replacing, securing, or tightening cables	26
jump starting	19
checking fluid level or adding water	19
unknown	5

Table 52 US statistics (1983-1992) on injuries from battery accidents

Type of accident	Percent
explosion or violent rupture	38
overheating	27
leak or mild rupture	23
flame or fire	12

An explosion of a lead-acid battery may be caused by attempting to recharge a battery with a dead cell or using too rapid a charging rate on a flat battery. In both cases, the water may be excessively electrolyzed into H_2 and O_2. This may raise internal temperatures sufficiently so that the lead plates buckle, contact each other, and produce an internal spark[540]. A spark may also be produced if the electrolyte level is allowed to drop below the base of the plates. A fire has been documented[622] where a wood shelf holding lead-acid batteries became sufficiently contaminated with battery acid as to become conductive. Contact of two electrodes with the shelf caused the wood to ignite.

Two explosions of automotive type, 12 volt batteries occurred at a battery manufacturing facility when a worker was peeling off a label attached to the side of the case[541]. The batteries were new and were sitting on a wood pallet, without any electrical hookup. Experiments conducted during the course of investigation showed that the battery case could be electrostatically charged up to 8 kV during the process of label removal. Battery cases are made of several pieces of plastic that are welded together. Further tests indicated that discharge into the interior of the battery is possible along minute defects present in a weld seam. Measurements indicated that the capacitance of the battery sitting on

a pallet is about 25 pF. When it was placed directly on earth, a value of 140 pF was found. If a fixed amount of charge is transferred during peeling the label, the battery can get charged to a higher voltage if its capacitance is low. In turn, the probability for an incendive discharge to occur is increased if the voltage is raised. Thus, the likelihood for this type of accident to occur is greater if the battery is situated so that its capacitance is low.

Attempts to recharge non-rechargeable batteries will lead to chemical reactions (evolution of H_2 and O_2) that take place in a way not anticipated by the manufacturer, consequently, an explosion may result[542]; the attempt may also result in metallic deposits being collected in such a way as to short out the cell. When subjected to fire, even a single 'D-size' dry cell can cause an explosion. In one case[543], an expended cell was put into a 55 gallon (208 L) steel drum used for burning trash. An explosion ripped apart the drum from top to bottom. Essentially any type of battery can be expected to rupture or explode if an attempt is made to incinerate it.

Hay et al.[544] determined that typical sparks resulting from loose battery connections on a motor vehicle battery are on the order of 0.5 J and 500 μs duration. Based on this, they designed a test apparatus for flame-arrester battery plugs. The latter are intended to eliminate the possibility of a spark outside the battery propagating fire into the battery, and causing an explosion inside. Since hydrogen/oxygen mixtures have an exceptionally low quenching diameter, these plugs are commonly constructed from sintered metal, which can more easily be manufactured with very small openings[545].

Batteries much smaller than those in motor vehicles can be involved in explosions. Accumulated hydrogen has caused hand-held flashlights to explode. NIOSH has documented that even a specialized flashlight used by divers which contains a chemical catalyst to recombine hydrogen has been subject to explosions[546]. Small 9-Volt alkaline batteries have exploded in airline luggage; this usually occurs due to shorting out of the terminals. Lithium batteries can explode internally, due to excessive rates of gas generation within. One explosion[547] of a small lithium battery (Color Plate 61) was severe enough that it "blew the Assistant Chief out the office door."

The Tokyo Fire Department investigated several fires caused by small batteries[548]. In one case, 2000 used coin-type lithium batteries (3.2 V) were thrown together into a cardboard box; the box ignited. In another case, a person's pocket ignited when a Ni-Cd battery (1.2 V, 600 mAH) used for powering handheld tape players shorted out. Testing showed that, when short-circuited by an external metallic object, the battery was able to pass about 18 – 20 A through test clips and staples and heat them red-hot. In a third case, a portable telephone left in a parked car started a fire. The cause was identified as being due to an internal failure of its lithium battery; the battery was improperly manufactured and had been the subject of a recall.

All electric batteries represent a form of stored chemical energy which can readily be converted to electric energy. The latter, in turn, may serve as an ignition source. Most batteries, however, will not contribute much fuel to the fire themselves. A different situation arises with lithium batteries, since the metal lithium is easily ignitable, will burn readily, will contribute appreciable heat to fire, and is not extinguishable by water, gaseous agents, or most dry chemicals. NTSB[549] documented a fire caused by rough handling of lithium batteries being shipped as air cargo. Ignition was found to readily occur upon mechanical abuse of the packages of batteries. Lithium batteries are classified as Division 9 (Miscellaneous Hazardous Material) under the UN and DOT classification system for hazardous materials. The UN Manual[550] provides a whole gamut of tests to be run on lithium batteries, however, these address only the issues of prudent manufacture and not of accidents due to abusive handling, e.g., dropping, crushing, or puncturing. Test standards dealing with end-user abuse have been issued by UL (UL 1642[551]) and by the US Navy[552] and results from a number of studies conducted by manufacturers or US military agencies that simulate abusive handling have been published[542].

Electric blankets and mattress pads

In old-style electric blankets, heating was provided by a resistive wire, and safety against overheating by thermostats. Multiple thermostats (often 12) were embedded in an effort to avoid overheating, nonetheless, these were not always successful. Apart from defective units, fires sometimes originated when the blanket was doubled over or tucked in, so that excessive heat was locally accumulated[271]. A CPSC study[553] on old-technology (pre-1982) blankets provided failure mode statistics shown in Table 52; comparable data on current-generation blankets are not available. UL has a test standard (UL 964) for electric blankets[554].

Since 1990, there has been only one manufacturer of electric blankets in the US. In 1981 they introduced the PTC (Positive Temperature Coefficient) technology. This is a self-regulating, conductive polymer—primarily polyethylene with carbon black—that operates much like self-

Table 53 Failure modes identified in a CPSC survey of fires originating in pre-1982 electric blankets

Failure mode	Percent
cord or cord/blanket connection	31
thermostat	27
heat entrapment (e.g., doubling-over)	18
short circuit	10
wiring	9
control unit	5

regulating heat tapes (see *Heat tapes and heat cables*). Discrete thermostats are not needed, since the entire heater itself functions as a thermostat. Unlike the old-style resistive arrangement, here the electrical topology is of parallel resistance between two good conductors. The latter are small-gauge wires, each of which is helically configured[555,556]. The technology has a certain resistance to aging-induced failures, since aging causes the equilibrium temperature to fall, not rise. Despite the improved safety of this technology, McLaughlin[557] reports that 500 fires per year are estimated to originate in blankets of the new technology. The failure mode has been described by Carlson[558] as: a break occurs in a conductor, arcing then occurs at the break, and the polymeric PTC material ignites from the arcing. McLaughlin points out that fuses or safety devices are provided, but that these only provide partial coverage, with faults beyond a certain distance along the conductor not being able to activate the device. Similar to certain heat tapes, "the PTC material acts as a fuel, burning and sparking much like the fuse of a fire cracker"[557]. But fires due to damage to the cord or to the control box may be more common than failures at the heating elements[559].

Blankets in other countries do not necessarily use the same technology. A 1999 British study[559] listed the causes of electric blanket fires as shown in Table 54. The appliance faults were found to be due mainly to deterioration or due to lack of adequate overheating protection (until the 1980s, there were a number of blanket models sold in the UK market without any overheat protection). Deterioration was commonly manifested as heating elements becoming detached due to excessive use, elements bending, and the consequent formation of hot spots. It was estimated that a flaming fire can occur about 2 h after a hot spot develops. Very old blankets were found to have yellowed or disintegrated polymeric material. Abusive uses included excessive folding, doubling, and use of blankets as mattress pads. British designs and customs were quite different from the US, since blankets were designed and intended only for pre-warming a bed, and were intended to be turned off during actual sleeping. Regulations in the UK governing electric blankets were tightened in 1990, and ignitions have been much decreased with newer-technology blankets. The earlier technology in the UK was badly antiquated, but post-1990 designs involve a sensor wire which is helically wrapped around the heating wire and separated from it by a polyethylene insulator which melts at a moderately overheated temperature. When contact between the sensor wire and the heating wire occurs, the control circuit deactivates the blanket. Earlier designs where PVC was the meltable polymer were found not to be reliable. The UK study concluded that the US-type PTC technology is probably significantly safer than the current UK technology.

Table 54 Causes of electric blanket fires in the UK

Cause	Percent
faulty appliance or cord	63
misuse of equipment	33
other accidental causes	3
other	1

Published information on fires associated with electric mattress pads (heating devices intended to be placed between the mattress and the bed sheet) is not available, but is sometimes believed that these are more prone to ignitions, since they have less extensive over-temperature protection and are more likely to be doubled over or tucked under by the user. In the US, the same electric heating technology as used for blankets is also used to produce heated 'throws,' 'cuddle-ups,' and heated comforters[560].

Electric circuit interruption devices

Circuit interruption devices are fuses and circuit breakers. Fuses are considered more reliable, since their failure modes are generally 'fail-safe,' while circuit breakers can 'fail-unsafe.' For fuses, unexpected circuit interruption can occur at currents below the rated capacity, if the fuse had been subjected to many overloads that did not quite blow the fuse. This is understood to be due to weakening of the metal fuse element by the excessive heating cycles. The forensic examination of fuses has been described by Twibell and Christie[561]. However, there is one important safety function which is customarily provided by circuit breakers that cannot be provided by fuses: simultaneous opening of all phases. If a fault occurs requiring the opening of a circuit interruption device and more than one phase conductor exists in the circuit, then current made available through the phase conductor which did not blow its fuse may still continue to cause damage. With circuit breakers, the problem is easily solved by mechanical or electrical means for gang-operation.

Expulsion fuses are the simplest form of high-voltage fuse and when they operate hot particles are discharged. Stokes[562] found that the greatest discharge of incandescent particles was when short-circuits currents of 50 – 200 A were used. The particles showed a range of diameters from 0.4 to 1.3 mm under those conditions. Color Plate 62 shows a shower of particles from a test conducted by Stokes. In that test, he placed an 0.7 × 1.0 m tray filled with hardwood twigs and leaves 2 m below the fuse. In 30 trials, there was only 1 ignition of the fuel bed by an ejected copper particle.

In a survey of low-income housing, CPSC found that 31% of circuits protected by circuits were overfused, compared to 12% for circuits protected by circuit breakers[563].

The role of a circuit breaker is a multiple one. If a modest overload is sustained over long periods of time, the circuit breaker must trip. But if a moderately high overload is presented for a short time, it must not trip. This is because electric motors present a very large load when first starting up, and circuit breakers would be constantly tripping if they did not permit such brief overloads. For highly excessive

overloads, however, a circuit breaker should trip nearly instantaneously. Modern circuit breakers are of the combined thermal/magnetic type. The thermal element is slow-acting and is designed to protect against sustained overload. Its action corresponds to the rated capacity of a circuit breaker, which specifies the current level at which tripping should occur for an overload of 'very long' duration. The magnetic portion responds very quickly to high-current faults. But the short-term tripping level is subject to the discretion of the manufacturer and is not marked on the device.

It is considered a good practice to periodically open and close circuit breakers, since it reduces the chance of a breaker being stuck in the closed position. Exercising breakers periodically cleans the contacts and verifies that the mechanism works.

Failure of a circuit breaker to open under electric fault conditions can be due to[564]:

- a defect in either design or manufacturing
- lack of maintenance
- inappropriate settings (on adjustable circuit breakers)
- fault current in excess of interruption rating
- insufficient fault current.

Early molded-case circuit breakers were of 'thermal' action alone. Some of these were subject to a failure mode if encountering a very large overload, under which condition the contacts would sometimes get welded shut, instead of opening. The commercialization of dual-mode (thermal/magnetic) circuit breakers has eliminated this failure mode (there are also some circuit breakers that only have magnetic action, but these are rare). Over the years, there have been a number of product recalls due to defects. Product defects leading to failure have included rusted parts, excessive mechanical friction, and contacts plated with a poorly-chosen metal, leading to excessive fouling in the presence of moisture and SO_2 in polluted air. Residential type circuit breakers connect to the supply bus by plugging on, rather than by being bolted down; there have been a number of failures at the supply-side connection, due to its limited robustness. Aronstein[565] presented laboratory studies showing failures due to other causes, such as improper oiling during manufacture and harsh climatic conditions. Some fires have been attributed to incendiarism, where an individual deliberately misadjusted an adjustable breaker to an excessive setting.

Some test data comparing various devices have been published by Franklin[566]. Franklin claimed that most arcs caused by short-circuiting in 120 VAC circuits range between 200 and 250 A, and that often a fire can get ignited from a short-circuit arc before a US-made circuit breaker will trip. To characterize the performance of a number of different types of circuit protection devices, he conducted tests specifically at 200 and 250 A. Table 55 indicates that the majority of breakers did not provide fast enough response in their supposedly-fast (magnetic trip) mode and that in most cases their instantaneous trip current exceeded the 200 A level characteristic of 120 VAC arcs. Franklin concluded that adequate protection can be obtained if the design of the European '5X' breakers was followed, which limits the instantaneous trip level to 5× the rated current.
Shefchick[567] investigated the realism of using the European

Table 55 The opening times for circuit protection devices under typical arc currents in 120 VAC circuits

Type	Rating (A)	Time to trip (s)		Instantaneous trip level (A)
		at 200 A	at 250 A	
ABC-8 glass fuse	8	0.005	0.003	NA
ABC-10 glass fuse	10	0.008	0.006	
MDA-15 glass fuse	15	0.015	0.008	
ABC-15 glass fuse	15	0.015	0.005	
AGC-20 glass fuse	20	0.033	0.021	
TL-15 plug fuse	15	0.025	0.012	
TL-20 plug fuse	20	0.063	0.016	
T-30 plug fuse	30	0.375	0.080	
European "5X" breaker	15	0.004	0.004	75
Brand A	15	0.008 – 0.075	0.008 – 0.032	120 – 180
	20	0.125 – 0.133	0.051 – 0.058	
Brand B	15	0.004 – 0.112	0.004 – 0.008	120 – 230
	20	0.008 – 0.275	0.004 – 0.152	
Brand C	15	0.310 – 0.450	0.192 – 0.256	325
	20	0.100 – 0.650	0.006 – 0.368	
Brand D	15	0.250	0.160	360
Brand E	15	0.360	0.230	360
Brand F	15	0.650	0.420	800+
Brand G	15	0.390	0.180	800+

breakers in North American power systems. He concluded that the design of the breakers was such that they can only be used successfully in the 240 VAC systems for which they were designed, and not in 120 VAC applications. This was because the contacts—which need to be more robust in lower-voltage systems—would not have withstood 120 VAC service. Also, the higher European voltage reduces starting currents, and permits use of breakers with lower instantaneous trip currents. If used in North America, nuisance tripping would result. If used to protect a 20 A circuit, a '5X' breaker would instantaneously trip at 100 A. This would cause unacceptable nuisance tripping, according to a study by UL[568]. They tested a vacuum cleaner, a circular saw, and an air compressor. These appliances drew steady-state currents of 7.4 – 11.4 A and, consequently, should properly be usable on 20 A branch circuits. But their inrush currents were measured to be 94 – 124 A, indicating that nuisance tripping would occur if a breaker instantaneously tripped at 100 A. In fact, the appliances would be unusable, since resetting the breaker and re-starting the appliance would repeat the cycle. Furthermore, the trend towards more efficient motors has adversely affected the situation, since efficiency is increased by decreasing the iron content of the motor and this leads to higher inrush currents during startup. UL also studied the consequences of re-powering entire branch circuits, for example, after a power outage. In these cases, inrush currents of 102 – 176 A were found for typical loads of electronics + lamps. The conclusion was that '10X' breakers would be practicable, but '5X' would not.

In testing, circuit breakers are only tested in ambient environment temperature. But the thermal-action portion of the circuit breaker is sensitive to ambient temperature, and the actual opening current will be raised if the breaker is in a cold environment (e.g., outdoors), or lowered if the breaker is in a hot environment (e.g., a panelboard full of other breakers drawing high currents. Thus, in order to avoid nuisance tripping under conditions where the panelboard is running hot, the NEC requires that "The rating of any one cord- and plug-connected utilization equipment shall not exceed 80% of the branch-circuit ampere rating." Branch-circuit circuit breakers are normally rated for an operating temperature range of –5 to +40ºC. Goodson et al.[569] conducted some tests to determine the effect of installation in some low temperature environments. Tests on 15 and 20 A rated breakers conducted at –14ºC and carrying a load 2× the breaker rating showed that trip times were increased, but remained below 120 s. By contrast, a 20 A breaker at –27ºC did not trip while carrying a current 3.1× its rated value.

Table 56 Available short circuit current in residential branch circuits

Available short circuit current (A)	15 A branch circuits	20 A branch circuits
average	300	467
minimum	77	81
maximum	1650	2260

The maximum current that can be delivered into a fault on a branch circuit will depend on the characteristics of the breaker and on the resistance of the wiring in between the breaker and the fault. A UL survey[568] of residential branch circuits gave the results shown in Table 56. These are not necessarily the current values pertinent to operation of a protective device, since if the short in an arcing short rather than a bolted short, the current in the circuit will be less than the available short-circuit current. For further details see: *Electric transmission and distribution systems*.

Circuit breakers have a finite capacity for sustaining over-current without damage—greatly excessive currents may lead to the destruction of the breaker. Reiter[570] conducted tests where the over-current failure of a 4000 A circuit breaker was simulated by presenting it with an internal phase-to-phase bolted short, located on a feed line capable of supplying 13,000 A short-circuit current. The fault current was sustained for approximately 10 cycles and the results are shown in Color Plate 65.

A circuit breaker may trip and clear the original fault, but the process can induce a new fault. Masumura et al.[571] studied this situation. The possibility arises because molded-case circuit breakers have a vent hole through which hot ionized gases are ejected. If these gases impinge across a narrow gap between two external electrodes, breakdown may be induced at that location. In limited experiments on a 110 VAC system using a circuit breaker with a short-circuit rating of 5000 A (rms) they placed the circuit breaker in a circuit having 24.5 kA short-circuit capacity and were able to induce an external fault; the measured arc current for the original circuit was 8.3 kA. Further modeling and testing produced a relation between the conductivity of the gases needed for breakdown, versus the voltage across the external electrodes. Over the range 150 – 350 V, the necessary conductance was 10^{-3} – 10^{-2} S.

Electric fences

Electric fences have been known to start grass fires in dry weather when vegetation contacts the conductor. The incendive ability presumably depends on circuit design details, which will not be identical for all units. Types using controllers described as 'weed clipping' or 'weed burning' are particularly liable to cause ignitions[572].

Electric lamps and lighting fixtures

Lamps* come in two basic types: (a) incandescent, and (b) arc discharge. An incandescent lamp is based on resistance

* The commercial terminology and the lay-person's terminology are confusingly different. The fixture itself is called a luminaire in commercial and engineering usage, but a lamp in lay usage. Meanwhile the lighting device that is inserted into the fixture is called a lamp in commercial/engineering usage, but a light bulb in lay usage. In addition, what is

heating of a tungsten filament. A sub-category which has recently become very popular is the *tungsten-halogen* type, also identified as *quartz-halogen*, or just *halogen*. Sealed lamps based on electric arc discharge are grouped into low-intensity and high-intensity types. Arc discharge lamps are not to be confused with traditional *arc lamps*, such as used in movie projectors. These involve an arc created in open air between two carbon electrodes and are not devices that are enclosed in a glass envelope.

ORDINARY INCANDESCENT LAMPS

Electric lamps, under certain circumstances, are known to be competent ignition sources. The effects of a lamp are two-fold: heating by direct conduction and radiative heating. If a lamp is not directly touching the potential target then, of course, conduction heat transfer will not exist. Convective heat transfer is present in all cases and is essential for cooling the glass envelope, but this only plays a limited role in ignition of combustibles. A number of sources list temperatures measured at various locations on lamps of various sizes. This type of information should only be used for very rough guidance, because the temperatures invariably are measured in free air. But except for very powerful lamps, ignition normally occurs only if a solid comes into direct contact with the lamp. As soon as a solid does come into contact with the glass envelope, however, the heat balance within the lamp changes significantly, since convective and radiative cooling is cut off at the location of the solid body. By simply comparing the tabulated values of lamp-surface temperatures with ignition temperatures of various solids, one would conclude that hardly anything can be ignited by an incandescent lamp—an incorrect conclusion!

Nonetheless, for the sake of completeness, some tabulated lamp-surface temperatures are given. Table 57 shows a large set of temperatures measured by one investigator for a variety of lamps[573]. These temperatures appear to be rather low, since one investigator[574] measured a peak temperature of 247ºC and another investigator[575] measured 263ºC for 100 W lamps. The temperatures at the lampholder are normally lower, for instance ca. 100ºC can be found for a 100 W lamp[576]. A peak temperature of only 89ºC has been reported[575] for 25 W lamps, yet decorative material was ignited in one fire from such a lamp. Even 89ºC is still above the rated temperature of general-purpose wires, so incandescent lighting fixtures often need to use high-temperature fixture wire.

Incandescent lamps are well-known as a cause of fires when placed in contact with towels, bedding, and similar low-density combustibles[522]. Incandescent lamps of a 50 W size or larger have also been known to cause fires when dropped into cellulosic attic insulation. A 75 W lamp has been documented to fully char through a plywood floor assembly[577] (Figure 26). If kindling or wind had been present, a flaming ignition, instead of full-depth charring might have been possible (although this was not demonstrated). Even 6 W night-light lamps have ignited highly insulative Dacron comforters[578], and manufacturers now offer 4 W lamps to reduce this risk.

commonly known as a lamp post is termed a light standard in commercial/engineering usage.

Table 57 Maximum temperatures measured for incandescent lamps in free air

Lamp type	Max. temp. (ºC)	Location of max. temp.
200 W clear	237	top, when lamp on its side
150 W clear	208	top, when lamp upright
100 W frosted	193	top, when lamp upright
75 W frosted	168	top, when lamp on its side
60 W frosted	145	top, when lamp on its side
40 W frosted	121	top, when lamp upright
250 W reflector flood	304	top, when lamp on its side
75 W reflector	213	top, when lamp upright
50 W reflector	196	top, when lamp upright
125 W infrared heat lamp	126	top, when lamp upright

An entirely different situation occurs when the glass envelope of a lamp is missing. Filaments are not designed to withstand the high-temperature oxidation which occurs in air, and a naked filament exposed to air will conduct electricity only for a short time before burning out. Its temperature, however, will be vastly greater than the surface temperature of the glass that is found in normal operation. Thus, arsonists are known[223] to have tried ignition devices where the glass envelope is carefully broken under de-energized conditions, then the lamp is positioned to ignite some flammable item immediately as the power is applied.

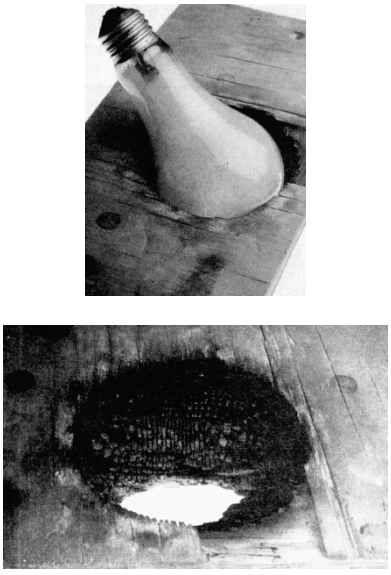


Figure 26 Charring of plywood floor from 75 W incandescent lamp
(Courtesy IAAI Fire & Arson Investigator)

During steady-state operation, the tungsten filament at 1800 – 2300ºC in a miniature incandescent lamp, around 2500ºC in larger lamps, and up to 3000ºC for special-purpose lamps. If the glass envelope is broken, the tungsten filament rapidly oxidizes, rises in temperature, and can actually flame for a short while before burning out[579]. When a filament burns out, an arc is sometimes formed across the gap. In the process of arcing, it will not necessarily be true that most of the original resistance of the filament will be available as a current-limiting series resistor. Thus, the arc can draw a substantial current. For this reason, manufacturers often incorporate a fuse in the wire leads going to the filament. This fuse can open up and arcing is then stopped. Occasionally, failure of lamps takes place in a manner not as anticipated by the manufacturer and the glass envelope shatters explosively. Incandescent debris can be ejected under such circumstances, and this may have a potential to ignite materials it lands upon.

Most incandescent lamps have short, straight filaments between the lead-in wires; however, some lamps, e.g., lamps for night lights and decor, have long, folded filaments which zig-zag between the lead-in wires. The filament folds are kept from touching and shorting out by supports. However, toward the end of life the filament may become weak, sag and stretch allowing the folds to touch. If they weld together, the normal wattage of the lamp may be increased by 50%. Series-connected street-light lamps often fail by arcing since the resistance of the other lamps in the series stabilizes the arc. The molten metal produced by the arcing can break the bulb and fall, igniting any combustible materials below[578].

An early investigation at the Bureau of Mines[580] examined the possibility for incandescent lamps to ignite methane/air mixtures upon the breaking of the glass envelope. They found that the probability of igniting the mixture depended on several factors:

- the way that the glass envelope was breached
- the diameter of the filament wire
- the over-voltage supplied
- lamp type, standard or miniature
- the type of filament used, carbon or tungsten.

Carbon filaments are no longer in common use, so their results are not reviewed here. Smashing the envelope usually broke the filament of standard lamps, but not of miniature lamps. In some cases, ignition was exacerbated because pieces of filament shorted together due to mechanical impact. Filaments were less likely to break in cases where a hole was made in the glass envelope, without shattering it. A higher probability of ignition was associated with filaments that did not quickly break. When an over-voltage was applied, not surprisingly the probability of ignition increased. At any given voltage rating, the probability of ignition increased with the wattage rating of the lamp. The diameter of the filament was seen to be a major factor, much as found in ignition testing with hot wires (Chapter 4). Ignition probability was high for wires of 0.17 mm or higher, and very low for 0.15 mm. The probability of ignition from very small (ca. 1 W) miniature lamps was much lower than from standard lamps. In another BM study[581], tests were conducted solely on miniature lamps used in mining applications. The glass envelopes were broken off the lamp before testing. Lamps rated for 3 – 6 W at 120 V were found to consistently ignite methane/air and coal dust/air mixtures when 120 V was applied. Likewise, a series of lamps rated 0.95 – 1.8 W at 2.38 – 28 V commonly caused ignitions when the design voltage was applied. A few types, however, did not cause ignition when supplied with the rated voltage, although these too led to ignitions if an over-voltage was applied. Lamps rated at 0.74 W or less never caused ignitions when supplied with the rated voltage, although, again, ignitions could be provoked by overload.

Similar systematic studies of lamps in larger wattage sizes intended for general illumination uses are not available. Normal, 75 and 100 W incandescent lamps, when dropped onto a floor and shattered, have been shown to readily ignite a gasoline spill[582]. Spraying water onto a hot bulb generally shatters the glass, but spraying gasoline may not, unless the spray is prolonged. The chances of igniting gasoline vapors are increased with 'rough service' lamps[499], since these have filaments which take longer to burn out when the glass envelope is shattered. Teflon-coated lamps were found not to break from liquid sprays and were quite resistant to impact breakage[582]. It has been found[583] that automotive taillight lamp filaments glow for about 7 s after the glass envelope is shattered, while those of sealed-beam headlights glow for about 5 s. Both of those 'immediately' ignite gasoline vapors.

In dust-laden environments, the insulating effect of a dust layer will cause temperatures of a lamp to rise. Likewise, deposits of dust on a protective globe can cause an increase in temperature; in one set of tests, the increase was measured to range between 22–34ºC for a globe over a 150W lamp averaging 130ºC in clean air[584]. The possibility of a breaking incandescent lamp igniting a dust cloud was tested by Morse[585], who used grain dust of an unspecified type but of small particle diameter (< 74 μm). She found that even a 6 W pilot light was able to cause an explosion, as were all higher wattage sizes tried.

Lamps made with a sub-standard sized insulator between the hot terminal and the ground threads have been known to cause fires[586]. This can occur when the defective (2-way) lamp is inserted into a 3-way socket. An intermittent short can then occur between the secondary hot terminal of the socket and the grounded screw base of the lamp, since the space that should be occupied by an insulator in a 2-way lamp or the secondary contact in a 3-way lamp is encroached upon by the metallic screw base.

Excessive temperatures and possible ignition may result if an infrared heat lamp is used in a lamp socket not designed

for the high base temperatures associated with this type of lamp[587].

Sanderson[588] tested the ability of 250 W infrared heat lamps to ignite various combustibles. When placed at distances of 50 – 130 mm above a wood stud, the lamps were able to create progressive charring within the wood, but a flaming ignition did not occur. A similar situation was also found for straw. But a cotton towel placed 50 mm below the lamp ignited in 3 min, while placed at 130 mm below the lamp it ignited in 4 min with a red lamp and 12 min with a clear lamp.

An incandescent lamp represents a resistive load, but with a non-constant resistance. The resistance is much lower when the filament is cold; as soon as it heats up, the resistance increases and the current drawn decreases. UL has measured the currents drawn by incandescent lamps[589] and determined that the peak inrush current is 10 – 15 times greater than the peak current that is found in steady state, when the lamp has equilibrated thermally. The large spike is present only in the first half-cycle, and by the second half cycle the value is only about twice the steady-state value. The exact value of the inrush current depends on when in the AC cycle the lamp is turned on. A much larger spike is found when a lamp's filament burns out. This was found to be 164 A for a 300 W lamp, and "in excess of 50 A" for a 75 W lamp.

In explosions involving flammable vapors or gases, broken incandescent lamps are sometimes found and it becomes of interest to determine whether the explosion was caused by a breaking lamp, or if the lamp simply broke due to being in an explosion. Allsop et al.[590] conducted experiments and examined the remains under a microscope. Their conclusions were:

- Filament broken when cold: the fracture is sharp-edged and there is no plastic flow of the tungsten. The surface resembles a bright steel wire.
- Filament broken due to natural burnout or due to overvoltage: the tungsten surfaces are bright and unoxidized; bright beads of molten metal are formed.
- Filament burned out due to shattering of glass envelope: a yellow or greenish-yellow deposit of tungsten oxide can be found on the supports of the filament; the metal ends at the filament gap are usually pointed, unless the lamp has been running at under-voltage prior to burnout, in that case there can be a thick deposit of tungsten oxide at the gap; the color of the filament ranges from steel gray (near the gap) to blue or blue-black near the supports, and it is rough-textured; beads of molten glass may adhere to the filament unless the glass was broken first and current only applied subsequently.
- Filament ignited vapors but did not burn out (possibly due to removal of power): the filament is covered by a film of blue-black oxide; if the filament broke subsequently (due to mechanical forces), the fractured ends are sharp-edged.

The condition of lamp filaments is also an important part of aircraft accident investigation, if examination of the filament can help to determine whether the lamp was illuminated or not at the time of impact, a Canadian guide[591] can be useful. The background document[592] to this guide contains much valuable forensic metallography information.

HALOGEN LAMPS

Halogen lamps were invented[593] in 1882, but were not commercialized for a long time, first coming onto the consumer market in the US in 1983. They operate with a tungsten filament, the same as common incandescent lamps. The differences are: (1) a halogen gas fills the envelope; (2) the envelope is made of fused quartz, not soda-lime glass; and (3) much higher surface temperatures can be reached by the lamp. Either iodine or bromine is used, filled to a very small pressure of 0.05 – 1.5 kPa. The filament in a standard incandescent lamp vaporizes a certain amount of tungsten, and the tungsten gets deposited on the glass walls, preventing small lamp sizes from being used. In a tungsten-halogen lamp, the halogen gas interacts with the tungsten vapor and an equilibrium is established which keeps the glass envelope largely free of metal deposit. In place of the argon which, along with nitrogen, is used to fill a standard incandescent lamp, a tungsten-halogen lamp commonly contains krypton or xenon, which reduce the rate of filament evaporation and extend its life. The envelope is usually made of vitreous fused quartz (which can operate at higher temperatures than glass), but sometimes from borosilicate glass or Vycor. Halogen lamps come in two types: (1) Lamps which comprise only a single quartz envelope. These must be used in fixtures with an external shield to prevent excessive UV radiation and minimize the danger of exploding fragments, should the lamp rupture. For many consumer applications, it is also desirable to have an outer wire-mesh shield which minimizes the possibilities of external combustibles contacting a hot surface. (2) Lamps with an inner quartz envelope which is enclosed within a thick glass outer envelope. These have PAR, MR, MB, TB, or BT industry designations and do not need any other shielding.

In a statistical study, CPSC noted 277 accidents during 1992-1997 with halogen lamps[594]. The breakdown was (numbers rounded to nearest percent): 29% fire due to ignition of nearby objects; 19% fire due to exploding lamp; 15% fire due to electrical short; 12% fire due to lamp tip-over; 11% fire, other; 3% exploding lamp, no fire; 4% shock or burn; 8% other.

In lab studies[595], CPSC measured typical equilibrium temperatures of 611ºC for a fixture using a 500 W halogen lamp, 585ºC for one with a 300 W lamp, and 602ºC for one with 250 W lamp. In comparative testing, a 150W incandescent lamp was found to indicate 284ºC, while a 100 W

incandescent lamp gave 224ºC. Industry sources report that some halogen lamps, however, can run at up to 900ºC. CPSC also conducted tests using cheese cloth and terry cloth material placed on top or near the lamp. From this testing, they concluded that if a 300 W lamp is used with a supplemental guard, ignition of most combustible materials which could come in contact with the lamp can be avoided. Lowe et al.[596] measured a temperature of 630ºC on the surface of a 300 W halogen lamp and 421ºC on the tempered-glass shield above the lamp.

A paper gives the results[597] of operating a 300 W halogen-lamp fixture within 229 mm (9 in) of walls and ceiling which were covered with cardboard. The highest temperature reached on the wall was 88ºC, with the ceiling being only 70ºC. No scorching occurred. At least one case has been documented where a halogen lamp placed under a low plywood-paneled ceiling caused a house fire[598]. Subsequent testing suggested that the fixture probably used a 500 W lamp and might have been as close as 0.1 m to the ceiling[599]. A house fire has been claimed to be started from a halogen lamp (300 or 500 W) igniting a fabric valence located 127 mm (5 in) away[600], but this has been legally disputed. Béland[601] reported some experiments where he placed strips of paper on a 300 W halogen torchère lamp. For paper strips placed on a hot lamp, ignition was "in seconds." For a condition where a paper strip was placed on a lamp, then the lamp was turned on, charring started in 2 min. Ignition did not always occur and sometimes the paper just charred. Béland did not specify the exact relation of paper to lamp, i.e., whether a guard was in place.

Halogen lamps may explode and act as ignition source. Ignition of bedding occurred when a halogen lamp exploded and deposited hot glass upon a bed[602]. The same author notes a case where an eyewitness observed a lamp explode as soon as its power was turned on; a fire was avoided in the second case. In another case[596], hot glass fragments from a halogen lamp that exploded ignited a carpet, which was extinguished by the owner.

CPSC's investigation of accidents associated with halogen floor lamps led to a number of changes in the standard (UL 153[603]) under which these devices are generally tested. The main changes were that 500 W lamps were no longer permitted, with 300 W being the largest allowed wattage. Also, a mechanical shield was required which is intended to keep combustible matter from coming too close to the hot lamp.

Holmes[604] reports that some tests have been made on the possibility of 300 W halogen lamps igniting gasoline/air atmospheres without shattering. This was normally not possible, but in one case when a fixture containing a halogen lamp was violently thrown against a concrete floor, an explosion did result. Examination of the lamp indicated that the filament did not have as many filament support wires as other makes of lamps and, consequently, the hot filament could deflect enough to cause a hot spot on the quartz envelope, with the flammable vapor mixture being ignited from that hot spot.

It is reported[605] that some halogen lamps have to be positioned within 5º of horizontal lest they shatter unexpectedly due to a phenomenon of halide migration.

ARC DISCHARGE LAMPS*

Arc discharge lamps are divided into two basic types: low-intensity and high-intensity. Low-intensity discharge lamps include low-pressure sodium and fluorescent types (the latter are discussed separately, below). High-intensity discharge (HID) lamps include mercury vapor, high-pressure sodium, and metal halide types. All discharge lamps require a ballast to start and stabilize the arc discharge. Mercury vapor and metal-halide HID lamps (Figure 27) have a tube made of fused quartz (silicon dioxide glass) that contains the arc discharge. The arc tube for high-pressure sodium HID lamps is made of polycrystalline alumina (aluminum oxide). In all three types of lamps, an outer glass envelope then surrounds the inner arc tube to prevent contamination and, for mercury vapor and metal-halide types, to absorb the intense ultra-violet radiation. The space between the arc tube and the outer glass envelope is filled with a small amount of dry nitrogen to prevent oxidation of the metal supports.

The arc tube operates at around 600 – 800ºC in mercury vapor lamps, 900 – 1100ºC in metal-halide lamps[606], and up to 1200ºC in high-pressure sodium lamps[607]. At operating temperature, the internal pressure in the arc tube can be as high as 7.5 atm and the outer glass envelope temperature[608] can be as high as 400ºC. The arc tube of HID lamps can unexpectedly rupture and shatter the outer glass envelope, resulting in the discharge of hot glass fragments and extremely hot particles of the arc tube. Arc tubes rupture from internal causes (such as manufacturing defects), from external causes (such as ballast failure, lamp misapplication, or injury to the outer glass envelope), and from old age.

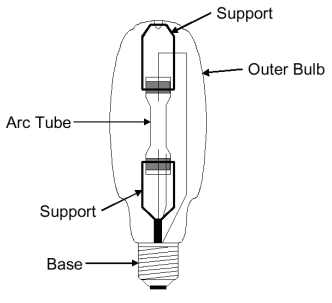


Figure 27 Construction of an HID lamp
(Copyright NEMA, used by permission)

* This section written by Ross F. Firestone.

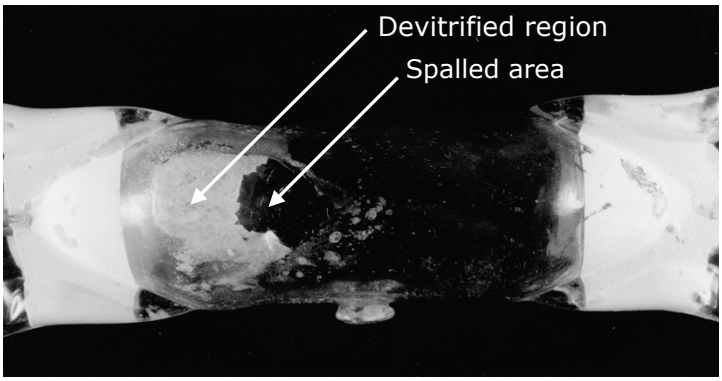


Figure 28 A 400 watt HID arc tube showing a devitrified region and a portion of that region that has spalled out
(Courtesy Ross F. Firestone)

In addition to their incandescent temperature, the amount of heat in the arc tube fragments is high, equivalent to 10 or 20 matches; thus, even after falling 7 – 9 m through the air they can ignite combustible materials, such as furniture and cardboard. If the lamp is enclosed in a fixture with a thermoplastic lens/diffuser, the arc tube fragments will melt and ignite the plastic causing flaming drops to cascade to the floor. These can ignite hardwood floors such as are used in basketball courts even when they are 9 m below the lamp.

Devitrification is a cause of rupture unique to lamps using fused quartz arc tubes. Fused quartz is a glass and, like all glass, is unstable. Over time it reverts to crystalline quartz from which it is made. This process is called devitrification. Normally this does not occur before the lamp has burned out from other causes, but it can occur in an operating lamp if the arc tube is contaminated with water vapor, sodium or other materials during manufacturing, or by the environment if the outer glass envelope is broken.

Devitrification starts at the surface of the arc tube from the formation of quartz crystals at a region of contamination. The crystals have a lower volume than fused quartz glass so devitrification causes the surface to contract and produces a network of cracks which appear frosty white (Figure 28; a normal arc tube is shown for comparison in Figure 29). The cracks grow along the tube surface and into the wall until the tube is so weakened that it ruptures from internal pressure.

The crystallized region undergoes several sudden volume shrinkages at different temperatures as it cools. If a lamp with a partially devitrified but intact arc tube is turned off, the arc tube will sometimes shatter as it cools, or the devitrified layer may exfoliate, exposing a network of cracks in the fused quartz glass. Devitrification is slow below 810ºC, hence it is more common in metal-halide arc tubes which operate as high as 1100ºC than in mercury vapor arc tubes which operate below 800ºC under normal conditions. The aluminum oxide arc tube used in high-pressure sodium lamps is crystalline and therefore immune to devitrification. In addition, it is 4 to 5 times stronger than a fused quartz arc tube[609].

Arc tubes may bulge and rupture if run under improper conditions due to:

- Incorrect or defective ballasts which operate the lamp at over or under the rated wattage or do not fully start the lamp (Figure 30).
- Fixtures with improperly designed reflectors which redirect energy directly onto the arc tube.
- Improper positioning of the lamp so that a "Base Up" lamp is burned in base-down position, or a vertical lamp is burned horizontally or visa versa.

Arc tube bloating is more common in mercury and metal-halide lamps because fused quartz[609] softens at approximately 1350°C while alumina[610], which is used in high pressure sodium lamps, does not weaken until approximately 1600°C. If the outer glass envelope of an HID lamp is broken, the lamp may continue to operate for weeks or even years. During this time the exposed arc tube produces hazardous ultra-violet radiation and also can be an ignition source for explosive concentrations of dust or gas in air.

Since a failure of an HID lamp can eject material at up to 1200ºC, there is a potential for ignition if a non-

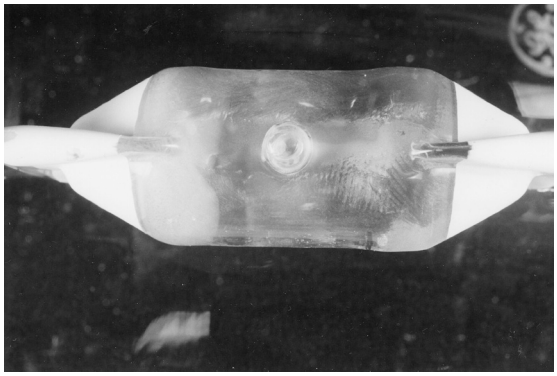


Figure 29 A normal arc tube from a 400 W HID lamp
(Courtesy Ross F. Firestone)

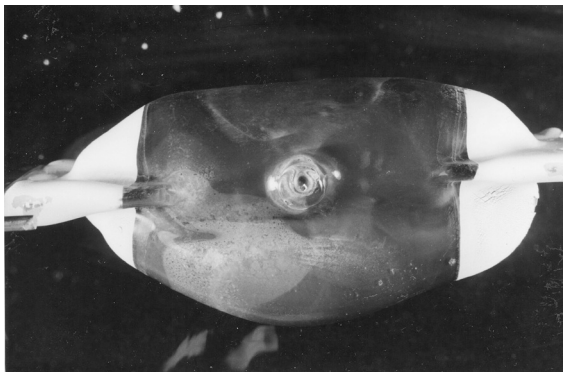


Figure 30 Bloated arc tube from 400 W HID lamp due to ballast failure
(Courtesy Ross F. Firestone)

combustible shield that can capture and retain any broken material is not installed below an HID lamp. There have been 29 losses at premises insured by FM Global during the 1990s due to ignitions from HID lamps[611]. Of these, 14 were metal halide, 12 mercury vapor, and 3 sodium vapor. In the US, the industry recognizes three types of lamps: E, S, and O types. E types must be used with a bottom shield, O types have an integral barrier within the lamp and consequently do not need a barrier, while S types are a low-cost choice which is approved for use in open-bottom fixtures. The electric industry trade association NEMA considers it to be acceptable risk[612] to use S-type lamps, although this is a decision that users must make for themselves. The risk is lower if lamps are systematically replaced after a certain number of hours, before end-of-life failure occurs. In addition, HID lamps may fracture due to overpressure if continuously operated. Manufacturers' recommendations are that the lamps be turned off once a week for at least 15 minutes; if overpressure has occurred, the lamp will not restart. Requirements for HID lamps used to be given in UL 1572; this was superceded in 2000 by UL 1598/CSA 250[613] which is a master standard governing a variety of lamp types.

Because sodium reacts pyrophorically with air and water, it has been shown that breaking a low-pressure sodium lamp not connected to an electric supply can result in the ignition of a methane/air mixture[581]. This is because these lamps contain up 1 g of sodium. However, high-pressure sodium lamps, which only contain about 8 mg sodium were found to be non-incendive.

FLUORESCENT LAMPS

Even though the temperatures developed by fluorescent lamps in normal operation are modest, this is not necessarily true if the lamp is used abusively, e.g., by covering it up with combustibles. A Japanese study documented that 300ºC can be reached from a 27 W compact fluorescent lamp that is covered up by bedding, and this corresponds to a fire that occurred under these circumstances[614]. Verweij[615] conducted tests on fluorescent lamps and classified ignitions of flammable atmospheres into the following categories:

- The glass envelope is broken, exposing the insides and extinguishing the electric discharge between the electrodes. The tungsten wire spiral preheating the electrodes is energized by the starter and begins to glow, rapidly oxidize, and break. When it breaks, an electric spark occurs and this can ignite a flammable atmosphere.
- In some exceedingly-flammable atmospheres (e.g., hydrogen in air), explosion may be caused merely by the residual heat of electrodes. This mechanism cannot ignite natural gas/air atmospheres, however.
- Likewise, only in exceedingly-flammable atmospheres explosion can be initiated by a shock-wave mechanism, due to rapid expansion of gases into the previously-evacuated space. In extreme cases, this can take place in a cold lamp.

LIGHTING FIXTURES: INCANDESCENT

Until the energy crisis of the 1970s, many attics were uninsulated; it was also uncommon to use recessed ceiling lights in residential-type construction. The energy crisis caused many owners to insulate their attics, and they often chose low-cost cellulose insulation. Also, recessed incandescent ceiling fixtures started becoming popular. The early fixtures were just a sheet metal can. Ignitions of combustible ceiling insulation started being reported from these fixtures. To avoid these ignitions, three solutions are possible: (1) box in an air space around the fixture; (2) make a double-walled fixture, possibly with non-combustible insulation in the gap; (3) provide a thermal cutout on the fixture. Solution #1 is labor-intensive, but can be effective. Solutions #2 and #3 have been present in the NEC since 1981 and have been incorporated in UL 1571, where detailed requirements for 'IC' fixtures are given. These are fixtures which have been tested and found to be safe in insulated-ceiling constructions. To also avoid direct ignition of wood members, the NEC requires either that the fixture have a 13 mm clearance from wood members, or that parts of the fixture in contact with the wood not rise above 90ºC. Non-IC-rated fixtures remain on the marketplace, since IC-rated ones are not necessary if combustible insulation is not placed in the ceiling.

Issen[218] reported on a special rig that was built at NIST in the 1970s to examine ignition of cellulose insulation by non-IC fixtures. The test was a simulated attic space where the attic temperature was maintained at 60ºC, representing high summer temperatures. For fixtures installed without protection, there was no cellulose insulation found that could be sufficiently FR-treated in order to not get ignited. Ignition times are not given, but the test time was always less than 7 h.

The hazard of ignition is directly increased if the fixture is 'over-lamped,' that is, operated with a lamp of greater wattage than the rating permits. Extensive testing at the Oak Ridge National Laboratory documented the increases in temperature for various over-lamping conditions[616]. Tests showed that ignition hazards from recessed ceiling fixtures are much lower when reflector lamps are used, rather than ordinary light lamps[617]. This is not surprising, since the reflector minimizes heat transfer upwards, where there is the highest potential for ignition.

While ignition of thermal insulation is the main hazard caused by improper installation of ceiling fixtures, it is also possible to ignite high-density combustibles such as solid wood. CPSC documented a fire[522] where solid wood was ignited from a 100 W lamp used in a fixture rated for 60 W, having the additional installation fault that the occupant had failed to install the heat shield that was a needed part of the light fixture. Cooksey[618] described tests where temperatures

were monitored in and around 150 W non-IC fixtures improperly covered with R-19 attic insulation. A peak temperature of 343ºC was reached at 105 minutes in one test, and wire insulation was found melted off the wires upon examination. In another test, a peak temperature of 482ºC was reached in 90 min, at which point the wood members ignited. Apart from these basic results, test details were not supplied.

A subtle form of hazard was also discovered in connection with non-recessed (i.e., *surface-mounted*) ceiling fixtures. NIST laboratory studies showed that addition of even a minimal thickness of thermal insulation directly above surface-mount fixtures holding two or more, properly sized lamps caused wire temperatures to exceed the 60ºC insulation rating[619]. Excessive wire temperatures can lead to thermal degradation and subsequent failure.

Failures of lamp sockets have been noted which were due to thermal effects destroying a good contact between an aluminum shell and a brass eyelet through which current was fed[710].

Cooper[622] has described an arc tracking failure of a phenolic lampholder. Arc tracking occurred between the pins due to a damp environment. The resistance was measured and indicated an acceptably high value, yet, upon reconnecting to the power source, a loud crack was heard. The lampholder was then studied by connecting it to a high impedance power source (which limits the available current). Under those conditions, it was possible to watch "a glowing thread gradually extend from one pin to the other."

See also: *Cellulose insulation.*

CHRISTMAS TREE LIGHTS

Christmas tree lights are a low-power device, with current products commonly being arranged as two or three strings joined in parallel, with each string containing 50 lights in series. The current drawn by a set of 100 lights is 0.3 – 0.4 A and each light is typically rated at 2.5 V and consumes about 0.4 W. It can be difficult to make miniature lights that are reliable from a fire safety point of view, and the industry has progressively made improvements. Thus, over the years, fused plugs were introduced, the light filament shape changed so to decrease the potential of a drooping filament contacting the glass envelope and creating a hot spot on it, and the contact configuration between the lamp base and the lampholder was improved (greater depth, use of ribs). With the current contact types, errant wires are less likely to make an unintended electrical contact. Despite their low power dissipation, Christmas tree lights continue to start house fires, and, CPSC requested UL to upgrade their standard for this product. Consequently, in 1997 a major revision was made to UL 588 to make it a tougher standard. The tightening up was done 'on general principles' and there was no specific experimental study program. The major changes in the UL standard governing products using push-in type lamps, which are the most popular in the marketplace, are summarized in Table 58. A small fraction of Christmas tree lights can be found in retail stores that are not compliant to UL 588; a much higher probability of ignition may be expected with those. Testing has indicated that the most likely ignition mode is one of a bad series-connection. A fault of this type effectively decreases, rather than increases, the current consumption, so fusing is ineffective against it. Using UL 588-conforming products, tests showed that as little as 1.25 W dissipated in a resistance connection can ignite notebook paper and 2.2 W dissipated in a similar connection can ignite the lampholder itself[623].

Table 58 Flammability-related changes in UL 588 for Christmas tree lights (series-connected, push-in type lamps)

Item	UL 588, 16th ed.[620] (1990)	UL 588, 17th ed.[621] (1997)
plug flammability	V-2	V-0
wire size, min.	24 AWG	22 AWG[b]
cord type	FXT	CXTW
wire insulation thickness, min.	0.51 mm	0.76 mm
wire temperature rating	60ºC	105ºC
wire flammability test		VW-1
wire environmental rating		"W" rating required for outdoor use; must pass sunlight & water resistance testing
lampholder/husk	phenolic or urea	V-1, or phenolic or urea, or meets UL 1694[c]
max. surface temperature	125ºC rise	65ºC rise anywhere; max 90ºC on lamp (absolute, not rise)
fuse[a]	3 A[d]	3 A
mechanical tests		added/upgraded

[a] both sides must be fused in non-polarized plugs; higher ratings allowed for larger wire gages
[b] 20 AWG min. if polarized plug
[c] for lampholders smaller than 2500 mm^3
[d] no fuse required in plug if a special design is used where the first and last lamps act as current-limiting devices.

LIGHTING FIXTURES: FLUORESCENT

A British study[624] provided a breakdown of the causes of fires due to fluorescent lighting fixtures (Table 59). Wiring failures were identified largely to be caused by overheating of the tube socket and resulting breakdown of insulation.

The main component in fluorescent lighting fixtures that has been associated with ignitions, especially of combustible-tile ceilings, is the ballast. A ballast raises the line voltage to a value sufficient to cause a gas discharge in the lamp; ballasts are needed for fluorescent fixtures operating at less than 277 VAC. The main component of a traditional

ballast was an iron-core inductor or transformer, potted in pitch and contained within a sheet-metal housing. The failure mode is normally a shorted turn in the inductor windings, which causes the device to overheat. If no protective measures are in place, ballasts have even directly ignited wood members[625]. The inside of the metal case of a ballast is filled with a pitch-like potting compound. The compound prevents ingress of moisture, reduces noise from the inductive components and acts as a heat sink. Problems arise if a temperature increase causes the potting compound to melt out of the enclosure. If the potting compound melts out, wire insulation often breaks down and the coils overheat. The overheating can cause a break in the wire, and a spark can be emitted as the break occurs. If the melted potting compound created sufficient flammable vapors, a fire can result.

In the US, in 1968 the NEC initially introduced requirements for 'Class P' ballasts. These are thermally-protected, using the requirements of UL 935[626]. The thermal protection is allowed to be of the cycling, self-resetting type. These fixtures are marked with a 'P' to identify the presence of a protective device[634]. Other safety features of fluorescent lighting fixtures apart from the ballast are covered in UL standard 1570[627]. Yarbrough et al.[628] studied temperatures of fluorescent fixtures equipped with Class P ballasts but not specifically designed for use with insulated ceilings. The thermal protection devices kept temperatures below 80ºC in all cases, but in one case ballast potting material was found to liquefy and melt out.

Ignitions occur most readily when the ballast is mounted directly onto the metal fixture housing, which in turn is directly mounted onto a combustible ceiling. Designs which use a spacer to keep the inductor away from the metal fixture housing are less likely to cause ignition of ceilings. An ongoing fire may damage the thermal cutouts of ballasts in the vicinity; thus, care is needed in investigating to determine whether a particular ballast was actually the cause of the fire. The ballast should be opened up and the overheat patterns examined inside. These can make it clear whether the fault was internal or due to external heating. Occasionally, excessive ballast temperatures cause an accumulation of vapors of the molten pitch, with a subsequent explosion[271]. There are alternate means for providing the needed voltage apart from an iron-core inductor. 'Electronic ballasts' have become common in recent years, and these replace much of the bulk of the iron-core inductor with an electronic circuit. Due to the history of ignition of combustible ceilings from ballast malfunctions, the NFPA Handbook[290] carries the warning: "Fixtures containing ballasts should not be mounted in contact with low-density, cellulose fiberboard, unless they are specifically listed by a qualified electrical testing laboratory for mounting in that manner."

Table 59 Causes of fires from fluorescent lighting fixtures

Cause	Percent
ballast	53
wiring	15
tube (overheated or in contact with combustibles)	8
transformer	8
starter	7
fitting, component	7
capacitor	2

Apart from shorts in the windings of the inductor, another way that fires can originate from a fluorescent lighting fixture is a failure of the capacitor, which is used in all but the simplest ballasts. Thermal cutouts are only rarely effective against failing capacitors[223].

An Australian investigation of fires caused by fluorescent lighting fixture starters identified a common failure mode[629]. A starter is a small cylindrical device whose primary active component is a glass bulb containing bimetallic contacts. The glass bulb is filled with a mixture of helium, hydrogen, and argon at low pressure, along with a radioactive material to facilitate ionization. When inactive, the contacts are in the open position. When voltage is first applied to the bimetallic contacts, a glow discharge occurs and the contacts begin getting heated and eventually close. This allows current to flow through the heating elements at the ends of the fluorescent tube and start heating it. A current flow occurs in the tube then and the voltage across its two ends (and across the starter) then drops and the starter's contacts open up. Tiny wire leads are attached to the glass bulb of the starter and initiation of the fires was found to involve a faulty design where wires have an excessively sharp bend (Color Plate 63), leading to failure at the bend. The heating of the wire at the failing spot ignites thermoplastic components of the starter. In turn, molten, burning material from the starter then falls onto a thermoplastic light diffuser, allowing it to ignite. These types of fires are avoided by use of properly manufactured starters where the lead wires do not contain sharp bends.

Another mechanism which has been identified as a potential cause of fluorescent lighting fixture fires is the thermal relaxation of the spring contacts in the lampholders[630]. A laboratory investigation in the aftermath of a fire revealed that, with certain lampholder designs, after sufficient aging and thermal stress, a spring no longer makes contact to the pin of the light. The fixture appears to operate normally, because current is carried by means of an arc over the gap. A glowing connection between the lampholder and the lamp's pin was also observed in some laboratory tests. Under such conditions of a glowing/arcing connection, the urea formaldehyde insulating material comprising the body of the lampholder gradually turned from white to brown to black, and eventually ignited in a smoldering mode. By contrast, virgin urea formaldehyde would not ignite in a

smoldering mode. This failure mechanism is specifically limited to certain models of 'push in' types of lampholders and does not apply to the more common 'twist in' type.

Overheating of the lamp base and lampholder can occur if fluorescent fixtures are improperly wired in converting fixtures from conventional ballasts to instant-start ballasts. The wiring must be such that the current of one lamp does not pass through the second lamp, and NEMA provides detailed instructions[631].

An ignition hazard can exist with certain compact fluorescent lamps that are a direct screw-in replacement for Edison-base incandescent lamps[632]. These come with a built-in electronic ballast in the base. Excessive heating and melting of the base can occur when the lamp reaches its end of life and the electronic circuit repeatedly attempts to unsuccessfully light it.

Electric motors

Motors are one of the few types of electric devices that are likely to fail due to insufficient, as opposed to excessive, voltage being supplied. There are two possibilities: (1) Low voltage. Below a certain voltage, many (but not all) types of motors will stall. If a motor stalls, it can no longer generate the back e.m.f., which is essential to limiting the current flow through it. Consequently, unless a protective device activates, damage and possibly fire[633] may result. (2) Single-phasing. Higher capacity motors are commonly 3-phase devices, dependent on current through 3 phase conductors being available. If one of the phases drops out, the motor may still turn as a single-phase device but overheat.

Failures of motors driven by electronic variable-speed controllers are sometimes found to be due to the overvoltage created by the spiky waveform generated by the controller[867].

Apart from electrical or mechanical faults which lead the motor to ignite itself, a motor may end up as an ignition source to external combustibles, especially dusts. Motors which are not fully-enclosed present a spark ignition hazard in cases where an explosible gas or dust atmosphere may be present. In addition, if used in a dusty atmosphere, a motor whose external surface would otherwise be at a low enough temperature may sustain a sufficient temperature rise to ignite combustible dust. In the same vein, some totally-enclosed, fan-cooled motors contain an outer annulus through which air is moved. In a dusty environment, this annulus may get plugged with dust, causing its ignition. Motors that are not fully enclosed and are used in a dusty atmosphere can get clogged within their operating innards and ignite themselves.

When compressors are of moderate size, the motors used to drive them are almost invariably a sealed unit, integral with the compressor. The experience is that, because they contain thermal protection devices and have a sealed construction, it is extremely unlikely that a fault within the motor would cause an external ignition[634].

Table 60 Failure modes of electric outlets studied by CPSC

Cause of failure	Percent
fire or flame	38
sparking	26
no longer functional	20
overheated	14
smoke emission	3

Electric outlets, plugs and connections

The ignition problems related to electric outlets (receptacles), electric plugs ('attachment plugs,' in UL's terminology), and various connections are often interrelated, thus they are considered jointly in this section. In the US, electric outlets are generally sold in four quality grades, which are, in descending order:

(1) hospital grade
(2) Federal Specification grade
(3) commercial/"specification" grade
(4) general/residential grade; often does not carry any designation of grade.

In an extensive study[635], CPSC collected 66 outlets with problems actually or potentially leading to fire. The causes of failures are given in Table 60.

In a 1995 Japanese study[636] some 28,112 wiring devices (outlets and plugs) that were located in moist places (kitchens or bathrooms) of residences were surveyed for deterioration and hazardous conditions. Out of the total, 27 devices were found to be damaged, most showing more than one type of damage. The gross damage rate was thus 1×10^{-3}. This rate, of course, is not for failures leading to fires, but only for damaged conditions that indicate a seriously diminished level of safety and could—given a combination of circumstances—eventually lead to fire. The results are

Table 61 Damages found in the 27 devices showing hazardous conditions in a Japanese survey

Damage found	Number of devices
charring around plug blades	17
plug blades discolored due to overheating	17
bent plug blades	11
arcing signs around plug blades	8
charring or melting around openings in receptacles	7
verdigris	6
charring between plug blades	5
discolored prongs of receptacles due to overheating	4
poor connections within screw-assembled plugs	3
poor connections of wires in receptacles	2
oily or dusty	2

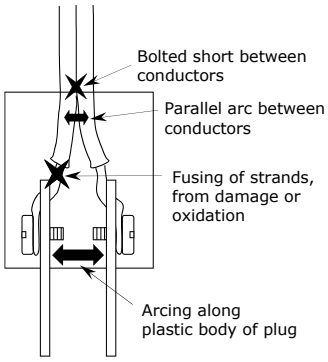


Figure 31 Four common failure locations at electric plugs
(Courtesy Yasuaki Hagimoto, NRIPS)

summarized in Table 61.

A Canadian survey of households[637] conducted in 1982 identified that 52% of the respondents had encountered problems in their households with poor mating contact at wall outlets, i.e., "contacts too loose." Even though the sample size was small (25) the finding was of serious concern, since it implied a lack of sufficiently rigorous standards for outlets and plugs to ensure that plug/outlet connections are sound and do not lead to overheating and possible fires. The study also noted that while higher grades of devices are available in the marketplace, they are difficult to sell, since the wiring device market is highly cost-competitive and consequently the least robust devices that can meet minimum standards predominate.

A NIST investigation[638,639] on the nature of failures of connections concluded that a reliable mechanical connection between two current-carrying metallic contacts is not trivial to make. The only thing preserving a mechanical (i.e., not welded or soldered) connection is spring force in one or more components of the connection. But spring force diminishes due to repeated heating, creep, and resultant stress relaxation. Due to thermal cycling occurring from variations in electric current, the wire connection undergoes a "squirming" micro-motion. The motion causes a buildup of metal oxide, which, in turn, increases the electric resistance of the connection. The probability of failure greatly increases with increasing ambient temperature. If all portions of the connection are not made of the same metal, then additional effects due to differential thermal expansion come into play and can further contribute to cold flow of components.

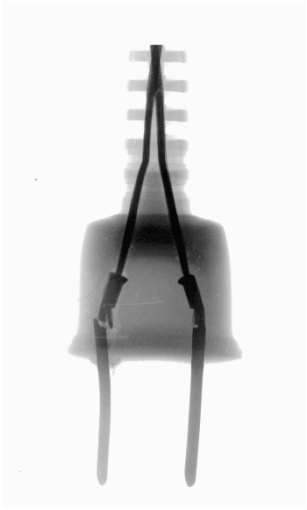


Figure 32 X-ray of molded plug at the end of a vacuum cleaner cord. The blade broke due to repeated stress of pulling on the cord sideways. Fire jetted out from the plug, but was noticed by the user.
(Courtesy T. Hijikata)

FAILURES AT PLUGS

An electric failure of a plug can originate in several ways:

- degradation due to excessive temperatures or excessive electrical loads, including 'hot-plugging' under high load
- mechanical damage
- defect in manufacturing, e.g., improper crimping
- insufficient tightening of screw connection
- poor contact with the mating female part
- contamination leading to arc tracking.

These failure modes have not all received equally extensive study, but sufficient studies (although mostly only in the Japanese literature) now exists so that general failure modes can be understood. Hagimoto et al.[640] consider that there are 4 locations at a male plug where failure is most likely (Figure 31).

Plugs associated with high-current devices are especially likely to sustain degradation which can later lead to a fire. Failure under 'hot-plugging' conditions was studied experimentally by Blades[641]. He repeatedly inserted and removed a plug to which was connected a 1500 W load. Initially, only brief, self-extinguishing arcing could be produced. But after about 10 min of continued insertions and removals, sustained arcing at the plug/outlet interface occurred. The arcing was sustained at that point and accompanied by voluminous emission of pyrolysis products from insulation materials. Inspection of the plug surface showed carbonization of insulation. Color Plate 64 shows a hair dryer plug which was found to be degraded due to normal use.

Mechanical damage is common in plugs, especially if they are removed by yanking or are subject to pounding from furniture, doors, etc. If a cord is yanked sufficiently frequently, wire strands inside may break, leading to overheating and possible failure. An example of the ultimate consequence of such repeated mistreatment is shown in Color Plate 66. Ignition due to failure of a blade from mechanical abuse is shown in Figure 32. Several researchers have conducted laboratory experiments to explore failures due to mechanical damage. Uchida et al.[642] found that the propen-

sity for separation of wires from the plug connection (only plugs with screw-attached wires were tested) depended greatly on the exact details of the cord and plug used. They conducted tests where the cord was repeatedly pulled until failure occurred. For some arrangements, 20,000 pullout cycles were successfully sustained. But when the wire was sloppily terminated in the plug, failures occurred in as few as 2000 cycles (no load) or 4000 cycles (7 A load). In their tests, the connection was not subjected to other stresses that can occur in real life, for example, shoving of objects against the plug, leading to a sharp bend in the wire. Thus, their numbers should be viewed as an upper limit. The failures in Uchida's tests all involved open-circuits rather than ignition.

Shimizu[643] also studied the failure at the cord/plug junction due to mechanical forces. In one series of tests, he bent the cord back and forth over a ±70º angle until strands broke. Using a 1 kg pulling force on the cord, it took 2000 cycles to break all 30 strands of a wire entering a molded plug. Two types of do-it-yourself plugs that attach by screwing together were also examined. For one it took 250 cycles, while for the other 2000 cycles. After the strands were broken, Shimizu conducted ignition tests by connecting an incandescent lamp load of 1000 W to each cord, bending the cord by hand back and forth at about 30 times per minute, and watching for ignition. For tests where PVC plugs and PVC-insulated cords were used, only arcing holes were made in the specimens, without flaming ignition. But for tests using (a) PVC plugs and rubber/cloth insulated cords (such as used for some heaters), and (b) PVC plugs and neoprene-insulated cords, flaming ignitions were recorded, with the duration of flaming being from 3 s to 2 minutes. Typical results are illustrated in Color Plate 68. Target fuels were not present, so ignition of other objects was not observed.

Shimizu then conducted a second series of tests where he abused the plugs by bending until a break was created at either **P** or **Q** (see Figure 33). He then maintained arcing at **P** or **Q** by moving the body of the plug back and forth by hand. Doing this, he documented ignitions accompanied by more extensive flaming in the second series. A typical experiment in this series proceeded as follows: Arcing was observed at the failure point after bending an average of 86 times. After 3 – 8 s, smoke jetted out from the root of the plug prongs and a 15 mm length of flame burst out through a 1 mm-diameter hole in the PVC body near the failure point. The flame height then decreased, but spread across the surface of the plug. After 1 – 7 minutes, the flame extinguished. A small current was still flowing through the carbonized PVC insulation. Some plugs restarted flaming by themselves. Others restarted both arcing and flaming when moved by hand a little. A test from this series (Color Plate 69) illustrates that a wood board was ignited from the burning cord.

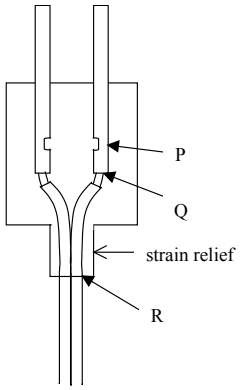


Figure 33 Failure points when electric plugs undergo mechanical stress
(Illustration courtesy Yasuaki Hagimoto)

The PVC-plug/PVC-cord, while evidently harder to ignite than other combinations, does get ignited, as demonstrated in the studies of Katayama et al.[644] They created wire failures at the cord/plug junction (point **R** in Figure 33) by repeatedly bending the plug over a ±60º angle, with a pulling force being created by an 0.5 kg weight attached to the cord (Figure 34). This method is a standard testing procedure described in a Japanese test standard[645]. After all of the wire strands in the wire had been broken in this manner, they conducted electric arcing/ignition tests by applying electrical loads at various power levels and bending the faulted wires by hand at a rate of about 30 cycles/minute. The results are shown in Figure 35. Not only were cord sets with PVC-insulated wires successfully ignited in this series of tests, but the amount of bending that it took to cause ignition was lower than for neoprene-insulated wires. Katayama additionally tested improved cord sets made from FR ethylene-propylene rubber and from FR PVC; none of these ignited in trials lasting 5000 cycles.

Plugs which have screw (as opposed to swaged) connections are susceptible to heating from a loose screw connection. Hagimoto[646] conducted experiments where a screw was loosened by one turn. A current of 10 A was then run for an extended period through the plugs. Temperatures around 200ºC were typically reached within about 1 h, with maximum temperatures ca. 400ºC being recorded. As discussed below, the degradation of PVC is severe once about 200ºC is exceeded. Uchida et al.[642] studied the same problem. Without load, even backing the screw off by a full 360º, they found that there was negligible increase in contact resistance (note that this pertains only to stranded conductors). They then conducted tests where a 12 A load was carried by the connections. Of 3 plug types tested, one led to failure when the screw was loosened by 90º, while a second type required 180º loosening; the third type tested did not fail for loosening up to 180ºC. Failure in all cases consisted of melting of conductors, sparking, and an open circuit being created. Fires were not initiated in the limited testing that was undertaken.

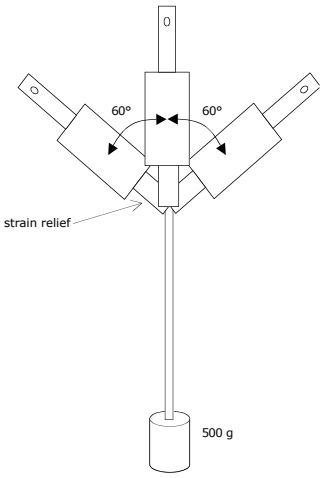


Figure 34 Arrangement used by Katayama et al. to break wires
(Illustration courtesy Yasuaki Hagimoto)

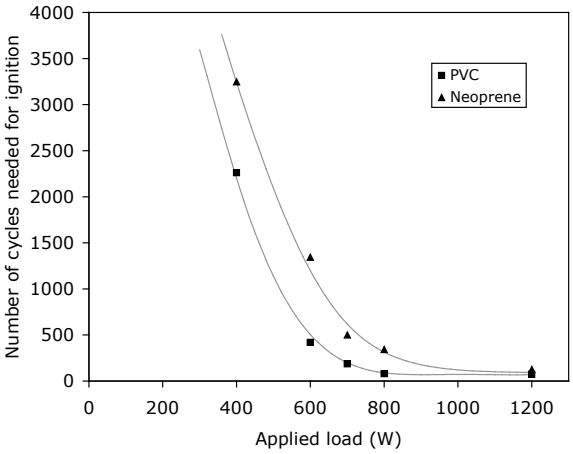


Figure 35 Number of cycles needed to cause ignition at cord/plug junction where all of the wire strands have already been broken by previous bending. Results for molded PVC plugs attached to cords insulated with two different polymers are shown.

Degradation can also be expected if the plug's prongs are not firmly gripped by the outlet; Color Plate 67 shows one such outcome. In running 20 A through molded PVC plugs, Hagimoto[646] found negligible heating if the removal force was 1 N or higher. But for a force of 0.1 – 0.2 N, serious heating was recorded, with temperature reaching 200ºC in the case of 0.1 N removal force. The same tests showed heating was negligible even at 0.1 N, if only 15 A was passed through the plug. As a basis for comparison, Japanese standards require that 10 N be available[647], thus a substantial safety factor should exist under normal conditions. Color Plate 70 shows a molded PVC plug which developed heating due to poor connection between the plug's prong and an outlet; a very similar outcome was found during laboratory testing (Color Plate 71).

Ultimate ignition at plugs is often preceded by arc tracking[648]. The insulation can become carbonized due to contaminants in the environment (electric plugs used near salt-water aquariums are notorious for this failure) or by thermal effects due to poor swaging, poor screw connection, etc. Ashizawa et al.[649] conducted studies to elucidate the details of the thermal degradation mechanism for the case when PVC is the insulation material. They determined that when PVC insulation breaks down due to heating at a poor contact, one of the reaction products is $CaCl_2$, with the calcium portion coming from the calcium carbonate normally used as a filler in PVC. The following sequence of steps was determined as leading to ignition:

(1) overcurrent and poor connection
(2) thermal degradation of PVC
(3) release of HCl gas from PVC (sometimes described as 'dehydrochlorination')
(4) formation of calcium chloride ($CaCl_2$) as a reaction product between PVC and calcium carbonate
(5) attraction of moisture to the highly hygroscopic $CaCl_2$
(6) initiation of surface and internal scintillations
(7) formation of carbonized paths in the PVC, both on the surface and internally
(8) arcing
(9) ignition.

As part of the study, laboratory aging and simulations were done. PVC plugs containing 20% calcium carbonate were oven-aged for several hundred hours. At 120ºC, no chemical activity was detected, but at 165ºC, over 20% mass gain occurred after 100 h of aging. This was moisture absorption due to the hygroscopic nature of calcium carbonate, which will absorb moisture during periods when there is no heating due to current flow. This absorbed moisture is later able to initiate the process of arc tracking. Typical test specimen conditions are shown in Color Plate 72 and Color Plate 73.

The authors next measured the drop in resistance between the blades at elevated temperatures. By 280ºC, the resistance had dropped to 100 kΩ; with further temperature rise, the resistance rose again, because the plastic could no longer sufficiently adhere to the metal contacts. The authors then conducted studies where the blades of the plug and the mating receptacle surfaces were initially degraded by inducing corrosion and oxidation. Using a load of 12 A, the plugs were then run for 1 week under these poor contact conditions, with additional heating applied externally. The results were variable, with the plugs developing temperatures of 250ºC or more in the worst case, and the plug's insulation resistance dropping to 100 kΩ. The plugs were then removed from the load carrying circuit and kept in the laboratory at ambient conditions for about 17 days. During this period, the moisture absorption increased significantly and the insulation resistance dropped to as low as 1 kΩ. For

the highly degraded specimens, the moisture pickup was not just a surface phenomenon, but involved in-depth absorption, including into the void spaces that had formed during thermal degradation. Finally, current (10 A, 100 VAC) was re-applied to the plugs to determine if ignition would occur. Plugs having an insulation resistance of 10 kΩ – 100 kΩ did not ignite, but the most degraded ones (1 kΩ) ignited under load (Color Plate 74), with scintillations preceding overt ignition. The degradation regimen used by the authors was clearly a very strenuous one, but necessary, in view of the probabilistic nature of failure and the impossibility of conducting a huge number of tests. Their reported temperature range for the initial degradation of PVC was very similar to that found by Van Luik[650], who reported that at 143ºC PVC degrades sufficiently to show a detectable mass loss rate.

Other insulation materials are also susceptible to arc tracking, although they have been less extensively studied. Plugs made from urea formaldehyde (UF), which are common as do-it-yourself items, are quite resistant to arc tracking, nonetheless exposure to prolonged heating can also lead to failure (Color Plate 76). Conversely, arc-tracking performance of old-style phenol-formaldehyde (Bakelite) plugs was found by Okamoto et al.[651] to be much worse than for plugs made of PVC or UF. They also conducted ASTM D 3638 Comparative Tracking Index tests on thermally-degraded material. Unaged materials, both PVC and UF, showed CTI > 600. The aging temperature used was 200ºC for PVC and 250ºC for urea. When aged for 1 h, the CTI for PVC dropped to 459 and for UF dropped to 116. When aged for 5 h, the respective values became 113 and 112.

FAILURES AT OUTLETS

The most common way that fire can originate at an electrical wall outlet is due to a poor connection at the screw terminals[652]; failures also occur due to improper grip of the prongs from the male plug. Other failure locations are more rare but can happen due to defects in manufacture. An actively glowing screw connection* is shown in Color Plate 75 in a test conducted by Reiter[570] where a receptacle was used to power a 120 VAC, 1500 W load for about 6 h. The type of damages that are seen from a glowing connection are illustrated in Color Plate 79. When investigating fires, it is important to distinguish between the damage caused to an outlet when one of its screws exhibits a glowing connection from the damage incurred when an outlet is heated externally by fire. Color Plate 77 and Color Plate 78 provide the comparison. It has been observed that most outlets recovered from fires and identified as the point of origin are found to have some missing metal, which implies that arcing may be common[652].

Meese and Beausoleil[653] conducted a series of experiments specifically focusing on glowing at the screw terminals of an AC duplex outlet. Glowing connections readily occurred when the screw was not tightly tightened. Visible glow occurred for currents carrying as little as 0.3 A in a 120 V circuit and also in low-voltage (3 – 4 V) circuits carrying less than 1 A. A poor connection which is glowing can re-establish the glow if the current is cut off and later turned back on. There does not appear to be any time limit for glows; in one experiment Meese and Beausoleil saw a connection glow for 129 h. In a circuit carrying 20 A, a glowing connection would dissipate 20 – 40 W, contrasted with 0.08 – 0.2 W for a good connection at the same current. Meese and Beausoleil also found that steel screws† are much more likely than brass screws to produce a glowing connection. This was attributed to the fact that the electrical conductivity of steel is about 1/10 that of brass, and the thermal conductivity of steel is about half that for brass. The higher conductivities of brass reduce ohmic heating and do not allow heat to be concentrated in one spot. The nature of the screw is crucially important since it was found that, with the devices tested, more than ¾ of the current from the wire flowed through the screw. The back plate carried much less current, since oxide was not being scraped off there in screwing down the connection. In their tests, which only used AC current, they could make copper-copper, copper-aluminum, and aluminum-aluminum contacts glow, but not copper-brass or aluminum-brass. In some additional explorations, they saw that glowing connections could readily scorch or char materials, but did not investigate circumstances leading to flaming fires.

Another NIST study[654] showed that for conventional outlets wired with 14 AWG copper wire, a minimum screw torque of about 0.7 N-m is necessary to achieve minimum heating at the connection; greater torques do not improve the reliability. Color Plate 80 shows an outlet where a fire originated due to a poor connection of an aluminum wire to a terminal screw.

In 1989 CPSC reported on investigations of outlets and the adequacy of the tenth edition of the UL 498 standard[635] then in force. In one series of tests, 25 insertions and removals were made while imparting bending and twisting forces to the mating plug (which may readily occur in usage, but is not simulated in the UL standard). Some outlet models sustained a 100% failure rate in this test. A number of other examples of inadequate design or poor manufacturing tolerances were found. The largest concerns of CPSC were with back-wired designs, and these are discussed below.

Similar findings concerning reliability of duplex outlets made according to the UL 498 standard were obtained by Aronstein in a 1993 study[655]. He documented that after less than 100 insertions of a male plug, some 3.5% of a test

* See Chapter 11 for basic information about glowing connections.

† Screws for electrical connections are often plated on the outside, but can be identified with a magnet.

sample of 200 positions (2 positions per duplex outlet, 100 outlets) effectively failed, by becoming palpably loose. Aronstein concluded that part of the problem was created when manufacturers reduced the thickness of metal in the duplex outlets as a cost-cutting measure. Outlets with this design were often unable to maintain adequate gripping force after a modest number of insertion/removal cycles. Using one model of a 'cost-cutting' 15 A outlet, he ran a 3-year test where a 10 A current flow was intermittently passed through the outlets, cycling no more frequently than 1 h on, ½ h off, with a total duty cycle of 5%. In that test, 4 out of 7 outlets developed failures. Most consisted of visible charring on the front face of the outlet, but in one case even the adjacent wall plate charred, albeit only in a non-flaming mode. In the worst case, the male/female contact became poor enough that the plastic of the male plug entirely melted away, the wire broke at the point of attachment to the male plug's prong, a break-arc was created, and the circuit opened up at that point. Another contributor to the problem has been inadequate tolerances on the thickness of the prongs of male plugs. Aronstein found male prong thicknesses ranging from 0.91 mm to 1.55 mm at the thinnest part, and concluded that the design of the mating female portion (outlet) cannot reliably cope with such variations. Plugs that had non-uniform prong thickness were considered to be the least reliable, because the thicker portion served to distend the mating female part, while presence of the thin portion made the grip poor, once the plug was fully inserted.

In North America, many duplex outlets available today either have a provision for *back-wiring* as an alternate to screw-termination, or are designed solely for back-wiring. A back-wiring design provides holes in the back of the outlet through which a straight, stripped wire can be inserted and held in solely by spring tension, without mechanical hold-down*. The relative safety of back-wiring versus use of screw terminals has been vigorously debated among fire investigators[656]. A limited CPSC-sponsored statistical survey[657] was only able to find a total of 11 overheating, copper-wired outlets in 130 homes surveyed. On this basis, a meaningful failure rate comparison could not be made between copper-wire back-wired and copper-wire screw-terminated outlets. However, two different series of laboratory tests have suggested that there is a distinct difference. Aronstein[655] conducted aging tests which showed that, after 9 years, the contact resistance was about 4× greater for the push-in type than for the screw-connected (copper wiring used for both). This was of concern, since the test program basically involved an idle circuit—current flow was for less than 2 h total, and never exceeded the rated device capacity. Peak temperatures of 98 – 111ºC were measured, in contrast to 27 – 28ºC for devices using screw-connections. The back-wired devices were approved under UL 498, since

* Some devices are available of a 'push-in, screw-tighten' variety, but these are uncommon, since spring-tension-retained arrangements are less costly.



Figure 36 Crack formation at a spring tab of a back-wired outlet
(Courtesy Jesse Aronstein)

they all passed a temperature rise limit of 30ºC during the first 30 days of use. The standard was consequently judged incapable of weeding out designs which deteriorate progressively over longer time periods. Aronstein concluded that back-wired connections are "unsuitable…for use as part of the permanent wiring system in buildings." An electron-microscope photograph of crack formation at a spring tab is shown in Figure 36; upon failure of the spring tab, there would no longer be an applied force to maintain a tight connection to the wire.

A CPSC study[635] subjected 275 back-wired, residential-grade outlets to a test program of approximately 1 year. During this time, cycling tests using 15 and 20 A currents were conducted using a duty cycle that was not particularly strenuous and would represent normal, not extreme, use conditions. Of the total, 10 specimens visibly failed due to arcing and overheating during the course of the tests. In addition, inspection after the test series was finished indicated that 31 other specimens had arced or overheated. Thus, a 15%/year failure rate was effectively observed. The high rate was presumably directly attributable to flimsiness of construction extensively documented for the lower grades of outlets. The CPSC study also noted that some outlet models were so poorly designed that even a single insertion and removal of a back-wired wire will lead to an inability of the outlet to retain any force on a wire inserted again. The CPSC study observed that 'screwless' outlet types (ones having 8 holes for backwiring, but no screw terminals at all), were the least reliable, to the point that some jurisdictions found them unacceptable. The study also documented how one outlet failed by arcing within 24 h, after a wire was inadvertently inserted into a release slot instead of a wire hole (the design of most outlets readily permits this mistake to be made, and presumably a certain fraction of outlet fires arises from this cause). As a consequence of the CPSC study, UL proposed a number of

changes for the 11th edition of UL 498, but there has not been a follow-up study to determine what improvements might have taken place.

An interesting failure of a back-wired outlet was reported by Graps[658]. The origin of a house fire was found to have been at a heating pad placed on a couch. Investigation revealed that the cause of the fire was not a malfunction of the pad. Instead, a daisy-chained outlet (which was of a back-wired-only type, having no provision for screw connections) exhibited a high-resistance connection. The resistance heating eventually caused a short to ground that vaporized the brass contact strip inside the outlet, partially burned the plug that was plugged into the outlet, shot out a jet of incandescent material from the ground pin opening and ignited a heating pad that was sitting on a nearby couch (Color Plate 81 – Color Plate 83). Figure 37 shows a X-ray of the failed outlet.

Despite their evidently inferior performance, back-wired outlets have not been prohibited by CPSC, and are still acceptable to UL. This is presumably because electric outlet failures are rare events and the risk of these failures—at this point—has not yet been deemed unacceptable. Similarly, despite Aronstein's warning, the unreasonable size variation found in male plug prong thicknesses has not been eliminated.

Not to be confused with back-wired outlets are outlets designed on the *insulation-displacement* principle[659-661]. A back-wired outlet requires that the wire be accurately stripped to a correct distance, then pushed into a provided hole. An insulation-displacement outlet does not require that the wire insulation be stripped. The wire is placed in a slot and a hinged cover is closed down upon it. In this process, sharp electrodes pierce the wire insulation and make contact with the conductor. Many commercial devices provide for a feed-through arrangement, so that if the outlet is in the middle of a daisy-chained run, the cable does not need to be chopped at the outlet. Conventional wiring practice for daisy-chained branch circuits can result in a heating connection (and potential ignition) occurring at an outlet to which no load is connected, with current merely being passed through the outlet and a faulty, high-resistance connection within it. But an insulation-displacement outlet cannot fail in this way, since current to the downstream device is passed through a solid copper wire, without any screw connections in series with the current flow. Devices of this type are commonly used in construction of manufactured homes. There are no known studies comparing the failure potential of this type of outlet to screw-terminated or back-wired outlets.

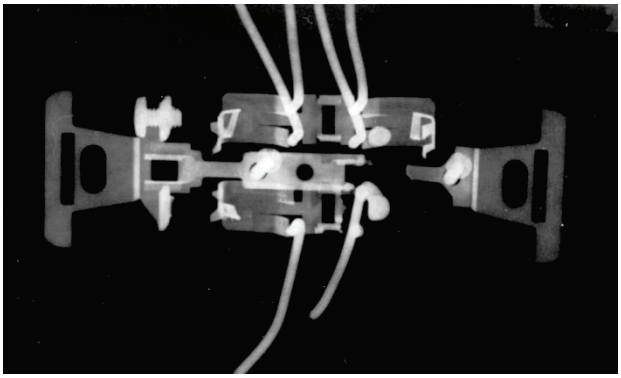


Figure 37 X-ray of failed outlet showing portion of hot-side contact strip that melted out
(Courtesy Al Graps, Electric Forensics, Inc.)

The potential for ignition from electric-outlet faults is discussed in some detail in connection with aluminum wiring, discussed below. Even though less studied, copper-wiring faults could presumably ignite the same combustibles. The propagation of fire from duplex outlets contained on the end of an extension cord was studied by Hagimoto[665]. He found that a long flame can be projected outside the device if an arc fault occurs inside the outlet box (Color Plate 84). Aronstein[662] states that he successfully ignited:

- Low thermal inertia furnishings (bedding, drapes, upholstery) placed directly against the face of an outlet, from a connection dissipating 28 W.
- Thermosetting-plastic receptacle cover plates, from a connection dissipating 30 W (thermoplastic cover plates, however, were prone to melt away rather than to ignite).
- Wood studs, from a connection dissipating 35 – 50 W.

Unfortunately, Aronstein gave few details of his experimental work. He did note that the burning of the thermosetting cover plates was a flameless, glowing combustion, and that a lightweight material (e.g., drapes) would have to be contacting the cover plate for further propagation to take place. In the case of ignitions of studs, again he found that initial ignition was of a glowing or smoldering type, but that this turned into flaming when it broke to the other side of the stud, or, in the case of wood paneling, when it broke through the front face of the paneling. Aronstein also reports that glowing connections were able to ignite:

- male plugs, cords, and small transformers plugged into the outlet,
- vapor barriers inside the wall cavity,

but he did not give details on the conditions needed for these ignitions to occur. He also found that a connection glowing at a 45 – 50 W level was able to melt aluminum wiring, and the globs of molten aluminum could ignite a cardboard box filled with papers.

Note that an electric outlet can be the cause of a fire *even if nothing is plugged into it*. In normal wiring practice, the wiring to outlets is daisy-chained, that is, many outlets are fed from an 'upstream' outlet, rather than directly from the panelboard. Apart from the special case of insulation-displacement outlets (discussed above), for a bad connection to develop at the outlet, it is not necessary that current be drawn by an item plugged into the outlet—current may

simply be drawn by a 'downstream' outlet. Of course, a faulty connection must exist at an outlet, for it to be a cause of fire.

MISCELLANEOUS CONNECTION FAILURES

The contacts of a switch, relay, thermostat, etc. can fail by becoming *welded* together (Color Plate 85) due to a combination of mechanical and electrical factors. But the fact the contacts of some circuit controlling a heat-producing device were found welded after a fire does not mean that this failure occurred prior to the fire, nor that the device started the fire. Béland pointed out that exposing contacts to an ongoing wood fire, without electric current flowing, is often sufficient to weld contacts together[663]. Especially notable was the finding that some bimetallic thermostats, which are designed to open their contacts upon reaching an elevated temperature, can respond in a fire environment by welding of their contacts (Color Plate 86 – Color Plate 88). Similarly, circuit breaker contacts can become welded due to an external fire exposure. Contacts welding due to external fire exposure can generally be identified by serious fire damage to the component, for example, a well-burned circuit breaker case.

Long-term failures of *twist-on connectors* (sometimes referred to by the trademarked term Wire Nuts) with copper wires was studied by Béland[663]. When a connector was poorly applied, without adequate tightening, he found that failures commonly occur due to metal loss, but this always occurred "several inches" away from the connector, not at the connector itself. This was discovered to be a corrosion problem. Overheating of the connector liberates HCl gas from the PVC wire; the gas is corrosive and attacks copper. Over long periods, metal loss occurs to the point that a connection can be completely severed.

Mechanical *vibration* can lead to failure of connections. CPSC has documented a case where the air bubbler of a spa caused a connection failure in a receptacle in an adjoining wall[522]. Some brass compositions, especially those containing over 15% zinc (by mass), are susceptible to *dezincification* when subjected to corrosive environments. If this occurs, the metal loses its strength and will not be able to function as an effective contact.

A significant fraction of fires originating in electrical appliances such as dishwashers and clothes washers was found to originate at internal wiring connections of the *quick-connect* (also called *push-on* or *push-in*) type[472]. These were either insecurely assembled originally or worked loose, resulting in a poor connection (Color Plate 89).

An investigation of a fire in Japan[664] documented the fire origin to be due to a glowing connection. Because of limited damage at the origin area, it was possible to use X-ray diffraction analysis on the components retrieved; this showed that the red-and-glassy material recovered was Cu_2O. Electrical analysis of the connection showed a negative temperature characteristic, which is typical of Cu_2O, but not of pure copper. Hagimoto[665] reports one unpublished experiment where a glowing connection was made in a knife switch. The switch was housed in a molded plastic case and attached to a wood board. After about 5 h of carrying 10 A, the wood had partly carbonized and a piece of plastic from the case melted, dropped onto the hot conductor, and ignited. This, in turn, caused the wood board to ignite.

THE ALUMINUM WIRING PROBLEM

Aluminum branch-circuit wiring, used by some contractors since 1964, increased in usage as a cost-saving measure due to the 1966-7 copper shortage. Many US houses and mobile homes were wired with aluminum wiring until about 1972, when sufficient problems were found with this wiring method for it to drop out of use. Connections where any kind of metallic conductor is connected to another conductor can be subject to failure. However, the problems associated with small-gauge aluminum wire have been sufficiently severe that numerous studies have been devoted to it. The problem was generally confined to AWG 10 and smaller connections, with large-size conductors—such as used for service-entrance wiring—not showing major problems. A 1977 CPSC survey[666] determined that—at that time—there was a very serious problem of overheating in aluminum wired receptacles (Table 62). The survey also found evidence of burning at outlets that had been replaced (due to some kind of fault) in 14% of the aluminum-wired houses, but in only 1% of the copper-wired houses. A laboratory study[653] showed that in 10,000 h, some 24% of screw connections with aluminum wire had failed, as contrasted to zero for copper and zero for copper-clad aluminum wire.

Color Plate 90 shows an incipient failure at an aluminum-wired duplex outlet. Color Plate 91 shows a gross failure, but note the cover plate of the same outlet (Color Plate 96)—almost no external signs are visible of the serious problem inside the electrical box. Color Plate 93 shows charring of wire insulation where one insulated conductor was touching another, but the insulation melted back from

Table 62 Measured temperatures found at outlets in survey houses when drawing a load equal to 75% of the rated circuit load

Connections	Percent of outlets	
	Over 75ºC	Over 100ºC
copper, screw-terminated	0	0
copper, back-wired	2.3	0.2
aluminum, screw-terminated	5.3	2.2
aluminum, back-wired	*	*

* - This combination was not permitted by NEC, but was found in 3.2% of surveyed houses; these outlets were not tested for overheating.

one insulator and has nearly charred through the insulation of the second.

In 1966 UL started to recognize wiring devices for use with aluminum wire and developed the "AL-CU" designation for connections deemed to be suitable[667]. Just as changing metal prices made aluminum wires attractive, rising prices for brass led to widespread shift in the mid-1960s to use of zinc-plated steel as connection screws. Unfortunately, the combination of aluminum wires and steel screws proved exceptionally prone to bad connections and ensuing fires. Because part of the problem was due to creep of aluminum wire, UL mandated that starting in May 1971 the exceedingly creep-prone EC-H19 aluminum alloy be no longer used for making wires; the UL procedures were further tightened in September 1972. The importance of this was confirmed in an NBS study on duplex outlets wired with aluminum wire[668] where a cyclic condition of moderate overload current was designed as a form of accelerated aging test. The duplex outlets were the older technology, prior to introduction of "CO/ALR" (copper/aluminum revised) devices. It was found that with wire made from the alloy EC-H19, failure occurred on the average in 18 cycles; the newer, more creep-resistant aluminum alloy required an average of 42 cycles for failure. Continuing problems with connecting aluminum branch-circuit wire to outlets and switches led UL to develop in 1972 the "CO/ALR" designation for wiring devices, which were designed for an improved connection to aluminum wire, and could also be used safely for copper wires. These devices were specified in UL 1567[669] and had a base plate with improved gripping capabilities, brass instead of steel screws, and indium plating. CPSC, however, concluded that there was little chance that a householder could correctly install these devices so that they would perform as intended[670]. Bunten et al.[667] published a history of aluminum wiring developments up to 1974 which provides many more details on problems and solutions.

While a reasonable conductor of electricity in the bulk, aluminum is a notoriously poor material for making reliable electrical contacts. This is due to a combination of several factors[671]:

(1) Upon exposure to oxygen, aluminum forms a tough layer of oxide which, unlike copper, does not readily pass an electric current by means of 'electron tunneling.' Conduction between an aluminum wire and a mating metallic surface occurs only at a sparse number of places where the oxide fractures. This weak connection is also susceptible to failure by electromigration[672].
(2) Aluminum is prone to creep and stress relaxation, which means that, with the passage of time and especially with an increase in temperature, connections which were initially tight become loose[673]. Not all alloys and grades of aluminum, however, are equally prone, and the grade EC-H19 used prior to 1972 was an exceptionally poor choice.
(3) Aluminum has a high coefficient of thermal expansion, which exacerbates the effect of creep, since screws were not used having a matching coefficient of thermal expansion.
(4) Because of the large heat of formation of aluminum oxide, when aluminum oxidizes, much more heat is liberated than when copper oxidizes. This heat becomes available towards accelerating the failure of a connection.

In addition, making connections at screw terminals with aluminum wire was more prone to failure than with copper wire since:

(a) The aluminum alloy used in making building wires prior to 1972 had an inappropriately high yield stress and resisted shaping itself to the mating surface so as to make a large contact area.
(b) A larger wire size needs to be used for the same current-carrying capacity with aluminum than with copper; combined with the previous factor, this meant that a much stiffer wire has to be looped and tightened than in the case of copper wire.
(c) Prior to the introduction of the serrated screw-connection baseplate design, there was no good means of breaking the surface oxide film in making a connection, since a 'wiping' action is hard to execute.
(d) The propensity for overheating of aluminum-wire connections can bring in a corrosion problem: If, as is most common, the building wire insulation is PVC, heating of the PVC will liberate HCl in the early stages of its decomposition. This is a corrosive gas which can then attack the connection and accelerate its worsening.
(e) Even without elevated temperatures, aluminum is prone to galvanic corrosion in high humidity locations, due to its highly-anodic ranking in the galvanic series. Aluminum wire connected to steel or brass screws or terminals, which was common before the recognition of the problem, is a particularly infelicitous combination.

The first experimental study of aluminum wire connectors was conducted by UL in 1954, but the report did not provide details of the connectors examined[780]. Later, Aronstein and Campbell studied the failures of twist-on connectors[674]. The connectors in their test series all had zinc- or tin-plated steel springs. Unlike several other studies, in this work the current rating of the conductor was *not* exceeded. A current of 13.5 A was run through wires rated at 15.0 A. The voltage drop across the connection was measured, and it was found that connections were stable if the drop was less than 0.04 V. If this drop was exceeded, the connection was found to start behaving erratically, and progressively developing ever higher drops with time. Overheating to the point of charred wire insulation occurred in numerous cases; actual ignition potential was not tested, since the splices were situated in open air, away from other combustibles. No failures during a 12 month testing period were found with cop-

per wires. For EC-H19 aluminum wires, failures predominated when the connectors were zinc-plated; failures were fewer, but not nil, for tin-plated connectors. Some shorter-term tests with the newer alloy wires showed improvements, but not full success. Improvements were also noted when using a larger-size wire connector. In a follow-on study[675], 'special-service' connectors were examined; these use a copper alloy, instead of steel, spring. The results indicated that this metallurgical improvement did not translate to connections which were reliable. The authors concluded that providing a copper cladding or plating may be the only means of achieving reliable field connections for building branch-circuit wiring with aluminum wires.

The effect of torque on the service life of an electrical connection was examined by Hicks[676]. The test program consisted of cycling the connections using a 3.5 h on/0.5 h off program using a modest over-current of 27.5 A. Twist-on connector pigtails using 14 AWG copper wire and 12 AWG aluminum wire were tested, as well as screw connections on a duplex outlet. The results are shown in Figure 38. The straight lines plotted have a slope of approximately 3, thus it was concluded that

$$\text{service life} \propto (\text{torque})^3$$

Apart from the service life issue, using both copper and aluminum wires, Hicks also examined the torque needed on a duplex outlet's screw connection in order to produce a low-resistance connection. With increasing torque, the resistance dropped greatly until about 0.4 N-m were reached. Further increase in torque caused little improvement in the connection, with thread stripping occurring at 1.7 – 2.1 N-m. The recommendation was to tighten screws to 1.0 – 1.6 N-m. For twist-on connectors, a good connection required > 0.2 N-m torque, with the recommended torque being 0.4 – 0.7 N-m. The completed connection must show twisting of wire in the portion not concealed by the connector for this torque to be achieved.

A similar study was conducted by Aronstein[677] using the worst-case combination of 12 AWG pre-1972 aluminum wire and outlets with steel screws. Running 12 A in a 1 h on/1 h off cycle he obtained overheating (as evidenced by charring of plastic parts) for connections that had been torqued to 0.45 N-m or less. At 0.45 N-m, 2 out of 40 connections overheated; at 0.23 N-m, 10 out of 40; and at 0.11 N-m, 22 out of 40. At a torque of 0.90 N-m, he observed no failures. By contrast, when using copper wire, there were no charred connections even at the lowest torque of 0.06 N-m.

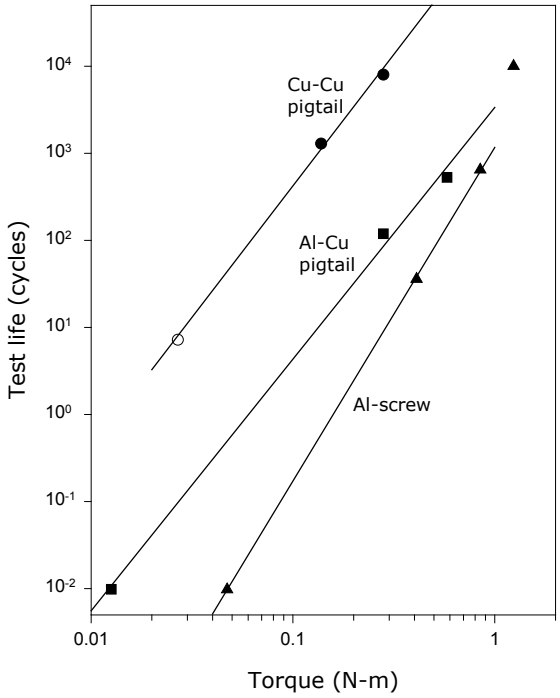


Figure 38 Effect of tightening torque on connector life (1 cycle: 3.5 h on/0.5 h off)

Prior to Hicks' study (see above), a common recommendation was to torque screws to 1.36 N-m (12 lb-in). This would seem to imply that a properly-torqued terminal will not fail. But Aronstein provided some further results which indicate that even if a screw is torqued down to 1.36 N-m, the subsequent manipulation of wires necessary to fit the outlet to the box generally results in an alarming loosening of pre-1972 aluminum wire and in occasional loosening of post-1972 wire. Aronstein also measured the temperatures at various locations. For an aluminum-wire connection dissipating 42 W, he found a peak temperature of 540ºC on the screw. Values in the vicinity of 200ºC were measured on the box and on the faceplate screw. When dissipating only 22 W, temperatures on the wire at 25 mm away from the terminal were also around 200ºC. He also found that a 12 AWG aluminum wire melted when poor-connection heating was increased to 50 W.

The effect of screw plating material was examined by Mastoris[678]. His results are summarized in Table 65. It is evident that zinc and nickel are unsuitable materials.

Table 63 Results from Ontario Hydro testing of duplex outlets with poor connections

Wall paneling	Insulation	Covering over outlet plate	Wiring method	Results
wood	cellulose	cotton blanket	screw	scorching only
wood	cellulose	cotton blanket	back-wired	wood paneling and cellulose insulation ignited after 4 cycles
wood	cellulose	cotton blanket	back-wired	fuse blew in 4th cycle; paneling and insulation ignited after current flow had ceased
gypsum wallboard	fiber glass	cotton drapery	back-wired	no ignitions after 42 cycles; plastic outlet parts charred

Table 64 Laboratory testing results on faulty duplex outlets

Power dissipated in connection (W)	Results
4 – 10	Arcing heard.
4	Newspaper over face; 425ºC measured at faceplate screw; slight charring only.
0.5 – 35	Charred bedspread
4 – 35	Face covered w. cotton bedspread; measured 450ºC at faceplate screw.
23	Measured 475ºC at faceplate screw.
34 – 57	Wire melted; wallpaper glowed and charred.
23 – 46	Insulation melted, wires shorted, melted, caused open circuit; towel against face charred.
4 – 9	Shorted wire due to melted insulation.
14 – 20	Flaming ignition of cotton towel against face.
12 – 46	Bedspread against face first smoldered then flamed; temperature at faceplate screw > 540ºC.
28 – 32	Bedspread ignited; 340ºC on faceplate screw.
29	Used 20 A current; ignition of wood members in 1 h.

Campbell and Ling[679] conducted glowing connection tests in aluminum-wired duplex outlets on behalf of CPSC and also developed a model for estimating the temperatures. Aluminum wires melted out when creating a connection that dissipated 40 W. Using lower dissipations of 20 – 27 W they successfully modeled the peak temperatures with a finite-element analysis computer code. Aronstein[680] conducted laboratory tests on duplex outlets provided by CPSC which had been removed from service as being 'failing' specimens. Connections were made by welding new wires onto the cut-off wire remnants. The current/time regimen was different for the various samples and typically comprised cycling up to the 12 – 15 A range. Some of his example data are summarized in Table 64.

Table 65 Effect of screw plating material on failures during a 2500 cycle test; values given are [failures/tests]

Screw plating material	Conductor	
	EC-grade aluminum	Copper
zinc	34/54	2/10
nickel	6/15	0/3
tin	0/30	0/4
silver	0/6	--

Ontario Hydro[681] conducted a series of tests using duplex outlets wired with aluminum wire and previously exposed to a modest overload of 27 A. The alloy composition of the wire and details of the outlet were not specified. In the test program, the outlets were cycled using a 15 A load applied for 3.5 h, then off for 0.5 h. A mockup up stud space was built, including thermal insulation inside the cavity and combustibles placed at the face. No male plug was used, the current being drawn by a daisy-chain connection. The results are summarized in Table 63. These results clearly indicate that back-wired connections are less robust than screw connections for aluminum wiring.

Currently, the National Electrical Code does not forbid the use of small-gauge aluminum wires for branch-circuit wiring, but many jurisdictions have local laws in force that preclude their usage and their use in new construction in the US is minimal. CPSC has issued a booklet[682] giving advice to homeowners whose residences have aluminum wiring. They recommend that the best solution is rewiring the building with copper wiring. Next best is crimping on copper splice wires using COPALUM connectors made by AMP/Tyco Electronics Corp.; these require a special tool and special training, so they can only be installed by electricians. CPSC does not consider pigtailing with copper splice wires using twist-on connectors (Color Plate 94), nor replacing switches and outlets with the CO/ALR variety acceptable, irrespective of whether they are approved by a testing laboratory. A solution that had been proposed and that met UL criteria, but was not accepted by CPSC, was a special wing nut filled with a corrosion-inhibitor compound. In laboratory testing[683], Aronstein concluded that the design was unlikely to be sufficiently robust. This was borne out in a follow-on field study[684], where he found that the connectors failed even during the first year after installation, with the failed units showing melting and charring that closely resembled the laboratory test failures.

Aluminum wire is very commonly used for high voltage wiring by electric utilities and for the service entrance cables that bring in the power to the distribution panel. Because of the large wire sizes involved, and since better connection mechanisms have always been available for service entrance cables, these connections have not been identified as a special fire problem. Nonetheless, a CPSC study on electric distribution system faults[522] did find some fires due to deteriorated connections to aluminum service entrance wiring at the distribution panel. A NIST investigation identified that twist-on connectors between AWG 8 stranded aluminum wires and AWG 12 or 14 solid wires were also prone to failure[685].

INCENDIARISM

Electric outlets, being a source of energy, are sometimes exploited by arsonists. Flocken and Bates[686] described a fire set by inserting two graphite pencil 'leads' into an electric outlet, then bridging across them with a third lead. The re-

sistance of the graphite was sufficient to cause heating, without drawing enough current to operate the circuit breaker.

Electric switches

Hagimoto et al.[687] investigated the ability of power switches used on domestic appliances to ignite flammable gas mixtures. They found that mixtures were readily ignited with the spark upon opening the switch. They were also able to find ignitions occurring during the closing of switches, but only when the switches were carrying approximately their maximum rated current. They also concluded that for the same spark energy, it was easier to ignite mixtures by opening the circuit to an inductive load than to a resistive one.

Electric transmission and distribution systems

In this section, large-current components are considered. Branch-circuit wiring and end-use device wiring are considered under *Electric wires and cables*.

TRANSFORMERS

Transformers in power systems can be cooled by a liquid (generally an oil), by air, or by another gas (e.g., sulfur hexafluoride); or, they may be potted in a resin, typically epoxy. Liquid cooling is required at higher voltages and capacities; air-cooled transformers are primarily found inside user facilities. Significant fire and explosion hazards are only associated with oil-filled transformers, since dry types have only a limited amount of combustible insulation material. Transformer fires or explosions can lead to major structure fires, apart from destroying the electrical equipment; as an example, a large warehouse was destroyed due to a transformer fire[688]. The nomenclature used for electric transformers by power utilities is confusing, since *distribution transformers* sensibly denotes transformers used in distributing energy to users, but *power transformers* is used as the term to refer to high-capacity network transformers that are employed in the power network prior to reaching the customer-distribution points. Distribution transformer ratings are commonly 50 to 2000 kVA, with 5 to 36 kV primary voltage. It must also be noted that power companies refer to the primary distribution voltage as *medium voltage* and the secondary (120 to 600 V) as *low voltage*.

Distribution transformers are generally highly reliable and failures are rare. Statistics vary widely among countries, but a probability of 0.1% for failure, per transformer, per year, is common[698]. Statistics are not available to indicate what fraction of failures result in fires or explosions. Cooper[622] examined a number of case histories and concluded that the following circumstances most commonly led to transformer fires or explosions:

- Failure of tap-changing mechanism; this is commonly caused by contacts that have become poorly conducting due to foreign deposits or carbonized oil deposits[689]
- Electric flashover above oil level (between leads, terminals, and ground), commonly due to overvoltage or internal arcing
- Inter-turn insulation failure
- Lead-in bushing failure (from lightning, overvoltage, or mechanical damage)
- Lightning damage
- Open-circuit arcing (loose connections, fractured conductors)
- Ignition of vapor above the oil level
- Puncturing of cooling tubes by ground leakage current
- Overloading.

In rural areas, damage due to snakes and birds is also a significant cause[693]. An insurance company survey[690] indicated that the top causes of transformer failures in 1998 were:

- Line surges, external short circuit
- Deterioration of insulation
- Lightning surges
- Inadequate maintenance
- Moisture
- Poor manufacturing workmanship
- Loose connections
- Overloading.

Sabotage or malicious mischief, which in the US were among the top causes in the 1970s and 1980s, became insignificant in the 1990s. These causes are still important in some other countries, however. In India it has been reported[691] that theft of transformer oil is one cause of transformer failures.



Figure 39 Experimental explosion in oil-filled pole-mount type transformer; 10 kA available fault current with a 25 mm arc
(© IEEE 1975)

Common faults that can lead to a transformer fire or explosion include[692,698]:

- Failure of inter-turn insulation in the main windings
  - relative movement between turns (due to faulty spacers, inadequate tightening of clamps, or overheating)
  - overheating due to overload or overvoltage (overvoltage on the primary side can lead to excessive primary current even in the absence of a secondary load)
  - overheating due to obstruction in oil circulation
  - overheating due to sludge accumulation
  - mechanical damage during manufacture (e.g., sharp edges on conductor)
  - local overheating due to proximity of steel and eddy currents due to stray magnetic flux
  - inadequate balancing and excessive heating of paralleled conductors
  - moisture penetration between turns
  - tracking across wood cleats
- Insulation failure between winding and transformer tank
  - aging or deterioration of insulation
  - moisture entry into oil
  - insufficient clearance between flexible lead and tank
  - tracking across wood cleats
- Failures of magnetic circuit, leading to excessive eddy currents in the core
  - shorting out of insulation one bolts holding together laminations
  - burrs on laminations, allowing their short-circuiting
  - metallic filings trapped between laminations
- External causes
  - steep-fronted surge voltages
  - external short circuit on the secondary side
  - heavy overload
  - rapidly fluctuating load
  - switching out of unloaded transformers (due to high induced voltages from inductive effect)
- Miscellaneous faults
  - failure at connections or bushings
  - loosening of laminations due to fault in clamping bolts (e.g., inadequate torquing)
  - inadequate spring tension on tap-changer contact springs
  - inadequate design, or a design unsuited to the service for which the transformer was installed.

Tracking across laminated wood cleats is often due a defect whereby a small air gap exists between laminations. Paper insulation is susceptible to mechanical damage and to thermal degradation. In addition, it releases moisture throughout its life, with chemical degradation being responsible for part of it, not just free moisture. Excessive arcing in oil-filled transformers causes bits of copper in the form of tiny balls to be formed from arced conductors. These balls then flow with the oil and can be deposited in places where further damage can result[693]. On rare occasions, catastrophic failure and explosion may be initiated by arcing of an internal fusible link, if the latter blows out of its housing, which can occur if the available fault current is greater than the interrupting capacity of the link[695].

More specialized causes of transformer failure include ferroresonance and geomagnetically-induced currents. Ferroresonance is a specialized form of fault which can be elicited by certain circuit configurations when the transformer is unloaded. Geomagnetically-induced currents are due to geomagnetic storms and cause a stray flux impingement which can develop a local hot spot, leading to breakdown[694].

Most transformer faults do not lead to an explosion, since the failure mechanism is progressive[695]. The initial fault commonly involves only a few turns of the winding and the fault energy is limited by the impedance of the undamaged portion of the winding. The fault may either cease to propagate or the current may increase until a protective device operates. A high energy fault is less common and it happens if there is a major insulation failure of a direct internal short to ground. Estimates of the arc energy that must be delivered to cause a catastrophic transformer failure vary from 30 kJ within one cycle, to 100 – 200 kJ of arc energy within a half-cycle. It is rare for a rupture to require more than 4.5 cycles. Oil-filled transformer failures, including explosions, are more likely in older units that do not have nitrogen blanketing (Figure 39[696]).

If an arcing fault occurs within the transformer, ejection of oil aerosol can occur, possibly accompanied by a physical explosion of the transformer housing. If the oil is ignitable, a serious fire or a vapor/mist explosion can happen. When an arc occurs in an ignitable oil, hydrogen and acetylene are the main gases produced; by contrast, breakdown of oil due to excessive conductor temperatures yields mostly ethane, ethylene, and methane, with smaller amounts of hydro-

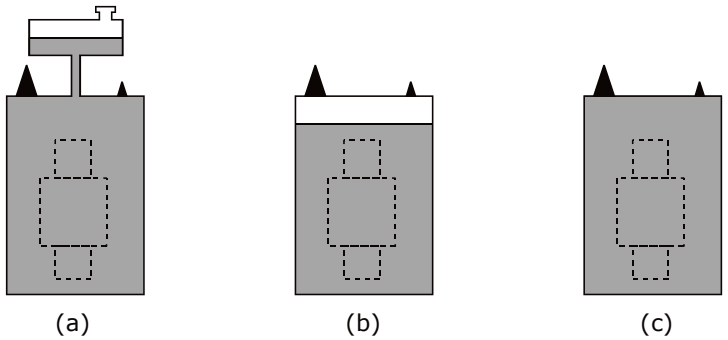


Figure 40 Three main types of liquid-filled distribution transformers: (**a**) open system with conservator; (**b**) hermetically sealed, with inert-gas blanketing; (**c**) hermetically-sealed system, with variable-volume tank and no gas cushion (after Rønningen)

gen[698]. A typical sequence of steps leading up to a transformer explosion is[697]:

- a heavy overload carbonizes the oil sufficiently to cause a fairly high leakage current
- the leakage current further degrades the insulation and eventually leads to a turn-to-turn or layer-to-layer fault
- the fault becomes large enough to cause the primary fused cutout to operate
- upon re-fusing and re-closing the cutout, the transformer insulation fully breaks down ('flashes over'), drawing a very large arc fault current
- the energy released from the arc gasifies the transformer oil, primarily into hydrogen and methane
- rapid pressure buildup from the gasification causes the transformer cover to be blown off
- the combustible escaping gases ignite either due to remaining arc energy or due to sparking associated with rapid metal breakage.

The flow chart developed by Rønningen[698] (Figure 41) is also useful. Pressure-relief devices are generally effective only for slow-rising overpressure events, thus they do not prevent serious explosions. A transformer explosion can almost be assured to happen if maintenance of oil is neglected. Oil degrades over time due to heat, moisture, arcing from on-line tap changing, and partial discharges. The Bureau of Reclamation makes available a short guide to transformer maintenance[699], while Myers[700] published an exceptionally extensive handbook on the subject.

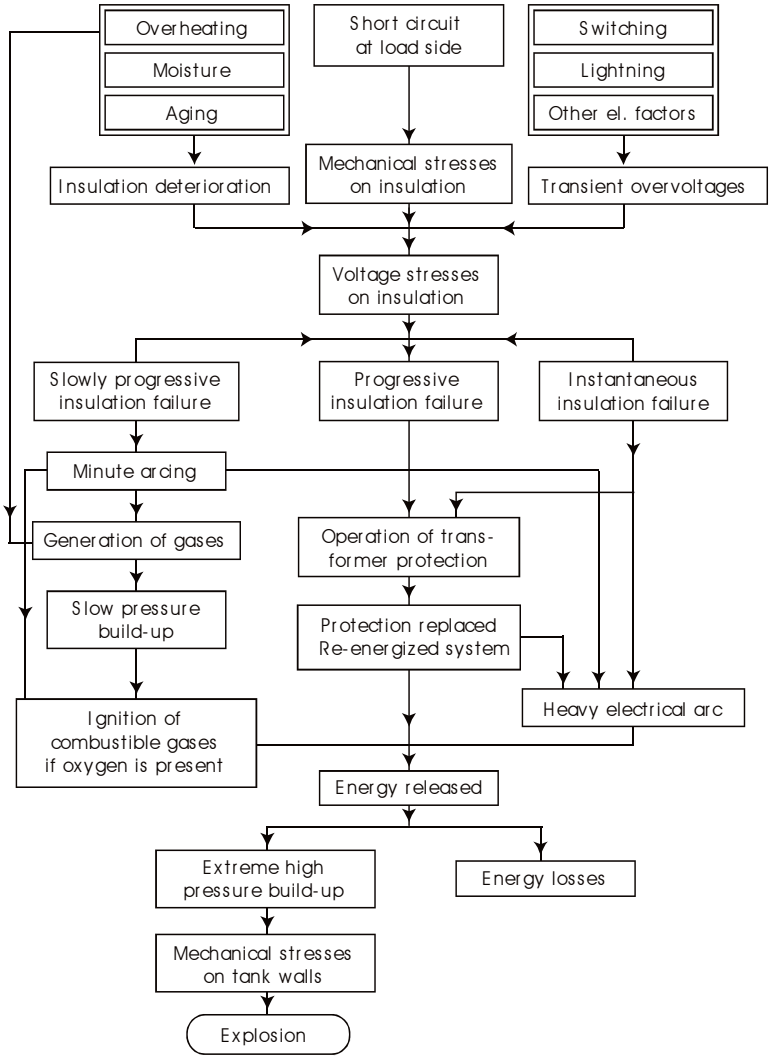


Figure 41 Sequence of events that can lead to a transformer explosion

Liquid-filled transformers come in several intrinsically different configurations (Figure 40), and these perform somewhat differently with regard to explosion potential. Type (b) is most common in the US, while types (a) and (c) are more prevalent in Europe; it is generally felt that type (c) is the most reliable. Oil-filled transformers are commonly equipped with a *Buchholz relay* for shutting down in case of a fault. This device comprises switches which are triggered by a dropping liquid level or by an excessive gas evolution from the oil. Thus, in principle, it is the transformer's first line of defense against an explosion.

All else being equal, the fire or explosion hazard is proportional to the flammability of the oil used. Silicone fluids have flashpoints of around 300ºC, much higher than the 150ºC or so for mineral oil. French explosion tests[701] on 100 kVA distribution transformers indicated that a serious explosion is most likely in the case of turn-to-turn fault in the secondary windings; lesser violence was normally found with turn-to-turn faults or phase-to-phase arcing on the primary side. With some transformer designs, the most vulnerable components are the wire links connecting the primary windings to the bushings—overcurrent sufficient to melt out this link usually leads to explosion.

When arcing takes place inside an oil-filled transformer, the outcome—modest damage versus serious explosion—is often determined by the clearing time of the circuit protection devices. For 'expulsion' type fuses, it is often assumed that the time is ½ cycle, but experiments indicate that actual arcing time may be longer[702]. Successful protection can be achieved by the use of 'current-limiting' fuses, which are able to open the circuit well before the first half-cycle of fault current has been passed[695]. If protection is by circuit breakers, then even the expected clearing time becomes much longer. Theories to predict the rupture (physical explosion) of oil-filled transformers (but not an ensuing chemical explosion or fire) were developed by Mahieu[696] and Barkan et al.[703] The two variables identified as controlling the process were I^2t and arc length. The quantity I^2t has units kJ/Ω and corresponds to the electrical energy dissipated per unit of resistance; with I = current and t = time.

A number of the failure mechanisms of oil-filled transformers are also common to other oil-filled high-voltage equipment such as capacitors, circuit-breakers, or reclosers. IEEE has published a guide to the investigation of transformer failures[704]. This manual contains a useful tutorial on transformer construction, but does not encompass fire/explosion as a failure mode.

Because they have large in-rush currents, and because transformers' short-term current carrying capacity is high in comparison to their continuous-duty rating, the primary side is typically fused with fuses much larger than the rated primary current, 250% being not untypical[705]. Consequently, arcing faults on the secondary side may not be protected against.

BUSBARS, SWITCHBOARDS, AND PANELBOARDS

The common ways by which an arc fault may occur on a *bare-metal electric bus* or other power distribution component are[706]:

- direct shorting by a metallic object, e.g., an electrician dropping a screwdriver.
- a loose connection causing progressive heating and minor arc formation. Over time, this may ionize the air in an enclosed space sufficiently that a general bus-to-bus or bus-to-ground arc occurs.
- surface conduction due to accumulation of dust or contamination[707], or due to a cracked porcelain insulator.
- conductive gases being discharged onto a bus conductor from a tripping circuit breaker or a blowing fuse. Arcing may occur if the conductors against which this flow occurs are not ones that have become de-energized.
- failure of a circuit interruption device upon short-circuit conditions.
- rodents or snakes entering into a space that should be an air insulator.

It has also been noted that some faults occur due to installations that leave inadequate clearances. Similarly, the main causes of ignitions originating at a residential 120/240 V panelboard are considered to be the following[708]:

- dirt and debris brought in by ingress of water or moisture
- rodents, insects
- mechanical abrasion of insulation
- resistance heating from loose connections
- improper wiring or overloaded circuit
- faulty circuit breaker.

In addition, the possibility of sabotage may have to be considered. Short-circuiting may be due to a faulty installation or may reflect a design problem. Color Plate 99 shows a panelboard fire which Lentini[709] identified as due to the use of a thermoplastic material to support the main power lugs. If these are insufficiently tightened, heating of the connection can then cause the hot lug to migrate through the plastic and to contact the metal rear wall of the enclosure.

The failure modes of residential panelboard circuit breakers that engage aluminum busbar contacts have been examined by Aronstein[710]. Even though the area of contact is large, he found that serious erosion is common. This was true not just for branch-circuit breakers, but was also documented for a 200 A main breaker. The primary factor was fretting, induced by microscopic interfacial motion. The latter can arise from thermal expansion, or from the forces involved in the circuit breakers, or from other forces. A fire within a panelboard can occur due to a poor connection of a primary conductor. Color Plate 100 shows melting and pulling back of insulation. If this continues, eventually the conductor is likely to short to the metal enclosure. Color Plate 101 shows a consequence of a fire in a panelboard.

An interesting case history documents a massive arcing fault and fire that occurred in an electric switchgear cabinet[711]. Due to an undersized transformer for a control circuit, a boiler-control relay lacked sufficient voltage for pull-in and was, instead, chattering. The arcing at the contacts due to the chattering caused sufficient ionization of the air that a breakdown ensued between conductors carrying high current.

Fires in panelboards can occur due to arc tracking. Aronstein[712] conducted experiments to simulate some events that took place during the Beverly Hills Supper Club fire. In that fire, some witnesses reported hearing bangs and flashes coming from various electrical panels. He was able to reconstruct the failure of an electric panel by arc tracking (Color Plate 102). It was sufficient to heat a section of conduit connected to the panel, but without heating the panel itself. Pyrolysis products from the overheated wire insulation traveled through the conduit and ended up in the electric panel, where they were deposited on the cold surfaces, including electrical insulation, thereby causing failure through arc tracking.

Arcing faults in secondary distribution systems can sometimes be hard to protect because the current levels under such fault conditions may be low enough not to trip circuit interruption devices. Voltage/current relationships for electrical arcs in general have been presented in Chapter 11. Here, some studies specific to distribution system arcing will be reviewed. Values of arc fault currents for typical circuit impedances were calculated by Kauffmann and Page[713] and widely publicized by Dunki-Jacobs[714], as shown in Table 66. The fault currents shown for the 208Y/120 V distribution system would be difficult to reliably detect and clear because they are so small. Sec. 230-95 of the National Electric Code requires ground-fault protection in 480Y/277 V systems that are rated at 1000 A or more. Thus, it might be expected that these devices would protect the circuit. However, both calculations and loss ex-

perience indicate that the arcing conditions may be such that the device is tripped late or not at all[706].

Table 66 Arc fault currents (rms) as a percent of symmetrical, 3-phase bolted-short current for two different secondary distribution systems, as calculated by Kauffmann and corrected by Dunki-Jacobs

Type of arcing fault	Secondary arrangement	
	480Y/277 V	208Y/120 V
three-phase	89%	12%
phase-phase	74%	2%
phase-ground	38%	--
multi-phase, w. one primary fuse open	80%	--

It is important to understand that values such as given in Table 66 are not absolute, mathematical constants. Instead, they came from calculations that were based on certain simplified assumptions:

- The circuit's impedance, apart from the arc, is wholly inductive and has no resistive component (0% power factor).
- After a voltage zero-crossing, current flow does not resume until the voltage rises to the value of the re-strike voltage, which is assumed to be 340 V except for the case of a phase-phase fault in the 208Y/120 system, where it is taken to be 275 V.
- Immediately upon restriking, the voltage across the arc drops to a fixed value and stays at that level until it extinguishes at the next current zero. This arc voltage is taken to be 140 V for a phase-ground fault and 275 V for a phase-phase fault. As shown in Chapter 11, the arc voltage depends mostly on the electrode gap, with a lesser dependence on current. If the busbars are spaced 100 mm apart, then an arc voltage gradient of 140/100 = 1.4 V mm^{-1} is, in fact, typical of experimental results. For the phase-ground fault, evidently Kauffmann assumed a larger gap of roughly 200 mm.

The computed current waveform is discontinuous and non-sinusoidal; the values tabulated represent the rms values of this computed waveform, compared to the rms bolted-short available current. Whether Kauffmann's assumptions were realistic must be determined from experiments. Wagner and Fountain[715] conducted experiments where arc faults were created across distribution system busbars for circuits with known values of symmetrical, 3-phase bolted-short currents. For 3-phase shorts across a 500 V busbar, arc currents during the first half-cycle were typically 0.7 – 1.0 of the symmetric, 3-phase bolted-short current. Single-phase shorts gave values in the range 0.5 – 1.0. For a 250 V busbar, both 3-phase and single-phase shorts gave widely scattered results, typically 0.3 – 1.0. During the initial half-cycle, a few values were slightly greater than 1.0; this is possible because the maximum asymmetric current flow that can be delivered is higher than the computed symmetric current value. The authors also pointed out that the distinction between a bolted fault and an arcing fault is not categorical—heavier shorts placed across the line start out with current characteristics of a bolted short, then progress to arcing characteristics. All of the Wagner and Fountain tests involved an ungrounded Δ-connected transformer secondary and busbars with a 100 mm conductor spacing.

Stanback[716] used a different arrangement, namely a single-phase fault between a busbar and a metal enclosure using 277 V with a power factor of 9 – 16%. His results showed a strong dependence on the electrode gap distance, as indicated in Table 67. Matters are somewhat complicated by the fact that there was also a current-level dependence in Stanback's results. Higher values of available bolted-short current led to arc-currents that were a smaller percent of the available current. However, this effect was not explored sufficiently to be able to produce a correlation. Stanback also measured arc voltages in his experiments; the values shown represent the average value of a nearly-flat-topped waveform; these can be compared to the peak-to-peak source voltage which is $\sqrt{2} \times 277 = 392$ V.

Another series of tests was conducted by Fisher[717], who examined arc fault currents for phase-ground faults in 277, 208, and 120 VAC circuits. In his tests, short-circuit currents ranged from 500 to 42,000 A, while the power factor varied from near-zero to 100%. Electrode spacings were 13 – 100 mm. His results (Table 68) show values that are similar to Stanback's at small electrode gaps, but do not drop as sharply with increasing gap distances. Fisher ran some additional tests using the 13 mm spacing but lower supply voltages (Table 69); at 120 V, the arcing was not sustained, but it was sustained at 146 V or higher. Additional testing indicated that the power factor, not surprisingly, has an effect on the outcome and that higher power factors lead to smaller arc currents. On the basis of this work, Fisher proposed that more realistic calculations should be done than are represented by Kauffmann's table. In his method, the resistance of the arc R_{arc} (Ω) is computed as

$R_{arc} = 4.96 \frac{\sqrt{L}}{I^{0.85}}$, where L = electrode gap (mm), and I = arc current (A). The equivalent circuit is expressed as a complex impedance $Z = R + jX$, where R = resistive component, $j = \sqrt{-1}$, and X = reactive impedance. The power supply voltage is a fixed, known value, while the total load

Table 67 Stanback's experimental results on phase-ground busbar faults at 277 VAC

Busbar-to-enclosure spacing (mm)	Arc fault curent, as % of bolted-short current	Arc voltage (V)	
		Average	Range
25	85%	109	91 – 153
50	70%	176	99 – 184
100	35%	268	207 – 342

is simply the vector sum of R_{arc} and Z. The desired value of arc current is obtained iteratively, by finding that value of I that gives $V = I \times (R_{arc} + Z)$ equal to the power supply voltage.

Table 68 Fisher's experimental results on phase-ground busbar faults at 277 VAC

Busbar-to-enclosure spacing (mm)	Arc fault current, as % of bolted-short current
13	92%
25	86%
51	80%
57	66%
89	50%
100	50%

Table 69 Fisher's results for 13 mm busbar-to-enclosure spacing and varying supply voltages

Voltage	Arc fault current, as % of bolted-short current
120	80%
146	87%
208	92%
277	92%

In real power systems calculating the available bolted-short current is not an easy task. Contributions to the short-circuit current come not only from the power utility connection but also from on-site motors. These contributions have different time response characteristics and this needs to be taken into account. A theoretical model for predicting arc currents in low-voltage (< 600 VAC) circuits has been described by Gammon and Matthews[718]. For design purposes, actual calculations are normally done with a computer program developed for these calculations. St. Pierre[719] has published a textbook devoted to the topic of short-circuit calculations.

In AC circuits, an arc extinguishes when the current waveform reaches a zero-crossing, but it can subsequently reignite when the voltage rises to a sufficient value. Kauffmann considered the *re-ignition voltage* (also called restrike voltage) to be 375 V. In principle, this would preclude sustaining an arc (arc re-ignition) for circuits with rms voltages less than $375/\sqrt{2} = 265$ V. In actual fact, the restrike voltage is highly dependent on the circuit parameters (i.e., resistance, capacitance, inductance), on gap size and arrangement, and on the timing when the voltage becomes available after the current zero-crossing. The dielectric strength of the ionized air starts to recover as soon as arcing stops, but the strength does not recover fully for a certain time period. In one study on low-current (< 25 A) arcs[720], restrike voltages of 320 – 400 V were found if the needed voltage could be supplied within the first 5 μs of the current zero-crossing. If voltage could not be supplied until 20 μs, then the range was 280 – 580 V, while at 200 μs, the needed voltage was 400 – 860 V. The value of 280 V was the minimum found in that study over all test conditions. In other tests[721], a restrike voltage of 160 – 240 V was found immediately after arc extinction, with the value again rising with time; however, it appears that the conditions needed to elicit these low restrike values would not be common in actual distribution systems. Thus, Kauffmann's assumed value falls somewhere within the experimental range, but the range is quite broad.

Case histories[722] indicate that arc faults in 480 V systems tend to last for minutes-to-hours and cannot be expected to self-extinguish or to trip circuit protection devices. Smolinski[705] found that sustaining an arc in a 240 VAC circuit is not easy, but is possible, and it could be sustained in circuit where the fault current was limited to as low as 30 A. Experience indicates that in 208 V systems there is a mixed probability as to whether an arc will self-extinguish or not[723]. As mentioned above, Fisher was able to sustain arcing at 146 V, but not at 120 V. Because of his and other studies, it has often been claimed that it is impossible to sustain arcing in 120 VAC circuits, but this is not true. Bruning[724] demonstrated that circuit parameters are crucial—a self-sustained arc is impossible for most circuit parameters, but there are conditions (inductance is especially critical) under which it becomes possible.

A limited amount of work has been done on arcing in higher-voltage busbar systems; for example, Klaus and Schau[725] reported brief results on experiments in 3 – 15 kV systems.

Most arc faults originate as phase-to-phase or phase-to-ground faults, then escalate to 3-phase faults in 5 to 15 ms[726]. In the case of *insulated* busbars in 480 VAC systems, tests indicate that it is very hard to sustain arcing[727]; similar results at higher voltages are not available. In the same vein, a phase-ground fault has a good chance of not escalating to a 3-phase fault on insulated busbars[723]. In general, single-phase arcing is much more difficult to sustain than 3-phase arcing, since on a single-phase line the current passes through zero twice a cycle, during which time production of arc plasma ceases and the breakdown strength of air can recover. But on a 3-phase bus, there is no interval when all current flow ceases, thus production of arc plasma also does not cease. Bus arcing faults in secondary systems of the ungrounded, delta-connected type (3-wire) are exceedingly rare, in comparison to the currently prevalent 480Y/277 V grounded system (4-wire)[714]. However, the latter is sensibly preferred due to its better performance in regards to transient overvoltages.

In the case of non-insulated busbars, arcing failures may be induced by an ongoing, non-electrical fire. This can take place in one of two different ways: (1) deposition of conductive soots into the busway; or (2) discharging of ionized gases into the busway.

Because of magnetic repulsion effects, an arc fault across a pair of busbars moves *away* from the source; the speed of motion is greater for higher arc-fault currents. During the travel, typically little damage is done because of the non-sustained nature at one place. Burndown damage is normally found once the arc stops moving upon encountering an obstacle. Stanback[716] conducted experiments to quantify the amount of metal destroyed in arc faults in single-phase 277 V-to-ground busbar faults. The natural magnetic effect propelled the arc to the end of the bus way, and the total amount of metal lost from the busbars and from the steel enclosure was measured. The empirical rule developed was:

$$V = kI_{arc}^{1.5}t$$

where V = volume of metal destroyed (mm^3), I_{arc} = arc current (kA), and t = time (s). The constant k = 0.025 for aluminum busbar, = 0.012 for copper busbar, and = 0.011 for steel enclosures. Studies have determined that the damage to a *switchboard* from bus arcing is proportional to the energy released[728]. Only cosmetic damage normally is seen for energies < 100 kJ; conversely for energies > 700 kJ, destruction is comprehensive. In examining 3-phase arc faults in circuits carrying from 380 to 726 V, the authors found that arc power has a rise time of about 7 ms and stabilizes to its ultimate power at about 15 ms. Thus, for event durations >> 15 ms, the arc energy becomes directly proportional to duration.

There are no systematic studies of ignition potential from distribution system arcing faults. A fairly detailed report has been published on an office building fire which led to 5 fatalities[729]. An electrician attempted to replace a 200 A fuse in a 480 VAC, 3-phase distribution panel without disconnecting the power. Apparently his fumbling created a violent arcing fault, which quickly escalated into a 3-phase fault, the failure of each phase being heard as an explosion. The fire originated in an electrical closet, then quickly ignited carpeting and wall coverings along the building's corridor, thereby trapping a number of occupants.

If aluminum wire or connections (lugs) are used, then special precautions are needed, lest the probability of failure rise dramatically. Pure (uncoated) aluminum lugs may lead to rapid failure. The current good practice is to use lugs that are first coated with copper or nickel, then flashed with tin or silver. Aluminum distribution wiring systems using these types of lugs are considered to be as reliable as all-copper systems[730].

INSULATED DISTRIBUTION CABLES

The nature of arc faults in underground distribution ducts was examined by Koch and Carpentier[731] in Montréal, where a three-phase 600/347 V distribution network is used. A modest overvoltage was used, comprising 635/367 V. Phase conductors were stranded aluminum, insulated with XLPE (cross-linked polyethylene); a bare-copper neutral was used. They found that arc behavior is governed by whether the interior of the duct is clean and dry, or not. For clean, dry conditions, phase-to-neutral or phase-to-ground arcs self-extinguished in only a few cycles, and very little damage was sustained. When dirty, moist conditions were created, arcing escalated to phase-to-phase and finally to a 3-phase fault. These arcs kept re-igniting and burned for up to 5 minutes, when the experiments were terminated due to gross overheating. Because the arcing was repetitive, rather than continuous, it would not have been possible for overcurrent protection on either the secondary or the primary to activate. The arc faults pyrolyzed large amounts of wire insulation, apart from what could be directly incinerated in the arc. The pyrolysis products were found to be quite flammable, and this accounts for a number of *manhole explosions* which the authors investigated. Oxygen supply within the duct was not sufficient to allow the pyrolysis products to burn, but burning was possible once they were ejected into manholes. The authors also report that use of direct-burial cable, without enclosure in a duct, does not eliminate the problem if arcing occurs close to a manhole or a transformer vault. Case histories are known where arc-fault induced explosions occurred with direct-burial cables running at the low voltage of 208/120.

As part of their study, Koch and Carpentier provided an estimating rule for the arc fault current of insulated distribution cables:

$$I = 120 + 0.64I_{sc}$$

where I_{sc} = bolted-short current (A). Schau[732] explored arc fault currents of 3-core, insulated distribution cables at 416 V. He found that the arc current was 69% of the bolted-short available current when the latter was 5 kA, dropping to 60% for 15 kA. Additional studies were reported by Ohnishi et al.[733]

SERVICE DROPS AND HIGH CURRENT CAPACITY CONDUITS

The service drop is the wiring that goes from the secondary of the power utility's transformer to the meter and panelboard of the user's building. This wiring is particularly vulnerable to starting fires if a fault condition occurs, since the protection given to it is very limited. Basically, the only protection that normally exists are the power utility's fuses on the primary side of the transformer. But since the transformer may be sized to feed quite a number of service drops, the fuses have to have a high rating and may allow very sizable fault currents to flow in the service drop of one particular user. The damage to be expected depends on whether the fault occurs in overhead/underground wiring, or in a service entrance conduit in the building itself. In the former case, damage is usually limited to the wiring. But the latter situation, while less common (since wire in conduit has fewer opportunities to be damaged) can be much more serious. Failure of wire insulation inside a steel conduit feeding the electric meter[734] can lead to a 'cutting-torch action,' similar to a welder's metal-cutting operation (see Figure 42). The progress rate of the electric arc cutting the

metal conduit has been timed at about 1 mm s^{-1}. Any nearby combustibles can then easily be ignited by the molten steel, as documented in several cases[734].

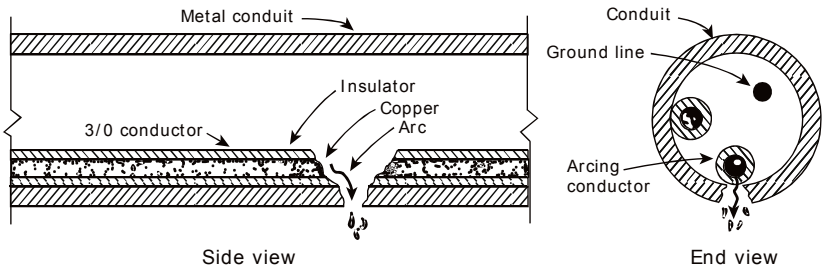


Figure 42 Arcing damage inside a service entrance conduit (after Sanford)

Another series of tests was conducted by the Kearney Co., in which ¾" (nominal 20 mm) and 1" (nominal 25 mm) conduits carrying AWG 8 copper wires or AWG 6 aluminum wires were tested[735]. In their tests, a 480 VAC power supply was provided, with resistors in line to limit current to 240 A. The fault comprised a stripped-bare wire across which were wound layers of 22 AWG copper wire, and then the assembly was wrapped with paper masking tape. The test program included steel (EMT) and PVC (ENMT) electric conduits and also schedule 40 PVC pipe. Using THW copper wires, no external damage was found with the EMT conduit and with the ¾" PVC pipe, but both sizes of the ENMT conduit showed external burn damage. Using RHW copper wires, a 75 mm long hole was melted through the ¾" EMT conduit, but no destruction of the 1" EMT conduit. Both sizes of the PVC pipe and the ENMT conduit showed external burn damage. With aluminum USE wires, all three conduits of both sizes showed external burn-through damage. Ignitability of external combustibles was not examined in the tests.

An unusual case of a circular hole of about 25 mm blown out of a service entrance conduit elbow fitting ('condulet') was studied[736]. It was found to be due to the high temperatures caused by internal arcing, combined with the low melting point of the aluminum alloy.

HIGH VOLTAGE INSULATORS

Arcing along high-voltage insulators is termed '*flashover*' by electrical engineers; this term is unrelated to its usage in fire science to denote a stage of a room fire. Electrical flashover typically occurs in wet or rainy weather, when a semi-conductive path can form along the surface of the insulator. It is facilitated by pollution, since pollutants in the atmosphere lower the resistivity of the water film. The process entails small leakage currents initially. Because of non-uniformities in this layer, preferential dry bands are established which have a higher resistivity than the rest of the layer. Local arcing along these dry bands occurs first, and this can then lead to a complete discharge path being established, electrode to electrode. The latter is designated as flashover. Electrical flashover resembles arc tracking in some of its basic features. In ceramic insulators, the material itself is not subject to charring, although pollution can deposit a film on the insulator which contains ionic dissolved solids. This film is not a perfect insulator, and when a low enough resistivity is attained, surface tracking can occur. The breakdown strength of a semiconducting pollution strip[737] is much lower than the breakdown strength of air: 50 – 70 kV m^{-1}, as opposed to 3 MV m^{-1}. Newer insulators made of silicone rubber or other elastomers show a slightly different behavior. In the case of silicone rubber, a strong role is played by oil that exudes from the material and, when present, keeps the surface hydrophobic[738]. Breakdown is facilitated by conditions that destroy this surface oil film. Rizk[739] has reviewed numerous theories for flashover along insulators. One of the simpler theories for flashover in AC circuits gives:

$$E = 102\bar{r}^{1/3}$$

where E = breakdown field strength (V m^{-1}) and $\bar{r}$ = resistance of pollutant film, per unit leakage length (Ω m^{-1}).

Electric wires and cables

In the US, testing of wires and cables is most commonly done under UL standards. A large number of different standards have been issued by UL for wires and cables of various types. The ones of most general interest include: UL 4[740] (armored cable), UL 44[741] (thermoset-insulated), UL 62[742] (specifications for flexible wires/cables), UL 83[743] (thermoplastic-insulated), UL 444[744] (communications cables), UL 493[745] (underground cables), UL 719[746] (nonmetallic-sheathed cables), UL 758[747] (appliance internal wiring), UL 817[748] (appliance cords and extension cords), UL 854[749] (service entrance cables), UL 1581[750] (general wire/cable fire tests), UL 1666[751] (vertical fire propagation test for cables in shafts), UL 1685[752] (vertical cable tray fire propagation test), UL 2196[753] (cables passing a fire-resistance test). The Steiner Tunnel test for plenum cables used to be UL 910[754], but in 2002 was withdrawn in favor of NFPA 262[755].

MODES OF IGNITION OF WIRING

It is no surprise that electric wiring* faults in buildings lead to fires. Yet, the mechanisms by which ignition occurs are not trivial and have only been explored in recent years. It is convenient to consider that ignition of electric insulation (or other nearby combustibles) can occur due the following causes:

- arcing
- excessive ohmic heating, without arcing
- external heat sources.

* 'Electric wiring' is considered here in the most general sense, encompassing wires, cables, and all other devices forming the current path.

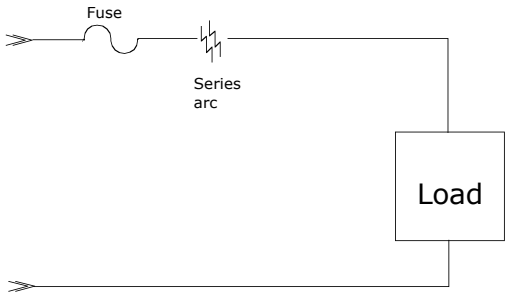


Figure 43 Series arc

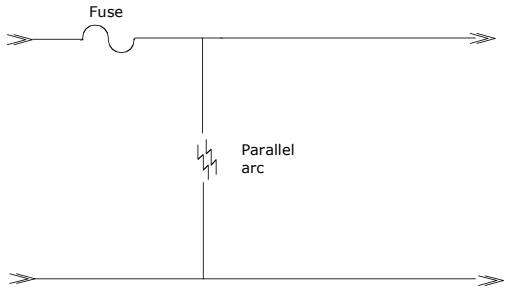


Figure 44 Parallel arc

ARCING

Topologically, an arc in a single-phase circuit* can be identified as a series arc (Figure 43) or a parallel arc (Figure 44).

A series arc cannot exist without a load. As Figure 43 indicates, if the load is turned off, then current flow through a series arc cannot occur. The presence of the load also means that it will be very rare that a series arc blows the fuse or trips the circuit breaker protecting the circuit. In a steady-state analysis, the presence of the arc *decreases* the current being drawn through the circuit, so if the circuit interruption device was appropriate to the load, introducing an arc will not trip it. Arcs in AC circuits have a highly transient characteristic, however, so if the load is sufficiently reactive (e.g., a large motor), the combination of the erratic waveform of the arc and the reactive load could possibly trip the interruption device, but this cannot be counted on.

In the case of branch circuits (as contrasted to service entrance wiring), it is also unlikely that a parallel arc will trip the protective device. There are three factors that come into play here: (1) the intermittent nature of current flow through the arc; (2) considerable resistance of branch circuit wiring; and (3) the time response characteristics of circuit interruption devices. All of these issues are considered in detail below.

* Some authors consider a third form of arc—line-to-ground—which is possible when the circuit contains a ground in addition to a neutral. The topological arrangement is identical to that of the parallel arc, since the load is not in series with the arc. Three-phase circuits can also exhibit phase-to-phase arcing.

The causes of arcs can be many, but the primary ones are:
(1) carbonization of insulation (arc tracking)
(2) externally induced ionization of air (created by flames or an earlier arc)
(3) metal-to-metal contact, i.e., short circuits
(4) poor connections.

The first three mechanisms are discussed in detail below; poor connections have been discussed in the *Electric outlets, plugs and connections* section. A sustained electric arc can ignite many substances, and general arc characteristics have been discussed in Chapter 11 and earlier in this Chapter under *Electric transmission and distribution systems.* Protective devices for detecting arc fault conditions are discussed in Chapter 12.

Carbonization of insulation (arc tracking)

In 120 VAC circuits, it is difficult to sustain arcing in air, but not difficult to sustain arcing over a carbonized conductive path. This is sometimes called 'arcing-across-char.' The mechanism has been known in electrical engineering for a very long time, but how a carbonized path gets established across an insulating material is not a trivial question. There turns out to be more than one way of creating such a path, with the most common being:

- applying an arc directly at the surface of the insulation, for example, by placing two electrodes on the insulator and applying a high voltage across them; this procedure is used in certain test methods;
- heating the insulation to excessive temperatures, as discussed earlier under *Electric outlets, plugs and connections*;
- combined effects of moisture and pollutants on the surface;
- fungal growth.

Carbonized insulation comprises a resistance which may be low enough to pass significant current and lead to ignition, yet not trip a circuit breaker. The basic principles of the arc tracking process have been discussed in Chapter 7. Color Plate 95 shows wire damage formed due to arcing across carbonized insulation[570] on an NM electric cable in a 15 A, 120 VAC branch circuit. Arcing went between the phase and the neutral conductors; the wire in between is the ground wire and this was cut afterwards, it was not involved in the arcing. Note that the statement made in Sec. 6-10.1 of NFPA 921[756] that arcing-through-char is "always a result of fire" is not correct, since carbonization of insulation can be produced by mechanisms other than fire†.

In a more elaborated scheme, UL considers that four mechanisms can cause carbonized insulation[757]:
(1) gradual breakdown of insulation due to repeated overvoltages;
(2) high voltage electrical tracking across the surface of solid insulation, due to repeated transient overvoltages;

† Referring to the 2001 edition; this statement may be removed in the next edition.

(3) deposition of contaminants and moisture on the surface;
(4) thermal decomposition of the insulation due to heat sources. These may include high-resistance series faults, break-arcs, or an existing fire impinging on wiring.

Electric insulation can carbonize due to fungal growth, since the extensive vascular system of the fungus provides a conductive string of paths[758]. This mechanism can only take place in wet environments. Fires due to carbonization of insulation are commonly seen on electrical devices near aquariums (Color Plate 96), especially ones using salt water, but whether fungal contributions are important to this ignition process has not been elucidated.

Hagimoto created a charred layer on a synthetic rubber surface, then used various metal electrodes for creating further arcing along the charred surface[525]. He found that in all cases the arcs were intermittent, with a very low on/off ratio, with brass showing a lower ratio than copper or iron. It was considered that the electromagnetic force tending to move the arc away from the source was at least one factor accounting for the intermittence[759].

Yereance[223] considers arc tracking to be a major source of residential fires of electrical origin and claims that the time period for arc tracking to lead to a fire can range from a few hours to forty years, but his study lacks specificity or details. He points out that common items such as cooking oil vapors, lint, and cat fuzz have been found not to be contaminants leading to arc tracking, but fails to identify ones that are. Béland, who unlike Yereance, conducted laboratory studies, agrees that arc tracking can happen in domestic wiring, but considers it rare, rather than common[760]. In testing, Béland examined the possibility that salt water at 120 V could cause a carbonized path when two electrodes are placed onto a Bakelite plastic surface. This proved possible to do for electrodes 2.5 mm apart, but not at 12.6 mm. In his arrangement, Béland required a minimum of 70 V for a carbonized track to occur; this is much higher than the 6 V documented in Chapter 7. He also found that results varied according to the particular type of Bakelite used. Material used for making circuit breakers was much more resistant to arc tracking than material used for switch plates. He also concluded that PVC was not able to exhibit arc tracking, which contradicts most other researchers.

Few illustrations are available for arc tracking in building wires. Welte[761] reported that prior to the 'B-grades' (NM-B and UF-B) being introduced in 1985*, it was not rare for electricians to come across house wiring cable that had carbonized. Neither damage, nor lightning, nor electrical overloads were considered to be the cause, but rather an intrinsic cable failure mechanism. Burnt cables were recovered showing that they were burned from the inside out (Figure 45). Welte reports[762] observing several accidental arc tracking fires that were either buzzing, without a visible flame, or were exhibiting localized flaming. After introduction of the B grades, instances of this type of failure became rare.

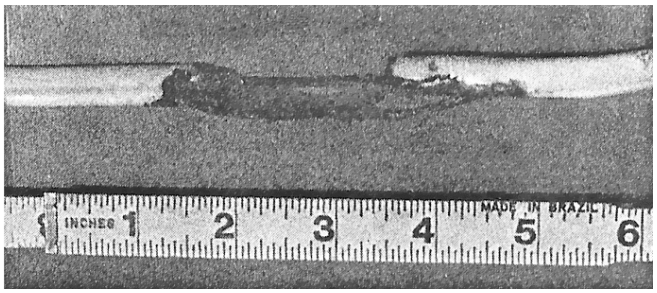


Figure 45 Non-metallic 12 AWG building cable which ignited "from inside out" due to arc tracking
(Courtesy *Air Conditioning, Heating & Refrigeration News*)

Reiter[763] reports investigating several fires that appeared to originate due to cable degradation of 60ºC-rated cables in attic spaces. Carrying of high currents and burial in thermal insulation were considered to be contributing causes.

Noto and Kawamura conducted experiments using the IEC 60112[764] apparatus and were able to obtain arc tracking on PVC-insulated cables[765] with a 100 V power supply. Using four different test arrangements, all on cables having 1.6 mm copper conductors, they were able to create arc tracking in all cases; however, only two of the four arrangements led to ignition. Ignition was preceded by intermittent arcing at ca. 5 s intervals. The PVC cables which ignited continued burning until the circuit was de-powered, at which point flaming stopped. Both plain and shielded cables could be ignited, but the ability to ignite proved to be dependent on exact details how the salt water was applied to a damaged cable location. The authors also did some experiments with flat plaques of PVC materials of various compositions. They discovered that calcium carbonate, an FR additive often added to PVC compositions as an HCl scavenger, actually promotes arc tracking failure, since early outgassing of HCl is helpful in forestalling arc ignition.

PVC insulated wire becomes semiconducting when charred. In an early study, Soma[766] examined the resistance of insulation of stranded-wire power cords when exposed in a furnace to various temperatures. Up to 200ºC, little change in resistance was found. But at 300ºC the resistance dropped dramatically. For higher temperatures, resistance further fell, until at 600ºC the resistance dropped to only 3 Ω. Tests by Hagimoto et al.[767] showed that leakage resistance of a power cord, originally ca. 10^{12} Ω prior to heating, dropped to 5×10^{5} Ω when heated for 1000 h at 180ºC and down to 10^{2} Ω at 190ºC. At a temperature of 250ºC, resistance values ca. 10^{5} Ω were reached in only 10 h. These results suggest that serious damage is already incurred at 180º.

* The 90ºC rated cables were introduced to replace the older 75ºC rated ones primarily due to thermal failures that were being experienced in wiring to incandescent lighting fixtures.

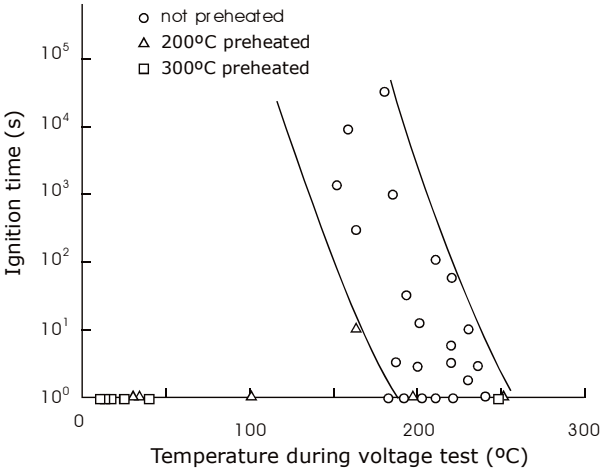


Figure 46 Effect of preheat temperature and test temperature on ignition of PVC wire insulation when subjected to 100 VAC across 1 mm insulation thickness

Even lower temperatures were found sufficient by Nagata and Yokoi[768,769]. When virgin PVC insulation was heated to about 160ºC, ignition occurred if a potential difference of 100 VAC was presented across an insulation thickness of 1 mm, which represents a common value of wire insulation thickness. If the insulation had previously been preheated to 200 – 300ºC, then ignitions occurred when the preheated insulation was raised to only very mild temperatures during the voltage test—from room temperature to 40ºC (Figure 46). To explain these results, the authors used the measured resistivity/temperature relations and applied thermistor theory to the material[770]. This showed that negative resistance characteristics are found once the applied voltage exceeds some rather modest threshold value and that the consequence is a thermal runaway of the material. In such a runaway, electrical resistance drops as temperature increases. This causes an increased current flow, which raises the temperature, which lowers the resistance, and the process escalates.

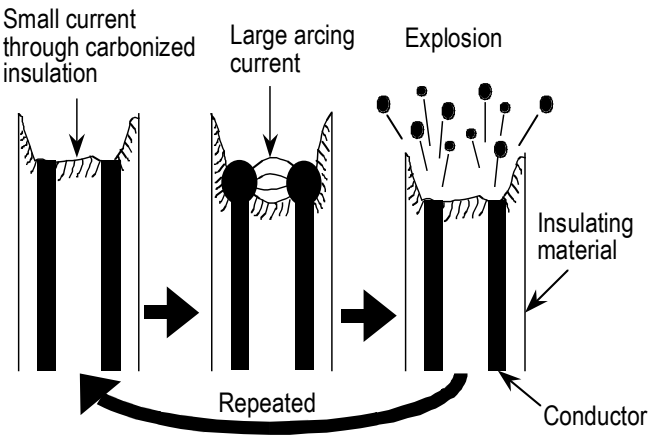


Figure 47 The discontinuous nature of an electrical cord or cable arcing fault (courtesy Hagimoto et al.)

When a Neoprene extension cord is heated to 336ºC with the exclusion of oxygen, this results in the carbonization of the insulation[771]. The conductivity of the insulation then becomes low enough so that arcing across the insulation is possible. The authors were also able to ignite cloth in a smoldering mode and carbonize the insulation of a Neoprene-insulated coiled cord, by simply covering the coiled cord with enough cloth while drawing 12.5 A through the cord. Temperatures over 300ºC were recorded. In similar experiments[772], they also obtained short circuits of PVC-insulated cords, when coiled three times, covered with a towel, and drawing 12.5 A. The wire size of the conductors was 0.75 mm^2 (18~19 AWG).

Hagimoto et al.[773] conducted laboratory studies simulating parallel-arcing faults of electrical cords and cables. They identified that the process typically proceeds in a repetitive, but irregular fashion. The basic steps are illustrated in Figure 47:

- initial current flow occurs due to a carbonized layer
- the current flow increases and results in local arcing
- the arcing causes melting of metal and expulsion of the molten pieces
- once the molten pieces are expelled, current flow drops
- continued current flow through carbonized material eventually leads again to a sizeable current flow.

The process repeats indefinitely. The authors tested four different sample types, as detailed in Table 70. The current waveforms, as determined during a 1 s duration measurement interval, are shown in Figure 48. (Note, of course, that the actual current values will depend on the resistance of the particular circuit tested).

The authors then examined the implications of the discontinuous nature of the arcing fault waveform on the time

Table 70 Construction of 2-conductor cords/cables tested by Hagimoto et al.

Specimen	Insulation material	Construction	Conductor
A	Neoprene	flat cord	0.18 mm Ø × 50; tot. area 1.25 mm^2
B	PVC	dumbbell-shaped cord	0.18 mm Ø × 50; tot. area 1.25 mm^2
C	PVC	2 insulated conductors; round jacket	0.18 mm Ø × 50; tot. area 1.25 mm^2
D	PVC	2 insulated conductors; flat jacket	1.6 mm Ø

required to trip a 10 A circuit breaker, Figure 49. It is clear that for the same peak value of current, a much longer time was needed when the waveform was not sustained. While the arcing waveform is irregular, Hagimoto et al. did find that the arcing frequency was correlated to the peak current, as shown in Figure 50. Arcing frequency was defined as $= \frac{\text{number of arcs}}{2 \times \text{number of cycles}} \times 100$. That higher currents should decrease the arcing frequency is not surprising in view of the mechanism described. Higher currents lead to more material being expelled, and this means that a longer time is required to re-create surface conditions suitable for arcing.

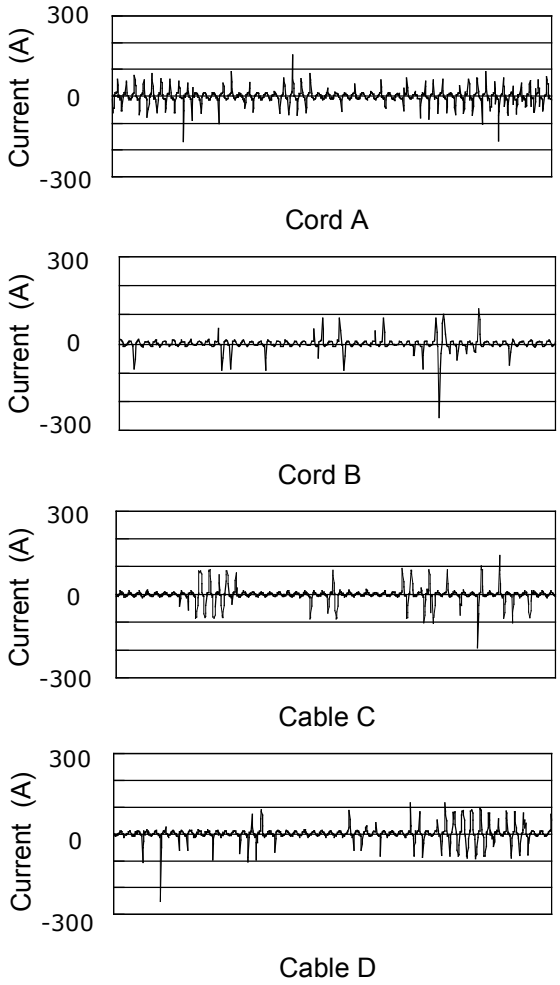


Figure 48 Current waveforms for four different specimens during 1 s measurement time
(Courtesy Hagimoto et al.)

Externally-induced ionization of air

The intrinsic dielectric strength of air is high (roughly 3 MV m^{-1}, except for very small gaps), but breakdown can occur at much lower values if the air space is ionized by some means. Two such means are flames and pre-existing arcs. If a serious arc-fault occurs, a large amount of ionized gases will be ejected. These can travel a certain distance,

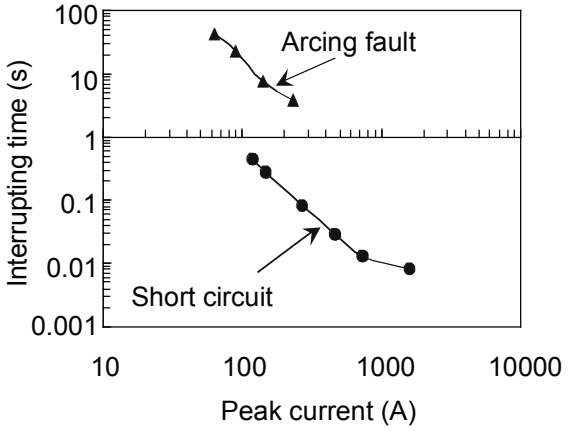


Figure 49 Interrupting characteristics of a 10 A circuit breaker for arcing faults and short circuits on Cord A
(Courtesy Yasuaki Hagimoto, NRIPS)

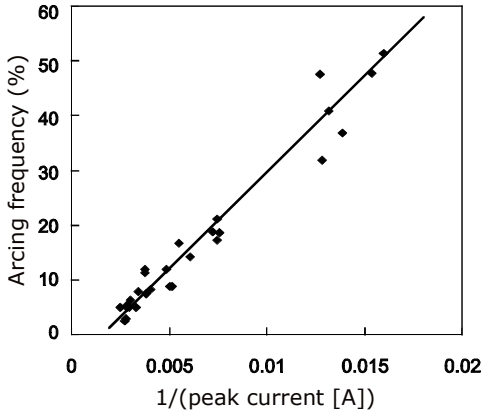


Figure 50 Arcing frequency, as determined by peak arcing current
(Courtesy Yasuaki Hagimoto, NRIPS)

and if they encounter another circuit, they can readily cause a breakdown and new arcing at the second location[706]. The decreased breakdown strength of air due to presence of flames has been documented in laboratory studies by Mesina[774], who showed that the dielectric strength of air drops to ca. 0.11 MV m^{-1} in flames. Mesina's study, however, only encompassed conditions at 1600 V and higher. A similar study was reported by Scott and Dolgos[775]. They conducted tests in an enclosure where explosions were ignited in a 9.8% methane/air mixture and the breakdown strength measured in an arc gap between two 12.5 mm brass sphere electrodes. Their results (Figure 51) show a somewhat higher than standard breakdown strength in normal air (4 MV m^{-1}) and a strength of 0.19 MV m^{-1} in the atmosphere undergoing a methane/air explosion. Bossert and Hurst[776] reported some similar data showing the reduced breakdown strength in various fuel-gas/air explosions. Their results

showed curves, rather than straight lines and also showed that some gas explosions, e.g., acetylene/air result in a lower breakdown strength than methane/air explosions. The fire does not have to be large in order to lower the breakdown strength of air. Baldo et al.[777] placed a Bunsen burner into 1.0 – 2.5 m long arc gaps and found that the breakdown strength was reduced by 30 – 50%.

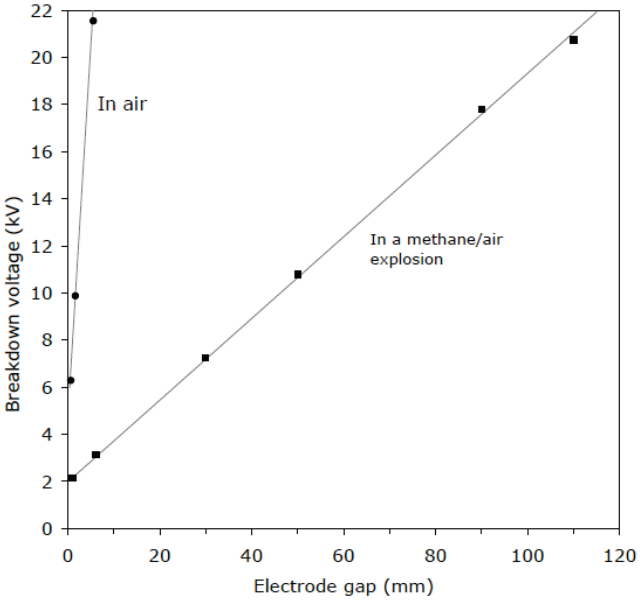


Figure 51 Breakdown strength in a methane/air explosion

There have also been limited studies in the fire investigations field[778] (see also Color Plate 97 and Color Plate 98), but many of the details of flame-induced arcing have not yet been elucidated. Arcing induced by local flaming may then cause further ignitions, either locally or elsewhere in the electric wiring. Thus, by far the most common situation for arcing to be encountered in fires is when the arc is caused by an ongoing fire[829].

It is often claimed that when evidence is found of arcing at multiple locations along a branch circuit conductor run and wires have physically broken apart at the arc locations, the initial arcing had to have occurred at the place most distant from the supply. Bernstein[779] points out that this is not true for circuits exposed to an intense fire—arcing can then occur more or less simultaneously along the entire branch circuit conductor run.

Short circuits

The term *short circuit* is commonly applied to the situation where a low-resistance, high-current fault suddenly develops in a circuit. This can take two forms: (1) a *bolted short* where a good metal-to-metal contact is made across a full-thickness section of metal; (2) an *arcing short*, where initial metal-to-metal contact is not sustained and current flows through an arc. In a bolted short, heating is not localized at the fault but distributed over the entire length of the circuit. A bolted short can readily be created by mis-wiring a circuit and then turning on the circuit breaker. The circuit breaker then typically trips before anything ignites.

An arcing short results from a momentary contact of two conductors. This causes melting of the material around the contact area. Magnetic forces tend to push the conductors apart, and the liquid bridge between them then gets broken. Electric breakdown across the gap created is then visible as the conductors separate. After an arcing short, large-diameter conductors can often be seen with a notch on the surface; smaller-diameter wires may be severed entirely; both results are illustrated in NFPA 921[756]. Color Plate 103 shows an arc created[570] by making a direct metallic short circuit across a 240 VAC line.

Color Plate 104 shows conductor damage that took place when a direct short circuit was created in a 240 VAC circuit[570]. In this case, both conductors were heavily damaged, but did not melt sufficiently to create a gap in the copper. Arcing ceased once metal was lost and remaining copper conductors became effectively further spaced.

In 120 VAC branch circuits protected by 15 – 20 A circuit interruption devices, it is exceedingly difficult to ignite a fire by means of short circuits. Short circuits will usually trip the circuit protection device, or blow out enough metal to clear the fault, or both. The amount of molten material ejected is usually small and it is difficult to ignite anything with it except 'tinder' type materials. UL testing showed that, upon creating a short circuit, wire insulation is usually 'blown away,' rather than getting ignited and burning[780]. Ettling tried igniting PVC wire insulation by creating short circuits[781], but his only successes were when a large overcurrent was created, not from bolted shorts or parting arcs.

Experiments have been performed, however, that illustrate the potential of tinder to get ignited from shorts. Hagimoto et al.[782] slowly crossed over two bare wires to make contact, with cheesecloth being placed below the location of the arcing short as an ignition target. Two types of wires were used, 1.6 mm solid conductors and 50×0.18 mm stranded. In their experiments, they used two different circuit breaker types, thermal-only and thermal/magnetic. Each was rated at 20 A. The thermal/magnetic breaker tripped in all cases, and in no case was there an ignition of the cheesecloth. Arc 'notches' were small and no wires melted through during these tests. The current at tripping ranged from 360 to 820 A. The thermal breaker did not trip in 40 trials, and tripped only in 4 trials. In two of those, the contacting wires became welded; in the remaining 38 trials, the wire melted through and broke. In every case where the thermal breaker was used, the cheesecloth target was ignited by ejected molten copper. The authors measured the current and voltage across the arc and determined that all cases of ignition involved arc energies > 100 J, while all cases of non-ignition had energies < 100 J. Similarly, using

I^2t as the test variable, ignitions occurred for $I^2t > 1500$ A^2 s, while non-ignition for $I^2t < 1500$ A^2 s. They also determined that, due to magnetic repulsion force, when the two wires were crossed over at an angle of 10º, an arc was more likely to be sustained longer than when crossed over at 90º. As for the types of wires, stranded wires had a tendency to sustain arcing longer than solid ones when a thermal breaker was used. The basic ignition/non-ignition outcome, however, was not affected by the wire type, nor by the angle of the wire crossing.

In similar experiments, Watanabe et al.[783] created short circuits by crossing two bare copper wires together, in a circuit protected by a 10 A circuit breaker of either the thermal-only or the thermal/magnetic type. Using target fuels of tissue paper and absorbent cotton, they were able to get ignitions when the peak current exceeded 260 A for the thermal circuit breaker, or 800 A for the thermal-magnetic circuit breaker. The corresponding I^2t values required were 250 A^2-s and 900 A^2-s. These are the minimum values seen for absorbent cotton, and ignition of tissue paper required somewhat higher currents.

Franklin[566] documented that fires are readily started in blankets and in paper, when a power cord is cut with diagonal cutters. The fires ignite from the molten copper droplets which are ejected. In such a situation, a bolted-short condition persists only very briefly, since the magnetic forces induced by the short circuit push the conductors apart, converting the bolted short into an arc. He was able to create up to 30 such short circuits on a power cord before a 20 A circuit breaker tripped. In laboratory measurements, Franklin documented that arcing across a 120 V circuit normally draws 200 – 250 A, but with some arcs as low as 150 A and others as high as 400 A. He reports that in creating hundreds of parallel arcs, currents below 100 A were never measured.

In circuits with larger circuit breakers, however, even high-density materials can ignite from arcing shorts. One such fire was documented in a Japanese investigation[784]. An arcing short occurred because a bolt pierced a power cable and made contact with a line conductor. The 100 VAC circuit was protected by a 150 A circuit breaker, but the actual current was only 4.5 A, because the bolt formed a poor ground connection. Laboratory tests replicating this arrangement produced an explosive sound, flames of about 0.4 m height, and heavy charring of nearby structural timber.

Plastic foam targets can be ignited in arcing faults of aircraft wire, described below under *Electric wiring in aircraft*.

High-voltage breakdown in low-voltage circuits

In 120 or 240 VAC circuits, arcing is normally initiated by metal-to-metal contact or by arcing across carbonized insulation. But direct arcing is possible if a high voltage is introduced into low-voltage wiring. If a sufficient high voltage is imposed on such wiring, then a breakdown of insulation can occur without previous carbonization or metal-to-metal contact. The exact breakdown voltage will depend on details of the devices (e.g., outlets) where the breakdown takes place, but experiments generally indicate[785] that 5000 – 7000 volts is needed for direct arcing; this is very similar to the 6500 V computed from Paschen's Law (see Chapter 11). This is because—unlike in HV wiring—insulation thicknesses in LV wiring are not selected simply on the basis of the voltage being carried (plus some safety factor), but rather are chosen for mechanical robustness and longevity. Extremely small insulation thicknesses would suffice were it desired just to withstand, say, 600 V.

EXCESSIVE OHMIC HEATING

Gross overloads

Excessive overload can lead to fires, but this condition is much rarer than is an arcing fault. It can arise if either a circuit breaker is faulty, or a cable is used which is of much smaller gauge than is the rating of the circuit breaker. Both of these situations are uncommon. Ampacity ratings of wires and cables are conservative enough that an overload of roughly 2× is not expected to create any significant problems, at least in the short term (long-term thermal degradation of insulation material is a separate issue). CPSC, however, has attributed some fires due to the use of 18 AWG extension cords* (rated at 10 A) in circuits protected by 20 A circuit protection devices[522]. In the case of a gross overload, CPSC found that a fire occurred where two refrigerators were plugged into a cube tap rated at 660 W; illustrating the long-term degradation issue, the fire happened only after 10 years of use. Another fire was investigated by NIST[521,786], where the cause was determined to be the use of steel-wire nonmetallic-sheathed cable in the 1948-vintage house. The branch-circuit wiring had functioned successfully until ca. 1980, when a window air conditioner was plugged into the outlet. The investigators speculated that some experimental cable had inadvertently been sold and used, and of course it did not have the same current-carrying capacity that a copper cable would have had. In addition, the 14 AWG cable was protected by a 20 A fuse, which would have been oversized even for a copper-wire circuit. Another fire originated in an attic space where a 14 AWG cable was found to be carrying 68 A. NIST investigation revealed that the homeowner had installed a 100 A subpanel, but fed it with a 14 AWG cable[786].

If a sufficiently overloaded condition persists, then cables may be able not just to ignite, but to create a propagating, self-sustained fire. Yamamoto et al.[787] investigated this situation. In testing Japanese cables, they found that for a self-sustained ignition to occur, an overload of 6× the rated

* The current edition of UL 817 requires that extension cords be a minimum of 16 AWG (rated at 13 A).

current had to occur for small gauge (3.5 mm^2) low voltage PVC cables, 5× for 600 V rated 200 mm^2 PVC power cables, and 3 – 4× for high voltage 200 mm^2 cross-linked polyethylene cables. In British tests[788] on a PVC extension cord rated at 7.8 A, fire occurred when a current of 55 A was passed through it, giving a ratio of 7×. This took 810 s to occur, and higher overloads resulted in fire occurring at shorter times. Gray et al.[789] tested extension cords rated at 5 A and found that a current of 35 A was needed for ignition, giving a ratio of 7×. At that current, ignition took 130 – 180 s. A thin (1 mm) PVC-insulated wire will ignite if sufficient current is passed through it to heat it to ca. 225ºC[768].

A test laboratory incident has been reported[665] where a PVC-insulated cable (ampacity = 19 A) was used to feed an electric heater drawing 60 A. The cable was hot, but still touchable, yet when it was accidentally stepped upon, a parallel arc resulted, and the arcing propagated about 3 m in less than 2 s. The insulation between the conductors was fully destroyed, but the rest of the material was not destroyed in the event, which comprised arcing but not flaming.

A moderate overload will not ignite an insulated wire, but it does raise the temperature of both the wire and the insulator. Old-style rubber-insulated wires used to be prone to a *sleeving* effect, whereby insulation closest to the wire is thermally degraded and shrinks back from the conductor. If sleeving is found, it can imply that overload conditions existed. For wires insulated with thermoplastic insulation* (which included the majority of today's common cable types), a somewhat different effect is found. Elevated temperatures cause copper to elongate, but the insulation to shrink. As a result, copper wires readily 'pop out' of the softened insulation (Color Plate 105). A direct metallic contact can then occur, with this short circuit being a localized place of ignition (Color Plate 106). Mazer[790] has provided some brief accounts of overcurrent experiments where ignition was preceded by short-circuiting.

Ignition in the excessive-overload mode cannot occur if the cable is in a circuit which is protected by a circuit breaker/fuse matched to the rating of the cable, since tripping would occur rapidly under 3× and greater overloads. But ignitions can readily occur if a much smaller gauge cable is used than corresponds to the rating of the circuit breaker. Béland[791] was able to get arcing to occur when nonmetallic sheathed 14 AWG cables, rated for 12 A, were used to carry very high currents (Figure 52). For the old style of cable

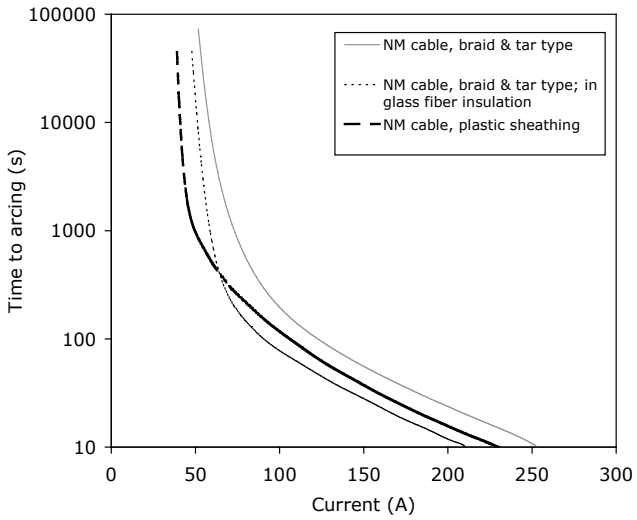


Figure 52 Time to arcing for AWG 14/2 cables with 125 V applied
(Copyright NFPA, used by permission)

which uses a braid with tar, arcing occurred at about 400ºC; for PVC constructions, at about 200ºC. In an attempt to produce an ignition of the building structure, Béland constructed a wall stud cavity, filled with thermal insulation, in which he ran an AWG 14/2 NM cable[792]. An equilibrium temperature of 370ºC was reached with 50 A. With 75 A, 520ºC was reached after 20 min, but the temperature was still climbing. Charring, but not flaming was seen, due to absence of oxygen entry into the cavity.

Excessive thermal insulation

The current required to cause sustained ignition will be less if the cable is buried in thermal insulation, where access to oxygen exists, but dissipation of heat is retarded. Béland[805] reports of a fire incident where a 12 AWG aluminum wire cable, rated for 15 A but fused at 30 A, was run for a long time at about the 30 A level, and was covered by combustible insulation. Eventually, a fire ensued. Béland also reported on arcing induced by placing an 18 AWG extension cord between a carpet and a carpet pad and running large currents through it[792]. At a borderline value of 21.5 A, no arcing occurred until the carpet was walked upon; when it was, arcing started. For a current of 27 A, arcing started in 8 min, without walking. The original data points were not provided, but Béland stated that in some cases, at a current of 40 – 50 A, it took "many days" for arcing to occur. Color Plate 107 shows a situation where a copper 14 AWG cable, rated for 15 A was run at 28 A and was covered with thermal insulation.

Theriault and Theriault[793] conducted studies on NM cables using a mockup stud cavity, framed in nominal 2"×4" studs, which was filled with mineral-wool insulation. 14 AWG cables were looped inside the cavity in various configurations to create more than one proximate path. When using

* The most common insulation for nonmetallic cable used in building wiring is PVC. The polymer is classified as a thermoplastic, i.e., a plastic which melts upon heating. Softening and melting is indeed what occurs due to medium-temperature (a few hundred °C) electric overcurrent. But if the cable is involved in a building fire (temperature of ca. 1000°C), the material typically intumesces and chars, rather than melting. The insulation normally contains not just pure PVC, but also various additives, including inorganic fillers such as calcium carbonate. These play a role in promoting high-temperature charring.

the Code-permitted 15 A current through the cables, a maximum temperature of 38ºC was recorded. Under the same conditions, but when the mineral-wool insulation was overpacked by installing twice the thickness intended for the cavity, a maximum temperature of 74ºC was recorded. This was high enough to perhaps shorten the lifetime of the cable, but not an immediate danger. The tests were repeated using 30 A, as an illustration of abusive over-fusing of branch circuits. In that case, a peak temperature of 89ºC was found using the normal insulation thickness. In the case of overpacked insulation, short circuits terminated testing in each of the tested configurations. Recorded temperatures at the time of short circuit were generally 150 – 200ºC, but these values are not necessarily indicative of temperatures at the short-circuit location, since short-circuits did not necessarily occur in those places where the thermocouples were mounted.

Table 71 Temperatures (ºC) recorded on the conductor surface of NM cables after 6 h of test in a wood-stud wall space

Wire size, AWG	No. of adjacent cables	Current (A)	No insulation	Fiber-glass	Poly-urethane
14	1	15 A (100% of rating)			173
	2				245
	3				294
	4				332
	1	18 A (120% of rating)			195
	2				308
	3				390
	4				417
12	1	20 A (100% of rating)			236
	2				267
	3				265
	4				290
	1	24 A (120% of rating)	114	131	
	2		131	206	
	3		141	211	
	4		146	215	

Heat dissipation is diminished if wires are bundled or grouped so that each wire is exposed to other wires also overheating, rather than to an environment where convective cooling is effective[772]. Several electric cables are commonly run next to each other in wiring of houses. The studies of Theriault involved some overlap and adjacency, but not much. Much higher temperatures were recorded by Goodson et al.[794] (Table 71). They conducted wall-cavity tests similar to Theriault, but Goodson used cables which were placed adjacent to each other for the entire length of the test jig. Goodson's tests used 90ºC-rated NM cables, placed in a cavity framed in by 2"×4" studs, with plywood on the other faces. The pertinent standard (UL 489[795]) does not require that a circuit breaker ever trip at its rated capacity, and only require tripping in 1 hour at 135% of the rating. Thus, Goodson conducted tests at 100% and 120% of the cable's rating, since a circuit breaker within its specifications would not be expected to trip at either of these levels. Table 71 shows that at 120% of rated ampacity, no thermal insulation, and no other nearby cables, a temperature of 114ºC was reached. This is not surprising for a cable rated at 90ºC when running a current of 100% of ampacity. Much more troubling are the results for cavities filled with polyurethane foam (for which Goodson used a foam-in-place product), since temperatures over 200ºC will lead to very rapid degradation. Goodson noted that his investigation was motivated by observing a house during construction where charring damage was already found on the insulation of NM cables. Likewise, his tests showed that for the cases of runs with 3 and 4 adjacent cables, actual charring was generally achieved during a 6 h run. His findings are especially troubling because a householder would have no way of knowing that a circuit is running at modestly overloaded conditions, since the circuit breaker will not trip. It should be noted that the NEC permits engineering calculations of ampacity derating, performed to reflect the actual thermal environment, but such calculations are almost never done except for industrial occupancies.

Prior to World War II, knob-and-tube wiring was common in the US. This form of wiring uses two separate conductors which are not grouped into a cable, but are individually strung on widely-spaced porcelain knobs. The current-carrying capacity of this form of wiring is dependent on there being unobstructed air cooling of the wires. Fires have occurred when the wires were buried in thermal insulation[522]. A similar problem can be encountered when extension cords, which are rated for exposed-air use, are buried under thermally-insulating objects.

Extension cords wrapped in cord reels or placed under rugs have much reduced dissipation of heat; see the sections below on *Appliance cords and extension cords* and *Impaired cooling*.

Stray currents and ground faults

Stray currents occur when circumstances cause current to flow through paths not intended to carry current. Ground faults are a well-known example[796,797]. They can occur if a conductor is abraded or damaged and contacts metal siding, roofing, etc. Jackson[798] described a particularly interesting case where an outlet was miswired so that the line and neutral conductors were switched. This would ordinarily not cause any problems, except in this case a heavy-duty extension cord was equipped with a separate grounding lug, intended to be fastened to an outlet plate screw. Instead, the lug contacted the 'neutral' prong of the plug, which was actually the line side. The extension cord fed a window air conditioner, and the spurious connection applied line voltage to the air conditioner housing. The latter, in turn, was

contacting the aluminum siding of the house. Current flowing over a high-resistance path through the siding ignited a wood-fiber sheathing board.

Kinoshita et al.[799] documented that only 5 A were required for ignition when a 3-conductor, PVC-insulated cable contacted a galvanized iron roof. In a limited study, voltage drops of around 1 – 5 V at each casual metal-to-metal contact were found when various metallic objects not of normal electrical function were inserted in series with a 120 V branch circuit[800]. In these laboratory experiments, it was difficult to find adventitious conductive components having enough resistance that a circuit breaker would not be rapidly tripped when the test arrangement was inserted in parallel across the line, instead of in series with a load. Nabours[801] has pointed out that fires are sometimes caused by improper wiring whereby an electrical conduit was pressed into duty as the neutral conductor, with a proper wire for that purpose not being provided. The load-carrying capacity of the conduit itself might be adequate, but connections are the weak point. On occasion, set-screw type couplings have been found where the set-screws were not tightened and the conduit itself fell out of good contact with the coupling, causing arcing at that location. CPSC has hypothesized that the Beverly Hills Supper Club fire, one of the deadliest US fires of the 20th century, was made possible by improper wiring of the neutral conductors and triggered by a ground fault that occurred[802].

An unusual mode of ignition from a ground fault is where current flows through a gas line. The current can cause overheating of the metal and lead to a rupture of the pipe[803]. Color Plate 108 shows such an outcome.

Another interesting type of ground fault was described in an incident where a downed power line contacted a corrugated steel fence[804]. Four different fires erupted in four buildings near the fence line. In each case, the fire started at the dielectric union installed ahead of the gas meter (Color Plate 109). A dielectric union is used to prevent galvanic corrosion of dissimilar metals. In this case, breakdown occurred across the dielectrics due to the high voltage (12 kV) of the power line.

In cold climates, it is not rare for individuals to thaw a frozen water pipe by attaching a welding transformer and passing current through it. Fires have resulted due the very large currents that are involved[805]. Sanderson[806] studied a case where thawing activity did not ignite the house that was being worked on, but caused ignition in six neighboring houses fed from the same power utility connection.

If a building has conductive components throughout it, such as metal lath, aluminum siding, etc., an electric fault can result in an *electrified house*. One case was already described above. Color Plate 110 shows how electrical contact with plaster mesh led to multiple ignitions of building paper and wood members. In another case[807], a 7620 VAC power line fell down and established contact with a house having aluminum siding. This ignited various locations having electrical contact to the siding. An additional consequence was that electric current also flowed through the water meter, blowing it out and creating a flood in the basement. In a similar case, a power line contacted a chain-link fence which was in contact with the aluminum siding of the house. In addition to fire damage (Color Plate 111), an explosion also resulted due to current flow induced in the gas piping.

Overvoltage and floating neutrals

All indications are that ignition from an overvoltage is rare, as concerns branch-circuit wiring. The materials used for wires and wiring devices are well able to withstand the normal surges that are a regular event in a power distribution system. To experience ignitions, one of these events is generally needed:

(a) lightning strike;
(b) a large voltage spike;
(c) accidental delivery of high voltage into low voltage wiring, or large surges on high-voltage wiring causing unexpectedly high voltages on 120/240 V wiring; or
(d) a floating neutral.

Lightning strikes can result in massive ignitions, not just of wiring, but of all sorts of combustibles. The problem has generally not been studied in connection with 120/240 V wiring systems.

Surprisingly large voltage spikes can be found on 120/240 V systems. Without any overt fault conditions, simply the operation of a motor controller can create a 2000 – 3000 V spike[808]. It seems entirely probable that repeated power line surges are responsible for substantial degradation of wire insulation and electrical components that are nominally designed for no more than 600 V operation (albeit with large safety margins). But no systematic study exists on dielectric failures—from any cause—in 120/240 V systems. As a rough approximation, a 1 mm thickness of many dielectric solids can withstand about 20,000 V. Thus, in principle, the insulation thicknesses would have to be exceptionally small or the spike voltages very large for immediate failure to occur, however, cumulative degradation effects may come into play. Also failure might occur at points of pinched insulation or at other installation abnormalities.

Occasional fire reports are encountered where, due to some malfunction in the power distribution network, high voltage

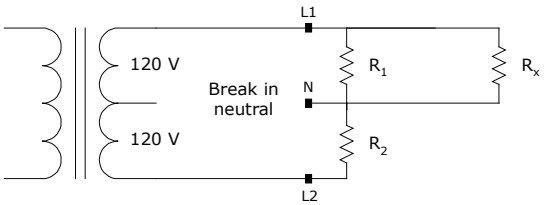


Figure 53 Floating neutral

got applied to wiring intended to carry only 120/240 V. A case is documented[809] where a utility transformer fault caused all the ground-fault circuit interrupter devices in a house to fail, along with igniting a fire due to an 'explosion' of a TV set. In another case, a faulty transformer caused the service entrance wires to ignite and burn inside a house. Such cases are rare enough that no systematic study exists.

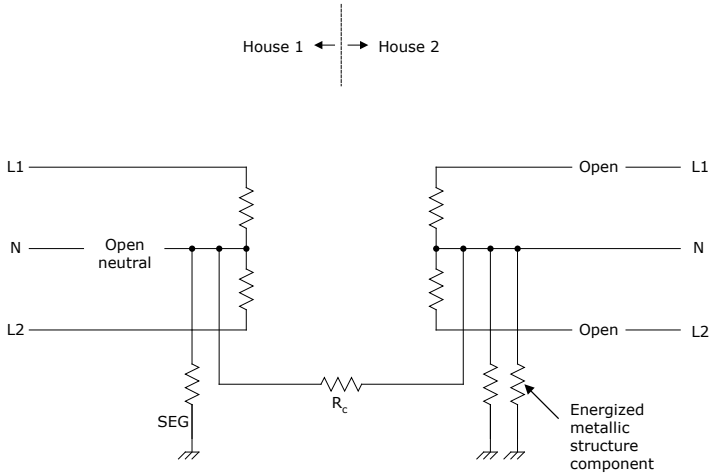


Figure 54 Ignition in house 2 (which had a pulled meter) due to open neutral in adjoining duplex house 1 (SEG = service entrance ground)

Floating neutral (sometimes called *open neutral*) problems are a bit less rare, but again, no systematic studies exist. This type of ignition occurs due to a specialized failure of 120/240 V wiring circuits[*]. In a single-phase service entrance, there are three current carrying wires: two 'hot' wires and one neutral. Figure 53 illustrates the normal feed from an outdoor transformer to the building. Inside the building, the system becomes effectively a 4-wire system, since a safety grounding wire is also run which is connected to the neutral and terminates at a ground rod[†]. All 240 V loads are directly connected across L1 and L2 and do not depend on the presence of the neutral. But 120 V loads are connected across N and either L1 or L2. If a neutral is in place, the loads will receive the intended 120 V voltage. However, if a break occurs in the neutral, the voltage delivered to 120 V loads can swing widely, in principle from barely above 0 to almost 240 V, although in practice the range is not quite as large. Figure 53 shows the circuit arrangement. The voltage present across a particular load R_x will be determined by the voltage divider action of other loads in the system, designated as R_1 and R_2. The voltage across R_x will be:

$$V_x = \frac{240}{1 + \frac{R_2}{R_1} + \frac{R_2}{R_x}}$$

Many electrical or electronic equipment can ignite if a voltage much in excess of the intended one is fed to it. Conversely, most devices will not ignite if the voltage delivered to them is too low. Electric motors, however, are an exception, and it has been experimentally demonstrated that flaming fires can result from motors running at a sufficiently under-voltage condition (see *Electric motors*).

An ignition due to under-voltage can also occur if one hot leg of a 240 V circuit is disconnected. If the circuit had any 240 V appliances and these are energized, then they can transfer power from the live leg to the disconnected leg. But the delivery will be through a sizeable resistance and much less than 120 V will be delivered.

The above discussion ignored the presence of the ground wire. According to the NEC, a 'grounding electrode' must be connected from the neutral to an earth ground at the service entrance. But, provided that the neutral is functioning properly, this ground wire serves no observable function. Consequently, there may be little to prevent its deterioration or abuse over the years. If a break in the neutral then occurs, a sizable current can flow through the ground wire. If the ground wire passes near or through combustibles, and an excess current ends up flowing through it, then an ignition might occur at that place. Fires have also been reported[810] in installations using armored cable, when a floating neutral occurred and current that would normally flow through the neutral instead flowed through the armor.

In rare cases, buildings with disconnected power (pulled meter) have sustained ignitions due to floating neutral problems[811]. Figure 54 shows how an open neutral in one house has led to an *energized neutral* in the second unit of a duplex and subsequent ignition. An open neutral exists is House 1, while the meter has been removed in House 2. Because of the break, the house-side of the neutral in House 1 has risen to a voltage substantially above 0 V. Because of high resistance in the service entrance grounds, current flows along the metallic power distribution conduit from House 1 to House 2, denoted as R_c. In House 2, the electrical conduit is touching metallic stucco mesh, which in turn has a path to ground. Consequently, a circuit is established for current to flow through the stucco mesh and ignition occurs at a poor connection along that path.

Harmonic distortion or overload

If a facility uses primarily 3-phase, non-electronic loads, then voltage and current waveforms generally remain close to the expected shape, a sine-wave. But some current-using devices are not constantly 'on' during an entire power cycle, for example:

- solid-state motor controls and variable-speed drives
- 'high-frequency' type power supplies for computer or electronic equipment
- electronic ballasts for fluorescent lighting fixtures

[*] The discussion here is based on electrical practice in North America.
[†] Mobile homes normally have a 4-wire service from pole to building.

Table 73 Results of Barnes et al. from various ignition tests on wire and cable specimens

ID No.	Glow wire ignition		Needle flame ignition		Setchkin furnace ignition		UL 94 V		
	Temp. (ºC)	Thick. (mm)	Edge/Face	Thick. (mm)	Piloted (ºC)	Auto (ºC)	1 mm	2 mm	3 mm
2	960	3	NI	1,3	400	410	V-0	V-0	V-0
3	960	1,3	NI	1,3	375	410	V-0	V-0	V-0
4	960	1,3	NI	1,3	400	430	V-0	V-0	V-0
5	960	3	NI	1,3	340	385	V-0	V-0	V-0
6	960	3	E (F)	1,3 (3)	330	385	V-1	V-2	V-0
7	960	1,3	NI	1,3	400	415	V-1	V-0	V-0
8	960	1,3	NI	1,3	530	540	V-0	V-0	V-0
9	850	1,3	E,F	1,3	350	370	fail	fail	fail
10	850	1,3	E,F	1,3	400	420	fail		
11	850	1,3	E (F)	1,3 (1)	390	420	fail		
12	850	1,3	E,F	1	390	420	V-1	V-0	V-0
13	850	1	E	1,3	405	420	fail	fail	fail
14			E	1	400	420			
15							V-0	V-0	V-0
18							fail	fail	fail
19	750	1	E	3			fail	fail	fail

- battery chargers
- arc welders.

The consequence is that the current and voltage waveforms in that circuit become distorted from a true sine-wave shape, a process termed harmonic distortion. Since the network is interconnected, this distortion then propagates to other parts of the network. The distortion is termed *harmonic* since any alteration of a sine wave produces a waveform which can be represented as the summation of a series of sine waves that includes the primary (the original sine-wave) frequency, plus additional frequencies that are harmonics (i.e., frequencies equal to 2×, 3×, etc. times the primary).

Table 72 Identification of specimens tested by Barnes et al.

ID No.	Composition	Density kg m^{-3}
2	PVC, FR A*	1580
3	PVC, FR B*	1560
4	PVC, FR C	1560
5	PVC, FR D*	1510
6	PVC, non FR	1480
7	chlorosulfonated polyethylene (Hypalon)	1580
8	PTFE (Teflon)	2160
9	polyethylene, non FR	920
10	EVA copolymer A†	1490
11	ethylene-propylene rubber†	1460
12	EVA copolymer B†	1590
13	EVA copolymer C†	1380
14	EVA copolymer D†	1570
15	fluorinated ethylene propylene (Teflon FEP)	1750
16	ethylene/maleic anhydride copolymer†	1570
18	polyphenylene oxide/polystyrene copolymer	1050
19	EVA copolymer E†	1560

* reduced acid emission formulation
† filled with aluminum trihydrate

Harmonic overload of the neutral conductor can take place if a system was designed for balanced, 3-phase loads initially, but waveform-distorting devices are subsequently hooked up. In a 3-phase system, the neutral does not need to carry much load, so a small-diameter wire can safely be used *if* harmonic distortion is not present. But in distorted-waveform networks, current flows up to 173% of the phase-conductor current can flow in the neutral[812]. If the neutral is under-sized, it may overheat or melt out, leading to possible ignition. If the neutral does open up, then floating-neutral problems can follow.

A high harmonic content can also cause overheating and failure of transformers. Transformers that are especially designed to withstand high harmonic-content conditions are termed 'K-rated' transformers, with the term coming from a calculational procedure used by UL for testing transformers[813]. K-rated transformers have the drawback of a higher inrush current, which by itself can lead to other problems. IEEE Std-579[814] is a standard on the subject of harmonic distortion.

IGNITION FROM EXTERNAL HEATING

Barnes et al.[815] reported on a series of extensive tests of wire and cables and also on tests using the plaques of the polymer material alone (not made up into wires). The specimen identifications are given in Table 72. Results from a variety of ignition tests are shown in Table 73. The glow-wire tests were conducted according to IEC 60695-2-1; the needle flame tests were according to IEC 60695-2-2. Most tests were run on 1 and 3 mm samples, but the UL 94 tests were also run on 2 mm plaques. Radiant ignition results are shown in Table 74. With the exception of the PTFE specimen (which required about 35 kW m^{-2}), all other samples

Table 74 Radiant ignition results of Barnes et al. on wire/cable insulation materials made up in the form of 3 mm thick plaques

ID No.	Cone Calorimeter				ISO 5657 test				
	Critical flux kW m^{-2}	Time at 30 kW m^{-2} (s)	Time at 40 kW m^{-2} (s)	Time at 50 kW m^{-2} (s)	Time at 10 kW m^{-2} (s)	Time at 20 kW m^{-2} (s)	Time at 30 kW m^{-2} (s)	Time at 40 kW m^{-2} (s)	Time at 50 kW m^{-2} (s)
2	9.4	110	59	38	NI	150	62	35	23
3	9.2	75	44	29	NI	130	48	30	17
4	15.1	82	63	39	NI	170	75	42	26
5	7.7	68	38	20	NI	125	53	32	19
6	5.9	64	30	23	NI	125	58	35	23
7	12.9	99	58	42	NI	190	83	53	28
8	25.4	NI	439	250	NI	NI	NI	330	193
9	9.8	103	67	50	NI	250	127	78	54
10	16.4	123	80	52	NI	250	137	85	63
11	12.9	105	60	48	NI	195	128	78	56
12	5.5	346	144	110	NI	650	230	135	100
13	13.6	231	139	97	NI	424	181	98	74
14	21.2	155	93	53	NI	300	143	83	60

NI – no ignition

showed a minimum flux for ignition in the vicinity of 15 kW m^{-2}.

Meyer et al. [816] reported on extensive small-flame tests conducted on a wide variety of wires and cables. They conducted tests in both vertical and horizontal orientation, but according to a protocol which did not follow any existing standards.

Some Cone Calorimeter data on ignition of electric cables were reported by Nakagawa[817], as shown in Table 75. The effect of FR formulations can be seen to prevent ignition at lower irradiance values. The results, however, do not indicate that the FR formulations were particularly effective in delaying ignition at irradiance values over the minimum required for ignition.

Table 75 Piloted ignition times for electric cables by Nakagawa

Wire insulation	Jacket	Ignition time (s) at specified flux (kW m^{-2})			
		20	30	40	50
PVC	PVC	61	34	17	13
PE	PE	395	142	54	35
PVC	PVC, FR	--	--	26	22
PE	PO, FR	--	123	46	30
XLPE	PVC	85	35	18	13
XLPE	PE	553	167	54	29
XLPE	PVC, FR	--	--	--	15
XLPE	PO, FR	--	126	53	31

PVC – polyvinylchloride
PE – polyethylene
FR – fire-retardant
PO – polyolefin
XLPE – crosslinked polyethylene

Andersson and Van Hees[818] exposed 4 types of data cables and power cables to Cone Calorimeter heating to determine heat flux levels needed to cause electric failure in the form of short-circuiting. The test cables were all multiconductor types, ranging from 24 conductors of 0.5 mm^2 to 7 conductors of 2.5 mm^2, with the insulation types used being PVC, polyolefin, and XLPE. For exposures of 1200 s or greater (but test time of 4800 s or less), 10 – 20 kW m^{-2} was needed to cause failure. For shorter times, higher fluxes could be withstood. During a 600 s exposure, typically 15 – 40 kW m^{-2} was needed for failure. Repeatability was generally very poor—identical tests often gave different results. This is presumably because short-circuiting involves mechanical contact between the conductors, but this is determined both by the stresses in the conductors and by the exact details of the melting of the polymer. Some tests were made to examine the effect of deliberately bending the cable prior to test, but the results were inconclusive. Generally, no current leakage was measured until shorting occurred. Visible damage (melting, or even insulation totally melting away in a portion of the cable) occurred in all cases before electric shorting. Ignition commonly occurred at the time of shorting, provided the heat flux was $\geq$ 15 kW m^{-2}. Sometimes ignition did not occur upon shorting and occasionally it occurred a short time before shorting. Typical ignition times for cables with a polyolefin were 103 s at 35 kW m^{-2} and 48 s at 50 kW m^{-2}. PVC-jacketed cables ignited more quickly: 21 – 32 s and 10 – 11 s, respectively. The test work involved both unloaded cables and cables carrying a 5.3 A current, but no significant difference between these two conditions was found. A few 'old' cables, one approximately 15 years old and one 20 years were also tested, but the results did not show a significant difference.

Bertrand et al.[819] ran room fire tests on PVC-insulated and jacketed cables arranged in full-scale cable trays. For tests of 1 h duration, cables short-circuited when their temperature reached 215 – 250ºC, which required a mean heat flux of only 5.3 – 5.4 kW m^{-2}. The failures occurred because at approximately 220ºC PVC softens sufficiently that mechanical stresses can move conductors into contact with each other. They then ran oven tests on individual cables and found that in a 250ºC oven short-circuiting occurred in 15 – 20 min. When tested in a 400ºC oven, however, the specimens ignited prior to short-circuiting.

Hoffmann et al.[820] conducted both radiant heat and flame tests on power cords using SPT-1 and SPT-2 type stranded, two-conductor cords. SPT-1 is 20 or 18 AWG and has 0.76 mm min. thermoplastic insulation thickness, while SPT-2 type is 18 or 16 AWG with 1.14 mm min. insulation thickness. The SPT-1 cords were also tested in a variant where a separate jacket is used, while the SPT-2 types were only tested as 'zip' cords. All radiant heat tests were at 40 kW m^{-2} irradiance, while flames were applied from a gas burner or from a wood crib. Electrical load on the cables was a 15 W lamp. When a section approximately 175 mm long was irradiated, 58% showed no electrical failure (shorting or opening), 25% tripped a 15 A circuit breaker, while 22% severed completely; less damage was recorded in another test series, where a shorter section of cord received 40 kW m^{-2} radiation. Times to failure when exposed to the radiant heat were typically 4 – 8 minutes. When a gas flame was applied to cords, 86% showed electrical failure (shorting or opening), 83% tripped the circuit breaker, while 27% severed completely. Times to failure were typically ca. 1 minute, but as short as 23 s for one type of test cord. When subjected to a wood crib fire, 100% of the test specimens showed electrical failure, 83% tripped the circuit breaker, while 22% severed completely. Failure times were longer, however, being typically 2 – 4 minutes. Severed conductors typically showed a bead at the ends (Color Plate 112 and Color Plate 113). Some cords showed arcing damage at multiple places along the length. The authors also noted that when exposed to radiant heat, some cables ignited but did not fail electrically, but did not provide details on specimen ignitions. Hagimoto et al.[821] also conducted radiant heating tests on a variety of cords and cables. They found that a wide spacing (8 mm) between conductors was helpful to avoiding initiation of arc tracking with PVC cords, but that there was little effect of the spacing on the behavior of rubber-insulated cords. Increasing the overall insulation thickness of rubber-insulated was helpful, however, and cords with 2.5 mm thick insulation proved to be resistant to arc tracking, even at the highest flux used, 40 kW m^{-2}.

Table 76 Highest heat flux at which no ignition (piloted) occurred, as measured by Factory Mutual

Wire insulation	Jacket	Highest flux at which no ignition observed (kW m^{-2})
PP, PES	PVC	10
PE (FR)	none	12
PVC	PVC	13 - 25
silicone, glass braid	asbestos	14
EP	PVC	15
PVC	EP	15
TPE	TPE	15
PE	PVC	15 - 20
XLPO, PVF	XLPO	15 - 20
silicone	PVC	19
EP	PE (FR)	18 - 25
EP (FR)	none	19 - 25
XLPE	Neoprene	20
XLPO	XLPO	20
XLPE	XLPO	20
EP	EP	20 - 23
XLPE	XLPE	20 - 25
XLPE	EVA	20 - 25
silicone	XLPO	20 - 25
ETFE	EA	22
TPE	PE (FR)	25
silicone, glass braid	none	29
silicone	XLPO, metal armor	30
PVC	PVF	30
FEP	FEP	30 - 36
PTFE	PTFE	43

EA: ethylene-acrylic
EP: ethylene-propylene
ETFE: ethylene-tetrafluoroethylene
EVA: ethylene-vinyl acetate
FEP: fluorinated ethylene propylene
FR: fire-retarded
PE: polyethylene
PES: polyester
PP: polypropylene
PVC: polyvinyl chloride
PVF: polyvinylidene fluoride
TPE: thermoplastic elastomer
XLPE: crosslinked polyethylene
XLPO: crosslinked polyolefin

Additional radiant ignition tests were reported by Factory Mutual[822,823], as shown in Table 76. The minimum heat flux values were not reported, but in most cases the heat fluxes were incremented by units of 5 kW m^{-2}. Thus, if the highest heat flux at which no ignition was observed was 20 kW m^{-2}, and the lowest heat flux at which ignition was observed was 25 kW m^{-2}, it would be concluded that $\dot{q}''_{\min} = 22.5$ kW m^{-2}.

Hasegawa et al.[824,825] examined a number of electric cables in a radiative heating apparatus where an impinging pilot was used. Minimum heat fluxes for ignition were found as shown in Table 77.

Electric cables generally behave so that, at room temperature, if a small flame applied directly to the cable, it does not lead to a propagating fire. But experience indicates that if the temperature of a PVC cable is raised to 60 – 100ºC, then propagation will occur. A limited amount of published

Table 77 Minimum flux for ignition of electric cables using an impinging pilot

Cable jacket material	Minimum flux for ignition (kW m^{-2})
ethylene propylene rubber	15
Hypalon (chlorosulfonated polyethylene) rubber	25
polyethylene	6 – 10
PVC	10

research also exists on the topic. In Sandia tests[826] (described in Chapter 11), where a glowing connection was simulated, it was also found that fire does not spread along non-preheated building wires. But when as little as 50 W was used to preheat a wire connection for 10 min, subsequent ignition allowed extensive fire propagation. Several studies where small-flame tests were conducted on wires/cables at elevated temperatures have been discussed in Chapter 7.

In actual fire incidents, there can be a wide variety of external heating circumstances that ignite electrical wiring. In one case studied by NIST[786], it was found that fire originated in branch circuit wiring midway between two outlets. Investigation showed that one side of the wall cavity was formed by the backside of a brick fireplace, which was being intensively used and led to ignition of the nonmetallic cable.

A European research project on large-scale fire testing of electric wires and cables also entailed collecting ignition data for a wide variety of specimens, as tested in the Cone Calorimeter[827]. Piloted ignition data at 35, 50, and 75 kW m^{-2} were reported. Ignition times at 35 kW m^{-2} ranged from 21 to 304 s, while at 75 kW m^{-2} the specimens ignited in 4 – 50 s. The authors also provided results from analyzing the data according to Janssens' thermally-thick procedure, but the applicability of the method is uncertain since the specimens may not be thermally-thick, they are invariably complex composites (including copper layers), and only 3 heat flux values were available.

CONTRIBUTORY FACTORS

MECHANICAL INJURY

Mechanical injury to wiring may be caused by any number of sources. CPSC identified[522] some interesting cases where a nonmetallic-sheathed cable had been draped against vibrating metal ducts. In time, the vibration caused the insulation to wear through and a fire to occur.

Major damage can be inflicted on wiring and other electrical installations by *vermin infestation*, e.g., rodents, snakes, insects. During the early part of the 20th century, 'rats chewing wires' became infamous as a fire cause determination by sloppy fire investigators. Consequently, this cause of fires was subsequently sometimes considered to be a myth. Yet, fires can start from rats chewing wires. It has also been sometimes considered that rodents will chew cotton-fabric insulation, but will not attack modern plastic insulations. This is incorrect, as shown in Color Plate 114. Even though ants are much smaller, the damage they can inflict can be disproportionate to their size, as shown in Color Plate 115. Fire ants are especially prone to causing damage to wiring. Both the bodies and the feces of vermin have sufficient electrical conductivity to create an electric fault; in the case of insulation chewed from wires, direct metallic contact also becomes possible.

Hosaka[828] established a flow chart of possibilities leading to ignition due to rodents (Figure 55). He then conducted laboratory experiments to quantify the phenomenon. In the first series of tests, he placed rats in a cage and supplied them with food and water *ad libitum*. He also enclosed samples of six different types of non-energized cables and 5 different types of stranded-conductor cords in the same cage. After a 10 day period, the weight of the wire insulation of the cables that remained was only about 10 – 40% of the original weight. For the cords, he was unable to measure the remaining weight of the wire insulation, since the stranded conductors were also being chewed and dispersed; using the gross weight of the assemblies, he found that the weight remaining ranged between 20 and 65%. He then conducted an arc tracking test on a partly-chewed cable containing two 1.6 mm conductors by energizing it in a 100 VAC circuit and applying one drop of rat urine to the damaged location every 30 s. Short-circuit current was limited to 10 A by a series resistance of 10 Ω. The specimen (Figure 56) showed sustained ignition in about 3.5 h.

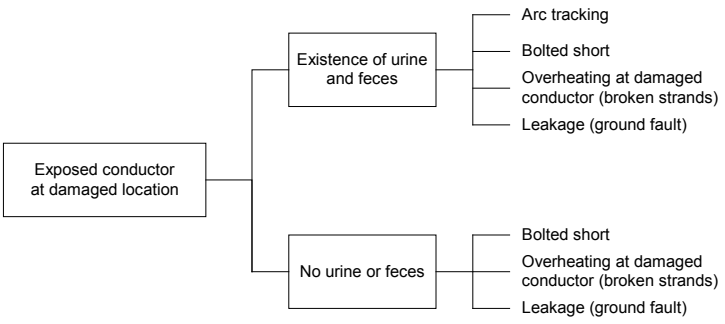


Figure 55 Flow chart of ignition possibilities upon rodent damage of an electrical cord or cable

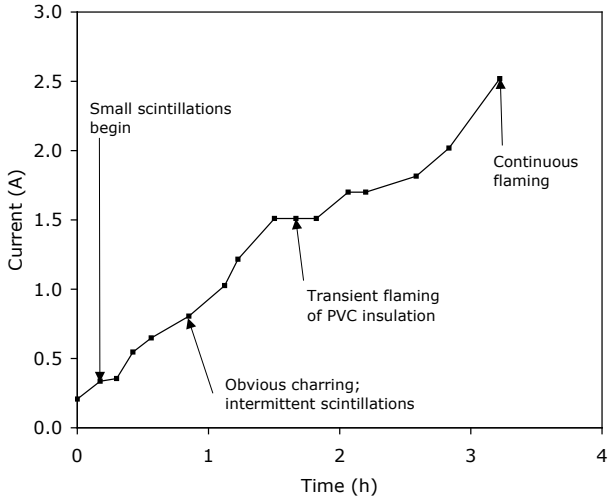


Figure 56 Arc tracking of a cable damaged by chewing of rats

Solid conductors—parallel arcing

Béland reports conducting numerous tests where cables, armored cables, and conduits were hammered until the circuit breaker opened[829]. These produced minimal mechanical sparks and could never ignite wood. In some cases loose fibers from wood fiberboard insulation could be ignited, however. He also reports that simply bringing two bare conductors together until a short resulted created even less propensity for ignition than did hammering. On the other hand, Kinoshita et al.[830] successfully ignited cotton gauze when creating bolted shorts with wires having 1.6 mm diameter solid conductors and also with ones using 1.25 mm^2 stranded conductors. In their experiments, this required a thermal-mode-only, 20 A circuit breaker; when using a 20 A thermal/magnetic breaker, ignitions were not observed. Clearly, it is difficult, but not impossible to start a fire from parallel arcing in a 120 VAC branch circuit. (See also: *Overdriven staples*).

Solid conductors—series arcing

Roberts[831] created series arcing by severing a conductor in a 14 AWG nonmetallic cable with a nail. Ignition of the cable and charring of the adjoining wood stud resulted. The fire self-extinguished after "a few minutes." This self-extinguishing might not happen if the cable were covered in a layer of dust or if other finely-divided combustibles were present. In another test, he was able to get self-sustained smoldering of the wood member, which he eventually manually extinguished. In a test using 12 AWG nonmetallic cable, he was able to get an arc which sustained itself for 1.25 h before the wire melted and the arc self-extinguished; however, in that test suitable ignition targets were not present. In none of the tests did the circuit breaker trip. Béland[829] also reported on similar experiments, but with negative results. Evidently, the probability of ignition is not so large for the severed-by-a-nail scenario.

Without an overload condition, solid conductors that are merely nicked or gouged, and not severed, are unlikely to lead to overheating conditions, much less ignition[832,833]; see however the discussion on the 'last-strand' problem for stranded conductors. If a sufficient overload is sustained, however, to cause wiring to melt, melting and arcing are expected to first occur at the reduced-section location.

Stranded conductors—parallel arcing

Nishida[834] found that cotton and paper (but not PVC) can be ignited when a single 0.18 mm strand contacts a strand from the other leg of a cable. In that case, the ignition was found to occur due to the high temperature reached by the strand and not through spark energy. A maximum of 35 J could be delivered through a short circuit of this type, but 0.3 J was found to suffice for the ignition of cotton.

The cutting of an energized electrical cord by an electric saw can result in ignition of nearby combustibles having a low thermal inertia. UL has a 'guillotine' test which simulates a sawing accident[757]. Cheesecloth is placed nearby as the ignition target. (See also: *Short circuits*).

Stranded conductors—series arcing (last strand problem)

Stranded wires used in power supply cords and extension cords are sometimes subject to abuse, leading to breakage and separation of conductor strands. This can occur due to various forms of mechanical damage, one specific case being the connection of wires into a male plug (see above). A stranded cord will overheat if strands are broken due to excessive bending and current is being carried by the last remaining strand. Color Plate 116 illustrates a cord on an electric foot warmer that failed after being used for only a few months.

Mitsuhashi et al.[835] conducted bending experiments where two types of stranded cords were repeatedly bent by 90º while under a tension load. The PVC-insulated cords were of the type SPT-1 and had 30×0.18 mm strands (rated 7 A) and 50×0.18 mm strands (rated 12 A). After the first 10% of strands were broken, the rate of breakage accelerated dramatically. It took about 900 cycles to break all except 1 strand on the 30-strand cord and about 1200 cycles on the 50-strand cord. For a one-remaining-strand condition to be

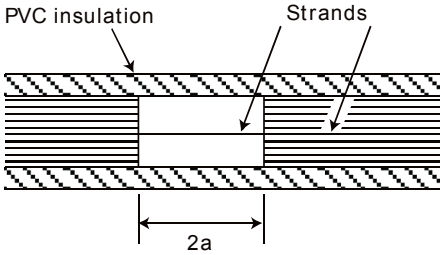


Figure 57 Geometry for last-strand failure

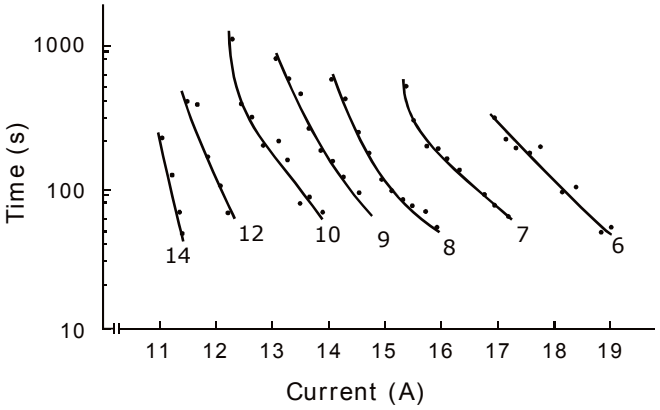


Figure 58 Relation between time and current needed for ignition of PVC to occur; numbers on curves refer to gap spacing (mm)

obtained, it was necessary to limit the tension so that the gap created at the broken strands (Figure 57) was 5 mm or less; otherwise all strands broke, rather than all-but-one. The PVC insulation was not degraded after the breaking was completed, as measured by a 5 kV DC dielectric withstand test. The authors then set up a last-strand-remaining experiment where AC current of 5 to 30 A was passed through the cord. It was found that ignition of the PVC insulation occurred only if the current was between 10 and 20 A. Currents smaller than 10 A equilibrated to steady-state temperatures of 100ºC or less and did not lead to fusing of the strand and ignition of the PVC. Conversely, currents over 20 A caused a rapid fusion of the strand, and consequently did not deliver sufficient energy into the already-broken strands to raise their temperature sufficiently to ignite the PVC.

The regions of ignition and non-ignition are shown in Figure 59. It is found necessary that the bulk copper temperature be raised above 100ºC during the overheating period, and that the last-remaining strand fuse and raise the temperature briefly to over 450ºC. The sequence of events for that strand, of course is: overheating → fusing → arcing → stopping of current flow. The ignition occurs initially at only a tiny spot, but because a certain portion of the cord has been preheated to over 100ºC, rapid flame spread can occur away from the ignition location. Conversely, if the cord has not been preheated to at least 100ºC, then only a tiny localized ignition—but no propagation—is possible. The authors did further heat transfer modeling and concluded that a gap of at least 1 mm is needed for ignition to occur.

Nagata also conducted experiments and theoretical modeling on the last-strand problem[836] (Figure 57). His experiments showed that heating of the PVC insulation proceeds in two steps: (1) gradual heating to about 100ºC due to excess current flowing through the remaining strand; and (2) abrupt heating due to explosion of the strand, with ignition of the PVC occurring at about 550ºC. His experimental results are shown in Figure 58. The least current is required at large gap spacings, since heat losses become smaller. However, as noted above, in their experiments, Mitsuhashi et al. found it impossible to create gap distances greater than 5 mm where one strand still remained. Clearly, they did not explore all mechanical deformation possibilities, so larger gap distances must still be considered as possible, although less probable. For such larger gaps, Nagata's results can offer guidance. In practice, it must not be concluded that ignitions will be limited to the current values reported by Mitsuhashi or Nagata, since other variables may well come into play; for example, in actual fires a portion of the cord is often placed against a surface rather than being suspended in air. Thus, the research results should be viewed only as qualitative guidance.

The UL standard for electric cords, UL 817[748], includes a 'mechanical drop' test which is done for 1300 cycles and an 'abrupt pull' test which is done for 5 cycles. Series-arc ignitions occur in the UL 'rotational flexing' test[757], where a stranded electrical cord is rotated enough times that one of the conductors suffers a break. Cheesecloth is the ignition target in that test.

Excessive pressure and creep of insulation

Plastics which are flexible enough to use as wire insulation show appreciable creep. That is, if a significant load is continuously applied, the plastic will exhibit cold-flow and the loaded section will permanently deform[837]. A cable which is pinched, by whatever means, might deform sufficiently over time that the insulation loses enough thickness so that failure occurs. The pinching can be an overdriven staple, an appliance leg improperly placed on top of a cord, a plastic cable tie excessively tightened around a bundle of wires,

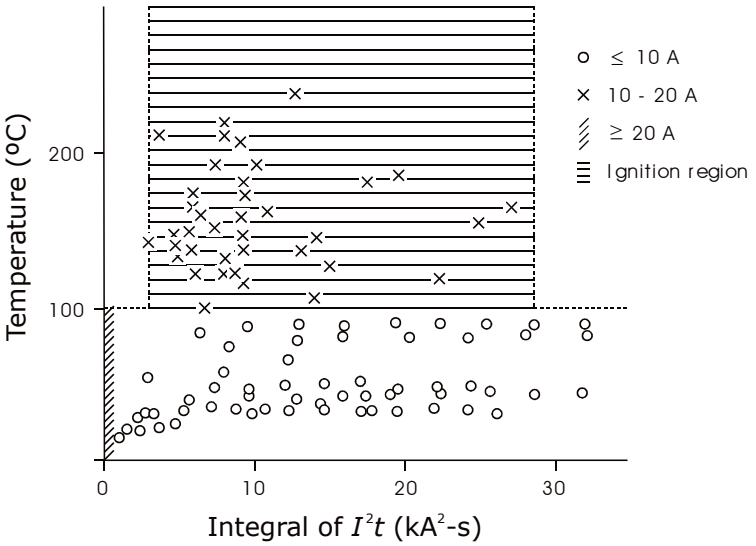


Figure 59 Ignition and non-ignition regions by fusing of the last-remaining strand

etc. CPSC[522] found a number of fires due to extension cords being pinched in doorways and other situations where a continued force was applied to the cord, but details were not documented.

The breakdown voltage of any insulator is dependent on the thickness. If the plastic insulation separating two conductors eventually gets thin enough that the breakdown voltage is lower than the actual voltage of the circuit, an arcing failure can occur. Matters are complicated by the fact that creep itself actually changes the electrical properties of the insulator, apart from the gross change in geometry[838]. Perhaps more likely is that sustained creep would cause a direct contact by a single wire strand with the opposing conductor. Such a fault would quickly be relieved by melting out of the strand but, in the meantime, high temperatures would be presented to the wire insulation. This could cause sufficient carbonizing of the insulation that arc tracking could be initiated. It has also recently been recognized[839] that excessive mechanical stress can lead to 'dielectric treeing' and eventually to gross failure. Unfortunately, as with most studies of the mechanisms of dielectric failure, few results are available below the kilovolt range.

Ignitions, in fact, are not rare when a heavy furniture or appliance item is placed on a power cord or a cord is pinched by a door. In one case known to the author, a fire took place when a heavy wooden cabinet was accidentally placed over a length of an NM-type house-wiring cable which was used instead of a cord to power some appliances. NM cables have solid conductors, so evidently the phenomenon does not intrinsically require stranded conductors. But apart from one unpublished paper[840] where an abortive attempt was made to study creep in PVC cords, laboratory studies do not exist. If the forces are such that a conductor actually breaks, then ignition may be caused largely by arcing. But if the conductors do not separate, then insulation creep is a possible—but unproven—means by which the process leads to these ignitions.

Overdriven staples

The possible ignition modes involved when staples used to secure wiring are 'overdriven' or otherwise improperly installed are not all fully elucidated, but the following mechanisms must be considered:

1. A staple is driven in so one leg contacts the hot conductor and the other the ground. In that case, immediate short-circuiting will become evident the first time that the circuit is turned on.
2. A staple fully severs one conductor, and the staple itself now bridges the two severed ends. The steel-to-copper connection resulting is likely to be a high-resistance joint, and progressive heating can be expected. See *Overheating electrical connections* in Chapter 11.
3. A staple is driven so as to nearly, but not quite, squeeze out the insulation from both conductors. This is an insulation creep situation, and breakdown of insulation can be expected to occur after a prolonged time of cold flow, as discussed above.
4. The staple pierces insulation from both conductors, and one leg of the staple contacts one conductor, while the second leg comes very close to the second conductor. The connection is exposed to an adverse environment and arc tracking eventually occurs.

In addition to the direct mechanisms, there can be at least two environmental effects:

(a) differential settlement of the structure may eventually cause a direct contact to occur where originally a small clearance existed;
(b) thermal cycling of the cable may eventually cause a direct contact to occur where originally a small clearance existed.

Tests have been reported[841] where it was endeavored to prove that a fire cannot start from an overdriven staple. However, Brugger[842] conducted a test where a staple piercing an NM cable eventually led to fire (Color Plate 120). The delayed nature of these failures was clearly identified by CPSC, who documented fires from overdriven staples in field investigations[522]. Dixon discusses a case where it took 15 hours from the turning on of power to the initiation of fire at an overdriven staple[843]. He considers that this was largely accounted for by thermal effects. A case incident of a mobile home fire is illustrated in Color Plate 121.

Perhaps the most specific case history where creep alone was involved comes from Keleher[844]. This electrician reported two different cases of creep failure. His observations are especially valuable since he was also the electrician who originally installed the wiring that failed. In both cases, the cable was 14/3 or 12/3 type NM-B, 600 volt, 90ºC rated, using THHN wire insulation. The installations were unusual, however, in that (a) the circuits were carrying 240, not 120 VAC; and (b) they were protected by 2 A, fast-blow fuses. In the first case, the electrician was called because of a blown fuse. He found failures at 5 different staple locations. In each case, no external charring was found and no mechanical damage was found. But when the cable was slit open, a 50 – 100 mm length of wire insulation was found charred. The second case was similar, except that the fault and the charring were found inside a 1/2" clamp connector (2-screw type). The wire insulation of the black wire was charred and the wire had shorted to the bare ground wire. Inspection revealed that the original installation was properly made. The higher voltage, while well within the rating, makes an insulation failure more probable, while the fast-blow fuses prevented sustained combustion and allowed the evidence to be preserved.

Driving *nails* into electric cables can lead to similar consequences as staples. In some cases, even driving the nail in is not necessary. A fire originated at a power cord that was strung over a nail (Color Plate 117). The cord spanned about 1.5 m unsupported under a desk and had been in place about a year. The investigator concluded that the insu-

lation degraded due to the hanging and vibratory forces. Copper wire melted onto a nail does not necessarily indicate an arcing event, however, as shown in Color Plate 118.

POOR SPLICES OR TERMINATIONS

CPSC found that, in a flagrant violation of both regulations and good sense, a number of fires have been caused by amateurs who made connections to building wires by simply twisting two wires together, and not by soldering or using a twist-on connector[522]. Similarly, individuals sometimes repair electric cords simply by twisting the wires together and insulating them with electrical tape. This leads to a poor connection, and Hijikata and Ogawara[845] measured the characteristics of some splices of this type at currents of 10 – 20 A. They found that the temperature of the splice increased linearly with current, typically being 50 – 95ºC for 10 A, and going up to 130 – 300ºC at 20 A. The cords were made up of 30 strands, each 0.18 mm diameter. The resistance of the splice increased less drastically with current, going from 2 – 8 mΩ at 10 A to 3 – 12 mΩ at 20 A.

On rare occasions, fires have occurred due to inadvertent presence of *process splices* in a power cable. In the manufacturing of cables, it is necessary to join conductors as a spool becomes exhausted. This is done with a splice that is not intended to be current-carrying and will normally be chopped out before packaging into shorter spools of cable for sales. But occasionally a spliced cable gets sold and subsequently is used without proper inspection. The heating process is similar to that discussed above.

DEGRADATION AND AGING OF INSULATION

Wiring is sometimes incorrectly perceived as inert and stationary and, therefore, having an infinite lifetime. If electrical insulators are made from inorganic materials (e.g., ceramic), then their lifetime is essentially infinite, provided that they are not physically damaged and that contaminants are not deposited on their surface. But for low-voltage applications, the most common insulators are polymers, which are organic substances and having a finite lifetime. Apart from mechanical insult, degradation can proceed due to the effect of heat, chemical reaction, or applied electric field. Aging consists of slow, irreversible changes in the properties of a substance. Generally, aging in polymeric materials involves on or more of these chemical mechanisms:

- Oxidation—attack of the substance by oxygen molecules. This often leads to formation of acid groups that increase the conductivity of the material. With some polymers, oxidation also leads to unwanted cross-linking, creating a more brittle material.
- Hydrolysis—interaction of the substance with hydrogen or hydroxyl radicals, with the latter commonly originating from dissociation of water.
- Pyrolysis—degradation due to heat.
- Loss of plasticizer. Many pure polymers, e.g., PVC, are unusable as electrical wire insulation, since they are hard and brittle. Consequently, organic molecules generically known as plasticizers are added which improve the physical properties. With some polymers, during aging, the plasticizer is readily lost. This can then lead to mechanical failure of the insulation due to embrittlement.

The first three of these processes modifies the polymer by breaking bonds in various ways. The consequences can be that small molecules are formed and possibly released as a vapor. The remaining segments will show a poorer performance. The consequences of these chemical changes are typically[846,847]:

(a) increase in the dielectric loss factor;
(b) decrease of dielectric breakdown strength;
(c) decreased resistance to partial discharges associated with the phenomenon of dielectric treeing; and
(d) degradation of mechanical properties.

Polymer degradation due to an applied electric field has mostly been studied theoretically and in connection with high-voltage equipment. The book by Dissado and Fothergill[848] presents the current-day theories, but it presumes a familiarity with advanced chemistry and physics of the solid state and the authors also forthrightly admit that it is difficult to apply most theories towards understanding actual field failures. Leaving aside pure theory, laboratory aging studies on various polymeric insulation materials[848] typically show that if the applied electric field is less than about 1 – 5 MV m^{-1}, then life is 'infinite.' This kind of laboratory conclusion, however, does not help interpret failures or ignitions resulting therefrom.

Natural rubber insulation used in the first half of the 20th century was exceptionally susceptible to aging, and would tend to fail in a catastrophic way—sufficient cracking would develop so that pieces of insulation could fall off an insulated wire[576]. Modern plastic insulation is more resistant to aging and does not fail by falling off in chunks, thus, studying the ways in which it does fail has been more difficult. In an interesting experiment, modern PVC-insulated cables were boiled for 15 minutes, then re-tested for electrical failure under high load, but did not indicate any changes attributable to boiling[849].

In commercial specifications, the aging problem is normally approached rather indirectly. Lifetime is normally not assessed *per se*, but a 'rating' temperature is reported. The latter is determined by a test protocol where some variable, such as ultimate strength or AC breakdown strength is measured as a function of time and 'failure' is declared when the value has dropped below a certain limit. An extrapolation is then made, commonly to 20,000 hours, and the temperature at which the material is deemed to be able to survive for that period is declared to be its rating temperature. Dakin[850] originally showed that most degradation processes can be represented reasonably well by Arrhenius-form kinetics and that, most often, first-order kinetics was realistic. The consequence is that plots of a measurable property (e.g., tensile strength or breakdown strength) can

be made as straight lines—for a specified temperature—if time is plotted on a linear x-axis and the performance measure on a logarithmic y-axis. More commonly, a decrease of the property down to a certain value is arbitrarily defined as end-of-lifetime. In that case, if $1/T$ is plotted on a linear x-axis, where T = absolute temperature (K) and lifetime is plotted on a logarithmic y-axis, again straight-line plots can be made. Bruning and Campbell[851] provide a good summary of some of the theoretical concepts used in laboratory studies of insulation aging. Mathes[852] has described the history of industrial standards (e.g., IEC 60085[853], IEEE Std-1[854]) by which temperature classes are established for electrical insulation material.

From the point of view of understanding electrical failures, this process is unsatisfactory, since no failure is actually ever evaluated. In an end-use article made from this material, mechanical strength is rarely challenged, while insulation thickness is commonly vastly greater than the minimum that would be needed if it were sized according to the limiting-value breakdown strength. This is because other factors generally govern, for example, wire insulation thickness must be sufficient so that moderate mechanical abrasion does not cause short circuits. Bajpai and Marlin[855] surveyed existing methods used to analyze aging effects in electric wiring and components and found a plethora of theories but essentially no validated studies, where actual failures under operating conditions (as opposed to extreme test conditions) would have been observed. UL has a procedure of long-standing, UL 746B[856], for the evaluating thermal aspects of aging of polymeric materials; this involves medium-term testing, along with extrapolations. But there is no known study which relates performance measures used in that standard to electric failures that result in ignitions. UL themselves have pointed out that since laboratory aging tests often involve subjecting a polymer to temperatures above its glass transition temperature, while the in-use conditions would involve temperatures below this value, the degradation chemistry deduced from accelerated aging tests may be inapplicable[857]. On the other hand, many polymers have a glass transition temperature below room temperature, so this limitation would not apply. IEC has a multipart series of standards—IEC 60216—which is similar to UL 746B; it is understood that eventually the two organizations may harmonize these standards.

There is no modern study which actually examines aging effects in connection with fire incidents. A British study[858] found that in the pre-World-War-II era there was a statistical correlation between incidence of electrical fires and age of installation. However, wires of that era were insulated with materials quite different from those in use today, thus failure modes would hardly be comparable. A recent survey of aircraft wiring does at least help to illustrate the problem, see *Electrical wiring in aircraft*. The combustion products of a fire, especially HCl released from burning PVC, can attack electrical insulation chemically and prematurely shorten its lifetime. Dervos and Vassiliou[859] found that in some circumstance even comprehensive cleaning of surfaces exposed to fire smoke failed to restore electrical resistivity to acceptable values (while creating a visually 'clean' appearance).

As shown in Table 43, deterioration due to aging accounts for about 14% of US fires originating in the electrical distribution systems of residences. The majority of the deterioration involves thermal insulation of wires and cables, with age, heating (including sunlight), moisture, and mechanical wear being the dominant deterioration mechanisms. CPSC specifically identifies moisture as being a problem in service entrance cables. When a fault occurs allowing rain to enter into the service entrance cable or conduit, resulting degradation has been found to be the cause of some fires. Voltage spikes have been proposed as another means of degradation[860]. Apart from several studies where insulation was degraded at very high temperatures (discussed below), there has been no laboratory research on other degradation factors in the context of building wires. Much military and industrial test data exists on laboratory degradation of wires, but neither the wire types, nor the test protocols there are applicable to building wiring.

Stricker[861] noted that "although cable life has not been defined, a life expectancy of 20 to 50 years is reasonable." In a short-term aging program, he then examined 90ºC and 105ºC rated PVC-insulated cables. The specimens were all heating cables, thus, sufficient lifetime under elevated temperature conditions was presumably a design objective. Eight different types were tested, some without jacket, others with PVC or nylon jackets. Significant plasticizer loss occurred for all types when conditioned at 71 – 77ºC for approximately 1 month. Stricker interpreted the plasticizer loss as the end of useful life for the cables, although further electrical or thermal testing was not done. He concluded that none of the specimens should be operated at over 71ºC; this was in sharp contrast to the 90 – 105ºC temperatures for which the cables were rated.

Sandia National Laboratories conducted several studies on the thermal degradation of insulation. Chavez[862] examined the electrical failure of two cables as a function of oven heating. Electrical failure was considered to be a short circuit or a low-resistance condition developed across the line; experiments were not conducted to actually elicit ignitions. The two cables were a 12/3 cable with cross-linked polyethylene insulation and a 12/3 cable with polyethylene/PVC wire insulation and PVC jacket. His results are given in Table 78.

Lukens[863] conducted limited testing on a 3-conductor, 12 AWG cable using polyethylene/PVC wire insulation and a PVC jacket. In short-term oven testing, no short circuits occurred in a 60 min test at 130ºC; 10% of specimens short-circuited when exposed to 150ºC for 60 min; 25% exposed to 170ºC for 30 min; and 33% exposed to 170ºC for 60 min. The test arrangement was not designed to elicit overt ignitions, since negligible current was passed through the conductors. In another Sandia study[864], the combined effects of thermal and nuclear radiation aging was examined on a series of electric cables. In complementary testing, the effect of submersion in an alkaline water solution was also explored. Neither electric failures nor overt ignitions were studied, with the only variables examined being the resistance and dielectric strength of the insulation. In yet another Sandia study[865], cables were subjected to accelerated aging at 125 – 150ºC, followed by high-temperature testing. In the high-temperature testing portion, cables were energized and failed electrically, leading to ignition of the insulating materials. The results indicated that the effect of the lower-temperature aging was small-to-insignificant. In the high-temperature tests, failure occurred at about 425ºC for a 10 min exposure, dropping to 330 – 365ºC for a 75 min exposure.

When recessed ceiling lighting fixtures are used that are intended to be buried in thermal insulation, some exceptionally high temperatures can be reached. Using a fixture carrying the IC (insulated ceiling) rating and specified for a 75 W lamp, Yarbrough and Toor[866] measured a maximum temperature of 123ºC on the building wiring connecting to the fixture. The installation, including lamp size, were in accordance with how the product was listed by the testing laboratory. Since building wiring may have a rated temperature as low as 60ºC temperature, they concluded that greatly shortened lifetimes must be anticipated in applications of this kind. A NIST study on lighting fixtures also examined the effect of over-temperatures on 60ºC-rated normal building wiring[619]. When overlamping of a fixture created 202 – 205ºC temperatures in the electrical junction box, failure occurred in less than 65 h. The wire insulation became brittle, cracked, fell away from the conductors, and this led to a short circuit.

See also: *Arc tracking* in Chapter 7; *Electrical wiring in airplanes* in this Chapter.

Table 78 The results of Chavez on time to electrical failure (min) at various temperatures

Temperature (ºC)	XLPE	PE/PVC
250		8.7
270	47	
350	13.2	4.2
450	4.0	2.0
500	3.3	

PARTIAL DISCHARGES

Partial discharges are partial breakdowns of an electrical insulation that occur when the electric field locally exceeds the breakdown field strength, but a full breakdown from electrode to electrode does not occur[867]. These discharges convert capacitively-stored energy into a heat, mechanical, or chemical form of energy which, in turn, acts to further degrade the insulation. If the process is sustained, it may eventually culminate in a gross breakdown of the insulation. Partial discharge is generally initiated by a transient overvoltage. The problem is especially acute in circuits, such as electronic variable-speed drives for motors, that create pulse-type voltages significantly greater than the nominal sinusoidal circuit voltage.

CHEMICAL DAMAGE

Oil or other chemicals can cause damage to wire insulation, leading to failure and possibly fire.

ALLOYING DURING MELTING

Damage due to alloying due to melting can be confused with damage due to arcing, so the process of alloying must be understood. Even though copper has a melting point of 1085ºC, pouring molten aluminum (T_{mp} 660ºC) on it will lead to melting of the copper and the formation of a copper/aluminum alloy[868]. This can take place because, under optimum conditions, copper and aluminum can form an alloy (33% copper, 67% aluminum) which has a melting point of only 548ºC. Color Plate 119 shows an example of typical damage to a copper conductor from alloying.

APPLIANCE CORDS AND EXTENSION CORDS

CPSC estimates[869] that there are about 7100 fires a year in US residences originating from electrical cords and plugs, along with 120 deaths. Of these, extension cords account for 3300 fires, along with 50 fatalities and 270 injuries[870]. A CPSC field study[871] on fires originating from appliance cords led to the statistics shown in Table 79 through Table 81. In the case of appliances rated at 1500 W or more, 74% of the fires involved failures of various kinds at the male plug end; failures along the cord were only 6.5%.

A parallel CPSC laboratory study[872] identified the most common failure modes as:

- Bad crimp within molded male plug or female cord connector. This is a manufacturing defect.
- Bad mating contact with wall outlet, extension cord, or male contacts of appliance. Usually a progressive failure due to wear.
- Flexure failure of cord, commonly at entry to plug or to appliance. Normally due to heavy use. Was a more serious problem before introduction of bend-relief reinforcements.
- Tension failure at plug; cord insulation separated from molded plug. Can sometimes be due to inadequate bonding of plug to cord insulation.

Table 79 Breakdown of appliance cord accidents according to accident type

Accident type	Percent
flaming fires	34
overheating: smoke, deformation	31
arcing	29
electric shock	3.6
mechanical damage of cord, without fire or electrical failure	3.2

Table 80 Breakdown of flaming fires caused by appliance cords according to appliance type

Appliance type	Percent
clothes irons	18
lamps & lighting fixtures, not hard-wired	15
fans	15
televisions and audio equipment	10
coffeemakers	9
electric heaters	8
hair dryers	6
air conditioners	6
curling irons	5
toasters	4
vacuum cleaners	3

Table 81 Location of failure point for fires originating from appliance cords

Failure point	Percent
along cord conductors	46
at connection to appliance	32
at connection between cord and male plug	10
male plug	5
at connection between male plug and extension cord	3.7
at connection between male plug and wall outlet	2.5
at male/female joint built into cord itself	1.2

- Plug blades pitted or arced, possibly due to withdrawal of plug under load. Was seen to be especially problematic with air conditioners.
- Flexure or abrasion failure of cord insulation, leading to arcing between conductors or to grounded objects.

The CPSC study focused on design and manufacturing issues, but clearly several of the failure types are likely to be caused by negligent or abusive usage. In some European countries, recessed wall outlets are used, where the male plug, when inserted, is flush with the surface, rather than protuberant. There are presumably fewer fires that result in those cases from furniture being shoved against plugs.

In a 1981 study on extension cords[873], CPSC determined that about 90% of extension cords on the US marketplace conform to UL 817[874]. But a 1999 study[869] concluded that only 28% met 'current safety standards.' This shift parallels the dominant role that imported articles (mostly Chinese) assumed during the same time period. Based on a number of fires examined in depth in the 1981 study, CPSC identified three main causes of fires from extension cords (Table 82). Improper alterations usually involved splicing of the cord. Age of extension cord was not necessarily correlated to failure, since some 35% of the incidents involved cords one year old or less.

Table 82 Factors leading to fires from extension cords

Factor leading to fire	Percent
overloading	48
physical damage or misuse	46
improper alterations	6

There has been a large number of product recalls by CPSC of improperly manufactured extension cords. By far the largest number has been due to undersized conductors. Other factors have been improperly polarized plugs, inadequate strain relief, or—in one case—use of a plastic that "once ignited, continues to burn and spread flames."

IMPAIRED COOLING

As discussed under *Excessive thermal insulation*, above, published current-carrying ratings ('ampacity' values) are based on certain assumptions of convective cooling. When the actual situation involves much poorer cooling, electric failures and possibly ignition can be anticipated. As an example, a case history[875] has been reported where a fire originated at an extension cord which was coiled upon itself and stuffed into a baseboard hot-water radiator. CPSC has explicitly warned[870] consumers not to place extension cords under rugs, since the reduced heat dissipation may cause ignition even if the cord is within its normal current rating.

Cord reels are a consumer item where an extension cord incorporates a permanently attached reel intended for storing the cord. As considered above, under normal circumstances, an overload must be exceedingly large before a cable will ignite. A fire and its subsequent investigation, however, revealed that cord reels do not comprise 'normal' circumstances. In the absence of adequate warnings, it is natural to use a cord reel by only unreeling a needed amount of cord and not the whole length. The cooling for the tightly-wound portion then becomes minimal. Tests[876] have been done on a 16 AWG cord reel, rated for 10 A. In ambient air, passing 9.5 A through the cord caused about 1ºC of temperature rise. But by passing 9.5 A through it for about 1.5 h, a fire resulted when the wire remained wound on the reel.

WIRES IN STEEL CONDUITS

Electrical branch-circuit conduits are sometimes found after fires to contain arc-fault damage. The cause of the fire might then be attributed to a wiring fault. This reasoning is rarely likely to be correct. Instead, the most common reason for arcing damage found on conduits is external heating of the conduit during fire[877]. Without providing external heat-

ing to a conduit, it is very hard to create a fault within it. Splices inside conduits are prohibited, so the only internal causes are limited to gross overloads or defective wire insulation (due to manufacture, installation, mechanical abuse, vibration, etc.). In either case, a short from a conductor to the conduit would lead to a high-current parallel arc and would likely cause quick tripping of the circuit breaker. For serious damage to occur*, it is necessary that either (1) the arcing be current-limited, or (2) an unsuitably high-rating circuit breaker be used. If an inappropriate circuit breaker was installed or some defect existed making the short-circuit current unreasonably small for the circuit, these factors would be expected to be found in the investigation after the fire. (Service entrance conduits, which effectively lack protection, are discussed in a separate section: *Service drops and high current capacity conduits*.)

If an external fire impinges on the conduit, however, the heat of the fire can char the wire insulation inside the conduit, creating a semi-conductive char through which arcing can occur locally. The resistance created is likely to be high enough that the circuit breaker will not be tripped (Figure 60)[878,879]. Color Plate 122 shows the consequence of an experiment where a propane burner was used to heat a steel conduit until the wiring inside it failed and arcing occurred.

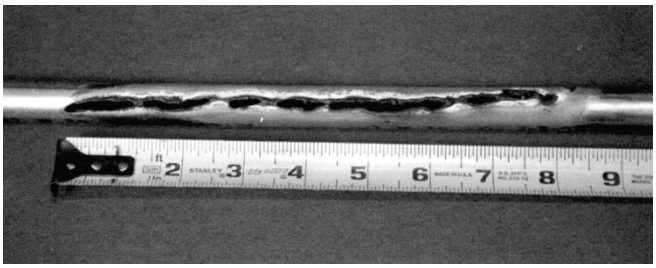


Figure 60 Damaged conduit due to arcing inside caused by external fire
(Copyright Fire Findings, LLC, reprinted by permission)

Fuller et al.[880] conducted experiments where a bare spot was created on a THHN 4 AWG copper wire which was run through a 32 mm (1-¼") EMT conduit. A 120 VAC supply was used, but current was deliberately limited to 20 – 80 A by a resistance inserted into the circuit. The authors found that three different results could be obtained:

(1) the wire would get spot welded to the conduit;
(2) a glow discharge would develop which could last indefinitely and would consume about 100 W, with a voltage drop of 0.14 to 1.4 V rms. This glow produced little heating outside the conduit and would not be an ignition source.
(3) an arc would be created. The arcs typically dissipated 1000 W, showed a voltage drop of 8 – 15 V rms, and drew 70 – 80 A. The arcs lasted less than 1 s, but they melted the zinc from the outside of the conduit. Ignition was achieved when cotton or paper was placed on the outside of the conduit at the place of the arcing.

Fuller's study involved essentially a series arc, since enough resistance was inserted into the circuit to avoid circuit breaker tripping. Under those conditions, they proved that arcs could cause lightweight kindling to be ignited. A parallel arc, by contrast, will normally present a great enough load to trip circuit breakers of 30 A or less before any significant damage is done[881]. The question then arises whether a 'poor contact' somewhere in the circuit can provide sufficient resistance for the arc to constitute a series arc. Ettling measured various poor (i.e., barely touching) contacts and found that they provided either low resistance (a voltage drop of only 1 – 5 V in a 120 VAC circuit), or else were fully open[800]. His study, then, suggests that poor contacts are unlikely to prevent a circuit breaker from functioning sufficiently quickly, but the study was not exhaustive.

ELECTRIC WIRING: CAUSE OR VICTIM?

ARC BEADS AND FIRE-MELTED WIRES

When an arc occurs in electrical wiring, portions of the conductors may melt since the temperature of an electric arc is over 6000 K (see Chapter 11), which is greatly in excess of the melting temperature of copper (1085ºC) or aluminum (660ºC). Upon cooling, the molten material often assumes a roughly-spherical shape (Color Plate 123, Color Plate 124) and consequently this re-solidified zone is termed an 'arc bead.' By contrast, the shape of the end of a copper wire that simply melted is likely to have a droopy look (Figure 61). Fire-melted artifacts are sometimes called 'globules,' as distinguished from 'beads.' An arc bead, however, does not necessarily have to be spherical (Color Plate 104). In the investigation of fires, arc beads are frequently encountered because electricity is available in most buildings undergoing a fire and if a fire is sizable, it is likely to burn wiring to the extent that short circuits occur. A single fire may generate a large number of arc beads in this manner, and such beads can be called 'victim' beads. Conversely, if a fire originated because an electric fault produced arcing, the beads from such an event can be called 'cause' beads because they actually correspond to the cause of the fire.

Visually, arc beads can often be distinguished from melt globules since they possess a sharp demarcation between a roughly-spherical bead and the cylindrical portion of the wire, while fire-melted wires do not show a sharp transition between molten/re-solidified and virgin material[756]. This criterion may not suffice for unequivocal determination and, in that case, microscopic examination is needed.

The crystal structure of copper changes with heating. Color Plate 126 shows examples of virgin and fire-exposed grain structure. Cracking often occurs along grain boundaries after a fire exposure (Figure 62). Unless heated to beyond about 300ºC, copper wire shows fine longitudinal striations

* Different considerations apply for conduits carrying large-diameter wires. In those cases, sufficient current may be available to cause serious damage before tripping of the circuit breaker.



Figure 61 Examples of melted copper wire beads caused by exposure to fire without arcing
(Courtesy Yasuaki Hagimoto)

caused by the wire-drawing process[882]. When heated to higher temperatures, fine-grain recrystallization appears, followed by the formation of some large-grain structures as temperatures over about 800ºC are attained. Shaw[883] proposed that, when examined under a microscope, arc beads exhibit a much finer, smoother grain structure than do the wires melting due to heating from fire alone. But he was rebutted by Levinson[884], who pointed out that copper melted in the presence of oxygen shows a pattern of pure copper grains interspersed with oxygen-containing material, irrespective of what was the cause of the melting. Singh[885] proposed that, if arcing was involved, there will be a pronounced CuO or Cu_2O grain structure near the end, progressively diminishing away from the end. On the other hand, if the wire was simply fire-exposed without arcing, there will be diverse grain patterns along the length, without a systematic gradient. Takaki[882] conducted more detailed experiments and concluded that arc beads commonly show three regions: (1) a surface layer containing numerous voids, (2) an intermediate layer that did not melt, but did recrystallize, and (3) a deep layer where the material neither melted nor recrystallized (Figure 63). By contrast, fire-melted beads tend to be uniformly recrystallized. Ettling[886] cautioned that no simple rule is likely to cover all cases, but also described a number of other qualitative differences that can help distinguish arcing from simple melting.

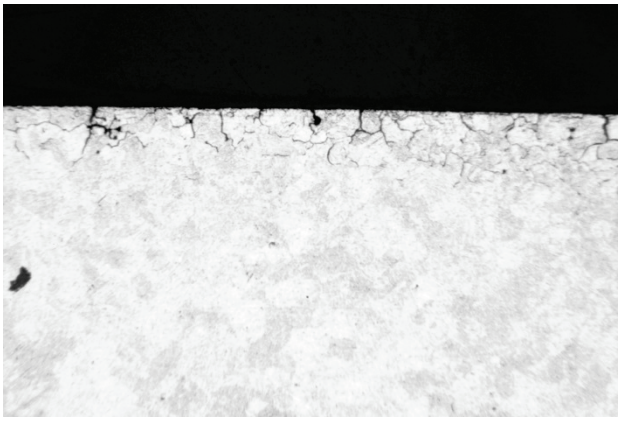


Figure 62 Grain structure of a copper wire after a fire. Note cracking at the grain boundaries.
(Courtesy Kevin Lewis, Schaefer Engineering Corp.)

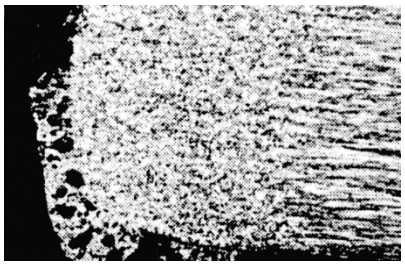


Figure 63 Arc bead showing the three metallographic zones (surface, intermediate, deep layers)
(Courtesy Akira Takaki)

The above discussion was limited solely to arc beads in copper conductors used in branch-circuit wiring. Arc beads in aluminum wiring commonly do not survive the temperatures of a room fire, while there has been no significant research on arc beads in large-diameter wires, such as used in the building service entrance. Wires that are tinned or solder-coated[884] behave differently from solid-copper wires and will also not be considered.

PROPOSED METHODS OF DISTINGUISHING 'CAUSE' FROM 'VICTIM' BEADS

If the melt feature on a conductor is due to arcing and not simply due to melting in a fire, investigators and forensic scientists have explored the notion that the two types of arc beads—'cause' and 'victim' beads—might be distinguished after the fire by some means of physical or chemical testing. If a particular bead could be demonstrated to have been the residue of an arc that caused the fire, this might enable the cause of a fire to be pinpointed which would otherwise be undetermined. Simple visual observation is not sufficient for this purpose, since two Japanese studies[887,888] showed that the following features do not discriminate between 'cause' and 'victim' beads, even when the former were not subjected to the ensuing fire:

- glossiness of the bead
- color of the bead
- shape of the bead
- surface smoothness or roughness
- size of the bead (although the very smallest beads of less than 1 mm tended to be 'cause' beads,

while the largest ones of over 3 mm tended to be 'victim' beads).

Consequently, a number of instrumental analysis techniques have been proposed, and these fall into three categories:

(i) microscopy
(ii) Raman spectroscopy and X-ray microanalysis
(iii) Auger electron spectroscopy (AES) and secondary ion mass spectrometry (SIMS).

In addition, testing for metal hardness was explored by Takaki[882], but he definitively demonstrated that all copper wires exposed to temperatures over about 250ºC showed greatly reduced hardness and this was independent of any details of arcing.

Microscopy methods

The simplest proposed methods claim that examination of a bead under a microscope (after preliminary preparation which may include cleaning or etching surfaces, and other techniques for preparing cross-sections) will suffice to make the distinction. The methods that have been suggested for differentiation are:

(1) 'cause' beads have square or rectangular pock marks, while 'victim' beads lack these structures;
(2) 'victim' beads show small surface-deposited particles, while 'cause' beads do not have these;
(3) 'cause' beads have small voids, while 'victim' beads have large ones;
(4) the number of voids or their total cross-sectional area is different in 'cause' beads than in 'victim' beads;
(5) 'cause' beads have a small dendrite-arm spacing, while 'victim' beads have a large spacing;
(6) based on examining long segments of wire and not just beads, if long segments are uniformly recrystallized, the wire suffered gross electrical overheating; this does not directly establish cause/victim status, but may be of help in assessing the sequence of events that transpired.

Method #1 was proposed by Gray et al.[789] in 1983. They presented results from one accidental fire and conducted a few experiments in the laboratory on flexible, PVC-insulated cords by passing excessive current through the cord until it shorted out and ignited (producing 'cause' beads) and by heating a cord carrying normal current in a fire until ignition (producing 'victim' beads). They then examined slices cut through the beads under a scanning electron microscope (SEM) and, on the basis of observed features, proposed that 'cause' beads show numerous square or rectangular pock marks, while 'victim' beads show few or none. It was not clear whether the pock marks observed represented impurity inclusions or merely regions of crystallization. No other investigators have reported finding these features, so presumably they were due to some rare combination of circumstances, rather than being a normal characteristic of 'cause' beads.

Method #2 was explored by Erlandsson and Strand[889]. In one set of experiments, they created shorts between copper conductors, then exposed the wires to a fire fueled by wood and PVC, the latter intended to simulate burning wire insulation. In another set of experiments, they created the short circuit within the fire environment. The 'victim' beads, when examined with SEM, showed a nearly uniform dispersion of small particles of about 2 μm size on the surface of the beads. Supplementary studies showed that particles of this type could also be created when arcing took place in an atmosphere containing pure HCl vapors, generated by evaporating liquid HCl and not by burning PVC. Small surface particles, by contrast, were absent in beads created by arcing of *bare* conductors prior to exposure to a wood/PVC fueled fire. Unfortunately, the latter test condition does not correspond to the normal creation of 'cause' beads. When the authors created 'cause' beads by shorting together *insulated* wires (by scraping away only small bits of insulation), they found that the bead surfaces contained small particles indistinguishable from those on the 'victim' beads.

A number of investigators explored voids in the bead as an indicator. Erlandsson and Strand[889] studied the cross-sections of beads created in several different ways. They found that in an air atmosphere, arc beads showed copious voids but beads formed by melting the copper by an overcurrent were without voids. In a reducing atmosphere (a gas flame), they found that a smaller number, but larger, voids were present, irrespective of whether the bead was created by arcing or simple melting. They also noted that an 'oxide wedge' could be found between the melted and the unmelted material when tests were run in air, but not in a reducing atmosphere. Tokyo Fire Department[890] conducted experiments which showed that, contrary to the findings of Erlandsson and Strand, voids can be created when copper beads are formed in an air atmosphere by an overcurrent melting process. They made beads by fusing wires with overcurrent in air and in atmospheres of N_2 and CO_2. The experiments were conducted in a tube furnace and the ambient temperature was also controlled. Voids were almost always present when beads were formed in air at 1000ºC, but almost never when in N_2 or CO_2 at the same temperature.

Method #3 was briefly explored by the Tokyo Fire Department[890]. On the basis of limited testing, they noted that voids in 'cause' beads are smaller than in 'victim' beads. They concluded that the voids in 'cause' beads are also more likely to be near the surface, while those in 'victim' beads deeper inside. They consider that the reason is because 'cause' beads tend to solidify more rapidly and oxygen has a lesser possibility of diffusing further inside, whereas 'victim' beads solidify more slowly and voids near the surface tend to migrate inwards and aggregate into larger voids inside, where the temperature is still high. Their testing was not extensive enough to draw statistical conclusions.

Method #4 was investigated by Ishibashi and Kishida[888] who examined 15 beads from fires where it was known whether the bead was the cause or the victim. They concluded that presence of voids is generally more plentiful in 'cause' beads than in 'victim' beads. Presumably this is because 'cause' beads are more likely to be formed in an oxidizing atmosphere and 'victim' beads in a reducing atmosphere, but differences did not support a firm distinction between the two types of beads. Mitsuhashi[891] created 'cause' beads by making current-limited shorts with a stranded-conductor cord and then placing the beads obtained in an oven heated to 400 – 1000ºC. The 'victim' beads were created by first exposing bare conductors to the oven-heating treatment, then covering them with PVC insulation and producing a current-limited short. Mitsuhashi counted micro-voids (0.5 to 1.0 μm) for each bead in three small areas near the center and found about double the number of voids in 'victim' beads than in 'cause' beads. But he also counted voids in 'cause' beads that were not exposed to any further heating after creation of the bead. In that case, the number of voids was roughly similar to the 'victim' beads. For forensic purposes, the method did not seem promising since, while the average number of voids was different for 'cause' versus 'victim' beads, the distributions were overlapping and a particular concentration of voids could be encountered for either case. Method #4 was also explored by Oba[892] who created 'cause' and 'victim' beads in the laboratory and, in each case, subjected them to various oven-heating regimes afterwards. Typically, 30 – 45% of the cross-section area comprised voids and this depended on the temperature of heating that was used after formation of the arc bead, but the distributions overlapped greatly and he concluded that void-area percent cannot be used as a tool for discrimination.

Both method #3 and #4 were studied by Miyoshi[893,894], who counted large voids and found that they were much more plentiful in 'victim' beads than in 'cause' beads. In his study, the 'victim' beads were created by burning a power cord in a burner flame until shorting occurred. But the 'cause' beads were created by shorting a wire together which was not subsequently placed in a fire; thus, his protocol did not attempt to simulate room-fire effects. Under these conditions, the maximum diameter of the voids in the 'victim' beads was typically 2 – 3 times larger than in the 'cause' beads. Similarly, the fraction of the total void area occupied by voids of 132 μm or larger diameter was 14% in the 'cause' beads and 72% in the 'victim' beads. Again, however, the actual distributions showed overlap and a particular void distribution could show up in either a 'cause' or a 'victim' bead, albeit with a higher probability in the one than in the other.

Seki et al.[887] focused on the presence of a dendritic crystal structure (Figure 64) in arc beads. They showed that the general presence or absence of dendrites in an arc bead cannot be used as a means of identification (Table 83),

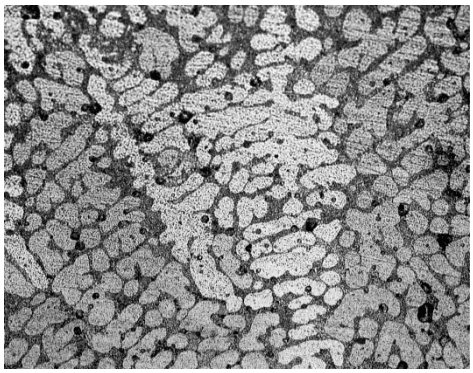


Figure 64 A copper wire bead showing a dendritic crystal structure
(Courtesy Yasuaki Hagimoto)

since it simply reflects the oxygen concentration in the bead. Near-zero O_2 concentration leads to no crystals, as does the eutectic concentration of 0.39 mass%. O_2 concentrations smaller than this produce primary crystals of Cu, while larger concentrations produce primary crystals of Cu_2O. But Seki et al., together with Lee et al.[895], proposed method #5, observing that, if a dendritic crystal structure is created, the spacing between the dendrite arms reflects the ambient temperature at which the bead solidified. In their view, a 'cause' bead will solidify at a near-ambient temperature (< 400ºC) and therefore have a small dendrite-arm spacing while a 'victim' bead will solidify at a fire-gas temperature (> 400ºC) and show a large spacing (unless it re-melts in the fire). On the other hand, the rate of cooling and the temperature of the environment prior to the formation of the bead were found not to affect the spacing. In support of their thesis, the authors produced experimental curves showing the spacing as a function of ambient temperature at solidification and of oxygen concentration, separately for Cu and Cu_2O dendrites. Based on their photographs, however, assigning a characteristic dendrite arm spacing to a particular bead appears to be a highly subjective determination. The authors performed extensive testing, but the description of their results does not make it clear if categorical classification of results as 'cause' or 'victim' was successful. In any case, the tests were primarily exposures in a small electric furnace and creating 'cause' beads which would then be subjected to a room fire was not undertaken. The method cannot be applied at all if the bead does not exhibit dendritic crystal structures and, as shown in Table 83, most beads do not.

Table 83 Dendritic crystal structure observed by Seki et al. in test arc beads

Bead	No dendritic crystals	Dendritic Cu crystals	Dendritic Cu_2O crystals
Cause	57%	38%	5%
Victim	92%	8%	0%

Method #6 was proposed by Levinson[884], who noted that if a substantial length of wire exhibits uniform recrystallization, this is most likely due to electrical overcurrent, rather than thermal heating from a fire, since the latter would be unlikely to heat a wire uniformly. Levinson carefully avoided claiming this distinction can be used as a proof of the origin of a fire, however, since the fire itself may have created conditions leading to an overcurrent.

Raman spectroscopy and X-ray microanalysis methods

On the basis of a very small number of tests, Tokyo Fire Department[890] noted that carbonaceous material is likely to be found inside 'victim' beads, but not inside 'cause' beads. Masui[896] used X-ray microanalysis to examine for the presence of carbon in arc beads that he created by (a) causing a series-arc failure in a cord; or (b) by first charring the wire insulation with a burner flame, then causing a series-arc. His results were only exploratory, but they did show a negligible amount of carbon in the first type of bead, which would correspond to a 'cause' bead. The analysis showed the second bead type to have nearly as high a local concentration of carbon as a pure carbon control sample. The second bead type, however, only partially represents a 'victim' bead in that insulation was charred prior to arcing, but the bead was not subsequently exposed to a fire.

Lee et al.[897,898] carried this idea further by examining the constitution of carbonaceous inclusions. They did not collect any data on what fraction of beads contains carbonaceous inclusions, but rather studied beads that did have these inclusions with Raman spectroscopy to distinguish between amorphous and graphitic carbon. This can be done on the basis of Raman spectra since amorphous carbon shows a broad peak at 1350 – 1360 cm^{-1}, while graphitic carbon has a sharp peak at 1580 cm^{-1}. The authors created 'cause' and 'victim' beads in the laboratory and found that 100% of the 'cause' beads always contained amorphous carbon but 27% of 60 samples also contained graphitic carbon. In all of 20 'victim' beads tested, amorphous carbon was detected; in none of them was graphitic carbon detected. The authors then examined 8 beads from actual fires where the status of the bead was established by other means. They were able to find graphitic carbon in 3 of the 5 'cause' beads. The authors hypothesized that the effect occurs because PVC is bodily conveyed into the interior of an arc bead. In their view, graphitic carbon is created inside the bead only if the sequence of creating the 'cause' bead is such that PVC insulation is slowly charred due to an electrical fault before final failure leading to arcing occurs. In a 'victim' bead or in a 'cause' bead where the fault rapidly leads to ignition, time required to form graphitic carbon is not available. 'Cause' beads of the latter type will occur when a large, rapid overcurrent melts the insulation and quickly creates a short circuit. It is not clear how the authors envision that carbon migrates into the copper, since they state that temperatures are only 110 – 250ºC when PVC is being charred. In any case, the method has a rather low probability of identifying a 'cause' bead of only 27 – 60%.

AES, SIMS, and ESCA methods

A number of techniques exist that allow the concentrations of certain elements in a metallic sample to be determined. These include Auger electron spectroscopy (AES), electron spectroscopy for chemical analysis (ESCA), and secondary ion mass spectrometry (SIMS). With any of these, a depth vs. concentration profile can be made by progressively etching away portions of the surface and examining a lower layer. Erlandsson and Strand used AES in connection with their experiments discussed above to quantify the chlorine present in the surface particles attached to the bead, but, as mentioned above, the presence of chlorine was found not to be uniquely associated with 'victim' beads and was equally-well found in 'cause' beads, if the 'cause' arcs were created by shorting together insulated, rather than bare, wires.

In 1980, MacCleary and Thaman postulated[899,900] that an arc bead formed without a pre-existing fire ('cause' bead) would be formed in an oxidizing atmosphere, while one that occurred after a fire was already ongoing ('victim' bead) would be formed in a reducing atmosphere. Consequently, they believed that profiles of the oxygen concentration, as a function of depth below the surface of the bead, would enable identification to be made. Their patent[900] envisions that AES, ESCA, or SIMS can be used for this purpose, but their own work they used only AES. Because of the limited sensitivity of their technique, they took the derivative of the signal data as the analysis variable and only sought relative magnitudes, not an absolute calibration of oxygen concentration. Figure 65 shows three samples they analyzed. The 'cause' bead was created by short-circuiting two conductors after preheating them for 15 s. The 'victim' bead was created by a small fire which short-circuited an NM cable. The 'overload' bead was created by producing a current-limited overload which heated the cable for some time (unspecified) before the conductor fused and arced. The authors also showed results from four beads taken from real fires where the fire cause was known. Their proposed scheme for identifying beads was to discard the first 5 nm of the surface (since it would likely reflect ambient oxidation of the copper) and to evaluate the remaining portion:

- if the concentration is generally low, the peak is found at 20 nm or less inside the surface, and concentrations beyond the peak become quite small, then this is a 'victim' bead;
- if the concentration is generally high, the peak is found at a depth of 20 – 200 nm, and the concentration decays slowly at greater depths, then this is a 'cause' bead;
- if the concentration is very high, and oxygen is detected to 2000 – 4000 nm, then this is a 'cause' bead where arcing was preceded by prolonged overheating.

The authors also pointed out that the method cannot be used if a re-melt occurred. To detect the latter, they proposed that a bead be cut in half and an AES scan be made across the diameter. If four, rather than two, peaks are found across the diameter, then a re-melt is indicated. Robertsson et al.[901] attempted to validate the MacCleary/Thaman method, but found that the oxygen profiles could not reliably distinguish 'cause' from 'victim' beads.

Satoh et al.[902] used AES and SIMS to obtain O, C, and Cl profiles on four specimens: a 'cause' and a 'victim' bead from actual fires and a 'cause' and a 'victim' bead produced in the laboratory. The 'cause' bead was created by short-circuiting a stranded-conductor cord, then exposing it in a burner flame, while the 'victim' bead was produced by placing the cord into a burner flame until it shorted. Depth profiles were obtained by etching the surface down with a cesium ion beam (for the SIMS) or an argon ion beam (for the AES). They plotted both the AES and the SIMS data in a way as to normalize the remaining elements to Cu, which was taken to have a constant depth profile. From these preliminary plots, they concluded that the primary feature of a 'cause' bead is an oxygen profile that rises to a peak at about 1000 nm beneath the surface, and only then proceeds to fall. By contrast, 'victim' beads showed O, C, and Cl concentrations that were all similarly-shaped decay curves, without any appreciable rising portion. By comparing AES and SIMS results, they concluded that AES is much less sensitive and incapable of good resolution deeper than about 1000 nm; thus they concluded that SIMS is the preferred technique. In a later study[903], they used only SIMS to examine 10 beads recovered from fires where the cause/victim identity of the beads was known (Figure 66). The fires however were all small and none had reached the fully-involved room stage. One of the beads was so heavily surface-damaged that it was considered not appropriate for analysis. Of the remaining 9 beads, all were correctly classified by adopting the following rule:

- if the (absolute) oxygen concentration at the 3000 nm depth is $<10^{17}$ atoms/mm^3, then it is a 'cause' bead;
- if the concentration is $>10^{17}$ atoms/mm^3, then it is a 'victim' bead.

They cautioned, however, that the results must only be viewed as preliminary. They hypothesized that the distinction arises because the environment temperature is high when a 'victim' bead is formed and this allows a greater amount of oxygen to diffuse into a piece of copper that has been preheated. It must be noted that this is the exact opposite of the MacCleary/Thaman classification, where low—not high—oxygen concentration denote a 'victim' bead, although Satoh et al. analyzed concentrations at much greater depths into the bead, while the MacCleary/Thaman technique had sufficient sensitivity to characterize only a shallower region. Satoh et al.[904] continued the research with 65 additional samples from real fires and then found that there was only a 39% agreement between their proposed technique and the conclusion from that particular fire investigation.

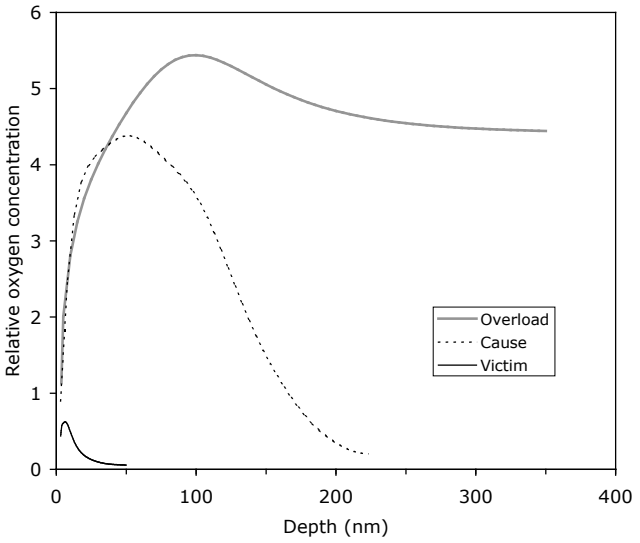


Figure 65 Oxygen concentration profiles shown in the patent by MacCleary and Thaman

MacCleary and Thaman did not pursue further the ideas of their patent, but since 1989 a method has been promoted by Anderson[905] that is similar to the MacCleary/Thaman idea in that it is proposed that AES depth profiles of certain elements can be used to establish the cause/victim status of an arc bead. Anderson noted that ambient air contains significant amounts only of oxygen and nitrogen. If an arc occurs between two wires in ambient air, then only oxygen can dissolve into the bead while the bead is in its molten state (nitrogen does not dissolve into copper). However, if the arc occurs in an atmosphere where there is an ongoing fire, then a number of other atoms will be found in the atmos-

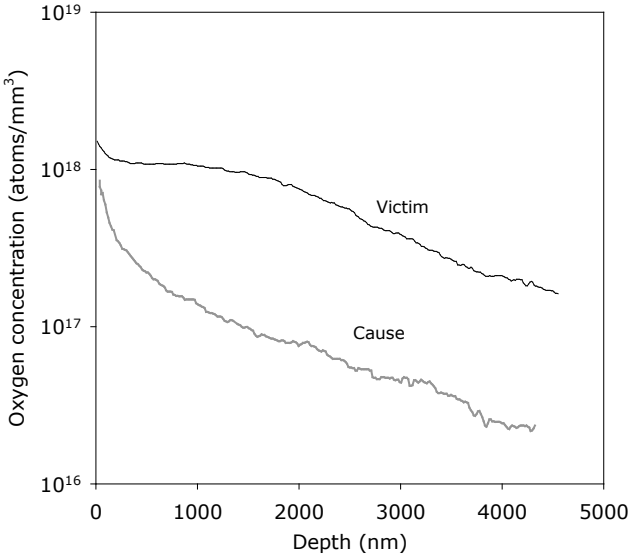


Figure 66 Oxygen concentration profiles, as measured by Satoh et al.

phere; these will also dissolve into the bead. Apart from oxygen, Anderson used carbon, chlorine, sulfur, calcium, zinc, iron, phosphorus, and chromium atom profiles. He did not propose any quantitative criteria for distinguishing between 'cause' and 'victim' beads, relying instead on a subjective evaluation, with apparently some emphasis placed on the carbon profile. Thus, a sizable concentration of carbon would indicate a 'victim' bead, while a lack thereof would suggest a 'cause' bead. Figure 67 shows a bead presented by Anderson[912] as a 'cause' bead, while Figure 68 shows a 'victim' bead.

The basic notion, however, that non-oxygen atoms will become available for incorporation only into 'victim' beads lacks foundation. In most practical cases, wires are insulated by a polymeric material, typically PVC. The polymer is in contact with the conductor and may be vaporized regardless of whether the arc bead was the first event of the fire, or if it occurred much later in the fire. Thus, it is not clear why a more copious presence of carbon or chlorine atoms would suggest a 'victim' bead. Similarly calcium carbonate is a common filler for plastics used in electrical wiring, so calcium may also be anticipated from either destruction of wire insulation as part of the initial arcing or from events much later in the fire.

One of the pivotal assumptions of the MacCleary/Thaman and Anderson theories is that the elemental profiles are frozen into the bead once the bead has cooled. Consequently, it is considered that once the arcing has stopped, further exposure to the fire atmosphere will not affect distribution of elements to be found within the bead (except possibly at the very surface, which is to be removed and discarded in their testing procedure). The principle is that the solubility of gases is much greater in liquid copper than in solid copper and, thus, the gases will be trapped after the bead solidifies and this distribution will be frozen in place and available for later study. Howitt[906] argued against this, but the basic concept that a substantial amount of oxygen can be dissolved in molten copper is correct[907,908]. Some gases can enter into copper while it is hot but not molten, however. This is the reason that stranded copper wires recovered from fire scenes often crumble to bits in the process of examination—the material has turned into copper oxide and no longer has mechanical strength. Howitt also conducted tests[909], but using energy-dispersive X-ray spectrometry (EDS), instead of AES. He was criticized by a laboratory offering AES services[910] for using a technique that is much less sensitive, but this does not seem germane, since his results showed adequate sensitivity. More problematic is the fact that a depth profile was not established, only a concentration within a relatively thick sub-surface layer. Howitt analyzed 13 samples obtained under various combustion and no-combustion conditions and noted that no systematic differences in C or O concentrations could be found that would be attributed to the presence of a pre-arc fire.

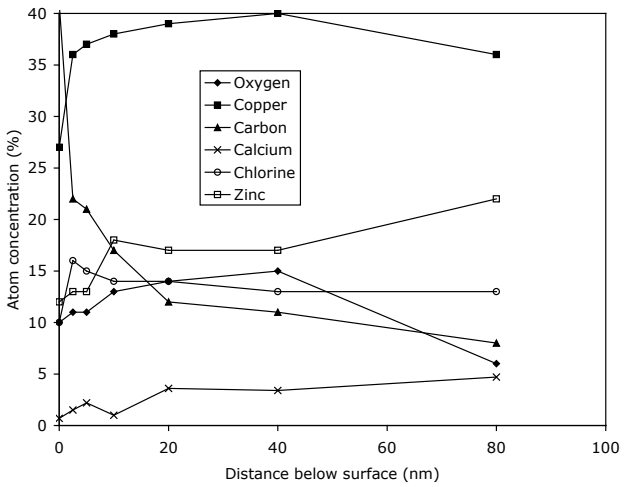


Figure 67 A 'cause' bead, Anderson's Case (graphs of results published by Anderson in the form of tables)

The use of Anderson's method for forensic purposes would require a quantitative protocol for analysis, specifically, concerning how the depth profile should be considered. Argon-ion sputtering is used in the Anderson method to remove the outer layer ("environmental cap" in his terminology). In his scheme, the cap comprises all the layers until a region is reached which has at least 60% copper. Consequently the disregarded environmental cap is stated in his reports as having widely-varying thicknesses: 2.5 nm[914], or 5 nm[911], 5 – 10 nm[912], or 5 – 20 nm[913]. But once the "environmental cap" has been removed, Anderson relies solely on a qualitative judgment that a 'victim' bead shows a profile where C, Cl, and Ca atoms are abundant to a greater sub-surface distance than in a 'cause' bead[914]; he does not appear to have been able to establish any quantitative criteria for making this distinction.

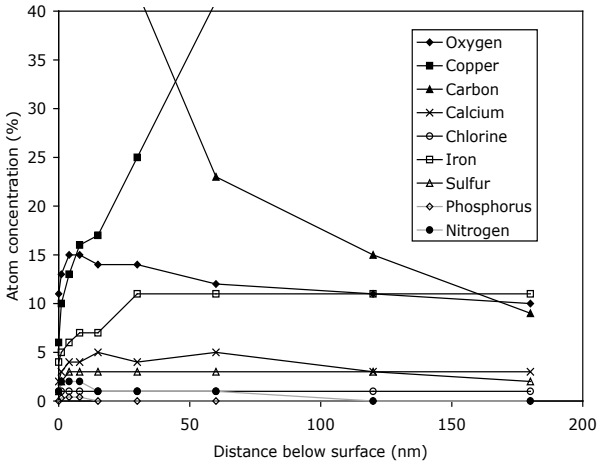


Figure 68 A 'victim' bead, Anderson's Case 3 (graphs of results published by Anderson in the form of tables)

Béland[915] pointed out that there is a significant statistical problem with the method even in a single laboratory: tests conducted on different portions of the same bead give substantially different results. An AES spectrometer can be operated in a raster-scan mode to characterize surface areas; however, no statistical technique has been demonstrated for obtaining characteristic averages in this way. He also pointed out[916] that Anderson's published work did not include even elementary descriptions of the tests performed, such as the exposure times for the specimens. Anderson claimed[913] that, in a fire litigation case, he was able to correctly distinguish 'cause' from 'victim' beads but Béland[916] argued that this was not done 'blind.'

Ettling[917] examined Anderson's data[905] and found numerous problems and inconsistencies. In his view, the basic problem is that in real fires—as opposed to Anderson's laboratory tests—a bead will most likely remain in a fire environment for an extended time, regardless of whether it is a 'cause' or a 'victim' bead. Thus, laboratory studies where a bead is created and then quickly removed from a fire environment do not present relevant information. Ettling also noted that in Anderson's study, the oxygen content of a bead formed in air was higher than for a bead formed in oxygen. No explanation was given by Anderson in his paper for this (nor did Anderson provide any description in his paper of specimen preparation or exposure procedures). Another questionable result was a bead from a 'victim' arc occurring near a gypsum wallboard which showed high amounts of sulfur. Electric arcs in branch circuit wiring do not normally vaporize gypsum wallboard, and there is negligible calcium sulfate liberated even as hydration water is lost during a post-flashover stage of fire. Thus, Ettling concluded that presence of sulfur is likely to indicate contamination to a hot bead, rather than being a useful tool for unraveling the early history of the fire.

Ettling also analyzed Anderson's later paper[912] where he presented AES results on beads recovered from three fires. In one case (Figure 67), the very deepest layer tested, 80 nm, showed zinc to be about 2/3 as plentiful as copper. Ettling points out that, at high temperatures, zinc oxidizes in air so readily that only zinc oxide should be available in the air, and the latter is unlikely to migrate into the bead. Thus, he concluded that this large amount of zinc came from a gross surface contamination of the bead. In another of Anderson's example cases (Figure 68), a power cord bead was examined from a failed electrical cooking pot. For layers below the "environmental cap," copper was the most abundant element, with iron being next. Anderson claims the iron came from the failed element, but would require that both the cord and the element be arcing at the same time, and that a huge fraction of the iron end up in the other bead. Equally problematic is that if the iron came from the heating element, no chromium or nickel (from the resistance wire itself) was recovered.

Henderson et al.[918] attempted a direct validation of Anderson's theory by preparing specimens under two conditions. The 'cause' beads were prepared by shorting together 18 AWG stranded copper wire in air; the 'victim' beads by placing the insulated, energized wire in a fire and waiting until an arc occurred. They found that the carbon profiles overlapped, and that there was no way to unambiguously differentiate between the two sets of results. Béland ran a similar set of experiments[915] and obtained the same conclusion in comparing the chlorine profiles of 'cause' and 'victim' beads.

Reese[919] pointed out that in dwellings, when a fire originates in branch circuit wiring and a bead is found, the event commonly involves arcing-through-char, not a simple metal-to-metal short. The latter would be likely to cause rapid tripping of the circuit breaker and would only rarely start a fire. Thus, while wire beads can be created readily in the laboratory by simply shorting two bare conductors against each other, this type of event is not common in accidental fires. If a fire originates from an electrical fault where charring occurred first, followed by shorting, then the AES test result will presumably be a false negative, since it will be formed in an environment containing reaction products from the charring of wire insulation. Fitz[920] pointed out a more fundamental logical concern with the AES scheme. In addition to arcing-through-char, a short circuit can happen due to radiant heat flux falling onto a thermoplastic cable or cord from an ongoing fire. When the insulation softens sufficiently for the conductors to make contact and produce a short circuit, there may not be any combustion or combustion products in the vicinity of this arc. This effect particularly may occur inside appliances, in engine compartments, or in wall cavities subjected to external heating. Thus, a positive AES result ("this bead was the cause of the fire") will be reported, despite the fact that the bead was the victim and not the cause.

For a laboratory technique that has been offered for forensic purposes, it is also a serious concern that the basic details of the phenomenon being utilized have not been studied scientifically. The non-copper elements identified in an AES spectrum must originally start out as atoms or molecules somewhere else. Through processes of transport and reaction, they end up embedded in the bead, but the chemical history that takes them there has not even been conjectured. Likewise, after they have entered the bead, no theory has been offered to provide a quantitative understanding of the depth profiles and of the lateral concentration variations in the bead.

Only one published study could be found supportive of Anderson's claims. Metson and Hobbis[921] performed an AES analysis on a single bead removed from the wall cavity of a fire scene, but suggested that reference to Anderson's work suffices to establish validity of results.

VIABILITY OF PROPOSED SCHEMES

Most of the proposed methods have been pure empiricisms, without any theoretical basis. Obviously, these could only be validated by a preponderance of empirical data. But some others refer to a theoretical principle, even though an actual quantitative theory has not been offered by any researcher. The relevant principles are necessarily based on some hypothesis that the chemical or the thermal histories of 'cause' and 'victim' beads form distinctly different populations. Concerning chemical histories, there have been only two hypotheses: (1) 'Cause' and 'victim' beads are uniquely associated with oxidizing and reduction atmospheres, respectively. In turn, the oxygen content of the bead will uniquely reflect this. But as Robertsson et al.[901] observed: "The oxygen content in the surface layer of a melt bead does not only depend on the type of damage but also on the thermal pre- and post-history of the electrical damage." In other words, once a bead is created—either a 'cause' or a 'victim' bead—it may remain for a long time in atmospheres that range from oxidizing (good supply of oxygen), to reducing (buried in oxygen-depleted, glowing or smoldering rubble). (2) The atmosphere surrounding a 'victim' bead will contain material that originated from decomposing solids nearby, while that around a 'cause' bead will not. Adequate amounts of this material (carbon, etc.) will then be found in the bead. This hypothesis is refuted, however, when it is considered that 'cause' arcs can and do occur in environments where the insulation already has been substantially degraded. Conversely, a short-circuit due to molten wire insulation can occur during a fire in a protected environment where there are no local combustion products and a minimum of pyrolysis products.

Thermal histories of arc beads can be diverse, but it is hard to envision any aspects that innately separate 'cause' from 'victim' beads. The temperature of an arc itself is vastly higher than the temperature of flames, but this is no help in making a distinction, since both arc temperatures and flame temperatures will have been attained at some time for beads of both types. Any bead can be expected to remain in a fire for a long time after it was formed—or a short time. An extended period of very high conductor temperatures, due to gross overload, may also precede the formation of an arc, irrespective of whether it is a 'cause' or a 'victim' arc. Remelting of an arc bead, of course, is universally agreed to eliminate any chance of deducing its prior history. One research group proposed that 'cause' beads, once formed, are likely to solidify at fairly low temperatures, while 'victim' beads will solidify at high temperatures. This presumes that fire heating will not be rapid, once a 'cause' bead initiates a fire. The hypothesis is questionable and, in any case, has not been experimentally examined apart from the authors' work.

Most of the techniques described in the literature have clearly been identified by their authors as being exploratory, initial investigations and not as finalized, validated methods. The one exception is Anderson's method, which he has claimed is sufficiently developed to be suitable for forensic purposes. But evidence does not support the idea that this method is ready for such usage. The main problems with the method are: (1) apart from the knowledge that oxygen and some other elements can dissolve into molten copper, there has been no chemical or metallurgical study that examines the details of the process and establishes a theoretical basis for concentration distributions to be expected in the solidified bead; (2) no quantitative criteria for distinguishing 'cause' from 'victim' beads have been developed; (3) even if post-fire contamination does not occur, subsequent and repeated heating in the fire environment makes interpretation of results uncertain; (4) the method is intrinsically subject to producing false positive and false negative results. False positives would indeed appear to be a problem, judging from Anderson's report[922] that he determined 1/3 of all the arc beads that he examined to be 'cause' beads. In the normal course of events, 'victim' beads should outnumber 'cause' beads by a huge fraction, since many fires cause extensive arcing, while generally there will only be one arc—at most—responsible for starting a fire.

In view of the above considerations, there is not much promise with any of the methods that have been proposed for distinguishing between 'cause' and 'victim' beads since:

(1) Most of the methods have been offered without any supporting theory. But the few theories that have been offered are inconsistent with the knowledge of the variety of behaviors that are found in room fires.
(2) With a few exceptions, the methods have been put forth as qualitative and subjective, without means of quantification.
(3) The methods typically have been based on studies using an extremely small number of experiments. In the few studies where sufficient samples were used to enable statistical conclusions to be drawn, the 'cause' and 'victim' bead populations showed sufficient overlap that only trends, not categorical distinctions, could be drawn. In the only study where comparison was made to a fairly large number of real-fire beads of known identity, the results were unacceptable (39% success).
(4) Almost all of the fire exposures for the laboratory-created beads have been very different from real room fires.
(5) None of the methods has been independently validated, although several validation attempts have been made and led to conclusions of irreproducibility.
(6) Most researchers proposing the various methods have suggested them in the spirit of ideas meriting further research, but Anderson has argued that his method is robust enough that it already should be accepted for forensic purposes. However, his

method does not appear to be more promising than any of the other methods.

In addition, serious doubt exists that any method could be developed in the future which is robust and reliable. This could only be possible if chemical or thermal exposure conditions were invariably different during the formation of 'cause' versus 'victim' arc beads. But distinctions of this kind have not been discovered.

Electric wiring and equipment in motor vehicles

The automotive environment presents increased possibilities of ignition, since electrical wiring and devices can be damaged both by collision and by vibration. Until the last few decades, automobile manufacturers used circuit protection devices only to a limited extent and it was not rare to encounter circuits that are totally without protection, or have inadequate protection. Short circuits by means of a relatively poor (high resistance) connection can also be more of a problem in motor vehicles than in house wiring, due to a ten-fold difference in voltages. For example, in one incident[923], a 5 A current was drawn due to a screw improperly driven into a cable bundle. At a 12 V supply voltage, this high-resistance short represents 2.4 Ω and the current will not trip a 10 to 30 A breaker. But if the voltage were 120 V, then the same 2.4 Ω resistance would draw 50 A and would be expected to trip a household 15 or 20 A breaker. Franklin[924] reported on tests conducted by General Motors, who documented that a faulty door lock switch can start an armrest fire and not blow a 20 A fuse used to protect the circuit. An arc in such a device can draw 12 to 24 A, and such arcs have been documented to be able to burn as long as 60 s prior to melting out a conductor.

Arc tracking is generally considered to be a lesser problem at low voltages, but a countervailing issue in motor vehicles is that the environment can contain pollutants (corrosives, soot, etc.) that promote arc tracking. Certain 1984-1993 models of Ford vehicles had ignition switches which were found to be a cause of fires (Color Plate 125). Investigations[925] determined this to be an arc-tracking problem inside the switch, exacerbated by the fact that the polymeric insulation between the metal contacts was grease-coated.

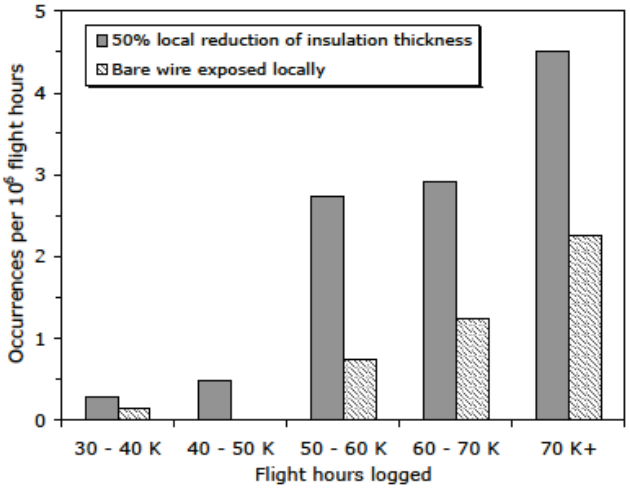


Figure 69 Aging of aircraft wiring

If the main ground strap going from the battery to the chassis develops a corrosion-caused high resistance, a fire can result if excessive current then flows through other paths to ground. A case of this type was documented by Sloan[926]. Battery acid is a relatively good conductor, thus, under unusual circumstances, battery acid can drip onto two exposed conductors and cause a temporary short. This short can then be the cause of an ignition[927].

As of the present time, the automotive industry is actively planning to raise system voltages from 12 volts nominal (14 V charging) to 36 volts nominal (42 V charging). The effect of this on ignition potential is yet to be determined.

Electric wiring in aircraft

The US National Transportation Safety Board[928] analyzed accidents or fires in commercial airplanes due to wiring faults from 1983 to 1999. The incidents identified involved:

- improperly routed wiring bundles shorted to various metallic objects (4 incidents)
- explosion in fuel tank due to degraded insulation from tank float switch wiring
- an excessively tight bend in a wiring bundle caused arcing; accumulated lint contributed to fire
- clearance was too small between electric wiring and hydraulic line; hydraulic fluid got ignited
- electrical arcing, not otherwise identified by NTSB (considered to be arc tracking by many private experts)
- unidentified electrical ignition event associated with fuel-level sensor wiring caused explosion in fuel tank. This was the famous TWA 800 flight of 17 July 1996.

Most of the above problems were due to faulty inspection or maintenance. An exception is arc tracking, which has been researched in depth during the past few decades.

One practical survey on degradation done on fuel tank wiring in Boeing 737 aircraft is at least illustrative[929]. Figure 69 shows that failure rates progressively increase as more aircraft hours are logged. The results imply that a useful service life of around 50,000 hours might be construed for these components.

Arc tracking was first noted in the aerospace industry around 1960. In the earliest research study[930], Elliott found that PVC cables carrying 28 VDC would readily undergo arc tracking. He also observed that electrolysis of water produces oxygen, which erodes copper and produces copper hydroxide and cuprous oxide. In a DC circuit, the process leads to conductive dendrites growing from the cathode to

the anode. Each dendrite can carry about 1 mA. The growth of dendrites is unique to DC circuits and does not occur when the polarity is changing. Arc tracking is especially problematic in aircraft, since each time an airplane descends from a high altitude into a warmer lower altitude, the chilled parts of the airplane may condense moisture.

The specifications for wiring in aerospace applications are different from that for building or electronics uses. It is essential to minimize both space and weight, whereas material cost is relatively secondary. For wiring, these objectives can be met if the insulation is made much thinner than found in other industries, down to about ¼ of such comparative thickness. Weight reduction is also helped by increasing the temperature rating to 200 – 260ºC, compared to normal ratings which are below 100ºC. Aromatic polyimide (Kapton™) and various types of fluorinated polymers (Tefzel™, Teflon™ etc.) were a suitable design solution[931]. Kapton has very good dielectric strength when dry and undegraded; unfortunately, due to its high water absorption factor, it proved to be highly prone to arc tracking. Color Plate 127 shows an example of mild arc tracking on Kapton aircraft wiring[932]. In cases of severe tracking, the whole bundle can be destroyed, not just individual wires[933].

Published research on arc tracking has mostly been due to FAA, NASA, and their contractors. The FAA ran tests on wires with various insulation types to determine their propensity for arc tracking[934]. In their tests, bundles of wire were coated on one end with powdered graphite, then an arc was deliberately created there. The test then consisted of determining whether 'dry' arc tracking would be observed to propagate or not. Tefzel (MIL-W-22759/16), PVC/nylon (MIL-W-5086/1), and cross-linked ETFE (MIL-W-22759/41 and also a proprietary grade) samples did not lead to arc tracking. Nor did an experimental construction comprising Teflon inner wrap/polyimide middle wrap/Teflon outer wrap. But Kapton (aromatic polyimide, MIL-W-81381/12) did, see Color Plate 128.

Ignition of electrical wiring occurred during 9 NASA space missions, of which 3 involved arc tracking. Consequently NASA sponsored three workshops on wiring for spacecraft applications[935-937]; in each, arc tracking of Kapton-insulated wires was a predominant concern. The most important technical conclusions to emerge from the workshops were that:

- circuit protection devices usually do not protect against arc tracking;
- the higher the voltage the easier it is to initiate arc tracking;
- arc tracking occurs less readily in vacuum than in air;
- the probability of an arc re-strike over a carbon path is proportional to the available Volt×Amp product. For three different wire types evaluated as improved replacements* for existing MIL-W-81381 Kapton-type wiring, the 50% probability of restrike was at V×A products in the range of 100 – 130 VA (tests run in air). Numerous restrike results were documented at circuit voltages as low as 20 V.
- for bends in the wire, arc-tracking probability is inversely proportional to bend radius;
- wires of 4 AWG (5.189 mm) or larger are unlikely arc track, due to heat sink effect of copper mass.

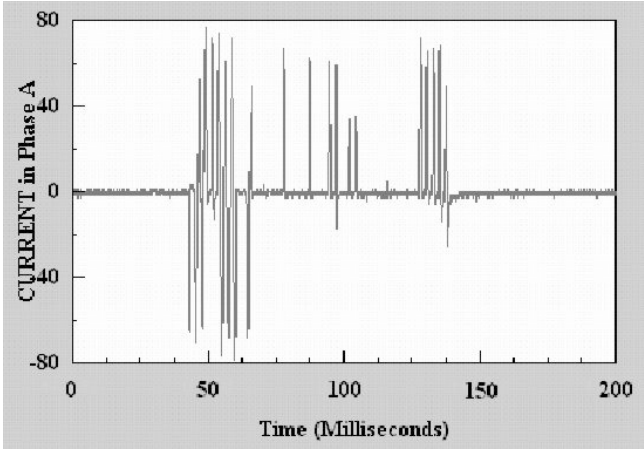


Figure 70 Waveform of flashing event

The workshops also documented that Kapton arc tracking problems have been severe in US Navy aircraft, and remediation measures within the Navy have been going on since the late 1980s.

Because of these problems, commercial aircraft makers have generally switched to XL-Tefzel (crosslinked ETFE) or TKT (MIL-W-22759, Teflon/Kapton/Teflon composite) in the mid-1990s; Airbus was still reported to be using Kapton wiring as of 1999[929]. Even though it contains a Kapton layer, in the TKT composite it is encapsulated between two other layers and the resultant composite does not show the problematic behavior of MIL-W-81381. Additional test data on composite wire insulation has been presented by Berkebile et al.[938]

A detailed laboratory investigation was conducted of arc tracking and other failure modes on exemplar aging aircraft wiring subsequent to the TWA 800 disaster[932]. An experimental arrangement patterned after Section 27 of the ASTM D 3032 wet-arc tracking test was used, with 3-phase, 208 VAC at 400 Hz being supplied. With this power supply, the study identified three stages of progressive electrical failure:

(1) Scintillations. These show up as pinpoints of light at damaged areas of insulation. During some scintillations, buzzing or crackling sounds could be heard. Peak

* The three systems were: (1) Kapton/extruded, crosslinked ethylene tetrafluoroethylene; (2) PFTE extrusion/Kapton/PTFE dispersion; and (3) modified PTFE tape/TPT tape/modified PTFE tape/PTFE dispersion.

current spikes are only about 20 A, consequently no circuit breakers trip.

(2) Flashing. These were noted as a white flash and audible popping, and tended to occur after scintillations had been going on for some time. They are isolated events, with seconds or minutes passing before the next event (Figure 70). The events last about 0.5 ms and show 8 kW peaks, with 4 J being dissipated. Arc voltages of ca. 100 V and peak currents up to 65 A were measured.

(3) Strong arcing. A bright flash that lasted up to 1 s or more, with intense hum or crackling. Arc power levels were ca. 10 kW, with peaks up to 15 kW; energy dissipated was ca. 5 kJ. Circuit breakers often tripped, since the circuit topology produces parallel arcing.

A series of tests was conducted by Cahill[939] to examine the potential of electrical faults for igniting kindling fuels. In her tests, bare sections of 20 AWG aircraft wires were intermittently touched. This tripped the 7.5 A breaker in only 1 of 25 trials, but ignited adjacent polyurethane foam (non-FR) in several trials.

Electronic components

Researchers at VTT conducted limited testing to examine the ignition behavior of electronic circuit boards subjected to power supply overvoltage or reversed polarity conditions[940]. Electric failures and smoke were readily produced, but flaming ignitions were less common and were barely sustained. Tantalum capacitors readily 'exploded,' but this did not lead to flaming fires or subsequent ignitions. In a few cases, the printed circuit board itself ignited, but flaming only lasted 25 – 70 s. See also: *Television sets and computer monitors*.

Engines, diesel

The operating temperatures on the metal surfaces of a small, 1-cylinder diesel engine have been measured[941]. These were found to be very much dependent on the engine rpm's. At 700 rpm, no temperatures exceeded 150ºC, while at 1400 rpm peak temperatures of 400ºC were measured on the muffler, and temperatures around 300ºC on the exhaust manifold. Larger diesel engines, in particular those that are turbocharged, may show exhaust component temperatures over 600ºC under heavy load conditions. These can readily act as ignition sources for many kinds of combustible liquids. For this reason, some heavy equipment designs use a firewall between the engine and the hydraulic pump. An incident has been reported[942] where diesel fuel was being accidentally sprayed onto the exhaust manifold of a diesel engine. Ignition occurred only upon shutting down the engine. The engine was equipped with a high-speed cooling fan and the air flow created by this fan helped limit the residence time of the fuel in the vicinity of the manifold. If the air intake for a diesel engine happens to become contaminated with flammable vapors, a runaway condition can be precipitated, due to this unexpected source of fuel delivery. Some two-stroke diesel engines can runaway if the air intake is occluded. This vacuum condition can cause motor oil to be sucked into the chambers and burned.

Ethers

Ethers are organic compounds where two functional groups (which may be aryls or alkyls) are linked together by an oxygen atom. Common ethers include diethyl ether ($C_4H_{10}O$), vinyl ether (C_4H_6O), furan (C_4H_4O), tetrahydrofuran (C_4H_8O), ethylene oxide (C_2H_4O), and 1,2-propylene oxide (C_3H_6O). Some cyclic ethers are linked by two oxygen atoms, e.g., 1,4-dioxane ($C_4H_8O_2$). The explosion hazard of ethers comes from their propensity to react with atmospheric oxygen, forming first a hydroperoxide, then further reacting to form polymeric 1-oxyperoxides. 1-Oxyperoxides are substances containing the group (O–C–OO–). Ethers can be photosensitive, with light serving to accelerate the generation of peroxides.

Diethyl ether, also called ethyl ether, or just "ether," was the first anesthetic to achieve widespread use; however, it has been replaced in modern medicine by anesthetics which have fewer medical side effects and are not as seriously flammable. It is used very widely in the chemical, plastics, and pharmaceutical industries. Some of diethyl ether's unusual problems stem from its boiling point (34ºC), which is barely above room temperature. The high density of diethyl ether vapors sometimes allows vapors to accumulate in low spots or to creep along the floor until they come in contact with a source of ignition. It has been reported[943] that diethyl ether vapors are susceptible to ignition if discharged into the air at high pressure, but the mechanism is not documented. The thermal decomposition kinetics has been discussed by Seres and Huhn[944].

The combustion of diethyl ether is specialized, since, apart from showing normal flames and cool flames, it can also show green flames in a certain temperature/pressure region[945]. The green-flame combustion can occur at 1 atm pressure and temperatures of 330 – 370ºC. At subatmospheric pressures, diethyl ether is also unusual in that it exhibits two, discontinuous regions of flammability. For instance, at 20ºC and 0.5 atm pressure, mixtures of 1 – 7.5% are flammable, as are ones of 20 – 27%, but mixtures between 7.5 and 20% are not. The lower-concentration region corresponds to normal flames and green flames, while the higher one to cool flames. According to the Bureau of Mines, at 25ºC and 1 atm, the limits of flammability of diethyl ether are considered to be 1.9 – 36%. Flame propagation does not occur[946] at pressures below about 0.2 atm. Cool-flame ignition, by itself, does not injure persons or ignite other combustibles such as paper. However, once diethyl ether is ignited in the cool-flame mode, it can transition to regular burning with normal, hot flames; this can lead to explosions and general fire involvement. Glass bottles of diethyl ether have been documented to explode spontaneously in storage[947]. Diethyl ether is an electrical insulator, which allows electrostatic charge buildup that may re-

sult in incendive sparks being formed. Shipping containers for diethyl ether normally contain stabilizers, which involve an oxidized metallic surface such as cuprous oxide or stannous oxide.

Diethyl ether is one of the easiest to ignite vapors, but its AIT has historically proven very difficult to measure accurately, and early studies showed extreme disparities. The first reliable studies are considered to be those of White[947], who used a heated-tube method and reported 187ºC. In a later study[948], however, he considered the value of 227ºC, obtained by Tizard and Pye, to be a more accurate determination. Later, Hsieh and Townsend[949] reported on experiments where they had no difficulty in observing autoignition at 200ºC, but did not explore lower temperatures. Mullins[950] gives the AIT as 186ºC in air and 178 – 182ºC in oxygen. In a 1965 compilation[4], the Bureau of Mines listed the AIT as 160ºC in air. A 1985 Bureau of Mines compilation[127] gives a value of 195ºC in air and 180ºC in oxygen, but another table in the same publication lists 160ºC in air. Neither compilation provides information as to the origin of the data. NFPA 325 considers the AIT in air to be 180ºC. Powell[17] specifies that the AIT is 102ºC, but without giving any details, and this should be considered a spurious value. Bull et al.[951] reported on experiments where a 7.2% diethyl ether/air mixture was heated by a 114 × 114 mm vertical aluminum plate. Cool, blue flames were first observed at a plate temperature of 267ºC, while a hot-flame ignition took place at 591ºC. On the other hand, Powell[17] reports that using a much smaller brass plate (26 × 16 mm), ignition was found to occur at 225ºC. Additional data in Chapter 6 indicate that diethyl ether is one of the few substances for which hot-surface ignition temperatures are only barely higher than the AIT.

A vapor cloud explosion of dimethyl ether took place at BASF, in Ludwigshafen, Germany in 1948 that killed 207. *Petroleum ether* is a chemical misnomer and the product is not an ether at all; it is a mixture of low-boiling-point hydrocarbons and is synonymous with petroleum naphtha. See also: *Ethylene oxide*; *Organic peroxides*; *Propylene oxide*.

Ethylene

Ethylene (C_2H_4) is a gas widely used in the chemical and plastics manufacturing industries. The limits of flammability are unusually wide: 2.7 – 36%. The UFL rises drastically with increased pressure, leading to potential hazards in processes where ethylene is used under pressure. In oxygen, the upper limit rises to 79.9%. The minimum oxygen concentration for combustion is 10%; this is lower than the 11.5% – 12% value found for most hydrocarbons. Its very small MESG value of 0.65 mm (British) to 0.69 mm (UL) places it among the most difficult to protect of gases from the point of view of designing explosionproof instrument enclosures. The double bond (C=C) is not strong and ethylene is prone to decomposition, in which carbon, methane and hydrogen are the main products. In the presence of certain catalysts, e.g., anhydrous aluminum chloride, ethylene can undergo explosive oligomerization[26]. Ethylene is also used for artificially ripening fruit and a number of explosions have taken place when flammable atmospheres were inadvertently created. Britton et al.[952] reviewed the ignition hazards of ethylene that are potentially encountered in chemical production facilities.

Ethylene glycol

An ethylene glycol/water mixture is the most common form of antifreeze agent and is used in transportation vehicles of various sorts. The antifreeze mixture will not ignite and burn by itself, but if it is spilled on a hot surface, the water fraction can first be driven off, with the residual glycol igniting at that point. Spills of the antifreeze on electrical parts can start an electrolysis action which has been reported to start fires in aircraft[953]. Under such circumstances, a period of many hours may be needed after the spill before ignition can occur.

Ethylene oxide

Ethylene oxide (C_2H_4O) is used in very large quantities as an intermediate in the chemical manufacturing industry; it is also used as a sterilization gas for surgical equipment. The molecule has the shape of a 3-membered ring and is a member of the chemical family of oxiranes. In air, its minimum spark ignition energy of 0.06 mJ is exceptionally low, thus nearly-imperceptible sparks can lead to ignition. The spark energy required to ignite ethylene oxide vapor decompositionally (in the absence of air) is vastly higher. Energies in the range 100 – 1000 mJ are typical, but depending strongly on pressure and temperature[962]. Ethylene oxide is considered stable if pure and at low temperatures, but is notorious for fire and explosion incidents under other conditions, e.g., leakage into contaminated atmospheres or ignition by localized heat. Pure ethylene oxide vapor can be readily ignited at 125ºC by electric spark[954]. Ethylene oxide reacts with most organic compounds, thus, care must be taken not to use inappropriate gaskets or seals. The flammable range of ethylene oxide is quoted as 3 – 100%, which is, of course, exceptionally broad. At 1 atm, there are two regions of combustion: between 3% and 65% C_2H_4O, a normal luminous flame is seen; for mixtures over 65%, a pale-blue flame occurs; for 100% C_2H_4O, a nearly-invisible decomposition flame is found[963]. The pale-blue flame and the decomposition flame are not cool flames, which also occur, but which do not lead to propagating-flame conditions. A pressure limit of 0.7 atm is reported[26]. Gustin[955] reviewed case histories for a number of explosions involving ethylene oxide.

Surprisingly small amounts of ethylene oxide vapor in air can lead to explosion if rapidly compressed. Griffiths and Perche[956] showed that less than 1% vapor suffice, under mild compression conditions where compression raises the gas temperature to 567 – 617ºC. In addition, they hypothesized, but did not demonstrate, that compression in oxygen-free environments can also lead to ignition.

Britton conducted a large number of decomposition-explosion tests using ethylene oxide/nitrogen mixtures in an 0.55 L sphere[962]. For near-ambient pressures, a temperature of ca. 500ºC was needed for explosion, dropping to about 450ºC at 13 atm. A value of $E \approx 260$ kJ mol^{-1} appears to reasonably capture the process, both for Britton's own data and for Japanese work that he cites. During decomposition, detonation can occur at low temperatures. Chen and Faeth[957] found that there were two distinct pressure regimes, within which the limits were insensitive to the actual pressure. At pressures of 2 – 12 atm, detonations in 100% ethylene oxide were observed for temperatures over 80 – 120ºC; at pressures over 20 atm, the minimum temperature dropped to as low as 28ºC. These results indicate that setting up processes to operate at pressures over 12 atm is inadvisable, unless reliable chilling can be provided.

Pure liquid ethylene oxide is considered highly stable, but, in the presence of other substances it is subject to polymerization, isomerization, and decomposition reactions. Polymerization in the presence of moisture produces tetraethylene glycol or low-molecular-mass polyethylene gly-

Table 84 Common names for pure explosives

Common name	Chemical name	Alternate names
AN	ammonium nitrate	
AP	ammonium perchlorate	
BTF	benzotris[1,2,5]oxadizole, 1,4,7-trioxide	benzotrifuroxan; hexanitrosobenzene
CP	5-cyanotetrazolpentaamine cobalt III perchlorate	
DADNPh	dinitrobenzenediazooxide	diazodinitrophenol
DATB	2,4,6-trinitro-1,3-benzenediamine	
DDNP	diazodinitrophenol	
DEGN	2,2'-oxybisethanol, dinitrate	diethyleneglycol dinitrate; dinitroglycol
DINA	N-nitrobis(2-hydroxyethyl)-amine dinitrate	diethanol-N-nitramine dinitrate
dinol	dinitrobenzenediazooxide	diazodinitrophenol
DIPAM	2,2',4,4',6,6'-hexanitro[1,1-biphenyl]-3,3'-diamine	diaminohexanitrophenyl; hexanitrodiphenyl
DNP	2,4-dinitrophenol	
DNPA	2-propenoic acid, 2,2-dinitropropyl ester	2,2-dinitropropyl acrylate monomer
DNT	1-methyl-x,x-dinitro-benzene, where x,x denotes one of 6 possible isomers	dinitrotoluene
EDNA	N,N'-dinitro-diaminoethane	ethylene dinitramine
EDNP	ethyl 4-4-dinitropentanoate	
Explosive D	ammonium picrate	Dunnite
hexyl	dipicrylamine	hexanitrodiphenylamine; 2,2',4,4',6,6'-hexanitrodiphenylamine
HMTD	hexamethylenetriperoxidediamine	
HMX	octahydro-1,3,5,7-tetranitro-1,3,5,7-tetrazocine	octogen
HNAB	hexanitroazobenzene	
HNS	1,1'-(1,2-ethenediyl)bis-[2,4,6-trinitrobenzene]	2,2',4,4',6,'-hexanitrostilbene
NC	partially nitrated cellulose	nitrocellulose; guncotton
NG	1,2,3-propanetriol, trinitrate	nitroglycerin
NM	nitromethane	nitrocarbol
NQ	nitroguanidine	Picrite
PA	2,4,6-trinitrophenol	picric acid; trinitrophenol
pDNPA	2-propenoic acid, 2,2-dinitropropyl ester polymer	dinitropropyl acrylate polymer
PETN	2,2-bis[(nitrooxy)methyl]-1,3-propanediol, dinitrate	pentaerythritol-tetranitrate; penthrite; TEN
PGDN	1,2-propanediol, dinitrate	1,2-propylene glycol dinitrate
RDX	hexahydro-1,3,5-trinitro-1,3,5-triazine	Cyclonite; hexogen; trinitrotrimethylene-triamine; Research Department Explosive
TATB	2,4,6-trinitro-1,3,5-benzene-triamine	1,3,5-triamino-2,4,6-trinitrobenzene
TATNB	1,3,5-triazido-2,4,6-trinitrobenzene	triazidotrinitrobenzene
TATP	triacetone triperoxide	
tetryl	N-methyl-N,2,4,6-tetranitro-benzenamine	N-methyl-N,2,4,6-tetranitroaniline; tetranitromethylaniline
TNA	2-methoxy-1,3,5-trinitro-benzene	methyl picrate
TNB	1,3,5-trinitrobenzene	
TNM	tetranitromethane	
TNRS	lead styphnate	
TNT	2-methyl-1,3,5-trinitrobenzene	

cols, while polyethylene oxide is produced under dry conditions. Exothermic activity for 5 g samples of pure ethylene oxide held in a glass vessel[958] was found to commence at around 80ºC. The polymerization process requires a catalyst, with either acids or bases being able to serve that role[959]. Iron oxides promote the isomerization of ethylene oxide, although the action is not that of a simple catalyst[962]; the two most hazardous forms[960] of iron oxide are γ-Fe_2O_3 and γ-FeO(OH). Isomerization produces acetaldehyde with the release of 115 kJ mol^{-1} of heat. Acetaldehyde has a much lower AIT than does ethylene oxide, and if acetaldehyde has been formed due to catalytic isomerization, the resultant mixture can show a large drop in AIT[962]. The presence of water greatly lowers the temperature at which exothermic activity occurs. Detectable heat release was found at 200ºC for pure ethylene oxide, but at 50ºC for 10% ethylene oxide/90% water mixture. Even a 1% addition of dimethylamine to ethylene oxide was found to reduce the threshold to 33ºC[962]. June and Dye[961] studied the lower limit in ethylene oxide/nitrogen systems for decomposition explosions, and provided data as a function of moderately elevated pressures and temperatures.

Ethylene oxide soaking into porous pipe insulation is a special problem. Exotherms are found below 100ºC with certain insulations[1663]. Porous insulation exacerbates the self-heating problems of ethylene oxide since it captures a certain amount of moisture from the air, which is then available to react with the ethylene oxide. Britton considered the case of ethylene oxide polymerizing into one of the glycols and conducted oven-cube tests on glycol-soaked insulation to determine the temperature below which runaway self-heating is unlikely to occur. He concluded that for practical insulation thicknesses, pipe temperatures below 60ºC were acceptable[1663].

The liquid is more stable than the gas, but under extremes of pressure and temperature, liquid ethylene oxide can show a flaming decomposition[962] and has been considered as a rocket monopropellant and gas generant at one time. The decomposition products are primarily CO and CH_4, but C_2H_4, H_2, and minor amounts of C_2H_6 can also be produced. The primary reactions are[963]:

$$C_2H_4O \rightarrow CH_4 + CO$$
$$2C_2H_4O \rightarrow C_2H_4 + 2CO + 2H_2$$

For pressures up to 1 MPa, it is recommended that process temperatures be held below 75ºC; for higher pressures, progressively lower temperatures are needed[964]. The mixing of ethylene oxide and water is an exothermic reaction. A case history is reported of an explosion which occurred when water was added to a tank car which was about 15% full of ethylene oxide[965]. The analysis of the incident indicated that the two liquids (which are 100% miscible) did not, in fact, mix but rather stratified due to the filling procedure. A reactive lay-

Table 85 Common designations for explosive mixtures

Designation	Component	Percent
Amatol 80/20	AN	80
	TNT	20
Baratol	$Ba(NO_3)_2$	76
	TNT	24
black powder (gunpowder)	KNO_3	75
	charcoal	15
	sulfur	10
CH-6	RDX	97.5
	calcium stearate	1.5
	polyisobutylene	0.5
	graphite	0.5
Composition A-3	RDX	91
	desensitizing wax	9
Composition A-5	RDX	98.5
	stearic acid	1.5
Composition B	RDX	59
	TNT	40
	wax	1
Composition B-3	RDX	60
	TNT	40
Composition C-4	RDX	91
	di(2-ethylhexyl)sebacate	5.3
	polyisobutylene	2.1
	motor oil	1.6
Cyclotol	RDX	75
	TNT	25
LX-04-1	HMX	85
	Viton A (vinylidine fluoride/ hexafluoropropylene copolymer, 60/40)	15
LX-09	HMX	93
	pDNPA	4.6
	FEFO: 1,1-dinitro-2-(2,2-dinitro-ethoxy)methoxy)-1-fluoro-ethane	2.4
LX-10	HMX	95
	Viton A	5
LX-15	HMX	95
	Kel-F 800 (chlorotrifluoroethylene/ vinylidene fluoride copolymer, 3:1)	5
LX-16	PETN	96
	FPC 461 (vinyl chloride/ chlorotrifluoro-ethylene copolymer, 3:2)	4
Octol	HMX	75
	TNT	25
PBX-9404	HMX	94
	NC (12.0%N)	3
	CEF (tris-δ-chloroethyl-phosphate)	3
PBXN-5	HMX	95
	fluoroelastomer	5
Pentolite	PETN	50
	TNT	50
Torpex	RDX	41
	TNT	41
	aluminum powder	18

er was formed which heated strongly and drove the rest of the system to explosive decomposition.

In 1997 there was a rash of ethylene oxide explosions and it was speculated that at least some of them were associated with catalytic combustion systems used for air pollution control purposes[966]. In older times, it used to be prescribed that copper should not be used in ethylene oxide systems, since small amounts of acetylene impurities were common and there was concern of creating highly explosive copper acetylide. Ethylene oxide currently produced is free of these impurities and consequently the advice is outdated[26].

Explosives

Explosives are classed by UN[1650] as Class 1 Dangerous Goods. This class is subdivided into 6 divisions; in addition, a letter designation is appended to the Division number which denotes a 'compatibility group.' All transportable Dangerous Goods are also assigned a "UN No." For pure chemicals, a UN number identifies a unique compound. But most explosives are not pure chemicals, and they are assigned group numbers. These are determined by both the composition and the functional nature of the item. Each UN number belongs to a single Division, but there are many UN numbers in each Division. Explosive substances are assigned UN Nos. 0000 through 0500, but not all numbers are currently in use. Dangerous Goods of classes other than Class 1 are assigned numbers 1000 and higher. National regulations are typically based on the UN scheme, but with local variations.

Since the chemical names of most explosives are lengthy, in the explosives profession there has arisen a standard set of abbreviations or common names; a selection is given in Table 84 and Table 85. Some additional designations exist in Europe that are not common in the US.

Each year, BATF attends about 1500 bombing incidents, 500 attempted bombings, 400 fire-bombings, and 180 attempted fire-bombings[967]. The explosives used in these incidents are shown in Table 86. The deaths and injuries from incidents[968] are shown in Table 87.

Table 86 Explosives used in bombings and attempted bombing incidents in the US during 1993 – 1997

Explosive	Percent
flammable liquid	30
"chemicals" (homemade devices producing gas from domestic materials)	26
pyrotechnics, flash powders	17
black powder	10
smokeless powder	8
match heads	2
commercial high explosives	1.1
military explosives, except C4 and TNT	1.1
blasting agents	0.2
C4 and TNT	0.1
other	5

Table 87 Deaths and injuries in the US during 1979 – 1995 from bombing incidents

Explosive	Percent	
	Deaths	Injuries
blasting agents	25.1	9.9
black powder, smokeless powder	20.0	17.5
flammable liquids	14.2	8.7
dynamites and water gels	13.6	4.3
pyrotechnics, flash powders	12.0	15.0
C4, TNT	4.0	0.2
other*	14.5	44.4

* includes match heads, flares, boosters, detonating cord, gases, blasting caps, military explosives other than C4 or TNT, model rocket propellants, and smoke grenades

Table 88 Ignition or explosion temperature for a number of explosives, as reported by Stecher

Substance	T_{ig} (°C)
black powder	270 – 300
cordite	225
guncotton	180 – 190
nitroglycerine	217
nitrostarch	175
picric acid	300
TNT	180

Table 89 Ignition temperatures reported by Urbański

Substance	T_{ig} (°C)
barium azide	190 – 200
black powder	300
calcium azide	171 – 176
copper acetylide	120 – 123
cupric azide	203 – 205
cyanuric triazide	205 – 208
dinitrodiethyloxamide	160
EDNA	180
EGDN	195 – 200
lead azide	332 – 359
lead styphnate	267 – 268
mercury fulminate	115
NC	165
NG	180 – 200
nitrogen selenide	230
nitrogen sulfide	207
PETN (penthrite)	205 – 225
picric acid	243 – 330
RDX (cyclonite)	229
silver acetylide	200
silver fulminate	170
smokeless powder, single-base	180
smokeless powder, double-base	200
strontium azide	190 – 202
tetrazene	< 115
tetryl	203
TNT	240

The oldest explosive is *black powder* (gunpowder) and for many centuries it was the *only* available explosive. Black powder normally contains 75% potassium nitrate, 15% charcoal, and 10% sulfur. Since it is a physical mixture made up of the three different materials, the method of preparation greatly influences the properties of the finished product. Furthermore, the nature of the ingredients themselves, e.g., what type of tree was burned to produce the charcoal, is also important. Maltitz[969] has written a book devoted solely to practical details, while Urbański[256] gives a more scientific review. The ignition temperature is typically cited as 300ºC, but this is preceded by several 'pre-ignition' steps. The process begins with melting of the sulfur at ca. 115ºC, then at ca. 150ºC the molten sulfur reacts with the hydrogen in charcoal to form H_2S. The H_2S reacts with the potassium nitrate to form potassium sulfate. The exothermicity of this reaction then leads to progressive melting of the KNO_3. Black powder still has significant uses in manufacture of fireworks, although it has long been replaced as a military propellant by smokeless powder. It sees use among enthusiasts of antique weapons, since these could not withstand the pressure created by smokeless powder. Some 'black powder' coming from China in recent years includes sodium chlorate, which produces a much more energetic (and dangerous) propellant[970]. Urbański[256] warns that substituting potassium chlorate for potassium nitrate in black powder will produce a mixture "exceptionally sensitive to impact and friction, and therefore too dangerous to manufacture." Even without this substitution, he notes that black powder is "highly sensitive to impact and friction." The wheel-lock weapon invented in the 16th century used a spark from a serrated wheel moving against iron pyrite to ignite black powder, clearly demonstrating that a modest mechanical spark suffices. A spark flying off a match head[315] has also been documented to ignite black powder. The energy required for spark ignition of black powder is 45 mJ, and one explosion in a black-powder manufacturing facility was attributed to low ambient temperatures, which caused low humidity levels and a high propensity towards static electrification[1436].

Stecher[443] supplied some very old values for ignition/explosion temperatures of a number of explosives, determined by an unspecified method (Table 88).

Urbański[256] has given ignition temperatures for various explosives (Table 89), obtained under short-term heating. For explosives lacking long-term stability, room temperature may effectively become their ignition temperature when they have sufficiently decomposed.

Hikita[971] reported T_{ig} and the activation energy, E, for a number of explosives in air. He also determined that, for the substances studied, there was no effect of oxygen concentration on the ignition temperature. Kayser[972] reported results from the NOL Thermal Sensitivity Test, which uses a sealed 'microbomb' to determined 'threshold' temperatures for the initiation of explosion. Both of these sets of data are given in Table 91.

Table 91 Properties as determined by Hikita and Kayser

Substance	T_{ig} (ºC)	E (kJ mol^{-1})	$T_{thres.}$ (ºC)
acrylonitrile			710
ammonium picrate	380		
chloropicrin			325
collodion cotton		197	
crotonaldehyde			780
DADNPh	150	219	
UDMH			515
m-dinitrobenzene	500		450
DNP			470
DNT	420		
dinitronaphthalene	380		
ethyl nitrate			375
guncotton		236	
hexyl	360		
hydrazine, 95%			827
hydrazine hydrate, 85%			920
lead picrate	230		
mercury fulminate		189	
NC (13.14% N)	170		
NG		179	220
nitrobenzene			530
NM			370
PETN	170	222	
picric acid	320		
PGDN		154	
TNA			411
TNB			460
tetryl	180		
RDX	260		
TNT	250		427

Table 90 Comparison of sensitivity test results for several explosives

Explosive	Min. detonating charge (g)	Impact (cm in drop-hammer test)		Explosion temp. (ºC)	Friction test
		BM	Picatinny Arsenal		
lead azide		75	7.6	340	explodes
lead styphnate	0.001		20.3	282	explodes
PETN	0.03		15.2	225	crackles
tetryl	0.10	26	20.3	257	crackles
HMX	0.30	60	22.9	327	explodes
TNT	0.27	> 95	35.6	475	unaffected
black powder		32	40.6	427	snaps
ammonium picrate	0.4	> 100	43.2	318	unaffected

Table 92 Spark ignition results from various studies on explosives

Substance	Ignition energy (J)			
	BM P = 0%		LANL P = 50%	NMIMT P = 50%[c]
	Unconfined	Confined[a]	Confined[b]	
AN				0.58
AP (90 μm)				0.41
AP (200 μm)				0.53
ammonium picrate (as received)	> 12.5	6.0		
ammonium picrate (< 80 or 100 mesh)	0.025	6.0		0.76
black powder (< 100 mesh)	>12.5	0.8		
HMX			0.23	0.21
lead azide	0.0070	0.0070		
lead styphnate	0.0009	0.0009		
LX-04			1.04	
magnesium powder, Grade B	0.007 to >12.5	>12.5		
mercury fulminate	0.025	0.025		
NC (13.4% N)	0.061	3.1		
NG	>12.5	0.90		
NQ				0.60
nitrostarch	0.007	1.0		
PBX-9404			0.42	
Pentolite			0.32	
PETN (as received)	>11.0	0.21	0.19	
PETN (< 100 mesh)	0.062	0.21		
RDX			0.21	0.15
TATB			4.25	2.56
tetryl (as received)	>11.0	4.68	0.54	
tetryl (< 100 mesh)	0.007	4.38		
TNT (as received)	>11.0	4.68	0.46	
TNT (< 80 or 100 mesh)	0.062	4.38		0.57

a – unspecified details
b – confined by 0.08 mm lead foil
c – only confined by a layer of 0.05 mm Mylar tape

The sensitivity of explosives to various forms of energy input varies a great deal, and even rank-ordering is not assured. Table 90 shows results for some common explosives[973]. The minimum detonating charge test uses lead azide as the detonator. The two drop-hammer tests, in principle, measure the same impact effect. Explosion temperature results were determined as 5-s exposures in an open cup. The friction test is a qualitative test at Picatinny Arsenal. Most of the tests rank-order explosives similarly, although with significant exceptions; however, the explosion temperature is clearly unrelated to the other results. A compilation of Bureau of Mines data from their versions of the card gap test and the projectile impact test has been published by Watson[974].

The Bureau of Mines (BM) reported ignition data on a series of explosives in a spark discharge test apparatus where the voltage was fixed at 5 kV and the capacitance varied[90]. In addition, confined and unconfined conditions were examined. Unlike most other procedures, the results were reported as P = 0% values, i.e., the highest energy for which no ignition will occur. Larson et al.[975] measured a number of explosives confined by thin foils at Los Alamos National Laboratory (LANL). In their study, they consistently found that greater thicknesses gave higher MIE values, thus only their thinnest foil results are presented here. Most recently, Skinner et al.[976] reported on a series of tests conducted at the New Mexico Institute of Mining and Technology (NMIMT) where the only confinement was a layer of Mylar tape. Some comparative results of these studies are given in Table 92. The agreement varies widely, but the two newer studies tend to agree better. Larson et al. also examined the effect of heated specimens on the MIE. At 175ºC, the MIE values typically dropped to about 50% compared to room temperature, although for a few specimens there was almost no decrease.

Several conclusions emerged from the Bureau of Mines study:

(1) The minimum spark ignition energy for unconfined mixtures usually increases greatly when the substance is pulverized to smaller than 100 mesh size.
(2) For confined conditions, the size of granules generally does not affect the minimum spark ignition energy needed.
(3) There is generally no relation between the confined and the unconfined results.

Table 93 Friction and impact sensitivity for various explosives (values given are for 50% probability level)

Substance	Friction sensitivity (kg)	Impact sensitivity (kg-m)
barium styphnate	1.7 – 2.0	0.113 – 0.122
CP	0.9 – 1.3	0.066 – 0.105
HMX	6.2	0.160 – 0.176
PBX of HMX (96% HMX, 4% FPC-461)	7.2	0.17
LX-15	> 36	> 0.250
LX-16	7.7	0.12
PETN	7.0 – 8.1	0.124 – 0.170
RX26BB (HMX/ TATB, 50/50)	13	> 0.250
TATB	> 36	> 0.250

(4) The above results pertain to 25ºC conditions; in separate testing, it was shown that for nitroglycerin under confined conditions at 60ºC, the minimum energy is greatly lower (0.056 J).

The values reported for lead azide are highly dependent on the test conditions. In other studies, MIE values have been lower, e.g., 0.002 mJ to 0.04 mJ. Dusts of black powder require 30 mJ for capacitive spark ignition, at the 50% probability level, while lead styphnate ($C_6H_3N_3O_9Pb$) requires[977] 0.052 mJ. A minimum ignition energy of 0.1 J has been reported for RDX[90]. Static electricity can readily cause explosion of detonators. Dale[67] and Demberg[978] described several accidents. In examining non-electric detonators using lead azide as the primary charge and various charges of secondary explosives, Demberg found that all incidents occurred within 72 h of manufacture. It was concluded that the most likely cause was electrostatic charge picked up during packaging, given the very high sensitivity of lead azide to electrostatic initiation. It was also concluded that safer detonators would result if fine particles of lead azide were eliminated from use.

Friction and impact sensitivities for a number of explosives were reported by Wang and Hall[979]. For friction sensitivity testing they used the Koenen/BAM test, while for impact sensitivity a drop-hammer test having an 0.5 m hammer drop distance and a 20 mg quantity of test substance. The results are shown in Table 93.

Table 94 Flash points for explosives

Substance	Flash point (ºC)
tetrazene	140
mercury fulminate	170 – 180
smokeless powder	180 – 200
tetryl	195 – 200
cellulose nitrate	195 – 200
nitroglycerin	200 – 205
RDX	215 – 230
lead styphnate	270 – 280
TNT	295 – 300
picric acid	300 – 310

Table 95 Critical energy fluence for shock initiation of some explosives

Substance	Density (kg m^{-3})	Critical energy fluence (kJ m^{-2})
Composition B	1730	1850
Composition B-3	1727	1381
DATB	1676	1632
HNS	1555	< 1422
lead azide	493	≈1.225
LX-04	1865	1090
LX-09	1840	962
NM	1130	≈17,000
PBX-9404 (HMX, NC, CEF)	1840	630
PETN	1000	84 – 120
	1600	≈167
RDX	1550	≈680
TATB	1762	3013 – 3682
	1930	≈9600
tetryl	1655	420
TNT (cast)	1600	≈4200
	1620	1339
TNT (pressed)	1645	1420

Using an adiabatic calorimeter, Gross et al.[980,981] determined the kinetic parameters of some common explosives (Table 98). Values from various sources[976,982,985] are shown in Table 100. The latter data are more current, thus can be expected to be more reliable than the work of Gross et al. Note however that Janswoude and Pasman[983] demonstrated that explosive substances typically do not show a behavior consistent with single-step Arrhenius kinetics over the entire temperature range of interest. Instead, as temperatures increase, the effective values of both *E* and *QA* fall.

Flash points for a number of explosives have been reported in the Russian literature[984]. The values shown in Table 94 were obtained in an open-cup, dynamic test method.

The minimum energy density (kJ m^{-2}) for shock initiation has been obtained for some explosives. Values are given in Table 95[985]. The term *critical energy fluence* is commonly used in the explosives field as a synonym for minimum energy density. The measuring techniques and the calculational formulas for obtaining these values are given by Walker and Wasley[986]. Results for liquid explosives (e.g., nitromethane; liquid TNT) are generally found not to obey a critical energy fluence relation[987].

The radiant ignition times of HMX, RDX, and tetryl at high irradiance values (> 300 kW m^{-2}) using a CO_2 laser has been reported by Vilyunov[234].

Table 96 Critical diameters for detonation of some pressed explosives

Explosive	Density (kg m^{-3})	Grain size (mm)	Critical diameter (mm)
AN	900 – 1000	0.05 – 0.2	100
AN/Al (80/20)	900 – 1000	0.05 – 0.2	12
AN/TNT (79/21)	900 – 1000	0.05 – 0.2	10 – 12
AN/TNT (90/10)	900 – 1000	0.05 – 0.2	15
lead azide	900 – 1000	0.05 – 0.2	0.01 – 0.02
lead picrate	750	0.01 – 0.05	1.45 – 1.53
	100	≈0.2	2 – 3
PETN	1000	0.025 – 0.05	0.7 – 0.9
	1000	0.05 – 0.1	1.0
	1000	≈0.25	2.1 – 2.2
picric acid	800	0.01 – 0.05	2.08 – 2.28
	950	0.1 – 0.75	8.9 – 9.25
potassium picrate	750	0.04 – 0.15	5.5 – 6.0
RDX	1000	0.025 – 0.15	1.0 – 1.15
	1000	≈0.2	1.5
TNT	850	0.01 – 0.05	4.5 – 5.4
	850	0.07 – 0.2	10.5 – 11.2

Table 97 Critical diameters for detonation of some liquid explosives

Explosive	Density (kg m^{-3})	Critical diameter (mm)
glycerol dinitrate	1520	8.0
nitric acid	1390	110.
nitroglycerine	1600	2.4
nitroglycide	1320	7.
nitromethane	1140	18.
nitromethane/acetone, 84/16	1080	80.
tetranitromethane	1640	16.

Critical diameters for detonation (not to be confused with critical diameters for decomposition) have been tabulated[90] for a number of explosives (Table 96). A larger compilation has been provided by Dobratz and Crawford[985]; they include information on effects of confinement, but not on grain size. Some critical diameters for liquid explosives (Table 97) have been presented by Dremin[988]. Heats of combustion, explosion, and detonation are shown for some explosives[90,989,990] in Table 99.

Table 99 Heats of combustion, explosion, and detonation for some explosives

Explosive	OB (%)	Heat of combustion (MJ kg^{-1})	Heat of explosion (MJ kg^{-1})	Heat of detonation (MJ kg^{-1})
NG	+3.5	6.76	6.69	6.22
PETN	–10.1	8.20	6.13	6.26
RDX	–21.6	9.53	5.72	6.08
HMX	–21.6	9.42	5.68	6.19
Pentolite	–42.0	11.67	4.09	
Tetryl	–47.4	12.24	3.90	4.77
TATB	–55.8	11.89	3.12	4.26
TNT	–74.0	15.15	2.78	4.57

Many explosives are prone to self-heating caused by decomposition, if stored above room temperature. For example, some limiting storage temperatures[232] are: mercury fulminate 50ºC, nitroglycerin 60ºC, PETN 65ºC, tetrazene 75ºC, although of course both the time and the quantity stored should also be taken into account. But others, such as tetryl, TNT, etc., are greatly more stable.

The US Department of Transportation regulates shipments by categorizing explosives as Forbidden, Acceptable, or New. Forbidden explosives include:

- materials showing a self-accelerating decomposition temperature (SADT) of 50ºC or less
- explosive mixtures or devices containing a chlorate and an ammonium salt or an acidic substance
- nitroglycerine, diethylene glycol dinitrate, or other liquid explosives, except as authorized by DOT
- leaking or damaged packages of explosives
- unstable, condemned or deteriorated propellants
- certain toy torpedoes
- fireworks containing yellow or white phosphorus
- initiating explosives, when dry
- all other substances identified as Forbidden in Par.172.101 (Hazardous Materials Table).

Table 98 Reaction properties determined by Gross and coworkers for some common explosives

Substance	Density (kg m^{-3})	Thermal conductivity (W m^{-1} K^{-1})	Heat capacity (kJ kg^{-1} K^{-1})	E (kJ mol^{-1})	AQ (kW kg^{-1})
AP	1830	0.40	1.20	172	5.61×10^{16}
Cyclotol	1700	0.25	1.08	155	2.54×10^{19}
DINA	1610	0.23	1.14	149	7.07×10^{16}
NC	820	0.21	1.42	176	1.24×10^{20}
RDX	1660	0.21	1.10	239	8.74×10^{24}
TNT	1570	0.19	1.10	155	2.08×10^{14}

Table 100 Kinetic and thermal properties of explosives

Substance	Q (kJ kg^{-1})	A (s^{-1})	E (kJ mol^{-1})	C (kJ kg^{-1} K^{-1})	ρ (kg m^{-3})	λ (W m^{-1} K^{-1})	Porosity (--)
AN		5.01×10^{12}	169	1.67		0.12 – 0.16	
AP		2.09×10^{9}	126	1.29		0.4 – 0.5	
Composition B	3171	4.62×10^{16}	180	1.13	1580	0.20	
DATB	1255	1.17×10^{15}	194	0.96	1740	0.25	
HMX	2092	5.0×10^{19}	221	1.65	1800	0.42 – 0.56	
NQ	2092	2.84×10^{7}	87	1.24	1700	0.21	
PBX 9404	2100	5.0×10^{19}	220	2.11	1800	0.39 – 0.43	0.32
PETN	1355	6.3×10^{19}	197	1.09	1740	0.25	0.135
RDX	2092	2.02×10^{18}	197	1.13	1800	0.11	
TATB	2510	3.18×10^{19}	251	1.05	1840	0.42	
Thermite ($2Al + Fe_2O_3$)	3800	1.0×10^{15}	320		4140		0.355
TNT (pressed)	1255	2.51×10^{11}	144	1.37	1570[a]	0.21	

a – varies widely for actual product

Although it is common for flammable gas/air explosions to cause fires, it is uncommon for explosions of solid explosives[180]. Forest fires have been repeatedly ignited by shooting enthusiasts using tracer, incendiary, or armor piercing ammunition. Numerous ignitions have been documented[991] due to use of Chinese bullets that have a steel 'penetrator core.' Firing high-power rifle bullets into cases of sporting ammunition causes only modest hazard. Hampton[992] fired 2 to 3 shots into various cases of ammunition and observed puffs of smoke. Some individual cartridges were found to be fired within, but there was no evidence of propagating explosion. He concluded that the hazard of mass detonating upon firing into ammunition cases is minimal. The *Handloader* magazine has published a book giving numerous details on essentially all commercially available powders for handloading of ammunition[993].

See also: *Ammonium nitrate and ANFO*; *Cellulose nitrate*; *Dusts*.

Table 101 Ignition source for incidents where clothing fabrics ignited

Ignition source	Percent
matches, lighters	28.5
kitchen range	21.1
open fires	17.4
cigarettes, cigars	5.7
engine	5.0
water heater	3.9
space heater	3.0
welding torch	2.3
furnace	2.0
appliance, other	1.9
electric wiring	1.9
candle	1.6
heater, unspecified	0.7
all others	5.1

Fabrics

Fabrics predominantly occur in draperies, other decorative applications (e.g., bunting), bedding, clothing, and as the cover material for upholstered furniture. Textiles can also be found in rugs and carpets, but these are generally treated as a separate commodity from the point of view of ignition testing and characterization.

An early study[994] provides US statistics on the ignition of clothing fabrics (Table 101). In 36% of the cases, a flammable liquid was involved as an 'intermediary material.' Gas ranges accounted for 65% of the kitchen range incidents. In another US study[995], the activities of victims leading to ignition were identified (Table 102).

Table 102 Activities of victims whose clothing got ignited

Activity	Percent
cooking	12.1
playing with matches	10.5
using matches or lighter	10.5
falling asleep with smoking material	7.6
working/repairing machine	6.1
smoking	5.8
tending open fire (not leaves or trash)	5.4
burning leaves or trash	4.8
sleeping	4.8
playing near open fire	2.8
cleaning with flammable liquid	2.7
helping another person	1.3
other	15.7

The US Federal standard regulating the flammability of apparel fabrics does very little to prevent injury from flammable fabrics. During 1965 – 1970, a Federal program was in place whereby 434 fabrics associated with burn injuries were tested[996]. Of those, only 5, or 1.2% failed the CS 191-53 (16 CFR 1610) method; this method is described in Chapter 7.

Fabrics are sometimes divided into those made of natural versus synthetic fibers. Cotton, wool, linen, silk and hemp are the dominant natural fibers, while synthetic fibers include nylon, polyester, acrylic, and a host of others. Rayon and cellulose acetate are made by chemical modification of natural materials, thus, they do not fully fall into either category. The earliest form of rayon fabrics were based on cellulose nitrate (see *Cellulose nitrate*). These were extremely flammable and such fabrics have not been made since the 1930s. The cellulose used today in making rayon fabrics is not nitrated.

Because of their light weight, the ignition of both charring and melting fabrics tends to involve complications. Most synthetic fibers (apart from acrylic and high-temperature fibers, e.g., Nomex) are thermoplastic. These types of fabrics generally show melting, drooping, and other large-geometry deformations prior to igniting. Thus, they may move out the igniter flame, if ignition is from a flaming source. If ignition is by radiant heat, the motion may change the effective heat flux that subsequently seen by the specimen.

Charring fabrics (e.g., cotton, wool) generally do not deform greatly prior to ignition. However, if heated slowly, they char and blacken, then possibly ignite in a glowing mode, prior to going into flaming ignition. In some unpublished testing on cotton fabrics using a hot air stream, the author found that the response to temperature of the test specimens was approximately as follows:

225 – 245ºC light brown
260 – 290ºC medium brown
300 – 340ºC dark brown/black
355 – 365ºC glowing ignition

Glowing ignition is readily recognizable as an abrupt turning red of a previously black place on the material. Often glowing ignition is highly localized, preferentially occurring at an edge or where fabric yarns have broken due to charring-induced tension. The temperature noted above is *not* the temperature of the glow, but the surface temperature of the material an instant before the glow appears; actual glow temperatures would be several hundred degrees higher. Under slow heating conditions, transition from glowing to flaming is highly unpredictable. In some cases, flaming occurs after only a slight additional heating (i.e., a surface temperature of 370 – 400ºC). But it may occur much later, when the surface is substantially hotter, or not at all, if the fabric is sufficiently consumed by means of glowing combustion. The above sequence of events appears to be relatively insensitive to the weight of the cotton fabric; however the temperatures reported should not be construed as minimum values.

Table 103 Ignition temperatures for fabrics measured in a modified Setchkin furnace

GIRCFF No.	Fabric type	Pilot ignition (ºC)	Auto-ignition (ºC)
4	cotton	280-290	280-297
9	cotton	297-290	297-308
18	cotton	278-294	301-311
5	cotton	301-311	301-327
10	cotton	339-351	429-443
19	cotton, FR	316-329	463-480
16	polyester/cotton, 50/50	353-360	466-473
1	polyester/cotton, 65/35	331-337	409-416
6	polyester/cotton, 65/35	337-345	409-416
8	polyester/cotton, 65/35	304-316	416-450
17	polyester/cotton, 65/35	368-384	463-480
15	polyester/rayon, 65/35	331-337	419-426
20	wool	316-329	463-480

Table 104 Ignition temperatures of various flame-retardant fabrics

Fabric	Ignition temperature (ºC)
cotton, FR	230
modacrylic	315
PVC	500
matrix (Kohjin, Cordelan)	500 – 540
wool, FR	570 – 595

Table 105 Fabric ignition temperatures reported by German investigators

Fabric	Piloted (ºC)	Auto-ignition (ºC)	Ref.
cellulose triacetate	325	490	1000
cotton	350	400	1000
	289	255	1001
Kynol	500	614	1000
Nomex	490	675	1000
	> 500	> 600	1001
nylon	390	510	1000
	354	425	1001
polyacrylonitrile	250	515	1000
	245	465	1001
polyester	390	508	1000
	372	485	1001
polyethylene terephthalate (Enkatherm)	560	637	1000
polypropylene	375	495	1000
	242	420	1001
polyurethane		415	1001
PVC	182	455	1001
Teflon		> 600	1001
wool	325	590	1000
	224	570	1001

Fabrics are perhaps the best example of a thermally-thin material. Thus, studies on fabrics may reveal, at least qualitatively, fire physics pertinent to other thin materials.

Charring or glowing of fabrics can be affected significantly by impurities present in the fabric, especially alkali metal ions. When cotton and similar fabrics are ignited in a flam-

Table 106 Effect of orientation on autoignition temperature of cotton/polyester fabrics

Fabric (cotton/polyester)	Autoignition temp. (ºC)	
	Horizontal	Vertical
100/0	< 500	< 350
50/50	500 – 550	375 – 400
35/65	500 – 550	400 – 450
12/88	500 – 550	400 – 450
0/100	500 – 550	400 – 450

Table 107 AIT values determined by Horrocks et al. in a tube furnace with an updraft

Fabric	AIT (ºC)
cotton	480
polyester	764
polyester/cotton (50/50 or 65/35)	574
silk, light	909
silk, heavy	655
wool	746

Table 108 Piloted (spark) ignition temperatures measured by Mórotz-Cecei and Beda

Fabric	T_{ig} (ºC)
cotton	278
polyester	379
viscose rayon	263
wool	310

ing mode, they typically do not burn for the entire burning time in a flaming mode, but later transition to glowing combustion.

See also: *Cotton*; *Fibers*; *Wool*. Oily rags are discussed under *Fibers covered with oil*. Ignitability of upholstered furniture and mattresses is considered under *Upholstered furniture*. Standard tests for fabrics are discussed in Chapter 7.

IGNITION TEMPERATURE

The ignition temperatures of fabrics, despite being studied by numerous investigators, are poorly known. The problem comes from the fact that very diverse results have been reported for the same fabric type, and it is not readily possible to ascribe these differences to peculiarities of the test method or the experimental technique. Consequently, the present section comprises a compilation of data from some of the better-known or more extensive literature sources, but none of the reported values should be viewed as definitive or as recommended.

The AIT[443] of several fabric types was reported by NIST in 1947 using a test method which was only described very sketchily, see *Wood* for details. The values given were: cotton 240ºC, nylon 475ºC, silk 570ºC, viscose rayon 280ºC, wool 205ºC. In 1949, Graf[997] reported on the autoignition temperatures of a number of fabrics. His typical values were: cotton 250ºC, linen 240ºC, rayon 300ºC, silk 232ºC, and wool 240ºC. His experimental technique, however, was poor (see *Wood*).

Wulff et al.[1032] conducted ignition tests in a modified ASTM D 1929 Setchkin furnace, with the modifications as described in Chapter 7. These results are shown in Table 103. For piloted ignition, there was little difference among the cotton specimens. But for autoignition, the differences were surprisingly large, apart from the FR cotton which would well be expected to diverge from other cotton specimens. The 'GIRCFF' numbers refer to a textile industry research program; the physical characteristics of these specimens have been studied in some detail[998], but ignition temperature differences are presumably due to chemical, not physical factors.

The NFPA Handbook[999] lists ignition temperatures for a number of FR fabrics and of fabrics that intrinsically resist high temperatures. These are shown in Table 104, but the measurement technique used to obtain the values is unknown. The temperature given for FR cotton seems questionable. Einsele[1000] and Rieber[1001] reported the ignition temperatures for a number of fabrics, using unspecified test methods (Table 105). Rieber's data for cotton are dubious, since a higher value is listed for piloted ignition than for autoignition.

Khattab[1002] studied the autoignition temperature of 25 × 25 mm fabric samples using a tube furnace. He found that higher ignition temperatures were recorded in the horizontal orientation than in the vertical (Table 106).

Horrocks et al.[1003] studied the autoignition temperatures of a number of fabrics in a vertical tube furnace, with the presence of an updraft. Their tabulated AIT values (Table 107) are notably high, as compared to values determined in other studies; this is presumably due to effects of the updraft.

Normal cotton fibers are about 95% cellulose. Davies et al.[199] conducted thermal analysis tests on cellulose purified from cotton (see *Cellulose*) and found that in a DTA apparatus autoignition occurs at 350ºC for a heating rate of 20ºC min^{-1}, going down to 290ºC at 1ºC min^{-1}. Repeating the experiments for cotton treated with a durable FR agent, they found[1004] an autoignition temperature of 310ºC at the 20ºC min^{-1} heating rate; a drop in ignition temperature is common for FR agents that work in the condensed phase. The ignition temperature of fabrics was studied by Mórotz-Cecei and Beda[1005] in a modified thermal analysis instrument which had been equipped for spark ignition, giving the results shown in Table 108.

Robinson et al.[1006] tested fluff created by grinding up rubberized cotton fabric and testing 'small samples' in a fur-

nace. No exothermic behavior was found at a furnace temperature of 200ºC; at 210ºC smolder could be initiated, but without visible glowing; at a 220ºC furnace temperature, glowing ignition was observed. The ignition temperature of white cotton terry-cloth towel was determined[1007] using the LIFT test to be 302ºC; as normal for reporting results from that test, the value is determined by a computation based on a theory and not by direct measurement.

FLAME IGNITION

A large number of studies are available on the flame ignition of fabrics, because burn injuries from clothing items most commonly occur when a flaming ignition source ignites the garment. Because of heat-sink effects, time to ignition is usually found to be proportional to the fabric's 'basis weight,' which is the mass per unit area (g m^{-2}). Exceptions commonly involve napped-surface fabrics such as terry cloth which are effectively 3-dimensional structures and less well idealized as being simply a plane sheet. Fabrics with napped or brushed surfaces may ignite much more readily than their weight might suggest, but such ignitions are sometimes only partial, that is, only the nap burns off and the base fabric fails to ignite.

A large ignitability study was performed at NIST on 58 fabrics in a wide variety of fiber types. The specimens were oriented at 45º and ignited by a small, diffusion flame from a butane burner. Apart from five that did not ignite (2 nylon, 1 polyester, 1 silk, 1 wool), the results are shown in Figure 71. The straight-line relation shown is:

$$t_{ig} = 0.0128\, w$$

where t_{ig} = ignition time (s) and w = basis weight (g m^{-2}).

A major study at FMRC[1008] gave the following conclusions concerning fabric ignitions from small flames of a laboratory burner:

- For most fabrics, ignition times did not change with fabric angle, for angles between 0º (horizontal) and 62º. The only exceptions were knit-brushed and terry cloth fabrics, which were much slower to ignite in the 0º position. (But note below that other researchers have disagreed).
- Ignition times were insensitive to flame height and burner tube diameter.
- For premixed flames, the equivalence ratio (normalized fuel/air ratio) had a significant effect, with fastest ignitions being near stoichiometric conditions.
- Ignition always occurred fastest when the luminous tip (for diffusion flames) or the tip of the inner cone (for premixed flames) was contacting the fabric. Ignition times increased when the flame was held closer or farther from the fabric than this distance.
- Premixed flames ignited fabrics about 2.5× faster than did diffusion flames. For very quickly ignitable fabrics (ignition times < 1 s with a diffusion flame), the ratio climbed even higher.
- Ignition times from a paper match were similar to ignition times when using a diffusion flame burner.
- A sizable fraction of thermoplastic-fiber fabrics tested melted but did not ignite when using a premixed flame burner; most of them did ignite when using the diffusion flame burner.
- Fabrics which had dissimilar front and back surfaces tended to show different ignition times for flames applied to back versus front.
- The presence of a skin-simulating heat sink close to the rear face of the fabric had only slight effects on ignition time.
- Fabric porosity did not affect the results.
- Over the range of RH values studied (15 to 85%), no effect was found of equilibrium relative humidity on the ignition time for thermoplastic fabrics. A minor effect was found for cotton and part-cotton fabrics, but this effect can become important in any particular test if the performance is otherwise borderline.

The FMRC ignition time data for cotton fabrics, when using a premixed methane flame could be predicted on the basis of the fabric weight as:

$$t_{ig} = 0.0055\, w$$

in other words, ignition was about twice as quick as found in the NIST tests for a diffusion flame. The FMRC correlation is restricted to cotton fabrics, since few thermoplastic specimens ignited when using the premixed flame burner.

Weaver[1009] conducted ignition tests using the CS 191-53 (16 CFR 1610) method (described in Chapter 7) with the modification that the flame was applied for varying lengths of time in 1-s increments. In his tests on cotton fabrics, he found a similar proportionality between the ignition time and the fabric weight. Corduroy and terry were the excep-

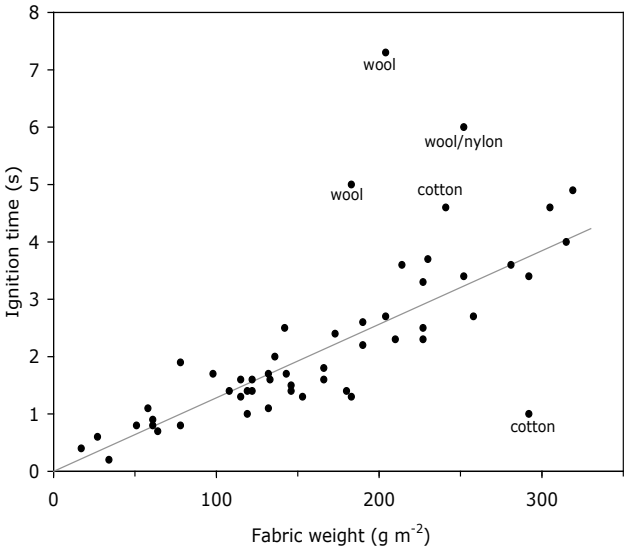


Figure 71 Ignition times for fabrics ignited with a small diffusion flame

Table 110 Results of ignition tests conducted by Irjala on bed linens

Fabric	Weight (g m^{-2})	NT Fire 037 Cigarette ign.	NT Fire 037 Butane flame	NT Fire 029 Butane flame Ign. time (s)
cotton	140	pass*	fail	2
cotton, FR (Proban)	175	pass*	pass	>20
cotton/polyester, 50/50	131	pass*	pass	2
cotton/polyester, 50/50, same as above, but used	138	pass*	fail	2
cotton/polyester, 50/50, satin stripes	152	pass*	fail	3
cotton/polyester, 50/50, satin stripes, same as above, but used	145	pass*	fail	2
polyester/cotton, 67/33	117	pass*	fail	2
polyester, FR	143	pass*	pass	>20
polyester/viscose, 67/33, FR	134	pass*	pass	2
* passed both cotton-sheet covered test and absorbent-cotton pad covered test				

tions to the general trend, igniting much faster than expected from their weight. Apparel cottons typically ignited in 1 – 2 s; twills, ducks, and denims ignited in 4 – 6 s; only one specimen out of 65 required more than 6 s for ignition.

Ward and Jaeckel[1010] tested a variety of fabrics by applying small flames to specimens oriented vertically, horizontally, and at 45º. For thermoplastic fabrics, ignition generally took much longer in the 45º orientation than for vertical or horizontal specimens. For cotton fabrics, the effect was unclear, since not enough data were collected. Not surprisingly, on the average, ignitions were fastest for the vertical orientation. In some tests, a flame is applied to the face of the cloth, while in others it is applied to the bottom edge of the fabric. A study[1011] showed that ignition times are roughly twice as long when the flame is applied to the face, as opposed to the edge. In some cases, ignition times are slightly different depending on the orientation of fabric, that is, whether the warp or the weft direction is placed vertically[1003]. Holmes[1012] pointed out that size of flame does not make much difference when igniting cellulosic fabrics, but that thermoplastic fabrics have a higher probability of ignition from a *smaller* flame, since a smaller flame is less likely to cause melting and retraction sufficient for the fabric to move away from the hot zone.

Durbetaki[1013] ignited clothing fabrics from the gas flame above a burner and examined the effect of the angle of the cloth. His results (Table 109) show that, with most fabrics, when the burner gas stream was not directly perpendicular, longer ignition times were found. For terry cloth, quickest ignition was at a 30º angle. This is due to the high pile structure of the cloth, which can 'capture' the gas stream.

Table 109 Results for fabric ignition times (s) from a gas flame

Fabric	Angle of cloth from horizontal			
	0º	30º	45º	60º
cotton denim, 296 g m^{-2}	4.0	5.1	7.3	--
cotton terry cloth, 265 g m^{-2}	3.7	1.0	1.9	2.6
batiste, 65% polyester/35% cotton, 86 g m^{-2}	1.2	1.8	3.1	3.8

Irjala[1014] conducted several Nordtest tests on bed linens. Her results are summarized in Table 110. The Nordtest NT Fire 037[1015] is a horizontal-test method that has three parts: cigarette ignition is tested in the horizontal orientation by placing the specimen on a mineral fiber board, placing a lighted cigarette on top, and covering it with (a) a cotton sheet; or (b) an absorbent cotton pad. Flaming ignition is tested by applying a butane flame for 20 s; ignition is reported if flaming continues for 150 s after removal of butane flame. Nordtest NT Fire 029[1016] is a 45º test slightly similar to CS 191-53. A flame is applied to the surface, near the bottom for varying lengths of time. If no ignition occurs for a 20 s application, ignition time is reported simply as greater than 20 s.

Injury from clothing textiles is often very serious because it takes a relatively long time for pain to be felt after the ignition of a fabric. Studies at FMRC[1017] showed that lightweight cotton fabrics ignited from a small flame in 1 – 2 s, but it took another 4 – 11 s before the wearer would have registered pain. By that time, flame spread may well have engulfed a large part of the garment and serious injury might be unavoidable. It has been suggested that this happens with cotton fabrics because, even though the thermally-thin assumption is generally reasonable, flaming commonly occurs on the outside of the fabric first, and does not break through to the inside until a sizable area has become flame-involved[1018].

A significant fraction of clothing ignitions occur when the victim, especially an elderly woman, is wearing a billowy-sleeve garment and is doing cooking on a gas stove. To address this issue, a possibly unique set of experiments[1019] was conducted by Gillette Research Institute. In these experiments, various fabrics were constructed in the shape of

Table 111 Burn injury from garment fabrics ranked according to fiber type, as proposed by Kadolph

Fiber type	Injury
FR types, various	least
wool	↓
nylon	
polyester	
acetate	
rayon	
cotton	greatest
acrylic	

Table 112 Burn injury from garment fabrics ranked according to fiber type, as measured by Bercaw and Jordan

Fiber type	Injury
FR types, various	almost none
nylon	
polyester	
wool	least
acrylic acetate	↓
polyester/cotton	
cotton	greatest

Table 113 Burn injury potential from garment fabrics potential, as determined in the MAFT test

Fiber type	Heat transfer rate ($kW\ m^{-2}$)
modacrylic	0.6
wool	0.7 – 1.3
heat resistant fibers: Nomex, Kynol, Kermel	1.0 – 1.8
wool, FR	1.2 – 1.6
cotton, viscose (FR)	1.8 – 19.3
nylon	4.4 – 5.1
polyester	4.1 – 5.7
cotton, viscose	4.4 – 38.8
polyester/cotton	19.2 – 28.7
acetate	26.7
acrylic	35.5 – 58.1

a sleeve and moved over a gas burner, maintaining various heights above the stove and times of exposure. Enough test runs were made so ignition propensity could be expressed as a probability of ignition. Fabrics which tend to melt and shrink performed well: polyesters showed nearly 0% probability of ignition, with nylon ranging 5-25% for a 15 s exposure. Wool showed a 30% probability for a 15 s exposure, while acrylic and acetate/nylon blends showed around 40%. Cotton, FR cotton*, and cotton/polyester blends showed very poor ignition performance, with most specimens showing an 85-100% probability for a 10 s exposure. Even at a 5 s exposure, these fabric types fared badly, with only a few heavyweight trouser fabrics showing less than 50% probability of ignition. Trousers, however, are rarely ignited on stovetops in actual incidents.

For applying ignition data to fire cases, it must be noted that ignition propensity is not the only factor affecting burn injury. Lightweight fabrics have the highest propensity to ignition. They also have the highest flame spread rate. However, their heat content is also the lowest, which means that at any given location such a material will present a briefer heat flux history to the skin, than does a heavier, slower-to-ignite material. In principle, a fabric could be so lightweight that it could burn up fully, yet not cause serious injury. In practice, Webster et al.[1020] estimated that a fabric would have to be 11 g m^{-2} or lighter in order to burn up without causing injury. This is not a viable weight for clothing textiles, since even a lightweight muslin is ca. 35 g m^{-2}.

In addition, it must be emphasized that while most thermoplastic fabrics are capable of being ignited by a small burner (e.g., as in the NIST study), this does not indicate that they will cause an appreciable burn injury. Arnold et al. conducted full-scale tests on dresses and concluded that nylon, polyester, and certain FR fabrics cannot sustain combustion, even when ignition is attempted with a large paper fuse[1021]. The question whether ignition leads to self-sustained combustion is a crucial feature of fabrics flammability, but is not incorporated into any standard test or regulation for fabric flammability. Based on further experimental work, Kadolph et al.[1022] proposed a rating scale (Table 111); her ratings are very similar to experimental observations of Krasny et al.[1023] and of Chouinard et al.[1024] These studies indicate that thermoplastic fibers which melt and pull away from the source of heat (such as nylon or polyester) are associated with low injury potential from garments. Conversely, acrylic fibers were found to be the most hazardous fiber type both by Kadolph and by Krasny. These plastic fibers, instead of melting and shrinking back, intumesce and burn in place.

Full-scale mannequin tests conducted by Bercaw and Jordan[1025], however, gave somewhat different results. Their testing, which used single-layer A-line dresses, gave the results shown in Table 112. Perhaps the most usable data are those obtained from NIST's Mushroom Apparel Flammability Test (MAFT) since they are measured quantitatively; some results[1026] are shown in Table 113. In some cases, an individual may wear cotton underwear, with a nylon or polyester outer garment. In that situation, there is no benefit from the melting behavior of the outer garment, and the two-layer combination can cause severe injury. Other heat transfer measurements were made by Chouinard et al.[1024], who measured the total heat transferred (as opposed to the heat transfer rate) to sensors located 6 mm

* It is noteworthy that the same FR cotton fabric which showed ignition behavior indistinguishable from non-FR specimens in the stovetop burner test showed "no ignition" results in Bunsen burner tests conducted at FMRC.

away from the back side of various fabrics. They determined that for cotton, acrylic, and wool fabrics:

$$q'' = (1.5 \text{ to } 2.1)W$$

where q'' = energy fluence (kJ m^{-2}), and W = basis weight (g m^{-2}).

The melting temperature of melting fabrics is invariably lower than the ignition temperature, and this is the main reason that melting fibers show relatively good performance with regard to burn injury. Table 114 shows some melting temperatures for various fibers[1001,1027]. But melting temperature alone does not determine whether the material will stay in place or fall off and the latter, as mentioned above, is an important factor.

Table 114 Melting temperatures of different fibers

Fiber	Melting temperature (ºC)
acrylic[a]	235 – 320
diacetate	255
modacrylic	160 – 190
nylon	160[b] – 260
polyester	252 – 292
polypropylene	164 – 170
PVC	100 – 160
triacetate	293
a – acrylics often shows no clear melting point b – value appears to be unreasonably low.	

Most ignition test methods used for fabrics are a variant of a Bunsen burner test, but there has been a very large variety of similar, but non-identical tests published by various standards bodies. The two mandatory Federal standards in the US concerning the ignitability of garment textiles are discussed in Chapter 7. Villa and Krasny[1028], Krasny[1029] and Carroll-Porczynksi[1030] reviewed a large number of other US and UK test methods. Vlot[1945] has reviewed laws and regulations governing the flammability of textile products from numerous countries.

RADIANT IGNITION

Radiant ignition occasionally occurs with garments, but is more important in other applications, e.g., theater curtains. Thus, a fair amount of research exists on this ignition mode. Wesson[1031] compared the piloted-ignition times for black and white fabrics using flame radiation and tungsten lamps. Since white fabrics have a low radiant absorptivity in the visible spectrum, but high in the infrared, the results (Figure 72) show that white fabric ignites more quickly when using a flame source than a tungsten lamp source. For black fabric, there was no detectable effect of radiation source. Wesson further showed that if the absorbed irradiance, rather than incident irradiance, were plotted on the x-axis, all of the data would collapse onto a single line. This data treatment will generally be impractical, however, since it requires having the complete spectral absorptivity curves of the test materials, along with the spectral characteristics of the radiant source. Wulff et al.[1032] studied the absorptivity of 20 different garment fabrics under two conditions: tungsten lamp source and infrared heater. For both sources, absorptivities were very low, typically 0.2, and higher than 0.26 in only 10% of the cases. This could be attributed to the diaphanous nature of most fabrics, with transmissivity typically being much greater than absorptivity.

Table 115 Piloted ignition times for terry cloth tested horizontally in the Cone Calorimeter

Heat flux (kW m^{-2})	20	30	45	60
Ignition time (s)	51	17	6.3	4.3

Table 116 Piloted ignition times (s) for fabrics tested at various heat fluxes in the Cone Calorimeter by Scudamore et al.

Fabric	Weight (g m^{-2})	Flux (kW m^{-2})			
		20	30	40	50
acrylic	400	52	28	16	19
wool	392	24	15	11	9

The piloted ignition of cotton fabrics exposed vertically to a radiant heat source was studied by Rangaprasad et al.[1033], who found a minimum heat flux for ignition of 12.6 kW m^{-2}. A white cotton terry-cloth towel was tested for piloted ignition in the LIFT test[1034]; it gave a minimum flux for ignition as 10 kW m^{-2} when tested with a non-combustible ceramic fiber backing board. Vodvarka[1035] conducted studies to determine the minimum radiant flux needed for autoignition of a muslin cotton bedsheet when exposed to quartz lamp radiation. He found a minimum flux of 40 kW m^{-2} was needed, but this dropped to 29 kW m^{-2} when a mattress was placed behind the bedsheet so it no longer received convective cooling on the unexposed face. Simms[1036] reported that 16 kW m^{-2} was needed for the autoignition of cotton cloth, provided that the exposed area was large (greater than about 0.05 m^2). For an exposed area of 50 × 50 mm, the value rose to 33 kW m^{-2}.

Ohlemiller conducted Cone Calorimeter tests on terry cloth and obtained the results shown in Table 115. Scudamore et al.[1673] tested two fabrics for piloted ignition in the Cone Calorimeter. The specimens were oriented horizontally, but further test details were not specified. The results are shown in Table 116. Holbrow et al.[1037] tested the autoignition of various fabrics in the Cone Calorimeter. The specimens were backed with 13 mm thickness of ceramic fiber blanket. Their results are shown in Table 117.

Mowrer[1038] explored the autoignition of several fabrics using the Cone Calorimeter in the horizontal orientation. Fabrics were desiccated then stretched over a dead air space. His results are shown in Table 118.

Table 117 Autoignition times for fabrics tested at various heat fluxes in the Cone Calorimeter by Holbrow et al.

Fabric	Flux (kW m^{-2})		
	35	50	75
disposable overalls	NI	23	12
nylon	NI	NI	13
polyester	NI	NI	10
polyester/cotton	NI	42	5
polyester/cotton, soaked in diesel fuel	NI	6	2
polyester/cotton, soaked in solvent	1	1	< 1
polyester/cotton, FR	NI	100	19
polyester/cotton, FR, soaked in diesel fuel	15	6	3
polyester/cotton, FR, soaked in solvent	2	1	1
wool	NI	NI	11
wool, soaked in diesel fuel	233	14	7
wool, soaked in diesel solvent	7	3	1
NI – no ignition.			

Table 118 Minimum flux for autoignition of various types of cotton fabrics

Fabric type	Basis weight (g m^{-2})	Min. flux for ignition (kW m^{-2})
cheesecloth	40	45.3
surgical cotton	72	25.2
canvas	273	16.2
blanket	285	22.2
towel, beige	356	17.9
towel, white	366	25.1

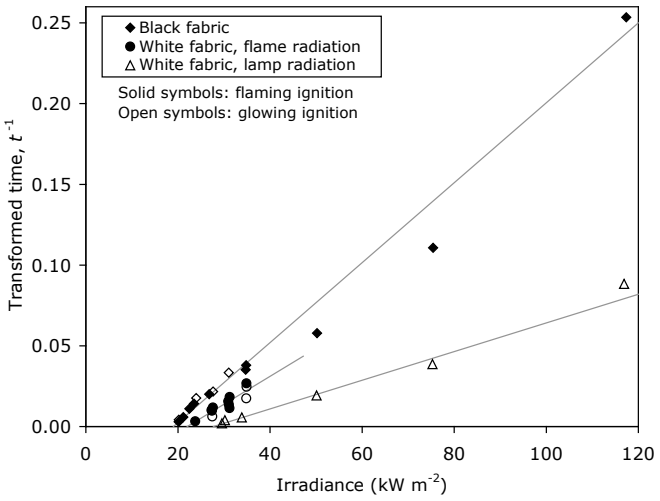


Figure 72 Effect of fabric radiant absorptivity (color) and radiation source type on the piloted ignition of cotton fabrics

Researchers at Japan's NRIFD reported an interesting study on fabrics in the Cone Calorimeter[1039]. They used the horizontal specimen orientation and the stretcher frame developed at NIST for testing fabrics over a dead-air space. Fabrics in the range of 70 to 538 g m^{-2} were tested. All fabrics ignited at a heat flux of 50 kW m^{-2}, one fabric (a 70 g m^{-2} nylon) did not ignite at 35 kW m^{-2}, while 4 fabrics did not ignite at 20 kW m^{-2}: the above nylon; a 77 g m^{-2} FR nylon; a 115 g m^{-2} polyester lace fabric; and a 118 g m^{-2} FR polyester lace. In addition, at 35 kW m^{-2}, the non-FR polyester lace ignited in only 1 of 3 trials. These results appear to be related to basis weight, since the 4 fabrics failing to ignite at 20 kW m^{-2} were the 4 lightest fabric samples examined. Times to ignition at 50 kW m^{-2} were very short (< 7 s) for most specimens, except the lightest and the heaviest. The specimens taking more than 7 s to ignite were the two lightweight polyester lace fabrics, plus a 409 g m^{-2} rayon and a 538 g m^{-2} FR rayon. Details of the ignition are not provided, but it may be that the very lightweight thermoplastic lace fabrics shrink and melt together at the edges, and only ignite there. If so, this would explain a long time to ignition, since the effective thickness of such a molten glob would be much greater than for the initial fabric.

Table 119 Ignition times (s) for autoignition of fabrics subjected to radiant heating from both sides

Fabric	Weight (g m^{-2})	Flux (kW m^{-2})	
		34	42
cotton	217	3	1
Kynol	159	7	2.5
Nomex/Kevlar, 95/5	180	35	21
PBI	153	25	19

Table 120 Electric arc energy fluence (kJ m^{-2}) needed to ignite various cotton fabrics

Fabric	Weight (g m^{-2})	Probability level			
		1%	10%	50%	90%
twill, blue (shirt)	176	209	238	265	289
twill, blue (shirt)	190	234	289	335	381
twill, black	234	289	310	331	347
twill, blue (shirt), over 156 g m^{-2} white jersey knit T-shirt	163	201	268	331	393
fleece, white (shirt)	316	389	448	502	556
sateen, white	400	493	607	711	816
duck, tan	414	510	628	736	845
denim, blue (pant)	546	673	736	795	849
denim, blue (pant)	570	703	753	799	845

The NRIFD researchers conducted all their tests with an unusual arrangement: underneath the fabric they placed a layer of aluminum foil (Figure 73). Thus, the tested specimens were a fabric-foil "sandwich," which was then stretched over the dead-air space in the specimen holder. This was done because they reported[1040] getting generally no ignitions without a foil backing; it is not clear how many fluxes or specimens were tried in the no-foil condition. The interpretation of such results is not necessarily obvious. Fabrics are porous substances and the lightweight ones are visibly porous. Possibly radiation reflected from the foil then serves to simultaneously heat the back face of the specimen. The flow of pyrolysis gases is also clearly affect-

ed, although this is harder to interpret. In any case, it is not very clear whether such results are applicable to any end-use situations.

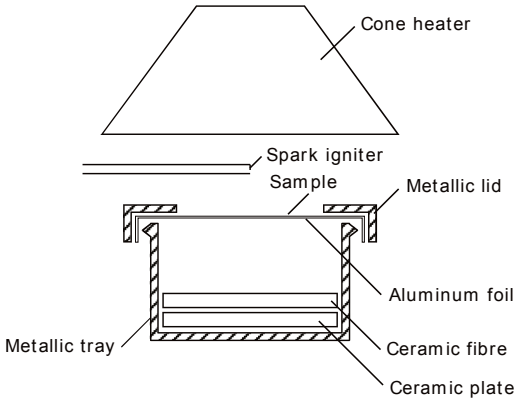


Figure 73 Arrangement for testing fabrics in the Cone Calorimeter used by researchers at NRIFD

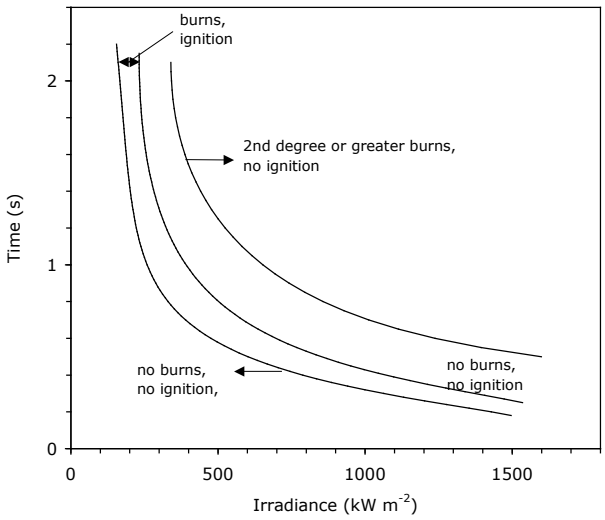


Figure 74 Regimes of radiant ignition found by Mixter for shirt fabric + underwear fabric system

Schopee et al.[1041] tested fabrics for autoignition with an unusual radiant heat apparatus where the specimen was simultaneously exposed by heaters from both sides. Their results are given in Table 119.

Wu et al.[1042] tested the ignitability of protective Army clothing by radiant heating. In their tests, two-layer (Nomex/Kevlar outer layer, aramid waffle-weave underwear) samples were tested on top of a block which has thermal properties roughly similar to human skin. At a flux of 84 kW m^{-2}, without a pilot there were no ignitions during the maximum exposure time of 10 s. Using a gas pilot, no specimens ignited for a 4 s exposure, but when exposed for 6 – 10 s, ignition did occur, but flaming was not sustained upon removal of the pilot.

Ward and Jaeckel[1010] studied the ignition of fabrics placed vertically 7 mm away from a radiant heater of unspecified heat flux. They found that cotton and FR cotton (but the FR cotton specimens ignited much faster than the non-FR) ignited in a few seconds, while cellulose triacetate, secondary cellulose acetate, acrylic, polyester/cotton blend, and all thermoplastic fiber fabrics did not ignite at all.

The clothing of electricians sometimes ignites when a high-current electric arc is caused in switchgear. Doughty et al.[1043] used an electric arc test apparatus to determine the energy needed to ignite cotton apparel fabrics of the kinds commonly used by workers. Their results are given in Table 120.

Under intense radiant heating, a fabric may be so rapidly pyrolyzed that sustained flaming becomes impossible. Mixter[1044] studied this phenomenon by exposing fabric systems comprising a cotton shirt fabric on top of an undershirt material to radiant heating from a carbon arc. Figure 74 shows that four regimes were found in this work:

- at lowest fluxes—no ignition, no burns
- at higher fluxes—ignition, burns
- at higher yet fluxes—no ignition, no burns
- at highest fluxes—no ignition, but burns occur.

This phenomenon, which is relevant only to very high heat fluxes, has not been studied for other fabric systems, so the results of Mixter should be viewed only as indicative. Burns are avoided in the third regime due to the endothermicity of the pyrolysis process.

CONVECTIVE HEATING

Hinkley et al.[196] conducted experiments on vertically-oriented white cotton fabric (120 g m^{-2}) by impinging an air stream from a hot-air blower onto the fabric. Their results are given in Table 121. Air flow velocities were not measured. It was found that fabrics ignited convectively by a hot air stream ignite substantially faster when oriented horizontally than when oriented vertically, but a general quantification of the effect was not undertaken[1045]. In another study[1046], it was found that cotton fibers (not woven into fabric) autoignited in a hot air stream at less than 370ºC.

Table 121 Autoignition of cotton fabric from a hot-air blower

Distance from outlet (mm)	Hot air temp. (ºC)	Ignition time (s)
25	876	3.1
51	849	3.5
76	705	5
102	545	17
114	470	N.I.

OTHER FORMS OF HEATING

It is extremely unlikely that a cigarette would ignite (either flaming or sustained smoldering) an item of clothing[317,1047]. This includes even fabrics which fail the CS 191-53 test. It was also found that a variety of contaminants (laundry softener, oily soil, cigarette ashes, and an ethanol/water mixture) placed on fabrics could not induce flaming from a cigarette[1048]. Smoldering which can later turn into flaming was found possible only in massed layers of fabrics, such as in storage. Smoldering ignition of folded denim clothing has been reported upon placing a lighted cigarette within the folds; in one test smoldering transitioned to flaming at 28 minutes[304].

Large burning wood brands (38 × 38 mm) readily ignite denim, burlap, gunny sack, and similar heavy cotton fabrics[1049]. For somewhat smaller wood brands, ignition probability is highly dependent on wind conditions. Lighter fabrics, such as broadcloth cotton shirt fabrics and wool fabrics, tend to burn through without sustained ignition, unless backed by some insulating material. Even with backing, they tend to resist ignition from smaller wood brands. However, it is rare that brands this large would land on persons. The hazards of burning wood brands only a few mm in size appear to be negligible. Molten copper ejected from a high-current electric fault has caused ignition of workers' clothing[1050]. Impact sparks and welding sparks (slag) have been documented to ignite clothing of workers, leading to fatal injuries. Molten material from arc welding will readily burn holes through clothing, but actual flaming ignitions are rare, and no laboratory study appears to exist of this topic.

Table 122 Hotplate ignition temperatures of some fabrics

Fabric	Temp. (ºC)
cotton	400
acetate	525
nylon 6	530
triacetate	540
acrylic	560
polypropylene	570
wool	600
modacrylic (Teklan - polyacrylonitrile/ polyvinylidene chloride, 50/50)	690

Table 123 Glow-bar ignition temperatures of some fire-improved fabrics

Fabric	Weight (g m^{-2})	Temp. (ºC)
cotton	155	< 820
FR cotton	155	820
Nomex (aromatic polyamide)	170	800
Nomex	220	850
Kynol (phenolic based)	240	790
Fypro (modified polyamide)	145	860
polybenzimidazole (PBI)	165	930

Hot-surface ignitions of fabrics have been studied by several workers. Sayers[1051] tested a number of fabrics by dropping specimens onto a hotplate. His results are given in Table 122 and these are not too different from ignition temperatures determined by other means. Kaswell[1052] tested some fire-improved fabrics by pressing a glowing metal bar against the fabric; his results are given in Table 123. Ward and Jaeckel[1010] attempted igniting various fabrics with a heated metal bar of an unspecified temperature. They found that cotton, FR cotton, secondary cellulose acetate, and cellulose triacetate specimens ignited, while wool and thermoplastic fiber fabrics did not.

Ignitions of fabrics from electric burners has been studied[1053]. No fabrics ignited when exposed to a burner at 370ºC (visible radiation is not seen at this temperature). For the two higher temperatures used, results are given in Table 124. Ignitions, when they did occur, took from 1 s to 30 s, with the exception of a single specimen that took 56 s. The results indicate that 100% thermoplastic fabrics are unlikely to ignite from an electric burner, but that cellulosic and part-cellulosic fabrics will usually ignite if brought into contact with a burner running at its high-heat setting. They may also ignite if held a short distance above such a burner.

Data on thermal exposures to parachutes from burning-aircraft fireballs have been analyzed by Thielman[1054], who also reports some tests on nylon, Nomex, Kevlar, and

Table 124 Ignition of fabrics from electric burner

Fabric	Maximum height above burner (mm) at which ignition occurs	
	510ºC (dull red)	590ºC (bright red)[c]
cotton, plain-weave, 306 g m^{-2}	0	5
cotton, plain-weave, 297 g m^{-2}	NI	0
cotton, flannel, 408 g m^{-2}	0	5
cotton, flannel, 422 g m^{-2}	0	0
polyester/cotton (65/35), plain-weave, 325 g m^{-2}	NI	0
polyester/viscose (52/48), plain-weave, 330 g m^{-2}	0	a
polyester/cotton (62/38), twill, 760 g m^{-2}	0	0
polyester/cotton (48/52), twill, 747 g m^{-2}	0	b
polyester, plain-weave, 185 g m^{-2}	NI	NI
polyester, plain-weave, 408 g m^{-2}	NI	NI
nylon 6,6, tricot, 320 g m^{-2}	NI	NI

NI – no ignitions
a – No ignitions for fabric touching burner; 1 out of 5 specimens ignited when 5 mm of fabric draped over burner.
b – No ignitions for fabric touching burner; 5 out of 5 specimens ignited when 5 mm of fabric draped over burner.
c – It is not clear if the temperatures were measured correctly, since a radiant source at 590ºC is not normally perceived as "bright red."

polybenzimidazole (PBI) parachute fabrics. Ignition of fabrics from nuclear weapons detonations has been studied by the Naval Applied Research Laboratory[1055].

Self-heating of (unoiled) fabrics is possible, although the temperatures and sizes involved preclude this from being a concern except at industrial processing establishments. Smedley and Wake[1056] reported on a study of a wool/nylon fabric which had led to a factory fire. Spontaneous combustion was found possible for a pile 0.85 × 0.6 × 0.49 m, if stacked at a hot-work temperature of 120ºC. Franke et al.[45] described a fire in a drum dryer used in the making of textiles from recycled fibers. This was found to be due to self-heating promoted by the use of 'unsuitable' spinning oils. They also documented fires repeatedly occurring in a vertical dryer used to dry nylon fibers at 165ºC. Glowing clusters of material would form, then drop down to ignite bulk material. They found out that if nylon fibers are rapidly heated, they melt upon reaching around 215ºC but do not show self-heating. But if heated slowly at 130 – 170ºC, the fibers char instead. Oven-basket tests of 100 mm cubes of the aged, charred material showed a critical temperature less than 170ºC; open flaming was not found, but glowing clusters did form.

ELEVATED OXYGEN CONDITIONS

In one case, an electrostatic spark from a workman who was wearing rubber-soled shoes ignited his trousers in oxygen-rich atmosphere[26]. In another case, the clothes of two workmen ignited with fatal consequences when they entered an environment where an oxygen-acetylene cutting torch had been used 2 days earlier and started up their torch[26]. For proper cutting, the torches release more oxygen than is actually reacted and the surplus oxygen can accumulate within a confined space. A confined environment is not necessary for ignitions of this type to occur. In one case, a workman died from ignition of his clothing when he was repairing a liquid oxygen tanker in the open air. There was a gaseous oxygen leak at the other end of the vehicle, but the exact cause why his clothing ignited was not established[26]. An insidious hazard of clothing fabrics when used by workers exposed to oxygen-enriched atmospheres (or to liquid oxygen) is that fabrics may retain a fairly high concentration of oxygen. It is reported that periods of up to ½ hour should be anticipated, and a number of industrial accidents have been documented when the oxygen-retention capability of fabrics was ignored[1057].

Voigtsberger[1058] studied the ignitability of a wide array of fabrics from electric spark discharges. He found that at 21% oxygen no fabric—clean or dirty—could be ignited, although some became locally singed or melted. Using a 100% oxygen atmosphere, however, nearly all clean specimens could be ignited with 193 J spark. Only silk, polyester, and nylon resisted ignition. Even at 0.45 mJ, 6 out of 17 specimens ignited. When dirty (oily), however, all of the fabrics ignited even from the 0.45 mJ spark. Repeating the tests with mechanical sparks produced from pressing a carbon-steel piece against a corundum grinding wheel, he found that no specimens ignited in 21% oxygen (although most were singed), but that all ignited in a 100% oxygen atmosphere, and it typically took only 1 s for ignition to be achieved. Fitt et al.[1059] undertook to reproduce Voigtsberger's experiments and discovered the crucial roles of two factors not treated by Voigtsberger: (1) the oxygen flow rate; and (2) spark duration. Increasing the flow through the experimental rig from stagnant to a high, but unspecified, velocity decreased the required energy for ignition by about a hundred-fold. Short-duration sparks were found incapable of igniting solid materials, simply because of inadequate time during which heat was being supplied. They only explored circuit parameters to a limited extent, but found that optimum spark duration was in excess of 100 ms. Plano[1060] conducted tests in a 100% oxygen atmosphere using 90 mJ sparks and determined a statistical probability of ignition for various fabrics: PVC 20%, wool 20%, tissue paper 10%, nylon 33%, PET/cotton 1%, cotton muslin 1%. Guest[1061] conducted tests in atmospheres of 52 – 64% oxygen and was unable to obtain any ignition of clean materials, but oily cotton could be ignited by 2.5 mJ sparks. Purser[1062] examined hyperbaric oxygen conditions and found that at 3 atm it was easier to ignite all materials than at 1 atm, but sufficient tests were not run to develop quantitative trends. A study[1063] has shown that for many fabrics, increasing the oxygen concentration beyond about 40% results in a very rapid increase in flame spread rate, which would presumably be reflected as increased injury potential.

EFFECTS OF TREATMENTS

Even small amounts of treatments can greatly affect the ignitability of fabrics. For instance, use of finishing agents, such as melamine resins or polysiloxanes, was found to make polyester fabrics ignitable that otherwise resisted ignition[1064].

Fire-retardant treatments are occasionally used for fabrics, although only in specialized applications, not for general wearing apparel. General principles of fire retardants for use with textiles has been reviewed by Gordon[1065]. Khattab et al.[1066] examined the effect on autoignition behavior of several water-soluble FR treatments for cotton fabrics, as tested in a crucible apparatus. A minimum loading of ca. 5 – 8% was found to be needed for useful improvement of ignition behavior. Smaller amounts of FR agents had no effect or even a deleterious effect. Reeves and Smitherman[1011] studied the effect of several different, non-soluble flame retardants added to cotton and cotton/polyester fabrics. For flame ignitions at both edge and surface, the effect on ignition time of the FR agent was negligible until some critical add-on percentage (typically 15 – 30%) was attained. For larger add-on values the effect was notable, but the authors only described these results as "ignition time > 3 s" rather than quantifying them. A handbook of fire-retardant formulations for fabrics was published by Reeves

et al.[1067] in 1974. While old, this collection describes in much detail the fire retardants available in that era.

Farm machinery

Striking of rocks with the cutter head of a combine can result in a field fire and some of these can be sufficiently rapid to destroy the combine itself. Other ignition modes include combustible debris on exhaust systems, leaking oils and hydraulic fluids, and electrical failures. Tracked equipment operated laterally on steep hillsides sustain large friction forces that may cause shearing off of hot metal particles.

Feedstuffs

A fire was reported due to spontaneous combustion of pallet-loads of stored bone meal, used as an animal feedstuff[1068]. Accompanying tests demonstrated the self-heating potential, but predictive constants were not evolved. See also: *Agricultural products*.

Felt

A 19th century treatise[1802] reports numerous fires that occurred due to self-heating of felt. Its use in today's economy is more limited and recent investigations do not exist.

Fertilizers

Most fertilizers are relatively resistant to ignition and applying a flame to a fertilizer will generally not result in combustion or other exothermic reactions. But some formulations, especially those containing ammonium nitrate, can undergo exothermic decomposition. The term 'compound fertilizer,' means that it contains ammonium nitrate and potash or a phosphate. If it contains all three, then the designation NPK is used (N = nitrogen, P = phosphorus, K = potassium).

Kiiski[1069] has summarized 11 major case histories involving decomposition of large quantities of fertilizers. The ignition source in these cases was typically a hot lamp or a welding spark. In most incidents involving decomposition, it was considered that a source of ignition was present, and that decomposition incidents were not solely due to self-heating. But when organic material is present in the mixture, then oxidation also becomes possible, not just thermal decomposition. At least one incident is reported of a true self-heating ignition for mixtures containing organic material[1073]. Médard[26] reviewed a number of fires associated with fertilizer production, storage, or shipping facilities. Self-heating was more of a problem in the 1960s and '70s, when the first compound fertilizers were introduced, than it is today. Improved understanding of the solid-state reactions, measures implemented to control the pH, and precautions in production facilities to prevent the transport of hot material (exceeding 50ºC) into storage all helped to reduce losses.

If a fertilizer mixture contains organic matter, not just nitrates, superphosphate and other inorganics, the potential exists for thermal runaway due to an exothermic oxidizing reaction between the nitrate and the organic matter. The tendency to self-heating is proportional to the acidity of the fertilizer—those with pH > 3.5 tend to have a reduced self-heating propensity, while for pH > 4.5 self-heating is unlikely[1075]. Adding sufficient ammonia to the mixture to neutralize it is an effective strategy, as is adding a material such as cyanamide which will liberate ammonia when heated. Lime or dolomite is sometimes added, but this is not the best strategy, since their reactivity is poor. Urea is commonly added to suppress self-heating. The hazard from ammonium nitrate is that it readily decomposes into ammonia and nitric acid, initially under the action of free phosphoric acid and, after some self-heating has occurred, due to thermal decomposition. Even though ammonia is being evolved in this process, with excessive free phosphoric acid present, the proportions are such that the resulting mixture's pH is excessively low. Nitric acid, a very powerful oxidizer, then acts on the organic matter, with the reactions being highly exothermic. For the latter process, there are various reaction variants possible, since the nitrogen may go into a variety of nitrogen-containing reaction products. Fertilizers containing more than 70% AN behave differently in that they normally melt; as the supporting matrix for decomposition is not present, the melting produces an endothermic effect and in most cases the decomposition stops. But if the melt flows to confinement (e.g. drains) and excessive heat is present, an explosion may occur. Raising the pH may not be feasible with some formulations, due to solubility problems of phosphates[1072].

Various organic substances have different potential towards contributing to thermal runaway. Unfortunately, most of the practical fertilizer components are of the problematic type. This includes activated sewage sludge, animal and garbage tankage, brown rotten wood, cane sugar, castor pomace, cocoa shell meal, cornstarch, cottonseed meal, dextrose, fishmeal, ground burlap, ground cork, ground Kraft paper, lignin, millet seed, oak heartwood, peanut-hull meal, peat, sawdust, soybean meal, and tobacco stems. Only dried blood, casein, ground filter paper, egg albumen, and lampblack were found to be less problematic. Fertilizers containing no carbon are not susceptible to self-heating[26], but practical source materials are rarely carbon-free.

The addition of ammonia during the compounding of a fertilizer in order to neutralize the mixture is itself an exothermic process. Thus, care must be taken that this be done under conditions such that the mixture has cooled down before being aggregated into large piles.

The modeling of the self-heating behavior of fertilizers has been attempted using the F-K theory of Chapter 9, but the efforts indicated that a much more complex model needs to be constructed in order to obtain realistic values[1075]. The problematic effects included multiple reactions, high variations in thermal conductivity, water transport, and melting. However, the modeling also indicated that while the F-K

theory cannot be applied correctly, results are empirically correlatable in the form of a graph where $1/T$ is plotted on the x-axis and $\ln(r_c)$ on the y-axis, where T is the temperature (K) and r_c is the critical radius (m). For example, Huygen and Perbal[1070] gave oven-basket self-heating data for a 12-13-6 fertilizer from which $E = 144$ kJ mol^{-1} and $P = 61.7$ may be derived. The problem with the application of such plots to real-life problems is that, lacking a theoretical justification, only modest extrapolations can prudently be made.

Self-sustained decomposition of a fertilizer requires[1070] that three ions be present: NO_3^-, NH_4^+, and Cl^-. This is a commercial concern, since chlorine is a commonly incorporated in a fertilizer by adding potassium chloride. The primary decomposition reactions are:

$$NH_4NO_3 \rightarrow NH_3 = HNO_3$$

$$NH_4NO_3 \rightarrow N_2O + 2H_2O$$

$$5NH_3 + 3HNO_3 \xrightarrow{Cl^-} 4N_2 + 9H_2O$$

The chlorine acts as a catalyst and is not consumed in the primary decomposition reactions, although numerous secondary reactions then take place wherein chlorine is consumed. Cobalt or chromium can play a similar role as chlorine. The actual exothermic event that takes place depends on the physical nature of the fertilizer. Decomposition generally starts at about 230ºC and products which melt below that temperature undergo 'liquid fume-off.' This is a violent reaction but liquid fume-off requires that a large amount of product first be melted, typically by an external fire. If the product does not melt before the decomposition temperature is reached, then 'cigar burning' can take place, which is an exothermic zone propagation within the solid material[1071]. Cigar burning can be started by a small ignition source, resembles smoldering combustion, and is non-explosive in nature. The temperature of the reaction front[1069] is about 300 – 500ºC, but in the presence of organic materials, it can exceed 1000ºC. Small amounts of copper are synergists to the reaction. The main hazard is high toxicity of the combustion products. The fertilizer industry sometimes describes mixtures prone to 'cigar burning' as 'capable of undergoing self-sustained decomposition.' A chlorine amount as small as 0.003% has been found sufficient to catalyze the decomposition reaction[1072]. For various primary fertilizer ingredients (e.g., NH_4NO_3, $NH_4H_2PO_4$, KCl, etc.) stability diagrams have been prepared[1069,1070,1072] which show the relative proportions that may lead to liquid fume-off, cigar burning, or no sustained self-decomposition. These types of diagrams alone do not fully express the hazardous regimes since, in some cases adding an inert substance such as diatomaceous earth can cause a fertilizer which would otherwise be in a non-burning regime to enter into the cigar-burning regime[1070]. This appears to be a physical effect having to do with absorbing liquid reaction products.

International and national shipping regulations for ammonium nitrate/ammonium sulfate fertilizers have varied over the years, but it is typically recognized that mixtures with less than 45% ammonium nitrate are of lowest hazard (although these are not automatically to be considered safe!), mixtures of 45 – 70% ammonium nitrate are of similar hazard to AN itself, while mixtures containing over 70% AN are more hazardous than pure AN[26]. Experiments have shown[1073,1074] that ammonium nitrate is more hazardous than sodium nitrate or potassium nitrate. It is commonly considered[1075] that compound fertilizers will not exhibit criticality if the ammonium nitrate content is below 15%. Fertilizers without AN are considered not to present an explosion hazard. A specific UN test for fertilizers—Test S1, the trough test—is discussed in Chapter 9. Kiiski tested a variety of fertilizer formulations using a modified UN Test S1 (trough test) and found temperatures of 210 – 310ºC to be the minimum needed for ignition. Unfortunately, he did not specify the layer depth, so the results cannot be quantitatively compared to other studies. Additional information is given under *Ammonium nitrate and ANFO*.

Fibers

Various fibers of both animal and vegetable origin are susceptible to self-heating. These include cotton, flax, hemp, shoddy, silk, and wool. Systematic differences in propensity are observed between the two classes, however. Vegetable fibers are hollow and they consequently tend to absorb oxidizing foreign material. Once ignited, vegetable-origin fibers tend to burn more vigorously than ones of animal origin. Also see: *Cotton; Fabrics; Jute; Marijuana and hemp; Wool.*

Fibers covered with oil

For self-heating to occur due to oxidation (some substances undergo non-oxidative exothermic reactions), a ready supply of air is necessary. This is not possible, for instance, with a bucket of linseed oil, since oxygen is only accessible at the surface. A rag covered with linseed oil, however, presents a very large surface where there is contact between air and oil. While it may be very difficult to actually measure the exposed surface area of an oil-covered rag, nonetheless it is clear that the surface/volume ratio is orders of magnitude greater than that for the bucket. The minimum amount of oil or of cloth needed to lead to spontaneous combustion in a room temperature environment has not been precisely explored, but it is reported that 25 g of cloth may give marginal conditions and 75 g of cloth a higher probability[445]. The optimum mass of oil is about 100% of the mass of cloth. A very old study[2056] suggests that 5% of oil by weight may be sufficient, but there has not been a recent study exploring this point.

Self-heating propensity is generally proportional to the degree of unsaturation of the oil, since this increases the ease of oxidation. Mineral oils are normally significantly less prone to causing self-heating, since they are not readily oxidizable, however Monakhov[1076] points out that petroleum products such as mineral oil, bitumen, and asphalt can self-heat when applied onto fibers. Thompson also reported

spontaneous combustion in mineral-oil soaked cotton, but he had to start at 150ºC instead of 100ºC in a modified Mackey tester to elicit the behavior[1082].

The effect of the type of fibers may be expected to have some effect on self-heating potential, but this is a second-order effect and has been explored only to a limited extent. Early studies by Mackey[1077,1078] on the effect of fiber type provided contradictory results. Cotton fibers in contact with fatty oils are more susceptible to self-heating than fibers of animal origin. Fibers of mineral origin, e.g., rock wool, are the least conducive to self-heating. Spontaneous combustion of linseed-oil soaked steel wool has readily been created in the laboratory[1079]. If self-heating ignition is to occur, rags soaked in boiled linseed oil need to be loosely packed. Laboratory tests have demonstrated that tightly-packed linseed-oil soaked rags tend not to reach runaway conditions[1080].

In view of the difficulties in realistically recreating the packing conditions of oil-soaked cloths, it may not be surprising that not much data have been published giving example values. Gross and Robertson[109] determined self-heating data for various oils soaked into cotton gauze (Table 125). They used a weight of oil equal to 1/6 the weight of cotton, so the condition most conducive to self-heating (about a 1:1 ratio) was not captured. An old study cited by Ellern[1407] gives Q = 962 kJ kg^{-1} for linseed oil, but it is not clear if this is a reliable value.

The data of Gross and Robertson are of limited practical interest because of the very low loading of oil used. But if it is assumed that the most hazardous loading of oil is 100% of the mass of cloth, and if the estimation method is used whereby the heat of reaction, Q, is taken to be proportional to the fraction of oil, then the Q must be multiplied by (6+1)/(1+1) = 3.5 to estimate the worst-case condition. Making this adjustment, the new value of P estimated is 50.8. Note, however, that Gross and Robertson only tested raw linseed oil, but in most wood-finishing applications boiled, not raw, linseed oil is used. Horrocks et al.[1081] conducted oven cube tests on cotton fabric soaked in vegetable oils. They only applied small amounts of oil and conducted tests solely in 102 mm size cube baskets. For both cottonseed and rapeseed oil, at a 10% loading of oil, the critical temperature was ca. 100ºC, while for a 5% loading it was ca. 140ºC. Thermal runaway generally took 1 – 3 h. Thompson studied linseed oil soaked cotton in a modified Mackey test, where 30 g of oil was applied to 30 g of cloth[1082]. His research indicated that the reaction is auto-catalytic, rather than following a simple first-order Arrhenius form. More modern data on this question are given in the section on *Oils*.

On a practical note, Taradoire[1083] found 75 g of cotton rags soaked in the same weight of linseed oil typically went to flaming in 1 to 6 hours, and that there was a strong acrid odor shortly before eruption of flaming. Browne[1172] soaked 50 g of cotton in 50 g of raw linseed oil to which 5 g of cobalt oleate had been added, effectively simulating boiled linseed oil. The temperature rose to 400ºC in 1.5 h, at which time flaming occurred "when a gentle air blast was applied." In another test[1084], one cotton towel and 16 paper towels were coated with linseed oil and bundled up. A flaming fire erupted in 90 min. Zicherman[1085] studied linseed-oil soaked rags which were dropped into open-top cardboard boxes. He found that there was a great deal of data scatter—a number of tests using 24 rags failed to go to thermal runaway, while other tests using only 10 rags did. Thermal runaway took 4 – 10 h, in the cases where it occurred; it was always preceded by copious, highly acrid smoke. In most cases, thermal runaway was not followed by overt flaming, even though the aftermath was a pile of black-charred residue. DeHaan[1086] found that waste containers filled with linseed-oil soaked cotton rags developed smoke and acrid odors in about 1 h. Eruption into flaming then followed after another 4 – 14 h. In a test[1087] where 100 g of jute fiber was soaked with 25 mL of raw linseed oil and 3 mL of a drying agent (together, those two ingredients were used to simulate boiled linseed oil), ignition occurred in 2 h from a starting temperature of 27ºC. Cloths soaked in a linseed-oil based stain ignited in 4.25 h and flamed for about 0.5 h in another test[1594]. Another author[1088] reported that it typically takes 4 – 8 h for flaming to erupt, but also documents one test where it took 31 h for ignition to occur after a floor mop soaked in a linseed oil based preparation was wrung out, rinsed, and hand-washed. A fire incident where the time interval was 19 hours has been reported[1089]. In cases where there is doubt if a drying oil was involved, it is often possible to analyze the fire debris for fatty acid residues; this is discussed under *Dryers and washers*.

The propensity of linseed-oil soaked rags for causing spontaneous combustion is generally well-known by lay per-

Table 125 Self-heating properties for oil-soaked cotton, as determined by Gross and Robertson

Material	E (kJ mol^{-1})	AQ (W kg^{-1})	ρ (kg m^{-3})	λ (W m^{-1} K^{-1})	C (J kg^{-1} K^{-1})	P 1:6	P 1:1
castor oil	116	1.1×10^{16}	314	0.046	1400	55.3	56.6
cottonseed oil	101	3.0×10^{15}	338	0.046	1400	53.9	55.2
linseed oil, raw	88	4.7×10^{13}	309	0.046	1400	49.6	50.8
neatsfoot oil	103	5.1×10^{14}	316	0.046	1400	52.1	53.4
olive oil	78	3.3×10^{11}	308	0.046	1400	44.5	45.7
rapeseed oil	84	8.1×10^{12}	316	0.046	1400	47.8	49.0
sperm oil	84	2.1×10^{11}	313	0.046	1400	44.1	45.4

sons. Thus, some arsonists will try to exploit this phenomenon. Gray[1090] reports an interesting case where an arsonist tried to create the impression that his 'careless' use of oiled rags led to an accidental fire occurrence, whereas the fire was caused in an entirely different manner. Gray used self-heating tests and theory to analyze the case. He used twice the amount of rags claimed by the individual to be present (in order to take a conservative upper limit) and then explored the amount of oil needed to cause maximum self-heating tendency. Under such optimal conditions, he was able to show that a minimum ambient temperature of 68ºC would have been needed to cause thermal runaway. This temperature was way beyond any possible ambient temperature in a residence.

Hill[1091] investigated the self-heating tendency of waste from a process where cotton buffing wheels are used with a polishing compound. The latter was only described generically as containing alumina, fatty acids, and water. Using the FRS procedure, he found that critical conditions corresponded to a cube dimension of 1.0 m for a starting temperature of 40ºC, or 2.3 m dimension for a starting temperature of 20ºC. The real accident conditions are reported to have corresponded to a cube size of 0.92 m at a temperature somewhere between 20ºC and 40ºC. This would suggest a good validation, except for the fact that no details of the actual occurrence are available. Also, the experimental work was based on fitting a straight line through only 3 data points, which would not normally be considered a sufficient number of data points to make usable predictions.

Prudent disposal measures for linseed-soaked cloths can include: (1) burying underground; (2) burning outdoors in a safe place; (3) packing into empty metal paint cans, tightly hammering the lids shut, then placing in a non-combustible outdoor refuse bin; (4) dispersing cloths individually outdoors on non-combustible surfaces and leaving them there until the oxidative polymerization reactions are finished.

Turpentine is also subject to self-heating, when rags are soaked in it[1092]. Likewise, rags soaked in *polyurethane*-based wood-finishing preparations are known to self-heat[1093], although this has not been studied in detail. See also: *Oils*; *Paints*.

Fire hoses

MIT professor Gill[1094] documented a case history where a nominal 64 mm (2-½") fire hose ignited due to friction while it was connected to a pumper and pumping water. The hose was constructed of an outer cotton jacket, a rubber lining, and an inner cotton jacket. Vibrations of the pumper produced sufficient chafing of the hose to lead to ignition. Remarkably, laboratory tests were largely able to reproduce this situation, although it appears (details were not given) that the test hoses only charred and did not flame.

Fishmeal

Fishmeal is the dried and ground residue of fish that has been cooked and has had the oil extracted. It has a known propensity for self-heating and has been the cause of a number of ship fires. The self-heating is attributed to a combination of oxidation of the residual oil and action of micro-organisms[1095]. It has been reported[1096] that Chilean fishmeal is particularly susceptible to spontaneous combustion due to the high fat content in anchovy fishmeal. Conversely, it was found self-heating has not been a problem with fishmeal produced in Northern Hemisphere countries. Standard safety recommendations for transporting fishmeal on ships are:

- to dry the meal to between 6% and 12% moisture
- to store it at least 21 days prior to loading
- to not exceed 11% of fat content in the fishmeal
- to store bags of fishmeal is ship holds in such a way that air can circulate between bags.

Floor buffers

Case histories have been reported[1097] of three individuals burned due to ignition of solvent vapors from a floor buffer. The fires involved use of flammable solvents to clean a floor, buffing it with electric floor buffers. The mechanism of ignition was sparking from the motor, not static electricity.

Floor coverings

In the US, the Federal government enforces a standard whereby carpets and rugs must resist ignition from a methenamine pill. The test method used, ASTM D 2859, is described in Chapter 7. The test specimen may ignite and burn in the immediate vicinity of the pill, but flames must not travel more than 75 mm from the ignition source. This ignition source produces exceptionally small and localized flames. DeHaan[1098] reported that many polypropylene carpets currently on the market will pass this test, but when presented with a slightly larger flaming ignition source, will show unlimited flame propagation. Such carpets tend to show flames that are only 50 – 75 mm high and burn at a slow rate (ca. 1 m^2 per hour). The most common outcome when one of these carpets is ignited is that the entire carpet will be consumed, but furniture in the room will not be ignited. The floor coverings industry in the US describes flexible sheet and tile products as 'resilient floor coverings,' which is a confusing nomenclature since carpets and rugs are resilient substances, yet are understood to be excluded from that definition.

Table 126 Hot surface ignition temperatures for carpets

Material	Temp. (ºC)
acrylic	710
nylon	660
polypropylene	735
viscose rayon	660
wool	760

Table 127 Floor coverings tested by Van Hees (courtesy Patrick Van Hees)

Specimen ID	Description	Thick. (mm)	Weight (kg m^{-2})
PVC 1	PVC-tile	2	4.3
PVC 2	PVC-tile	2	4.3
PVC 3	soft PVC	2	1.8
PVC 4	PVC	2	3.3
PVC 5	PVC	2	2.8
linoleum	linoleum	2.5	3.1
parquet 1	oak on soft wood board	13	7.6
parquet 2	oak	22	18.8
parquet 3	laminate	8	8.0
cork FR	coated cork tile	4	1.8
carpet 1	nylon*	9	2.6
carpet 2	nylon, FR*	6	1.8
carpet 3	wool*	10	2.3
carpet 4	polypropylene*	9.3	1.9
carpet 5	nylon*	7.2	2.1
carpet 6	needle-felt polypropylene	6.4	1.5
rubber	rubber tile	3	5.6
* with polypropylene backing			

Table 128 Cone Calorimeter piloted ignition results, uncorrected (courtesy Patrick Van Hees)

Specimen ID	Ignition times (s) for exposure at various heat fluxes (kW m^{-2})							
	10	12	15	20	25	30	35	50
PVC 1				NI	NI	83	72	41
PVC 2			NI	1188	616	320	262	59
PVC 3	NI	116	108	83	27	16	15	7
PVC 4	NI	177	146	80	55	46	39	18
PVC 5	NI	236	176	97	76	52	45	16
linoleum		NI	298	167	127	83	69	41
parquet 1			NI	496	228	113	82	31
parquet 2			NI	575	276	146	103	45
parquet 3		NI	1161	725	498	325	177	92
cork FR			NI	62	36	27	16	6
carpet 1				NI	246	126	72	41
carpet 2				NI	387	145	82	11
carpet 3			NI	95	64	49	27	9
carpet 4	NI	304	205	185	84	62	42	24
carpet 5			NI	430	186	114	81	38
carpet 6	NI	364	162	108	68	47	35	13
rubber		NI	778	362	241	186	124	75
NI – no ignition								

Palmer et al.[1938] examined the small-flame ignitability of carpets, carpet underlayments, and carpet tiles. They found that cigarettes and matches could not ignite any specimens. When ignited with a 200 × 300 mm piece of paper, folded up, 1 of 2 acrylic carpets and also latex foam and rubber underlayments suffered sustained ignition. Wool, rayon, and a number of blended-fiber carpets ignited but did not sustain burning. Polypropylene and nylon carpets, fiber felt underlayment and all carpet tiles did not ignite at all. When presented with a 15 g fiberboard crib or a larger wood crib, more ignitions were found. Acrylic, polypropylene and nylon specimens performed worst against crib ignitions, since at least some showed total destruction. A majority of carpets proved resistant to full burning, even when confronted with the largest source used, the wood crib; damaged areas were typically less than 0.5 m across. Settle[1099] tested carpets by using a 24 × 28 mm stainless steel plate electrically heated to a high temperature (Table 126).

Table 129 Effective material properties derived by Van Hees

Specimen ID	$\dot{q}''_{cr}$ (kW m^{-2})	$\lambda\rho C$ (kJ^2 s K^{-1} m^{-4})	T_{ig} (^{o}C)
PVC 1	16.78	0.426	395
PVC 2	14.93	0.991	373
PVC 3	6.13	0.399	222
PVC 4	2.42	4.169	119
PVC 5	4.74	1.480	189
linoleum	3.48	5.182	150
parquet 1	13.22	0.558	350
parquet 2	12.28	0.879	337
parquet 3	8.15	3.421	267
cork FR	15.80	0.080	383
carpet 1	14.98	0.529	373
carpet 2	21.57	0.091	450
carpet 3	13.06	0.177	348
carpet 4	4.11	2.385	172
carpet 5	11.42	0.808	324
carpet 6	6.66	0.737	233
rubber	4.51	5.969	183

The most extensive radiant ignition results on floor coverings were obtained by Van Hees, in the course of his doctoral research[1100]. Descriptions of the test specimens are given in Table 127, with results obtained from tests in the Cone Calorimeter given in Table 128. Van Hees also developed a model for correcting the data for heat conduction effects of the wire grid used to retain the specimens during testing and for differences in the substrate, compared to accompanying real-scale tests that he also conducted. For bench-scale testing, the wire grid was necessary because most floor coverings are only a few mm thick and show shrinking behavior, while some also show excessive swelling. Fiber cement boards were used in the real-scale tests, but these showed inconsistent data due to their water content and erratic spalling. In view of these factors, to obtain bench-scale data which would more reliably reflect the real-scale environment, Van Hees adopted the following procedure:

- Tests were conducted on floor coverings without backing board, but wrapped in aluminum foil. Beneath the foil only the ceramic wool specified in ISO 5660 was placed. The tests were conducted with grid and retainer frame.

Table 130 Cone Calorimeter piloted ignition results, corrected (courtesy Patrick Van Hees)

Specimen ID	Ignition times (s) for exposure at various heat fluxes (kW m^{-2})							
	10	**12**	**15**	**20**	**25**	**30**	**35**	**50**
PVC 1				NI	NI	124	108	60
PVC 2			NI	2990	1589	791	644	113
PVC 3	NI	249	233	180	56	33	30	26
PVC 4	NI	292	240	132	85	76	64	30
PVC 5	NI	414	310	171	133	91	79	28
linoleum		NI	610	343	261	171	142	84
parquet 1			NI	2387	945	426	293	81
parquet 2			NI	1877	813	369	227	62
parquet 3		NI	2644	1769	1319	870	467	239
cork FR			NI	115	48	31	16	6
carpet 1				NI	1073	496	265	140
carpet 2				NI	1699	681	336	11
carpet 3			NI	390	238	165	59	9
carpet 4	NI	1334	900	813	364	268	147	100
carpet 5			NI	1529	723	436	303	135
carpet 6	NI	1430	621	413	255	173	127	42
rubber		NI	1242	575	381	294	196	119
NI – no ignition								

Table 131 Radiant piloted ignition of carpets

Carpet	Pile height (mm)	$\dot{q}''_{\min}$ (kW m^{-2})	$\dot{q}''_{cr}$ (kW m^{-2})	B_{ig}
polypropylene (PP)	4	< 9	0	232
polypropylene (PP)	1	< 9	2.5	200
acrylic	6	10	–0.7	266
acrylic FR	7.5	10	2.8	174
nylon	shag	19	*	*
nylon, FR	6	19	4.2	299
wool	7	12	*	*
polyester (PES)	10	24	4.5	323
polyester/acrylic 50/50	4	14	5.4	185
polypropylene/nylon 50/50	4.5	< 9	0.6	269
polyester/modacrylic 65/35	8.5	13	5.6	188
* data do not conform to thermally-thick material theory				

- With a 1-dimensional heat transfer model, the corresponding temperature of the floor covering was determined at the time of ignition. The numerical heat transfer model used a Crank-Nicolson solver and included convection and radiation losses at the surface. The grid was simulated by a thin steel plate. As steel has a high heat conduction coefficient, heat conduction is only affected to a limited extent, but radiation losses at the surface, which were found to be important, are taken into account. The λ, ρ and C input values for the model were determined by obtaining a value of $\lambda\rho C$ using the Janssens method (see Chapter 7). Separate values for λ were determined by using C values from literature for the material. Knowing ρ for the material, the value of λ can be determined. Constant, non-temperature-dependent λ, ρ and C values were used.
- The above thermal properties include the contributing effect of the backing board. Thus, a new simulation was performed using the backing board and no grid (since the latter is not present in the real-scale). From this simulation new ignition times were obtained using the temperature of the floor covering, determined in the first simulation as trigger point for ignition. These ignition times were then used to determine the ignition temperature T_{ig} and effective $\lambda\rho C$ by the Janssens method.

Before this model was applied to all floor coverings in the study, the model was first validated by means of tests where different sample preparations were compared. The simulation method showed satisfactory results, despite the limitations of the method, being 1-dimensional and based on temperature-invariant material properties. The corrected values are shown in Table 130. Shown in Table 129 are

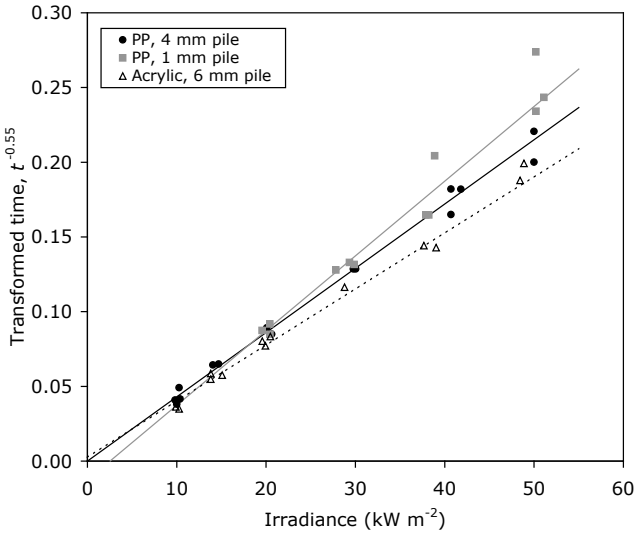


Figure 75 Carpet ignition (Yanai)

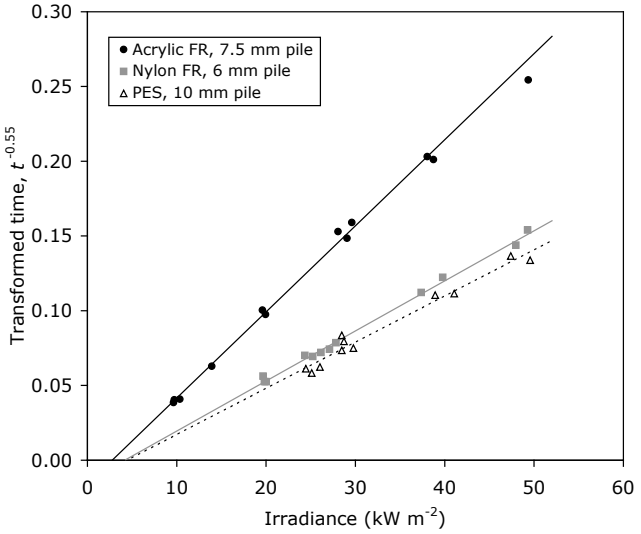


Figure 76 Carpet ignition (Yanai)

$\dot{q}''_{cr}$, the critical heat flux (kW m^{-2}); $\lambda\rho C$, the effective thermal inertia; and T_{ig}, the computed ignition temperature (ºC). As discussed in Chapter 7, ignition temperatures obtained by such calculational procedures are not always realistic, and values below about 300ºC must be viewed as artifacts.

The minimum flux[1102] for vertically oriented vinyl-asbestos tile of unspecified thickness was found to be 72 kW m^{-2} for autoignition and 38 kW m^{-2} for piloted ignition. Using specimens in the horizontal orientation, a minimum flux for radiant, piloted ignition of 14.5 kW m^{-2} was found[1101] for vinyl-asbestos tile. The tile was 2.4 mm thick, with a basis weight of 480 g m^2. Long[1102] measured the ignitability of carpets in a vertical orientation using a developmental NIST

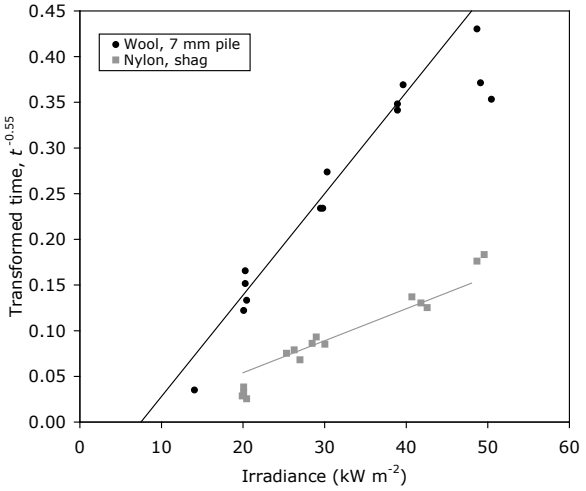


Figure 77 Carpet ignition—examples of specimens not conforming to thermally thick theory

Table 132 The ignitability of some carpets as determined by Long

Fiber	Pile height (mm)	Basis weight of pile (g m^{-2})	Minimum flux for ignition (kW m^{-2})	
			Piloted	Auto.
acrylic	6	1300	43	46
acrylic, with pad	6[a]	1300	<27	36
acrylic	2 – 8[b]	1100	42	47
acrylic, with pad	2 – 8	1100	41	46
nylon	3	680	15	31

a – pad of rubberized hair/jute
b – pile cut in pattern

heat release rate apparatus. His results are given in Table 132. Hirschler[1103] tested the ignitability of nylon carpet tile using the Cone Calorimeter in the horizontal orientation. All of the specimens ignited (piloted ignition) at the lowest fluxes used, 20 or 25 kW m^{-2}. Ignition times at 25 kW m^{-2} flux were 69 – 212 s. Hilado and Murphy[1903] tested the autoignition of carpets in the vertical orientation. They found no ignitions at a flux of 25 kW m^{-2}. Polyester, nylon, and acrylic samples did ignite at 58 kW m^{-2}, which was the next higher flux used. Wool did not ignite at 58 kW m^{-2}, but ignited at 81 kW m^{-2}. The test apparatus used was of poor quality, so the results should be viewed as only semi-quantitative. Tomann[1104] gave results on piloted ignition in the Cone Calorimeter for 4 different carpets tested at a flux of 35 kW m^{-2}.

The radiant, piloted ignitability of carpets was tested by Yanai[1105], who used the ISO 5657 test apparatus (Table 131). The specimens shown in Figure 75 and Figure 76 conform rather well to thermally-thick materials theory. The wool and the shag nylon data shown in Figure 77 do not. Carpet construction is highly non-uniform with respect to density—at the very top are some fluffy fibers, then more

solid yarns below, then finally a backing which has a different yet construction. Thus, it may be somewhat surprising that the data for the majority of carpets follows the thermally-thick relation. Apart from shag carpets, pile height evidently has almost no effect on ignitability, as seen by comparing the two PP results. The data indicate that PP carpets ignite at lower heat fluxes than do other types, although acrylics are close.

Foodstuffs

Peacock and Vaishnav[1106] tested a series of generically-described foodstuffs for ignitability. Using the CPSC test procedure, which involves applying a candle flame for 5 s to the surface, they did not find any foodstuffs that ignited. The tested foodstuffs that did not ignite were:

- flour
- fruit cereal
- instant chocolate drink
- instant coffee
- instant tea
- rice
- sugar.

Manufactured foodstuffs, unlike raw agricultural products, are rarely associated with self-heating events, possibly because they are commonly not piled in substantial-size piles. But spontaneous combustion cases have been reported for noodles, potato chips, and deep-fat fried Indian foods. Gray[1090] described a case where pallets of shrink-wrapped '1-minute noodles' stored in a noodle factory underwent spontaneous combustion. The fire took place when production was sped up, so that the product was being packaged at 113ºC, instead of at 81ºC, as previously. Tests indicated that 1.24 m^3 pallet-loads had a critical hot-work temperature of 106ºC. Potato chip wastes have self-heated to ignition when stored in 1.5 × 1.5 × 2.0 m wire-mesh containers[1107]. The wastes were simply pieces that were broken or undersized in the production of potato chips. Subsequent oven testing in wire-mesh spheres was done to obtain the self-heating characteristics of the material. The following values were derived: E = 126 kJ mol^{-1}; ρ = 150 to 300 kg m^{-3} Q = 740 to 1220 kJ kg^{-1}; λ = 0.076 to 0.101 W m-1 K^{-1}, $A = 2.4\times10^{12}$ s^{-1}. The laboratory tests showed that at 40ºC the critical diameter is about 0.15 m, so the material can readily go into thermal runaway when in meter-size volumes. Coffee beans, powdered coffee, and powdered chicory exhibited strong self-heating tendencies in laboratory experiments[1108]. Dixon[1109] reported a case where a fire occurred about 8 h after an Indian food preparation made mostly from flour deep fried in rapeseed oil self-heated to ignition as it was draining in a large (size unspecified) colander after having been fried. Dixon determined the iodine value of the used oil, using an unburned oil sample, as 116. He then conducted a test where a bucket of the material was placed in an oven at 130ºC. Thermal runaway, but without flames, was observed in about 24 h. Self-heating was probably promoted in this case by the fact that a high surface/volume ratio—the foodstuff was described as being breadcrumb-like in appearance. Nelson conducted oven-basket tests to determine the self-heating properties of wheat flour[1597]. His results were: E = 129.2 kJ mol^{-1}, P = 58, λ = 0.060 to 0.177, and C = 1.49 to 3.14 kJ kg^{-1} K^{-1} ; the latter two variables being in the range over 50 – 140ºC. Takai[1110] reported studies on the self-heating of roast cocoa powder and soybean flour. The cause of some explosions in chocolate candies was found to be fermentation due to anaerobic bacteria[1111].

Forest materials, vegetation, and hay

The top causes of forest fires depend on the locale, but are commonly:

- lightning
- incendiarism
- careless use of heat or fire. The latter includes cigarettes and matches, campfires, machinery, uncontrolled agricultural burning, and badly executed prescribed burns.

Statistics[1112] for the US are given in Figure 78 and Figure 79. In most years, debris burning, arson, and lightning are typically the top three causes leading to the most fires, but the most destructive fires are from lightning, by far.

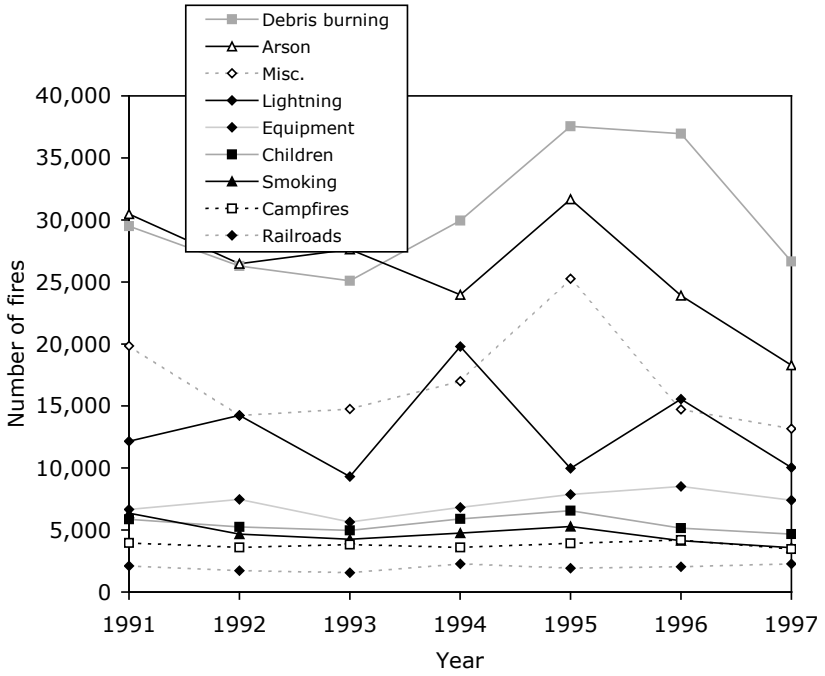


Figure 78 US wildland statistics for 1991 – 1997, based on number of fires

Table 133 Types of equipment leading to forest fire ignitions in California survey

Equipment type		Percent
Road vehicles		**68.1**
automobiles	30.4	
trucks	23.8	
motorcycles	4.8	
other	1.7	
unspecified	7.4	
Farm equipment		**16.8**
harvesters	6.3	
tractors	7.1	
other farm equipment	3.4	
Power tools		**7.4**
welding torches	4.3	
saws	1.1	
other	2.0	
Stationary engines		**3.1**
Highway maintenance or construction equipment		**2.3**
Other		**2.3**

Weber[1113] compiled data showing lightning was the top cause in some regions, but accounted for less that 5% in other regions. Apart from the above causes, the only other cause of some general prevalence is associated with high-voltage transmission lines and ancillary equipment, but this is inevitably a small percentage. In the US national statistics, it is simply grouped into 'Miscellaneous.' A category

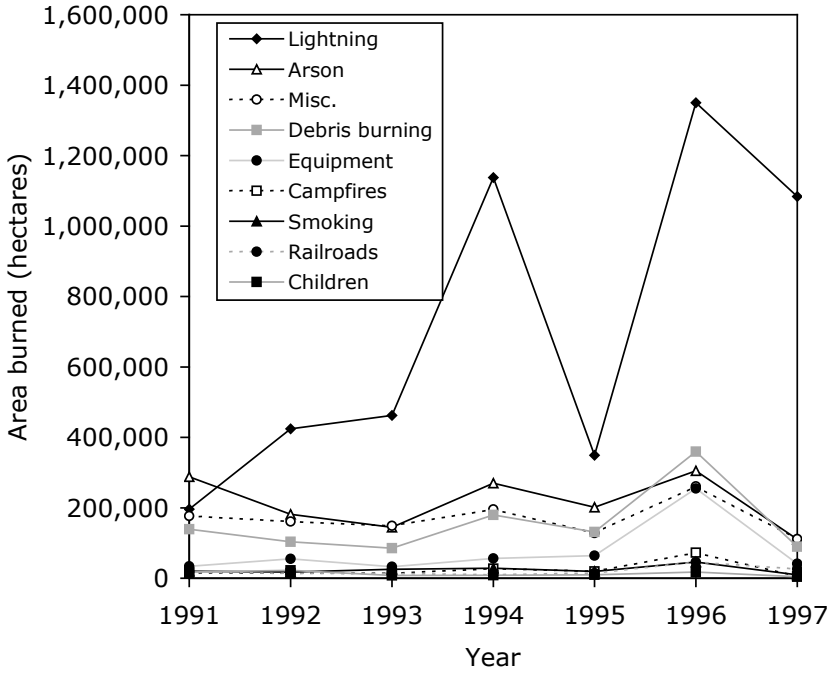


Figure 79 US wildland statistics for 1991 – 1997, based on hectares burned

Table 134 Causes of forest fire ignitions due to equipment use in California survey

Cause	Percent
exhaust sparks	39.5
friction	16.2
wiring	9.9
gas leak	9.7
other	22.4
not stated	2.3

of more readily preventable fires involves those due to use of equipment. 'Equipment use' is typically defined by forest fire specialists as any mechanical or electrical equipment except railroads or electric distribution systems. Some statistics on fires from equipment use in California have been published for 1962 – 1971, when it accounted for 28% of forest fire ignitions. Bernardi[1114] analyzed details of these fires, and the results are given in Table 133. The specific causes leading to ignition are identified in Table 134. During 1975 – 1979 California forest fires due to equipment use accounted for 39% of the land area burned[1115].

Prescribed burns that are improperly executed and then lead to major conflagrations of inhabited areas are another type of fire of special interest. The most notable such fire in recent years in the US was the Cerro Grande fire of May 2000 which grew into the largest wildfire in New Mexico's history and destroyed hundreds of homes and portions of the Los Alamos National Laboratory—several reports were written analyzing the failures involved[1116,1117].

Scientists commonly distinguish three types of forest (or wildland) fires[1118]:

(1) Ground fires. This type of fire burns in duff, organic soils, roots, rotten buried logs, etc.
(2) Surface fires. A surface fire burns fuels that are above the ground but below the canopy. The fuels comprise needles, leaves, grass, downed wood, shrubs, and short trees.
(3) Crown fires. A crown fire burns in the elevated canopy fuels. Apart from the rarely-seen 'independent' crown fire, crown fires are subdivided into active and passive. An active crown fire involves a solid wall of flame from near-ground level through the top of the canopy and encompasses many trees burning en masse. A passive crown fire involves only one or a small number of trees, with solid flame not consistently maintained in the canopy.

The ignition of vegetation is greatly influenced by its moisture content, *MC*. This is

measured on an oven-dry weight (ODW) basis and is defined as:

$MC = \frac{\text{mass of water}}{\text{mass of dry fuel}}$. For living vegetation, MC > 70% and for some species may reach 400%. The fiber saturation point corresponds to 30 – 35% MC, so dead vegetation that has not been flooded or recently rained upon will normally be below this value. In the absence of flood or rain, the MC of dead vegetation is established by atmospheric temperature and RH conditions.

The US Forest Service uses the concept of *moisture of extinction*, which is the maximum moisture that vegetation can have and still support a propagating fire. Its ue[1119-1121] depends on the type of vegetation, being typically 12 – 15% for light, airy fuels; 15 – 20% for dead grasses, 15 – 25% for logging slash; 20% for chaparral and brush, 25 – 30% for pine needles; 30% for forest litter, 40% for palmetto understory, and over 100% for many types of live timber stands. Matters are complicated by the fact, however, that wind speed must also be taken into account. Figure 80 shows the predicted combined effects of fuel moisture and wind speed on fire types, as developed by Scott and Reinhardt[1118]. Not surprisingly, the combination of dry fuel and high wind speed is seen to allow the most dangerous fire type—the active crown fire—to occur. Ground fires[1121], however, can propagate in some extremely wet materials, as much as 90% MC. All of the information on moisture contents needed to achieve a sustained ignition is unfortunately anecdotal and systematic research is absent. Thus, for example, Ford[1153] reports that 18 – 22% moisture content is needed to ensure that a fire will not propagate through fine fuels, which is substantially higher than the USFS values cited above. The moisture of extinction concept is based on the presence of sizable flames. When ignition is by flying brands, lower moisture contents are required. McArthur[1122] found that in eucalyptus litter at MC > 7% "only very large flaming brands will be effective in starting new fires," but at MC ≤ 4% "even the very smallest of burning embers have a high probability of starting a fresh fire." When using the concept of the moisture of extinction, it must be recognized that, for higher MC values, a fire may get ignited, but its HRR is likely to be so low that the hazard associated with such a fire will be small. Luke and McArthur[1141] consider fire hazard to be low if fine-fuel MC > 15%. They also consider that the probability of a fire starting becomes small for MC > 9% and very small for MC > 15%. Viegas[1123] categorized the hazard of surface or crown fires as:

- fine-fuel MC < 10%: extreme hazard exists
- fine-fuel MC > 20%: hazard is low (< 10 hectares can be expected to burn)
- fine-fuel MC > 40%: only trivial fires are possible.

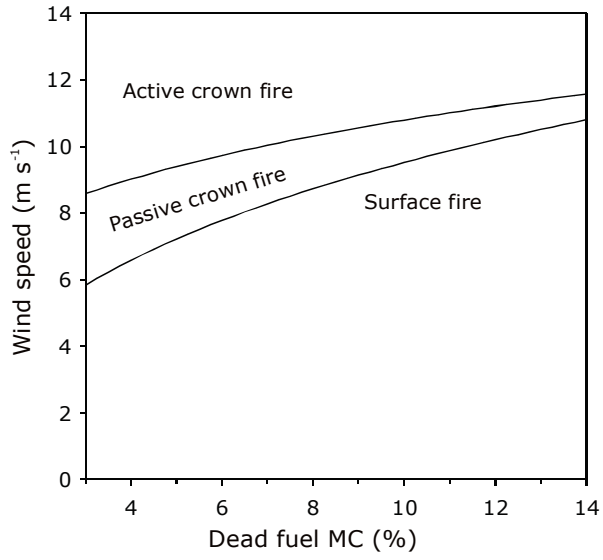


Figure 80 Effect of wind speed and fuel MC on the type of forest fire possible (this is an example calculation only; actual values are affected by the detailed fuel characteristics)

Another set of expressions[1124] has been derived empirically based on experience with grassland fires in Australia:
for $MC < 18.8\%$:

$$F = 3.35W \exp(-0.0897MC + 0.145V)$$

for $18.8\% \le MC < 30\%$:

$$F = 0.299W(30 - MC)\exp(-1.686 + 0.145V)$$

where W = fuel load (tonnes ha^{-1}), V = wind speed (m s^{-1}), and MC = fuel moisture content. F is a fire danger index which evaluates the probability that a fire can spread significantly from an initial ignition source. For moisture content over 30%, ignition and spread is held unlikely.

IGNITION BY HOT GASES AND HOT SURFACES

Ignition temperatures of vegetation have been measured by numerous researchers, as detailed below. However, the reported values are widely discordant. It is first necessary to ask whether there should be differences in ignition temperatures of vegetation of various types. Since the chemical composition varies somewhat, the answer must be Yes, but generally one would expect that most vegetation of a particular type (e.g., deciduous leaves, needles, grass, etc.) would show ignition temperature variations only within a modest range. Another variable that is important is the moisture content of the material since live vegetation can have MC values over 100%. However, MC should not have an effect if a thin specimen is heated for a long time at a heat flux close to its minimum ignition flux—in that case, all of the moisture should be evaporated before ignition takes place. A major complication is that many of the reported results have been obtained by foresters, botanists and other workers who may not be well-versed in physics or chemistry and have never conducted ignition experiments on any other substance. Thus, the equipment used has generally been uniquely-designed and not calibrated with any reference materials. A physical complication is that inadequate specimen size may have been used. Since practical

ignition usually involve a substantial bed of material, rather than an isolated needle, twig, etc., some reported T_{ig} values are undoubtedly too high to represent such realistic fuel beds. The best recommendation that can be offered at the present time is to consider that the ignition temperature of vegetation is essentially identical to that of whole wood, as described later in this Chapter under *Wood*. The results of Di Blasi, which are recent and obtained by a combustion specialist, are highly suggestive that this is a reasonable conclusion.

Di Blasi et al. tested the ignition of beds of straw in a convective-heating apparatus where both the air stream temperature and its velocity could be varied. Their results are considered in detail in Chapter 7, but the basic finding was that T_{ig} = 250ºC when the specimens were heated using the lowest temperature air stream. At higher heat fluxes, the values of T_{ig} rose. This phenomenon is identical to the one described for solid wood later in this Chapter.

The ignition temperature of pine duff was tested at the Forest Products Laboratory of Canada using an unspecified technique[1125]. They reported flashing ignition at 166ºC and sustained flaming at 177ºC. Bowes[1126] assessed the ignition temperature of dried (6% MC) grass to be 249ºC by using a crossing-point technique. Using a hot-air apparatus, Yamashita[1127] measured the autoignition temperatures for a variety of leaves and branches. Leaves typically showed an AIT of 375 – 400ºC, although some types required up to 600ºC for ignition. Small branches gave results as low as 350 – 375ºC and as high as 650 – 675ºC. Johnson et al.[1128] measured the autoignition temperatures for several botanic materials (Table 135). Their technique involved declaring ignition when a certain rate of temperature rise was exceeded, and visual observation of ignition was not made. Shu et al.[1129] reported ignition temperatures for leaves and twigs from 12 species of Chinese trees using a Chinese test apparatus. For leaves the range was 210 – 254ºC (average: 240ºC), while for twigs it was 228 – 244ºC (average: 236ºC); the moisture content of most of the specimens was ca. 50%.

Stockstad tested ponderosa pine needles in a horizontal tube furnace[1130]. A tiny amount of specimen was lashed onto a rod and held in the middle of the cavity; a maximum exposure time of 3 min was used. A minimum furnace temperature of 280ºC was found for piloted ignition, and a minimum of 365ºC for autoignition. The effect of moisture content was also explored, and the wettest specimens (MC = 33%) required a temperature of 350ºC for piloted ignition and 390ºC for autoignition. In his test procedure, he did not differentiate between glowing and flaming ignitions. Using the same technique, he also tested cheatgrass[1131]. A minimum furnace temperature of 380ºC was found for piloted ignition, and a minimum of 450ºC for autoignition. These values seem excessively high, but the reason for this is not clear.

Table 135 Ignition temperatures of several botanic materials measured by Johnson et al.

Substance	AIT (ºC)
corn 'beeswings'	302
fir sawdust	313
locust sawdust	291
tobacco	272
willow oak leaves	282

Table 136 Effect of species on ignitability at 400ºC

Probability of ignition at 400ºC	Percent of species tested	
	Fresh leaves	Oven-dried
100%	66%	82%
90%	14%	4%
80%	4%	6%
70%	8%	2%
60%	0	2%
50%	2%	0
40%	2%	0
30%	0	0
20%	2%	0
10%	0	2%
0	2%	0

A number of workers examined ignition/non-ignition of specimens using only a single furnace temperature. Mutch[1132] examined the ignitability of ponderosa pine needles (MC 5 – 6%) and sphagnum moss (MC 19 – 20%) by dropping them into the Jentzsch tester, which is a heated crucible used in the early years of the 20th century for testing of liquids. Running tests only at 320ºC, he found that autoignition of pine needles took 36 – 39 s, while the moss ignited in 19 – 20 s. Liodakis et al.[1133] tested for the autoignition of pine (*pinus halepensis*) needles using 0.2 – 1.0 g samples placed into an oven. At an oven temperature of 500ºC, ignition time was 59 s; no ignition was found at lower oven temperatures.

Gill and Moore[1134] tested the leaves of 50 different Australian plants (which came from 19 botanical families) in a muffle furnace. Their tests all used spark ignition and most tests were conducted at 400ºC, although a small number of difficult-to-ignite specimens were re-tested at 500ºC. Using 10 replicates per plant type, they obtained ignition at 400ºC in 89.6% of the trials when using fresh leaves, and in 95.2% of the trials when using oven-dried leaves. Most species showed a 100% probability of ignition, but 17 species (for fresh leaves) and 9 species (oven-dried) showed probabilities of less than 100%. Species effects are summarized in Table 136. The authors repeated their tests at 500ºC using the five least ignitable species. At the higher temperature of 500ºC, still not all specimens ignited. Two species (*Myoporum acuminata* and *Geijera parviflora*) exhibited less than 100% ignitions when fresh, and one species (*Amyema*

cambagei) showed only 50% ignitions at 500ºC when oven-dried. The latter species was peculiar, in that at both temperatures a lower probability of ignition was found for oven-dried samples than for fresh ones. The authors also found that leaves with higher surface/volume ratios were more easily ignited, and, surprisingly, that ones with a higher mineral content were also more readily ignitable. Ignition times at 400ºC were typically 4× greater for fresh specimens than for oven-dried ones, although there was significant scatter from this trend. No specimen that did ignite required more than 57 s to ignite, with the minimum being 3.2 s.

Xanthopoulos and Wakimoto[1135] tested conifer needles for piloted ignition using a vertical tube furnace. They reported that almost no specimens ignited for furnace temperatures below 400ºC, while most ignited for temperatures of 440ºC and over. They did not specify their time of exposure nor the location of the pilot, leading to the possible conclusion that the surprisingly high temperatures reported might have been due to inadequate exposure time or due to poor location of the pilot. Montgomery and Cheo[1136] ignited leaves from plants of 32 different species in a furnace held at 750ºC and found that the ignition time would be represented as:

$$t_{ig} = 1.02 + 3.40d$$

where t_{ig} = ignition time (s) and d = thickness (mm). This linear increase with thickness indicates a thermally-thin behavior, which is consistent with the 0.05 – 0.58 mm range of thicknesses in their study.

A number of workers conducted tests where a sizable *hot surface* (ignition by brands is discussed separately later) was pressed into the vegetation and the temperature needed of the hot surface for ignition was determined. Results of this kind depend strongly on the size of the hot object, but most of the workers either did not specify the size or used irregular-shaped heaters. Wright[1125] dropped heated iron discs of about 6.5 cm^2 area and 45 g mass onto pine duff. No ignition was observed at 625ºC, but flaming ignition was found at 725ºC. Fairbank and Bainer[1137] conducted tests where simulated hot exhaust manifolds were used to test the ignitability of vegetation. The lowest temperature at which an ignition occurred was 448ºC for dry oats; a two-minute exposure was required. For temperatures over 600ºC, ignition was nearly instantaneous. Pine needles and dry, rotten wood (punk wood) required 760ºC, while dry grass ignited at 663ºC. Harrison pressed a rod-shaped electric heating element against forest fuels and determined their short-duration ignition temperatures[1138]. He first determined that a wind velocity of 0.9 m s^{-1} (2 mph) was optimum, then using this velocity found that 350ºC was needed to ignite dry pine needles and 400ºC to ignite dry grass for a 4 min exposure (Figure 81). Four minutes is a short exposure time, as indicated by the results obtained by Kaminski[1139], which showed lower temperatures. He conducted tests where a hot chain-saw muffler was pressed against various forest materials. Using an ambient temperature of 35.6ºC and a test time of 10 min, he found that punky (partly rotten) wood and bark underwent a glowing ignition at a surface temperature of 270ºC. With a temperature of 300ºC and a light wind, flaming ignition was observed. Cheat grass required 330ºC for a glowing ignition. Upon rerunning the tests with a pilot flame, cheat grass produced a flaming ignition at 270ºC, and sawdust at 260ºC. Rallis and Mangaya[1140] placed "fine, dry veld grass" on a hotplate and observed that glowing ignition required a hotplate temperature of 250 to 350ºC. For a hotplate temperature of 400ºC, it was possible to obtain a flaming fire by gently blowing on the specimen.

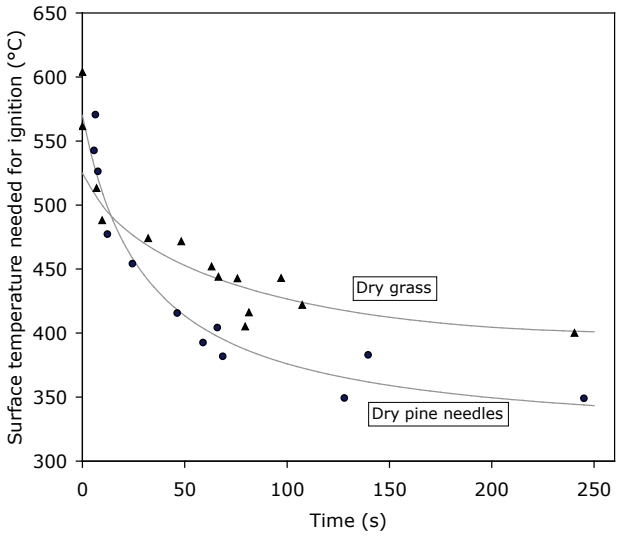


Figure 81 Hot surface temperatures needed for ignition of forest materials in Harrison's tests

IGNITION BY MATCHES AND SMALL FLAMES

Green grasses may have moisture contents as high as 350% and, for practical purposes, cannot be ignited. As a rule of thumb, moisture content must drop to the range of 20 – 25% for fine forest or grassland fuels to be ignitable[1141]. Sale[1370] conducted experiments on the ignition of dried grass by matches. The moisture content of the grass was ca. 5%. Matches were either dropped or thrown onto the grass. When dropped from a distance of 0.9 m, 80% of matches caused ignitions, but at a distance of 3 m the probability went down to 25%. Matches that were thrown, rather than dropped, showed a slightly smaller probability of ignition. Curiously, the ignition percentages from using larger wood matches were lower. An old US Forest Service report[1142] which has been widely cited advises that dropped matches will not ignite forest fires at wind speeds above 1.8 m s^{-1} (4 mph), but the author provides no experimental data and the conclusion is questionable.

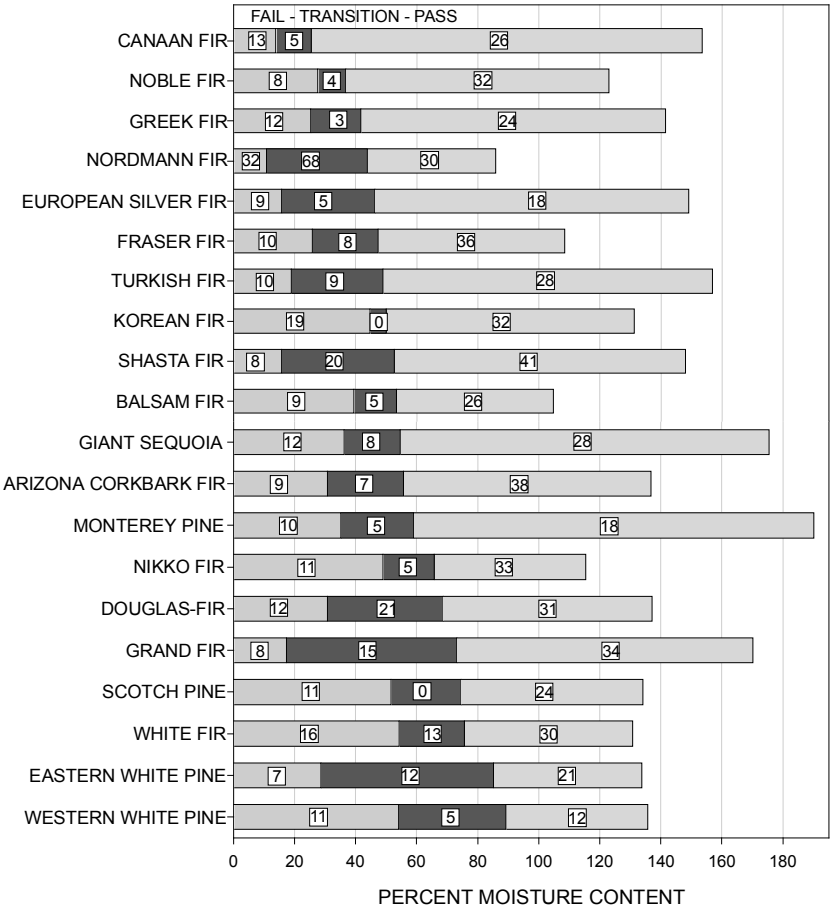


Figure 82 Effect of moisture content on ability of branches from 20 different species of Christmas trees to pass a modified California State Fire Marshal's flammability test. Bars show the moisture range where samples pass or fail the test as well as the size of the transition zone where some samples pass and some fail. Numbers in small boxes are the number of samples tested.
(Courtesy Gary Chastagner)

The effect of moisture on the ignitability of forest-floor pine-needle litter was studied by Blackmarr[1143]. He used three different wood match igniters: (1) a miniature match; (2) kitchen match; and (3) three kitchen matches tied together. The results focused on the role of moisture content for needles of *pinus elliottii* (slash pine), and it was found that there is a relatively narrow range of moisture contents over which the probability of ignition goes from near-zero to near-100%. For the miniature match, the 50% probability of ignition corresponded to 19.3% moisture content, for the kitchen match to 21.5%, and for the three-match set to 29.9%. The matches were used as ignition sources not because matches are a major form of forest material ignition, but simply as a surrogate for flaming brands of various sizes. Gill et al.[1144] conducted experiments where they ignited various specimens with 'large-headed' matches. Unfortunately, they did not record observed ignition but, rather, declared ignition to have occurred when 1 g of specimen mass was lost (their specimens were generally in the 10 – 40 g range). Their 'ignition time' results showed a modest influence of moisture for MC ≤ 11.1%, but nearly a doubling of ignition time when going from 11.1% to 16.6% MC.

The ignition behavior of *Christmas trees* is determined mostly by the moisture content. A fresh-cut Christmas tree will show moisture in the vicinity of 100 – 150%. The moisture loss is small while it is still baled and is stored in a cold place, and one study[1145] found that even after storage for 6.5 weeks in an unheated shelter (average temperature – 4ºC), the MC only dropped from 120% to 100%. But moisture levels can drop precipitously if a tree is brought into a heated room and not watered properly. Example data for Douglas fir[1146] are shown in Figure 83. Douglas fir is probably the worst Christmas tree from the viewpoint of 'keepability,' since under dry conditions Figure 83 indicates an MC loss of about 11% per day. Some other species[1145] show losses of only 4 – 6%.

For many years, the California State Fire Marshal had regulations requiring that Christmas trees used in certain occupancies be fire-retardant treated, with a small burner test

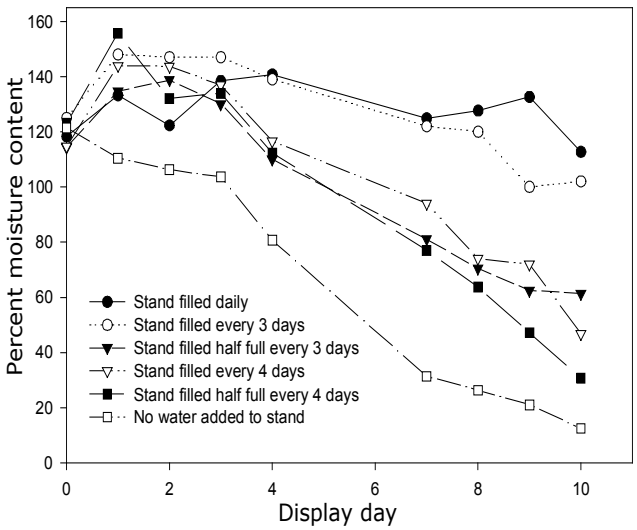


Figure 83 Effect of display care on changes in the moisture content of Douglas fir trees
(Courtesy Gary Chastagner)

being used to determine compliance[1147]. The test is to be performed 30 days after application of the FR agent. A diffusion flame from a Bunsen burner is applied to a branch for 12 s, with the flame adjusted to be 38 mm high. The specimen passes if fire does not spread and if afterflame time is ≤ 10 s. Using a similar small flame but applying it for 5 s, Chastagner[1148] examined the ignitability of non-FR Christmas trees of various species, as a function of the moisture content. His results, shown in Figure 82, indicate that there is a large species effect. Some conifers, e.g., Noble fire and Canaan fir, can more safely be used as Christmas trees since they are ignition-resistant down to much lower moisture contents. Chastagner[1146] also examined FR-treated trees and found that applications of the FR agent damaged the needles on many of the trees. Furthermore, the FR agents did not make the trees significantly more resistant to small-flame ignition, thus Chastagner concluded that trees must be diligently watered, but that applying FR treatments is counterproductive. A related study showed that resistance to small flames does not imply a Christmas tree cannot be ignited from a larger source[1149]. All test trees, even substantially wet ones, could be ignited and burned fairly completely if they were ignited with either flaming gift packages at the base of the tree or with a small burning toy. In those cases, there was a progressive involvement mechanism, whereby the initial ignition source preheats and dries out the tree locally, at which point the branches become able to burn; the drying/burning zone then proceeds to circle around the tree.

IGNITION BY CIGARETTES

Hoffheins et al.[314,1150] conducted experiments on the ignition of grass and forest duff and litter by cigarettes. For grass samples of 7 – 9% moisture content and 43 kg m^{-3} density, he found that ignition probability P depended on the wind velocity. At velocities ≤ 0.7 m s^{-1}, P = 0; at 1.4 m s^{-1}, P = 5%; at 2.0 m s^{-1}, P = 30%; and at 2.8 m s^{-1}, P = 50%. For velocities greater than 3 m s^{-1}, there was no further effect on ignition probability. Grass samples at greater packing density showed a higher probability of ignition. At 99 kg m^{-3} density, P ≈ 80% for the higher wind velocities. Ignition times, using 32 mm long cigarette butts, were about 5 – 11 min, with shorter times corresponding to higher wind velocities. Cigars were found to show roughly half the probability of ignition of cigarettes, under identical circumstances. For forest floor duff and litter, again wind velocity played a similar role, although, the exact nature of the vegetation was also of importance. The moisture content clearly plays an important role, but in these tests was controlled only indirectly, with solely the short-term RH being reported. In any case, probabilities approaching 100% were found for a variety of materials under wind conditions of around 3 m s^{-1}.

A later study on cheat grass and wild oats was conducted by Countryman[1151,1152]. In preliminary testing, he identified that grass is unlikely to ignite if a cigarette falls on stalks of grass that support the cigarette above the actual litter layer. Thus, he then focused on ignitions solely by applying cigarettes directly on the litter layer. His tests were all conducted at a temperature of 27ºC and with a wind of 1.3 m s^{-1} (3 mph), since limited testing indicated lower ignitability for smaller wind speeds. The cigarettes were pre-burned to a 50 mm length prior to placing on the bed. The ignition results were found to depend greatly on whether the fuel was coarse or fine. For fine fuel, ignition readily occurred for moisture contents up to 13%, with marginal ignitions up to about 14 – 15% and none beyond. Coarse fuel was not possible to ignite even for the lowest moisture tested, 1.9%. Medium fuel gave erratic results, but was less readily ignitable than fine fuel. Fine fuel is likely to occur in areas where foot or vehicular traffic repeatedly crushes the grass. In his main tests, no flaming ignitions occurred, the ignited fuels were solely consumed in smoldering combustion. Some further exploratory testing indicated that smoldering-to-flaming transitions occurred when a non-uniformity in the fuel bed was encountered by the smolder front. Countryman also found that the cigarette direction where the lit end faces into the wind is more likely to lead to ignition. Depth of the fuel bed had only a small effect on ignitability, with a 13 mm thickness showing slightly increased ignitability than a 6 mm thickness. From his study it can be concluded that there are two, related fuel effects:

(1) a minimum contact area must exist between the fuel and the cigarette; coarse fuel or geometries where the cigarette is supported at only a few spots prevents sufficient heat transfer for ignition to occur;
(2) the fuel array itself must not be so sparse or thin that initial points of ignition fail to propagate fire to the remaining mass of fuel.

Ford[1153] reported that, under some circumstances, vegetation with moisture contents of 18 – 22% is ignitable by cig-

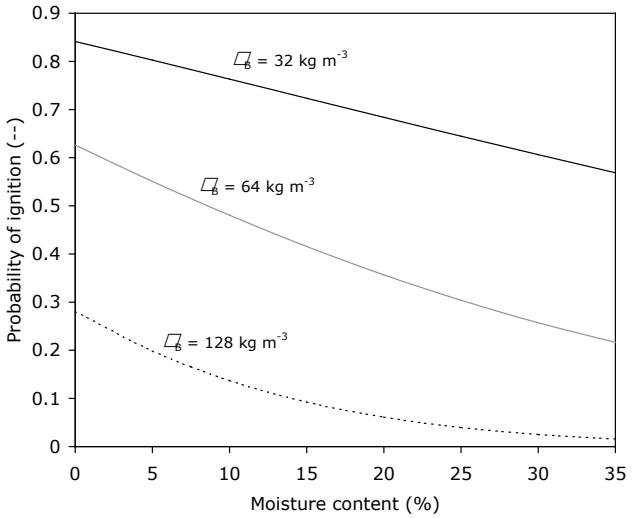


Figure 84 Effect of fuel moisture and density on the probability of ignition by lightning

arettes, but provided no details on vegetation type nor on wind conditions. He also concluded that the cigarette must contact fine vegetation for at least 1/3 of its perimeter for ignition to be possible. Markalas[1154] studied the potential of cigarettes to ignite foliage of various types. For materials dried to 4.5 – 6.5% MC, he found that: (a) no ignition could be achieved without wind; (b) with wind, ignition probability depended greatly on the species; (c) filter cigarettes were slightly less likely to cause ignition; and (d) thicker layers of vegetation were more readily ignited than thinner ones. Pine needles were least likely to ignite, while *Quercus coccifera L.* was most likely. Hardwood leaves only ignited when chopped into small pieces and compressed.

IGNITION BY LIGHTNING

Latham and coworkers conducted extensive studies into the ignition of vegetation by lightning. Because of the nature of the variables involved, the formulation of their models was presented in probabilistic terms. In an early study[1155], they concluded that 20% of cloud-to-ground discharges comprise 'long continuing current' (LCC) discharges, and that only the latter are likely to be incendive. The probability of fuel ignition, given an LCC discharge, was modeled as:

$$P_{ig} = \left[1 + \left(\frac{\rho_B [0.17 + 0.0062MC]}{2822} \right)^{1.44} \right]^{-1402}$$

where P_{ig} = probability of ignition (--),ρ_B = fine fuel bulk density (kg m^{-3}), and MC = moisture content (%). Example plots are given in Figure 84, with density data being shown in Table 137. Other submodels were also created to estimate the ignitions expected per area of ground surface, given various characteristics of storms.

In a later study[1156], they concluded that positive and negative discharges have different probabilities. For either, the lighting discharge parameter governing the process is duration, not energy flux. The relative importance of fuel parameters varied with the type of forest floor material—for some moisture content was found to be the most important, for others depth of the layer or density of the material. For positive discharges, the optimal duration was found to be 50 ms, while for negative discharges it was 110 ms. At their respective optimal discharge durations, however, positive discharges were 3× more incendive than negative ones.

Table 137 Bulk densities of various fine forest fuels

Forest fuel type	Bulk density (kg m^{-3})
Alaskan black spruce	128
Eastern pine	64
pine-grass	64
sagebrush-grass	32
short-needle	128
tundra	32
Western annual grass	32
Western long-needled conifer	64

Actual data[1157] show the probability of starting a fire in North America, per flash (not per LCC flash), ranges from about 0.04% for grass to 5% for Douglas fir forests; most other fuel types show probabilities of 1.5 – 3% with an average of around 2.4%. These data reflect an overall statistic and are not differentiated with regards to fuel moisture. The main ignition mode in Douglas fir forests is when a lightning strike ignites the needles on the ground—actual ignition of a tree is rare and may not lead to a propagating fire. Furthermore, lightning strikes generally lead to ignitions which are smoldering first, and transition to flaming only later. Laboratory experiments led Latham to conclude that layers of Douglas fir duff need to be at least 28 mm thick before an ignition can take place.

A study of lightning-caused fires in Yosemite National Park[1158] showed that: (a) likelihood of ignition from a lightning strike greatly increases if larger-diameter dead and downed fuels have < 13% MC; (b) lightning is more likely to ignite fires in old-growth areas; and (c) for unexplained reasons, Douglas fir stands sustained an average incidence of lightning ignitions, but these led to fewer than expected crown fires.

IGNITION FROM CONTACT WITH POWER LINES

When trees or other vegetation contact electric power lines, there can be diverse outcomes with respect to the ignition potential. Stokes[1159] studied this situation in the laboratory and also summarized experiences learned by electrical utilities. His conclusions were that there is a minimal danger of ignition from live, growing vegetation contacting power lines. Under conditions where vegetation encroaches onto a power line, the contact is likely to be made by leaves or twigs. The consequence of this contact with an 11 kV power line is a current flow of typically 10 – 50 mA through the

vegetation. The flowing current through the vegetation heats it up and when the vegetation reaches around 70ºC it has been destroyed and will eventually die, even though it may appear for a while to still be 'green.' After some days, it then loses its 'green vitality' and shows a dull appearance. Then, after a further interval between many days to a month or so, the leaves finally turn brown and are blown off in strong winds. Stokes referred to the process as 'electrical pruning.' The process requires several thousand volts, and vegetation can be in indefinite contact with 415 V power lines without any visible effect. For a detectable fire hazard to exist, Stokes found that contact of relatively large (> 10 mm) branches was needed, as can happen when large branches or whole trees fall onto a power line. In such cases, the ignition sources that can be created include:

(1) Falling incandescent particles;
(2) Flames generated due to combustion of oily material, leading to falling flaming material;
(3) Carbonization of a branch and its smoldering ignition; the branch can then fall down and lead to ignition of ground-level material. This process takes place only within a narrow range of current values and Stokes found it necessary to 'fine-tune' the current to obtain the phenomenon in laboratory testing.

Whether or not a fire ensues will, of course, be strongly governed by the type and moisture content of the ground-level fuel. In many cases, when a branch falls down on a power line, none of the ignition sources will be generated, instead, the branch will be severed at the point of contact and fall down without leading to fire. The events in general depend both on the voltage of the power line and on the form of contact between the vegetation or branches and the power line—sustained or intermittent. If sustained contact is made with power lines carrying over 100 kV, a steam explosion can result. This is dramatic but does not, by itself, create a fire hazard. In addition, sustained contact may be accompanied by an electrical 'flashover' which of course entails extremely high temperatures. But Stokes found that the flashover events were not able to ignite combustible target solids, which he speculated was due to pressure effects associated with the breakdown process blowing out any incipient flame. However, if the sustained contact also creates ignition sources such as those listed above, then ignition of ground-level fuels can be possible. Ignition from particles ejected by conductor clashing is discussed below under *Brands and hot particles*. A related ignition hazard is from the operation of expulsion fuses that are used to protect HV power lines; this is discussed under *Electric circuit interruption devices*. The arc tracking process in trees is discussed under *Wood and related products*.

RADIANT IGNITION

Stokes[562] ignited beds of various forest-floor materials using the ISO 5657 test. The specimens were collected in the field under 'high fire danger' conditions but were not further dried in the laboratory. Table 138 shows the ignition time results. Except at the highest flux, all of the ignitions began as glowing ignitions, with transition to flaming occurring only later; at 50 kW m^{-2}, the ignition mode was not specified.

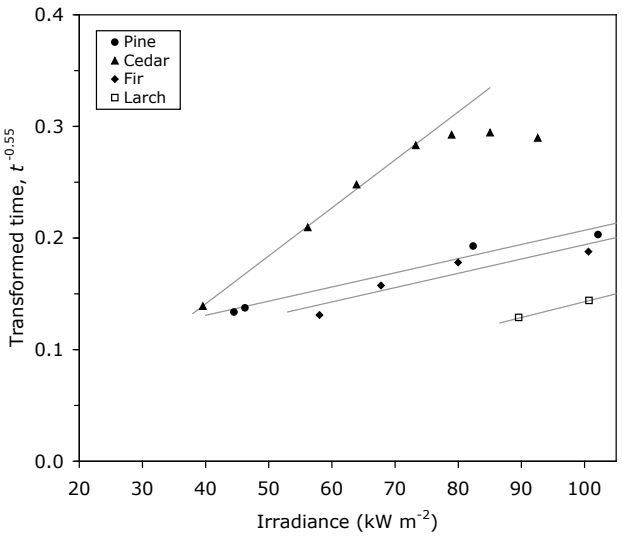


Figure 85 Radiant autoignition of conifer needles

Table 138 Ignition times (s) for the autoignition of various forest-floor materials

Substance	Heat flux (kW m^{-2})			
	10	15	30	50
hardwood litter	50, 600		14, 20, 36, 37	7
barley grass	47, 300	115	16	2, 6
pine needles				4

Filippov[1160] measured the radiant flux needed for autoignition of a variety of forest materials; his results are shown in Figure 85 through Figure 87. Moisture contents were not specified, but presumably were typical for the Russian climate. The lines fitted through the data give the parameters

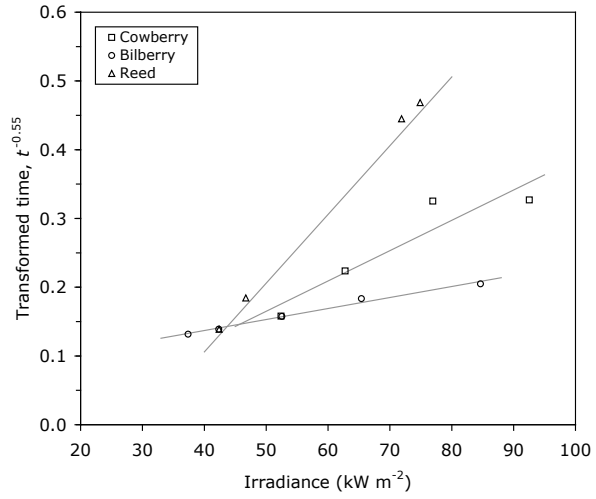


Figure 86 Radiant autoignition of shrubs

Table 139 Ignition properties of forest materials tested by Filippov

Material	Critical flux (kW m^{-2})	B_{ig}
aspen leaves	-0.21	161
birch leaves	1.9	177
pine needles	-63.0	787
cedar needles	7.2	233
fir needles	-51.6	781
larch needles	-5.2	735
reeds	29.4	100
cowberry	12.6	227
bilberry	-45.6	625
club moss	-14.0	398
sphagnum moss	53.0	175
Schrebers moss	14.3	172
alpine lichens	27.6	112

listed in Table 139.

White et al.[1161] conducted piloted Cone Calorimeter tests at a 25 kW m^{-2} irradiance on branches from various coniferous trees—balsam fir, blue spruce, Fraser pine, Norway pine, red pine, Scotch pine, white pine, and white spruce. Their results (Figure 88) show that increasing moisture delays ignition, but clearly other factors are also involved. Not enough samples were tested from any single species to enable botanical differences to be studied. Trabaud[1162] exposed a variety of vegetation types to a radiant heat flux of about 25 kW m^{-2} and measured the autoignition time as a function of moisture content. Typical ignition times at 0% MC were 10 – 20 s, increasing to 50 – 70 s at 20% and then rapidly increasing, so that MC=35% material typically took 300 – 400 s to ignite.

Dimitrakopoulos and Papaioannou[1163] tested the piloted ignitability of vegetation using the ISO 5657 test method, but using only a single irradiance value of approx. 45 kW m^{-2}. Their main objective was to determine the moisture content necessary so that no ignition would occur during a 300 s exposure period. For 24 species tested, this value turned out to be typically 60 – 140%. At the given irradiance, they found that the ignition time results could be represented by $t_{ig} = a + b\ MC$, where MC = moisture content (%), and a and b are constants. There was a wide disparity of results among the species, and some species took 4 – 5 times longer to ignite at a given moisture content than did others.

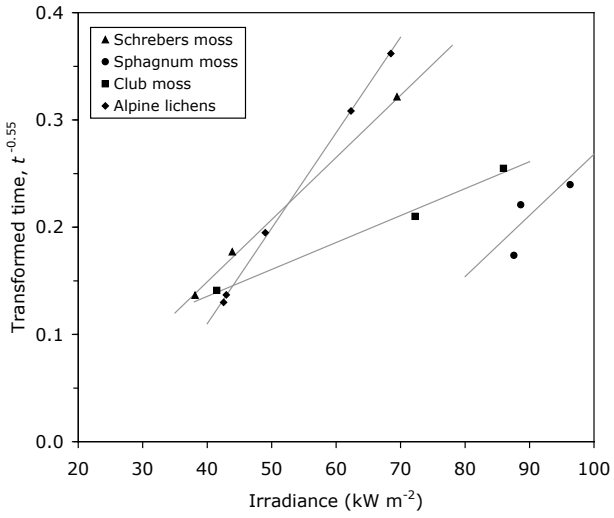


Figure 87 Radiant autoignition of mosses and lichens

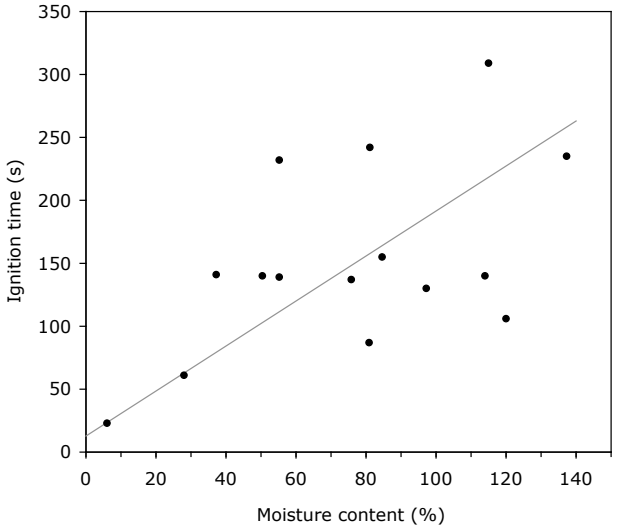


Figure 88 Piloted radiant ignition of conifer branches as a function of moisture

IGNITION BY BRANDS OR SMALL HOT PARTICLES

The experience of the US Forest Service is that a glowing brand only tens of milligrams in mass can start a smoldering fire in a highly susceptible target fuel[1164]. This is consistent with the laboratory results cited in the section on *Brands ejected from fireplace* in Chapter 11 which showed that burning coal particles of only 5 mg (about 2 mm diameter) inevitably cause ignition when dropped onto cotton wool. The investigators found that cotton wool was exceptionally easy to ignite, but other studies show that fine, dry vegetation material is not much more difficult to ignite, as discussed later in this Section.

Once a fuel bed starts smoldering, there is no definite time limit when—if at all—flaming may occur, since this depends on details of the fuel bed, its moisture, and the prevalent wind and temperature conditions. In extreme cases, when smoldering is initiated in combustible subsurface layers, punky portions of trees, etc., months may elapse (see *Ignitions from lightning* in Chapter 11). Pockets of smoldering material have also been undetected and stayed buried under a cover of snow during winter, only to turn into a flaming fire the following summer[1165].

Despite the importance of the firebrand mechanism in igniting or propagating forest fires, not much laboratory work is available on the subject. Several studies using engine exhaust particles were discussed in Chapter 11. More recently, Ellis[1166] tested the ignitability of pine needles using brands made of eucalyptus (*Eucalyptus obliqua*) bark cut into specimens of approximate size 50×15×5 mm and having a mass of 0.7 – 1.8 g. Both flaming and glowing brands were used. Under still air conditions and for rather-dry target conditions (MC ≤ 9%), when flaming brands were used, 100% of the targets ignited, all in a flaming mode. For glowing brands and no wind, it was impossible to achieve flaming ignition, but many tests resulted in a glowing ignition of the target fuel. When a wind of 1 m s^{-1} was applied, the probability of a flaming ignition from a glowing brand was found to be related to the fuel MC, as shown in Figure 89. It is of interest to note that these experiments were done under mild laboratory conditions—temperature was typically 22ºC and humidity 30% RH.

Wildland fires are occasionally ignited from high-voltage power lines when *conductor clashing* occurs (due to creep, ice storms, etc.) or some other arcing event that ejects molten aluminum or copper particles. Rowntree and Stokes[1167] published some data on the ignitability of oven-dried barley grass from molten *aluminum particles*. The study (Figure 90) grouped results into three groups—definite ignition, possible ignition, and no ignition. Two different theories have been proposed to predict this type of ignition: (1) minimum ignition energy; and (2) hot inert sphere ignition. The minimum ignition energy theory is less a theory than an arbitrary hypothesis, presumably formulated on the basis that if MIE is a useful predictor for the ignition of gases, it can also be applied to solids. The hot inert sphere ignition theory, on the other hand, is based on physics, as developed

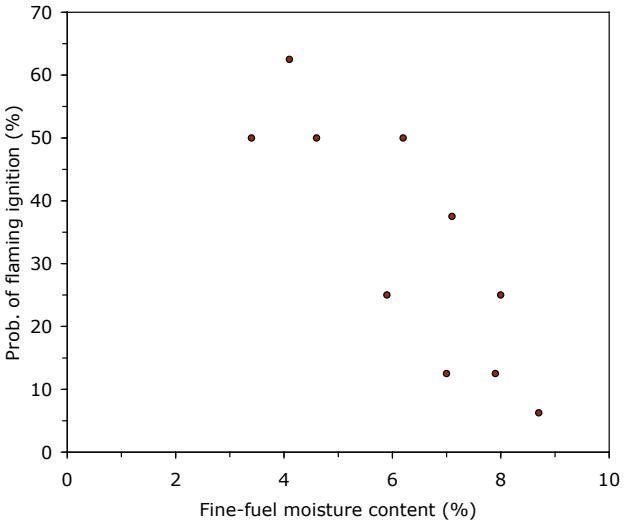


Figure 89 Effect of fine-fuel moisture content on the ignitability of pine needles from small glowing brands

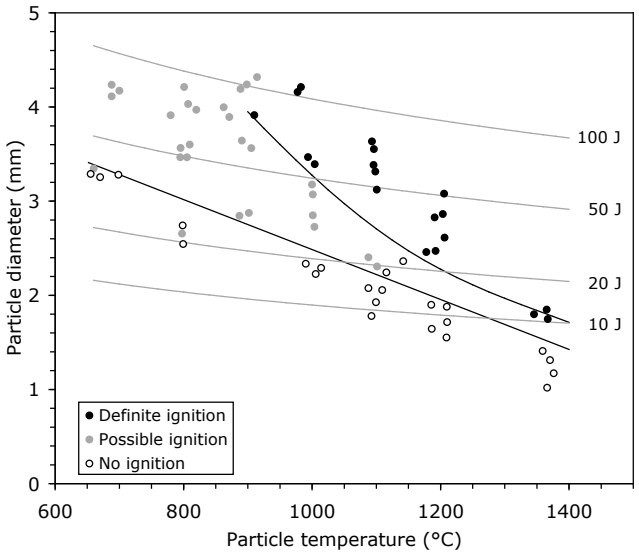


Figure 90 Experimental data on ignition of oven-dried barley grass from molten aluminum particles; also shown are data-envelope contours, fitted to the experimental results by eye (black lines) and contours of constant MIE (gray lines), indicating that MIE is not a viable criterion for ignition of beds of porous materials of this type.

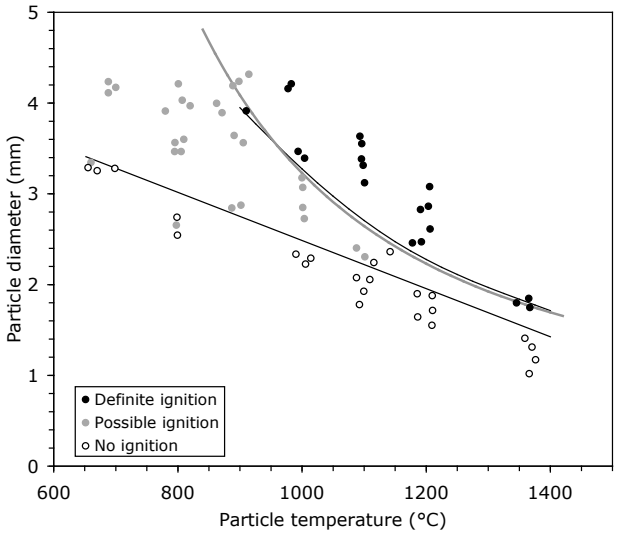


Figure 91 Comparison of Gol'dshleger's theory (thick gray line) to experimental results.

by Gol'dshleger (see Chapter 9). Since Rowntree and Stokes proposed that the experimental data can be adequately correlated by the MIE theory, Figure 90 shows the results of these calculations. The theory is based on computing the stored thermal energy in a sphere that can be delivered by cooling it down from its original temperature to the ignition temperature of the fuel. Since aluminum melts at 660ºC, the initial cooling from high temperatures will be for a liquid, followed by recovery of the heat of fusion at 660ºC, then cooling a solid material below this temperature.

The constant-energy lines in Figure 90 were computed by assuming that density = 2380 kg m^{-3}, heat capacity (which is similar for solid and liquid aluminum) = 1110 J kg^{-1} K^{-1}, and T_{ig} = 300ºC. It can also be shown that changing T_{ig} over a range of physically plausible values, say 250 to 600ºC, does not improve the correlation. The results from applying Gol'dshleger's theory are shown in Figure 91. Here, it was assumed that T_o = 293 K, ρ_h = 2380 kg m^{-3}, λ_h = 80 W m^{-1} K^{-1}, C_h = 1110 J kg^{-1} K^{-1}, ρ = 120 kg m^{-3}, λ = 0.043 W m^{-1} K^{-1}, and C = 2000 J kg^{-1} K^{-1}. Values of the chemical kinetics constants E and P are not known for barley grass, so a best-fit to the data was made, giving E = 70 kJ mol^{-1} and P = 36.2. In contrast to the MIE theory, the Gol'dshleger theory is able to predict slopes which are roughly similar to the experimental ones. These deduced values of E and P are quite close to measured values for some plant material studied by Jones (see *Self-heating* section below), suggesting that the chemistry of Gol'dshleger's theory may be reasonable. The 'possible ignition' regime may not be amenable to theoretical analysis, since the effects are likely to be created by local inhomogeneities of the fuel bed. Rountree and Stokes also presented some summary data indicating that other vegetation types—such as pine needles, and mixed forest floor litter (leaves, twigs, bark) from two different forest types—are less readily ignitable than is barley grass. Stokes[1168] also studied the ability of *copper particles* to ignite vegetation. The particles were created by an electric arc and fell only a short distance onto a fuel bed. The particle temperature was not measured but was presumed to be close to the melting point (1085ºC). Particles smaller than 1 mm showed essentially zero probability of igniting barley grass or forest litter from a hardwood forest, and only a small probability (< 1%) of igniting cotton wool. Particles with a maximum size of 2.5 mm showed about a 10% probability of igniting barley grass. The sizes refer to the maximum size within the shower of particles and most particles were much smaller than the maximum size.

Stokes also conducted some experiments[562] where steel and copper particles were emitted from an electric arc located 0.9 m above a bed of oven-dried fuel and were tested using two wind conditions: still air and a velocity of 2 m s^{-1}. Incandescent particle sizes were not measured in these experiments. Table 140 shows that steel particles were much more likely to cause flaming ignition than copper particles and, surprisingly, that a low-velocity wind decreased the probability. It is also interesting that cotton lint proved to be much more readily ignitable than did forest-floor materials. Stokes noted that some samples which did not yield flaming ignitions produced smoke, but did not assess the probability of smoldering ignitions.

In a second series of tests, Stokes characterized the particle size distribution of the incandescent particles, but the tests were conducted solely in still air. The particle sizes were typically 0.5 – 2.0 mm and the results from these tests are shown in Table 141. These results clearly established a rank order for incendivity as: steel (most), aluminum, copper, brass (least). The boiling points of the metals are all roughly similar, the volumetric heat capacity is similar for all except aluminum (which is about 100× lower), while the thermal inertia ranks, high-to-low: copper/brass, steel, aluminum. Thus, it is not clear what thermal properties actually are dominant in establishing the incendivity. Stokes also took photographs indicating that qualitatively the radiance of the spark showers was: aluminum (highest), copper, steel (least). Stokes also presented data on the effect of particle size on ignition, but these results cannot be readily interpreted since temperature was an uncontrolled variable—smaller particles are also cooler, but he was not able to control the temperatures. In addition, Stokes noted that particles have a varying propensity to break up upon hitting a fuel bed, but this trait depends on details of the fuel bed.

Table 140 Number of flaming ignitions in 10 trials for steel and copper incandescent particles falling onto various materials

Substance	Steel		Copper	
	No wind	2 m s^{-1}	No wind	2 m s^{-1}
cotton lint	10	10	10	10
barley grass	10	6	3	0
hardwood, sieved	8	7	3	0
hardwood, coarse	7	3	3	1
pine needles, fresh	10	2	0	0
pine needles, decomposed	10	9	3	0

Table 141 Probability (%) of flaming ignition in 50 – 100 trials for various incandescent particles falling onto ignitable materials

Substance	Alum.	Brass	Copper	Steel
cotton lint		0		
barley grass			48	
hardwood litter	58		8	90
pine needles, fresh	84		0	94
pine needles, decomposed	44		56	90

Two theories have been published[1169,1170] for predicting ground-fuel ignition distances from particles ejected due to conductor clashing. But these require making numerous assumptions of uncertain validity and experimental data are lacking to judge their realism.

SPOTTING FIRES

If a wildland fire carries brands which start new fires at distances remote from the ongoing fire, the ignition mechanism is called spotting. The propensity for spotting is determined largely by three factors: (1) fuel type; (2) wind speed; and (3) relative humidity. The first factor cannot be easily generalized and depends on local fuel characteristics. The effects of wind speed and RH, however, can be illustrated by trends observed in one geographic area[1171] (Figure 92).

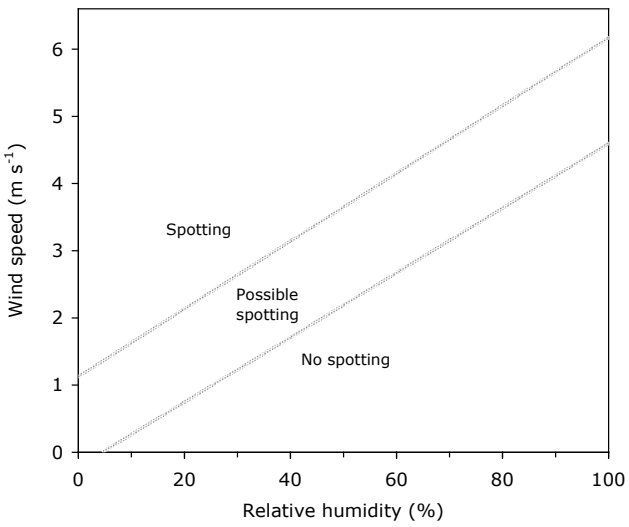


Figure 92 Effect of wind speed and RH on spotting potential in Florida wildlands

SELF-HEATING

Fires in haystacks due to self-heating was already a problem known by the Romans[266,1172], and hay is one of the earliest substances which was studied for its self-heating propensities. Chemical consideration of the problem was undertaken by Ranke in 1873[1173]. The role of microbial action was also appreciated surprisingly early—Medem[35] speaks of it in 1898—although this understanding was not quantitative. The problem of self-heating in hay was of such practical importance that as early as 1907 an entire book on the topic of self-heating of hay was published in Germany[1174]. The earliest explanations of the phenomena, however, that would be consistent with modern science did not take place until around 1930[266,1172, 1175].

Firth and Stuckey[1176] report that spontaneous combustion fires in haystacks most typically break out at 5 – 10 weeks from stacking, although times as short as 10 days or as long as 3 months are known. Drysdale[1177] states that the most common interval is 2 – 6 weeks after storage. According to Firth and Stuckey, if it takes more than 3 months for fire to break out after stacking, this is due to the hay having gotten wetted in the interim. The pivotal role of moisture in actual fire incidents of self-heating of hay was documented after a Vermont flood, when piles of hay started self-heating 2 – 3 days after being flooded, and in one case caught fire after 4 days[1178]. During self-heating prior to runaway conditions being reached, the odor is described as caramel-like[1179]. If visible wisps of 'steam' rise from haystacks, that is also a danger sign. The odor of spontaneously combusted haystacks is aromatic, resembling tobacco or tea leaves; it is different from the acrid smell of a haystack ignited externally[1176].

It is considered that the self-heating of hay generally progresses through three stages. In the first stage, the biological respiration of the plant material still continues and provides heat. In the second stage, fungi and bacteria can flourish, and these provide additional heating. Their action can be complicated since one of the effects of microbial decomposition of carbohydrates is the production of water, thus changing the moisture balance of the material. The final stage occurs after temperatures have risen enough to kill off microorganisms. This involves the chemical oxidation reaction of the hay itself.

Firth and Stuckey[1180] consider that there is significant similarity between the self-heating of haystacks and the production of silage. The latter is produced in silos where air flow is excluded. In the early stages, cell respiration provides self-heating. Cell activity stops when the air is exhausted or when a combination of cell respiration and microorganism action raises temperatures beyond about 40ºC. At that point, cells die and microorganisms start to multiply, deriving nourishment from the dead cells. Fungi are probably dominant at lower temperatures and bacteria at higher ones. The process results in breakdown of carbohydrates (and possibly proteins) and the production of CO_2, alcohol, organic acids, and unsaturated organic compounds. Oxidation does not play a significant role, due to low oxygen levels. In well-made haystacks, the process is basically similar, except air is not excluded and moisture levels are lower. Activity of the microorganisms ceases when the water supply becomes exhausted, and temperatures do not continue to rise. Runaway self-heating of a haystack occurs when moisture does *not* get exhausted, yet air is present. As the self-heating process develops, chemical heating starts becoming important at about 70 – 75ºC, and at around 76ºC bacterial activity stops, even of high-temperature tolerant, thermophilic bacteria. From that level up to about 170ºC, chemical decomposition reactions take place which are dependent on the presence of moisture. Some of the decompositions reactions become autocatalytic, which accelerates the process. Above about 170ºC, oxidation reactions predominate, and these continue to the point of thermal runaway. With oxygen continuing to be available, open flaming may eventually erupt.

Rothbaum[1181] discovered an important limit to the starting conditions of the hay, if thermal runaway is to occur. Bacteria metabolize strongly only at RH values over 95%. Thus, haystacks with RH > 95% would be the main ones vulnerable. There is an upper limit also. As RH approaches 100%, the thermal conductivity of porous materials begins to show a very rapid increase, and this increase gets progressively more so at higher temperatures. Since high thermal conductivity reduces self-heating, the humidity range where actual self-heating fires are expected to occur is confined to RH values of 95 – 97%. Expressed as moisture content of the hay, the critical range is about 39 – 49%. Rothbaum proved his hypothesis in laboratory testing. Hussain[1182] agreed that

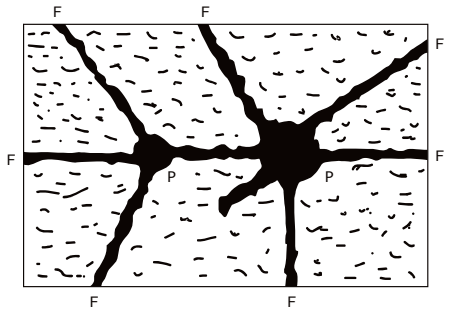


Figure 93 Pattern of flues (**F**) and pockets (**P**) formed in the interior of a haystack that self-heated to the point of charring

45% is the worst-case moisture content, but in his experiments runaway self-heating was possible for hay having moisture as low as 25%. Firth and Stuckey noted that MC = 25% is also the lower limit of moisture content found for actual case incidents, although Rothbaum considers the limit to be 33%. Rothbaum's basic findings were recently confirmed by Miao et al.[1183] They tested hay packed at a density of 50 kg m^{-3} in a temperature-controlled reactor and demonstrated that initial conditions of T = 110ºC, RH = 5% do not lead to detectable self-heating, nor does T = 50ºC and RH = 95%. But T = 70ºC and RH = 95% leads to runaway conditions (Figure 94). Thus, they showed the necessity of both (a) an RH value around 95% and an elevated temperature starting at around 70ºC. The latter, of course, validates the concept that biological heating (cell respiration + microorganisms) is needed to cause the initial stage of self-heating. They also elucidated that there is a contribution from the heat of sorption, since specimens which were initially at a higher moisture content showed less self-heating than did originally-drier specimens, when subjected to an environment of the same RH. In a follow-on study[1184], the authors concluded that the chemical self-heating of hay involves three separate groups of reactions: (1) decomposition; (2) oxidation; and (3) Maillard reactions. The latter involve condensation of carbohydrate decomposition products with protein or amino acids to form a dark-colored, insoluble polymer.

The theory that biological heating is an essential step of the process, while generally agreed to, has been questioned by one research group. In a series of oven tests at 104ºC, moistened bales of hay were found to ignite in 3 to 60 hours[1185]. The authors consider that the oven environment was ramped up so rapidly that any biological activity would have ceased very quickly and would not have contributed measurably under their conditions. On the basis of spontaneous combustion statistics, it has been argued that excessive *compression* of hay promotes self-heating[1186]. It was also observed that adequate ventilation is required in order to avoid self-heating problems[1187]. The role of ventilation in the self-heating process is a double one: (1) it provides a bulk flow cooling effect through the mass; this is normally ignored in simplified self-heating theory, but is non-

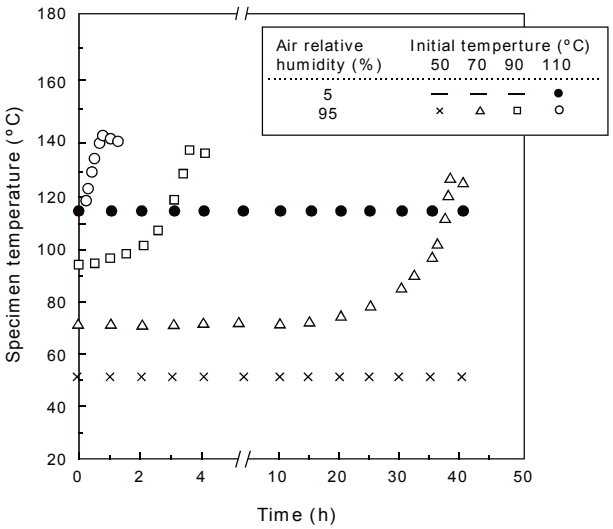


Figure 94 Effect of temperature and RH on self-heating of hay
(Copyright ASAE, reprinted by permission)

negligible at high enough ventilation rates; and (2) it suppresses the growth of thermophilic microorganisms.

Numerical calculations of the self-heating of hay have not produced adequately realistic results. This is due to the fact that the multiple exothermic processes which occur in an overlapping manner are difficult to accommodate in a theory simple enough to lead to solutions. Additional complications come from the need to model the flow of moisture and the need to represent accurately the thermal conductivity, which varies widely with moisture. In laboratory tests where small quantities of hay were initially exposed to a room-temperature environment, the time to thermal runaway was typically 15 – 40 days[1181,1182,1188]. Since this is similar to the range of spontaneous combustion times found for real haystacks, it is quite evident that time-to-runaway does not follow F-K theory (which would predict increasing times with increasing size).

As with any product susceptible to self-heating, the charring in a self-heating-caused fire is from the inside out, while if the haystack is ignited externally, charring is from the outside in. Firth and Stuckey also recommend that the investigator cut apart a suspect haystack (having a water hose ready to extinguish flaming, if flaming erupts during this process). Upon cutting through the center, if the haystack was self-heating to the point of charring, a gradation of damage should be seen, where going from the outside in, the color goes: greenish-brown → gold-brown → dark brown → chocolate → black hay still retaining structure → fine black powder. In addition, if a pattern of charred flues and pockets is found (Figure 93), this is indicative of charring due to self-heating. These flues will be surrounded by part-charred material; and should not be confused with crevices formed due to vigorous external burning. In the latter case, the crevices will only be charred to one side, and

not surrounded by charred material. Haystacks that have spontaneously combusted sometimes leave a glassy material as residue. These 'clinkers' are not a suspicious device, but rather are formed from the minerals contained in plants[1189].

Recommendations for optimum storage of hay are to keep it at 12 – 22% moisture content[1179,1190]; values over 25% may lead to spontaneous combustion (and to moldy conditions), while hay at very low moisture contents is nutritionally poor. It is reported that hay from clover or alfalfa is more prone to self-heating than from grasses[1191]. *Straw* is much less prone to self-heating, nonetheless recorded incidents do exist of spontaneous combustion of piles of straw bales[1192]. For sufficient self-heating to occur, fungal action is necessary, and the latter requires nitrogen-rich conditions.

When stored in *silos*, hay is optimally at 50 – 65% MC when put into a top-unloading silo and 45 – 55% for a bottom-unloading silo[1193]. Self-heating is most likely to occur for somewhat dry hay, at about 30%; this may occur due to air leaking in through cracks in walls or doors. Very dry hay at around 20% will not self-heat due to lack of conditions suitable to microbial heating. A fire is made more likely if the hay is improperly packed so that it is not tight against the silo walls—this condition makes it easier for air to reach the interior of the silage. Spontaneous combustion is less likely in silos constructed to be oxygen-limiting, compared to ones with more significant air leakage. Some practical aspects of fires in silos have been presented by Maloney[1194] and the US Fire Administration[1195].

Grasses of all kinds, even those not suitable for fodder, generally show similar behavior to hay. Rothbaum[1196] examined the self-heating propensity of Moroccan esparto grass. The crucial difference is that esparto grass takes up significantly less moisture for a given RH value, in comparison to hay. In the critical region of 95 – 97% RH, where chemical self-heating becomes important, the moisture content of esparto grass is 25 – 27%, compared to 66 – 71% for hay. In adiabatic calorimeter tests starting with an ambient temperature of 20ºC, self-heating of esparto grass was nil for specimens at less than 90% RH. Because of the smaller moisture take-up, esparto grass is considered to be less prone to self-heating than hay under otherwise similar circumstances.

A case incident is reported[1197] where a pile of spruce bark heaped up against a wood door self-heated and ignited the wood door even though the pile was only ca. 1 m in size. Eucalyptus leaves are quite prone to self-heating, much more than are chips of the eucalyptus wood itself. Jones and Raj[1198] reported results which produce the values E = 71 kJ mol^{-1} and P = 38.3 for leaves at a density of 140 kg m^{-3}. Jones et al.[1199] studied the self-heating of forest floor material. Their two data sets can, on the average be represented by E = 82 kJ mol^{-1}, P = 41; and E = 91 kJ mol^{-1}, P = 44. Jones[1200] also speculated that relatively minor concentrations of *inorganic materials* may play a role in the smolder-ignition propensity of vegetative materials, but did not present quantitative data. Earlier, Rudge[1201] claimed that spontaneous combustion in forest or vegetative matter is promoted by a chalk or limestone subsoil. In his view, moisture played a major role and the exothermicity of some calcium reactions could appreciably aid self-heating.

Fuel oil

Fuel oil consists of a wide variety of hydrocarbons; it does not show a unique boiling point, but rather a temperature range over which evaporation (fractional distillation) progressively occurs. Table 142 indicates some typical values[134]. The primary variable used to distinguish fuel oil grades is viscosity, with the higher-number grades being more viscous. Other properties tend to track with viscosity. In the US, characteristics of fuel oils are governed by ASTM D 396[1202]. The ignition temperature for small drops of heavy (residual) fuel oil follows the relation[1203]:

$$T_{ig} = \frac{76.6}{d} + 218$$

where T_{ig} = ignition temperature (ºC) and d = diameter (mm).

Table 142 Fractional distillation features of fuel oils

Fuel oil	Temperature (ºC) at which given % has evaporated		
	0%	50%	100%
No. 1	180	225	280
No. 2	190	265	330
No. 4	215	290	365

Furnaces and boilers

Boiler explosions[1204] are generally due to two causes: (1) a fuel gas/vapor explosion within the combustion space; or (2) a massive leak of steam into the combustion area from the rupture of a large tube or header. In the latter case, a physical explosion of the boiler takes place because steam enters the boiler so fast that the available openings are insufficient to stop the pressure rise.

Numerous fires occur when furnaces or boilers are placed improperly on the floor so that excessive temperatures can be developed on wood flooring materials. Schwalje[1205] documented a number of fires and near-misses due to this cause. In one near-miss case, he found a 25 mm layer of cement board under a boiler, underneath which was an OSB wood subfloor. A thermocouple reading at the interface between the cement board and the OSB subfloor indicated over 172ºC at the time of measurement, however, an identical installation in another building had resulted in fire. Further aspects of low-temperature, long-term ignition of wood materials are discussed under *Wood and related products*. Maintenance and troubleshooting of boiler low-water cut-off switches is described by Certuse[1206].

Arsonists have been known to rig furnaces to fail and thereby cause a fire. One method which has been described for a hot-air furnace involves disabling the mechanical operation of the fan, possibly by breaking the fan belt, then rigging the high-limit switch so that the wiring effectively bypasses the switch contacts[1207]. This form of incendiarism, of course, is not difficult to detect.

GAS-FIRED

Ostroot[1208] surveyed 116 explosions in industrial gas-fired furnaces and identified the causes (Table 143). Same as gas-fired water heaters, a gas-fired furnace or boiler needs adequate combustion air. If it is improperly installed so that combustion air is inadequate, flame 'rollout' can occur. This happens when air supply is too limited to allow proper inflow into the combustion chamber. A lazy flame can then leave the combustion chamber. Combustibles located nearby the furnace can get ignited in a 'rollout' event. Some recently-made furnaces have been equipped with thermal devices at the edge of the air opening which sense an abnormal temperature increase and cut off the fuel supply[1209]. Flame rollout can also occur due to flue blockage or blockage at the heat exchanger within the furnace.

Table 143 Causes for explosions of industrial gas-fired furnaces

Cause	Percent
gas leakage into furnace due to faulty shutoff valve	26
delayed ignition, miscellaneous reasons	28
inadequate air supply or unstable gas supply	16
inadequate purging, miscellaneous reasons	15
attempted lighting by hand or lance	9
repeated attempts to light pilot without intermediate purging	7

Nearby combustibles were ignited in a series of furnace failures involving a furnace improperly designed to reduce NOx emissions under California regulations[1210]. It was found that excessive temperatures were created within the combustion chamber which the metalwork could not withstand. Consequently, the heat exchanger would crack and rupture, and eventually flames would issue from exterior furnace openings due to action of the air blower, leading to ignition of external objects. Overfiring, and a possible fire, will occur if a furnace or boiler is converted from natural gas to propane service and a smaller-size orifice is not installed.

OIL-FIRED

Ostroot[1208] surveyed 98 explosions in industrial oil-fired furnaces and identified the causes (Table 144). Blum[1211] describes the following as being the main causes for fires originating from residential oil-fired furnaces:

- Clogged heat exchanger or flue pipe. A large number of faults can cause grossly poor combustion, leading to clogging.
- Puffback explosion. This happens if there is a substantial delay between introducing oil into the combustion chamber and igniting the mixture. The overpressure can crack lightweight furnace components or flue pipe parts, with the result that fire or hot gases can escape. Causes of delayed ignition include defective ignition transformer, worn or dirty electrodes, cracked electrode insulators, loose ignition wiring, low oil pressure, water in the oil, or a faulty nozzle.
- External oil leak which ignites.
- Firebox deterioration, leading to an opening being formed. This can be caused by flame impingement or by use of corrosive cleaning agents.

Table 144 Causes for explosions in industrial oil-fired furnaces

Cause	Percent
delayed ignition, miscellaneous reasons	51
defective ignition system	32
inadequate purge	12
improper fuel/air ratio	5

Sokalski[1212] reviewed fires originating at residential oil-fire furnaces and considers that common causes or contributing factors include:

- worn-out oil pump
- burner tip worn or clogged
- improperly adjusted burner
- failure of safety control circuits
- plugged flue, or defective or improperly installed barometric damper
- lack of an oil safety valve (OSV)
- clogged air filters
- miscellaneous electrical or mechanical failures.

One specific failure mode that can be a ready cause of fires is a failure of an elastomeric pump diaphragm in installations where (a) the fuel tanks are above the burner level and (b) an OSV is absent. In these cases, the static pressure of the oil in the tank will create an excessive supply of oil into the burner, which can lead to runaway combustion. An OSV is a form of check valve which can be placed in the fuel line from the tanks. The valve keeps the fuel line shut except when there is a negative pressure on its downstream side, created by the operation of the pump. When the pump stops, a negative pressure is no longer generated, and the check valve closes.

Another failure mode involves the cutoff valve. The pressure regulator typically contains a cutoff valve, the function of which is to close the flow of oil into the burner as soon as the pump is stopped. If this valve leaks, fuel will drip into the combustion chamber and an excess may build up, leading to an overfiring upon startup.

An unusual cause of over-firing an oil burner can be due to improper switching to a more viscous grade of fuel oil. If

the same regulator pressure is maintained, it is natural to presume that a lower flow would emerge from the nozzle when using a more viscous oil. However, the design of some nozzles is such that the flow rate is actually increased. This has been hypothesized to be related to the swirl-inducing characteristics, but details are not researched. The problem can also arise even without switching grades of oil if a much colder oil (which is more viscous) is introduced into a system set up to operate at a higher temperature. An additional effect of improperly introducing a more viscous grade of fuel oil is that it will have a higher heat of combustion. This means that, for a given air supply, longer flames will be generated.

NFPA 31 provides guidance on safe installation of oil-burning equipment[1213].

Furniture

Palmer et al.[1938] tested plastic furniture parts for ignitability with matches and found that for ABS, polypropylene, polystyrene, and polyurethane (rigid foam) specimens ignitions generally were possible only at an edge. Upholstered furniture is discussed under *Upholstered furniture and mattresses*.

Gas meters, regulators, and piping

A gas meter explosion has been described that occurred due to electrical causes[1214]. An electric power utility was repairing power lines after a storm and erroneously crossed over a hot line to feed the neutral. Above-ground-potential voltage now existed at the neutral of the service entrance of the building. The neutral-to-ground connection at the service entrance was defective, so electric current flowed through another connection that existed between the neutral and the gas piping. The gas meter was electrically insulated from the gas piping in the building by a thin washer (this is done in order that cathodic protection could be provided to the underground piping). The current arced across the dielectric, blew a hole in the gas piping and caused a gas/air explosion.

Fires caused by failures of gas lines due to ground faults have been documented[803]. The faults caused by excess flow of electric current resembled hacksaw marks in some cases, requiring careful efforts to avoid mis-identification. For flexible tubing, the failure is often near the connection (Color Plate 129), because the metal narrows down at that point. Another ground-fault ignition near gas meters is described under *Electric wires and cables: Stray current and ground faults*. A case has also been described[1215] where a building exploded due an accumulation of natural gas. The gas entered the building from a leaking gas pipe, and the leak in the gas pipe was caused by an electric fault which originated when a bird short-circuited a high-voltage power line.

Gas pipes can fail because of metal alloying. A case is reported where a small, round hole was found in a copper propane pipe[1216]. Investigation showed that aluminum had melted onto the pipe and created a low-melting-point alloy.

The forensic examination and testing of gas pressure regulators has been described by Cox[1217]. Regulators sometimes develop a small leak so that the valve does not mate in a gas-tight way against the seat. Under those conditions, if the regulator does not have a pressure relief vent, or if the vent becomes blocked (due to ice, paint, insects, flood waters, or other causes), the pressure on the outlet side can rise to the inlet pressure[1218]. Excessive pressure sent to the furnace or appliance control valves can then cause leakage or failure. In propane systems, failures have been observed where all the gas-using appliances were shut off, a leaky regulator led to excess pressures in the system, and this caused propane to re-liquefy in a cool portion of the piping[1219]. Upon turning on an appliance, the presence of liquid propane continues to sustain excessive pressures. Regulator failures can be hard to document, since often the cause of the valve not seating properly is a small piece of debris being caught there. When the gas supply is turned off in connection with the fire, the valve rises and the debris falls away.

Sanderson[1219] points out that house fires sometimes occur when a new owner first turns on a gas appliance, not realizing that the previous owner removed a gas appliance (e.g., dryer) and both failed to properly cap the outlet and had previously failed to install the mandatory separate shutoff for the dryer.

Gasoline

Gasoline is a blend of hydrocarbons of various types (primarily in the C_4 to C_{10} range), plus additives. On the order of 200 different chemical species may be found in gasoline. These different constituents have different vapor pressures. The technical specifications of gasoline in the US are governed by ASTM D 439[1220]. The vapor pressure of gasoline must stay within certain bounds, especially it must not be so high as to lead to vapor lock nor so low that it ceases to flow properly. Consequently, ASTM D 439 establishes five volatility classes, with Reid vapor pressure values ranging from 62 to 108 kPa. Vendors must then select the appropriate volatility class to sell, depending on the climate of the locale and the month of the year. However, the ASTM specification does not end up governing the gasoline that is sold, since stricter vapor pressure limits are generally set by the Environmental Protection Agency[1221]. When exposed to air, gasoline will 'weather,' which means that the constituents having higher vapor pressures will preferentially evaporate first. Thus, the fraction that remains will progressively show a lower vapor pressure and will comprise compounds of higher molar mass. Eaton[1222] has tabulated various other properties of gasoline. *White gasoline* (white gas) is an unleaded, uncracked gasoline which is sold as fuel in motorboats, stoves and lanterns. The additives contained in this fuel are primarily for anti-gumming.

The American Petroleum Institute[1223] considers that the flammable range for commercial gasoline is 1 – 7%; another source[1224] lists 1.4 – 7.6%. LFL values as low as 0.6% have been reported, but these are evidently erroneous. Frobese[1225] measured the flammability limits of gasoline vapors actually collected from the vapor space of a filling station tank and found a flammable range of 1.3 – 7.7%. The detonation limits[1226] are 1.1 – 3.3%. The minimum oxygen concentration[142] for a gasoline/air mixture is 11.6%, when dilution from 21% oxygen is by means of adding N_2, and is 14.4% when diluting with CO_2. The pressure limit[1227] of gasoline, at room temperature, is 4.0 kPa, that is, if a gasoline/air mixture has a total pressure below this value, flame propagation within the mixture is impossible, at least for ignition sources that are comparable in strength to what was used in testing. A complete gasoline/air/inert diagram for various diluents is shown in Figure 95.

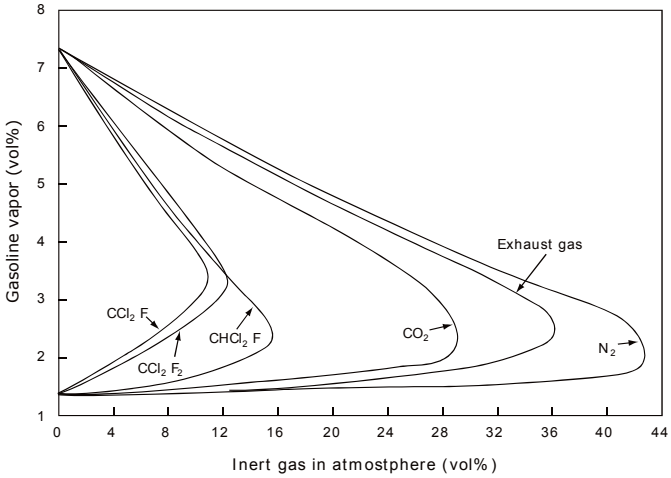


Figure 95 Inerting requirements for a gasoline/air mixture at 25ºC

The flash point of gasoline is typically around –45ºC. However, when stored for a long time in a closed container, an effective LTL of –65ºC has been found. This is because the flash point test apparatus does not represent the same heating and vaporizing conditions which occur under long-term storage conditions. The MIE of gasoline is 5 mJ at its flash point. In one study[1228], it was found that the MIE of gasoline sprays decreases for temperatures higher than the flash point, and reaches about 0.6 mJ at 10ºC.

The autoignition temperature of gasoline depends on the octane number. Ignition at a low temperature leads to 'knock' and consequently higher-grade gasolines are formulated to raise the AIT value. Using a 1 L flask test at NBS[1229], the AIT was found to be 248ºC for 65-octane gasoline, 258ºC for 73-octane, and 412ºC for 87 octane. The above values were determined at the concentration showing the lowest AIT, which was about 0.15 g L^{-1}. The temperatures take a jump upwards at higher octane numbers since the ignition mechanism changes. A red flame and a puff was seen at the lower octane values, but a blue flame (and much shorter ignition times) for the higher octane values. The dependence of ignition time on the temperature of the flask is shown in Figure 96. Modern-day, high-octane automotive gasoline typically has an AIT of 440 – 450ºC, although Hawksworth[1230] found values as low as 350ºC. The AIT of gasoline in oxygen at a pressure of 25 atm is less than 100ºC[1231].

Husa and Runes[1232] examined the possibility of igniting the vapors above large open pans of gasoline by an electrically heated pipe of 114 mm diameter and 1.2 m long. Temperatures in excess of 600ºC failed to ignite the vapors.

In fire incidents, gasoline vapors have been ignited by sparks from hammers, from boot nails on a concrete floor, and from metal tools dropped onto concrete[1233]. In laboratory tests, gasoline vapors have been marginally ignitable by sparks produced by grinding mild steel with an abrasive wheel, with much preheating of the steel being required; in many test conditions, negative results are reported[1234]. In actual fire incidents, grinding sparks have ignited ethylene, methanol, and oil vapor[1233]. These substances are of similar ignitability as gasoline, so grinding sparks should also be expected to ignite gasoline vapors in actual incidents. Steel tools cutting into quartz-bearing rocks readily ignite gasoline vapors, but this does not occur with other rocks[1235]. Bronze, brass, copper-beryllium, or aluminum tools are unlikely to ignite gasoline vapors.

The vapor pressure of gasoline is so high that, in most circumstances, the concentration in a vehicle's fuel tank and the appurtenant plumbing is above the UFL, and consequently, no ignition or explosion is possible. Frobese[1236] investigated experimentally the conditions under which this assumption might prove to be false. The problem was of special concern, since in 1993 European regulations were

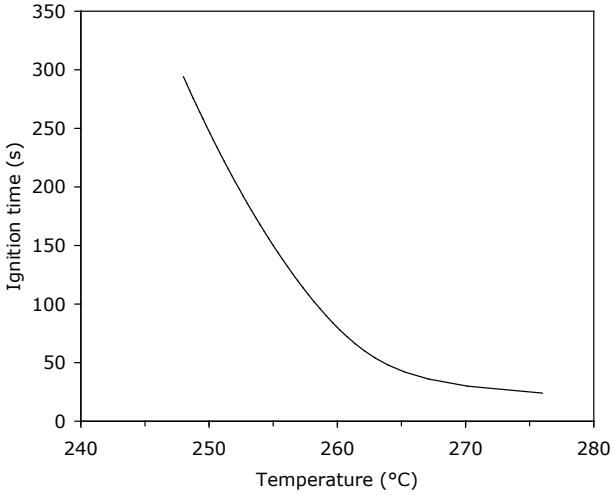


Figure 96 Ignition time of 65-octane gasoline, as determined by Setchkin in a 1 L heated-flask test

changed so the lower RVP limit of summer gasoline was dropped from 68 to 35 kPa, and of winter gasoline from 88 to 55 kPa. At a temperature of –20ºC, the 55 kPa RVP gasoline showed a fuel tank concentration of 6.0 vol%, which is within the flammable range; by contrast the 88 kPa RVP gasoline showed a concentration of 8.6 vol% at the same temperature. In the case of the 55 kPa RVP gasoline, for a flammable mixture to be attained (i.e., the UTL to be reached), required reducing the temperature to only –8ºC. In simulated vehicle-operation experiments, Frobese also found that the lower boiling-point fractions get preferentially decreased. This is primarily caused by temperature cycling of the vehicle, which produces a rise in pressure and a venting of the lighter fractions. Summer fuels, both new and old, showed negligible changes in RVP after the simulated vehicle-operation tests. But the old winter fuel decreased from 88 to 60 kPa, while the new one from 55 to 44 kPa. Frobese also conducted some ignition tests to determine the UFL for the fuels. A minimum-violence deflagration was found at concentrations as high as 8.4 vol%, although to achieve rapid and complete combustion required a concentration below about 6.7 vol%.

If the atmosphere within the gasoline tank is flammable, then it has been found that the spark energy from a breaking wire of an in-tank fuel pump is sufficient to cause ignition, but a break in the fuel tank gauge sender wiring is not[1237].

Gasoline is undoubtedly the most dangerous substance that is routinely handled by untrained individuals. Consequently, numerous accidents occur due to improper fueling, storage, or use. In many cases, individuals apparently forget that gasoline vapors are flammable and easily ignitable. Some details are discussed below and under *Water heaters: Gas-fired water heaters*. The issue of whether gasoline vapors can be ignited by cigarettes is discussed under *Cigarettes*.

GASOLINE SUBSTITUTES

In recent decades, concerns over air pollution and, to a lesser extent, over fuel availability have led to fuels being delivered at filling stations which are other than normal gasoline; these are sometimes referred to as *reformulated gasoline*. This is a generic term and it does not specify the chemical composition of the fuel. The Reid vapor pressure of reformulated gasoline is lower than for standard gasoline; one study reports values of only 46 – 48 kPa[1238]. The relative safety of vehicle gasoline tanks depends on the fact that, except at extreme winter temperatures, the atmosphere within the tank is non-flammable since the fuel concentration is above the UFL. A study by Vaivads et al.[1239] determined the UTL values for a variety of other fuels using a realistic tank geometry and a moderately large, 0.25 J ignition source. The results (Table 145) show that pure alcohols would be categorically hazardous. There is evidently no increased hazard with the reformulated gasolines under summer conditions, but reformulated winter fuels could be significantly more hazardous in cold climates. The small amount of tank fill was selected to represent worst-case conditions. For a half-full tank, the UTL values dropped by 2 – 10ºC. In related work, the authors[1240] provided flammability limits estimating rules for reformulated gasoline:

$$LFL = 0.58C_{st}$$

$$ULF = 2.8C_{st}$$

where C_{st} = stoichiometric concentration (g m^{-3}) and the units of LFL and UFL are g m^{-3}.

Table 145 Values of UTL determined in a fuel tank 1/30-filled with various fuels

Fuel type	Fuel is below UTL for temperatures under:
Winter fuels	
winter gasoline	–22
90 gasoline/10 ethanol	–26
85 gasoline/15 ethanol	–8
85 gasoline/15 methanol	–5
Summer fuels	
summer gasoline	–17
90 gasoline/10 ethanol	–14
85 gasoline/15 ethanol	0
85 gasoline/15 methanol	+1
Pure fuels	
ethanol	+38
methanol	+37

When ethanol is added to gasoline, the Reid vapor pressure rises until about 5 – 10 vol% is added, at which point a plateau is reached that is about 8% higher than for pure gasoline[1241]. Increasing the ethanol fraction further causes a monotonic decrease in RVP. For pure ethanol, RVP = 15.9 kPa. The peak occurs because it is easier for ethanol to evaporate from gasoline than from itself; this phenomenon is termed the 'hydrogen bonding dilution effect.'

FILLING OF PORTABLE GASOLINE CONTAINERS

Filling of portable gasoline containers ('jerry cans') at filling stations sometimes leads to an electrostatically-ignited fire. CPSC at one time waged an effort to reduce these incidents, which has resulted in signs being posted at the pumps that give warnings on this. Smoot[1242] studied the problem and concluded that the four main factors which increase the likelihood of a fire are:

- filling the container while it is sitting on a surface that is a good electrical insulator (the bed of a pickup truck having a polyethylene truck-bed liner, a carpet, etc.)
- use of a metal, rather than plastic, container
- failure of the user to make contact between the (grounded) nozzle and the container
- using a large fuel flow rate.

The atmosphere in the container will normally be above the UFL, but filling it with liquid causes vapors to be forced out; these can then accumulate on the truck bed. Ignition most commonly takes place when a spark passes between

the nozzle and the container. This will normally lead to only a small, non-violent fire, but victims sometimes panic and attempt to lift up the container, leading to a large spill and becoming injured in the process. Smoot concluded that the high-density polyethylene typically used to make truck bed liners is an unfortunate material choice, since it has an extremely high electrical resistivity and the layer of plastic reduced the effective container+truck capacitance from around 180 pF, which is measured on trucks without a liner, to around 70 pF. Metal containers are more hazardous since they are more likely to undergo a spark discharge between the nozzle and the container than are plastic ones. The charge accumulation from the streaming current associated with the gasoline flow depends only on the filling rate. Smoot measured streaming current values ca. 1.7×10^{-9} A for a filling rate of 19 L min^{-1} to ca. 6.8×10^{-9} A for 38 L min^{-1}. A lower capacitance leads to higher hazard, since a smaller charge suffices for a critical discharge voltage to be reached. Pratt[1243] presented a calculational example for the problem.

Experiments have been conducted to determine the minimum conditions needed for an incendive spark discharge between a metal gasoline can pouring spout and a container filled with gasoline[1244]. The necessary voltage V to ignite gasoline vapors was found to be:

$$V = 6.5\,C^{-0.3}$$

where V = volts (peak), and C = capacitance (F). Note that this equation does not represent a constant-energy relation. The equation given is a lower bound, and actual data points ranged up to a factor of 2 higher. Lowest values were obtained when slowly withdrawing the spout from a gasoline container in good contact with earth. If a typical capacitance of a person is taken as being 220×10^{-12} F, then 5100 V is needed to ignite gasoline and the ignition energy needed is 3 mJ. If discharge is not from a spout but from a needle point, the required voltage was found to be 65% of that given in the above equation. The lower-bound equation given above represents testing on a warm sunny day. For tests run at 9ºC, the needed voltage was about double that indicated.

A case history is reported of an individual who got burned due to the unexpected ignition when transferring gasoline outdoors from one plastic container (an approved, conductive-plastic type) to another in the absence of any overt ignition sources other than static created by the person's movements[1245]. The temperature was 25ºC and the humidity 65%.

Actual explosions of portable gasoline containers are rare, because this requires that the vapors inside be below the UFL. This can happen in extremely cold climates. It has been claimed that explosions can occur in temperate climates while emptying a container, due to entry of ambient air into the container. This is not supported by the published literature. There have been no case histories published where an event of this kind would have been documented. In addition, there have been no experiments that would support this suggestion; instead, experimental work has shown the opposite, that containers will not explode (J. D. DeHaan, Kirk's Fire Investigation, 6th ed., Pearson Education, 2006, pp. 70-71).

FUELING VEHICLES AT FILLING STATIONS

It has been reported that during the 1990s there was a large increase in static ignition accidents at gasoline filling stations in Europe[1246]. The frequency of incidents was related to times of low humidity. Studies and data reports indicated that a sizeable fraction of the cases have a common theme: at a self-service station the customer starts filling the tank and uses the 'latch-on' feature of the nozzle. She then sits down in the car seat and gets up when the filling is finished*. The sitting/rising action causes static charging which is discharged as she contacts the nozzle. PTB conducted laboratory studies[1247] on the problem and found that sparks could be created in several ways, most commonly for some car models at the location between the filler spout and conductive rubber membrane connected to the car body. Color Plate 130 shows a spark at this location that required only 3 kV. The study also showed that the charge that can be built up as a consequence of pumping the gasoline depends on the conductivity of the gasoline. But it was found that commercial gasolines show a huge range in conductivity of 8 to 760 pS m^{-1}. Since a car body represents a capacitance of around 1 nF, in the worst case 20 mJ energy could be stored, which is roughly 100× the minimum needed to ignite a gasoline/air mixture. The study identified the major factors leading to ignitions as being:

- Cars using plastic filler tubes without proper bonding straps between metal parts of the filler neck and the car body. Flow of only a few liters of fuel was sufficient to create a voltage over 4 kV in this type of design.
- Ground surfaces that are of excessively high electrical resistivity (often due to use of sealers).
- Use of new tire formulations that are vulcanized with SiO_2 and have very high resistivity.
- Inadequate grounding of the filling hose nozzle.
- Failure to use anti-static seats in cars, allowing high charge to be built up on people as they exit the car.

The first of these factors was found to be the most significant in actual field incidents. As an aftermath, some cars in Germany that had plastic filler tubes without necessary bonding straps were recalled. Claims have also been made that certain ignitions were due to personal electronics devices (e.g., pagers, cell phones), but these appear to be spurious and unsupported.

During 1999 similar problems started becoming of more concern in the US and the Petroleum Equipment Institute

* These incidents appear to be more common with women, because they are more likely to re-enter the vehicle during the course of the fueling.

issued an advisory report[1248]. It is currently estimated that there are about 150 – 200 such incidents per year in the US. Most of the incidents here too occurred in winter months because of the low humidity (absolute, not RH) prevalent in cold weather. A substantial number of the fires occurred while the person was in the process of removing the filler cap, prior to actual commencement of refueling. Also, a significant fraction reproduced the German scenario of the individual who re-enters and re-exits the vehicle during the refueling operation. A sizable fraction of US incidents involved certain Japanese car models from 1991 – 1996; the lack of significant representation of later-model cars suggests that manufacturers may have solved these design problems. The vintages involved of US-make cars were highly varied, with no clear trends. The study identified only a single incident involving a European-make vehicle (the car model in Germany that was subject to recall had not been exported to the US).

Since (with rare exceptions in very cold climates) the interior of the fuel tank is above the UFL and the outside atmosphere is below the LFL, somewhere between the tank interior and the outside world, concentrations must exist which are within the flammable range. Pidoll[1224] studied the effect of filler design and vapor recovery system details on this flammable zone. The vapor recovery mechanism of the gasoline pump can be set to recover a varying fraction of the fuel vapor. When set to recover at 150% (for reduced pollutant emission), he found that the flammable zone migrates down into the filler tube and this, under some circumstances, might increase the risk of explosion.

For environmental and other reasons, gasoline filling stations are nowadays likely to have plastic, rather than metal, piping installed for conveying the product. Hearn[1249] conducted full-scale tests on a nylon-lined polyethylene piping system intended to simulate an arrangement similar to what can be found underground at a filling station. A maximum potential of –8 kV was induced due to fuel flow in these experiments, which is significantly below the 20 – 25 kV needed for a brush discharge. Hearn concluded that, based on these results, there is not much danger of an electrostatic ignition in the piping system simply from the flow of liquid.

FILLING STATION TANKS

A localized flammable atmosphere may be created near vent pipes of underground storage tanks at a gasoline filling station due to pumping out of the liquid. German regulations had assumed that, so long as (a) the tank is covered by at least 0.8 m of earth, (b) the UTL of the gasoline is below –4ºC, (c) pumping is not continuous, and (d) the pumping rate is below 200 L min^{-1}, this condition cannot arise. However, Frobese[1225,1250] conducted tests using 10 and 20 m^3 tanks and discovered that these conditions do not prevent the possibility of a flammable atmosphere. Using a gasoline having a Reid vapor pressure of 75 – 85 kPa, he found that whether the upper portion of the vapor stayed above the UFL depended on both the pumping-out rate and the size of the vent pipe. Using a 40 mm diameter vent pipe, only at a 400 L min^{-1} rate did the top portion of the vapor space stay above the UFL; for rates of 200 L min^{-1} and lower, the tank stayed above the UFL only when it was nearly full. The vent pipe diameter is critical, because, for larger diameters, the velocity is slow enough so that the incoming air forms a layer on top of the gasoline vapors and does not adequately mix. At a low flow rate of 50 L min^{-1}, even using a very small 25 mm pipe did not suffice to maintain the tank above the UFL. Frobese concluded that no reasonable combination of pumping rate and vent pipe diameter can lead to an assurance that the tank's atmosphere will not be within the flammable range. However, he pointed out that the consequence of an underground tank explosion is likely to be minimal; in addition, ignition sources within the tank or at the vent pipe are uncommon. Yallop[180] has documented one fire that occurred when a vent pipe discharge was located too close to a source of ignition.

Ground fault circuit interrupters

GFCIs are intended to prevent electric shock (and, to a limited extent, certain types of fire ignitions) by removing power from circuits when a ground leakage current is detected. They also have the potential of being ignition sources themselves. Five cases have been documented[1251] where GFCIs located in public toilets suffered extensive corrosion due to water splashing from nearby plumbing fixtures. The corrosion was sufficient to create an overheating situation inside the GFCI but without activating the tripping function. Consequently, burning of plastic parts of the GFCIs occurred (Color Plate 131).

Gypsum wallboard

Janssens[1252] tested the ignitability of paper-faced gypsum wallboard in the LIFT test (Figure 97). His data give $\dot{q}''_{\min} =$ 26 kW m^{-2}, $\dot{q}''_{cr} =$ 9.3 kW m^{-2} and $B_{ig} =$ 311. As pointed out

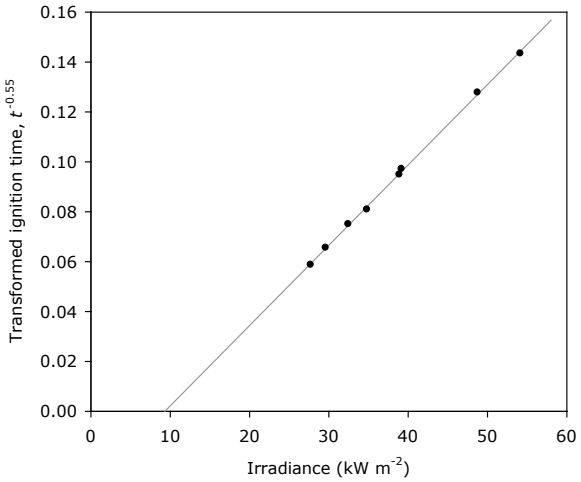


Figure 97 The radiant ignition of paper-faced gypsum wallboard, as measured in the LIFT apparatus

in Chapter 7, the product acts as a thermally-thick substance, despite the thinness of the combustible facing. The effect of the product density[1253] on the time to ignition was examined using Cone Calorimeter tests at an irradiance of 50 kW m^{-2}. Over the range $638 \leq \rho \leq 1173$ kg m^{-3}, the relation was:

$$t_{ig} = 0.1078\rho - 42.163$$

These results and others obtained on the ignition of gypsum wallboard must be taken not as precise, but only as broadly indicative. There is a significant variation in the thickness of the paper face among different manufacturers and even among different production plants of the same manufacturer.

Painting a gypsum wallboard surface generally has a negligible effect on ignitability unless blistering occurs. When many coats are present or when the wallboard is heated at a high heat flux, however, blistering may occur. In that case, the paint detaches locally from the substrate and acts as a thermally-thin material, giving much shorter ignition times. Mowrer[1254] obtained the Cone Calorimeter results shown in Table 146.

Table 146 Radiant ignitability of painted gypsum wallboard

Heat flux kW m^{-2}	Coats needed to blister	Ignition time (s)	
		Not blistered	Blistered
35	8	60 – 110	18 – 22
50	4	35 – 42	10 – 12
75	2	17 – 23	5 – 6

Hair

Peacock and Vaishnav[1106] developed a test method for examining the ignitability of substances by a small electric arc discharge. Surprisingly, they found that human hair ignited in 0.1 s, which was the same time as needed for black powder and smokeless powder. Most other consumer goods, including tissue paper, took about 0.5 to 1.0 s.

Hairdresser chemicals

A fire has been reported[1255] where rags soaked in thioglycolic acid (mercaptoacetic acid, $C_2H_4O_2S$) and sodium bromate ($NaBrO_3$) self-heated to ignition.

Heat guns

The peak temperature of the air coming out of a heat gun has been measured at about 580ºC at the nozzle[1256]. Clearly this can ignite numerous combustibles. Heat guns are commonly used to strip paint from wood, and an insidious form of ignition has been reported[1257] where smoldering was started inside a wall cavity while using the gun against exterior boards.

Heat tapes and heat cables

Heat tapes, heating tapes, heat cables are all terms for electric cables sold for do-it-yourself heating of pipes and surfaces. The term 'cable' is more commonly used when the device has an approximately round cross-section, while 'tape' often refers to devices having a shape of a flattened dumbbell, but the terms will be used interchangeably in this section (CPSC also considers these terms as interchangeable, although the manufacturers generally do not). The devices are commonly used to heat pipes subject to freezing (especially underneath mobile homes) and also to melt snow from the eaves of roofs in cold climates.

Heat tapes are generally rated at 16.4 – 23.0 W m^{-1} (5 – 7 W/foot) and normally plug into a 120 V outlet. The oldest variety, used in the 1930s, comprised a small-diameter heating wire, looped together and fitted with a plug; this variety is uncommon today. During the 1960s, a type became available which consists of two insulating filaments, separated by about 10 mm. Around each filament a fine gauge heating wire is wrapped helically, and the whole assembly is encapsulated in PVC. At one end, a length of unheated cord is supplied to be plugged into an outlet. The far end requires a termination to join the two runs of heating wire together. This termination must exclude moisture and some fires have occurred due to improper field termination. This type of heat tape is called a 'series resistance' design.

David C. Smith investigated thousands of heat tape failures[1258,1259] and reports that there are two different failure modes of series resistance heat tapes: (1) burnout, and (2) thermal decomposition. Burnout tends to occur due to aging of the PVC insulation or when a slightly excessive amount of thermal insulation has been applied. This raises temperatures higher than intended and the PVC (which is typically rated at only 75º, 90º or 105ºC) progressively loses its plasticizers, embrittles, and chars. Excessive temperatures then cause geometry changes of the heating wires and this causes further localized heating and charring. Smith reports that this failure mode occurs only when the heating wires are wound more finely than 1 turn per mm (24 turns per inch). Burnout causes failure of the heat tape and burns out a tiny section of heat tape, but normally does not cause fires. CPSC was able to create this type ignition in the laboratory by an accelerated aging program where a heat tape was operated at 150ºC for two weeks[1260]. This resulted in enough degradation to cause ignition.

Fires are much more likely to be caused by the thermal decomposition mode, even though, according to Smith, this failure mode accounts for only 5% of heat tape failures. This mode commonly occurs when a heat tape has been greatly overinsulated or has been doubled over itself, but such abuse is not a prerequisite. In this mode, significant arcing occurs, and the arcing can 'leapfrog' back to the power source. Flames of around 80 mm high are commonly seen and these can ignite nearby combustibles. The burning process is slow, and the heat tape is only consumed at about 150 mm per hour. Smith believes that ignition of fires has been facilitated by a change in the formulation of PVC

commonly used for the insulation around 1970, since heat tapes in the 1960s were not causing fires.

Once a failure has occurred at a certain point on the heat tape, it tends to propagate since the two polyester cords (around which the heating wire is wrapped) shrink when overheated[1261]. The shrinking is generally non-uniform, and this results in the heat tape twisting. Twisting promotes additional localized heating, and the fault thereby propagates towards the power supply. Twisting is reduced if the tape is equipped with a grounded copper braid.

Normal 15 or 20 A circuit breakers are not effective in preventing heat tape failure and possible ignitions, since a failed cable does not draw enough current to trip the breaker. What is effective, is using a GFCI in conjunction with an outer copper braid. Shorting of either conductor to the braid will then trip the GFCI. Many heat tapes are not supplied with thermostats, and tapes are often not turned off by the user in the summertime. The higher temperatures thus sustained serve to reduce the life of the heat tape.

A newer variety of heat tape is of a parallel-resistance design. In this type, two 12 AWG copper wires run down the length of the heat tape. Spirally wrapped around the bus wires is a thin Nichrome heating wire, which contacts the bus wires only every so often; for the rest of the length, the bus wires are insulated with a fluoropolymer insulation. The outer jacket is also made of a fluoropolymer. This type of product is generally marketed for industrial, not consumer, use.

The latest type of parallel-resistance heat cable was invented by Raychem, who developed a conductive polymer which has a negative temperature coefficient. In such cables, two long copper wires are used, and the polymer is used to bridge between the two wires. The heating is provided by the polymer, not by the two wires. Not only is no thermostat needed, but since the temperature is controlled locally, it is possible to double-up or loop the heat cable without causing an abnormal increase in temperature. These cables are called 'self-regulating.' The failure of such cables normally occurs due to ingress of moisture. This can occur due to improper end termination, burial in moist soil, or use in wet environments. The wet exposure causes arc tracking to progressively occur. Such arc tracking failure is termed 'wet fire' and resembles a series of firecrackers going off along the length of the cable. This occurs as the bus wires progressively short out along the length. Newer versions of this design have an improved jacket formulation intended to resist moisture ingress and improved end termination design. The latter is crucial, since if the end seal does not remain moisture-tight, failure can start there. A fuse built into the heat tape may not be effective against a wet fire, since it has been reported[1262] that "a full arcing fire could be sustained with currents as low as 40 mA."

Smith[1263] pointed out that, because of the thermal aging problem, most units have a field life of three years or less, but "none of the manufacturers state this fact on their instruction sheets." Apart from thermal aging, faulty installation, and physical damage, some mobile home heat tape fires are caused by animal damage. Smith also noted that some failures heat tape failures are due to creep, wherein the resistance wire migrates through the insulation due to prolonged mechanical stress. In cold climates, PVC insulation is apt to crack due to mechanical impact at installation or during its lifetime. In his 1974 paper, Smith also recommended that a grounding braid be used by manufacturers.

CPSC concluded that about 2/3 of the fires due to heat tapes could be attributed to improper installation[1264]. Improper installation was about twice as likely to be made with series-resistance tapes as with self-regulating designs. This is because doubling over the product, or over-insulating it, are not dangerous with the self-regulating type. Once failure occurs, it was found that in 42% of the cases, a wood material was the first item to ignite, and in 24% of the cases it was paper backing on fiberglass insulation. It was also found that about 60% of the heat tape fire incidents investigated with series-resistance tapes involved tapes less than 3 years old; by contrast, only 10% of the self-regulating tape incidents involved tapes less than 3 years old.

In 1988, prior to widespread adoption of UL standards by the industry, CPSC also found out[1265] that none of 12 commercial heat tapes they tested could meet the UL 94 V-0 test. In muffle furnace testing, it was determined that most heat tapes exhibited a thermoplastic behavior, softening at 107 – 113ºC and melting at 210 – 260ºC. One out of 11 specimens, however, did not melt but rather ignited at 400ºC; ignition temperatures for others were not determined. In tests with energized heat tapes improperly installed (adjacent turns abutted), it was found[1266] that temperatures in the range of 111 – 113ºC led to melting and charring, although tests were not run long enough to fail electrically. Since a worst-case mis-installation, such as might result from doubling of the recommended thermal insulation thickness, would result in heat tape temperatures of ca. 150ºC, CPSC engineers suggested that PVC material of 150ºC rating could significantly reduce ignition potential.

A test program on heat tapes was conducted by UL for CPSC[1267]. It found that an effectively grounded braid, in combination with a GFCI device, was the best protection. Other results were that longer runs of heat tape are more hazardous than short ones (because the probability of operating a fuse or circuit breaker is lower if the cable presents a higher resistance load), and that 'wet fire' failures are easily produced in the laboratory with older-generation self-regulating cables, but not with 1993 vintage specimens. It was also found that a 10 A fuse built into the heat tape was useful for self-regulating heat cables, but that a 30 A panel-

board fuse never opened. For series-resistance types, a 10 A fuse did not enhance protection.

Experience has shown that the grounding braid should be made of copper, and that aluminum braids are much less satisfactory. For this reason, aluminum braids, which earlier were used, are now generally obsolete. Even with a copper braid, however, there can be little assurance against ignition unless a GFCI is used.

According to CPSC, until 1991, some 90 – 95% of heat tapes sold were not tested nor Listed by any safety organization. Starting in 1991, virtually all products are labeled according to UL (UL 1462[1268] or UL 2049[1269]) or CSA (C 22.2 No. 130) requirements. Neither organization implements a scheme for ensuring that a minimum service life would be obtained, during which a cable would not self-ignite. However, even despite that omission there is reason to believe that newer heat tapes are generally less prone to ignitions than previous ones.

Long heating elements are also very common in the chemical manufacturing industries, however, in such applications they are generally termed 'heat tracing,' and can comprise steam tracing, not just electric resistance heating. Electric heat tracing products are tested and specified according to IEEE 515[1270].

Heat transfer liquids

Lee and Walton[1271] characterized a series of heat transfer liquids used for solar collectors, but which represent chemical families which may also find application in other heat-transfer applications. Their results are shown in Table 147.

Table 147 Flash points and fire points (ºC) for heat transfer liquids

Liquid	Flash point		Fire point
	Pensky-Martens	Cleveland open cup	
alkylated aromatic	57	63	71
diphenyl/diphenyl oxide	116	129	135
ethylene glycol	118	121	135
extracted naphthenic	138	163	177
hydrocarbon oil (light)	52	71	82
paraffinic base A	135	152	168
paraffinic base B	163	182	193
paraffinic base C	199	235	254
polyalkylene glycol	249	291	316
silicone oil	285	318	> 371

Heaters, catalytic

Catalytic heaters are ones which utilize flameless combustion on a platinum-coated porous panel. The panel incorporates an auxiliary electric heater, since catalytic combustion cannot start from room temperature. A pilot flame is used for initial ignition, but not for subsequent operation. The operating temperature of the panel is normally around 400 – 500ºC. The fuel gas can be butane or propane. Use of methane is, in principle, also feasible, but a much higher panel temperature would be required. The potential of catalytic heaters to cause unwanted ignitions was examined by Rogowski and Pitt[1272]. In their tests, the heaters were run at their maximum output setting, giving a 525ºC panel temperature. Diethyl ether, hexane, and petroleum ether (VM&P naphtha) readily ignited when squirted upon the panel, but 100-octane gasoline did not. Jets of hydrogen readily ignited when directed against the panel, ethylene only under limited conditions, and propane only on 1 of 3 test heaters. Hydrogen jets also ignited on the platinum surface when the panel was not heated at all and was simply at room temperature. The ignitability of thin solids was more variable. One heater ignited cotton fabric, newsprint, and paper tissue. But a second type of heater only caused glowing, not flaming, ignitions, while a third type showed no glowing or flaming ignitions, except for the cotton cloth. Cellulose acetate and nylon test fabrics melted and charred, but did not ignite.

Heaters, electric

BUILT-IN HEATERS

According to Fitz[1273], the main safety features that should be incorporated into a built-in heater in order to minimize the chance of fire are:

- Normal discharge temperature to be less than 120ºC.
- Under transient conditions (e.g., when the high-limit switch is being activated), discharge temperatures should not exceed 175ºC for 30 s.
- A high-limit switch that detects discharge (not intake) air temperature across the entire discharge area (e.g., a capillary tube device) and that is manually, not automatically, reset.
- Any portions of a high limit switch exposed to discharge air should robustly resist high temperatures and not be damaged by over-temperature conditions.
- Means must be provided to prevent lint buildup.

Ignitions of combustibles from heaters built into walls come from four main failure modes: (1) a failure of both the thermostat and the high-limit switch; (2) designs where the high-limit switch is ineffective against certain modes of overheating (e.g., failure of fan motor, a partial blockage of airflow); (3) excessive accumulations of dust within the unit; and (4) ignition due to combustibles placed too close to the heater or actually introduced into the heater. UL standard UL 2021[1274] (previously UL 1025[1275]) is normally relied upon by manufacturers. These standards examine a variety of overheating modes, but not all possible modes are examined. Specifically, the test sequences do not examine the effects of partial blockage due to dust buildup (although some UL testing apparently involves this mode), failure of wiring due to vibration or temperature, nor the effects of failure of fan motor (apart from open circuit conditions). The standards also permit self-resetting high-limit switches that only give a pilot-light warning. Thus, a user may con-

clude that a heater which, due to some fault, is 'running on the high-limit' is simply lighting the pilot light to indicate 'heat on' rather than 'malfunction.'

Most built-in heaters do not contain a built-in on-off switch since this is not required by UL or NEC. The only control mechanism readily accessible to the householder is usually the wall thermostat, but, with some models, the latter may only be decreased to a low temperature, not turned off. Thus, unexpected activation of heater can take place, and this can create a hazard if combustibles have been piled at the heater, on the assumption that the heater will not operate. Such a thermostat function is useful if it is necessary to prevent water pipes from freezing. However, not all thermostats having a 'Low' setting actually keep temperature above freezing; in some models the temperature setpoint at that marking is much lower, e.g., one model has been measured to be at about – 23ºC. In some cases, units have a 'High/Low' switch, and fires have been reported[1276] where the occupant believed the unit to be turned off, not realizing that the switch position provides 'Low' heat, not 'Off.'

Built-in heaters typically have heating elements of one of three styles:

(1) zigzag Nichrome wire wound on several closely-spaced insulator boards;
(2) long helices of Nichrome wire; or
(3) tubular heating elements that contain a heating wire, a grounded outer shell made of stainless steel or similar material, and magnesium oxide packing as the insulator in between the two.

The type with zigzag elements may involve an air path having close spacings between adjacent elements; in such a case, there can be a potential for clogging with dust. The tubular heating element type is generally robust, but it can have a failure mode similar to the failure of a heating element in an electric oven: a short between the center conductor and the outer shell leads to an 'arc cutting' mode, whereby the outer shell is progressively ripped open by electric arc action and metal pieces are simultaneously ejected.

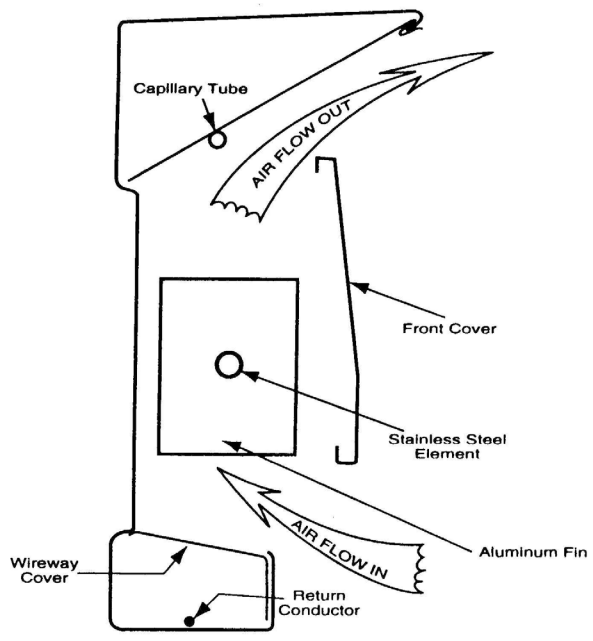


Figure 98 Baseboard heater cross-section
(Courtesy CAFI and Daniel B. Langlois)

Details of some failure modes were elucidated in the course of CPSC's investigation of a large US manufacturer of in-wall heaters[1277]. CPSC identified 134 instances where heaters smoked, sparked, caught fire, emitted flame or ejected burning particles. The remedial actions to be taken by the manufacturer included upgraded specifications of the high-limit switch; adoption of high-limit switches that provide an audible alarm or require manual resetting, rather than being self-resetting without audible alarm (note that CPSC does not consider visual alarms sufficient); improvement of blower wheels and wire crimping procedures; affixing of labels advising users of hazards of impeded airflow (due to lint or debris), of objects placed too close to heater, and of installation in insulated walls; and setting up of a quality assurance program.

Baseboard heaters are less prone to ignite combustibles because they are generally designed as convective rather than radiative devices, with lower heating element temperatures. A typical design uses cylindrical heating elements with convection-enhancing fins. In such a design, apart from the generally-lower temperatures, the fins tend to keep combustibles away from the hottest portion, which is the tubular element itself. Nonetheless, designs have been recalled from the marketplace where the thermostats themselves overheated and caused fires[1278]. A study on baseboard heaters[1279] concluded that both a failed high-limit switch and combustibles blocking air flow passages would normally be needed in order for an ignition potential to arise. A common type of baseboard heaters uses a heat element which is a resistance wire surrounded by magnesium oxide insulation, covered by an outer stainless steel sheath. These occasionally fail in a dramatic 'arc cutting' mode, as discussed above[1280]. Fires have occurred when individuals bypassed the high limit switch and subsequently created a blockage with combustibles[1281]. Fires have also occurred because a heater was installed upside down. Figure 98 shows that a typical heater has a thermostat sensing element (capillary tube) located near the top of the unit, so that it is properly positioned in the warm air outflow. If a heater is installed upside down, then the capillary tube senses the cold air coming into the bottom, instead. Laboratory testing showed that cheesecloth and bed sheets draped over its face are readily ignited by a properly functioning heater when it has been improperly installed upside down[1282].

Goodson et al.[1283] examined the fire-causing potential when electric wire (typically, Nichrome) heating elements fail. Because heating creates an elevated temperature of the met-

al, the rate of oxidation increases and eventually even a properly-installed element can fail. Failure can manifest itself either as sagging or as breaking open. In either case, contact by the sagged or broken location can be made to a grounded surface. For heating elements that are supplied from 240 VAC power, in the North American wiring scheme* neither leg is grounded. Thus, it suffices for either of the broken legs to contact a grounded surface for current flow through the element to resume. This current flow may be higher than intended, which can directly cause overheating, or result in a second failure of the element. Arcing associated with a failure can spatter hot metal, leading to ignition of combustibles that may be within the area. Goodson et al. further considered that a large fraction of failures is due to improper installation of replacement elements. Usually, the instructions do not make clear that coils of wire must be uniformly spaced throughout. Local bunching will lead to overheating and an earlier failure can be expected. In addition, if a failure occurs where the element breaks open, with one broken end then shorting to ground, any thermal protection device will be nullified if it is located in the leg that is open, rather than shorted. Consequently, a design is needed (and must not be circumvented by repair work) whereby each leg is protected by an over-temperature device.

PORTABLE HEATERS

Portable heaters come in two basic varieties, radiant and convection. Heaters with a visible glowing element are classed as radiant, the others as convection. In 1986 CPSC conducted an in-depth field investigation of fires originating at portable heaters[1284]. For radiant heaters, ignition of too-close combustibles was the predominant hazard pattern. But unless the heater sustains a failure, the peak temperatures at convection heaters will be below the ignition temperature of household solid combustibles. Thus, these fires (which were only about 1/5 as numerous as from radiant heaters) primarily involved malfunctions of heaters, typically of wiring or controls. Only one case was listed of a fire due to combustibles being too close and details were not supplied.

Radiant electric heaters commonly produce a heat flux around 10 kW m^{-2} at the face of the grille and the value drops rapidly with distance. Unless overt electrical failure occurs, it can be assumed that there is no source of pilot ignition. The question of interest then becomes what materials might autoignite at a heat flux of 10 kW m^{-2} or lower. Fabric and paper goods generally require substantially higher heat fluxes for autoignition. But cardboard can be ignited at fluxes below 10 kW m^{-2} (see *Paper products*). Of course, pushing any combustibles up to the face of a radiant heater is a misuse of the heater and, in that same vein, more abusive misuses are possible: stuffing material inside the grille or blocking the entire face of the heater. In the latter case, however, a properly designed thermal cutout should operate.

HOUSE FURNACES

Some fires have been caused due to ignition of the manufacturer's operating instructions, which were located inside the furnace.

Numerous fires have been reported due to the failure of electric heating elements dropping hot particles into combustible ducting located below the element.

Electric duct heaters can be ignition sources in the event the high limit switch and the airflow switch fail.

Heating equipment (general statistics)

NFPA statistics[1285] of home heating equipment fires are given in Table 148 and Table 149. FEMA statistics on the material first ignited[1286] in portable heater fires are given in Table 150. NFPA estimated the risk of fire (that is, the likelihood of having a fire, if a certain equipment is installed) for the various heating equipment types, as shown in Table 151. The NFPA report also contains details on the cause of fire and on the material first ignited; these are presented separately for each equipment category but not pooled. Kerosene heaters have a reputation for being high-risk devices, but the NFPA statistics indicate that wood stoves and fireplaces are vastly more risky. See also specific equipment: *Chimneys and flues*; *Furnaces and boilers*; *Heaters, catalytic*; *Heaters, electric*; *Wood-burning appliances*.

High-temperature accelerants

Accelerants for incendiary fires are commonly hydrocarbon liquids—gasoline, kerosene, paint thinners, solvents, and similar liquids. But occasionally incendiary fires[1287] have been observed where the ignition source shows unique characteristics:

- very high heat fluxes of 250 – 300 kW m^{-2}, and possibly up to 700 kW m^{-2};
- a huge heat release rate of about 10 MW m^{-2};
- enormous charring rates of wood, up to 10 mm per minute;
- very rapid or extensive destruction of concrete;
- melting or burning of iron and steel.

These traits are inconsistent with those of liquid accelerants. But a research program[1288] showed that a formulation similar to what could be used as rocket propellant (ammonium perchlorate, powdered aluminum, eutectic salts, and diesel fuel) produced in experiments similar outcomes to those seen in incendiary fires started with high-temperature accelerant (HTA) materials. Color Plate 132 shows scenes from a full-scale test burn where an empty retail store building was ignited at locations next to three columns.

A simpler form of HTA is thermite, and this has occasionally been used as an incendiary material. Color Plate 133

* In other parts of the world, 240 VAC power supplies are configured in an end-grounded, not center-grounded, topology.

Table 148 Home heating equipment fires for 1998, categorized according to function of equipment

Equipment	Percent
fixed space heater	23.5
central heating unit	17.0
chimney	16.8
water heater	15.4
indoor fireplace	12.6
portable space heater	6.9
chimney connector	4.8
heat transfer system	0.8
unclassified	2.1

Table 149 Home heating fires for 1998, categorized according to type of energy used

Type of energy	Percent
solid fuel	46.2
gas fuel	23.3
electricity	21.3
liquid fuel	9.2

Table 150 Material first ignited in portable heater fires

Material	Percent
fabric	35
wood or paper	22
combustible liquids	13
plastics	8

Table 151 Comparative risk of various domestic heating equipment, expressed as fires per 10,000 households

Type of equipment		Risk
central heating unit	gas fuel	1.06
	liquid fuel	3.68
	electricity	4.35
fireplace	solid fuel	15.38
fixed space heater	gas fuel	7.52
	solid fuel	33.45
	electricity	5.42
portable space heater	liquid fuel	3.00
	electricity	1.72
water heater	gas fuel	1.99
	electricity	0.49

shows the results of testing to recreate an incendiary fire where thermite was used to burn a kitchen range.

Hops

Baled hops are known for their self-heating potential. The severity of the problem depends on the variety, and 'super-high alpha' types are particularly susceptible. In addition to self-heating, it appears that sufficient vapors may be produced so that gas-phase explosions are possible; this was experienced in at least one fire[1289]. Hops are processed by being kiln-dried after harvesting, then packed into bales of about 0.6 × 0.6 × 1.2 m long, weighing about 90 – 100 kg. The self-heating potential is so high that hops must be stored in a refrigerated warehouse, with the normal storage temperature being –2ºC. Moisture is critical to self-heating of hops and hops at 8 – 10% MC show the least propensity for self-heating; bales that are much drier or much wetter than this are less stable[1290]. Some large-scale testing suggested that, if all other factors are optimum, bales can be warehoused at a temperature of 35ºC, while bales with improper moisture content, but otherwise properly processed, may be acceptably stored at 24ºC. But fires have been experienced even at the standard storage temperature of –2ºC, implying improper processing or plant material variations. The kiln drying conditions were also found to be important, especially the temperature of the material that is being baled, which should generally be below 40ºC. Additional data were reported by Jones and Raj[1291], but they did not have the opportunity to examine the varieties especially-prone to self-heating. A bale which was found to be self-heating and was set aside without being sent to the warehouse is shown in Color Plate 134. Smoldering bales pulled from a warehouse[1292] are shown in Color Plate 135. The stack height in this fire was 3.0 m high, although similar facilities stack the product up to 6.1 m high.

Humans

Few topics in fire investigation have inspired as much controversy or emotion as the issue of 'spontaneous human combustion' (SHC), there being fundamental doubt about the existence of such a phenomenon. The normal fire fatality who caught clothing on fire arrives at the hospital or morgue with skin destroyed, but very recognizably human. However, throughout history a number of fatalities have been recorded where the circumstances typically include near-total incineration of everything except the extremities. Near-total incineration might be expected from victims who were, for example, trapped in warehouse fire which burned for a day or so. However, deaths claimed to be caused by spontaneous human combustion involve very little burning in the vicinity of the victim. Such reported cases tend to share a number of characteristics (although not every incident possesses all of them)[1293-1295]:

- The victim is unrecognizable, with all of the body except the legs (sometimes also arms and head) being reduced to ash.
- The room where the incident occurred has suffered minimal fire damage; in some cases furniture, bedding, etc., within a very close proximity to the victim is unburned. Flashover (full room involvement) has not occurred.
- An oily residue is often found to cover the room surfaces, and the smell, if any, is described as "sweet," while it is claimed that in a normal-fire case the smell would be foul. The latter claim, however, is unsupported.
- No reasonable ignition source can be identified.
- The time scale varies, but in the more perplexing cases can be minutes rather than hours.

In addition, older writers commonly claimed that the victim is disproportionately likely to be female, elderly, or corpulent. However, Arnold[1294] compiled a large database which shows that there is no preference towards females in the cases of claimed SHC.

In essence, it is claimed that there are two puzzles concerning such victims:

(1) No source of ignition can be identified.
(2) The human body is a 'low-grade' fuel. Low-grade fuels (ones that are wet or have a low heat of combustion) burn only in environments where significant external heat can be supplied. Clothing items have little mass and can only burn for a short time. Even if a victim catches clothing on fire and can take no action (drunk, etc.), it has been difficult to envision starting and sustaining combustion of a human body with such a short-lasting source of heat.

There is also the subsidiary problem in that victims of 'normal' fires tend to have their extremities burned more, not less, than the other body parts. In 'normal' fires, this is due to heat transfer, in that the central portions of the body represent the maximum heat sink, with thinner portions being more readily raised in temperature, for a given incident heat flux.

When a solitary victim has been found fully cremated, it may be difficult to conclusively rule out external ignition sources. In a number of cases, however, the victim was known as a non-smoker, and evidence suggests the victim was not using candles or other forms of heat or flame, and was not close enough to any electrical equipment that might have been malfunctioning. The apparent lack of an ignition source, however, can simply be an indication of poor fire investigation or scene preservation. In some cases, no nearby ignition source exists because the victim moved some distance after catching fire before succumbing. Perhaps most perplexing have been the cases that do *not* lead to death, with the victim surviving his or her burns. But none of these reported cases appear to be comprehensively documented by credible individuals.

If one believes that the victims were not ignited from normal ignition sources, then it is necessary to posit one or more abnormal sources. This has been a point of considerable difficulty to the believers of SHC. It has been asserted that the cause may be related to ball lightning[1293,1294], but there are very few adequately-documented cases of any injuries from this source, much less cremation. Another phenomenon which is considered as a possibility is kundalini energy[1294]. This enters the realm of the metaphysical—an internal 'fire energy' is not the study matter of physics or chemistry. Arnold[1294] presents an extensive catalogue of other potential chemical, electrical, geological, atomic-particle, etc. causes. These do not find acceptance among orthodox scientists as potential ignition sources and all of them lack any documentation of causality.

Fire specialists have generally taken the view that SHC cannot occur. The debunkers of the 19th century often used to insist that the victims were all drunk and that this was sufficient to sustain combustion of a body which would normally not burn. This hypothesis was refuted in mid-19th century when experiments by the German chemist Justus von Liebeg showed that soaking flesh in alcohol is not sufficient to make it undergo sustained burning[1293]; other researchers also came up with the same conclusion[1294]. In the 20th century, UK Home Office forensic scientist J. B. Firth proposed the hypothesis that a 'wick effect' is responsible, and this was not too different from the conclusion reached by the French surgeon Guillaume Dupuytren in 1830. This was subsequently pursued by D. J. Gee[1296], who conducted small-scale experiments demonstrating that while human fat requires a temperature ≈ 250ºC to melt when heated directly, human fat made into a sausage with cloth casing acting as a wick can burn up completely in ambient air. Prof. D. D. Drysdale later illustrated this with a sausage-shaped piece of animal fat[1293]. These small demonstrations did not prove quantitatively an analogy to human bodies, however, since only roughly ¼ of the body mass is fat, the remainder being muscle, organs, blood, bone, etc. British researcher Stan Ames[1293] increased the realism of such studies by conducting an experiment burning in a fireplace an entire 70-kg pig chopped into pieces. Burning the chunks over a fire of British-type 'smokeless fuel' (coal with volatiles boiled out) during a 13 h period he succeeded in reducing the pig to ashes with just a few small bone and teeth fragments. His study was directed toward a particular criminal case where a victim was chopped up and burned. But success in obtaining complete combustion under those circumstances was not necessarily directly pertinent to SHC.

Ettling[1297] endeavored to recreate an automobile fire by use of large sheep. His first test was brief, but in the second test he used a 77-kg sheep, soaked in gasoline and placed on a car seat. At the end of the test, the remains of the sheep were only about 23 kg, and only the skull and the abdominal and pelvic regions were not fully burned. The burning process was one of fat rendering, with the body being supported on metal seat springs and dripping melted fat onto embers on the floor, where the fat would ignite and provide heat to render more fat out of the body. In his research, Ettling also discovered that Nazi extermination camps knew about this technique and suspended bodies on racks, with a fire underneath serving to render the fat.

DeHaan[1298] investigated a case where a sheriff's deputy discovered a woman burning in the woods, lying face-down on a layer of leaves. The deputy was able to photograph small flames about 0.35 m high licking above the body (Color Plate 136). Leaves directly next to the victim were charred, but there was no other fire damage. The body, however, had large portions of its middle section reduced to powder. Examination of the victim revealed stab wounds at the shoulder. The victim was burning for less than five

hours when discovered. The investigation developed that she was first murdered then set on fire. To reproduce such events in the laboratory, DeHaan conducted several experimental studies.

In the first study[1299], he conducted preliminary bench-scale testing with the Cone Calorimeter. For such samples, he established that at a 35 kW m^{-2} irradiance, bare pig* flesh can be ignited and feebly burned, but self-extinguished upon removal of the radiant source. When the experiment was repeated with the pig flesh covered with a cotton cloth, steady combustion was produced which continued to render fat and to burn the flesh. Next, he conducted a series of larger scale experiments, where he burned chunks of pork fat wrapped in fabric and measured the mass loss and the HRR. Finally, he placed small whole pig carcasses on a thermoplastic-fiber carpet, dressed in polyester/cotton garments, and ignited with 1 L of gasoline. These larger scale tests revealed that fat renders out relatively easily upon modest heating, but that it forms a pool of liquid with a high flash point which does not ignite and burn of its own. Sustained ignition becomes possible in the presence of a wick formed by the porous char of the fabric. The pig carcasses burned for around 1 to 2 hours, but did not fully burn up. DeHaan determined this to be because the mass (all less than 53 kg) was smaller than that for a typical human victim. Thus, in a follow-on study[1300] he used a pig carcass of 95 kg. This carcass burned at 55 – 65 kW for most of the 6.5 h test period. Flames of only 70 – 250 mm height were seen on and around the burning carcass. When the fire was extinguished, more than half of the carcass had been consumed; in the burned portion, bones burned also, since they become friable and fell apart upon applying slight pressure. The time scale seems consistent with Gee's credibly documented case[1296], where a woman's limbs burned up fully in 3 hours. DeHaan also noted that soot and unburned pyrolysates were produced in large amounts during the burning process which would be available for coating room surfaces. DeHaan also conducted additional Cone Calorimeter tests comparing pork fat and human fat. The two materials showed similar combustion and relatively similar HRR values. Finally, to rebut claims that self-sustained, wick-fed combustion could not take place without ignition from a flammable liquid, DeHaan conducted a small-scale demonstration[1301] where a cotton-wrapped piece of pork fat was ignited directly at the cloth without use of liquids. The outcome was also a self-sustained combustion.

Bohnert et al.[1302] observed the commercial cremation process for a number of bodies and reviewed similar earlier literature. Typically, after about 50 minutes, the major features of the body had been consumed and only larger bones remained. Christensen[1303] also reported on some studies related to combustion of humans. She first consulted with crematoria operators and learned that times needed to incinerate the human body vary widely, with elderly often being cremated in less than 1 h, while youthful individuals take up to 3.5 h. Her initial experiment involved burning of amputated human flesh. This gave a heat of combustion of 17 MJ kg^{-1} obtained by crudely estimating the HRR from flame heights. She then conducted cremation experiments on normal and osteoporotic tibia bones. She noted that most of the active burning took place between 625 and 790ºC and that the osteoporotic bones, which were originally about half the mass of normal bones, lost a somewhat higher fraction of their mass during the cremation. Thus, there would be a significantly smaller mass of bone left after a given thermal exposure from osteoporotic bones, as compared to normal bones. Her conclusion was that the propensity of elderly, corpulent females to become more fully burned in fires is physically explainable—they have a higher fat content and a lower bone mass due to osteoporosis.

Leitch[1304] did not conduct experiments, but he studied numerous fire fatalities and documented that the near-total burning up of the body is not unphysical. In the cases he studied, he concluded that physical causes of ignition were invariably present.

The conclusion to be drawn from these scientists' studies is that, starting with a normal ignition, human bodies can indeed be burned to a condition which resembles that of the victims identified as purported SHC victims. A means for sustained wicking is necessary for extensive combustion to take place. The wicking can be supplied by cotton clothes, charred leaves, or other appropriate adjacent objects. Combustion must be supported by such means until the flesh can shrink, split, and start the rendering process. Thus, quick-lived ignition sources such as flammable-liquid spills are neither necessary nor sufficient. The low *average* heat of combustion of the human body is not relevant, since combustion is initiated and sustained by the burning of bodily fats, which have an adequate heat of combustion. Concerning the availability of ignition sources, scientific studies can neither explain nor preclude metaphysical or supernatural causes, if these indeed sometimes play a role. However, recourse to such explanations would be needed only if there were cases which were thoroughly investigated by fire investigation *professionals*, who then concluded that there was no external ignition source. Such cases do not appear to exist.

HUMAN SKIN

Durfee[1305] conducted tests on human flesh, attempting to ignite it in a pure-oxygen atmosphere with an electric arc discharge from an electrode to the skin. Burn-off of hair could be achieved, but bulk ignition of skin did not take place. He points out that similar experiments conducted in the UK where ignition was reported to be possible were

* Pigs are often the preferred experimental animal for burn-injury studies because their skin is considered a reasonably close equivalent to human skin in regards to thermal injury. They also have a close resemblance to humans with regards to body size and fat distribution. Note however the results of Durfee which suggest that pig skin is easier to burn than human skin.

flawed due to direct exposure of fat to the ignition source. He also concluded that skin of suckling pigs, often used as a human-skin simulant in studies of burn injury, did not behave similarly to human skin with regards to ignitability: pig skin could be ignited in circumstances where human skin could not. An incident is reported[1306] where it is stated that a man's skin ignited during a fire in hypobaric oxygen chamber running at 0.34 atm pressure, but it is not clear how accurate the reported details may be.

HVAC equipment

All furnaces and other heat-producing equipment can be potential sources of ignition in certain cases, as can all manner of electrical motors, etc. used in non-heating air moving. There are cases however, of burning brand ignitions from such devices. Yereance[223] has reported on three types: (1) Evaporative coolers ('swamp coolers') are devices sometimes used in the desert areas of the US which provide cooling simply by adding moisture to air and then circulating it through a building. These are typically located on rooftops and have ducting discharging to various rooms. Water is applied onto pads and a blower then carries this wet air throughout the building. The pads are typically made of combustible material, which is not a problem unless the water supply pump fails to apply water. Cases are found where such pumps fail and start burning. This ignites the then-dry pads which burn and release firebrands into the air-moving system. The result is a number of spot fires that start simultaneously in different rooms. (2) While uncommon, there are residential furnaces so arranged that there is foam insulation inside the blower area. If this material is ignited and starts burning, a ready mechanism exists whereby firebrands are spread throughout the house and start spot fires in various rooms. (3) Occasional rooftop air conditioning units also have combustible thermal insulation inside the air path and have been documented to spread burning brands throughout a house.

Hydraulic fluids

Traditionally, the most common hydraulic fluid in aircraft applications was MIL-H-5606, which is a naphthenic, mineral oil that is usable over a wide range of operating temperatures, but which is also very easily ignitable. During the 1980s, this was largely replaced by MIL-H-83282, which is a synthetic hydrocarbon-based (hydrogenated poly-α-olefin oligomer) fluid with improved fire properties and usable as a direct replacement for MIL-H-5606. For new applications, designs have commonly used phosphate ester fluids, which are significantly less flammable. Snyder et al.[1307] compiled data on a number of aircraft hydraulic fuels (Table 152). The flash point values are from the Cleveland Open Cup test, the AIT values from ASTM D 2155, the hot surface ignition values from Federal Test Method Standard 791 (Method 6053), while the gunfire ignition test is from MIL-H-83282 specifications, which entails firing 50-caliber incendiary ammunition into part-filled aluminum canisters containing the test fluid; the results reported as the number of ignitions per 5 trials.

Table 152 Ignition characteristics of aircraft hydraulic fluids

Fluid	Flash point (ºC)	Fire point (ºC)	AIT (ºC)	Hot surf. ign. (ºC)	Ht. comb. (MJ kg^{-1})	Gunfire ignition
MIL-H-5606	102	113	232	388	42.3	5/5
phosphate ester	170	188	524	760	29.7	0/5
silicate ester	190	210	400	371	34.0	3/5
MIL-H-83282	230	254	354	322	41.0	1/5
silicone	276	343	409	477	22.6	0/5
chlorofluorocarbon	>500	>500	630	927	5.6	0/0
fluoroalkyl ether	>500	>500	669	927	4.1	0/0

Khan[1308] examined the pilot, radiant ignitability of various hydraulic fluids that are commonly used in mining industries. His study gives results at irradiance values over the range 30 – 60 kW m^{-2}; studies where low irradiances or $\dot{q}''_{\min}$ values would have been examined are not available. Khan also measured the fire points of a number of hydraulic fluids, using the ASTM D 92 method (Table 153). The mineral oil was for comparison purposes and would not ordinarily be used as a hydraulic fluid in mining machinery.

Table 153 Fire points of some hydraulic fluids

Type	Fire point (ºC)	
	Complete range	Typical values
organic/polyol esters	202 – 303	275 – 300
phosphate esters	163 – 320	310 – 320
mineral oil	252	252

Hydrazine

Hydrazine (N_2H_4) is a liquid which is widely used as a monopropellant and bipropellant fuel in rocketry and which also has uses as a boiler feed water additive, and as an intermediate in the plastics, pharmaceutical and agricultural chemical industries. Commercially, hydrazine is available as an aqueous solution (hydrazine monohydrate, hydrazine hydrate, $N_2H_4 \cdot H_2O$). The basic chemistry of hydrazine has been described by the Bureau of Mines[1309], along with a discussion of its hazards. The LFL of hydrazine in air is 4.7%, but the UFL is 100%, because hydrazine is able to decompose without the presence of an oxidizer. In nitrogen, the LFL of hydrazine is 38%. Decomposition occurs in two stages:

$$2N_2H_4 \rightarrow 2NH_3 + N_2 + H_2$$
$$2NH_3 \rightarrow N_2 + 3H_2$$

In practice, the second reaction is never complete, thus ammonia always remains among the products. Determining the ignition temperature of hydrazine is problematic, with erratic results commonly being observed[1309]. When tested in

pure glassware, an ignition temperature of 270ºC in air and 204ºC in oxygen was found. But when a platinum surface was introduced the ignition temperature in oxygen dropped to 30ºC. Upon introduction of ferric oxide, hydrazine ignited pyrophorically at room temperature. The combination was not pyrophoric at the dry ice temperature of –78.5ºC. Black iron and stainless steel were not pyrophoric and hydrazine showed ignition temperatures over 130ºC in these cases. Apart from iron rust, the decomposition of hydrazine can be catalyzed by chromium, copper, and iridium. Thus, hydrazine can spontaneously decompose if stored in a vessel which has such metallic impurities[142]. Hydrazine vapor is detonable at partial pressures down to 2.39 kPa; liquid hydrazine is not detonable at room temperature. Since hydrazine is a strong reducing agent, when used as a fuel in rocket propulsion, it is combined with an oxidizer such as dinitrogen tetroxide (N_2O_4) or hydrogen peroxide (H_2O_2) and it reacts hypergolically with strong oxidizers. Rags or paper tissues used to wipe up small anhydrous hydrazine spills will often autoignite in air if carelessly thrown into a wastebasket. Unnoticed and uncorrected accidental hydrazine leaks and spills will often result in autoignition by contact with contaminants on the floor. Even contact with vermiculite—a recommended packaging material in US Federal regulations (49CFR173.276)—will result in ignition. Anhydrous hydrazine must be stored under a nitrogen gas blanket. Accidental pressurization of hydrazine tanks with air or oxygen will result in explosions. There is an old monograph on hydrazine by Audrieth[1310], a monograph on hydrazine safety by Pedley et al.[1311], and a recently revised comprehensive study by Schmidt[1312].

Hydrocarbon gases

Certain simple hydrocarbon gases can, under pressure, decompose exothermically and thereby explode. These include not only acetylene, but also ethylene, propylene, cyclopentadiene, and cyclohexadiene, for all of which such accidents have been reported[1313]. The conditions leading to explosion have not been extensively documented, but in one case propylene was compressed to 955 atm at 327ºC, while ethylene has been observed to explode at 54 atm and 460ºC, and also at 254 atm at 331ºC.

Hydrogen

The AIT value for hydrogen has been controversial. In an early survey (1907) of studies of $H_2 - O_2$ mixtures (i.e., with no nitrogen), Falk[1314] found reported values to range from 518 to 845ºC, with most of the values being in the range 580 – 700ºC. Falk himself measured 523ºC at the optimum H_2/O_2 ratio of 50:50. In their 1952 compilation of flammability data[1315], the Bureau of Mines cites an AIT value of 585ºC for hydrogen in air. The value dropped to 400ºC in the 1965 compilation[4], while in their final (1985) compilation[127], the Bureau of Mines quoted a value of 520ºC. Unlike for much of their other data, none of the BM compilations provide a documentation as to the experimental basis of the hydrogen AIT values that were cited. Speaking specifically to the 400ºC value, Woinsky[1316] points out that "the Bureau of Mines has not been able to reproduce this temperature," and this value must be considered an error. According to the classic textbook of Lewis and von Elbe[1317], there is an effect of the diameter of the test vessel, with AIT = 596ºC for a 39 mm vessel and 558ºC for a 74 mm vessel. The standard German compilation of flammability data[1318] gives a value of 560ºC and this appears to be the value that is most consistent with the bulk of experimental results. A history of hydrogen accidents sustained by NASA has been published[1319].

The quenching distance for hydrogen in air is a minimum of 0.63 mm at the fuel concentration of 29.5%, and this value is quite close to the minimum for any concentration. In pure oxygen, a quenching distance of 0.19 mm has been reported at the stoichiometric concentration[1322].

The flammability limits of hydrogen are commonly quoted as 4 – 75%. The exact value of the LFL has been controversial. Using an 8 L test chamber, Hertzberg[1320] showed that the LFL ≈ 7% for a quiescent mixture, falling to ≈ 5% under turbulent conditions. The lowest reported values appear to be an artifact of a too-small size of test apparatus, since repeating the same experiments in a 12 L chamber (which is still much smaller than real-scale problems), he found LFL ≈ 8.1% for quiescent mixtures. Hydrogen is among the easier fuels to detonate. If mixed in suitable concentration (18 – 59%) in air, detonations within pipelines[1226] may take place if the length of pipe is 100× its diameter, or greater.

The ignition properties of hydrogen are exceptionally sensitive to the amount of turbulence, unlike most other gases, which do not show a major turbulence effect. Because of the low MIE value for hydrogen, a number of accidents have taken place in chemical manufacturing facilities where hydrogen accidentally ignited in a vent stack. Britton[1321] reviewed various theories, but concluded that good explanations were generally lacking.

Drell and Belles[1322] published a report that comprehensively covers flammability properties of hydrogen, although it is now quite old. Another extensive study was done by the Bureau of Mines[1323], where the work focused on spills and pool fires of liquid hydrogen. A more recent (though hardly current) review is by Hord[1226]. Even small spills were shown to create quite tall regions of flammable mixture. The maximum height at which a flammable mixture existed was found to be about twice as high for spills on gravel as on smooth macadam. For a 3 L spill on macadam in quiescent air, flammable mixtures were found at heights up to 4.1 m, which was about 50% greater than the height of the visible cloud. When ignited, the pools showed a momentary yellow flash and then burned with a non-luminous flame.

EXPLOSIONS DUE TO ADVENTITIOUS HYDROGEN PRESENCE

Hydrogen/air explosions sometimes occur not where hydrogen is deliberately used, but rather when hydrogen is accidentally created in an unwanted chemical reaction. Médard[26] reviewed a number of incidents of this kind and Schneider[1324] discussed one incident in detail. Baker and Willis[1325] investigated the possibility that sufficient hydrogen could be generated for an explosion by electrolysis when performing electrical arc welding on chemical plant equipment where aqueous solutions are in steel containers. They concluded that this is not possible for an all-metal system, but could conceivably be possible if welding current is passed through an insulating joint in metal piping. An interesting case has been reported where a workman was injured due to a dishwasher explosion[1326]. An inspection was being performed prior to placing into service a dishwasher at an apartment complex. When the knob was rotated to start the cycle, an explosion ensued shortly thereafter. Investigation revealed that the water heater was in service but water was not being used. The water heater contained a magnesium anode for corrosion control purposes, and this allowed a sizeable amount of hydrogen gas to accumulate and to disperse into the water piping. A similar case of a dishwasher explosion was documented by the US Navy[1327]. The explosion destroyed the dishwasher and caused structural damage in a vacant Naval housing unit. When a plumbing system is in regular use, the small amount of hydrogen generated is dissipated from faucets. But if an apartment in unoccupied, yet the heater continues to operate, hazardous levels of hydrogen may accumulate in the piping. Hydrogen hazards due to improper operation of sacrificial anodes are known in other contexts[1328].

Hydroxylamine

Hydroxylamine, $HO–NH_2$, is a highly unstable compound used in semiconductor manufacturing. In its anhydrous form, it is usually stored at 10ºC to minimize the decomposition hazard[3]. Small amounts of impurities, especially iron, can violently catalyze the decomposition reaction[1329]. In commercial applications, it is often used as a 50 mass% solution in water. Of the three hydroxylamine manufacturing facilities formerly in existence, Concept Sciences, Inc. was destroyed by explosion in 1999 and Nisshin Chemical in 2000, leaving solely BASF as the remaining maker[1330]. Studies of the decomposition kinetics were made by Cisneros et al.[1329] and by Iwata et al.[1331], but they did not explain the conditions leading to the accidents.

Incendiary timing, delay, and actuation devices

Arsonists often do not wish to be present while the fire they are setting starts. This can be either to give themselves an alibi or else to avoid personal injury, especially if flammable liquids or explosions are contemplated. This requires either a timing device or a remote-actuation device to ignite the fire. In case of flammable-liquid ignited fires, an arsonist may simply ignite a 'trailer,' which is commonly a roll of toilet paper, toweling, lengthwise-wadded newspaper, etc., leading from the safe point of ignition into the to-be-ignited interior.

A recent review of timing devices[1332] used suggests that the most common one is simply a cigarette which is lighted, then its unlit end is placed in a book of matches, between the match heads and the cover; kindling is placed around the match book. A delay of 10 – 20 minutes is obtained this way, but the start of a fire is not necessarily reliable. Electric timers of various sorts are often used, but they leave metal parts that are not destroyed by a fire. Attempts are sometimes made to not have the incongruity of a timing device noticed by utilizing a device which contains both a time-dependent function and a heating mechanism. One example is placing combustible fuels at a furnace, where they will be ignited when the main burner comes on, but not ignited from a pilot light. Another example is timed baking in an oven, where some readily ignitable substance is placed inside.

Remote-actuated devices are less commonly used, but may typically involve a radio receiver or an electronic circuit connected onto a telephone line. Swab[1333] published a book giving details of various incendiary devices.

Insecticides, pesticides, fungicides

These substances come from a wide variety of chemical families. Some exhibit self-heating. EPA investigated an explosion[1334] caused by moderate heating of an organophosphorus insecticide. A safe storage temperature of 26ºC was found for 'supersack' quantities of the material. Agricultural insecticides are often formulated as dusts or wettable powders in which the active ingredient is mixed in with a finely-ground clay. Such clay-diluted chlorinated insecticides can show self-heating when decomposing. The decomposition is promoted by acid sites on the clay[1335]. This problem is normally addressed by the use of clay deactivators such as urea or hexamethylenetetramine. A case history is reported[1336] where self-heating of Perthane powder [diethyl diphenyl dichloroethane; 1,1-dichloro-2,2-bis(4-ethylphenyl) ethane; $C_{18}H_{20}Cl_2$] caused a large warehouse fire. Because of the huge variety of chemicals used for these purposes, individual testing is necessary to determine actual self-heating properties.

Iron sulfides

Iron sulfides are a family of inorganic compounds which have long been known to be susceptible to pyrophoric action. These compounds are FeS, FeS_2, Fe_2S_3, and Fe_3S_4. When found as a mineral, iron disulfide (FeS_2) is termed *pyrite* (or somewhat redundantly as *iron pyrite*), the term directly implying its potential to cause fire. The most exothermically-reactive sulfur-bearing mineral is pyrrhotite[1337]. It has the empirical formula Fe_nS, where n = 0.8 to 1.0. Case histories on the spontaneous combustion in mines of iron-sulfide-containing minerals have been collected by

Ninteman[1338]; a more recent bibliography was published by Wu et al.[1339]

In petroleum processing equipment, crude oil, bitumen, etc., may contain sulfur. Either sulfur or H_2S that is formed may react with iron or iron rust (Fe_2O_3), to form FeS, FeS_2, or Fe_2S_3. Anaerobic conditions are required for these reactions to occur[1340]. But the iron sulfides which are formed inside pipes, vessels, etc., may then self-heat to ignition when piping is drained or air is introduced. The reaction of FeS_2 with atmospheric oxygen is:

$$FeS_2 + O_2 \rightarrow FeS + SO_2$$

Moisture promotes pyrophoric reactivity, and in the presence of moisture, another reaction can occur:

$$2FeS_2 + 7O_2 + 2H_2O \rightarrow 2FeSO_4 + 2H_2SO_4$$

In the case of mineral form pyrites, the ferrous sulfate that is formed then attacks the pyrite, causing its decomposition and accelerating the reaction. The FeS form can react with oxygen in two different ways:

$$4FeS + 3O_2 \rightarrow 2Fe_2O_3 + 4S$$

$$4FeS + 7O_2 \rightarrow 2Fe_2O_3 + 4SO_2$$

Finely-divided iron sulfides are more prone to react pyrophorically.

A special rust-related problem has been the cause of several explosions in crude oil tankers, where a pyrophoric reaction was determined to be the reason[1341]. A laboratory investigation determined that the chain of events begins with fine particles of hydrated α-ferric oxide, α-FeO(OH), sometimes known as goethite. The primary steps involved are sulfide formation:

$$FeO(OH) + H_2S \rightarrow Fe_2S_3 + H_2O$$

followed by oxidation:

$$Fe_2S_3 + O_2 \rightarrow Fe_2O_3 + S$$

The reaction was found to be pyrophoric at temperatures as low as 25ºC, although only under certain conditions. The sulfide formation proceeded actively only at low oxygen concentrations, while the pyrophoric oxidation required oxygen concentrations > 11%; lower oxygen concentrations led to slow heating only. The fact that one step of the reaction occurs only under high oxygen conditions and another under minimal oxygen, helps to explain why the problem is relatively rare in practice. The sulfur needed for the reaction comes from the crude oil itself, and it is common for tanker atmospheres to have H_2S concentrations up to 3.5%. An explosion occurs because the oxidation reaction can produce incandescent-hot particles. The authors speculated that similar reactions might also account for some boiler explosions that were never otherwise satisfactorily explained. Walker et al.[1342-1344] have further studied pyrophoric reactions with various iron sulfides.

Jute

Jute, if clean, has been found to have negligible self-heating. However, baled jute has been known to self-heat if contaminated with the fats or oils of agricultural products, especially if micro-organisms are present[1345]; a number of ship fires have been recorded due to this cause[347]. Following a series of unexplained fires of jute cargo in steam ships, NIST conducted tests on jute[1087]. Using the Mackey tester, no self-heating was indicated, except for samples which had been contaminated with drying oils. This was confirmed in some larger size bundles tested in ovens. No ignitions were obtained, although some self-heating was observed. It was concluded that either very large piles would be required or contamination with drying oils would be needed for spontaneous combustion to be a problem. In some simple ignition tests with cigarettes, bales of jute ignited in 2 of 12 trials, but "loosely piled" jute did not ignite in 20 trials, although the test arrangement was not clear.

A limited amount of self-heating occurs in connection with wetting. In an early study[1346], it was documented that wet bales of jute commonly show 'heart damage,' which apparently consisted of self-heating, but short of thermal runaway. For the damage to occur, moisture had to exceed 25%. A level this high requires soaking with liquid water, it is not achievable by an equilibrium process with moisture in the air.

Kerosene

Kerosene (also spelled 'kerosine') is a petroleum distillate product which represents the fraction between gasoline and gas oil (diesel oil). It originally came into use in the 1840s as a lamp oil, but later became common—in various grades—as a heater fuel and as a fuel for jet engines). Chemically, kerosene can contain all of the main petroleum distillate families: paraffins, naphthenes, and aromatics, although the aromatics are removed for certain applications and paraffins in general tend to predominate. The dominant constituents[1347] are in the C_8 to C_{11} range. The kerosene that is used for space heaters and similar applications is known as 1-K grade (or Ultrasene) and is desulfurized, with sulfur < 0.04 mass%. The specification for this grade is governed by ASTM D 3699[1348]. Visually, this grade cannot be distinguished from 2-K, which may not be used in unvented heaters. A Chinese study[470] determined the minimum flux for piloted ignition of kerosene to be 2.9 kW m^{-2}. Even though, by law, the flash point of kerosene in most countries is above room temperature, by applying a small flame to a 90 mm pan of kerosene held in open air for about 4 minutes it was found possible to achieve ignition[463]. This pre-warmed the fuel locally so that sufficient vapors were produced for ignition.

Kerosene heaters

Portable kerosene heaters are devices that typically have a heat output of 2.2 – 4.4 kW at maximum setting. Their design has changed over the last few decades, with safety features now being much more robust than previously. During the 1970s and '80s, CPSC encouraged the manufacturers to upgrade the safety of kerosene heaters. Consequently, kerosene heaters today have safety features which did not exist in earlier decades:

- improved guards or grilles that reduce the risk of accidental contact burns;
- a manual shut-off device which allows for a quick shut-off during an emergency situation;
- a wick-stop mechanism which prevents the wick from being retracted to a hazardously low setting;
- labels that stress the use of 1-K fuel and the importance to not mis-fuel with gasoline.

In the US, kerosene heaters are commonly manufactured to conform to UL 647[1349]. It is interesting, however, to consider a statistical breakdown of kerosene heater fires[1350] compiled in Great Britain in 1960-61 (Table 154), since they indicate a large component of human carelessness which better engineering may not necessarily prevent.

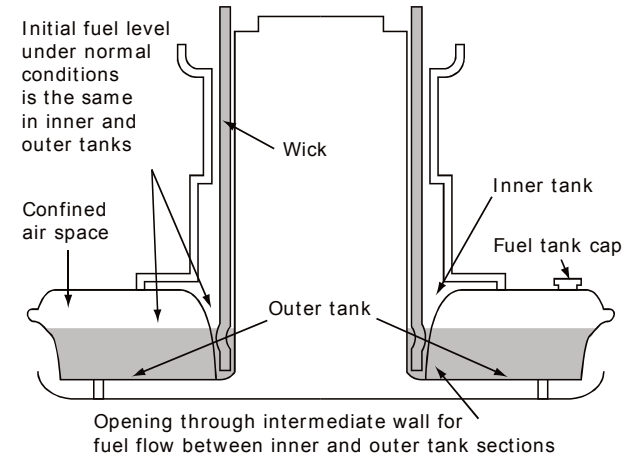


Figure 99 Failure mode for bottom-fed kerosene heater mis-fueled with high-vapor-pressure fuel
(Copyright Fire Findings, LLC, reprinted by permission)

Table 154 Breakdown of UK kerosene heater fires, 1960-61

Cause	Percent
overheated or flared up	24.8
turned too high	16.4
leakage or flooding	13.0
overfilled or spilled	12.2
too near combustibles	11.3
overturned or dropped	10.4
other or unknown	7.7
filling while alight	3.5
exploded	0.5

The two most common fuel-feed systems for kerosene heaters are the bottom feed and the cartridge-type fuel tank. The bottom-feed fuel system presumes that only the correct fuel, kerosene, will be introduced into the heater. Too often users erroneously introduce gasoline, or kerosene contaminated with a fuel having a high vapor pressure, such as mineral spirits or turpentine. The consequence[1351,1352] of this fueling error is likely to be a "heater enveloped in flames" (Figure 99). Cartridge-type heaters will overflow and show catastrophic flaming when fed with a fuel of the wrong vapor pressure. In addition, overflow can also result if the fuel cartridge develops a leak. A device has been described which can mitigate the effects of leaks in fuel cartridges and prevent flareups[1353].

Lambswool pads, imitation

A study[2087] found that some commercial imitation lambswool pads, such as are used to prevent bedsores or for automobile driver's comfort, were highly susceptible to self-heating. In one case, the pad was put into a sterilizer, and in another case it was put through a clothes dryer.

Lawn mowers

Exhaust system temperatures have been measured on one small, 3.5 horsepower lawn mower[1354]. A maximum temperature 350ºC of was found on the outside of the muffler, while the exhaust gases measured 370ºC at the discharge.

Lime

Unslaked lime ('quicklime,' CaO) reacts highly exothermically with moisture to form $Ca(OH)_2$. Rossotti[1355] relates that this was already known to ancient Greeks, who would smear quicklime with some readily combustible substance such as sulfur or crude oil on enemy buildings, then wait for rains to cause ignition. Fires due to accidental contact of moisture with quicklime have been reported[1453].

LNG and LPG

LNG is liquefied natural gas and comprises mostly methane. LPG is liquefied petroleum gas and comprises propane, butane, and small amounts of propylene, butylene, ethane, and other gases. In addition, an odorant is added to gas sold to consumers. The actual composition of LPG is highly dependent on the country in which it is produced. In the US, LPG is predominantly propane, while in some Eu-

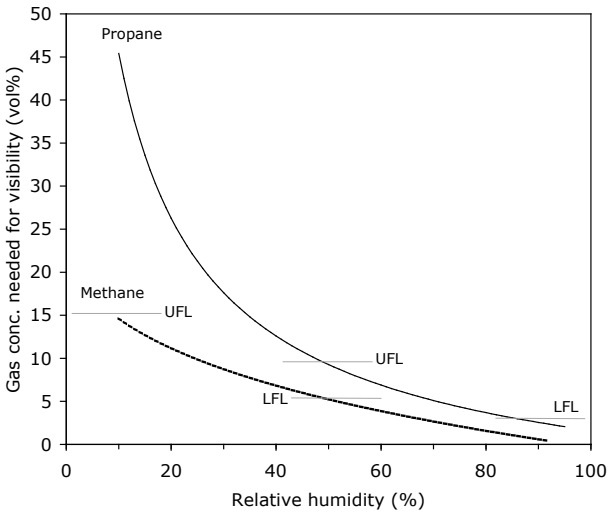


Figure 100 Relation of RH to visibility of liquefied gas plumes in air

ropean countries the major constituent is butane. LPG used for motor vehicle engines is produced to a specification known as HD5 which requires a propane content of at least 90% and a propylene content no more than 5%.

When LPG is sold in portable containers, the container is supposed to be filled only to 80% of capacity. Fires have been numerous when containers have been overfilled. When a container was filled in a cold environment and is then brought into a warm environment, if sufficient vapor space is not available in the container, expansion of the liquid will raise the vapor pressure sufficiently to expel the vapor from the safety relief, whereupon it can potentially ignite if ignition sources are present outside. The problem largely arises because liquid propane has an exceptionally high coefficient of thermal expansion, which is roughly 100× that of steel. Under some conditions (if the temperature change is extreme, or if the container is tilted), liquid—not only vapor—can be expelled. de Nevers has presented detailed calculations on the thermal expansion process[1356].

Modern, portable propane cylinders are likely to contain safety features which were historically not present. The background and features of quick-closing couplings[1357] (QCC) and overfill protection devices[1358] (OPD) have been documented. OPD valves have been used by US manufacturers of 1.8 – 18 kg (4 to 40 lb) cylinders since 1998 and have been required by NFPA 58[1359] since the 1998 edition of that document. These devices comprise a tank valve which has a special float which rises during refilling to block the filling process when the tank is 80% full. The valve handle on OPD-equipped cylinders is triangular shaped, as contrasted to round or star-shaped ones used previously. Propane cylinder BLEVEs are discussed in Chapter 13.

Liquefied natural gas occasionally autoignites when spilled on water. The Bureau of Mines[1360] documented several such instances in the course of laboratory testing, but did not produce a definitive explanation. It appeared that the explosions most probably were akin to steam explosions (physical, rather than chemical, explosions), possibly involving ice formation. For cryogenic temperatures, the effect of temperature on the LFL of methane[1361] has been determined to be:

$$LFL_T = 5 + 0.0052(298 - T)$$

where T = temperature (K). Large shipments of LNG and LPG are usually carried by refrigerating the gas below its boiling point, rather than by enclosing it in a pressure vessel. If a spill of refrigerated LNG or LPG cargo occurs, a visible plume will be seen in the atmosphere. The actual fuel gases are invisible at any temperature, but introducing a cold gas into the atmosphere causes local condensation of moisture. Blackmore et al.[1362] studied the relation between the relative humidity in the air and the fuel gas concentration in the spill plume at which the plume becomes visible. Figure 100 shows that propane plumes are difficult to see, and at 50% RH only that part of a plume which is over the UFL would be visible. For methane, on the other hand, a concentration essentially equal to the LFL can be seen in a 50% RH environment.

Marijuana and hemp

The marijuana (*Cannabis sativa*) plant contains from 25 to 40% hempseed oil and the latter is rich in fatty acids. The iodine number of hempseed oil is typically in the range of 145 to 167, which is only slightly lower than that of linseed oil. Consequently, the plant shows a pronounced self-heating tendency. Two cases have been reported where small quantities (one or several garbage bags) containing marijuana underwent thermal runaway in Canadian police stations[1363]. In one case, the self-heating progressed to a flaming fire. Thermal runaway is readily evident due to strong odor, even if flaming does not occur. The storage time in one case was only 1 – 2 days and was probably only somewhat longer in the other. More than 100 years ago, Moore[257] recorded that moist hemp has "been known to take fire spontaneously" but did not give details.

Matches and lighters

PROPERTIES OF MATCHES

In the history of technology, matches existed even in the times of the Romans, but prior to the 1800s, matches were either devices for propagation—rather than initiating—fire, or else were part of some wet-chemistry scheme, typically involving sulfuric acid[1364]. The current-day matches are pyrotechnic devices, with the material of the match head being a pyrotechnic mixture, where ignition and initial combustion is based on a solid-state reaction. Oxygen from the air is not involved except when the match stem ('splint') begins to burn. Apart from head and splint, a modern match has the top 15 mm or so of the splint dipped in paraffin wax

in order to make sure that the burning of the head ignites the wood splint. Conversely, the entire splint is also treated with a fire-retardant agent to suppress after-glow, once flaming is extinguished.

A match head composition originating from Vienna in 1820 comprised[1364]:

33% potassium nitrate
33% manganese oxide
10% phosphorus (P_4)
24% gum arabic.

Despite the early description, it is not clear when matches of this nature were actually commercialized. The first pyrotechnic-mixture based matches known to have been commercialized were those produced in 1826 by the apothecary John Walker[1365]. His match heads comprised potassium chlorate, antimony sulfide, gum, and starch. They were ignited by rubbing against sandpaper. The addition of sulfur to the composition by Isaac Holden in 1829 made ignition more efficient and practical. Early matches also had splints treated with sulfur, rather than wax. Safety matches were invented in 1844 by Swedish professor Gustaf Pasch, and were commercialized in the same year, although the initial product was not very satisfactory. The head contained mainly potassium chlorate and antimony sulfide, while the active ingredient in the friction strip was red phosphorus. Worldwide commercialization of safety matches is considered to have been started in 1855 by the brothers Johan and Carl Lundström, at the Jönköping Match Factory in Sweden. Consequently, during the 19th century safety matches were often called 'Swedish matches.'

Nineteenth century strike-anywhere matches were based on white phosphorus; its use presented toxicity problems and fire hazards in transportation and storage. This was solved by the development of phosphorus sesquisulfide. One formulation of a strike-anywhere match head involved:

28% potassium chlorate
13% phosphorus sesquisulfide (P_4S_3)
14% animal glue
15% ferric oxide
10% zinc oxide
20% ground glass.

The animal glue also serves as fuel, not just as binder. Physically, modern strike-anywhere matches use two different layers of pyrotechnic composition, one applied on top of the other; the tip has a high content of P_4S_3 for easy ignitability, while the base has more fuel in order to avoid premature extinguishment[1436].

The typical composition of a safety match head commonly includes red phosphorus, powdered glass, and glue, along with smaller quantities of other substances. The friction strip against which safety matches are lighted has typically about 50% amorphous red phosphorus, about 20% of an adhesive, and a smaller amount of abrasive, such as glass powder. Paper, i.e., 'book' matches, were invented in 1892 by Joshua Pusey and commercialized in 1894 by the Diamond Match Company.

Cooke and Ide[605] report that the ignition temperature of British safety matches is 180 – 200ºC and that of strike-anywhere matches is 120 – 150ºC; their book also contains much useful guidance for forensic investigations involving matches. An old study by Lucas[449] found an AIT of 40 – 85ºC for strike-anywhere matches and 120 – 175ºC for safety matches. His values for strike-anywhere matches are exceedingly low and apparently pertain to matches produced in Egypt in the 1920s. Phosphorus sesquisulfide itself has an AIT around 100ºC and this governs the rather low AIT value for strike-anywhere matches[1436]. The AIT of American strike-anywhere matches[443] was reported by NIST in 1947 as being 163ºC. Latham[1366] determined the ignition temperature of American and Australian strike-anywhere matches to be 215ºC, but with a very large standard deviation of ⌖50º. The temperatures at the head and at several places along the splint have been measured on burning book matches and wood (box) matches[1367]. The peak surface temperatures were found to be in the range of 800 – 900ºC, both at the head and also along the splint at up 10 mm away from the head. No significant differences in peak temperature were found between book and box matches. Actual flame temperatures have been reported[1368] to be in the range 1350 – 1930ºC, with most values being in the range of 1400 – 1500ºC. Since the peak temperatures in the similar flame of a candle are 1400ºC, the values at the high end of this range are probably in error, as is the low reported value[311] of 1130ºC.

The ignition process that occurs upon striking a match head upon a suitable surface and the subsequent combustion of match head and stem are complex and have not been studied in a quantitatively satisfactory way. Finch and Ramachandran[1365] consider that there are at least 8 steps involved in the combustion process.

CPSC has reported tests on matches[1369]. Their results are shown in Table 155. In some cases the matches went out before being consumed (for the dropped ones) or got too hot to hold (for the held ones). The drop distance was 457 mm and a significant number—but highly variable (12% to 58%)—of them self-extinguished during, or upon landing. These were not included in the burn time averages.

Table 155 Average burn times (s) for various matches

Orientation	**Book match** (35 mm long)	**Wood match** (40 mm long)	**Wood kitchen match** (55 mm long)
held horizontal	22.9	16.4	31.4
dropped on glass fiber board	42.6	41.5	40.2
dropped on cotton duck fabric	12.1	12.2	10.4
held vertical, head-up	31.0	28.3	28.8

The total burn time (non-hand-held) of American kitchen matches held head-up was determined to be 52 s, but Australian matches, which were slightly shorter (42 mm) burned up in 28 s[1366]. The difference appears to stem from the fact that they were also thinner and weighted 0.11 g, compared to 0.24 for the American ones. Burning time of matches held head-down were studied by Sale[1370], who found burn times of 13 s for a 49 mm wooden safety match, 16 s for a 63 mm kitchen match, and 18 s for a paper book match. The time taken to light a cigarette using a match is about 5 s, but about 10 s is needed to light a cigar or a pipe. For the latter articles, there was quite a wide spread found in the lighting times, with 95% of the data falling between 6 and 14 s.

After the head has burned off, a paper (book) match burns at a HRR of about 45 W, a wood kitchen match at about 100 W[1371]. Latham found that for kitchen matches placed vertically, head-up, an adjacent match has to be 8 – 9 mm away for it to autoignite by radiation[1366]. Matchbooks occasionally ignite when placed in airline luggage. Documented cases include match heads from one book rubbing against the striker of another book, and match heads rubbing against an emery board[1372]. In Latin American countries, *vesta* matches are sometimes encountered. These do not have a wood or cardboard stem, but rather resemble a miniature candle—there is cotton wick at the center, surrounded by paper rolled around it, with the latter being then impregnated in wax. In enriched-oxygen atmospheres, matches can burn up very quickly. Wharton[331] showed that a match burning downwards at 1.5 mm s^{-1} in a normal atmosphere burned at about 12 mm s^{-1} in 50% O_2.

IGNITION POTENTIAL OF BLOWN-OUT MATCHES

The problem of inadvertent ignitions from 'extinguished' matches dates to the very early days of match production. In 1868 S. Howse already received a British patent for impregnating chemicals to be used to reduce the afterglow tendency[1365]. In current manufacture, stems are treated with an after-glow suppressant such as a 1.5% solution of H_3PO_4. A consumer protection agency in Canada[1367] studied the temperatures of contemporary blown-out matches and found that some matches required more than 4 s to drop to a temperature of 400ºC and 5 – 6 s to drop down to 350ºC. Highest temperatures were reached at the midpoint of the head and for a 10 s pre-burn time. Shorter pre-burn times of other measuring locations showed lower values.

In Canada, FR agents used to suppress after-glow are often ammonium dibasic phosphate or ammonium polyphosphate. A study[1373] examined the effect of these agents on potential ignitions through afterglow. Of matches obtained in the Canadian marketplace, the afterglow at the head in some cases ranged to over 36 s, but was typically < 15 s. Afterglow at the splint was < 3 s in 91% of cases. For certain imported matches which did not have FR treated splints, 40% showed afterglow times of 15 – 35 s, while 60% showed times over 36 s. The authors then conducted target-item ignition tests. No ignitions of petroleum ether vapors were possible, nor were there any ignitions of lint or crumpled facial tissue, although in some tests up to 250 s of smoldering was observed, before smoldering self-terminated. As a worst case situation, ground-up facial tissue was used. Out of 23 tests with this target material, 20 trial resulted in self-terminating smoldering of less than 190 s duration. In one case, smoldering lasted for 10 min. In two other cases, smoldering transitioned to flaming when the specimens were covered with the target combustible and a mild draft applied. The times for transition to flaming were 12 and 15 min. The positive results were all obtained from afterglow of splints; no positive results were obtained from afterglow of heads.

In a further study, the same agency examined paper book matches[1374]. Untreated splints showed afterglow times of 22 – 60 s, while treated ones had times of 5 – 17 s. The matches that were not FR treated showed a strong tendency to re-light after being blown out, with only 16% of the matches tested not re-lighting. Of the untreated splints, no flaming ignitions occurred for: cotton lint; a cotton pad; paper towels; shredded newspaper; or petroleum ether vapors; smoldering times, if any, were short. When specimens were surrounded by ground-up facial tissue, flaming ignitions did not occur, but smoldering lasted up to 10 min. When specimens were placed within dried ground leaves, one out of 3 specimens initiated self-sustained smoldering that transitioned to flaming in 20 min. The most sensitive target fuel proved to be ground up newsprint. For one type of untreated splints, 100% went to flaming, which occurred in only 16 – 28 s. For another type, 20 out of 50 initiated self-sustained smoldering that transitioned to flaming in 15 – 35 s. For FR-treated splints, only 1 out of 50 samples initiated self-sustained smoldering; this specimen went to flaming after 36 s.

LIGHTERS

CPSC found that maximum burn times for disposable cigarette lighters ranged from 200 s to 960 s, depending on the size and design[1369]. For two out of four tested, the reported burn time was due to the lighter becoming too hot to hold, the others ran out of fuel. When ignited in an enriched-oxygen atmosphere, a butane lighter[331] will ignite with a 'pop' at 30% O_2 and a loud 'pop' at 45% O_2. ASTM F 400[1375] is the ASTM standard on lighters.

Metal alkyls

Metal alkyls are compounds of the general formula $M_x(C_nH_{2n+1})_y$, where 'M' stands for a metal. Examples include *n*-butyllithium, diethylzinc, triethylaluminum, and triethylborane. Many metal alkyls are either pyrophoric or require only moderately elevated temperatures for ignition. Marsel and Kramer[1376] studied the autoignition properties of several metal alkyls and Ellern[1407] summarized available information on others. When metal alkyls are diluted with

hydrocarbon solvents, they may still retain their pyrophoric properties, if present in a high enough concentration. Mudry et al.[1377] studied the behavior of such solutions. To characterize their relative pyrophoric hazards, they developed a simple test where a small amount of solution is dropped on a cellulose filter paper and a 'pyrophoric concentration' is declared to be the minimum concentration that causes the paper to be charred in 45 s.

Metal alloys

Certain metal alloys are pyrophoric or water-reactive. These include[3]:

- aluminum-lanthanum-nickel alloy ($AlLaNi_4$)
- a wide variety of cerium alloys, especially with mercury
- lead-zirconium alloys containing 10 – 70% zirconium (they pulverize and ignite on impact)
- silver-thorium alloy
- zinc-mercury amalgam.

Metal carbonyls

Many metals can form a compound of the general formula $M_x(CO)_y$, where 'M' stands for a metal and 'x' and 'y' vary according to the valence of the metal atom. More complex molecules incorporating several different metals in one molecule are also possible. The metal carbonyls where the metal is an alkali metal (lithium, sodium, potassium, rubidium, cesium) are generally pyrophoric, but carbonyls formed with other metals may also be. Examples include: iron pentacarbonyl ($Fe(OC)_5$), potassium carbonyl (KCO), sodium tetracarbonylferrate ($Na_2[Fe(CO)_4]$). Urben[3] provides extensive listings along with literature references.

Metal hydrides

Hydrides in general are divided into three categories, depending on the type of chemical bonds holding the hydrogen atom to its partner:

(1) Covalent hydrides contain covalent bonds, such as those in hydrocarbons and hydronitrogens.
(2) Saline or ionic hydrides contain hydrogen in the form of a negatively charged hydride ion H^-, such as in lithium hydride or sodium hydride.
(3) Metallic hydrides are formed by absorption of hydrogen into the electron cloud surrounding atoms in metals. The compounds are electrical conductors and are nonstoichiometric, allowing a wide variation of hydrogen contents. Many metals become embrittled as the result of inadvertent hydrogen absorption.

Many metallic hydrides are highly reactive. Examples with pyrophoric tendencies include aluminum hydride (AlH_3), barium hydride (BaH_2), lithium hydride (LiH), lithium aluminum hydride ($LiAlH_4$), magnesium hydride (MgH_2), potassium hydride (KH), sodium hydride (NaH), thorium dihydride (ThH_2), thorium hydride (ThH_4), uranium hydride (UH_3; UH_4). Urben[3] provides extensive listings along with literature references. Tests by the Bureau of Mines[1378] showed that 5 g quantities of powdered sodium hydride and lithium hydride ignite in air at 54ºC, but not at 32ºC. Moisture is necessary to elicit the pyrophoric behavior of some metal hydrides.

Metal oxides

Some metal oxides are oxygen-rich and can act as oxidizers, these include PbO_2, MnO_2, and CrO_3. Médard[26] reports that contact of oil with CrO_3 causes a near-instant ignition.

Metals

ALUMINUM

Because aluminum combustion has significant applications in the rocket propulsion field, its combustion has been studied in more depth than that of any other metal. The details of aluminum's ignition process have been described by Price[1379]. Ignition of aluminum does not require oxygen. Reaction can occur with halogenated hydrocarbons and some other compounds that are explosive in nature. NFPA has a standard, NFPA 651[1380], covering the safety precautions of working with aluminum powders. Werley et al.[1381] published an extensive review paper that discusses many specialized ignition modes, e.g., friction and impact.

BULK MATERIAL

Bulk aluminum is difficult to ignite. Grosse and Conway[1382] found that aluminum pools in pure oxygen at 1 atm in a high-temperature furnace did not ignite* at a temperature of 1000ºC. Brzustowski and Glassman[1383] ignited aluminum ribbons by resistance heating and found that the surface temperature at ignition was 1752ºC.

Zhu et al.[1384] explored the ignition of large specimens (10 mm diameter) of aluminum at the very low pressure of 8 kPa. As with any non-protected aluminum, the surface was originally oxidized, that is, converted to Al_2O_3. When approaching the ignition temperature, the oxide layer began to crack and separate. Ignition occurred in the *gas phase*, with initial flaming occurring at the cracked areas. At a constant heating rate of ca. 4ºC s^{-1} supplied by inductive heating, the ignition temperature of 1900ºC was nearly independent of oxygen concentration over the range of 20 – 100%. The measured ignition temperature was lower than the boiling point at 8 kPa (2035ºC) and also lower than the melting point of Al_2O_3, which is 2042ºC. When ignition occurred, a diffusion flame of Al vapor was formed about 2 – 4 mm above the specimen surface. After ignition, the temperature of the specimen continued to rise, and it eventually exploded due to trapped gases inside. In a related study[1385], the authors varied the heating rate. The ignition temperature was seen to be inversely dependent on the heating rate. For a heating rate < 2ºC s^{-1}, the ignition temperature approached the melting point temperature for Al_2O_3 of 2042ºC. At a heating rate of 2ºC s^{-1}, an ignition temperature around

* Their finding has been misreported in several surveys, where it is incorrectly given that 1000ºC is the ignition temperature.

1750ºC was found. The authors also studied the ignition of aluminum cylinders which did not have the natural coating of aluminum oxide. At 1 atmosphere pressure and an unspecified heating rate, the ignition temperature ranged from ca. 1550ºC (for near-zero air flow) to ca. 1670ºC (for air flow rates over 4 m s^{-1}). Such temperatures are, of course, well below both the boiling point of Al and the melting point of Al_2O_3. Zhu concluded that the *mechanism* of ignition of aluminum depends on the surface conditions. For an *unoxidized* surface, if the temperature is high enough, vaporization of Al proceeds at a sufficient rate that a gas phase flame can form. Conversely, if the temperature and vaporization rate are insufficient, O_2 diffuses easily to the metal surface and an oxide layer forms instead of ignition occurring. Ignition can occur subsequently at a higher temperature corresponding to oxidized-surface ignition. For an *oxidized* surface, the ignition temperature is lower than the melting point, because of reactivity. At elevated temperatures, surface heating occurs due to the reaction between the metal and the oxidizer. This is why the ignition temperature is progressively lower for higher heating rates. In cases where the oxide is forcibly stripped off the metal, e.g., by frictional rubbing, a vastly lower T_{ig} value is found. Benz and Stoltzfus[1386] found a value of 375 – 425ºC under these circumstances.

Liedtke and Rhein[1387] studied the ignition and combustion of aluminum/lithium alloys (typ. 90%+ Al; 2.5% Li; 1% Cu, 1-2% Mg) and found that the presence of lithium, in many cases, defeats the protective oxide layer of aluminum and enhances ignitability and combustion. Their study also showed strong reactivity of these alloys with certain salts. Notably, the extinguishing powder Met-L-X, used for extinguishing certain metal fires, was found to promote combustion of Al/Li alloys.

SINGLE PARTICLES

Friedman and Maček studied the ignition of single particles of aluminum by use of propane flat-flame burner[1388]. They found that even at zero oxygen concentration, ignition of 23 and 35 µm aluminum spheres was possible in the high-temperature combustion product stream of the propane burner (the particles spent a negligible time period in the flame itself). Furthermore, the ignition temperature hardly varied with O_2 concentration, being 2000ºC at 0% O_2 and 1940ºC at 36% O_2. These are temperatures that are very close to the melting point of Al_2O_3, 2030ºC. The induction period varied with particle diameter according to:

$$t_{ig} = 2.6 \times 10^{-3} d^2$$

where d = diameter (µm). When ignited, a flame temperature of ca. 2500 K was noted[1389]. Maček[1390] studied aluminum spheres of 35 – 45 µm diameter and found that a gas temperature of 2000ºC was needed at 1 atm and near-zero oxygen concentration. As the partial pressure of oxygen was raised to 1.7 atm, the temperature dropped to 1870ºC. The effect of total pressure appears to be larger, however. Kuehl[1391] studied 0.5 mm diameter aluminum wires and found, at 0.3 atm and higher, a constant value of 2050ºC. But for lower pressures, the temperature needed for ignition dropped significantly, reaching 1500ºC at 0.03 atm.

Frolov et al.[1392] summarized results from experimental studies conducted by several Russian research groups on the ignition of individual particles of aluminum. In experiments using very small particle sizes, for the smallest diameter tested, 7 µm, ignition was at 710ºC in air, rising to 930ºC for 10 µm and 1320ºC for 19 µm. But in another series, T_{ig} decreased with increasing particle size over the experimental of 80 – 250 µm. Frolov did not provide a consistent explanation for these trends.

Merzhanov and coworkers[1393] studied the ignition in pure O_2 of very fine electrically heated aluminum wires. The wire diameters ranged from 30 to 50 µm. The ignition temperature was found to depend on the heating rate. For high heating rates, a value around 1650ºC was found, while for the smallest heating rates a value around 1970ºC was seen, with a transition region joining these two temperature plateaus. By providing a gas velocity of 0.5 m s^{-1}, the ignition temperature dropped by 200 – 350ºC. Results for ignition in a CO_2 atmosphere were very similar. The authors provided an accompanying theoretical model, which includes both chemical kinetics and heat loss effects; this theory, however, does not seem to have seen further use by other researchers.

An explosion hazard can be created if powdered aluminum is mixed with a solvent that contains both halogen and hydrogen atoms[1644]. The reaction produces gaseous hydrogen and this may lead to a hydrogen explosion, in the presence of a suitable ignition source. Similarly, powdered aluminum moistened with alkaline water may release hydrogen and autoignite in air; this reaction is accelerated by traces of mercury.

DUST CLOUDS AND LAYERS

According to Hartmann et al.[1394], aluminum dust in air will autoignite at 645ºC. The temperature is size-dependent, and Maranda et al.[1395] found an AIT of 600ºC for particles of 11 µm mass-mean diameter, but over 1030ºC for 68 µm. Ignition temperatures of very small particles[1402] (< 0.1 µm) were reported to be 410 – 585ºC. The spark ignitability of aluminum dust is also highly dependent on particle size. At room temperature, an MIE of 20 mJ was found for particles of 11 µm mass-mean diameter, but rising to 246 mJ for 68 µm mass-mean diameter[1395]. Aluminum without an oxide coating is considered to be pyrophoric in sizes less than 0.03 µm[1459]; however, it must be noted that this is an exceedingly small particle size. *Flake aluminum* is more readily ignitable than atomized aluminum or other more compact particle shapes. This is due to the greater surface/volume ratio for flakes.

In a CO_2 atmosphere, aluminum powder (ultra fine, 0.03 μm size) was found to ignite at 360 – 420ºC[1396]. It appears that aluminum powder can ignite at 800 – 900ºC in a nitrogen atmosphere, although experimental results are highly inconsistent[1397]. If aluminum powder is moistened, it may ignite spontaneously in air[1398].

ALUMINUM IN PHYSICAL MIXTURES

Powdered aluminum is often used in propellants and in pyrotechnic mixtures. Ignition in such mixtures can be achieved at temperatures much below those needed for igniting pure aluminum. Nir[1399] studied the ignition of aluminum particles mixed with ammonium perchlorate oxidizer. He found that the aluminum ignites below 1000ºC, and he attributed this to a reaction between aluminum oxide and a gaseous combustion product of ammonium perchlorate.

ANTIMONY

Grosse and Conway[1382] found an ignition temperature of 650ºC for solid antimony burning in pure oxygen at 1 atm.

BARIUM

Grosse and Conway[1382] found an ignition temperature of 175ºC for solid barium burning in pure oxygen at 1 atm. Laurendeau and Glassman[1400] found an ignition temperature of 550ºC for solid barium burning in pure oxygen at 1 atm. Laurendeau and Glassman attribute this very large difference due to atmospheres used in the test work—the Gross and Conway experiments preheated the specimens under inert conditions, then applied an oxygen stream. The Laurendeau and Glassman procedure involved inductive heating of the specimen from room temperature in the pure-oxygen atmosphere. This results in a thick coat of oxide being built up on the surface. In addition, barium undergoes a great deal of self-heating before ignition, which was also considered to be a factor in explaining the difference. For applications where a protective oxide coating is not deliberately minimized, the Laurendeau and Glassman results would be more relevant. Finely-divided barium is spontaneously flammable in moist air[1398].

BERYLLIUM

Maček et al.[1401] found that single particles of beryllium (30 – 45 μm size) autoignite in an atmosphere of 21% oxygen at a temperature of about 2300ºC. There is a slight dependence on the oxygen partial pressure, and for an O_2 partial pressure of 5 atm the temperature drops to about 2100ºC. Beryllium powder (< 0.1 μm size) was found to spontaneously ignite at room temperature in air[1402] and in a CO_2 atmosphere[1396]; in a nitrogen atmosphere ignition temperatures of 504 – 527ºC were found[1403].

BISMUTH

Grosse and Conway[1382] found an ignition temperature of 775ºC for solid bismuth burning in pure oxygen at 1 atm. Laurendeau and Glassman[1400] found an ignition temperature of 735ºC for solid bismuth burning in pure oxygen at 1 atm.

BRASS

Brass powder can readily smolder. In hotplate tests on powder of unspecified particle diameter[1404], a hot-surface temperature needed for ignition was found to be 160ºC for 12.7 mm layer, 140ºC for 25.4 mm, and 135ºC for 38.1 mm. The authors pointed out that the stearic acid coating placed on brass powder to prevent rapid oxidation clearly affects the process, but uncoated powder would not be a stable item.

CADMIUM

Grosse and Conway[1382] found an ignition temperature of 760ºC for solid cadmium burning in pure oxygen at 1 atm.

CALCIUM

Grosse and Conway[1382] found an ignition temperature of 550ºC for solid calcium burning in pure oxygen at 1 atm. Laurendeau and Glassman[1400] found an ignition temperature of 790ºC for solid calcium burning in pure oxygen at 1 atm. Calcium powder (< 45 μm size) was found to ignite in air[1402] at 222 – 236ºC, and in a CO_2 atmosphere at 293ºC[1396]; in a nitrogen atmosphere, ignition temperatures of 327 – 671ºC were found[1403].

CERIUM, PYROPHOR, AND CIGARETTE-LIGHTER 'FLINTS'

According to one source[3], cerium ignites in air at 160ºC, but according to another[1405], a temperature of 400ºC is needed before cerium pellets ignite in air, and even then it is a mild glow type of ignition. Cerium has been the basis of 'pyrophoric alloys,' first described in 1903 by Carl Auer von Welsbach, and sometimes called *Auer metal*. These comprise about 70 – 80% *misch metal* and about 15 – 30% iron. Misch metal, in turn, contains mainly cerium and lanthanides; a typical composition[90] is Ce 49%, La 25.6%, Nd 16.0%, Pr 4.6%, Sm 2.0%, Tb 1.0%, Y 1.0%, and Fe 0.8%. The term 'pyrophoric' here is a misnomer. The material does not simply ignite upon exposure to air, instead, it functions as an igniter since it is very brittle and easily fractures; filing or scratching produces small readily burning particles. After Auer's invention, cigarette lighter 'flints' were usually produced of Auer metal; these are sometimes known as *pyrophor bars*. Rae[1406] dropped small particles of pyrophor bar onto a heated plate and found that the minimum temperature for ignition was 178 – 207ºC, with most results being around 180ºC. Amalgams of cerium and mercury are pyrophoric[1407].

Cerium powder (< 45 μm size) was found to ignite in air[1402] at 106 – 115ºC, in a CO_2 atmosphere at 172 – 190ºC[1396,1403] and in a nitrogen atmosphere at 216 – 230ºC [1403]. In a nitrogen atmosphere, fine cerium wires were found to ignite at 850ºC[1397].

CESIUM

Cesium is pyrophoric in air or oxygen and violently reactive with water[3].

CHROMIUM

In a CO_2 atmosphere, chromium powder (< 45 μm size) did not visibly ignite, but at 870ºC a slow glowing reaction was found to start[1396]. Fine chromium particles are pyrophoric[1407].

COBALT

Fine cobalt particles are pyrophoric[1407]. Cobalt finds use as a catalyst for polyester resins or drying oils such as linseed or tung oils.

COPPER

Jakowsky and Butzler[1408] ignited copper in an oxygen bomb and found an ignition temperature of 1050ºC at 1 atm, going down to 825ºC at 109 atm. Using a radiant heat source, Abbud-Madrid et al.[1409] ignited bulk copper in an O_2 atmosphere at 1 atm. The surface temperature at ignition was 1087ºC. Because of its very low heat of combustion, copper is difficult to ignite and burn, and most other investigators have reported 'no ignition.' Copper powder of very small diameters (0.01 – 0.03 μm) is pyrophoric[1410].

HAFNIUM

Hafnium dusts are prone to room temperature autoignition[1411].

IRON AND STEEL

Iron is one of the few metals which burns only heterogeneously (at the surface), showing no gas-phase flame. The main reaction takes place at the metal/oxide interface:

$$Fe + Fe_3O_4 \rightarrow 4FeO$$

Grosse and Conway[1382] found an ignition temperature of 930ºC for solid iron burning in pure O_2 at 1 atm. The identical ignition temperature was earlier reported by Jakowsky and Butzler[1408], who also found 600ºC at a pressure of 136 atm. Abbud-Madrid et al.[1409] ignited iron rods in a 1 atm O_2 atmosphere and found a surface temperature of 1197ºC at ignition. Sato et al.[1412] heated up iron rods in an inert atmosphere, then plunged them into a hyperbaric O_2 atmosphere. When plunged into an atmosphere at 5 MPa pressure, a minimum initial specimen temperature of 1280ºC was needed for ignition. Specimens at lower initial temperatures self-heated to an appreciable extent, but no ignition was observed except for tests where the specimen attained a surface temperature of 2930ºC or more. It is not clear why Sato needed higher temperatures for ignition when using hyperbaric oxygen, compared to 1 atm oxygen used by Grosse. Using a very different experiment of an electrically-heated wire, an identical ignition temperature was found by Jakowsky and Butzler[1413], who also documented a nearly linear drop with pressure, the value at 136 atm being 600ºC. Laurendeau and Glassman[1400] found an ignition temperature of 1315ºC for solid iron burning in pure oxygen at 1 atm. White and Ward reported that steel requires 1200 – 1300ºC for ignition in oxygen at ambient pressure[1445]; ignition in air was considered to occur at similar temperatures. Reynolds found that mild steel ignited at 1225 – 1275ºC in air[1414]. He also found that stainless steel ignited at 1350 – 1365ºC in oxygen, but melted without igniting in air. Schutt et al.[1415] found that, with heat generated by rotating stainless steel against stainless steel, an ignition temperature of 1232ºC was obtained in an oxygen atmosphere at 6.8 atm. Accidental ignitions of bulk steel members are rare, but one case has been described where carbon steel heat recovery unit tube fins started burning after long exposure to high temperatures[1416].

Grosse and Conway also measured an ignition temperature of 315ºC for iron powder. Commercial steel wool is ignitable with a match[1417]. Karim and Mehta[1418] tested the autoignition of steel wool in a wind tunnel at an air flow velocity of 4 m s^{-1}. The samples were solvent-cleansed of oil and contaminants before testing and packed to a density of 285 kg m^{-3} in wire baskets. For commercial grade 0 fibers (61 μm dia.) an ignition temperature of 417ºC was found, while for grade 0000 (20 μm dia.) the temperature was 377ºC, with intermediate temperatures for intermediate fiber diameters. Iron powder of very small diameters (0.01 – 0.03 μm) is pyrophoric[1410]. The ignition of small iron particles as function of their specific surface area (area per unit mass of particle) was studied by Evans et al.[1419], with their results given in Figure 101. Particles with a specific surface area higher than about 6 m^2 g^{-1} are pyrophoric, i.e., ignite at or below room temperature. The theory discussed in Chapter 8 indicates that this kind of result is also controlled by another dimension, the size of the pile being tested. Evans et al. describes their vessel only as being of 1 cm^3 volume. This is a very small volume, so much lower temperatures would be expected if a sizable pile were assembled. Stainless steel particles are also pyrophoric, when milled under exclusion of oxygen (i.e., covered with a hydrocarbon liq-

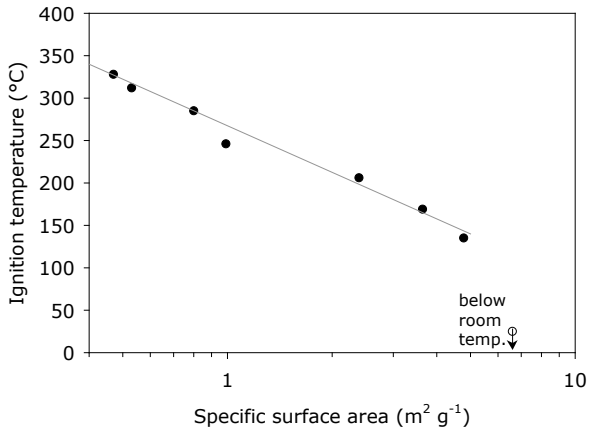


Figure 101 Ignition temperature of fine iron particles, as a function of the specific surface area

uid)[1407]. Ferrous oxide (FeO) is also pyrophoric in small sizes[1407], since it is only partially oxidized; ferrous hydroxide, $Fe(OH)_2$, is even more pyrophoric.

Sponge iron, also known as *direct-reduced iron*, generally produced in lump, pellet, or briquette form, has a notable propensity for self-heating. This is due to its physical form, which is porous and has a very high surface/volume ratio and low thermal conductivity. The density of sponge iron is about half that of pure, non-porous iron. The specific surface area is typically around 1 $m^2\ g^{-1}$. Because of this high surface area, ignition is possible when a pile is stored at ambient temperature[1420]; numerous fires in sea shipments have occurred[1421]. The lump form is somewhat more self-heating prone than the pellet form; the briquette form—especially if hot-molded rather than cold-molded—has the lowest specific surface area and is the least susceptible. Moisture plays a crucial role in self-heating of sponge iron. Alabi[1421] conducted an extensive study on the self-heating of sponge iron. The process involves a multiplicity of reactions and no simple expression for self-heating could be derived. Part of the complication stems from the fact that hydrogen is liberated in low-temperature reactions with moisture, and the hydrogen then reacts with the metal in dry zones, creating a highly activated iron which then leads to thermal runaway upon its oxidation. Additional kinetic studies were reported by Sraku-Lartey et al.[1422] Burning sponge iron does not produce a flame, but rather a red-hot glowing region[1423]. The propagation of reaction is very slow, much as for other smoldering-type reactions. Because of this slow burning rate, a fire can often be controlled simply by pulling out the burning material from the rest of the pile. The hazard of ignition can be reduced by using a similar strategy as in the production of charcoal—weathering the newly-made material in small layers until the surface is somewhat oxidized. Commercial coatings are also available to minimize the hazard. Sometimes ship cargoes are inerted with nitrogen as a safety measure.

Iron powder can ignite at temperatures below 400ºC when combined with a solid oxidizing chemical (e.g., BaO_2, $KMnO_4$, $K_2Cr_2O_7$, etc.) and pressed into pellets[1424]. A number of other elements react in a similar way to iron.

LEAD

Grosse and Conway[1382] found an ignition temperature of 870ºC for solid lead burning in pure oxygen at 1 atm. Laurendeau and Glassman[1400] found an ignition temperature of 850ºC for solid lead burning in pure O_2 at 1 atm. Fine lead particles are pyrophoric, as originally described by Michael Faraday[174].

LITHIUM

Lithium melts at 180ºC and ignites (apart from finely-divided powders) at a higher temperature than its melting point. What that temperature might be, has been an unsettled issue. Grosse and Conway[1382] found an ignition temperature of 190ºC for lithium burning in pure oxygen at 1 atm, but Rhein's survey[1425] found values in the very wide range of 180 – 640ºC. Moisture in air facilitates the ignition of lithium; at relative humidities above 90%, oxidation can be explosive[1425]. The combustion products are Li_2O, LiOH, $LiOH{\cdot}H_2O$, and Li_3N. In nitrogen, ignition temperatures from 170 to 600ºC have been reported. Molten lithium is extremely reactive and is very difficult to extinguish if ignited. Extinguishing agents containing water, foam, CO_2, halons, or the common types of dry powders accelerate combustion[3]. The primary useful extinguishants are those based on graphite powders[1425]. Lithium is a water-reactive substance, with the reaction being:

$$Li + H_2O \rightarrow LiOH + \tfrac{1}{2}H_2$$

but water does not necessarily cause an actual ignition. In one test, lithium at 248ºC was ignited by a water spray[1425]. Lithium reacts either vigorously or pyrophorically with most halogens and halogenated compounds at ambient temperature. Finely divided lithium is pyrophoric in air, water, and argon. In a CO_2 atmosphere, lithium powder (100 μm size) was found to ignite at 330ºC[1396].

MAGNESIUM

Grosse and Conway[1382] found an ignition temperature of 623ºC for solid magnesium and 520ºC for magnesium powder burning in pure oxygen at 1 atm. Laurendeau and Glassman[1400] found an ignition temperature of 635ºC for solid magnesium burning in pure oxygen at 1 atm. Magnesium alloys generally ignite at 500 – 600ºC[1445]. A survey[1426] of other results shows most data to lie between 591ºC and 645ºC, which is just slightly below the melting point of 650ºC. There does not appear to be any significant difference between the ignition temperature in air and that in oxygen. Abbud-Madrid et al.[1409] ignited magnesium rods by radiant heating in 1 atm O_2 atmosphere and found a surface temperature of 977ºC at ignition; this is much higher than obtained by other investigators and presumably was due to the heating technique used. Peloubet has described a study of flashing occurring upon machining magnesium stock[1427]; none of the experiments conducted led to any bulk ignition of material.

The ignition temperature of aluminum is much higher than of magnesium, but tests indicate that magnesium/aluminum alloys have ignition temperatures similar to pure magnesium if they contain about 10% or more of magnesium. For lower magnesium contents the ignition temperature climbs steeply up to the pure-aluminum value[1428]. Etching of magnesium/aluminum alloys in chromic acid has been found to produce a pyrophoric surface which can spark or explode on contact[1455]. This has been attributed to the creation of a powdery condition on the surface.

Ignition of magnesium particles in air was studied by Cassel and Liebman[1429]. For single particles burning in air, they found an inverse relation between particle size and ignition temperature. Particles of 15 μm size required 780ºC, while

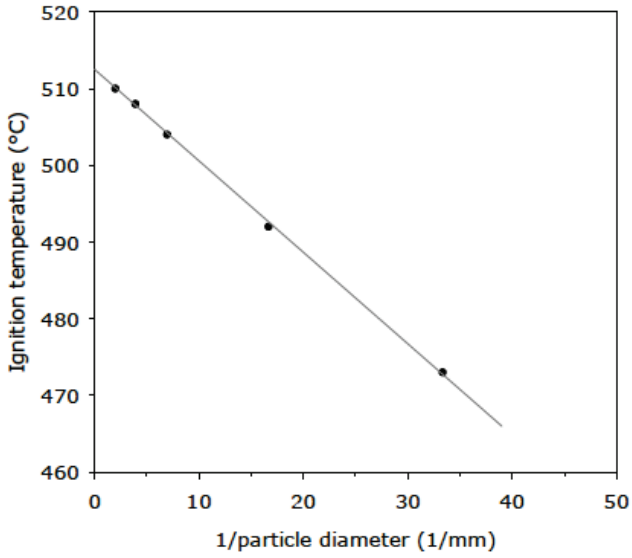


Figure 102 Effect of particle size on the ignition temperature of magnesium

55 µm particles ignited at 650ºC, with intermediate sizes igniting at intermediate temperatures. In dust clouds, lower temperatures suffice for ignition. A cloud of 7 µm particles at a concentration of 165 g m^{-3} ignited at only 525ºC. Magnesium dusts can burn in a CO_2 atmosphere, when ignited by an electric spark. Sparks from grinding operations have been shown to ignite a layer of magnesium dust which was at room temperature[1430].

The effect of particle size on the ignition temperature of magnesium was studied by NBS[191], as shown in Figure 102. Bulk material, described as small pieces of magnesium ribbon, showed an ignition temperature of 540ºC in the same tests. Actual test details, especially the size of pile tested, were not given.

Liebman et al.[1431] studied the ignition of single magnesium particles by laser radiation. They found that the heat flux necessary for ignition was directly proportional to the particle diameter, with

$$\dot{q}'' \approx 10^4 D$$

where $\dot{q}''$ = heat flux (kW m^{-2}) and D = particle diameter (µm). The experimental range covered by this relation was 28 – 130 µm. Laser ignition was different in nature from ignition by hot gases, since ignition did not occur until the particle reached the boiling point and started vaporizing; at that point, the vapors ignite.

In a CO_2 atmosphere, magnesium powder (< 45 µm size) was found to ignite at 749ºC[1396]. In a nitrogen atmosphere (oxygen content < 0.5%), magnesium powder (< 150 µm) was found to ignite at 530ºC[1397]. In another study (< 45 µm size), no ignition was found at temperatures up to 1071ºC[1403]. Magnesium powder is spontaneously flammable when combined with moist iron and chlorine and explodes if combined with chloroform or methyl chloride[1398]. Magnesium powder mixed with silver nitrate does not react, but bursts into flame if water is added to the mixture[1436]. Applying water onto finely-divided magnesium is likely to cause a fire or explosion, due to the exothermicity of the oxidation reaction $Mg + H_2O \rightarrow MgO + H_2$. The hydrogen gas liberated can then burn in a second stage of the reaction. This has led to exacerbation of fires in pyrotechnic manufacturing facilities that were not suitably fought. Magnesium however is not classified as water-reactive because the reaction only takes place in a pre-heated environment, not from ambient temperature. Applying CO_2 to burning magnesium promotes combustion, due to exothermicity of the reaction $2Mg + CO_2 \rightarrow 2MgO + C(s)$. NFPA 480[1432] contains guidance on the flammability of magnesium.

MANGANESE

Grosse and Conway[1382] found an ignition temperature of 450ºC for manganese powder burning in pure oxygen at 1 atm. Eckhoff[512] found that manganese dust in air has an MIE of only around 1 mJ, which means that it is extremely easily ignitable. Fine manganese and manganese nitride particles are pyrophoric[1407]. In a CO_2 atmosphere, manganese powder (< 45 µm size) was not able to ignite in a flaming mode, but at 696ºC it started glowing[1396].

MOLYBDENUM

Grosse and Conway[1382] found an ignition temperature of 750ºC for solid molybdenum burning in pure oxygen at 1 atm. Laurendeau and Glassman[1400] found an ignition temperature of 780ºC for solid molybdenum burning in pure oxygen at 1 atm. A value of 725ºC has also been reported[1426]. A dust layer ignition temperature of 360ºC has been found[1433]. Fine molybdenum particles are pyrophoric[1407].

NICKEL

Nickel powder of very small diameters (0.01 – 0.03 µm) is pyrophoric[1410]. 'Raney nickel' is sometimes described as a nickel/aluminum alloy, but this is only the starting material. In 1927 Murray Raney invented a process[1434] whereby a nickel/aluminum or nickel/aluminum/silicon alloy is pulverized, then leached in a strong sodium hydroxide solution. This dissolves out the aluminum, leaving a highly porous, pyrophoric nickel powder. The powder can be stored indefinitely in a hydrogen atmosphere, but Lee[1435] found that if liquid oxygen is admitted to a vessel that contains Raney nickel and hydrogen, then ignitions at cryogenic temperatures are possible. The lowest temperature at which he documented autoignition was 57 K (–216ºC), but this was limited by the apparatus design and ignition at lower yet temperatures may also be possible. A similar pyrophoric product can be made by alloying nickel, iron, or cobalt with zinc, then dissolving out the zinc[1436]. It has been claimed[1407] that Raney nickel is no longer pyrophoric if aluminum and hydrogen impurities are removed from it, but the validity of this claim is unclear.

PLUTONIUM

Plutonium is considered to be pyrophoric and, under some circumstances, mass plutonium has been known to ignite at room temperatures[1451].

POTASSIUM

Potassium is exothermically reactive with a wide variety of chemicals. It is not pyrophoric in completely dry air, but can pyrophorically ignite in moist air[3]. Grosse and Conway[1382] found an ignition temperature of 69ºC for solid potassium burning in pure oxygen at 1 atm. When exposed to air, the surface of potassium can become oxidized to potassium superoxide, and this compound is highly susceptible to explosion (see *Peroxides*). If dropped into water, potassium ignites and burns, undergoing an analogous reaction to sodium. Potassium is normally stored in kerosene, or a similar substance, to avoid reactions with air.

RARE EARTH ELEMENTS

Rare earth elements are 15 metallic elements with rather similar chemical properties: lanthanum (^{57}La), cerium (^{58}Ce), praseodymium (^{59}Pr), neodymium (^{60}Nd), promethium (^{61}Pm), samarium (^{62}Sm), europium (^{63}Eu), gadolinium (^{64}Gd), terbium (^{65}Tb), dysprosium (^{66}Dy), holmium (^{67}Ho), erbium (^{68}Er), thulium (^{69}Tm), ytterbium (^{70}Yb), and lutetium (^{71}Lu). These elements can show an explosive reaction with halogenated solvents. One study was prompted by an explosion in a grinding mill where the atmosphere consisted of nitrogen and Freon 113 ($C_2Cl_3F_3$). The study concluded that the exothermic halogenation reaction is autocatalytic, and this was seen to be the main reason for the violence of explosion[1437]. Dusts of some rare-metal alloys ($Sm_2Fe_{17}N_3$ in a 2 μm size and $Sm_2Co_{17}Fe_3Cu_4Ce_2$ in a 7 μm size) have been found to explode spontaneously upon dispersion into an explosion test vessel, without use of an ignition source[1438]. *Cerium* is discussed individually above.

RUBIDIUM

Rubidium is pyrophoric and explosively water-reactive; the latter reaction liberates hydrogen gas, which autoignites[3].

SODIUM

Sodium is highly reactive and may, under some circumstances, be pyrophoric; it has a low melting point of 98ºC. Grosse and Conway[1382] found an ignition temperature of 118ºC for sodium burning in pure oxygen at 1 atm. However, the Bureau of Mines[1378] tested 4 g quantities of sodium and found that it ignited in air at 54ºC, but not at 32ºC. Small droplets apparently require a higher ignition temperature, since Richard et al.[1439] found ignition to occur at 200ºC when testing 1 – 3 mm droplets. Yuasa[1440] measured ignition temperatures of sodium exposed to forced air flow in a stagnation-point geometry and found a strong effect of moisture. He reported an ignition temperature of 210ºC for a water vapor pressure of 133 Pa, rising to 290ºC for water vapor pressure of 1370 Pa. Neither the effects of air flow rate nor of specimen size were explored. Akita and Yamashika[1441] conducted experiments where they noted that a protective oxide layer is formed on the surface. When the oxide film was not disturbed, ignition temperatures for cube-shaped samples were found to be 300 – 400ºC, being above the melting point of the oxide (290ºC). However, when the oxide film was mechanically disrupted, ignition temperatures in the range 140 – 210ºC were obtained. Saito et al.[1442] measured the ignition temperature of sodium pools in moving air streams. Flow velocity raised the observed T_{ig} and the lowest value found in air was 115ºC at a flow rate of 5 L min^{-1}. They also produced a relation between the temperature and the oxygen concentration needed for extinction. For 115ºC, oxygen needed to be reduced to 6% for extinction. Below this concentration, there was an inverse linear relation between temperature and oxygen concentration—at 600ºC, the MOC was 2%. There were some anomalous results, however, and it proved possible to ignite the material at 450ºC and 0.5% O_2. They also found that reignition could occur even when the temperature was lowered to 50ºC in nitrogen.

If dropped into water, sodium ignites and burns violently. Three reactions are involved[1443]:

$$Na + H_2O \rightarrow NaOH + ½\ H_2 \quad \text{(evolution of hydrogen)}$$
$$2H_2 + O_2 \rightarrow H_2O \quad \text{(combustion of hydrogen)}$$
$$4Na + O_2 \rightarrow 2Na_2O \quad \text{(combustion of metallic Na)}$$

STRONTIUM

Laurendeau and Glassman[1400] found an ignition temperature of 1075ºC for solid strontium burning in pure oxygen at 1 atm. Finely-divided strontium ignites upon exposure to air[1398].

TANTALUM

According to Reynolds[1414], bulk tantalum ignites at 1240 – 1280ºC in air. Matsuda and Yamaguma[1444] studied the ignitability of fine tantalum powder (polydisperse, with a mass-mean diameter of 31 μm). Using an unspecified test method, they found a layer ignition temperature of 300ºC and a dust cloud ignition temperature of 610ºC. Using a test method somewhat similar to the Hartmann apparatus, but having a flat baseplate, they placed a conical heap of powder (1 – 2 g) upon the flat base and discharged a spark through the middle of the pile. Under those conditions, they found an MIE of less than 0.2 mJ, the latter being the lowest energy level that could be created with their discharge circuit. Repeating the MIE experiments on different types of tantalum dust samples, they obtained 1.3 mJ for one of 70 μm size and 30 mJ for flat particles of 25 μm diameter. In the MIE experiments, they found that the spark did not 'blow away' the dust particles, but explosion was not immediate. At first, a glow formed, and this propagated into a flash only after 1 – 2 s. They also conducted MIE experiments on dust clouds and found a value of 14 mJ for the original 31 μm material.

THORIUM

Grosse and Conway[1382] found an ignition temperature of 500ºC for solid thorium burning in pure oxygen at 1 atm. Under rare circumstances, mass thorium has been known to ignite at room temperatures[1451]. Thorium fires are likely to result in explosion[1451]. Some thorium/silver alloys are pyrophoric[1407]. In air[1402], ignition temperatures of 280 – 466ºC have been reported for particles sizes of 7.2 – 45 µm. In a CO_2 atmosphere, thorium powder (< 45 µm size) was found to ignite at 330ºC[1396]; in a nitrogen atmosphere, an ignition temperature of 620ºC was found[1403].

TIN

Grosse and Conway[1382] found an ignition temperature of 865ºC for solid tin burning in pure oxygen at 1 atm. Abbud-Madrid et al.[1409] ignited tin rods by radiant heating in 1 atm O_2 atmosphere and found a surface temperature of 883ºC at ignition. Laurendeau and Glassman[1400] found an ignition temperature of 940ºC for solid tin burning in pure oxygen at 1 atm. Finely-divided tin may be spontaneously flammable[1398].

TITANIUM

Titanium is one of the few metals where, as the temperature is raised, the metal oxide dissolves in the molten metal. In air, the AIT of bulk titanium is in the range 1200 – 1600ºC[1449,1447]. At ambient pressure, the ignition temperature in air and in oxygen is similar. The ignition temperature decreases with increasing oxygen pressure, going down to about 800ºC in pure oxygen at 20 atm. The ignition temperature is lowered if the material is thin and is being subjected to a very rapid heating rate. In a study on 0.1 mm thick strips (surface/volume ratio = 20 mm^{-1}), an empirical equation was proposed:

$$T_{ig} = 338 + 4.97 \times 10^5 \dot{T}^{-2}$$

where $\dot{T}$ = heating rate (ºC s^{-1}). The mechanism is suggested to be the formation of local hot spots under these conditions. Specimens with surface/volume ratio greater than about 5 to 10 mm^{-1} should be considered as 'thin' and therefore igniting at a lower temperature, but the size effect has been quantified neither for constant-temperature nor rapid-heating conditions. At the extremely small sizes comprising powders or dusts, reported ignition temperatures are very low. Bulk titanium sheets can be ignited at ambient oxygen conditions and room temperature and pressure by discharging a 1 – 10 J spark onto the surface[1445].

In pure oxygen atmospheres at high pressures, bulk titanium can ignite at room temperature or lower[1446], but these may be piloted forms of ignition, rather than autoignitions due to a uniform rise in temperature. It can be spark ignited at ambient pressure and temperature in an oxygen atmosphere. At room temperature, but in high-pressure gaseous oxygen, titanium can be ignited by projectiles or mechanical impact[1447].

The ignition temperature of fine titanium particles was characterized by Evans et al.[1419] as shown in Figure 103. The powder was tested in a tiny vessel of 1 cm^3 capacity, so much lower temperatures would be anticipated if a sizable pile were assembled.

Titanium sponge[1405] ignites (glowing ignition) at 580ºC. Grosse and Conway[1382] found an ignition temperature of 480ºC for titanium powder burning in pure oxygen at 1 atm. In air at ambient temperature, titanium dust can be ignited by an electric spark of 25 mJ[1433]. Strobridge et al. reported that fine titanium powder can ignite spontaneously in air at room temperature and pressure[1449], however according to a survey by Rhein and Baldwin[1447], most of the reported temperatures for ignition of the powder in air are in the range of 250 – 600ºC.

When used in systems which also contain iron, titanium may undergo a thermite reaction:

$$Fe_3O_4 + 2Ti \rightarrow 2TiO_2 + 3Fe$$

This has been the cause of some accidents where oxyacetylene cutting torches were used on equipment made of titanium and steel[1448]. The primary combustion product is TiO_2, although TiO and various other oxides are also found.

The combustion of titanium used in aircraft gas turbine engines has been studied by Strobridge et al.[1449] They point out that under normal operating conditions, titanium components will not ignite, since the service temperature to which titanium parts are designed is about 427ºC, which is significantly lower than the temperature at which titanium ignites in air. Nonetheless, during 1957 – 1979, at least 144 titanium engine combustion incidents were recorded. The incidents arise due to mechanical heating, such as rubbing, or due to stall conditions.

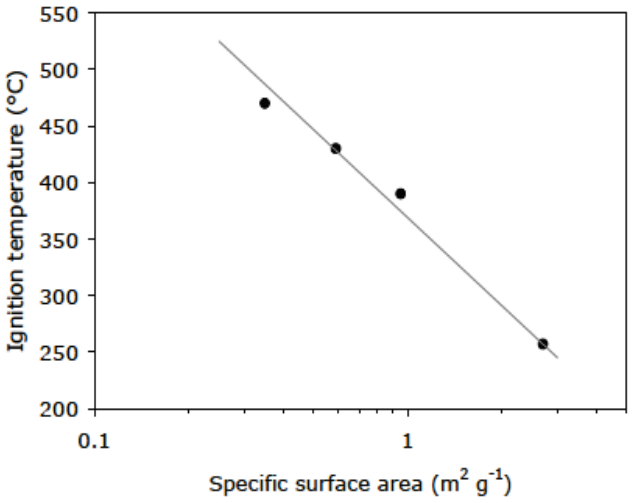


Figure 103 Effect of particle specific area on the ignition temperature of fine titanium particles

Titanium can also ignite in atmospheres of CO_2 or nitrogen. Titanium/aluminum alloys are generally more resistant to ignition than is pure titanium. In a CO_2 atmosphere, titanium powder (1 – 5 µm size) was found to ignite at 670ºC[1396]. In a nitrogen atmosphere, titanium powder was found to ignite at 760 - 800ºC[1397]. The ignition of titanium and its alloys under specialized conditions of impact, explosive loading, or liquid oxygen has been reviewed by White and Ward[1445].

Most conventional extinguishing agents cannot be used on titanium fires. Effective extinguishants[1447] include argon, trimethoxyboroxine, sodium chloride, graphitic powders, sodium or calcium carbonate, silica, and possibly TEC (20 mass% NaCl, 20% KCl, 51% $BaCl_2$).

TUNGSTEN

Reynolds[1414] found that tungsten ignited at 1240 – 1275ºC in air.

URANIUM

In one study, bulk uranium was reported[1414] to ignite at 320ºC in oxygen, and in another study[1450] at 500 – 600ºC in air or oxygen, but such elevated temperatures are normally not needed. In fact, uranium is so pyrophoric that it has been documented to ignite spontaneously at room temperature, while resting on dry ice, under vacuum, and even under water[1451]. On the other hand, experiments have been conducted where it has been heated to its melting point without igniting. In air[1402], ignition temperatures of 100 – 157ºC have been reported for powders in the range of 10.8 – 75 µm size. Tetenbaum et al.[1452] developed a theory for the ignition of uranium powder and this has been presented in Chapter 8. Self-heating theory indicates that, for a pile of material, an ignition temperature cannot be uniquely associated with a particle size, but, rather, also depends on the size of the bulk volume. When tested in a 9.5 mm diameter crucible, their smallest particles (specific surface area of 72 m^2 kg^{-1}) ignited at 245ºC. In a CO_2 atmosphere, depleted uranium powder (< 75 µm size, coated with 2% Viton) was found to ignite at 235ºC[1396]; in a nitrogen atmosphere, ignition temperatures of 354 – 360ºC were found[1403]. Carbides and nitrides of uranium are known to be pyrophoric, as are many intermetallic uranium compounds, including UBi, UBi_2, U_5Sn_4, U_3Sn_5, UPb and UPb_3.

ZINC

Grosse and Conway[1382] found an ignition temperature of 900ºC for solid zinc burning in pure oxygen at 1 atm. Abbud-Madrid et al.[1409] ignited zinc rods by radiant heating in 1 atm O_2 atmosphere and found a surface temperature of 787ºC at ignition. Laurendeau and Glassman[1400] found an ignition temperature of 905ºC for solid zinc burning in pure oxygen at 1 atm. Etching of zinc/aluminum castings in chromate solutions has been found to lead to pyrophoric ignition upon drying[1455]. This has been attributed to the creation of a residue of aluminum powder on the surface. Zinc powder can self-heat if exposed to moisture; fires due to this cause have been known since at least 1876[1453].

ZIRCONIUM

The melting point of its oxide is higher than that of the metal, and, as the temperature is raised, the melting oxide tends to dissolve in the molten metal. Abbud-Madrid et al.[1409] ignited zirconium rods by radiant heating in 1 atm O_2 atmosphere and found a surface temperature of 1282ºC at ignition. Beal et al.[1454] found that 854ºC is the ignition temperature for zirconium wires, both in air and in pure oxygen. They also found that molten drops of zirconium, dropped in either oxygen or air atmospheres, explode after they have fallen for a short distance. Explosions have also occurred in accidents where zirconium has caught fire[1451]. Grosse and Conway[1382] found that zirconium powder will ignite at room temperature in pure oxygen at 1 atm, although another study claims that an elevated pressure is needed[1446]. Testing in room air at 54 and 82ºC showed no reaction[1581], but there are some reports that ignition is possible in room temperature air in the presence of a spark[170]. Ignition temperatures in air have been reported as 210ºC (for < 45 µm particles) and 190 – 240ºC (for 3.0 – 3.3 µm particles)[1402]. Friction has been sufficient to ignite zirconium in air, at room temperature[1451]. Some of the zirconium accidents have been attributed to effects of moisture.

Zirconium sponge[1405] ignites (glowing ignition) at 870ºC. Finely divided zirconium can ignite at room temperature[1455]. The pyrophoricity of zirconium powder is highly dependent on particle size—powder of 3 µm is highly pyrophoric in air, while 12 µm size "does not catch fire at red heat"[1410]. To prevent unwanted ignitions, fine-size zirconium powder is stored under water. Zirconium powder is no longer pyrophoric and shows an ignition temperature of 300 – 400ºC, instead of 20ºC if it has[1456] (a) moisture content

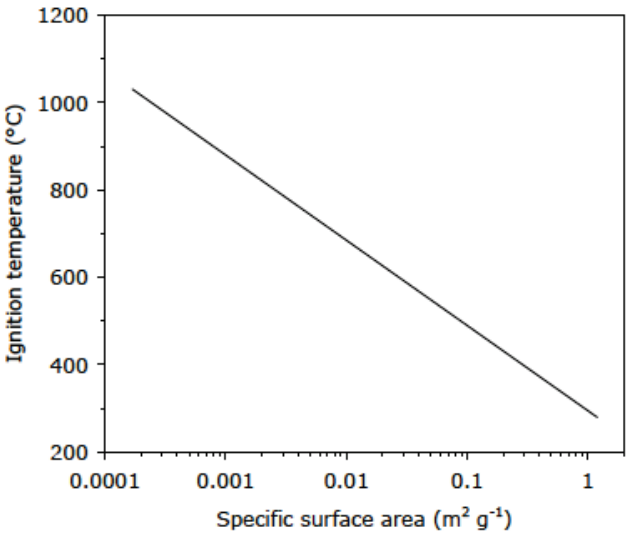


Figure 104 Effect of particle specific area on the ignition temperature of fine zirconium particles

greater than about 4%; or (b) ZrO_2 mass fraction greater than 45%; or (c) the oxygen content is reduced to about 10%. The effect of particle size, expressed as the specific area, on the AIT of zirconium powders is shown in Figure 104 from the work of Schnitzlein[1457], although his study did not extend down into the pyrophoric regime. Anderson and Belz[1458] also reported studies of this kind. The ignition temperature, using a 1 g quantity of material placed in a crucible, ranged from around 135 to 214ºC for material of 1 – 3 $m^2 g^{-1}$; the spread was due to differences in purity and preparation of the samples and did not correlate just to the specific surface area.

Zirconium powders and dusts may also ignite in atmospheres of CO_2 and of nitrogen. In a CO_2 atmosphere, zirconium powder (3 μm size) was found to ignite at 363 – 366ºC[1396]. In a nitrogen atmosphere, zirconium powder (< 45 μ) was found to ignite at 530ºC[1397]. Dust clouds of zirconium are considered especially hazardous, since static electricity generated in their dispersal may be sufficient to ignite them[1459]. Some alloys of zirconium with gold, silver, or copper can ignite upon rubbing[1407].

Methane and natural gas

For many years, incorrectly low values of the AIT have been published for methane in various compilations. Recent work indicates that the value is 600ºC or higher. Using a spherical vessel of 0.8 L, Robinson and Smith[1460] determined the value to be 601ºC for a boric-acid coated vessel and 612ºC for plain stainless steel. The minimum AIT was found at a methane concentration of 7% and ignition time was 17 – 20 s at the AIT. The effect of concentration was found to be very small, however, with mixtures of 2.7% and 10.0% both igniting at 616ºC in the stainless steel sphere. BM[1463] examined the effect of elevated pressure on the AIT of natural gas. At a pressure of 610 atm (the only pressure studied), the results were found to be strongly dependent on the gas concentration. At a 2.2% concentration, an AIT value of 319ºC was found, dropping to 242ºC for 14%.

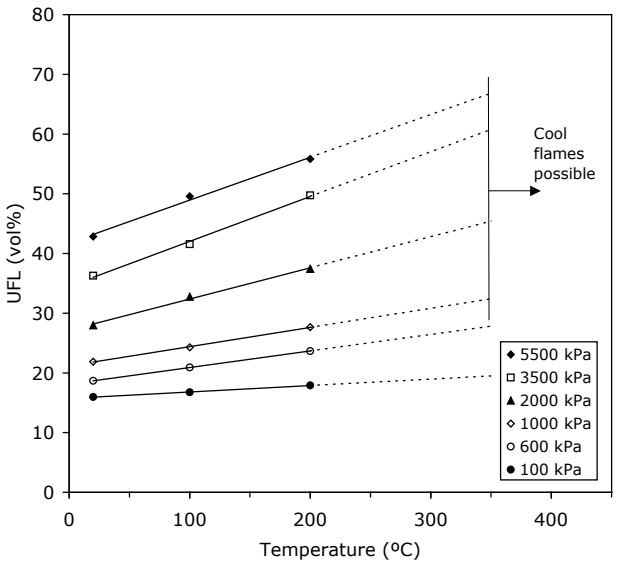


Figure 106 The effect of elevated pressure and temperature on the UFL of methane/air mixtures

Cashdollar et al.[1461] reported a recent series of measurements on the flammability limits of methane in air, and these confirm the traditionally-reported limits of 5% and 15%. The flammable and non-flammable zones of methane in air[1462] are shown in Figure 105.

Raising the pressure, temperature, or both will expand the

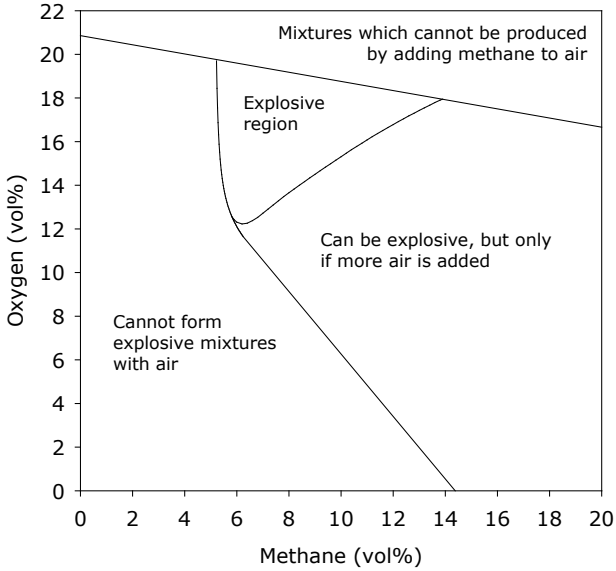


Figure 105 The limits of flammability of methane in air (nitrogen % = 100% – oxygen % – methane %)

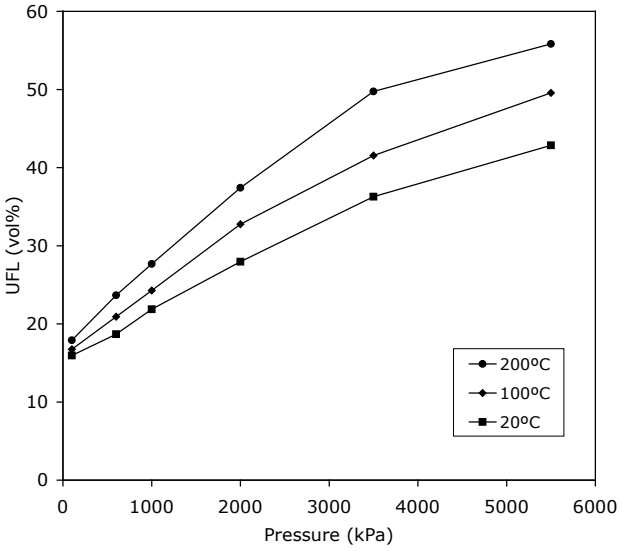


Figure 107 The dependence of the UFL of methane/air mixtures on pressure

flammable region. Data obtained by BM[1463] on natural gas show that for a pressure of 680 atm, the LFL drops to 2.3 vol%; for pressures between 1 atm and 680 atm, a linear dependence on pressure is seen. For the UFL, Vanderstraeten et al.[1464] obtained the results shown in Figure 106, which show a linear dependence on temperature. The same results plotted as a function of pressure (Figure 107) shows a dependence which is not linear. It can also be shown that these results can be linearly fitted by an ln(*P*) function at high pressures, but a logarithmic function would not represent well the lower-pressure regime. The pressure dependence of methane's UFL is *not* identical to that for natural gas, which shows values substantially higher at 20ºC, the only temperature for which data have been published (see Chapter 4).

Using the same apparatus, Caron et al.[1465] examined methane/air mixtures containing 30 – 85% methane at pressures of 500 – 2700 kPa. Even though their lowest concentration studied, 30%, is above the 1-atm UFL, they were able to get both normal flame and cool flame ignitions. At a vessel temperature of 410ºC, it was possible to obtain cool flame ignitions for fuel concentrations over 40 vol% and pressures over 500 kPa. At the same temperature, normal flame autoignitions were documented for system pressures over about 700 kPa. The optimum fuel concentration for normal flame ignition was 40%, with lower and higher concentrations requiring greater pressures. System temperatures above 410ºC did not change the outcome substantively, but for lower temperatures some very high pressures were required. For example, at 350ºC, about 3500 kPa was required for a cool-flame ignition. In general, their results suggested that above about 350ºC, cool-flame ignitions are possible at elevated pressures which are not extremely high, as indicated in Figure 106. For a fuel concentration of 60%, the authors provided two Semenov-type correlating equations:

$$\ln\left(\frac{p_i}{T_{cf}}\right) = \frac{14.53\times10^3}{T_{cf}} - 21.42$$

or

$$\ln(p_i) = \frac{13.88\times10^3}{T_{cf}} - 13.92$$

where p_i = initial pressure (kPa), and T_{cf} = sub-ignition temperature (minimum temperature for a cool flame ignition). Similar expressions were not provided for any other fuel concentration values. Melvin[1466] provided some limited data showing that at 10.4 MPa and 351ºC, even mixtures containing 90% methane are flammable.

The detonation limits of methane in air are approximately 6.3 – 13.5%. Pure methane[26] does not detonate in air, at 1 atm, unless the diameter of the pipe or vessel exceeds about 0.15 m. It should not be inferred from this that a similar limit pertains to natural gas; as discussed in Chapter 4, natural gas is easier to detonate than pure methane. Nitrogen dioxide (NO_2) has a strong effect in lowering the ignition temperature of methane[1467]. Adding 0.1% NO_2 to a methane/air mixture was found to lower the ignition temperature by roughly 120ºC.

See also: *LNG and LPG*.

Methyl bromide

Methyl bromide, CH_3Br, has sometimes been used as an extinguishing agent. In the standard Bureau of Mines 50 mm flame propagation tube it does not show any flammable range. Measured in a 2.5 L bell jar, an LFL of 13.5% and a UFL of 14.5% were reported[1468]. This would seem to imply very limited combustibility, but the idea was proven wrong by an explosion of a large storage tank containing methyl bromide and air under pressure[1469]. It turns out that at larger diameters the flammability limits are about 10 – 15% at 1 atm. But the flammability limits are strongly affected by pressure, and at 5 atm the range becomes 8 – 20%.

Methylene chloride

Methylene chloride, CH_2Cl_2, is a solvent commonly used as paint stripper. It is often described as "non-flammable," but this should not be taken literally. According to Coffee et al.[1470], violent explosions are possible at elevated temperatures or pressures. At a 1 atm pressure, the lowest temperature for flammability is 103ºC, at which the LFL and the UFL are identical at 15.1%. The flammability limits broaden at higher temperatures and at 258ºC the LFL is 13.1% while the UFL is 20.6%. Flammable behavior is also found at room temperature if the pressure is raised to 1.7 atm or higher. Methylene chloride is also flammable at 1 atm and 25ºC if it is present in a pure-oxygen atmosphere[1471]; in that case, the LFL is 13.5%. Many other chlorinated solvents that are "non-flammable" under ordinary circumstances are similarly flammable if temperature, pressure, or oxygen concentration are raised. Kuchta et al.[1471] give these details for a number of such solvents.

Microwave ovens

Miyazaki[1472] measured the time that it takes for small (40 – 80 g) portions of various foods to ignite when heated in a 500 W microwave oven. For the items that did ignite, ignition took 9 – 28 minutes. A correlation was found between ignition time and the water content of the food, with dry foods igniting quickest. It has been reported that broken carrots ignite particularly easily in microwave ovens and it has been speculated that this may be due to either their relatively high content of metals or else due to sharp edges distorting the electric field, but scientific studies are not available on this point. Sloan[1473] documented the ignition of a microwave oven in which the owner inadvertently set the timer for 40 min, instead of 4 min, in order to heat a small dish of food. The top of the cooling cavity had a thermoplastic liner and this ignited from the flaming food.

Mineral wool

This term is used somewhat differently in North America (and in this book) versus in Europe. In North America, it

means a product made from molten basalt or other minerals that has a softening point of 1000 – 1100ºC. In Europe, that particular product is known as *stone wool*, while mineral wool is a more general term that encompasses both stone wool (also called rock wool) and glass wool. The latter has a softening point of 700 – 800ºC and is made from glass (typically from silica, sodium carbonate, and calcium carbonate). Mineral wool insulation has a low organic content (ca. 5%) of a binder, commonly phenol formaldehyde. Even though the organic content is low, the thermal conductivity is also low, thus self-heating is possible and spontaneous combustion has occurred in stored stocks which have not been adequately cooled. The material can also smolder under some circumstances if subjected to external ignition sources. The exothermic mechanism is considered to be primarily a polycondensation of phenolic alcohols, although oxidation is also involved[1474]. Typical values are: $\lambda = 0.06$ W m^{-1} K^{-1}, $\rho = 175$ kg m^{-3}, $E = 56.54$ kJ mol^{-1}, $P = 35.4$, $QA = \beta \cdot 2.3\times10^{9}$ W kg^{-1}, β = organic fraction (--), and $C = 920$ J kg^{-1} K^{-1}.

Motor vehicles

The vast majority of motor vehicle fires[1475] involve passenger cars, as shown in Table 156.

Statistics[1476] for the cause and origin of automobile fires are shown in Table 157 and Table 158; 'Accidental, non-vehicular' typically means a structure fire that ended up burning a vehicle. Vehicle fires represent about 20% of all reported fires in the US and 24% in the UK. Unintentional automobile fires peak during the evening rush hour, while incendiary fires peak around midnight[1475]. Only about 0.1% of reported automobile collisions involve a fire, although the statistics on this point are fairly scattered[1477].

In more recent years, intentionally-set automobile fires have dramatically increased in the UK, with the 1998 statistics indicating that 67% of automobile fires are now deliberate[1478]. Of the accidental fires, smokers' materials account for about 10%.

Table 156 US motor vehicle fires, 1994 – 1998

Vehicle type	Percent
passenger automobile	82.5
freight road transport vehicle	9.3
heavy equipment vehicle	1.6
motor home	0.7
all-terrain vehicle (motorcycle, golf cart, snow-mobile, dune buggy, etc.)	0.7
bus or trackless trolley	0.6
boat	0.4
travel trailer	0.3
train	0.2
mobile home	0.1
camping trailer	0.1
airplane	0.1
special vehicle	0.5
unclassified or unknown	18.6

Table 158 Percent of automobile fires, by cause

Cause	US 1980-1992	UK 1978-1988
incendiary	17	31
accidental, electrical	21	27
accidental, non-electrical	48	32
accidental, non-vehicular	12	7
collision	2	3

Table 157 Percent of automobile fires, by area of origin

Area of origin	US	UK
engine compartment	70	67
passenger compartment	20	20
underside or rear	10	13

In 1988 Cole collected statistics on the cause of over 200 automobile fires investigated by his firm that involved neither arson nor collision[1479]. The results are given in Table 159. A very substantial number of the fires was because of faulty or amateur repairs. Many were due to persons making repairs improperly reconnecting lines carrying ignitable fluids. Others were due to leaving wire bundles or combustible hoses close to heat-producing parts. One interesting fire was identified due to: "Shop left rag in engine compartment." Curiously, in his sample no fires were attributed to accidental ignitions by occupants of upholstery or other combustible interior finishes.

Cole also reports on the results of an insurance company survey in California in the mid-1980s[1480]. Of 1448 incidents examined, the cause could not be determined for 778; the results for the ones where the cause was successfully determined are given in Table 160. Note that arson, collision, and structure fires are not excluded from this tabulation. An official California state report[1481] for 1975 gave the breakdown shown in Table 161.

The above two studies do not identify any causes as being

Table 159 Causes of automobile fires investigated by Cole

Cause	Percent
electric short	42
leak at carburetor or at its inlet	18
fuel line leak	14
fuel injection system leak	6
propane leak	6
transmission fluid	5
oil leak	5
power steering fluid	5
vapor recovery canister	4
catalytic converter	3
overheated engine	3
overheated plastic part in engine compartment	2
hydraulic line	2
turbo charger	2

Table 160 The breakdown of known causes of vehicle fires in the mid-1980s in California

Cause	Percent
engine compartment (fuel related)	47.8
electrical	22.2
arson	7.3
garage fire	7.2
catalytic converter	2.4
cigarette or smoldering material	2.4
muffler or exhaust system	1.5
propane or butane	1.2
power steering	0.9
oil	0.9
friction	0.9
refrigerator in motor home	0.9
transmission	0.7
paper in motor home or van	0.7
fueling	0.6
fire in pickup bed	0.4
collision	0.4
brush fire	0.4
air conditioning compressor	0.3
welding activity	0.3
tire fire	0.1
rag in engine compartment	0.1
ether spray on engine	0.1

Table 161 California automobile fire statistics for 1975

Cause	Percent
fuel leaks	57.6
people-caused, accidental or incendiary	31.7
electrical short circuits	4.0
brake and friction	3.5
exhaust system	1.3
overheated engines	0.6
oil leaks on exhaust parts	0.5
power steering fluid leaks on exhaust parts	0.5
catalytic converter-related	0.1
other	0.2

due to backfiring of the engine. Statistics from the State of Florida listed 10% of vehicle ignitions as being due to backfire[1482], while national US statistics indicate 11.5%[1475]. A US Federal government survey[1483] identified that 0.18% of collisions result in a fire and that 20% of these fires involve a fuel leak. Most collision-induced fuel leaks do not lead to a fire, in fact, in the survey it was found that only 7.5% did. Within the US[1484], an average of 2.7% of motor vehicle fatalities involve fire, but there is a tremendous variation state-by-state, with the range being 0.1 to 5.3%.

The question is often raised whether vehicle age or model year have a significant effect on ignition of automobile fires. The last study[1485] on this topic is now fairly old, covering only pre-1985 vehicles. It was also limited solely to collision-caused fires. In that study, there was negligible effect of car age, but a strong effect of model year. 1969 year vehicles had 2.6 times the probability of fire, per collision, than did 1984 year vehicles, with intervening years showing intermediate results.

If an automotive fire occurs shortly after a vehicle is stopped, there is a good possibility that the cause is a fuel leak[924]. In numerous cases, if a fuel system leak occurs and the vehicle is moving, air flow may blow away the fuel. However, once motion stops, fuel may start to accumulate in locations where a hot surface can cause ignition. In actual automobile fire tests, it is found that gasoline or brake fluid leaking onto a hot manifold will not ignite without a flame or spark (e.g., errant spark plug wire), but that automatic transmission fluid and power steering fluid will[1480]. Engine oil can also be ignited in the same manner.

Fires ignited from electrical faults in the dash are likely to end up consuming most of the vehicle combustibles, but fires originating in engine-compartment faults are more likely to be confined solely to the engine compartment[1486]. In the case of more severe engine compartment fires, ignition of passenger cabin materials is more likely to occur if the windshield breaks out.

In field tests, it was shown[1506] that it is not difficult for an abusively stalled automatic transmission to set the engine compartment on fire. It was also claimed that it is not possible to create a sustained fire by overheating a rear wheel bearing, however, there is positive experience to the contrary, where an overheating bearing ignited a tire[1487].

Motor vehicles used in fighting wildland fires have been known to burn down due to embers being sucked in with the combustion air supply and igniting a paper or plastic air filter[1488]. Ember separators are required by NFPA 1901[1489], but are not always fitted.

An in-depth study of 21 collision-caused fires[1490] indicated that the most common location for the initial ignition is the engine compartment, but that passenger compartment combustibles are subsequently ignited very quickly, most commonly "immediately" to within 5 minutes.

While fuel tanks may contain a sizable amount of fuel, the fraction of automobile fires which originate in the fuel tank area is small, estimated[1491] to be 2.2% in the US. For automobile fires due solely to collisions, about 9% originate in the fuel tank area. Also, despite repeated portrayals in films, it is exceedingly rare that a gasoline tank will explode. Perhaps surprisingly, this also includes modern polypropylene tanks. Hollywood stunt technicians typically blow cars up by using a detonating cord to shatter a concealed firebomb (Molotov cocktail)[1492]. The primary reason is because the tank's air space will be above the UFL, except in extremely cold climates. This has been demonstrated by throwing lighted matches into the filler neck. The tank is also not built to withstand significant pressure, and if external

flames impinge upon it, venting will occur. This behavior has been demonstrated in a number of full-scale ies[1493-1495]. About the only simple way to explode a tank is to drain it of all the liquid. The vapor remaining will then likely be within the flammable region and could be exploded. This has also been demonstrated in numerous accidents where welding was attempted on an 'empty' tank. In a serious automobile fire, while the gasoline tank is unlikely to explode, the gasoline will likely become eventually involved. This occurs when the fuel pipe or the filler pipe fail, or when the tank itself begins to leak fuel. Crashes that destroy the integrity of automotive gasoline tanks are of two basic types: (1) compression of tank, resulting in a violent expulsion of contents (in this mode commonly the first release of fuel is through a popped-off sender unit); or (2) a simple puncture, resulting primarily in gravity drainage. Unfortunately, a NIST study[1496] indicated that ignition of the fuel is readily likely in both scenarios.

A vehicle may be fueled with relatively cold gasoline, then brought into a warmer environment. If the tank is overfilled, the liquid will expand and liquid or vapor will be expelled, depending on fuel system particulars. A case is reported where a car in this condition was parked in a garage where an extension cord was shorting out[1497]. Vapors coming out from the overfilled tank then ignited at the cord fault. An unusual incident occurred with a vehicle towing a boat up a long, steep hill when a broken muffler allowed exhaust gases to directly impinge on a metal fuel tank[1498]. The filler neck ruptured, allowing fuel to get ignited. The entire vehicle was engulfed in flames in a few seconds.

If an automobile is ignited and others are parked nearby, it is likely that radiation from the original fire will ignite the other automobiles, although the process generally progresses slowly. Joyeux[1499] conducted fire tests on a variety of European cars of 1980s – 90s vintage. The tires of a nearby car typically ignited in 10 – 20 minutes after the ignition of car #1, even though the fire spread in car #1 was rapid, since a window was left open and a seat cushion was ignited in a flaming mode. Tires were invariably the first portion of car #2 to ignite. Target tires were also exposed that were not affixed onto vehicles. These ignited at the maximum distance explored, 1.25 m. See also: *Tires and wheels*.

FLAMMABILITY OF INTERIOR COMBUSTIBLES

The flammability of passenger compartment materials used in automobiles is measured in the US by the MVSS 302 test discussed in Chapter 7. This is a remarkably lax test standard and materials passing the test may be exceptionally easily ignitable (and exhibit rapid flame spread and high HRR). Data to illustrate this point were collected by Hirschler[1500], as shown in Table 162. At both the higher irradiance (40 kW m^{-2}) and the lower (20 or 25 kW m^{-2}), the ignition times for the general-purpose plastics were much longer.

Table 162 Median piloted ignition times (s) for specimens tested in the Cone Calorimeter

Specimens	Heat flux	
	20–25 kW m^{-2}	40 kW m^{-2}
general-purpose plastics	479	85
automotive passenger compartment materials	59	26

AUTOMOBILE EXHAUST SYSTEMS

Exhaust systems of automobiles have the potential to ignite dry vegetation. Ignition can occur due to two different mechanisms: (a) contact of vegetation with heated automobile surfaces; or (b) ejection of hot material (e.g., broken pieces of catalytic converters) from the tailpipe. Automobile manufacturers normally consider the region up to 300 mm above ground the level as the zone where exhaust system temperatures should be restricted in order to minimize vegetation ignitions. Ignitability testing of forest fuels (see *Forest materials, vegetation, and hay*) showed that dry vegetation at 550ºC ignites within a few seconds, as would occur during driving. Conversely, when exposure times are of many minutes, temperatures of 350 – 400ºC suffice. Depending on the type of vegetation, some material can be loose and land on or be trapped on hot parts of the system (e.g., while driving over a cut field of hay or grain). With an extended residence time, this vegetation can be ignited, then drop down and ignite the field material.

In a typical exhaust system, temperatures gradually decrease down the length, although the catalytic converter may be a localized hot spot, since additional oxidation is being promoted there. Bends in the exhaust pipe also correspond to temperature deviations, thus often the highest temperature is found near the first bend of the exhaust pipe. Of course, actual temperatures vary widely with load, driving conditions, and engine conditions (e.g., malfunctions). In one study[1501], values from 174ºC to 457ºC were measured on exhaust systems, with the bulk of the temperatures being in the 200º – 400ºC range. In another study[1502], peak temperatures of 450 – 600ºC were recorded under difficult driving conditions. These US studies did not identify the heights at which different temperatures were observed. An Australian study[1503], however, did specifically examine temperatures at heights ≤ 300 mm from the ground. With the exception of one vehicle (an old, Wankel engine model) that showed a peak of 548ºC, the peak temperatures on other automobiles were found to be in the range 290 – 468ºC during strenuous uphill driving. The authors also conducted laboratory tests on exhaust systems that were brought to a certain temperature and then allowed to cool down naturally as vegetation was applied to the surface. The results were highly variable, but both glowing and ignitions were found when the metal starting temperature was 400ºC or higher. Glowing was usually reported as "immediate," but flaming always took at least 20 s to develop, even at a starting tem-

perature of 525ºC. There appeared to be no significant difference between the ignitability of grass at 0% and 11% moisture.

The conclusion from the above studies is that driving almost any automobile in vegetation of moderate (under 300 mm) height is unlikely to result in ignitions, but parking on dry vegetation could cause ignitions, as could driving in very high (> 300 mm) vegetation. Further conclusions from a California study were[1504]:

- under normal engine operating conditions, catalyst-equipped cars do not show higher exhaust system temperatures then older non-catalyst cars;
- under misfire conditions, catalyst cars develop higher exhaust temperatures than non-catalyst cars, but misfire is relatively rare in modern cars;
- the highest exhaust system temperature occur during misfire and not due to other problems (overly rich mixture, timing errors, excessive cranking);
- radiant heat from a catalytic converter is too low to ignite grasses, actual contact is needed;
- highest exhaust system temperatures occur with ignition misfires at high speed under high load; however, the motion of the vehicle under those conditions is fast enough that ignition will not occur.

The highest exhaust system temperature recorded during strenuous uphill driving in the California study was 604ºC under normal conditions and 688ºC under misfire conditions; these temperatures were within 300 mm of the ground. Claims that asphalt could be damaged by stopped catalytic-converter equipped cars were said to be disproved, since only an 8ºC rise was found under severe conditions. But the value appears to be very low and it may be that much greater temperatures occur under conditions somewhat different from those tested.

A modest temperature *rise* can occur in the peak catalytic converter temperature after the engine has been turned off; Hoffman et al.[1505] report measuring a rise in the vicinity of 40ºC. Field tests[1506] showed that, while an overheated catalytic converter may ignite dry grass, unless large amounts of vegetation are present, this fire will normally not propagate to ignite combustible parts of the vehicle.

Bertagna[1507] studied catalytic converter caused fires which originated from expulsion of hot material from the tailpipe and provided details on 39 fires investigated during 1985-1996. In a majority of the incidents, the vehicle caused more than one fire, with hot particles being repeatedly ejected as the vehicle traveled along a vegetated area. A typical failure of a converter is precipitated by an electronic ignition system malfunction; this leads to raw fuel being sent into the exhaust system. Temperature rise of the catalytic converter is proportional to the amount of material reacting within it, but the design of these devices only anticipates that minor amounts of unburned combustion products will enter into the converter, not sizable quantities of gasoline. Consequently, the unit overheats and melts down. The effect has been described as "fusees being thrown out of the vehicle" or "a steady stream of fire coming out of the exhaust system." Possible signs of a catalytic converter melt-down include:

- vehicle runs very rough
- backfiring
- vehicle seems to lose power.

The vehicle does not have to be old for this failure mode, with some failures being found on vehicles of less than 15,000 km. Identifying catalytic converter pieces can be difficult for the fire investigator, because the particles are non-magnetic and may resemble a light-grey pebble. The pieces range in size from very small up to 25 × 50 mm. Pieces have been found as much as 10 m away from the edge of the road, although most pieces are found within 1.5 m. Unlike fires caused by overheated metal-work, converter melt-down fires are not related to driving conditions such as pulling a heavy load or driving up a long hill. Apart from fires caused by expulsion of hot materials, Bertagna also documented that hot-surface ignitions of vegetation occur "instantaneously" once the vehicle comes to stop on dry grass. In several cases, occupants exited the vehicle as flames were already appearing underneath it because the vegetation was on fire.

A catalytic converter can also overheat due to an improperly functioning engine and ignite undercoating or carpeting inside the vehicle. A fire was documented originating from a converter that was missing a heat shield which allowed ignition of carpet at the front passenger seat location[1508]. Another case involved a car that was started in cold weather with a manual choke. The car was allowed to run for 30 minutes with the choke on. The converter overheated, melting carpeting and items in the car directly above it.

AUTOMOTIVE AIR BAGS

The first experimental airbags tested in the 1970s used compressed gas to rapidly inflate airbags in the steering wheel or in the dashboard to cushion the impact of drivers or passengers in the event of frontal collisions. Many compressed gas systems use a pyrotechnic charge to rupture the burst disc and also as a heat source to compensate for the adiabatic cooling during expansion of the compressed gas. These 'hybrid' units are still in use in some older automobiles. The first experimental all-pyrotechnic inflators used a double-base rocket propellant with a liquid fluorocarbon coolant, similar to slide inflators on the early models of Boeing 747 airplanes. The first all-solid propellant gas generators used sodium azide with iron(III) oxide or potassium nitrate as the oxidizer. The advantage of sodium azide-based gas generators is the clean nitrogen exhaust they produce, meeting all exhaust gas specifications issued by the automobile manufacturers. Sodium azide is very toxic and may form friction-sensitive metal azides when in contact with copper or lead. During the 1990s, sodium azide began to be gradually replaced by non-azide inflators in

new vehicles. Only after the automotive manufacturers relaxed their CO emission restrictions, was the inflator industry able to supply non-azide inflators, mostly based on high-nitrogen organic solids.

Currently used non-azide gas generators include:

a) 5-aminotetrazole with sodium nitrate or strontium nitrate as the oxidizer.
b) nitrocellulose/nitroglycerin extrudates.
c) copper hydroxide nitrate + cobalt(III) hexammino nitrate extrudates.
d) guanidinium nitrate/copper hydroxide nitrate/copper(II) oxide/sodium nitrate-ammonium perchlorate.
e) azodicarbonamide/alkali metal nitrates.
f) silicone/sodium nitrate-ammonium perchlorate.
g) stabilized ammonium nitrate/HMX/binder.

In addition, current-generation gas generators use typically boron/potassium nitrate as initiating material in the ignition train.

The pyrotechnic material inside an automotive air bag is heat sensitive, and it is normally expected that it will activate during a vehicle fire, since the critical temperature of 150 – 175ºC will be exceeded. What is not normally expected is a violent projectile, but at least one case has been documented in detail. In that incident[1509], the main steel portion of the inflator assembly created a large divot in the vehicle's roof, then was expelled some 4.5 m away from the vehicle. Meanwhile, two large rivets pierced the roof like bullets. ISO has produced a draft standard (ISO CD 12097-3[1510]) for airbags that entails an exposure-fire test; passing such a test would minimize the likelihood of dangerous projectiles.

FLAMMABLE REFRIGERANTS

In most countries, traditionally automotive refrigerant fluids were required to have low flammability. But after concerns were raised about ozone depletion, some regulations were relaxed and highly-flammable refrigerants are found in automobiles in certain countries*. These are typically mixtures of alkanes and can, in fact, be simply LP gas. Historically, most automotive air conditioning systems used R12 (CCl_2F_2). This has generally been replaced by ozone-friendly R134a ($C_2H_2F_4$), however, the latter is significantly more expensive than LP gas. R134a is 'practically non-flammable' in that it has no flammability limits in air at normal pressure and has an exceptionally high AIT of 743ºC. By contrast, alkanes are flammable over a wide range of concentrations, as shown in Chapter 15. Elias[1511] conducted a theoretical modeling study and concluded that a turbulent jet fire resulting from a break in the piping system is impossible and flames would either blow off due to excessive velocity or else a fire would be unsustained, if a large hole emptied the system rapidly. Elias did no experiments, however, and accidents indicate that the actual situation is not as benign as Elias hypothesized. Sloan[1512] reported that some used automobiles have been imported into New Zealand from Japan which had their air conditioning systems charged with LP gas. He describes one collision where rapid and extremely destructive combustion took place once the escaping gas was ignited by an electric spark. In that collision, the refrigerant's combustion did not cause passenger injuries, but refrigerant piping must necessarily extend into the dashboard area and introducing a flammable substance at high pressure into the passenger compartment creates a new and worrisome hazard. Maclaine-cross and Leonardi[1513] conducted a study which claimed that LP gas released within a passenger compartment cannot be ignited by electrical sources and argued that, expressed on a risk basis, the new hazard should be completely negligible, but they did not study actual accidents. Several manufacturers of LP-gas type refrigerants have also published papers claiming risks are minuscule.

* They are also found in some countries in domestic refrigerators.

Neon lighting

The high voltage for neon lighting comes from a transformer with a loose-coupled secondary. This means that the secondary voltage under normal load conditions is about half of the open-secondary voltage. It also means that the transformer is relatively invulnerable to thermal problems from shorts or other faults in the HV circuit. Instead, problems are generally found to lie in the installation of the HV cabling and associated connections[1514]. Fires are common when neon signs are improperly installed next to wooden members and arc tracking results[2089]. Tracking damage and ignition of a wood board from a 9 kV neon transformer circuit[570] is shown in Color Plate 137.

Nitrates

Deposits of sodium nitrate and wood dust have been known to ignite solely from heating of the sun[26]. If mixed with cellulosic materials, magnesium nitrate also promotes combustion. A molten mixture of $NaNO_3$ and KNO_3, along with a small amount of $NaNO_2$, is used as a heat-treatment bath for certain metals. Médard[26] reports that "it is not unusual for the operation to give rise to an explosion." Explosions can be steam explosions, or arise due to introduction of an organic contaminant, or due to overheating of the bath.

Nitric acid and nitrogen oxides

Nitric acid is considered to be the foremost chemical involved in reactive chemicals incidents[3]. Apart from its reactivity with a gigantic list of chemical laboratory substances, it can readily cause ignition of wood, sawdust, hay, and other cellulosic substances. Concentrated acid (greater than 43.6%[1515]) is necessary, however. *White fuming nitric acid* is a term describing acid that is at least 97.5% pure, although concentrations as low as 70% fume in air. Nitric acid decomposes into NO_2, H_2O and oxygen. A concentrated solution containing 82 – 85% HNO_3 and the remainder mostly NO_2 is termed *red fuming nitric acid*; the reddish color comes from the NO_2 dimer, N_2O_4, which is also pre-

sent. The red variety is even more reactive than the white and has seen use in rocket propulsion. In earlier years, nitric acid used to be shipped in glass carboys wrapped with straw, and ignition incidents were common if the container broke or spilled. Arsonists with some chemistry knowledge have on occasion been discovered using nitric acid for fire-setting. Nitric acid can also react explosively with rubber, due to the presence of sulfur compounds[3]. Explosions involving nitric acid oxidizing some other substance are often detonations, not just deflagrations[1516].

All nitrogen oxides (N_2O, NO, N_2O_3, NO_2, and N_2O_4) are oxidizers and can be involved in ignitions or explosions under some circumstances. Nitrogen dioxide (NO_2) is a stronger oxidizing agent than oxygen. Some nitrogen oxides, e.g., nitrous oxide (N_2O), are also mild explosives on their own right, since they can decompose exothermically. Médard[26] has reviewed a number of ignition/explosion accidents involving nitrogen oxides.

Nitrides

Nitrides comprise a wide-ranging chemical family, with some, but not all, of the members showing pyrophoric tendencies. Examples include: calcium nitride (Ca_3N_2), disulfur dinitride (S_2N_2), lithium nitride (Li_3N), potassium nitride (K_3N), silver nitride (Ag_3N), and uranium nitride (UN). Disulfur dinitride may detonate spontaneously at ambient temperature. Urben[3] provides extensive listings along with literature references.

Nitrogen, liquid

Liquid nitrogen (LN_2) is readily appreciated as being potentially hazardous if allowed to contact the skin, since a freezing injury will result. It is much more rarely that its use would lead to ignition of fire. Yet, Cooke and Ide[605] report of an incident in a food processing facility where LN_2 was used to as part of a food grinding operation. The supply of LN_2 ran out, and a lethal explosion occurred. This was identified due to the difference in boiling point of liquid nitrogen (–196ºC), versus liquid oxygen (–183ºC). When the flow of LN_2 stopped, liquid nitrogen was no longer available to keep the surface inert. But since oxygen will condense into liquid form below –183ºC, it meant that the product became flooded not with an inert gas, nor with an atmosphere of 21%, but with a layer of 100% oxygen. The frictional heating of the process was then sufficient to cause an ignition of the substance in a 100% oxygen environment. In general, oxygen impurities in the LN_2 tank may also need to be taken into account; these will evaporate last and the mixture will effectively become oxygen enriched at the end.

Table 164 Ignition properties of vegetable oils as determined by Koseki et al.

Oil	Flash point (ºC)	AIT (ºC)
castor	307	415
coconut	294	360
cottonseed	333	420
linseed	334	415
rapeseed	321	405
sesame	336	419
soybean	320	400

Oils

Animal and vegetable oils exposed to air are oxidizable and consequently can self-heat. This tendency is much accelerated if the surface area is increased by applying oils onto rags (see under *Fibers covered with oil*, above) or onto sawdust (see under *Wood—Oiled sawdust*, below). Under most circumstances, mineral oils do not show self-heating.

VEGETABLE AND ANIMAL OILS

Ignition problems with cooking oils fall into two areas: autoignition of improperly operated cooking pans, and self-heating, commonly due to soaking of cloths in oils. The flash points of cooking fats were measured at FRS by Stark and Mulliner, who also took into account the effect of repeated use of the fats[1517]. Their results are given in Table 163; it may be noted that the results obey quite well the rule-of-thumb that a hot surface must exceed the AIT by about 200ºC for ignition to be likely (see Chapter 7). They also conducted some tests where food cooking, not just solely heating/cooling cycles were used. These tests gave results nearly identical to the cycling tests without food.

Table 163 Properties of cooking fats measured at FRS

Fat	Flash point (ºC)		Fire point (ºC)		AIT (ºC)		Hot surface ignition temp. (ºC)	
	Virgin	After 8 heating cycles	Virgin	After 8 heating cycles	Virgin	After 8 heating cycles	Virgin	After 8 heating cycles
corn oil	254	227	NA	321	309	283	526	542
drippings	254	241	NA	331	348	276	553	537
hydrogenated cooking fat	260	210	NA	331	355	273	568	554
lard	249	218	NA	326	355	282	541	568
olive oil	234	218	NA	316	340	280	562	543
peanut oil	260	243	347	335	342	280	552	535

The maximum temperature to which cooking fats should be raised for proper cooking is around 205ºC, thus serious temperature excesses must be incurred before ignition can be anticipated. The test results also indicate that differences among various types of cooking fats can typically be ignored. It can also be concluded that, for any type of fat, used cooking fats are slightly more hazardous than virgin ones.

Several other investigators have also reported flash points or AIT values for cooking fats[1518,1519]; their results and conclusions are broadly similar to the FRS study, which has been the most ambitious. More recently, researchers at Japan's National Research Institute of Fire and Disaster[1520] measured properties for a number of vegetable cooking oils (Table 164); their data are probably more reliable than older data, much of which is collected in Chapter 15.

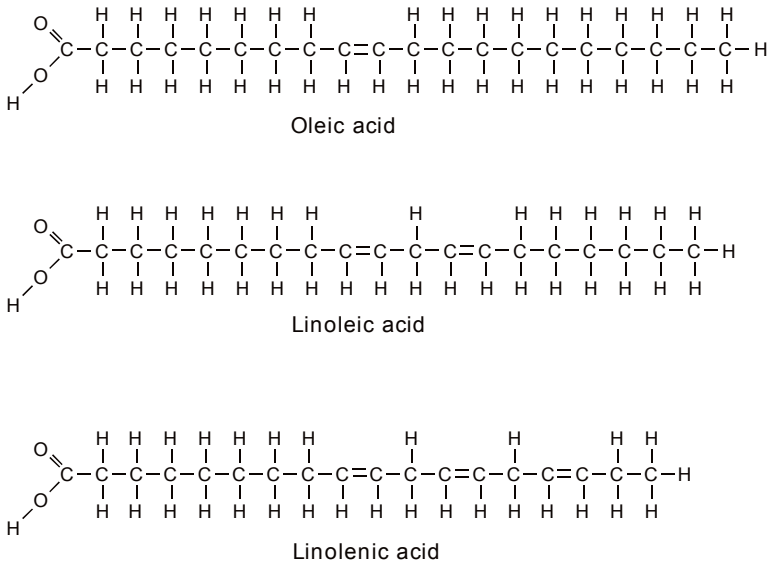


Figure 108 Fatty acids found in linseed oil (all shown as *cis* isomers)

Stark and Mulliner also noted the sequence of events leading to ignition of fats in a cooking pan. In their experiments, they brought the test substance up to temperature exceeding the AIT with a lid closed on the pan. Upon lifting the lid, vapors at first ascended as a simple rising plume. Shortly before ignition, the pattern acquired a toroidal aspect, with vapors rising upward from the edge of the pan and descending towards the center of the pan. A relatively clear central zone was formed, apparently due to air entrainment. The vapors then became more opaque and whiter, and ignition occurred. No frothing, boiling, or ejection of liquids was noted. None of the tests showed a piloted-ignition character, that is, the gas flame below the pan did not cause the ignition.

Chemically, oils of vegetable and animal origin are mixtures of glycerides of fatty acids. The common fatty acids include palmitic ($C_{15}H_{31}COOH$), stearic ($C_{17}H_{35}COOH$), linolenic ($C_{17}H_{29}COOH$), linoleic ($C_{17}H_{31}COOH$), and oleic ($C_{17}H_{33}COOH$). The propensity to self-heating of the glycerides of these acids is directly related to their ease of oxidation. The latter, in turn, is determined by the number of unsaturated bonds (C=C bonds) present, since oxygen most readily attacks the double bond. Palmitic and stearic acids are saturated and thus tend not to self-heat. Oleic acid has one C=C bond, linoleic acid has two, while linolenic acid has three. Since animal and vegetable-origin oils had been available for a long time, their self-heating problem was one of the earlier ones studied. The first studies of self-heating of oil-soaked rags, as discussed in Chapter 9, date to 1781 and involved boiled hempseed oil and pine soot.

Starchy foodstuffs cooked in *rapeseed (canola) oil* and left in a colander have been documented to be the cause of a self-heating fire which occurred in a restaurant specializing in (East) Indian foods[1521]. The foodstuffs had the consistency of dry breadcrumbs. A sample of the batch that was unburned was tested in a laboratory oven at 140ºC and led to a smoldering ignition. Used rapeseed oil was determined to have an iodine number of 103. Some *essential oils* (these are oils obtained from odorous plant materials) have been reported to be quite prone to self-heating, when dispersed onto fibers or similar substances[1522].

Linseed oil is perhaps the substance that is most famous for causing self-heating ignitions. It is not edible, but is extensively used in the paints industry and also is occasionally found in cosmetics. Linseed oil is obtained from crushing the seeds of the flax plant. Since it is a natural product, its composition can vary significantly. It is largely made up of the glycerides of three unsaturated acids: linolenic, oleic, and linoleic acids (Figure 108), with a small amount (6 – 10%) of saturated acids. There is typically[1523] about 15% of linoleic acid, 20 – 25% of oleic acid, while the fraction of linolenic acid depends on the iodine number (see below) and ranges from about 48% (for iodine number of 175) to 60% (for iodine number of 195). Linseed oil has traditionally been the most preferred vegetable oil in the paint industry since other oils have a much smaller, if any, fraction of linolenic oil. The oxidation potential is increased by having a concentration of the double bonds close to each other. When linseed oil undergoes 'drying,' the side-chains of the fatty acid react with oxygen by crosslinking (polymerizing)[1524]. The oxidized, cross-linked linseed oil becomes hard and this elastomeric substance that is formed is known as linoxyn. The chemical reactions involved are numerous and complicated and many details are still not solved[1525,1526,1527]. The reaction proceeds in three basic steps:

(1) Initially, naturally-present antioxidants (primarily tocopherols) are consumed; this is not accompanied by visible physical changes.

(2) Then a period of rapid oxygen consumption ensues, leading to the creation of hydroperoxides and conjugated dienes.
(3) Finally, a complex series of autocatalytic reactions takes place, during which hydroperoxides are consumed and the cross-linked film is formed. In addition, cleavage reactions produce some low-molecular-mass byproducts in this stage. Cleavage and cross-linking reactions continue even after the material 'dries' and leads to eventual browning and embrittlement.

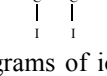
Sastry[1528] gives extensive details on the reactions involved. From a functional point of view, the polymerization is precisely what is desired, since it makes this a 'drying' oil. But the reaction generates heat and this can lead to spontaneous combustion. When the oil has 'dried,' it is no longer soluble in organic solvents; thus, if hardened residues are sampled, an identification of the original linseed oil will not be possible. Linseed oil gains weight in hardening, since oxygen is taken up from the air; when hardened, the weight will typically increase by around 14%[1527]. The oxidation process evolves a modest amount of CO_2 (about 5% of the original mass) and about a similar amount of volatile acids. Fully-dried linseed oil has a composition of approximately $C_{57}H_{96}O_{20}$.

The drying characteristics of fatty acids, including but not limited to those in linseed oil, depend on: (1) the number of double bonds present; this is sometimes equivalently stated as the number of ethylene groups; (2) the isomeric form of the ethylene groups, whether *cis* or *trans*; and (3) the relationship of the ethylene groups to each other—conjugated or isolated. The double bonds are conjugated if they are separated by one single C–C bond. Greater drying propensity is associated with a higher number of double bonds, conjugated arrangement, and a *trans* isomerism. *Tung oil* exhibits self-heating behavior similar to linseed oil but its reaction mechanisms are different and tung oil takes up only 3% oxygen upon drying[1527]. This is due to the fact that the primary constituent of tung oil is *α*-eleostearic acid, $CH_3(CH_2)_3CH{=}CH{-}CH{=}CH{-}CH{=}CH(CH_2)_7COOH$ and it has conjugated bonds.

For use in paints, linseed oil is usually sold as '*boiled*.' Boiled linseed oil used to be heat processed in the presence of a suitable metal salt. This would liberate acetic acid and form linoleates (salts of linoleic acid). Product labeled as 'boiled linseed oil' today is normally not actually boiled, but merely catalyzed using catalysts ('driers') such as salts of cobalt, copper, zirconium, chromium, or manganese, which serve the same purpose[1529]. Lead is particularly effective as a drier, but is no longer used in consumer paints due to toxicity reasons. The metal salts are often accompanied by an organic peroxide as an oxidizing agent, and function by inactivating the naturally-present antioxidants (tocopherols) in the oil. There is also a variety of linseed oil known as 'burnt,' which has been used in the printing industry and has less of a self-heating tendency than raw or boiled linseed oils[1530]. It has often been stated that addition of iron or iron rust to linseed oil exacerbates its self-heating potential. There is some very old work[1531] to support this notion, but the idea cannot be viewed as quantified. Apart from boiled linseed oil, commercial wood-finishing preparations usually also contain mineral spirits.

The oxidation of *peanut oil* has been studied using a dynamic DSC technique[1532] and showed a first-order reaction, with E = 62.2 kJ mol^{-1}, $A = 3.43\times10^4$ s^{-1}, and C = 2300 J kg^{-1} K^{-1}. However, the same authors[1533] then did more extensive studies on several vegetable oils (rapeseed, corn, soybean, and peanut) comparing isothermal and dynamic DSC techniques and found that the data produced by the two techniques are notably dissimilar, with imputed E values differing by up to 20 kJ mol^{-1}. The conclusion was that the process has to be treated as autocatalytic. A more detailed study on mustard oil[1534] showed that the oxidation needs to be modeled as two sequential reactions, with the first reaction being autocatalytic and the second being a first-order reaction. They then studied[1535] linseed and three other oils and also found that their reactions are strongly autocatalytic. Similar studies on individual fatty acids[1536] also showed two peaks in the DSC curves and an autocatalytic character. The first peak corresponds to the formation of hydroperoxides, while the second to the further oxidation of the initially-formed reaction products[1537]. The process cannot be represented by a single activation energy. For linseed oil, they found three different values of E: 132.7 kJ mol^{-1} (at onset), 73.1 kJ mol^{-1} (first peak), and 75.7 kJ mol^{-1} (second peak). Corresponding values of pre-exponential factors were: 1.92×10^{14}, 1.83×10^{6}, and 8.08×10^{5} s^{-1}.

THE IODINE NUMBER TEST

The oldest technique for characterizing the self-heating potential of vegetable and animal oils is the *iodine number* (also called *iodine value*) test[1538]. In this test, an iodine solution is added to the drying oil until a permanent mauve color is observed. The iodine acts only on the double C=C bonds, converting them to  bonds. If the oil sample is 100 g, the number of grams of iodine necessary for the color to break through is defined as the iodine number and it corresponds to the concentration of C=C bonds. If all the bonds are saturated, then the substance should show a zero iodine number. But the number of C=C bonds, while indicative of self-heating potential, is not the only factor governing self-heating. The iodine number test is usually conducted using the Wijs[1539] modification of the Hübl method. It was developed over 100 years ago; the current procedures are specified as the American Association of Oil Chemists' Method Tg 1-64. The test is sensitive to small details of procedure and the standard must be followed if reproducible results are to be obtained. Experimental comparisons between self-heating results in the Mackey tester and iodine number values confirmed that other factors must be considered[1078,1540], including the position of the double bond and

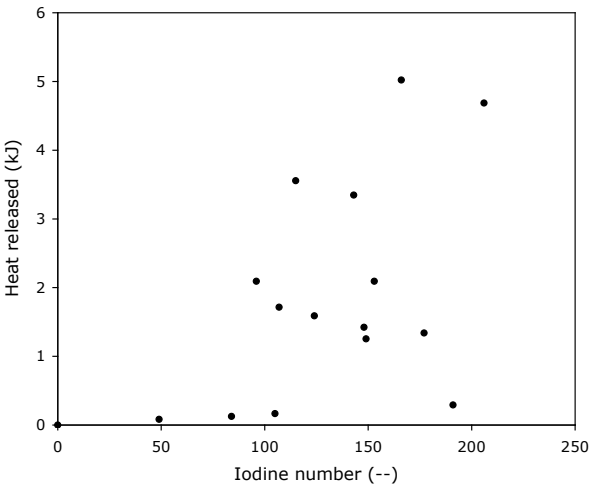


Figure 109 Relation for various oils between iodine number and heat released in a test where air is bubbled through a 20 g sample held at 100ºC

steric factors. For example, boiled linseed oil is more prone to self-heating than raw linseed oil, yet its iodine number is lower. Additionally, the iodine number indicates the *amount* of oxidation possible, whereas the kinetics of the problem, i.e., the *rate* of oxidation, also needs to be considered.

Perilla oil has an iodine number of 196-201, linseed oil 175-195, tung oil 163-173, hempseed oil 145-167, menhaden oil 139-180, poppyseed oil 133-143, soybean oil 137-143, safflower oil 129-150, sunflower oil 119-135, rosin oil 112-115, corn oil 111-130, cottonseed oil 108-110, mustard oil 96-107, peanut oil 97, castor oil 82-86, olive oil 79-88, neatsfoot oil 70, butter 26-42, and coconut oil 8-10[1521,1541,1542]. Peanut and corn oils are claimed to self-heat to criticality only if starting from a warm condition, while coconut oil has not been found to exhibit self-heating problems[1092]. Palm kernel fat has an iodine number of 15 – 18, yet sacks of palm kernels are known to have sustained self-heating fires[43]. When a drying oil has hardened, not all of the bonds become saturated; an iodine number of 31 has been reported for hardened linseed oil[1538].

Animal oils usually have iodine numbers around 50 and tend not to have self-heating problems; it is noted, however, that lard oil (iodine number 56-74) does tend to self-heat[1542]. The oils of marine animals, however, while showing some very high iodine numbers (e.g., cod liver oil has 160-180), are generally of low hazard with regards to self-heating since they contain large amounts of natural anti-oxidants. Lewis[1542], however, notes that fish oil is susceptible to self-heating.

Recently, Schildhauer[1543] proposed that chemiluminescence be used as a superior technique to replace the iodine number test in characterizing vegetable oils. It has been known since the 1970s that vegetable oils undergoing oxidation produce a weak chemiluminescence. Since this is a measure of the actual reaction rate (rather than the potential for a reaction to occur), he considers it to be a more direct measurement. The merit of this scheme will be better assessed once other laboratories undertake to reproduce his findings.

Virtala et al.[1197] developed a technique to measure the heat release of oils in a calorimeter where air was bubbled

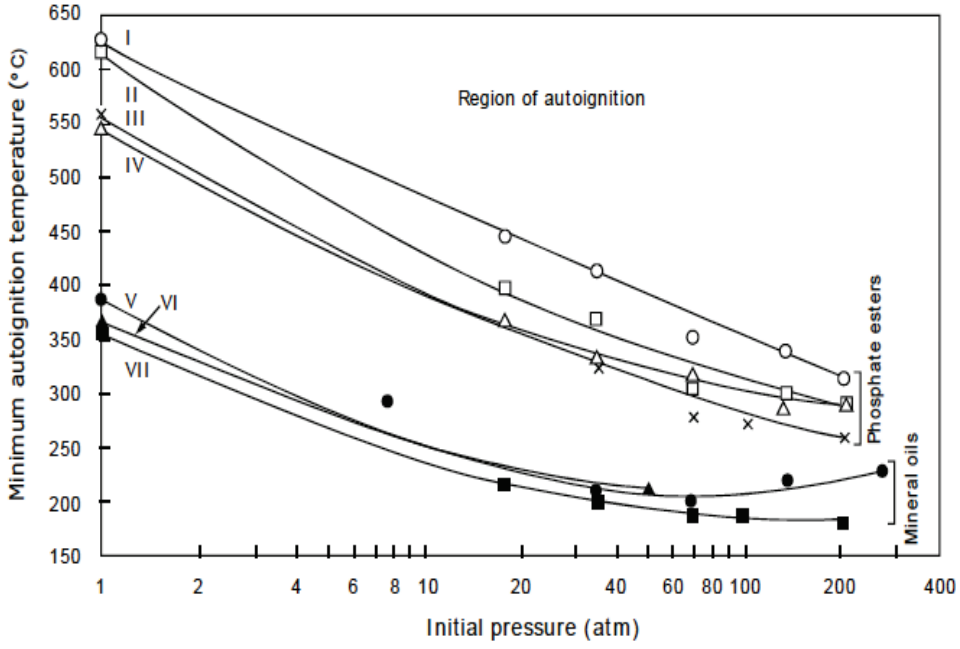


Figure 110 The effect of pressure on the AIT of mineral and synthetic oils[4]. Roman numerals identify different commercial products.

through the test oil; they also obtained iodine number values for the same substances. The results (Figure 109) indicate that iodine number is, at best, only a qualitative indicator of self-heating propensity. Today, the most common way to examine oils is the way that actual accidents will probably occur: as oiled rags.

MINERAL AND SYNTHETIC OILS

The AIT of oils generally decreases with increasing pressure (Figure 110). This characteristic especially emphasizes the hazards of industrial processes where oils are used under combined high pressure and high temperature. If extrapolations are needed to be made from such experimental data, linear relationships can often be obtained if P/T is plotted as a function of $1/T$, where T is expressed as absolute temperature (K).

Ohlemiller and Cleary[123] investigated the effect of contamination with gasoline on the flash point and fire point of motor oil. Using a non-standard open-cup test apparatus, they found that the flash point dropped from 165ºC for pure motor oil to room temperature (22ºC) when 10 – 17 vol% of the mixture was gasoline. The fire point dropped from 215ºC for pure motor oil to 22ºC for a mixture with 20 vol% gasoline. Dissolving as little as 0.3% methane[461] into motor oil (which readily happens at increased pressures) lowers the AIT to 130ºC. Dissolving 5% diesel fuel into motor oil lowers the flash point from 220ºC to 170ºC. Ferguson[457] conducted similar tests for diesel oil mixed into an additive-type paraffinic-base lubricating oil. His results (Figure 111) show that for contamination levels up to 20% there is negligible effect on the AIT, but that the open-cup flash point drops rapidly.

Modak[1544] attempted to ignite 50 mm deep layers of several oils with welding spatter. A steel rod located 0.5 m above the liquid pool was continually melted with an oxyacetylene torch for 60 s. No. 6 fuel oil briefly ignited, but only flamed for 10 s. No. 2 fuel oil, SAE 30 motor oil, turbine lubricating oil, and a fire-retardant grade of hydraulic fluid did not ignite at all. Modak then repeated the tests using thinner layers of 4 mm depth. Again, no ignitions observed. Ignitions also did not occur by directly playing an *oxyacetylene torch flame* on the surface of the four shallow pools for 15 seconds.

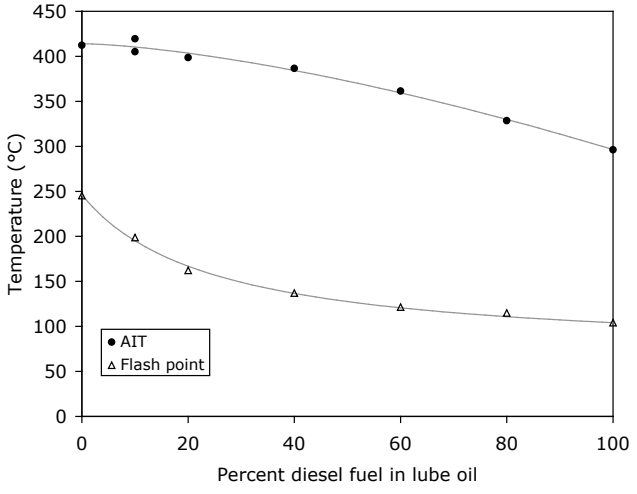


Figure 111 Effect of adding various amount of diesel fuel to lubricating oil

A large compilation of ignition data for commercial oils and lubricants on the marketplace prior to 1968 has been published by Kuchta and Cato[1518]. The relationship between molecular structure and AIT of a variety of lubricating oils was explored by Frank et al.[1545] See also: *Air compressors and compressed air systems*; *Diesel fuel*; *Fuel oil*.

Oil-water emulsions

Oil spills from marine accidents may become emulsified. Such an emulsion is expected to have different ignition properties than pure oil. An experimental ignition study of diesel-oil-water emulsions using the Cone Calorimeter was reported by Moghtaderi and coworkers[1546]. It was found that emulsion layer thickness within the range of 10 to 40 mm did not affect ignition times. The emulsions behaved as thermally thick materials, with a critical heat flux of 6 kW m^{-2} when plotting irradiance versus ignition time to the –0.5 power. For irradiance values lower than about 20 kW m^{-2}, boiling set in prior to ignition. Increasing the water fraction in the emulsion caused longer times to ignition.

Organometallic compounds

A wide variety of organometallic compounds are pyrophoric or highly reactive. Examples include triethyl aluminum ($C_6H_{15}Al$), trimethyl aluminum (C_3H_9Al), and ferrocene ($C_{10}H_{10}Fe$). Urben[3] provides extensive listings along with literature references. Also see: *Metal carbonyls*

Otto fuel II

This liquid monopropellant, named after its developer Otto Reitlinger, is composed of propylene glycol dinitrate ($C_3H_6N_2O_6$), 2-nitrodiphenylamine ($C_{12}H_{10}N_2O_2$), and dibutyl sebacate ($C_{18}H_{34}O_4$) and is used by the US Navy to propel certain torpedoes. Its fire point[1644] is reported as 129ºC.

Oxidizing chemicals

There is a very wide assortment of chemical that act as oxidizers and many of these are able to cause fires or explosions, if inappropriately combined with certain combustibles. In this section, some oxidizers are discussed which have proven to be especially problematic. Potassium permanganate, $KMnO_4$, is a solid which can ignite various organic liquids if it comes into contact with them. The strongest reactions are with glycols, sugars, aldehydes, and methenamine[26]. Capsules containing potassium permanganate and ethylene glycol are used in Australia as incendiary devices for starting prescribed-burn fires from airplanes[1141]. Calcium permanganate, $Ca(MnO_4)_2$, is used for water sterilization, as a disinfectant, deodorant, and for various uses in

manufacturing industry. It behaves similarly to potassium permanganate, but is even more reactive[1547]. Dinitrogen tetroxide, N_2O_4, also called nitrogen tetroxide, is a liquid rocket oxidizer which is used in expendable and reusable launch vehicles (Ariane-4, Delta-2, Space Shuttle). When mixed with a number of fuels, including aniline, ethylene glycol, furfuryl alcohol, hydrazine, methylhydrazine (MMH), or UDMH, a hypergolic ignition or an explosion may ensue[1644].

See also: *Ammonium perchlorate*; *Metal oxides*; *Nitric acid and nitrogen oxides*; *Perchloric acid*; *Peroxides*; *Sodium chlorate and sodium chlorite*. General safety principles concerning ignition in pure-oxygen or oxygen-enriched atmospheres are presented in Chapter 13.

HALOGEN FLUORIDES

The powerful oxidizing agents chlorine trifluoride (ClF_3) and chlorine pentafluoride (ClF_5) react hypergolically with many metals and organic materials. Wood, paper, and cotton invariably ignite[3]. The agents are also able to ignite when coming into contact with asbestos, glass wool, sand, or refractory materials. Both compounds are gases at room temperature and pressure. They have potential application in aerospace applications for purposive ignitions[1548]. Other halogen fluorides with generally similar oxidizing properties include chlorine fluoride (ClF) and perchloryl fluoride (ClO_3F).

GASEOUS FLUORINE

Fluorine (F_2) is, in principle, one of the most powerful oxidizers, but it only rarely presents an ignition problem since it is rarely used in its pure, uncombined form. Ellern[1407] reports that its ignition potential for organic combustibles is erratic—clothing may ignite when hit by a stream of the gas, while sugar will not.

LIQUID CHLORINE

Chlorine is a powerful oxidizer and is incompatible with many materials. After a serious explosion where Cl_2 reacted with a polypropylene filter, E. I. Du Pont de Nemours & Co. Inc. advised against use of any organic materials in chlorine service without careful testing[1549]. It was judged that the reaction was catalyzed by a zinc contaminant.

WATER PURIFYING AND BLEACHING CHEMICALS

Calcium hypochlorite, $Ca(ClO)_2$, often called 'cal hypo,' is one of the most powerful oxidants that is in commercial use. Its primary uses are as a bleaching powder and as a water purification and swimming pool treatment. For use as bleaching powder, it is normally used in mild concentrations below 39% and was originally known as '*chloride of lime.*' Higher calcium hypochlorite concentrations of 65% – 78% are contained in products to be used as swimming pool treatment chemicals and for water purification purposes. These latter products are sometimes designated "70% available chlorine," but this is a chemical misnomer. It originated due to an old chemical analysis method where atomic chlorine (rather than Cl_2) was presumed to be the reactant. The mass fraction of chlorine in pure $Ca(ClO)_2$ is 50%, thus, even pure calcium hypochlorite cannot release more than 50% chlorine. Instead, "70% available chlorine" must be understood to mean that the product contains 70% $Ca(ClO)_2$ and 30% of impurities. Cal hypo containing approximately 70% $Ca(ClO)_2$ is often commercially designated as "high-test calcium hypochlorite," HCH. The material is also produced in a hydrated form and then contains approximately 65% $Ca(ClO)_2$ and 5 – 8% H_2O. Apart from water, the impurities are mostly NaCl, $CaCl_2$, $Ca(ClO_3)_2$, $Ca(OH)_2$, $CaCO_3$, and H_2O. Bleaching powder grade material commonly contains $CaCl_2{\cdot}Ca(OH)_2{\cdot}H_2O$, CaO, and $CaCl_2O_4$ as impurities. Calcium hypochlorite is normally packaged for sale as granules or pellets. The determination of "available chlorine" is described in ASTM D 2022[1550].

Commercially, low-strength calcium hypochlorite is most commonly found as the anhydrous product, but high-strength product is most commonly sold in the form of the dihydrate, $Ca(ClO)_2{\cdot}2H_2O$, and labeled as "65% available chlorine." Under the UN scheme[1650], if the anhydrous product contains over 39% chlorine, it is identified as UN 1748, while if it has 10 – 39%, it is identified as 'bleaching powder,' and classed as UN 2208. The hydrated product is classed as UN 2880 if it contains 5.5 – 10% moisture. If it contains more than 10% moisture, shipping regulations permit it to be classified as UN 1479 (miscellaneous oxidizing solids). Less strict regulations pertain to this class, although, as shown below, the moister material is more prone to self-heating.

Anhydrous calcium hypochlorite was found to be the most reactive oxidizer in a test program that compared the performance of 16 oxidizers[1551]. But it is not necessary for a partner fuel to be present in order for an exothermic reaction to occur. Calcium hypochlorite is a self-heating substance and elevated temperature or excessive storage sizes can cause thermal runaway without need for a reaction partner. Some metal contaminants (iron, manganese, cobalt, magnesium) can accelerate self-heating. The spontaneous decomposition of cal hypo in storage is known to manufacturers, who estimate that 2 – 5% of chlorine is lost per year in storage[1553].

It is reported that potential for calcium hypochlorite to cause unexpected ignitions was already being studied in 1878[353]. In manufacturing, the product is produced in slurry form and then dried. Explosions during drying have been noted[1552]. Fire incidents on land have been less common with the bleaching powder grade. But numerous fires and explosions have been reported in connection with shipping and warehousing of swimming pool grade material[1553]. A certain number of incidents have been identified as being due to a hypergolic reaction between calcium hypochlorite and some other substance. These include soap, various oils,

gasoline, turpentine, other diverse organic liquids, and a wide array of other substances[3,26]. A large warehouse burned down when a small amount of cal hypo was spilled on a wood pallet[1554]. Even though the spill was cleaned up, the pallet ignited about 40 minutes later. Ignitions have also been reported from the use of a dirty scoop[1558]. A single drop of glycerin is enough to ignite the bulk material, as is the application of a lit cigarette[1553,1555]. A fireball is produced if cal hypo is combined with brake fluid[1556]; this is perhaps the most energetic reaction partner identified. In other fires, however, self-heating of the material itself has been the cause.

Large-scale rack storage fire tests have indicated that, once ignited, combustible materials in contact with calcium hypochlorite burn exceptionally fiercely[1557]. Applying small quantities of water to calcium hypochlorite fires has been known to make them worse. Wetting is also exothermic and can cause violent reactions; this is avoided in the use of the product by adding it to water, not vice versa. A comprehensive literature review of reactions, hazards, and case incidents has been published[1557]. A number of explosions have occurred when workers removed lids from drums, there having been no previous indication that the contents were unstable and would explode[1565]. Clancey[1558] studied a dozen fires and explosions that occurred in ships carrying anhydrous calcium hypochlorite during 1967-1973. The explosions are typically quite weak, with peak over-pressures of only ca. 1 atm. Investigations suggested that the primary cause of the accidents was impurities in the product, but details were not elucidated. Products from factories producing higher purity product appeared to rarely, if ever, spontaneously ignite in shipping.

For a number of years subsequently, there were not many serious marine losses. But the problem returned with grave severity in the 1990s. Between 1991 and 1999, eight ships suffered fires or explosions due to self-heating of cal hypo—MV RECIFE, TIGER WAVE (MAAS), CONTSHIP FRANCE, MAERSK MOMBASA, SEA EXPRESS, DG HARMONY, ACONCAGUA, and CMA DJAKARTA. The cargoes were commonly the hydrated form, although not in all cases. Packaging was typically as drums stored in standard shipping containers of 6 m length. The basic problem appears to stem from the misclassification by UN of the cal hypo family as 'oxidizing solids,' Class 5.1, rather than as 'self-reactive solids,' Class 4.1 or 'substances liable to spontaneous combustion,' Class 4.2. This classification creates the incorrect impression that the material is stable in the absence of a reaction partner. As a consequence of this classification, the IMDG Code permitted at the time of these incidents a maximum packaging of 180 kg in fiber drums and 250 kg in steel drums and specifically permitted storage in below-deck areas. The anhydrous product had to be stowed "away from sources of heat," whereas the hydrated product could be stored where temperatures did not exceed 55ºC for more than 24 h. These packages are also allowed to be stored in containers of up to 40-ft size.

The International Group of P&I Clubs (IGP&IC), which represents shipping insurance companies, responded to the marine disasters by recommending[1559] to IMO that the Code be changed so that the material could only be shipped in drums and not bags or sacks, that drum size be limited to 45 kg, that temperatures not be allowed to exceed 35ºC, that drums not be shipped in containers over 20-ft size (and be stored clear of living quarters), and that the material to be transported be tested and certified as free from dangerous contaminants. By use of drums, a certain amount of ventilation is inherently provided, due to the circular shape. IGP&IC considered also asking that steel drums be used, but concluded that the advantage of non-combustibility is offset by the fact that the material can cause steel to rust, and rust promotes decomposition reaction. IGP&IC also noted[1560] that test results were available showing the SADT for a single 45 kg package is about 52ºC and that the value would be much lower for a container holding a number of these packages. Thus, in their view, even according to existing IMDG Code provisions, cal hypo should be transported according to Control and Emergency Temperature requirements, which come into effect if a 50 kg package has an SADT of 55ºC or less. Some of the larger packages transported had SADTs of less than 50ºC, which would require temperature control according to US regulations.

The US delegation to IMO[1561] endeavored to minimize the implications of the problem and argued against making restrictions on package size, on limiting the temperature at the place onboard ship where the product is to be stored (while agreeing to restrictions on keeping goods away from heaters and steam pipes), and on purity certification for products. Remarkably, they argued against the recommendations to stow clear of living quarters. Part of their argument rested on the facts uncovered in the investigation of two of the ship fires which implied that the product was placed too close to a source of heat onboard; however, the argument did not explain the other six fires. The Canadian delegation[1562] also argued against any increased requirements in the Code on the basis that they disbelieved that cal hypo was a self-heating material. The European Chemical Industry Association (CEFIC) also argued that no changes were needed[1560]. Despite the re-iterated urging of a group[1563] representing essentially all of the world's marine insurance interests (International Union of Marine Insurance, International Chamber of Shipping, and IGP&IC), IMO instead adopted the mild provisions suggested by Germany. These changes, adopted in 2000 as Amendment 30-00 to the IMDG Code, specifically forbade bags, IBCs and bulk packagings, and required segregation from certain other cargoes, but did not reduce the permissible size of drums nor establish a more realistic temperature limit. Requirements were also made that the material not be transported below-deck.

The self-heating properties of 72.5% anhydrous commercial calcium hypochlorite in granular form were studied by Uehara et al.[1564]. Multiple reactions were found possible:

$$Ca(ClO)_2 \rightarrow CaCl_2 + O_2$$

$$3\ Ca(ClO)_2 \rightarrow 2CaCl_2 + Ca(ClO_3)_2$$

followed by:

$$Ca(ClO_3)_2 \rightarrow CaCl_2 + 3O_2$$

and in the presence of moisture:

$$Ca(ClO)_2 + CaCl_2 + 2H_2O \rightarrow 2Ca(OH)_2 + 2Cl_2$$

Of these, however, the first one was found to be, by far, the dominant one. Other studies have identified that, under some circumstances, chlorine monoxide (dichlorine oxide), Cl_2O, is formed, with the latter being a violently unstable gas[1565]. For a flaming ignition to be seen, it was found necessary that organic material be present. Explosive decomposition, however, could occur upon heating with or without organic partners. Based on oven-cylinder testing, Uehara's results give E = 123 kJ mol^{-1}, QA = 6.48 × 10^{17} kW kg^{-1}, and P = 58.35. They also determined the values Q = 608 kJ kg^{-1}, C = 1088 J kg^{-1} K^{-1}, λ = 0.437 W m^{-1} K^{-1}, and ρ = 1000 kg m^{-3}. Given these constants, for a 1 m^3 cube, critical conditions would be reached for an ambient temperature of 58ºC, which is not much above normal room temperature. For packaging in 0.4 × 0.4 × 0.4 m cubes, however, the critical temperature would be 73ºC, which should be well above any room temperature. Clancey[1553] has pointed out that these results should not be viewed as 'typical,' since Uehara obtained very different values in additional testing that was published only in Japanese.

For the hydrated product, Gray et al.[1566] consider that the primary reaction is two-step, with the first step being:

$$Ca(ClO)_2 \rightarrow CaCl_2 + O_2$$

followed by:

$$Ca(ClO)_2 + CaCl_2 + 2CO_2 \rightarrow 2CaCO_3 + 2Cl_2$$

under dry conditions, with the CO_2 coming from atmospheric sources. Under moist conditions, the second step is:

$$Ca(ClO)_2 + CaCl_2 \rightarrow 2CaO + Cl_2$$

The hydrated form, $Ca(ClO)_2 \cdot 2H_2O$, was originally promoted by Mandell[1567] as being more stable and safer than the anhydrous. But in a recent extensive study, Gray and Halliburton[1568] concluded that Mandell's small-scale tests on which this conclusion was based were poorly designed, and that the hydrated form is actually less stable and is more dangerous in shipping and storage. This is consistent with the findings from several research groups[1552,1569] who conducted a variety of thermal analysis tests and concluded that the presence of moisture in cal hypo accelerates decomposition and lowers the temperature at which exothermic activity starts. However, Gray et al. note that, while more dangerous for decomposition, the hydrated form is safer when acting solely as an oxidizer and reacting with a fuel[1568]. Gray and Halliburton determined that heating-rate dependences made it impossible to successfully predict real-scale performance from micro-scale thermal analysis measurements and that larger-scale self-heating tests needed to be done. Their extensive test program ranged from cylindrical oven baskets of 9.25 mm diameter to 200 kg drums of material. The results (Figure 112) show that there are two temperature regimes. The high temperature regime above about 117ºC exhibits characteristics roughly similar to those that Uehara found for the anhydrous product. But in the low-temperature/large-size regime that is relevant to actual transport and storage issues, E = 48.5 kJ mol^{-1}, P = 33.33, QA = 7.19×10^6 W kg^{-1}, and $QA\rho$ = 7.48×10^9 W m^{-3}. The authors also found that ρ = 1040 kg m^{-3}, λ = 0.142 W m^{-1} K^{-1} at 20ºC and 0.147 W m^{-1} K^{-1} at 35ºC for the commercial granulated form. They did obtain some data for times to ignition, but cautioned against making extrapolations from those results, since there is a possibility of chain reactions that would make extrapolations incorrect. The largest specimen tested by Gray and Halliburton, a 200 kg fiber drum (0.55 m diameter), showed a critical ambient temperature of 43.4ºC, when tested inside an external enclosure, which limits the cooling available and simulates the conditions when the drum is stored inside a shipping container. Thus, they concluded that there is an overt hazard of runaway occurring during transit through hot climates. A comparison using a polyethylene 40 kg drum (0.35 m diameter) showed a critical ambient temperature of 60ºC when tested inside a circulating laboratory oven and 55.2ºC when tested surmounted by a steel box. Halliburton[1570] then estimated (but did not validate) that the critical ambient temperature for a 20-ft shipping container filled

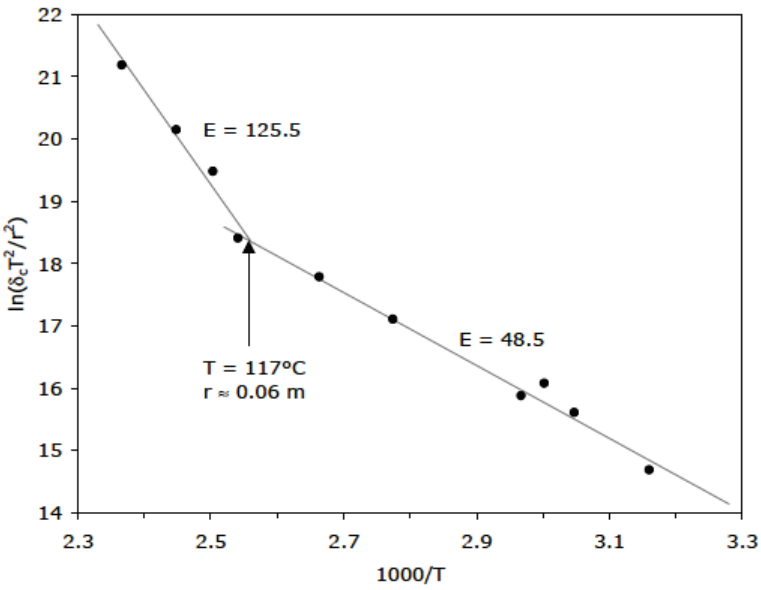


Figure 112 Hydrated calcium hypochlorite oven test results of Gray and Halliburton

with 40 kg drums would be 42.6ºC, while if the container were filled with 200 kg drums, the value would drop to 31ºC. Gray et al.[1568] further concluded that the UN SADT test (see Chapter 9) gives misleadingly unconservative results for cal hypo.

Gray and Halliburton also pointed out shortcomings in Uehara's study on the anhydrous form, noting that (1) they used a value of δ_c pertinent to infinite cylinders, not the relevant short cylinders; (2) their assumption of infinite Biot number is inappropriate; and (3) thermal conductivity was determined on finely-ground material, not on the commercially-produced granular material.

Gray et al.[1568] also noted that unpublished results that showed that a 45 kg keg of hydrated cal hypo went into thermal runaway in 3 days when held at 57ºC but that when held at 50°C it survived for 3 weeks (longer times were not tested). This contrasted sharply with the results of Uehara for the anhydrous material, where 75ºC was required for thermal runaway of a 50 kg drum. Other unpublished tests on the hydrated product showed thermal runaway in 20 min for a 50 kg container at 64ºC and 13 h for a 10 kg container at the same temperature. Small-scale tests on 400 g of material showed thermal runaway at 60ºC for one material, but no runaway for another manufacturer's sample. Simultaneously with Gray's research, a Japanese group[1571] conducted a study which was not based on self-heating theory and came forth with a benign conclusion. The Japanese workers took the IMDG Code prescription literally, conducted tests for 24 h at 55ºC, and found no thermal runaway. Behavior during a 24 h period, of course, does not suffice to determine what will happen during a weeks-long journey. The Japanese group then further stated[1560] that they also conducted testing which showed that a 50 kg plastic drum was safe at 40ºC for a 3-month period, but did not provide details.

Earlier, Clancey had reported on some large scale tests of drums of cal hypo[1553]. Upon being placed in a bonfire, a 50 kg drum exploded. This drum had a plastic liner. When tested without a liner, the lid blew off but the explosion was not as violent. Results of testing that product with the UN SADT test indicated a critical temperature of 64ºC, but from additional testing Clancey concluded that drum-sized containers could safely be exposed to a temperature of no more than 50ºC.

Other oxidizing chemicals in common use for swimming pool treatment are:

- dichlor ($C_3Cl_2N_3O_3.Na$; sodium dichloro-s-triazinetrione; sodium dichloroisocyanurate; 1,3-dichloro-1,3,5-triazinetrione, sodium salt)
- trichlor ($C_3Cl_3N_3O_3$; 1,3,5-trichloro-1,3,5-triazinetrione, trichloroisocyanuric acid)

While intended for the same purpose, calcium hypochlorite and sodium dichloro-s-triazinetrione react violently if mixed together[1572].

CARBON TETRACHLORIDE

Carbon tetrachloride (CCl_4) used to be commonly employed as a fire extinguishing agent and as a solvent. Its toxicity has eliminated it from the former role and highly restricted its use in the latter. It is also a powerful oxidizing agent, when combined with certain classes of compounds. These include boranes, several metals, metal alloys, or metal oxides, along with some compounds themselves classed as oxidizers (e.g., calcium hypochlorite, dinitrogen tetroxide, etc.). Fires or explosions can occur with such combinations[3].

AIRCRAFT OXYGEN GENERATION CANISTERS

In older days, oxygen sometimes used to be produced by 'oxygen candles' or 'chlorate candles.' The primary ingredient in these is sodium or potassium chlorate which decomposes exothermically to yield oxygen. For stable decomposition, it is also necessary to include a catalyst, which can be iron powder. An early paper[1573] describes candles cast as cylinders from these ingredients, along with barium peroxide and powdered glass fiber. The barium peroxide reacts with chlorine to avoid the production of chlorine gas, while the glass fiber helps to avoid cracking during burning. Another formulation used sodium chlorate, with 4% manganese dioxide (as reaction stabilizer) and 2.5% charcoal (as fuel)[26]; charcoal is undesirable, however, because it leads to the production of carbon monoxide.

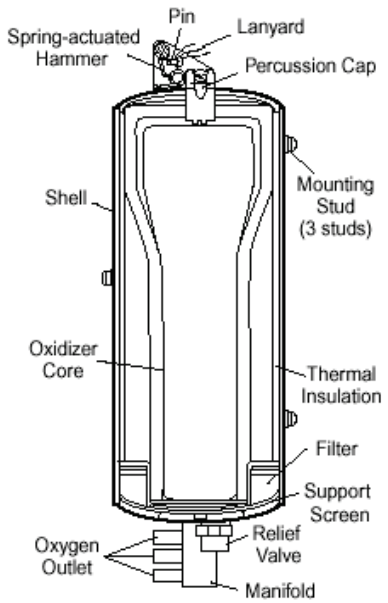


Figure 113 Chemical oxygen generator for aircraft passenger use
(Source: Flight Safety Foundation and NTSB)

To save weight, oxygen for passenger use aboard aircraft is delivered not by means of compressed gas cylinders, but rather by generating from modern-day version of the chlorate candle (for crew use, compressed gas cylinders are used). There have been approximately 20 fires[1574], including a DC-9 where 110 lives were lost[1575], when improperly stored oxygen generation canisters being transported in a cargo hold ignited and then ignited other substances. Illustrated in Figure 113, a canister (also called 'chemical oxygen generator') contains a chemical core of sodium chlorate and powdered iron, an igniter cap containing a primary explosive, a mechanical firing pin, filter media, and hopcalite (a granular mixture of oxides of copper, cobalt, manganese, and silver) to remove any CO which is formed. By replacing charcoal with iron or manganese, the formation of chlorine is avoided. The decomposition reaction is:

$$2NaClO_3 \rightarrow 2NaCl + 3O_2$$

which is exothermic and gives 92 kJ mol^{-1}. A typical canister generates oxygen for 800 – 1000 s, after which the device starts to cool down. Within the reaction zone[1575], temperatures of 550 – 850ºC can be found, but temperatures are lower on the exterior. Shafirovich et al.[1576] conducted some more fundamentally based modeling and also measured similar reaction temperatures. In FAA testing[1577], temperatures on the outside of the stainless steel canisters of only 150 – 200ºC were typically measured. However, when packed in cardboard, polyurethane foam, or polyethylene bubble pack packaging, the canisters were able to ignite the packing materials in several, but not all, trials. Independent testing[1575] showed that when a canister was wrapped in an inorganic insulating blanket, 350 – 400ºC was measured on the exterior of the canister, thus ignition of packing materials is not surprising. In actual testing of generators wrapped in bubble wrap and stored in cardboard boxes, upon triggering the generator, 9 out of 21 trials led to a flaming ignition of the cardboard box, with 2 out of 21 trials leading to a mass discharge of the generators. The initial fire developed slowly, with peak HRR not being attained until about 10 minutes after triggering the initial generator. Once ignition occurs, the subsequent fire hazard is greatly exacerbated because pure oxygen is being delivered from the canister to the nearby area. Normal operating instructions specify that a safety cap must be fitted to an oxygen generator that is shipped, moved, or stored; this cap prevents the triggering of the firing pin. The accidents became possible when these instructions were disregarded. Subsequent to the 1996 fatal crash, FAA banned passenger aircraft from carrying the canisters as cargo.

There is an unrelated category of products which are sometimes erroneously also called oxygen generators, but are properly termed oxygen concentrators. These use a molecular sieve (commonly zeolite) to separate oxygen from nitrogen in the air and do not involve high-temperature reactions.

COMPRESSED GASEOUS OXYGEN

There are numerous case incidents where unexpected ignitions occurred in the use of pure-O_2 or oxygen-enriched mixtures, e.g., Urben's compilation[3]. NFPA 53[1578], which is a general safety guide for enriched-oxygen systems, contains a number of case histories of accidental ignitions. Even simple systems, with few chances for contamination or introduction of combustible foreign matter have led to explosions. In one case, an explosion occurred when oxygen was added to a methane cylinder at a cylinder filling facility[22]. An identification of the ignition mechanism is not available for most incidents. In many cases, adiabatic compression, mechanical sparks, or static electricity have been surmised to be the ignition mechanism. In quite a few cases, the incident arose because of inadvertent substitution of an oxygen cylinder or hoseline for one of air or nitrogen. The generally-incomplete understanding of ignitions under oxygen-enriched conditions is largely due to the violent destruction which is associated with the incidents, along with the fact that much smaller energy sources may suffice for ignition than is customary under 21% oxygen conditions.

LIQUID OXYGEN

Liquid oxygen at 1 atm boils at –183ºC. Its critical temperature is –119ºC, meaning that, at any pressure, it will it be a gas at this, or higher temperatures. Bringing together liquid oxygen (LOX) with many combustible substances offers a probability that an explosion will occur. Detonations can result if liquid oxygen is mixed with powdered metals. Various incidents have been reported where a spill of liquid oxygen on an oily road surface leads to violent explosions upon accompanying mechanical impact[3]. In many cases, simply the friction of tires suffices for ignition, if LOX was spilled on an asphalt road surface[26]. In one case, an explosion occurred due to a person walking across gravel on which LOX had been spilled before[26] . NASA conducted tests[1579] to simulate the spillage of LOX on asphalt paving. The results demonstrated that explosions can readily occur, but required that the asphalt be on a firm base—when the asphalt was on a soft base, explosions did not occur. When explosions occurred, violent combustion of the asphalt consumed nearly the entire top layer. Wood can absorb a large amount of LOX and this can cause an explosion. Charcoal that contains small amounts of iron rust impurities explodes in an autoignition mode if it comes in contact with LOX, even if both substances are at the low LOX temperature[26]. Many plastics have been found to be susceptible to explosions when subjected to impact in the presence of LOX[1580]. In most cases, the explosions had a moderately low probability, with only 1 out of 10 or 20 trials leading to explosion. Curiously, the highest probabilities for explosion were almost never associated with the highest drop-hammer energies used. In the absence of impact, LOX combined with sawdust does not lead to an ignition[1581].

The violent results that can be obtained should not be surprising in view of the existence of LOX-based explosives.

These were invented in 1895 and achieved significant usage in the World War I era, with commercial applications persisting through the 1950s[90]. The fuel portion is generally any porous, absorbent combustible—charcoal, carbonized cork, lampblack, woodmeal, and others having been used. Some compositions are highly sensitive to impact, friction, static electricity and other forms of ignition. *Liquid air*, although less effective, can be used for making LOX-type explosives, so the hazards of accidental explosions with liquid air also exist.

Oxygen pumps

Centrifugal pumps for liquid oxygen sometimes ignite or explode while in service. Laboratory tests to characterize these conditions were conducted by Bauer et al.[1582]. The testing identified that factors which can lead to ignition include (a) the presence of gas in the liquid and (b) tramp metal. Ignitions, however, were impossible to provoke when the pump casings and impellers were made of bronze, thus the authors recommended the use of this metal. The possibility of tramp metal can be minimized by fitting the inlet to the pump with a strainer.

Oxygen regulators

Explosions originating in pressure regulators for gaseous oxygen (e.g., for welders' use) are unfortunately not rare. A study[1583] has identified that most accidents involve two factors: (1) heating due to adiabatic compression; and (2) the unanticipated presence of an easily-ignitable material, typically a contaminant, in the system. The two most important precautions pertinent to the user are: (a) before opening the cylinder valve, make sure that the pressure-adjusting screw is fully backed out; (b) open the cylinder valve slowly. It was also determined that safer designs use a bursting disc rather than a relief valve, since the latter contains more ignitable material that can contribute to the severity of the accident. Furthermore, it was found that 'attached-stem' designs are more accident-prone than designs where the valve stem is separate from the diaphragm assembly. Newton et al.[1584] reported that use of a polychloroprene diaphragm in oxygen regulators is likely to exacerbate an accident, in comparison with a stainless steel diaphragm. But Gusky[1583] concluded replacing a polymeric diaphragm with a stainless steel one does not necessarily improve fire safety, since a steel diaphragm can also get ignited, and if it does, it burns at a higher temperature than does a polymeric one. Of commercial designs surveyed, a 'heavy-duty,' two-stage type was found to show the least potential for operator injury.

Some designs of oxygen regulators for medical equipment use aluminum as the material from which most of the regulator's parts are made. Earlier safety recommendations[1585] considered this to be an acceptable material, but experience has indicated that ignitions, explosions, and tragic burn injuries are encountered with such designs[1586-1588]. The ignitions are considered to involve one of the following mechanisms: (1) galling of metal by opening the post valve in an aluminum-bodied cylinder; (2) particle impact; or (3) a frictional mechanism. Aluminum used in oxygen service is particularly vulnerable to ignition from all of these mechanisms. Consequently, NIOSH has recommended that aluminum not be used for this purpose[1586]. The investigation of one of the incidents also suggested that bronze sintered-metal filters used in an effort to prevent particle-impact ignitions may be ineffectual. In contrast to aluminum, NIOSH concluded that bronze or brass regulators are unlikely to ignite/explode in medical-oxygen applications. As a result of NIOSH studies, which identified 16 ignitions/explosions over a 5 year period, aluminum-bodied regulators are largely being discontinued from medical-oxygen service[1589]. ASTM recently developed a forced-ignition test, ASTM PS 127[1590] to determine the vulnerability of various medical oxygen regulator designs to catastrophic burn-through.

Paints, dyes, and related substances

Dreisbach[1591] studied the piloted ignition of paints applied onto concrete-block surfaces using the Cone Calorimeter. All paint systems included a primer coat, plus the specified number of finish coats. His results are shown in Table 165 and Table 166.

Drying oils are used in stains, alkyd ('oil-base') paints, and other surface coatings. The self-heating properties of drying oils are described in detail under *Oils*. In this section, ignition hazards associated with surface coatings are considered, both due to use of drying oils and from other causes.

Table 165 Piloted ignition times (s) in the Cone Calorimeter for latex paint on a concrete-block substrate

Coats	Heat flux (kW m^{-2})							
	35	50	55	60	65	70	75	85
2	NI	NI					NI	NI, 106
4	NI	NI			NI	NI	NI,70,87,121	
6	NI	NI			147		79,97,114	
8	NI	NI	171	107,150,198	103,113		62,69	
10	NI	NI			123,127		64,65	
NI – no ignition								

Table 166 Piloted ignition times (s) in the Cone Calorimeter for alkyd enamel paint on a concrete-block substrate

Coats	Heat flux (kW m^{-2})							
	45	50	55	60	65	70	75	85
4		NI		NI	283		109,132,212	
6		NI	327				30,85,100	21,22,26
8	NI	NI,324	180		38,41,109		28,32	
10	NI	234,240			33,33,45		19,29,33	
NI – no ignition								

As discussed in Chapter 9, by the late 18th century, the problems of spontaneous combustion of paint products were being researched. Moore's 1877 book[1592] mentions losses of ships due to spontaneous combustion of stains containing rapeseed oil and fir-wood soot. Much of the problem of spontaneous combustion of paints is directly connected to the 'drying' process. The latter, for non-water-based paints, is somewhat of a misnomer, since no migration of any water is involved. Conventional ('oxidizing') alkyd paints stop being 'tacky' due to oxidative polymerization of the drying oil contained in the formulation. This type of reaction is deliberately promoted by the inclusion of a catalyst in the formulation, otherwise the paint could be impractical to use. Traditionally, catalysts have included a combination of a metallic compound (e.g., manganese naphthenate), and an amine (e.g., 1,10-phenanthroline)[1593]; the amine is sometimes termed the 'accelerator,' to distinguish it from the metallic compound. More recently, 'non-oxidizing' alkyds have been available. These types of alkyds are typically used as a plasticizer in nitrocellulose-based lacquers. They are not subject to the self-heating hazard associated with oxidative polymerization, since the oil used is non-drying (e.g., castor or coconut oil) and polymerization is accomplished by cross-linking hydroxyl groups with melamine-formaldehyde, urea-formaldehyde, or polyisocyanate resins.

The actual reactions taking place in commercial products can be complicated. For instance, some wood stains contain roughly equal parts of boiled linseed oil and mineral spirits. The mineral spirit component vaporizes at a lower temperature, and since vaporization is an endothermic process, for an initial time period this will serve to counteract the self-heating tendency of the linseed oil reaction[1594].

In addition to drying oils, some pigments themselves are prone to self-heating. Binswanger[1595] mentions lampblack, Prussian blue, chrome green, toluidine, and para reds. Chrome yellow (lead chromate, $PbCrO_4$) and chrome orange (lead dichromate, $PbCr_2O_7$) are not much used now, but these pigments can react explosively with some organics[943]. Cooke and Ide[605] report that a number of self-heating ignitions in paint spray shops have been associated with a self-heating reaction between primer containing chrome yellow and a polyester resin containing styrene monomer and an organic peroxide hardener, when both were put into one waste bin. Theoretical modeling of the self-heating of organic pigments has been presented by De Faveri et al.[1596] Sulfur-black dye is highly prone to self-heating[1790]. A wide variety of other unstable, easily oxidizable or readily decomposing materials tend to be used in paint and dye industries. Smart[347] discusses a variety of incidents. Copper phthalocyanine ($C_{32}H_{16}CuN_8$) is used in the manufacture of dyestuffs, and it has been implicated in a number of smoldering fires[1597]. Gibson et al.[1598] conducted oven-basket self-heating tests on two dyestuffs (identified only as 'synthetic dye') and found that neither obeyed the standard F-K self-heating theory. Paints containing zinc have been found to cause ignitions of grass[1599]. The reaction was taken to be:

$$Zn + H_2O \rightarrow ZnO + H_2$$

Flash point information is normally provided by the paint manufacturer. Latex paints are normally described as having no flash point. However, once water is evaporated, the remaining paint film is an organic substance and can be ignited, but ignition temperatures have not been reported for latex paint films.

Two-part paint systems that use a *hardener* involve an exothermic polymerization reaction, and this can lead to ignition, in some cases. A fire in extreme heat of the summer in a closed car was identified as being due to the reaction between polyester paint resin and hardener; laboratory testing showed that mixing 15 g paint with 15 g hardener at an ambient temperature of 50ºC sufficed to lead to spontaneous combustion[1600]. Inadvertent reactions can occur between a lacquer and a varnish, leading to spontaneous combustion in a spray booth[1601], but details have not been provided. Similarly, reactions between lacquer and alkyd paints have been known to lead to fire, due to the action of the not-yet-reacted catalyst contained in the alkyd paint upon the lacquer.

With certain particularly-exothermic paint products, *overspray*, even in small quantities, may lead to fire. Anderson[1602] documented case histories where overspray from a lacquer caused numerous spontaneous combustion fires. He also conducted tests which showed that three cups of lacquer dust mixed with one cup of sawdust led to a flaming fire in about 1.5 h. Lacquers can contain a wide variety of constituents and the chemical composition in Anderson's tests was unknown. A combination of exothermic reactions from polymerization of alkyd resins, and the decomposition of a cellulose nitrate component may be the cause. Anderson demonstrated that lacquer dust alone, placed in a paper bag, also went into spontaneous combustion, but about 3.5 h were required. The Fire Research Station investigated a series of fires due to self-heating of paint dust[1603]. It was found that paint dust resulting from the sanding of newly-painted metal surfaces was highly prone to self-heating. This included both finish coat and primer coat layers, but the investigation did not delve into the chemical nature of the paints, except to identify that a wide variety of different products were showing the same problem. In spray booth applications, spontaneous combustion fires are known to occur due to self-heating of deposits on filters, if these are not properly cleaned.

Experience indicates that *quick-drying* paints (including as overspray, upon rags, etc.) are more susceptible to self-heating. Such paints are formulated so that the exothermic 'drying' reaction would be quicker, raising their HRR, and all else being equal, raising the HRR of a self-heating-prone substance directly increases its spontaneous combustion hazard.

Eckhoff et al.[1604] studied the explosibility characteristics of polyester and epoxy powders used in electrostatic powder coating applications. When tested in the closed Hartmann bomb and using the CMI spark generator (see Chapter 5), minimum ignition energies were found to range from 'less than 3 mJ' to 25 mJ. LFL values ranged from 33 to 67 g m^{-3}. The LFL value was found to be determined by the organic content of the powder, with all specimens showing a value ≈ 33 g m^{-3}, when taking into account solely the combustible fraction of the mass. No relation was found between the MIE and the organic content, however.

Electrostatically-sprayed paints can create flammable atmospheres even if they have a fairly high water content. On the basis of experimental studies, it has been proposed[1605] that flammable atmospheres will not be present if *WC*, the water percent in the mixture (by mass) exceeds:

$$WC > 1.70\,SV + 0.96\,SO$$

where *SV* = organic solvent content (% by mass) and *SO* = organic solids content (% by mass). Electrostatic charging during *airless spraying* produces currents which are about a factor of 10 higher than during paint spraying with an air compressor[1606]. Incendive sparks can readily occur if the operator or the gun are not properly grounded. Relative humidity was found not to play a role in the electrification produced.

Aluminum-based paints are susceptible to a special hazard—if struck by a rusty steel object, a thermite reaction can cause sparks of very high temperature to be emitted. This has been a concern in mining and other industries where flammable atmospheres might exist and become ignited. Since the thermite reaction involves iron oxide, not pure iron, a thermite reaction will not occur if the steel is not rusted. Kingman et al.[1607] conducted numerous tests with various aluminum-based paints. Except for nitrocellulose-containing products, they found that preheating the painted surface to 200ºC or more was needed for obtaining incendive sparks in hydrogen/air atmospheres. Gasoline vapors in air were not ignitable at all, except from a preheated surface coated with nitrocellulose-containing paint. The reason why the non-metallic components of the paint played an important role was not made clear.

Practical advice on avoiding fires in spraying operations is given in NFPA 33[1608]. See also: *Gypsum wallboard*; *Wood and wood products*.

Paper products

PAPER

Paper is a substance where great variations are possible. Tissue paper, newsprint, glossy magazine stock, and manila (folder) paper are all papers, but their properties relevant to ignition are dissimilar. Basis weight (that is, g m^{-2}) and percent inorganic content are two significant variables. The latter is important because some paper types, mainly gloss stock, are highly loaded with clay or similar minerals. This component is not combustible and to a certain extent it serves to inhibit combustion of the remainder.

Newsprint is produced by mechanical pulping of softwood followed by bleaching. Inks, of course, may be applied to the surface. Smith[1609] measured the ignition temperature of newspaper want ads by an optical pyrometer and reported values of 260 – 290ºC, independent of flux and independent of whether test runs were piloted or not. Almost identical temperatures of 260ºC for tissue paper and 280ºC for crepe paper were obtained much earlier by C. L. Dows using an unspecified technique, as cited by Brown[189]. Since Smith's values are the only published values where a reasonably reliable testing technique was used, they should be considered authoritative. A wide variety of values were obtained by other researchers using unspecified or poor experimental techniques. These are summarized here for reference; some more extensive review of old and poor testing techniques is given under *Wood*. Graf[997] measured the AIT for a wide variety of paper types. Apart from oiled papers and Kraft paper, all others showed ignition at around 225 – 240ºC. Kraft paper ignited at 320 – 370ºC. Using an even-poorer technique, Brown[189] obtained an AIT of 184ºC for newsprint. A NIST study[1610] gave the ignition temperature of paper as 123ºC and asphalt-impregnated Kraft paper as 203ºC, but details were not given and values below 200ºC must be judged to be erroneous. The pyrolysis and combustion chemistry of newsprint was studied in a TGA apparatus[1611]. It was found that ignition for non-inked surfaces occurred at 290ºC, for black inked at 310ºC, and for colored inks at 270ºC. In follow-on experiments[1612] on the char formed by anaerobic pyrolysis of the virgin material, it was found that char of non-inked surfaces ignited at 442ºC, for black inked at 449ºC, and for colored inks at 428ºC. In was also found that washing the newsprint in water prior to testing had negligible effect on both sets of results. In an earlier study[2084], the authors examined TGA heating rates from 1ºC min^{-1} to 50ºC min^{-1} and determined that, within that range, the heating rate had no influence on the results.

More extensive and reliable data are available for the ignition temperature of wood. Paper—unless highly treated or modified—is chemically similar to wood and can be considered to ignite at the same temperature, as detailed under *Wood and wood products*, below.

For a heated metal bar to ignite paper, a temperature of 695ºC was found to be needed[1613]. Mechanical sparks from steel against a carborundum grinding wheel were found to ignite tissue paper in a flaming mode, but no ignitions could be obtained from sparks of steel-against-steel[1614]. Telephone directory pages, both flat and crumpled, are readily ignited by 38 mm fire brands; 19 mm brands can only marginally ignite this form of paper when some wind is present[1049].

Minimum irradiance values needed for the autoignition of paper products has been studied using a high-temperature tungsten-lamp heat source[1615]. Single sheets of newspaper classified ads required 38 kW m^{-2}, while a stack of multiple layers only required 19 – 24 kW m^{-2}. This is because of poor thermal contact between sheets of newspaper, with the backing sheets acting as thermal insulation, not as a heat sink. Crumpled newspaper sheets needed 25 kW m^{-2}. For alpha-cellulose filter paper, values were generally similar to newspaper sheets. White facial tissue required 59 – 67 kW m^{-2} for ignition, reflecting the very low absorptivity (estimated at 0.09) for the high-temperature radiation. The low absorptivity is due, in good measure, to the diathermancy (semi-transparent nature) of the material. Using a quartz-lamp radiant heat source[1035], stacks of 6 telephone directory pages required 21 kW m^{-2} for autoignition.

Mowrer[1038] studied the autoignition of paper products using the Cone Calorimeter in a horizontal orientation, with a dead air space located below the specimen. For tissue, he found the minimum flux of ignition to be 35.6 kW m^{-2}, while for paper towel it was 30.6 kW m^{-2} and for newsprint 27.8 kW m^{-2}. Lee[1616,1617] placed crumpled newspaper on the floor in room fire tests and found that about 20 – 30 kW m^{-2} flux was needed for ignition; however, because the flux in that environment is non-uniform both in space and time, results can only be viewed as semi-quantitative.

Several studies on the ignition of waste paper baskets from cigarettes have been discussed under *Cigarettes*, above. Holleyhead tested 20 wastebaskets stuffed with paper tissues and obtained flaming ignitions in 4 instances, with times to flaming ranging from 16 to 26 minutes[304]. In a single test, he was able to ignite a cardboard tube from a toilet paper roll by placing a cigarette inside it. Flaming occurred in 37.5 minutes. In another test series, he placed cigarettes on upper surfaces of rolls of toilet paper; 3 flaming ignitions were found during 28 trials. The times to flaming were 92, 98, and 102 minutes. Holleyhead also reported being unable to ignite corrugated cardboard in the horizontal orientation, but that a cigarette placed between vertical cardboard pieces led to flaming in 15 minutes. Cooke and Ide[605], however, obtained a flaming ignition when a cigarette was placed on horizontal cardboard in the presence of a 1 m s^{-1} wind; the ignition took 5 minutes.

Large rolls of paper are known to occasionally undergo spontaneous combustion in transit or storage. Causes include over-drying the material[1618] or storing it too hot[1619]. Spontaneous combustion is less likely to occur if moisture levels over 5% are maintained. As with many other manufactured materials, it is important to avoid storing large piles of material which is initially at an elevated temperature. Hirst[1620] mentions that "soggy heaps of waste paper" have been found to undergo spontaneous combustion; he considers that moisture is necessary and that bacterial action may be involved. Little quantitative information is available on the subject, apart from one old study. Rosenhain and Gemmell[264] conducted experiments in 1913 which were a cruder version of the FRS oven-basket testing method. Using 0.305 m cube baskets, they filled them with torn up pieces of Kraft paper and found that an oven temperature of 195ºC was needed for thermal runaway. An interesting case of spontaneous combustion of paper towels was investigated at Lawrence Livermore National Laboratory[1621]. A sealed, unopened package of paper towels was found smoldering on a storeroom shelf (Color Plate 138). The investigation determined that an unknown contaminant had been present in the unopened package. Carbon paper has been found to be exceptionally easily ignitable in a smoldering mode[317]. Eruption into flaming is possible by gently blowing[304]. Autoignition of scrap paper was reported to occur[1197] when placed around a steam pipe having a temperature of 210ºC.

CARDBOARD

Tests at the Fire Research Station[1622] indicated that the minimum flux for radiant ignition of corrugated cardboard is 17 kW m^{-2} for autoignition and 15 kW m^{-2} for piloted ignition. No effect of thickness or number of walls (2 or 3) was found. Lattimer[1623] conducted unpiloted Cone Calorimeter tests on 4 mm thick corrugated cardboard and found a minimum flux of 8.5 kW m^{-2} for igniting in a smoldering mode. At fluxes of 15 – 23 kW m^{-2} two-stage ignitions were seen, with smoldering being followed by flaming. At higher fluxes, single-stage flaming ignitions were observed. Using piloted test conditions, single-stage, direct-flaming ignitions required a minimum flux of 8.5 kW m^{-2}. Tests at NIST[1624] using the LIFT apparatus indicated a minimum flux of 14 kW m^{-2} for piloted ignition. For fluxes somewhat lower than this, no flaming occurred, but the specimen was fully consumed in a smoldering ignition; the minimum flux for smoldering ignition was not established. Cone Calorimeter ignition results obtained by Grant and Drysdale[1625] for corrugated cardboard are given in Chapter 7 as one of the example graphs and show $\dot{q}''_{\min}$ = 12.5 kW m^{-2} for piloted ignition. The authors also measured T_{ig} in their experiments and obtained 362ºC at 15 kW m^{-2} and 325ºC at 20 kW m^{-2} (average values from 3 tests). In some long-exposure tests, Shoub and Bender[1626] exposed 10 mm thick, primed or painted paperboard samples to a heat flux of 4.3 kW m^{-2}. The specimens autoignited in 0.58 – 4.75 h. Test details are discussed in Chapter 7. Smith[1609] measured the piloted ignition temperature of cardboard by an optical pyrometer and reported a value of 320ºC, independent of the heat flux over the range 21 – 105 kW m^{-2}; his reported values under autoignition conditions were evidently incorrect.

Corrugated cardboard is ignitable by fire brands of 19 mm size if a modest wind is present; 38 mm brands cause ignition without a wind[1049]. A case history was reported[45] where autoignition of cardboard drums occurred due to filling with a hot product at 160 – 200ºC. The authors label this as a self-heating occurrence, but the temperature is high enough

that external heating alone might be considered the primary cause, with contributions from self-heating.

PAPER VAPOR BARRIER

A case has been reported where a bituminized Kraft paper vapor barrier ignited from the friction of a workman's drill and caused a house fire[1627].

Peat and organic soils

Organic soil* and peat are roughly interchangeable terms and are defined as soils with an organic content greater than 20% and a layer thickness greater than 0.41 m. Peat will commonly have organic contents in excess of 90% and be found in layers more than 1.5 m thick. It often has a moisture content over 100%, yet is fairly prone to ignition by lightning[1157].

Fresh peat comprises, by mass, about 48 – 50% carbon, 5% hydrogen, 0.5 – 1% nitrogen, 0.5 – 1% hydrogen, 38 – 42% oxygen, and 3 – 10% ash. As plant matter, it decomposes in storage. Aged peat will contain approximately 58 – 60% carbon, 5% hydrogen, 1 – 3% nitrogen, and 30 – 35% oxygen. Thus, with decomposition the carbon content rises, oxygen content falls, and the heat of combustion also rises. The net heat of combustion of dry peat is approximately 20 – 23 MJ kg^{-1}. Peat deposits are often ignited from an ongoing wildland fire. The burning is of a smoldering type, with much smoke but little visible flames being seen. Peak temperatures of only ca. 475ºC are found[1628]. Salgado et al.[1629] measured the ignition temperatures of several organic soils and reported values of 230 – 236ºC. But since they conducted their tests in a thermal analysis apparatus using a poorly described technique, not much confidence can be placed in these values.

High organic content, low moisture content, and low density are the main factors which influence the ease of igniting organic soil from an ongoing above-surface fire. A number of studies have been published where the maximum moisture content permitting ignition to take place was explored, but the data are extremely variable. As a rough predictor, it has been suggested[1630] that for soils of around 110 kg m^{-3} density, ignition can take place if:

$$MC < 110 - 25R_I$$

where MC = moisture content (mass percent, dry basis), and R_I = inorganic ratio = inorganic mass /dry organic mass. Thus, for example, if inorganic ratio were 3.0, then only soils with MC < 35 would be expected to ignite, while if R_I = 0.2, then all soils with MC < 105 would be expected to ignite.

The above predictive equation is simple, but it does not work very well when soil density varies. Hartford proposed a relation that takes density into account and also acknowledges the probabilistic nature of the ignition problem. Her equation is:

$$P_{ig} = 1/\left[1 + \exp\left(-19.3 + 0.17MC + 1.72R_I + 0.0231\rho_B\right)\right]$$

where P_{ig} = probability of ignition (--), and ρ_B = bulk density (kg m^{-3}) of soil. Later, Frandsen[1631] and Lawson et al.[1632] conducted probabilistic evaluations of the ignition problem. Unfortunately, a different predictive equation was needed for each type of organic soil, implying that some important variable was still unaccounted for. Figure 114 shows the moisture dependence of 6 different organic soils according to the equations of Lawson. The values for inorganic content and density were set equal to average values for the soil type studied.

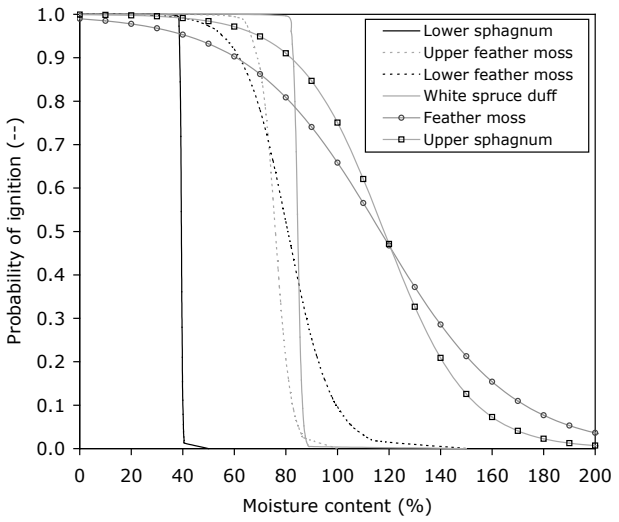


Figure 114 Probability of ignition of various organic soil types, as a function of moisture content

Peat does not require an external source of ignition to ignite and, in fact, is one of the substances well known to undergo self-heating. The self-heating of peat is a complex phenomenon because it involves chemical exothermicity, moisture

Table 167 Peat samples tested in a microcalorimeter by Jones

Sample	Mass tested (mg)	Condition	Temp. range (ºC)	E (kJ mol^{-1})	A (s^{-1})
C	660	as received	28 – 46	101	4×10^{7}
D	950	as received	25 – 60	99	2×10^{7}
F	1190	as received	28 – 79	61	6
J	870	as received	30 – 58	101	2×10^{7}
E	510	as received	40 – 65	84	5×10^{4}
H	320	as received	40 – 70	111	8×10^{8}
G	1200	as received	40 – 75	66	54
B	350	oven dried	30 – 64	41	4×10^{-3}
A	120	oven dried	40 – 80	41	4×10^{-3}

* Soil which is not organic soil is referred to as *mineral soil*.

effects, and biological heating. The latter takes place below about 80ºC only, while chemical heating effects are mainly found above 100ºC. Since peat is used in some places as a commercial fuel, most of the reported work has focused on pressed and powdered peat, not peat in nature. Most of the research on peat self-heating has been done in Russia and this work is not readily available in English. The most comprehensive study, which references a number of the key Russian findings is a report from the national fire research laboratory of Finland[1633]. One of the chemical reactions that contributes to self-heating is a dry distillation. This produces not only CO_2, but also methane and other combustible hydrocarbon gases. A series of small-scale measurements on the self-heating properties of peat were reported in an earlier study[1634] from the same Finnish laboratory. The density and the moisture content affect the results, and the authors found that a single correlating variable was useful: $r\rho(0.9 - MC/100)$, where r = radius (m) of the pile, ρ = density (kg m^{-3}), and MC = moisture content (%). Piles as small as 4.9 liters were seen to have critical temperatures of 120 – 140ºC.

Jones[1635] measured the self-heating properties of Irish peat using a microcalorimeter. His results are summarized in Table 167. It is clear that oven-drying greatly alters the self-heating behavior. For the 'as-received' specimens, however, he found a huge variation in the values of E and A, and this most likely is because, due to multiple reactions present, use of F-K theory is inappropriate.

For large piles, self-heating tends to be concentrated in a zone which is 0.5 – 1.0 m below the surface[1633]. This is due to the fact that deeper regions do not get adequate oxygen supply, while the region very close to the surface receives adequate convective cooling. The self-heating zone then moves toward the surface, where open fire can break out. Fire spots also tend to appear in cracks, if the pile has cracks.

One technique that is suitable to restrict the potential for runaway heating is the use of airtight plastic film for covering the material. This is especially helpful since the bacteria involved are aerobic[1633]. Another technique, as with all materials, is to restrict the pile size. Since biological activity can occur up to 80ºC, the pile size should be limited by limiting the critical temperature to a value suitably in excess of 80ºC. For a spherical pile, such a limit may be reached at a radius of around 22 cm. This is a very small pile size, and this indicates that other measures need to also be considered to prevent spontaneous combustion. Wetting down a pile is a questionable strategy; thermal conductivity and, therefore, heat losses may be increased. However, biological activity is also encouraged.

Tests have shown that welding sparks and cigarettes both were able to ignite 15 out of 20 specimens, which comprised 6 different peat types. Peat dust layers show an ignition temperature of 210 – 270ºC[1633] during short-term heating. If a layer is heated for more than two hours, the ignition temperature drops to 150 – 160ºC, due to chemical changes within the material that are not well characterized. The ignition times for radiant heating of a peat dust layer depend greatly on the nature of the specimen. The results for two types are shown in Table 168.

Table 168 Ignition times for 5 mm peat dust layers

Heat flux (kW m^{-2})	Ignition time (s)	
	Type Oulu	Type Hämeenlinna
10	230	N.I.
20	31	45
30	7	7

Several cases have been reported of small flower pots undergoing spontaneous combustion. In one case[1636] a 4-inch flower pot holding a dead plant is reported to have spontaneously combusted in a locked house when the owners were away. It is said that, in a careful investigation, all other causes were ruled out, including smoking materials or intruders. Attending firefighters found a vigorously smoking pot, which erupted into open flaming when they broke it apart. In a similar case[1637], a dead plant in a 1-gallon container was found to be the origin of a fire. In another case[1638], fire originated in a 12-inch pot that only contained 1-year old potting soil. The latter was identified to consist of peat, perlite, dolomite lime, and possibly copper or aluminum flakes. While organic soils can readily self-heat, the small sizes of the containers, combined with the limited ambient temperatures that can be reached in the home, suggest that flower pots will not go into spontaneous combustion to due the self-heating of organic soils. Contaminants or ingredients having very strong self-heating properties would be needed to cause self-heating in these small-size containers, but studies to explore this possibility have not been made. Cases are well-known where disposal of a cigarette into a flower pot caused a smoldering ignition. Planting mixes comprising mainly peat moss, along with perlite or vermiculite and a fertilizer, are especially prone to being ignited from cigarettes[1639].

Perchloric acid

Anhydrous perchloric acid, $ClHO_4$, is unstable in air and consequently is not used in that form. Commercial grades are water solutions containing 60 – 72%, by mass, of perchloric acid. The substance does not burn by itself, but it is a strong oxidizer and is often used in laboratories for that purpose. Because of its oxidation potential, a number of explosions have been documented[1640]. Laboratory testing using small quantities in test tubes showed that combinations of perchloric acid with a wide variety of organic solids commonly led to ignition temperatures in the range of 130 – 200ºC. Small amounts of iron added to the mixture often lowered the ignition temperature substantially, in some cases down to 90ºC. A number of the mixtures exhibited high-

order detonations upon ignition. Diluting the acid down to a 40% concentration tended not to reduce the ignition hazard, although mixtures that detonated using a 60% acid concentration did not detonate at lower concentrations. At concentrations greater than 77%, room-temperature ignitions are possible, but concentrations this high are not commercially distributed[26].

Perfluorocarbons

Perfluorocarbons, which are substances with the general formula C_xF_{2x+2}, function as extinguishant agents in atmospheres where oxygen and hydrocarbon fuels are present. But in a study on one of the perfluorocarbons, perfluorobutane (C_4F_{10}), Ohtani[1641] found that in other atmospheres, explosions have occurred. In the presence of silane, perfluorobutane acts as an oxidizer, while in a fluorine/nitrogen atmosphere, the compound acts as a fuel. In the latter case, it is oxidized by fluorine to yield CF_4.

Peroxides

Peroxides are compounds that contain the –O–O– structure, which is a relatively unstable configuration for a molecule. Peroxide compounds are grouped into inorganic and organic peroxides. The latter are generally more hazardous, since the molecule contains a fuel portion, not just an oxidizer.

INORGANIC PEROXIDES

Hydrogen peroxide, H_2O_2, is the most common inorganic peroxide, and is used for antiseptic purposes, hair bleaching, and various industrial applications. It decomposes as:

$$2H_2O_2 \rightarrow 2H_2O + O_2$$

The decomposition properties have been studied by Liaw et al.[1642], who determined that the reaction is of first order, with $E = 91.8$ kJ mol^{-1}, and $A = 2.15\times10^9$ s^{-1}. If the reaction is solely decomposition, i.e., fuel is not available for further reaction with the liberated oxygen, only a very low adiabatic flame temperature of 1000ºC can be reached[26]. Under some cases, liquid hydrogen peroxide can be made to detonate, but this requires a concentration greater than ca. 92%. Solid crystallized hydrogen peroxide can also be detonated, but neither type of explosion is likely to be accident-caused. Concentrated H_2O_2 vapors can be exploded and marginally detonated[26]. The perception that hydrogen peroxide is an unstable compound that readily decomposes stems from experiences with impure material, since many impurities catalyze decomposition; highly purified H_2O_2 has good stability. Small amounts of rust falling into a container of H_2O_2 with greater than 70% concentration can lead to a violent decomposition.

Ignitions or explosions involving hydrogen peroxide are much more likely to happen in the presence of a fuel, rather than as a pure decomposition event. If concentrated H_2O_2 is spilled onto rusted iron, concrete, dust, or clothing, a fire may result; an explosion is possible if the liquid is partially confined[157]. Breakage of a container with a 70% solution and subsequent reaction with a lubricant caused a sizable fire and explosion[26]. The National Transportation Safety Board[1643] reports a flaming fire with a 50% solution and a smoldering fire with a 35% solution that were caused due to breakages or spills on board airliners. Spills of 32% or greater concentration solutions onto combustibles can lead to ignition if the ambient temperature is 25ºC or higher and humidity is low[26]. The drugstore variety is generally a 3% concentration and poses no hazards. Hydrogen peroxide is compatible with certain aluminum alloys, polyethylene, PTFE, and Kel-F plastics. Extensive listings of incompatible materials have been published in a US military handbook[1644]. The loss of the Russian submarine KURSK has been blamed on the use of hydrogen peroxide in a torpedo drive unit. In the US, hydrogen peroxide is recently making a comeback as a rocket propellant because it is advertised as "nontoxic" (in comparison to dinitrogen tetroxide).

The peroxides of a number of metals—sodium, lithium, and barium—show strong oxidizing or explosive properties. Potassium superoxide, KO_2, is a more potent oxidizer than potassium peroxide (K_2O_2). Some explosions have occurred when this compound formed simply by exposing potassium to air[26]. Médard[26] reviews the explosion hazards of a number of other, less common, inorganic peroxides and related compounds.

ORGANIC PEROXIDES

Organic peroxides are substances with the formula R–O–O–R'. They tend to be thermally unstable and decompose into two fragments:

$$R–O–O–R' \rightarrow R–O^{\bullet} + R'–O^{\bullet}$$

The fragments are free radicals which can react further. Organic peroxides are classed as oxidizing agents, since the decomposition fragments react by oxidizing other substances. Organic peroxides are widely used in the polymer industry, where they can serve as initiators of polymerization, since they produce radicals needed to start the reaction. When used as a component in a multi-component adhesive or coating, the organic peroxide is often called a *hardener*. Organic peroxides may be liquids, powders, or pastes. When in paste form, explosions are generally less severe than for the dry solid. Decomposition of organic peroxides can be accelerated by the presence of catalysts such as $AlCl_3$ or iron salts. A huge variety of organic peroxides could be synthesized, but only a modest number are useful as commercial products. Castranas et al.[1645] published a general safety survey, with known hazards briefly described and extensive references supplied. Peroxides are sometimes ranked according to their active oxygen content, which is the percent of the compound (by mass) represented by the –O–O– groups. The US Dept. of Transportation forbids shipment of certain organic peroxides that have an active oxygen content greater than 9%. Phlegmatizers are sometimes added to organic peroxides to reduce their explosive potential. These are substances—commonly phthalates, phosphates, or maleates—that reduce the vapor pressure, raise the flash point, and decrease the sensitivity to shock.

Bowes reported on self-heating and thermal decomposition studies of benzoyl peroxide[1646] and lauroyl peroxide[1647]. The reactions are complex and not fully quantified; the reaction products include both liquid and gaseous components. Thus, the thermal history of the material does not follow a simple, single-reaction theory. In later work, Bowes concluded[445] that experimental explosion results for benzoyl peroxide could be adequately represented by the use of the self-heating constants E = 183.3 kJ mol^{-1}, P = 83.78; however, since the response clearly does not conform to the theory, the usefulness of such treatment is dubious. Data from large-scale burns of organic peroxides have been published[1648] with the specific details being given on radiative fraction, in order to enable calculations to be made of target ignitions from such burning fuels.

Kayser[1649] examined the self-heating of several organic peroxides using small samples placed in an oven for 20 h at 55ºC. Lauroyl peroxide sustained thermal runaway in an 0.5 g quantity. Benzoyl peroxide, *tert*-butyl acetate, *tert*-butyl hydroperoxide, di-*tert*-butyl peroxide, cyclohexanone peroxide, and methyl ethyl ketone peroxide were stable in 1.0 g quantities. She also determined that polyethylene material was non-reactive with the peroxides and did not act to promote exothermic behavior.

The UN Model Regulations[1650] contain a table giving extensive properties and safety measures for most commercially common organic peroxides. Bond[1651] has tabulated self-heating and other properties for a variety of organic peroxides. Tamura et al.[1652] reported on a large series of organic peroxides tested in the Japanese Revised Time-Pressure Test. Zitrin[1653] reports that the organic peroxide TATP (triacetonetriperoxide, $C_9H_{18}O_6$) has been used by some terrorist groups. Médard[26] provides an extensive discussion of the properties of organic peroxides, along with reports of accidental explosions.

Pharmaceuticals

Koltsov[1654] has reported on Russian research where the self-heating of a large number of powdered vitamins and pharmaceuticals was studied using oven tests with cubic baskets. Unfortunately, only data reduced according to a crude Russian estimating formula were provided.

Phosphines

Phosphine, PH_3, is spontaneously flammable in the air if there are even traces of diphosphine, P_2H_4, present[1655], or if it is moisture-free[3]. Diphosphine is also spontaneously flammable by itself. At room temperature and pressure, it has been found[1781] that pyrophoric ignition will occur if the ratio of phosphine to oxygen (assuming the remainder to be nitrogen) exceeds a certain value. The authors' data can be represented as:

$$phosphine\ \% \geq 0.28 + 3.57\left(oxygen\ \%\right)^{0.62}$$

The above relation specifies the maximum amount of oxygen that can exist for pyrophoric ignition to occur and is applicable for phosphine volume fractions of 6.5% or less. Clearly, there also has to be some minimum of oxygen, greater than zero, but this limit was not explored, nor were phosphine levels over 6.5%. Thin, ghostly flames are sometimes seen above marshes and are known as *marsh gas*, will o' the wisp, foxfire, or jack o' lantern. The fuel gases causing these flames comprise methane, phosphine and diphosphine[1398]. Fires onboard ships have been reported[1656] due to excessive generation of phosphine from *magnesium phosphide*, which is used as a fumigant.

Phosphorus

White or yellow phosphorus oxidizes rapidly in air, and can ignite at slightly above room temperature. There are two oxidation modes—in the slow mode a green glow is seen, while the fast mode gives a yellow flame. The slow oxidation mode takes place at 16 – 38ºC if the air is adequately moist[1657]. Above 38.5ºC, flaming occurs. The ignition temperature is pressure sensitive, and decreases if pressure is lowered. In one series of tests, the Bureau of Mines[1378] tested 4 g quantities of white phosphorus and found that it ignited in air at the lowest temperature used, 32ºC. The oxidation reaction is:

$$4P + 5O_2 \rightarrow 2P_2O_5$$

Contact with finely divided charcoal or lampblack promotes ignition. An incendiary preparation, sometimes known as Fenian Fire, can be made with phosphorus by dissolving it in carbon disulfide. The dissolved solution is applied as a film and resists igniting only until the CS_2 evaporates, at which point spontaneous combustion occurs. Rat poisons containing phosphorus used to be common, and cases have been reported where a small amount of phosphorus reacted with organic materials to cause a fire[2078]. Phosphorus fires are difficult to extinguish and tend to re-erupt after initial extinguishment.

Red phosphorus is an allotrope which is prepared by anaerobic heating to 240 – 253ºC. It is not pyrophoric, but can be ignited by impact or friction[3]. It has been reported[943] that its ignition temperature is 240ºC. Powders of red phosphorus are subject to oxidative self-heating, consequently, antioxidants have been developed specifically for red phosphorus[1658]. Other allotropic forms of phosphorus, such as violet or black, are rarely encountered.

Pillows

Ramsay and McArthur studied the ignition of pillows[1659]. All pillows were tested covered with 50/50 polyester/cotton pillow cases of 172 g m^{-2} weight and placed on sheets of similar fabric located atop a simulated polyurethane foam mattress. Their results are summarized in Table 169. The authors concluded that details of the coverings mattered little, with behavior being determined by the fillings.

Table 169 Ignitability of pillows

Filling	Covering	Ignition from cigarette		Ignition from methenamine pill	
		on top surface	underside of edge	on top surface	underside of edge
PUR foam	cotton, 93 g m^{-2}	no	no	flaming of cover and case only	flaming at 3.5 min
PUR foam	cotton, 163 g m^{-2}	no	no	flaming at 7 min	flaming at 3.5 min
PUR foam, high resilience	cotton, 93 g m^{-2}	no	no	flaming at 9 min	flaming at 4 min
PUR foam (crumb)	cotton, 99 g m^{-2}	no	no	flaming at 4.5 min	flaming at 1 min
latex foam	nylon, 67 g m^{-2}	no	yes (smolder)	flaming at 2.5 min	flaming at 1 min
polyester fibers	cotton, 121 g m^{-2}	no	no	flaming at 5 min	flaming at 2 min
duck feathers	cotton, 154 g m^{-2}	no	no	flaming of cover and case only	flaming of cover and case only

Pipe insulation

The theory of self-heating-caused ignitions of pipe insulation is presented in Chapter 9. Here, some experimental findings and some practical advice are provided. Bowes[1660] reported on oven-cube tests and on 'pipe simulator' tests with two different pipe insulations, a mineral wool and a calcium silicate/asbestos type. Both were coated with a low-viscosity transformer oil not containing antioxidants. The tests were difficult to conduct in a repeatable manner, since a uniform coating of oil is not possible to achieve. Some pipe insulation systems use a fabric-type cover on the outside. In pipe simulator experiments with such specimens, self-heating could not induce glowing, much less flaming ignition, at pipe temperatures up to 300ºC. This demonstrates the importance of restricting oxygen supply in order to control self-heating.

Gugan[1661] reviewed a number of case histories of self-heating fires associated with pipe insulation. He pointed out that the oils or other materials likely to contaminate pipe insulation in real-fire incidents are rarely distributed in a uniform manner, and this fact can significantly diminish the ability to use laboratory tests for prediction. Furthermore, he pointed out that the standard theory requires assuming a known value for λ, the thermal conductivity of the contaminated insulation material. It is well-known that the effective thermal conductivity of porous insulation materials increases greatly with temperature[1662]. The conductivity to consider, by the way, must be the 'effective' one, which includes contributions from convection and radiation taking place within the porous structure, since the latter two effects are not negligible in lightweight, porous insulations. The problem is especially difficult in the pipe insulation case due to the strong temperature gradients necessarily present, even before any self-heating has started.

The amount of liquid which is deposited on the insulation material clearly will influence the self-heating process. A small amount of liquid will not provide much HRR; a very large amount, however, will tend to fill the pore structure and prevent oxidation. Thus, for oxidizable liquids, an intermediate loading should exist which creates the worst-case condition. But Britton[1663] showed that, within limits, actual self-heating results are not highly sensitive to the amount of liquid loading; he considers loadings of 150 – 350%, by mass, to be appropriate for test purposes. This lack of major sensitivity explains why there is significant disagreement in the literature concerning how much liquid corresponds to a worst-case loading. He also reports an extensive set of experimental data on various liquids soaked into calcium silicate and mineral wool insulation. The variables included loading and temperature, but all tests were run only with 51 mm cubes; thus the standard variables E and P could not be deduced. The fluids included amines, glycols, organosilane esters, and a variety of heat transfer fluids. Britton concluded that the results of the self-heating tests could be roughly correlated by Lindner's[1664] variable Z:

$$Z = \frac{AIT}{AIT - FP}$$

where AIT is the autoignition temperature (ºC), and FP is the flash point (ºC). Generally, liquids with $Z < 1.35$ did not show self-heating in the oven-cube tests, while those with $Z > 1.61$ did. The region of $1.35 < Z < 1.61$ was a zone where rankings were contradictory. Britton attributes this to the use of NFPA 325 values for the AIT. The latter are compiled as the 'lowest published values,' which means there are significant inconsistencies due to different experimental techniques or laboratory variations. Fluids which have a low Z are ones which have either a low flash point, a high AIT, or both. Liquids having a low flash point show a *lower* self-heating hazard because such liquids are also very prone to evaporate. If the liquid readily evaporates, then enough of it will not remain in the insulation in order to undergo thermal runaway.

Two categories of liquids are special cases and Z values for them should not be expected to give indicative results. (1) liquids which react with ambient air moisture (e.g., trichlorosilane), since these can generate products which are less volatile than the parent compound. (2) liquids which react to form peroxides (e.g., tetralin and 2-ethyl hexaldehyde).

Britton also reports case histories where methyldiethanolamine soaked into calcium silicate insulation and high molar

Table 170 Plastic materials comprising the first item ignited in fires

Plastic article ignited	Percent
bowl, bucket, container	18.7
furniture, furnishings	9.1
toys, games	7.6
electrical insulation	6.6
external/internal fittings	6.6
sheet, covering	4.5
packaging, wrapping	3.5
waste bin	4.0
tray	4.0
wall or ceiling linings	3.0
electric plug, outlet, switch	3.0
domestic equipment components	3.0
thermal insulation	2.5
fan	2.5
hair curlers	2.0
other (known)	17.7
unspecified or unknown	2.0

mass polyethylene glycols soaked into mineral wool insulation caused fires. Another fire involved tetralin used as a heat transfer fluid on an unspecified insulation. Tetralin is particularly problematic since it forms tetralin hydroperoxide upon exposure to air, with the latter being an unstable compound which shortly decomposes.

In some cases, the evaporation behavior, and not just oxidation, of the liquid can play a strong role in determining conditions for thermal runaway. Effectively, if the fuel can vaporize faster than it self-heats, then it will not create a thermal runaway hazard. Brindley et al.[1665,1666] performed modeling where fuel vaporization effects were included. This work indicated that the classical Frank-Kamenetskii theory is only applicable to low-volatility, highly-exothermic fluids; if applied to situations where this is not true, grossly over-conservative predictions may be obtained. In the Brindley theory, a large number of physicochemical constants are needed to perform the computation, and the values for quite a few of them will generally be difficult to get. Thus, a practical hazard-computation scheme has not yet emerged, although there is an expectation that further analysis of experimental results could produce one.

Hilado[1667] reports on tests where fourteen different insulation types were soaked in ethylene oxide. The order, best to worst, when tested for the self-heating propensity was: glass beads, glass fibers, mineral wool, perlite, and calcium silicate. Quantitative conclusions are hard to draw, however, because non-standard testing techniques were used. A way by which the self-heating problem can be eliminated is to use *cellular glass* insulation, since this material does not have a pore structure into which a liquid can penetrate. However, it is expensive, difficult to work with, and in some industrial situations it may not be usable because it

Table 171 Sources of ignition for plastics

Source of ignition	Percent	
cooking appliances		**25.2**
electric	14.1	
gas	11.1	
space heating		**20.2**
electric	7.6	
solid fuel (fire in grate)	6.1	
gas	4.0	
oil	2.5	
electric appliances, other		**19.7**
wire and cable	9.6	
washing machine	3.5	
immersion heater	1.5	
kettle	1.5	
other	3.5	
smoking materials		**8.6**
ashes and soot		**4.6**
candle		**4.6**
children with fire		**4.0**
chimney, flue		**3.0**
matches, open flame		**2.5**
other (known)		**7.1**
unknown		**0.5**

cannot achieve a fire endurance rating due the melting temperature of glass. For ordinary insulation, installing an impermeable cover on the surface can help. Another material which can help is a perlite insulation which is treated with a water-repellant; however, water repellants on mineral wool are not effective and do not eliminate wicking[1663].

Plastics

A British survey examined the ignition of plastic materials in residences[1668]. A total of 396 incidents that occurred in 1969 in which plastic was the material first ignited were studied. The salient findings are shown in Table 170 and Table 171. A number of authors have reported ASTM D 1929 (Setchkin furnace) data on plastics, and many of these

Table 172 Ignition properties of FR and non-FR polymers

Material	T_{ig} (°C)	Ignition times (s) for various heat fluxes					
		25 kW m^{-2}		50 kW m^{-2}		75 kW m^{-2}	
		Flash	S.F.	Flash	S.F.	Flash	S.F.
ABS	410	NF	111	NF	38	14	17
ABS, FR	420	98	120	27	34	15	17
HIPS	410	176	206	NF	52	21	24
HIPS, FR	390	149	304	40	106	20	25
PC/ABS	440	NF	189	NF	49	NF	21
PC/ABS, FR	440	211	267	51	53	26	28
polyester		107	119	40	42		
polyester, FR		NF	∞	150	159	37	79
XLPE		NF	86	33	37		
XLPE, FR		155	162	61	63	33	37

HIPS – high-impact polystyrene
NF – no flashing
PC/ABS – polycarbonate/ABS copolymer
S.F. – sustained flaming
XLPE – cross-linked polyethylene

Table 173 Setchkin furnace values of ignition temperature, as determined in roundrobin tests

Material	Piloted ignition (ºC)			Autoignition (ºC)		
	T_{ig}	s_r	s_R	T_{ig}	s_r	s_R
nylon 6	413	2.8	13.6	439	11.2	20.1
phenol formaldehyde, solid	430	3.3	41.7	482	5.0	36.8
polyester resin (sheet)	380	3.2	20.1	451	4.1	27.6
polystyrene, high-impact (granules)	378	3.5	9.8	458	4.4	21.1
polystyrene, high-impact, FR (granules)	370	4.7	18.7	422	5.1	16.7
" " (second trial)	377	3.6	16.8	426	2.9	35.7
polyurethane foam, flexible	349	4.1	23.6	370	3.9	21.6
" " (second trial)	363	3.1	13.4	378	5.0	7.9
polyurethane foam, rigid	378	4.9	14.7	502	4.7	10.8
PVC, unplasticized	441	4.9	14.7	474	4.7	10.8
PVC, film	327	3.8	16.2	438	4.8	22.9
" " (second trial)	308	4.9	14.7	454	2.7	27.6

s_r – repeatability standard deviation
s_R – reproducibility standard deviation

results are tabulated in Chapter 15 without further elaboration. For most of these data, repeatability and reproducibility are unknown. Masařík[1669-1671] reported on several roundrobins where precision of results was determined. These results are shown in Table 173.

The ignition temperatures of thermoplastics are typically 150 – 300ºC higher than their melting points, and no specific relation exists between these two properties[1672]. The decomposition temperature, by contrast, is typically only slightly lower than T_{ig}. However, decomposition temperature is not a basic property of plastics but, rather, depends greatly on the apparatus used and the definition adopted, thus, it is not much used in fire safety studies.

Several studies on the radiant ignition of plastics have been used as examples in Chapter 7, and detailed information is given there. Hallman[440] conducted extensive tests on the piloted, radiant ignition of plastics using radiation from a flame source. His primary results are summarized in Chapter 15. Also given are the values of B_{ig} and $\dot{q}''_{cr}$ derived from his data. Apart from the few specimens indicated, Hallman generally did not explore the minimum flux for ignition. Most of his results provided good fits to the thermally-thick data plotting procedure of Janssens. A few materials showed deviations at the high or the low end of the heat flux scale. Those cases are noted in the Table. The 3 mm

Table 174 Ignitability of PVC materials

Flux (kW m^{-2})	Flexible floor covering			Floor tile			Sheet material		
	Cone piloted	EU piloted	EU auto	Cone piloted	EU piloted	EU auto	Cone piloted	EU piloted	EU auto
10	69	95	NI						
15	37	45	NI						
20	20	19	NI				562	NI	NI
25	13	17	NI	67	75	NI			
30			NI	45	53	NI	420	NI	NI
40			11	29	35	NI	335	455	NI
50				19	22	NI			NI
60						34			NI

NI – no ignition in 30 min period

Table 175 Comparison of ignitability of several plastics in various tests

Material	Glow wire ignition			Methenamine pill	Ign. time (s) with needle flame	Ign. time (s) in Cone Calorimeter at 50 kW m^{-2} flux
	750ºC	850ºC	960ºC			
PMMA, 1.5 mm	no	yes	yes	33	92	19
polycarbonate, 1.5 mm	no	no	yes	no	116	37
polystyrene, 1.5 mm	no	yes	yes	44	20	35
PVC, 1 mm	no	no	no	no	no	38
PVC, prismatic*	no	no	no	no	no	53

* a light diffuser with prismatic surface, thickness of 1.5 to 3.0 mm

Table 176 Minimum flux for ignition of electrical PVC materials

	Flux (kW m^{-2})	
	Auto-ignition	Piloted ignition
flexible PVC tubing	35	15
rigid PVC conduit	35	15

Table 177 Autoignition times for several plastics in the Cone Calorimeter

Material	Ignition time (s) at heat fluxes indicated		
	35 kW m^{-2}	50 kW m^{-2}	75 kW m^{-2}
polycarbonate	NI	99	44
polyethylene, high-density	141	70	35
PVC	485	421	69

thick specimens were analyzed as thermally thin. In addition to the data shown, Hallman also obtained ignition results for several proprietary formulations and for exposure conditions where the specimens were heated with high-temperature (3000 K) lamps. Also provided in Chapter 15 is a table of extensive results obtained in the Cone Calorimeter by Scudamore et al.[1673]

Grand[1674] compared the radiant ignition behavior of FR plastics to their non-FR counterparts using the Cone Calorimeter. His results are shown in Table 172. For several of these materials, he also determined the piloted ignition temperature in the ASTM D 1929 test.

Morimoto et al.[1675] reported autoignition temperature data for a large collection of polymers. Their results are not listed in Chapter 15, because their values were typically on the order of 100ºC higher than those of most other workers. Their test rig was roughly similar to the Setchkin furnace, but they used very small samples (0.2 g), and apparently this caused unduly high T_{ig} values to be reported. No polymer in their study showed T_{ig} < 430ºC, and most showed values of 500 – 700ºC.

Table 178 Comparison of ignitability of several plastics in various tests

Material	Glow wire (ºC)	UL 94V tests		Needle flame	Min. heat flux (kW m^{-2})
		1 mm thick	2 mm thick		
chlorosulfonated polyethylene	960	V-1	V-0	NI	16
EVA, cross-linked, ATH filled	750	fail	fail	I	13
EVA, thermoplastic, ATH filled	850	fail	fail	I	16
PTFE	960	V-0	V-0	NI	33
PVC	850	V-1	V-2	I	8
PVC, FR	960	V-0	V-0	NI	11
I – ignited; NI – not ignited					

Table 179 Hot-surface ignition temperatures of plastics

Material	Ignition temp. (ºC)	
	For 1 s contact	For 10 s contact
cellulose acetate	595	480
cellulose acetate butyrate	620	425
cellulose nitrate	370	315
phenol formaldehyde, asbestos filled, molded	775	650
phenol formaldehyde, cast	860	590
phenol formaldehyde, mica-filled, molded	815	650
phenol formaldehyde, paper-based, laminated	595	480
phenol formaldehyde, wood-flour filled	705	540
PMMA	620	480
polystyrene, clear, injection molded	730	565
polyvinyl chloride acetate	480	370
urea formaldehyde, molded	815	705

Starchville conducted Cone Calorimeter tests on electrical tubing and conduit, as discussed in Chapter 7. His results for minimum flux for ignition are given in Table 176. Holbrow et al.[1037] tested several 3 mm thick plastics in the Cone Calorimeter for autoignition. They obtained the results shown in Table 177.

The fire properties of PMMA have been more extensively studied than for any other plastic. Kashiwagi and Omori[1676] studied the piloted ignition of PMMA and found that the ignition temperature depended on the molar mass of the material—a low molar mass specimen showed 330ºC, while a high one gave 265ºC. This trait was polymer-specific, and molar mass was not found to affect the results for polystyrene (365ºC). The molar mass effect was not related to thermal properties, but was identified, instead, to be due to multiple, exothermic decomposition reactions in the high molar mass material. In Chapter 7, results of Babrauskas indicated $\dot{q}''_{min}$ = 8 kW m^{-2} for PMMA, while two different types of PMMA tested by Thomson[1677] showed values of 9.5 and 10.6 kW m^{-2}. The values of piloted T_{ig} measured by Thomson under various conditions were very close to 311ºC. Hopkins and Quintiere[1678] found ignition temperatures of 250 – 355ºC; this wide spread of data apparently repre-

Table 180 Results of Hedges et al. for hot-surface heating of plastics of two thicknesses

Material	Ignition temperature (ºC)	
	25 – 50 µm	125 µm
nylon 6,6	482	435
polyethylene	378	365
PET	481	440
PVC	NA	260

Table 181 Minimum temperature needed for ignition of various plastics by a 1 s application of a Nichrome heater

Material	Ign. temp. (ºC)
Nylon	1075
PMMA	1050
polycarbonate	1125
polyethylene	1055
POM	975
PS	1000
PVC	1260

Table 182 Ignition properties of plastic foam reported by the PRC

Foam	AIT (ºC)	Min. flux for ignition (kW m^{-2})	
		Piloted	Auto-ignition
polyisocyanurate			23 – 24
polystyrene, expanded	440 – 448		27
polystyrene, expanded, FR	405 – 429		
polyurethane, flexible	426 – 445	16.4	16.4
polyurethane, flexible, FR	430 – 450	21.4	20.0
polyurethane, flexible, high resilience	413 – 429	18.7	
polyurethane, flexible, high resilience, FR	431 – 453	19.4	
polyurethane, rigid	457 – 494		22 – 26
polyurethane, rigid, FR			26

sents different testing conditions, rather than different samples, but details were not given. Henderson[2111] reported T_{ig} = 345ºC in the Cone Calorimeter, but with few details being given. For the thermochemical properties of PMMA, Staggs[1679] recommends the following values: $A = 1.0226\times10^6$ s^{-1}, E = 97.02 kJ mol^{-1}, ρ = 1190 kg m^{-3}, λ = 0.22 W m^{-1} K^{-1}, C = 2104 J kg^{-1} K^{-1}, ε = 0.95, H_v = 420 kJ kg^{-1}.

Braun and Allen[1770] reported $\dot{q}''_{min}$ = 30 kW m^{-2} for polycarbonate tested in the LIFT apparatus and the identical value was also reported by Quintiere and Harkleroad[2113]. Wang et al. examined the ignitability of several grades of PVC in the Cone Calorimeter and in the Edinburgh University apparatuses[1680]. Their results are given in Table 174. Clearly, there are huge differences between the grades.

O'Neill[1681] reported test results on several plastics which were tested in a variety of test methods, including the minimum heat flux, as determined by the Cone Calorimeter, the IEC 60695-2-13 glow-wire test[1682], the to IEC 60695-2-2 needle flame test[1683] and UL 94. The needle flame and glow-wire tests were conducted on 1 mm thick samples, the thickness for the Cone Calorimeter tests was not specified. The results are shown in Table 178.

Briggs and Morgan[1684] conducted a variety of ignition tests on 5 different plastics. Their results are given in Table 175. The glow wire test was according to IEC 60695-2-13 test[1682], while the needle flame test was according to IEC 60695-2-2[1683]. The results do not suggest that there is a great deal of correlation among results from the diverse tests, thus, use of a test that reasonably simulates the desired fire condition is important.

In an early study, Delmonte and Azam[1685] characterized the hot-surface ignitability of plastics by holding plastic samples for different times to molten sodium hydroxide. The latter substance was picked as giving more reproducible results than molten metals. Their results are shown in Table 179.

Hedges et al.[1686] tested several plastic films for hot-surface ignitability by gluing them onto metal strips that were resistively heated at high rates. In addition, a pilot flame was located in the pyrolysate stream. Their results are shown in Table 180. Filippov et al.[1687] tested the ignitability of plastics by pressing a 2.5 mm Nichrome heater onto their surface; their results are given in Table 181. Another study[1688] by the same authors showed that there is only a small difference of the heater diameter, for example, when the diameter was increased to 3.9 mm, the ignition temperature for polycarbonate dropped from 1125 to 1110ºC.

Table 183 Piloted ignition times (s) for foams tested using the ISO 5657 test method

Foam	Density (kg m^{-3})	Irradiance (kW m^{-2})						
		10	15	20	25	30	40	50
phenolic	35		NI	NI	201	8	8.5	
phenolic	35		NI	NI	159	82	9.9	3.0
phenolic	43		NI	NI	NI	75	7.7	
phenolic	45		NI	NI	296	218	40	10.8
phenolic	57		NI	NI	NI	276	54	13
PUR	30	43	10.4	6.2	4.9	2.3	1.5	
PUR/PIR	35	51	10.5	6.6	5.8	2.2	1.5	
PIR	40	134	33	10.0	6.1	4.1	2.5	
EPS	15	NI	148	18.6	4.5			
EPS	20	NI	131	3.7				
EPS, FR	20	252	70	37	23.4	14.7		

SELF-HEATING OF SOLID PLASTICS

Monomers used for making plastics (e.g., styrene, methyl methacrylate, vinyl acetate, ethylene oxide, etc.) polymerize exothermically upon initiation. Heat, light, shock, or a catalyst can serve as initiators[2087]. In general, polymerization reactions in plastics-manufacturing are exothermic, so they can only be conditionally stable: an upset to operating temperatures, flow rates, etc. can cause thermal runaway and ignition. Biesenberger et al.[1689] presented a theoretical model and experimental results for thermal runaway of styrene polymerization. Acrylic resin monomers are especially reactive and a history of fires and explosions in chemical plants involving these resins has been published[1690]. Some thermoset plastics require heat curing for their manufacture. The curing process is exothermic and the potential exists for thermal runaway. Buckmaster and Vedarajan[1691] presented a modified Frank-Kamenetskii theory for analyzing such processes.

A case history has been documented[45] of autoignition events in a continuous vertical drier processing nylon flock for carpets. Most of the events occurred as glowing hot spots, which fell and ignited other material. Tests elucidated that if high temperatures are rapidly reached, melting occurs and self-heating is precluded. But if nylon fibers are exposed over a longer period of time to temperatures of 130 – 170ºC, charring occurs and a matrix is preserved which is air-permeable. Using oven tests at 170ºC of 100 mm cubes, it was shown that in thermally-aged specimens glowing hot spots formed in 6 h.

The process of making *fiberglass* with polyester resins has been known to lead to self-heating problems, since the curing reactions involving an organic peroxide (e.g., methyl ethyl ketone peroxide) catalyst and a cobalt 'accelerator' are exothermic. Several fire investigators[1692,1693] published results of limited testing where they documented that they could create self-heating but not spontaneous combustion by over-catalyzing the resin. The temperatures reported in tests have been high enough, however, being 200ºC in one series of tests[1694], that conditions may not need to be much different for overt flaming to occur. In any case, such attempts at negative proof must be viewed with caution. Brydson's treatise on plastics[1695] points out that catalyst and accelerator coming into direct contact can form an explosive mixture. Thus, fires may also be due to accidental direct mixing of catalyst and accelerator, rather than over-catalyzing of the resin.

Jones[1696] studied the exothermic oxidation of *polystyrene* in a microcalorimeter and found that detectable heat output was seen starting about at 55ºC, but that the reaction rate was several orders of magnitude less than in materials with a pronounced self-heating tendency, such as coals, carbons, and cellulosics. Mok et al.[1697] studied the self-heating of methacrylate-butadiene-styrene powder and reported self-heating variables E = 138 kJ mol^{-1}, and P = 62.0; the latter value, however, is very high and may not be correct. ABS resin in powder form can smolder and shows autocatalytic behavior in thermal decomposition[1597]. Oven-basket testing indicated a critical temperature in the range of 110 – 125ºC for 50 mm cubes. Self-heating of ABS resin has caused a warehouse fire and a Japanese report has been published[1698].

A case history is reported where a quilt made of *polypropylene* fibers self-heated to a smoldering ignition in a clothes dryer[1699]. Laboratory tests at the American Institute of Laundering were able to reproduce the conditions.

ELASTOMERS AND FOAMS

An elastomer is defined as[1700] "A macromolecular material that returns rapidly at room temperature to approximately its initial dimensions and shape after substantial deformation by a weak stress and subsequent release of the stress." In everyday English usage, elastomers are called "rubber" or "flexible plastic foam." Plastic foams may also be rigid, and in that form are commonly used as thermal insulation.

A large number of tests on foam plastics were reported by the Products Research Committee[1701], a US plastics industry effort in the 1970s that was coordinated by the National Bureau of Standards. Their ignitability results are given in Table 183. Cleary and Quintiere[1706] reported that 15 kW m^{-2} was needed in the Cone Calorimeter under piloted conditions for the ignition of rigid polyurethane foams, both regular and FR.

Fernando et al.[1702] measured the ignition of a non-FR, furniture-grade polyurethane foam in the Cone Calorimeter. They found a minimum flux for ignition of 7 kW m^{-2} for piloted tests and 28 kW m^{-2} for autoignition. At the low flux of 7 kW m^{-2}, it was noted that there was some surface discoloration directly below the spark electrode, indicating that at such a low flux there may be some local heating from the spark. Kallonen[1703] tested a variety of rigid foam plastics using the ISO 5657 test method. Her results are given in Table 182.

Table 184 Piloted ignition properties of several polyurethane foam types

Type	Density (kg m^{-3})	Crit. MLR (g m^{-2} s^{-1})	T_{ig} (ºC)	Ignition time (s) at various fluxes			
				10	15	26	37
non-FR	21	0.61	324		29	9	4
non-FR	30	0.47	326	49	25	8	2
FR (graphite)	75	0.32	306		31	8	4
FR (graphite)	37	0.51	310	59	28	8	3
FR (melamine)	25	2.51	306[a]		NI	112	61
FR (ATH)	35	3.01	319[a]		NI	152	88
non-FR, solid	1040	1.21	271		205	57	21

NI – no ignition
a – flash point value; surface temperature at sustained ignition not given

Annamalai and Sibulkin[1704] tested a number of plastic foams for ignitability with a very small (25 W) propane flame applied to the specimens. Polystyrene and polyethylene foams did not ignite due to melting—the foam melted out of the reach of the flame. Latex foam ignited in 0.5 s, and non-FR flexible polyurethane foams ignited in 2 – 10 s. Non-FR rigid polyurethane foams ignited in 0.3 – 2 s. A sample of flexible PVC foam ignited in 38 s. FR polyurethane and polyisocyanurate foams did not ignite from the flame. When a radiant flux of 2 kW m^{-2} was added, some of the FR foams which did not ignite from the gas flame alone then did ignite. In the case of one rigid FR polyurethane foam, it required a radiant flux of 6 kW m^{-2} before ignition was achieved.

Values of $\dot{q}''_{\min}$ for polystyrene foams, both expanded and extruded, regular and FR, are typically[1706] 15 kW m^{-2}, although values from 8 to 23 kW m^{-2} have been reported[2121].

Drysdale and Thomson[1705] tested the piloted ignition properties of several polyurethane foams using the Edinburgh University radiant heat apparatus, which is similar to ISO 5657 test and has been described in Chapter 7. Their results are shown in Table 184. The mass loss rates found at ignition for many of the samples were surprisingly lower than values determined in the same apparatus by Thomson for other plastics, as discussed in Chapter 7; the reason for this is not clear. Polyisocyanurate and phenol formaldehyde (phenolic) foams are moderately difficult to ignite in a radiant-heating mode. The minimum heat flux was found to be 21 kW m^{-2} for polyisocyanurate[1706,2113] and 30 kW m^{-2} for phenol formaldehyde[1706]. But UK tests[224] showed that phenol formaldehyde insulating foams can readily start smoldering from a cigarette, even though they do not ignite from a match or an electric arc; polyisocyanurate insulating foams are capable of sustaining smoldering, but need an ignition source greater than a cigarette to start smoldering. Saito et al.[1707] dropped 10 – 14 mm steel balls heated to 700 – 1300ºC onto phenolic and polyurethane foams from a height of 1 m. No ignitions were achieved with a 10 mm ball heated to 700ºC, but a 10 mm ball heated to 1000ºC sufficed to cause ignition.

A variety of elastomers tend to show *self-heating* problems. These primarily occur under three types of conditions:

(1) when processing machinery is run at excessive temperatures;
(2) when the product is mal-formulated or processed improperly (apart from excessive temperatures);
(3) when the product is stored too hot or in too large a volume.

A case has been reported[1708] where an improperly-manufactured batch self-heated instead of cooling down upon leaving the production line and led to a large-loss fire. In another case[1709], polyurethane foam ignited in a manufacturing facility since an inhibitor was accidentally omitted from the formulation. Fires have also occurred when the materials were in storage[1710] although details are not available. Oxidative self-heating of such substances has long been known. For example, a 1967 study[1711] identified that self-heating can occur due to oxidation of diene and triene bonds in rubbers.

A detailed case history of a self-heating fire in a rubber-manufacturing factory was reported by the Hungarian researcher Pap in 1965[1712]. Pap studied the specific material (not fully identified) that caused the fire, plus several commercial formulations. Thermal analysis tests were performed on natural rubber, polychloroprene, an SBR rubber and a polybutadiene rubber. The thermal analysis tests showed that polychloroprene rubber starts exothermic decomposition at around 200ºC, natural rubber at around 230ºC, polybutadiene rubber (BR) at 370ºC, and styrene-butadiene rubber (SBR) at 380ºC. Tire-making rubbers that contained carbon black and an oil were found to start decomposing at 200ºC. He noted that the thermal decomposition process involves both exothermic (oxidation, cyclization) and endothermic (depolymerization, evaporation) reactions, and the actual self-heating process will depend strongly on the heat balance established within the material. For the material involved in the factory fire, he showed that oxidative reactions predominate, and that fire would not occur if oxygen were excluded. But the temperatures found in micro-scale thermal analysis tests do not replicate the temperatures at which thermal runaway occurs in larger samples. The manufacturing process wherein the fire occurred involved a mixer operated at 150 – 160ºC. Pap simulated this environment with a 200 L drum sample. Thermal runaway in this large-scale test did not take place at 180ºC, but did take place at 200ºC, implying a critical temperature of around 190ºC for the 200 L size. Pap also documented that the self-heating of the rubber was not uniform throughout, and he found red-hot nodules upon taking apart the self-heating material; once in contact with free air, these turned into an intensely flaming fire.

Kuzminskii published a review paper on self-heating of elastomers[1713] where he noted that polydiene elastomers do not need oxygen for self-heating, since the process of cyclization can occur anaerobically. But, with access to oxygen, polydiene elastomers are "extremely unstable." Vinyl-cyclohexene was found to be the predominant cyclization product. He concluded that copolymerization is the most effective way of stabilizing the product, with as little as 10% of copolymer serving to prevent development of a cyclization chain reaction. Copolymerization, in his assessment, is much more effective than active fillers, stabilizers, or cross-linking agents in reducing self-heating. Metals such as iron or cobalt act as catalysts to promote self-heating of polydiene elastomers. He also found that the self-heating of silicone rubbers is more pronounced under low-oxygen conditions. This is because their self-heating is dominated by hydrolysis and access to copious oxygen helps to remove moisture from the material.

Table 186 Self-heating properties for elastomers determined by Gross and Robertson

Material	E (kJ mol^{-1})	AQ (W kg^{-1})	ρ (kg m^{-3})	λ (W m^{-1} K^{-1})	C (J kg^{-1} K^{-1})
crepe rubber	98	4.8×10^{9}	920	0.12	2100
GRS rubber	99	4.2×10^{10}	1100	0.13	2100
foam rubber, natural	116	2.9×10^{15}	108	0.040	2100
foam rubber, synthetic	110	1.6×10^{14}	129	0.04	2100

Emmons[1714] examined whether Goodyear's SBR rubber Plioflex was prone to spontaneous combustion while in storage. In small-scale tests using 70 mm cubes in the oven-basket method he found a critical temperature of 300ºC; he also noted that below about 220ºC the specimen's behavior was endothermic and that standard F-K theory would not be applicable to the material, due to the presence of the endothermic reaction. The SBR bales come wrapped in polyethylene film, so Emmons also conducted experiments where the oven cube sample was wrapped in polyethylene film. These tests revealed minimal endothermic behavior, showing that the endothermic reaction was being suppressed by not allowing the vapors to exude from the specimen faces. He also conducted large-scale experiments using a 'hot work' mode. In one case he loaded a 1-m cube box with the SBR material at 74ºC, then placed it outdoors for 14 days. Internal thermocouples showed cooling rather than self-heating. In another test, he placed an instrumented box of the SBR material at 74ºC initial temperature into a warehouse, surrounded by other boxes of the same material. Likewise, in that case there was cooling rather than self-heating. The conclusion was that the material can be safely stored at 74ºC in sizes up to the ones tested.

Weickert[1715] reported on DTA tests done to characterize the self-heating of an SBR rubber. In the DTA graphs, he identified two peaks, the first being due to oxidation and the second due to decomposition. He also showed that when the rubber is ground up, the oxidation peak is increased and the onset of exothermicity takes place earlier. Exothermic activity was generally first seen in DTA tests on SBR at around 110ºC and he found that the self-heating kinetics could be represented by a 2nd-order Arrhenius expression.

Shikhanov and co-workers briefly examined the spontaneous combustion hazards associated with a spontaneous polymerization which can occur in the processing equipment for diene thermoplastic elastomers in general and specifically butadiene, isoprene, and butadiene-piperylene rubbers[1716,1717]. Using a Russian test method that involved oven-testing of 35 mm cubes and failure criterion of 100ºC, they tested numerous scrapings of polymerized material from processing machinery and found that more than half showed critical temperatures below 100ºC. The conclusion was that, compared to the highly hazardous ones, moderately hazardous elastomers show a smaller number of C=C bonds, more extensive cross-linking, and a higher molar mass. Further quantifying behavior by using oven-basket tests of varying sizes, they concluded that 'highly hazardous' materials were ones where a 0.7 mm thick layer was able to go to a thermal runaway situation in 200 h or less at ambient air conditions. The production wastes of the kind examined by Shikhanov were clearly highly prone to self-heating, but it must be noted that these were not products whose manufacture was completed.

Self-heating data based on a small-specimen study in an adiabatic furnace were obtained by Gross and Robertson[109]. Their results are shown in Table 185.

During the 1950s, *latex foam* (foam rubber) became popular in consumer items such as pillows, pads, toys, upholstered furniture, and ladies undergarments. Some of these items are intended to be washed, and if subsequently dried in clothes dryers, self-heating fires occurred[1718] and NFPA issued a warning advisory[1719]. By the 1970s, latex foam was replaced by polyurethane foam in most applications, with the latter not showing these problems. Fabrics coated with

Table 185 Self-heating parameters for polyurethane foams

Spec. ID	ρ (kg m^{-3})	C (J kg^{-1} K^{-1})	λ (W m^{-1} K^{-1})	E (kJ mol^{-1})	QA (W kg^{-1})
C32	270	1600	0.023	47.3	3.17×10^{6}
C42	300	1600	0.023	51.4	8.24×10^{6}
F32	340	1600	0.023	51.4	2.56×10^{7}
F42	320	1600	0.023	59.0	1.67×10^{8}
G32	290	1600	0.023	74.0	9.87×10^{9}
G42	290	1600	0.023	69.4	1.98×10^{9}
H32	340	1600	0.023	51.0	2.89×10^{7}
H42	360	1600	0.023	61.0	3.34×10^{8}

latex can self-heat, if copper impurities have become mixed into the latex. Case histories of this have been reported[1720] and it was found that copper is such a powerful catalyst for the oxidation of latex that large temperature excursions were registered in the Mackey test.

A warehouse fire was found to have occurred due to self-heating of polychloroprene patient examination gloves[1721-1723]. Laboratory testing produced an estimate that an 0.325 m cube of material would be sufficient to lead to thermal runaway at 35ºC. This small critical size suggests that the material may have been improperly formulated or manufactured. In coal mines, conveyor belts made of polychloroprene are often used. Because of the size and configuration, the belts do not exhibit self-heating problems. However, roller wear causes polychloroprene dust particles to accumulate, and such layers can self-heat. Wachowicz[1724] investigated this self-heating for three different formulations of polychloroprene and found exothermic peaks at 230ºC, 320ºC, and higher. When subjected to some *ad hoc* self-heating tests, the material showed thermal runaway, with glowing occurring at ca. 550ºC. Open flaming, however, never erupted, which the authors attribute to the presence of large amounts of FR agents in the elastomers.

Polyurethane foams can self-heat to ignition, but reported incidents are typically limited to (1) mis-formulated or mis-manufactured batches[1725,1726]; (2) stacking of not yet fully-reacted product in excessively large stacks[2087]; or (3) use as insulation materials in solar collectors. The warm-material stacking situation occurs because the foaming reaction is highly exothermic and runaway can occur if the volume is too large before the reaction has run to completion. In a Canadian study[1727] it was concluded that a sphere of $r = 10$ m would be required for critical conditions to be reached in an unspecified type of polyurethane foam stored at 40ºC. Fires have occurred with polyurethane foam insulations used in solar collectors, and Loftus investigated the self-heating characteristics of foams in that connection[1728]. The temperatures reached in the collectors vary greatly, but in the worst case, under no-water-flow conditions, temperatures of ca. 200ºC are possible. The self-heating situation in solar collectors is complicated, since plywood is used atop the foam, and this is also a substance that can show exothermic behavior. Loftus evaluated the materials individually, using an adiabatic calorimeter. The results for 8 different polyurethane foams are given in Table 186. The results indicate a high possibility of criticality. For example, for specimen H42 at 120ºC the critical thickness is only around 50 mm.

Franke et al.[45] reported a case history of spontaneous combustion involving a rubber formulation based on butadiene-acrylonitrile rubber and PVC granules. A fire occurred due to a blockage of a mixer, with material of around 165ºC being plugged up. This material presumably did not require oxygen for self-heating, since access of air to a closed mixer is limited.

Taken together, the studies on self-heating of elastomers point to the following conclusions:

- Most elastomers show exothermic temperature regimes and thus may be capable of self-heating under certain circumstances. The propensity to self-heating depends on the chemical nature of the elastomer, on its additives (e.g., inhibitors), and on any self-heating promoters that may be present, e.g., iron, copper, or cobalt. In addition, as with any self-heating material, the amount of material and the storage temperature are crucial factors.
- Chemical reactions which may cause self-heating include:
  –oxidation of diene and triene bonds
  –formation of hydroperoxides
  –epoxidation of double bonds, and the crosslinkages resulting from it
  –formation and decomposition of polymeric peroxides
  –oxidative cleavages of C–C bonds via ketone and alcohol formation;
  –hydrolysis.
- When elastomers self-heat, they commonly do this in a non-homogeneous way, that is, isolated hot spots or nodules become generated within the material.

See also: *Tires* and *Upholstered furniture and mattresses*.

Potassium chlorate

Potassium chlorate, $KClO_3$, is a powerful oxidizer commonly used in pyrotechnics. The decomposition of potassium chlorate produces oxygen and this property has occasionally been exploited. Pure potassium chlorate is non-detonable, but it can react explosively with a number of substances. A mixture of potassium chlorate and sulfur explodes[26] if heated to about 160ºC. In olden times, this mixture was used as a pyrotechnic formulation, until its hazard became known. Similar hazards exist in use of potassium chlorate with aluminum powder. Potassium chlorate is less stable than sodium chlorate, and numerous explosions have occurred with it, caused by shock, friction, or heating. In practice, this combination is highly hazardous at any temperature, unless passivated by including a carbonate or bicarbonate in the mixture[1436]. The presence of moisture causes the chlorate* to react, yielding ClO_2, Cl_2, and O_2, and these oxidizing agents then react with the sulfur. Other contaminants besides moisture may also be involved. Reactions with most organic and many inorganic substances are likely to be explosive. Spills[1729] on the floor of potassium chlorate powder can be ignited by action of footsteps, if organic dust is also present. Conversely, $KClO_3$ can be used as an extinguishing agent, if applied to flames in the form of a fine powder. The action here involves the activity of the K^+ ion. Potassium chlorate and red phosphorus, when

* This type of reaction is a hazard with a wide variety of chlorates, not just potassium chlorate.

brought together dry in powdered form, react explosively[1436]; they are not likely to explode on contact if combined moist, however. See also: *Pyrotechnics*.

Potassium perchlorate has similar properties, but is more stable. In one case, however, a wood ventilation hood self-ignited after a long-term exposure to potassium perchlorate dust[26]. Potassium bromate is more reactive than potassium chlorate, but is less commonly used.

Powdered milk

In factories producing milk powder, the dominant causes for fires[1730] are: (1) self-heating; (2) friction or external heating; (3) malfunction of equipment; and (4) improper operating or control procedures. The final step in producing milk powder is spray-drying at an elevated temperature. This has caused a number of dryer fires due to the self-heating properties of milk powder[1731]. Explosions are also not rare in the industry, especially dryer explosions[1731]. Fires in storage silos sometimes are due to introduction of smoldering clumps of material[1732]. External ignition of milk powder has only been studied by Raemy et al.[1733], who found an AIT of 150ºC under 25 atm of pure oxygen and 170ºC under 5 atm. Studies do not exist on the AIT in normal air. The self-heating of milk powder has been studied by numerous researchers, as compiled in Table 187. Part of the reason why rather different results were obtained may be due to differences in the particle size distribution of the samples tested. In addition to the data summarized here, Duane et al.[1734] also examined a variety of milk powders with various fats added. The added fats affected the self-heating properties, but it was found that this could not be correlated to their values of iodine number. A higher fraction of unsaturated fats was found to lead to lower critical temperatures of self-heating. Raemy et al.[1733] studied in more detail some of the exothermic reactions occurring in milk powders. O'Connor conducted testing using DSC and determined Q = 421 to 582 kJ kg^{-1} (depending on product type) and that the order of the reaction is 0.6; however, the chemical constants obtained with DSC were rather different from values obtained with oven-basket testing. Gray[1735] noted that the parameters derived from self-heating tests can be strongly influenced by moisture; Rivers et al.[1736] performed numerical modeling of the problem and demonstrated that even 1 – 3% moisture of the powder is highly beneficial towards reducing the self-heating hazard.

Power steering fluid

Ohlemiller and Cleary[123] investigated the effect on the flash point and fire point of power steering fluid when contaminated with gasoline. Using a non-standard open-cup test apparatus, they found that the flash point dropped from 170ºC for pure power steering fluid, to room temperature (22ºC) when 14 vol% of the mixture was gasoline. The fire point dropped from 210ºC for pure power steering fluid to 22ºC for a mixture with 17 –19 vol% gasoline.

Propane

Okamoto et al.[1739] conducted experiments to determine the hot-surface ignition temperature for propane/air mixtures. Using a 5 vol% concentration of propane, they found that a temperature of 780ºC was needed for ignition. Such results are dependent on the size of the heated surface and their experiments were conducted using a heated glass cylinder of 12.5 mm diameter and 250 mm length, having an exposed surface area of 9818 mm^2. See also: BLEVEs in Chapter 13 and *LNG and LPG* in this chapter.

Propylene oxide

Propylene oxide (C_3H_6O) is a member of the chemical family of oxiranes and generally has similar properties to ethylene oxide. It is subject to exothermic polymerization and can be detonated[3]. For 5 g pure propylene oxide samples heated in a glass vessel[958] exothermic activity was found to commence at around 100ºC.

Pyrotechnics

Pyrotechnics is a general term of which fireworks is only a subset. Pyrotechnic devices that are not fireworks include such items as automotive airbag inflators, which are discussed above. Unwanted ignitions of pyrotechnics are generally of two general types: (1) Ignition and fire or explosion in connection with manufacturing, shipping, or handling. (2) A normal activation of a pyrotechnic device which results in some undesired ignition, for instance of clothing. McIntyre and Rindner[1740] collected statistics on accidents in the course of manufacturing military pyrotechnics (Table 189). Friction initiations were commonly due to

Table 187 Self-heating constants for milk powder

Powder	Temp. range (ºC)	ρ (kg m^{-3})	λ (W m^{-1} K^{-1})	C (J kg^{-1} K^{-1})	E (kJ mol^{-1})	P	AQ (W kg^{-1})
skim milk[1737]	135 - 170	670	0.33	1949	97.1	40.0	9.43×10^{12}
skim milk[1731]	142 - 171				79.0	48.5	4.16×10^{13}
skim milk[1732]	138 - 173	600	0.072	1547	79.3	42.5	3.52×10^{10}
whole milk[1737]	130 - 145	551	0.16	2012	160.4	59.3	8.63×10^{20}
	145 - 165				75.3	34.3	2.41×10^{10}
milk w. 30% fat added[1738]	130 - 200				81.1	43.2	
milk w. 44% fat added[1734]	135 - 175	508	0.127		99.6	48.0	1.46×10^{13}

problems in reaming or die-pressing operations. In the accidents, fires outnumbered explosions by more than 4 : 1.

The contents of fireworks are sometimes taken out and utilized in efforts to manufacture homemade bombs. The Royal Canadian Mounted Police[1741] provided the statistics given in Table 188. As can be seen, accidental explosions were far outnumbered by criminal actions. In the majority of the bombings, the filler material was identified as black powder, so it is not clear whether this necessarily came from disassembly of fireworks or from other sources.

Table 188 Breakdown of RCMP-attended pyrotechnics incidents in 1991, excluding thefts and recoveries

Activity	Percent
bombing	45
attempted bombing	17
hoax device	17
IED found	13
attack on safe or deposit box	5
accidental explosion	3.2

Most countries these days use the UN Regulations[1650] in classifying pyrotechnics. In the UN scheme, pyrotechnics fall under the general category of explosives (see *Explosives*). Pyrotechnics will not fall under the most-hazardous classes of explosives and would only be classified as 1.3G, 1.4G, or 1.4S. Division 1.3 comprises substances which show major hazards of radiant heat or violent burning, but only minor blast or projectile hazard. Division 1.4 comprises explosives with only small hazard in the event of ignition or initiation during transport. The 'G' designation indicates a 'small' hazard outside the package, in case of inadvertent activation during transport, while 'S' denotes no hazard outside the package, except if under external fire attack. Actual testing (which has some subjective aspects) and classification is done by the national government. Thus, for example, in The Netherlands[1742] most pyrotechnics are classified into Division 1.4S. Rockets which can produce fiery projectiles for a distance more than 15 m are classed into Division 1.3G, however, these can also be shipped as 1.4S if packages are overwrapped with wire mesh to restrain projectile action. In the US, by contrast, consumer fireworks are normally classed as 1.4G, while display fireworks as 1.3G; a minor amount of pyrotechnics not sold to consumers are considered theatrical or special-effects fireworks and are classed as 1.4S.

Table 189 Accidents in US manufacturing of military pyrotechnics, 1950 – 1976

Source of initiation	Percent
friction	54
impact	11
static electricity	8
pressure	6
heat	2
chemical reactions	2
electric (other than static electricity)	2
undetermined	15

Many of the reactions that fireworks can undergo are not fully understood. One major difficulty arises from the fact that a pyrotechnic composition is a physical mixture of two or more chemical compounds. Chemical compounds are reproducible entities. That is, if a laboratory makes an experiment with compound "A," and a second laboratory repeats the experiment with compound "A," the results should very closely agree, provided both have used substances of high purity. Physical mixtures, however, are not very well reproducible and depend on grain size, grain shape, the state of homogeneity of the mixture, etc. Moisture sorption from the air is often a particular difficulty, since a number of pyrotechnic substances are sensitive to moisture. Self-heating reactions are known to occur (e.g., with mixtures of ammonium perchlorate and magnesium powder), but systematic self-heating studies have rarely been made.

Some substances used for manufacture of pyrotechnic devices also show unwanted ignition problems as a pure material, before mixing or preparation. Such substances include very finely divided metals, which can self-heat due to oxidation from atmospheric oxygen.

Of even greater safety concern than oxidative self-heating is a propensity of some molecules to break up into two fragments, since no reaction partner is required for this. Most pyrotechnic oxidizers show endothermic decomposition characteristics, that is, external energy input is required for the decomposition to occur. But some exhibit exothermic decomposition; for example, potassium chlorate is subject to the exothermic decomposition reaction:

$$2\,KClO_3 \rightarrow 2KCl + 3O_2$$

Acids, sulfur, and metal oxides (e.g., manganese dioxide) tend to accelerate such decomposition of potassium chlorate and, in some circumstances, can cause an unwanted explosion. Mixtures of potassium chlorate with red phosphorus explode readily upon the slightest friction or impact[1755]. Mixtures of potassium chlorate with Al or Mg powders are likewise highly hazardous. If potassium chlorate is combined with sulfur, a hazardous mixture can result, and such combinations have been banned in England since 1894. Chapman et al.[1743] studied these mixtures, in various proportions, to determine the ignition temperatures. They found the lowest value, 120ºC, for 8 – 10% sulfur. Using their technique, pure $KClO_3$ showed ca. 150ºC, while pure S was not measured. Tanner[1744] explained the mechanism of the reaction between sulfur and potassium chlorate. He noted that problems rarely occur with crude sulfur. This is the raw product and it has a purity of 99.8 to 99.9%, but still possess a residual surface coating of asphalt. This surface impurity minimizes the oxidation at the surface. If refined sulfur ('flowers of sulfur') is used, reactivity with

$KClO_3$ becomes much greater. The refined product, when exposed to moist air, forms a layer of polythionic acid on the surface. The latter is $H_2S_nO_6$, with *n* typically being 3 to 5. Its role is the liberation of SO_2, which is needed in the further reaction steps. The whole sequence is:

$$H_2S_nO_6 \rightarrow H_2SO_4 + SO_2 + (n–2)S$$
$$SO_2 + 2KClO_3 \rightarrow 2CLO_2 + K_2SO_4$$
$$2ClO_2 + 4S \rightarrow 2SO_2 + S_2Cl_2$$

The last two equations represents a chain propagation reaction with respect to SO_2, since its presence is needed for initiation, but afterwards more is produced than is consumed. The first equation is the chain initiation step. Some sulfur compounds, e.g., thiourea, exhibit similar sensitivity as do formulations using elemental sulfur[1745]. Tests for mixtures of potassium chlorate with 15 – 25% thiourea indicated ignition temperatures of 142 – 153ºC, vastly lower than for the two constituents, neither one of which was ignitable, by itself, below 400ºC. In the opinion of Hardt[1436], the single most-hazardous and unpredictable pyrotechnic mixture which is in current-day use is the one contained in toy caps, which comprises potassium chlorate, red phosphorus, and a calcium carbonate inhibitor.

Since potassium chlorate has intrinsic stability problems and requires care in preparation and use, where possible, it is recommended that preparations use potassium perchlorate instead[1746]. But despite these concerns, it must be noted that it is one of the most common ingredients in the manufacture of matches, so there is no doubt that mixtures using it can be designed to be safe.

Mixtures containing both ammonium and chlorate salts are classified as forbidden explosives by the US Dept. of Transportation due to their hazard. This is because an exchange reaction can occur in which ammonium chlorate is formed. For example, ammonium nitrate and potassium chlorate could react to form some ammonium chlorate. The latter is an unstable compound and could lead to an unwanted explosion.

Mixtures containing titanium and black powder can readily be ignited by impact (for Ti > 20%) and by friction (for 3% < Ti < 70%); this sensitivity has led to accidents in the UK[1745].

Firecrackers, as originally produced in China, traditionally contained 80 mg of black powder, but currently are more likely to contain flash powder than black powder[1747]. M80 was a Dept. of Defense designation for firecrackers in military applications. The composition is potassium perchlorate (64%), aluminum (22.5%), sulfur (10%), and antimony sulfide (3.5%).

Snap caps (also called snappers, pop-pop snappers, bang snaps, etc.) are tiny noise-making devices consisting of a few grains of gravel dipped in a silver compound and hand-wrapped in cigarette paper. They have only a limited burning capability, since they contain a minuscule amount of pyrotechnic composition which is usually silver fulminate, $Ag_2(CNO)_2$. For snap caps sold in California, regulations[1748] require them to contain no more than 0.25 grams of gravel impregnated with no more than 1 mg of pyrotechnic compositions; they also require that the paper wrapping be fire-retardant, but there does not seem to be any evidence that regular paper could ignite upon discharge of the device. In retail sales, snap caps are commonly packed in small cardboard boxes holding about 50 individual devices, cushioned with sawdust.

In an interesting study, Conkling[1749] devised twenty different tests for examining whether snap caps could ignite clothing. The tests included throwing an entire boxload of 50; burning a display pack of 40 boxes on a barbecue grill; dropping display packs from a height of 15 feet onto a brick surface; discharging poppers into a gasoline-covered metal pan; throwing single and multiple poppers against dry vegetation. No ignition could be obtained of any combustible target presented in these tests. For clothing testing, Conkling wrapped 50 poppers in a T-shirt, placed it on a brick and hammered it; this was done twice, with and without packaging sawdust around the poppers. No charring or ignition of the fabric resulted. McLain[1750] additionally points out that (a) snap caps are not capable of igniting vapors of diethyl ether nor of petroleum ether (a solvent of relatively low flash point); (b) heating snap caps for 2 hours in an oven at 75ºC does not set them off; and (c) no burns or injury results even if one goes off while being handled.

A series of tests examining whether common consumer fireworks would ignite shredded newspaper has been reported[1751]. Bottle rockets, Jumping Jacks, smoke bombs, and sparklers caused ignition; firecrackers (32 to 38 mm long varieties) and snap caps did not.

A number of pyrotechnic compositions are subject to spontaneous combustion if moisture enters a mixture. For instance, zinc powder and $CaSi_2$ both react exothermically with water.

Conkling provided ignition results for some pyrotechnics[1752]. Table 191 shows spark sensitivity, as measured in the BM apparatus[1753], while Table 192 gives ignition temperatures as measured in a DTA apparatus. Conkling[1754] also reported ignition energies for a number of potassium nitrate/metal and potassium perchlorate/metal compositions, where the metals used were flake aluminum and magnesium/aluminum (50/50) alloy. In this study, the ESD ignition energies obtained were much lower, typically 15 – 500 mJ, with the actual value depending greatly on the physical details. Adding 10% sulfur lowered some values further. Conkling concluded that electrostatic discharge from a person might suffice to explode some of these compositions.

Table 190 Hazard rating scheme for pyrotechnics proposed by McLain

Mix	Uses	Class
$KClO_3$, Al or Mg, Sb_2S_3	salute mix	6A
$KClO_3$, Al, S	salute mix	6A
$KClO_3$, Al or Mg, As_2S_3	salute mix	6A
$KClO_3$, C, S	chlorate explosive	6A
$KClO_3$, S, sand	torpedo mix	6A
$KClO_4$, Zr	'instantaneous' squib; relay powder	6A
$KClO_3$, C, S	squib	6B
$KClO_4$, Al or Mg	photoflash	6B
$KClO_4$, Al or Mg, $Ba(NO_3)_2$	photoflash	6B
$KClO_4$, Al or Mg, S	flash and sound; firecrackers	6B
$KClO_4$, Al or Mg, Sb_2S_3	flash and sound; firecrackers	6B
$KClO_4$, Al or Mg, As_2S_3	flash and sound; firecrackers	6B
PbO_3, Zr or ZrH_4	'instantaneous' squib	6B
PbO_3, Ti	'instantaneous' squib	6B
PbO_3, B	'instantaneous' squib	6B
Pb_3O_4, Zr	'instantaneous' squib	6B
Pb_3O_4, Ti or B	'instantaneous' squib	6B
$PbCrO_4$, Ti or B	'instantaneous' squib	6B
picrate + oxidizer	whistle mix	6B
gallate + oxidizer	whistle mix	6B
salicylate + oxidizer	whistle mix	6B
KNO_3, C, S	black powder	5A
KNO_3, B	igniter	5A
PbO_2, Si	millisecond delay	5A
$KClO_4$, Mg	tracer mix	5B
$Ba(NO_3)_2$, Mg	tracer mix	5B
$BaCrO_4$, Zr	heat mix	5B
Fe_2O_3, Zr	starter mix	5B
$(C_2F_4)_n$, Mg	IR flares	5B
$KClO_3$, $NaHCO_3$, S, dye	military colored smoke	4A*
$KClO_3$, lactose, dye	military colored smoke	4A*
$BaCrO_4$, Mg	igniter	4A
$PbCrO_4$, Mg, Si	flash igniter	4A
$KClO_3$, flour, dye	fireworks colored smoke	4B*
$KClO_4$, Mg, $Ba(NO_3)_2$	military stars	4B
$KClO_4$, Mg, $Sr(NO_3)_2$	military stars	4B
$BaCrO_4$, B	igniter and delay	4B
$NaNO_3$, Mg, binder	illuminating flare mix	4B
$KClO_4$, Mo	millisecond delay	4C
$KClO_4$, salts of Sr, Ba, Na, powdered Al, Mg, or Zn, gums	fireworks stars	3A
Fe_2O_3, Zr, Ti	flash igniter	3B
Fe_2O_3, Ti	starter	3B
$KMNO_4$, Ag	smoke puff	3B
KNO_3, C, S (unmilled)	candle or rocket mix	2A
PbO_2, Si, CuO	starter	2A
Pb_3O_4, Fe_2O_3, Si, Ti	starter	2A
$K_2Cr_2O_7$, B, Si	delay	2A
$KClO_4$, Al, $Sr(NO_3)_2$, dextrin	colored sparklers	2A
KNO_3, Al, Fe_3O_4, C, Si	smoke starter	2B
$KMnO_4$, Sb	delay	2B
$KMnO_4$, Mn	delay	2B
$NaNO_3$, C, sugar	starter	2B
$K_2Cr_2O_7$, Ti	delay	2C
Fe_2O_3, Al, Ni	Pyronol torch	2D
$KClO_4$, Zr/Ni alloy, $BaCrO_4$	grenade delay	1A
$KClO_4$, $Sr(NO_3)_2$, S, sawdust	fusee mix	1A
Pb_3O_4, Si, kaolin	delay	1A
$KClO_4$, W, $BaCrO_4$	long delay	1B
$KClO_4$, Cr, $BaCrO_4$	delay	1B
$KMnO_4$, W, $BaCrO_4$	long delay	1B
PbO, Si	delay	1B
$CaSi_2$, Fe_3O_4	food can heater	1B
Bi_2O_3, B, $K_2Cr_2O_7$	delay	1B
$BaCrO_4$, $PbCrO_4$, Mn	D16 delay	1C
Bi_2O_3, B	delay	1C
Fe_3O_4, Al	thermite	1D
$Ba(NO_3)_2$, Fe, Al, dextrin	gold sparkler	1D
ZnO, Al, C_2Cl_6	HC smoke	1D

* In bulk and unpressed in containers; when pressed and in containers, downgrade to Class 2.

Table 191 Electrostatic spark discharge sensitivity of several pyrotechnic compositions

Composition	Min. energy (J)
red stars: potassium perchlorate, strontium carbonate, red gum, charcoal	0.69
green stars: potassium perchlorate, barium nitrate, red gum, charcoal	1.6
silver cone fountain: potassium nitrate, charcoal, sulfur, flitter aluminum	1.8
gold comet: potassium nitrate, charcoal, sulfur	2.2
black powder	3.1

Table 192 Ignition temperatures for several pyrotechnic compositions

Composition	Temp. (°C)
Chinese firecracker composition: potassium chlorate, sulfur, aluminum	150
potassium chlorate, sugar	200
black powder	340
flash powder: potassium perchlorate, sulfur aluminum	450
gold sparkler: barium nitrate, aluminum, dextrin, iron filings	> 500

Table 193 Ignition temperatures for stoichiometric binary pyrotechnic mixtures

Oxidizer	Fuel	Temp. (ºC)
potassium chlorate	aluminum	785
	antimony	295
	charcoal	335
	colophony (rosin)	335
	graphite	890
	Iditol (phenol formaldehyde resin)	345
	lactose	195
	magnesium	540
	shellac	345
	sulfur	220
potassium nitrate	aluminum	890
	charcoal	415
	lactose	390
	magnesium	565
	sulfur	440
potassium perchlorate	aluminum	765
	charcoal	460
	lactose	315
	magnesium	460
	sulfur	560

McLain proposed[1750] that the hazard of pyrotechnic mixes be classified by a two-way matrix scheme. The sensitivity to ignition of a mix is denoted by a letter, A being most sensitive and D being least sensitive. The destructiveness to be expected if an ignition occurs is denoted by a number for 6 (most hazardous) to 1 (least hazardous). The physical hazards associated with the numeric ratings are:

6 Detonates from open burning. Small critical mass. Capable of sympathetic detonation.
5 Relatively unconfined burning (e.g. in open-end mixers or a small building) can produce low-order but destructive explosions.
4 Bulk powder subject to deflagration progressing to low-order explosion.
3 Large and quick fireball.
2 Fire hazard to personnel.
1 Slight fire hazard to building and surroundings.

Pyrotechnic mixes as classified by McLain are given in Table 190.

Shidlovskiy[1755] reported ignition temperatures for a number of binary oxidizer/fuel mixtures (Table 193). Practical formulations, of course, generally involve more than two reactants, but these simplest mixtures give some idea of trends to be expected. The mixtures were all in ratios so as to be oxygen-balanced, but other details of the preparations were not specified. The results show that—when combined with most fuels—potassium chlorate produces much lower ignition temperatures than the other oxidizers. Apart from compositions involving metal or graphite dusts/powders, the other values are fortuitously similar to ignition temperatures of pyrolyzing solids, despite an entirely dissimilar mode of ignition. Shidlovskiy also reported that the ignition temperature of black powder is 310ºC, but details were not given.

Radiant heating in different parts of the spectrum for ignition of pyrotechnics was attempted by de Yong and Lui[1756] using a xenon lamp source and spectral filters. With samples being 30 mg pills, they reported either non-ignitions or enormous minimum heat fluxes (hundreds of kW m^{-2}) and the authors were not able to explain these results. With non-pyrotechnic solids, such results would suggest an insufficiency of mass for generating a combustible fuel/air mixture. But since pyrotechnic compositions supply their own oxidizer, the interpretation is not clear.

A large compilation of ESD data was presented by McIntyre[1740]. Values typically ranged from 0.225 J to greater than could be measured in his apparatus (11.02 J). The exceptions are given in Table 194.

Table 194 Pyrotechnic compositions found by McIntyre to be exceptionally easily ignited by electrostatic discharge

Composition	ESD energy (J)
67% potassium perchlorate, 33% titanium	0.005
65% potassium perchlorate, 32% antimony sulfide, 5% gum arabic	< 0.05
64% potassium perchlorate, 22.5% flake aluminum, 10% sulfur, 3.5% antimony sulfide	< 0.1

McLain conducted hot-spot ignition tests on a number of pyrotechnic compositions by touching an incandescent Pt-Ir wire to the surface of the test substance. Their results were described in terms of power needed for supplying the hot wire. For 9 compositions tested, all of the results were within the range of 2.5 to 6.3 W. He also obtained ignition temperatures which ranged from 450 to 630ºC. These values are all quite high and reflect the difficulty in igniting a solid at a single hot point. For radiant ignition, he reported an ignition temperature of 321ºC for black powder, but few

Table 195 Pyrotechnic compositions tested for cookoff behavior

Composition	Test results
aluminum (20%), copper oxide (80%)	no damage
aluminum (15%), lead chromate (85%)	no damage
aluminum (40%), ammonium nitrate (60%)	no damage
aluminum (60%), potassium perchlorate (40%)	destroyed
magnesium (50%), sodium nitrate (50%)	mild damage in one test, destroyed in another
magnesium (39%), sodium nitrate (50%), EVA (11%)	mild damage
magnesium (61%), Teflon (34%), Viton (5%)	no damage
potassium chlorate (22%), lactose (21%), kaolin (12%), orange dye (45%)	no damage

other values were provided.

Pyrotechnic compositions using gum arabic are subject to spontaneous combustion due to bacterial activity. Bacterial action on aging gum arabic causes generation of acetic acid, which ignites the fuel/oxidizer composition[323].

Pyrotechnics are mostly insensitive to cookoff. That is, if confined within a pipe bomb or similar arrangement, a violent explosion will occur with only a few types of compositions. de Yong and Redman[1757] tested a wide variety of compositions and obtained the results indicated in Table 195.

Radio and audio equipment

The flammability of radio and audio equipment in the US is governed by one of three UL standards, as described in Table 196. This table summarizes the requirements for non-high-voltage equipment. The requirements for the latter (i.e., televisions receivers) are discussed under *Television sets and computer monitors*. UL 1270[1758] has been withdrawn as of January 2002 and, in 2006, UL 1492[1759] will also be phased out. UL 6500[1760] is derived from IEC 60065[1761], but the flammability requirements are completely different. The requirements for enclosure materials in the UL standards are not necessarily evident from the wording of the standard and have been subject to interpretation by the Laboratory. For UL 1270, the V-2 specification only refers to "required parts" and generally manufacturers have been permitted to use HB materials. It is understood that according to UL 1492 and UL 6500, enclosures are more likely to be made of V-2 materials, even though the wording of UL 6500 is not especially restrictive.

Table 196 Main flammability provisions of UL standards for plastic parts in radio and audio equipment

Component	UL 1270	UL 1492	UL 6500
enclosure	V-2, 12 mm flame, 20 mm flame[a]	V-2	V-2
any plastic housing that has a separate interior fire enclosure for line-voltage parts			HB
in contact w. live electric parts in circuits		V-2	V-2
all other plastics	HB		HB

[a] – the 12 mm flame and 20 mm flame tests, per UL 746C are equivalent only to an HB, not a V-2 performance

Railroads

The propensity for railroads to cause vegetation fires was studied by Cowles[1762]. He found the major categories to be:

- hot brake shoes
- engine exhaust particles
- journal boxes
- welding and grinding associated with track repairs.

Brake shoe fragments have been found up to "several inches long." Composition brake shoes were found less likely to act as ignition sources than older cast iron shoes. Exhaust particles have been found to be cast up to 12 –15 m away from the engine. Journal box overheating was found to be on the decline, since roller bearings have been replacing journal bearings. In addition, Cowles found that railroad rights-of-way create a microclimate more conducive to ignitions. Temperatures are higher and humidities lower and, in addition, wind effects are sometimes increased. DeBernardo[1763] identified the following as additional, relatively minor ignition sources associated with railroads:

- engine-powered equipment (e.g., bulldozers) and tools (e.g., chainsaws)
- signal flares
- smoking materials.

Hot particles are ejected due to wheel slip against the track. But these long, slim steel shavings normally fall down at the track, do not get propelled significant distances, and are rarely a cause of fire[1764]. Dynamic braking involves running the traction motors as generators and dissipating the produced power in a resistor grid. A resistor grid can fail by explosive arcing and shower molten metal up to 30 m or so.

Rayon

Walker et al.[197] studied self-heating of viscose rayon in an oven test and saw critical self-heating at around 169ºC oven temperature for a 6 L cylinder. They also refer to a fire in Germany where staple rayon ignited when trapped in a drier for a long time at 150ºC. See also: *Fabrics*.

Refrigerators

Compared to other types of electric appliances, refrigerators are more likely to have metallic construction and minimal number of heat-producing parts. Common causes of ignition of refrigerators include: (a) failure of the appliance cord or receptacle; (b) failure of the defrost heater igniting combustible materials; and (c) failure of the condenser motor or attached wiring, igniting lint or nearby combustibles. A drain pan made of ABS is commonly found under the condensor and it can get ignited in the latter case. An unusual ignition source led to a rash of fires in Europe and Japan during the mid-1990s. This anomaly was due to faulty starting devices that were fitted to compressors by a manufacturer holding a large share of the market for refrigerator compressors[1765]. These small devices, made largely of plastic, contain a Positive Temperature Coefficient (PTC) thermistor which is wired in series with the starting winding of the compressor. At room temperature, the device represents a low resistance, but the resistance increases greatly when

hot, reducing the current to the starting winding. The failures were found to involve largely older units which were sitting in moist environments. The ceramic thermistor element itself would overheat and ignite the surrounding plastic, from which a jet of flame would spurt out, since plastic was being pyrolyzed at the ceramic/plastic interface and had to develop an overpressure before it could escape to the atmosphere. Even though the PTC device is only about 40 g (Color Plate 139) a sizable fire could result (Color Plate 140). A laboratory study[1766] confirmed the tendency of these PTC devices to fail in an arc-tracking mode. The problem was solved when the manufacturer redesigned the starting devices in 1999.

Since the adoption internally of policies to eliminate ozone-destroying chemicals, changes to refrigerants have been made. In Europe, small refrigerators and air conditioners nowadays commonly use isobutane as the refrigerant. Propane has also been used in various countries as a refrigerant fluid. These are notably flammable hydrocarbons, but a systematic fire incident study is unavailable. A research study[1767], however, has been published that examines a number of leak scenarios, accompanied by measurements of concentrations. In many cases, even very small (5 g min^{-1}) leaks produced gas concentrations that were within the flammable range, at least at some location within the room and during some time period after the start of the leak.

Rice husks

The self-heating of rice husks was examined by Raj and Jones[1768], who conducted small-scale oven cube tests. Their results were: ρ = 140 kg m^{-3}; E = 105 kJ mol^{-1}; P = 46.31.

Roofing materials

The minimum flux for piloted ignition of asphalt roofing shingles has been reported as 12.6 kW m^{-2} in one study[1769], 13.0 in a second[1998], and 14.5 kW m^{-2} in third[1770]. For fiberglass shingles, a value of 23.0 kW m^{-2} was found[1770]. When the shingles are in an orientation other than horizontal, the asphalt tends to melt and slide off the shingle at a heat flux[1998] of about 2.5 kW m^{-2}, which is much lower than needed for ignition; consequently, the sloughed material may ignite later in a different place.

When roof coverings on flat roofs are installed, the two ways that this is most commonly done is by (a) torch-down, or (b) mop-applied operations. Torch-down is an operation where a special propane torch is used to apply a flame to the underside of a single-ply roofing membrane, which is thereby partly melted and consequently adheres when laid down upon the substrate. The roofing membrane is designed so that it does not catch fire itself, but ignition problems commonly arise with the substrate. The membrane is usually torched-down onto an insulating board which may be wood fiber or 'perlite.' Wood fiberboard is readily ignited in a smoldering mode, and this has often proven to be unnoticed by workmen[1771]. "Losses from torch-related fires have indeed been enough for some insurance companies to stop underwriting torch-applied modified bitumen jobs"[1772]. While perlite is an inorganic, mineral material, the boards described as 'perlite' in the construction industry, in fact, contain a sizeable proportion of wood fibers. Thus, they are also subject to smoldering ignition. Since many hours may elapse before a smoldering fire becomes visible, a fire watch is mandated for torch-down roofing operations. NFPA 241[1773] mandates a 1 h fire watch. It is not at all clear that any material that was ignited in a smoldering mode would necessarily exhibit observable combustion within a 1 h period, and some jurisdictions sensibly require a longer time period.

Conventional multi-ply, built-up roofing is mop-applied, whereby a mop soaked in hot asphalt is used. In normal used, the mop temperatures are not sufficient to ignite common combustibles. However, asphalt-saturated mops have been known to undergo spontaneous tion[1773,1774]. This usually requires that the mop strings be spread out to allow access to air, and overt flaming usually does not happen in the absence of wind. Generally, petroleum products show a low potential for self-heating, but the high temperature at which the mop is used (and may be left at the end of the day) is presumably the reason why runaway self-heating is possible. Moore[262] noted that tarred felt is subject to spontaneous combustion, but did not provide details.

Roofers' tar kettles occasionally are cleaned of the carbonaceous deposits that build up along their inner surfaces. Spontaneous combustion incidents have occurred in the process where thin layers of the built-up material were partly dislodged by water streams and left overnight[1775]. It was speculated that a reactive char had formed in these layers that proceeded to oxidize upon exposure to oxygen. Other modes of ignition for tar kettles have been discussed by Hill[1776].

Polymeric-membrane type roof coverings are applied by an electric heat 'welder;' smoldering ignition case histories have not been reported with these systems.

Sanding machines

Tests have been reported on a disc-type sanding machine to see if sanding certain materials might result in incendive sparks[1006]. When carbon-steel or mild-steel pieces were held against the sanding wheel, sparks caught on fluff were able to ignite the fluff in a smolder mode. The fluff was obtained from a sanding operation on a rubberized-cotton conveyor belt. Sanding of carbon-steel pieces on a coarse disc was also able to ignite methane/air atmospheres. The potential for sanded material removed from painted surfaces to self-heat is discussed under *Paints, dyes, and related substances*.

Saunas

Saunas in the home are popular in the Nordic countries. Their interiors are constructed of wood planks and modern-day saunas typically employ an electric heater, thus ignitions commonly reflect some malfunction, misuse, or misinstallation of the heater. The high humidity environment makes reliability of electrical devices especially challenging. Finnish statistics[1777] indicate that saunas are the second-most likely electric appliance to result in fire, preceded only by electric stoves.

Shredded materials

Radiant ignition tests on excelsior (long shavings of softwood) were performed by Garg and Stewart[1778], and their results are discussed in Chapter 7, as illustrative of porosity effects. Peacock and Vaishnav[1106] tested numerous types of Easter grasses (artificial decorative grass) for ignitability with a wooden match. They found that untreated cellulosic grasses ignited readily, but ones treated with FR agents did not ignite at all. Polypropylene grasses—both untreated and treated—ignited with some difficulty. The untreated ones burned to completion, while the treated ones did not sustain ignition after the match flame went out.

Siding, plastic

Luzik[115] reported on the radiant, piloted ignitability of fiberglass-type (glass-reinforced polyester) siding that is used for industrial buildings. The basis weight of the product was 1870 g m^{-2}. Using the Factory Mutual apparatus, data obtained are shown in Table 197. Flame spread testing on the same siding indicated exceptionally rapid flame spread rates.

Table 197 Ignition times for fiberglass siding

Heat flux (kW m^{-2})	Ignition time (s)
20	141
30	55
40	33
50	22
60	15

Dietenberger[1779] measured the radiant, piloted ignitability of 0.9 mm thick PVC siding. For a heat flux of 55 kW m^{-2}, t_{ig} = 18 s was found. Flaming ignition was also obtained at higher heat fluxes. But for heat fluxes below 55 kW m^{-2}, the product shrank to a charred mass, then the charred mass ignited much later. At 35 kW m^{-2} (the lowest flux tested), t_{ig} was 380 s.

Silane and chlorosilanes

Silane (SiH_4) and chlorosilanes (SiH_nCl_{4-n}) are widely used in semiconductor manufacturing. Under certain conditions, silane is pyrophoric in air and can autoignite at temperatures as low as ca. –100ºC[1780]. Pyrophoric ignition can occur even at very low oxygen concentrations. At room temperature, but for very low oxygen concentrations, it was found that pyrophoric ignition controlled by the silane/oxygen ratio[1781], assuming that the remainder is nitrogen. Over the range of 0 to 0.3% oxygen, it was found that pyrophoric ignition occurs if the silane/oxygen ratio (vol/vol) exceeds 9.5.

It has also been found that pyrophoric ignition occurs when silane is discharged at *low* velocities into air, but not at high ones. Silicon dioxide and water are the primary combustion products when burning in air; however, under some conditions hydrogen is formed. Water vapor acts as an inhibitor of the silane + oxygen reaction. For mixtures which are not pyrophoric, the flammability limits of silane are ca. 1.37 – 96%. For highly rich mixtures, the reaction is exothermic decomposition instead of oxidation. If silane is added to a hydrogen/air mixture, even small amounts can increase hydrogen's flammability limits to about 1.37 – 98%. It is considered that silane/air mixtures can detonate, but in most case histories it is not clear if detonation or merely very rapid deflagration had occurred. Silane reacts with halocarbons and halogenated refrigerants, so use of a halon extinguisher would lead to exacerbation instead of extinguishing of the fire. At high temperatures, silane can undergo decomposition reactions in which elemental silicon, in the form of a fine powder, is the reaction product. Such silicon powder is highly flammable in air. When the latter burns, SiO is formed as one combustion product. SiO itself is pyrophoric in air. Other explosion studies have been reviewed[1782].

Monochlorosilane is not commonly used, but mixtures of chlorosilanes which include monochlorosilane are pyrophoric in air, and this tendency has been exploited as one technique of skywriting[1780]. Dichlorosilane (SiH_2Cl_2) has flammability limits of 4.7 – 96% and is not pyrophoric in air. Its AIT using ASTM E 659 method is 44ºC for a worst-case quantity of 4.5 mL used. For less rich samples, the AIT rises rapidly, being 120ºC for 0.5 mL. Upon contact with certain contaminants, a violent explosion can result even from tiny quantities of dichlorosilane. Its minimum spark ignition energy is 0.0154 mJ and it is considered liable to detonate under certain conditions. Trichlorosilane ($SiHCl_3$) has flammable limits of 7.0 – 83%. The AIT is 182ºC. Britton[1780] points out that the statement made in the 1988 edition of Sax's **Dangerous Properties of Industrial Materials** concerning trichlorosilane (and also dichlorosilane) being pyrophoric is erroneous, as is the very low AIT published there. The minimum spark ignition energy for trichlorosilane is 0.017 mJ.

Hsieh et al.[1783] obtained AIT values for a series of substituted trichlorosilanes: ethyltrichlorosilane ($C_2H_5SiCl_3$) 405ºC, *n*-propyltrichlorosilane ($C_3H_7SiCl_3$) 360ºC, isobutyltrichlorosilane ($C_4H_9SiCl_3$) 329ºC, octyltrichlorosilane ($C_8H_{17}SiCl_3$) 221ºC, vinyltrichlorosilane ($C_2H_3SiCl_3$) 263ºC, phenyltrichlorosilane ($C_6H_5SiCl_3$) 544ºC, and 3-chloropropyltrichlorosilane ($ClC_3H_6SiCl_3$) 396ºC. Some

substances can decompose to produce silane. One such substance, triethoxysilane, $HSi(C_2H_5O)_3$, has been documented to cause fires or explosions in a disproportionation reaction that produces SiH_4[1784]. The Uniform Fire Code has a special standard[1785] governing installations using silane.

Since germanium and silicon have rather similar chemical properties, *germanes* tend to behave similarly to silanes, although they have not been studied much since the semiconductor industry no longer has much use for germanium. Digermane, Ge_2H_6, may ignite at room temperature[1407].

Silicon

Grosse and Conway[1382] found an ignition temperature of 775ºC for silicon powder burning in pure oxygen at 1 atm. Silicon dust in air[1394] can be ignited at 775ºC. Matsuda presented extensive explosibility studies of silicon dusts conducted in several Japanese test methods, along with the Hartmann apparatus[1786].

Silicone fluids and polymers

Silicones are compounds which have a structure with a backbone comprising silicon and oxygen atoms. Common formulations are of the type $(CH_3)_3Si\text{-}O\text{-}Si(CH_3)_2\text{-}O\text{-}\ldots\text{-}Si(CH_3)_3$. The radiant ignition of silicones has been extensively studied[1787]. For liquids, the minimum heat flux for ignition varies with the viscosity (or molar mass) of the fluid, ranging from 0.5 kW m^{-2} for a fluid with viscosity of 1×10^{-6} m^2 s^{-1}, to 15 kW m^{-2} for a fluid with a viscosity of 1×10^{-3} m^2 s^{-1}. Unmodified elastomers can show $\dot{q}''_{\min}$ = 11 to 14 kW m^{-2}, but with FR additives this can rise to ca. 20 kW m^{-2}. Hshieh has published large tabulations of the flash points[1788] and LFL values[1789] for silicone compounds.

Skins and leathers

The ignition of leather-upholstered furniture is discussed under *Upholstered furniture and mattresses*. Leather shrinks appreciably when exposed to heat and this can affect its ignition performance, both in testing and under actual fire conditions. Smoldering ignition of leather can occur from dropped cigarettes. A case is reported where transition to flaming took about 5 hours[304]. Animal skins can self-heat by a mechanism similar to that described under *Wool*. Self-heating fires in tanneries have been attributed to a combination of use of neatsfoot oil in conjunction with chromium-based preparations, which promote catalytic oxidation[1790].

Soaps

Soaps are alkali metal salts of long-chain monocarboxylic acids. It has been reported[40] that soap flakes used for clothes washing are prone to self-heating. This is primarily of historical interest, since synthetic detergents, instead of soap flakes, are used these days for clothes washing. Soap flakes made from olive oil are known to self-heat[40]. In addition, cases are known of spontaneous combustion of soap flakes containing only saturated fatty acids; the latter was attributed to over-drying, followed by exothermic uptake of moisture.

Sodium chlorate and sodium chlorite

Sodium chlorate, $NaClO_3$, is an oxidizer which is used in matches, oxygen candles, explosives, leather tanning, weed killing, and bleaching. It is susceptible to exothermic decomposition upon shock or heating. Explosions can occur due to accidental mixing with sugar, which may not be distinguished by eye from the white-powder appearance of sodium chlorate. If involved in fire, sodium chlorate is likely to explode[1791]. Sodium chlorate is highly reactive with organic substances and many inorganic ones. A mixture of sodium chlorate and nitrobenzene has sometimes been used as a terrorist explosive; home-made bombs are sometimes constructed using a sodium-chlorate based weed killer and sugar[1792]. A Japanese fire has been attributed to a reaction between a pesticide powder containing sodium chlorate with another powder containing sulfur[1793]. The S.S. MAHIA exploded in 1947 when its sodium chlorate cargo was ignited by unknown means[1794]. An explosion destroyed a ship in 1971 when vegetable oil seeped into a cargo of sodium chlorate[26]. Thomson reviewed a number of other accidents[1792]. Many properties of sodium chlorate are similar to those of potassium chlorate. HSE subjected sodium chlorate to a large assortment of reactivity and explosion tests and surveyed the literature for other findings[1795]. The results indicated that the substance, alone or in combination with fuels, is not particularly explosive, but can detonate if combined with a fuel under some circumstances. It is not fully clear why it has been somewhat hard to cause explosions with sodium chlorate in laboratory testing, but unfortunately not so hard in various accidents. Aggressive measures (e.g., detonators) have *not* been needed in the latter. Using an Accelerating Rate Calorimeter and assuming first-order decomposition kinetics, kinetic constants E = 300 kJ mol^{-1}, $A = 1.9\times10^{20}$ s^{-1}, and Q = 284 kJ kg^{-1} were found, but the actual order of the reaction was considered to be closer to 1.44. Another kinetics study showed E = 297 kJ mol^{-1} and $A = 2.3\times10^{18}$ s^{-1}. The material is only modestly reactive until rather high temperatures are reached, with around 550ºC needed for rapid reaction. Rust, in addition to fuels, promotes violence of reaction.

In most respects, sodium chlorite, $NaClO_2$, exhibits similar reactivity and combustion/explosion hazards. Sodium chlorite is primarily used as a bleaching agent. Sodium chlorite is non-explosive by itself, but a mixture of sodium chlorite and sawdust has been found to be about as sensitive as TNT to detonation in the drop-weight test[26].

An case of friction-caused ignition has been documented by Yallop[323]. A man playing tennis suddenly found his leg enveloped in flame. It turns out that the tennis court had been treated with sodium chlorate for killing weeds, and his rubber-soled shoes caused enough frictional heating to create a reaction between the rubber (fuel) and sodium chlorate (ox-

idizer). In another case[3], a shoe contaminated with sodium chlorate weed killer exploded when a welding spark fell onto it.

Sodium dithionite

Sodium dithionite (sodium hydrosulfite, $Na_2S_2O_4$) may ignite due to a violent reaction with water[3]. In addition, it is a self-heating powder which shows a complicated reaction, even though no atmospheric oxygen is consumed in the reaction. Henderson and Tyler[1796,1797] studied the material in hotplate tests and found a critical temperature for self-heating of ca. 188ºC for a 5 mm layer. They also found that it exhibits two exothermic peaks and cannot correctly be treated by standard self-heating theory. Additional studies have been reported by Reddy et al.[1798] Decomposition, fire, or explosion accidents involving sodium dithionite are not rare—EPA[1799] catalogued 17 such incidents in one 11-year period. Many of these started when water leaked into a container where sodium dithionite was stored.

Solder and soldering irons

Carroll[1800] attempted to ignite excelsior, wood shavings, oily rags and newspaper with molten solder and reported that they could not be ignited, even with 'large quantities' of solder being poured on them.

Soldering irons can easily cause smoldering ignitions of smolderable substances. Tests have also been reported on soldering irons placed against wood boards[271]. A unit running at 325ºC was not able to ignite a wood board, but an iron at 425ºC caused flaming in 3.5 h when the smolder front broke through to the back of the board. Using a soldering iron at 400ºC caused a paper towel to start flaming in 12 minutes[1801].

Soots, lampblack, other 'blacks'

Soots of various sorts include lampblack (made by burning low-grade heavy oils in limited oxygen conditions), carbon black (from natural gas or liquid hydrocarbons), vegetable black (made by burning and grinding plant matter), and bone black (prepared by anaerobic heating of animal bones and hoofs). These substances are less common today, but were widely used in the 19th century in paints and as clarifying media. In the 19th century literature[1802] their self-heating propensities have commonly been discussed. Some of the problems apparently were when oils prone to self-heating would be mixed into a porous soot material. Even apart from acting as substrates, the porous nature of soots suggests that their self-heating propensities might share some similarities with those of charcoal. They share the trait that, when freshly made, they must be 'weathered' if they are not to be excessively prone to self-heating[943]. The latter is simply a process whereby volumes smaller than would dangerously self-heat are exposed to air, allowed to undergo exothermic sorption of moisture and oxygen onto the large surface area of the substance, then cooled off.

Soybeans

Soybeans and soybean products are highly prone to self-heating. Self-heating at lower temperatures is due to microbial heating. At higher temperatures, exothermic reactions are due to oxidation and thermal polymerization of their unsaturated oils, in which they are exceptionally rich[38]. When charred soybeans are encountered, agronomists distinguish two types of damage. *Binburned* soybeans are those which attained elevated temperatures only due to microbial heating, while *fireburned* soybeans have been chemically oxidized or polymerized[1803]. Soybeans which sustained a maximum temperature less than 195ºC are considered to be only binburned. The distinction is important because insurers may pay for fireburned product, but not binburned. A UL study examined the self-heating and dust explosion hazards of various forms of soybean products[34].

Spas

A number of fires in spas were found in New Zealand. Investigation[1804] revealed two common modes of failure: (1) An air lock develops in the heater unit in a product designed so that the heating element and the temperature high-limit switch are both located at the top of the pipework. The heater then overheats and the plastic casing ignites. (2) Water flow stops due to pump failure. This condition is supposed to be sensed by a pressure switch, which is intended to disconnect the heating element if the pressure drops, but the switch may not respond due to an air lock condition or a piping blockage.

Stearic acid

Despite its very low iodine number (1 – 3), Monakhov[1076] reports that this fatty acid can self-heat when fibers are coated with it.

Steel turnings

Steel turnings generated in machine shop operations, also other processes which produce steel in finely divided form can lead to self-heating problems. Water is ineffective towards the extinguishment of such fires, since at high temperatures iron reacts with water to produce hydrogen gas, which itself is flammable.

Styrene

Styrene (C_8H_8) is an organic liquid that is used to manufacture polystyrene and related plastics. By itself, it has a propensity to exothermic polymerization, while in the presence of oxygen an explosive interpolymeric peroxide may be produced[3] if styrene is heated to 40 – 60ºC. The critical temperature of a railcar load of styrene is at or below room temperature[1805]. The reactivity problems are normally avoided by adding a small amount of 4-*tert*-butyl catechol as an inhibitor. The latter is effective only if there is some dissolved oxygen in the liquid styrene, thus industrial storage schemes often involve an aeration procedure. Styrene vapor is liable to autoignite in the presence of polymerizing

liquid, but the vapor is relatively unreactive if no liquid phase is present[1806].

Sugar

Refined sugar melts at 160ºC and decomposes (caramelizes) at 170-180ºC. The sugar itself does not ignite, but the decomposition products of caramelized sugar ignite at about 460ºC. Raw sugar, however, is stated to be able to burn directly[1807]. Refined sugar has not been found to be prone to self-heating[1808].

Sulfur

Sulfur (S_8) is a unique substance with several physical forms ('allotropes') and with varied chemical traits. With the right chemical partners, it is able to act as either fuel or oxidizer. For pyrotechnic purposes, only the α allotrope is used. Furthermore, the grade known as "sulfur flour" is normally specified. It is a highly pure form, crystallized from molten sulfur. Sulfur purified by sublimation—termed "flowers of sulfur"—is a highly pure form, but its purity makes it much more reactive than the crude grade[1746]. Hazards of sulfur reaction with potassium chlorate are discussed under *Pyrotechnics*, above.

Sulfur liquefies at 95 – 120ºC, depending on the allotrope[90]. All forms have a boiling point of 444.7ºC. Liquid sulfur is easily ignited in air, but there is not good agreement on the exact values of the flash point nor the AIT. Urben[3] reports that the flash point of pure sulfur is 188ºC, but impure sulfur may ignite at 168ºC. Fedoroff[90] reports an open cup flash point of 207ºC, closed cup 227ºC, and an autoignition temperature of 232ºC. Shimizu[1809] reports an AIT of 223ºC. Lancaster reports an AIT of 260ºC for flowers of sulfur and 190ºC for sulfur flour. Liquid sulfur accidents most commonly occur in the course of transportation accidents involving the molten material. Molten sulfur is transported at 150 – 200ºC, thus in a road tanker collision[1810] when spillage occurred, the sulfur ignited "immediately."

The major causes of sulfur dust fires are: autoignition, static electricity, metallic sparking, bare electricity-carrying wires, and open flames[90]. Sulfur dust has a reported minimum ignition energy of 3 mJ, which is a very low value for dusts. Sulfur dust is so easily ignitable from electrostatic discharge that ignitions have occurred simply during sieving of the dust[1811]. The flammability limits for the dust are approximately 35 – 1400 g m^{-3} . An AIT of 167ºC in the Godbert-Greenwald furnace has been reported for dust clouds of 20 µm particles[1812].

At elevated temperatures, sulfur reacts violently with many metals, especially if they are in finely-divided form—aluminum, copper, iron, tin, zinc, etc. Incandescence, ignition, or explosion can take place. These reactions are exploited in some pyrotechnic and propellant formulations, but will be a hazard if unexpected. Water can initiate some of these reactions with metals. With some metals, e.g., copper, iron, magnesium, or mercury, an exothermic reaction can take place starting from room temperature[3]. Reactions with some non-metals—boron, phosphorus, lamp black—that lead to spontaneous combustion can occur at room temperature. In general, sulfur can react exothermically with almost any element apart from gold, platinum, iridium and the inert gases. In 1822 a sulfur-bearing soil was identified which was prone to spontaneous combustion[1813]; this was attributed to reactivity with metals. Sulfur in its mineral form used to be known as *brimstone*, suggesting the reactivity that occurs. A fire occurred when paper sacks containing sulfur and sodium nitrite were placed into a rubbish container[3]. NFPA has a standard, NFPA 655[1814], which gives advice on the safe handling of sulfur.

Surge suppressor MOV devices

Surge suppressors are any devices which are intended to reduce the damaging potential to electronic equipment of excessively high voltage power line spikes. The most common and lease expensive variety relies on metal-oxide varistors (MOVs). These devices are sacrificial and will fail (and may self-ignite) after absorbing a certain amount of excess-voltage spikes. Olson[1815] conducted testing showing that the failure can result in the device dropping down to about 15 Ω resistance, which is sufficient to cause ignition of plastic casings, but does not result in circuit breaker tripping. Open flaming resulted in less than 5 min when an MOV device exhibited such medium-resistance failures. Their failure modes have also been described by Goodson[1816]. One way of minimizing the potential for such fires is by installing a TCO close to the MOV device. UL has a standard on the construction of MOVs[1817]. Expensive surge protectors usually use other technologies that do not entail sacrificial behavior or potential fires.

Surgical tubing

A number of accidents occur in hospital operating rooms where oxygen is supplied to a patient via tracheal tubing and the tubing ignites. Wolf et al.[1818] measured the AIT of several tubing types in a 100% oxygen atmosphere (Table 198).

Table 198 Ignition temperatures in pure O_2 for several types of surgical tubing

Rubber	AIT (ºC)
PVC	428
PVC*	397
red rubber	371
silicone rubber	381
* industrial, not surgical, grade	

Tanks

It has been pointed out in endless instructional materials (e.g., Smart[347]) that tanks which have held an ignitable liquid cannot be safely readied for welding, brazing, etc. by simply running water through them, although this does not stop accidents of this type from occurring. Liquid residue is likely to remain, and it takes very little residue for the LFL to be attained, especially if the temperature is raised. NFPA

327[1819] describes safe ways that steam cleaning or chemical cleaning can be accomplished.

ASPHALT STORAGE TANKS

Ignitions in asphalt storage tanks can occur due to a wide variety of causes, as described in a recent survey[1820]. Many occur due to faults of heaters, welding operations, ignition sources being present near the tank's vapor vent, etc. However, a number of fires and explosions have been found perplexing, since overt causes were not identified. Asphalt storage tanks are specialized in that they must be heated to 190 – 230ºC in order to keep the asphalt sufficiently fluid. The closed-cup flash point of asphalt is normally around 260ºC, so if tank temperatures are significantly lower than that, explosions should not result. Investigations have shown[1821] that flash-point testing of asphalts can often produce unconservative results due to losses of light fractions in sampling. Explosions have occurred even in tanks that are normally inerted (with nitrogen, steam, or flue gases), since opening to air is required in cleaning operations. Industry experience has led to a rule of thumb that oxygen concentrations should not be dropped below 5%, since anaerobic conditions promote the formation of pyrophoric iron sulfides[1820]. Because elevated temperatures are needed for normal tank operation, it was hypothesized that self-heating might be causing the unexplained ignitions, but tests indicated minimal exothermic activity in the temperature region of interest[1822]. Instead, it was concluded that the smoldering-type reactions that occur on a tank's inside surfaces decrease the available oxygen and foster anaerobic conditions suitable towards the generation of pyrophoric iron sulfides. An actual ignition can then result when the tank is opened up, additional oxygen becomes available, and it can react with the iron sulfides. A mathematical model has been proposed[1823] for treating the self-heating aspects, but it has not been validated. The best preventive measure is considered to be regular tank cleaning, which will not allow significant deposits to build up that could form iron sulfides. See also: *Iron sulfides*.

Tar (wood)

Pine tar has a flash point of 54ºC and has a self-heating propensity[1542]. Its boiling range is 240 – 400ºC.

Telephones, cellular

In recent years it has sometimes been claimed that use of cellular telephones can cause ignitions in flammable-vapor atmospheres, e.g., at filling stations. Tokyo Fire Department conducted extensive experiments[1824] to simulate such a scenario. Six models of cellular telephones were operated by a remote control device in an atmosphere containing 12% methanol vapor. No ignitions occurred during this series of experiments which included 924 outgoing transmissions, 800 incoming calls, and 3000 times of removing (with phone energized in standby mode) and reattaching the phone's battery. A further test series involving 1000 removals and reattachments of a phone's battery in a carbon disulfide/air mixture, also did not cause ignition. These findings are not surprising, in view of: (1) The devices use a low voltage battery, typically in the range 3 – 6 V. These are very marginal voltages for igniting a flammable mixture by means of a contact spark. For a resistive circuit, Figure 43 in Chapter 4 suggests that a current of around 25 A would be needed; this level of current is simply unavailable from a battery of a cellular telephone. Due to physical size reasons, the device cannot have large capacitors or inductors. For a capacitive circuit, Figure 39 in Chapter 4 again indicates that ignition is not expected, due to absence of either a huge capacitance or a large voltage. Similar data for an inductive circuit are shown in Figure 41. (2) While not specifically designed for flame arrester action, nonetheless the close spacings within a cellular telephone suggest that even if an incendive spark could be generated, there is likely to be an effectively flame-trapped path between it and the exterior environment.

Television sets and computer monitors

In Japan, informal statistics showed that consumer complaints of fire hazards from television sets far exceeded those for any other category of electrical appliance[1825]. It was also found that the two highest causes of fires with television sets involved (1) high-voltage transformer failures, and (2) cracks occurring at soldered joints. A study examining TV fires throughout Europe[1826] identified predominant causes:

Main causes

- bad solder joints
- worn power switches
- failures of heavy (over 10 g) components subjected to line voltage or high voltage and to electromechanical stress
- overheating caused by an imbalance in the thermal expansion coefficients of circuit components.

Secondary causes

- line-voltage filter capacitors, possibly breaking down due to power supply instability
- power transformer
- cathode ray tube, including coil and high voltage connector
- power cord.

The study pointed out that failures of soldered joints often involve a crystallization which takes place gradually over time; however, the exact metallurgical process is not well understood.

In Denmark, a study was made on used TV sets of 3 – 20 years which had *not* been involved with fire[1827]. In nearly 1/3 of the specimens, faults were found which could lead to a subsequent fire. The faults included cracked insulation on electric wires (29% of the sets), defective solder and cold solder joints (29%), incipient breakdown of components (9%), and signs of overheating (6%). In addition, 14% of the sets were found to have such high levels of dust accumulation that safety concerns were registered. The authors

concluded that the dust hazard was indirect—if ignited, a dust layer would cause such a short-lasting fire that components of the TV set would not be ignited. Instead, the hazard is because of the hygroscopic properties of dust layers, which can cause leakage currents in moist environments and consequent fires due to arc tracking. The Danish study also reports that bad solder connections have been noted in actual TV fires, but the investigations have not been broad enough to draw statistical conclusions.

Table 199 Characteristics of ignition sources used by Troitzsch

Ignition source	Mass (g)	Flame height (mm)	Burn time (s)	HRR (W)
methenamine pill	0.15	5 – 10	80 – 105	40 – 55
small candle (tea candle)	14	10 – 15	NA	30
regular candle, 21 mm Ø	53	15 – 30	NA	60
rag soaked in isopropanol	413	200 –300	210 – 240	1600 – 1900
isopropanol, 200 mL	160	600 – 800	120 – 180	2700 – 4000
NA – not available				

A US study[855] done in the 1970s identified that, at that time, the top two ignition sources were high-voltage transformers and switches/relays/plugs/sockets. Laboratory tests on TV chassis (i.e., excluding cabinets) showed that local ignition sources failed to propagate fire through chassis components. The authors also studied the effects of dust, lint, grease, and fluff deposits in televisions sets. They found that the heat of combustion of this material averaged 20 MJ kg^{-1}. Testing showed that the material only exhibited transient flashing and did not lead to sustained burning. Another study on circuit malfunctions in television sets conducted in the 1970s[1828] showed that temperatures of 200 – 500ºC are often found on circuit components (e.g., resistors) under malfunction conditions. At the higher end of this temperature scale, however, temperatures tend not to be sustained, since a fuse blows or the part burns out and circuit continuity is lost. The authors, however, were apparently not aware of the arc tracking potential identified by the Danish researchers.

When a fire impinges on a picture tube, the outcome may be an implosion, but it may simply crack and fill with air and not be a violent event. If an implosion does occur, however, it may impel burning material from the immediate vicinity of a burning TV set onto other objects, thereby causing secondary ignitions. A UK test[1829] demonstrated that the implosion of a TV picture tube led to the ignition of a couch about 1 m away.

In the US, in the early 1970s CPSC found that 20,000 TV fires per year and 800 life-threatening ones comprised an "unreasonable risk." UL responded by requiring enclosures rated V-2 under the UL 94 test in 1975, V-1 in 1977 and V-0 in 1979. By 1994, the number of TV fires had dropped to 1300/year. The requirement pertains only to fire enclosures, not necessarily external cabinetry, although typically TV sets in the US market have had V-0 rated cabinets. The same does not hold true for rear-projection televisions, where the outer cabinet is normally not considered a fire enclosure and which consequently is only HB-rated. UL standards governing TV sets changed through the years. Originally, it was UL 492, then UL 1410. UL 1492 is currently in effect, but in 2006 it will be withdrawn and re-

Table 200 Test results on television sets and PC monitors

ID	UL 94 rating	Thick. (mm)	Meth. pill	Small candle	Reg. candle	Rag on top	Rag below	200 mL alcohol	Notes
TV-01-28-28	HB	3.2	Y						
TV-03-25	HB	3.2	Y						p
TV-04-25	HB	3.2	Y						p
TV-02-25	V-2	2.6	Y						F/O
TV-06-14	V-2	2.0	Y						
TV-09-25-JAP	V-2	2.4	N	N	N	N	N		
TV-07-25-US	V-2[X]	3.0	N	N	N	N	N	N	
TV-05-25	V-1	2.9	N	N	N	N	N		
TV-08-25-US	V-0	3.2	N	N	N	N	N	N	
PC2	V-2	3.2	N	N	N	N	N	Y	c
PC4	V-1	3.2	N	N	N	N	N	Y	c; s
PC3	V-0	2.4	N	N	N	N	N	Y	c
PC5	V-0	3.0	N	N	N	N	Y		v
PC1	V-0	3.1	N	N	N	N	Y		a

Y – ignited
N – did not ignite
(blank) – not examined
[X] – slightly short of V-2 performance
F/O – room flashover
a – ABS
c – PC/ABS
p – polystyrene
q – unknown material
s – especially severe fire
v – PVC

placed by UL 6500[1760] which is already in use. The latter two standards are not just for TVs but also encompass radio/audio equipment, while UL 6500 further adds musical instrument equipment. The flammability of wood cabinets, except for the back panel, is unregulated. Computer monitors are treated by UL separately under UL 1950; this has been described above under: *Computer and information technology equipment*.

In Europe, the pertinent standard is IEC 60065[1761], and that standard currently has no flammability requirements for enclosures, provided that certain high voltage and other electrical components have internal protection. Traditionally, manufacturers there produced televisions with V-0 or V-1 rated cabinets. But a campaign against fire-retardant agents organized by political/environmental groups caused this to change and by 1995 most manufacturers had removed FR agents from their plastics. Furthermore, revisions were made to IEC 60065 to take away even the HB requirement which existed earlier. Fire statistics indicate this disparity in ignition performance: the number of television fires, per million TV sets, is about 30 times higher in Europe than in the US[1830]. UL 6500 is largely based on IEC 60065, but the flammability requirements are different and UL 6500 retains a requirement for V-0 rated cabinets. Eventually, it is projected that IEC 60065 and IEC 60950 (on computer equipment) will be merged into a document that is patterned after ECMA-287[1831].

An extensive study of fire tests on TV sets and computer monitors was run by Troitzsch[1832], who presented a graded series of ignition sources to full-size test articles (Table 199). But if a specimen failed a smaller ignition source, larger sources were not tested. He also conducted tests using the UL 94 series. The results are given in Table 200. Unless specified, all cabinets were made of high-impact polystyrene (HIPS). The data show that a V-1 rating is needed so that reasonable resistance to the smallest flaming ignition source, the methenamine pill, would be obtained. With regard to differences between V-1 and V-0 ratings, the results are unclear. In general, it appears that the UL 94 series is not a consistent determinant of performance when actual end-use articles are presented with realistic flame sources. The ratings in class V-2 are especially glaring, since it seems that almost any level of performance might be found in products rated V-2. As a safety minimum, the test results do indicate that TV sets, computer monitors and probably other appliances with plastic housings rated V-0 can be expected, to a high probability, to resist flaming sources the size of candle flames, or smaller.

Similar testing was also done by Simonson[1833]. She tested three computer monitors using V-0 rated enclosures, one HB-rated, and one that failed to meet V-2 but was not tested for HB requirements. She also tested a computer keyboard meeting V-0 requirements. The V-0 rated equipment did not propagate fire when tested with a match, a candle, and a small wad of burning paper. The monitors rated HB (or lower) led to a severe room fire when ignited with a match.

Tents

The ignitability of tent fabrics is commonly tested by the industry standard CPAI 84[1834]; ASTM D 4372[1835] is similar. Tent fabrics are also tested by NFPA 701[1836], which is not similar.

Textile wall coverings

Harkleroad conducted LIFT tests on a series of textile wall coverings[1837]. These are products that visually resemble carpets, but are not identified as such by the manufacturing industry, due to different testing and marketing requirements. The majority of the specimens showed very similar ignitability properties. Minimum heat fluxes for piloted ignition were 19 – 26 kW m^{-2}, computed T_{ig} values 440 – 490ºC, and effective thermal inertias of 0.7 to 0.9 $kJ^2\ m^{-4}\ s^{-1}\ K^{-2}$.

Thatch

The effect of an FR treatment on the ignition of roof thatch was explored by Eboatu et al.[1838], who studied four different grasses commonly used in Nigeria for thatching roofs, along with calcium phosphate-calcium sulfate monohydrate as the FR agent. Non-FR specimens could be ignited with a cigarette lighter flame instantaneously. By applying the FR treatment at a 16 g L^{-1} concentration, ignition times were raised to over 20 s. The ignition times of the FR specimens depended strongly on the type of grass used.

Thermostats

See: *Electric appliances and electronic equipment: High-limit switches* and *Electric outlets, plugs and connections: Miscellaneous connection failures*.

Tinder

Nowadays, the term 'tinder' is applied to any lightweight, easily ignitable materials. But until the 19th century, tinder was a vital component of making fire, and it came in one of two variants[1364]. The most useful type was known by the French term *amadou*, and was prepared from one of two fungi, *fomes fomentarius* or *phellinius igniarius*. These fungi grow on trees, and the tinder was prepared by treating with lye, then beating and rubbing. Sometimes *amadou* was treated with chemicals to make it more flammable. *Amadou* was sometimes also known as *punk*. A less desirable tinder was made from carbonized linen or cotton.

Tires and wheels

Tests by the Ontario Fire Marshal's office[1839] showed that an automobile tire could be ignited by a match, applied to the bottom of the tire for only 8 s. However, the small-flame ignition of tires will depend on the chemical composition of the rubber and the geometry of the tread, and some tires may be difficult to ignite. The same authors also demonstrated that flames from newspapers, a grass fire, and a gasoline fire can ignite tires. In some early tests, the Fire

Research Station[1840] determined that the minimum heat flux for ignition of rubber tires is 16.5 kW m^{-2} under piloted conditions and 40 kW m^{-2} for autoignition. The latter value is probably inaccurate, for the same reason that early FRS data on the autoignition of wood are systematically high. Jurng et al.[1841] tested the ignitability of small (0.7 g) chips of tire rubber in a high-temperature convective furnace and found an AIT of 527ºC. Brookes[1846] found the AIT of truck-tire rubber to be 422ºC at 1 atm, but this dropped to 240 – 270ºC at 6.9 atm. White[1842] tested a tire sample using the ICAL apparatus and obtained an AIT of 550ºC when exposed at 60 kW m^{-2} and 600ºC when exposed at 40 kW m^{-2}; he also reported a piloted ignition temperature of 396ºC when exposed at 25 kW m^{-2}.

Fires of heavy-equipment (truck, bus, etc.) tires[605] tend to occur due to failed wheel bearings, brake dragging, or excessive rubber flexing when the tires are underinflated or the vehicle is overloaded. Flaming is prone to break out when the vehicle has stopped, since at that point the convective cooling stream of the air flowing by has stopped. Due to the extremely high loads, ignition from friction can be a serious problem for aircraft tires. High ambient temperatures and underinflation of tires are the most common factors leading to ignition or explosion. For example, a DC-8-61 charter flight leaving Jeddah, Saudi Arabia on 11 July 1991 sustained a tire fire due to underinflation, with a loss of 261 persons on board. Investigation suggested that pressures recorded in tire maintenance records had been altered[1843]. Tire fires due to overinflation have also been reported[1844]. Another loss due a tire fire was on 31 March 1986 when 166 persons died in a Mexicana Airlines B-727-264 which was departing the Mexico City airport. In this incident, a tire exploded due to overheating of the left main-gear brake. Investigation revealed that the tire had been inflated with air rather than nitrogen, making an internal tire ignition easier. In some cases, tire fires lead to only minor losses. Emergency braking of a Delta Air Lines Flight 54 at Honolulu Airport on 7 August 1997 started a tire fire. Only minor injuries were sustained and the airplane was repaired.

A small fraction of tire explosions involve combustion effects and not simply a physical explosion. A number of such incidents been reported in heavy construction and mining equipment when the equipment accidentally contacts a high-voltage power line[1845]. Current flowing to the ground through tires—which have an appreciable conductivity due to carbon black—causes heating and pyrolysis of the rubber material, leading to a combustible atmosphere being formed in the void space which then explodes.

Several explosions have been caused by welding truck rims without first having removed the tire. In one incident, the tire was neither deflated nor removed before the welding commenced. An explosion took place about 3 – 5 minutes after the work was finished, killing two workers[1846]. It was determined that the tire was lubricated with a compound, based largely on alcohol, that had a low flash point (56ºC). Laboratory reconstruction determined that the high temperatures created by the welding were sufficient to ignite a quantity of the lubricant that was on the inside of the rim. The burning lubricant then heated other portions of the inside of the wheel and pyrolyzed enough tire rubber to create a flammable mixture not in direct contact with the burning zone. The mixture later ignited and this caused the explosion. In another incident, welding was conducted on a truck rim where the tire had been deflated, but not dismounted. The tire was then reinflated and an explosion occurred shortly thereafter. The investigation revealed that rim temperatures were high enough (over 700ºC) as a result of the welding that pyrolysis started once the tire was remounted. Explosion was possible because increasing the pressure lowered the AIT of the pyrolysate. Pyrolysis-caused explosions need oxygen, and tires that are nitrogen filled (aircraft, F-1 race cars) are not subject to this mechanism.

Numerous fires or explosions have occurred due to the use of a product to repair and repressurize a punctured tire. These products used to consist of an aerosol can containing a flammable gas (a non-flammable gas is used in current products) and leak sealant substance. This creates a flammable atmosphere within the tire, and accidents generally coincided with a further repair operation being performed on the tire.

Tire shavings are subject to spontaneous combustion[1847]. Shredded tires can self-heat and lead to fire, if stacked in sufficient quantities. This has happened both in production facilities and in places where tire shreds are used as a road fill. In one case investigated by the author, a facility was producing tire shreds by grinding tires into pieces of about 12 mm size. The grinding process raises the temperature of the rubber and exit temperatures were about 115ºC. A pile about 1.2 – 1.8 m high and 3.0 – 3.6 m wide was stacked. About 4-½ days later fire erupted. Humphrey[1848] reported four cases of thermal runaway in production facilities, but these did not lead to open flaming. The stack heights in these were much higher (6 – 15 m), but the materials were more coarse (50 – 100 mm size). He also reports two cases of fires in road fills and one case of thermal runaway that did not lead to flaming. Stack heights ranged from about 2 m to 13 m. Apart from the basic exothermicity of the oxidation of rubber (see *Plastics: Foams and elastomers*), Humphrey suggests that several additional factors can be involved: (1) Oxidation of iron. Iron will be present unless all fragments of steel in the tire can be removed from the scrap. (2) Microbial oxidation of sulfur (which is a component of tire rubber) and iron. (3) Microbial oxidation of petroleum products, possible if contamination is present. Microbes may also play a role once sufficient heating has taken place so that a pyrolysate liquid flows out of the pile. It has also been observed[1849] that rainfall may promote the thermal runaway of tire scrap piles. This can enhance both rusting of the iron and biological reactions, the latter possi-

bly due to flow of nutrients. The problem of self-heating of road fill made from shredded tires was considered to be sufficiently serious that an industry recommendation[1850] has been published urging heights no more than 3 m, along with minimizing the amount of finely-ground material and limiting oxygen ingress. Limiting the height (and not stacking hot material) is essential. However the roles of particle size and oxygen access are more debatable. Hermetic sealing would prevent oxidative self-heating, but this is unlikely to be practical. Ventilation increases the availability of oxygen but also carries heat away from the reaction. Thus, its role is complex and it may not be possible to give a reliable rule-of-thumb. Similarly, up to a certain point, making the material finer increases the surface area and increases the access to air. But further reduction in diameter of the particles can reduce the air flow through the pile and limit self-heating due to limiting oxygen availability.

Toasters

Toasters may ignite kitchen cabinets or other nearby combustibles if a food item is overheated and begins to flame. Commonly, toasters are equipped with a bimetallic thermostat that is supposed to operate the pop-up mechanism. Occasionally, the mechanism fails. The consequences of failure have been documented to be particularly severe in the case of jelly-filled snack foods. Flames of 0.5 – 0.75 m high have been documented to emanate from the toaster under these conditions[1851]. According to Fitz[1852], to provide adequate safety against unwanted ignitions, toasters should have both a bimetallic thermostat and a timing device. Either of these devices must activate a trip-free mechanism that will de-energize the toaster in the event the bread carriage is jammed in the down position. The timing device is needed because the bimetallic thermostat may not sense sufficient heating if one of several heating elements becomes de-energized, yet the product being toasted continues to be heated to flaming by the remaining elements.

Town gas

Town gas is manufactured gas, derived from coal or oil. It used to be common in the UK until the 1960s and was also used in some locations in the US prior to World War II. The primary constituents are CO and H_2, with small amounts of saturated hydrocarbons, and very small quantities of CO_2 and unsaturated hydrocarbons. A typical composition included about 40 – 60% H_2 and 10 – 25% CO; in the US, the fraction of CO was less, 6 – 12%. The explosive range of US-type town gas[1853] was considered to be 6 – 36%. Up until quite recent times, a number of Bunsen burner-type fire tests (e.g., by the Federal Aviation Administration) used a mixture called *B-gas*. This was a standardized version of town gas, comprising 55% H_2, 18% CO, 24% methane, and 3% ethane.

Turpentine

Turpentine is hazardous because of its very low LFL, which is 0.7%[4] and its tendency towards self-heating when dispersed (e.g., when applied to rags). In an early study[1197] of various paints, varnishes, and oils, turpentine was found to have the highest iodine number (206), the second-highest heat of reaction (234 kJ kg^{-1}), and the greatest tendency to react with oxygen from the air.

Unsymmetrical dimethylhydrazine

UDMH, $C_2H_8N_2$, is a liquid fuel for rockets; its ignitability characteristics have been studied by the Bureau of Mines[1854]. Its LFL is 2.3% and the LTL is –15ºC. The UTL is nearly identical to its boiling point, 63ºC. For UDMH vapor, the LFL is 1.9% at 100ºC and 1.8% at 200ºC. The UFL at 100ºC is 92%, rising to 99% at 200ºC. The AIT is 250ºC at ambient pressure, dropping to 148ºC at 14.6 atm. According to the Bureau of Mines, UDMH is not prone to autodecomposition and is insensitive to initiation by shock. The main hazard is associated with the very wide flammability range.

Upholstered furniture and mattresses

NFPA estimates[1855] that ignition of upholstered furniture or mattresses comprises some 33% of the fire fatalities in the US. While US fire deaths have dropped dramatically in the last 25 years, the proportion of deaths attributed to upholstered furniture ignitions has additionally decreased. In 1976 it was estimated[1856] that this fraction was 54%. CPSC estimates[1857] that US fire deaths for upholstered furniture ignited by cigarettes, cigars and similar non-flaming sources dropped from 1150 during 1980 to 340 during 1998. Similarly, flaming-ignition fire deaths dropped from 110 to 80.

Upholstered furniture and mattresses (for purposes of examining the ignitability behavior, these two categories of goods are commonly treated as one category) ignite in practice from four main types of sources:

(1) smoldering cigarettes
(2) small flames (children playing with fire; electrical faults)
(3) radiant heat (too close to heaters; on-going room fire)
(4) burning brands (houses exposed to wildland fires; wartime activities; on-going room fire)

Regulatory concern has mostly focused on #1 and #2. Source #3 may be important in individual fire histories, but has not been seen as an important factor in overall loss statistics. There is a sizable amount of research data available on the radiant ignition of upholstered composites, however. Very little research is available on #4.

SMOLDERING AND IGNITION FROM CIGARETTES

Certain types of both fabrics and foams used in upholstery are susceptible to smoldering. Cigarettes are the primary smoldering ignition source for furniture materials, although other causes (e.g., glowing electrical connections) are possible. Ignitability from cigarettes is largely correlated to presence of cellulosic materials in the construction. As with most fire properties of upholstered furniture materials, it normally requires the testing of a realistic, composite as-

sembly. Individual testing of fabric or padding layers may not give predictive results, although several test methods are based on individual-component testing. The ignitability of upholstered items from cigarettes has been reviewed extensively by Babrauskas and Krasny[1858], Krasny[1859], and Krasny, Parker, and Babrauskas[1860].

Damant studied a large amount of data collected from composite mockup tests conducted on over 1200 commercial furniture samples in California[1861]. His salient conclusions were:

- Thermoplastic fabrics tested over untreated cotton battings showed a 15% probability of cigarette ignition.
- Cellulosic fabrics tested over untreated cotton battings showed a 94% probability of cigarette ignition.
- For thermoplastic fabrics tested over untreated cotton battings, the probability of cigarette ignition is inversely related to fabric weight. Fabrics over 400 g m^{-2} showed a 0% probability, while those under 300 g m^{-2} showed a 24% probability.
- Fabrics that are of mixed cellulosic/thermoplastic fibers tend to respond according to the fiber proportion. Fabrics having a 50/50 mix showed a 50% probability of ignition when tested over untreated cotton battings.
- When tested over a variety of paddings (market mix, but predominantly polyurethane foams), thermoplastic fabrics showed about a 5% probability of ignition. There was no significant effect of fabric weight. On this point, industry sources[1862] estimate that, for current-day materials, the probability is actually below 2%.
- When tested over a variety of paddings (market mix, but predominantly polyurethane foams), cellulosic fabrics showed results that depended on fabric weight. Fabrics over 440 g m^{-2} had an 86% probability of ignition, fabrics of 300 – 440 g m^{-2} had 57%, while those under 300 g m^{-2} had a 43% probability. Industry sources[1862], however, consider that other factors (e.g., the type of weave) can be controlling and that fabric weight alone is a poor predictor of ignitability.

In another study, Damant[1863] showed that the presence of a fabric is essential for a cigarette to induce smoldering in a smolderable polyurethane—no ignitions could be achieved without a fabric. Even in tests where a cigarette was placed directly on polyurethane foam blocks, then covered on top with fabric (as opposed to being placed on a fabric/foam composite) ignitions were very rare. Conversely, it is easy to get cellulosic fabrics smoldering even if the substrate (e.g., fiberglass) is noncombustible[1864]. For untreated cotton fabrics, smolder propensity is directly related to its basis weight, but the phenomenon is essentially go/no-go, and the maximum basis weight that can be used without leading to smoldering ignition is also dependent on the substrate. In one study[1865], it was found that fabric weights > 280 g m^{-2} led to smoldering when used over a fiberglass substrate, weights > 350 – 400 g m^{-2} led to smoldering over polyurethane foam, and weights > 400 g m^{-2} led to smoldering over FR treated cotton batting. When smoldering did occur, smolder rates of 150 – 300 mm h^{-1} were typically found.

The high ignition propensity of heavy-weight cellulosic fabrics have been identified to be almost entirely due to the presence of alkali metal ions in the material; well-washed cellulosic fabrics do not show a propensity to ignition from cigarettes, regardless of weight[1860].

Wool fabrics, which are neither cellulosic nor thermoplastic, show low probability of cigarette ignition. Paddings made from other natural fibers (hemp, coir, etc.) have similar smoldering tendencies as cotton batting. Resistance to cigarette ignition is typically imparted to cotton batting by treating with 8 to 12% boric acid crystals. Polyester padding is naturally resistant to smoldering; latex foam is highly smolder prone. Some grades of leather upholstery are resistant to cigarette ignition[1866], although this material has received only very limited study.

It is perhaps surprising that some polyurethane foams can smolder because smoldering requires the material to char and not to melt—otherwise melting would destroy the large pore area needed for a smolder front to propagate. It turns out that when presented with a low heat flux, some polyurethane foams can char. There is a narrow range of heating conditions over which this happens, with lower fluxes leading to extinction and higher fluxes leading to melting. The topic was studied to a limited extent by Rogers and Ohlemiller[1867,1868].

Most cigarette ignition testing is done under quiescent air flow conditions. Limited test results (discussed in Chapter 7) indicate that modest air flow velocities increase the propensity to smoldering ignition. Almost all testing for the cigarette ignitability has been done using actual cigarettes. Cerra and Ramsay proposed[1869] that statistical variations in the burning of cigarettes could be avoided by use of a Nichrome wire glowing igniter, and Ortiz-Molina et al.[1870] used exactly such an arrangement. Opposite to Damant's conclusion, they found that the most smolder-prone foam (of three tested) was able to smolder without any fabric covering. Their least smolder-prone foam required a heavy-weight cotton fabric to smolder. Another study[1871] also demonstrated that some polyurethane foams can be induced to smolder in the absence of a smolderable cover fabric, but in this case the heater had to be applied by a long time, 3000 s.

The transition from smoldering to flaming of upholstered furniture items has been studied statistically by Babrauskas[1872]. From a database of 102 full-scale tests on chairs, sofas, and mattresses, it was found that 32% burned up or went out without erupting in flaming, 64% transitioned to flaming, with 4% undetermined or manually extinguished. Of the items that did transition to flaming, the

mean time for flaming to erupt was 88 minutes, with the total experimental range being 22 to 306 min. These studies were all based on testing in an open laboratory environment. If furniture starts smoldering in a tightly closed space, it may smolder for a very long time.

Test results show that furniture composites which will not get ignited from a cigarette placed open on the surface, may get ignited if the cigarette is covered by a bedsheet[1873]. This is the reason that the standard test method for mattresses (see Chapter 7) involves use of a sheet over the cigarette. Bed sheets are rarely used on top of upholstered chairs or sofas, thus testing the latter is normally done without a bedsheet. However, pillows, 'throws,' and other accessories are sometimes used in a living room, and a cigarette slipping under one of these articles would create a condition not anticipated by standard test methods.

THE POSSIBILITY OF SAFER CIGARETTES

The ignition of upholstered furniture from cigarettes requires that the cigarette be ignition-capable, and that the upholstered furniture item be ignitable. The bulk of research and regulation, on a worldwide basis, has been addressed to second requirement. But since ignitions could also be avoided if cigarette characteristics were altered to make them no longer competent ignition sources, this alternative was explored in the US during two research projects. Both projects were specifically legislated by Congress, with the overall responsibility falling to CPSC and the technical research portion being organized by NIST. Both projects included economic studies, which are not within the scope here. Actual ignitability results obtained from research under the Cigarette Safety Act of 1984 were in the form of two technical reports[313,1874] and two papers[1875,1876]. The first study identified that there were negligible differences among commercial US cigarettes in regards to their ability to act as competent ignition sources. After this was found out, NIST turned to examining patented and specially-fabricated cigarettes. It was concluded that cigarette design aspects leading to a lowered propensity to ignite furnishings are:

- lower packing density of tobacco
- lower paper permeability
- a smaller diameter, e.g., 21 and not 25 mm
- avoidance of citrates in the paper wrappers
- use of a filter tip.

The type of tobacco was found not to have a significant effect. Some cigarettes having these design features were prone to self-extinguishing in air (which might be objectionable to smokers) but others were not. In addition, many of the patented designs were found to be promising.

The primary results from NIST studies done under the Fire Safe Cigarette Act of 1990 emerged as a report documenting the development of two test methods[1877], along with two papers[1878,1879]. The two methods developed in the study were:

(1) A Mock-up Ignition Test Method that uses three different weight standardized cotton-duck fabrics and a polyurethane foam padding. The least ignition-susceptible fabric also uses a layer of thermoplastic film underneath the fabric.
(2) A Cigarette Extinction Test Method that uses layers of cellulose filter paper as the smolderable substrate. The three levels of test comprise 3, 10, or 15 layers. The method is easier to conduct and to standardize than the one using simulated furniture constructions.

The study also identified 4 experimental cigarette types that rarely ignited the most-difficult-to-ignite composite and had tar, nicotine, and CO yields similar to best-selling commercial cigarettes. Hirschler conducted a follow-on study that demonstrated the relation between Mock-up Test results and results with an extensive collection of 500 fabrics[1880]. The US tobacco industry vigorously opposed the proposed test methods, generally on the grounds that they found imperfections in the procedures[1881-1885]; however, no alternative test methods have been put forth by the industry. Most regulatory fire safety tests are designed to eliminate the worst-performing products, not to guarantee a minimum level of performance. The latter is rarely possible, since there are too many end-user variables that are not under the control of the product maker. The tobacco industry position, summarized briefly, was that no test method should be promulgated since none can always correctly predict the in-use behavior. In 2002, the Cigarette Extinction Test Method was standardized as ASTM E 2187[1886].

The NIST Mock-up Ignition Test Method is based solely on using polyurethane foam as the padding material, since this is the most common padding used in the US. In the UK, however, latex and cotton batting paddings still see fairly common use, thus Paul[1887] conducted extensive tests with various cigarettes using the British BS 5852[1888] mockup rig and a variety of padding materials. He also reported on tests with beds. His 'improved' cigarettes were normal marketplace, slim types, so the improvements offered over ordinary cigarettes were found to be modest.

In early studies, it had often been tacitly assumed that if a cigarette is designed so that—in air—it would cease burning if not puffed, then such a 'self-extinguishing' cigarette would also not ignite furniture materials. Unfortunately, research proved otherwise, so actual testing by placing cigarettes on furniture remains necessary[1889].

In July 2000, the Philip Morris company started producing fire-improved Merit-brand cigarettes by using a patented cigarette paper, PaperSelect, that has rings to periodically slow down the burning rate. NIST tests[1890] indicated that the cigarette does indeed show a reduced ignition potential, but the probability of ignition was still 3 – 50%, depending on the test substrate.

Table 201 Performance of European furniture composites when subjected to various ignition sources

Construction	No. 2 butane flame	No. 3 butane flame	No. 5 crib	No. 7 crib	20 g paper pillow	100 g paper pillow
FR polyester fabric HR PUR foam	N	N	M	Y	M	Y
cotton fabric graphitic PUR foam	Y	Y	M	M	M	M
wool fabric graphitic PUR foam	N	N	N	N	N	M
acrylic fabric melamine PUR foam	N	N	N	Y	N	Y
FR PVC covering HR PUR foam	N	N	N	Y	N	Y
FR polyester fabric FR cotton interliner melamine PUR foam	N	N	M	Y	N	M

HR – high resilience
PUR – polyurethane
Y – generally ignited (flaming)
M – mixed results
N – generally did not ignite (flaming)

- FR but non-HR foams showed a mixed record of ignition/non-ignition. The foam densities were 19 – 45 kg m^{-3}.

Matches, hot wires, candles, and small cribs were found to readily ignite uncovered polyurethane foams of various densities, as well as latex foam[1893]. When PVC or wool fabrics were used to cover the foams, the probability of ignition decreased. For composites involving fabrics other than these two, match ignition nearly always occurred. When the foam was an FR-grade* and was covered with PVC or wool fabric, ignition probability further decreased; however, a substantial number of ignitions were still found. Generally similar observations were also made by Woolley et al.[1894], who saw less benefit in wool or PVC coverings, but found that if certain interliners (fiberglass or FR cotton) were used, then frequently only the fabric would become ignited and burn off, but the foam underneath would not undergo sustained combustion.

IGNITION FROM SMALL FLAMES

Very little of furniture available in 2003 to consumers in the US will resist a small flame, if the flame is applied for more than a few seconds. Considering fabrics alone, wool, FR cellulosic, and heavily PVC-coated fabrics tend to resist a 20-s application of a match-size flame[1860]. Polyester and nylon fabrics tend to shrink away from the heat source instead of igniting. Apart from the California TB 117 procedures (see below), paddings are normally not tested for ignitability from flames, since they are not directly exposed to external flames. Results on composites are discussed in several sections below.

When using a methenamine pill, one set of tests[1891] indicated that ordinary furniture-grade polyurethane foams not containing any FR agents did not ignite. But a more extensive study[1892] showed that:

- All conventional (non-FR, non-HR) foams ignited and burned up. The foam densities were 19 – 30 kg m^{-3}.
- No high-resilience (HR) foams ignited, even though some were FR and some non-FR. The foam densities were 32 – 48 kg m^{-3}.

Table 202 Supplemental radiant heat flux needed to cause ignition of upholstered furniture composites from a methenamine pill

Fabric	Heat flux needed (kW m^{-2})
none (bare foam)	0
cotton corduroy	0
polyester	< 2
rayon/nylon	< 2
FR cotton drill	6
wool	8

Prior to the introduction of British regulations requiring that furniture resist small flames, Raftery[1895] tested 10 full-scale furniture items for match flame and small burner flame ignitability. The furniture samples included convoluted styles with various crevices and re-entrant corners. Ignitions were invariably obtained, except for one item with a PVC covering and a polyurethane padding foam covered by a polyester batting 'topper' layer.

When upholstered furniture mockups were subjected to ignition from burning, balled-up newspaper, FR wool-covered composites were found to resist ignition, and 60% of non-FR wool composites resisted, but PVC-covered composites ignited[1896]. Wool-covered composites commonly, but not always, resist ignition from the smallest wood crib ignition source ('No. 4 crib') described in the British standard BS 5852, discussed below, but ignite from all larger cribs[1897]. Leather upholstery, when used in the thicker grades, generally resists ignition from match-sized flames[1866].

A roundrobin was organized in Europe which tested several composites, when exposed to a variety of ignition sources[1898]. The butane flames and the wood cribs followed the specifications given in the British standard BS 5852. The results are shown in Table 201. The foam types are common in the UK but not elsewhere. The results only refer to flaming ignitions. A number of specimens showed smoldering, but not flaming, ignitions. It often happens that fire exposure involves both a small flame and radiant heating. Moulen et al.[1899] ran tests using the smallest available flam-

* Results in the literature attributed to "FR foams" must be viewed with caution, since FR formulations of polyurethane foams can range all the way from ineffectual to highly effective.

ing ignition source, the methenamine pill, supplemented by a radiant heater. The criterion for ignition was visible flame propagation away from the ignition source. The fabrics were in all cases on top of 23 kg m^{-3} PUR foam. The results (Table 202) show that adding a radiant heat flux of 1 – 2 kW m^{-2} will lead to ignite of a numerous upholstered items that might not otherwise ignite from a tiny flame alone.

IGNITABILITY FROM RADIANT HEAT

Both the minimum heat flux for ignition and the time to ignite under a given irradiance have been used to determine ignitability of fabric/padding composites. This is relevant to the scenario in which an upholstered item is exposed to the radiant heat from other burning items or from the heated walls, ceiling, or upper hot gas layer. Radiant ignition can take place under piloted or unpiloted conditions, but few unpiloted tests have been run on furniture assemblies.

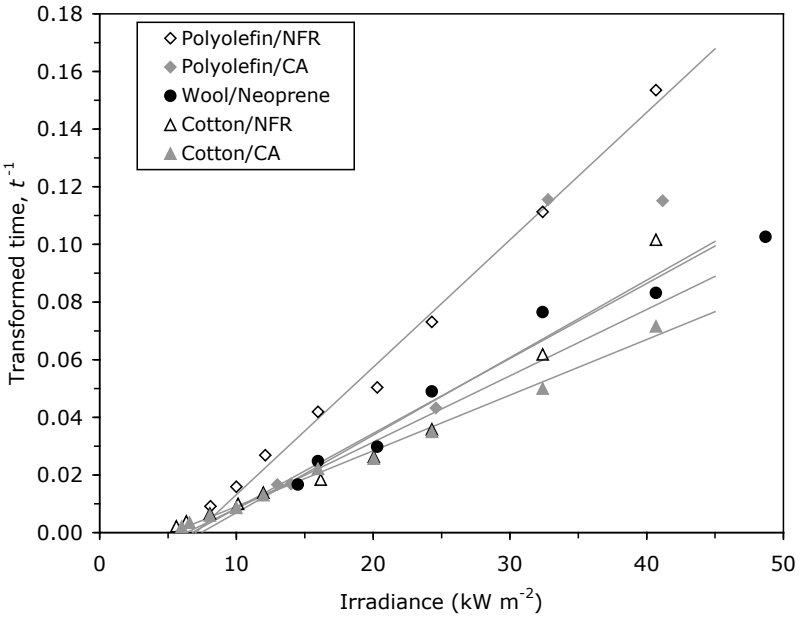


Figure 115 Cone Calorimeter ignition results for upholstered furniture specimens tested at NIST (first designation refers to fabric type, second to foam type: NFR = normal, CA = TB 117-compliant)

A number of researchers have reported radiant ignition data for furniture foams. This information is usually of limited value, since the contributions of foam and fabric cannot be integrated except by testing composites. Nonetheless, some typical data are the following. Palmer and Taylor[1893] tested the autoignition of uncovered polyurethane foams at a radiant heat exposure of 7.2 kW m^{-2}. Half of the tested specimens ignited at this flux and half did not. Of the ones that ignited, higher foam densities led to longer ignition times. The authors also found that the ignitability depended on the thickness of the foam, with around 200 mm needed for ignition at the 7.2 kW m^{-2}, but details of this thickness exploration were not furnished. The maximum time duration of the experiments was not specified, but in one case an ignition was recorded at 145 min. Smith[1609] tested the piloted ignition of an unspecified polyurethane foam by exposing it to tungsten lamp radiation. The specimen ignited in 220 s at a flux of 5.2 kW m^{-2}; lower fluxes were not tried. Foley and Drysdale[1900] conducted piloted ignition tests in the Cone Calorimeter and found that, for most furniture foams tested, the minimum flux for ignition was below 15 kW m^{-2}. But for two samples of mel-

Table 203 Cone Calorimeter piloted ignition times for CBUF upholstered furniture specimens

Fabric	Interliner	Foam	Min. flux for ignition (kW m^{-2})	Propagating fire ?
cotton, FR	--	PUR, HR	6.5	Y
acrylic/cellulosic, FR	--	PUR, HR	7	Y
cotton	Kevlar	PUR, HR	7	Y
acrylic/cellulosic, FR	polyester[a]	PUR, CMHR (UK)	7.5	Y
PVC, FR	--	PUR, CMHR (UK)	< 8	N
cotton, FR	--	PUR, HR	< 10	Y
polyester	Unigard	polyether	< 10	[b]
wool	--	PUR, CMHR (UK)	12.5	N
wool	Springs F187	PUR, HR	13.5	N
polyester, FR	--	PUR, HR	15.5	Y
leather	--	PUR, HR	16	Y
wool, FR	--	PUR, impregnated type FR	21	N

PUR – polyurethane
HR – high resilience
CMHR (UK) – combustion modified, high-resilience, UK type
[a] – ordinary polyester batting for style reasons, not an interliner for fire safety
[b] – propagating resulted due to manufacturing fault

Table 204 Effect of padding material on piloted ignition time (s) of upholstery composites

Fabric	Weight (g m^{-2})	Flux = 20 kW m^{-2}					Flux = 50 kW m^{-2}				
		MF	PUR	LF	CB	WB	MF	PUR	LF	CB	WB
substrate alone	--	NI	30	23	37	NI	NI	5	5	4	10
cotton	149	31	28	25	29	37	7	7	8	7	7
nylon-backed PUR	183	NI	49	42	43	NI	10	8	11	8	6
cotton	319	39	41	46	40	52	10	9	11	11	9
55/45 cotton/linen	348	56	50	54	54	48	12	11	13	13	11
rayon	438	57	51	57	67	70	17	16	17	13	ES
wool	458	NI	NI	NI	69	NI	20	19	20	21	19
cotton-backed PVC	661	36	28	38	38	52	7	6	6	7	6
55/45 rayon/wool	773	83	80	103	89	116	32	28	22	24	ES

MF – mineral fiber
PUR – polyurethane
LF – latex foam
CB – cotton batting
WB – wool waste batting
NI – no ignition
ES – excessive swelling

amine-treated polyurethane foam, the values were ca. 17.5 and 25 kW m^{-2}.

Turning now to tests on composites, in a 1954 study[1901] FRS researchers found that upholstered chairs autoignited at a heat flux of 8.7 kW m^{-2} during a 25-minute exposure. The construction was not specified, but the study predates the use of foams in furniture. Hilado et al.[1902,1903] tested vertically-oriented foam/fabric composites in front of a radiant heater and obtained problematic results, since many fabrics melted out of the specimen holder prior to ignition. In general, they found no autoignitions at 25 kW m^{-2}, but most specimens autoignited at 58 kW m^{-2}.

A series of fabric/foam composites were tested at NIST in the Cone Calorimeter using spark ignition[1858]. Figure 115 shows the results when plotted as for thermally-thin materials. Some results produced a straight line, while others showed a fair bit of deviation. Four of the 5 specimens showed a slope which is probably identical to within experimental error. This implies that the differences in their effective thermal properties were insignificant. These properties are dominated by the behavior of the fabric and the basis weights of the fabrics were relatively similar. The densities of the paddings were grossly different (Neoprene 115 kg m^{-3}, polyurethanes 17 and 21 kg m^{-3}), but their effect is minimal. The reason for the unusual behavior of the polyolefin/NFR composite is not clear. The minimum heat flux for ignition varied from 5.6 kW m^{-2} (for cotton/NFR) to 14.5 kW m^{-2} (for wool/Neoprene). The two specimens with polyolefin fabrics required 8.1 and 13.0 kW m^{-2}.

A similar search for the minimum heat flux for ignition was undertaken as part of the CBUF study[1904], although only a portion of the total specimen collection was tested for ignitability. The results (Table 203) show the lowest flux was 6.5 kW m^{-2}, surprisingly for a construction using FR cotton fabric. The specimens showing values of $\dot{q}''_{\min} > 10$ kW m^{-2} were construction types uncommon in residential furniture, apart from leather which has been rising in popularity. The FR polyester was a polyester fabric with inherent FR qualities, not one with added FR agents. The results show that there is no discernable relation between $\dot{q}''_{\min}$ and the propensity of furniture presented with a 30 kW burner flame to propagate or not propagate fire. It also indicates that while protective interliners can be helpful in reducing the HRR of furniture, they do little to forestall ignition. This should not be surprising, since they are situated *underneath* the top (fabric) layer.

Chen[1905] tested the ignition of composites using a modified ISO 5657 test where ignition was with an electric spark, not a gas pilot. All tests were conducted over a single type of polyurethane foam. For 14 different fabrics used, values of $\dot{q}''_{\min}$ ranged from 6.5 kW m^{-2} to 17.5 kW m^{-2}, but the major fraction (57%) gave 7.5 kW m^{-2}. The unusually hard-to-ignite specimen was a nylon pile fabric. She also noted that for melting fabrics, at any given flux, if ignition occurred at all, it took place in 190 s or less. This was not true for charring fabrics and one such specimen took 778 s to ignite. Values of critical heat flux, using a thermally-thin fuel model were typically 1 kW m^{-2} lower than $\dot{q}''_{\min}$. She also determined that values of $L\rho C$ ranged from 0.89 to 2.17 kW m^{-2} K^{-1}, but with most values being around 1.3 kW m^{-2} K^{-1}. This grouping of constants in an effective fire property for a thermally thin material (see Chapter 7), with L = thickness (m), ρ = density (kg m^{-3}) and C = heat capacity (kJ kg^{-1} K^{-1}). For the specimens tested (which were mainly thermoplastic and did not include any FR grades), she recommended that ignition time t_{ig} (s), as a function of irradiance $\dot{q}''_e$ (kW m^{-2}) can be estimated as:

$$t_{ig} = \frac{338}{\dot{q}''_e - 7.8}$$

The effect of padding material on the radiant, piloted ignition of upholstery composites was specifically investigated by Moulen and Grubits[1906] and Table 204 shows that it is generally small-to-nil. In some cases, the composites using mineral fiber or wool batting showed somewhat longer times, but in other instances no effect could be seen. This question was further explored by Forsten[1907], who ran Cone

Table 205 Cone Calorimeter piloted ignition times (s) for school bus seat specimens

Covering	Padding	Heat flux (kW m^{-2})								
		2.5	3.5	5	7.5	10	15	35	50	75
Standard, 870 g m^{-2}	Rebonded PUR, 73 kg m^{-3}	--	--	NI	NI	83.4	35.2	8.5	5.0	2.5
Kevlar backed, 830 g m^{-2}	Rebonded PUR, 73 kg m^{-3}	--	--	--	--	99.0	42.5	8.2	4.3	2.1
UMTA, 770 g m^{-2}	Melamine treated PUR, 85 kg m^{-3}	NI	462	174	--	48.6	21.8	4.1	2.1	2.1
UMTA, 770 g m^{-2}	CMHR PUR, 49 kg m^{-3}	NI	736	260	--	50.4	21.8	4.1	2.0	1.7
UMTA, 770 g m^{-2}	Polychloroprene foam, 145 kg m^{-3}	NI	546	233	--	48.8	--	4.0	2.2	1.0
UMTA, 770 g m^{-2}	Rebonded FR PUR, 90 kg m^{-3}	NI	510	208	--	49.2	22.1	3.8	2.2	1.4

Standard – PVC backed with polyester scrim
Kevlar backed – same as 'Standard,' except nonwoven Kevlar interliner laminated to back.
UMTA – same as 'Standard,' except claimed to meet UMTA flammability guidelines
'--' – denotes not tested at this heat flux.
NI – no ignition.

Calorimeter tests on composites formed from 14 fabrics combined with polyurethane foams that were either TB 117-compliant or of the melamine type and an optional light-weight Kevlar interliner. Use of melamine foam increased the ignition time by an average of 20%, that of the interliner by about 10%.

Upholstered furniture composites of the type used on school buses were tested by Braun et al.[1908] using the Cone Calorimeter (Table 205). Note that the padding densities used in this application are much higher than for domestic furnishings, where they typically range from about 16 to 32 kg m^{-3}. It is interesting to note the very low values of minimum flux for ignition obtained in these tests. Four of the 6 constructions showed 3.0 kW m^{-2}. Braun also repeated the tests with the LIFT procedure and obtained values of $\dot{q}''_{\min}$ = 9.0 kW m^{-2} for the first assembly, 13.0 for the second, and 3.0 for the four remaining. Apart from the second value, these results show a good agreement with Cone Calorimeter data. Plots of the school bus seat results show that the data conform neither to thermally-thin nor to thermally-thick behavior. The explanation possibly lies in the fact that for a physically-thin substance such as a PVC fabric, when very long ignition times are involved, the material becomes sufficiently thermally degraded so that it cannot be represented by a single set of effective properties (T_{ig}, etc.).

The conclusion from the above studies is that the majority of upholstered furniture composites in common use for residential applications show minimum heat flux values in the range of 6 – 10 kW m^{-2}. The results from studies done on bare foams do not have much practical application to upholstered furniture problems, since (1) foam is never used in furniture uncovered; and (2) there does not exist any means whereby bare-foam ignitability could be correlated to some performance aspect of the actual composite. Despite a shortage of autoignition tests on furniture composites, experience indicates that, at flashover, upholstered furniture items not yet burning will normally ignite. This can be taken to mean that if a heat flux of roughly 20 kW m^{-2} is applied, then autoignition is in most cases assured. But it is not necessary for a room to reach flashover before significant flaming and high heat fluxes can be found in localized places. Thus, upholstered furniture may well ignite from radiant heating occurring prior to flashover. In addition, NIST and CBUF testing indicated that, if one arm of an upholstered chair or sofa is flaming, the other arm commonly ignites from radiant heating, not by surface flame spread.

IGNITION FROM BURNING BRANDS

An old study indicates that upholstered furniture of the 1960s was relatively resistant to being ignited by burning brands, although with cotton fabrics and large brands (38 mm size) some ignitions did occur[1049]. A study on this topic has not been performed with modern furniture. Furniture fires have been started in houses exposed to wildland fires, where window glass broke and brands entered the premises, but research has not been reported to quantify this ignition scenario.

IGNITABILITY MODE COMPARISONS

Ramsay and McArthur[1909] examined the effect of various ignition sources on four bean-bag chairs. The specimens were all filled with expanded polystyrene foam beads and the coverings were heavy, PVC-coated fabrics. The beads of two chairs were FR and were non-FR for the other two. Neither cigarettes nor methenamine pills could ignite any specimens. Wood safety matches, 43 mm long, were able to ignite the chairs only when buried into folds; limited burning occurred even in the worst case. Crumpled balls of newspaper (100 g) ignited all specimens. When a radiant electric room heater was placed directly up to the chair, somewhat buried into it, and energized for 195 s, ignition and full consumption occurred for all specimens.

Several studies have examined the ignitability differences between radiant heating and a wood crib. In one study[1910] using a variety of furniture composites, it was found that the BS 5852 Crib No. 5 was less severe than a radiant exposure of 25 kW m^{-2}. Relatively similar results were found in another study[1911].

In a NIST study, five different chairs were exposed to a variety of ignition sources[1912]. A TB 133 gas burner ignited all chairs; a 1.5 kW radiant heater directed at the front of

Table 206 Comparison of flaming ignition sources to Cone Calorimeter results

Fabric	Padding	Cone t_{ig} (s) at flux of:		Ignition with flaming sources			
		10	15	(1)	(2)	(3)	(4)
polyolefin, 360 g m^{-2}	cotton batting, 27 kg m^{-3}	70	25	Y	Y	--	--
polyolefin, 360 g m^{-2}	PUR foam, 17 kg m^{-3}	85	30	Y	Y	--	--
polyolefin, 360 g m^{-2}	Neoprene, 142 kg m^{-3}	140	45	½	½	--	--
cotton velvet, 560 g m^{-2}	cotton batting, 27 kg m^{-3}	125	55	SE	Y	--	--
wool, 480 g m^{-2}	cotton batting, 27 kg m^{-3}	N	50	N	N	N	SE
Haitian cotton, 650 g m^{-2}	PUR foam, 17 kg m^{-3}	115	65	N	SE	Y	--
Haitian cotton, 650 g m^{-2}	cotton batting, 27 kg m^{-3}	110	65	N	SE	SE	SE
wool, 480 g m^{-2}	Neoprene, 142 kg m^{-3}	N	100	N	N	N	SE, N
Haitian cotton, 650 g m^{-2}	Neoprene, 142 kg m^{-3}	195	125	N	SE,N	SE,N	--
wool, 480 g m^{-2}	PUR foam, 17 kg m^{-3}	N	85	N	N	Y	Y
nylon, 450 g m^{-2}	exptal. foam, 45 kg m^{-3}	N	85	N	N	Y	Y
nylon, 285 g m^{-2}	exptal. foam, 45 kg m^{-3}	N	100	Y	Y	--	--
nylon, 285 g m^{-2}	CMHR foam, 76 kg m^{-3}	N	140	SE	SE	--	--
cotton velvet, 560 g m^{-2}	Neoprene, 142 kg m^{-3}	N	170	N	N	N	½
nylon, 450 g m^{-2}	CMHR foam, 76 kg m^{-3}	N	N	SE	SE	--	--

Y – ignited
N – did not ignite
½ - one out of 2 specimens ignited
SE – ignited but self-extinguished

the chairs caused only slight pyrolysis in 30 min, but when it was then tipped forward, the pyrolysis gases ignited in presence of an electric spark; a focused quartz/halogen reading lamp used as the heater caused only ignition of the acrylic fabric covered chair; the BS 5852 Flame No.1 did not ignite the cotton covered and the expanded vinyl covered chairs; and the cigarette ignited only the cotton covered chair.

Krasny and Huang[1913] tested a series of upholstered furniture composites using four flame sources:
(1) methenamine pill. Specimens tested horizontally.
(2) 97 W burner flame, applied for 20 s. Specimens oriented vertically, with flame applied to face at 25 mm above the bottom.
(3) 210 W burner flame, applied for 20 s. Same specimen conditions as above.
(4) 210 W burner flame, applied for 40 s. Same specimen conditions as above.

Cone Calorimeter tests examining piloted radiant ignitability at two heat flux levels were also conducted on the same materials. Table 206 gives the results obtained. A qualitative relation between ignition resistance for the two types of ignition sources could be seen, but not firm enough to be quantitative.

EFFECT OF WEAR AND SOILING

Ignitability is rarely tested for other than virgin material. In one study where mechanical cycling was done to simulate in-use wear conditions[1914], it was found that 6 out of 7 specimens were no longer able to pass the BS 5852 small-flame test after cycling. CPSC conducted limited testing to examine a series of related issues. They found small or no effect on ignitability from spilled beverages[1915]; soiling with greasy material[1916]; and pounding (to simulate wear), professional cleaning, or home cleaning[1917]. In industry testing[1914], it was found that cigarette ashes, when used to soil a fabric which originally passed the cigarette ignition test, caused it to fail. Cigarette ashes also caused a TB 117-complying foam to no longer pass the TB 117 test. Similarly, a TB 117 complying-foam, when soaked in human urine and then dried out not longer passed the test.

UFAC AND BIFMA REQUIREMENTS FOR IGNITABILITY

From 1976 to 1981, the US Consumer Product Safety Commission (CPSC) considered the possibility of adopting a mandatory standard for the cigarette ignition resistance of upholstered furniture, much as it already had inherited (from the Department of Commerce) a mandatory standard for mattresses. CPSC asked NIST to develop a method, and NIST produced a long study and a proposed method[1918]. The work resulted in the publication of ASTM E 1352[1919], which involves placing lit cigarettes on a fairly large mockup of the intended construction. The industry was opposed to having a mandatory requirement and, in 1981, CPSC accepted the counter-proposal from industry that they will form an entity, the Upholstered Furniture Action Council (UFAC) which will vigorously promote a test on a voluntary-compliance basis. A special tag was developed to identify the complying furniture, with the notion that this would call the attention of the consumer to the benefits of improved fire performance. Since it was felt that testing all fabrics over all paddings would be onerous, a classification scheme was adopted, whereby fabrics are tested over a standard polyurethane foam and classified as Class I or

Class II. Class I fabrics do not permit ignition of the polyurethane foam during the test, while Class II fabrics do. However, Class II fabrics may be used to make furniture if a suitable barrier is used between the fabric and the polyurethane foam. Similarly, battings and other filling and padding materials are tested separately underneath a standard fabric. Some of the UFAC procedures have been standardized as ASTM E 1353[1920], but the ASTM version has not been much used. Further description of details has been published[1860]; actual UFAC requirements change on a periodic basis and are obtained from the organization itself[1921]. The UFAC requirements pertain only to cigarette ignitions; there is no testing from flaming sources. The Business and Institutional Furniture Manufacturer's Association (BIFMA) published a standard[1922] for furniture intended for the business and institutional markets which essentially represents the combination of ASTM E 1352 for cigarette resistance of composites and CS 191-53 for flaming performance of fabrics.

CALIFORNIA TB 117 STANDARD FOR IGNITABILITY

The Cal. TB 117 standard[1923], which came into effect in 1977 and is mandatory in the State of California, comprises separate test procedures for flaming ignition of fabrics, flaming ignition of paddings, and smolder-resistance of padding materials. There is no control over the cigarette-ignition propensity of fabrics, even though smolderable fabrics have been a larger problem than smolderable paddings. The State has published a separate method TB 116, which addresses the cigarette ignition resistance of as-built mockups, but this method is non-mandatory. The test procedure for the smolder-resistance of paddings is similar to that in ASTM E 1353. The Cal. TB 117 procedures concerning smolderability of paddings are, effectively, a subset of the UFAC requirements; thus, UFAC-complying furniture items would meet the California requirements in that regards.

For flaming ignition regulation, the California procedures do not examine the actual-use composite. Instead, foam and fabric are subjected to separate tests. The test for the fabric is the CS 191-53 (16 CFR 1610) test (see *Fabrics*). Almost any fabric that is suitable as an upholstery material can pass this very lenient test, although rare failures occur. The foam test is more demanding, and some FR agents have to be added in order to meet it. Since almost any fabric will pass the Cal. TB 117 test and since, in actual ignitions, the fabric is the material which is closest to the flame, common sense would indicate that the test method does nothing to reduce the potential of small-flame ignitions. Engineering tests confirm this. In tests using a 70 W ignition flame (corresponding approximately to the output of a cigarette lighter)[1924], it was found that real chairs made with Cal. TB 117 complying materials readily ignited. CPSC conducted extensive testing[1925] and concluded: "TB 117 component results were not predictive of full scale performance"; and "TB 117…would not, if federally mandated, ensure a substantial reduction in the risk of small open flame ignition of finished articles of furniture." CPSC also documented that small-flame ignitability of upholstered furniture is governed mostly by the performance of the fabric. Talley[1926] further demonstrated that furniture made to the Cal. TB 117 standard ignites readily from small ignition sources and shows ignitability behavior identical to regular commercial furniture not made to the Cal. TB 117 standard. His study is especially noteworthy since he used the very small methenamine pill ignition source.

The TB 117 test for flammability of foam exposes vertically-oriented specimens 76 mm wide × 304 mm tall × 13 mm thick to a 12 s burner flame applied at the bottom edge. Specimens pass if the maximum char length is not over 203 mm, the average char length for 5 specimens not over 152 mm, the maximum afterflame time not over 10 s, and the maximum afterglow time not over 15 s. Usually, a small amount of FR additives must be added to polyurethane foams to meet this requirement, but in some cases even ordinary furniture foams without any FR additives pass the test[1891].

In 1999 California Bureau of Home Furnishings and Thermal Insulation announced that the TB 117 standard will be substantively revised. It appears, at this point, that when the revised method is published (anticipated for 2003), it will retain the component-testing features and add a procedure for testing composites, roughly modeled on the British BS 5852 standard.

FLAMING-SOURCE IGNITION EXPERIMENTS AND PROPOSED TEST BY CPSC

In examining small-flame ignition hazards to upholstered furniture, CPSC concluded[1927] that nearly all products in the marketplace as of 1996 ignite when exposed for a short time of 5 – 20 s. In their study[1928] CPSC used a 96 W butane diffusion flame simulating a match to ignite full-scale chairs. A total of 27 different furniture specimens were tested: 9 made to the Cal. TB 117 standard, 9 made to UFAC requirements, and 9 to the British BS 5852 standard. Two locations were tested: at the seat/back juncture and at the seat/arm juncture. Of the 54 total specimen/location tests, ignition occurred in 100% of the specimens. Of these, 3 occurred in 5 s, 44 in 15 s, and 7 in 20 s (a 10 s exposure condition was not attempted). There is probably little actual difference between 15 s and 20 s ignitions. But two of the 5-s ignitions were for Cal. TB 117 specimens, one for a BS 5852 specimen, and none for the UFAC specimens. Since the UFAC procedures make no restrictions on open-flame ignition performance, while Cal. TB 117 test method has a requirement for open-flame testing of upholstery fabrics, it can be concluded that the California procedure is ineffectual. The tests were terminated once ignition was established and did not go on to examine further burning. CPSC also undertook to verify that the test conformance claimed was

met. Upon performing the pertinent tests, however, they found that several of the filling materials for chairs claimed to conform to Cal. TB 117 did not meet the test requirement. None of the chairs claimed to meet BS 5852 were found to meet it 100%, but this perhaps reflects the fact that the specimens were not of UK manufacture. In one *ad hoc* test, it was found that a glass cloth interliner, while having no effect on ignition of the fabric, was successful in preventing ignition of the underlying foam from a 96 W flame.

In preparation for regulatory action, in 2001 CPSC proposed[1929] that a test rig similar to the BS 5852 rig be used*, that composites be tested comprising that fabric, standard foam (although actual foam is permitted as an option), and optionally a barrier. A 96 W butane flame is applied for 20 s, since this time length is typical of the burning time of a match. Flames from cigarette lighters may, of course, be applied by a small child for longer than 20 s. They also proposed that a fabric passes if flaming self-extinguishes within 120 s and smoldering within 15 min, and the burned area does not extend to the edge of the mockup; no ignition time limits, per se, were proposed. A separate test is provided for dust covers, which are typically non-woven fabrics used to close in the bottom of the furniture item. An optional test is included for assemblies containing interliners or barrier fabrics; it is based on Crib No. 5 of BS 5852. Of 50 fabrics tested by CPSC, they found that 29 would pass the proposed test. All except two of these were either intrinsically-FR or FR-treated. They also then procured some commercial chairs actually manufactured in the UK and found that, of 27 specimens, 21 met the requirements of the proposed test and 16 showed no ignitions in full-scale testing.

CPSC received public comments in 2002 on its 2001 proposal and expects to make a revised proposal in 2003.

UK FURNITURE REGULATIONS

The current UK fire regulations concerning upholstered furniture were promulgated in 1988, with minor changes made subsequently[1930]. The requirements are roughly based on the British standard BS 5852[1888] but do not follow it in all respects. BS 5852 was originally published in two parts, but the 1990 edition consolidated all tests into a single document. The actual furniture composite is required to pass a cigarette-resistance test. For flaming-source performance, polyurethane foam is tested as a composite, over a standard FR-polyester fabric, and exposed to a No. 5 crib. Other filling materials are only tested with a small gas flame. It has especially been of serious concern that latex foam, which is typically more hazardous than polyurethane foam, is treated much more leniently. The small-flame ignition resistance of fabrics is tested using a composite with a standard polyurethane foam. Welt cords are not subjected to test, despite the fact that this is a preferred place for cigarettes to cause ignition.

MATTRESSES

The ignition characteristics of mattresses are generally nearly identical to those of upholstered seating. The two main differences are: (1) an absence of non-planar surfaces; (2) the universal use of sheets and bedding in connection with the product. Extraneous items, e.g., quilts, pillows, are also often used in conjunction with seating furniture, but this interaction has generally been ignored in testing and in regulations. Recent US statistics involving mattresses are shown in Table 207. These were obtained from a special study of four cities[1931] where more detailed information was elicited than normally reported; the data include fires where either the mattress or bedding was the first-ignited item. The open-flame ignitions (matches, lighters, candles) comprise 39.6% and exceed the 36.4% reported for cigarettes. By contrast, statistics[1932] published in 1972, prior to the 1973 introduction of the Federal standard mandating cigarette-ignition resistance for mattresses, showed that 65.9% of mattress ignitions were from cigarettes. This improvement is not all due to the standard, since during the 1970s cotton-batting was largely superceded by polyurethane foam for mattress padding. Mattresses made with untreated cotton batting will almost invariably ignite from a cigarette, while a large fraction of PUR-foam upholstery systems will not, so some of the improvement would have occurred solely to this marketplace change.

Technically, the same principles govern the ignitability of mattresses and upholstered furniture, so below we summarize only a selection of mattress-specific research. A cigarette placed on a mattress will typically burn about 20 min. It has been found that self-sustained ignition of the mattress tends to occur at about the time that the cigarette is nearly finished burning[1933]. Balls of crumpled up newspaper (100 g) placed in between two cotton sheets on top of a mattress were found to readily ignite four different types of cotton ticking/polyurethane foam mattresses[1934]. In a test series[1935] where mattress padding materials were tested alone, without a mattress ticking, it was found that:

- crumpled newspapers ignited all paddings

Table 207 Fires originating in mattresses or bedding, arranged by ignition source, as obtained in a study of four US cities during 1996-1997

Ignition source	Percent
cigarette	36.4
match	21.4
lighter	15.5
candle	2.7
heater	2.7
electric blanket	0.9
other	16.4
unknown	4.1

* Even though the proposed CPSC tests are based on a rig evolved from BS 5852, the proposal does not share much in common with the UK regulations.

- a paper match ignited latex foam paddings
- a paper match ignited non-FR polyurethane foam paddings, but 1 out of 4 self-extinguished
- a paper match only ignited 1 out of 8 FR-polyurethane foam paddings, and that specimen self-extinguished
- a paper match did not ignite a Neoprene foam padding
- a paper match did not ignite a boric-acid treated cotton batting padding.

In the same study, the resistance to crumpled newspaper ignition sources was also examined for several complete mattresses, with ticking. Using an FR-polyurethane foam, ignition was achieved when a nylon-reinforced PVC ticking was used, but not for an FR-cotton ticking. Also, the newspaper source was not able to ignite a mattress that had an FR-cotton ticking and an FR-cotton batting. Details of the FR treatments were not given. In another study on boric-acid treated cotton batting[454], it was found that neither paper nor wood matches produced sustained ignitions, with the fire dying out after leaving a small burned area.

Latex foam (an SBR elastomer) mattresses were found by Hilado to be readily ignitable in a smolder mode from cigarettes[1936], although earlier Swanson and Adolph[1937] were not able to achieve that. Palmer et al.[1938] subsequently clarified that latex foams are ignitable by cigarettes in a smolder mode if: (a) the foam is bare; or (b) the fabric itself smolders; or (c) the fabric melts away, shrinks away, or burns through under the cigarette. Ignitions were found not to occur when PVC or wool fabrics were used. Unpublished NIST work showed that latex foam is almost inextinguishable once ignited and continues to smolder even if surface flaming is extinguished with water. A methenamine pill may cause either a smoldering or a flaming ignition of latex foam mattresses[1936]. For polyurethane foam mattresses, whether or not a methenamine pill will cause a flaming ignition tends to depend on the ticking material[1936].

If furniture starts smoldering in a tightly closed space, it may smolder for a very long time. A case is documented[1939] where a victim was murdered in bed and the bed lit (in a flaming mode) by the perpetrator. After a time, the bed fire went to smoldering due a lack of oxygen and smoldered for "two or three days" before someone entered the house to investigate the foul smell coming from the victim. Upon opening the door, smoldering transitioned to flaming.

In the US, mattresses made since June 1973 have had to comply with a test method in the Federal regulations. Originally, the test method[1940] was developed by NIST, but after the establishment of CPSC it was taken over by CPSC. The pertinent test is still commonly known by its original designation as FF 4-72. The test is on a full-size article and involves placing 9 cigarettes on the bare mattress and 9 more sandwiched in between two sheets placed on the mattress. In late 2001, CPSC announced that it may institute another standard for mattresses, this one to require open-flame resistance. Also in 2001, the State of California passed a law which will require mattresses sold there to be resistant to open flames, starting in 2004. Their proposed TB 603 standard is expected to contain testing methods that are similar to a scheme developed at NIST[1941], whereby two T-shaped burners are used to expose the edge of the mattress to fairly large flames. The criteria are to be based on HRR and ignitability is not directly involved.

Since the Federal test only uses two bed sheets, it may be speculated that if a full set of winter bedding is present on the bed and a lighted cigarette is introduced atop the top sheet, the likelihood of ignition will be greater. CPSC conducted unpublished research in 1984 which explored this effect to a limited extent. They concluded that complying mattresses will not be ignited if the bedding is mainly thermoplastic, but may be ignited if it is primarily cotton. They also speculated that when ignition of complying mattresses occurs, this may be because it is easier to ignite rumpled beds than beds with flat and smooth bedding; however, this conjecture was not explored in the laboratory.

Mattress test requirements in the UK have a complex legislative history, but in practice testing is normally done under the 'low hazard' section of BS 7177[1942]. This standard contains both a cigarette ignition portion and a test using a small gas flame; the same standard also contains specifications for higher-performance contract furniture. The current version of the British tests follows the European standards EN 597-1[1943] and EN 597-2[1944]. Many other countries have mattress ignition standards, commonly only against cigarette ignition, and a number of those have been reviewed[1858,1945]. European countries, however, are now coming to use the EN standards.

The safety of bedding on ships is governed by IMO, which has a test standard that includes a smoldering and a flaming ignition source[1946]. The smoldering source is unique in that the cigarette is placed on the mattress (a mockup of 450 × 350 mm is used) and is covered, not by a sheet, but by a layer of cotton wool. As with most non-US standards, the IMO standard ignores the possibility that the welt cord may be the most smolder-prone component in the assembly. US Coast Guard testing showed that the cotton-wool scheme is much more stringent, since 9 of 9 test specimens passed the test requirements when covered by a sheet (a draft IMO requirement that was dropped), while only 3 out of 9 passed the cotton-wool-cover procedure[1947]. The test method also differs from US procedures, in that the failure criterion for smoldering is an ill-defined "progressive smoldering," rather than a more quantifiable length of char. The flame source is a small gas burner flame of about 80 W.

Vacuum cleaners

Sloan[1948] reports of an incident where an industrial-type 'wet-or-dry' vacuum cleaner ignited while stored inside a truck. There was a large buildup of dust and oil in the motor area, causing the motor to overheat. It was concluded that

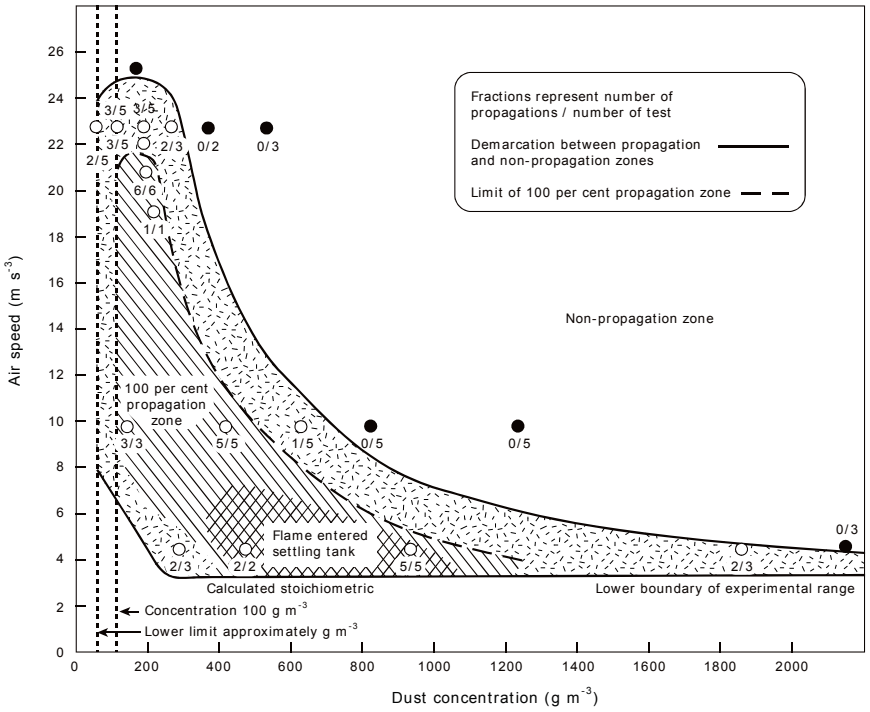


Figure 116 Conditions in vacuum cleaner suction hose for which an explosion of coal dust is possible
(Copyright HMSO, used by permission)

smoldering started in this material while the unit was still being used, but later erupted into flaming when no longer energized.

SMRE[1949] conducted a study where explosions in vacuum cleaner suction hoses were studied for coal dust being vacuumed. For a 50 mm diameter hose, the regime in which explosion is possible—given an ignition source—is delineated in Figure 116.

Wastes

The fire aspects of wastes have been studied by various researchers focusing on either issues arising in waste incineration, or else use of wastes as fuel. Cone Calorimeter ignitability studies have been reported by Hirunpraditkoon and coworkers[1950]. They studied dry wastes and wastes with 22% and 38% moisture. The effective heat of combustion of these fuels varied somewhat according to the test irradiance, but were approximately 17 MJ kg^{-1} for the dry material, 16 MJ kg^{-1} for the 22% moisture samples, and 8 MJ kg^{-1} for the 38% moisture samples. Using a data reduction method similar to Janssens' for thick fuels, their results are given in Table 208. Minimum flux values for ignition were not specified, however.

Table 208 Ignition of wastes, as a function of moisture content

MC (%)	Critical flux (kW m^{-2})	T_{ig} (°C)	$\lambda\rho C$ (kJ^2 m^{-4} K^{-2} s^{-1})
0	7±2	214±67	0.13±0.10
22	7±2	208±76	0.15±0.13
38	9±2	267±47	0.22±0.10

Water heaters

ELECTRIC WATER HEATERS

Despite the fact that electric water heaters are devices that can draw heavy power (typ. 3.5 to 11 kW), they are rarely a cause of ignition. Goodson[1951] has described the operation of electric water heaters and their possible failure modes. He investigated close to 40 fires which were considered to have possibly been caused by an electric water heater, but did not find a single incident where a detailed investigation supported this hypothesis. He concluded that the only significant probability of ignition involves faults in the branch-circuit wiring or in poor connections of the supply leads at the heater terminals.

GAS-FIRED WATER HEATERS

The most serious fire scenario involving water heaters is when the flame of the water heater serves to ignite gasoline vapors and a flash fire or explosion results. This scenario typically takes place in a garage, but on some occasions, flammable vapors are introduced into a basement, utility room, etc., where a water heater had been installed. According to CPSC estimates[1952], approximately 2000 fires each year result from ignition of flammable vapors by gas-fired water heaters. Gas-fired water heaters are the primary cause for ignition of gasoline vapors in dwellings[1953], accounting for 66% of such cases; the remaining 34% of cases are distributed among a wide variety of causes.

US building codes require that if a gas-fired water heater is placed in a garage, it must be raised 457 mm (18") off the floor. Gasoline tank leaks, fueling operations, and any number of thoughtless actions by occupants can result in gasoline vapors being introduced into the space. Gasoline vapors are heavier than air, and will normally accumulate at floor level. With sufficient stirring, heavy vapors can, of course, be mixed into the entire air space. But spills normally occur near floor level and it is reasonable to presume that significant stirring is not common in most situations. Thus, the building code requirement, while not offering absolute certainty, at least endeavors to minimize the risk. Unfortu-

nately, many home owners do not install water heaters at a code-complying height. Talbott and Beckham[1954] documented full-scale tests performed to determine the effectiveness of the 457 mm requirement. They spilled an unspecified quantity of gasoline from a 2-gallon container and observed that ignition of vapors took place for the unit without the raised legs, but not for the one located so that the burner was 457 mm above the floor. A combustible gas detector also indicated high concentrations at 152 mm and undetectable at 457 mm. Tests were conducted by CPSC[1955] where gasoline was spilled at 0.46 m away from the centerline of the heater and gas concentrations monitored at the location of the pilot flame. The results, shown in Table 209, while not extensive, suggest that even raising the heater as little as 0.15 m (6") improves the chances significantly of avoiding a vapor ignition.

Table 209 Results from CPSC test on gasoline spills close to gas-fired water heaters

Height of heater above floor (m)	Amount spilled (mL)	Results at location of pilot	Conditions
0	450	reached LFL in 2/4 trials	still air
0	2000	reached LFL in 1 trial	still air
0.15	2000	did not reach LFL in 5 trials	still air
0.15	2000	did not reach LFL in 2 trials	forced air ventilation, pilot cover off
0.30	1000	did not reach LFL in 1 trial	forced air ventilation

Following several years of study by CPSC and by industry groups, a standard (ANSI Z21.10.1-2001[1956]) was adopted in 2001 which will require designs that are resistant towards acting as an ignition source for flammable vapors[1957]. The provisions of this standard will be phased in during 2003 – 2005. The earliest such model was already produced in 1999 and comprised a combustion chamber that is sealed, except for a path for incoming combustion air that enters through flame arresters. The design also includes a non-resettable thermal sensor within the combustion chamber that shuts off the gas supply if abnormal temperatures are sensed. Designs that comply with the new standard will also have to make provisions against failure due to clogging from lint, dust, or oil deposits that may accumulate on flame arrester surfaces. Water heaters made to this new standard will generally not require to be installed on raised legs.

In a gas-fired water heater, the combustion system sits at the bottom of the unit. Without additional legs installed, the combustion chamber is raised from the floor by short legs of 70 – 100 mm. If the floor is made of wood particleboard and a leak occurs in the heater, the wood may rot out underneath and the heater drop down to the point that the combustion chamber is contacting the particleboard. Fires have been documented to occur under these conditions, since the bottom of the chamber runs at temperatures much higher than can safely be placed against wood[1958]. Another failure mode that sometimes occurs is when burner orifices become blocked and flames get directed downward instead of up.

Under some circumstances, water heater burner flames may 'roll out' and burn outside the combustion chamber, setting fire to surrounding combustibles[1959]. There are four possible causes of rollout:

(1) Excessive burning within the combustion chamber. This can happen if anything greatly increases the burning rate within the combustion chamber, such as a failure to maintain fuel gas at a suitable pressure. But case histories also are known of rollout due to product defects that cause soot to accumulate within the combustion chamber. When this happens, it is possible for the soot eventually to catch fire *en masse*.
(2) Inadequate air supply for combustion. Commonly, this will occur if the heater is improperly closed in within a small room that lacks door louvers or other means of obtaining combustion air. It can also occur due to blockage of the air ports into the burner. Running the heater in this way will cause serious soot buildup in the flue tube, which may eventually clog. If this happens, sooty yellow flames may roll out of the burner[1960].
(3) Faulty venting. If the burning fuel gas cannot properly move up a vent pipe, flames may leave the combustion chamber by other means.
(4) Negative pressure conditions in the house. A NIST study[1961] documented that negative pressure conditions can cause an absence of upward draft when the burner is first started up, leading to roll-out. A tightly-constructed house can achieve a negative pressure due to action of exhaust fans, furnaces, fireplaces, or similar devices.

A number of heaters have combustion chamber doors designed in such a way as to make it difficult to replace them, once they are removed. Leaving off the combustion chamber doors will not lead to roll-out of flames by itself. But if conditions occur that are conducive to flame roll-out, absence of doors will increase the chances of a roll-out and of possible external ignitions. The NIST study[1961] also documented that some water heater designs are much more prone to flame roll-out than others, although it did not try to identify the reasons for poor performance. Gas-fired water heaters are generally highly reliable appliances, but are sometimes chosen by arsonists desiring to stage an 'accidental' fire. Thus, the possibility of the appliance being deliberately sabotaged, or foreign objects introduced for them to get ignited, needs to be considered by fire investigators.

Excessive combustion, possibly leading to external fire, can be expected if a water heater designed for natural-gas service is hooked up to an LPG supply without making the necessary combustion system modifications. The same factor can of course come into play for any gas-fired appliance. The maximum combustion rate (kilowatts) of an appliance is fixed by its design, while the rate of fuel delivery, in simple domestic appliances, is controlled by an orifice. This flow then is determined by the orifice diameter and the supply pressure (back pressure upon the orifice). For an orifice diameter much smaller than the pipe diameter:

$$\dot{Q} = \Delta h_c \frac{AP}{RT}\sqrt{\frac{2P}{\rho}}$$

where $\dot{Q}$ = HRR (kW), Δh_c = heat of combustion (kJ mol^{-1}), A = orifice area (m^2), P = pressure (Pa), R = 8.314 Pa m^3 mol^{-1} K^{-1}, and ρ = density (kg m^{-3}). If the temperature is kept constant, then the scaling relation for different fuel gases is:

$$\frac{\dot{Q}_2}{\dot{Q}_1} = \frac{\Delta h_{c(2)}}{\Delta h_{c(1)}}\frac{A_2}{A_1}\left(\frac{P_2}{P_1}\right)^{3/2}\sqrt{\frac{M_1}{M_2}}$$

where M = molar mass (g mol^{-1}), and 1 and 2 denote the two fuel gases. Thus, if propane were substituted for methane without changing the orifice size or the supply pressure, the HRR would increase by a factor of 1.54. When expressed in Imperial units, this relation is sometimes called the Wobbe Index.

Welding*

Welding can cause fires by many ignition modes and in each welding incident the factors involved must be analyzed. There are two main heat sources used for welding—gas and electric. Welding can be further subdivided by the type of process, such as joining or cutting, and by material, such as aluminum or steel, and further by the type and size of spatter that is created during the process. Spatter is used here to include all of the material that is created during the welding process and includes incandescent particles of base material, the filler material, slag or other inert materials, and pieces that may be cut from the object. Each has its own specific hazards which will be generalized in this section. The discussion is based primarily on common gas torch and electric stick welding techniques and does not include specialized welding processes such as plasma arc, TIG, MIG, laser, explosive, friction, magnesium cutting bars, spot, or submerged arc.

Because the function of welding is to melt the parent material, all welding processes will be competent ignition sources to flammable mixtures at the point of welding since it generally involves open flame or an open arc. Numerous examples of explosions caused by cutting or welding on containers that had previously held flammable material can testify to this hazard. Sometimes welding is done in a mixture above the UFL, for example to repair natural gas leaks. The effect of an inert gas local atmosphere (cone) used in MIG or TIG welding has not been specifically tested but the presence of incandescent spatter that exits the gas cone would indicate that an ignition source is present.

Direct ignition of combustible materials in contact or proximity to the heated base material is common and is seen in shipboard fires. It is common to see steel glowing red on the back side of a bulkhead, indicating temperatures in excess of 600ºC. Procedures to minimize fires are specified in numerous standards and codes and include the removal of combustibles, direct observation of the materials including the opposite side and fire watches intended to suppress delayed ignition. Most fire watch requirements are for 30 minutes but situations involving thick materials with high heat input or materials that are prone to smoldering may require longer observation times. Investigation of these fires should include determination of the orientation, thickness and type of base materials, the type and size of the filler material (rod or wire) and the settings on the heat source such as amperage, range, polarity, voltage, speed, pressure, flow, and other factors specific to the welding equipment. In some cases the parent material, ignited materials and welder have been secured for laboratory or *in-situ* testing with instrumentation to determine the exact temperatures reached.

Spatter produced from the cutting process probably causes more fires. With gas cutting, commonly utilizing propane or acetylene in the US, steel is heated to a high temperature, at which time a high pressure stream of oxygen is directed onto the preheated metal. The resulting oxidation of the steel melts the adjacent material which is then blown away and also helps keeps the process continuing. The oxygen pressure is a function of the tip type and the material thickness and generally ranges from 1.3 to 10 atm gauge. The spatter that is produced can contain drops of molten steel as large as 8 mm. With electric arc cutting, several processes can be used. Electrodes with a special coating create a directional arc jet that will melt the material and blow it away from the electrode. Or, a carbon rod can be used with an air jet in a special holder in a process called air-arc. The arc is struck and the high pressure (5.4 – 6.8 atm gauge) air jet blows the molten material out of the arc. When cutting, pieces of base material can be produced that may weigh in excess of 500 g and be cherry red. Typical parts in the field include bolts, nuts and rivets and would be extremely competent ignition sources. Characteristics of welding slag are discussed in Chapter 11.

* This section was written by Michael M. Fitz.

Wood and related products

See also *Charcoal* and *Paper products.*

WHOLE WOOD

PROPERTIES OF WOOD AND ITS DEGRADATION AND COMBUSTION

The density of natural wood is highly dependent of the species, the growing conditions, the part of the tree from which the timber was taken, and the moisture content. Very roughly, density* ranges from 300 to 550 kg m^{-3} for common woods, but some rare tropical species exceed 1000 kg m^{-3}. Density is best determined by actually weighing a specimen, since there is a fair bit of variability within each species. Several sources exist[1962,1963] where densities are tabulated for a wide range of species. The thermal and diffusional properties of wood are highly anisotropic (different in different directions): the main permeability is through the end-grain and not through side/longitudinal grain.

The elemental composition of wood, by mass, is 47 – 53% C, 40 – 44% O, 6% H, 0.1 – 0.2% N, and 0.1 – 0.6% total for the trace amounts of various other elements[1964]. The heat capacity of wood can be represented by:

$$C = \frac{0.1031 + 0.003867\,T + 4.19M}{1+M} + \left(0.02355T - 1.32M - 6.191\right)M$$

where C = heat capacity (kJ kg^{-1} K^{-1}); M = moisture content (--), expressed as a fraction (not percent) of dry weight; and T = temperature (K). For charred wood, reported values[1965] range from a constant C = 1.0 to a much higher, temperature-dependent expression:

$$C = 1.39 + 0.00036\,T$$

The thermal conductivity of wood in the direction perpendicular to the grain (in either the radial or the tangential direction) can be expressed as:

$$\lambda = S\left(0.1941 + 0.4064M\right) + 0.01864$$

where λ = thermal conductivity (W m^{-1} K^{-1}) and S = specific gravity (--). The latter can be taken as roughly = ρ/1000, where ρ = oven-dry density (kg m^{-3}).

For room-conditioned wood, a good fit to experimental data is obtained by[1966]:

$$\lambda = (0.195\rho + 25.5)/1000$$

The thermal conductivity in the direction along the grain is about 1.8 times greater than in the perpendicular direction. For charred material,

$$\lambda = 0.67S - 0.071$$

The thermal diffusivity α is defined as:

$$\alpha = \lambda / \rho\, C$$

But since thermal conductivity is roughly proportional to density, the thermal diffusivity for woods is almost independent of species and density; values of 1.4 – 1.8 × 10^{-7} m^2 s^{-1} are typical[1981]. Some more detailed expressions than the above, including shrinkage and density changes, have been given by Janssens[1967] and by Yuen[1968].

The surface of wood is not opaque to thermal radiation, but, rather, a certain amount of radiation is absorbed in depth[1969]; the property of non-opaqueness is called 'diathermancy.' Gardon measured the diathermancy of two wood species across the visible spectrum[1970]. The values of the effective in-depth absorption coefficient were progressively smaller at longer wavelengths, dropping to 1.3 – 4.5 mm^{-1}, depending on the species, at a wavelength of 0.7 μm. For most accidental ignitions, the wavelengths in the infrared will be of primary importance, but infrared diathermancy of wood has been less studied. A single graph by Gardon shows values of ca. 1.0 mm^{-1} for 0.7 – 1.3 μm, and ca. 3.5 mm^{-1} for 1.4 – 1.9 μm. Russian researchers[1971] have reported a coefficient of 4.0 – 5.0 mm^{-1} for a radiant source at 4500ºC, and values of 2.5 – 4.5 mm^{-1} at a wavelength of 0.7 μm. The effects of diathermancy on the ignition properties of wood are generally ignorable, except perhaps in the case of ignitions from nuclear weapons[1972].

Timber is relatively light-colored and, consequently, the absorptivity is 0.3 – 0.4 in the visible spectrum[1970]. Accidental ignitions, however, commonly involve radiation that is primarily infrared, not visible. A typical value of the absorptivity of a virgin wood surface for infrared radiation is 0.76, but this reaches close to 1.0 at the moment of ignition; thus it is recommended that a value of 0.88 be used for modeling the ignition of wood[1252]. Because of the surface absorptivity changes with prolonged exposure, accurately separating the effects of absorptivity from in-depth absorption effects would not be easy.

Chemically, the main components of wood are cellulose, hemicellulose, and lignin. In addition, wood contains lesser amounts of extractives (substances in wood, not an integral part of the cellular structures, that can be removed by solution in hot or cold water, ether, benzene, or other solvents that do not react chemically with wood substances), mineral matter (reported as 'ash' in chemical analysis), and water. The chemistry of wood's thermal degradation (pyrolysis) and self-heating is surprisingly poorly known and controversial. A multitude of reactions occur, some of them competing or only occurring under certain conditions of heating rate or specimen temperature. The kinetics of the thermal degradation of wood has been studied by numerous re-

* The density of wood, of course, depends on its moisture content. In the wood industry, *specific gravity* is often reported instead of density using a peculiar definition: $S = \frac{\text{oven-dry mass}}{\text{actual volume}} \times \frac{1}{1000}$. Since wood shrinks when dried, the consequence is that S quoted at moist conditions is a slightly lower number than for oven-dry conditions. True density, on the other hand, increases with increasing moisture content. The wood industry also uses the equally peculiar 'basic density,' which is the same as S, but without the factor of 1000.

Table 210 The results of exposure of matchstick-sized wood samples to elevated temperatures for long periods

Temp.	Time (days)	Condition
107ºC	1050	light chocolate color
120ºC	1235	brittle, dark-chocolate color
140ºC	320	lost 45% of weight, became like charcoal
150ºC	165	lost 65% of weight, became like charcoal

searchers. It is quite clear that a single, global expression for reaction kinetics does not capture the rudiments of the chemistry. In an early study, Akita[1973] showed that an effective value of activation energy is determined as 105 kJ mol^{-1} if temperatures below 400ºC are studied, $E \approx 75$ kJ mol^{-1} at 400 – 470ºC, and $E \approx 54$ kJ mol^{-1} at 470 – 720ºC. Studied on the self-heating behavior of wood in finely divided form (see below) show $E \approx 100$ kJ mol^{-1}; but studies on the pyrolysis of whole wood[1974] generally show $E \approx 125$ kJ mol^{-1}. Apart from the basic oversimplification in representing the degradation by a single-step, global kinetics expression, possibly the higher E for whole-wood heating implies that is more difficult to pyrolyze wood when access to oxygen is poor, as it is in slab-form samples.

In a comprehensive review of wood degradation, Antal[1975] points out that there are several tiers of competing degradation mechanisms, which makes any engineering treatment very difficult without making gross, questionable simplifications. Vovelle et al.[198] proposed a simplification where there are two simultaneous reactions (essentially, one representing cellulose and the other the remaining wood components) and two mass loss regimes, the first from virgin material down to about 40% mass, with the second continuing to the end. The second mass loss regime, of course, is not relevant to ignition studies. For the first regime, cellulose is taken to show a first-order reaction, with $E = 250$ kJ mol^{-1}, and $A \approx 10^{19}$. The non-cellulose component reacts in a zero-order reaction, $E = 84$ kJ mol^{-1}, and $A \approx 10^{4}$. Even though such a two-reaction scheme is greatly simplified from reality, it still would not be trivial to make computations using it. Furthermore, even though more realistic than a representation using a single, one-step chemical reaction, the Vovelle model is grossly simplified, and it is not clear what its limits of validity might be. Russian researchers[1976] have concluded that the pyrolysis of wood and cellulose is an autocatalytic process and provided kinetic constants pertinent to a first-order autocatalytic reaction. Wichman and Oladipo[1977] reviewed several schemes and concluded that the 3-step kinetics of Broido[1978] offers a reasonable balance between simplicity and tractability.

When wood burns, there are two different mechanisms of oxidation. During initial combustion, volatiles are pyrolyzed out of the wood and burn in the gas phase, with a flame. Once this process is finished, a char still remains. The char then oxidizes heterogeneously, showing surface glowing, but not flame. There is an intermediate period of time when both processes occur. The gross heat of combustion of whole wood is around 19.3 to 21.6 MJ kg^{-1}; the heat of combustion of the volatiles is around 16.4 to 18.3 MJ kg^{-1}, while for the char[1979] it is around 30 MJ kg^{-1}. The gross heat of combustion is not realized in fire exposure, and is generally around 10 – 15 MJ kg^{-1} during early burning, approaching 30 MJ kg^{-1} when charring is nearly complete.

It is sometimes suggested[1980] that wood chars upon reaching a specified temperature, for example, 288ºC. But such a simplification will be valid only over limited circumstances—typically only high heat flux exposures, such as from a fire resistance test furnace, are considered. Even then, the demarcation between charred and non-charred material is often very gradual and indistinct[1981]. Long-exposure studies have shown that degradation first becomes visible when the wood (not the environment) reaches a temperature around 100ºC[1618]. McNaughton at the Forest Products Laboratory exposed small (3 × 6 × 76 mm) wood wedges to slightly elevated temperatures for long periods[1982]. His results are shown in Table 210. At the same institution, MacLean[1983] exposed woods of various types to high-humidity environments. He reports that specimens showed "very pronounced" charring after long heating periods at ca. 93ºC. Unlike McNaughton, however, he did not further specify the resulting color. Comparing the results of MacLean to those of McNaughton, the conclusion could be drawn that even lower temperatures suffice to cause charring in high-humidity environments than in normal ones. This was, in fact, a conclusion explicitly noted by MacLean, although without additional quantitative comparison.

In general, the relation between temperature, color, and state of degradation of wood is time-dependent. In short-term heating of white pine shavings, Vandaveer found the first color change at 170ºC, with the wood turning light brown at 190ºC and dark brown at 260ºC. White and Nordheim[1984] consider that wood has charred when it first attains a temperature of 288ºC. Kubler concluded[1619] that when exposed over many years, even moderate temperatures around 120ºC suffice for the decomposition of all wood components; on the other hand, wood heated rapidly under exclusion of oxygen reaches relatively high temperatures prior to disintegrating to the charcoal stage. Regardless of the time scale, if wood reaches temperatures above 300ºC, it is inevitably carbonized and black[1964]. It is important to realize that the above experimental results only deal with tiny samples for which any self-heating effects are limited. Thus, for such conditions, around 120ºC is expected to be the minimum temperature at which dark char would be found. If the size of the member is large enough so that self-heating cannot be ignored, the effective interior temperatures will rise to a higher value than is the externally imposed temperature. Thus, it will be possible to find dark char in larger members, even though externally they were heated to less than 120ºC.

Table 211 Summary of ignition temperature results for wood

Year	Investigator	Specimen size	Ignition temp. (ºC)		Comments
			Piloted	Auto-ignition	
1887	Hill[254]	0.5-15 g		**220–300**	measured air temperature near sample
1910	Bixel, Moore[263]	35 mm ?		200–250	measured oven temperature; scant details
1922	Banfield, Peck[1985]	50×50× 200 mm		302–308	measured surface temperature
1934	Brown[189]	1–5 g		**220–250**	measured oven temperature; tiny samples; unsound ignition criterion
1936	VanKleeck[1986]	chips		**235**	measured specimen temperature; unsound ignition criterion
1947	NIST[1987]	shavings		**228–264**	softwood shavings in test tube; criterion—glowing or flaming
1949	Graf[997]	7–13 g		**232–245**	measured oven temperature; tiny samples; unclear ignition criterion
1949	Angell[1988]	13×19v 51 mm		204	measured gas temperature close to specimen
1950	Fons[255]	2-9 mm cylinders		343	measured oven temperature; solved inverse problem
1958	Narayanamurti [1989]	?	228		measured oven temperature
1959	Thomas et. al. [1990] (based on 1915 data of Prince[1991])	32v32v 102 mm	210		measured oven temperature; solved inverse problem
1959	Akita[1973]	20×20× 1.8 mm	450	489	measured oven temperature; solved inverse problem
			< 350		measured oven temperature only
1960	Simms[1992]	8 mm ø		545	calculated from correlation; error found in calculations by Koohyar
1960	Moran[1993]	50×50× 6.4 mm		255	at flux = 25 kW m^{-2}; measured surface temperature
1961	Patten[1994]	3 g shavings	**260**	**260**	measured oven temperature (Setchkin test)
1961	Buschman[1995]	57×57× 8 mm	369		calculated from correlation; fluxes 14.3 to 37.2 kW m^{-2}
1964	Shoub, Bender[1626]	920×920 mm		254	measured surface temperature
1964	Tinney[1996]	≥6 mm ø		350	measured oven temperature
1967	Simms, Law[1997]	76×76× 19 mm	380		calculated from correlation
1967	Muir[1998]	80 × 160 mm	364-384		measured surface temperature; flux range 15 – 25 kW m^{-2}
1967	Koohyar[1981]	100×100 × 12-19 mm	361	402	measured surface temperature; flux range 18 – 35 kW m^{-2}
1969	Melinek[1999]	100×100 ×13 mm	353	382	calculated from correlation
1969	Jach[2000]	few grams		**260–290**	measured oven temperature
1970	Smith[1609]	75×75× 19 mm	350	413–714	temperatures measured by optical pyrometry; autoignition values dubious
1983	Atreya[2001]	64 mm ø × 19 mm	370		temperatures measured, but below surface; flux = 18 kW m^{-2}
			350		temperatures measured, but below surface; flux ⌑ 30 kW m^{-2}
1986	Atreya et al.[2002]	75×75 ×19 mm	330–405		temp. measured, but below surface

? – denotes unknown measurements

Table 211 - continued Summary of ignition temperature results for wood

Year	Investigator	Specimen size	Ignition temp. (ºC)		Comments
			Piloted	Auto-ignition	
1988	Abu-Zaid[2003]	150×75 ×37 mm	420		forced-air flow; temp. measured but below surface; flux = 18.5 kW m^{-2}
			350		forced-air flow; temp. measured but below surface; flux > 25 kW m^{-2}
				530	flux = 40 kW m^{-2}
1991	Janssens[1252]	100×100 ×17 mm	300–364		surface temp. measured; fluxes 25 to 35 kW m^{-2}
1992	Li, Drysdale[2004]	64×64 ×18 mm	411–497		temp. measured but below surface; flux < 20 kW m^{-2}
			353–397		temp. measured but below surface; flux > 20 kW m^{-2}
1993	Masařík[2005]	2.5 g	**220–240**		tested wood fiberboard; measured oven temperature (Setchkin test)
1996	Fangrat[2006]	100×100 mm	296–330		surface temp. measured; fluxes ¤ 25 kW m^{-2}
1997	Moghtaderi[2007]	100×100 ×19 mm	332		temp. measured but below surface; at 20 kW m^{-2}
			297		temp. measured but below surface; at 60 kW m^{-2}
2001	Boonmee[2008]	40×40 ×40 mm		650	measured w. infrared camera; at 40 kW m^{-2}
				400	measured w. infrared camera; at 75 kW m^{-2}
? – denotes unknown measurements					

In terms of radiative heating, if the heat flux is less than 4 kW m^{-2}, then lengthy exposure (hours) can occur without darkening of the surface[2009]. Conversely, at 12 kW m^{-2}, the surface becomes charred black in about 10 min.

The pyrolysis of wood is, to a certain extent, oxidative. Moghtaderi[2010] has provided data on the mass loss rate of wood specimens prior to ignition. An oxygen-concentration effect is seen, which implies an oxidative reaction of the solid.

IGNITION TEMPERATURE OF WOOD

The ignition temperature of wood was recently surveyed by Babrauskas[2011] and this section summarizes the review. The topic addressed here is ignition during short-term heating. Slow heating over protracted time periods (months, years) is treated separately below. As can be seen in Table 211, studies on the ignition temperature of wood go back well into the 19th century and have continued until the present time. The spread of data is clearly enormous. Excluding one value, the results in Table 211 span 210 – 497ºC for piloted ignition and 200 – 510ºC for autoignition. Babrauskas considered the following reasons that might account for the spread:

- the definition of ignition that is used
- piloted vs. autoignition conditions
- the design of the test apparatus and its operating conditions
- specimen conditions (e.g., size, moisture, orientation)
- species of wood.

The design of the test apparatus may have a significant influence. The majority of devices fall into one of two types: (1) a furnace into which a small specimen is bodily plunged; or (2) a specimen sitting in the open air and being radiatively heated, e.g., the Cone Calorimeter. But this basic division is confounded by the fact that there is a preferred specimen type for each test: specimens of only a few grams are normally put into a furnace that exposes the whole specimen bodily, while specimens placed in front of radiant heaters are typically on the order of 100 g and of sizeable dimensions in at least two directions. The results from Type 1 tests are indicated in **bold** in Table 211 while Type 2 are underlined.

An analysis of the results indicated that disparities arise because Type 1 tests are normally conducted at heat fluxes near the minimum flux for ignition, while Type 2 tests are normally conducted at higher fluxes. But essentially all of the data become consistent when it is realized that if a wood specimen is ignited under external heating barely sufficient to ignite it, it will ignite at ca. 250ºC regardless of the type of heating arrangement. The data also indicate the same 250ºC value is found irrespective of whether a pilot is used or not. The reason is because ignition at minimum-flux heating is always initially a glowing ignition, and only later, if at all, it may transition to flaming*.

By comparison, materials that are not susceptible to glowing ignition (e.g., thermoplastics), show a substantially

* This characteristic is also shared with other combustibles that are capable of glowing, but available data on this point for most other combustibles are sparse.

Table 212 Summary of ignition temperature results

	Flux		
	Minimum	**Low**	**Medium**
Ignition type	glowing	glowing or glowing/flaming	flaming
T_{ig} (ºC), piloted	250	350 – 400 peak, lower for fluxes close to minimum.	300 – 310 hardwoods 350 – 365 softwoods
T_{ig} (ºC), autoignition	250	no data	400 ??

lower T_{ig} in the Setchkin furnace for piloted than for autoignition conditions. The glowing ignition temperature must not be confused with the temperature of the glowing spot. In a glowing ignition, a glow begins at one spot and very quickly reaches red-hot conditions (over 600ºC). This high temperature is not the glowing ignition T_{ig}; instead the latter must be determined either by a thermocouple reading just before a steep jump takes place or by a thermocouple on the same surface but away from the spot of initial glow.

As the heat flux is raised above the minimum value, there is a certain flux range (whose limits have not been sufficiently well studied thus far) where the ignition temperature rapidly increases with only small increases in heat flux. Moran's data are instructive here. Although intermediate data were scattered, as the flux was raised from 25 kW m^{-2} to 29 kW m^{-2}, the ignition temperature rose from 255ºC to 301ºC while the ignition time dropped by 33%. The 300ºC value is significant, since wood pyrolysis involves competing mechanisms, with temperatures under 300ºC leading largely to charring, while over 300ºC gasification being favored[2012]. Thus, if heating conditions are such that the material does not exceed 300ºC, a glowing ignition is favored.

At higher heat fluxes, 2-stage (glowing, followed by flaming) ignitions are not found and specimens, instead, ignite directly in a flaming mode. For piloted ignition, $T_{ig} \approx 300$ – 350ºC adequately represents most of the results from most of the studies. Janssens[1252] noted that the range can be further shrunk by considering the slight but systematic effect of *wood type*. His results for oven-dried specimens were:

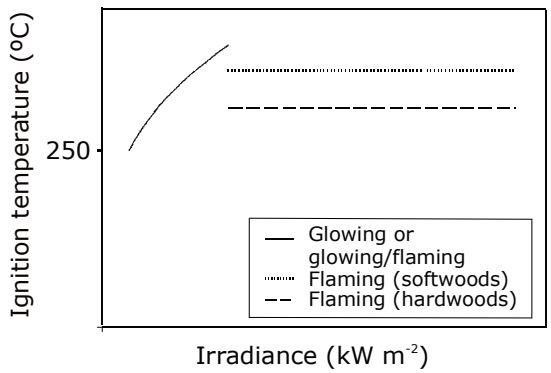


Figure 117 Summary of ignition temperature trends for piloted ignition of wood

hardwoods 300 – 311ºC; softwoods 349 – 364ºC. The effect is attributed to the differences in wood composition between hardwoods and softwoods. As indicated below, hemicellulose ignites at the lowest temperature, cellulose higher, and lignin higher yet. Compared to hardwoods, softwoods have a smaller fraction of hemicellulose and a higher fraction of lignin, thus accounting for their higher T_{ig}.

Concerning *moisture*, as would be expected, at the minimum flux condition Moran found no difference in T_{ig} between oven-dried and room conditioned specimens. In the medium flux regime under piloted conditions, Janssens[2013] concluded that T_{ig} rises by 2ºC for each percent of moisture content increase. This will normally be insignificant for practical moisture contents. *Grain orientation* (i.e., along-grain versus end-grain exposure) may also have an effect on T_{ig}, but good enough data are not available to explore the issue. Almost all existing experimental data deal with along-grain exposures, which are also common in accidental fires.

The basic ignition temperature conclusions are summarized in Table 212 and Figure 117. The data of Koohyar, Li, and Boonmee suggest that the dividing line between 'low' and 'medium' fluxes may be around 22 kW m^{-2} for piloted ignition and 33 – 40 kW m^{-2} for autoignition, but the scatter is quite large. The survey indicated that very few data are available for high fluxes (over 80 kW m^{-2}), thus no conclusions at all are drawn concerning ignition temperatures in that regime.

IGNITION FROM RADIANT HEAT FLUX

Experimental results on piloted ignition

In Chapter 7 Janssens' method for correlating results obtained from radiant-heating tests on thermally-thick substances was presented. It entails plotting the ignition time raised to the –0.55 power on the y-axis and the external imposed heat flux (irradiance) on the x-axis, and is illustrated with Janssens' own data in Figure 118. For the example wood species studied, the equation describing the data plot is:

$$t_{ig}^{-0.55} = \left[\dot{q}''_e - \dot{q}''_{cr}\right] / B_{ig}$$

where the two material constants are $\dot{q}''_{cr}$ = 9.3 kW m^{-2} and B_{ig} = 201 kW m^{-2} s$^{+0.55}$. An equation of this type is specific to a particular species of wood, tested under one set of conditions (e.g., orientation, moisture, etc.). The question then

becomes, is it possible to obtain an equation which would be generally predictive of the piloted ignition of wood, without having to have test results for a particular species? Koohyar[1981] studied this question as early as 1967, but this was prior to the availability of current-day equipment for making radiant-heating ignition tests. Babrauskas[2011] reviewed the question recently, and his results will be summarized here.

Since different wood species differ mostly in the values of density and thermal conductivity, it was considered that these are the primary factors to be treated. Density is easy to measure for any specimen, but thermal conductivity is not. Fortunately, within a given chemical family, thermal conductivity is generally a direct function of density. The other variable of significant importance is moisture. To make an accurate treatment of moisture, the extremes of green wood to oven-dried wood would have to be considered. Green wood can have MC > 100%, but there are no available ignition data on it, with the literature containing data only for oven-dried specimens and ones that are equilibrated to room conditions. For room-conditioned wood specimens, MC is commonly in the 9–12% range, which is actually close to zero, if the whole range of possible MC values were considered. Thus, correlations were sought on the basis of capturing density, moisture, and orientation (horizontal or vertical) effects, with data available on densities over the range 170 – 850 kg m^{-3}. A density effect was statistically identified, but moisture and orientation effects were swamped by data scatter. To eliminate systematic effects of test apparatus, only tests run in the Cone Calorimeter were analyzed. Based on 254 data points, a correlation was evolved:

$$t_{ig} = \frac{130\rho^{0.73}}{\left(\dot{q}''_e - 11.0\right)^{1.82}}$$

where ρ = density (kg m^{-3}), $\dot{q}''_e$ = heat flux (kW m^{-2}), and t_{ig} = ignition time (s). An 0.73 power for the density factor seems low from a theoretical viewpoint, but Kelley[2014] also found a low value, 0.9 in his case; Harada[2015] used 1.0, but with an offset, i.e., $t_{ig} \propto \left(\rho - 105\right)^{1.0}$. The goodness of fit is shown in Figure 119. The root-mean-square error of the predictions is 64%, which indicates that predicting times to ignition can only be done semi-quantitatively, but this must also be placed in the context that experimental data went from 2.5 to 4200 s, or a range of 1 : 1680. A close inspection of the figure also reveals that below about 15 kW m^{-2} the points deviate systematically above the straight line. This is as might be expected, since the theory is based on a thermally thick material, and wood specimens 12–25 mm thick no longer behave in a thermally thick manner when heated for a long time. Recently Harada[2016] offered another prediction method based on a similar concept of relating species effects solely to density. Using his method (and correcting for a missing factor of 10^6), however, the rms error is 77%.

The *minimum flux* for ignition is often a quantity of interest. In 1965, McGuire[2017] suggested that this value can be taken as ca. 12.5 kW m^{-2} for most wood materials apart from low-density fiberboard. A value of 12.5 kW m^{-2} has subsequently been used for design purposes in many countries. This is indeed the value that is customarily obtained in the Cone Calorimeter and in other test methods where the time allotted for observation of ignition is 10 – 20 minutes. But lower values have been found, although not widely publicized. Spearpoint[2018] recently conducted Cone Calorimeter tests of longer duration. For side-grain exposures, Spearpoint found $\dot{q}''_{\min}$ = 12.5 kW m^{-2} for redwood and somewhat less than 12 kW m^{-2} for maple (Figure 120). Ignition of maple at 12 kW m^{-2} required 4200 s. However, since the minimum flux needed for piloted ignition cannot be higher than that need-

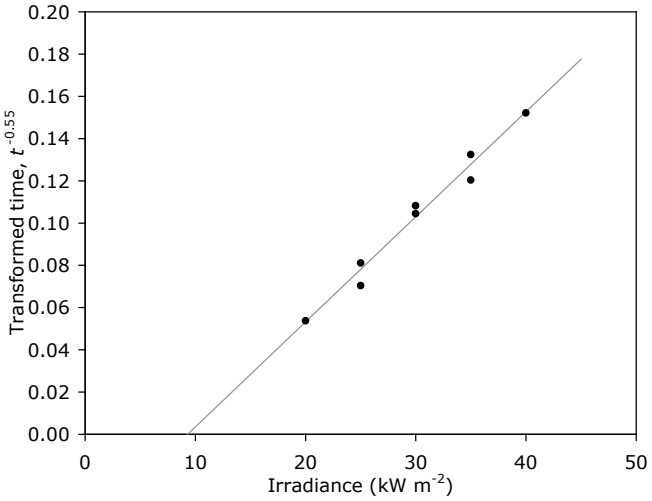


Figure 118 Janssens' piloted ignition results for Blackbutt, oven-dried, vertical orientation

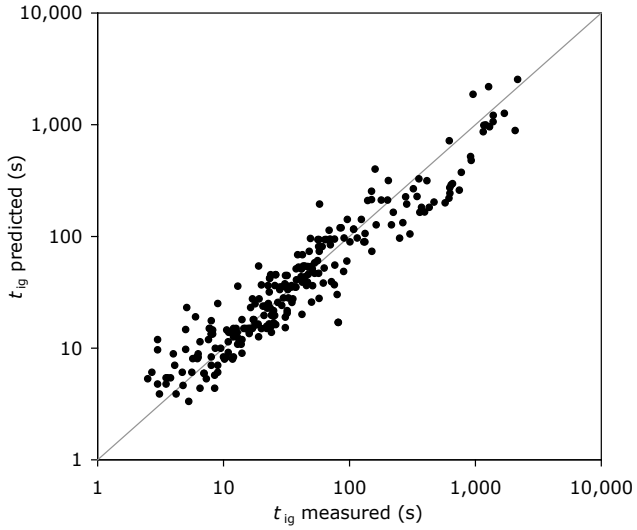


Figure 119 Goodness of fit for equation for estimating the piloted ignition time of wood

ed for autoignition, and the latter value (from Shoub and Bender, as discussed above and further discussed below) has been reported as 4.3 kW m^{-2}, the minimum flux for piloted ignition can also be taken as being approximately 4.3 kW m^{-2}.

Grain orientation has a strong effect on ignition. Ignition data for wood are normally presented with heating being in the perpendicular-to-the-grain ('side grain') direction, since end grains are not so commonly exposed to early ignition in building fires. However, as noted above, the thermal properties of wood are decidedly anisotropic, and this influences ignition. In his tests, Spearpoint also examined end-grain ignitions. At high fluxes, due to the greater thermal conductivity, the end-grain ignitions, not surprisingly, took longer (Figure 120); however, at low heat fluxes, the results were reversed. This is possibly connected in some way with the fact that end-grain surfaces tend to have an intrinsic irregularity, but the exact reason has not been elucidated; possibly, this could also be related to the nature of the specimens tested at the low fluxes, which was a sandwich laid up of four 12.5 mm layers. For end-grain ignition of maple, the lowest flux at which ignition occurred was 8 kW m^{-2}, with no ignition at 7 kW m^{-2}, making $\dot{q}''_{\min}$ = 7.5 kW m^{-2}. The minimum flux for end-grain ignition of redwood was not fully explored, but was found to be below 9 kW m^{-2}. For ignitions occurring at fluxes below 10 kW m^{-2}, a glowing spot was first seen to occur on the surface (Color Plate 141), with the glowing spot later catching flames. Unlike at higher fluxes, after this first flaming occurred, flames spread only slowly over the rest of the exposed surface. The above results would suggest that, for end-grain ignition, $\dot{q}''_{\min} \approx 7.5$ kW m^{-2}. However, the true value is presumably lower, since his finding was that a lower flux suffices for end-grain than for side-grain ignition, and 4.3 kW m^{-2} suffices for side-grain ignition of wood products (see below).

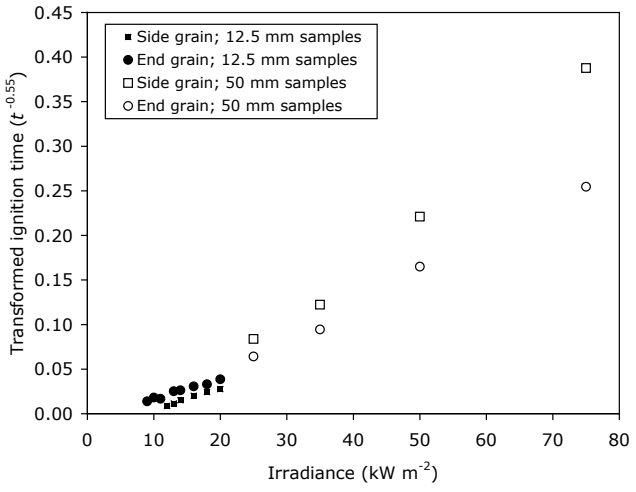


Figure 120 Grain-orientation effect on the piloted ignition of horizontal Douglas fir specimens

Earlier, Vyas[2019] studied the piloted ignition of wood, when exposed to the end grain. In his study, he determined that for fluxes in the range 37 – 109 kW m^{-2}, the ignition times in the end-grain orientation were 2× those found for side-grain exposure. He did not, however, investigate the value of the minimum flux for ignition.

Generally, 'piloted ignition' means the presence of a flame or a spark in the gas phase where pyrolysates accumulate. But it is also possible to apply a gas flame directly onto a surface as an *impinging pilot*, in which case much less radiant heating is needed to achieve ignition since a local heat flux concentration is created. An old FRS study[2020] showed $\dot{q}''_{\min}$ = 5 kW m^{-2} for Western red cedar and Douglas fir. No other published studies exist. Apart from surface-applied pilots, both the type of pilot and its location can affect ignition times. Several studies[2021,2022] produced limited data—more studies would be needed to quantify trends reliably. It is also possible to heat a wood surface by applying a relatively-uniform 'wall of flame' onto it, and this is discussed later.

Experimental results on autoignition

Unlike piloted ignition, autoignition of wood under radiant heating conditions has been studied by only a few researchers, most notably Simms, who conducted various experiments at FRS in the 1950s and '60s. In a 1952 study, he tested 6 different species of wood using 19 mm thick specimens[2023]. The results, including the correction for a 20% flux mis-calibration[2024], are shown in Table 213. In a 1961 study[2025], he reported an enormous value of up to 117 kW m^{-2} for autoignition of blackened oak and cedar specimens. In a 1967 study[1997], he reported minimum fluxes for piloted ignition that were similar to the corrected 1952 values, but autoignition values reported were quite a bit higher, being ca. 40–50 kW m^{-2}. In his 1961 study, Simms noted that a draft strong enough to be turbulent was helpful in reducing the $\dot{q}''_{\min}$. This was evidently a gas-phase effect, but even today there is no systematic knowledge on this topic. In another study[1992], Simms concluded that the quantitative effect of the rather small exposure size of 8 mm is nearly negligible, so presumably the enormous $\dot{q}''_{\min}$ values in the 1961 study were mainly due to insufficiently long test time. Moran[1993] examined the ignition of vertical panels of 6.4 mm thick ponderosa pine using an electric radiant panel and found $\dot{q}''_{\min}$ = 25 kW m^{-2}. Shields et al.[2021] examined the autoignition of Sitka spruce in the Cone Calorimeter and in the ISO 5657 apparatus. They exposed specimens in increments of 10 kW m^{-2}, so their results were only approximate. Since the heater arrangements have some similarity, it is not clear why the values obtained in the Cone Calorimeter and the ISO 5657 apparatus were not closer. Shields' data do illustrate that it is much more difficult to achieve autoignition in the vertical orientation than in the horizontal orientation. The above studies were all of less than 20 minutes duration. Boonmee[2008] tested vertically-oriented redwood

Table 213 Minimum flux for autoignition of wood, as reported by various researchers

Study	Orient.	MC (%)	Draft	Specimen size exposed	Max. time of test	$\dot{q}''_{min}$ (kW m^{-2})	Notes
Lawson, Simms (1952)	V	0	N	50 × 50 mm	20 min	29–33	
Simms (1961)	V	0	Y	8 mm ø	14 s	75–100	blackened surface
			N		18 s	117	
Simms, Law (1967)	V	0	N	76 × 76 mm	70 s	46	
				150 × 150 mm	79 s	42	
Moran	V	0	Y	50 × 50 mm	9 min	25	
Shields et al.	H	≈10	N	100 × 100 mm	96 s	30–40	
	V				59 s	40–50	
	H	≈10	N	165 × 165 mm	12 min	< 20	ISO 5657 test
Boonmee	V	6	N	100 × 100 mm	22 min	38	but lower for glowing-only ignition mode
Shoub, Bender	V	≈10	N	920 × 920 mm	3.9–5.2 h	4.3	

samples in the Cone Calorimeter and found a minimum flux of 34 kW m^{-2} for producing flaming ignition in the side-grain orientation and 38 kW m^{-2} for end-grain. Glowing-only ignitions were possible at lower fluxes, but he did not explore the limit. Only the study by Shoub and Bender[1626] involved exposures extending into hours. They used an electric radiant panel operating at an effective black-body face temperature of 273ºC and producing a heat flux of 4.3 kW m^{-2} at the center of the specimen, and lower heat fluxes at the edges. While they did not test any whole woods, they tested 13 mm plywood. It ignited at the 4.3 kW m^{-2} flux, but required waiting over 5 hours. In their tests, they also documented that the face temperatures of the specimens in some cases reached temperatures higher than that of the radiant source, indicating that self-heating of the material was important and that assuming an inert solid would not be appropriate. The conclusion is that wood will autoignite at about 4.3 kW m^{-2}, if exposed for hours, rather than minutes. For short-term exposures, a value of 20 kW m^{-2} perhaps best captures the research results. Experiments should be made to replicate Shoub and Bender's findings, but the value appears to be reasonable. If the autoignition temperature of wood at the minimum flux is taken to be 250ºC, then a simple estimate can be made by assuming that for the surface to be brought up to 250ºC, it must be irradiated by a heater which is at least at a temperature of 250ºC. The radiant heat flux coming from an infinitely large black body at 250ºC is $= 5.67 \times 10^{-11} (250 + 273)^4 = 4.2$ kW m^{-2}. Thus, an experimental value of 4.3 kW m^{-2} is plausible, since the simple estimate ignores the contribution of both self-heating (which will lower the needed flux) and convective cooling (which will raise it).

At any given irradiance, if ignition occurs under both autoignition and piloted ignition conditions, it is evident that ignition times for the latter will be shorter (unless the pilot is badly placed). A tractable theory, such as Janssens', models only the solid phase, so the presumed conclusion would be that ignition times do not change. A more refined point of view would be to assume that for autoignition, heating up the solid to the same temperature suffices as for the piloted case, but that afterwards a delay time must be added to account for gas-phase events. A theory of this sort has not been developed, however. Experimentally, even though there is a great deal of scatter the results of Shields et al. can be used to derive an equation:

$$t_{ig}\ (autoignition) = \left(2.86 - 0.0172\, \dot{q}_e'' \right) \times t_{ig}\ (spark)$$

Thus, for example, at a flux of 25 kW m^{-2}, under autoignition, ignition times can be expected to be 2.43× those for the spark-ignition case, while at 50 kW m^{-2} the factor drops down to 2.0×. Since the highest experimental flux was 70 kW m^{-2}, the rule should not be extrapolated to greatly higher fluxes. Also, due to the data scatter, the guidance is only semi-quantitative.

Other radiant ignition effects

The minimum heat flux needed for wood to stay ignited (*sustained flaming*) has been studied very little. Babrauskas[2026] examined the piloted ignition of 18.3 mm thick red oak specimens in the Cone Calorimeter. At an imposed heat flux of 20 kW m^{-2}, all specimens burned essentially to completion (> 90% mass lost) when tested in the horizontal orientation. But when tested vertically, two out of three specimens self-extinguished in the middle of the test. Mass loss values at the end of the test were 30%, 38%, and 78%. In a radiant test apparatus, the heat flux received by the specimen after ignition includes both the externally imposed flux and the flux from the flame. But the flame flux is higher in the horizontal orientation, leading to a higher heat release rate. A minimum heat release rate, in turn, can be viewed as the actual criterion that should determine whether burning continues. There is also a wood species effect: 19.1 mm thick white pine specimens burned to completion in both orientations at the 20 kW m^{-2} flux. The species effect can most likely be ascribed to density, the red oak being 660 – 860 kg m^{-3}, white pine 400 – 410 kg m^{-3}. Parker[2027] considers that for wood the question of sustained flaming is affected by cracking. After the initial peak in heat release from a wood specimen, flaming becomes no longer uniform and is localized, instead, to the places where there are fissures. Thus, the minimum heat for sustained

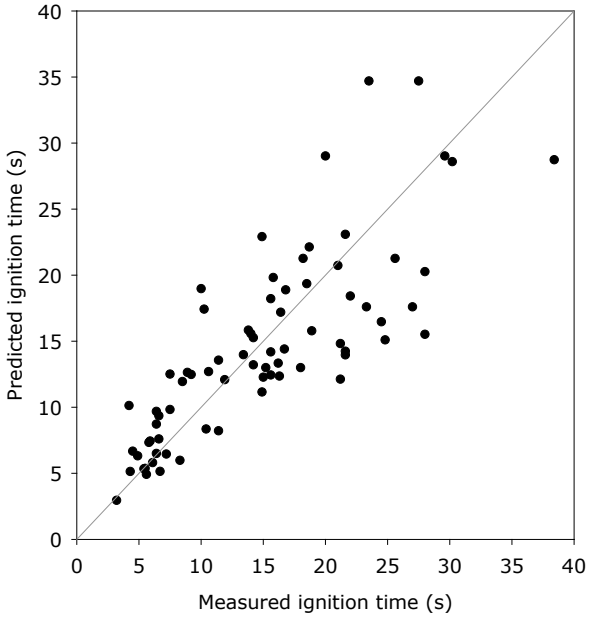


Figure 121 Prediction of ignition time from flame contact

flaming can be expected to depend on the grain orientation, among other factors.

Ignition with *laser radiation* produces very different results than radiation from flames or grey-body radiators. Kashiwagi[2028] exposed horizontally-oriented red oak specimens to laser radiation at 10.6 μm and found $\dot{q}''_{\min} \approx 80$ kW m^{-2} for autoignition and 55 kW m^{-2} for piloted ignition. These values are, of course, much higher than those obtained using normal radiant heaters.

IGNITION FROM FLAMES

When a thin piece of wood is lit at the bottom, burning may continue to completion. But a thick piece of wood will not undergo self-sustained combustion under the same circumstances. Bryan[2029] reported that the maximum thickness for self-sustained burning, given a flaming ignition at the bottom of a vertical piece, is about 19 mm. Tuyen et al.[2030] found that 14 × 14 mm or larger sticks would not continue burning, but smaller ones would. Ignitability of wood boards has been examined[2031] using the ISO 11925-2 small-burner test. Using a 30 s flame exposure to the surface, ignition rarely occurred and never spread to the 150 mm limit, even with specimens as thin as 2 mm. For 30 s bottom-edge impingement, specimens of 18 mm thickness or less commonly ignited, but only ones of 10 mm thickness or less generally reached the 150 mm mark. Using the methenamine pill test (a standard test for floor coverings), it was found[2032] that no ignition occurred for any of a wide variety of wood products tested in thicknesses of 10 – 21 mm. Friedman[2033] claimed (without explaining the basis) that a piece of wood must attain an average temperature of at least 320ºC for self-sustained flaming to continue. The latter criterion, even if correct, would not be easy to apply, since simple methods do not exist for estimating the average temperature of a specimen burning on all sides.

The earliest study where wood was ignited by direct exposure of flames to the entire specimen face was by Bamford et al. and is discussed in Chapter 7. Later data were collected at the University of Oklahoma by Ebeling[2034] who tested oak, white pine, redwood, and yellow pine. From his results it is possible to derive the correlation:

$$t_{ig} = 41.3\rho^{0.94}\left(\dot{q}''_e\right)^{-1.82}$$

where ρ = density (kg m^{-3}) and $\dot{q}''_e$ = irradiance (kW m^{-2}). The results of this predictive equation are shown in Figure 121. The equation captures the basic trends, but the fit is only fair. The above equation implies that the critical flux for ignition (the x-axis intercept if flux is plotted against $t_{ig}^{-0.55}$) is identically zero. This is somewhat different from the results obtained from non-flame radiant sources, where values substantially above zero are normally found. The flame used by Welker et al. was a liquid fuel/oxygen flame and this may make the results systematically different than from flames in normal building fires. In any case, their flame ignition times were a fair bit shorter than times found when applying the same heat flux in radiant heating tests. This is at least partly due to the fact that there is no convective cooling of the surface in a flame-ignition test.

GLOWING OR SMOLDERING IGNITION AND IGNITION BY FIREBRANDS

Glowing and smoldering are similar, but not identical mechanisms of ignition. Smoldering is, by definition, a self-sustained process. Ignition and consumption of a wood material by glowing, on the other hand, can occur if it is subject to sufficient radiant or convective heating, without a requirement that the process continue, should the external heat source be removed. Firebrands themselves may be flaming or glowing, and they may, in some cases, initially cause flaming in the target fuel, although a smoldering ignition is the usual concern.

Self-sustained smoldering occurs easily in various wood products which are highly porous or finely divided (fiberboard, wood shavings, rotted wood, etc.). Whole wood, however, is only slightly porous to the inflow of oxygen. Whole wood will not smolder as a single surface facing open air. Ohlemiller[2035] reports that by supplying external heating of ca. 10 kW m^{-2}, wood can be made to burn in a glowing mode; this of course is not smoldering, since it is not self-sustained. But by preheating the bulk of the wood sufficiently, self-sustained combustion can be obtained. This can be seen in a fireplace where individual pieces may continue glowing even after a 'three-log' effect no longer exists.

Only a limited number of experimental studies exist on the question of minimum conditions necessary to start wood

smoldering. Ohlemiller[2036] conducted experiments where smoldering was achieved by providing a 'three-log' arrangement (Figure 122). In these experiments, three pieces of wood were used to form a U-shaped channel with an air space of 51 mm. Even with this optimal geometry, to achieve smoldering required (a) applying an electrical igniter for 1.5 hours; and (b) blowing air through the channel, with the flow velocity being maintained over a narrow range. A minimum air flow of ca. 0.08 m s^{-1} was needed to sustain smoldering, while velocities over 0.22 m s^{-1} led to flaming, rather than smoldering. Increasing air velocities led to increasing temperatures of glowing wood, and the transition to flaming was found to occur when the glow-front temperature reached about 700ºC. The smolder front propagation rate along the interior surface of the channel was 20 – 70 mm h^{-1} for forward smoldering and 30 – 40 mm h^{-1} for reverse smoldering. In an earlier study, Ohlemiller and Rogers[2037] found that it is also possible to initiate smoldering in white pine arranged in a vertical-channel geometry with only one or two wood slabs. Again, ignition was by flat electric heaters, applied for a long but unspecified time. Smoldering ignition required that a temperature of 310 – 360ºC be reached, but the authors noted that the results were not well repeatable. Dependence on air flow rate was noted, but not quantified in these tests.

Solid wood is most commonly ignited by firebrands during wildland fires. Some statistical information on this topic is given in Chapter 13. It can be seen there that a wide variety of wood structural and trim items have been ignited by firebrands in actual fire incidents. Humidity plays a strong role in the process, and wildland fires often involve extremes of high temperature, low humidity, and strong wind gusts. Several laboratory studies also exist on the ignitability of solid wood by firebrands.

In Australia, there are numerous timber bridges and these often ignite in wildfires, leading CSIRO to study this particular ignition target. Dowling[2038] conducted both field and laboratory experiments on this ignition process. In laboratory experiments conducted at 20ºC and 65% RH and still-air conditions, mockup structures made up of weathered bridge beams removed from service were tested. Wood cribs of 200 g or greater showed a high probability of causing self-sustained ignitions, while 150 g cribs only showed limited charring. Cribs were placed over 5 – 10 mm gaps between two wood members, and when smoldering was produced, it started at the edges and corners of the gaps. In another series of laboratory tests, wood cribs were burned up until they produced a mass of embers, then the embers were poured into a 10 mm gap between wood bridge members; 7 g of embers produced from the burning of a 150 g crib sufficed to start self-sustained smoldering. In field experiments conducted at 16 – 19ºC, 52 – 87% RH and typical wind speeds of 0.5 m s^{-1}, ignitions were not obtained when gaps between wood members were smaller than 10 mm. But for gaps of 10 mm or greater, a 300 g crib, producing 20 g of

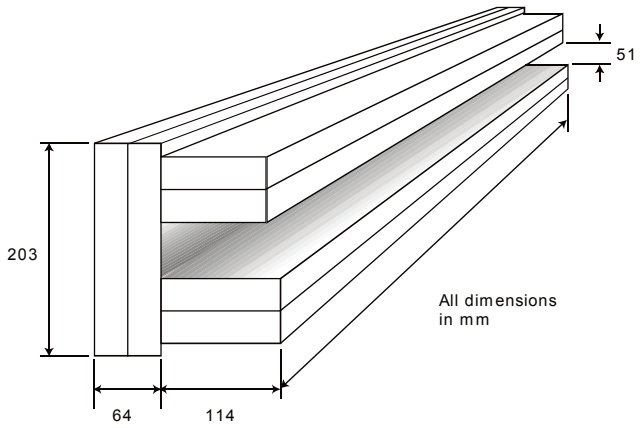


Figure 122 U-shaped arrangement used by Ohlemiller to create smoldering in wood

embers, was found sufficient to cause a smoldering ignition of a 40-year old deck. The differences between laboratory and field results were ascribed to weather conditions. Dowling also concluded that timbers that are rotted or heavily fissured are much more prone to ignition than sound timbers. He also found that flames from large (6 kg) wood cribs placed below the bridge structure and impinging flames up on it, simulating a wildfire below the deck, were sometimes able to cause a smoldering ignition of bridge timbers.

Even smaller ignition sources sufficed in another CSIRO study by McArthur and Lutton[2039] who tested the ignitability of wood siding from very small (0.8 – 12 g) wood cribs and piles of leaves and twigs under an elevated ambient temperature (40ºC) and extremely dry conditions (10% RH) that are commonly associated with wildland fires. Dry specimens (5% MC) generally showed flame spread over most of their 0.5 m height (Color Plate 142), while moist ones (MC ≥ 12%) showed only localized charring. Even cribs as small as 0.8 g were able to cause ignition and substantial charring height. An inside-corner ('re-entrant corner') geometry of the siding was especially conducive to ignition. The specimens were extinguished when maximum char zone extent was recorded, so continued burning was not examined. In both CSIRO test programs, the target woods were hardwoods (*Eucalyptus*) and it is not known if any significant differences would be seen for softwoods.

Hamada[2040] studied the effect of wind and RH on the ignitability of wood by incandescent-red firebrands. Under no-wind conditions, brands of about 5 mm diameter were needed, but for an 8 m s^{-1} wind, even brands of 2.5 mm were likely to cause ignition. Low RH values (20%) were needed for this to occur. At an RH of 80%, even with a high wind of 8 m s^{-1}, it required a brand size of about 8 mm. In Waterman's study[1049], larger brands were needed than those used by Hamada, but Waterman did not measure or control the RH in his experiments. In a reported incident[2041], welding slag that dropped down on wood scaffolding planks

resulted in a smoldering ignition of the wood, which subsequently turned to flaming. It is unlikely that such a piece of slag would be greater than a few millimeters.

The present author conducted unpublished experiments examining the ignitability of wood studs (nominal 2×4") by applying the flame from an acetylene/air plumber's torch directly onto studs for periods of 1 – 5 minutes. It was found that this produces transient flaming, but combustion dies out after the flame is removed and smoldering is not initiated. Even in a 'chimney' geometry of two, closely spaced studs and in a corner geometry of a stud meeting a sill plate, sustained combustion could not be initiated. This does not rule out ignition in geometries more unusual than those tried, but it would appear that fire incidents attributed to plumbers' torches most likely involve the additional presence of other materials that can sustain smoldering, e.g., fiberboard, sawdust, cellulosic insulation, etc.

Sufficient results are evidently not available from these studies to be able to derive quantitative guidance on the minimum conditions needed to ignite solid wood in a smoldering mode or by firebrands. In general, it appears that a hot solid object is necessary; applying small flames—even very hot ones—to wood is unlikely to result in sustained smoldering once the source is taken away. Some exceptionally small brands can ignite wood under ideal conditions: very low moisture, and a geometry where the surfaces 'view' each other. Air velocity has a strong effect, both on the probability of initiating smoldering and on transitioning from smoldering to flaming. Ignition by heating sources sustained for very long periods of time (months) is considered separately below. A *cigarette* has been shown[2042] not to be capable of igniting solid wood or plywood surfaces, at least in still air.

IGNITION FROM OTHER EXTERNAL HEATING SOURCES

Ignition from nuclear weapons was studied by the Naval Applied Science Laboratory[2043]. A radiant exposure from an arc-image furnace was applied over a circular area of approximately 17 mm. The results for the brief, high-intensity pulses were expressed in terms of energy fluence. Very weathered Douglas fir, 19 mm thick, showed no ignition at 385 kJ m^{-2}, (equivalent to 65 kt bomb*) and transient ignition for pulses of 500 kJ m^{-2} (equivalent to 115 kt) or higher. No sustained flaming was observed under any exposure. Punky (i.e., partly rotted) Douglas fir also showed no sustained flaming; transient flaming followed by smoldering required in the range of 385 to 540 kJ m^{-2}. By contrast, when testing 13 mm thick fresh Douglas fir, transient flaming was observed at 1090 kJ m^{-2} (480 kt) and sustained flaming at 1300 kJ m^{-2} (1180 kt) or higher. Yellow poplar of 1.6 mm thickness also showed sustained flaming at 1090 kJ m^{-2}, but no transient flaming regime. Excelsior showed no ignition up to 540 kJ m^{-2}, smoldering ignition starting at 750 kJ m^{-2}, and flaming ignition at 1210 kJ m^{-2}. Except for one trial, sawdust showed no flaming ignitions, but transient ignition followed by smoldering required as little as 270 kJ m^{-2}; the lower limit was not explored.

Hinkley et al.[196] conducted autoignition experiments on wood planks (13 mm thick, 520 kg m^{-3}) and wood fiberboard (25 mm thick, 260 kg m^{-3}) by impinging an air stream from a hot-air blower onto vertically-oriented specimens. Their results are given in Table 121. Air flow velocities were not measured.

Table 214 Autoignition of whole wood and wood fiberboard from a hot-air blower

Distance from outlet (mm)	Hot air temp. (°C)	Ignition time (s)	
		Whole wood	Fiberboard
25	876	13.5	4
76	705	18	6
102	545	37	13
114	470	84	
127	413	300	57
152	292		208
178	210		NI

EFFECTS OF VARIOUS FACTORS ON EXTERNAL IGNITION OF WOOD

Fire retardants

The efficacy of fire retardants is varied; likewise any given FR agent may be applied by various methods and at various loadings. Thus, it is hard to make any general statements about 'fire-retardant treated' wood. At the good end of the scale, Gardner and Thomson[2044] showed that FR pine (pressure-impregnated) can have a minimum flux for ignition > 60 kW m^{-2}, pertinent to a 10-min test. On the other hand, a pine that was surface-coated with an different FR agent had a minimum flux for ignition of < 20 kW m^{-2}. Richardson[2045] reported that Southern yellow pine boards ignited in 36 s at a flux of 50 kW m^{-2}, but when FR-treated the ignition took 217 s. Spruce boards treated with a commercial FR agent were found to be greatly improved in their ignition properties[2046]. A 16% loading of the retardant raised minimum flux for ignition to about 35 kW m^{-2}, as measured during 10-minute tests in the Cone Calorimeter. Increasing the loading to 21% raised the minimum flux value to over 50 kW m^{-2}. A review of available literature[2047] showed that the effects on T_{ig} are small or inconsistent, with some retardants raising the ignition temperature, while others serving to lower it. The inconsistent test results must be considered from the point of view that FR agents are generally added to wood in order to improve the flame spread, heat release rate, or fire endurance properties; any improvements in ignition performance are normally a by-product, not the primary function. The use of many common types of FR agents in wood products is complicated by the fact that

* For atomic weapons, yield is expressed in equivalents of TNT, using the US ton (2000 lb) as the measure of mass of TNT.

many of them cause a progressive hydrolysis of the wood, making it lose strength over time. This can limit the applicability of products with these treatments to uses where loadbearing strength requirements are modest.

In recent years, it has been proposed that certain fire retardants, some of them water-soluble, might be applied on an emergency basis onto wooden sidings of houses in imminent danger from wildland fires. Some ignitability tests[2048] on several systems showed that ignition times at a 25 kW m^{-2} irradiance could be prolonged by about 5 – 10 minutes, but that minimum heat flux for ignition was not affected. The latter is simply because these surface-applied treatments are consumed during the heat exposure period.

Treatment with preservatives

In an early study, Weiss[2049] determined the piloted ignition temperature of Eastern hemlock using a vertical tube furnace. For untreated wood, he established an ignition temperature of 320ºC. Various inorganic preservatives had an insignificant effect on the temperature, although for a number of them Weiss remarked "hard to ignite"—perhaps this referred to time needed for ignition, which was unspecified. Organic preservatives invariably lowered the ignition temperature, with various tars and creosotes giving 217 – 243ºC ignition temperatures.

Impurities

Limited studies have suggested that certain metallic ions present in wood can affect the ignition temperature. Hshieh and Richards[1611] concluded that the natural presence of large concentrations of calcium and potassium is important in determining the glowing or smoldering ignition of wood. When those ions were artificially removed, specimens proved to be much harder to ignite. Adding cobalt (present naturally only in minuscule concentrations) significantly enhanced ignitability. Older studies[1618,2134] indicated that iron also plays a catalytic role in enhancing ignitability. None of the above studies, however, were conducted under conditions representative of radiant heating in real fires, so quantitative conclusions cannot be drawn from them.

Charring

Wood and other materials capable of charring are irreversibly altered when subjected to elevated temperatures. Thus, a practical question arises: Will wood ignite more, or less, readily if it is first pre-charred by exposing it to temperatures sufficient to cause degradation, but not enough for ignition? There are two competing effects when pre-charring occurs: (1) density and thermal conductivity are lowered; and (2) flammable volatiles are driven off. Lowering the density and conductivity lower the thermal inertia which, in turn, makes it easier for a given heat source to raise the face temperature of the material[292,2050]. But driving off volatiles makes it harder to cause ignition, since it becomes more difficult to generate enough volatiles to sustain a flame. Experimentally, it has been demonstrated that the latter effect dominates over the former and pre-charring makes it harder, not easier, to reach ignition. The Bureau of Mines[2051] conducted flame spread tests which showed reduced flame spread of pre-charred specimens. These results can be interpreted as pertaining to ignition since flame spread can be viewed as a succession of ignitions. More direct studies were done at the Fire Research Station[2052] where 50 × 50 × 12 mm thick oak specimens were baked at 120ºC for up to 72 days, at 150ºC for up to 36 days, and at 180ºC for up to 12 days. Autoignition tests on these samples indicated no change of ignition time for a given heat flux. The minimum ignition flux was raised, however, and the increase was linearly proportional to the fraction of mass that was lost in the pre-charring, up to 30% mass loss (Figure 123). The absolute values of $\dot{q}''_{\min}$ are systematically high in many series of FRS tests, as discussed above. However, a relative relation can usefully be derived as:

$$\dot{q}''_{\min}(\text{charred}) = \dot{q}''_{\min}(1 + 0.018ML)$$

where ML = mass lost (%). Thus, if ML = 30%, the minimum flux will increase by a factor of 1.54. Ignition time was raised in piloted Cone Calorimeter tests run at 50 kW m^{-2} by Akizuki et al.[2053] For 27 mm thick red cedar, they found an ignition time of 15 s for virgin material and 23 – 32 s for pre-charred material. When painted wood surfaces are subjected to pre-charring, however, the results are variable[2054].

The above findings must not be applied to situations where self-heating dominates. If ignition requires days-to-years, rather than minutes or hours, then self-heating—rather than external heating—is the dominant source of heat. This is discussed in the *Self-heating* section, below.

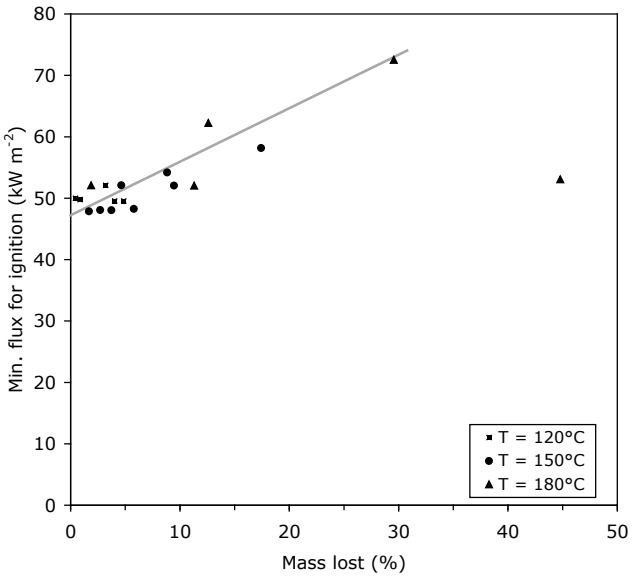


Figure 123 Effect of pre-charring oak on the minimum flux for ignition

Table 215 Autoignition temperatures determined by Hill

Wood	Autoignition temp. (ºC)	
	Sound wood	Decayed wood
hemlock–heartwood	255	208 – 285
hemlock–sapwood	220 – 235	223
pine–heartwood	238 – 300	NA
pine–sapwood	239	218 – 230

Table 216 Hill's results on the effect of specimen size on the ignition of decayed wood

Mass (g)	Autoignition temp. (ºC)
0.5	204
3.0	181
9.0	175
15.8	158

Weathering, aging, decay, and rot

The effect of weathering on cedar samples was examined by Muir[1998]. Using piloted ignition in a radiant panel apparatus, he found that unweathered cedar ignited in 126 s at 20 kW m^{-2}, but cedar weathered in 3 months of outdoor exposure took 328 s. At lower fluxes, however, the effect became progressively smaller; for example, at 16 kW m^{-2}, the results were 802 and 1097 s, respectively. He did not investigate the effect further, but it would appear that it may be related to a loss of potentially flammable volatiles from the outer layer of wood. The most noticeable effect which occurs when wood weathers is that the color darkens, but if the effect were mainly a raising of the surface absorptivity, the ignition times would fall, not rise. In any case, the absorptivity changes primarily in the visible part of the spectrum, and for realistic ignition sources the infrared part of the spectrum is important, not the visible.

It is sometimes claimed that *old wood* is more readily ignited than fresh wood. Kawasaki[2058] considers that the mechanism for this is the preferential decomposition of cellulose, with more of the wood now comprising the more-readily ignitable lignin. The only available data on this point[346] are shown in Table 217 and they do not indicate that there is any significant effect. The specimens listed as 'oven-dried' were dried for 83 days at 105ºC. Note also the results of Muir (above), where he found that weathered wood became *harder* to ignite.

Table 217 Effect of age and drying on the AIT of wood

Specimen	AIT (ºC)
white pine drillings (fresh)	285
wood, oven-dried	270
wood, 3 years old	240 – 264
wood, 20 years old	252 – 261
wood, 20 years old, oven-dried	254 – 267
knot, 20 years old	242
knot, 20 years old, oven-dried	270

Hill[254] compared the autoignition temperatures of sound and decayed wood, using a convective heating arrangement and measuring temperatures in the air space near the specimen surface. His results are summarized in Table 215. It appears that decayed wood ignites at a slightly lower temperature than sound wood, but the difference is only about 10ºC. In an interesting further exploration, Hill then examined the specimen mass effect on a decayed hemlock heartwood sample that he recorded as igniting initially (for an unspecified mass) at 220ºC. These results are shown in Table 216. The decrease in the required air or furnace temperature with increasing specimen mass is due to a modest self-heating effect; note, however that the actual values reported in Table 216 are implausibly low.

Rotted wood was later studied by Angell et al.[1988] They exposed small (13 × 19 × 51 mm) specimens to convective, short-term heating. In comparing fresh and rotted southern yellow pine, they found an ignition temperature (as measured in the air near the specimen) to be 204ºC for sound wood, but only 149ºC for rotted wood. The test paradigm used temperature steps of 14ºC, thus the 149ºC reported value indicates that ignition occurred at 149ºC, but did not occur at 135ºC. Thus, their data suggest that rotted wood has an ignition temperature of about 50ºC lower than fresh wood. The ignition times were 427 s for the sound wood and 105 s for the rotted. Again, the very low values reported should be viewed as reflecting inaccuracies in measurement.

Stockstad studied the ignitability of several types of rotted wood in a horizontal tube furnace, but without a comparative study on sound samples[2055]. Specimen size was 2.5 × 2.5 × 25 mm, with a maximum test time of 3 min (this seems very short, but the small specimen size has to be taken into account). Table 218 shows the main results. The temperatures reported are those of the furnace. In a few cases, Stockstad also measured temperatures in the gas space close to the specimen; these averaged 18ºC lower than the furnace temperatures. The effect of moisture content was also examined, but with anomalous results—increasing moisture content over the range of 5 – 23% increased ignition times for autoignition, but not for piloted ignition.

The ignitability of rotted wood (unspecified species) by glowing, non-flaming juniper brands was studied by Bunting and Wright[504]. Using cylindrical-shaped brands, for the largest size used, 5 × 20 mm, they found that ignition re-

Table 218 Stockstad's tube-furnace ignition results for rotted wood specimens

Wood	Density (kg m^{-3})	T_{ig} (ºC) autoignition	T_{ig} (ºC) piloted
Douglas fir	247 – 332	260	250
ponderosa pine	234 – 457	270	260
subalpine fir	NA	300	NA

Table 219 Low-temperature, long-term ignitions of wood studied by the Swedish Fire Protection Association

Hot object	Ignited	Estimated peak temp.	Estimated time
insulated steam boiler return pipe	25 mm thick floor board	90 – 100ºC, rarely up to 120ºC	unknown
steam boiler return pipe	sawdust & shavings	70 – 100ºC	unknown
condensate water	insulation comprising cardboard + 12 mm wood	90ºC	unknown
high pressure steam pipe*	wood scaffolding	200ºC	2 h
pickling tank	floor under tank	112ºC	1 yr
low pressure steam pipe	cardboard + mineral wool	106ºC	< 1 yr

* This incident does not comprise low-temperature, long-term heating but is included here to present the entire table published by the original authors.

quired a minimum air temperature of 0ºC but that there were few ignitions until 4ºC was reached. Also, fuel moisture content of < 15% was found to be a prerequisite for ignition. Unlike for ignitions of fine-size fuels by brands, wind velocity and RH did not affect the results significantly. When brand size was varied, ignitions were found to regularly occur even for the smallest brands used, 2 × 10 mm.

Rosenhain and Gemmell[264] conducted experiments in 1913 which were a cruder version of the FRS oven-basket testing method. Using 0.305 m cubes of solid, but 'somewhat decayed' wood, they found that an oven temperature of 178 – 180ºC was needed for thermal runaway.

Rotting also removes mass and thus lowers the density and presumably the thermal conductivity. Thermal inertia of rotted woods have not been characterized, however. Rudge[1201] speculated that inorganic constituents in soil, especially calcium, play a strong role in lowering the ignition temperature of rotted wood.

SELF-HEATING, 'PYROPHORIC CARBON,' AND IGNITIONS FROM HOT PIPES

As already discussed at the start of this Section, wood is a very complex substance. Certain aspects of its chemistry have been studied at some length, but these studies normally do not help in solving practical ignition problems. Most of the problems of self-heating of wood arise in connection with porous forms of it, for example, wood fiberboard or wood sawdust. The chemical reactions leading to exothermic phenomena are, of course, the same, irrespective of the physical form of the substance. But when, as in the case of wood, self-heating involves an oxidation reaction (oxygen from the air reacts with the substance) then access of air to the interior of the material is necessary. This is readily feasible for porous forms and more difficult in the case of 'solid' wood. Yet already in 1902 Schwartz[2056] wrote: "Beams of timber may become capable of spontaneous ignition when exposed to prolonged influence of moderate warmth, even below 100ºC." A century later, this issue remains controversial and not fully resolved, as will be explored in this section. The controversies have centered around two related issues: (1) are ignitions possible from heat sources, such as low-pressure steam pipes* (which operate in the region of 100 – 120ºC); and (2) the character and role of char formation and char oxidation in this process. The controversies arise because, unlike piles of sawdust or wood fiberboard, structural members will commonly be no more than 150 to 300 mm thick in their thinnest dimension and, as discussed in Chapter 9, self-heating shows a very strong size dependence. An additional issue of controversy has been whether whole wood is sufficiently permeable to oxygen that a process of continued oxidation could be sustained.

Ever since about 1900, case reports have been published of wood members igniting after a long period of heating by steam pipes, hot water pipes, and other hot surfaces that have temperatures of 100 – 150ºC or, in some cases, lower yet. Since the autoignition temperature of wood, as discussed above, is 250ºC or higher, such cases are not just external ignitions—self-heating has to play a dominant role. In 1910, Bixel and Moore[263] reported details of more than 40 fires where the origin was identified to be a wood beam igniting from an uninsulated steam pipe which had been drilled through it. For most, the time required for ignition was unknown, but the two known cases involved 3 months and 3 years of steam heating prior to the occurrence of fire. Additional cases were collected by Matson et al.[2057]; of special interest is a case where it took 15 years for the condition to lead to a fire. In 1967, Kinbara[2058], a professor at Tokyo's Sophia University, studied two cases in Japan, one where the steam pipe temperature was just over 100ºC, the second estimated to be 140 – 150ºC. The question of the steam pipe temperature is, of course, very important. Low-pressure steam lines will run below 120ºC, while high-pressure steam lines might typically run at 170ºC. In some cases, the hot-surface temperature has been lower. Matson reports a fire where wood members in contact with a water tank ignited, and the latter could not have exceeded 100ºC and another where a steam return pipe could not have exceeded 100ºC. A fire in joists adjacent to a hot-water radia-

* Low-pressure steam is customarily defined as being below 2 atm absolute; steam at the latter pressure is at 120ºC temperature.

tor running at ca. 82ºC has been reported in relatively recent times[2059]. In this case, it was clear that the thickness of wood was greater than just one beam's worth. The actual arrangement involved 50 × 300 mm beams, along the bottom of which was clamped a radiator; below the radiator was a makeshift enclosure. One important practical observation in Matson's study was that in a number of the incidents where the fire was promptly discovered and extinguished, other wood members exposed to similar conditions were cut apart as part of the investigation. These commonly showed that the wood members had become charred black and charcoal-like near the places where they abutted the steam pipes.

In 1960, the Swedish Fire Protection Association published an assessment of the problem[2060]. The case histories surveyed are summarized in Table 219. The last case listed is especially interesting, since the author notes: "The fire [started] when the charring reached a gap with access to air." A recent case history was documented in an apartment house fire in Winnipeg, Canada in 2001. Fire investigation revealed the point of origin at an 1-¼" hot water supply pipe (left pipe in Color Plate 143 and Color Plate 144; the right pipe is an 1-½" return pipe), where it passed from one storey to the next within a wall cavity[2061]. The furnace was producing water at 88 – 93ºC and was checked out to be in proper operational order. The pipe was mostly insulated by 25 mm thickness of fiberglass insulation, but the insulation was omitted at the area of floor penetration. The pipe penetrated an assembly which consisted of 15.9 mm thick OSB sub-floor, on top of which was a 38.1 mm thick wall plate. The investigation was carefully done and all alternative fire causes were ruled out. In this situation, the heating conditions would not be conceptualized as a single hot surface on a body otherwise at ambient temperature. The floor-ceiling space was a small, closed volume and the trapped air space heated up to a temperature higher than ambient.

The fire incident with the lowest measured temperature known to the author involved a fire that occurred on 4 February 1972 in Van Nuys, California[2062]. The fire was found to have originated at a header in a wall cavity (of 2×4" timber construction) where a hot-water pipe passed through. To reduce the potential for vibrations, the plumber had forced a red cedar wedge into the aperture surrounding the pipe, so that good contact was made between the wood and the pipe. The fire broke out some time after numerous individuals of a large family had finished taking showers. During the investigation of the fire, the investigator measured the temperature of the hot water pipe as 77ºC, which is much higher than common for domestic hot water, but in this case was set to enable a large family to not run out of hot water.

Some reported cases should not be considered as solid-wood ignitions, since other substances, such as sawdust or oils, were also present. Other cases need to be excluded since investigation revealed that some heating malfunction had occurred and substantially higher temperatures were reached than are found in normally operating low-pressure steam pipes. In a rare quantitatively documented example[2063] it was noted that fire broke out where steam pipes penetrated walls, but it broke out at 10 places simultaneously. Molten lead in the flanges of the pipe system indicated that steam temperatures had surpassed 320ºC, and the investigators correctly determined the cause to be the failure of a pump in the steam system. It is possible that some fraction of incidents where the fire origin was attributed to normally-operating, low-pressure steam pipes, in fact, involved excessively high temperatures due to gross malfunction. However, it does not seem credible that *all* fires ascribed to low-temperature, long-term ignition of wood involved incompetent fire investigation.

If it is taken that low-temperature, long-term ignitions can occur, then of course there is an interest in explaining the phenomenon. In 1873 the German pharmacologist H. von Ranke[1173] proposed a theory of self-heating of haystacks where he concluded that *pyrophoric carbon* gets formed by self-heating, then this highly-reactive carbon is the substance which subsequently ignites. The term was selected because Ranke believed that the carbonized matter was particularly easy to ignite. The actual sequence of spontaneous combustion of haystacks was more successfully quantified later, and has been discussed above under *Forest materials, vegetation, and hay*. In his 1902 book, Schwartz applied the term and idea of 'pyrophoric carbon' to low-temperature, long-term ignitions of wood[2056]. The term 'pyrophoric carbon' (or 'pyrophoric char') has since been used widely in the fire investigation community. Fire investigators, however, have tended to use the term simply as a synonym for 'low-temperature, long-term ignition of wood,' not necessarily ascribing a particular chemical explanation to the phenomenon.

In 1908 Brooks and McCreary[2064], two students at Case School of Applied Science, conducted the first experiments to examine the potential for steam pipes to ignite wood. They constructed a test rig which surrounded a steam pipe with several boxes into which were placed various test materials. The experiment was conducted for 35 days, during which time steam heating was provided only about 11.5 h per day, with pipe temperatures being about 150 – 160ºC while steam was being provided. In the course of a single day, they obtained ignition in one box, which was packed with charcoal. But they got no ignition during the entire 35 day period in a second charcoal-packed box, nor in boxes filled with sawdust, pine chips, 'wastes' coated in machine oil, wood shavings coated in machine oil, or solid blocks of pine. They concluded that their testing was insufficiently long, and that future researchers should (a) conduct experiments for a whole year, and (b) examine more closely the issue of temperature cycling.

Table 220 Self-heating properties for wood products

Substance	ρ kg m^{-3}	E kJ mol^{-1}	P ln(K^2 m^{-2})	QA W kg^{-1}	QA/C K s^{-1}
various solid woods[2069]		104.6 – 123.4			
Douglas fir, solid[2070]		126			
solid wood[2058]		149			
Douglas fir chips, virgin[2050]		68.60	37.51		5.89×10^{5}
Douglas fir chips, pre-charred[2050]		80.45	39.98		5.93×10^{6}
wood sawdust[2071]	140			6.11×10^{13}	
hardwood chips[1768]	145	102	46.26		
Monterey pine sawdust[2072]	222	90		3.19×10^{11}	1.88×10^{8}
wood sawdust[445]	260	108.33	48.77		
wood sawdust[2073]	210	100		2.7×10^{12}	
wood fiberboard[445]	270	100.97	48.37		1.10×10^{10}
charcoal briquettes (high wood char)[275]		98.94	46.3		
charcoal briquettes (high wood char, in polyethylene bag)[275]		83.14	42.32		
activated charcoal[445]	370	97.02	49.72		

The first theoretically-based study of the problem was presented in 1967 by Kinbara[2058], who assumed wood sawdust behaves identically to whole wood, tested spheres of sawdust for self-heating, then applied simple F-K theory (Chapter 9) and concluded that a temperature of 130ºC would be needed to cause thermal runaway. Shortly thereafter, Handa et al.[2065] conducted tests and modeled a sphere of whole wood, as opposed to sawdust. Their study, however, does not have much generality since to represent certain features of a fire they wanted to reconstruct, they coated the test spheres with plaster or with fiberglass insulation. Later, Handa et al.[2066] conducted 300 h furnace tests on wood blocks and used the data to validate a two-dimensional theoretical model. Their experimental data showed 50 mm thick blocks igniting at a furnace temperature of 190ºC, decreasing to 155ºC for 200 mm thick blocks; the actual ignition times were not stated. A value of E = 149 kJ mol^{-1} was derived from the experimental results.

In more recent years, two researchers—Bowes and Cuzzillo—studied the problem and attempted to disprove either the possibility of low-temperature, long-term ignitions, or some aspects thereof. Bowes[445] started by reviewing data obtained from heating of whole-wood specimens in the kinds of experiments that are discussed in Chapter 9. There had not been many studies, but Bowes found two examples. Topf[2067] examined the effect of percent lignin content on the critical temperature for self-heating of wood using cylindrical specimens of 67 mm dia. and 90 mm height. His test condition was peculiar, however, in that the specimens were insulated with a 50 mm layer of mineral wool before being placed in a constant-temperature oven. As lignin content increased from 20% to 37%, Topf found that the critical temperature dropped from 155ºC to 136ºC. For the same tests repeated in a pure oxygen atmosphere, the critical temperature dropped from 149ºC to 130ºC. Heinrich and Kaesche-Krischer[2068] also used a very similar arrangement, with 60 mm specimen cubes, covered with a 60 mm outer layer of mineral wool. For solid-wood cubes, the lowest critical temperature value was 130ºC, for a highly-resinous Scotch pine sample; a comparable sample of normal Scotch pine gave 180ºC. In cube-tests on shavings of Scotch pine, the temperatures were 180ºC for normal and 100ºC for highly-resinous. The lowest temperature for normal solid wood was 160ºC for Norway pine. Criticality was reached in these tests in 11 – 23 h. Heinrich then ran self-heating tests on resins extracted from the woods, mixed with an inert substrate, and placed in 40 mm diameter cylinders. Critical temperatures as low as 70ºC were found in those tests. The authors also conducted unique tests where they tested beech specimens at 190ºC in a nitrogen atmosphere and found no evidence of exothermicity. Under the same conditions, but in air, thermal runaway was reached in 11 h. In a further test, they kept a specimen in nitrogen for 15 h, then admitted air into the oven, at which point thermal runaway took place.

Bowes analyzed in some detail both of these studies and estimated that about 30ºC needed to be added to Topf's values in order to represent the self-heating of uninsulated specimens. With this correction, he considered that cubes or short cylinders of 60 – 70 mm size are to be viewed as showing critical temperatures of 165 – 185ºC. Bowes also compared these results to studies which examined wood sawdust and observed that such critical temperature values are essentially identical to those found for wood cubes of the same dimensions. He concluded that, at least for cubes of 60 – 70 mm, this was indirect evidence that oxygen is able to diffuse through solid wood and become available for reaction in essentially an indistinguishable manner from

what occurs in wood sawdust. But the geometry of a steam pipe passing through a wood beam is different from any of the standard geometries considered in self-heating theory. Thus, Bowes performed specific calculations for the hole-in-slab geometry. Based on those results, he concluded that a pipe temperature of approximately 200ºC is required to cause thermal runaway.

More recently, Cuzzillo reported the results of several lab studies[2050,2074]. He placed an 89 mm cube of solid Douglas fir in an oven; it reached thermal runaway after being held at 200ºC for around 250 min. A 200 mm cube held at the same temperature for around 12 h was close to the runaway condition. When he sealed the end grain surfaces, however, a 200 mm cube then took some 9.2 days to reach criticality. Earlier, Kubler[2075] had argued that oxygen access into the interior of pieces of whole wood is essentially nil. But Cuzzillo's results indicated that oxygen *can* enter into the interior, primarily through the end grain, but also sufficiently through the side grain so that slow oxidation can take place. Furthermore, it is evident that extended exposure of wood to elevated temperatures *creates* porosity. Thus, the self-heating process of whole wood includes a secondary positive-feedback mechanism—the creating of porosity due to self-heating, with porosity then further promoting self-heating. In another series of tests, Cuzzillo conducted experiments where the self-heating properties of virgin wood chips (as expressed by F-K theory constants) were compared to wood chips which had been pre-charred for 8 days at 198ºC. His results, along with those from several other studies, are compared in Table 220.

Cuzzillo's results showed that, in his tests, the pre-charred chips had a slightly lower, not a higher, self-heating propensity. According to these results, for thermal runaway, a pre-charred 150 mm thick slab would require a temperature about 20ºC higher than a virgin layer. It should be noted that, despite sizeable differences in the individual data constants, many of the results in Table 220 are broadly consistent. As Cuzzillo pointed out, when a limited, realistic range is considered for the problem variables, agreement is good since pairs of different E and P values can lead to the same prediction of critical temperature versus size.

Kubler also argued that, for solid wood, because of the poor access of oxygen into the interior, hydrolysis and pyrolysis reactions, rather than oxidation, dominate. If the governing reactions, then, are chemically different, it would also be expected that the self-heating constants for whole wood would be different than for porous wood products, where oxygen is readily available and oxidation reactions dominate. Cuzzillo did not test enough cubes of solid wood, so his work did not prove or disprove Kubler's claim. But the values of E in Table 220 are rather higher for solid wood than for wood in more porous configurations.

Since his experimental results indicated that pre-charred chips show a slightly smaller, not larger, self-heating propensity in oven-basket testing, Cuzzillo concluded that he thereby disproved the theory of 'pyrophoric carbon.' While Cuzzillo did not specifically perform these calculations, it is also clear from either one of his results—virgin or pre-charred—that, if self-heating calculations were performed using the simple F-K theory, a broadly similar conclusion to Bowes' would follow: it would be 'proved' to be impossible to ignite wood members with low-temperature, long-term heating. But unlike Bowes, Cuzzillo did not specifically draw that conclusion. Instead, he concluded that low-temperature ignitions of wood members may occur, but would occur since the thermal inertia of charred wood is much lower than that of virgin wood. The latter claim, while true, is irrelevant for self-heating, because thermal inertia is a variable that only governs ignition from external heating, not from self-heating.

Neither Bowes nor Cuzzillo (1) conducted any chemistry studies on the reactions of wood, nor (2) conducted tests where a wood member would be subjected to conditions reasonably simulating the ones that have been involved in fires. Thus, neither of these studies have been directly helpful towards quantifying the conditions needed for low-temperature, long-term ignition of wood. It might be observed, furthermore, that use of the F-K theory is clearly inappropriate, in view of the time frames involved. Laboratory tests of the various researchers on small cubes and other similar samples showed that thermal runaway, if it happens, happens in a matter of hours or days. For example, in his test of longest duration, Cuzzillo obtained a thermal runaway time of 9 days for a 200 mm cube. Thus, it should be clear that the physicochemical mechanisms which are operating in incidents where it takes months-to-years for fire to break out are not ones within the scope of the simple F-K theory.

Turning now to other investigations and theories, Cuzzillo's experiments showing that pre-charring creates a less self-heating-prone situation is the opposite of what was found by Palmer earlier[2076] in tests of virgin and pre-charred sawdust. Palmer tested layers of sawdust on a hotplate, determining the minimum hotplate temperature needed for the ignition of a layer of a given depth. His results are shown in Table 221. The temperature needed for the ignition of the carbonized material was found to be 30ºC lower than for the virgin wood sawdust. Thus, the effect found by Palmer was about of the same magnitude, but in the opposite direction, as found by Cuzzillo. Palmer's trends were confirmed during recent testing by Fitz[2077], who conducted hotplate tests on pre-charred sawdust and obtained results nearly identical to Palmer's. Since the self-heating process involves a solid-state oxidation and not combustion of volatiles, it can be concluded that removing some of the volatiles by pre-charring aids, not hinders, the self-heating process. But in any case, neither sawdust nor wood-chip exper-

iments have direct applicability to ignitions of solid wood members.

McGuire[2017] reported on a study where temperatures of ca. 121ºC were maintained for 4 years on both whole wood and wood fiberboard specimens. Charring was found, but not a flaming ignition; however, the paper provided no details on experiments conducted.

There are a number of hints in the literature that the self-heating ignitions of wood members which take months-to-years are highly dependent on oxygen conditions, specifically, that ignitions of this type are promoted when oxygen is excluded from the wood member by a physical barrier such as a sheet-metal or a tile cover over wood. Already in 1922, Wedger[2078] wrote that "pyrophoric carbon" is preferentially formed "where there is no circulation of air." In current times, this has been illustrated by DeHaan[322] and others[2079]. It is not rare to find low-temperature, long-term ignitions under boilers where the unit has a solid-metal base in contact with wood flooring[2080]. Even without such overt devices restricting the availability of oxygen from the wood member, when a steam pipe or similar metallic member at an elevated temperature is located adjacent to a wood member, oxygen delivery into the interface will be restricted. Progressive charring causes shrinkage, so the exclusion effect would appear to diminish with time, but actual gas concentrations in these environments have never been studied.

To unravel details relating to the role of oxygen, it would be helpful if the chemistry of the pyrolysis and charring of wood were understood. The late Prof. Fred Shafizadeh, who was considered to be the foremost expert on the subject of pyrolysis of cellulosic materials, made an effort to do exactly that. He produced cellulose chars at various temperatures in an anaerobic process[2081]. Then, he conducted thermal

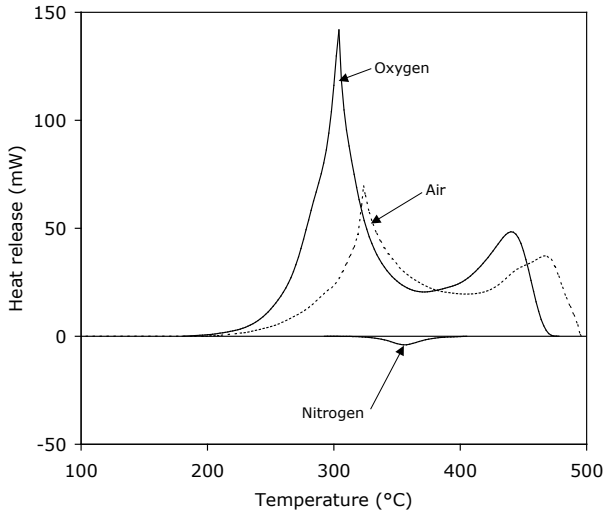


Figure 124 DSC curves for oven-dried Douglas fir
(Courtesy Frank C. Beall)

Table 221 Palmer's hotplate ignition tests on wood sawdust

Specimen	Density kg m^{-3}	Min. hotplate temperature needed for ignition (ºC)	
		Depth 25 mm	Depth 50 mm
wood sawdust	200	270	240
carbonized wood sawdust	200	240	210

analysis tests on these specimens and found that the chars produced at lower temperatures showed a pronounced exothermic peak occurring at a low temperature value; this exothermic peak was not present for chars produced at temperatures over 375ºC. This implied that chars produced at low temperatures are substantially more reactive than those produced under higher temperatures. The reactivity manifests itself as an exothermic chemisorption of oxygen onto the freshly-formed char. The chemisorption was found[2082] to produce up to 460 kJ per mole of O_2 and led Shafizadeh to refer to write that: "This gives credibility to Ranke's theory of pyrophoric char and his explanation of spontaneous ignition"[2083]. In 1989, Shafizadeh's student, Hsieh[2084] attempted to repeat these experiments at lower temperatures, but obtained negative results. No further investigations in this area have been reported since then.

As the review of McNaughton's work in the preceding Section has shown, the charring of wood already takes place at 107ºC and is full-fledged at 120ºC. Kollmann and Topf[2085] summarized several German DTA studies and found that the lowest temperature at which an exothermic behavior was detected ranged from 105ºC to 208ºC. The lower values from this study are quite consistent with McNaughton's results. The higher values would seem to reflect limitations in measuring technology. Even today, the ability to measure chemical activity at low temperatures is limited. Differential scanning calorimetry (DSC) plots for oven-dried Douglas fir taken on a modern instrument are shown in Figure 124. No detectable response is seen below about 180ºC. Thus, the paucity of chemistry studies is not surprising, in view of the fundamental difficulty of measuring reaction rates at low temperatures.

Considering Shafizadeh's and DeHaan's findings, plus the plethora of case histories, it is possible to speculate about the nature of the ignition mechanism. It appears that char is initially formed under conditions of very limited access to oxygen. It is well known that char shrinks and cracks under extended heating. Both of these factors will play some role in the chemistry, but the details are not known. It is possible that ultimate flaming ignition follows a time period when larger cracking took place. Cyclic aspects of the flow of heat, moisture, and oxygen may play a role. In many cases, low-temperature ignitions involved a heat source which is cyclic. This aspect has largely been ignored in recent inves-

tigations. However, early in the 20th century, Prof. Ira Woolson (considered to be America's first fire scientist), felt that low-temperature ignitions of wood are particularly liable to occur when steam pipes are in a heat/cool cycle[2086]. Much more recently, chemists at the National Research Council of Canada[2087] published a study giving an essentially identical opinion. It has often been noted that low-temperature wood ignition fires can occur after wetting of wood. But Woolson suggested that a water/air mechanism may apply to steam pipes. When steam heating is cyclic, ambient moisture may condense on pipes during periods of non-use. This will contribute to the exothermic heat of wetting to the self-heating process. When heating is restarted, a drying cycle occurs, in which there is an endothermic contribution from drying moisture, but an exothermic contribution from oxygen being made again available to char pores which were previously moisture-laden. Moore[262] speculated there may be a further mechanism involved, an interaction between wood and iron. For a variety of reactions, iron oxide acts as a catalyst, and he thought this should also be explored in connection with steam pipe ignitions.

As discussed earlier in this Chapter, wood is an extraordinarily complex substance, possibly the most complex substance which tends to get involved in accidental fires. Its enormously complicated degradation chemistry is known today only in its roughest outline. The standard self-heating theory (F-K theory), on the other hand, assumes that the substance is the simplest substance conceivable, not showing two-step reactions, parallel reactions, or effects of oxygen or moisture flow, and certainly no effects of thermomechanical phenomena such as cracking. Thus, it should be no surprise that the theory does not cope with the low-temperature, long-term ignition phenomenon. What has been missing—and is very much needed—is an experimental study where the low-temperature, long-term ignition of wood would be examined in a realistic environment. This should include a pipe which is cycled in temperature between, say, ambient and 120ºC. Experiments where oven samples are uniformly heated do not constitute a realistic representation of the fire cases that are of practical interest. In 1960 Östlin[2060] observed that, in practice, wood members have ignited at temperatures down to ca. 100ºC and pointed out: "That ignition did not occur in the laboratory attempts can be assumed to depend on the fact that these did not contain all the necessary conditions for ignition." This observation remains true today.

A more complex problem is *flue-pipe* ignitions. Here, it is generally difficult to estimate what the temperature of the pipe was. In addition, the heat transfer situation is normally complicated, since even in imprudent installation, flue pipes are not necessarily butted up to a wood member, but may be located some distance away. Thus, the boundary conditions at the high-temperature surface involve radiation and convection, not a fixed temperature surface. Even though the radiant/convective transfer situation entails a thermal resistance, which is zero in the fixed-temperature boundary-condition case, flue pipes are likely to be heated to significantly higher temperatures than steam pipes. The same questions of long-term, low-temperature ignitions exist, however. Handa et al.[2088] attempted to elucidate the mechanism of ignition whereby a fire in a Japanese hotel originated at a wood pillar that was located close to a flue pipe. The actual system was complex, including layers of plaster, metal, and two different woods, and the authors did not succeed in replicating the ignition by laboratory testing.

Self-heating of *porous wood products* (sawdust, wood fiberboard, etc.) where there is good access of oxygen into the entire volume of the product is a different problem. For sawdust surrounding hot pipes or vessels, a temperature as low as 65ºC was found to suffice[1197]. If ignition occurs within a short time of creating the pile, then use of F-K theory, along with the constants given in Table 220, should be sufficient to enable calculations to be made. This would not apply, of course, to situations where long-term heating took place, but there do not exist sufficient case histories nor experimental data to enable such possibilities to be considered. Further aspects of self-heating for porous materials are discussed below.

IGNITION BY ARC TRACKING

When an electric current is made to flow across a tree or a wood member, an arc tracking process can take place under some circumstances. Wood first dries out at the electrodes, then a carbonized channel starts to form. Given enough time and voltage, sufficient heating of the carbonized track takes place that the electric current passing through the track heats up the wood to ignition. The presence of contaminants in the water greatly lowers the voltage necessary to initiate arc tracking (Figure 125). Because of the anisotropic nature of wood, the carbonized tracks can appear in the interior of the material, not necessarily on the surface. Kinbara et al.[2089,2090] documented that wet wood is more easily ignited by the electric carbonization process than is dry wood, and also that ignition is more likely to occur if

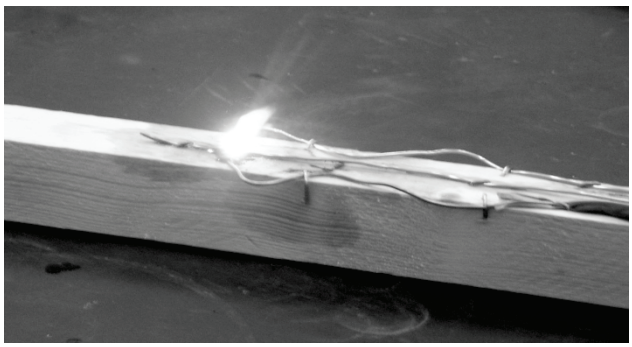


Figure 125 Arc tracking-induced ignition upon contact with wood by bare conductors carrying 120 VAC and wetting the surface with contaminated water.
(Courtesy Michael M. Fitz, MDE Engineers)

point electrodes are used instead of plate electrodes, since a higher current density is created with the former. Sanderson[2091] has reproduced some of these main findings. Fires due to wet arc tracking are common in the case of faulty installations of neon signs where high-voltage leads can contact wood.

In the case of high voltage power distribution lines, much higher voltages and currents are possible than with neon transformers. Ross[2092] studied the ignition of wood crossarms in power distribution systems. He found that the conditions most conducive to ignition involve a dry member that then receives moisture from a drizzle or fog. Under these conditions, patches of dry surface exist, and high electric potentials are then impressed upon these small areas. Leakage currents flowing through the dry patches then cause charring or ignition. Laboratory tests indicated that surprisingly little leakage current (10 mA at 12 kV) suffices to cause flaming ignition. Both testing and field experience, however, indicate that, because of the large wood member sizes, once ignited, the fires usually self-extinguish and the members are only partially burned.

Living or green trees have a much lower resistivity and are semiconductors, while dry trees are reasonably good insulators. Thus, Blackburn and Pau[2093] conducted tests with freshly-cut Eucalyptus trees to simulate a tree creating a high-impedance fault across a power distribution line. Cylindrical wood samples of various diameters and 0.4 m length were placed across a bare-conductor line and voltage was slowly raised across the line. Current flow was limited by a series resistor. It was found that ignition occurred in all cases below 0.5 A; a typical experimental result is shown in Figure 126. If a current limiting resistor was not used, they found that eventually the faults escalated to a short-circuit condition, which would have possibly tripped a circuit protection device. The high-impedance faults, however, clearly could not trip protection devices when currents were below 0.5 A. Blackburn and Pau also determined that the resistivity of undamaged (that is, without significant current flow) wood was 10 – 14 kΩ-m, and was independent of impressed voltage over the range 500 – 5000 V. As charring starts to develop, the resistivity drops rapidly until runaway conditions are reached. In the course of their experiments, they also noted that hot embers were dropped to the ground for a considerable period before short-circuit conditions were ultimately reached. Since the peak voltage across the specimens in their tests was measured at around 1700 V, it was concluded that the hazard is clearly demonstrated for voltage over 1700 V. But the authors considered it likely that, for long duration exposures, ignitions and short-circuit conditions could be experienced for voltages as low as 415 V. The pattern of charring was found to be initially concentrated near the two contacts, at which highest electric field values were recorded. Later in the test, the pattern of charring became more uniform along the length as did the electric field.

Both trees and wood poles are at high risk of ignition[1244] if the potential drop across the tree, induced from a high-voltage transmission line, exceeds about 100 kV, but of course the other results cited above indicate that ignition may occur at vastly lower voltages. Some additional studies on ignition of wood poles and crossarms were reviewed by Darveniza et al.[2094]

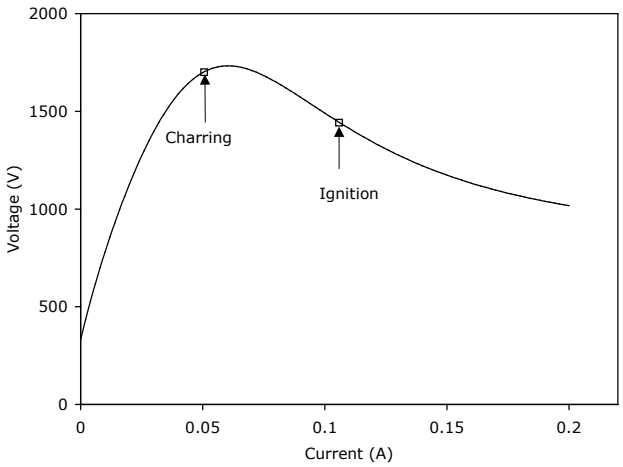


Figure 126 Voltage-current characteristic for Eucalyptus tree specimen bridged across a power line

WOOD COMPONENTS

A limited number of studies of the oxidation or ignition of wood components have been reported. Handa and coworkers[2095] conducted experiments to quantify the relative contributions of the three main constituents of wood: cellulose, hemicellulose, and lignin. They found that at 200ºC, if the HRR developed in the oxidation of cellulose is normalized to 1.0, then the HRR of hemicellulose is 2, the HRR of lignin is 12, while the HRR of wood (birch) is 4. Softwoods have a higher percentage of cellulose than do hardwoods, thus the implication is that they oxidize less readily. The results in this type of study, however, depend both on the temperature used and on experimental details. Roberts[2096] reviewed some other studies and these showed that hemicellulose invariably has a higher HRR than cellulose, but in most other studies the HRR of lignin was found to be much lower than what was determined by Handa, in some cases being lower than the HRR of cellulose. More extensive studies are available in the literature on pure cellulose, but since its oxidation is not the dominant factor in the self-heating of wood, extrapolations should not be made from studies on cellulose to the behavior of wood. Using their oxygen consumption technique, Handa et al. were able to measure the HRR of wood at temperatures as low as 150ºC, but found that up to 180ºC the HRR was quite small. From 180 to 210ºC there was a large jump in the HRR, with a subsequent tapering off (perhaps due to depletion of reactants). Using thermal analysis, they also demonstrated that, in the absence of oxygen, pyrolysis of wood is endothermic over its entire temperature range. They also observed that

even small amounts of moisture (1 – 3% MC) had very strong effects on the reactivity of char, tending to interfere with the consumption of oxygen and promote a closing down of opened-up pore structures. Similar studies were also made by Smith[2097], who studied fibers from numerous woods and found that the reaction rate was strongly affected by the percent of extractives in the fiber (the fraction extractable with an alcohol/benzene solution). For example, as extractives increased from 2.56% (cottonwood) to 7.03% (Ponderosa pine), the reaction rate increased 7-fold.

Buchanan[2098] studied the autoignition of wood components. Hemicellulose was found to ignite at 170 – 180ºC, lignin at 180 – 185ºC, and cellulose at 260ºC. DTA[2099,2100] and TGA[2101] studies conducted in an air atmosphere confirm that exothermicity is initially shown by hemicellulose at the lowest temperature, followed by lignin, followed by cellulose at the highest temperature. The phenol groups in lignin are considered to act as antioxidants[2102], but this fact alone does not give it an especially high ignition temperature. However, Kuriyama[2103] heated wood components in an aluminum retort and concluded that, under his test conditions, lignin had to be heated to a higher temperature in order to produce flammable decomposition products than did hemicellulose. As mentioned in the self-heating section above, limited studies indicate that resinous woods are much more prone to self-heating than non-resinous species. But data do not exist on this point for external-heating ignitions.

PAINTED WOOD

FRS studied the radiant ignition of wood surfaces painted with ordinary house paints[2104]. They found that there were two distinctly different ignition events—first the paint layer ignited, then substantially later the wood itself ignited. They also examined the effectiveness of various fire-retardant paints applied to low-density fiberboard, where they found that for untreated samples the critical flux for piloted ignition was 6.3 kW m^{-2} but that it was 8.4 – 41 kW m^{-2} for samples coated with various FR coating systems. Muir[1998] conducted piloted ignition tests on painted and unpainted cedar and found that oil-base paints slightly increased ignition times, but latex paint or spar varnish showed the opposite effect. In all cases the effect was quite small. The most extensive study so far has been by Staggs et al.[2105], who primed plywood and particleboard surfaces with a water-based primer then coated them with coats of alkyd enamel. Piloted ignition tests with the Cone Calorimeter at a 35 kW m^{-2} irradiance showed that one coat of enamel greatly increased the ignition time, two coats slightly increased the ignition time, while applying a larger number of coats caused a drastic decrease in ignition time (about 7-fold, compared to uncoated wood). A theoretical model was offered which can explain the basic trends. The authors consider that the increase in ignition time comes from a decrease in the surface absorptivity due to paint, while the increase is simply associated with volatile materials being pyrolyzed from the paint.

HARDBOARD

Hallman[440] examined the piloted, radiant ignition of hardboard (Masonite) samples of 1203 kg m^{-3} density and 3.2 mm thickness. His data show $\dot{q}''_{cr}$ = 9.7 kW m^{-2}, B_{ig} = 323. den Braven[1101] tested 6 mm thick hardboard and found $\dot{q}''_{min}$ = 11 kW m^{-2}. In a series of long-exposure experiments, Shoub and Bender[1626] exposed a 6 mm hardboard sample to a very low heat flux of 4.3 kW m^{-2}; autoignition occurred in 3.93 h. Test details are discussed in Chapter 7. Using the LIFT test[2113], $\dot{q}''_{min}$ was found to be 10 kW m^{-2} for 6.4 mm thick specimens and 14 kW m^{-2} for 3.2 mm thick ones. Painted specimens[1779,2113] showed slightly higher $\dot{q}''_{min}$ values of 14.7 – 17.0 kW m^{-2}. This included even a specimen painted with nitrocellulose paint (17.0 kW m^{-2}).

Tran et al.[2106] conducted large-scale mockup tests on wood siding made from hardboard. By placing 40 or 160 kW diffusion-flame burners adjacent to the siding, ignition was obtained in about 1 min. But ignition was not self-sustained and the fire went out when the igniting burner was shut off.

FIBERBOARD

Wood fiberboard (also called cellulose insulation board, even though it does not comprise pure cellulose) is made by interfelting wood fibers. The fibers do not have to come from trees, and a significant fraction is made from bagasse, which remains after sugar cane is processed. Although binders may be added, the felting process is mechanical, augmented by the ability of the lignin component to rebond when heated. The density range for wood fiberboard is 20 to 500 kg m^{-3}, although commercially densities of 180 to 300 kg m^{-3} are the most common. Even though wood fiberboard of 240 kg m^{-3} has half the density of whole wood, which might be 480 kg m^{-3}, its perpendicular-to-the-grain thermal conductivity (ca. 0.035 W m^{-1} K^{-1}) is only about 30% of whole wood's. Fiberboard is commonly used as sheathing board, for insulation of roofs, and as ceiling tiles.

Zicherman and Allard[2107] tested the ignition of fiberboard in the Setchkin furnace (Table 222). Their value for glowing-ignition temperature is essentially identical to the 250ºC recommended above for whole wood. They also measured the thermal conductivity of the FR specimens to be 0.053 W m^{-1} K^{-1} at 28ºC and 0.052 W m^{-1} K^{-1} at 93ºC. The FR treatment was boric acid, present in the specimen at a level of 7%. Much earlier (1947), the AIT of wood fiberboard[443] was reported by NIST as being 216 – 229ºC, but this does not appear to be a reliable value.

Ignition of wood fiberboard does not occur from very small flames such as the methenamine pill test[2032], but commonly occurs from plumbers' torches. Often the smoldering initiation is not observed until flaming breaks out, which can be from a half hour to several hours after initial ignition[2108]. It has been experimentally demonstrated[2109] that an ordinary Bunsen burner is also sufficient for ignition. The investigators found that, using a laboratory pre-burning procedure, only 2 out of 4 types of wood fiberboard tested could be ignited so that, after extinguishing visible flames, progressive smoldering would continue. Both asphalt-coated and uncoated specimens smoldered. However, the specimens which smoldered had densities of 240 and 245 kg m^{-3}, while the ones which did not had densities of 325 and 433 kg m^{-3}. This implies that the probability of initiation of smoldering is inversely related to density. Specimens that did smolder had a smoldering velocity of 66 – 71 mm h^{-1} in still air. These values are very close to the 57 – 79 mm h^{-1} velocities earlier measured by Palmer[2110]. When wind-blown, velocities can increase several-fold over the above values.

Ignitability of wood fiberboard from small-burner flames of the ISO 11925-2 test has been studied[2031]. Except for a very dense grade (443 kg m^{-3}) of fiberboard, ignition always occurred using a 15 s application of flame either to the surface or to the bottom edge, with flame always spreading farther than the 150 mm mark. The ignition temperature of medium-density (exact density unspecified) fiberboard was measured to be 330ºC in Cone Calorimeter testing[2111]. Using the LIFT test, the ignition temperature was measured to be 290ºC on fiberboard of unspecified density[2112].

In Cone Calorimeter tests, the minimum flux for piloted radiant ignition of low-density (270 kg m^{-3}) wood fiberboard was found to be 8 kW m^{-2} (see the example in Chapter 7). In one NIST study[1770] using the LIFT apparatus, the minimum flux for piloted radiant ignition of high-density (900 kg m^{-3}) wood fiberboard, was found to be 9.7 kW m^{-2} using the LIFT apparatus. In another study[2113] a minimum flux of 12 kW m^{-2} was reported for a low-density fiberboard. In a study by Shoub and Bender[1626] where long exposure times were used, it was found that 13 mm thick, 290 kg m^{-3} bagasse-fiber fiberboard autoignited in 0.92 h when exposed to a heat flux of 4.3 kW m^{-2}. Its face temperature was 260ºC at the time of ignition. Test details are discussed in Chapter 7.

Wood fiberboard can self-heat, however, it needs to be stacked into imprudently huge piles to self-heat at ambient temperature conditions. Although the initial temperature of the pile is not known, Mitchell[156] reports of an incident where a fire resulted when a pile of 680 m^3 was created. More numerous are incidents[445] where ignition takes place because the product was not allowed to cool down after manufacture before being stacked. Under such improper cooling conditions, truck-load quantities can ignite. A rough recommendation[1618] is that the product must be cooled down below 80ºC before stacking. Oven-dry fiberboard will adsorb moisture from the air. This is an exothermic process and contributes to self-heating of the material. Moisture effects cannot be included in simple F-K theory, and existing studies on moisture effects with fiberboard are mainly exploratory in nature, but they indicate that the effect can be serious[2115,2114]. Thus, a safety precaution in addition to cooling is to moisten the manufactured product to 8 – 9% moisture before stacking it[2115].

Table 222 Wood fiberboard results tested in the Setchkin furnace.

Specimen	Ignition temperature (ºC)		
	Glow	Flaming piloted	Flaming autoignition
untreated	249	310	377
FR-treated	318	310	427
FR-treated, painted	248	343	438

Thomas and Bowes[2116] re-analyzed the data of Mitchell[156] and Gross and Robertson[109] using a more refined formulation of self-heating theory. Their results (presented as a calculational example in Chapter 9) showed that ignition data of oven samples can be readily correlated in straight lines, just as the theory would predict. However, they then went on to compare the temperature rise predicted in the center of the sample under *subcritical* conditions to the theoretically computed value. The experimental value was about 10× the theoretical value (Figure 127). Thus, they concluded that at least two different exothermic reactions must be taken into account. The first reaction was consid-

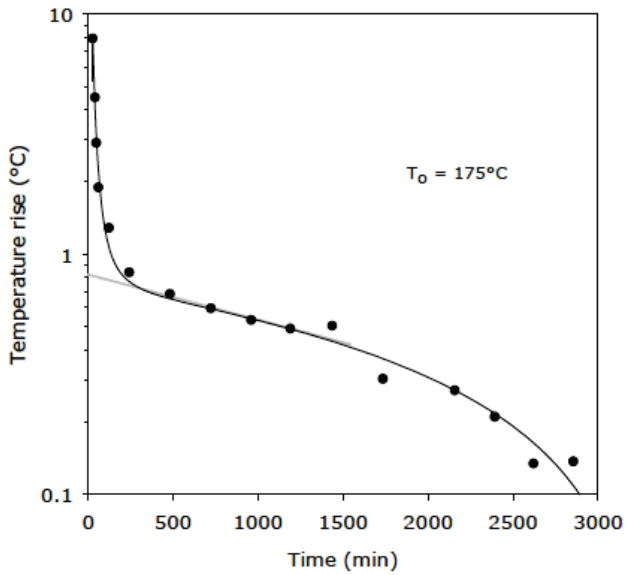


Figure 127 The self-heating of a 25 mm cube of wood fiberboard (gray line indicates extrapolated trend if only a single reaction were present)
(Copyright BRE Ltd.; reproduced by permission)

Table 223 Piloted radiant ignition results for plywood conditioned to room moisture and tested in the horizontal orientation in the Cone Calorimeter

Plywood	Thick. (mm)	Dens.	Ignition time (s) at various fluxes (given in kW m^{-2})											
			15	20	25	30	33	35	40	50	60	65	70	75
lauan[2118]	4	580			112			49		30				
hoop pine, FR[2118]	4	580			116			548		18				
plywood[2006]	5.5	600			158		81			28				
plywood[2006]	9	450			273		48			31				
Douglas fir[2119]	11.5	540	991	481	142	62		46	30	17		9		
Douglas fir[2119]	12	515			178	74		53	40	15		7		
Douglas fir, FR[2119]	11.8	560		840	423	181		129	44	30		21		
plywood, FR[2119]	11.5	600			621	222		181	42	28		22		
plywood[2006]	12	550			160		63			28				
plywood[2006]	18	520			268		79			33				
birch[425]	12	680			352					28				
plywood, FR[425]	9	620			100					25				
Gaboon[2021]	12	625		135		53			32	22	15		11	
plywood[2120]	9.4	630			476					47				12
plywood[2121]	15	440			72			34	21	16				
plywood, FR[2121]	15	460			301			12	8	5.5				

ered to be short-lasting, but with a high peak HRR, while the 'main' reaction was much slower. Their conclusion was that the total heat of reaction for either reactions was about 335 kJ kg^{-1}, but disagreement on this value among investigators has been vast. By using the simplest assumption of there being only one exothermic reaction, they assigned an activation energy of about 106 kJ mol^{-1}. Other wood materials results are tabulated in Table 220. Walker et al.[2117] reviewed the Thomas and Bowes findings and concluded: "It is unlikely that any natural organic solid material would oxidize by one single oxidation mechanism."

Walker and Harrison[2122] determined that there is some species effect on the self-heating propensity of wood fiberboard, with Monterey pine being less prone to self-heating than slash pine or European black pine (*pinus nigra*). Oxidation studies showed that there is no significant difference during later periods of thermal exposure, but that at the early stages there is more HRR from slash pine than from Monterey pine. They concluded that the differences can be attributed to the extractives content, which is higher for slash pine.

PLYWOOD

The thermal and ignition properties of plywood are roughly similar to that of whole wood. Thermal conductivity is generally found to be lower for plywood than for whole wood.

Janssens[1252] reported a minimum flux of 15.1 kW m^{-2} for 11 – 12 mm Douglas fir and Southern pine plywood specimens, both at 9% moisture content; the measured ignition temperature was 368ºC. He also found $\dot{q}''_{\min}$ = 24 kW m^{-2} for FR Southern pine plywood. Ignition times of plywood measured in the Cone Calorimeter by various investigators are given in Table 223. Note that ignition times for FR plywood are typically either similar to non-FR specimens, or shorter. Yet, full-scale tests indicate that room fire hazard development is much slower with FR plywood[2118], where its lower HRR plays the key role.

In a series of long-exposure experiments, Shoub and Bender[1626] exposed 13 mm thick, 630 kg m^{-3} plywood to a heat flux of 4.3 kW m^{-2} and found autoignition in 5.17 h. A T_{ig} of 254ºC was measured. The test details are described in Chapter 7.

Loftus conducted measurements self-heating measurements on two grades of plywood using an adiabatic calorimeter[1728]. From his results (Table 224), the computed critical thickness for a slab at 100ºC is 72 mm for plain plywood, while for FR plywood it is 68 mm. Loftus' measurements would imply that the self-heating propensity of plywood is higher than for wood sawdust and chips

Table 224 Self-heating parameters for plywood

Material	ρ (kg m^{-3})	C (J kg^{-1} K^{-1})	λ (W m^{-1} K^{-1})	E (kJ mol^{-1})	QA (W kg^{-1})
plywood	470	2300	0.107	87.9	4.18×10^{12}
FR plywood	590	2300	0.107	96.2	4.85×10^{13}

but this has not been compared under identical conditions of test.

PARTICLEBOARD AND ORIENTED STRAND BOARD

A value of $\dot{q}''_{min}$ = 19.7 kW m^{-2} was determined in the LIFT test[1252] for particleboard of 7% moisture content, and 13 mm thickness; the measured ignition temperature was 422ºC. Other values reported for this material[2113,2123] were $\dot{q}''_{min}$ = 15.5 – 16 kW m^{-2}. It was found the FR particle board required 25 kW m^{-2} for ignition in the Cone Calorimeter[2124]. Using the ICAL test, Urbas and Parker[2125] measured a piloted-ignition temperature for 13 mm Douglas fir particleboard of 270ºC at a flux of 15 kW m^{-2}. For heat fluxes of 30 – 50 kW m^{-2}, T_{ig} rose to 300 – 330ºC.

A value of $\dot{q}''_{min}$ = 14.8 kW m^{-2} was determined in the LIFT test[1252] for oriented strand board of 7% moisture content, 585 kg m^{-3} density, and 11.4 mm thickness; the measured ignition temperature was 364ºC.

WOOD SAWDUST, CHIPS, AND WASTES

Typical thermal properties for wood sawdust are: ρ = 70 – 260 kg m^{-3} (but normally at the low end of this range if the material is not tightly packed); λ = 0.035 – 0.064 W m^{-1} K^{-1}; C = 1700 – 1840 J kg^{-1} K^{-1}. Piloted Cone Calorimeter testing[2126] of wood chips (particle density = 650 kg m^{-3}; bulk density = 200 kg m^{-3}) gave an ignition time of 27 s at 35 kW m^{-2} irradiance and 20 s at 50 kW m^{-2}; these values are not too different from results obtained on very light weight solid wood samples. The Bureau of Mines[346] obtained AIT values of 270ºC for oak sawdust, 279ºC for red cedar sawdust, and 225ºC for bark removed from a 3-year old wood post. Bowes[2127] tested the autoignition of shavings from 6 species of woods in a tube furnace and found T_{ig} values of 238 – 248ºC. For a heated metal bar to ignite pine sawdust, a temperature of 648ºC was found to be needed[1613]. Pryce and Cole[2128] reported on a wide variety of ignition tests with large-scale wood chip piles. Generally, ignition was difficult to achieve since relative humidity was typically 70 – 80% during their tests.

Table 225 Effect of wood species on the self-heating of sawdust

Species	T_o (ºC)*	ρ kg m^{-3}	α (m^2 s^{-1})	E kJ mol^{-1}
Zelkova	118	279	2.3×10^{-7}	99
Telaling	119	214	2.5×10^{-7}	114
Western red cedar	124	153	2.7×10^{-7}	104
Sawara cedar	125	173	2.7×10^{-7}	104
Douglas fir	127	197	2.3×10^{-7}	103
Meranti	130	185	2.5×10^{-7}	133
Port Orford cedar	131	138	2.8×10^{-7}	116
Japanese cedar	132	145	3.0×10^{-7}	116
Palulownia	133	173	2.8×10^{-7}	109
Japanese red pine	133	253	2.2×10^{-7}	137
Eli ayanskya	135	138	2.7×10^{-7}	120
Alaska yellow cedar	136	138	2.8×10^{-7}	134
Japanese cypress	138	131	2.7×10^{-7}	147
Western hemlock	141	131	2.8×10^{-7}	137
Sitka spruce	142	131	2.8×10^{-7}	142

* - critical ambient temperature for an 0.61 m thick slab

Kotoyori[2129] conducted adiabatic furnace self-heating experiments on 15 different species of wood sawdusts and found distinct species differences, as shown in Table 225. There is a substantial difference between the least-safe and most-safe species, and this difference is not accounted for solely by density or E, but includes also the effect of QA, values of which were not tabulated by the author.

Sawdust and wood chip piles are known to show tendencies to self-heat. An experimental pile 7 m high reached spontaneous combustion in 9 months[2130]. However, standard recommendations for maximum safe storage heights of wood chip piles[1618] range from 8 to 18 m, depending on the type of wood. Self-heating in wood chips occurs through direct respiration of living cells, microbial action and fungal growth, and direct chemical oxidation of unsaturated fatty acids and other organic components. Fungal growth tends to be seen only after prolonged storage outdoors. A number of case histories of self-heating wood dust and chips have been collected[42]. It is reported[347] that a 30 m high pile of Douglas fir sawdust is likely to "ignite in a few months." Three piles of approximately 19 m high ignited in Sweden after rainy weather; presumably rain aided microbial growth[2131]. A detailed case history of a self-heating fire which occurred in a 250,000 m^3 pile of wood chips has been reported[2132]. The cause was assigned to an unusually high fraction of *resin* and to a presence of some very *fine-size* material. The former has been identified as a factor which tends to lower wood's ignition temperature. The contributing role of the fines was felt to be because they formed a blanketing layer near the outside of the pile, thereby decreasing the availability of convective cooling. Whether this is true is unclear, since if convective cooling is disrupted, so will the flow of oxygen to the center, and reducing oxygen inflow serves to reduce, not increase, the tendency to self-heating. It has also been stated[2133], somewhat more generally, that piles which contain material of varying sizes are found to self-heat more readily than piles of only coarse or only fine material, but a reason is not given. Rain promotes self-heating in wood chip piles, as does tramp metal, due to a catalytic action of iron[1618,2134]. Sawdust from seasoned lumber is less likely to self-heat than sawdust from green trees[2135]; this is presumably due to higher levels of microorganisms in freshly-cut timber.

A qualitative study[2136] has shown that whole-wood chips have a much more pronounced tendency toward self-

heating than do debarked chips. A ranking was established for self-heating as:

debarked chips < whole-wood chips < bark < foliage.

A case history was also reported for a production facility that monitored self-heating in a large pile of about 11 m high. The pile contained 30% whole-wood chips and 70% debarked chips. At 10 days after pile completion, a peak temperature of 97ºC was recorded. The temperature then dropped and leveled off at 57ºC. But one month later, a second rise began, reaching 102ºC. After a brief plateau, the temperature finally rose to 115ºC on the 49th day, at which the experiment was stopped. These results indicate that moisture appears to play a very strong role and that simple Frank-Kamenetskii theory is not appropriate. This was noted by Walker and Manssen[2137], who cited a case of a wood-chip pile where the interior temperature reached 90ºC, but actual fire did not break out until close to 1 year later. They concluded that a sizable moisture effect on the thermal conductivity of the material makes F-K theory inapplicable, and that a pile of sawdust or chips must dry out to below about 98% RH before thermal runaway becomes possible. They also stated that 75ºC is a critical temperature: most piles of sawdust, wood chips or wastes only self-heat to or below this value, with the exothermicity in this regime being due to microorganisms. But if rising temperatures over 75ºC are found, this indicates that chemical self-heating has taken over. There is no natural stopping temperature for chemical self-heating, in the way that bacterial growth stops at ca. 75ºC. Thus, if 75ºC is surpassed, the likelihood becomes significant that thermal runaway has started.

A case has been reported[1197] where filling material comprising sawdust and wood chips ignited from a steam pipe which was at 100ºC. The dimensions of the space occupied by the filling material was not specified, but clearly it was of modest size. In another case, the same authors investigated a fire around a condensate water tank, which was surrounded by wood boards and then with wood shavings. The case is of interest since the temperature of the tank could not have exceeded 100ºC. In another case, the authors describe the ignition of the wood shavings that formed a ceiling insulation around a vent pipe which did not exceed 65ºC. Not involving any elevated temperatures was a series of fires in the 1920s that occurred in icehouses insulated with wood sawdust and shavings[2138]. The wall cavity thicknesses were only 0.3 m, so presumably some contamination played a role.

Springer et al.[2139] conducted laboratory studies on chips of aspen and Douglas fir. For samples that were steam sterilized, killing both bacteria and living cells, no oxygen consumption or CO_2 release could be found below 35 – 40ºC. By contrast, samples free of microorganisms but with living cells not destroyed, showed strong oxidation from room temperature to ca 40ºC, then tapering off to zero as high temperatures killed cell activity when ca. 55ºC was reached. Beyond this temperature, chemical oxidation was seen as the only mechanism available for self-heating. Walker and Harrison[2134] studied the self-heating of wet sawdust and found a large catalytic effect of iron—in the presence of iron compounds, reaction rates approximately doubled. They considered it a relevant factor in spontaneous combustion of wood-wastes, where materials such as lengths of broken wire rope, may often be found.

Bowes and Thomas[2140] reported some self-heating properties of wood sawdust, obtained from a combination of testing, theory, and estimation. They assigned an activation energy E of 96 kJ mol^{-1} for the reaction. The order of the reaction was determined to be n = 2/3. Other results on wood sawdust are listed in Table 220 above. Sopping-wet sawdust cannot smolder. In bench-scale tests, it was found that at 40% MC, sawdust would no longer smolder. At 5% MC, a smolder velocity of 0.55 mm min^{-1} was found, dropping to 0.23 mm min^{-1} at 35% MC.

OILED SAWDUST

The self-heating tendency is exacerbated when the wood material is mixed or contaminated with vegetable or animal oils, nitric acid, and certain glues and organic dyes. Ettling and Adams made a study of sawdust mixed with boiled linseed oil[2141]. In one set of experiments, they found that an 80 g pile of sawdust+oil, mixed in a 1:1 weight ratio, was the minimum weight needed to lead to runaway at an ambient temperature of 22ºC. The time to reach critical conditions was ca. 28 h. At 30ºC, the time dropped to 9 h. A 1:1 mixture was close to the worst condition and increasing the proportion of oil beyond that decreased the amount of self-heating. The 1:1 mixture was also about the maximum amount of oil that will be readily absorbed by sawdust without dripping of excess; the amount of oil which can be absorbed, however, decreases with increasing pile sizes of sawdust. In another series of experiments, where the material was arranged differently, 24 g sufficed to lead to runaway. Moisture in the sawdust was found to reduce the self-heating, but the effect of contaminants, such as metal and floor sweepings was insignificant.

Sawdust mixed with raw linseed oil was studied by Napier and Vlatis[2142]. In their work, they ran both oven-cube tests and hotplate tests on sawdust+oil layers. They found that an oil content of 35 – 40% led to the greatest self-heating, which is not too different from the 50% seen in Ettling's study. They also found that very thin layers (5 mm) tend to crack when self-heating, which affects the heat transfer of the layer. In attempting to reduce their data according to standard self-heating theory, they found that the activation energy depended greatly on the moisture content of the mixture. For predictive applications, data would be needed in a form which accounts for both the loading percent of oil and the moisture content, but the work was not carried to that stage.

It has been suggested that propionic acid could be used to retard the self-heating effects in oiled sawdust, however, this is unlikely to be an economical solution.

WOOD PULP

Buchanan[2098] reported values of 210 – 265ºC for the AIT of various types of wood pulp.

SHINGLES AND SHAKES

Roofing shingles (produced by sawing) and shakes (produced by splitting) that are not fire-retardant treated are ignitable by 38 mm fire brands, but with a probability of significantly less than 100%[1049]. When shingles/shakes are weathered, they become more readily ignitable.

Wood-burning appliances

Wood-burning appliances include fireplaces, wood-burning stoves, wood-burning fireplace inserts, and similar devices. Pellet stoves, which burn small pellets compressed from wood sawdust, are a specialized form of wood-burning appliance. US statistics[289] on fires from these appliances are shown in Table 226 and Table 227.

An early study by Voigt [2143] showed that flue pipe temperatures typically ranged up to 450 – 480ºC. Temperatures on the metal base of stoves went up to 500 – 600ºC. Based on his test results, Voigt recommended that clearances of 300 mm be observed from wood ceilings or joists. For single-wall flue pipes passing through combustible walls, he recommended that either a ventilated air space of 100 mm be provided, or else that the annulus size could be reduced to 50 mm if it was packed with thermal insulation. Peacock[296] examined the results from a number of laboratory studies and concluded that peak external surface temperatures of wood-burning appliances may reach up to 300 – 450ºC, with flue gas temperatures reaching to about 700ºC. However, under improper use conditions, i.e., overfiring, the temperatures can be higher. Figure 128 shows the consequence of overfiring a fireplace with too much wood—a structural wood member inside the wall was ignited right above the fireplace.

Table 226 Equipment involved in wood-burning appliance fires

Source of fire	Percent
appliance	55
chimney	35
chimney connector	10

Table 227 Causes of wood-burning appliance fires

Cause	Percent
improper maintenance	27.5
combustibles (occupant goods) too close	18.1
improper equipment design	10.0
exterior fire from sparks	9.2
improper operation	7.5
ignition of structure	6.7
improper fueling technique	5.5
equipment malfunction	4.4
improper installation	2.4
improper chimney	1.3
use of flammable liquids	1.2
chimney fire	0.2
other	0.3



Figure 128 Ignition of wood wall-framing member from an overfired fireplace
(Courtesy Tim Bradley)

The process of burning wood pellets creates small burning embers which go up the chimney. Roof fires have occurred when such embers leaving the chimney landed on a wood-shake roof[2144].

Wool

The AIT of wool blankets[443] was reported by NIST in 1947 as being 205ºC. The method used, however, appears to give anomalously low values with other materials. Lawson[2145] reported that the minimum flux for ignition of wool fabrics is about 33 kW m^{-2} for piloted ignition and 84 kW m^{-2} for autoignition, but it is not clear what measurements were made to obtain the values.

Self-heating fires are known to occur in bales of greasy wool[1710]. Walker and coworkers examined the problem in a series of very extensive studies[2146-2149]. Self-heating problems do not occur with wool that is sheared—only with wool removed by chemical means or by a rotting process. For the latter, again no problems have been found for grease-free and completely dry wool; however wet (with water in excess of that needed to saturate the interstitial atmosphere) or moist (water content below that needed for saturation) wool will self-heat. The amount of water required to cause interstitial saturation is about 33%, dry basis ('re-gain'), but 'wet' wool can easily contain 100% moisture. Bales of wool at around 400 kg m^{-3} density may show significant, albeit sub-critical, self-heating if they have as little as 18% moisture and are thus substantially below the moisture needed for saturation. Significantly accelerated

self-heating starts for wool under conditions of RH > 85%, with an 85% RH corresponding to about 18% regain. Under most circumstances, self-heating stops at a temperature of around 76ºC, which is indicative of the death of microorganisms. Two types of bacteria are involved in the process—mesophilic ones dominating at lower temperatures and thermophilic ones at higher. Both are aerobic, since no self-heating is found under inert atmospheres. In a few laboratory tests, self-heating up to the vicinity of 100ºC was observed. The exothermicity at such higher temperatures is presumed to be of chemical, rather than biological, nature, but details have not been understood yet. It is also suggested that molds may contribute to the heating process. The balance between biological and chemical reactions is also not fully understood. In terms of moisture, the requirements are opposite: high moisture contents are conducive to bacterial heating, but deleterious to chemical oxidation, since water saturation reduces the supply of oxygen to the interior of the bale. The main chemical effect is considered to be the oxidation of unsaturated fatty acids. Trace amounts of iron and manganese may also act as catalysts. The self-heating of bales of wool is due to the subcutaneous fats that are mixed in, rather than the fibers themselves. Thus, self-heating problems can generally be eliminated by adoption of processing methods which are designed to minimize contamination of the wool with the fats[2150]. A small amount of grease in wool (about 1%) does not contribute to self heating—such wool exhibits self-heating characteristics that are essentially identical to Soxhlet extracted samples[2151].

Self-heating may also occur for bales of wool that are not greasy due to moisture of sorption effects, and Back noted that bales of wool coming from a dry climate have ignited when transported to a humid harbor area[2115]. Karim and Mehta[1418] found that clean wool samples start to smolder at about 200ºC. Jones reported results on standard oven-cube tests on greasy-fleece Merino wool specimens[2152]. For wool at 114 kg m^{-3} density, his data gives E = 91.5 kJ mol^{-1} and P = 42.5. While bulk density, of course, is one of the major variables governing self-heating, it was shown that for wool the fiber diameter does not affect self-heating results[2153]. It has been shown that the energy of compressing wool for shipping has a negligible effect on self-heating. There do not appear to be problems of wool textiles undergoing self-heating except in commercial cleaners' drying facilities, where higher ambient temperatures are attained[2154].

Further readings

Two NFPA publications contain extensive tabulated data. Hazardous Chemicals Data (NFPA 49) is essentially a compilation of brief-form MSDS information; flash points, flammability limits, and AIT values are given where available. Guide to Fire Hazard Properties of Flammable Liquids, Gases, and Volatile Solids (NFPA 325) presents similar information as does NFPA 49, but arranged in tabular format, without narratives. A larger number of chemicals are collected here than in NFPA 49.

P. G. Urben, ed., **Bretherick's Handbook of Reactive Chemical Hazards: An Indexed Guide to Published Data**, 2 vol. set, 5th edition, Butterworth-Heinemann, Oxford (1995). Bretherick's compilation of hazards of reactive chemicals is the most comprehensive collection on this topic. It is especially useful because references are given to primary literature sources for each material discussed. A chemical explanation is generally provided *why* a hazardous reaction occurs, a feature absent in most other hazardous materials handbooks. Of additional interest is Louis Médard's **Accidental Explosions**, 2 vols., Ellis Horwood, Chichester, England (1989). The second volume of this monograph is a handbook of reactive substances; the number of compounds covered is much smaller than in Urben's work, but extensive narrative information is provided for each.

Recommendations on the Transport of Dangerous Goods: Model Regulations, United Nations, New York. The periodically-revised UN compilation is the basis for regulations established in the US by the Dept. of Transportation governing shipping requirements, test methods, and prohibitions. Most common chemicals which are reactive, unstable, etc. are included in the compilation. The listing gives transportation restrictions, but does not provide a chemical description of the hazard.

T. E. Daubert, **Physical and Thermodynamic Properties of Pure Chemicals**, 4 loose-leaf vols. plus annual supplements. Taylor & Francis, Bristol PA (1995). This compilation of thermochemical data is based on the results from an AIChE research project and is an excellent reference for heats of formation of a wide array of pure chemical substances. From the heats of formation, heats of combustion can be computed.

Fire Test Standards, 5th ed., ASTM (1999). Most—but not all—of the ASTM standards that deal with fire performance are collected in this massive, but reasonably priced tome. Apart from the ASTM tests discussed in the present work, this tome contains the full texts of many other test methods dealing with ignition properties in specialized applications.

References

1. Armstrong, A., Armstrong Forensic Laboratory, private communication (2001).
2. Gohar, M. M., Accelerant Behavior in Fire, *Fire & Arson Investigator* **34**:2, 29-32 (Dec. 1983).
3. Urben, P. G., ed., **Bretherick's Handbook of Reactive Chemical Hazards: An Indexed Guide to Published Data**, 2 vols., 5th ed., Butterworth-Heinemann, Oxford (1995).
4. Zabetakis, M. G., Flammability Characteristics of Combustible Gases and Vapors (Bulletin 627), Bureau of Mines, Pittsburgh (1965).
5. Calcote, H. F., Gregory, C. A. jr, Barnett, C. M., and Gilmer, R. B., Spark Ignition: Effect of Molecular Structure, *Ind. and Eng. Chem.* **44**, 2656-2662 (1952).
6. Litchfield, E. L., Hay, M. H., and Cohen, D. J., Initiation of Spherical Detonation in Acetylene-Oxygen Mixtures (RI 7061), Bureau of Mines, Pittsburgh (1967).
7. Sutherland, M. E., and Wegert, H. W., An Acetylene Decomposition Incident, *Chem. Eng. Prog.* **69**:4, 48-51 (1973).
8. Miller, S. A., **Acetylene, Its Properties, Manufacture and Uses**, 2 vols., Academic, New York (1965).
9. Williams, A., and Smith, D. B., The Combustion and Oxidation of Acetylene, *Chem. Reviews* **70**, 267-293 (1970)
10. Jones, G. W., Kennedy, R. E., and Spolan, I., Effect of Hydrocarbons and Other Gases upon the Explosibility of Acetylene (RI 4196), Bureau of Mines, Pittsburgh (1948).
11. Nelson, H. H., The Effect of Pipe Diameter on the Thermal Decomposition of Acetylenes, pp. 823-827 in *6th Symp. (Intl.) on Combustion*, The Combustion Institute, Pittsburgh (1956).
12. Detz, C. M., and Sargent, H. B., Acetylene: Physical and Chemical Properties and Explosive Behavior, pp. 192-203 in **Kirk-Othmer Encyclopedia of Chemical Technology**, 3rd ed., vol. 1, Wiley, New York (1978).
13. Detz, C. M., Threshold Conditions for the Ignition of Acetylene Gas by a Heated Wire, *Combustion and Flame* **26**, 45-55 (1976).
14. Miller, S. A., and Penny, E., Hazards in Handling Acetylene in Chemical Processes Particularly under Pressure, pp. 87-94 in *Proc. Symp. on Chemical Process Hazards with Special Reference to Plant Design*, Institution of Chemical Engineers, London (1960).
15. Brameld, V. F., Clark, M. T., and Seyfang, A. P., Copper Acetylides, *J. Soc. Chemical Industry* **66**, 346-353 (1947).
16. Ness, C., **The Safe and Efficient Handling of Acetylene**, Linde Div., Union Carbide Corp. (1958).
17. Powell, F., Ignition of Gases and Vapours by Hot Surfaces and Particles—A Review, pp. 267-299 in *Report of the 9th Intl. Symp. on Prevention of Occupational Accidents and Diseases in the Chemical Industry*, Intl. Social Security Assn., Lucerne (1984).
18. Ashmore, F. S., Dealing with Acetylene, *Fire Prevention*, No. 204, 37-38 (Nov. 1987); also, Anon., Better Guidance Needed, Inquest Told, *ibid.*, p. 39.
19. Fire Tests on Acetylene Cylinders (unpublished reports on Project R05.050), Health & Safety Laboratory, Health and Safety Executive, Buxton, England (1994-95).
20. **AGA Gas Handbook**, K. Ahlberg, ed., AGA AB, Lidingö, Sweden (1985).
21. Jones, B., Home Office Procedure for Dealing with Acetylene Cylinders in Fire—Paradox or Paradigm? *Fire Research and Management* **5**, 39-45 (1999).
22. Fowler, A. H. K., and Baxter, A., Fires, Explosions and Related Incidents at Work in Great Britain in 1996/97 and 1997/98, *J. Loss Prevention in the Process Industries* **13**, 547-554 (2000).
23. Price, J. W. H., An Acetylene Gas Cylinder Explosion, *J. Pressure Vessel Technology* **120**, 62-68 (1998).
24. Bjerketvedt, D., Bakke, J. R., and van Wingerden, K., Gas Explosion Handbook, *J. Hazardous Materials* **52**, 1-150 (1997).
25. Carver, F. W. S., Hards, D. J., and Hunt, K., The Explosibility of Some Unsaturated C4 Hydrocarbon Fractions, pp. 99-116 in *Proc. Symp. on Chemical Process Hazards with Special Reference to Plant Design—V* (Symp. Series 39a), The Institution of Chemical Engineers, London (1974).
26. Médard, L. A., **Accidental Explosions**, 2 vols., Ellis Horwood, Chichester, England (1989).
27. DeHaan, J. D., and Howard, W. A., Combustion Explosions Involving Household Aerosol Products, pp. 67-71 in *20th Intl. Conf. on Fire Safety*, Product Safety Corp., Sunnyvale, CA (1995).
28. Krämer, H., and Fröchtenigt, H., Electrostatic Charging of Spray Cans, *J. Electrostatics* **30**, 159-164 (1993).
29. Accidents Caused by Ignition of Aerosols, Sambrook Research Intl. for Dept. of Trade and Industry, London (1997).
30. Fox, M., unpublished information.
31. *The Irish Emigrant* [Galway, Ireland], Bits and Pieces, No. 547 (28 July 1997).
32. Miura, H., and Hirata, K., Dangerous Properties of Pressurized Containers such as Spray and Liquid Butane Gas Bomb, *Annual Report of the Fire Research Laboratory, Nagoya City Fire Dept.* **18**, 36-57 (1989).
33. Hawthorne, C., and Blake, D., Performance of Improved Aerosol Cans Subjected to an Aircraft Fire (DOT/FAA/AR-TN98/78), Federal Aviation Admin., Atlantic City NJ (1995).
34. Dufour, R. E., and Clogston, C. C., The Spontaneous Ignition and Dust Explosion Hazards of Certain Soybean Products (Bull. of Research 47), Underwriters' Laboratories, Inc., Chicago (1953).
35. Medem, R., **Die Selbstentzündung von Heu und Steinkohlen** (1895). Second ed.: **Die Selbstentzündung von Heu, Steinkohlen und geölten Stoffen**, Julius Abel, Greifswald (1898).
36. Bailey, C. H., The Moisture Content of Heating Wheat, *J. Amer. Soc. Agronomy* **9**, 248-251 (1917).
37. Bailey, C. H., The Handling and Storage of Spring Wheat, *J. Amer. Soc. Agronomy* **9**, 275-281 (1917).
38. Milner, M., and Geddes, W. F., Grain Storage Studies. IV. Biological and Chemical Factors Involved in the Spontaneous Heating of Soybeans, *Cereal Chemistry* **23**, 449-470 (1946).
39. Sallans, H. R., Sinclair, G. D., and Larmour, R. K., The Spontaneous Heating of Flaxseed and Sunflower Seed Stored under Adiabatic Conditions, *Canadian J. Research* **22F**, 181-190 (1944).
40. Better, E. J., Spontaneous Combustion in the Oil and Soap Industries, *The Industrial Chemist* **15**, 361-362 (1939).
41. Kubler, H., Self-Heating of Lignocellulosic Materials, pp. 429-449 in *Fire and Polymers—Hazards Identification and Prevention* (Symp. Series 425), American Chemical Society, Washington (1990).

42. van Wingerden, K., and Alfert, F., Detection and Suppression of Smouldering Fires in Industrial Plants (Report CMR-94-F25068). Christian Michelsen Research AS, Bergen, Norway (1994).
43. Bowes, P. C., Burgoyne, J. H., Hilditch, T. P., and Thomas, A., Spontaneous Heating and Ignition of Stored Palm Kernels. *J. Science Food Agric.* **1**, 360-366 (1950); **2**, 8-30; 79-91 (1951).
44. Walker, I. K., Spontaneous Ignition of Spent Brewing Grains, *New Zealand J. Sci.* **4**, 230-247 (1961).
45. Franke, A., Stiegler, R., and Werner, D., Selbstentzündung—eine oftmals unterschätzte Zundquelle Beispiele aus der Praxis [Spontaneous Ignition—An often Underestimated Source of Ignition—Examples from Practice], *Brandschutz, Explosionsschutz* **18**, 126-134 (1989).
46. Mills, J. T., Spoilage and Heating of Stored Agricultural Products (Publ. 1823E), Research Branch, Agriculture Canada, Ottawa (1989).
47. Cotton Gin Fires Caused by Static Electricity (Departmental Circular 28), Dept. of Agriculture, Washington (1919).
48. Dahn, J. C., Electrostatic Characterization of Grain Products (SMS-80-046), National Grain and Feed Assn., Washington (1980).
49. Singh, S., Cartwright, P., and Thorpe, D., Silo Electrostatic Hazards (SMS-84-052), National Grain and Feed Assn., Washington (1984).
50. Compressed-Air Line Explosions, *Power Generation* **52**, 86-89 (Jan. 1948).
51. Raivo, B. D., Baker, E. L., and Green, R. C., Guidance for Oil Flooded Rotary Screw Air Compressors, Lockheed Martin Idaho Technologies Co. (1999).
52. Fowle, T. I., Air Compressor Fires and Explosions, *Fire Prevention Science and Technology*, No. 7, 20-27 (1973).
53. Burgoyne, J. H., and Craven, A. D., Fire and Explosion Hazards in Compressed Air Systems, *7th Loss Prevention Symp.*, AIChE (1972).
54. Schmitt, D. W., Compressor Test Facility Explosion, pp. 59-63 in **Fire Protection Manual for Hydrocarbon Processing Plants**, vol. 1, C. H. Vervalin, ed., 2nd ed., Gulf Publishing, Houston (1973).
55. Perlee, H. E., and Zabetakis, M. G., Compressor and Related Explosions (RI 8187), Bureau of Mines, Pittsburgh (1963).
56. Fitz, M. M., MDE Engineers, private communication (2002).
57. Chase, J. D., Evaporation and Ignition in Air of a Surface Oil Film Following Adiabatic Compression, *Combustion and Flame* **10**, 315-329 (1966).
58. Chase, J. D., Ignition Caused by the Adiabatic Compression of Air in Contact with Lubricating-Oil Wetted Surfaces, *Proc. Instn. Mech. Engineers* **181**, Part 1, 243-258 (1966/67).
59. Burgoyne, J. H., and Craven, A. D., Fire and Explosion Hazards in Compressed Air Systems, pp. 79-87 in *7th Loss Prevention Symp.*, AIChE (1972).
60. Busch, H. W., Berger, L. B., and Schrenk, H. H., The Carbon-Oxygen Complex as a Possible Initiator of Explosions and Formation of Carbon Monoxide in Compressed-Air Systems (RI 4465), Bureau of Mines, Pittsburgh (1949).
61. Laing, P. D., and Russell, A. G., Fires in Oil Injected Screw Compressors–Their Prediction, Analysis and Prevention, Paper C146/80, pp. 19-25 in *Fluid Machinery Failures–Prediction, Analysis and Prevention*, Institution of Mechanical Engineers, London (1980).
62. Loison, R., The Mechanism of Explosions in Compressed-Air Pipe Ranges, paper No. 26 in *7th Intl. Conf. of Directors of Safety in Mines Research*, SMRE (1952).
63. Matsui, H., and Komamiya, K., An Experimental Study of Soot Film Detonations, pp. 559-570 in *Prog. in Astronautics and Aeronautics*, Vol. 106, AIAA, New York (1986).
64. Ostroot, G. jr., Lessons Learned from a Coupling Failure and Lube Oil Fire, *1st Loss Prevention Symp.*, AIChE (1967).
65. Jones, S., The Ignition Hazard from Leaks of Compressed Air (Research Report 137), Safety in Mines Research Establishment, Sheffield, England (1956).
66. Luzik, S. J., How to Limit Fire and Explosion Hazards with Oil-flooded Rotary Screw Compressors, *Mining Engineering* (Littleton CO) **40**, 881-884 (Sep. 1988).
67. Dale, R. A., Electrostatic Hazards in Coal Mining (SMRE Research Report 118), Safety in Mines Research Establishment, Sheffield, England (1955).
68. Thompson, W., and Titman, H., Incendivity of Frictional Sparks Produced within a Compressed-Air Motor and Expelled in the Exhaust (Research Report 60), Safety in Mines Research Establishment, Sheffield, England (1953).
69. Faeth, G. M., Thermal Environment of Combustibles During Pneumatic Charging Processes, *Naval Engineers J.* **77**, 299-307 (1965).
70. Ridgway, R. S., The Mechanism of Explosions in Starting Air Lines, *Petroleum Refiner* **37**:6, 171-174 (1958).
71. Harkleroad, M. F., Ignition and Flame Spread Measurements of Aircraft Lining Materials (NBSIR 88-3773), NBS (1988).
72. Newman, M. M., and Robb, J. D., Investigation of Minimum Corona Type Currents for Ignition of Aircraft Fuel Vapors (NASA TN D-440), NASA, Washington (1960).
73. Harrison, L. P., Lightning Discharges to Aircraft and Associated Meteorological Conditions (NACA TN 1001), NACA, Washington (1946).
74. Robb, J. D., Hill, E. L., Newman, M. M., and Stahmann, J. R., Lightning Hazards to Aircraft Fuel Tanks (NACA TN 4326), NACA, Washington (1958).
75. Oh, L. L., and Schneider, S. D., Lightning Strike Performance of Thin Metal Skin, *Lightning and Static Electricity Conf.*, Royal Aeronautical Society, London (1975).
76. Robb, J. D., Stahmann, J. R., Chen, T., and Mudd, C. P., Swept Lightning Stroke Effects on Painted Surfaces and Composites of Helicopters and Fixed Wing Aircraft, *Lightning and Static Electricity Conf.*, Royal Aeronautical Society, London (1975).
77. Alcoholic Beverages Burn Efficiently, but Don't Prove to be Very Effective Accelerants, *Fire Findings* **6**:3, 1-3 (Summer 1998).
78. Guide to Fire Hazard Properties of Flammable Liquids, Gases, and Volatile Solids (NFPA 325), NFPA.
79. Britton, L. G., Flammability of Lower Aliphatic Aldehydes at Elevated Pressure and Temperature, *Process Safety Progress* **17**, 138-148 (1998).
80. Khan, A. S., Kelley, R. D., and Chapman, K. S., Flammability Limits of Ammonia-Air Mixtures, *ASHRAE Trans.* **101**, Part 2, 454-462 (1995).
81. Ginsburgh, I., and Bulkley, W., Industrial Aspects of Hydrocarbon-Air Detonations, pp. 198-205; 220 in **Fire Protection Manual for Hydrocarbon Processing Plants**, vol. 1, C. H. Vervalin, ed., 2nd ed., Gulf Publishing, Houston (1973).

82. Explosion of Ammonia-Air Mixture, *J. Royal Inst. Chem.* **80**, 663-664 (1956).
83. Ammonia Explosion, $200,000 Loss, Jackson, Miss., *Fire J.* **73**:5, 13 (Sep. 1979).
84. McRae, M. H., Ammonia Explosion Destroys Ice Cream Plant, *Fire Command* **51**:4, 36-37 (Apr. 1984).
85. Klem, T. J., Explosion in Cold Storage Kills Fire Fighter, *Fire J.* **79**:2, 43-46, 79-80 (Mar. 1985).
86. Colley, K., Explosions and Fire Scuttle Homer, AK Seafood Plant, *American Fire J.* **51**:1, 6-8 (Jan. 1999).
87. Scott, G. S., and Grant, R. L., Ammonium Nitrate: Its Properties and Fire and Explosion Hazards (IC 7463), Bureau of Mines, Pittsburgh (1948).
88. Kintz, G. M., Jones, G. W., and Carpenter, C. B., Explosions of Ammonium Nitrate Fertilizer on Board the S.S. Grandcamp and the S.S. Highflyer at Texas City, Tex., April 16, 17, 1947 (RI 4245), Bureau of Mines, Pittsburgh (1948).
89. van der Steen, A., Groothuizen, D., and de Jong, E., Detonation Properties of Industrial Substances, pp. 105-118 in *Proc. Intl. Workshop on Safety in the Transport, Storage and Use of Hazardous Materials*, National Research Institute of Fire and Disaster, Tokyo (1998).
90. **Encyclopedia of Explosives and Related Items**, B. T. Fedoroff, et al., eds., Picatinny Arsenal, Dover NJ (1960-1983).
91. Van Dolah, R. W., Mason, C. M., Perzak, F. J. P., Hay, J. E., and Forshey, D. R., Explosion Hazards of Ammonium Nitrate under Fire Exposure (RI 6773), Bureau of Mines, Pittsburgh (1966).
92. Van Dolah, R. W., Gibson, F. C., and Murphy, J. N., Sympathetic Detonation of Ammonium Nitrate and Ammonium Nitrate-Fuel Oil (RI 6746), Bureau of Mines, Pittsburgh (1966).
93. Arai, H., et al., Detonation Behaviour of ANFO in Resin Tubes, pp. 29-32 in *APSS2001—Proc. Asia Pacific Symp. on Safety*, Vol. 2, Japan Soc. for Safety Engineering, Yokohama (2001).
94. Cook, M. A., Explosives: A Survey of Technical Advances, *Ind. and Eng. Chem.* **60**, 44-55 (July 1968).
95. Burns, J. J, Scott, G., S., Jones, G. W., and Lewis, B., Investigations on the Explosibility of Ammonium Nitrate (RI 4994), Bureau of Mines, Pittsburgh (1953).
96. Findlay, A., and Rosebourne, C., Note on the Decomposition and Stability of Ammonium Nitrate in the Presence of Oxidisable Material, *J. Soc. Chemical Ind.* **41**, 58T-59T (1922).
97. Lewis, B., Report of Research and Technologic Work on Explosives, Explosions, and Flames—Fiscal Years 1947 and 1948 (RI 4502), Bureau of Mines, Pittsburgh (1947).
98. Progress Report. Study of Marking, Rendering Inert, and Licensing of Explosive Materials, Dept. of Treasury, Washington (1997).
99. Watson, R. W., Hay, J. E., and Becker, K. R., Sensitivity of Some Ammonium Nitrate Based Explosive Compositions (RI 7840), Bureau of Mines, Pittsburgh (1974).
100. Nabiullah, M., Gupta, R. N., and Singh, B., An Investigation into the Thermal Behaviour of Emulsion Explosive and Detonating Fuse, pp. 702-712 in *Proc. 23rd Intl. Conf. Safety in Mines Research Institutes*, Bureau of Mines, Washington (1989).
101. Rogers, R. N., Janney, J. L., and Loverro, N. P. jr., Thermal Stability and Compatibility Predictions for the Explosive EAK, *J. Energetic Materials* **2**, 293-330 (1984).
102. Hainer, R. M., The Application of Kinetics to the Hazardous Behavior of Ammonium Nitrate, pp. 224-230 in *5th Symp. (Intl.) on Combustion*, Reinhold, New York (1954).
103. Finger, M., et al., Characterization of Commercial, Composite Explosives, pp. 729-739 in *Proc. 6th Symp. (Intl.) on Detonation*, Office of Naval Research, Dept. of the Navy, Arlington VA (1976).
104. Cook, M. A., **The Science of Industrial Explosives**, Ireco Chemicals, Salt Lake City (1974).
105. Code for the Storage of Ammonium Nitrate (NFPA 490), NFPA.
106. Explosive Materials Code (NFPA 495), NFPA.
107. Jacobs, P. W. M., and Whitehead, H. M., Decomposition and Combustion of Ammonium Perchlorate, *Chem. Reviews* **69**, 551-590 (1969).
108. Solymosi, F., and Fógany, K., Effect of Cadmium Oxide and Cadmium Perchlorate on the Decomposition and Ignition of Ammonium Perchlorate, pp. 429-437 in *11th Symp. (Intl.) on Combustion*, The Combustion Institute, Pittsburgh (1966).
109. Gross, D., and Robertson, A. F., Self-Ignition Temperatures of Materials from Kinetic-Reaction Data, *J. Research NBS* **61**, 413-417 (1958).
110. Jacobs, P. W. M., and Russell-Jones, A., The Thermal Decomposition and Ignition of Mixtures of Ammonium Perchlorate + Copper Chromite, pp. 457-462 in *11th Symp. (Intl.) on Combustion*, The Combustion Institute, Pittsburgh (1966).
111. Powling, J., Experiments Relating to the Combustion of Ammonium Perchlorate-Based Propellants, pp. 447-456 in *11th Symp. (Intl.) on Combustion*, The Combustion Institute, Pittsburgh (1966).
112. Levy, J. B., and Friedman, R., Further Studies of Pure Ammonium Perchlorate Deflagration, pp. 663-672 in *8th Symp. (Intl.) on Combustion*, The Combustion Institute, Pittsburgh (1960).
113. McIntyre, F. L., Westover, D., and Caltagirone, J., Hazards Testing of Ammonium Perchlorate (ARLCD-CR-82026), US Army Armament R&D Command, Dover NJ (1982).
114. Routley, J. G., Fire and Explosions at Rocket Fuel Plant, Henderson, Nevada (Report 021), Fed. Emergency Management Agency, Emmitsburg MD (1988).
115. Luzik, S. J., Fire and Explosion Investigation—Pacific Engineering and Production Co. of Nevada, May 4, 1988, Bruceton Safety Technology Center, Mine Safety and Health Administration, Pittsburgh [n.d.].
116. Bogg, T. L., ed., Response of Ammonium Perchlorate to Thermal and Mechanical Shock Stimuli (NWC TP 7053), Naval Weapons Center, China Lake CA (1990).
117. Mniszewski, K. R., The Pepcon Plant Fire/Explosion. A Rare Opportunity in Fire/Explosion Investigation, *J. Fire Protection Engineering* **6**, 63-78 (1994).
118. Cole, L. S., **Investigation of Motor Vehicle Fires**, 4th ed., Lee Books, San Anselmo CA (2001).
119. Zündquelle: Stofflichen Funken (Nr. 1.3) [Sources of ignition: Material sparks], *Unabhängige Brandschutzzeitschrift*, Heft 05/91 (1991).
120. Canon, V., private communication (2003).
121. Iwata, Y., and Koseki, H., Combustion Characteristics of Asphalt and Sodium Compounds, pp. 224-229 in *Proc. 3rd Intl. Symp. on Hazards, Prevention, and Mitigation of Industrial Explosions*, Tsukuba, Japan (2000).
122. Kemp, S. P., and Linden, J. L., Physical and Chemical Properties of a Typical Automatic Transmission Fluid (SAE

Technical Paper 902148), Society of Automotive Engineers, Inc., Warrendale PA (1990).
123. Ohlemiller, T. J., and Cleary, T. G., Aspects of the Motor Vehicle Fire Threat from Flammable Liquid Spills on a Road Surface (NISTIR 6147), NIST (1998).
124. Fitz, M. M., MDE Engineers, unpublished test results (1992).
125. Transmission Fluid Fires, *The Vehicle Fire Reporter* **9**, 1, 4-8 (Summer 1999).
126. Cole, L. S., Transmission Fires—A Misunderstood Fire Source, *Fire & Arson Investigator* **39**:2, 32 (Dec. 1988).
127. Kuchta, J. M., Investigation of Fire and Explosion Accidents in the Chemical, Mining, and Fuel-Related Industries—A Manual (Bulletin 680). Bureau of Mines, Pittsburgh, PA (1985).
128. Violi, A., et al., Experimental Formulation and Kinetic Model for JP-8 Surrogate Mixtures, *Combustion Science and Technology* **174**:11/12, 399-417 (2002).
129. Ural, E. A., Zalosh, R. G., and Tamanini, F., Ignitability of Jet-A Fuel Vapors in Aircraft Fuel Tanks, pp. 14-1 to 14-13 in *Aircraft Fire Safety* (AGARD Conf. Proc. No. 467), AGARD (1989).
130. Ott, E. E., Effects of Fuel Slosh and Vibration on the Flammability Hazards of Hydrocarbon Turbine Fuels within Aircraft Fuel Tanks (AFWAL-TR-70-65), Air Force Aero Propulsion Laboratory, Wright-Patterson AFB, OH (1970).
131. Standard Specification for Aviation Gasolines (ASTM D 910), ASTM.
132. Standard Specification for Aviation Turbine Fuels (ASTM D 1655), ASTM.
133. Sochet, I., and Gillard, P., Flammability of Kerosene in Civil and Military Aviation, *J. Loss Prevention in the Process Industries* **15**, 335-345 (2002).
134. Barnett, H. C., and Hibbard, R. R., Properties of Aircraft Fuels (Tech. Note 3276), NACA, Washington (1956).
135. Bustin, W. M., and Dukek, W. G., **Electrostatic Hazards in the Petroleum Industry**, Research Studies Press, Letchworth, Herts., England (1983).
136. Shepherd, J. E., Krok, J. C., and Lee, J. L., Jet A Explosion Experiments: Laboratory Testing (Explosion Dynamics Lab. Report FM97-5), Graduate Aeronautical Laboratories, California Institute of Technology, Pasadena (1997).
137. Carhart, H. W., Jet Fuel Safety and Flash Point, pp. 35-45 in **Factors in Using Kerosine Jet Fuel of Reduced Flash Point** (ASTM STP 688), ASTM (1979).
138. Zabetakis, M., and Rosen, B. H., Considerations Involved in Handling Kerosine, *Proc. Amer. Petroleum Inst.* **37**(III), 296-306 (1957).
139. Fire Protection Research Program for Supersonic Transport (APL 564-105), Wright-Patterson Air Force Base, Ohio (1964).
140. Johnson, A. M., Roth, A. J., and Moussa, N. A., Hot Surface Ignition Tests of Aircraft Fluids (AFWAL-TR-88-2101), Air Force Wright Aeronautical Labs., Wright-Patterson AFB, OH (1988).
141. Gould, G., The Limiting Surface Temperature for Spontaneous Ignition of Fuel Vapour/Air Mixtures in High Speed Aircraft (Tech. Note Mech. Eng. 339), Royal Aircraft Establishment, Farnborough, UK (1961).
142. Kuchta, J. M., and Clodfelter, R. G., Aircraft Mishap Fire Pattern Investigations (AFWAL-TR-85-2057), Aero Propulsion Laboratory, Air Force Systems Command, Wright-Patterson AFB OH (1985).
143. Hill, R., ed., A Review of the Flammability Hazard of Jet A Fuel Vapor in Civil Transport Aircraft Fuel Tanks (DOT/FAA/AR-98/26), Federal Aviation Admin., Atlantic City NJ (1998).
144. Davies, K., and Gerken, S., Charging and Ignition of Sprayed Fuel, *J. Electrostatics* **49**, 139-150 (2000).
145. Atkinson, A. J., and Eklund, T. I., Crash Fire Hazard Evaluation of Jet Fuels (FAA-RD-70-72), Federal Aviation Admin., Washington (1971).
146. Leonard, J. T., and Bogardus, H. F., Pro-static Agents in Jet Fuels (NRL Report 8021), Naval Research Lab., Washington (1976).
147. Leonard, J. T., and Affens, W. A., Electrostatic Charging of JP-4 Fuel on Polyurethane Foams (NRL Report 8204), Naval Research Lab., Washington (1978).
148. Dukek, W. G., Strauss, K. H., and Leonard, J. T., Charge Generation by U.S. Commercial Aircraft Fuels and Filter-Separators, *Lightning and Static Electricity Conf.*, Royal Aeronautical Society, London (1975).
149. Bachman, K. C., Variables Which Influence Spark Production Due to Static Electricity in Tank Truck Loading, *Lightning and Static Electricity Conf.*, Royal Aeronautical Society, London (1975).
150. Leonard, J. T., and Carhart, H. W., Electrical Discharges from a Fuel Surface, pp. 100-111 in *Proc. 2nd Conf. on Static Electrification* (Conf. Series No. 4), The Institute of Physics, London (1967).
151. Pollock, B. D., Fisco, W. J., Kramer, H., and Forsyth, A. C., Handling, Storability, and Destruction of Azides, pp. 73-109 in **Energetic Materials**, vol. 2: Technology of the Inorganic Azides, H. D. Fair and R. F. Walker, eds., Plenum Press, New York (1977).
152. Dixon, T. F., Spontaneous Combustion in Bagasse Stockpiles, *Proc. Australian Soc. of Sugar Cane Technologists* **10**, 53-61 (1988).
153. Gray, B. F., Griffiths, J. F., and Hasko, S. M., Spontaneous Ignition Hazards in Stockpiles of Cellulosic Materials: Criteria for Safe Storage, *J. Chem. Tech. and Biotech.* **34A**, 453-463 (1984).
154. Macaskill, C., Sexton, M. J., and Gray, B. F., A Reaction-Diffusion Model of Stored Bagasse (Report 98-33), School of Mathematics and Statistics, The University of Sydney, Sydney (1998).
155. Gray, B. F., Sexton, M. J., Halliburton, B., and Macaskill, C., Wetting Induced Ignition in Cellulosic Materials, *Fire Safety J.*, **37**, 465-479 (2002).
156. Mitchell, N. D., New Light on Self-Ignition, *NFPA Q.* **45**, 165 (1951).
157. **Combustion Processes**, B. Lewis, et al., eds., Princeton University Press, Princeton (1956).
158. Primer on Spontaneous Heating and Pyrophoricity (DOE-HDBK-1081-94), Dept. of Energy, Washington (1994).
159. Talley, C. P., The Combustion of Elemental Boron, pp. 279-285 in **Solid Propellant Rocket Research**, Academic Press, New York (1960).
160. Maček, A., and Semple, J. M., Combustion of Boron Particles at Elevated Pressures, pp. 859-868 in *13th Symp. (Intl.) on Combustion*, The Combustion Institute, Pittsburgh (1970).
161. Maček, A., Combustion of Boron Particles: Experiment and Theory, pp. 1401-1411 in *14th Symp. (Intl.) on Combustion*, The Combustion Institute, Pittsburgh (1972).

162. Yeh, C. L., and Kuo, K. K., Ignition and Combustion of Boron Particles, *Prog. Energy and Combustion Science* **22**, 511-541 (1996).
163. King, M. K., A Review of Studies of Boron Ignition and Combustion Phenomena at Atlantic Research Corporation over the Past Decade, pp. 1-80 in **Combustion of Boron-Based Solid Propellants and Solid Fuels**, K. K. Kuo, ed., CRC Press, Boca Raton FL (1993).
164. Li, S. C., and Williams, F. A., Ignition and Combustion of Boron in Wet and Dry Atmospheres, pp. 1147-1154 in *23rd Symp. (Intl.) on Combustion*, The Combustion Institute, Pittsburgh (1990).
165. Yuasa, S., Yoshida, T., Kawashima, M., and Isoda, H., Effects of Pressure and Oxygen Concentration on Ignition and Combustion of Boron in Oxygen/Nitrogen Mixture Streams, *Combustion and Flame* **113**, 380-387 (1998).
166. Glassman, I., Princeton University, private communication (2001).
167. Mohan, G., and Williams, F. A., Ignition and Combustion of Boron in O_2/Inert Atmospheres, *AIAA J.* **10**, 776-783 (1972).
168. Glassman, I., Williams, F. A., and Antaki, P., A Physical and Chemical Interpretation of Boron Particle Combustion, pp. 2057-2064 in *20th Symp. (Intl.) on Combustion*, The Combustion Institute, Pittsburgh (1984).
169. Zhou, W., Yetter, R. A., Dryer, F. L., Rabitz, H., Brown, R. C., and Kolb, C. E., Multi-Phase Model for Ignition and Combustion of Boron Particles, *Combustion and Flame* **117**, 227-243 (1999).
170. Gaydon, A. G., and Wolfhard, H. G., **Flames: Their Structure, Radiation and Temperature**, 4th ed., Chapman and Hall, London (1979).
171. Matsko, A. M., and Zolotko, A. N., The Ignition of Boron-Magnesium Dust Clouds, pp. 485-495 in **Combustion of Boron-Based Solid Propellants and Solid Fuels**, K. K. Kuo, ed., CRC Press, Boca Raton FL (1993).
172. DeHaan, J. D., The Reconstruction of Fires Involving Highly Flammable Hydrocarbon Liquids (Ph.D. dissertation), Univ. Strathclyde, Glasgow, UK (1995).
173. Sanderson, J. L., Candle Fires, *Fire Findings* **5**:4, 7-11 (Fall 1997).
174. Faraday, M., **The Chemical History of a Candle**, reprint ed., Cherokee Publ. Co., Atlanta GA (1993).
175. Special Data Information Package—Candle Fires in U.S. Homes and Other Occupancies, Fire Analysis & Research Div., NFPA (2001).
176. Provisional Standard Fire Specification for Candles (ASTM PS 59), ASTM (2002).
177. Singh, H., Hazard Report on Candle-Related Incidents, US Consumer Product Safety Commission, Washington (1998).
178. Zündquelle: Kerze Nr. 1.2 [Ignition source: Candle], *Unabhängige Brandschutzzeitschrift* No. 04 (1991).
179. Fires Associated with the Use of Night Lights and Ceramic Burners, Consumer Safety Research, Dept. of Trade and Industry, London (1996).
180. Yallop, H. J., **Fire Investigation**, Alan Clift Associates, Edinburgh, Scotland (1984).
181. Dillon, S. E., and Hamins, A., Ignition Propensity and Heat Flux Profiles of Candle Flames for Fire Investigation, pp. 363-376 in *Fire and Materials 2003*, Interscience Communications Ltd., London (2003).
182. Lentini, J., private communication (1999).
183. Townsend, D., unpublished report, London Fire Brigade (1999).
184. Townsend, D., Fires and Tea Light Candles, *Fire Engineers J.* **60**, 23-26 (Jan. 2000).
185. Daéid, N. N., and Thain, E., Measurement of Temperature Rise over Time for Commercially Available Night Lights (Tea Lights), *Fire Safety J.* **37**, 329-336 (2002).
186. The Holland Tunnel Chemical Fire, New Jersey – New York, May 13, 1949. National Board of Fire Underwriters, New York [n.d.].
187. Kilchyk, V., and Wierzba, I., Flammability Limits of Carbon Monoxide-Water Vapor Mixtures at Moderately Elevated Temperatures, pp. 465-470 in *Fire & Explosion Hazards—Proc. 3rd Intl. Symp.*, Univ. Central Lancashire, Preston, England (2000).
188. Weatherford, W. D., jr., Sheppard, D. M., and Valtierra, M. L., An Experimental and Mathematical Study of the Mechanism of Wood Ignition (SwRI Report No. RS-472), Southwest Research Institute, San Antonio TX (1965).
189. Brown, C. R., The Determination of the Ignition Temperatures of Solid Materials (D.Sc. thesis), The Catholic University of America, Washington (1934).
190. Holm, H., Über Entzündungstemperaturen (Zündpunkte) besonders von Brennstoffen [On the Kindling Temperatures of Combustible Materials], *Zeitschrift für angewandte Chemie* **26**, 273-279 (1913).
191. Self-ignition Temperature of Cellulose and Magnesium, *J. Franklin Institute* **234**, 492-493 (1942).
192. Shivadev, U. K., and Emmons, H. W., Thermal Degradation and Spontaneous Ignition of Paper Sheets by Irradiation, *Combustion and Flame* **22**, 223-236 (1974).
193. Martin, S. B., and Alvares, N. J., Ignition Thresholds for Large-yield Nuclear Weapons (USNRDL/TR-1007), Naval Radiological Defense Laboratory, San Francisco CA (1966).
194. Martin, S. B., Diffusion-Controlled Ignition of Cellulosic Materials by Intense Radiant Energy, pp. 877-896 in *10th Symp.(Intl.) on Combustion*, The Combustion Institute, Pittsburgh (1964).
195. Weatherford, W. D. jr., and Valtierra, M. L., Piloted Ignition of Convection-Heated Cellulose Slabs, *Combustion and Flame* **10**, 279-286 (1966).
196. Hinkley, P. L., Theobald, C. R., and Carter, S., Some Experiments with a Domestic Electric Firelighter (F.R. Note 536), Fire Research Station, Borehamwood, UK (1964).
197. Walker, I. K., Harrison, W. J., and Read, A. J., The Effect of Dry Heat on the Ignition Temperature of Cellulose, *New Zealand J. Science* **12**, 98-110 (1969).
198. Vovelle, C., Mellottée, H., and Delbourgo, R., Kinetics of the Thermal Degradation of Cellulose and Wood in Inert and Oxidative Atmospheres, pp. 797-805 in *19th Symp. (Intl.) on Combustion*, The Combustion Institute, Pittsburgh (1982).
199. Davies, D., Horrocks, A. R., and Greenhalgh, M., Ignition Studies on Cotton Cellulose by DTA, *Thermochimica Acta* **63**, 351-362 (1983).
200. Horrocks, A. R., Davies, D., and Greenhalgh, M., The Use of DTA to Study Spontaneous Ignition of Cellulose, *Fire and Materials* **9**, 57-64 (1985).
201. Standard Test Method for Critical Radiant Flux of Exposed Attic Floor Insulation Using a Radiant Heat Energy Source (ASTM E 970), ASTM.
202. Standard Specification for Cellulosic Fiber (Wood-Base) Loose-Fill Thermal Insulation (ASTM C 739), ASTM.

203. Kokkala, M., Fire Tests on Loose-Fill Insulation Materials (Research Reports 485), Valtion Teknillinen Tutkimuskeskus, Espoo, Finland (1989).
204. Siddiqui, S. A., Hillier, R. L., and Damant, G. H., Effect of Fire Retardant Formulations on the Fire Properties of Cellulose Insulation, pp. 15-24 in Fire Safety Progress in Regulations, Technology and New Products, Fire Retardant Chemicals Assn., Lancaster, PA (1987).
205. Siddiqui, S. A., **A Handbook on Cellulose Insulation**, Robert E. Krieger, Malabar FL (1989).
206. Ohlemiller, T. J., Smoldering Combustion Hazards of Thermal Insulation Materials (NBSIR 81-2350), NBS (1981).
207. Gustin, B., How to Avoid Rekindle Fires, *Fire Engineering* **153**, 69-73 (Nov. 2000).
208. Choi, J. H., Hong, K., and Ok, R. K., The Particle Size Effect on Combustion Behavior of Cellulose Insulation, pp. 185-192 in *Intl. Symp. on Fire Science and Technology*, Korean Institute of Fire Science & Engineering, Seoul (1997).
209. Grand, A. F., Final Report—Survey on Fires Involving Cellulose Loose-fill Insulation, Project No. 13220-94648 on behalf of N. American Insulation Manufacturers Assn., Omega Point Laboratories, Elmendorf TX (1993).
210. Tremblay, K. J., Furniture Store Destroyed by Sparks for Circular Saw, *NFPA J.* **96**:4, 16-18 (Jul./Aug. 2002).
211. Belles, D. W., Loose-Fill Cellulose Insulation—An Aging Problem, *J. Applied Fire Science* **3**, 295-303 (1993/94).
212. Katz, D., and Siddiqui, S. A., Cellulose Insulation Issue in Palo Alto—History and Current Status, pp. 43-74 in *2nd California Thermal Insulation Conf.*, Bureau of Home Furnishings and Thermal Insulation, North Highlands CA (1989).
213. Davie, B. W., jr., Cellulose Insulation, *The Alberta Fire News* **15**:2, 7-8 (Nov. 1994).
214. Lawson, J. R., Environmental Cycling of Cellulosic Thermal Insulation and Its Influence on Fire Performance (NBSIR 84-2917), NBS (1984).
215. Yarbrough, D. W., and Graves, R. S., Review of Cellulose Insulation Fire Safety, pp. 113-119 in *Proc. 23rd Intl. Conf. on Fire Safety*, Product Safety Corp., Sissonville WV (1997).
216. Fischer, S. J., Hillier, R. L., and Damant, G. H., Long Term Aging Studies on Loose-Fill Cellulose Insulation—Part IV, pp. 101-123 in *7th Intl. Conf. on Thermal Insulation*, Product Safety Corp., Millbrae CA (1991).
217. Koffer, W., A Possible Explanation Why Cellulose Insulation in Simulated Attic Test Fail the Critical Radiant Flux Test, pp. 259-264 in *Fire Safety '91* Volume 4, Polyplastex Intl., Pinellas Park FL (1991).
218. Issen, L. A., Fire Performance of Loose Fill Cellulosic Insolation in Residential Occupancies—A Progress Report (NBSIR 80-2085), NBS (1980).
219. Rogers, F. E., and Ohlemiller, T. J., Cellulosic Insulation Material. I. Overall Degradation Kinetics and Reaction Heats, *Combustion Science and Technology* **24**, 129-137 (1980).
220. Ohlemiller, T. J., and Rogers, F. E., Cellulosic Insulation Material. II. Effect of Additives on Some Smolder Characteristics, *Combustion Science and Technology* **24**, 139-152 (1980).
221. Ohlemiller, T. J., and Rogers, F. E., Smoldering Combustion Hazards of Thermal Insulation Materials, Final Report on Contract ORNL/7686, Guggenheim Laboratories, Princeton University, Princeton NJ (1979).
222. Analysis of Fires Involving Thermal Insulation Materials, Consumer Product Safety Commission, Washington (1980).
223. Yereance, R. A., **Electrical Fire Analysis**, 2nd ed., Charles C. Thomas, Springfield IL (1995).
224. Malhotra, H. L., Sutcliffe, R. J., Rogowski, B., and Ramaprasad, R., Possible Fire Hazards of Loft Insulating Materials (CP 2/80), Fire Research Station, Borehamwood, UK (1980).
225. Miles, F. D., **Cellulose Nitrate: The Physical Chemistry of Nitrocellulose, its Formation and Use**, Oliver and Boyd, London (1955).
226. Rideal, E. K., and Robertson, A. J. B., The Spontaneous Ignition of Nitrocellulose, pp. 536-544 in *Third Symp. on Combustion and Flame and Explosion Phenomena*, Williams and Wilkins, Baltimore (1949).
227. van de Putte, T., Determination of the Thermal Stability of Unstable Substances, pp. 179-190 in *Selfheating of Organic Materials*, Intl. Symp. 18th and 19th February 1971, Delft. Delft University (1971).
228. Rushbrook, F., **Fire Aboard**, 3rd ed., Brown, Son & Ferguson, Ltd., Glasgow (1998).
229. Gamble, S. G., **A Practical Treatise on Outbreaks of Fire**, Charles Griffin & Co., London (1926).
230. Storm, C. G., The Decomposition of Smokeless Powder, *Army Ordnance* **9**, 230-234 (1929).
231. Leider, H. R., and Pane, A. J., Evidence of Differences in Stability between Nitrate Ester Positions on the Cellulose Nitrate Ring, pp. 231-236 in *Symp. on Compatibility of Plastics and Other Materials with Explosives, Propellants, Pyrotechnics & Processing of Explosives, Propellants and Ingredients*, American Defense Preparedness Assn. (1986).
232. Lindner, V., Explosives, pp. 561-620 in **Kirk-Othmer Encyclopedia of Chemical Technology**, 3rd ed., Vol. 9, Wiley, New York (1980).
233. Van Geel, J. L. C., Investigations into the Self-ignition Hazard of Nitrate Ester Propellants (Ph.D. dissertation), De Technische Hogeschool Delft. Published by Technological Laboratory RVO-TNO, Rijswijk, Netherlands (1969).
234. Vilyunov, V. N., and Zarko, V. E., **Ignition of Solids**, Elsevier, Amsterdam (1989).
235. Fifer, R. A., Chemistry of Nitrate Ester and Nitramine Propellants, pp. 177-237 in **Prog. in Astronautics and Aeronautics**, vol. 90: Fundamentals of Solid-Propellant Combustion, AIAA, New York (1984).
236. Brill, T. B., and Gongwer, P. E., Thermal Decomposition of Energetic Materials. 69. Analysis of the Kinetics of Nitrocellulose at 50ºC – 500ºC, *Propellants, Explosives, Pyrotechnics* **22**, 38-44 (1997).
237. Hartgerink, J. W., Investigation into the Cause of an Explosion during the Drying of Porous Nitrocellulose Powder, pp. 125-132 in *Proc. Symp. on Chemical Process Hazards with Special Reference to Plant Design—V* (Symp. Series 39a), The Institution of Chemical Engineers, London (1974).
238. Grossman, E. D., and Rele, P. J., Ignition of Cellulose Nitrate by High Velocity Particles, *Combustion Science and Technology* **9**, 55-60 (1974).
239. Lenchitz, C., Hayes, E., Velicky, R. W., Schlosberg, L., and Suh, N. P., The Ignition Characteristics of Nitrocellulose Films, *Combustion Science and Technology* **7**, 1-11 (1973).

240. Millet, M. A., et al., Kinetics of the Thermal Degradation of Cellulose Nitrate as Measured by an Improved Taliani Procedure, *TAPPI* **44**, 636-647 (1961).
241. Jones, J. C., **Combustion Science: Principles and Practice**, Millennium Books, Newtown NSW, Australia (1993).
242. Proc. of a Board of the Chemical Warfare Service Appointed for the Purpose of Investigating Conditions Incident to the Disaster at the Cleveland Hospital Clinic, Cleveland, Ohio, on May 15, 1929, U.S. Government Printing Office, Washington (1929).
243. Stokes, H. N., and Weber, H. C. P., Effects of Heat on Celluloid and Similar Materials (Tech. Paper No. 98), [U.S.] Bur. Stand., Washington (1917).
244. Akita, A., and Arai, H., A Study on Spontaneous Ignition of Celluloid. Part 2. Ignitability of Celluloid, *Report of the Fire Research Institute* [Japan], **1**:3, 18-36 (1950).
245. Cummings, J.W., Hutton, A. C., and Silfin, H., Spontaneous Ignition of Decomposing Cellulose Nitrate Film, *J. SMPTE* **54**, 268-274 (1950).
246. Merrifield, R., and Roberts, T. A., Thermal Radiation Hazards and Separation Distances for Industrial Cellulose Nitrate, *J. Loss Prevention in the Process Industries* **5**, 311-319 (1992).
247. Ryan, J. V., Cummings, J. W., and Hutton, A. C., Fire Effects and Fire Control in Nitrocellulose Photographic-Film Storage (BMS 145), [U.S.] Natl. Bur. Stand., Washington (1956).
248. Nitrocellulose, *Fire Prevention* No. 155, 49-50 (1982).
249. Code for the Storage of Pyroxylin Plastic (NFPA 40E), NFPA.
250. Standard for the Storage and Handling of Cellulose Nitrate Motion Picture Film (NFPA 40), NFPA.
251. Standard for the Manufacture of Organic Coatings (NFPA 35), NFPA.
252. Hägglund, E., **Chemistry of Wood**, Academic Press, New York (1951).
253. Davy, H., On the Fire-Damp of Coal Mines, and on Methods of Lighting the Mines so as to Prevent Its Explosion, *Phil. Trans. Royal Soc.* 1-24 (1816).
254. Hill, H. B., On the Behavior of Sound and Decayed Wood at High Temperatures, *Proc. Amer. Acad. Arts and Sciences* **22**, 482-492 (1887).
255. Fons, W. L., Heating and Ignition of Small Wood Cylinders, *Ind. and Eng. Chem.* **42**, 2130-2133 (1942).
256. Urbański, T., **Chemistry and Technology of Explosives**, vols. 1-4, Methuen/Pergamon, New York (1964-84).
257. Burgoyne, J. H., and Richardson, J. F., The Influence of Zinc Chloride on the Ignition of Scotch Pine and Its Charcoal, *Fuel* **30**, 13-16 (1951).
258. Bergström, H., Träkols självantändning [Spontaneous ignition of charcoal], *Jernkontorets Annaler* **107**, 309-350 (1923).
259. Bergström, H., Träkols antändningstemperatur [Ignition temperature of charcoal], *Jernkontorets Annaler* **109**, 90-92 (1925).
260. Beistle, C. P., Spontaneous Heating and Ignition in Transportation by Railroad, pp. 40-45 in Report of Conf. on Spontaneous Heating and Ignition of Agricultural and Industrial Products, NFPA and US Dept. of Agriculture, Washington (1929).
261. Blench, E. A., and Garner, W. E., The Heat of Adsorption of Oxygen by Charcoal, *J. Chemical Soc.* **125**, 1288-1295 (1924).
262. Moore, F. C., **Fire Insurance and How to Build**, Baker & Taylor, New York (1903).
263. Bixel, E. C., and Moore, H. J., Are Fires Caused by Steam Pipes? (B.S. thesis), Case School of Applied Science, Pittsburgh (1910).
264. Rosenhain, W., and Gemmell, W., An Investigation into the Inflammability of Flake Charcoal, Decayed Wood and Insulating Papers, pp. 207-228 in **Collected Researches of the National Physical Laboratory**, vol. 10, London (1913).
265. Laupper, G., Die Schaden der Landwirtschaft infalge Selbstentzündung der Heustacke [The Losses to Farming as a Result of Spontaneous Combustion of Haystacks], *Materiaux pour l'étude des calamités*, 112-140 (Jul./Sep. 1926).
266. Laupper, G., Die neuesten Ergebnisse der Heubrandforschung [The Latest Results of Research on Hay Fires], *Landwirtschaftliches Jahrbuch der Schweiz* **34**, 1-54 (1920).
267. Blayden, H. E., Riley, H. L., and Shaw, F., A Study of Carbon Combustibility by a Semi-micro Method, *Fuel in Science and Practice* **22**, 32-38; 64-71 (1943).
268. Beistle, C. P., p. 95 in Report of Conf. on Spontaneous Heating and Ignition of Agricultural and Industrial Products, NFPA and US Dept. of Agriculture, Washington (1929).
269. Ford, R. T. sr., Glow Temperature and Heat Retention of Barbecue Briquets, *Fire & Arson Investigator* **44**:3, 16-19 (Mar. 1994).
270. Charcoal Briquettes Remain Hot Longer than 26 Hours, *Fire Findings* **2**:3, 13 (Summer 1994).
271. Stickney, C. W., Recognizing Where Arson Exists. II., *Fire & Arson Investigator* **35**, 10-20 (Sept. 1984).
272. Wolters, F. C., Pagni, P. J., Frost, T. R., and Vanderhoof, D. W., The Effect of Wetting on Self-Ignition Temperatures of Charcoal Briquettes, unpublished paper, [1989?].
273. Spontaneous Ignition of Charcoal, *Fire J.* **67**, 70 (July 1973).
274. Beatty, T., private communication (2001).
275. Wolters, F. C., Pagni, P. J., Frost, T. R., and Vanderhoof, D. W., Size Constraints on Self-ignition of Charcoal Briquettes, Clorox Technical Center, Pleasanton, CA (1987).
276. Shea, F. L. jr., and Hsu, H. L., Self-heating of Carbonaceous Materials, *Ind. and Eng. Chem.—Product Res. Dev.* **11**, 184-187 (1972).
277. Bowes, P. C., and Cameron, A., Self-Heating and Ignition of Chemically Activated Carbon, *J. Appl. Chem. Biotechnology* **21**, 244-250 (1971).
278. Boden, N., Cullis, C. F., and Fish, A., Spontaneous Ignition in Carbon Absorption Beds, *J. Appl. Chem.* (London) **12**, 145-148 (1962).
279. Activated Charcoal Filter Fire, *Loss Prevention Bulletin* No. 105, 15 (1992).
280. Cameron, A., and MacDowall, J. D., The Self Heating of Commercial Powdered Activated Carbons, *J. Appl. Chem. Biotechnology* **22**, 1007-1018 (1972).
281. Jones, J. C., Towards an Alternative Criterion for the Shipping Safety of Activated Carbons, *J. Loss Prevention in the Process Industries* **11**, 407-411 (1998).
282. Jones, J. C., Indirect Evidence of Relatively High Thermal Conductivities in Powdered Activated Carbons, *Fuel* **77**, 1679-1681 (1998).
283. Bigg, S., and Street, P. J., Predicting Spontaneous Ignition and Combustion in Fixed Beds of Activated Carbon, *Combustion Science and Technology* **65**, 245-262 (1989).

284. Hardman, J. S., Lawn, C. J., and Street, P. J., Further Studies of the Spontaneous Ignition Behaviour of Activated Carbon, *Fuel* **62**, 632-638 (1983).
285. Standard Test Method for Ignition Temperature of Granular Activated Carbon (ASTM D 3466), ASTM.
286. Freeman, W. P., Hunt, J. R., and Kovach, J. L., Ignition Properties of Nuclear Grade Activated Carbons, pp. 317-334 in *CSNI Specialist Meeting on Interaction of Fire and Explosion with Ventilation Systems in Nuclear Facilities*, vol. 2, Los Alamos National Laboratory, Los Alamos NM (1983).
287. Suzin, Y., Buettner, L. C., and LeDuc, C. A., Characterizing the Ignition Process of Activated Carbon, *Carbon* **37**, 335-346 (1999).
288. Itagaki, H., and Matsuda, T., Thermal Ignition of Activated Carbon Dusts, pp. 141-145 in *Proc. 6th Intl. Colloquium on Dust Explosions*, Northeastern Univ. Press, Shenyang, China (1994).
289. Peacock, R. D., Review of Fire Incidents Related to Wood-Burning Appliances, *Fire J.* **74**, 58-63, 93 (Nov. 1980).
290. Cote, A. E., and Linville, J. L., eds., **Fire Protection Handbook**, 18th ed., NFPA (1997).
291. Standard for Chimneys, Fireplaces, Vents, and Solid Fuel-Burning Appliances (NFPA 211), NFPA.
292. Neale, J. A., Clearances and Insulation of Heating Appliances (Bull. of Research No. 27), Underwriters' Laboratories, Chicago (1943).
293. Lawson, K. I., Fox, L. L., and Webster, C. T., The Heating of Panels by Flue Pipes (Fire Research Special Report No. 1), Dept. of Scientific and Industrial Research and Fire Offices' Committee, HMSO, London (1952).
294. Kline, L. M., and Witte, H., Performance of Type B Gas Vents for Gas-Fired Appliances (Bull. of Research No. 51), Underwriters' Laboratories, Chicago (1959).
295. Loftus, J. J., and Peacock, R. D., Clearances and Methods of Protection for Wall and Ceiling Surfaces Exposed to Radiant Heating Appliances (Tech. Note 1205), NBS (1984).
296. Peacock, R. D., Thermal Performance of Masonry Chimneys and Fireplaces (NBSIR 87-3515), NBS (1987).
297. Shoub, H., Survey of Literature on the Safety of Residential Chimneys and Fireplaces (NBS Misc. Pub. 252), NBS (1963).
298. Loftus, J. J., Evaluation Tests on Factory-Built Insulated Chimneys used for Venting Solid Fuel Burning Appliances (Memorandum to CPSC), NBS (22 Feb. 1985).
299. Sanderson, J. L., Masonry Fireplaces: Improper Construction Years Ago May Lead to Fires Today, *Fire Findings* **11**:1, 1-3 (Winter 2003).
300. Yoshida, T., Wada, Y., and Foster, N., **Safety of Reactive Chemicals and Pyrotechnics**, Elsevier, Amsterdam (1995).
301. Subject 411—Outline of Investigation for Artificial Christmas Trees, 2nd ed., UL (1991).
302. Harwood, B., Kissinger, T. L., Karter, M. J., jr., Miller, A. L., Fahy, R. F., Hall, J. R., jr., Eisenhower, D., Forbes, P., and Hall, J., Cigarette Fire Incident Study, vol. 4 of Final Report. Fire Safe Cigarette Act of 1990, Consumer Product Safety Commission, Washington (1993).
303. Karter, M. J. jr., Kissinger, T. L., Miller, A. L., Harwood, B., Fahy, R. H., and Hall, J. R. jr., Cigarette Characteristics, Smoker Characteristics, and the Relationship to Cigarette Fires, *Fire Technology* **30**, 400-431 (1994).
304. Holleyhead, R., Ignition of Solid Materials and Furniture by Lighted Cigarettes: A Review, *Science and Justice* **39**, 75-102 (1999).
305. Countryman, C. M., Some Physical Characteristics of Cigarettes as Firebrands, Forest Service Contract 43-9AD6-0-755, Pacific Southwest Forest & Range Expt. Sta., Riverside CA (1980).
306. Cigarette Delays Don't Always Work, But When They Do… *Fire Findings* **2**:2, 14-15 (Spring 1994).
307. Plencner, L. A., and Donahue, R. L., Fact-Finding Report on Comparative Fire Testing of Two Mobile Home Living Room Sections With Representative Interior Finish Materials and Furnishings (File MH10498, 76NK1062), UL (1978).
308. Damant, G. H., The Cigarette as an Ignition Source, *Proc. 4th Intl. Conf. on Fire Safety*, Univ. San Francisco (1979).
309. Baker, R. R., Temperature Distribution Inside a Burning Cigarette, *Nature* **247**, 405-406 (1974).
310. Holleyhead, R., Ignition of Flammable Gases and Liquids by Cigarettes: A Review, *Science and Justice* **36**, 257-266 (1996).
311. Béland, B., On the Measurement of Temperature, *Fire & Arson Investigator* **45**:1, 27, 30-31, 34-35 (Sep. 1994).
312. Egerton, A., Gugan, K., and Weinberg, F. J., The Mechanism of Smouldering in Cigarettes, *Combustion and Flame* **7**, 63-78 (1963).
313. Gann, R. G., Harris, R. H., jr., Krasny, J. F., Levine, R. S., Mitler, H. E., and Ohlemiller, T. J., The Effect of Cigarette Characteristics on the Ignition of Soft Furnishings (Tech. Note 1241), NBS (1988).
314. Sale, P. D,. and Hoffheins, F. M., Cigarettes and Cigars, Fire Hazard Tests, *NFPA Q*. **21**, 237-246 (Jan. 1928).
315. Harrington, D., and Parker, D. J., Explosions in Coal Mines Caused by Smoking (IC 7141), Bureau of Mines, Pittsburgh (1941).
316. Strese, G., Zündmöglichkeit von brennbaren Gasen und Dämpfen durch glimmenden Tabak, *Sonderdruck aus Bundesarbeitsblatt—Fachteil Arbeitsschutz* **3**, 66-70 (1970).
317. Yockers, J. R., and Segal, L. S., Cigarette Fire Mechanisms, *NFPA Q*. **49**, 213-222 (Jan. 1956).
318. Hards, D. J., Examination of the Effect of Lighted Cigarettes on Flammable Vapour-Air Mixtures (Section Paper IR/L/IN/83/1), Health and Safety Executive, Harpur Hill, England (1983).
319. Nii, R., Ignition of Combustible Liquids by Heat Sources of Solids of Small Sizes, Part 2, *Report of the Fire Research Institute* [Japan] **6**:2, 31-43 (1955).
320. Hagimoto, Y., and Kinoshita, K., Ignition Possibility of Inflammable Mixtures with Burning Cigarettes, *J. Japan Soc. for Safety Engrg.* **20**, 197-202 (1981).
321. Harris, R. J., **The Investigation and Control of Gas Explosions in Buildings and Heating Plant**, E&FN Spon, London (1983).
322. DeHaan, J. D., **Kirk's Fire Investigation**, 4th ed., Brady/Prentice-Hall, Englewood Cliffs, NJ (1997).
323. Yallop, H. J., **Explosion Investigation**, The Forensic Science Society, Harrogate/Scottish Academic Press, Edinburgh (1980).
324. DeHaan, J. D., private communication (2001).
325. North, M. A., The Relative Fire Hazard of Plain and Tipped Cigarettes (Fire Research Note 593), Fire Research Station, Borehamwood, UK (1968).

326. Cigarette Fires in Paper Trash, *Fire Findings* **6**:1, 1-3 (Winter 1998).
327. Zündquelle: Tabakglut Nr. 1.4 Bl. 2 [Ignition source: Glowing tobacco], *Unabhängige Brandschutzzeitschrift* No. 07 (1991).
328. Wilk, E., private communication (2002).
329. Raftery, M. M., Ignition and Burning Behavior of Continental Quilts (IP 9/82), Building Research Establishment, Garston, UK (1982).
330. Mitler, H. E., and Walton, G. N., Modeling the Ignition of Soft Furnishings by a Cigarette (SP 852), NIST (1993).
331. Wharton, R. K., The Anomalous Burning Behaviour of Some Smokers' Materials in Oxygen-Enriched Atmospheres, *J. Occupational Accidents* **4**, 25-32 (1982).
332. Operating Temperatures of an Electric Iron, *Fire Findings* **1**:1, 5 (Spring 1993).
333. Béland, B., and Gamache, D., Irons as Causes of Fires, *Fire & Arson Investigator* **38**:2, 39-41 (Dec. 1987).
334. Guess What? Some 168 Hours Later, the Iron Still Didn't Start a Fire, *Fire Findings* **6**:4, 4-5 (Fall 1998).
335. Zündquelle: Elektrische Heizgeräte Nr. 2.8 [Ignition source: Electrical heating apparatus], *Unabhängige Brandschutzzeitschrift* No. 07 (1992).
336. Knowles, R. E., Discussion, *Trans. Inst. Marine Engineers* **77**, 137-138 (1965).
337. Leonard, J. T., and Clark, R. C., Ignition of Flammable Vapors by CO_2 Fire Extinguishers, *J. Fire & Flammability* **8**, 131-134 (1977).
338. Haessler, W. M., Static Electricity Generation by Carbon Dioxide Extinguishers, *NFPA Q.* **56**, 221-226 (Jan. 1963).
339. Cockram, R. W. J., The Generation of Static Electricity during Discharge of Liquified CO_2 Gas, pp. 155-165 in *Conf. on Electrical Safety in Hazardous Environments* (Conf. Publ. No. 74), Institution of Electrical Engineers, London (1971).
340. Butterworth, G. J., Electrostatic Ignition Hazards Associated with the Preventative Release of Fire Extinguishing Fluids, pp. 161-169 in *Electrostatics 1979* (Conf. Series No. 48), The Institute of Physics, London (1979).
341. Morgan, V. T., Collocott, S. J., and Morrow, R., The Electrification of Operating Portable CO_2 Fire Extinguishers, *J. Electrostatics* **9**, 201-210 (1980).
342. Van Krevelen, D. W., **Coal**, Elsevier, Amsterdam, Amsterdam (1961).
343. Singer, J. M., and Tye, R. P., Thermal, Mechanical, and Physical Properties of Selected Bituminous Coals and Cokes (RI 8364), Bureau of Mines, Pittsburgh (1979).
344. Mahajan, O. P., and Walker, P. J. jr., Water Adsorption on Coals, *Fuel* **50**, 308-317 (1971).
345. Hottel, H. C., and Stewart, I. M., Space Requirements for the Combustion of Pulverized Coal, *Ind. and Eng. Chem.* **32**, 719-730 (1940).
346. Jones, G. W., and Scott, G. S., Chemical Considerations Relating to Fires in Anthracite Refuse (RI 3468), Bureau of Mines, Pittsburgh (1939).
347. Smart, R. C., **The Technology of Industrial Fire and Explosion Hazards**, 2 vols., Chapman & Hall, London (1947).
348. Rowan, T., **Coal Spontaneous Combustion and Explosions—Occurring in Coal Cargoes—Their Treatment and Prevention**, E&FN Spon, London & New York (1882).
349. Report of the Royal Commissioners Appointed to Enquire into the Spontaneous Combustion of Coal in Ships, London (1876).
350. Thomas, J. W., **A Treatise on Coal, Mine-gases, and Ventilation**, with copies of researches 'On the Gas enclosed in Coal,' &c. Longmans, Green and Co., London (1878).
351. Fayol, H., Études sur l'alteration et la combustion spontanée de la houille exposée à l'air, *Bull. Soc. de l'Industrie Minérale*, Ser. 2^e, **8**, III (1979).
352. Threlfall, R., The Spontaneous Heating of Coal, Particularly during Shipment, *J. Soc. Chemical Industry* **28**, 759-773 (1909).
353. Hexamer, C. J., **A Collection of Essays on Spontaneous Combustion**, The Spectator Co., New York (1888).
354. Scott, G. S., Anthracite Coal Mine Fires: Their Behavior and Control (Bulletin 455), Bureau of Mines, Pittsburgh (1944).
355. Coward, H. F., Research on Spontaneous Combustion of Coal in Mines. A Review (SMRE Research Report 142), Safety in Mines Research Establishment, Sheffield, England (1957).
356. Banerjee, S. C., **Spontaneous Combustion of Coal and Mine Fires**, A. A. Balkema, Rotterdam (1985).
357. Braun, E., Self Heating Properties of Coal (NBSIR 87-3554), NBS (1987).
358. Jones, J. C., and Vais, M., Factors Influencing the Spontaneous Heating of Low-Rank Coals, *J. Hazardous Materials* **26**, 203212 (1991).
359. Jones, J. C., The Accidental Ignition of Stockpiled Low-rank Coal by Proximity to Active Combustion, *J. Hazardous Materials* **49**, 49-56 (1996).
360. Tognotti, L., Petarca, L., and Zanelli, S., Spontaneous Combustion in Beds of Coal Particles, pp. 201-210 in *22nd Symp. (Intl.) on Combustion*, The Combustion Institute, Pittsburgh (1988).
361. Smith, A. C., and Lazzara, C. P., Spontaneous Combustion Studies of U.S. Coals (RI 9079), Bureau of Mines, Pittsburgh (1987).
362. Nugroho, Y. S., McIntosh, A. C., and Gibbs, B. M., Low-temperature Oxidation of Single and Blended Coals, *Fuel* **79**, 1951-1961 (2000).
363. Berkowitz, N., and Schein, H. G., Heats of Wetting and Spontaneous Ignition of Coal, *Fuel* **30**, 94-96 (1951).
364. Bhattacharyya, K. K., The Role of Sorption of Water Vapor in the Spontaneous Heating of Coal, *Fuel* **50**, 367-380 (1971).
365. Vance, W. E., Chen, X. D., and Scott, S. C., The Rate of Temperature Rise of a Subbituminous Coal during Spontaneous Combustion in an Adiabatic Device: The Effect of Moisture Content and Drying Methods, *Combustion and Flame* **106**, 271-270 (1996).
366. Hodges, D. J., Spontaneous Combustion: The Influence of Moisture in the Spontaneous Ignition of Coal, *Colliery Guardian* **207**, 678-682 (1963).
367. Stott, J. B., Influence of Moisture on the Spontaneous Heating of Coal, *Nature* **188**, 54 (1960).
368. Bhattacharyya, K. K., Hodges, D. J., and Hinsley, F. B., Influence of Humidity on the Initial Stages of the Spontaneous Heating of Coal, *Mining Engineer* **128**, 275-283 (1969).
369. Feng, K. K., Chakravorty, R. N., and Cochrane, T. S., Spontaneous Combustion—A Coal Mining Hazard, *The Canadian Mining and Metallurgical (CIM) Bulletin*, 75-84 (October 1973).
370. Hardy, V. O., The Smouldering of Coal Dust and the Effect of Lubricants (Research Report 136), Safety in Mines Research Establishment, Sheffield, England (1956).

371. Hensel, W., The Dependence of Self-Ignition Temperatures of Dusts upon Grain Size, *Archivum Combustionis* **7**, 45-57 (1987).
372. Carras, J. N., and Young, B. C., Self-heating of Coal and Related Materials: Models, application and test methods, *Prog. Energy Combustion Science* **20**, 1-15 (1994).
373. Handa, T., Morita, M., Sugawa, O., Ishii, T., and Hayashi, K., Computer Simulation of the Spontaneous Combustion of Coal Storage, *Fire Science and Technology* **3**, 13-24 (1983).
374. Jones, J. C., Anomalies in the Self-Heating Temperature Histories of a Higher Rank Coal, *J. Fire Sciences* **13**, 378-385 (1995).
375. Miron, Y., Smith, A. C., and Lazzara, C. P., Sealed Flask Test for Evaluating the Self-Heating Tendencies of Coals (RI 9330), Bureau of Mines, Pittsburgh (1990).
376. Schmal, D., Spontaneous Heating of Stored Coal, pp. 133-215 in **Chemistry of Coal Weathering**, Nelson, C. R., ed., Elsevier, Amsterdam (1989).
377. Salinger, A. G., Aris, R, and Derby, J. J., Modeling the Spontaneous Ignition of Coal Stockpiles, *AIChE J.* **40**, 991-1004 (1994).
378. Monazam, E. R., Shadle, L. J., and Shamsi, A., Spontaneous Combustion of Char Stockpiles, *Energy & Fuels* **12**, 1305-1312 (1998).
379. Safety in Mines Research 1953, Thirty-second Annual Report, Safety in Mines Research Establishment, HMSO, London (1954).
380. Zalosh, R. G., Review of Coal Pulverizer Fire and Explosion Incidents, pp. 191-201 in **Industrial Dust Explosions** (ASTM STP 958), ASTM (1987).
381. Carini, R. C., and Hules, K. R., pp. 202-216 in **Industrial Dust Explosions** (ASTM STP 958), ASTM (1987).
382. Bloom, J., and Bloom, C., Coffeemaker Fires, *Fire & Arson Investigator* **43**:3, 35-37 (Spring 1993).
383. Household Electric Coffeemakers and Brewing Type Appliances (UL 1082), UL.
384. Finneran, J. M., Coffeemaker Fires, *Fire Findings* **4**:1, 7-10 (Winter 1996).
385. Delayed Ignition Devices: Do You Have One in Your Home? *Fire Findings* **1**:2, 1-2 (Summer 1993).
386. Brown, J. E., Braun, E., and Twilley, W. H., Cone Calorimeter Evaluation of the Flammability of Composite Materials (NBSIR 88-3733). NBS (1988).
387. Brown, J. E., Cone Calorimeter Method for Determining the Flammability of Composite Materials, pp. 141-150 in *How to Apply Advanced Composites Technology (Proc. 4th Annual Conf. on Advanced Composites)*, ASM International, Dearborn MI (1988).
388. Scudamore, M. J., Fire Performance Studies on Glass-reinforced Plastic Laminates, *Fire and Materials* **18**, 313-326 (1994).
389. Nyden, M. R., and Brown, J. E., Investigation into the Flammability Properties of Honeycomb Composites (NISTIR 5509), NIST (1994).
390. Egglesonte, G. T., and Turley, D. M., Flammability of GRP for Use in Ship Superstructures, *Fire and Materials* **18**, 255-260 (1994).
391. Brown, J. R., Fawell, P. D., and Mathys, Z., Fire-Hazard Assessment of Extended-chain Polyethylene and Aramid Composites by Cone Calorimetry, *Fire and Materials* **18**, 167-172 (1994).
392. Ramsay, G. C., Dowling, V. P., McKechnie, B., and Leonard, J., Methods for Assessing the Fire Performance of Phenolic Resins and Composites, pp. 355-366 in *Fire Science and Technology—Proc. 2nd Asia-Oceania Symp*., Asia-Oceania Assn. for Fire Science and Technology, Khabarovsk State University of Technology, Khabarovsk, Russia (1995).
393. Hshieh, F.-Y., and Beeson, H. D., Evaluation of the Controlled-Atmosphere Cone Calorimeter for Determining Fire Properties of Materials According to NASA Handbook 8060.1C Test 2 (NASA Reference Publication 1345; also Technical Memorandum TM-104809), National Aeronautics and Space Administration, Washington (1995).
394. Hshieh, F.-Y., and Beeson, H. D., Cone Calorimeter Testing of Epoxy/Fiberglass and Brominated Epoxy/Fiberglass Composites in Normal Oxygen and Oxygen-Enriched Environments, pp. 152-167 in *7th Intl. Symp. of Flammability and Sensitivity of Materials in Oxygen-Enriched Atmospheres* (1995).
395. Brown, N., Linnert, E., and Bühl, D., New Generation of Fire-retarded Polyester Composite for Mass Transportation, *Composites* No. 14 (Mars-Avril 1996).
396. Hshieh, F.-Y., and Beeson, H. D., Flammability Testing of Flame-retarded Epoxy Composites and Phenolic Composites, *Fire and Materials* **21**, 41-49 (1997).
397. Grenier, A. T., and Janssens, M. L., Improved Method for Analyzing Ignition Data of Composites, pp. 253-264 in *23rd Intl. Conf. on Fire Safety*, Product Safety Corporation, Sissonville WV (1997).
398. Janssens, M. L., and Dillon, S. E., Predictions Based on Quintiere's Model of ISO 9705 Room Fire Test Performance of Marine Composites (SwRI Project No. 01-2854-001), prepared for US Coast Guard, Southwest Research Institute, San Antonio TX (1999).
399. Setchkin, N. P., A Method and Apparatus for Determining the Ignition Characteristics of Plastics, *J. Research NBS* **43**, 591-608 (1949).
400. Setchkin, N. P., Discussion of Paper on the Ignition Temperature of Rigid Plastics, *ASTM Bull.* No. 151, 66-69 (1948).
401. Brown, J. R., and Gellert, E. P., The Combustion of Organic Polymeric Materials—Ignition Properties (Tech. Note MRL-TN-414), Materials Research Laboratories, Dept. of Defence, Ascot Vale, Vic., Australia (1978).
402. Fire and Toxicity Test Methods and Qualification Procedure for Composite Material Systems used in Hull, Machinery, and Structural Applications inside Naval Submarines, MIL-STD-2031 (SH). Dept. of Defense, Philadelphia (1991).
403. Sorathia, U., Fire Resistant Barriers for Composites (DTRC/SME-88-28), David Taylor Research Center, Bethesda MD (1988).
404. Sorathia, U., Survey of Resin Matrices for Integrated Deckhouse Technology (DTRC SME-88-52), David Taylor Research Center, Bethesda MD (1988).
405. Sorathia, U., Dapp, T., Kerr, J., and Wehrle, J., Flammability Characteristics of Composites (DTRC SME-89/90), David Taylor Research Center, Bethesda MD (1989).
406. Sorathia, U., Dapp, T., and Kerr, J., Fire Barriers for Composite Structures (DTRC SME-90-13), David Taylor Research Center, Bethesda MD (1990).
407. Sorathia, U., Dapp, T., and Kerr, J., Flammability Characteristics of Composites for Shipboard and Submarine Internal Applications, *Intl. SAMPE Symp. and Exhibition ("How Concept Becomes Reality")* **36** (Part II), 1868-1878, SAMPE (1991).

408. Sorathia, U., Rollhauser, C. M., and Hughes, W. A., Improved Fire Safety of Composites for Naval Applications, *Fire and Materials* **16**, 119-125 (1992).
409. Sorathia, U., Dapp, T., and Beck, C., Fire Performance of Composites, *Materials Engineering* **109**, 10-12 (Sept. 1992).
410. Sorathia, U., and Beck, C., Fire-Screening Results of Polymers and Composites, pp. 93-114 in *Improved Fire- and Smoke-Resistant Materials for Commercial Aircraft Interiors: A Proceedings* (Publ. NMAB-477-2). National Materials Advisory Board/National Research Council. National Academy Press, Washington (1995).
411. Sorathia, U., Telegadas, H., and Bergen, M., Mechanical and Flammability Characteristics of Phenolic Composites for Marine Applications, pp. 82-93 in *20th Intl. Conf. on Fire Safety*, Product Safety Corp., Millbrae CA (1995).
412. Sorathia, U., and Beck, C., Fire Protection of Glass/Vinyl Ester Composites for Structural Applications, pp. 687-697 in *41st Intl. SAMPE Symp.*, SAMPE (1996).
413. Sorathia, U., Lyon, R., Gann, R. G., and Gritzo, L., Materials and Fire Threat, *Fire Technology* **33**, 260-275 (1997).
414. Lyon, R. E., Balaguru, P. N., Foden, A., Sorathia, U., Davidovits, J., and Davidovics, M., Fire-resistant Aluminosilicate Composites, *Fire and Materials* **21**, 67-73 (1997).
415. Sastri, S. B., Armistead, J. P., Keller, T. M., and Sorathia, U., Flammability Characteristics of Phthalonitrile Compounds, pp. 1032-1038 in *42nd Intl. SAMPE Symp.*, SAMPE (1997).
416. Sorathia, U., Lyon, R. E., Ohlemiller, T. J., and Grenier, A., Review of Fire Test Methods and Criteria for Composites, *SAMPE J.* **33**:4, 23-31 (Jul./Aug. 1997).
417. Kim, P. K., Pierini, P., and Wessling, R., Thermal and Flammability Properties of Poly(*p*-phenylene-benzobisoxazole), *J. Fire Sciences* **11**, 296-307 (1993).
418. Stevanovic, A., Mehta, S., Walther, D. C., and Fernandez-Pello, A. C., The Effect of Fiberglass Concentration on the Piloted Ignition of Polypropylene/Fiberglass Composites, *Combustion Science and Technology* **174**:11/12, 171-186 (2002).
419. Brinton, W. F., jr., Evans, E., and Brinton, R. B., Standardized Test for Evaluation of Compost Self-Heating, *BioCycle* **36**, 64-69 (Nov 1995).
420. Rynk, R., Fires at Composting Facilities: Causes and Conditions, *BioCycle* **41**, 54 (Jan. 2000).
421. James, L. H., Bidwell, G. L., and McKinney, R. S., An Observed Case of "Spontaneous" Ignition in Stable Manure, *J. Agricultural Res.* **36**:5 (March 1, 1928).
422. Fitz, M. M., MDE Engineers, private communication (2002).
423. Zabetakis, M. G., Biological Formation of Flammable Atmospheres (RI 6127), Bureau of Mines, Pittsburgh (1962).
424. Shields, T. J., Azhakesan, M. A., and Silcock, G. W. H., The Creation, Development and Application of a Strategy for the Classification of Building Materials Using a Cone Calorimeter, Appendix 2, Fire SERT Centre, Univ. Ulster, Carrickfergus, Co. Antrim, N. Ireland (1995).
425. Tsantaridis, L., and Mikkola, E., Cone Calorimeter Results for Four Nordic Materials Tested Earlier in Full Scale (Rapport L 9010052), TräteknikCentrum, Stockholm (1990).
426. Östman, B. A.-L., and Tsantaridis, L. D., Ignitability in the Cone Calorimeter and the ISO Ignitability Test, pp. 175-182 in *Interflam '90,* Interscience Communications Ltd., London (1990).
427. Safety of Information Technology Equipment, Including Electrical Business Equipment (IEC 60950), International Electrotechnical Commission, Geneva.
428. Safety of Information Technology Equipment, Including Electrical Business Equipment (UL 1950), UL.
429. Wadehra, I., Fire Safety Concerns Play Key Role in the Material Selection Process, presented at Bromine Science and Environmental Forum Seminar, Tokyo (1997).
430. Simonson, M., Fire tests conducted for the National Association of Fire Marshals, SP, Borås, Sweden (2000).
431. Wilcox, W., Robertson, W. M., Tideswell, F. V., and Jones, S., Ignition of Conveyor Belts by Frictional Heating (Research Report 20), Safety in Mines Research Establishment, Sheffield, England (1951).
432. Bradford, C., Static Electricity Considerations in the Grain Industry—Preliminary Data on Conveyor and Elevator Belting, pp. 100-126 in *Proc. Intl. Symp. on Grain Dust Explosions*, Grain Elevator and Processing Society, Minneapolis (1977).
433. Hall, J. R. jr., U.S. Home Cooking Fire Patterns and Trends, Fire Analysis & Research Div., NFPA (2001).
434. Hogg, J., Fires Associated with Electrical Cooking Appliances (Fire Research Technical Paper 9), Fire Research Station, Borehamwood, UK (1963).
435. Smith, L., Monticone, R., and Gillum, B., Range Fires, Consumer Product Safety Commission, Washington (1999).
436. Kitchen Fires: It Pays to Know What's Cooking, *Fire Findings* **1**:1, 13 (Spring 1993).
437. Kitchen Fires: Electric Range Tests Produce Results Similar to 1993 Gas Range Experiment, *Fire Findings* **5**:3, 6 (Summer 1997).
438. How Hot Does It Get? *Fire Findings* **2**:1, 5 (Winter 1994).
439. Grill Fires, Topical Fire Research Series, Vol. 2, Issue 3, US Fire Administration, Emmitsburg MD (2001).
440. Hallman, J. R., Ignition Characteristics of Plastics and Rubber (Ph.D. dissertation), Univ. Oklahoma, Norman (1971).
441. Cain, M. W., An Investigation into the Ignitability Characteristics of Several Common Materials (IR/L/FR/85/10), HSE, Buxton, UK (1985).
442. Hensel, W., Entzündung abgelagerter Stäube, *VDI Berichte Nr. 701*, 143-166 (1988).
443. Stecher, G. E., and Lendall, H. N., **Fire Prevention and Protection Fundamentals (Comburology)**, The Spectator, Philadelphia (1953).
444. Wakelyn, P. J., and Hughs, S. E., Evaluation of the Flammability of Cotton Bales, *Fire and Materials* **26**, 183-189 (2002).
445. Bowes, P. C., **Self-Heating: Evaluating and Controlling the Hazards**, Her Majesty's Stationery Office, London (1984). Also published by Elsevier Science.
446. The Spontaneous Heating and Ignition of Wet Cotton Bales, *J. Textile Institute* **47**, P1024-1025 (1956).
447. Fire by Freight, *Ind. and Eng. Chem.* **44**: 3, 11A (Mar. 1952).
448. Abbott, R. E., p. 47 in Report of Conference on Spontaneous Heating and Ignition of Agricultural and Industrial Products, NFPA and US Dept. of Agriculture, Washington (1929).
449. Lucas, A., **Forensic Chemistry and Scientific Criminal Investigation,** 4th ed., Edward Arnold, London (1946).
450. Bowes, P. C., The Spontaneous Heating and Ignition of Wet Cotton Bales (FR Note 126), Fire Research Station, Borehamwood (1954).

451. Chan, T.-K., and Napier, D. H., Smoldering and Ignition of Cotton Fibres and Dust, *Fire Prevention Science and Technology*, No. 4, 13-23 (Feb.1973).
452. Gray, B. F., Little, S. G., and Wake, G. C., The Prediction of a Practical Lower Bound for Ignition Delay Times and a Method of Scaling Times-to-Ignition in Large Reactant Masses from Laboratory Data—II., pp. 1785-1791 in *24th Symp. (Intl.) on Combustion*, The Combustion Institute, Pittsburgh (1992).
453. Jones, J. C., Thermal Calculations on the Ignition of a Cotton Bale by Accidental Contact with a Hot Particle, *J. Chem. Tech. and Biotech.* **65**, 176-178 (1996).
454. Knoepfler, N. B., Gentry, W. T., and Madacsi, J. P., Resistance of Mattresses Containing Boric Acid Treated Cotton Batting to Open Flame Ignition, *J. Consumer Product Flammability* **4**, 169-187 (1977).
455. Mansfield, W. P., Crankcase Explosions: Development of New Protective Devices, *Proc. Instn. Mech. Engineers* **170**, 825-862 (1956).
456. Lamb, J., Explosions in Enclosed Crankcases of Reciprocating Engines: Their Cause, Effect, and Possible Remedy, *Proc. Instn. Mech. Engineers* **166**, 327-349 (1952).
457. Ferguson, G. W., Diesel Engine Crankcase-Explosion Investigation, *Trans. ASME* **74**, 7-21 (1952).
458. Hoare, D. J., and Conybeare, A. M., Crankcase Explosions, pp. 735-758 in *Premier Congrès International des Moteurs à Combustion Interne*, vol. 2, Paris (1951).
459. Davies, D. H. J., Crankcase Protection and Oil Mist Phenomena, *The Motor Ship*, 69-74 (Aug. 1978).
460. Burgoyne, J. H., and Newitt, D. M., Crankcase Explosions in Marine Engines, *Trans. Inst. Marine Engineers* **67**, 255-270 (1955).
461. Smedley, G. P., Risk of Crankcase Explosions in Oil Engines and Dual-fuel Engines, *Trans. Inst. Marine Engineers* **97**, Paper 8 (1985).
462. Redwood, B., **Petroleum**, 3rd ed., vol. 1, London, Charles Griffin, London (1913).
463. Iwata, Y., Koseki, H., Janssens, M. L., and Takahashi, T., Comparison of Combustion Characteristics of Crude Oils, *Fire and Materials* **25**, 1-7 (2001).
464. Elam, S. K., Altenkirch, R. A., Saito, K., and Arai, M., Cone Heater Ignition Tests of Liquid Fuels, *Fire Safety J.* **16**, 65-84 (1990).
465. How Hot Does It Get? *Fire Findings* **1**:3, 3 (Fall 1993).
466. Goodale, T., Ignition Hazard to Urban Interiors During Nuclear Attack Due to Burning Curtain Fragments Transported by Blast (URS 7030-5; Modification P616-1), URS Research Co., San Mateo CA (1971).
467. Shipp, M., private communication (2000).
468. **The Science of Petroleum**, vol. 4, A. E. Dunstan et al., eds., Oxford Univ. Press, London (1938).
469. Standard Specification for Diesel Fuel Oil (ASTM D 975), ASTM.
470. Li, J.-H., and Huang, Z.-H., Study on the Correlation of Ignition Time for Liquid Fuels and Heat Radiation, pp. 108-116 in *Symp. for '97 FORUM—Applications of Fire Safety Engineering*, Tianjin, China (1997).
471. Paul, K. T., and Hough, M. C., Fires in Dishwashers (CTR 26150), RAPRA Technology Ltd. for Dept. of Trade and Industry, London (1995).
472. Dishwashers/Washing Machines (Europe), Sambrook Research Intl. for Dept. of Trade and Industry, London (1995).
473. Fires Involving Dishwashers in the United Kingdom, Metra Martech Ltd. for Dept. of Trade and Industry, London (1995).
474. Kadambi, S., Report on Electric and Gas Clothes Dryers, Clothes Dryer Project, Consumer Product Safety Commission (1999).
475. Electric and Gas Clothes Dryers—Staff Evaluation and Contractor Report (memorandum to Commission), Consumer Product Safety Commission (2000).
476. Gas Clothes Dryers, vol. 1. Type I Clothes Dryers (ANSI Z21.5.1), American National Standards Institute, New York (1995).
477. Electric Clothes Dryers (UL 2158), UL.
478. Fire Hazards Associated with Household Clothes Dryers (Communiqué No. 96-031), Ontario Fire Marshal, Toronto (1996).
479. Clean Those Lint Traps, *The Code Authority*, Underwriters Laboratories Inc., **8**:2 1, 5 (2000).
480. Fitz, M. M., MDE Engineers, private communication (2001).
481. Laundry Rooms Posing Potential Hazards, *Canadian Assn. of Fire Investigators The/Le Journal*, 7-9 (Mar. 1991).
482. Sanderson, J. L., Clothes Dryers Fires. Part I, *Fire Findings* **4**:3, 7-11 (Summer 1996).
483. Sanderson, J. L., Clothes Dryers Fires. Part II, *Fire Findings* **4**:4, 7-11 (Fall 1996).
484. Tumbler Fires, *Textile Notes*, No. TN-143, Intl. Fabricare Institute, Silver Spring MD (1986).
485. Monroe, G., and Wuepper, J., Spontaneous Combustion of Vegetable Oils on Fabrics (report prepared for CPSC), Whirlpool Corp., R&D Center, Benton Harbor MI (1991).
486. Harris, E. E., Fire! *Textile Rental* 61-70 (Aug. 1983).
487. Fire Incidents: Mopheads Spontaneously Ignite; $25,000 Damage, *Code Red (Bull. of the Health Care Section of NFPA)* No. 31 (Sep. 1984).
488. Jones J. C., A Theoretical Examination of the Possibility of Spontaneous Combustion of Laundry in Tumble Dryers, *J. Fire Sciences* **19**, 181-189 (2001).
489. Jones J. C., A Theoretical Examination of the Possibility of Spontaneous Combustion of Laundry in Tumble Dryers. Part 2: The Role of Reactive Contaminants, *J. Fire Sciences* **19**, 335-339 (2001).
490. Dixon, B. M., The Role of Self-heating as a Cause of Laundry Fires, presented at the meeting of the Canadian Society of Forensic Sciences, Vancouver BC (1994).
491. Dixon, B. M., Spontaneous Combustion Part II, *Canadian Assn. of Fire Investigators The/Le Journal*, 14-15 (March 1994).
492. Removal of Cooking Oil from Cotton Terry Cloth Towels, The Soap and Detergent Assn., n.p. (1996).
493. Sanderson, J., Clothes Dryer Lint: Part II. Testing Reaffirms Spontaneous Heating of Lint is Unlikely, *Fire Findings* **7**:1, 12-14 (Winter 1999).
494. Coulombe, R., Chemical Analysis of Vegetable Oils Following Spontaneous Ignition, *J. Forensic Sciences* **47**, 195-201 (2002).
495. Mann, D. C., and Fitz, M. M., Dryer Fire Investigations: An Alternative Sampling Protocol to Recover Oils Which May Spontaneously Heat, *The Fire Place* (Washington State IAAI Chapter Newsletter), 12-14 (Dec. 1999/Jan. 2000).
496. Code Red!, Bulletin of the Health Care Section of the National Fire Protection Association, No. 31 (Sept. 1984).

497. Reese, N. D., et al., Clothes Dryer Fires, *Fire & Arson Investigator* **48**:4, 17-19 (July 1998).
498. Sanderson, J. L., and Schudel, D., Clothes Dryer Lint: Spontaneous Heating Doesn't Occur in Any of 16 Tests, *Fire Findings* **6**:4, 1-3 (Fall 1998).
499. Dryer, F. L., private communication (1999).
500. Lasseran, J.-C., Grain Drier Fires: Their Cause and Prevention, *The Agricultural Engineer* **42**, 132-135 (Winter 1987).
501. Gibson, N., and Schofield, F., Fire and Explosion Hazards in Spray Dryers, pp. 57-66 in *Proc. 6th Intl. Symp. on Chemical Process Hazards with Special Reference to Plant Design* (Symp. Series No. 49), The Institution of Chemical Engineers, Rugby (1977).
502. Beever, P. F., Hazards in Drying Thermally Unstable Powders, pp. 223-231 in *Hazards X: Process Safety in Fine and Specialty Chemical Plants* (Symp. Series No. 115), Institution of Chemical Engineers, Rugby (1989).
503. Abbott, J. A., **Prevention of Fires and Explosions in Dryers—A User Guide**, 2nd ed., Instn. Chemical Engineers, Rugby, England (1990).
504. Bunting, S. C., and Wright, H. A., Ignition Capabilities of Non-Flaming Firebrands, *J. Forestry* **72**, 646-649 (1983).
505. Casey, H., Dirty Diaper Ignites Texas Blaze, *Fire & Arson Investigator* **51**:1, 12 (Oct. 2000).
506. van Laar, G. F. M., De ontstekingsmogelijkheid van explosieve stof-luchmengels door sigaren, sigaretten en glimnestern (PML 1980-118), Prins Maurits Laboratorium TNO, Rijswijk, Netherlands (1981).
507. Glinka, W., Klemens, R., and Wolański, P., Experimental and Theoretical Studies on Radiative Ignition of Dust Layer, *14th Intl. Colloquium on Dynamics of Explosions and Reactive Systems*, Univ. Coimbra, Portugal (1993).
508. Leisch, S. O., Kauffman, C. W., and Nicholls, J. A., Smoldering Combustion as Related to Grain Elevator Safety, National Grain and Feed Assn., Washington (1982).
509. Xu, B.-W., Zheng, H.-J., and Xu, W.-Q., The Effect of Particle Size of Fibre Dust LEL, pp. 237-246 in *Proc. 5th Intl. Colloquium on Dust Explosions*, Pultusk near Warsaw (1994).
510. Palmer, K. N., Interim Report on the Ignition of Tea Fluff (FR Note 167), Fire Research Station, Borehamwood, UK (1955).
511. Kauffman, C. W., Recent Dust Explosion Experience in the U.S. Grain Industry, pp. 243-264 in **Industrial Dust Explosions** (ASTM STP 958), ASTM (1987).
512. Eckhoff, R. K., **Dust Explosions in the Process Industries**, 2nd ed., Butterworth-Heinemann, Oxford (1997).
513. van Wingerden, K., Dust Explosions in the Wood Processing Industry, Christian Michelsen Research AS, Bergen, Norway [199?].
514. Thorpe, D. G. L., Singh, S., Cartwright, P., and Bailey, A. G., Electrostatic Hazards in Sugar Dust in Storage Silos, *J. Electrostatics* **16**, 193-207 (1985).
515. Chiotti, P., An Overview of Grain Dust Explosion Problems, pp. 13-36 in *Proc. Intl. Symp. on Grain Dust Explosions*, Grain Elevator and Processing Society, Minneapolis (1977).
516. Matsuda, T., Dust Explosibility of Fine Ceramic Powders, *Specific Report of the Research Institute of Industrial Safety* No. 12, 49-55 (1993).
517. Matsuda, T., Evaluation of Dust Explosibility by a Testing Method, *Specific Report of the Research Institute of Industrial Safety* No. 12, 71-76 (1993).
518. Suzuki, K., Matsubara, Y., Iwami, T., Hokugo, A., and Murosaki, Y., Causes and Progress of Fires following the 1995 Southern Kyogo Prefecture Earthquake, pp. 157-164 in *Proc. 14th Joint Panel Mtg. UJNR Panel on Fire Research and Safety*, Building Research Institute, Tsukuba, Japan (1998).
519. Fire in the United States 1985-1994, 9th ed., US Fire Administration, Emmitsburg MD (1997).
520. Hall, J. R. jr., private communication (2001).
521. Hall, J. R. jr., Bukowski, R. W., and Gomberg, A., Analysis of Electrical Fire Investigations in Ten Cities (NBSIR 83-2803), NBS (1983).
522. Smith, L. E., and McCoskrie, D., What Causes Wiring Fires in Residences, *Fire J.* **84**, 19-24, 69 (Jan/Feb 1990).
523. Smith, L., and McCoskrie, D., Residential Electrical Distribution System Fires, Consumer Product Safety Commission, Washington (1987).
524. Peck, G. C., Fire and Explosion Hazards of Liquid-filled Electrical Equipment. Part 1: An Overview (ITB-R84/108), The Insurance Technical Bureau, London (1984).
525. 2000 Annual Fire Report, National Fire Defence Agency, Tokyo (2002).
526. Smelkov, G. I., and Pekhotikov, V. A., On the Assessment of an Electrical Fire Risk, VNIIPO MVD RF, Balashikha, Moscow (1998).
527. Sletback, J., Kristensen, R., Sundklakk, H., Nåvik, G., and Munde, R., Glowing Contact Areas in Loose Copper Wire Connections, pp. 244-248 in *Proc. 37th IEEE Holm Conf. on Electrical Contacts*, IEEE (1991).
528. Rohr, K., US Home Product Report, 1992-1996: Appliances and Equipment, NFPA (1998).
529. Losinger, W. C., Estimated Fire Losses Involving Electrical Equipment–1990, Consumer Product Safety Commission, Washington (1992).
530. Eaton, T. E., **Notes on Electrical Fires**, 3rd ed. and 1990 supplement, Eaton Engineering Co., Nicholasville, KY (1989).
531. Malik, H. A., Assessment of Flammability of Plastic Materials Used as Electrical Appliance Enclosures (CPSC/ES/TR-98/001), Consumer Product Safety Commission, Washington (1998).
532. Standard for Safety of Household and Similar Electrical Appliances, Part 1: General Requirements (IEC 60335-1), International Electrotechnical Commission, Geneva.
533. Safety of Household and Similar Appliances. Part 1: General Requirements (IEC 60335-1), International Electrotechnical Commission, Geneva.
534. Fire Hazard Testing – Part 2-11 Glowing/Hot Wire Based Test Methods—Glow-Wire Flammability Test Method for End Products (IEC 60695-2-11), International Electrotechnical Commission, Geneva.
535. Fire Hazard Testing – Part 2-12 Glowing/Hot Wire Based Test Methods—Glow-Wire Flammability Test Method for Materials (IEC 60695-2-12), International Electrotechnical Commission, Geneva.
536. Wagner, M., Stricter Fire Standards for Appliances Require Higher-Performance Grades, *Modern Plastics* **80**:2, 62-63 (Feb. 2003).
537. Massar, J. C., and Catanesco, M. A., Hermetically Sealed Temperature Sensitive Non-Resettable Relay, US Patent No. 2,934,628 (1960).
538. Injuries Associated with Hazards Involving Motor Vehicle Batteries (Research Note), Natl. Center for Statistics &

Analysis, Natl. Highway Traffic Safety Admin., Washington (1997).
539. Info & Requests, *The Vehicle Fire Reporter* **9**, 3, 12 (Summer 1999).
540. Adams, J. Maxwell, **Electrical Safety: A Guide to the Causes and Prevention of Electrical Hazards** (IEE Power Series 19), Instn. Electrical Engineers, London (1994).
541. Tolson, P., and Tomlinson, R., Explosion of a Lead/Acid Battery due to Electrostatic Charging, *J. Electrostatics* **30**, 149-158 (1993).
542. Levy, S. C., and Bro, P., **Battery Hazards and Accident Prevention**, Plenum Press, New York (1994).
543. Townsend, J. S., Dry Cell Batteries: A Big Bang in a Little Box, *Industrial Fire World* **15**:3, 51, 53 (May/June 2000).
544. Hay, N., Kubba, B., and Shayler, P. J., Safety Assessment of Flame-arresting Battery Plugs, *J. Hazardous Materials* **6**, 309-317 (1982).
545. Hay, N., Kubba, B., and Shayler, P. J., Flame-arresting Performance of Round Holes and Porous Discs for Battery Vent Plugs, *J. Hazardous Materials* **6**, 299-308 (1982).
546. Exploding Flashlights: Are They a Serious Threat to Worker Safety? (NIOSH Fact Sheet/DHHS Publ. 97-149), NIOSH, Washington (1997).
547. Two Firefighters Injured When an Automated External Defibrillator Battery Exploded or Ruptured During Testing—Florida, *NIOSH Injury in the Line of Duty…*99F-39 (10 Apr. 2000).
548. Tokyo Fire Department, Fire Report: Fires of Small Battery, *J. Japan Assn. of Fire Science and Engineering* **44**:5, 57-60 (Oct. 1994).
549. Safety Recommendations A-99-80 through -84, National Transportation Safety Board, Washington (1999).
550. **Recommendations on the Transport of Dangerous Goods: Manual of Tests and Criteria**, 2nd ed., United Nations, New York (1995).
551. UL Standard for Safety for Lithium Batteries (UL 1642), UL.
552. Technical Manual for Batteries, Navy Lithium Safety Program Responsibilities and Procedures, NAVSEA S9310-AQ-SAF-010, Naval Sea Systems Command, Washington (1988).
553. Briefing Package on the Electric Blanket Project, US Consumer Product Safety Commission, Washington (1982).
554. Standard for Safety for Electrically Heated Bedding (UL 964), UL.
555. McLaughlin, G. E., Electric Blanket Fires, *Fire Findings* **8**:4, 7-11 (Fall 2000).
556. Hull, W., and Pippen, D. L., Electric Blanket Fires, *Fire Findings* **11**:1, 7-10 (Winter 2003).
557. McLaughlin, G. E., Fire in the Night, unpublished paper [1999?].
558. Carlson, G., Electric Blanket Safety Circuit, US Patent 4,436,986, assigned to Sunbeam Corp. (1984).
559. Electric Blanket Fires & Related Injuries (URN 99/1061), Sambrook Research Intl. for Dept. of Trade and Industry, London (1999).
560. McLaughlin, G. E., Electric Blanket Fires, *Trial* 53-55 (Nov. 1999).
561. Twibell, J. D., and Christie, C. C., The Forensic Examination of Fuses, *Science and Justice* **35**, 141-149 (1995).
562. Stokes, A. D., Fire Ignition by Electrically Produced Incandescent Particles (Dept. report), Dept. of Electrical Engineering, Univ. Sydney, Australia (2001).
563. Harwood, B., Residential Electrical Wiring Systems and Thermal Insulation, Consumer Product Safety Commission, Washington (1979).
564. Jacobs, M. B., and Kusko, A., Litigating Uninterrupted Arcing Faults in Electrical Equipment, unpublished paper (1999).
565. Aronstein, J., Evaluation of Residential Circuit Breaker Panel (Report to CPSC, Contract CPSC-C-81-1455), Wright-Malta Corp., Ballston Spa NY (May 10, 1984).
566. Franklin, F. F., Circuit Breakers: The Myth of Safety, *Fire & Arson Investigator* **41**, 42-45 (June 1991).
567. Shefchick, T. P., Comparison of American and European Residential Circuit Breakers, presented at American Academy of Forensic Sciences Conf. (1995).
568. Wagner, R. V., Fact-Finding Report on An Evaluation of Branch-Circuit Circuit-Breaker Instantaneous Trip Levels (Project 92ME51901), UL (1993).
569. Goodson, M. E., Perryman, T., and McKinney, K., Circuit Breaker Performance in Depressed Atmospheres, *Fire & Arson Investigator* **51**:4, 13-16 (July 2001).
570. Reiter, D., Verité Forensic Engineering, private communication (2001).
571. Matsumura, T., et al., Thermal Model Criteria of Short-Circuit Fault Induced in Hot Gas Ejected from a Molded-Case Circuit Breaker, pp. I-58 to I-61 in *Proc. 11th Intl. Conf. on Gas Discharges and Their Applications (GD '95)*, The Institute of Electrical Engineers of Japan, Tokyo (1995).
572. NWCG Wildfire Cause Determination Handbook (PMS 412-1, NFES 1874), National Interagency Fire Center, Boise ID (1978).
573. How Hot Does It Get? *Fire Findings* **1**:2, 5 (Summer 1993).
574. Pocket Guide to Arson and Fire Investigation, 5th ed., FM Global, Johnston RI (1999).
575. Freytag, H. H., **Handbuch der Raumexplosionen**, Verlag Chemie, Weinheim, Germany (1965).
576. Morgan, P. D., Taylor, H. C., and Lethersich, W., The Heating of Domestic Pendant Lighting Fittings and their Connecting Leads, *J. IEE* **73**, 545-568 (1933).
577. Gruehn, R. L., To Be Prepared Is Everything, *Fire & Arson Investigator* **39**:1, 54 (Sep. 1988).
578. Firestone, R. F., private communication (2002).
579. Allsop, G., and Thomas, T. S. E., The Ignition of Firedamp by the Filaments of Broken Electric Lamp Bulbs (Paper 80), Safety in Mines Research Board, London (1933).
580. Clark, H. H., and Ilsley, L. C., Ignition of Mine Gas by the Filaments of Incandescent Electric Lamps (Bull. 52), Bureau of Mines, Government Printing Office, Washington (1913).
581. Litchfield, E. L, Kubala, T. A., Schellinger, T., Perzak, F. J., and Burgess, D., Practical Ignition Problems Related to Intrinsic Safety in Mine Equipment: Four Short-Term Studies (RI 8464), Bureau of Mines, Pittsburgh (1980).
582. Swatko, T., Bowerman, R., Hedjuk, G., and Evans, S., Trouble Light Ignition Fire Tests, *Canadian Assn. of Fire Investigators The/Le Journal*, 9-12 (June 1999).
583. Severy, D. M., Blaisdell, D. M., and Kerkhoff, J. F., Automotive Collision Fires, pp. 113-199 in *Proc. 18th Stapp Car Crash Conf.*, Society of Automotive Engineers, Warrendale PA (1974).
584. Schram, P. J., Ignition Temperature of Gases and Vapors as Applied to Electrical Equipment for Use in Hazardous Locations, pp. 47-59 in **Electrical Safety Practices** (Monograph 113), Instrument Society of America, Pittsburgh (1972).

585. Morse, A. R., Ignition of Grain-dust Clouds by Electric Lightbulbs and Motors (NRC No. 4411, ERB-430), National Research Council of Canada, Ottawa (1956).
586. Baum, K., Investigators' Discovery of Hazardous Lightbulb Results in Grocers Pulling from Shelves Statewide, *Fire & Arson Investigator* **44**:1, 8 (Sept. 1993).
587. Harkness, K. A., Electrical System Fire Hazards, *Fire & Arson Investigator* (Oct./Dec. 1961).
588. Sanderson, J. L., Heat-bulb Testing: Wood, Straw and Towels Respond Differently at Close Distances to Lamps, *Fire Findings* **8**:4, 1-3 (Fall 2000).
589. Dini, D. A., Skuggevig, W., Wagner, R., Boden, P. J., and Dubiel, D. G., Report of Research on Arc-Fault Detection Circuit Breakers for National Electrical Manufacturers Association (Project 95NK6832), UL (1996).
590. Allsop, G., and Wheeler, R. V., The Ignition of Firedamp by Broken Electric Lamp Bulbs: The Appearance of the Filaments (Paper 89), Safety in Mines Research Board, London (1935).
591. Poole, M. R., and Vermij, M., A Guide to Lightbulb Analysis in Support of Aircraft Accident Investigation (TP 6255E), Transportation Safety Board of Canada, Ottawa (1991).
592. Poole, M. R., and Vermij, M., Lightbulb Filament Impact Dynamics Study in Support of Aircraft Accident Investigation (TP 6254E), Transportation Development Centre, Transport Canada, Ottawa (1985).
593. Coaton, J. R., Lamp Materials, *The Metallurgist and Materials Technologist* **7**, 510-514 (Oct. 1975).
594. Long, K., Data Summary on Halogen Torchiere-Style Floor Lamps (memorandum), Consumer Product Safety Commission, Washington (1997).
595. Torchiere Lamps Test Protocol—Halogen & Incandescent—Phase I (memorandum), Consumer Product Safety Commission, Washington (April 22, 1996).
596. Lowe, R. E., Lowe, D. A., and Lowe, J. A., Halogen Lamps: Clearly a Bright and Present Danger, *Fire & Arson Investigator* **47**:3, 14-15 (Mar. 1997).
597. Béland, B., Halogen Lamps as a Cause of Fires, *Fire & Arson Investigator* **49**, 6-8 (April 1999).
598. House for Sale—Buyers' Remorse Rarely the Reason for Fire, *Fire Findings* **4**:2, 6 (Spring 1996).
599. Calls Prompt Halogen Lamp Tests, *Fire Findings* **4**:3, 14 (Summer 1996).
600. Rakosnik, R., Torchère Lamps, *Fire Engineering* **150**, 20-21 (Jan. 1997).
601. Béland, B., Right or Wrong?…Depends on the Test Conditions, *Fire & Arson Investigator* **48**, 4-5 (July 1998).
602. Paul, D., Letter to the Editor, *Fire & Arson Investigator* **47**:4, 4 (June 1997).
603. Portable Electric Lamps (UL 153), UL.
604. Holmes, D. L., private communication (2000).
605. Cooke, R. A., and Ide, R. H., **Principles of Fire Investigation**, The Institution of Fire Engineers, Leicester, England (1985).
606. Best Practices for Metal Halide Lighting Systems, Lamp and Luminaire Sections, National Electrical Manufacturers Association, Rosslyn VA (2000).
607. Zollweg, R. J., The Alumina Arc Tube Wall Temperature of High Pressure Sodium Lamps, *J. Illuminating Engineering Soc.* **12**, 275-281 (1983).
608. High Intensity Discharge Metalarc® Lamps (Engineering Bull. HID-011-0995), Osram Sylvania (1998).
609. Elenbaas, W., et al., **High Pressure Mercury Vapour Lamps and Their Applications**, pp. 114-146, Philips, Eindhoven, Netherlands (1965).
610. Firestone, R. F., Distribution of Strength Controlling Flaws in Polycrystalline Ceramics, *Bull. Amer. Ceramic Soc.* **55**, 397 (1976).
611. HID Lighting Advisory, *NFPA SectioNews* **1**:5, 5 (Apr./May 2001).
612. Questions and Answers about Lamp Ruptures in Metal Halide Lighting Systems, Lamp and Luminaire Sections, National Electrical Manufacturers Association, Rosslyn VA (2000).
613. Standard for Safety for Luminaires (UL 1598/CSA 250), UL and Canadian Standards Assn.
614. Shinomiya, K., Kashiwagi, N., Kodera, T., and Sakamoto, N., An Investigation of a Fire Caused by an Fluorescent Lamp Covered with Quilts, *Summary of 4th Mtg. Japanese Assn. Science and Technology for Identification*, 104 (1998).
615. Verweij, W., The Ignition of Explosive Gas Mixtures following Breakage of Fluorescent Lamps, Paper. no. 7 in *9th Intl. Conf. of Directors of Safety in Mines Research.*, Sheffield, England (1959).
616. Yarbrough, D. W., Yoo, K. T., and Koneru, P. B., Recessed Light Fixture Test Facility (ORNL/SUB-7504/3), Oak Ridge Natl. Lab., Oak Ridge TN (1979).
617. Recessed Light Fixtures, *Fire Findings* **2**:4, 7-10 (Fall 1994).
618. Cooksey, P. N., Recessed Lighting, Insulation, and Fire, *International Fire Chief* **46**:9, 50-51 (Sept. 1980).
619. Fulcomer, P. M., Temperature Measurement on Operating Surface Mounted Lighting Fixtures (NBSIR 79-1912), NBS (1979).
620. Christmas-Tree and Decorative-Lighting Outfits (UL 588), 16th ed., UL.
621. Seasonal and Holiday Decorative Products (UL 588), 17th ed., UL.
622. Cooper, W. F., and Jones, D. A. D., **Electrical Safety Engineering**, 3rd ed., Butterworth-Heinemann, Oxford (1993).
623. Clayton, J. W. jr., private communication (2002).
624. Fire Hazard of Fluorescent Lighting Fittings, *Fire Prevention* No. 93, 15 (May 1973).
625. Tremblay, K. J., Fluorescent Light Ballast Ignites Blaze in Yarn Dyeing Plant: Georgia, *NFPA J.* **89**, 32 (Mar/Apr. 1995).
626. Fluorescent-Lamp Ballasts (UL 935), UL.
627. Fluorescent Lighting Fixtures (UL 1570), UL.
628. Yarbrough, D. W., and Toor, I. A., Operating Temperatures of Recessed Fluorescent Fixtures with Thermal Insulation (ORNL/SUB-7715/4), Oak Ridge Natl. Lab., Oak Ridge TN (1981).
629. Cooper, R., private communication, Scientific Services Laboratory, Port Melbourne, Vic., Australia (2000).
630. Zicherman, J., Technical Note: The Fire Performance of Electrical Insulating Materials Used in Fluorescent Lighting Fixtures, *Fire and Materials* **25**, 209-213 (2001).
631. Application Note: Wiring Requirements for T-8 Lamps with Instant-Start Ballasts, Lamp Section, National Electrical Manufacturers Association, Rosslyn VA (1998).
632. Beliveau, D. W., Potential Fire Hazard: Compact Fluorescent Lamps and High Frequency Electronic Ballast, *Fire & Arson Investigator* **47**:4, 28 (June 1997).
633. Béland, B., Floating Neutral as a Cause of Fires, *Fire & Arson Investigator* **36**, 9-12 (Sept. 1985).

634. Ettling, B. V., Electrical Fire Cause: Further Comments and Cautions, *Fire & Arson Investigator* **36**:2, 37-39 (Dec. 1985).
635. Biss, A. A., Evaluation of Design and Operating Characteristics of 15 Ampere 125 Volt Receptacle Outlets, Consumer Product Safety Commission, Washington (1989).
636. Results of the Investigation on Plugs and Receptacles Damaged by Tracking (Interim Report), Assn. of Electrical Inspectors in Kanto District, Japan (March 1995).
637. BC Research, Performance of Residential Electrical Wiring System Component Parts (Report 000 U 114), Canadian Electrical Assn., Montreal (1982).
638. Rabinow, J., Some Thoughts on Electrical Connections (NBSIR 78-1507), NBS (1978).
639. Aluminum Branch Circuit Wiring in Residences. Summary Report for the Consumer Product Safety Commission. January-September 1974 (NBS 75-723), NBS (1975).
640. Hagimoto, Y., Watanabe, N., and Okamoto, K., Considerations in Ignition Process of Electrical Plug on the Side of Cord, pp. 254-257 in *Abstracts of the Annual Meeting of the Japan Assn. for Fire Science and Engineering* (2000).
641. Blades, R., The Real Cause of Electrical Fires, RB Laboratories, Boulder CO (1993).
642. Uchida, M., Saito, H., Watanabe, S., and Sassa, Y., Experiments on the Heat due to Poor Connections inside a Male Plug and on the Breaking of Wires due to Repeated Pulling Out, *Report of the Fire Science Laboratories of the Tokyo Fire Department*, No. 18, 8-16 (1981).
643. Shimizu, Y., A Study on Ignition of Wiring Devices (Cord Plugs), unpublished report, Forensic Science Laboratory, Oita Prefectural Police Headquarters, Oita, Japan (1984).
644. Katayama, S., Endo, S., Okumura, K., Fujio, N., and Wakita, S., Ignition by Sparks of Appliance Cords and Its Prevention, *Abstracts of the 11th Symp. on Safety Engineering (Japan)*, 57-60 (1981).
645. Testing Methods for Wiring Devices (JIS C 8306), Japanese Industrial Standard.
646. Hagimoto, Y., Watanabe, N., Okamoto, K., and Sato, H., Fire Causes in Electrical Plugs, pp. 1211-1216 in *Interflam 2001—Proc. 9th Intl. Conf.*, Interscience Communications Ltd., London (2001).
647. Okamoto, K., Watanabe, N., and Hagimoto, Y., Fire Hazard Caused by Thermal Degradation of Organic Insulating Materials at Plug and Receptacle Connection, pp. 203-214 in *Fire and Materials 2003*, Interscience Communications Ltd., London (2003).
648. Hijikata, T., Fire Causes at Electrical Wiring Devices, *J. Japanese Assn. Fire Science & Engrg.* **46**, No. 2, 13-17 (1996).
649. Ashizawa, K., and Omata, K., Property of Ignition Mechanism Caused by Thermal Degradation on Plug, *Abstracts of Annual Meeting of JAFSE*, Paper C-22, 386-389 (1997).
650. Van Luik, F. W. jr., Characteristics of Invisible Particles Generated by Precombustion and Combustion, *Fire Technology* **10**, 129-139 (1974).
651. Okamoto, K., Watanabe, N., and Hagimoto, Y., Deterioration of Tracking Resistance of Dielectric Materials Caused by Thermal Degradation, pp. 231-234 in *Proc. 1st Conf. of the Assn. of Korean-Japanese Safety Engineering Society*, Kyongju, Korea (1999).
652. Cowan, J. D., jr., Arc, Beads and Other Electrical Things, *Fire & Arson Investigator* **34**:2, 32-35 (Dec. 1983).
653. Meese, W. J., and Beausoliel, R. W., Exploratory study of Glowing Electrical Connections (NBS BSS 103), NBS (1977).
654. Burns, G. W., Scroger, M. G., Evans, G. A., Beausoleil, R. W., and Meese, W. J., Experimental Determinations of Temperatures and Power Losses at the Electrical Connections of Some Duplex Receptacles (NBSIR 77-1380), NBS (1978).
655. Aronstein, J., Evaluation of Receptacle Connections and Contacts, pp. 253-260 in *Proc. 39th IEEE Holm Conf. on Electric Contacts*, IEEE (1993).
656. Rakosnik, R. J., Back Wiring Poses Fire Hazard, *Fire & Arson Investigator* **47**:2, 13-14 (Dec. 1996).
657. National Controlled Study of Relative Risk of Overheating of Aluminum Compared with Copper Wired Electrical Receptacles in Homes and Laboratory (Tech. Report F-C4812-01), Franklin Research Center, Philadelphia (1979).
658. Graps, A., private communication (2000).
659. Kloth, J. A., Parsons, S. L., Zimmerman, J. A. jr., and Vigeant, G. H., Method and Apparatus for a Wiring System Utilizing Wiring Devices, US Patent 3,860,739 (1975).
660. Bromberg, M., Electrical Receptacle, US Patent 3,951,489 (1976).
661. Bromberg, M., Electrical Receptacle, US Patent 3,957,336 (1976).
662. Aronstein, J., Fire Due to Overheating Aluminum-Wired Branch Circuit Connections, Wright Malta Corp., Ballston Spa NY (1983).
663. Béland, B., Behaviour of Electrical Contacts under Fire Conditions, *Fire & Arson Investigator* **38**, 38-41 (Sept. 1987).
664. Okada, M., Takahashi, T., Ebina, K., and Taniguchi, M., An Investigation of a Fire Concluded to be Caused by Glowing Connection, *Summary of 5th Mtg. Japanese Assn. Science and Technology for Identification*, 98 (1999).
665. Hagimoto, Y., National Research Institute of Police Science, private communication (2000).
666. Newman, R., and King, W. H. jr., Pilot Survey of Branch Wiring Systems in Montgomery County, Maryland, Consumer Product Safety Commission, Bethesda (1977).
667. Bunten, E., Donaldson, J. L., and McDonald, E. C., Hazard Assessment of Aluminum Electrical Wiring in Residential Use (NBSIR 75-677), NBS (1974).
668. Laug, O. B., Evaluation of Selected Connectors for Aluminum Wire in Residential Structures (NBSIR 76-1039), NBS (1976).
669. Standard for Receptacles and Switches Intended for Use with Aluminum Wire (UL 1567), UL.
670. Affidavit of William H. King jr., (26 Oct. 1977).
671. Campbell, W. E., Final Report on Study of Aluminum Wire Binding-Screw Connections for House Wiring (CPSC Order No. 75144800), report to CPSC (1977).
672. Aronstein, J., Electromigration Failure of Aluminum Contact Junctions, pp. 10-16 in *Proc. 41st IEEE Holm Conference on Electrical Contacts*, IEEE, Piscataway NJ (1995).
673. Braunovic, M., Stress Relaxation of Aluminum Wire Conductors, pp. 239-251 in *Proc. 1998 44th IEEE Holm Conf. on Electrical Contacts*, IEEE, Piscataway NJ (1998).
674. Aronstein, J., and Campbell, W.E., Failure and Overheating Failures of Aluminum-Wired Twist-on Connectors, *IEEE Trans. Components, Hybrids, and Mfg. Tech.* **CHMT-5**, 42-50 (1982).
675. Aronstein, J., and Campbell, W.E., Overheating Failures of Aluminum-Wired Special Service Connectors, *IEEE Trans.*

Components, Hybrids, and Mfg. Tech. **CHMT-6**, 8-15 (1983).
676. Hicks, R. L., The Effect of Installation Torque on Residential Branch Circuit Connection Life (Report 78-155-K), Ontario Hydro, Toronto (1974).
677. Aronstein, J., Behavior of Overheating Aluminum Wired Branch Circuit Connections Under Normal Loads, pp. 117-131 in *Proc. 26th Annual Holm Conference on Electrical Contacts*, Illinois Institute of Technology, Chicago (1980).
678. Mastoris, S., Heat Cycling of Duplex Receptacle Connections to Aluminum Wiring (Report 76-189-X), Ontario Hydro, Toronto (1976).
679. Campbell, W. E., and Ling, F. F., Temperature Analysis of an Overheating Aluminum Wire Termination to a Steel Binding Screw Contact (Contract CPSC-C-76-0116), report to CPSC (1977).
680. Aronstein, J., Investigation of Fire Hazards in Field Samples of Aluminum-Wired Devices (Contract CPSC-C-76-0115), report from Wright Malta Corp. to CPSC (1977); and supplements.
681. Oda, S. J., Progress Report—Fire Initiation Potential of Failing Electrical Receptacles (Report 78-92-K), Ontario Hydro, Toronto (1978).
682. Repairing Aluminum Wiring (CPSC #516), Consumer Product Safety Commission, Washington (1994).
683. Aronstein, J., Evaluation of a Twist-on Connector for Aluminum Wire, pp. 45-56 in *Proc. 1997 43rd IEEE Holm Conf. on Electrical Contacts*, IEEE, Piscataway NJ (1997).
684. Aronstein, J., Analysis of Field Failures of Aluminum-Copper Pigtail Splices Made with Twist-on Connectors, pp. 87-93 in *Proc. 1999 45th IEEE Holm Conf. on Electrical Contacts*, IEEE, Piscataway NJ (1999).
685. Sorrells, J. R., Visit to Rossmoor Community (Memo for files), NBS (28 Jan. 1975).
686. Flocken, J., and Bates, R., The "Write" Way to Start a Fire, pp. 241-244 in *Proc. Intl. Symp. on the Forensic Aspects of Arson Investigations*, FBI, Washington (1995).
687. Hagimoto, Y., Possibility of Gas Explosions Caused by the Electric Sparks of Domestic Switches, *J. Japan Soc. for Safety Engrg.* **20**, No. 3, 127-132 (1981).
688. Aircraft Spares Store in £72.5 Million Blaze, *FPA J.* No. 136, 36-38 (June 1980).
689. Peck, G. C., Fire and Explosion Hazards of Liquid-filled Electrical Equipment. Part 6: Tap-Changing Gear (ITB-R84/113), The Insurance Technical Bureau, London (1984).
690. Bartley, W. H., An Analysis of Transformer Failures. Part 1—1988 through 1997. Part 2—Causes, Prevention and Maximum Service Life, *The Locomotive*, Hartford Steam Boiler Inspection and Insurance Co. (1997/8).
691. Murthy, H. V. V., and Buch, N. J., Failure Analysis of Distribution Transformer during Testing, pp. I-17 to I-31 in *Proc. Seminar on Distribution Transformers—Failures & New Developments*, Central Board of Irrigation and Power, New Delhi (1997).
692. Hattangadi, A. A, **Electrical Fires and Failures**, McGraw-Hill, New York (2000).
693. Parish, C. W., Fundamentals and Failures of Transformers and Motors, *Fire & Arson Investigator* **22**:3, 50-58 (1973).
694. Kappenman, J. G., Geomagnetic Storms and Impacts on Power Systems: Lessons Learned from Solar Cycle 22 and Outlook for Solar Cycle 23, *IEEE Power Engineering Review* **16**, 5-8 (May 1996).
695. Ristuccia, D. J., Prevention of Catastrophic Transformer Failures, *Power Engineering* **75**, 42-44 (Jan. 1971).
696. Mahieu, W. R., Prevention of High-Fault Rupture of Pole-Type Distribution Transformers, *IEEE Trans. Power Apparatus and. Systems* **PAS-94**, 1698-1707 (1975).
697. Benton, R. E., and Ristuccia, D. J., Arcing Faults Cause Transformer Failures, *Electrical World* (New York) **179**, 44-45 (1 April 1973).
698. Rønningen, T., Internal Faults in Oil-Filled Distribution Transformers: Fault Mechanisms and Choice of Protection (Ph.D. dissertation), Norges Tekniske Høgskole, Trondheim, Norway (1993).
699. Transformer Maintenance (FIST 3-30), Hydroelectric Research and Technical Services Group, Bureau of Reclamation, Denver (2000).
700. Myers, S. D., et al., **Transformer Maintenance Guide**, 2nd ed., S.D. Myers Inc., Tallmadge OH (2001).
701. Raux, C., Leconte, C.-J., and Gibert, T., Resistance of Transformers to Internal Faults: Synthesis of Experimental Results, pp. 71-75 in *10th Intl. Conf. on Electricity Distribution* (Conf. Publ. No. 305 Pt 1), IEE, Stevenage, England (1989).
702. Cuk, N. P., Analysis and Evaluation of Internal Arcing Faults in Distribution Transformers, *Trans. Canadian Electrical Association. Engineering and Operation Division* **28**, Pt. 1, 89-D-45 (1989).
703. Barkan, P., Damsky, B. L., Ettlinger, L. F., and Kotski, E. J., Overpressure in Distribution Transformers with Low Impedance Faults: Experiment and Theory, *IEEE Trans. Power Apparatus and Systems* **PAS-95**, 37-48 (1976).
704. IEEE Guide for Failure Investigation, Documentation, and Analysis for Power Transformers and Shunt Reactors (IEEE C57.125-1991), IEEE, New York (1992).
705. Smolinski, W. J., Requirements for Distribution Transformer Protection against Destructive Arcing Faults (Paper 77-D-40), *Trans. Engineering & Operating Div., Canadian Electrical Assn.* **16**, Part 1 (1977).
706. Dunki-Jacobs, J. R., The Escalating Arcing Ground-Fault Phenomenon, *IEEE Trans. Ind. Appl.* **IA-22**, 1156-1161 (1986).
707. Brown, L. R., Electrical Fire Opinions, *Fire & Arson Investigator* **44**:2, 36-37 (Dec. 1993).
708. Panelboard Examinations. Part II. Looking at Potential Fire Causes in and around the Panel Area, *Fire Findings* **8**:2, 1-4 (2000).
709. Lentini, J., private communication (2002).
710. Aronstein, J., Failure of Aluminum Connections in Residential Applications, pp. 271-277 in *Proc. 37th IEEE Holm Conf. on Electrical Contacts*, IEEE (1992).
711. Rummer, D., Case of the Chronic Boiler Burndown, *EC&M* **101**:10, 12-14 (Oct. 2002).
712. Aronstein, J., private communication (2002).
713. Kauffmann, R. H., and Page, J. C., Arcing Fault Protection for Low-Voltage Power Distribution Systems—Nature of the Problem, *AIEE Trans.***79** Part III, 160-167 (June 1960).
714. Dunki-Jacobs, J. R., The Effects of Arcing Ground Faults on Low-Voltage System Design, *IEEE Trans. Ind. Appl.* **IA-8**, 223-230 (1972).
715. Wagner, C. F., and Fountain, L. L., Arcing Fault Currents in Low-voltage A-C Circuits, *AIEE Trans.* **67**, 166-174 (1948).
716. Stanback, H. I. jr., Predicting Damage from 277 V Single Phase to Ground Arcing Faults, *IEEE Trans. Ind. Appl.* **IA-13**, 308-314 (1977); and **IA-14**, 93-95 (1978).

717. Fisher, L. E., Resistance of Low-Voltage AC Arcs, *IEEE Trans. Ind. Appl.* **IA-6**, 607-616 (1970).
718. Gammon, T., and Matthews, J., Instantaneous Arcing-fault Models Developed for Building System Analysis, *IEEE Trans. Industry Applications* **37**, 197-203 (2001).
719. St. Pierre, C., **A Practical Guide to Short-Circuit Current Calculations**, Electric Power Consultants, LLC, Schenectady NY (2001).
720. Attwood, S. S., Dow, W. C., and Krausnick, W., Reignition of Metallic A-C Arcs in Air, *Trans. AIEE* **50**, 854-870 (1931).
721. Slepian, J., and Strom, A. P., Arcs in Low-Voltage A-C Networks, *AIEE Trans.* **50**, 847-853 (Sep. 1931).
722. Shields, F. J., The Problem of Arcing Faults in Low-Voltage Power Distribution Systems, *IEEE Trans. Ind. and Gen. Appl.* **IGA-3**, 15-25 (Jan./Feb. 1967).
723. Kaufmann, R. H., and Page, J. C., Arcing Fault Protection for Low Voltage Power Distribution Systems—Nature of the Problem, *AIEE Trans.* **79**, 160-167 (June 1960).
724. Bruning, A. M., Discussion, *IEEE Trans. Power Delivery* **7**, 1431-1432 (1992).
725. Klaus, A., and Schau, H., An Approach for Calculating the Active Power of Arcing Faults in MV Busbar Systems, Based on Power Arc Tests, *SCC 2000—9th Intl. Symp. on Short-Circuit Currents in Power Systems*, Institute of Electrical Power Engineering, Lodz, Poland (2000).
726. Schau, H., and Stade, D., Requirements to Be Met by Protection and Switching Devices from the Arcing Protection Point of View, pp. 15-22 in *Proc. 5th Intl. Conf. on Electric Fuses and Their Applications (ICEFA)*, Ilmenau, Germany (1995).
727. Jones, R. A., et al., Staged Tests Increase Awareness of Arc-Flash Hazards in Electrical Equipment, *IEEE Trans. Industry Applications* **36**, 659-667 (2000).
728. Schau, H., Stade, D., and Wey, P., A New Concept of Arcing Fault Protection in Low Voltage Switchgear, pp. 4.11.1 to 4.11.8 in *6th Intl. Symp. on Short-Circuit Currents in Power Systems*, Liège, Belgium (1994).
729. Jennings, C., Five-Fatality High-Rise Office Building Fire, Atlanta, Georgia (June 30, 1989), Report 033, Federal Emergency Management Agency, Emmitsburg MD [1989?].
730. Paschal, J., Copper or Aluminum: How Should You Decide? *EC&M* **99**, 50-54 (Sep. 2000).
731. Koch, B., and Carpentier, Y., Manhole Explosions due to Arcing Faults on Underground Secondary Distribution Cables in Ducts, *IEEE Trans. Power Delivery* **7**, 1425-1433 (1992).
732. Schau, H., Effects of Arcing Faults in Low-Voltage Cables, pp. 985-988 in *Proc. 31st Universities Power Engineering Conf.*, Technological Educational Institute, Iraklio (1996).
733. Ohnishi, H., Urano, H., Hasegawa, S., Morita, T., and Nakajima, M., Measurement of Arc Resistance and Dielectric Breakdown Voltage at Intermittent Grounding of 6.6 kV Distribution CVT Cable, *IEEE Trans. Power Delivery* **3**, 363-367 (1988).
734. Sanford, R. S., Fire Hazards and Welding Action in Service-Entrance Conductors, *IEEE Trans. Ind. Appl.* **IA-18**, 479-484 (1982).
735. Summary Report—Comparative Performance of Electrical Conduit Under Conditions of Internal Arcing (Report #M-1143), Kearney Co., Electrical Research Lab., McCook IL (1982).
736. Béland, B., and Saucier, D., Deformation of Conduit Fittings by Fire and Electrical Activity, *Fire & Arson Investigator* **38**:1, 60-61 (Sept. 1987).
737. Wilkins, R., Flashover Voltage of High-Voltage Insulators with Uniform Surface-Pollution Films, *Proc. IEE* **116**, 457-465 (1969).
738. Karady, G. G., Flashover Mechanism of Non-ceramic Insulators, *IEEE Trans. on Dielectrics and Electrical Insulation* **6**, 718-723 (1999).
739. Rizk, F. A. M., Modèles mathématiques du contournement des isolateurs sous pollution/Mathematical Models for Pollution Flashover, *Electra* No. 78, 71-103 (1981).
740. Armored Cable (UL 4), UL.
741. Thermoset-Insulated Wires and Cables (UL 44), UL.
742. Flexible Cord and Fixture Wire (UL 62), UL.
743. Thermoplastic-Insulated Wires and Cables (UL 83), UL.
744. Communications Cables (UL 444), UL.
745. Thermoplastic-Insulated Underground Feeder and Branch-Circuit Cables (UL 493), UL.
746. Nonmetallic-Sheathed Cables (UL 719), UL.
747. Appliance Wiring Material (UL 758), UL.
748. Cord Sets and Power-Supply Cords (UL 817), UL.
749. Service-Entrance Cables (UL 854), UL.
750. Reference Standard for Electrical Wires, Cables, and Flexible Cords (UL 1581), UL.
751. Test for Flame Propagation Height of Electrical and Optical-Fiber Cables Installed Vertically in Shafts (UL 1666), UL.
752. Standard for Vertical-Tray Fire-Propagation and Smoke-Release Test for Electrical and Optical-Fiber Cables (UL 1685), UL.
753. Standard for Tests of Fire Resistive Cables (UL 2196), UL.
754. Test for Flame-Propagation and Smoke-Density Values for Electrical and Optical-Fiber Cables Used in Spaces Transporting Environmental Air (UL 910), UL.
755. Standard Method of Test for Flame Travel and Smoke of Wires and Cables for Use in Air-Handling Spaces (NFPA 262), NFPA.
756. Guide for Fire and Explosion Investigations (NFPA 921), NFPA.
757. Wagner, R. V., Boden, P. J., Skuggevig, W., and Davidson, R. J., Technology for Detecting and Monitoring Conditions That Could Cause Electrical Wiring System Fires (UL Project NC233, 94ME78760), UL (1995).
758. Reed, A., private communication (2001).
759. Hagimoto, Y., Watanabe, N., and Kinoshita, K., Effect of Electromagnetic Force on the Arcing Current, p. 54 in *Abstract of the 1994 Biennial Meeting of Forensic Fire and Explosion Investigation*, National Institute of Police Science, Tokyo (1994).
760. Béland, B., and Fortier, C., Arc Tracking in Relation to Fire Investigation, *Fire & Arson Investigator* **45**, 27-29 (March 1995).
761. Welte, S., Power Arcs and Other Hot Flashes, *Air Conditioning, Heating & Refrigeration News* p. 23 (13 July 1987).
762. Welte, S., private communication (2001).
763. Reiter, D., Verité Forensic Engineering, private communication (2002).
764. Method for Determining the Comparative and the Proof Tracking Indices of Solid Insulating Materials under Moist Conditions (IEC 60112), International Electrotechnical Commission, Geneva (1979).
765. Noto, F., and Kawamura, K., Tracking and Ignition Phenomena of Polyvinyl Chloride Resin Under Wet Polluted

Conditions, *IEEE Trans. Electr. Insul.* **EI-13**, 418-425 (1978).
766. Soma, S., Change of Electric Resistance of Vinyl Cord Covering through Heating, *Bull. Fire Prevention Soc. of Japan* **13**:2, 42-48 (Aug. 1965).
767. Hagimoto, Y., Watanabe, N., and Okamoto, K., Electrical Fault of PVC-Insulated Cords at Loose Connections within Rated Current, *Proc. APSS2001 Asia Pacific Symp. on Safety*, Japan Soc. for Safety Engineering (2201).
768. Nagata, M., and Yokoi, Y., Firing Phenomena of Polyvinyl Covering Cords Caused by High Temperature Deterioration, *Trans. IEE Japan* **103-A**, No. 12, 51 (1983).
769. Nagata, M., and Yokoi, Y., Deterioration and Firing Properties of Polyvinyl Chloride Covering Cords at Elevated Temperatures, *Bull. Japan Assn. of Fire Science and Engineering* **33**:2, 25-29 (1983).
770. Nagata, M., Thermal Runaway of Polyvinyl Chloride Covering Cords Caused by High Temperature Deterioration, *Trans. IEE Japan* **104-A**:3, 173 (1984).
771. Hagimoto, Y., and Kinoshita, K., Fire Hazard of a Coiled Electric Cord Insulated with Synthetic Rubber, *22nd Symp. on Safety Engineering (Japan)* (1992).
772. Hagimoto, Y., and Kinoshita, K., Temperature Measurements of Extension Electrical Cords Using a Thermal Camera, pp. 98-99 in *Abstracts of the Annual Meeting of the Japan Assn. for Fire Science* (1994).
773. Hagimoto, Y., Watanabe, N., and Okamoto, Arcing Faults on PVC-covered Electrical Cords, pp. 221-224 in *Proc. 1st Conf. of the Assn. of Korean-Japanese Safety Engineering Society*, Kyongju, Korea (1999).
774. Mesina, J. G., Determination of Electrical Clearances for Permissible Equipment Operating in Gassy Mines and Tunnels, *IEEE Trans. Industry Applications* **IA-30**, 1339-1350 (1994).
775. Scott, L. W., and Dolgos, J. G., Electric Arcing at High Voltage during Methane-Air Explosions inside Explosion-Proof Enclosures (Tech. Progress Rep. 115), Bureau of Mines, Pittsburgh (1982).
776. Bossert, J., and Hurst, R., **Hazardous Locations**, Canadian Standards Assn., Rexdale, Ont. (1986).
777. Baldo, G., Diaz, R. R., and Pesavento, G., The Effects of Flames on Discharge Characteristics in Air Gaps, pp. 954-957 in *Proc. 10th Intl. Conf. on Gas Discharges and Their Applications (GD '92)*, Univ. College of Swansea, Swansea, UK (1992).
778. Béland, B., Examination of Electrical Conductors Following a Fire, *Fire Technology* **16**, 252-258 (1980).
779. Bernstein, T., Electrical Fires: Causes, Prevention, and Investigation, pp. 116-134 in Greenwald, E.K., ed., **Electrical Hazards and Accidents: Their Cause and Prevention,** Van Nostrand Reinhold, New York (1991).
780. Zimmerer, C. W., and Neumer, F., Aluminum Building Wires and Connectors (Bull. of Research No. 48), Underwriters Laboratories Inc., Chicago (1954).
781. Ettling, B. V., Ignitability of PVC Electrical Insulation by Arcing, *IAAI—Oregon Chapter Newsletter*, 6 (Mar. 1997).
782. Hagimoto, Y., Watanabe, N., and Kinoshita, K., Fire Hazard of Short Circuits on Electrical Wirings, *Abstracts of the Annual Meeting of the Japan Assn. for Fire Science and Engineering* (1995).
783. Watanabe, N., Okamoto, K., Hagimoto, Y., and Kinoshita, K., Minimum Ignition Energy of Flammables by Short Circuits on Electrical Wirings, *Proc. 1999 Annual Mtg. Japan Assn. Fire Science and Engrg*., 4-5 (1999).
784. Nakahara, T., and Hagiwara, T., An Experiment of Electrical Fire Caused by Leakage Current from a PVC Power Cable to a Grounded Bolt, *Summary of 6th Mtg. Japanese Assn. Science and Technology for Identification*, 103 (2000).
785. Olson, D. B., private communication (2002).
786. Bukowski, R. W., private communication (2000).
787. Yamamoto, T., et al., A Test on Cables on Fire from Over Electric Current, *Mitsubishi Cable Industries Review*, No. 92, 41-47 (June 1997).
788. Lawson, D. I., McGuire, J. H., Fires Due to Electric Cables (FR Note 55), Fire Research Station, Borehamwood, UK (1953).
789. Gray, D. A., Drysdale, D. D., and Lewis, F. A. S., Identification of Electrical Sources of Ignition in Fires, *Fire Safety J.* **6**, 147-150 (1983).
790. Mazer, W. M., **Electrical Accident Investigation Handbook**, 3 vols., Electrodata, Inc., Glen Echo MD (var. dates).
791. Béland, B., Considerations on Arcing as a Fire Cause, *Fire Technology* **18**, 188-202 (1982).
792. Béland, B., The Overloaded Circuit as a Fire Source, *Fire & Arson Investigator* **31**, 13-18 (June 1981).
793. Theriault, M. G., and Theriault, A. J., Effects of Mineral Wool Insulation on Electric Cables in Buildings, *Fire Technology* **28**, 228-239 (1992).
794. Goodson, M., Perryman, T., and Colwell, K., Effects of Polyurethane Foam Systems on Wiring Ampacity, *Fire & Arson Investigator* **52**:4, 47-50 (July 2002).
795. Molded-Case Circuit Breakers, Molded-Case Switches, and Circuit-Breaker Enclosures (UL 489), UL.
796. Béland, B., Fires of Electrical Origin, *Fire & Arson Investigator* **43**, 35-41 (Dec. 1992).
797. Béland, B., Ground Fault in Flexible Exhaust Duct, *Fire & Arson Investigator* **44**, 44-45 (June 1994).
798. Jackson, A. L., Fire Investigation: You Can Learn From Every Fire, *Fire Engineering* **148**:3, 80-81 (Mar. 1995).
799. Kinoshita, K., Hagiwara, T., and Kinbara, J., Ignitability of VVF Cable in Contact with Grounded Object, *J. Japanese Assn. Fire Science & Engrg.* **28**, No. 3, 30-37 (1978).
800. Ettling, B. V., Electrical Path through Poor Contacts, *Fire & Arson Investigator* **36**:3, 29-30 (Mar. 1986).
801. Nabours, R. E., Heat and Arcing Fire Causation at Conduit Connections, *J. Natl. Acad. of Forensic Engineers* **10**:1, 63-76 (June 1993).
802. U.S. Consumer Product Safety Commission Staff Report on the Beverly Hills Supper Club Fire of May 28, 1977, CPSC, Washington [n.d.].
803. Goodson, M., Sneed, D., and Keller, M., Electrically Induced Fuel Gas Fires, *Fire & Arson Investigator* **49**:4, 10-12 (1999).
804. Prosser, H. F., The Case of the Recurring 911 Call, *EC&M* **99**, 20-21 (Oct. 2000).
805. Béland, B., Some Fires of Electrical Origin, *Fire & Arson Investigator* **37**:2, 37-38 (Dec. 1986).
806. Sanderson, J. L., private communication (2000).
807. Loud, H., Expect the Unexpected: An Electrified House, *Firehouse* 66-67 (June 2001).
808. Turkel, S., In Search of Transients, *EC&M* **99**, 16, 18 (Oct. 2000).
809. Davis, K. F., Building Fires Attributed to Be Caused by Electrical Wiring Faults, pp. 101-110 in *Proc. 27th Intl.*

Conf. on Fire Safety, Product Safety Corp., Sissonville WV (1999).
810. Cushing, P., BX Cable and Fire Cause Determination, *Fire Engineering* **153**, 46 (July 2000).
811. Weintraub, L., Open Electrical Neutral Hazards and Pyrophoric Carbonization Phenomenon, *Fire & Arson Investigator* **44**:2, 11-13 (Dec. 1993).
812. Ling, P. J. A., and Eldridge, C .J., Designing Modern Electrical Systems With Transformers That Inherently Reduce Harmonic Distortion in a PC-Rich Environment, unpublished paper.
813. Dry-Type General Purpose and Power Transformers (UL 1561), UL
814. IEEE Recommended Practice and Requirements for Harmonic Control in Electrical Power Systems (IEEE Std-519), IEEE, New York.
815. Barnes, M.. A., Briggs, P. J., Hirschler, M. M., Matheson, A. F., and O'Neill, T. J., A Comparative Study of the Fire Performance of Halogenated and Non-Halogenated Materials for Cable Applications. Part I. Tests on Materials and Insulated Wires, *Fire and Materials* **20**, 1-16 (1996). Part II. Tests on Cables, **20**, 17-37 (1996).
816. Meyer, L. E., Taylor, A. M., and York, J. A., Electrical Insulation Fire Characteristics. Vol. 1. Flammability Tests (UMTA-MA-06-0025-79-1,1), Urban Mass Transit Admin., Washington (1990).
817. Nakagawa, Y., A Comparative Study of Bench-Scale Flammability Properties of Electric Cables with Different Covering Materials, *J. Fire Sciences* **16**, 179-205 (1998).
818. Andersson, P., and Van Hees, P., Performance of Cables Subject to Thermal Radiation (SP Report 2000:24), Swedish National Testing and Research Institute, Borås (2000).
819. Bertrand, R., et al., Behaviour of French Electrical Cables under Fire Conditions, pp. 219-227 in *Fire Science and Technology—Proc. 5th Asia-Oceania Symp.*, Univ. Newcastle, Australia (2001).
820. Hoffmann, J. M., Hoffmann, D. J., Kroll, E. C., Wallace, J. W., and Kroll, M. J., Electrical Power Cord Damage from Radiant Heat and Fire Exposure, *Fire Technology* **37**, 129-141 (2001).
821. Hagimoto, Y., Watanabe, N., and Okamoto, K., Watanabe, N., Short-Circuit Faults in Electrical Cables and Cords Exposed to Radiant Heat, pp. 215-226 in *Fire and Materials 2003*, Interscience Communications Ltd., London (2003).
822. Tewarson, A., and Khan, M. M., Electrical Cables—Evaluation of Fire Propagation Behavior and Development of Small-Scale Test Protocol (FMRC J.I. 0M2E1.RC), Factory Mutual Research Corp., Norwood MA (1989).
823. Tewarson, A., Lee, J. L., and Pion, R. F., Categorization of Cable Flammability. Part 1: Laboratory Evaluation of Cable Flammability Parameters (EPRI NP-1200 Part 1). Electric Power Research Institute, Palo Alto (1979).
824. Hasegawa, H. K., Staggs, K., and Fernandez-Pello, A. C., Procedure for Ranking Fire Performance of Electrical Cables (UCRL-93936). Lawrence Livermore National Laboratory, Livermore CA (1986).
825. Hasegawa, H. K., et al., Fire Protection Research for DOE Facilities: FY 84 Year-End Report (UCRL-53179-84), Lawrence Livermore Natl. Lab., Livermore CA (1985).
826. Spletzer, B. L., and Horine, F., Description and Testing of an Apparatus for Electrically Initiating Fires Through Simulation of a Faulty Connection (NUREG/CR-4570; SAND86-0299), Sandia Natl. Labs., Albuquerque NM (1986).
827. Grayson, S. J., et al., Fire Performance of Electric Cables—New Test Methods and Measurement Techniques (Contract no. SMT4-CT96-2059), final report to the European Commission. Interscience Communications Ltd., London (2000).
828. Hosaka, M., Rodents' Habit of Eating/Damaging Insulated Wires and Ignition Possibility due to the Damage, *Proc. 1984 Annual Mtg. Japan Assn. Fire Science and Engrg.*, 97-98 (1984).
829. Béland, B., Electrical Damages—Cause or Consequence? *J. Forensic Sciences* **29**, 747-761 (1984).
830. Kinoshita, K., Hagimoto, Y., and Watanabe, N., Investigation Reports and Igniting Experiments on the Electrical Causes of Many Fires Started after the Big Earthquake in Kobe Area in 1995, published in Urgent Study Reports on the Hanshin-Awaji Big Earthquake, Science and Technology Agency of Japan, Tokyo (1995).
831. Roberts, E. W., The Ground-Fault Circuit Interrupter and Fire Prevention, Electrical Fires Conference, Univ. Wisconsin, Madison (April 3, 1986).
832. Ettling, B. V., Arc Marks and Gouges in Wires and Heating at Gouges, *Fire Technology* **17**, 61-68 (1981).
833. Béland, B., Heating of Damaged Conductors, *Fire Technology* **18**, 229-236 (1982).
834. Nishida, Y., Ignition Hazard by Short Circuit between Element Wires of a Stranded Cord, *Reports of the National Research Institute of Police Science* **45**:4, 57 (Nov. 1992).
835. Mitsuhashi, N., Yokoi, Y., Nagata, M., and Isaka, K., Concerning the History of Deterioration in Insulated Electric Wires and Fire Hazards, *J. Japanese Assn. for Fire Science & Engrg.* **31**, No. 1, 11-19 (1981).
836. Nagata, M., Firing Current and Energy Input of Polyvinyl Chloride Covered Cords Having Disconnected Element Wires, *Bull. Japanese Assn. Fire Science and Engrg.* **33**:1, 1-7 (1983).
837. Pichugina, S. V., et al., Deformability of Polyvinyl Chloride in Creep Conditions, *Polymer Science USSR* **24**, 1261-1268 (1983).
838. Van Turnhout, J., Klaase, P. Th. A., Ong, P. H., and Struik, L. C. E., Physical Aging and Electrical Properties of Polymers, *J. Electrostatics* **3**, 171-179 (1977).
839. Varlow, B. R., and Auckland, D. W., Mechanical Aspects of Electrical Treeing in Solid Insulation, *IEEE Electrical Insulation Magazine* **12**:2, 21-26 (Mar./Apr. 1996).
840. Howitt, D. G., The Creep of Electrical Appliance Cords, paper presented at *21st Intl. Conf. on Fire Saf*ety, Product Safety Corp. (1996).
841. Ettling, B. V., The Overdriven Staple as a Fire Cause, *Fire & Arson Investigator* **44**:3, 51-53 (Mar. 1994).
842. Brugger, R. D., Glowing Electrical Connections, *J. Natl. Academy of Forensic Engineers* **9**, 21-33 (1992).
843. Dixon, H. S., Simultaneous Multiple Points of Origin: Incendiary or Electrical? *J. Natl. Acad. of Forensic Engineers* **1**:2, 21-33 (Oct. 1984).
844. Keleher, P., Romex Failures: Summary of Observations, Paul Keleher Electrical Services, Berlin MA (2000).
845. Hijikata, T., and Ogawara, A., Research on Thermal Phenomena of Twist Joint Point of PVC Insulated Flexible Cords, *Summary of 1992 Annual Mtg. of Japan Assn. of Fire Science and Engineering* 204-205 (1992).
846. Grzybowski, S., Zubielik, P., and Kuffel, E., Changes of Thermoplastic PE Cable Insulation Properties Caused by the Overload Current, *IEEE Trans. Power Delivery* **4**, 1507-1512 (1989).

847. Toop, D. J., Theory of Life Testing and Use of Thermogravimetric Analysis to Predict the Thermal Life of Wire Enamels, *IEEE Trans. Electrical Insulation* **EI-6**, 2-14 (1971).
848. Dissado, L. A., and Fothergill, J.C., **Electrical Degradation and Breakdown in Polymers**, Peter Peregrinus, London (1992).
849. Lawson, D. I., and Fry, J. F., Fires of Electrical Origin, *Proc. IEE* **104A**, 185, 531 (1957).
850. Dakin, T. W., Electrical Insulation Breakdown Treated as a Chemical Rate Phenomenon, *Trans. AIEE* **67**, 113-122 (1948).
851. Bruning, A. M., and Campbell, F. J., Aging in Wire Insulation under Multifactor Stress, *IEEE Trans. Electrical Insulation* **EI-28**, 729-754 (1993).
852. Mathes, K. N., Thermal Aging of Electrical Insulation—Technology and Standardization, *IEEE Electrical Insulation Magazine* **1**:1, 29-35 (Sep. 1985).
853. Thermal Evaluation and Classification of Electrical Insulation (IEC 60085), International Electrotechnical Commission, Geneva.
854. IEEE Recommended Practice—General Principles for Temperature Limits in the Rating of Electric Equipment and for the Evaluation of Electrical Insulation (IEEE Std-1), IEEE, Piscataway NJ.
855. Bajpai, S. N., and Marlin, P. G., Analysis of the Flammability of Television Receiver Chassis and Components (FMRC J.I. 1A7N1.RC), Prepared for CPSC under contract CPSC-C-77-0093, Factory Mutual Research Corp., Norwood MA (1979).
856. Polymeric Materials—Long Term Property Evaluation (UL 746B), UL.
857. Report of the Meeting of the Industry Advisory Group of UL Plastic Materials, October 16, 1999, Underwriters Laboratories Inc., Melville NY (1999).
858. Gosland, L., Age and the Incidence of Fires in Electrical Installations, *Proc. IEE* **103A**, 271-284 (1956).
859. Dervos, C. T., and Vassiliou, P., Aging of Solid Insulators Exposed to Toxic Fire Byproducts, pp. 599-602 in *Conf. Record of the 1998 IEEE Intl. Symp. on Electrical Insulation*, IEEE, Piscataway NJ (1998).
860. Armstrong, R. W., Voltage Spike Failure of Building Wire Insulation as a Fire Cause, *J. Natl. Acad. of Forensic Engineers* **8**:1, 59-66 (June 1001).
861. Stricker, S., Thermal Design of PVC-Insulated Heating Cable (Report 74-26-K), Ontario Hydro, Toronto (1974).
862. Chavez, J. M., Steady-State Environment Cable Damage Testing (Quick Look Test Report), Sandia Natl. Labs., Albuquerque NM (1984).
863. Lukens, L. L., Nuclear Power Plant Electrical Cable Damageability Experiments (SAND82-0236), Sandia National Labs., Albuquerque NM (1982).
864. Jacobus, M. J., and Fuehrer, G. F., Submergence and High Temperature Steam Testing of Class 1E Electrical Cables (SAND90-2629; NUREG/CR-5655). Sandia National Laboratories, Albuquerque NM (1991).
865. Nowlen, S. P., An Investigation of the Effects of Thermal Aging on the Fire Damageability of Electric Cables (SAND90-0696; NUREG/CR-5546). Sandia National Labs., Albuquerque NM (1991).
866. Yarbrough, D. W., and Toor, I., Operating Temperatures for a Convectively Cooled Recessed Incandescent Light Fixture (ORNL/SUB-7715/1), Oak Ridge Natl. Lab., Oak Ridge TN (1980).
867. Kaufhold, M., Börner, G., Eberhardt, M., and Speck, J., Failure Mechanism of the Interturn Insulation of Low Voltage Electric Machines Fed by Pulse-Controlled Inverters, *IEEE Electrical Insulation Magazine* **12**:5, 9-16 (Sep./Oct. 1996).
868. Béland, B., Roy, C., and Tremblay, M., Copper-Aluminum Interaction in Fire Environments, *Fire & Arson Investigator* **37**:3, 52-55 (Mar. 1987).
869. CPSC Warns Consumers About Faulty Extension Cords, Power Strips and Surge Protectors (Release #99-069), Consumer Product Safety Commission, Washington (1999).
870. Extension Cord Fact Sheet (CPSC Document #16), Consumer Product Safety Commission, Washington.
871. Smith, L., Electrical Hazards involving Appliance Cords, Consumer Product Safety Commission, Washington (1990).
872. McCoskrie, D., Technical Analysis of Failing Cords and Plugs: 1988 – 1989, Consumer Product Safety Commission, Washington (1989).
873. Smith, L., and McGee, L., Hazard Analysis—Fires Associated with Extension Cords, Consumer Product Safety Commission, Washington (1981).
874. Cord Sets and Power-Supply Cords (UL 817), UL.
875. Rakosnik, R., Fire Investigation: Mennonite Church, *Fire Engineering* **154**, 113-114 (Jan. 2001).
876. Popular Extension Cord Reels Can Be Real Dangerous, *Fire Findings* **2**:1, 13 (Winter 1994).
877. Béland, B., Electricity…The Main Fire Cause? *Fire & Arson Investigator* **32**, 18-22 (Jan./Mar. 1982).
878. Arc Mapping May Provide Valuable Clues of Fire's Origin, *Fire Findings* **7**:2, 12-13 (Spring 1999).
879. Béland, B., Behaviour of Cables under Fire Conditions, *Canadian Assn. of Fire Investigators The/Le Journal*, 12-18 (Sep. 1997).
880. Fuller, J. F., Hanna, W. J., and Kallenbach, G. A., Arcing Faults in Metallic Conduit at 120 and 240 V, *IEEE Trans. Ind. Appl.* **IA-21**, 820-825 (1985).
881. Arcing in Conduit Is Generally the Result of the Fire, Not the Cause, *Fire Findings* **7**:2, 13 (Spring 1999).
882. Takaki, A., On the Effect of Thermal Histories upon the Metallographic Structure of Electric Wires, *Reports of the National Research Institute of Police Science* **24**:2, (48-56) 84-92 (June 1971).
883. Shaw, C. E., Fire Marshals on Duty, *NFPA J.* **59**, 26-27 (July 1965); 96-97 (Nov. 1965).
884. Levinson, D. W., Copper Metallurgy as a Diagnostic Tool for Analysis of the Origin of Building Fires, *Fire Technology* **13**, 211-222 (1977).
885. Singh, R. P. Scanning Electron Microscopy of Burnt Electric Wires, *Scanning Microscopy* **1**:4, 1539-1544 (1987).
886. Ettling, B. V., Electrical Wiring in Building Fires, *Fire Technology* **14**, 317-325 (1978).
887. Seki, T., Hasegawa, H., Imada, S., and Isao, Y., Determination between Primary and Secondary Molten Marks on Electric Wires by DAS, National Institute of Testing and Evaluation, Kiryu, Gunma, Japan (2000).
888. Ishibashi, Y., and Kishida, J., Research on First and Second Fused Mark Discrimination of Electric Wires, pp. 83-90 in *1990 Annual Mtg. Japan Assn. for Fire Science and Engrg.* (1990).
889. Erlandsson, R., and Strand, G., An Investigation of Physical Characteristics Indicating Primary or Secondary Electrical Damage, *Fire Safety J.* **8**, 97-103 (1984/85).

890. Tokyo Fire Department, Investigation Section, Research on First and Second Fused Mark Discrimination of Electric Wires, *J. Japan Assn. for Fire Science and Engrg.* **42**, No. 2, 15-20 (1992).
891. Mitsuhashi, N., Discrimination between Primary and Secondary Arc Marks on Electric Wires by Micro-void Distribution, *Reports of the National Research Institute of Police Science* **48**:1, 20-26 (1995).
892. Oba, K., Identification of Melting Marks of Electric Wires (unpublished report), Yamagata Prefecture Police Headquarters, Criminal Scientific Laboratory, Japan (1980).
893. Miyoshi, S., Internal Cavity Analysis of Electrical Arc Beads, presented at *15th Mtg. Intl. Assn. of Forensic Sciences*, Los Angeles (1999).
894. Miyoshi, S., Internal Cavity Analysis of Electrical Arc Beads, pp. 653, 656 in *Proc. 4th Asia-Oceania Symp. on Fire Science & Technology*, Asia-Oceania Assn. for Fire Science & Technology/Japan Assn. for Fire Science & Engineering, Tokyo (2000).
895. Lee, E.-P., et al., Discrimination between Primary and Secondary Molten Marks on Electric Wires by DAS, *J. Applied Fire Science* **9**, 361-379 (1999/2000).
896. Masui, M., Possibility of Carbon Inclusion in the Molten Mark of Polyvinyl Chloride Insulated Cords due to a Fire, *Trans. IEE Japan* **112A**:1, 78-79 (1992).
897. Lee, E., Ohtani, H., Matsubara, Y., Seki, T., Hasegawa, H., and Imada, S., Study on Primary and Secondary Molten Marks, pp. 209-212 in *Proc. 1st Conf. Assn. Korean-Japanese Safety Engineering Society*, Korean Institute for Industrial Safety (1999).
898. Lee, E.-P., Ohtani, H., Matsubara, Y., Seki, T., Hasegawa, H., Imada, S., and Yashiro, I., Study on Discrimination between Primary and Secondary Molten Marks Using Carbonized Residue, *Fire Safety J.* **37**, 353-368 (2002).
899. Did the Short Cause the Fire or Did the Fire Cause the Short? *Fire & Arson Investigator* **30**:1, 57-58 (Jul/Sep 1979).
900. MacCleary, R. C., and Thaman, R. N., Method for Use in Fire Investigation, US Patent 4,182,959 (1980).
901. Robertsson, A., Karlsson, S. E., Strand, G., and Nilsson, G., Smältskador på elektriska ledare Melt Damages on Electric Wires. (Rapport 20), Centrum för Forensisk Vetenskap, Linköping, Sweden (1988).
902. Satoh, K., Sugisaki, M., Kakizaki, S., Itoh, C., Saitoh, K., and Iwaki, M., Secondary Ion Mass Spectroscopy (SIMS) and Auger Electron Spectroscopy (AES) Applied to the Fire Investigation for Short Circuit, pp. 282-285 in *Proc. 1996 Annual Mtg. of Japan Assn. for Fire Science and Engrg.* (1996).
903. Satoh, K., Fukusima, H., Sigeru, S., and Iwaki, M., Verification SIMS Applied to the Fire Investigation for Short Circuit, pp. 336-336 in *Proc. 1998 Annual Mtg. of Japan Assn. for Fire Science and Engrg.* (1998).
904. Kitamura, Y., and Satoh, K., Progress of the Study on Electrical Beads (No. 2), *Japanese J. Science and Technology for Identification* **6**, Suppl., 105 (Oct. 2001).
905. Anderson, R. N., Surface Analysis of Electrical Arc Residues in Fire Investigation, *J. Forensic Sciences* **34**, 633-637 (1989).
906. Howitt, D. G., The Surface Analysis of Copper Arc Beads—A Critical Review, *J. Forensic Science* **42**, 608-609 (1997).
907. Massalski, T. B., ed., **Binary Alloy Phase Diagrams**, 2nd ed., ASM International, Materials Park OH (1990).
908. Kattner, U. R., NIST, private communication (2001).
909. Howitt, D. G., The Chemical Composition of Copper Arc Beads—A Red Herring for the Fire Investigator, *Fire & Arson Investigator* **48**:3, 34-39 (Mar. 1998).
910. Hirt, D., Letter to the Editor: At Best 'Junk Science' and at Worst Deliberately Misleading, *Fire & Arson Investigator* **48**:4, 5, 63 (July 1998).
911. Anderson, R. N., Brosz, H. G., Posey, E., and Schefelbein, B., Recent Advances in Auger Analysis of Electrical Arc Residues, pp. 162-166 in *13th Meeting, Intl. Assn. of Forensic Sciences* (1993).
912. Anderson, R. N., Which Came First…The Arcing or the Fire? Review of Auger Analysis of Electrical Arc Residues, *Fire & Arson Investigator* **46**:3, 38-40 (Mar. 1996).
913. Anderson, R. N., Letter to the Editor, *Fire & Arson Investigator* **45**:2, 44-45 (Dec. 1994).
914. Anderson, R. N., Scientific Examination of Electrical Arc Residues to Determine Fire Cause, *Fire & Arson Investigator* **42**:3, 58-59 (Mar. 1992).
915. Béland, B., Examination of Arc Beads, *Fire & Arson Investigator* **44**:4, 20-22 (June 1994).
916. Béland, B., Further Comments on Arc Bead Examination, *The Fire Place* Washington State IAAI Chapter newsletter., 24-28 (Apr./May 1997).
917. Ettling, B. V., Problems with Surface Analysis of Copper Beads Applied to the Time of Arcing, *The Fire Place* Washington State IAAI Chapter newsletter., 21-24 (Oct./Nov. 1997).
918. Henderson, R., Manning, C., and Barnhill, S., Questions Concerning the Use of Carbon Content to Identify "Cause" vs. "Result" Beads in Fire Investigations, *Fire & Arson Investigator* **48**:3, 26-27 (July 1998).
919. Reese, N. D., Letter to the Editor: Arc Beads, *Fire & Arson Investigator* **48**:4, 63-64 (July 1998).
920. Fitz, M. M., MDE Engineers, private communication (2001).
921. Metson, J. B., and Hobbis, C. M., The Use of Auger Electron Spectroscopy in Fire Investigations, *Chemistry in New Zealand* 7-9 (July 1994).
922. Anderson, R. N., What Came First? The Arc Bead or the Fire? *EC&M* **100**, 20-21 (July 2001).
923. Turkel, S., Clean Power to Go: PQ in the SUV Age, *EC&M* **100**, 14, 16, 18 (July 2001).
924. Franklin, F. F., Vehicle Short Circuit Fires and Their Prevention, *Professional Safety*, 38-40 (Aug. 1993).
925. Bloom, J., and Bloom, C., Ford Ignition Switch Overheating and Fires, *Fire & Arson Investigator* **47**:3, 10-11 (Mar. 1997).
926. Sloan, P. A., Beware: Corroded Earth Straps in Motor Vehicles Can Set off a Fire, *Fire & Arson Investigator* **50**, 58-59 (Jan. 2000).
927. Brugger, R. D., "Short Circuit" by Battery Acid, *Fire & Arson Investigator* **34**:2, 18-19 (Dec. 1983).
928. Testimony of Bernard Loeb, Director, Office of Aviation Safety, National Transportation Safety Board, before the Subcommittee on Oversight, Investigations, and Emergency Management, Committee on Transportation and Infrastructure, House of Representatives. Regarding: Aging Aircraft Wiring (Sept. 15, 1999).
929. Smith, C. D., FAA Aging Nonstructural Systems Research, *Third Joint FAA/DoD/NASA Conf. on Aging Aircraft* (1999).

930. Elliott, D. K., Wet-Wire Fires, pp. 124-127 in Conf. on Electrical Insulation, Annual Report 1963 (NRC Publ. 1141), National Research Council, Washington DC (1964).
931. Dricot, F., and Reher, H. J., Survey of Arc Tracking on Aerospace Cables and Wires, *IEEE Trans. Dielectrics and Electrical Insulation* **1,** 896-903 (1994).
932. Electrical Arcing of Aged Aircraft Wire (Report N191-RPT4AU99), Report to NTSB under Order No. NTSB18-99-SP0127, Lectromechanical Design Co., Sterling VA (1999).
933. Campbell, F. A., Flashover Failures from Wet-Wire Arcing and Tracking (NRL Memorandum Report 5508), Naval Research Lab., Washington (1984).
934. Cahill, P., Flammability, Smoke, and Dry Arc Tracking Tests of Aircraft Electrical Wire Insulations (DOT/FAA/CT-89/21). Federal Aviation Administration, Atlantic City Airport NJ (1989).
935. First NASA Workshop on Wiring for Space Applications, 1991 (NASA CP-10145), NASA Lewis, Cleveland OH (1994).
936. Second NASA Workshop on Wiring for Space Applications, 1993 (NASA CP-3244), NASA Lewis, Cleveland OH (1994).
937. Third NASA Workshop on Wiring for Space Applications, 1995 (NASA CP-10177), NASA Lewis, Cleveland OH (1995).
938. Berkebile, D. H., Cahill, P. L., and LaCourt, P. R., The Increased Safety Factor with Hybrid Wire Constructions, *Aerospace Electronics Interconnect Systems Conf.* (1995).
939. Cahill, P., Electrical Short Circuit and Current Overload Tests on Aircraft Wiring (DOT/FAA/CT-TN94/55), Federal Aviation Administration, Atlantic City NJ (1995).
940. Keski-Rahkonen, O., Mangs, J., and Turtola, A., Ignition of and Fire Spread on Cables and Electronic Components (VTT Publications 387), Valtion Teknillinen Tutkimuskeskus, Espoo, Finland (1999).
941. Tonkin, P. S., and Berlemont, C. F. J., Surface Temperatures of a Diesel Engine and Its Exhaust System (FR Note 917), Fire Research Station, Borehamwood, UK (1971).
942. Fitz, M. M., MDE Engineers, private communication (2002).
943. Cameron, A. M., **Chemistry in Relation to Fire Risk and Fire Extinction**, 3rd ed., Pitman, London (1948).
944. Seres, I., and Huhn, P., Radical Steps in Diethyl Ether Decomposition, *Intl. J. Chemical Kinetics* **18**, 829-836 (1986).
945. Townsend, D. T. A., and Chamberlain, E. A. C. The Influence of Pressure on the Spontaneous Ignition and Limits of Inflammability of Ether-Air Mixtures, *Proc. Royal Soc. London* **A158**, 415-429 (1937).
946. Viallard, R., Donnés relatives à l'inflammation des mélanges gazeux combustibles par l'étincelle électrique, *J. de Chimie Physique* **40**, 101-108 (1943).
947. White, A. G., and Price, T. W., The Ignition of Ether-Alcohol-Air and Acetone-Air Mixtures in Contact with Heated Surfaces, *J. Chem. Soc.* **115**, 1462-1505 (1919).
948. White, A. G., Limits for the Propagation of Flame in Inflammable Gas-Air Mixtures. Part III. The Effect of Temperature on the Limits, *J. Chem. Soc.* **127**, 672-684 (1925).
949. Hsieh, M. S., and Townsend, D. T. A., An Examination of the Mechanism by Which "Cool" Flames Give Rise to "Normal" Flames. Part I. The Inflammation Ranges of Ether-Air Mixtures in Closed Vessels, *J. Chem. Soc.* 337-345 (1939).
950. Mullins, B. P., **Spontaneous Ignition of Liquid Fuels**, AGARDograph no. 4. Butterworths, London (1955).
951. Bull, D. C., Cairnie, L. R., Harrison, A. J., and Morgan, P. A., Influence of Natural Convection on the Critical Conditions for Hot Surface Autoignition, pp. 8/634-8/646 in *3rd Intl. Symp. on Loss Prevention and Safety Promotion in the Process Industries*, Swiss Society of Chemical Industries, Zürich (1980).
952. Britton, L. B., Taylor, D. A., and Wobser, D. C., Thermal Stability of Ethylene at Elevated Pressures, *Plant/Operations Progress* **5**, 239-251 (1986).
953. Matzkin, L., Meckel, J., and Raymond, R. J., Ignition in Electrical Circuitry Induced by Glycol-Water Solutions (PF-1483), Raytheon Co., West Andover MA (1975).
954. Burgoyne, J. H., Betts, K. E., and Muir, R., The Explosive Decomposition of Ethylene Oxide Vapour under Pressure, pp. 31-36 in *Symp. on Chemical Process Hazards*, Institution of Chemical Engineers, Rugby (1960).
955. Gustin, J. L., Influence of Trace Impurities on Chemical Reaction Hazards, *J. Loss Prevention in the Process Industries* **15**, 37-48 (2002).
956. Griffiths, J. F., and Perche, A., The Spontaneous Decomposition, Oxidation and Ignition of Ethylene Oxide under Rapid Compression, pp. 893-901 in *18th Symp. (Intl.) on Combustion*, The Combustion Institute, Pittsburgh (1980).
957. Chen, L.-D., and Faeth, G. M., Initiation and Properties of Decomposition Waves in Liquid Ethylene Oxide, *Combustion and Flame* **40**, 13-28 (1981).
958. Hill, D. N., and O'Connell, D. C., Limited Comparative Studies of the Thermal Behaviour of Ethylene Oxide and Propylene Oxide (IR/L/EN/91/11), HSE, Buxton, UK (1991).
959. Gupta, A. K., The Explosive Poly-condensation of Ethylene Oxide, *J. Soc. Chemical Industry*, **68**, 179-183 (1949).
960. Ream, B. C., Thorsteinson, E. M., Chippett, S., Schreck, D. J., Cropley, J. B., and Elder, G. B., Ethylene Oxide Explosion at Seadrift, Texas. Part III – Iron Oxide Chemistry, *27th Loss Prevention Symp.*, AIChE (1993).
961. June, R. K., and Dye, R. F., Explosive Decomposition of Ethylene Oxide, *Plant/Operations Progress* **9**, 67-74 (Apr. 1990).
962. Britton, L. B., Thermal Stability and Deflagration of Ethylene Oxide, *Plant/Operations Progress* **9**, 75-86 (Apr. 1990).
963. Burden, F. A., and Burgoyne, H. J., The Ignition and Flame Reactions of Ethylene Oxide, *Proc. Royal Soc. London* **A199**, 328-351 (1949).
964. Cawse, J. N., et al., Ethylene Oxide, pp. 432-471 in **Kirk-Othmer Encyclopedia of Chemical Technology**, 3rd ed., vol. 9, Wiley, New York (1980).
965. Vanderwater, R. G., Case History of an Ethylene Oxide Tank Car Explosion, *Chem. Eng. Prog.* **85**, 16-20 (Dec. 1989).
966. Raber, L., Four Explosions Halt Ethylene Oxide Rule, *Chemical & Engineering News* **75**, 11 (11 Aug. 1997).
967. 1997 Arson and Explosives Incidents Report, Bureau of Alcohol, Tobacco and Firearms, Washington (1999).
968. Wilson, H., ATF Explosives Taggant Study, pp. 433-468 in *Proc. 4th Intl. Symp. on Fireworks*, Minister of Public Works and Government Service Canada, [n.p.] (1998).
969. Maltitz, I. von, **Black Powder Manufacture Methods & Techniques**, American Fireworks News, Dingmans Ferry PA (1997).

970. Weeth, C. P., A Case Study of a 6" Aerial Shell Malfunction in an HDPE Mortar Mounted in an Above-ground Wooden Rack during a Manually Ignited Display, pp. 495-515 in *Proc. 4th Intl. Symp. on Fireworks*, Minister of Public Works and Government Service Canada, [n.p.] (1998).
971. Hikita, T., Thermal Decomposition of Some Explosive Compounds, *Japan Sci. Rev. Engng. Sci.* **2**, 23-28 (1950).
972. Kayser, E. G., The Thermal Decomposition of Thirty Commercially Available Materials at 300ºC (Report No. TES-20-74-1; NOLTR 74-44). Naval Ordnance Laboratory, Silver Spring MD (1974).
973. Avrami, L., and Hutchinson, R., The Sensitivity to Impact and Friction, pp. 111-162 in **Energetic Materials**, Vol. 2: Technology of the Inorganic Azides, H. D. Fair and R. F. Walker, eds., Plenum Press, New York (1977).
974. Watson, R. W., Card-Gap and Projectile Sensitivity Impact Measurements, A Compilation (IC 8605), Bureau of Mines, Pittsburgh (1973).
975. Larson, T. E., Dimas, P., and Hannaford, C. E., Electrostatic Sensitivity Testing of Explosives at Los Alamos, Paper 16 in *9th Symp. (Intl.) on Detonation*, Naval Surface Warfare Center, White Oak MD (1989).
976. Skinner, D., Olson, D., and Block-Bolten, A., Electrostatic Discharge Ignition of Energetic Materials, *Propellants, Explosives, Pyrotechnics* **23**, 34-42 (1998).
977. Li, G., and Wang, C., Comprehensive Study on Electric Spark Sensitivity of Ignitable Gases and Explosive Powders, *J. Electrostatics* **11**, 319-332 (1981).
978. Demberg, E., Spontaneous Detonation of Initiators, paper No. 36 in *Proc. 8th Symp. on Explosives and Pyrotechnics*, The Franklin Research Center, Philadelphia (1974).
979. Wang, P. S., and Hall, G. F., Friction and Impact Sensitivities for High Explosives, pp. 417-439 in Minutes of the Twenty-Second Explosives Safety Seminar, vol. I, Dept. of Defense Explosives Safety Board, Alexandria VA (1986).
980. Gross, D., and Amster, A. B., Thermal Explosions: Adiabatic Self-Heating of Explosives and Propellants, pp. 728-734 in *8th Symp. (Intl.) on Combustion*, The Combustion Institute, Pittsburgh (1960).
981. Loftus, J. J., and Gross, D., Thermal and Self Ignition Properties of Ammonium Perchlorate and PETN Explosive (NBS 7012), NBS (1960).
982. Maiden, D. E., A Model for Calculating the Threshold for Shock Initiation of Pyrotechnics and Explosives (UCRL-96360), Lawrence Livermore National Lab., Livermore CA (1987).
983. Janswoude, J. J., and Pasman, H. J., Decreasing Progression of the Decomposition Rate of Explosive Substances at High Temperatures, pp. 515-521 in **Fast Reactions in Energetic Systems**, C. Capellos and R. F. Walker, eds., D. Reidel, Dordrecht (1981).
984. Dorofeyev, A. N., Kuznetsov, V. A., and Sarkisyan, R. S., Aviation Ammunition, FTD-ID(RS)T-0459-85, Foreign Technology Div., Air Force Systems Command, Wright-Patterson AFB (1986). Russian original: **Aviatsionnyye Boyepripasy** (1960).
985. Dobratz, B.M., and Crawford, P.C., LLNL Explosives Handbook: Properties of Chemical Explosives and Explosive Simulants (UCRL 52997 Change 2), Lawrence Livermore National Laboratory, Livermore CA (1985).
986. Walker, F. E., and Wasley, R. J., Critical Energy for Shock Initiation of Heterogeneous Explosives, *Explosivstoffe* **17**, 9-13 (1969).
987. de Longueville, Y., Fauquignon, C., and Moulard, H., Initiation of Several Condensed Explosives by a Given Duration Shock Wave, pp. 105-114 in *Proc. 6th Symp. (Intl.) on Detonation*, Office of Naval Research, Dept. of the Navy, Arlington VA (1976).
988. Dremin, A. N., **Toward Detonation Theory**, Springer-Verlag, New York (1999).
989. Köhler, J., and Meyer, R., **Explosives**, 4th ed., VCH, Weinheim, Germany (1993).
990. Baroody, E. E., and Peters, S. T., Heat of Explosion, Heat of Detonation, and Reaction Products: Their Estimation and Relation to the First Law of Thermodynamics (IHTR 1340), Naval Ordnance Station, Indian Head MD (1990).
991. Libershal, B., Target Shooting, Automatic Rifles and Steel Core Bullets, *Wildfire Strikes Home* **3**:1, 8-9 (1989).
992. Hampton, H., Facts About Sporting Ammunition Fires, *Fire J.* **71**:1, 5-9,29 (Jan. 1977).
993. **Propellant Profiles**, 4th ed., Wolfe Publishing Co., Prescott AZ (1999).
994. Tovey, H., and Giroux, R. R., Ignition Sources in Accident Cases Involving Flammable Fabrics (NBS 10 629), NBS (1971).
995. Third Annual Report to the President and the Congress on the Studies of Deaths, Injuries and Economic Loses Resulting from Accidental Burning of Products, Fabrics, or Related Materials—Fiscal Year 1971, Publication DHEW (FDA) 72-7013, Dept. of Health, Education, and Welfare, Washington (1972).
996. Second Annual Report to the President and the Congress on the Studies of Deaths, Injuries and Economic Losses Resulting from Accidental Burning of Products, Fabrics or Related Materials—Through June 1970, The Secretary of Health, Education, and Welfare, Washington (1971).
997. Graf, S. H., Ignition Temperatures of Various Papers, Woods, and Fabrics (Oregon State College Bull. 26), Oregon State College, Corvallis (1949).
998. Backer, S., Tesoro, G. C., Toong, T. Y., and Moussa, N. A., **Textile Fabric Flammability**, The MIT Press, Cambridge MA (1976).
999. Fibers and Textiles, S. A. Chines, ed., **Fire Protection Handbook**, A. E. Cote, and J. L. Linville, eds., 18th ed., NFPA (1997).
1000. Einsele, U., Über das Brennverhaltan und den Brennmechanismus von Synthesefasern [On Reduction of Flammability and Combustion Mechanisms of Synthetic Fibers], *Melliand Textilberichte* **53**, 1395-1402 (1972).
1001. Rieber, M., Über die Brennbarkeit von synthetischen Textilien, *Chemiefasern* **5**, 375-378 (1969).
1002. Khattab, M. A., Spontaneous Ignition Behavior of Cotton Fabric Having Different Amounts of Polyester, *J. Applied Polymer Science* **62**, 1503-1507 (1996).
1003. Horrocks, A. R., Gawande, S., Kandola, B., and Dunn, K. W., The Burning Hazard of Clothing—The Effect of Textile Structures and Burn Severity, *11th Annual BCC Conf. on Flame Retardancy: Recent Advances in Flame Retardancy of Polymeric Materials*, Business Communications Co., Norwalk CT (2000).
1004. Khattab, M. A., Price, D., and Horrocks, A. R., The Inhibition of Spontaneous Ignition by Flame-Retarding Cotton Fabrics, *J. Applied Polymer Science* **41**, 3069-3078 (1990).
1005. Mórotz-Cecei, K., and Beda, L., Comparative Testing of the Flammability of Upholstery Textiles, *J. Thermal Analysis* **32**, 901-908 (1987).

1006. Robinson, H., Smith, P. B., and Williams, H. L., Ignition Hazards Associated with the Use of a Buffing Machine Underground (Research Report 15), Safety in Mines Research Establishment, Sheffield, England (1951).
1007. Ohlemiller, T. J., and Villa, K. M., Material Flammability Test Assessment for Space Station Freedom (NISTIR 4591; NASA CR-187115), NIST (1991).
1008. Heskestad, G., Ease of ignition of Fabrics Exposed to Flaming Heat Sources (FMRC Serial 19967, RC73-T-4), Factory Mutual Research Corp., Norwood MA (1973).
1009. Weaver, J. W., Rate of Burning of Apparel Fabrics, *Textile Chemist and Colorist* **8**, 176-181 (Nov. 1976).
1010. Ward, C. D., and Jaeckel, S. M., Measurement of the Flammability of Apparel Fabrics, *J. Textile Institute* **67**:9, 309-318 (1976).
1011. Reeves, W. A., and Smitherman, J. E., Ignition Characteristics of Fire Retardant Cotton and Polyester/Cotton Fabrics, *American Dyestuff Reporter* **67**:9, 64-66, 68-69, 71, 85 (1978).
1012. Holmes, F. A., Flammability Testing of Apparel Fabrics, pp. 317-324 in *International Symposium: Fire Safety of Combustible Materials*, Edinburgh (1975).
1013. Durbetaki, P., Fundamental Studies on Fabric Ignition, pp. 243-254 in 10th Annual Mtg., Information Council on Fabric Flammability, New York (1976).
1014. Irjala, B.-L., Method for Determination of the Ignitability of Bed Linen (Nordtest Project Nr. 750-88), Valtion Teknillinen Tutkimuskeskus, Espoo, Finland (1989).
1015. Bedding Components: Ignitability (Nordtest NT Fire 037), Nordtest, Espoo, Finland (1988).
1016. Textile Fabrics: Ignition and Flame Spread (Nordtest NT Fire 029), Nordtest, Espoo, Finland (1987).
1017. Heskestad, G., and Kung, H. C., Pain Time Versus Fabric Ignition Time for Exposure to Flame. Technical Memorandum (FMRC Serial No. 19967), Factory Mutual Research Corp., Norwood MA (1971).
1018. Knapp, L. W. jr., and Lazar, A. J., Pilot Study of Clothing Ignition (Contract No. CPF69-35, Food and Drug Administration), College of Medicine, Univ. Iowa, Iowa City (1970).
1019. Fourt, L., Study of Ignition and Exposure. Conducted by Gillette Research Institute, Rockville, MD. NTIS No. COM-73-10958. NBS (1971).
1020. Webster, C. T., Wraight, H. G. H., and Thomas, P. H., Heat Transfer from Burning Fabrics, *J. Textile Inst. Trans.* **53**, T29-T37 (1962).
1021. Arnold, G., Fisher, A., and Frohnsdorff, G., Hazards from Burning Garments, Final Report for GIRCFF, Gillette Research Institute, Rockville MD (1973).
1022. Kadolph, S. J., Johnson, R. F., and Jordan, K. A., A Flammability Hazard Rating and Index for Women's Apparel, *J. Consumer Studies and Home Economics* **11**, 165-181 (1987).
1023. Krasny, J. F., Braun, E., and Peacock, R. D., Synthesis of a General Apparel Flammability Standard, pp. 171-184 in *Proc. 10th Annual Mtg., Information Council on Fabric Flammability,* New York (1976).
1024. Chouinard, M. P., Knodel, D. C., and Arnold, H. W., Heat Transfer from Flammable Fabrics, *Textile Research J.* **43**, 166-175 (1973).
1025. Bercaw, J. R., and Jordan, K. G., Use of "Thermo-Man" for Estimating Injury From Burning Garments, pp. 214-239 in *Proc. 8th Annual Mtg.*, Information Council on Fabric Flammability, Galveston TX (1974).
1026. Pakkala, L., The Flammability of Different Textiles and Its Influence on the Severity of Skin Burns, *Annales Chirurgiae et Gynaecologiae* **69**, 240-243 (1980).
1027. Benisek, L., Development of Flame-Resist Treatments for Wool, *Wool Science Review* No. 52, 30-63 (1976).
1028. Villa, K. M., and Krasny, J. F., Small-Scale Vertical Flammability Testing for Fabrics, *Fire Safety J.* **16**, 229-241 (1990).
1029. Krasny, J. F., Flammability Evaluation Methods for Textiles, pp. 155-200 in **Flame-Retardant Polymeric Materials**, vol. 3, M. Lewin et al., eds. Plenum Publishing Corp., New York (1982).
1030. Carroll-Porczynksi, C. Z., **The Flammability of Composite Fabrics**, Chemical Publishing Co.., New York (1976).
1031. Wesson, H. R., The Piloted Ignition of Wood by Radiant Heat (D. Eng. dissertation), Univ. Oklahoma, Norman (1970).
1032. Wulff, W., Zuber, N., Alkidas, A., and Hess, R. W., Ignition of Fabrics under Radiative Heating, *Combustion Science and Technology* **6**, 321-334 (1973).
1033. Rangaprasad, N., Sliepcevich, C. M., and Welker, J. R., The Piloted Ignition of Cotton Fabrics, *J. Fire and Flammability* **5**, 107-115 (1974).
1034. Ohlemiller, T. J., and illa, K. M., Material Flammability Test Assessment for Space Station Freedom (NISTIR 4591; NASA CR-187115), NIST (1991).
1035. Vodvarka, F. J., Full-scale Burns in Urban Areas. Part I. Fire Spread between Structures (IITRI Project J6009; OCD Contract N00228-68-C-2368), IIT Research Institute, Chicago (1969).
1036. Simms, D. L., The Minimum Intensity for the Spontaneous Ignition of Cellulosic Materials (FR Note 361), Fire Research Station, Borehamwood (1958).
1037. Holbrow, P., Hawksworth, S. J., and Tyldesley, A., Thermal Radiation from Vented Dust Explosions, *J. Loss Prevention in the Process Industries* **13**, 467-476 (2000).
1038. Mowrer, F. W., Ignition Characteristics of Various Fire Indicators Subjected to Radiant Heat Fluxes, pp. 81-92 in *Fire and Materials 2003*, Interscience Communications Ltd., London (2003).
1039. Suzuki, T., Yanai, E., and Yamada, T., A Study of the Flammability of Textile Products by Using Cone Calorimeter, pp. 115-123 in *Proc. 14th Joint Panel Mtg. UJNR Panel on Fire Research and* Safety, Building Research Institute & National Research Institute of Fire and Disaster, Tsukuba, Japan (1998).
1040. Suzuki, T., National Research Institute of Fire and Disaster, private communication (1998).
1041. Schopee, M. M., Welsford, J. M., and Abbott, N. J., Protection Offered by Lightweight Clothing Materials to the Heat of a Fire, pp. 340-357 in **Performance of Protective Clothing** (ASTM STP 900), ASTM (1986).
1042. Wu, P. K. S., Lee, C., and Kim, I.-Y., A Simple Method for Evaluation of Thermal Protective Clothing, pp. 631-643 in *Interflam 2001—Proc. 9th Intl. Conf.*, Interscience Communications Ltd., London (2001).
1043. Doughty, R. L., Neal, T. E., Dear, T. A., and Bingham, A. H., Testing Update on Protective Clothing & Equipment for Electric Arc Exposure (IEEE Paper PCIC-97-35), Institute of Electrical and Electronics Engineers, New York (1997).

1044. Mixter, G., Thermal Radiation Burns Beneath Fabric Systems, *Annals of the New York Academy of Sciences* **82**, 701-713 (1959).
1045. Durbetaki, P., Chang, H., Matson, G. L., and Tincher, W. C., Ignition Characteristics of Flame Retardant Fabrics, *J. Fire and Flammability* **10**, 105-128 (1979).
1046. Karim, G. A., and Mehta, S., The Behavior of Compacted Cotton Fibers in Hot Low Velocity Air Stream, *J. Fire and Flammability* **4**, 216-228 (1986).
1047. Vickers, A. K., Kitchen Ranges in Fabic Fires (Tech. Note 817), NIST (1974).
1048. Slutz, J. F., and Word, E. L., Cigarettes as an Ignition Source for Apparel Fabrics, *Textile Chemist and Colorist* **12**, 225-226 (1980).
1049. Waterman, T. E., and Takata, A. N., Laboratory Study of Ignition of Host Materials by Firebrands (Project J6142, OCD Work Unit 2539A), IIT Research Institute, Chicago (1969).
1050. Lee, R., Pressures Developed by Arcs, *IEEE Trans. Ind. Appl.* **IA-23**, 760-764 (1987).
1051. Sayers, L. W., Flammability of Fibers, Fabrics, and Garments, *Textile Institute and Industry* **3**, 168-171 (1965).
1052. Kaswell, E. R., Some Thoughts and Information on Nonflammable Products, *J. Amer. Assn. Textile Chemists and Colorists* **4**, 33-40 (1972).
1053. Blankenbaker, S. W., and Word, E. L., Flammability Study: Electric Burners as Ignition Sources for Apparel Fabrics, *Textile Chemist and Colorist* **13**, 151-155 1981).
1054. Thielman, G. W., Comparison of Parachute Fabric Response to Radiation Heat Transfer, AIAA paper 97-0810, Amer. Inst. of Aeronautics and Astronautics (1997).
1055. Critical Radiant Exposures for Ignition of Tinder and Combustible Materials (Part II – Cloth), Naval Applied Science Lab., Brooklyn NY (1965).
1056. Smedley, S. I., and Wake, G. C., Spontaneous Ignition: Assessment of Cause, paper presented at the Annual Meeting of the Institute of Loss Adjusters of New Zealand (Inc.), Palmerston North (1987).
1057. Wilk, I. J., Dangers Due to Increased Flammability of Materials in Oxygen-Enriched Atmospheres, *J. Chem. Educ.* **45**, A547-A548; A550-A551 (1968).
1058. Voigtsberger, P., Die Entzündung von sauerstoffgetränkten Geweben durch elektrostatische und mechanisch erzeugte Funken [The Ignition of Oxygen-Impregnated Fabrics by Electrostatic and Mechanically-Produced Sparks], *Moderne Unfallverhütung* No. 7, 66-70 (Winter 1962/63). SMRE Translation No. 5005, Safety in Mines Research Establishment, Sheffield, England.
1059. Fitt, P. W., Collings, N., and O'Neill, D., The Ignition of Solid Materials in Oxygen by Electrical Sparks, *J. Fire and Flammability* **4**, 185-196 (1973).
1060. Plano, R. J., Tests Evaluate Fire Hazard of Static Sparks, *The Modern Hospital* **95**, 154, 156 (Sept. 1960).
1061. Guest, Paul G., Oily Fibers May Increase Oxygen Tent Fire Hazard, *The Modern Hospital* **104**, 180, 182 (May 1965).
1062. Purser, P. R., Ignition by Electrostatic Sparks in Hyperbaric Oxygen, *Lancet*, 1405-1406 (24 Dec. 1966).
1063. Coleman, E. H., Effects of Compressed and Oxygen-Enriched Air on the Flammability of Fabrics, *British Welding J.* **6**, 406-410 (Sep. 1959).
1064. Aenishaenslin, R., and Mayer, F., Physical Factors Affecting the Burning Behavior of Fabrics, *Textilveredlung* **11**, 329-35 (1976).
1065. Gordon, P. G., Flame Retardants and Textile Materials, *Fire Safety J.* **4**, 109-123 (1981).
1066. Khattab, M. A., Kandil, S. H., Gad, A. M., El-Latif, M., and Morsi, S. E., Effect of Condensed-Phase and Gas-Phase Flame Retardants on the Ignition Behaviour of Cotton Fabric, *Fire and Materials* **16**, 23-28 (1992).
1067. Reeves, W. A., Drake, G. L. jr., and Perkins, R. M., **Fire Resistant Textiles Handbook**, Technomic Pub. Co., Westport CT (1974).
1068. Tokyo Fire Dept., Spontaneous Ignition of Bone Meal for Livestock Fodder, *Kasai* [J. Japan Assn. for Fire Science and Engineering] **28**:6, 28-30 (1978).
1069. Kiiski, H., Self Sustaining Decomposition of Ammonium Nitrate Containing Fertilisers, paper presented in *2000 IFA Conf.*, Intl. Fertilizer Industry Association, Paris (2000).
1070. Huygen, D. G., and Perbal, G., The Decomposition of Compound Fertilisers, LEE/65/XIII, *1965 Technical Conf.*, International Fertilizer Industry Assn., Paris (1965).
1071. Parker, A. B., and Watchorn, N., Self-propagating Decomposition in Organic Fertilisers Containing Ammonium Nitrate, *Journal of the Science of Food and Agriculture* **16**, 355-368 (1965).
1072. Barclay, K. S., Physical-Chemical Studies on Decomposition Reactions and the Safe Handling of Ammonium Nitrate-Bearing Fertilizers, pp. 31-48 in *Proc. 17th International Congress "Chemistry Days 1966" on Chemical Fertilizers*, Pergamon Press, Oxford [1968]
1073. Davis, R. O. E., and Hardesty, J. O., Organic Material and Ammonium Nitrate in Fertilizer Mixtures, *Ind. and Eng. Chem.* **37**, 59-63 (1945).
1074. Hardesty, J. O., and Davis, R. O. E., Spontaneous Development of Heat in Mixed Fertilizers, *Ind. and Eng. Chem.* **38**, 1298-1303 (1945).
1075. Perbal, G., Selfheating of Compound Fertilizers Containing Ammonium Nitrate, pp. 198-223 in *Selfheating of Organic Materials*, Intl. Symp. 18th and 19th February 1971, Delft. Delft University (1971).
1076. Monakhov, V. T., **Metody issledovaniya pozharnoi ospasnosti veshchestv**, Khimya, Moscow (1972). English translation: **Methods for Studying the Flammability of Substances**, published for U.S. National Bureau of Standards by Amerind Publishing Co., New Delhi, India (1985).
1077. Mackey, W. M., Spontaneous Combustion of Oils Spread on Cotton. II, *J. Soc. Chemical Industry* **14**, 940-941 (1895).
1078. Mackey, W. M., Note on the Behaviour of Some Oils and Fatty Acids in Mackey's Cloth Oil Tester, *J. Soc. Chemical Industry* **34**, 595-597 (1915).
1079. Radford, A. S., Spontaneous Combustion and Its Early Detection, *Paint Technology* **20**, 317-323 (1956).
1080. Choudry, Q., Fire Investigation Report. Examination of Spontaneous Combustion. Fire at Seneca Manufacturing Ltd., Office of the Fire Marshal, Ontario, Canada (1991).
1081. Horrocks, A. R., Moss, W. A., and Edwards, N. C., The Spontaneous Ignition Behaviour of Oil-contaminated Cotton, *Polymer Degradation and Stability* **33**, 295-305 (1991).
1082. Thompson, N. J., Statement of N. J. Thompson, pp. 29-34 in *Report of Conf. on Spontaneous Heating and Ignition of Agricultural and Industrial Products*, NFPA and US Dept. of Agriculture, Washington (1929).
1083. Taradoire, F., L'inflammation spontanée du coton, *La Revue des produits chimiques* **28**, 114-115 (28 Feb. 1925).

1084. Spontaneous Combustion Test: Outside of Linseed Oil Bundle Was Room Temp., but Inside Was Hot, *Fire Findings* **4**:4, 4 (Fall 1996).
1085. Zicherman, J. B., private communication (2000).
1086. DeHaan, J. D., Spontaneous Ignition. Part II: Investigation, *Fire & Arson Investigator* **46**, 8-11 (June 1996).
1087. Obold, W. L., Hoffheins, F. M., Ingberg, S. H., and James, L. H., Heating and Ignition Tests With Jute, National Fire Protection Assn., Boston (1934).
1088. Abraham, C. J., A Solution to Spontaneous Combustion in Linseed Oil Formulations, *Polymer Degradation and Stability* **54**, 157-166 (1996).
1089. Gale, M. J., A Close Look at Spontaneous Combustion, *Fire & Arson Investigator* **38**:4, 8 (June 1988).
1090. Gray, B. F., Arson and Spontaneous Combustion—Can They Be Confused?, lecture notes, n.d.
1091. Hill, S. M., Investigating Materials from Fires Using a Test Method for Spontaneous Ignition: Case Studies (M.S. thesis), Univ. Maryland, College Park (1997).
1092. Demidov, P. G., **Goreniye i svoystva goryuchikh veshchestv**, Izdatel'stvo Ministerstva Kommunal'nogo Khozyaystva RSFSR, Moskva (1962). English translation: **Combustion and Properties of Combustible Substance**, NTIS No. AD 621 738, National Technical Information Service, Springfield VA (1965).
1093. Carson, P. A., and Mumford, C. J., Fires without External Ignition Sources. Part I. Spontaneous Combustion, *Loss Prevention Bulletin* No. 108, 1-16 (Dec. 1992).
1094. Gill, A. H., The Ignition of Fire Engine Hose When in Use, *J. Industrial and Engineering Chemistry* **13**, 168 (1921).
1095. Bowes, P. C., Spontaneous Heating and Ignition of Fishmeal, *FPA J.*, No. 27, 285-289 (Oct. 1954).
1096. Fishmeal Strikes Again, *Hazardous Cargo Bull.* **4**:2, 20, 24 (1983).
1097. Still, J. M., Orlet, H. K., Law, E. J., and Pickens, H. C., Burns Due to Flammable Solvents Ignited with Floor Buffers, *J. Burn Care & Rehabilitation* **17**, 188-190 (1996).
1098. DeHaan, J. D., Our Changing World: Part 1. Furnishings, *The Fire Place* (Washington State IAAI Chapter newsletter), 13-15 (June/Aug. 2001).
1099. Settle, G. E., Temperature of Instantaneous Ignition, *Fire and Materials* **4**, 163 (1980).
1100. Van Hees, P., Meestroomvlamuitbreiding bij vloerbekledingen. Ontwikkeling en validatie van grootschalige en kleinschalige meettechnieken (Ph.D. dissertation), Faculteit Toegepaste Wetenschappen, Universiteit Gent, Belgium (1995).
1101. den Braven, K., Radiative Ignition of Some Typical Floor Covering Materials (NBSIR 75-967), NBS (1975).
1102. Long, M. E., Heat Release and Ignition Characteristics of Floor Coverings Used in the NBS Corridor Tests (NBS 10 497), NBS (1971).
1103. Hirschler, M. M., Smoke and Heat Release Following the Burning of Carpet Tiles, *Fire Safety J.* **18**, 305-324 (1992).
1104. Tomann, J., Comparison of Nordtest FIRE 007, CEN Draft Proposal (Radiant Panel) and Cone Calorimeter Methods in the Fire Testing of Floor Coverings, *Fire and Materials* **17**, 185-190 (1993).
1105. Yanai, E., Ignitability of Carpets Using Cone Type Flammability Test Method (ISO/DTR 5657), *Report of Fire Research Institute of Japan* No. 62, 23-31 (1986).
1106. Peacock, R. D., and Vaishnav, M. P., Flammability Testing of Solids Under the Federal Hazardous Substances Act (NBSIR 78-1580), NBS (1980).
1107. Sugawa, O., Short Communication on Self-Ignition of Potato Chip Waste, *Fire Science and Technology* **12**, 1-6 (1992).
1108. Raemy, A., and Lambelet, P., A Calorimetric Study of Self-Heating in Coffee and Chicory, *J. Food Technology* **17**, 451-460 (1982).
1109. Dixon, B. M., The Potential for Self-Heating of Deep-Fried Food Products, pp. 227-288 in *Proc. Intl. Symp. on the Forensic Aspects of Arson Investigations*, FBI, Washington (1995).
1110. Takai, S., Ignition of Powder Foods, Annual Report of Fire Research Laboratory, Nagoya City Fire Dept. No. 20 (1991).
1111. Weinzirl, J., Sugar as Source of Anaerobes Causing Explosion of Chocolate Candies, *J. Bacteriology* **13**, 203-207 (1927).
1112. 1991 – 1997 Wildland Fire Statistics, Fire and Aviation Management Staff, US Forest Service, [n.p.] (1998).
1113. Weber, R., Bushfire Causes, paper presented at *Bushfire 1999*.
1114. Bernardi, G. C., Fires Caused by Equipment Used during Critical Fire Weather in California, 1962-1971 (Research Note PSW-289), Pacific Southwest Forest and Range Experiment Station, US Forest Service, Berkeley CA (1974).
1115. McCurnin, J. J., Equipment as an Ignition Source, *Fire Prevention Notes* No. 17, Calif. Dept. of Forestry, Sacramento (Dec. 1981).
1116. Investigation Report—Cerro Grande Prescribed Fire, May 4-8, 2000. Fire Investigation Team, National Interagency Fire Center, Boise ID (2000).
1117. Board of Inquiry, Cerro Grande Prescribed Fire—Final Report, National Park Service, Washington (2001).
1118. Scott, J. H., and Reinhardt, E. D., Assessing Crown Fire Potential by Linking Models of Surface and Crown Fire Behavior (Research Paper RMRS-RP-29), Rocky Mountain Research Station, US Forest Service, Fort Collins CO (2001).
1119. Albini, F. A., Estimating Wildfire Behavior and Effects (Gen. Tech. Report INT-30), Intermountain Forest and Range Experiment Station, US Forest Service, Ogden UT (1976).
1120. Andrews, P. L., BEHAVE: Fire Behavior Prediction and Fuel Modeling System—BURN Subsystem, Part 1 (Gen. Tech. Report INT-194), Intermountain Forest and Range Experiment Station, US Forest Service, Ogden UT (1986).
1121. Albini, F. A., Wildland Fires, *American Scientist* **72**, 590-597 (1984).
1122. McArthur, A. G., Fire Behaviour in Eucalypt Forests (Leaflet No. 107), Forestry & Timber Bureau, Dept. of Natural Development, Canberra, Australia (1967).
1123. Viegas, D. X., Weather, Fuel Status and Fire Occurrence: Predicting Large Fires, pp. 31-48 in **Large Forest Fires**, J. M. Moreno, ed., Backhuys Publishers, Leiden (1998).
1124. Noble, I. R., Bary, G. A. V., and Gill, A. M., McArthur's Fire-Danger Meters Expressed as Equations, *Australian J. Ecology* **5**, 201-203 (1980).
1125. Wright, J. G., Forest Fire Hazard Research, *The Forestry Chronicle* **8**, 133-151 (1932).
1126. Bowes, P.C., Determination of Ignition Temperature of Dried Grass (F.C. Note No. 47), Fire Research Station, Borehamwood, UK (1951).

1127. Yamashita, K., Measurement of Flaming Ignition Temperature of Forest Materials Heated in Hot Air Stream—Comparison of Coniferous Tree and Broadleaf Tree, *Kasai* [J. Japan Assn. for Fire Science and Engineering] **36**:5, 12-18 (1986).
1128. Johnson, A. T., Schlosser, A. D., Kirk, G. D., and Long, G. L., Automatic Determination of Ignition Temperature, *Fire Technology* **16**, 181-191 (1980).
1129. Shu, L., Tian, X., and Kou, X., Studies on Selection of Fire Resistance Tree Species for Sub-tropical Area of China, pp. 181-190 in *Proc. 4th Asia-Oceania Symp. on Fire Science & Technology*, Asia-Oceania Assn. for Fire Science & Technology/Japan Assn. for Fire Science & Engineering, Tokyo (2000).
1130. Stockstad, D. S., Spontaneous and Piloted Ignition of Pine Needles (Res. Note INT-194), US Forest Service, Intermountain Forest & Range Expt. Sta., Ogden UT (1974).
1131. Stockstad, D. S., Spontaneous and Piloted Ignition of Cheatgrass (Res. Note INT-204), US Forest Service, Intermountain Forest & Range Expt. Sta., Ogden UT (1976).
1132. Mutch, R. W., Ignition Delay of Ponderosa Pine Needles and Sphagnum Moss, *J. Applied Chemistry (London)* **14**, 271-275 (1964).
1133. Liodakis, S., Bakirtzis, D., Lois, E., and Gakis, D., The Effect of $(NH_4)_2HPO_4$ and $(NH_4)_2SO_4$ on the Spontaneous Ignition Properties of *Pinus Halepensis* Pine Needles, *Fire Safety J.* **37**, 481-494 (2002).
1134. Gill, A. M., and Moore, P. H. R., Ignitability of Leaves of Australian Plants, A Contract Report to the Australian Flora Foundation, CSIRO Plant Industry, Canberra, Australia (1996).
1135. Xanthopoulos, G., and Wakimoto, R.H., A Time to Ignition–Temperature–Moisture Relationship for Branches of Three Western Conifers, *Canadian J. Forest Research* **23**, 253-258 (1993).
1136. Montgomery, K. R., and Cheo, P. C., Effect of Leaf Thickness on Ignitability, *Forest Science* **17**, 475-478 (1971).
1137. Fairbank, J. P., and Bainer, R., Spark Arresters for Motorized Equipment, *Bulletin* 577, pp. 3-42, University of California Experiment Station (1934).
1138. Harrison, R. T., Danger of Ignition of Ground Cover Fuels by Vehicle Exhaust Systems (ED&T Project 1337), US Forest Service, Equipment Development Center, San Dimas CA (1970).
1139. Kaminski, G. C., Ignition Time vs. Temperature for Selected Forest Fuels, Project Record, US Forest Service, San Dimas Equipment Development Center, San Dimas CA (1974).
1140. Rallis, C. J., and Mangaya, B. M., Ignition of Veld Grass by Hot Aluminium Particles Ejected from Clashing Overhead Transmission Lines, *Fire Technology* **38**, 81-92 (2002).
1141. Luke, R. H., and McArthur, A. G., **Bushfires in Australia**, Australian Government Publishing Office, Canberra (1978).
1142. Keetch, J. J., Smoker Fires and Firebrands (Tech. Note No. 49), Appalachian Forest Experiment Station, Asheville NC (1941).
1143. Blackmarr, W. H., Moisture Content Influences Ignitability of Slash Pine Litter (Res. Note SE-173), US Forest Service, Southeastern Experiment Station, Asheville NC (1972).
1144. Gill, A. M., Trollope, W. S. W., and MacArthur, D. A., Role of Moisture in the Flammability of Natural Fuels in the Laboratory, *Australian Forest Research* **8**, 199-208 (1978).
1145. Van Wagner, C. E., Flammability of Christmas Trees (Publ. 1034), 2nd ed., Forestry Branch, Dept. Forestry and Rural Development, Ottawa (1967).
1146. Chastagner, G., Effect of Fire Retardant Application and Display Care on the Postharvest Quality of Douglas-fir Christmas Trees, paper presented at the 2001 IAAI Annual Seminar, Atlantic City NJ (2001).
1147. California Flame Retardant Handbook: Laws and Regulations, California State Fire Marshal, Sacramento [199?].
1148. Chastagner, G., Factors Affecting the Moisture Levels of Cut Christmas Trees, paper presented at the 2001 IAAI Annual Seminar, Atlantic City NJ (2001).
1149. Babrauskas, V., The Heat Release Rate Hazard of Christmas Trees, paper presented at the 2001 IAAI Annual Seminar, Atlantic City NJ (2001).
1150. Hoffheins, F. M., Fire Hazard Tests with Cigarettes, *NFPA Q.* **27**, 132-140 (Oct. 1933).
1151. Countryman, C. M., Ignition of Grass Fuels by Cigarettes, Forest Service Contract 43-9AD6-1-617, Pacific Southwest Forest & Range Expt. Sta., Riverside CA (1982).
1152. Countryman, C. M., Ignition of Grass Fuels by Cigarettes, *Fire Management Notes* **44**:3, 3-7 (1983).
1153. Ford, R. T. sr., **Investigation of Wildfires**, privately published, Sunriver OR (1995).
1154. Markalas, S., Laboruntersuchungen über die Rolle weggeworfener Zigarettenstummel als Zündursache von Waldbränden [Laboratory experiments on the role of burning cigarette ends in igniting forest fires], *Allgemeine Forst und Jagdzeitung* **156**, 193-197 (1985).
1155. Fuquay, D. M., Baughman, R. G., and Latham, D. J., A Model for Predicting Lightning-Fire Ignition in Wildland Fuels (Res. Paper INT-217), US Forest Service, Intermountain Forest & Range Expt. Sta., Ogden UT (1979).
1156. Latham, D. J., and Schlieter, J. A., Ignition Probabilities of Wildland Fuels Based on Simulated Lightning Discharges (Res. Pap. INT-411), US Forest Service Intermountain Research Station, Ogden UT (1989).
1157. Latham, D., and Williams, E., Lightning and Forest Fires, pp. 375-418 in **Forest Fires: Behavior and Ecological Effects**, E. A. Johnson and K. Miyanishi, eds., Academic Press, San Diego (2001).
1158. Renkin, R.A., Fuel Moisture, Forest Type, and Lightning-caused Fire in Yellowstone National Park, *Canadian J. Forest Research* **22**, 37-45 (1992).
1159. Stokes, A. D., Fire Ignition by Contact between Green Vegetation and High Voltage Conductors (Dept. report), Dept. of Electrical Engineering, Univ. Sydney, Australia (2001).
1160. Filippov, A. V., The Pyrological Properties of Some Combustible Forest Materials, pp. 96-106 in **Problems in Combustion and Extinguishment—Collection of Articles**, I. V. Ryabov et al., eds., TT-71-58001, National Technical Information Service, Springfield VA (1974).
1161. White, R. H., DeMars, D., and Bishop, M., Flammability of Christmas Trees and Other Vegetation, pp. 99-110 in *24th Intl. Conf. on Fire Safety*, Product Safety Corp., Sissonville WV (1997).
1162. Trabaud, L., Inflammabilité et combustibilité des principales espèces des garrigues de la région mediterranéene, *Oecologia Plantarum* **11**, 117-136 (1976).
1163. Dimitrakopoulos, A. P., and Papaioannou, K. K., Flammability Assessment of Mediterranean Forest Fuels, *Fire Technology* **37**, 143-152 (2001).
1164. Albini, F. A., private communication (2001).

1165. Canon, V., Nevada County Consolidated Fire District, private communication (2003).
1166. Ellis, P. F., The Aerodynamic and Combustion Characteristics of Eucalypt Bark—A Firebrand Study (Ph.D. dissertation), Australian National Univ., Canberra (2000).
1167. Rowntree, G.W.G., and Stokes, A.D, Fire Ignition by Aluminium Particles of Controlled Size, *J. Electrical and Electronics Engineering, Australia* **14**, 117-23 (1994).
1168. Stokes, A. D., Fire Ignition by Copper Particles of Controlled Size, *J. Electrical and Electronics Engineering, Australia* **10**, 188-194 (1990).
1169. Mills, A. F., and Hang, X., Trajectories of Sparks from Arcing Aluminum Power Cables, *Fire Technology* **20**:2, 5-14 (May 1984).
1170. Tse, S. D., and Fernandez-Pello, A. C., On the Flight Paths of Metal Particles and Embers Generated by Powerlines in High Winds—Potential Source of Wildland Fires, *Fire Safety J.* **30**, 333-356 (1998).
1171. Florida Division of Forestry, Simulator Training Is Refined in Florida, *Fire Control Notes* **32**:3, 11-12 (Summer 1971).
1172. Browne, C. A., The Spontaneous Combustion of Hay (Tech. Bull. 141), US Dept. of Agriculture, Washington (1929).
1173. Ranke, H. von, Experimentaller Beweis der Möglichkeit der Selbstentzündung des Heues (Grummets), *Justus Liebigs Annalen der Chemie* **167**, 361-368 (1873).
1174. Miehe, H., **Die Selbsterhitzung des Heues: Eine biologische Studie**, G. Fischer, Jena (1907).
1175. Browne, C. A., The Spontaneous Combustion and Ignition of Hay and Other Agricultural Products, *Science* **77**, 223-229 (1933).
1176. Firth, J. B., and Stuckey, R. E., The Spontaneous Combustion of Hay, *J. Soc. Chemical Industry* **64**, 13-15 (1945); and **65**, 275-277 (1946).
1177. Drysdale, D. D., Chemistry and Physics of Fire, pp. 1-55 to 1-68 in **Fire Protection Handbook**, 18th ed., A. E. Cote and J. L. Linville, eds., NFPA (1997).
1178. James, L. H., and Price, D. J., Observations on Heating Hay in the Flooded Regions of Northern Vermont, *Science* **67**, 322-324 (23 Mar. 1928).
1179. Clarke, S., Silo and Hay Mow Fires on Your Farm (Agdex No. 732), Ontario Ministry of Agriculture, Food and Rural Affairs, Kemptville, Canada (1983).
1180. Firth, J. B., and Stuckey, R. E., Spontaneous Combustion of Hay, *Nature* **159**, 624-626 (1947).
1181. Rothbaum, H. P., Spontaneous Combustion of Hay, *J. Applied Chemistry* **13**, 291-302 (1963).
1182. Hussain, H., Investigations of the Biological Self-heating of Hay and Its Experimental Reconstruction up to Self-Ignition, pp. 111-126 in *Selfheating of Organic Materials*, Intl. Symp. 18th and 19th February 1971, Delft. Delft University (1971).
1183. Miao, Y., and Yoshikazi, S., Mechanism of Spontaneous Heating of Hay. Part 1. Necessary Conditions and Heat Generation from Chemical Reactions, *Trans. ASAE* **37**, 1561-1566 (1994).
1184. Miao, Y., Amaeri, M., and Yoshikazi, S., Mechanism of Spontaneous Heating of Hay. Part 2. Chemical Changes in Spontaneously Heated Hay, *Trans. ASAE* **37**, 1567-1570 (1994).
1185. Koegel, R. G., and Bruhn, H. D., Inherent Causes of Spontaneous Ignition in Solids, Paper 69-164 presented at *1969 Annual Mtg. American Society of Agricultural Engineers*, West Lafayette, IN (1969).
1186. Jach, W., The Influence of Agricultural Structural Fluctuations on the Self-ignition of Hay, pp. 96-110 in *Selfheating of Organic Materials*, Intl. Symp. 18th and 19th February 1971, Delft. Delft University (1971).
1187. Rész, A., The Influence of Ventilation on the Microbial Activity in Hay, pp. 127-138 in *Selfheating of Organic Materials*, Intl. Symp. 18th and 19th February 1971, Delft. Delft University (1971).
1188. Currie, J.A., and Festenstein, G.N., Factors Defining Spontaneous Heating and Ignition of Hay, *J. Science of Food and Agriculture* **22**, 223-230 (1971).
1189. Hicks, A. A., Hay Clinker as Evidence of Spontaneous Combustion, *Fire & Arson Investigator* **48**, 10-13 (July 1998).
1190. Mickan, F., What Happens When Hay Heats (AG0206), State of Victoria Dept. of Natural Resources and Environment, Australia (1999).
1191. Lamb, A. R., Spontaneous Combustion as a Cause of Fires (Circular 36). Iowa Agricultural Experiment Station, Iowa State College of Agriculture and Mechanic Arts (1917).
1192. Walls, H. J., An Unusual Case of Apparent Spontaneous Combustion, *J. Forensic Science Society* **2**, 82-84 (1962).
1193. Campbell, J. K., Who Wants a 20 by 60 Fireplace? *Hoard's Dairyman* 677, 684 (May 1973).
1194. Maloney, T. J., Combating Agricultural Silo Fires, *Speaking of Fire* **5**:2, 10-23 (Oct. 1997).
1195. Clark, A., Kimball, J., and Stambaugh, H., The Hazards Associated with Agricultural Silo Fires, US Fire Administration, Emmitsburg MD (1998).
1196. Rothbaum, H. P., Self-Heating of Esparto Grass, *J. Applied Chemistry* **14**, 436-439 (1964).
1197. Virtala, V., Oksanen, S., and Fridlund, F., Om självantändlighet, dess bestämning och förekomst [On spontaneous ignition and its occurrence; methods for the determination of the tendency to spontaneous ignition] (Julkaisu 14), Valtion Teknillinen Tutkimuslaitos, Helsinki (1949).
1198. Jones, J. C., and Raj, S. C., The Self-heating and Ignition of Vegetation Debris, *Fuel* **67**, 1208-1210 (1988).
1199. Jones, J. C., et al., The Self-Heating and Thermal Ignition Propensity of Forest Floor Litter, *J. Fire Sciences* **8**, 207-223 (1990).
1200. Jones, J. C., and Richards, G. N., On the Possible Role of Inorganics in the Ignition of Lignocellulosic Materials, *J. Fire Sciences* **15**, 91-94 (1997).
1201. Rudge, E. A., An Inquiry into the Mechanism of Decay of Wood, *J. Soc. Chemical Industry* **53**, 282T-288T (1934).
1202. Standard Specification for Fuel Oils (ASTM D 396), ASTM.
1203. Taylor, R. A., and Burgess, A. R., Particulate Formation in Fuel Oil Combustion, *Fuel Science & Technology Intl.* **6**, 41-81 (1988).
1204. Strehlow, R., Accidental Explosions, *American Scientist* **68**, 420-428 (1980).
1205. Schwalje, F., Combustible Flooring Fires under Boilers, *Fire & Arson Investigator* **51**:1, 41-43 (Oct. 2001).
1206. Certuse, J., Residential Steam Boilers, *Fire Findings* **9**:4, 7-11 (Fall 2001).
1207. Flocken, J., and Bates, R., The "Write" Way to Start a Fire, pp. 241-244 in *Proc. Intl. Symp. on the Forensic Aspects of Arson Investigations*, FBI, Washington (1995).
1208. Ostroot, G. jr., Explosions in Gas or Oil-Fired Furnaces, *6th Loss Prevention Symp.*, AIChE (1971).
1209. Flame Rollout Switch Guards Against Elevated Temperatures, *Fire Findings* **4**:2, 4 (Spring 1996).

1210. Zaminski, G. F., Consolidated Furnace Failures, *The California Fire-Arson Investigator* 1, 4, 9 (Mar. 2001).
1211. Blum, F. M., Oil Burner Fires, *Fire & Arson Investigator* **33**:4, 12-14 (June 1983).
1212. Sokalski, M. A., Fuel Oil Furnace Fires, *Fire & Arson Investigator* **51**:1, 41-44 (Oct. 2000).
1213. Standard for the Installation of Oil-Burning Equipment (NFPA 31), NFPA.
1214. Rosenhan, A. K., An Ice Storm, the Gas Meter, and Electricity, *Fire & Arson Investigator* **46**:1, 16 (Sept. 1995).
1215. Olson, D., Quoth the Raven "Nevermore," *The Fire Place [Washington State IAAI newsletter]* 9 (Sep./Dec. 2002).
1216. McVicar, M. J., The Perforation of a Copper Pipe During a Fire, *Canadian Assn. of Fire Investigators The/Le Journal*, 14-16 (June 1991).
1217. Cox, D. E., Gas Regulator Lock-ups, *Fire Findings* **10**:3, 7-11 (Summer 2002).
1218. Caskanette, R., Fires Attributable to Pressure Regulator Failures on Residential Natural Gas Services, *Canadian Assn. of Fire Investigators The/Le Journal*, 7-10 (3rd Quarter 1988).
1219. Sanderson, J. L., Investigation of Gas & Electric Appliance Fires Seminar, Fire Findings Laboratory, LLC, Benton Harbor MI [n.d.].
1220. Standard Specification for Automobile Gasoline (ASTM D 439), ASTM.
1221. Regulation of Fuels and Fuel Additives (40 CFR Ch. 1 Part 80), Code of Federal Regulations.
1222. Eaton, T., Physical Properties of Gasoline, *J. Applied Fire Science* **1**, 175-183 (1990/91).
1223. Safe Entry and Cleaning of Petroleum Storage Tanks (API Publ. 2015), 4th ed., American Petroleum Institute, Washington (1991).
1224. Davis, D. J., Davis, J. A., and Christianson, G. T., **Firefighter's Hazardous Material Reference Book and Index**, 2nd ed., Van Nostrand Reinhold, New York (1993).
1225. Frobese, D.-H., Investigations into the Distribution of Hydrocarbon Concentrations in Underground Tanks of Petrol Stations, *J. Hazardous Materials* **42**, 1-14 (1995).
1226. Hord, J., Is Hydrogen Safe? (Tech. Note 690), NBS (1976).
1227. Jones, G. W., and Spolan, I., Inflammability of Gasoline Vapor-Air Mixtures at Low Pressures (RI 3966), Bureau of Mines, Pittsburgh (1946).
1228. Liebman, I., Spolan, I., Kuchta, J. M., and Zabetakis, M. G., Ignition of Tank Atmospheres During Fuel Loading, 30th Midyear Meeting, American Petroleum Institute, Montreal, Canada (11 May 1965).
1229. Setchkin, N. P., Self-Ignition Temperatures of Combustible Liquids, *J. Research NBS* **53**, 49-66 (1954).
1230. Hawksworth, S., Appendix 6 in Carleton, F. B., Bothe, H., Proust, Ch., and Hawksworth, S., Prenormative Research on the Use of Optics in Potentially Explosive Atmospheres—PROPEX (EUR 19617 EN), European Commission, Luxembourg (2000).
1231. Brown, G. R., pp. 46-47 in Report of Conference on Spontaneous Heating and Ignition of Agricultural and Industrial Products, NFPA and US Dept. of Agriculture, Washington (1929).
1232. Husa, H. W., and Runes, E., How Hazardous Are Hot Metal Surfaces?, *The Oil and Gas J.* **61**, 180, 182 (11 Nov. 1963).
1233. Billinge, K., Frictional Ignition Hazard in Industry: A Survey of Reported Incidents From 1958 to 1978, *Fire Prevention Science and Technology*, No. 24, 13-19 (1981).
1234. Bernstein, H., and Young, G. C., Sparking Characteristics and Safety Hazards of Metallic Materials (NGF-T-1-57, NAVORD Report 5205), US Naval Gun Factory, Washington (1957).
1235. Powell, F., Ignition of Gas and Vapors*, Ind. and Eng. Chem*. **61**, 29-37 (Dec. 1969).
1236. Frobese, D.-H., Safety Aspects of Petrol Vehicle Tanks, *Erdöl und Kohle—Erdgas—Petrochemie vereinigt mit Brennstoff-Chemie* **48**:3, 146-150 (1995).
1237. Vaivads, R. H., Bardon, M. F., Rao, V. K., and Battista, V., Flammability Tests of Alcohol/Gasoline Vapours (SAE Paper 950401), Society of Automotive Engineers, Warrendale PA (1995).
1238. Sawyer, R. F., Reformulated Gasoline for Automotive Emission Reduction, pp. 1423-1432 in *24th Symp. (Intl.) on Combustion*, The Combustion Institute, Pittsburgh (1992).
1239. Vaivads, R., Bardon, M. F., Rao, V. K., and Battista, V., Flammability of Alcohol-Gasoline Blends in Fuel Tanks, pp. 575-586 in *Fire Safety Science—Proc. 4th Intl. Symp.*, Intl. Assn. for Fire Safety Science (1994).
1240. Vaivads, R. H., Rao, V. K., Bardon, M. F., and Battista, V., Volatility and Flammability of Variable Fuel Vehicle Tank Contents (SAE Paper 932776), Society of Automotive Engineers, Warrendale PA (1993).
1241. Aulich, T. R., He, X., Grisanti, A. A., and Knudson, C. L., Gasoline Evaporation—Ethanol and Nonethanol Blends, *Air & Waste* **44**, 1004-1009 (1994).
1242. Smoot, L. D., personal communication (2002).
1243. Pratt, T. H., **Electrostatic Ignitions of Fires and Explosions**, Burgoyne Inc., Marietta GA (1997).
1244. Deno, D. W., and Zaffanella, L. E., Field Effects of Overhead Transmission Lines and Stations, Chapter 8 in **Transmission Line Reference Book, 345 kV and Above**, 2nd rev. ed., Prepared by Project UHV, General Electric Co. Electric Power Research Institute, Palo Alto CA (1987).
1245. Fuel Containers Ignite, *Flight Safety Australia*, 10 (Nov. 1998).
1246. Thompson, J., Report on Refuelling Ignitions on Petrol Filling Stations in Europe, *APEA Bull.* **35** (Aug. 1997).
1247. Pidoll, U. von, Krämer, H., and Bothe, H., Avoidance of Electrostatic Hazards during Refuelling of Motorcars, *J. Electrostatics* **40/41**, 523-528 (1997).
1248. Renkes, R. N., Special Report: Fires at Refueling Sites that Appear to Be Static Related, Petroleum Equipment Institute, Tulsa OK (2000).
1249. Hearn, G. L., Electrostatic Ignition Hazards Arising from Fuel Flow in Plastic Pipelines, *J. Loss Prevention in the Process Industries* **15**, 105-109 (2002).
1250. Förster, H., Frobese, D.-H., and Finnern, S., Untersuchungen der Kohlenwasserstoffkonzentration im Dampfraum unterirdischer Lagertanks für Ottokraftstoff [Investigation of the Hydrocarbon Concentration in the Vapor Space of Underground Storage Tanks for Gasoline] (DGMK-Projekt 462), Deutsche Wissenschaftliche Gesselschaft für Erdöl, Erdgas und Kohle E.V., Hamburg (1992).
1251. Vander Plas, B., and Lewis, K., Corroded GFCIs Create Fire Hazard, *Fire & Arson Investigator* **49**:2, 10-13 (Jan. 1999).
1252. Janssens, M. L., Fundamental Thermophysical Characteristics of Wood and Their Role in Enclosure Fire Growth (Ph. D. dissertation), Universiteit Gent, Belgium (1991).

1253. Tsantaridis, L. D., Östman, B. A.-L., and König., J., Short Communication: Fire Protection of Wood by Different Gypsum Plasterboards, *Fire and Materials* **23**, 45-48 (1999).
1254. Mowrer, F. W., The Effect of "Blistering" on the Ignition and Flammability of Painted Gypsum Wallboard, pp. 197-208 in *Proc. Fire and Materials 2001 Conf.*, Interscience Communications Ltd., London (2001).
1255. Bowen, J. E., Phenomenon of Spontaneous Ignition Is Still Misunderstood by Some, *Fire Engineering* **135**:5, 42, 45-46 (May 1982).
1256. Hot Air Gun Can Start Fire, but It's Undependable as an Ignition Device, *Fire Findings* **2**:2, 5 (Spring 1994).
1257. Sloan, P., Beware! *Fire & Arson Investigator* **50**:1, 9 (Oct. 1999).
1258. Smith, D. C., Electric Heat Tape Failures. Why Do they Occur, and What Is the Effect of Moisture? DCS Alaska, Juneau (1989).
1259. Smith, D. C., Heat Tape and Cable Fires, *Fire & Arson Investigator* **39**, 38-40 (March 1989).
1260. Mogan, N., Engineering Sciences Heat Tape Activities Fiscal Years 1991 & 1992, U.S. Consumer Product Safety Commission, Washington (October 1992).
1261. Moskowitz, L., Short Circuit Tests of Resistive Heat Tape, Engineering Laboratories Report 551665, Consumer Product Safety Commission, Washington (October 1992).
1262. Smith, D. C., Wet-Fire Phenomena: Cause of Most Heat Tape Failures and All Heat Cable Fires, *Natl. Fire & Arson Report* **10**, No. 1/2, 1-3 (1992).
1263. Smith, D. C., An New Look at the Hazards of Electric Heat Tape and Cables, *Fire J.* **68**, 11-13 (Sep. 1974).
1264. Losinger, W. C., Investigations of Heat Tape Fires, 1991-1992, Division of Hazard Analysis, Consumer Product Safety Commission, Washington (March 1993).
1265. Hogarth, A., and Franklin, T., Heat Tape Safety (CPSC Contract no.: CPSC-C-86-1161; MET report no.: 18709N-88), MET Electrical Testing Co., Inc., Baltimore (1988).
1266. Moskowitz, L., and Garrett, R., Engineering Laboratories Report—Results of the Abnormal Installation of Resistive Heat Tape (Doc. 551652), Consumer Product Safety Commission, Washington (1992).
1267. Hallerberg, D. A., Heat Tape Safety Measures Study, Final Report under Contract No. CPSC-C-93-1126 for Consumer Product Safety Commission. UL (1993).
1268. Mobile Home Pipe Heating Cables (Outline of Investigation 1462), UL (1990).
1269. Residential Pipe Heating Cables (UL 2049), UL (1991).
1270. Recommended Practice for the Testing, Design, Installation, and Maintenance of Electrical Resistance Heat Tracing for Industrial Applications (IEEE 515), IEEE, New York (1989).
1271. Lee, B. T., and Walton, W. D., Fire Experiments and Flash Point Criteria for Solar Heat Transfer Liquids (NBSIR 79-1931), NBS (1979).
1272. Rogowski, Z. W., and Pitt, A., Ignition of Flammable Vapours, Gases and Sheet Materials by Catalytic Heaters (Fire Research Note 1023). Fire Research Station, Borehamwood, UK (1975).
1273. Fitz, M. M., MDE Engineers, private communication (2002).
1274. Fixed and Location-Dedicated Electric Room Heaters (UL 2021), UL.
1275. Electric Air Heaters (UL 1025), UL.
1276. Bloom, C. J., unpublished information (1999).
1277. Consent Agreement and Order, CPSC Docket No. 99-1 (In the Matter of Cadet Manufacturing Co.), Consumer Product Safety Commission, Washington (1999).
1278. CPSC, Honeywell Announce Revised Rating and Recall of Electric Baseboard Heater Thermostats (News Release #98-139), Consumer Product Safety Commission, Washington (1998).
1279. Sanderson, J. L., Electric Baseboard Heaters not Always the Fire Cause Culprits, *Fire Findings* **1**:1, 1-3 (Spring 1993).
1280. Electric Baseboard Heaters Revisited: Radiating Fins Are the Key to Uncovering Failure, *Fire Findings* **1**:2, 6 (Summer 1993).
1281. Baseboard Heaters, *Fire & Arson Investigator* **35**:3, 51-52 (Mar. 1985).
1282. Langlois, D. B., Fire Investigation Report on an Electric Baseboard Heater, *Canadian Assn. of Fire Investigators The/Le Journal*, 9-15 (June 1995).
1283. Goodson, M., Perryman, T., and Colwell, K., Fires Caused by Fractured Resistance Heating Elements, *Fire & Arson Investigator* **53**:1, 43-45 (Oct. 2002).
1284. Smith, L., and Kramer, J., Fires Associated with Portable Electric Heaters, Consumer Product Safety Commission, Washington (1986).
1285. Hall, J. R., jr., U.S. Home Heating Fire Patterns and Trends, Fire Analysis & Research Div., NFPA (2001).
1286. Portable Heating Fires in Residential Structures, Topical Fire Research Series, Vol. 1, Issue 10, US Fire Administration, Emmitsburg MD (2000).
1287. Russo, W. P., Northwest Battles High-Tech Arsonist, *NFPA J.* **86**:6, 67-69, 72-73 (Nov./Dec. 1992).
1288. Keltner, N. R., Hasegawa, H. K., and White, J. A. jr., High-Temperature Accelerant Arson—Revisited, pp. 41-54 in **Very Large-Scale Fires** (ASTM STP 1336), ASTM (1998).
1289. Buhler, M., Yakima Hop Fire Investigation, *The Fire Place* (Washington State Chapter IAAI newsletter) 10-15 (Sep./Nov. 2001).
1290. White, J. A., and Cuzzillo, B. R., Study of the Prevention of Ignition by Self Heating of Hops—Harvest 2001, Western Fire Center, Inc., Kelso WA (2002).
1291. Jones, J. C., and Raj, S. C., The Self-heating and Ignition of Hops, *J. Institute Brewing* **94**, 139-141 (1988).
1292. Rodriguez, G., Hop Fires, *The Fire Place [Washington State IAAI newsletter]* 20-21 (Mar.-May 2001).
1293. Randles, J., and Hough, P., **Spontaneous Human Combustion**, Dorset Press, New York (1992).
1294. Arnold, L. E., **Ablaze! The Mysterious Fires of Spontaneous Human Combustion**, M. Evans and Co., New York (1995).
1295. Harrison, M., **Fire from Heaven: A Study of Spontaneous Combustion in Human Beings**, Methuen, New York (1978).
1296. Gee, D. J., A Case of "Spontaneous Combustion," *Medicine, Science and the Law* **5**, 37-38 (Jan. 1965).
1297. Ettling, B. V., Consumption of an Animal Carcass in a Fire, *J. Criminal Law, Criminology and Police Science* **60**, 131-321 (1969).
1298. DeHaan, J. D., A Case of Not-so-spontaneous Human Combustion, *Fire & Arson Investigator* **47**, 14-16 (June 1997).
1299. DeHaan, J. D., Campbell, S. J., and Nurbakhsh, S., Combustion of Animal Fat and Its Implications for the Consumption of Human Bodies in Fires, *Science and Justice* **39**, 27-38 (1999).

1300. DeHaan, J. D., and Nurbakhsh, S., Sustained Combustion of an Animal Carcass and Its Implications for the Consumption of Human Bodies in Fire, *J. Forensic Sciences* **46**, 1076-1081 (2001).
1301. DeHaan, J. D., private communication (2001).
1302. Bohnert, M., Rost, T., and Pollak, S., The Degree of Destruction of Human Bodies in Relation to the Duration of the Fire, *Forensic Science International* **95**, 11-21 (1998).
1303. Christensen, A. M., Debunking the Spontaneous Human Combustion Myth: Experiments in the Combustibility of the Human Body (M.S. thesis), Univ. Tennessee, Knoxville (2000).
1304. Leitch, D., **A Guide to Fatal Fire Investigations**, Institute of Fire Engineers, Leicester, England (1993).
1305. Durfee, R. L. The Flammability of Skin and Hair in Oxygen-Enriched Atmospheres (SAM-TR-68-130), USAF School of Aerospace Medicine, Brooks AFB, Texas (1968). NTIS No. AD688920.
1306. Sheffield, P. J., and Desautels, D. A., Hyperbaric and Hypobaric Chamber Fires: A 73-year Analysis, *Undersea & Hyperbaric Medicine* **24**, 153-164 (1997).
1307. Snyder, C. E. jr, Krawetz, A. E., and Tovrog, T., Determination of the Flammability characteristics of Aerospace Hydraulic Fluids, *Lubrication Engineering* **37**, 705-714 (Dec. 1981).
1308. Khan, M. M., Spray Flammability of Hydraulic Fluids and Development of a Test Method (FMRC J.I. 0T0W3.RC), Factory Mutual Research Corp., Norwood MA (1991).
1309. Scott, F. E., Burns, J. J., and Lewis, B., Explosive Properties of Hydrazine (RI 4460), Bureau of Mines, Pittsburgh (1949).
1310. Audrieth, L. F., and Ogg, B. A., **The Chemistry of Hydrazine**, Wiley, New York (1951).
1311. Pedley, M. D., Baker, D. L., Beeson, H. D., Wedlich, R. C., Benz, F. J., Bunker, R. L., and Martin, N. B., Fire, Explosion, Compatibility, and Safety Hazards of Hydrazine (RD-WSTF-0002), NASA JSC White Sands Test Facility, Las Cruces NM (1990).
1312. Schmidt, E. W., **Hydrazine and Its Derivatives: Preparation, Properties, Applications**, 2nd ed., Wiley, New York (2001).
1313. Explosive Decomposition of Propylene, *Chem. and Eng. News* **30**, 1239 (1952).
1314. Falk, K. G., The Ignition Temperature of Hydrogen-Oxygen Mixtures, *J. Amer. Chem. Soc.* **28**, 1517-1534 (1906).
1315. Coward, H. F., and Jones, G. W., Limits of Flammability of Gases and Vapors (Bull. 503), Bureau of Mines, Pittsburgh (1952).
1316. Woinsky, S. G., Predicting Flammable-Material Classifications, *Chemical Engineering* **79,** 81-86 (Nov. 27, 1972).
1317. Lewis, B., and von Elbe, G., **Combustion, Flames and Explosions in Gases**, 3rd ed., Academic Press, Orlando, FL (1987).
1318. Nabert, K., and Schön, G., **Sicherheitstechnische Kennzahle brennbarer Gase und Dämpfe** [Safety Characteristics of Flammable Gases and Vapors], 2nd ed., Deutscher Eichverlag, Berlin (1963).
1319. Ordin, P. M., Review of Hydrogen Accidents and Incidents in NASA Operations (NASA-TM-X-71565), NASA Lewis Research Center, Cleveland OH (1974).
1320. Hertzberg, M., The Flammability Limits of Gases, Vapors and Dusts: Theory and Experiment, pp. 3-48 in **Fuel-Air Explosions**, J. H. S. Lee and C. M. Guirao, eds., Univ. Waterloo Press, Waterloo, Canada (1982).
1321. Britton, L. G., **Avoiding Static Ignition Hazards in Chemical Operations**, AIChE (1999).
1322. Drell, I. L., and Belles, F. E., Survey of Hydrogen Combustion Properties (NACA Report 1383), NACA, Washington (1958).
1323. Zabetakis, M. G., and Burgess, D. S., Research on the Hazards Associated with the Production and Handling of Liquid Hydrogen (RI 5707), Bureau of Mines, Pittsburgh (1961).
1324. Schneider, R. L., Fundamentals of Fire and Explosion Hazards Recognition and Control in Fireworks Manufacturing, pp. 346-377 in *Proc. 1st Intl. Symp. on Fireworks*, Minister of Supply and Services Canada, [n.p.] (1992).
1325. Baker, A. R., and Willis, C. H. H., A Preliminary Assessment of the Explosion Hazard from Hydrogen and Other Fuels During Electric Arc Welding (IR/L/IN/82/04), HSE, Buxton, UK (1982).
1326. Blair, M., Dishwasher Explosion Proves Perplexing, *Fire & Arson Investigator* **46**:2, 21-22 (Dec. 1995).
1327. Cook, R., The Dishwasher Exploded, unpublished case history (2001).
1328. Foley, R. T., and Brown, B. F., Corrosion and Corrosion Inhibitors, pp. 113-142 in **Kirk-Othmer Encyclopedia of Chemical Technology**, vol. 7, 3rd ed., Wiley, New York (1979).
1329. Cisneros, L. O., Rogers, W .J., and Mannan, M .S., Adiabatic Calorimetric Decomposition Studies of 50-wt% Hydroxylamine/Water, *J. Hazardous Materials* **82**, 13-24 (2001).
1330. Chemical Explosion in Japan Kills Four, *Chemical & Engineering News*, p. 15 (19 June 2000).
1331. Iwata, Y., Koseki, H., and Hosoya, F., Study on Decomposition of Hydroxylamine/Water Solution, *J. Loss Prevention in the Process Industries* **16**, 41-53 (2003).
1332. Delayed Ignition Devices, *Fire Findings* **8**:4, 4-6 (Fall 2000).
1333. Swab, S. E., **Incendiary Fires**, Robert J. Brady Co., Bowie MD (1983).
1334. EPA/OSHA Joint Chemical Accident Investigation Report. BPS, Inc., West Helena, Arkansas (EPA 550-R-99-003), Environmental Protection Agency, Washington (1999).
1335. Fowkes, F. M., et al., Clay-Catalyzed Decomposition of Insecticides, *Agricultural & Food Chemistry* **8**, 203-210 (1960).
1336. Unstable Insecticide, *Fire J.* **62**, 5-9 (Mar. 1968).
1337. Rosenblum, F., and Spira, P., Evaluation of Hazard from Self-heating of Sulphide Rock, *CIM Bulletin* **88**, 44-49 (April 1995).
1338. Ninteman, D. J., Spontaneous Oxidation and Combustion of Sulfide Ores in Underground Mines (IC 8775), Bureau of Mines, Pittsburgh (1978).
1339. Wu, C., Li, Z. J., and Zhou, B., A Simple Method for Predicting the Spontaneous Combustion Potential of Sulfide Ores at Ambient Temperature, pp. 19-22 in *APSS2001—Proc. Asia Pacific Symp. on Safety*, vol. 1, Japan Soc. for Safety Engineering, Yokohama (2001).
1340. Davie, F. M., Nolan, P. F., and Hoban, T. W. S., Study of Iron Sulfide as a Possible Ignition Source in the Storage of Heated Bitumen, *J. Loss Prevention in the Process Industries* **6**, 139-143 (1993).
1341. Hughes, R. I., Morgan, T. D. B., and Wilson, R. W., The Generation of Pyrophoric Material in the Cargo Tanks of

Crude Oil Carriers, *Trans. Inst. Marine Engineers* **88**, 153-161 (1976).
1342. Walker, R., Steele, A. D., and Morgan, T. D. B., The Formation of Pyrophoric Iron Sulphide from Rust, *Surface and Coatings Technology* **31**, 183-197 (1987).
1343. Walker, R., Steele, A. D., and Morgan, T. D. B., Pyrophoric Oxidation of Iron Sulphide, *Surface and Coatings Technology* **34**, 163-175 (1988).
1344. Walker, R., Steele, A. D., and Morgan, D. T. B., Pyrophoric Nature of Iron Sulfides, *Ind. and Eng. Chem. Res.* **35**, 1747-1752 (1996).
1345. Bowes, P. C., Spontaneous Heating and Ignition in Stored Palm Kernels. V. A Study of the Self-heating of the Palm Kernels and the Jute Bags in the Presence of Moisture, *J. Science Food Agric.* **2**, 79-91 (1951).
1346. Finlow, R. S., Heart Damage in Baled Jute, *Memoirs of the Department of Agriculture in India, Chemistry Series* **5**, 33-68 (1918).
1347. SubbaRao, L. D., Measurement of Vapor Concentrations in Heated Combustible Liquid Storage Tanks (M.S. thesis), Worcester Polytechnic Institute, Worcester MA (1996).
1348. Standard Specification for Kerosine (ASTM D3699), ASTM.
1349. Standard for Unvented Kerosene-Fired Room Heaters and Portable Heaters (UL 647), UL.
1350. Fry, J. F., and Lustig, R. E., Fires Associated with Kerosine-Burning Appliances in Dwellings, June 1960—May 1961 (Fire Research Technical Paper 4), Fire Research Station, Borehamwood (1962).
1351. Lentini, J. J., Vapor Pressures, Flash Points and the Case Against Kerosene Heaters, *Fire & Arson Investigator* **40**:3, 16-18 (March 1990).
1352. Lehman, D., Portable Kerosene Heaters, *Fire Findings* **1**:3, 7-10 (Fall 1993).
1353. Henderson, R. W., and Lightsey, G. R., An Anti-Flareup Device for Barometric Kerosene Heaters, *Fire & Arson Investigator* **45**:2, 8-9 (Dec. 1994).
1354. Mowers Get Hot but Seldom Cause Fires, *Fire Findings* **4**:3, 5 (Summer 1996).
1355. Rossotti, H., **Fire**, Oxford University Press, Oxford (1993).
1356. de Nevers, N., Propane Overfilling Fires, *Fire J.* **81**, 80-82 (Sept./Oct. 1987).
1357. Proposed UL Standards Lead to Important Propane Valve Safety Changes, *Fire Findings* **3**:3, 12-13 (Summer 1995).
1358. Cox, D. E., LP Gas Cylinders, *Fire Findings* **5**:3, 7-10 (Summer 1997).
1359. Liquefied Petroleum Gas Code (NFPA 58), NFPA.
1360. Burgess, D. S., Murphy, J. N., and Zabetakis, M. G., Hazards Associated with the Spillage of Liquefied Natural Gas on Water (RI 7448), Bureau of Mines, Pittsburgh (1970).
1361. Burgess, D. S., and Zabetakis, M. G., Fire and Explosion Hazards Associated with Liquefied Natural Gas (RI 6099), Bureau of Mines, Pittsburgh (1962).
1362. Blackmore, D. R., Eyre, J. A., and Summers, G. G., Dispersion and Combustion Behavior of Gas Clouds Resulting from Large Spillages of LNG and LPG onto the Sea, *Trans. Inst. Marine Engineers* **94**, Paper No. 29 (1982).
1363. Merkley, D. J., Fire Facts Inc., private communication (2003).
1364. Johansson, S. R., On the History of Fire Tools and Matches, pp. 1-104 in *Pyroteknikdagen 1983*, Sektionen för Detonik och Förbränning, Royal Academy of Sciences, Sundbyberg, Sweden (1985).
1365. Finch, C. A., and Ramachandran, S., **Matchmaking: Science, Technology and Manufacture**, Ellis Horwood, Chichester, England (1983).
1366. Latham, D. J., Australian-American Match Tests (Res. Note INT-RN-426), Intermountain Research Station, US Forest Service, Missoula MT (1995).
1367. Mehkeri, K. A., and Dhawan, K. L., An Evaluation of Matches for a Potential Ignition Hazard, *Fire Technology* **18**, 152-161 (1982).
1368. Arditti, R., Gaudry, H., and Laure, Y., Mesure des températures de combustion des pâtes de'allumettes [Determination of the flame temperatures of match heads], *Comptes Rendus Academie Sciences Paris* **226**, 1179-1180 (1948).
1369. Murphy, J. R., and Khanna, R., Match Burn Times (Memorandum to File), Consumer Product Safety Commission, Washington DC (1995).
1370. Sale, P. D., Matches, Fire Hazard Tests, *NFPA Q.* **21**, 331-337 (1928).
1371. Fitz, M. M., MDE Engineers, private communication (1995).
1372. Kershaw, R., Matchbooks in Luggage a Real Danger, *Fire & Arson Investigator* **47**:4, 28 (June 1997).
1373. Bang, W., Hazard Assessment of Afterglow of Matches, Consumer & Corporate Affairs Canada, Ottawa (1989).
1374. Bang, W., Ghosh, R., and Grinshpon, R., Hazard Assessment of Afterglow of Paper Book Matches, Consumer & Corporate Affairs Canada, Ottawa (1991).
1375. Standard Consumer Safety Specification for Lighters (ASTM F 400), ASTM.
1376. Marsel, J., and Kramer, L., Spontaneous Ignition Properties of Metal Alkyls, pp. 906-912 in *7th Symp. (Intl.) on Combustion*, Butterworths, London (1959).
1377. Maudry, W. L., Burleson, D. C., Malpass, D. B., and Watson, S. C., A Simple Method for Gauging the Pyrophoricity of Metal Alkyl Solutions, *J. Fire & Flammability* **6**, 478-487 (1975).
1378. Kuchta, J. M., and Smith, A. F., Classification Test Methods for Flammable Solids (RI 7593), Bureau of Mines, Pittsburgh (1972).
1379. Price, E. W., Combustion of Metallized Propellants, pp. 479-513 in **Progress in Astronautics and Aeronautics**, vol. 90: Fundamentals of Solid-Propellant Combustion, AIAA, New York (1984).
1380. Standard for the Manufacture of Aluminum Powder (NFPA 651), NFPA.
1381. Werley, B. L., et al., A Critical Review of Flammability Data for Aluminum, pp. 300-345 in **Flammability and Sensitivity of Materials in Oxygen-Enriched Atmospheres** (ASTM STP 1197), ASTM (1993).
1382. Grosse, A. von, and Conway, J. B., Combustion of Metals in Oxygen, *Ind. and Eng. Chem.* **50**, 663-672 (1958).
1383. Brzustowski, T. A., and Glassman, I., Vapor-phase Diffusion Flames in the Combustion of Magnesium and Aluminum. II. Experimental Observations in Oxygen Atmospheres, pp. 117-158 in **Heterogeneous Combustion**, Academic Press, New York (1964).
1384. Zhu, Y., and Yuasa, S., Effects of Oxygen Concentration on Combustion of Aluminum in Oxygen/Nitrogen Mixture Streams, *Combustion and Flame* **115**, 327-334 (1998).
1385. Yuasa, S., Zhu, Y., and Sogo, S., Ignition and Combustion of Aluminum in Oxygen/Nitrogen Mixture Streams, *Combustion and Flame* **108**, 361-388 (1997).

1386. Benz, F. J., and Stoltzfus, J. M., Ignition of Metals and Alloys in Gaseous Oxygen by Frictional Heating, pp. 38-58 in **Flammability and Sensitivity of Materials in Oxygen-Enriched Atmospheres**, Second Volume (ASTM STP 910), ASTM (1986).
1387. Liedtke, L. L., and Rhein, R. A., The Combustion of Lithium-Aluminum Alloy, unpublished paper, Naval Weapons Center, China Lake CA (1989).
1388. Friedman, R., and Maček, A., Ignition and Combustion of Aluminium Particles in Hot Ambient Gas, *Combustion and Flame* **6**, 9-19 (1962).
1389. Friedman, R., and Maček, A., Combustion Studies of Single Aluminum Particles, pp. 703-709 in *9th Symp. (Intl.) on Combustion*, The Combustion Institute, Pittsburgh (1963).
1390. Maček, A., Fundamentals of Combustion of Single Aluminum and Beryllium Particles, pp. 203-217 in *11th Symp. (Intl.) on Combustion*, The Combustion Institute, Pittsburgh (1966).
1391. Kuehl, D. K., Ignition and Combustion of Aluminum and Beryllium, *AIAA J.* **3**, 2239-2247 (1965).
1392. Frolov, Yu. V., Pokhil, P. F., and Logachev, V. S., Ignition and Combustion of Powdered Aluminum in High-Temperature Gaseous Media and in a Composition of Heterogeneous Condensed Systems, *Combustion, Explosion, and Shock Waves* **8**, 168-187 (1972).
1393. Merzhanov, A. G., Grigorjev, Yu. M., and Gal'chenko, Yu. A., Aluminium Ignition, *Combustion and Flame* **29**, 1-14 (1977).
1394. Hartmann, I., Nagy, J., and Brown, H.R., Inflammability and Explosibility of Metal Powders (RI 3722), Bureau of Mines, Pittsburgh (1943).
1395. Maranda, A., et al., Some Aspects of Fire and Explosion Hazards in Comminution of Flaked Aluminum Powders, *Archivum Combustionis* **6**, 39-49 (1986).
1396. Rhein, R. A., Preliminary Experiments on Ignition of Metal Powder in Carbon Dioxide, pp. 76-78 in Space Programs Summary No. 37-28, Vol. IV, Jet Propulsion Lab., Pasadena CA (1964).
1397. Rhein, R. A., A Review of Some Reactions of Molecular Nitrogen (Section Report 384-2), Jet Propulsion Lab., Pasadena CA (1964).
1398. Gibson, J. R., and Weber, J. D., Handbook of Selected Properties of Air- and Water-reactive Materials (RDTR 144), US Naval Ammunition Depot, Crane IN (1969).
1399. Nir, E. C., Combustion of Powdered Metals in Contact with a Solid Oxidizer (Ammonium Perchlorate), pp. 1019-1029 in *13th Symp. (Intl.) on Combustion*, The Combustion Institute, Pittsburgh (1970).
1400. Laurendeau, N. M., and Glassman, I., Ignition Temperatures of Metals in Oxygen Atmospheres, *Combustion Science and Technology* **3**, 77-82 (1971).
1401. Maček, A., Friedman, R., and Semple, J. M., Techniques for the Study of Combustion of Beryllium and Aluminum Particles, pp. 3-16 in **Heterogeneous Combustion**, Academic Press, New York (1964).
1402. Rhein, R. A., The Utilization of Powdered Metals as Fuels in the Atmospheres of Venus, Earth, and Mars (Tech. Report 32-1073), Jet Propulsion Lab., Pasadena CA (1967).
1403. Rhein, R. A., The Combustion of Powdered Metals in Nitrogen and Carbon Dioxide, *Pyrodynamics* **4**, 161-166 (1966).
1404. Miron, Y., and Lazzara, Hot-Surface Ignition Temperatures of Dust Layers, *Fire and Materials* **12**, 115-126 (1988).
1405. Hillstrom, W. W., Thresholds for the Initiation of Pyrophoric Sparking, *4th Intl. Pyrotechnics Seminar*, Steamboat Village CO (1974).
1406. Rae, D., The Ignition of Explosive Gas Mixtures by Small Combustible Particles. Part 1. Ignition by Particles of Pyrophor Bar (Research Report 129), Safety in Mines Research Establishment, Sheffield, England (1956).
1407. Ellern, H., **Military and Civilian Pyrotechnics**, Chemical Publishing, New York (1968).
1408. Jakowsky, J. J., and Butzler, E. W., Spontaneous Ignition of Metals in Oxygen under Pressure (RI 2521), Bureau of Mines, Pittsburgh (1923).
1409. Abbud-Madrid, A., Branch, M. C., Feiereisen, T. J., and Daily, J. W., Ignition of Bulk Metals by a Continuous Radiation Source in Pure Oxygen Atmosphere, pp. 211-222 in **Flammability and Sensitivity of Materials in Oxygen-Enriched Atmospheres** (ASTM STP 1197), ASTM (1993).
1410. Kopelman, B., and Compton, V. B., Spontaneous Combustion of Metal Powders, *Metal Progress* **63**, 77-79 (Feb. 1953).
1411. Hertzberg, M., Cashdollar, K. L., Zlochower, I. A., and Green, G. M., Explosives Dust Cloud Combustion, pp. 1837-1843 in *24th Symp. (Intl.) on Combustion*, Combustion Institute, Pittsburgh (1992).
1412. Sato, J., Ohtani, H., and Hirano, T., Ignition Process of a Heated Iron Block in High-Pressure Oxygen Atmosphere, *Combustion and Flame* **100**, 376-383 (1995).
1413. Jakowsky, J. J., and Butzler, E. W., Oxygen-Oil Explosions (Serial 2521), Bureau of Mines, Pittsburgh (1923).
1414. Reynolds, W. C., Investigation of Ignition Temperatures of Solid Metals (Tech. Note D-182), NASA, Washington (1966).
1415. Schutt, H. U., Knapp, R. H., and Schmeal, W. R., Ignition of Some Common Engineering Alloys – The Critical Energy Concept and Effects of Oxygen Pressure, Preprint 14 in *Corrosion 76*, National Association of Corrosion Engineers, Houston TX (1976).
1416. Bailey, B. W., Iron Fire in a Heat Recovery Unit, *24th Loss Prevention Symp.*, AIChE (1990).
1417. Kingman, F. E., and Coleman, E. H., Ignition of Steel Wool, *FPA J.* No. 21, 53-54 (1953).
1418. Karim, G. A., and Mehta, S. A., An Investigation of the Ignition and Combustion of Loosely Compacted Commercial Steel Wool, *J. Fire Sciences* **5**, 272-285 (1987).
1419. Evans, J. D., Borland, W., and Mardon, P. G., Pyrophoricity of Fine Metal Powders, *Powder Metallurgy* **19**, 17-21 (1976).
1420. Ganguly, A., and Bandyopadhyay, A., Self-ignition Tendency—A Hazard for Sponge Iron Producer and User, *Tool and Alloy Steels* **22**:1, 19-26 (1988).
1421. Alabi, A. F., The Mechanism of Auto-Ignition of Direct Reduced Iron (DRI), Ph.D. dissertation, Univ. Pittsburgh (1988).
1422. Sraku-Lartey, K., Parker, R. H., and Hawkins, R. J., Oxidation of Sponge Iron Particles and Pellets Produced by Reduction of Hematite in Hydrogen, *Ironmaking & Steelmaking* **11**:1, 23-33 (1984).
1423. Hunter, R., Handling and Shipping of DRI/HBI, Midrex Technologies, Inc., unpublished paper.
1424. Spice, J. E., and Staveley, L. A. K., The Propagation of Exothermic Reactions in Solid Systems, *J. Soc. Chemical Industry* **68**, 313-319; 349-355 (1949).

1425. Rhein, R. A., Lithium Combustion: A Review (NWC TP 7087), Naval Weapons Center, China Lake CA (1990).
1426. Mellor, A. M., and Glassman, I., A Physical Criterion for Metal Ignition, *Pyrodynamics* **3**, 43-64 (1965).
1427. Peloubet, J. A., Machining Magnesium—A Study of Ignition Factors, *Fire Technology* **1**, 5-14 (1965).
1428. Shoshin, Y. L., Mudryy, R. S., and Dreizin, E. L., Preparation and Characterization of Energetic Al-Mg Mechanical Alloy Powders, *Combustion and Flame* **128**, 259-269 (2002).
1429. Cassel, H. M., and Liebman, I., The Cooperative Mechanism in the Ignition of Dust Dispersions, *Combustion and Flame* **3**, 467-475 (1959).
1430. Margerson, S. N. A., Robinson, H., and Wilkins, H. A., The Ignition Hazard from Sparks from Magnesium-base Alloys (Research Report 75), Safety in Mines Research Establishment, Sheffield, England (1953).
1431. Liebman, I., Corry, J., and Perlee, H. E., Ignition and Incendivity of Laser Irradiated Single Micron-size Magnesium Particles, *Combustion Science and Technology* **5**, 21-30 (1972).
1432. Standard for the Storage, Handling, and Processing of Magnesium Solids and Powders (NFPA 480), NFPA.
1433. Jacobson, M., Cooper, A. R., and Nagy, J., Explosibility of Metal Powders (RI 6516), Bureau of Mines, Pittsburgh (1964).
1434. Raney, M., US Patent 1,628,190 (1927).
1435. Lee, W. B., Cryogenic Ignition of Hydrogen and Oxygen with Raney Nickel, *Ind. and Eng. Chem.—Product Res. Dev.* **6**, 59-64 (1967).
1436. Hardt, A. P., **Pyrotechnics**, Pyrotechnica Publications, Post Falls ID (2001).
1437. Kotoyori, T., and Ando, T., Explosion Reaction of Rare Earth Elements with a Halogen-Containing Solvent, *Specific Report of the Research Institute of Industrial Safety* No. 12, 15-21 (1993).
1438. Matsuda, T., Dust Explosion Hazards of New Magnetic Materials, *Specific Report of the Research Institute of Industrial Safety* No. 12, 39-48 (1993).
1439. Richard, J. R., Delbourgo, R., and Laffitte, P., Spontaneous Ignition and Combustion of Sodium Droplets in Various Oxidizing Atmospheres at Atmospheric Pressure, pp. 39-48 in *12th Symp. (Intl.) on Combustion*, The Combustion Institute, Pittsburgh (1968).
1440. Yuasa, S., Spontaneous Ignition of Sodium in Dry and Moist Air Streams, pp. 1869-1876 in *20th Symp. (Intl.) on Combustion*, The Combustion Institute, Pittsburgh (1984).
1441. Akita, K., and Yamashika, S., Ignition of a Sodium Piece in Air, *Report of Fire Research Institute of Japan*, No. 24, 38-43 (Mar. 1964).
1442. Saito, N., Liao, C., and Tsuruda, T., Ignition and Extinguishment of Sodium Fires in Air Diluted by Nitrogen, pp. 285-294 in *Fire Science and Technology—Proc. 5th Asia-Oceania Symp.*, Univ. Newcastle, Australia (2001).
1443. Markowitz, M. M., Alkali Metal-Water Reactions, *J. Chem. Educ.* **40**, 633-636 (1963).
1444. Matsuda, T., and Yamaguma, M., Tantalum Dust Deflagration in a Bag Filter Dust-Collecting Device, *J. Hazardous Materials* **A77**, 33-42 (2000).
1445. White, E. L., and Ward, J. J., Ignition of Metals in Oxygen (DMIC Report 224), Battelle Memorial Institute, Columbus OH (1966).
1446. Markstein, G., Combustion of Metals, *AIAA J.* **1**, 550-562 (1963).
1447. Rhein, R. A., and Baldwin, J. C. Literature Review on Titanium Combustion and Extinction (NWC TP 6167 rev.1), Naval Weapons Center, China Lake CA (1984).
1448. Prine, B. A., Analysis of Titanium/Carbon Steel Heat Exchanger Fire, *25th Loss Prevention Symp.*, AIChE (1991).
1449. Strobridge, T. R., Moulder, J. C., and Clark, A. F., Titanium Combustion in Turbine Engines (FAA-RD-79-51; NBSIR 79-1616), Federal Aviation Administration, Washington (1979).
1450. Solbrig, C. W., Heat Release Rate from the Combustion of Uranium, pp. 963-974 in **Transport Phenomena in Combustion**, vol. 2, S. H. Chen, ed., Taylor & Francis, Washington (1996).
1451. Smith, R. B., Pyrophoricity—A Technical Mystery Under Vigorous Attack, *Nucleonics* **14**, 23-33 (1956).
1452. Tetenbaum, M., Mishler, L., and Schnizlein, G., Uranium Powder Ignition Studies, *Nuclear Science & Engineering* **14**, 230-238 (1962).
1453. Smith, W., Spontaneous Combustion, *J. Royal Soc. of Arts* **67**, 500-507 (1919).
1454. Beal, J. L., Brown, W. R., and Vassallo, F. A., Oxidation and Explosion of Drops of Molten Zirconium Metal, *Pyrodynamics* **3**, 135-160 (1965).
1455. Brown, H. R., How to Control Spontaneous Ignition of Pyrophoric Materials, *Safety Maintenance* **116**, 46, 49-52 (Sep. 1958).
1456. Matsuda, T., Yashima, M., Nifuku, M., and Enomoto, H., Some Aspects in Testing and Assessment of Metal Dust Explosions, pp. 92-97 in *Proc. 3rd Intl. Symp. on Hazards, Prevention, and Mitigation of Industrial Explosions*, Tsukuba, Japan (2000).
1457. Schnitzlein, J. G., Ignition Behavior and Kinetics of Oxidation for Reactor Metals U, Zr, Pu, Th, and Binary Alloys of Each (ANL-5974), Argonne National Laboratory, Lemont IL (1959).
1458. Anderson, H. C., and Belz, L H., Factors Controlling the Combustion of Zirconium Powders, *J. Electrochemical Soc.* **100**, 240-249 (1953).
1459. Dahn, C. J., Explosivity and Pyrophoricity of Metal Powders, pp. 194-200 in **Metals Handbook**, 9th ed., Vol. 7, American Society for Metals, Metals Park OH (1978).
1460. Robinson, C., and Smith, D. B., The Auto-Ignition Temperature of Methane, *J. Hazardous Materials* **8**, 199-203 (1984).
1461. Cashdollar, K. L, Zlochower, I. A., Green, G. M., Thomas, R. A., and Hertzberg, M., Flammability of Methane, Propane, and Hydrogen Gases, *J. Loss Prevention in the Process Industries* **13**, 327-340 (2000).
1462. Coward, H. F., and Ramsay, H. T., Ignition of Firedamp by Means Other Than Electricity and Explosives: A Review (Research Report 231), Safety in Mines Research Establishment, Sheffield, England (1965).
1463. Hanna, N. E., Zabetakis, M. G., Van Dolah, R. W., and Damon, G. H., Potential Ignition Hazards Associated with Compressed-Air Blasting Using a Compressor Underground (RI 5223), Bureau of Mines, Pittsburgh (1956).
1464. Vanderstraeten, B., Tuerlinkckx, D., Berghmans, J., Vliegen, S., Van't Oost, E., and Smit, B., Flammability Limits of Methane/Air Mixtures at Elevated Pressure and Temperature, *J. Hazardous Materials* **56**, 237-246 (1997).

1465. Caron, M., Goethals, M., De Smedt, G., Berghmans, J., Vliegen, S., Van't Oost, E., and van den Aarssen, A., Pressure Dependence of the Auto-ignition Temperature of Methane/Air Mixtures, *J. Hazardous Materials* **65**, 233-244 (1999).
1466. Melvin, A., Spontaneous Ignition of Methane-Air Mixtures at High Pressure: I. The Ignition Delay Preceding Explosion, *Combustion and Flame* **10**, 120-128 (1966).
1467. Coward, H. F., and Wheeler, R. V., The Ignition of Firedamp (Paper 53), Safety in Mines Research Board, London (1929).
1468. Jones, G. W., The Flammability of Refrigerants: Mixtures of Methyl and Ethyl Chlorides and Bromides, *Ind. and Eng. Chem.* **20**, 367-370 (1928).
1469. Hill, H. W., Methyl Bromide-Air Explosion, *Chem. Eng. Prog.* **58**:8, 46-49 (Aug. 1962).
1470. Coffee, R. D., Vogel, P. C., and Wheeler, J. J., Flammability Characteristics of Methylene Chloride (Dichloromethane), *J. Chem. and Eng. Data* **17**, 89-93 (1972).
1471. Kuchta, J. M., Furno, A. L., Bartkowiak, A., and Martindill, G. H., Effect of Pressure and Temperature on Flammability Limits of Chlorinated Hydrocarbons in Oxygen-Nitrogen and Nitrogen Tetroxide-Nitrogen Atmospheres, *J. Chem. and Eng. Data* **13**, 421-428 (1968).
1472. Miyazaki, N., Ignition of Food Heated by Microwave Oven, *Report of Fire Science Laboratories, Kobe City Fire Dept.* No. 8, 25-28 (1994).
1473. Sloan, P. A., Beware: Unattended Microwave Ovens Can Be Dangerous, *Fire & Arson Investigator* **51**:4, 19 (July 2001).
1474. Spokoinyi, F. E., and Eidukyavicius, K. K., Mechanism of Spontaneous Ignition during Storage of Mineral Wool Objects, *Combustion, Explosion and Shock Waves* **24**, 649-651 (1988).
1475. Ahrens, M., U.S. Vehicle Fire Trends and Patterns, NFPA (2001).
1476. Hrynchuk, R. J., CAFI Vehicle Fire Investigation Techniques, Toronto, Ont. (1998).
1477. Warner, C. Y., James, M. B., and Woolley, R. L., A Perspective on Automobile Crash Fires, *SAE Trans.* **93**, 1.530-1.543 (1985).
1478. Cole, L. S., Vehicle Fires—Differences between the UK and US, *The Vehicle Fire Reporter* **10**, 1, 4-8 (Winter 1999).
1479. Cole, L. S., **A Survey of Vehicle Fire Causes**, Lee Books, [n.p.] (1988).
1480. Cole, L. S., **Investigation of Motor Vehicle Fires**, 3rd ed., Lee Books, Novato CA (1992).
1481. Catalytic Converter Investigation—Task Force Report, California State Fire Marshal, Sacramento CA (1976).
1482. Radwan, E. E., Al-Deek, H., Garib, A. M., and Ishak, S. S., Motor Vehicle Fires—Trends and Characteristics, Univ. Central Florida, published by AAA Foundation for Traffic Safety, Washington (1993).
1483. Tessmer, J., An Analysis of Fires in Passenger Cars, Light Trucks, and Vans (DOT HS 808 208), National Highway Traffic Safety Administration, Washington (1994).
1484. Griffin, L. I., III, An Assessment of the Reliability and Validity of the Information on Vehicle Fires Contained in the Fatal Accident Reporting System (FARS), Texas Transportation Institute, Texas A&M University, College Station (1997).
1485. Malliaris, A. C., Impact-Induced Car Fires—A Comprehensive Investigation, *Accident Analysis and Prevention* **23**, 257-273 (1991).
1486. Hrynchuk, R. J., A Study of Automobile Fires, *Can. Soc. Forensic Sci. J.* **11**, 15-21 (1978).
1487. Fitz, M. M., MDE Engineers, private communication (2002).
1488. Gholson, G., Fire Apparatus Ember Protection Guidelines, *Firehouse* 44-45 (Sept. 2002).
1489. Standard for Automotive Fire Apparatus (NFPA 1901), NFPA.
1490. Scheibe, R. R., Shields, L. E., and Angelos, T. E., Field Investigation of Motor Vehicle Collision Fires, *SAE Trans.* **108**, 119-135 (1999).
1491. Steilen, K., Analysis of Motor Vehicle Fuel Tank-Related Fires (EPA-AA-SDSB-8805), Standards Development and Support Branch, Environmental Protection Agency, Ann Arbor MI (1988).
1492. Murray, C. J., The Real Story Behind Car Fires: Overdesign Prevents Cars from Exploding, *Design News* **49**:19, 114-120 (4 Oct. 1993).
1493. Mangs, J., and Keski-Rahkonen, O., Characterization of the Fire Behaviour of a Burning Passenger Car. Part I: Car Fire Experiments, *Fire Safety J.* **23**, 17-35 (1994).
1494. Shipp, M., and Spearpoint, M., Measurements of the Severity of Fires Involving Private Motor Vehicles, *Fire and Materials* **19**, 143-151 (1995).
1495. Ward, B., Fire Dynamics 1994-1995, Manitoba Public Insurance, Winnipeg, Manitoba (1995).
1496. Cleary, T. G., and Gann, R. G., Effect of Fuel Tank Rupture Mode of the Ignitability of Expelled Fuel, NIST (1993).
1497. Courtney, N., Fumes Ignite in Garage: Kentucky, December 1985, *Fire J.* **80**:6, 12 (Nov. 1986).
1498. Fitz, M. M., MDE Engineers, private communication (2002).
1499. Joyeux, D. Natural Fires in Closed Car Parks: Car Fire Tests (INC-96/294d-DJ/NB), Centre Technique Industriel de la Construction Métallique (CTICM), Maizières-lès-Metz, France (1997).
1500. Hirschler, M. M., Fire Hazard of Automotive Interiors, pp. 164-195 in *Proc. Fire Risk & Fire Hazard Assessment Research Application Symp.*, National Fire Protection Research Foundation, Quincy MA (1998).
1501. Catalytic Converter Retrofit Program—Used Vehicles Retrofitted with Universal Oil Products Catalytic Converters, Air Resources Board, El Monte CA (1975).
1502. Harrison, R. T., Catalytic Converter Temperature Tests (SAE 760781), Society of Automotive Engineers, Warrendale PA (1976).
1503. Knight, I. K., and Hutchings, P. T., Ignition of Bushfires by Hot Exhaust Surfaces (DFR User Series No. 12), Forest Research, CSIRO, Canberra, Australia (1987).
1504. Catalytic Converter Temperature Study—Field Test of Exhaust System Temperatures of 200 Catalyst and Non-catalyst Vehicles, Project M298, California Air Resources Board, Sacramento (1975).
1505. Hoffman, J. M., Hoffman, D. J., and Kroll, M. J., Letter to the Editor, *Fire & Arson Investigator* **47**:3, 4 (Mar. 1997).
1506. Hrynchuk, R. J., ed., A Study of Vehicle Fires of Known Ignition Source, Alberta Chapter, Intl. Assn. of Arson Investigators, Edmonton, Alberta (1983).
1507. Bertagna, P. J., Catalytic Converter Caused Fires, pp. 135-141 in Industrial Operations Fire Prevention Field Guide, Office of State Fire Marshal, Dept. of Forestry and Fire Protection, Sacramento CA (1999).

1508. Fitz, M. M., MDE Engineers, private communication (2002).
1509. Hollins, L. T., Air Bag Inflator Explosions, *Fire Engineering* **149**, 33-35 (Dec. 1996).
1510. Road Vehicles—Airbag Components—Part 3: Testing of Inflator Assemblies (ISO CD 12097-3), International Organization for Standardization, Geneva.
1511. Elias, N. N., Ignition of High Speed Hydrocarbon Leaks from Car Air-Conditioning Systems (B.Eng. thesis), Univ. New South Wales, Sydney, Australia (1996).
1512. Sloan, P. A., Beware: LPG in Motor Vehicle Air Conditioning Systems Can Be Lethal, *Fire & Arson Investigator* **51**:2, 13 (Jan. 2002).
1513. Maclaine-cross, I. L. and Leonardi, E., Hydrocarbon Refrigerant Risk in Car Air-Conditioners, *1995 Intl. CFC and Halon Alternatives Conf.*, Washington (1995).
1514. Kilgore, W. R., Neon Signs as a Fire Cause, *Fire & Arson Investigator* **45**:2, 23-25 (Dec. 1994).
1515. Archbutt, L., Note on the Ignition of Sawdust by Nitric Acid, *J. Soc. Chemical Industry* **15**, 84-85 (1896).
1516. Van Dolah, R. W., Detonation Potential of Nitric Acid Systems, *3rd Loss Prevention Symp.*, AIChE (1969).
1517. Stark, G. W. V., and Mulliner, W., The Fire Properties of Fats (FR Note 610), Fire Research Station, Borehamwood, UK (1965).
1518. Kuchta, J. M., and Cato, R. J., Ignition and Flammability Properties of Lubricants, *SAE Trans.* **77**, 1008-1020 (1968).
1519. Water-mist Fire-Suppression Systems Offer Excellent Protection for Commercial Cooking Areas, *Construction Innovation* (Natl. Res. Council of Canada) **4**:3, 1; 11 (Spring/Summer 1999).
1520. Koseki, H., Natsume, Y., and Iwata, Y., Combustion of High Flash Point Materials, pp. 339-349 in *Proc. Fire and Materials 2001 Conf.*, Interscience Communications Ltd., London (2001).
1521. Dixon, B. M., The Potential for Self Heating of Deep Fried Food Products, poster presented at FBI Workshop of Fire Investigation, Fairfax VA (1995).
1522. Bowes, P. C., and Langford, B., Spontaneous Ignition of Oil-soaked Lagging, *Chemical & Process Engineering (London)* **49**, 108-116 (1968).
1523. Hutchinson, G. H., Some Recent Advances in the Chemistry and Technology of Drying Oils, *J. Oil & Colour Chemists' Assn.* **41**, 474-492 (1958).
1524. Lazzari, M., and Chiantore, O., Drying and Oxidative Degradation of Linseed Oil, *Polymer Degradation and Stability* **65**, 303-313 (1999).
1525. Wicks, Z. W. jr., Jones, F. N., and Pappas, S. P., **Organic Coatings: Science and Technology**, 2 vols., Wiley, New York (1992-1994).
1526. **Bailey's Industrial Oil and Fat Products**, 5th ed., vol. 5, Y. H. Hui, ed., Wiley, New York (1996).
1527. Hutchinson, G. H., Some Aspects of Drying Oils Technology, *J. Oil & Colour Chemists' Assn.* **56**, 44-53 (1973).
1528. Sastry, G. M., Studies on Derivatives of Hydroxy Unsaturated Oils (Ph.D. dissertation), North Dakota State Univ., Fargo (1966).
1529. Abraham, C. J., Howitt, D. G., Rosen, M., and Tanyzer, H., Linseed Oil: A Hazardous but Necessary Ingredient? Presented at *Recent Advances in Flame Retardancy of Polymeric Materials, 5th Annual BCC Conf. on Flame Retardancy*, Business Communications Co., Norwalk CT (1994).
1530. Smith, W. H., Iodine Number of Linseed and Petroleum Oils (Tech. Paper No. 37), [U.S.] Bur. Stand., Washington (1914).
1531. Thompson, N. J., The Spontaneous Heating of Oils, *Oil & Fat Industries* ***5***, 317-326 (1928).
1532. Kasprzycka-Guttman, T., Jarosz-Jarszewska, M., and Litwinienko, G., Specific Heats and Kinetic Parameters of Thermo-oxidative Decomposition of Peanut Oil, *Thermochimica Acta* **250**, 197-205 (1995).
1533. Litwinienko, G., Kasprzycka-Guttman, T., and Jarosz-Jarszewska, M., Dynamic and Isothermal DSC Investigation of the Kinetics of Thermooxidative Decomposition of Some Edible Oils, *J. Thermal Analysis* **45**, 741-750 (1995).
1534. Litwinienko, G., and Kasprzycka-Guttman, T., A DSC Study on Thermoxidation Kinetics of Mustard Oil, *Thermochimica Acta* **319**, 185-191 (1998).
1535. Kasprzycka-Guttman, T., and Odzeniak, D., Isothermal DSC Investigation of the Kinetics of Thermooxidative Decomposition of Some Edible Oils, *J. Thermal Analysis* **39**, 217-220 (1993).
1536. Litwinienko, G., and Kasprzycka-Guttman, T., Study on Autoxidation Kinetics of Fats by Differential Scanning Calorimetry. 2. Unsaturated Fatty Acids and Their Esters, *Ind. and Eng. Chem. Res.* **39**, 13-17 (2000).
1537. Litwinienko, G., Autooxidation of Unsaturated Fatty Acids and Their Esters, *J. Thermal Analysis and Calorimetry* **65**, 639-646 (2001).
1538. Morrell, R. S., and Wood, H. R., **The Chemistry of Drying Oils**, Van Nostrand, New York (1925).
1539. Wijs, J. J. A., The Reactions in Hübl's Method of Iodine Absorption, *J. Soc. Chemical Industry* **17**, 698 (1898).
1540. Hyland, J., and Lloyd, L. L., The Oxidation of Oils and of Fatty Acids, *J. Soc. Chemical Industry* **34**, 62-65 (1915).
1541. Lewkowitsch, J., **Chemical Technology and Analysis of Fats, Oils, and Waxes**, 3 vols., 6th ed., G. H. Warburton, ed., Macmillan, London (1921-23).
1542. Lewis, R J. sr., **Hawley's Condensed Chemical Dictionary**, 14th ed., Wiley, New York (2001).
1543. Schildhauer, P., Selbstentzündung ungesättigter Pflanzenöle auf saugfähigen Trägerstoffen [Autoigition of unsaturated vegetable oils on absorbent slow-acting materials] (Ph.D. dissertation, Bergische Universität Gesamthochschule Wuppertal), VDS Schadenverhütung Verlag, Köln (2001).
1544. Modak, A. T., Ignitability of High-Fire-Point Liquid Spills (EPRI NP-1731), Electric Power Research Inst., Palo Alto, CA (1981).
1545. Frank, C. E., Blackham, A. U., and Swarts, D. E., Investigation of Spontaneous Ignition Temperatures of Organic Compounds With Particular Emphasis on Lubricants (NACA TN 2848), National Advisory Committee for Aeronautics, Washington (1952).
1546. Moghtaderi, B., Pope, D. M., Dlugogorski, B. Z., and Kennedy, E. M., Piloted Ignition of Oil-in-Water Emulsions, *Chemeca '98—26th Australian and New Zealand Chemical Engineering Conf.* (1998).
1547. Calcium Permanganate, *Fire Prevention* No. 145, 47-48 (1981).
1548. Rhein, R. A., Ignition of Metals with ClF3 and ClF5 for Use as Spacecraft Chemical Heaters, *J. Spacecraft and Rockets*, **6**, 1328-1329 (1969).
1549. Statesir, W. A., Explosive Reactivity of Organics and Chlorine, *7th Loss Prevention Symp.*, AIChE (1972).

1550. Standard Test Methods of Sampling and Chemical Analysis of Chlorine-Containing Bleaches (ASTM D 2022), ASTM.
1551. King, P. V., Sr., and Lasseigne, A. H., Hazard Classification of Oxidizing Materials and Flammable Solids for Transportation: Evaluation of Test Methods (TES-20-72-6). Dept. of Transportation, Washington (1972).
1552. Cardillo, P., and Nebuloni, M., Reactivity and Thermal Stability of Calcium Hypochlorite, *La Rivista dei Combustibili* **48**, 300-305 (1994).
1553. Clancey, V. J., Calcium Hypochlorite—A Fire and Explosion Hazard, pp. 11-23 in *Hazards from Pressure: Exothermic Reactions, Unstable Substances, Pressure Relief, and Accidental Discharge* (IChemE Symp. Series No. 102), The Institution of Chemical Engineers, Rugby, England; and Pergamon Press, Elmsford NY (1987).
1554. Armstrong, B. S., Fire in Auckland, New Zealand, *Loss Prevention Bulletin* No. 84, 23-31 (1988).
1555. DeHaan, J. D., private communication (2002).
1556. Kirkbride, K. P., and Kobus, H. J., The Explosive Reaction between Swimming Pool Chlorine and Brake Fluid, *J. Forensic Sciences* **36**, 902-907 (1991).
1557. Nugent, D. P., Sheppard, D., and Steppan, D. R., National Oxidizing Pool Chemicals Storage Fire Test Project, National Fire Protection Research Foundation, Quincy MA (1998).
1558. Clancey, V. J., Fire Hazards of Calcium Hypochlorite, *J. Hazardous Materials* **1**, 83-94 (1975/76).
1559. Sub-Committee Doc. DSC 5/3/6, Sub-Committee on Dangerous Goods, Solid Cargoes and Containers, Intl. Maritime Organization, London (1999).
1560. Report to the Maritime Safety Committee, Sub-Committee Doc. DSC 5/13, Sub-Committee on Dangerous Goods, Solid Cargoes and Containers, Intl. Maritime Organization, London (2000).
1561. Sub-Committee Doc. DSC 5/3/30, Sub-Committee on Dangerous Goods, Solid Cargoes and Containers, Intl. Maritime Organization, London (1999).
1562. Sub-Committee Doc. DSC 5/3/31, Sub-Committee on Dangerous Goods, Solid Cargoes and Containers, Intl. Maritime Organization, London (1999).
1563. Sub-Committee Doc. DSC 5/3/10, Sub-Committee on Dangerous Goods, Solid Cargoes and Containers, Intl. Maritime Organization, London (1999).
1564. Uehara, Y., Uematsu, H., and Saito, Y., Thermal Ignition of Calcium Hypochlorite, *Combustion and Flame* **32**, 85-94 (1978).
1565. Cane, R. F., Calcium Hypochlorite—A Potentially Hazardous Product, *Chemistry in Australia* **45**, 313-314 (1978).
1566. Gray, B. F., Holleyhead, R., and Halliburton, B., A Study of the Thermal Properties of Hydrated Calcium Hypochlorite (UN 2880), Annex to Sub-Committee Doc. DSC 5/3/6, Sub-Committee on Dangerous Goods, Solid Cargoes and Containers, Intl. Maritime Organization, London (1999).
1567. Mandell, H. C. jr., A New Calcium Hypochlorite and a Discriminatory Test, *Fire Technology* **7**, 157-161 (1971).
1568. Gray, B. F., and Halliburton, B., The Thermal Decomposition of Hydrated Calcium Hypochlorite (UN 2880), *Fire Safety J.* **35**, 223-239 (2000).
1569. Bibby, D. M., and Milestone, N. B., The Decomposition of High Grade Bleaching Powder, *J. Chem. Tech. and Biotech.* **34A**, 423-430 (1984).
1570. Halliburton, B. W., Investigation of Spontaneous Combustion Phenomenology of Bagasse and Calcium Hypochlorite (Ph.D. dissertation), Macquarie Univ., Sydney, Australia (2002).
1571. Annex to Sub-Committee Doc. DSC 5/INF.6, Sub-Committee on Dangerous Goods, Solid Cargoes and Containers, Intl. Maritime Organization, London (1999).
1572. Mixing Pool Chemicals, *NFPA J.* **94**, 8 (Mar./Apr. 2000).
1573. Schechter, W. H., et al., Chlorate Candles as a Source of Oxygen, *Ind. and Eng. Chem.* **42**, 2348-2358 (1950).
1574. Federal Aviation Administration Docket No.29318, Notice No. 98-12, Prohibition on the Transportation of Devices Designed as Chemical Oxygen Generators as Cargo in Aircraft, Federal Aviation Administration, Washington (21 Aug. 1998).
1575. Alvares, N. J., and White, J. A. jr., Oxygen Accelerated Fires in Passenger Aircraft Cargo Compartments, pp. 721-731 in *Fire & Explosion Hazards—Proc. 3rd Intl. Symp.*, Univ. Central Lancashire, Preston, England (2000).
1576. Shafirovich, E., et al., Mechanism of Combustion in Low-Exothermic Mixtures of Sodium Chlorate and Metal Fuel, *Combustion and Flame* **128**, 133-144 (2002).
1577. O'Connor, T. R., and Hagen, E. L., Activation of Oxygen Generators in Proximity to Combustible Materials (DOT/FAA/AR-TN99/9), Federal Aviation Administration, Atlantic City NJ (1999).
1578. Guide on Fire Hazards in Oxygen-Enriched Atmospheres (NFPA 53), NFPA.
1579. Gayle, J. B., Explosions Involving Liquid Oxygen and Asphalt, *Fire J.* **67**, 12-13 (May 1973).
1580. Hauser, R. L., and Rumpel, W. F., Reactions of Organic Materials with Liquid Oxygen, *Advances in Cryogenic Engineering* **8**, 242-250 (1962).
1581. Hough, R., Lasseigne, A. H., and Pankow, J., Hazard Classification of Flammable and Oxidizing Materials for Transportation: Evaluation of Test Methods. Phase 2 (TES-20-73-1), Dept. of Transportation, Washington (1973).
1582. Bauer, H., Wegener, W., and Windgassen, K. F., Fire Tests on Centrifugal Pumps for Liquid Oxygen, *Cryogenics* **10**:3, 241-248 (June 1970).
1583. Gusky, F. J., Oxygen Regulator Myths, pp. 359-367 in **Flammability and Sensitivity of Materials in Oxygen-Enriched Atmospheres** (ASTM STP 986), ASTM (1988).
1584. Newton, B. E., Langford, R, K., and Meyer, G. R., Promoted Ignition of Oxygen Regulators, pp. 241-266 in **Flammability and Sensitivity of Materials in Oxygen-Enriched Atmospheres: Fourth Volume** (ASTM STP 1040), ASTM (1989).
1585. Clark, A. F., and Hust, J. G., A Review of Compatibility of Structural Materials with Oxygen, *AIAA J.* **12**, 441-454 (1974).
1586. Emergency Medical Technician Receives Serious Burns from an Oxygen Regulator Flash—South Carolina, *NIOSH Injury in the Line of Duty*…98/F-25 (13 Sep. 1999).
1587. Oxygen Regulator Flash Severely Burns One Fire Fighter—Florida, *NIOSH Injury in the Line of Duty*…98/F-23 (5 Feb. 1999).
1588. Aluminum Regulator Fire Injures One Fire Fighter—Nevada, *NIOSH Injury in the Line of Duty*…99/F-07 (6 Jan. 2000).
1589. FDA and NIOSH Public Health Advisory: Explosions and Fires in Aluminum Oxygen Regulators, US Food and Drug Administration, Rockville MD (Feb. 1999).
1590. Standard Test Method for Evaluating the Ignition Sensitivity and Fault Tolerance of Oxygen Regulators Used for Medical

and Emergency Applications (ASTM PS 127), ASTM (2000).
1591. Dreisbach, J., Flammability Characteristic of Painted Concrete Blocks (NIST GCR 02-832), NIST (2002).
1592. Moore, F. C., **Fires: Their Causes, Prevention and Extinction**, The Continental Insurance Co. of New York, New York (1877).
1593. Wheeler, G. K., Canty, W. H., and Myers, R. R., Drier Catalyst Activity of 1,10-phenanthroline in Organic Coatings, *Ind. and Eng. Chem. Product Res. Develop.* **1**, 52-56 (1962).
1594. Howitt, D. G., Zhang, E., and Sanders, B. R., The Spontaneous Combustion of Linseed Oil, pp. 34-38 in *Proc. 20th Intl. Conf. on Fire Safety*, Product Safety Corp., Sunnyvale, CA (1995).
1595. Binswanger, J., Spontaneous Combustion of Colors, Dry and Mixed with Oils, pp. 292-293 in Circular 184, Paint Manufacturers Assn. of the U.S. (1923).
1596. De Faveri, D. M., Zonato, C., Pagella, C., Vidili, A., and Ferraiolo, G., Runaway Reaction and Safety Measures in Organic Processes, pp. 155-175 in *Intl. Symp. on Runaway Reactions*, AIChE (1989).
1597. Nelson, M., Detection and Extinction of Fire and Smouldering in Bulk Powder, pp. 64-139 in British Materials Handling Board, CREDIT Project Report, EV5V-CT92-0082 (1992).
1598. Gibson, N., Harper, H. J., and Rogers, R. L., Evaluation of the Fire and Explosion Risk in Drying Powders, *Plant/Operations Progress* **4**, 181-189 (1985).
1599. Spontaneous Ignition of Zinc-rich Coatings, *Fire J.* **64**, 63-64 (July 1970).
1600. Usami, A., The Danger of Combustion when Mixing Polyester Resin Paint with a Hardener, *Annual Report of the Fire Research Laboratory, Nagoya City Fire Dept.* **29**, 44-47 (2000).
1601. Waste Reduction Guide—Wood Furniture Industries, Tennessee Valley Authority, [n.p.], (1994?).
1602. Anderson, D., Tests Confirm Fire Cause in Spray Booths, *Western Fire J.* **30**, 19-20 (Dec. 1978).
1603. Spontaneous Ignition of Paint Dust, *BRE News of Fire Research* 1 (May 1984).
1604. Eckhoff, R. K., Pedersen, G. H., and Arvidsson, T., Ignitability and Explosibility of Polyester/Epoxy Resins for Electrostatic Powder Coating, *J. Hazardous Materials* **19**, 1-16 (1988).
1605. Pidoll, U. von, and Krämer, H., Flammability Characteristics of Sprays of Water-based Paints, *Fire Safety J.* **29**, 27-39 (1997).
1606. Lundquist, S., Fredholm, O., and Lövstrand, K. G., Dangerous Electrostatic Charging during Airless Spray Painting, pp. 260-269 in *Proc. 3rd Conf. on Static Electrification* (Conf. Series No. 11), The Institute of Physics, London (1971).
1607. Kingman, F. E. T., Coleman, E. H., and Rogowski, Z. W., The Ignition of Flammable Gases from Sparks from Aluminium, Paint, and Rusty Steel, *J. Applied Chemistry (London)* **2**, 449-455 (1952).
1608. Standard for Spray Application Using Flammable or Combustible Materials (NFPA 33), NFPA.
1609. Smith, W. K., and King, J. B., Surface Temperatures of Materials during Radiant Heating to Ignition, *J. Fire & Flammability* **1**, 272-288 (1970). Also: Smith, W. K., and Schilberg, L. E., Surface Temperature History of Materials during Radiant Heating to Ignition (Tech. Note 40604-9), Naval Weapons Center, China Lake CA (1969).
1610. Gross, D., Ignition Temperature Tests of Combustible Material—Asphalt Treated Weatherproof Paper (NBS 1498), NBS (1952).
1611. Hshieh, F. Y., and Richards, G. N., Factors Influencing Chemisorption and Ignition of Wood Chars, *Combustion and Flame* **76**, 37-47 (1989).
1612. Hshieh, F. Y., and Richards, G. N., Factors Influencing Oxygen Chemisorption and Ignition of Chars from Newsprint, *Combustion and Flame* **76**, 49-56 (1989).
1613. Guest, P. G., Ignition of Natural Gas-Air Mixtures by Heated Surfaces (Tech. Paper 475) Bureau of Mines, Washington (1930).
1614. Burgess, M. J., and Wheeler, R. V., The Ignition of Firedamp by the Heat of Impact of Metal against Rock (Paper 54), Safety in Mines Research Board, London (1929).
1615. Martin, S. B., and Alvares, N. J., Critical Irradiance for Ignition of Cellulosic Fuels (WSCI-66-23), 1966 Spring Meeting, Western States Section, The Combustion Institute, Pittsburgh (1966).
1616. Lee, B. T., and Steel, J. S., Standard Room Fire Test Research at the National Bureau of Standards, unpublished study (1987).
1617. Lee, B. T., Standard Room Fire Test Development at the National Bureau of Standards, pp. 29-44 in **Fire Safety: Science and Engineering** (ASTM STP 882), ASTM (1985).
1618. Cunningham, M. B., Self Heating of Paper, *TAPPI* **44**, 194A-197A (1961).
1619. Kubler, H., Heat Generating Processes as Cause of Spontaneous Ignition in Forest Products, *Forest Products Abstracts* **10**, 299-327 (1987).
1620. Hirst, R., **Underdown's Fire Precautions**, 3rd ed., Gower Publishing Co., Aldershot, UK (1989).
1621. Alvares, N. J., private communication.
1622. Wraight, H., Ignition of Corrugated Fiberboard ('Cardboard') by Thermal Radiation (FR Note 1002), Fire Research Station, Borehamwood, UK (1974).
1623. Lattimer, B., Hughes Associates, private communication (2003).
1624. Hamins, A., and McGrattan, K., Reduced-scale Experiments to Characterize the Suppression of Rack-Storage Commodity Fires (NISTIR 6439), NIST (1999).
1625. Grant, G. B., and Drysdale, D. D., The Use of Ignitability Data from the Cone Calorimeter to predict T_{ig}, the Surface Temperature at Ignition for Cellulosic Packaging Materials, pp. 35-63 in *Industrial Fires: Workshop Proceedings* (EUR 15340 EN). Published for the Commission of the EC, Apeldoorn, Netherlands (1993).
1626. Shoub, H., and Bender, E. W., Radiant Ignition of Wall Finish Materials in a Small Home (NBS 8172), NBS (1964).
1627. Timber Home Fire Reveals New Risk, *Building (London)* **248**, 7 (15 Feb. 1985).
1628. Hungerford, R. D., Frandsen, W. H., and Ryan, K. C., Ignition and Burning Characteristics of Organic Soils, pp. 78-91 in *Proc. 19th Tall Timbers Fire Ecology Conf.*, Tall Timbers Research Station, Tallahassee FL (1995).
1629. Salgado, J., et al., Loss of Organic Matter in Atlantic Forest Soils due to Wildfires. Calculation of the Ignition Temperature, Thermochimica Acta **259**, 165-175 (1995).
1630. Frandsen, W. H., The Influence of Moisture and Mineral Soil on the Combustion Limits of Smoldering Forest Duff, *Canadian J. Forest Research* **17**, 1540-1544 (1987).

1631. Frandsen, W. H., Ignition Probability of Organic Soils, *Canadian J. Forest Research* **27**, 1471-1477 (1997).
1632. Lawson, B. D., Frandsen, W. H., Hawkes, B. C., and Dalrymple, G. N., Probability of Sustained Smoldering Ignition for Some Boreal Forest Duff Types (Forest Mgt. Note No. 63), Northern Forestry Centre, Edmonton, Alberta (1997).
1633. Weckman, H., Hyvärinen, P., Olin, J., Rautalin, A., and Vuorio, M., Reduction of Fire and Explosion Hazards at Peat Handling Plants (Research Report 2/1981), Palotekniikan laoratorio, Valtion Teknillinen Tutkimuskeskus, Espoo, Finland (1981).
1634. Vuorio, M., and Weckman, H., Measurements on the Self-Ignition of Peat (Tiedonanto 20), Palotekniikan laoratorio, Valtion Teknillinen Tutkimuskeskus, Espoo, Finland (1980).
1635. Jones, J. C., On the Low-temperature Oxidation of Processed Peat, *J. Fire Sciences* **15**, 162-171 (1997).
1636. Raftery, W. J., The Burning Bush, *Fire Engineering* **150**, 103-108 (Mar. 1997).
1637. Madden, J. J., Potted Plant Fires, *The California Fire-Arson Investigator* 8 (Mar. 2001).
1638. Keller, F., Organic Potting Soil Considered Source of Spontaneous Ignition, *The Fire Place* (Washington State IAAI Chapter newsletter), 6-7 (Dec. 2001/Feb. 2002).
1639. Spurrell, A. N., 'Suspicious' Fire in a Planter?, *Canadian Assn. of Fire Investigators The/Le Journal*, 9-11 (Mar. 2000).
1640. Elliott, M. A., and Brown, F. W., Investigations of Explosion Hazards of Perchloric Acid and Mixtures of Perchloric Acid and Organic Materials (RI 4169), Bureau of Mines, Pittsburgh (1948).
1641. Ohtani, H., Experimental Study on Flammability Characteristics of Perfluorocarbons, pp. 245-254 in *Fire Safety Science—Proc. 6th Intl. Symp.*, Intl. Assn. for Fire Safety Science (2000).
1642. Liaw, H.-J., Yur, C.-C., and Lin, Y.-F., A Mathematical Model for Predicting Thermal Hazard Data, *J. Loss Prevention in the Process Industries* **13**, 499-507 (2000).
1643. Safety Recommendation A-00-51 through 53, National Transportation Safety Board, Washington (2000).
1644. Hazards of Chemical Rockets and Propellants Handbook. Vol. III. Liquid Propellant Handling, Storage and Transportation (CPIA-194), Chemical Propulsion Information Agency, Silver Spring MD (1972).
1645. Castranta, H. M., Banerjee, D. K., and Noller, D. C., **Fire and Explosion Hazards of Peroxy Compounds** (ASTM STP 394), ASTM (1965).
1646. Bowes, P. C., Thermal Explosion of Benzoyl Peroxide, *Combustion and Flame* **12**, 289-310 (1968).
1647. Bowes, P. C., and Harris, J., Thermal Decomposition of Lauroyl Peroxide (Fire Research Note 684), Fire Research Station, Borehamwood, UK (1967).
1648. Roberts, T. A., Merrifield, R., and Tharmalingam, S., Thermal Radiation Hazards from Organic Peroxides, *J. Loss Prevention in the. Process Industries* **3**, 244-252 (1990).
1649. Kayser, E. G., Effect of Container Material on Several Organic Peroxides at 130°F (NOLTR 73-89), Naval Ordnance Laboratory, White Oak MD (1973).
1650. **Recommendations on the Transport of Dangerous Goods: Model Regulations**, 10th ed., United Nations, New York (1997).
1651. Bond, J., **Sources of Ignition**, Butterworth-Heinemann, Oxford (1991).
1652. Tamura, M., et al., Evaluation of the Deflagration Hazards of Organic Peroxides by the Revised Time-Pressure Test, *J. Hazardous Materials* **17**, 89-98 (1987).
1653. Zitrin, S., Analysis of Explosives by Infrared Spectrometry and Mass Spectrometry, pp. 267-314 in **Forensic Investigation of Explosions**, A. Beveridge, ed., Taylor & Francis, London (1998).
1654. Koltsov, K. S., Thermal Spontaneous Combustion of Dispersed Solid Biologicals, *Soviet Biotechnology* **6**, 87-89 (1989).
1655. Budavari, S., et al., eds., **The Merck Index**, 12th ed., Merck & Co., Whitehouse Station NJ (1996).
1656. Inglis, D. B., private communication (1998).
1657. The Glow and Slow Oxidation of Phosphorus, pp. 237-267 in **Supplement to Mellor's Comprehensive Treatise on Inorganic and Theoretical Chemistry**, vol. 8, supl. 3, Longman, London.
1658. Silverstein, M. S., et al., Stable Red Phosphorus, *Ind. and Eng. Chem.* **40**, 301-303 (1948).
1659. Ramsay, G. C., and McArthur, N. A., Studies on the Fire Behaviour of Some Pillows (DBR Report R86/2), CSIRO, Highett, Vic., Australia (1986).
1660. Bowes, P. C., Fires in Oil Soaked Lagging (CP 35/74), Building Research Establishment, Garston (1974).
1661. Gugan, K., Lagging Fires: The Present Position, pp. 28-43 in *Proc. Symp. on Chemical Process Hazards with Special Reference to Plant Design—V* (Symp. Series 39a), The Institution of Chemical Engineers, London (1974).
1662. Bankvall, C., Heat Transfer in Porous Materials, *J. Testing and Evaluation* **1**, 235-243 (1973).
1663. Britton, L. G., Spontaneous Fires in Insulation, *Plant/Operations Progress* **10**, 27-44 (1991).
1664. Lindner, H., and Seibring, H., Selbstentzündung organisher Substanzen an Isoliermaterial [Spontaneous Combustion of Organic Substances in Insulation Materials] *Chemie-Ingenieur-Technik* **39**, 667-671 (1967).
1665. Brindley, J., Griffiths, J. F., Zhang, J., Hafiz, N. A., and McIntosh, A. C., Critical Criteria for Ignition of Combustible Fluids in Insulation Materials, *AIChE J.* **44**, 1027-1037 (1998).
1666. Brindley, J., Griffiths, J. F., Hafiz, N., McIntosh, A. C., and Zhang, J., Criteria for Autoignition of Combustible Fluids in Insulation Materials, *Trans. Instn. Chem. Engrs.* **77B**, 61-68 (1999).
1667. Hilado, C. J., Self-Heating of Organic Compounds with Thermal Insulation, *J. Fire and Flammability* **5**, 321-333 (1974).
1668. Chandler, S. E., The Ignition of Plastic Materials in Dwellings (FR Note No. 883), Fire Research Station, Borehamwood, UK (1971).
1669. Masařík, I., Interlaboratory Trials of Ignition Temperatures—Report for ISO TC 61/SC4/WG1, Fire Technical Institute, Praha (1992).
1670. Masařík, I., Final Report on Interlaboratory Trials (for the ISO TC 61/SC4/WG1 meeting), Fire Technical Institute, Praha (1994).
1671. Masařík, I., Final Report on Interlaboratory Tests (for the ISO TC 61/SC4/WG1 meeting), Fire Technical Institute, Praha (1999).
1672. Tewarson, A., Abu-Isa, I. A., Cummings, D. R., and LaDue, D. E., Characterization of the Ignition Behavior of Polymers Commonly Used in the Automotive Industry, pp. 991-1002

in *Fire Safety Science—Proc. 6th Intl. Symp.*, Intl. Assn. for Fire Safety Science (2000).
1673. Scudamore, M. J., Briggs, P. J., and Prager, F. H., Cone Calorimetry—A Review of Tests Carried Out on Plastics for the Association of Plastic Manufacturers in Europe, *Fire and Materials* **15**, 65-84 (1991).
1674. Grand, A. F., The Use of the Cone Calorimeter to Assess the Effectiveness of Fire Retardant Polymers under Simulated Real Fire Test Conditions, pp. 143-152 in *Interflam '96*, Interscience Communications Ltd., London (1996).
1675. Morimoto, T., Mori, T., and Enomoto, S., Ignition Properties of Polymers Evaluated From Ignition Temperature and Ignition Limiting Oxygen Index, *J. Applied Polymer Science* **22**, 1911-1918 (1978).
1676. Kashiwagi, T., and Omori, A., Effects of Thermal Stability and Melt Viscosity of Thermoplastics on Piloted Ignition, pp. 1329-1338 in *22nd Symp. (Intl.) on Combustion*, The Combustion Institute, Pittsburgh (1988).
1677. Thomson, H. E., Ignition Characteristics of Plastics (Ph.D. dissertation), Univ. Edinburgh, Scotland (1988).
1678. Hopkins, D. jr., and Quintiere, J. G., Material Fire Properties and Predictions for Thermoplastics, *Fire Safety J.* **26**, 241-268 (1996).
1679. Staggs, J. E. J., A Theory for Quasi-steady Single-step Thermal Degradation of Polymers, *Fire and Materials* **22**, 109-118 (1998).
1680. Wang, Z., Fan, W., Wang, Q., and Yuan, H., Ignitability of Polyvinyl Chloride Materials, pp. 73-79 in *Symp. for '97 FORUM—Applications of Fire Safety Engineering*, Tianjin, China (1997).
1681. O'Neill, T., The Heat & Flame Response of Flame Retardant Halogenated and Non-Halogenated Polymers & Compounds, pp. 43-52 in *Flame Retardants '90*, Elsevier, London (1990).
1682. Fire Hazard Testing—Part 2-13: Glowing/hot Wire Based Test Methods—Glow-wire Ignitability Test Method for Materials (IEC 60695-2-13), International Electrotechnical Commission, Geneva.
1683. Fire Hazard Testing - Part 2: Test Methods - Section 2: Needle-flame Test (IEC 60695-2-2), International Electrotechnical Commission, Geneva (1991).
1684. Briggs, P., and Morgan, A., The Potential Fire Hazard of Lighting Assemblies, *Fire Safety Engineering* **6**, 18-20 (Aug. 1999).
1685. Delmonte, J., and Azam, M. A., Ignition Points of Plastic Materials, *Modern Plastics* **20**, 88, 122, 124 (Feb. 1943).
1686. Hedges, J. H., Baer, A. D., and Ryan, N. W., Pyrolysis and Ignition of Polymers under Approximated Fire Conditions, pp. 1173-1181 in *17th Symp. (Intl.) on Combustion*, The Combustion Institute, Pittsburgh (1978).
1687. Filippov, A. A., Khalturinskii, N. A., and Berlin, A. A., Experimental Study of the Inflammability of Polymeric Materials with Low-Calorific Sources, *Polymer Science USSR* **27**, 1327-1333 (1985).
1688. Khalturinsky, N. A., and Berlin, Al. Al., pp. 145-294 in **Degradation and Stabilization of Polymers**, H. H. G. Jellinek, ed., Elsevier, Amsterdam (1989).
1689. Biesenberger, J. A., Capinpin, R., and Yang, Y. C., A Study of Chain Addition Polymerizations with Temperature Variations, *Polymer Engrg. and Science* **16**, 101-123 (1976).
1690. Kao, C.-S., Hu, K.-H., and Lee, C., Fire and Explosion of an Acrylic Resin Plant, pp. 15-18 in *APSS2001—Proc. Asia Pacific Symp. on Safety*, vol. 1, Japan Soc. for Safety Engineering, Yokohama (2001).
1691. Buckmaster, J., and Vedarajan, T.G., Self-Heating Effects in Thermoset Composites, *J. Composite Materials* **31**, 2-21 (1997).
1692. Curing Fiberglass Resin: Creates Chemical Reaction but No Fire, *Fire Findings* **5**:1, 6 (Winter 1997).
1693. Herrera, F., Testing the Fire Cause Hypothesis, *The California Fire-Arson Investigator* 1, 6 (Nov. 2001).
1694. Tokyo Fire Dept., Fire Report—Fire Caused by Polymerization Heat of Fire Protective Coating, *J. Japan Assn. Fire Science and Engrg.* **49**:4, 63-66 (1999).
1695. Brydson, J. A., **Plastics Materials**, 6th ed., Butterworth-Heinemann, Oxford (1995).
1696. Jones, J. C., The Behaviour of Polystyrene in a Microcalorimeter at Temperatures up to 353 K, *Intl. J. on Engineering Performance-Based Fire Codes* **2**, 90-93 (2000).
1697. Mok, Y.-S., Lee, D.-H., Choi, J.-W., and Lim, W.-S., The Effect of Humidity in Dust Explosion and the Autoignition Characteristics of MBS Copolymer, pp. 11-14 in *APSS2001—Proc. Asia Pacific Symp. on Safety*, Vol. 1, Japan Soc. for Safety Engineering, Yokohama (2001).
1698. Shibata, Y., Spontaneous Ignition of ABS Resin in Recycling Process, *Kasai* [J. Japan Assn. for Fire Science and Engineering] **35**:5, 15-25 (1985).
1699. Spontaneous Heating of Polypropylene, *Fire J.* **64**, 66 (July 1970).
1700. Standard Terminology Relating to Plastics (ASTM D 883), ASTM.
1701. Products Research Committee, Materials Bank Compendium of Fire Property Data, NBS (1980).
1702. Fernando, A., Leonard, J., Webb, A., Bowditch, P., and Dowling, V., Experimental Derivation of Material Combustion Properties for Flame Spread Models, pp. 315-326 in *Proc. Fire and Materials 2001 Conf.*, Interscience Communications Ltd., London (2001).
1703. Kallonen, R., Test Methods for Fire Hazards of Construction Plastics (Research Reports 542), Valtion Teknillinen Tutkimuskeskus, Espoo, Finland (1988).
1704. Annamalai, K., and Sibulkin, M., Ignition and Flame Spread Tests of Cellular Plastics, *J. Fire & Flammability* **9**, 445-458 (1978).
1705. Drysdale, D. D., and Thomson, H. E., Ignition of PUFs: A Comparison of Modified and Unmodified Foams, pp. 191-205 in *Flame Retardants '90*, Elsevier, London (1990).
1706. Cleary, T. G., and Quintiere, J. G., Flammability Characterization of Foam Plastics (NISTIR 4664), NIST (1991).
1707. Saito, J., Yamamoto, Y., and Sugahara, S., Study on the Evaluating Method of Combustibility of Thermal Insulation Materials—Flammability Experiment Using a Constant Volume Heat Source of Steel Ball, *Report of Fire Science Laboratories, Tokyo Fire Dept.* No. 36, 1-10 (1999).
1708. Stevens, J. B., Ohio: $4 Million Fire Strikes Tire Plant, *Firehouse* **7**:2, 16-17 (Feb. 1982).
1709. Tremblay, K. J., Fire Damages Foam Manufacturing Plant: California, *NFPA J.* **92**:6, 21 (Nov./Dec. 1998).
1710. Marryatt, H. W., **Fire—A Century of Automatic Sprinkler Protection in Australia and New Zealand**, 2nd ed., Australian Fire Protection Assn., N. Melbourne (1988).
1711. Walker, I. K., The Role of Water in Spontaneous Combustion of Solids, *Fire Research Abstracts and Reviews* **9**, 5-22 (1967).

1712. Pap, Z., Kaucsukok és nyers kaucsukkeverékek öngyulladási viszonyainak tanulmányozása [The Examination of Spontaneous Combustion of Rubber and Rubber Mixtures], *Műanyag és Gumi* **7**, 243-248 (1970).
1713. Kuzminskii, A. S., Some Urgent Problems in the Ageing and Stabilization of Elastomers. Review. *Polymer Science USSR* **19**, 2509-2523 (1977).
1714. Emmons, H. W., Spontaneous Ignition of Styrene-Butadiene Rubber, *J. Applied Polymer Science* **26**, 2447-2457 (1981).
1715. Weickert, G., Zur reaktionstechnischen Untersuchung des Sebstentzündungsverhaltens einer polymeren Schüttung [A Reaction Kinetics Study of the Spontaneous Ignition Behavior of a Polymeric Feedstock] *Chem. Techn. (Leipzig)* **40**, 469-473 (1988).
1716. Shikhanov, V. A., Komarovsky, N. A., Kriger, T. V., Penkina, O. P., Vasilyeva, T. M., Ossipova, A. A., and Rodionova, N. M., An Evaluation of the Fire and Explosion Hazards of Thermopolymers of Diene Hydrocarbons. Report 1. A Study of the Thermal Indications of the Fire and Explosion Hazards of Thermopolymers, *Proizvod. Ispol'z. Elastomerov*, No. 8; 12-15 (1992).
1717. Shikhanov, V. A., Komarovsky, N. A., Kriger, T. V., and Vasilyeva, T. M., An Evaluation of the Fire And Explosion Hazards of Thermopolymers of Diene Hydrocarbons. Report 2. A Study of the Critical Conditions of Spontaneous Combustion in Thermopolymers, *Proizvod. Ispol'z. Elastomerov* No. 9; 9-11 (1992).
1718. The Fire Risks to Industry from Spontaneous Heating, *Fire Prevention* No. 126, 26-29 (1978).
1719. Foam Rubber Products, *Fire News*, No. 467, 2 (Aug./Sept. 1957).
1720. Fol, J. G., and Visser, W. de, Latex Contaminated with Copper Compounds as a Source of Danger of Fire, *Bull. Rubber Growers Assn*., **10** 124-127 (1928).
1721. FDA Public Health Advisory: Potential Risk of Spontaneous Combustion in Large Quantities of Patient Examination Gloves, US Food and Drug Administration, Rockville MD (27 June 1996).
1722. Spontaneous Combustion of Exam Gloves, *Infection Control and Hospital Epidemiology* **17**, 624 (1996).
1723. Hill, S. M., and Quintiere, J. G., Investigating Materials from Fires Using a Test Method for Spontaneous Ignition, *Fire and Materials* **24**, 61-66 (2000).
1724. Wachowicz, J., Investigations of the Phenomenon of Spontaneous Heating of Chloroprene Cover Wear-off in Fire-resistant Conveyor Belts, *Fire and Materials* **23**, 7-12 (1999).
1725. Ramsay, G. C., and Nicholl, P. R., The Ignitability of Flexible Cellular Plastics and Their End Products, CSIRO, Highett, Vic., Australia (1978).
1726. Tremblay, K. J., Fire Damages Manufacturing Plant, *NFPA J.* **92**, 21 (Nov./Dec. 1998).
1727. Sumi, K., and Tsuchiya, Y., Spontaneous Ignition—Relation Between Ambient Temperature and Size of Specimen (Building Res. Note 115), Natl. Res. Council of Canada, Ottawa (1976).
1728. Loftus, J. J., Self-Heating to Ignition Measurements and Computation of Critical Size for Solar Energy Collector Materials (NBSIR 85-3122), NBS (1985).
1729. Walker, G. H. P., Spontaneous Combustion, *NFPA Q.* **11**, 32-39 (1917).
1730. Synnott, E. C., and Duane, T. C., Fire Hazards in Spray-Drying of Milk Products, in **Concentration and Drying of Foods**, D. A. McCarthy, ed., Elsevier, London (1986).
1731. Beever, P. F., Spontaneous Ignition of Milk Powders in a Spray-Drying Plant, *J. Dairy Technology* **37**, 68-71 (1984).
1732. O'Connor, J. F., Self-Heating and Self-Ignition in Dairy Powders (Ph.D. dissertation), Michigan State Univ., East Lansing (1991).
1733. Raemy, A., Hurrell, R. F., and Löliger, J., Thermal Behaviour of Milk Powders Studied by Differential Thermal Analysis and Heat Flow Calorimetry, *Thermochimica Acta* **65**, 81-92 (1983).
1734. Duane, T. C., and Synnott, E. C., Ignition Characteristics of Spray-Dried Milk Product Powders in Oven Tests, *J. Food Engineering* **17**, 163-176 (1992).
1735. Gray, B. F., Spontaneous Combustion and Self-Heating, in **SFPE Handbook of Fire Protection Engineering**, 3rd ed., NFPA (2002).
1736. Rivers, C. M., Wake, G. C., and Chen, X. D., The Role of Drying in the Spontaneous Ignition of Moist Milk Powder, *Mathematical Engineering in Industry* **6**, 1-14 (1996).
1737. Chong, L. V., Chen, X. D., and Mackereth, A. R., Effect of Ageing and Composition on the Ignition Tendency of Dairy Powders, *J. Food Engineering* **39**, 269-276 (1999).
1738. O'Mahony, J. G., and Synnott, E. C., Influence of Sample Shape and Size on Self-Ignition of a Fat-Filled Milk Powder, *J. Food Engineering* **7**, 271-280 (1988).
1739. Okamoto, K., Satoh, H., Watanabe, N., and Hagimoto, Y., Study on Ignition of Propane-Air Mixture by a Glass Tube Heater, *Proc. APSS2001 Asia Pacific Symp. on Safety*, Japan Soc. for Safety Engineering (2201).
1740. McIntyre, F. L., and Rindner, R. M., A Compilation of Hazard and Test Data for Pyrotechnic Compositions (ARLCD-CR-80047), US Army Armament R&D Command, Dover NJ (1980). NTIS No. ADA096248.
1741. Pelletier, Y., Criminal Activities Using Fireworks and Pyrotechnics, pp. 19-26 in *Proc. 1st Intl. Symp. on Fireworks*, Minister of Supply and Services Canada, [n.p.] (1992).
1742. Kodde, H. H., Groothuizen, T. M., and Mul, J. M., Transport Classification of Common Fireworks, pp. 161-174 in *Proc. 1st Intl. Symp. on Fireworks*, Minister of Supply and Services Canada, [n.p.] (1992).
1743. Chapman, D., Wharton, R. K., Fletcher, J. E., and Webb, A. E., Studies of the Thermal Stability and Sensitiveness of Sulfur/Chlorate Mixtures. Part 3. The Effects of Stoichiometry, Particle Size and Added Materials, *J. Pyrotechnics* No. 11, 16-24 (Summer 2000).
1744. Tanner, H. G., Instability of Sulfur-Potassium Chlorate Mixture—A Chemical Review, *J. Chem. Educ.* **36**, 58-59 (1959).
1745. Wharton, R. K., Observations on the Sensitiveness and Reactivity of Certain Pyrotechnic Mixes That Have Been Involved in Ignition Accidents, pp. 339-345 in *Proc. 1st Intl. Symp. on Fireworks*, Minister of Supply and Services Canada, [n.p.] (1992).
1746. Conkling, J. A., **Chemistry of Pyrotechnics: Basic Principles and Theory**, Marcel Dekker, New York (1985).
1747. Bowes, R. A., The Evaluation of Low Hazard Fireworks ("Family Fireworks"), pp. 12-18 in *Proc. 1st Intl. Symp. on Fireworks*, Minister of Supply and Services Canada, [n.p.] (1992).
1748. California Code of Regulations, Title 19, Subchapter 6, section 986.8.

1749. Conkling, J. A., Snap Cap Tests – 1994 (unpublished report), Chestertown MD (1994).
1750. McLain, Joseph H., **Pyrotechnics: From the Viewpoint of Solid State Chemistry**, The Franklin Institute Press, Philadelphia (1980).
1751. Fireworks—Not Just Personal Injury—Fire Risk Also Associated with Many, *Fire Findings* **5**:3, 1-3 (Summer 1997).
1752. Conkling, J. A., Ignition Sensitivity of Fireworks Compositions, pp. 36-45 in *Proc. 1st Intl. Symp. on Fireworks*, Minister of Supply and Services Canada, [n.p.] (1992).
1753. Brown, F. W., Kusler, D. J., and Gibson, F. C., Sensitivity of Explosives to Initiation by Electrostatic Discharge (RI 5002), Bureau of Mines, Pittsburgh (1953).
1754. Conkling, J. A., and Jacobson, D. P., Investigation of the Spark Sensitivity of Oxidizer/Aluminum Compositions, pp. 55-63 in *Proc. 5th Intl. Symp. on Fireworks*, Minister of Public Works and Government Service Canada, [n.p.] (2000).
1755. Shidlovskiy, A. A., **Principles of Pyrotechnics**, 3rd ed., American Fireworks News, [Dingmans Ferry PA] (1997).
1756. de Yong, L., and Lui, F., Radiative Ignition of Pyrotechnics: Effect of Wavelength on Ignition Threshold, *Propellants, Explosives, Pyrotechnics* **23**, 328-332 (1998).
1757. de Yong, L., and Redman, L. D., Cookoff Behaviour of Pyrotechnics (MRL-TR-91-44), Materials Research Lab., Defence Science and Technology Organisation, Maribyrnong, Vic., Australia (1992).
1758. Radio Receivers, Audio Systems, and Accessories (UL 1270), UL.
1759. Standard for Audio-Video Products and Accessories (UL 1492), UL.
1760. Audio/Video and Musical Instrument Apparatus for Household, Commercial, and Similar General Use (UL 6500), UL.
1761. Audio, Video and Similar Electronic Apparatus - Safety Requirements (IEC 60065), International Electrotechnical Commission, Geneva.
1762. Cowles, F. R., Railroad-Caused Fires: What Starts Them, What Keeps Them Going, *Fire Control Notes* **33**:2, 12-15 (Spring 1972).
1763. DeBernardo, L. U., Fire Start Potential of Railroad Equipment (ED&T Project 1801; 7951 1206), San Dimas Equipment Development Center, San Dimas CA (1979).
1764. Railroad Fire Prevention Field Guide, Office of State Fire Marshal, Dept. of Forestry and Fire Protection, Sacramento CA (1999).
1765. Erlandsson, U., private communication, Rädningsverket, Växjö, Sweden (2001).
1766. Hasegawa, S., Ignition Mechanism Caused by Tracking on Starting Relay (PTC Thermistor), *Proc. 1999 Annual Mtg. Japan Assn. Fire Science and Engrg*., 10-13 (1999).
1767. Clodic, D., Leak Flow Rates and Measurement of Concentration Gradients of Flammable Refrigerants, Centre d'Energétique, Ecole des Mines de Paris, France (1997).
1768. Raj, S. C., and Jones, J. C., Self-Heating in the Oxidation of Natural Materials from Fiji, *New Zealand J. Technology* **3**, 199-203 (1987).
1769. Moysey, E., and Muir, W., Pilot Ignition of Building Materials by Radiation, *Fire Technology* **4**, 46-50 (1968).
1770. Braun, E., and Allen, P. J., Flame Spread on Combustible Solar Collector Glazing Materials (NBSIR 84-2887), NBS (1984).
1771. Rinck, R. R., jr., and Fantigrossi, P., Torch-Down Roofing: An Unrecognized Hazard? *Speaking of Fire* 4 (Summer 1992).
1772. Shaw, W., Modified Bitumen Allies Rally to Cause of Torching Safety, *RSI Roofing, Siding, Insulation* **63**, 32-36; 91-92 (Aug. 1986).
1773. Standard for Safeguarding Construction, Alteration, and Demolition Operations (NFPA 241), NFPA.
1774. Loeb, D. L., Roofing Equipment May Include Unexpected Hazard, *Fire Chief* **30**, 47-48 (Sep. 1986).
1775. Armstrong, A., Armstrong Forensic Laboratory, private communication (2000).
1776. Hill, H., Tar Kettle Fires, *Firehouse* **14**, 74-75 (June 1989).
1777. Nurmi, V.-P., Electrical Fire Risks, pp. 1515-1520 in *Interflam 2001—Proc. 9th Intl. Conf.*, Interscience Communications Ltd., London (2001).
1778. Garg, D. R., and Steward, Pilot Ignition of Cellulosic Materials Containing High Void Spaces, *Combustion and Flame* **17**, 287-294 (1971).
1779. Dietenberger, M. A., Ignitability Analysis of Siding Materials Using Modified Protocol for LIFT Apparatus, pp. 297-306 in *20th Intl. Conf. on Fire Safety*, Product Safety Corp., Sunnyvale CA (1995).
1780. Britton, L. G., Combustion Hazards of Silane and Its Chlorides, *Plant/Operations Progress* **9**, 16- (1990).
1781. Kondo, S., Tokuhashi, K., Nagai, H., Iwasaka, M., and Kaise, M., Spontaneous Ignition Limits of Silane and Phosphine, *Combustion and Flame* **101**, 170-174 (1995).
1782. Fthenakis, V. M., and Moskowitz, P. D., Assessment of Silane Hazards, *Solid State Technology* **33**, 81-85 (1990).
1783. Hshieh, F.-Y., Hirsch, D. B., and Williams, J. H., Short Communication: Autoignition Temperature of Trichlorosilanes, *Fire and Materials* **26**, 289-290 (2002).
1784. Buchwald, S. L., Silane Disproportionation Results in Spontaneous Ignition, *Chem. & Eng. News* **71**, 2 (29 Mar. 1993).
1785. Storage, Dispensing and Use of Silane and Its Mixtures (Uniform Fire Code Standard 80-1), Uniform Fire Code, International Conference of Building Officials, Whittier CA (1997).
1786. Matsuda, T., Dust Explosion Hazards of Metallic Silicon, *Specific Report of the Research Institute of Industrial Safety* No. 12, 57-69 (1993).
1787. Hshieh, F.-Y., and Julien, C. J., Experimental Study on the Radiative Ignition of Silicones, *Fire and Materials* **22**, 179-185 (1998).
1788. Hshieh, F.-Y., Note: Correlation of Closed-Cup Flash Points with Normal Boiling Points for Silicone and General Organic Compounds, *Fire and Materials* **21**, 277-282 (1997).
1789. Hshieh, F.-Y., Predicting Heats of Combustion and Lower Flammability Limits of Organosilicon Compounds, *Fire and Materials* **23**, 79-89 (1999).
1790. Mowry, C. W., Spontaneous Heating and Ignition in the Manufacturing Industries, pp. 59-64 in Report of Conference on Spontaneous Heating and Ignition of Agricultural and Industrial Products, NFPA and US Dept. of Agriculture, Washington (1929).
1791. Sodium Chlorate Risks to Be Reconsidered, *Fire Engineers J.* **39**, 14 (June 1979).
1792. Thomson, B. J., Synopsis of Fires and Explosions involving Sodium Chlorate (IR/L/HM/83/11), HSE, Buxton, UK (1983).
1793. Spontaneous Ignition of Pesticides, *Bosai Kenkyu* [Annual Report] No. 15, 74-77, Yokohama City Fire Bureau, Yokohama, Japan (1985).
1794. Recent Port and Ship Fires and Explosions, *NFPA Q.* **41**:2, 108-121 (1947).

1795. Thomson, B. J., Freeder, B. G., Heathcote, N. L., Pickering, D. H., and Roberts, T. A., Experimental Work on the Explosion Hazard of Sodium Chlorate (IR/L/HM.EX/85/01), HSE, Buxton, UK (1985).
1796. Henderson, D. K., and Tyler, B. J., Dual Ignition Temperatures for Dust Layers, *J. Hazardous Materials* **19**, 155-159 (1988).
1797. Tyler, B. J., and Henderson, D. K., Spontaneous Ignitions in Dust Layers: Comparison of Experimental and Calculated Values, pp. 45-59 in *Hazards from Pressure: Exothermic Reactions, Unstable Substances, Pressure Relief, and Accidental Discharge* (IChemE Symp. series no. 102), Institution of Chemical Engineers, Rugby, England; and Pergamon Press, Elmsford NY (1987).
1798. Reddy, P. D., Amyotte, P. R., and Pegg, M. J., Effects of Inerts on Layer Ignition Temperatures of Coal Dust, *Combustion and Flame* **114**, 41-53 (1998).
1799. EPA/OSHA Joint Chemical Accident Investigation Report—Napp Technologies, Inc., Lodi, New Jersey (EPA 550-R-97-002), Environmental Protection Agency, Washington (1997).
1800. Carroll, J. R., **Physical and Technical Aspects of Fire and Arson Investigation**, Charles C. Thomas, Springfield IL (1979).
1801. Tip of Soldering Iron Reaches Very High Temperatures, *Fire Findings* **9**:1, 5 (Winter 2001).
1802. Phillips, H. J., **Handling of Dangerous Goods**, Crosby Lockwood and Son, London (1896).
1803. Christensen, C. M., Meronuck, R. A., Steele, J. A., and Behrens, J. C., Some Morphological and Chemical Characteristics of Binburned and Fireburned Soybeans, *Trans. Amer. Soc. Agricultural Engineers* **16**, 899-901 (1973).
1804. The Spa Pools that Catch Fire, *Consumer [New Zealand]* No. 260, 110-111 (May 1988).
1805. Hofelich, T. C., and LaBarge, M. S., On the Use and Misuse of Detected Onset Temperature of Calorimetric Experiments for Reactive Chemicals, *J. Loss Prevention in the Process Industries* **15**, 163-168 (2002).
1806. Cullis, C. F., and Kurmanadhan, S., Studies of the Vapour-Phase Polymerisation and Oxidation of Styrene, *Combustion and Flame* **31**, 1-5 (1978).
1807. High Flash-Point Liquids and Low Melting Point Solids, Fire Prevention, No. 107, 31-35 (Feb. 1975).
1808. Zitkowski, H. E., pp. 111-112 in Report of Conference on Spontaneous Heating and Ignition of Agricultural and Industrial Products, NFPA and US Dept. of Agriculture, Washington (1929).
1809. Shimizu, T., **Fireworks: The Art, Science and Technique**, Pyrotechnica Publications, Austin TX (1996).
1810. Molten Sulphur Spillage, *Loss Prevention Bulletin* No. 78, 23-25 (1987).
1811. Jones, E., and White, A. G., Gas Explosions and Dust Explosions—A Comparison, pp. 129-139 in *Dust in Industry*, Society of Chemical Industry, Leeds, England (1948).
1812. van der Wel, P. G. J., Ignition and Propagation of Dust Explosions (Ph.D. dissertation), Delft University Press, Delft, Netherlands (1993).
1813. Murray, J., On a Species of Earthy Matter Spontaneously Combustible, *Edinburgh Philosophical J.* **7**, 105-107 (1822).
1814. Standard for Prevention of Sulfur Fires and Explosions (NFPA 655), NFPA.
1815. Olson, D. B., Surge Suppressors: Real Protection or Potential Hazards? *Fire Findings* **7**:2, 1-4 (Spring 1999).
1816. Goodson, M. E., Surge Suppressor Fires, *Fire & Arson Investigator* **50**, 10-11, 14-16 (Jan. 2000).
1817. Transient Voltage Surge Suppressors (UL 1449), UL.
1818. Wolf, G. L., McGuire, J. G., Nolan, P. F., and Sidebotham, G. W., Spontaneous Ignition Temperature of Tracheal Tubes, pp. 57-65 in **Flammability and Sensitivity of Materials in Oxygen-Enriched Atmospheres** (ASTM STP 1197), ASTM (1993).
1819. Standard Procedures for Cleaning or Safeguarding Small Tanks and Containers Without Entry (NFPA 327), NFPA.
1820. Davie, F. M., Nolan, P. F., and Hoban, T. W. S., Case Histories of Incidents in Heated Bitumen Storage Tanks, *J. Loss Prevention in the Process Industries* **7**, 217-221 (1994).
1821. Dimpfl, L. H., Study Gives Insight into Asphalt Tank Explosions, *Oil and Gas J.* **29**, 180-185 (29 Dec. 1980).
1822. Davie, F. M., Mores, S., Nolan, P. F., and Hoban, T. W. S., Evidence of Oxidation of Deposits in Heated Bitumen Storage Tanks, *J. Loss Prevention in the Process Industries* **6**, 145-150 (1993).
1823. Davie, F. M., Nolan, P. F., and Tucker, R. F., Mathematical Model for the Self-Heating of Deposits Found in Heated Bitumen Storage Tanks, *J. Loss Prevention in the Process Industries* **6**, 203-208 (1993).
1824. Tokyo Fire Department, Possibility of Ignition with Cellular Phone in Flammable Mixture, *J. Japan Assn. Fire Science and Engrg*. **50**:1, 76-79 (2000).
1825. Fire Hazard of a Television, Center for Better Living, Tsukuba, Japan (1994).
1826. TV Fires (Europe), Sambrook Research Intl., Newport, Shropshire, United Kingdom (1996).
1827. Television Fires, Danish Electrical Equipment Control Office (DEMKO), Denmark (1995).
1828. Rogers, G. J., and Evans, D. D., Characterization of Electrical Ignition Sources within Television Receivers (Tech. Note 1109), NBS (1979).
1829. Front Room Fire 2 (video), BRE Ltd., Garston, UK (2001).
1830. De Poortere, M., Schonbach, C., and Simonson, M., The Fire Safety of TV Set Enclosure Materials: A Survey of European Statistics, *Fire and Materials* **24**, 53-60 (2000).
1831. Safety of Electronic Equipment (ECMA-287), European Computer Manufacturers Association, Geneva (1999).
1832. Troitzsch, J. H., Fire Safety of TV-Sets and PC-Monitors, Report for European Flame Retardants Assn., Fire Protection Service, Wiesbaden, Germany (1998).
1833. Simonson, M., Fire tests conducted for the National Association of Fire Marshals, SP, Borås, Sweden (1999).
1834. A Specification for Flame Resistant Materials Used in Camping Tentage (CPAI 84), Canvas Products Assn. Intl., St. Paul MN (1976). The organization is currently named the Industrial Fabrics Assn. Intl.
1835. Standard Specification for Flame-Resistant Materials Used in Camping Tentage (ASTM D 4372), ASTM.
1836. Standard Methods of Fire Test for Flame-Resistant Textiles and Films (NFPA 701), NFPA.
1837. Harkleroad, M. F., Fire Properties Database for Textile Wall Coverings (NISTIR 89-4065), NIST (1989).
1838. Eboatu, A. N., Birnin-Kebbi, F., and Shebu, D., Note: Fire-retardant Treatment of Roofing Thatch, *Fire and Materials* **16**, 155-158 (1992).
1839. Large, M., and McNeil, M., Tire Fire Investigation (OFC 9002), Office of Fire Marshal, Ontario, Canada [n.d.].
1840. Wraight, H., Ignition of Motor Tire Samples (FR Note 742), Fire Research Station, Borehamwood, UK (1969).

1841. Jurng, J., Park, E.-S., Park, J. W., and Lee, G. W., Burning Characteristics of a Waste Tire Chip in High Temperature Environments, pp. 341-351 in **Transport Phenomena in Combustion**, vol. 1, S. H. Chen, ed., Taylor & Francis, Washington (1996).
1842. White, J. A., Western Fire Center, private communication (2001).
1843. Garstang, J. H., Aircraft Explosive Sabotage Investigation, pp. 133-182 in **Forensic Investigation of Explosions**, A. Beveridge, ed., Taylor & Francis, London (1998).
1844. NTSB incident report BFO85IA035, Scheduled 14 CFR 121 operation of People Express (d.b.a. North Terminal), Apr-12-85 at Chantilly, VA (1985).
1845. Glenn, W., Exploding Tires—The Hazard Nobody's Heard of, *OHS Canada* (Mar. 1997).
1846. Brookes, F. R., Explosions Initiated by Welding the Rims of Wheels Fitted with Tubeless Tyres, *J. Occupational Accidents* **5**, 149-160 (1983).
1847. Satoru, T., Spontaneous Combustion of Five Materials, *Annual Report of Fire Research Laboratory, Nagoya City Fire Dept.* No. 27, 57-69 (1998).
1848. Humphrey, D. N., Investigation of Exothermic Reaction in Tire Shred Fill Located on SR 100 in Ilwaco, Washington, prepared for Federal Highway Administration, Washington (1996).
1849. Rings of Fire: Fire Prevention & Fire Suppression of Scrap Tire Piles, Office of State Fire Marshal, State of California, Sacramento [1994?].
1850. Design Guidelines to Minimize Internal Heating of Tire Shred Fills, Intl. Tire & Rubber Assn. Foundation, Inc., Louisville KY (1997).
1851. Pop Tarts Fuel Faulty Toasters and Produce Burning Results, *Fire Findings* **1**:3, 13 (Fall 1993).
1852. Fitz, M. M., MDE Engineers, private communication (2002).
1853. Parker, D. J., and Owings, C. W., Gas Explosions in Buildings: Their Cause and Prevention (IC 7142), Bureau of Mines, Pittsburgh (1941).
1854. Herickes, J. A., Damon, G. H., and Zabetakis, M. G., Determining the Safety Characteristics of Unsymmetrical Dimethylhydrazine (RI 5635), Bureau of Mines, Pittsburgh (1960).
1855. Hall, J. R. jr., Targeting Upholstered Furniture Fires, *NFPA J.* **95**, 57-60 (Mar./Apr. 2001).
1856. Clarke, F., and Ottoson, J., Fire Death Scenario and Firesafety Planning, *Fire J.* **70**, 20-22, 117-118 (May 1976).
1857. Ault, K., and Levinson, M. S., Upholstered Furniture Fire Loss Estimates 1980 – 1998, Consumer Product Safety Commission, Washington (2001).
1858. Babrauskas, V., and Krasny, J. F., Fire Behavior of Upholstered Furniture (NBS Monograph 173), NBS (1985).
1859. Krasny, J. F., Cigarette Ignition of Soft Furnishings—A Literature Review With Commentary (NBSIR 87-3509), NBS (1987).
1860. Krasny, J. F., Parker, W. J., and Babrauskas, V., **Fire Behavior of Upholstered Furniture and Mattresses**, William Andrew Publishing, Norwich NY (2000).
1861. Damant, G. H., Cigarette Ignition of Upholstered Furniture, *J. Fire Sciences* **13**, 337-349 (1995).
1862. Talley, T. H., private communication (2002).
1863. Damant, G. H., Cigarette Induced Smoldering of Flexible Polyurethane Foam (Lab. Report SP-75-2), Californian Bureau of Home Furnishings, Sacramento (1975).
1864. Donaldson, D. J., Yeadon, D. A., and Harper, R. J. jr., Smoldering Characteristics of Cotton Upholstery Fabrics, *Textile Research J.*, **51**, 196-202 (1981).
1865. Donaldson, D. J., Yeadon, D. A., and Harper, R. J. jr., Smoldering Phenomenon Associated with Cotton, *Textile Research J.* **53**, 160-164 (1983).
1866. Prime, D. M., Ignitability and Leather Upholstery, *Cabinet Maker and Retail Furnisher*, 39 (26 Mar. 1982).
1867. Rogers, F. E., Ohlemiller, T. J., Kurtz, A., and Summerfield, M., Studies of the Smoldering Combustion of Flexible Polyurethane Cushioning Materials, *J. Fire and Flammability* **9**, 5-13 (1978).
1868. Rogers, F. E., and Ohlemiller, T. J., Smolder Characteristics of Flexible Polyurethane Foams, *J. Fire and Flammability* **11**, 32-44 (1980).
1869. Cerra, A. P., and Ramsay, G. C., A Protocol for Assessment of Smouldering Behaviour of Upholstery Combinations (DBR Report R85/2), CSIRO, Highett, Vic., Australia (1985).
1870. Ortiz-Molina, M. G., Toong, T. Y., Moussa, N. A., and Tesoro, C., Smoldering Combustion of Flexible Polyurethane Foams and Its Transition to Flaming or Extinguishment, pp. 1191-1200 in *17th Symp. (Intl.) on Combustion*, The Combustion Institute, Pittsburgh (1978).
1871. Tse, S. D., and Fernandez-Pello, A. C., Some Observations of Two-dimensional Smoldering and the Transition to Flaming, pp. 689-700 in **Transport Phenomena in Combustion**, vol. 1, S. H. Chen, ed., Taylor & Francis, Washington (1996).
1872. Babrauskas, V., and Krasny, J. F., Upholstered Furniture Transition from Smoldering to Flaming, *J. Forensic Sciences* **42**, 1029-1031 (1997).
1873. Hoschke, B. N., A Critical Appraisal of Some Features of ISO DP8191/1 and 2: "Furniture Burning Behaviour—Assessment of the Ignitability of Upholstered Furniture," unpublished study (1983).
1874. Krasny, J. F., and Gann, R. G., Relative Propensity of Selected Commercial Cigarettes to Ignite Soft Furnishings Mockups (NBSIR 86-3421), NBS (1986).
1875. Krasny, J. F., Harris, R. H., Jr., Levine, R. S., and Gann, R.G., Cigarettes with Low Propensity to Ignite Soft Furnishings, *J. Fire Sciences* **7**, 251-288 (1989).
1876. Gann, R. G., Harris, R. H., Jr., Krasny, J. F., Levine, R. S., Mitler, H. E., and Ohlemiller, T. J., Cigarette Ignition of Soft Furnishings, pp. 77-86 in *Fire Safety Science, 2nd Intl. Symp.*, Hemisphere, New York (1989).
1877. Ohlemiller, T. J., Villa, K. M., Eberhardt, K. R., Harris, R. H., jr., Lawson, J. R., and Gann, R. G., Test Methods for Quantifying the Propensity of Cigarettes to Ignite Soft Furnishings (NIST SP 851), NIST (1993).
1878. Ohlemiller, T. J., Villa, K. M., Braun, E., Eberhardt, K. R., Harris, R. H., jr., Lawson, J. R., and Gann, R. G., Quantifying the Ignition Propensity of Cigarettes, *Fire and Materials* **19**, 155-169 (1995).
1879. Eberhardt, K. R., Levenson, M. S., and Gann, R. G., Fabrics for Testing the Ignition Propensity of Cigarettes, *Fire and Materials* **21**, 259-264 (1997).
1880. Hirschler, M. M., Comparison of the Propensity of Cigarettes to Ignite Upholstered Furniture Fabrics and Cotton Ducks (500-Fabric Study), *Fire and Materials* **21**, 123-141 (1997).

1881. Spears, A. W., Rhyne, A. L., and Norman, V., Factors for Consideration in a Test for Cigarette Ignition Propensity on Soft Furnishings, *J. Fire Sciences* **13**, 59-84 (1995).
1882. Lewis, L. S., Morton, M. J., Norman, V., Ihrig, A. M., and Rhyne, A. L., The Effects of Upholstery Fabric Properties on Fabric Ignitabilities by Smoldering Cigarettes. II., *J. Fire Sciences* **13**, 445-471 (1995).
1883. Lewis, L. S., Nestor, T. B., and Townsend., D. E., A Comparative Ignition Propensity Study of Foreign and US Cigarettes Using the NIST Cotton Duck Mockup Ignition Test Method, *J. Fire Sciences* **13**, 386-398 (1995).
1884. Greear, L. C., Hudson, W. Z., Jupe, R., Pinion, D. O., and Wanna, J. T., Ignition Responses of Fifty Upholstery Fabrics to Commercial Cigarettes, *J. Fire Sciences* **14**, 413-425 (1996).
1885. Rhyne, A. L., Short Communication: Comparison of the Propensity of Cigarettes to Ignite Upholstered Furniture Fabrics and Cotton Ducks (500-Fabric Study): A Second Opinion, *Fire and Materials* **22**, 175-178 (1998).
1886. Standard Test Method for Measuring the Ignition Strength of Cigarettes (ASTM E 2187), ASTM.
1887. Paul, K. T., Assessment of Cigarettes of Reduced Ignition Power and Their Role to Reduce Fire Risks of Upholstered Seating, Mattresses, and Bed Assemblies, *J. Fire Sciences* **18**, 28-73 (2000).
1888. Methods of Test for the Ignitability of Upholstered Seating by Smouldering and Flaming Ignition Sources (BS 5852), British Standards Institution, London (1990).
1889. Krasny, J. F., Allen, P. J., Maldonado, A., and Juarez, N., Development of a Candidate Test Method for the Measurement of the Propensity of Cigarettes to Cause Smoldering Ignition of Upholstered Furniture and Mattresses (NBSIR 81-2363), NBS (1981).
1890. Gann, R. G., et al., Relative Ignition Propensity of Test Market Cigarettes (Tech Note 1436), NIST (2001).
1891. Szabat, J. F., Combustibility Aspects of Polyurethane Foams for Mattresses, *J. Consumer Product Flammability* **5**, 82-95 (1978).
1892. Damant, G. H., Flammability Aspects of Flexible Polyurethane Foams Commonly Used in Upholstered Furniture (Lab. Report SP-76-3), California Bureau of Home Furnishings, Sacramento (1976).
1893. Palmer, K. N., and Taylor, W., Fire Hazards of Plastics in Furniture and Furnishings: Ignition Studies (CP 14/74), Building Research Establishment, Borehamwood, UK (1974).
1894. Woolley, W. D., Ames, S. A., Pitts, A. I., and Buckland, K., The Ignition and Burning Characteristics of Fabric Covered Foams, *Fire Safety J.* **2**, 39-59 (1979/80).
1895. Raftery, M. M., Ignition Response and Fire Test Behaviour of Modern Upholstered Furniture (IP 17/82), Building Research Establishment, Garston, England (1982).
1896. Ingham, P. E., Goddard, J. M. and Grueber, A. L., The Influence of Fabric Coverings on the Flammability of Polyurethane Upholstered Furniture (Communication No. 66), Wool Research Organisation of New Zealand, Christchurch (1979).
1897. Ingham, P. E., The Flammability of Polyurethane Upholstered Furniture. Part II. Tests with Larger Ignition Sources and 'Improved' Foams (Communication No. 72), Wool Research Organisation of New Zealand, Christchurch (1981).
1898. Agreed Summary and Conclusions on Interlaboratory Experiment on Larger Flame Sources (ISO/TC136/SC1/WG4/N188), Technical Committee 136, International Organization for Standardization (1992).
1899. Moulen, A. W., Grubits, S., and Miles, P. A., Tests on Upholstery to Grade Horizontal Flame Spread (Technical Record 450), Experimental Building Station, N. Ryde, NSW, Australia (1979).
1900. Foley, M., and Drysdale, D. D., The Use of Small Scale Fire Test Data for the Hazard Assessment of Bulk Materials, Contract 3115/R04.41, Health and Safety Executive, Sheffield, England (1995).
1901. Fire Research 1954 (Report of the Director of Fire Research for 1954), pp. 10-11, HMSO, London (1955).
1902. Hilado, C. J., and Brauer, D. P., Effect of Construction, Substrate, and Piloting on Ignitability of Furniture Upholstery Fabrics, *J. Fire and Flammability* **10**, 26-40 (1979).
1903. Hilado, C. J., and Murphy, R. M., Ignitability by Radiant Heat of Some Materials in Home Furnishings, *J. Consumer Product Flammability* **5**, 68-81 (1978).
1904. Sundström, B., ed., Fire Safety of Upholstered Furniture—The Final Report on the CBUF Research Programme (Report EUR 16477 EN), Interscience Communications Ltd, England (1995).
1905. Chen, F. F., Radiant Ignition of New Zealand Upholstered Furniture Composites (M.S. thesis), Univ. Canterbury, Christchurch, New Zealand (2001).
1906. Moulen, A. W., and Grubits, S., Fire Properties of Some Commonly Used Upholstery Materials (Technical Record TR 44/153/412), Experimental Building Station, N. Ryde, NSW, Australia (1973).
1907. Forsten, H. H., Cone Calorimeter Studies of Furniture Component Systems, pp. 105-113 in **Fire and Flammability of Furnishings and Contents of Buildings** (ASTM STP 1233), ASTM (1994).
1908. Braun, E., Davis, S., Klote, J. H., Levin, B. C., and Paabo, M., Assessment of the Fire Performance of School Bus Interior Components (NISTIR 4347), NIST (1990).
1909. Ramsay, G. C., and McArthur, N. A., Studies on the Fire Behaviour of Some Bean Bag Chairs (DBR Report R86/3), CSIRO, Highett, Vic., Australia (1986).
1910. Vanspeybroeck, R., Van Wesemael, E., Van Hees, P, and Vandevelde, P., Calorimetric Combustion Assessment of Polyurethane Flexible Foam and Fabric Composites, *Fire and Materials* **17**, 155-166 (1993).
1911. Hirschler, M. M., and Smith, G. F., Flammability of Fabric/Foam Combinations for Use in Upholstered Furniture, *Fire Safety J.* **16**, 13-31 (1990).
1912. Cleary, T. G., Ohlemiller, T. J., and Villa, K. M., The Influence of Ignition Source on the Flaming Fire Hazard of Upholstered Furniture (NISTIR 4847), NIST (1992).
1913. Krasny, J. F., and Huang, D., Small Flame Ignitability and Flammability Behavior of Upholstered Furniture Materials (NBSIR 88-3771), NBS (1988).
1914. Ziolkowski, J., and Talley, H., The Durability of FR Treatments on Upholstery Fabrics Using the BS 5852 Small Open Flame Test and Effects of Immersion Treatment/Ammonia Curing on Cigarette Ignition Propensity of 100% Cotton Fabrics and the Effects of FR Backcoating on the Cigarette Ignition Propensity of 100% Cotton Fabrics, *AFMA Flammability Conf.* (1999).
1915. Bernatz, A. J., Effects of Beverages on the Flammability of Upholstery Fabrics, CPSC (2000).
1916. Tao, W., Effects of Soiling on the Flammability of Upholstery Fabrics, CPSC (2000).

1917. Tao, W., et al., Cleaning and Wear Effects on Upholstery Fabric Flammability, CPSC (2000).
1918. Loftus, J. J., Back-Up Report for the Proposed Standard for the Flammability (Cigarette Ignition Resistance) of Upholstered Furniture, PFF 6-76 (NBSIR 78-1438), NBS (1978).
1919. Standard Test Method for Cigarette Ignition Resistance of Mock-up Upholstered Furniture Assemblies (ASTM E 1352), ASTM.
1920. Standard Test Method for Cigarette Ignition Resistance of Components of Upholstered Furniture Assemblies (ASTM E 1353), ASTM.
1921. Upholstered Furniture Action Council, High Point NC.
1922. The Business and Institutional Furniture Manufacturer's Association First Generation Voluntary Upholstered Furniture Flammability Standard for Business and Institutional Markets (F-1-1978), BIFMA, Grand Rapids MI (1978).
1923. Flammability Information Package (Contains Technical Bulletins 116, 117, 121, 106 and 26). Bureau of Home Furnishings and Thermal Insulation, Dept. of Consumer Affairs, State of California, North Highlands (1992).
1924. Schuhmann, J. G., and Hartzell, G. E., Flaming Combustion Characteristics of Upholstered Furniture, *J. Fire Sciences* **7**, 368-402 (1989).
1925. Medford, R. L., and Ray, D. R., Upholstered Furniture Flammability: Fires Ignited by Small Open Flames and Cigarettes, Consumer Product Safety Commission, Washington DC (Oct. 24, 1997).
1926. Talley, T. H., Phases 1&2, UFAC Small Open Flame Tests and Cigarette Ignition Tests, *AFMA Flammability Conf.* (1995).
1927. Regulatory Options Briefing Package on Upholstered Furniture Flammability, Consumer Product Safety Commission, Washington (1997).
1928. Fansler, L., et al., Upholstered Furniture Flammability Testing: Full Scale Open Flame Data Analysis, Consumer Product Safety Commission, [Bethesda MD] (1996).
1929. Briefing Package on Upholstered Furniture Flammability: Regulatory Options, CPSC (2001).
1930. Consumer Protection: The Furnishings and (Fire) (Safety) Regulations 1988, No. 1324; and The Furniture and Furnishings (Fire) (Safety) (Amendment) Regulations 1989, No. 2358, HMSO, London.
1931. Wide Awake: A Study of 220 Fires Involving Mattresses, Natl. Assn. of State Fire Marshals and Sleep Products Safety Council, [n.p.] (1997).
1932. Frye, R. E., Vickers, A. K., and Tyrrell, E. A., Analysis of Accident Data on Mattress Fires (NBS 10 820), [U.S.] Natl. Bur. Stand., Washington (1972).
1933. Kinoshita, K., Hagimoto, Y., and Tanimoto, M., Studies on the Ignitability of Inflammables by a Smoldering Cigarette. 2. The Ignitability of a Quilt and Mattress, *Natl. Res. Inst. of Police Science Reports—Research on Forensic Science* **41**, 45-54 (Feb. 1988).
1934. Ramsay, G. C., and McArthur, N. A., Studies on the Fire Behaviour of Some Mattresses (DBR Report R86/1), CSIRO, Highett, Vic., Australia (1986).
1935. Williams, M. J., and Campbell, H. J., Flammability of Mattress Materials, *Canadian J. Criminology* **21**, 16-21 (1979).
1936. Hilado, C. J., Fire Studies of Bedding Materials, *J. Fire and Flammability* **4**, 235-277 (1973).
1937. Swanson, A. L., and Adolph, G. A., Comparing Mattresses for Flammability Potential, *Hospitals* **37**, 37-40 (Sept. 1, 1963).
1938. Palmer, K. N., Taylor, W., and Paul, K. T., Fire Hazards of Plastics in Furniture and Furnishings: Characteristics of the Burning (CP 3/75), Building Research Establishment, Borehamwood, UK (1975).
1939. Rethoret, H., **Fire Investigations**, Recording and Statistical Corp. Ltd., Toronto (1945).
1940. Standard for the Flammability of Mattresses and Mattress Pads (FF 4-72), 16 CFR 1632, Code of Federal Regulations, Consumer Product Safety Commission.
1941. Ohlemiller, T. J., Shields, J. R., McLane, R. A., and Gann, R. G., Flammability Assessment Methodology for Mattresses (NISTIR 6497), NIST (2000).
1942. Specification for Resistance to Ignition of Mattresses, Divans and Bed Bases (BS 7177), British Standards Institution, London.
1943. Furniture. Assessment of the Ignitability of Mattresses and Upholstered Bed Bases. Ignition Source: Smouldering Cigarette (EN 597-1), Comité Europeén du Normalisation, Brussels.
1944. Furniture. Assessment of the Ignitability of Mattresses and Upholstered Bed Bases. Ignition Source: Match Flame Equivalent (EN 597-2), Comité Europeén du Normalisation, Brussels.
1945. Vlot, I., Fire Safety of Textile Products—Legislation and Standardization (Report 48), Consumer Safety Institute, Amsterdam (1989).
1946. Fire Test Procedures for Ignitability of Bedding Components, Res. A.688(7), **FTP Code—International Code for Application of Fire Test Procedures**, International Maritime Organization, London (1998).
1947. Nash, L., Testing of an Ignitability Standard for Bedding Components (DG-D-18-98), US Coast Guard R&D Center, Groton CT (1998).
1948. Sloan, P. J., Beware, *Fire & Arson Investigator* **51**:1, 45 (Oct. 2000).
1949. Safety in Mines Research 1954, Thirty-third Annual Report, Safety in Mines Research Establishment, HMSO, London (1955).
1950. Hirunpraditkoon, S., Moghtaderi, B., Dlugogorski, B. Z., and Kennedy, E. M., Combustion Properties of a Surrogate Refuse-derived Fuel under Fire Conditions, *Chemeca '98—26th Australian and New Zealand Chemical Engineering Conf.* (1998).
1951. Goodson, M. E., Electric Water Heater Fires, *Fire & Arson Investigator* **51**:1, 17-20 (Oct. 2000).
1952. Medford, R. L., and Switzer, D. W., Status Report on Gas-fired Water Heater Ignition of Flammable Vapors, Consumer Product Safety Commission, Washington (1996).
1953. Briefing Package for Gas-fired Water Heater Ignition of Flammable Vapors, Consumer Product Safety Commission, Washington (1994).
1954. Talbott, J. A., and Beckham, W. M., Garage Fire Caused by Ignition of Aspirated Gasoline Vapors, paper presented at 42nd Annual Meeting of the American Academy of Forensic Sciences, Cincinnati OH (1990).
1955. Fandey, J. Z., Water Heater Test Project (Memorandum, April 14, 1994), Consumer Product Safety Commission, Washington (1994).
1956. Gas Water Heaters. Volume 1. Storage Water Heaters with Input Ratings of 75,000 BTU per Hour or Less (ANSI

Z21.10.1), American Natl. Standards Institute, New York (2001).
1957. A New Design for Gas Water Heaters: Flammable Vapor Ignition Resistant Gas Water Heaters Will Be in the Marketplace Soon, *Plumbing & Mechanical* 50-59 (Jan. 2003).
1958. Gas Water Heater Fires, *Fire Findings* **1**:1, 7-10 (Spring 1993).
1959. Lentini, J. J., Letter to the Editor, *Fire Findings* **1**:2, 14-15 (Summer 1993).
1960. Hanko, J. C., Another Cause of Rollout, *Fire & Arson Investigator* **50**:4, 25 (July 2000).
1961. Kao, J. Y., Ward, D. B., and Kelly, G. E., Flame Roll-out Study for Gas Fired Water Heaters (NBSIR 88-3724), [U.S.] Natl. Bur. Stand., Washington (1988).
1962. Kukachka, B. F., Properties of Imported Tropical Woods (FPL 125), US Forest Service, Forest Products Laboratory, Madison WI (1970).
1963. Strength and Related Properties of Woods, **International Critical Tables of Numerical Data, Physics, Chemistry, and Technology**, McGraw-Hill, New York (1927).
1964. Ragland, K. W., and Aerts, D. J., Properties of Wood for Combustion Analysis, *Bioresource Technology* **37**, 161-168 (1991).
1965. Bilbao, R., et al., Experimental and Theoretical Study of the Ignition and Smoldering of Wood Including Convective Effects, *Combustion and Flame* **126**, 1363-1372 (2001).
1966. Nagaoka, T., Kodaira, A., and Uehara, S., Relationship between Density and the Ignitability and Combustibility of Wood, pp. 197-208 in *Fire Science and Technology—Proc. Third Asia-Oceania Symp.*, Asia-Oceania Assn. for Fire Science and Technology (1998).
1967. Janssens, M., Thermo-Physical Properties for Wood Pyrolysis Models, pp. 607-618 in *Pacific Timber Engineering Conf.*, vol. 1, Gold Coast, Australia (1994).
1968. Yuen, R. K.-K., Pyrolysis and Combustion of Wood in a Cone Calorimeter (Ph.D. dissertation), The University of New South Wales, Australia (1998).
1969. Simms, D. L., Damage to Cellulosic Solids by Thermal Radiation, *Combustion and Flame* **6**, 303-318 (1962).
1970. Gardon, R., Temperatures Attained in Wood Exposed to High Intensity Thermal Radiation (Ph.D. dissertation), University of London, England (1959).
1971. Aleksandrov, V. V., and Aravin, G. S., The Role of Wood Transparency in Ignition by a Radiant Flux: Methods of Determination (Translation No. OOENV TR-937), Environment Canada (1975).
1972. Hottel, H. C., and Williams, C. C., Transient Heat Flow in Organic Materials Exposed to High Intensity Thermal Radiation, *Ind. and Eng. Chem.* **47**, 1136-1143 (1955).
1973. Akita, K., Studies on the Mechanism of Ignition of Wood, *Report of the Fire Research Institute of Japan* **9**, 1-44, 51-54, 77-83, 99-105 (1959).
1974. Hostikka, S., and McGrattan, K. B., Large Eddy Simulation of Wood Combustion, pp. 755-765 in *Interflam 2001—Proc. 9th Intl. Conf.*, Interscience Communications Ltd., London (2001).
1975. Antal, M. J. jr., Biomass Pyrolysis: A Review of the Literature. Part II. Lignocellulose Pyrolysis, pp. 175-255 in **Advances in Solar Energy**, vol. 2, American Solar Energy Society, New York (1985).
1976. Rubtsov, Yu. I., Kazakov., A. I., Andrienko, L. P., and Manelis, G. B., Kinetics of Heat Release during Decomposition of Cellulose, *Combustion, Explosion, and Shock Waves* **29**, 710-713 (1993).
1977. Wichman, I. S., and Oladipo, A. B., Examination of Three Pyrolytic Reaction Schemes for Cellulosic Materials, pp. 313-323 in *Fire Safety Science—Proc. 4th Intl. Symp.*, Intl. Assn. for Fire Safety Science (1994).
1978. Broido, A., and Nelson, M. A., Char Yield on Pyrolysis of Cellulose, *Combustion and Flame* **24**, 263-268 (1975).
1979. Shafizadeh, F., and Bradbury, A. G. W., Smoldering Combustion of Cellulosic Materials, *J. Thermal Insulation* **2**, 141-152 (1979).
1980. Richardson, L. R., and Batista, M., Fire Resistance of Timber Decking for Heavy Timber Construction, pp. 33-45 in *Proc. 29th Intl. Conf. on Fire Safety*, Product Safety Corp., Sissonville WV (2000).
1981. Koohyar, A. N., Ignition of Wood by Flame Radiation (Ph.D. dissertation), Univ. Oklahoma, Norman (1967).
1982. McNaughton, G. C., Ignition and Charring Temperatures of Wood, *Wood Products* **50**, 21-22 (1945).
1983. MacLean, J. D., Rate of Disintegration of Wood under Different Heating Conditions, *Proc. American Wood Preservers Assn.* **47**, 155-168 (1951).
1984. White, R. H., and Nordheim, E. V., Charring Rate of Wood for ASTM E 119 Exposure, *Fire Technology* **28**, 5-30 (1992).
1985. Banfield, W. O., and Peck, W. S., The Effect of Chemicals on the Ignition Temperature of Wood, *Canadian Chemistry and Metallurgy* **6**, 172-176 (Aug. 1922).
1986. VanKleeck, A., A Preliminary Study of Ignition Temperatures of Finely Chopped Wood (Project L-179), Forest Products Lab., Madison WI (1936).
1987. As cited in: Wood and Wood-Based Products, J. M. Cholin, ed., **Fire Protection Handbook**, A. E. Cote, and J. L. Linville, eds., 18th ed., NFPA (1997).
1988. Angell, H. W., Gottschalk, F. W., and McFarland, W. A., Ignition Temperature of Fireproofed Wood, Untreated Sound Wood and Untreated Decayed Wood, *British Columbia Lumberman* **33**, 57-58, 70-72 (Sept. 1949).
1989. Narayanamurti, D., A Note on Pyrolysis and Ignition of Wood, *Current Science* **27**, 22-23 (1956).
1990. Thomas, P. H., Simms, D. L., and Theobald, C. R., The Interpretation of Some Experimental Data on the Ignition of Wood (Fire Research Note No. 411), Fire Research Station, Borehamwood, UK (1959).
1991. Prince, R. E., Tests on the Inflammability of Untreated Wood and of Wood Treated with Fire-Retarding Compounds, *Proc. NFPA* **19**, 108-158 (1915).
1992. Simms, D. L., Ignition of Cellulosic Materials by Radiation, *Combustion and Flame* **4**, 293-300 (1960).
1993. Moran, H. E., jr., Effectiveness of Water Mists for Protection from Radiant Heat Ignition (NRL Report 5439), US Naval Research Laboratory, Washington (1960).
1994. Patten, G. A., Ignition Temperatures of Plastics, *Modern Plastics* **38**, 119-122, 180 (July 1961).
1995. Buschman, A. J., Ignition of Some Woods Exposed to Low Level Thermal Radiation (NBS Report 7306), NBS (1961).
1996. Tinney, E. R., The Combustion of Wooden Dowels in Heated Air, pp. 925-930 in *10th Symp. (Intl.) on Combustion*, The Combustion Institute, Pittsburgh (1964).
1997. Simms, D.L., and Law, M., The Ignition of Wet and Dry Wood by Radiation, *Combustion and Flame* **11**, 377-388 (1967).

1998. Muir, W. E., Studies of Fire Spread between Buildings (Ph.D. dissertation), Univ. Saskatchewan, Saskatoon, Canada (1967).
1999. Melinek, S. J., Ignition Behaviour of Heated Wood Surfaces (FR Note 755), Fire Research Station, Borehamwood, UK (1969).
2000. Jach, W., Das Verhalten von Holz und Holzwerkstoffen bei Dauereinwirkung von Temperaturen unterhalb des Flamm- und Brennpunktes, *Mitteilungen der deutschen Gesellschaft für Holzforschung*, Nr. 56, 12-17 (1969).
2001. Atreya, A., Pyrolysis, Ignition and Fire Spread on Horizontal Surfaces of Wood (Ph.D. dissertation), Harvard Univ., Cambridge MA (1983).
2002. Atreya, A., Carpentier, C., and Harkleroad, M., Effect of Sample Orientation on Piloted Ignition and Flame Spread, pp. 97-109 in *Fire Safety Science — Proc. 1st Intl. Symp.*, Hemisphere, Washington (1986).
2003. Abu-Zaid, M., Effect of Water on Ignition of Cellulosic Materials (Ph.D. thesis), Michigan State Univ., East Lansing MI (1988).
2004. Li, Y., and Drysdale, D., Measurement of the Ignition Temperature of Wood, pp. 380-385 in *Fire Science and Technology—Proc. First Asian Conf.*, Intl. Academic Publishers, Beijing (1992).
2005. Masařík, I., Ignitability and Burning of Plastic Materials: Testing and Research, pp. 567-577 in *Interflam '93*, Interscience Communications Ltd., London (1993).
2006. Fangrat, J., Hasemi, Y., Yoshida, M., and Hirata, T., Surface Temperature at Ignition of Wooden Based Slabs, *Fire Safety J.* **27**, 249-259 (1996); **28**, 379-380 (1997).
2007. Moghtaderi, B., Novozhilov, V., Fletcher, D. F., and Kent, J. H., A New Correlation for Bench-scale Piloted Ignition Data of Wood, *Fire Safety J.* **29**, 41-59 (1997).
2008. Boonmee, N., Radiant Auto-Ignition of Wood (M.S. thesis), Univ. Maryland, College Park (2001).
2009. Griffiths, L. G., and Heselden, A. J. M., The Use of Wooden Blocks as Simple Radiometers (Fire Research Note No. 648), Fire Research Station, Borehamwood (1967).
2010. Moghtaderi, B., Short Communication: Effects of Char Oxidation on Re-ignition Characteristics of Wood-Based Materials, *Fire and Materials* **24**, 303-304 (2000).
2011. Babrauskas, V., Ignition of Wood: A Review of the State of the Art, *J. Fire Protection Engineering* **12**, 163-189 (2002).
2012. Shafizadeh, F., Utilization of Biomass by Pyrolytic Methods, pp. 191-199 in *Proc. TAPPI 1997 Joint Forest Biology/Wood Chemistry Mtg.*, Madison WI (1977).
2013. Janssens, M., Piloted Ignition of Wood: A Review, *Fire and Materials* **15**, 151-167 (1991).
2014. Kelley, C. S., Piloted Ignition Times for Cellulosic Solids Exposed to Time-Dependent Heat Fluxes (EATR 4539), Edgewood Arsenal MD (1971).
2015. Harada, T., Charring of Wood with Thermal Radiation. II. Charring Rate Calculated from Mass Loss Rate, *Mokuzai Gakkaishi* **42**:2, 194-201 (1996).
2016. Harada, T., Time to Ignition, Heat Release Rate and Fire Endurance Time of Wood in Cone Calorimeter Test, *Fire and Materials* **25**, 161-167 (2001).
2017. McGuire, J. H., Limiting Safe Surface Temperature of Combustible Materials, *Fire Technology* **5**, 237-241 (1969).
2018. Spearpoint, M. J., Predicting the Ignition and Burning Rate of Wood in the Cone Calorimeter Using an Integral Model (NIST GCR 99-775), NIST (1999).
2019. Vyas, R. J., End-Grain Piloted Ignition of Wood by Flame Radiation (M.S. thesis), Univ. Oklahoma, Norman (1973).
2020. Pickard, R. W., Simms, D. L., and Walters, J. E. L., The Ignition by Radiation of Wood Protected by Some Common Paints (FPE Note No. 61/1951), Fire Research Station, Borehamwood (1951).
2021. Shields, T. J., Silcock, G. W., and Murray, J. J., The Effects of Geometry and Ignition Mode on Ignition Times Obtained using a Cone Calorimeter, *Fire and Materials* **17**, 25-32 (1993).
2022. Simms, D. L., and Hird, D., On the Pilot Ignition of Materials by Radiation (FR Note 365), Fire Research Station, Borehamwood, UK (1958).
2023. Lawson, D. I., and Simms, D. L., The Ignition of Wood by Radiation, *Brit. J. Appl. Phys.* **3**, 288-292 (1952).
2024. Simms, D. L., On the Pilot Ignition of Wood By Radiation, *Combustion and Flame* **7**, 253-261 (1963).
2025. Simms, D. L., Experiments on the Ignition of Cellulosic Materials by Thermal Radiation, *Combustion and Flame* **5**, 369-375 (1961).
2026. Babrauskas, V., unpublished Cone Calorimeter tests at NIST (1982).
2027. Parker, W. J., private communication (2000).
2028. Kashiwagi, T., Experimental Observation of Radiative Ignition Mechanisms, *Combustion and Flame* **34**, 231-244 (1979).
2029. Bryan, J., The Fire Hazard, *Wood* **8**, 260-262 (1943).
2030. Tuyen, B., Loof, R., and Bhattacharya, S. C., Self-sustained Flaming Combustion and Ignition of Single Wood Pieces in Quiescent Air, *Combustion Science and Technology* **110/111**, 53-65 (1995).
2031. Tsantaridis, L., CEN Ignitability Test Results for Wood Building Products (L-Rapport 9702010), Trätek, Stockholm (1997).
2032. Tsantaridis, L., CEN Tablet Test Results for Wood Floorings (L-Rapport 9702009), Trätek, Stockholm (1997).
2033. Friedman, R., Ignition and Burning of Solids, pp. 91-111 in **Fire Standards and Safety** (ASTM STP 614), ASTM (1976).
2034. Ebeling, K. L., Ignition of Wood by Direct Flame Contact (M.S. thesis), Univ. Oklahoma, Norman (1973).
2035. Ohlemiller, T. J., Smoldering Combustion (NBSIR 85-3294), NBS (1986).
2036. Ohlemiller, T. J., Smoldering Combustion Propagation on Solid Wood, pp. 565-574 in *Fire Safety Science—Proc. 3rd Intl. Symp.*, Elsevier, New York (1991).
2037. Ohlemiller, T. J., and Rogers, F. E., Smoldering Combustion Studies of Rigid Cellular Plastics (Report No. 1432), Dept. of Mechanical and Aerospace Engineering, Princeton University, Princeton NJ (1979).
2038. Dowling, V. P., Ignition of Timber Bridges in Bushfires, *Fire Safety J.* **22**, 145-168 (1994).
2039. McArthur, N. A., and Lutton, P., Ignition of Exterior Building Details in Bushfires: An Experimental Study, *Fire and Materials* **15**, 59-64 (1991).
2040. Hamada, M., et al., Experiments on the Ignition due to Fire Brands, Fire Research—Reports from the Fire Science Research Committee, Property and Casualty Insurance Rating Organization of Japan, Tokyo (1951).
2041. Safety Advice Follows Utilities Shaft Fire, *Petroleum Review* **40**, 38 (Apr. 1986).

2042. Tanaka, M., Ignition Hazard of Cigarettes in Still Air, *Kasai* [J. Japan Assn. for Fire Science and Engineering], **9**:2, 92-95 (1959).
2043. Critical Radiant Exposures for Ignition of Tinder and Combustible Materials (Part I – Wood), Naval Applied Science Lab., Brooklyn NY (1965).
2044. Gardner, W. D., and Ross, C. R., Ignitability and Heat-release Properties of Forest Products, *Fire and Materials* **15**, 3-9 (1991).
2045. Richardson, L. R., Assessing Fire Performance of Claddings Using the ICAL (Intermediate-Scale Calorimeter), pp. 240-252 in *Proc.23rd Intl. Conf. on Fire Safety*, Product Safety Corp., Sissonville WV (1997).
2046. Kristofferson, B., Hansen, A. S., and Hovde, P. J., Optimization of Fire Retardant Treated Wood, pp. 173-184 in *Proc. Fire and Materials 2001 Conf.*, Interscience Communications Ltd., London (2001).
2047. Holmes, C. A., The Fire Performance of Wood and Its Improvement by Fire-Retardant Treatments, *Proc. American Wood Preservers Assn.* **70**, 95-102 (1974).
2048. Grand, A. F., and Mehrafza, M., Evaluation of the Effectiveness of Fire Resistant Durable Agents on Residential Siding Using an ICAL-Based Testing Protocol, pp. 241-248 in *Proc. Fire and Materials 2001 Conf.*, Interscience Communications Ltd., London (2001).
2049. Weiss, H. F., Tests to Determine the Commercial Value of Wood Preservatives. A Progress Report, *8th Intl. Congress of Applied Chemistry*, Rumford Press, Concord (1911).
2050. Cuzzillo, B. R., Pyrophoria (Ph.D. dissertation), Univ. California, Berkeley (1997).
2051. Lee, C. K., Chaiken, R. F., and Singer, J. M., Wood Precharring: A Novel Fire-Retardancy Technique (RI 8299), Bureau of Mines, Pittsburgh (1978).
2052. Simms, D. L., and Roberts, V. E., Effect of Prolonged Heating on the Subsequent Spontaneous Ignition of Oak, *J. Inst. Wood Science* **5**, 29-37 (1960).
2053. Akizuki, M., Hasemi, Y., et al., Fire Safety Studies in the Restoration of a Historic Wooden Townhouse in Kyoto—Fire Safety Experiments on Japanese Traditional Wood-Based Constructions, pp. 329-340 in *Fire Science and Technology—Proc. 5th Asia-Oceania Symp.*, Univ. Newcastle, Australia (2001).
2054. Pickard, R. W., and Simms, D. L., The Effectiveness of Fire Retardant Paints, *Industrial Finishing* (Oct. 1955).
2055. Stockstad, D. S., Spontaneous and Piloted Ignition of Rotten Wood (Res. Note INT-267), US Forest Service, Intermountain Forest & Range Expt. Sta., Ogden UT (1979).
2056. Schwartz, E. von, **Fire and Explosion Risks**, Charles Griffin & Co., Ltd., London (1904). Original German edition: **Handbuch zur Erkennung, Beurtheilung und Verhütung der Feuer- und Explosionsgefahr chemisch-technischer Stoffe und Betriebsanlagen**, Ackermann, Konstanz (1902).
2057. Matson, A. F., Dufour, R. E., and Breen, J. F., Survey of Available Information on Ignition of Wood Exposed to Moderately Elevated Temperatures, Part II of Performance of Type B Gas Vents for Gas-Fired Appliances (Bull. of Research 51), Underwriters' Laboratories, Inc., Chicago (1959).
2058. Kinbara, T., and Kawasaki, A., Spontaneous Ignition of Wooden Materials Heated for a Long Time at a Low Temperature, *Bull. Fire Prevention Soc. of Japan* **16**, No. 2, 9-16 (Jan. 1967).
2059. Nailen, R. L., Carbonized Wood Ignition Determined in 4-Alarm Fire, *Fire Engineering* **134**, 30-31 (Jun. 1981).
2060. Östlin, B., Antändning av trä vid temperaturer under den normala tändpunkten [Ignition of Wood at Temperatures below the Normal Ignition Point], *Svenska Papperstidning* **63**:7, 225-227 (15 April 1960).
2061. Swan, K., Office of Fire Commissioner, Manitoba, private Communication (2001).
2062. VanderLaan, J., private communication (2002).
2063. Knudsen, H. P., Lavtryksdampkedel som brandstifter [Low pressure steam boiler as fire starter], *Fyring* **13**, 27-32, 39-41 (1954).
2064. Brooks, C. K., and McCreary, A.R., Are Steam Pipes Responsible for Fires? (B.S. thesis), Case School of Applied Science, Pittsburgh (1908).
2065. Handa, T., Suzuki, H., Takahashi, A., and Morita, M., Checks on Possibilities for the Spontaneous Combustion of Wood, Part II, *Bull. Fire Prevention Soc. of Japan* **21**:1, 9-16 (1971).
2066. Handa, T., Morita, M., Sugawa, O., Ishii, T., and Hayashi, K., Computer Simulation of the Oxidative Pyrolysis of Wood, *Fire Science & Technology* **2**, 109-116 (1982).
2067. Topf, P., Untersuchungen über die thermische Zersetzung von Holz in oxidierender Atmosphäre bei Temperaturen bis 180 Grad, Institut für Holzforschung, Ludwig-Maximilian-Universität, München (1970).
2068. Heinrich, H. J., and Kaesche-Krischer, B., Beitrag zur Aufklärung der Selbstentzündung von Holz, *Brennstoff-Chemie* **43**, 142-148 (1962).
2069. Stamm, A. J., Thermal Degradation of Wood and Cellulose, *Ind. and Eng. Chem.* **48**, 413-417 (1956).
2070. Parker, W J, Prediction of the Heat Release Rate of Douglas Fir, pp. 337-346 in *Fire Safety Science—Proc. 2nd Intl. Symp.*, Hemisphere, New York (1989).
2071. Kinbara, T., and Akita, K., An Approximate Solution of the Equation for Self-Ignition, *Combustion and Flame* **4**, 173-180 (1960).
2072. Chong, L. V., Shaw, I. R., and Chen, X. D., Thermal Ignition Kinetics of Wood Sawdust Measured by a Newly Devised Experimental Technique, *Process Safety Progress* **14**, 266-270 (1995).
2073. Jones, J. C., On the Extrapolation of Results from Oven Heating Tests for Propensity to Self-Heating, *Combustion and Flame* **124**, 334-336 (2001).
2074. Cuzzillo, B. R., and Pagni, P. J., The Myth of Pyrophoric Carbon, pp. 301-312 in *Fire Safety Science—Proc. 6th Intl. Symp.*, Intl. Assn. for Fire Safety Science (2000).
2075. Kubler, H., Role of Oxygen Diffusion in Self-Heating of Forest Products, *Wood and Fiber Science* **16**, 97-105 (1984).
2076. Palmer, K. N., and Tonkin, P. S., The Ignition of Dust Layers on a Hot Surface, *Combustion and Flame* **1**, 14-18 (1957).
2077. Fitz, M. M., MDE Engineers, private communication (2003).
2078. Wedger, W. L., Spontaneous Combustion and Friction, *Fire and Water Engrg.* **71**, 603-604; 614 (1922).
2079. Martin, J.-C., and Margot, P., Approche thermodynamique de la recherche des causes des incendies. Inflammation du bois. I., *Kriminalistik und forensische Wissenschaften* **82**, 33-50 (1994).
2080. Brittingham, C. W., Short Cuts Can Be Deadly, *Fire & Arson Investigator* **47**:1, 24-25 (Sept. 1996).

2081. Shafizadeh, F., and Seguchi, Y., Oxidation of Chars during Smoldering Combustion of Cellulosic Materials, *Combustion and Flame* **55**, 171-179 (1984).
2082. Shafizadeh, F., Chemistry of Pyrolysis and Combustion of Wood, pp. 746-771 in *Proc. 1981 Intl. Conf. on Residential Solid Fuels—Environmental Impacts and Solutions*, Oregon Graduate Center, Beaverton OR (1981).
2083. Bradbury, A. G. W., and Shafizadeh, F., Role of Oxygen Chemisorption in Low-Temperature Ignition of Cellulose, *Combustion and Flame* **37**, 85-89 (1980).
2084. Hshieh, F.-Y., and Richards, G. N., The Effect of Preheating of Wood on Ignition Temperature of Wood Char, *Combustion and Flame* **80**, 395-398 (1989).
2085. Kollmann, F. F. P., and Topf, P., Exothermic Reactions of Wood at Elevated Temperatures, *J. Fire & Flammability* **2**, 231-239 (1971).
2086. Low Temperature Ignition of Wood, *NFPA Q.* **19**, 159-167 (1925).
2087. Tsuchiya, Y., and Sumi, K., Spontaneous Ignition (Canadian. Bldg. Digest 189), National Research Council of Canada, Ottawa (1977).
2088. Handa, T., Suzuki, H., Origasa, R., and Takahashi, A., Checks on the Possibilities for the Spontaneous Combustion of Wood, Part I, *Bull. Fire Prevention Soc. of Japan* **20**:1, 11-30 (1970).
2089. Kinbara, T., and Sue, S., On the Outbreak of Fire Due to Leakage of Electricity from Neon Transformer through Planking, *Bull. Fire Prev. Soc. of Japan* **2**:2, 39-41 (1953).
2090. Kinbara, T., and Takizawa, K., Ignition of a Salt-soaked Wooden Board by an Electric Current Through It, *Bull. Fire Prev. Soc. of Japan* **11**:2, 26-31 (Dec. 1961).
2091. Sanderson, J. L., Carbon Tracking: Poor Insulation Combined with Contaminants is Potential Fire Cause, *Fire Findings* **8**:3, 1-3 (2000).
2092. Ross, P. M., Burning of Wood Structures by Leakage Currents, *AIEE Trans.* **66**, 279-287 (1947).
2093. Blackburn, T. R., and Pau, L. T., Characteristics of a Simulated High Impedance Fault, pp. 301-304 in *Electric Energy Conf. 1985*, Newcastle, Australia (1985).
2094. Darveniza, M., Limbourn, G. J., and Prentice, S. A., Line Design and Electrical Properties of Wood, *IEEE Trans. Power Appar. Syst.***PAS-86**, 1344-1353 (1967).
2095. Handa, T., et al., Thermal Processes in the Smoldering of Wood, pp. 308-366 in *Fire Research and Safety—Proc. 5th Joint Panel Mtg. US-Japan Cooperative Program in Natural Resources* (Spec. Pub. 639), NBS (1982).
2096. Roberts, A. F., A Review of Kinetics Data for the Pyrolysis of Wood and Related Substances, *Combustion and Flame* **14**, 261-272 (1970).
2097. Smith, K. N., Self-heating of Wood Fiber, *TAPPI* **42**, 869-872 (1959).
2098. Buchanan, M. A., The Ignition Temperature of Certain Pulps and Other Wood Components, *TAPPI*, **35**, 209-211 (1952).
2099. Beall, F. C., and Eickner, H. W., Thermal Degradation of Wood Components: A Review of the Literature (Res. Paper FPL 130), Forest Products Lab., US Forest Service, Madison WI (1970).
2100. Shafizadeh, F., The Chemistry of Pyrolysis and Combustion, pp. 489-529 in **The Chemistry of Solid Wood** (Advances in Chemistry Series 207), R. Rowell, ed., American Chemical Society, Washington (1984).
2101. Beall, F. C., Thermogravimetric Analysis of Wood Lignin and Hemicelluloses, *Wood & Fiber* **1**, 215-226 (1969).
2102. Kasprzycka-Guttman, T., and Odzeniak, D., Antioxidant Properties of Lignin and Its Fractions, *Thermochimica Acta* **231**, 161-168 (1994).
2103. Kuriyama, A., A Study on the Carbonization Process of Wood, *Bull. Forestry and Forest Products Research Institute* No. 304, 7-76 (Mar. 1979).
2104. Simms, D. L., Fire Hazards of Timber, *Record of the 1st Annual Convention of the British Wood Preserving Assn.* (1951).
2105. Staggs, J. E. J., Phylaktou, H. N., and McCreadie, R. E., The Effect of Paint on the Ignition Resistance of Plywood and Chipwood, *Fire Safety Science—Proc. 7th Intl. Symp.*, Intl. Assn. for Fire Safety Science (2002).
2106. Tran, H. C., Cohen, J. D., and Chase, R. A., Modeling Ignition of Structures in Wildland/Urban Interface Fires, pp. 253-262 in *Proc. First Intl. Fire and Materials Conf.*, Interscience Communications Ltd, London (1992).
2107. Zicherman, J. B., and Allard, D. L., Fire Performance of Fire-retardant Wood Fiberboard Ceiling Tile, *Fire and Materials* **16**, 187-196 (1992).
2108. LaCosse, R. A., Insulation Board Industry and Sound-Deadening Board, *Fire J.***70**, 45-48 (May 1976).
2109. Brenden, J. J., and Schaffer, E. L., Smoldering Wave-Front Velocity in Fiberboard (Research Pap. FPL 367), Forest Products Lab., Madison WI (1980).
2110. Palmer, K. N., Smouldering Combustion in Dusts and Fibrous Materials, *Combustion and Flame* **1**, 129-154 (1957).
2111. Henderson, A., Predicting Ignition Time under Transient Heat Flux Using Results from Constant Heat Flux Experiments (Report 98/4), School of Engineering, Univ. Canterbury, Christchurch, New Zealand (1998).
2112. Quintiere, J. G., Simplified Theory for Generalizing Results from a Radiant Panel Rate of Flame Spread Apparatus, *Fire and Materials* **5**, 52-60 (1981).
2113. Quintiere, J. G., and Harkleroad, M. F., New Concepts for Measuring Flame Spread Properties (NBSIR 84-2943), NBS (1984).
2114. Mehaffey, J. R., Richardson, L. R., Batista, M., and Guerguiev, S., Self-heating and Spontaneous Ignition of Fibreboard Insulating Panels, *Fire Technology* **36**, 226-235 (2000).
2115. Back, E. L., Autoignition in Hygroscopic, Organic Materials—Especially Forest Products—as Initiated by Moisture Absorption from the Ambient Atmosphere, *Fire Safety J.* **4**, 185-196 (1981/82).
2116. Thomas, P. H., and Bowes, P. C., Some Aspects of the Self-heating and Ignition of Solid Cellulosic Materials, *British J. Applied Physics* **12**, 222-229 (1961).
2117. Walker, I. K., Harrison, W. J., and Hooker, C., N., The Heat Balance in Spontaneous Ignition. Part 3. Application of Ignition Theory to a Porous Solid, *New Zealand J. Sci.* **8**, 319-332 (1965).
2118. Dowling, V. P., McArthur, N. A., Webb, A. K., Leonard, J. E., and Blackmore, J. M., Large-scale Fire Tests on Three Building Materials, pp. 217-227 in *ICFRE3 – Proc. 3rd Intl. Conf. on Fire Research and Engineering*, Society of Fire Protection Engineers, Bethesda MD (1999).
2119. Grexa, O., Janssens, M., and White, R., Analysis of Cone Calorimeter Data for Modeling of the Room/Corner Test on Wall Linings, pp. 63-71 in *Proc. 4th Intl. Fire and Materials Conf.*, Interscience Communications Ltd., London (1995).

2120. Chew, M. Y. L., HRR, Smoke and Toxicity of Ceiling and Wall Linings and Finishes, *Intl. J. on Engrg. Performance-Based Fire Codes* **1**, 204-212 (1999).
2121. Dillon, S. E., Kim, W. H., and Quintiere, J. G., Determination of Properties and the Prediction of the Energy Release Rate of Materials in the ISO 9705 Room-Corner Test. Appendices (NIST-GCR-98-754), NIST (1998).
2122. Walker, I. K., and Harrison, W. J., Exothermic Aerial Oxidation of Wood-Fibre Insulating Board, *New Zealand J. Sci.* **21**, 527-536 (1978).
2123. Harkleroad, M. F., Quintiere, J. G., and Walton, W. D., Radiative Ignition and Opposed Flow Flame Spread Measurements on Materials (DOT/FAA/CT-83/28), Federal Aviation Administration, Atlantic City Airport NJ (1983).
2124. Dillon, S. E., Analysis of the ISO 9705 Room/Corner Test: Simulations, Correlations and Heat Flux Measurements (M.S. Thesis), Univ. Maryland, College Park (1998).
2125. Urbas, J., and Parker, W. J., Impact of Air Velocity on Ignition in the Intermediate Scale Calorimeter (ICAL), *Fire and Materials* **21**, 143-151 (1997).
2126. Bhargava, A., Dlugogorski, B. Z., and Kennedy, E. M., Fire Properties of Wood Chips, pp. 1343-1348 in *Interflam 2001—Proc. 9th Intl. Conf.*, Interscience Communications Ltd., London (2001).
2127. Bowes, P. C., The Determination of the Ignition Temperature of Solids by a Rising Temperature Method (F.R. Note 10), Fire Research Station, Borehamwood, UK (1952).
2128. Pryce, J. N., and Cole, A. H., Wood-Chip Pile Burning Tests at the Restigouche Mill of Fraser Companies Limited, *Pulp & Paper Magazine of Canada* **64**, T389-T399 (1963).
2129. Kotoyori, T., Critical Ignition Temperatures of Wood Sawdusts, pp. 463-471 in *Fire Safety Science — Proc.1st Intl. Symp.,* Hemisphere, Washington (1986).
2130. Bowes, P. C., Spontaneous Heating and Ignition in Heaps of Sawdust (FR Note 187), Fire Research Station, Borehamwood (1955).
2131. Bergström, H., The Spontaneous Ignition of Wood and the Origin of Fusain, pp. 787-796 in *Proc. 3rd Intl. Conf. on Bituminous Coal*, Carnegie Institute of Technology, Pittsburgh (1932).
2132. Bergman, Ö., Thermal Degradation and Spontaneous Ignition in Outdoor Chip Storage, *Svensk Papperstidning* **77**:18, 681-684 (1974).
2133. Manssen, N. B., and Walker, I. K., Self-heating of Wet Wood. 3. Spontaneous Ignition of Chip Piles and Wood-Waste Dumps, *New Zealand J. Science* **22**, 105-112 (1979).
2134. Walker, I. K., and Harrison, W. J.., Self-heating of Wet Wood. 1. Exothermic Oxidation of Wet Sawdust, *New Zealand J. Science* **20**, 191-200 (1977).
2135. Haldane, J. S., and Makgill, R. H., The Spontaneous Oxidation of Coal and Other Organic Substances, *J. Soc. Chem. Industry* **53**, 359T-367T (1934).
2136. Springer, E. L., Should Whole-Tree Chips for Fuel be Dried before Storage? (Res. Note FPL-0241), Forest Products Lab., Madison WI (1980).
2137. Walker, I. K., and Manssen, N. B., Self-heating of Wet Wood. 2. Ignition by Slow Thermal Explosion, *New Zealand J. Science* **22**, 99-103 (1979).
2138. Sherrard, F. C., Sawdust, pp. 96-99 in Report of Conference on Spontaneous Heating and Ignition of Agricultural and Industrial Products, NFPA and US Dept. of Agriculture, Washington (1929).
2139. Springer, E. L., and Hajny, G. J., Spontaneous Heating in Piled Wood Chips. I. Initial Mechanism, *TAPPI* **53**, 85-86 (1970). II. Effect of Temperature, **54**, 589-591 (1971).
2140. Bowes, P. C., and Thomas, P. H., Ignition and Extinction Phenomena Accompanying Oxygen-dependent Self-heating of Porous Bodies, *Combustion and Flame* **10**, 221-230 (1966).
2141. Ettling, B. V., and Adams, M. F., Spontaneous Combustion of Linseed Oil in Sawdust, *Fire Technology* **7**, 225-236 (1971).
2142. Napier, D. H., and Vlatis, J., Safety Considerations in the Self-Heating of Two Component Systems, pp. 2/F:1 to 2/F:16 in *Runaway Reactions, Unstable Products and Combustible Powders* (Symp. Series No. 68), The Institution of Chemical Engineers, London (1981).
2143. Voigt, G. Q., Fire Hazard of Domestic Heating Installations, *Bureau of Standards J. of Research* **11**, 353-372 (1933).
2144. Fitz, M. M., MDE Engineers, private communication (2002).
2145. Lawson, D. I., Fire Accidents—The Contribution of Some Textiles, *Research* **11**, 126-133 (1958).
2146. Walker, I. K., and Harrison, W. J., The Self-Heating of Wet Wool, *New Zealand J. Agricultural Research* **3**, 861-895 (1960).
2147. Walker, I. K., and Williamson, H. M., The Spontaneous Ignition of Wool. I. The Causes of Spontaneous Fires in New Zealand Wool, *J. Applied Chemistry* **7**, 468-480 (1957).
2148. Rothbaum, H. P., and Dye, M. H., Self-Heating of Damp Wool. Part 3. Self-Heating of Damp Wool under Isothermal Conditions, *New Zealand J. of Science* **7**, 119-146 (1964).
2149. Walker, I. K., and Harrison, W. J., The Reaction between Pie Wool and Oxygen, *New Zealand J. Science* **4**, 26-54 (1961).
2150. Carrie, M. S., Walker, I. K., and Harrison, W. J., The Spontaneous Ignition of Wool. II. A New Process for Wool Removal from Sheepskin Pieces, *J. Applied Chemistry* **9**, 608-615 (1959).
2151. Walker, I. K., Harrison, W. J., and Patterson, G. F., Ignition of Wool in Air. Part 3—Ignition in Heated Room Air, *New Zealand J. Science* **11**, 380-393 (1968).
2152. Jones, J. C., The Self-Heating of Wool and Its Conformity to Ignition Theory, *Wool Tech. & Sheep Breeding* 137-141 (Dec. 1988/Jan. 1989).
2153. Read, A. J., Harrison, W. J., and Walker, I. K., Ignition of Wool in Air. Part 2—Effects of Sample Size, *New Zealand J. Science* **10**, 964-978 (1967).
2154. Perdue, G. R., Spontaneous Combustion: How It Is Caused and How to Prevent It Occurring, *Power Laundry* 599 (5 Oct. 1956); and 689 (19 Oct 1956).

Copyright © 2003, 2014 Vytenis Babrauskas

Chapter 15. Tables

Introduction **1022**
Pure chemical substances **1024**
Mixtures and commercial products **1056**
Aviation hydraulic fluids and lubricating oils **1059**
Refrigerants **1060**
NEC Groups according to chemical families **1061**
Dusts **1062**
Ignition temperatures of solids **1066**
Radiant ignition of plastics and elastomers **1070**
Miscellaneous thermophysical properties of solids **1072**
Further readings **1077**
References **1077**

Introduction

A number of tables are provided in this Chapter to serve as a convenient reference. The user must strongly keep in mind that many industrial ignition hazards occur at elevated pressures or in atmospheres substantially different from ambient. Thus, in assessing specific hazards, recourse should preferably be had to original research literature where hazards of a particular compound or reaction have been studied in detail. Even at a given ambient condition, measurements are notably dependent on test apparatus vagaries. Thus, above all, the reader is cautioned to keep the words of Magison[1] in mind: "*There are few absolute numbers in combustion and ignition studies*."

For the data given in Tables 1 and 2, the following explanation notes are pertinent. The data have been compiled primarily from BM[2,3,4] and NIST[5,6] publications. AIT values in air[*] are mostly from NFPA 325[7]. AIT values in oxygen are mostly from Mullins[8]. Data were also used from Pedley[9], Budaveri[10], Lide[11], Dean[12], Helwig[13], Britton[14],

[*] The values in NFPA 325 generally represent a compilation of the lowest values found in the literature. Thus, these values are best viewed as conservative bounds, not as best-estimate values. In some cases, the values given in NFPA 325 may be in serious error. For instance, the value for methane, reported for many years as 537ºC is actually 640ºC, according to latest and most reliable study (see Chapter 14).

Yaws[15], NACA[16], CPIA[17], Hertzberg[18], Burgoyne[19], Jones[20], Lambourne[21], Lewis[22], Dillon[23], and Snyder[24]. Notation: **g** - the substance is a gas at 25ºC, **s** - the substance is a solid at 25ºC, **e** - estimated value, **pyr** - pyrophoric, **exp** - explodes. Flammability limits in *italics* denote that the substance is flammable only at temperatures higher than ambient, consequently the data were obtained at a temperature higher than 25ºC; the original BM references can be consulted for details of test conditions. NEC Group information is from NFPA 497M[25]. The suffix '**t**' designates a value obtained by test, '**c**' by committee action without testing. Some substances have a dual designation, e.g., B/C. This denotes that the substance is in Group C, as determined by its MESG value, but in Group B, as determined by maximum pressure rise. Vapor pressures at the flash point are from Kueffer and Donaldson[26]. The values cited as 'Calcote' are from Calcote et al.[27] The flanged electrode data (rather than plain) are normally used, since these correspond more closely to the experimental arrangement subsequently used by the Bureau of Mines. Quenching diameters are listed from Grove[28]. The IEC MESG values are as tested by PTB[29]; where unavailable, values from HSE[30] were used. The values cited by NFPA 497 (not shown) are typically similar to the IEC values. The UL MESG values are from UL Bull. 58[31]. UK MIC values are from Slack and Woodhead[32] or from Magison[1] and refer to a circuit with an inductance of 95 mH. None of the values are available as *evaluated* or *best-estimate* constants, that is, having undergone a systematic review process wherein values obtained with poor experimental techniques are rejected in preference to values obtained from experiments judged to be of higher accuracy.

The reader will note that, in a number of cases, lower values are reported for AIT in air than in oxygen. This, of course, does *not* mean that these substances are less readily ignitable in pure oxygen than in air. The anomaly arises because data from different workers or different test rigs have been presented. If experiments are conducted in a single apparatus, the ignition temperatures measured will be lower in oxygen (or, in some cases, equal) than in air.

CAS (Chemical Abstracts Service) registry numbers are provided, since they are a unique identifier for chemical substances. A pure substance may be known by many different names, but it will not have multiple CAS numbers. Conversely, each CAS number denotes a unique chemical substance (there are limited exceptions, primarily for mixtures of isomers that are normally not available individually). The UN (United Nations) designation numbers are also provided, where they are relatively unique. In the UN system, many compounds are not assigned a unique number, but fall into broad categories, for example, "UN 3180: Flammable solid, corrosive, inorganic, n.o.s." These lumped categories have not been listed in Table 1.

Table headings are as follows:
CAS No. – Chemical Abstracts Service registry number
UN No. – United Nations designation
Formula – chemical formula of substance
MW – molecular mass
Δh_f – heat of formation
Δh_c – heat of combustion
C_{st} – stoichiometric volume concentration of fuel
LFL – lower flammability limit
UFL – upper flammability limit
AIT – autoignition temperature
NEC group – National Electrical Code Group
LTL – lower temperature limit
BP – boiling point
P_{vap} – vapor pressure at flash point
MIE – minimum ignition energy
Quench dist. – quenching distance
MESG – maximum experimental safe gap
MIC – minimum igniting current
T_{ad} at LFL – adiabatic flame temperature at the LFL
T_{ad} at stoich – adiabatic flame temperature at stoichiometry

For additional details on these variables, the reader should consult Chapters 3 and 4.

Pure chemical substances

Table 1A Pure chemical substances

Substance	CAS No.	UN No.	Formula	MW	Δh_f kJ mol^{-1}	Δh_c (upper) kJ mol^{-1}	Δh_c (lower) kJ mol^{-1}	Δh_c (lower) MJ kg^{-1}
acetal (1,1-diethoxyethane)	105-57-7	1088	$C_6H_{14}O_2$	118.18	-420.6	3941.3	3633.2	30.74
acetaldehyde (g)	75-07-0	1089	C_2H_4O	44.05	-170.7	1188.0	1100.0	24.97
acetanilide (s)	103-84-4		C_8H_9NO	135.17	-209.5	4224.9	4026.8	29.79
acetic acid	64-19-7	1842	$C_2H_4O_2$	60.05	-483.52	875.2	787.1	13.11
acetic anhydride	108-24-7	1715	$C_4H_6O_3$	102.09	-575.7	1855.9	1723.8	16.89
acetone	67-64-1	1090	C_3H_6O	58.08	-249.4	1788.7	1656.6	28.52
acetonitrile (methyl cyanide)	75-05-8	1648	C_2H_3N	41.05	40.56	1256.3	1190.3	28.99
acetophenone	98-86-2		C_8H_8O	120.15	-142.5	4148.9	3972.9	33.07
acetylacetone (2,4-pentadione)	123-54-6	2310	$C_5H_8O_2$	100.12	-423.8	2687.1	2511.0	25.08
acetyl chloride	75-36-5	1717	C_2H_3ClO	62.50	-272	967.5	923.5	14.78
acetylene (g)	74-86-2	1001	C_2H_2	26.04	226.7	1299.6	1255.5	48.22
acrolein	107-02-8	1092	C_3H_4O	56.06	-81	1671.2	1583.2	28.24
acrylic acid (2-propenoic acid)	79-10-7	2218	$C_3H_4O_2$	72.06	-383.8	1368.4	1280.4	17.77
acrylonitrile (vinyl cyanide)	107-13-1	1093	C_3H_3N	53.06	140	1749.3	1683.3	31.72
adipic acid (s)	124-04-9		$C_6H_{10}O_4$	146.14	-989.5	2800.8	2580.7	17.66
adiponitrile	111-69-3	2205	$C_6H_8N_2$	108.14	84.9	3589.3	3413.2	31.56
aldol	107-89-1	2839	$C_4H_8O_2$	88.11	-430.5	2286.9	2110.8	23.96
allyl alcohol (2-propenol)	107-18-6	1098	C_3H_6O	58.08	-171.8	1866.3	1734.2	29.86
allyl amine	107-11-9	2334	C_3H_7N	57.10	10	2191.0	2036.9	35.68
allyl bromide	106-95-6	1099	C_3H_5Br	120.98	20	1893.4	1805.3	14.92
allyl carbinol	627-27-0		C_4H_8O	72.11				
allyl chloride	107-05-1	1100	C_3H_5Cl	76.53	-0.63	1918.2	1830.2	23.92
allyl glycidyl ether	106-92-3	2219	$C_6H_{10}O_2$	114.14				
ammonia (g)	7664-41-7	1005	NH_3	17.03	-45.94	382.8	316.8	18.60
ammonium nitrate (s)	6484-52-2	var.	$H_4N_2O_3$	80.04	-365.56	206.1	118.1	1.48
ammonium perchlorate (s)	7790-98-9	1442	H_4NO_4Cl	117.49	-295.77	299.6	233.6	1.99
n-amyl acetate	628-63-7	1104	$C_7H_{14}O_2$	130.19	-505.5	4250.0	3941.8	30.28
sec-amyl acetate	626-38-0	1104	$C_7H_{14}O_2$	130.19				
amyl alcohol (1-pentanol)	71-41-0	1105	$C_5H_{12}O$	88.15	-351.62	3331.0	3066.9	34.79
tert-amyl alcohol	75-85-4	1105	$C_5H_{12}O$	88.15	-379.5	3303.1	3039.0	34.48
n-amyl amine	110-58-7	1106	$C_5H_{13}N$	87.16	-438.5	3387.0	3100.9	35.58
n-amyl bromide	110-53-2		$C_5H_{11}Br$	151.05	-170.4	3347.5	3127.4	20.71
n-amyl chloride	543-59-9	1107	$C_5H_{11}Cl$	106.59	-213.4	3350.0	3129.9	29.36
tert-amyl chloride	594-36-5		$C_5H_{11}Cl$	106.59	-235	3328.4	3108.3	29.16
n-amylene (1-pentene)	513-35-9	1108	C_5H_{10}	70.13	-68.6	3328.2	3108.1	44.32
n-amyl ether (pentyl ether)	693-65-2		$C_{10}H_{22}O$	158.28	-435.22	6644.1	6159.9	38.92
n-amyl nitrate	1002-16-0	1112	$C_5H_{11}NO_3$	133.15				
n-amyl nitrite	463-04-7	1113	$C_5H_{11}NO_2$	117.15	-215.4	3324.3	3082.2	26.31
amyl propionate	624-54-4		$C_8H_{16}O_2$	144.21				
aniline	62-53-3	1547	C_6H_7N	93.13	31.3	3392.8	3238.7	34.78
anisole	100-66-3	2222	C_7H_8O	108.14	-114.8	3783.1	3607.1	33.36
anthracene (s)	120-12-7		$C_{14}H_{10}$	178.23	125.54	7063.9	6843.8	38.40
arsine (g)	7784-42-1	2188	AsH_3	77.95	66.44	209.4	187.4	
benzaldehyde	100-52-7	1989	C_7H_6O	106.12	-87.1	3525.0	3392.9	31.97
benzene	71-43-2	1114	C_6H_6	78.11	48.95	3267.5	3135.5	40.14
1,4-benzenediamine (s)	106-50-3	1673	$C_6H_8N_2$	108.14	6.3	3510.7	3334.6	30.84
benzoic acid (s)	65-85-0	9094	$C_7H_6O_2$	122.12	-384.8	3227.3	3095.2	25.35
benzonitrile	100-47-0	2224	C_7H_5N	103.12	163.2	3632.4	3522.3	34.16
benzotrifluoride	98-08-8	2338	$C_7H_5F_3$	146.12	-620.45	3376.9	3332.9	17.01
benzyl alcohol	100-51-6		C_7H_8O	108.14	-194.9	3703.0	3527.0	32.61
benzyl benzoate	120-51-4		$C_{14}H_{12O2}$	212.25	-272.4	6951.8	6687.7	31.51
benzyl chloride	100-44-7	1738	C_7H_7Cl	126.59	-33	3745.7	3613.7	28.55

Table 1B Pure chemical substances

Substance	C_{st} (vol%)	LFL (vol%)	LFL (g m^{-3})	UFL (vol%)	AIT (ºC) in air	AIT (ºC) in O_2	NEC Group	Flash point (ºC)	LTL (ºC)	BP (ºC)	P_{vap} at FP (atm)
acetal (1,1-diethoxyethane)	2.41	1.6	77.3	10	230	174		36	37	103	
acetaldehyde (g)	7.74	4.0	72.0	60	175	160	Ct	-38		21	0.051
acetanilide (s)	2.10	1.1e		6.9e	540			173		304	
acetic acid	9.49	*5.4*	132.6	*16*	465	490	Dt	43	40	118	0.046
acetic anhydride	4.98	*2.7*	112.7	*10.3*	392	361	Dc	54	47	140	0.038
acetone	4.98	2.6	61.7	12.8	465	445	Dt	-18		56	0.036
acetonitrile (methyl cyanide)	7.08	4.4	73.8	16	524		Dc	13		82	
acetophenone	2.16	1.1e		6.7e	571			82 oc		202	0.015
acetylacetone (2,4-pentadione)	3.38	2.4	98.2	11.6	493			34		140	
acetyl chloride	7.74	*5.0*	127.8	15.6e	390			4		52	
acetylene (g)	7.74	2.5	26.6	100	305	296	At			-83	
acrolein	5.65	2.8	64.2	31	278		B/C	-26		52	
acrylic acid (2-propenoic acid)	6.53	2.4	70.7	20.2	438		Dc	48		141	
acrylonitrile (vinyl cyanide)	5.29	3.0	65.1	17	481	460	Dt	0	-6	113	0.039
adipic acid (s)	3.12	1.6	95.6	9.6	420			196		337	
adiponitrile	2.55	1.7	75.2	5	550		Dc	93		295	
aldol	4.02	2.1e		12.2e	250			66 oc		171e	
allyl alcohol (2-propenol)	4.98	2.5	59.4	18	378	348	Ct	21	22	97	0.025
allyl amine	4.23	2.2	51.4	22	375			-28		53	
allyl bromide	5.29	4.4	217.6	7.3	295			-1		70	
allyl carbinol	3.67	4.7	138.6	34				38		112	
allyl chloride	4.98	2.9	90.7	11.2	487	404	Dc	-32	-32	45	0.032
allyl glycidyl ether	2.72						B/Cc	48		154	
ammonia (g)	21.85	15	104.4	28	651		Dt			-33	
ammonium nitrate (s)										dec	
ammonium perchlorate (s)										dec	
n-amyl acetate	2.16	*1.0*	53.2	*7.1*	399	235	Dc	25	25	149	
sec-amyl acetate	2.16	1.1	58.5	7.5	343		Dc	32		134	
amyl alcohol (1-pentanol)	2.72	*1.4*	50.5	*10*	427	332	Dt	32	38	137	
tert-amyl alcohol	2.72	1.2	43.2	9	437			20		102	0.011
n-amyl amine	2.48	2.2	78.4	22				4		104	
n-amyl bromide	2.81							31		130	
n-amyl chloride	2.72	*1.6*	69.7	*8.6*	260			11		107	
tert-amyl chloride	2.72	*1.5*	65.4	7.4	343			-9	-12	93	
n-amylene (1-pentene)	2.72	1.4	40.1	8.7	275			-45		39	
n-amyl ether (pentyl ether)	1.38	*0.7*	45.3	5.5e	170			57		190	
n-amyl nitrate	3.25	*1.1*	59.9		195			48		155	
n-amyl nitrite	3.01	1.0e			210					104	
amyl propionate	1.87	1.0e			380			41 oc		169	
aniline	2.63	*1.2*	45.7	*8.3*	530	530	Dc	70		184	0.014
anisole	2.41	1.3e		9.0e	475			41		154	
anthracene (s)	1.25	*0.65*	47.4	*5.3*	472	580		121		340	0.001
arsine (g)	45.61	5.1	162.5	78						-62	
benzaldehyde	2.55	1.3	56.4	7.8e	192	168		64		179	
benzene	2.72	*1.3*	41.5	*7.9*	580	566	Dt	-11		80	0.018
1,4-benzenediamine (s)	2.55	1.5	66.3	9.8e				156		267	
benzoic acid (s)	2.72	1.4e		8.0e	573	556		121		249	
benzonitrile	2.48	1.3e		8.0e				71		191	
benzotrifluoride	2.72			8.4e				12		101	
benzyl alcohol	2.41	1.7	75.2	15	428	373		94		205	
benzyl benzoate	1.29	0.7e		4.5e	480			147		323	
benzyl chloride	2.41	*1.1*	56.9	*7.1*	627		Dc	67		179	

Table 1C Pure chemical substances

Substance	MIE (mJ), plain Calcote	MIE (mJ), flanged Calcote	MIE (mJ), air other	MIE (mJ), O_2 other	Quench dist. (mm)	Quench dia. (mm) Grove	MESG [IEC] (mm)	MESG [UL] (mm)	MIC [UK] (mA)	T_{ad} at LFL (K)	T_{ad} at stoich (K)
acetal (1,1-diethoxyethane)											
acetaldehyde (g)	0.376	0.57	0.38				0.92	0.43	163	1675	2300
acetanilide (s)											
acetic acid						5.59	1.76	1.45	390		
acetic anhydride							1.23				
acetone	1.15	2.15	1.15	0.0024			1.04		170	1700	2210
acetonitrile (methyl cyanide)	2.8	6.0					1.50				
acetophenone											
acetylacetone (2,4-pentadione)							0.99				
acetyl chloride											
acetylene (g)	0.02	0.03	0.017	0.0002	0.65	0.85	0.37	0.08	60	1275	2580
acrolein	0.137	0.175	0.13					0.46		1540	2340
acrylic acid (2-propenoic acid)											
acrylonitrile (vinyl cyanide)			0.16		1.5		0.87	0.81	131		
adipic acid (s)											
adiponitrile											
aldol											
allyl alcohol (2-propenol)							0.84	0.66			
allyl amine											
allyl bromide											
allyl carbinol											
allyl chloride	0.775	1.35	0.78				1.17		210		
allyl glycidyl ether											
ammonia (g)			680			22.1	3.18	0.99	1070		
ammonium nitrate (s)											
ammonium perchlorate (s)											
n-amyl acetate						2.95	1.02				
sec-amyl acetate											
amyl alcohol (1-pentanol)					1.8		1.02				
tert-amyl alcohol							0.96				
n-amyl amine											
n-amyl bromide											
n-amyl chloride											
tert-amyl chloride											
n-amylene (1-pentene)											
n-amyl ether (pentyl ether)											
n-amyl nitrate											
n-amyl nitrite											
amyl propionate											
aniline											
anisole							0.82				
anthracene (s)											
arsine (g)											
benzaldehyde											
benzene	0.55	0.91	0.22		1.95		0.99		158	1715	2340
1,4-benzenediamine (s)											
benzoic acid (s)											
benzonitrile							0.89				
benzotrifluoride							1.40				
benzyl alcohol											
benzyl benzoate											
benzyl chloride											

Table 1A Pure chemical substances

Substance	CAS No.	UN No.	Formula	MW	Δh_f kJ mol^{-1}	Δh_c (upper) kJ mol^{-1}	Δh_c (lower) kJ mol^{-1}	Δh_c (lower) MJ kg^{-1}
bicyclohexyl	92-51-3		$C_{12}H_{22}$	166.31	-276.4	7590.0	7105.7	42.73
biphenyl (s)	92-52-4		$C_{12}H_{10}$	154.21	96.73	6248.1	6028.0	39.09
bromobenzene	108-86-1	2514	C_6H_5Br	157.01	58.6	3112.5	3024.5	19.26
1,3-butadiene (g)	106-99-0	1010	C_4H_6	54.09	108.8	2540.4	2408.3	44.52
2,3-butadione (diacetyl)	431-03-8	2346	$C_4H_6O_2$	86.09	-365.5	2066.1	1934.0	22.46
butane (g)	106-97-8	1011	C_4H_{10}	58.12	-127.1	2876.1	2656.0	45.70
1-butanol (*n*-butanol)	71-36-3	1120	$C_4H_{10}O$	74.12	-327.01	2676.2	2456.1	33.14
2-butanol (*sec*-butanol)	78-92-2	1120	$C_4H_{10}O$	74.12	-342.7	2660.5	2440.4	32.92
tert-butanol	75-65-0	1120	$C_4H_{10}O$	74.12	-359.2	2644.0	2423.9	32.70
2-butene (g)	107-01-7		C_4H_8	56.11	-7.1	2710.3	2534.2	45.17
1-butene (butylene) (g)	106-98-9	1012	C_4H_8	56.11	-0.63	2716.8	2540.7	45.28
n-butyl acetate	123-86-4	1123	$C_6H_{12}O_2$	116.16	-609.6	3466.5	3202.4	27.57
sec-butyl acetate	105-46-4	1123	$C_6H_{12}O_2$	116.16	-503.8	3572.3	3308.2	28.48
tert-butyl acetate	540-88-5	1123	$C_6H_{12}O_2$	116.16	-554.5	3521.6	3257.5	28.04
n-butyl acrylate	141-32-2	2348	$C_7H_{12}O_2$	128.17	-422.6	4047.0	3782.9	29.51
butyl amine (1-butanamine)	109-73-9	1125	$C_4H_{11}N$	73.14	-127.7	3018.5	2776.4	37.96
tert-butyl amine	75-64-9		$C_4H_{11}N$	73.14	-150.6	2995.6	2753.5	37.65
n-butyl benzene	104-51-8	2709	$C_{10}H_{14}$	134.22	-62.9	5873.1	5564.9	41.46
sec-butyl benzene	135-98-8	2709	$C_{10}H_{14}$	134.22	-17.6	5918.4	5610.2	41.80
tert-butyl benzene	98-06-6	2709	$C_{10}H_{14}$	134.22	-70.8	5865.2	5557.0	41.40
n-butyl bromide	109-65-9	1126	C_4H_9Br	137.02	-148	2690.6	2514.5	18.35
butyl cellosolve (ethylene glycol monobutyl ether, EGME)	111-76-2	2369	$C_6H_{14}O_2$	118.18	-812	3549.9	3241.8	27.43
n-butyl chloride	109-69-3	1127	C_4H_9Cl	92.57	-188.15	2695.9	2519.8	27.22
butyl ether	142-96-1	1149	$C_8H_{18}O$	130.23	-378	5342.6	4946.5	37.98
butyl formate	592-84-7	1128	$C_5H_{10}O_2$	102.13	-593	2803.8	2583.7	25.30
n-butyl glycidyl ether	2426-08-6		$C_7H_{14}O_2$	130.19	-345.3	4410.2	4102.0	31.51
butyl glycolate	7397-62-8		$C_6H_{12}O_3$	132.16				
butyl mercaptan	109-79-5	2347	$C_4H_{10}S$	90.18	-88.3	3516.9	3340.8	37.05
butyl methacrylate	97-88-1	2227	$C_8H_{14}O_2$	142.20	-413.1	4735.9	4427.7	31.14
butyl stearate	123-95-5		$C_{22}H_{44}O_2$	340.59	-973	13972.7	13004.3	38.18
p-tert-butyltoluene	98-51-1	2667	$C_{11}H_{16}$	148.25	-56.9	6558.4	6206.3	41.86
butyraldehyde (butanal)	123-72-8	1129	C_4H_8O	72.11	-245.4	2472.0	2295.9	31.84
butyric acid	107-92-6	2820	$C_4H_8O_2$	88.11	-533.92	2183.5	2007.4	22.78
γ-butyrolactone	96-48-0		$C_4H_6O_2$	86.09	-419	2012.6	1880.5	21.84
camphene (s)	79-92-5		$C_{10}H_{16}$	136.24	-75	6146.8	5794.7	42.53
camphor (s)	76-22-2	2717	$C_{10}H_{16}O$	152.24	-319	5902.8	5550.7	36.46
carbon disulfide	75-15-0	1131	CS_2	76.13	89.41	1686.9	1774.9	23.31
carbon monoxide (g)	630-08-0	1016	CO	28.01	-110.53	283.0	283.0	10.10
carbon subnitride (2-butynedinitrile)	1071-98-3		C_4N_2	76.06	500.4	2074.4	2074.4	27.27
carbonyl sulfide (g)	463-58-1	2204	COS	60.07	-138.4	857.1	901.1	15.00
chloroacetaldehyde	107-20-0	2232	C_2H_3ClO	78.50	-191	1048.5	1004.5	12.80
chloroacetylene (g)	593-63-5		C_2HCl	60.48	213.8	1167.4	1167.4	19.30
chlorobenzene	108-90-7	1134	C_6H_5Cl	112.56	11.5	3110.9	3022.8	26.86
2-chloro-2-butene	4461-41-0		C_4H_7Cl	90.55				
chlorodifluoroethane (Freon 142b)	75-68-3	2517	$C_2H_3ClF_2$	100.50	-502	1089.6	1089.6	9.15
1-chloro-2,4-dinitrobenzene	97-00-7		$C_6H_3ClN_2O_4$	202.55	-73.3e	2740.2e	2696.2e	13.31e
2-chloroethanol (ethylene chlorohydrin)	107-07-3	1135	C_2H_5ClO	80.51	-294	1231.3	1143.3	14.20
chloromethoxymethane	107-30-2	1239	C_2H_5ClO	80.51	-236e	1289.3e	1201.3e	14.92e

Table 1B Pure chemical substances

Substance	C_{st} (vol%)	LFL (vol%)	LFL (g m^{-3})	UFL (vol%)	AIT (ºC) in air	AIT (ºC) in O_2	NEC Group	Flash point (ºC)	LTL (ºC)	BP (ºC)	P_{vap} at FP (atm)
bicyclohexyl	1.18	*0.65*	44.2	*5.1*	244	232		92	74	238	
biphenyl (s)	1.43	*0.6*	37.8	*5.8*	577			113	110	255	0.011
bromobenzene	3.01	*1.5*	96.3	*9.1*	565			51		155	
1,3-butadiene (g)	3.67	2.0	44.2	12	418	335	B/Dt	-76		-4.4	
2,3-butadione (diacetyl)	4.45							6		88	
butane (g)	3.12	1.8	42.8	8.4	408	283	Dt	-60	-72	-0.6	0.049
1-butanol (*n*-butanol)	3.38	*1.7*	51.5	*12*	365	328	Dt	29		117	0.052
2-butanol (*sec*-butanol)	3.38	*1.7*	51.5	*9.8*	414	377	Dt	24	21	100	0.022
tert-butanol	3.38	*1.9*	57.6	*9*	478	460		11	11	82	0.021
2-butene (g)	3.38	1.7	39.0	9.7	325			-73		3.7	
1-butene (butylene) (g)	3.38	1.6	36.7	10	384	310	Dc	-79		-6.3	
n-butyl acetate	2.55	*1.4*	66.5	*7.6*	421		Dt	22		125	0.012
sec-butyl acetate	2.55	*1.7*	80.7	*7.6*	423		Dc	16		113	0.013
tert-butyl acetate	2.55	1.3e		7.3e			Dc	15		98	
n-butyl acrylate	2.28	1.5	78.6	9.9	345	328	Dc	39		145	
butyl amine (1-butanamine)	3.01	1.7	50.8	9.8	312		Dc	-12		77	0.015
tert-butyl amine	3.01	*1.7*	50.8	*8.9*				-9		45	
n-butyl benzene	1.53	*0.82*	45.0	*5.8*	410			59		183	
sec-butyl benzene	1.53	0.77	42.3	*5.8*	418			45		173	
tert-butyl benzene	1.53	0.8	43.9	5.6	445			44		169	
n-butyl bromide	3.52	*2.5*	140.0	*6.6*	265			13		101	
butyl cellosolve (ethylene glycol monobutyl ether, EGME)	2.41	*1.1*	53.1	*11*	238		Cc	61		171	
n-butyl chloride	3.38	1.8	68.1	*10.1*	250	245		-9		78	0.027
butyl ether	1.72	1.5	79.9	*7.6*	194			25		141	
butyl formate	3.12	1.7	71.0	8.2	322			18		107	
n-butyl glycidyl ether	2.16						B/Cc	54		169	
butyl glycolate	2.72							68		180	
butyl mercaptan	2.55	1.4e		11.3e	272e		Cc	2		97	
butyl methacrylate	1.96	2.0	116.3	8.0				41		163	
butyl stearate	0.65	0.3e		2.3e	355			160		223	
p-tert-butyltoluene	1.38	*0.8*	48.5	5.1e			Dc	54		190	
butyraldehyde (butanal)	3.67	2.5	73.7	12.5	218	206	Ct	-7		76	
butyric acid	4.02	*2.0*	72.0	*10*	450		Dc	69		164	
♈o-butyrolactone	4.45	*2.0*	70.4	*12.6*				98		204	
camphene (s)	1.48	0.8e		6.7e				36		114	
camphor (s)	1.53	0.6	37.3	3.5	466			66		207	
carbon disulfide	4.98	1.3	40.5	50	100	< 105	none	-30		46	0.029
carbon monoxide (g)	29.54	12.5	143.1	74	609	588	Ct			-192	
carbon subnitride (2-butynedinitrile)	4.98									77	
carbonyl sulfide (g)	9.49	11.9	292.2	29						-50	
chloroacetaldehyde	9.49	5.7e		18.4e			Cc	88		85	
chloroacetylene (g)	9.49			100						-30	
chlorobenzene	2.91	1.4	64.4	7.1	674		Dc	29	21	132	0.019
2-chloro-2-butene	3.67	2.9	107.4	9.3				-19		71	
chlorodifluoroethane (Freon 142b)	9.49	6.2	254.7	17.9	632					-9	
1-chloro-2,4-dinitrobenzene	4.45	1.9	157.3	22	432			194		315	
2-chloroethanol (ethylene chlorohydrin)	7.74	*4.9*	161.3	*15.9*	425			41		130	
chloromethoxymethane	7.74	4.5e		22.8e				-18		59	

Table 1C Pure chemical substances

Substance	MIE (mJ), plain Calcote	MIE (mJ), flanged Calcote	MIE (mJ), air other	MIE (mJ), O_2 other	Quench dist. (mm)	Quench dia. (mm) Grove	MESG [IEC] (mm)	MESG [UL] (mm)	MIC [UK] (mA)	T_{ad} at LFL (K)	T_{ad} at stoich (K)
bicyclohexyl											
biphenyl (s)											
bromobenzene											
1,3-butadiene (g)	0.175	0.235	0.13		1.25	2.13	0.79	0.79	129	1590	2365
2,3-butadione (diacetyl)	0.41	0.64									
butane (g)			0.26	0.009	2.4		0.98	0.99	162	1765	2280
1-butanol (*n*-butanol)					2.69	0.94	0.91	1.07			
2-butanol (*sec*-butanol)								1.07			
tert-butanol											
2-butene (g)							0.89		161		
1-butene (butylene) (g)							0.94				
n-butyl acetate							1.02		175		
sec-butyl acetate											
tert-butyl acetate											
n-butyl acrylate											
butyl amine (1-butanamine)							1.16		193		
tert-butyl amine											
n-butyl benzene											
sec-butyl benzene											
tert-butyl benzene											
n-butyl bromide											
butyl cellosolve (ethylene glycol monobutyl ether, EGME)											
n-butyl chloride	1.24	2.35	0.33	0.0007	2.2		1.06				
butyl ether							0.88		150		
butyl formate											
n-butyl glycidyl ether											
butyl glycolate							0.88				
butyl mercaptan											
butyl methacrylate							0.94				
butyl stearate											
p-tert-butyltoluene											
butyraldehyde (butanal)							0.92	0.48			
butyric acid											
γ-butyrolactone											
camphene (s)							0.90				
camphor (s)											
carbon disulfide	0.015	0.039	0.015		0.55		0.34	0.05	72	1030	2250
carbon monoxide (g)					1.73		0.94	0.64	158		
carbon subnitride (2-butynedinitrile)											
carbonyl sulfide (g)							1.35				
chloroacetaldehyde											
chloroacetylene (g)											
chlorobenzene											
2-chloro-2-butene											
chlorodifluoroethane (Freon 142b)											
1-chloro-2,4-dinitrobenzene											
2-chloroethanol (ethylene chlorohydrin)											
chloromethoxymethane							1.00				

Table 1A Pure chemical substances

Substance	CAS No.	UN No.	Formula	MW	Δh_f kJ mol^{-1}	Δh_c (upper) kJ mol^{-1}	Δh_c (lower) kJ mol^{-1}	Δh_c (lower) MJ kg^{-1}
chloroprene	126-99-8	1991	C_4H_5Cl	88.54	43.4e	2355.7e	2267.7e	25.61e
2-chloropropene (g)	557-98-2	2456	C_3H_5Cl	76.53	-24.7	1894.1	1806.1	23.60
chlorotrifluoroethylene (g)	79-38-9	1082	C_2ClF_3	116.48	-505.5	833.4	921.4	7.91
m-cresol	108-39-4	2076	C_7H_8O	108.14	-193.3	3704.6	3528.6	32.63
o-cresol	95-48-7	2076	C_7H_8O	108.14	-202	3695.9	3519.9	32.55
crotonaldehyde (2-butenal)	4170-30-3	1143	C_4H_6O	70.09	-146.9	2284.7	2152.6	30.71
cumene (isopropyl benzene)	98-82-8	1918	C_9H_{12}	120.19	-41.2	5215.4	4951.3	41.19
cyanamide (s)	420-04-2		CH_2N_2	42.04	58.79	738.1	694.1	16.51
cyanogen (g)	460-19-5	1026	C_2N_2	52.04	309.07	1096.1	1096.1	21.06
cyanogen chloride (s)	506-77-4	1589	CClN	61.47	137.8	555.0	577.0	9.39
cyclobutane (g)	287-23-0	2601	C_4H_8	56.11	28.4	2745.8	2569.7	45.80
cycloheptane	291-64-5	2241	C_7H_{14}	98.19	-156.4	4599.1	4290.9	43.70
cyclohexane	110-82-7	1145	C_6H_{12}	84.16	-157.7	3918.4	3654.3	43.42
cyclohexanol	108-93-0		$C_6H_{12}O$	100.16	-352	3724.1	3460.0	34.54
cyclohexanone	108-94-1	1915	$C_6H_{10}O$	98.14	-276.1	3514.2	3294.1	33.56
cyclohexene	110-83-8	2256	C_6H_{10}	82.15	-37.82	3752.4	3532.3	43.00
cyclohexene oxide	286-20-4		$C_6H_{10}O$	98.14	-166	3624.3	3404.2	34.69
cyclohexylacetate	622-45-7	2243	$C_8H_{14}O_2$	142.20	-558.9	4590.1	4281.9	30.11
cyclopentadiene (1,3-cyclopentadiene)	542-92-7	2048	C_5H_6	66.10	105.9	2931.0	2798.9	42.34
cyclopentane	287-92-3	1146	C_5H_{10}	70.13	-105.6	3291.2	3071.1	43.79
cyclopropane (g)	75-19-4	1027	C_3H_6	42.08	39.3	2077.4	1945.3	46.23
p-cymene	99-87-6	2046	$C_{10}H_{14}$	134.22	-78.03	5858.0	5549.8	41.35
decaborane	17702-41-9	1868	$B_{10}H_{14}$	122.21	-7.1	3978.9	4331.0	35.44
n-decaldehyde (1-decanal)	112-31-2		$C_{10}H_{20}O$	156.27	-330.91	6462.6	6022.4	38.54
decalin	91-17-8	1147	$C_{10}H_{18}$	138.25	-169	6338.7	5942.5	42.98
decane	124-18-5	2247	$C_{10}H_{22}$	142.28	-301	6778.3	6294.1	44.24
1-decanol	112-30-1		$C_{10}H_{22}O$	158.28	-478.1	6601.2	6117.0	38.65
decene	25339-53-1		$C_{10}H_{20}$	140.27	-173.8	6619.7	6179.5	44.05
DEGDN (diethyleneglycol dinitrate)	693-21-0		$C_4H_8N_2O_7$	196.12	-433	2284.4	2108.3	10.75
deuterium (g)	7782-39-0	1957	D_2	4.03	0	285.8	241.8	60.00
diacetone alcohol	123-42-2	1148	$C_6H_{12}O_2$	116.16	-592.8	3483.3	3219.2	27.71
diborane (g)	19287-45-7	1911	B_2H_6	27.67	41	1295.5	1295.5	46.83
di-*tert*-butyl peroxide (DTBP)	110-05-4	2102	$C_8H_{18}O_2$	146.23	-380.8	5339.8	4943.7	33.81
dichlorodimethylsilane	75-78-5	1162	$C_2H_6Cl_2Si$	129.06	-495.4	2100.0	2012.0	15.59
1,2-dichlorobenzene	95-50-1	1591	$C_6H_4Cl_2$	147.00	-17.4	2962.7	2918.7	19.85
1,2-dichloroethylene	540-59-0	1150	$C_2H_2Cl_2$	96.94	-169.7	950.6	950.6	9.81
2,2-dichloroethyl ether	1191-17-9		$C_4H_6Cl_4O$	211.90				
1,1-dichloro-1-nitroethane	594-72-9	2650	$C_2H_3Cl_2NO_2$	143.96				
1,3-dichloropropene	542-75-6	2047	$C_3H_4Cl_2$	110.97	-71	1728.6	1684.6	15.18
dichlorosilane	4109-96-0	2189	Cl_2H_2Si	30.10	-320.49	868.8	824.8	27.40
dicyclopentadiene (s)	77-73-6	2048	$C_{10}H_{12}$	132.20	-110	5540.1	5276.0	39.91
diethyl carbonate	105-58-8	2366	$C_5H_{10}O_3$	118.13	-639.1	2757.7	2537.6	21.48
diethylamine	109-89-7	1154	$C_4H_{11}N$	73.14	-72.4	3073.8	2831.7	38.72
2-diethylaminoethanol	100-37-8	2686	$C_6H_{15}NO$	117.19	-309.5	4195.4	3865.2	32.98
2,6-diethyl aniline	579-66-8	2432	$C_{10}H_{15}N$	149.24	1.8	6080.7	5750.6	38.53
p-diethyl benzene	105-05-5		$C_{10}H_{14}$	134.22	-22.2	5913.8	5605.6	41.76
diethylcyclohexane	1331-43-7		$C_{10}H_{20}$	140.27	-298	6495.5	6055.3	43.17

Table 1B Pure chemical substances

Substance	C_{st} (vol%)	LFL (vol%)	LFL (g m^{-3})	UFL (vol%)	AIT (ºC) in air	AIT (ºC) in O_2	NEC Group	Flash point (ºC)	LTL (ºC)	BP (ºC)	P_{vap} at FP (atm)
chloroprene	4.02	4.0	144.8	20			Dc	-16		59	
2-chloropropene (g)	4.98	4.5	140.8	16				-4		23	
chlorotrifluoroethylene (g)	17.33	24.0	1142.8	40.3						-28	
m-cresol	2.41	*1.1*	48.6	*7.6*	626		Dc	86		202	
o-cresol	2.41	1.4	61.9	7.6	559			81		191	0.016
crotonaldehyde (2-butenal)	4.02	2.1	60.2	*15.5*	232		Ct	13		102	
cumene (isopropyl benzene)	1.72	*0.88*	43.2	*6.5*	467		Dc	36	31	152	0.013
cyanamide (s)	12.26							141			
cyanogen (g)	9.49	6.6	140.4	32	850			-62		-22	
cyanogen chloride (s)	21.85			24e						14	
cyclobutane (g)	3.38	1.8	41.3	11.1e	427e			-64		12	
cycloheptane	1.96	1.1	44.2	6.7	155e			6		118	0.010
cyclohexane	2.28	1.3	44.7	7.8	259	296	Dc	-18		81	0.012
cyclohexanol	2.41	*1.2*	49.1	*9.3*	300	350	Dc	68		161	
cyclohexanone	2.55	*1.1*	44.1	*8.8*	420	453	Dc	46		156	
cyclohexene	2.41	*1.2*	40.3	10.1e	310			-20	-16	83	
cyclohexene oxide	2.55							27		130	
cyclohexylacetate	1.96	*1.0*	58.1		330	335		58		172	
cyclopentadiene (1,3-cyclopentadiene)	3.12	1.7e		14.6e	503	510	Cc	32		42	
cyclopentane	2.72	1.5	43.0	9.4e	385			-37		49	0.017
cyclopropane (g)	4.45	2.4	41.3	10.4	498	454	Dt			-33	
p-cymene	1.53	*0.85*	46.6	*6.5*	445		Dc	47	49	177	
decaborane	1.12	0.2	10.0					80		213	
n-decaldehyde (1-decanal)	1.43	0.8e		5.4e			Cc	85		209	
decalin	1.43	*0.71*	40.1	*4.9*	250	236		57	57	196	
decane	1.33	*0.75*	43.6	*5.6*	232	202		46	46	174	0.007
1-decanol	1.38	0.7e		5.5e	288		Dc	82		231	
decene	1.38	0.7e		5.9e	235		Dc			171	
DEGDN (diethyleneglycol dinitrate)	7.74										
deuterium (g)	29.54	4.9	8.1	75	400e					-249	
diacetone alcohol	2.55	1.8	85.5	6.9	603		Dc	52		166	
diborane (g)	4.45	0.84	9.5	98	pyr.			-90		-93	
di-*tert*-butyl peroxide (DTBP)	1.79	0.8	47.8	88				18		expl.	
dichlorodimethylsilane	4.98	3.4	179.4	>9.5				-16		70	
1,2-dichlorobenzene	3.12	*2.2*	132.2	*9.2*	647		Dc	66		181	0.019
1,2-dichloroethylene	9.49	9.7	384.4	12.8	460		Dc	6		60	
2,2-dichloroethyl ether	4.98	2.7	233.9	7.9	403		Dt	55		179	
1,1-dichloro-1-nitroethane	14.36						Cc			124	
1,3-dichloropropene	5.65	2.6	118.0	7.8			Dc	27		108	
dichlorosilane	12.26	4.7	57.8	96	44					8	
dicyclopentadiene (s)	1.59	1.0		8.3e	510			26		170	
diethyl carbonate	3.38	1.7e		12.4e	334e			25		126	
diethylamine	3.01	1.8	53.8	10.1	312		Ct	-23		57	
2-diethylaminoethanol	2.22	1.2e		8.4e				60		163	
2,6-diethyl aniline	1.50	*0.8*	48.8	5.4	630			97	80	215	
p-diethyl benzene	1.53	*0.8*	43.9	*6.1*	430		Dc	57		183	
diethylcyclohexane	1.38	*0.8*	45.9	*6*	240			49		174	

Table 1C Pure chemical substances

Substance	MIE (mJ), plain Calcote	MIE (mJ), flanged Calcote	MIE (mJ), air other	MIE (mJ), O_2 other	Quench dist. (mm)	Quench dia. (mm) Grove	MESG [IEC] (mm)	MESG [UL] (mm)	MIC [UK] (mA)	T_{ad} at LFL (K)	T_{ad} at stoich (K)
chloroprene											
2-chloropropene (g)											
chlorotrifluoroethylene (g)											
m-cresol											
o-cresol											
crotonaldehyde (2-butenal)							0.81	0.48			
cumene (isopropyl benzene)											
cyanamide (s)											
cyanogen (g)											
cyanogen chloride (s)											
cyclobutane (g)											
cycloheptane											
cyclohexane	1.38	2.65	0.22		3		0.94		160	1670	2225
cyclohexanol											
cyclohexanone							0.98				
cyclohexene	0.525	0.86			2.1				162		
cyclohexene oxide	0.74	1.3					0.74				
cyclohexylacetate											
cyclopentadiene (1,3-cyclopentadiene)	0.67	1.14	0.67								
cyclopentane	0.54	0.83	0.24				1.01			1675	2235
cyclopropane (g)	0.24	0.34	0.18	0.001	1.8		0.91	0.86	146	1650	2080
p-cymene											
decaborane											
n-decaldehyde (1-decanal)											
decalin											
decane					2.06		1.05				
1-decanol											
decene											
DEGDN (diethyleneglycol dinitrate)											
deuterium (g)											
diacetone alcohol											
diborane (g)											
di-*tert*-butyl peroxide (DTBP)	0.41	0.65	0.41				0.84				
dichlorodimethylsilane											
1,2-dichlorobenzene											
1,2-dichloroethylene											
2,2-dichloroethyl ether								0.76			
1,1-dichloro-1-nitroethane											
1,3-dichloropropene											
dichlorosilane			0.015								
dicyclopentadiene (s)							0.91				
diethyl carbonate							0.83				
diethylamine								0.69			
2-diethylaminoethanol							0.79				
2,6-diethyl aniline											
p-diethyl benzene											
diethylcyclohexane											

Table 1A Pure chemical substances

Substance	CAS No.	UN No.	Formula	MW	Δh_f kJ mol^{-1}	Δh_c (upper) kJ mol^{-1}	Δh_c (lower) kJ mol^{-1}	Δh_c (lower) MJ kg^{-1}
diethyl dichlorosilane	1719-53-5	1767	$C_4H_{10}Cl_2Si$	157.12				
diethylene glycol monobutyl ether	112-34-5		$C_8H_{18}O_3$	162.23	-606	5114.6	4718.5	29.09
diethylene glycol monoethyl ether	111-90-0		$C_6H_{14}O_3$	134.17	-565	3796.9	3488.8	26.00
diethylene glycol monomethyl ether	111-77-3		$C_5H_{12}O_3$	120.15	-670.3	3012.3	2748.2	22.87
diethyl ether (ether; ethyl ether)	60-29-7	1155	$C_4H_{10}O$	74.12	-271.2	2732.0	2511.9	33.89
diethyl ketone	96-22-0	1156	$C_5H_{10}O$	86.13	-296.51	3100.2	2880.1	33.44
diethyl oxalate	95-92-1	2525	$C_6H_{10}O_4$	146.14	-809.73	2980.5	2760.4	18.89
3,3-diethyl pentane	1067-20-5		C_9H_{20}	128.26	-231.8	6168.2	5728.0	44.66
diethyl sulfate	64-67-5	1594	$C_4H_{10}O_4S$	154.18	-812.91	2792.3	2616.2	16.97
dihydropyran (3,4-dihydro-2H-pyran)	110-87-2	2376	C_5H_8O	84.12	-147.73	2963.2	2787.1	33.13
diisobutylcarbinol	108-82-7		$C_9H_{20}O$	144.26	-910	5490.0	5049.8	35.01
diisobutylene	107-39-1	2050	C_8H_{16}	112.21	-45.9	5388.9	5036.7	44.88
diisobutyl ketone	108-83-8	1157	$C_9H_{18}O$	142.24	-408.6	5705.6	5309.4	37.33
diisopropylamine	108-18-9	1158	$C_6H_{15}N$	101.19	-171	4333.9	4003.7	39.57
diketene	674-82-8	2521	$C_4H_4O_2$	84.07	-233.1	1912.6	1824.6	21.70
1,1-dimethoxyethane	534-15-6	2377	$C_4H_{10}O_2$	90.12	-420.6	2582.6	2362.5	26.21
1,2-dimethoxyethane	110-71-4	2252	$C_4H_{10}O_2$	90.12	-601.3	2401.9	2181.8	24.21
dimethoxymethane (formal; methyl formal; methylal)	109-87-5	1234	$C_3H_8O_2$	76.10	-377.8	1946.1	1770.0	23.26
dimethyl acetylene (2-butyne)	503-17-3	1144	C_4H_6	54.09	146.31	2577.9	2445.8	45.22
dimethylamine (g)	124-40-3	1032	C_2H_7N	45.08	-18.8	1768.7	1614.6	35.81
N,N-dimethyl aniline	121-69-7	2253	$C_8H_{11}N$	121.18	47.7	4767.9	4525.8	37.35
2,2-dimethylbutane (neohexane)	75-83-2	1208	C_6H_{14}	86.18	-213.4	4148.5	3840.4	44.56
2,3-dimethylbutane	79-29-8	2457	C_6H_{14}	86.18	-207.0	4154.9	3846.8	44.64
dimethyl decalin	1618-22-0		$C_{12}H_{22}$	166.31	-266	7600.4	7116.1	42.79
N,N-dimethylformamide	68-12-2	2265	C_3H_7NO	73.09	-239.4	1941.6	1787.5	24.45
2,3-dimethylpentane	565-59-3		C_7H_{16}	100.20	-233.5	4807.8	4455.6	44.47
2,2-dimethylpropane (neopentane) (g)	463-82-1	2044	C_5H_{12}	72.15	-167.9	3514.7	3250.6	45.05
dimethyl sulfate	77-78-1	1595	$C_2H_6O_4S$	126.13	-735.3	1511.2	1423.2	11.28
dimethyl sulfide	75-18-3	1164	C_2H_6S	62.13	-65.4	2181.1	2093.1	33.69
dimethyl sulfoxide	67-68-5		C_2H_6SO	78.13	-203.4	2043.1	1955.1	25.02
p-dioxane (1,4 dioxane)	123-91-1	1165	$C_4H_8O_2$	88.11	-355.13	2362.3	2186.2	24.81
diphenyl methane	101-81-5		$C_{13}H_{12}$	168.24	97.1	6927.8	6663.7	39.61
4-diphenylamine (s)	92-67-1		$C_{12}H_{11}N$	169.23	201.7	6495.9	6253.8	36.96
2-diphenylamine (s)	90-41-5		$C_{12}H_{11}N$	169.23	121.8	6416.0	6173.9	36.48
diphosphine	13445-50-6		P_2H_4	65.98	-5	566.7	478.6	
n-dipropylamine	142-84-7	2383	$C_6H_{15}N$	101.19	-154.6	4350.3	4020.1	39.73
dipropylene glycol monomethyl ether	34590-94-8		$C_7H_{16}O_3$	148.20	-660.8e	4380.5e	4028.3e	27.18e
disulfur dichloride	10025-67-9	1828	Cl_2S_2	135.03	-58.16	1193.2	1325.2	9.81
di-*tert*-butyl ether	6163-66-2		$C_8H_{18}O$	130.23	-399.6	5321.0	4924.9	37.82
divinyl ether (vinyl ether)	109-93-3	1167	C_4H_6O	70.09	-39.7	2391.9	2259.8	32.24
DNT (2,4-dinitrotoluene) (s)	121-14-2	2038	$C_7H_6N_2O_4$	182.14	-66.4	3545.7	3413.6	18.74
n-dodecane	112-40-3		$C_{12}H_{26}$	170.34	-352.1	8085.9	7513.7	44.11
dodecene	25378-22-7		$C_{12}H_{24}$	168.32	-226.2	7926.0	7397.8	43.95
eicosane	112-95-8		$C_{20}H_{42}$	282.55	-556.5	13316.3	12391.9	43.86
epichlorohydrin	106-89-8	2023	C_3H_5OCl	92.52	-149	1769.8	1681.8	18.18

Table 1B Pure chemical substances

Substance	C_{st} (vol%)	LFL (vol%)	LFL (g m^{-3})	UFL (vol%)	AIT (ºC) in air	AIT (ºC) in O_2	NEC Group	Flash point (ºC)	LTL (ºC)	BP (ºC)	P_{vap} at FP (atm)
diethyl dichlorosilane	2.91							27		130	
diethylene glycol monobutyl ether	1.87	0.9	59.7	24.6	228		Cc	100		231	
diethylene glycol monoethyl ether	2.55	1.2	65.8	10.4	204			83		197	
diethylene glycol monomethyl ether	3.12	1.4	68.8	22.7	241		Cc	83		193	
diethyl ether (ether; ethyl ether)	3.38	1.9	57.6	36	195	180	Ct	-45		35	0.018
diethyl ketone	2.91	1.6	56.3	8	452			12		101	0.024
diethyl oxalate	3.12	1.5e		8.4e				76		186	
3,3-diethyl pentane	1.48	*0.7*	36.7	*5.7*	290			21		146	
diethyl sulfate	3.38	1.6e			436			104		208	
dihydropyran (3,4-dihydro-2H-pyran)	3.12							-9		86	
diisobutylcarbinol	1.53	*0.82*	48.4	*6.1*				66		179	
diisobutylene	1.72	1.1	50.5	6	470		Dt	-5		101	
diisobutyl ketone	1.59	*0.8*	46.5	*6.2*	396		Dc	49		168	
diisopropylamine	2.10	0.8	33.1	7.1	316		Cc	-7		84	
diketene	4.98	2.5e		16.8e	310			34		126	
1,1-dimethoxyethane	3.67							-17		64	
1,2-dimethoxyethane	3.67	1.9e		18.7e	202			-6		85	
dimethoxymethane (formal; methyl formal; methylal)	4.98	2.2	68.4	13.8	237		Ct	-32		43	
dimethyl acetylene (2-butyne)	3.67	1.4	31.0	41.8e	323e			-31		27	
dimethylamine (g)	5.29	2.8	51.6	14.4	400	346	Cc	-56		7	0.017
N,N-dimethyl aniline	1.91	1.0	49.5	6.4	371			63		194	
2,2-dimethylbutane (neohexane)	2.16	1.2	42.3	7.0	425	310		-48		50	
2,3-dimethylbutane	2.16	1.2		7.0	415			-29		58	
dimethyl decalin	1.18	*0.67*	45.6	*5.4*	235			84		232	
N,N-dimethylformamide	4.70	*1.8*	53.8	*14*	435		Dc	57	57	149	
2,3-dimethylpentane	1.87	1.1	45.1	6.8	337			-6		90	0.017
2,2-dimethylpropane (neopentane) (g)	2.55	1.4	41.3	7.5	450			<-7		7	
dimethyl sulfate	6.53	2.9e			188		Dc	83		188	
dimethyl sulfide	4.02	2.2	55.9	20	206			-34		37	
dimethyl sulfoxide	4.45	*2.6*	83.0	*28.5*	215			95	84	189	
p-dioxane (1,4 dioxane)	4.02	2.0	72.0	22	266		Cc	12		101	0.027
diphenyl methane	1.29	0.7e		5.2e	485			127		264	
4-diphenylamine (s)	1.40	0.7e		5.5e	635			153		302	
2-diphenylamine (s)	1.40	0.8e								299	
diphosphine	17.33									64	
n-dipropylamine	2.10	1.1e		7.7e	299		Cc	3		110	
dipropylene glycol monomethyl ether	2.16	1.1e		10.9e			Cc	85 oc		190	
disulfur dichloride	7.74				230					138	
di-*tert*-butyl ether	1.72	0.9e		6.8e				-3e		107	
divinyl ether (vinyl ether)	4.02	1.7	48.7	27	360	165		<-30		28	
DNT (2,4-dinitrotoluene) (s)	3.12	1.4e		8.2e				207		300	
n-dodecane	1.12	*0.6*	41.8	*4.7*	204			74	74	215	
dodecene	1.15	0.6e		5.4e	255		Dc	49		214	
eicosane	0.68	0.4	46.2	4.9e	240					343	
epichlorohydrin	5.65	3.8	143.7	21	411		Ct	33		115	

Table 1C Pure chemical substances

Substance	MIE (mJ), plain Calcote	MIE (mJ), flanged Calcote	MIE (mJ), air other	MIE (mJ), O_2 other	Quench dist. (mm)	Quench dia. (mm) Grove	MESG [IEC] (mm)	MESG [UL] (mm)	MIC [UK] (mA)	T_{ad} at LFL (K)	T_{ad} at stoich (K)
diethyl dichlorosilane											
diethylene glycol monobutyl ether							1.11				
diethylene glycol monoethyl ether							0.94				
diethylene glycol monomethyl ether											
diethyl ether (ether; ethyl ether)	0.49	0.79	0.2	0.0013	1.85	2.62	0.87	0.64	145	1610	2305
diethyl ketone							0.90				
diethyl oxalate							0.97				
3,3-diethyl pentane											
diethyl sulfate							1.11				
dihydropyran (3,4-dihydro-2H-pyran)	0.365	0.56	0.36							1740	2230
diisobutylcarbinol							0.93				
diisobutylene	0.96	1.75	0.96		3.2		0.98	0.81		1825	2290
diisobutyl ketone											
diisopropylamine											
diketene							0.80				
1,1-dimethoxyethane							0.86				
1,2-dimethoxyethane							0.76				
dimethoxymethane (formal; methyl formal; methylal)	0.42	0.66	0.42					0.58			
dimethyl acetylene (2-butyne)											
dimethylamine (g)							1.15				
N,N-dimethyl aniline											
2,2-dimethylbutane (neohexane)	1.64	3.3								1705	2220
2,3-dimethylbutane											
dimethyl decalin											
N,N-dimethylformamide							1.08				
2,3-dimethylpentane											
2,2-dimethylpropane (neopentane) (g)	1.57	3.1								1740	2220
dimethyl sulfate											
dimethyl sulfide	0.48	0.76	0.48								
dimethyl sulfoxide											
p-dioxane (1,4 dioxane)							0.70				
diphenyl methane											
4-diphenylamine (s)											
2-diphenylamine (s)											
diphosphine											
n-dipropylamine											
dipropylene glycol monomethyl ether											
disulfur dichloride											
di-*tert*-butyl ether											
divinyl ether (vinyl ether)											
DNT (2,4-dinitrotoluene) (s)											
n-dodecane											
dodecene											
eicosane											
epichlorohydrin	0.29	0.43					1.00	0.56			

Table 1A Pure chemical substances

Substance	CAS No.	UN No.	Formula	MW	Δh_f kJ mol^{-1}	Δh_c (upper) kJ mol^{-1}	Δh_c (lower) kJ mol^{-1}	Δh_c (lower) MJ kg^{-1}
ethane (g)	74-84-0	1035	C_2H_6	30.07	-83.85	1560.7	1428.6	47.51
ethanol	64-17-5	1170	C_2H_6O	46.07	-277	1367.5	1235.5	26.82
ethanolamine (monoethanolamine)	141-43-5	2491	C_2H_7NO	61.08	-507.5	1280.0	1125.9	18.43
ethoxy ethane	109-92-2	1302	C_4H_8O	72.11	-166.6	2550.8	2374.7	32.93
2-ethoxyethyl acetate (cellosolve acetate)	111-15-9	1172	$C_6H_{12}O_3$	132.16	-926	3150.1	2886.0	21.84
ethyl acetate	141-78-6	1173	$C_4H_8O_2$	88.11	-480.57	2236.8	2060.8	23.39
ethyl acetoacetate	141-97-9		$C_6H_{10}O_3$	130.14	-640.4	3149.9	2929.8	22.51
ethyl acetylene (1-butyne) (g)	107-00-6	2452	C_4H_6	54.09	165.2	2596.8	2464.7	45.57
ethyl acrylate	140-88-5	1917	$C_5H_8O_2$	100.12	-370.6	2740.3	2564.2	25.61
ethylamine (g)	75-04-7	1036	C_2H_7N	45.08	-84.5	1703.0	1548.9	34.36
ethylbenzene	100-41-4	1175	C_8H_{10}	106.17	-12.5	4564.8	4344.7	40.92
ethyl benzoate	93-89-0		$C_9H_{10}O_2$	150.18	-284.	4686.8	4466.7	29.74
ethyl bromide	74-96-4	1891	C_2H_5Br	108.97	-95.52	1384.3	1296.3	11.90
2-ethyl-1-butanol	97-95-0	2275	$C_6H_{14}O$	102.18	-326.1	4035.8	3727.7	36.48
ethyl butyl ketone (3-heptanone)	106-35-4	1224	$C_7H_{14}O$	114.19	-300.45	4455.0	4146.9	36.32
ethyl cellosolve (2-ethoxyethanol; ethylene glycol monoethyl ether)	110-80-5	1171	$C_4H_{10}O_2$	90.12	-400	2603.2	2383.1	26.44
ethyl chloride (g)	75-00-3	1037	C_2H_5Cl	64.51	-136.8	1388.5	1300.5	20.16
ethyl cyclobutane	4806-61-5		C_6H_{12}	84.16	-58.95	4017.2	3753.0	44.59
ethyl cyclohexane	1678-91-7		C_8H_{16}	112.21	-213	5221.8	4869.6	43.40
ethyl cyclopentane	1640-89-7		C_7H_{14}	98.19	-163.5	4592.0	4283.8	43.63
ethylene (g)	74-85-1	1962	C_2H_4	28.05	52.47	1411.2	1323.1	47.16
ethylene diamine (1,2-ethanediamine)	107-15-3	1604	$C_2H_8N_2$	60.10	-63.01	1867.4	1691.3	28.14
ethylene dichloride (1,2-dichloroethane)	107-06-2	1184	$C_2H_4Cl_2$	98.96	-169.7	1236.4	1192.4	12.05
ethylenedinitramine (EDNA) (s)	505-71-5		$C_2H_6N_4O_4$	150.09	-689	955.5	823.5	5.49
ethylene glycol	107-21-1		$C_2H_6O_2$	62.07	-460	1184.5	1052.5	16.96
ethylene glycol monobutyl ether acetate (butyl glycol acetate)	112-07-2		$C_8H_{16}O_3$	160.21	-710.3e	4724.5e	4372.3e	27.29e
ethylene oxide (g)	75-21-8	1040	C_2H_4O	44.05	-52.63	1306.1	1218.0	27.65
ethylenimine	151-56-4	1185	C_2H_5N	43.07	91.9	1593.5	1483.5	34.44
ethyl ethoxyacetate	817-95-8		$C_6H_{12}O_3$	132.16	-639.5	3436.6	3172.5	24.01
ethyl formate	109-94-4	1190	$C_3H_6O_2$	74.08	-394.17	1643.9	1511.8	20.41
2-ethylhexaldehyde	123-05-7		$C_8H_{16}O$	128.21	-348.6	5086.2	4734.0	36.92
2-ethyl hexanol	104-76-7		$C_8H_{18}O$	130.23	-432.9	5287.7	4891.6	37.56
2-ethylhexyl acrylate	103-11-7		$C_{11}H_{20}O_2$	184.28	-470	6717.0	6276.8	34.06
ethylidene chloride (1,1-dichloroethane)	75-34-3	2362	$C_2H_4Cl_2$	98.96	-158.4	1247.7	1203.7	12.16
ethyl lactate	97-64-3	1192	$C_5H_{10}O_3$	118.13	-663.6	2733.2	2513.1	21.27
ethyl mercaptan (ethanethiol)	75-08-1	2363	C_2H_6S	62.13	-46.15	2200.4	2112.3	34.00
ethyl methacrylate	97-63-2	2277	$C_6H_{10}O_2$	114.14	-381	3409.3	3189.2	27.94
n-ethylmorpholine	100-74-3		$C_6H_{13}NO$	115.17				
1-ethylnaphthalene	1127-76-0		$C_{12}H_{12}$	156.23	96.65	6533.8	6269.7	40.13
ethyl nitrate	625-58-1		$C_2H_5NO_3$	91.07	-190.4	1311.2	1201.2	13.19
ethyl nitrite (g)	109-95-5	1194	$C_2H_5NO_2$	75.07	108	1609.6	1499.6	19.98
ethyl propionate	105-37-3	1195	$C_5H_{10}O_2$	102.13	-505.59	2891.2	2671.1	26.15
ethyl propyl ether	628-32-0	2615	$C_5H_{12}O$	88.15	-303.6	3379.0	3114.9	35.34

Table 1B Pure chemical substances

Substance	C_{st} (vol%)	LFL (vol%)	LFL (g m^{-3})	UFL (vol%)	AIT (ºC) in air	AIT (ºC) in O_2	NEC Group	Flash point (ºC)	LTL (ºC)	BP (ºC)	P_{vap} at FP (atm)
ethane (g)	5.65	3.0	36.9	12.4	515	506	Dt	-135	-130	-89	
ethanol	6.53	3.3	62.2	*19*	365	375	Dt	13		79	
ethanolamine (monoethanolamine)	6.06	3.1	77.4	17	410		Dc	85		170	
ethoxy ethane	3.67	1.7	50.1	28	202			-45		36	0.017
2-ethoxyethyl acetate (cellosolve acetate)	2.72	1.7	91.9	12.7	285		Dc	51		156	
ethyl acetate	4.02	2.2	79.2	11.5	427		Dt	-4		77	0.028
ethyl acetoacetate	2.91	1.4	74.5	9.5	295			84		181	
ethyl acetylene (1-butyne) (g)	3.67	2.0e		32.9e	319e			<-7		8	
ethyl acrylate	3.38	1.4	57.3	9.3	372		Dt	10		99	
ethylamine (g)	5.29	3.5	64.5	14	385		Dt	-50		17	0.217
ethylbenzene	1.96	*1.0*	43.4	*6.7*	477	468	Dc	15		136	
ethyl benzoate	1.96	1.0	61.4	6.1e	490			88		213	
ethyl bromide	7.08	6.7	298.5	11.3	511			-23		39	0.065
2-ethyl-1-butanol	2.28	1.2e		8.3e	304		Dc	57		146	
ethyl butyl ketone (3-heptanone)	2.05	1.1e		7.3e	410e		Dc	41		148	
ethyl cellosolve (2-ethoxyethanol; ethylene glycol monoethyl ether)	3.67	*1.8*	66.3	*14*	235		Ct	94		135	
ethyl chloride (g)	6.53	3.8	100.2	15.4	519	470	Dc	-50		12	
ethyl cyclobutane	2.28	1.2	41.3	7.7	210					71	
ethyl cyclohexane	1.72	*0.95*	43.6	*6.6*	260			18		132	
ethyl cyclopentane	1.96	1.1	44.2	6.7	260					103	
ethylene (g)	6.53	2.7	31.0	36	449	485	Ct	-136		-104	
ethylene diamine (1,2-ethanediamine)	4.98	4.2	103.2	14.4	385		Dt	34		116	
ethylene dichloride (1,2-dichloroethane)	7.74	*4.5*	182.1	*17.3*	440	430	Dt	13		84	0.057
ethylenedinitramine (EDNA) (s)	12.26										
ethylene glycol	7.74	*3.5*	88.8	21.6	400	413		114		198	0.037
ethylene glycol monobutyl ether acetate (butyl glycol acetate)	1.96	0.5	32.7	3.7	340		Cc	88		192	
ethylene oxide (g)	7.74	3.6	64.8	100	429		B/Ct	-20		14	0.260
ethylenimine	6.06	3.6	63.4	46	322		Ct	-11		56	
ethyl ethoxyacetate	2.72									158	
ethyl formate	5.65	2.8	84.8	16	455		Dc	-20		55	0.031
2-ethylhexaldehyde	1.79	0.9	47.2	7.93	163		Ct	50		163	
2-ethyl hexanol	1.72	0.9	47.9	9.7	231		Dc	73		185	
2-ethylhexyl acrylate	1.38	0.7	52.7	8.2	252		Dc	71		217	
ethylidene chloride (1,1-dichloroethane)	7.74	5.4	218.5	11.4	438		Dc	-5		57	
ethyl lactate	3.38	*1.5*	72.4	10.6	400			46		151	
ethyl mercaptan (ethanethiol)	4.02	2.8	71.1	18	299	261	Ct	-17		35	
ethyl methacrylate	2.72	1.8	84.0	9.6	370e			15		117	
n-ethylmorpholine	2.34						Cc	27		139	
1-ethylnaphthalene	1.38	0.7e		5.2e	480			107		258	
ethyl nitrate	10.70	4.0	148.9					10		87	
ethyl nitrite (g)	8.52	3.0	92.1	50	90			-35		17	
ethyl propionate	3.12	1.8	75.2	11	476	440		12		99	0.023
ethyl propyl ether	2.72	1.7	61.3	9	225e			-20		64	

Table 1C Pure chemical substances

Substance	MIE (mJ), plain Calcote	MIE (mJ), flanged Calcote	MIE (mJ), air other	MIE (mJ), O_2 other	Quench dist. (mm)	Quench dia. (mm) Grove	MESG [IEC] (mm)	MESG [UL] (mm)	MIC [UK] (mA)	T_{ad} at LFL (K)	T_{ad} at stoich (K)
ethane (g)	0.285	0.42	0.26	0.002	1.5		0.91			1600	2195
ethanol					1.71	2.97	0.91				
ethanolamine (monoethanolamine)											
ethoxy ethane											
2-ethoxyethyl acetate (cellosolve acetate)							0.97				
ethyl acetate	1.42	2.8			2.5	3.12	0.95			1705	2125
ethyl acetoacetate							1.04				
ethyl acetylene (1-butyne) (g)							0.71				
ethyl acrylate							0.86	0.81			
ethylamine (g)	2.4	5.2						0.99			
ethylbenzene											
ethyl benzoate											
ethyl bromide											
2-ethyl-1-butanol											
ethyl butyl ketone (3-heptanone)											
ethyl cellosolve (2-ethoxyethanol; ethylene glycol monoethyl ether)							0.84	0.46	169		
ethyl chloride (g)									200		
ethyl cyclobutane											
ethyl cyclohexane											
ethyl cyclopentane											
ethylene (g)	0.096	0.114	0.07	0.001	1.22	1.75	0.65	0.69	108	1475	2340
ethylene diamine (1,2-ethanediamine)							1.55	0.74			
ethylene dichloride (1,2-dichloroethane)					4.57		1.82	0.99			
ethylenedinitramine (EDNA) (s)											
ethylene glycol											
ethylene glycol monobutyl ether acetate (butyl glycol acetate)											
ethylene oxide (g)	0.087	0.105	0.062		1.18	1.37	0.59	0.33	101	1515	2425
ethylenimine	0.48	0.78						0.61			
ethyl ethoxyacetate							0.95				
ethyl formate							0.94				
2-ethylhexaldehyde								0.33			
2-ethyl hexanol											
2-ethylhexyl acrylate											
ethylidene chloride (1,1-dichloroethane)											
ethyl lactate											
ethyl mercaptan (ethanethiol)							0.90		148		
ethyl methacrylate							1.01				
n-ethylmorpholine											
1-ethylnaphthalene											
ethyl nitrate											
ethyl nitrite (g)	0.17	0.23					0.96				
ethyl propionate											
ethyl propyl ether											

Table 1A Pure chemical substances

Substance	CAS No.	UN No.	Formula	MW	Δh_f kJ mol^{-1}	Δh_c (upper) kJ mol^{-1}	Δh_c (lower) kJ mol^{-1}	Δh_c (lower) MJ kg^{-1}
ethyl *sec*-amyl ketone	541-85-5		$C_8H_{16}O$	128.21				
ethyl selenide	627-53-2		$C_4H_{10}Se$	137.08				
ethyl silicate	78-10-4	1292	$C_8H_{20}O_4Si$	208.33				
formaldehyde (g)	50-00-0	1198	CH_2O	30.03	-115.9	563.5	519.4	17.30
formic acid	64-18-6	1770	CH_2O_2	46.03	-425.09	254.3	210.2	4.57
furan	110-00-9	2389	C_4H_4O	68.08	-62.34	2083.4	1995.3	29.31
furfural (2-furaldehyde)	98-01-1	1199	$C_5H_4O_2$	96.09	-200.2	2339.0	2251.0	23.43
furfuryl alcohol (2-furanmethanol)	98-00-0	2874	$C_5H_6O_2$	98.10	-276.4	2548.7	2416.6	24.63
glycerol (glycerin; 1,2,3-propanetriol)	56-81-5	1760	$C_3H_8O_3$	92.09	-669.6	1654.3	1478.2	16.05
heptane	142-82-5	1206	C_7H_{16}	100.20	-224.4	4816.9	4464.7	44.56
1-heptanol	111-70-6		$C_7H_{16}O$	116.20	-403.4	4637.9	4285.7	36.88
2-heptanone (methyl *n*-amyl ketone)	110-43-0	1110	$C_7H_{14}O$	114.19	-300.45	4455.0	4146.9	36.32
1-heptene	592-76-7	2278	C_7H_{14}	98.19	-97.7	4657.8	4349.6	44.30
2-heptene	592-77-8		C_7H_{14}	98.19	-107	4648.5	4340.3	44.20
1-heptyne	628-71-7		C_7H_{12}	96.17	-62.8	4406.8	4142.7	43.08
hexadecane (cetane)	544-76-3		$C_{16}H_{34}$	226.44	-456.35	10699.1	9950.8	43.94
hexamethyldisilazane	999-97-3		$C_6H_{19}NSi_2$	161.39	-476.6	6406.9	5988.7	37.11
hexamethyldisiloxane	107-46-0		$C_6H_{18}OSi_2$	162.38	-532	6208.6	5812.4	35.80
hexane	110-54-3	1208	C_6H_{14}	86.18	-198.7	4163.2	3855.1	44.73
hexanol	111-27-3	2282	$C_6H_{14}O$	102.18	-377.5	3984.4	3676.3	35.98
1-hexene	592-41-6	2370	C_6H_{12}	84.16	-72.34	4003.8	3739.6	44.43
hexyl ether	112-58-3		$C_{12}H_{26}O$	186.34	-1054	7384.0	6811.8	36.56
HMX (cyclotetramethylene tetramine) (s)	2691-41-0	226	$C_4H_8N_8O_8$	296.16	75	2792.4	2616.3	8.83
hydrazine	302-01-2	2029	N_2H_4	32.05	50.63	622.3	534.3	16.67
hydrazoic acid	7782-79-8		HN_3	43.03	264	406.9	384.9	8.95
hydrogen (g)	1333-74-0	1049	H_2	2.02	0	285.8	241.8	119.96
hydrogen cyanide	74-90-8	1051	HCN	27.03	135.14	671.6	649.6	24.03
hydrogen selenide (g)	7783-07-5	2202	H_2Se	80.98	29.7	315.5	271.5	
hydrogen sulfide (g)	7783-06-4	1053	H_2S	34.08	-20.6	867.2	867.2	25.45
isoamyl acetate	123-92-2	1104	$C_7H_{14}O_2$	130.19	-511.9	4243.6	3935.4	30.23
isoamyl alcohol (isopentanol)	123-51-3	1105	$C_5H_{12}O$	88.15	-355.9	3326.7	3062.6	34.74
isoamyl chloride	107-84-6		$C_5H_{11}Cl$	106.59	-208	3355.4	3135.3	29.41
isoamylene oxide	51109-21-8		$C_5H_{10}O$	86.13				
isoamyl formate	110-45-2	1109	$C_6H_{12}O_2$	116.16				
isobutane (g)	75-28-5		C_4H_{10}	58.12	-134.99	2868.3	2648.2	45.56
isobutyl acetate	110-19-0	1213	$C_6H_{12}O_2$	116.16	-518.8	3557.3	3293.2	28.35
isobutyl acrylate	106-63-8	2527	$C_7H_{12}O_2$	128.17	-394	4075.6	3811.5	29.74
isobutyl alcohol	78-83-1	1212	$C_4H_{10}O$	74.12	-334.6	2668.6	2448.5	33.03
isobutylbenzene	538-93-2		$C_{10}H_{14}$	134.22	-69.9	5866.1	5557.9	41.41
isobutyl chloride	513-36-0		C_4H_9Cl	92.57	-159.4	2724.6	2548.5	27.53
isobutylene (g)	115-11-7	1055	C_4H_8	56.11	-37.5	2679.9	2503.8	44.63
isobutyl formate	542-55-2	2393	$C_5H_{10}O_2$	102.13	-436.3	2960.5	2740.4	26.83
isobutyl methacrylate	97-86-9	2283	$C_8H_{14}O_2$	142.20	-465.2e	4683.8e	4375.6e	30.77e
isobutyraldehyde	78-84-2	2045	C_4H_8O	72.11	-247.3	2470.1	2294.0	31.81
isobutyric acid	79-31-2	2539	$C_4H_8O_2$	88.11	-717	2000.4	1824.3	20.71
isobutyronitrile	78-82-0	2284	C_4H_7N	69.11	-13.8	2560.7	2406.6	34.82
isocrotyl bromide	3017-69-4		C_4H_7Br	135.00				
isocrotyl chloride	513-37-1	2554	C_4H_7Cl	90.55				

Table 1B Pure chemical substances

Substance	C_{st} (vol%)	LFL (vol%)	LFL (g m^{-3})	UFL (vol%)	AIT (ºC) in air	AIT (ºC) in O_2	NEC Group	Flash point (ºC)	LTL (ºC)	BP (ºC)	P_{vap} at FP (atm)
ethyl *sec*-amyl ketone	1.79						Dc			160	
ethyl selenide	3.12	2.5	140.1							108	
ethyl silicate	1.72	1.3	110.7	23			Dc	52		169	
formaldehyde (g)	17.33	7.0	85.9	73	430		Bc	-19		-19	
formic acid	29.54	18	338.7	57	504		Dc	47		101	0.356
furan	4.45	2.3	64.0	14.3				-36		31	
furfural (2-furaldehyde)	4.02	*2.1*	82.5	*19.3*	316		Ct	60		161	0.025
furfuryl alcohol (2-furanmethanol)	3.67	*1.8*	72.2	*16.3*	391	364	Cc	75	72	171	
glycerol (glycerin; 1,2,3-propanetriol)	5.65	2.7e		19.0e	370	320		160		290	
heptane	1.87	1.05	43.0	6.7	223	209	Dt	-4	-4	98	0.012
1-heptanol	1.96	1.0e		7.2e	282e			73		176	
2-heptanone (methyl *n*-amyl ketone)	2.05	1.1	51.4	7.9	393		Dc	39		150	
1-heptene	1.96	1.0e		8.0e	260		Dc	-1		94	
2-heptene	1.96	1.1e		7.8e						98	
1-heptyne	2.05	1.1e		7.2e	255e			-2		98	
hexadecane (cetane)	0.85	0.43e		4.7e	230			126	126	287	
hexamethyldisilazane	1.62	0.8	52.8	31	368			9		127	
hexamethyldisiloxane	1.72	1.3	86.3	18.6	341			-1		101	
hexane	2.16	1.2	42.3	7.4	223	220	Dt	-23	-26	69	0.015
hexanol	2.28	*1.2*	50.1	7.7	300		Dc	63		157	
1-hexene	2.28	1.2e		9.2e	272		Dc	-26		63	
hexyl ether	1.15	0.6e		5.5e	185			77 oc		229	
HMX (cyclotetramethylene tetramine) (s)	9.49										
hydrazine	17.33	*4.7*	61.6	*100*	270	150	Cc	38		114	0.040
hydrazoic acid	45.61					expl.				36	
hydrogen (g)	29.54	4.0	3.3	75	520	400	Bt			-253	
hydrogen cyanide	14.36	5.6	61.9	40	538		Ct	-18		26	0.138
hydrogen selenide (g)	29.54						Cc			-41	
hydrogen sulfide (g)	9.49	4.0	55.7	44	260	220	Ct			-61	
isoamyl acetate	2.16	*1.1*	58.5	*7.5*	378		Dc	25	25	142	
isoamyl alcohol (isopentanol)	2.72	*1.4*	50.5	*9*	343		Dc	43		130	0.017
isoamyl chloride	2.72	1.5	65.4	7.4							
isoamylene oxide	2.91										
isoamyl formate	2.55	1.7	80.7	10	320			22		124	
isobutane (g)	3.12	1.8	42.8	8.4	462	319		-81	-81	-12	
isobutyl acetate	2.55	2.4	114.0	10.5	421		Dt	18		117	
isobutyl acrylate	2.28	2.0e		8.0e	427		Dc	31		132	
isobutyl alcohol	3.38	*1.7*	51.5	*11*	427	364		28		108	
isobutylbenzene	1.53	*0.82*	45.0	*6*	430			55		173	
isobutyl chloride	3.38	2.0	75.7	8.8	414e			-18		46	
isobutylene (g)	3.38	1.8	41.3	8.8	465			-76		-7	
isobutyl formate	3.12	1.7	71.0	8	320			10		97	
isobutyl methacrylate	1.96	1.0e		7.4e	390			46		155	
isobutyraldehyde	3.67	1.6	47.2	10.6	196		Cc	-24		64	
isobutyric acid	4.02	2.0	72.0	9.2	502			55		155	0.014
isobutyronitrile	3.52	1.9e		11.5e				8		107	
isocrotyl bromide	3.84	6.4	353.2	12							
isocrotyl chloride	3.67	4.2	155.5	19						68	

Table 1C Pure chemical substances

Substance	MIE (mJ), plain Calcote	MIE (mJ), flanged Calcote	MIE (mJ), air other	MIE (mJ), O_2 other	Quench dist. (mm)	Quench dia. (mm) Grove	MESG [IEC] (mm)	MESG [UL] (mm)	MIC [UK] (mA)	T_{ad} at LFL (K)	T_{ad} at stoich (K)
ethyl *sec*-amyl ketone											
ethyl selenide											
ethyl silicate											
formaldehyde (g)							0.57				
formic acid							1.86				
furan	0.225	0.328					0.68			1540	2390
furfural (2-furaldehyde)							0.94	0.41			
furfuryl alcohol (2-furanmethanol)											
glycerol (glycerin; 1,2,3-propanetriol)											
heptane	0.7	1.15			2.2		0.91		174	1980	2275
1-heptanol							0.94				
2-heptanone (methyl *n*-amyl ketone)											
1-heptene							0.85				
2-heptene							0.97				
1-heptyne	0.56	0.931			1.85						
hexadecane (cetane)											
hexamethyldisilazane											
hexamethyldisiloxane							0.73				
hexane			0.29	0.006	1.5		0.93		164		
hexanol							0.98				
1-hexene											
hexyl ether											
HMX (cyclotetramethylene tetramine) (s)											
hydrazine											
hydrazoic acid											
hydrogen (g)	0.02	0.03	0.017	0.0012	0.64	0.9	0.29	0.23	75	985	2345
hydrogen cyanide							0.80				
hydrogen selenide (g)											
hydrogen sulfide (g)	0.068	0.077	0.077					0.66			
isoamyl acetate							0.99				
isoamyl alcohol (isopentanol)											
isoamyl chloride											
isoamylene oxide							0.82				
isoamyl formate											
isobutane (g)	0.52	0.85			2.2					1680	2260
isobutyl acetate											
isobutyl acrylate											
isobutyl alcohol						2.9	0.94				
isobutylbenzene											
isobutyl chloride											
isobutylene (g)							1.00				
isobutyl formate											
isobutyl methacrylate							0.96				
isobutyraldehyde							>0.92				
isobutyric acid											
isobutyronitrile							1.00				
isocrotyl bromide											
isocrotyl chloride											

Table 1A Pure chemical substances

Substance	CAS No.	UN No.	Formula	MW	Δh_f kJ mol^{-1}	Δh_c (upper) kJ mol^{-1}	Δh_c (lower) kJ mol^{-1}	Δh_c (lower) MJ kg^{-1}
isodecaldehyde	1321-89-7		$C_{10}H_{20}O$	156.27				
isooctaldehyde (6-methyl-1-heptanal)	63885-09-6		$C_8H_{16}O$	128.21				
iso-octane	540-84-1	1262	C_8H_{18}	114.23	-259.3	5461.3	5065.2	44.34
iso-octyl alcohol	26952-21-6		$C_8H_{18}O$	130.23	-839	4881.6	4485.5	34.44
isopentane	78-78-4	1265	C_5H_{12}	72.15	-178.2	3504.4	3240.3	44.91
isophorone	78-59-1		$C_9H_{14}O$	138.21	-251	5291.5	4983.3	36.06
isoprene (2-methyl-1,3-butadiene)	78-79-5	1218	C_5H_8	68.12	75.7	3186.6	3010.5	44.20
isopropenyl acetate	108-22-5	2403	$C_5H_8O_2$	100.12	-386.4	2724.5	2548.4	25.45
isopropyl acetate	108-21-4	1220	$C_5H_{10}O_2$	102.13	-518.8	2878.0	2657.9	26.02
isopropylacetone (methyl isobutyl ketone)	108-10-1	1245	$C_6H_{12}O$	100.16	-388.7	3687.4	3423.3	34.18
isopropylamine	75-31-0	1221	C_3H_9N	59.11	-112.3	2354.5	2156.4	36.48
2-isopropyl bicyclohexyl	66374-73-0		$C_{15}H_{28}$	208.39	229.7	10134.1	9517.8	45.67
2-isopropyl biphenyl	25640-78-2		$C_{15}H_{16}$	196.29	49.4	8238.8	7886.6	40.18
isopropyl chloride	75-29-6	2356	C_3H_7Cl	78.54	-172.3	2032.4	1900.3	24.20
isopropyl ether (diisopropyl ether)	108-20-3	1159	$C_6H_{14}O$	102.18	-351.5	4010.4	3702.3	36.23
isopropyl glycidyl ether	4016-14-2		$C_6H_{12}O_2$	116.16	-342.9	3733.2	3469.1	29.86
isopropyl mercaptan	75-33-2	2703	C_3H_8S	76.16	-106.6	2819.3	2687.2	35.29
isopropyl nitrate	1712-64-7	1222	$C_3H_7NO_3$	105.09	-229.8	1951.2	1797.1	17.10
isopropyl nitrite	541-42-4		$C_3H_7NO_2$	89.09	-164	2017.0	1862.9	20.91
limonene (dipentene)	138-86-3	2052	$C_{10}H_{16}$	136.24	-54.5	6167.3	5815.2	42.68
maleic anhydride (s)	108-31-6	2215	$C_4H_2O_3$	98.06	-470.41	1389.5	1345.5	13.72
mesityl oxide	141-79-7	1229	$C_6H_{10}O$	98.14	-220.98	3569.3	3349.2	34.13
methane (g)	74-82-8	1971	CH_4	16.04	-74.873	890.3	802.3	50.01
methanol	67-56-1	1230	CH_4O	32.04	-238.4	726.8	638.8	19.93
methenamine (s)	100-97-0		$C_6H_{12}N_4$	140.19	124.1	4200.2	3936.1	28.08
methoxypropanol	1320-67-8		$C_4H_{10}O_2$	90.12				
methyl acetate	79-20-9	1231	$C_3H_6O_2$	74.08	-445.89	1592.2	1460.1	19.71
methyl acetoacetate	105-45-3		$C_5H_8O_3$	116.12	-623.31	2487.6	2311.5	19.91
methyl acetylene (propyne) (g)	74-99-7	1060	C_3H_4	40.06	185.4	1937.6	1849.6	46.16
methyl acrylate	96-33-3	1919	$C_4H_6O_2$	86.09	-362.2	2069.4	1937.3	22.50
methylallyl chloride	563-47-3	2554	C_4H_7Cl	90.55				
methylamine (g)	74-89-5	1061	CH_5N	31.06	-47.3	1060.8	950.8	30.61
methyl amyl alcohol (methyl isobutyl carbinol)	108-11-2	2053	$C_6H_{14}O$	102.18	-394.7	3967.2	3659.1	35.81
methyl bromide (g)	74-83-9	1062	CH_3Br	94.94	-34.3	766.2	722.2	7.61
3-methyl-1-butene (g)	563-45-1	2561	C_5H_{10}	70.13	-51.6	3345.2	3125.1	44.56
methyl butyl ketone (2-hexanone)	591-78-6		$C_6H_{12}O$	100.16	-330.1	3746.0	3481.9	34.76
methyl cellosolve (2-methoxyethanol)	109-86-4	1188	$C_3H_8O_2$	76.10	-422.04	1901.9	1725.8	22.68
methyl cellosolve acetate	110-49-6	1189	$C_5H_{10}O_3$	118.13	-622.8	2774.0	2553.9	21.62
methyl chloride (g)	74-87-3	1063	CH_3Cl	50.49	-80.83	765.1	721.1	14.28
methyl chlorocarbonate	79-22-1	1238	$C_2H_3ClO_2$	94.50	-476	763.5	719.5	7.61
methylcyclohexane	108-87-2	2296	C_7H_{14}	98.19	-154.8	4600.7	4292.5	43.72
methylcyclohexanol	25639-42-3	2617	$C_7H_{14}O$	114.19	-415	4340.5	4032.3	35.31
2-methylcyclohexanone	583-60-8	2297	$C_7H_{12}O$	112.17	-288.1	4181.5	3917.4	34.92

Table 1B Pure chemical substances

Substance	C_{st} (vol%)	LFL (vol%)	LFL (g m^{-3})	UFL (vol%)	AIT (ºC) in air	AIT (ºC) in O_2	NEC Group	Flash point (ºC)	LTL (ºC)	BP (ºC)	P_{vap} at FP (atm)
isodecaldehyde	1.43						Cc	85		197	
isooctaldehyde (6-methyl-1-heptanal)	1.79							40		152	
iso-octane	1.65	0.95	44.4	6	415	283		-12		99	
iso-octyl alcohol	1.72	0.9	47.9	5.7	277		Dc	82		186	
isopentane	2.55	1.4	41.3	7.6	420			-56	-56	28	0.014
isophorone	1.72	*0.84*	47.5	*3.8*	462	322	Dc	84 oc		215	
isoprene (2-methyl-1,3-butadiene)	2.91	2.0	55.7	9	460	440	Dt	-54		34	0.011
isopropenyl acetate	3.38							10		94	
isopropyl acetate	3.12	1.8	75.2	8.0	460		Dc	4		88	
isopropylacetone (methyl isobutyl ketone)	2.41	1.4	57.3	7.5	460		Dt	18		117	0.017
isopropylamine	3.84	2.0	48.3	10.4	402		Dc	-37		32	
2-isopropyl bicyclohexyl	0.94	*0.52*	44.3	*4.1*	230			124		283	
2-isopropyl biphenyl	1.09	*0.53*	42.5	*3.2*	445			140		269	
isopropyl chloride	4.45	2.8	89.9	10.7	593			-32		35	0.042
isopropyl ether (diisopropyl ether)	2.28	1.4	58.5	7.9	443		Dt	-28		69	0.010
isopropyl glycidyl ether	2.55						Cc	33		137	
isopropyl mercaptan	3.12	1.8e						-35		53	
isopropyl nitrate	6.06									101	
isopropyl nitrite	5.29	2.6	94.7	11.0	428			24		40	
limonene (dipentene)	1.48	*0.75*	41.8	*6.1*	237		Dc	46	45	176	
maleic anhydride (s)	6.53	*1.4*	56.1	*7.1*	477			102		202	
mesityl oxide	2.55	1.4	56.2	7.2	344		Dt	31		130	
methane (g)	9.49	5.0	32.8	15	640	556	Dt	-188	-187	-164	
methanol	12.26	6.7	87.8	*36*	470	461	Dt	11		65	0.082
methenamine (s)	2.28	1.1e		3.6e				250		subl.	
methoxypropanol	3.67	1.9	70.0	18.1	286			34		125	
methyl acetate	5.65	3.2	96.9	16	502		Dc	-9		57	0.049
methyl acetoacetate	3.67	1.8e		8.8e	280			70		170	
methyl acetylene (propyne) (g)	4.98	1.7	27.8	12.5	340		Ct			-24	
methyl acrylate	4.45	2.8	98.5	*25*	468		Dc	-3		80	
methylallyl chloride	3.67	2.3	85.1	8.1				-12		72	
methylamine (g)	8.52	4.9	62.2	20.7	430	400	Dc	-58e		-6.3	
methyl amyl alcohol (methyl isobutyl carbinol)	2.28	*1.0*	41.8	*5.5*	306		Dc	41	40	133	
methyl bromide (g)	14.36	10	388.1	15	537			-40		3.6	0.127
3-methyl-1-butene (g)	2.72	1.5	43.0	9.1	365e			-56		20	0.022
methyl butyl ketone (2-hexanone)	2.41	*1.2*	49.1	*8*	533		Dc	25		127	
methyl cellosolve (2-methoxyethanol)	4.98	*2.5*	77.8	*20*	380			46	46	125	
methyl cellosolve acetate	3.38	*1.7*	82.1	*8.2*				44		145	
methyl chloride (g)	12.26	10.7	220.9	17.4	632			-40		-24	0.480
methyl chlorocarbonate	12.26	6.7	258.8	15.6	504			15		70	
methylcyclohexane	1.96	1.1	44.2	6.7	250	285	Dc	-4		101	0.013
methylcyclohexanol	2.05	*1.0*	46.7	7.7e	296		Dc	65		155-180	
2-methylcyclohexanone	2.16				598		Dc	48		163	

Table 1C Pure chemical substances

Substance	MIE (mJ), plain Calcote	MIE (mJ), flanged Calcote	MIE (mJ), air other	MIE (mJ), O_2 other	Quench dist. (mm)	Quench dia. (mm) Grove	MESG [IEC] (mm)	MESG [UL] (mm)	MIC [UK] (mA)	T_{ad} at LFL (K)	T_{ad} at stoich (K)
isodecaldehyde											
isooctaldehyde (6-methyl-1-heptanal)											
iso-octane	1.35	2.9			3.47	2.97	1.04			1825	2210
iso-octyl alcohol											
isopentane	0.7	0.96	0.25		1.78		0.98			1660	2250
isophorone											
isoprene (2-methyl-1,3-butadiene)							0.81	0.86			
isopropenyl acetate							0.98				
isopropyl acetate											
isopropylacetone (methyl isobutyl ketone)							1.01				
isopropylamine			2.0								
2-isopropyl bicyclohexyl											
2-isopropyl biphenyl											
isopropyl chloride	1.55	3.1	1.08				1.32				
isopropyl ether (diisopropyl ether)	1.14	2.14			3.0		0.94	1.04		1735	2250
isopropyl glycidyl ether											
isopropyl mercaptan	0.53	0.87									
isopropyl nitrate									130		
isopropyl nitrite							0.98				
limonene (dipentene)							1.18				
maleic anhydride (s)											
mesityl oxide								0.84			
methane (g)	0.37	0.71	0.3	0.003	2.03	3.53	1.14	1.12	195	1650	2200
methanol	0.215	0.3	0.14		1.5	2.69	0.92		167		
methenamine (s)											
methoxypropanol											
methyl acetate							0.97		178		
methyl acetoacetate							0.84				
methyl acetylene (propyne) (g)	0.152	0.2	0.115		1.15		0.74	0.64	116	1600	2450
methyl acrylate							0.85		161		
methylallyl chloride											
methylamine (g)							1.10				
methyl amyl alcohol (methyl isobutyl carbinol)											
methyl bromide (g)											
3-methyl-1-butene (g)											
methyl butyl ketone (2-hexanone)											
methyl cellosolve (2-methoxyethanol)							0.85				
methyl cellosolve acetate											
methyl chloride (g)							1.00				
methyl chlorocarbonate							1.85				
methylcyclohexane			0.27								
methylcyclohexanol											
2-methylcyclohexanone											

Table 1A Pure chemical substances

Substance	CAS No.	UN No.	Formula	MW	Δh_f kJ mol^{-1}	Δh_c (upper) kJ mol^{-1}	Δh_c (lower) kJ mol^{-1}	Δh_c (lower) MJ kg^{-1}
methyl-1,3-cyclopentadiene	26519-91-5		C_6H_8	80.13	15	3519.4	3343.3	41.72
methylcyclopentane	96-37-7	2298	C_6H_{12}	84.16	-137.7	3938.4	3674.3	43.66
2-methyl-1,3-dioxolane	497-26-7		$C_4H_8O_2$	88.11	-386.9	2330.5	2154.4	24.45
methylene chloride	75-09-2	1593	CH_2Cl_2	84.93	-124.3	602.5	602.5	7.09
methyl ether (dimethyl ether) (g)	115-10-6	1033	C_2H_6O	46.07	-184.1	1460.4	1328.4	28.83
methyl ethyl ether (g)	540-67-0	1039	C_3H_8O	60.10	-216.4	2107.5	1931.4	32.14
methyl ethyl ketone (2-butanone)	78-93-3	1193	C_4H_8O	72.11	-273.3	2444.1	2268.0	31.45
methyl ethyl ketone peroxide	1338-23-4	2550	$C_8H_{16}O_4$	176.21				
methyl formate	107-31-3	1243	$C_2H_4O_2$	60.05	-365.9	992.8	904.8	15.07
methylhydrazine (monomethylhydrazine)	60-34-4	1244	CH_6N_2	46.07	54.14	1305.2	1173.1	25.46
methylisocyanate	624-83-9	2480	C_2H_3NO	57.05	-57.78	1158.0	1092.0	19.14
methylisopropenyl ketone	814-78-8	1246	C_5H_8O	84.12	-391	2719.9	2543.8	30.24
methyl lactate	547-64-8		$C_4H_8O_3$	104.11	-637.2	2080.2	1904.1	18.29
methyl mercaptan (g)	74-93-1	1064	CH_4S	48.10	-22.8	1544.4	1500.3	31.19
methyl methacrylate	80-62-6	1247	$C_5H_8O_2$	100.12	-382.4	2728.5	2552.4	25.49
1-methylnaphthalene	90-12-0		$C_{11}H_{10}$	142.20	56.2	5814.0	5593.9	39.34
methyl nitrate	598-58-3		CH_3NO_3	77.04	-156.3	666.0	599.9	7.79
2-methyl pentane	107-83-5	2462	C_6H_{14}	86.18	-204.3	4157.6	3849.5	44.67
3-methyl pentane	96-14-0	2462	C_6H_{14}	86.18	-202.0	4159.9	3851.8	44.70
methyl propionate	554-12-1	1248	$C_4H_8O_2$	88.11	-427.5	2289.9	2113.8	23.99
2-methyl pyridine (a-picoline)	109-06-8	2313	C_6H_7N	93.13	-68.99	3292.5	3138.4	33.70
3-methyl pyridine	108-99-6	2313	C_6H_7N	93.13	61.1	3422.6	3268.5	35.10
a-methyl styrene	98-83-9	2303	C_9H_{10}	118.18	70.5	5041.3	4821.2	40.80
methyl *tert*-butyl ether (MTBE)	1634-04-4	2398	$C_5H_{12}O$	88.15	-313.6	3369.0	3104.9	35.22
monoisopropanolamine	78-96-6		C_3H_9NO	75.11	-239	2227.8	2029.7	27.02
monomethyl aniline (methyl aniline)	100-61-8	2294	C_7H_9N	105.14	33.4	3788.4	3634.3	34.57
morpholine	110-91-8	2054	C_4H_9NO	87.12	-186.7	2673.6	2475.5	28.41
naphthalene (s)	91-20-3	1334	$C_{10}H_8$	128.17	87.17	5165.6	4989.6	38.93
nicotine	54-11-5	1654	$C_{10}H_{14}N_2$	162.23	42.7	5978.7	5670.5	34.95
nitrobenzene	98-95-3	1662	$C_6H_5NO_2$	123.11	12.5	3088.2	2978.1	24.19
nitroethane	79-24-3	2842	$C_2H_5NO_2$	75.07	-144	1357.6	1247.6	16.62
nitroglycerin	55-63-0		$C_3H_5N_3O_9$	227.09	-371.1	1524.0	1414.0	6.23
nitromethane	75-52-5	1261	CH_3NO_2	61.04	-113	709.3	643.2	10.54
1-nitropropane	108-03-2	2608	$C_3H_7NO_2$	89.09	-167	2014.0	1859.9	20.88
2-nitropropane	79-46-9	2608	$C_3H_7NO_3$	89.09	-140.2	2040.8	1886.7	21.18
2-nitrotoluene	88-72-2	1664	$C_7H_7NO_2$	137.14	-1.7	3753.3	3599.2	26.25
nonane	111-84-2	1920	C_9H_{20}	128.26	-274.7	6125.3	5685.1	44.33
1-nonanol (nonyl alcohol)	143-08-8		$C_9H_{20}O$	144.26	-453.6	5946.4	5506.2	38.17
1-nonene	124-11-8		C_9H_{18}	126.24	-103.51	6010.6	5614.5	44.47
octane	111-65-9	1262	C_8H_{18}	114.23	-250.3	5470.3	5074.2	44.42

Table 1B Pure chemical substances

Substance	C_{st} (vol%)	LFL (vol%)	LFL (g m^{-3})	UFL (vol%)	AIT (ºC) in air	AIT (ºC) in O_2	NEC Group	Flash point (ºC)	LTL (ºC)	BP (ºC)	P_{vap} at FP (atm)
methyl-1,3-cyclopentadiene	2.55	*1.3*	42.6	*7.6*	445			49		72	
methylcyclopentane	2.28	1.2e		8.4e	323	329		-6		72	0.039
2-methyl-1,3-dioxolane	4.02							-2		81	
methylene chloride	17.33	*15.9*	552.1	*19.1*	556	535		ca. -9		40	
methyl ether (dimethyl ether) (g)	6.53	3.4	64.0	27	350		Ct	-41		-23	
methyl ethyl ether (g)	4.45	2.0	49.1	10.1	190			-37		10	
methyl ethyl ketone (2-butanone)	3.67	1.9	56.0	11	516		Dt	-6		80	0.029
methyl ethyl ketone peroxide	2.05				390				40	expl.	
methyl formate	9.49	5.0	122.8	23	465		Dc	-19		32	
methylhydrazine (monomethylhydrazine)	7.74	2.5	47.1	97	185		Cc	18		88	0.008
methylisocyanate	8.52	5.3	123.6	26	534		Dc	-18		40	
methylisopropenyl ketone	3.12	1.8	61.9	9						98	
methyl lactate	4.45	*2.2*	93.6		385			49		145	
methyl mercaptan (g)	5.65	3.9	76.7	21.8	325e		Cc	-18		6	
methyl methacrylate	3.38	2.1	86.0	12.5	422		Dc	10		101	
1-methylnaphthalene	1.53	*0.8*	46.5	5.3e	529			82		241	
methyl nitrate	45.61									expl.	
2-methyl pentane	2.16	1.2	42.3	7.0	306			-23		60	
3-methyl pentane	2.16	1.2	42.3	7.0	300			<-20		63	
methyl propionate	4.02	2.4	86.4	13	469			-2		80	
2-methyl pyridine (a-picoline)	2.63	1.4	53.3	8.6	535			27		128	
3-methyl pyridine	2.63	1.4e		11.9e	537e			40		144	
a-methyl styrene	1.79	*1.9*	91.8	*6.1*	495		Dc	45	49	165	
methyl *tert*-butyl ether (MTBE)	2.72	2.0	72.1	15.1	224			-28		55	
monoisopropanolamine	4.23	2.2	67.6	12	374		Dc	74		160	
monomethyl aniline (methyl aniline)	2.34	1.2e		7.4e	482		Cc			196	
morpholine	3.52	2.0	71.2	11.2	310		Ct	37		128	
naphthalene (s)	1.72	*0.88*	46.1	*5.9*	526	560		79		218	
nicotine	1.53	*0.75*	49.7	*4*	244	235		101	79	246	
nitrobenzene	3.25	*1.8*	90.6	*9.1*	482		Dc	87		211	
nitroethane	8.52	3.4	104.3	17.2	414		Cc	28	30	115	
nitroglycerin					270			expl		expl.	
nitromethane	21.85	*7.3*	182.2	*22.2*	419		Cc	35	33	101	0.074
1-nitropropane	5.29	*2.2*	80.1	*13.8*	417		Cc	33	34	131	
2-nitropropane	5.29	*2.5*	91.1	*11*	428		Ct	30	27	120	
2-nitrotoluene	2.63	2.2	123.3	7.6	305			106		222	
nonane	1.48	0.85	44.6	5.6	205		Dc	32	31	151	0.008
1-nonanol (nonyl alcohol)	1.53	0.8	47.2	6.1	277e		Dc	74		215	
1-nonene	1.53	0.8e		6.4e	237e		Dc	25		147	
octane	1.65	0.95	44.4	*6.5*	220	208	Dt	14	13	126	

Table 1C Pure chemical substances

Substance	MIE (mJ), plain Calcote	MIE (mJ), flanged Calcote	MIE (mJ), air other	MIE (mJ), O_2 other	Quench dist. (mm)	Quench dia. (mm) Grove	MESG [IEC] (mm)	MESG [UL] (mm)	MIC [UK] (mA)	T_{ad} at LFL (K)	T_{ad} at stoich (K)
methyl-1,3-cyclopentadiene											
methylcyclopentane											
2-methyl-1,3-dioxolane							0.83				
methylene chloride			10000		5.46						
methyl ether (dimethyl ether) (g)	0.29	0.45					0.84	0.36	140		
methyl ethyl ether (g)											
methyl ethyl ketone (2-butanone)	0.68	1.1	0.53		2		0.85		159	1650	2210
methyl ethyl ketone peroxide											
methyl formate	0.4	0.62			1.65		0.94				
methylhydrazine (monomethylhydrazine)											
methylisocyanate							1.14				
methylisopropenyl ketone											
methyl lactate											
methyl mercaptan (g)							1.18				
methyl methacrylate							0.95				
1-methylnaphthalene											
methyl nitrate											
2-methyl pentane											
3-methyl pentane											
methyl propionate											
2-methyl pyridine (a-picoline)											
3-methyl pyridine											
a-methyl styrene							0.88				
methyl *tert*-butyl ether (MTBE)							1.00				
monoisopropanolamine											
monomethyl aniline (methyl aniline)											
morpholine							0.95	0.43			
naphthalene (s)											
nicotine											
nitrobenzene							0.94				
nitroethane	0.22	0.31					0.87				
nitroglycerin											
nitromethane							1.17		167		
1-nitropropane							0.84				
2-nitropropane								0.53			
2-nitrotoluene											
nonane											
1-nonanol (nonyl alcohol)											
1-nonene											
octane							0.94				

Table 1A Pure chemical substances

Substance	CAS No.	UN No.	Formula	MW	Δh_f kJ mol^{-1}	Δh_c (upper) kJ mol^{-1}	Δh_c (lower) kJ mol^{-1}	Δh_c (lower) MJ kg^{-1}
1-octanol	111-87-5		$C_8H_{18}O$	130.23	-426.6	5294.0	4897.9	37.61
1-octene	111-66-0		C_8H_{16}	112.21	-121.8	5313.0	4960.8	44.21
paraformaldehyde (polyoxymethylene) (s)	30525-89-4	2213	$(CH_20)_n$	30.03	-171.3	508.1	464.0	15.45
paraldehyde	123-63-7	1264	$C_6H_{12}O_3$	132.16	-681.8	3394.3	3130.2	23.68
pentaborane	19624-22-7	1380	B_5H_9	63.12	42.8	2321.6	2453.7	38.87
pentanal (*n*-valeraldehyde)	110-62-3	2058	$C_5H_{10}O$	86.13	-267.2	3129.6	2909.5	33.78
pentane	109-66-0	1265	C_5H_{12}	72.15	-173.5	3509.1	3245.0	44.98
2-pentanol (*sec*-amyl alcohol)	6032-29-7	1105	$C_5H_{12}O$	88.15	-365.2	3317.4	3053.3	34.64
2-pentanone (methyl propyl ketone)	107-87-9	1249	$C_5H_{10}O$	86.13	-258.6	3138.2	2918.1	33.88
trans-2-pentene	646-04-8		C_5H_{10}	70.13	-58.24	3338.5	3118.4	44.46
PETN (pentaerythritol-tetranitrate) (s)	78-11-5		$C_5H_8N_4O_{12}$	316.14	-538.5	2572.4	2396.3	7.58
phenol (s)	108-95-2	1671	C_6H_6O	94.11	-165	3053.6	2921.5	31.04
phenyl ether (diphenyl ether)	101-84-8		$C_{12}H_{10}O$	170.21	-14.6	6136.7	5916.6	34.76
phenylhydrazine	100-63-0	2572	$C_6H_8N_2$	108.14	141	3645.4	3469.3	32.08
phosphine (g)	7803-51-2	2199	PH_3	34.00	5.4	5.4	5.4	
phthalic anhydride (s)	85-44-9	2214	$C_8H_4O_3$	148.12	-460.37	3259.4	3171.4	21.41
picric acid (s)	88-89-1	1344	$C_6H_3N_3O_7$	229.11	-216.33	2573.5	2507.5	10.94
pinane	473-55-2		$C_{10}H_{18}$	138.25				
♋-pinene	80-56-8	2368	$C_{10}H_{16}$	136.24	-16.4	6205.4	5853.3	42.96
potassium nitrate (s)	7757-79-1	1486	KNO_3	101.10	-494.63	-494.6	-494.6	
potassium perchlorate (s)	7778-74-7	1489	$KClO_4$	138.55	-432.75	-409.1	-387.0	
1,2-propadiene (allene) (g)	463-49-0	2200	C_3H_4	40.06	190.92	1943.1	1855.1	46.30
propane (g)	74-98-6	1978	C_3H_8	44.10	-104.7	2219.2	2043.1	46.33
propanoic acid (propionic acid)	79-09-4	1848	$C_3H_6O_2$	74.08	-510.8	1527.3	1395.2	18.83
propanoic anhydride (propionic anhydride)	123-62-6	2496	$C_6H_{10}O_3$	130.14	-679.1	3111.2	2891.1	22.21
2-propanol (isopropyl alcohol)	67-63-0	1219	C_3H_8O	60.10	-317	2006.9	1830.8	30.46
1-propanol (*n*-propyl alcohol)	71-23-8	1274	C_3H_8O	60.10	-302.54	2021.4	1845.3	30.71
2-propanone (acetone cyanohydrin)	75-86-5	1541	C_4H_7NO	85.11	-120.9	2453.6	2299.5	27.02
propargyl alcohol (2-propyn-1-ol)	107-19-7		C_3H_4O	56.06	42.2	1794.4	1706.4	30.44
propargyl bromide	106-96-7	2345	C_3H_3Br	118.96	167	1754.5	1710.5	14.38
propargyl chloride	624-65-7		C_3H_3Cl	74.51	129.5e	1762.5e	1718.5e	23.06e
propiolactone	57-57-8		$C_3H_4O_2$	72.06	-333.2	1419.0	1331.0	18.47
propionaldehyde (propanal)	123-38-6	1275	C_3H_6O	58.08	-218.3	1819.8	1687.7	29.06
propionitrile	107-12-0	2404	C_3H_5N	55.08	15.5	1910.6	1800.6	32.69
n-propyl acetate	109-60-4	1276	$C_5H_{10}O_2$	102.13	-464.8	2932.0	2711.9	26.55
propylamine	107-10-8	1277	C_3H_9N	59.11	-101.5	2365.3	2167.2	36.66
propyl benzene	103-65-1	2364	C_9H_{12}	120.19	-38.4	5218.2	4954.1	41.22
propyl bromide	106-94-5	2344	C_3H_7Br	122.99	-124.4	2034.8	1902.8	15.47
n-propyl chloride	540-54-5	1278	C_3H_7Cl	78.54	-160.5	2044.2	1912.1	24.35
propylene (propene) (g)	115-07-1	1077	C_3H_6	42.08	20.41	2058.5	1926.4	45.78
propylene dichloride (propylene chloride)	78-87-5	1279	$C_3H_6Cl_2$	112.99	-165.7	1919.8	1831.7	16.21
propylene glycol	57-55-6		$C_3H_8O_2$	76.10	-501	1822.9	1646.8	21.64

Table 1B Pure chemical substances

Substance	C_{st} (vol%)	LFL (vol%)	LFL (g m^{-3})	UFL (vol%)	AIT (ºC) in air	AIT (ºC) in O_2	NEC Group	Flash point (ºC)	LTL (ºC)	BP (ºC)	P_{vap} at FP (atm)
1-octanol	1.72	0.9e		6.4e	282			81		195	
1-octene	1.72	0.9e		7.1e	230		Dc	13		121	
paraformaldehyde (polyoxymethylene) (s)	17.33				300			71		dec	
paraldehyde	2.72	1.3	70.2	16.2	237			27		124	
pentaborane	2.10	0.42	10.8	98	pyr					58	
pentanal (*n*-valeraldehyde)	2.91	1.5e		9.5e	222		Cc	12		103	
pentane	2.55	1.4	41.3	7.8	260	258	Dt	-49	-48	36	0.014
2-pentanol (*sec*-amyl alcohol)	2.72	1.2	43.2	8e	343		Dc	34		119	
2-pentanone (methyl propyl ketone)	2.91	1.6	56.3	8.2	505		Dc	7		102	0.017
trans-2-pentene	2.72	1.4e		10.6e	285e			-48e		36	
PETN (pentaerythritol-tetranitrate) (s)	17.33									expl.	
phenol (s)	2.91	1.8	69.3	8.6	715	500		79		182	
phenyl ether (diphenyl ether)	1.48	*0.8*	55.7	*1.5*	618			115		259	0.010
phenylhydrazine	2.55	1.3e		9.5e	174		Dc	88		240	
phosphine (g)	100.00	1.0			100					-88	
phthalic anhydride (s)	2.72	*1.2*	72.7	*9.2*	570	556		152	140	295	
picric acid (s)	6.06				300			150		expl.	
pinane	1.43	*0.74*	41.8	*7.2*						169	
♋-pinene	1.48	*0.7*	39.0	6.6e	255	263		33		156	
potassium nitrate (s)										dec	
potassium perchlorate (s)											
1,2-propadiene (allene) (g)	4.98	2.2	36.0	12						-35	
propane (g)	4.02	2.1	37.9	9.5	500	466	Dt	-104	-102	-42	
propanoic acid (propionic acid)	5.65	2.9	87.8	14.8	466		Dc	52		139	0.025
propanoic anhydride (propionic anhydride)	2.91	1.3	69.2	11.9	285		Dc	63		167	
2-propanol (isopropyl alcohol)	4.45	2.2	54.1	*12*	399	512	Dt	12		82	
1-propanol (*n*-propyl alcohol)	4.45	*2.2*	54.1	*14*	439	328	Dt	15		97	0.013
2-propanone (acetone cyanohydrin)	3.84	*2.2*	76.5	*12*	688		Dc	74		82	
propargyl alcohol (2-propyn-1-ol)	5.65	*2.2*	50.4	*14*	115			36		114	
propargyl bromide	6.06	3.0	145.9	100	324			18		90	
propargyl chloride	5.65	3.4	103.6	41				18		65	
propiolactone	6.53	*2.9*	85.4	*25.1*			Dc	74		162	
propionaldehyde (propanal)	4.98	2.9	68.9	17	207	108	Cc	-9		49	
propionitrile	4.70	3.1	69.8	14.0	512			2		97	
n-propyl acetate	3.12	1.8	75.2	*8*	450	388	Dc	14		102	0.020
propylamine	3.84	2.0	48.3	10.4	318			-37		47	0.014
propyl benzene	1.72	0.8	39.3	6.0	450e			39		159	
propyl bromide	4.70	2.7e		9.2e	490			14		71	
n-propyl chloride	4.45	2.6	83.5	11	520			<-18		47	
propylene (propene) (g)	4.45	2.4	41.3	11	458	423	Dt	-108		-47	
propylene dichloride (propylene chloride)	4.98	3.4	157.1	14.5	557		Dc	16		96	
propylene glycol	4.98	*2.6*	80.9	*12.5*	371	392		99		187	0.030

Table 1C Pure chemical substances

Substance	MIE (mJ), plain Calcote	MIE (mJ), flanged Calcote	MIE (mJ), air other	MIE (mJ), O_2 other	Quench dist. (mm)	Quench dia. (mm) Grove	MESG [IEC] (mm)	MESG [UL] (mm)	MIC [UK] (mA)	T_{ad} at LFL (K)	T_{ad} at stoich (K)
1-octanol							1.05				
1-octene											
paraformaldehyde (polyoxymethylene) (s)							0.57				
paraldehyde											
pentaborane											
pentanal (*n*-valeraldehyde)											
pentane	0.51	0.82			2.07		0.93	0.56	164	1635	2275
2-pentanol (*sec*-amyl alcohol)											
2-pentanone (methyl propyl ketone)							0.99				
trans-2-pentene										1650	2320
PETN (pentaerythritol-tetranitrate) (s)											
phenol (s)											
phenyl ether (diphenyl ether)											
phenylhydrazine											
phosphine (g)											
phthalic anhydride (s)											
picric acid (s)											
pinane											
♋-pinene	1.4	2.7					0.86				
potassium nitrate (s)											
potassium perchlorate (s)											
1,2-propadiene (allene) (g)											
propane (g)	0.305	0.5	0.26	0.002	1.75		0.92	0.94	146	1640	2260
propanoic acid (propionic acid)											
propanoic anhydride (propionic anhydride)											
2-propanol (isopropyl alcohol)	0.65	1.11					1.00				
1-propanol (*n*-propyl alcohol)							0.89		166		
2-propanone (acetone cyanohydrin)											
propargyl alcohol (2-propyn-1-ol)	0.21	0.30									
propargyl bromide											
propiolactone											
propargyl chloride											
propionaldehyde (propanal)	0.325	0.49			1.75		0.83			1565	2310
propionitrile											
n-propyl acetate							1.05				
propylamine							1.13				
propyl benzene											
propyl bromide											
n-propyl chloride	1.08	2									
propylene (propene) (g)	0.282	0.418	0.28				0.90	0.89		1610	2320
propylene dichloride (propylene chloride)											
propylene glycol											

Table 1A Pure chemical substances

Substance	CAS No.	UN No.	Formula	MW	Δh_f kJ mol^{-1}	Δh_c (upper) kJ mol^{-1}	Δh_c (lower) kJ mol^{-1}	Δh_c (lower) MJ kg^{-1}
propylene glycol monomethyl ether (1-methoxy-2-propanol)	107-98-2	3092	$C_4H_{10}O_2$	90.12	-447.7e	2555.5e	2335.4e	25.91e
propylene glycol monomethyl ether acetate (methoxypropyl acetate)	108-65-6		$C_6H_{12}O_3$	132.16	-663.2e	3412.9e	3148.8e	23.83e
propylene oxide	75-56-9	1280	C_3H_6O	58.08	-122.6	1915.5	1783.4	30.71
propyl ether (dipropyl ether)	111-43-3	2384	$C_6H_{14}O$	102.18	-328.8	4033.1	3725.0	36.46
n-propyl nitrate	627-13-4	1865	$C_3H_7NO_3$	105.09	-174.1	2006.9	1852.8	17.63
pyridine	110-86-1	1282	C_5H_5N	79.10	99.96	2782.1	2672.1	33.78
pyrrole	109-97-7		C_4H_5N	67.09	63.1	2351.7	2241.7	33.41
quinoline	91-22-5	2656	C_9H_7N	129.16	141.2	4683.2	4529.2	35.07
RDX (cyclotrimethylene trinitramine) (s)	121-82-4		$C_3H_6N_6O_6$	222.12	71.55	2109.6	1977.5	8.90
silane (g)	7803-62-5	2203	H_4Si	32.12	34.3	1509.5	1421.4	44.26
stearic acid (s)	57-11-4		$C_{18}H_{36}O_2$	284.48	-912.07	11316.2	10523.9	36.99
styrene	100-42-5	2055	C_8H_8	104.15	103.4	4394.8	4218.8	40.51
sucrose (s)	57-50-1		$C_{12}H_{22}O_{11}$	342.30	-2221.2	5645.2	5160.9	15.08
sulfamic acid (s)	5329-14-6	2967	H_3NO_3S	97.09	-674.9	355.8	333.8	3.44
sulfur (s)	7704-34-9	1350	S	32.06	0	602.0	646.0	20.15
p-terphenyl (s)	92-94-4		$C_{18}H_{14}$	230.31	163	9247.1	8938.9	38.81
tetraborane (g)	18283-93-7		B_4H_{10}	53.32	66.1	2289.3	2333.4	43.76
tetradecane	629-59-4		$C_{14}H_{30}$	198.39	-403.3	9393.4	8733.1	44.02
tetraethyl lead	78-00-2	1649	$C_8H_{20}Pb$	323.44	53.0	6059.5	5619.3	17.37
tetrafluoroethylene (g)	116-14-3		C_2F_4	100.02	-658.56	832.7	920.7	7.29
tetrahydrofuran	109-99-9	2056	C_4H_8O	72.11	-216.2	2501.2	2325.1	32.25
tetrahydrofurfuryl alcohol	97-99-4		$C_5H_{10}O_2$	102.13	-435.6	2961.2	2741.1	26.84
tetrahydropyran	142-68-7		$C_5H_{10}O$	86.13	-254.8	3142.0	2921.9	33.92
tetrahydrothiophene	110-01-0	2412	C_4H_8S	88.17	-72.8	3246.6	3114.5	35.33
tetralin (tetrahydronaphthalene)	119-64-2		$C_{10}H_{12}$	132.20	-28.6	5621.5	5357.4	40.52
tetramethyl lead	75-74-1	1649	$C_4H_{12}Pb$	267.34	98.1	3387.2	3123.1	11.68
2,2,3,3-tetramethyl pentane	7154-79-2		C_9H_{20}	128.26	-237.2	6162.8	5722.6	44.62
tetramethyl silane	75-76-3	2749	$C_4H_{12}Si$	88.22	391	4583.6	4319.5	48.96
tetranitromethane	509-14-8	1510	CN_4O_8	196.03	38	431.5	431.5	2.20
tetryl (s)	479-45-8		$C_7H_5N_5O_8$	287.15	33.76	3502.9	3392.9	11.82
thiophene	110-02-1	2414	C_4H_4S	84.14	80.96	2828.7	2784.6	33.10
TNT (2,4,6-trinitrotoluene) (s)	118-96-7	1356	$C_7H_5N_3O_6$	227.13	-63.2	3406.0	3295.9	14.51
toluene	108-88-3	1294	C_7H_8	92.14	12	3909.9	3733.9	40.52
2,4-toluene diisocyanate	584-84-9	2078	$C_9H_6N_2O_2$	174.16	-163	4236.1	4104.1	23.57
1,2,4-trichlorobenzene	120-82-1	2321	$C_6H_3Cl_3$	181.45	-50.21	2810.7	2810.7	15.49
1,1,1-trichloroethane (methyl chloroform)	71-55-6	2831	$C_2H_3Cl_3$	133.40	-174	1112.9	1112.9	8.34
trichloroethylene	79-01-6	1710	C_2HCl_3	131.39	-53.1	947.9	992.0	7.55
trichloromethylsilane	75-79-6	1250	CH_3Cl_3Si	149.48				
1,2,3-trichloropropane	96-18-4		$C_3H_5Cl_3$	147.43	-230.	1736.2	1692.2	11.48
trichlorosilane	10025-78-2	1295	Cl_3HSi	135.45	-539.3	578.2	622.2	4.59
1-tridecene	2437-56-1		$C_{13}H_{26}$	182.35	-185.98	8645.6	8073.3	44.27
triethyl amine	121-44-8	1296	$C_6H_{15}N$	101.19	-169	4335.9	4005.7	39.59
triethylene glycol	112-27-6		$C_6H_{14}O_4$	150.17	-804.2	3557.7	3249.6	21.64
trimethoxymethane	149-73-5		$C_4H_{10}O_3$	106.12	-570	2433.2	2213.1	20.85
trimethylamine	75-50-3	1297	C_3H_9N	59.11	-45.73	2421.1	2223.0	37.61
2,2,3-trimethylbutane (triptane)	464-06-2		C_7H_{16}	100.20	-236.9	4804.4	4452.2	44.43
trimethylene glycol	504-63-2		$C_3H_8O_2$	76.10	-480.8	1843.1	1667.0	21.91

Table 1B Pure chemical substances

Substance	C_{st} (vol%)	LFL (vol%)	LFL (g m^{-3})	UFL (vol%)	AIT (ºC) in air	AIT (ºC) in O_2	NEC Group	Flash point (ºC)	LTL (ºC)	BP (ºC)	P_{vap} at FP (atm)
propylene glycol monomethyl ether (1-methoxy-2-propanol)	3.67	1.9e		16e				33		120	
propylene glycol monomethyl ether acetate (methoxypropyl acetate)	2.72	1.3	70.2	13.1	354			42		146	
propylene oxide	4.98	2.8	66.5	37	464		B/Ct	-37		34	0.027
propyl ether (dipropyl ether)	2.28	1.3	54.3	7	188		Ct	-28		90	
n-propyl nitrate	6.06	*1.8*	77.3	100	175		Bt	20	21	110	
pyridine	3.25	*1.8*	58.2	*12.4*	482		Dt	20		115	0.021
pyrrole	3.84	2.0	54.9	12				33		130	
quinoline	1.91	1.0e		7.8e	480			101		238	
RDX (cyclotrimethylene trinitramine) (s)	12.26									expl.	
silane (g)	9.49	1.0	13.1	100	-100					-112	
stearic acid (s)	0.80	0.4e		4.9e	395			196		361	
styrene	2.05	*1.1*	46.8	*6.1*	490	450	Dt	31	28	145	0.012
sucrose (s)	1.72	0.8e		9.5e	385	378				dec	
sulfamic acid (s)	21.85	9.3e								dec	
sulfur (s)	12.26	2.0	26.2		232			168	247	445	
p-terphenyl (s)	0.97	0.5e		3.7e	535			207 oc		376	
tetraborane (g)	2.41	0.4	8.7							16	
tetradecane	0.97	0.5	40.6	4.7	200			107		253	
tetraethyl lead	1.59	1.8	238.0					80		183	
tetrafluoroethylene (g)	17.33	10	408.9	50	218					-76	
tetrahydrofuran	3.67	2.0	59.0	11.8	321		Ct	-14		66	
tetrahydrofurfuryl alcohol	3.12	1.5	62.6	9.7	282	273		74		178	
tetrahydropyran	2.91							-20		88	
tetrahydrothiophene	2.72	1.5	54.1	9				13		119	
tetralin (tetrahydronaphthalene)	1.59	*0.84*	45.4	*5*	384	266	Dc	71	71	208	
tetramethyl lead	2.91	1.8	196.7		127		Cc	38		110	
2,2,3,3-tetramethyl pentane	1.48	0.8	41.9	*4.9*	430			16		140	
tetramethyl silane	2.55	1.5	54.1		177			-27		27	
tetranitromethane										126	
tetryl (s)	4.70							135		187	
thiophene	3.12	1.6e		14.9e				-6		84	
TNT (2,4,6-trinitrotoluene) (s)	3.84									expl.	
toluene	2.28	*1.2*	45.2	*7.1*	480	516	Dt	4		111	
2,4-toluene diisocyanate	2.16	0.9	64.1	9.5				121	120	251	
1,2,4-trichlorobenzene	3.38	2.5	185.5	6.6	571			105		214	0.032
1,1,1-trichloroethane (methyl chloroform)	9.49	6.8	370.9	10.5	485	470		-1e		74	
trichloroethylene	12.26	8	429.7	10.5	419	405		32	30	87	
trichloromethylsilane		5.1	311.7	> 20	404			8		66	
1,2,3-trichloropropane	5.65	3.2	644.6	12.6	304			74		156	
trichlorosilane	29.54	7	387.6	83	182			-13		32	
1-tridecene	1.06	0.6e		5.4e	237e		Dc	79		233	
triethyl amine	2.10	1.2	49.6	8	249		Ct	-11		89	
triethylene glycol	2.72	0.9	55.3	9.2	370			177		291	
trimethoxymethane	4.02							13		101	
trimethylamine	3.84	2.0	48.3	11.6	190			-6		7	0.693
2,2,3-trimethylbutane (triptane)	1.87	1.0	41.0	6.1e	454					81	
trimethylene glycol	4.98	2.6	80.9	16.6e	378			131		214	

Table 1C Pure chemical substances

Substance	MIE (mJ), plain Calcote	MIE (mJ), flanged Calcote	MIE (mJ), air other	MIE (mJ), O_2 other	Quench dist. (mm)	Quench dia. (mm) Grove	MESG [IEC] (mm)	MESG [UL] (mm)	MIC [UK] (mA)	T_{ad} at LFL (K)	T_{ad} at stoich (K)
propylene glycol monomethyl ether (1-methoxy-2-propanol)							0.88				
propylene glycol monomethyl ether acetate (methoxypropyl acetate)							0.84				
propylene oxide	0.19	0.21	0.14		1.3		0.70	0.53	108	1555	2360
propyl ether (dipropyl ether)								0.31			
n-propyl nitrate											
pyridine								0.84			
pyrrole	1.7	3.4									
quinoline											
RDX (cyclotrimethylene trinitramine) (s)											
silane (g)											
stearic acid (s)											
styrene								0.94	210		
sucrose (s)											
sulfamic acid (s)											
sulfur (s)											
p-terphenyl (s)											
tetraborane (g)											
tetradecane											
tetraethyl lead											
tetrafluoroethylene (g)			3.5				0.60				
tetrahydrofuran	0.54	0.89					0.87	0.61		1900	2430
tetrahydrofurfuryl alcohol							0.85				
tetrahydropyran	1.21	2.3	0.22		1.8					1900	2270
tetrahydrothiophene							0.99				
tetralin (tetrahydronaphthalene)											
tetramethyl lead											
2,2,3,3-tetramethyl pentane											
tetramethyl silane							0.65				
tetranitromethane											
tetryl (s)											
thiophene	0.39	0.6					0.92				
TNT (2,4,6-trinitrotoluene) (s)											
toluene	1.3	2.5	0.24				1.06				
2,4-toluene diisocyanate											
1,2,4-trichlorobenzene											
1,1,1-trichloroethane (methyl chloroform)											
trichloroethylene			295	18							
trichloromethylsilane											
1,2,3-trichloropropane											
trichlorosilane											
1-tridecene											
triethyl amine	0.75	1.3	1.15					0.53			
triethylene glycol											
trimethoxymethane							0.79				
trimethylamine							1.05				
2,2,3-trimethylbutane (triptane)	1.0	1.82	1.0								
trimethylene glycol											

Table 1A Pure chemical substances

Substance	CAS No.	UN No.	Formula	MW	Δh_f kJ mol^{-1}	Δh_c (upper) kJ mol^{-1}	Δh_c (lower) kJ mol^{-1}	Δh_c (lower) MJ kg^{-1}
1,3,5-trioxane	110-88-3		$C_3H_6O_3$	90.08	-522.33	1515.7	1383.7	15.36
tripropylamine	102-69-2	2260	$C_9H_{21}N$	143.27	-206.9	6336.0	5873.8	41.00
tripropylene	13987-01-4	2057	C_9H_{20}	128.26				
n-undecane	1120-21-4	2330	$C_{11}H_{24}$	156.31	-327.2	7431.5	6903.3	44.16
1-undecene	821-95-4		$C_{11}H_{22}$	154.29	-144.77	7328.1	6843.9	44.36
unsymmetrical dimethylhydrazine (UDMH)	57-14-7	1163	$C_2H_8N_2$	60.10	48.33	1978.7	1802.6	29.99
urea (s)	57-13-6		CH_4N_2O	60.06	-333.11	632.1	544.0	9.06
valeric acid	109-52-4		$C_5H_{10}O_2$	102.13	-560.2	2836.6	2616.5	25.62
vinyl acetate	108-05-4	1301	$C_4H_6O_2$	86.09	-350.8	2080.8	1948.7	22.64
vinyl acetylene (g)	689-97-4		C_4H_4	52.08	295	2440.7	2352.7	45.18
vinyl bromide (g)	593-60-2	1085	C_2H_3Br	106.95	79.2	1273.2	1229.2	11.49
vinyl chloride (g)	75-01-4	1086	C_2H_3Cl	62.50	29	1268.5	1224.5	19.59
vinylidene chloride (1,1-dichloroethene)	75-35-4	1303	$C_2H_2Cl_2$	96.94	-24.3	1096.0	1096.0	11.31
vinyl methyl ether (g)	107-25-5	1087	C_3H_6O	58.08	-186	1852.1	1720.0	29.61
vinyl toluene (mixed isomers of *m*,*o*,*p*-methyl styrene)	25013-15-4	2618	C_9H_{10}	118.18	-151	4819.8	4599.7	38.92
m-xylene	108-38-3	1307	C_8H_{10}	106.17	-25.4	4551.9	4331.8	40.80
o-xylene	95-47-6	1307	C_8H_{10}	106.17	-24.4	4552.9	4332.8	40.81
p-xylene	106-42-3	1307	C_8H_{10}	106.17	-24.4	4552.9	4332.8	40.81

Table 1B Pure chemical substances

Substance	C_{st} (vol%)	LFL (vol%)	LFL (g m^{-3})	UFL (vol%)	AIT (ºC) in air	AIT (ºC) in O_2	NEC Group	Flash point (ºC)	LTL (ºC)	BP (ºC)	P_{vap} at FP (atm)
1,3,5-trioxane	6.53	*3.6*	132.6	*29*	414			45		155	
tripropylamine	1.45	0.8	46.9	5.4			Dc	29		156	
tripropylene	1.48										
n-undecane	1.22	0.68	43.5	4.8e	202e			60		196	
1-undecene	1.25	0.7e		5.6e	237		Dc	71		193	
unsymmetrical dimethylhydrazine (UDMH)	4.98	2.3	56.5	*95*	250		Ct	-15	-15	63	
urea (s)	12.26	0.9	22.1	98.0	52			-90		dec	
valeric acid	3.12	1.6e		9.6e	400			86		186	
vinyl acetate	4.45	2.6	91.5	13.4	427		Dt	-8		72	
vinyl acetylene (g)	4.02	2.2	46.8	31.7				<-5		5.1	
vinyl bromide (g)	8.52	3.6	157.4	33	472			5		16	
vinyl chloride (g)	7.74	3.6	92.0	33	472		Dt	-78 oc		-14	
vinylidene chloride (1,1-dichloroethene)	9.49	7.3	289.3	16	570		Dc	-15		32	
vinyl methyl ether (g)	4.98	2.6	61.7	39	287			-51		7	
vinyl toluene (mixed isomers of *m*,*o*,*p*-methyl styrene)	1.79	0.8	38.7	11	494		Dc	49		170	
m-xylene	1.96	*1.1*	47.7	*6.4*	465		Dt	25		139	0.010
o-xylene	1.96	*1.1*	47.7	*6.4*	475		Dt	32		144	0.013
p-xylene	1.96	*1.1*	47.7	*6.5*	496		Dt	27		138	0.013

Table 1C Pure chemical substances

Substance	MIE (mJ), plain Calcote	MIE (mJ), flanged Calcote	MIE (mJ), air other	MIE (mJ), O_2 other	Quench dist. (mm)	Quench dia. (mm) Grove	MESG [IEC] (mm)	MESG [UL] (mm)	MIC [UK] (mA)	T_{ad} at LFL (K)	T_{ad} at stoich (K)
1,3,5-trioxane							0.75		138		
tripropylamine											
tripropylene							0.89				
n-undecane											
1-undecene											
unsymmetrical dimethylhydrazine (UDMH)								0.46			
urea (s)											
valeric acid											
vinyl acetate	0.7	1.2	0.7		2.35		0.94	1.04			
vinyl acetylene (g)	0.0822	0.095									
vinyl bromide (g)											
vinyl chloride (g)					1.93	2.72	0.99	0.74	180		
vinylidene chloride (1,1-dichloroethene)							3.91				
vinyl methyl ether (g)											
vinyl toluene (mixed isomers of *m*,*o*,*p*-methyl styrene)											
m-xylene			0.2			3.1	1.09				
o-xylene			0.2			3.1	1.09				
p-xylene			0.2			3.1	1.09	1.22			

Mixtures and commercial products

Table 2 Properties of selected mixtures and commercial products

Substance	LFL (vol%)	UFL (vol%)	AIT (ºC) in air	AIT (ºC) in O_2	Flashpoint (ºC)	Fire point (ºC)	BP (ºC)	MIE (mJ), air	MESG (UL)	MESG (UK)	NEC Group
asphalt					197 - 204						
automatic transmission fluid: Dextron II			212		186						
automatic transmission fluid: Dextron IIE			210 - 214		183- 193						
automatic transmission fluid: Ford					175						
automatic transmission fluid, unspecified					199	210					
aviation fuel AvGas 100/130	1.3	7.15	440	315	-45		116				
aviation fuel AvGas 115/145	1.2	7.1	470		-45		120				
aviation fuel Jet A	0.6	4.7	225		41 - 58		249				
aviation fuel Jet B	1.3	8.2	230		-23 to -1		199				
aviation fuel JP-1	0.67	5.0	230		46		210				
aviation fuel JP-3	0.9	6.2	240				227				
aviation fuel JP-4	0.8	5.6	240		-27 to -7		199				
aviation fuel JP-5	0.6	4.5	225		60 - 67		238				
aviation fuel JP-6	0.6	3.7	232	224	36 - 43	43	260				
aviation fuel JP-7	0.6	4.5	241		> 60						
aviation fuel JP-8	0.6	4.7	225		41 - 58	68	238				
brake fluid					115 - 179						
camphor oil					47		175-200				
carnauba wax					282						
castor oil			415-449		229-307		313				
coconut oil			360		216-294						
cod liver oil					211						
Coleman fuel; white gas					< -18						
corn oil			393		254						
cottonseed oil			343-420		252-333						
creosote, coal tar			335		75		200-325				
creosote, wood			360		92		200-240				
crude oil					-23 to +32						
cutting oil					166						
diesel fuel (41 cetane)			233								
diesel fuel (55 cetane)			230								
diesel fuel (60 cetane)			225		40 to 55		325				
diesel fuel (68 cetane)			226								

Table 2 continued

Substance	LFL (vol%)	UFL (vol%)	AIT (ºC) in air	AIT (ºC) in O_2	Flashpoint (ºC)	Fire point (ºC)	BP (ºC)	MIE (mJ), air	MESG (UL)	MESG (UK)	NEC Group
diesel fuel 2D			256		min. 52; typ. 96						
ethylene glycol/water mixture (50/50)			484								
fish oil					216						
fuel oil, No. 1	0.58	4.45	254		> 38; typ. 60						Dc
fuel oil, No. 2	0.52	4.09	233 - 260		> 38; typ. 58-124	90 - 129					Dc
fuel oil, No. 4	0.45	3.71	263		> 54; typ. 96						Dc
fuel oil, No. 5					> 54; typ. 143						Dc
fuel oil, No. 6			332 - 407		> 66; typ. 95-146	177					Dc
gas oil			338		> 66						
gasoline	1	7	300 - 350		-43		18 - 127	0.24	0.74		Dt
gasoline, 65 octane	1.4	7.6	248								Dt
gasoline, 75 octane			258								Dt
gasoline, 87 octane			412								Dt
gasoline, 92 octane	1.5	7.6	390		-42 to -45						Dt
gasoline, 100 octane	1.4	7.4	429		-38						
gear oil					264						
hydraulic fluid, AS1241			524		170	188					
hydraulic fluid, Fyrquel 220			366		257	313					
hydraulic fluid, MIL-H-5606			232		89-102	110					
hydraulic fluid, MIL-H-83282			354		210-221	235					
hydraulic fluid, MIL-H-87257			243		166	191					
hydraulic fluid, MIL-H-53119			643		none	none					
isoparaffinic solvent					52 - 66						
kerosene	1	5	227	216	38 - 74		150 - 300			1.05	
lacquer diluent					-18						
lard oil					260						
linseed oil			415-438		224-334	279					
liquefied petroleum gas											Dc
lubricating oil, MIL-L-7808					235						
lubricating oil, SAE 10			382		171	193					
lubricating oil, SAE 60			410		249	327					
lubricating oil, turbine, Mobil DTE 797			366		207	224					
olive oil			441		225						
mineral oil					193	252	360				
mineral spirits, incl. some lighter fluids and charcoal lighters			242		> 40		149				

Table 2 continued

Substance	LFL (vol%)	UFL (vol%)	AIT (ºC) in air	AIT (ºC) in O_2	Flashpoint (ºC)	Fire point (ºC)	BP (ºC)	MIE (mJ), air	MESG (UL)	MESG (UK)	NEC Group
missile fuel JP-9					23						
missile fuel JP-10			250		53						
missile fuel RJ-4			245		71						
missile fuel RJ-5			329		104						
missile fuel RJ-6			234		61						
motor oil, SAE 30			232		216	241					
motor oil, SAE 5W-30					166						
motor oil, unspecified, Ohlemiller/Cleary						215					
naphtha	1.1	5.9	232 - 288		< -18		95-140				Dc
natural gas	4.8	13.5	500								
neatsfoot oil			442		243						
olive oil			343-441		225						
palm oil			343		162-203						
paraffin wax			245		204 -271	238-263					
peanut oil			445		282						
perilla oil					272						
petroleum ether (benzine)	1.1	5.9	228-329		-46 to -18		35-60	0.25			
pine oil					59-78		186-226				
power steering fluid					177	210					
rapeseed oil (canola oil)			315-447		163-321						
sesame oil			419		255-336						
Solvasol			276	258							
soybean oil			400-445		220 - 320						
Stoddard solvent (white spirit)	1.1	6	149 - 232		38 - 60						
sunflower oil					320						
tallow					265						
tallow oil					256						
transformer oil, naphthenic distillate					132-150						
tung oil			457		289						
turbine oil					248						
turpentine	0.8		252		35		150				Dc
varsol			235								
VM&P naphtha	0.9	6.7	232-257		-2 to 29		100-177				

Aviation hydraulic fluids and lubricating oils

Properties for aviation hydraulic fluids and lubricating oils have been compiled by the US Air Force[33]; these are given in Table 3.

Table 3 Properties of aviation hydraulic fluids and lubricating oils

Fluid	AIT (ºC)	Flash point (ºC)	Fire point (ºC)
Aromatic ethers			
5P4E (polyphenoxy)	610	293	349
MCS-293	490	220	270
OS-124 (polyphenyl)	600	288	349
Chlorinated silicones and hydrocarbons			
Arachlor	640	193	>315
MLO-53-446 (silicone)	420	304	377
Pydraul A-200 (hydrocarbon)	650	177	360
Glycols			
Houghto-Safe 271 (water-glycol)	410		
propylene glycol	445	110	113
Ucon 50 HB-260 (polyglycol)	395	235	260
Mineral oils or hydrocarbons			
MIL-H-5606 (oil)	225	90	107
MIL-2190 (oil)	350	232	
MLO-60-294 (oil)	370	196	221
Mobil DTE-103 (oil)	370	199	
MIL-H-83282 (synthetic)	354	196	
Pyrogard D (invert emulsion)			>315
Phosphate esters			
Cellulube 220 (ester base)	560	235	352
Houghto-Safe 1055 (aryl ester)	550	263	360
Pydraul 150 (ester base)	525	193	243
Pydraul AC (ester base)	595	232	396
Skydrol 500B (ester base)	510	182	243
Tricresyl phosphate	600	243	
Polyol and dibasic acid esters			
MIL-L-7808 (acid diester)	390	225	238
MIL-L-9236	390	221	246
MIL-L-23699B (polyol ester)	385	227	
MLO-54-581 (acid diester)	390	224	246
Plexol 201 (acid diester)	380	216	232
Silanes			
MLO-56-280 (diphenyl-dodecyl)	415	291	329
MLO-56-610 (decyl-dodecyl)	400	279	302
Silicates and silicones			
Dow Corning 400 (siloxane)	320	124	138
Dow Corning 500 (siloxane)	480	243	
Dow Corning 550 (siloxane)		316	
MLO-54-540 (silicate)	375	163	221
MLO-54-856 (silicate)	380	157	227
Oronite 8200 (silicate)	380	196	227
Versilube F-50 (silicone)	480	288	338

Refrigerants

The flammability of various refrigerants, as measured in the ASTM E 681 apparatus, was reported by Richard and Shankland[34]. They explored many ignition sources for use within the apparatus; their results using a match are listed in Table 4. In most cases, the differences in the flammability limits due to different ignition sources were very slight, but in one case, R-161, there was a major difference, which was not explained by the authors: LFL = 3.0% (match), and = 14.2% (spark). UFL = 18.0% (match), and = 43.7% (spark).

Table 4 Flammability limits for some refrigerants

Formula	Compound	ASHRAE No.	LFL (vol%)	ULF (vol%)
C_4F_8	octafluorocyclobutane	C-318	none	none
CCl_3F	trichlorofluoromethane	R-11	none	none
$CHClF_2$	chlorodifluoromethane	R-22	none	none
CH_2Cl_2	methylene chloride	R-30	14.6	21.8
CH_2F_2	difluoromethane	R-32	12.7	33.5
$C_2Cl_3F_3$	1,1,2-trichloro-1,2,2-trifluoroethane	R-113	none	none
$C_2HCl_2F_3$	2,2-dichloro-1,1,1-trifluoroethane	R-123	none	none
$C_2HCl_2F_3$	1,2-dichloro-1,1,2-trifluoroethane	R-123a	none	none
C_2HClF_4	chlorotetrafluoroethane	R-124	none	none
C_2HF_5	pentafluoroethane	R-125	none	none
$C_2H_2F_4$	1,1,2,2-tetrafluoroethane	R-134	none	none
$C_2H_2F_4$	1,1,1,2-tetrafluoroethane	R-134a	none	none
$C_2H_3Cl_3$	1,1,1-trichloroethane	R-140a	7.4	16.5
$C_2H_3Cl_2F$	1,1-dichloro-1-fluoroethane	R-141b	7.9	17.0
$C_2H_3ClF_2$	1-chloro-1,1-difluoroethane	R-142b	7.2	18.2
$C_2H_3F_3$	1,1,2-trifluoroethane	R-143	5.8	24.4
$C_2H_3F_3$	1,1,1-trifluoroethane	R-143a	7.0	19.0
$C_2H_4F_2$	1,2-difluoroethane	R-152	3.6	21.8
$C_2H_4F_2$	1,1-difluoroethane	R-152a	4.0	20.8
C_2H_5F	fluoroethane	R-161	3.0	18.0
C_3F_8	octafluoropropane	R-218	none	none
NH_3	ammonia	R-717	14.8	33.4

NEC Groups according to chemical families

The classification of compounds into Groups by the NEC can be roughly predicted according to chemical families. Table 5 shows the proposal according to NMAB 353-1[35].

Table 5 NEC Groups: prediction according to chemical families

Group	Classes of compounds
B	ethers w. 3-membered ring
C	acetylenes, higher alcohols, small unsaturated aldehydes amines, secondary and tertiary ethers containing $–CH_2$ or $–CH_3$ ethers, cyclic, larger than 3-membered ring glycol ethers mercaptans nitro compounds, aliphatic nitrogen compounds, aliphatic heterocyclic organo lead compounds sulfides (except CS_2)
D	aliphatic hydrocarbons alicyclic hydrocarbons alcohols (exc. those in Group C) amides amines, primary aromatic hydrazines aromatic hydrocarbons chlorinated hydrocarbons esters ethers not containing $–CH_2$ or $–CH_3$ glycols and glycol esters ketones nitro compounds, aromatic nitrogen compounds: cyanides, isocyanates nitrogen compounds: aromatic heterocyclic olefins, higher (most) organic acids organo phosphates organo sulfates and sulfones phenols

Dusts

Dusts of numerous substances have been studied by the Bureau of Mines[36- 45]. Illustrative data from these studies are given in the tables below. The ignition temperatures were determined in the Godbert-Greenwald vertical tube furnace. For dust cloud tests, 0.1 g was dispersed into the furnace. For layer ignition tests, wire baskets 12.7 mm deep and 25.4 mm diameter were used. The LFL values were determined in the 1.23 L Hartmann tube using a 23.5 mA inductive spark. Note that all of these data are highly dependent of the test apparatus and test conditions used. Especially, the discussion in Chapter 5 needs to be considered, where it is pointed out that reported LFL values below 30 g m^{-3} are suspect. Thus, the tabulated results should only be used as relative indications, not as absolute values. The layer ignition temperature testing method used by the Bureau of Mines was roughly similar to performing an oven-cube test for self-heating *at one specimen size*. The limitations of a strategy of this kind must be considered in the context of the principles developed in Chapter 9.

Much more recently, the Bureau of Mines[46] conducted a series of tests on dusts of metals and other pure elements using their 20 L test apparatus. The test apparatus uses extremely powerful pyrotechnic igniters, so the data should be viewed only as relative indications—actual ignition sources may not be so powerful. These results are given in Table 12.

The characteristics of dust clouds for a series of explosives was examined by the Bureau of Mines[47] using their 20 L chamber and a 2500 J pyrotechnic igniter. The results are shown in Table 6. For the loadings examined, all of the dusts produced only deflagrations and not detonations; although the authors considered it likely that if very high concentrations had been tested, detonations would have been seen. The size effect for the dusts of explosives is notably different from that for most other dusts (see Chapter 5): the smallest diameters show a higher, not a lower, LFL value compared to mid-range diameters. In general, the most explosible diameter for these substances is in the range of 10 – 50 μm. As far as actual LFL values are concerned, it is striking to note that these are not particularly low. The authors' analysis indicates that the data become highly consistent with that of common organic molecules if it is assumed that the $–NO_2$ groups in these molecules make *no* contribution to the explosibility and merely act as an inert fraction. The effective volatile fuel fraction is then only 22 – 46% for the explosives examined. Additional testing showed that HMX and RDX dusts, but not the other compounds shown in Table 6, were also explosible in a nitrogen atmosphere. In those cases, the $–NO_2$ groups do play a role, since they provide the only oxidizer available.

Field[48] evaluated a great deal of test data obtained at the Fire Research Station in the UK and considers that, under most circumstances, the dusts listed in Table 14 are non-explosible. A slightly different list has been published by the Bureau of Mines[44].

Table 6 Flammability limits for dusts of explosives

Explosive	Solid density (kg m^{-3})	Diameter (μm)	LFL (g m^{-3})
HMX	1900	7	240
		20 – 40	190
		40 – 80	170
		100 – 150	160
		250 – 350	160
HNAB	1780	47	190
HNS	1740	2	350
		10 – 40	140
		40 – 80	140
PETN	1770	19	210
picric acid	1760	46	320
RDX	1800	12	260
		20 – 40	170
		100 – 150	180
		150 – 250	170
TATB	1940	5	270
		7	300
		20 – 40	100
		40 – 90	120
		80 – 120	80
tetryl	1740	48	140
TNT	1650	24	130
		39	110
		150 – 250	120

Table 7 Ignition properties of dusts of metal and selected non-metal elements

Element [a]	Ignition temp. (ºC)		Dust cloud MIE (mJ)	LFL (g m^{-3})
	Layer	Dust cloud		
aluminum	490	670	50	85 - 120
antimony	330	420	1920	420
boron	400	470	60	120
cadmium	250	570	4000	> 2000
carbon				90 - NF
chromium	400	580	140	230
cobalt	370	760		> 2000
copper		700		NF
hafnium				200
iron	290	320		105 – 500
lead	270	710		NF
magnesium	430	560	40	30 – 60
manganese	240	460	305	125 – 245
molybdenum	360	720		NF
niobium				420
silicon	950	780	100	110 – 245
sulfur	220	190		100
tantalum	300	630	120	400
thorium	280	270	5	75
tin	430	630	80	190
titanium	380-510	330-590	25	70
tungsten	430			700 - NF
uranium	100	20	45[b]	60
vanadium	490	500	60	220
zinc	540	690	960	300 - NF
zirconium	190-320	20	15[b]	45

[a] – for 200-mesh particles (< 74 μm)
[b] – amounts greater than 1 g ignited spontaneously in air
NF - nonflammable

Table 8 Ignition properties of carbonaceous dusts

Substance [a]	Ignition temp. (ºC)		Dust cloud MIE (mJ)	LFL (g m^{-3})
	Layer	Dust cloud		
charcoal	180 - 250	530 - 730	20	140
charcoal, activated	340 - 380	470 - 670		
coal dust, Pittsburgh coal	233	560	250	130
graphite	540 - 600	730 - 970		
lampblack	520	730 - 850		
lignite	180 - 200	390 - 440		25 - 50
road tunnel dust	200 - 220	360 - 600		
soot	390	600		2000

[a] – for 200-mesh particles (< 74 μm)

Table 9 Ignition properties of agricultural dusts

Substance [a]	Ignition temp. (ºC)		Dust cloud MIE (mJ)	LFL (g m^{-3})
	Layer	Dust cloud		
alfalfa meal	220 - 260	470 - 620	320 - 5100	105
cinnamon	230	440	30	60
cocoa	200 - 390	420 -510	100 - 180	45 - 75
coffee	270	720	160	85 - 150
cork	210 - 280	460 - 490	35 - 100	35 - 50
cornstarch	330 - 380	380 - 430	30 - 60	45 - 55
cotton linters		520	1920	50
flour, cake	230 - 320	450 - 490	25 - 80	55 - 65
grain dust	230	430	30	55
grass seed	180	490 -530	60-260	140-290
lycopodium	310	420	50	70
peat, dried	240	460 - 470		
potato starch		440	25	45
rice	220 - 480	440 - 520	40 - 120	50 - 180
soy flour	190 - 340	540 -550	100 - 460	60 - 140
sugar, powdered	400	370	30	45
wheat starch	360 - 440	380 - 440	25 - 60	45
wood bark	250 - 270	450 - 540	40 - 60	20
wood flour	260 - 300	430 - 470	30 - 40	35 - 50
yeast	260	520	50	50

[a] – for 200-mesh particles (< 74 μm)

Table 10 Ignition properties of plastics dusts

Substance [a]	Ignition temp. (ºC)		Dust cloud MIE (mJ)	LFL (g m^{-3})
	Layer	Dust cloud		
ABS		470	30	20
cellulose acetate	390 - 430	410 - 480	20 - 50	40
melamine formaldehyde		790 - 810	50 - 320	65
nylon	430	500 - 540	20 - 30	30 - 50
phenol formaldehyde	180 - 320	460 - 730	10 - 6000	25 - 250
PMMA		440 - 480	15 - 20	30
polyacrylonitrile	460	500	20	25
polycarbonate		710	25	25
polyethylene	380	395	70	45
polyethylene terephthalate		500	35	40
polypropylene		420 - 460	25 - 400	20 - 55
polystyrene	470	490 - 560	40 - 120	15 - 25
polyvinylidene chloride	390	830 - 900		> 2000
polyvinyl acetate		550	160	40
polyvinyl acetate alcohol	440	520	120	35
polyvinyl butyral		390	10	20
polyvinyl chloride	400 - 500	660 - 730		> 2000
PTFE	570	670		> 2000
rayon	250 - 280	520 - 530	240	55
SAN		500	30	35
urea formaldehyde		450 - 530	80 - 1280	70 - 165

[a] – for 200-mesh particles (< 74 μm)

Table 11 Ignition properties of miscellaneous dusts

Substance [a]	Ignition temp. (ºC)		Dust cloud MIE (mJ)	LFL (g m^{-3})
	Layer	Dust cloud		
ammonium nitrate		400		
ammonium perchlorate	260			
aspirin		660-670	25-30	35-50
bone meal	230-250	490-560		
detergents, various	250-390	510-660		130
dextrin	440	410	40	50
guano, bat	240	460		
paper dust	170-270	390-440	20-60	55-70
pyrethrum	210	460	80	100
rubber dust, from tires		530-540		
soap powder	310-600	430-650	60-120	45-85

[a] – varies, but mostly for 200-mesh particles (< 74 μm)

Table 12 Recent Bureau of Mines data on dusts of metals and selected non-metal elements

Element	Diameter range (μm)	LFL (g m^{-3})		Stoich. conc. C_{st} (g m^{-3})
		for 2500 J igniter	for 5000 J igniter	
aluminum	3 – 30 p	90	75	310
	5 – 15	90	90	
	20 – 100	120	90	
boron	1 – 40	120	85	126
carbon (graphite)	4 – 10 p	350	70	105
	10 – 200 p		NF	
copper	10 – 50		NF	1111
hafnium	4 – 30	200		1563
iron	2 – 8	230	160	652
	10 – 80	700	400	
lead	20 – 60		NF	3628
magnesium	20 – 60 p	60	50	425
niobium	20 – 60	450	400	651
silicon	5 – 50	200	190	246
tantalum	2 – 30	400		1268
titanium	20 – 70	80	65	419
tungsten	⭘ 1	800		1073
	5 – 25		NF	
zinc	10 – 50 p	320	230	1250
	10 – 100		NF	

p – platelike form
NF – non-flammable

Table 13 Ignition properties of explosives dusts

Substance [a]	Ignition temp. (°C)		Dust cloud MIE (mJ)	LFL (g m^{-3})
	Layer	Dust cloud		
black powder	340		320	120
dinitrobenzamide	500		45	40
dinitrobenzoic acid	460		45	50
dinitro-sym-diphenylurea	550		60	95
dinitrotoluamide	500		15	50
guanidine nitrate	850			
NQ	400		< 7200	
nitrostarch	190	165	40	70
TNT			75	70
[a] – particle sizes varied from sub-74 μm to sub-840 μm				

Table 14 Dust found to be non-explosible by Field

acetamide	copper (foundry dust)	nickel permalloy
alizarine (yellow G)	cupric oxide	oxalic acid
alumina	3,5-diacetylamine 2,4,6-tri-iodo benzoic acid	plumbago
aluminum dichromate	diaminostilbene disulfonic acid	polytetrafluoroethylene
aluminum silicate	dicyandiamide	polyvinylidene chloride
amaranth lake (food red 9)	digitalis lanata leaf	potassium perchlorate
ammonium carbonate	era chrome brown	Prussian blue
ammonium nitrate	era chrome green	seaweed
ammonium perchlorate	erythrosine lake (food red 14)	selenium
bismuth salicylate	ferrous sulfate	sewage sludge, dried
bone charcoal	foundry blacking	shoddy
boron carbide	fuel ash, pulverized	silica
brass dross	graphite	sodium dihydroxy naphthalene-disulfonic acid
bronze	hammerscale	sodium di-isobutyl sulfosuccinate
cadmium red	herring meal	sodium perborate
cadmium sulfide	indigo carmine lake (food blue 1)	sodium trichloro ethyl phosphate
cadmium sulfoselenide	ivory and mineral black	sunset yellow lake (food yellow 3)
cadmium zinc sulfide	lampblack	talc
calcium borate	lead phosphate, basic	tartrazine lake (food yellow 4)
calcium carbonate	lead zirconate titanate	thiourea dioxide
calcium citrate	magnesium oxide	tomato base, spray dried
calcium gluconate	manganese dioxide	trichloro isocyanuric acid
carbon, activated (some)	molybdenum disulfide	tungsten
carbon black (some)	myrobalan and valonia nuts	urea
castor oil meal	naphthionic acid, crude	zinc oxide
coke		

Ignition temperatures of solids

For solids, the ignition temperatures compiled have been determined mainly with the Setchkin furnace (ASTM D 1929) or similar arrangements (Table 15). The reported ignition temperature in that test is the minimum temperature of the *air* near the specimen that is necessary for ignition to occur. A small number of ignition temperatures of solids have also been measured in the ASTM D 2155 test (see Chapter 6); that test was developed for liquids, but solids can also be tested. Available values are given in Table 16; it is evident that the AIT values are substantially higher than those found in the ASTM D 1929 test.

Table 15 Ignition temperatures for a number of solid substances, determined in the ASTM D 1929 test or similar test environments.

Substance	Ignition temp. (°C)		Ref.
	Piloted	Auto-ignition	
ABS		362	49
	410		50
		466	51
		530	52
ABS, FR	420		50
ABS/PVC blend		531 – 543	52
acetal: *See* polyoxymethylene			
cellulose acetate	305	475	53
cellulose nitrate	141	141	53
cotton	254	254	54
	230-270	250	55
epoxy, amine-cured	355		55
epoxy, anhydride-cured	385		55
epoxy, anhydride-cured, 60% mineral filled	410-415	500-505	55
epoxy resin	315	429	56
ethyl cellulose	291	296	54
ethylene-propylene rubber	378	413	57
	180		58
fiberboard	310		55
Hypalon (chlorosulfonated polyethylene) rubber	380	384	57
latex (natural rubber) adhesive	289	330	56
latex foam (natural rubber)	274	310	56
melamine formaldehyde		600	59
		729	52
melamine formaldehyde, w. glass reinforcement	475-500	623-645	53
melamine formaldehyde, w. mineral filler	481	610	60
	313	455	53
melamine formaldehyde, w. paper reinforcement	398	433	56
melamine formaldehyde, w. paper reinforcement, FR	554	559	56
mineral fiber marine board (w. organic binder)	494	494	56
Neoprene: *See* polychloroprene			
newsprint	229	229	54
nitrile rubber		310	61
nylon 6		328	49
		489	52
	413	439	62
	497		63
nylon 6,6	420-450	425-480	55
		492	52
	421	424	59
	500		64
nylon 11		476	65
phenol formaldehyde		510	59
		614	52
	430	482	62

Table 15 continued

Substance	Ignition temp. (°C)		Ref.
	Piloted	Auto-ignition	
phenol formaldehyde, w. paper reinforcement	300-311	367-430	53
phenol formaldehyde, w. glass reinforcement	520-540	571-580	53
phenolic (*See*: phenolformaldehyde)			
polyacrylonitrile	331		65
polycarbonate		516	49
	522	550	59
		580	52
	467	580	75
	440		63
polychloroprene rubber (Neoprene)	300		58
	307	390	57
		300	66
polychloroprene rubber, FR	321	424	57
polyester, unsaturated	350-410	420-500	55
	352-394	447-488	67
	380	451	62
polyester, glass reinforced	346-394	447-488	53
	399	484	59
polyetherimide	520	535	75
polyethersulfone		490	49
	560	560	75
polyethylene	270		58
	340 – 430	350-450	55
		430	52
	340	349	54
		398	49
	408	457	57
	315 – 330		64
	443		63
polyethylene terephthalate (PET)	374		63
polymethylmethacrylate (PMMA)		392	49
	280 – 300	450 – 462	53
		520	52
	250 – 355		64
	273		68
	378		63
	313 – 323	377 – 407	69
polymethylmethacrylate (PMMA), high molecular weight	265		70
polymethylmethacrylate (PMMA), low molecular weight	330		70
polymethylmethacrylate (PMMA), commercial grade (Plexiglas G, Lucite)	275		71
polyoxymethylene		488	52
polypropylene	325 – 343	325 – 388	59
	350 – 370	370 – 410	55
	342	364	56
	250 – 360		64
		440	52
	443		63
polypropylene, FR		440 – 533	52

Table 15 continued

Substance	Ignition temp. (°C)		Ref.
	Piloted	Auto-ignition	
polystyrene		416	49
	365		70
		518	52
	360	496	54
polystyrene, beads	296	491	54
polystyrene, compression molded	345	488	56
polystyrene, expanded	346	491	54
polystyrene, expanded (FR grade EPS)	380 – 405		55
	366	470	72
polystyrene, high impact (HIPS)	378	458	62
		528	52
	410		50
polystyrene, high impact, FR	370 – 377	422 – 426	62
		470 – 523	52
	390		50
polystyrene/polymethylmethacrylate copolymer	329	484	54
polytetrafluoroethylene (Teflon)		504	65
		530	53
poly(trifluorochloroethylene) (CTFE)		349 – 390	61
polyurethane, foam		528	59
polyurethane, FR foam, 50% Cl		528	59
polyurethane, FR foam, 5% P, 50% Cl		554	59
polyurethane, FR foam, 10% P		638	59
polyurethane foam, flexible	335	335	56
	349 – 363	370 – 378	62
polyurethane foam, flexible, non-FR	324 – 326		73
polyurethane foam, flexible, FR	306 – 310		73
polyurethane, rigid foam		550	74
	378	502	62
polyurethane, rigid foam (polyether)	310	416	54
polyurethane, solid (not foam)	271		73
polyvinyl acetate		520	65
polyvinyl fluoride	420	480	75
polyvinylidene chloride	> 532	> 532	54
		469	65
PVC, pure, without plasticizer		600	76
		600	74
	441	474	62
PVC, unspecified grade	390	454	54
	357 – 374		63
PVC, flexible		441	52
PVC film	308 – 327	438 – 454	62
PVC, with 50 phr dioctyl phthalate plasticizer	340		55
PVC, with 50 phr dioctyl phthalate plasticizer and FR agent	400		55
PVC, semi-rigid, with 40 phr dioctyl phthalate plasticizer	240	294	57
PVC, flexible, with 50 phr dioctyl phthalate plasticizer	277	311	57

Table 15 continued

Substance	Ignition temp. (ºC)		Ref.
	Piloted	Auto-ignition	
PVC, flexible	250-280		58
	422	424	
PVC, flexible, wire-insulation grade		263	66
PVC, rigid	360 – 430	480-550	55
		502	52
PVC, rigid, FR		571	52
PVC floor tiles	370-410		55
PVC foam, flexible	441	441	56
SAN (styrene/acrylonitrile copolymer)	366	454	54
		542	52
	329	485	54
SBR (styrene-butadiene rubber)	360	450	75
silicone, w. glass reinforcement	490-527	550-564	53
urea formaldehyde		540	59
		630	52
vinyl asbestos	431	434	56
vinyl epoxy adhesive	333	414	56
XLPE (crosslinked polyethylene)	374	427	57
XLPE , FR	352	383	57

Table 16 Autoignition temperatures, as determined in the ASTM D 2155 test

Substance	AIT (ºC)	Ref.
ABS, pellets	479	77
polyester, glass reinforced	396	77
polyethylene, bottles	443-491	77
polyethylene, pellets	446	77
polypropylene	435-466	77
polystyrene, foam	521-532	77
polystyrene, solid	516-524	77
polyurethane foam, rigid	518	77
PVC, bottles	571	77
PVC, wrapping film	504	77

Radiant ignition of plastics and elastomers

Radiant ignition properties for a number of plastics are given in Chapters 7 and 14. Here, data from two major studies are provided, those of Hallman[78] (Table 17) and Scudamore et al.[79] (Table 18). Hallman's tests were using radiation from a specially-built flame source, while Scudamore used the Cone Calorimeter.

Table 17 Hallman's results on the radiant ignition of plastics and elastomers

Material, density, thickness	**Data used**	B_{ig}	$\dot{q}''_{cr}$	**Ignition data pairs First line: flux (kW m^{-2}). Second line: time (s)**								
ABS	Omit: 1at H	382	8.8	27.6	37.7	51.5	64.0	75.7	90.4	103.8	124.3	
1029 kg m^{-3}, 13.2 mm				186	110	57.5	40.3	22.5	16	12.5	9.8	
butyl rubber (isobutylene/ isoprene copolymer)	Omit: 6 at H	166	19.4	26.4	32.6	38.1	48.5	60.2	75.3	92.9	105.9	125.5
1093 kg m^{-3}, 10.9 mm				304	103	52	53.3	28	13.2	7.8	4.2	2.7
cellulose acetate butyrate	All*	794	35.2	37.7	50.6	62.8	78.7	94.1	111.3	125.5		
1199 kg m^{-3}, 3.2 mm		*	*	NI	48	28	19.4	13.6	11	8.5		
cellulose acetate butyrate	All	318	24.0	31.8	42.7	54.4	65.3	87.0	103.3	120.1		
1211 kg m^{-3}, 12.7 mm				NI	136	110.5	33.7	21	11.8	9		
chloroprene rubber	All	120	8.1	53.1	61.1	72.4	92.9	120.1				
275 kg m^{-3}, 12.7 mm				NI	4.1	3.2	2	1.1				
chloroprene rubber	All	89	42.9	45.2	46.9	59.4	73.2	80.3	92.9	108.4	116.3	131.8
564 kg m^{-3}, 12.7 mm				NI	238	29.6	6	4.4	3.8	1.5	1.3	1.1
chloroprene rubber	All; poor fit	214	33.4	39.7	51.0	59.4	64.4	73.6	94.1	110.5	125.9	
804 kg m^{-3}, 12.2 mm				NI	193	192	15.2	15.5	10.5	6.1	5	
chloroprene rubber	Omit: 2 at H	183	37.2	45.6	53.1	61.9	72.4	92.9	108.4	127.6		
1478 kg m^{-3}, 13.7 mm				158	224	33	17.7	9.1	7.9	5.1		
melamine formaldehyde (Formica)	Omit: 3 H	224	25.1	37.7	48.1	61.9	76.6	89.5	108.4	125.5		
1392 kg m^{-3}, 12.7 mm				148	81.5	24.5	14.5	12.4	8.3	6.9		
nitrile rubber (buna-N)	Omit: 1 H	295	26.3	36.0	52.7	64.0	73.6	95.0	108.4	133.1		
1596 kg m^{-3}, 12.2 mm				300.0	105.0	55.0	22.0	16.0	9.7	2.5		
nylon 6,6	Omit: 1L, 2 H	418	27.6	36.8	48.5	56.9	62.8	78.7	89.1	107.1	124.3	
1116 kg m^{-3}, 13.0 mm				383	220	146	75.5	51	31	23.8	19	
phenol formaldehyde (phenolic, Bakelite)	All	429	26.0	45.2	50.2	60.7	81.6	89.1	100.8	109.6	118.4	
1368 kg m^{-3}, 13.7 mm				196	255	96	47	30	23.5	20	16	
PMMA, black	All	290	9.0	27.6	38.5	52.7	64.0	73.6	95.0	103.8	107.9	118.8
1264 kg m^{-3}, 6.4 mm				137	61	30	21.2	15.3	10.2	7.6	7	5.5
PMMA, black	All	353	7.2	36.8	37.7	51.9	62.8	79.9	92.9	108.4	125.1	
1290 kg m^{-3}, 12.7 mm				101	91.5	41.2	26	17.6	14.3	9.5	7.4	
PMMA, white	Omit: 1 L, 1 H	375	18.6	33.5	49.0	61.9	76.6	93.7	109.2	128.9		
1194 kg m^{-3}, 6.4 mm				161	99	56.5	26.5	18.1	13.8	10.7		
PMMA, white	All	402	22.3	37.2	51.9	59.8	80.8	91.2	109.6	126.4		
1158 kg m^{-3}, 12.7 mm				302	122	100	30.5	23.7	15.4	12.2		
PMMA, clear	All	410	5.7	33.1	50.6	69.0	79.1	92.9	110.0	119.7		
1173 kg m^{-3}, 6.4 mm				127	75	25	22	17	13	10		
PMMA, clear	Omit: 2 H	402	7.1	27.6	38.1	50.6	63.2	77.0	87.9	104.6	126.4	
1187 kg m^{-3}, 12.7 mm				232	104	67	29	25.2	19	15.9	9.3	
polycarbonate (Lexan)	All	662	11.5	52.7	65.3	73.2	92.0	103.8	124.3			
1193 kg m^{-3}, 13.0 mm				NI	92	76	49.7	33.6	25.2			
polyethylene	All	575	8.0	33.1	49.0	63.2	77.8	92.9	110.0	123.0		
930 kg m^{-3}, 12.0 mm				264	130	68	47	33	24.5	17.5		
polyoxymethylene	All	518	6.2	37.7	52.3	75.3	87.0	106.3	120.5			
1437 kg m^{-3}, 13.2 mm				181	78	37	28.5	21.3	15.3			
polyphenylene oxide	All	323	19.3	36.0	51.0	57.7	64.4	86.2	95.0	110.0	120.5	
1095 kg m^{-3}, 12.7 mm				169	68	53	33	19.6	14.3	10.4	7.6	
polypropylene	Omit: 1 L	549	1.0	52.3	62.8	79.1	80.3	87.0	97.9	116.3	121.3	
907 kg m^{-3}, 12.7 mm				207	54	31.8	32.8	34.5	22.7	16.5	16.3	
polystyrene, white	All*	741	41.9	50.2	60.7	73.2	93.3	102.9	112.1			
1001 kg m^{-3}, 3.2 mm		*	*	97.4	35.5	23	15.7	12.5	10			
polystyrene, white	All	336	11.1	28.0	42.3	52.7	62.8	79.1	93.7	115.1	124.7	
1092 kg m^{-2}, 12.7 mm				140	73.5	51.5	32.5	19.9	13.7	7.3	7.4	
polystyrene, clear	All	526	6.0	30.1	37.7	46.9	63.6	74.5	92.9	111.3	123.8	127.6
1051 kg m^{-3}, 12.7 mm				350	182	123	49.3	34	24.5	21	15	15

Table 17 continued

Material, density, thickness	Data used	B_{ig}	$\dot{q}''_{cr}$	Ignition data pairs First line: flux (kW m^{-2}). Second line: time (s)								
polyurethane elastomer	All	347	22.5	37.7	50.6	62.8	81.6	94.6	110.0	128.0		
1200 kg m^{-3}, 14.2 mm				275	137	46	24	16	11.9	9.3		
PVC, gray	Omit: 2 H	364	27.5	44.8	59.8	73.6	92.0	106.3	117.2			
1433 kg m^{-3}, 13.2 mm				197	100	44	22.2	5.7	4.9			
PVC, clear	All*	546	52.8	60.2	64.9	76.1	92.9	107.9	125.5			
1384 kg m^{-3}, 3.1 mm		*	*	NI	46	25.3	12.7	10	7.6			
PVC, clear	All	319	20.5	35.1	48.1	55.2	64.9	75.3	93.3	105.9	128.4	
1478 kg m^{-3}, 13.2 mm				161	124	62	60	19	12.5	10.5	7.9	
rubber, natural	Omit: 4 H	294	17.1	31.8	44.8	62.8	82.4	94.1	112.1	126.4	134.7	
990 kg m^{-3}, 12.7 mm				206	77	31.3	15	8.6	4.5	3.02	4.5	
silicone rubber	Omit: 2 H	429	34.1	54.8	66.5	75.3	86.2	108.8	129.3			
1749 kg m^{-3}, 12.2				736	170	95	67	52	36			

NI – no ignition
* – analyzed as thermally thin

Table 18 Radiant ignition results on plastics from Scudamore et al.

Material	Thick. (mm)	Density (kg m^{-3})	Ignition time (s)			
			20 kW m^{-2}	30 kW m^{-2}	40 kW m^{-2}	50 kW m^{-2}
ABS	6	970	299	130	68	43
epoxy	11	1195	337	172	100	62
epoxy/glass	11	1917	320	120	75	57
modacrylic/glass	3	1445	553	252	148	101
nylon 6	6	1130	700	193	115	74
PEEK	3	1427	NI	NI	390	142
phenolic foam, filled	14	250	NI	NI	NI	28
phenolic/glass	3	1600	NI	423	214	165
polyester (isophthalic)	10	1199	256	115	59	38
polyester (isophthalic)/glass	11	1926	480	172	91	77
polyester/glass	3	1537	NI	NI	309	109
polyethylene	6	970	403	171	91	58
polypropylene			120	63	35	27
polystyrene foam, EPS			NI	73	28	18
polystyrene foam, EPS FR			NI	77	40	24
polyvinyl ester	10	1192	441	120	77	38
polyvinyl ester/glass	11	1837	646	235	104	78
PVC, flexible			119	61	41	25
PVC, flexible FR A			136	84	64	37
PVC, flexible FR B			278	103	69	45
PVC, flexible FR C			114	72	49	35
PVC, rigid A	3		NI	487	277	86
PVC, rigid B	6	1388	NI	320	153	87

NI – no ignition

Miscellaneous thermophysical properties of solids

Miscellaneous computed ignition properties for various solids are presented in Table 19. They have typically been obtained by running either Cone Calorimeter or LIFT tests. The properties obtained are 'effective' and were obtained by calculations according to a simplified ignition model and not by direct measurement (except for measured T_{ig} values, where given). The notation used is as follows: MC = moisture content; Thick = thickness of sample (mm); ρ = density (kg m^{-3}); λ = thermal conductivity (kW m^{-1} K^{-1}); C = heat capacity (kJ kg^{-1} K^{-1}); Eff. $\lambda\rho C$ = effective thermal inertia (kJ^2 m^{-4} s^{-1} K^{-2}) ; B_{ig} = ignition parameter, see Chapter 7; α = thermal diffusivity (m^2 s^{-1}); ε_s = radiant absorptivity (--); h_{ig} = effective convective heat transfer coefficient for ignition (W m^{-2} K^{-1}); T_{ig} meas = measured ignition temperature (ºC); T_{ig} comp = computed ignition temperature (ºC); q_{cr} = critical heat flux for ignition (kW m^{-2}); q_{min} = minimum heat flux for ignition (kW m^{-2}).

Table 19 Miscellaneous ignition properties of various solids

Material	Ref.	Test	Thick	ρ	λ	C	Eff. $\lambda\rho C$	B_{ig}	α	ε_s	h_{ig}	T_{ig} meas	T_{ig} comp	q_{cr}	q_{min}
ABS/PVC (80%/20%)	80	LIFT	1.5				0.76						388		16
aircraft honeycomb: epoxy, fiberglass, Nomex	80	LIFT					0.174						438		20
aircraft honeycomb: epoxy, Kevlar, Nomex	80	LIFT					0.188						465		23
aircraft honeycomb: phenolic, fiberglass, Nomex	80	LIFT					0.107						570		36
aircraft honeycomb: phenolic, graphite, Nomex	80	LIFT					0.186						570		36
aircraft honeycomb: phenolic, Kevlar, Nomex	80	LIFT					0.133						558		34
asphalt shingle	81	LIFT					0.7						378		15
carpet, acrylic	81	LIFT					0.42						300		10
" "	82	LIFT					0.7						300		10
carpet, nylon	82	LIFT					0.96						405		18
carpet, polypropylene	82	LIFT					0.86						300		14
carpet, wool	81	LIFT					0.11 - 0.25						435 - 465		20 - 23
carpet, wool	82	LIFT					0.86 - 1.14						365 - 415		14 - 18.5
carpet, wool/nylon blend	83	LIFT	6.3										395		
ceiling tile, wood fiberboard	81	LIFT					0.24 - 0.28						500 - 520		27 - 29
charcoal briquettes	84	NA			2.60×10^{-4}	1.2									
dimethylsilicone	85	NA													
fabric: white cotton terry cloth towel	86	LIFT	7				0.46						302		10
fiberboard	87	Cone					0.238						334	7.7	
" "	81	LIFT					0.46						355		14
" "	88	LIFT										290			19
fiberboard, low density	81	LIFT											330		12
fiberboard, medium density	89	Cone					1.377	340				330		1.6	
fiberboard, medium density 0% MC	90	Cone		280	1.18×10^{-4}	2.7	0.089								
fiberboard, high density	91	LIFT	6.4	900									307		10
grass	92	NA								0.97					
gypsum wallboard	81	LIFT	12.7				0.45						565	35	
gypsum wallboard	93	Cone	12.5	720			0.549						515		26
gypsum wallboard - Type X	94	Cone	16.5	755			0.457				34.5		341	12.6	
gypsum wallboard - Type X	95	Cone					0.451		3.74×10^{-7}	0.9			336		
gypsum wallboard - Type X	81	LIFT	12.7				0.4						510		28
hardboard	87	Cone					0.629						392	11.1	
hardboard	94	Cone	6	1026			0.277				38.9		393	16.5	
hardboard	95	Cone					0.763		1.50×10^{-7}	0.88			281		
hardboard	81	LIFT	6.4				1.87						298		10
hardboard	81	LIFT	3.2				0.88						365		14
hardboard (primer paint) 0% MC	96	LIFT	10	730	2.37×10^{-4}				1.76×10^{-7}				299		15
hardboard (primer paint) 7.9% MC	96	LIFT	6.4	730	2.73×10^{-4}				1.56×10^{-7}				308		15

Table 19 continued

Material	Ref.	Test	Thick	ρ	λ	C	Eff. $\lambda\rho C$	B_{ig}	α	ε_s	h_{ig}	T_{ig} meas	T_{ig} comp	q_{cr}	q_{min}
hardboard (gloss paint)	81	LIFT	3.2				1.22						400		17
hardboard (nitrocellulose paint)	81	LIFT					0.79						400		17
leaves	92	NA								0.96					
melamine-faced chipboard	87	Cone					0.575						463	16.6	
needle foliage	92	NA								0.97					
nylon 6,6	64	Cone			3.29×10^{-4}	2.27	0.874					500	380		
oriented strand board	94	Cone	11	643			0.21				36.5		365	14.3	
oriented strand board	95	Cone					0.217		9.32×10^{-9}	0.88			348		
oriented strand board 7% MC	64	LIFT	11.4	585	3.10×10^{-4}		0.252				37.8	364			15
particleboard	95	Cone					1.09		3.79×10^{-7}	0.88			257		
particleboard 7% MC	97	LIFT	13		2.50×10^{-4}		0.277				43.1	422			20
particleboard, D. fir	81	LIFT	12.7				0.94						382		16
particleboard, D. fir	23	LIFT	12.8												16
particleboard, FR	93	Cone		805			4.024						505		25
peat 7% MC	98	NA			5.60×10^{-5}							150			
peat 15% MC	98	NA			9.30×10^{-5}							150			
peat 20% MC	98	NA			1.00×10^{-4}							150			
peat 45% MC	98	NA			2.00×10^{-4}							150			
peat 55% MC	98	NA			2.60×10^{-4}										
phenolic foam	99	Cone	50	42			0.11						524		30
plywood	87	Cone					0.526						386	10.7	
plywood	81	LIFT	6.3 - 12.7				0.46 - 0.54						390		16
plywood	93	Cone	15	440			0.633						290		8
plywood	81	LIFT					0.76						620		44
plywood	95	Cone					0.373		1.57×10^{-7}	0.9			373		
plywood: D. fir (ASTM; 5 plies)	94	Cone	11.5	541			0.236				35.6		355	13.6	
plywood: D. fir (ASTM)	95	Cone					0.254		1.60×10^{-7}	0.9			336		
plywood: D. fir (MB; 3 plies)	94	Cone	12	513			0.194				37		369	15.2	
plywood: D. fir (MB)	95	Cone					0.259		1.60×10^{-7}	0.9			326		
plywood: D. fir 9% MC	97	LIFT	11.9	525	4.21×10^{-4}		0.326				38.2	368			15
plywood: D. fir FR (ASTM; 5 plies)	94	Cone	11.8	558			0.453				36.1		362	14	
plywood: D. fir -- FR	94	Cone					0.453				36.1		362	14	
plywood: D. fir -- FR	95	Cone					0.308		1.60×10^{-7}	0.9			387		
plywood, FR	93	Cone	15	460			0.105						480		22
plywood: oak veneer (For-intek; 5 plies)	94	Cone	13	479			0.465				30.1		280	8.9	
plywood: oak veneer	95	Cone					0.171		1.44×10^{-7}	0.9			357		
plywood: Southern pine	95	Cone					0.335		1.57×10^{-7}	0.88			323		
plywood: Southern yellow pine 9% MC	97	LIFT	10.9	600	2.20×10^{-4}		0.259				38.2	368			15
plywood: Southern pine FRT (5 plies)	94	Cone	11.5	599			0.449				39.8		403	17.3	
plywood: Southern yellow pine FR 9% MC	97	LIFT	12.1	580											24
PMMA: black, Polycast	81		25		4.32×10^{-4}	4.12	2.12					250 - 355	180		
PMMA: Type G	81	LIFT	12.7				1.02						378		15
PMMA: Polycast	81	LIFT	16				0.73						278		9
PMMA: clear glazing	93	Cone	3	1150			2.957						195	4	

Table 19 continued

Material	Ref.	Test	Thick	ρ	λ	C	Eff. $\lambda\rho C$	B_{ig}	α	ε_s	h_{ig}	T_{ig} meas	T_{ig} comp	q_{cr}	q_{min}
PMMA: clear glazing	91	LIFT	1.6	1350									289		9
PMMA: unspecified	89	Cone					1.228					345			
polyamide-imide	100	Cone	12.5				0.41						625	49	
polycarbonate	81	LIFT					1.16						528		30
polycarbonate	91	LIFT	1.5	1220									561		30
polycarbonate	101	HIFT					1.75						455 - 464	23	12 - 15
polycarbonate (Lexan 9034)	100	Cone	12.5				0.62						485	26	
polycarbonate/ polyeth-erimide	80	LIFT	1.5				0.84						518		29
polycarbonate, FR, hollow inside	93	Cone	16	1200			1.472						495		24
polycarbonate/ABS	102	Cone	NA				0.861					440			
polycarbonate/ABS, FR	106	Cone	NA				1.12					440			
polyetheretherketone (Ket-ron 1000)	100	Cone	12.5				0.91						631		
polyetherimide (Ultem 1000)	100	Cone	12.5				0.49						658	43	
polyetherimide (Ultem 1000)	50	HIFT					2.72						507	28	24
polyethylene	64	Cone			6.39×10^{-4}	3	1.834					315 - 330	300		
polyethylenenaphthalene	103	Cone					0.45						640	46	
polyisocyanurate foam	81	LIFT					0.02						445		21
polyisocyanurate foam	24	HIFT	50	26			0.03						445		21
polyphenylenesulfide (Techtron)	100	Cone	12.5				1.03						596	38	
polyphenylsulfone	103	Cone	3				1.03						596	38	
polypropylene	97	Cone			3.81×10^{-4}	6.27	2.15					250 - 360	210		
polystyrene, high-impact	106	Cone	NA				1.17					410			
polystyrene, high-impact, FR	106	Cone					1.16					390			
polystyrene foam, EPS	99	Cone	50	32			0.58						376		15
polystyrene foam, FR EPS	99	Cone	50	16			0.96						376		15
polystyrene foam, FR EPS	99	Cone	50	32			0.91						376		15
polystyrene foam, FR EPS	93	Cone	40	30			1.594						295		8
polystyrene foam, FR EPS	93	Cone	80	30			0.557						490		23
polystyrene foam, FR XPS	99	Cone	50	32			0.91						376		15
polysulfone (Udel P-1700)	100	Cone	12.5				0.45						640	46	
polyurethane foam -- FR	94	Cone					0.042				29.5		272	8.4	
polyurethane foam -- FR	95	Cone					0.02		1.46×10^{-6}	0.68			416		
polyurethane foam, rigid, FR, spray-applied	99	Cone	50	38			0.037 - 0.051						376		15.1
polyurethane foam, rigid, spray-applied	99	Cone	50	42			0.036						370		15
polyurethane foam w. Al. face	93	Cone	41	38											
PVC siding	96	LIFT	0.3	1890					8.70×10^{-8}				427		
PVC, FR	93	Cone	3	1505			1.306						415		16
PVC/acrylic (Kydex)	86	LIFT	1.6				1.4						376		15
roof shingles, asphalt	91	LIFT	3.2	1420											15

Table 19 continued

Material	Ref.	Test	Thick	ρ	λ	C	Eff. $\lambda\rho C$	B_{ig}	α	ε_s	h_{ig}	T_{ig} meas	T_{ig} comp	q_{cr}	q_{min}
roof shingles, fiberglass	91	LIFT	2.5	1780											23
roof shingles, fiberglass	81	LIFT					0.5						445		21
soil	92	NA								0.95-0.99					
trees	92	NA								0.96					
waferboard	95	Cone					0.325		1.57×10^{-7}	0.88			315		
wood: basswood 8.1% MC	104	OSU	64	420			0.141	109					298	10	< 15
wood: beech	94	Cone	15	749			0.504				35.8		358	13.7	
wood: beech	105	Cone					0.783						246	7.5	
wood: beech 9% MC	89	Cone					0.463	246				380		12.7	
wood: Blackbutt 0% MC	97	Cone	17.4	810			0.394				31.4	300		10	
wood: blue gum	106	Cone		850			0.91						309	9.3	
wood: Douglas fir 0% MC	97	Cone	16.8	465			0.159				35.2	350		13.2	
wood: heart rimu 10% MC	89	Cone					0.548					355		12.6	
wood: macracarpa 10% MC	89	Cone					0.376	214				402		11.1	
wood: mahogany	82	LIFT					0.512						407		18
wood: Monterey pine 0% MC	107	Cone					0.111								
wood: Monterey pine 0% MC	97	Cone	17.5	460			0.156				35.1	349		13.1	
wood: Monterey pine 15% MC	107	Cone					0.269								
wood: Monterey pine 22% MC	107	Cone					0.359								
wood: Monterey pine 30% MC	107	Cone					0.478								
wood: Monterey pine 11% MC	89	Cone					0.593	228				340		10.8	
wood: northern white cedar 2% MC	96	LIFT	18.5	310	1.34×10^{-4}				1.87×10^{-7}				314		15
wood: northern white cedar 10% MC	96	LIFT	7.7	310	1.44×10^{-4}				1.72×10^{-7}				362		20
wood: oak	105	Cone					0.447						301	10.6	
" "	82	LIFT					0.528						455		
wood: Pacific maple 10-12%MC	107	Cone					0.213								
wood: Pacific maple	106	Cone		544			0.676						313	9.5	
wood: pine 0% MC	90	Cone		510	1.85×10^{-4}	1.8	0.170								
wood: poplar	105	Cone					0.101						356	14.5	
wood: ponderosa pine 2% MC, rough surface	96	LIFT	18.5	420	1.58×10^{-4}				1.76×10^{-7}				288		14
wood: ponderosa pine 9.3% MC, rough surface	96	LIFT	17.9	420	1.83×10^{-4}				1.64×10^{-7}				367		21
wood: red oak 8.5% MC	104	OSU	64	660			0.36	194					315	10.5	< 16
wood: redwood	94	Cone	19	421			0.184				38.4		388	16	
wood: redwood	95	Cone					0.129		1.25×10^{-7}	0.86			365		
wood: redwood 6% MC side grain	108	mod. Cone	40				0.076								
wood: redwood 6% MC end grain	108	mod. Cone	40				0.068								
wood: redwood 8.3% MC	104	OSU	64	312			0.073	100					363	12.4	< 16
wood: redwood 2% MC	96	LIFT	19.1	410			0.152		1.81×10^{-7}			287			13
wood: redwood 7.4% MC	96	LIFT	17	410					1.65×10^{-7}				358		19
wood: redwood 0% MC	97	Cone	19	430			0.143				36.3	364		14.2	

Table 19 continued

Material	Ref.	Test	Thick	ρ	λ	C	Eff. $\lambda\rho C$	B_{ig}	α	ε_s	h_{ig}	T_{ig} meas	T_{ig} comp	q_{cr}	q_{min}
wood: rimu 10% MC	89	Cone					0.548	245				355		10.4	
wood: Southern pine	95	Cone					0.27		1.60×10^{-7}	0.88			367		
wood: Southern pine 9.7% MC	104	OSU	64	508			0.183	136					320	10.7	< 15
wood: spruce	94	Cone	15	468			0.208				38.1		375	15	
wood: spruce	95	Cone					0.214		1.63×10^{-7}	0.88			358		
wood: spruce	105	Cone					0.181						352	14.1	
wood: spruce 0% MC	90	Cone		440	1.25×10^{-4}	1.8	0.099								
wood: sugar pine 10-12% MC	107	Cone					0.071								
wood: sugar pine	106	Cone		430			0.509						309	9.2	
wood: tawa 12% MC	89	Cone					1.048	307				340		10.3	
wood: varnished	93	Cone	9				0.53						330		10
wood: Victorian ash 0% MC	97	Cone	17.2	640			0.261				32.2	311		10.6	
wood: western red cedar 0% MC	97	Cone	17	330			0.088				35.5	354		13.5	

Further readings

Guide to Fire Hazard Properties of Flammable Liquids, Gases, and Volatile Solids (NFPA 325), NFPA, Quincy MA. This compilation gives listings for close to 2000 pure or commercial (but not trademarked) products. Flash points are included for most listed compounds, with AIT values and flammability limits provided for a fraction of those.

Flash Point Index of Trade Name Liquids, 9th ed., NFPA, Boston (1978). This valuable compilation of over 8800 products is no longer published and the ninth was the final edition.

References

1. Magison, E. C., **Electrical Instruments in Hazardous Locations**, 4th ed., ISA, Research Triangle Park NC (1998).
2. Coward, H. F., and Jones, G. W., Limits of Flammability of Gases and Vapors (Bull. 503), Bureau of Mines, Pittsburgh (1952).
3. Zabetakis, M. G., Flammability Characteristics of Combustible Gases and Vapors (Bulletin 627), Bureau of Mines, Pittsburgh (1965).
4. Kuchta, J. M., Investigation of Fire and Explosion Accidents in the Chemical, Mining, and Fuel-Related Industries—A Manual (Bulletin 680), Bureau of Mines, Pittsburgh (1985).
5. Wagman, D. D., et al., The NBS Tables of Chemical Thermodynamic Properties. Selected Values for Inorganic and C_1 and C_2 Organic Substances in SI Units, *J. Phys. and Chem. Ref. Data* **11**, Supplement 2 (1982).
6. NIST Chemistry WebBook (1991-2001).
7. Guide to Fire Hazard Properties of Flammable Liquids, Gases, and Volatile Solids (NFPA 325), NFPA.
8. Mullins, B. P., **Spontaneous Ignition of Liquid Fuels**, AGARDograph no. 4. Butterworths, London (1955).
9. Pedley, J. B., **Thermochemical Data and Structures of Organic Compounds**, vol. 1. CRC Press, Boca Raton FL (1994).
10. Budavari, S., et al., eds., **The Merck Index**, 12th ed., Merck & Co., Whitehouse Station NJ (1996).
11. Lide, D. R., **CRC Handbook of Chemistry and Physics**, 76th ed., CRC Press, Boca Raton FL (1995).
12. Dean, J. A., **Lange's Handbook of Chemistry**, 15th ed., McGraw-Hill, New York (1999).
13. Helwig, N., and Nabert, K., Zusammenhänge zwischen Kenngrössen für explosionsgeschützte Betriebsmittel [Correlation between Characteristic Values for Explosion Safety of Materials], PTB Mitteilungen, *PTB-Mitteilungen* 287-293 (April 1968).
14. Britton, L. B., Using Material Data in Static Hazard Assessment, *Plant/Operations Progress* **11**, 56-70 (1992).
15. Yaws, C. L., **Chemical Properties Handbook**, McGraw-Hill, New York (1999).
16. Basic Considerations in the Combustion of Hydrocarbon Fuels with Air (NACA Report 1300), NACA, Washington (1957).
17. Hazards of Chemical Rockets and Propellants Handbook. Vol. III. Liquid Propellant Handling, Storage and Transportation (CPIA-194), Chemical Propulsion Information Agency, Silver Spring MD (1972).
18. Hertzberg, M., The Flammability Limits of Gases, Vapors and Dusts: Theory and Experiment, pp. 3-48 in **Fuel-Air Explosions**, J. H. S. Lee and C. M. Guirao, eds., University of Waterloo Press, Waterloo, Canada (1982).
19. Burgoyne, J. H., Roberts, A. F., and Quinton, P. G., The Spread of Flame Across a Liquid Surface. I. The Induction Period, *Proc. Royal Soc. London* **A308**, 39-53 (1968).

20. Jones, J. C., and Godefroy, J., Anomalies in the Flash Points of Four Common Organic Compounds, *J. Loss Prevention in the Process Industries* **15**, 245-247 (2002).
21. Paint and Surface Coatings: Theory and Practice, 2nd ed., R. Lambourne and T.A. Strivens, eds., William Andrew Pub., Norwich NY (1999).
22. Lewis, R J. sr., **Hawley's Condensed Chemical Dictionary**, 14th ed., Wiley, New York (2001).
23. Dillon, S. E., and Hamins, A., Ignition Propensity and Heat Flux Profiles of Candle Flames for Fire Investigation, pp. 363-376 in *Fire and Materials 2003*, Interscience Communications Ltd., London (2003).
24. Snyder, C. E. jr., and Gschwender, L. J., Fire Resistant Hydraulic Fluids and Fire Resistance Test Methods Used by the Air Force, pp. 72-77 in Fire Resistance of Industrial Fluids (ASTM STP 1284), ASTM (1996).
25. Manual for Classification of Gases, Vapors, and Dusts for Electrical Equipment in Hazardous (Classified) Locations (NFPA 497M), NFPA.
26. Kueffer, J., and Donaldson, A. B., Correlation of Flash Point Data with Lower Flammability Limit, pp. 119-124 in *Proc. 1997 Tech. Mtg., Central States Section, The Combustion Institute* (1997).
27. Calcote, H. F., Gregory, C. A. jr, Barnett, C. M., and Gilmer, R. B., Spark Ignition: Effect of Molecular Structure, *Ind. and Eng. Chem.* **44**, 2656-2662 (1952).
28. Grove, J. R., The Measurement of Quenching Diameters and Their Relation to the Flameproof Grouping of Gases and Vapours, pp. 51-54 in *Proc. 3rd Symp. on Chemical Process Hazards with Special Reference to Plant Design* (Symp. Series No. 25), The Institution of Chemical Engineers, London (1968).
29. Brandes, E., PTB, private communication (2001).
30. Lunn, G. A., The Influence of Chemical Structure and Combustion Reactions on the Maximum Experimental Safe Gap of Industrial Gases and Liquids, *J. Hazardous Materials* **6**, 341-359 (1982).
31. Bartkus, A. A., et al., An Investigation of Flammable Gases or Vapors with Respect to Explosion-proof Electrical Equipment (Tech. Rept. No. 58), UL (1993).
32. Slack, C., and Woodhead, D. C., Correlation of Ignitabilities of Gases and Vapours by a Break Spark and at a Flange Gap, *Proc. IEE* **113**, 297-301 (1966).
33. Kuchta, J. M., and Clodfelter, R. G., Aircraft Mishap Fire Pattern Investigations (AFWAL-TR-85-2057), Aero Propulsion Laboratory, Air Force Systems Command, Wright-Patterson AFB OH (1985).
34. Richard, R. G., and Shankland, I. R., Flammability of Alternative Refrigerants, *ASHRAE J.* **34**:4, 20-23 (1992).
35. Matrix of Combustion-Relevant Properties and Classification of Gases, Vapors, and Selected Solids (NMAB 353-1), National Materials Advisory Board, National Academy of Sciences Press, Washington (1979).
36. Kuchta, J. M., Fire And Explosion Manual for Aircraft Accident Investigators (AFAPL-TR-73-74). Prepared by Bureau of Mines, Pittsburgh, for Air Force Aero Propulsion Laboratory, Wright-Patterson Air Force Base, Ohio (1973).
37. Cashdollar, K. L., Flammability of Metals and Other Elemental Dust Clouds, *Process Safety Progress* **13**, 139-145 (1994).
38. Jacobson, M., Cooper, A. R., and Nagy, J., Explosibility of Metal Powders (RI 6516), Bureau of Mines, Pittsburgh (1964).
39. Jacobson, M., Nagy, J., Cooper, A. R., and Ball, J. J., Explosibility of Agricultural Dusts (RI 5753), Bureau of Mines, Pittsburgh (1961).
40. Hartmann, I., Nagy, J., and Jacobson, M., Explosive Characteristics of Titanium, Zirconium, Thorium, Uranium, and their Hydrides (RI 4835), Bureau of Mines, Pittsburgh (1951).
41. Nagy, J., Dorsett, H. G. jr., and Cooper, A. R., Explosibility of Carbonaceous Dusts (RI 6597), Bureau of Mines, Pittsburgh (1965).
42. Dorsett, H. G., jr., and Nagy, J., Dust Explosibility of Chemicals, Drugs, Dyes, and Pesticides (RI 7132), Bureau of Mines, Pittsburgh (1968).
43. Jacobson, M., Nagy, J., and Cooper, A. R., Explosibility of Dusts used in the Plastics Industry (RI 5971), Bureau of Mines, Pittsburgh (1961).
44. Nagy, J., Cooper, A. R., and Dorsett, H. G., Explosibility of Miscellaneous Dusts (RI 7208), Bureau of Mines, Pittsburgh (1968).
45. Hertzberg, M., Conti, R. S., and Cashdollar, K. L., Electrical Ignition Energies and Thermal Autoignition Temperatures for Evaluating Explosion Hazards of Dusts (RI 8988), Bureau of Mines, Pittsburgh (1985).
46. Hertzberg, M., Zlochower, I. A., and Cashdollar, K. L., Metal Dust Combustion: Explosion Limits, Pressures, and Temperatures, pp. 1827-1835 in *24th Symp. (Intl.) on Combustion*, Combustion Institute, Pittsburgh (1992).
47. Hertzberg, M., Cashdollar, K. L., Zlochower, I. A., and Green, G. M., Explosives Dust Cloud Combustion, pp. 1837-1843 in *24th Symp. (Intl.) on Combustion*, Combustion Institute, Pittsburgh (1992).
48. Field, P., **Dust Explosions**, Elsevier, Amsterdam (1982).
49. Hilado, C. J., and Kosola, K. L., A Laboratory Technique for Determining Ignition Temperatures of Materials, *Fire Technology* **14**, 291-296 (1978).
50. Grand, A. F., The Use of the Cone Calorimeter to Assess the Effectiveness of Fire Retardant Polymers under Simulated Real Fire Test Conditions, pp. 143-152 in *Interflam '96*, Interscience Communications Ltd., London (1996).
51. Hilado, C. J., **Flammability Handbook for Plastics**, 5th ed., Technomic, Lancaster PA (1998).
52. Morimoto, T., Mori, T., and Enomoto, S., Ignition Properties of Polymers Evaluated from Ignition Temperature and Ignition Limiting Oxygen Index, *J. Applied Polymer Science* **22**, 1911-1918 (1978).
53. Setchkin, N. P., A Method and Apparatus for Determining the Ignition Characteristics of Plastics, *J. Research NBS* **43**, 591-608 (1949).
54. Patten, G. A., Ignition Temperatures of Plastics, *Modern Plastics* **38**, 119-122, 180 (July 1961).
55. Pál, G., and Macskásy, H., **Plastics: Their Behaviour in Fires**, Elsevier Science Publishers, Amsterdam (1991).
56. Brown, J. R., and Gellert, E. P., The Combustion of Organic Polymeric Materials—Ignition Properties (Tech. Note MRL-TN-414), Materials Research Laboratories, Dept. of Defence, Ascot Vale, Vic., Australia (1978).
57. Yoshida, S., Ito, K., Tamamoto, Y., Aida, F., and Hosokawa, E., Flash and Ignition Characteristics of Flame Retardant Materials, pp. 318-325 in *Proc. 38th Intl. Wire and Cable Symp.*, US Army Communications-Electronics Command, Fort Monmouth NJ (1989).
58. Fernandez-Pello, A. C., Hasegawa, H., Staggs, K., Lipska-Quinn, A. E., and Alvares, N. J., A Study of the Fire Per-

formance of Electrical Cables, pp. 237-347 in *Fire Safety Science—Proc. Third Intl. Symp.*, Elsevier Applied Science, London (1991).
59. Aseeva, R. M., Zaikov, G. E., **Combustion of Polymers**, Karl Hanser Verlag, München (1986).
60. Setchkin, N. P., Discussion of Paper on the Ignition Temperature of Rigid Plastics, *ASTM Bull.* No. 151, 66-69 (1948).
61. Standard Guide for Evaluating Nonmetallic Materials for Oxygen Service (ASTM G 63), ASTM.
62. Masařík, I., unpublished data from roundrobin tests conducted for ISO.
63. Tewarson, A., Abu-Isa, I. A., Cummings, D. R., and LaDue, D. E., Characterization of the Ignition Behavior of Polymers Commonly Used in the Automotive Industry, pp. 991-1002 in *Fire Safety Science—Proc. 6th Intl. Symp.*, Intl. Assn. for Fire Safety Science (2000).
64. Hopkins, D. jr., and Quintiere, J. G., Material Fire Properties and Predictions for Thermoplastics, *Fire Safety J.* **26**, 241-268 (1996).
65. Kishore, K., Nagarajan, R., and Mohandas, K., Polymer Ignition – A Review, *Polymer Engineering Reviews* **2**, 257-293 (1983).
66. Hertzberg, M., Litton, C. D., and Garloff, R., Studies in Incipient Combustion and Its Detection (RI 8206), Bureau of Mines, Pittsburgh (1977).
67. Stark, H. J., Ignition and Burning Characteristics of Polyester, Phenolic and Melamine Fibrous Glass Laminates, *ASTM Bull.* 55-58 (Dec. 1949).
68. Long, R. T. jr., Torero, J. L., Quintiere, J. G., and Fernandez-Pello, A. C., Scale and Transport Considerations on Piloted Ignition of PMMA, pp. 567-578 in *Fire Safety Science—Proc. 6th Intl. Symp.*, Intl. Assn. for Fire Safety Science (2000).
69. Tsai, T.-H., Li, M.-J., Shih, I-Y., Jih, R., and Wong, S.-C., Experimental and Numerical Study of Autoignition and Pilot Ignition of PMMA Plates in a Cone Calorimeter, *Combustion and Flame* **124**, 466-480 (2001).
70. Kashiwagi, T., and Omori, A., Effects of Thermal Stability and Melt Viscosity of Thermoplastics on Piloted Ignition, pp. 1329-1338 in *22nd Symp. (Intl.) on Combustion*, The Combustion Institute, Pittsburgh (1988).
71. Kashiwagi, T., Inaba, A., and Brown, J. E., Differences in PMMA Degradation Characteristics and Their Effects on Its Fire Properties, pp. 483-493 in *Fire Safety Science—Proc. 1st Intl. Symp.*, Hemisphere Publishing Corp., Washington (1986).
72. Unpublished data, Omega Point Laboratories, Inc.
73. Drysdale, D. D., and Thomson, H. E., Ignition of PUFs: A Comparison of Modified and Unmodified Foams, pp. 191-205 in *Flame Retardants '90*, Elsevier, London (1990).
74. Babrauskas, V., Harris, R. H., Jr., Braun, E., Levin, B. C., Paabo, M., and Gann, R. G., The Role of Bench-Scale Test Data in Assessing Full-Scale Fire Toxicity (NIST Tech. Note 1284), NIST (1991).
75. Landrock, A. H., **Plastics Flammability and Combustion Toxicology**, Noyes Publications (1983).
76. Delfosse, L., Study of Self-Ignition of PVC, *J. Macromol. Sci.—Chemistry* **A11**, 1491-1501 (1977).
77. Dean, R. K., Stored Plastics Test Program (FMRC Serial No. 20269), Factory Mutual Research Corp., Norwood MA (1975).
78. Hallman, J. R., Ignition Characteristics of Plastics and Rubber (Ph.D. Dissertation), Univ. Oklahoma, Norman (1971).
79. Scudamore, M. J., Briggs, P. J., and Prager, F. H., Cone Calorimetry—A Review of Tests Carried Out on Plastics for the Association of Plastic Manufacturers in Europe, *Fire and Materials* **15**, 65-84 (1991).
80. Harkleroad, M. F., Ignition and Flame Spread Measurements of Aircraft Lining Materials (NBSIR 88-3773), NBS (1988).
81. Quintiere, J. G., and Harkleroad, M. F., New Concepts for Measuring Flame Spread Properties (NBSIR 84-2943), NBS (1984).
82. Harkleroad, M., unpublished NIST data.
83. Harkleroad, M. F., Quintiere, J. G., and Walton, W. D., Radiative Ignition and Opposed Flow Flame Spread Measurements on Materials (DOT/FAA/CT-83/28), Federal Aviation Administration, Atlantic City Airport NJ (1983).
84. Wolters, F. C., Pagni, P. J., Frost, T. R., and Vanderhoof, D. W., Size Constraints on Self-ignition of Charcoal Briquets, Clorox Technical Center, Pleasanton CA (1987).
85. Page, W. C., and Buch, R. R., Recent Studies on the Fire Behavior of Silicones, pp. 185-188 in *Proc. 21st Intl. Conf. on Fire Safety*, Product Safety Corp., Sissonville WV (1996).
86. Ohlemiller, T. J., and Villa, K. M., Material Flammability Test Assessment for Space Station Freedom (NISTIR 4591; NASA CR-187115), NIST (1991).
87. Azhakesan, M. A., Shields, T. J., and Silcock, G. W. H., Ignition and Opposed Flow Flame Spread Utilising a Reduced Scale Attachment to the Cone Calorimeter, *Fire Technology* **34**, 99-115 (1999).
88. Quintiere, J. G., Simplified Theory for Generalizing Results from a Radiant Panel Rate of Flame Spread Apparatus, *Fire and Materials* **5**,52-60 (1981).
89. Henderson, A., Predicting Ignition Time under Transient Heat Flux Using Results from Constant Heat Flux Experiments (Report 98/4), School of Engineering, Univ. Canterbury, Christchurch, New Zealand (1998).
90. Mikkola, E., Thermal Properties of Wood for Modeling, Second Intl. Cone Calorimeter Workshop, Univ. Kent, England (1990).
91. Braun, E., and Allen, P. J., Flame Spread on Combustible Solar Collector Glazing Materials (NBSIR 84-2887), NBS (1984).
92. Grishin, A. M., **Mathematical Modeling of Forest Fires and New Methods of Fighting Them**, Publishing House of the Tomsk State University, Tomsk, Russia (1997), p. 18. Also note extensive tables of radiative properties of leaves and needles on pp. 151-152.
93. Dillon, S. E., Analysis of the ISO 9705 Room/Corner Test: Simulations, Correlations and Heat Flux Measurements (M.S. thesis), Univ. Maryland, College Park (1998).
94. Grexa, O., Janssens, M., White, R., and Dietenberger, M., Fundamental Thermophysical Properties of Materials Derived from Cone Calorimeter Measurements, pp. 139-147 in *Wood & Fire Safety: 3rd Intl. Scientific Conf.*, The High Tatras, Slovak Republic (1996).
95. Dietenberger, M., and Grexa, O., Analytical Model of Flame Spread in Full-scale Room/Corner Tests (ISO 9706), pp. 211-222 in *Fire & Materials '99, 6th Intl. Conf.*, Interscience Communications Ltd., London (1999).

96. Dietenberger, M. A., Ignitability Analysis of Siding Materials Using Modified Protocol for LIFT Apparatus, *Fire and Materials* **20**, 115-121 (1996).
97. Janssens, M. L., Fundamental Thermophysical Characteristics of Wood and Their Role in Enclosure Fire Growth (Ph. D. dissertation), Univ. Gent, Belgium (1991).
98. Weckman, H., Hyvärinen, P., Olin, J., Rautalin, A., and Vuorio, M., Reduction of Fire and Explosion Hazards at Peat Handling Plants (Research Report 2/1981). Palotekniikan laoratorio. Valtion Teknillinen Tutkimuskeskus, Espoo, Finland (1981).
99. Cleary, T. G., and Quintiere, J. G., Flammability Characterization of Foam Plastics (NISTIR 4664), NIST(1991).
100. Gandhi, S., Walters, R. N., and Lyon, R. E., Fire Performance Study of Advanced Engineering Thermoplastics, pp. 119-126 in *Fire & Materials '99, 6th Intl. Conf*., Interscience Communications Ltd., London (1999).
101. Kashiwagi, T., and Cleary, T. G., Effects of Sample Mounting on Flammability Properties of Intumescent Polymers, *Fire Safety J*. **20**, 203-225 (1993).
102. Grand, A. F., The Use of the Cone Calorimeter to Assess the Effectiveness of Fire Retardant Polymers under Simulated Real Fire Test Conditions, pp. 143-152 in *Interflam '96*, Interscience Communications Ltd., London (1996).
103. Gandhi, S., Study of Advanced Fire-Resistant Materials for Aircraft Applications, pp. 191-204 in *ICFRE3 – Proc. 3rd Intl. Conf. on Fire Research and Engineering*, Society of Fire Protection Engineers, Bethesda MD (1999).
104. Tran, H. C., and White, R. H., Burning Rate of Solid Wood Measured in a Heat Release Rate Calorimeter, *Fire and Materials* **16**, 197-206 (1992).
105. Grexa, O., Horváthová, E., and Osvald, A., Cone Calorimeter Studies of Wood Species, pp. 77-84 in *Intl. Symp. on Fire Science and Technology*, Korean Institute of Fire Science & Engineering, Seoul (1997).
106. Dlugogorski, B., Pope, D. M., Moghtaderi, B., Kennedy, E. M., and Lucas, J. A., A Study on Fire Properties of Australian Eucalyptus, pp. 57-72 in *Wood & Fire Safety—4th Intl. Scientific Conf*., The High Tatras, Slovak Republic (2000).
107. Moghtaderi, B., Novozhilov, V., Fletcher, D. F., and Kent, J. H., A New Correlation for Bench-scale Piloted Ignition Data of Wood, *Fire Safety J.* **29**, 41-59 (1997).
108. Boonmee, N., Radiant Auto-Ignition of Wood (M.S. thesis), Univ. Maryland, College Park (2001).

Copyright © 2003, 2014 Vytenis Babrauskas

Index

Numbers in bold indicate the primary reference. Alphabetization is according to the scheme where spaces are not used in sorting.

12 mm Flame Test 326
20 mL Sphere Test 127-128
20 mm Flame Test 326, 741, 918
Abbreviations 20-22
Abel Flash Point Test 223, 226
Ablation 242, 468, 542
ABS 20, 286, 290, 307, 309, 628, 849, 905, 909, 918, 925, 1064, 1067, 1070-1073, 1075
Absorptivity (radiant) 102, 255, 257, 261, 264, 275-276, 296, 305-308, 310, 332, 373, 409, 522, 571, 573, 705, 821-822, 899, 942, 954, 962, 1072
Abuse 686, 732, 742-743, 757, 783, 788, 795, 854
Accelerants 683
Accelerants, high-temperature 672, 858-859
Accelerating Rate Calorimeter (ARC) 20, **425-428**, 714, 921
Acceleration of gravity, effect of 78-79, 253, 304, 483, 526
Access of air, effect of 396-397
Acetal 1024-1026, 1067
Acetaldehyde 31, 45, 60, 594, 809, 1024-1026
Acetamide 1066
Acetanilide 1024, 1025, 1026
Acetic acid 888, 918, 1024-1026
Acetic anhydride 1024-1026
Acetone cyanohydrin 1048-1050
Acetone 31, 58, 113, 115, 119, 225, 469, 507, 511-512, 558, 561, 566, 613, 683, 685-686, 717, 814, 1024-1026
Acetonitrile 1024-1026
Acetophenone 1024-1026
Acetyl chloride 1024-1026
Acetylacetone 1024-1026
Acetylene 5, 26, 31, 44, 75-76, 78, 87, 104, 109-110, 113, 121-124, 145, 226, 331, 447, 561, 566, 594-595, 597, 599, 619, **683-686**, 717, 767, 778, 810, 825, 863, 941, 952, 1024-1026
Acetylenic compounds 111, 452, 686
Acrolein 597, 620, 717, 1024-1026
Acronyms 20-22
Acrylic 166, 269, 286, 299, 506, 786, 816, 820-821, 823-824, 829-832, 931-932, 935, 1073, 1075
Acrylic acid 477, 1024-1026
Acrylic batting 506
Acrylonitrile 20, 811, 912, 1024-1026, 1070
Activated carbon 159, 160, 399, 417, **714**, 1066
Adhesives 184, 708
Adiabatic calorimeters 421-425, 428, 721, 813, 847, 912
Adiabatic compression 219-220, 460, 466, 483, 625, 627, 690, 895-896
Adiabatic decomposition temperature 432
Adiabatic flame temperature 9, 30-32, 37, 67, 69, 108, 114-115, 144-145, 150, 255, 473, 480, 526, 615-616, 902, 1023
Adiabatic Storage Test 421-422
Adipic acid 1024-1026
Adiponitrile 1024-1026
Aerial bombs 454
Aerodynamic heating 576
Aerosol cans 575, **686-687**, 767, 927
Aerosols 29, 43, 64, 68, 102, 114, 116, 151, 183, 186, 188-189, **190-192**, **202-207**, 219, 449, 464, 475, 515, 554-555, 563, 565-566, 575, 594, 623, 686-687, 697, 767, 927
AES 20, 797, 799-802
Afterflame 241, 291, 320, 322, 325-327, 839, 936
Afterglow 320, 325-327, 706, 869, 936
Aging, effect of **310**, 323, 706, 733, 738, 744, 754, 758, 759-760, 763, 767, **791-793**, 805, 854-855, 918, **954**
Agricultural products 20, 244, 303, 308, 316, 369, 371, 374, 396, 404, **687-688**, 736, 833, 865
Air bags 884-885
Air compressors 57, 64, **688-689**
Aircraft 219, 311, 328, 570, 575-576, 594, 687, **690-691**, 696-699, 725, 749, 779, 792-793, 804-807, 824, 862, 877, 884, 894-895, 927, 1073
Aircraft, wiring in 804-806
Aircraft honeycomb 690, 1073
Aircraft oxygen generation canisters 894-895
Aircraft wall panels 690
Air flow rate, effect of 63, 79, 116, 166, 297-299
Air/fuel ratio 28-29, 78
Air-gap Sensitivity Test 488
Airless spraying 898
Airline pilots 571
Airplanes (*see* Aircraft)
Air terminals (lightning protection devices) 592-593
Alcoholic beverages 691
AL-CU wiring devices 763

Aldehydes 45, 109, 562, 691, 890, 1061
Aldol 1024-1026
Alfalfa meal 1064
Alizarine 1066
Alkali-metal carbides 452
Alkanes ... 54-55, 76, 109, 110, 185, 196, 683, 696, 856, 865
Alkyd paints 896-897, 962
Alkylation 6, 451
Alkyl-metal compounds 452
Allene 686, 1048-1050
Alloying 480, 667, **793**, 849, 875
Allyl alcohol 1024-1026
Allyl amine 1024-1026
Allyl bromide 1024-1026
Allyl carbinol 1024-1026
Allyl chloride 1024-1026
Allyl glycidyl ether 1024-1026
Alternators 738
Alumina 308, 314, 750, 751, 829, 1066
Aluminum 59, 72, 83, 86, 89, 149, 151, 161, 163, 165, 168, 211, 307, 319, 328, 353, 355-356, 358, 359, 393, 409, 419, 432, 454-455, 469, 472, 474-475, 480-482, 487-488, 508-517, 526, 534, 549, 552, 561, 572, 593-594, 601, 626-628, 690, 695, 703-704, 706, 719, 733, 753, 759, 769, 772-773, 780, 782, 784, 793, 795, 809, 822, 830, 844, 849-850, 856, 858, 862, **870-872**, 874-875, 878, 890, 896, 901-902, 912, 915-917, 923, 941, 962, 1063, 1065
Aluminum alkyl compounds 452
Aluminum bronze 513
Aluminum chloride 807
Aluminum dichromate 1066
Aluminum electrodes 546
Aluminum facings 307-08
Aluminum hydride 870
Aluminum oxide 357, 511, 517, 550, 750-751, 763, 871-872
Aluminum paints 510, 898
Aluminum particles 74, 500, 510, 514, 517, 553, 843, 872
Aluminum siding 666, 782
Aluminum silicate 1066
Aluminum tanks 624
Aluminum wiring 660, 662, 761, **762-765**, 796
Alva Cape (tanker) 719
Amalgam 870
Amaranth lake 1066
Ammonia 28, 31, 44, 82, 100, 121-122, 452, 476, 620, 623, **691**, 717, 826, 862, 1024-1026, 1060
Ammoniated polyphosphoric acid 706
Ammonium carbonate 1066
Ammonium nitrate 454, 471-472, 474-475, **691-694**, 808, 826-827, 885, 915, 917, 1024-1026, 1065-1066
Ammonium perchlorate 304, 475, 477, 479, 480-482, 484, **694-695**, 808, 858, 872, 885, 914, 1024-1026, 1065-1066
Ammonium perchromate 468
Ammonium phosphate 319, 562
Ammonium picrate 808, 811-812
Ammonium sulfate 562, 692-693, 706, 827
Ampacity 18, 549, 780-781, 794
Ampacity derating 781
n-Amyl acetate 1024-1026
sec-Amyl acetate 1024-1026
Amyl alcohol 1024-1026
sec-Amyl alcohol 1048-1050
tert-Amyl alcohol 1024-1026
n-Amyl amine 1024-1026
n-Amyl bromide 1024-1026
n-Amyl chloride 1024-1026
tert-Amyl chloride 1024-1026
n-Amylene 1024-1026
n-Amyl ether 1024-1026
n-Amyl nitrate 1024-1026
n-Amyl nitrite 1024-1026
Amyl propionate 1024-1026
ANFO 446, 453, 455, 459, 474, 490, **691-694**, 815, 827
Aniline 891, 1024-1026
Animal glue 868
Animal oils 886, 888, 966
Anisole 1024-1026
Anode 313, 466, 534, 539-540, 543, 546, 805, 864
ANSI Z21.10.1 940
Antennas, adventitious 572-573
Anthracene 480, 1024-1026
Anthraquinone 170, 526
Anti-caking agents 692
Antifreeze 226, **695**, 807
Antimony 319, 353, **872**, 1063
Antimony sulfide 472, 868, 915, 917
Antioxidants **400**, 404, 414, 723, 888, 903-904, 962
Antoine equation 185, 192, 199
Ants 667, 787
Apparatus dependence 9, 311
Apparel 321, 559-560, 703, 815, 823, 825
Appliance cords 655-656, 666, 773, **793-794**
APTAC Test 426
Aquariums 663, 758, 775
Arachlor 1059
Arc beads 795-804
Arc fault circuit interrupters 604
Arc flash 545, 642, 665
Arcing across a carbonized path 20, 237, **312-315**, 333-334, 663-664, 671, 673, 725, 732, 753, 756, 758-759, 769, 773-775, 786-787, 790, 804-805, 841, 855, 885, 925, 960
Arcing fault (*see* Electric arcs)
Arcing short 746, 774-779
Arc power (*see* Electric arcs: arc power)
Arc pressure 548
ARC Test (*see* Accelerating Rate Calorimeter)
Arc tracking 20, 237, **312-315**, 333-334, 663-664, 671, 673, 725, 732, 753, 756, 758-759, 769, 773-775, 786-787, 790, 804-806, 841, 855, 885, 925, 960

Arc welding 499, 506-507, 824, 864
Armchairs (*see* Upholstered furniture)
Aromatic hydrocarbons 865
Arrhenius kinetics 47, 60, 120, 247, 252-253, 281-284, 377, 391, 393-394, 405, 419, 426, 451, 458, 469, 488, 705, 723, 813
Arsenic compounds 695
Arsine 1024-1026
Arsonists 575, 725, 747, 765, 829, 864, 940
Aryl-metals compounds 452
AS1241 hydraulic fluid 1057
Asbestos 312, 501, 630, 685, 786, 832, 891, 904, 907
Asbestos-cement 630
Ashes 5, **695**, 711-712, 824, 860, 905, 935
Ashes (*see also* Embers)
Aspen 842, 966
Asphalt 328, 371, 475, 502, 515, 629-630, **696**, 754, 780, 827, 865, 884, 895, 898, 914, 919, 924, 930, 963, 1056, 1075
Asphalt shingles 499, 501, 1073
Aspirin 1065
ASTM C 739 ..... 335, 706
ASTM D 56 ..... 199, 218, 224
ASTM D 86 ..... 114, 202
ASTM D 92 ..... 15, 225, 862
ASTM D 93 225
ASTM D 240 39
ASTM D 286 ..... 53, 220, 221, 222, 338, 629
ASTM D 439 849
ASTM D 495 333-334
ASTM D 975 732
ASTM D 1230 321
ASTM D 1310 ..... 195, 225
ASTM D 1692 ..... 322, 323
ASTM D 1929 ..... 15, 241, 243, 278, 336-338, 817, 905, 907, 1066-1067
ASTM D 2015 39
ASTM D 2132 333
ASTM D 2155 ..... 222, 862, 1066, 1070
ASTM D 2303 333
ASTM D 2512 628
ASTM D 2539 484
ASTM D 2540 483
ASTM D 2633 327
ASTM D 2859 ..... 321, 829
ASTM D 2863 ..... 338, 629
ASTM D 2883 432
ASTM D 3032 ..... 327, 334, 805
ASTM D 3243 226
ASTM D 3278 ..... 224, 225
ASTM D 3466 714
ASTM D 3638 ..... 334, 759
ASTM D 3828 226
ASTM D 3874 336
ASTM D 3934 226
ASTM D 3941 ..... 224, 226
ASTM D 4206 226
ASTM D 4372 926
ASTM D 4809 39
ASTM D 5238 335
ASTM D 6194 336
ASTM E 84 327
ASTM E 108 ..... 335, 502, 582, 630, 640
ASTM E 136 ..... 241, 337
ASTM E 144 39
ASTM E 162 327
ASTM E 476 434
ASTM E 487 432
ASTM E 502 224-225
ASTM E 537 432
ASTM E 582 127
ASTM E 659 ..... 222, 920
ASTM E 681 ..... 125-126, 1060
ASTM E 698 431-432
ASTM E 771 434
ASTM E 789 172
ASTM E 793 ..... 431, 432
ASTM E 918 126
ASTM E 970 ..... 706, 707
ASTM E 1226 175
ASTM E 1231 432
ASTM E 1232 ..... 125, 175
ASTM E 1321 ..... 262-263, 311, 331-332, 818, 821, 853, 926, 963, 1072
ASTM E 1352 935
ASTM E 1353 936
ASTM E 1354 ..... 217, 249, 252-253, 260-262, 265, 268, 272-273, 290-291, 293-299, 304, 306, 309-311, 317, 326, **330-331**, 333, 338, 344, 725-726, 729, 731, 785, 787, 821-823, 830-832, 842, 854, 861, 883, 890, 896, 899, 906-909, 932-935, 939, 945, 947-949, 952-953, 962-965, 1070, 1072
ASTM E 1491 170
ASTM E 1515 ..... 17, 24, 126, 173
ASTM E 1623 333
ASTM E 1641 431
ASTM E 2019 170
ASTM E 2021 419
ASTM E 2058 332
ASTM E 2079 126
ASTM E 2187 930
ASTM F 400 869
ASTM G 72 627-628
ASTM G 74 627-628
ASTM G 86 628-629
ASTM G 124 628
ASTM G 125 629
ASTM PS 59 702
Atomization 124, 563
Attachment plugs 655, 657-658, 660, 755
Attics 629, 630, 707, 752
Audio equipment 740, 794, **918**, 926
Auger electron spectroscopy (*see* AES)
Autocatalytic reactions 34, 376, 386, 387, 393, 424,

429, 888
Autoignition 6, 10, 13, 16, 18-19, 36, 43, 45, **46-65**, 69, 88, 100, 104, 120, 123, 128, 147-149, 153, 170, 183, 186-187, 189, 191, 209, 212-213, 219-222, 238-239, 241-242, 248-249, 250-255, 266, 268, 275-281, 288, 292-294, 298-304, 311-312, 337, 364, 371, 404, 445, 521, 530, 616, 627-628, 690, 704-705, 711, 714, 716, 720, 725, 729, 807, 817, 821-823, 825, 832, 836, 841-842, 850, 858, 863, 869, 873, 875, 886, 895, 899, 904, 907, 909, 923, 927, 932, 934, 944-945, 946, 948, 949-950, 952, 954-955, 962-965, 967, 1023
Autoignition temperature 13, 16, 18-19, 43, 52, 104, 123, 128, 147-149, 153, 170, 183, 187, 212-213, 220, 222, 239, 241-242, 276, 303, 627-628, 704, 711, 714, 817, 836, 850, 904, 907, 923, 949, 954-955, 1023
Automatic Pressure Tracking Adiabatic Calorimeter (APTAC).....426
Automatic transmission fluid 21, 199, **696**, 882, 1056
Auto-oxidation 144
Available chlorine 891
Available energy of explosion 28
Avgas 697
Aviation fuels.....114, 198, 212, 217, **696-700**
Aviation gasoline 119, 209, 212, 690, 696-697, 699
Aviation hydraulic fluids 1059
Aviation lubricating oils 1059
Azides 446, 455, 457, 468-469, **700**, 884
Backdraft..... 617-618, 647
Back emf 547
Backfiring 881, 884
Bad-connection Test 336
Bagasse 312, 371, 399, 417, **700-701**, 962, 963
Bales 729, 846, 847, 859, 865, 911, 967, 968
Ball lightning 570-571
Ballasts..... 750-754
BAM 21, 149, 153-154, 156, 168, 170-172, 175-176, 459, 483-485, 639, 693, 813
BAM furnace (BAM oven) 153, 156, 171, 176, 637
Barium 168, 319, 353, 481, 813, **872**, 894, 902
Barium azide 810
Barium hydride 870
Barium nitrate 174, 472, 476, 526, 916
Bark 373, 396, 501, 503-504, 569, 729, 837, 843-844, 847, 965-966
Barley.....687
Barley grass..... 500, 841, 843-844
Basic density 942
Basis weight.....268, 317, 705, 732, 818, 821-822, 832, 920, 929, 933
Basswood.....1076
Bathrooms.....755
Batteries (*see* Electric batteries)
Beads..... 665-667, 670, 786, 795-803
Bed linens 560, 819
Beds 937-938
Beech 271, 286, 401, 402, 957, 1076
Beeswings 836
Belt rubbing 508
Benzaldehyde 452, 1024-1026
Benzene 110, 115, 117, 119, 198, 221, 224, 468, 507, 512, 525, 562-563, 713, 717, 808, 942, 962, 1024-1026
1,4-Benzenediamine 1024-1026
Benzene diammonium nitrate 468
Benzoic acid 1024-1026
Benzonitrile 1024-1026
Benzotrifluoride.....1024-1026
Benzoyl peroxide.....371, 448, 903
Benzyl alcohol 1024-1026
Benzyl benzoate.....1024-1026
Benzyl chloride.....1024-1026
Beryllium..... 72, 95, 355, 357, 512, 514, 550, **872**
Bicyclohexyl.....194, 1027-1029
BIFMA 935-936
Biot number.....378-383, 398, 409-410, 412, 419, 549, 894
Biphenyl 808, 1027-1029
Bis(2-chlorobenzoyl)peroxide 386-387
Bis(2-methoxyethyl)phthalate 45
Bismuth.....353, **872**
Bismuth salicylate.....1066
Bisphenylethynylanthracene.....481
Bitumen (*see* Asphalt)
Blackbutt.....947, 1076
Black Canyon powder 475
Black powder.....457, 459-460, 464, 470, 472-473, 475, 482, 641, 693, 809-810, **811**, 812-813, 846, 854, 914-918, 1066
Blacks 922
Blankets 560, 739, 743, 744, 779
Blasting agents.....474, 810
Blasting caps.....14, 459, 467, 472-474, 487-488, 571, 573, 692-693, 810
Blasting circuits 573
Blasting explosives 474
Blasting gelatin 459
Bleaching powder 891
BLEVEs..... 13, 524-525, **619-625**, 631-632, 641, 649, 867, 913
Blood 826, 860
Blue gum 1076
Boiler explosions 865
Boilers 14, 847, 858, 959
Boiling point.....15, 17, 27, 60, 73, 83, 86, 111, 114-115, 184-186, 191, 194, 196-197, 202, 207, 215, 354-355, 428, 449, 451, 466, 478, 540-541, 543, 547, 602, 623, 695, 697, 701, 704, 806, 844, 847, 867, 870, 875, 886, 923, 928, 1023
Bolted short 544, 746, 770-772, 778-779, 788
Bombing 455, 810, 914
Bonding 32, 591, 793, 852
Bone charcoal 1066
Bone meal 826, 1065
Book cases 521
Boot nails.....508, 513, 850
Borane 701

Boranes 452, 701, 894
Borax 320, 706, 707, 712
Boric acid 318, 319, 320, 706-707, 730, 929, 962
Boron 319, 354-355, **701-702**, 885, 923, 1063, 1065
Boron carbide 1066
Bottles 575
Bourdon gages 684
Bowls 575
Brake fluid 199, 210, **702**, 882, 892, 1056
Brake shoes 918
Brass 59, 87, 316, 419, 508, 510, 512-515, 546, 550-552, 558, 602, 614, 626, 685, 703-704, 711, 723, 753, 759, 761-763, 775, 777, 807, 844, 850, **872**, 896
Brass dross 1066
Brassieres 733
Break-flash Apparatus No. 3 ..... 100, 603
Breaking wires 70, 80
Break-spark 10, 70-73, 77, 80-81, 127, 546, 602-603
Brewing grains 687
Broken pipes 614
Bromobenzene 1027-1029
Bronze 514, 515, 685, 896, 1066
Brush discharge 555-556, 562, 690, 699
BS 3442 226
BS 3900 226
BS 4790 336
BS 5852 ..... 287, 519, 930-931, 934-937
Bubbles 207, 460-461, 518, 554, 565, 567, 594, 620, 622-624, 627, 694
Buchholz relays 768
Bulking discharge 556, 561-562
Bulldozers 918
Bullets, armor-piercing 621
Bullets, tracer 686
Buna-N rubber 627
Bunsen burner 35, 37, 286, 290, 322-323, 327-328, 433, 435, 507, **518-519**, 778, 820-821, 838, 928, 963
Buoyancy 64, 107, 116, 117, 403, 504, 525, 538, 539, 541, 544, 567, 610
Bureau of Mines 13, 21, 37, 45, 56-57, 60-62, 69, 76, 83, 116-117, 124-128, 146-148, 151, 156, 159-160, 170-174, 204, 221-223, 230, 322, 334-335, 401, 420, 435, 474-475, 484-486, 488-490, 495, 511-512, 514, 538-539, 596, 604, 619, 634, 688-689, 692-693, 717, 719-721, 723, 748, 806-807, 812, 862-863, 867, 870, 880, 928, 953, 986, 1023, 1062, 1065, 1086
Bureau of Mines 1.2 L furnace 171
Bureau of Mines flammability tube 124-125
Burlap 502, 730, 824, 826
Burning buildings 527-531
Burning forests and vegetation 531
Burning particles 74
Burning vehicles 532
Burning velocity 17, 35, 74, 79, 108, 121, 144, 731
Burn injury potential, from fabrics 819-821
Busbars 545, 769-772
1,3-Butadiene 620, 1027-1029
2,3-Butadione 1027-1029
Butanal 1027-1029
1-Butanamine 1027-1029
Butane 28, 31, 55, 56, 60, 62, 64, 89-90, 111, 119, 122, 216, 321, 447, 519-520, 524-525, 566, 594, 612-613, 619-620, 623, 686, 717, 818-819, 856, 866, 869, 882, 931, 936-937, 1027-1029
n-Butanol 194, 196, 199, 209, 1027-1029
2-Butanol 194, 1027-1029
sec-Butanol 194, 1027-1029
tert-Butanol 1027-1029
2-Butanone 1045-1047
2-Butenal 1030-1032
1-Butene 31, 119, 1027-1029
2-Butene 1027-1029
Butter 889
n-Butyl acetate 200, 1027-1029
sec-Butyl acetate 1027-1029
tert-Butyl acetate 903, 1027-1029
n-Butyl acrylate 1027-1029
Butyl amine 1027-1029
tert-Butyl amine 1027-1029
n-Butyl benzene 1027-1029
sec-Butyl benzene 1027-1029
tert-Butyl benzene 1027-1029
n-Butyl bromide 1027-1029
Butyl cellosolve 1027-1029
n-Butyl chloride 1027-1029
Butylene 119, 151, 717, 866, 1027-1029
Butyl ether 1027-1029
Butyl formate 1027-1029
n-Butyl glycidyl ether 1027-1029
Butyl glycol acetate 1036-1038
Butyl glycolate 1027-1029
tert-Butyl hydroperoxide 903
Butyllithium 869
Butyl mercaptan 1027-1029
Butyl methacrylate 1027-1029
tert-Butylperoxybenzoate 451
Butyl rubber 307, 628, 1071
Butyl stearate 1027-1029
p-tert-Butyltoluene 1027-1029
1-Butyne 1036-1038
2-Butyne 1033-1035
2-Butynedinitrile 1027-1029
Butyraldehyde 691, 1027-1029
Butyric acid 1027-1029
Butyrolactone 1027-1029
C4 explosive 55, 684, 810, 849, 986
Cacodyl 695
Cadmium 72-73, 83, 86, 168, 353, 512, 546, 550, 572, 602, **872**, 1063
Cadmium red 1066
Cadmium sulfide 1066
Cadmium sulfoselenide 1066
Cadmium zinc sulfide 1066
Calcined coke 713

Calcium....319, 353, 357-358, 481, 512, 526, 800, 802, 847, **872**, 886, 926, 953, 955
Calcium azide 810
Calcium borate 1066
Calcium carbonate 308, 758, 775, 780, 801, 878, 881, 915, 1066
Calcium chloride 758
Calcium citrate 1066
Calcium gluconate 1066
Calcium hypochlorite 371, 430, **891-894**
Calcium permanganate 452
Calcium resinate 702
Calcium silicate 331, 685, 716, 904, 905
Calcium stearate 515, 809
California TB 117 .....931, 936
California TB 603 938
Calorimeter tests 27-28, 422-425
Campers 532, 610
Campfires 503, 833
Camphene 1027-1029
Camphor 224, 472, 708, 709, 1027-1029
Camphor oil 1056
Camping fuel 613, 702
Candles 4, 326, 499, **702-704**, 860, 894, 931, 937
Canola oil 887, 1058
Canola oil (*see also* Rapeseed oil)
Canopy fuels 834
Canyons 630
Capacitance 70, 73, 79-80, 127, 163-164, 170, 280, 409, 467, 547, 548, 557-561, 592-593, 601, 719, 743, 771, 812, 852, 924
Capacitors 80, 165, 738, 739, 769, 806, 924
Carbohydrates 729, 845
Carbon..... **359-364**
Carbon, activated 159, 160, 399, 417, **714**, 1066
Carbon black 103, 314, 597, 744, 910, **922**, 927, 1066
Carbon disulfide 31, 87, 100, 103-104, 111, 115, 119, 447, 508, 512, 562, 594, 599, **704**, 717, 903, 924, 1027-1029
Carbonization 312, 314, 362-363, 663-664, 671, 673, 710-711, 713, 756, 774-776, 779, 960
Carbonization of insulation 312-315, 663-664, 671, 673, 756, 774-775
Carbon monoxide 15, 31, **54**, 89, 119, 122, 328, 689, **704**, 894, 1027-1029
Carbon subnitride 31, 1027-1029
Carbon tetrachloride 123, 201, **894**
Carbonyl sulfide 1027-1029
Carborundum 511, 512, 898
Carboxylate ester hydraulic fluids 210
Carburetors 185, 881
Cardboard 250, 269, 286, 399, 502, 506, 522, 575, 696, 706, 710, 718, 728, 743, 750-751, 761, 828, 858, 869, 895, **898-900**, 915, 955
Card-gap tests 461, 484
Carnauba wax 1056
Carpets (*see* Floor coverings)
Casein 323, 826
Castings 454, 878
Castor oil 708, 828, 886, 889, 1056, 1066
Castor oil meal 1066
Castor pomace 826
Catalysts 34, 38-39, 84, 89, 105, 481, 695, 713, 743, 809, 827, 873, 884, 894, 897, 909, 912, 960
Catalytic combustion 8, 38, 810, 856
Catalytic converters 39, 84, 881, 882, 883, 884
Catalytic cracking 6
Catalytic heaters 91
Catalytic ignition 8, 38, **89-91**
Catechins 729
Cat fur 557
Cathode 313, 466, 534-537, 539, 540-541, 546, 547, 805
Cathode ray tubes 924
Cats 557
Cavitation 621, 622
Cellosolve acetate 1036-1038
Cell size (detonations) 122
Cellular glass 905
Celluloid 707-710
Cellulose ...242, 246, 253, 266-267, 275, 290, 300-303, 311, 318-319, 338, 700, **704-705**, 706-707, 729, 817, 899, 930, 942-943, 946, 954, 959, 961-962
Cellulose acetate 289, 559, 709, 710, 816, 823, 824, 907, 1064, 1067
Cellulose acetate butyrate 307, 559, 907, 1071
Cellulose insulation 317-319, 335, 419, 619, **705-707**, 752, 764, 962
Cellulose nitrate 288-289, 433-459, 475, 480, 488, 559, 582, **707-710**, 808-814, 816, 897, 885, 897-898, 907, 962, 1067, 1086
Cellulose triacetate 816, 823-824
Cellulube 220 1059
CENELEC 596
Cerium 205, 359, 509, 512, 513, 516, 870, **872**, 876
Cesium 358, 800, **873**
Cetane 46, 50, 208, 210, 216, 219, 1039-1041, 1056
Cetones 562
Chain reactions 7, 33-34, 47, 53, 59, 200, 469, 893
Chain-reaction explosions 20, 53
Chainsaws 596, 918
Char 8, 147, 237, 238, 244, 246, 255, 283, 287, 292, 309, 312-315, 317, 319, 322-323, 327, 359, 361-363, 414, 503, 520, 545, 569, 747, 759, 774, 795, 802, 816, 825, 861, 898, 919, 929, 936, 938, 943, 951, 955-957, 959, 962
Charcoal 143, 159, 184, 241, 316, 353, 370, 372-374, 405, 414, 417, 460, 475, 480-481, 597, 685, **710-714**, 721-722, 809, 811, 874, 894-896, 903, 916-917, 922, 943, 956-957, 1063, 1066, 1073
Charcoal, activated 405, 414, 417, **713-714**
Charcoal briquettes **712-713**, 957, 1073
Charcoal scrubbers 713
Charge relaxation 558, 563, 567

Charge separation 553, 554, 562
Charred materials 310
Charring 237, 244-245, 268, 271, 283, 285, 309-310, 313-315, 321, 335, 394, 399, 434, 485, 719, 730-731, 747, 749-750, 755, 760, 762, 764-765, 773, 779-781, 788, 790, 799, 802, 816, 846, 854-855, 858, 909, 915, 933, 943, 946, 951, 953, 956, 958-959, 961
Cheat grass 505, 837, 839
Chemical damage, to electrical insulation 793
Chemical decomposition tests 485
Chemical lighting devices 481
Chemical nature of fuel, effect of (*see* Molecular structure, effect of)
Chemical Reactivity Test 486
Chemiluminescence 96, 889
CHETAH program 446
Chimneys ... 4-5, 22, 395, 434, 570, 618, 624, **715**, 859, 905, 952, 967
Chlorate candles 894
Chloride of lime 891
Chlorine 16, 198, 200, 480, 620, 623, 799-802, 827, 875, **891**, 894-895
Chlorine fluoride 891
Chlorine monoxide 893
Chlorine pentafluoride 891
Chlorine trifluoride 452, 476, 891
Chloroacetaldehyde 1027-1029
Chloroacetylene 113, 686, 1027-1029
Chlorobenzene 1027, 1028, 1029
2-Chloro-2-butene 1027-1029
Chlorodifluoroethane 1027-1029, 1060
1-Chloro-1,1-difluoroethane 1027-1029, 1060
Chlorodifluoromethane 1060
1-Chloro-2,4-dinitrobenzene 1027-1029
2-Chloroethanol 1027-1029
Chloromethoxymethane 1027-1029
Chloroprene rubber 307, 1030-1032, 1071
2-Chloropropene 1030-1032
Chlorosilanes 920-921
Chlorotetrafluoroethane 1060
5-Chloro-1,2,3-thiadiazole 715-716
Chlorotrifluoroethylene 717, 809, 1030-1032
Chocolate candies 833
Chocolate drink 833
Christian Michelsen Research 128, 165, 175, 335
Christmas tree lights 238, 753
Christmas trees, artificial 716
Christmas trees, natural 838-839
Chromium 72, 221, 318, 514, 801-802, 827, 863, **873**, 888, 921, 1063
Cigar burning (fertilizers) 827
Cigarettes ... 10, 287, 316, 335, 499, 503, 518, 712, **716-719**, 729-730, 735, 815, 830, 833, 839, 851, 865, 899, 901, 921, 928-930, 934-935, 937-938
Cigarettes, safer 719, 930
Cigars 503, 716-717, 815, 928
Cinnamon 1064
Circuit boards 806
Circuit breaker panels (*see* Electric panelboards)
Circuit breakers 541, 604, 654, 737-739, **744-746**, 762, 766, 768-769, 774-775, 777-782, 786, 788, 795, 802, 806, 855, 923
Circuit topology, effect of 79-80, 163-166
Claddings (of houses) 455, 465, 629, 631, 764
Clapeyron equation 185-186, 201-202, 613
Class A brand 335-336
Class B brand 335-336, 640
Class C brand 335-336, 502, 640
Clausius-Clapeyron equation 185-186, 201-202, 613
Clay tiles 629-630
Clearance distance 314
Cleveland Hospital Clinic fire 709
Closed cup (flash point testing) 21, 196, 923
Closed vessels 215-217
Clothes irons **719**, 740-741, 794
Clover 687, 847
Club moss 153, 842
CMHR foams 21, 932, 934-935
CMI mechanical impact test 176
CO/ALR wiring devices 763, 765
CO_2 extinguishers 719
Coal 33, 66, 74, 102, 143-144, 146-147, 149-151, 154, 156-162, 164, 167-169, 174, 289, 316, 318, **360-364**, 371-374, 394, 396-402, 415-416, 420, 488, 507, 512-513, 515, 526, 596-597, 601, 711-712, **719-724**, 736, 748, 842, 860, 928, 939, 1056, 1063
Coal mines 70, 143, 151, 169, 371, 470, 473, 509, 603, 912
Coal mining machinery 509, 511
Coal pulverizers 724
Cobalt 319, 400, 625, 683, 808, 828, **873**, 875, 885, 888, 891, 895, 909-910, 912, 953, 1063
Cocoa 316, 401, 402, 403, 826, 833, 1064
Cocoa powder 401-403, 833
Cocoa shell meal 826
Coconut oil 886, 889, 897, 1056
Coconut waste 417
Cod liver oil 889, 1056
Coffee 373, 718, 725, 1064
Coffee, instant or powdered 515, 833
Coffeepots 725
Co-generation plants 726
Coke 316, 359, **360-364**, 399, 597, 710, 712-713, 1066
Coking 6
Cold work 389-390
Coleman fuel 1056
Collisions 507, 510, 517, 534, 719, 804, 881-882, 885, 923
Collodion cotton 811
Combines (farm machinery) 826
Combs 708
Combustible liquids 14-16, 183, 186, 193, 217, 224, 730, 806, 859
Combustion air 329, 734, 848, 882, 940

Composite materials..... 269, **725-726**
Composite propellants 475, 479
Compost.....374, 726
Compressed air systems..... 688-690, 890
Compression 36, 38, **64-65**, 124, 164, 219-220, 457, 460, 462, 466-467, 469, **517-518**, 546, 625-627, 684, 688-689, 807, 846, 883, 1069
Compression ignition.....64, 220, 466, 517, 518, 627, 689
Compressors.....6, 688-690, 755, 890, 918
Computer equipment..... 726-727
Computer monitors 326, 727, 741, 806, 918, 924, 926
Computer methods..... 11-12
Concentric tube tests.....46
Concrete.... 152-153, 218, 506, 508-509, 515-516, 568, 592, 613, 685, 704, 717, 750, 850, 858, 896, 902
Condensation 26, 190, 398, 399, 451, 567, 700, 711, 723, 846, 867
Condensation mists.....190
Condensation reactions.....683
Condensed phase.....27, 240, 449, 456, 476, 817
Conductance.....542, 746
Conductor clashing 841, 843-844
Conduits.....597, 670, 772, 773, 788, 794-795
Cone.....226-227, 327, 328, 381, 407, 518, 592, 723, 818, 916, 941
Cone Calorimeter..... 217, 249, 252-253, 260-262, 265, 268, 272-273, 290-291, 293-299, 304, 306, 309-311, 317, 326, **330-331**, 333, 338, 344, 725-726, 729, 731, 785, 787, 821-823, 830-832, 842, 854, 861, 883, 890, 896, 899, 906-909, 932-935, 939, 945, 947-949, 952-953, 962-965, 1070, 1072
Cone discharge.....556
Connections 314, 336, 549-553, 600, 731-732, 734, 738-739, 741-743, **755-765**, 766-767, 769, 772, 774, 782, 790-791, 885, 925-926, 928, 939
Contact arcs..... 546-548
Contact discharge.....467, 540
Contacts (*see* Electric contacts)
Contaminants or impurities..... 57, 102, 308, 312-315, 318-319, 361, 374, **400-401**, 472, 481-482, 548, 563-565, 625, 627, 684, 694, 701, 704, 714, 723, 758, 775, 791, 810, 816, 824, 863-864, 873, 876, 886, 891-892, 895, 902, 912, 920, 953, 960, 966
Continuously-stirred tank reactors.....449
Convective heating **277-281**, 288, 297-298, 320, 477, 520, 710, 823, 950, 954
Conveyor belts.....557, 558, **727**, 912, 919
Cooking appliances..... 727-729, 905
Cooking fats..... 886-887
Cooking pans 519, 886-887
Cookoff (explosives)..... 464-465, 474, 487, 917-918
Cool flames.....8, 14, 44, **45**, 54, 57-59, 64, 93, 105, 114, 222, 250, 300, 460, 806-807
Coolite.....481
COPALUM connectors.....765
Copper.... 59, 70, 72, 84, 86, 94-96, 209, 221, 313-314, 319, 334-336, 393, 400, 402, 409, 417, 472, 474-475, 487, 508, 510-514, 534, 536, 540-543, 545-552, 569, 593, 602, 625-626, 670, 695, 703, 744, 759, 760-767, 772-773, 775, 778-781, 787, 789-790, 793, 795-803, 805, 824, 827, 849-850, 855-856, 863, **873**, 879, 884-885, 888, 895, 901, 912, 917, 923, 1063, 1065-1066
Copper acetylide.....468, 684-685, 810
Copper azide.....700
Copper-beryllium alloys.....510, 513, 850
Copper particles.....843-844
Copra 687
Cord reels.....781, 794
Cordelan 816
Cordite 810
Cork 161, 164, 307, 318, 401-403, 407, **729**, 826, 830-831, 896, 1064
Corn 144, 516, 526, 687, 688, 728, 734, 735, 836, 886, 888-889, 1056
Corn dust 508, 515-516
Corn oil..... 728, 734, 886, 889, 1056
Cornstarch.....144-145, 147, 149, 152, 156, 161-163, 165, 168, 448, 826, 1064
Corona discharge.....82, 312, 553-555, 560, 562, 565-566, 569-570, 592, 625, 644, 699-700
Corrugated iron.....630
Corundum.....511, 825
Cosmic radiation.....534, 571
Cosmic rays 534, 571
Cotton...8, 227, 268-269, 289, 301, 304, 311, 314, 316-319, 321, 324-327, 335, 370, 372-373, 401, 410, 433-434, 452, 505-507, 560, 574-575, 614, 619, 708, 716, 718-719, **729-731**, 734, 736, 749, 764, 765, 779, 787-788, 795, 816-829, 842, 844, 856, 861, 868-869, 891, 903-904, 919, 926, 929-938, 1064, 1067, 1073
Cotton, absorbent.....729, 779, 819
Cotton batting 335, 729-730, 929-930, 933, 935, 937, 938
Cotton gins.....507, 688
Cotton linters 1064
Cottonseed meal 826
Cottonseed oil.....828, 886, 889, 1056
CPAI 84.....926
Crankcase explosions 730-731
Crazing 404
Creamer, non-dairy.....515
Creep 549, 756, 763, 789-790, 843, 855
Creepage distance.....314
Creosote.....715, 1056
Crepe rubber.....911
m-Cresol 1030-1032
o-Cresol 1030-1032
Cribs (wood piles) ...335, 518, 521, **523-524**, 527, 617, 931, 951
Crimping.....756, 765, 857
Critical ambient temperature ...370, 375, 381, 400, 425-426, 893, 965
Critical diameter 68, 188, 470-472, 481, 692-693, 695, 814, 833

Critical flux.....217-218, 260, 265, 291-292, 706, 726, 950, 962
Critical stacking temperature.....370, 375, 426
Crossing-point methods.....414-417
Crown fires.....504, 834, 835-840
Crude oil.....197, 217-218, 524, 562, **731**, 865-866, 1056
Crude oil tankers.....865
Crystal growth.....457, 469
CS 191-53.....321, 815, 818-819, 824, 936
CSA C22.2 No. 950.....326
ČSN 64 0149.....337
CTI ratings (UL).....334
Cu_2O breeding process.....550-551, 643
Cube.....213, 318, 370, 379-381, 388-389, 403, 406, 408-409, 411-413, 415-418, 421, 511, 713-714, 779, 809, 828-829, 876, 893, 899, 904, 911-912, 919, 957-958, 963, 966, 968, 1062
Cumene.....200, 1030-1032
Cupric azide.....810
Cupric oxide.....1066
Curling irons.....**731**, 740, 794
Curtains.....265, 310, 322, 527, 571, 630, **731-732**, 821
Cutting oil.....205, 1056
Cyanamide.....826, 1030-1032
Cyanogen.....1030-1032
Cyanogen chloride.....1030-1032
Cyanuric triazide.....810
Cyclobutane.....1030-1032
Cycloheptane.....1030-1032
Cyclohexadiene.....863
Cyclohexane.....28, 62, 115, 122, 193, 562, 619, 623, 717, 1030-1032
Cyclohexanol.....1030-1032
Cyclohexanone.....903, 1030-1032
Cyclohexanone peroxide.....903
Cyclohexene.....1030-1032
Cyclohexene oxide.....1030-1032
Cyclohexylacetate.....1030-1032
Cyclones.....596
Cyclonite.....454, 810
1,3-Cyclopentadiene.....863, 1030-1032
Cyclopentane.....1030-1032
Cyclopropane.....119, 597, 717, 1030-1032
Cyclotetramethylene tetramine.....1039-1041
Cyclotol.....809, 814
Cyclotrimethylene trinitramine.....455, 1051-1053
Cylinder, hollow.....403
Cylinder, infinite.....52, 285, 378-381, 383, 388-391, 395, 894
p-Cymene.....1030-1032
D 495 ratings (UL).....334
DADNPh.....808, 811
Damages from gas explosions.....614-615, 646
Damköhler number.....92, 278, 379
Dart leader.....568
DDNP.....472, 808
Decaborane.....1030-1032
Decabromodiphenylether.....310
Decahydronaphthalene.....46
n-Decaldehyde.....1030-1032
Decalin.....194, 1030-1032
1-Decanal.....1030-1032
Decane.....46, 58, 85, 109, 114, 120, 188, 190, 194-195, 208, 246-248, 1030-1032
1-Decanol.....1030-1032
Decayed materials.....837, 842, **954-955**
Decene.....1030-1032
Decomposition temperature.....814, 827, 906
Deflagration.....14-15, 17, 37-38, 121, 404, 449-450, 459, 461, 469-471, 595, 619, 684-685, 851, 917, 920
DEGDN.....1030-1032
Dehydrochlorination.....758
Delichatsios' procedure.....265
Dendrites.....553, 798, 805
Denim.....502, 574, 819, 822, 824
Denitration.....708
Density.....150, 318, 358, 362-363, 377, 394, 400, 407, **408**, 410-411, 692-693, 695, 704, 706-707, 723, 729, 730, 735, 839-840, 854, 900-901, 930, 942, 947, 950, 953, 955, 962
Depressurization.....621-622, 624
Deradiation.....290
Derivatization.....734
Desensitizers.....472, 474
Detergents.....732, 734, 921, 1065
Detonating fuses.....472
Detonation.....14, 17, 28, 32, 36, 37-38, 44, 121-123, 152, 404, 446, 452, 454, 456-457, 459-461, 465, 469-474, 482-483, 487-488, 571, 574, 594-596, 619, 683-685, 689, 692-693, 695, 708-709, 808, 814, 850, 880, 917, 920-921
Detonation induction distance.....121
Detonation limits.....122-123
Detonators.....18, 469, 472, 474, 484, 571, 812
Deuterium.....1030-1032
Devitrification.....751
Dewar tests.....420-421, 429
Dextrin.....482, 916, 1065
Dextron IIE.....1056
Dextrose.....826
Dezincification.....762
Diacetate.....159, 821
Diacetone alcohol.....1030-1032
Diacetyl.....1027-1029
3,5-Diacetylamine 2,4,6-tri-iodo benzoic acid.....1066
Diaminostilbene disulfonic acid.....1066
Diapers.....**732**, 735
Diathermancy.....255-256, 277, 306-307, 478, 479, 899, 942
Diatomaceous earth.....485, 685, 692-693, 827
Diazobenzene perchlorate.....468
Diborane.....701, 1030-1032
Dibromoacetylene.....686
Dichlor.....894
Dichlorine oxide.....893

1,2-Dichlorobenzene 1030-1032
Dichlorodimethylsilane 1030, 1031, 1032
1,1-Dichloroethane 454, 864, 1036-1038
1,2-Dichloroethane 1036-1038
1,2-Dichloroethylene 1030-1032
2,2-Dichloroethyl ether 1030-1032
1,1-Dichloro-1-fluoroethane 1060
1,1-Dichloro-1-nitroethane 1030-1032
1,3-Dichloropropene 1030-1032
Dichlorosilane 920, 1030-1032
1,2-Dichloro-1,1,2-trifluoroethane 1060
2,2-Dichloro-1,1,1-trifluoroethane 1060
Dicyandiamide 475, 1066
Dicyclopentadiene 1030-1032
Dielectric strength 535-536, 556, 771, 777, 793, 805
Dielectric unions (for gas piping) 666, 782
Diesel engines 505, 806
Diesel fuel 218, **732**, 1056-1057
1,1-Diethoxyethane 1024-1026
Diethylamine 1030-1032
2-Diethylaminoethanol 1030-1032
2,6-Diethyl aniline 1030-1032
p-Diethyl benzene 1030-1032
Diethyl carbonate 1030-1032
Diethylcyclohexane 1030-1032
Diethyl dichlorosilane 1033-1035
Diethylene glycol monobutyl ether 1033-1035
Diethylene glycol monoethyl ether 1033-1035
Diethylene glycol monomethyl ether 1033-1035
Diethyleneglycol dinitrate 808, 1030-1032
Diethyl ether 45, 59, 86-87, 94-95, 100, 103-104, 115, 119, 208-209, 220, 511-512, 563, 594, 597, 620, 717, **806-807**, 915, 1033-1035
Diethyl ketone 1033-1035
Diethyl oxalate 1033-1035
3,3-Diethyl pentane 1033-1035
Diethyl sulfate 1033-1035
Diethylzinc 869
Diffusion of flammable vapors 612-614
1,1-Difluoroethane 1060
1,2-Difluoroethane 1060
Difluoromethane 1060
Digitalis lanata leaf 1066
Dihydropyran 1033-1035
3,4-Dihydro-2H-pyran 1033-1035
Diisobutyl ketone 1033-1035
Diisobutylcarbinol 1033-1035
Diisobutylene 1033-1035
Diisopropylamine 1033-1035
Diisopropyl ether 1042-1044
Diketene 447, 1033-1035
Diluents 28, 31, 75-76, 82, 111, 118-119, 124, 167-169, 300, 850
1,1-Dimethoxyethane 1033-1035
1,2-Dimethoxyethane 1033-1035
Dimethoxymethane 87, 1033-1035
Dimethyl acetylene 1033-1035
Dimethylamine 809, 1033-1035
n,*n*-Dimethyl aniline 1033-1035
2,2-Dimethylbutane 1033-1035
2,3-Dimethylbutane 1033-1035
Dimethyl decalin 1033-1035
Dimethyl-dinitrobutane 454
Dimethyl ether 31, 101, 686, 717, 807, 1045-1047
n,*n*-Dimethylformamide 1033-1035
1,1-Dimethylhydrazine 476
2,3-Dimethylpentane 1033-1035
2,2-Dimethylpropane 1033-1035
Dimethylsilicone 1073
Dimethyl sulfate 1033-1035
Dimethyl sulfide 1033-1035
Dimethyl sulfoxide 452, 1033-1035
DINA 429, 461, 808, 814
Dinitrobenzamide 1066
Dinitrobenzoic acid 1066
Dinitrodiethyloxamide 810
Dinitronaphthalene 811
Dinitrosopentamethylenetetramine 732
Dinitro-*sym*-diphenylurea 1066
Dinitrotoluamide 1066
2,4-Dinitrotoluene 1033-1035
Dioxane 101, 562-563, 717, 806, 1033-1035
p-Dioxane 101, 562-563, 717, 806, 1033-1035
1,4 Dioxane 101, 562-563, 717, 806, 1033-1035
Dipentene 1042-1044
Diphenylamine 458, 708
2-Diphenylamine 1033-1035
4-Diphenylamine 1033-1035
Diphenyl ether 1048-1050
Diphenyl methane 1033-1035
Diphosphine 903, 1033-1035
DIPPR 111-112, 198
n-Dipropylamine 1033-1035
Dipropylene glycol monomethyl ether 1033-1035
Dipropyl ether 1051, 1052, 1053
Direct-reduced iron 874
Dishwashers 5, **732**, 740, 762, 864
Dissociation 31, 353-355, 537, 539, 554, 791
Dissolved acetylene 566, 685-686
Disulfur dichloride 1033-1035
Di-*tert*-butyl ether 1033-1035
Divinyl ether 45, 1033-1035
DNP 808, 811
DNT 808, 811, 1033-1035
Döbereiner's lamp 38, 638
n-Dodecane 46, 190, 1033-1035
Dodecene 1033-1035
Double bonds 62, 313, 807, 887, 888, 889, 912
Double-base powder 475
Double-base propellants 475, 478-479
Double-layer charging 553, 557
Douglas fir 250, 292, 311, 574, 838-840, 948, 952, 954, 957-959, 964-966, 1076
Dow Corning 400 1059

Dow Corning 500 1059
Dow Corning 550 1059
Downconductors....592
Drain systems 700
Drop-hammer tests 457, 461-462, 466, 483, 640, 812
Dropped objects, as ignition mechanism 517
Drops, ignition of.... 187-192, 202-213
Drums, shipping 558, 563, 693, 695, 743, 892-894, 899, 910
Dryers, clothes....91, 651, **732-734**, 740, 911
Dryers, process 734-735
Dry-tracking 313
DSC ... 21, 338, 423, 425-432, 447, 458, 582, 888, 913, 959
DTA 21, 241, 301, 311, 338, 416, 427, 429, 431, 432, 693, 694, 817, 911, 915, 959, 962
DTBP....1030-1032
Duff 316, 569, 834, 836-837, 839-840
Dung....735
Dust clouds 142-176
Dust explosions **142-181**, 515, 526, 600, 637, **735-736**
Dust layers..... 143, 276, 316, 318, 320, 334, 358, 382, **401-402**, 418-419, 435, 516, 723, **735-736**, 901, 925
Dyes 307, **896-898**, 919, 966
Dynamite 454-455, 459, 474, 693
Dysprosium....876
Earthquakes 737
Easter grasses....920
Eaves 529, 630, 631, 854
ECMA-287 926
Eddy currents....571-572, 767
EDNA....488, 808, 810, 1036-1038
Effective heat of combustion....28, 291-292, 939
EGDN....456, 810
Egg albumen....826
EGME....1027-1029
Eicosane....1033-1035
Elastomers 241, 299, 773, **909-912**, 921, 927, 1067-1072, 1074-1075
Electrical breakdown 16, 534
Electrical breakdown (*see al*so Dielectric strength)
Electrical conductivity..... 84, 310, 554, 558, 562, 759, 787
Electrical conductivity of liquids....562
Electrical heating....39, 402, 449
Electrical heating (*see also* Heaters, electric)
Electrical insulators 553, 791, 806, 851
Electrical pruning 841
Electric appliances....728, 737, 740, 905, 918
Electric arcs 13, 19, 86, 175, 227, 313, 335, 466, 499, 507, 534, **540-548**, 571, 599, 601, 732, 747, 757, 773-774, 795, 823, 844, 854, 857, 861, 910, 941
Electric arcs: arc current..... 541-577, 745-746, 770-772
Electric arcs: arc power 542, 544-545, 772
Electric arcs: arc voltage..... 542-548, 770-772
Electric batteries 687, 739, **742-743**, 804, 925
Electric batteries, adventitious....553
Electric batteries, lithium....743
Electric blankets 740, 743-744
Electric cables 310, 312, 327, 332, 334, 766, **773-806**, 849
Electric cables: insulated distribution cables..... 772
Electric circuit interruption devices....744-746
Electric conduits....772-773
Electric condulets 773
Electric contacts 65, **70-73**, 74, 80-81, 466, 540-541, 546-551, 603, 725, 733, 740, 742, 745-746, 754, 756, 758-759, 762-763, 766, 769, 781, 788, 790, 793, 795, 804, 855
Electric current 14, 84, 402, 472, 480, 499, 534, **548-553**, 571, 756, 762-763, 782, 849, 960
Electric equipment....740-741
Electric equipment (*see also* specific equipment)
Electric fences 746
Electric heaters (*see* Heaters, electric)
Electric lamps, arc discharge....750-752
Electric lamps, fluorescent 739, 752, 755
Electric lamps, halogen 749, 750
Electric lamps, incandescent 709, 747-749, 755
Electric lamps, mercury vapor....750
Electric lamps, sodium 750-752
Electric matches 482, 701
Electric mattress pads....744
Electric motors 755
Electric outlets.....10, 643, 655, 658-662, 731, 738-739, **755-766**, 774, 779, 787, 794, 926
Electric outlets, backwired 660, 759-765
Electric outlets, duplex....643, 658-662, 759-765
Electric plugs....653, 655-658, 660, **755-766**
Electric panelboards 654, 664, **769-772**
Electric service drops 772-773
Electric service entrance....772-773
Electric sparks 14, 65, 118, 126, 145, 153, 170, 172, 175, 205, 210, 225, 273, 293-295, 298, 311, 331, 334, 446, 466-467, 514-515, **537-540**, 554, 625, 685, 752, 807, 825, 875, 877, 885, 933, 935
Electric squibs 472, 476, 482
Electric statistics....737-740
Electric switchboards 769-772
Electric switches....766
Electric transformers 766-769
Electric transmission and distribution systems....766-773
Electric wires..... 4, 304, 310, 534, 552, 568-569, 706, 728, 738, **773-806**, 815, 924
Electric wires, fire melted 795-796
Electrified houses 666, 782
Electrodes....71, 79-83, 127, 165-166, 170, 176, 313, 334-335, 467, 486, 534-536, 540-543, 545, 551, 554-556, 560, 566, 572, 602, 699-700, 770, 773, 783, 793, 848, 861, 909, 941
Electrodes, flanged 68, 69, 82, 83, 127, 104, 1023
Electromagnetic waves....571-574
Electromigration....763
Electronic ballasts 755, 784
Electronic components 806
Electronic equipment..... 327, 336, 374, 593, 740-741, 783,

784, 923, 926
Electronic equipment (*see also* specific equipment)
Electron tunneling....763
Electron volt....534
Electrostatic charging of granular materials 561-562
Electrostatic charging of liquids 562-567
Electrostatic charging of persons and apparel.... 559-561
Electrostatic charging of solids 557-559
Electrostatic discharge 146, 152-53, 166, 466, 476, 539-540, 554-555, 559, 561, 563-566, 592, 719, 736, 915, 917, 923
Electrostatic eliminators....592
Electrostatic sensitivity of explosives 466-467, 476, 486
Elements, ignition of 352-364
Elevators, grain....736
Elovich kinetics....714
Embers 2, 6, 152, 237, 292, 503, 629, 630, 695, 835, 860, 882, 951, 961, 967
Embers (*see also* Ashes)
Emissive power.... 305, 523-527, 529-530, 710
Emulsions 189, 454, 474, 694, 890
EN 50281-1-2 420
Encapsulation....600
Enclosures....18, 44, 96, 310, 327, 572, 600-601, 603, 610, 612, 727, 740-741, 772, 807, 918, 925-926
Endothermic compounds 445, 447
Endothermic reactions 14, 694, 911
Energy fluence 274-275, 291, 461, 463-465, 471, 477-478, 482, 574, 705, 709, 813, 821-822, 952
Energy of detonation....28, 814
Energy of explosion 28, 453, 814
Engine nacelles 211-212
Engines 26, 39, 55, 64, 124, 209-213, 223, 505-506, 517, 537-538, 691, 695, 730-731, 802, 806, 815, 834, 843, 865, 867, 877, 881-884, 918
Engines, diesel 806
Enkatherm....816
Enthalpy ... 25-27, 30-31, 255, 354, 356, 358, 376, 427, 447, 450, 455
Epichlorohydrin 1033-1035
Epoxidation....912
Epoxy....167, 218, 300, 323, 475, 509, 690, 725-726, 766, 898, 1067, 1072-1073
Equicylinders 379-381, 391, 475, 730
Equivalence ratio **29-30**, 50, 56, 61, 75-77, 81, 85, 89, 107, 116, 124, 147-148, 163, 190-191, 203-204, 211, 250, 538, 616, 688-689, 818
Era chrome brown....1066
Era chrome green....1066
Erbium 876
Erythrosine lake 1066
ESCA 21, 799
Essential oils 887
Esterification....451, 707
Ethane 15, 31, 55, 60, 62-63, 69, 76, 91, 109, 119, 121-122, 328, 767, 809, 864, 866, 928, 1036-1038
1,2-Ethanediamine 1036-1038
Ethanethiol....1036-1038
Ethanol.... 31, 59, 94, 101, 115, 119, 120, 122, 194, 196, 209, 506, 512, 562, 713, 717, 824, 851, 1036-1038
Ethanolamine 1036, 1037, 1038
Ether extraction 734
Ethers.... 109, 221, 562, **806**, 1059, 1061
Ethoxy ethane 1036-1038
2-Ethoxyethanol....1036-1038
2-Ethoxyethyl acetate 1036-1038
Ethyl acetate 31, 113, 115, 717, 1036-1038
Ethyl acetoacetate....1036-1038
Ethyl acetylene 1036-1038
Ethyl acrylate....1036-1038
Ethyl alcohol (*see* Ethanol)
Ethylamine....1036-1038
Ethylbenzene 119, 1036-1038
Ethyl benzoate 1036-1038
Ethyl bromide 1036-1038
2-Ethyl-1-butanol....1036-1038
Ethyl butyl ketone....1036-1038
Ethyl cellosolve 1036-1038
Ethyl cellulose 161, 1067
Ethyl chloride 1036-1038
Ethyl cyclobutane 1036-1038
Ethyl cyclohexane....1036-1038
Ethyl cyclopentane 1036-1038
Ethylene....28, 31, 53, 60, 64, 75-76, 87, 89, 101, 103-104, 113, 119, 121-122, 447, 508, 511, 513-514, 525, 572, 599, 620, 623, 717, 767, **807**, 850, 863, 888, 1027-1029
Ethylene chlorohydrin 1027-1029
Ethylene diamine....1036-1038
Ethylene dichloride....119, 1036-1038
Ethylenedinitramine.... 1036, 1037, 1038
Ethylene glycol.....64, 199-200, 225, 594, 695, **807**, 856, 890, 1027-1029
Ethylene glycol monobutyl ether....200, 1027-1029
Ethylene glycol monobutyl ether acetate....1036-1038
Ethylenimine....1036-1038
Ethylene oxide 53, 60, 87, 113, 122, 403, 447, 597, 619-620, 717, 806, **807-810**, 905, 909, 913, 1036-1038
Ethylene-propylene rubber 757, 784, 1067
Ethyl ethoxyacetate....1036-1038
Ethyl formate 1036-1038
Ethyl glycol mononitrate 454
2-Ethylhexaldehyde....904, 1036-1038
2-Ethyl hexanol 1036-1038
2-Ethylhexyl acrylate....1036-1038
Ethylidene chloride....1036-1038
Ethyl lactate 1036-1038
Ethyl mercaptan....1036-1038
Ethyl methacrylate....1036-1038
N-Ethylmorpholine....1036-1038
1-Ethylnaphthalene....1036-1038
Ethyl nitrate 447, 811, 1036-1038
Ethyl nitrite....1036-1038

Ethyl propionate 1036-1038
Ethyl propyl ether 1036-1038
Ethyl *sec*-amyl ketone 1039-1041
Ethyl selenide 1039-1041
Ethyl silicate 1039-1041
Eucalyptus 503, 843, 847, 951, 961
Europium 876
EVA 21, 246, 784, 786, 907, 917
Exhaust ducts 733
Exhaust manifolds 209, 210, 806, 837, 883-884
Exhaust particles 499, **505-506**, 843, 918
Exhaust systems 596, 826, 883-884
Exothermic reactions 6, 9, 14-15, 19, **44-46**, 47, 282, 288, 315, 353, 357, 369, 371, 394, 431, 445, 451-452, 455, 468, 480, 683, 689, 694, 696, 705, 809, 826-827, 891, 897, 913, 922-923, 963
Exploding bridgewires 21, 86, 472, 571
Exploding wires 21, 86, 472, 571
Explosion limits 15, 17, 20, 105
Explosion severity 598
Explosionproof equipment 96, 149, 205, 597-601, 603-604, 807
Explosions 6, 10, 13-15, 17, 20, 22, 24, 28, 36-37, 43-44, 73, 78, 96-99, 105-107, 120-123, 128, 142-146, 150-151, 153, 159-162, 167, 173-177, 184, 193, 205-206, 209, 215, 217, 223, 249, 319, 359-360, 364, 377, 405-406, 420-421, 428, 435, 445, 448, 450-457, 459-460, 463-464, 466, 468, 470, 472-473, 482-483, 486-488, 509, 512, 515, 526, 553-554, 564, 573-574, 595-598, 600-602, 604, 609-610, 612, 614-615, 617-622, 627, 683-686, 688-695, 709-710, 719-721, 724, 726-727, 730-732, 736, 739, 742-743, 748-750, 752, 766-769, 772, 778, 782-783, 789, 804, 806-815, 826-827, 847-850, 853, 863-865, 871, 875-876, 880, 885-886, 891, 894-895, 902-903, 913-915, 917-918, 920-923, 927, 939
Explosions, damages from 614-615
Explosions, heterogeneous 449
Explosions, manhole 772
Explosions, physical 9, 14, 620, 767-768, 847, 927
Explosions, primary 128, 144, 146
Explosions, secondary 144, 146
Explosions in buildings 609-612, 646-647
Explosives, chemistry of 455-456
Explosive substances 28, 425, 429, **445-490**, 692, 808-815, 1062
Extension cords 666, 738-739, 761, 773, 776, 779, 780-782, 788, 790, 793-794, 883
Extinguishers 719
Extractives 942, 962, 964
Extremely insensitive detonating substances 484
Extrusions 454
Fabrics 15, 268, 280, 301, 304, 310, 315, 317, 321-322, 337, 373, 502, 520, 559, 575, 591, 719, 733, **815-826**, 856, 926, 928-931, 933, 934-938, 967
Factory Mutual tests 227, 264, 332-333
Faraday cage 593
FAR Bunsen Burner Test 328
Farm machinery 826
Fecal matter 735, 787
Feedstuffs 826
Felt 826
Ferric hydrate 689
Ferric oxide 480, 863, 865, 868
Ferrosilicon 452
Ferrous sulfate 865, 1066
Fertilizers 371, 435, 687, **826-827**
FF 3-71 322
FF 4-72 938
FF 5-74 322
Fiber saturation point 835
Fiberboard 269, 293, 312, 316, 328, 337, 399-400, 410-413, 446, 468, 619, 701, 754, 788, 830, 919, 945, 947, 950, 952, 955, 959-960, **962-964**, 1067, 1073
Fiberglass 21, 171, 314, 513, 690, 699, 725, 855, 909, 919-920, 929, 931, 956-957, 1073, 1076
Fiber-reinforced plastics (*see* Fiberglass)
Fibers 154, 308, 319, 397, 404, 434-435, 560, 597, 619, 685, 701, 708, 711, 719, 730, 788, 816, 817, 820-821, 823, 825, 827-828, 832, 873, 887, 904-905, 909, 919, 922, 929, 962, 968
Fibers covered with oil 827-829
Filling stations 851-853, 924
Filter paper 253, 329, 485, **704-705**, 729, 826, 870, 899, 930
Filters 563-565, 688, 699, 736, 848, 896-897, 917
Finishing agents (for fabrics) 825
Fir 836, 838-840, 842, 897, 952, 954, 1074
Fire **15**
Fireballs 154, 456, **524-527**, 533, 536, 570, 574, 614-617, 619-620, 622-623, 641, 648-649, 687, 824, 892, 917
Firebrands 74, 240, 499, **500-505**, 507, 528, 596, 629, 650, 735, 842-844, 857, 862, 872, 934, 950-952
Firecrackers 482, 855, 915-916
Firedamp 83
Fire enclosures 727, 925
Fire extinguishers, carbon dioxide 719
Fire extinguishers, dry chemical 562
Fire guards 596
Fire hoses 829
Fireplaces 507, 596, 715, 858, 940, 967
Fire point 15-16, 18, 183, 192, **193-194**, 195, 198-199, 219, 225, 239, 247, 301, 618, 696, 702, 704, 856, 862, 890, 913
Fire retardants, effect of 308-309, 905, 908-909, 952-953, 1067-1070, 1072, 1074-1075
Fire spread, probability 6, 529, 844-845
Fire tetrahedron 7
Fire triangle 6-7, 10, 24, 105
Fire whirl 504
First fire 482, 960
Fishmeal 687, 826, **829**
Fish oil 889, 1057
FIST Test 332

Flame 6, 8, 14-16, 32, 43-45, 64-66, 74, 77, 84, 96, 105, 108, 120-121, 144, 152, 172, 206, 208-209, 237-240, 242, 244, 248, 250, 253, 266, 272, 286-287, 289, 293, 305, 307, 315, 320, 322-323, 326, 328-329, 332, 369-370, 457, 464, 470, 473, 518-524, 527-530, 532-533, 538, 574, 595, 612, 615-618, 620, 624-625, 631, 642, 683-684, 702-703, 716, 724, 728, 730, 741, 774, 777, 779, 786, 794, 803, 806-807, 818-819, 829, 833, 835, 837, 839, 848-849, 860, 866, 882-885, 900, 903, 912, 926, 928, 931, 938, 940, 948, 950-952, 963
Flame acceleration 121, 154, 619
Flame arresters 44, 594-596, 604, 940
Flame cap 65
Flame-ignition tests 329
Flame kernel 18, 66-67, 70, 79, 81-83, 95, 104, 120, 127, 203, 250, 254, 538-539, 555
Flames, as an ignition mechanism 73-74, 286-287, 289, 518-532
Flame speed 35-36
Flame stretch 32, 67, 107, 117
Flame traps 594
Flame velocity 17, 107, 207, 595
Flammability limits 104-120, 145-148
Flammability limits (*see also* specific substances)
Flammable atmospheres..... 10, 73, 85-86, 96-97, 147, 470, 473, 510, 512, 517, 538, 546, 555, 561, 565-567, 572, 596-604, 625, 686, 719, 752, 807, 853, 898, 927
Flammable atmospheres, equipment for 596-604
Flammable liquids.... 4, 14-18, 116, 184-186, 200, 206, 215, 506, 515, 564, 565, 697, 728, 810, 815, 861, 864, 967
Flammable solids 15, 322
Flammable Solids Test 322
Flanges 82-83, 98-100, 128, 149, 558, 600-601
Flannel 304, 505, 824
Flares 472, 479, 482, 527, 726, 810, 916, 918
Flashback 79, 127, 594, 596, 685, 686
Flash fires 142, 208, 615, 619, 939
Flashing..... 8, 15, 193, 201, 215, 223, 239, 244, 247, 253, 287, 288, 290, 309, 575, 621, 805, 836, 874, 905, 925
Flashlights 743
Flashover (combustion) 16, 307, 529, 532, 534, 615-616, 766, 802, 841, 925, 934
Flashover (electrical) 16, 773
Flash point 14-17, 21, 110, 114-115, 183-184, 187-188, **192-202**, 205-206, 210, 212-218, 223-225, 239, 246-247, 301, 338, 506, 631, 691, 695-698, 702-704, 731-732, 850, 861-862, 865-887, 890, 897, 903-904, 909, 913, 915, 921-924, 927, 968, 1023
Flash powder 153, 810, 915-916
Flash vaporization 623
Flax 736, 827, 887
Flea foggers 686
Flexible couplings 690
Flexible intermediate bulk containers 556
Flexing 731, 789, 927
Flints (cigarette lighter)..... 509, 513, **872**
Floating neutral 782-783
Flock 154, 166
Floor area, effect on ignition probability 4
Floor buffers 829
Floor coverings 292, 507, 640, **829-831**, 950
Flour 153, 167-168, 482, 515, 526, 687, 833, 907, 916, 923, 1064
Flower pots 901
Flow rate 35, 63, 74, 96, 126, 143, 209, 211-212, 227, 248, 250, 297-298, 311, 359, 370, 397, 562, 611, 704, 723, 825, 849, 851, 853, 871, 876, 909, 951
Flow velocity 36, 59-60, 79, 85-86, 89, 93, 97-98, 207, 211, 213, 252, 278, 281, 294, 297, 299, 337, 359-360, 409, 418, 538, 542, 563-564, 567, 594-595, 610, 873, 951
Flue-pipe ignitions 960
Flueric ignition 518
Flues **715**, 846, 858
Fluidic ignition 518
Fluorine..... 16, 452, **891**, 902
Fluoroethane 1060
Flux-time product 259
Flying brands 74, 37, 335, 499-500, 615, 629, 835
Flying brands (*see also* Firebrands)
FM Fire Propagation Apparatus 264, 332
Foam rubber 911
Foams 21, 206, 271, 310, 316, 908, **909-912**, 928-929, 931-934, 936
Fodder 687, 847
Fog 535, 618, 961
Food blue 1 1066
Food red 9 1066
Food red 14 1066
Foodstuffs 833
Food yellow 3 1066
Food yellow 4 1066
Forced ignition..... 18, 65, 239, 451
Forest materials 833-847
Forests 503, 531, 569, 629, 840
Formaldehyde 45, 111, 755, 759, 897, 910, 1039-1041
Formic acid 1039-1041
Forward smolder 316, 317, 319, 951
Foundry blacking 1066
Fourier number 283
Foxfire 903
FR-1 Test 327
Fractional distillation 186, 847
Frank-Kamenetskii (F-K) theory 93, 358, **374-383**, 394, 403, 406, 428, 457, 723, 905, 909, 966
Frank-Kamenetskii, David..... 47, 374
Frank-Kamenetskii number 379
Freon..... 686, 876, 1027-1029
Freon 142b..... 1027-1029
Fretting 769
Friction 6, 15, 20, 74, 152-153, 322, 353, 457, 459-461, 466, 472, 476, 482, 484-485, 488, 499, **507-516**, 553-554, 560, 570, 625-626, 693, 695, 700, 716, 721, 727,

729, 733, 736-737, 745, 811-813, 826, 829, 834, 868, 870, 882, 884, 895-896, 900, 912-915, 921, 927, 941
Friction coefficient 508, 626
Friction sensitivity tests 484, 813
Froths 206
Frozen liquid droplets 206
Fruit cereal 833
Fuel-air explosives 619
Fuel ash, pulverized 1066
Fuel concentration, effect of 56-57, 73, 76-77, 154, 161, 191, 211, 215-216
Fuel exhaustion 268
Fuel oil 187, 194, 206, 218-219, 225, 565, 683, 692-694, **847**, 848, 890, 1057
Fuel tanks 215-217, 594, 690, 698-699, 848, 882
Fuel type, effect of (*see* Molecular structure)
Fundamental flame speed 17, 35
Fungal growth 774-775, 965
Fungicides 864
2-Furaldehyde 1039-1041
Furan 806, 1039-1041
2-Furanmethanol 1039-1041
Furfural 1039-1041
Furfuryl alcohol 891, 1039-1041
Furnaces 91, 156, 190, 277, 364, 739, **847-849**, 858, 862, 940
Furniture 269, 271, 287, 503, 519-521, 527, 615-616, 703, 719, 726, 728, 730-731, 751, 756, 790, 794, 817, 829, 849, 859, 905, 909, 912, 921, 928-938
Fuse cord 482
Fused-wire ignition 94-96
Fuses 95, 321, 738, **744**, 768, 769, 772, 790
Fuses, expulsion type 652, 768, 841
Fusible pellet 742
Fusible plugs 685
Fypro 824
Fyrquel 220 hydraulic fluid 1057
Gadolinium 876
Galling 896
Gamma rays 574
Garages 734, 882-883, 939
Garbage 726, 826, 867
Gardening equipment 596
Gas connectors (*see* Gas lines, flexible)
Gas lines, flexible 665, 671, 782
Gas discharge 524, 534, 540, 555, 573, 753
Gas discharge tubes 593
Gases 43-128
Gas explosions, damages from 614
Gas jets 91, 97, 461, 479, 519-520, 527, 614
Gas leaks 834, 848
Gas meters 849
Gas oil 206, 732, 865, 1057
Gasoline 8, 45, 55, 84, 106, 119-120, 184, 193, 199, 209-210, 215-216, 219, 221, 239, 453, 506-508, 515, 523, 525, 562, 594, 596-597, 612-613, 620, 631, 683, 690, 692, 696-697, 702, 717, 733, 748, 750, **849-853**, 856, 858, 860-861, 865-866, 882-884, 890, 892, 913, 915, 926, 939-940, 1057
Gasoline containers 851-852
Gasoline filling stations 852-853
Gasoline filling station tanks 853
Gasoline spills 219, 613, 940
Gasoline substitutes 851
Gas piping 609, 782, 849
Gas regulators 849
Gear oil 1057
Gel candles 704
Gels 454, 474
Generators 571, 603, 738, 739, 884, 885, 895, 918
Germanes 921
Gerstein anomaly 201-202
GFCI devices 671, **853**, 855-856
Gibbs free energy 217
GIRCFF 816-817
Glass 59, 66, 82-83, 87, 95, 124-127, 195, 205, 219, 221-222, 421, 433, 460, 472, 485, 513, 527-528, 520, **533-534**, 559, 565, 571, 575, 576, 618, 628-631, 691, 693-694, 702, 709, 745, 747-752, 754, 806, 809, 868, 886, 905, 913, 934
Glass, Pyrex 559
Glass jugs 575
Glass wool 881, 891
Gloves 592, 912
Glow 8, 16, 45, 54, 91, 160, 172, 205, 225, 249, 301, 315, 320, 336, 534, 537, 547-548, 550-552, 555, 570, 573, 705, 741, 748, 752, 754, 759, 785, 795, 816, 868-869, 872, 876, 903, 908, 946, 951
Glow discharge 534, 537, 547-548, 570, 573-754, 795
Glowing combustion 299, 315, 337, 353, 503, 504-505, 761, 816-817
Glowing connections (*see* Overheating electrical connections)
Glowing ignition 91, 238, 245, 278, 297-298, 302, **315**, 575, 674, 704, 710, 729, 816, 818, 837, 841, 843, 877-878, 945-946
Glowing nests 153, 403
Glow-Wire Flammability Index 741
Glow-Wire Ignition Test 327, 336
Glycerides 887
Glycerin 194, 452, 481, 814, 892, 1039-1041
Glycerol (*see* Glycerin)
Glycols 45, 808-809, 890, 904, 1061
Godbert-Greenwald furnace 153, 156, **170-171**, 176, 419, 435, 598, 638, 923
Gold 84, 94, 353, 512, 517, 546, 553, 846, 879, 916, 923
Golden powder 475
Grain 143, 152-153, 318-319, 405, 461-463, 470-471, 479, 480, 502, 508, 516, 687, 734-736, 748, 795, 796, 814, 883, 914, 942, 946-950, 958, 962, 1064, 1076
Grain dust 152-153, 405, 508, 735-736, 748, 1064
Grain elevators 736
Grain orientation 948-950
Grain size 463, 470-471, 479, 480, 814, 914

Grandcamp (steamship) 692
Granular materials... 143, 315, 369, 373, 398, 410, 451, 467, 474, 561, 562
Graphite 25, 86, 144, 146, 306, **359-360**, 526, 690, 765, 805, 809, 874, 909, 917, 1063, 1065-1066, 1073
Grass 298, 318, 502, 506, 574, 630, 735, 746, 834, 835-837, 839-840, 844, 847, 884, 897, 920, 926, 1064, 1073
Grasslands....531, 629
Grass seed 1064
Gravity 64, 89, 113, 116, 191, 304, 539, 617, 883
Great Hakodate Fire....501
Grills 739
Grinding 152-153, 175, 205, 360, 475, 508-509, 511-512, 514-516, 561, 739, 817, 825, 850, 875-876, 886, 898, 918, 922, 927
Grinding wheels....509, 512, 515-516, 825, 898
Ground fault circuit interrupters (*see* GFCI devices)
Ground faults 18, 604, 728, 738, 740, 770-771, **781-783**, 849
Grounding 10, 16, 18, 562, 565, 567, 591, 688, 719, 782, 783, 852, 855, 856
GRS rubber 911
Guanidine nitrate....1066
Guano, bat....1065
Gum arabic..... 868, 917-918
Guncotton 453, **707-710**, 808, 810-811
Gunny sacks....824
Gunpowder (*see* Black powder)
GWIT ratings (UL) 336
Gypsum wallboard.....269, 312, 764, 802, **853-854**, 1073
Gypsum wallboard, Type X....1073
Hafnium 359, 1063, 1065
HAI ratings (UL) 334
Hailstones 557
Hairdresser chemicals 854
Hair dryers 653, **731**, 739-740, 794
Hair 335, 571, 614, 756, 832, **854**, 861, 902, 905
Half-time....393, 405, 420
Halogenated hydrocarbons....562, 870
Halogenated substances 7, 108, 111, 118, 125-126, 157, 168, 193, 200-201, 237, 240-241, 308-309, 331, 447, 562, 686, 870, 874, 876, 920
Halogenation....451, 876
Halogen fluorides....891
Halogens 16, 27, 59, 74, 110, 118, 157, 200, 323, 747, 749-750, 871, 891, 935
Halons....118, 920
Hammerscale 1066
Hand tools....152, 508, 515
Hardboard 242, 286, 293, 295, 312, **962**, 1073-1074
Hardeners....897, 902
Hardening 404, 888
Harmonic distortion 783-784
Hart heat flux calorimeter 428
Hartmann apparatus 160, 172, 638, 898
Hartmann bomb (*see* Hartmann apparatus)
Harvesters....834
Hastelloy alloys 626
Hay 238, 241, 289, 369, 371-373, 390, 399, 446, 540, 687, 716, 718, **833-847**, 883, 885, 956
Haystacks....371, 398, 845-846, 956
HDPE....559
Heart rimu....1076
Heat Accumulation Storage Test 422
Heat cables....744, **854-856**
Heated tube tests....124
Heaters, catalytic 856
Heaters, electric 222, 643, 738, 794, **856-858**, 951
Heaters, portable....858
Heat exchangers....6
Heat flux 16
Heat flux calorimeter 428
Heat flux density....16
Heat guns 854
Heating elements 59, 171, 719, 733, 744, 754, 802, 837, 856-858, 922, 928
Heating equipment..... 6, 736, 739-740, **858-859**
Heat of combustion.....25-28, 30, 39, 67, 110, 147, 196-197, 204, 227, 248, 255, 291, 353-354, 356, 404, 453, 475, 500, 512, 519, 524, 619, 701, 710, 719, 723, 849, 860-861, 873, 900, 925, 941, 943, 1023
Heat of condensation 399
Heat of decomposition....15, 354, 447-449
Heat of detonation 28
Heat of explosion....28, 447, 456
Heat of formation.....25-27, 74, 354, 356, 358, 445, 447, 763, 1023
Heat of sorption 399, 721, 846
Heat release rate....21, 35, 121, 155, 227, 291-292, 309-310, 326, 328, 330, 332, 445, 449, 458, 466, 476, 504, 518-525, 537, 567, 616, 631, 700-701, 727, 733, 740, 809, 832, 835, 858, 861, 869, 883, 889, 895, 897, 904, 925, 933, 938, 941, 949, 952, 959, 961, 964
Heat tapes 740, 744, **854-856**
Heat tracing 856
Heat transfer liquids....856
Hemicellulose 704, 942, 946, 961-962
Hemp 373, 687, 816, 827, **867**, 929
Hempseed oil 371, 867, 887, 889
Henkin Test 487-488
Heptane..... 31, 46, 53, 61-63, 86, 87, 104, 115, 119, 188, 190-191, 194, 196, 203, 208-209, 562, 563, 717, 719, 1039-1041
1-Heptanol 1039-1041
2-Heptanone 1039-1041
3-Heptanone 1036-1038
1-Heptene 1039-1041
2-Heptene 1039-1041
1-Heptyne 1039-1041
Herring meal....1066
Heterogeneous explosions 449
Heterogeneous reactions..... 315, 358, 396, 449, 476, 683
Hexaborane....701

Hexadecane 46, 187-191, 1039-1041
Hexamethyldisilazane 562, 563, 1039-1041
Hexamethyldisiloxane 1039-1041
Hexamethylenetetramine 864
Hexamethylene triamine trinitrate 454
Hexamethylenetriperoxidediamine 455, 808
Hexamethylnitratodialuminate salts 452
Hexane 31, 43, 56, 57, 85, 86, 88, 90, 113, 115, 119, 120, 122, 194, 196, 220, 305, 525, 562, 702, 717, 856, 1039-1041
Hexanitrosobenzene 455, 808
Hexanol 195, 1039-1041
2-Hexanone 1042-1044
1,3,5-Hexatriyne 686
1-Hexene 31, 1039-1041
Hexyl 808, 811
Hexyl ether 1039-1041
HIFT Test 332
High-Current Arc Ignition Test 334
High explosives 454, 470, 473, 571, 619, 622, 810
High Flyer (steamship) 692, 693
High-limit switches 651-652, 725, 731, 733, **741-742**, 752, 754, 848, 856-858, 922
High-temperature accelerants (*see* Accelerants, high temperature)
High-Voltage Arc Resistance Test 334
High-Voltage Arc-Tracking-Rate Test 334
High voltage insulators 773
HIPS 309-310, 905, 926, 1069
HMX 394, 458-461, 464, 469, 517, 808-809, 811-815, 885, 1039-1041, 1062
HNAB 808, 1062
HNS 808, 1062
Hobnails 513
Holland Tunnel fire 704
Holmium 876
Homogeneous ignition 190, 360-362, 396
Homogeneous reactions 448
Honeycomb 329, 594, 690
Hops 673, **859**
Hoses 518, 565, 627, 686, 829, 881, 939
Hot bodies, as an ignition mechanism 287-289, 465-466, 499-516
Hot bolts (lightning) 569
Hot Flaming Oil Test 327
Hot gases, as an ignition mechanism 96-101, 154
Hotplate tests ... 393, 401, 409, **418-419**, 724, 730, 824, 872, 922, 958, 966
Hot rivet tests 336
Hot spots 390-391, 402-403
Hot surface ignition 43, 65, **83-94**, 102, 124, 148, 153, 184, 207-213, 288, 289, 354, 598, 599, 699, 807, 824, 829, 862, 871, 884, 886, 907, 913
Hot surfaces 6, 13, 43, 87-88, 142, 153, 183, 184, 207, 209, 213, 288, 317, 332, 500, 598, 723-724, 731, 736, 835, 955
Hot work 387-389, 413-414
Houghto-Safe 271 ..... 1055, 1059
Houses 501-502, 575, 611, 629-631, 686, 762, 781-782, 928, 934, 953
HSE 6, 21, 59, 87, 99, 100, 128, 154, 227, 572, 602, 685, 921, 1023
HSE 20 mL Sphere Test 128
Human skin 823, 861-862
Humans, combustion of 561, 859-861
Humans, electrostatic charging of 559
Humidity 21, **302-304**, 399, 535, 557, 559, 591, 735, 763, 811, 818, 843-845, 852, 867, 898, 902, 920, 943, 951, 965
HVAC equipment 862
HVAR ratings (UL) 334
HVTR ratings (UL) 334
HWI ratings (UL) 336
Hybrid explosions 143, 151-152
Hydraulic diameter 595
Hydraulic fluids 193, 210, 212, 226, 227, 826, **862**, **1059**
Hydrazine 447, 452, 454, 476, 811, **862-863**, 891, 1039-1041
Hydrazoic acid 459, 1039-1041
Hydrocarbon gases 863
Hydrogen 25-26, 28, 38, 43, 53-54, 61, 66, 69, 76, 78-82, 84-87, 89, 91, 94, 97, 99-100, 102-105, 110-111, 115, 118-122, 145, 149, 152, 198, 294, 311, 319, 328, 359-361, 462, 476, 508-511, 513, 525, 536, 539, 542, 558, 560-561, 572-573, 594, 597, 599, 612, 619, 620, 623, 685, 690-691, 710, 719, 726, 732, 742-743, 752, 754, 767-768, 791, 807, 811, 851, 856, **863-864**, 870-871, 874-876, 898, 900, 920, 922, 1039-1041
Hydrogen, explosions due to adventitious presence 864
Hydrogenation 451
Hydrogen bonding dilution effect 851
Hydrogen chloride 27, 452, 758, 762-763, 775, 792, 797
Hydrogen cyanide 1039-1041
Hydrogen peroxide 206, 447, 452, 481, 554, 863, 902
Hydrogen selenide 1039-1041
Hydrogen sulfide 31, 53, 111, 119, 717, 1039-1041
Hydrolysis 399, 451, 700, 708-710, 912, 953, 958
Hydrotreating 6
Hydroxylamine 864
Hydroxyl-terminated polybutadiene (HTPB) 278, 475
Hypalon 784, 787, 1067
Hypergolic reactions 16, 24, 254, 434-435, 452, 476-477, 489, 499, 891
ICAL test (*see* ASTM E 1623)
ICBO Urban-Wildland Interface Code 631
IC-rated lighting fixtures 752, 793
Ideal Gas Law 37, 52, 114
Ideal mixtures 199
IEC 60065 918
IEC 60079 ..... 128, 222, 536, 599-604
IEC 60112 ..... 24, 314, 334, 775
IEC 60216 792
IEC 60332-1 328
IEC 60332-2 328

IEC 60335-1 741
IEC 60587 333
IEC 60695-2-2 ..... 326, 336, 785, 908
IEC 60695-2-3 336
IEC 60695-2-11 741
IEC 60695-2-12 741
IEC 60695-2-13 ..... 336, 908
IEC 60695-11-10 ..... 323, 326
IEC 60695-11-20 ..... 323, 326
IEC 60950 ..... 326, 727, 926
IEC 61024 594
IEC 61241 ..... 175, 599
IEC 61241-2-3 175
IEC 707 336
IEC Groups 87, 599
IEC/PTB break-flash apparatus 70-71, 73, 100-101, 128, 149, 546, **602**, 603
IED 21, 455, 914
IEEE Std-1 792
IEEE Std-142 594
IEEE Std-579 784
IEEE Std-515 856
IEEE Std-1100 594
Ignitability 16
Ignitable 16
Ignitable liquids 14-16, 184, 187, 193, 239, 563, 683, 923
Ignite 16
Ignited 16
Igniters 118, 126, 146, 160, 172, 174, 333, 472, 476, 695, 701, 837
Igniters, pyrotechnic 118, 146, 147, 157, 160, 168, 169, 174, 175, 476, 1062
Ignition, multi-stage 63
Ignition, two-stage 57, 58, 64, 188, 250, 300, 899
Ignition sensitivity 598
Ignition sources 3, 7, 10-11, 13, 15, 17-19, 37, 65, 77, 98, 114, 116, 118, 121, 145-146, 148, 150, 152-154, 157, 160, 166, 170, 172, 174-175, 184-185, 192, 196, 202, 206, 213-214, 219, 225, 227, 237, 251, 268, 275-277, 286-287, 320-321, 326, 335, 337, 434, 452, 476, **498-576**, 611-613, 617, 619, 625, 627, 684, 686, 712, 716, 718, 735, 737, 740-741, 743, 747, 750-751, 755, 795, 806, 818, 826, 827, 829, 835, 838-839, 841, 850-853, 858-862, 867, 871, 876, 881, 910, 918, 924-926, 928, 930-931, 934-941, 951, 954, 1060-1062
Ignition switches (motor vehicle) 670, 804
Ignition temperature 13, 15-21, 43-46, 52, 56, 59-60, 64, 85-87, 89-91, 94, 97, 99, 152, 184, 186-187, 191, 206, 209, 211-213, 219-220, 222, 237, 240-249, 256, 259, 263, 274, 277, 279-280, 282-283, 288, 297, 301, 303, 308-309, 311, 317, 336-338, 353-354, 356-357, 359-364, 402, 455, 464, 478, 480-481, 518, 552, 598, 615, 626, 689, 693-695, 701-702, 704-705, 707, 709-711, 714, 720, 724, 730, 741, 747, 811, 816-818, 821, 824, 831-832, 835-837, 843, 847, 855, 858, 863, 868, 870-878, 880, 897, 898, 900-901, 903, 906-908, 914-915, 917, 921, 944-946, 952-955, 962-965, 1023, 1062, 1066, 1072
Ignition temperatures, multiple 45-46
Ignition time 17
Impact 3, 77, 152, 176, 211, 290, 310, 454, 457, **459-464**, 466, 470-472, 474, 476, 482-486, 489-499, 507-516, **517**, 565, 625-628, 695, 700, 709, 716, 724, 729, 748, 749, 811-813, 855, 870, 878, 884, 895-896, 903, 905-906, 914-915, 926, 1069, 1075
Impact angle 511
Impinging pilot 292, 786-787, 948
Improper alterations 738, 794
Improvised explosive devices 21, 455
Impurities (*see* Contaminants)
Incendiarism 4, 745, 765, 833, 848
Incendiary devices 765, 864
Incendiary fires 3, 683, 858, 881
Incendive 17, 70, 72-73, 80, 84, 97, 101-102, 153-154, 165, 508, 510-516, 534, 546, 548, 554-555, 558-560, 562, 564-567, 572, 600, 602-603, 625, 687, 698, 743, 746, 752, 807, 840, 852, 898, 919, 924
Incendivity 17, 72, 86, 153, 509, 511-516, 555, 562, 566, 572, 699, 844
Inconel alloys 59, 94, 514, 626, 627
Indigo carmine lake 1066
Inductance 70-73, 79-81, 165-166, 176, 547, 571, 601-603, 771, 1023
Induction 156, 166, 402, 553, 572
Induction period 43, 45, 47, 50, 59, 61, 63, 65, 69, 84, 87, 124, 187, 189, 213, 250, 282, 292, 392, 426, 432, 473, 488, 717, 871
Inerting 10, 106, 143, 169, 300, 398, 404, 565, 591
Information technology equipment 726-727, 926
Initiating devices 454, 473, 574, 902
Initiation 6-8, 13, 15, 17, 33, 68, 102, 319, 450, 457, 459-469, 472-473, 483-485, 487-488, 571, 574, 621, 624, 689, 692, 694, 733, 754, 758, 786, 790, 811, 813, 909, 914-915, 928, 963
Initiators 454, 473, 574, 902
Inks 708, 898
Insecticides 864
Insects 769, 787, 849
Insensitive munitions 446, 474
Insulating powders 555, 557, 562
Insulation, electrical (*see* Arcing across a carbonized path)
Insulation, in self-heating problems 398, 403-404, 707, 904-905
Insulation displacement outlets 761
Insulation failure 766-767, 790
Insulators, high-voltage 773
Interhalogens 714
Intermediate thickness solids 272-274, 303
Intermetallic reactions 480
Intermittent Break-flash Apparatus 71, 603
Intermolecular explosives 453
Intrinsically safe circuits 17
Intrinsically safe equipment 17, 597, 599-603

Intrinsically safe systems....601
Intumescent coatings....624
Inverse problem....242, 944
Iodine....452, 749, 833
Iodine number....433, 434, 867, 887-890, 913, 922, 928
Iodine value (*see* Iodine number)
Ionization....81, 83, 102, 165, 405, 534, 536, 547, 564, 754, 769, 774, 777
Ionizing radiation....468, 574
IP 33....226
IP 170....226
IP 303....224
IP 304....224
Iron or steel....37, 59, 72, 77, 82, 83-84, 86, 89, 94, 124, 126-127, 152-153, 165, 172-174, 205, 209-211, 216, 218, 221-223, 227, 288, 321, 330-331, 333-335, 337, 353, 373, 400, 406, 419, 433-435, 460, 472, 474-475, 483-484, 486-489, 506-517, 514, 516, 519, 525, 530, 536, 541, 546, 550, 552-553, 564, 572, 598, 602, 615, 620-621, 624-629, 631, 683, 685-686, 688-689, 693-695, 710-711, 729-730, 732, 743, 749, 759, 763-764, 767, 772-773, 775, 779, 782, 790, 794-795, 801-802, 815, 825, 828, 830-831, 837, 844, 850, 857-858, 863-864, **873-874**, 875, 877, 879, 885, 888, 890-893, 894-896, 898, 901, 910, 912, 916, 918-919, 922-923, 927, 941, 953, 960, 966, 968, 1063, 1065
Iron oxide....102-103, 328-329, 400, 480, 506, 509, 510, 512-514, 516, 572, 684-685, 688-691, 704, 720, 745, 809, 863, 865, 888, 892, 895, 898, 902, 921, 927, 960
Iron pentacarbonyl....329, 870
Iron pyrite....396, 400, 512, 514, 811, 864-865
Ironstone....510
Iron sulfides....396, 400, 512, 514, 811, **864-865**
ISA RP12.4....603
ISA S12.12....603
ISA S12.16....603
Isentropic compression....517
Isentropic expansion....622
ISO 871....337
ISO 1210....323
ISO 1516....226
ISO 1523....226
ISO 2678....333
ISO 3679....226
ISO 3680....226
ISO 3795....328
ISO 5657....269, 270, 272, 293-298, 311, 330-331, 729, 732, 785, 832, 841-842, 908-910, 933, 948, 949
ISO 5660 (*see* Cone Calorimeter)
ISO 6184-1....175
ISO 9772....323, 326
ISO 9773....323, 326
ISO 10351....323
ISO 11358-2....429
ISO 11925-2....328, 329, 950, 963
ISO 12097-3....885
ISO 15029....226-227
Isoamyl acetate....1039-1041
Isoamyl alcohol....215, 1039-1041
Isoamyl chloride....1039-1041
Isoamylene oxide....1039-1041
Isoamyl formate....1039-1041
Isobutane....119, 611, 686, 919, 1039-1041
Isobutyl acetate....1039-1041
Isobutyl acrylate....1039-1041
Isobutyl alcohol....197, 1039-1041
Isobutylbenzene....1039-1041
Isobutyl chloride....1039-1041
Isobutylene....119, 307, 1039-1041, 1071
Isobutyl formate....119, 1039-1041
Isobutyl methacrylate....1039-1041
Isobutyraldehyde....1039-1041
Isobutyric acid....1039-1041
Isobutyronitrile....1039-1041
Isocrotyl bromide....1039-1041
Isocrotyl chloride....1039-1041
Isodecaldehyde....1042-1044
Isomerization....8, 197, 373, 376, 448, 451, 808
Iso-octaldehyde....1042-1044
Iso-octane....31, 55, 189, 209, 1042-1044
Iso-octyl alcohol....1042-1044
Isoparaffinic solvent....683, 1057
Isopentane....119, 1042-1044
Isopentanol....1039-1041
Isoperibolic....406, 423
Isophorone....1042-1044
Isoprene....307, 911, 1042-1044, 1071
Iso-propanol (*see* Isopropyl alcohol)
Isopropenyl acetate....1042-1044
Isopropyl acetate....1042-1044
Isopropylacetone....1042-1044
Isopropyl alcohol....221, 562, 717, 1048-1050
Isopropylamine....1042-1044
Isopropyl benzene....1030-1032
2-Isopropyl bicyclohexyl....1042-1044
2-Isopropyl biphenyl....1042-1044
Isopropyl chloride....1042-1044
Isopropyl ether....1042-1044
Isopropyl glycidyl ether....1042-1044
Isopropyl mercaptan....1042-1044
Isopropyl nitrate....101, 454, 1042-1044
Isopropyl nitrite....1042-1044
Isothermal calorimeter....422
Isothermal Storage Test....432
Jack o' lantern....903
Janssens' procedure....260-262
Jentzsch tester....220-221, 836
Jerry cans....851-852
Jet A fuel....193, 202, 211, 562, 695-698, 1056
Jet A-1 fuel....695, 697
Jet B fuel....211, 696-697, 1056
Jet flames....520, 524
Journal boxes....918

JP-1 fuel 211, 696, 698, 1056, 1058
JP-3 fuel 119, 696, 1056
JP-4 fuel 119-120, 196, 211-214, 223, 515, 522-523, 690, 696-699, 1056
JP-5 fuel 188, 196, 212, 213, 217, 690, 696-699, 1056
JP-6 fuel 88, 194, 697, 1056
JP-7 fuel 696, 1056
JP-8 fuel 223, 522, 695-698, 1056
JP-9 fuel 1058
JP-10 fuel 1058
Jump starting 742
Juniper 735, 955
Jute 241, 397, 400, 828, 832, **865**
Kaolin 692, 916-917
Kapton 805
Kerosene 3, 58, 62, 184, 199, 201, 204-207, 209, 215, 218, 223, 226, 476, 506, 515, 523, 525, 562-563, 565-566, 613, 624, 631, 683, 696-697, 732, 858, **865**, 866, 876, 1057
Kerosene heaters 865-866
Ketron 1000 1075
Kevlar 269, 326, 690, 822-824, 932, 934, 1073
Kitchens 519, 755
Kleinbrenner Test 329, 519
Knob-and-tube wiring 781
Knock (in engines) 55, 64, 185, 850
Koenen/BAM Friction Sensitivity Test 466, 483-484
Kohjin 816
Kraft paper 712, 826, 898-900
Krakatoa 14
Kühner, Adolph (equipment makers) 176
Kynol 816, 820, 822, 824
Lacquer diluent 1057
Lacquers 482, 508, 710, 897
Lagging (*see* Pipe insulation)
Lambswool pads, imitation 866
Laminar flame speed 35, 67-68, 74-75, 122, 196
Lampblack 373, 826, 896, 897, 903, **922**, 1063, 1066
Lampholders 753-754
Lamps (*see* Electric lamps)
Landfills 726
Langmuir-Hinshelwood kinetics 361
Lanthanum 509, 870, 876
Lard 886, 889
Lard oil 889, 1057
Lasers 86, **101-104**, 146, 154, 218, 242, **275-277**, 290, 300, 305, 362-363, 465, 478-479, 536, 571, 627, 813, 875, 941, 950
Last strand problem 667, 788
Latex foam 316, 336, 619, 830, 904, 911, 929, 931, 933, 937-938, 1067
Lattice looseness 481
Lauan plywood 519
Laundries 560, 733-734, 824
Lauroyl peroxide 903
Lawn mowers 866
Layer ignition temperature 21, 401, 418, 435, 598, 599, 730, 875, 876, 1062
Lead 353, 742, 870, **874**, 889
Lead azide 448, 454-455, 459, 461, 467, 468, 472, 484, 488, 700, 810-814
Lead chromate 897, 917
Lead dichromate 897
Lead phosphate 1066
Lead picrate 811, 814
Lead styphnate 454, 472, 808, 810-813
Lead zirconate titanate 1066
Leathers 921
Le Chatelier's Law 111, 151, 199
Leidenfrost temperature 207-208
Lenses 575
Lexan 9034 1075
Lichtenberg discharge 554, 556-557
LIFT Test (*see* ASTM E 1321)
Light bulbs (*see* Lamps)
Light energy 32, 457, 468-469, **575-576**
Lighters 5, 702, 718, 815, 867, 869, 937, 1057
Lighting fixtures 738, 740, **746-755**, 753-775, 784, 793-794
Lightning 4-5, 13, 468, 554, 557, **567-571**, 576, 592-594, 644-646, 690, 736, 740, 766, 775, 782, 833-834, 840, 842
Lightning arresters 593
Lightning flash 568-569
Lightning-like discharge 554, 557
Lightning protection 576, 592-594
Lightning rods 13, 569, 592-593
Lightning strike 568-569, 592-593, 690, 782, 840
Lignin 704, 729, 826, 942, 946, 954, 957, 961-962
Lime 749, **866**, 901
Limit flame temperature 31, 97, 145, 291, 338
Limonene 1042-1044
Line thermals 504
Linoleic acid 887-888
Linolenic acid 887
Linoleum 830-831
Linseed oil 370, 373, 397, 401, 827-828, 867, **886-889**, 897, 966, 1057
Lint traps 733-734
Liquefied natural gas (*see* LNG)
Liquefied petroleum gas (*see* LPG)
Liquid-liquid reactions 449
Liquids 183-227
Liquids, self-heating in 402, 448-451
Lithium 353, 358, 446, 743, 871, **874**, 886, 902
Lithium aluminum hydride 870
Lithium batteries (*see* Electric batteries, lithium)
Lithium hydride 870
LNG 523, **866-867**, 880, 913
Local ignition 518, 617, 690, 925
Locomotives 505, 596
Locust wood 836
Long arcs 540, 543-544, 778
Long-term radiant exposures 312

Lower explosive limit 21
Lower flammability limit 17, 21, 44, 105-106, 111, 114, 145, 148, 170, 199, 1023
Lower flammability limit (*see also* specific substances)
Lower temperature limit 21, 114, 125, 697, 698, 1023
Low explosives 453-454
LOX 454, 476, 626, 629, **895-896**
LPG 4-6, 63, 508, 523, 620, 623-624, **866-867**, 880, 913, 941, 1057
Lubricant sprays 687
Lubricating oils 45, 193, 209, 223, 515, 688-690, 731-732, 890, 1057, 1059
Lucite 308, 1068
Lugs 769, 772
Luminaires 746, 752
Lumped-capacitance model 420
Lutetium 876
Luxembourg report 226
Lycopodium 153, 158, 164-165, 167, 170, 173, 316, 419, 1064
Mackey Test 400, **433-434**, 734, 828, 865, 889, 912
Macracarpa wood 1076
Magnesium 73, 151, 308, 316, 319, 353, 355, 357, 400, 452, 480-481, 499, 509-510, 512-516, 526, 561, 602, 626, 628, 695, 701-702, 812, 857, 864, 870, **874-875**, 885, 891, 903, 914-915, 917, 923, 941, 1063, 1065-1066
Magnesium alloys 510, 512
Magnesium hydride 870
Magnesium oxide 857, 1066
Magnetic repulsion effect 772, 779
Mahogany 245, 1076
Maleic anhydride 784, 1042-1044
Malt 687
Manganese 400, 514, 868, **875**, 888, 891, 894-895, 897, 914, 968, 1063, 1066
Manganese dioxide 894, 914, 1066
Manganese naphthenate 897
Manganese oxide 868
Manhole explosions 772
Manufactured homes (*see* Mobile homes)
Manure 726
MAPP gas 122, 686
Marijuana 867
Marsh gas 903
Mass loss rate 246-248
Mass of sample, effect of 311
Matches 5, 185, 326, 479, 499, 503, 518, 702, 718, 730, 751, 815, 830, 833, 837, 849, 864, **867-869**, 882, 905, 915, 921, 937-938
Matheson B-gas 328
Matrix (fabric type) 816
Mattresses 287, 321, 335, 719, 730, 817, 849, 912, 921, **928-938**
Mattress pads 743-744
Maximum experimental safe gap (*see* MESG)
Mechanical sparks 19, 87, 146, 153, **507-516**, 551, 553, 706, 736, 788, 811, 825, 895
Mechanical injury 787-791
Melamine formaldehyde 289, 307, 559, 726, 1064, 1067, 1071
Menhaden oil 889
Mercaptoacetic acid 854
Mercuric azide 468
Mercury fulminate 468
MESG 21, 43, 65, 78, 87, **96-101**, 103, 128, 148-149, 207, 597, 599-601, 603, 807, 1023, 1026, 1029, 1032, 1035, 1038, 1041, 1044, 1047, 1050, 1053, 1055-1058
Mesh 123, 149, 170, 174, 322, 406, 418-419, 434-435, 565, 594, 629, 735, 749, 782, 783, 812, 833, 914, 1063-1065
Mesityl oxide 1042-1044
Metal alkyls 869-870
Metal alloys 355, 870, 876, 894
Metal and non-metal hydrides 452, 870
Metal carbonyls 452, 870
Metal foam 594
Metal hydrides 870
Metal oxides 28, 354, 356, 553, 870, 894, 914
Metals, ignition of 352-364, 870-879
Metal sulfides 452
Metal tools 74, 508, 850
Methane 10, 15, 25-26, 28-31, 33, 35, 38, 43-45, 53-56, 60-61, 64-66, 69, 70-107, 109, 112-113, 116-124, 143-144, 146, 151-152, 154, 159, 164, 167, 169, 174, 184, 447, 470, 473-474, 488, 509-515, 520, 524-525, 536-539, 548, 558, 560-, 572, 573, 599, 601, 610-611, 617, 619, 690, 694, 710, 717-718, 726, 731, 740, 748, 752, 767-768, 777-778, 807, 818, 856, 866-867, **879-880**, 895, 901, 903, 919, 928, 941, 1042-1044
Methanol 87, 101, 115, 119-122, 184, 192, 194-197, 199-200, 209-210, 216, 507, 511, 514, 521, 525, 562, 594, 717, 850-851, 924, 1042-1044
Methenamine 321, 518, 727, 829, 904, 925-926, 931, 934-936, 938, 950, 963, 1042-1044
2-Methoxyethanol 1042-1044
Methoxypropanol 1042-1044
1-Methoxy-2-propanol 1051-1053
Methoxypropyl acetate 1051-1053
Methyl acetate 119, 1042-1044
Methyl acetoacetate 1042-1044
Methyl acetylene 113, 447, 686, 1042-1044
Methyl acrylate 1042-1044
Methylal 1033-1035
Methyl alcohol (*see* Methanol)
Methylallyl chloride 1042-1044
Methylamine 1042-1044
Methyl amine nitrate 454
Methyl amyl alcohol 1042-1044
Methyl *n*-amyl ketone 1039-1041
Methyl aniline 1045-1047
Methyl bromide 620, **880**, 1042-1044
2-Methyl-1,3-butadiene 1042-1044
3-Methyl-1-butene 119, 1042-1044

Methyl butyl ketone 58, 1042-1044
Methyl cellosolve 1042-1044
Methyl cellosolve acetate 1042-1044
Methyl chloride 27, 717, 1042-1044
Methyl chlorocarbonate 1042-1044
Methyl chloroform 1051-1053
Methyl cyanide 1024-1026
Methylcyclohexane 1042-1044
Methylcyclohexanol 1042-1044
2-Methylcyclohexanone 1042-1044
Methyl-1,3-cyclopentadiene 1045-1047
Methylcyclopentane 1045-1047
2-Methyl-1,3-dioxolane 1045-1047
Methylene chloride 201, 717, **880**, 1045-1047, 1060
Methyl ether 104, 1045-1047
Methyl ethyl ether 1045-1047
Methyl ethyl ketone 58, 115, 119, 613, 903, 909, 1045-1047
Methyl ethyl ketone peroxide 903, 909, 1045-1047
Methyl formal 1033-1035
Methyl formate 119, 1045-1047
6-Methyl-1-heptanal 1042-1044
Methylhydrazine 891, 1045-1047
Methyl isobutyl carbinol 1042-1044
Methyl isobutyl ketone 200, 1042-1044
Methylisocyanate 1045-1047
Methylisopropenyl ketone 1045, 1046, 1047
Methyl lactate 1045-1047
Methyl mercaptan 1045-1047
Methyl methacrylate 89, 909, 1045-1047
1-Methylnaphthalene 1045-1047
Methyl nitrate 1045-1047
2-Methyl pentane 1045-1047
3-Methyl pentane 1045-1047
Methyl propionate 1045-1047
Methyl propyl ketone 1048-1050
2-Methyl pyridine 1045-1047
3-Methyl pyridine 1045-1047
Methyl styrene 1054-1055
α-methyl styrene 1045-1047
Methyl *tert*-butyl ether 1045-1047
Met-L-X extinguishing powder 871
Microballoons 454-455, 472, 694
Microbial activity 701
Microcalorimeter 387, 425, 429, 900-901, 909
Microflora 687
Microgravity 89, 108, 191
Micronizing 561
Microorganisms 687, 701, 845-846, 965-966, 968
Microscopy 797-799
Microwave ovens 5, 573, 687, 739, **880**
Microwaves 5, 571-573, 687, 739, 880
MIG 941
Mike 3 test apparatus 175
MIL-2190 1059
MIL-H-5606 .....45, 205, 210-212, 223, 862, 1057, 1059
MIL-H-53119 1057
MIL-H-83282 ..... 45, 205, 210, 223, 862, 1057, 1059
MIL-H-87257 1057
Milk (*see* Powdered milk)
MIL-L-7808 ..... 45, 223, 1057, 1059
MIL-L-9236 1059
MIL-L-23699B 1059
Millet seed 826
MIL-STD-650 .....485-486, 488
MIL-STD-1751 (USAF) 485
MIL-STD-2223 334
MIL-W-81381 805
Mineral oils 210, 435-454, 594, 688-689, 704, 731, 768, 827, 862, 886, 890, 1057
Mineral spirits 683, 866, 888, 897, 1057
Mineral wool 403, 408, **881-882**, 904-905, 955, 957
Minimum energy for detonation 123
Minimum explosible concentration 21, 145, 174, 598
Minimum flux for ignition 217, 253, **259-260**, 262-265, 268, 272, 275-277, 293-295, 297-298, 304, 308, 311, 317, 521, 530, 616, 631, 695-696, 729, 785, 821, 865, 899, 906-907, 909, 919, 933-934, 945-948, 952-953, 963-964, 967
Minimum ignition energy **66-69**, 73-83, 95, 100, 102, 104, 116, 120, 122, 126-127, 149, 151-154, 161-166, 167-168, 170-173, 176, 202-205, 301, 335, 467, 515-516, 554-556, 558, 560, 563, 566, 598, 625, 683, 691, 698, 717, 736, 812-813, 843, 850, 863, 871, 875-876, 898, 1023, 1026, 1029, 1032, 1035, 1038, 1041, 1044, 1047, 1050, 1053, 1055-1058, 1063-1066
Minimum oxygen concentration 118-120, 156, 167-169, 299-300
Mirrors 242, 575
Misch metal 509, 872
Mists 116, 206, 211, 224, 554, 565, 620, 688, 698, 731, 767
Mixture KD 454
Mixtures 60, 198-202
MLO-53-446 1059
MLO-54-540 1059
MLO-54-581 1059
MLO-54-856 1059
MLO-56-280 1059
MLO-56-610 1059
MLO-60-294 1059
Mobil DTE 103 1059
Mobil DTE 797 1057
Mobile homes 532, 761-762, 790, 854, 855, 881
Modacrylic 560, 725, 816, 820-821, 824, 831, 1072
Moisture content 9, 21, 156, 158, 159, 162, 245, 273, **302-304**, 374, 398-400, 414, 434, 481, 506, 574, 687, 719, 734, 735, 834-843, 845, 847, 859, 878, 900-901, 939, 942, 946, 954-955, 964-966, 968, 1072
Moisture of extinction 835
Molecular dynamics 446, 469
Molecular explosives 453
Molecular structure, effect of 55, 61-63, 74-75, 189, 395
Molybdenum 84, 96, 319, 353, 514, 515, 541, **875**, 1063

Molybdenum disulfide....1066
Monel....84, 514, 517, 626
Monochloroacetylene....447
Monoethanolamine....1036-1038
Monoisopropanolamine....1045-1047
Monomethyl aniline....1045-1047
Monomethylhydrazine....1045-1047
Monomolecular explosives....453
Monopropellants....476, 694, 809, 862, 890
Monterey pine....245, 271, 304, 503, 957, 964, 1076
Moore's tester....220-221
Mops....919
Morpholine....1045-1047
Moss....501, 836, 842, 901
Motorcycles....834
Motor oil...194, 209-210, 217-218, 221, 454, 505, 806, 809, 890, 1058
Motor starters....738
Motor vehicles....3, 738, 743, 804, **881-885**
Motor vehicles, electric wiring in....804
Movement of surface, effect of....309-310
MSHA permitted explosives....473
MSHA spray test....227
MTBE....1045-1047
Mufflers....596
Multi-component explosives....453
Multiple packing, effect of....398
Mushroom Apparel Flammability Test....820
Mustard oil....888-889
MVSS 302....328, 883
Myrobalan and valonia nuts....1066
Nail polish....708
Nails....552, 573, 667, 788, 790
Naphtha....683, 807, 1058
Naphthalene....185, 224, 480, 1045-1047
Naphthionic acid, crude....1066
NASA Handbook NHB 8060....333
National Electrical Code....17, 21, 24, 128, 591, 596-602, 604, 606, 746, 752, 754, 762, 781, 783, 857, 765, 1023, 1025, 1028, 1031, 1034, 1037, 1040, 1043, 1046, 1049, 1052, 1054, 1056-1058, 1061
Natural gas....37, 43, 53, 84-85, 94, 99, 112-113, 116, 119, 122, 151, 293, 328, 518, 525, 560, 609-611, 615, 695, 717, 752, 848-849, 866-867, **879-880**, 922, 941, 1058
Natural rubber....301, 910, 1067
NC (*see* Cellulose nitrate)
Neatsfoot oil....828, 889, 921, 1058
NEC (*see* National Electrical Code)
NEC Groups....597-599, 1061
Needle flame....326, 519, 732, 785, 908
Needle-flame Test....326
Needles....143, 205, 501, 555, 574, 834-844
Negative proof....9-10
Negative temperature coefficient....45, 855
Neodymium....509, 876
Neohexane....1033-1035
Neon lighting....673, **885**, 961
Neopentane....1033-1035
Neoprene....301, 302, 314, 559, 627, 628, 776, 786, 933, 935, 938, 1067-1068
Neutralization....451, 564
Newsprint....241, 507, 856, 869, **898-899**, 1067
NFPA 30....14, 15, 24, 193
NFPA 31....18, 24, 849
NFPA 33....898
NFPA 35....710
NFPA 40....710
NFPA 40E....710
NFPA 44A....490
NFPA 49....18, 24, 490, 603, 968, 1023
NFPA 53....19, 24, 625, 895
NFPA 58....867
NFPA 77....17, 19, 24, 576
NFPA 211....715
NFPA 325....13, 24, 128, 219, 224, 598, 807, 904, 968, 1077, 1086
NFPA 327....924
NFPA 490....694
NFPA 495....18, 24, 490, 694
NFPA 497....598, 599, 1023
NFPA 499....598
NFPA 651....870
NFPA 701....322, 926
NFPA 705....322
NFPA 780....576, 593
NFPA 921....1, 7, 13, 24, 312, 617, 774
NFPA 1123....490
NFPA 1124....490
NFPA 1125....490
NFPA 1126....490
NFPA 1127....490
NFPA 1144....631
NG (*see* Nitroglycerin)
Nichrome....85, 171, 213, 293, 336, 434, 472, 485, 857, 929
Nickel....72, 84, 86, 124, 209, 319, 337, 338, 354, 359, 512, 514, 546, 550, 625, 626, 683, 764, 765, 772, 802, 870, **875-876**
Nickel permalloy....1066
Nicotine....930, 1045-1047
Niobium....466, 1063, 1065
NIST....21, 124, 126, 222, 298, 306, 322, 330, 335, 362, 518-520, 701, 706, 715, 719, 729, 752-753, 756, 759, 765, 779, 793, 817-818, 820, 822, 832, 865, 868, 883, 898-899, 930, 932-935, 938, 940, 944, 962-963, 967, 1086
NIST electric arc method....335
Nitramine....455, 476, 808
Nitrate esters....446, 475
Nitrates....885
Nitration....451, 694, 707, 708
Nitric acid....452, 454, 476, 485, 692, 708, 814, 826, **885-886**, 966
Nitrides....736, 875, 878, 886
Nitrile rubber....307, 628, 1067, 1071

Nitrobenzene 811, 921, 1045-1047
Nitrocellulose (*see* Cellulose nitrate)
Nitroethane 1045-1047, 1074
Nitrogen, liquid 886
Nitrogen dioxide 452, 708, 714
Nitrogen iodide 468
Nitrogen oxides 885-886
Nitrogen selenide 810
Nitrogen sulfide 810
Nitrogen tetroxide 476, 891
Nitroglycerin 454-455, 457, 459-460, 466, 474-475, 487-488, 708, 808, 810-814, 885, 1045-1047
Nitroglycide 814
Nitroglycol 474
Nitroguanidine 475, 808, 812, 815, 1066
Nitromethane 454, 692-693, 774-775, 780-781, 790, 799, 808, 811, 813-814, 1045-1047
1-Nitropropane 1045-1047
2-Nitropropane 1045-1047
Nitrostarch 810, 812, 1066
2-Nitrotoluene 1045-1047
NM (*see* Nitromethane)
No. 1 Wheeler Test 153
NOL Thermal Sensitivity Test 488
Nomex 690, 816, 820, 822-824, 1073
Nonane 194, 196, 200, 732, 1045-1047
1-Nonanol 1045-1047
1-Nonene 1045-1047
Non-premixed gases, ignition of 120-121
Non-sparking tools 510
Nonyl alcohol 1045-1047
Noodles 833
Nordtest 15 L apparatus (NT Fire 011) 146, 175
Nordtest NT Fire 016 335
Nordtest NT Fire 045 417
Normal combustion velocity 17
Northern white cedar 1076
NQ (*see* Nitroguanidine)
Nuclear power plants 714
Nuclear weapons 285, 290, 307, 571, **574**, 825, 942, 952
Nusselt number 92, 357-358, 595
Nylon (unspecified type) 298-299, 322, 558-560, 619, 741, 792, 805, 816-822, 825, 829-832, 853, 856, 904, 909, 931, 933, 935, 938, 1064, 1073
Nylon 6 ..... 824, 906, 1067, 1072
Nylon 6,6 ..... 279, 286, 301-302, 307, 310, 628, 824, 907, 1067, 1071, 1074
Nylon 11 1067
Oak 241-242, 245, 272-273, 276, 286, 292, 296-298, 489, 729, 826, 830, 836, 948-950, 953, 965, 1074, 1076
Oats 156, 315, 837, 839
Ocean Liberty (steamship) 692
Octafluorocyclobutane 1060
Octafluoropropane 1060
Octane ... 31, 62, 85, 115, 120, 122, 191, 194, 196, 199, 623, 717, 856, 1045-1047
Octane number 55, 850, 1057
1-Octanol 207, 1048-1050
1-Octene 62, 1048-1050
Octogen 454, 808
Odors 828, 845, 867
Ohmic heating 237, 467, 759, 773, 779
Oils 5, 7, 88, 184, 187-188, 190-191, 194, 197, 199, 204-206, 209-211, 215, 217-2220, 223, 454, 505-506, 514-515, 519, 525, 544, 562, 565-566, 572, 594, 600, 603, 625, 627, 683, 685, 687-690, 692, 694-695, 708, 711, 728, 730-734, 740, 766-769, 773, 775, 793, 806, 809, 827-829, 833, 847-850, 856, 862, 865-867, 870, 873, 881-882, **886-890**, 896-897, 904-905, 910, 921, 928, 938, 940, 956, 962, 966, 1056, 1057-1059, 1066
Oil safety valve 848
Oil-water emulsions 890
Oleic acid 887
Olive oil 379, 434, 687, 828, 886, 889, 921, 1057-1058
Open cup (flash point testing) ... 21, 194, 196, 210, 225, 226, 506, 703, 812, 856, 923
Oppau (explosion) 692-693
Ordway Test 433
Organic peroxides 15, 225, 406, 446, 522, 902-903
Organic soils 316, 834, **900-901**
Organometallic compounds 452, 455, **890**
Orientation, effect of 294-295
Oriented strand board 965, 1074
Oronite 8200 1059
Oscillatory combustion 45, 54
Osteoporotic bones 861
Otto fuel II 890
Outlets, electric (*see* Electric outlets)
Oven basket tests 389, 393, 397, 398-399, 403-404, **406-418**, 419, 429, 451, 700, 712-713, 721-723, 730, 827, 833, 897, 899, 911, 913, 955, 958
Ovens 409, 710, 728, 865, 880
Overcurrent 19, 312, 546, 549, 737, 739, 758, 768, 772, 780, 797, 799
Overfill protection devices 867
Overfiring 848, 967
Overfusing 744
Overheated bearings 507, 731
Overheating 4, 6, 18, 85, 175, 312, 336, 338, 374, 402, 507-08, 518, 549, 550, 552, 619, 685, 688, 706, 715, 727, 731-734, 737, 742-744, 753-756, 760, 762-764, 767, 769, 772, 781-782, 784, 788-789, 794, 797, 799, 853, 855-857, 858, 866, 881-882, 884-885, 918, 924, 927, 928
Overheating electrical connections 313, 548-553, 643, 658-660, 754, 759, 761-762, 765, 787
Overheating wires 549
Overinflation 927
Overload 18-19, 696, 738, 744-745, 748, 763, 765-780, 783-784, 788, 794, 799, 803
Overspray 897
Overvoltage 749, 755, 766, 767, 772, 782, 793, 806
Oxalic acid 1066

Oxidation 7-8, 14, 19, 31, 33-34, 44-46, 52-54, 63, 95, 104-105, 144, 184, 186, 212, 237, 238, 299, 310, 315, 317, 353, 355, 357-359, 369, 373, 376, 396-397, 399-401, 403, 426, 435, 451, 456, 469, 478-479, 507-509, 512, 515, 550-551, 561, 683, 687, 688, 700-701, 705, 707, 711, 713, 720-723, 736, 747, 750, 758, 791, 799, 826-827, 829, 845-846, 858, 865, 872, 874-875, 881, 883, 887-889, 901, 903-905, 909-912, 914, 920-922, 927, 941, 943, 955, 958, 961, 964-966, 968
Oxidizing chemicals 890-896
Oxidizing solids 434, 485, 489, 891-892
Oxiranes 807, 913
Oxosalts 714
Oxy-acetylene cutting 506, 507
Oxy-acetylene torches 518, 735
Oxygen, gaseous 28, 38, 452-453, 478, 626, 825, 877, **895**, 896
Oxygen, liquid 446, 454, 476, 629, 711, 719, 825, 875, 878, 886, **895-896**
Oxygen balance 28, 456, 462, 473, 479
Oxygen candles 894, 921
Oxygen chemisorption 689
Oxygen concentration 46, 57-58, 62, 75, 76, 88-92, 97, 101, 103, 112, 118-120, 149, 156, 159, 162-63, 167-170, 174, 190-191, 203, 207, 248, 253-254, 278, 281, 288, 299-301, 315, 317, 332, 338, 358-362, 364, 370, 397-398, 465, 470, 477, 556, 617, 625, 627-628, 691, 703, 705, 731, 798-800, 807, 811, 825, 865, 870-871, 876, 880, 920, 924
Oxygen consumption calorimetry 435
Oxygen-enriched atmospheres **625-629**, 719, 825, 891
Oxygen index 63, 75-77, 118, 338, 629
Oxygen pumps 896
Oxygen regulators 627, 896
Ozone 118, 447, 592, 686, 885, 919
Packing density (*see* Density)
Pacific maple 271, 1076
Paint (effect of) 307, 962
Paints 290, 307, 428, 510, 557, 702, 887-888, **896-898**, 922, 928, 962
Paints, aluminum-based 898
Paints, quick-drying 897
Paint thinners 201-202, 858
Palladium 84, 455, 480, 512, 546, 628
Palmitic acid 887
Palm kernels 687, 889
Palm oil 1058
Panelboards (*see* Electric Panelboards)
Paper 238, 241, 253, 265-267, 269, 289-291, 297, 303-304, 306, 311-312, 314, 316, 327-329, 452, 482, 485, 518, 520, 530, 557-559, 570, 574-575, 614-615, 693-694, 703-706, 709, 712, 716, 718, 726, 728-729, 736, 740, 750, 753, 761, 765, 767, 773, 779, 782, 788, 795, 806, 820, 825-826, 828, 830, 853-856, 858-859, 863-864, 870, 882, 891, 897, **898-900**, 907, 915, 922-923, 926, 930-931, 934, 937-938, 1065, 1067-1068
Paper, in rolls 558, 899
Paper dust 1065
PaperSelect 930
Paraffin-series compounds (*see* Alkanes)
Paraffin wax 712, 867, 1058
Paraformaldehyde 168, 1048-1050
Paraldehyde 1048-1050
Parallel arcs 774, 776, 779-780, 788, 795, 806
Para-mononitrotoluene 454
Parasitic inductance 176, 547
Parquet 219, 830-831
Partial discharges 768, 791, **793**
Particle diameter or size 74, 94, 143, 150, 155, 157-159, 161-162, 164, 169, 203-204, 207, 318, 358, 360, 362-363, 396, 504, 506, 556, 561, 596, 695, 706, 735, 748, 871, 872, 875
Particle impact 627, 896
Particulate radiation 571
Paschen's Law 70, 127, **535-536**, 546-547, 779
PCTFE (*see* Polychlorotrifluoroethylene)
Peanut-hull meal 826
Peanut oil 205, 886, 888-889, 1058
Peat 316, 429, 687, 736, 826, **900-01**, 1064, 1074
Peat, dried 1064
Peclet number 68
PEEK 21, 628, 1072
PEEK (*see also* Polyetheretherketone)
Pellet stoves 647, 967
Pencils 765
Pensky-Martens Test 195, 224-226, 639
Pentaboranes 701, 1048-1050
2,4-Pentadione 1024-1026
Pentaerythritol-tetranitrate 455, 808, 1048-1050
Pentafluoroethane 1060
Pentanal 1048-1050
Pentane 31, 55, 62-63, 78, 86-87, 103-104, 117, 119-120, 196, 510, 599, 613, 717, 731, 1048-1050
1-Pentanol 1024-1026
2-Pentanol 1048-1050
2-Pentanone 58, 1048-1050
1-Pentene 251, 1024-1026
Pentyl ether 1024-1026
PEPCON (explosion) 695
Perchloric acid 485, 901-902
Perchloryl fluoride 891
Percussion primers 472
Perfluorobutane 902
Perfluorocarbons 902
Perforated metal 594-595
Performance Level Categories (PLC) 333-334
Perilla oil 1058
Perlite 901, 905, 919
Permissible explosives 73, 77, 470, 473-474, 488
Peroxides 714, 806-807, **902-903**, 904, 912
Persons, electrostatic charging of 559
Perthane 864
Pesticides 864
PET 21, 558, 559, 825, 907, 1068

Peters, Julius (friction test) 484
PETN 454-455, 458, 460-461, 464, 468, 470-472, 478, 484, 561, 808-815, 1048-1050, 1062
Petroleum Act of 1862 223
Petroleum distillates 202
Petroleum ether 856, 869, 915, 1058
PGDN 808, 811
Pharmaceuticals 903
Phase diagrams 184, 355
1,10-Phenanthroline 897
Phenol 759, 962, 1048-1050
Phenol formaldehyde (*see* Phenolic)
Phenolic (phenol formaldehyde) 169, 289, 291, 307, 313, 316, 323-334, 408, 482, 690, 725-726, 753, 824, 881, 906-908, 910, 917, 1064, 1067-1068, 1071-1074
Phenyl ether 1048-1050
Phenylhydrazine 1048-1050
PHI-TEC Adiabatic Calorimeter 428
Phlegmatizers 472
Phosphate ester hydraulic fluids 210, 862
Phosphine 717, 903, 1048-1050
Phosphines 452, 903
Phosphoric acid 713, 826, 869
Phosphorus 319, 352, 482, 801, 814, 826, **903**, 912, 914-915, 923
Phosphorus sesquisulfide 868
Photoflash mixture 453
Phthalic anhydride 110, 1048-1050
Physical damage 794, 855
Picoline 1045-1047
Picric acid 448, 454, 683, 808, 810-811, 813-814, 1048-1050, 1062
Piezoelectrification 553
Pigs 860-862
Pigtailing 765
Pile size, effect of 395-396
Pillows **903-904**, 911, 930, 937
Pilot, effect of 292-294
Piloted ignition 9, 13, 16, 43, **65-104**, 120, 217, 239, 241-242, 245-250, 252, 255, 259, 268, 276-277, 292-293, 295, 298-304, 308-309, 312, 333, 337-338, 445, 521, 530, 615-616, 628, 631, 690, 705, 726, 729, 731-732, 817, 821-822, 830-832, 836-837, 865, 883, 896, 899, 907, 910, 919, 926-927, 932-934, 945-950, 953-954, 962, 967
Piloted ignition temperature 16, 245, 277, 337-338, 899, 907, 927, 953
Pilot flames 16, 19-20, 65, **73-74**, 192-193, 195, 201, 205, 213, 215, 226, 239, 251, 293-294, 331, 337, 731, 837, 856, 908, 940
Pinane 1048-1050
Pine 241, 245, 292, 298-299, 328, 371, 501, 504, 574, 835-837, 840-844, 887, 943, 949-952, 954, 956-957, 962, 964-965, 1074, 1076
Pine oil 1058
Pinene 1048-1050
Pipe insulation 288, 371, 381, 383, 403, 809, **904-905**
Pipes, broken 614
Pistols 143
Pitch (*see* Asphalt)
Pittsburgh coal 170, 173-174, 395, 396, 401-402, 419, 598, 724, 1063
Plasma arc 941
Plastic explosives 454-455
Plasticizers 454, 791, 792, 897, 1069
Plastics 558, 725-726, 905-912, 1064, 1067-1076
Plastics (*see also* individual substances)
Plastics, fiber-reinforced 725-726
Plastics, laminates 726
Plastics, self-heating of 909-912
Plastics, sheets 558
Platinum 8, 38-39, 59, 83-84, 86, 89-91, 94, 96, 105, 124, 160, 176, 277, 334, 353-354, 480, 512, 546, 553, 683-684, 735, 856, 863, 923
Plexiglas G 1068
Plexol 201 1059
Plumbago 1066
Plumes 218, 246, 251, 253-254, 275, 315, 330, 353, 500, 504, 527-529, 610, 867, 887
Plutonium 356, 452, **876**
Plywood 271-274, 312, 328, 519, 521, 530, 560, 574, 715, 747, 750, 781, 912, 949, 952, 962, **964-965**, 1074
PMMA 21, 147, 157, 172, 239, 242, 244, 246-248, 250, 252, 265, 268-270, 273, 275-281, 289, 294-301, 305-307, 308-311, 323, 328, 484, 559, 693, 906-908, 1064, 1068, 1071, 1074-1075
Pneumatic transfer 561
Pockets 145, 509, 846
Point discharge 555, 569, 592
Point source radiation model 522, 527
Polarization 553
Pollution 38, 546, 773, 810, 851
Polonium 592
Polyacrylonitrile 164, 280, 313, 816, 824, 1064, 1068
Polyamide 334, 824, 1075
Polyamide-imide 1075
Polybenzimidazole 21, 326, 824-825
Polybutadiene-acrylic acid (PBAA) 281, 477
Polybutadiene rubber 910
Poly-1-butene 251
Polybutylene terephthalate 334
Polycarbonate 286, 290, 297, 307, 334, 461, 559, 628, 905-908, 1064, 1068, 1071, 1075
Polychloroprene 896, 910, 912, 1067-1068
Polychlorotrifluoroethylene (PCTFE) 21, 323, 559, 628
Polycondensation 881
Polyester 21, 161, 167, 289-290, 304, 309, 322, 328, 334, 559-560, 719, 725, 732, 734, 741, 786, 816-825, 831, 855, 861, 898, 903-905, 920, 931-934, 937, 1072
Polyester, glass reinforced 559, 1068, 1070
Polyester, unsaturated 1068
Polyester resin 873, 897, 906, 909
Polyetheretherketone 21, 628, 1075
Polyetheretherketone (*see also* PEEK)

Polyetherimide....628, 1068, 1075
Polyethersulfone....628, 1068
Polyethylene....21-22, 146, 148, 151, 157, 160-161, 168-169, 239, 246, 248, 251, 262-264, 270, 273, 286, 290, 297, 301, 307, 310, 313, 475, 526, 558, 561, 565, 614, 627-628, 688, 695, 699, 712, 744, 772, 780, 784-787, 792-793, 808, 851-853, 893, 895, 902-905, 907-908, 910-911, 957, 1064, 1067-1068, 1070-1072, 1075
Polyethylenenaphthalene....1075
Polyethylene terephthalate....21, 313, 628, 816, 1064, 1068
Polyisobutylene....215, 454, 809
Polyisocyanurate....21, 908
Polyisocyanurate foam....300, 910, 1075
Polymerization....8, 104, 369, 373, 448, 451, 683, 687, 808, 829, 888, 897, 902, 909, 913, 922
Polymer structure, effect of....308
Polymethylmethacrylate (*see* PMMA)
Poly-4-methyl-1-pentene....251
Polyoxymethylene....246, 248, 265, 270, 289, 307, 908, 1048-1050, 1067-1068, 1071
Polyphenylene oxide....307, 628, 784, 1071
Polyphenylenesulfide....1075
Polyphenylsulfone....326, 1075
Polypropylene....21, 238, 246, 248, 251, 270, 286, 287, 298-299, 307, 309, 559, 627-628, 725-726, 730, 786, 816, 821, 824, 829, 830-831, 849, 882, 891, 909, 1064, 1068, 1070-1073, 1075
Polysaccharides....707
Polystyrene....21-22, 163-165, 200, 246, 248, 270, 286, 289-290, 293, 299, 307, 309-310, 312-313, 323, 461, 475, 478, 506, 559, 628, 704, 718, 784, 849, 905-910, 922, 925-926, 934, 1064, 1069-1072, 1075
Polysulfide....304, 475
Polysulfone....1075
Polytetrafluoroethylene (*see* PTFE)
Poly(trifluorochloroethylene)....1069
Polyurethane....21, 269, 291, 307, 316-318, 454, 460-461, 475, 477, 506, 559, 594, 619, 628, 716, 730, 781, 806, 829, 849, 895, 903, 906, 908-912, 929-934, 936-938, 1069-070, 1072, 1075
Polyvinyl acetate....1064, 1069
Polyvinyl acetate alcohol....1064
Polyvinyl butyral....1064
Polyvinyl chloride (*see* PVC)
Polyvinyl ester....1072
Polyvinylidene chloride....825, 1064, 1066, 1069
POM (*see* Polyoxymethylene)
Ponderosa pine....242, 304, 836, 948, 954, 1076
Pools, liquid....213-215, 521-524
Poplar....242, 952, 1076
Poppyseed oil....889
Porosity....218, 308, 311, 316, 318, 359, 384, 394-396, 399, 410, 471, 618
Potash....826
Potassium....319, 353, 358, 400, 434, 460, 485, 512, 711, 814, 826, **876**, 886, 953
Potassium carbonyl....870
Potassium chlorate....452, 454, 472, 480-482, 811, 868, 894, **912-913**, 914-917, 921, 923
Potassium fluoride....474
Potassium hydride....870
Potassium nitrate....460, 475, 480-481, 526, 701, 811, 827, 868, 884-885, 915-917, 1048-1050
Potassium perchlorate....475, 480-482, 526, 913, 915-917, 1048-1050, 1066
Potassium permanganate....452, 481, 890
Potassium peroxide....902
Potassium superoxide....876
Potato starch....1064
Pouring....196, 485, 555, 561, 688, 702, 793, 852
Powder heap discharge....554, **556**, 644
Powdered metals....561, 871-879, 895
Powdered metals (*see also* specific metal)
Powdered milk....913
Power cables....402, 544, 780, 785, 719, 732, 739, 775, 779, 786, 790, 798, 802, 924
Power lines....572, 592-593, 840-841, 843-844
Power steering fluid....199, 881, 882, **913**, 1058
Praseodymium....509, 876
Pre-charring, effect of....310, 953, 958
Pre-flash 'halo'....194
Prescribed burns....833
Preservatives, effect of....953
Pressure, effect of....45, 49-52, 57, 63, 68-69, 78, 97, 99-100, 112-114, 120-123, 158, 162, 188-189, 191, 205, 208, 212, 289, 301-302, 447, 451, 464, 470, 476, 478, 504, 508-511, 517-518, 535, 625-628, 683-686, 689, 691, 693-694, 697-698. 789-790, 807-809, 850, 863, 873, 877, 879-880, 889-890, 903, 927-928, 940-941
Pressure, excessive....172, 849
Pressure gradient....78
Pressure limit....113, 117, 686, 691, 807, 849, 850
Pressure piling....**37**-**38**, 100, 611
Pressurized enclosures....603
Preventive measures....404-405, 576, **591**-**604**, 624
Primacord....472
Primary explosives....459, 461, 466, 468, 471, 488, 559, 574, 700
Primers....11, 372, 472, 482, 896-897, 962, 1073
Priming mix....482
Probabilistic aspects....9-10, 528, 759, 900
Probability level....98, 157, 170, 175, 462, 486, 572, 813
Proban....819
Process splices....791
Promethium....876
Proof Tracking Index....334
1,2-Propadiene....145, 1048-1050
Propagating brush discharge....554-557, 644
Propanal....1048-1050
Propane....28, 31, 38, 54-5, 62-63, 69, 74-77, 79, 81-82, 85, 87, 89-93, 103-104, 107-109, 111, 113, 116, 118-122, 152, 210, 227, 287, 331, 337, 447, 489, 508, 511, 513-

514, 519-599, 609-612, 619-624, 686, 717, 795, 848-849, 856, 866-867, 871, 881-882, 910, **913**, 919, 941, 1048-1050
1,2,3-Propanetriol 808, 1039-1041
Propanoic acid..... 1048-1050
Propanoic anhydride 1048-1050
1-Propanol..... 1048-1050
2-Propanol..... 103-104, 1048-1050
2-Propanone..... 1048-1050
Propargyl alcohol..... 1048-1050
Propargyl bromide 447, 1048-1050
Propargyl chloride..... 1048-1050
Propellants 290, 304, 453, 456, 458-461, 466-468, **475-479**, 686, 694, 695, 709, 811, 858, 884, 902, 923
Propene 1048-1050
2-Propenoic acid 808, 1024-1026
2-Propenol..... 1024-1026
Propiolactone 1048, 1049, 1050
Propionaldehyde 104, 691, 110, 1048-1050
Propionic acid 687, 967, 1048-1050
Propionic anhydride..... 1048-1050
Propionitrile 1048-1050
n-Propyl acetate 1048-1050
n-Propyl alcohol..... 1048-1050
Propylamine..... 1048-1050
Propyl benzene..... 1048-1050
Propyl bromide 1048-1050
n-Propyl chloride 1048-1050
Propylcyclopentane.....46
Propylene ...31, 47, 54, 89-90, 113, 119, 122, 620, 623, 686, 717, 863, 866, 1048-1050
Propylene chloride..... 1048-1050
Propylene dichloride..... 1048-1050
Propylene glycol 808, 890, 1048-1053, 1059
Propylene glycol monomethyl ether 1051-1053
Propylene glycol monomethyl ether acetate 1051-1053
Propylene oxide 110, 119, 122, 448, 507, 511, 597, 717, 806, **913**, 1051-1053
Propyl ether..... 1051-1053
n-Propyl nitrate 101, 1051-1053
Propyne (*see* Methyl acetylene)
2-Propyn-1-ol..... 1048-1050
Protective clothing 545
Prussian blue 897, 1066
PRV..... 21, 620-622, 624
PTC devices 673-674, 918-919
PTFE (polytetrafluoroethylene; Teflon) 21, 300, 302, 313-314, 323, 558-559, 627-628, 748, 784-786, 805, 816, 902, 907, 917, 1064, 1066, 1069
Puffing combustion.....617
Pumps 6, 851, 862, 896
Push-on connectors 662, 741, 762
Putty.....454
PVC.... 22, 152, 157, 237-238, 241, 286, 289, 293, 299-301, 307, 309, 311, 313, 323, 328, 475, 526, 559, 575, 614, 627-628, 657, 663, 665, 716, 726, 744, 757-759, 762-763, 773, 775-778, 780, 782, 784-793, 797-801, 804-805, 816, 821, 825, 830-831, 854-855, 906-908, 910, 912, 920, 923, 925, 931-934, 938, 1064, 1067, 1069, 1070, 1072-1075
Pydraul 150.....1059
Pydraul A-200 1059
Pydraul AC 1059
Pyrethrum 1065
Pyridine.....1051-1053
Pyrite 396, 400, 512, 514, 811, 864-865
Pyro aluminum 482
Pyrodex.....475
Pyroelectrification 554
Pyrofuze.....455, 480, 628
Pyrogard D.....1059
Pyrogen igniters.....476
Pyrolysates.....238, 252, 292, 295, 299-300, 330, 468, 617, 908, 927
Pyrolysis ... 7, 18-19, 144, 146-148, 150, 161, 185, 238-240, 249, 252, 257, 260, 277, 281, 283, 285, 287-288, 290, 292, 295, 299, 304, 317, 319, 360, 363, 369, 370, 412, 429, 453, 468, 500, 503, 617, 756, 772, 803, 822-823, 898, 927, 935, 942-943, 945-946, 958-959, 961
Pyrolysis, oxidative 7
Pyrophor bar 509, 512-514, **872**
'Pyrophoric carbon' 674, 955-960
Pyrophoric liquids.....485
Pyrophoric materials.....18-19, 354-355, 358, 373, 452, 484-485, 490, 499, 598, 695, 863-865, 869-878, 886, 890, 903, 920, 924, 955-960, 1023
Pyrotechnics 7, 9, 18, 28, 144, 238, 335, 452-453, 455, 472, 476, **479-482**, 489-490, 517, 526, 810, 912, **913-918**
Pyrotechnics, chemistry of.....480-481
Pyroxylin 707
Pyrrole 1051-1053
Quartz 59, 77, 86, 89, 305-306, 332, 510-511, 515-517, 747, 749-751, 821, 850, 899, 935
Quartz, fused.....513, 749-751
Quartzitic rocks 510-511, 513, 515-516
Quaternary mixtures 106-107
Quench layer height.....195, 196
Quenching distance or diameter 44, 65-66, 68-69, 74-75, 77-83, 97-100, 103-104, 117, 127, 145-146, 148-149, 151, 166, 196, 251, 370, 376, 395, 554, 594, 683, 743, 863, 1023
Quicklime 866
Quinoline 1051-1053
Quintiere's procedure 262-263
Radiant ignition of explosives and propellants.....465, 478-479
Radiant ignition of fabrics 821-823
Radiant ignition of liquids 217-219
Radiant ignition of plastics 905-910, 1071-1076
Radiant ignition of solids..... 250-277, 292-312
Radiant ignition of upholstery 932-934
Radiant ignition of vegetation 841-842
Radiant ignition of wood 946-950

Radiata pine (*see* Monterey pine)
Radiators 330, 532, 794, 956
Radio receivers 740, 864, **918**
Radio transmitters 469, 571-574
Rail cars 406, 507, 622, 624
Railroads 372-373, 520, 834, **918**
Rain 398-400, 557, 562, 570, 721, 792, 835, 965
Ramjet fuel 699, 701
Rangetops 727-728
Rapeseed oil 734, 828, 833, 886, 887, 897, 1058
Rapeseeds 687, 735
Rapid compression machines 64, 123-124
Rare earth elements 513, **876**
R134a refrigerant 885
Rats 666, 787-788
Rayon 321, 371, 373, 507, 574, 716, 816-817, 820, 822, 829-830, 918, 931, 933, 1064
RDX 389, 453-455, 458-460, 464-465, 471-472, 476, 478-479, 484, 808-815, 1051-1053, 1062
Reaction kinetics 24, **32-35**, 57, 64, 105, 108, 149, 283, 394, 430, 942
Reactive substances 452
Readily combustible solids 484
Receptacles, electrical (*see* Electric outlets)
Reclaimer pads 688
Reclosers 769
Rectangular brick 413
Red cedar 290, 292, 503, 948, 953, 956, 965, 1077
Red gum 480, 482, 916
Reduction reactions 18
Redundancy 10
Redwood 298, 502, 569, 947-950, 1076
Reflux heat flow calorimeter 428
Reforming 6
Reformulated gasoline 851
Refrigerants 1060
Refrigerants, flammable 885
Refrigerators 5, 674, 739, 740, 779, 882, 885, **918-919**
Reid vapor pressure 15, 17, 18, 22, 216, 696-697, 699, 702, 849, 851, 853
Re-ignition 311, 362, 618-619, 771, 876
Reina del Pacifico (explosion) 731
Rekindle **618-619**, 706
Relaxation time 127, 558, 561, 563, 564
Residence time 60, 83, 155-156, 170, 211, 219
Resins 480, 825, 897, 909, 957
Resins (*see also* Plastics)
Resistors 734, 773, 925
Resonance 518, 624
Resonant circuits 81, 548
Restricted breathing apparatus 600
Restrike voltage 548, 770-771
Retorts 710
Return stroke (lightning) 568, 592
Reverse smolder 316-317, 319-320, 951
RF initiation of explosives 469
Rice 739, 833, 919, 1064
Rice husks 919
Rinse-aid 732
Risk of house destruction 629-630
RJ-4 1058
RJ-5 1058
RJ-6 1058
Road tunnel dust 1063
Rock wool 403, 828, 881
Rodents 666, 769, 787
Rollout (of flames) 848, 940
Roofing materials 310, 502, 631, 919
Roof shingles 501, 631, 1075-1076
Roof tile 629, 631
Room fires 32, 264, 332, 532, **615-617**, 703, 803
Room fresheners 686
Rosin 708, 889, 917
Rosin oil 889
Rot 162, 940, 954
Roundrobin tests 173, 221, 334, 906, 931
RP-1 kerosene 476
Rubber (*see* Elastomers)
Rubber dust, from tires 1065
Rubber hammers 510
Rubber, chlorinated 559
Rubber, hard 559
Rubbish 5, 718, 923
Rubidium 358, 870, 876
Rugs (*see* Floor coverings)
Runaway exothermic reactions 451
Run-up distance 121
Rust 102-103, 328-329, 400, 480, 506, 509, 510, 512-514, 516, 572, 684-685, 688-691, 704, 720, 745, 809, 863, 865, 888, 892, 895, 898, 902, 921, 927, 960
Ruthenium 455
SADT 405-406, 422, 426-428, 433
SAE 5W-30 motor oil 1058
SAE 10 lubricating oil 688, 1057
SAE 30 motor oil 217, 218, 890, 1058
SAE 60 lubricating oil 1057
SAE J335 596
Safety film 709, 710
Safety fuses 472, 488
Safety matches 868, 934
Safety measures 113, 567, 903
Safflower oil 889
Sagebrush 840
Sakata City Fire 501
Salt water 775
Samarium 356, 509, 876
SAN 1064, 1070
Sand bomb test 488
Sanding dust 897
Sanding machines 919
Sandpaper 466, 486, 868
Sandstone 510-513, 515-516
Saponification 734

SASIN....469
Saturated vapor pressure....186, 192
Saunas....617, 920
Sauter mean diameter.... 150, 163, 203-204
Sawdust (*see* Wood dust)
Saws....834
SBR....314, 371, 910, 911, 938, 1070
School buses....934
Schramm-Zebrowski Incandescent Rod Test....336
Scintillations....312, 758, 759, 806
Screens.... 329, 533-534, 596, 630
Screw connections....756-759, 761-762, 764-765
Screwdrivers....508, 769
Scrim....507, 934
Scroll feed transfer....561
Sealed equipment....603
Seaweed....1066
Secondary explosives.... 459-460, 464, 466, 468, 470-472, 813
Seebeck coefficient.... 88-89
Seeds....35, 373, 687
Selenium....1066
Self-heating.... 9, 11, 14-15, 19-21, 36, 43, 54, 143, 237-238, 241, 243, 245, 249, 282, 288-289, 312, 318, 320, 335, 337, 353, 356, 360, 362, **369-436**, 446, 448-452, 457-500, 538, 618-619, 687-688, 692-694, 696, 700-702, 705, 707-714, 720-724, 726, 729-730, 732-736, 809, 814, 825-829, 833, 845-847, 859, 864-867, 872, 874, 881, 886-905, 909-914, 918-919, 921-924, 928, 942-943, 949, 953-968, 1062
Self-ignition.... 16, 18-19
Self-ignition temperature....16, 19
Semenov, Nikolai....47, 374
Semenov number....48, 393, 450
Semenov theory....**46-51**, 91, 149, 191, 220, 360, 375, 403, 420-421, 426, 428, 449-450
Semtex....454
Sensitivity....19, 82, 152, 167, 281, 337, 416, 422, 427-430, 433-434, 446-447, 455, 457, 459, 461-462, 466-469, 472-474, 476, 482-487, 489, 517, 574, 598, 602, 626, 692-693, 695, 709, 799-801, 811-813, 903-904, 915-917
Sensitizers....472, 694
Series arcs....546, 774, 788, 795
Service drops....772
Sesame oil....886, 1058
Setaflash Test.... 193, 224-226
Setaram C80 calorimeter....428
Setaram MS80 calorimeter....428
Setchkin flask Test.... 222-223
Setchkin furnace (*see* ASTM D 1929)
Sewage....726, 826, 1066
Sewage sludge....826, 1066
Shampoo....686
Shear....459, 460, 462
Sheep....860
Shellac....480, 917
Shingles....241, 290, 501-503, 629, 630, 919, 967
Shock....10, **64-65**, 66, 101, 281, 446, **461-465**, 476, 477, 484, 559, 561, 684, 719, 749, 752, 794, 813, 853, 903, 909, 912, 921, 928
Shock waves....14, 36, 38, 66, 68-69, 97, 219, 449, 451, 454, 457, 459, 461, 463-464, 469, 470, 472, 487, 517, 537, 544, 568, 571, 621, 627
Shoddy....827, 1066
Shoes....560, 592, 825, 918, 921
Short arcs....536, 540
Short circuits.... 13, 18, 334, 553, 569, 728, 740, 743, 746, 766-767, 774, 776-781, 788, 792-793, 795, 797, 799, 802, 882
Shrapnel....454, 474, 622-623
Shredded materials....920
Shrubs....630, 834, 841
Siding.... 241, 290, 310, 528, 631, 674, 781-782, 920, 951, 962, 1075
Sieving....170, 174, 561, 923
Silage....845, 847
Silane (or silanes)....452, 902, **920-921**, 1051-1053
Silica.... 187, 485, 878, 881, 1066
Silicon.... 104, 526, 750, 875, 920, **921**, 1063, 1065
Silicon carbide....91, 104, 336, 511
Silicone fluids....921
Silicone oil....210, 211, 856
Silicone polymers....921
Silk....373, 816-818, 825, 827
Silos....555-557, 561, 736, 845, 847, 913
Silver 59, 72, 83-84, 353-354, 512, 536, 546, 765, 772, 879
Silver acetylide....469, 810
Silver azide....459, 468, 700
Silver fulminate....468, 810, 915
Silver nitrate....452, 469, 875
Silver nitride....468, 886
SIMS....22, 797, 799-800
Single-base powder....475
Single-compartment model....611
Single-component explosives....453, 467
Siwek 20 L sphere....174
Skin effect (electricity)....549, 573, 593
Skins....921
Skydrol 500B....1059
Slab, infinite....260, 380-381, 383, 390
Sleeving....780
Slosh....116, 217, 697
Sludge....553, 767
Slurries....454, 459, 694
Smoke bombs....915
Smoke explosions....617-618, 647
Smokeless powder....335, 468, 470, 475, 708, 810-811, 813, 854
Smoldering....8-9, 19, 144, 175, 237-238, 284, 288, **315-320**, 335, 369, 376, 390, 395, 399, 401-403, 484, 499, 505, 516, 569, 596, 617-618, 630, 650, 695, 706-707, 712, 716-718, 724, 729-732, 735-736, 755, 761,

776, 788, 803, 824, 827, 839-842, 844, 854, 869, 874, 882, 887, 897, 899-902, 909, 910, 913, 919, 922, 924, 928-929, 931, 937-939, 941, 950-953, 963
Smoldering to flaming transition 319-320, 395, 929, 952
Smolder inhibitors 318-319
SMRE 70-72, 171, 512, 603, 939
Snakes 766, 769, 787
Snap caps 915
Soap 891, 921, 1065
Soap powder 1065
Sodium 353, 358, 400, 481, 696, 706, 711, 750-752, **876**, 895, 902, 923
Sodium azide 455, 700, 884
Sodium benzoate 475
Sodium bicarbonate 474, 562
Sodium bromate 854
Sodium carbonate 708, 881
Sodium chlorate 485, 811, 894, 895, 912, **921-922**
Sodium chloride 474, 878
Sodium chlorite 891, 921-922
Sodium dichloro-s-triazinetrione 894
Sodium dihydroxy naphthalene-disulfonic acid 1066
Sodium di-isobutyl sulfosuccinate 1066
Sodium dithionite 371, 387, 401, 419, **922**
Sodium hydride 870
Sodium hydroxide 452, 875, 908
Sodium nitrate 526, 712, 827, 885, 917
Sodium perborate 1066
Sodium peroxide 452
Sodium tetracarbonylferrate 870
Sodium trichloro ethyl phosphate 1066
Soil 316, 824, 834, 855, **900-901**, 923, 955, 1076
Soiling 533, 935
Solar heating 396
Solder 221, 796, 922, 924
Soldered joints 924
Soldering irons 922
Solids 237-338
Solvasol 1058
Solvents 151, 184, 201, 310, 709, 713, 829, 858, 870, 876, 880, 888, 942
Solvents (*see also* Chapter 15)
Solvents, chlorinated 200-202, 880
Soot films 690
Soots 689, 772, 922
Southern pine 964, 1074, 1077
Soybean meal 735, 826
Soybean oil 734, 886, 889, 1058
Soybeans 687, 922
Soy flour 833, 1064
Spalding B-number 151, 204, 227
Spandrel panels 528, 531
Spark arresters 506, 596
Spark duration, effect of 72, 80-81, 163-164, 205, 825
Spark gaps 79, 593
Spark guards 596
Sparklers 915-916
Sparks 2, 13-19, 43-44, 47, 54-55, 65-84, 95-96, 98, 101-104, 106, 114-115, 117-118, 120-121, 124-127, 146, 153, 159-161, 163-166, 170, 172, 192, 196, 202-207, 213-214, 216-217, 239, 252, 293-294, 296-297, 311-312, 322, 331, 334-335, 337, 467-468, 481, 506-516, 534, 536-540, 546-547, 551, 554-555, 557-563, 566, 572, 593-594, 596, 602-603, 614, 644, 683-684, 686, 690, 699-700, 727, 731, 736-737, 742-743, 754-755, 766, 788, 807, 811-813, 817, 825-826, 836, 844, 851-852, 871, 874, 876-877, 882, 898, 909, 915-916, 920, 922, 924, 933, 948-949, 1060, 1062
Spark Test Apparatus (STA) 216, 602
Spas 922
Specific gravity 197, 942
Specimen area, effect of 295-297
Specimen orientation, effect of 294
Spectral absorptivity 305-308, 821
Spectral emissive power 306
Spedding steel mill 509-510
Sperm oil 828
Spheres 45, 51-52, 54, 66-67, 69, 85, 91-92, 94, 99, 107, 117-118, 120, 125-128, 146, 159, 166-170, 173-176, 207, 288-289, 359, 378-381, 384-385, 388-392, 395, 402, 414, 416, 421, 425, 450, 467, 504-505, 538-539, 558, 570, 592, 699-700, 733, 777, 843, 879, 912, 957
Spills (of flammable liquids) 612-614
Splash loading 206, 565, 567
Sponge iron 372, 874
Spontaneous combustion 1, 4-7, 9, 11, 19, 36, 243, **369-436**, 687-688, 700, 708, 711-712, 720-721, 723, 726, 729, 734, 736, 826-829, 833, 845-847, 864-865, 881, 888, 892, 897, 899, 901, 903, 909, 911-912, 915, 918-919, 921, 923, 927, 956, 965-966
Spontaneous human combustion 372, 673, 859-861
Spontaneous ignition 16, 19-20, 43, 337, 485, 955, 959
Spontaneous ignition temperature 16, 19, 43
Spontaneous polymerization 448, 911
Spotting fires, spotting distances 503-505, 844-845
Spray electrification 565
Sprays 83, 190-192, 202, 204-207, 209, 211-212, 219, 226-227, 513, 565-566, 748, 850
Sprengel explosives 454
Spruce 242, 272-273, 840, 842, 847, 948, 965, 1077
Squibs 701
St. Elmo's fire 555, 569, 690
Stab igniters 472
Stability of explosives 457-459, 485-486
Stabilizers 400, 807, 910
Stab initiation 466
Staples, overdriven 668-669, 790
Starch 103, 516, 687, 712, 868
Starch paste 712
Starter mix 482, 916
Starters 653, 738, 754
Static electricity 6, 20, 123, 160, 167, 534, **553-567**, 591, 697-698, 736, 829, 879, 895-896, 914, 923
Statistics 2-6, 146, 172, 373, 473, 528, 557, 569-570,

629-630, 702-703, 727-729, 732, 737-740, 742-743, 793, 815, 833-834, 846, 858, 881-882, 913-914, 920, 924, 926, 928, 937
Statistics, international 3
Statistics, US national 2-4
Steam 14, 24, 36, 106, 434, 558, 565, 574, 704, 709, 713-714, 725, 730, 841, 845, 847, 856, 865, 867, 885, 892, 899, 924, 955-956, 958, 959, 960, 966
Steam ejectors 558
Steam explosions 14, 36, 841, 867, 885
Steam explosions (*see also* Explosions, physical)
Steam pipe ignitions 674, 955-960
Stearic acid 419, 694, 809, 872, 887, **922**, 1051-1053
Steel (*see* Iron and steel)
Steel, mild 509, 512-513, 516, 850, 873
Steel, silver 513
Steel, ultimate strength of 621, 624, 791
Steel bands 729
Steel decks 630
Steel turnings 922
Steel wool 828, 873
Stefan problem 195, 613
Steiner Tunnel 327, 727, 773
Stepped leader 568, 592
Steven Test 489
Stoddard solvent 205, 1058
Stoichiometric mixture 14, 20, **29**, 53, 76, 84, 107, 164, 614
Stone wool 881
Straw 278-279, 687, 718, 749, 836, 847, 886
Stray currents 20, 781-783
Streaming current 564-565, 852
Stress relaxation 756, 763
Strontium 353, 481-482, **876**, 885, 916
Strontium azide 810
Structure fires 2-3, 371-372, 737-738, 740, 766, 881
Styrene 20, 115, 119, 159, 209, 314, 448, 454, 562, 563, 897, 909, 910, **922**, 1051, 1052, 1053, 1070
Subcritical 375-376, 379, 383, 387-389, 407, 963
Sub-ignition 8, 45, 63-64, 250, 880
Submerged arc 941
Sucrose 448, 1051-1053
Sugar 161, 452, 481, 508, 687, 700, 736, 826, 833, 890-891, 916, 921, 923, 962
Sugar, powdered 1064
Sugar dust 508, 736
Sugar pine 271, 1077
Sulfamic acid 1051-1053
Sulfonation 451
Sulfur 59, 109-110, 149, 165, 168, 198, 319, 352, 374, 396, 455, 460, 475, 480-482, 512, 515, 526, 556, 559, 563, 623, 693, 710, 719-720, 766, 800, 802, 809, 811, 864-866, 868, 886, 912, 914, 915-917, 921, **923**, 927, 1051-1053, 1063
Sulfur dioxide 711, 745
Sulfuric acid 38, 452, 481, 707-708, 867
Sunflower oil 889, 1058
Sunset yellow lake 1066
Supercritical 375, 379, 383, 387-388, 392, 395, 407-408, 413, 415
Superficial decomposition 251
Superheat limit temperature 22, 622
Surface absorptivity 305-308
Surface flash 20, 321, 354
Surface roughness, effect of 310
Surge suppressor MOV devices 923
Surgical tubing 923
Suspicious fires 3-4
Sustained flaming 8, 15, 20, 193, 239, 242, 244, 246-247, **290-292**, 301, 309, 335, 650, 823, 836, 905, 949-950, 952
Swamp coolers 862
Switchboards 740, 769, 772
Switches, electric 540, 546
Switchgear 738, 769, 823
Sympathetic explosions 457
Synthetic oils 890
Tagliabue Test 223-225
Talc 1066
Taliani Test 485, 709
Tallow 1058
Tallow oil 1058
Tank resonance 548
Tanks 114, 121, 184, 202, 215-216, 476, 521, 564-567, 612, 620-624, 690, 697, 699, 738, 848, 851, 853, 863, 882, **923-924**
Tanks, asphalt storage 924
Tank trucks 558, 567
Tannins 729
Tantalum 356, 465, **876**, 1063, 1065
Tap-changing mechanisms 766
Tapers 5
Tapioca 735
Tar (*see* Asphalt)
Tar, wood 924
Tar kettles 919
Tar paper 502
Tartrazine lake 1066
TATB 394, 808, 812, 813, 814, 815, 1062
Tawa 1077
Tea, instant 833
Tea candles 704
Teapots 725
Techtron 1075
Teflon (*see* PTFE)
Tefzel (ethylene/tetrafluoroethylene copolymer) 628, 805
Telephones, cellular 924
Television receivers 5, 310, 704, 740, **924-926**
Temperature, effect of 77-78, 114-116, 158, 162, 207-213, 304, 396
Temperature, high ambient 499
Temperature limits of flammability 113, 183, 563
Tents 926
Terbium 876

Terminology 13-22
p-Terphenyl 1051-1053
Terrazzo 592
Tessenderloo (explosion) 692
Tetraborane 701, 1051-1053
Tetracene 472
Tetradecane 1051-1053
Tetraethyl lead 1051-1053
1,1,1,2-Tetrafluoroethane 1060
1,1,2,2-Tetrafluoroethane 1060
Tetrafluoroethylene 86, 786, 805, 1051-1053
Tetrahydrofuran 104, 806, 1051-1053
Tetrahydrofurfuryl alcohol 1051-1053
Tetrahydronaphthalene 1051-1053
Tetrahydropyran 1051-1053
Tetrahydrothiophene 1051-1053
Tetralin 194, 203-204, 206, 207, 219, 904-905, 1051-1053
Tetramethyldiarsane 695
Tetramethyl lead 1051-1053
2,2,3,3-Tetramethyl pentane 1051-1053
Tetramethyl silane 1051-1053
Tetranitromethane 808, 814, 1051-1053
Tetrazene 454, 810, 813-814
Tetryl 122, 459, 471-472, 488, 808, 810-814, 1051-1053, 1062
Textile wall coverings 926
Tewarson's procedure 264
Thatch 926
Thermal Activity Monitor 22, 428
Thermal analysis tests 338, 412, 414, 416, 423, 425, **428-433**, 705, 707, 714, 715, 817, 893, 900, 910, 961
Thermal arrest 400
Thermal conductivity 35, 50-51, 67, 79, 92, 127, 204, 209, 224, 226, 243, 255, 257, 265-266, 269, 274, 288-289, 291, 303, 315, 337, 358-359, 371, 374, 377, 390, 393, 395, 398, 402, 408-409, **410**, 411-412, 414-415, 417, 419, 422, 426, 432, 449, 455, 462, 465-466, 477, 500, 508, 549, 552, 626, 685, 695, 701, 703-704, 714, 719, 723, 759, 826, 845-846, 874, 881, 894, 901, 904, 942, 947-948, 953, 955, 962, 966, 1072-1077
Thermal cutout devices 651-652, 725, 731, 733, **741-742**, 752, 754, 848, 856-858, 922
Thermal degradation 240, 313, 707, 753, 758-759, 767, 779, **791-793**, 942
Thermal diffusivity ...36, 67-68, 93, 396, 403, 409, 415-417, 517, 942, 1072
Thermal explosions 15, 24, 37, 47, 53, 282, 377, 403-404, 448-449, 457, 462-463
Thermal inertia 219, 243-244, 262-264, 269, 271, 292-293, 306, 308, 310, 332, 426, 477, 479, 500, 618, 761, 788, 832, 844, 926, 953, 958, 1072
Thermal insulation (*see* Mineral wool; Plastics)
Thermal insulation, excessive 780-781
Thermal lagging (*see* Pipe insulation)
Thermally-thick solids 256-259, 263, 265-269, 271-275, 297, 303, 332, 468, 477, 479, 481, 574, 787, 831-832, 853, 906, 934, 946
Thermally-thin solids 247, 253, 259, 263, 265-269, 272-275, 284, 297, 303, 309, 332, 574, 816, 819, 837, 854, 933, 934
Thermal penetration depth 271, 303, 500
Thermal protection 624, 725, 754-755, 858
Thermal response parameter 22, 259, 264
Thermal runaway 19-20, 43, 47-49, 52, 95, 358, 369-370, 373, 374, 377, 378, 380, 385, 389, 391, 395-396, 398-399, 402-403, 405-406, 408-409, 413-414, 417, 421, 430, 450, 457, 459, 687, 693, 710, 712, 714, 722-723, 725, 730, 733, 776, 826, 828-829, 833, 845-846, 865, 867, 874, 891, 894, 899, 903-905, 909-912, 927, 955, 957-958, 966
Thermal siphons 715
Thermite 480-481, 508-509, 512, 627, 672, 858, 877, 898, 916
Thermochemistry **24-32**, 422, 425, 447
Thermostats 661-662, 719, 725, 728, 732-733, 741-744, 762, 855-857, 928
Thickness, effect of 272-274
Thioglycolic acid 854
Thiophene 1051-1053
Thiourea dioxide 1066
Thomas, Philip 374, 489
Thorium 353, 359, 452, 509, 512, 870, **877**, 1063
Thorium dihydride 870
Thulium 876
Thunder 570
Thunderstorms 568, 570
TIG 941
Tiles 219, 293, 312, 502, 629, 753, 829-830, 832, 906, 959, 1073
Time of storage 396
Tin 72, 86, 319, 353, 512, 546, 625, 711, 763, 765, 772, **877**, 923, 1063
Tinder 38, 507, 517, 778, **926**
Tires 883, 895, **926-928**
Tires, shredded 927-928
Titanium 86, 89, 124, 153, 353, 355, 356, 359, 481, 509, 512, 514, 515-516, 625-626, 690, **877-878**, 915, 917, 1063, 1065
TNA 808, 811
TNB 462, 808, 811
TNT 433, 453-456, 458-459, 462-464, 471-472, 478, 484, 559, 574, 619, 622, 718, 808-815, 921, 952, 1051-1053, 1062, 1066
Toasters 739, 741, 794, **928**
Tobacco 241, 687, 716, 826, 836, 845, 930
Tocopherols 888
Toe puffs 708
Toilet paper 864, 899
Toluene 115, 119, 507, 558, 562-563, 594, 683, 717, 1051-1053
2,4-Toluene diisocyanate 1051-1053
Tomato base, spray dried 1066

Torque....759, 764
Towels....401, 673, 712, 718, 731, 733-734, 747, 749, 765, 776, 818, 821-822, 828, 869, 899, 922, 1073
Town gas....87, 93, 94, 508-510, 557, 717, **928**
Townsend discharge....534
Tracking....13, 20-21, 120, 309, 312-314, 326, 333-334, 499, 663-664, 671, 753, 759, 767, 769, 773-775, 786, 788, 793, 804-805, 855, 919, 960
Tractors....596, 834
Tramp metal....152-153, 175, 508, 896, 965
Trans-2-pentene....1048-1050
Transformer oil....544, 566, 766, 768, 904, 1058
Transformers (*see* Electric transformers)
Transient flaming....20, 239, 290, 952
Transient ignition....8, 242, 275, 328, 650, 735, 952
Transitory flaming....20
T-rating....597
Treeing (of electrical insulation)....312, 790-791
Trees....313, 503, 569, 630, 716, 834, 836, 839-842, 926, 961-962, 965, 1076
Triacetate....821, 824
Triacetone triperoxide....455, 808, 903
Triboelectric series....554
Tricalcium phosphate....694
Trichlor....894
1,2,4-Trichlorobenzene....1051-1053
Trichlorocarbobutoxyphenyl oxalate....481
1,1,1-Trichloroethane....1051-1053, 1060
Trichloroethylene....1051-1053
Trichlorofluoromethane....1060
Trichloro isocyanuric acid....1066
Trichloromethylsilane....1051-1053
1,2,3-Trichloropropane....1051-1053
Trichlorosilanes....31, 904, 920, 1051-1053
1,1,2-Trichloro-1,2,2-trifluoroethane....1060
Tricresyl phosphate....1059
1-Tridecene....1051-1053
Triethylaluminum....869
Triethyl amine....1051-1053
Triethylborane....869
Triethylene glycol....1051-1053
1,1,1-Trifluoroethane....1060
1,1,2-Trifluoroethane....1060
Trimethoxymethane....1051-1053
Trimethylamine....1051-1053
2,2,3-Trimethylbutane....1051-1053
Trimethylene glycol....1051-1053
2,4,6-Trinitrotoluene....448, 455, 1051-1053
1,3,5-Trioxane....1054-1055
Triple bonds....683
Triple-base powder....475
Triple-base propellants....458
Tripropylamine....1054-1055
Tripropylene....1054-1055
Triptane....1051-1053
Tris(2,3-dibromopropyl)phosphate....322
True vapor pressure....216, 697
Tundra....840
Tung oil....873, 888, 889, 1058
Tungsten....70, 73, 84-86, 94-96, 163, 176, 218, 272-273, 297, 305-306, 332-333, 335, 354-355, 541, 546, 602, 705, 747-749, 752, 821, **878**, 899, 932, 1063, 1065, 1066
Tungsten carbide....513-514
Turbine oil....209, 211, 218, 1058
Turbulence....36, 38, 59-60, 68, 79, 116, 118, 121, 144-145, 149, 156, 163, 166, 207, 249, 252, 515, 542, 565, 568, 595, 612, 619, 863
Turnings....922
Turpentine....184, 562, 683, 866, 892, 928, 1058
TV antennas....569
TV sets (*see* Television receivers)
Twisting....731, 759, 764, 791, 855
Twist-on connectors....663, 762-765
Type of pilot....292-294, 948
Ucon 50 HB-260....1059
Udel P-1700....1075
UDMH....119, 476, 811, 891, **928**, 1054-1055
UFAC....935-936
UL 4....773
UL 44....327, 773
UL 62....327, 773
UL 83....327, 773
UL 94....287, 309-310, **323-328**, 727, 741, 784-785, 855, 907-908, 925-926
UL 96A....594
UL 411....716
UL 444....773
UL 489....781
UL 492....925
UL 493....773
UL 498....759-761
UL 525....596
UL 588....753
UL 698....603
UL 719....773
UL 746A....327, 333-334
UL 746B....792
UL 746C....326-327, 740-741, 918
UL 758....773
UL 790....335
UL 817....773, 779, 794
UL 854....773
UL 910....773
UL 913....17, 24, 597, 602
UL 964....743
UL 1082....725
UL 1203....601
UL 1270....918
UL 1462....856
UL 1492....918, 925
UL 1567....763
UL 1571....752
UL 1581....327, 334, 773

UL 1642 743
UL 1666 773
UL 1685 773
UL 1694 ..... 326, 753
UL 1950 ..... 326, 327, 334, 727, 926
UL 2049 856
UL 2196 773
UL 6500 ..... 918, 926
UL 60335-1 741
Ultem 1000 1075
Unary reactions 104, 448, 451
Unconfined vapor cloud explosions 152, 619
1-Undecene 1054-1055
n-Undecane 1054-1055
Unified theories of gas ignition 120
Unimolecular reactions 376
Unpiloted ignition 19-20, 250, 292
UN Recommendations 405-406
Unreported fires 3, 5
Unstable substances 445-489
Unsymmetrical dimethylhydrazine (*see* UDMH)
UN Test 1(a) 484
UN Test 2(a) 484
UN Test 7(b) 484
UN Test H1 406
UN Test H2 ..... 421, 433
UN Test H3 ..... 432, 457
UN Test H4 422
UN Test N1 ..... 176, 640
UN Test N4 ..... 418, 730
UN Test N5 485
UN Test O1 ..... 434, 485
UN Test O2 ..... 435, 485
UN Tests 405, 484
UN Test S1 ..... 435, 827
Upholstered furniture 287, 317, 331, 502, 519, 521, 619, 703, 716, 719, 730, 815, 817, 911, 921, **928-938**
Upper flammability limit 22, 44, 77, 110, 148, 1023
Upper flammability limit (*see also* specific substances)
Upper flash point 193, 201
Upper temperature limit 22, 114, 193
Uranium 358, 359, 452, 509, 870, **878**, 886, 1063
Uranium hydride 452, 870
Urea 753, 864, 897, 1054-1066
Urea formaldehyde 323, 658, 754, 759, 907, 1064, 1070
Urea nitrate 455
Urine 787, 935
UVCE (*see* Unconfined vapor cloud explosions)
n-Valeraldehyde 1048-1050
Valeric acid 1054-1055
Vacuum cleaners 938-939
Vapor-freeing 215
Vapor pressure 15, 17, 18, 22, **184-186**, 192, 216, 696-697, 699, 702, 849, 851, 853
Vapor recovery canister 881
Variable Confinement Cookoff Test 487
Varistors 593, 923
Varnishes 226, 373, 428, 482, 897, 962
Varsol 1058
VCHZ Synthesia 454
VDI 3673 175
Vegetable oil 369, 400, 519, 733, 828, 886-889, 921
Vegetation 238, 289, 302, 390, 500-506, 531, 540, 574, 596, 630-631, 687, 716, 735, 738, 746, **833-847**, 883-884, 915, 918, 956
Vehicles 4, 532, 700, 739, 804, 807, 834, 852, 881-885, 891
Veld grass 837
Vent Sizing Package (VSP) 428
Vermin infestation 666-667, 787
Versilube F-50 1059
Vessel size, effect of 58-59, 157
Vibration 457, 517-518, 548, 734, 762, 787, 795, 804, 856
Victorian ash 1077
Vinyl acetate 21, 246, 786, 909, 1054-1055
Vinyl acetylene 447, 686, 717, 1054-1055
Vinyl asbestos 1070
Vinyl bromide 1054-1055
Vinyl chloride 28, 119, 620, 717, 809, 1054-1055
Vinyl cyanide 1024, 1025, 1026
Vinyl epoxy adhesive 1070
Vinyl ether 806, 1033-1035
Vinylidene chloride 119, 1054-1055
Vinyl methyl ether 1054, 1055
Vinyl toluene 119, 1054-1055
Viscous flow 459
Vitamins 903
VM&P naphtha 856, 1058
Volatile content, effect on dust cloud explosions 146-147, 154-155
Volume resistivity 152, 167, 558
Volumetric decomposition 251
VW-1 Test 327, 334, 753
Waferboard 1076
Wall material, effect of 59, 79, 87-89, 221
Wardrobes 521
Washers, clothes (*see* Washing machines)
Washing machines 5, 686, **733-734**, 762, 739-740, 905
Wastebaskets 718, 899
Wastes 726, 833, 911, **939**, 956, 965-966
Water, acid rain 562
Water, deionized 562
Water, effect of 310
Waterfalls 565
Water gel 810
Water heaters 5, 612, 739, 848, 851, **939-941**
Water-reactive materials 452
Wax 184, 472, 475, 482, 484, 693, 703-704, 728-729, 809, 868-869
Wear 513, 592, 787, 792-793, 820, 912, 935
Weathering 310, 713, 720-722, 874, 954
Wedge Test 487
Weed killer 921-922

Welded contacts 661, 762
Welders, arc 735, 784
Welding 4-5, 44, 152, 173, 184, 215, 237, 287, 452, 500, 506-507, 625, 685-686, 726, 736, 738-739, 762, 765, 782, 815, 824, 826, 834, 864, 882-883, 890, 901, 918, 922-924, 927, **941**, 952
Welding, ultrasonic 459
Welding slag 237, 287, 506-507, 941, 952
Welding spatter 500, 506-507, 726, 890
Welding torches 173, 452, 815, 834
Westerberg apparatus 99, 128, 597
Wet fire 855
Wetting by water, effect of 310
Wet-tracking 313
Wheat 153, 156, 168, 516, 687, 688, 833
Wheat starch 1064
Wheeler Test (No. 1) 153
Wheels 829, 857, 883, 927
White gasoline 702
White spirit 1058
Wildland-urban interface 629-631
Will o' the wisp 903
Window frames 569, 629, 649-650
Window glass 533-534
Wire (*see* Electric cables; Electric wires)
Wire gauge sizes ..... endpaper
Wire gauze 406, 433, 594
Wire Nuts (*see* Twist-on connectors)
Wood 9, 144, 168, 219, 237-246, 248-249, 251-253, 255, 257, 261, 269, 271-274, 286-287, 289-290, 292-293, 295, 297-300, 303-304, 309-312, 315-316, 318-320, 326, 335, 338, 369, 371, 379, 385, 387, 389, 395, 397-402, 410-413, 453, 455, 457, 501-506, 515, 518-521, 523-524, 527-531, 546, 552, 558-559, 569, 571, 574, 617-618, 629-631, 695, 701, 704-707, 710, 712-713, 715-716, 718, 736, 742, 749, 752-754, 757, 761-762, 764-765, 767, 781-782, 786, 788, 797, 824, 826, 830, 837, 847, 855, 858-859, 868, 885, 891, 892, 895, 897, 913, 919-920, 922, 924, 926, 931, 934, 940, **942-967**, 1064, 1073, 1076-1077
Wood, arc tracking 960-961
Wood, glowing or smoldering 950-952
Wood, ignition from flue pipes 960
Wood, ignition from hot pipes 674, 955-960
Wood, ignition temperature 944-946
Wood, old 954, 965
Wood, painted 962
Wood, self-heating of 955-960, 963-967
Wood bark 1064
Wood-burning appliances 967
Wood chips 370, 398, 847, 944, 956-958, **965-966**
Wood components 943, 961-962
Wood distillation 710
Wood dust 144, 155, 168, 370, 379, 389, 397, 401, 506-507, 712, 826, 836-837, 885, 895, 897, 915-916, 921, 952, 955-960, **965-967**
Wood dust, oiled 966-967
Wood fiberboard (*see* Fiberboard)
Wood flour 155, 1064
Wood pulp 967
Wood sawdust (*see* Wood dust)
Wood shakes 502, 967
Wood shavings 506, 718, 922, 950, 956, 966
Wood shingles 502, 967
Wood stains 897
Wood wastes 966
Wool 289, 372, 379, 391, 408, 410, 433, 502, 506-507, 558, 708, 736, 781, 816-818, 820-822, 824-825, 827, 829-832, 842, 844, 880-881, 905, 931-932, 933, 935, 938, 957, **967-968**, 1073
Wrenches 508
Wrist straps 592
XLPE 22, 772, 785, 786, 793, 905, 1070
X-rays 21, 469, 550, 571, 574, 709-710, 756, 761-762, 797, 799, 801
Xylene 115, 122, 200, 562
m-Xylene 194, 1054-1055
o-Xylene 194, 1054-1055
p-Xylene 194, 1054-1055
Yeast 687, 1064
Yellow G 1066
Yellowing 404
Ytterbium 876
Yttrium 509
Zinc 38, 72-73, 86, 89, 319, 353, 359, 512, 514, 546, 602, 624, 626, 685, 693, 713, 762-765, 795, 801-802, 868, 870, 875, **878**, 891, 897, 915, 923, 1063, 1065, 1066
Zinc chloride 713
Zinc oxide 802, 868, 1066
Zinc powder 915
Zirconium 174, 353, 355-356, 358-359, 509, 512, 514, 541, 870, **878-879**, 888, 1063

Copyright © 2003, 2014 Vytenis Babrauskas

Constants

e = 2.718 (base of Napierian logarithms)
$\varepsilon_o = 8.845\times10^{-12}$ F m^{-1} (electrical permittivity of a vacuum)
$\sigma = 5.67\times10^{-11}$ kW m^{-2} K^{-4} (Stefan-Boltzmann radiation constant)
R = 8.314 J mol^{-1} K^{-1} (universal gas constant)
R = 8.314 Pa m^3 mol^{-1} K^{-1} (universal gas constant, using alternate units)
$R = 82.1\times10^{-6}$ m^3 atm K^{-1} mol^{-1} (universal gas constant, using alternate units)
Molar volume = 22.414 L mol^{-1} (at 1 atm and 0°C)
Molar volume = 24.055 L mol^{-1} (at 1 atm and 20°C)
Molar mass of dry air = 28.96 g mol^{-1}
Density of air (kg m^{-3}) at 1 atm pressure = 353/T , where T = temperature (K)
Density of any gas (kg m^{-3}) at 1 atm pressure = 12.18 M/T,
where M = molar mass (g mol^{-1}), T = temperature (K)
Fraction of oxygen in dry air = 20.95 vol%

Volumes and areas

Sphere: $V = (4/3)\pi r^3$ $A = 4\pi r^2$
Cylinder: $V = \pi r^2 L$ $A = 2\pi r L$

Conversion factors

Density
1 PCF = 16.03 kg m^{-3}
Distance
1 in = 25.4 mm
1 ft = 0.3048 m
Electric charge
1 C = 1 A•s
Energy
1 J = 1 N•m = 1 kg m^2 s^{-2}
1 BTU = 1055 J
1 cal = 4.184 J
Power
1 BTU/h = 0.293 W
Mass
1 lb = 0.454 kg
Pressure
1 atm = 101,300 Pa = 101.3 kPa
1 psi = 0.068 atm = 6888 Pa = 6.888 kPa
1 bar = 100,000 Pa = 100 kPa = 0.987 atm
Surface weight
1 oz yard^{-2} = 33.93 g m^{-2}
Sprinkler density
1 GPM ft^{-2} = 679 g m^{-2} s^{-1} = 0.679 mm s^{-1} = 40.7 mm min^{-1}
Temperature
K = °C + 273
°F = (9/5)°C + 32
Volume
1 gallon (US) = 3.785 L

Copyright © 2003, 2014 Vytenis Babrauskas

American Wire Gauge sizes

AWG	Diameter (mm)	Area (mm^2)
50	0.0254	0.000507
48	0.0305	0.00073
46	0.0406	0.00130
44	0.0508	0.00203
42	0.0635	0.00317
40	0.0787	0.00487
38	0.102	0.00811
36	0.127	0.0127
34	0.160	0.0201
32	0.203	0.0324
30	0.254	0.0507
28	0.320	0.0804
26	0.404	0.128
24	0.511	0.205
22	0.643	0.324
20	0.813	0.519
18	1.02	0.823
16	1.29	1.31
14	1.63	2.08
12	2.05	3.31
10	2.588	5.26
8	3.264	8.37
6	4.115	13.30
4	5.189	21.15
2	6.543	33.62
1	7.348	42.41
1/0	8.252	53.49
2/0	9.266	67.43
3/0	10.40	85.01
4/0	11.68	107.2